

ORGANOMETALLICS

Volume 14, Number 10, October 1995

© Copyright 1995
American Chemical Society

Communications

Formation of the Metal-Coordinated Chelating Bis-Phosphorus Ligand $\text{Ph}_2\text{PN}(\text{Et})\text{C}(\text{O})\text{PPh}_2$ via a Novel [3 + 2] Cycloaddition between the Phosphenium Complexes $\text{Cp}(\text{CO})(\text{HPh}_2\text{P})\text{M}=\text{PPh}_2$ ($\text{M} = \text{Mo}, \text{W}$) and Ethyl Isocyanate¹

Wolfgang Malisch* and Helmut Pfister

*Institut für Anorganische Chemie der Universität Würzburg, Am Hubland,
D-97074 Würzburg, Germany*

Received May 23, 1995[®]

Summary: Convenient access to the unusual hydrido complexes $\text{Cp}(\text{CO})(\text{H})\text{MPPh}_2\text{C}(\text{O})\text{N}(\text{Et})\text{PPh}_2$ ($\text{M} = \text{Mo}$ (**4a, a'**), W (**4b, b'**)), obtained as mixtures of two isomers, is established via cycloaddition between the phosphenium complexes $\text{Cp}(\text{CO})(\text{HPh}_2\text{P})\text{M}=\text{PPh}_2$ (**2a, b**) and EtNCO (**3**). Reaction of **4a, b** with carbon tetrachloride yields the analogous chloro complexes $\text{Cp}(\text{CO})(\text{Cl})\text{MPPh}_2\text{C}(\text{O})\text{N}(\text{Et})\text{PPh}_2$ (**5a, a'**, **5b, b'**); **5b'** has been characterized by X-ray analysis.

In keeping with our studies concerning the reactivity of the secondary phosphine substituted phosphenium complexes $\text{Cp}(\text{CO})(\text{HPh}_2\text{P})\text{M}=\text{PPh}_2$ ($\text{M} = \text{Mo}$ (**2a**), W (**2b**)), characterized by a stereogenic metal center, we have described the chemo- and regioselective [2 + 2] cycloaddition with isothiocyanates.² In analogy to the reactions of the basic system $\text{Cp}(\text{CO})_2\text{M}=\text{PPh}_2$ ($\text{M} = \text{Mo}, \text{W}$)³ the cycloadducts contain the four-membered-ring skeleton $\text{M}-\text{P}-\text{C}-\text{S}$.

In this communication we present the reaction of these phosphenium complexes with ethyl isocyanate (**3**), which dramatically deviates from the known pattern.

It yields five-membered diphosphetacycles via a novel type of [3 + 2] cycloaddition between the central P—M—P bonding system of **2a, b** and the C=N bond of ethyl isocyanate (**3**).

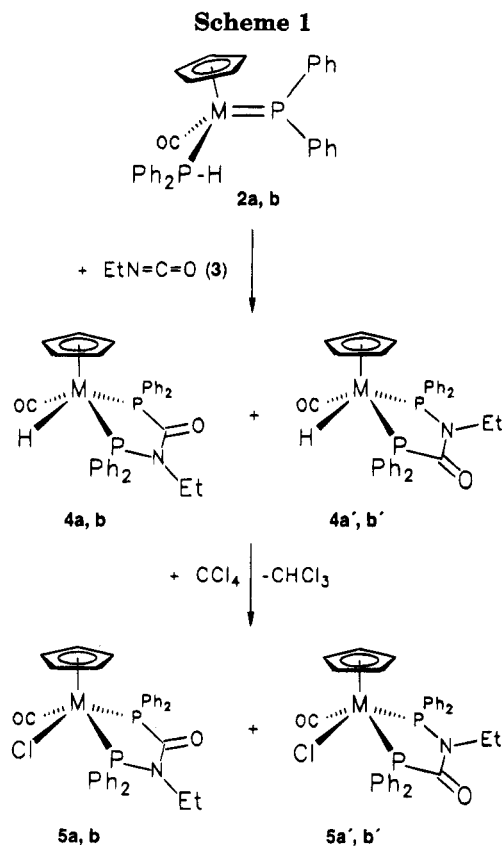
Addition of **3** to a freshly prepared solution of the phosphenium complexes **2a, b**² in toluene, generated by dehydrochlorination of $\text{Cp}(\text{CO})(\text{HPh}_2\text{P})_2\text{MCl}$ (**1a, b**) with 1,8-diazabicyclo[5.4.0]undec-7-ene (DBU), causes a slow change of the color from green (**2a**) or blue (**2b**) to brown. After a reaction period of 1 (**4a**) or 4 days (**4b**) the hydrido complexes **4a, b** are obtained after chromatographic purification as pale yellow microcrystalline powders, showing moderate solubility in aromatic solvents.⁴ Complexes **4a, b** can be described as the product of a formal [3 + 2] cycloaddition, accompanied by a shift of the P-bonded hydrogen to the metal (Scheme 1).

Addition of ethyl isocyanate (**3**) occurs chemoselectively at the C=N double bond, creating a new kind of PNCP-chelating ligand, which to our knowledge has so far not been accessible in the free state. The NMR spectra reveal the existence of mixtures of two diaster-

(3) (a) Fried, A.; Malisch, W.; Schmeusser, M.; Weis, U. *Phosphorus, Sulfur Silicon Relat. Elem.* **1992**, 65, 75. (b) Malisch, W.; Hirth, U.-A.; Fried, A.; Pfister, H. *Phosphorus, Sulfur Silicon Relat. Elem.* **1993**, 77, 17. (c) Spörl, A.; Hindahl, K.; Fried, A.; Pfister, H.; Malisch, W. In *Selective Reactions of Metal-Activated Molecules*, Werner, H., Griesbeck, A. G., Adam, W., Bringmann, G., Kiefer, W., Eds.; Vieweg: Braunschweig, Germany, 1992; p 191. (d) Fried, A.; Hahner, C.; Malisch, W. In ref 1c, p 195.

[®] Abstract published in *Advance ACS Abstracts*, August 15, 1995.
(1) Phosphenium Transition Metal Complexes. 36. Part 35: Guntzelmann, N.; Fey, O.; Malisch, W. *J. Organomet. Chem.*, submitted for publication.

(2) Pfister, H.; Malisch, W. *J. Organomet. Chem.* **1992**, 439, C11.



eomers **4a,a'** (ratio 5:2) and **4b,b'** (ratio 2:1), indicating that both modes of the C=N bond addition to the two phosphorus atoms have been realized, leading to a product with the hydrido ligand in a position *cis* either to the nitrogen or to the carbon-bonded phosphorus.

(4) Experimental details are given in the supporting information. Analytical and spectroscopic data are as follows. **[1,2-Bis(diphenylphosphino)-1-ethyl-2-oxo-1-azaethane-P,P']carbonyl(η^5 -cyclopentadienyl)hydridomolybdenum(II) (4a,a')**: mp 202 °C dec. Diastereomeric ratio: 5:2 (determined as for the following compounds by integration of the H_5C_5 NMR signal). Main diastereomer (**4a**): 1H NMR (400.1 MHz/ D_6]benzene) δ 8.50–6.91 (m, 20 H, H_5C_5), 4.36 (s, 5H, H_5C_5), 3.68 (m, 1 H, H_2C), 3.02 (m, 1 H, H_2C), 0.25 (m, 3 H, H_3C), –8.10 ppm (dd, $^2J_{PMoH} = 80.1$ Hz, $^2J_{PNMoH} = 19.2$ Hz, 1 H, HMo) (N-bonded phosphorus marked as P^a and C-bonded as P^b); ^{13}C NMR (100.6 MHz/ D_6]benzene) δ 237.27 (br, OCMo), 185.55 (br, C(O)), 141.00–126.00 (C_6H_5), 86.89 (s, C_5H_5), 40.98 (s, CH_2), 10.93 ppm (s, CH_3); ^{31}P NMR (162.0 MHz/ D_6]benzene): δ 131.53 (d, $^2J_{PMoP} = 77.1$ Hz, PN), 87.06 ppm (d, $^2J_{PMoP} = 77.1$ Hz, PC); IR (toluene) ν 1864 (vs, CO), 1644 (m, C(O)) cm^{-1} . Minor diastereomer (**4a'**): 1H NMR (400.1 MHz/ D_6]benzene) δ 8.50–6.91 (m, 20 H, H_5C_5), 4.29 (s, 5 H, H_5C_5), 3.57 (m, 1 H, H_2C), 3.02 (m, 1 H, H_2C), 0.20 (m, 3 H, H_3C), –8.15 ppm (d, br, $^2J_{PMoH} = 60.0$ Hz, 1 H, HMo); ^{31}P NMR (162.0 MHz/ D_6]benzene) δ 141.54 (d, $^2J_{PMoP} = 79.5$ Hz, PN), 90.35 ppm (d, $^2J_{PMoP} = 79.5$ Hz, PC); IR (toluene) ν 1864 (vs, CO), 1644 (m, C(O)) cm^{-1} . Anal. Calcd for $C_{33}H_{31}MoNO_2$ (631.5): C, 62.76; H, 4.95; N, 2.22. Found: C, 62.54; H, 5.12; N, 2.08. **[1,2-Bis(diphenylphosphino)-1-ethyl-2-oxo-1-azaethane-P,P']carbonyl(η^5 -cyclopentadienyl)hydridotungsten(II) (4b,b')**: mp 210 °C dec. Diastereomeric ratio: 2:1. Main diastereomer (**4b**): 1H NMR (400.1 MHz/ D_6]benzene) δ 8.05–6.90 (m, 20 H, H_5C_5), 4.32 (s, 5 H, H_5C_5), 3.67 (dq, $^2J_{HCH} = 13.2$ Hz, $^3J_{HCH} = 7.0$ Hz, $^3J_{PNCH} = 6.6$ Hz, 1 H, H_2C), 3.14 (dq, $^2J_{HCH} = 13.2$ Hz, $^3J_{HCH} = 6.9$ Hz, $^3J_{PNCH} = 3.3$ Hz, 1 H, H_2C), 0.18 (t, $^3J_{HCH} = 6.9$ Hz, 3 H, H_3C), –7.80 ppm (dd, $^2J_{PWH} = -72.9$ Hz, $^2J_{PNWH} = 18.5$ Hz, 1 H, HW); ^{13}C NMR (100.6 MHz/ D_6]benzene) δ 228.23 (d, $^2J_{PWC} = 12.85$ Hz, OCW), 180.76 (d, $^1J_{PC} = 53.9$ Hz, C(O)), 140.76–126.64 (C_6H_5), 84.90 (s, C_5H_5), 40.90 (dd, $^2J_{PNC} = 4.2$ Hz, $^3J_{PCNC} = 4.2$ Hz, CH_2), 10.91 ppm (s, CH_3); ^{31}P NMR (162.0 MHz/ D_6]benzene) δ 100.43 (d, $^2J_{PWP} = 56.4$ Hz, $^1J_{WP} = 283.1$ Hz, PN), 59.64 ppm (d, $^2J_{PWP} = 56.4$ Hz, $^1J_{WP} = 297.8$ Hz, PC); IR (toluene) ν 1853 (vs, CO), 1651 (m, C(O)) cm^{-1} . Minor diastereomer (**4b'**): 1H NMR (400.1 MHz/ D_6]benzene) δ 8.05–6.90 (m, 20 H, H_5C_5), 4.18 (s, 5H, H_5C_5), 3.42 (dq, $^2J_{HCH} = 13.3$ Hz, $^3J_{HCH} = 6.9$ Hz, $^3J_{PNCH} = 6.7$ Hz, 1 H, H_2C), 3.05 (dq, $^2J_{HCH} = 13.3$ Hz, $^3J_{HCH} = 6.9$ Hz, $^3J_{PNCH} = 2.7$ Hz, 1 H, H_2C), 0.09 (t, $^3J_{HCH} = 6.9$ Hz, 3 H, H_3C), –8.00 ppm (dd, $^2J_{PWH} = 58.2$ Hz, $^2J_{PNWH} = 12.6$ Hz, 1 H, HW); ^{13}C NMR (100.6 MHz/ D_6]benzene) δ 230.77 (d, $^2J_{PWC} = 15.2$ Hz, OCW),

The structure of **4a,a'** and **4b,b'** follows especially from the 1H NMR spectra,⁴ exhibiting two M–H resonances at approximately –8.0 ppm, with a coupling constant $^2J_{PWH}$ of about 75 (**4a,b**) or 60 Hz (**4a',b'**) to the *cis*-positioned phosphorus and of 20 Hz (maximum) to the *trans*-positioned phosphorus.^{5,6} Further evidence is given by the off-resonance-decoupled ^{31}P NMR spectra, showing a splitting of the P(N) signal in the main diastereomer **4a,b** or the P(C) signal in the minor diastereomer **4a',b'**, due to coupling with the *cis* hydrido ligand.

A reasonable explanation for the unexpected behavior of the phosphonium complexes **2a,b** is based on an equilibrium between **2** and its tautomer **A**, which is the result of a P → M hydrogen shift (Scheme 2). **A** is characterized by two electronically different phosphorus atoms, one of the phosphido (nucleophilic) and one of the phosphonium type (electrophilic), suggesting 1,3-dipolar behavior.

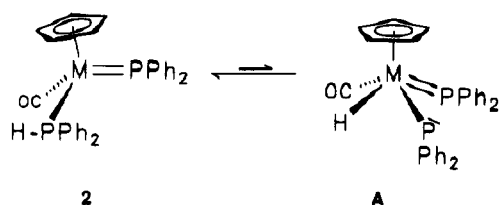
Although **A** is not observable in solution even at –60 °C by NMR spectroscopy, indicating extremely low concentration in the equilibrium (Scheme 2), support

181.07 (d, $^1J_{PC} = 53.9$ Hz, C(O)), 140.76–126.64 (C_6H_5), 85.38 (s, C_5H_5), 41.49 (dd, $^2J_{PNC} = 3.8$ Hz, $^3J_{PCNC} = 3.8$ Hz, CH_2), 10.46 ppm (s, CH_3); ^{31}P NMR (162.0 MHz/ D_6]benzene) δ 110.91 (d, $^2J_{PWP} = 61.2$ Hz, $^1J_{WP} = 319.4$ Hz, PN), 61.21 ppm (d, $^2J_{PWP} = 61.2$ Hz, $^1J_{WP} = 268.2$ Hz, PC); IR (toluene) ν 1853 (vs, CO), 1651 (m, C(O)) cm^{-1} . Anal. Calcd for $C_{33}H_{31}NOP_2W$ (719.41): C, 55.10; H, 4.31; N, 1.95. Found: C, 55.30; H, 4.15; N, 1.71. **[1,2-Bis(diphenylphosphino)-1-ethyl-2-oxo-1-azaethane-P,P']carbonylchloro(η^5 -cyclopentadienyl)molybdenum(II) (5a,a')**: mp 96 °C dec. Diastereomeric ratio: 3:2. Main diastereomer (**5a**): 1H NMR (400.1 MHz/ $CDCl_3$) δ 8.03–7.01 (m, 20 H, H_5C_5), 4.30 (d, $^3J_{PMoCH} = 2.2$ Hz, 5 H, H_5C_5), 3.83 (dq, $^2J_{HCH} = 13.4$ Hz, $^3J_{HCH} = 6.7$ Hz, $^3J_{PNCH} = 6.7$ Hz, 1 H, H_2C), 3.02 (dq, $^2J_{HCH} = 13.4$ Hz, $^3J_{HCH} = 6.7$ Hz, $^3J_{PNCH} = 6.7$ Hz, 1 H, H_2C), 0.14 ppm (t, $^3J_{HCH} = 6.7$ Hz, 3 H, H_3C); ^{13}C NMR (100.6 MHz/ $CDCl_3$) δ 248.04 (d, $^2J_{PMoC} = 24.1$ Hz, OCMo), 180.86 (dd, $^1J_{PC} = 43.1$ Hz, $^2J_{PNC} = 28.1$ Hz, C(O)), 141.00–127.27 (C_6H_5), 94.89 (s, C_5H_5), 42.57 (dd, $^2J_{PNC} = 4.0$ Hz, $^3J_{PCNC} = 4.0$ Hz, CH_2), 11.67 ppm (s, CH_3); ^{31}P NMR (162.0 MHz/ $CDCl_3$) δ 115.91 (d, $^2J_{PMoP} = 76.7$ Hz, PN), 88.14 ppm (d, $^2J_{PMoP} = 76.6$ Hz, PC); IR (toluene) ν 1892 (vs, CO), 1647 (m, C(O)) cm^{-1} . Minor diastereomer (**5a'**): 1H NMR (400.1 MHz/ $CDCl_3$) δ 8.03–7.01 (m, 20 H, H_5C_5), 4.35 (d, $^3J_{PMoCH} = 2.0$ Hz, 5 H, H_5C_5), 3.24 (dq, $^2J_{HCH} = 13.5$ Hz, $^3J_{HCH} = 6.7$ Hz, $^3J_{PNCH} = 3.7$ Hz, 1 H, H_2C), 2.92 (dq, $^2J_{HCH} = 13.5$ Hz, $^3J_{HCH} = 6.7$ Hz, $^3J_{PNCH} = 4.1$ Hz, 1 H, H_2C), –0.08 ppm (t, $^3J_{HCH} = 6.7$ Hz, 3 H, H_3C); ^{13}C NMR (100.6 MHz/ $CDCl_3$) δ 251.24 (d, $^2J_{PMoC} = 27.2$ Hz, OCMo), 181.37 (dd, $^1J_{PC} = 43.0$ Hz, $^2J_{PNC} = 25.7$ Hz, C(O)), 141.00–127.27 (C_6H_5), 95.89 (s, C_5H_5), 42.78 (dd, $^2J_{PNC} = 3.7$ Hz, $^3J_{PCNC} = 3.7$ Hz, CH_2), 11.14 ppm (s, CH_3); ^{31}P NMR (162.0 MHz/ $CDCl_3$) δ 144.35 (d, $^2J_{PMoP} = 91.7$ Hz, PN), 63.42 ppm (d, $^2J_{PMoP} = 91.7$ Hz, PC); IR (toluene) ν 1892 (vs, CO), 1647 (m, C(O)) cm^{-1} . Anal. Calcd for $C_{33}H_{30}ClMoNO_2P_2$ (665.95): C, 59.52; H, 4.54; N, 2.10. Found: C, 59.04; H, 4.54; N, 1.76. **[1,2-Bis(diphenylphosphino)-1-ethyl-2-oxo-1-azaethane-P,P']carbonylchloro(η^5 -cyclopentadienyl)tungsten(II) (5b,b')**: mp 106 °C dec. Diastereomeric ratio: 1:1. Diastereomer **5b**: 1H NMR (400.1 MHz/ $CDCl_3$) δ 8.05–7.15 (m, 20 H, H_5C_5), 4.39 (d, $^3J_{PWCH} = 2.4$ Hz, 5 H, H_5C_5), 3.88 (dq, $^2J_{HCH} = 13.5$ Hz, $^3J_{HCH} = 6.7$ Hz, $^3J_{PNCH} = 6.7$ Hz, 1 H, H_2C), 3.24 (dq, $^2J_{HCH} = 13.4$ Hz, $^3J_{HCH} = 6.7$ Hz, $^3J_{PNCH} = 6.7$ Hz, $^3J_{PCPNCH} = 2.7$ Hz, 1 H, H_2C), 0.16 ppm (t, $^3J_{HCH} = 6.7$ Hz, 3 H, H_3C); ^{13}C NMR (100.6 MHz/ $CDCl_3$) δ 237.35 (d, $^2J_{PCW} = 17.3$ Hz, OCW), 183.06–181.02 (C(O)), 141.00–126.93 (C_6H_5), 91.57 (s, C_5H_5), 41.58 (s, CH_2), 10.23 ppm (s, CH_3); ^{31}P NMR (162.0 MHz/ $CDCl_3$) δ 90.17 (d, $^2J_{PWP} = 48.9$ Hz, $^1J_{WP} = 313.1$ Hz, PN), 56.42 ppm (d, $^2J_{PWP} = 48.9$ Hz, $^1J_{WP} = 254.3$ Hz, PC); IR ($CHCl_3$) ν 1881 (vs, CO), 1652 (s, C(O)) cm^{-1} . Diastereomer **5b'**: 1H NMR (400.1 MHz/ $CDCl_3$) δ 8.05–7.15 (m, 20 H, H_5C_5), 4.46 (d, $^3J_{PWCH} = 2.1$ Hz, 5 H, H_5C_5), 3.56 (dq, $^2J_{HCH} = 13.8$ Hz, $^3J_{HCH} = 6.7$ Hz, $^3J_{PNCH} = 6.9$ Hz, 1 H, H_2C), 2.89 (dq, $^2J_{HCH} = 13.5$ Hz, $^3J_{HCH} = 6.7$ Hz, $^3J_{PNCH} = 6.5$ Hz, $^3J_{PCPNCH} = 2.1$ Hz, 1 H, H_2C), –0.07 ppm (t, $^3J_{HCH} = 6.7$ Hz, 3 H, H_3C); ^{13}C NMR (100.6 MHz/ $CDCl_3$) δ 240.99 (d, $^2J_{PCW} = 19.8$ Hz, OCW), 183.06–181.02 (C(O)), 141.00–126.93 (C_6H_5), 92.61 (s, C_5H_5), 41.98 (s, CH_2), 10.71 ppm (s, CH_3); ^{31}P NMR (400.1 MHz/ $CDCl_3$) δ 110.42 (d, $^2J_{PWP} = 62.7$ Hz, $^1J_{WP} = 276.6$ Hz, PN), 38.66 ppm (d, $^2J_{PWP} = 62.7$ Hz, $^1J_{WP} = 280.8$ Hz, PC); IR ($CHCl_3$) ν 1881 (vs, CO), 1652 (s, C(O)) cm^{-1} . Anal. Calcd for $C_{33}H_{30}NOP_2W$ (753.86): C, 52.58; H, 4.01; N, 1.86. Found: C, 52.70; H, 4.40; N, 1.29.

(5) Alt, H. G.; Engelhardt, H. E.; Kläui, W.; Müller, A. *J. Organomet. Chem.* **1987**, *331*, 317.

(6) Baker, R. T.; Calabrese, J. C.; Harlow, R. L.; Williams, I. D. *Organometallics* **1993**, *12*, 812.

Scheme 2



for its intermediate existence is given by Baker's results for the related system $(\eta^5\text{-Me}_5\text{C}_5)(\text{Me}_3\text{P})(\text{HPh}_2\text{P})\text{W}=\text{PPh}_2$, where a type **A** tautomer has been identified by NMR spectroscopy and X-ray analysis.⁶

Treatment of the hydrido complexes **4a,a'** and **4b,b'** with carbon tetrachloride in dichloromethane at room temperature leads to quantitative H/Cl exchange at the metal to give the analogous chloro complexes (Scheme 1) in a diastereomeric ratio of 3:2 (**5a,a'**) or 1:1 (**5b,b'**).⁴

The complexes **5**, obtained as orange to red microcrystalline powders, show nearly the same spectroscopic data as **4**, suggesting analogous structures. In the case of **5b,b'** slow evaporation of a benzene solution yields crystals of pure **5b'** (chlorine *cis* to C-bound phosphorus) suitable for X-ray analysis. The result confirms the proposed bis-phosphorus chelate structure, presumably also valid for the original cycloadducts **4'** (Figure 1).

The tungsten atom exhibits pseudo-square-monopyramidal coordination geometry with the cyclopentadienyl ligand in the apical position. The two phosphorus atoms adopt a *cis* arrangement at the metal with an P–W–P angle of 76.39(8)° and define together with the CN unit of the former ethyl isocyanate the 1-metalla-2,5-diphospha-3-azapentane cycle. The phenyl groups above the tetragonal base are aligned synperiplanar toward the cyclopentadienyl ring. The chelate system P1–N1–C2–P2 shows planarity with a torsion angle of 2.4(11)°. The length of the endocyclic carbon–nitrogen bond of 1.346(12) Å is significantly shorter than the C–N σ -bond distance,⁸ found for exocyclic N1–C8 (1.494(11) Å). This fact, together with the planarity of the nitrogen atom (sum of angles 358.9°), indicates a significant π -interaction between N1 and C2.

Further investigations will deal with analogous reac-

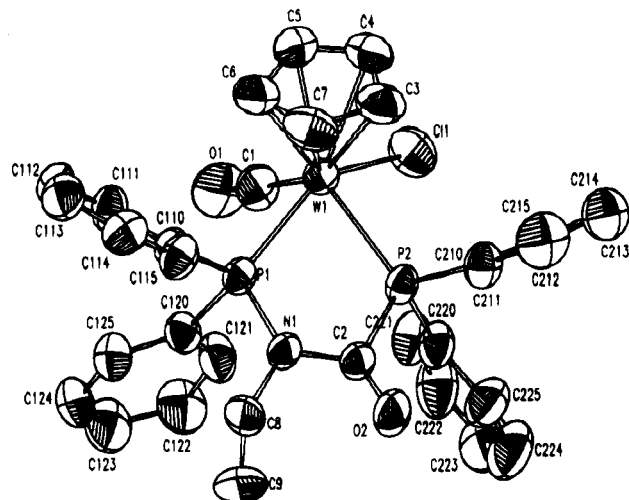


Figure 1. Crystal structure of **5b'**. Selected bond lengths (Å): W1–P1 = 2.410(2), W1–P2 = 2.420(3), W1–Cl1 = 2.506(3), W1–C1 = 1.943(11), P1–N1 = 1.737(8), P2–C2 = 1.892(7), O2–C2 = 1.190(8), N1–C2 = 1.362(8), N1–C8 = 1.476(9), C8–C9 = 1.48(1). Selected bond angles (deg): P1–W1–P2 = 76.41(6), W1–P1–N1 = 113.8(2), N1–P1–C110 = 102.6(3), W1–P2–C2 = 111.6(2), P1–N1–C2 = 119.5(4), P1–N1–C8 = 123.9(5), P2–C2–N1 = 113.6(5), O2–C2–N1 = 123.8(6), N1–C8–C9 = 114.8(8). Selected dihedral angles (deg): P2–W1–P1–N1 = 19.77(0.41), P1–W1–P2–C2 = –17.92(0.43), W1–P1–N1–C2 = –18.82(1.03), W1–P2–C2–N1 = 14.33(1.01), P1–N1–C2–P1 = 2.58(1.24), C2–N1–C8–C9 = 96.84(1.49). Hydrogen atoms have been omitted for clarity.

tions of P–H-functionalized phosphonium complexes of the type $\text{Cp}(\text{CO})[\text{H}(\text{Ph})(\text{R})\text{P}]\text{M}=\text{P}(\text{Ph})\text{R}$ (M = Mo, W; R = alkyl), with different organic substituents attached to the phosphorus, in order to realize stereocontrolled coupling of the two P(Ph)(R) moieties by isocyanates and other polar double-bond systems.

Acknowledgment. Generous support of these studies by the Deutsche Forschungsgemeinschaft (SFB 347: "Selektive Reaktionen Metall-aktiverter Moleküle") and the Fonds der Chemischen Industrie is gratefully acknowledged.

Supporting Information Available: Text giving experimental procedures and spectroscopic data for **4a,a'**, **4b,b'**, **5a,a'**, and **5b,b'** and tables giving crystal data and refinement parameters, positional and thermal parameters, and bond distances and angles for **5b'** (11 pages). Ordering information is given on any current masthead page.

OM950379B

(7) Crystallographic data for **5b'**: hexagonal, $P6_5$ (No. 170), $Z = 6$, $a = 23.708(4)$ Å, $b = 23.708(5)$ Å, $c = 10.113(6)$ Å, $V = 4923(3)$ Å³, $\rho_{\text{calcd}} = 1.528$ g cm⁻³; Enraf-Nonius CAD4 diffractometer, Mo $K\alpha$ radiation ($\lambda = 0.7093$ Å), 3407 independent reflections with $3^\circ < 2\theta < 52^\circ$ collected, 3085 reflections used in refinement with $I > 2\sigma(I)$; $R = 0.027$, $R_w = 0.084$. In the detected space group $P6_5$ (No. 170) the single molecules are arranged in a helical structure. As a result of the symmetrical properties of this space group and the chirality of the molecule, every crystal contains only one definite enantiomer. Because of the lower R value of the structure determination in space group $P6_5$ (No. 170) in comparison to that for the mirror symmetric space group $P6_1$ (No. 169), **5a** will be described in the first group.

(8) (a) Häfelinger, G. *Chem. Ber.* **1970**, *103*, 2902. (b) Pauling, L. *Die Natur der chemischen Bindung*; Verlag Chemie: Weinheim, Germany, 1964.

P-Functionalized Cyclic Phosphinidenemetallophosphoranes

Cp(CO)₂W-P(X)(*t*-Bu)-P(*t*-Bu) (X = Cl, H): Direct Formation from Metallophosphines and Transformation Reactions¹

Bernd K. Schmiedeskamp,[†] Joachim G. Reising,[†] Wolfgang Malisch,^{*,†}
Kathrin Hindahl,[†] Rudolf Schemm,[†] and William S. Sheldrick[‡]

*Institut für Anorganische Chemie der Universität Würzburg, Am Hubland,
D-97074 Würzburg, Germany, and Lehrstuhl für Analytische Chemie der
Ruhruniversität Bochum, Universitätsstrasse 150, D-44780 Bochum, Germany*

Received May 23, 1995[⊗]

Summary: The functionalized tungsten phosphines Cp(CO)₃WP(X)-*t*-Bu (**1a**, X = Cl; **1b**, X = H) convert in a controlled manner to the cyclized phosphinidenemetallophosphoranes Cp(CO)₂W-P(X)(*t*-Bu)-P(*t*-Bu) (**2a**, X = Cl; **2b**, X = H), which have been structurally determined by X-ray analysis. **2b** can be transformed to Cp(CO)₂W-P(*t*-Bu)(R)-P(*t*-Bu) (**4a**, R = Me; **4b**, R = CH₂CH=CH₂) via lithiation followed by alkylation. **4a** is quaternized with methyl iodide to give the cationic η²-diphosphine complex {Cp(CO)₂[η²-Me(*t*-Bu)P-P(*t*-Bu)-Me]W}I (**5**).

Metallophosphines of the type Cp(CO)₃M-PR₂ are characterized by a high Lewis basicity, which guarantees their facile quaternization, oxidation, and coordination.² In the case where bulky organic groups are attached at phosphorus, a high tendency for the formation of the corresponding phosphonium complexes Cp(CO)₂M=PR₂ (R = *t*-Bu, Mes) is observed,³ arising from an intramolecular ligand exchange, leading to CO elimination. These kinds of complexes, conceivable as phosphorus analogues of carbene complexes,⁴ represent, due to the high reactivity of the M=P bond, excellent starting materials for the generation of phosphametalloacycles.^{3,5} In keeping with studies concerning the transformation of metallophosphines into M=P com-

plexes, we have investigated the decarbonylation of the functionalized species Cp(CO)₃W-P(X)-*t*-Bu (**1a**, X = Cl; **1b**, X = H) and observed controlled, stereospecific formation of a cyclized phosphinidenemetallophosphorane, containing a hydrogen- or chlorine-substituted phosphorus, useful for further derivatization.

The metallophosphines **1a,b** are generated by metalation of *t*-BuPCl₂ with Na[W(CO)₃Cp] in benzene (**1a**) or via deprotonation of the cationic complex [Cp(CO)₃(*t*-BuH₂P)W]BF₄ with triethylamine in toluene (**1b**), respectively. Both compounds analogously convert in solution (**1a**, 24 h, benzene, room temperature; **1b**, 3.5 h, toluene, 80 °C) to the three-membered diphosphametalloacycles **2a,b** and the chloro/hydrido tungsten complex **3a,b** (Scheme 1). **2a,b** can easily be separated by extraction with pentane (**2a**) or column chromatography (**2b**).⁶

The generation of **2a,b** is explained via decarbonylation of **1a,b**, leading to the M=P intermediates Cp(CO)₂W=P(X)-*t*-Bu (X = Cl, H) and simultaneous decomposition to **3a,b**, with elimination of "tert-butylphosphinidene", which immediately adds to the M=P bond. Evidence for this reaction mechanism is provided by the easy transfer of the "MeP" moiety to the stable phosphonium complexes Cp(CO)₂W=PR₂ (R = *t*-Bu, *o*-Tol) using (MeP)₅.⁷ An additional access to **2b** is offered by treatment of **2a** with LiAlH₄ in benzene.⁶

According to NMR spectroscopy (¹H, ¹³C, ³¹P)⁶ the compounds **2a,b** exist only as one diastereomer, indicating stereocontrolled coupling of the phosphonium ligand and the "tert-butylphosphinidene" unit. The stereochemistry of **2a,b** has been proven by X-ray analysis,⁸ illustrated in Figures 1 and 2. It reveals that the tert-butyl groups, in agreement with the steric requirement, are located on different sides of the ring plane. The H or Cl atom at the phosphorane phosphorus P1 is in a position *anti* to the Cp ligand, while the lone pair at the phosphinidene phosphorus P2 in that respect adopts a *syn* orientation.⁹ In addition the X-ray study provides support for our description of **2a,b** as cyclic phosphinidenemetallophosphoranes, in which the metal acts as a coordination center for the phosphinidene phosphorus P2 as well as a σ-bonded ligand to P1.¹⁰ The diverse kinds of bonding of the phosphinidene-phosphorane unit to the metal are documented by the significantly different W-P1 and W-P2 distances in **2a,b**. While

[†] Universität Würzburg.

[‡] Ruhruniversität Bochum.

[⊗] Abstract published in *Advance ACS Abstracts*, September 1, 1995.

(1) Phosphenium Transition Metal Complexes. 34. Part 33: Malisch, W.; Hahner, C.; Grün, K.; Reising, J.; Goddard, R. *Inorg. Chim. Acta*, in press.

(2) (a) Malisch, W.; Maisch, R.; Colquhoun, I. J.; McFarlane, W. J. *Organomet. Chem.* **1981**, *220*, C1. (b) Maisch, R.; Ott, E.; Buchner, W.; Malisch, W. *J. Organomet. Chem.* **1985**, *286*, C31.

(3) (a) Malisch, W.; Jörg, K.; Hofmocker, U.; Schmeusser, M.; Schemm, R.; Sheldrick, W. S. *Phosphorus Sulfur Relat. Elem.* **1987**, *30*, 205. (b) Malisch, W.; Reich, W. to be submitted for publication.

(4) (a) Schrock, R. R. *Acc. Chem. Res.* **1986**, *19*, 342. (b) Dötz, K. H.; Fischer, H.; Hofmann, P.; Kreissl, F. R.; Schubert, U.; Weiss, K. *Transition Metal Carbene Complexes*; Verlag Chemie: Weinheim, Germany, 1983.

(5) (a) Fried, A.; Malisch, W.; Schmeusser, M.; Weis, U. *Phosphorus, Sulfur Silicon Relat. Elem.* **1992**, *65*, 75. (b) Malisch, W.; Märkl, M.; Amann, S.; Hirth, U.; Schmeusser, M. *Phosphorus, Sulfur Silicon Relat. Elem.* **1990**, *49/50*, 441. (c) Hirth, U.-A.; Malisch, W.; Käß, H.; Bright, T. A. *J. Organomet. Chem.* **1992**, *439*, C20. (d) Pfister, H.; Malisch, W. *J. Organomet. Chem.* **1992**, *439*, C11. (e) Spörl, A.; Hindahl, K.; Fried, A.; Pfister, H.; Malisch, W. In *Selective Reactions of Metal-Activated Molecules*; Werner, H.; Griesbeck, A. G.; Adam, W., Bringmann, G., Kiefer, W., Eds.; Vieweg: Braunschweig, Germany, 1992; p 191. (f) Fried, A.; Hahner, C.; Malisch, W. In ref 5e, p 195.

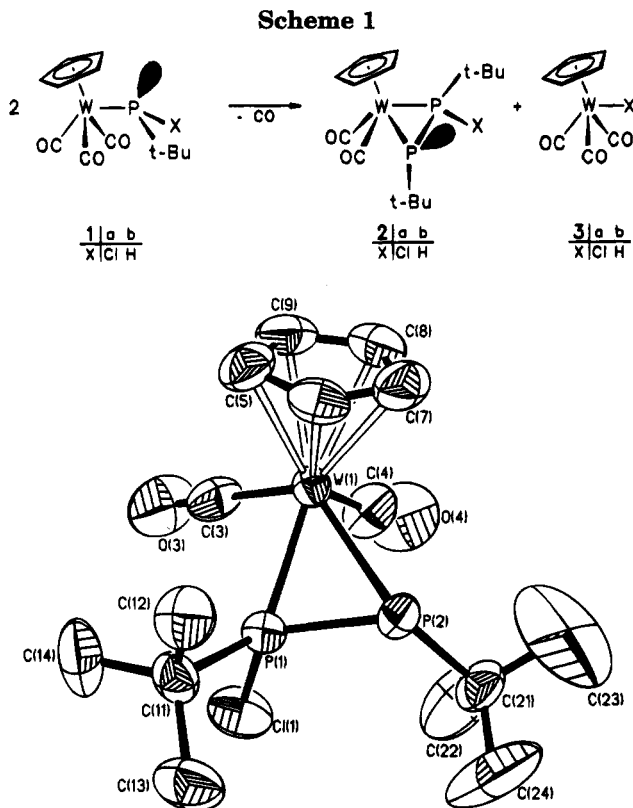


Figure 1. Drawing of **2a**. Selected bond lengths (Å): W1–P1 = 2.355(2), W1–P2 = 2.572(2), P1–P2 = 2.101(3), C11–P1 = 2.059(3). Selected bond angles (deg): P1–W1–P2 = 50.25(7), W1–P1–P2 = 70.25(8), W1–P2–P1 = 59.50(8). Hydrogen atoms are omitted for clarity.

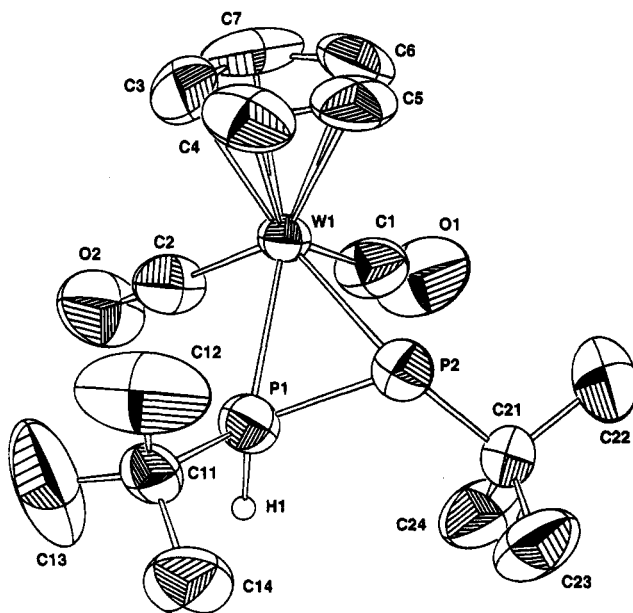


Figure 2. Drawing of **2b**. Selected bond lengths (Å): W1–P1 = 2.411(3), W1–P2 = 2.576(3), P1–P2 = 2.095(4), P1–H1 = 1.27(4). Selected bond angles (deg): P1–W1–P2 = 49.54(9), W1–P1–P2 = 69.33(11), W1–P2–P1 = 61.13(10). Hydrogen atoms (except for H1) are omitted for clarity.

the metal–phosphorane phosphorus distances W–P1 of 2.355(2) Å (**2a**)/2.411(3) Å (**2b**) lie between those of W–P double and single bonds,¹¹ the values of W–P2 bonds (2.572(2) Å (**2a**)/2.576(3) Å (**2b**)) are comparable to those of metal–phosphorus single bonds in the phosphido complexes Cp(CO)₂(L)W–PPh₂ (*d*(W–P) = 2.615–

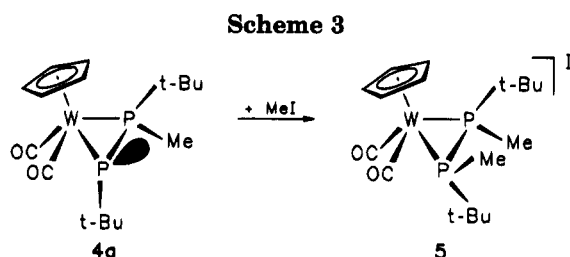
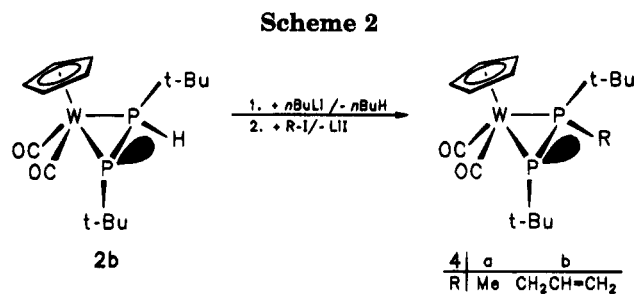
(3) Å (L = CO), 2.545(2) Å (L = PMe₃)).¹² A considerable double-bond character of the P–P unit is established

(6) Experimental details are given in the supporting information. Analytical and spectroscopical data are as follows. **tert-Butylchloro-tricarbonyl(η⁵-cyclopentadienyl)tungsteniophosphine (1a)**: mp 51 °C dec; ¹H NMR (60 MHz, C₆H₆) δ 4.80 (d, ³J_{PWCH} = 1.9 Hz, 5H, C₅H₅), 1.39 ppm (d, ³J_{PCC} = 13.3 Hz, 9H, (H₃C)₃C); ³¹P{¹H} NMR (36.2 MHz, C₆D₆) δ 197.1 ppm (s, ¹J_{WP} = 29.8 Hz); IR (pentane) ν(CO) 2012 (vs), 1952 (s), 1927 cm⁻¹ (vs); MS (based on ³⁵Cl and ¹⁸⁴W) *m/e* 456 (M⁺). Anal. Calcd for C₁₂H₁₄ClO₃PW (456.53): C, 31.57; H, 3.09; Cl 7.77. Found: C, 30.70; H, 3.10; Cl, 8.00. **[Tricarbonyl(η⁵-cyclopentadienyl)tungsteni]tert-butylphosphine (1b)**: ¹H NMR (200.1 MHz, C₆D₆) δ 4.59 (d, ³J_{PWCH} = 1.8 Hz, 5H, C₅H₅), 3.95 (d, ¹J_{PH} = 212.2 Hz, 1H, PH), 1.43 ppm (s, ³J_{PCC} = 12.5 Hz, 9H, (H₃C)₃C); ³¹P{¹H} NMR (36.2 MHz, C₆D₆) δ -71.6 ppm (s, ¹J_{WP} = 52.8 Hz); IR (pentane) ν(CO) 2001 (s), 1935 (s), 1920 cm⁻¹ (vs), ν(PH) 2259 cm⁻¹ (w). **Dicarbonyl(η⁵-cyclopentadienyl)[η²-(tert-butylphosphinidene)-tert-butylchlorophosphorane-P,P']tungsten(II) (2a)**: mp 93 °C; ¹H NMR (here and in the following compounds the tetravalent phosphorus is assigned as P^a and the trivalent phosphorus as P^b) (60 MHz, C₆H₆) δ 4.84 (dd, ³J_{P^aWCH} = 1.4 Hz, ³J_{P^bWCH} = 0.6 Hz, 5H, H₅C₅), 1.44 (dd, ³J_{P^bCCH} = 13.9 Hz, ⁴J_{P^aP^bCCH} = 1.3 Hz, 9H, H₃CCP^a), 1.26 ppm (dd, ³J_{P^aCCH} = 21.2 Hz, ⁴J_{P^aP^bCCH} = 0.3 Hz, H₃CCP^b); ³¹P{¹H} NMR (36.2 MHz, C₆D₆) δ 118.58 (d, ¹J_{P^aP^b} = 549.1 Hz, P^a), -196.86 ppm (d, ¹J_{P^bP^a} = 549.1 Hz, P^b); ¹³C{¹H} NMR (22.6 MHz, C₆D₆) δ 228.3 (dd, ²J_{P^bWC} = 29.6 Hz, ²J_{P^aWC} = 2.3 Hz, CO^a), 29.8 (s, br, CO^b), 89.0 (d, ²J_{P^aWC} = 2.9 Hz, C₅H₅), 40.8 (d, ¹J_{P^aC} = 22.9 Hz, (H₃C)₃CP^a), 32.3 (dd, ¹J_{P^bC} = 59.4 Hz, ²J_{P^aP^bC} = 6.8 Hz, (H₃C)₃CP^b), 32.4 (dd, ²J_{P^aCC} = 18.4 Hz, ³J_{P^aP^bCC} = 5.2 Hz, (H₃C)₃CP^a), 27.3 ppm (dd, ²J_{P^aCC} = 5.5 Hz, ³J_{P^aP^bCC} = 3.7 Hz, (H₃C)₃CP^a); IR (pentane) ν(CO) 1959 (vs), 1883 cm⁻¹ (s); MS (based on ³⁵Cl and ¹⁸⁴W) *m/e* 517 (M⁺). Anal. Calcd for C₁₅H₂₀Cl₂O₂P₂W (516.60): C, 34.88; H, 4.49; Cl, 6.86. Found: C, 35.01; H, 4.67; Cl, 7.14. **Dicarbonyl(η⁵-cyclopentadienyl)[η²-(tert-butylphosphinidene)-tert-butylphosphorane-P,P']tungsten(II) (2b)**: mp 110 °C; ¹H NMR (200.1 MHz, C₆D₆) δ 5.24 (dd, ¹J_{P^aH} = 415.0 Hz, ²J_{P^bP^aH} = 3.4 Hz, 1H, P^aH), 4.85 (d, ³J_{P^bWCH} = 1.3 Hz, 5H, H₅C₅), 1.22 (dd, ³J_{P^bCCH} = 13.8 Hz, ⁴J_{P^aP^bCCH} = 1.8 Hz, 9H, (H₃C)₃CP^b), 0.93 (d, ³J_{P^aCCH} = 19.2 Hz, 9H, (H₃C)₃CP^a); ³¹P{¹H} NMR (36.2 MHz, C₆D₆) δ -26.1 (¹J_{P^aP^b} = 489.8 Hz, P^a), -191.6 ppm (¹J_{P^bP^a} = 489.8 Hz, P^b); ¹³C{¹H} NMR (100.6 MHz, C₆D₆) δ 231.86 (dd, ²J_{P^bWC} = 23.8 Hz, ²J_{P^aWC} = 2.9 Hz, CO^a), 224.55 (s, br, CO^b), 87.96 (d, ²J_{P^aWC} = 2.9 Hz, C₅H₅), 31.81 (dd, ¹J_{P^aC} = 16.8 Hz, ²J_{P^bP^aC} = 4.9 Hz, (CH₃)₃CP^a), 29.25 (dd, ²J_{P^aCC} = 4.7 Hz, ³J_{P^aP^bCC} = 1.8 Hz, (CH₃)₃CP^a), 27.52 (dd, ¹J_{P^bC} = 50.3 Hz, ²J_{P^aP^bC} = 4.9 Hz, (CH₃)₃CP^b), 27.47 ppm (d, ²J_{P^bCC} = 29.8 Hz, (CH₃)₃CP^b); IR (pentane) ν(PH) 2319 (w), ν(CO) 1942 (s), 1870 (s) cm⁻¹; MS (based on ¹⁸⁴W) *m/e* 482 (M⁺), 425 (M⁺ - C₄H₉), 397 (M⁺ - C₄H₉ and CO), 339 (M⁺ - 2 C₄H₉ - CO - H), 311 (C₆H₅WP₂⁺), 57 (C₄H₉⁺). Anal. Calcd for C₁₅H₂₄O₂P₂W (482.16): C, 37.37; H, 5.02. Found: C, 36.72; H, 4.98. **Dicarbonyl(η⁵-cyclopentadienyl)[η²-(tert-butylphosphinidene)-methyl-tert-butylphosphorane-P,P']tungsten(II) (4a)**: mp 133 °C; ¹H NMR (400.1 MHz, C₆D₆) δ 4.90 (s, 5H, H₅C₅), 1.81 (d, ²J_{P^aCH} = 11.0 Hz, 3H, H₃CP^a), 1.23 (d, ³J_{P^bCCH} = 13.4 Hz, 9H, (H₃C)₃CP^b), 0.86 ppm (d, ³J_{P^aCCH} = 16.9 Hz, 9H, (H₃C)₃CP^a); ³¹P{¹H} NMR (162.0 MHz, C₆D₆) δ -5.07 (d, ¹J_{P^aP^b} = 534.2 Hz, ¹J_{W^aP^a} = 169.5 Hz, P^a), -180.8 ppm (d, ¹J_{P^bP^a} = 534.2 Hz, P^b); ¹³C{¹H} NMR (100.6 MHz, C₆D₆) δ 234.00 (d, ²J_{P^bWC} = 24.8 Hz, CO^a), 224.87 (s, CO^b), 89.66 (d, ²J_{P^aWC} = 3.0 Hz, C₅H₅), 32.87 (dd, ²J_{P^bCC} = 18.2 Hz, ³J_{P^aP^bCC} = 4.8 Hz, (CH₃)₃CP^b), 30.63 (dd, ¹J_{P^bC} = 58.1 Hz, ²J_{P^aP^bC} = 6.8 Hz, (CH₃)₃CP^b), 30.18 (dd, ¹J_{P^aC} = 26.1 Hz, ²J_{P^aP^bC} = 2.0 Hz, (CH₃)₃CP^a), 27.99 (dd, ²J_{P^aCC} = 4.0 Hz, ³J_{P^aP^bCC} = 3.9 Hz, (CH₃)₃CP^a), 12.56 ppm (dd, ¹J_{P^aC} = 27.7 Hz, ²J_{P^bP^aC} = 3.6 Hz, CH₃P^a); IR (pentane) ν(CO) 1933 (s), 1860 (s) cm⁻¹. Anal. Calcd for C₁₆H₂₆O₂P₂W (496.18): *m/e* C, 38.73; H, 5.28. Found: C, 38.67; H, 5.52. **Dicarbonyl(η⁵-cyclopentadienyl)[η²-tert-butylphosphinidene)allyl-tert-butylphosphorane-P,P']tungsten(II) (4b)**: mp 94 °C; ¹H NMR (400.1 MHz, [D₃]toluene, 203 K) δ 6.40 (m, 1H, H^aC=CH₂), 5.14 (d, ³J_{H^aCCH^b} = 9.7 Hz, 1H, H^bC=CH^a), 5.04 (d, ³J_{H^aCCH^c} = 15.2 Hz, 1H, H^bC=CH^c), 4.86 (s, 5H, H₅C₅), 3.61 (dd, ²J_{H^aCH} = 14.6 Hz, ³J_{H^aCH^c} = 8.3 Hz, 1H, H^c), 3.26 (dd, ²J_{H^aCH} = 14.4 Hz, ³J_{H^aCH^b} = 4.8 Hz, 1H, H^c), 1.56 (d, ³J_{P^bCCH} = 10.3 Hz, 9H, (H₃C)₃CP^b), 1.20 ppm (d, ³J_{P^aCCH} = 16.7 Hz, 9H, (H₃C)₃CP^a); ³¹P{¹H} NMR (162.0 MHz, C₆D₆) δ 0.74 (d, ¹J_{P^aP^b} = 537.1 Hz, ¹J_{W^aP^a} = 170.1 Hz, P^a), -169.84 ppm (d, ¹J_{P^bP^a} = 537.1 Hz, P^b); ¹³C{¹H} NMR (100.6 MHz, C₆D₆) δ 234.56 (d, ²J_{P^bWC} = 26.5 Hz, CO^a), 224.67 (s, CO^b), 135.40 (d, ²J_{P^aCC} = 8.0 Hz, CH^a=CH^bH^c), 118.18 (d, ³J_{P^aCC} = 12.0 Hz, CH^a=CH^bH^c), 88.66 (d, ²J_{P^bWC} = 3.2 Hz, C₅H₅), 37.75 (dd, ¹J_{P^aC} = 78.2 Hz, ²J_{P^bP^aC} = 3.6 Hz, CH₂), 32.85 (dd, ²J_{P^bCC} = 18.8 Hz, ³J_{P^aP^bCC} = 4.7 Hz, (CH₃)₃CP^b), 32.28 (dd, ¹J_{P^aC} = 27.9 Hz, ²J_{P^bP^aC} = 2.4 Hz, (CH₃)₃CP^a), 31.45 (dd, ¹J_{P^bC} = 60.9 Hz, ²J_{P^aP^bC} = 7.3 Hz, (CH₃)₃CP^b), 29.40 ppm (d, ²J_{P^aCC} = 3.7 Hz, (CH₃)₃CP^a); IR (petroleum ether, 40–60 °C) ν(CO) 1933 (vs), 1859 (s) cm⁻¹. Anal. Calcd for C₁₈H₂₈O₂P₂W (522.22): C, 41.40; H, 5.40. Found: C, 40.98; H, 5.03. **Dicarbonyl(η⁵-cyclopentadienyl)[η²-1,2-di-tert-butyl-1,2-dimethyldiphosphine]tungsten(II) iodide (5)**: mp 171 °C; ¹H NMR (CD₃NO₂) δ 5.83 (t, ³J_{PWCH} = 0.3 Hz, 5H, H₅C₅), 2.29 (vt, N = 1.9 Hz, 6H, H₃CP), 1.42 ppm (vt, N = 19.8 Hz, 18H, (H₃C)₃C); ³¹P{¹H} NMR (CD₃NO₂, 245 K, AB spectrum) δ_A -84.2 (¹J_{AB} = 384.1 Hz, ¹J_{WP} = 128.0 Hz), δ_B -97.2 ppm (¹J_{AB} = 384.1 Hz, ¹J_{WP} = 153.3 Hz); IR (acetonitrile) ν(CO) 1984 (vs), 1904 (s) cm⁻¹. Anal. Calcd for C₁₇H₂₉I₂O₂P₂W (638.12): C, 32.00; H, 4.58; I, 19.89. Found: C, 32.21; H, 4.71; I, 19.64.

by the P1–P2 distances (2.101(3) Å (**2a**)/2.095(4) Å (**2b**)), similar to what has been found for comparable systems prepared by different routes.¹³ Further evidence for this fact is given by the high value of the coupling constant $^1J_{PP} = 549.3$ Hz (**2a**)/489.8 Hz (**2b**).

Due to its PH functionality, **2b** opens up the possibility of phosphorus metallation. The spontaneous reaction of **2b** with *n*-BuLi already occurs at -78 °C in THF, yielding the lithiated species $\text{Li}[\text{Cp}(\text{CO})_2\text{W}-\text{P}(t\text{-Bu})-\text{P}(t\text{-Bu})]$,¹⁴ which reacts "in situ" with methyl or allyl iodide to give the methyl- or allyl-substituted phosphinidenemetallophosphoranes **4a,b** (Scheme 2), purified by column chromatography. Alkylation proceeds presumably with retention of configuration at the phosphorane phosphorus, evident by comparison of ³¹P NMR parameters of **4a,b** with those of **2b**.

In accordance with the trivalency of the phosphinidene phosphorus, **4a** is quaternized with methyl iodide in toluene at room temperature, yielding the pale yellow



(7) Malisch, W.; Hindahl, K.; Schemm, R. *Chem. Ber.* **1992**, *125*, 2027.

(8) **2a**: orange crystals of **2a**, suitable for X-ray analysis, were obtained by low-temperature crystallization from pentane at -40 °C; $\text{C}_{15}\text{H}_{23}\text{ClO}_2\text{P}_2\text{W}$, $M = 516.60$. Crystallographic data for **2a**: monoclinic, $P2_1/n$, $Z = 4$, $a = 11.888(3)$ Å, $b = 11.103(3)$ Å, $c = 14.798(4)$ Å, $\beta = 94.32(2)^\circ$, $V = 1947.6(16)$ Å³, $\rho_{\text{calc}} = 1.76$ g cm⁻³; Enraf-Nonius CAD4 diffractometer, Mo K α radiation ($\lambda = 0.71093$ Å); 3419 independent reflections with $3.0^\circ < 2\theta < 50.0^\circ$ collected, 2756 reflections used in refinement (F^2) with $I > 2\sigma(I)$; $R = 0.033$, $R_w = 0.035$; empirical absorption correction (ψ scan). **2b**: yellow crystals of **2b**, suitable for X-ray analysis were obtained by low-temperature crystallization from pentane at -78 °C; $\text{C}_{15}\text{H}_{24}\text{O}_2\text{P}_2\text{W}$, $M = 482.16$. Crystallographic data for **2b**: monoclinic $P2_1/n$, $Z = 4$, $a = 9.731(9)$ Å, $b = 15.647(3)$ Å, $c = 12.092(4)$ Å, $\beta = 94.61(4)^\circ$, $V = 1835(2)$ Å³, $\rho_{\text{calc}} = 1.752$ g cm⁻³; Enraf-Nonius CAD4 diffractometer, Mo K α radiation ($\lambda = 0.71093$ Å); 2548 independent reflections with $2.13^\circ < \theta < 22.91^\circ$ collected, 2548 reflections used in refinement (F^2) with $I > 3\sigma(I)$; $R = 0.0351$, $R_w = 0.0413$; empirical absorption correction (ψ scan).

(9) The compound $\text{Cp}(\text{CO})_2\text{Mo}-\text{P}(\text{H}(\text{R}))-\text{P}(\text{R})$ ($\text{R} = 2,4,6\text{-}(t\text{-Bu})_3\text{C}_6\text{H}_2$), an analogue to **2a,b**, has been prepared by Cowley et al. from the reaction of $\text{R}(\text{Cl})\text{P}-\text{P}(\text{H})\text{R}$ with $\text{K}[\text{Mo}(\text{CO})_5\text{Cp}]$. However, the M–P distances and the ³¹P NMR resonances have not been correctly assigned: Arif, A. M.; Cowley, A. H.; Pakulski, M.; Thomas, G. J. *Polyhedron* **1986**, *5*, 1651.

(10) Lindner, E.; Stängle, M.; Hiller, W.; Fawzi, R. *Chem. Ber.* **1989**, *122*, 823.

(11) Jörg, K.; Malisch, W.; Meyer, A.; Schubert, U. *Angew. Chem.* **1986**, *98*, 103; *Angew. Chem., Int. Ed. Engl.* **1986**, *25*, 367.

(12) Malisch, W.; Fried, A., manuscript in preparation.

(13) (a) Yoshifuji, M.; Shima, I.; Inamoto, N.; Hirotsu, K.; Higuchi, T. *J. Am. Chem. Soc.* **1981**, *103*, 4587. (b) Niecke, E.; Rüger, R.; Lysek, M.; Pohl, S.; Schoeller, W. *Angew. Chem.* **1983**, *95*, 495; *Angew. Chem., Int. Ed. Engl.* **1983**, *22*, 486.

(14) The metalation product is stable only for a short period in solution at low temperature; characterization was made by ³¹P NMR spectroscopy (162.0 MHz, [D_8]toluene/THF/pentane (3/1/1), 203 K) AB system, $\delta_A -39.25$ ppm ($^1J_{AB} = 430.9$ Hz), $\delta_B -53.45$ Hz ($^1J_{AB} = 430.9$ Hz)).

diphosphine complex **5** (Scheme 3), which precipitates from the reaction mixture. **5** contains a diastereomeric diphosphine, coordinated in an η^2 fashion. Its PP coupling constant of 384.1 Hz is indicative of some degree of P–P double-bond character.

The reaction presented in this communication opens up a facile route for highly selective coupling of phosphinidene and phosphinidene units at the metal, starting with metallophosphines available by convenient routes. Further investigations concerning the diverse reactivity of **2b** and related functionalized diphosphametallacycles with respect to controlled insertion of unsaturated organic substrates into the P–H and/or P–P bonds¹⁵ are in progress.

Acknowledgment. Support of this research by the Deutsche Forschungsgemeinschaft (SFB 347, "Selektive Reaktionen Metall-aktivierter Moleküle") and the Fonds der Chemischen Industrie is gratefully acknowledged.

Supporting Information Available: Text giving full experimental details and analytical data for **1a,b**, **2a,b**, **4a,b**, and **5** and tables of crystal data, atomic positions, anisotropic thermal parameters, bond distances, bond angles, and hydrogen atom coordinates for **2a,b** (17 pages). Ordering information is given on any current masthead page.

OM950378J

(15) For examples see: (a) Lindner, E.; Heckmann, M. *Chem. Ber.* **1991**, *124*, 1715. (b) Hou, Z.; Breen, T. L.; Stephan, D. W. *Organometallics* **1993**, *12*, 3158.

Synthesis of Dumbbell-Shaped Organometallics: Synthesis of a Peralkynylated Dinuclear Cyclobutadiene Complex

Jutta E. C. Wiegelmann-Kreiter and Uwe H. F. Bunz*

Max-Planck-Institut für Polymerforschung, Ackermannweg 10, 55021 Mainz, FRG

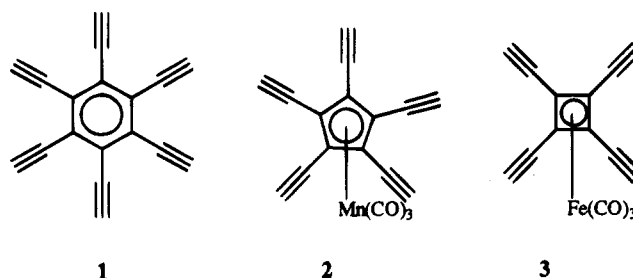
Received June 16, 1995[®]

Summary: With a tricarbonyl(diethynylcyclobutadiene)-iron complex as starting material, **7** is prepared in a stepwise fashion by a repetitive deprotonation/iodination/coupling sequence; **7** is a precursor to the dumbbell-shaped peralkynylated organometallics **8**, which are obtained by coupling of **7** with a ditin alkyne or butadiyne.

Interest in the synthesis of carbon-rich compounds has risen considerably during the last few years.¹⁻³ In particular, highly ethynylated compounds⁴⁻⁷ have attracted much attention, because they are viable monomers for the preparation of high carbon polymers, fullerene precursors, or fullerenyne segments. The synthesis of all-carbon molecules¹⁻³ and two-dimensional carbon nets is now an established (but not yet mastered) subfield of organic chemistry. To perform the controlled assembly of carbon molecules and all-carbon nets, it will be necessary to construct them from small units to form consecutively larger and more complex segments.

We have identified an organometallic all-carbon net consisting of organometallic (CpCo, (CO)₃Fe)-stabilized cyclobutadiene and alkyne or butadiyne bridges as targets and are involved in a program aiming at the

synthesis of fragments of this net.⁸ Linear,⁹ star-shaped (such as **3**),⁸ and *ortho* diethynylated¹⁰ segments have been synthesized in our laboratory in addition to multiply alkynylated derivatives of cymantrene (**2**) which can be considered as parts of metal-complexed fullerenynes.¹¹



To date the only known perethynylated organic moieties are Vollhardt's hexaethynylbenzene⁴ (**1**) and tetraethynylethylene⁶ and compounds further derived therefrom by Diederich;² they also represent the only known oligomers of peralkynylated moieties. Surprisingly, dimeric or oligomeric species of **1-3** have been hitherto unknown, even though they represent structurally unusual and attractive synthetic goals. We here wish to report the synthesis of the peralkynylated dumbbell-shaped complex **8**, which represents a persilylated dimer of **3**.

Reaction of **4**^{10,15,16} with *sec*-BuLi (THF, -78 °C) for 15 min led to the formation of the desired lithiated species. Quenching by addition of 1,2-diiodoethane and subsequent flash chromatography (silica gel; pentane) gave **5** in 89% yield. Due to the stereochemical equivalence of the cyclobutadiene protons in **4**, the usual precautions needed for selective *ortho* lithiation (very slow addition of *sec*-BuLi, careful control of the temper-

* To whom correspondence should be addressed. E-mail: Bunz@max.mpip-mainz.mpg.d400.de.

[®] Abstract published in *Advance ACS Abstracts*, September 15, 1995.

(1) Bunz, U. H. F. *Angew. Chem., Int. Ed. Engl.* **1994**, *33*, 1073.

(2) (a) Diederich, F.; Rubin, Y. *Angew. Chem., Int. Ed. Engl.* **1992**, *31*, 1101. Diederich, F. *Nature* **1994**, *369*, 199 and references cited therein. (b) Anthony, J.; Knobler, C. B.; Diederich, F. *Angew. Chem., Int. Ed. Engl.* **1993**, *32*, 406. Anderson, H. L.; Faust, R.; Rubin, Y.; Diederich, F. *Angew. Chem., Int. Ed. Engl.* **1994**, *33*, 1366. (c) An, Y.-Z.; Rubin, Y.; Schaller, C.; McElvany, S. W. *J. Org. Chem.* **1994**, *59*, 2927. (d) Xu, Z.; Moore, J. S. *Angew. Chem., Int. Ed. Engl.* **1993**, *32*, 1354 and references cited therein. (e) Fritch, J. R.; Vollhardt, K. P. C. *Organometallics* **1982**, *1*, 590.

(3) (a) Beck, W.; Niemer, B.; Wieser, M. *Angew. Chem., Int. Ed. Engl.* **1993**, *32*, 923 and references cited therein. (b) Weng, W.; Bartik, T.; Gladysz, J. A. *Angew. Chem., Int. Ed. Engl.* **1994**, *33*, 2199. (c) Gloaguen, B.; Astruc, D. *J. Am. Chem. Soc.* **1990**, *112*, 4607. Moulines, F.; Djakovitch, L.; Boese, R.; Gloaguen, B.; Thiel, W.; Fillaut, J.-L.; Delville, M.-H.; Astruc, D. *Angew. Chem., Int. Ed. Engl.* **1993**, *32*, 1075 and references cited therein.

(4) (a) Hexaethynylbenzene: Diercks, R.; Armstrong, J. C.; Boese, R.; Vollhardt, K. P. C. *Angew. Chem., Int. Ed. Engl.* **1986**, *25*, 268. Hexabutadiynylbenzene: Boese, R.; Green, J. R.; Mittendorf, J.; Mohler, D. L.; Vollhardt, K. P. C. *Angew. Chem., Int. Ed. Engl.* **1992**, *31*, 1643. (b) Other examples of polyethynylated arenes: Neenan, T. X.; Whitesides, G. M. *J. Org. Chem.* **1988**, *53*, 2489. Rutherford, D. R.; Stille, J. K. *Macromolecules* **1988**, *21*, 3530. Hyatt, J. A. *Org. Prep. Proced. Int.* **1992**, *23*, 460. Präfcke, K.; Kohne, B.; Singer, D. *Angew. Chem., Int. Ed. Engl.* **1990**, *29*, 177. Laschewsky, A. *Angew. Chem., Int. Ed. Engl.* **1989**, *28*, 1745.

(5) Hashmi, A. S. K.; Vollmer, A.; Szeimies, G. *Liebigs Ann. Chem.* **1995**, 471. Hashmi, A. S. K.; Szeimies, G. *Chem. Ber.* **1994**, *127*, 1075.

(6) (a) Kozhushkov, S. I.; Haumann, T.; Boese, R.; De Meijere, A. *Angew. Chem., Int. Ed. Engl.* **1993**, *32*, 401. (b) Hopf, H.; Kreutzer, M.; Jones, P. G. *Chem. Ber.* **1991**, *124*, 1471. (c) Vollhardt, K. P. C.; Winn, L. S. *Tetrahedron Lett.* **1985**, 709.

(7) Pericyclines: Scott, L. T. In *Modern Acetylene Chemistry*; Stang, P. J., Diederich, F., Eds.; VCH: Weinheim, Germany in press.

(8) (a) Bunz, U. H. F.; Enkelmann, V. *Angew. Chem., Int. Ed. Engl.* **1993**, *32*, 1653. (b) Bunz, U. H. F.; Enkelmann, V. *Organometallics* **1994**, *13*, 3823.

(9) (a) Wiegelmann, J. E. C.; Bunz, U. H. F. *Organometallics* **1993**, *12*, 3792. (b) Altmann, M.; Bunz, U. H. F. *Makromol. Chem., Rapid Commun.* **1994**, *15*, 785.

(10) Wiegelmann, J. E. C.; Bunz, U. H. F.; Schiel, P. *Organometallics* **1994**, *13*, 4649.

(11) (a) Bunz, U. H. F.; Enkelmann, V.; Räder, J. *Organometallics* **1993**, *12*, 4745. (b) Bunz, U. H. F.; Enkelmann, V.; Beer, F. *Organometallics* **1995**, *14*, 2490. (c) Bunz, U. H. F. *J. Organomet. Chem.* **1995**, *494*, C8.

(12) (a) Lo Sterzo, C.; Stille, J. K. *Organometallics* **1990**, *9*, 687 and references cited therein. (b) Viola, E.; Lo Sterzo, C.; Crescenzi, R.; Frachey, G. *J. Organomet. Chem.* **1995**, *493*, 55. Viola, E.; Lo Sterzo, C.; Crescenzi, R.; Frachey, G. *J. Organomet. Chem.* **1995**, *493*, C9.

(13) Beletskaya, I. P. *J. Organomet. Chem.* **1983**, *250*, 551 and references cited therein.

(14) Farina, V.; Krishnan, B. *J. Am. Chem. Soc.* **1991**, *113*, 9585 and references cited therein.

The complete functionalization of a cyclobutadiene complex in a merry-go-round fashion as achieved here should not only be applicable to the synthesis of peralkynylated species but may also serve as a starting point for the preparation of other fourfold-substituted tricarbonyl(cyclobutadiene)irons. These compounds have not attracted much interest (an exception being tricarbonyl(tetramethylcyclobutadiene)iron, easily available by Criegee's route¹⁷), probably due to the absence of

simple synthetic pathways to these complexes. The future direction of our work will be to use **7** as an end-capping agent in an attempt to build up a cyclobutadiene-ethynylene copolymer decorated by alkyne groups.

OM950460E

(17) Criegee, R. *Org. Synth.* **1966**, *46*, 34.

Phosphine-Substituted Silsesquioxanes as Building Blocks for Organometallic Gels

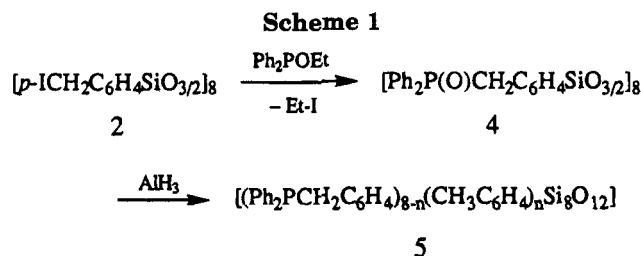
Frank J. Feher,* Joseph J. Schwab, Shawn H. Phillips, Andy Eklund, and Eduardo Martinez

Department of Chemistry, University of California, Irvine, California 92717-2025

Received June 7, 1995[⊗]

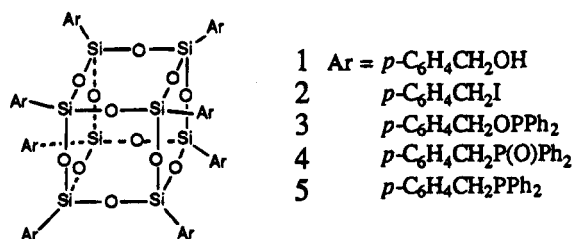
Summary: A new approach is described for the preparation of organometallic gels containing large amounts of potentially catalytically active metal centers. This approach uses nonchelating, phosphine-substituted silsesquioxane frameworks as rigid spacers to connect phosphine complexes of late transition metals. The synthesis, characterization, and reactivity of an organometallic gel obtained from the reaction of **5** with $[Rh(CO)_2Cl]_2$ (2 P/Rh) are described.

The development of late-transition-metal phosphine complexes to catalyze organic reactions represents one of the most important achievements of modern organometallic chemistry, and highly selective catalysts are now available to catalyze an impressive range of reactions.¹ The vast majority of these catalysts are soluble (i.e., homogeneous) catalysts, but several strategies have been proposed for preparing stoichiometrically similar insoluble (i.e., heterogeneous) catalysts, which in principle offer both the chemical selectivity of homogeneous catalysts and the engineering benefits of heterogeneous catalysts. Traditional strategies for immobilizing homogeneous catalysts have relied on phosphine-modified solids (e.g., cross-linked polystyrene or silica gel).^{2,3} More recently, dendrimeric polyphosphines⁴ have emerged as an interesting class of ligands which might be capable of achieving many of the same end results.⁵ We have been exploring the possibility of using nonchelating polyphosphines as building blocks for transition-metal-containing gels. Our goal is to promote the formation of organometallic gels with high surface areas and good porosity by using octafunctional silsesquioxane frame-



works as rigid spacers to connect catalytically active phosphine complexes of late transition metals. The results from our preliminary work in this area are reported here.

Of the large number of known octameric silsesquioxanes and spherosilicates,⁶⁻⁸ few possess the functionality required to attach trivalent phosphorus tether groups in a straightforward manner. Our initial efforts to synthesize phosphorus-substituted silsesquioxanes sought to use $[(p\text{-HOCH}_2\text{C}_6\text{H}_4)_8\text{Si}_8\text{O}_{12}]$ (**1**), which can



be obtained via $[(p\text{-ICH}_2\text{C}_6\text{H}_4)_8\text{Si}_8\text{O}_{12}]$ (**2**) in three steps from $p\text{-ClCH}_2\text{C}_6\text{H}_4\text{SiCl}_3$.⁸ Unfortunately, attempts to prepare phosphinites (e.g., **3**) by reacting **1** with chlorophosphines (e.g., Ph_2PCl) were only marginally successful. The reactions worked well when performed on a very small scale in dilute solutions (e.g., NMR tube reactions), but they could not be scaled up. We eventually succeeded in preparing synthetically useful quantities of a silsesquioxane with benzylic phosphine appendages via the approach outlined in Scheme 1.⁹

The multiple-Arbusov reaction of **2** with Ph_2POEt is remarkably efficient and affords a quantitative yield of **4**, which is surprisingly difficult to reduce because of its total insolubility in most common solvents except

(6) Reviews concerning silsesquioxanes: (a) Voronkov, M. G.; Lavrent'yev, V. I. *Top. Curr. Chem.* **1982**, *102*, 199-236. (b) Burgy H.; Calzaferri, G.; Herren, D.; Zhdanov, A. *Chimia* **1991**, *45*, 3-8.

(7) (a) Frye, C. L.; Collins, W. T. *J. Am. Chem. Soc.* **1970**, *92*, 5586-5588. (b) Day, V. W.; Klemperer, W. G.; Mainz, V. V.; Millar, D. M. *J. Am. Chem. Soc.* **1985**, *107*, 8262-8264. (c) Agaskar, P. A. *Colloids Surf.* **1992**, *63*, 131-138. (d) Agaskar, P. A. *Inorg. Chem.* **1990**, *29*, 1603. (e) Voronkov, M. G.; Martynova, T. N.; Mirskov, R. G.; Belyi, V. I. *Zh. Obshch. Khim.* **1979**, *49*, 1522-1525. (f) Martynova, T. N.; Korshkov, V. P.; Semyannikov, P. P. *J. Organomet. Chem.* **1983**, *258*, 277-282.

(8) Feher, F. J.; Budzichowski, T. A. *J. Organomet. Chem.* **1989**, *379*, 33-40.

(9) Experimental procedures and characterization data are provided in the supporting information.

[⊗] Abstract published in *Advance ACS Abstracts*, September 1, 1995.

(1) (a) Parshall, G. W.; Ittel, S. D. *Homogeneous Catalysis*, 2nd ed.; Wiley: New York, 1992. (b) Pignolet, L. H., Ed. *Homogeneous Catalysis with Metal Phosphine Complexes*; Plenum Press: New York, 1983. (c) Collman, J. P.; Hegedus, L. S.; Norton, J. R.; Finke, R. G. *Principles and Applications of Organotransition-Metal Chemistry*, 2nd ed.; University Science Books: Mill Valley, CA, 1987.

(2) (a) Pittman, C. U. In *Comprehensive Organometallic Chemistry*; Wilkinson, G., Ed.; Pergamon: New York, 1982; Vol. 8, pp 553-611. (b) Pittman, C. U. In *Polymer Supported Reactions in Organic Synthesis*; Hodge, P., Sherrington, D. C., Eds.; Wiley: New York, 1980, p 249. (c) Hartley, F. R. *Supported Metal Complexes*; Reidel: Boston, MA, 1985. (d) Iwasawa, Y., Ed. *Tailored Metal Catalysts*; Reidel: Boston, MA, 1986. (e) Yermakov, Y. I.; Kuznetsov, B. N.; Zakharov, V. A. *Catalysis by Supported Complexes*; Elsevier: New York, 1981.

(3) (a) Jongsma, T.; van Aert, H.; Fossen, M.; Challa, G.; van Leeuwen, P. W. N. M. *J. Mol. Catal.* **1993**, *83*, 37-50. (b) Grubbs, R. H. *CHEMTECH* **1977**, *7*, 512-518. (c) Hartley, F. R.; Vezey, P. N. *Adv. Organomet. Chem.* **1977**, *15*, 189-234. (d) Bailar, J. C. *Catal. Rev. - Sci. Eng.* **1974**, *10*, 17-36. (e) Leznoff, C. C. *Chem. Soc. Rev.* **1974**, *3*, 65-85. (f) Chauvin, Y.; Commereuc, D.; Dawans, F. *Prog. Polym. Sci.* **1977**, *5*, 95-221.

(4) Miedaner, A.; Curtis, C. J.; Barkley, R. M.; DuBois, D. L. *Inorg. Chem.* **1994**, *33*, 5482-5490.

(5) (a) Knapen, J. W. J.; van der Made, A. W.; de Wilde, J. C.; van Leeuwen, P. W. N. M.; Wihkens, P.; Grove, D. M.; van Koten, G. *Nature* **1994**, *372*, 659-663. (b) Tomalia, D. A.; Dvornic, P. R. *Nature* **1994**, *372*, 617-618. (c) van der Kuil, L. A.; Grove, D. M.; Zwickler, J. W.; Jenneskens, L. W.; Drenth, W.; van Koten, G. *Chem. Mater.* **1994**, *6*, 1675-1683.

trifluoroacetic acid. Several common reagents (e.g., $\text{HSiCl}_3/\text{Et}_3\text{N}$)¹⁰ did not react at all with **4**, while a variety of others (e.g., LiAlH_4 , Red-Al, $(i\text{-Bu})_2\text{AlH}$)¹¹ could not effect reduction without destroying the Si/O framework or cleaving benzylic C–P bonds. We eventually found that AlH_3 was able to reduce **4** with a minimum number of side reactions.¹² Some reduction of $\text{CH}_2\text{P}(\text{O})\text{Ph}_2$ groups to CH_3 groups was observed (~5%), but the overall yield of CH_2PPh_2 groups was quite good. For convenience, we refer to this product as **5**, but it is important to recognize that the actual product derived from the AlH_3 reduction of **4** is a mixture of many cuboctameric silsesquioxanes with randomly and statistically distributed $\text{C}_6\text{H}_4\text{CH}_3$ (and $\text{C}_6\text{H}_4\text{CH}_2\text{PPh}_2$) groups.

The addition of $[(\text{CO})_2\text{RhCl}]_2$ (0.0672 mmol) to a solution of **5** (0.0336 mmol) in benzene (25 mL) results in the immediate formation of a bright yellow gel which occludes the entire volume of solvent. This gel does not settle noticeably over several hours, but it quickly collapses to a pale yellow powder when the solvent is evaporated in vacuo or when the reaction mixture is filtered. Filtrates are colorless, and elemental analysis¹³ of the yellow powder (C, H, Cl, P) agrees reasonably well with the formula $5 \cdot [\text{Rh}(\text{CO})\text{Cl}]_4$, suggesting that virtually all of the Rh from $[(\text{CO})_2\text{RhCl}]_2$ is incorporated into the product. The surface area calculated by the BET equation (nitrogen) was 120–150 m^2/g , and the average pore diameter was calculated to be 285 Å. Thermogravimetric analysis and differential scanning calorimetry indicate that the dry gel is stable under nitrogen up to 260 °C. Between 260 and 500 °C, the sample gradually loses 25% of its mass. Over this temperature range the DSC curve exhibits a very slight overall endotherm with a small exotherm at ~400 °C.

In light of our elemental analysis data, the known reactivity of rhodium carbonyl chlorides with phosphines,^{14,15} and our previous work with P(III)-containing silicates derived from $[(\text{Me}_3\text{SnO})_8\text{Si}_8\text{O}_{12}]$,¹⁶ we expected our Rh-containing gel to contain a large fraction of *trans*- $\text{P}_2\text{Rh}(\text{CO})\text{Cl}$ groups. Consistent with this expectation, an IR spectrum of the gel exhibits a single carbonyl absorbance at 1969 cm^{-1} , which is very similar to the CO absorbances observed for a variety of *trans*- $(\text{RPPH}_2)_2\text{Rh}(\text{CO})\text{Cl}$ complexes.^{14,17} Quite remarkably, no other absorbances are observed in the carbonyl region of the spectrum. This suggests that the fraction of metal centers containing two CO ligands (e.g., “dangling” $\text{PRh}(\text{CO})_2\text{Cl}$ end groups) must be small, which in turn militates against the formation of many Rh centers with three phosphine ligands.

(10) Naumann, K.; Zon, G.; Mislow, K. *J. Am. Chem. Soc.* **1969**, *91*, 7012–7023.

(11) Hartley, F. R., Ed. *The Chemistry of Functional Groups: The Chemistry of Organophosphorus Compounds*; Wiley: New York, 1990; Vol. 1, Chapter 7, and references cited therein.

(12) Brown, H. C.; Yoon, N. M. *J. Am. Chem. Soc.* **1966**, *88*, 1464–1472.

(13) Anal. Calcd. for $5 \cdot [\text{Rh}(\text{CO})\text{Cl}]_4$ ($\text{C}_{156}\text{H}_{128}\text{Cl}_4\text{O}_{16}\text{P}_8\text{Rh}_4\text{Si}_8$): C, 57.07 (55.94); H, 3.93 (3.26); Cl, 4.26 (4.51); P, 7.55 (6.70).

(14) Hughes, R. P. In *Comprehensive Organometallic Chemistry*; Wilkinson, G., Ed.; Pergamon: New York, 1982; Vol. 5, pp 296–313, and references cited therein.

(15) (a) Sohn, Y. S.; Balch, A. L. *J. Am. Chem. Soc.* **1972**, *94*, 1144–1148. (b) Sanger, A. R. *J. Chem. Soc., Dalton Trans.* **1977**, 120–129. (c) Siegl, W. O.; Lapporte, S. J.; Collman, J. P. *Inorg. Chem.* **1971**, *10*, 2158–2165.

(16) Feher, F. J.; Weller, K. J. *Chem. Mater.* **1994**, *6*, 7–9.

(17) *trans*- $(\text{RPPH}_2)_2\text{Rh}(\text{CO})\text{Cl}$ complexes typically exhibit CO absorbances at $\sim 1970\text{ cm}^{-1}$. Stoichiometrically analogous *cis* isomers typically exhibit CO absorbances at $\sim 2010\text{ cm}^{-1}$. The CO absorbances for five-coordinate $\text{P}_3\text{Rh}(\text{CO})\text{Cl}$ complexes are typically $< 1960\text{ cm}^{-1}$.

A number of attempts were made to use solid-state NMR techniques to determine both the fraction of phosphine appendages attached to Rh and the relative populations of various Rh coordination environments. In the case of ^{31}P , the large chemical anisotropy of phosphorus and extensive spin-spin coupling produce very complex spectra. In contrast, the ^{13}C CPMAS NMR spectrum exhibits two broad, featureless resonances centered at δ 121 and 24. The very broad resonance at δ 121 is assignable to the overlapping ^{13}C resonances for the aromatic ring, while the resonance at δ 24 is assignable to benzylic CH_2 groups attached to phosphorus. The lack of any discernible shoulders on the resonance at δ 24 is consistent with our assertion that the vast majority of phosphine moieties are attached to Rh in chemically similar environments. Unfortunately, this lack of spectroscopic detail provides no basis for assessing the relative populations of various Rh coordination environments which might be reasonably expected to form.

Preliminary attempts to use our Rh-containing gels as catalysts for olefin isomerization, hydroformylation, and hydrogenation have been disappointing. Both the dry gel and swollen gels prepared in benzene via the reaction of $[(\text{CO})_2\text{RhCl}]_2$ with **5** failed to react with 1-pentene at 65 °C and pressures as high as 60 psi (H_2 and/or CO). At higher pressures (700 psig), some hydroformylation of 1-pentene by the swollen gel was observed, but the activity was very low and the selectivity was poor (~3:1 n/iso). The origin of this activity is not clear, but mass transport through the gel appears to be facile. We suspect that the catalytic activity observed at high pressure results from small amounts of soluble Rh complexes generated by the reaction of the gel with CO. Our belief is that dissociation of phosphine from Rh is required for catalytic activity in this system; this is very difficult and unfavorable in a network structure.

In conclusion, we have described an interesting new approach for preparing organometallic gels containing large amounts of potentially catalytically active metal centers. These gels, which contain the same metal–ligand environments present in many well-defined homogeneous catalysts, offer a number of interesting possibilities as catalysts, but only if phosphine dissociation is not part of the catalytic cycle. Forthcoming work from our group will describe practical syntheses of other phosphine-substituted silsesquioxanes and demonstrate that organometallic gels are indeed capable of catalysis.¹⁸

Acknowledgment. We gratefully acknowledge Dr. Jiejun Wu (UCI) for his generous help with the solid-state NMR studies and Mr. James H. Small (UCI) for performing BET analyses. This work was supported by the National Science Foundation. Acknowledgment is also made to the donors of the Petroleum Research Fund, administered by the American Chemical Society, for partial support of this research.

Supporting Information Available: Text describing the syntheses and characterization of **3**, **4**, **5**, and $5 \cdot [\text{Rh}(\text{CO})\text{Cl}]_4$, including detailed procedures and spectroscopic and analytical data (5 pages). Ordering information is given on any current masthead page.

OM950430B

(18) Manuscript in preparation.

Preparation and Structure of $\text{Cp}^*2\text{Ru}_2(\mu\text{-Cl})(\mu\text{-X})(\text{C}_{60})$, $\text{X} = \text{H}$ and Cl . Novel Dinuclear Fullerene Complexes with and without Direct Ruthenium-Ruthenium Bonding

Ipe J. Mavunkal, Yun Chi, Shie-Ming Peng, and Gene-Hsiang Lee

Organometallics, 1995, 14 (10), 4454-4456 • DOI: 10.1021/om00010a005 • Publication Date (Web): 01 May 2002

Downloaded from <http://pubs.acs.org> on March 9, 2009

More About This Article

The permalink <http://dx.doi.org/10.1021/om00010a005> provides access to:

- Links to articles and content related to this article
- Copyright permission to reproduce figures and/or text from this article



ACS Publications
High quality. High impact.

Preparation and Structure of $\text{Cp}^*_2\text{Ru}_2(\mu\text{-Cl})(\mu\text{-X})(\text{C}_{60})$, $\text{X} = \text{H}$ and Cl . Novel Dinuclear Fullerene Complexes with and without Direct Ruthenium–Ruthenium Bonding

Ipe J. Mavunkal,[†] Yun Chi,^{*,†} Shie-Ming Peng,^{*,‡} and Gene-Hsiang Lee[‡]

Departments of Chemistry, National Tsing Hua University,
Hsinchu 30043, Taiwan, Republic of China, and National Taiwan University,
Taipei 10764, Taiwan, Republic of China

Received June 13, 1995[§]

Summary: Treatment of C_{60} with stoichiometric amounts of both $[\text{Cp}^*\text{Ru}(\mu\text{-H})_2]_2$ and $[\text{Cp}^*\text{RuCl}_2]_2$ produced $\text{Cp}^*_2\text{Ru}_2(\mu\text{-H})(\mu\text{-Cl})(\text{C}_{60})$ (**2**), which contains a Ru_2 fragment bound to two conjugated C–C π -bonds. The related C_{60} derivative $\text{Cp}^*_2\text{Ru}_2(\mu\text{-Cl})(\text{C}_{60})$ (**3**) was obtained by using 2 equiv of $[\text{Cp}^*\text{RuCl}_2]_2$. Formation of a transient cationic species $[\text{Cp}^*\text{RuC}_{60}]^+$ is suggested on the basis of FAB mass analysis of **2** and **3**.

Transition metal fullerene complexes have contributed immensely to the understanding of the derivative chemistry of this fascinating allotrope of carbon.¹ The first structurally characterized C_{60} derivative, $(t\text{-BuC}_5\text{H}_5\text{N})_2\text{OsO}_4(\text{C}_{60})$,² provided the impetus for the synthesis of fullerene derivatives with direct M–C(C_{60}) π -interactions.³ Single-crystal X-ray determinations of the multinuclear C_{60} complexes show that the metal fragments tend to adopt positions which are further away from each other,⁴ due to a combined effect of reduced steric repulsion, low solubility, and high symmetry.⁵ The only compound reported so far in which the metal atoms occupy the adjacent π -bonds of a six-membered ring of C_{60} is the chloro-bridged iridium complex $\text{C}_{60}\{\text{Ir}_2\text{Cl}_2(1,5\text{-COD})_2\}_2$ (**1**).⁶ Herein, we report the synthesis and crystallographic characterization of two dinuclear derivatives $\text{Cp}^*_2\text{Ru}_2(\mu\text{-H})(\mu\text{-Cl})(\text{C}_{60})$ (**2**) and $\text{Cp}^*_2\text{Ru}_2(\mu\text{-Cl})(\text{C}_{60})$ (**3**). To the best of our knowledge, complex **2** is the first example of a transition-metal C_{60} derivative containing a direct Ru–Ru bonding interaction.

The title complex **2** was synthesized by heating a 1:1 mixture of $[\text{Cp}^*\text{Ru}(\mu\text{-H})_2]_2$ and C_{60} in toluene (90 °C, 10 h), followed by addition of 1 equiv of $[\text{Cp}^*\text{RuCl}_2]_2$ and continued heating for another 1.5 h. The resulting solution was passed through an alumina column eluting with toluene, producing a greenish band which was closely followed by a second brownish band. Dark-green crystals of **2** in 18% yield were obtained from the greenish fraction upon standing over a period of 12 h.⁷ Attempts to isolate pure crystalline material for the second fraction were unsuccessful. However, a FAB mass analysis of the brownish fraction indicated the presence of a mixture of C_{60} complexes with four Cp^*Ru fragments.⁸ Alternatively, complex **2** can be prepared by reacting equimolar amounts of C_{60} , $[\text{Cp}^*\text{Ru}(\mu\text{-H})_2]_2$, and $[\text{Cp}^*\text{RuCl}_2]_2$ in toluene (90 °C, 2.5 h) and purified by extraction with excess CS_2 solvent; yield 24%.

Complex **2** is stable in air and dissolves sparingly in common organic solvents, such as CS_2 , CH_2Cl_2 , benzene, and toluene. The negative ion FAB mass analysis showed a molecular ion at m/z 1230 corresponding to a composition $\text{Ru}_2\text{ClC}_{80}\text{H}_{31}$. The ^1H NMR spectrum of **2** in $\text{CS}_2/\text{C}_6\text{D}_6$ showed a Cp^* signal at δ 2.05 and a hydride resonance at δ –14.51. Although the ^{13}C NMR spectrum could not be obtained due to poor solubility (~ 0.33 mg/mL in CS_2), a formulation $\text{Cp}^*_2\text{Ru}_2(\mu\text{-H})(\mu\text{-Cl})(\text{C}_{60})$ was proposed on the basis of the available spectral data. Crystals suitable for X-ray diffraction studies were grown from a mixture of CS_2 /toluene at room temperature, and the structure was unambiguously established by single-crystal X-ray determination.⁹

[†] National Tsing Hua University.

[‡] National Taiwan University.

[§] Abstract published in *Advance ACS Abstracts*, September 15, 1995.

- (1) (a) Fagan, P. J.; Calabrese, J. C.; Malone, B. *Acc. Chem. Res.* **1992**, *25*, 134. (b) Bowser, J. R. *Adv. Organomet. Chem.* **1994**, *36*, 57. (c) Balch, A. L.; Catalano, V. J.; Lee, J. W.; Olmstead, M. M.; Parkin, S. R. *J. Am. Chem. Soc.* **1991**, *113*, 8953. (d) Hirsch, A. *Angew. Chem., Int. Ed. Engl.* **1993**, *32*, 1138. (e) Zhang, S.; Brown, T. L.; Du, Y.; Shapley, J. R. *J. Am. Chem. Soc.* **1993**, *115*, 6705.
- (2) Hawkins, J. M.; Meyer, A.; Lewis, T. A.; Loren, S.; Hollander, F. *J. Science* **1991**, *252*, 312.
- (3) (a) Balch, A. L.; Ginwalla, A. S.; Lee, J. W.; Noll, B. C.; Olmstead, M. M. *J. Am. Chem. Soc.* **1994**, *116*, 2227. (b) Schreiner, S.; Gallaher, T. N.; Parsons, H. K. *Inorg. Chem.* **1994**, *33*, 3021. (c) Douthwaite, R. E.; Green, M. L. H.; Stephens, A. H. H.; Turner, J. F. C. *J. Chem. Soc., Chem. Commun.* **1993**, 1522. (d) Crane, J. D.; Hitchcock, P. B. *J. Chem. Soc., Dalton Trans.* **1993**, 2537. (e) Koefod, R. S.; Hudgens, M. F.; Shapley, J. R. *J. Am. Chem. Soc.* **1991**, *113*, 8957. (f) Green, M. L. H. *Pure Appl. Chem.* **1995**, *67*, 249. (g) Park, J. T.; Cho, J.-J.; Song, H. *J. Chem. Soc., Chem. Commun.* **1995**, 15. (h) Balch, A. L.; Lee, J. W.; Noll, B. C.; Olmstead, M. M. *Inorg. Chem.* **1994**, *33*, 5238. (i) Shapley, J. R.; Du, Y.; Hsu, H. F.; Way, J. J. *Proc. Electrochem. Soc.* **1994**, *94*, 1255.
- (4) (a) Fagan, P. J.; Calabrese, J. C.; Malone, B. *J. Am. Chem. Soc.* **1991**, *113*, 9408. (b) Balch, A. L.; Lee, J. W.; Noll, B. C.; Olmstead, M. M. *J. Am. Chem. Soc.* **1992**, *114*, 10984.
- (5) Balch, A. L.; Lee, J. W.; Noll, B. C.; Olmstead, M. M. *Inorg. Chem.* **1994**, *33*, 5238.
- (6) Rasinkangas, M.; Pakkanen, T. T.; Pakkanen, T. A.; Ahlgren, M.; Rouvinen, J. *J. Am. Chem. Soc.* **1993**, *115*, 4901.

(7) Spectral data for **2**: MS (negative ion FAB, ^{102}Ru) m/z 1230 $[(\text{C}_{60}\text{Cp}^*_2\text{Ru}_2\text{HCl})^-]$; ^1H NMR ($\text{CS}_2/\text{C}_6\text{D}_6$, 293K) δ 2.05 (s, 30H), –14.51 (s, 1H); IR (KBr pellet) 2987 (w), 2955 (w), 2897 (m), 1568 (w), 1516 (s), 1456 (s), 1418 (m), 1373 (m), 1337 (m), 1188 (w), 1177 (w), 1074 (w), 1022 (s), 773 (w), 761 (w), 706 (w), 668 (w), 586 (w), 579 (m), 533 (m), 527 (s), 518 (m), 499 (m) cm^{-1} . Anal. Calcd for $\text{Ru}_2\text{C}_{80}\text{H}_{31}\text{Cl}\cdot\text{CS}_2$: C, 74.50; H, 2.39. Found: C, 73.68; H, 2.58.

(8) MS (FAB, ^{102}Ru): m/z 720 $[(\text{C}_{60})^-]$, 957 $[(\text{C}_{60}\text{Cp}^*\text{Ru})^+]$, 1194 $[(\text{C}_{60}\text{Cp}^*_2\text{Ru}_2)^-]$, 1230 $[(\text{C}_{60}\text{Cp}^*_2\text{Ru}_2\text{HCl})^-]$, 1466 $[(\text{C}_{60}\text{Cp}^*_3\text{Ru}_3\text{HCl})^+]$, and 1739 $[(\text{C}_{60}\text{Cp}^*_4\text{Ru}_4\text{H}_2\text{Cl}_2)^+]$.

(9) Crystal data for **2**: $\text{Ru}_2\text{C}_{80}\text{H}_{31}\text{Cl}\cdot\text{C}_7\text{H}_8$, $M = 1321.85$, monoclinic, space group $P2_1/n$, $a = 18.378(5)$ Å, $b = 13.307(5)$ Å, $c = 21.482(4)$ Å, $\beta = 99.97(2)^\circ$, $V = 5174(3)$ Å³, $Z = 4$, $\rho_{\text{calcd}} = 1.697$ g cm^{-3} , $F(000) = 2654$, $\lambda(\text{Mo K}\alpha) = 0.7107$ Å, $T = 298$ K, $\mu = 6.792$ cm^{-1} . The intensities were measured on a Nonius CAD4 diffractometer on a crystal with dimensions $0.05 \times 0.25 \times 0.50$ mm. An absorption correction based on ψ scans was applied. Three standard reflections were monitored every 3600 s with intensity variation <2%. Of the 9090 unique reflections collected, 6143 reflections with $I > 2\sigma(I)$ were used for the refinement. The structure was solved by the NRCC-SDP-VAX package and refined to $R_F = 0.045$, $R_w = 0.040$, and $\text{GOF} = 2.46$ for 753 parameters, weighting scheme $w^{-1} = \sigma^2(F_o) + 0.00001F_o^2$, and highest Δ/σ ratio 0.01. All non-hydrogen atoms were refined anisotropically. A difference map following convergence showed residual electron density within the range $-0.70/0.74$ e/Å³ (min/max). The toluene molecule is found to be distorted due to the partial replacement with CS_2 solvents during recrystallization.

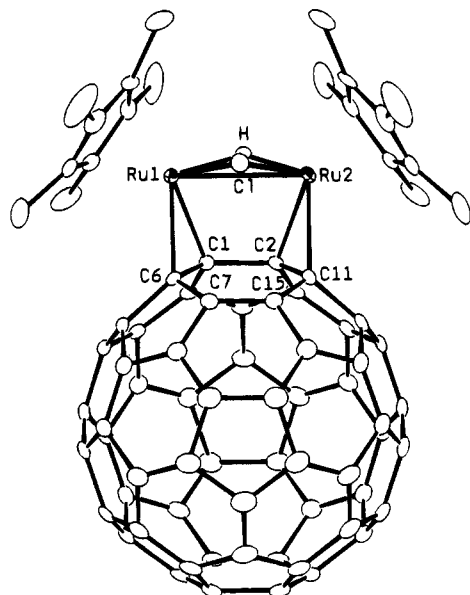


Figure 1. Molecular structure of **2** and selected bond lengths (Å): Ru(1)–Ru(2) = 2.9554(9), Ru(1)–C1 = 2.412(2), Ru(2)–C1 = 2.414(2), Ru(1)–H = 1.86(5), Ru(2)–H = 1.74(4), Ru(1)–C(1) = 2.168(6), Ru(1)–C(6) = 2.218(6), Ru(2)–C(2) = 2.187(6), Ru(2)–C(11) = 2.227(6), C(1)–C(2) = 1.491(8), C(1)–C(6) = 1.460(8), C(2)–C(11) = 1.456(8), C(6)–C(7) = 1.482(8), C(11)–C(15) = 1.478(9), C(7)–C(15) = 1.384(8).

The molecular structure of **2** is shown in Figure 1 together with selected bond distances. It possesses two Ru atoms coordinated to two adjacent 6–6 junctions of the C₆₀ molecule. Each Ru atom is further coordinated by a Cp* ligand, a bridging hydride, and a bridging chloro ligand. The observed Ru(1)–Ru(2) distance (2.9554(9) Å) is well within the range expected for a formal Ru–Ru single bond.¹⁰ The inner Ru–C bond distances, Ru(1)–C(1) = 2.168(6) and Ru(2)–C(2) = 2.187(6) Å, are slightly shorter than the outer Ru–C bond distances, Ru(1)–C(6) = 2.218(6) and Ru(2)–C(11) = 2.227(6) Å, and are within the range observed for the M–C(olefin) distances reported for ruthenium–olefin η^2 bonds.¹¹ Assuming that the C₆₀ fragment serves as a four-electron-donor, this molecule contains 34 valence electrons, which is in good agreement with the electron counting for dinuclear complexes having one metal–metal bond.

Interestingly, the related dichloro complex **3** was obtained along with **2** when C₆₀ was reacted with [Cp*Ru(μ -H)₂]₂ and [Cp*RuCl₂]₂ in the molar ratio 1:1:2 under identical conditions.¹² Single crystals suitable for X-ray diffraction study were obtained from the reaction mixture after filtering off the precipitated **2**, followed by passing the resultant filtrate through a short neutral alumina column and standing at room temperature for several days. The key features of **3**, which was un-

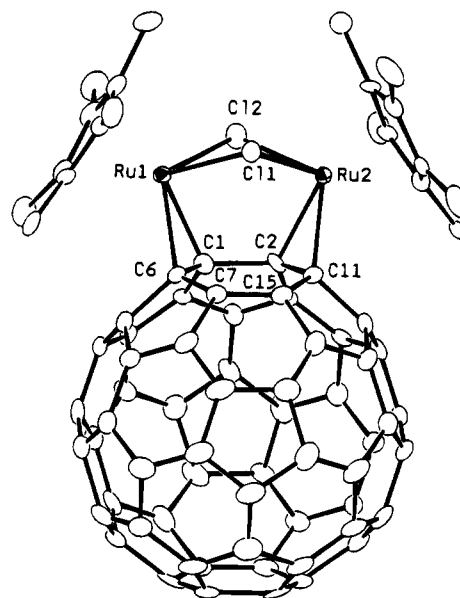


Figure 2. Molecular structure of **3** and selected bond lengths (Å): Ru(1)–Ru(2) = 3.461(2), Ru(1)–Cl(1) = 2.434(3), Ru(2)–Cl(1) = 2.420(3), Ru(1)–Cl(2) = 2.439(3), Ru(2)–Cl(2) = 2.458(3), Ru(1)–C(1) = 2.20(1), Ru(1)–C(6) = 2.208(9), Ru(2)–C(2) = 2.173(9), Ru(2)–C(11) = 2.217(9), C(1)–C(2) = 1.55(1), C(1)–C(6) = 1.41(1), C(2)–C(11) = 1.44(1), C(6)–C(7) = 1.47(1), C(11)–C(15) = 1.50(1), C(7)–C(15) = 1.40(1).

equivocally established by X-ray diffraction study,¹³ resemble those of **2** as indicated from its ORTEP diagram (Figure 2): both the ruthenium atoms of the Cp*₂Ru₂(μ -Cl)₂ fragment are coordinated to two adjacent 6–6 junctions of C₆₀, and the Ru–C distances and all C–C distances of the C₆₀ ball are within the ranges observed for compound **2**. The notable difference is the elongation of Ru(1)–Ru(2) distance (3.461(2) Å) in **3** as a consequence of a bridging chloro ligand replacing the hydride in **2**, which added two additional valence electrons to balance the electron deficiency caused by lengthening of the Ru–Ru bond. Similar alteration of M–M bond distance by varying the donor ability of ancillary ligands has been observed in the triosmium cluster compounds Os₃(CO)₁₀(μ -H)₂, Os₃(CO)₁₀(μ -H)(μ -X), and Os₃(CO)₁₀(μ -X)₂, X = Cl and OMe.¹⁴

After completing the discussion of their solid state structures, we focused on the fragmentation behavior in gaseous phase. The positive ion FAB mass spectrum of complex **2** is noteworthy. In contrast to the negative ion experiment which exhibited peaks due to the molecular ion and the C₆₀ anion, the positive ion FAB analysis showed an additional peak at *m/z* 957, corre-

(10) (a) Suzuki, H.; Omori, H.; Lee, D. H.; Yoshida, Y.; Fukushima, M.; Tanaka, M.; Moro-oka, Y. *Organometallics* **1994**, *13*, 1129. (b) Koelle, U.; Kossakowski, J.; Klaff, N.; Wesemann, L.; Englert, U.; Heberich, G. E. *Angew. Chem., Int. Ed. Engl.* **1991**, *30*, 690.

(11) Koelle, U.; Kang, B. S.; Englert, U. *J. Organomet. Chem.* **1991**, *420*, 227.

(12) Spectral data for **3**: MS (negative ion FAB, ¹⁰²Ru) *m/z* 1265 [(C₆₀Cp*₂Ru₂Cl₂)⁻]; ¹H NMR (CS₂/C₆D₆, 293 K) δ 1.69 (30H); IR (KBr pellet) 2987 (w), 2954 (w), 2902 (m), 1372 (m), 1338 (w), 1186 (w), 1020 (s), 693 (w), 582 (w), 525 (s), 518 (m), 501 (w), 457 (w), 418 (m), 397 (m) cm⁻¹.

(13) Crystal data for **3**: Ru₂C₆₀H₃₀Cl₂·2C₂H₆, *M* = 1321.85, monoclinic, space group *P*2₁/*n*, *a* = 16.173(5) Å, *b* = 23.247(4) Å, *c* = 16.305(5) Å, β = 106.48(3)°, *V* = 5878(3) Å³, *Z* = 4, ρ_{calcd} = 1.637 g cm⁻³, *F*(000) = 2919, λ (Mo K α) = 0.7107 Å, *T* = 298 K, μ = 6.398 cm⁻¹. The intensities were measured on a crystal with dimensions 0.02 × 0.25 × 0.75 mm. Of the 7666 unique reflections collected, 3846 reflections with *I* > 2 σ (*I*) were used for the refinement. The structure was refined to *R*_F = 0.048, *R*_w = 0.045, and GOF = 1.33 for 883 parameters, weighting scheme $w^{-1} = \sigma^2(F_o) + 0.00001F_o^2$, and highest Δ/σ ratio 0.04. A difference map following convergence showed residual electron density within the range -0.71/0.85 e/Å³ (min/max).

(14) (a) Broach, R. W.; Williams, J. M. *Inorg. Chem.* **1979**, *18*, 314. (b) Churchill, M. R.; Lashewycz, R. A. *Inorg. Chem.* **1979**, *18*, 3261. (c) Churchill, M. R.; Wasserman, H. J. *Inorg. Chem.* **1980**, *19*, 2391. (d) Churchill, M. R.; Lashewycz, R. A. *Inorg. Chem.* **1979**, *18*, 1926. (e) Allen, V. F.; Mason, R.; Hitchcock, P. B. *J. Organomet. Chem.* **1977**, *140*, 297. (f) Einstein, F. W. B.; Jones, T.; Tyers, K. G. *Acta Crystallogr.* **1982**, *B38*, 1272.

sponding to a cationic fragment $[\text{C}_{60}\text{RuCp}^*]^+$. We presume that the C_{60} unit in this transient fragment is coordinated to the Ru atom via a hexahapto bonding similar to that observed for $[\text{Cp}^*\text{Ru}(\text{C}_6\text{H}_6)]^+$,¹⁵ although theoretical studies indicate C_{60} an inferior ligand compared to benzene.¹⁶ Interestingly, Fagan et al. reported that a similar reaction between C_{60} and excess of $[\text{Cp}^*\text{Ru}(\text{CH}_3\text{CN})_3][\text{O}_3\text{SCF}_3]$ yielded cationic complexes $\{[\text{Cp}^*\text{Ru}(\text{CH}_3\text{CN})_2]_x(\text{C}_{60})\}[\text{O}_3\text{SCF}_3]_x$, $x = 3$ or 4 , in which the Ru atoms are linked to the C_{60} molecule in a dihapto fashion, as the metal retains two weakly coordinated acetonitrile molecules.¹⁷ The FAB mass spectra of **3** showed similar pattern as that of **2** although the intensity of the peak due to the fragment $[\text{C}_{60}\text{RuCp}^*]^+$ in the positive ion FAB mass spectrum was much smaller than that of **2**.

In conclusion, we report the first example of a structurally characterized C_{60} derivative which contain a direct metal-metal interaction and present preliminary evidence for the existence of hexahapto bonding for a C_{60} complex. The disposition of metals in **2** provide a good comparison with the earlier reported tetrairidium

adduct **1** and diruthenium complex **3**.⁶ In the latter case, the presence of two bridging chloro ligands push the metal atoms away from each other and each transition-metal atom can be considered as an independent 18-electron mononuclear fragment. Finally, the isolation of **1-3** suggest that the C_{60} molecule utilizes its adjacent C-C double bonds of a hexagonal ring to form stable dinuclear complexes; therefore, the formation of a triangular M_3C_{60} cluster with unique $\mu_3\text{-}\eta^2, \eta^2, \eta^2$ interaction similar to that observed for the Os_3 , Ru_3 , and Co_3 arene clusters can be envisioned.¹⁸

Acknowledgment. This work was supported by the National Science Council, Taiwan, Republic of China (Grant No. NSC 84-2113-M007-034CC).

Supporting Information Available: Text describing experimental procedures for the synthesis of **2** and **3** and tables of crystal data, bond distances, atomic coordinates and B values, and anisotropic thermal parameters for **2** and **3** (26 pages). Ordering information is given on any current masthead page.

OM950453Q

(15) Fagan, P. J.; Ward, M. D.; Calabrese, J. C. *J. Am. Chem. Soc.* **1989**, *111*, 1698.

(16) Rogers, J. R.; Marynick, D. S. *Chem. Phys. Lett.* **1993**, *205*, 197.

(17) Fagan, P. J.; Calabrese, J. C.; Malone, B. *Science* **1991**, *252*, 1160.

(18) (a) Gomez-Sal, M. P.; Johnson, B. F. G.; Lewis, J.; Raithby, P. R.; Wright, A. H. *J. Chem. Soc., Chem. Commun.* **1985**, 1682. (b) Braga, D.; Grepioni, F.; Johnson, B. F. G.; Lewis, J.; Housecroft, C. E.; Martinelli, M. *Organometallics* **1991**, *10*, 1260. (c) Wadepohl, H.; Buchner, K.; Herrmann, M.; Pritzkow, H. *Organometallics* **1991**, *10*, 861.

New and Convenient Synthesis of Lithiated Allenes and Ketenimines Based on Readily Available Aryl-Substituted Ketones and Amides

Dietmar Seyferth,^{*,1a} Peter Langer,^{1a,b} and Manfred Döring^{1a,c}

Department of Chemistry, Massachusetts Institute of Technology, Cambridge, Massachusetts 02139, Institut für Organische Chemie, Universität Hannover, 30167 Hannover, Germany, and Institut für Anorganische und Analytische Chemie, Friedrich-Schiller-Universität, 07743 Jena, Germany

Received June 12, 1995[®]

Summary: The action of 3 molar equiv of *i*-Pr₂NLi on silyl enol ethers of type Ph₂C=C(CH₃)(OSiMe₂Bu-*t*) and PhCH=C(CH₂R)(OSiMe₂Bu-*t*) (R = Ph, CH₃) results in formation of Ph₂C=C=CLi₂ and Ph(Li)C=C=C(Li)R, respectively, via initial allylic lithiation, subsequent elimination of *t*-BuMe₂SiOLi, and finally, lithiation of the allene thus formed. Reactions of the dilithioallenes with chlorosilanes, Me₃SnCl, (CH₃O)₂SO₂, and a proton source were carried out.

Silyl enol ethers are valuable reagents in organic synthesis.² By far the major interest has been in their reactions with electrophiles, but there are a few reports of their reactions with carbon nucleophiles or bases. One reaction of interest is the displacement of the Me₃SiO group of a trimethylsilyl enol ether by Grignard reagents in the presence of a Ni(II) catalyst, which represents a synthesis of di- or trisubstituted ethylenes.³ Corey and Rücker have reported an interesting conversion of silyl enol ether anions, via a silyl 1,3 O → C migration, to the respective α-silyl ketone anions when the silyl group is the bulky *i*-Pr₃Si.⁴ This conversion requires an excess of Lochmann's base (2 equiv of *n*-BuLi + 2.5 equiv of Me₃COK) in hexane at room temperature for 24 h.

During the course of our studies of the organometallic chemistry of ambident acetone dianions,^{5,6} we had occasion to investigate the action of lithium diisopropylamide (LDA) on 1,1-diphenylacetone-derived silyl enol ethers of the type Ph₂C=C(CH₃)(OSiR₃). These, via methyl group metalation, were expected to give an allylic lithium species which should be a useful synthetic reagent.

Treatment of 1,1-diphenylacetone in THF with 1 molar equiv of KH, followed by addition of Me₃SiCl, gave Ph₂C=C(CH₃)(OSiMe₃) (**1**) in 79% yield.⁷ Quenching of the enolate anion solution with *t*-BuMe₂SiCl gave Ph₂C=C(CH₃)(OSiMe₂Bu-*t*) (**2**, 82%). Treatment of **1** with 1 molar equiv of LDA in THF, followed by addition of Me₂HSiCl, resulted in formation of Ph₂C=C(CH₂-SiMe₃)(OSiMe₂H) (**3**) as the major product. Some start-

ing material also was recovered (**3**:**1** = 2 in the final product mixture). The formation of **3** can be explained in terms of a 1,3 O → C migration of the Me₃Si group in the initially formed anion,⁸ Ph₂C=C(CH₂)⁻(OSiMe₃), giving Ph₂C=C(CH₂SiMe₃)(O⁻), followed by reaction of the latter with the added Me₂HSiCl. Except for the rearrangement, this was the expected chemistry.

Completely different and unexpected results were obtained when the hindered *tert*-butyldimethylsilyl enol ether **2** was used instead of the Me₃Si derivative **1**. Instead of the expected (on the basis of the reaction above) Ph₂C=C(CH₂SiMe₂Bu-*t*)(OSiMe₂H), the major product was an allene, Ph₂C=C=C(SiMe₂H)₂ (**4**). Here also, some starting material was recovered (**4**:**2** = 2 in product mixture). A new and simply effected allene synthesis was of interest, and further experiments were carried out in which, in view of the information gained in the above reaction with **2**, 3.3 molar equiv of LDA was used (rather than only **1**) in the reaction with **2**, followed by addition of 3.5 molar equiv of a chlorosilane. Addition of the LDA to **2** in THF resulted in a deep red solution whose color was discharged when the chlorosilane was added. Such reactions gave the respective 1,1-diphenyl-3,3-bis(silyl)allenes Ph₂C=C=C(SiMe₂R)₂ (R = H, CH₃) and Ph₂C=C=C(SiPh₂CH₃)₂ in generally good (60–80%) yield.⁹ The reaction course which must lead to formation of the allenes is shown in Scheme 1. Elimination of *t*-BuMe₂SiOLi (whose intermediacy was proven by isolation of *t*-BuMe₂SiOSiPh₂CH₃ from the Ph₂CH₃SiCl quench) could occur directly from

(8) We use the "anion" terminology, although we recognize that this and related species discussed in this report are allylic lithium reagents.

(9) Formation of polyolithioallenes is a facile process: (a) Jaffe, F. J. *Organomet. Chem.* **1970**, *23*, 53. (b) Chwang, T. L.; West, R. J. *Am. Chem. Soc.* **1973**, *95*, 3324. (c) West, R.; Carney, P. A.; Mineo, J. C. *J. Am. Chem. Soc.* **1965**, *87*, 3788. (d) Priester, W.; West, R.; Chwang, T. L. *J. Am. Chem. Soc.* **1976**, *98*, 8413.

(10) All reactions were carried out on a 4–10 mmol scale under an atmosphere of argon or prepurified nitrogen. The generally used procedure was as follows. A 250 mL round-bottom Schlenk flask equipped with a magnetic stirbar and a rubber septum was charged with diisopropylamine (3.3 molar equiv) and 40 mL of dry THF. To this solution was added 3.3 molar equiv of *n*-BuLi in hexane with stirring. The resulting solution was stirred for 1 h and cooled to 0 °C, and then 1 molar equiv of the respective *tert*-butyldimethylsilyl enol ether was added by syringe to the LDA solution. The solution was stirred at room temperature for about 10 h, during which time it became deep red. Subsequently, it was cooled to 0 °C and the respective chlorosilane (3.5 molar equiv) was added by syringe; this mixture was stirred at room temperature for 14–48 h. During this time the red color was discharged and a white precipitate and a pale yellow solution resulted. The solvent was removed from the reaction mixture *in vacuo* without heating, and the residue, after it had been maintained *in vacuo* for 6 h, was extracted with three 40 mL portions of hexane. The extracts were filtered through Celite, the hexane was removed *in vacuo*, and the product was isolated. Purification was effected by column chromatography, crystallization, distillation, or GLC.

[®] Abstract published in *Advance ACS Abstracts*, September 1, 1995.

(1) (a) Massachusetts Institute of Technology. (b) Universität Hannover. (c) Friedrich-Schiller-Universität Jena.

(2) (a) Reetz, M. T. *Angew. Chem., Int. Ed. Engl.* **1982**, *21*, 96. (b) Brownbridge, P. *Synthesis* **1983**, *1*, 85.

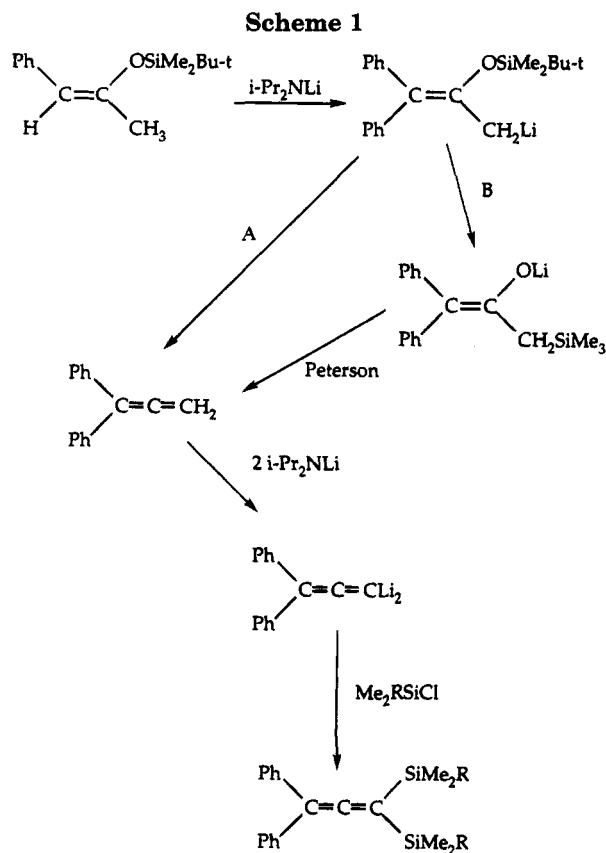
(3) Ryu, I.; Murai, S.; Niwa, I.; Sonoda, N. *Synthesis* **1977**, 874.

(4) Corey, E. J.; Rücker, C. *Tetrahedron Lett.* **1984**, *25*, 4345.

(5) Seyferth, D.; Wang, T.; Davis, W. B. *Organometallics* **1994**, *13*, 4134.

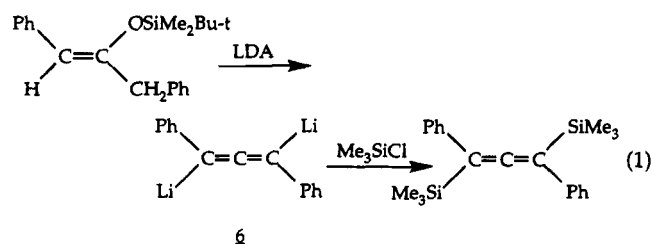
(6) Seyferth, D.; Wang, T.; Ostrander, R. L.; Rheingold, A. L. *Organometallics* **1995**, *14*, 2136.

(7) Details of product characterization are given in the supporting information.

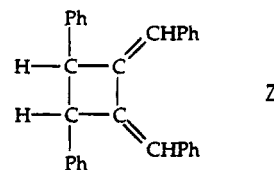


the C-lithiated silyl enol ether (path A) or *via* a 1,3 C \rightarrow O silyl migration/Peterson reaction sequence (path B). A requirement for this silanolate elimination reaction appears to be that the silyl group be bulky. It also was observed with $\text{Ph}_2\text{C}=\text{C}(\text{CH}_3)(\text{OSiPr-}i)_3$, but not with **1**. Once formed, 1,1-diphenylallene (**5**) is easily lithiated by LDA to give $\text{Ph}_2\text{C}=\text{C}=\text{CLi}_2$ (**6**).^{9,10} Addition of the chlorosilane then gives the final product, $\text{Ph}_2\text{C}=\text{C}=\text{C}(\text{SiMe}_2\text{R})_2$.

$\text{Ph}_2\text{C}=\text{C}=\text{CLi}_2$, in other experiments, was intercepted by addition of ethanol, giving $\text{Ph}_2\text{C}=\text{C}=\text{CH}_2$, and Me_3SnCl , giving $\text{Ph}_2\text{C}=\text{C}=\text{C}(\text{SnMe}_3)_2$ (60%). Reaction of $\text{Ph}_2\text{C}=\text{C}=\text{CLi}_2$ with dimethyl sulfate gave not $\text{Ph}_2\text{C}=\text{C}=\text{C}(\text{CH}_3)_2$ but rather the isomeric $\text{Ph}_2\text{CCH}_3\text{CC}=\text{CCH}_3$ (42%). It would appear that the reaction of the second C–Li bond with $(\text{CH}_3\text{O})_2\text{SO}_2$ is sufficiently slow so that the initially formed $\text{Ph}_2\text{C}=\text{C}=\text{C}(\text{CH}_3)\text{Li}$ can rearrange to the more highly stabilized $\text{Ph}_2(\text{Li})\text{CC}=\text{CCH}_3$ before introduction of the second CH_3 group. In contrast, in view of the products obtained, reactions of the intermediate $\text{Ph}_2\text{C}=\text{C}=\text{C}(\text{Z})\text{Li}$ ($\text{Z} = \text{R}_3\text{Si}, \text{Me}_3\text{Sn}, \text{H}$) with the second equivalent of the respective electrophile must be quite rapid, faster, in any case, than the $\text{Ph}_2\text{C}=\text{C}=\text{C}(\text{Z})\text{Li}$ to $\text{Ph}_2(\text{Li})\text{CC}=\text{CZ}$ rearrangement. Similar chemistry was observed with the 1,3-diphenylacetone-derived $\text{PhCH}=\text{C}(\text{CH}_2\text{Ph})(\text{OSiMe}_2\text{Bu-}t)$; e.g., eq 1.

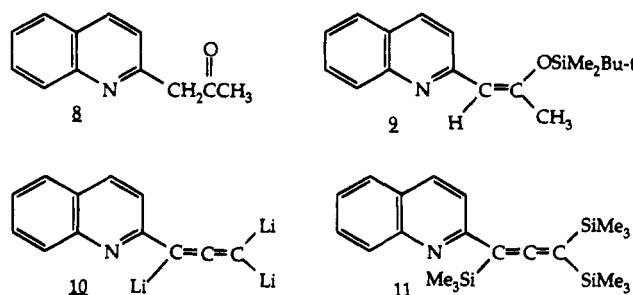


Reactions of dilithioallene **6** with Me_3SnCl and with $(\text{CH}_3\text{O})_2\text{SO}_2$ gave $\text{Ph}(\text{Me}_3\text{Sn})\text{C}=\text{C}=\text{C}(\text{SnMe}_3)\text{Ph}$ (53%) and a 2:1 mixture (47%) of $\text{Ph}(\text{CH}_3)_2\text{CC}=\text{CPh}$ and $\text{Ph}(\text{CH}_3)\text{C}=\text{C}(\text{CH}_3)\text{Ph}$, respectively. In the latter reaction the relative rates of the reaction of the initially formed $\text{Ph}(\text{Li})\text{C}=\text{C}=\text{C}(\text{CH}_3)\text{Ph}$ with dimethyl sulfate and its rearrangement to $\text{Ph}(\text{CH}_3)(\text{Li})\text{CC}=\text{CPh}$ must be more nearly comparable. The relatively unhindered $\text{PhCH}=\text{C}=\text{CHPh}$ obtained in the protonolysis of $\text{Ph}(\text{Li})\text{C}=\text{C}=\text{C}(\text{Li})\text{Ph}$ dimerized, and **7**¹² was isolated in 51% yield.



The silyl enol ether prepared from 1-phenyl-2-butanone, $\text{PhCH}=\text{C}(\text{C}_2\text{H}_5)(\text{OSiMe}_2\text{Bu-}t)$ (a 1:1 mixture of *E* and *Z* isomers), also reacted with 3.3 molar equiv of LDA, giving a dilithioallene, $\text{Ph}(\text{Li})\text{C}=\text{C}=\text{C}(\text{CH}_3)\text{Li}$. Its reaction with Me_3SiCl afforded $\text{Ph}(\text{Me}_3\text{Si})\text{C}=\text{C}=\text{C}(\text{CH}_3)\text{SiMe}_3$ in 19% yield. However, application of the reaction sequence LDA/ Me_3Si to the *tert*-butyldimethylsilyl enol ether prepared from $\text{C}_2\text{H}_5\text{C}(\text{O})\text{C}_2\text{H}_5$ produced a complex mixture of products whose spectra gave no evidence for the presence of an allene. It would appear that at least one aryl substituent, preferably two, are required on the carbon atoms adjacent to the carbonyl group of the ketone if this chemistry is to be observed.

Of particular interest is the case of the quinolyl-substituted acetone **8**, which was converted to silyl enol ether **9**. Treatment of **9** with 3.3 molar equiv of LDA



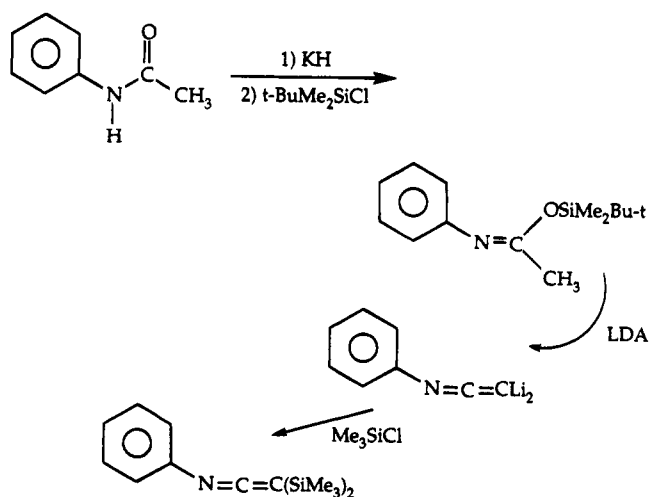
did not give a clean reaction mixture, but addition of 4.4 molar equiv of LDA to a THF solution of **9** must have resulted in clean trillithiation, giving **10**, since the isolated product, after addition of Me_3SiCl to the solution, was **11**, obtained in 85% yield. Trillithiation very likely was facilitated by interaction of the neighboring quinolyl nitrogen lone electron pair with the approaching lithium amide species and by its interaction with the β -Li in **10**.

This new chemistry not only is applicable to silyl enol ethers derived from appropriately substituted ketones

(11) Binger et al. had proposed earlier that $\text{Ph}_2\text{C}=\text{C}=\text{CLi}_2$ had been formed by the rearrangement of 1,2-dilithio-3,3-diphenylcyclopropene, the latter having been generated by the dilithiation of 3,3-diphenylcyclopropene by butyllithium: Binger, P.; Müller, P.; Wenz, R.; Mynott, R. *Angew. Chem., Int. Ed. Engl.* **1990**, *29*, 1037.

(12) The spectroscopic properties and melting point (194–196 °C) were identical with those of *cis*-1,2-diphenyl-*anti*-3,4-dibenzylidene-cyclobutane (mp 197 °C), which was prepared by heating 1,3-diphenylallene in refluxing benzene: Dehmlow, E. V. *Chem. Ber.* **1967**, *100*, 3260.

Scheme 2



but also was observed in the case of **12**, the silyl imino ether derived from acetanilide (Scheme 2).

It is clear that the chemistry described here will be applicable to the synthesis of diverse substituted allenes, provided that, at least according to our initial observations, one aryl group (preferably two) is present on the carbon atom α to the carbonyl group of the ketone. The extension of this chemistry to silyl imino ethers opens further synthetic vistas. In our initial studies, for the sake of convenience of isolation and

characterization, we have chosen for the most part to convert the polyolithiated intermediates to organosilicon products. Also, silyl-substituted allenes have demonstrated utility in organic synthesis,¹³ as do stannyl-substituted allenes.¹⁴

Our current work is aimed at defining and expanding the scope of this new and useful chemistry and at obtaining further information concerning questions of mechanism.

Acknowledgment. We are grateful to the National Science Foundation for support of this work and thank the Studienstiftung des deutschen Volkes for the award of a fellowship to P.L. and the Deutsche Forschungsgemeinschaft for the award of a Habilitanden Fellowship to M.D.

Supporting Information Available: Text giving analytical and spectroscopic characterization data for all new compounds (5 pages). Ordering information is given on any current masthead page.

OM950439D

(13) (a) Danheiser, R. L.; Carini, D. J. *J. Org. Chem.* **1980**, *45*, 3925. (b) Montury, M.; Psaume, B.; Gore, J. *Tetrahedron Lett.* **1980**, 163. (c) Danheiser, R. L.; Carini, D. J.; Basak, A. *J. Am. Chem. Soc.* **1981**, *103*, 1604. (d) Jellal, A.; Santelli, M. *Tetrahedron Lett.* **1980**, 4487.

(14) (a) Marshall, J. A.; Wang, X. *J. Org. Chem.* **1992**, *57*, 1242. (b) Haruta, J.; Nishi, K.; Matsuda, S.; Akai, S.; Tamura, Y.; Kita, Y. *J. Org. Chem.* **1990**, *55*, 4853.

Synthesis, Structure, and Reactions of the First Stable Dimercaptoborane¹

Norihiro Tokitoh, Mitsuhiro Ito, and Renji Okazaki*

Department of Chemistry, Graduate School of Science, The University of Tokyo,
7-3-1 Hongo, Bunkyo-ku, Tokyo 113, Japan

Received May 25, 1995[⊗]

Summary: The first stable dimercaptoborane, $\text{TbtB}(\text{SH})_2$ (**1**), was synthesized by the sulfurization of the corresponding overcrowded lithium aryltrihydroborate bearing a 2,4,6-tris[bis(trimethylsilyl)methyl]phenyl (Tbt) group. Dilithiation of **1** followed by treatment with $\text{Cp}_2\text{-TiCl}_2$ resulted in the isolation of a novel metallacycle, 1,3,2,4-dithiaboratitanetane **2**, as stable red crystals. Molecular structures of the novel organoboron compounds **1** and **2** were both determined by X-ray crystallographic analysis.

In contrast to the extensive studies carried out for heteroatom-containing organoboranes such as aminoboranes, haloboranes, and boronic acid derivatives,² the chemistry of organoboranes incorporating sulfur functionalities has been less well investigated in the past though they are also considered to be an important class of organoboron compounds. Meanwhile, we have recently developed a new and effective steric protection group, 2,4,6-tris[bis(trimethylsilyl)methyl]phenyl (denoted as Tbt hereafter), and reported its high efficiency in the isolation of highly reactive chemical species such as novel cyclic polychalcogenides,³ highly strained tin-containing small ring compounds,⁴ and heavy congeners of ketones (silanethione,⁵ germanethione,⁶ and germaneselonone⁷). Here, we present an application of the Tbt group to the stabilization of unstable sulfur-containing organoboron compounds leading to the first isolation of a stable aryl-dimercaptoborane, $\text{TbtB}(\text{SH})_2$ (**1**), and a novel boron-containing metallacycle, 1,3,2,4-dithiaboratitanetane derivative **2**.

Treatment of Tbt-substituted dimethoxyborane **3**, which was readily prepared by the reaction of TbtLi

with trimethyl borate, with excess lithium aluminum hydride in THF resulted in a quantitative formation of the corresponding lithium hydroborate **4**. Pure **4** was isolated as an air- and moisture-sensitive white solid by concentration of the reaction mixture after solvent exchange into hexane, followed by filtration of insoluble materials. The structure of **4** was confirmed by the characteristic signals in ¹¹B NMR [δ -30.7 (q, $^1J_{\text{BH}} = 74.4$ Hz)] and ¹H NMR spectra, the latter of which showed not only the signals of the BH protons at δ 0.90 (3H, $^1J_{\text{BH}} = 74.4$ Hz) but also those of three molecules of THF coordinated to lithium. In the IR spectra **4** showed characteristic absorptions at 2080 and 2190

(10) In the following are shown experimental procedures for the preparation of **1**, **2**, and **5** together with their spectral and analytical data. Since the analytically pure samples of **1** and **5** were obtained by a reprecipitation procedure (addition of ethanol to their hexane solutions), they contained crystalline water the existence of which was evidenced by ¹H NMR spectroscopy and elemental analysis (*vide infra*). We have often experienced that Tbt-substituted compounds are liable to include crystalline water.¹¹ **Preparation of 1:** A mixture of **3** (1.40 g, 2.23 mmol) and LiAlH_4 (533 mg, 14.0 mmol) in THF (15 mL) was stirred at room temperature for 7 h. After solvent exchange into hexane, insoluble materials were filtered off with Celite. The filtrate was evaporated to give **1** as a white solid, to which was added 15 mL of THF and elemental sulfur (1.35 g, 5.31 mmol as S_8), and the solution was stirred for 30 min. The reaction mixture was treated with aqueous NH_4Cl and then extracted with hexane. Concentration of the organic layer gave a pale yellow crude oil, which was subjected to flash column chromatography ($\text{SiO}_2/\text{hexane}$) followed by HPLC separation to afford **1** (300 mg, 21% from **3**) as white crystals. **1:** mp 184 °C (dec); ¹H NMR (500 MHz, CDCl_3) δ 0.04 (s, 18H), 0.05 (s, 36H), 1.33 (s, 1H), 1.52 (s, 3H, H_2O), 1.56 (s, 2H), 2.88 (s, 2H), 6.23 (brs, 1H), 6.35 (brs, 1H); ¹³C NMR (125 MHz, CDCl_3) δ 0.64 (q), 0.90 (q), 1.02 (q), 29.20 (d), 29.67 (d), 30.20 (d), 121.02 (d), 125.45 (d), 133.56 (brs, ipso-arom), 144.07 (s), 144.37 (s); ¹¹B NMR (86.4 MHz, CDCl_3) δ 67.5; HRMS (70 eV) m/z found 628.2950 [M^+], calcd for $\text{C}_{27}\text{H}_{61}\text{BS}_2\text{Si}_6$ 628.2923. Anal. Calcd for $\text{C}_{27}\text{H}_{61}\text{BS}_2\text{Si}_6 \cdot 1.5\text{H}_2\text{O}$: C, 49.42; H, 9.89; S, 9.77. Found: C, 49.19; H, 9.51; S, 10.43. **Preparation of 2:** To a THF solution (10 mL) of **1** (316 mg, 0.502 mmol) was added *n*-BuLi (1.67 M in hexane, 0.6 mL, 2.0 equiv) at -78 °C. After being stirred for 2 h, to the reaction mixture was added $\text{Cp}_2\text{-TiCl}_2$ (182 mg, 0.73 mmol, 1.45 equiv) in portions from a bent tube to give a dark-red solution. Gradual warming to room temperature followed by evaporation of the solvent afforded a reddish brown solid, which was separated by flash column chromatography ($\text{SiO}_2/\text{hexane}:\text{CH}_2\text{Cl}_2 = 4:1$) to give **2** (283 mg, 70%) as red crystals. **2:** mp > 300 °C; ¹H NMR (500 MHz, CDCl_3) δ 0.03 (s, 18H), 0.10 (s, 36H), 1.25 (s, 1H), 1.38 (s, 2H), 6.19 (brs, 1H), 6.31 (brs, 1H), 6.39 (s, 10H); ¹³C NMR (125 MHz, CDCl_3) δ 0.68 (q), 1.05 (q), 1.18 (q), 28.88 (d), 29.30 (d), 29.48 (d), 117.68 (d, Cp), 121.73 (d), 124.00 (brs, ipso-arom), 126.21 (d), 141.11 (s), 146.11 (s); ¹¹B NMR (86.4 MHz, CDCl_3) δ 47.0; HRMS (FAB) m/z found 804.2985 [M^+], calcd for $\text{C}_{39}\text{H}_{69}\text{BS}_2\text{Si}_6\text{Ti}$ 804.3029. Anal. Calcd for $\text{C}_{39}\text{H}_{69}\text{BS}_2\text{Si}_6\text{Ti}$: C, 55.19; H, 8.64; S, 7.96. Found: C, 55.12; H, 8.43; S, 7.88. **Preparation of 5:** To a THF solution (3 mL) of **1** (56.0 mg, 0.089 mmol) was added *n*-BuLi (1.64 M in hexane, 0.11 mL, 2.0 equiv) at -78 °C. After being stirred for 2 h, to the reaction mixture was added methyl iodide (0.10 mL, 1.60 mmol, 18 equiv) by means of a syringe. Gradual warming to room temperature followed by evaporation of the solvent afforded a white solid, which was separated by column chromatography ($\text{SiO}_2/\text{hexane}$) to give **5** (52.6 mg, 90%) as white crystals. **5:** mp 168.5-170 °C; ¹H NMR (500 MHz, CDCl_3) δ 0.04 (s, 18H), 0.05 (s, 36H), 1.32 (s, 1H), 1.54 (s, 2H, H_2O), 1.63 (brs, 2H), 2.18 (s, 6H), 6.20 (brs, 1H), 6.36 (brs, 1H); ¹³C NMR (125 MHz, CDCl_3) δ 0.71 (q), 1.64 (q), 14.13 (q), 28.50 (d), 30.13 (d), 121.49 (d), 126.21 (d), 130.95 (s), 143.50 (s), 145.92 (s); ¹¹B NMR (86.4 MHz, CDCl_3) δ 67.6; HRMS (EI, 70 eV) m/z found 656.3235 [M^+], calcd for $\text{C}_{29}\text{H}_{65}\text{BS}_2\text{Si}_6$ 656.3236. Anal. Calcd for $\text{C}_{29}\text{H}_{65}\text{BS}_2\text{Si}_6 \cdot \text{H}_2\text{O}$: C, 51.58; H, 10.00; S, 9.50. Found: C, 51.95; H, 10.14; S, 9.92.

* Abstract published in *Advance ACS Abstracts*, September 15, 1995.

(1) Dedicated to Prof. Dr. Richard Neidlein of the University of Heidelberg on the occasion of his 65th birthday.

(2) Odum, J. D. In *Comprehensive Organometallic Chemistry*, Wilkinson, G., Stone, F. G. A., Abel, E. W., Eds.; Pergamon Press: Oxford, U.K., 1982; Vol. 1, Chapter 5.1, p 253.

(3) (a) Tokitoh, N.; Suzuki, H.; Matsumoto, T.; Matsuhashi, Y.; Okazaki, R.; Goto, M. *J. Am. Chem. Soc.* **1991**, *113*, 7047. (b) Tokitoh, N.; Matsuhashi, Y.; Okazaki, R. *Tetrahedron Lett.* **1991**, *32*, 6151. (c) *Ibid.* **1992**, *33*, 5551. (d) Tokitoh, N.; Matsumoto, T.; Okazaki, R. *Ibid.* **1991**, *32*, 6143. (e) *Ibid.* **1992**, *33*, 2531. (f) Matsuhashi, Y.; Tokitoh, N.; Okazaki, R.; Goto, M.; Nagase, S. *Organometallics* **1993**, *12*, 1351.

(4) (a) Tokitoh, N.; Matsuhashi, Y.; Okazaki, R. *J. Chem. Soc., Chem. Commun.* **1993**, 407. (b) Matsuhashi, Y.; Tokitoh, N.; Okazaki, R. *Organometallics* **1993**, *12*, 2573.

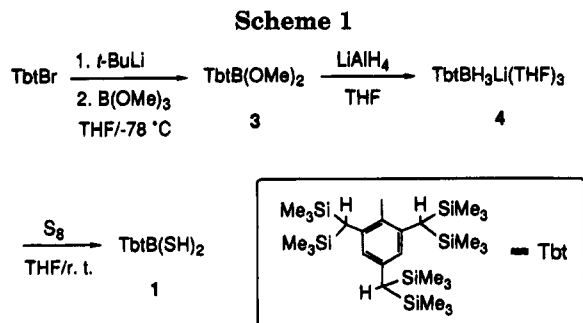
(5) Suzuki, H.; Tokitoh, N.; Nagase, S.; Okazaki, R. *J. Am. Chem. Soc.* **1994**, *116*, 11578.

(6) Tokitoh, N.; Matsumoto, T.; Manmaru, K.; Okazaki, R. *J. Am. Chem. Soc.* **1993**, *115*, 8855.

(7) Matsumoto, T.; Tokitoh, N.; Okazaki, R. *Angew. Chem.* **1994**, *106*, 2418; *Angew. Chem., Int. Ed. Engl.* **1994**, *33*, 2316.

(8) Eaborn et al. have already reported the X-ray structural analysis of [(THF)₂Li(μ -H)BC(SiMe₂Ph)₃] together with its spectroscopic data [IR ν_{BH} 2085, 2200 cm^{-1} ; ¹¹B NMR(C_6D_6) δ -30.2, $^1J_{\text{BH}}$ 80 Hz]: Eaborn, C.; El-Kheili, M. N. A.; Hitchcock, P. B.; Smith, J. D. *J. Chem. Soc., Chem. Commun.* **1984**, 1673.

(9) (a) Cole, T. E.; Bakshi, R. K.; Srebni, M.; Singaram, B.; Brown, H. C. *Organometallics* **1986**, *5*, 2303. (b) Brown, H. C.; Salunkhe, A. M.; Singaram, B. *J. Org. Chem.* **1991**, *56*, 1170.



cm^{-1} which are similar to those given for the crystallographically analyzed lithium alkyltrihydroborate $[(\text{THF})_3\text{Li}(\mu\text{-H})_3\text{BC}(\text{SiMe}_2\text{Ph})_3]$.⁸ An attempt to convert **4** into the corresponding dihydroborane by the reaction with hydrochloric acid or chlorotrimethylsilane⁹ failed, while the direct reaction of **4** with elemental sulfur followed by treatment with saturated aqueous NH_4Cl resulted in the isolation of the Tbt-substituted dimercaptoborane **1** as white crystals (21% from **3**) after chromatographic separation on silica gel.¹⁰ Compound **1** was found to be quite stable toward air and moisture and showed satisfactory spectral and analytical data, e.g., a singlet signal in the ^{11}B NMR [$\delta_{\text{B}}(\text{CDCl}_3)$ 67.5] attributable to the boron atom connecting two mercapto groups and a singlet signal in the ^1H NMR spectrum assignable to the two SH protons (Scheme 1).

The formation of **1** is worthy of note as the first example of a stable dimercaptoborane, and the molecular structure was definitively determined by X-ray crystallographic analysis (Figure 1).¹² Even in the solid state **1** showed no significant intermolecular interaction, and the geometry around the central boron atom was found to be completely trigonal planar. The dihedral angle between the plane defined by $\text{C}(1)\text{-B}(1)\text{-S}(1)\text{-S}(2)$ and the aromatic ring plane of the Tbt group is 86.0° , suggesting no essential conjugative interaction of π -electrons on the Tbt group with the dimercaptoboryl group. The $\text{B}(1)\text{-C}(1)$ bond length [1.53(2) Å] in **1**, however, was somewhat shorter than those of the related monomeric boron-sulfur compounds, $\text{TipB}(\text{SPh})_2$ [1.574(8) Å] and Mes_2BSPH (1.556 Å).¹⁴

With the stable dimercaptoborane **1** in hand, we next examined its further molecular transformation via lithiation of the mercapto groups. Thus, treatment of

(11) For example, see: Matsushashi, Y.; Tokitoh, N.; Okazaki, R.; Goto, M.; Nagase, S. *Organometallics* **1993**, *12*, 1351.

(12) Crystallographic data for **1**: $\text{C}_{27}\text{H}_{61}\text{BS}_2\text{Si}_6 \cdot 0.5\text{C}_7\text{H}_8$, $M = 676.3$, monoclinic, space group $C2/c$, $a = 40.605(7)$ Å, $b = 11.14(1)$ Å, $c = 20.270(6)$ Å, $\beta = 104.36(2)^\circ$; $V = 8881(6)$ Å³, $Z = 8$, $\rho_{\text{calcd}} = 1.011$ g cm^{-3} , $\mu = 2.99$ cm^{-1} , R (R_w) = 0.067 (0.073). Crystallographic data for **2**: $\text{C}_{37}\text{H}_{69}\text{BS}_2\text{Si}_6\text{Ti} \cdot \text{C}_6\text{H}_6$, $M = 844.35$, triclinic, space group $P1$, $a = 13.378(4)$ Å, $b = 17.720(3)$ Å, $c = 13.039(5)$ Å, $\alpha = 110.38(2)^\circ$, $\beta = 119.21(2)^\circ$, $\gamma = 81.35(2)^\circ$, $V = 2528(1)$ Å³, $Z = 2$, $\rho_{\text{calcd}} = 1.109$ g cm^{-3} , $\mu = 4.19$ cm^{-1} , R (R_w) = 0.079 (0.095). The intensity data were collected on Rigaku AFC7R (for **1**) and AFC5R (for **2**) diffractometers with Mo K α radiation ($\lambda = 0.71069$ Å, graphite monochromator), and the structures were solved by direct methods with SHELXS-86.¹³ All nonhydrogen atoms except for the solvents were refined anisotropically. The final cycles of full-matrix least-squares refinement were based on 1575 (for **1**) and 2378 (for **2**) observed reflections [$I > 4.00\sigma(I)$] and 339 (for **1**) and 431 (for **2**) variable parameters, respectively.

(13) Sheldrick, G. M. SHELXS-86; University of Göttingen: Göttingen, Germany, 1986.

(14) Wehmschulte, R.; Ruhlandt-Senge, K.; Olmstead, M. M.; Petrie, M. A.; Power, P. P. *J. Chem. Soc., Dalton Trans.* **1994**, 2113.

(15) An example of a dithiaborametallene derivative containing two iron tricarbonyl units, $\text{Me}_2\text{NBS}_3[\text{Fe}(\text{CO})_3]_2$, has already been reported. See: Nöth, H.; Schuchardt, U. *Z. Anorg. Allg. Chem.* **1975**, *418*, 97.

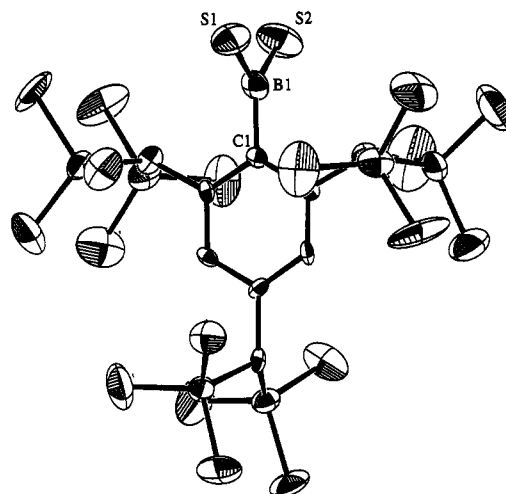


Figure 1. ORTEP drawing of TbtB(SH)_2 (**1**) with thermal ellipsoids plotted at 30% probability. The fragment of solvated toluene was omitted for clarity. Selected bond lengths (Å) and angles (deg): $\text{B}(1)\text{-C}(1)$ 1.53(2), $\text{B}(1)\text{-S}(1)$ 1.80(2), $\text{B}(1)\text{-S}(2)$ 1.81(2); $\text{C}(1)\text{-B}(1)\text{-S}(1)$ 122(1), $\text{C}(1)\text{-B}(1)\text{-S}(2)$ 121(1), $\text{S}(1)\text{-B}(1)\text{-S}(2)$ 115(1).

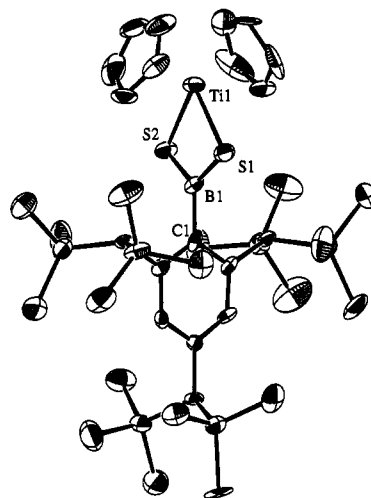
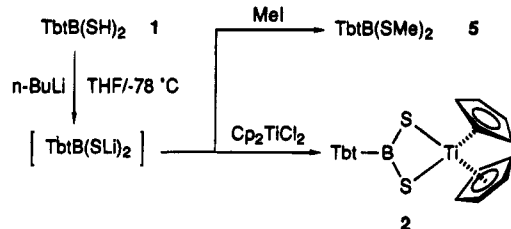


Figure 2. ORTEP drawing of $\text{TbtBS}_2\text{TiCp}_2$ (**2**) with thermal ellipsoids plotted at 30% probability. The fragment of solvated benzene was omitted for clarity. Selected bond lengths (Å) and angles (deg): $\text{B}(1)\text{-C}(1)$ 1.57(3), $\text{B}(1)\text{-S}(1)$ 1.80(2), $\text{B}(1)\text{-S}(2)$ 1.84(2), $\text{Ti}(1)\text{-S}(1)$ 2.422(5), $\text{Ti}(1)\text{-S}(2)$ 2.409(7); $\text{C}(1)\text{-B}(1)\text{-S}(1)$ 120(1), $\text{C}(1)\text{-B}(1)\text{-S}(2)$ 120(1), $\text{S}(1)\text{-B}(1)\text{-S}(2)$ 118(1), $\text{B}(1)\text{-S}(1)\text{-Ti}(1)$ 80.3(8), $\text{B}(1)\text{-S}(2)\text{-Ti}(1)$ 80.7(6), $\text{S}(1)\text{-Ti}(1)\text{-S}(2)$ 80.5(2).

1 with $n\text{-BuLi}$ (2.0 equiv) in THF at -78°C followed by addition of methyl iodide (2.0 equiv) resulted in the formation of the corresponding bis(methylthio)borane **5** in 90% yield, while the use of bis(cyclopentadienyl)titanium dichloride (1.45 equiv) instead of methyl iodide gave a novel boron-containing titanacycle, 1,3,2,4-dithiaboratitanetane derivative **2** [$\delta_{\text{B}}(\text{CDCl}_3)$ 47.0] (70%), as very stable red crystals.^{10,15} X-ray crystallographic analysis of **2** was also performed to reveal that its geometry around the boron atom was not much affected as compared to that of **1** in spite of being embedded in the ring system (Figure 2).¹² The four-membered dithiaboratitanetane ring was found to be almost planar and perpendicular to the aromatic ring of Tbt (dihedral angle 84.4°) as in the case of **1** (Scheme 2).

The successful isolation and noticeable stability of dimercaptoborane **1** and dithiaboratitanetane **2** here

Scheme 2



obtained are obviously due to the steric demand of the Tbt group. Since it is well-known that bis(cyclopentadienyl)titanium–chalcogen bonds in some other ring systems have a versatile reactivity toward electrophiles,¹⁶ dithiaboratitanetane **2** is expected to be useful as a stable, overcrowded boron dithiolate unit in the

synthesis of new types of highly reactive organoboron compounds. Further investigation on the reactivities of **1** and **2** is currently in progress.

Acknowledgment. This work was partly supported by the Sumitomo Foundation (N.T.) and a Grant-in-Aid for Scientific Research (No. 05236102) from the Ministry of Education, Science, and Culture of Japan. We also thank Shin-etsu Chemical and Tosoh Akzo Co., Ltd., for the generous gifts of chlorosilanes and alkyllithiums, respectively.

Supporting Information Available: ORTEP diagrams and tables of crystal data and structural refinement details, positional and thermal parameters, and bond lengths and angles for **1** and **2** (61 pages). Ordering information is given on any current masthead page.

(16) (a) Albertsen, J.; Steudel, R. *Phosphorus, Sulfur, Silicon* **1992**, 65, 165. (b) Steudel, R. *The Chemistry of Inorganic Ring Systems*; Steudel, R., Ed.; Elsevier: Amsterdam, 1992; p 233.

OM950390B

Synthesis and Structural Characterization of the First Pentacarbon Metallacarborane Complex: *nido-2-(η^5 -C₅H₅)Fe-7-CH₃-7,8,9,10,12-C₅B₆H₁₀*

Beverly A. Barnum, Patrick J. Carroll, and Larry G. Sneddon*

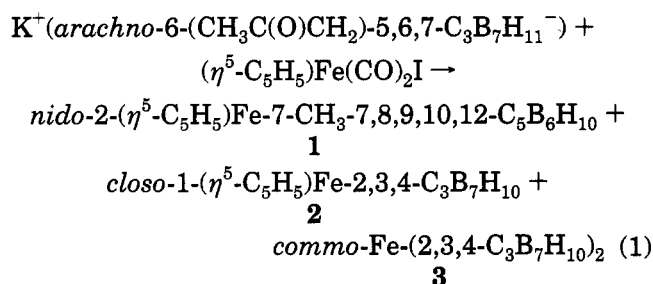
Department of Chemistry, University of Pennsylvania, Philadelphia, Pennsylvania 19104-6323

Received August 11, 1995[§]

Summary: The reaction of the *arachno-6*-(CH₃C(O)CH₂)-5,6,7-C₃B₇H₁₁⁻ tricarbaborane monoanion with CpFe(CO)₂I yields the first example of a metallacarborane complex containing five cage carbon atoms: *nido-2*-(η^5 -C₅H₅)Fe-7-CH₃-7,8,9,10,12-C₅B₆H₁₀ (**1**). A single-crystal X-ray study established that, in agreement with its 28-skeletal-electron count, the cage adopts a *nido*-type structure based on a 13-vertex dicosahedron missing one six-coordinate vertex. All five carbons are situated on the open six-membered face and exhibit carbon-carbon and boron-carbon distances in the normal ranges found in metallacarboranes.

The development of polyhedral carborane chemistry has been dominated by studies of the dicarbon cage systems, since these are the most readily accessible carboranes. The more recent syntheses of carborane clusters with higher numbers of cage carbons, including tri-^{1,3} and tetracarbon⁴ carboranes, as well as their derived metallacarborane complexes, have demonstrated that a continuum of carboranes with increasing carbon compositions should be achievable. However, although such species have been long anticipated, no neutral⁵ carboranes or metallacarboranes with greater than four cage carbons have been synthesized. In this communication, we report the synthesis and structural characterization of the first such higher-carbon boron cluster, the *pentacarbon* metallacarborane complex *nido-2*-(η^5 -C₅H₅)Fe-7-CH₃-7,8,9,10,12-C₅B₆H₁₀ (**1**).

The complex was isolated along with the parent derivatives of two known ferratricarbaborane complexes,² **2** and **3**, from the reaction of the *arachno-6*-(CH₃C(O)CH₂)-5,6,7-C₃B₇H₁₁⁻ tricarbaborane monoanion^{1b,c} with CpFe(CO)₂I as shown in eq 1.



Separation by thin-layer chromatography (silica gel/hexane-CH₂Cl₂ (5:3), R_f 0.48) gave **1** as a red-pink

crystalline solid in 13% isolated yield.⁶ An exact mass determination on the parent ion and the ¹¹B NMR spectrum, which showed only six intensity 1 doublets, indicated that loss of a "BOH" unit from the starting carborane cage had occurred upon formation of the complex. The ¹H NMR spectrum showed, in addition to cyclopentadienyl and methyl resonances, four intensity 1 singlets with line widths and chemical shifts consistent with cage-carbon C-H resonances. A single-crystal X-ray study confirmed that **1** was indeed a *pentacarbon* ferracarborane complex, with the structure shown in the ORTEP drawing in Figure 1.⁷

Consistent with its 28-skeletal-electron count, the cage adopts an open *nido*-type structure, based on a 13-vertex dicosahedron missing one six-connected vertex, similar to those found for other isoelectronic 12-vertex cage systems, including 2-(η^5 -C₅H₅)Fe-1,7,8,9-(CH₃)₄C₄B₇H₈,⁸ 2,4-(η^5 -C₅H₅)₂C₀-7,10,11,12-C₄B₆H₁₀,⁹ and 2-(η^5 -C₅H₅)Co-7,9,11,12-(CH₃)₄C₄B₇H₇.¹⁰ The six-membered open face of the cage contains the five carbon atoms and one boron atom, with all four of the four-

(3) (a) Stibr, B.; Holub, J.; Teixidor, F.; Viñas, C. *J. Chem. Soc., Chem. Commun.* **1995**, 795–796. (b) Shedlow, A. M.; Carroll, P. J.; Sneddon, L. G. *Organometallics* **1995**, *14*, 4046–4047. (c) For references to older tricarbaboranes, see footnotes 3–8 in ref 2b above.

(4) (a) Grimes, R. N. *Adv. Inorg. Chem. Radiochem.* **1983**, *26*, 55–115 and references therein. (b) Grimes, R. N. *Acc. Chem. Res.* **1978**, *11*, 420–427 and references therein.

(5) The monoboron pentacarbon cation [1-RBC₅(CH₃)₅]⁺ has been synthesized and structurally characterized. See: (a) Jutzi, P.; Seufert, A. *J. Organomet. Chem.* **1978**, *161*, C5–C7. (b) Jutzi, P.; Seufert, A.; Buchner, W. *Chem. Ber.* **1979**, *112*, 2488–2493. (c) Dohmeier, C.; Köpcke, R.; Robl, C.; Schnöckel, H. *J. Organomet. Chem.* **1995**, *487*, 127–130.

(6) Spectroscopic data: ¹¹B NMR (160.5 MHz, CD₂Cl₂) δ 9.5 (d, B6, J_{BH} = 135 Hz), -1.6 (d, B3, J_{BH} = 153), -10.1 (d, B4, J_{BH} = 161), -18.4 (d, B11, J_{BH} = 145), -21.8 (d, B5, J_{BH} = 144), -33.8 (d, B1, J_{BH} = 143); two-dimensional ¹¹B-¹¹B NMR established the connectivities B1–B3, B1–B4, B1–B5, B1–B6, B3–B4 (weak), B4–B5, B5–B6, B5–B11, B6–B11 (weak); ¹³C{¹H} NMR (50.3 MHz, CD₂Cl₂, -60 °C) δ 94.8 (C7), 80.4 (Cp), 38.9 (cage-CH), 34.6 (cage-CH), 29.5 (cage-CH), 28.9 (cage-CH), 18.0 (CH₃); ¹H{¹¹B} NMR (200 MHz, CD₂Cl₂) δ 4.52 (s, 5H, Cp), 3.65 (br s, 1H, BH), 3.04 (br s, 1H, BH), 2.76 (s, 3H, CH₃), 2.66 (br s, 1H, CH), 2.12 (br s, 1H, CH), 1.57 (br s, 1H, BH), 1.38 (br s, 1H, BH), 1.16 (br s, 2H, BH), 1.07 (br s, 1H, CH), 0.88 (s, 1H, CH); HRMS (CI⁻) calcd for ¹²C_{11¹H₁₈¹¹B₆⁶⁶Fe₁ 272.1316, found 272.1318; mp 153 °C; IR (NaCl windows, CCl₄) 3040 (m), 2975 (m), 2898 (w), 2840 (w), 2530 (s, br), 2295 (w), 1415 (w), 1370 (w), 1260 (s), 1115 (vw), 1080 (w), 1055 (vw, br), 1030 (w), 1018 (vw), 1000 (w), 990 (sh), 985 (vw), 925 (w) 855 (w), 840 (w), 740 (m, br).}

(7) Structural data: space group P $\bar{1}$ (No. 2), *a* = 7.7398(6) Å, *b* = 12.9563(7) Å, *c* = 6.8563(3) Å, *V* = 642.73(7) Å³, *Z* = 2, and *D*_{calcd} = 1.404 g/cm³. The structure was solved by direct methods (SIR92). Refinement was by full-matrix least-squares techniques based on *F* to minimize the quantity $\sum w(|F_o| - |F_c|)^2$ with *w* = 1/*σ*²(*F*). Non-hydrogen atoms were refined anisotropically, and hydrogen atoms were refined isotropically, except for the cyclopentadienyl hydrogens, which were included as constant contributions to the structure factors and were not refined. Refinement converged to *R*₁ = 0.0327 and *R*₂ = 0.0368.

(8) Maxwell, W. M.; Bryan, R. F.; Grimes, R. N. *J. Am. Chem. Soc.* **1977**, *99*, 4008–4015.

(9) Wong, K.-S.; Bowser, J. R.; Pipal, J. R.; Grimes, R. N. *J. Am. Chem. Soc.* **1978**, *100*, 5045–5051.

(10) Maynard, R. B.; Sinn, E.; Grimes, R. N. *Inorg. Chem.* **1981**, *20*, 1201–1206.

[§] Abstract published in *Advance ACS Abstracts*, September 15, 1995.
(1) (a) Kang, S. O.; Furst, G. T.; Sneddon, L. G. *Inorg. Chem.* **1989**, *28*, 2339–2347. (b) Su, K.; Barnum, B.; Carroll, P. J.; Sneddon, L. G. *J. Am. Chem. Soc.* **1992**, *114*, 2730–2731. (c) Su, K.; Carroll, P. J.; Sneddon, L. G. *J. Am. Chem. Soc.* **1993**, *115*, 10004–10017.
(2) (a) Plumb, C. A.; Carroll, P. J.; Sneddon, L. G. *Organometallics* **1992**, *11*, 1666–1671. (b) Plumb, C. A.; Carroll, P. J.; Sneddon, L. G. *Organometallics* **1992**, *11*, 1672–1680.

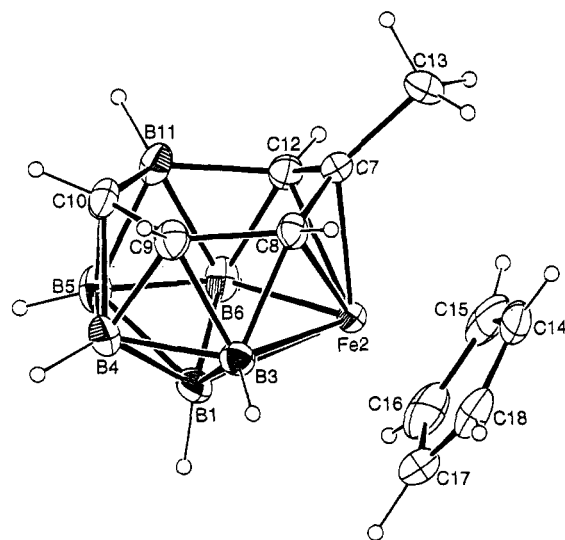


Figure 1. ORTEP drawing of the molecular structure of *nido-2-(η^5 -C₅H₅)Fe-7-CH₃-7,8,9,10,12-C₅B₆H₁₀* (**1**). Selected bond lengths (Å) and angles (deg): C7–C8, 1.441(4); C8–C9, 1.543(4); C9–C10, 1.525(4); C10–B11, 1.571(4); B11–C12, 1.645(4); C7–C12, 1.423(4); C7–Fe2, 1.989(2); C8–Fe2, 2.135(3); C12–Fe2, 2.106(3); B3–Fe2, 2.128(3); B6–Fe2, 2.158(3); B1–Fe2, 2.165(4); C8–C7–C12, 117.2(2); C9–C10–B11, 121.3(3); C7–C8–C9, 120.8(2); C8–C9–C10, 115.9(3); C10–B11–C12, 113.3(3); B11–C12–C7, 117.0(3).

coordinate carbon atoms and one boron atom forming a plane. The unique three-coordinate methyl-substituted carbon atom, C7, is distorted out of this plane by 0.46 Å. Given the high carbon content of the cage, deviation from the nonclassical bonding observed in the polyhedral boranes to a more classical organic structure might be expected; however, all of the intracage distances and angles are in the normal ranges observed in metallacarborane clusters. That all five cage carbon atoms are on the open face is consistent with the well-known preference of carbon atoms to occupy lower coordinate vertices in carborane clusters,¹¹ and, indeed, no further carbon skeletal rearrangements for **1** were observed even upon heating a sample to 240 °C *in vacuo*. Consistent with the carbon bonding interactions with the iron atom, the distances between the three carbon atoms C7, C8, and C12 are somewhat shortened (C7–C8, 1.441(4) Å; C7–C12, 1.423(4) Å) compared to those between the non-metal-coordinated C9 and C10 carbon atoms (C9–C10, 1.525(4) Å; C9–C8, 1.543(4) Å). The iron atom occupies a six-coordinate position bound to three carbon atoms and three boron atoms. Again, five of the ring atoms form a plane with the C7 carbon atom distorted out of this plane 0.35 Å toward the iron atom. As a consequence, the Fe–C7 distance (1.989(2) Å) is shortened relative to Fe–C8 (2.135(3) Å) and Fe–C12 (2.106(3) Å), as well as in comparison to the Fe–B1, –B3, and –B6 distances. The cyclopentadienyl ring and the C8–B3–B1–B6–C12 plane are parallel (dihedral angle 3.1°), with the iron atom sandwiched between the two planes (1.69 and 1.40 Å, respectively).

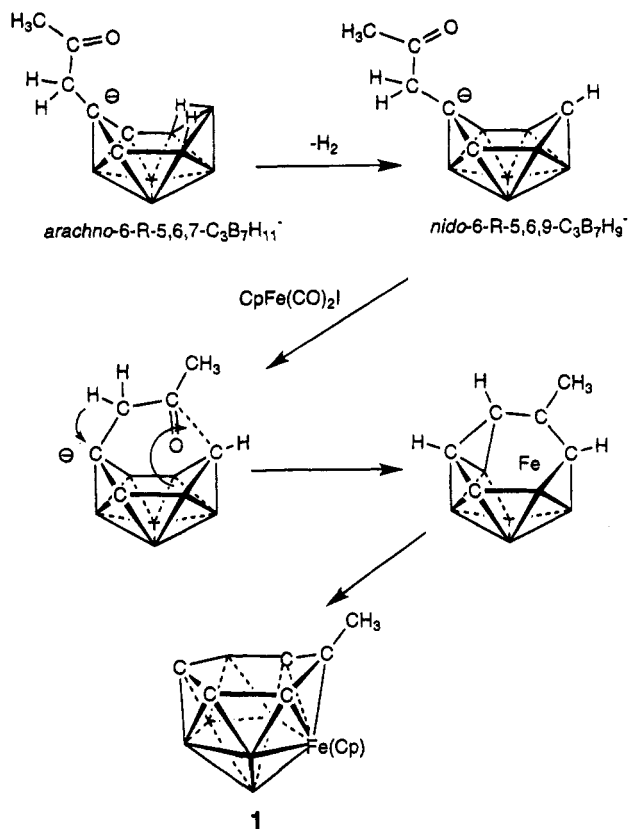


Figure 2. Possible reaction sequence leading to the formation of *nido-2-(η^5 -C₅H₅)Fe-7-CH₃-7,8,9,10,12-C₅B₆H₁₀* (**1**).

Although the mechanism for the formation of **1** is not yet known, a comparison of the compositions and structures of the starting *arachno-6-(CH₃C(O)CH₂)-5,6,7-C₃B₇H₁₁*[−] anion and **1** suggests that the carbon atoms of the ketone side chain of the anion become incorporated into the final cage structure of **1**. When the reaction was monitored by ¹¹B NMR, it was found that the *arachno-6-(CH₃C(O)CH₂)-5,6,7-C₃B₇H₁₁*[−] anion readily converts to the *nido-6-(CH₃C(O)CH₂)-5,6,9-C₃B₇H₉*[−] anion. Subsequent reaction of the ketone oxygen with a boron atom on the open face of the cage of this anion, followed by cyclization of the carbon framework in the manner shown in Figure 2, could, in fact, generate the structure observed for **1** in a straightforward fashion. Such a process may be metal-promoted, since control reactions carried out in the absence of CpFe(CO)₂I showed no evidence of pentacarbon cage products. We are now investigating the detailed mechanism of this reaction, as well as the development of new routes for the synthesis of even higher-carbon carboranes and metallacarboranes that may provide more links between the polyhedral carboranes and classical carbon cage compounds.

Acknowledgment. We thank the National Science Foundation for support of this work.

Supporting Information Available: Tables listing atomic coordinates, bond distances and angles, least-squares planes, and thermal parameters for **1** (10 pages). Ordering information is given on any current masthead page.

(11) Williams, R. E. *Adv. Inorg. Chem. Radiochem.* **1976**, *18*, 67–142.

Articles

Face Selectivity of the C–H Bond Activation of Cyclohexane by the “Bare” First-Row Transition-Metal Cations Sc⁺–Zn⁺Katrin Seemeyer,[†] Detlef Schröder,^{*,†} Martin Kempf,[‡] Olaf Lettau,[‡] Jörn Müller,[‡] and Helmut Schwarz^{*,†}

Institut für Organische Chemie and Institut für Anorganische und Analytische Chemie, Technische Universität Berlin, Strasse des 17. Juni 135, 10623 Berlin, Germany

Received April 19, 1995[®]

The ability of the first-row, atomic transition-metal cations from Sc⁺ through Zn⁺ to activate C–H and C–C bonds in cyclohexane has been examined by means of ion cyclotron resonance and sector-field mass spectrometry. Three types of reactions can be distinguished. (i) The early-transition-metal cations Sc⁺, Ti⁺, and V⁺ mediate multiple dehydrogenation of cyclohexane to yield benzene/M⁺ as the major product ion. (ii) For the late, group 8 transition-metal cations Fe⁺, Co⁺, and Ni⁺ single dehydrogenation is observed preferentially, and for Co⁺ and Ni⁺ the formation of M(C₃H₆)⁺ complexes demonstrates that these metal ions also activate C–C bonds of cyclohexane. (iii) For Cr⁺, Mn⁺, Cu⁺, and Zn⁺ there is no indication of any C–H or C–C bond activation. The stereochemistry of the C–H bond activation of cyclohexane/M⁺ was explored by investigating specifically labeled [*all-cis*-1,2,3,4,5,6-D₆]-cyclohexane. For all transition-metal cations studied here, the first dehydrogenation occurs stereospecifically in terms of a *syn* elimination. In the subsequent dehydrogenations this stereospecificity is maintained for the early transition metals Sc⁺, Ti⁺, and V⁺, whereas the group 8 transition metals Fe⁺, Co⁺, and Ni⁺ induce H/D exchange processes involving both faces of the cycloalkane ring; most probably, acyclic intermediates are involved.

Introduction

The gas-phase ion chemistry of “bare” and partially ligated transition-metal ions has attracted considerable interest over the last two decades.¹ This originates from the possibility of evaluating reaction mechanisms and characterizing intermediates of transition-metal-mediated C–H and C–C bond activation processes. Often, these aspects cannot be assessed in condensed-phase chemistry. In this context the reactions of hydrocarbons are particularly important, since in these substrates only C–H and C–C bonds are available. While for many substrates isotopic labeling has proven to give profound insight into mechanistic features, the elucidation of the metal-mediated dehydrogenation mechanism of hydrocarbons is difficult on the following grounds: (i) H/D equilibration reactions,² (ii) competition of different mechanisms, and (iii) metabolic switching³ may play a role. Consequently, detailed studies on the stereochemical course of metal-ion-mediated C–H and C–C bond activations of hydrocarbons are relatively scarce.^{4–6}

Here, we report the gas-phase reactions of the first-row transition-metal cations from Sc⁺ through Zn⁺ with

cyclohexane (1). This substrate, and in particular its isotopologue [*all-cis*-1,2,3,4,5,6-D₆]cyclohexane⁶ (**1a**), is of interest on the following grounds. Recently, we have demonstrated that the stereochemistry of the metal-ion-induced (M = Fe, Co) single and double dehydrogenation of tetralin in the gas phase follows a *syn*-1,2-pathway.^{4d,e,h} In this molecule, during the whole reaction sequence the metal ion remains bound to that π -face of the aromatic ring to which it was originally attached. Consequently, as there is hardly any chance for the metal ion to switch from one π -site of the arene to the other, the exclusive *syn* stereoselectivity observed for this substrate cannot be generalized to exist for saturated hydrocarbons as well. In contrast, in the reactions of metal ions with an alkane, e.g. cyclohexane, the metal

(4) Hydrocarbons: (a) Whiteside, T. H.; Arhad, R. W. *Tetrahedron Lett.* **1972**, 74, 297. (b) Prüsse, T. Ph.D. Thesis, Technische Universität Berlin D83, 1991. (c) Nekrasov, S.; Zagorevskii, D. V. *Org. Mass Spectrom.* **1991**, 26, 733. (d) Seemeyer, K.; Prüsse, T.; Schwarz, H. *Helv. Chim. Acta* **1993**, 76, 113. (e) Seemeyer, K.; Schwarz, H. *Helv. Chim. Acta* **1993**, 76, 2384. (f) Raabe, N.; Karrass, S.; Schwarz, H. *Chem. Ber.* **1994**, 127, 261. (g) Reference 6. (h) Seemeyer, K.; Hertwig, R. H.; Hrušák, J.; Koch, W.; Schwarz, H., *Organometallics*, in press. (5) Hetero compounds: (a) Schröder, D.; Schwarz, H. *J. Am. Chem. Soc.* **1993**, 115, 8818. (b) Schröder, D.; Zummack, W.; Schwarz, H. *J. Am. Chem. Soc.* **1994**, 116, 5857. (c) Hornung, G.; Schröder, D.; Schwarz, H. *J. Am. Chem. Soc.*, in press. (d) Schwarz, J.; Schwarz, H. *Helv. Chim. Acta* **1995**, 78, 1013. (e) Reference 3.

(6) (a) Huang, Y.; Profilet, R. D.; Ng, J. H.; Ranasinghe, Y. A.; Rothwell, I. P.; Freiser, B. S. *Anal. Chem.* **1994**, 66, 1050. (b) Freiser, B. S. *Acc. Chem. Res.* **1994**, 27, 353. (c) It should be mentioned that in the experiments reported in ref 6a,b the reactions of “bare” Co⁺ with mixtures of cyclohexane isotopologues were probed by MS/MS experiments.

[†] Institut für Organische Chemie.

[‡] Institut für Anorganische und Analytische Chemie.

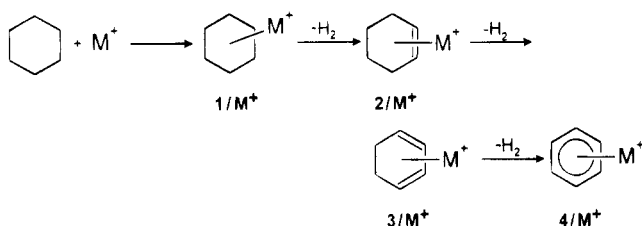
[®] Abstract published in *Advance ACS Abstracts*, August 15, 1995.

(1) (a) Eller, K.; Schwarz, H. *Chem. Rev.* **1991**, 91, 1121. (b) Eller, K. *Coord. Chem. Rev.* **1993**, 126, 93.

(2) For an extreme example of H/D equilibration, see: Schwarz, J.; Schwarz, H. *Chem. Ber.* **1993**, 126, 1257.

(3) (a) Prüsse, T.; Fiedler, A.; Schwarz, H. *Helv. Chim. Acta* **1991**, 74, 1127. (b) Seemeyer, K.; Prüsse, T.; Schwarz, H. *Helv. Chim. Acta* **1993**, 76, 1632.

Scheme 1



ion is not fixed to a particular face of the molecule. In fact, as a consequence of the more or less isotropic van der Waals spheres, the initial coordination of the metal ion to a particular region of the alkanes occurs almost statistically.⁷ The idea to study [*all-cis*-1,2,3,4,5,6- D_6]-cyclohexane (**1a**) rather than an acyclic alkane is related to the amply demonstrated fact that in metal-ion-induced reactions of isotopically labeled, flexible hydrocarbons often extensive H/D exchange processes precede dissociation.^{2,8} These hamper the analysis of the experimental data with respect to the stereo- and regioselectivity of the reactions of interest. However, in the case of **1a**, due to the well-defined stereochemical relationship of the two faces of the molecule, the observation of metal-ion-induced H/D loss would have significant implications for the dehydrogenation mechanism. For example, loss of HD from **1a** would imply that dehydrogenation no longer occurs with *syn* stereochemistry from an intact cyclohexane skeleton; rather, sequential C-H(D)/C-C bond activation may take place, resulting in an apparent switch of the metal ion from one face of the ring to the other. Alternatively, facile H/D equilibration processes are feasible when an electron is transferred from the hydrocarbon (or the corresponding radical) to the metal cation (or a cationic metal hydride); this follows from the propensity for hydrogen scrambling in ionized cycloalkanes. However, for the system under study this possibility is not really relevant on energetic grounds (see below).⁹

Experimental Section

Most of the experiments were performed with a Spectrospin CMS 47X Fourier transform ion cyclotron resonance (FTICR) mass spectrometer, which has been described in detail elsewhere.¹⁰ In brief, M^+ cations were formed by laser desorption/laser ionization¹¹ of a pure metal target in the external ion source of the instrument. By a system of electric potentials and lenses the ions so formed were transferred to the analyzer cell, which is located within a superconducting magnet (maximum field strength 7.05 T). Subsequently, the metals' most abundant isotopes were mass-selected using the FERETS technique,¹² a computer-controlled ion-ejection protocol which combines single-frequency ion-ejection pulses with frequency sweeps to optimize ion isolation. Due to the injection of the ions from the external ion source into the FTICR cell, the mass-selected ions are kinetically excited, as compared to thermal

motion. In order to afford thermalization of M^+ , argon was pulsed in several times to allow ca. 200 collisions and then pumped out, and the M^+ ions were again mass-selected.¹³

Cyclohexane (**1**) and [*all-cis*-1,2,3,4,5,6- D_6]cyclohexane (**1a**) were introduced in the FTICR cell via a leak valve at typical pressures of ca. 8×10^{-9} mbar. Reaction rate constants and branching ratios were derived from the analysis of the pseudo-first-order reaction kinetics and are reported with a relative error of $\pm 25\%$. Note, however, that the relative rate constants reported here are not subject to systematic errors such as calibration; consequently, the error of the relative rate constants is as low as $\pm 10\%$.¹⁴ For the conversion of the experimentally measured rate constants to absolute values, the measured pressures were corrected according to the relative sensitivity of the ion gauge, which was calibrated using data reported for well-known ion/molecule processes.¹⁵ For the evaluation of precise intensities in the case of isobaric multiplets (e.g. 2H_2 and D_2 losses, $\Delta m = 4.032$ and 4.028 amu, respectively), exact ion masses were determined by high-resolution experiments ($m/\Delta m > 200\,000$), and intensities were derived from the absolute amplitude of the transients.² We wish to mention that for such overlapping multiplets the peak heights obtained in the broad-band spectra result from an accidental data overlap of both signals and do not reflect real intensities. Furthermore, all product ion intensities were deconvoluted for natural abundances of all relevant isotopes and the incompleteness of the deuterium labeling for **1a** (see below). All data were accumulated and on-line processed using an ASPECT 3000 minicomputer.

Additional experiments were performed with a modified four-sector tandem mass spectrometer of BEBE configuration (B stands for magnetic and E for electric sector), in which MS-I is an VG ZAB-HF-2F and MS-II an AMD 604 mass spectrometer. As the experimental setup of the sector-field mass spectrometer has also been described previously,¹⁶ a brief description may suffice: a ca. 1:1 mixture of a suitable precursor for the metal ion¹⁷ (e.g. $\text{Cr}(\text{CO})_6$, $\text{Mn}_2(\text{CO})_{10}$, $\text{Fe}(\text{CO})_5$, $\text{Co}(\text{CO})_3\text{NO}$, NiCp_2 , and $\text{Cu}(\text{acac})_2$) and cyclohexane **1** or its isotopologue **1a** was bombarded with 100-eV electrons in the chemical ionization source (repeller voltage ca. 0 V), the organometallic complexes of the transition-metal ions and **1** or **1a**, having 8 keV translational energy, were mass-selected by means of B(1)E(1), and the unimolecular reactions occurring in the field-free region between E(1) and B(2) were recorded by scanning B(2). Unfortunately, no appropriate precursors for complexes of bare Sc^+ , Ti^+ , and V^+ with **1** were available. Although the actual mechanism by which the complexes $1/\text{M}^+$ and $1a/\text{M}^+$ are formed is unknown, the pressure in the ion source is high enough to permit collisional cooling, thus increasing the lifetime of the complexes to such an extent that time-delayed decomposition reactions after ca. $1 \mu\text{s}$ take place; these will be referred to as metastable ion (MI) dissociations. Spectra were recorded on-line by using signal-averaging techniques employing the AMD Intectra data system. In typical experiments, 15–20 spectra were accumulated.

For the synthesis of **1a**, [D_6]benzene (Aldrich, 99.5 % atom % D) has been hydrogenated under the conditions of homogeneous catalysis using (η^3 -2-propenyl)tris(trimethyl phosphite)cobalt ($(\eta^3\text{-C}_3\text{H}_5)\text{Co}(\text{P}(\text{OCH}_3)_3)_3$). This complex, which is known to bring about stereoselective *all-cis* hydrogenation of

(7) Henkinson, D. J.; Allison, J. J. *Phys. Chem.* **1987**, *91*, 5307.

(8) See, for example: Houriet, R.; Halle, L. F.; Beauchamp, J. L. *Organometallics* **1983**, *2*, 1818.

(9) Lias, S. G.; Bartmess, J. E.; Liebman, J. F.; Holmes, J. L.; Levin, R. D.; Mallard, W. G. *J. Phys. Chem. Ref. Data Suppl.* **1988**, *17* (suppl. 1).

(10) (a) Eller, K.; Schwarz, H. *Int. J. Mass Spectrom. Ion Processes* **1989**, *93*, 243. (b) Eller, K.; Zummack, W.; Schwarz, H. *J. Am. Chem. Soc.* **1990**, *112*, 621.

(11) (a) Freiser, B. S. *Talanta* **1985**, *32*, 697. (b) Freiser, B. S. *Anal. Chim. Acta* **1985**, *178*, 137.

(12) Forbes, R. A.; Laukien, F. H.; Wronka, J. *Int. J. Mass Spectrom. Ion Processes* **1988**, *83*, 23.

(13) (a) Schröder, D.; Fiedler, A.; Ryan, M. F.; Schwarz, H. *J. Phys. Chem.* **1994**, *98*, 68. (b) Chen, Y.-M.; Clemmer, D. E.; Armentrout, P. B. *J. Am. Chem. Soc.* **1994**, *116*, 2815. (c) Fiedler, A.; Schröder, D.; Shaik, S.; Schwarz, H. *J. Am. Chem. Soc.* **1994**, *116*, 10734.

(14) Schröder, D. Ph.D. Thesis, TU Berlin D83, 1993.

(15) Bartmess, J. E.; Georgiadis, R. M. *Vacuum* **1983**, *33*, 149.

(16) (a) Srinivas, R.; Sülzle, D.; Koch, W.; DePuy, C. H.; Schwarz, H. *J. Am. Chem. Soc.* **1991**, *113*, 5970. (b) Srinivas, R.; Sülzle, D.; Weiske, T.; Schwarz, H. *Int. J. Mass Spectrom. Ion Processes* **1991**, *107*, 369.

(17) Prüsse, T.; Schwarz, H. *Organometallics* **1989**, *8*, 2856.

arenes,^{18,19} has been synthesized in three steps by starting from CoCl_2 and $\text{P}(\text{OCH}_3)_3$ and following literature procedures.²⁰ As the catalyst performance deteriorated in the presence of free $\text{P}(\text{OCH}_3)_3$,^{19b} the product was carefully purified by repeated chromatography ($\text{Al}_2\text{O}_3/5\% \text{H}_2\text{O}/n\text{-pentane}$) and recrystallized three times from $n\text{-pentane}$ at -78°C . For the hydrogenation a 25:1 mixture of C_6D_6 and catalyst^{19b} was reacted at room temperature for 6 days under slightly elevated^{19c} hydrogen atmosphere pressure ($p_{\text{H}_2} = 3\text{--}4 \text{ bar}$).²¹ The crude reaction product was purified by vacuum distillation, and in line with literature data¹⁹ the GC/MS analysis indicates that ca. 50% of the initial C_6D_6 had been converted to the required product. We did not find evidence that at conversion rates exceeding 5% the hydrogenated product is inhomogeneous due to H/D exchange processes. We suppose that the reported^{19c} H/D exchange is caused by the higher temperature (80°C rather than room temperature as used in the present experiment). Finally, the sample of **1a**, which still contained a spurious amount of solvent as well as C_6D_6 , was purified by preparative gas chromatography (CP-WAX 51).

Results and Discussion

The products of the ion/molecule reactions of **1** with M^+ cations ($\text{M} = \text{Sc}\text{--}\text{Zn}$) and the reaction efficiencies ϕ , defined as the ratio of the measured reaction rate constant k_R to the collision rate constant k_C ,²² are given in Table 1; the magnitude of ϕ represents a measure for the relative reactivity of a particular transition-metal cation toward cyclohexane.²³ The MI data of the cyclohexane/ M^+ complexes **1a**/ M^+ ($\text{M} = \text{Cr}\text{--}\text{Cu}$) are given in Table 2. The results of the sector-field mass-spectrometer experiments are quite similar to the FTICR experiments as far as the occurrence or absence of bond activation is concerned; however, multiple dehydrogenation does not take place in the former. The reason for the absence of multiple dehydrogenation is twofold. First, the unimolecular dissociations in the ion-beam mass spectrometer are monitored in the microsecond time frame, while in the ICR setup reaction times are much longer, extending to the microsecond and second time regime. Therefore, consecutive processes may be too slow to be observed in the MI spectra but gain in importance in ICR experiments. Second, in the low-pressure regime prevailing in the ICR

Table 1. Relative Amounts of Single, Double, and Triple Dehydrogenation as Well as Losses of Propene and Reaction Efficiencies ϕ in the Ion/Molecule Reaction of Cyclohexane with "Bare" Metal Cations M^+ ^a

M^+	adduct	H_2	2H_2	3H_2	C_3H_6	ϕ (%)
Sc^+				100 ^b		50
Ti^+				100		100
V^+			48	52		50
Cr^+						<0.2
Mn^+						<0.1
Fe^+		77	18	5		100
Co^+		57	26	3	14	100
Ni^+		74	21		5	100
Cu^+	100 ^c					10
Zn^+						<0.1

^a Intensities are normalized to 100%. ϕ is defined as the ratio of the measured rate constant k_R and the collision rate constant k_C . ^b See ref 23d. ^c Also $\text{Cu}(\text{H}_2\text{O})^+$ is formed as a consecutive product in the reaction of $1/\text{Cu}^+$ with background water.^{23f}

Table 2. Unimolecular Losses (MI) of Dihydrogen and Propene Isotopologues from [*all-cis*-1,2,3,4,5,6- D_n]Cyclohexane/ M^+ Complexes in the Sector-Field Mass Spectrometer^a

M^+	H_2	HD	D_2	$\text{C}_3\text{H}_4\text{D}_2$	$\text{C}_3\text{H}_3\text{D}_3$	$\text{C}_3\text{H}_2\text{D}_4$	1a ^b	KIE ^c
Cr^+							100	
Mn^+							100	
Fe^+	96		4					24
Co^+	72	4	16	2	4	2		4,5
Ni^+	77		19	1	2	1	<1	4,1
Cu^+							100	

^a Intensities are normalized to 100%. ^b This entry corresponds to the unimolecular loss of the entire cyclohexane ligand to yield M^+ . ^c The kinetic isotope effect refers to the first dehydrogenation, i.e. $k_{\text{H}_2}/k_{\text{D}_2}$. The mixed isotopomers have been neglected.

machine the encounter complexes $1/\text{M}^+$ are rovibrationally excited by the amount of binding energy of M^+ to the alkane; in contrast, the metastable ions of $1/\text{M}^+$ sampled in the ion-beam instrument possess less internal energy for several reasons (e.g. collisional stabilization in the ion source prompt decay). These energetic differences also account for the absence of consecutive processes, as has been discussed in detail elsewhere.²⁴

Apparently, the gas-phase chemistry of cyclohexane²³ with the first-row transition-metal cations M^+ can be divided into three groups. (i) The early transition-metal cations from Sc^+ through V^+ induce multiple dehydrogenation of cyclohexane to yield benzene/ M^+ as the predominant product; in the case of V^+ also a significant amount of the double-dehydrogenation product is observed.²⁵ (ii) The late group 8 transition-metal cations Fe^+ , Co^+ , and Ni^+ preferentially give rise to a single dehydrogenation to form cyclohexene/ M^+ ; products due to multiple dehydrogenation are less abundant. For Co^+ and Ni^+ also C-C bond activation to yield $\text{M}(\text{C}_3\text{H}_6\text{--}n\text{D}_n)^+$ complexes ($n = 2\text{--}4$) is observed to some extent. (iii) The transition metals Cr^+ , Mn^+ , and Zn^+ are unreactive toward cyclohexane, and for Cu^+ the slow formation of the adduct complex $1/\text{Cu}^+$ is observed exclusively.^{23f} The

(18) (a) Muetterties, E. L.; Hirsekorn, F. J. *J. Am. Chem. Soc.* **1974**, *96*, 4063. (b) Muetterties, E. L.; Rakowski, M. C.; Hirsekorn, F. J.; Larson, W. D.; Basus, V. J.; Anet, F. A. *J. Am. Chem. Soc.* **1975**, *97*, 1266. (c) For mechanistic aspects of the catalytic cycle, see ref 20.

(19) (a) Muetterties, E. L.; Bleeke, J. R. *Acc. Chem. Res.* **1979**, *12*, 324. (b) Bleeke, J. R.; Muetterties, E. L. *J. Am. Chem. Soc.* **1981**, *103*, 556. (c) Blum, J.; Amer, I.; Vollhardt, K. P. C.; Schwarz, H.; Hönhe, G. *J. Org. Chem.* **1987**, *52*, 2804.

(20) (a) Muetterties, E. L.; Hirsekorn, F. J. *J. Am. Chem. Soc.* **1974**, *96*, 7920. (b) Rakowski, M. C.; Hirsekorn, F. J.; Stuhl, L. S.; Muetterties, E. L. *Inorg. Chem.* **1976**, *15*, 2379.

(21) In view of the H/D exchange reactions occurring at elevated temperature,^{19c} we have not attempted to accelerate the reaction by conducting the hydrogenation of C_6D_6 at higher temperatures. Similarly, increase of the H_2 pressure^{19c} does not necessarily improve the yield of **1a** as the catalyst decomposes at ca. 35 bar.

(22) Su, T.; Bowers, M. T. *Int. J. Mass Spectrom. Ion Phys.* **1973**, *12*, 347.

(23) For earlier studies of reactions of first-row transition-metal cations with unlabeled cyclohexane, see: (a) Armentrout, P. B.; Beauchamp, J. L. *J. Am. Chem. Soc.* **1981**, *103*, 6628. (b) Byrd, G. D.; Burnier, R. C.; Freiser, B. S. *J. Am. Chem. Soc.* **1982**, *104*, 3565. (c) Jacobson, D. B.; Freiser, B. S. *J. Am. Chem. Soc.* **1983**, *104*, 7492. (d) Schilling, J. B.; Beauchamp, J. L. *J. Am. Chem. Soc.* **1988**, *110*, 15. (e) Schilling, J. B.; Beauchamp, J. L. *Organometallics* **1988**, *7*, 194. (f) Dahrouch, A.; Mestdag, H.; Rolando, C. *J. Chim. Phys. Phys.-Chim. Biol.* **1994**, *91*, 443. (g) Reference 9. (h) For the dehydrogenation of cyclohexane by $\text{Ni}(\text{C}_5\text{H}_5)^+$, one of the earliest examples of a gas-phase C-H bond activation reaction, see: Müller, J.; Goll, W. *Chem. Ber.* **1973**, *106*, 1129.

(24) (a) Schalley, C. A.; Wesendrup, R.; Schröder, D.; Schwarz, H. *J. Am. Chem. Soc.*, in press. (b) Schröder, D.; Schwarz, H. *Int. J. Mass Spectrom. Ion Processes*, in press.

(25) In ref 23d Sc^+ is reported to yield also ca. 10% double-dehydrogenation product. Unfortunately, in our experiments complete thermalization of scandium cation was not possible since the argon, which was used for thermalization, possessed significant amounts of oxygen-containing compounds, which irreversibly react with Sc^+ to yield the corresponding oxide cation ScO^+ . However, the incomplete thermalization will not affect the qualitative stereochemical outcome of the current study.

Table 3. Isotope Distribution in the Multiple Dehydrogenations of [all-cis-1,2,3,4,5,6-D₆]Cyclohexane by the Early-Transition-Metal Cations Sc⁺-V⁺ and Associated Kinetic Isotope Effects (KIEs)^{a,c}

M ⁺	2H ₂	2D ₂	3H ₂	(2H ₂ + D ₂)	(H ₂ + 2D ₂)	3D ₂	KIE ^b
Sc ⁺			77	4	2	17	4.5 ^c
Ti ⁺			74			26	2.8
V ⁺	25	23	45			7	2.3

^a Intensities are normalized to 100%. All data were corrected for natural abundances of ¹³C isotopomers as well as the incompleteness of the deuterium labeling in **1a** (99.6 atom % D; see text); no other isotopomers were observed. ^b Here, the kinetic isotope effect refers to the overall ratio of C-H versus C-D bond activation in all multiple-dehydrogenation events. ^c The mixed isotopomers have been neglected.

fact that these last metal cations do not activate C-H or C-C bonds of alkanes has been attributed to their respective electronic ground states, which exhibit empty, filled, or half-filled valence shells, i.e. Cr⁺ (4s⁰3d⁵), Mn⁺ (4s¹3d⁵), Cu⁺ (4s⁰3d¹⁰), and Zn⁺ (4s¹3d¹⁰). Note that these trends in reactivity as a function of the electronic structures of M⁺ have been discussed previously and were analyzed in detail.^{23,26} Therefore, these aspects will not be pursued further in the discussion; rather, we will focus on the *stereochemical* features of C-H bond activation of cyclohexane by the remaining first-row transition-metal cations.

Early Transition Metals Sc⁺, Ti⁺, and V⁺. Table 3 displays the experimental findings for the multiple dehydrogenations of **1a** by Sc⁺, Ti⁺, and V⁺. It is apparent from the data that all dehydrogenation steps occur with a high degree of stereoselectivity, in that sequential losses of H₂ or D₂, respectively, take place; products due to the elimination of HD losses are absent. Before going into a more detailed analysis of the isotope distributions, it is mandatory to verify the isotopomeric and, in particular, the stereogenic purity of **1a**. In this case, standard spectroscopic techniques such as IR, NMR, or conventional MS are quite limited in providing this information and, as suggested by Freiser and co-workers,^{6a,b} "bare" metal-ion chemistry may complement these analytical methods.

With respect to the structural analysis of **1a**, its reactions with "bare" Ti⁺ turned out to be useful. As can be seen in Figure 1, the exclusive reaction products correspond to Ti(C₆H₆)⁺ and Ti(C₆D₆)⁺, which are formed together with their ¹³C isotopomers. Of particular interest is the signal for Ti(C₆HD₅)⁺. A quantitative analysis of the peak heights of the signals shown in Figure 1 together with corrections for the ¹³C isotopes reveals that **1a** contains 99.6 atom % D. Within experimental error this figure corresponds to the isotopomeric purity of [D₆]benzene (99.5 atom % D), which was used as a precursor in the synthesis of **1a**. Thus, we conclude that the isotopomeric purity of [D₆]benzene was completely conserved in the hydrogenation; from the virtual absence of any H/D exchange product we further conclude that the hydrogenation C₆D₆ + 3H₂ → C₆D₆H₆ occurred with practically 100% stereoselectivity.

From Figure 1 we also conclude that for Ti⁺ triple dehydrogenation of **1a** in the gas phase occurs stereospecifically in an *all-cis* fashion to yield exclusively [D₀]benzene or [D₆]benzene/Ti⁺. In addition, the rela-

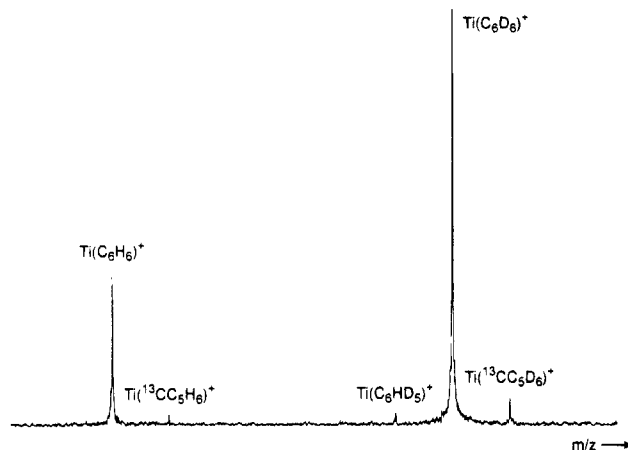
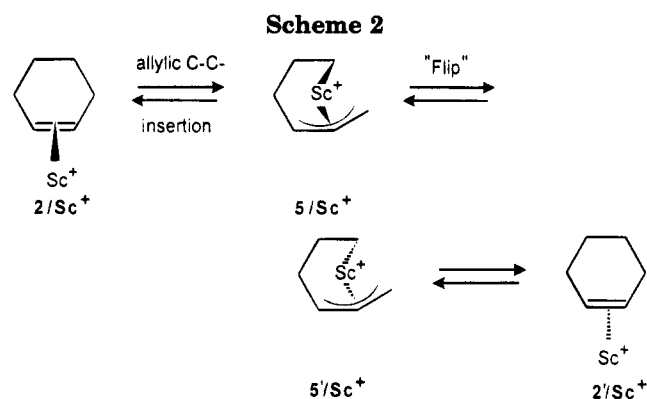


Figure 1. Partial FTICR mass spectrum of the triple-dehydrogenation region for the reaction of **1a** with "bare" Ti⁺ cations at 30% conversion. The spectrum was acquired with 64K data points and zero-filled to 128K prior to Fourier transformation.



tive abundances of both products imply the operation of an average kinetic isotope effect (KIE) of 2.8 for multiple C-H versus C-D bond activation.

"Bare" Sc⁺ behaves similarly to Ti⁺, generating Sc(C₆H₆)⁺ and Sc(C₆D₆)⁺ as the most dominant products by far. As compared to Ti⁺, for scandium the overall KIE is somewhat larger (4.1), which may in part be due to the lower efficiency for Sc⁺ (50% versus 100%) but reflects the operation of a different intrinsic KIE. Interestingly, non-negligible amounts of Sc(C₆H₄D₂)⁺ and Sc(C₆H₂D₄)⁺ are also observed, whereas product ions containing odd numbers of H and D atoms are absent. Thus, in the case of Sc⁺ a minor, additional mechanism for consecutive dehydrogenation must be operative, which permits a stereoselective dehydrogenation of *both* sides of **1a** without involving H/D exchange processes.

As a plausible reaction mechanism we propose a ring-flipping process in which after the first dehydrogenation (1/Sc⁺ → 2/Sc⁺) the metal changes the coordination site via an allylic C-C bond insertion to yield 5/Sc⁺ (Scheme 2). Subsequently, 5/Sc⁺ can undergo a ring inversion ("flip") to 5'/Sc⁺, which may then reclose to its ring-inverted isomer 2'/Sc⁺; as a net result a degenerate rearrangement has taken place in which the metal ion gains access to either surface. Alternatively, the empty 3d orbitals of Sc⁺ may allow for the direct interconversion 2/Sc⁺ ⇌ 2'/Sc⁺ with a planar coordination of the metal to the C-C double bond as a transition structure. The direct migration of the metal cation through the

(26) For trends in the periodic table, see: Armentrout, P. B.; Georgiadis, R. *Polyhedron* **1988**, *7*, 1573.

Table 4. Isotope Distribution in the Multiple Dehydrogenations of [*all-cis*-1,2,3,4,5,6-D₆]Cyclohexane (1a) by the Group 8 Transition-Metal Cations Fe⁺–Ni⁺ and Kinetic Isotope Effects Associated with the First Dehydrogenation Step^{a,b}

M ⁺	H ₂	HD ^c	D ₂	2H ₂	(H ₂ + HD)	(H ₂ + D ₂)	(D ₂ + HD)	3H ₂	(2H ₂ + HD)	(2H ₂ + D ₂)	(H ₂ + HD + D ₂)	(H ₂ + 2D ₂)	KIE ^d
Fe ⁺	67	<0.4	10	12	4	2	<1	1	2	1	1		6.7
Co ⁺	48	2	16	15	9	5	1	<1	1	2	1	<1	3.0 ^e
Ni ⁺	62	<0.3	16	12	6	3	1						3.9

^a Intensities are normalized to 100%. All data were corrected for natural abundances of ¹³C isotopomers as well as the incompleteness of the deuterium labeling in 1a (99.6 atom % D; see text); for the sake of clarity, in the multiple dehydrogenations some isotopomers of intensities much less than 1% have been neglected. ^b Due to the overlapping isobaric multiplets in the broad-band spectra (e.g. loss of 2H₂ versus D₂), the intensities were derived from high-resolution mass spectra (for experimental details see ref 2). ^c The relative abundances of the HD losses were derived from the measured heights of the [1a/M⁺ – 3] peaks after subtraction of the portion which can be traced back to the incompleteness of the labeling in 1a; ¹³C contributions were completely mass-resolved. ^d Here, the kinetic isotope effect refers to the first dehydrogenation, i.e. k_{H_2}/k_{D_2} . ^e The loss of HD was neglected.

plane of the six-membered ring can be excluded on energetic grounds.²⁷

Vanadium cations also mediate multiple C–H/C–D bond activation of 1a to yield V(C₆H₆)⁺ and V(C₆D₆)⁺, respectively. The smaller reaction efficiency (50%) and the observation of the double-dehydrogenation products indicate that V⁺ is somewhat less reactive toward cyclohexane as compared to its congeners Sc⁺ and Ti⁺.²⁸ However, as far as the face selectivity is concerned, dehydrogenation occurs stereospecifically without involving any H/D exchange processes. Noteworthy is the isotopically sensitive branching³ for V⁺: while the ratio for the losses of 2H₂/3H₂ amounts of 0.55, that for 2D₂/3D₂ losses is as large as 3.3 (Table 3). This large difference in terms of rate constants is not necessarily caused primarily by an intrinsically high KIE associated with the third dehydrogenation step,²⁹ rather, it may be the result of the interplay of the KIE with the lifetime of the rovibrationally excited cyclohexadiene/V⁺ intermediate; the lifetime will increase when multiple dehydrogenation is hampered by a KIE. As a consequence, the probability for a third D₂ loss is significantly lower as compared to that of H₂, and a relatively large fraction of excited V(C₆H₆D₂)⁺ undergoes radiative or collisional cooling³⁰ to yield the stable ion instead of losing another D₂ molecule to form V(C₆H₆)⁺. In contrast, consecutive loss of H₂ from excited V(C₆D₆H₂)⁺ is more facile, such that V(C₆D₆)⁺ is produced preferentially.

Group 8 Transition Metals Fe⁺, Co⁺ and Ni⁺. The behavior of the group 8 transition metals is distinct from that of the early transition metals, in that single dehydrogenation predominates, while double and triple dehydrogenations are much less intense. In addition, for Co⁺ and Ni⁺ also C–C bond activation takes place (Table 1) to yield M(C₃H₆)⁺, most probably propene complexes. With respect to the stereoselectivity of the dehydrogenation processes, the following conclusions can be drawn from the experimental data (Table 4). For the group 8 metal cations the first dehydrogenation (1a/M⁺ → 2/M⁺) hardly involves any H/D exchange processes between both faces of 1a, and only from 1a/Co⁺ is a

somewhat enhanced loss of HD observed. The KIEs associated with the first dehydrogenation in the ICR experiment amount to 6.7 (24), 3.0 (4.5), and 3.9 (4.1) for Fe⁺, Co⁺, and Ni⁺, respectively (data in parentheses refer to MI processes). Due to the fact that these figures result from several competing processes, as outlined above for the vanadium cation, and the different time scales of both instruments, as well as varying amounts of internal energy content, we cannot directly compare the KIEs. Nevertheless, in a qualitative sense, the KIE for Fe⁺ is significantly higher than those for Co⁺ and Ni⁺, which indicates that different steps in the overall reaction sequence of dehydrogenation may be rate-determining for Fe⁺ as compared to Co⁺ and Ni⁺. In contrast to the high site specificity of single dehydrogenation, H/D exchange processes are significant in the second dehydrogenation (2/M⁺ → 3/M⁺), indicating partial equilibration of both sides of the cyclohexene substructure. In terms of a possible reaction mechanism, here one cannot invoke the same scenario as proposed for the scandium cation (Scheme 2), since this would not account for the losses of mixed isotopomers, e.g. (H₂ + HD). Furthermore, the observation of C–C bond activation products indicates that quite a different reaction mechanism is operative which involves sequential breaking and formation of C–C and C–H bonds.

As a plausible reaction mechanism we propose (Scheme 3) that the cyclohexene/M⁺ complex 2/M⁺ which is formed in the first dehydrogenation step can subsequently undergo facile allylic C–H bond activation and consecutive β-H transfer to lose another dihydrogen molecule (2/M⁺ → 3/M⁺); this scenario, of course, conserves the complete *syn* stereochemistry of the dehydrogenation process. In contrast, allylic C–C bond activation followed by several steps involving reversible β-H transfer may lead to an acyclic hexadiene complex, 6/M⁺, which can subsequently eliminate dihydrogen to yield either acyclic 7/M⁺ or 3/M⁺ via an electrocyclic ring closure. Due to the acyclic structure of the intermediate 6/M⁺, partial or even complete H/D equilibration of both faces can take place via rotations as well as reversible C–H bond insertion and β-H transfer steps. Of course, in this reaction sequence a variety of many other intermediates are conceivable, and we have chosen 6/M⁺ in order to emphasize the possibility of complete H/D equilibration in acyclic isomers.

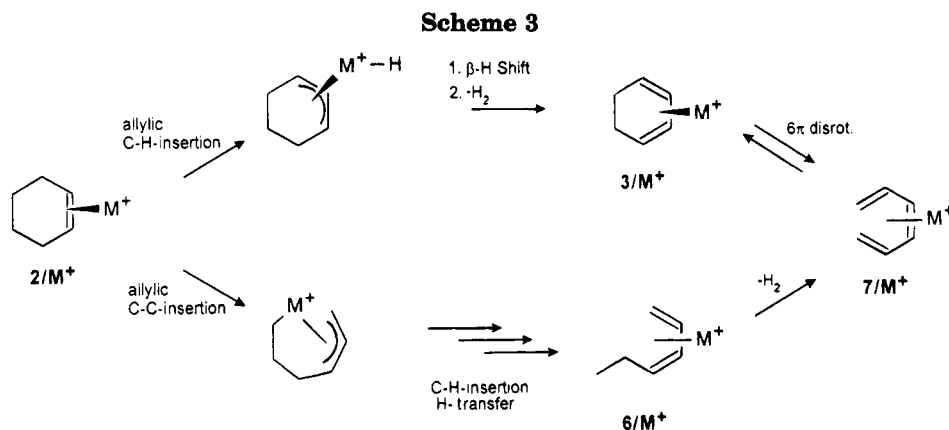
An alternative mechanism that would account for the H/D equilibration involves the reversible formation of the bis(propene) complex M(C₃H_{6-n}D_n)₂⁺, in which the hydrogen atoms can easily be equilibrated via reversible

(27) For example, for the passage of the much smaller helium atom through the plane of a benzene ring, the activation barrier exceeds 180 kcal/mol: (a) Hrušák, J.; Schwarz, H. *Chem. Phys. Lett.* **1992**, *193*, 97. (b) Sprang, H.; Mahlkow, A.; Campbell, E. E. B. *Chem. Phys. Lett.* **1994**, *227*, 91.

(28) Toibert, M. A.; Beauchamp, J. L. *J. Am. Chem. Soc.* **1986**, *108*, 7509.

(29) Thibblin, A.; Ahlberg, P. *Chem. Soc. Rev.* **1989**, *18*, 209.

(30) (a) Dunbar, R. C. *Int. J. Mass Spectrom. Ion Processes* **1990**, *100*, 423. (b) Smith, D. *Int. J. Mass Spectrom. Ion Processes* **1993**, *129*, 1. (c) Stöckigt, D.; Hrušák, J.; Schwarz, H. *Int. J. Mass Spectrom. Ion Processes*, in press.



allylic C–H bond activation processes.³¹ In fact, it is tempting to apply this mechanism to the H/D exchange in the Co^+ system, as for this metal a significant amount of H/D equilibration in the first dehydrogenation parallels the amount of C–C bond activation to yield $\text{M}(\text{C}_3\text{H}_{6-n}\text{D}_n)^+$.

Finally, in the third dehydrogenation, which is of fairly low intensity for Fe^+ and Co^+ and not observed at all for Ni^+ , the isotope distribution is more or less statistical, which is in line with a mechanism invoking acyclic isomers as outlined above. As far as the C–C bond activation for Co^+ and Ni^+ is concerned, the isotope distributions of the $\text{M}(\text{C}_3\text{H}_{6-n}\text{D}_n)^+$ product ions are identical for both metals in the range of experimental error, i.e. $[\text{D}_2]:[\text{D}_3]:[\text{D}_4] = 1:2:1$, which is in line with a statistical equilibration of H/D atoms prior to dissociation.

Conclusions

The use of the stereospecifically labeled cyclohexane **1a** turns out to be extremely beneficial for the understanding of important details of C–H bond activation processes by “bare” first-row transition-metal cations. By examining [*all-cis*-1,2,3,4,5,6- D_6]cyclohexane it becomes possible to distinguish between the “top” and the “bottom” of the hydrocarbon surfaces and to decide whether C–C activation processes take place or not during the reaction.

Furthermore, the present study reveals that, for the particular purpose of comparing relative reactivities of different metal cations, the approach used in ICR mass spectrometry is much more valuable as compared to sector-field experiments, not only with respect to mass resolution and flexibility for the various metal cations, but also as far as relative energetics and kinetic isotope and lifetime effects are concerned. Interestingly, the outcome of the synthesis of **1a**, in which a cobalt(I) catalyst was employed to hydrogenate benzene, is in sharp contrast to the gas-phase chemistry of “bare” cobalt cation: while in the condensed phase the hydrogenation of benzene occurs with almost 100% *cis* stereoselectivity, in the gas phase Co^+ (and also Fe^+ and Ni^+) mediates H/D equilibration between both faces of the cyclohexane backbone. In marked contrast, the “bare” metal cations of the early transition metals Sc, Ti, and V exhibit a high face selectivity in cyclohexane dehydrogenation.³²

Acknowledgment. Financial support by the Deutsche Forschungsgemeinschaft and the Fonds der Chemischen Industrie is gratefully acknowledged.

OM950284+

(31) Jacobson, D. B.; Freiser, B. S. *J. Am. Chem. Soc.* **1985**, *107*, 72.

(32) For a similar phenomenon, see: Eller, K.; Schröder, D.; Schwarz, H. *J. Am. Chem. Soc.* **1992**, *114*, 6173.

Redox Properties of Cationic Vanadium(IV): [Cp₂VCH₃(CH₃CN)]⁺[BPh₄]⁻

Robert Choukroun,* Bénédicte Douziech, Cheng Pan, Françoise Dahan, and Patrick Cassoux

Equipe Précurseurs Moléculaires et Matériaux, Laboratoire de Chimie de Coordination du CNRS, 205 route de Narbonne, 31077 Toulouse Cedex, France

Received December 29, 1994[®]

The cationic vanadium complexes [Cp₂VCH₃(CH₃CN)]⁺ and [Cp₂V(THF)]⁺ with [BPh₄]⁻ as counterion are obtained from Cp₂VMe₂ and [NHMe₂Ph]BPh₄ in CH₃CN or THF, respectively; in CH₂Cl₂, chloride abstraction from the solvent occurs via a redox decomposition, evidenced by the X-ray crystal structure of [N(CH₂Cl)Me₂Ph]BPh₄ and the formation of Cp₂VCl. In presence of the phosphine PMe₂Ph, [Cp₂VCH₃(CH₃CN)]⁺ affords the intermediate species [Cp₂VCH₃(PMe₂Ph)]⁺ (characterized by the EPR spectrum with resolved methyl hyperfine interaction) followed by a disproportionation and a redox reaction with [BPh₄]⁻, giving Cp₂VMe₂ and [Cp₂V(PMe₂Ph)]⁺. Preliminary studies show that [Cp₂VCH₃]⁺ is unreactive toward ethylene polymerization.

The chemistry of cationic transition metals of group 4 has challenged both experimentalists and theoreticians due to its importance with regard to Ziegler–Natta or Kaminsky catalysts.¹ The extreme reactivity of the 14-electron species [Cp₂MR]⁺ (M = Ti, Zr) allowed only occasional isolation of such compounds, stabilized by trapping with a donor. The synthesis of these stable 16-electron species is now well documented.² In contrast to the well-developed field of cationic dicyclopentadienyl–Ti and –Zr complexes,³ the chemistry of cationic vanadium complexes has attracted much less attention.⁴ In order to extend the cationic chemistry already described for Ti and Zr to V, we studied the protonolysis of Cp₂VMe₂ (1) with [NHMe₂Ph]BPh₄.

Results and Discussion

The general procedure used in the synthesis of the 16-electron compounds [Cp₂MR(L)]⁺ and base-free 14-electron compounds [Cp₂MR]⁺ (M = Ti, Zr) was used

for the synthesis of analogues of vanadium.^{5,6} Reaction of Cp₂VMe₂ (1) with [NHMe₂Ph]BPh₄ in CH₃CN at room temperature afforded a nearly quantitative precipitate of pale violet [Cp₂VCH₃(CH₃CN)]BPh₄ (2). The presence of the methyl group in 2 was confirmed by evolution of CH₄ (characterized by IR and mass spectra) on adding HCl to a suspension of 2 in THF. The adduct is paramagnetic, with one unpaired electron and a formal oxidation state of IV for the vanadium ($\mu = 1.88 \mu_B$). The IR spectrum showed bands due to CH₃CN at 2308 and 2279 cm⁻¹ (free CH₃CN bands at 2287 and 2251 cm⁻¹).

When the reaction was carried out in THF at room temperature or at –80 °C, 1 equiv of methane was evolved and a blue-violet precipitate of [Cp₂V(THF)]BPh₄ (3) was obtained, identified by elemental analysis, magnetism ($\mu = 2.75 \mu_B$, indicating two unpaired electrons), and ¹H NMR spectroscopy. The filtrate contains unreacted 1 and biphenyl (by EPR⁷ and ¹H NMR and GC/MS, respectively). No CH₄ was observed on acidic hydrolysis of 3, verifying the absence of the methyl group. The yield of the reaction was roughly 50% based on vanadium. We propose a disproportionation and a redox reaction⁸ between V^{IV} and [BPPH₄]⁻. It is reasonable to assume that the intermediate [Cp₂VMe(THF)]BPh₄ disproportionates to [Cp₂V(THF)₂](BPh₄)₂ and Cp₂VMe₂, the [Cp₂V(THF)₂]²⁺ oxidizing the counteranion [BPh₄]⁻ to BPh₃ and PhPh. Compound 3 was also obtained from 1 and 2 equiv of the ammonium salt. In this case, 2 equiv of CH₄ and nearly 100% of 3

[®] Abstract published in *Advance ACS Abstracts*, September 1, 1995.

(1) For leading references to cationic group 4 metal alkyl complexes see: (a) Dyachkovskii, F. S. In *Coordination Polymerization*; Chien, J. C. W., Ed. Academic Press: New York, 1975; p 199. (b) Jordan, R. F. *Adv. Organomet. Chem.* **1991**, *32*, 325. (c) Marks, T. J. *Acc. Chem. Res.* **1992**, *25*, 57 and references cited therein. (d) Spaleck, W.; Küber, F.; Winter, A.; Rohrmann, J.; Bachmann, B.; Anterg, M.; Dolle, V.; Paulus, E. F. *Organometallics* **1994**, *13*, 954 and references cited therein. (e) Stehling, U.; Diebold, J.; Kirsten, R.; Rol, W.; Brintzinger, H.; Jüngling, S.; Mülhaupt, R.; Langhauser, F. *Organometallics* **1994**, *13*, 964 and references cited therein. (f) Andersen, A.; Cordes, H. G.; Herwig, J.; Kaminski, W.; Merck, A.; Mottweiler, R.; Pein, J.; Sinn, H.; Vollmer, H. J. *Angew. Chem., Int. Ed. Engl.* **1976**, *15*, 630. (g) Sinn, H.; Kaminsky, W. *Adv. Organomet. Chem.* **1980**, *18*, 99. (h) Kaminsky, W.; Külper, K.; Brintzinger, H. H.; Wild, F. R. W. P. *Angew. Chem., Int. Ed. Engl.* **1985**, *24*, 507.

(2) (a) Bochmann, M.; Lancaster, S. J.; Hursthouse, M. B.; Abdul Malik, K. M. *Organometallics* **1994**, *13*, 2235 and references cited therein. (b) Bochmann, M.; Lancaster, S. J. *Organometallics* **1993**, *12*, 633. (c) Röttger, D.; Erker, G.; Grehl, M.; Fröhlich, R. *Organometallics* **1994**, *13*, 3897. (d) Jia, L.; Yang, X.; Stern, C.; Marks, T. J. *Organometallics* **1994**, *13*, 3755.

(3) (a) Pellechia, C.; Grassi, A.; Zambelli, A. *Organometallics* **1994**, *13*, 298. (b) Guo, Z.; Swenson, D. C.; Jordan, R. F. *Organometallics* **1994**, *13*, 1424. (c) Guo, Z.; Swenson, D. C.; Guram, A. S.; Jordan, R. F. *Organometallics* **1994**, *13*, 766. (d) Yang, X.; Stern, C. L.; Marks, T. J. *J. Am. Chem. Soc.* **1994**, *116*, 10015.

(4) Fachinetti, G.; DelNero, S.; Floriani, C. J. *Chem. Soc., Dalton Trans.* **1976**, 1046.

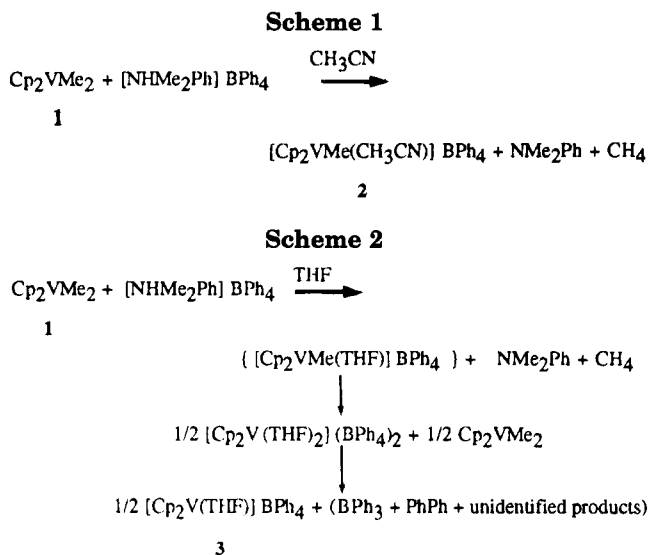
(5) Yang, X.; Stern, C. L.; Marks, T. J. *J. Am. Chem. Soc.* **1991**, *113*, 3623.

(6) Bochmann, M.; Lancaster, S. J.; Hursthouse, M. B.; Abdul Malik, K. M. *Organometallics* **1994**, *13*, 2235 and references therein.

(7) Razuvaev, G. A.; Latyaeva, V. N.; Vishinskaya, L. I.; Cherkasov, V. K.; Korneva, S. E.; Spiridonova, N. N. *J. Organomet. Chem.* **1977**, *129*, 169.

(8) (a) Abley, P.; Halpern, J. *J. Chem. Soc. D* **1971**, 1238. (b) Eisch, J. J.; Shah, J. H.; Boleslawski, M. P. *J. Organomet. Chem.* **1994**, *464*, 11. (c) Crowther, D. J.; Jordan, R. F.; Branziger, N. C.; Verma, A. *Organometallics* **1990**, *9*, 2574.

(9) (a) Alelyulas, Y. W.; Guo, Z.; LaPointe, R. E.; Jordan, R. F. *Organometallics* **1993**, *12*, 544. (b) Erker, G.; Schlund, R.; Kruger, C. *Organometallics* **1989**, *8*, 2349. (c) Pellechia, C.; Immirzi, A. *Organometallics* **1993**, *12*, 4473. (d) Eshuis, J. J. W.; Tan, Y. Y.; Teuben, J. H. *J. Mol. Catal.* **1990**, *62*, 277.



are obtained. Attempts to improve the mass balance of the reaction described in Scheme 2 by quantification of liberated PhPh was impossible (attributable to the formation of other unidentified boron species^{8b,10} which leads us to underestimate PhPh), even through a quantitative yield of **3** is observed.

The instability of the THF intermediate adduct $[\text{Cp}_2\text{VMe(THF)]BPh}_4$ was demonstrated on treating complex **2**. A characteristic EPR spectrum for vanadium(IV) was obtained in THF, where **2** is slightly soluble, consistent with the suggested species $[\text{Cp}_2\text{VMe(THF)]BPh}_4$ ($I = 7/2$, $g = 1.995$, $A(^{51}\text{V}) = 69.7$ G; no hyperfine coupling to the methyl group). Development of the EPR spectrum into the characteristic EPR spectrum of $\text{Cp}_2\text{V(CH}_3)_2$ occurs over 2 days, with formation of $[\text{Cp}_2\text{V(THF)]BPh}_4$, which was transformed after workup in acetone and identified by ^1H NMR spectroscopy as $[\text{Cp}_2\text{V(OCMe}_2)]\text{BPh}_4$.⁴ A similar disproportionation redox reaction occurs when **2** is treated with PR_3 (PMePh_2 or PMe_2Ph). Addition of PR_3 to a CH_3CN suspension or a THF solution of **2** slowly displaced the CH_3CN and generated a spectrum attributable to $[\text{Cp}_2\text{VCH}_3(\text{PR}_3)]\text{BPh}_4$. The unpaired electron interacts with the ^{51}V ($I = 7/2$) nucleus and one ^{31}P ($I = 1/2$) nucleus of the phosphine, giving a doublet of octets ($[\text{Cp}_2\text{VCH}_3(\text{PMePh}_2)]\text{BPh}_4$: $g = 2.007$, $a(^{31}\text{P}) = 23.3$ G, $A(^{51}\text{V}) = 66.7$ G). In the case of PMe_2Ph in CH_3CN (Figure 1), the methyl group on the vanadium gave a hyperfine coupling to the three protons of the methyl, observed as a quartet ($[\text{Cp}_2\text{VCH}_3(\text{PMe}_2\text{Ph})]\text{BPh}_4$: $g = 1.999$, $a(^{31}\text{P}) = 30.8$ G, $a(^1\text{H}) = 6.25$ G, $A(^{51}\text{V}) = 61.2$ G). The change from $[\text{Cp}_2\text{VCH}_3(\text{PMe}_2\text{Ph})]\text{BPh}_4$ to $\text{Cp}_2\text{V(CH}_3)_2$ occurs over 3–4 days with concomitant formation of $[\text{Cp}_2\text{V(PMe}_2\text{Ph)]BPh}_4$, identified after workup by ^1H and ^{31}P NMR spectroscopy and by comparison with an authentic sample prepared *in situ* from **3** and PMe_2Ph in CD_3CN (the relative intensities of liberated THF and PMe_2Ph signals show the formation of the mono(phosphine) adduct; ^1H NMR (ppm) 140 (Cp), 3.68, 1.83 (free THF), 1.75 ($J_{\text{PH}} = 13$ Hz, $\text{V(PMe}_2\text{Ph)}$), 1.42 (free PMe_2Ph); ^{31}P NMR (ppm) 37.9). All these reactions leading to **1** and $[\text{Cp}_2\text{V(L)]BPh}_4$ ($\text{L} = \text{THF}, \text{PR}_3$) suggest that the intermediate complexes ($[\text{Cp}_2\text{VCH}_3(\text{L)]BPh}_4$) are probably kinetic products rather than thermodynamic ones, as for **2**. Exchanges of the THF in **3** with

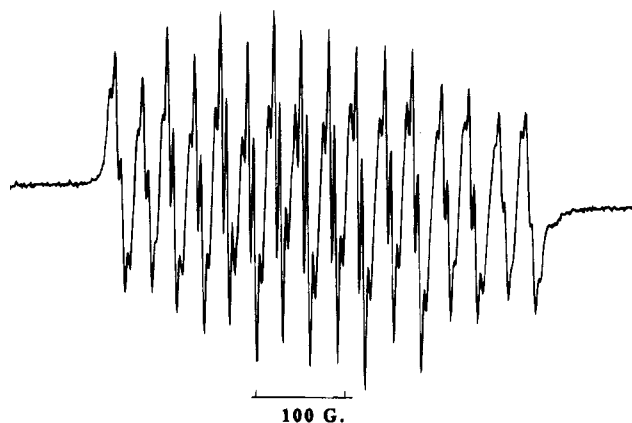


Figure 1. EPR spectrum in CH_3CN at room temperature of **2** in the presence of an excess of PMe_2Ph .

acetone and acetonitrile were followed by ^1H NMR spectroscopy and give the corresponding adducts $[\text{Cp}_2\text{V(L)]BPh}_4$ ($\text{L} = \text{OCMe}_2, \text{CH}_3\text{CN}$) and free THF. The similar species $[\text{Cp}_2\text{V(L)]BPh}_4$ ⁴ were previously isolated, but the THF adduct was not obtained from Cp_2VCl by the chemical procedure used.

It was recently shown that base-free 14-electron alkyl cations of titanium and zirconium in weakly coordinating solvents such as dichloromethane are active in the homogeneous polymerization of olefins.^{5,6} Although the ammonium salt is known to be modestly stable in solution,¹⁰ treatment of **1** and solid $[\text{NHMe}_2\text{Ph}]\text{BPh}_4$ in CH_2Cl_2 at -80 °C or at room temperature leads to a blue-green solution and a vanadium-free microcrystalline product in approximately 5–10% yield, depending on the experiment. An X-ray diffraction analysis showed this to be $[\text{N(CH}_2\text{Cl)Me}_2\text{Ph}]\text{BPh}_4$, instead of the expected V^{IV} complex. The salt has a classical ammonium structure in which the CH_2Cl fragment is the most significant (see the supporting information). Chloride abstraction from CH_2Cl_2 occurs frequently with 14- or 16-electron cationic zirconium or titanium complexes;⁹ however, we have been able to trap the carbocation $[\text{CH}_2\text{Cl}]^+$ formed from the supposed transient adduct $[\text{Cp}_2\text{VCH}_3(\text{CH}_2\text{Cl}_2)]^+$. We believe that the reaction of the ammonium salt with **1** competes with its decomposition in CH_2Cl_2 .¹⁰ A similar reaction involving nucleophilic attack of NR_3 at a $\text{Zr}-\text{ClCH}_2\text{Cl}$ adduct, leading to a chloromethylammonium salt and a chlorozirconium complex, was recently reported by Jordan et al.¹¹ In our experiments, the formation of the neutral Cp_2VCl was observed by ^1H NMR spectroscopy and by comparison with an authentic sample. After the reaction, the solution was EPR silent and no CH_4 evolution was observed when HCl was added to the reaction mixture. The mechanism of the reaction, a disproportionation and a redox reaction between V^{IV} , $[\text{BPh}_4]^-$, and CH_2Cl_2 , giving respectively V^{III} , BPh_3 (and other unidentified boron species), and $[\text{N(CH}_2\text{Cl)Me}_2\text{Ph}]^+$, was not studied in detail.

Since Cp_2VCl_2 in the presence of alkylaluminum halide as cocatalyst yields catalytic systems able to polymerize ethylene,¹² we have performed different

(11) Tjaden, E. B.; Swenson, D. C.; Jordan, R. F.; Petersen, J. L. *Organometallics* **1995**, *14*, 371.

(12) (a) Breslow, D. S. U.S. Patent 2 924 593; *Chem. Abstr.* **1960**, *54*, 11573. (b) Karapinka, G. L.; Carrick, W. L. *J. Polym. Sci.* **1961**, *55*, 145.

ethylene polymerization tests with **1** containing the counteranions $[\text{NHMe}_2\text{Ph}]\text{B}(\text{C}_6\text{F}_5)_4$ and $\text{B}(\text{C}_6\text{F}_5)_3$ in various solvents (THF, toluene, CH_3CN , CH_2Cl_2 , and $\text{ClCH}_2\text{CH}_2\text{Cl}$), at different temperatures (-30 , 20 , 40 °C) and pressures (2, 20, and 40 bar of C_2H_2), without success. Although the participation of cationic d^0Ti and Zr complexes in Ziegler–Natta catalysis is well established, inclusion of cationic vanadium $[\text{Cp}_2\text{VMe}]^+$ within this framework has failed and will require additional effort. Our results seem to confirm that the presence of the intact Cp_2V unit in the catalyst inhibits polymerization, as was previously observed.¹²

Experimental Section

All manipulations were carried out under argon by conventional Schlenk tube techniques or using a drybox (Vacuum Atmosphere Dri-Lab) filled with argon. Liquids were transferred *via* syringe or cannula. All solvents were dried by conventional methods, distilled under argon, and degassed before use: THF is distilled from sodium/benzophenone, toluene from sodium/potassium alloy, and CH_2Cl_2 from calcium dihydride. Cp_2VMe_2 ,¹³ $[\text{NHMe}_2\text{Ph}]\text{BPh}_4$,¹⁴ $[\text{NHMe}_2\text{Ph}]\text{B}(\text{C}_6\text{F}_5)_4$,¹⁵ and $\text{B}(\text{C}_6\text{F}_5)_3$ ¹⁶ were prepared and isolated via procedures described elsewhere. ^1H and ^{31}P NMR spectra were recorded on a Bruker WM 250 spectrometer (values of ^1H and ^{31}P chemical shifts are positive downfield from SiMe_4 or 85% H_3PO_4 in D_2O , respectively). Magnetic susceptibility measurements were carried out by Faraday's method. EPR spectra were recorded on a Bruker ER 200 T spectrometer. Elemental analyses were performed by the Service Central de Microanalyse du CNRS.

$[\text{Cp}_2\text{VMe}(\text{CH}_3\text{CN})]\text{BPh}_4$ (2**).** A 10 mL CH_3CN solution of $[\text{NHMe}_2\text{Ph}]\text{BPh}_4$ (800 mg, 1.81 mmol) was added to Cp_2VMe_2 (380 mg, 1.80 mmol) dissolved in 10 mL of CH_3CN at 20 °C. Gas evolution was monitored by means of a Toepler pump, the gas being identified as CH_4 by IR and MS (approximately 1 equiv), and a purple solid formed. After 12 h of stirring, the purple mixture was filtered, leading to a brown filtrate and a violet solid which was washed with CH_3CN and dried under vacuum; yield 80%. Anal. Calcd for $\text{C}_{37}\text{H}_{36}\text{BNV}$: C, 79.86; H, 6.52; N, 2.52; V, 9.15. Found: C, 79.42; H, 6.22; N, 2.46; V, 9.17.

Attempts to crystallize the compound by different experiments at lower temperature (-20 °C) with slow addition of the ammonium salt led to a similar precipitate of **2**.

$[\text{Cp}_2\text{V}(\text{VHF})]\text{BPh}_4$ (3**).** A freshly prepared solution of $[\text{NHMe}_2\text{Ph}]\text{BPh}_4$ (585 mg, 1.33 mmol) in THF (10 mL) was added to Cp_2VMe_2 (280 mg, 1.33 mmol) in 10 mL of THF at 20 °C. Gas evolution was monitored by means of a Toepler pump (approximately 1 equiv of CH_4 identified by IR and MS), and a purple solid was formed. After 12 h, the mixture was filtered, giving a brown filtrate and purple solid **3**, which was washed with THF and dried under vacuum; yield 50%. The filtrate was identified by EPR spectroscopy as **1**. Acid hydrolysis of the solution gave the expected evolution of CH_4 , whereas a suspension of **3** did not. GC/MS analysis of the filtrate confirmed the presence of biphenyl in the solution.

(13) Foust, D. F.; Rausch, M. D.; Samuel, E. *J. Organomet. Chem.* **1980**, *193*, 209.

(14) (a) Bochmann, M.; Wilson, L. *J. Chem. Soc., Chem. Commun.* **1986**, 1610. (b) Crane, F. E., Jr. *Anal. Chem.* **1956**, *28*, 1794.

(15) (a) Turner, H. W.; Hlatki, G. G. Eur. Patent Appl. 0,277,003, 1982. (b) Turner, H. W. Eur. Patent Appl. 0,277,004, 1988.

(16) Massey, A. G.; Park, A. J. *J. Organomet. Chem.* **1964**, *2*, 245.

Attempts to crystallize **3** in experiments at -80 °C with slow addition of solid ammonium salt (1 or 2 equiv per V atom) led to the same purple powder **3**. ^1H NMR (250 MHz, δ in ppm): in $[\text{H}_6]\text{acetone}$, δ 140.5 (broad signal, $\Delta\nu_{1/2} = 1170$ Hz, Cp), 7.45, 7.06, 6.9 (s, t, t, BPh_4), 3.74, 1.90 (free THF in acetone); in $[\text{H}_3]\text{acetonitrile}$, δ 138.7 ((broad signal, $\Delta\nu_{1/2} = 1160$ Hz, Cp), 7.27, 7.0, 6.85 (s, t, t, BPh_4), 3.64, 1.80 (free THF in acetonitrile). Anal. Calcd for $\text{C}_{38}\text{H}_{38}\text{BOV}$: C, 79.72; H, 6.64, V, 8.91. Found: C, 79.68; H, 6.59; V, 8.60.

Reaction of $[\text{Cp}_2\text{VCH}_3(\text{CH}_3\text{CN})]\text{BPh}_4$ (2**), $[\text{Cp}_2\text{V}(\text{THF})]\text{BPh}_4$ (**3**), and PMe_2Ph .** In a typical reaction, an NMR tube was charged with **3** (55 mg, 0.1 mmol), $[\text{H}_6]\text{acetone}$ (0.5 mL), and a slight excess of PMe_2Ph (200 mg, 1.48 mmol). The reaction was monitored by ^1H and $^{31}\text{P}\{^1\text{H}\}$ spectroscopy. Formation of $[\text{Cp}_2\text{V}(\text{PMe}_2\text{Ph})]\text{BPh}_4$ was observed immediately. ^1H NMR (250 MHz, δ in ppm): in $[\text{H}_6]\text{acetone}$, δ 140 (broad signal, $\Delta\nu_{1/2} = 1170$ Hz, Cp), 6.8–8.2 (m, Ph, BPh_4), 3.74, 1.90 (free THF in acetone), 1.74 (d, $J_{\text{PH}} = 13$ Hz, PMe_2Ph), 1.42 (free PMe_2Ph); in $[\text{H}_3]\text{acetonitrile}$, δ 140 (broad signal, $\Delta\nu_{1/2} = 1170$ Hz, Cp), 6.8–8.2 (m, Ph, BPh_4), 3.68, 1.83 (free THF in acetonitrile), 1.67 (d, $J_{\text{PH}} = 13$ Hz, PMe_2Ph), 1.33 (broad signal, free PMe_2Ph). ^{31}P NMR (81 MHz): δ 37.9 (free PMe_2Ph , -40.2).

Reaction of Cp_2VMe_2 and $[\text{NHMe}_2\text{Ph}]\text{BPh}_4$ in CH_2Cl_2 . Solid $[\text{NHMe}_2\text{Ph}]\text{BPh}_4$ (345 mg, 0.781 mmol) was added to Cp_2VMe_2 (172 mg, 0.781 mmol) in 10 mL of CH_2Cl_2 at -80 °C. The reaction mixture was warmed slowly to room temperature. After 12 h, the mixture was filtered, leading to a blue-green solution and a crystalline solid, which was washed with CH_2Cl_2 and dried under vacuum. The solid was identified as $[\text{N}(\text{CH}_2\text{Cl})\text{Me}_2\text{Ph}]\text{BPh}_4$ by an X-ray structure determination (the description of the data collection and structural analysis as well as the structural results are in the supporting information). A part of the filtrate was evaporated to dryness and dissolved in CD_2Cl_2 . The ^1H NMR spectrum showed a broad peak at 130 ppm, identified by comparison with an authentic sample as Cp_2VCl . ^{11}B NMR spectroscopy showed peaks at -5 and 70 ppm due to $[\text{BPh}_4]^-$ and BPh_3 , respectively, and a third unidentified peak at 46 ppm. GC/MS analysis of the remaining filtrate confirmed the presence of biphenyl in the solution as well as the decomposition of the ammonium salt.¹⁰

General Procedure for Polymerization Reactions. A 75 mL autoclave with a magnetic stirrer was connected via a pressure regulator to a 125 mL tank of ethylene. The tests were made according to the procedure described previously.^{2b} In a typical run, aliquots of toluene solutions of **1** (80 mg, 0.378 mmol) and $[\text{NHMe}_2\text{Ph}]\text{B}(\text{C}_6\text{F}_5)_4$ (150 mg, 0.187 mmol) were injected into the autoclave, previously charged with toluene saturated with ethylene, at the required temperature. After 2 h the reaction was terminated by injecting 5 mL of methanol. In any case, no polymer was observed in the solution. Experimental conditions: (i) solvents toluene, THF, CH_2Cl_2 , and $\text{ClCH}_2\text{CH}_2\text{Cl}$; (ii) temperatures -20 , 20 , and 40 °C; (iii) ethylene pressure 1, 2, and 20 bar.

Supporting Information Available: Tables giving details on the data collection and structure of $[\text{N}(\text{CH}_2\text{Cl})\text{Me}_2\text{Ph}]\text{BPh}_4$, all atomic coordinates, thermal parameters, bond distances, bond angles, and least-squares-planes equations and deviations therefrom and an ORTEP plot of the structure (10 pages). Ordering information is given on any current masthead page.

OM9409985

Synthesis of Heterobimetallic Complexes from (η^4 -MeC₅H₅)Fe(CO)₂(η^1 -PPh₂CH₂PPh₂)

Ling-Kang Liu,^{*,1a,b} Lung-Shiang Luh,^{1a,b} Yuh-Sheng Wen,^{1a} Uche B. Eke,^{1a,c} and M. Adediran Mesubi^{1c}

Institute of Chemistry, Academia Sinica, Taipei, Taiwan 11529, Republic of China, Department of Chemistry, National Taiwan University, Taipei, Taiwan 10767, Republic of China, and Department of Chemistry, University of Ilorin, Ilorin, Nigeria

Received December 20, 1994[®]

The ring alkylation of (η^5 -C₅H₅)Fe(CO)₂I with MeLi in the presence of PPh₂CH₂PPh₂ (=dppm) at -78 °C yields a novel monodentate dppm complex (η^4 -MeC₅H₅)Fe(CO)₂(η^1 -dppm) (**1**) that is used in this study as a mononuclear precursor for the construction of dimetallic complexes with dppm as a stabilizing backbone. Compound **1** reacts with (C₄H₈S)AuCl in THF at -30 °C to give a heterobimetallic complex (η^4 -MeC₅H₅)Fe(CO)₂(μ - η^1 : η^1 -dppm)AuCl (**4**), whose Au-Cl moiety could be attacked nucleophilically by MeLi to result in (η^4 -MeC₅H₅)Fe(CO)₂(μ - η^1 : η^1 -dppm)AuMe (**5**). When complex **4** is treated with equimolar Ph₃C⁺PF₆⁻, the *endo*-H atom abstracted^{*} complex [(η^5 -MeC₅H₄)Fe(CO)₂(μ - η^1 : η^1 -dppm)AuCl]⁺PF₆⁻ (**6**) is obtained. Compound **1** does not participate in the methyl migratory insertion of (η^5 -C₅H₅)Fe(CO)₂Me to produce (η^4 -MeC₅H₅)Fe(CO)₂(μ - η^1 : η^1 -dppm)(η^5 -C₅H₅)Fe(CO)C(O)Me (**2**) even after refluxing in MeCN for 24 h. Interestingly, when the monodentate dppm complex **1** is allowed to react with [Rh(CO)₂Cl]₂ in THF/*n*-hexane at room temperature, a novel heterobimetallic complex (η^5 -MeC₅H₄)Fe(μ -CO)₂(μ - η^1 : η^1 -dppm)RhCl₂ (**9**) could be isolated in excellent yields. This immediately formed complex **9** sums up sequentially a PPh₂ ligation, an *endo*-H-atom elimination, and post rearrangements in one treatment.

Introduction

Heterobimetallic complex synthesis has been of constant interest in view of incorporation of site-selective reactivity and synergistic effects to the bimetallic system, especially the ones with catalytic potential.² Recently, a novel monodentate dppm complex-(η^4 -MeC₅H₅)Fe(CO)₂(η^1 -PPh₂CH₂PPh₂) (**1**)-has been successfully synthesized in good yields.³ The reactivity of this novel monodentate dppm toward a second metal center has been studied, aiming to construct dinuclear especially heterobimetallic systems, as reported here.

Results and Discussion

At -78 °C, the reaction of equimolar (η^5 -C₅H₅)Fe(CO)₂X with RLi in the presence of 1 equiv of PR'₃ has been found to cause ring alkylation, which effectively changes the η^5 -C₅H₅ bonding mode in (η^5 -C₅H₅)Fe(CO)₂X to η^4 -RC₅H₅ bonding in (η^4 -RC₅H₅)Fe(CO)₂(PR'₃).⁴ The similar ring alkylation of (η^5 -C₅H₅)Fe(CO)₂I with MeLi in the presence of PPh₂CH₂PPh₂ (=dppm) at -78 °C yields only the single-end alkylation product (η^4 -MeC₅H₅)Fe(CO)₂(η^1 -dppm) (**1**) with no double-end

alkylation observed.³ There seems to be a high barrier to bring two [(η^4 -MeC₅H₅)Fe(CO)₂] units into close proximity. An organometallic complex containing a pendant dppm ligand is considered to be a mononuclear precursor to react with a second metal center for the stepwise construction of a dinuclear complex in which dppm serves as a stabilizing backbone, and in many instances metal-metal interaction results.⁵ Accordingly, the novel compound **1** with pendant dppm fragment is thought to possess a potentially rich chemistry.

The phosphine-assisted Me-migratory insertion reaction of (η^5 -C₅H₅)Fe(CO)₂Me has been known to be very facile.⁶ With a dangling PPh₂ in compound **1**, the 1-induced methyl migratory insertion of (η^5 -C₅H₅)Fe(CO)₂Me had been attempted, expecting the formation of a complex (η^4 -MeC₅H₅)Fe(CO)₂(μ - η^1 : η^1 -dppm)(η^5 -C₅H₅)Fe(CO)C(O)Me (**2**) in which (η^4 -MeC₅H₅)Fe(CO)₂ and (η^5 -C₅H₅)Fe(CO)C(O)Me are linked by a dppm bridge (see Scheme 1). Nonetheless, refluxing equimolar amounts of (η^5 -C₅H₅)Fe(CO)₂Me and **1** in MeCN for 24 h recovered only the reactants. The IR spectroscopic data of the crude revealed four ν_{CO} bands at 2006, 1963, 1947, and 1903 cm⁻¹. Those at 2006 and 1947 cm⁻¹ belonged to (η^5 -C₅H₅)Fe(CO)₂Me whereas the pair at 1963 and 1903 cm⁻¹ belonged to compound **1**. The ³¹P NMR spectrum had two doublets at δ 66.38 and -25.65 with ²J_{PP} = 80.2 Hz, comparing favorably well with those recorded for compound **1**. It was, however, remarkable to note that the novel compound **1** (mp 91-

* Author to whom correspondence should be addressed. Fax: 886-2-783 1237. E-mail: liuu@chem.sinica.edu.tw.

[®] Abstract published in *Advance ACS Abstracts*, August 15, 1995.
(1) (a) Institute of Chemistry, Academia Sinica. (b) Department of Chemistry, National Taiwan University. (c) Department of Chemistry, University of Ilorin.

(2) (a) Shore, N. E.; Hope, H. *J. Am. Chem. Soc.* **1980**, *102*, 4251. (b) Casey, C. P.; Bullock, R. M. *Organometallics* **1982**, *1*, 1591. (c) Bahsoun, A. A.; Osborn, J. A.; Bird, P. H.; Nucciarone, D.; Peters, A. V. *J. Chem. Soc., Chem. Commun.* **1984**, 72.

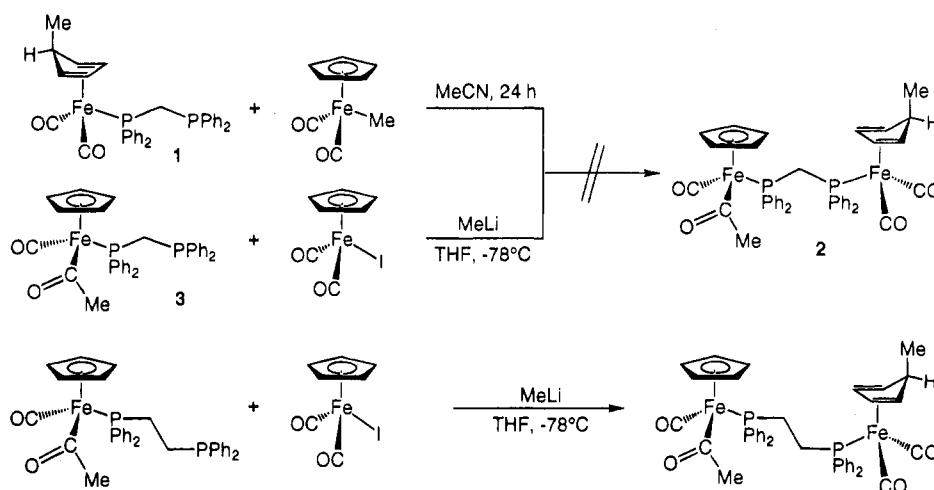
(3) Liu, L.-K.; Luh, L.-S.; Eke, U. B. *Organometallics* **1995**, *14*, 440.

(4) (a) Liu, L.-K.; Luh, L.-S. *Organometallics* **1994**, *13*, 2316. (b) Luh, L.-S.; Liu, L.-K. *Bull. Inst. Chem., Acad. Sinica* **1994**, *41*, 39.

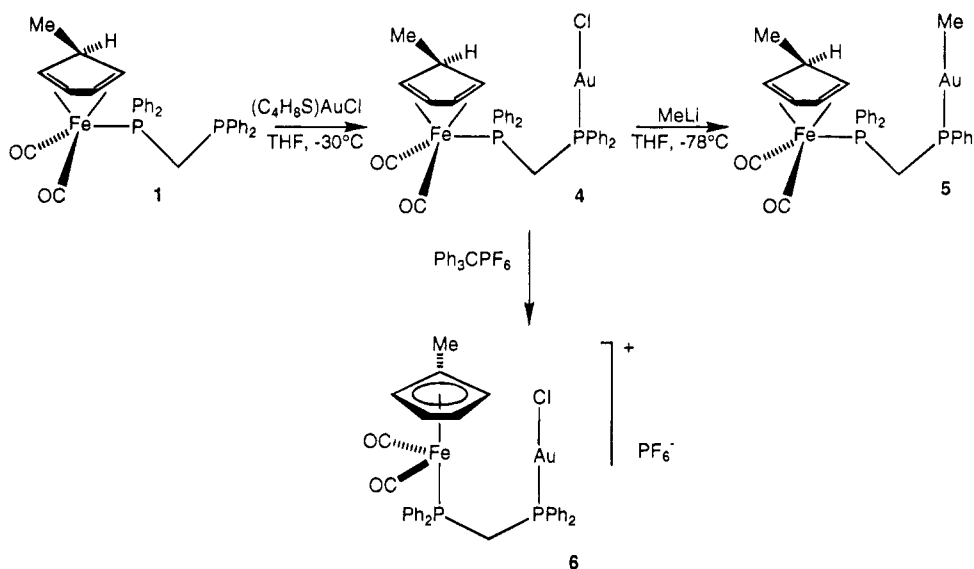
(5) (a) Puddephatt, R. *J. Chem. Soc. Rev.* **1983**, *12*, 99. (b) Chaudret, B.; Delavaux, B.; Poilblanc, R. *Coord. Chem. Rev.* **1988**, *86*, 191. (c) Braunstein, P.; de Meric de Bellefon, C.; Oswald, B. *Inorg. Chem.* **1993**, *32*, 1638. (d) Braunstein, P.; Knorr, M.; Strampfer, M.; Dusausoy, Y.; Bayeul, D.; DeCian, A.; Fischer, J.; Zanello, P. *J. Chem. Soc., Dalton Trans.* **1994**, 1533.

(6) Bibler, J. P.; Wojciki, A. *Inorg. Chem.* **1966**, *5*, 889.

Scheme 1



Scheme 2



92 °C) and $(\eta^5\text{-C}_5\text{H}_5)\text{Fe}(\text{CO})_2\text{Me}$ (mp 80–83 °C) withstood the refluxing temperature of MeCN (bp 81 °C) for 24 h. In a separate experiment, the ring alkylation reaction³ of $(\eta^5\text{-C}_5\text{H}_5)\text{Fe}(\text{CO})_2\text{I}$ with MeLi in the presence of $(\eta^5\text{-C}_5\text{H}_5)\text{Fe}(\text{CO})_2\text{C}(\text{O})\text{Me}(\eta^1\text{-dppm})$ (**3**) (as a phosphine source) at -78 °C was also performed in a hope to produce **2** (see Scheme 1). Synthetic manipulations and chromatography following the usual low-temperature, three-component reaction procedure gave just small amounts of orange, waxy, de-insertion complex $(\eta^5\text{-C}_5\text{H}_5)\text{Fe}(\text{CO})_2\text{Me}$ along with three other low-yield compounds with spectroscopic data (IR, ³¹P, and ¹H NMR) not informative enough for identification.⁷ Similar strategy works for the dppe analog with excellent yields (see also Scheme 1), however.⁸

In addition to the attempts to construct above mentioned dppm-linked diiron complexes, other dinuclear systems were explored. For instance, equimolar amounts of **1** and $(\text{C}_4\text{H}_9\text{S})\text{AuCl}$ [or $(\text{Me}_2\text{S})\text{AuCl}$] were reacted in THF at -30 °C to give the heterobimetallic complex $(\eta^5\text{-C}_5\text{H}_5)\text{Fe}(\text{CO})_2(\mu\text{-}\eta^1\text{-}\eta^1\text{-dppm})\text{AuCl}$ (**4**) in 68.7% yields

(Scheme 2). After purification on a column of nonactivated alumina, crystals suitable for X-ray diffraction were grown from a $\text{CH}_2\text{Cl}_2/n\text{-hexane}$ mixture. A $\text{d}^{10}\text{-Au}_2$ fragment has formed successfully at the originally pendant PPh_2 end. The ³¹P NMR resonance of P–(Au) at δ 19.06 shows a δ 44.66 downfield coordination shift (cf. δ -25.60 in compound **1**). The 14 electron P–Au–Cl unit is known a common configuration of $\text{d}^{10}\text{-Au}$ core.⁹ The ³¹P NMR chemical shifts have been reported ranging δ 14.6–32.3 in P–(Au) systems where a bridging dppm is present.¹⁰ In complex **4**, the ³¹P NMR chemical shift of PPh_2 connected to Fe is virtually unchanged at δ 65.78 (cf. δ 66.38 in compound **1**). The IR spectrum of **4** reveals the presence of two terminal CO stretching bands at 1966 and 1906 cm^{-1} (1963 and 1902 cm^{-1} in the parent compound), exhibiting a slight reduction in electron density at the Fe center. The ¹H NMR spectrum is made up of multiplets at δ 7.5–7.3

(7) The species found are more than likely the decomposed/degraded products, for instance, dppm, $[(\eta^5\text{-C}_5\text{H}_5)\text{Fe}(\text{CO})_2]_2$, etc., in addition to $(\eta^5\text{-C}_5\text{H}_5)\text{Fe}(\text{CO})_2\text{Me}$.

(8) Luh, L.-S.; Liu, L.-K. *Organometallics* **1995**, *14*, 1514.

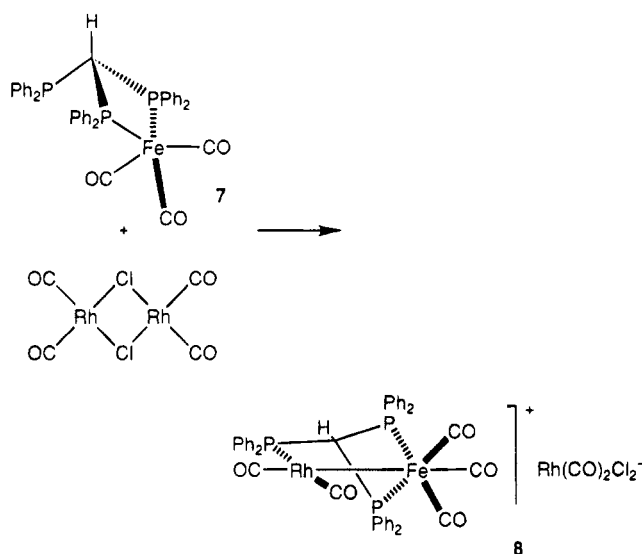
(9) (a) Hitchcock, P. B.; Pye, P. L. *J. Chem. Soc., Dalton Trans.* **1977**, 1457. (b) Cooper, M. K.; Mitchell, L. E.; Hendrick, K.; McPartlin, M.; Scott, A. *Inorg. Chim. Acta* **1984**, *84*, L9. (c) Hill, D. T.; Girard, G. R.; McCabe, F. L.; Johnson, R. K.; Stupik, P. D.; Zhang, J. H.; Reiff, W. M.; Egleston, D. S. *Inorg. Chem.* **1989**, *28*, 3529. (d) Ni Dhubbghaill, O. M.; Sadler, P. J.; Kuroda, R. *J. Chem. Soc., Dalton Trans.* **1990**, 2913. (e) Schmidbaur, H.; Stutzer, A.; Bissinger, P. *Z. Naturforsch.* **1992**, *47B*, 640. (f) Schmidbaur, H.; Bissinger, P.; Lachmann, J.; Steigelmann, O. *Z. Naturforsch.* **1992**, *47B*, 1711.

for Ph protons; δ 4.80, 2.56, and 2.27 for the H_{2,3}, H₅, and H_{1,4} atoms in ratio of 2:1:2; δ 3.39 for methylene H atoms; and a doublet at δ 0.27 for Me protons. The ¹³C NMR data is in accordance with the pattern and assignments observed for the precursor compound **1**. The observed spectroscopic data are in agreement with the X-ray-deduced structure.

The Au–Cl moiety of complex **4** is easily subjected to a nucleophilic substitution. When treated with MeLi at -78°C in THF for 4 h, complex **4** proceeds smoothly, as shown in Scheme 2, with a replacement of Cl by Me to give ($\eta^4\text{-MeC}_5\text{H}_5$)Fe(CO)₂($\mu\text{-}\eta^1\text{:}\eta^1\text{-dppm}$)AuMe (**5**) in 74.0% yields. By comparison of the IR and ³¹P NMR data of **4** and **5**, it is concluded that no significant chemistry takes place around the Fe coordination sphere when MeLi reacts with **4**. For instance, the ν_{CO} bands at 1966 and 1906 cm⁻¹ in the precursor are found at 1962 and 1902 cm⁻¹ in the product. The ³¹P NMR studies of **5** reveal the P–(Fe) resonance at δ 65.36 and that of P–(Au) is at δ 34.30 whereas in **4** P–(Fe) resonances at δ 65.78 and P–(Au) at δ 19.04. The 15.26 δ units downfield shift of ³¹P–(Au) resonance on formation of **5** is regarded as a direct evidence for the Me⁻ nucleophilic substitution at the Au atom. The ¹H and ¹³C NMR data of **5** are very similar to those of **4**, the only difference being the presence of the newly added Me on Au atom—at δ 0.02 (³J_{PH} = 8.1 Hz) in ¹H NMR and at δ 1.02 in ¹³C NMR. The observed spectroscopic data also conform to the X-ray structure in the solid state.

The *endo* H-atom of the $\eta^4\text{-MeC}_5\text{H}_5$ ring has been confirmed to be hydridic in nature. When complex **4** was treated with equimolar Ph₃C⁺PF₆⁻ in CH₂Cl₂ at 0 °C, a novel complex [($\eta^5\text{-MeC}_5\text{H}_4$)Fe(CO)₂($\mu\text{-}\eta^1\text{:}\eta^1\text{-dppm}$)-AuCl]⁺PF₆⁻ (**6**) resulted in 86% yields (Scheme 2). A hydridic H-atom is known to be abstracted by a triphenylmethane cation Ph₃C⁺ to produce a triphenylmethane Ph₃CH.¹¹ The bonding mode of the ($\eta^4\text{-MeC}_5\text{H}_5$) ring in **4** thus changes to ($\eta^5\text{-MeC}_5\text{H}_4$) in **6**. Such a transformation is equivalent to the oxidation of the d⁸-Fe in zero valence to a d⁶-Fe in +2 valence, the neutral complex **4** finalizing as the cationic complex **6**. A reduction of electron density at the Fe center in **6** is evidenced with a blue shift of the IR ν_{CO} bands from 1966 and 1906 cm⁻¹ in **4** to 2050 and 2007 cm⁻¹ in **6**. Complex **6** reveals in ³¹P NMR the presence of three nonequivalent P atoms in the molecule: P–(Fe), δ 56.48; P–(Au), δ 20.68; and P–(F), δ -143.38 (septet, ¹J_{PF} = 711 Hz). The assignment of the P–(Fe) and P–(Au)

Scheme 3



peaks has been done by comparison with those of the precursor **4**. In the ¹H NMR spectrum, the features of ($\eta^4\text{-MeC}_5\text{H}_5$) ring in **4** are now replaced by two peaks at δ 4.9 (2H) and 4.8 (2H) of the new ($\eta^5\text{-MeC}_5\text{H}_4$) ring in **6**. The assignment of these peaks to H_{2,5} and H_{3,4} atoms, however, are still not unambiguous. The methylene H atoms of dppm and the methyl H atoms of the $\eta^5\text{-MeC}_5\text{H}_4$ ring in **6** occur at δ 4.01 and 1.83, respectively, both resonances experiencing substantial downfield shifts from δ 3.37 and 0.27 in **4**. The ¹³C NMR data are also consistent with the assigned formula of complex **6**.

With Ph₃C⁺PF₆⁻ externally eliminating the *endo*-H atom of **4**, the resulting **6** shows no Fe–Au bond formation because neither ²⁺³J_{PP} coupling nor ³¹P shift due to a ring formation could be recorded— δ 19.04 (s) *vs* δ 20.68 (s) before and after *endo*-H atom abstraction experiment. The P–(Au) local environment remains unchanged in the conversion from **4** to **6**. The experimental results suggest that, in the Fe–Au heterobimetallic system, the monodentate dppm ligation to the Au center followed by *endo*-H atom elimination of the ($\eta^4\text{-MeC}_5\text{H}_5$) ring does not lead to an Fe–Au bond formation.

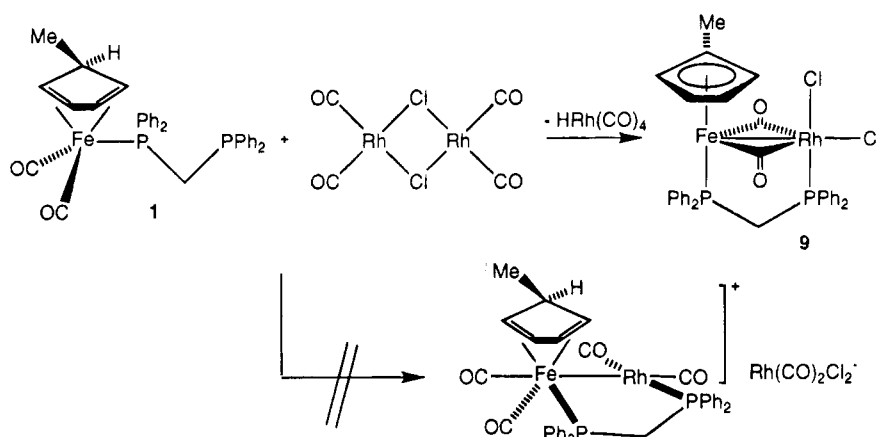
In the literature, Osborn *et al.* reacted [$\eta^2\text{-HC(PPh}_2)_3$]Fe(CO)₃ (**7**) with [Rh(CO)₂Cl]₂ in THF to produce {(CO)₃Fe[$\mu\text{-}\eta^2\text{:}\eta^1\text{-HC(PPh}_2)_3$]Rh(CO)₂}⁺[Rh(CO)₂Cl]₂⁻ (**8**),¹² whose X-ray structure indicated an Fe–Rh bond and an unsymmetric bridging HC(PPh₂)₃, the reaction being drawn in Scheme 3. The monodentate triphosphine **7** has a pentacoordinate Fe(0) center and a dangling PPh₂, very similar to the monodentate dppm **1**. Therefore, it was thought worthwhile to react **1** with [Rh(CO)₂Cl]₂. When compound **1** is allowed to react with [Rh(CO)₂Cl]₂, interestingly ($\eta^5\text{-MeC}_5\text{H}_4$)Fe($\mu\text{-CO}$)₂($\mu\text{-}\eta^1\text{:}\eta^1\text{-dppm}$)RhCl₂ (**9**) forms in 88% yields, instead of an imagined complex [($\eta^4\text{-MeC}_5\text{H}_5$)Fe(CO)₂($\mu\text{-}\eta^1\text{:}\eta^1\text{-dppm}$)Rh(CO)₂]⁺[Rh(CO)₂Cl]₂⁻ (Scheme 4). The immediately formed Fe–Rh heterobimetallic complex **9** sequentially sums up a PPh₂ ligation, an *endo*-H atom elimination, and post rearrangements in one treatment. The results here are completely different from the

(10) (a) Schmidbaur, H.; Wohlleben, A.; Wagner, F.; Orama, O.; Huttner, G. *Chem. Ber.* **1977**, *110*, 1748. (b) Briant, C. E.; Hall, K. P.; Mingos, D. M. P. *J. Chem. Soc., Chem. Commun.* **1983**, 843. (c) Uson, R.; Laguna, A.; Fornies, J.; Valenzuela, I.; Jones, P. G.; Sheldrick, G. M. *J. Organomet. Chem.* **1984**, *273*, 129. (d) Jones, P. G. *J. Organomet. Chem.* **1988**, *345*, 405. (e) Kim, H. P.; Fanwick, P. E.; Kubiak, C. P. *J. Organomet. Chem.* **1988**, *346*, C39. (f) Manojlovic-Muir, L.; Henderson, A. N.; Treurnicht, I.; Puddephatt, R. J. *Organometallics* **1989**, *8*, 2055. (g) Alvarez, S.; Rossell, O.; Seco, M.; Valls, J.; Pellinghelli, M. A.; Tiripicchio, A. *Organometallics* **1991**, *10*, 2309. (h) Stutzer, A.; Bissinger, P.; Schmidbaur, H. *Chem. Ber.* **1992**, *125*, 367. (i) Jones, P. G.; Thone, C. *Acta Cryst.* **1992**, *C48*, 1312. (j) Lin, I. J.-B.; Liu, C.-W.; Liu, L.-K.; Wen, Y.-S. *Organometallics* **1992**, *11*, 1447. (k) Braunstein, P.; Knorr, M.; Tiripicchio, A.; Camellini, M. T. *Inorg. Chem.* **1992**, *31*, 3685. (l) Balch, A. L.; Noll, B. C.; Olmstead, M. M.; Toronto, D. V. *Inorg. Chem.* **1992**, *31*, 5226. (m) Davila, R. M.; Elduque, A.; Grant, T.; Staples, R. J.; Fackler, J. P., Jr. *Inorg. Chem.* **1993**, *32*, 1749.

(11) (a) Fieser, L. F.; Fieser, M. *Reagents for Organic Synthesis*; Wiley: New York, 1967–70; Vol. 1, pp. 1256–1258; Vol. 2, p454; Vol. 3, p330. (b) Deeming, A. J.; Ullah, S. S.; Domingos, A. J. P.; Johnson, B. F. G.; Lewis, J. J. *Chem. Soc., Dalton Trans.* **1974**, 2093.

(12) Bahsoun, A. A.; Osborn, J. A.; Bird, P. H.; Nucciarone, D.; Peter, A. Av. *J. Chem. Soc., Chem. Commun.* **1984**, 72.

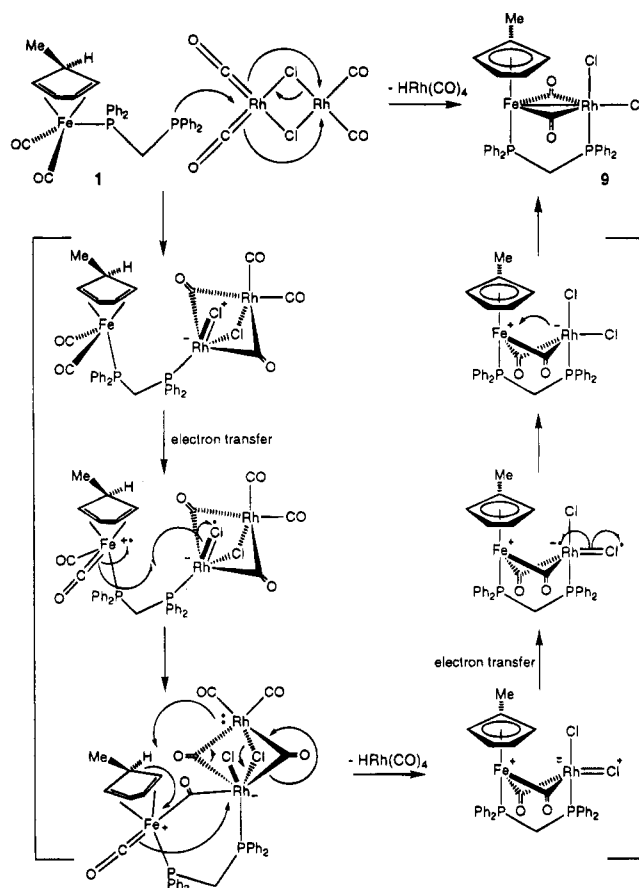
Scheme 4



general reaction of $[\text{Rh}(\text{CO})_2\text{Cl}_2]_2$ with a monodentate PR_3 : $[\text{Rh}(\text{CO})_2\text{Cl}_2]_2$ reacts with a variety of tertiary PR_3 ligands to give (halo)(carbonyl)(phosphine)rhodium complexes. Many confusing reports exist in the literature concerning the mechanism and intermediates involved. Depending on the molar ratio PR_3 to Rh, the final products could either be the chloro-bridged dimer *cis-/trans*- $[\text{RhCl}(\text{CO})\text{PR}_3]_2$ with a PR_3 to Rh ratio of one or *trans*- $\text{Rh}(\text{CO})_2(\text{PR}_3)_2$ with a PR_3 to Rh ratio greater than one.¹³ Complex **9** exhibits in the IR spectrum ν_{CO} bands at 1853 and 1809 cm^{-1} , indicating that only bridging carbonyl ligands are present. The characteristic pattern of 2:1:2 integration ratio for the ($\eta^4\text{-MeC}_5\text{H}_5$) fragment of **1** disappears in the ^1H NMR spectrum of **9**, in which two new chemical shifts with equal intensity typical for a ($\eta^5\text{-MeC}_5\text{H}_4$) moiety are observed at δ 4.86 (2H) and 4.43 (2H). The methylene H atoms of dppm and the methyl H atoms of $\eta^5\text{-MeC}_5\text{H}_4$ ring in **9** occur at δ 2.25 and 1.92, respectively. The methylene H resonance shows a substantial upfield shift from δ 3.0 in **1** whereas the methyl H resonance shows a substantial downfield shift from δ 0.27 in **1**. The methylene H atoms in **9** are apparently very different in local environment from the corresponding methylene H atoms in **6** which has also the ($\eta^5\text{-MeC}_5\text{H}_4$) ring attached to Fe atom. Complex **9** exhibits in the ^{31}P NMR spectrum chemical shifts at δ 77.78 (d) and 47.03 (dd), the initial peaks at δ 66.38 and -25.60 in compound **1** being replaced completely. The ^{31}P peak pattern at δ 47.03 (dd) illustrates couplings to both Rh atom and the remaining P atom with $^1J_{\text{RHP}} = 127.2$ Hz and $^{2+3}J_{\text{PP}} = 71.8$ Hz. Shown in Figure 3 is the single-crystal X-ray structure of **9** which reveals in the solid state two crystallographically independent molecules per asymmetric unit. On the basis of the spectroscopic and crystallographic results, the molecular structure of complex **9** is found to realize the formation of an Fe–Rh bond and the change of the $\eta^4\text{-MeC}_5\text{H}_5$ bonding mode in **1** to $\eta^5\text{-MeC}_5\text{H}_4$ bonding in **9**. To the best of our knowledge, this is the first reported transformation from (cyclopentadiene)–Fe(0) to (cyclopentadienyl)–Fe(I) with simultaneous formation of an Fe–Rh bond.

The ($\eta^5\text{-C}_5\text{H}_5$) $\text{Fe}(\mu\text{-CO})_2(\mu\text{-}\eta^1\text{-}\eta^1\text{-dppm})\text{Rh}$ skeleton was reported by Shaw *et al.* in their treatment of ($\eta^5\text{-C}_5\text{H}_5$) $\text{Fe}(\text{CO})\text{C}(\text{O})\text{Me}(\eta^1\text{-dppm})$ with $[\text{Rh}(\text{CO})_2\text{Cl}_2]$ to give

Scheme 5



($\eta^5\text{-C}_5\text{H}_5$) $\text{Fe}(\mu\text{-CO})_2(\mu\text{-}\eta^1\text{-}\eta^1\text{-dppm})\text{Rh}(\text{COMe})\text{Cl}$, whose slow decarbonylation in acetone deposited ($\eta^5\text{-C}_5\text{H}_5$) $\text{Fe}(\mu\text{-CO})_2(\mu\text{-}\eta^1\text{-}\eta^1\text{-dppm})\text{Rh}(\text{Me})\text{Cl}$ and ($\eta^5\text{-C}_5\text{H}_5$) $\text{Fe}(\mu\text{-CO})_2(\mu\text{-}\eta^1\text{-}\eta^1\text{-dppm})\text{RhCl}_2$ in the ratio 0.4:0.6.¹⁴

One of the possible mechanisms concerning the formation of an Fe–Rh complex is outlined in Scheme 5. Although detailed mechanistic studies are yet to pursue, the authors currently speculate that, after the monodentate dppm coordination to Rh atom, a single electron transfer step proceeds before the *endo*-H atom abstraction and the $\text{HRh}(\text{CO})_4$ extrusion. By stoichiometry, there would be 1 equiv of byproduct $\text{HRh}(\text{CO})_4$ which has not been isolated experimentally, partly because

(13) Hughes, R. P. In *Comprehensive Organometallic Chemistry*; Wilkinson, G., Stone, F. G. A., Abel, E. W., Eds.; Pergamon Press: Oxford, U.K., 1982; Vol. 5, pp 277–540.

(14) Shaw, B. L.; Smith, M. J.; Stretton, G. N.; Thornton-Pett, M. *J. Chem. Soc., Dalton Trans.* **1988**, 2099.

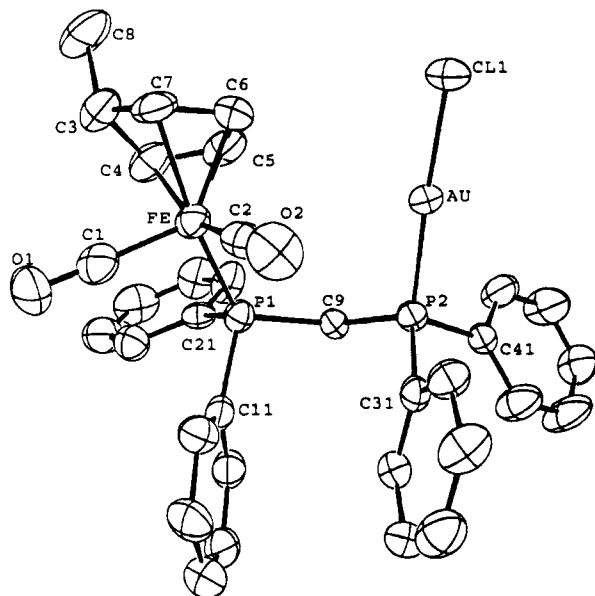


Figure 1. Molecular plot of complex **4** with the atomic numbering sequence. The thermal ellipsoids are drawn at the 50% level. The H atoms are omitted for clarity. Selected bond lengths (Å): Au–P2, 2.226(22); Au–Cl, 2.290(2); Fe–P1, 2.217(3); Fe–C1, 1.747(10); Fe–C2, 1.765(11); Fe–C4, 2.120(9); Fe–C5, 2.036(9); Fe–C6, 2.040(9); Fe–C7, 2.105(8); P1–C9, 1.855(8); P2–C9, 1.829(8); O1–C1, 1.158(12); O2–C2, 1.138(13). Selected bond angles (deg): P1–Fe–C1, 95.4(3); P1–Fe–C2, 96.6(3); C1–Fe–C2, 101.5(4); P2–Au–Cl, 176.44(8); P1–C9–P2, 120.4(4); Au–P2–C9, 112.4(3); Fe–P1–C9, 124.1(3).

HRh(CO)₄ aggregates quickly to clusters.¹⁵ Only spectroscopic evidence for rhodium clusters was obtained. The *endo*-H atom abstraction here could be viewed as an oxidative addition of the unique *endo*-C–H unit to Fe and Rh centers simultaneously with aromatization of cyclopentadiene ring as a driving force, eventually leading to the formation of an Fe–Rh bond. Such a speculation comes in passively because, in the Fe–Au heterobimetallic system, the monodentate dppm ligation to Au center followed by the *endo*-H atom elimination of the (η^4 -MeC₅H₅) ring using Ph₃C⁺PF₆[−] does not lead to an Fe–Au bond formation. The *endo*-H atom in the Fe–Rh system is likely eliminated in a manner different from being a hydride.

Crystallography. Complex **4** crystallizes with the occlusion of 1 mol of CH₂Cl₂ in the monoclinic space group P2₁/n. As shown in Figure 1, the X-ray structure of **4** gives no evidence of an Fe–Au bond [Fe··Au distance = 4.081(2) Å]. The two metal centers are only linked together by the dppm bridge. The Fe–P1–C9, P1–C9–P2, and Au–P2–C9 angles of 124.1(3), 120.4(5), and 112.4(3)°, respectively, result in the formation of a slightly distended W-shaped Fe–P1–C9–P2–Au fragment. The Cl atom is atop the Au atom [Au–Cl = 2.290(2) Å] from a near linear angle [\angle Cl–Au–P2 = 176.5(1)°]. The Fe–P1 length of 2.218(3) Å is similar to the those of closely related Fe–P bonds in the literature: for example 2.202(2) Å in (η^4 -MeC₅H₅)Fe(CO)₂(PMePh₂) and 2.208(1) Å in [(η^4 -MeC₅H₅)Fe(CO)₂]₂(μ -dpppe).² The Au–P2 length of 2.226(2) Å is in

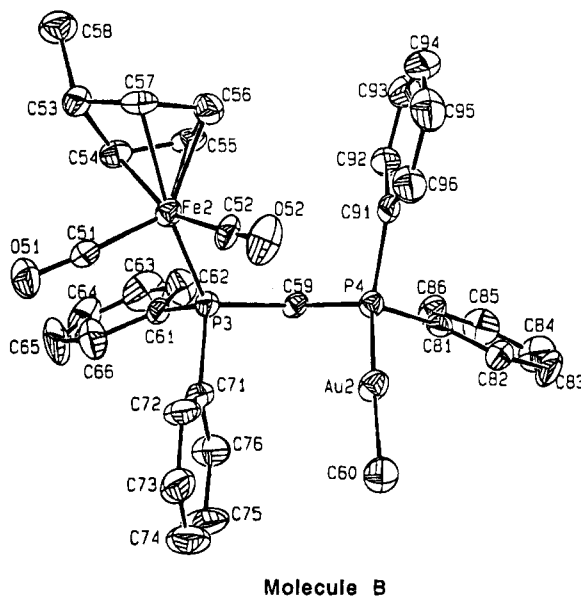
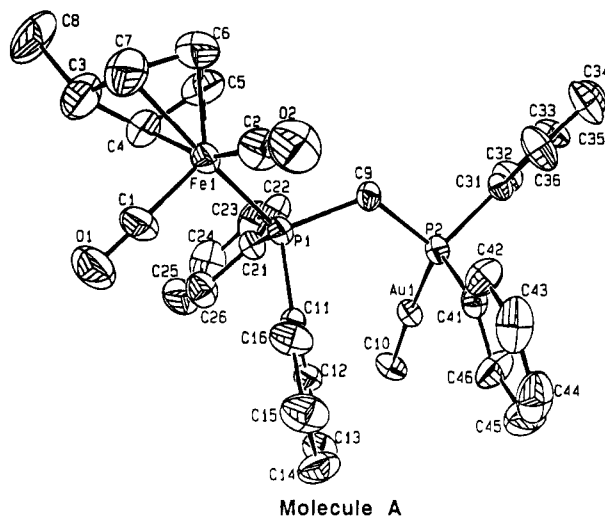


Figure 2. Molecular plot of complex **5** with atomic numbering sequence. The thermal ellipsoids are drawn at the 50% level. The H atoms are omitted for clarity. Selected bond lengths (Å): Au1–P2, 2.291(3); Au1–C10, 2.053(11); Fe1–P1, 2.212(3); Fe1–C1, 1.727(11); Fe1–C2, 1.732(14); Fe1–C4, 2.116(15); Fe1–C5, 2.021(13); Fe1–C6, 1.998(14); Fe1–C7, 2.099(15); P1–C9, 1.842(10); P2–C9, 1.849(10); Au2–P4, 2.284(3); Au2–C60, 2.112(10); Fe2–P3, 2.204(3); Fe2–C51, 1.735(11); Fe2–C52, 1.769(11); Fe–C54, 2.110(10); Fe2–C55, 2.057; Fe2–C56, 2.055; Fe2–C57, 2.076(9); P3–C59, 1.852(9); P4–C59, 1.810(10). Selected bond angles (deg): P2–Au1–C10, 177.3(4); P1–Fe1–C1, 97.1(4); P1–Fe1–C2, 95.1(5); Fe1–P1–C9, 113.5(4); P1–C9–P2, 121.5(6); Au1–P2–C9, 117.8(3); P4–Au2–C60, 175.1(3); P3–Fe2–C51, 96.5(3); P3–Fe2–C52, 95.2(3); Fe2–P3–C59, 120.7(3); P3–C59–P4, 118.4(5); Au2–P4–C59, 116.1(3).

agreement with the 2.238 Å found in (dppm)Au₂Cl₂¹⁶ and in [(dppm)₂Au₃Cl₂]⁺[Au(C₆H₅)₃Cl][−]¹⁷ but considerably shorter than the 2.391 Å found in (dppm)₃Au₄I₂.¹⁸ The ring Me group is *exo* on the cyclopentadiene from Fe. The coordination geometry around Fe may be

(16) Schmidbaur, H.; Wohlleben, A.; Wagner, F.; Orama, O.; Huttner, G. *Chem. Ber.* **1977**, *110*, 1748.

(17) Uson, R.; Laguna, A.; Laguna, M.; Fernandez, E.; Villacampa, M. D.; Jones, P. G.; Sheldrick, G. M. *J. Chem. Soc., Dalton Trans.* **1983**, 1679.

(18) van der Velden, J. W. A.; Bour, J. J.; Pet, R.; Bosman, W. P.; Noordik, J. H. *Inorg. Chem.* **1983**, *22*, 3112.

(15) (a) Vidal, J. L.; Walker, W. E. *Inorg. Chem.* **1981**, *20*, 249. (b) Vidal, J. L.; Schoening, R. C.; Walker, W. E. *A. C. S. Symp. Ser.*, **155** (*React. Met.-Met. Bonds*) 61–83, 1981.

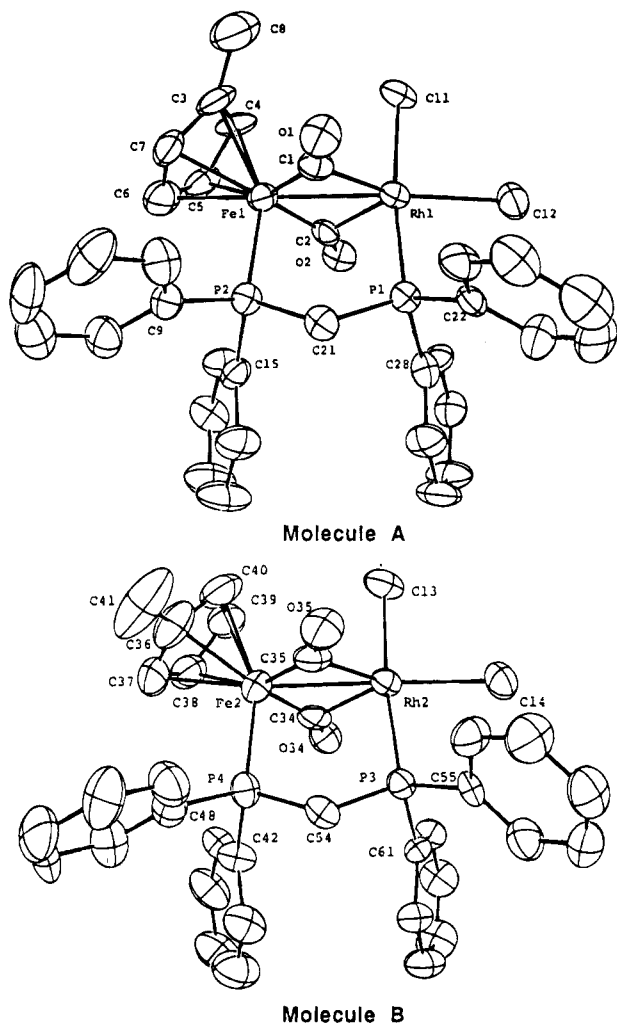


Figure 3. Molecular plots of complex **9** with atomic numbering sequence. The thermal ellipsoids are drawn at the 50% probability level. The H atoms are omitted for clarity. Selected bond lengths (Å): Rh1-Fe1, 2.611(2); Rh1-P1, 2.262(3); Rh1-C11, 2.390(3); Rh1-C12, 2.340(3); Rh1-C1, 2.057(9); Rh1-C2, 2.050(8); Rh2-Fe2, 2.613(2); Rh2-P3, 2.261(3); Rh2-C13, 2.396(3); Rh2-C14, 2.334(3); Rh2-C34, 2.049(9); Rh2-C35, 2.042(9); Fe1-P2, 2.211(3); Fe2-P4, 2.233(3). Selected bond angles (deg): Fe1-Rh1-P1, 94.59(7); Fe1-Rh1-C11, 92.25(8); Fe1-Rh1-C12, 173.30(8); P1-Rh1-C11, 173.14(9); P1-Rh1-C12, 84.56(9); P1-Rh1-C1, 88.8(3); P1-Rh1-C2, 92.9(2); C11-Rh1-C12, 88.72(9); C11-Rh1-C1, 95.7(3); C11-Rh1-C2, 92.5(2); C1-Rh1-C2, 88.2(4); Fe2-Rh2-P3, 94.44(7); Fe2-Rh2-C13, 92.19(8); Fe2-Rh2-C14, 177.18(9); P3-Rh2-C13, 173.3(1); P3-Rh2-C14, 85.68(9); P3-Rh2-C34, 92.4(2); P3-Rh2-C35, 89.0(3); C13-Rh2-C14, 87.7(1); C13-Rh2-C34, 91.9(2); C13-Rh2-C35, 96.2(3); C34-Rh2-C35, 88.5(4); Rh1-Fe1-P2, 96.40(8); P2-Fe1-C1, 90.2(3); P2-Fe1-C2, 92.3(3); C1-Fe1-C2, 102.7(4); Rh2-Fe2-P4, 96.44(8); P4-Fe2-C34, 91.3(3); P4-Fe2-C35, 91.3(3); C34-Fe2-C35, 102.1(4); Rh1-C1-Fe1, 84.1(4); Rh1-C2-Fe1, 84.5(4); Rh2-C34-Fe2, 84.6(4); Rh2-C35-Fe2, 84.4(4). Selected torsion angles (deg): P1-Rh1-Fe1-P2, -1.6(1); P3-Rh2-Fe2-P4, -2.4(1); Rh1-Fe1-centroid1-C3, -51.1(4); Rh2-Fe2-centroid2-C36, -108.8(5). Selected interplanar angles (deg): [Rh1, Fe1, C1, O1, C2, O2]-[Rh1, Fe1, P1, C11, C12], 93.4(1); [Rh2, Fe2, C34, O34, C35, O35]-[Rh2, Fe2, P3, C13, C14], 87.1(1).

described as a distorted square pyramid with one of the CO ligands at the apical position. The second CO ligand is in the basal plane *trans* to one of the double bonds, and the $\text{PPh}_2\text{CH}_2^-$ ligand is *trans* to the second double

bond. The diene atoms C4, C5, C6, and C7 are coplanar within 0.001(15) Å. The plane made up with C8, C3, Fe, C1, and O1 is planar to within 0.005(13) Å making an interplanar angle of 91.7(4)° with the plane of C4-C7. The apical CO ligand is seemingly farther away from the Fe core [Fe-C2 = 1.764(11) Å] than the basal CO [Fe-C1 = 1.746(10) Å].

Slow evaporation of a $\text{CH}_2\text{Cl}_2/n$ -hexane solution of **5** gave crystals suitable for X-ray structure analysis revealing two crystallographically independent molecules. The structural parameters of **5** are similar to those of **4** except for the Me replacement of Cl and the distended W-shaped dppm on attachment of Fe and Au atoms. For **5**, the coordination geometry around the Fe atom may also be described as a distorted square pyramid, the same as in **4**. The diene atoms C4, C5, C6, and C7 and C54, C55, C56, and C57 are respectively coplanar to within 0.002(22) and 0.004(14) Å. The plane of C8, C3, Fe1, C1, O1 (deviations 0.0182 Å) and that of C58, C53, Fe2, C51, O51 (deviations 0.012 Å) are each perpendicular to the connecting diene planes C4-C7 and C54-C57, with interplanar angles of 89.3(5) and 87.8(4)°, respectively. That is, the planar diene skeleton is orthogonal to the plane made up of the *exo*-C atom, the unique C atom of the cyclopentadiene ring, Fe, and the apical CO ligand. The X-ray structure gives no evidence of a direct Fe-Au bond, Fe...Au distances being 6.300(2) and 4.916(2) Å for the two independent molecules. The two metals are simply linked by dppm. The Au-P lengths are considerably elongated compared to the corresponding values in the Au-Cl analog. The structural parameters obtained for the two crystallographically independent molecules are very similar except the torsion angles Fe1-P1...P2-Au1 = -158.1(2)° and Fe2-P3...P4-Au2 = 90.8(1)°.

Shown in Figure 3 are the ORTEP molecular drawings of the Fe-Rh heterobimetallic complex **9**. The complex reveals, in the solid state X-ray structure, two CO bridges and a direct Fe-Rh bond in addition to the dppm bridge, the five-membered ring Fe-P-C-P-Rh being approximately orthogonal to the plane made of CO bridges. Crystallized in the monoclinic space group $P2_1/a$ with 8 molecules per unit cell, complex **9** gives two crystallographically independent molecules that are similar in structural parameters and different only in the orientation of the ring Me group with respect to Fe-Rh bond. The torsion angles of C3-Fe1-Rh1-C11 and C36-Fe2-Rh2-C13 are -30.2(2) and -55.5(3)°, respectively, and the torsion angles of C3-centroid1-Fe1-Rh1 and C36-centroid2-Fe2-Rh2 are 146.9(6) and 140.5(7)°, respectively, where centroid1 and centroid2 are the centers of gravity of the respective rings. The distances of Fe-Rh are 2.611(2) and 2.613(2) Å for the two molecules. Such bond lengths are shorter than the reported 2.699(4) Å in $\text{Fe}(\text{CO})_4(\mu\text{-dppm})\text{RhCl}(\text{CO})$,¹⁹ 2.762(2) Å in $(\text{CO})_2\text{Fe}(\mu\text{-CO})(\mu\text{-C}_7\text{H}_7)\text{Rh}(\text{dppe})$,²⁰ and 2.776 Å in **8**¹³ but longer than 2.557(2) Å in $(\text{C}_4\text{H}_4)(\text{CO})_3\text{FeRh}(\eta^5\text{-C}_5\text{H}_5)$.²¹ The average Rh-CO and Fe-CO bond distances are 2.049 and 1.832 Å, respectively,

(19) Jacobsen, G. B.; Shaw, B. L.; Thomson-Pett, M. *J. Chem. Soc., Chem. Commun.* **1986**, 13.

(20) Ball, R. G.; Edelmann, F.; Kiel, G.-Y.; Takats, J.; Drews, R. *Organometallics* **1986**, *5*, 829.

(21) King, M.; Holt, E. M.; Radnia, P.; McKennis, J. S. *Organometallics* **1982**, *1*, 1718.

Table 1. Final Fractional Coordinates and B Values (Å²) for Non-H Atoms of Complex 4, (η⁴-MeC₅H₅)Fe(CO)₂(μ-η¹:η¹-dppm)AuCl-CH₂Cl₂

atom	x	y	z	B _{iso}	atom	x	y	z	B _{iso}
Au	0.93956(3)	0.08920(1)	0.03346(2)	2.88(2)	C15	1.3076(9)	0.3063(4)	0.3458(6)	4.0(5)
Fe	1.06755(12)	0.05617(5)	0.30102(7)	3.04(5)	C16	1.3127(9)	0.2436(4)	0.3171(5)	3.6(4)
P1	1.2058(2)	0.1240(1)	0.2663(1)	2.7(1)	C21	1.3662(7)	0.0946(4)	0.3072(5)	2.9(4)
P2	1.0752(2)	0.1688(1)	0.0683(1)	2.7(1)	C22	1.4204(9)	0.1023(4)	0.3979(6)	4.2(5)
Cl1	0.7918(2)	0.0116(1)	-0.0079(2)	4.3(1)	C23	1.5350(11)	0.0745(5)	0.4331(7)	5.6(6)
Cl2	0.5303(4)	0.2061(2)	0.1088(3)	10.2(2)	C24	1.5966(10)	0.0391(5)	0.3807(8)	6.0(6)
Cl3	0.4790(3)	0.0847(2)	0.0254(2)	8.2(2)	C25	1.5430(10)	0.0302(5)	0.2911(7)	5.1(5)
O1	1.1179(8)	0.0855(3)	0.4916(4)	6.4(4)	C26	1.4284(9)	0.0580(5)	0.2557(6)	4.4(5)
O2	0.8420(7)	0.1299(3)	0.2375(4)	5.4(4)	C31	1.0070(8)	0.2407(4)	0.1038(5)	2.7(4)
C1	1.0967(9)	0.0754(4)	0.4151(6)	3.9(4)	C32	0.8776(8)	0.2465(4)	0.0834(6)	3.4(4)
C2	0.9329(9)	0.1022(4)	0.2591(6)	3.7(4)	C33	0.8205(9)	0.3031(4)	0.0994(6)	4.5(5)
C3	1.0890(10)	-0.0592(4)	0.3753(6)	4.4(5)	C34	0.8930(11)	0.3536(4)	0.1375(6)	4.7(5)
C4	1.1812(9)	-0.0260(4)	0.3296(6)	4.2(5)	C35	1.0209(11)	0.3475(4)	0.1595(6)	4.4(5)
C5	1.1264(11)	-0.0199(4)	0.2381(7)	4.7(5)	C36	1.0786(8)	0.2391(4)	0.1422(5)	3.5(4)
C6	0.9959(11)	-0.0214(4)	0.2278(6)	4.8(5)	C41	1.1400(8)	0.1938(4)	-0.0276(5)	2.9(4)
C7	0.9737(9)	-0.0290(4)	0.3175(6)	4.1(4)	C42	1.1777(11)	0.1490(4)	-0.0808(6)	4.9(5)
C8	1.0879(12)	-0.1324(4)	0.3729(7)	6.5(6)	C43	1.2268(12)	0.1660(5)	-0.1544(7)	6.2(6)
C9	1.2158(7)	0.1454(4)	0.1497(5)	2.7(3)	C44	1.2400(10)	0.2275(5)	-0.1752(6)	5.0(5)
C11	1.2112(8)	0.2036(4)	0.3166(5)	2.9(4)	C45	1.1986(13)	0.2731(5)	-0.1249(7)	6.5(7)
C12	1.1092(8)	0.2263(4)	0.3485(5)	3.6(4)	C46	1.1486(11)	0.2566(4)	-0.0512(6)	5.5(6)
C13	1.1055(10)	0.2890(4)	0.3771(6)	4.4(5)	C50	0.5861(10)	0.1316(6)	0.0898(7)	6.3(6)
C14	1.2037(11)	0.3291(4)	0.3731(6)	4.7(5)					

whereas the average bond angles of Rh-C-O and Fe-C-O are 124.3 and 150.9°, respectively, indicative of the semibridging nature of CO ligands. The two Cl ligands coordinated to Rh are *cis*, one *trans* to Fe and the other *trans* to P. Rh1, Fe1, Cl1, Cl2, and P1 are coplanar (± 0.109 Å). So are Rh2, Fe2, Cl3, Cl4, and P2 (± 0.076 Å). The Cp rings C3-C8 and C36-C41 are respectively planar (to within 0.0046 and 0.064 Å), with coordinated Fe atoms displaced by 1.739(5) and 1.737(6) Å. The overall bonding geometry around Fe could be described as an octahedron with a dative bond toward Rh which partially returns electron density *via* the semibridging CO ligands. In the solid state, there are 2 CH₂Cl₂ solvate molecules for each Fe-Rh complex.

Experimental Section

General Methods. All manipulations were performed under an atmosphere of prepurified nitrogen with standard Schlenk techniques. All solvents were distilled from an appropriate drying agent.²² Infrared spectra were recorded in CH₂Cl₂ using CaF₂ optics on a Perkin-Elmer 882 spectrophotometer. The ¹H NMR and ¹³C NMR spectra were obtained on Bruker AC200/AC300 spectrometers, with chemical shifts reported in δ values relative to the residual solvent resonance of CDCl₃ (¹H 7.24 ppm, ¹³C 77.0 ppm). The ³¹P{¹H} NMR spectra were obtained on Bruker AC200/AC300 spectrometers using 85% H₃PO₄ as an external standard (0.00 ppm). The melting points (uncorrected) were determined on a Yanaco MPL melting-point apparatus. Compound **1**³ and (η⁵-C₅H₅)Fe(CO)₃¹²³ were prepared according to the literature procedure. Other reagents were obtained from commercial sources e.g. Aldrich, Merck, and used without further purification.

Synthesis of (η⁴-MeC₅H₅)Fe(CO)₂(μ-η¹:η¹-dppm)AuCl (4). (C₄H₉S)AuCl (0.278 g, 0.868 mmol) and (η⁴-MeC₅H₅)Fe(CO)₂(η¹-dppm) (0.50 g, 0.868 mmol) were placed in a flask and cooled to -30 °C. THF (30 mL) also cooled to -30 °C was transferred into the reaction flask *via* cannula. The reaction mixture was stirred at -30 °C for 30 min before being warmed up to room temperature and stirred overnight. The mixture was then filtered through a pad of Celite and the

solvent removed on a rotary evaporator. The resultant greenish-yellow solids were prepared for chromatography on a column of nonactivated alumina, eluting with 1:4 ethyl acetate/*n*-hexane to obtain one yellow band. The yellow solution was collected which, after solvent removal, gave yellow, powdery **4** (0.482 g, 68.7%). Crystals suitable for X-ray crystallography were grown from a CH₂Cl₂/*n*-hexane mixture by slow evaporation. **4**: mp 103-105 °C; IR (CH₂Cl₂) ν_{CO} 1966 (vs), 1906 (vs) cm⁻¹; ³¹P NMR (CDCl₃) δ 65.78 (s), 19.04 (s); ¹H NMR (CDCl₃) δ 7.50-7.31 (m, 20H, Ph), 4.87 (s, 2H, -CH=CHCHMe), 3.39 (b, 2H, PCH₂P), 2.56 (s, 1H, -CH=CHCHMe), 2.27 (s, 2H, CH=CHCHMe), 0.26 (d, 3H, ³J_{PH} = 9 Hz, Me); ¹³C NMR (CDCl₃) δ 219.3 (s, CO), 133.7-128.6 (m, Ph), 82.3 (s, -CH=CHCHMe), 58.4 (s, -CH=CHCHMe), 51.1 (s, -CH=CHCHMe), 32.2 (s, PCH₂P), 28.1 (s, Me); MS (FAB) *m/z* 774 (M⁺ - Cl). Anal. Calcd for C₃₃H₃₀AuClFeO₂P₂: C, 48.99; H, 3.74. Found: C, 48.49; H, 3.92.

Reaction of 4 with MeLi. Complex **4** (0.194 g, 0.240 mmol) was dissolved in dry THF (20.0 mL) and cooled to -78 °C. Excess MeLi (1.0 mL, 1.6 M in ether) diluted in ether (10.0 mL) and kept at -78 °C was dropwise added to the stirring solution over a period of 10 min. The mixture was stirred at -78 °C for 1 h and gradually warmed up to room temperature with continued stirring for a further 3 h. The solution was then filtered on a glass frit through a short plug of alumina. The resultant clear yellow solution gave a yellow powdery material after solvent removal on a rotary evaporator. The solid material was redissolved in a minimum amount of CH₂Cl₂ and applied to the top of a column of alumina. The column was eluted with 10% ethyl acetate in *n*-hexane to yield a bright yellow solid of (η⁴-MeC₅H₅)Fe(CO)₂(μ-η¹:η¹-dppm)AuMe (**5**) (0.14 g, 74.0%) after solvent removal. Crystals suitable for X-ray crystallography were grown from a mixture of CH₂Cl₂/*n*-hexane by slow evaporation. **5**: mp 141-142 °C; IR (CH₂Cl₂) ν_{CO} 1962 (vs), 1902 (vs) cm⁻¹; ³¹P NMR (CDCl₃) δ 65.36 (s), 34.30 (s); ¹H NMR (CDCl₃) δ 7.61-6.96 (m, 20H, Ph), 4.86 (s, 2H, -CH=CHCHMe-), 3.37-3.32 (m, 2H, PCH₂P), 2.59 (b, 1H, -CH=CHCHMe-), 2.28 (s, 2H, -CH=CHCHMe-), 0.27 (d, ⁴J_{PH} = 9 Hz, 3H, Me-), 0.02 (d, ³J_{PH} = 8.1 Hz, 3H, AuMe); ¹³C NMR (CDCl₃) δ 1.02 (s, AuMe), 28.16 (s, Me), 30.35 (s, PCH₂P), 51.08 (s, -CH=CHCHMe-), 58.12 (s, -CH=CHCHMe-), 82.22 (s, -CH=CHCHMe-), 134.5-125.5 (m, Ph), 219.4 (b, CO); MS (FAB) *m/z* 775 (M⁺ - Me). Anal. Calcd for C₃₄H₃₃AuFeO₂P₂: C, 51.78; H, 4.23. Found: C, 52.22; H, 4.53.

Synthesis of [(η⁵-MeC₅H₄)Fe(CO)₂(μ-η¹:η¹-dppm)AuCl]⁺PF₆⁻ (6**).** Complex **4** (0.80 g, 0.989 mmol) dissolved in CH₂-

(22) Perrin, D. D.; Armarego, W. L. F.; Perrin, D. R. *Purification of Laboratory Chemicals*; Pergamon Press: Oxford, U.K., 1981.

(23) (a) Dombek, B. D.; Angelici, R. J. *Inorg. Chim. Acta* **1973**, *7*, 345. (b) Meyer, T. J.; Johnson, E. C.; Winterton, N. *Inorg. Chem.* **1971**, *10*, 1673. (c) *Inorg. Synth.* **1971**, *12*, 36. (d) *Inorg. Synth.* **1963**, *7*, 110.

Table 2. Final Fractional Coordinates and B Values (Å²) for Non-H Atoms of Complex 5, (η^4 -MeC₅H₅)Fe(CO)₂(μ - η^1 : η^1 -dppm)AuMe

atom	x	y	z	B _{iso}	atom	x	y	z	B _{iso}
Au1	0.13000(3)	0.49479(2)	0.07305(2)	3.90(2)	C41	0.2275(6)	0.6620(6)	0.1064(5)	4.2(6)
Au2	0.71292(3)	0.68954(2)	0.22459(2)	4.18(2)	C42	0.2756(7)	0.7163(7)	0.1407(5)	5.7(6)
Fe1	0.40996(9)	0.50225(9)	0.31310(7)	4.43(8)	C43	0.3165(7)	0.7676(7)	0.1106(7)	7.6(8)
Fe2	0.54586(8)	0.90630(8)	0.14703(7)	3.34(7)	C44	0.3097(8)	0.7650(7)	0.0471(7)	8.2(9)
P1	0.3267(2)	0.5031(2)	0.2206(1)	3.7(1)	C45	0.2611(10)	0.7139(8)	0.0130(7)	8.7(9)
P2	0.1723(2)	0.5901(2)	0.1411(1)	3.7(1)	C46	0.2214(8)	0.6610(7)	0.0421(6)	6.7(7)
P3	0.6767(2)	0.8891(1)	0.1447(1)	3.2(1)	C51	0.5106(6)	0.8951(6)	0.0669(5)	4.1(5)
P4	0.7392(2)	0.8028(2)	0.2706(1)	3.2(1)	C52	0.5298(6)	0.8166(6)	0.1752(5)	4.2(5)
O1	0.5524(5)	0.4413(6)	0.2725(5)	9.8(7)	C53	0.4458(6)	1.0223(6)	0.1264(5)	4.5(5)
O2	0.4468(6)	0.6573(5)	0.3146(5)	10.5(7)	C54	0.5400(6)	1.0225(5)	0.1387(5)	4.4(6)
O51	0.4856(5)	0.8919(5)	0.0128(3)	6.8(5)	C55	0.5675(6)	1.0004(6)	0.2009(5)	4.7(6)
O52	0.5118(4)	0.7606(4)	0.1926(4)	6.4(5)	C56	0.5066(6)	0.9577(6)	0.2208(5)	4.5(6)
C1	0.4940(7)	0.4650(7)	0.2878(6)	6.7(8)	C57	0.4418(6)	0.9570(6)	0.1677(5)	4.0(5)
C2	0.4287(8)	0.5965(7)	0.3144(7)	7.5(8)	C58	0.4062(7)	1.0921(6)	0.1452(6)	6.1(7)
C3	0.4529(10)	0.3934(9)	0.3966(7)	9.6(10)	C59	0.7525(5)	0.8783(5)	0.2184(5)	3.2(5)
C4	0.3791(8)	0.3971(8)	0.3447(6)	7.9(8)	C60	0.6994(7)	0.5828(6)	0.1844(5)	5.2(6)
C5	0.3286(8)	0.4533(8)	0.3589(6)	7.6(9)	C61	0.7220(6)	0.9672(6)	0.1100(5)	3.8(5)
C6	0.3782(9)	0.5058(9)	0.3978(7)	9.3(10)	C62	0.7683(7)	1.0212(6)	0.1446(6)	5.6(7)
C7	0.4617(8)	0.4780(10)	0.4069(7)	10.1(11)	C63	0.7978(8)	1.0801(7)	0.1159(7)	8.1(9)
C8	0.4507(12)	0.3459(11)	0.4554(8)	14.4(15)	C64	0.7825(7)	1.0870(8)	0.0524(7)	8.4(9)
C9	0.2400(6)	0.5676(5)	0.2166(5)	3.9(5)	C65	0.7339(8)	1.0359(9)	0.0164(6)	8.5(9)
C10	0.0892(6)	0.4129(6)	0.0092(6)	5.2(6)	C66	0.7040(7)	0.9751(7)	0.0451(6)	6.5(7)
C11	0.3707(6)	0.5252(5)	0.1514(5)	3.8(5)	C71	0.7030(6)	0.8116(6)	0.0978(5)	4.4(5)
C12	0.3410(6)	0.4976(6)	0.0917(5)	4.5(6)	C72	0.6465(6)	0.7588(6)	0.0732(6)	5.1(6)
C13	0.3752(7)	0.5174(7)	0.0396(6)	6.4(7)	C73	0.6683(7)	0.7008(7)	0.0389(6)	6.5(7)
C14	0.4395(8)	0.5666(7)	0.0473(6)	6.9(8)	C74	0.7447(8)	0.6962(8)	0.0264(6)	7.9(8)
C15	0.4684(8)	0.5940(8)	0.1053(7)	7.8(8)	C75	0.8032(8)	0.7472(8)	0.0489(7)	8.9(9)
C16	0.4363(7)	0.5746(7)	0.1574(6)	5.9(7)	C76	0.7814(6)	0.8052(7)	0.0860(6)	6.2(7)
C21	0.2791(5)	0.4139(5)	0.1999(5)	3.6(5)	C81	0.8371(5)	0.8009(6)	0.3252(4)	3.6(5)
C22	0.2013(6)	0.3955(6)	0.2094(5)	4.9(6)	C82	0.8618(7)	0.7356(6)	0.3548(5)	5.2(6)
C23	0.1671(7)	0.3251(7)	0.1966(6)	7.0(7)	C83	0.9354(8)	0.7343(7)	0.3976(6)	7.1(7)
C24	0.2130(8)	0.2735(7)	0.1736(7)	7.9(8)	C84	0.9824(7)	0.7948(8)	0.4093(6)	7.5(8)
C25	0.2904(9)	0.2891(7)	0.1650(7)	7.5(8)	C85	0.9605(7)	0.8596(7)	0.3807(6)	6.5(7)
C26	0.3234(7)	0.3585(6)	0.1776(6)	5.9(7)	C86	0.8863(6)	0.8638(6)	0.3389(5)	4.7(6)
C31	0.0845(6)	0.6347(5)	0.1671(5)	3.6(5)	C91	0.6704(5)	0.8380(6)	0.3205(4)	3.6(5)
C32	0.0123(7)	0.5994(6)	0.1580(6)	5.3(6)	C92	0.6816(7)	0.9062(6)	0.3478(5)	5.0(6)
C33	-0.0559(7)	0.6319(7)	0.1762(6)	6.0(7)	C93	0.6332(7)	0.9298(7)	0.3895(6)	6.1(7)
C34	-0.0499(7)	0.6976(7)	0.2040(6)	6.6(7)	C94	0.5709(7)	0.8853(8)	0.3996(6)	7.5(8)
C35	0.0230(8)	0.7335(7)	0.2149(7)	7.5(9)	C95	0.5588(7)	0.8156(8)	0.3736(6)	6.8(8)
C36	0.0912(7)	0.7024(7)	0.1969(7)	7.2(8)	C96	0.6096(6)	0.7930(7)	0.3331(5)	5.5(7)

Cl₂ (15 mL) was treated with Ph₃C⁺PF₆⁻ (0.384 g, 0.989 mmol) in CH₂Cl₂ (15 mL) at 0 °C. The reaction mixture was stirred at 0 °C for 30 min before being gradually warmed up to room temperature and was stirred for a further 2.5 h. The solution was then filtered on a pad of Celite. The solvent was reduced to a small volume on a rotary evaporator. After the addition of anhydrous Et₂O, complex **6** precipitated as a light green solid material which was collected by filtration and recrystallized from CH₃CN (yield: 0.811 g, 86.0%). **6**: mp 160–162 °C; IR (CH₂Cl₂) ν_{CO} 2050 (vs), 2007 (vs) cm⁻¹; ³¹P NMR (CDCl₃) δ 56.48 (s), 20.68 (s), -143.38 (sept, ¹J_{PF} = 711 Hz); ¹H NMR (CDCl₃) δ 7.80–7.45 (m, 20H, Ph), 4.90 (s, 2H, Cp'-β), 4.87 (s, 2H, Cp'-α), 4.01 (m, 2H, PCH₂P), 1.83 (s, 3H, Me); ¹³C NMR (CDCl₃) δ 218.22 (s, CO), 133.86–129.70 (m, Ph), 107.36 (s, Cp'_{ipso}), 89.01 (s, Cp'-β), 87.39 (s, Cp'-α), 31.57 (s, PCH₂P), 22.64 (s, Me); MS (FAB) m/z 808 (M⁺ - PF₆). Anal. Calcd for C₃₃H₂₉AuClF₆O₂P₃: C, 41.59; H, 3.07. Found: C, 41.65; H, 3.36.

Reaction of Compound 1 and [Rh(CO)₂Cl]₂. Compound **1** (0.115 g, 0.2 mmol) and [Rh(CO)₂Cl]₂ (0.085 g, 0.2 mmol) were dissolved in 15 mL of THF/30 mL of *n*-hexane. The color of solution changed gradually from yellow to red when red precipitates appeared in 10 min. The mixture was stirred for an additional 1 h, and then the solution was cannula transferred. The precipitate was washed with *n*-hexane (30 mL × 3) to give red (η^5 -MeC₅H₄)Fe(μ -CO)₂(μ - η^1 : η^1 -dppm)RhCl₂ (**9**) (0.088 g, 88%). **9**: mp 189–190 °C (dec); IR (CH₂Cl₂) ν_{CO} 1854 (w), 1809 (s) cm⁻¹; ³¹P NMR (CDCl₃) δ 77.78 (d, ²J_{PP} = 71.8 Hz), 47.03 (dd, ²J_{PP} = 71.8 Hz, ¹J_{RhP} = 127.2 Hz); ¹H NMR (CDCl₃) δ 1.92 (b, 3H, Me), 2.25 (b, 2H, Ph₂PCH₂PPh₂), 4.43 (b, 2H, Cp'-α), 4.86 (b, 2H, Cp'-β), 7.19–7.47 (m, 20H, Ph); ¹³C NMR (CDCl₃) δ 12.0 (s, Me), 28.6 (m, Ph₂PCH₂PPh₂), 53.4 (s,

Cp'-α), 77.2 (s, Cp'-β), 88.6 (s, Cp'-*ipso*), 128.2–133.2 (m, Ph), 219.8 (dd, CO, ²J_{PC} = 14.2 Hz, ⁴J_{PC} = 1.85 Hz); MS (m/z) 767 (M⁺). Anal. Calcd for C₃₅H₃₅Cl₂FeO₂P₂Rh: C, 44.85; H, 3.55. Found: C, 45.22; H, 3.61.

X-ray Structure Analyses of Complexes 4, 5, and 9. Diffraction intensities were measured with background counts made for half the total scan time on each side of peak. Three standard reflections, remeasured after every 1 h, showed no significant decrease in intensity during data collection. Data were corrected for Lorentz–polarization and absorption (empirical ψ corrections). The structure was solved by direct methods with MULTAN.²⁴ Calculations and full matrix least-squares refinements were performed utilizing the NRCVAX program package.²⁵ All non-H atoms were refined with anisotropic thermal parameters with all hydrogen atoms idealized (C–H = 1.00 Å). Scattering factor curves of Fe, P, O, C, and H were taken from the ref 26. Final fractional coordinates of complexes **4**, **5**, and **9**, respectively, are given in Tables 1–3. Relevant structural parameters are listed in the captions of Figures 1–3, the molecular plots of complexes **4**, **5**, and **9**, respectively.

(24) Main, P. In *Crystallographic Computing 3: Data Collection, Structure Determination, Proteins and Database*; Sheldrick, G. M., Krueger, C., Goddard, R., Eds.; Clarendon: Oxford, U.K., 1985; pp. 206–215.

(25) Gabe, E. J.; Le Page, Y.; Lee, F. L. In *Crystallographic Computing 3: Data Collection, Structure Determination, Proteins and Database*; Sheldrick, G. M., Krueger, C., Goddard, R., Eds.; Clarendon: Oxford, U.K., 1985; pp. 167–174.

(26) Ibers, J. A., Hamilton, W. C., Eds. *International Tables for X-ray Crystallography*; Kynoch: Birmingham, U.K. (current distributor D. Reidel, Dordrecht, The Netherlands), 1974; Vol. 4, Tables 2.2A and 2.3.1D.

Table 3. Final Fractional Coordinates and B Values (Å²) for Non-H Atoms of Complex 9, (η⁵-MeC₅H₄)Fe(μ-CO)₂(μ-η¹:η¹-dppm)RhCl₂·2CH₂Cl₂

atom	x	y	z	B _{iso}	atom	x	y	z	B _{iso}
Rh1	0.53935(4)	0.27155(4)	0.46664(3)	2.67(4)	C26	0.3397(6)	0.0606(6)	0.3373(5)	5.8(7)
Rh2	-0.04770(4)	0.23217(4)	0.97577(3)	2.91(4)	C27	0.3531(6)	0.1327(5)	0.3576(4)	4.7(6)
Fe1	0.54925(8)	0.32864(7)	0.56864(6)	2.88(7)	C28	0.3440(5)	0.2926(5)	0.3959(4)	3.0(5)
Fe2	0.03488(8)	0.17328(8)	1.07573(6)	3.41(8)	C29	0.3640(5)	0.3502(5)	0.3680(4)	3.1(5)
P1	0.41580(14)	0.23576(13)	0.44587(11)	2.74(12)	C30	0.3088(6)	0.3948(5)	0.3308(4)	4.0(5)
P2	0.42937(15)	0.30593(13)	0.56367(11)	2.83(14)	C31	0.2328(6)	0.3821(6)	0.3219(5)	5.1(6)
P3	0.05487(14)	0.26103(13)	0.94813(11)	2.80(12)	C32	0.2100(5)	0.3237(6)	0.3487(5)	5.0(7)
P4	0.14874(15)	0.18775(14)	1.06285(11)	3.18(14)	C33	0.2656(6)	0.2801(5)	0.3851(4)	4.3(6)
Cl1	0.66959(14)	0.30201(13)	0.47801(12)	3.94(14)	C34	-0.0053(5)	0.1316(5)	1.0028(4)	3.3(5)
Cl2	0.52366(15)	0.23295(15)	0.37021(11)	4.28(14)	C35	0.0109(5)	0.2687(5)	1.0590(4)	3.7(5)
Cl3	-0.16550(15)	0.20643(14)	0.99393(13)	4.73(16)	C36	0.0479(7)	0.1856(6)	1.1659(4)	6.0(7)
Cl4	-0.12205(15)	0.27922(16)	0.88428(12)	4.84(15)	C37	0.0859(6)	0.1234(7)	1.1575(5)	6.0(7)
O1	0.5770(4)	0.1739(3)	0.5668(3)	4.5(4)	C38	0.0306(6)	0.0768(6)	1.1201(5)	5.0(6)
O2	0.5024(3)	0.4220(3)	0.4648(3)	3.4(3)	C39	-0.0394(6)	0.1091(6)	1.1061(5)	5.3(7)
O34	-0.0209(4)	0.0801(3)	0.9721(3)	4.0(4)	C40	-0.0304(7)	0.1760(6)	1.1335(5)	6.1(8)
O35	0.0106(4)	0.3290(3)	1.0748(3)	5.1(4)	C41	0.0802(10)	0.2462(9)	1.2063(5)	11.3(12)
C1	0.5620(5)	0.2343(5)	0.5517(4)	3.1(5)	C42	0.1891(5)	0.1134(5)	1.0332(4)	3.4(5)
C2	0.5183(5)	0.3706(5)	0.4956(4)	2.6(5)	C43	0.1619(6)	0.0431(5)	1.0350(4)	4.2(6)
C3	0.6612(5)	0.3251(5)	0.6336(4)	4.4(5)	C44	0.1957(6)	-0.0134(5)	1.0167(5)	5.7(7)
C4	0.6536(5)	0.3877(5)	0.5989(4)	4.0(5)	C45	0.2559(7)	-0.0017(6)	0.9952(6)	6.8(8)
C5	0.5933(6)	0.4287(5)	0.6064(4)	4.2(6)	C46	0.2813(7)	0.0664(6)	0.9919(6)	6.7(8)
C6	0.5641(6)	0.3899(5)	0.6440(4)	4.5(6)	C47	0.2494(6)	0.1239(5)	1.0125(5)	4.9(7)
C7	0.6052(6)	0.3257(6)	0.6606(4)	4.1(6)	C48	0.2295(6)	0.2142(5)	1.1274(4)	3.9(5)
C8	0.7224(7)	0.2681(7)	0.6434(5)	7.2(8)	C49	0.2847(6)	0.1637(6)	1.1570(5)	5.5(7)
C9	0.4228(5)	0.2756(5)	0.6338(4)	3.2(5)	C50	0.3457(7)	0.1852(7)	1.2069(5)	6.6(7)
C10	0.3945(6)	0.3201(6)	0.6686(4)	4.5(6)	C51	0.3515(7)	0.2542(7)	1.2266(4)	6.9(8)
C11	0.3962(7)	0.2977(6)	0.7242(5)	5.5(7)	C52	0.2971(7)	0.3040(6)	1.1970(5)	6.4(8)
C12	0.4243(7)	0.2328(7)	0.7454(4)	6.3(7)	C53	0.2364(6)	0.2842(6)	1.1481(4)	5.2(6)
C13	0.4520(7)	0.1879(6)	0.7125(5)	6.2(7)	C54	0.1431(5)	0.2625(5)	1.0116(4)	3.0(5)
C14	0.4520(6)	0.2095(5)	0.6571(4)	4.5(6)	C55	0.0534(5)	0.3517(5)	0.9200(4)	2.9(5)
C15	0.3581(5)	0.3773(5)	0.5405(4)	3.1(5)	C56	0.0659(6)	0.3682(5)	0.8683(5)	4.4(6)
C16	0.3814(5)	0.4479(5)	0.5408(4)	3.7(6)	C57	0.0667(7)	0.4390(6)	0.8497(5)	5.5(7)
C17	0.3269(6)	0.5023(5)	0.5276(5)	4.7(7)	C58	0.0523(6)	0.4932(5)	0.8828(5)	5.3(7)
C18	0.2505(6)	0.4862(6)	0.5145(5)	5.5(7)	C59	0.0393(7)	0.4787(5)	0.9341(5)	5.6(7)
C19	0.2268(6)	0.4168(6)	0.5132(6)	6.0(8)	C60	0.0380(6)	0.4079(5)	0.9526(4)	4.5(6)
C20	0.2801(5)	0.3615(5)	0.5271(5)	4.6(6)	C61	0.0752(5)	0.2020(5)	0.8945(4)	2.8(5)
C21	0.3886(5)	0.2315(5)	0.5129(4)	2.9(5)	C62	0.1454(6)	0.2063(5)	0.8842(4)	4.0(6)
C22	0.3950(5)	0.1449(5)	0.4171(4)	3.0(5)	C63	0.1619(6)	0.1597(6)	0.8459(5)	5.0(7)
C23	0.4236(6)	0.0858(5)	0.4538(4)	4.1(6)	C64	0.1080(7)	0.1082(6)	0.8174(5)	5.6(7)
C24	0.4089(7)	0.0167(5)	0.4329(5)	5.2(7)	C65	0.0380(6)	0.1030(6)	0.8269(5)	4.9(6)
C25	0.3673(7)	0.0047(6)	0.3746(5)	5.9(8)	C66	0.0225(5)	0.1503(5)	0.8658(4)	3.4(5)

Crystal Data for 4·CH₂Cl₂: C₃₄H₃₂AuCl₃FeO₂P₂, MW = 893.74, monoclinic, space group *P*₂₁/*n*; *a* = 10.896(2), *b* = 21.064(6), *c* = 15.212(3) Å; β = 101.86(2)°, *V* = 3417(1) Å³; *Z* = 4, *F*(000) = 1572, *D*_{calcd} = 1.738 g/cm³; Nonius CAD-4 data, Mo radiation, λ = 0.710 69 Å, μ = 5.06 mm⁻¹; minimum and maximum transmission factors 0.479–0.999. The structure was solved by heavy atom methods and refined by full-matrix least squares (all non-hydrogen atoms anisotropic and hydrogen atoms idealized with C–H = 1.00 Å). *R* = 0.031, *R*_w = 0.039, and GOF = 1.86 with 75 atoms and 389 parameters for 3578 out of 4454 measured reflections, cut off *I*_o > 2.5σ(*I*_o).

Crystal Data for 5: C₃₄H₃₃AuFeO₂P₂, MW = 788.39, monoclinic, space group *P*₂₁/*n*; *a* = 16.606(2), *b* = 18.086(3), *c* = 21.629(5) Å; β = 100.62(1)°, *V* = 6384.8(20) Å³; *Z* = 8, *F*(000) = 3103, *D*_{calcd} = 1.640 g/cm³; Nonius CAD-4 data, Mo radiation, λ = 0.710 69 Å, μ = 5.16 mm⁻¹; minimum and maximum transmission factors 0.499–1.000. The structure was solved by heavy atom methods and refined by full-matrix least squares (all non-hydrogen atoms anisotropic and hydrogen atoms idealized with C–H = 1.00 Å). *R* = 0.034, *R*_w = 0.036, and GOF = 1.17 with 146 atoms and 722 parameters for 4809 out of 8324 measured reflections, cut off *I*_o > 2.5σ(*I*_o).

Crystal Data for 9·2CH₂Cl₂: C₃₅H₃₃Cl₆FeO₂P₂Rh, MW = 919.05, monoclinic, space group *P*₂₁/*a*; *a* = 18.406(3), *b* = 18.606(2), *c* = 23.915(4) Å; β = 109.28(2)°, *V* = 7731(2) Å³; *Z* = 8, *F*(000) = 3695.67, *D*_{calcd} = 1.579 g/cm³; Nonius CAD-4 data, Mo radiation, λ = 0.710 69 Å, μ = 1.33 mm⁻¹; minimum and maximum transmission factors 0.777–1.000. The structure was solved by direct methods and refined by full-matrix least squares (all non-hydrogen atoms anisotropic and hydrogen atoms idealized with C–H = 1.00 Å). *R* = 0.041, *R*_w = 0.041, and GOF = 1.53 with 176 atoms and 819 parameters for 5508 out of 10 086 unique reflections, cut off *I*_o > 2.5σ(*I*_o).

Acknowledgment. The authors take this chance to thank Academia Sinica and the National Science Council, ROC, for the kind financial supports.

Supporting Information Available: For the structures of 4, 5, and 9, listings of crystallographic data and refinement details, positional and anisotropic thermal parameters, and bond distances, angles, and structural parameters (43 pages). Ordering information is given on any current masthead page.

OM9409736

**Versatility in Phenolate Bonding in Organoaluminum
Complexes Containing Mono- and Bis-*ortho*-Chelating
Phenolate Ligands. X-ray Structures of
Al{OC₆H₂(CH₂NMe₂)₂-2,6-Me-4}₃,
Al(Me)₂{OC₆H₂(CH₂NMe₂)₂-2,6-Me-4}·N-AlMe₃, and
Al(Me)₂{OC₆H₂(CH₂NMe₂)₂-2,6-Me-4}·N-AlMe₃·O-AlMe₃**

Marinus P. Hogerheide,[†] Maurits Wesseling,[†] Johann T. B. H. Jastrzebski,[†]
Jaap Boersma,[†] Huub Kooijman,[‡] Anthony L. Spek,^{‡,§} and Gerard van Koten^{*,†}

*Debye Institute, Department of Metal Mediated Synthesis, and Bijvoet Center for
Biomolecular Research, Laboratory of Crystal and Structural Chemistry, Utrecht University,
Padualaan 8, 3584 CH Utrecht, The Netherlands*

Received April 28, 1995[®]

The effect of intramolecular coordination on both the structure and the Lewis acidity of aluminum phenolates has been studied. The mono-*ortho*-amino-substituted phenol HOC₆H₄(CH₂NMe₂)₂ (**3**) reacts with AlMe₃ to produce the substitution products AlMe_{3-x}(OC₆H₄(CH₂NMe₂)₂)_x (*x* = 1 (**1a**), 2 (**1b**), and 3 (**1c**)) and the trimethylaluminum adduct AlMe₂(OC₆H₄(CH₂NMe₂)₂)·O-AlMe₃ (**1d**), all in high yield. For the bis-*ortho*-amino-substituted phenol HOC₆H₂(CH₂NMe₂)₂-2,6-Me-4 (**4**) the substitution products AlMe_{3-x}(OC₆H₂(CH₂NMe₂)₂-2,6-Me-4)_x (*x* = 2 (**2b**) and 3 (**2c**)) were obtained, as well as the mono- and bis(trimethylaluminum) adducts AlMe₂(OC₆H₂(CH₂NMe₂)₂-2,6-Me-4)·N-AlMe₃ (**2d**) and AlMe₂(OC₆H₂(CH₂NMe₂)₂-2,6-Me-4)·N-AlMe₃·O-AlMe₃ (**2e**). The mono(phenolate) dimethylaluminum complexes (**1a** and **2a**) easily undergo an inter- (**1a**) or an intramolecular (**2a**) Lewis base induced ligand exchange to give the bis(phenolate) complexes (**1b** and **2b**, respectively) and trimethylaluminum. The aluminum phenolate complexes were characterized by variable-temperature NMR and single-crystal structure determinations (**2c–e**). The solid state structure of **2c** contains the aluminum surrounded by two bidentate, *O,N*-bonded, phenolate ligands and one monodentate, *O*-bonded, phenolate ligand in a trigonal bipyramidal coordination geometry, with the oxygen atoms in the trigonal plane and the two coordinating nitrogen atoms in the apical positions. The molecular structure of **2d** contains one AlMe₂ moiety which is bidentate, *O,N*-coordinated by the phenolate ligand, in a distorted tetrahedral geometry. The second amino substituent forms a Lewis acid–base complex with a molecule AlMe₃, also with a distorted tetrahedral geometry around the aluminum. The structure of **2e** is similar to that of **2d** but contains an additional molecule of AlMe₃, which forms a Lewis acid–base complex with a lone pair of the phenolate oxygen atom, resulting in a distorted tetrahedral geometry around the aluminum. NMR spectroscopy shows the solution structures to be closely related to those established in the solid state.

Introduction

Monomeric aluminum phenolate complexes with bulky *ortho*-substituents (^tBu, Ph) have found applications in the stereo- and regioselective activation of carbonyl groups,¹ the reduction of coordinated benzophenone,² and transfer of alkyl groups from aluminum to main-group chlorides.³ The bulky *ortho*-substituents present in the phenolate ligands prevent association, which is

normally found for aluminum phenolate complexes with less sterically demanding *ortho*-substituents.⁴ Accordingly, the aluminum centers in these complexes have a free—be it sterically restricted—coordination site available, which enables them to act as Lewis acids.^{5–8}

* To whom correspondence should be addressed. e-mail: vankoten@xray.chem.ruu.nl.

[†] Debye Institute.

[‡] Bijvoet Center for Biomolecular Research.

[§] Address correspondence regarding the crystallography to this author.

[®] Abstract published in *Advance ACS Abstracts*, August 1, 1995.

(1) (a) Maruoka, K.; Itoh, T.; Sakurai, M.; Nonoshita, K.; Yamamoto, H. *J. Am. Chem. Soc.* **1988**, *110*, 3588. (b) Maruoka, K.; Saito, S.; Yamamoto, H. *J. Am. Chem. Soc.* **1992**, *114*, 1089.

(2) Power, M. B.; Nash, J. R.; Healy, M. D.; Barron, A. R. *Organometallics* **1992**, *11*, 1830.

(3) Healy, M. D.; Ziller, J. W.; Barron, A. R. *Organometallics* **1992**, *11*, 3041.

(4) (a) Pasynkiewicz, S.; Starowieyski, K. B.; Skowrońska-Ptasińska, M. *J. Organomet. Chem.* **1973**, *52*, 269. (b) Starowieyski, K. B.; Skowrońska-Ptasińska, M.; Muszyńska, J. *J. Organomet. Chem.* **1978**, *157*, 379. (c) Starowieyski, K. B.; Pasynkiewicz, S.; Skowrońska, M. D. *J. Organomet. Chem.* **1971**, *31*, 149.

(5) (a) Shreve, A. P.; Mulhaupt, R.; Fultz, W.; Calabrese, J.; Robbins, W.; Ittel, S. D. *Organometallics* **1988**, *7*, 409. (b) Healy, M. D.; Barron, A. R. *Angew. Chem., Int. Ed. Engl.* **1992**, *31*(7), 921. (c) Healy, M. D.; Wierda, D. A.; Barron, A. R. *Organometallics* **1988**, *7*, 2543. (d) Starowieyski, K. B.; Pasynkiewicz, S.; Skowrońska-Ptasińska, M. *J. Organomet. Chem.* **1975**, *90*, C43. (e) Maruoka, K.; Nagahara, S.; Yamamoto, H. *J. Am. Chem. Soc.* **1990**, *112*, 6115.

(6) Healy, M. D.; Ziller, J. W.; Barron, A. R. *J. Am. Chem. Soc.* **1990**, *112*, 2949.

(7) Healey, M. D.; Mason, M. R.; Gravelle, P. H.; Bott, S. G.; Barron, A. R. *J. Chem. Soc., Dalton Trans.* **1993**, 441.

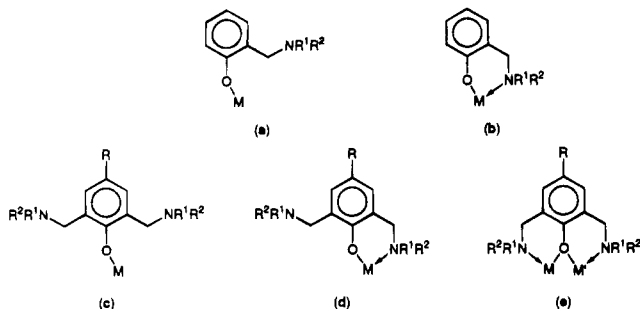


Figure 1. *ortho*-Chelating phenolate ligands and their coordination possibilities: Monodentate (**a**, **c**), bidentate (**b**, **d**),^{9,10} and bridging between identical ($M = M'$)^{11,12} or different ($M \neq M'$)¹³ metal centers (**e**).

The use of phenolates with potentially intramolecularly coordinating *ortho*-substituents provides an attractive alternative to steric bulk. When coordinated, these substituents combine steric shielding of the metal center with electron donation to the metal center. When pendant, they provide steric shielding. For example, the monoanionic 2-[(dimethylamino)methyl]phenolate (see Figure 1a,b) can serve either as an *ortho*-hindered monodentate or as a bidentate ligand, depending on the steric and electronic requirements of the metal center. Introduction of a second *ortho*-amino substituent as in monoanionic 2,6-[(dimethylamino)methyl]-4-methylphenolate (see Figure 1c–e) essentially brings in a second *ortho*-hindering substituent but also another Lewis basic functional group when the ligand coordinates in bidentate fashion, a feature that will be shown to be of importance in the chemistry presented below.

In this paper we report the first results of the systematic study of the effect of *ortho*-chelation on the structure in solution as well as in the solid state and the reactivity of aluminum phenolates.

Experimental Section

General Methods. All reactions were performed in an atmosphere of dry, oxygen-free dinitrogen using standard Schlenk and syringe techniques. All solvents were carefully dried and distilled prior to use. AlMe_3 was used as a 2.0 M solution in hexane as obtained from Aldrich. The phenols $\text{HOC}_6\text{H}_4(\text{CH}_2\text{NMe}_2)_2$ (**3**) and $\text{HOC}_6\text{H}_2(\text{CH}_2\text{NMe}_2)_2$ -2,6-Me-4 (**4**) were synthesized according to literature procedures.¹¹ Elemental analyses were performed by H. Kolbe, Mikroanalytisches Laboratorium, Mülheim, Germany. ¹H and ¹³C NMR data were collected on Bruker AC200 and AC300 spectrometers.

$\text{AlMe}_2\{\text{OC}_6\text{H}_4(\text{CH}_2\text{NMe}_2)_2\}$ (**1a**). To a stirred solution of AlMe_3 (9.0 mmol; 4.5 mL of a 2.0 M hexane solution) in hexane

(25 mL) a solution of $\text{HOC}_6\text{H}_4(\text{CH}_2\text{NMe}_2)_2$ (1.36 g; 9.0 mmol) was added dropwise at 0 °C. While methane gas evolved from the mixture, a white precipitate was formed. After the mixture was stirred for an additional 2 h at room temperature the solvent was removed *in vacuo* and the product washed once with pentane (30 mL). Complex **1a** was obtained as a white powder in quantitative yield. Recrystallization from hexane afforded **1a** as colorless hexagonal crystals. Mp: 125 °C.

¹H NMR data (C_6D_6 , 200 MHz, 298 K) (δ)SPCLN 7.13 (m, 2H, ArH); 6.69 (m, 2 H, ArH); 3.05 (s, 2 H, CH_2N); 1.60 (s, 6 H, NMe_2); -0.56 (s, 6H, AlMe_2). ¹³C NMR data (C_6D_6 , 50 MHz, 298 K) (δ)SPCLN 160.37 (CO); 130.89, 129.43, 120.40, 117.23 (Ar); 120.70 (CCH_2); 62.39 (CH_2N); 44.33 (NMe_2). Anal. Calcd for $\text{C}_{11}\text{H}_{18}\text{NOAl}$: C, 63.75; H, 8.75; N, 6.76. Found: C, 63.88; H, 8.83; N, 8.82.

$\text{AlMe}\{\text{OC}_6\text{H}_4(\text{CH}_2\text{NMe}_2)_2\}_2$ (**1b**). The preparation of **1b** was analogous to that of **1a**. Addition of $\text{HOC}_6\text{H}_4(\text{CH}_2\text{NMe}_2)_2$ (2.72 g; 18 mmol) to a stirred solution of AlMe_3 (4.5 mL; 9.0 mmol) at 0 °C afforded **1b**, after workup, in quantitative yield. Mp: >200 °C.

¹H NMR data (C_6D_6 , 200 MHz, 298 K) (δ)SPCLN 7.23 (m, 2 H, ArH); 6.89 (d, 2 H, ³ $J_{\text{HH}} = 7.9$ Hz, ArH); 6.80 (m, 4 H, ArH); 3.68 (d, 2 H, ³ $J_{\text{HH}} = 13.5$ Hz, CH_2N); 3.15 (d, 2 H, $J_{\text{HH}} = 13.5$ Hz, CH_2N); 2.12 (s, 6 H, NMe_2); 1.98 (s, 6 H, NMe_2); -0.63 (s, 3 H, AlMe). ¹³C NMR data (C_6D_6 , 50 MHz, 298 K) (δ): 160.16 (CO); 129.45, 129.28, 122.96, 119.54, 117.29 (Ar); 62.59 (CH_2N); 45.69 (NMe_2). Anal. Calcd for $\text{C}_{19}\text{H}_{27}\text{N}_2\text{O}_2\text{Al}$: C, 66.65; H, 7.95; N, 8.18. Found: C, 66.20; H, 7.40; N, 8.06.

$\text{Al}\{\text{OC}_6\text{H}_4(\text{CH}_2\text{NMe}_2)_2\}_3$ (**1c**). The preparation of **1c** was analogous to that of **1a**. Addition of $\text{HOC}_6\text{H}_4(\text{CH}_2\text{NMe}_2)_2$ (3.63 g; 24 mmol) to a stirred solution of AlMe_3 (4.0 mL; 8.0 mmol) at room temperature afforded **1c** in quantitative yield. Crystallization from hexane at -30 °C resulted in the formation of colorless, hexagonal crystals. Mp: 165 °C (dec).

¹H NMR data (C_6D_6 , 200 MHz, 298 K) (δ): 7.38 (d, 1 H, ³ $J_{\text{HH}} = 7.4$ Hz, *o*-H); 7.25 (m, 1 H, ArH); 6.96 (m, 3 H, ArH); 6.77 (m, 7 H, ArH); 3.89 (br, 2 H, CH_2N); 3.53 (d, 1 H, ² $J_{\text{HH}} = 12.4$ Hz, CH_2N); 3.26 (m, 3 H, CH_2N); 2.23 (s, 6 H, NMe_2); 2.14 (s, 6 H, NMe_2); 2.09 (s, 6 H, NMe_2). ¹³C NMR data (C_6D_6 , 50 MHz, 298 K) (δ): 159.73, 159.18 (CO); 129.56, 129.15, 128.85, 123.02, 119.62, 117.94, 117.61 (Ar); 62.94, 59.53 (CH_2N); 46.72, 45.92, 45.57 (NMe_2). Anal. Calcd for $\text{C}_{27}\text{H}_{36}\text{N}_3\text{O}_3\text{Al}$: C, 67.90; H, 7.60; N, 8.80. Found: C, 67.75; H, 7.54; N, 8.78.

$\text{AlMe}_2\{\text{OC}_6\text{H}_4(\text{CH}_2\text{NMe}_2)_2\}\text{AlMe}_3$ (**1d**). The preparation of **1d** was analogous to that of **1a**. Addition of $\text{HOC}_6\text{H}_4(\text{CH}_2\text{NMe}_2)_2$ (1.97 g; 13 mmol) to a stirred solution of AlMe_3 (20 mL; 40 mmol) at 0 °C afforded **1d**, after workup, in quantitative yield. Mp: 90 °C.

¹H NMR data (C_6D_6 , 200 MHz, 298 K) (δ): 7.16 (m, 1 H, ArH); 7.00 (m, 1 H, ArH); 6.75 (m, 1 H, ArH); 6.57 (m, 1 H, ArH); 2.98 (s, 2 H, CH_2N); 1.52 (s, 6 H, NMe_2); -0.29 (s, 9 H, AlMe_3); -0.63 (s, 6 H, AlMe_2). ¹³C NMR data (C_6D_6 , 50 MHz, 298 K) (δ): 153.17 (CO); 131.05, 130.02, 124.72, 124.14, 123.72 (Ar); 61.71 (CH_2N); 46.58 (NMe_2); -5.10 (AlMe_3); -9.67 (AlMe_2). Anal. Calcd for $\text{C}_{14}\text{H}_{27}\text{NOAl}_2$: C, 60.20; H, 9.74; N, 5.01. Found: C, 60.09; H, 9.70; N, 5.09.

$\text{AlMe}\{\text{OC}_6\text{H}_2(\text{CH}_2\text{NMe}_2)_2$ -2,6-Me-4 $\}_2$ (**2b**). The preparation of **2b** was analogous to that of **1a**. Addition of $\text{HOC}_6\text{H}_2(\text{CH}_2\text{NMe}_2)_2$ -2,6-Me-4 (3.45 g; 15.5 mmol) to a stirred solution of AlMe_3 (4.0 mL; 8.0 mmol) at 0 °C resulted in the formation of a slightly yellow, clear solution. Complex **2b** was obtained, after workup, as a yellow powder or oil in essentially quantitative yield. The product contained some unidentified impurities that could not be removed.

¹H NMR data (C_6D_6 , 200 MHz, 298 K) (δ): 7.30 (s, 2 H, ArH); 6.58 (s, 2 H, ArH); 3.54 (br, 4 H, CH_2N); 2.9–1.9 (m, 35 H, CH_2N , NMe_2 , *p*-Me); -0.57 (s, 3 H, AlMe_2). ¹³C NMR data (C_6D_6 , 50 MHz, 298 K) (δ): 156.44 (CO); 131.72, 124.89, 122.62 (Ar); 62.80, 60.10 (CH_2N); 45.72 (NMe_2); 20.71 (*p*-Me).

$\text{Al}\{\text{OC}_6\text{H}_2(\text{CH}_2\text{NMe}_2)_2$ -2,6-Me-4 $\}_3$ (**2c**). After the addition of $\text{HOC}_6\text{H}_2(\text{CH}_2\text{NMe}_2)_2$ -2,6-Me-4 (6.00 g; 27.0 mmol) to a

(8) For a review on sterically crowded aluminum phenolate complexes see: Healy, M. D.; Power, M. B.; Barron, A. R. *Coord. Chem. Rev.* **1994**, *130*, 63.

(9) van der Schaaf, P. A.; Boersma, J.; Smeets, W. J. J.; Spek, A. L.; van Koten, G. *Inorg. Chem.* **1993**, *32*, 5108.

(10) Alsters, P. L.; Teunissen, H. T.; Boersma, J.; Spek, A. L.; van Koten, G. *Organometallics* **1993**, *12*, 4691.

(11) (a) van der Schaaf, P. A.; Jastrzebski, J. T. B. H.; Hogerheide, M. P.; Smeets, W. J. J.; Spek, A. L.; van Koten, G. *Inorg. Chem.*, **1993**, *32*, 4111. (b) Hogerheide, M. P.; Ringelberg, S. N.; Janssen, M. D.; Boersma, J.; Spek, A. L.; van Koten, G. To be published.

(12) (a) van der Schaaf, P. A.; Hogerheide, M. P.; Grove, D. M.; Spek, A. L.; van Koten, G. *Chem. Soc., Chem. Commun.* **1992**, 1703. (b) Tesh, K. F.; Hanusa, T. P. *J. Chem. Soc., Chem. Commun.* **1991**, 879. (c) Gultneih, Y.; Farooq, A.; Liu, S.; Karlin, K. D.; Zubietta, J. *Inorg. Chem.* **1992**, *31*, 3607. (d) Teipel, S.; Griesar, K.; Haase, W.; Krebs, B. *Inorg. Chem.* **1994**, *33*, 456.

(13) Hogerheide, M. P.; Jastrzebski, J. T. B. H.; Boersma, J.; Smeets, W. J. J.; Spek, A. L.; van Koten, G. *Inorg. Chem.* **1994**, *33*, 4431.

Table 1. Crystallographic Data for the Complexes 2c-e

	complex		
	2c	2d	2e
Crystal Data			
formula	C ₃₉ H ₆₃ N ₆ O ₃ Al	C ₁₈ H ₃₆ N ₂ OAl ₂	C ₂₁ H ₄₅ N ₂ OAl ₃
M _n	690.97	350.46	422.55
cryst system	monoclinic	orthorhombic	monoclinic
space group	C2/c	Pbca	P2 ₁ /c
a, Å	26.831(2)	12.014(2)	11.5731(17)
b, Å	23.904(3)	15.496(1)	19.893(3)
c, Å	12.9273(16)	24.078(4)	14.5892(13)
β, deg	107.354(9)	90	129.036(11)
V, Å ³	7913.7(16)	4482.6(11)	2608.9(7)
D _{calc} , g cm ⁻³	1.160	1.038	1.076
Z	8	8	4
F(000), e	3008	1536	928
μ, cm ⁻¹	0.9	1.3	1.5
cryst size, mm	0.10 × 0.23 × 0.38	0.12 × 0.30 × 0.60	0.70 × 0.40 × 0.40
Data Collection			
T, K	150	150	150
radiation, λ, Å	Mo Kα, 0.170 73 (graphite monochr)	Mo Kα, 0.710 73 (graphite monochr)	Mo Kα, 0.710 73 (graphite monochr)
Δω, deg	0.60 + 0.35 tan θ	0.99 + 0.35 tan θ	0.54 + 0.35 tan θ
hor, ver aperture, mm	3.00, 4.00	2.60, 4.00	3.00, 4.00
ref reflens	225, 10, 2, 2 622	241, 225, 062	253, 124, 042
data set, hkl	-34:34, 0:31, -16:16	-15:0, -20:13, -31:0	-15:14, -25:0, -18:18
tot. unique data	9073	5127	5947
obsd data	4358 (I > 3σ(I))	2141 (I > 2σ(I))	3638 (I > 2.5σ(I))
Refinement			
no. of refined params	450	218	285
final R ^a	0.064	0.098 [2141 F > 4σ(F)]	0.0542
final wR ₂ ^b		0.256	
final R _w ^c	0.050		0.0449
weighting scheme ^d	[σ ² (F)] ⁻¹	[σ ² (F) + (0.1136P) ²] ⁻¹	[σ ² (F)] ⁻¹
(Δ/σ) _{av} , (Δ/σ) _{max}	0.03, 0.7	0.00, 0.011	0.9877, 0.0152
min and max resid density, e Å ⁻³	-0.47, 0.72	-0.45, 0.50	-0.32, 0.33

$$^a R = \sum |F_o| - |F_c| / \sum |F_o|. \quad ^b wR_2 = [\sum [w(F_o^2 - F_c^2)^2] / \sum [w(F_o^2)^2]]^{1/2}. \quad ^c R_w = [\sum [w(|F_o| - |F_c|)^2] / \sum [w(F_o^2)]]^{1/2}. \quad ^d P = (\max(F_o^2, 0) + 2F_c^2) / 3.$$

stirred solution of AlMe₃ (4.5 mL; 9.0 mmol), the mixture was heated under reflux for 48 h. The usual workup (cf. **1a**), followed by purification of the crude product by recrystallization from toluene, afforded **2c** as a yellow powder in 60–80% yield. Mp: 170 °C (dec).

¹H NMR data (C₆D₆, 200 MHz, 298 K) (δ): 7.42 (s, 2 H, ArH); 7.25 (s, 2 H, ArH); 6.58 (s, 2 H, ArH); 3.65 (br, 2 H, CH₂N); 3.47 (br, 6 H, CH₂N); 2.6–2.0 (m, 49 H, CH₂N, NMe₂, p-Me). ¹³C NMR data (C₆D₆, 50 MHz, 298 K): δ 156.09 (CO); 154.17 (CO); 131.69, 130.27, 125.97, 125.44, 122.61 (Ar); 63.71, 60.35, 59.24 (CH₂N); 45.86, 45.75 (br, NMe₂); 21.10, 20.73 (p-Me). Anal. Calcd for C₃₉H₆₃N₆O₃Al: C, 67.80; H, 9.19; N, 12.16. Found: C, 67.77; H, 9.10; N, 12.11.

AlMe₂{OC₆H₂(CH₂NMe₂)₂-2,6-Me-4}·N-AlMe₃ (**2d**). Addition of HOC₆H₂(CH₂NMe₂)₂-2,6-Me-4 (2.22 g; 10.0 mmol) to a stirred solution of 2 molar equiv of AlMe₃ (10 mL; 20 mmol) at 0 °C resulted in the formation of a white precipitate. After the mixture was stirred for an additional 1 h, the product was centrifuged off and dried *in vacuo*. Recrystallization from warm hexane afforded **2d** as a white crystalline solid in 90% yield. Mp: 125 °C.

¹H NMR data (C₆D₆, 300 MHz, 298 K) (δ): 6.72 (s, 1 H, ArH); 6.43 (s, 1 H, ArH); 4.03 (s, 2 H, CH₂N); 3.01 (s, 2 H, CH₂N); 2.19 (s, 6 H, NMe₂); 2.16 (s, 3 H, p-Me); 1.58 (s, 6 H, NMe₂); -0.31 (s, 9 H, AlMe₃); -0.62 (s, 6 H, AlMe₂). ¹³C NMR data (C₆D₆, 75 MHz, 298 K) (δ): 157.12 (CO); 134.92, 130.62, 125.31 (Ar); 62.24, 54.65 (CH₂N); 44.29, 42.83 (NMe₂); 20.47 (p-Me); -9.18, -11.41 (AlMe). Anal. Calcd for C₁₈H₃₆N₂OAl₂: C, 61.69; H, 10.35; N, 7.99. Found: C, 61.54; H, 10.28; N, 7.85.

AlMe₂{OC₆H₂(CH₂NMe₂)₂-2,6-Me-4}·(N-AlMe₃)(O-AlMe₃) (**2e**). The preparation of **2e** was analogous to that of **2d**. Addition of HOC₆H₂(CH₂NMe₂)₂-2,6-Me-4 (2.22 g; 10.0 mmol) to a stirred solution of 4 equiv of AlMe₃ (20 mL; 40 mmol) at 0 °C resulted in the formation of a white precipitate.

Workup afforded **2e** as a white crystalline solid in 92% yield. Mp: 115 °C.

¹H NMR data (C₆D₆, 200 MHz, 298 K) (δ): 6.93 (s, 1 H, ArH); 6.39 (s, 1 H, ArH); 4.14 (s, 2 H, CH₂N); 3.03 (s, 2 H, CH₂N); 2.23 (s, 6 H, NMe₂); 2.13 (s, 3 H, p-Me); 1.55 (s, 6 H, NMe₂); -0.26 (s, 9 H, AlMe₃); -0.35 (s, 9 H, AlMe₃); -0.59 (s, 6 H, AlMe₂). ¹³C NMR data (C₆D₆, 50 MHz, 298 K) (δ): 153.43 (CO); 135.87, 131.40, 130.45, 123.98 (Ar); 62.16, 55.71 (CH₂N); 46.04, 43.83 (NMe₂); 20.44 (p-Me); -5.21, -8.55, -9.23 (AlMe). Anal. Calcd for C₂₁H₄₅N₂OAl₃: C, 59.69; H, 10.73; N, 6.63. Found: C, 59.55; H, 10.62; N, 6.67.

X-ray Data Collection and Structure Refinement. Colorless crystals of **2c–e** were sampled directly into a viscous oil, glued on top of a glass fiber, and transferred into the cold nitrogen stream on an Enraf-Nonius CAD4T rotating anode diffractometer for data collection. Accurate unit-cell parameters were determined by least squares treatment of 25 well-centered reflections (SET4) in the range 11 < θ < 14°. All data were collected with the ω/2θ scan mode. Crystal data and details on data collection and refinement are collected in Table 1. Data were corrected for Lp effects, for the observed linear decay of the reference reflections, and for absorption (**2e**, DIFABS;¹⁴ correction range 0.798–1.191). The structures were solved using direct methods (**2c**, SIR92;¹⁵ **2d,e**, SHELXS86¹⁶) and subsequent difference Fourier techniques. Refinement was carried out by full-matrix least squares techniques on F (**2c,e**, SHELX76)¹⁷ or on F² (**2d**, SHELXL92).¹⁸

(14) Walker, N.; Stuart, D. *Acta Crystallogr., Sect. A* **1983**, *39*, 158.

(15) Altomare, A.; Casciarano, G.; Giacovazzo, C.; Guagliardi, A. *J. Appl. Crystallogr.* **1993**, *26*, 343.

(16) Sheldrick, G. M. *SHELXS86. Program for crystal structure determination*; University of Göttingen, Göttingen, Federal Republic of Germany, 1986.

Table 2. Final Coordinates and Equivalent Isotropic Thermal Parameters of the Non-Hydrogen Atoms for 2c

atom	x	y	z	$U_{eq},^a \text{Å}^2$
Al	0.26480(5)	0.10502(5)	0.77401(10)	0.0187(3)
O(1)	0.32714(9)	0.13085(10)	0.78296(19)	0.0214(9)
O(2)	0.20576(10)	0.14157(10)	0.7566(2)	0.0199(8)
O(3)	0.26228(11)	0.03367(10)	0.7865(2)	0.0258(9)
N(1)	0.27906(12)	0.11772(12)	0.9397(2)	0.0188(10)
N(2)	0.37826(12)	0.21969(14)	0.6703(3)	0.0253(11)
N(3)	0.25081(12)	0.10608(13)	0.6073(2)	0.0200(10)
N(4)	0.11736(12)	0.16686(13)	0.8817(3)	0.0254(11)
N(5)	0.40620(13)	-0.04883(15)	0.8530(3)	0.0360(12)
N(6) ^b	0.11773(18)	-0.0432(2)	0.7135(4)	0.0409(19)
C(1)	0.37168(15)	0.13955(15)	0.8642(3)	0.0211(12)
C(2)	0.37586(15)	0.12513(16)	0.9715(3)	0.0216(12)
C(3)	0.42227(15)	0.13588(16)	1.0520(3)	0.0252(14)
C(4)	0.46515(16)	0.15960(17)	1.0305(3)	0.0275(14)
C(5)	0.46000(15)	0.17233(17)	0.9221(3)	0.0277(14)
C(6)	0.41418(15)	0.16296(16)	0.8394(3)	0.0237(12)
C(7)	0.51530(15)	0.17258(18)	1.1192(3)	0.0388(17)
C(8)	0.41240(15)	0.17347(16)	0.7224(3)	0.0270(14)
C(9)	0.39600(18)	0.27207(17)	0.7262(3)	0.0431(17)
C(10)	0.37809(16)	0.22355(18)	0.5576(3)	0.0344(16)
C(11)	0.33157(14)	0.09550(16)	0.9987(3)	0.0229(12)
C(12)	0.23963(14)	0.08893(16)	0.9802(3)	0.0253(14)
C(13)	0.27764(16)	0.17842(15)	0.9657(3)	0.0574(17)
C(14)	0.16065(15)	0.14410(16)	0.6753(3)	0.0204(12)
C(15)	0.15411(15)	0.11762(16)	0.5754(3)	0.0225(12)
C(16)	0.10652(15)	0.12128(17)	0.4954(3)	0.0276(16)
C(17)	0.06456(15)	0.15015(18)	0.5094(3)	0.0289(14)
C(18)	0.07193(15)	0.17725(17)	0.6081(3)	0.0278(16)
C(19)	0.11895(15)	0.17464(16)	0.6911(3)	0.0216(12)
C(20)	0.01318(15)	0.1542(2)	0.4212(3)	0.0456(19)
C(21)	0.19721(14)	0.08314(16)	0.5540(3)	0.0233(12)
C(22)	0.28808(15)	0.06957(17)	0.5732(3)	0.0290(14)
C(23)	0.25444(15)	0.16374(15)	0.5680(3)	0.0249(14)
C(24)	0.12455(15)	0.20410(16)	0.7973(3)	0.0250(12)
C(25)	0.13006(17)	0.19588(17)	0.9858(3)	0.0363(17)
C(26)	0.06367(15)	0.14712(18)	0.8527(3)	0.0397(17)
C(27)	0.26263(16)	-0.02211(15)	0.7798(3)	0.0206(11)
C(28)	0.21558(15)	-0.05146(17)	0.7690(3)	0.0227(14)
C(29)	0.21592(16)	-0.10918(17)	0.7655(3)	0.0270(16)
C(30)	0.26113(18)	-0.13938(15)	0.7726(3)	0.0263(14)
C(31)	0.30689(16)	-0.10975(17)	0.7837(3)	0.0253(14)
C(32)	0.30845(15)	-0.05169(16)	0.7864(3)	0.0205(14)
C(33)	0.26034(18)	-0.20283(15)	0.7695(3)	0.0401(16)
C(34)	0.35825(14)	-0.02031(16)	0.7940(3)	0.0271(12)
C(35)	0.41109(17)	-0.0519(2)	0.9682(3)	0.0501(19)
C(36)	0.45137(17)	-0.0192(2)	0.8376(4)	0.054(2)
C(37)	0.16719(14)	-0.01929(19)	0.7690(3)	0.0357(16)
C(38)	0.11145(18)	-0.0440(2)	0.5939(4)	0.056(2)
C(39) ^b	0.0758(2)	-0.0096(3)	0.7330(5)	0.067(3)

^a $U_{eq} = 1/3$ of the trace of the orthogonalized U. ^b Major disorder form (77%).

Hydrogen atoms were introduced on calculated positions (C-H = 0.98 Å) and included in the refinement riding on their carrier atoms. All non-hydrogen atoms were refined with anisotropic thermal parameters. The structure determination for **2c** showed some disorder in the positions of N(6) and C(39), which was modeled and refined using fractional site occupation factors and anisotropic thermal parameters for the major positions only. The hydrogen atoms of **2d** were refined with a fixed isotropic thermal parameter related to the value of the equiv isotropic thermal parameter of their carrier atoms by a factor of 1.5 for the methyl hydrogen atoms and by a factor of 1.2 for the other hydrogen atoms. Weights were introduced in the last refinement cycles. Positional parameters are listed in Tables 2–4 for **2c–e**, respectively. Neutral atom scattering factors were taken from Cromer and Mann¹⁹ and corrected for anomalous dispersion²⁰ for **2c,e**. Neutral atom scattering factors and anomalous dispersion corrections were taken from

(17) Sheldrick, G. M. *SHELXL76. Crystal structure analysis package*; University of Cambridge: Cambridge, England, 1976.

(18) Sheldrick, G. M. *SHELXL-93. Program for crystal structure refinement*; University of Göttingen: Göttingen, Germany, 1993.

Table 3. Final Coordinates and Equivalent Isotropic Thermal Parameters of the Non-Hydrogen Atoms for 2d

atom	x	y	z	$U_{eq},^a \text{Å}^2$
Al(1)	0.35656(12)	0.18802(10)	0.28920(6)	0.0281(5)
Al(2)	0.38159(14)	0.37959(11)	0.05168(6)	0.0334(5)
O(1)	0.3946(3)	0.1866(2)	0.21905(13)	0.0317(12)
N(1)	0.3098(3)	0.0645(3)	0.2911(2)	0.0267(12)
N(2)	0.3573(3)	0.2560(3)	0.0787(2)	0.0280(12)
C(11)	0.4257(4)	0.1207(3)	0.1863(2)	0.0250(14)
C(12)	0.4268(4)	0.0352(3)	0.2063(2)	0.0237(14)
C(13)	0.4625(4)	-0.0304(3)	0.1710(2)	0.0293(17)
C(14)	0.4994(5)	-0.0147(3)	0.1181(2)	0.0357(17)
C(15)	0.4970(4)	0.0697(3)	0.0994(2)	0.0283(17)
C(16)	0.4590(4)	0.1373(3)	0.1320(2)	0.0263(17)
C(17)	0.5424(5)	-0.0863(3)	0.0809(2)	0.0390(17)
C(18)	0.4013(4)	0.0128(3)	0.2662(2)	0.0283(16)
C(19)	0.2949(5)	0.0342(4)	0.3495(2)	0.0397(19)
C(21)	0.4842(5)	0.1971(4)	0.3393(2)	0.0447(19)
C(22)	0.2293(5)	0.2626(4)	0.3023(3)	0.053(2)
C(31)	0.3757(6)	0.4489(4)	0.1199(2)	0.055(3)
C(32)	0.2553(6)	0.4009(4)	0.0016(2)	0.058(3)
C(33)	0.5275(5)	0.3738(4)	0.0142(3)	0.063(3)
C(110)	0.2058(4)	0.0496(4)	0.2604(3)	0.045(2)
C(111)	0.4604(4)	0.2277(3)	0.1099(2)	0.0280(17)
C(112)	0.2576(4)	0.2516(4)	0.1151(2)	0.045(2)
C(113)	0.3379(5)	0.1998(4)	0.0294(2)	0.0427(17)

^a $U_{eq} = 1/3$ of the trace of the orthogonalized U.

Table 4. Final Coordinates and Equivalent Isotropic Thermal Parameters of the Non-Hydrogen Atoms for 2e

atom	x	y	z	$U_{eq},^a \text{Å}^2$
Al(1)	1.19453(10)	0.17654(4)	0.86513(8)	0.0185(3)
Al(2)	0.91802(10)	0.11896(4)	0.59235(8)	0.0197(3)
Al(3)	0.64736(11)	0.03741(5)	0.79631(8)	0.0218(3)
O(1)	0.9936(2)	0.17126(9)	0.73656(16)	0.0156(6)
N(1)	1.2261(3)	0.27074(12)	0.8328(2)	0.0202(8)
N(2)	0.7487(3)	0.12893(12)	0.8258(2)	0.0192(8)
C(1)	0.9099(3)	0.22667(14)	0.7250(2)	0.0159(8)
C(2)	0.7836(3)	0.21824(14)	0.7168(2)	0.0160(9)
C(3)	0.7055(3)	0.27665(14)	0.7014(3)	0.0194(9)
C(4)	0.7498(3)	0.34070(14)	0.6983(3)	0.0184(9)
C(5)	0.8761(3)	0.34660(14)	0.7069(3)	0.0192(9)
C(6)	0.9543(3)	0.28997(14)	0.7180(2)	0.0168(9)
C(7)	0.6667(4)	0.40242(14)	0.6892(3)	0.0262(11)
C(8)	1.0854(3)	0.29597(14)	0.7192(3)	0.0191(9)
C(9)	1.2705(4)	0.31950(16)	0.9286(3)	0.0317(11)
C(10)	1.3458(3)	0.27158(17)	0.8211(3)	0.0336(11)
C(11)	0.7248(3)	0.15046(14)	0.7163(3)	0.0182(9)
C(12)	0.6851(4)	0.17797(15)	0.8603(3)	0.0371(13)
C(13)	0.9100(3)	0.12278(18)	0.9248(3)	0.0360(11)
C(14)	1.3127(3)	0.11399(16)	0.8528(3)	0.0278(11)
C(15)	1.2396(3)	0.18179(17)	1.0185(3)	0.0263(10)
C(16)	1.0199(3)	0.15469(16)	0.5329(3)	0.0266(10)
C(17)	0.9708(4)	0.02664(15)	0.6524(3)	0.0339(11)
C(18)	0.7034(3)	0.14050(16)	0.4787(3)	0.0289(11)
C(19)	0.4378(4)	0.05351(18)	0.6592(3)	0.0407(12)
C(20)	0.6890(4)	0.01895(16)	0.9476(3)	0.0338(11)
C(21)	0.7498(5)	-0.02523(16)	0.7637(4)	0.0444(16)

^a $U_{eq} = 1/3$ of the trace of the orthogonalized U.

ref 21 for **2d**. All calculations were carried out on a DECstation 5000 cluster. Geometrical calculations (including the ORTEP plots) were done with PLATON.²²

Results and Discussion

Syntheses. By reaction of trimethylaluminum with 1, 2, or 3 equiv of $\text{HOC}_6\text{H}_4(\text{CH}_2\text{NMe}_2)_2$ (**3**), all three

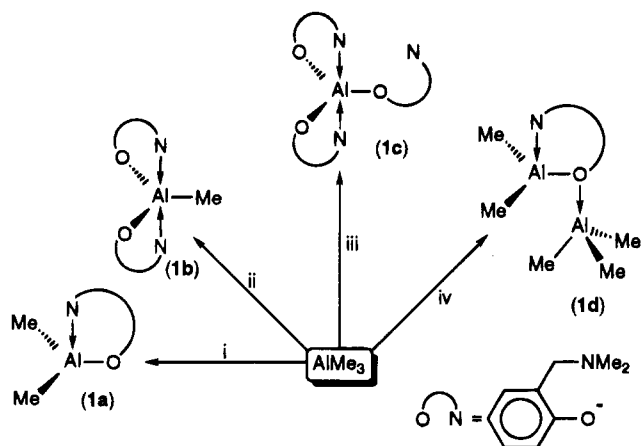
(19) Cromer, D. T.; Mann, J. B. *Acta Crystallogr., Sect. A* **1968**, *24*, 321.

(20) Cromer, D. T.; Liberman, D. *J. Chem. Phys.* **1970**, *53*, 1891.

(21) Wilson, A. J. C., Ed. *International Tables for Crystallography*; Kluwer Academic Publishers: Dordrecht, The Netherlands, 1992; Vol. C.

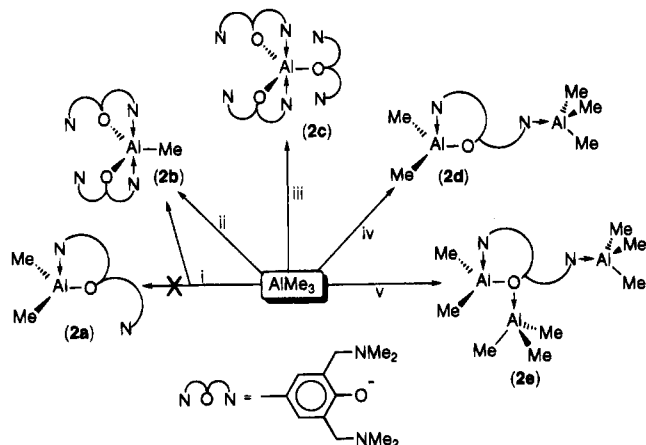
(22) Spek, A. L. *Acta Crystallogr., Sect. A* **1990**, *46*, C34.

Scheme 1. Synthesis and Schematic Structures of the Aluminum Complexes of the Mono-*ortho*-Substituted Phenolate 3^a



^a Key: (i) 1 equiv of $\text{HOC}_6\text{H}_4(\text{CH}_2\text{NMe}_2)_2$, hexane, 0 °C; (ii) 2 equiv of $\text{HOC}_6\text{H}_4(\text{CH}_2\text{NMe}_2)_2$, hexane, 0 °C; (iii) 3 equiv of $\text{HOC}_6\text{H}_4(\text{CH}_2\text{NMe}_2)_2$, hexane, RT; (iv) 0.5 equiv of $\text{HOC}_6\text{H}_4(\text{CH}_2\text{NMe}_2)_2$, hexane, 0 °C.

Scheme 2. Synthesis and Schematic Structures of the Aluminum Complexes of the Bis-*ortho*-Substituted Phenolate 4^a



^a Key: (i) 1 equiv of $\text{HOC}_6\text{H}_2(\text{CH}_2\text{NMe}_2)_2$ -2,6-Me-4, hexane, 0 °C; (ii) 2 equiv of $\text{HOC}_6\text{H}_2(\text{CH}_2\text{NMe}_2)_2$ -2,6-Me-4, hexane, 0 °C; (iii) 3 equiv of $\text{HOC}_6\text{H}_2(\text{CH}_2\text{NMe}_2)_2$ -2,6-Me-4, hexane, reflux; (iv) 0.5 equiv of $\text{HOC}_6\text{H}_2(\text{CH}_2\text{NMe}_2)_2$ -2,6-Me-4, hexane, 0 °C; (v) 0.33 equiv of $\text{HOC}_6\text{H}_2(\text{CH}_2\text{NMe}_2)_2$ -2,6-Me-4, hexane, 0 °C.

substitution products were prepared in high yield (see Scheme 1).

In the case of $\text{HOC}_6\text{H}_2(\text{CH}_2\text{NMe}_2)_2$ -2,6-Me-4 (**4**), only the trisubstituted product could be obtained pure and in high yield (see Scheme 2). The disubstituted product was also obtained, but due to its high solubility in both polar and apolar solvents and the fact that it was usually obtained as an oil, we were unable to purify it. The monosubstituted product appeared not to be stable: from the 1:1 reaction of AlMe_3 and **4**, $\text{AlMe}(\text{OAr})_2$ and free AlMe_3 were obtained in a 1:1 ratio (*vide infra* and Scheme 2).

However, when an excess of AlMe_3 was used, the monosubstituted product could be obtained as a Lewis acid–base complex with one or two additional molecules of AlMe_3 (see Scheme 2). Similarly, reaction of phenol **3** with an excess of trimethylaluminum afforded a Lewis acid base complex of the mono(phenolate) complex with an additional molecule AlMe_3 (see Scheme 1).

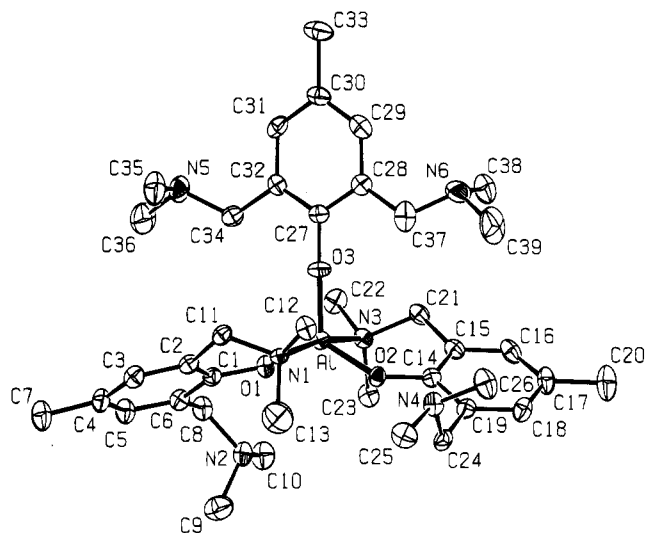


Figure 2. ORTEP representation of $\text{Al}\{\text{OC}_6\text{H}_2(\text{CH}_2\text{NMe}_2)_2$ -2,6-Me-4 $\}_3$ (**2c**) with the adopted numbering scheme. Hydrogen atoms have been omitted for clarity.

Table 5. Selected Bond Distances (Å) and Angles (deg) for Complex 2c

Distances			
Al–O(1)	1.754(3)	Al–N(3)	2.074(3)
Al–O(2)	1.764(3)	O(1)–C(1)	1.351(5)
Al–O(3)	1.716(3)	O(2)–C(14)	1.347(5)
Al–N(1)	2.083(3)	O(3)–C(27)	1.336(4)
Angles			
O(1)–Al–O(2)	129.53(13)	O(1)–Al–N(1)	90.10(13)
O(1)–Al–O(3)	114.02(15)	O(1)–Al–N(3)	86.43(13)
O(2)–Al–O(3)	116.43(15)	O(2)–Al–N(1)	86.65(13)
Al–O(1)–C(1)	135.3(2)	O(2)–Al–N(3)	89.09(13)
Al–O(2)–C(14)	133.3(2)	O(3)–Al–N(1)	92.77(13)
Al–O(3)–C(27)	169.8(3)	O(3)–Al–N(3)	96.31(13)
N(1)–Al–N(3)	170.91(13)		

Crystallographic and Spectroscopic Characterization. Selected X-ray structure determinations were carried out for a number of key compounds, which, in combination with spectroscopic data, provided insight into the structural features of these complexes, both in solution and in the solid state. Because of the obvious role that the second *ortho*- CH_2NMe_2 substituent plays in both the instability of the $\text{AlMe}_2(\text{OR})$ and the tendency to capture up to two additional AlMe_3 molecules by this complex, we concentrated on obtaining X-ray structures of the aluminum phenolate complexes of **4**.

Tris(phenolato)aluminum Complexes. The structure in the solid state of $\text{Al}\{\text{OC}_6\text{H}_2(\text{CH}_2\text{NMe}_2)_2$ -2,6-Me-4 $\}_3$ (**2c**) is shown in Figure 2; selected bond distances and angles are given in Table 5. The structure determination reveals the aluminum atom to be surrounded by three phenolate ligands, bonded through oxygen. Two phenolate ligands each have one amino substituent coordinated to the aluminum, while the second one is pendant. In contrast, both amino substituents of the third phenolate ligand are pendant. Accordingly, two of the binding modes shown in Figure 1, *i.e.* *O,N*-bidentate (**c**) and *O*-monodentate (**d**), are present. The geometry around aluminum is slightly distorted trigonal bipyramidal (28% on the Berry pseudorotation path between D_{3h} and C_{4v}), with the three oxygen atoms forming the trigonal plane (the Al is situated 0.007(18) Å out of this plane, $\Sigma(\text{O}–\text{Al}–\text{O}) = 359.98(15)^\circ$); the two coordinating amino substituents occupy the apical posi-

tions ($\angle \text{N}(1)\text{-Al-N}(3)$ is $170.91(13)^\circ$). This geometry around aluminum is general for five-coordinate aluminum complexes containing three normal and two dative bonds.²³ The Al-N distances of the *O,N*-bidentate bonded phenolate ligands are almost equal at 2.083(3) and 2.074(3) Å and lie in the range usually found for amino ligands bound to aluminum (1.957(3)-2.238(4) Å).^{8,24-26} The O-Al-O angle involving the oxygen atoms of the two *O,N*-bidentate ligands is larger at $129.53(13)^\circ$ than the O-Al-O angles involving the oxygen atoms of each of the *O,N*-bidentate ligands and the *O*-monodentate ligand, which are $114.02(15)$ and $116.43(13)^\circ$. This opening of the O-Al-O bond between the two bidentate ligands is probably caused by steric interference between a methyl group of a coordinated amino substituent and the pendant amino substituent on the other bidentate ligand. When this second, pendant substituent is absent, as in the trigonal bipyramidal complex $\text{AlMe}[\text{O}=\text{C}(\text{OMe})\text{C}_6\text{H}_4\text{-}o\text{-O}]_2$ (**5**),²⁷ bond angles in the trigonal plane are close to 120° ($118.28(10)$ - $120.86(7)^\circ$).

The Al-O bond lengths (1.716(3)-1.764(3) Å) are in the range normally found for aluminum phenolates (1.640(5)-1.773(2) Å).⁵⁻⁸ The Al-O bond lengths with the two bidentate, *O,N*-coordinated ligands are in the upper part of this range (1.754(3) and 1.764(3) Å). This is the result of (a) the presence of two coordinating amino substituents, which reduces the Lewis acidity of the metal center, and (b) the formation of the six-membered chelate ring, which pulls the ligand over, leading to relatively small Al-O-C bond angles ($135.3(2)$ and $133.3(2)^\circ$), and reduces the s character in the Al-O bond. Both effects are also present in **5**,²⁷ leading to an Al-O bond length of 1.773(2) Å. As expected, with both amino substituents pendant, the Al-O(3) bond length for the monodentate *O*-bonded ligand is somewhat shorter at 1.716(3) Å and the Al-O(3)-C(27) bond angle is nearly linear ($169.8(3)^\circ$). This near linear Al-O-C bond angle is most probably a result of steric interference caused by the two pendant amino substituents.

As a result of fluxional processes, the room-temperature ^1H NMR spectra of the complexes **2b,c**, containing the bis-*ortho*-chelating phenolate ligand, show relatively broad signals that are difficult to interpret. However, the room-temperature ^{13}C NMR spectrum of the tris(phenolate) $\text{Al}\{\text{OC}_6\text{H}_2(\text{CH}_2\text{NMe}_2)_2\text{-}2,6\text{-Me-}4\}_3$ (**2c**) contains two signals for both the *ipso*-carbon and the *para*-methyl substituent, both in a 2:1 ratio, which shows that two of the three phenolate ligands are identical. The presence in the ^1H NMR spectrum of three separate signals for the benzylic carbon atoms in a 1:1:1 ratio, as well as three separate signals for the aromatic protons, which all integrate for two protons, indicates that there are two ligands with one amino substituent coordinating to the metal center and a pendant one, as well as one ligand of which both substituents are pendant. These observations suggest that the structure found in the solid state for **2c** is retained in solution. In

addition, the presence of three separate signals for the aromatic protons at room temperature indicates that rotation of the ligands around the Al-O bond is slow on the NMR time scale at that temperature, which is probably due to a strong Al-N interaction. The analogous complex $\text{Al}\{\text{OC}_6\text{H}_4(\text{CH}_2\text{NMe}_2)_2\}_3$ (**1c**), which contains the mono-*ortho*-chelating phenolate ligand **3**, shows very similar spectroscopic data. The ^1H NMR spectrum of **1c** at room temperature shows three signals for the dimethylamino protons of the phenolate ligand. The signals for the benzylic protons consist of one sharp AB pattern, integrating for 2 protons, and one broad AB pattern, integrating for 4 protons. Assuming a trigonal bipyramidal geometry around aluminum (see Scheme 1 and Figure 2), the sharp AB pattern can be assigned to the benzylic protons of the pendant amino substituent and the broad AB pattern to the benzylic protons of the coordinated amino substituents. This view is supported by the ^{13}C NMR spectrum, which shows two signals for the benzylic carbon atoms in a 2:1 ratio, with the most intense at lower field, indicating two coordinated and one pendant amino substituent. This implies that exchange between coordinated and pendant amino substituents is slow on the NMR time scale at room temperature. Heating a toluene-*d*₈ solution of **1c** to 370 K causes coalescence of the benzylic proton signals, which indicates that this process only exists at elevated temperatures. This process most probably involves Al-N bond dissociation/association equilibria.

Bis(phenolato)aluminum Methyl Complexes. The ^{13}C NMR spectrum of the bis(phenolate) $\text{AlMe}\{\text{OC}_6\text{H}_2(\text{CH}_2\text{NMe}_2)_2\text{-}2,6\text{-Me-}4\}_2$ (**2b**) at room temperature shows one signal for the aromatic carbon attached to the oxygen, indicating both phenolate ligands to be identical. The presence of two separate signals for the benzylic carbon atoms shows that one amino substituent of each ligand is coordinated to the aluminum, while the other is not.

For the related bis(phenolate) $\text{AlMe}\{\text{OC}_6\text{H}_4(\text{CH}_2\text{NMe}_2)_2\}_2$ (**1b**) the ^1H NMR spectrum at 300 K shows two doublets (AB pattern) for the benzylic protons and a broad signal for the methyl protons. Slight cooling of a toluene-*d*₈ solution of **1b** to 295 K leads to splitting of the signal for the methyl protons into two separate signals ($\Delta G^\ddagger = 14.6$ kcal/mol), while raising the temperature to 370 K only leads to sharpening of the signal for the methyl protons. This indicates that on the NMR time scale a fast Al-N dissociation/association process, in combination with inversion of configuration on nitrogen, takes place. The AB pattern for the benzylic protons remains even at 370 K, which suggests a trigonal bipyramidal geometry around aluminum, with the two nitrogen donors in the apical positions and a *C*₂-axis through the methyl to aluminum bond, as is general for this coordination geometry around aluminum.²³ In this description the two phenolate ligands are equiv, but the benzylic hydrogen atoms diastereotopic (see Scheme 1). For the AB pattern to coalesce, a fast interchange of the positions of the two amino substituents would have to take place. This implies simultaneous dissociation of the Al-N dative bonds and the existence of a three-coordinate intermediate, which is very unlikely. The proposed trigonal bipyramidal geometry is similar to that of the complexes **2c** and **1c**,

(23) Haaland, A. In *Coordination Chemistry of Aluminum*; Robinson, G. H., Ed.; VCH: New York, 1993; pp 1-51.

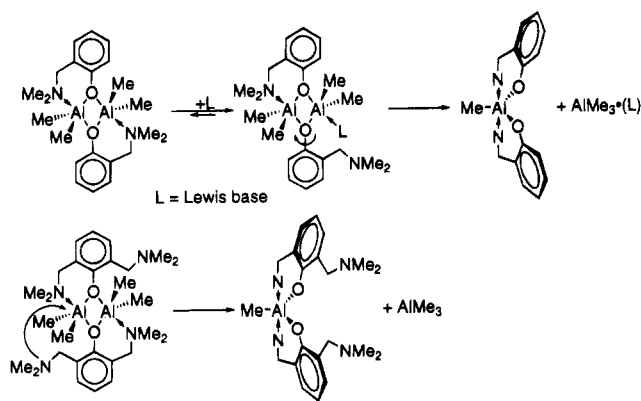
(24) Hill, J. B.; Eng, S. J.; Pennington, W. T.; Robinson, G. H. *J. Organomet. Chem.* **1993**, *445*, 11.

(25) Müller, G.; Krüger, C. *Acta Crystallogr., Sect. C* **1984**, *40*, 628.

(26) Kumar, R.; Sierra, M. L.; Oliver, J. P. *Organometallics* **1994**, *13*, 4285.

(27) Lewiński, J.; Zachara, J.; Mańk, B.; Pasykiewicz, S. *J. Organomet. Chem.* **1993**, *454*, 5.

Scheme 3. Proposed Mechanism for the Lewis Base induced Ligand Exchange



the monodentate phenolate ligand being replaced by a methyl substituent.

Mono(phenolato)dimethylaluminum Complexes. The ^1H NMR of the mono(phenolato) $\text{AlMe}_2\{\text{OC}_6\text{H}_4(\text{CH}_2\text{NMe}_2)_2\}$ (**1a**) shows singlets for both the benzylic and methyl protons of the ligand, as well as for the methyl groups on aluminum. This indicates either a monomeric structure, with a four-coordinate aluminum (cf. ref 3), or a dimeric structure with bridging phenolate ligands (cf. ref 1a). In view of the stabilization of monomeric mono(phenolato)aluminum bis(alkyl) complexes by coordination of a Lewis base,^{7,8} we assume that **1a** is monomeric.

Attempts to isolate the mono(phenolato) $\text{AlMe}_2\{\text{OC}_6\text{H}_2(\text{CH}_2\text{NMe}_2)_2, 2,6\text{-Me-4}\}$ (**2a**) led to disproportionation into the bis(phenolato) **2b** and AlMe_3 . This ligand exchange may be the result of a Lewis base induced ligand exchange involving the pendant dimethylamino group present.⁷ This view is supported by the observation that mono(phenolato) **1a**, which does not contain a pendant dimethylamino group, also disproportionates to give the bis(phenolato) and free AlMe_3 upon addition of a Lewis base like THF. In addition, the disproportionation of **2a** is blocked by the presence of a second equiv of AlMe_3 , and the AlMe_3 -adduct $\text{AlMe}_2\{\text{OC}_6\text{H}_2(\text{CH}_2\text{NMe}_2)_2, 2,6\text{-Me-4}\}\cdot\text{N-AlMe}_3$ (**2d**) is formed. For this exchange of ligands between two aluminum centers to take place, a transition state has to be formed in which the phenolate ligands bridge between the two aluminum centers (see Scheme 3). The proposed structure for this transition state comprises the geometry found earlier for $[\text{tBu}_2\text{AlOCH}_2\text{-2-C}_5\text{H}_4\text{N}]_2$,²⁸ i.e. the anionic C- and O-ligand forming the trigonal plane, with the neutral N-donor of the first and the anionic oxygen of the second phenolate ligand occupying the apical positions in a distorted trigonal bipyramidal geometry around each aluminum (see Scheme 3). We propose that the role of the Lewis base in the exchange reaction of **1a** is to make it possible for an amino substituent to dissociate from one aluminum center and, after rotation about the C–O bond of the ligand, make a nucleophilic attack on the other aluminum center, causing a methyl shift and expelling $\text{Al}(\text{Me})_3(\text{L})$ from the newly formed bis(phenolato). In the case of complex **2a** no rotation of the ligand is necessary, because the pendant amino substituent can make a nucleophilic attack on one aluminum center, while the

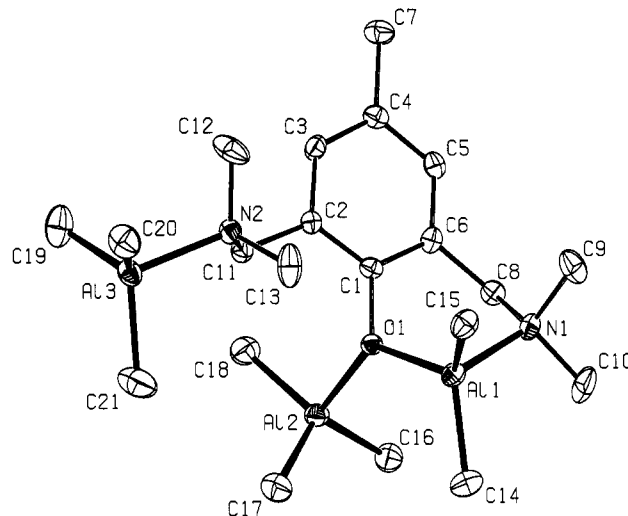


Figure 3. ORTEP representation of $\text{AlMe}_2\{\text{OC}_6\text{H}_2(\text{CH}_2\text{NMe}_2)_2, 2,6\text{-Me-4}\}\cdot\text{N-AlMe}_3$ (**2d**) with the adopted numbering scheme. Hydrogen atoms have been omitted for clarity.

Table 6. Selected Bond Distances (Å) and Angles (deg) for Complex 2d

Distances			
Al(1)–O(1)	1.750(3)	Al(2)–N(2)	2.044(5)
Al(1)–N(1)	1.995(5)	Al(2)–C(31)	1.964(6)
Al(1)–C(21)	1.956(6)	Al(2)–C(32)	1.966(7)
Al(1)–C(22)	1.942(6)	Al(2)–C(33)	1.974(7)
O(1)–C(11)	1.343(6)		
Angles			
O(1)–Al(1)–N(1)	94.80(18)	N(2)–Al(2)–C(31)	104.0(2)
O(1)–Al(1)–C(21)	113.0(2)	N(2)–Al(2)–C(32)	104.0(2)
O(1)–Al(1)–C(22)	111.7(3)	N(2)–Al(2)–C(33)	103.3(2)
N(1)–Al(1)–C(21)	106.0(2)	C(31)–Al(2)–C(32)	113.2(3)
N(1)–Al(1)–C(22)	110.2(2)	C(31)–Al(2)–C(33)	116.1(3)
C(21)–Al(1)–C(22)	118.3(3)	C(32)–Al(2)–C(33)	114.4(3)
Al(1)–O(1)–C(11)	130.5(3)		

other amino substituent dissociates from the other, making the methyl transfer possible (see also Scheme 3). It is interesting to note that in this case the AlMe_3 formed during the ligand exchange does not form a Lewis acid–base complex with one of the two pendant amino substituents in **2b**, as is the case in both **2d** and **2e**. This may be due to steric interference.

Trimethylaluminum Adducts of the Mono(phenolato)dimethylaluminum Complexes. The X-ray structure of $\text{AlMe}_2\{\text{OC}_6\text{H}_2(\text{CH}_2\text{NMe}_2)_2, 2,6\text{-Me-4}\}\cdot\text{N-AlMe}_3$ (**2d**) is shown in Figure 3, and a selection of bond distances and angles are collected in Table 6. The structure contains an AlMe_2 moiety and a molecule AlMe_3 , both bonded to the ligand. The AlMe_2 moiety is bonded to the phenolate oxygen, with one of the dimethylamino groups coordinating to the metal center, leading to a distorted tetrahedral geometry around Al(1). The molecule AlMe_3 forms a Lewis acid–base complex with the second, pendant amino substituent, which also results in a distorted tetrahedral geometry around Al(2). Such distorted geometries, with the most acute angles associated with the coordinating Lewis base (N(1) for Al(1) and N(2) for Al(2)), have been observed previously.^{7,8} In addition, the geometry around each aluminum atom is very similar to that found for other four-coordinate aluminum phenolates, as is shown by the sum of the angles around Al (excluding those connected with the coordinating Lewis base), which amounts to $343.0(3)^\circ$ for Al(1) and to $343.7(9)^\circ$ for Al(2) (literature range: $343.7(6)–346.6(7)^\circ$).⁷ It is interesting

(28) van Vliet, M. R. P.; van Koten, G.; de Keijser, M. S.; Vrieze, K. *Organometallics* **1987**, *6*, 1652.

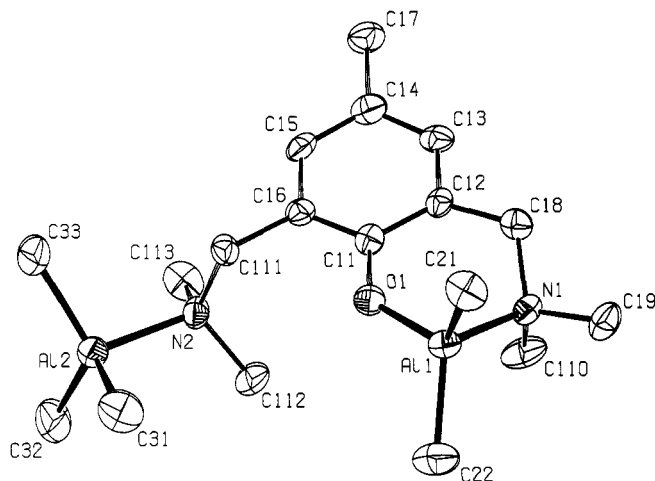


Figure 4. ORTEP representation of $\text{AlMe}_2\{\text{OC}_6\text{H}_2(\text{CH}_2\text{NMe}_2)_2\text{-}2,6\text{-Me-}4\}\text{-N-AlMe}_3\text{-O-AlMe}_3$ (**2e**) with the adopted numbering scheme. Hydrogen atoms have been omitted for clarity.

to note that the presence of an intramolecularly coordinating substituent leads to this, generally observed, geometry for four-coordinate aluminum complexes, which illustrates the flexibility of the ligand system. Apparently the coordination geometry is determined by the metal center and not by the rigidity or the spatial arrangement of the O- and two N-donor atom sites of ligand **4**. The Al–O bond length (1.750(3) Å) and the Al–O–C bond angle (130.5(3)°) are comparable to those of $\text{Me}_2\text{Al}(2S,3R)\text{-}(+)\text{-}4\text{-}(\text{dimethylamino})\text{-}1,2\text{-diphenyl-}3\text{-methyl-}2\text{-butanoxide}$ (**6**) (1.726(3) Å and 132.7(3)°, respectively),²⁶ which also contains a six-membered chelate ring. However, the combination of the Al–O bond length and Al–O–C bond angle in **2d** does not fit the trend observed for other four-coordinate aluminum phenolates $\text{AlR}_2(\text{BHT})(\text{L})$ (R = alkyl; BHT = $\text{OC}_6\text{H}_3\text{-Bu-}2,6$; L = Lewis base).⁸ In these complexes the relatively short Al–O bond lengths, also observed in **2d**, are connected to larger Al–O–C angles, which is described as resulting from π -donation from the oxygen p orbitals to the Al–C and Al–Y σ^* orbitals.^{6,8,26,29} The Al–C bond lengths in **2d** are in the range observed previously (1.90–2.01 Å)^{5–7,24} but slightly longer around Al(2) (1.964(6)–1.974(7) Å) than around Al(1) (1.942(6) and 1.956(6) Å), as may be expected from the different Lewis acidities of aluminum in ArOAlMe_2 vs AlMe_3 . The same is true for the Al–N dative bond, which is also slightly longer for Al(2) (2.044(5) Å) as compared to Al(1) (1.995(5) Å). These bond lengths are also in the normal range of 1.957(3)–2.238(4) Å.^{6,7,24–26}

The solid state structure of $\text{AlMe}_2\{\text{OC}_6\text{H}_2(\text{CH}_2\text{NMe}_2)_2\text{-}2,6\text{-Me-}4\}\text{-N-AlMe}_3\text{-O-AlMe}_3$ (**2e**) is shown in Figure 4, with selected bond distances and angles collected in Table 7. The structure of this complex is similar to that of **2d**, with an additional molecule of AlMe_3 forming a Lewis acid–base complex with one of the lone pairs on the phenolate oxygen atom. This leads to an almost perfectly trigonal planar surrounded oxygen atom O(1), with the sum of the angles amounting to 354.6(2)° (O(1) is 0.232(2) Å out of the plane defined by Al(1), Al(2),

Table 7. Selected Bond Distances (Å) and Angles (deg) for Complex **2e**

Distances			
Al(1)–O(1)	1.855(2)	Al(2)–C(18)	1.979(4)
Al(1)–N(1)	2.021(3)	Al(3)–N(2)	2.059(3)
Al(1)–C(14)	1.939(4)	Al(3)–C(19)	1.968(4)
Al(1)–C(15)	1.954(4)	Al(3)–C(20)	1.975(4)
Al(2)–O(1)	1.989(2)	Al(3)–C(21)	1.974(6)
Al(2)–C(16)	1.984(4)	O(1)–C(1)	1.406(4)
Al(2)–C(17)	1.959(3)		
Angles			
O(1)–Al(1)–N(1)	96.44(11)	C(17)–Al(2)–C(18)	116.81(18)
O(1)–Al(1)–C(14)	112.21(13)	N(2)–Al(3)–C(19)	104.10(14)
O(1)–Al(1)–C(15)	114.92(16)	N(2)–Al(3)–C(20)	103.00(13)
N(1)–Al(1)–C(14)	109.36(17)	N(2)–Al(3)–C(21)	105.01(19)
N(1)–Al(1)–C(15)	105.10(13)	C(19)–Al(3)–C(20)	116.3(2)
C(14)–Al(1)–C(15)	116.44(16)	C(19)–Al(3)–C(21)	113.61(19)
O(1)–Al(2)–C(16)	106.77(13)	C(20)–Al(3)–C(21)	113.03(18)
O(1)–Al(2)–C(17)	102.23(12)	Al(1)–O(1)–C(1)	114.02(16)
O(1)–Al(2)–C(18)	104.88(14)	Al(2)–O(1)–C(1)	118.20(15)
C(16)–Al(2)–C(17)	115.3(2)	Al(1)–O(1)–Al(2)	122.36(14)
C(16)–Al(2)–C(18)	109.52(16)		

and C(1)). Compared to the geometry around this oxygen in **2d**, this can be seen as a rehybridization from sp^3 to sp^2 , caused by the formation of a Lewis acid–base complex of one of the lone pairs with the AlMe_3 molecule. In accordance with this description, the most acute angles in the distorted tetrahedral geometry around Al(2) are those associated with O(1). The resulting geometry around O(1) is very similar to that found in $\text{Me}_2\text{Al}(\text{t-Bu})\text{N}=\text{CHC}(\text{Me})_2\text{OAlMe}_3$ (**7**),³⁰ which also contains a bidentate monoanionic N,O-ligand with an additional molecule AlMe_3 coordinated to the oxygen.

The similarity of the coordination geometries of the four-coordinated aluminum atoms in **2e** is shown by the sum of the angles around Al, excluding those connected with the coordinating Lewis base, which amount to 343.6(2)° for Al(1), 341.6(2)° for Al(2), and 342.9(2)° for Al(3). Both the lengthening of the Al(1)–O bond to 1.855(2) Å and the more acute Al(1)–O–C(1) bond angle of 114.02(16)°, as compared to **2d** (1.750(3) Å and 130.5(3)°, respectively), are to be expected by the coordination of AlMe_3 to the phenolate oxygen and the resulting rehybridization.

In conclusion, the structures found in the solid state for the trimethylaluminum adducts **2d,e** are retained in solution, as observed by NMR spectroscopy. The ¹H NMR of the mono(trimethylaluminum) adduct **2d** shows two separate singlets for both the benzylic and NMe_2 protons, as well as for the methyl groups on aluminum, which integrate for nine (–0.31 ppm) and six (–0.62 ppm) protons, respectively. The AlMe_3 moiety in this complex may form a Lewis acid–base complex with either the amino function or a lone pair on the oxygen in the mono(phenolate). However, on account of the basicity of the amino function and the above mentioned inhibition of the (intramolecular) Lewis base induced ligand exchange, it is to be expected that the AlMe_3 moiety is attached to the second amino substituent and not to the phenolate oxygen, *i.e.* as found in the crystal structure of **2d** (see Figure 3). The two separate peaks for the AlMe_3 and AlMe_2 moieties remain present even at 80 °C in benzene, so no exchange of methyl groups takes place on the NMR time scale between the two

(29) (a) Barron, A. R.; Dobbs, K. D.; Francl, M. M. *J. Am. Chem. Soc.* **1991**, *113*, 39. (b) Lichtenberger, D. L.; Hogan, R. H.; Healy, M. D.; Barron, A. R. *J. Am. Chem. Soc.* **1990**, *112*, 3369. (c) Lichtenberger, D. L.; Hogan, R. H.; Healy, M. D.; Barron, A. R. *Organometallics* **1991**, *10*, 609.

(30) van Vliet, M. R. P.; van Koten, G.; Rotteveel, M. A.; Schrap, M.; Vrieze, K.; Kojić-Prodić, B.; Spek, A. L.; Duisenberg, A. J. M. *Organometallics* **1986**, *5*, 1389.

aluminum centers. The $^1\text{H-NMR}$ of the bis(trimethylaluminum) adduct **2e** is similar to that of **2d**, but it shows three singlets for the methyl groups attached to aluminum. These integrate for 9 (-0.26 ppm), 9 (-0.35 ppm), and 6 protons (-0.59 ppm), respectively, corresponding with a Lewis acid-base complex of two separate AlMe_3 moieties with both the pendant amino substituent and a lone pair on the oxygen of the ligand, in accord with the crystal structure (see Figure 4). Here also, the three separate peaks for the methyl groups on the aluminum centers are still present at 80 °C in benzene, indicating that exchange of methyl groups between the aluminum centers does not take place on the NMR time scale. Finally, the $^1\text{H NMR}$ spectrum of the mono(phenolate) **1d** shows singlets for both the benzylic and NMe_2 protons, and two separate singlets for methyl groups attached to aluminum, integrating for nine (-0.29 ppm) and six (-0.36 ppm) protons, respectively. A Lewis acid-base complex with a lone pair on the oxygen as found in the crystal structure of **2e** seems likely.

General Properties. With the exception of the bis(phenolate) **2b**, all complexes are slightly soluble in hexane at room temperature but readily dissolve upon warming, making (re)crystallization from hexane a suitable purification method. They also dissolve readily in aromatic and ethereal solvents, with the exception of the mono(phenolate) **1a**, which undergoes a ligand exchange in the presence of a coordinating solvent (*vide supra*). The bis(phenolate) **2b** is very soluble in apolar, aromatic, and ethereal solvents. This high solubility makes purification of this complex difficult and up to now we have not been able to obtain material sufficiently pure for elemental analyses.

All complexes, except the tris(phenolates) **1c** and **2c**, are air and moisture sensitive due to the presence of an aluminum to methyl bond. Especially the trimethylaluminum adducts **1d** and **2d,e** readily burn on exposure to air and react vigorously with moisture.

The AlMe_3 -adducts **1d** and **2d,e**, as well as the mono(phenolate) **1a**, melt without decomposition at relatively low temperatures (90, 125, 115, and 85 °C, respectively), showing the stability of the ligand to metal bonding. The bis(phenolate) **1b** has a melting point higher than 200 °C. In contrast, the tris(phenolate) complexes **1c** and **2c** decompose at 165 and 170 °C, respectively, which may be due to the presence of pendant amino substituents, which introduce additional reactivity, as apparent from the intramolecular Lewis base induced ligand exchange of **2a**.

Both the bis- and tris(phenolates) fail to show interaction with Lewis bases like THF, indicating that the Lewis acidic character of the Al^{3+} ion is strongly reduced by the intramolecular coordination. This is also apparent from the finding that coordination of a third amino substituent to give an octahedral coordination geometry does not occur, as is in principle possible in the complexes **1c** and **2c** (see Figure 2). Such an octahedral geometry around aluminum is found in $\text{Al}(\text{moz})_3$ [$\text{Hmoz} = 2$ -(2'-hydroxy-3'-methylphenyl)-2-oxazoline], where all three ligands are bidentate, O,N-bonded.³¹

The relatively facile synthesis of the tris(phenolate) complexes **1c** and **2c** reported here contrasts with the elaborate route used for the synthesis of the first reported aluminum tris(phenolate) complex $\text{Al}(\text{BHT})_3$ (**8**).^{5b} The synthesis of the latter complex involved the separation of an equimolar mixture of $\text{AlH}(\text{BHT})_2$ and $\text{Li}(\text{BHT})$, formed upon reaction of LiAlH_4 with 3 equiv of $(\text{BHT})\text{H}$, through fractional crystallization. Reaction of $\text{AlH}(\text{BHT})_2$ with an additional 1 equiv of $(\text{BHT})\text{H}$, at reflux temperature in toluene, then afforded **8**. Attempts to synthesize **8** in one step invariably afforded $\text{AlR}(\text{BHT})_2$, even under extreme conditions.^{5b} The relatively mild conditions that are sufficient for the syntheses for the tris(phenolate) complexes **1c** and **2c** (room temperature and reflux temperature in hexane, respectively) may be accounted for by (a combination of) two effects. First, the amino substituents present in the phenolate ligands **3** and **4** are less sterically demanding than the *tert*-butyl substituents in BHT. Moreover, in **1c**, each phenolate ligand contains only one *ortho*-amino substituent, leading to considerably less steric congestion. Second, the substitution of the methyl group in the bis(phenolate) complexes **1b** and **2b** may be assisted by coordination of the incoming phenol, *via* an amino substituent, to the aluminum center in the bis(phenolate) complexes. This brings the acidic hydrogen in close proximity to the aluminum to methyl bond.

Conclusions

The crystal structure of **2c** and the structures in solution of the bis- and tris(phenolates) as determined by NMR spectroscopy, show that intramolecular coordination has a positive influence on the stability of monomeric aluminum phenolates. The combination of electronic saturation and steric shielding provided by the *ortho*-amino substituents in **3** and **4** leads to the isolation of aluminum bis- and tris(phenolates), which are monomeric in the solid state, as well as in solution (*vide supra*). Furthermore, the ligands **3** and **4** show great flexibility in their coordination modes, as evidenced by the crystal structures of **2c-e**. For mono-*ortho*-substituted **3**, both bidentate *O,N*-coordination and monodentate *O*-coordination have been observed, while the oxygen in the bidentate mode retains its Lewis basic properties (*cf.* the formation of the AlMe_3 -adduct **1d**). For bis-*ortho*-substituted **4**, the second *ortho*- $\text{CH}_2\text{-NMe}_2$ substituent can be just an *ortho*-hindering substituent as shown by the solid state structure of **2c** and the structure in solution of both **2c** and **2b**. On the other hand, its Lewis basicity can play a crucial role in the stability of the complexes, as shown by the instability of **2a** and the isolation of **2d** when the Lewis basicity is blocked through a Lewis acid-base complex. Another striking example of this cooperation between anionic and neutral Lewis basic properties is found in the lanthanide phenolate complex $\text{Na}[\text{Ln}\{\text{OC}_6\text{H}_2(\text{CH}_2\text{NMe}_2)\text{-2,6-Me-4}\}_3\text{Cl}]$ ($\text{Ln} = \text{Lu}, \text{Y}$), in which preorganization of the ligand systems, caused by coordination of chloride anion to a neutral lanthanide tris(phenolate), leads to cooperation between pendant amino substituents and the phenolate oxygen atoms to form a six-coordinate cage for the sodium ion.¹³

The similarity of the coordination geometry around the O,N-chelate bonded aluminum centers in **2d,e** (Al -

(31) (a) Hoveyda, H. R.; Karunaratne, V.; Rettig, S. J.; Orvig, C. *Inorg. Chem.* **1992**, *31*, 5408. (b) Hoveyda, H. R.; Rettig, S. J.; Orvig, C. *Inorg. Chem.* **1993**, *32*, 4909. (c) Liu, S.; Rettig, S. J.; Orvig, C. *Inorg. Chem.* **1992**, *31*, 5400.

(1) in both complexes) with that of reported four-coordinate mono(phenolato)aluminum complexes⁷ shows the flexibility of the ligand backbone connecting the anionic and neutral Lewis basic sites. This flexibility allows the coordination geometry to be determined by the metal center and not by the interconnectedness of the different binding sites of the ligand. A similar effect is found with respect to the trigonal bipyramidal coordination geometry found for the tris(phenolates) **1c** and **2c**, where electronic saturation of the metal center causes additional potentially intramolecularly coordinating amino substituents to remain pendant where an octahedral geometry with three amino substituents coordinating is in principle possible.³¹

Acknowledgment. This work was supported in part (H.K., A.L.S.) by the Netherlands Foundation for Chemical Research (SON) with financial aid from the Netherlands Organization for Scientific Research (NWO) and financially supported (M.P.H.) by the Innovation Oriented Research Program on Catalysis (IOP-Katalyse).

Supporting Information Available: Further details on the structure determinations, including tables of X-ray parameters, atomic coordinates, bond lengths and angles, and thermal parameters for **2c-e** (26 pages). Ordering information is given on any current masthead page.

OM950312O

**Oxo Complexes of Tungstenocene via Oxidation of
[W(η^5 -C₅H₅)₂(OCH₃)(CH₃)] and Related Reactions:
Synthesis, Structural Characterization, and
Photodisproportionation of the Spin-Paired d¹-d¹
Oxo-Bridged Dimer [W(η^5 -C₅H₅)₂(CH₃)₂(μ -O)]²⁺ and
Synthesis and Characterization of the d⁰ Terminal Oxo
Complex [W(η^5 -C₅H₅)₂(O)(CH₃)]⁺ †**

Peter Jernakoff,[‡] James R. Fox,[‡] Jeffrey C. Hayes,[‡] Samkeun Lee,[§]
Bruce M. Foxman,^{||} and N. John Cooper^{*,‡}

*Departments of Chemistry, University of Pittsburgh, Pittsburgh, Pennsylvania 15260,
Taejon University, 96-3 Young-dong Tong-gu, South Korea, and Brandeis University,
Waltham, Massachusetts 02254*

Received November 30, 1994[®]

Oxidation of [W(η^5 -C₅H₅)₂(OCH₃)(CH₃)] (1) with ferrocenium hexafluorophosphate in methyl ethyl ketone at room temperature leads to a 76% yield of the W(V) oxo complex [W(η^5 -C₅H₅)₂(CH₃)₂(μ -O)]²⁺ (2²⁺), established by a single-crystal X-ray diffraction study of the PF₆⁻ salt to contain two d¹ [W(η^5 -C₅H₅)₂(CH₃)₂]²⁺ moieties connected by a linear oxo bridge such that the W atoms, the bridging oxygen atom, and the methyl groups are coplanar with an *anti* orientation of the methyl groups. The molecule is diamagnetic in the solid state and in solution, implying spin pairing of the metal centers through a π -interaction involving the oxo bridge, and exhibits a strong absorption in the visible region (λ_{max} 525 nm, $\epsilon = 23\,600\text{ L mol}^{-1}\text{ cm}^{-1}$) assigned to a transition with some MLCT character from a nonbonding level formed by the π -interaction to an empty antibonding level with π^* character. The oxo-bridged dimer 2²⁺ is photosensitive and photodisproportionates in CH₃CN to give the d⁰ terminal oxo complex [W(η^5 -C₅H₅)₂(O)(CH₃)]⁺ (3⁺) and the d² solvent-trapped methyl complex [W(η^5 -C₅H₅)₂(NCCH₃)(CH₃)]⁺ (4⁺). The W(IV) acetonitrile complex 4⁺ has been independently isolated and characterized following photolysis of [W(η^5 -C₅H₅)₂(CH₃)₂] (7) with NH₄PF₆ in CH₃CN. The W(VI) oxo complex [W(η^5 -C₅H₅)₂(O)(CH₃)]PF₆ (3[PF₆]) has been prepared in 74% yield by photolysis of 4[PF₆] in acetone under O₂. An X-ray diffraction study of the I⁻ salt 3[I] has established that 3⁺ is a terminal oxo complex. The oxo complex is not formed in the absence of O₂, even when 4[PF₆] is heated in the presence of water, and it is proposed that 3⁺ is formed via addition of O₂ to transient "[W(η^5 -C₅H₅)₂(CH₃)]⁺" to form the reactive peroxy intermediate [W(η^5 -C₅H₅)₂(CH₃)(η^2 -O₂)]⁺. Photolysis of 2[PF₆] in the weakly coordinating solvent acetone under O₂ results in clean conversion to 3⁺ by a sequence presumed to involve photodisproportionation of 2²⁺ to give some 3⁺ directly, together with "[W(η^5 -C₅H₅)₂(CH₃)]⁺", which is then oxidized to 3⁺. Ferrocenium oxidation of 1 in CH₂Cl₂ results in formation of the radical cation [W(η^5 -C₅H₅)₂(CH₃)Cl]⁺, independently prepared and characterized as a PF₆⁻ salt by ferrocenium oxidation of [W(η^5 -C₅H₅)₂(CH₃)Cl], which is in turn prepared by protolysis of 7 with NH₄Cl.

Introduction

There was remarkable growth throughout the 1980s in the chemistry of transition-metal oxo complexes.¹ This began with the recognition of the role of the oxo functionality as a "spectator" ligand in catalytic alkene metathesis² and has been fueled by developments in the chemistry of transition-metal porphyrin oxo complexes³ (including their roles in hydrocarbon oxidations and in alkene epoxidation and hydroxylation reactions), by

continuing rapid evolution of our understanding of biologically relevant oxo transfer reactions,⁴ by advances in the use of oxo complexes as catalysts for alkene hydroxylation⁵ and epoxidation,⁶ and by the remarkable catalytic activity demonstrated by high-valent rhenium

(2) (a) Rappe, A. K.; Goddard, W. A., III. *Nature* **1980**, *285*, 311. (b) Rappe, A. K.; Goddard, W. A., III. *J. Am. Chem. Soc.* **1980**, *102*, 5114. (c) Rappe, A. K.; Goddard, W. A., III. *J. Am. Chem. Soc.* **1982**, *104*, 448.

(3) (a) Mimoun, H. In *Comprehensive Coordination Chemistry*: Wilkinson, G., Gillard, R. D., McCleverty, J. A., Eds.; Pergamon: Oxford, U.K., 1987; Vol. 6, Section 61.3. (b) Meunier, B. *Chem. Rev.* **1992**, *92*, 1411.

(4) (a) Holm, R. H. *Chem. Rev.* **1987**, *87*, 1401. (b) Holm, R. H. *Coord. Chem. Rev.* **1990**, *100*, 183.

(5) Sharpless, K. B.; Amberg, W.; Bennani, Y. L.; Crispino, G. A.; Hartung, J.; Jeong, K.-S.; Kwong, H.-L.; Morikawa, K.; Wang, Z.-M.; Xu, D.; Zhang, X.-L. *J. Org. Chem.* **1992**, *57*, 2768 and references therein.

† Taken in part from the Ph.D. Thesis of Peter Jernakoff, Harvard University, 1986.

‡ University of Pittsburgh.

§ Taejon University.

|| Brandeis University.

® Abstract published in *Advance ACS Abstracts*, July 15, 1995.

(1) For a general introduction see: Nugent, W. A.; Mayer, J. M. *Metal-Ligand Multiple Bonds*; Wiley: New York, 1988.

oxo alkyls.⁷ These developments have been paralleled by significant advances in the syntheses of oxo complexes, including the preparations of "low-valent" oxo complexes⁸ and of high-valent oxo alkyl complexes,^{7,9} and by extensions of the rational synthesis of organometallic oxo complexes.¹⁰

Our own work with oxo alkyl complexes began with the modest observation that although most tungstenocene complexes (except the dihalides¹¹) are relatively weakly colored, we sometimes observed the formation in this system of traces of purple complexes which we suspected were oxo complexes. We have now been able to confirm this by determining that ferrocenium oxidation of $[\text{W}(\eta^5\text{-C}_5\text{H}_5)_2(\text{O}(\text{CH}_3)(\text{CH}_3))]^{2+}$ (1) in undried methyl ethyl ketone (MEK) gives a red-purple crystalline material in good yield, which we have determined is an oxo complex in which the chromophore is a $d^1\text{-}d^1$ linear oxo bridge within the diamagnetic $[\{\text{W}(\eta^5\text{-C}_5\text{H}_5)_2(\text{CH}_3)_2(\mu\text{-O})\}^{2+}]^{2+}$ (2^{2+}) cation. The most distinctive feature of the chemistry of this complex observed to date is the facility with which it photo-disproportionates in CH_3CN to give the W(VI) oxo complex $[\text{W}(\eta^5\text{-C}_5\text{H}_5)_2(\text{O})(\text{CH}_3)]^+$ (3^+) and the W(IV) acetonitrile complex $[\text{W}(\eta^5\text{-C}_5\text{H}_5)_2(\text{NCCH}_3)(\text{CH}_3)]^+$ (4^+). Both 3^+ and 4^+ have been independently prepared as shown in Scheme 1, which summarizes the major synthetic observations to be reported.

Experimental Section

General Data. All transformations and manipulations involving air-sensitive compounds were performed under an atmosphere of prepurified nitrogen or argon unless otherwise noted, using either standard Schlenk techniques or a Vacuum Atmospheres drybox. Glassware was flame-dried under vacuum or dried in an oven (>4 h, 120°C) before use.

Solvents and Reagents. Tetrahydrofuran (THF) and diethyl ether were predried over sodium wire and then distilled from sodium/benzophenone ketyl under nitrogen. Ligroin ($90\text{--}120^\circ\text{C}$ boiling range, Mallinckrodt) was dried over sodium wire before use. Reagent grade acetone (Mallinckrodt) and benzene (Mallinckrodt) were used as received. Toluene was predried over sodium wire and distilled from CaH_2 under nitrogen. Methyl ethyl ketone (MEK, Eastman Kodak) and acetonitrile (Mallinckrodt) were reagent grade and were used as received. Dichloromethane was distilled from CaH_2 under a CaSO_4 drying tube. Water was deionized. Ammonium chloride (Aldrich), sodium iodide (Aldrich), and ammonium hexafluorophosphate (Aldrich) were used as received. Ferrocenium hexafluorophosphate (FcPF_6) was prepared from ferrocene (Aldrich) by a literature procedure.¹³ Triphenylmethyl hexafluorophosphate (trityl- PF_6 , Alfa) was recrystallized twice

(6) (a) Jorgenson, K. A. *Chem. Rev.* **1989**, *89*, 431. (b) Jorgenson, K. A.; Schiott, B. *Chem. Rev.* **1990**, *90*, 1483.

(7) (a) Herrmann, W. A.; Wagner, W.; Flessner, U. N.; Volkhardt, U.; Kombe, H. *Angew. Chem., Int. Ed. Engl.* **1991**, *30*, 1636. (b) Herrmann, W. A.; Fischer, R. W.; Marz, D. W. *Angew. Chem., Int. Ed. Engl.* **1991**, *30*, 1638. (c) Herrmann, W. A.; Wang, M. *Angew. Chem., Int. Ed. Engl.* **1991**, *30*, 1641.

(8) Spaltenstein, E.; Mayer, J. M. *J. Am. Chem. Soc.* **1991**, *113*, 7744 and references therein.

(9) Herrmann, W. A. *J. Organomet. Chem.* **1986**, *300*, 111.

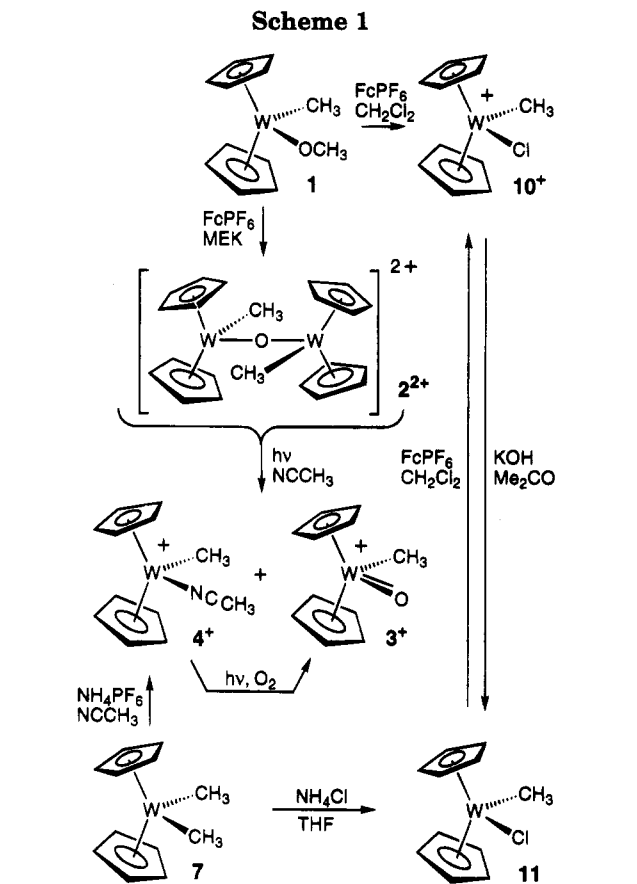
(10) Bottomley, F.; Sutin, L. *Adv. Organomet. Chem.* **1988**, *28*, 339.

(11) (a) Cotton, F. A.; Wilkinson, G. *Z. Naturforsch.* **1954**, *9B*, 417. (b) Cooper, R. L.; Green, M. L. H. *J. Chem. Soc. A* **1967**, 1155.

(12) (a) Farrugia, L.; Green, M. L. H. *J. Chem. Soc., Chem. Commun.* **1975**, 416. (b) Hayes, J. C.; Cooper, N. J. To be submitted for publication.

(13) Yang, E. S.; Chan, M. S.; Wahl, A. C. *J. Phys. Chem.* **1975**, *79*, 2049.

(14) Benfield, F. W. S.; Green, M. L. H. *J. Chem. Soc., Dalton Trans.* **1974**, 1324.



from CH_3CN that had been distilled from CaH_2 . $[\text{W}(\eta^5\text{-C}_5\text{H}_5)_2(\text{CH}_3)_2]^{14}$ and $[\text{W}(\eta^5\text{-C}_5\text{H}_5)_2(\text{O}(\text{CH}_3)(\text{CH}_3)]^{12}$ were prepared from $[\text{W}(\eta^5\text{-C}_5\text{H}_5)_2\text{H}_2]$ by established procedures.

Spectroscopy and Analysis. ^1H NMR spectra were recorded on a Varian CFT-80 (80 MHz), a Bruker AM-300 (300 MHz), or a Bruker WM-300-WB (300 MHz) NMR spectrometer. Perdeuterioacetone, perdeuterioacetonitrile, perdeuteriodimethyl sulfoxide (all 99.5+ atom %) were purchased from Merck, Sharpe, and Dohme or from Cambridge Isotopes and were used as received. Chemical shifts are reported in δ using the residual proton resonances of the deuterated solvents as internal standards (acetone- d_6 , δ 2.04; acetonitrile- d_3 , δ 1.93; dimethyl sulfoxide- d_6 , δ 2.49). ^{13}C NMR spectra were obtained on a Bruker AM-300 (75.5 MHz) or a Bruker WM-300-WB (75.5 MHz) NMR spectrometer. Chemical shifts are reported in δ using the ^{13}C chemical shift of the deuterated solvent as an internal standard (dimethyl sulfoxide- d_6 , δ 39.5). Infrared spectra were obtained using KBr pellets or Nujol mulls on a Perkin-Elmer 683 grating infrared spectrometer with the 1601 cm^{-1} band of polystyrene as an external reference. Mass spectra were recorded on a Kratos MS-9 spectrometer. Mass spectral patterns which exhibited the W isotope envelope are reported as the values of m/e corresponding to the ion containing ^{184}W . EPR spectra were recorded on a Varian E-109 spectrometer in a $60 \times 10 \times 0.25$ mm quartz flat cell and were calibrated against the sharp line ($g = 2.0036$) of a sample of 2,2-diphenyl-1-picrylhydrazyl (DPPH)¹⁵ in a sealed capillary attached externally to the flat cell. Solid-state magnetic susceptibilities were determined by the Guoy method¹⁶ on a Bruker Research B-E15 B8 magnet equipped with a Cahn RG electrobalance and a Hewlett-Packard Model 3465A digital multimeter. The sample holder was a 5 mm borosilicate NMR tube cut to a length of 2 cm and fitted with a plastic cap to which was glued (epoxy) a platinum loop. The sample holder

(15) Hutchinson, C. A.; Pastor, R. L. *Phys. Rev.* **1951**, *81*, 282.

(16) Mulay, L. N. *Magnetic Susceptibility*; Wiley: New York, 1963; p 1782.

was calibrated with $\text{HgCo}(\text{SCN})_4$. Microanalyses were carried out by Dornis und Kolbe, Mülheim a.d. Ruhr, Germany.

[$[\text{W}(\eta^5\text{-C}_5\text{H}_5)_2(\text{CH}_3)_2(\mu\text{-O})][\text{PF}_6]_2$ (2[PF_6])₂]. A 0.028 M solution of ferrocenium hexafluorophosphate in methyl ethyl ketone (30 mL, 0.84 mmol) was added to a stirred dark orange solution of $[\text{W}(\eta^5\text{-C}_5\text{H}_5)_2(\text{OCH}_3)(\text{CH}_3)]$ (0.30 g, 0.83 mmol) in MEK (30 mL) to give, after 10 min, a deep cherry red solution and a flocculent purple-red precipitate. After 24 h the precipitate was collected by decantation, washed with MEK (2×5 mL), and dried in vacuo to yield spectroscopically pure $[\text{W}(\eta^5\text{-C}_5\text{H}_5)_2(\text{CH}_3)_2(\mu\text{-O})][\text{PF}_6]_2$ (0.31 g, 0.32 mmol; yield 76%) as a dark red-purple powder. The complex could be recrystallized as small red-brown needles (ca. 80% recovery) by slowly concentrating a saturated acetone/toluene solution (5/1 v/v) of the complex under reduced pressure. Analytically pure material was obtained as hexagonal plates by slow vapor diffusion in the dark of diethyl ether into a saturated acetone solution of the complex. ^1H NMR (300 MHz, acetonitrile- d_3): δ 6.09 (s, 20H, $4\text{C}_5\text{H}_5$), 0.88 (s, satellites $J_{\text{W-H}} = 2.4$ Hz, 6H, 2CH_3). ^1H NMR (300 MHz, acetone- d_6): δ 6.48 (s, 20H, $4\text{C}_5\text{H}_5$), 1.18 (s, satellites $J_{\text{W-H}} = 3.4$ Hz, 6H, 2CH_3). ^{13}C NMR (75.5 MHz, gated decoupled, dimethyl- d_6 sulfoxide): δ 104.2 (d, $^1J_{\text{C-H}} = 185.0$ Hz, $4\text{C}_5\text{H}_5$), 3.89 (q, $^1J_{\text{C-H}} = 133.2$ Hz, 2CH_3). IR (KBr): 3138 ms, 2961 mw, 2900 m, 2812 w, 1440 s, 1431 s, 1420 ms, 1382 m, 1206 m, 1128 w, 1084 m, 1022 m, 850 vs br, 741 ms, 702 m, 552 vs, 409 m, 349 m cm^{-1} . Anal. Calcd for $\text{C}_{22}\text{H}_{26}\text{F}_{12}\text{P}_2\text{O}_2$: C, 27.41; H, 2.72. Found: C, 27.43; H, 2.83.

[$[\text{W}(\eta^5\text{-C}_5\text{H}_5)_2(\text{NCCH}_3)(\text{CH}_3)]\text{PF}_6$ (4[PF_6])₂]. A saturated solution (10 mL, ca. 0.1 M, 1 mmol) of NH_4PF_6 in acetonitrile was added to $[\text{W}(\eta^5\text{-C}_5\text{H}_5)_2(\text{CH}_3)_2]$ (0.103 g, 0.30 mmol). The mixture was swirled, and the resulting clear, red solution was left to stand undisturbed for 30 min at room temperature. The solvent was then removed under reduced pressure (37 °C) and the orange-brown solid was washed with toluene (3×5 mL) and then dried under vacuum (3 h). Acetone and water (10 mL each) were added to give an orange solution, from which the acetone was removed under reduced pressure to precipitate an orange-brown solid. The orange mother liquor was filtered off, and the solid was washed with water (3×5 mL) and dried under vacuum (50 °C, 1 h) to give $[\text{W}(\eta^5\text{-C}_5\text{H}_5)_2(\text{NCCH}_3)(\text{CH}_3)]\text{PF}_6$ as orange-brown "spaghetti-like" crystals (0.108 g, 0.21 mmol; yield 70%). A sample of these crystals was unchanged in appearance after exposure to air for 10 min. ^1H NMR (300 MHz, acetonitrile- d_3): δ 5.18 (s, 10H, $2\text{C}_5\text{H}_5$), 2.61 (s, 3H, NCCH_3), 0.25 (s, satellites $J_{\text{W-H}} = 5.3$ Hz, 3H, W-CH_3). ^1H NMR (300 MHz, acetone- d_6): δ 5.38 (s, 10H, $2\text{C}_5\text{H}_5$), 2.82 (s, 3H, NCCH_3), 0.30 (s, satellites $J_{\text{W-H}} = 5.6$ Hz, 3H, WCH_3). IR (KBr): 3218 m, 3135 br s, 3005 m, 2947 s, 2900 s, 2853 m, 2823 ms, 2415 br w, 2320 vw, 2280 w, 1461 m sh, 1439 s, 1437 s, 1427 s sh, 1420 s, 1385 s, 1368 ms sh, 1218 ms, 1117 m, 1080 br m, 1030 ms, 1019 ms, 998 s, 950 s, 938 br s, 848 vs, 825 br vs, 744 ms, 607 m, 596 m, 554 vs, 484 w, 380 w, 357 m, 349 m cm^{-1} . Anal. Calcd for $\text{C}_{13}\text{H}_{16}\text{F}_6\text{NPW}$: C, 30.31; H, 3.13. Found: C, 30.43; H, 3.25.

[$[\text{W}(\eta^5\text{-C}_5\text{H}_5)_2(\text{O})(\text{CH}_3)]\text{PF}_6$ (3[PF_6])₂]. A stirred orange solution of $[\text{W}(\eta^5\text{-C}_5\text{H}_5)_2(\text{NCCH}_3)(\text{CH}_3)]\text{PF}_6$ (0.30 g, 0.58 mmol) in acetone (30 mL) was irradiated for 1 h under oxygen with a 150 W sunlamp. The resulting yellow solution was filtered to remove a small amount of a grayish precipitate and the solvent removed under reduced pressure to give spectroscopically pure $[\text{W}(\eta^5\text{-C}_5\text{H}_5)_2(\text{O})(\text{CH}_3)]\text{PF}_6$ as yellow flakes (0.21 g, 0.43 mmol; yield 74%). Analytically pure material could be obtained (ca. 68% recovery) by slow concentration under reduced pressure of a saturated acetone/toluene solution (1/2 v/v) of the complex. ^1H NMR (300 MHz, acetone- d_6): δ 6.90 (s, 10H, $2\text{C}_5\text{H}_5$), 2.30 (s, satellites $J_{\text{W-H}} = 7.9$ Hz, 3H, WCH_3). ^1H NMR (300 MHz, acetonitrile- d_3): δ 6.58 (s, 10H, $2\text{C}_5\text{H}_5$), 2.16 (s, 3H, satellites $J_{\text{W-H}} = 7.8$ Hz, WCH_3). ^{13}C NMR (75.5 MHz, gated decoupled, dimethyl- d_3 sulfoxide): δ 113.7 (d, $^1J_{\text{C-H}} = 185.5$ Hz, $2\text{C}_5\text{H}_5$), 5.34 (q, $^1J_{\text{C-H}} = 136.4$ Hz, WCH_3). IR (KBr): 3125 s, 2992 w, 2920 mw, 1456 m, 1428 ms, 1382 m, 1217 w, 1132 mw, 1071 mw, 1032 m, 1009 mw, 850 vs br, 740

m, 551 s, 350 mw br cm^{-1} . Anal. Calcd for $\text{C}_{11}\text{H}_{13}\text{OF}_6\text{PW}$: C, 26.96; H, 2.68. Found: C, 27.04; H, 2.78.

[$[\text{W}(\eta^5\text{-C}_5\text{H}_5)_2(\text{O})(\text{CH}_3)]\text{I}$ (3[I])₂]. An orange solution of $[\text{W}(\eta^5\text{-C}_5\text{H}_5)_2(\text{NCCH}_3)(\text{CH}_3)]\text{PF}_6$ (0.28 g, 0.54 mmol) in acetone (70 mL) was stirred in air in a well-lit laboratory for 24 h. The resulting pale yellow solution was decreased in volume to ca. 20 mL under reduced pressure, filtered, and cooled to 0 °C. This was added to 5.0 mL of a 0.33 M solution of NaI in acetone (0.25 g, 1.65 mmol) also at 0 °C. Swirling precipitated $[\text{W}(\eta^5\text{-C}_5\text{H}_5)_2(\text{O})(\text{CH}_3)]\text{I}$ as spectroscopically pure golden yellow flakes in an orange solution. The flakes were collected by decantation, washed with 0 °C acetone (1×10 mL) and diethyl ether (2×10 mL), and dried in vacuo (0.20 g, 0.42 mmol; yield 78%). Analytically pure material could be obtained in low yield as yellow blocks and needles by slow vapor diffusion of diethyl ether into a saturated acetone solution of the complex. ^1H NMR (300 MHz, acetonitrile- d_3): δ 6.61 (s, 10H, $2\text{C}_5\text{H}_5$), 2.17 (s, 3H, satellites $J_{\text{W-H}} = 7.5$ Hz, WCH_3). ^{13}C NMR (75.5 MHz, gated decoupled, dimethyl- d_3 sulfoxide): δ 113.6 (d, $^1J_{\text{C-H}} = 185.5$ Hz, $2\text{C}_5\text{H}_5$), 5.36 (q, $^1J_{\text{C-H}} = 136.4$ Hz, WCH_3). IR (KBr): 3100 ms, 3055 s, 2972 w, 2918 w, 1451 m, 1422 s, 1382 mw, 1365 w br, 1260 mw, 1214 mw, 1130 mw, 1079 mw, 1053 mw, 1031 m, 1023 m, 1004 m, 974 mw, 880 sh, 867 vs, 838 s, 798 w, 588 w, 499 w cm^{-1} . Anal. Calcd for $\text{C}_{11}\text{H}_{13}\text{IOW}$: C, 27.99; H, 2.78. Found: C, 27.93; H, 2.79.

[$[\text{W}(\eta^5\text{-C}_5\text{H}_5)_2(\text{CH}_3)\text{Cl}]$ (11)]. A dark red solution of $[\text{W}(\eta^5\text{-C}_5\text{H}_5)_2(\text{CH}_3)_2]$ (0.63 g, 1.83 mmol) and NH_4Cl (2.0 g, 37.4 mmol) in THF (20 mL) was heated at 56 °C for 23 h. The solvent was removed under reduced pressure and the solid residue extracted with benzene (1×25 mL, 3×10 mL). Ligroin was then added (50 mL) and the solvent mixture filtered. Slow concentration under reduced pressure to ca. 15 mL yielded dark brown crystals of spectroscopically pure $[\text{W}(\eta^5\text{-C}_5\text{H}_5)_2(\text{CH}_3)\text{Cl}]$. The crystals were collected by decantation, washed with cold ligroin (0 °C, 3×10 mL), and dried in vacuo (0.41 g, 1.12 mmol; yield 61%). Analytically pure material could be obtained as dark brown needles (ca. 40% recovery) by slow concentration of a saturated diethyl ether solution of the complex. ^1H NMR (80 MHz, acetone- d_6): δ 4.96 (s, 10H, $2\text{C}_5\text{H}_5$), 0.37 (s, 3H, satellites $J_{\text{W-H}} = 4.8$ Hz, WCH_3). IR (KBr): 3110 m br, 2940 m br, 2885 m, 2820 mw br, 1422 ms, 1385 w, 1360 mw, 1250 w br, 1191 m, 1112 m, 1074 mw, 1063 mw, 1010 ms, 994 ms, 943 m, 872 ms, 837 s, 793 ms, 588 ms, 478 ms, 393 m, 364 ms, 339 ms cm^{-1} . Mass spectrum (molecular ion, ^{184}W): m/e 364. Anal. Calcd for $\text{C}_{11}\text{H}_{13}\text{ClW}$: C, 36.24; H, 3.60. Found: C, 36.36; H, 3.58.

[$[\text{W}(\eta^5\text{-C}_5\text{H}_5)_2(\text{CH}_3)\text{Cl}]\text{PF}_6$ (10[PF_6])₂]. A 0.016 M solution of FcPF_6 in CH_2Cl_2 (30 mL, 0.48 mmol) was added to a stirred dark orange-red solution of $[\text{W}(\eta^5\text{-C}_5\text{H}_5)_2(\text{CH}_3)\text{Cl}]$ (0.18 g, 0.49 mmol) in CH_2Cl_2 (15 mL). Within 1 min the solution had lightened to a bright orange and had deposited an orange precipitate. The solvent was removed under reduced pressure and the solid residue triturated with toluene (4×30 mL) to yield $[\text{W}(\eta^5\text{-C}_5\text{H}_5)_2(\text{CH}_3)\text{Cl}]\text{PF}_6$ as a spectroscopically pure orange powder after vacuum drying (0.23 g, 0.45 mmol; yield 92%). Analytically pure material could be obtained as clusters of small orange needles (ca. 80% recovery) via slow concentration of a saturated CH_2Cl_2 solution of the complex. EPR (acetone, 25 °C, 9.389 GHz): $g = 2.006$ (q, $a_{\text{H}} = 4.0$ G). IR (KBr): 3130 s, 2955 m, 2915 ms, 2856 m, 1440 s, 1428 s, 1382 mw, 1340 w, 1261 w, 1212 w, 1128 mw, 1078 mw, 1030 m, 1017 mw, 980 w br, 924 ms, 850 vs br, 743 m, 552 s, 310 s cm^{-1} . Anal. Calcd for $\text{C}_{11}\text{H}_{13}\text{ClF}_6\text{PW}$: C, 25.93; H, 2.58. Found: C, 25.64; H, 2.64.

Reduction of $[\text{W}(\eta^5\text{-C}_5\text{H}_5)_2(\text{CH}_3)\text{Cl}]\text{PF}_6$. An orange solution of $[\text{W}(\eta^5\text{-C}_5\text{H}_5)_2(\text{CH}_3)\text{Cl}]\text{PF}_6$ (0.11 g, 0.22 mmol) in acetone (30 mL) was vigorously stirred with a saturated solution of aqueous KOH (30 mL) at room temperature for 1.5 h. The cherry red organic layer was decanted off and the solvent removed under reduced pressure to give a brown-red solid. Extraction with CH_2Cl_2 (35 mL) gave a red-orange solution which was filtered. Removal of the solvent under reduced

pressure gave an oily brown powder which was shown to be $[\text{W}(\eta^5\text{-C}_5\text{H}_5)_2(\text{CH}_3)\text{Cl}]$ (0.04 g, 0.11 mmol; yield 50%) by comparison ($^1\text{H NMR}$ and mass spectroscopy) with an authentic sample.

X-ray Diffraction Studies of $[\{\text{W}(\eta\text{-C}_5\text{H}_5)_2(\text{CH}_3)\}_2(\mu\text{-O})]\text{-}[\text{PF}_6]_2$ (2 $[\text{PF}_6]_2$) and $[\text{W}(\eta\text{-C}_5\text{H}_5)_2(\text{O})(\text{CH}_3)]\text{I}$ (3 $[\text{I}]$). Crystals of 2 $[\text{PF}_6]_2$ and 3 $[\text{I}]$ for diffraction studies were obtained by vapor diffusion of diethyl ether into a saturated acetone solution of the complexes. Crystals were mounted in glass capillary tubes and flame sealed under argon. Data were collected on a Nicolet R3 diffractometer using graphite-monochromatized Mo K α radiation (50 kV, 30 mA). Data collection was controlled by the Nicolet P3 program,¹⁷ and structures were solved using SHELXTL.¹⁸ Refinement was carried out using either the SHELXTL package¹⁸ or the Oxford University CRYSTALS program.^{19a} Diffractometer data were processed with FOXTAPE, a local modification of the Nicolet program XTAPE. Empirical absorption corrections were performed by the program XEMP (Nicolet), while drawings were generated by the program SNOOPI (part of the Oxford University CHEMGRAF Suite package)^{19b} or by XPLOR (Nicolet). All molecular calculations were performed with the aid of the program XP (Nicolet). Atomic scattering factors were based on literature values.²⁰ Weights were taken as $[\sigma^2(F) + gF^2]^{-1}$. Crystal data, details of the data collection, and final agreement parameters are summarized in Table 1.

For both structures, unit cell dimensions were obtained by a least-squares fit of 25 reflections with $18^\circ < 2\theta < 31^\circ$. No significant variation in the intensities of the standard reflections was observed. Lorentz and polarization corrections were applied to the data. Data were corrected for absorption by an empirical procedure which employed six refined parameters to define a pseudoellipsoid. Hydrogen atoms were placed in idealized positions in both structures. At the conclusion of refinement, there were no unusual trends in observed and calculated structure factors vs $\sin \theta$, Miller indices, or reflection parity.

Initial examination of the data and rotation photographs for 2 $[\text{PF}_6]_2$ indicated mmm diffraction symmetry. A number of possible solutions were attempted in the orthorhombic crystal system, but it was not possible to solve the structure in an orthorhombic space group. Fortunately, two octants of data had been collected, and careful reinspection of these data (the mmm symmetry was very close but not exact) suggested to us that the true crystal system was monoclinic, space group $P2_1/c$. The data were reprocessed, and the structure was solved by using the Patterson function and successive ΔF syntheses. The monoclinic crystal is twinned; the refinement^{19a} was carried out by hypothesizing that the crystal was composed of two twin elements related by a 2-fold rotation about the crystallographic a axis. The rotation matrices for these two elements are then $(100/010/001)$ and $(100/0\bar{1}0/00\bar{1})$. During the refinement the sum of the scale factors for the two elements was constrained to be 1.0. At convergence ($R_F = 0.031$; $R_{wF} = 0.031$), the scale factor for the parent crystal element $(100/010/001)$ had a value of 0.422(6). A value of 0.5 would lead to the condition that $I(hkl) = (h\bar{k}\bar{l})$; thus, the reason for the near-orthorhombic symmetry is obvious.

After initial examination of rotation photographs and systematic absences, the space group of 3 $[\text{I}]$ was determined

Table 1. Summary of Crystallographic Data for $[\{\text{W}(\eta^5\text{-C}_5\text{H}_5)_2(\text{CH}_3)\}_2(\mu\text{-O})][\text{PF}_6]_2$ (2 $[\text{PF}_6]_2$) and $[\text{W}(\eta^5\text{-C}_5\text{H}_5)_2(\text{O})(\text{CH}_3)]\text{I}$ (3 $[\text{I}]$)

	2 $[\text{PF}_6]_2$	3 $[\text{I}]$
Crystal Data		
color	dark red-purple	bright yellow
shape	hexagonal plates	cubes
dimens (mm)	$0.10 \times 0.20 \times 0.50$	$0.30 \times 0.30 \times 0.30$
formula	$\text{C}_{22}\text{H}_{26}\text{F}_{12}\text{O}_2\text{P}_2\text{W}_2$	$\text{C}_{11}\text{H}_{13}\text{IO}_2$
cryst syst	monoclinic	cubic
space group	$P2_1/c$	$Ia\bar{3}$
a (Å)	7.246(3)	24.601(4)
b (Å)	18.796(6)	(24.601(4))
c (Å)	9.438(4)	(24.601(4))
β (deg)	89.98(2)	(90)
V (Å ³)	1285(3)	14 889(7)
Z	2	48
d_c (g/mL)	2.49	2.53
μ (cm ⁻¹)	93.6	119.4
T (°C)	23	23
Data Collection		
λ (Å)	0.710 69	0.710 69
scan type	$\theta-2\theta$	$\theta-2\theta$
2θ range (deg)	3.5–60	3.5–60
variable scan speed (deg/min)	2.55–14.65	2.93–14.65
data collected	$+h,+k,\pm l$	$+h,+k,+l$
no. of std rflns; period	60; 3	60; 3
no. of rflns measd	4287; 3900 in unique set	8316; 2216 in unique set
no. of data used in refinement	3505 with $I > 2.5\sigma(I)$	1768 with $I > 2.5\sigma(I)$
Agreement Parameters		
R_{int} for merged data ^a	0.022	0.051
R_F (%) ^b	0.031	0.065
R_{wF} ^c	0.031	0.060
max residue peak (e/Å ³)	0.44	0.53
weighting factor, g	0.0008	0.0008

^a $R_{\text{int}} = \sum |F_o|^2 - (F_o^2)_{\text{mean}} / \sum |F_o|^2$. ^b $R_F = \sum ||F_o| - |F_c|| / \sum |F_o|$. ^c $R_{wF} = \{ \sum w[|F_o| - |F_c|]^2 / \sum w|F_o|^2 \}^{1/2}$.

to be $Ia\bar{3}$; this choice was consistent with application of both the P3 program and TRACER.²¹ The W and I atoms in 3 $[\text{I}]$ were located using the direct methods program SOLV; the remaining non-hydrogen atoms were located from subsequent ΔF syntheses.

The dication in 2 $[\text{PF}_6]_2$ resides on an inversion center with the bridging oxygen atom at $(\frac{1}{2}, \frac{1}{2}, 0)$. The hexafluorophosphate anion is ordered and well-behaved. The asymmetric unit of 3 $[\text{I}]$ contains three iodide anions, I(1), I(2), and I(3), at special positions with site occupancy factors of $\frac{1}{6}$, $\frac{1}{2}$, and $\frac{1}{3}$, respectively, together with a molecule of the 3^+ cation in a general position. Final atomic positional parameters for 2 $[\text{PF}_6]_2$ and 3 $[\text{I}]$ are presented in Tables 2 and 3, respectively, and anisotropic thermal parameters are given in Tables SI and SII, respectively, of the supporting information.

Results and Discussion

The methoxy complex $[\text{W}(\eta^5\text{-C}_5\text{H}_5)_2(\text{OCH}_3)(\text{CH}_3)]$ (1) is readily prepared from $[\text{W}(\eta^5\text{-C}_5\text{H}_5)_2(\text{CH}_3)(\text{OCOPh})]^{22}$ by reaction with excess NaOCH_3 in CH_3OH ,^{12b} and our interest in the oxidation chemistry of 1 began when we included the complex in an electrochemical study of one-

(17) P3/R3 Data Collection Manual; Nicolet Instrument Corp.: Madison, WI, 1983.

(18) Sheldrick, G. M. *SHELXTL User Manual, Version 4*; Nicolet Instrument Corp.: Madison, WI, 1983.

(19) (a) Watkin, D. J.; Carruthers, J. R.; Betteridge, P. W. *CRYSTALS User Guide*; Chemical Crystallography Laboratory, University of Oxford: Oxford, U.K., 1985. (b) Davies, C. E. K. *CHEMGRAF Program Suite*; Chemical Crystallography Laboratory, University of Oxford: Oxford, U.K., 1982.

(20) Cromer, D. T.; Waber, J. T. In *International Tables for X-ray Crystallography*; Ibers, J. A., Hamilton, W. C., Eds.; Vol. IV, Kynoch Press: Birmingham, England, 1974; Vol. IV, pp 99–101. Cromer, D. T.; Ibers, J. A. *Ibid.*, pp 148–150.

(21) Lawton, S. L. *TRACER II, A FORTRAN Lattice Transformation-Cell Reduction Program*; Research Department, Mobil Oil Corp.: Paulsboro, NJ, 1967 (as adapted by Professor B. M. Foxman, Brandeis University).

(22) Cooper, N. J.; Green, M. L. H.; Mahtab, R. *J. Chem. Soc., Dalton Trans.* **1979**, 1557.

(23) Asaro, M. F.; Cooper, S. R.; Cooper, N. J. *J. Am. Chem. Soc.* **1986**, *108*, 5187.

Table 2. Fractional Atomic Coordinates ($\times 10^4$) for $[\{W(\eta^5-C_5H_5)_2(CH_3)\}_2(\mu-O)]PF_6$

atom	<i>x/a</i>	<i>y/b</i>	<i>z/c</i>
W(1)	4707.0(4)	4245.7(1)	1327.1(3)
C(1)	1703(11)	4451(5)	1043(10)
O(1)	5000(0)	5000(0)	0000(0)
C(11)	4358(17)	2988(4)	1443(14)
C(12)	6213(14)	3140(5)	1272(15)
C(13)	6519(14)	3479(6)	12(12)
C(14)	4762(14)	3507(4)	-675(8)
C(15)	3495(13)	3208(5)	184(10)
C(21)	6698(13)	4315(6)	3262(8)
C(22)	6287(16)	5001(6)	2841(7)
C(23)	4406(11)	5111(5)	3070(7)
C(24)	3673(11)	4513(5)	3621(9)
C(25)	5171(14)	3966(5)	3781(8)
P(1)	-16(2)	1593(1)	1241(2)
F(1)	-2198(6)	1619(3)	1331(10)
F(2)	2166(6)	1557(3)	1166(9)
F(3)	-143(8)	796(3)	723(6)
F(4)	107(7)	2384(3)	1767(6)
F(5)	75(11)	1323(4)	2804(5)
F(6)	-118(13)	1858(4)	-315(5)

Table 3. Fractional Atomic Coordinates ($\times 10^4$) for $[W(\eta^5-C_5H_5)_2(O)(CH_3)]I$

atom	<i>x/a</i>	<i>y/b</i>	<i>z/c</i>
W	1553.0(3)	6136.6(2)	1311.7(3)
I(1)	2500(0)	2500(0)	2500(0)
I(2)	2500(0)	4810(1)	0(0)
I(3)	1187(1)	1187(1)	1187(1)
O(1)	1089(5)	6509(5)	1664(5)
C(1)	928(7)	5622(7)	914(9)
C(11)	1573(10)	5607(11)	2124(11)
C(12)	1607(12)	5262(9)	1734(13)
C(13)	2056(13)	5282(10)	1463(9)
C(14)	2361(8)	5749(16)	1645(14)
C(15)	2016(11)	5921(9)	2085(9)
C(21)	1752(13)	6225(11)	359(10)
C(22)	1415(9)	6743(13)	568(10)
C(23)	1818(10)	6977(8)	908(9)
C(24)	2213(9)	6674(8)	977(13)
C(25)	2237(11)	6246(9)	614(9)

electron oxidation of d^2 tungstenocene derivatives $[W(\eta^5-C_5H_5)_2XY]^{23}$. It has been known for many years that such complexes are readily oxidized to give an extensive and remarkably stable class of organometallic radicals containing $d^1 [W(\eta^5-C_5H_5)_2XY]^+$ cations,^{11,22,24,25} but our electrochemical study established that **1** was unique among the d^2 tungstenocene substrates examined in exhibiting two electrochemically reversible one-electron oxidations at -402 and +431 mV vs SCE. It seemed probable that the products of these oxidations were the 17-electron radical cation $[W(\eta^5-C_5H_5)_2(OCH_3)(CH_3)]^+$ and the formally 16-electron dication $[W(\eta^5-C_5H_5)_2(OCH_3)(CH_3)]^{2+}$,²³ and the isolation of either of these complexes would be of interest. Hydrogen atom abstraction from the methyl group of the monocation could result in an unprecedented insertion of a cationic methylidene ligand into a metal-oxygen bond,²⁵ while hydrogen atom abstraction from the methoxy group of

the monocation could give an unusual cationic formaldehyde complex of tungstenocene.²⁶ The dication is also of interest in that no dicationic derivatives of tungstenocene have been previously isolated, and these considerations led us to examine chemical oxidation of $[W(\eta^5-C_5H_5)_2(OCH_3)(CH_3)]$.

Oxidation of $[W(\eta^5-C_5H_5)_2(OCH_3)(CH_3)]$ in Methyl Ethyl Ketone: Formation of $[\{W(\eta^5-C_5H_5)_2(CH_3)\}_2(\mu-O)]PF_6$. Initial oxidation experiments involved the reaction of **1** with the one-electron oxidants ferrocenium hexafluorophosphate ($[Fe(\eta^5-C_5H_5)_2]PF_6$; $FcPF_6$) and trityl hexafluorophosphate ($[Ph_3C]PF_6$) in CH_2Cl_2 at -78 °C, conditions which we have previously found convenient for one-electron oxidation of $[W(\eta^5-C_5H_5)_2-RR']$ complexes to the corresponding radical cations.²⁵ With **1**, however, the products obtained by oxidation in CH_2Cl_2 were quite dependent on the precise reaction conditions (some of these products will be discussed later) and we turned instead to the use of ketonic solvents, particularly methyl ethyl ketone (MEK). This is the solvent of choice for oxidation of **1** because it is sufficiently polar to dissolve $FcPF_6$ and the primary oxidation product of **1** is insoluble in MEK while the oxidation byproducts are soluble.

Addition of 1 equiv of $FcPF_6$ to an orange MEK solution of $[W(\eta^5-C_5H_5)_2(OCH_3)(CH_3)]$ at room temperature resulted in an immediate reaction, as evidenced by a solution color change to cherry red. Within 10 min a dark red-purple flocculent solid began to precipitate from the solution. After the reaction mixture had been stirred overnight, the air-stable solid was isolated by decantation, washed with a small amount of MEK, and dried under vacuum.

¹H and ¹³C NMR spectra of the purple solid (CD_3CN) established the presence of the $[\{W(\eta^5-C_5H_5)_2(CH_3)\}]$ moiety. The material was only soluble in the most polar solvents (acetone, acetonitrile), suggesting an ionic formulation, and IR spectra of a Nujol mull of the material established the presence of the PF_6^- anion. No other functional groups could be readily identified spectroscopically, but it did prove feasible to obtain dark red-purple hexagonal plates of the complex suitable for X-ray diffraction.

Molecular Structure of $[\{W(\eta^5-C_5H_5)_2(CH_3)\}_2(\mu-O)]PF_6$. A single-crystal X-ray diffraction study of the product of oxidation of **1** in MEK established that the reaction had produced the dimeric W(V) dication $[\{W(\eta^5-C_5H_5)_2(CH_3)\}_2(\mu-O)]^{2+}$ shown in Figure 1, in which two $[W(\eta^5-C_5H_5)_2(CH_3)]^{2+}$ fragments are linked in a centrosymmetric fashion by a bridging oxygen atom such that the methyl groups adopt an *anti* orientation. Bond lengths and angles within the cation are summarized in Tables 4 and 5, respectively. Combustion analysis data for the diffraction-quality crystals are in accord with the formulation of the complex determined by the diffraction study. The ligand geometry about the unique tungsten atom in the dimer is analogous to that

(24) (a) Lindsell, W. E. *J. Chem. Soc., Dalton Trans.* **1975**, 2548. (b) Green, M. L. H.; Lindsell, W. E. *J. Chem. Soc. A* **1967**, 1455. (c) Harriss, M. G.; Green, M. L. H.; Lindsell, W. E. *J. Chem. Soc. A* **1969**, 1453. (d) Gore, E.; Green, M. L. H.; Harriss, M. G.; Lindsell, W. E.; Shaw, H. *J. Chem. Soc. A* **1969**, 1981. (e) Green, M. L. H.; Lindsell, W. E. *J. Chem. Soc. A* **1969**, 2150, 2215.

(25) (a) Hayes, J. C.; Pearson, G. D. N.; Cooper, N. J. *J. Am. Chem. Soc.* **1981**, *103*, 4648. (b) Hayes, J. C.; Cooper, N. J. *J. Am. Chem. Soc.* **1982**, *104*, 5570. (c) Hayes, J. C.; Cooper, N. J. *Organometallic Compounds: Synthesis, Structure and Theory*; Texas A&M University Press: College Station, TX, 1983; p 353. (d) Hayes, J. C.; Jernakoff, P.; Miller, G. A.; Cooper, N. J. *Pure Appl. Chem.* **1984**, *56*, 25. (e) Jernakoff, P.; Cooper, N. J. *Organometallics* **1986**, *5*, 747.

(26) For examples of formaldehyde complexes see: (a) Brown, K. L.; Roper, W. R.; Clark, G. R.; Headford, C. F. L.; Marsden, K. *J. Am. Chem. Soc.* **1979**, *101*, 503. (b) Berke, H.; Bankhardt, W.; Huttner, G.; Seyerl, J.; Zsolnai, L. *Chem. Ber.* **1981**, *114*, 2754. (c) Buhro, W. E.; Patten, A. T.; Strouse, C. E.; Gladysz, J. A.; McCormick, F. B.; Etter, M. C. *J. Am. Chem. Soc.* **1983**, *105*, 1056. (d) Gamarotta, S.; Floriani, C.; Chiesi-Villa, A.; Guastini, C. *J. Am. Chem. Soc.* **1985**, *107*, 2985.

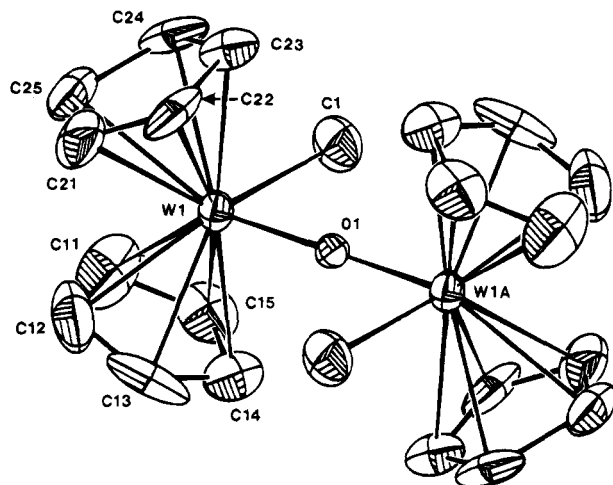


Figure 1. Molecular structure of the $[\{W(\eta^5\text{-C}_5\text{H}_5)_2(\text{CH}_3)\}_2(\mu\text{-O})]^{2+}$ cation in $2[\text{PF}_6]_2$ (50% probability ellipsoids).

Table 4. Bond Lengths (Å) within $[\{W(\eta^5\text{-C}_5\text{H}_5)_2(\text{CH}_3)\}_2(\mu\text{-O})]^{2+}$

W(1)–C(1)	2.227(8)	C(11)–C(12)	1.383(14)
W(1)–O(1)	1.904(1)	C(12)–C(13)	1.367(15)
W(1)–C(11)	2.379(8)	C(13)–C(14)	1.430(13)
W(1)–C(12)	2.349(9)	C(14)–C(15)	1.348(11)
W(1)–C(13)	2.311(9)	C(15)–C(11)	1.404(14)
W(1)–C(14)	2.345(7)	C(21)–C(22)	1.382(14)
W(1)–C(15)	2.396(8)	C(22)–C(23)	1.395(12)
W(1)–C(21)	2.331(8)	C(23)–C(24)	1.347(12)
W(1)–C(22)	2.317(9)	C(24)–C(25)	1.503(13)
W(1)–C(23)	2.323(8)	C(25)–C(11)	1.376(13)
W(1)–C(24)	2.345(8)		
W(1)–C(25)	2.399(7)		

Table 5. Bond Angles (deg) within $[\{W(\eta^5\text{-C}_5\text{H}_5)_2(\text{CH}_3)\}_2(\mu\text{-O})]^{2+}$

C(11)–C(12)–C(13)	111(1)	C(21)–C(22)–C(23)	108(1)
C(12)–C(13)–C(14)	106(1)	C(22)–C(23)–C(24)	109(1)
C(13)–C(14)–C(15)	109(1)	C(23)–C(24)–C(25)	109(1)
C(14)–C(15)–C(11)	109(1)	C(24)–C(25)–C(21)	103(1)
C(15)–C(11)–C(12)	106(1)	C(25)–C(21)–C(22)	112(1)
C(1)–W(1)–O(1)	84.3(3)	W(1)–O(1)–W(1A)	180(0)
Cp(1) ^a –W(1)–Cp(2) ^b	129.5	Cp(2)–W(1)–C(1)	104.3
Cp(1)–W(1)–C(1)	103.5	Cp(2)–W(1)–O(1)	111.0
Cp(1)–W(1)–O(1)	113.0		

^a Cp(1) is the centroid of the cyclopentadienyl ligand containing C(11)–C(15). ^b Cp(2) is the centroid of the cyclopentadienyl ligand containing C(21)–C(25).

found in other $[W(\eta^5\text{-C}_5\text{H}_5)_2\text{X}_2]$ systems²⁷ and consists of an approximately tetrahedral arrangement of two slightly staggered η^5 -cyclopentadienyl rings, the bridging oxygen atom, and a methyl group around the tungsten atom. If the two ring centroids, the oxygen atom, and the methyl carbon atom are taken to define

(27) (a) Prout, K.; Miao, F. M. *Acta Crystallogr., Sect. B* **1982**, *B38*, 945. (b) Cowie, M.; Gauthier, M. D. *Inorg. Chem.* **1980**, *19*, 3142. (c) Davis, B. R.; Bernal, I. *J. Cryst. Mol. Struct.* **1972**, *2*, 135. (d) Debaerdemaeker, T.; Kutoglu, A. *Acta Crystallogr., Sect. B* **1973**, *B29*, 2664. (e) Prout, K.; Rees, G. V. *Acta Crystallogr., Sect. B* **1974**, *B30*, 2717. (f) Prout, K.; Gale, G. D.; Forder, R. A. *Acta Crystallogr., Sect. B* **1975**, *B31*, 307. (g) Prout, K.; Jefferson, I. W.; Forder, R. A. *Acta Crystallogr., Sect. B* **1975**, *B31*, 618. (h) Kochi, J. K.; Huffman, J. C.; Klingler, R. J. *J. Am. Chem. Soc.* **1980**, *102*, 208. (i) Wolczanski, P. T.; Threlkel, R. S.; Bercaw, J. E. *J. Am. Chem. Soc.* **1979**, *101*, 218. (j) Alcock, N. W.; Howarth, O. W.; Moore, P.; Morris, G. E. *J. Chem. Soc., Chem. Commun.* **1979**, 1160. (k) Sutton, D.; Einstein, F. W. B.; Hanlan, A. J. L.; Jones, T. J. *J. Chem. Soc., Chem. Commun.* **1980**, 1078. (l) Caulton, K. G.; Huffman, J. C.; Foltz, K.; Marsella, J. A. *J. Am. Chem. Soc.* **1981**, *103*, 5596. (m) Prout, C. K.; Cameron, T. S.; Forder, R. A.; Critchley, S. R.; Denton, B.; Rees, G. V. *Acta Crystallogr., Sect. B* **1974**, *B30*, 2290.

a distorted tetrahedron, then the angles about the tungsten atom display a maximum and minimum deviation from the ideal tetrahedral value (109°) of 21 and 2° , respectively (see Table 5).

The tungsten–cyclopentadienyl carbon bond distances are not all equal within experimental error: the distances generally become longer as one moves around the rings away from the methyl group. Within Cp(1) the difference between the longest (W–C(15)) and the shortest (W–C(13)) distance is 0.085(12) Å; within Cp(2), the difference between the longest (W–C(25)) and shortest (W–C(22)) distance is 0.082(12) Å. The average values for the tungsten–cyclopentadienyl carbon bond distances (2.356(4) Å for Cp(1) and 2.343(4) Å for Cp(2)) can be compared with the 2.26–2.35 Å range observed for the analogous average distances in other $[W(\eta^5\text{-C}_5\text{H}_5)_2]$ -containing complexes.²⁷ The observed deviation in these distances indicates a slight tilting of the cyclopentadienyl rings away from perfect η^5 bonding, which may serve to reduce some of the steric strain introduced by the unsymmetrical ligand environment around the tungsten atom.

The perpendicular distances from the cyclopentadienyl mean ring planes to the tungsten atoms (2.038 Å for Cp(1) and 2.017 Å for Cp(2) and the angle between the ring normals (49.1°) lie just outside the 1.93–2.01 Å and 34 – 49° ranges, respectively, observed for the analogous values in other tungstenocene complexes.²⁷

The W(1)–O(1) bond length of 1.904(1) Å is shorter than the 2.05–2.13 Å range observed for the molybdenum–oxygen single-bond length in closely related d^2 complexes of molybdenocene²⁸ (the ionic radii of W^V and Mo^IV are essentially identical²⁹) and is indicative of some partial double-bond character arising from π -interaction between the oxygen p orbital and the two $[W(\eta^5\text{-C}_5\text{H}_5)_2(\text{CH}_3)]^{2+}$ fragment HOMO's (vide infra).

The bridging oxygen atom O(1) is located at a crystallographic center of symmetry, and the W(1)–O(1)–W(1A) group is therefore exactly linear. The dihedral angle between the plane defined by C(1), W(1), and O(1) and the plane defined by C(1A), W(1A), and O(1) is similarly required to be 180° .

Reduction of $[\{W(\eta^5\text{-C}_5\text{H}_5)_2(\text{CH}_3)\}_2(\mu\text{-O})][\text{PF}_6]_2$. Although 2^{2+} is not particularly oxygen sensitive (at least in the dark; vide infra), in sharp contrast with the recently reported isoelectronic niobium complex $[\{\text{Nb}(\eta^5\text{-C}_5\text{H}_5)_2(\text{SnMe}_3)_2(\mu\text{-O})\}]$,³⁰ the complex reacts readily under a wide range of reducing conditions, including KOH/H₂O/acetone, Li[BEt₃H], Na/Hg, and K/benzophenone in THF. These reactions were of interest, given the possibility of reducing 2^{2+} to the unknown d^2 – d^2 dimer “[$\{W(\eta^5\text{-C}_5\text{H}_5)_2(\text{CH}_3)\}_2(\mu\text{-O})$],” but no tractable products could be isolated under any of the conditions examined.

Electronic Structure of $[\{W(\eta^5\text{-C}_5\text{H}_5)_2(\text{CH}_3)\}_2(\mu\text{-O})]^{2+}$. The W(V) centers in 2^{2+} are formally d^1 , but the chemical shifts of the cyclopentadienyl and methyl ligands are within normal ranges for a diamagnetic tungstenocene complex, and the complex was deter-

(28) (a) Daran, J.; Prout, K.; Adam, G. J. S.; Green, M. L. H.; Sala-Pala, J. *J. Organomet. Chem.* **1977**, *131*, C40. (b) Kubas, G. J.; Ryan, R. R. *Inorg. Chem.* **1984**, *23*, 3181.

(29) Greenwood, N. N.; Earnshaw, A. *Chemistry of the Elements*; Pergamon Press: Oxford, U.K., 1984, p 1170.

(30) Green, M. L. H.; Hughes, A. K.; Mountford, P. *J. Chem. Soc., Dalton Trans.* **1991**, 1407.

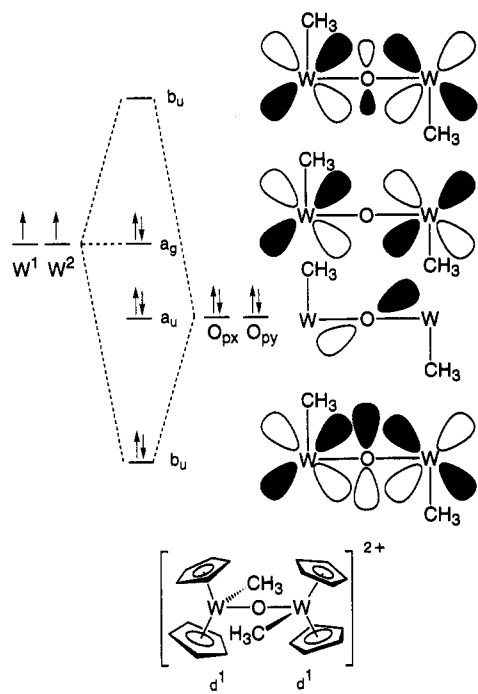


Figure 2. Frontier orbitals of $[\{W(\eta^5\text{-C}_5\text{H}_5)_2(\text{CH}_3)_2(\mu\text{-O})\}]^{2+}$ (idealized C_{2h} symmetry).

mined to be diamagnetic in the solid state at room temperature by the Gouy method ($\chi_m \sim -4.5 \times 10^{-4}$ cgsu). This observed diamagnetism can be rationalized by invoking the presence of three-center delocalized molecular orbitals formed from the overlap of the singly occupied $[W(\eta^5\text{-C}_5\text{H}_5)_2(\text{CH}_3)_2]^{2+}$ fragment HOMO's with a single p orbital of the bridging oxygen atom (Figure 2).

Spin pairing via the π -interactions in a linear oxo bridge was first invoked by Dunitz and Orgel to explain the diamagnetism of the $d^5\text{-}d^5$ dimer $[\text{Cl}_5\text{Ru}-\text{O}-\text{RuCl}_5]^{4-}$,³¹ and the concept was then used by Cotton and co-workers to explain the diamagnetism and conformations of $d^1\text{-}d^1$ dimer complexes containing linear $\text{Mo}^V(\text{O})-\text{O}-\text{Mo}^V(\text{O})$ linkages.³² These $[\text{Mo}^V_2\text{O}_3]^{4+}$ complexes provide the earliest and best known models in the literature for the molecular and electronic structure of a $d^1\text{-}d^1$ oxo bridged dimer such as 2^{2+} ,³³ and Cotton used a simple Hückel molecular orbital treatment to show that, neglecting exchange effects and destabilizing steric repulsions, the interaction between the two d orbitals and a single oxygen p orbital (corresponding to

a $\text{Mo}(\text{O}_t)(\text{O}_b)-\text{Mo}(\text{O}_t)(\text{O}_b)$ dihedral angle of 0 or 180°) is energetically more favorable than two separate d-p interactions (corresponding to a $\text{Mo}(\text{O}_t)(\text{O}_b)-\text{Mo}(\text{O}_t)(\text{O}_b)$ dihedral angle of 90° and giving rise to a triplet structure).³² Since it is well-established that the frontier orbital containing the odd electron in d^1 bent metallocene complexes of the $[\text{M}(\eta^5\text{-C}_5\text{H}_5)_2\text{XY}]$ type is a mixture of d_{z^2} and $d_{x^2-y^2}$ located within the MXY plane with its major radial extent outside the XMY angle,^{23,34} such a three-center π -interaction leads, as shown in Figure 2, to the observed structure in which the W atoms, the bridging O atom, and the methyl groups all lie in a plane with an anti orientation for the methyl groups. The W frontier orbitals and the two oxygen p orbitals form one bonding, two nonbonding, and one antibonding orbital, and low spin population of these orbitals leads to a singlet ground state and a W-O bond order of 1.5, consistent with the short W-O bond length.

Similar bonding descriptions have been advanced to account for the diamagnetism of several $d^1\text{-}d^1$ dimers of bent niobocene derivatives established crystallographically to have linear oxo bridges between the Nb(IV) centers.^{10,30} These include $[\{\text{Nb}(\eta^5\text{-C}_5\text{H}_5)_2(n\text{-Bu})\}_2(\mu\text{-O})]$,³⁵ $[\{\text{Nb}(\eta^5\text{-C}_5\text{H}_4\text{Me})_2\text{Cl}\}_2(\mu\text{-O})]$,³⁶ and $[\{\text{Nb}(\eta^5\text{-C}_5\text{H}_5)_2(\text{SnMe}_3)_2\}_2(\mu\text{-O})]$,³⁰ and the structures of these complexes and of 2^{2+} provide an interesting contrast with the structures of $d^0\text{-}d^0$ bent metallocene dimers containing oxo bridges. As summarized in Table 6, the $d^0\text{-}d^0$ dimers all have M-O-M' groups which approach linear geometries (reported M-O-M angles range from $165.8(0)^\circ$ to 177.0°) and relatively short M-O bonds, characteristics which both suggest significant π -donation of the oxygen nonbonding electrons into the same (but now empty) metallocene frontier orbital in the MXY plane. There is now, however, a dihedral angle of $54\text{-}77^\circ$ between the MXO and the M'X'O planes, in sharp contrast with the 180° dihedral angle in the $d^1\text{-}d^1$ cases and consistent with strong π -interactions between the metal centers and both of the oxygen electron pairs in orthogonal p-orbitals.

The description of the electronic structure of 2^{2+} embodied in Figure 2 accounts well for its unusual electronic spectrum, shown in Figure 3. Most tungstenocene complexes are d^0 , d^1 , or d^2 systems with yellow, orange, or red colors arising from strong UV absorptions with tails in the visible or relatively weak, high-energy visible absorptions. The only common exceptions contain halide ligands, in which case the

(31) Dunitz, J. D.; Orgel, L. E. *J. Chem. Soc.* **1953**, 2594.

(32) Blake, A. B.; Cotton, F. A.; Wood, J. S. *J. Am. Chem. Soc.* **1964**, *86*, 3024.

(33) Analogous $[\text{W}^V_2\text{O}_3]^{4+}$ complexes have only recently been reported: (a) Yu, S.-B.; Holm, R. H. *Inorg. Chem.* **1989**, *28*, 4385. (b) Lee, S.; Staley, D. L.; Rheingold, A. L.; Cooper, N. J. *Inorg. Chem.* **1990**, *29*, 4391.

(34) (a) Green, J. C.; Green, M. L. H.; Prout, C. K. *J. Chem. Soc., Chem. Commun.* **1972**, 421. (b) Green, M. L. H. *Pure Appl. Chem.* **1972**, *30*, 373. (c) Prout, C. K.; Cameron, T. S.; Forster, R. A.; Critchley, S. R.; Denton, B.; Rees, G. V. *Acta Crystallogr., Sect. B* **1974**, *B30*, 2290. (d) Petersen, J. F.; Dahl, L. F. *J. Am. Chem. Soc.* **1974**, *96*, 2248. (e) Petersen, J. F.; Dahl, L. F. *J. Am. Chem. Soc.* **1975**, *97*, 6416. (f) Petersen, J. F.; Dahl, L. F. *J. Am. Chem. Soc.* **1975**, *97*, 6422. (g) Petersen, J. F.; Lichtenberger, D. L.; Fenske, R. F.; Dahl, L. F. *J. Am. Chem. Soc.* **1975**, *97*, 6433. (h) Green, J. C.; Jackson, S. E.; Higginson, B. *J. Chem. Soc., Dalton Trans.* **1975**, 403. (i) Lauher, J. W.; Hoffman, R. *J. Am. Chem. Soc.* **1976**, *98*, 1729. (j) Clark, J. P.; Green, J. C. *J. Less-Common Met.* **1977**, *54*, 63. (k) Cauletti, C.; Clark, J. P.; Green, J. C.; Jackson, S. E.; Fraga, I. L.; Ciliberto, E.; Coleman, A. W. *J. Electron. Spectrosc. Relat. Phenom.* **1980**, *18*, 61. (l) Bruce, M. R. M.; Kenter, A.; Tyler, D. R. *J. Am. Chem. Soc.* **1984**, *106*, 639.

(35) Kirillova, N. I.; Lemenovski, D. A.; Baukova, T. V.; Struchkov, Yu. T. *Sov. J. Coord. Chem. (Engl. Transl.)* **1977**, *3*, 1254.

(36) (a) Skripkin, Yu. V.; Evemenko, I. L.; Pasynskii, A. V.; Volkov, O. G.; Bakun, S. I.; Porai-Koshits, M. A.; Antsyshkina, A. S.; Dikareva, L. M.; Ostrikova, V. N.; Sakharov, S. G.; Struchkov, Yu. T. *Sov. J. Coord. Chem. (Engl. Transl.)* **1985**, *3*, 570. (b) Lemenovskii, D. A.; Urazowski, I. F.; Nifant'ev, I. E.; Perevalova, E. G. *J. Organomet. Chem.* **1985**, *292*, 217.

(37) Thewalt, U.; Keibel, B. *J. Organomet. Chem.* **1978**, *150*, 59.

(38) Thewalt, U.; Schleussner, G. *Angew. Chem., Int. Ed. Engl.* **1978**, *17*, 531.

(39) LePage, Y.; Heyding, R. D.; Hunter, B. K.; McCowan, J. D. *J. Organomet. Chem.* **1980**, *193*, 201.

(40) Rausch, M. D.; Sikora, D. J.; Hrnrcir, D. C.; Hunter, W. E.; Atwood, J. L. *Inorg. Chem.* **1980**, *19*, 3817.

(41) Fronczek, F. R.; Baker, E. C.; Sharp, P. R.; Raymond, K. N.; Alt, H. G.; Rausch, M. D. *Inorg. Chem.* **1976**, *15*, 2284 and references therein.

(42) Clarke, J. F.; Drew, M. G. B. *Acta Crystallogr., Sect. B* **1974**, *B30*, 2267.

(43) Hunter, W. E.; Hrnrcir, D. C.; Bynum, R. V.; Penttila, R. A.; Atwood, J. L. *Organometallics* **1983**, *2*, 750.

(44) Peterson, J. L. *J. Organomet. Chem.* **1979**, *166*, 179.

Table 6. Selected Molecular Parameters for Bridging-Oxo Metallocene Complexes of the Type $[\{M(\eta^5-C_5H_5)_2X\}_2(\mu-O)]^{n+}$ ($n = 0, 2$)

complex	electron count	M-O-M' angle (deg)	dihedral angle ^a (deg)	M-O bond length (Å)
$[\{Ti(\eta^5-C_5H_5)_2(OH_2)\}_2(\mu-O)][ClO_4]_2^{27}$	d ⁰ -d ⁰	175.8(5)	74.1	1.829(2)
$[\{Ti(\eta^5-C_5H_5)_2(OH_2)\}_2(\mu-O)][S_2O_6]^{38}$	d ⁰ -d ⁰	177.0	74.1	1.834
$[\{Ti(\eta^5-C_5H_5)_2Cl\}_2(\mu-O)]^{39}$	d ⁰ -d ⁰	173.8	75.4	1.837(2)
$[\{Ti(\eta^5-C_5H_5)_2(C\{CF_3\}H)\}_2(\mu-O)]^{40}$	d ⁰ -d ⁰	170.0(2)	53.9 (avg)	1.856(6)
$[\{Hf(\eta^5-C_5H_5)_2(CH_3)\}_2(\mu-O)]^{41}$	d ⁰ -d ⁰	173.9(3)	75.4	1.941(3)
$[\{Zr(\eta^5-C_5H_5)_2Cl\}_2(\mu-O)]^{42}$	d ⁰ -d ⁰	168.9(8)	74.3	1.94(1)
$[\{Zr(\eta^5-C_5H_5)_2(CH_3)\}_2(\mu-O)]^{43}$	d ⁰ -d ⁰	174.1(3)	76.6	1.948(1)
$[\{Zr(\eta^5-C_5H_5)_2(SPh)\}_2(\mu-O)]^{44}$	d ⁰ -d ⁰	165.8(8)	61.7	1.966(3) (avg)
$[\{Nb(\eta^5-C_5H_5)_2Cl\}_2(\mu-O)][BF_4]_2^{27m}$	d ⁰ -d ⁰	169.3(8)	72.5	1.88(1)
$[\{Nb(\eta^5-C_5H_5)_2(C_4H_9)\}_2(\mu-O)]^{35}$	d ¹ -d ¹	180	180	1.926(2)
$[\{Nb(\eta^5-C_5H_5)_2(SnMe_3)\}_2(\mu-O)]^{30}$	d ¹ -d ¹	180	180	1.9434(4)
$[\{Nb(\eta^5-C_5H_4Me)_2Cl\}_2(\mu-O)]^{36}$	d ¹ -d ¹	180	180	na ^b

^a Defined as the angle between the X-M-O and X'-M'-O planes. A value of 0° would correspond to a *syn* orientation of the X and X' ligands. ^b na = not available from published data.

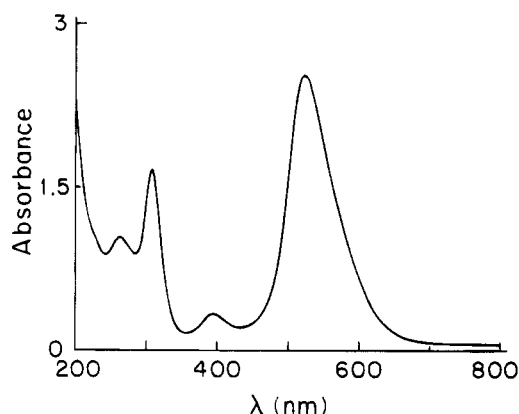
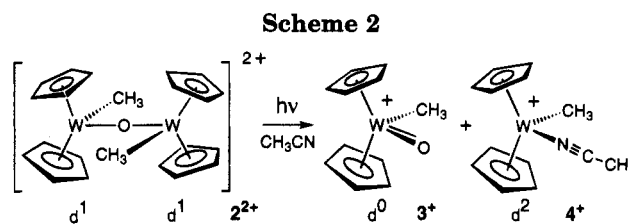


Figure 3. Electronic spectrum of a 1.2×10^{-4} mole L^{-1} solution of $[\{W(\eta^5-C_5H_5)_2(CH_3)_2(\mu-O)\}][PF_6]_2$ in CH_3CN .

complexes are more intensely colored (often green), probably as a consequence of LMCT absorptions in the visible region. Complex 2^{2+} is, however, unique in having a spectrum dominated by a very strong visible absorption at 525 nm ($\epsilon = 23\,600\text{ L mol}^{-1}\text{ cm}^{-1}$), which gives solutions of this material an intense red-purple color. This band is very similar to the strong absorptions at ca. 500 nm, which are a common,⁴⁵ if not universal,⁴⁶ characteristic of d¹-d¹ dimers containing $[MoV_2O_3]^{4+}$ cores with linear oxo bridges and can be assigned to promotion from the a_g nonbonding orbital to the b_u antibonding orbital in Figure 2. A small energy gap would be expected between these orbitals, consistent with the low energy of the absorption, and the transition would have some MLCT character which would account for the intensity of the absorption.

The validity of this interpretation of the electronic spectrum of 2^{2+} is supported by the observation that the closely related d¹-d¹ dimer $[\{Nb(\eta^5-C_5H_5)_2(SnMe_3)\}_2(\mu-O)]$, in which the metal centers are similarly spin-paired through the linear oxo bridge, is described as forming an "intensely blue solution" consistent with the presence of similar intense absorptions in the visible region.³⁰ In sharp but not surprising contrast, the closely related d⁰-d⁰ dimer of niobium $[\{Nb(\eta^5-C_5H_5)_2Cl\}_2(\mu-O)][BF_4]_2$ is orange,^{27m} while most of the group 4 d⁰-d⁰ dimers in Table 6 are colorless.

Photodisproportionation of $[\{W(\eta^5-C_5H_5)_2(CH_3)_2(\mu-O)\}][PF_6]_2$. The bridging oxo dimer 2^{2+} is quite



photosensitive, and the purple color of a solution of $2[PF_6]_2$ in acetonitrile was discharged and replaced with a pale orange color after ca. 1.5 h of irradiation with a sunlamp. A 1H NMR spectrum of the solid obtained from such a reaction (acetone- d_6) contained singlet resonances of equal intensity in the cyclopentadienyl region at δ 6.90 and 5.38, together with two new methyl peaks at δ 2.30 and 0.30 with satellites indicative of bonding to W (^{183}W , $I = 1/2$, 14% abundance) and a resonance at δ 2.82 assigned to coordinated acetonitrile. This spectrum suggested that 2^{2+} had undergone the photodisproportionation reaction shown in Scheme 2 to give the novel terminal oxo complex $[W(\eta^5-C_5H_5)_2(O)(CH_3)]^+$ (3^+) and the tungstenocene methyl complex $[\{W(\eta^5-C_5H_5)_2(CH_3)\}^+]$,⁴⁷ trapped by the coordinating solvent acetonitrile as the 18-electron complex $[W(\eta^5-C_5H_5)_2(NCCH_3)(CH_3)]^+$ (4^+).

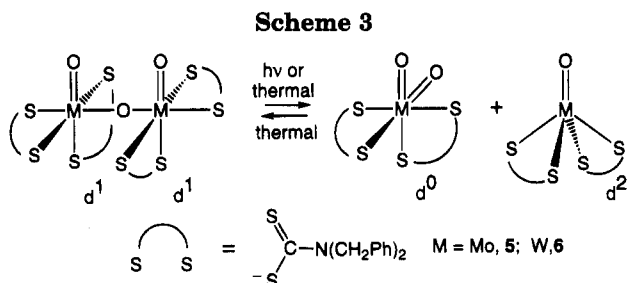
It is well-established that many of the d¹-d¹ oxo-bridged dimers containing $[MoV_2O_3]^{4+}$ cores participate in facile thermal disproportionation equilibria which give d⁰ and d² monomers containing $[Mo^{IV}O_2]^{2+}$ and $[Mo^{IV}O]^{2+}$ cores,^{45,48} and we have recently reported that at least two examples of such molecules, the dithiocarbamate complex $[Mo_2O_3\{S_2CN(CH_2Ph)_2\}_4]$ (**5**) and its tungsten analog **6**, exhibit marked photochromism because the disproportionation equilibria can be accessed both thermally and photochemically; i.e., irradiation

(47) It is still unresolved whether this species is a 16-electron cationic alkyl complex, an 18-electron agostic alkyl complex, or a methylenide hydride complex as originally proposed: Cooper, N. J.; Green, M. L. H. *J. Chem. Soc., Dalton Trans.* **1979**, 1121. See also discussion in: McNally, J. P.; Cooper, N. J. *J. Am. Chem. Soc.* **1989**, *111*, 4500.

(48) For examples see: (a) Chen, G. J. J.; McDonald, J. W.; Newton, W. E. *Inorg. Chem.* **1976**, *15*, 2612. (b) Tanaka, T.; Tanaka, K.; Matsuda, T.; Hashi, K. In *Molybdenum Chemistry of Biological Significance*; Newton, W. E.; Otsuka, K.; Eds.; Plenum Press: New York, 1980; p 361. (c) Hyde, J.; Venkatasubramanian, K.; Zubietta, J. *Inorg. Chem.* **1978**, *17*, 414. (d) Newton, W. E.; Corbin, J. L.; Bravard, D. C.; Searles, J. E.; McDonald, J. W. *Inorg. Chem.* **1974**, *13*, 1100. (e) Tatsumisago, M.; Matsubayashi, G.; Tanaka, T.; Nishigaki, S.; Nakatsu, K. *J. Chem. Soc., Dalton Trans.* **1982**, 121. (f) Barral, R.; Bocard, C.; Séré de Roch, I.; Sajus, L. *Tetrahedron Lett.* **1972**, 1693. (g) Matsuda, T.; Tanaka, K.; Tanaka, T. *Inorg. Chem.* **1979**, *18*, 454.

(45) Stiefel, E. I. *Prog. Inorg. Chem.* **1977**, *22*, 1.

(46) Craig, J. A.; Harlan, E. W.; Snyder, B. S.; Whitener, M. A.; Holm, R. H. *Inorg. Chem.* **1989**, *28*, 2082.



tion of **5** and **6** induces disproportionation which is then reversed thermally (Scheme 3).^{33b}

The photodisproportionation in Scheme 2 provides an intriguing complement to reactions such as those shown in Scheme 3, since the tungstenocene complex **2**²⁺ provides the first example in which disproportionation of a d¹-d¹ dimer with a linear oxo bridge can be photochemically induced but is not observed thermally at room temperature. This led us to undertake a detailed study (on which we have already made a report^{49a}) of the photochemical and thermal disproportionation of **2**²⁺. This study has provided information on the quantum yield for the photodisproportionation and the kinetic parameters of the thermal disproportionation, but a prerequisite for the physical studies was the unambiguous characterization of **3**⁺ and **4**⁺, and this led us to attempt independent syntheses to confirm the identity of **3**⁺ and **4**⁺. The successful syntheses described below allowed us to confirm the hypothesis in Scheme 2 by comparison of the NMR characteristics of the pure complexes with those of the materials formed by photolysis of **2**²⁺.

Synthesis of the Acetonitrile-Methyl Cation $[\text{W}(\eta^5\text{-C}_5\text{H}_5)_2(\text{NCCH}_3)(\text{CH}_3)]^+$. It has been known since 1979 that monomethyl tungstenocene complexes such as the benzoate $[\text{W}(\eta^5\text{-C}_5\text{H}_5)_2\{\text{OC}(\text{O})\text{Ph}\}(\text{CH}_3)]$ can be prepared by treatment of the dimethyl complex $[\text{W}(\eta^5\text{-C}_5\text{H}_5)_2(\text{CH}_3)_2]$ (**7**) with a protonic acid (benzoic acid in this case), in a sequence which presumably involves protolytic removal of one of the methyl groups as methane.²² We have extended this approach to the synthesis of the acetonitrile methyl cation $[\text{W}(\eta^5\text{-C}_5\text{H}_5)_2(\text{NCCH}_3)(\text{CH}_3)]^+$ (**4**⁺) by reacting **7** with $[\text{NH}_4]\text{PF}_6$ in acetonitrile (Scheme 1). The ammonium ion is a strong enough acid to protonate **7**, and in the absence of a coordinating anion such as benzoate, the 16-electron $[\text{W}(\eta^5\text{-C}_5\text{H}_5)_2(\text{CH}_3)]^{+47}$ cation is trapped by the coordinating solvent as **4**⁺. This cation was isolated as the hexafluorophosphate salt **4** $[\text{PF}_6]$ in 70% yield and was fully characterized by combustion analysis and spectroscopy as described in the Experimental Section. Comparison of the NMR characteristics of **4**⁺ with those of a solution of **2** $[\text{PF}_6]_2$ in CD_3CN following photolysis confirmed that the higher field cyclopentadienyl and methyl resonances in the photolyzed solution had been correctly assigned to **4**⁺.

Synthesis and Structural Characterization of the d⁰ Oxo-Methyl Cation $[\text{W}(\eta^5\text{-C}_5\text{H}_5)_2(\text{O})(\text{CH}_3)]^+$. The acetonitrile ligand in the complex **4**⁺ is substitutionally labile both thermally and photochemically, so that **4**⁺ is a convenient starting material for a number of tungstenocene methyl complexes of the $[\text{W}(\eta^5\text{-C}_5\text{H}_5)_2$

$(\text{CH}_3)\text{X}]$ and $[\text{W}(\eta^5\text{-C}_5\text{H}_5)_2(\text{CH}_3)\text{L}]^+$ types (X⁻ and L represent anionic and neutral two-electron ligands, respectively).^{49b} This led us to examine photolysis of **4**⁺ under O₂, and we have observed that this provides a convenient route to the d⁰ oxo methyl complex $[\text{W}(\eta^5\text{-C}_5\text{H}_5)_2(\text{O})(\text{CH}_3)]^+$.

Photolysis of **4**⁺ under O₂ was conveniently carried out in acetone, and after ca. 1 h irradiation with a sunlamp the orange color of **4**⁺ had been discharged from a solution of **4** $[\text{PF}_6]$ and replaced by a pale yellow color. Filtration and removal of the solvent gave spectroscopically pure yellow crystalline flakes which could be recrystallized as lemon yellow flakes by slow concentration of a saturated acetone/toluene solution of the material under reduced pressure. Combustion analysis was consistent with a C₁₁H₁₃WOPF₆ stoichiometry, and a ¹H NMR spectrum in CD₃CN contained resonances at δ 6.58 and 2.16, the latter with tungsten satellites, which were integrated as 10 and 3 protons, respectively, consistent with the presence of a complex containing a $[\text{W}(\eta^5\text{-C}_5\text{H}_5)_2(\text{CH}_3)]$ moiety. The complex was insoluble in aromatic and ethereal solvents, and the presence of the characteristic IR absorptions of PF₆⁻ confirmed that the compound was a salt.

The spectroscopic and analytical data were consistent with formulation of the oxidation product as the terminal-oxo methyl complex $[\text{W}(\eta^5\text{-C}_5\text{H}_5)_2(\text{O})(\text{CH}_3)]\text{PF}_6$ (**3** $[\text{PF}_6]$), but it was not feasible on the basis of the available spectroscopic data to rule out formulation of the product as a dimer with a double oxo bridge, viz. $[\{\text{W}(\eta^5\text{-C}_5\text{H}_5)_2(\text{CH}_3)(\mu\text{-O})\}_2]^{2+}$. Either formulation would account for the stoichiometry of the complex, and there is literature precedent for double oxo bridges between d⁰ metal centers.⁵⁰ This ambiguity led us to attempt to characterize the complex crystallographically, but initial efforts were frustrated by the high solubility of the complex in polar solvents, which negated attempts to grow diffraction-quality crystals of the PF₆⁻ salt via layer diffusion, vapor diffusion, or low-temperature recrystallization.

The crystallization problems were circumvented by exchange of I⁻ for the PF₆⁻ counterion to give a salt of **3**⁺ with reduced solubility in polar nonaqueous solvents. The exchange was carried out by addition of a 0 °C solution of **3** $[\text{PF}_6]$ in acetone to a 0 °C solution of NaI in acetone to precipitate **3** $[\text{I}]$ as golden crystalline flakes. IR spectra of these flakes suggested that the desired exchange reaction had probably occurred, since the absorption bands characteristic of the PF₆⁻ anion were not observed, while the presence of a relatively strong and sharp band at 867 cm⁻¹ (previously masked by the 840 cm⁻¹ absorption of PF₆⁻) was consistent with the presence of a terminal tungsten-oxo bond within the exchanged complex.¹ This value is somewhat below the 900–1100 cm⁻¹ range usually cited for terminal metal oxo groups⁵¹ but is similar to the value of 789–879 cm⁻¹ previously reported for the W=O stretch in $[\text{W}(\eta^5\text{-C}_5\text{H}_5)_2(\text{O})]$.⁵² ¹H and ¹³C NMR spectra of the flakes confirmed that the tungstenocene cation had remained intact during the anion exchange.

(50) (a) Smith, C. J.; Caughlin, C. N.; Campbell, J. A. *Inorg. Chem.* **1972**, *11*, 2989. (b) Bottomley, F.; Egharevba, G. O.; Lin, I. J. B.; White, P. S. *Organometallics* **1985**, *4*, 550.

(51) Barraclough, C. G.; Lewis, J.; Nyholm, R. S. *J. Chem. Soc.* **1959**, 3552.

(52) Green, M. L. H.; Lynch, A. H.; Swanwick, M. G. *J. Chem. Soc., Dalton Trans.* **1972**, 1445.

(49) (a) Thompson, R. L.; Hopkins, M. D.; Cooper, N. J.; Lee, S. *Organometallics* **1995**, *14*, 1969. (b) Hayes, J. C.; Jernakoff, P.; Cooper, N. J. To be submitted for publication.

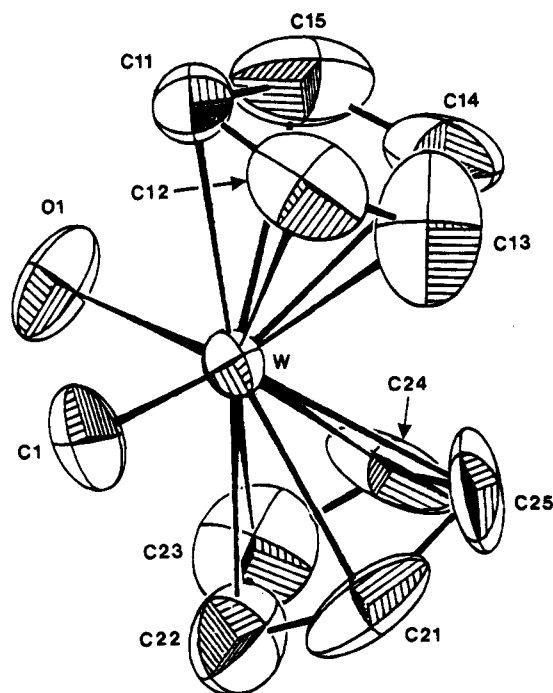


Figure 4. Molecular structure of the $[\text{W}(\eta^5\text{-C}_5\text{H}_5)_2(\text{O})(\text{CH}_3)]^+$ cation in **3**[I] (50% probability ellipsoids).

Table 7. Bond Lengths (Å) within $[\text{W}(\eta^5\text{-C}_5\text{H}_5)_2(\text{O})(\text{CH}_3)]^+$

W-C(1)	2.219(16)	C(11)-C(12)	1.285(31)
W-O(1)	1.700(11)	C(12)-C(13)	1.289(31)
W-C(11)	2.386(23)	C(13)-C(14)	1.442(37)
W-C(12)	2.392(20)	C(14)-C(15)	1.437(34)
W-C(13)	2.467(19)	C(15)-C(11)	1.338(30)
W-C(14)	2.352(21)	C(21)-C(22)	1.605(34)
W-C(15)	2.280(18)	C(22)-C(23)	1.419(30)
W-C(21)	2.403(20)	C(23)-C(24)	1.235(26)
W-C(22)	2.385(19)	C(24)-C(25)	1.382(29)
W-C(23)	2.384(19)	C(25)-C(21)	1.347(29)
W-C(24)	2.250(21)		
W-C(25)	2.418(20)		

Bright yellow cubes of **3**[I] suitable for a diffraction study were obtained via vapor diffusion of diethyl ether into a saturated acetone solution of the complex, and single-crystal X-ray diffraction was used to characterize one of the cubes structurally as described in the Experimental Section. The displacement coefficients for the C and O atoms in the structure are somewhat high, limiting the precision of the derived bond lengths and angles, but the diffraction study does unambiguously establish that **3**[I] contains the terminal oxo alkyl complex $[\text{W}(\eta^5\text{-C}_5\text{H}_5)_2(\text{O})(\text{CH}_3)]^+$ as the discrete, monomeric cation illustrated in Figure 4 and characterized by the bond lengths and angles in Tables 7 and 8.

The niobocene complex isoelectronic with 3^+ , $[\text{Nb}(\eta^5\text{-C}_5\text{H}_5)_2(\text{O})(\text{CH}_3)]$, is known,⁵³ together with the related complexes $[\text{Nb}(\eta^5\text{-C}_5\text{H}_5)_2(\text{O})(\text{X})]$ (X = Cl, $\alpha\text{-C}_4\text{H}_3\text{S}$, $\alpha\text{-CH}_2\text{-C}_5\text{H}_4\text{N}$),⁵⁴ and the decamethyltungstenocene analog $[\text{W}(\eta^5\text{-C}_5\text{Me}_5)_2(\text{O})(\text{CH}_3)]^+$,⁵⁵ but $[\text{Nb}(\eta^5\text{-C}_5\text{H}_4\text{SiMe}_3)_2(\text{O})(\text{CH}_3)]$,⁵⁶ $[\text{Mo}(\eta^5\text{-C}_5\text{H}_4\text{CH}_3)_2(\text{O})]$,⁵⁷ and $[\text{Ta}(\eta^5\text{-C}_5\text{Me}_5)_2\text{-}$

Table 8. Bond Angles (deg) within $[\text{W}(\eta^5\text{-C}_5\text{H}_5)_2(\text{O})(\text{CH}_3)]^+$

C(11)-C(12)-C(13)	115(3)	C(21)-C(22)-C(23)	99(2)
C(12)-C(13)-C(14)	108(2)	C(22)-C(23)-C(24)	113(2)
C(13)-C(14)-C(15)	99(2)	C(23)-C(24)-C(25)	114(3)
C(14)-C(15)-C(11)	111(2)	C(24)-C(25)-C(21)	107(3)
C(15)-C(11)-C(12)	106(3)	C(25)-C(21)-C(22)	106(2)
C(1)-W-O(1)	93.8(7)		
Cp(1) ^a -W-Cp(2) ^b	128.6	Cp(2)-W-C(1)	104.2
Cp(1)-W-C(1)	100.2	Cp(2)-W-O(1)	111.7
Cp(1)-W-O(1)	111.0		

^a Cp(1) is the centroid of the cyclopentadienyl ligand containing C(11)-C(15). ^b Cp(2) is the centroid of the cyclopentadienyl ligand containing C(21)-C(25).

(O)H]⁵⁸ are the only other crystallographically characterized terminal-oxo complexes of metallocenes.

The 3^+ cation contains an approximately tetrahedral arrangement of two η^5 -cyclopentadienyl rings, a terminally bound oxygen atom, and a methyl group bound to a central tungsten atom. If the two ring centroids, the oxygen atom, and the methyl carbon atom are used to determine a distorted tetrahedron, then the angles about W display a maximum and minimum deviation from the tetrahedral value (109°) of 20 and 2°, respectively (see Table 8).

The tungsten-cyclopentadienyl carbon bond distances are not all equal within experimental error: the distances become progressively longer as one moves around the rings away from the terminal oxo ligand. The difference between the longest (W-C(13)) and the shortest (W-C(15)) distance within Cp(1) is 0.186(26) Å; the difference between the longest (W-C(25)) and the shortest (W-C(24)) distance within Cp(2) is 0.166(29) Å. The average values of the tungsten-cyclopentadienyl carbon bond distances (2.375(9) Å for Cp(1) and 2.368(9) Å for Cp(2)) lie just outside the 2.26–2.35 Å range typically observed for the analogous values in other $[\text{W}(\eta^5\text{-C}_5\text{H}_5)_2]$ -containing complexes.²⁷

The cyclopentadienyl rings within the structure are tilted slightly away from perfect η^5 bonding, as manifested in values for the angles between the ring normals and the corresponding tungsten ring centroid vectors of 5.3° for Cp(1) and 1.2° for Cp(2). The origin and significance of this tilt are, however, unclear, given the level of precision of the present crystallographic study. The perpendicular distances from the cyclopentadienyl mean ring planes to the tungsten atoms (2.067 Å for Cp(1) and 2.049 Å for Cp(2)) and the angle between the ring normals (52.6°) lie somewhat outside the 1.93–2.01 Å and 34–49° ranges, respectively, observed for the analogous values in other tungstenocene complexes.²⁷ The dihedral angle between the plane defined by the two ring centroids and W and the plane defined by C(1), W, and O(1) is 88.4°, a value consistent with the pseudotetrahedral structure of the cation.

The $\text{W}^{\text{VI}}\text{-CH}_3$ σ bond length of 2.219(16) Å cannot be distinguished from the $\text{W}^{\text{V}}\text{-CH}_3$ σ bond of 2.227(8) Å in 2^{2+} , but may be shorter than the values of 2.25(2) and 2.25(2) Å in the literature for the $\text{W}^{\text{IV}}\text{-C}$ σ bonds in tungstenocene alkyls such as $[\text{W}(\eta^5\text{-C}_5\text{H}_5)_2(\text{CH}_2\text{C}_6\text{H}_3\text{-Me}_2)_2]^{27g}$ and $[\text{W}(\eta^5\text{-C}_5\text{H}_5)_2(\text{CH}_2\text{CH}_2\text{PMe}_2\text{Ph})(\text{CH}_3)]^+$.^{27f}

(53) Middleton, A. R.; Wilkinson, G. *J. Chem. Soc., Dalton Trans.* **1980**, 1888.

(54) (a) Lemenovskii, D. A.; Baukova, T. V.; Knizhnikov, V. A.; Perevalova, E. G.; Nesmeyanov, A. N. *Dokl. Chem. (Engl. Transl.)* **1976**, *226*, 65. (b) Broussier, R.; Normand, H.; Gautheron, B. *J. Organomet. Chem.* **1978**, *155*, 347.

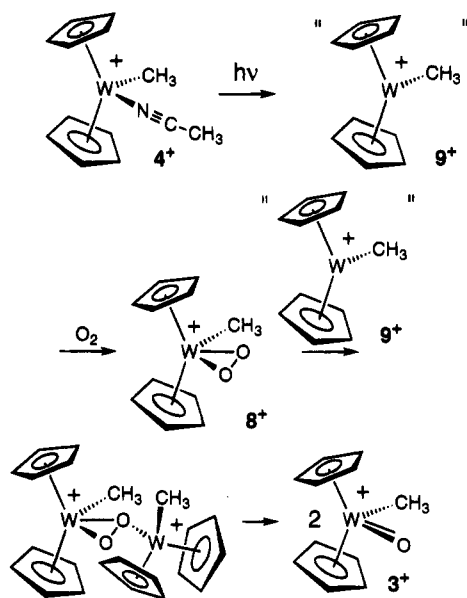
(55) Parkin, G.; Bercaw, J. E. *Polyhedron* **1988**, *7*, 2053.

(56) Antinolo, A.; de Ilarduya, J. M.; Otero, A.; Royo, P.; Lanfredi, A. M. M.; Tiripicchio, A. *J. Chem. Soc., Dalton Trans.* **1988**, 2685.

(57) Tyler, D. R.; Chiang, M. Y.; Silavwe, N. D. *Inorg. Chem.* **1985**, *24*, 4219.

(58) Parkin, G.; van Asselt, A.; Leahy, D. J.; Whinnery, L.; Hua, N. G.; Quan, R. W.; Hemling, L. M.; Schaefer, W. P.; Santarsiero, B. D.; Bercaw, J. E. *Inorg. Chem.* **1992**, *31*, 82.

Scheme 4



The $W^{VI}-CH_3$ bond in 3^+ is, however, somewhat longer than W^{VI} -alkyl σ bonds in some other ligand environments such as that in $[W_2O_3(CH_2CMe_3)_6]$ (2.134(8) Å).⁵⁹

The W-O(1) bond distance of 1.700(11) Å falls within the 1.66–1.73 Å range observed for the M=O bond distances in d^0 and d^1 complexes of Mo and W (the ionic radii of these two metals are essentially identical in both oxidation states²⁹). The C(1)-W-O(1) bond angle of 93.8(7)° falls just within the 93–98° range observed for the XMX angle in d^0 bent metallocene complexes.²⁷

With $3[I]$ fully characterized structurally and spectroscopically, we were able to confirm by comparison with the 1H NMR spectra of an isolated sample that the lower field cyclopentadienyl and methyl resonances in the solution formed by photolysis of 2^{2+} in CH_3CN had been correctly assigned to 3^+ and that Scheme 2 does describe the photolysis reaction.

Mechanism of the Oxidation of $[W(\eta^5-C_5H_5)_2(NCCH_3)(CH_3)]^+$ to $[W(\eta^5-C_5H_5)_2(O)(CH_3)]^+$. It was clear from the reaction conditions that molecular oxygen was the source of the oxo ligand in 3^+ , and 3^+ could not be formed from 4^+ in the absence of oxygen or air. We also examined the reaction of 4^+ with excess water under nitrogen in acetone—only traces of 2^{2+} were formed when this mixture was gently heated, and formation of 3^+ was not observed.

Deliberate irradiation is not essential for the oxidation of 4^+ to 3^+ , and the reaction typically proceeds in good yield when a solution of $4[PF_6]$ in acetone is stirred under air or oxygen for 1 day. The reaction is, however, less reproducible under these conditions (presumably as a consequence of variations in laboratory illumination), and use of a sunlamp is recommended to allow a more convenient reaction time and to ensure reproducibility. Irradiation of 4^+ probably induces dissociation of the acetonitrile ligand and generates coordinatively unsaturated $[W(\eta^5-C_5H_5)_2(CH_3)]^+$,⁴⁷ which can complex molecular oxygen (Scheme 4). Details of subsequent steps have not been established, but a reasonable possibility,³ as shown in Scheme 4, is that the O_2 adduct is the 18-electron peroxide complex 8^+ and peroxo

cleavage is induced by coordination of a second $[W(\eta^5-C_5H_5)_2(CH_3)]^+$ (9^+) fragment. Circumstantial support for this mechanism is provided by the report of the structural characterization of $[Nb(\eta^5-C_5H_5)_2(\eta^2-O_2)Cl]$, isoelectronic with 8^+ , as an η^2 -peroxo complex.⁶⁰

If the role of 4^+ is solely that of a source of 9^+ , we should be able to prepare 3^+ from other 9^+ sources. We have confirmed that this is indeed the case, most intriguingly in the present system by examining the photolysis of the bridging oxo complex 2^{2+} in acetone. Under nitrogen, this gave a complex mixture of tungstenocene derivatives, including 3^+ , $[W(\eta^5-C_5H_5)_2(C_2H_4)H]^+$, and at least five other tungstenocene derivatives (1H NMR). Under air, however, the purple color of 2^{2+} was rapidly replaced by a pale yellow color and 1H NMR analysis indicated essentially quantitative conversion to 3^+ , consistent with photochemical disproportionation of 2^{2+} to a mixture of 3^+ and 9^+ and subsequent oxidation of the 9^+ to 3^+ by molecular oxygen.

Mechanism of the Oxidation of $[W(\eta^5-C_5H_5)_2(OCH_3)(CH_3)]$ to $[W(\eta^5-C_5H_5)_2(CH_3)_2(\mu-O)]^{2+}$ in MEK. The origin of the bridging oxo group in 2^{2+} is an obvious question posed by the oxidation of 1 to 2^{2+} , but it is one to which we do not have an answer. Adventitious oxygen is not the source (since oxidation proceeds reliably in good yield under anaerobic conditions), and it must derive from the oxygen of the methoxy ligand, from trace water in the ketonic solvent, or from the oxygen of the solvent itself. The last possibility arises because aldol dimerization of MEK and subsequent dehydration of the dimer (aldol condensation), releasing one of the ketonic oxygen atoms as water, could be catalyzed by acidic species formed under the oxidation conditions.^{61,62} This scenario significantly complicates the potential design of any labeling study aimed at determination of the origin of the bridging oxygen atom. Such a study would in any case be difficult to analyze, since none of the straightforward NMR techniques (e.g. 1H or ^{13}C) are applicable and no neutral derivatives of 2^{2+} suitable for mass spectrometry are available; no labeling study was attempted.

The electrochemistry of 1 suggests that the first step in its reaction with ferrocenium is probably electron transfer to form 1^+ , but conversion of such a radical to 2^{2+} must involve a number of further steps. Some of these may be bond homolyses (e.g. there might be loss of a methoxy radical prior to formation of an intermediate aquo complex), but there could also be heterolytic pathways in which radical transfers are achieved in two steps involving, for example, proton transfer followed by electron transfer. A mechanism with more than one electron transfer step would require an efficient series of redox equilibria to complete the reaction with the observed stoichiometry (consumption of a single equivalent of ferrocenium).

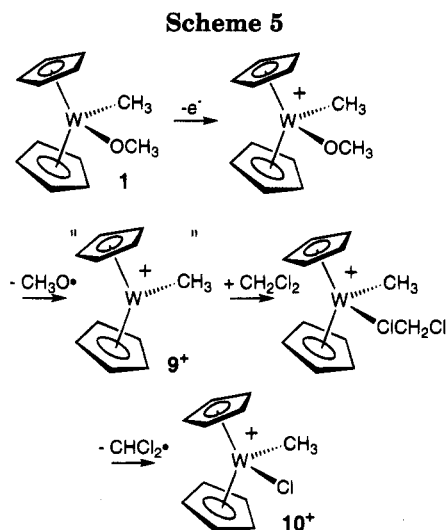
Oxidation of $[W(\eta^5-C_5H_5)_2(OCH_3)(CH_3)]$ in CH_2Cl_2 . The bridging oxo complex 2^{2+} can be formed from 1 in CH_2Cl_2 in moderate yield (53% by quantitative 1H NMR,

(60) Bkouche-Waksman, I.; Bois, C.; Sala-Pala, J.; Guerschais, J. E. *J. Organomet. Chem.* **1980**, *195*, 307.

(61) March, J. *Advanced Organic Chemistry*, 4th ed.; Wiley: New York, 1992; Reaction 6–39.

(62) Perrin, D. D.; Armarego, W. L. F. *Purification of Laboratory Chemicals*, 3rd ed.; Butterworth-Heinemann: Oxford, U.K., 1988; pp 68, 107.

(59) Feinstein-Jaffe, I.; Gibson, D.; Lippard, S. J.; Schrock, R. R.; Spool, A. *J. Am. Chem. Soc.* **1984**, *106*, 6305.



together with 10% 3^+) if the ferrocenium oxidation is carried out at -78°C . Under these conditions there were obvious visual indications that this is a complex reaction; the material obtained after -78°C oxidation and solvent removal at -45°C was brown, and did not acquire the characteristic purple of 2^+ until it had been dried under vacuum.

The course of the oxidation reaction in CH_2Cl_2 is sensitive to the reaction conditions, and room-temperature ferrocenium oxidation of **1** in CH_2Cl_2 does *not* give 2^+ but instead leads to only small quantities of diamagnetic products (as determined by quantitative ^1H NMR in CD_3CN with $^t\text{BuOH}$ as internal standard); the major product is a paramagnetic complex with an EPR signal with quartet hyperfine structure ($a = 4.0$ G) indicative of the presence of a methyl group and an isotropic g value of 2.006 intermediate between the typical values observed for 17-electron dihalo^{24b} and dialkyl^{25b} tungstenocene derivatives. A number of paramagnetic tungstenocene complexes of the general type $[\text{W}(\eta^5\text{-C}_5\text{H}_5)_2\text{-XY}]^+$ have been reported, but it is unusual to observe resolved hyperfine coupling to the X or Y ligands,^{24b} and this distinctive hyperfine "finger print" enables us to assign the EPR resonance unambiguously to $[\text{W}(\eta^5\text{-C}_5\text{H}_5)_2(\text{CH}_3)\text{Cl}]^+$ (10^+), a previously unknown tungstenocene radical which we have been able to prepare independently from **7** as shown in Scheme 1.

(63) Kulawiec, R. J.; Crabtree, R. H. *Coord. Chem. Rev.* **1990**, *99*, 89.

The first step in the independent preparation of 10^+ involves a variation on the conversion of **7** to 4^+ by ammonium ion protolysis in which the use of NH_4Cl leads to the formation of $[\text{W}(\eta^5\text{-C}_5\text{H}_5)_2(\text{CH}_3)\text{Cl}]$ (**11**), following coordination of the chloride counterion to the intermediate $[\text{W}(\eta^5\text{-C}_5\text{H}_5)_2(\text{CH}_3)]^+$. The methyl chloride complex **11** was characterized spectroscopically and analytically as described in the Experimental Section and was conveniently oxidized with ferrocenium to the radical cation 10^+ in excellent yield. The paramagnetism of 10^+ limited the spectroscopic tools available for its characterization, but in addition to combustion analysis and EPR data, formulation of $10[\text{PF}_6]$ as $[\text{W}(\eta^5\text{-C}_5\text{H}_5)_2(\text{CH}_3)\text{Cl}]\text{PF}_6$ is strongly supported by reduction of the salt back to **11** in 50% yield using the $\text{KOH}/\text{acetone}$ mixture, which we have previously found to be a convenient reductant in the tungstenocene system.²⁵

Formation of 10^+ by oxidation of **1** in CH_2Cl_2 must again involve several steps— it is reasonable, particularly in light of the recent establishment of a number of classes of halocarbon complexes,⁶³ that a CH_2Cl_2 complex such as $[\text{W}(\eta^5\text{-C}_5\text{H}_5)_2(\text{Cl}_2\text{CH}_2)\text{CH}_3]^+$ is an intermediate in the reaction, but subsequent conversion to 10^+ must involve at least one further homolysis. One possible pathway is shown in Scheme 5.

Conclusions

Oxidation of $[\text{W}(\eta^5\text{-C}_5\text{H}_5)_2(\text{OCH}_3)(\text{CH}_3)]$ (**1**) with ferrocenium ion in MEK gives the bridging oxo complex $\{[\text{W}(\eta^5\text{-C}_5\text{H}_5)_2(\text{CH}_3)]_2(\mu\text{-O})\}^{2+}$ (2^{2+}), in which the formally d^1 metal centers are spin-paired through a linear oxo bridge. This chromophore gives rise to a distinctive and strong visible absorption at 525 nm which is responsible for the purple color of 2^{2+} . The dimer photodisproportionates in CH_3CN to the W(VI) oxo complex $[\text{W}(\eta^5\text{-C}_5\text{H}_5)_2(\text{O})(\text{CH}_3)]^+$ (3^+) and the W(IV) acetonitrile complex $[\text{W}(\eta^5\text{-C}_5\text{H}_5)_2(\text{NCCH}_3)(\text{CH}_3)]^+$ (4^+), as confirmed by independent synthesis.

Acknowledgment. This work was supported in part by the Office of Naval Research. We thank Professor Steven Geib for helpful discussions of the X-ray analyses.

Supporting Information Available: Anisotropic displacement coefficients for $2[\text{PF}_6]_2$ and $3[\text{I}]$ (Tables S-I and S-II) and calculated hydrogen atom parameters for $2[\text{PF}_6]_2$ and $3[\text{I}]$ (Tables S-III and S-IV) (2 pages). Ordering information is given on any current masthead page.

OM9409175

Organometallic Chemistry of a Titanium(IV) *meso*-Octaethylporphyrinogen Complex: Carrier Properties of Polar Organometallics and Their Behavior in Insertion Reactions

Stefania De Angelis, Euro Solari, and Carlo Floriani*

Institut de Chimie Minérale et Analytique, BCH, Université de Lausanne, CH-1015 Lausanne, Switzerland

Angiola Chiesi-Villa and Corrado Rizzoli

Dipartimento di Chimica, Università di Parma, I-43100 Parma, Italy

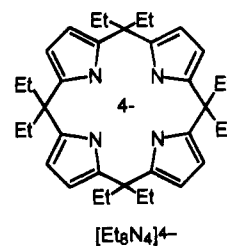
Received May 5, 1995[⊗]

The reaction of lithium organometallics with the (*meso*-octaethylporphyrinogenato)titanium complex $[(\eta^1:\eta^1:\eta^1:\eta^1\text{-Et}_8\text{N}_4)\text{Ti}(\text{THF})_2]$ (**2**), which acts as a bifunctional carrier, led to the formation of dimetallic Li-Ti organometallics, where the original LiR unit is present in the ion-separated form. These compounds contain the alkyl or aryl groups bonded to titanium, while the lithium cation remains bonded to the porphyrinogen periphery, $[(\eta^1:\eta^1:\eta^1:\eta^1\text{-Et}_8\text{N}_4)\text{-Ti-R}]\text{[Li}(\text{THF})_2]$ (R = Me, **3**; R = Ph, **4**). The dissolution of **3** in Et₂O led to the separation of Li⁺ from the porphyrinogen and the formation of $[(\eta^1:\eta^1:\eta^1:\eta^1\text{-Et}_8\text{N}_4)\text{Ti-Me}]\text{[Li}(\text{Et}_2\text{O})_3]^+$ (**5**). The migratory aptitude of the methyl group has been observed in the reaction of **5** with Bu^tNC, which leads to the corresponding η^2 -iminoacyl $[(\eta^1:\eta^1:\eta^1:\eta^1\text{-Et}_8\text{N}_4)\text{Ti}(\eta^2\text{-C}(\text{CH}_3)=\text{NBu}^t)]\text{[Li}(\text{THF})_2]$ (**6**). The reaction of **5** with carbon monoxide proceeds *via* a very reactive η^2 -acetyl intermediate. The carbenium ion nature of the η^2 -acyl group favors the attack on one of the pyrrolyl anions, which is homologated to a 4-methylpyridine unit. This reaction requires the complete cleavage of the Cd=O bond, leading to a titanyl complex, which has been recrystallized from pyridine as $[(\eta^1:\eta^1:\eta^1:\eta^1\text{-Et}_8(\text{C}_4\text{H}_2\text{N})_3(4\text{-MeC}_5\text{H}_2\text{N}))\text{Ti}=\text{O} \cdot \cdot \text{Li}(\text{py})_3]$ (**8**).

Introduction

The titanium-carbon bond functionality, which has been one of the most widely investigated bonds, is found associated mainly with cyclopentadienyls.¹ Attempts to mimic the stereoelectronic properties of the Cp₂M moiety have led several groups to investigate a range of ancillary ligands such as bulky alkoxides² and amides³ and polydentate ligands such as Schiff bases,⁴ tetraaza[14]annulenes,⁵ porphyrinogens,⁶ and porphyrins.⁷ Macrocyclic ligands, however, suffer from the fact that the alkyl functionality can migrate to some elec-

trophilic sites of the ligand structure;^{4,5} thus, reactivity studies are rather limited. In this context the study of the organometallic chemistry of titanium(IV) bonded to a *meso*-octaalkylporphyrinogen tetraanion⁸ introduced some novel aspects.



This kind of ancillary ligand has a number of peculiarities appropriate for studying the organometallic

* To whom correspondence should be addressed.
[⊗] Abstract published in *Advance ACS Abstracts*, August 15, 1995.
 (1) (a) Reetz, M. T. *Organotitanium Reagents in Organic Synthesis*; Springer: Berlin, Germany, 1986. (b) Wailes, P. C.; Courts, R. P.; Weigold, H. *Organometallic Chemistry of Titanium, Zirconium and Hafnium*; Academic: New York, 1974. (c) Cardin, D. J.; Lappert, M. F.; Raston, C. L. *Chemistry of Organozirconium and Hafnium Compounds*; Wiley: New York, 1986. (d) Buchwald, S. L.; Nielsen, R. B. *Chem. Rev.* **1988**, *88*, 1047. (e) Reetz, M. T. In *Organometallics in Synthesis*; Schlosser, M., Ed.; Wiley: New York, 1994; Chapter 3. (f) Duthaler, R. O.; Hafner, A.; Riediker, M. In *Organic Synthesis via Organometallics*; Dötz, K. H., Hoffmann, R. W., Eds.; Vieweg: Braunschweig, Germany, 1991; p 285. (g) Negishi, E.-I. In *Comprehensive Organic Synthesis*; Paquette, L. A., Ed.; Pergamon: Oxford, U.K., 1991; Vol. 5, p 1163. (h) Grossman, R. B.; Buchwald, S. L. *J. Org. Chem.* **1992**, *57*, 5803 and references therein. (i) Negishi, E.-I.; Takahashi, T. *Acc. Chem. Res.* **1994**, *27*, 124 and references therein. (j) Schore, N. E. In *Comprehensive Organic Synthesis*; Paquette, L. A., Ed.; Pergamon: Oxford, U.K., 1991; Vol. 5, p 1037. (k) Erker, G.; Krüger, C.; Müller, G. *Adv. Organomet. Chem.* **1985**, *24*, 1 and references therein. (l) Swanson, D. R.; Negishi, E. *Organometallics* **1991**, *10*, 825. (m) Erker, G.; Pfaff, R.; Krüger, C.; Werner, S. *Organometallics* **1993**, *12*, 3559. (n) Erker, G.; Noe, R.; Krüger, C.; Werner, S. *Organometallics* **1992**, *11*, 4174. (o) Erker, G.; Pfaff, R. *Organometallics* **1993**, *12*, 1921. (p) Jordan, R. F. *Adv. Organomet. Chem.* **1991**, *32*, 325.

(2) (a) Chisholm, M. H.; Rothwell, I. P. In *Comprehensive Coordination Chemistry*; Wilkinson, G.; Gillard, R. D., McCleverty, J. A., Eds.; Pergamon: Oxford, U.K., 1988; Vol. 2, Chapter 15.3. (b) Chamberlain, L. R.; Durfee, L. D.; Fau, P. E.; Fanwick, P. E.; Kobriger, L.; Latesky, S. L.; McMullen, A. K.; Rothwell, I. P.; Foltling, K.; Huffman, J. C.; Streib, W. E.; Wang, R. *J. Am. Chem. Soc.* **1987**, *109*, 390, 6068 and references therein. Durfee, L. D.; Fanwick, P. E.; Rothwell, I. P.; Foltling, K.; Huffman, J. C. *J. Am. Chem. Soc.* **1987**, *109*, 4720. (c) Zambrano, C. H.; Fanwick, P. E.; Rothwell, I. P. *Organometallics* **1994**, *13*, 1174. (d) Hill, J. E.; Bailich, G.; Fanwick, P. E.; Rothwell, I. P. *Organometallics* **1993**, *12*, 2911. (e) Bailich, G.; Fanwick, P. E.; Rothwell, I. P. *J. Am. Chem. Soc.* **1993**, *115*, 1581. (f) Hill, J. E.; Bailich, G.; Fanwick, P. E.; Rothwell, I. P. *Organometallics* **1991**, *10*, 3428. (g) Lubben, T. V.; Wolczanski, P. T. *J. Am. Chem. Soc.* **1987**, *109*, 424 and references therein. (h) Floriani, C.; Corazza, F.; Lesueur, W.; Chiesi-Villa, A.; Guastini, C. *Angew. Chem., Int. Ed. Engl.* **1989**, *28*, 66.

chemistry of titanium. These peculiarities have been recently discovered in an extended study on zirconium chemistry;⁶ among them, the following should be mentioned.

(i) The macrocycle does not contain any electrophilic or reactive site which can compete with the metal for nucleophilic substrates.^{4,5}

(ii) The four pyrrolyl anions, due to the conformational flexibility assured by the *meso* sp³ carbons, can adapt their bonding mode η^1 , η^3 , or η^5 to the electronic requests by the metal.^{6b,9}

(iii) The three-dimensional structure of the ligand engenders a kind of a protecting cavity for very reactive species formed on the metal.^{6e,f}

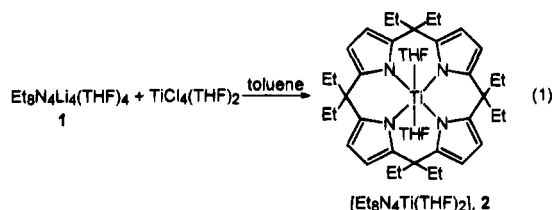
(iv) The bifunctional nature of early-transition-metal complexes, where the central metal acts as a Lewis acid and the electron-rich periphery can bind,^{6,10} for instance, alkali-metal cations, allows one to use them as bifunctional carriers of polar organometallics.^{6b}

Here we report the synthesis of lithium alkyl adducts formed from the reaction of LiR with the (*meso*-octa-

ethylporphyrinogenato)titanium(IV) complex¹¹ and their reaction with isocyanides and carbon monoxide. The latter produced a reactive η^2 -acyl complex which evolves to a titanyle species and to the homologation of one of the pyrrolyl anions to pyridine.

Results and Discussion

The parent compound **2**, which was considered for the study of the organometallic chemistry of titanium(IV), supported by the *meso*-octaethylporphyrinogen anion, has been synthesized by the general procedure published by this group some years ago and is shown in reaction 1.^{6,8,10}



(3) Lubben, T. V.; Wolczanski, P. T.; Van Duyne, G. D. *Organometallics* **1984**, *3*, 977. Lubben, T. V.; Wolczanski, P. T. *J. Am. Chem. Soc.* **1987**, *109*, 424. Andersen, R. A. *Inorg. Chem.* **1979**, *18*, 2928. Cummins, C. C.; Schaller, C. P.; Van Duyne, G. D.; Wolczanski, P. T.; Chan, A. W. E.; Hoffman, R. *J. Am. Chem. Soc.* **1991**, *113*, 2985.

(4) (a) Floriani, C.; Solari, E.; Corazza, F.; Chiesi-Villa, A.; Guastini, C. *Angew. Chem., Int. Ed. Engl.* **1989**, *28*, 64. (b) Corazza, F.; Solari, E.; Floriani, C.; Chiesi-Villa, A.; Guastini, C. *J. Chem. Soc., Dalton Trans.* **1990**, 1335. (c) Rosset, J.-M.; Floriani, C.; Mazzanti, M.; Chiesi-Villa, A.; Guastini, C. *Inorg. Chem.* **1990**, *29*, 3991. (d) Solari, E.; Floriani, C.; Chiesi-Villa, A.; Rizzoli, C. *J. Chem. Soc., Dalton Trans.* **1992**, 367 and references therein. (e) Tjaden, E. B.; Swenson, D. C.; Jordan, R. F.; Petersen, J. L. *Organometallics* **1995**, *14*, 371.

(5) (a) Ciurli, S.; Floriani, C.; Chiesi-Villa, A.; Guastini, C. *J. Chem. Soc., Chem. Commun.* **1986**, 1401. (b) Floriani, C.; Ciurli, S.; Chiesi-Villa, A.; Guastini, C. *Angew. Chem., Int. Ed. Engl.* **1987**, *26*, 70. (c) Floriani, C.; Mazzanti, M.; Ciurli, S.; Chiesi-Villa, A.; Guastini, C. *J. Chem. Soc., Dalton Trans.* **1988**, 1361. (d) Solari, E.; De Angelis, S.; Floriani, C.; Chiesi-Villa, A.; Rizzoli, C. *Inorg. Chem.* **1994**, *33*, 2204. (g) Giannini, L.; Solari, E.; De Angelis, S.; Ward, T. R.; Chiesi-Villa, A.; Rizzoli, C. *J. Am. Chem. Soc.* **1995**, *117*, 5801. (h) Uhrhammer, R.; Black, D. G.; Gardner, T. G.; Olsen, J. D.; Jordan, R. F. *J. Am. Chem. Soc.* **1993**, *115*, 8493. (i) Goedken, V. L.; Ladd, J. A. *J. Chem. Soc., Chem. Commun.* **1981**, 910; **1982**, 142. Housmekerides, C. E.; Pilato, R. S.; Geoffroy, G. L.; Rheingold, A. L. *J. Chem. Soc., Chem. Commun.* **1991**, 563. Yang, C. H.; Ladd, J. A.; Goedken, V. L. *J. Coord. Chem.* **1988**, *18*, 317. (j) Floriani, C. *Polyhedron* **1989**, *8*, 1717.

(6) (a) Jacoby, D.; Floriani, C.; Chiesi-Villa, A.; Rizzoli, C. *J. Chem. Soc., Chem. Commun.* **1991**, 790. (b) Jacoby, D.; Floriani, C.; Chiesi-Villa, A.; Rizzoli, C. *J. Am. Chem. Soc.* **1993**, *115*, 3595. (c) Jacoby, D.; Floriani, C.; Chiesi-Villa, A.; Rizzoli, C. *J. Am. Chem. Soc.* **1993**, *115*, 7025. (d) Solari, E.; Musso, F.; Floriani, C.; Chiesi-Villa, A.; Rizzoli, C. *J. Chem. Soc., Dalton Trans.* **1994**, 2015. (e) Jacoby, D.; Isoz, S.; Floriani, C.; Chiesi-Villa, A.; Rizzoli, C. *J. Am. Chem. Soc.* **1995**, *117*, 2793. (f) Jacoby, D.; Isoz, S.; Floriani, C.; Chiesi-Villa, A.; Rizzoli, C. *J. Am. Chem. Soc.* **1995**, *117*, 2805.

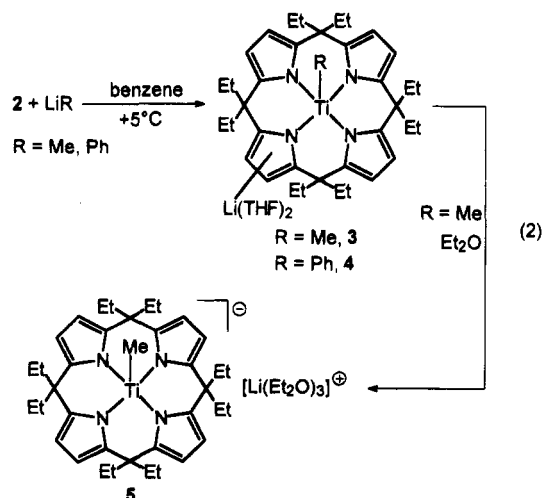
(7) (a) Dawson, D. Y.; Brand, H.; Arnold, J. *J. Am. Chem. Soc.* **1994**, *116*, 9797. (b) Brand, H.; Arnold, J. *Angew. Chem., Int. Ed. Engl.* **1994**, *33*, 95. (c) Arnold, J.; Hoffman, C. G.; Dawson, D. Y.; Hollander, F. *J. Organometallics* **1993**, *12*, 3645. (d) Brand, H.; Arnold, J. *Organometallics* **1993**, *12*, 3655. (e) Martin, P. C.; Arnold, J.; Bocian, D. F. *J. Phys. Chem.* **1993**, *97*, 1332. (f) Kim, H.-J.; Whang, D.; Kim, K.; Do, Y. *Inorg. Chem.* **1993**, *32*, 360. (g) Arnold, J.; Johnson, S. E.; Knobler, C. B.; Hawthorne, M. F. *J. Am. Chem. Soc.* **1992**, *114*, 3996. (h) Brand, H.; Arnold, J. *J. Am. Chem. Soc.* **1992**, *114*, 2266. (i) Shibata, K.; Aida, T.; Inoue, S. *Chem. Lett.* **1992**, 1173. (j) Schaverien, C. J.; Orpen, A. G. *Inorg. Chem.* **1991**, *30*, 4968. (k) Arnold, J.; Hoffman, C. G. *J. Am. Chem. Soc.* **1990**, *112*, 8620.

(8) De Angelis, S.; Solari, E.; Floriani, C.; Chiesi-Villa, A.; Rizzoli, C. *J. Chem. Soc., Dalton Trans.* **1994**, 2467 and references therein. (9) Rosa, A.; Ricciardi, G.; Rosi, M.; Sgamellotti, A.; Floriani, C. *J. Chem. Soc., Dalton Trans.* **1993**, 3759.

(10) (a) De Angelis, S.; Solari, E.; Floriani, C.; Chiesi-Villa, A.; Rizzoli, C. *J. Am. Chem. Soc.* **1994**, *116*, 5691. (b) *J. Am. Chem. Soc.* **1994**, *116*, 5702. (c) Jubb, J.; Jacoby, D.; Floriani, C.; Chiesi-Villa, A.; Rizzoli, C. *Inorg. Chem.* **1992**, *31*, 1306.

Complex **2** can be isolated as dark green crystals.¹¹ The bonding mode of the porphyrinogen anion, unlike the case for other high-valent early transition metals, is $\eta^1:\eta^1:\eta^1:\eta^1$ both in solution at room temperature, as proved by NMR, and in the solid state. A variable-temperature NMR study did not show any other accessible bonding mode. Complex **2**, like the zirconium porphyrinogen complex, can function as a carrier for polar or ionic substrates, having titanium acting as a Lewis acid center and the pyrrolyl anions as basic sites. A major difference exists, however, between zirconium- and titanium-porphyrinogen derivatives, besides the bonding mode of the porphyrinogen, the titanium being easily reducible by a number of polar organometallics.

Reduction of titanium(IV) to the corresponding titanium(III) has been observed in the reaction of **2** with NaH.¹² In the reaction of **2** with LiR, however, under the conditions specified in the Experimental Section, no reduction was observed.



Complex **2** functions as a bifunctional carrier binding the alkyl or aryl group at the metal and the lithium

(11) The structure of **2** has been briefly communicated: De Angelis, S.; Solari, E.; Floriani, C.; Chiesi-Villa, A.; Rizzoli, C. *Angew. Chem., Int. Ed. Engl.* **1995**, *34*, 1092.

(12) Floriani, C.; et al., unpublished results.

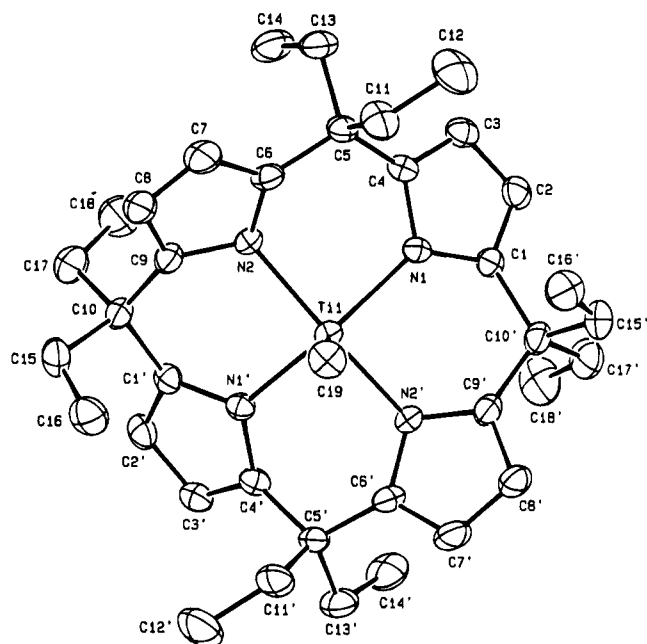


Figure 1. ORTEP drawing of the anion in complex **5** (30% probability ellipsoids). The prime denotes a transformation of $-x, y, 0.5 - z$.

Table 1. Selected Bond Distances (Å) and Angles (deg) for Complex 5^a

Ti1-N1	2.057(3)	C1-C2	1.361(5)
Ti1-N2	2.048(3)	C2-C3	1.414(5)
Ti1-C19	2.077(5)	C3-C4	1.376(4)
N1-C1	1.416(4)	C6-C7	1.372(6)
N1-C4	1.403(5)	C7-C8	1.401(7)
N2-C6	1.390(5)	C8-C9	1.381(6)
N2-C9	1.400(4)		
N2-Ti1-C19	100.0(1)	C1-C2-C3	108.0(3)
N1-Ti1-C19	104.1(1)	C2-C3-C4	106.9(3)
N1-Ti1-N2	87.6(1)	N1-C4-C3	110.2(3)
N1-Ti1-N1'	151.8(1)	C3-C4-C5	127.7(3)
N2-Ti1-N2'	160.0(1)	N1-C4-C5	120.3(3)
Ti1-N1-C4	124.0(2)	N2-C6-C5	124.5(3)
Ti1-N1-C1	125.5(2)	C5-C6-C7	125.6(3)
C1-N1-C4	104.9(3)	N2-C6-C7	109.1(3)
Ti1-N2-C9	117.8(2)	C6-C7-C8	108.4(4)
Ti1-N2-C6	114.6(2)	C7-C8-C9	106.8(4)
C6-N2-C9	106.4(3)	N2-C9-C8	109.3(3)
N1-C1-C10'	121.4(3)	C8-C9-C10	126.0(3)
N1-C1-C2	109.9(3)	N2-C9-C10	123.7(3)
C2-C1-C10'	126.8(3)		

^a Prime denotes a transformation of $-x, y, 0.5 - z$.

cation at the periphery. The complexed separated ion pair can be transformed in a coordinating solvent into a truly ionic form, lithium being the countercation. The proposed structure of **3** and **4** has been based on a number of results obtained for several metal complexes which bind the alkali-metal cations at the porphyrinogen periphery.^{6,10} The recrystallization of **3** in Et₂O, however, gave the ion separated form **5**. The ¹H NMR spectra showed the constant $\eta^1:\eta^1:\eta^1:\eta^1$ bonding mode of the porphyrinogen in solution for **4** and **5**, while the intermediate **3** has not been characterized. A common feature of the ¹H NMR spectra is the presence of two sets of triplets and quartets for the meso-ethyls, approaching a C₂ symmetry in the orientation of the ethyl groups toward the metal. A view of the anion of **5** is shown in Figure 1, while a selection of structural parameters is listed in Table 1. Both anion and cation possess a crystallographic C₂ symmetry. The 2-fold axis

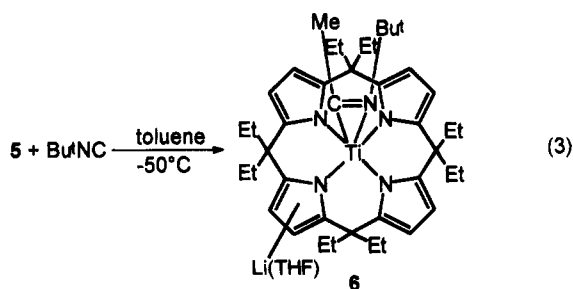
Table 2. Comparison of Structural Parameters within the Ti-Porphyrinogen Units for Compounds 5, 6 and 8

	5	6	8
(a) Distances of Atoms from the N ₄ Core, (Å)			
dist of Ti from N ₄ ^a plane	0.429(1)	0.642(1)	0.498(1)
dist of N1 from N ₄ plane	-0.073(3)	-0.001(4)	-0.096(5)
dist of N2 from N ₄ plane	0.073(3)	0.001(4)	0.096(5)
dist of N3 from N ₄ plane		-0.001(4)	-0.090(5)
dist of N4 from N ₄ plane		0.001(4)	0.087(5)
(b) Distances of Ti from the Pyrrole Rings, (Å)			
dist of Ti from A ^b plane	0.816(1)	0.382(1)	0.249(1)
dist of Ti from B plane	1.419(1)	1.195(1)	0.671(1)
dist of Ti from C plane	0.816(1)	0.430(1)	0.808(1)
dist of Ti from D plane	1.419(1)	1.738(1)	1.720(1)
(c) Relevant dihedral angles, (deg)			
dihedral angle A-C	105.1(1)	110.3(2)	115.2(3)
dihedral angle B-D	111.6(1)	110.7(7)	118.9(3)
dihedral angle N ₄ -A	142.6(1)	147.0(2)	155.2(2)
dihedral angle N ₄ -B	145.8(1)	152.8(2)	159.1(2)
dihedral angle N ₄ -C	142.6(1)	143.1(2)	145.8(2)
dihedral angle N ₄ -D	145.8(1)	136.7(2)	146.3(3)

^a N₄ refers to the least-squares mean plane defined by N1, N2, N3, and N4. ^b A, B, C and D refer to the least-squares mean planes defined by the pyrrolic rings containing N1, N2, N3, N4, respectively. For complex **5**, the C and D rings are the symmetry-related ones.

is perpendicular to the N₄ core, which implies that the methyl hydrogens are statistically distributed over two positions. The porphyrinogen shows the saddle-shaped conformation¹⁰ expected for the $\eta^1:\eta^1:\eta^1:\eta^1$ bonding mode, the four pyrrole rings being tilted alternatively up and down with respect to the N₄ plane. Bond distances within the pyrrolyl anion show a double C=C bond localization; thus, the nitrogen atoms have a pyramidal geometry. N1 and N2 are displaced by 0.217(3) and 0.424(3) Å, respectively, from the plane through the three bonded atoms. The differences in the distances of Ti from the plane of the pyrrole rings [0.816(1) and 1.419(1) Å from the A and B rings, respectively; Table 2] reflect the fact that the titanium atom is out of plane from the N₄ core. The Ti-C bond distance (2.077(5) Å) is significantly shorter than the usual Ti-Me distances.^{4e} The structure of [(Et₂O)₃Li]⁺ cation is reported in the supporting information.

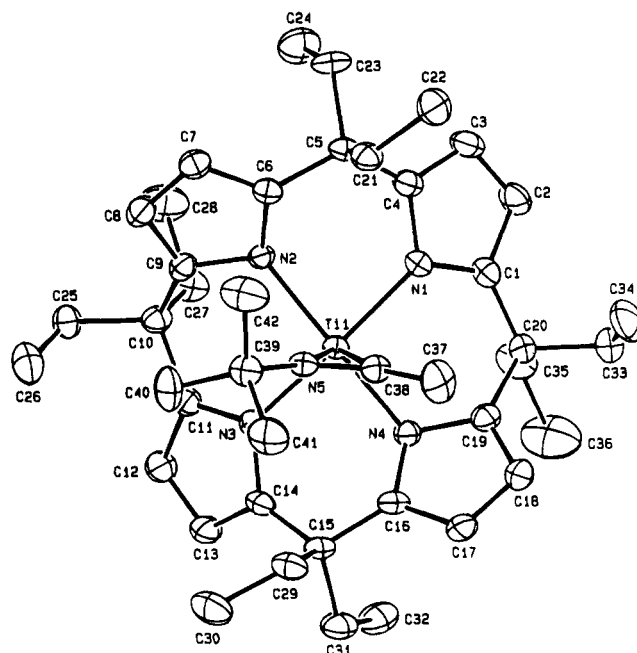
Complex **5** has been engaged in insertion reactions with isocyanide and carbon monoxide.¹³ The migratory insertion of BuⁿNC into the Ti-Me bond proceeds smoothly, leading to the η^2 -iminoacyl derivative **6**.^{13,14}



Complex **6** has been isolated as red crystals. The imino band is at 1650 cm⁻¹ in the IR spectrum. The ¹H NMR spectrum at room temperature shows the $\eta^1:\eta^1:\eta^1:\eta^1$ bonding mode of the porphyrinogen along with the usual structural characteristics observed for complexes **2** and **5**, with regard to the meso-ethyl groups, which appear as two kinds of methylene and methyl

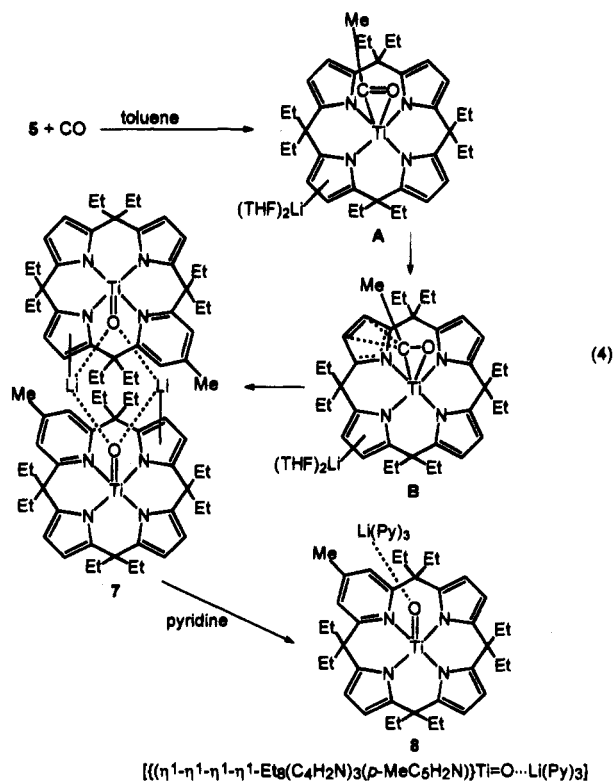
Table 3. Selected Bond Distances (Å) and Angles (deg) for complex 6

Ti1-N1	2.078(4)	N4-C19	1.398(6)
Ti1-N2	2.057(4)	N5-C38	1.248(6)
Ti1-N3	2.137(4)	N5-C39	1.500(7)
Ti1-N4	2.102(4)	C1-C2	1.378(8)
Ti1-N5	2.043(4)	C2-C3	1.372(9)
Ti1-C38	2.023(6)	C3-C4	1.375(8)
Li1-O1	1.888(14)	C6-C7	1.374(8)
Li1-N3	2.194(17)	C7-C8	1.414(8)
Li1-N4	2.381(18)	C8-C9	1.361(7)
Li1-C14	2.185(15)	C11-C12	1.372(8)
N1-C1	1.381(6)	C12-C13	1.387(9)
N1-C4	1.390(7)	C13-C14	1.362(8)
N2-C6	1.382(7)	C16-C17	1.376(9)
N2-C9	1.394(6)	C17-C18	1.406(8)
N3-C11	1.399(6)	C18-C19	1.366(8)
N3-C14	1.397(7)	C37-C38	1.496(9)
N4-C16	1.412(7)		
N5-Ti1-C38	35.7(2)	C5-C6-C7	126.7(5)
N3-Ti1-N4	78.8(1)	N2-C6-C7	109.4(5)
N2-Ti1-N4	143.8(1)	C6-C7-C8	107.3(5)
N2-Ti1-N3	87.4(1)	C7-C8-C9	107.0(5)
N1-Ti1-N4	89.9(1)	N2-C9-C8	109.8(4)
N1-Ti1-N3	144.5(1)	C8-C9-C10	128.7(5)
N1-Ti1-N2	82.2(1)	N2-C9-C10	119.6(4)
Ti1-N1-C4	125.0(3)	N3-C11-C10	123.8(4)
Ti1-N1-C1	127.4(3)	C10-C11-C12	127.3(5)
C1-N1-C4	106.5(4)	N3-C11-C12	108.7(5)
Ti1-N2-C9	122.8(3)	C11-C12-C13	108.3(5)
Ti1-N2-C6	116.7(3)	Li1-C13-C12	84.3(6)
C6-N2-C9	106.4(4)	C12-C13-C14	107.5(5)
Ti1-N3-C14	124.9(3)	Li1-C13-C14	58.1(5)
Ti1-N3-C11	128.1(3)	N3-C14-C13	109.7(5)
C11-N3-C14	105.7(4)	Li1-C14-C13	89.9(5)
Ti1-N4-Li1	90.5(5)	Li1-C14-N3	71.7(5)
Ti1-N4-C19	113.0(3)	C13-C14-C15	129.1(5)
Ti1-N4-C16	105.9(3)	N3-C14-C15	121.0(5)
C16-N4-C19	105.7(4)	Li1-C14-C15	108.2(7)
Ti1-N5-C39	154.0(3)	N4-C16-C15	123.4(5)
Ti1-N5-C38	71.2(3)	C15-C16-C17	126.5(5)
C38-N5-C39	134.7(4)	N4-C16-C17	108.9(5)
N1-C1-C20	124.7(5)	C16-C17-C18	107.9(5)
N1-C1-C2	108.4(5)	C17-C18-C19	107.5(5)
C2-C1-C20	126.8(5)	N4-C19-C18	110.0(5)
C1-C2-C3	108.6(5)	C18-C19-C20	128.7(5)
C2-C3-C4	107.3(5)	N4-C19-C20	121.0(4)
N1-C4-C3	109.1(5)	N5-C38-C37	133.5(5)
C3-C4-C5	127.5(5)	Ti1-C38-C37	153.4(5)
N1-C4-C5	123.0(5)	Ti1-C38-N5	73.0(3)
N2-C6-C5	122.8(5)		

**Figure 2.** ORTEP drawing of the anion in complex 6 (30% probability ellipsoids).

90.4(1)°) to the planar N4 core, from which titanium protrudes by 0.642(1) Å. The other structural parameters (Ti-C38, 2.023(6) Å; C38-N5, 1.248(6) Å; Ti-N5, 2.043(4) Å) do not reveal any significant carbenoid nature of the η^2 -iminoacyl,¹³ and this is in accordance with the spectroscopic and chemical data. These carbenium ion characteristics¹⁵ are much enhanced when one moves from the η^2 -iminoacyl to a η^2 -acyl group. This is the plausible explanation for the occurrence of reaction 4.

groups. A view of 6 is shown in Figure 2, while a selection of bond distances is reported in Table 3. The [(Et₅N₄)Ti] fragment maintains the saddle-shaped conformation (Table 2), though with important distortions due to the sterically hindered η^2 -iminoacyl group, and the lithium cation is bound at the periphery. The Ti-N3 and Ti-N4 distances are lengthened and the titanium atom is displaced from the pyrrole rings. The porphyrinogen binds in a $\eta^1:\eta^1:\eta^1:\eta^1$ fashion to the metal, though some π delocalization has been observed for pyrroles A and C, confirmed by the lower pyramidalities of N1 and N3, the out-of-plane distance from the three bonded atoms being 0.098(4) and 0.105 Å, respectively. Titanium is 2.835(6) and 2.945(5) Å away from C16 and C19, suggesting a tendency of the A pyrrole ring to move to a η^3 interaction mode. The binding of lithium to the porphyrinogen occurs via N4 (Li-N4, 2.381(2) Å) and a η^2 mode to N3-C14 (Li-N3, 2.194(2) Å; Li-C14, 2.185(2) Å). The plane of the (η^2 -iminoacyl)titanium fragment (Ti, N5, C38) is perpendicular (dihedral angle



The reaction of 5 with carbon monoxide in toluene at room temperature led almost quantitatively to 7, which

derives from the homologation¹⁶ of one pyrrole to a pyridine¹⁷ and the consequent cleavage of the C=O multiple bond with formation of an oxotitanium(IV) functionality. The homologation of a pyrrole to a pyridine ring within the porphyrinogen skeleton has been observed in the reaction of carbon monoxide with alkylzirconium–porphyrinogen complexes.^{6c,e} As in the latter case, though the oxophilicity of titanium is lower than that of zirconium, we envisage that the reaction proceeds via a η^2 -acyl intermediate which has carbenium ion properties¹⁵ suitable for attack of one of the pyrrole rings. This attack is followed by the cleavage of the C–O bond driven by the oxophilicity of both the titanium and lithium. A major difference is seen between titanium and zirconium in the regiochemistry of the homologation reaction,^{6e} 3,5-substituted pyridines are obtained in the case of zirconium, while 4-substituted pyridines are formed in the case of titanium and niobium.^{6e} This difference may arise from the different bonding mode of the pertinent pyrrole. In the case of zirconium and hafnium, it can be assumed that the 3,5-regiochemistry can be explained by assuming an attack of the carbenium ion on a η^5 -bonded pyrrolyl anion.^{6e} In the case of titanium, it can be assumed that the 4-regiochemistry derives from the attack on a η^3 -bonded pyrrolyl anion. A η^3 -bonding mode is very easily accessible, due to the conformational flexibility of the porphyrinogen tetraanion. In a number of cases the fluxional behavior of the porphyrinogen ligand and a facile change of the bonding modes has been observed.⁶ On the other hand, in the case of the X-ray structure of complex **6** we observed that one of the pyrrolyl anions is close to change from a η^1 - to a η^3 -bonding mode. In addition, complex **6** is modeling the first step of the reaction with carbon monoxide. The proposed structure of **7**, which forms in toluene solution, is based on those which have been determined by X-ray analysis on the homologated complexes of zirconium^{6e} and is further supported by the similar spectroscopic data. The crystallization of **7** in pyridine breaks down the dimeric structure via the solvation of the lithium cation, affording the monomeric titanyl complex **8**.

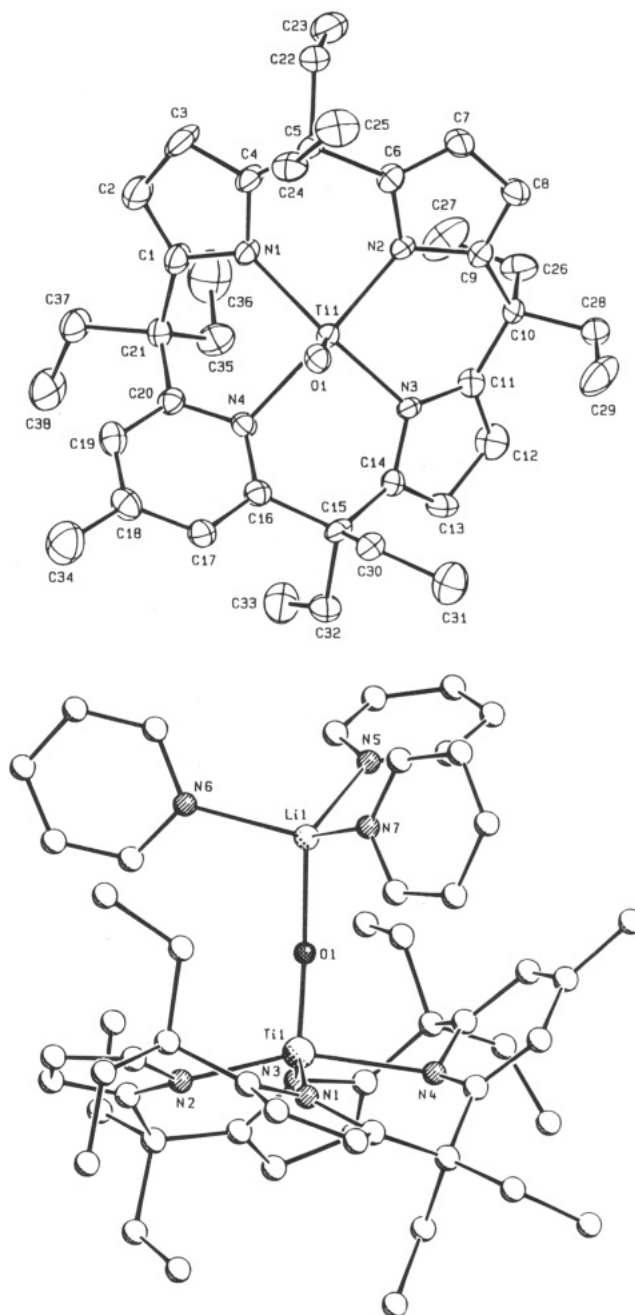


Figure 3. (A, top) ORTEP drawing of the anion in complex **8** (30% probability ellipsoids). (B, bottom) SCHAKAL perspective view of complex **8**.

Crystals of **8** suitable for an X-ray analysis have been obtained from crystallization in pyridine. Complex **8** crystallizes with disordered pyridine solvent molecules in a 1:1 molar ratio. Views of the complex are given in parts A and B of Figure 3. The tris(pyrrole) fragment is $\eta^1\text{:}\eta^1\text{:}\eta^1$ -bonded to the titanium atom through the three nitrogens at Ti–N distances ranging from 2.023(5) to 2.063(5) Å (Table 4). These distances are comparable to those present in complexes **5** and **6**, while the pyridine fragment interacts at a much longer Ti–N distance (Ti–N4, 2.278(5) Å). The four nitrogen atoms show remarkable tetrahedral distortions, the titanium atom being displaced by 0.498(1) Å toward the oxygen atom. The twisting of the opposite pyrrole rings and the presence of pyridine give rise to a very distorted saddle-shaped conformation (Table 3). The Ti=O distance (1.652(5) Å) clearly supports the existence of a Ti=O double

(14) An iminoacyl group formed from migratory insertion of RNC into M–C bonds is a well-known reaction: Singleton, E.; Ossthnizen, H. E. *Adv. Organomet. Chem.* **1983**, *22*, 209. Otsuka, S.; Nakamura, A.; Yoshida, T.; Naruto, M.; Ataba, K. *J. Am. Chem. Soc.* **1973**, *95*, 3180. Yamamoto, Y.; Yamazaki, H. *Inorg. Chem.* **1974**, *13*, 438. Aoki, K.; Yamamoto, Y. *Inorg. Chem.* **1976**, *15*, 48. Bellachioma, G.; Cardaci, G.; Zanazzi, P. *Inorg. Chem.* **1987**, *26*, 84. Maitlis, P. M.; Espinet, P.; Russell, M. J. H. In *Comprehensive Organometallic Chemistry*; Wilkinson, G., Stone, F. G. A., Abel, E. W., Eds.; Pergamon: London, 1982; Vol. 8, Chapter 38.4. Crociani, B. In *Reactions of Coordinated Ligands*; Braterman, P. S., Ed.; Plenum: New York, 1986; Chapter 9.

(15) Tatsumi, K.; Nakamura, A.; Hofmann, P.; Stauffert, P.; Hoffmann, R. *J. Am. Chem. Soc.* **1985**, *107*, 4440. Martin, B. D.; Matchett, S. A.; Norton, J. R.; Anderson, O. P. *J. Am. Chem. Soc.* **1985**, *107*, 7952. Roddick, D. M.; Bercau, J. E. *Chem. Ber.* **1989**, *122*, 1579. Hoffmann, P.; Stauffert, P.; Frede, M.; Tatsumi, K. *Chem. Ber.* **1989**, *122*, 1559. Hoffmann, P.; Stauffert, P.; Tatsumi, K.; Nakamura, A.; Hoffmann, R. *Organometallics* **1985**, *4*, 404. Tatsumi, K.; Nakamura, A.; Hoffmann, P.; Hoffmann, R.; Moloy, K. G.; Marks, T. J. *J. Am. Chem. Soc.* **1986**, *108*, 4467. Fanwick, P. E.; Kobriger, L. M.; McMullen, A. K.; Rothwell, I. P. *J. Am. Chem. Soc.*, **1986**, *108*, 8095. Arnold, J.; Tilley, T. D.; Rheingold, A. L. *J. Am. Chem. Soc.* **1986**, *108*, 5355.

(16) For a general review on the homologation reaction of alcohols and related species, see: Chiusoli, G. P.; Salerno, G.; Foa, M. In *Reactions of Coordinated Ligands*; Braterman, P. S., Ed.; Plenum: New York, 1986; Vol. 1, Chapter 7. Parshall, G. W.; Ittel, S. D. *Homogeneous Catalysis*, 2nd ed.; Wiley: New York, 1992. Colquhoun, H. M.; Thompson, D. J.; Twigg, M. V. *Carbonylation*; Plenum: New York, 1991.

(17) Jones, R. L.; Rees, C. W. *J. Chem. Soc. C* **1969**, 2249, 2255 and references therein. Fowler, F. W. *Angew. Chem., Int. Ed. Engl.* **1971**, *10*, 135.

Table 4. Selected Bond Distances (Å) and Angles (deg) for Complex 8

Ti1-O1	1.652(5)	C18-C19	1.373(12)
Ti1-N1	2.063(5)	C18-C34	1.486(12)
Ti1-N2	2.023(5)	C19-C20	1.368(11)
Ti1-N3	2.035(4)	N3-C11	1.390(8)
Ti1-N4	2.278(5)	N3-C14	1.378(9)
Li1-O1	1.913(14)	N4-C16	1.337(9)
Li1-N5	2.072(15)	N4-C20	1.346(10)
Li1-N6	2.102(15)	C1-C2	1.338(11)
Li1-N7	2.035(14)	C1-C21	1.530(10)
N1-C1	1.397(9)	C2-C3	1.421(14)
N1-C4	1.379(9)	C3-C4	1.388(10)
N2-C6	1.389(9)	C6-C7	1.373(10)
N2-C9	1.394(9)	C7-C8	1.431(11)
C13-C14	1.362(10)	C8-C9	1.344(10)
C16-C17	1.370(10)	C11-C12	1.379(11)
C17-C18	1.416(12)	C12-C13	1.438(12)
N3-Ti1-N4	84.5(2)	C11-N3-C14	108.6(5)
N2-Ti1-N4	158.1(2)	Ti1-N4-C20	116.8(4)
N2-Ti1-N3	90.2(2)	Ti1-N4-C16	109.8(4)
N1-Ti1-N4	88.3(2)	C16-N4-C20	118.9(5)
N1-Ti1-N3	146.6(2)	N1-C1-C21	119.4(6)
N1-Ti1-N2	84.5(2)	N1-C1-C2	109.5(7)
O1-Ti1-N4	95.0(2)	C2-C1-C21	131.0(7)
O1-Ti1-N3	106.2(2)	C1-C2-C3	108.2(7)
O1-Ti1-N2	106.8(2)	C2-C3-C4	106.5(8)
O1-Ti1-N1	106.8(2)	N1-C4-C3	108.7(6)
Ti1-O1-Li1	173.7(5)	C3-C4-C5	124.6(7)
Ti1-N1-C4	123.1(4)	N1-C4-C5	126.5(6)
Ti1-N1-C1	129.2(4)	N2-C6-C5	124.4(6)
C1-N1-C4	107.1(5)	C5-C6-C7	126.2(6)
Ti1-N2-C9	126.0(4)	N2-C6-C7	109.4(6)
Ti1-N2-C6	122.9(4)	C6-C7-C8	106.1(6)
C6-N2-C9	106.9(5)	C7-C8-C9	108.4(6)
Ti1-N3-C14	122.0(4)	N2-C9-C8	109.2(6)
Ti1-N3-C11	123.4(4)	C8-C9-C10	126.9(6)
N2-C9-C10	122.1(6)	C15-C16-C17	118.9(6)
N3-C11-C10	126.9(6)	N4-C16-C17	122.5(7)
C10-C11-C12	124.9(7)	C16-C17-C18	118.4(6)
N3-C11-C12	107.9(6)	C17-C18-C34	120.2(7)
C11-C12-C13	107.1(7)	C17-C18-C19	117.3(7)
C12-C13-C14	107.3(7)	C19-C18-C34	122.5(8)
N3-C14-C13	109.0(6)	C18-C19-C20	121.3(7)
C13-C14-C15	128.6(7)	N4-C20-C19	120.5(6)
N3-C14-C15	121.7(6)	C19-C20-C21	123.5(6)
N4-C16-C15	118.3(6)	N4-C20-C21	116.0(6)

bond.¹⁸ The Li cation interacts strongly with the oxo group (1.913(14) Å) to give a Ti-O-Li angle of 173.7(5)°. The tetrahedral coordination around lithium is completed by the nitrogen atoms from three pyridine molecules. Bond distances and angles within the three pyrrole rings are consistent with a significant double-bond localization, in agreement with the pyramidal nature of the N1, N2, and N3 nitrogen atoms, which are displaced by 0.067(5), 0.188(5), and 0.221(5) Å, respectively, from the planes through the three bonded atoms. The N4 nitrogen atom of the pyridine ring shows a pronounced pyramidal nature, being 0.343(6) Å out of the plane through the three bonded atoms.

The titanyl unit is rare in titanium-oxo chemistry, some significant examples having appeared very recently.¹⁸ The binding of the lithium cation emphasizes

the high basicity of the titanyl group compared to the corresponding vanadyl.¹⁹ It should be mentioned that in complex 8 the titanyl unit is synthetically quite easily accessible for reactivity studies.^{18g}

Experimental Section

General Procedure. All reactions were carried out under an atmosphere of purified nitrogen. Solvents were dried and distilled before use by standard methods. The synthesis of complex 1 has been carried out according to a reported procedure.⁸ Infrared spectra were recorded with a Perkin-Elmer FT IR 1600 spectrophotometer; ¹H NMR spectra were measured on a 200-AC Bruker instrument.

Synthesis of 2. TiCl₄(THF)₂ (8.9 g, 26.8 mmol) was added to a colorless toluene (350 mL) solution of 1 (22.8 g, 26.8 mmol). The resulting dark green-black solution was stirred at room temperature for 1 day; then LiCl was removed by filtration. After evaporation of the solvent and trituration of the residue with pentane (120 mL), a dark green crystalline solid was filtered off and dried *in vacuo* (12 g, 62%). ¹H NMR (C₆D₆, 200 MHz, room temperature): δ 5.98 (s, C₄H₂N, 8 H), 3.40 (m, THF, 8 H), 1.93 (q, CH₂, 16 H, *J* = 7.2 Hz), 1.18 (m, THF, 8 H), 0.90 (t, CH₃, 24 H, *J* = 7.2 Hz). The ¹H NMR spectrum does not change in a range of temperature from 293 to 223 K in C₇D₈ solution. IR (Nujol): 1314 (s), 1294 (s), 1246 (s), 1197 (s), 1128 (s), 1081 (s), 1010 (s), 948 (m), 766 (s), 562 (m), 527 (w) cm⁻¹. Anal. Calcd for 2, C₄₄H₆₄N₄O₂Ti: C, 72.50; H, 8.85; N, 7.69. Found: C, 72.69; H, 8.93; N, 7.89.

Synthesis of 4. Solid PhLi (0.75 g, 7.5 mmol) was added to a frozen solution of 2 (4.5 g, 6.2 mmol) in benzene. The mixture was warmed to room temperature with stirring. After a few hours an emerald green suspension was obtained, which was stirred for 1 day. The small amount of solid was filtered out; then the emerald green solution was evaporated to dryness and the residue collected (90%). ¹H NMR (C₆D₆, 400 MHz, room temperature): δ 6.78 (m, Ph, 5 H), 6.22 (s, C₄H₂N, 8 H), 3.08 (m, broad, THF, 8 H), 2.00 (q, CH₂, 8 H, *J* = 7 Hz), 1.92 (s, CH₂, 8 H), 1.12 (m, broad, THF, 8 H), 0.86 (t, CH₃, 12 H, *J* = 7 Hz), 0.82 (t, CH₃, 12 H, *J* = 7 Hz). Anal. Calcd for 2, C₅₀H₆₉LiN₄O₂Ti: C, 73.87; H, 8.56; N, 6.89. Found: C, 73.72; H, 8.25; N, 6.78.

Synthesis of 5. MeLi (24 mL sol 0.10 M in Et₂O, 2.4 mmol) was added dropwise to a dark green solution of 2 (1.5 g, 2.0 mmol) in frozen benzene. No reaction took place at low temperature. The mixture was warmed to room temperature, resulting in a purple solution which was stirred at room temperature for 4 h. After evaporation of the solvent, Et₂O (70 mL) was added to the purple solid and the solution was allowed to remain at -20 °C for 2 days. A crop of purple X-ray suitable crystalline solid was collected and dried *in vacuo* (0.6 g, 36%). The product can be obtained in near quantitative yield by removal of the mother liquor (85%). ¹H NMR (C₆D₆, 400 MHz, room temperature): δ 6.30 (s, C₄H₂N, 8 H), 3.03 (q, Et₂O, 12 H, *J* = 6.8 Hz), 2.15 (q, CH₂, 8 H, *J* = 7.6 Hz), 1.92 (m, CH₂, 8 H, *J* = 7.6 Hz), 1.29 (s, CH₃, 3 H), 0.96 (t, CH₃, 12 H, *J* = 7.6 Hz), 0.90 (t, Et₂O, 18 H, *J* = 6.8 Hz), 0.77 (t, CH₃, 12 H, *J* = 7.6 Hz). Anal. Calcd for 3, C₄₉H₅₁LiN₄O₃Ti: C, 70.99; H, 9.85; N, 6.75. Found: C, 70.71; H, 9.63; N, 6.95.

Synthesis of 6. To a stirred blue-violet solution of complex 5 (3.2 g, 3.9 mmol) in toluene (100 mL) was added dropwise a toluene (50 mL) solution of Bu^tNC (0.5 mL, 4.4 mmol) at -50 °C. No immediate reaction took place. The mixture was warmed to room temperature and stirred for 1 day to give a dark red solution. After removal of the solvent under reduced pressure, THF (5 mL) and hexane (40 mL) were added to the red solid. After standing overnight at -4 °C, a red solid was collected and dried (2.0 g, 67%). (Note: THF is necessary to substitute Et₂O in the coordination of lithium, to make the compound crystallize more easily). Recrystallization of the

(18) (a) Olmstead, M. M.; Power, P. P.; Viggiano, M. *J. Am. Chem. Soc.* **1983**, *105*, 2927. (b) Willey, G. R.; Palin, J.; Drew, M. G. B. *J. Chem. Soc., Dalton Trans.* **1994**, 1799. (c) Wieghardt, K.; Quilitzsch, U.; Weiss, J.; Nuber, B. *Inorg. Chem.* **1980**, *19*, 2514. (d) Bodner, A.; Jeske, P.; Weyhermüller, T.; Wieghardt, K.; Dubler, E.; Schmalle, H.; Nuber, B. *Inorg. Chem.* **1992**, *31*, 3737. (e) Jeske, P.; Haselhorst, G.; Weyhermüller, T.; Wieghardt, K.; Nuber, B. *Inorg. Chem.* **1994**, *33*, 2462. (f) Smith, M. R.; Matsunaga, P. T.; Andersen, R. A. *J. Am. Chem. Soc.* **1993**, *115*, 7049. (g) Housmekerides, C. E.; Ramage, D. L.; Kretz, C. M.; Shontz, J. T.; Pilato, R. S.; Geoffroy, G. L.; Rheingold, A. L.; Haggerty, B. S. *Inorg. Chem.* **1992**, *31*, 4453.

(19) Comba, P.; Merbach, A. *Inorg. Chem.* **1987**, *26*, 1315.

Table 5. Experimental Data for the X-ray Diffraction Studies on Crystalline Compounds 5, 6, and 8

	5	6	8
chemical formula	C ₄₉ H ₈₁ LiN ₄ O ₃ Ti	C ₄₆ H ₆₆ LiN ₅ OTi	C ₅₃ H ₆₆ LiN ₇ OTi·C ₅ H ₅ N
a (Å)	11.361(6)	18.196(2)	17.019(2)
b (Å)	26.446(4)	19.054(3)	23.435(3)
c (Å)	16.812(2)	12.408(3)	13.474(1)
α (deg)	90	90	90
β (deg)	97.74(2)	90	90
γ (deg)	90	90	90
V (Å) ³	5005(3)	4301.9(13)	5374.0(10)
Z	4	4	4
fw	829.1	761.9	951.1
space group	C2/c (No. 15)	P2 ₁ 2 ₁ 2 (No. 18)	P2 ₁ 2 ₁ 2 ₁ (No. 19)
t (°C)	22	22	22
λ (Å)	0.710 69	1.541 78	1.541 78
ρ _{calcd} (g cm ⁻³)	1.100	1.176	1.176
μ (cm ⁻¹)	2.12	19.66	16.86
transmn coeff	0.954–1.000	0.881–1.000	0.822–1.000
R1 ^b	0.052	0.047 [0.073] ^a	0.049 [0.071]
wR2 ^c	0.154	0.136 [0.199]	0.134 [0.177]

^a Values in square brackets refer to the "inverted structure". ^b $R = \sum |\Delta F| / \sum |F_o|$, calculated for the unique observed data. ^c $wR2 = [\sum w(\Delta F^2)^2] / \sum w(F_o^2)^2$, calculated for the unique total data.

powder from hexane gave crystals suitable for X-ray analysis. ¹H NMR (C₆D₆, 400 MHz, room temperature): δ 6.26 (s, C₄H₂N, 8 H), 3.05 (m, THF, 4 H), 1.96 (q, CH₂, 8 H, *J* = 7.2 Hz), 1.95 (s, Me, 3 H), 1.90 (q, CH₂, 8 H, *J* = 7.2 Hz), 1.06 (t, CH₃, 12 H, *J* = 7.2 Hz), 1.05 (s, Bu^t, 9 H), 1.05 (m, THF, 4 H), 0.79 (t, CH₃, 12 H, *J* = 7.2 Hz). IR (Nujol; C=N): 1650 (vs) cm⁻¹. Anal. Calcd for **6**, C₄₂H₆₀LiN₅Ti·C₄H₈O: C, 72.52; H, 9.00; N, 9.19. Found: C, 72.50; H, 9.03; N, 9.14.

Synthesis of 7 and 8. Complex **5** (3.3 g, 4.0 mmol) was dissolved in freshly distilled toluene (100 mL) to obtain a purple solution. The reaction vessel was then evacuated, and CO was added at room temperature. The mixture was stirred for 3 days under an atmosphere of CO, resulting in a red solution. After removal of the solvent and trituration with hexane (30 mL) a maroon solid was collected (2.2 g, 87%). ¹H NMR (acetone-*d*₆, 200 MHz, room temperature): δ 7.50 (s, pyridine ring, 2 H), 6.04 (d, C₄H₂N, 2 H), 5.96 (s, C₄H₂N, 2 H), 5.88 (d, C₄H₂N, 2 H), 2.61 (s, Me, 3 H), 2.3–1.98 (m, CH₂, 16 H), 0.93 (t, CH₃, 12 H), 0.64 (t, CH₃, 6 H), 0.52 (t, CH₃, 6 H). IR (Nujol): 1608 (s), 879 (s), 780 (s), 748 (s), 577 (s) cm⁻¹. Anal. Calcd for **7**, C₃₈H₅₁LiN₄OTi: C, 71.91; H, 8.10; N, 8.83. Found: C, 71.08; H, 8.04; N, 8.52. Recrystallization of **7** from pyridine gave after standing at -20 °C for 2 days crystals of complex **8** suitable for X-ray analysis (72%). Microanalysis and NMR spectra have been carried out on a sample dried in vacuo for a long time, while the X-ray analysis has been performed on a sample containing pyridine of crystallization. ¹H NMR (acetone-*d*₆, room temperature): δ 8.67 (m, 6 H), 7.99 (m, 3 H), 7.48 (m, 8 H), 6.04 (d, C₄H₂N, 2 H), 5.96 (s, C₄H₂N, 2 H), 5.88 (d, C₄H₂N, 2 H), 2.54 (s, Me, 3 H), 2.3–1.98 (m, CH₂, 16 H), 0.93 (t, CH₃, 12 H), 0.64 (t, CH₃, 6 H), 0.52 (t, CH₃, 6 H). Anal. Calcd for **8**, C₅₃H₆₆LiN₇OTi: C, 73.00; H, 7.63; N, 11.24. Found: C, 73.55; H, 7.57; N, 11.50.

X-ray Crystallography for Complexes 5, 6, and 8. Suitable crystals were mounted in glass capillaries and sealed under nitrogen. The reduced cells were obtained with use of TRACER.²⁰ Crystal data and details associated with data collection are given in Tables 5 and S1 (Table S1 is supporting information). Data were collected at room temperature (295 K) on a Rigaku AFC6S single-crystal diffractometer. For intensities and background the individual reflection profiles were analyzed.²¹ The structure amplitudes were obtained after the usual Lorentz and polarization corrections,²² and the absolute scale was established by the Wilson method.²³ The crystal quality was tested by ψ scans showing that crystal

absorption effects could not be neglected. Data were then corrected for absorption using a semiempirical method.²⁴ The function minimized during the least-squares refinement was $\sum w(\Delta F^2)^2$. Anomalous scattering corrections were included in all structure factor calculations.^{25b} Scattering factors for neutral atoms were taken from ref 25a for nonhydrogen atoms and from ref 26 for H. Structure solutions were based on the observed reflections ($I > 2\sigma(I)$). Structure refinements were carried out using the unique total reflections for all complexes.

The structures were solved by the heavy-atom method starting from three-dimensional Patterson maps. Refinements were done by full-matrix least-squares first isotropically and then anisotropically for all the non-H atoms, except for the disordered atoms. In complex **5** an ethylic chain (C24, C25) of a diethyl ether molecule was found to be disordered over two positions (A and B), isotropically refined with a site occupation factors of 0.7 and 0.3, respectively. In complex **8** the pyridine molecule of crystallization (C61··C66) was found to be statistically distributed over two positions (A and B) isotropically refined with a site occupation factor of 0.5. We did not have any possibility of distinguishing between carbon and nitrogen.

All hydrogen atoms, except those associated with the disordered molecules, which were ignored, were located from difference Fourier maps and introduced in the subsequent refinements as fixed atom contributions with isotropic *U*'s fixed at 0.10 for all complexes. In complex **5** the hydrogen atoms associated with the C19 methyl carbon lying over a C2 axis were also ignored, being required to be statistically distributed over two positions.

In the last stage of refinement the weighting scheme $w = 1/[\sigma^2(F_o)^2 + (aP)^2]$ ($P = (F_o^2 + 2F_c^2)/3$) with $a = 0.0752, 0.0751$, and 0.0471 for **5**, **6**, and **8** respectively) was applied. During the refinement of complex **5**, the C–O and C–C bond distances involving the disordered diethyl ether molecule were constrained to be 1.48(1) and 1.54(1) Å, respectively.

The crystal chirality of complexes **6** and **8**, which crystallize in polar space groups, was tested by inverting all the coordi-

(20) Lawton, S. L.; Jacobson, R. A. *TRACER (a Cell Reduction Program)*; Ames Laboratory, Iowa State University of Science and Technology: Ames, IA, 1965.

(21) Lehmann, M. S.; Larsen, F. K. *Acta Crystallogr., Sect. A: Cryst. Phys., Diffraction, Theor. Gen. Crystallogr.* **1974**, *A30*, 580–584.

(22) Wilson, A. J. C. *Nature* **1942**, *150*, 151.

(23) North, A. C. T.; Phillips, D. C.; Mathews, F. S. *Acta Crystallogr., Sect. A: Cryst. Phys., Diffraction, Theor. Gen. Crystallogr.* **1968**, *A24*, 351.

(24) (a) *International Tables for X-ray Crystallography*; Kynoch Press: Birmingham, U.K., 1974; Vol. IV, p 99. (b) *Ibid.*, p 149.

(25) Stewart, R. F.; Davidson, E. R.; Simpson, W. T. *J. Chem. Phys.* **1965**, *42*, 3175.

(26) Sheldrick, G. M. *SHELX76: Program for Crystal Structure Determination*; University of Cambridge: Cambridge, U.K., 1976.

(27) Sheldrick, G. M. *SHELX92: Program for Crystal Structure Refinement*; University of Göttingen, Göttingen, Germany, 1992.

nates ($x, y, z \rightarrow -x, -y, -z$) and refining to convergence again. The resulting R values quoted in Table 5 in brackets indicated that the original choice should be considered the correct one.

All calculations were performed by using SHELX76 for the early stages of solution and SHELXL92 for the refinements. The final difference maps showed no unusual features, with no significant peak above the general background. Final atomic coordinates are listed in Tables S2–S4 for non-H atoms and in Tables S5–S7 for hydrogens. Thermal parameters are given in Tables S8–S10 bond distances and angles in Tables S11–S13.²⁹

(29) See paragraph at the end regarding supporting information.

Acknowledgment. We thank the “Fonds National Suisse de la Recherche Scientifique” (Grant No. 20–40268.94) and Ciba-Geigy SA (Basel, Switzerland) for financial support.

Supporting Information Available: Tables of experimental details associated with data collection and structure refinement, final atomic coordinates, thermal parameters, and bond distances and angles for **5**, **6**, and **8** (17 pages). Ordering information is given on any current masthead page.

OM950326U

Variable-Energy Photoelectron Spectroscopy of $(\eta^5\text{-C}_5\text{H}_5)\text{M}(\eta^3\text{-C}_3\text{H}_5)$ (M = Ni and Pd): Molecular Orbital Assignments

Xiaorong Li,[†] J. S. Tse,[‡] G. M. Bancroft,^{*,†,§} R. J. Puddephatt,^{*,†} and K. H. Tan[§]

Department of Chemistry, The University of Western Ontario, London, Canada N6A 5B7, Canadian Synchrotron Radiation Facility, Synchrotron Radiation Centre, University of Wisconsin–Madison, Stoughton, Wisconsin 53589, and Steacie Institute for Molecular Sciences, National Research Council of Canada, Ottawa, Ontario, Canada K1A 0R6

Received April 11, 1995[®]

Variable-energy photoelectron spectra have been recorded between 21.2 and 70 eV photon energies for $(\eta^5\text{-C}_5\text{H}_5)\text{Ni}(\eta^3\text{-C}_3\text{H}_5)$ and between 21.2 and 60 eV photon energies for $(\eta^5\text{-C}_5\text{H}_5)\text{-Pd}(\eta^3\text{-C}_3\text{H}_5)$. The ground-state electronic structures have been calculated with the X α –SW method. Photoionization cross sections (σ) have also been calculated for the valence ionizations using both the Gelius and X α –SW methods, and the theoretical branching ratios ($\sigma_i/\sum\sigma$) have been compared with the observed photoelectron branching ratios ($A_i/\sum A$, A = band area). The assignments of the photoelectron spectra are based on comparison of the experimental and theoretical band energies and intensities. For both molecules, the lowest binding energy peak is assigned to the HOMO with mainly metal d–Cp π_2 bonding character. The higher IP's for the Pd 4d electrons lead to a different assignment for the second peaks in the two compounds; this orbital has mainly Ni 3d character for M = Ni but has high π -allyl character for M = Pd. The metal d orbitals and ligand π orbitals follow at higher binding energies.

Introduction

$(\eta^5\text{-C}_5\text{H}_5)\text{M}(\eta^3\text{-C}_3\text{H}_5)$ (M = Ni and Pd) are mixed-sandwich organometallic compounds whose photoelectron spectra and electronic structures have not been reported. With the advent of synchrotron radiation sources, it has become possible in the last 10 years to obtain high-quality valence band photoelectron spectra at continuously variable photon energy for small inorganic molecules¹ and transition metal complexes.^{2,3} Because photoionization cross sections for different atomic and molecular orbital vary greatly with photon energy (due, for example, to delayed onsets, shape resonances, Cooper minima, and many body effects),⁴

the relative intensities of photoelectron peaks usually vary markedly with photon energy. Comparison of the experimental intensities (or relative intensities) with theoretical values usually enables a much more confident assignment of the photoelectron peaks than is possible just using experimental and theoretical energies.^{1–3} In this paper, we have carried out a variable-energy gas phase photoelectron study of these complexes using He I and monochromatized synchrotron radiation sources. We have also performed X α –SW ground-state calculations and have compared the experimental relative intensity (branching ratio) variations with the ones from both the Gelius model and from X α –SW photoionization cross section calculations. On the basis of these comparisons, spectral assignments have been made for these compounds.

Experimental Section

The compounds were synthesized by methods in the literature.⁵ Samples were purified by vacuum sublimation before recording the NMR and PE spectra and were stored at –78 °C under an inert atmosphere. The ¹H NMR spectra confirm the purity of the samples used in our work.

All samples were introduced into the gas cell of the photoelectron spectrometers by sublimation. The sublimation temperatures were 0 °C for both compounds. The He I spectra of the compounds were obtained using an ESCA 36 spectrometer with a resolution of ~20 meV.⁶ The variable-energy spectra (between 30 and 70 eV for the Ni compound and between 35 and 60 eV for the Pd compound) were obtained at the Canadian Synchrotron Radiation Facility (CSRFB) at the Aladdin storage ring using modified ESCA 36 spectrometer fitted

[†] The University of Western Ontario.

[‡] Steacie Institute for Molecular Science, National Research Council.

[§] Canadian Synchrotron Radiation Facility.

[®] Abstract published in *Advance ACS Abstracts*, August 15, 1995.

(1) For example: (a) Yates, B. W.; Tan, K. H.; Bancroft, G. M.; Coatsworth, L. L.; Tse, T. S. *J. Chem. Phys.* **1985**, *83*, 4906. (b) Yates, B. W.; Tan, K. H.; Bancroft, G. M.; Coatsworth, L. L.; Tse, T. S.; Schrobilgen, G. J. *J. Chem. Phys.* **1986**, *84*, 3603. (c) Addison-Jones, B. M.; Tan, K. H.; Yates, B. W.; Cutler, J. N.; Bancroft, G. M.; Tse, J. S. *J. Electron Spectrosc. Relat. Phenom.* **1989**, *48*, 155. (d) Bozek, J. D.; Cutler, J. N.; Bancroft, G. M.; Tan, K. H.; Yates, B. W.; Tse, J. S. *J. Chem. Phys.* **1989**, *132*, 257.

(2) (a) Cooper, G.; Green, J. C.; Payne, M. P.; Dobson, B. R.; Hillier, I. H. *J. Am. Chem. Soc.* **1987**, *109*, 3836. (b) Cooper, G.; Green, J. C.; Payne, M. P. *Mol. Phys.* **1988**, *63*, 1031. (c) Didziulis, S. V.; Cohen, S. L.; Butcher, K. D.; Solomon, E. I. *Inorg. Chem.* **1988**, *27*, 2238. (d) Didziulis, S. V.; Cohen, S. L.; Gerwith, A. A.; Solomon, E. I. *J. Am. Chem. Soc.* **1988**, *110*, 250. (e) Butcher, K. D.; Didziulis, S. V.; Briat, B.; Solomon, E. I. *J. Am. Chem. Soc.* **1990**, *112*, 2231. (f) Brennan, J. G.; Green, J. C.; Redfarn, C. M. *J. Am. Chem. Soc.* **1989**, *111*, 2373. (g) Brennan, J. G.; Green, J. C.; Redfarn, C. M.; MacDonald, M. A. *J. Chem. Soc., Dalton Trans.* **1990**, 1907. (h) Lichtenberger, D. L.; Ray, C. D.; Stepiak, F.; Chen, Y.; Weaver, J. H. *J. Am. Chem. Soc.* **1992**, *114*, 10492. (i) Green, J. C.; Kaltsoyannis, N.; Sze, K. H.; MacDonald, M. *J. Am. Chem. Soc.* **1994**, *116*, 1994.

(3) Li, X.; Bancroft, G. M.; Puddephatt, R. J.; Liu, Z. F.; Hu, Y. F.; Tan, K. H. *J. Am. Chem. Soc.* **1994**, *116*, 9543.

(4) Berkowitz, J. *Photoabsorption, Photoionization, and Photoelectron Spectroscopy*; Academic Press: New York, 1979; pp 35–72.

(5) McClellan, W. R.; Hoehn, H. H.; Cripps, H. N.; Muetterties, E. L.; Howk, B. W. *J. Am. Chem. Soc.* **1961**, *83*, 1601.

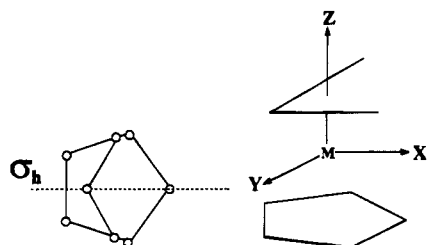
(6) Bancroft, G. M.; Bristow, D. J.; Coatsworth, L. L. *Chem. Phys. Lett.* **1981**, *82*, 344.

with a Quantar no. 36 position sensitive detector.^{3,7,8} The Grasshopper grazing incidence monochromator has been previously described.⁹ Many broad scan and narrow scan variable-energy spectra were recorded at a resolution of <100 meV. The He I spectrum was calibrated with the Ar 3p_{3/2} line at 15.759 eV. For the synchrotron radiation spectra, the Xe 5s band at 23.397 eV was used as the calibrant.

For the cross section analyses, many of the spectra were fit to Gaussian-Lorentzian line shapes using an iterative procedure.^{3,10} Peak positions, widths, and shapes were normally constrained to obtain consistent fits from one photon energy to another. Correction of the areas for the electron analyzer transmission was performed by dividing the computed area by the kinetic energy of the band. Experimental branching ratios (BR_i) were obtained using the resulting band areas (A_i) and the branching ratio formula, BR_i = A_i/ΣA.

Computational Details

Valence orbital energies and compositions of (η⁵-C₅H₅)M(η³-C₃H₅) (M = Ni, and Pd) were calculated using the Xα-SW method as described earlier.¹¹ Structural parameters for (η⁵-C₅H₅)Pd(η³-C₃H₅) were taken from the reported crystallographic data.¹² Since no structural information is available for (η⁵-C₅H₅)Ni(η³-C₃H₅), ligand parameters were used as for (η⁵-C₅H₅)-Pd(η³-C₃H₅), but the distance between the Ni atom and each ligand was decreased by 0.17 Å, the difference in atomic radii between Pd and Ni.¹³ C_s symmetry was assumed for both compounds, shown as follows:



Electronic structures for the fragments (η⁵-C₅H₅)M (M = Ni and Pd, in C_{5v} symmetry) and η³-C₃H₅ (in C_{2v} symmetry) were also calculated respectively using the Xα-SW method. The structural parameters used for them were the same as those of these fragments in the (η⁵-C₅H₅)M(η³-C₃H₅) molecules. For (η⁵-C₅H₅)M(η³-C₃H₅) structures, the y-axis was assumed to be perpendicular to the mirror plane (σ_h), and z-axis perpendicular to the cyclopentadienyl ring, with the metal atom

located at the origin. The exchange α-parameters used in each atomic region were taken from Schwarz's tabulation,¹⁴ except for hydrogen, for which 0.77725 was used. Overlapping atomic sphere radii were used with the outer sphere radius tangent to the outermost atomic spheres. An l_{max} of 4 was used around the outer-sphere region, whereas an l_{max} of 3, 1, and 0 was used around M (= Ni and Pd), C, and H atoms, respectively. Photoionization cross sections were calculated for the outer valence levels of (η⁵-C₅H₅)M(η³-C₃H₅) using the Xα-SW cross section program of Davenport.¹⁵ The calculations were performed with the converged Xα-SW HOMO transition state potential, modified with a Latter tail to correct for large r behavior. In addition to the parameters used in the Xα-SW calculations on molecular orbitals, the maximum azimuthal quantum number, l_{max}, for final states were extended to 7, 4, 2, and 1 around outer-sphere, metals, carbon, and hydrogen regions, respectively. In calculations of transition states, half of an electron is removed from the uppermost molecular orbitals. All symmetry-allowed photoionization processes based on the dipolar selection rule were included in the calculations.

Results

(a) Photoelectron Spectra. In this paper, only the photoelectron spectra in the outer valence region for (η⁵-C₅H₅)M(η³-C₃H₅) will be considered, since the relative energies of the nine valence orbitals of the 18-electron metal centers are of greatest interest. These orbitals are formed by combination of metal orbitals (s, p, and d) with ligand π orbitals. All ligand σ MO's are omitted from the discussion since they have lower ground-state energies and there is much overlapping of the bands so that a reliable assignment cannot be made. For future discussion, the energy region encompassing the outer nine valence orbitals will be termed, somewhat arbitrarily, the "bonding valence region".

The broad range He I spectra of the Ni and Pd compound are shown in Figures 1a and 2, respectively. The first challenge is to determine which bands comprise the "bonding valence region". It can be assumed, on the basis of the Xα-SW calculations to be discussed (Tables 1-3) and on several precedents,^{16,17} that the MO with mainly Cp-π₁ character (11a') should have the highest binding energy among the nine outermost MO's. Hence, once the Cp-π₁ band is located, the "bonding valence region" can be defined. In the literature, this Cp π₁ MO in the photoelectron spectra of (η⁵-C₅H₅)M-(CO)₂ (M = Co and Rh)¹⁶ and (η⁵-C₅H₅)NiNO¹⁷ is assigned to bands at ca. 12 eV and the band energy is expected to be similar in the spectra of (η⁵-C₅H₅)M(η³-C₃H₅). Therefore, band 7 of (η⁵-C₅H₅)Ni(η³-C₃H₅) (12.20 eV) and band 9 of (η⁵-C₅H₅)Pd(η³-C₃H₅) (11.99 eV) are assigned to the Cp-π₁ MO. Thus the "bonding valence region" for (η⁵-C₅H₅)M(η³-C₃H₅) comprises bands 1-7 for M = Ni and bands 1-9 for M = Pd. Hence, when M

(7) Bozek, J. D.; Cutler, J. N.; Bancroft, G. M.; Coatsworth, L. L.; Tan, K. H.; Yang, D. S. *Chem. Phys. Lett.* **1990**, *165*, 1.

(8) Liu, Z. F.; Coatsworth, L. L.; Tan, K. H. *Chem. Phys. Lett.* **1993**, *203*, 337.

(9) (a) Tan, K. H.; Bancroft, G. M.; Coatsworth, L. L.; Yates, B. W. *Can. J. Phys.* **1982**, *60*, 131. (b) Bancroft, G. M.; Bozek, J. D.; Tan, K. H. *Phys. Can.* **1987**, 113.

(10) Bancroft, G. M.; Adams, J.; Coatsworth, L. L.; Bennwitz, C. D.; Brown, J. D.; Westwood, W. D. *Anal. Chem.* **1975**, *47*, 586.

(11) (a) Yang, D. S.; Bancroft, G. M.; Puddephatt, R. J.; Bozek, J. D.; Tse, J. S. *Inorg. Chem.* **1989**, *28*, 1. (b) Yang, D. S.; Bancroft, G. M.; Puddephatt, R. J.; Bursten, B. E.; McKee, S. D. *Inorg. Chem.* **1989**, *28*, 872. (c) Yang, D. S.; Bancroft, G. M.; Puddephatt, R. J. *Inorg. Chem.* **1990**, *29*, 2118. (d) Yang, D. S.; Bancroft, G. M.; Dignard-Bailey, L.; Puddephatt, R. J.; Tse, J. S. *Inorg. Chem.* **1990**, *29*, 2487. (e) Yang, D. S.; Bancroft, G. M.; Puddephatt, R. J.; Tse, J. S. *Inorg. Chem.* **1990**, *29*, 2496. Yang, D. S.; Bancroft, G. M.; Puddephatt, R. J.; Tan, K. H.; Cutler, J. N.; Bozek, J. B. *Inorg. Chem.* **1990**, *29*, 4956.

(12) Minasyants, M. Kh.; Struchkov, Yu. T. *Zh. Strukt. Khim.* **1968**, *9*, 481 (in Russian); *J. Struct. Chem. (Engl. Transl.)* **1968**, *9*, 406.

(13) Sargent-Welch Scientific Com. *Table of Periodic Properties of the Elements*; Sargent-Welch: Skokie, IL, 1980.

(14) (a) Schwarz, K. *Phys. Rev. B* **1972**, *5*, 2466. (b) Schwarz, K. *Theoret. Chim. Acta (Berl.)* **1974**, *34*, 225.

(15) (a) Davenport, J. W. Ph.D. Dissertation, University of Pennsylvania, 1976. (b) Davenport, J. W. *Phys. Rev. Lett.* **1976**, *36*, 945.

(16) Lichtenberger, D. L.; Calabro, D. C.; Kellogg, G. E. *Organometallics* **1984**, *3*, 1623.

(17) Evans, S.; Guest, M. F.; Hiller, I. H.; Orchard, A. F. *J. Chem. Soc., Faraday 2*, **1974**, *70*, 417.

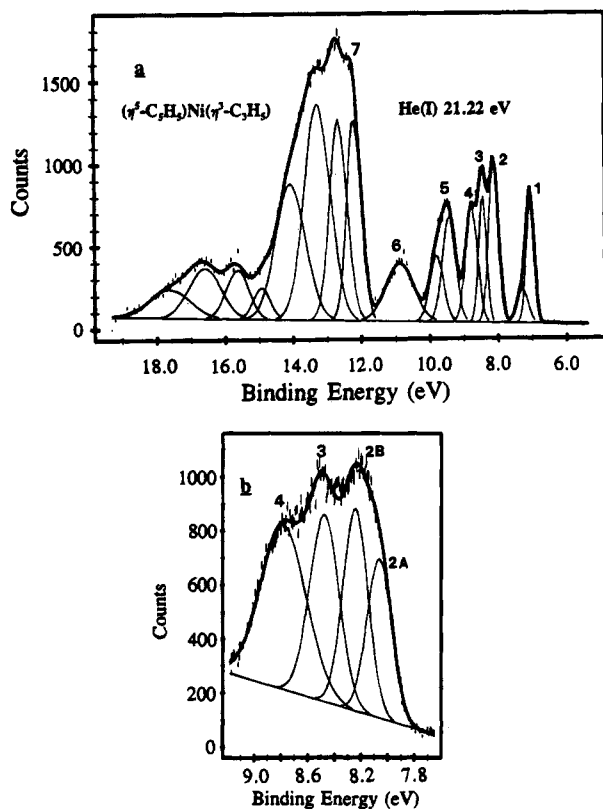


Figure 1. (a) Broad range He I photoelectron spectrum of $(\eta^5\text{-C}_5\text{H}_5)\text{Ni}(\eta^3\text{-C}_3\text{H}_5)$. Bands 1–7 are corresponding to the “bonding valence region”. The small fitted peak in band 1 is due to the vibrational splitting. (b) Narrow range He I photoelectron spectrum of $(\eta^5\text{-C}_5\text{H}_5)\text{Ni}(\eta^3\text{-C}_3\text{H}_5)$, which shows bands 2–4. Band 2 is fitted into peaks 2A and 2B.

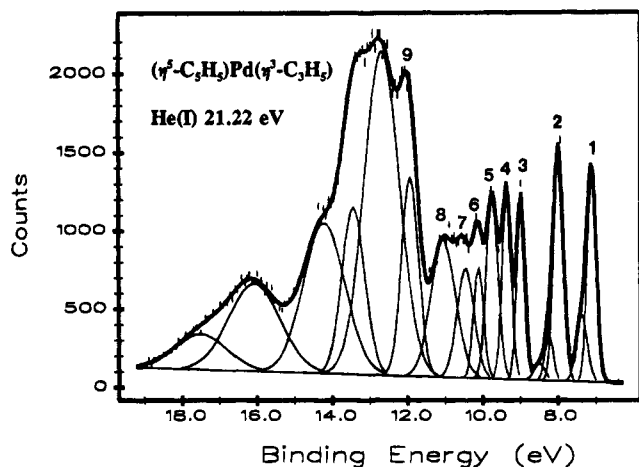


Figure 2. Broad range He I photoelectron spectrum of $(\eta^5\text{-C}_5\text{H}_5)\text{Pd}(\eta^3\text{-C}_3\text{H}_5)$.

= Pd, there is a one-to-one relationship between the number of bands and the number of MO's in the outer valence region. But, when $\text{M} = \text{Ni}$, the number of bands (seven) is less than the number of MO's (nine). This means that overlapping of bands occurs for $\text{M} = \text{Ni}$, in agreement with the general observation that the PE bands are less widely separated for first-row transition metal molecules than second row.³

Representative variable-energy spectra for the Ni and Pd compounds are shown in Figures 3 and 4, respectively, and show dramatic intensity variations as a function of photoelectron energy. A qualitative estimate of the atomic orbital composition for each MO repre-

Table 1. X α -SW MO Energies and Compositions (%) for MCp ($\text{M} = \text{Ni}$ and Pd) Fragments ($n = 3$ for Ni, $n = 4$ for Pd)

orbital	energy (eV)	M ($n + 1$)p	M ($n + 1$)s	M nd	C 2p	C 2s	inter ^a	outer ^a
NiCp								
6e ₁	-3.35	4.9		63.6	31.3		20.5	4.7
4a ₁	-4.64		1.4	97.5	0.5		7.0	0.7
1e ₂	-4.82			98.0	2.7		6.4	0.5
5e ₁	-5.78	1.3		53.6	44.4	0.5	18.6	0.7
3a ₁	-8.82	2.3	11.1	0.7	85.6	0.2	30.7	1.1
PdCp								
6e ₁	-3.11	15.3		53.1	31.4	0.1	17.7	5.7
4a ₁	-4.81	0.5	3.9	94.0	0.8	0.1	5.2	1.1
1e ₂	-5.14			97.3	2.5		3.9	0.5
5e ₁	-6.22	2.3		56.6	40.0	0.8	10.2	0.7
3a ₁	-8.86	7.2	15.3	3.1	74.1	0.3	16.3	0.9

^a inter = intersphere; outer = outer sphere.

sented by its ionization band can be made very quickly on the basis of the comparison of the observed band intensity variation with Yeh and Lindau's cross-section curve for atomic subshells (Figure 5).¹⁸ Orbitals with mostly ligand C 2p character are expected to give bands whose intensities fall at higher photon energy. It is apparent from Figure 3 that the relative intensity of bands 1, 3, and 6 of the Ni compound and bands 1, 2 and 8 of the Pd compound decrease with increasing photon energy, suggesting that they arise from the MO's with mostly ligand character. Also, the relative intensity of bands 2 and 4 of the Ni compound and bands 3–5 of the Pd compound increase with photon energy, indicating that they should be assigned to orbitals with mostly metal d character. The trend of intensity variations of band 5 of the Ni compound and bands 6 and 7 of the Pd compound are intermediate between the variations of the above two groups, showing that they are from MO's with mixed-metal d and ligand C 2p character.

Although the intensity of both bands 1 and 2 of the Pd compound decrease with photon energy relative to bands 3–5, the first band shows an increase in intensity relative to the second band, demonstrating that the orbital associated with the second band has more ligand character than that of the first band.

(b) Electronic Structures of $(\eta^5\text{-C}_5\text{H}_5)\text{M}(\eta^3\text{-C}_3\text{H}_5)$ ($\text{M} = \text{Ni}$ and Pd) from X α -SW Calculations. The X α -SW orbital energies and compositions for $\text{M}(\eta^5\text{-C}_5\text{H}_5)$ ($\text{M} = \text{Ni}$ and Pd) fragments (with C_{5v} symmetry) in the outer valence are listed and plotted in Table 1 and Figures 6 and 7. The MO's in these regions are formed mainly between metal nd ($n = 3$ for Ni, $n = 4$ for Pd) and Cp π_1 (a_1 symmetry), Cp π_2 (e_1 symmetry, doubly degenerate) MO's, with a small amount of metal ($n + 1$)s and ($n + 1$)p also involved. The calculated electron configurations for $\text{M}(\eta^5\text{-C}_5\text{H}_5)$ are as follows: (core)(3a₁)²(5e₁)⁴(1e₂)⁴(4a₁)²(6e₁)³. There are three types of orbital interactions (π , σ , and δ) for $\text{M}(\eta^5\text{-C}_5\text{H}_5)$.¹⁹ Among them, 4a₁ and 3a₁ are σ type MO's, with 4a₁ having mainly metal nd_{z^2} character; and 3a₁ having mainly Cp- π_1 character with some metal s, p constitution. The metal nd_{z^2} orbital is essentially nonbonding. The 1e₂ MO's are of δ -symmetry with predominant

(18) Yeh, J. J.; Lindau, I. *At. Nucl. Data Tables* **1985**, *32*, 1.

(19) Elschenbroich, C.; Salzer, A. *Organometallics: A Concise Introduction*, 2nd ed.; VCH Publishers Inc.: New York, 1992; pp 318–319.

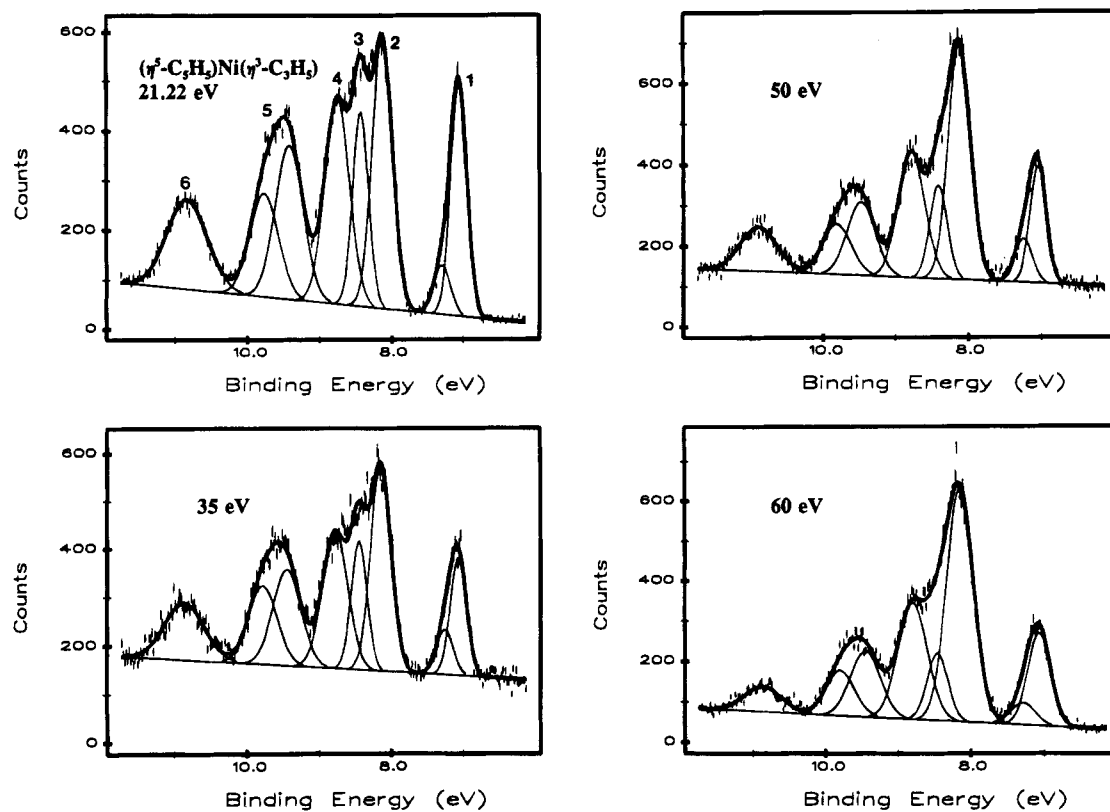


Figure 3. Representative variable-energy photoelectron spectra of $(\eta^5\text{-C}_5\text{H}_5)\text{Ni}(\eta^3\text{-C}_3\text{H}_5)$ of the first six bands at 21.2, 35, 50, and 60 eV photon energies.

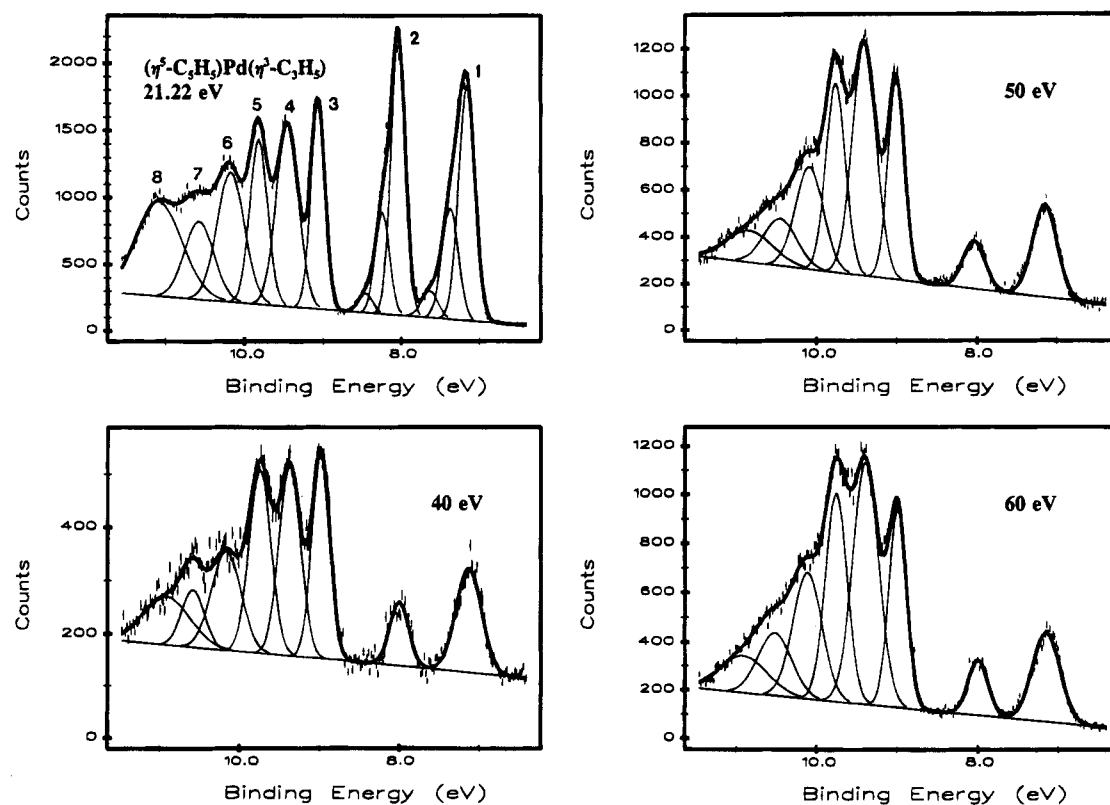


Figure 4. Representative variable-energy photoelectron spectra of $(\eta^5\text{-C}_5\text{H}_5)\text{Pd}(\eta^3\text{-C}_3\text{H}_5)$ of the first eight bands at 21.2, 40, 50, and 60 eV photon energies.

metal $nd_{x^2-y^2}/nd_{xy}$ character. They remain mainly non-bonding because the δ -type overlap with the Cp π -orbitals is weak. The MO's $6e_1$ and $5e_1$ have π symmetry. They have significant metal nd_{xz}/nd_{yz} and ligand C 2p character, suggesting that $6e_1$ is the out-of-phase and

$5e_1$ is the in-phase interaction between metal nd_{xz}/nd_{yz} and Cp e_1 orbitals. The electronic structure of the $\text{M}(\eta^5\text{-C}_5\text{H}_5)$ fragment has been discussed before, and the orbital ordering from our X α calculation is in agreement with the literature.²⁰

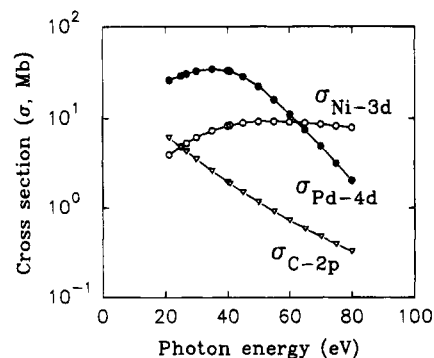


Figure 5. Photoionization cross sections of Ni 3d, Pd 4d, and C 2p atomic subshells from Yeh and Lindau's calculation.¹⁸

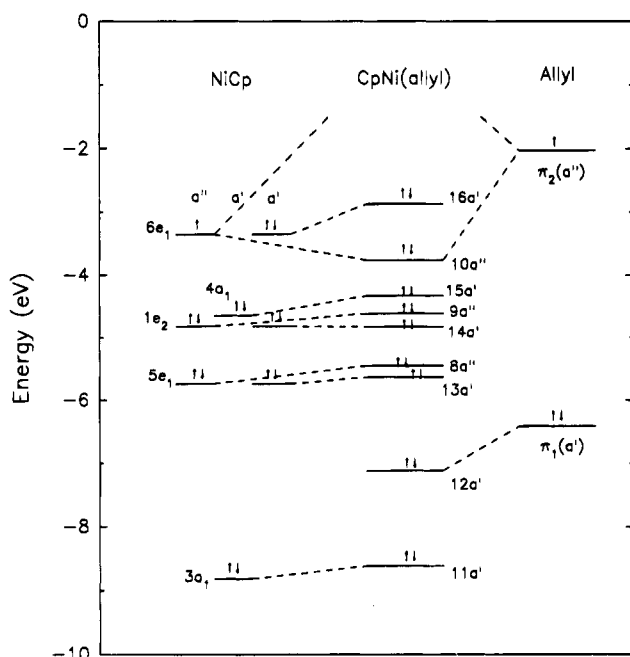


Figure 6. Molecular orbital diagrams of $(\eta^5\text{-C}_5\text{H}_5)\text{Ni}$, $\eta^3\text{-C}_3\text{H}_5$, and $(\eta^5\text{-C}_5\text{H}_5)\text{Ni}(\eta^3\text{-C}_3\text{H}_5)$ from X α -SW calculations. Dashed lines show the orbital correspondence due to bonding.

The molecule $(\eta^5\text{-C}_5\text{H}_5)\text{M}(\eta^3\text{-C}_3\text{H}_5)$ has C_s symmetry. The correlation of $\text{M}(\eta^5\text{-C}_5\text{H}_5)$ MO's on going from $C_{5v} \rightarrow C_s$ symmetry is $a_1 \rightarrow a'$ and $e \rightarrow a' + a''$. The configuration of π -allyl fragments in C_s symmetry is $(\text{core})(a'')^2(a'')^1$ or $(\text{core})(\pi_1)^2(\pi_2)^1$. In forming $(\eta^5\text{-C}_5\text{H}_5)\text{M}(\eta^3\text{-C}_3\text{H}_5)$ from the $\text{M}(\eta^5\text{-C}_5\text{H}_5)$ and $\eta^3\text{-C}_3\text{H}_5$ fragments, no cross-interactions ($a'-a''$) are allowed. From the data in Tables 2 and 3 and Figures 6 and 7, it is clear that $12a'$, $10a''$, and $8a''$ of $(\eta^5\text{-C}_5\text{H}_5)\text{M}(\eta^3\text{-C}_3\text{H}_5)$ have more π -allyl ligand character. Since the $nd_{x^2-y^2}/nd_{xy}$ orbitals ($9a''$ and $14a'$, corresponding to e_2 symmetry of $\text{M}(\eta^5\text{-C}_5\text{H}_5)$) are approximately perpendicular to the plane of the allyl and Cp ligands, they cannot interact effectively with the ligand orbitals. These two orbitals remain essentially nonbonding with metal d character. Besides the symmetry-match requirement, the energy of the interacting orbitals should be close. On the basis of these conditions, an orbital interaction occurs between the π_2 -allyl and an a'' MO's of $\text{M}(\eta^5\text{-C}_5\text{H}_5)$ which were

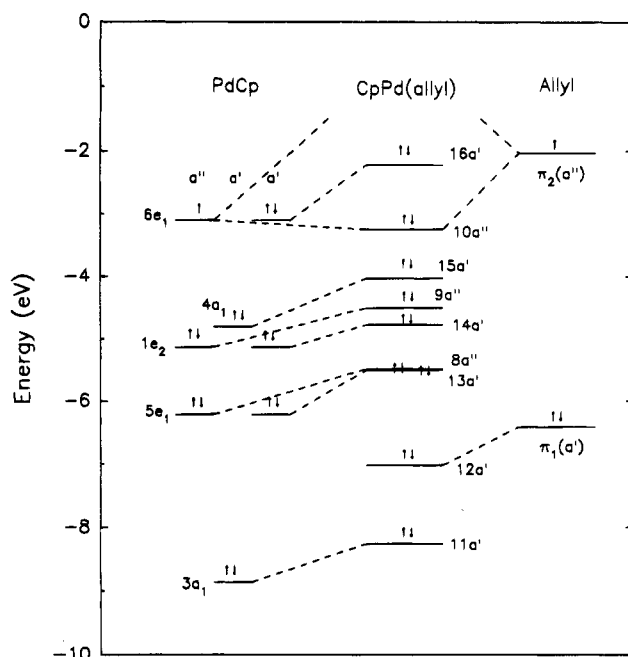


Figure 7. Molecular orbital diagrams of $(\eta^5\text{-C}_5\text{H}_5)\text{Pd}$, $\eta^3\text{-C}_3\text{H}_5$, and $(\eta^5\text{-C}_5\text{H}_5)\text{Pd}(\eta^3\text{-C}_3\text{H}_5)$ from X α -SW calculations. Dashed lines show the orbital correspondence due to bonding.

originally the $6e_1$ orbital in C_{5v} symmetry. There are two MO's formed for $(\eta^5\text{-C}_5\text{H}_5)\text{M}(\eta^3\text{-C}_3\text{H}_5)$ by this interaction. They are $10a''$ and a virtual MO in a'' symmetry (Figures 6 and 7). The remaining valence molecular orbitals, $16a'$, $15a'$, $8a''$, and $13a'$ for $(\eta^5\text{-C}_5\text{H}_5)\text{M}(\eta^3\text{-C}_3\text{H}_5)$, are mainly $\text{M}(\eta^5\text{-C}_5\text{H}_5)$ orbitals and have little allyl character. The $12a'$ and $11a'$ MO's are mainly π_1 orbitals of allyl and Cp, respectively, with small interactions with frontier metal d, s, and p orbitals in a' symmetry.

The X α -SW calculations show that, for the ligand orbitals, the π_2 orbitals of Cp and allyl are largely involved in the bonding, and the π_1 orbitals are less involved. The crystal structure of $(\eta^5\text{-C}_5\text{H}_5)\text{Pd}(\eta^3\text{-C}_3\text{H}_5)$ has shown that the planes of the allyl and cyclopentadienyl ligands are not parallel; the angle between them is 19.5° . The end carbon atoms of the allyl group are 0.24 \AA closer to the cyclopentadienyl plane than the middle one,¹² suggesting that the π_2 orbital of allyl, whose electron cloud is mainly located at the end carbons, is largely involved in the bonding.

(c) Theoretical Calculations for Photoelectron Branching Ratios. We obtained theoretical valence molecular orbital photoionization cross sections using both the Gelius²¹ and X α methods,¹⁵ and then obtained branching ratios ($\text{BR}_i = \sigma_i/\Sigma\sigma$), where σ_i is the calculated cross section for the i th orbital, to compare with the experimental BR_i values ($A_i/\Sigma A$). In the Gelius treatment, the cross section of an individual MO is assumed to be proportional to the sum of the atomic cross sections (σ_{A_j}) of its components weighted by the "probability" (P_{A_j}) _{i} of finding in the i th molecular orbital an electron belonging to the atomic orbital A_j :

(20) Albright, T. A.; Burdett, J. K.; Whangbo, M.-H. *Orbital Interactions in Chemistry*; John Wiley & Sons: New York, 1985; pp 387-388.

(21) Gelius, U. *Electron Spectroscopy*; Shirley, D. A., Ed.; North Holland: Amsterdam, 1972; pp 311. (b) Bancroft, G. M.; Malmquist, P.-Å.; Svensson, S.; Bailier, E.; Gelius, U.; Siegbahn, K. *Inorg. Chem.* **1978**, *17*, 1595.

Table 2. X α -SW MO Energies and Compositions (%) for CpNi(allyl) ("Bonding Valence")

orbital	energy (eV)	Ni			Cp			allyl			inter.	outer.
		4p	4s	3d	C 2p	C 2s	H 1s	C 2p	C 2s	H 1s		
16a'	-2.86	2.6	0.6	63.2	27.8	0.1		4.8		0.8	17.7	0.4
10a''	-3.76	9.0		16.5	39.4			33.8	0.6	0.8	34.2	4.4
15a'	-4.32	0.3	3.4	92.2	0.9		0.3	2.1		0.6	9.0	0.2
9a''	-4.61	0.3		95.0	3.2			0.8		0.6	6.9	0.2
14a'	-4.82	0.2		95.0	2.2		0.1	2.3		0.1	7.7	0.2
8a''	-5.45	0.3		63.8	25.0	0.5	0.1	9.2	0.3	0.8	15.9	0.7
13a'	-5.63	2.5	0.4	46.9	46.0	0.4		3.5		0.2	23.0	1.6
12a'	-7.12	6.9	1.8	12.4	16.5	0.1		61.6	0.3	0.3	26.4	2.8
11a'	-8.62	1.1	13.3	2.6	70.0	0.3	0.2	12.0	0.5		32.2	2.4

Table 3. X α -SW MO Energies and Compositions (%) for CpPd(allyl) ("Bonding Valence")

orbital	energy (eV)	Pd			Cp			allyl			inter.	outer.
		5p	5s	4d	C 2p	C 2s	H 1s	C 2p	C 2s	H 1s		
16a'	-2.22	6.5	0.8	57.6	28.0	0.1		5.8	0.1	1.2	12.0	8.2
10a''	-3.25	20.0		10.9	35.3			31.9	0.7	1.1	21.4	5.1
5a'	-4.03	1.1	10.2	82.4	1.6		0.5	3.2	0.2	1.0	7.6	0.7
9a''	-4.51	0.9		91.4	4.7	0.1		1.5	0.1	1.3	3.9	0.3
14a'	-4.78	0.7	0.1	93.0	2.9			2.9		0.3	4.2	0.3
8a''	-5.49	0.6		59.6	24.2	0.9	0.2	13.3	0.7	1.5	7.4	1.3
13a'	-5.51	6.2	0.5	43.9	41.4	0.7		6.5	0.1	0.7	11.5	2.1
12a'	-7.02	13.2	2.2	14.9	11.7	0.1		56.3	0.8	0.7	6.6	2.7
11a'	-8.26	4.0	16.2	4.9	65.8	0.6	0.1	7.9	0.4	0.1	13.8	2.7

$$\sigma_i \alpha \sum_j (P_{Aj})_i \sigma_{Aj} \quad (1)$$

where $(P_{Aj})_i$ is given approximately by the orbital composition from our X α calculations, and σ_{Aj} are the theoretical atomic cross sections as a function of photon energy. In this work, Yeh and Lindau's data,¹⁸ obtained by the Hartree-Slater central field method, were used. A qualitative guide to the variations in molecular cross sections and branching ratios can be obtained by looking at the important atomic cross sections in Figure 5. Thus all metal d orbitals show a large increase in cross section above threshold, before decreasing in markedly different ways at higher energies. In contrast, the C 2p orbital shows a monotonic decrease in cross section over the whole range. This behavior gives rise to the changes in the ratio of the M nd/C 2p cross sections, which are reflected in the branching ratio changes.

The theoretical branching ratios for MO's in the valence spectra of $(\eta^5\text{-C}_5\text{H}_5)\text{M}(\eta^3\text{-C}_3\text{H}_5)$ are plotted in Figures 8 and 9 (solid line, X α calculation; dashed line, Gelius model treatment). They demonstrate that the general trends of experimental and theoretical branching ratios of the metal d based MO's (15a', 9a'', and 14a') increase from 21.2 to 70 eV, and the curves for the other MO's either decrease or show little change on going from low to high photon energy.

Discussion

(a) Spectral Assignment. The spectral assignments are based on the generally good agreement between the trends of theoretical branching ratios (Gelius and X α -SW) with the experimental ones (Table 4 and Figures 8 and 9). The agreement is just as good as we have observed in previous studies.^{1-3,11}

The assignments for M = Pd are more straightforward and so are discussed first. It is clear from Figures 4 and 9 that bands 3-5 increase in intensity with increasing photon energy and they must be assigned to the MO's 15a', 9a'', and 14a' which are calculated to have >80% Pd 4d character. Bands 1, 6, and 7 have

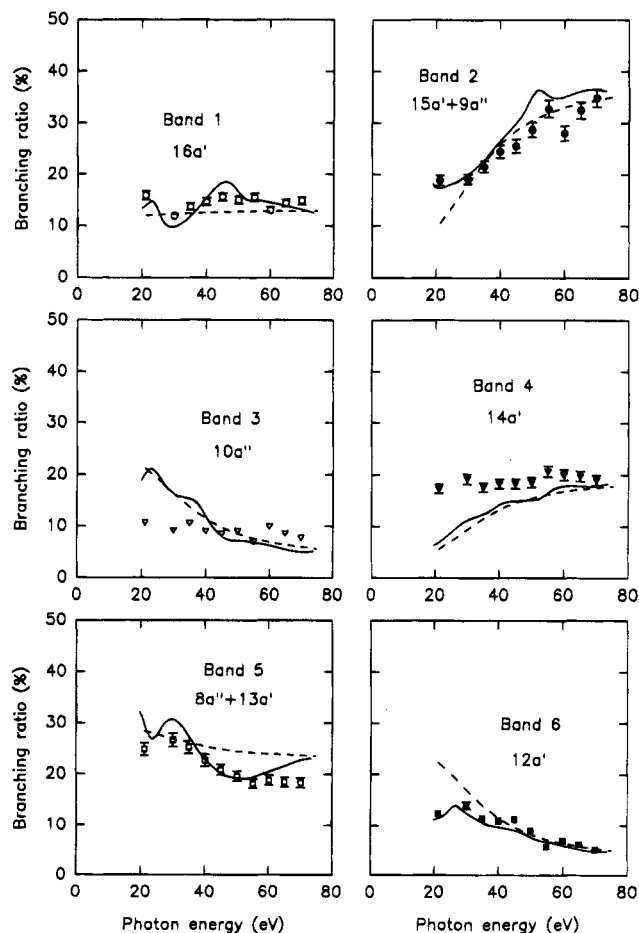


Figure 8. Experimental branching ratios of PES bands and theoretical branching ratios of molecular orbitals for $(\eta^5\text{-C}_5\text{H}_5)\text{Ni}(\eta^3\text{-C}_3\text{H}_5)$ (circles, triangles, and squares, experimental data; solid line, X α -SW data; dashed line, Gelius model treatment).

intensities which are less dependent on photon energy and so are assigned to MO's 16a', 8a'', and 13a' which are calculated to have 44-60% Pd 4d character and have metal ligand bonding character. Bands 2, 8, and 9 show the greatest decrease in intensity with photon

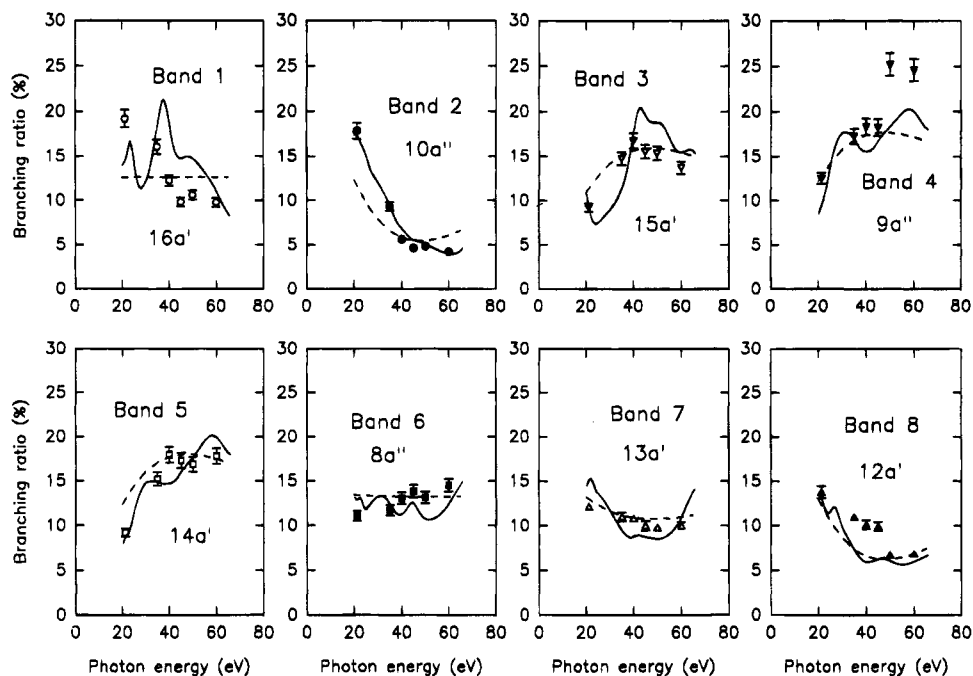


Figure 9. Experimental branching ratios of PES bands and theoretical branching ratios of molecular orbitals for $(\eta^5\text{-C}_5\text{H}_5)\text{Pd}(\eta^3\text{-C}_3\text{H}_5)$ (circles, triangles, and squares, experimental data; solid line, X α -SW data; dashed line, Gelius model treatment).

Table 4. Assignments for Photoelectron Spectra of CpM(allyl) (M = Ni and Pd)

molecular orbital	X α ground-state energy (eV)	band assgnt	vertical IP (± 0.01 eV)
CpNi(allyl)			
16a'	-2.86	1	7.06
10a''	-3.76	3	8.43
15a'	-4.32	2A	8.02
9a''	-4.61	2B	8.10
14a'	-4.82	4	8.76
8a''	-5.45	5A	9.42
13a'	-5.63	5B	9.77
12a'	-7.12	6	10.84
11a'	-8.62	7	12.20
CpPd(allyl)			
16a'	-2.22	1	7.10
10a''	-3.25	2	7.99
15a'	-4.03	3	8.99
9a''	-4.51	4	9.36
14a'	-4.78	5	9.74
8a''	-5.49	6	10.10
13a'	-5.51	7	10.45
12a'	-7.02	8	11.05
11a'	-8.26	9	11.99

energy and are assigned to the ligand bands 10a'', 12a', and 11a', respectively. Figure 9 shows that this assignment gives good agreement between the observed and calculated branching ratios, while Table 4 indicated a perfect correlation between the sequences of experimental and calculated MO energies. Both the energy and intensity calculations put this assignment on a very firm footing.

The assignments for M = Ni are more difficult. Because of band overlaps, deconvolution of the bands is necessary and creates some uncertainty in the experimental branching ratios. However, from Figures 3 and 8 it is clear that band 2 gives the greatest increase in intensity with photon energy and that band 4 is the only other band to show an overall increase in intensity. Band 2 (peaks 2A and 2B in Figure 1b) is assigned to both MO's 15a' and 9a'', while band 4 is assigned to MO

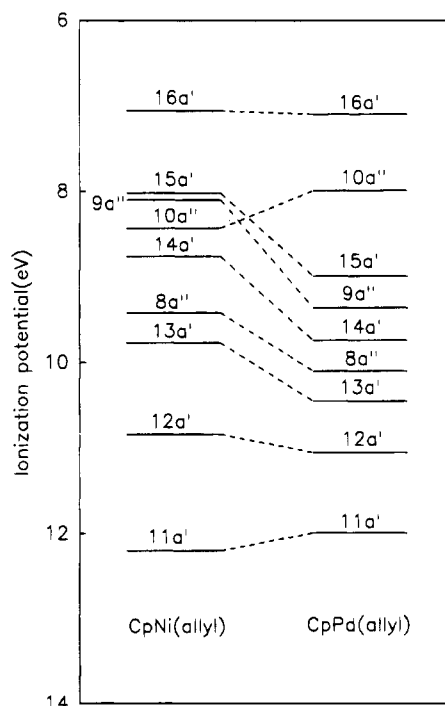


Figure 10. Correlation of the ionization potentials for the complexes with M = Ni and Pd.

14a'. These are all calculated to have 92–95% Ni 3d character. Bands 1 and 5 do not change in intensity greatly as a function of photon energy and are assigned to MO's 16a' and 8a'' + 13a', respectively, having 47–64% Ni 3d character. Bands 3, 6, and 7, which decrease in intensity with increasing photon energy, are then assigned to MO's 10a'', 12a', and 11a', respectively, having $\leq 16\%$ Ni 3d character.

(b) A Comparison of the Assignments for M = Ni and Pd. A correlation of the MO energies for the complexes with M = Ni and Pd is shown in Figure 10.

The relative IP's for $M = \text{Ni}$ are therefore

$$16a' > 15a', 9a'' > 10a'' > 14a' > 8a'', 13a' > 12a' > 11a'$$

In contrast, the calculated $X\alpha$ sequence for $M = \text{Ni}$ and Pd , and experimental IP sequence for $M = \text{Pd}$, are

$$16a' > 10a'' > 15a' > 9a'' > 14a' > 8a'' > 13a' > 12a' > 11a'$$

The major energy differences between the two compounds are for the MO's with greatest metal nd character, especially for the MO's $15a'$, $9a''$, and $14a'$. These differences are not predicted by the ground-state $X\alpha$ calculations (Tables 2–4). There are two possible explanations. First, it is possible that relaxation effects are greater for the Ni 3d MO's than for the Pd 4d MO's. There is support for this interpretation from studies of photoelectron spectra of organometallic derivatives of other first- and second-row transition metal complexes.^{16,22} The second interpretation is that the ground-state energies are actually Ni 3d > Pd 4d and that the $X\alpha$ calculations fail to reflect this difference. Support for this interpretation is found from a study of the photoelectron spectra of $M(\eta^3\text{-C}_3\text{H}_5)_2$ ($M = \text{Ni}, \text{Pd}$, and

Pt).³ Of course, it is also possible that both factors play a part.

Conclusion

The photoelectron spectra of $(\eta^5\text{-C}_5\text{H}_5)M(\eta^3\text{-C}_3\text{H}_5)$ ($M = \text{Ni}$ and Pd) have been recorded and assigned by using the variable-energy technique and the theoretical calculations. Both experimental and theoretical relative intensities for the mainly ligand and metal valence photoionizations show distinct trends, which puts the spectral assignments on a firm footing. The comparison of the assignments for $M = \text{Ni}$ and Pd (in this work and our previous work³) suggests that the orbital relaxation and ground-state energy orderings (both are Ni 3d > Pd 4d) may play parts for the observed ionization difference between Ni 3d and Pd 4d.

Acknowledgment. We are very grateful for the financial support of NSERC (Canada), for the continued assistance from the staff at the Aladdin Synchrotron, and for the other assistance from Mr. Y. F. Hu. We also acknowledge the support of NSR Grant No. DMR-9212658 to the Synchrotron Radiation Centre.

OM9502603

(22) (a) Calabro, D. C.; Lichtenberger, D. L. *Inorg. Chem.* **1980**, *19*, 1732. (b) Lichtenberger, D. L.; Kellogg, G. E. *Acc. Chem. Res.* **1984**, *3*, 1623.

Rhodium-Catalyzed Reaction of Benzoic Anhydride with Styrene under Molecular Hydrogen

Ken Kokubo, Masahiro Miura,* and Masakatsu Nomura

Department of Applied Chemistry, Faculty of Engineering, Osaka University,
Suita, Osaka 565, Japan

Received May 18, 1995[®]

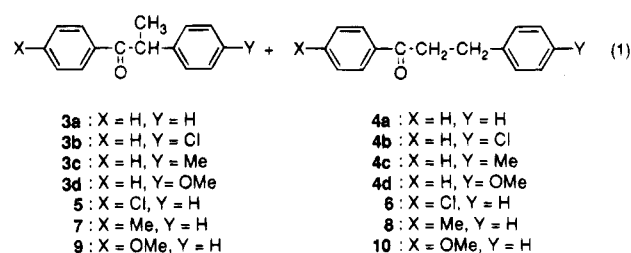
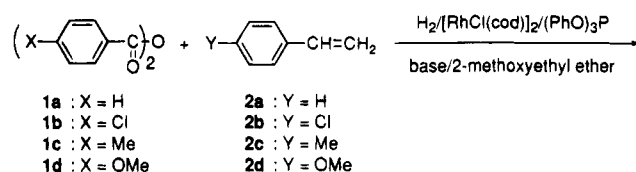
It has been found that styrene undergoes intermolecular hydrobenzoylation by benzoic anhydride under a normal pressure of molecular hydrogen in the presence of a tertiary amine and a catalytic amount of $[\text{RhCl}(\text{cod})]_2$ and a phosphorous ligand to give a mixture of 1,2- and 1,3-diphenyl-1-propanones. The catalyst efficiency has been observed to be a marked function of the ligand employed; triphenylphosphite appears to be one of the favorable ones. The reaction using deuterium has also been carried out to obtain insight into the reaction mechanism.

Introduction

Transition metal complex catalyzed hydroacylation of alkenes may provide an attractive tool for the preparation of ketones. One of the most effective metals for the reaction with aldehydes as both the acyl and hydrogen moieties appears to be rhodium, and the intramolecular reaction of 4-pentenals to produce cyclopentanones,¹ especially using cationic rhodium complexes,² has been successfully developed. However, the intermolecular reaction has been less explored,^{3,4} while catalytic example for the reaction of benzaldehyde with ethylene using an indenylrhodium complex has been described.⁵ One of the major reasons for the limited intermolecular studies may be due to formation of catalytically inactive carbonylrhodium species.

On the other hand, it has been reported that hydroacylation of ethylene takes place by using acyl halides and a stoichiometric amount of $\text{HRh}(\text{CO})(\text{PPh}_3)_3$.⁶ We conceived that such a reaction could be made catalytic if it is performed in the presence of an appropriate hydrogen source and a base. Indeed, it has been observed that hydroaroylation of 4-substituted styrenes with 4-substituted benzoic anhydrides as the acyl moieties efficiently proceeds in the presence of $[\text{RhCl}(\text{cod})]_2$ and a phosphorous ligand using a tertiary amine under a normal pressure of hydrogen (eq 1), while aroyl

$[\text{RhCl}(\text{cod})]_2$ and a phosphorous ligand using a tertiary amine under a normal pressure of hydrogen (eq 1), while aroyl



halides were ineffective.^{7,8} Consequently, a detailed investigation has been carried out to elucidate the factors affecting the reaction. The results are described herein.

Results and Discussion

Reaction of Benzoic Anhydride with Styrene.

The reaction of benzoic anhydride (1a; 2 mmol) with styrene (2a; 8 mmol) in the presence of $[\text{RhCl}(\text{cod})]_2$ (0.01 mmol), triphenylphosphine (0.04 mmol), and diisopropylethylamine (4 mmol) in 2-methoxyethyl ether at 100 °C for 20 h under 1 atm of hydrogen gave 1,2-diphenyl-1-propanone (3a) as the major product along with 1,3-diphenyl-1-propanone (4a) in a total ketone yield of 17% based on 1a used (eq 1 and Table 1). When the ligand employed was varied, the product yield as

(7) A relevant palladium-catalyzed intermolecular reaction of aroyl chlorides with dienes in the presence of a disilane has been reported, while it accompanies decarbonylation: Obora, Y.; Tsuji, Y.; Kawamura, T. *J. Am. Chem. Soc.* **1993**, *115*, 10414.

(8) Effective radicalic intermolecular hydroacylations of alkenes using (a) selenoesters and (b) organic iodides under carbon monoxide as acyl moieties in the presence of a tin hydride as hydrogen source have also been developed: (a) Boger, D. L.; Mathvink, R. J. *J. Org. Chem.* **1989**, *54*, 1779. (b) Ryu, I.; Kusano, K.; Yamazaki, H.; Sonoda, N. *J. Org. Chem.* **1991**, *56*, 5003.

[®] Abstract published in *Advance ACS Abstracts*, August 15, 1995.

(1) (a) Sakai, K.; Ide, J.; Oda, O.; Nakamura, N. *Tetrahedron Lett.* **1972**, *13*, 1287. (b) Lochow, C. F.; Miller, R. G. *J. Am. Chem. Soc.* **1976**, *98*, 1281. (c) Larock, R. C.; Oertle, K.; Potter, G. F. *J. Am. Chem. Soc.* **1980**, *102*, 190. (d) Campbell, R. E., Jr.; Miller, R. G. *J. Organomet. Chem.* **1980**, *186*, C27. (e) Campbell, R. E., Jr.; Lochow, C. F.; Vora, K. P.; Miller, R. G. *J. Am. Chem. Soc.* **1980**, *102*, 5824. (f) Milstein, D. *J. Chem. Soc., Chem. Commun.* **1982**, 1357. (g) Sakai, K. *J. Synth. Org. Chem. Jpn.* **1993**, *51*, 733; *Chem. Abstr.* **1993**, *113*, 270830g.

(2) (a) Fairlie, D. P.; Bosnich, B. *Organometallics* **1988**, *7*, 936. (b) Fairlie, D. P.; Bosnich, B. *Organometallics* **1988**, *7*, 946. (c) Wu, X.-M.; Funakoshi, K.; Sakai, K. *Tetrahedron Lett.* **1992**, *33*, 6331. (d) Barnhart, R. W.; Wang, X.; Noheda, P.; Bergens, S. H.; Whelan, J.; Bosnich, B. *J. Am. Chem. Soc.* **1994**, *116*, 1821.

(3) (a) Vora, K. P.; Lochow, C. F.; Miller, R. G. *J. Organomet. Chem.* **1980**, *192*, 257. (b) Okano, T.; Kobayashi, T.; Konishi, H.; Kiji, J. *Tetrahedron Lett.* **1982**, *23*, 4967. (c) Rode, E.; Davis, M. E.; Hanson, B. E. *J. Chem. Soc., Chem. Commun.* **1985**, 716.

(4) Ruthenium-catalyzed intermolecular hydroacylation: (a) Isnard, P.; Denise, B.; Sneed, R. P. A.; Congnion, J. M.; Durual, P. *J. Organomet. Chem.* **1982**, *240*, 285. (b) Kondo, T.; Tsuji, Y.; Watanabe, Y. *Tetrahedron Lett.* **1987**, *28*, 6229. (c) Kondo, T.; Akazome, M.; Tsuji, Y.; Watanabe, Y. *J. Org. Chem.* **1990**, *55*, 1286.

(5) Marder, T. B.; Roe, D. C.; Milstein, D. *Organometallics* **1988**, *7*, 1451.

(6) Schwartz, J.; Cannon, J. B. *J. Am. Chem. Soc.* **1974**, *96*, 4721.

Table 1. Reaction of 1a with 2a using Various Phosphorus Ligands^a

ligand	temp (°C)	yield of 3a + 4a (%) ^b	3a:4a
Ph ₃ P	100	17	92:8
(n-Bu) ₃ P	100	8	54:46
(EtO) ₃ P	100	11	80:20
(PhO) ₃ P	100	46	68:32
(PhO) ₃ P ^c	100	26	50:50
(PhO) ₃ P ^d	100	25	68:32
(PhO) ₃ P ^e	100	28	68:32
(PhO) ₃ P ^f	100	39	67:33
(o-MePhO) ₃ P	100	43	65:35
(o-t-BuPhO) ₃ P	100	36	64:36
(PhO) ₃ P	80	52	73:27
(PhO) ₃ P	65	59	75:25
(PhO) ₃ P ^g	65	66	72:28
(PhO) ₃ P	50	40	73:27

^a The reaction was carried out in 2-methoxyethyl ether for 20 h under H₂ (1 atm). [[RhCl(cod)]₂:ligand]:[1a]:[2a]:[Et(i-Pr)₂N] = 0.01:0.04:2:8:4 (in mmol). ^b GC yield based on 1a used. ^c [ligand] = 0.02 mmol. ^d [ligand] = 0.06 mmol. ^e [2a] = 4 mmol. ^f [2a] = 16 mmol. ^g [[RhCl(cod)]₂:ligand]:[2a] = 0.02:0.08:16 (in mmol).

Table 2. Reaction of 1a with 2a using Various Bases^a

base	yield of 3a + 4a (%) ^b	3a:4a
Et ₃ N ^c	31	71:29
Et(i-Pr) ₂ N	46	68:32
(n-Bu) ₃ N	21	57:43
K ₂ CO ₃ ^d	28	75:25
Li ₂ CO ₃ ^d	20	60:40
pyridine	3	67:33
DBU	0	

^a The reaction was carried out in 2-methoxyethyl ether at 100 °C for 20 h under H₂ (1 atm). [[RhCl(cod)]₂:(PhO)₃P]:[1a]:[2a]:[base] = 0.01:0.04:2:8:4 (in mmol). ^b GC yield based on 1a used. ^c Reaction at 65 °C. ^d [base] = 2 mmol.

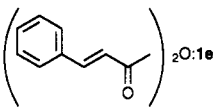


well as the product composition was significantly affected. Among the phosphorus ligands examined, (PhO)₃P gave the most favorable result with respect to the product yield. The ratios of (PhO)₃P/Rh and 2a/1a and the reaction temperature were also found to be important functions: favorable results were obtained at approximately (PhO)₃P/Rh = 2, 2a/1a = 4, and 60–80 °C (Table 1). A reasonable ketone yield of 66% was attained by using 0.02 mmol of [RhCl(cod)]₂ at 65 °C. It has been reported that, in the rhodium-catalyzed hydroformylation of alkenes using phosphite ligands, hindered phosphites enhance the reaction.⁹ Consequently, (o-MePhO)₃P and (o-t-BuPhO)₃P were tested; however, no considerable influence on the reaction was observed.

The effect of base employed is indicated in Table 2. While tertiary amines and inorganic carbonates could be used, the hindered organic base Et(i-Pr)₂N was found to be favorably used. Stronger and weaker nitrogen-bases, DBU and pyridine, were almost ineffective. Although the solvent effect for this reaction was examined using heptane, toluene, acetonitrile, and DMF, none of them was superior to 2-methoxyethyl ether.

Reaction of Various Acid Anhydrides with Alkenes. The reactions of 4-substituted benzoic anhydrides (1b–d) with 2a and of 1a with 4-substituted styrenes (2b–d) gave 1,2-diaryl-1-propanones together with the corresponding 1,3-diaryl isomers in good yields

(9) (a) Van Leeuwen, P. W. N. M.; Roobeek, C. F. *J. Organomet. Chem.* **1983**, *258*, 343. (b) Van Rooy, A.; Orij, E. N.; Kamer, P. C. J.; Van Leeuwen, P. W. N. M. *Organometallics* **1995**, *14*, 34.

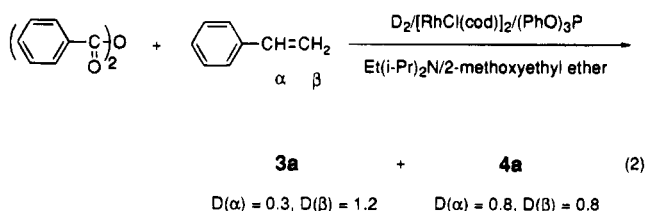
Table 3. Reaction of Various Acid Anhydrides 1 with Alkenes 2a

substrates		ketone yield (%) ^b
1	2	
1a	2a	66 (3a/4a = 73:27)
1b	2a	54 (5/6 = 67:33)
1c	2a	47 (7/8 = 68:32)
1d	2a	52 (9/10 = 71:29)
	2a	21 (11/12 = 62:38) ^f
		
(Ac) ₂ O:1f	2a	18 (13/14 = 39:61) ^d
1a	2b	47 (3b/4b = 81:28)
1a	2c	71 (3c/4c = 68:32)
1a	2d	58 (3d/4d = 74:26)
1a ^e	(EtO) ₃ Si-2e	27 (15) ^f
1a ^e		23 (16) ^g
1a ^{e,h}		20 (17) ⁱ

^a The reaction was carried out in 2-methoxyethyl ether at 65 °C for 20 h under H₂ (1 atm). [[RhCl(cod)]₂:(PhO)₃P]:[1]:[2]:[Et(i-Pr)₂N] = 0.02:0.08:2:16:4 (in mmol). ^b GC yield based on 1 used. ^c 11, 1,4-diphenyl-1-penten-3-one; 12, 1,5-diphenyl-1-penten-3-one. ^d 13, 3-phenyl-2-butanone; 14, 4-phenyl-2-butanone. ^e Reaction at 100 °C. ^f 15, 1-phenyl-3-(triethoxysilyl)-1-propanone. ^g 16, exo-2-benzoylnorbornane. ^h Under 5 atm of H₂. ⁱ 17, cyclopentyl phenyl ketone.

(eq 1 and Table 3). Cinnamic anhydride (1e) and acetic anhydride (1f) could also be reacted with 2a, although the product yields were reduced. The anhydride 1a reacted with triethoxyvinylsilane (2e), 2-norbornene (2f), and cyclopentene (2g) to give ketones 15–17, whereas with 1-octene only a few percent of the corresponding products were detected by GC–MS. It is noted that the reaction with 2e gave 1-phenyl-3-(triethoxysilyl)-1-propanone (15) as the single detectable hydrobenzoylated product.

Reaction Scheme. To obtain insight into the mechanism of the present reaction, the reaction of 1a with 2a was carried out under deuterium. The numbers of deuterium atoms introduced into products 3a and 4a determined by ¹H NMR are indicated in eq 2. The



reaction may be considered to involve initial styrene insertion to a hydridorhodium species generated in situ to form 1- and 2-phenethylrhodium complexes. The incorporation of deuterium in both the olefinic carbons in styrene may indicate that the insertion is reversible, as is the usual rhodium-catalyzed hydroformylation of alkenes.¹⁰ The facts that (a) the numbers of deuterium incorporated into both 3a and 4a were more than unity and (b) the recovered styrene was estimated to contain 1.7 deuterium atoms by GC–MS may suggest that the

(10) Brown, C. K.; Wilkinson, G. *J. Chem. Soc. A*, **1970**, 2753.

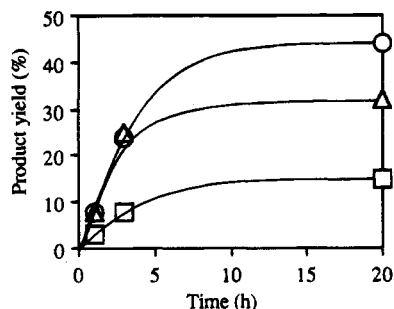
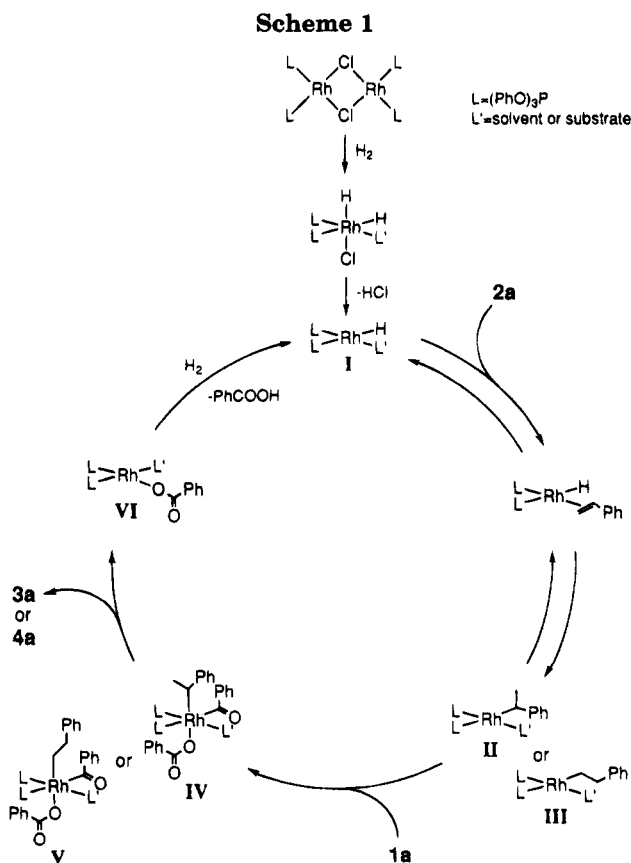


Figure 1. Time course of the reaction of **1a** with **2a** showing yields of **3a** (O), **4a** (□), and ethylbenzene (Δ, yield based on **2a** used). Reaction conditions: $[\text{RhCl}(\text{cod})_2]$ (0.01 mmol), $(\text{PhO})_3\text{P}$ (0.04 mmol), **1a** (2 mmol), **2a** (8 mmol), $\text{Et}(\text{i-Pr})_2\text{N}$ (4 mmol), in 2-methoxyethyl ether under H_2 (1 atm) at 65°C .



coordination of the alkene to the hydridorhodium species is also reversible.

It should also be noted that (a) during the reaction of **1a** with **2a**, the product ratio of **3a** to **4a** was essentially constant and (b) ethylbenzene was formed as the predominant byproduct whose amount increased as the hydrobenzoylation proceeded (Figure 1).

On the basis of the above results, a plausible catalytic cycle for the reaction of **1a** with **2a** is illustrated in Scheme 1. Reaction of $[\text{RhCl}(\text{cod})_2]$ with hydrogen in the presence of $(\text{PhO})_3\text{P}$ and a base may generate a catalytically active hydridorhodium species (I). Insertion of styrene to I affords either 1- (II) or 2-phenethylrhodium complex (III), and the successive oxidative addition of **1a** may produce benzoyl(1- or 2-phenethyl)rhodium species (IV or V). Reductive elimination of product **3a** or **4a** gives benzoyloxrhodium species VI which may react with hydrogen to regenerate the hydridorhodium complex I. The requirement of more

than a stoichiometric amount of a base may imply that it acts as a trap of benzoic acid as well as that of HCl in the initial generation of I. The hindered base $\text{Et}(\text{i-Pr})_2\text{N}$ appears to be less ligative, and hence the coordination of the substrates to the metal may be less inhibited. The fact that **3a** was the major product suggests that the formation of complex II is relatively more favorable than that of III.^{9b} The deuterium distribution in **3a** could also indicate that II is the kinetically major intermediate and, therefore, that deuterium is preferentially introduced into the methyl group. On the other hand, the comparable incorporation of deuterium in the two methylene groups in **4a** may imply that a significant part of III, which reacts with **1a** to give **4a**, comes via II. The byproduct ethylbenzene may be produced via oxidative addition of hydrogen to intermediate II or III, competitively with that of **1a**. Although the reason why $(\text{PhO})_3\text{P}$ is significantly superior to Ph_3P for this reaction is not definitive at the present stage, the better π -acceptor property of the phosphite ligand would ease the coordination of **2a** to I to enhance the reaction.^{9b}

When the reaction of benzoyl chloride in place of **1a** was carried out with **2a**, benzoyl chloride was gradually consumed to give benzoic anhydride (possibly by participation of adventitious water) together with small amounts of benzaldehyde, benzophenone, and other minor unidentified products. After the complete disappearance of the chloride, the formation of **3a** and **4a** was observed. This would imply that benzoyl chloride reacts with I more faster than **2a**. In turn, the reason why the tandem reaction of hydrogen, **1a**, and **2a** around the rhodium species proceeds smoothly may be largely owing to the reactivity order toward I.⁶

Experimental Section

^1H NMR spectra were recorded at 400 MHz for CDCl_3 solutions. MS data were obtained by EI. GC analysis was carried out using a silicone OV-17 glass column (ϕ 2.6 mm \times 1.5 m) or a CBP-1 capillary column (ϕ 0.5 mm \times 25 m). Benzoic anhydrides **1b-d**¹¹ and **1e**¹² were prepared by the methods reported previously. Other starting materials were commercially available. The following experimental details given below may be regarded as typical in methodology and scale.

Reaction of Benzoic Anhydride (**1a**) with Styrene (**2a**).

To a flask containing $[\text{RhCl}(\text{cod})_2]$ (4.9 mg, 0.01 mmol) under hydrogen (with a balloon) was added a solution of **1a** (452 mg, 2 mmol), **2a** (832 mg, 8 mmol), $(\text{PhO})_3\text{P}$ (12.4 mg, 0.04 mmol), $\text{Et}(\text{i-Pr})_2\text{N}$ (516 mg, 4 mmol), and 1-methylnaphthalene (ca. 100 mg) as an internal standard in 2-methoxyethyl ether (5 mL), and the resulting mixture was stirred at 65°C for 20 h. GC and GC-MS analyses of the mixture confirmed formation of **3a** (185 mg, 44%) and **4a** (63 mg, 15%). Products **3a** and **4a** were also isolated by column chromatography on silica gel using hexane-dichloromethane as eluent. Data for compound **3a**: mp $49-50^\circ\text{C}$ (lit.¹³ $52-53^\circ\text{C}$); ^1H NMR δ 1.53 (d, 3H, $J = 6.8$ Hz), 4.68 (q, 1H, $J = 6.7$ Hz), 7.18-7.30 (m, 5H), 7.37 (t, 2H, $J = 7.6$ Hz), 7.47 (t, 1H, $J = 7.3$ Hz), 7.95 (d, 2H, $J = 7.3$ Hz); MS m/z 210 (M^+). Compound **4a**: mp $71-71.5^\circ\text{C}$ (lit.¹⁴ $70-71^\circ\text{C}$); ^1H NMR δ 3.07 (t, 2H, $J = 7.6$ Hz), 3.30 (t, 2H, J

(11) Berliner, E.; Altschul, L. H. *J. Am. Chem. Soc.* **1952**, *74*, 4110.

(12) Baumgarten, H. E. *J. Am. Chem. Soc.* **1953**, *75*, 1239.

(13) Newman, M. S.; Linsk, J. *J. Am. Chem. Soc.* **1949**, *71*, 936.

(14) Perold, G. W.; von Reiche, F. V. K. *J. Am. Chem. Soc.* **1957**, *79*, 465.

= 7.6 Hz), 7.20–7.32 (m, 5H), 7.45 (t, 2H, $J = 7.6$ Hz), 7.55 (t, 1H, $J = 7.3$ Hz), 7.96 (d, 2H, $J = 6.8$ Hz); MS m/z 210 (M^+).

Other products **3b**,¹⁵ **4b**,¹⁶ **3c**,¹⁷ **4c**,¹⁸ **3d**,¹⁹ **4d**,¹⁸ **5**,¹⁵ **6**,²⁰ **7**,¹⁵ **8**,¹⁶ **9**,²⁰ **10**,²¹ **11**,²² **12**,²³ **13**,²⁴ **14**,²⁵ **15**,²⁶ **16**,²⁷ and **17**²⁸ are also known and were compared with those authentic specimens.

Acknowledgment. The present work was partly supported by a Grant-in-Aid for Scientific Research from

(15) Kunieda, N.; Endo, H.; Hirota, M.; Kodama, Y.; Nishio, M. *Bull. Chem. Soc. Jpn.* **1983**, *56*, 3110.

(16) Burton, H.; Ingold, C. K. *J. Chem. Soc.* **1928**, 904.

(17) Curtin, D. Y.; Pollak, P. I. *J. Am. Chem. Soc.* **1951**, *73*, 992.

(18) Pratt, E. F.; Evans, A. P. *J. Am. Chem. Soc.* **1956**, *78*, 4950.

(19) Curtin, D. Y.; Crew, M. C. *J. Am. Chem. Soc.* **1955**, *77*, 354.

(20) Krans, M. A.; Patchornik, A. *J. Am. Chem. Soc.* **1971**, *93*, 7325.

the Ministry of Education, Science and Culture of Japan.

OM9503609

(21) Rothstein, E. *J. Chem. Soc.* **1951**, 1459.

(22) Pisano, C.; Mezzetti, A.; Consiglio, G. *Organometallics* **1992**, *11*, 20.

(23) Fonken, G. S.; Johnson, W. S. *J. Am. Chem. Soc.* **1952**, *74*, 831.

(24) Cragoe, E. J., Jr.; Pietruszkiewicz, A. M.; Robb, C. M. *J. Org. Chem.* **1958**, *23*, 971.

(25) Carroll, M. F. *J. Chem. Soc.* **1940**, 1266.

(26) Komarov, N. V.; Roman, V. K.; Komarova, L. I. *Izv. Akad. Nauk SSSR, Ser. Khim.* **1966**, 1464; *Chem. Abstr.* **1967**, *66*, 55546a.

(27) Lewis, F. D.; Johnson, R. W.; Ruden, R. A. *J. Am. Chem. Soc.* **1972**, *94*, 4292.

(28) Triford, C. H.; van Campen, M. G., Jr. *J. Am. Chem. Soc.* **1954**, *76*, 2431.

Oxidative Addition of Catecholborane to IrX(CO)(dppe) Complexes

Brian P. Cleary and Richard Eisenberg*

Department of Chemistry, University of Rochester, Rochester, New York 14627

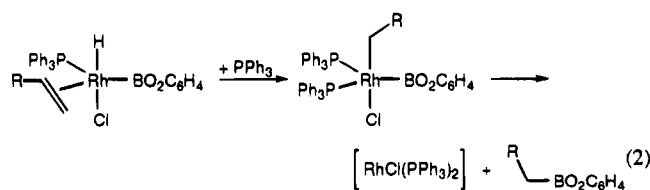
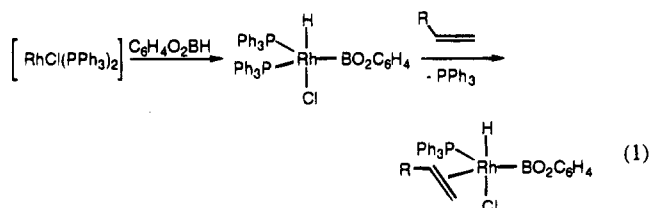
Received February 1, 1995*

The oxidative addition of catecholborane (1,3,2-benzodioxaborole) to the Ir(I) *cis*-phosphine complexes IrX(CO)(dppe) (X = Br, I, H, BO₂C₆H₄; dppe = 1,2-bis(diphenylphosphino)ethane) has been found to proceed stereoselectively under kinetic control. Of the four complexes that can be formed by *cis* oxidative addition of the B-H bond to IrBr(CO)(dppe), the one having hydride trans to phosphorus and boron trans to bromide is formed in >99% yield while addition to IrI(CO)(dppe) occurs similarly but with only 90% stereoselectivity. Isomerization of the initially formed diastereomers to thermodynamically less stable diastereomers which display hydride trans to halide and boron trans to phosphorus occurs after 1 day. The mechanism for the isomerism for X = Br has been determined to proceed via reductive elimination/oxidative addition processes. The oxidative addition reactions of catecholborane to [IrH(CO)(dppe)] and [Ir(BO₂C₆H₄)(CO)(dppe)], generated from IrH₃(CO)(dppe) and IrH₂(BO₂C₆H₄)(CO)(dppe), respectively, also occur in a *cis* fashion with 99% stereoselectivity yielding Ir(III) products with hydride trans to CO and boron trans to phosphorus. The observed stereoselectivity for catecholborane addition to IrX(CO)(dppe) (X = Br, I) is reversed with respect to addition to IrX(CO)(dppe) (X = H, BO₂C₆H₄) and is accounted for by electronic factors involving the π -basicity of the halide ligands.

Introduction

The activation of small molecules via oxidative addition at d⁸ metal centers is of fundamental importance in homogeneous hydrogenation, hydrosilation, and hydroformylation catalysis.^{1,2} Recently, there has been a renewed interest surrounding the chemistry of transition metal-catalyzed olefin hydroborations and, in particular, those reactions catalyzed by Rh(I) species.³⁻¹¹ For example, RhCl(PPh₃)₃ efficiently catalyzes hydroboration reactions between olefins and catecholborane (1,3,2-benzodioxaborole) at ambient temperatures, while the uncatalyzed reactions proceed only at temperatures at or above 70 °C.^{12,13} In addition to rate enhancement, transition metal catalysts can also alter the chemo-, regio-, and enantioselectivities of organic products formed during hydroboration relative to the uncatalyzed

reaction.^{3,5,14-18} Männig and Nöth have postulated a mechanism to account for olefin hydroborations catalyzed by RhCl(PPh₃)₃.¹³ In this mechanism, hydroboration is initiated by oxidative addition of the B-H bond of catecholborane to [RhCl(PPh₃)₂] (generated via PPh₃ loss from RhCl(PPh₃)₃) to yield a Rh(III) boryl hydride complex that coordinates olefin after dissociation of PPh₃ (eq 1). Hydride migration, possibly promoted by phosphine ligation, then produces a Rh(III) alkyl boryl intermediate from which B-C reductive elimination occurs to form the organic product and the catalyst [RhCl(PPh₃)₂] as in eq 2.



* Abstract published in *Advance ACS Abstracts*, August 15, 1995.

(1) Cotton, F. A.; Wilkinson, G. *Advanced Inorganic Chemistry*, 5th ed.; John Wiley and Sons, Inc.: New York, 1988; p 1455.

(2) Collman, J. P.; Hegedus, L. S.; Norton, J. R.; Finke, R. G. *Principles and Applications of Organotransition Metal Chemistry*; University Science Books: Mill Valley, CA, 1987.

(3) Burgess, K.; Ohlmeyer, M. J. *Chem. Rev.* **1991**, *91*, 1179-1191.

(4) Hoveyda, A. H.; Evans, D. A.; Fu, G. C. *Chem. Rev.* **1993**, *93*, 1307-1370.

(5) Westcott, S. A.; Blom, H. P.; Marder, T. B.; Baker, R. T. *J. Am. Chem. Soc.* **1992**, *114*, 8863-8869.

(6) Burgess, K.; van der Donk, W. A.; Westcott, S. A.; Marder, T. B.; Baker, R. T.; Calabrese, J. C. *J. Am. Chem. Soc.* **1992**, *114*, 9350-9359.

(7) Evans, D. A.; Fu, G. C.; Anderson, B. A. *J. Am. Chem. Soc.* **1992**, *114*, 6679-6685.

(8) Evans, D. A.; Fu, G. C.; Hoveyda, A. H. *J. Am. Chem. Soc.* **1992**, *114*, 6671-6679.

(9) Ruffing, C. J. *Aldrichim. Acta* **1989**, *22*, 80-81.

(10) Westcott, S. A.; Marder, T. B.; Baker, R. T. *Organometallics* **1993**, *12*, 975-979.

(11) Brown, J. M.; Lloyd-Jones, G. C. *J. Am. Chem. Soc.* **1994**, *116*, 866-878.

(12) Brown, H. C.; Gupta, S. K. *J. Am. Chem. Soc.* **1971**, *93*, 1816-1818.

(13) Männig, D.; Nöth, H. *Angew. Chem., Int. Ed. Engl.* **1985**, *24*, 878-879.

(14) Matsumoto, Y.; Naito, M.; Uozumi, Y.; Hayashi, T. *J. Chem. Soc., Chem. Commun.* **1993**, 1468-1469.

(15) Sato, M.; Miyaura, N.; Suzuki, A. *Tetrahedron Lett.* **1990**, *31*, 231-234.

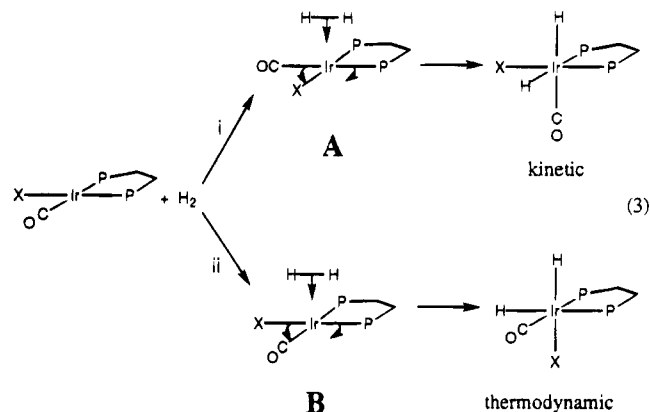
(16) Zhang, J.; Lou, B.; Guo, G.; Dai, L. *J. Org. Chem.* **1991**, *56*, 1670-1672.

(17) Kocienski, P.; Jarowicki, K.; Marczak, S. *Synthesis* **1991**, 1191-1200.

(18) Brands, K. M. J.; Kende, A. S. *Tetrahedron Lett.* **1992**, *33*, 5887-5890.

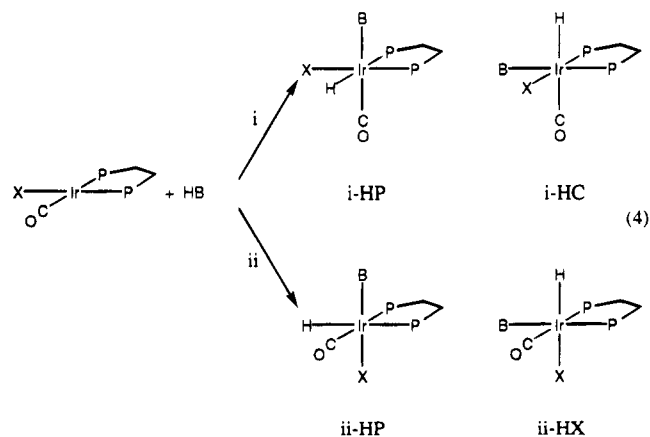
Accompanying the efforts aimed at expanding the breadth of synthetic methodology of transition metal-catalyzed hydroborations are reports which have emphasized the characterization and structure determination of metal-boryl complexes synthesized from stoichiometric oxidative addition reactions with R_2BH^{19-29} and the estimation of transition metal-boryl covalent bond energies.³⁰ However, little attention has been paid to the effects that specific ligands impart on the stereochemistry of products formed by the cis-oxidative additions of boranes to four coordinate transition metal compounds. In order to extend studies elucidating the extent and basis of kinetically controlled diastereoselectivity in B-H oxidative addition reactions, we have examined the reaction chemistry between catecholborane and $IrX(CO)(P^*P)$, where $P^*P = 1,2$ -bis(diphenylphosphino)ethane (dppe) and (2*S*,3*S*)-bis(diphenylphosphino)butane (chiraphos) and $X = Br, I,$ and H , in a manner which complements previous reports from our laboratory (*vide infra*) describing the kinetic stereoselectivities of hydrogen, silane, and hydrogen halide oxidative additions to $IrX(CO)(dppe)$ ($X = Cl, Br, I, CN$) complexes.³¹⁻³⁴

We have demonstrated previously that, for concerted cis-oxidative additions to $IrX(CO)(dppe)$ complexes, a direct comparison of the electronic and steric effects of the X and CO ligands can be made because the phosphine donors are constrained to be in mutually cis positions and will therefore exert the same influence for each of the two stereochemical pathways of addition.^{32,33} For the concerted oxidative addition of hydrogen to $IrX(CO)(dppe)$, two pathways can be followed which lead to different diastereomers as shown in eq 3.³² For addition along pathway i, hydrogen approaches $IrX(CO)(dppe)$ over the $OC-Ir-P$ axis (A) yielding an Ir(III) product with one hydride ligand trans to CO and the other trans to phosphorus while, for addition along pathway ii, hydrogen approaches $IrX(CO)(dppe)$ over the $X-Ir-P$ axis (B) forming an Ir(III) product with one hydride trans to X and the other trans to phosphorus.



Although both oxidative addition products of eq 3 form, only the dihydride product corresponding to pathway i is generated *initially*. Slow conversion of this isomer to an equilibrium distribution of products that is mainly the *other* isomer of eq 3 reveals the kinetic control of the oxidative addition reaction. The origin of the kinetic selectivity is electronic in nature and arises from the relative propensity of mutually trans ligands in $IrX(CO)(dppe)$ to bend away from the incoming hydrogen molecule upon oxidative addition. Qualitatively, approach A is favored over B as trans CO and P ligands preferentially bend away from the approaching H_2 molecule. The basis of the diastereoselectivity results from the carbonyl ligand being able to stabilize the transition state through the removal of electron density from the $Ir d_{z^2}$ orbital, thereby reducing the repulsive $4e^-$ interaction between d_{z^2} and $\sigma^b(H_2)$.

For the concerted oxidative addition of unsymmetrical $Y-H$ bonds to $IrX(CO)(dppe)$ complexes, a similar stereochemical analysis can be applied with the additional consideration of the *regiochemistry* of the $Y-H$ addition.³³ As shown in eq 4 for the cis oxidative



addition of catecholborane to $IrX(CO)(dppe)$, the asymmetry of the substrate $B-H$ bond increases the number of diastereomers that can be formed from two to four. The identity of these diastereomers can be designated according to the pathway (i or ii) and the nature of the ligand which is trans to hydride in the product. For example, for oxidative addition along the $OC-Ir-P$ axis (pathway i), when hydride is trans to P , the diastereomer is designated as *i-HP*, and when hydride is trans to CO , the diastereomer is indicated as *i-HC*. We will follow this manner of designation in the present paper. In concerted oxidative addition reactions, diastereomers

(19) Gilbert, K. B.; Boocock, S. K.; Shore, S. G. In *Comprehensive Organometallic Chemistry: The Synthesis, Reactions and Structures of Organometallic Compounds*; Wilkinson, S. G., Ed.; Pergamon Press: Oxford, U.K., 1982; Vol. 6.

(20) Schmid, G. *Angew. Chem., Int. Ed. Engl.* **1970**, *9*, 819-916.

(21) Hartwig, J. F.; De Gala, S. R. *J. Am. Chem. Soc.* **1994**, *116*, 3661-3662.

(22) Hartwig, J. F.; Huber, S. *J. Am. Chem. Soc.* **1993**, *115*, 4908-4909.

(23) Westcott, S. A.; Marder, T. B.; Baker, R. T.; Calabrese, J. C. *Can. J. Chem.* **1993**, *71*, 930-936.

(24) Nguyen, P.; Blom, H. P.; Westcott, S. A.; Taylor, N. J.; Marder, T. B. *J. Am. Chem. Soc.* **1993**, *115*, 9329-9330.

(25) Baker, R. T.; Calabrese, J. C.; Westcott, S. A.; Nguyen, P.; Marder, T. B. *J. Am. Chem. Soc.* **1993**, *115*, 4367-4368.

(26) Westcott, S. A.; Taylor, N. J.; Marder, T. B.; Baker, R. T.; Jones, N. J.; Calabrese, J. C. *J. Chem. Soc., Chem. Commun.* **1991**, 304-305.

(27) Baker, R. T.; Overnall, D. W.; Calabrese, J. C.; Westcott, S. A.; Taylor, N. J.; Williams, I. D.; Marder, T. B. *J. Am. Chem. Soc.* **1990**, *112*, 9399-9400.

(28) Baker, R. T.; Overnall, D. W.; Harlow, R. L.; Westcott, S. A.; Taylor, N. J.; Marder, T. B. *Organometallics* **1990**, *9*, 3028-3030.

(29) Knorr, J. R.; Merola, J. S. *Organometallics* **1990**, *9*, 3008-3010.

(30) Rablen, P. R.; Hartwig, J. F.; Nolan, S. P. *J. Am. Chem. Soc.* **1994**, *116*, 4121-4122.

(31) Johnson, C. E.; Fisher, B. J.; Eisenberg, R. *J. Am. Chem. Soc.* **1983**, *105*, 7772-7774.

(32) Johnson, C. E.; Eisenberg, R. *J. Am. Chem. Soc.* **1985**, *107*, 3148-3160.

(33) Johnson, C. E.; Eisenberg, R. *J. Am. Chem. Soc.* **1985**, *107*, 6531-6540.

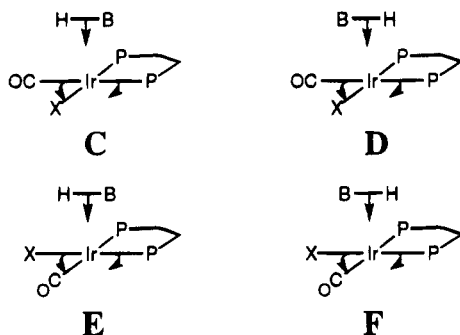
(34) Kunin, A. J.; Farid, R.; Johnson, C. E.; Eisenberg, R. *J. Am. Chem. Soc.* **1985**, *107*, 5315-5317.

Table 1. ^1H NMR Spectroscopic Data for Complexes 1–10^a

complex	$\delta(\text{Ir-H})$	$^2J_{\text{H-P}}$	$\delta(\text{CH}_2 \text{ of dppe})$	$\delta(o\text{-Ph of dppe})^b$
IrH(BO ₂ C ₆ H ₄)Br(CO)(dppe), 1	-7.52	dd, 128.5, 16.9	2.67 (4H)	7.87 (2H), 7.69 (2H), 7.48 (2H), 7.28 (2H)
IrH(BO ₂ C ₆ H ₄)Br(CO)(dppe), 2	-16.18	dd, 15.7, 8.1	2.67 (1H), 2.49 (1H), 1.94 (1H), 1.68 (1H)	7.78 (2H), 7.68 (2H), 7.63 (2H), 7.42 (2H)
IrH(BO ₂ C ₆ H ₄)I(CO)(dppe), 3	-8.38	dd, 126.5, 17.0	2.73 (4H)	7.73 (2H), 7.59 (2H), 7.46 (2H), 7.31 (2H)
IrH(BO ₂ C ₆ H ₄)I(CO)(dppe), 4	-9.47	t, 17.5	2.10 (2H), 1.75 (2H)	7.95 (2H), 7.83 (2H), 7.71 (2H), 7.32 (2H)
IrH(BO ₂ C ₆ H ₄)I(CO)(dppe), 5	-14.29	dd, 15.9, 8.3	2.68 (3H), 1.78 (1H)	7.51 (2H), 7.11 (2H) ^c
IrH ₂ (BO ₂ C ₆ H ₄)CO(dppe), 6	-9.12, -10.04	dd, 114.8, 12.6; t, 18.8	2.19 (2H), 1.95 (2H)	7.87 (2H), 7.77 (2H), 7.69 (2H), 7.48 (2H)
IrH(BO ₂ C ₆ H ₄) ₂ (CO)(dppe), 7	-9.08	t, 18.0	2.13 (2H), 1.89 (2H)	7.76 (4H), 7.58 (4H)
IrH(BO ₂ C ₆ H ₄)Br(CO)(chiraphos), 8a ^d	-7.20	dd, 122.4, 14.4	e	f
IrH(BO ₂ C ₆ H ₄)Br(CO)(chiraphos), 8b ^d	-7.65	dd, 127.0, 13.8	e	f
IrH(BO ₂ C ₆ H ₄)Br(CO)(chiraphos), 9a ^d	-8.19	dd, 20.5, 13.2	e	f
IrH(BO ₂ C ₆ H ₄)Br(CO)(chiraphos), 9b ^d	-8.33	dd, 23.3, 15.3	e	f
IrH(BO ₂ C ₆ H ₄)Br(CO)(chiraphos), 10a ^d	-16.11	dd, 18.8, 5.9	g	h
IrH(BO ₂ C ₆ H ₄)Br(CO)(chiraphos), 10b ^d	-16.28	dd, 12.9, 10.6	g	h

^a ^1H NMR (400.13 MHz) spectra are reported in ppm downfield of tetramethylsilane in C₆D₆ unless otherwise noted. ^b $^2J_{\text{H-P}}$ are reported in Hz. ^c The *o*-phenyl resonances of dppe are generally downfield of the corresponding meta and para resonances. ^d The remaining two *o*-Ph dppe resonances were not located due to overlap with the Ph resonances of **4**. ^e Spectra obtained in toluene-*d*₆. ^f Seven resonances were observed for the chiraphos methylene protons for complexes **8** and **9** but were not assigned. ^g Six overlapping resonances are observed between 8.25 and 7.40 ppm attributed to *o*-Ph protons of chiraphos. ^h Chiraphos methylene protons not assigned. ⁱ Chiraphos *o*-Ph protons not assigned.

i-HP and *i*-HC correlate respectively with B-H approaches to IrX(CO)(dppe) that are shown as **C** and **D**, whereas diastereomers *ii*-HP and *ii*-HX arise from approaches **E** and **F**, respectively.



In the present paper we report the results of a systematic study of the oxidative addition of catecholborane to the Ir(I) *cis*-phosphine complexes IrX(CO)(dppe) and IrBr(CO)(chiraphos) complexes.

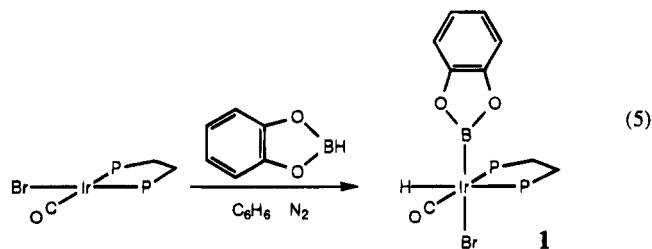
Results and Discussion

All of the catecholborane oxidative addition reactions with IrX(CO)(dppe) and IrBr(CO)(chiraphos) and subsequent reaction chemistry of the Ir(III) products were monitored by infrared and NMR spectroscopies. The stereochemistries of the six-coordinate Ir(III) diphosphine oxidative addition products were established unambiguously by determining the ^1H , ^{31}P , and ^{13}C chemical shifts and coupling constants of the hydride, carbonyl, and phosphine ligand nuclei of the Ir(III) products.

For the *cis* addition of catecholborane to the Ir(I)-(P)(P) complexes, four different stereoisomers can be envisaged in principle as shown in eq 4. The resonances of the hydride ligand in stereoisomers *i*-HP and *ii*-HP will be similar and appear as a doublet of doublets with a large *trans* $^2J_{\text{H-P}}$ coupling (110–130 Hz) and a smaller *cis* $^2J_{\text{H-P}}$ (5–20 Hz). For the two stereoisomers *i*-HC and *ii*-HX, only smaller *cis* $^2J_{\text{H-P}}$ couplings will be seen, and for *ii*-HX only, a distinctive upfield shift in the

hydride chemical shift indicative of hydride-*trans*-to-halide will occur. Moreover, the orientation of the catecholboranyl ligand will be established through the influence of the boron nucleus (spin $3/2$, 80.4% natural abundance; spin 3, 19.6% natural abundance) on the ^1H , ^{13}C , or ^{31}P resonance of the hydride, carbonyl, or phosphine ligand *trans* to it since the resonance of the spin $1/2$ nucleus in that position will display significant broadening due to quadrupolar coupling.³⁵

Oxidative Addition of C₆H₄O₂BH to IrBr(CO)(dppe). Facile Stereochemical Isomerization of IrH(BO₂C₆H₄)Br(CO)(dppe). A new six-coordinate Ir^{III}(dppe) boryl-hydride complex (**1**) is obtained by treating a benzene solution of IrBr(CO)(dppe) with 5 equiv of C₆H₄O₂BH (catecholborane) under N₂ as shown in eq 5. After precipitation with hexanes and recrystallization from CH₂Cl₂/hexanes, the analytically pure product is isolated in 81% yield as an air sensitive, cream colored powder.



Complex **1** has been characterized spectroscopically (Tables 1 and 2 list spectroscopic data for all new complexes). The solution infrared spectrum of **1** in benzene exhibits a single terminal ν_{CO} at 2052 cm^{-1} while the $^{13}\text{C}\{^1\text{H}\}$ NMR spectrum shows the carbonyl ligand as a doublet of doublets ($^2J_{\text{C-P}} = 120.6$, 5.1 Hz) at 175.5 ppm, where, on the basis of the very different $^2J_{\text{C-P}}$ values, CO resides *trans* and *cis* to the two dppe phosphorus nuclei. The $^{31}\text{P}\{^1\text{H}\}$ NMR spectrum of **1** displays two doublets at 34.12 ppm and 20.90 ppm

(35) Harris, R. K. *Nuclear Magnetic Resonance Spectroscopy*; Longman Scientific and Technical: Essex, U.K., 1986.

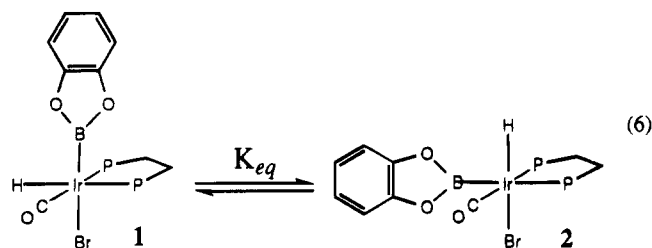
Table 2. Infrared, $^{31}\text{P}\{^1\text{H}\}$, and $^{13}\text{C}\{^1\text{H}\}$ Spectroscopic Data for Complexes 1–10^a

complex	ν_{CO} (cm ⁻¹)	$\delta(\text{P})$ ($^2J_{\text{P-P}}$)	$\delta(\text{CO})$ ($^2J_{\text{C-P}}$)
IrH(BO ₂ C ₆ H ₄)Br(CO)(dppe), 1	2052	34.1, 20.9 (d, 7.3)	175.5 (dd, 121, 5)
IrH(BO ₂ C ₆ H ₄)Br(CO)(dppe), 2		25.0 (d, 9.0), 24.0 (broad, $\omega_{1/2}$ = 60 Hz)	174.3 (dd, 120, 6)
IrH(BO ₂ C ₆ H ₄)I(CO)(dppe), 3	2049	27.5, 14.7 (d, 7.4)	174.3 (dd, 119, 5)
IrH(BO ₂ C ₆ H ₄)I(CO)(dppe), 4		29.5 (d, 2.5), 7.1 (broad, $\omega_{1/2}$ = 37 Hz)	
IrH(BO ₂ C ₆ H ₄)I(CO)(dppe), 5		20.4 (d, 9.4), 17.7 (broad, $\omega_{1/2}$ = 53 Hz)	
IrH ₂ (BO ₂ C ₆ H ₄)(CO)(dppe), 6	1984	28.12 (AB quartet)	178.3 (t, 5)
IrH(BO ₂ C ₆ H ₄) ₂ (CO)(dppe), 7	1995	26.1 (broad, $\omega_{1/2}$ = 40 Hz)	
IrH(BO ₂ C ₆ H ₄)Br(CO)(chiraphos), 8a^b		30.5, 19.3 (d, 12.2)	174.6 (dd, 117, 7)
IrH(BO ₂ C ₆ H ₄)Br(CO)(chiraphos), 8b^b		29.8, 23.9 (d, 13.0)	173.9 (dd, 120, 6)
IrH(BO ₂ C ₆ H ₄)Br(CO)(chiraphos), 9a^b		37.1 (d, 3.8), 22.0 (broad, $\omega_{1/2}$ = 71 Hz)	176.7 (t, 3)
IrH(BO ₂ C ₆ H ₄)Br(CO)(chiraphos), 9b^b		32.9 (d, 4.9), 18.7 (broad, $\omega_{1/2}$ = 56 Hz)	176.3 (dd, 5, 3)
IrH(BO ₂ C ₆ H ₄)Br(CO)(chiraphos), 10a^b		20.2 (d, 17.1), 27.8 (broad, $\omega_{1/2}$ = 55 Hz)	
IrH(BO ₂ C ₆ H ₄)Br(CO)(chiraphos), 10b^b		31.45 (d, 18.6), 12.5 (broad, $\omega_{1/2}$ = 58 Hz)	

^a Infrared spectra are reported in benzene solution. $^{31}\text{P}\{^1\text{H}\}$ (161.98 MHz) and $^{13}\text{C}\{^1\text{H}\}$ (161.98 MHz) NMR spectra are reported in ppm down field of external 85% phosphoric acid and tetramethylsilane in C₆D₆ solution unless otherwise noted. $^2J_{\text{P-P}}$ and $^2J_{\text{C-P}}$ are reported in Hz. ^b Spectra recorded in toluene-*d*₈.

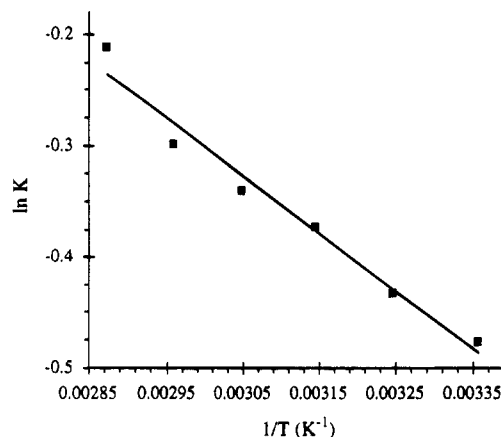
($^2J_{\text{P-P}}$ = 7.3 Hz) consistent with two inequivalent *cis*-phosphorus nuclei. In the ^1H NMR spectrum, the hydride ligand resonates at -7.52 ppm as a doublet of doublets ($^2J_{\text{H-P}}$ = 128.5, 16.9 Hz) with the larger $^2J_{\text{H-P}}$ coupling establishing that the hydride is *trans* to one dppe phosphorus nucleus. Also in the ^1H NMR spectrum, four sets of dppe *o*-phenyl protons are observed at 7.87, 7.69, 7.48, and 7.28 ppm. From these results, **1** is assigned unambiguously as IrH(BO₂C₆H₄)Br(CO)(dppe) with hydride and carbonyl ligands *trans* to dppe phosphine donors.

An equilibrium between **1** and a new hydride-containing complex (**2**) is established in benzene after 24 h, eq 6. In the ^1H NMR spectrum, the hydride



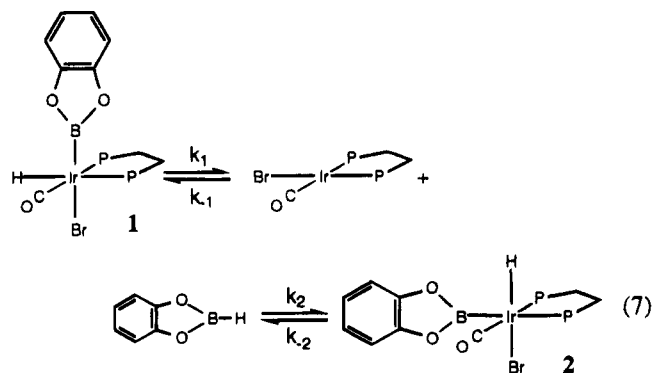
resonance of **2** appears at -16.18 ppm as a doublet of doublets ($^2J_{\text{H-P}}$ = 15.7, 8.1 Hz). Since the hydride resonance of **2** shows a characteristic upfield chemical shift and two small $^2J_{\text{H-P}}$ couplings, it is assigned to be *trans* to bromide and *cis* to two inequivalent phosphorus nuclei. Confirmation of this arrangement is obtained from both ^{31}P and ^{13}C NMR spectroscopy. The $^{31}\text{P}\{^1\text{H}\}$ NMR spectrum shows two phosphorus resonances at 25.0 and 24.0 ppm with the former appearing as a doublet ($^2J_{\text{P-P}}$ = 9 Hz) and the latter as a broad singlet ($\omega_{1/2}$ = 60 Hz) due to *trans* coupling to boron, while the $^{13}\text{C}\{^1\text{H}\}$ NMR spectrum shows the carbonyl ligand at 174.28 ppm as a doublet of doublets ($^2J_{\text{C-P}}$ = 120, 6 Hz) with $^2J_{\text{C-P}}$ values establishing that it is both *trans* and *cis* to the phosphorus nuclei of dppe.

While in theory **2** can form by the direct oxidative addition of catecholborane to IrBr(CO)(dppe) via pathway ii with B-H orientation leading to the HX diastereomer (eq 4), the fact that **1** is formed with >99% stereoselectivity indicates that the catecholborane oxidative addition to IrBr(CO)(dppe) proceeds under kinetic control via pathway i with HP orientation and that this reaction route is favored over the pathway leading to ii-HX by ≥ 2.7 kcal mol⁻¹.

Temperature Dependence of K_{eq} for the Equilibrium Between **1** and **2****Figure 1.** Van't Hoff plot for the equilibrium of **1** and **2**.

At 298 K, K_{eq} for the equilibrium depicted in eq 6 is 0.62 which corresponds to a free energy difference between **1** and **2** of 0.29 kcal mol⁻¹ and establishes that **1** is slightly more stable than **2** in addition to being the kinetically preferred isomer. A plot of K_{eq} vs $1/T$ (Figure 1) is linear over the temperature range 298–350 K and yields $\Delta H = 1.04 \pm 0.04$ kcal mol⁻¹ and $\Delta S = 2.5 \pm 0.1$ eu.

Isomerization Mechanism for the Interconversion of **1 to **2**.** A kinetic study of the isomerization of IrH(BO₂C₆H₄)Br(CO)(dppe) from **1** to **2** in C₆D₆ has been carried out using ^1H NMR spectroscopy to monitor the progress of the reaction. Relative amounts of **1** and **2** were determined by recording the integrated intensities of the hydride resonances for both complexes. At 338 K and *early* kinetics, the isomerization follows first-order kinetics. Two possible mechanisms to account for the observed first-order kinetics are (1) a simple intramolecular rearrangement and (2) a two-step process involving catecholborane reductive elimination/oxidative addition as shown in eq 7. For the mechanism in eq 7 to satisfy first-order kinetics, the rate of reductive elimination of catecholborane must be significantly faster than the rate of isomerization. Since **1** is obtained uniquely from the addition of catecholborane to IrBr(CO)(dppe) with greater than 99% stereoselectivity, the ratio of the oxidative addition rate constants, k_{-1}/k_2 , must be greater than or equal to 100. If the rate-determining step for the isomerization is assumed to be catecholborane oxidative addition leading to **2**, the



steady state approximation can be applied to IrX(CO)(dppe) at early reaction times when $k_{-2}[2]$ is negligible (reaction times prior to $\sim 40\%$ conversion). The first-order rate expression describing the disappearance of 1 (eq 8) is thus obtained. Given the requirement that $k_{-1}/k_2 \geq 100$, the rate expression requires that $k_1 > 100k_{\text{obs}}$, where k_{obs} is the observed rate constant for the isomerization.

$$-\frac{d[1]}{dt} = k_{\text{obs}}[1] = \frac{k_1 k_2}{k_{-1} + k_2}[1] = \frac{k_1}{k_{-1}/k_2 + 1}[1] \quad (8)$$

Two experiments were performed to test the notion that isomerization between 1 and 2 proceeds via catecholborane reductive elimination from 1 and subsequent oxidative addition to give the resulting IrH(BO₂C₆H₄)Br(CO)(dppe) product, ii-HX. In the first, the reaction between a benzene solution of IrD(BO₂C₆H₄)Br(CO)(dppe) (1-*d*₁) and 10 equiv of catecholborane-*d*₀ at 25 °C was monitored using ¹H NMR spectroscopy. Formation of 1-*d*₀ was observed to be complete after 3 min and occurs without any observation of 2 over *ca.* 5 h. In the second, the reaction between an equilibrium mixture of IrD(BO₂C₆H₄)Br(CO)(dppe) (1-*d*₁ and 2-*d*₁) and catecholborane-*d*₀ at 55 °C was monitored by ¹H NMR spectroscopy. As shown in Figure 2, ¹H NMR spectra of the hydride region for both isomers obtained during the reaction show that hydride incorporation into 1-*d*₁ is facile and complete before the first scan can be acquired (<30 s) while hydride incorporation into 2-*d*₁ is slower and takes nearly 1 h. Given the results from both experiments, we conclude that the requirement of $k_1 > 100k_{\text{obs}}$ is satisfied and that all of the kinetic data are consistent with the reductive elimination/oxidative addition mechanism shown in eq 7. While simple

intramolecular rearrangement for eq 6 cannot be unambiguously eliminated, it seems improbable given the facility of B-H reductive elimination and oxidative addition involving 1. Our conclusion is in accord with results reported previously for isomerization via a reductive elimination/oxidative addition mechanism in related Ir^{III}(dppe) systems.^{32,33}

The approach to equilibrium for the conversion of 1 to 2 was monitored by ¹H NMR spectroscopy between 333 and 348 K over the entire course of the isomerization and yielded linear plots of $\ln(([1]_0 - [1]_{\infty})/([1] - [1]_{\infty}))$ vs time as shown in Figure 3. The full integrated rate equation for this isomerization which allows for reductive elimination from 2 is shown as eq 9 and is

$$\ln(([1]_0 - [1]_{\infty})/([1] - [1]_{\infty})) = k_{\text{obs}}'t = ((k_1 k_2 + k_{-1} k_{-2})/(k_2 + k_{-1}))t \quad (9)$$

derived in the Appendix. From the measured values of the equilibrium constant K_{eq} and the first-order rate constant k_{obs}' for the approach to equilibrium that are given in Table 3, it is possible to extract additional information about the rate constants of eq 7. Specifically, on the basis of the observed diastereoselectivity of catecholborane oxidative addition that leads to the relationship $k_{-1} \geq 100k_2$, the isomerization rate constant k_{obs}' can be approximated as in eq 10, where K_{eq}

$$k_{\text{obs}}' = (K_{\text{eq}} + 1)k_{-2} \quad (10)$$

is simply $(k_1 k_2)/(k_{-1} k_{-2})$. With experimental determination of both K_{eq} and k_{obs}' , we can obtain values for the reductive elimination rate constant k_{-2} from eq 11

$$k_{-2} = k_{\text{obs}}'/(K_{\text{eq}} + 1) \quad (11)$$

at different temperatures, and these values are given in Table 3. In addition, a lower bound for the reductive elimination rate constant k_1 can be calculated based on eq 12 which arises from expression of K_{eq} in terms of the kinetic parameters of eq 7 and the relationship that $k_{-1} \geq 100k_2$. These values are also given in Table 3.

$$k_1 > 100K_{\text{eq}}k_{-2} \quad (12)$$

The temperature dependence of k_{-2} allowed for the calculation of the kinetic activation parameters for the k_{-2} step. A linear plot of $\ln k_{-2}/T$ vs $1/T$ was obtained and is shown in Figure 4. For the k_{-2} step, $\Delta H^\ddagger = 28.4 \pm 1.4$ kcal mol⁻¹ and $\Delta S^\ddagger = 7.6 \pm 4.1$ eu. A similar temperature dependence for the lower limit of k_1 was also obtained, yielding $\Delta H^\ddagger = 29.9 \pm 1.4$ kcal mol⁻¹.

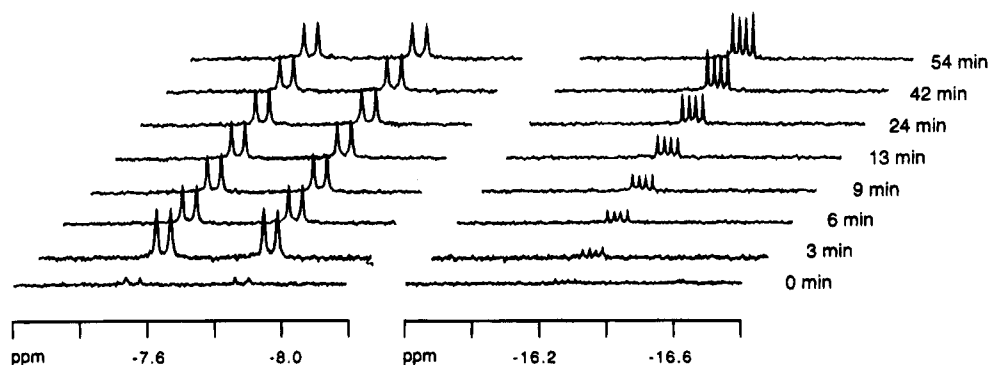


Figure 2. ¹H NMR spectra for the reaction of (1-*d*₁ + 2-*d*₁) + catecholborane-*d*₀. The hydride for 1 is shown at -7.52 ppm as a doublet of doublets (²J_{H-P} = 128.5, 16.9 Hz). The hydride for 2 is shown at -16.18 ppm as a doublet of doublets (²J_{H-P} = 15.7, 8.1 Hz).

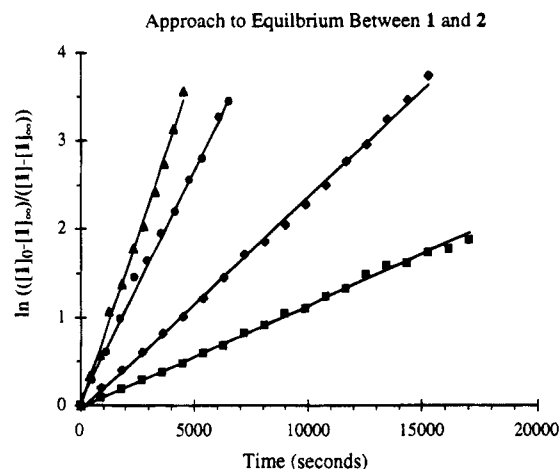


Figure 3. Plots for the approach to equilibrium for the isomerization of **1** to **2**, where $n = 333$ K, $u = 338$ K, $l = 343$ K, and $s = 348$ K.

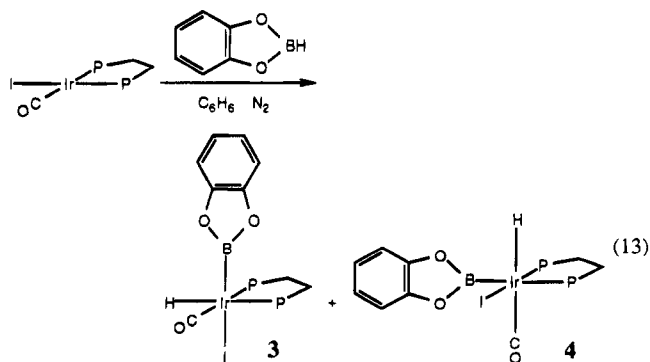
Table 3. Equilibrium and Rate Constants for the Interconversion of **1 to **2**^a**

temp (K)	K_{eq}	$10^4 k_{obs}$ (s ⁻¹) ^b	$10^3 k_1$ (s ⁻¹)	$10^5 k_{-2}$ (s ⁻¹)
333	0.739 ± 0.006	1.17 ± 0.01	>4.96 ± 0.2	6.7 ± 0.2
338	0.742 ± 0.006	2.42 ± 0.03	>10.3 ± 0.4	13.9 ± 0.4
343	0.773 ± 0.007	5.26 ± 0.09	>22.9 ± 1.3	29.7 ± 0.9
348	0.809 ± 0.006	7.7 ± 0.1	>34.5 ± 1.9	42.6 ± 1.2

^a Reaction conditions: $[1] = 0.024$ M in C₆D₆. Values obtained from least squares fit of lines from plots of $\ln([1]_0/[1]_t) / ([1]_0/[1]_t - [1]_t/[1]_t)$ vs time. ^b $k_{obs} = (k_1 k_2 + k_{-1} k_{-2}) / (k_2 + k_{-1})$.

However, since the actual values of k_1 are not known, this value for ΔH^\ddagger should be viewed as an upper limit and the value of ΔS^\ddagger is not strictly obtainable. On the basis of all of these results, a reaction coordinate diagram for the isomerization of **1** to **2** at 298 K can be constructed as shown in Figure 5.

Oxidative Addition of C₆H₄O₂BH to IrI(CO)(dppe). The reaction of IrI(CO)(dppe) with catecholborane leads initially to the formation of two diastereomers of IrH(BO₂C₆H₄)Br(CO)(dppe) (**3** and **4**) in a 9:1 ratio, respectively. The assignment of structure **3** (shown in eq 13) is based on the magnitude of $^2J_{H-P}$ for



the hydride ligand and $^2J_{C-P}$ for the carbonyl group in the ¹H and ¹³C{¹H} NMR spectra respectively (see Tables 1 and 2) and by analogy with the observed spectroscopic data and structural assignment made for complex **1**. In the ¹H NMR spectrum of complex **4**, the hydride ligand appears as a pseudotriplet at -9.47 ppm, and on the basis of a $^2J_{H-P}$ of 17.5 Hz and its chemical shift, the hydride ligand is assigned as cis to both

Eyring Plot for the Reductive Elimination of Catecholborane From **2.**

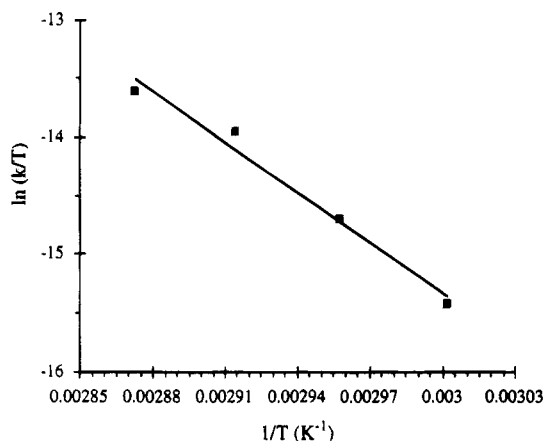


Figure 4. Eyring plot for the reductive elimination of catecholborane from **2**, where $n = k_{-2}$ step.

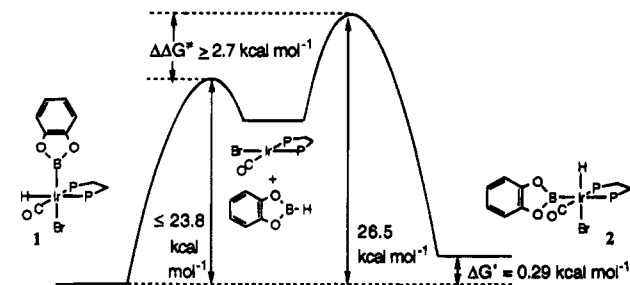
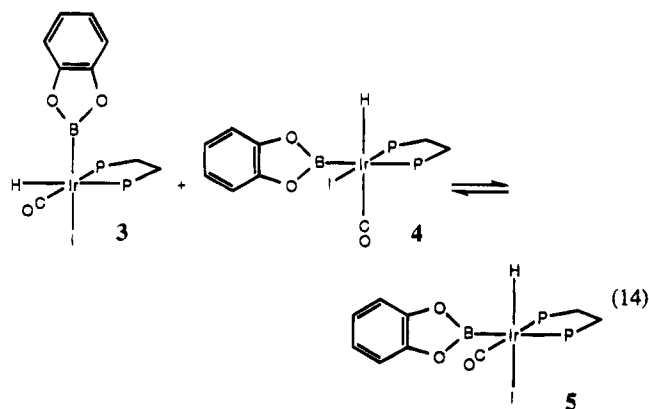


Figure 5. Reaction profile for the equilibrium between **1** and **2** at 298 K.

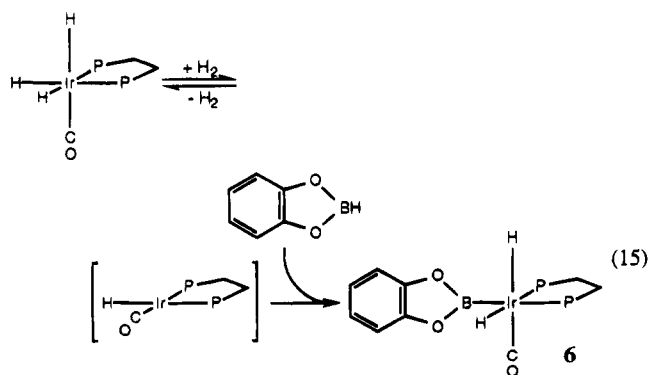
phosphorus nuclei and trans to CO. The ³¹P{¹H} NMR spectrum for **4** shows two phosphorus signals at 29.5 and 7.1 ppm with the former as a doublet due to *cis*-phosphorus coupling and the latter exhibiting significant broadening ($\omega_{1/2} = 37$ Hz) due to *trans* coupling to boron. Thus, the oxidative addition of catecholborane to IrI(CO)(dppe) shows a 90% stereoselectivity with the formation of **3** favored over **4** by 1.3 kcal mol⁻¹.

After 1 day at ambient temperature, a new hydride complex (**5**) is observed to form at the expense of both **3** and **4**. The hydride resonance of **5** appears at -14.29 ppm in the ¹H NMR spectrum as a doublet of doublets with two small *cis*-phosphorus couplings. As was observed for **2**, the hydride resonance of **5** shows a characteristic upfield chemical shift which indicates that it resides *trans* to iodide. The ³¹P{¹H} NMR spectrum of **5** displays two resonances: a doublet at 20.4 ppm that shows a typical *cis* $^2J_{P-P}$ of 9.4 Hz and a broad signal at 17.7 ppm with $\omega_{1/2} = 40$ Hz for phosphorus *trans* to boron. On the basis of the spectroscopy and comparison to **2**, the coordination geometry of **5** is assigned to that shown in eq 14.

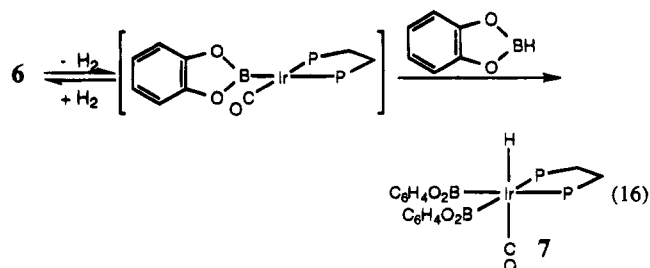
Oxidative Addition of C₆H₄O₂BH to [IrH(CO)(dppe)] and [Ir(BO₂C₆H₄)(CO)(dppe)]. The 4-coordinate complex [IrH(CO)(dppe)] has been proposed to be generated photolytically and thermally as an intermediate during reactions of IrH₃(CO)(dppe) with D₂ and ethylene yielding IrD₂H(CO)(dppe) and Ir(C₂H₅)(η^2 -C₂H₄)(CO)(dppe), respectively.^{32,36} In order to study the stereoselectivity of borane addition to [IrH(CO)(dppe)],



a reaction between $\text{IrH}_3(\text{CO})(\text{dppe})$ and catecholborane was carried out. When a benzene solution of $\text{IrH}_3(\text{CO})(\text{dppe})$ was photolyzed ($h\nu > 300 \text{ nm}$) or heated to 60°C in the presence of 1 equiv of catecholborane, a new Ir(III) product (**6**) was formed after *ca.* 2 h. Examination of the ^1H NMR spectrum of **6** shows two hydride resonances, a doublet of doublets at -9.12 ppm ($^2J_{\text{H-P}} = 114.8, 12.6 \text{ Hz}$) and a triplet at -10.04 ppm ($^2J_{\text{H-P}} = 18.8 \text{ Hz}$), indicating that the former is *trans* and *cis* to dppe phosphorus nuclei while the latter is *cis* to both dppe phosphorus atoms. Four sets of *o*-phenyl dppe ^1H resonances are assignable while the remaining dppe *m*- and *p*-phenyl ^1H resonances overlap with resonances attributed to the catecholate moiety of the boryl ligand. Terminal CO coordination is established by a single ν_{CO} at 1984 cm^{-1} and by $^{13}\text{C}\{^1\text{H}\}$ NMR spectroscopy which shows the carbonyl carbon as a triplet at 178.3 ppm ($^2J_{\text{C-P}} = 5 \text{ Hz}$), thereby fixing its orientation as *cis* to both dppe phosphorus nuclei. In the $^{31}\text{P}\{^1\text{H}\}$ NMR spectrum, an AB quartet is observed for the two dppe phosphorus nuclei. On the basis of the spectroscopic data, **6** is assigned as $\text{IrH}_2(\text{BO}_2\text{C}_6\text{H}_4)_2(\text{CO})(\text{dppe})$. Although *no* quadrupolar coupling to boron is observed in any of the NMR spectra, the geometry of **6** is unambiguously assigned as that shown in eq 15 from the coupling constants of the hydride, carbonyl, and phosphine ligands and the fact that the catecholate protons are observed in the ^1H NMR spectrum indicating boryl coordination.



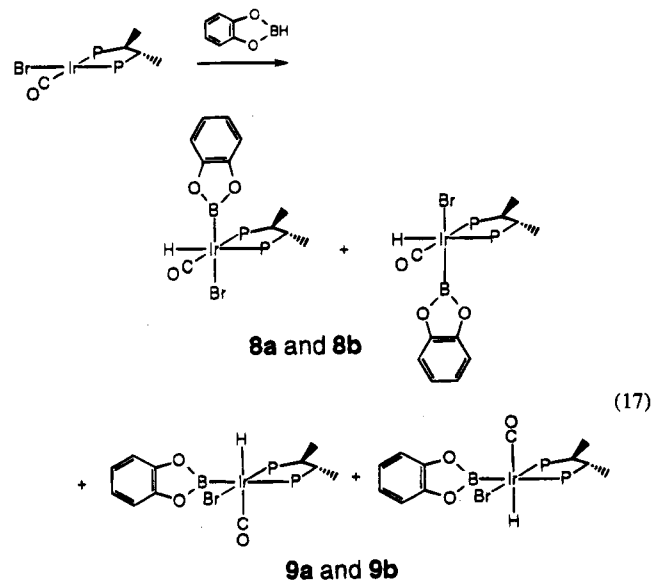
A reaction at 60°C , or by irradiation ($h\nu > 300 \text{ nm}$), between a benzene solution of **6** and 5 equiv of catecholborane yields a new complex (**7**) after *ca.* 2 h (eq 16). The ^1H NMR spectrum confirms the presence of the hydride as a triplet at -9.08 ppm with a small *cis*-phosphorus coupling constant at 18.0 Hz . Terminal CO coordination is established from ν_{CO} at 1995 cm^{-1} while



the $^{31}\text{P}\{^1\text{H}\}$ NMR spectrum shows one broad resonance at 26.1 ppm ($\omega_{1/2} = 40 \text{ Hz}$) confirming that both phosphorus nuclei of dppe are *trans* to boron. On the basis of these results, complex **7** is assigned as the bis-(boryl) derivative $\text{IrH}(\text{BO}_2\text{C}_6\text{H}_4)_2(\text{CO})(\text{dppe})$ with the C_s structure shown in eq 16.

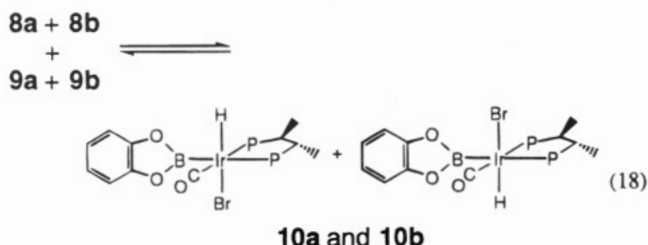
Oxidative Addition of $\text{C}_6\text{H}_4\text{O}_2\text{BH}$ to $\text{IrBr}(\text{CO})(\text{dppe})$ (chiraphos). As described above, the oxidative addition of catecholborane to $\text{IrBr}(\text{CO})(\text{dppe})$ proceeds under kinetic control with initial formation of a single isomer (**1**) that subsequently equilibrates with a less stable isomer (**2**). In analyzing the stereochemistry of concerted oxidative addition reactions by eqs 3 and 4, we have noted previously that substrate approach from either side of the square planar Ir(I) dppe complex are equivalent and that the oxidative addition reaction thus generates a racemic mixture of Ir(III) products. Through the use of a chiral diphosphine, the degeneracy of substrate approach from either side of the square planar complex is removed, leading to possible diastereoselectivity in the oxidative addition reaction. Indeed, such diastereoselectivity in both H_2 and silane oxidative additions to the chiral complex $\text{IrBr}(\text{CO})(\text{chiraphos})$ has been observed and reported previously.³⁴ In view of the kinetic stereoselectivity of catecholborane oxidative addition to $\text{IrBr}(\text{CO})(\text{dppe})$ (eq 1), a series of experiments were run with $\text{IrBr}(\text{CO})(\text{chiraphos})$ in order to assess possible diastereoselectivity in the oxidative addition process. However, instead of observing any diastereoselectivity, we found a surprising *absence of kinetic selectivity*.

As shown in eq 17, $\text{IrBr}(\text{CO})(\text{chiraphos})$ reacts with 5 equiv of catecholborane in toluene- d_8 at -30°C to

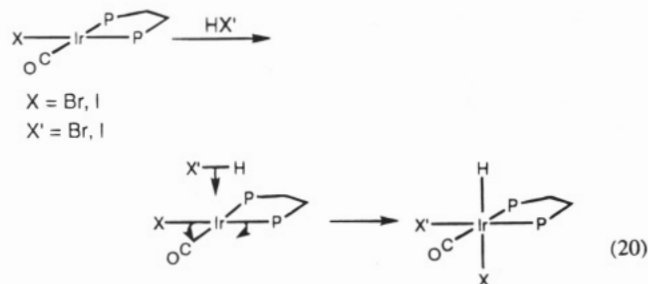
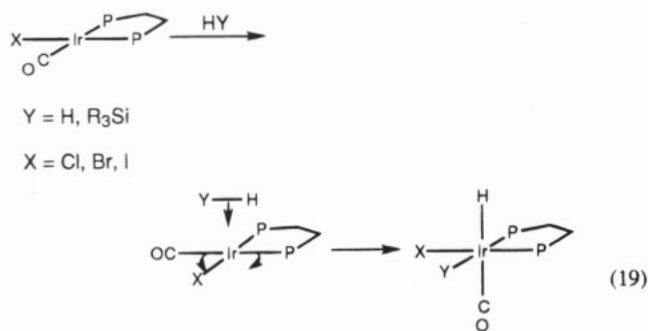


yield two sets of diastereomers (**8a,b** and **9a,b**) in a 1:1:

1:0.5 ratio as determined by NMR spectroscopy (see Tables 1 and 2). Diastereomers **8a,b** display hydride signals in the ^1H NMR spectrum at -7.20 and -7.65 ppm, respectively, with large trans $^2J_{\text{H-P}}$ and terminal CO resonances in the $^{13}\text{C}\{^1\text{H}\}$ NMR spectrum at 174.6 and 173.9 ppm, respectively, with large trans $^2J_{\text{C-P}}$. When the solution is allowed to react for 1 day at 25°C , an equilibrium is observed to form between the diastereomeric pairs **8** and **9** and a new set of diastereomers **10a,b**, as shown in eq 18. The conversion of diastereomers **8** and **9** to a set of diastereomers with hydride trans to bromide is similar to that observed for the dppe analogs in the equilibrium between **1** and **2** (eq 6).



Comments on the Mechanism of Catecholborane Oxidative Addition. To rationalize the results obtained here for catecholborane oxidative additions to $\text{IrX}(\text{CO})(\text{dppe})$ complexes, it is necessary to review the results and conclusions made for hydrogen, silane, and hydrogen halide (HX') oxidative additions to $\text{IrX}(\text{CO})(\text{dppe})$ complexes.^{32,33} The cis oxidative addition of H_2 and R_3SiH to $\text{IrX}(\text{CO})(\text{dppe})$ proceeds stereospecifically along pathway i (yielding the product i-HC for silane addition) (eq 19) while HX' reacts oppositely along

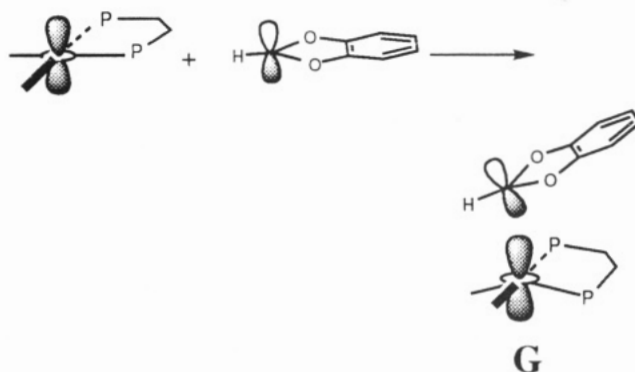


pathway ii with HX' orientation yielding product ii-HX (eq 20). Since both H_2 and R_3SiH add to $\text{IrX}(\text{CO})(\text{dppe})$ complexes as nucleophiles, the additions occur over the $\text{OC}-\text{Ir}-\text{P}$ axis because π^*_{CO} is able to stabilize the developing transition state by removal of electron density from the Ir d_{z^2} orbital, thus reducing the repulsive $4e^-$ interaction between the filled d_{z^2} and $\sigma^{\text{b}}(\text{H}_2)$ and $\text{R}_3\text{Si}-\text{H}$ orbitals. For R_3SiH addition, preference

for silane orientation leading to product i-HC is probably steric in nature, involving minimization of nonbonded interactions between the silyl and dppe phenyl groups.

While H_2 and R_3SiH approach the metal center as nucleophiles, the hydrogen halides approach $\text{IrX}(\text{CO})(\text{dppe})$ in aprotic media as electrophiles. Therefore, interactions that retain or enhance electron density at the metal center will favor addition along that pathway. Pathway ii is preferred for HX' additions because bending of the $\text{X}-\text{Ir}-\text{P}$ axis effects an antibonding interaction between an occupied p_z orbital of X and the d_{z^2} orbital of Ir, thus enhancing the ability of X to donate electrons to the incoming electrophile.³⁷ Preference for HX' orientation leading to the ii-HX diastereomer is likely to be steric in nature involving minimization of nonbonded contacts.

Catecholborane oxidative addition to $\text{IrX}(\text{CO})(\text{dppe})$ complexes (X = Br, I) resembles HX' additions since the initially formed products, **1** (>99%) and **3** (90%), correspond to addition via pathway ii although the relative orientation of the B-H bond is reversed in both instances to that of the H-X' bond. This result implies that catecholborane approaches the metal center as an electrophile in accord with the view that the vacant B p_z orbital can overlap with the filled d_{z^2} of Ir (**G**).



Rearrangement of **1** to **2** and of **3** to **5** occurs via catecholborane reductive elimination and subsequent oxidative addition along pathway ii, with the regiochemistry of B-H addition reversed such that the B-H orientation is the same as that observed during HX' oxidative additions.

For catecholborane oxidative addition to $[\text{IrH}(\text{CO})(\text{dppe})]$ and $[\text{Ir}(\text{BO}_2\text{C}_6\text{H}_4)(\text{CO})(\text{dppe})]$, and for the minor isomer **4** (10%) of catecholborane addition to $\text{IrI}(\text{CO})(\text{dppe})$, diastereomers are obtained corresponding to addition along pathway i with B-H orientation so as to yield product i-HC. The formation of these diastereomers is similar to the products obtained from H_2 and R_3SiH additions to $\text{IrX}(\text{CO})(\text{dppe})$ via pathway i with addition over the $\text{OC}-\text{Ir}-\text{P}$ axis of the four-coordinate complex. The change in kinetic selectivity for catecholborane addition to $[\text{IrH}(\text{CO})(\text{dppe})]$ and $[\text{Ir}(\text{BO}_2\text{C}_6\text{H}_4)(\text{CO})(\text{dppe})]$ relative to that seen for $\text{IrBr}(\text{CO})(\text{dppe})$ may arise from the fact that, with the former compounds, the ligand interaction with Ir d_{z^2} that increases the complex's basicity upon bending is absent. Thus the addition proceeds more in accord with the factors that control nucleophilic additions of H_2 and silanes. The regiochemistry of the addition to give i-HC products

(37) Sargent, A. L.; Hall, M. B.; Guest, M. F. *J. Am. Chem. Soc.* **1992**, *114*, 517-522.

rather than *i*-HP products is apparently determined by minimization of nonbonded interactions.

The observation that oxidative addition of catecholborane to IrBr(CO)(chiraphos) leads to the formation of both *ii*-HP and *i*-HC diastereomers in nearly equal proportions is, at this time, very puzzling. While we expected the chiraphos ligand to impart subtle preferences upon the facial diastereoselectivity of the oxidative addition,³⁴ it was not expected to influence the stereoselectivity of the addition in terms of pathway *ii* vs *i* relative to that seen with IrBr(CO)(dppe). The initially formed pairs of diastereomers, however, indicate the absence of kinetic selectivity (pathway *ii* vs pathway *i*) as well as facial diastereoselectivity. On the basis of these results, we conclude that a fine balance between steric and electronic factors influences the stereoselectivity and diastereoselectivity of catecholborane oxidative addition reactions to IrX(CO)(P[∧]P) complexes. Additional studies with other systematically varied complexes and computational studies are necessary to fully comprehend the factors governing borane additions to Ir(I) centers.

Experimental Section

Reactions and sample preparations were performed in a nitrogen filled glovebox or under the appropriate gas using a high-vacuum line or Schlenk line. All solvents were reagent grade or better and were dried and degassed prior to use by accepted methods. Catecholborane-*d*₁³⁸ and the complexes IrBr(CO)(dppe) and IrI(CO)(dppe),³¹ IrH₃(CO)(dppe),³⁹ and IrBr(CO)(chiraphos)³⁴ were prepared according to literature procedures. The identities of all complexes are determined solely by spectroscopic methods. Microanalysis has also been included for **1**.

NMR samples were prepared using resealable NMR tubes fitted with J Young Teflon valves (Brunfeldt) and high-vacuum line adapters. ¹H, ¹³C, and ³¹P NMR spectra were recorded at 400.13, 100.62, and 161.98 MHz, respectively, on a Bruker AMX 400 NMR spectrometer. Temperature control was achieved using a B-VT 1000 variable-temperature unit, a Cu-constantan temperature sensor, and calibration for high and low temperatures using ethylene glycol and methanol standards, respectively. ¹H NMR chemical shifts are reported in ppm downfield of tetramethylsilane but measured from residual ¹H signal in the deuterated solvents. ¹³C NMR spectra are reported in ppm downfield of tetramethylsilane and referenced to a known carbon signal in the solvent. ³¹P NMR spectra are reported in ppm downfield of an external 85% solution of phosphoric acid. Benzene-*d*₆ (MSD) and toluene-*d*₈ (Cambridge) were dried and distilled from purple solutions of sodium benzophenone ketyl. Methylene chloride-*d*₂ (Cambridge) was dried and distilled from a calcium hydride suspension. Solution and KBr (Aldrich) mull infrared spectra were recorded on a Matteson 6020 Galaxy FT infrared spectrometer. Elemental analysis was performed by Desert Analytics Laboratory, Tucson, Az.

IrH(BO₂C₆H₄)Br(CO)(dppe), 1. To a 50 mL benzene solution of IrBr(CO)(dppe) (75 mg, 0.107 mmol) was added 5 equiv of catecholborane (57 μL, 0.535 mmol). The solution was stirred for 10 min after which the volume was reduced to 15 mL. The addition of 50 mL of hexanes induced precipitation of the crude product. Recrystallization from methylene chloride and hexanes yielded the analytically pure **1** in 81% yield. See Tables 1 and 2 for spectroscopic characterization. Anal. Calcd for C₃₃H₂₉BBIrO₃P₂: C, 48.43; H, 3.57. Found: C, 48.19; H, 3.51.

IrD(BO₂C₆H₄)Br(CO)(dppe), 1-*d*₁. A similar procedure was used to prepare **1-*d*₁** using IrBr(CO)(dppe) and catecholborane-*d*₁.³⁸ Recrystallization from methylene chloride and hexanes afforded **1-*d*₁** in 78% yield.

IrH(BO₂C₆H₄)I(CO)(dppe), 3 and 4. In a nitrogen-filled glovebox, a resealable NMR tube was charged with IrI(CO)(dppe) (3 mg, 4 × 10⁻³ mmol) and 0.5 mL of a 8 × 10⁻³ mM C₆D₆ solution of catecholborane (1 equiv, 4 × 10⁻³ mmol) delivered by a 0.5 mL syringe. The NMR tube was sealed and shaken to ensure complete mixing. After 5 min the colorless solution was analyzed by infrared and NMR spectroscopies (see Tables 1 and 2).

IrH₃(BO₂C₆H₄)(CO)(dppe), 6. In a nitrogen-filled glovebox, a resealable NMR tube was charged with 8 mg of IrH₃(CO)(dppe) (0.013 mmol) and 0.5 mL of a 0.026 mM C₆D₆ solution of catecholborane (1 equiv, 0.013 mmol) delivered by a 0.5 mL syringe. The NMR tube was shaken to ensure complete mixing and either photolyzed (*hν* > 300 nm) at ambient temperature or warmed to 60 °C for 2 h. The formation of **6** was confirmed by infrared and NMR spectroscopies (see Tables 1 and 2).

IrH₂(BO₂C₆H₄)₂(CO)(dppe), 7. To an opened resealable NMR tube containing **6** in a nitrogen-filled glovebox was added 5 equiv (7 μL, 0.065 mmol) of catecholborane. The tube was sealed, shaken, and either photolyzed (*hν* > 300 nm) or heated at 60 °C for 2 h. The formation of **7** was observed by infrared and NMR spectroscopies (see Tables 1 and 2).

Kinetic Studies of the Interconversion of 1 to 2. In a nitrogen-filled glovebox, a resealable NMR tube was charged with 0.5 mL of a standard C₆D₆ solution of **1** (0.024 M) delivered by a 0.5 mL syringe, sealed, and inserted into a preheated NMR probe. The interconversion of **1** to **2** was monitored using ¹H NMR spectroscopy by measuring the integrated intensities of the hydride ligands due to **1** (-7.52 ppm, dd, ²J_{H-P} = 128.5, 16.9 Hz) and **2** (-16.18 ppm, dd, ²J_{H-P} = 15.7, 8.1 Hz). The reactions were monitored until equilibrium was reached in the temperature range 333–348 K. Plots of ln([**1**]₀ - [**1**]_e)/([**1**] - [**1**]_e) vs *t* yielded straight lines with the slope equal to the first-order rate constant *k*_{obs}' (*K*_{obs}' = (*k*₁*k*₂ + *k*₋₁*k*₋₂)/(*k*₂ + *k*₋₁); see Appendix).

Incorporation of Catecholborane-*d*₀ into 1-*d*₁ and 2-*d*₁. To an open resealable NMR tube in a nitrogen-filled glovebox was added 10 mg (0.012 mmol) of **1-*d*₁** and 0.5 mL of C₆D₆. The tube was sealed, removed from the glovebox, and heated overnight at 75 °C to ensure an equilibrium solution was obtained. After the equilibrium was established, the tube was transferred into the glovebox where 10 equiv (13.0 mL, 0.12 mmol) of catecholborane-*d*₀ was added to the tube. The tube was immediately removed from the box and placed into a preheated (55 °C) NMR probe. The incorporation of catecholborane-*d*₀ into **1-*d*₁** and **2-*d*₁** was monitored by ¹H NMR spectroscopy for 1 h.

Acknowledgment. We wish to thank the National Science Foundation (Grants CHE 89-09060 and CHE 94-04991) for support of this work and the Johnson Matthey Co. Inc. for a generous loan of iridium trichloride. B.P.C. gratefully acknowledges Sherman Clarke, Bristol Myers-Squibb, and Arnold Weissberger Fellowships.

Appendix

In view of the fact that the dissociative isomerization mechanism shown in eq 7 is not routinely treated in standard kinetics references, we outline the mathematical treatment of the approach to equilibrium of this reaction. Since the studies were performed in the absence of excess borane, it is clear from the stoichiometry of eq 7 that the concentrations of IrBr(CO)(dppe) and catecholborane are equal. If we represent their

(38) Newsom, H. C.; Woods, W. G. *Inorg. Chem.* **1968**, *7*, 177–178.

(39) Fisher, B. J.; Eisenberg, R. *Organometallics* **1983**, *2*, 764–767.

concentrations as $[x]$, then the differential rate law for the disappearance of **1** is given by eq A.1. Similarly, the rate law for the appearance of **2** is eq A.2 and for the time dependence of $[x]$ is eq A.3.

$$-d[1]/dt = k_1[1] - k_{-1}[x]^2 \quad (\text{A.1})$$

$$d[2]/dt = -k_{-2}[2] + k_2[x]^2 \quad (\text{A.2})$$

$$d[x]/dt = k_1[1] + k_{-2}[2] - (k_2 + k_{-1})[x]^2 \quad (\text{A.3})$$

Application of the steady state approximation for $[x]$ yields eq A.4, and by substitution into eq A.1 and

$$x = ((k_1[1] + k_{-2}[2]) / (k_2 + k_{-1}))^{1/2} \quad (\text{A.4})$$

$$-d[1]/dt = (k_1k_2[1] - k_{-1}k_{-2}[2]) / (k_2 + k_{-1}) \quad (\text{A.5})$$

rearrangement, eq A.5 is obtained. At time $t = 0$, $[1] = [1]_0$ and $[2] = [1]_0 - [1]$ so that the rate law becomes as follows:

$$-d[1]/dt = ((k_2k_1 + k_{-1}k_{-2}) / (k_2 + k_{-1})) [1] - ((k_{-1}k_{-2}) / (k_2 + k_{-1})) [1]_0 \quad (\text{A.6})$$

At equilibrium, $t \rightarrow \infty$, $[1] = [1]_e$ and $d[1]/dt = 0$. Therefore

$$-d[1]/dt = 0 = ((k_2k_1 + k_{-1}k_{-2}) / (k_2 + k_{-1})) [1]_e - ((k_{-1}k_{-2}) / (k_2 + k_{-1})) [1]_0 \quad (\text{A.7})$$

and

$$[1]_0 = ((k_2k_1 + k_{-1}k_{-2}) / (k_{-1}k_{-2})) [1]_e \quad (\text{A.8})$$

Substitution of the expression for $[1]_0$ into eq A.6 yields eq A.9,

$$-d[1]/dt = ((k_2k_1 + k_{-1}k_{-2}) / (k_2 + k_{-1})) ([1] - [1]_e) \quad (\text{A.9})$$

$$\ln((([1]_0 - [1]_e) / ([1] - [1]_e)) / (([1]_0 - [1]_e) / ([1] - [1]_e))) = ((k_1k_2 + k_{-1}k_{-2}) / (k_2 + k_{-1})) t = k_{\text{obs}}' t \quad (\text{A.10})$$

which may then be integrated to yield eq A.10. A linear plot of $\ln((([1]_0 - [1]_e) / ([1] - [1]_e)) / (([1]_0 - [1]_e) / ([1] - [1]_e)))$ vs t then yields the first-order rate constant $k_{\text{obs}}' = ((k_1k_2 + k_{-1}k_{-2}) / (k_2 + k_{-1}))$.

On the basis of the experimental results that indicate $k_{-1} \gg k_2$ and the equilibrium constant in terms of the kinetic parameters of eq 7, we obtain the equation for estimating k_{-2} in terms of k_{obs}' and K_{eq} , eq A.11.

$$k_{-2} = k_{\text{obs}}' / (K_{\text{eq}} + 1) \quad (\text{A.11})$$

The lower limit value of k_1 is based on the fact that that $k_{-1} > 100k_2$ which by substitution into $K_{\text{eq}} = k_1k_2 / k_{-1}k_{-2}$ leads to the inequality of eq A.12.

$$k_1 > 100K_{\text{eq}}k_{-2} \quad (\text{A.12})$$

OM950084Y

Reactions of Heteronuclear Dimetalated Olefin Complexes. Reactions of $\text{CpFe}(\text{CO})_2[\mu\text{-(Z)}\text{-(MeO}_2\text{C)C=C(CO}_2\text{Me)}]\text{Re}(\text{CO})_4$ with CO and *p*-Tolyl Isothiocyanate

Richard D. Adams* and Mingsheng Huang

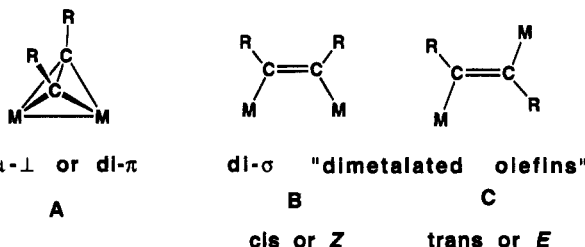
Department of Chemistry and Biochemistry, University of South Carolina, Columbia, South Carolina 29208

Received May 22, 1995*

Addition of CO to the dimetalated olefin complex $\text{CpFe}(\text{CO})_2[\mu\text{-(Z)}\text{-(MeO}_2\text{C)C=C(CO}_2\text{Me)}]\text{Re}(\text{CO})_4$, **1**, at 25 °C/700 psi of CO resulted in the formation of the adduct $\text{CpFe}(\text{CO})_2[\mu\text{-(E)}\text{-(MeO}_2\text{C)C=C(CO}_2\text{Me)}]\text{Re}(\text{CO})_5$, **2**, in 52% yield by cleavage of the Re–O bond to the coordinated carboxylate group. In contrast the reaction of **1** with CO at 70 °C/900 psi of CO provided the new compound $\text{CpFe}(\text{CO})_2[\mu\text{-(Z)}\text{-C=O(MeO}_2\text{C)C=C(CO}_2\text{Me)}]\text{Re}(\text{CO})_4$, **3**, in 77% yield. Compounds **2** and **3** were characterized by single-crystal X-ray diffraction analyses. Compound **2** is a Z-dimetalated olefin formed by addition of CO to the $\text{Re}(\text{CO})_4$ group in **1**, C–C = 1.35(1) Å. Compound **3** is an isomer of **2** in which a CO was added to **1** and inserted into the iron–carbon bond to the alkyne. The oxygen atom of the inserted CO grouping is coordinated to the rhenium atom, C–C = 1.349(7) and Re–O = 2.154(4) Å. Compound **2** loses CO spontaneously but slowly at room temperature to return to **1**, but compound **3** does not even under forcing conditions. When treated with EtNH_2 , the $\text{CpFe}(\text{CO})_2$ group in **3** was replaced by a EtNH grouping to yield the trisubstituted vinyl ligand in the complex $(\text{EtNHC=O})(\text{MeO}_2\text{C)C=C(CO}_2\text{Me)}]\text{Re}(\text{CO})_4$, **5**, in which carbonyl oxygen atom of the amido grouping is coordinated to the rhenium atom. Compound **1** reacts with EtNH_2 or H_2O to yield the new compound $\text{CpFe}(\text{CO})_2[(\text{MeO}_2\text{C)C=C(CO}_2\text{Me)(H)}]$, **6**, by the cleavage of the rhenium grouping from the molecule. The reaction with H_2O is catalyzed by silica gel. The reaction of **1** with *p*-tolyl isothiocyanate provided the iron–rhenium complex $\text{CpFe}(\text{CO})(\mu\text{-CO})[\mu\text{-CC(CO}_2\text{Me)}_2\text{C=SN}(p\text{-MeC}_6\text{H}_4\text{)C=O}]\text{Re}(\text{CO})_3$, **7** (17% yield), that was shown crystallographically to contain heterocycle $\text{CC(CO}_2\text{Me)}_2\text{C=SN}(p\text{-MeC}_6\text{H}_4\text{)C=O}$ formed by the coupling of the isothiocyanate molecule to a CO ligand and a rearranged form of the alkyne group. Crystal data for **2**: space group = $P2_1/c$, $a = 15.386(3)$ Å, $b = 7.520(2)$ Å, $c = 18.862(2)$ Å, $\beta = 107.66(1)^\circ$, $Z = 4$, 1750 reflections, $R = 0.024$. For **3**: space group = $P2_1/c$, $a = 14.285(2)$ Å, $b = 7.335(1)$ Å, $c = 20.943(4)$ Å, $\beta = 104.60(1)^\circ$, $Z = 4$, 2214 reflections, $R = 0.022$. For **7**: space group = $P\bar{1}$, $a = 10.655(2)$ Å, $b = 13.828(2)$ Å, $c = 9.626(1)$ Å, $\alpha = 109.53(1)^\circ$, $\beta = 98.23(1)^\circ$, $\gamma = 91.83(1)^\circ$, $Z = 2$, 3311 reflections, $R = 0.020$.

Introduction

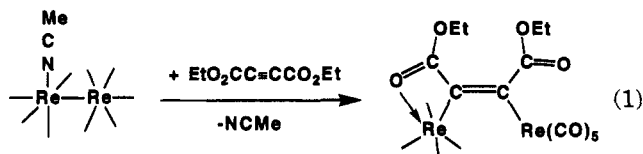
The activation of alkynes by metal complexes is an important method for converting these molecules to new organic molecules.¹ In dinuclear metal complexes, alkynes generally coordinate in the well-known $\mu\text{-}\perp$, di- π mode **A**;² however, the number of examples of di- σ -coordinated alkynes **B** and **C**, also known as dimetalated olefins, has been steadily increasing in recent years.^{3,4}



We have recently described the preparation of a number of new examples of dimetalated olefin complexes by the insertion of carboxylate-substituted alkynes into the metal–metal bonds of activated dimanganese and dirhenium carbonyl complexes (e.g., eq 1).^{3,5–9}

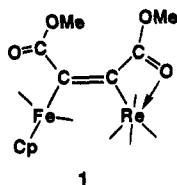
(4) (a) Hoffman, D. M.; Hoffmann, R. *J. Chem. Soc., Dalton Trans.* **1982**, 1471. (b) Hoffman, D. M.; Hoffmann, R. *Organometallics* **1982**, *1*, 1299.

* Abstract published in *Advance ACS Abstracts*, September 1, 1995.
 (1) (a) Shore, N. E. *Chem. Rev.* **1988**, *88*, 1081. (b) Colquhoun, H. M.; Thompson, D. J.; Twigg, M. V. *Carbonylation. Direct Synthesis of Carbonyl Compounds*; Plenum Press: New York, 1991. (c) Pino, P.; Braca, G. In *Organic Synthesis via Metal Carbonyls*; Wender, I., Pino, P., Eds.; Wiley: New York, 1977; Vol. 2, pp 420–516.
 (2) (a) Hoffman, D. M.; Hoffmann, R.; Fisel, C. R. *J. Am. Chem. Soc.* **1982**, *104*, 3858 and references therein.
 (3) Adams, R. D. *Chem. Soc. Rev.* **1994**, 335.



The coupling of CO to alkynes is one of the principal methods for functionalizing the alkyne group in metal complexes.^{1,6,10-13} It has been found that the coupling of CO to alkynes in dinuclear manganese-carbonyl complexes produces ligands in which the oxygen atom of the CO grouping is usually coordinated to one or more of the manganese atoms.^{6,11-13}

We have recently prepared the new heteronuclear Fe-Re dimetalated olefin complex, CpFe(CO)₂[μ-(Z)-(MeO₂C)C=C(CO₂Me)]Re(CO)₄, **1**.¹⁴ In this report the



results of our investigations of the reactions of **1** with CO and *p*-tolyl isothiocyanate are described. Carbonyl addition proceeds in two ways depending upon the conditions. At room temperature addition occurs at the rhenium atom, but at 70 °C an addition product that formed by the insertion of CO into the iron-carbon bond was obtained. We have found that the iron grouping can be cleaved from the latter product by a primary amine to yield a rhenium complex containing a trisubstituted vinyl ligand that is coordinated to the metal atom at two sites.

Experimental Section

Unless specified otherwise, all reactions were carried out under an atmosphere of nitrogen. Hexane was dried over sodium and freshly distilled under nitrogen prior to use. CH₂Cl₂ was dried over CaH₂. EtNH₂ (70 wt %) and *p*-tolyl isothiocyanate (97% purity) were purchased from Aldrich Co.

(5) (a) Adams, R. D.; Chen, L. *Organometallics* **1994**, *13*, 1264. (b) Adams, R. D.; Chen, L.; Wu, W. *Organometallics* **1993**, *12*, 1257.

(6) (a) Adams, R. D.; Chen, L.; Huang, M. *Organometallics* **1994**, *13*, 2696. (b) Adams, R. D.; Chen, L. *J. Am. Chem. Soc.* **1994**, *116*, 4467.

(7) (a) Adams, R. D.; Chen, L.; Wu, W. *Organometallics* **1994**, *13*, 1257. (b) Adams, R. D.; Chen, L.; Wu, W. *Organometallics* **1993**, *12*, 4962.

(8) Adams, R. D.; Chen, L.; Wu, W. *Organometallics* **1993**, *12*, 4112. (9) Adams, R. D.; Huang, M. *Organometallics* **1995**, *14*, 506.

(10) (a) Dyke, A. F.; Knox, S. A. R.; Naish, P. J.; Taylor, G. E. *J. Chem. Soc., Dalton Trans.* **1982**, 1297. (b) Finimore, S. R.; Knox, S. A. R.; Taylor, G. E. *J. Chem. Soc., Dalton Trans.* **1982**, 1783. (c) Hogarth, G.; Kayser, F.; Knox, S. A. R.; Morton, D. A. V.; Orpen, A. G.; Turner, M. L. *J. Chem. Soc., Chem. Commun.* **1988**, 358. (d) Gracey, B. P.; Knox, S. A. R.; Macpherson, K. A.; Orpen, A. G.; Stobart, S. R. *J. Chem. Soc., Dalton Trans.* **1985**, 1935. (e) Dickson, R. S. *Polyhedron* **1991**, *10*, 1995. (f) Johnson, K. A.; Gladfelter, W. L. *Organometallics* **1992**, *11*, 2534. (g) Takats, J. *J. Cluster Sci.* **1992**, *3*, 479. (h) Lemke, F. R. Szalda, D. J.; Bullock, R. M. *J. Am. Chem. Soc.* **1991**, *113*, 8466.

(11) (a) Adams, R. D.; Chen, G.; Chen, L.; Wu, W.; Yin, J. *Organometallics* **1993**, *12*, 3431.

(12) (a) Adams, R. D.; Chen, G.; Chen, L.; Wu, W.; Yin, J. *J. Am. Chem. Soc.* **1991**, *113*, 9406. (b) Adams, R. D.; Chen, L.; Wu, W. *Organometallics* **1993**, *12*, 4112.

(13) (a) García Alonso, F. J.; Riera, V.; Ruiz, M. A.; Tiripicchio, A.; Camellini, M. T. *Organometallics* **1992**, *11*, 370. (b) Derunov, V. V.; Shilova, O. S.; Batsanov, A. S.; Yannovskii, A. I.; Struchkov, Yu. T.; Kolobova, N. E. *Metalloorg. Khim.* **1991**, *4*, 1166.

(14) Adams, R. D.; Huang, M. *Organometallics* **1995**, *14*, 2887.

and were used without further purification. TLC separations were performed in air by using silica gel (60 Å, F₂₅₄) on plates (Whatman, 0.25 mm). IR spectra were recorded on a Nicolet 5DXB FT-IR spectrophotometer. ¹H NMR spectra were taken at 400 MHz on a Bruker AM-400 spectrometer. Elemental analyses were performed by Desert Analytics, Tucson, AZ. Mass spectra were run on a VG model 70SQ mass spectrometer by direct inlet using electron impact ionization. High-pressure reactions were performed in a 15-cc glass-lined Parr high-pressure reaction vessel. CpFe(CO)₂[μ-(Z)-(MeO₂C)C=C(CO₂Me)]Re(CO)₄, **1**, was prepared by our previously reported procedure.¹⁴

Preparation of CpFe(CO)₂[μ-(Z)-(MeO₂C)C=C(CO₂Me)]Re(CO)₅, **2.** A 50.0-mg amount (0.081 mmol) of **1** was dissolved in 5 mL of CH₂Cl₂ and placed in a Parr high-pressure reaction vessel. The vessel was pressurized to 700 psi with CO and stirred at 25 °C for 12 h. After the vessel had been vented, the solvent was removed, the residue was redissolved in a minimum amount of hexane, and the product was obtained by recrystallization by cooling the solution to -14 °C overnight. This yielded 27.2 mg of pale yellow crystals of CpFe(CO)₂[μ-(Z)-(MeO₂C)C=C(CO₂Me)]Re(CO)₅, **2**, in 52% yield. Spectral data for **2**: IR (ν_{CO} in hexane, cm⁻¹), 2134 (w), 2064 (w), 2040 (s), 2022 (m), 2007 (s), 1988 (s), 1969 (s), 1697 (w, br); ¹H NMR (δ in C₆D₆, ppm), 4.33 (s, 5H, C₅H₅), 3.47 (s, 3H, OCH₃), 3.46 (s, 3H, OCH₃). Anal. Calcd (found): C, 33.50 (33.17); H, 1.72 (1.69).

Preparation of CpFe(CO)₂[μ-C=O(MeO₂C)C=C(CO₂Me)]Re(CO)₄, **3.** A 52.0-mg amount (0.084 mmol) of **1** was dissolved in 5 mL of hexane and placed in a Parr high-pressure reaction vessel. This was pressurized to 900 psi with CO and then placed in an oil bath at 70 °C for 24 h. After the vessel had been cooled slowly and vented, the mother liquor was decanted and the yellow crystalline product CpFe(CO)₂[μ-(Z)-C=O(MeO₂C)C=C(CO₂Me)]Re(CO)₄, **3**, was removed from the vessel and washed with four 2-mL portions of hexane. Yield: 41.7 mg, 77%. The mother liquor was concentrated and separated by TLC using a hexane/CH₂Cl₂ (1/1) solvent mixture to yield 0.7 mg of pale yellow CpFe(CO)₂[μ-(E)-(MeO₂C)C=C(CO₂Me)]Re(CO)₄,¹⁴ **4** (1%) and 1.0 mg of **3** (2%). Spectral data for **3**: IR (ν_{CO} in hexane, cm⁻¹): 2105 (w), 2051 (w), 2042 (m), 2004 (s), 1996 (s), 1950 (s), 1724 (w, br), 1718 (w, br); ¹H NMR (δ in C₆D₆, ppm), 4.03 (s, 5H, C₅H₅), 3.63 (s, 3H, OCH₃), 3.46 (s, 3H, OCH₃). Anal. Calcd (found): C, 33.50 (33.19); H, 1.72 (1.78).

Reaction of 3 with EtNH₂. A 26.0-mg amount (0.040 mmol) of **3** was dissolved in 30 mL of CH₂Cl₂, and a 326.0-μL amount of EtNH₂/H₂O (70% by wt, 4.0 mmol) was added via syringe. The mixture was stirred at room temperature for 6 h. The solvent was removed in vacuo, and the residue was separated by TLC using a hexane/CH₂Cl₂ 1/2 solvent mixture to yield, in order of elution, 13.6 mg of pale yellow [EtNHC=O(MeO₂CC=CCO₂Me)]Re(CO)₄, **5** (66%), and 2.4 mg of unreacted **3**. Compound **5** was obtained as an oil and could not be crystallized at room temperature. Spectral data for **5**: IR (ν_{CO} in hexane, cm⁻¹), 2103 (m), 2004 (s), 1996 (s), 1949 (s), 1728 (w, br), 1695 (m), 1597 (m), 1559 (w, br); ¹H NMR (δ in C₆D₆, ppm), 8.97 (br, 1H, NH), 3.68 (s, 3H, OCH₃), 3.25 (s, 3H, OCH₃), 2.72 (dq, ³J_{H-H} = 7.3 Hz, ³J_{H-H} = 7.3 Hz, 2H, NHCH₂-Me), 0.52 (t, ³J_{H-H} = 7.3 Hz, CH₃). The mass spectrum for **5** showed the parent ion *m/e* 513 (for ¹⁸⁷Re) and ions corresponding to the loss of each of the four carbonyl ligands. Anal. Calcd (found): C, 30.47 (31.49); H, 2.36 (2.32); N, 2.73 (2.73).

Synthesis of CpFe(CO)₂[(MeO₂C)C=C(CO₂Me)(H)], **6.** (a) Reaction of **1** with EtNH₂: A 30.0-mg amount (0.049 mmol) of **1** was dissolved in 40 mL of hexane. To this solution was added a 393.0-μL amount of EtNH₂/H₂O (70% by wt, 4.9 mmol). The mixture was stirred at room temperature for 4 h. After the solvent was removed in vacuo, the residue was separated by TLC using CH₂Cl₂ solvent to give 13.5 mg of CpFe(CO)₂[(MeO₂C)C=C(CO₂Me)(H)], **6**, as a dark yellow oil in 87% yield. Spectral data for **6**: IR (ν_{CO} in hexane, cm⁻¹),

2043 (sh), 2037 (s), 1991 (s), 1746 (w), 1712 (w), 1583 (w, br); ^1H NMR (δ in C_6D_6 , ppm), 6.24 (s, 1H, CH), 4.05 (s, 5H, Cp), 3.75 (s, 3H, OMe), 3.40 (s, 3H, OMe). The mass spectrum (chemionization using NH_3) for **6** showed the parent ion in two forms: m/e 321 (MH^+) and m/e 338 ($\text{M}(\text{NH}_4)^+$).

(b) Reaction of **1** with H_2O : The direct reaction of **1** with H_2O is very slow; however, it is catalyzed by silica gel. A silica gel treatment procedure is given here: A 15.0-mg amount of **1** (0.024 mmol) was dissolved in a minimum amount of CH_2Cl_2 and transferred to a silica gel TLC plate. Elution with CH_2Cl_2 yielded 7.5 mg of yellow **6**, 96%.

(c) Reaction of **1** with D_2O : To a 5-mm NMR tube were added 3.0 mg (0.0049 mmol) of **1**, 10 μL of D_2O , and 0.5 mL of C_6D_6 . The reaction was monitored by ^1H NMR spectroscopy. After 10 days, compound **1** was completely converted into $\text{CpFe}(\text{CO})_2\text{-(MeO}_2\text{C)C=C(CO}_2\text{Me)(D)}$, **6-d**, as indicated by the absence of the resonance at 6.24 ppm and the presence of the resonances at 4.05, 3.75, and 3.40 ppm.

Decarbonylation of 2. A 15.0-mg amount of **2** was dissolved in 30 mL of hexane in a 50-mL three-neck flask wrapped with aluminum foil to protect it from light. The mixture was stirred under a slow purge with nitrogen at room temperature for 24 h. The solvent was then removed, and the residue was dissolved in about 1 mL of C_6D_6 . ^1H NMR spectrum of this sample showed the presence of compound **1** in $\approx 66\%$ of the total and compound **6** in $\approx 34\%$ of the total based on ^1H NMR integration.

Preparation of $\text{CpFe}(\text{CO})(\mu\text{-CO})[\mu\text{-CC}(\text{CO}_2\text{Me})_2\text{C=SN}(p\text{-MeC}_6\text{H}_4)\text{C=O}]\text{Re}(\text{CO})_3$, **7.** A 30.0-mg amount (0.048 mmol) of **1** and a 631.0-mg amount (4.23 mmol) of $p\text{-MeC}_6\text{H}_4\text{-NCS}$ were dissolved in 40 mL of hexane. The solution was heated to 50 $^\circ\text{C}$ for 44 h. The solvent was removed under vacuum, and the unreacted $p\text{-MeC}_6\text{H}_4\text{NCS}$ was separated from the product on a silica gel column by eluting with a hexane/ CH_2Cl_2 4/1 solvent mixture. The product was then eluted from the column using a 1/2 hexane/ CH_2Cl_2 solvent mixture. This yielded a red band containing 6.4 mg of $\text{CpFe}(\text{CO})(\mu\text{-CO})[\mu\text{-CC}(\text{CO}_2\text{Me})_2\text{C=SN}(p\text{-MeC}_6\text{H}_4)\text{C=O}]\text{Re}(\text{CO})_3$, **7** (17%). Spectral data for **7**: IR (ν_{CO} in hexane, cm^{-1}), 2047 (vs), 2000 (sh), 1990 (s), 1980 (s), 1973 (sh), 1961 (w), 1942 (s), 1824 (s), 1756 (w, br), 1723 (w, br), 1623 (w, br). ^1H NMR (δ in C_6D_6 , ppm), 7.70 (d, $^3J_{\text{H-H}} = 9.0$ Hz, 2H, C_6H_4), 7.08 (d, $^3J_{\text{H-H}} = 9.0$ Hz, 2H, C_6H_4), 4.68 (s, 5H, C_5H_5), 3.17 (s, 3H, OCH_3), 3.05 (s, 3H, OCH_3), 2.03 (s, 3H, $\text{C}_6\text{H}_4\text{CH}_3$). Anal. Calcd (found): C, 39.17 (38.93); H, 2.37 (2.17); N, 1.83 (1.83).

Crystallographic Analysis. Crystals of **2** suitable for X-ray diffraction analysis were obtained by recrystallization from solution in hexane solvent by cooling to -14 $^\circ\text{C}$. Crystals of **3** suitable for X-ray diffraction analysis were obtained by recrystallization from solution in a hexane/ CH_2Cl_2 1/1 solvent mixture by cooling to -4 $^\circ\text{C}$. Crystals of **7** were obtained by slow evaporation of solvent from solutions in a hexane/ CH_2Cl_2 1/1 solvent mixture at 25 $^\circ\text{C}$. All crystals that were used in diffraction intensity measurements were mounted in thin-walled glass capillaries. Diffraction measurements were made on a Rigaku AFC6S fully automated four-circle diffractometer by using graphite-monochromated Mo $\text{K}\alpha$ radiation. The unit cells were determined and refined from 15 randomly selected reflections obtained by using the AFC6 automatic search, center, index, and least-squares routines. All data processing was performed on a Digital Equipment Corp. VAXstation 3520 computer by using the TEXSAN motif structure solving program library obtained from Molecular Structure Corp., The Woodlands, TX. Neutral atom scattering factors were calculated by the standard procedures.^{15a} Anomalous dispersion corrections were applied to all non-hydrogen atoms.^{15b} Lorentz/polarization (Lp) and absorption corrections were applied to the data for each analysis. Full-matrix least-squares refine-

Table 1. Crystal Data for Compounds **2**, **3**, and **7**

compd	2	3	7
formula	$\text{ReFeO}_{11}\text{C}_{18}\text{H}_{11}$	$\text{ReFeO}_{11}\text{C}_{18}\text{H}_{11}$	$\text{ReFeSO}_{10}\text{NC}_{25}\text{H}_{18}$
fw	645.33	645.33	766.53
cryst syst	monoclinic	monoclinic	triclinic
lattice params			
<i>a</i> (\AA)	15.386(3)	14.285(2)	10.655(2)
<i>b</i> (\AA)	7.520(2)	7.335(1)	13.828(2)
<i>c</i> (\AA)	18.862(2)	20.943(4)	9.627(1)
α (deg)			109.53(1)
β (deg)	107.66(1)	104.60(1)	98.23(1)
γ (deg)			91.83(1)
<i>V</i> (\AA^3)	2079.3(6)	2123.4(5)	1318.2(3)
space group	$P2_1/c$ (No. 14)	$P2_1/c$ (No. 14)	$P\bar{1}$ (No. 14)
<i>Z</i> value	4	4	2
ρ_{calcd} (g/cm^3)	2.06	2.02	1.93
μ (Mo $\text{K}\alpha$) (cm^{-1})	65.7	64.4	52.8
temp ($^\circ\text{C}$)	20	20	20
$2\theta_{\text{max}}$ (deg)	42.0	45.0	46.0
no of obsd ($I > 3\sigma$)	1750	2214	3311
goodness of fit	1.25	1.28	1.36
residuals: ^a <i>R</i> ; <i>R</i> _w	0.024; 0.025	0.022; 0.023	0.020; 0.023
abs corr	empirical	empirical	empirical
largest peak final diff map (e/\AA^3)	0.72	0.35	0.48

$$^a R = \frac{\sum_{hkl} (||F_o| - |F_c||)}{\sum_{hkl} |F_o|}; R_w = \frac{[\sum_{hkl} w(|F_o| - |F_c|)^2]}{\sum_{hkl} w|F_o|^2}^{1/2}, w = 1/\sigma^2(F_o); \text{GOF} = \frac{[\sum_{hkl} (|F_o| - |F_c|/\sigma(F_o))]^2}{(n_{\text{data}} - n_{\text{vari}})}$$

ments minimized the function $\sum_{hkl} w(|F_o| - |F_c|)^2$, where $w = 1/\sigma(F_o)^2$, $\sigma(F_o) = \sigma(F_o^2)/2F_o$, and $\sigma(F_o^2) = [\sigma(I_{\text{raw}})^2 + (0.02I_{\text{net}})^2]^{1/2}/L_p$. All structures were solved by a combination of direct methods (MITHRIL) and difference Fourier syntheses. Crystal data and results of the analyses are listed in Table 1.

Compounds **2** and **3** crystallized in the monoclinic crystal system. The space group $P2_1/c$ was identified uniquely for both compounds from the patterns of systematic absences observed in the data. Least-squares refinements were performed using anisotropic thermal parameters for all non-hydrogen atoms. The positions of all hydrogen atoms were calculated by assuming idealized geometries about the carbon atoms and C-H distances of 0.95 \AA . The scattering contributions of the hydrogen atoms were added to the structure factor calculations, but their positions were not refined.

Compound **7** crystallized in the triclinic crystal system. The space group $P\bar{1}$ was assumed and confirmed by the successful solution and refinement of the structure. Least-squares refinements were performed using anisotropic thermal parameters for all non-hydrogen atoms. The positions of all hydrogen atoms were calculated by assuming idealized geometries about the carbon atoms and C-H distances of 0.95 \AA . The scattering contributions of the hydrogen atoms were added to the structure factor calculations, but their positions were not refined.

Results and Discussion

The reaction of **1** with CO at 700 psi and 25 $^\circ\text{C}$ for 12 h yielded the new compound $\text{CpFe}(\text{CO})_2[\mu\text{-}(Z)\text{-(MeO}_2\text{C)C=C(CO}_2\text{Me)}]\text{Re}(\text{CO})_5$, **2** (52% yield), as pale yellow crystals. Compound **2** was characterized by IR, ^1H NMR (δ 4.33 (s, Cp), 3.47 (s, OMe), 3.46 (s, OMe)), and single-crystal X-ray diffraction analyses. An ORTEP diagram of the molecular structure of **2** is shown in Figure 1. Final atomic positional parameters are listed in Table 2. The compound is a simple *Z*-dimetalated olefin complex. The Fe-C and Re-C bond distances to the "olefinic" group, Fe-C(2) = 2.037 (5) and Re-C(1) = 2.247(4) \AA , are similar to those observed in **1** (Fe-C(2) = 2.007(5) and Re-C(1) = 2.211(6) \AA) and its *E*-isomer **4** (Fe-C(2) = 2.007(6) and Re-C(1) = 2.175(5) \AA), both of which have an oxygen atom of one of the carboxylate groups coordinated to the rhenium atom.¹⁴ The C-C double bond, C(1)-C(2) = 1.35(1) \AA , is similar

(15) (a) *International Tables for X-ray Crystallography*; Kynoch Press: Birmingham, England, 1975; Vol. IV, Table 2.2B, pp 99-101. (b) *Ibid.*, Table 2.3.1, pp 149-150.

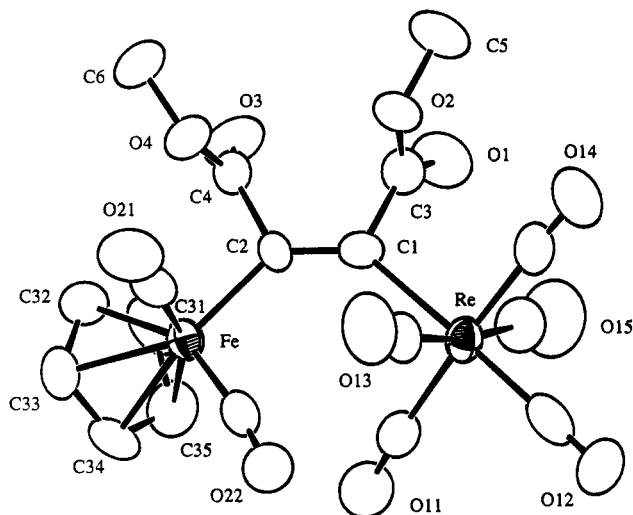


Figure 1. ORTEP diagram of $\text{CpFe}(\text{CO})_2[\mu\text{-}(Z)\text{-}(\text{MeO}_2\text{C})\text{C}=\text{C}(\text{CO}_2\text{Me})]\text{Re}(\text{CO})_5$, **2**, showing 50% probability thermal ellipsoids. Selected bond distances (Å) and angles (deg) are as follows: $\text{Fe}-\text{C}(2) = 2.037(5)$, $\text{Re}-\text{C}(1) = 2.247(4)$, $\text{C}(1)-\text{C}(2) = 1.35(1)$, $\text{C}(1)-\text{C}(3) = 1.48(1)$, $\text{C}(2)-\text{C}(4) = 1.49(1)$, $\text{C}(3)-\text{O}(1) = 1.20(1)$, $\text{C}(4)-\text{O}(3) = 1.196(8)$; $\text{Re}-\text{C}(1)-\text{C}(2) = 134.2(5)$, $\text{Fe}-\text{C}(2)-\text{C}(1) = 135.6(6)$, $\text{Re}-\text{C}(1)-\text{C}(3) = 107.3(5)$, $\text{Fe}-\text{C}(2)-\text{C}(4) = 108.8(5)$, $\text{C}(2)-\text{C}(1)-\text{C}(3) = 118.3(7)$, $\text{C}(1)-\text{C}(2)-\text{C}(4) = 115.4(6)$.

Table 2. Positional Parameters and $B(\text{eq})$ Values (Å²) for **2**

atom	<i>x</i>	<i>y</i>	<i>z</i>	<i>B</i> (eq)
Re	0.60074(2)	0.18387(5)	0.67492(2)	3.22(2)
Fe	0.79812(7)	0.3002(2)	0.86524(6)	2.85(4)
O(1)	0.7992(4)	0.063(1)	0.6016(3)	6.6(4)
O(2)	0.7889(4)	-0.1607(9)	0.6762(3)	4.5(3)
O(3)	0.9527(4)	0.1086(8)	0.7645(3)	5.1(3)
O(4)	0.9125(3)	-0.0527(8)	0.8482(3)	3.7(2)
O(11)	0.6230(5)	0.574(1)	0.7106(4)	6.2(4)
O(12)	0.3933(4)	0.257(1)	0.5760(3)	6.2(4)
O(13)	0.5759(4)	-0.023(1)	0.7834(4)	6.3(4)
O(14)	0.5696(5)	-0.187(1)	0.5702(4)	6.3(4)
O(15)	0.6524(5)	0.344(1)	0.5128(4)	8.4(4)
O(21)	0.8027(5)	-0.016(1)	0.9541(4)	5.9(4)
O(22)	0.6066(4)	0.3494(9)	0.8485(3)	5.1(3)
C(1)	0.7474(5)	0.120(1)	0.7074(1)	2.7(3)
C(2)	0.8035(5)	0.150(1)	0.7768(4)	2.5(3)
C(3)	0.7821(5)	0.012(1)	0.6563(5)	4.0(4)
C(4)	0.8963(5)	0.070(1)	0.7937(4)	3.2(4)
C(5)	0.8176(7)	-0.280(2)	0.6286(6)	7.4(6)
C(6)	1.0016(5)	-0.131(1)	0.8722(5)	5.0(4)
C(11)	0.6165(5)	0.429(1)	0.6910(5)	3.8(4)
C(12)	0.4709(7)	0.231(1)	0.6018(5)	4.6(4)
C(13)	0.5825(5)	0.059(1)	0.7363(5)	3.8(4)
C(14)	0.5828(6)	-0.053(1)	0.5997(5)	4.3(4)
C(15)	0.6351(6)	0.285(1)	0.5614(5)	5.2(5)
C(21)	0.8011(6)	0.103(1)	0.9178(5)	3.6(4)
C(22)	0.6815(6)	0.323(1)	0.8501(4)	3.4(3)
C(31)	0.9009(7)	0.456(1)	0.8430(6)	4.9(5)
C(32)	0.9338(5)	0.379(1)	0.9138(6)	4.5(4)
C(33)	0.8802(6)	0.441(1)	0.9566(5)	4.6(4)
C(34)	0.8156(6)	0.557(1)	0.9127(6)	4.8(5)
C(35)	0.8270(7)	0.563(1)	0.8423(6)	5.3(5)

in length to that found in **1** (1.332(8) Å) and **4** (1.344(8) Å). The bond angles involving the *cis* metal groups are large ($\text{Re}-\text{C}(1)-\text{C}(2) = 134.2(5)^\circ$ and $\text{Fe}-\text{C}(2)-\text{C}(1) = 135.6(6)^\circ$) probably due to steric effects between the large metal-containing groupings. Correspondingly large angles were also observed in **1** ($\text{Re}-\text{C}(1)-\text{C}(2) = 146.3(4)^\circ$ and $\text{Fe}-\text{C}(2)-\text{C}(1) = 127.8(4)^\circ$).¹⁴ The bond angles in *(Z)*-**4** were closer to the 120° value expected for

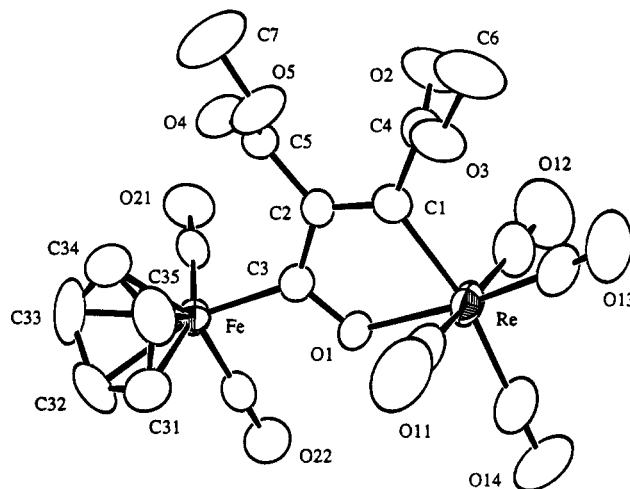
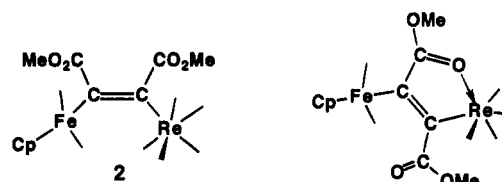


Figure 2. ORTEP diagram of $\text{CpFe}(\text{CO})_2[\mu\text{-}(Z)\text{-}\text{C}=\text{O}-(\text{MeO}_2\text{C})\text{C}=\text{C}(\text{CO}_2\text{Me})]\text{Re}(\text{CO})_4$, **3**, showing 50% probability thermal ellipsoids. Selected bond distances (Å) and angles (deg) are as follows: $\text{Re}-\text{O}(1) = 2.154(4)$, $\text{Fe}-\text{C}(3) = 1.923(5)$, $\text{Re}-\text{C}(1) = 2.139(5)$, $\text{C}(1)-\text{C}(2) = 1.349(7)$, $\text{C}(2)-\text{C}(3) = 1.481(7)$, $\text{C}(1)-\text{C}(4) = 1.487(8)$, $\text{C}(3)-\text{O}(1) = 1.278(6)$, $\text{C}(4)-\text{O}(2) = 1.185(7)$, $\text{C}(2)-\text{C}(5) = 1.494(7)$, $\text{C}(5)-\text{O}(5) = 1.189(7)$; $\text{Re}-\text{C}(1)-\text{C}(2) = 116.6(4)$, $\text{Re}-\text{O}(1)-\text{C}(3) = 120.6(3)$, $\text{Fe}-\text{C}(3)-\text{C}(2) = 128.2(4)$, $\text{Re}-\text{C}(1)-\text{C}(4) = 122.3(4)$, $\text{Fe}-\text{C}(3)-\text{O}(1) = 118.8(4)$, $\text{C}(1)-\text{C}(2)-\text{C}(3) = 116.0(4)$, $\text{C}(2)-\text{C}(3)-\text{O}(1) = 112.9(4)$.

trigonal planar carbon atoms in olefins: $\text{Re}-\text{C}(1)-\text{C}(2) = 119.0(4)^\circ$ and $\text{Fe}-\text{C}(2)-\text{C}(1) = 129.8(4)^\circ$. The dihedral angle between the planes $\text{Re}-\text{C}(1)-\text{C}(3)$ and $\text{Fe}-\text{C}(2)-\text{C}(4)$ is 3.6° . A slightly larger value, 7.8° , was observed in **1**.

Although it can be isolated in a pure form, **2** readily



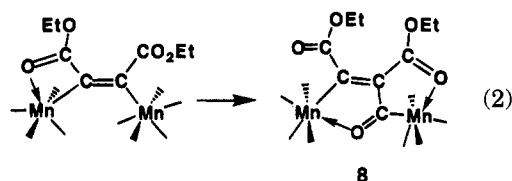
loses 1 equiv of CO at room temperature in air or under a nitrogen atmosphere. Compound **1** is regenerated, but **1** itself decomposes fairly readily on standing, so the yield of **1** that is formed is not high ($\approx 66\%$).

When solutions of **1** were heated to 70 °C for 24 h under 900 psi of CO, the new compound $\text{CpFe}(\text{CO})_2[\mu\text{-}(Z)\text{-}(\text{O}=\text{C})(\text{MeO}_2\text{C})\text{C}=\text{C}(\text{CO}_2\text{Me})]\text{Re}(\text{CO})_4$, **3**, was obtained in 79% yield together with a small amount of **4** ($\approx 1\%$). Compound **3** was characterized by IR, ¹H NMR (δ 4.03 (s, Cp), 3.63 (s, OMe), 3.46 (s, OMe)), and single-crystal X-ray diffraction analyses. An ORTEP diagram of the molecular structure of **3** is shown in Figure 2. Final atomic positional parameters are listed in Table 3. This compound is a carbonylated form of **1** formed by the addition and insertion of a CO group into the Fe-C bond of **1**. The oxygen atom of the inserted CO ligand is coordinated to the rhenium atom. The $\text{O}=\text{C}(\text{MeO}_2\text{C})\text{C}=\text{C}(\text{CO}_2\text{Me})$ group can be viewed as a dimetalated enone. A similar dimetalated enone complex $\text{Mn}_2(\text{CO})_8[\mu\text{-}(\text{EtO}_2\text{C})\text{C}=\text{C}(\text{CO}_2\text{Et})\text{C}=\text{O}]$, **8**, was obtained by the intramolecular insertion of CO into one of the manganese-carbon bonds in the complex $(\text{OC})_4\text{Mn}[\mu\text{-}(\text{EtO}_2\text{C})\text{C}=\text{C}(\text{CO}_2\text{Et})]\text{Mn}(\text{CO})_5$, **8**, at room tempera-

Table 3. Positional Parameters and $B(\text{eq})$ Values (\AA^2) for **3**

atom	<i>x</i>	<i>y</i>	<i>z</i>	<i>B</i> (eq)
Re	0.69116(2)	0.02461(4)	0.71677(1)	3.66(1)
Fe	0.94365(6)	-0.2195(1)	0.62562(4)	2.82(3)
O(1)	0.8205(3)	-0.0938(5)	0.6993(2)	3.5(2)
O(2)	0.6406(3)	0.3817(6)	0.5664(2)	5.7(2)
O(3)	0.5342(3)	0.1550(6)	0.5614(2)	4.6(2)
O(4)	0.8583(3)	0.1406(6)	0.5205(2)	4.5(2)
O(5)	0.7025(3)	0.0736(7)	0.4842(2)	5.2(2)
O(11)	0.5760(5)	-0.325(1)	0.6585(3)	9.3(4)
O(12)	0.7776(4)	0.4045(9)	0.7638(3)	8.2(33)
O(13)	0.4947(4)	0.192(1)	0.7160(3)	9.3(4)
O(14)	0.7314(4)	-0.1266(9)	0.8600(2)	8.4(3)
O(21)	1.0623(3)	0.0968(6)	0.6167(2)	4.8(2)
O(22)	1.0249(3)	-0.2695(6)	0.7658(2)	5.5(2)
C(1)	0.6940(4)	0.1011(7)	0.6187(2)	3.0(2)
C(2)	0.7694(4)	0.0395(7)	0.5969(2)	2.7(2)
C(3)	0.8390(4)	-0.0792(7)	0.6429(2)	2.7(2)
C(4)	0.6226(4)	0.230(1)	0.5785(3)	3.6(3)
C(5)	0.7846(5)	0.0898(7)	0.5311(3)	3.2(3)
C(6)	0.4584(5)	0.270(1)	0.5251(4)	7.0(4)
C(7)	0.7037(6)	0.138(1)	0.4192(3)	8.6(5)
C(11)	0.6208(6)	-0.202(1)	0.6799(3)	5.6(4)
C(12)	0.7509(5)	0.262(1)	0.7481(3)	5.0(4)
C(13)	0.5693(6)	0.130(1)	0.7190(3)	5.6(4)
C(14)	0.7146(5)	-0.073(1)	0.8073(3)	5.7(4)
C(21)	1.0137(4)	-0.0237(8)	0.6202(3)	3.2(3)
C(22)	0.9923(4)	-0.2487(8)	0.7104(3)	3.4(3)
C(31)	0.8921(6)	-0.4848(9)	0.6065(3)	4.7(3)
C(32)	0.9883(5)	-0.4805(9)	0.6049(4)	5.1(3)
C(33)	0.9979(7)	-0.363(1)	0.5559(4)	6.4(4)
C(34)	0.9038(8)	-0.294(1)	0.5258(3)	6.5(4)
C(35)	0.8403(5)	-0.376(1)	0.5575(4)	5.4(3)

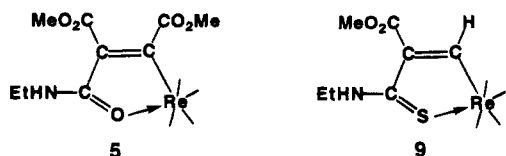
ture, eq 2.⁶



8

(2)

Compound **3** was found to react with EtNH_2 at room temperature to yield the new compound $[\text{EtNHC}=\text{O}(\text{MeO}_2\text{C})\text{C}=\text{C}(\text{CO}_2\text{Me})]\text{Re}(\text{CO})_4$, **5**, in 66% yield. Compound **5** could not be obtained in a crystalline form. Its IR spectrum exhibits four terminal CO absorptions that are characteristic of a cis-disubstituted $\text{M}(\text{CO})_4$ grouping. The ^1H NMR spectrum shows resonances due to a EtNH grouping (8.97 (br, NH) and 2.72 (dq, $^3J_{\text{H-H}} = 7.3$ Hz, $^3J_{\text{H-H}} = 7.3$ Hz, NHCH_2Me), 0.52 (t, $^3J_{\text{H-H}} = 7.3$ Hz, CH_3)) and due to two carboxylate methyl groups (3.68 (s, OCH_3), 3.25 (s, OCH_3)). The mass spectrum for **5** showed the parent ion m/e 513, characteristic of the expected parent ion, and ions corresponding to the loss of each of the four carbonyl ligands. On the basis of this data the structure **5** is proposed to be the trisubstituted alkenyl complex shown below.



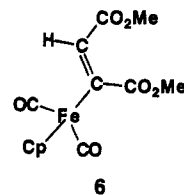
5

9

In the absence of a crystal structure analysis, an alternative structure with trans carboxylate groups having one coordinated group would be spectroscopically

acceptable but seems most unlikely in view of the established structure of **3**. The related compound $[\text{EtNHC}=\text{S}(\text{MeO}_2\text{C})\text{C}=\text{CH}]\text{Re}(\text{CO})_4$, **9**, containing a coordinated thioamido grouping has recently been structurally characterized.¹⁶ It is believed that an amido group was formed by the attack of the amine upon the acyl carbon atom in **3** with displacement of the $\text{CpFe}(\text{CO})_2$ grouping and loss of one hydrogen atom for the amine. The expelled groups might have been eliminated as $\text{CpFe}(\text{CO})_2\text{H}$, but this molecule is known to be unstable and was not observed here. The formation of amido groupings by the attack of amines on transition metal acyl groups has been observed previously.¹⁷

Compound **1** was found to react with H_2O to yield the new compound $\text{CpFe}(\text{CO})_2[(\text{MeO}_2\text{C})\text{C}=\text{C}(\text{CO}_2\text{Me})(\text{H})]$, **6**. We have not been able to establish the fate of the rhenium-containing grouping. The reaction is very slow on its own but is strongly promoted by silica gel, and thus **1** cannot be purified by chromatography over such materials. The yield of **6** can be as high as 96% when **1** is passed through silica gel on TLC plates. Compound **6** is a dark yellow oil at room temperature. On the basis of a combination of IR, ^1H NMR (6.24 (s, 1H), 4.05 (s, 5H), 3.75 (s, 3H), 3.40 (s, 3H)), mass spectra, and elemental analyses, compound **6** is assigned the structure with cis carboxylate groups shown below.



6

A structure with trans carboxylate groups cannot be ruled out by the spectroscopic data, but this structure would require the occurrence of a cis \rightarrow trans isomerization of the double bond during the reaction since the carboxylate groups are cis in **1**. Compound **6** can also be obtained from the reaction of **1** with aqueous EtNH_2 . When **1** was allowed to react with D_2O in benzene- d_6 solvent, compound **6-d**₁ was formed with the deuterium atom located exclusively on the alkenyl carbon atom.

The reaction of **1** with a large excess of *p*-tolyl isothiocyanate provided the addition product $\text{CpFe}(\text{CO})$ -

$(\mu\text{-CO})[\mu\text{-CC}(\text{CO}_2\text{Me})_2\text{C}=\text{SN}(p\text{-MeC}_6\text{H}_4)\text{C}=\text{O}]\text{Re}(\text{CO})_3$, **7**, in a 17% yield. Compound **7** was characterized by a single-crystal X-ray diffraction analyses. An ORTEP diagram of the molecular structure of **7** is shown in Figure 3. Final atomic positional parameters are listed in Table 4. Selected bond distances and angles are listed in Tables 5 and 6, respectively. Compound **7** contains a $\text{CpFe}(\text{CO})$ grouping connected to a $\text{Re}(\text{CO})_3$ grouping by an Fe-Re metal-metal bond, 2.7048(7) \AA . This distance is similar to that found in the compound $\text{CpFeRe}(\text{CO})_4[\mu\text{-C}(\text{CO}_2\text{Me})\text{C}(\text{CO}_2\text{Me})\text{C}(\text{CO}_2\text{Me})\text{C}(\text{CO}_2\text{Me})]$, **10**, $\text{Re-Fe} = 2.717(1)$ \AA .¹⁴ The Re-Fe bond is bridged by a carbonyl ligand on one side and a hetero-

cycle $\text{CC}(\text{CO}_2\text{Me})_2\text{C}=\text{SN}(p\text{-MeC}_6\text{H}_4)\text{C}=\text{O}$ with the ring atoms C(1)-C(2)-C(6)-N-C(5) that contains a thio-

(16) Adams, R. D.; Chen, L.; Huang, M. *J. Chin. Chem. Soc.* **1995**, *42*, 11.

(17) Adams, R. D.; Chodosh, D. F.; Golembeski, N. M. *Inorg. Chem.* **1978**, *17*, 266.

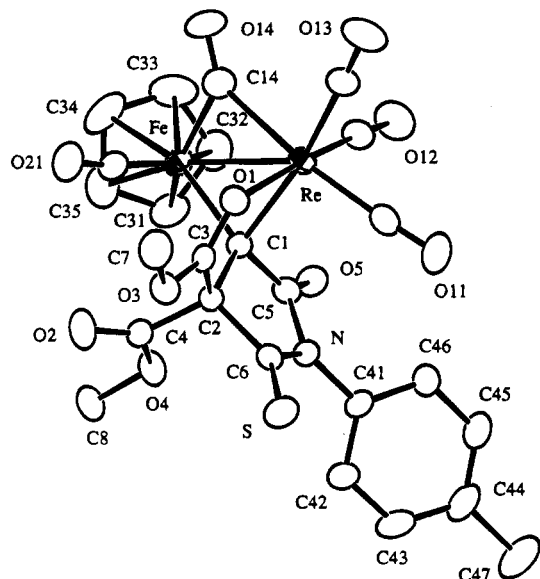


Figure 3. ORTEP diagram of $\text{CpFe}(\text{CO})(\mu\text{-CO})[\mu\text{-CC}(\text{CO}_2\text{Me})_2\text{C}=\text{SN}(p\text{-MeC}_6\text{H}_4)\text{C}=\text{O}]\text{Re}(\text{CO})_3$, **7**, showing 50% probability thermal ellipsoids.

Table 4. Positional Parameters and $B(\text{eq})$ Values (\AA^2) for **7**

atom	<i>x</i>	<i>y</i>	<i>z</i>	<i>B</i> (eq)
Re	0.30571(2)	0.22465(1)	0.02313(2)	2.823(7)
Fe	0.28853(6)	0.41354(4)	0.22235(7)	3.00(2)
S	-0.1321(1)	0.09205(9)	0.0179(1)	4.10(5)
O(1)	0.2428(3)	0.1641(2)	0.1894(3)	3.1(1)
O(2)	-0.0016(4)	0.3419(3)	0.4012(4)	4.8(2)
O(3)	0.0890(3)	0.1503(2)	0.3163(3)	3.5(1)
O(4)	-0.0789(3)	0.3846(2)	0.2041(3)	4.1(1)
O(5)	0.0727(3)	0.3689(2)	-0.1185(3)	3.4(1)
O(11)	0.1509(4)	0.0541(3)	-0.2515(4)	5.4(2)
O(12)	0.3653(4)	0.3136(3)	-0.2124(4)	6.1(2)
O(13)	0.5453(4)	0.1021(3)	-0.0073(5)	6.6(2)
O(14)	0.5458(4)	0.3504(3)	0.2529(5)	5.8(2)
O(21)	0.2988(4)	0.3703(3)	0.4991(4)	5.2(2)
N	-0.0425(3)	0.2386(2)	-0.0788(4)	2.7(1)
C(1)	0.1467(4)	0.3108(3)	0.0913(4)	2.5(1)
C(2)	0.0588(4)	0.2537(3)	0.1585(4)	2.6(1)
C(3)	0.1376(4)	0.1852(3)	0.2245(4)	2.8(2)
C(4)	-0.0098(4)	0.3304(3)	0.2726(5)	3.0(2)
C(5)	0.0629(4)	0.3167(3)	-0.0406(5)	2.7(2)
C(6)	-0.0431(4)	0.1917(3)	0.0249(5)	2.7(2)
C(7)	0.1655(6)	0.0868(4)	0.3838(6)	4.7(2)
C(8)	-0.1481(5)	0.4639(4)	0.2946(5)	4.6(2)
C(11)	0.2067(5)	0.1142(4)	-0.1449(6)	3.5(2)
C(12)	0.3451(5)	0.2808(4)	-0.1199(6)	3.9(2)
C(13)	0.4555(5)	0.1447(4)	0.0019(5)	4.0(2)
C(14)	0.4382(5)	0.3391(4)	0.1990(6)	4.0(2)
C(21)	0.2879(4)	0.3830(3)	0.3869(5)	3.5(2)
C(31)	0.1896(5)	0.5307(3)	0.1698(7)	4.6(2)
C(32)	0.2980(6)	0.5141(4)	0.1000(6)	4.9(2)
C(33)	0.4054(6)	0.5359(4)	0.2120(9)	5.8(3)
C(34)	0.3650(7)	0.5634(4)	0.3488(7)	6.0(3)
C(35)	0.2320(7)	0.5608(4)	0.3226(7)	5.2(3)
C(41)	-0.1333(4)	0.2132(3)	-0.2134(5)	2.9(2)
C(42)	-0.2610(5)	0.2076(3)	-0.2069(5)	3.7(2)
C(43)	-0.3474(5)	0.1801(4)	-0.3384(6)	4.8(2)
C(44)	-0.3087(6)	0.1608(4)	-0.4755(6)	4.7(2)
C(45)	-0.1807(6)	0.1700(4)	-0.4781(5)	4.2(2)
C(46)	-0.0915(5)	0.1958(3)	-0.3490(5)	3.6(2)
C(47)	-0.4064(7)	0.1310(5)	-0.6161(7)	7.7(3)

imide grouping $\text{O}=\text{CN}(p\text{-MeC}_6\text{H}_4)\text{C}=\text{S}$. The carbon C(1) is a carbene center that bridges the metal-metal bond, $\text{Re}-\text{C}(1) = 2.155(4)$ and $\text{Fe}(1)-\text{C}(1) = 2.003(4)$ Å. The ring has a nonplanar envelope conformation with a dihedral angle of 23° between the planes formed by

Table 5. Intramolecular Distances for **7^a**

Re-Fe	2.7048(7)	O(5)-C(5)	1.215(5)
Re-O(1)	2.208(3)	O(11)-C(11)	1.150(6)
Re-C(1)	2.155(4)	O(12)-C(12)	1.167(6)
Re-C(11)	1.954(5)	O(13)-C(13)	1.138(6)
Re-C(12)	1.880(5)	O(14)-C(14)	1.171(6)
Re-C(13)	1.966(5)	O(21)-C(21)	1.142(5)
Re-C(14)	2.179(5)	N-C(5)	1.450(5)
Fe-C(1)	2.003(4)	N-C(6)	1.361(5)
Fe-C(14)	1.925(5)	N-C(41)	1.433(5)
Fe-C(21)	1.771(5)	C(1)-C(2)	1.545(5)
Fe-C(Cp av)	2.103(5)	C(1)-C(5)	1.472(6)
S-C(6)	1.624(4)	C(2)-C(3)	1.518(6)
O(1)-C(3)	1.233(5)	C(2)-C(4)	1.539(6)
O(2)-C(4)	1.185(5)	C(2)-C(6)	1.540(6)
O(3)-C(3)	1.297(5)	C-C(Cp av)	1.396(8)
O(3)-C(7)	1.460(5)	C-C(C ₆ av)	1.381(7)
O(4)-C(4)	1.328(5)	C(44)-C(47)	1.510(7)
O(4)-C(8)	1.450(5)		

^a Distances are in angstroms. Estimated standard deviations in the least significant figure are given in parentheses.

Table 6. Intramolecular Bond Angles for **7^a**

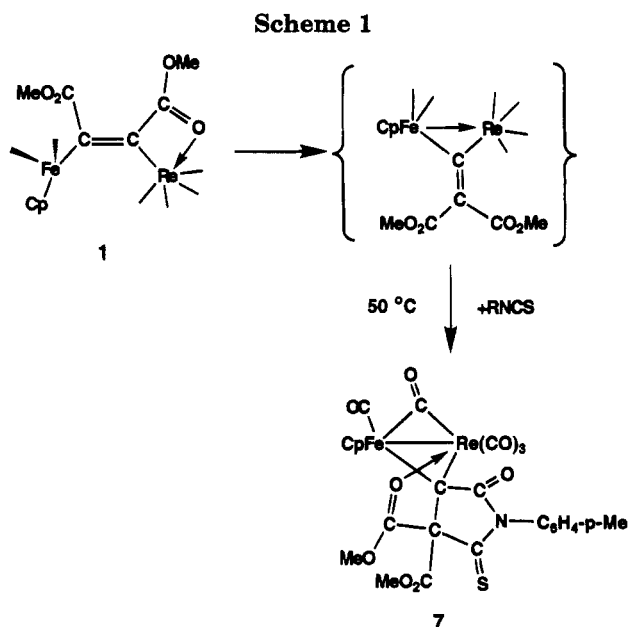
Fe-Re-O(1)	85.94(7)	C(4)-C(2)-C(6)	107.3(3)
O(1)-Re-C(1)	75.8(1)	O(1)-C(3)-O(3)	122.6(4)
Re-Fe-C(1)	51.9(1)	O(1)-C(3)-C(2)	120.0(4)
Re-Fe-C(14)	52.9(2)	O(3)-C(3)-C(2)	117.3(4)
C(1)-Fe-C(14)	104.1(2)	O(2)-C(4)-O(4)	124.7(4)
Re-O(1)-C(3)	117.4(3)	O(2)-C(4)-C(2)	126.4(4)
C(5)-N-C(6)	112.6(3)	O(4)-C(4)-C(2)	108.8(3)
C(5)-N-C(41)	122.8(3)	O(5)-C(5)-N	120.3(4)
C(6)-N-C(41)	124.6(3)	O(5)-C(5)-C(1)	131.7(4)
Re-C(1)-Fe	81.1(2)	N-C(5)-C(1)	107.9(3)
Re-C(1)-C(2)	111.6(2)	S-C(6)-N	129.0(3)
Re-C(1)-C(5)	109.9(3)	S-C(6)-C(2)	124.8(3)
Fe-C(1)-C(2)	120.8(3)	N-C(6)-C(2)	106.2(3)
Fe-C(1)-C(5)	127.5(3)	Re-C(11)-O(11)	173.9(4)
C(2)-C(1)-C(5)	103.0(3)	Re-C(12)-O(12)	177.3(5)
C(1)-C(2)-C(3)	108.5(3)	Re-C(13)-O(13)	177.1(5)
C(1)-C(2)-C(4)	110.8(3)	Re-C(14)-Fe	82.2(2)
C(1)-C(2)-C(6)	104.2(3)	Re-C(14)-O(14)	139.3(4)
C(3)-C(2)-C(4)	113.1(3)	Fe-C(14)-O(14)	138.5(4)
C(3)-C(2)-C(6)	112.6(3)	Fe-C(21)-O(21)	172.8(4)

^a Angles are in degrees. Estimated standard deviations in the least significant figure are given in parentheses.

the atoms C(1)-C(2)-C(5) and C(5)-N-C(6)-C(2). Most interestingly, both carboxylate groups are coordinated to the same carbon atom C(2) and the carbonyl group of one of these is coordinated to the rhenium atom by its oxygen atom, $\text{Re}-\text{O}(1) = 2.208(3)$ Å. The imido nitrogen atom N links the thiocarbonyl group C(6)-S to the carbonyl group C(5)-O(5), $\text{C}(6)-\text{S} = 1.624(4)$ and $\text{C}(5)-\text{O}(5) = 1.215(5)$ Å. The C(6)-N distance is significantly shorter than the C(5)-N distance, 1.361-(5) versus 1.450(5) Å, suggesting greater unsaturation between the atoms C(6) and N than between C(5) and N. The presence of both carboxylate groups on the same carbon atom suggests a rearrangement in which one carboxylate group is shifted to the carbon atom containing the other carboxylate group and could imply the formation of a species containing a substituted vinylidene ligand, see Scheme 1. The transformation of various types of alkynes into vinylidene ligands has been observed previously¹⁸ and is not uncommon in complexes containing dimanganese and dirhenium groupings.^{5b,19} We suspect that the formation of the heterocycle in **7** has occurred by the coupling of such

(18) (a) Bruce, M. I. *Chem. Rev.* **1991**, *91*, 197. (b) Bruce, M. I.; Swincer, A. G. *Adv. Organomet. Chem.* **1983**, *22*, 59.

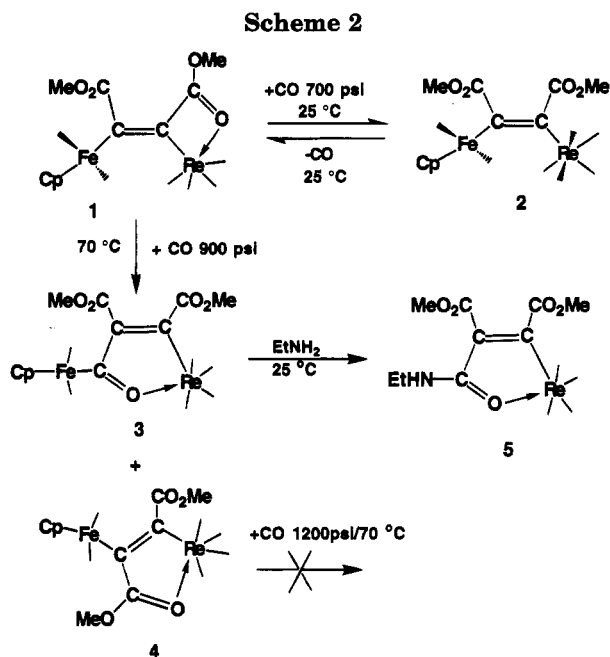
(19) (a) Adams, R. D.; Chen, G.; Chen, L.; Pompeo, M. P.; Yin, J. *Organometallics* **1992**, *11*, 563. (b) Garcia Alonso, F. J.; Riera, V.; Ruiz, M. A.; Tiripicchio, A.; Camellini, M. T. *Organometallics* **1992**, *11*, 370.



an unobserved vinylidene-containing intermediate to a CO ligand and the isothiocyanate molecule. Such a combination is here to fore unprecedented although it has been shown previously that CO ligands can be coupled to vinylidene ligands and the combination of alkynes with CO^{5b,20} and that isocyanates in the presence of iron pentacarbonyl will yield succinimide complexes.²¹ Due to the low yield of **7**, further analysis of the mechanism of its formation has not been possible.

A summary of the results of the reactions of **1** with CO is shown in Scheme 2. The room temperature addition of CO to **1** is analogous to that of the addition of CO to $\text{Re}(\text{CO})_5[\mu\text{-}(Z)\text{-(MeO}_2\text{C)C=C(CO}_2\text{Me)Re}(\text{CO})_4]$.^{5a} The coordinated oxygen atom of the carboxylate group is displaced, and the CO group is added to the rhenium. We have shown previously that **1** will also add $\text{MeO}_2\text{CC}\equiv\text{CCO}_2\text{Me}$ with coupling to the alkyne ligand to yield the complex **10**, which contains a tetracarboxylate-substituted rheniacyclopentadienyl group that is π -bonded to the iron atom.¹⁴ Complex **2** loses CO with surprising ease at 25 °C to regenerate to **1**, 66% yield, in 24 h.

The formation of **3** under more forcing conditions appears to involve an addition of CO to the iron atom



accompanied by a CO insertion into the iron-carbon bond and a subsequent coordination of the acyl oxygen atom to the rhenium atom. Assuming that the migration mechanism is operative in this reaction, then the inserted CO group would not be the CO group that was added but instead would be one of the originally coordinated CO groups on the iron atom in **1**.²² It seems most likely that the process probably involves an initial addition of CO to the rhenium atom followed by the addition and insertion at the iron atom which, in turn, is followed by a CO elimination at the rhenium atom and coordination of the acyl oxygen atom, that is, **2** is probably an intermediate in the formation of **3**.

Acknowledgment. This research was supported by the Office of Basic Energy Science of the U.S. Department of Energy.

Supporting Information Available: Tables of hydrogen atom positional parameters, anisotropic thermal parameters, and bond distances and angles for all three structural analyses (19 pages). Ordering information is given on any current masthead page.

OM950368I

(20) Birk, R.; Berke, H.; Huttner, G.; Zsolnai, L. *Chem. Ber.* **1988**, *121*, 471.

(21) Ohshiro, Y.; Kinugasa, K.; Minami, T.; Agawa, T. *J. Org. Chem.* **1970**, *35*, 2136.

(22) Collman, J. P.; Hegedus, L. S.; Norton, J. R.; Finke, R. G. *Principles and Applications of Organotransition Metal Chemistry*; University Science Books: Mill Valley, CA, 1987; Chapter 6.

Thiolato Ligand Transfer from Bis(thiolato)titanocenes to Platinum(II) Complexes

Kohtaro Osakada,* Yasuharu Kawaguchi, and Takakazu Yamamoto*

Research Laboratory of Resources Utilization, Tokyo Institute of Technology,
4259 Nagatsuta, Midori-ku, Yokohama 226, Japan

Received May 26, 1995[®]

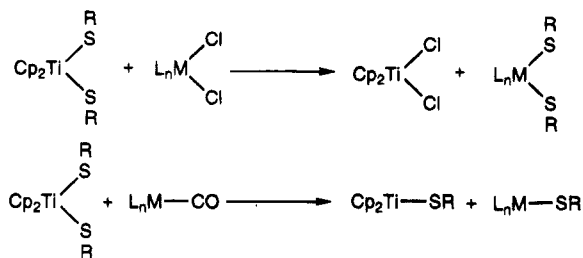
Reactions of $\text{Cp}_2\text{Ti}(\text{SEt})_2$ (**1a**) and $\text{Cp}_2\text{Ti}(\text{S-}i\text{-Pr})_2$ (**1b**) with equimolar $\text{PtCl}_2(\text{cod})_2$ give bis(thiolato)platinum complexes, $[\text{Pt}(\text{SEt})_2]_n$ (**2a**) and $[\text{Pt}(\text{S-}i\text{-Pr})_2]_n$ (**2b**), respectively, accompanied by formation of Cp_2TiCl_2 . Complexes **2a,b**, which are insoluble in common organic solvents, are characterized by elemental analyses and by CP-MAS ^{13}C NMR spectra in the solid state. $\text{Cp}_2\text{Ti}(\text{SC}_6\text{H}_4\text{-}p\text{-Me})_2$ (**1c**), $\text{Cp}_2\text{Ti}(\text{SPh})_2$ (**1d**), $\text{Cp}_2\text{Ti}(\text{S}_2\text{C}_6\text{H}_4)$ (**1e**), and $\text{Cp}_2\text{Ti}(\text{S}_2\text{C}_2\text{H}_4)$ (**1f**) react with equimolar $\text{PtCl}_2(\text{cod})$ smoothly to give mixtures of Cp_2TiCl_2 and (thiolato)platinum complexes with the cod ligand, $\text{Pt}(\text{SC}_6\text{H}_4\text{-}p\text{-Me})_2(\text{cod})$ (**3c**), $\text{Pt}(\text{SPh})_2(\text{cod})$ (**3d**), $\text{Pt}(\text{S}_2\text{C}_6\text{H}_4)(\text{cod})$ (**3e**), and $\text{Pt}(\text{S}_2\text{C}_2\text{H}_4)(\text{cod})$ (**3f**), respectively. Reactions of **1a** with excess $\text{PtCl}_2(\text{cod})$ in THF and in CH_2Cl_2 cause a color change of the solution indicating initial formation of $\text{Cp}_2\text{TiCl}(\text{SEt})$ followed by its further reaction with Pt complexes to give Cp_2TiCl_2 . The latter step, which is much slower than the former, obeys pseudo-first-order kinetics with respect to $[\text{Cp}_2\text{TiCl}(\text{SEt})]$. The observed rate constants, k_{obsd} , of the reaction in CH_2Cl_2 are proportional to $[\text{PtCl}_2(\text{cod})]$. Temperature dependence of the rate constants in THF gives the kinetic parameters $E_a = 57.4 \text{ kJ mol}^{-1}$, $\Delta H^\ddagger = 54.8 \text{ kJ mol}^{-1}$, $\Delta S^\ddagger = -106 \text{ J mol}^{-1} \text{ K}^{-1}$, and $\Delta G^\ddagger = 86.3 \text{ kJ mol}^{-1}$ at 298 K. Reaction of **1b** with excess $\text{PtCl}_2(\text{cod})$ also gives Cp_2TiCl_2 through $\text{Cp}_2\text{TiCl}(\text{S-}i\text{-Pr})$. The kinetic parameters of the reaction are $E_a = 62.3 \text{ kJ mol}^{-1}$, $\Delta H^\ddagger = 59.8 \text{ kJ mol}^{-1}$, $\Delta S^\ddagger = -124 \text{ J mol}^{-1} \text{ K}^{-1}$, and $\Delta G^\ddagger = 96.7 \text{ kJ mol}^{-1}$ at 298 K. The absorption spectrum of a reaction mixture of **1f** with excess $\text{PtCl}_2(\text{cod})$ shows a decrease in the peak due to **1f** with concomitant growth of a peak due to Cp_2TiCl_2 . The reaction obeys 0.5th-order kinetics with respect to **1f**. Reactions of **1c,d** with equimolar $\text{PtCl}_2(\text{cod})$ in toluene give the complexes formulated as $[\text{Cp}_2\text{Ti}(\text{SAr})_2\text{PtCl}_2(\text{cod})]$ (**4c**, Ar = $\text{C}_6\text{H}_4\text{-}p\text{-Me}$; **4d**, Ar = Ph), which are characterized by elemental analyses and ^{13}C NMR spectra in the solid state. Dissolution of **4c,d** in THF causes formation of a mixture of Cp_2TiCl_2 with **3c,d**, respectively.

Introduction

Bis(thiolato)titanocene complexes react with group 9 and 10 transition metal complexes to cause thiolato ligand transfer to give thiolato complexes of the late transition metals (Scheme 1).¹⁻⁴ The thiolato ligand transfer from Ti to late transition metals provides a useful synthetic tool for (dithiolene)rhodium complexes⁴ and for multinuclear Ni or Pd complexes with thiolato ligands.^{3b} Occurrence of the reaction seems to have the thermodynamic reason that hard and soft mismatching of coordination between titanocene and thiolato in the starting materials is more unfavorable than the coordination of Cl to Ti in the product, Cp_2TiCl_2 .

The previous studies on the above thiolato transfer reaction leave several mechanistic issues unclarified. The reaction is believed to proceed through an associative pathway involving a heterobimetallic intermediate with bridging thiolato ligands because an alternative dissociation pathway requires initial thiolato ligand

Scheme 1. Thiolato Ligand Transfer



dissociation from the Ti center to result in formation of a coordinatively unsaturated titanocene compound with a 14 electron metal center. The above observation seems to be reasonable although there have been no reports to afford experimental evidence to support the pathway. Furthermore, it is not clear whether the rate-determining step of the associative ligand transfer involves initial formation of heterobimetallic intermediate or cleavage of Ti-S bond from the preformed heterobimetallic intermediate. Facile formation of many heterobimetallics containing titanocene and late transition metals bridged by thiolato ligands might suggest the latter mechanism. On the other hand, reactivity toward the ligand transfer was not compared among various (thiolato)titanocene complexes. Elucidation of the above mechanistic details of the ligand transfer reaction would be of interest in relation to preparation

[®] Abstract published in *Advance ACS Abstracts*, September 1, 1995.

(1) Bolinger, C. M.; Rauchfuss, T. B. *Inorg. Chem.* **1982**, *21*, 3947.

(2) Shaver, A.; Morris, S.; Turrin, R.; Day, V. W. *Inorg. Chem.* **1990**, *29*, 3622.

(3) (a) Wark, T. A.; Stephan, D. W. *Can. J. Chem.* **1990**, *68*, 565. (b) Huang, Y.; Drake, R. J.; Stephan, D. W. *Inorg. Chem.* **1990**, *29*, 3622.

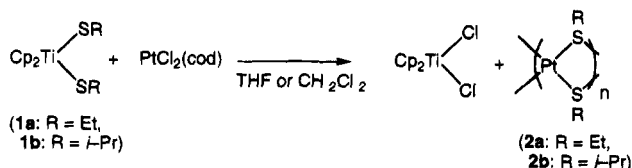
(4) Yamaguchi, A.; Fujita, T.; Kajitani, M.; Akiyama, T.; Sugimori, A. *Abstracts of Papers*; 65th Annual Meeting of Chemical Society of Japan; Chemical Society of Japan: Tokyo, 1993; 2P08.

of late transition metal thiolato complexes from a thiolato group transfer reaction. We report here reactions of bis(thiolato)titanocene complexes with $\text{PtCl}_2(\text{cod})$ to give (thiolato)platinum complexes, $[\text{Pt}(\text{SR})_2]_n$ or $\text{Pt}(\text{SR})_2(\text{cod})$, as well as results of the kinetic study of the reaction.

Results

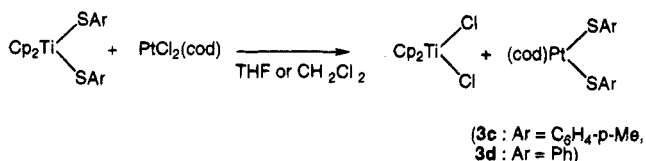
Reaction of $\text{PtCl}_2(\text{cod})$ with $\text{Cp}_2\text{Ti}(\text{SR})_2$ in THF.

Reactions of $\text{PtCl}_2(\text{cod})_2$ with equimolar $\text{Cp}_2\text{Ti}(\text{SEt})_2$ (**1a**) and $\text{Cp}_2\text{Ti}(\text{S-}i\text{-Pr})_2$ (**1b**) proceed smoothly to give mixtures of Cp_2TiCl_2 and polynuclear bis(thiolato)platinum complexes formulated as $[\text{Pt}(\text{SEt})_2]_n$ (**2a**) and $[\text{Pt}(\text{S-}i\text{-Pr})_2]_n$ (**2b**), respectively. The solid state ^{13}C NMR

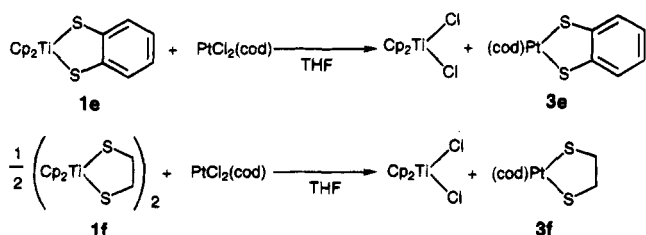


spectrum of **2a** shows peaks at 24.7 and 30.1 ppm which are assigned to CH_3 and CH_2 carbons of the ethanethiolato ligand, respectively. The peaks due to carbons of cod or Cp ligands are not observed at all. Similar homoleptic thiolato complexes of Ni and Pd such as $[\text{Ni}(\text{SR})_2]_n$ ($n = 6, 8$) and $[\text{Pd}(\text{SR})_2]_6$ were characterized by X-ray crystallography.⁵ Poor solubility of complexes **2a,b** in organic solvents prevents further characterization by NMR in solution or X-ray diffraction of the single crystals and determination of molecular weight of the complexes. $\text{PtMe}_2(\text{cod})$ does not react with **1a** at all either at room temperature or at 60 °C.

Reactions of $\text{PtCl}_2(\text{cod})$ with equimolar $\text{Cp}_2\text{Ti}(\text{SC}_6\text{H}_4\text{-}p\text{-Me})_2$ (**1c**) and with $\text{Cp}_2\text{Ti}(\text{SPh})_2$ (**1d**) give mixtures of Cp_2TiCl_2 and bis(arenethiolato)platinum complexes with cod ligand, $\text{Pt}(\text{SC}_6\text{H}_4\text{-}p\text{-Me})_2(\text{cod})$ (**3c**) and $\text{Pt}(\text{SPh})_2(\text{cod})$ (**3d**), respectively. The Pt-containing products, **3c,d**, are separated out from the reaction mixtures and characterized by comparison of the NMR (^1H and ^{13}C) spectra with authentic samples.



$\text{Cp}_2\text{Ti}(\text{S}_2\text{C}_6\text{H}_4)$ (**1e**) with a chelating dithiolato ligand reacts with $\text{PtCl}_2(\text{cod})$ to give a mixture of Cp_2TiCl_2 and $\text{Pt}(\text{S}_2\text{C}_6\text{H}_4)(\text{cod})$ (**3e**). Although the ^1H and ^{13}C NMR



spectra of **3e** agree well with those of an authentic sample (cf. Experimental Section), the NMR results are not helpful to determine whether the complex has a mononuclear structure or another dinuclear structure

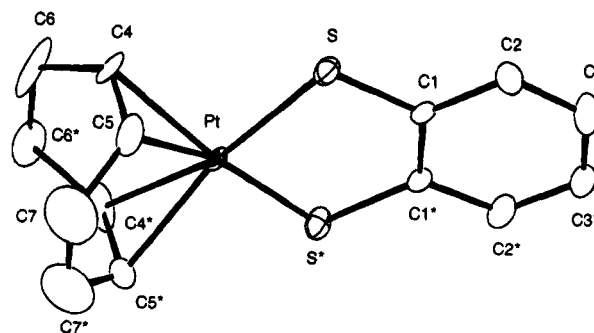


Figure 1. ORTEP drawing of $\text{Pt}(\text{o-SC}_6\text{H}_4\text{S})(\text{cod})$ at the 30% ellipsoidal level. The atoms with asterisks are crystallographically equivalent to those with the same numbering without asterisks.

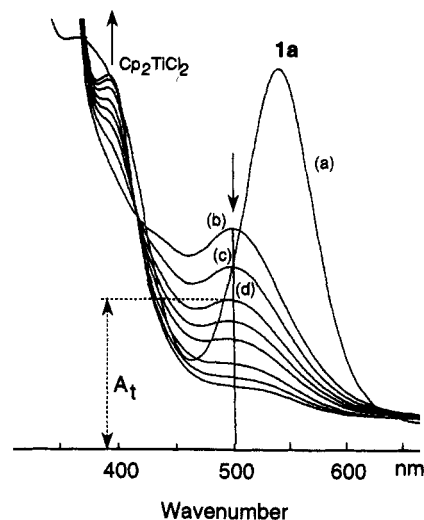


Figure 2. Change in the absorption spectra of a reaction mixture of **1a** (0.35 mM) and $\text{PtCl}_2(\text{cod})$ (3.5 mM) in THF at 9 °C: (a) before addition of $\text{PtCl}_2(\text{cod})$; (b) at $t = 0$ after addition of the Pt complex; (c) at $t = 220$ (s); (d) at $t = 460$ (s).

containing two bridging bis(thiolato) ligands. X-ray crystallography of the complex is examined to determine the structure of the complex. Figure 1 shows the molecular structure of **3e** which has a square planar coordination around Pt center. No intermolecular interaction between S and Pt atoms is observed similarly to $\text{Pt}(\text{SCH}_2\text{CH}_2\text{S})(\text{PR}_3)_2$.⁶ The Pt–S bond distance (2.264 Å) is within the range of already reported (thiolato)platinum(II) complexes (2.276–2.374 Å).⁷ Reaction of $[\text{Cp}_2\text{Ti}(\text{SCH}_2\text{CH}_2\text{S})]_2$ (**1f**) with $\text{PtCl}_2(\text{cod})$ gives a mixture of Cp_2TiCl_2 and $\text{Pt}(\text{SCH}_2\text{CH}_2\text{S})(\text{cod})$ (**3f**) as revealed by comparing the ^1H and ^{13}C NMR spectra of the reaction mixture with those of a mixture of the two complexes.

Kinetic Studies on Reactions of $\text{PtCl}_2(\text{cod})$ with **1a,b,e.** Addition of 10 equiv of $\text{PtCl}_2(\text{cod})$ to a THF or CH_2Cl_2 solution of **1a** causes a color change of the

(5) (a) Woodward, P.; Dahl, L. F.; Abel, E. W.; Crosse, B. C. *J. Am. Chem. Soc.* **1965**, *87*, 5251. (b) Abel, E. W.; Crosse, B. C. *J. Chem. Soc. A* **1966**, 1377. (c) Kunchur, N. R. *Acta Crystallogr. B* **1968**, *24*, 1623. (d) Gould, R. O.; Harding, M. M. *J. Chem. Soc. A* **1970**, 875. (e) Dance, I. G.; Scudder, M. L.; Secomb, R. *Inorg. Chem.* **1985**, *24*, 1201.

(6) Rauchfuss, T. B.; Roundhill, D. M. *J. Am. Chem. Soc.* **1975**, *97*, 3386.

(7) (a) Bulman Page, P. C.; Klair, S. S.; Brown, M. P.; Harding, M. M.; Smith, C. S.; Maginn, S. J.; Muley, S. *Tetrahedron Lett.* **1988**, *29*, 4477. (b) Briant, C. E.; Gardner, C. J.; Andy Hor, T. S.; Howells, N. D.; Mingos, D. M. P. *J. Chem. Soc., Dalton Trans.* **1984**, 2645.

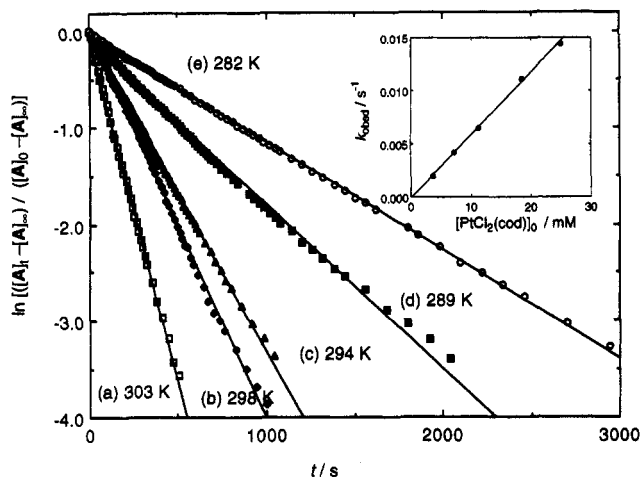
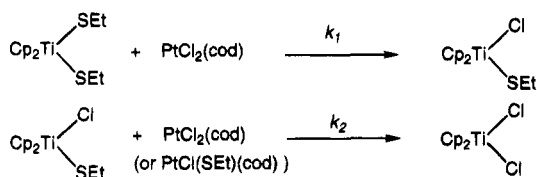


Figure 3. Pseudo-first-order plots of the reaction of **1a** and $\text{PtCl}_2(\text{cod})$ in THF at several temperatures. The reaction was followed by the decrease in the peak due to $\text{Cp}_2\text{TiCl}(\text{SEt})$ during the reaction. The dependence of k_{obsd} on $[\text{PtCl}_2(\text{cod})]_0$ in CH_2Cl_2 at 27 °C is shown in inset. Detailed kinetic data are summarized in Table 1.

solution from purple to red. The absorption spectrum of the solution after completion of the reaction shows a peak at 370 nm that is assigned to Cp_2TiCl_2 . Figure 2 shows change of the absorption spectra during the reaction of **1a** with 10 equiv of $\text{PtCl}_2(\text{cod})_2$ (3.5 mM) at 9 °C. The peak at 530 nm due to **1a** disappears immediately on addition of $\text{PtCl}_2(\text{cod})_2$ to give rise to a new peak at 500 nm which decreases gradually in intensity accompanied by growth of the peak due to Cp_2TiCl_2 . An isosbestic point at 420 nm is observed throughout the reaction. The peak at 500 nm observed during the reaction is assigned to $\text{Cp}_2\text{TiCl}(\text{SEt})$ since the complex prepared independently from the reaction of Cp_2TiCl_2 and NaSEt also shows a peak at the same position. On the basis of these observations, the whole reaction is considered to involve initial formation of $\text{Cp}_2\text{TiCl}(\text{SEt})$ and the ensuing reaction of the complex with $\text{PtCl}_2(\text{cod})$ or $\text{PtCl}(\text{SEt})(\text{cod})$ to give Cp_2TiCl_2 .



The former reaction occurs too fast to be followed by the corresponding spectroscopic change, while the latter reaction proceeds with a moderate reaction rate that can be estimated by decrease of the peak due to $\text{Cp}_2\text{TiCl}(\text{SEt})$ in the reaction mixture. Figure 3 shows pseudo-first-order plots which keep good linearity until ca. 85% conversion. The rate constants under various conditions are summarized in Table 1. The observed kinetic constants, k_{obsd} , are proportional with initial concentration of $\text{PtCl}_2(\text{cod})$, indicating that the reaction obeys first-order kinetics both with respect to $[\text{Cp}_2\text{TiCl}(\text{SEt})]$ and $[\text{PtCl}_2(\text{cod})]$.⁸ The kinetic parameters of the reac-

tion are obtained from the temperature dependence of the rate constants as $E_a = 57.4 \text{ kJ mol}^{-1}$, $\Delta H^\ddagger = 54.8 \text{ kJ mol}^{-1}$, $\Delta S^\ddagger = -106 \text{ J mol}^{-1} \text{ K}^{-1}$, and $\Delta G^\ddagger = 86.3 \text{ kJ mol}^{-1}$ at 298 K. Interpolation of the Arrhenius plots shows that the k_{obsd} value of the reaction of **1a** with excess $\text{PtCl}_2(\text{cod})$ (3.5 mM) at 22.7 °C should be 3.85 (s^{-1}). On the other hand, reaction of $\text{Cp}_2\text{TiCl}(\text{SEt})$, prepared separately, with $\text{PtCl}_2(\text{cod})$ under similar conditions proceeds with pseudo-first-order kinetics with k_{obsd} of 4.02 (s^{-1}). Similarity of the rate constants of both reactions indicates that the reaction of **1a** with $\text{PtCl}_2(\text{cod})$ does involve intermediate $\text{Cp}_2\text{TiCl}(\text{SEt})$ whose reaction with Pt complex giving Cp_2TiCl_2 is the rate-determining step of the whole reaction.

Reaction of **1b** with excess $\text{PtCl}_2(\text{cod})$ proceeds similarly to give Cp_2TiCl_2 , although both formation of $\text{Cp}_2\text{TiCl}(\text{S-}i\text{-Pr})$ and subsequent reaction giving Cp_2TiCl_2 proceed more slowly than the corresponding reactions observed with **1a** and $\text{PtCl}_2(\text{cod})$. Spectroscopic study reveals that conversion of $\text{Cp}_2\text{TiCl}(\text{S-}i\text{-Pr})$ into Cp_2TiCl_2 obeys pseudo-first-order kinetics to give kinetic parameters of $E_a = 62.3 \text{ kJ mol}^{-1}$, $\Delta H^\ddagger = 59.8 \text{ kJ mol}^{-1}$, $\Delta S^\ddagger = -124 \text{ J mol}^{-1} \text{ K}^{-1}$, and $\Delta G^\ddagger = 96.7 \text{ kJ mol}^{-1}$ at 298 K, respectively.

Kinetic study on reaction of **1e** with $\text{PtCl}_2(\text{cod})$ was not feasible, since the spectroscopic change of the reaction was completed within a few seconds even below 10 °C. Reaction of **1f** with excess $\text{PtCl}_2(\text{cod})$ in THF is slower than that of **1e**. Figure 4 shows spectroscopic change involving a simple decrease of the peak at 535 nm due to **1f** accompanied by concomitant growth of a peak at 370 nm assigned to Cp_2TiCl_2 . It is contrast with the reactions of **1a,b** which show stepwise spectroscopic change. Decrease in the peak intensity at constant temperature indicates that the reaction obeys 0.5th-order kinetics with respect to **1f** rather than simple first-order kinetics. Figure 5 shows linear plots of the reaction according to the 0.5th-order kinetics.⁹ Previous studies have already revealed that **1f** has a structure containing two $\text{Cp}_2\text{Ti}(\text{SCH}_2\text{CH}_2\text{S})$ units which are bound to each other through two $\text{S} \cdots \text{Ti}$ bonds.^{10,11} Although **1f** undergoes rapid and reversible dissociation of two $\text{Cp}_2\text{Ti}(\text{SCH}_2\text{CH}_2\text{S})$ units and their reassociation the equilibrium favors the dimer structure in the solution. On the basis of these observations, the kinetic results are interpreted by assuming that the reaction involves initial dissociation of $\text{Cp}_2\text{Ti}(\text{SCH}_2\text{CH}_2\text{S})$ units from **1f** as the rate-determining step. The ensuing ligand exchange proceeds much more rapidly since no peaks other than those for **1f** and Cp_2TiCl_2 are observed during the reaction.

Reaction of $\text{PtCl}_2(\text{cod})$ with $\text{Cp}_2\text{Ti}(\text{SR})_2$ in Toluene. Although equimolar reactions of the bis(thiolato)-titanocene complexes with $\text{PtCl}_2(\text{cod})$ in THF or CH_2Cl_2 cause thiolato ligand transfer from Ti to Pt centers as shown above, similar reactions in *toluene* lead to forma-

(9) Attempts to determine the relationship between k_{obsd} and $[\text{PtCl}_2(\text{cod})]_0$ were not successful since the reaction is completed in few seconds in CH_2Cl_2 , which dissolves sufficient amounts of $\text{PtCl}_2(\text{cod})$. It is not clear why the reaction rates differ remarkably depending on the solvent used, while reaction of **1a** with $\text{PtCl}_2(\text{cod})$ shows similar rate constants in CH_2Cl_2 and in THF.

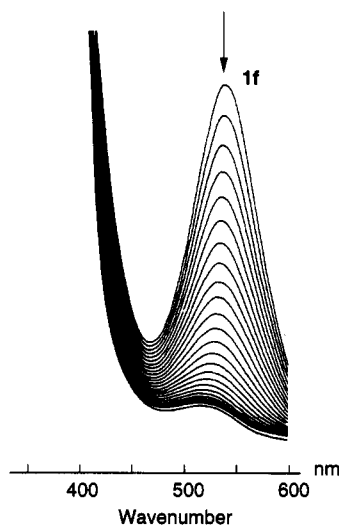
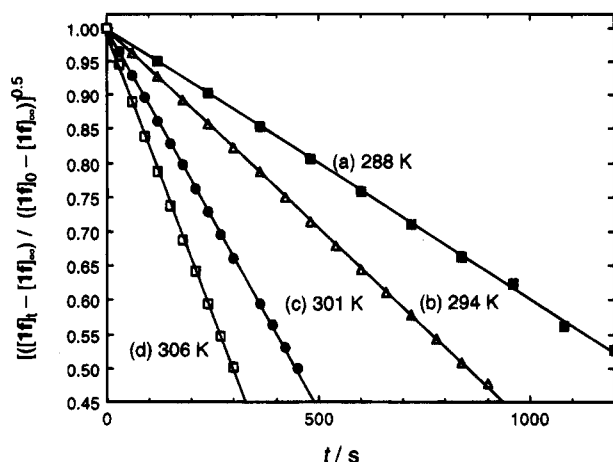
(10) Nadasdi, T. T.; Stephan, D. W. *Organometallics* **1992**, *11*, 116.

(11) $\text{Cp}_2\text{Ti}(\text{SEt})_2$ has a mononuclear structure in the solid state. See: Calhorda, M. J.; de C. T. Carrondo, M. A. F.; Dias, A. R.; Frazão, C. F.; Hursthouse, M. B.; Martinho Simões, J. A.; Teixeira, C. *Inorg. Chem.* **1988**, *27*, 2513.

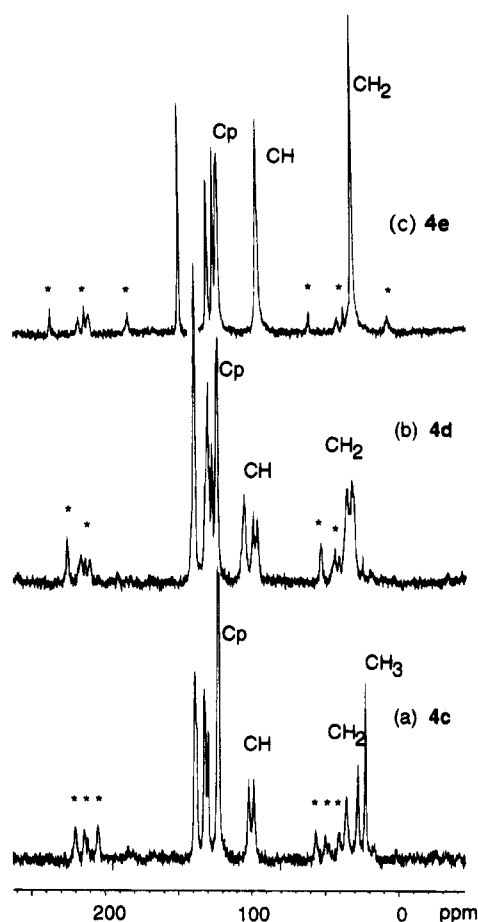
(8) Measurement on the temperature dependence of rate constants was carried out in THF, while the relationship of proportionality between the rate constants and $[\text{PtCl}_2(\text{cod})]$ was confirmed by kinetic results of the reaction in CH_2Cl_2 due to the limited solubility of the Pt complex in THF.

Table 1. Observed Rate Constants k_{obsd} , of Reactions of $\text{PtCl}_2(\text{cod})$ with **1a,b**

run	no., $[\text{Cp}_2\text{Ti}(\text{SR})_2]_0$ (M)	$[\text{PtCl}_2(\text{cod})]_0$ (M)	solvent	temp (K)	k_{obsd} (s^{-1})	$k_{\text{obsd}}/[\text{PtCl}_2(\text{cod})]_0$
1	1a , 0.347×10^{-3}	3.47×10^{-3}	THF	281.5	1.15×10^{-3}	3.31×10^{-1}
2	1a , 0.345×10^{-3}	3.48×10^{-3}	THF	283.6	1.56×10^{-3}	4.48×10^{-1}
3	1a , 0.297×10^{-3}	3.53×10^{-3}	THF	288.6	1.92×10^{-3}	5.44×10^{-1}
4	1a , 0.358×10^{-3}	3.51×10^{-3}	THF	293.6	3.55×10^{-3}	1.01
5	1a , 0.349×10^{-3}	3.47×10^{-3}	THF	298.2	3.86×10^{-3}	1.11
6	1a , 0.353×10^{-3}	3.38×10^{-3}	THF	303.0	7.65×10^{-3}	2.26
7	1a , 0.347×10^{-3}	3.75×10^{-3}	CH_2Cl_2	300.7	1.96×10^{-3}	5.23×10^{-1}
8	1a , 0.345×10^{-3}	7.24×10^{-3}	CH_2Cl_2	300.7	4.17×10^{-3}	5.76×10^{-1}
9	1a , 0.349×10^{-3}	1.13×10^{-2}	CH_2Cl_2	300.7	6.43×10^{-3}	5.69×10^{-1}
10	1a , 0.341×10^{-3}	1.84×10^{-2}	CH_2Cl_2	300.7	1.11×10^{-2}	6.03×10^{-1}
11	1a , 0.349×10^{-3}	2.49×10^{-2}	CH_2Cl_2	300.7	1.44×10^{-2}	5.78×10^{-1}
12	2a , 0.342×10^{-3}	3.44×10^{-3}	THF	300.7	8.78×10^{-6}	2.55×10^{-2}
13	2a , 0.353×10^{-3}	3.41×10^{-3}	THF	309.7	1.72×10^{-4}	5.04×10^{-2}
14	2a , 0.355×10^{-3}	3.44×10^{-3}	THF	312.4	2.42×10^{-4}	7.03×10^{-2}
15	2a , 0.351×10^{-3}	3.41×10^{-3}	THF	318.6	3.48×10^{-4}	1.02×10^{-1}

Figure 4. Change in the absorption spectra of the reaction mixture of **1f** (0.35 mM) and $\text{PtCl}_2(\text{cod})$ (3.5 mM) in THF at 20 °C.Figure 5. Plots of the reaction of **1f** (0.35 mM) with $\text{PtCl}_2(\text{cod})$ (3.5 mM) at several temperatures according to 0.5th-order kinetics.

tion of the complexes containing both Pt and Ti centers. Reactions of **1c,d** with equimolar $\text{PtCl}_2(\text{cod})$ in toluene cause deposition of pale yellow solids formulated as $\text{Cp}_2\text{Ti}(\text{SC}_6\text{H}_4\text{-}p\text{-Me})_2\text{PtCl}_2(\text{cod})$ (**4c**) and $\text{Cp}_2\text{Ti}(\text{SPh})_2\text{PtCl}_2(\text{cod})$ (**4d**), respectively. Elemental analyses of the products agree well with the proposed formula. Figure 6 shows CP-MAS ^{13}C NMR spectra of **4c,d** in the solid state. The signal due to Cp carbons appear as a single peak. The CH carbon signal of the cod ligand of **4c**

Figure 6. CP-MAS ^{13}C NMR spectra of (a) **4c**, (b) **4d**, and (c) **4e** (67.5 MHz). The peaks with asterisks are due to spinning side bands.

appear as two peaks with equal intensity, while the corresponding signal of **4d** is separated into three peaks with a ca. 2:1:1 peak area ratio. Both complexes show two peaks with equal intensity due to magnetically nonequivalent CH_2 carbons. The above NMR data of carbons of the cod ligand indicate unsymmetrical coordination around the Pt center. Further characterization of the complexes by ^1H and ^{13}C NMR in solutions was not feasible because dissolution of **4c,d** in THF or CH_2Cl_2 caused gradual color change of the solutions to give a mixture of Cp_2TiCl_2 and **3c** or **4c** as the final product. On the basis of the above analytical and solid state NMR spectra of the complexes, several structures could be proposed for **4c,d** although it is not possible at present to determine the molecular structures unambiguously.

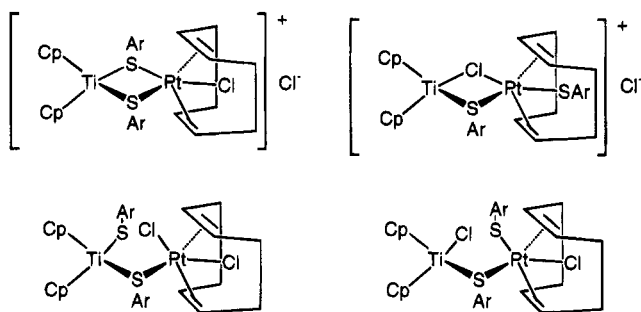
Chart 1. Proposed Structures for **4c,d**

Chart 1 summarizes possible structures of the complexes containing both the titanocene and Pt(cod) units. The Ti and Pt centers seem to be bonded through one or two bridging thiolato ligands since there have been a number of stable heterobimetallic complexes containing early and late transition metals which are bonded through bridging thiolato ligands.¹²⁻¹⁸ Both of the above cationic structures containing two bridging ligands and those with one bridging thiolato ligand have pentacoordinated Pt center. These structures agree with the ¹³C NMR spectra of the complexes showing unsymmetrical coordination around the Pt center. The other neutral structure with two bridging Cl or SAr ligands is much less plausible since it requires a hexacoordinated Pt(II) center with 20 electrons.

Reaction of **1e** with equimolar PtCl₂(cod) in toluene also affords Cp₂Ti(SC₆H₄S)PtCl₂(cod) (**4e**) which gives satisfactory analytical results. The ¹³C NMR spectrum in Figure 6c shows simple peaks due to carbons of the cod ligands. It is not clear whether **4e** has a structure similar to **4c,d**.

Discussion

Reaction of bis(thiolato)titanocene complexes with PtCl₂(cod) causes a smooth reaction involving thiolato transfer regardless the kind of the thiolato groups. Complexes **1a,b** react with PtCl₂(cod) to give multinuclear homoleptic (thiolato)platinum(II) complexes formulated as [Pt(SR)₂]_n, while similar reactions of **1c,d** give mononuclear Pt complexes, Pt(SAr)₂(cod). The difference in the products depending on the thiolato group is caused by the higher basicity of SET and S-*i*-Pr ligands, which have a greater tendency to coordinate as bridging ligands than SAr ligands. Kinetic studies on reactions of **1a,b** with PtCl₂(cod) under pseudo-first-order conditions have revealed several characteristics of the thiolato ligand transfer to give chlorotitanocene complexes. These results indicate that the transfer of the remaining thiolato ligand in Cp₂TiCl(SR) is caused

(12) Cameron, T. S.; Prout, C. K.; Rees, G. V.; Green, M. L. H.; Joshi, K. K.; Davies, G. R.; Kilbourn, B. T.; Braterman, P. S.; Wilson, V. A. *J. Chem. Soc., Chem. Commun.* **1971**, 14.

(13) Sato, M.; Yoshida, T. *J. Organomet. Chem.* **1975**, *94*, 403.

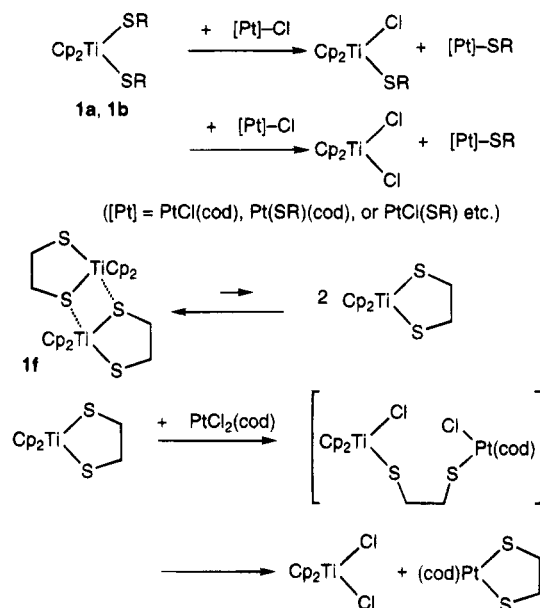
(14) Werner, H.; Ulrich, B.; Schubert, U.; Hofmann, P.; Zimmer-Gasser, B. *J. Organomet. Chem.* **1985**, *297*, 27.

(15) Ruffing, C. J.; Rauchfuss, T. B. *Organometallics* **1985**, *4*, 524.

(16) Douglas, W. E.; Green, M. L. H. *J. Chem. Soc., Dalton Trans.* **1972**, 1796.

(17) Darensbourg, M. Y.; Pala, M.; Houliston, S. A.; Kidwell, K. P.; Spencer, D.; Chojnacki, S. S.; Reibenspies, J. H. *Inorg. Chem.* **1992**, *31*, 1487.

(18) (a) White, G. S.; Stephan, T. W. *Organometallics* **1987**, *6*, 2169. (b) Wark, T. A.; Stephan, D. W. *Inorg. Chem.* **1987**, *26*, 363. (c) *Organometallics* **1989**, *8*, 2836. (d) Rousseau, R.; Stephan, D. W. *Organometallics* **1991**, *10*, 3399. (e) Wark, T. A.; Stephan, D. W. *Inorg. Chem.* **1990**, *29*, 1731. (f) *Inorg. Chem.* **1994**, *33*, 1532.

Scheme 2. Pathways for Reactions of **1a,b,f** with PtCl₂(cod)

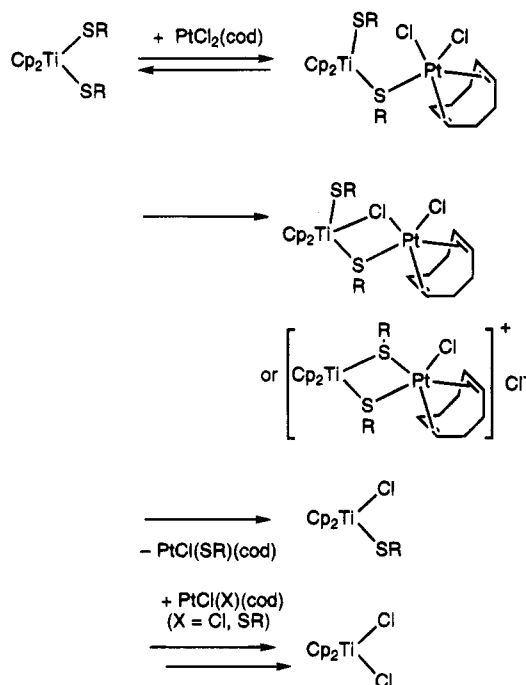
by interaction with the Pt complexes.¹⁹ Reaction of Cp₂TiCl(SEt) with PtCl₂(cod) is faster than that of Cp₂TiCl(S-*i*-Pr) due to smaller steric hindrance of the SEt ligand than the S-*i*-Pr ligand. Large negative entropy values of both reactions agree well with an associative pathway of the reaction in which a complex with bridging thiolato ligands plays an important role as the intermediate or the transition state.

Kinetic study on reaction of **1f** with PtCl₂(cod) revealed 0.5th-order kinetics with respect to [**1f**], indicating that the rate-determining step of the reaction involves dissociation of two Cp₂Ti(SCH₂CH₂S) units from dinuclear **1f**. The net reaction rate of thiolato ligand transfer from Cp₂Ti(SCH₂CH₂S) was not determined since the preceding dissociation from the dimer is slower even than SET group transfer from Cp₂TiCl(SEt) to PtCl₂(cod) as judged from comparison of half-life time of the reactions under similar conditions. On the other hand, reactions of **1e** with PtCl₂(cod) and of **1f** with PtCl₂(cod) in THF are completed within a few seconds below 10 °C to give Cp₂TiCl₂. The corresponding spectroscopic change does not show any peaks due to intermediate titanocene complexes in the reaction mixture. All these results indicate that transfer of the chelating thiolato ligand occurs rapidly. Scheme 2 compares pathways of the reaction of the chelating and non-chelating bis(thiolato)titanocene complex. Reaction of PtCl₂(cod) with **1f** involves initial transfer of a coordinated sulfur atom on Ti to the Pt center to give Cp₂TiCl(μ-SCH₂CH₂S)PtCl(cod) that undergoes facile intramolecular transfer of the second sulfur atom on Ti to Pt.

On the basis of the kinetic results, thiolato ligand transfer from Cp₂TiCl(SR) (R = Et, *i*-Pr) to PtCl₂(cod) proceeds through associative transition state. Reactions of Cp₂Ti(SR)₂ with PtCl₂(cod) giving Cp₂TiCl(SR) also

(19) Poor reactivity of PtMe₂(cod) with **1a** may suggest the pathway of the reaction of **1a** with PtCl₂(cod) involving a cationic intermediate because neutral heterobimetallics containing Ti(IV) and Pt(II) centers bridged by Me ligand are stable to some extent. See: Ozawa, F.; Park, J. W.; Mackenzie, P. B.; Schaefer, W. P.; Henling, L. M.; Grubbs, R. H. *J. Am. Chem. Soc.* **1989**, *111*, 1319.

Scheme 3. Proposed Mechanism of the Thiolato Ligand Transfer



seem to proceed through an associative pathway. Scheme 3 shows a possible reaction mechanism of thiolato ligand transfer from $\text{Cp}_2\text{Ti}(\text{SR})_2$ to Pt complex to give $\text{Cp}_2\text{TiCl}(\text{SR})$. The most convincing mechanism involves metathesis-like ligand exchange through a four-membered ring transition state containing Pt, S, Ti, and Cl atoms. Another mechanism through a cationic intermediate containing Ti and Pt centers which are bonded through two bridging thiolato ligands is also possible. According to the mechanism, $[\text{Cp}_2\text{Ti}(\text{SR})]^+$ formed after transfer of one thiolato ligand would react with Cl^- dissociated from the complex to give $\text{Cp}_2\text{TiCl}(\text{SR})$.²⁰

Reactions of **1c,d** with $\text{PtCl}_2(\text{cod})$ in *toluene* give heterobimetallic complexes **4c,d**, which release Cp_2TiCl_2 and $\text{Pt}(\text{SAr})_2(\text{cod})$ on dissolution in THF or in CH_2Cl_2 . The results indicate facile formation of heterobimetallics containing Ti(IV) and Pt(II) centers bridged by thiolato ligands, while it is not clear at present whether **4c,d** are actual intermediates of thiolato transfer in the reaction of **1c,d** with $\text{PtCl}_2(\text{cod})$ in THF and in CH_2Cl_2 .

Experimental Section

General Materials and Measurements. All the manipulations of the complexes were carried out under nitrogen or argon using standard Schlenk technique. The solvents were dried by the usual method, distilled, and stored under nitrogen. Complexes **1a-f**, $\text{Cp}_2\text{TiCl}(\text{SEt})$, $\text{PtCl}_2(\text{cod})$, and $\text{PtMe}_2(\text{cod})$ were prepared according to the literature.²¹⁻²⁴ (Thiolato)-platinum complexes **3c,e,f** were prepared from reaction of $\text{PtCl}_2(\text{cod})$ with sodium thiolate or thiol in the presence of NET_3

(20) The kinetic results do not agree with another pathway involving initial disproportionation of $\text{Cp}_2\text{TiCl}(\text{SR})$ followed by further reaction of formed $\text{Cp}_2\text{Ti}(\text{SR})_2$ with Pt complexes.

(21) (a) Köpf, H.; Schmidt, M. *J. Organomet. Chem.* **1965**, *4*, 426. (b) *Ibid.* *Z. Anorg. Allg. Chem.* **1965**, *340*, 139. (c) Klapötke, T.; Köpf, H. *Inorg. Chim. Acta* **1987**, *133*, 115.

(22) Coutts, R. S. P.; Surtees, J. R.; Swan, J. M.; Wailes, P. C. *Aust. J. Chem.* **1966**, *19*, 1377.

(23) Chaudhari, M. A.; Stone, F. G. A. *J. Chem. Soc. A* **1966**, 838.

(24) Giddings, S. A. *Inorg. Chem.* **1967**, *6*, 849.

in order to compare spectroscopic data with the reaction product. Analytical and spectroscopic results of new complexes are as follows. **3c**: Anal. Calcd for $\text{C}_{22}\text{H}_{26}\text{PtS}_2$: C, 48.1; H, 4.8. Found: C, 48.2; H, 5.3. ^1H NMR (C_6D_6): δ 2.31 (s, 6H, CH_3), 1.9–2.7 (m, 8H, CH_2), 4.62 (br, 4H, CH, $J(\text{PtH}) = 53$ Hz), 7.03 (d, 4H, $J = 7$ Hz, aromatic), 7.34 (d, 4H, aromatic). ^{13}C NMR (CD_2Cl_2): δ 21.1 (CH_3), 30.6 (CH_2), 99.5 (CH, $J(\text{PtH}) = 120$ Hz), 129.3, 132.8, 136.4, and 137.0 (aromatic). **3e**: ^1H NMR (C_6D_6): δ 2.57 and 2.68 (m, 8H, CH_2), 5.50 (br, 4H, CH, $J(\text{PtH}) = 54$ Hz), 5.89 and 7.49 (ABq, 4H, aromatic). ^{13}C NMR (CD_2Cl_2): δ 30.4 (CH_2), 92.5 (CH, $J(\text{PtH}) = 116$ Hz), 122.9, 127.9, and 145.9 (aromatic). **3f**: Anal. Calcd for $\text{C}_{10}\text{H}_{16}\text{PtS}_2$: C, 30.4; H, 4.1. Found: C, 30.3; H, 4.7. ^1H NMR (C_6D_6): δ 2.43 and 2.55 (m, 8H, cod CH_2), 2.70 (s, 4H, SCH_2 , $J(\text{PtH}) = 52$ Hz), 5.10 (br, 4H, CH, $J(\text{PtH}) = 54$ Hz). ^{13}C NMR (CD_2Cl_2): δ 30.5 (CH_2), 40.6 (s, SCH_2), 94.9 (CH, $J(\text{PtH}) = 111$ Hz). IR spectra were recorded on a JASCO-IR810 spectrophotometer. NMR spectra (^1H and ^{13}C) were recorded on JEOL EX-90 and GX-500 spectrometers. CP-MAS ^{13}C NMR spectra were obtained on a JEOL GX-270 spectrometer. Absorption spectra were obtained by a Hitachi 200-20 spectrophotometer equipped with a thermostated control for the water jacket. Elemental analyses were carried out by a Yanagimoto Type MT-2 CHN autocorder.

Reactions of $\text{PtCl}_2(\text{cod})$ with **1a,b in THF.** To a mixture of $\text{PtCl}_2(\text{cod})$ (95 mg, 0.25 mmol) and **1a** (77 mg, 0.26 mmol) was added THF (3 mL) at room temperature. The purple reaction mixture was soon turned into a red solution from which was gradually deposited a pale yellow solid. After further reaction for 12 h the formed solid was filtered out, washed repeatedly with Et_2O , and dried in vacuo to give $[\text{Pt}(\text{SEt})_2]_n$ (**2a**) (65 mg, 82%). Anal. Calcd for $(\text{C}_4\text{H}_{10}\text{PtS}_2)_n$: C, 15.1; H, 3.2. Found: C, 16.9; H, 3.1.²⁵ ^{13}C NMR (in the solid state using the CP-MAS technique): δ 24.7 (CH_3), 30.1 (CH_2). The ^1H NMR spectrum of the filtrate shows formation of Cp_2TiCl_2 in a high yield (>90%).

Similar reaction with **1b** gave **2b** (63%). Anal. Calcd for $(\text{C}_6\text{H}_{14}\text{PtS}_2)_n$: C, 20.9; H, 4.1. Found: C, 21.4; H, 3.7. ^{13}C NMR (in the solid state using the CP-MAS technique): δ 41.2 (CH), 26.5 (CH_3).

Reaction of $\text{PtCl}_2(\text{cod})$ with **1c,d in THF.** To a mixture of **1c** (200 mg, 0.47 mmol) and $\text{PtCl}_2(\text{cod})$ (180 mg, 0.48 mmol) was added THF (5 mL) at room temperature. The color of the solution soon turned from purple to orange. On further stirring an orange solid was gradually deposited. After reaction for 24 h, the formed solid was filtered out, washed with hexane, and dried in vacuo to give **3e** (260 mg, 96%). The ^1H and ^{13}C NMR spectra agreed with authentic samples of **3e**. The ^1H NMR spectrum of the filtrate indicates formation of Cp_2TiCl_2 in high yield (>90%).

Reaction with **1d** was carried out analogously to give a mixture of Cp_2TiCl_2 and $\text{Pt}(\text{SPh})_2(\text{cod})$ (**3e**).

Reactions of $\text{PtCl}_2(\text{cod})$ with **1e,f in THF.** To a mixture of $\text{PtCl}_2(\text{cod})$ (66 mg, 0.18 mmol) and **1e** (56 mg, 0.18 mmol) was added THF (5 mL) at room temperature. The color of the solution changed from deep green to red in 5 min. A yellow solid which was deposited within 1 h from the reaction mixture was filtered out and dried in vacuo (44 mg). The ^1H and ^{13}C NMR spectra of the product indicated the presence of **3e** and a small amount of Cp_2TiCl_2 based on comparison of the spectra with those of authentic sample.

Reaction with **1f** was carried out similarly to give an orange solid after stirring for 12 h. The ^1H NMR spectrum showed the presence of Cp_2TiCl_2 and **3e** in almost quantitative yields although isolation of the complexes by fractional crystallization was not feasible due to similar solubilities of the complexes.

Crystallographic Study of **3e.** A yellow single crystal with dimension of $0.2 \times 0.4 \times 0.4$ mm obtained from a THF-

(25) Elemental analyses of **2a** always show somewhat higher carbon content than calculated based on the formula. This may be due to the presence of a small amount of THF that is hardly removed probably due to strong interaction with the complex.

hexane mixture was sealed in a capillary under argon. Crystal data: $C_{14}H_{16}PtS_2$, $M_w = 443.49$, orthorhombic, space group *Pnma* (No. 62), $a = 14.187(8)$ Å, $b = 11.534(5)$ Å, $c = 8.262(5)$ Å, $V = 1351$ Å³, $Z = 4$, $D_c = 2.179$ g cm⁻³, $\mu(\text{Mo K}\alpha) = 106.20$ cm⁻¹ (graphite monochromated), $\lambda = 0.71069$ Å, $F(000) = 840$. The data were collected on a Rigaku AFC5R diffractometer at ambient temperature (288 K) using the ω scan mode ($2\theta \leq 55^\circ$). The data were corrected for Lorentz and polarization effects, and an empirical absorption correction (ψ scan) was carried out. The structure was solved by direct methods (SAPI 91). Of the unique 1812 reflections, 1352 reflections with $I > 3\sigma(I)$ were used in the refinement. A total of 79 parameters were refined, and the structure converged to $R = 0.064$ and $R_w = 0.078$.

Kinetic Measurements. An optical cell equipped with an Ar inlet and rubber septum containing a THF (3 mL) solution of **1a** (0.35 mM) was set in a spectrometer with a thermostated water jacket. After the cell was kept at a constant temperature for 2 h, a solution of **1a** was injected by a syringe through rubber septum. The spectroscopic change was followed by measurement of intensity of absorption at a fixed wavelength.

Reactions of $PtCl_2(\text{cod})$ with **1c,d in Toluene.** To a mixture of $PtCl_2(\text{cod})$ (160 mg, 0.43 mmol) and **1c** (180 mg, 0.42 mmol) was added toluene (7 mL) at room temperature. Stirring the mixture at room temperature for 16 h caused a color change of the mixture from purple to red accompanied by a pale red solid. Filtration of the solid followed by repeated washing with hexane gave $Cp_2Ti(\text{SC}_6\text{H}_4\text{-}p\text{-Me})_2PtCl_2(\text{cod})$ (**4c**) (300 mg, 89%) as a pink solid. Anal. Calcd for $C_{32}H_{36}Cl_2PtS_2Ti$: C, 48.1; H, 4.5. Found: C, 48.1; H, 4.7. ¹³C NMR (in the solid state using the CP-MAS technique): δ 22.4 (CH₃), 27.5 and 35.9 (CH₂), 98.2 and 101.8 (CH), 122.1 (Cp), 129.5, 132.0, and 138.3 (aromatic).

Similar reaction with **1d** gave $Cp_2Ti(\text{SPh})_2PtCl_2(\text{cod})$ (**4d**) (77%). Anal. Calcd for $C_{30}H_{32}Cl_2PtS_2Ti$: C, 46.8; H, 4.2.

Found: C, 47.2; H, 4.0. ¹³C NMR (in the solid state using the CP-MAS technique): δ 40.4 and 33.6 (CH₂), 94.7, 97.5, and 103.8 (CH), 122.1 (Cp), 125.8, 128.5, and 138.1 (aromatic).

Reaction of $PtCl_2(\text{cod})$ with **1e in Toluene.** To a mixture of **1e** (98 mg, 0.31 mmol) and $PtCl_2(\text{cod})$ (120 mg, 0.31 mmol) was added toluene (5 mL) at room temperature. Stirring the mixture at room temperature for 15 min caused a color change of the mixture from green to brown. Further stirring for 12 h caused precipitation of an orange solid which was filtered out, washed with hexane, and dried in vacuo to give $Cp_2Ti(\text{SC}_6\text{H}_4\text{S})PtCl_2(\text{cod})$ (**4e**) (200 mg, 93%). Anal. Calcd for $C_{24}H_{26}Cl_2PtS_2Ti$: C, 41.6; H, 3.8. Found: C, 41.5; H, 3.7. ¹³C NMR (in the solid state using the CP-MAS technique): δ 30.4 (CH₂), 95.7 (CH), 122.0 (Cp), 125.3, 129.6, 148.9 (aromatic).

Acknowledgment. This work was supported by a Grant-in-Aid for Scientific Research from the Ministry of Education, Science, and Culture of Japan. The authors are grateful to Dr. Yoshiyuki Nakamura for the helpful measurement of CP-MAS ¹³C NMR spectra and to Dr. Masako Tanaka for the crystallographic study.

Supporting Information Available: Tables of crystallographic data for complex **3e** including atom coordinates, thermal parameters, and bond distances and angles (4 pages). This material is contained in many libraries on microfiche, immediately follows this article in the microfilm version of the journal, and can be ordered from the ACS; see any current masthead page for ordering information.

OM950394G

Synthesis and Structures of Trans-Chelating Chiral Diphosphine Ligands Bearing Aromatic *P*-Substituents, (*S,S*)-(*R,R*)- and (*R,R*)-(*S,S*)-2,2''-Bis[1-(diarylphosphino)ethyl]-1,1''-biferrocenes (ArylTRAPs), and Their Transition Metal Complexes

Masaya Sawamura,^{*,†} Hitoshi Hamashima, Masanobu Sugawara, Ryoichi Kuwano, and Yoshihiko Ito*

Department of Synthetic Chemistry and Biological Chemistry, Kyoto University, Kyoto 606-01, Japan

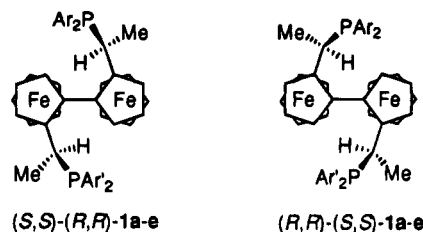
Received March 21, 1995[⊗]

The trans-chelating chiral phosphine ligand (*S,S*)-(*R,R*)-2,2''-bis[1-(diphenylphosphino)ethyl]-1,1''-biferrocene (**1a**, abbreviated to PhTRAP) was synthesized from (*S*)-1-(*N,N*-dimethylamino)ethylferrocene (**2**) in four steps in 51% overall yield. (*R,R*)-(*S,S*)-PhTRAP and other arylTRAP derivatives (**1b**, AnisTRAP; **1c**, Cl-PhTRAP, **1d**, FurTRAP; **1e**, Tol-PhTRAP) were synthesized in a similar manner. Through-space ³¹P–³¹P spin couplings were observed indirectly in the ¹H and ¹³C{¹H} NMR spectra of **1a–e** and directly in the ³¹P{¹H} NMR spectrum of asymmetrical TRAP **1e**, indicating that the two phosphorus atoms of the ligands are in close proximity. Results of NOE experiments showed that PhTRAP is a fairly rigid molecule and in a conformation favorable for trans-chelation. As square planar transition metal complexes bearing arylTRAPs as trans-chelating ligands, *trans*-[PdX₂{(*S,S*)-(*R,R*)-PhTRAP}] (**7**, X = Br; **8**, X = I; **9**, X = Cl), *trans*-[PtCl₂{(*R,R*)-(*S,S*)-PhTRAP}] (**10**), *trans*-[PtCl₂{(*S,S*)-(*R,R*)-**1e**}] (**11**), *trans*-[IrCl(CO){(*S,S*)-(*R,R*)-PhTRAP}] (**12**), *trans*-[RhCl(CO){(*S,S*)-(*R,R*)-PhTRAP}] (**13**), and *trans*-[RhCl(CO){(*S,S*)-(*R,R*)-FurTRAP}] (**14**) were prepared and fully characterized. X-ray crystal structures were determined for the palladium complex **7** and the rhodium complex **14**.

Introduction

Asymmetric synthesis catalyzed by chiral phosphine–transition metal complexes is an area of research that has been attracting a great deal of interest due to its high efficiency for the synthesis of optically active compounds.¹ Recent progress in this area has been prompted mostly by the molecular design and synthesis of new effective chiral phosphine ligands. Earlier, we reported the synthesis of trans-chelating chiral diphosphine, (*R,R*)-(*S,S*)-2,2''-bis[1-(diphenylphosphino)ethyl]-1,1''-biferrocene (**1a**, abbreviated to PhTRAP), which possesses planar chiralities as well as stereogenic centers, and this ligand proved to coordinate to palladium and platinum in bidentate trans-chelation manner.^{2–4} High chiral recognition ability of this ligand was demonstrated in the Rh-catalyzed asymmetric

Michael reaction of 2-cyanopropionates.⁵ Later, TRAP derivatives bearing flexible alkyl substituents on phosphorus atoms (alkylTRAPs) were prepared, and some of those were shown to be effective chiral ligands for the Rh-catalyzed asymmetric hydrosilylation of simple ketones.⁶ In this paper we wish to report the syntheses and structures of several TRAP derivatives bearing aromatic substituents on phosphorus atoms (**1a–e**, arylTRAPs) and their transition metal complexes.



- a: Ar = Ar' = Ph (PhTRAP)
 b: Ar = Ar' = *p*-MeO-Ph (AnisTRAP)
 c: Ar = Ar' = *p*-Cl-Ph (Cl-PhTRAP)
 d: Ar = Ar' = 2-Furyl (FurTRAP)
 e: Ar = Ph, Ar' = *p*-Tol (Tol-PhTRAP)

[†] Present address: Department of Chemistry, School of Science, The University of Tokyo, Tokyo 113, Japan.

[⊗] Abstract published in *Advance ACS Abstracts*, September 1, 1995.
 (1) For reviews, see: (a) Ojima, I., Ed. *Catalytic Asymmetric Synthesis*; VCH Publishers: New York, 1993. (b) Ojima, I.; Clos, N.; Bastos, C. *Tetrahedron* **1989**, *45*, 6901. (c) Noyori, R.; Kitamura, M. In *Modern Synthetic Methods*; Scheffold, R., Ed.; Springer-Verlag: Berlin, 1989; Vol. 5, p 115.

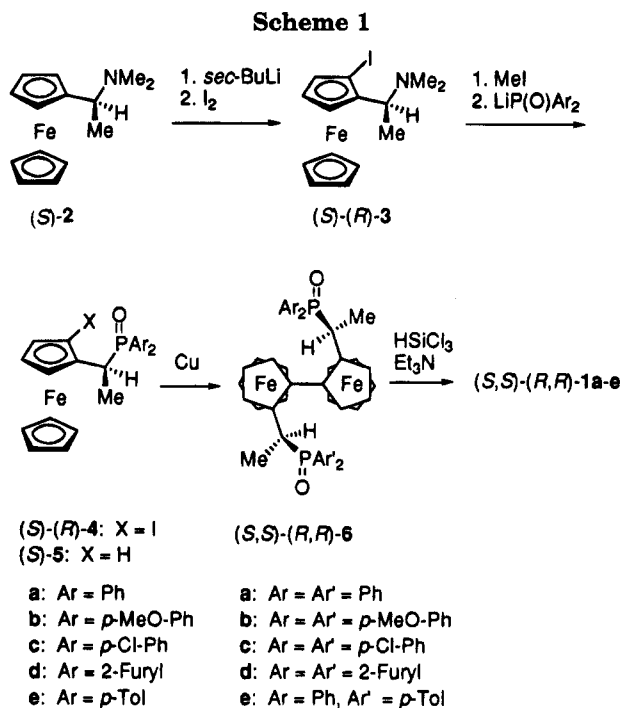
(2) Sawamura, M.; Hamashima, H.; Ito, Y. *Tetrahedron: Asymmetry* **1991**, *2*, 593.

(3) For terdentate chiral phosphine ligands spanning trans-positions, see: (a) Brown, J. M.; Chaloner, P. A.; Descotes, G.; Glaser, R.; Lafont, D.; Sinou, D. *J. Chem. Soc., Chem. Commun.* **1979**, 611. (b) Descotes, G.; Lafont, D.; Sinou, D.; Brown, J. M.; Chaloner, P. A.; Parker, D. *Nouv. J. Chim.* **1981**, *5*, 167. (c) Burk, M. J.; Feaster, J. E.; Harlow, R. L. *Tetrahedron: Asymmetry* **1991**, *2*, 569. (d) Gorla, F.; Venanzi, L. M. *Organometallics* **1994**, *13*, 43. (e) Gorla, F.; Togni, A.; Venanzi, L. M.; Albinati, A.; Lianza, F. *Organometallics* **1994**, *13*, 1607.

(4) For an achiral trans-chelating diphosphine, see: (a) DeStefano, N. J.; Johnson, D. K.; Venanzi, L. M. *Angew. Chem., Int. Ed. Engl.* **1974**, *13*, 133. (b) Bürgi, H.-B.; Murray-Rust, J.; Camalli, M.; Caruso, F.; Venanzi, L. M. *Helv. Chim. Acta* **1989**, *72*, 1293 and references cited therein.

(5) Sawamura, M.; Hamashima, H.; Ito, Y. *J. Am. Chem. Soc.* **1992**, *114*, 8295. (b) Sawamura, M.; Hamashima, H.; Ito, Y. *Tetrahedron* **1994**, *50*, 4439.

(6) Sawamura, M.; Kuwano, R.; Ito, Y. *Angew. Chem., Int. Ed. Engl.* **1994**, *33*, 111.



Results and Discussion

Synthesis of ArylTRAPs. The synthesis of (*S,S*)-(*R,R*)-arylTRAPs bearing different aromatic *P*-substituents is outlined in Scheme 1. For the synthesis of (*S,S*)-(*R,R*)-PhTRAP (**1a**), optically pure (*S*)-1-(*N,N*-dimethylamino)ethylferrocene (**2**)⁷ was converted into iodoferrrocene derivative (*S*)-(*R*)-**3** via diastereoselective ortholithiation with *sec*-BuLi and subsequent reaction with iodine [(*S*)-(*R*)-:*(S)*-(*S*) = 42:1].⁸ The crude mixture of **3** was treated with MeI and was then subjected to the substitution reaction with lithium diphenylphosphinite in refluxing MeCN to give a mixture of phosphine oxides (*S*)-(*R*)-**4a** and (*S*)-**5a**. The nucleophilic substitution reaction proceeded with complete retention of configuration at the stereogenic center.⁹ The homocoupling of **4a** was best performed with activated copper powder¹⁰ at 130 °C (neat), producing *C*₂-symmetric biferrocene (*S,S*)-(*R,R*)-**6a**. Finally, reduction of the phosphine oxide with HSiCl₃/Et₃N¹¹ afforded (*S,S*)-(*R,R*)-PhTRAP (**1a**) as an orange powder. Thus, the chiral ligand was synthesized in four steps in 51% overall yield starting with (*S*)-1-(*N,N*-dimethylamino)ethylferrocene (**2**),⁷ which is easily obtainable in large quantities in optically pure form for both enantiomers. The crude compounds **3** and **4a** were used for any further synthetic transformations. (*R,R*)-(*S,S*)-PhTRAP and other arylTRAP derivatives, which have *p*-methoxyphenyl (**1b**, AnisTRAP), *p*-chlorophenyl (**1c**, Cl-PhTRAP), or 2-furyl (**1d**, FurTRAP) groups on the phosphorus atoms, were synthesized in a similar man-

ner. For the synthesis of unsymmetrical TRAP **1e**, an equimolar mixture of **4a** and **4e** was subjected to the copper-promoted coupling. HPLC separation of three statistically formed coupling products gave pure **6e**.

Structure of ArylTRAPs. Full assignment of the ¹H (400 MHz) and ¹³C{¹H} (100 MHz) NMR spectra of (*S,S*)-(*R,R*)-PhTRAP (**1a**) in CDCl₃ has been done with the aid of ¹H{¹H} NOE (Table 1, Figure 1), HETCOR, HMBC, and ¹³C INADEQUATE (see supporting information for details of the assignment). Reflecting the *C*₂ symmetry of the molecule, each 2-[1-(diphenylphosphino)ethyl]ferrocenyl unit is equivalent in both ¹H and ¹³C{¹H} NMR spectra. In the ³¹P{¹H} NMR spectra (81 MHz, 85% H₃PO₄) of **1a** in CDCl₃ the resonance for two phosphorus atoms appeared at δ 2.19 ppm as a broad singlet. It is noteworthy that the resonance for the side chain α-methyl protons does not appear as a simple doublet and that most of the ¹³C resonances split into multiplet. Aromatic region of the ¹³C{¹H} NMR is shown in Figure 2. These data suggest that there exists a through-space ³¹P–³¹P spin coupling due to the close proximity of the two phosphorus atoms.^{12,13} The ³¹P–³¹P spin coupling was directly observed in the ³¹P{¹H} NMR spectrum of unsymmetrical TRAP **1e**, where the resonances for two phosphorus atoms appeared separately at δ 0.4 and 2.6 ppm as a set of doublets with a ³¹P–³¹P coupling constant of 22.0 Hz. Since the two phosphorus atoms are connected through seven σ-bonds, spin coupling through the bonds should not be taken into consideration. Such close proximity seems to be possible only for the conformation where the lone pairs of the two phosphorus atoms converge in the cavity created by four aromatic *P*-substituents and biferrocene backbone as depicted in Figure 1.

The NOE technique was used not only for the assignment of the ¹H NMR spectrum of (*S,S*)-(*R,R*)-PhTRAP (**1a**) but also for the conformational study in solution. Observed NOEs are summarized in Table 1. Figure 1 shows the view of the ligand in a conformation which is consistent with the NOEs. Selected NOEs are also shown in Figure 1. The irradiation of methyl protons (*H*_{Me}) gave rise to large NOE enhancements at ferrocenyl protons *H*₃ (18%) and at protons on unsubstituted Cp rings *H*_{Cp} (18%) together with a weak enhancement at *H*₅ (4%). On the other hand, the irradiation of *H*_α caused no NOE at *H*₃ while giving a large NOE enhancement at *H*₅ (12%) and a weak enhancement at *H*_{Cp} (3%). Upon irradiation of *H*₅ was obtained an NOE of 7% at *H*_α together with a large NOE at *H*_{Cp} (15%). The NOEs between the ferrocenyl protons *H*₅ and side chain protons (*H*_α, *H*_{Me}) should be attributed to the NOEs caused by the relaxation toward the other 2-[1-(diphenylphosphino)ethyl]ferrocenyl components. The large NOE from *H*₅ to *H*_{Cp} is also explained by considering the contribution of relaxation toward the *H*_{Cp} of the other ferrocenyl moiety. These NOEs described above and all other NOEs summarized in Table 1 are in good agreement with the conformation predicted in an earlier paper.²

(7) Marquarding, D.; Klusacek, H.; Gokel, G.; Hoffmann, P.; Ugi, I. *J. Am. Chem. Soc.* **1970**, *92*, 5389.

(8) Watanabe, M.; Araki, S.; Butsugan, Y.; Uemura, M. *J. Org. Chem.* **1991**, *56*, 2218.

(9) (a) Gokel, G. W.; Marquarding, D.; Ugi, I. *J. Org. Chem.* **1972**, *37*, 3052. (b) Hayashi, T.; Mise, T.; Fukushima, M.; Kagotani, M.; Nagashima, N.; Hamada, Y.; Matsumoto, A.; Kawakami, S.; Konishi, M.; Kamamoto, K.; Kumada, M. *Bull. Chem. Soc. Jpn.* **1980**, *53*, 1138.

(10) Fuson, R. C.; Cleveland, E. A. *Organic Syntheses*; Wiley: New York, **1955**; Collective Vol. 3, p. 339.

(11) Naumann, K.; Zon, G.; Mislow, K. *J. Am. Chem. Soc.* **1969**, *91*, 7012.

(12) Redfield, D. A.; Cary, L. W.; Nelson, J. H. *Inorg. Chem.* **1975**, *14*, 50.

(13) For through-space ³¹P–³¹P coupling, see: (a) Haenel, M. W.; Fieseler, H.; Jakubik, D.; Gabor, B.; Goddard, R.; Krüger, C. *Tetrahedron Lett.* **1993**, *34*, 2107. For through-space ¹⁹F–¹⁹F coupling, see: (b) Mallory, F. B.; Mallory, C. W.; Ricker, W. M. *J. Org. Chem.* **1985**, *50*, 457.

Table 1. $^1\text{H}\{^1\text{H}\}$ NOEs of (*S,S*)-(*R,R*)-PhTRAP (1a) in CDCl_3^a

irradiated position	enhancement, % ^b						
	H _{Me} (δ 1.35)	H α (δ 3.49)	H ₃ (δ 3.79)	H ₄ (δ 4.12)	H ₅ (δ 4.55)	H _{Cp} (δ 4.29)	H _{Ph} (δ 7.05–7.40)
H _{Me} (δ 1.35)		+15.9	+17.6	-1.8	+3.5	+17.6	+15.9
H α (δ 3.49)	+7.6		c	-0.8	+11.9	+3.4	+23.7, -3.4
H ₃ (δ 3.79)	+4.8	c		+12.8	-0.5	+3.7	+1.6
H ₄ (δ 4.12)	c	c	+11.4		+8.6	c	c
H ₅ (δ 4.55)	c	+6.9	-1.0	+12.9		+14.9	c

^a The experiment was performed at 200 MHz at ambient temperature. ^b Reduced values to one irradiated proton. ^c NOE was not observed.

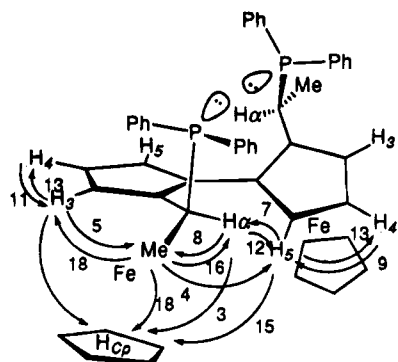


Figure 1. Selected $^1\text{H}\{^1\text{H}\}$ NOEs (% enhancement) of (*S,S*)-(*R,R*)-PhTRAP (1a) in CDCl_3 .

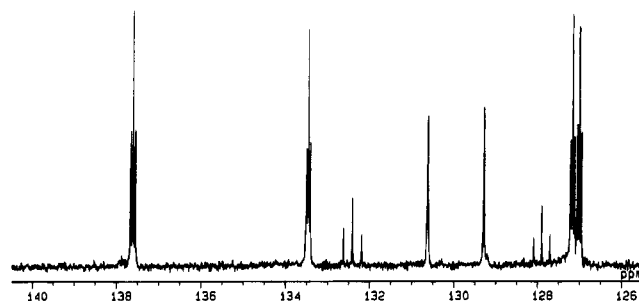


Figure 3. $^{13}\text{C}\{^1\text{H}\}$ NMR (100 MHz) spectrum of *trans*-[$\text{PdBr}_2\{(\text{S,S})\text{-}(\text{R,R})\text{-PhTRAP}\}$] (7) in CDCl_3 (phenyl region).

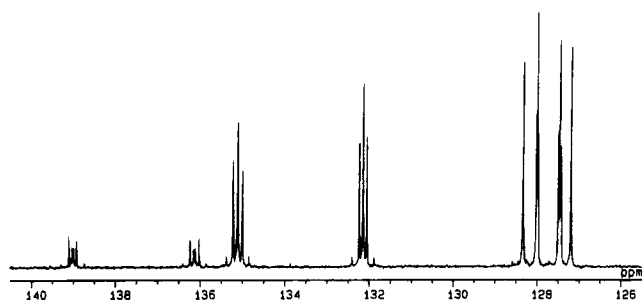


Figure 2. $^{13}\text{C}\{^1\text{H}\}$ NMR (100 MHz) spectrum of (*S,S*)-(*R,R*)-PhTRAP (1a) in CDCl_3 (phenyl region).

Although efforts to obtain an X-ray crystal structure were unsuccessful, results of the NOE study and the existence of through-space ^{31}P - ^{31}P spin coupling indicate that arylTRAPs are fairly rigid molecules and in a conformation favorable for *trans*-chelation.

Palladium Complexes. Reaction of (*S,S*)-(*R,R*)-PhTRAP with PdBr_2 in CH_2Cl_2 at room temperature formed *trans*-[$\text{PdBr}_2\{(\text{S,S})\text{-}(\text{R,R})\text{-PhTRAP}\}$] (7) exclusively. Two 2-[1-(diphenylphosphino)ethyl]ferrocenyl units were equivalent in both ^1H (400 MHz) and $^{13}\text{C}\{^1\text{H}\}$ (100 MHz) NMR spectra. The $^{31}\text{P}\{^1\text{H}\}$ NMR (81 MHz) showed a singlet peak at δ 29.9 ppm. In the $^{13}\text{C}\{^1\text{H}\}$ NMR spectrum, phosphorus-coupled resonances split into a 1:2:1 triplet (Figure 3). Such a triplet could be observed when a ^{13}C nucleus and two ^{31}P nuclei form an AXX' spin system and the two ^{31}P nuclei couple to each other with a large coupling constant.¹² Although the ^{31}P - ^{31}P coupling constant cannot be directly determined, the characteristic splitting of $^{13}\text{C}\{^1\text{H}\}$ NMR spectrum clearly indicates that the two chemically equivalent phosphorus atoms are bound to palladium in a *trans* manner. *trans*-[$\text{PdI}_2(\text{PhTRAP})$] (8) and *trans*-[$\text{PdCl}_2(\text{PhTRAP})$] (9) were similarly prepared from PdI_2 and $\text{PdCl}_2(\text{MeCN})_2$, respectively.

Trans-chelation of PhTRAP was confirmed by the X-ray crystal structure analysis of *trans*- $\text{PdBr}_2\{(\text{S,S})\text{-}(\text{R,R})\text{-PhTRAP}\}$ (7). An ORTEP drawing with atom-

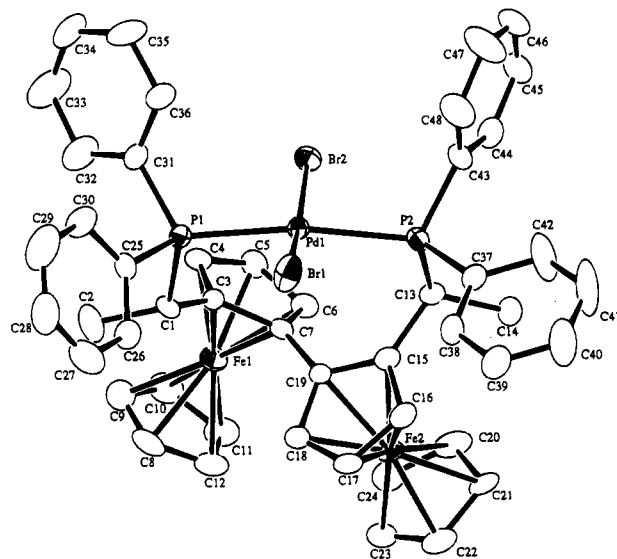


Figure 4. ORTEP drawing (30% probability level) and atom-labeling scheme for *trans*-[$\text{PdBr}_2\{(\text{S,S})\text{-}(\text{R,R})\text{-PhTRAP}\}$] (7) (hydrogen atoms are omitted for clarity).

labeling scheme is shown in Figure 4. Bond distances and angles are given in Table 2. The environment of the Pd atom is described as slightly distorted square planar with two *trans* phosphorus atoms and two *trans* bromine atoms. Bond angles P(1)-Pd(1)-P(2) and Br(1)-Pd(1)-Br(2) are 163.6(1) and 167.44(8)°, respectively. The bond distances of two Pd-P bonds and two Pd-Br bonds are normal. Two phosphorus atoms are located in the exo region of ferrocene, dihedral angles P(1)-C(1)-C(3)-C(7) and P(2)-C(13)-C(15)-C(19) being 92(1) and 100(1)°, respectively. The angle between the least-squares planes through the two linked Cp rings (C3-C7, C15-C19) is 121.4°. Another view normal to the virtual square plane is shown in Figure 5, where the deviation from C_2 symmetry is well visualized. For example, the orientation of four Ph groups is asymmetrical, and the σ -bonds connecting the two ferrocene units are not positioned on the imaginary C_2 axis. Such a deviation seems to be caused by the

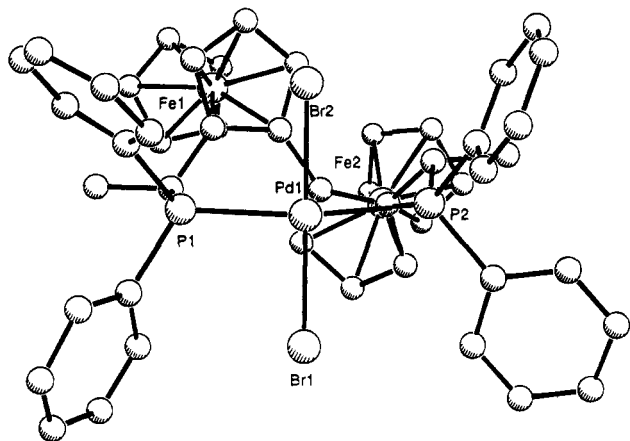


Figure 5. View of $trans$ -[PdBr₂{(S,S)-(R,R)-PhTRAP}] (7) normal to the virtual square plane (hydrogen atoms are omitted for clarity).

Table 2. Selected Bond Lengths (Å) and Angles (deg) of 7

Bond Lengths (Å)			
Pd(1)–Br(1)	2.414(2)	Pd(1)–Br(2)	2.432(2)
Pd(1)–P(1)	2.327(4)	Pd(1)–P(2)	2.341(4)
P(1)–C(1)	1.87(1)	P(1)–C(25)	1.81(1)
P(1)–C(31)	1.85(2)	P(2)–C(13)	1.86(1)
P(2)–C(37)	1.83(2)	P(2)–C(43)	1.81(2)
Angles (deg)			
Br(1)–Pd(1)–Br(2)	167.44(8)	Br(1)–Pd(1)–P(1)	93.0(1)
Br(1)–Pd(1)–P(2)	96.5(1)	Br(2)–Pd(1)–P(1)	88.3(1)
Br(3)–Pd(1)–P(2)	85.4(1)	P(1)–Pd(1)–P(2)	163.6(1)
Pd(1)–P(1)–C(1)	106.4(5)	Pd(1)–P(1)–C(25)	117.5(5)
Pd(1)–P(1)–C(31)	116.5(5)	C(1)–P(1)–C(25)	101.4(7)
C(1)–P(1)–C(31)	110.9(7)	C(25)–P(1)–C(31)	103.1(7)
Pd(1)–P(2)–C(13)	104.8(5)	Pd(1)–P(2)–C(37)	125.5(5)
Pd(1)–P(2)–C(43)	111.8(5)	C(13)–P(2)–C(37)	104.3(7)
C(13)–P(2)–C(43)	108.4(7)	C(37)–P(2)–C(43)	101.1(7)

steric bulkiness of Ph groups. Two bromine atoms on Pd are deeply buried in the chiral cavities created by the biferrocenyl backbone and Ph groups, suggesting a high degree of chiral recognition ability of PhTRAP as a chiral ligand for catalytic asymmetric synthesis.

Platinum Complexes. The reaction of (R,R)-(S,S)-PhTRAP (1a) with 1 equiv of PtCl₂(MeCN)₂ in CHCl₃ at 40 °C for 12 h gave two platinum species in a ratio of 20:1. The ³¹P{¹H} NMR spectrum (CDCl₃, 85% H₃PO₄) of the major product (δ 21.41) was accompanied by its ¹⁹⁵Pt satellite with a $J_{^{195}\text{Pt}-^{31}\text{P}}$ value of 2612 Hz, indicating the trans geometry of two phosphorus atoms.¹⁴ On the other hand, the minor product was deduced to have a cis geometry from a larger $J_{^{195}\text{Pt}-^{31}\text{P}}$ value (3668 Hz). The ¹H and ¹³C{¹H} NMR spectra of the major product were similar to those of $trans$ -[PdX₂(PhTRAP)]. These species were easily separated by column chromatography (silica gel, CH₂Cl₂; R_f 0.94 for trans, 0.20 for cis). The chelated mononuclear structure of the $trans$ -[PtCl₂(PhTRAP)] (10) was concluded from FAB-mass spectra and from a molecular weight determination by VPO analysis (MW calcd 1060.5, obsd 1120 in CHCl₃). Reaction of unsymmetrical TRAP 1e with PtCl₂(MeCN)₂ at 35 °C for 30 min gave $trans$ -PtCl₂1e (11) as a single isomer. The ³¹P{¹H} NMR spectrum (202 MHz) showed an AB quartet with a ³¹P–³¹P coupling constant of 490 Hz. Such a large value was in agreement with the trans geometry.

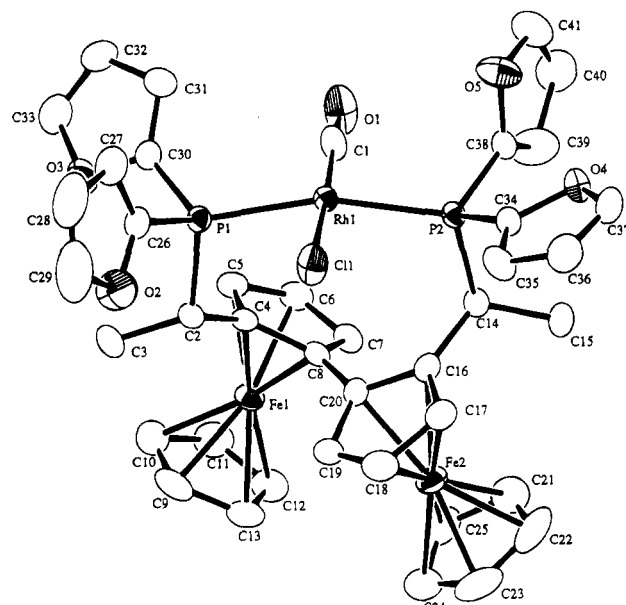


Figure 6. ORTEP drawing (30% probability level) and atom-labeling scheme for $trans$ -[RhCl(CO){(S,S)-(R,R)-FurTRAP}] (14) (hydrogen atoms are omitted for clarity). Only one of the two molecules in a unit cell is shown. The second molecule is in essence a rotamer in which O3 and C31 and O5 and C39 are interchanged.

Iridium Complex. Vaska-type complex $trans$ -[IrCl(CO){(S,S)-(R,R)-PhTRAP}] (12) was prepared by the reaction of (S,S)-(R,R)-PhTRAP with dicarbonylchloro-(*p*-toluidine)iridium(I). Because of the chirality of PhTRAP, resonances of the two phosphorus atoms of 12 appeared with different chemical shifts (21.0 and 40.4 ppm) and coupled with each other with a $J_{\text{P-P}}$ value of 344 Hz. Such asymmetry was also observed in both ¹H and ¹³C{¹H} NMR spectra. From the large ³¹P–³¹P coupling constant, the iridium complex was deduced to have trans geometry.

Rhodium Complexes. Reaction of (S,S)-(R,R)-PhTRAP with [Rh(CO)₂]₂(μ -Cl)₂ proceeded at room temperature with evolution of carbon monoxide to give $trans$ -[RhCl(CO){(S,S)-(R,R)-PhTRAP}] (13). The ³¹P{¹H} NMR spectrum showed a pair of double doublets due to ³¹P–³¹P (J = 355 Hz) and ¹⁰³Rh–³¹P coupling (J = 129 and 126 Hz). The ¹H and ¹³C{¹H} NMR spectra were similar to those of iridium complex 12.

X-ray crystal structures have been determined for $trans$ -[RhCl(CO){(S,S)-(R,R)-FurTRAP}] (14), each unit cell containing a set of independent molecules. An ORTEP drawing with atom-labeling scheme for one of the two molecules is shown in Figure 6.¹⁵ Bond distances and angles are given in Table 3. The environment of Rh is almost the same as that of Pd in PhTRAP–Pd complex 7. Bond angles P(1)–Rh(1)–P(2) and Cl(1)–Rh(1)–C(1) are 161.06(4) and 176.2(2)°, respectively. Dihedral angles P(1)–C(2)–C(4)–C(8) and P(2)–C(14)–C(16)–C(20) are 100.9(4) and 92.8(5)°, respectively. The angle between the least-squares planes through the two linked Cp rings (C4–C8, C16–C20) is 124.7°. Contrary to PhTRAP coordinating to the Pd atom, FurTRAP adopts essentially C₂ symmetrical conformation in coordination to the Rh atom (compare

(15) The structure of another molecule is similar to that shown in Figure 6. Crystallographic data were deposited with the Cambridge Crystallographic Data Centre.

(14) Rahn, J. A.; Baltusis, L.; Nelson, J. H. *Inorg. Chem.* **1990**, *29*, 750 and references cited therein.

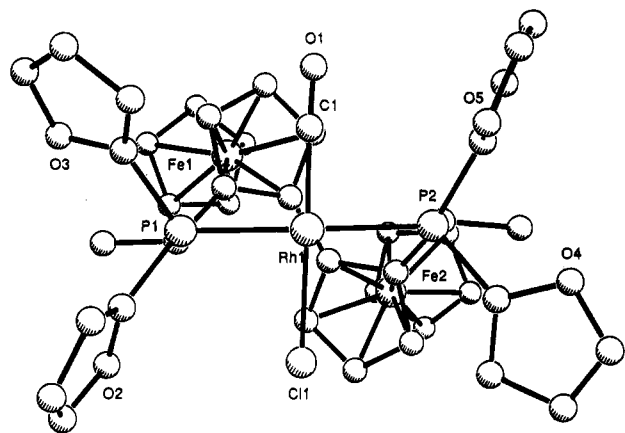


Figure 7. View of *trans*-[RhCl(CO){(*S,S*)-(*R,R*)-FurTRAP}] (**14**) normal to the virtual square plane (hydrogen atoms are omitted for clarity).

Table 3. Selected Bond Lengths (Å) and Angles (deg) of 14

Bond Lengths (Å)			
Rh(1)–Cl(1)	2.365(2)	Rh(1)–P(1)	2.301(1)
Rh(1)–P(2)	2.300(1)	Rh(1)–C(1)	1.807(1)
P(1)–C(2)	1.859(1)	P(1)–C(26)	1.806(5)
P(1)–C(30)	1.799(5)	P(2)–C(14)	1.864(4)
P(2)–C(34)	1.796(5)	P(2)–C(38)	1.815(5)
Angles (deg)			
Cl(1)–Rh(1)–P(1)	86.78(5)	Cl(1)–Rh(1)–P(2)	93.81(5)
Cl(1)–Rh(1)–C(1)	176.2(2)	P(1)–Rh(1)–P(2)	161.06(4)
P(1)–Rh(1)–C(1)	92.6(2)	P(2)–Rh(1)–C(1)	88.0(2)
Rh(1)–P(1)–C(2)	105.5(1)	Rh(1)–P(1)–C(26)	118.9(2)
Rh(1)–P(1)–C(30)	118.0(2)	C(2)–P(1)–C(26)	103.4(2)
C(2)–P(1)–C(30)	108.7(2)	C(26)–P(1)–C(30)	101.1(2)
Rh(1)–P(2)–C(14)	109.7(1)	Rh(1)–P(2)–C(34)	121.5(2)
Rh(1)–P(2)–C(38)	114.7(2)	C(14)–P(2)–C(34)	104.3(2)
C(14)–P(2)–C(38)	101.4(2)	C(34)–P(2)–C(38)	102.9(2)

Figure 7 with Figure 5). The difference in conformation between PhTRAP–Pd complex **7** and FurTRAP–Rh complex **14** may be attributed to the difference in steric bulkiness of the aryl substituents on the phosphorus atoms.

Experimental Section

General Procedures. Optical rotations were measured with a Perkin-Elmer 243 polarimeter. NMR spectra were obtained with JEOL JNM-A500 (^1H , 500.16 MHz; ^{13}C , 125.77 MHz; ^{31}P , 202.46 MHz), JEOL JNM-A400 (^1H , 399.78 MHz; ^{13}C , 100.53 MHz; ^{31}P , 161.83 MHz), and Varian VXR-200 (^1H , 200.06 MHz; ^{13}C , 50.31 MHz; ^{31}P , 80.98 MHz) spectrometers. Most of the ^1H and ^{13}C NMR spectra of new compounds described below were measured at two different frequencies to determine coupling constants with ^{31}P . ^1H NMR spectra were recorded in δ ppm relative to internal Me_4Si (δ 0). ^{13}C - $\{^1\text{H}\}$ NMR spectra were recorded in δ ppm relative to CDCl_3 (δ 77.0). $^{31}\text{P}\{^1\text{H}\}$ NMR spectra were recorded in δ ppm relative to external 85% aqueous H_3PO_4 (δ 0). IR spectra were recorded with a Hitachi 270–30 spectrophotometer. High-resolution mass spectra (HRMS) were obtained with JEOL JMS-DX300 and JEOL JMS-SX102A spectrometers. Preparative high-performance liquid chromatography (HPLC) was performed with a YMC SH043-5 (silica gel, 20 mm \times 250 mm) column.

Materials. (*R*)- and (*S*)-**2**,⁷ diarylphosphine oxides ($\text{Ar}_2\text{P}(\text{O})\text{H}$): Ar = Ph, 4-MeOC₆H₄, 4-ClC₆H₄, 4-MeC₆H₄,¹⁶ and [IrCl(CO)₂(*p*-toluidine)]¹⁷ were prepared according to the literature

procedures. $\text{PdCl}_2(\text{MeCN})_2$ was prepared by boiling a suspension of PdCl_2 in MeCN. $[\{\text{Rh}(\text{CO})_2\}_2(\mu\text{-Cl})_2]$ was purchased and used without purification.

(*R*)-2-[(*S*)-1-(*N,N*-Dimethylamino)ethyl]-1-iodoferrocene [(*S*)-(*R*)-3**]** was prepared from (*S*)-**2** according to the literature procedure.⁸ The product was obtained as a mixture with the starting material (87% conversion, (*S*)-(*R*)-**3**/*S*)-(*S*)-**3**/*S*)-**2** in an 85/2/13 molar ratio) and was used without further purification: brown solid; mp 45–48 °C; ^1H NMR (200 MHz, CDCl_3) δ 1.50 (d, J = 6.8 Hz, 3 H), 2.15 (s, 6 H), 3.62 (q, J = 6.8 Hz, 1 H), 4.12 (s, 5 H), 4.15 (dd, J = 2.6 and 1.2 Hz, 1 H), 4.24 (t, J = 2.6 Hz, 1 H), 4.46 (dd, J = 2.6 and 1.2 Hz, 1 H); ^{13}C NMR (50 MHz, CDCl_3) δ 15.94, 41.16 (2 C), 45.44, 57.52, 65.52, 68.13, 71.61 (Cp), 74.25, 90.11; HRMS (EI) calcd for $\text{C}_{14}\text{H}_{18}\text{FeIN}$, 382.9830, found (m/z) 382.9824.

(*R*)-2-[(*S*)-1-(Diphenylphosphinyl)ethyl]-1-iodoferrocene [(*S*)-(*R*)-4a**]**: In a nitrogen atmosphere, was added dropwise 1.6 M *n*-butyllithium/hexane (13.0 mL) to an ice-cooled solution of diphenylphosphine oxide (4.05 g, 20.0 mmol) in dry THF (50 mL) over 2 min. The brown solution was stirred at room temperature for 1.5 h. The solvent was evaporated, and the remaining lithium diphenylphosphinite was dried in vacuo.

(*S*)-(*R*)-**3** in another reaction flask was dissolved in CH_2Cl_2 (10 mL), and iodomethane (8.0 g, 56 mmol) was added with ice cooling. The mixture was stirred at room temperature for 30 min. The solvent was evaporated, and the remaining ammonium salt was dried in vacuo. The ammonium salt was dissolved in dry MeCN (110 mL), and the solution was transferred to the phosphinite salt at room temperature. The mixture was refluxed for 1 h and was cooled to room temperature. After dilution with 100 mL of water, the mixture was extracted twice with ether. The organic layer was washed twice with saturated NaCl and dried over MgSO_4 . The residue was passed through a column of alumina (EtOAc /diethylamine = 15/1) to give a mixture of **4a** and **5a**, which was formed mainly by the reaction of **2** (5.37 g, **4a**/**5a** = 4.5/1, quantitative yield, the yield from **3** to **4a** was 96%). This crude product was used without further purification: viscous oil; $[\alpha]_D^{25}$ –17.9 (for pure **4a**, c 0.504, CHCl_3); ^1H NMR (400 MHz, CDCl_3) δ 1.68 (dd, $J_{\text{P-H}}$ = 15.4 and $J_{\text{H-H}}$ = 7.3 Hz, 3 H), 3.29 (dq, $J_{\text{P-H}}$ = 6.5 and $J_{\text{H-H}}$ = 7.3 Hz, 1 H), 4.16 (s, 5 H), 4.28 (dd, $J_{\text{H-H}}$ = 2.5 and 1.4 Hz, 1 H), 4.31 (dt, $J_{\text{P-H}}$ \approx 0.5 and $J_{\text{H-H}}$ = 2.5 Hz, 1 H), 4.55 (ddd, $J_{\text{P-H}}$ = 1.3, $J_{\text{H-H}}$ = 2.5 and 1.4 Hz, 1 H), 7.14–7.25 (m, 4 H), 7.31–7.36 (m, 1 H), 7.54–7.63 (m, 3 H), 7.90–7.97 (m, 2 H); ^{13}C NMR (100 MHz, CDCl_3) δ 16.13 (d, $^2J_{\text{P-C}}$ = 1.8 Hz), 34.29 (d, $^1J_{\text{P-C}}$ = 65.9 Hz), 47.04 (d, $^3J_{\text{P-C}}$ = 2.4 Hz), 66.61 (d, $^3J_{\text{P-C}}$ or $^4J_{\text{P-C}}$ = 1.9 Hz), 68.90, 71.34 (Cp), 73.23, 89.21, 127.69 (d, $^3J_{\text{P-C}}$ = 11.6 Hz, meta), 128.66 (d, $^3J_{\text{P-C}}$ = 11.0 Hz, meta), 130.82 (d, $^1J_{\text{P-C}}$ = 92.8 Hz, ipso), 131.40 (d, $^4J_{\text{P-C}}$ = 3.0 Hz, para), 131.59 (d, $^1J_{\text{P-C}}$ = 98.3 Hz, ipso), 131.64 (d, $^2J_{\text{P-C}}$ = 8.6 Hz, ortho), 131.81 (d, $^2J_{\text{P-C}}$ = 9.2 Hz, ortho), 131.84 (d, $^4J_{\text{P-C}}$ = 3.1 Hz, para); ^{31}P NMR (81 MHz, CDCl_3) δ 34.40; HRMS (EI) calcd for $\text{C}_{24}\text{H}_{22}\text{FeIOP}$, 539.9800, found (m/z) 539.9793.

(*R*)-2-[(*S*)-1-{Bis(4-methoxyphenyl)phosphinyl}ethyl]-1-iodoferrocene [(*S*)-(*R*)-4b**]** was prepared from (*S*)-(*R*)-**3** and bis(4-methoxyphenyl)phosphine oxide as a mixture with **5b** as described for the preparation of **4a** and was used without further purification (total 91%, the yield from **3** to **4b** was 72%): viscous oil; ^1H NMR (200 MHz, CDCl_3) δ 1.65 (dd, $J_{\text{P-H}}$ = 15.2 and $J_{\text{H-H}}$ = 7.2 Hz, 3 H), 3.19 (dq, $J_{\text{P-H}}$ = 6.6 and $J_{\text{H-H}}$ = 7.2 Hz, 1 H), 3.74 (s, 3 H), 3.89 (s, 3 H), 4.15 (s, 5 H), 4.31 (AA'X system, d, 2 H), 4.51 (AA'X system, t, $^1J_{\text{H-H}}$ + $^2J_{\text{H-H}}$ = 4.2 Hz, 1 H), 6.68 (pseudo-dd, 2 H), 6.9–7.2 (m, 4 H), 7.83 (pseudo-dd, 2 H); ^{13}C NMR (50 MHz, CDCl_3) δ 16.05 (d, $^2J_{\text{P-C}}$ = 2.0 Hz), 34.67 (d, $^1J_{\text{P-C}}$ = 67.1 Hz), 47.29 (d, $^3J_{\text{P-C}}$ = 2.8 Hz), 55.17, 55.32, 66.51 (d, $^3J_{\text{P-C}}$ or $^4J_{\text{P-C}}$ = 2.3 Hz), 68.80, 71.31 (Cp), 73.16, 89.34 (d, $^2J_{\text{P-C}}$ = 1.2 Hz), 113.19 (d, $^3J_{\text{P-C}}$ = 12.6 Hz, meta), 114.15 (d, $^3J_{\text{P-C}}$ = 12.1 Hz, meta), 121.95 (d, $^1J_{\text{P-C}}$ = 99.1 Hz, ipso), 123.32 (d, $^1J_{\text{P-C}}$ = 104.8 Hz, ipso), 133.34 (d, $^2J_{\text{P-C}}$ = 9.6 Hz, ortho), 133.61 (d, $^2J_{\text{P-C}}$ = 10.6 Hz,

(16) (a) Hunt, B. B.; Saunders, B. C. *J. Chem. Soc.* **1957**, 2413. (b) Grayson, M.; Farley, C. E.; Streuli, C. A. *Tetrahedron* **1967**, 23, 1065. (17) Kläubunde, U. *Inorg. Synth.* **1974**, 15, 82.

ortho), 161.98 (d, $^4J_{P-C} = 2.8$ Hz, para), 162.28 (d, $^4J_{P-C} = 3.0$ Hz, para); ^{31}P NMR (81 MHz, $CDCl_3$) δ 34.30; HRMS (EI) calcd for $C_{26}H_{26}FeIO_3P$, 600.0014, found (m/z) 599.9988.

(R)-2-[(S)-1-(Bis(4-chlorophenyl)phosphinyl)ethyl]-1-iodoferrocene [(S)-(R)-4c] was prepared from (S)-(R)-3 and bis(4-chlorophenyl)phosphine oxide as a mixture with 5c as described for the preparation of 4a and was used without further purification (total 93%, the yield from 3 to 4c was 82%): orange amorphous solid; mp 63–65 °C; 1H NMR (200 MHz, $CDCl_3$) δ 1.67 (dd, $J_{P-H} = 15.7$ and $J_{H-H} = 7.3$ Hz, 3 H), 3.24 (dq, $J_{P-H} = 6.5$ and $J_{H-H} = 7.3$ Hz, 1 H), 4.17 (s, 5 H), 4.32 (AA'X system, d, 2 H), 4.50 (AA'X system, t, $|^1J_{H-H} + ^2J_{H-H}| = 4.2$ Hz, 1 H), 7.0–7.2 (m, 4 H), 7.5–7.6 (m, 2 H), 7.8–7.9 (m, 2 H); ^{13}C NMR (100 MHz, $CDCl_3$) δ 15.92 (d, $^2J_{P-C} = 2.2$ Hz), 34.38 (d, $^1J_{P-C} = 66.9$ Hz), 46.88 (d, $^3J_{P-C} = 3.0$ Hz), 66.49 (d, $^3J_{P-C}$ or $^4J_{P-C} = 2.1$ Hz), 69.07, 71.44 (Cp), 73.39, 88.54 (d, $^2J_{P-C} = 1.2$ Hz), 128.09 (d, $^3J_{P-C} = 12.2$ Hz, meta), 128.92 (d, $^1J_{P-C} = 93.7$ Hz, ipso), 129.17 (d, $^3J_{P-C} = 11.7$ Hz, meta), 129.73 (d, $^1J_{P-C} = 99.9$ Hz, ipso), 132.91 (d, $^2J_{P-C} = 9.3$ Hz, ortho), 133.08 (d, $^2J_{P-C} = 10.2$ Hz, ortho), 138.19 (d, $^4J_{P-C} = 3.4$ Hz, para), 138.74 (d, $^4J_{P-C} = 3.4$ Hz, para); ^{31}P NMR (81 MHz, $CDCl_3$) δ 32.87; HRMS (EI) calcd for $C_{24}H_{20}Cl_2FeIO$, 607.9023, found (m/z) 607.8995.

(R)-2-[(S)-1-(Di-2-furylphosphinyl)ethyl]-1-iodoferrocene [(S)-(R)-4d]. To a solution of furan (10.36 g, 152 mmol) in 90 mL of ether was added dropwise 1.57 M *n*-BuLi/hexane (65 mL, 102 mmol) at 0 °C over 1 h, and the mixture was refluxed for 2 h. A solution of diethyl phosphite (4.22 g, 31 mmol) in 20 mL of ether was added dropwise to the mixture at 0 °C over 30 min. The mixture was stirred at room temperature for 1 h and was then evaporated in vacuo. The reaction of the residual solid [lithium bis(2-furyl)phosphinite] with the ammonium salt prepared from 6.90 g (14.4 mmol) of crude (S)-(R)-3 (80 mol % purity) gave a mixture of (S)-(R)-4d and 5d (6.86 g, 4d/5d = 10/1 in a molar ratio, yield from 3 to 4d was 95%, which was used without further purification: 1H NMR (400 MHz, $CDCl_3$) δ 1.71 (dd, $J_{P-H} = 17.1$ and $J_{H-H} = 7.3$ Hz, 3 H), 3.34 (dq, $J_{P-H} = 11.1$ and $J_{H-H} = 7.4$ Hz, 1 H), 4.14 (s, 5 H), 4.20 (m, 1 H), 4.24 (t, $J = 2.5$ Hz, 1 H), 4.36 (m, 1 H), 6.35 (m, 1 H), 6.51 (m, 1 H), 6.70 (m, 1 H), 7.18 (m, 1 H), 7.54 (m, 1 H), 7.71 (m, 1 H); ^{13}C NMR (100 MHz, $CDCl_3$) δ 15.51, 35.62 (d, $J_{C-P} = 75.7$ Hz), 45.46 (d, $J_{C-P} = 3.0$ Hz), 66.20 (d, $J_{C-P} = 2.5$ Hz), 68.82, 71.43, 73.72, 88.12, 110.08 (d, $J_{C-P} = 8.0$ Hz), 110.73 (d, $J_{C-P} = 8.5$ Hz), 122.63 (d, $J_{C-P} = 18.3$ Hz), 123.36 (d, $J_{C-P} = 17.7$ Hz), 145.87 (d, $J_{C-P} = 133.7$ Hz), 146.06 (d, $J_{C-P} = 138.0$ Hz), 147.68 (d, $J_{C-P} = 7.3$ Hz), 148.02 (d, $J_{C-P} = 7.3$ Hz); ^{31}P NMR (81 MHz, $CDCl_3$) δ 14.68; HRMS (EI) calcd for $C_{20}H_{18}FeIO_3P$, 519.9410, found (m/z) 519.9408.

(R)-2-[(S)-1-(Bis(4-methylphenyl)phosphinyl)ethyl]-1-iodoferrocene [(S)-(R)-4e] was prepared from (S)-(R)-3 and bis(4-methylphenyl)phosphine oxide as a mixture with 5e as described for the preparation of 4a and was used without further purification (quantitatively, the yield from 3 to 4e was 88%): orange crystals; mp 180–185 °C (decomp); 1H NMR (200 MHz, $CDCl_3$) δ 1.66 (dd, $J_{P-H} = 15.3$ and $J_{H-H} = 7.3$ Hz, 3 H), 2.27 (s, 3 H), 2.45 (s, 3 H), 3.23 (dq, $J_{P-H} = 6.7$ and $J_{H-H} = 7.3$ Hz, 1 H), 4.15 (s, 5 H), 4.30 (AA'X system, d, 2 H), 4.52 (AA'X system, t, $|^1J_{H-H} + ^2J_{H-H}| = 3.8$ Hz, 1 H), 6.9–7.2 (m, 4 H), 7.3–7.4 (m, 2 H), 7.7–7.8 (m, 2 H); ^{13}C NMR (50 MHz, $CDCl_3$) δ 16.19 (d, $^2J_{P-C} = 2.0$ Hz), 21.49 (d, $^5J_{P-C} = 1.3$ Hz), 21.62 (d, $^5J_{P-C} = 1.3$ Hz), 34.35 (d, $^1J_{P-C} = 66.3$ Hz), 47.18 (d, $^3J_{P-C} = 2.9$ Hz), 66.57 (d, $^3J_{P-C}$ or $^4J_{P-C} = 2.3$ Hz), 68.79, 71.31 (Cp), 73.12, 89.37 (d, $^2J_{P-C} = 1.1$ Hz), 127.64 (d, $^1J_{P-C} = 95.2$ Hz, ipso), 128.37 (d, $^3J_{P-C} = 12.0$ Hz, meta), 128.48 (d, $^1J_{P-C} = 100.7$ Hz, ipso), 129.33 (d, $^3J_{P-C} = 11.5$ Hz, meta), 131.57 (d, $^2J_{P-C} = 8.9$ Hz, ortho), 131.75 (d, $^2J_{P-C} = 9.9$ Hz, ortho), 141.59 (d, $^4J_{P-C} = 2.9$ Hz, para), 142.09 (d, $^4J_{P-C} = 2.8$ Hz, para); ^{31}P NMR (81 MHz, $CDCl_3$) δ 34.59; HRMS (EI) calcd for $C_{26}H_{26}FeIO$, 568.0115, found (m/z) 568.0104.

(R,R)-2,2'-Bis[(S)-1-(diphenylphosphinyl)ethyl]-1,1'-biferrocene [(S,S)-(R,R)-6a]. To a CH_2Cl_2 (25 mL) solution of (S)-(R)-4a (4.32 g, 6.84 mmol for 4a, 4a/5a = 82/18 in molar

ratio) was added activated copper powder¹⁰ (25 g), and the solvent was evaporated. The remaining mixture was heated under an argon atmosphere at 130 °C for 12 h and was cooled to room temperature. Organic materials were extracted with CH_2Cl_2 . The solvent was evaporated, and the residue was chromatographed on silica gel (benzene/EtOAc = 2/1). Fractions containing 6a were collected and concentrated. Recrystallization from toluene gave 2.11 g (64%) of (S,S)-(R,R)-6a (toluene)_{1.5}: orange crystals; mp 245–250 °C (decomp); $[\alpha]^{25}_D + 130$ (c 1.02, $CHCl_3$); 1H NMR (400 MHz, $CDCl_3$) δ 1.65 (dd, $J_{P-H} = 16.8$ and $J_{H-H} = 7.4$ Hz, 6 H), 3.81 (dq, $J_{P-H} = 11.0$ and $J_{H-H} = 7.4$ Hz, 2 H), 4.01 (m, 2 H), 4.08 (t, $J_{H-H} = 2.6$ Hz, 2 H), 4.35 (s, 10 H), 4.35 (m, 2 H), 6.99–7.06 (m, 4 H), 7.28–7.33 (m, 2 H), 7.40–7.52 (m, 6 H), 7.60–7.68 (m, 4 H), 7.77–7.84 (m, 4 H); ^{13}C NMR (100 MHz, $CDCl_3$) δ 19.14, 30.23 (d, $^4J_{P-C} = 69.0$ Hz), 65.39, 68.32 (d, $^3J_{P-C}$ or $^4J_{P-C} = 5.5$ Hz), 69.36 (Cp), 72.56, 84.48 (d, $^2J_{P-C}$ or $^3J_{P-C} = 6.8$ Hz), 90.58, 128.07 (d, $^3J_{P-C} = 11.0$ Hz, meta), 128.18 (d, $^3J_{P-C} = 11.6$ Hz, meta), 130.95 (d, $^4J_{P-C} = 2.4$ Hz, para), 131.22 (d, $^4J_{P-C} = 3.0$ Hz, para), 131.36 (d, $^2J_{P-C} = 9.1$ Hz, ortho), 132.03 (d, $^1J_{P-C} = 94.0$ Hz, ipso), 132.25 (d, $^2J_{P-C} = 8.5$ Hz, ortho), 133.85 (d, $^1J_{P-C} = 94.6$ Hz, ipso); ^{31}P NMR (81 MHz, $CDCl_3$) δ 35.59. Anal. Calcd for $C_{58.5}H_{56}Fe_2O_2P_2$: C, 72.83; H, 5.85. Found: C, 72.95; H, 5.79.

(R,R)-2,2'-Bis[(S)-1-(bis(4-methoxyphenyl)phosphinyl)ethyl]-1,1'-biferrocene [(S,S)-(R,R)-6b] was prepared as described for the preparation of 6a and was purified by flash chromatography (silica gel, benzene/EtOAc): 32% yield; orange amorphous solid; mp 170–174 °C; $[\alpha]^{25}_D + 65.8$ (c 1.00, $CHCl_3$); 1H NMR (500 MHz, $CDCl_3$) δ 1.63 (dd, $J_{P-H} = 16.6$ and $J_{H-H} = 7.3$ Hz, 6 H), 3.70 (s, 6 H), 3.72 (m, 2 H, α -CH), 3.84 (s, 6 H), 4.08 (m, 4 H), 4.28 (m, 2 H), 4.34 (s, 10 H), 6.56 (pseudo-dd, 4 H), 6.95 (pseudo-dd, 4 H), 7.52 (pseudo-dd, 4 H), 7.69 (pseudo-dd, 4 H); ^{13}C NMR (125 MHz, $CDCl_3$) δ 19.33 (d, $^2J_{P-C} \approx 0.5$ Hz), 30.35 (d, $^1J_{P-C} = 68.7$ Hz), 55.06, 55.20, 65.37, 68.23 (d, $^3J_{P-C}$ or $^4J_{P-C} = 5.4$ Hz), 69.27 (Cp), 72.20, 84.47 (d, $^2J_{P-C}$ or $^3J_{P-C} = 6.1$ Hz), 90.72, 113.61 (d, $^3J_{P-C} = 12.2$ Hz, meta), 113.69 (d, $^3J_{P-C} = 12.2$ Hz, meta), 123.30 (d, $^1J_{P-C} = 100.6$ Hz, ipso), 125.35 (d, $^1J_{P-C} = 100.7$ Hz, ipso), 133.16 (d, $^2J_{P-C} = 10.7$ Hz, ortho), 133.92 (d, $^2J_{P-C} = 9.9$ Hz, ortho), 161.56 (d, $^4J_{P-C} = 2.3$ Hz, para), 161.88 (d, $^4J_{P-C} = 2.3$ Hz, para); ^{31}P NMR (81 MHz, $CDCl_3$) δ 35.64; HRMS (FAB) calcd for $C_{52}H_{52}Fe_2O_6P_2$, 946.1938, found (m/z) 946.2012.

(R,R)-2,2'-Bis[(S)-1-(bis(4-chlorophenyl)phosphinyl)ethyl]-1,1'-biferrocene [(S,S)-(R,R)-6c] was prepared as described for the preparation of 6a, except that the coupling was performed at 170 °C for 8 h and purified by column chromatography (silica gel, benzene/EtOAc): 37% yield; orange amorphous solid; mp 137–139 °C; $[\alpha]^{25}_D + 189$ (c 1.04, $CHCl_3$); 1H NMR (500 MHz, $CDCl_3$) δ 1.59 (dd, $J_{P-H} = 17.4$ and $J_{H-H} = 7.3$ Hz, 6 H), 3.69 (dq, $J_{P-H} = 11.9$ and $J_{H-H} = 7.3$ Hz, 2 H), 3.89 (br s, 2 H), 4.13 (t, $J_{H-H} = 2.5$ Hz, 2 H), 4.35 (s, 10 H), 4.46 (br s, 2 H), 6.94 (pseudo-d, 4 H), 7.41 (pseudo-dd, 4 H), 7.60 (pseudo-dd, 4 H), 7.69 (pseudo-dd, 4 H); ^{13}C NMR (125 MHz, $CDCl_3$) δ 19.04, 29.79 (d, $^1J_{P-C} = 70.7$ Hz), 65.56, 67.95 (d, $^3J_{P-C}$ or $^4J_{P-C} = 4.3$ Hz), 69.43, 72.93, 84.34 (d, $^2J_{P-C}$ or $^3J_{P-C} = 7.5$ Hz), 90.35, 128.48 (d, $^3J_{P-C} = 11.8$ Hz, meta), 128.63 (d, $^3J_{P-C} = 11.8$ Hz, meta), 130.17 (d, $^1J_{P-C} = 96.4$ Hz, ipso), 131.84 (d, $^1J_{P-C} = 95.3$ Hz, ipso), 132.70 (d, $^2J_{P-C} = 9.7$ Hz, ortho), 133.65 (d, $^2J_{P-C} = 9.6$ Hz, ortho), 137.92 (d, $^4J_{P-C} = 3.3$ Hz, para), 138.09 (d, $^4J_{P-C} = 3.2$ Hz, para); ^{31}P NMR (81 MHz, $CDCl_3$) δ 34.77. Anal. Calcd for $C_{48}H_{40}Cl_4Fe_2O_2P_2$: C, 59.79; H, 4.18. Found: C, 59.94; H, 4.30.

(R,R)-2,2'-Bis[(S)-1-(di-2-furylphosphinyl)ethyl]-1,1'-biferrocene [(S,S)-(R,R)-6d] was prepared as described for the preparation of 6a and was purified by a column chromatography on alumina (EtOAc/Et₂NH = 15/1) followed by a recrystallization from CH_2Cl_2 /hexane: 65% yield; orange crystals; mp 140–145 °C; $[\alpha]^{25}_D - 408$ (c 0.2, $CHCl_3$); 1H NMR (200 MHz, $CDCl_3$) δ 1.79 (dd, $J_{P-H} = 18.6$ Hz, $J_{H-H} = 7.4$ Hz, 6 H), 3.9–4.1 (m, 2 H), 4.15 (m, 2 H), 4.28 (m, 2 H), 4.35 (m, 12 H), 6.36 (m, 2 H), 6.57 (m, 2 H), 6.68 (m, 2 H), 7.20 (m, 2

H), 7.57 (m, 2 H), 7.77 (m, 2 H); ^{13}C NMR (50 MHz, CDCl_3) δ 18.70, 32.34 (d, $J_{\text{C-P}} = 76.9$ Hz), 66.41, 67.33 (d, $J_{\text{C-P}} = 5.0$ Hz), 69.32, 71.28, 84.25, (d, $J_{\text{C-P}} = 4.8$ Hz), 87.70, 110.83 (d, $J_{\text{C-P}} = 8.3$ Hz), 111.15 (d, $J_{\text{C-P}} = 8.5$ Hz), 122.23 (d, $J_{\text{C-P}} = 18.3$ Hz), 124.27 (d, $J_{\text{C-P}} = 17.2$ Hz), 145.98 (d, $J_{\text{C-P}} = 133.6$ Hz), 147.38 (d, $J_{\text{C-P}} = 8.0$ Hz), 147.67 (d, $J_{\text{C-P}} = 134.3$ Hz), 147.87 (d, $J_{\text{C-P}} = 7.0$ Hz); ^{31}P (81 MHz, CDCl_3) δ 15.6. Anal. Calcd for $\text{C}_{40}\text{H}_{36}\text{O}_6\text{P}_2\text{Fe}_2\text{CH}_2\text{Cl}_2$: C, 56.52; H, 4.40. Found: C, 56.80; H, 4.46.

(R,R)-2-[(S)-1-(Diphenylphosphinyl)ethyl]-2'-[(S)-1-(bis(4-methylphenyl)phosphinyl)ethyl]-1,1'-biferrocene [(S,S)-(R,R)-6e] was prepared from (S)-(R)-4a (1.02 g, containing 1.61 mmol of 4a) and (S)-(R)-4e (1.02 g, containing 1.91 mmol of 4e) as described for the preparation of 6a. The crude product was purified by PTLC (silica gel, hexane/EtOAc = 1/3) followed by HPLC (hexane/1,2-dichloroethane/ethanol = 24/8/1) to give 0.156 g of 6e (23%); orange amorphous solid; mp 166–170 °C; $[\alpha]_D^{25} +116$ (c 1.01, CHCl_3); ^1H NMR (500 MHz, CDCl_3) δ 1.61 (dd, $J_{\text{P-H}} = 16.8$ and $J_{\text{H-H}} = 7.3$ Hz, 3 H), 1.66 (dd, $J_{\text{P-H}} = 16.8$ and $J_{\text{H-H}} = 7.3$ Hz, 3 H), 2.27 (s, 3 H, tol-1- CH_3), 2.39 (s, 3 H, tol-2- CH_3), 3.68 (dq, $J_{\text{P-H}} = 11.6$ and $J_{\text{H-H}} = 7.3$ Hz, 1 H), 3.87 (dq, $J_{\text{P-H}} = 10.5$ and $J_{\text{H-H}} = 7.3$ Hz, 1 H), 3.99 (m, 1 H), 4.07 (t, $J_{\text{H-H}} = 2.6$ Hz, 1 H), 4.08 (t, $J_{\text{H-H}} = 2.6$ Hz, 1 H), 4.10 (m, 1 H), 4.31 (m, 2 H), 4.33 (s, 5 H), 4.35 (s, 5 H), 6.86 (pseudo-dd, 2 H, tol-1-meta), 6.97 (pseudo-td, 2 H, Ph-1-meta), 7.24 (pseudo-dd, 2 H, tol-2-meta), 7.27 (pseudo-td, 1 H, Ph-1-para), 7.42 (pseudo-dd, 2 H, Ph-2-meta), 7.46 (pseudo-td, 1 H, Ph-2-para), 7.47 (pseudo-dd, 2 H, tol-1-ortho), 7.65 (pseudo-dd, 4 H, Ph-1-ortho and tol-2-ortho), 7.83 (pseudo-dd, 2 H, Ph-2-ortho); the coupling network was deduced by an ^1H - ^1H COSY experiment; ^{13}C NMR (125 MHz, CDCl_3) δ 19.20 (d, $^2J_{\text{P-C}} = 1.1$ Hz), 19.23, 21.44 (d, $^5J_{\text{P-C}} = 1.3$ Hz), 21.56 (d, $^5J_{\text{P-C}} = 1.3$ Hz), 30.06 (d, $^1J_{\text{P-C}} = 68.6$ Hz), 30.39 (d, $^1J_{\text{P-C}} = 69.4$ Hz), 65.35, 65.42, 68.05 (d, $^3J_{\text{P-C}}$ or $^4J_{\text{P-C}} = 4.6$ Hz), 68.56 (d, $^3J_{\text{P-C}}$ or $^4J_{\text{P-C}} = 5.3$ Hz), 69.30 (Cp), 69.34 (Cp), 72.35, 72.49, 84.31 (d, $^2J_{\text{P-C}}$ or $^3J_{\text{P-C}} = 6.9$ Hz), 84.63 (d, $^2J_{\text{P-C}}$ or $^3J_{\text{P-C}} = 5.4$ Hz), 90.66 (2C), 128.07 (d, $^3J_{\text{P-C}} = 11.5$ Hz, meta), 128.08 (d, $^3J_{\text{P-C}} = 10.7$ Hz, meta), 128.36 (d, $^1J_{\text{P-C}} = 96.7$ Hz, ipso), 128.79 (d, $^3J_{\text{P-C}} = 12.2$ Hz, meta), 128.94 (d, $^3J_{\text{P-C}} = 11.5$ Hz, meta), 130.65 (d, $^1J_{\text{P-C}} = 96.9$ Hz, ipso), 130.77 (d, $^4J_{\text{P-C}} = 2.3$ Hz, para), 131.13 (d, $^4J_{\text{P-C}} = 2.3$ Hz, para), 131.35 (d, $^2J_{\text{P-C}} = 9.1$ Hz, ortho), 131.42 (d, $^2J_{\text{P-C}} = 9.2$ Hz, ortho), 132.09 (d, $^2J_{\text{P-C}} = 8.4$ Hz, ortho), 132.37 (d, $^1J_{\text{P-C}} = 94.6$ Hz, ipso), 132.39 (d, $^2J_{\text{P-C}} = 9.1$ Hz, ortho), 133.92 (d, $^1J_{\text{P-C}} = 93.8$ Hz, ipso), 141.15 (d, $^4J_{\text{P-C}} = 3.0$ Hz, para), 141.52 (d, $^4J_{\text{P-C}} = 2.3$ Hz, para); ^{31}P NMR (81 MHz, CDCl_3) δ 35.77, 35.83; HRMS (FAB) calcd for $\text{C}_{50}\text{H}_{48}\text{Fe}_2\text{O}_2\text{P}_2$, 854.1828, found (m/z) 854.1875.

(R,R)-2,2'-Bis[(S)-1-(diphenylphosphino)ethyl]-1,1'-biferrocene [(S,S)-(R,R)-PhTRAP (1a)]. In a glass tube was placed 918 mg (0.952 mmol) of (S,S)-(R,R)-4a (toluene) $_{1.5}$. After benzene (2.5 mL), Et_3N (1.1 mL, 7.9 mmol), and HSiCl_3 (0.6 mL, 5.9 mmol) were successively added, the tube was cooled with dry ice-acetone, sealed in vacuo, and heated at 100 °C for 10 h. The reaction mixture was cooled to room temperature, 30% aqueous NaOH was carefully added to the mixture, and the whole was warmed at 60 °C for 5 min to dissolve silicon-containing precipitate. After the mixture had cooled to room temperature, the organic layer was separated, washed once with water, once with brine, and dried over MgSO_4 . Purification by column chromatography (alumina, benzene) gave 741 mg (98%) of 1a: orange amorphous solid; mp 98–103 °C; $[\alpha]_D^{25} +426$ (c 0.51, CHCl_3); ^1H NMR (400 MHz, CDCl_3) δ 1.35 (pseudo-t, 6 H, CH_3), 3.49 (q, $J_{\text{H-H}} = 6.9$ Hz, 2 H, α -CH), 3.79 (dd, $J_{\text{H-H}} = 2.5$ and 1.4 Hz, 2 H, H-3 and H-3'), 4.12 (t, $J_{\text{H-H}} = 2.5$ Hz, 2 H, H-4 and H-4'), 4.29 (s, 10 H, Cp), 4.55 (dd, $J_{\text{H-H}} = 2.5$ and 1.4 Hz, 2 H, H-5 and H-5'), 7.05–7.40 (m, 20 H, phenyl); ^{13}C NMR (100 MHz, CDCl_3) δ 17.03 (t, $^2J_{\text{P-C}} + ^3J_{\text{P-C}} = 2.2$ Hz, CH_3), 29.25 (split into six lines, $^1J_{\text{P-C}} + ^2J_{\text{P-C}} = 17.1$ Hz, α -CH), 65.36 (C-4 and C-4'), 68.05 (t, $^3J_{\text{P-C}} + ^4J_{\text{P-C}} = 6.8$ Hz, C-3 and C-3'), 69.32 (Cp), 71.67 (t, $^4J_{\text{P-C}} + ^5J_{\text{P-C}} = 2.3$ Hz, C-5 and C-5'), 84.37 (t, $^3J_{\text{P-C}} + ^4J_{\text{P-C}} = 4.2$ Hz, C-1 and C-1'), 93.08 (quint, $^2J_{\text{P-C}} + ^3J_{\text{P-C}} = 20.2$ Hz, C-2 and

C-2'), 127.19 (Ph-1-para), 127.46 (t, $^3J_{\text{P-C}} + ^4J_{\text{P-C}} = 6.7$ Hz, Ph-2-meta), 128.00 (t, $^3J_{\text{P-C}} + ^4J_{\text{P-C}} = 4.8$ Hz, Ph-1-meta), 128.33 (Ph-2-para), 132.14 (quint, $^2J_{\text{P-C}} + ^3J_{\text{P-C}} = 18.3$ Hz, Ph-1-ortho), 135.11 (quint, $^2J_{\text{P-C}} + ^3J_{\text{P-C}} = 21.4$ Hz, Ph-2-ortho), 136.13 (split into six lines, $^1J_{\text{P-C}} + ^2J_{\text{P-C}} = 21.3$ Hz, Ph-2-ipso), 139.01 (split into six lines, $^1J_{\text{P-C}} + ^2J_{\text{P-C}} = 18.9$ Hz, Ph-1-ipso); ^{31}P NMR (81 MHz, CDCl_3) δ 2.19; full assignment of the spectra has been done with the aid of $^1\text{H}\{^1\text{H}\}$ NOE (Table 1, Figure 1), HETCOR, HMBC, and ^{13}C INADEQUATE (see supporting information for the 2D NMR experiments). Anal. Calcd for $\text{C}_{48}\text{H}_{44}\text{Fe}_2\text{P}_2$: C, 72.56; H, 5.58. Found: C, 72.68; H, 5.40.

Although product 1a can be recrystallized from $\text{CH}_2\text{Cl}_2/\text{EtOH}$, benzene/EtOH, etc. to give solvent-containing orange crystals, the amounts of crystallization solvent were nonspecific.

NOE Experiment on 1a. The $^1\text{H}\{^1\text{H}\}$ NOE experiment was performed at 200 MHz with 20 mg of (S,S)-(R,R)-1a in CDCl_3 (0.6 mL) at room temperature. The decoupler was set to the resonance of α -methyl proton and was turned on for 16 s. The power of irradiation was set so that the intensity of the signal saturated might become around 70% of the original intensity. This preirradiation period was followed by a short (0.05 s) switching time to prevent the occurrence of unwanted decoupling immediately followed by a 90°-acquisition pulse and a 4-s acquisition. Eight transients were acquired with the decoupler on resonance. Next, for each α -H, H-3, H-4, and H-5, eight transients were acquired by the same procedure. Reference spectra were obtained in a similar manner with the decoupler frequency set to an empty region of the spectrum, and eight reference transients were acquired. A series of the above procedures was repeated eight times; a total of 384 transients were collected. Percent NOE enhancements were determined by integration of the difference spectra as totals of the enhancements for all equivalent protons.

(R,R)-2,2'-Bis[(S)-1-(bis(4-methoxyphenyl)phosphino)ethyl]-1,1'-biferrocene [(S,S)-(R,R)-AnisTRAP (1b)] was prepared as described for the preparation of 1a: 85% yield; orange amorphous solid; mp 104–108 °C; $[\alpha]_D^{25} +321$ (c 0.53, CHCl_3); ^1H NMR (500 MHz, CDCl_3) δ 1.36 (pseudo-t, 6 H), 3.36 (q, $J_{\text{H-H}} = 7.2$ Hz, 2 H), 3.67 (s, 6 H), 3.75 (dd, $J_{\text{H-H}} = 2.4$ and 1.4 Hz, 2 H), 3.77 (s, 6 H), 4.07 (t, $J_{\text{H-H}} = 2.4$ Hz, 2 H), 4.30 (s, 10 H), 4.52 (dd, $J_{\text{H-H}} = 2.4$ and 1.4 Hz, 2 H), 6.60 (pseudo-d, 4 H), 6.76 (pseudo-d, 4 H), 7.18–7.28 (m, 8 H); ^{13}C NMR (125 MHz, CDCl_3) δ 18.01 (t, $^2J_{\text{P-C}} + ^3J_{\text{P-C}} = 5.0$ Hz), 29.10 (split into six lines, $^1J_{\text{P-C}} + ^2J_{\text{P-C}} = 14.1$ Hz), 54.99, 55.08, 65.07, 68.28 (t, $^3J_{\text{P-C}} + ^4J_{\text{P-C}} = 9.4$ Hz), 69.16 (Cp), 72.24 (t, $^4J_{\text{P-C}} + ^5J_{\text{P-C}} = 2.3$ Hz), 84.19 (t, $^3J_{\text{P-C}} + ^4J_{\text{P-C}} = 4.0$ Hz), 93.63 (split into six lines, $^2J_{\text{P-C}} + ^3J_{\text{P-C}} = 18.6$ Hz), 113.33 (t, $^3J_{\text{P-C}} + ^4J_{\text{P-C}} = 7.9$ Hz, meta), 113.74 (t, $^3J_{\text{P-C}} + ^4J_{\text{P-C}} = 5.5$ Hz, meta), 127.42 (split into six lines, $^1J_{\text{P-C}} + ^2J_{\text{P-C}} = 17.7$ Hz, ipso), 130.13 (split into six lines, $^1J_{\text{P-C}} + ^2J_{\text{P-C}} = 14.4$ Hz, ipso), 133.38 (quint, $^2J_{\text{P-C}} + ^3J_{\text{P-C}} = 20.2$ Hz, ortho), 136.65 (quint, $^2J_{\text{P-C}} + ^3J_{\text{P-C}} = 22.8$ Hz, ortho), 158.93 (para), 160.20 (para); ^{31}P NMR (81 MHz, CDCl_3) δ 0.30. Anal. Calcd for $\text{C}_{52}\text{H}_{52}\text{Fe}_2\text{O}_4\text{P}_2$: C, 68.29; H, 5.73. Found: C, 68.06; H, 5.69.

(R,R)-2,2'-Bis[(S)-1-(bis(4-chlorophenyl)phosphino)ethyl]-1,1'-biferrocene [(S,S)-(R,R)-Cl-PhTRAP (1c)] was prepared as described for the preparation of 1a: 87% yield; orange amorphous solid; mp 115–119 °C; $[\alpha]_D^{25} +459$ (c 0.43, CHCl_3); ^1H NMR (400 MHz, CDCl_3) δ 1.30 (split into six lines, 6 H), 3.35 (q, $J_{\text{H-H}} = 7.0$ Hz, 2 H), 3.87 (dd, $J_{\text{H-H}} = 2.5$ and 1.4 Hz, 2 H), 4.23 (t, $J_{\text{H-H}} = 2.5$ Hz, 2 H), 4.28 (s, 10 H), 4.55 (dd, $J_{\text{H-H}} = 2.5$ and 1.4 Hz, 2 H), 7.00–7.07 (m, 8 H), 7.11–7.19 (m, 8 H); ^{13}C NMR (100 MHz, CDCl_3) δ 15.49, 30.22 (dd, $^1J_{\text{P-C}} + ^2J_{\text{P-C}} = 21.0$ Hz), 65.75, 67.58 (t, $^3J_{\text{P-C}} + ^4J_{\text{P-C}} = 5.1$ Hz), 69.55 (Cp), 71.14, 84.46 (t, $^3J_{\text{P-C}} + ^4J_{\text{P-C}} = 5.1$ Hz), 92.11 (t, $^2J_{\text{P-C}} + ^3J_{\text{P-C}} = 20.4$ Hz), 127.60 (t, $^3J_{\text{P-C}} + ^4J_{\text{P-C}} = 6.4$ Hz, meta), 128.43 (t, $^3J_{\text{P-C}} + ^4J_{\text{P-C}} = 5.1$ Hz, meta), 133.63 (t, $^2J_{\text{P-C}} + ^3J_{\text{P-C}} = 19.7$ Hz, ortho), 133.89 (para), 134.06 (dd, $^1J_{\text{P-C}} + ^2J_{\text{P-C}} = 24.1$ Hz, ipso), 134.32 (para), 135.42 (t, $^2J_{\text{P-C}} + ^3J_{\text{P-C}} = 12.2$ Hz, ortho), 136.89 (dd, $^1J_{\text{P-C}}$

+ $^2J_{P-C}$) = 19.9 Hz, ipso); ^{31}P NMR (81 MHz, $CDCl_3$) δ -0.82. Anal. Calcd for $C_{48}H_{40}Cl_4Fe_2P_2$: C, 61.84; H, 4.32. Found: C, 62.08; H, 4.58.

(R,R)-2,2'-Bis[(S)-1-(di-2-furylphosphino)ethyl]-1,1'-biferrocene [(S,S)-(R,R)-FurTRAP (1d)] was prepared as described for the preparation of **1a**: 88% yield; orange amorphous solid; mp 115–127 °C; [α] $^{25}_D$ +444 (c 0.28, $CHCl_3$); 1H NMR (400 MHz, $CDCl_3$) δ 1.56 (dt, $J_{H-H} = 7.2$ Hz, $J_{P-H} = 6.5$ Hz, 6 H), 3.27 (q, $J_{H-H} = 7.2$ Hz, 2 H), 3.84 (dd, $J_{H-H} = 2.7$ and 1.4 Hz, 2 H), 4.15 (t, $J_{H-H} = 2.7$ Hz, 2 H), 4.25 (s, 10 H), 4.46 (dd, $J_{H-H} = 2.7$ and 1.4 Hz, 2 H), 6.33 (m, 4 H), 6.53 (dd, $J_{H-H} = 3.2$ and 0.8 Hz, 2 H), 6.68 (ddd, $J_{H-H} = 3.2$ and 0.8 Hz, $J_{P-H} = 1.9$ Hz, 2 H), 7.60 (dd, $J_{H-H} = 1.8$ and 0.8 Hz, 2 H), 7.66 (dd, $J_{H-H} = 1.8$ and 0.8 Hz, 2 H); ^{13}C NMR (100 MHz, $CDCl_3$) δ 19.23, 31.77 (t, $J = 12.9$ Hz), 65.79, 66.66 (t, $J = 5.9$ Hz), 69.38, 70.69 (t, $J = 4.7$ Hz), 83.98 (t, $J = 3.9$ Hz), 92.15 (t, $J = 20.2$ Hz), 110.34 (t, 7.7 Hz), 110.35 (t, $J = 4.7$ Hz), 119.31 (t, $J = 20.4$ Hz), 123.22 (t, $J = 32.5$ Hz), 146.07 (t, $J = 2.4$ Hz), 146.75, 150.04 (dd, $J_{C-P} = 15.6$ and 14.2 Hz), 152.37 (dd, $J_{C-P} = 8.7$ and 7.9 Hz); ^{31}P NMR (81 MHz, $CDCl_3$) δ -42.7. Anal. Calcd for $C_{40}H_{38}Fe_2O_4P_2$: C, 63.69; H, 4.81. Found: C, 63.39; H, 4.63.

(R,R)-2-[(S)-1-(Diphenylphosphino)ethyl]-2'-[(S)-1-{bis(4-methylphenyl)phosphino}ethyl]-1,1'-biferrocene (1e) was prepared as described for the preparation **1a**: 90% yield; orange amorphous solid; mp 71–75 °C; [α] $^{25}_D$ +405 (c 0.51, $CHCl_3$); 1H NMR (500 MHz, $CDCl_3$) δ 1.36 (pseudo-t, 6 H), 2.24 (s, 3 H), 2.28 (s, 3 H), 3.44 (q, $J_{H-H} = 7$ Hz, 1 H), 3.49 (q, $J_{H-H} = 7$ Hz, 1 H), 3.75 (m, 1 H), 3.82 (m, 1 H), 4.098 (t, $J_{H-H} = 2.4$ Hz, 1 H), 4.103 (t, $J_{H-H} = 2.4$ Hz, 1 H), 4.29 (s, 5 H), 4.30 (s, 5 H), 4.54 (m, 1 H), 4.56 (m, 1 H), 6.88 (br d, 2 H), 6.98 (br d, 2 H), 7.11–7.22 (m, 8 H), 7.22–7.33 (m, 6 H); ^{13}C NMR (125 MHz, $CDCl_3$) δ 17.15 (d, $^2J_{P-C} = 1.8$ Hz), 17.55 (d, $^2J_{P-C} = 3.3$ Hz), 21.13, 21.26 (d, $^5J_{P-C} \approx 0.5$ Hz), 29.04 (dd, $^1J_{P-C} = 19.6$ and $^2J_{P-C} = 2.1$ Hz), 29.06 (dd, $^1J_{P-C} = 18.4$ and $^2J_{P-C} = 2.6$ Hz), 65.25, 65.28, 68.08 (d, $^3J_{P-C} = 6.8$ Hz), 68.24 (d, $^3J_{P-C} = 7.8$ Hz), 69.25 (Cp), 69.27 (Cp), 71.70 (d, $^4J_{P-C} = 2.5$ Hz), 71.78 (d, $^4J_{P-C} = 2.7$ Hz), 84.21 (d, $^3J_{P-C} = 3.9$ Hz), 84.38 (dd, $^3J_{P-C} = 3.9$ and $^4J_{P-C} \approx 0.5$ Hz), 93.12 (d, $^2J_{P-C} = 19.5$ Hz), 93.45 (d, $^2J_{P-C} = 19.6$ Hz), 127.11 (d, $^4J_{P-C} \approx 0.5$ Hz, para), 127.47 (d, $^3J_{P-C} = 6.8$ Hz, meta), 128.00 (d, $^3J_{P-C} = 4.5$ Hz, meta), 128.34 (d, $^3J_{P-C} = 6.8$ Hz, meta), 128.44 (d, $^4J_{P-C} \approx 0.5$ Hz, para), 128.77 (d, $^3J_{P-C} = 4.9$ Hz, meta), 132.05 (dd, $^2J_{P-C} = 16.1$ and $^3J_{P-C} = 1.9$ Hz, ortho), 132.10 (dd, $^2J_{P-C} = 16.6$ and $^3J_{P-C} = 2.2$ Hz, ortho), 132.91 (d, $^1J_{P-C} = 20.0$ Hz, ipso), 135.08 (dd, $^2J_{P-C} = 19.5$ and $^3J_{P-C} = 2.4$ Hz, ortho), 135.29 (dd, $^2J_{P-C} = 19.5$ and $^3J_{P-C} = 2.5$ Hz, ortho), 135.55 (dd, $^1J_{P-C} = 18.3$ and $^2J_{P-C} = 1.7$ Hz, ipso), 136.01 (d, $^1J_{P-C} = 21.4$ Hz, ipso), 136.80 (d, $^4J_{P-C} \approx 0.5$ Hz, para), 138.22 (d, $^4J_{P-C} \approx 0.5$ Hz, para), 139.05 (dd, $^1J_{P-C} = 20.2$ and $^2J_{P-C} = 1.5$ Hz, ipso); ^{31}P NMR (81 MHz, $CDCl_3$) δ 0.40 and 2.58 (ABq, $J = 22.0$ Hz). Anal. Calcd for $C_{50}H_{48}Fe_2P_2$: C, 73.01; H, 5.88. Found: C, 73.06; H, 6.01.

trans-[PdBr₂]{(S,S)-(R,R)-PhTRAP} (7). To a suspension of $PdBr_2$ (81.3 mg, 0.305 mmol) in CH_2Cl_2 (2 mL) was added a solution of (S,S)-(R,R)-**1a** (200.0 mg, 0.252 mmol) in CH_2Cl_2 (2 mL) at room temperature. The deep orange solution was stirred for 30 min. After the remaining $PdBr_2$ was filtered off, the resulting solution was concentrated. Ether was slowly added to the solution, and the orange precipitate that formed was collected and dried in vacuo: yield, 237.4 mg (89%); orange crystals; mp 250–255 °C (decomp); [α] $^{20}_D$ +644 (c 0.232, $CHCl_3$); 1H NMR (200 MHz, $CDCl_3$) δ 1.68 (td, $^3J_{P-H} + ^5J_{P-H} = 12.0$ and $|J_{H-H}| = 7.2$ Hz, 6 H), 3.92 (dd, $J_{H-H} = 2.4$ and 1.4 Hz, 2 H), 4.10 (tq, $^2J_{P-H} + ^4J_{P-H} = 7.1$ and $|J_{H-H}| = 7.2$ Hz, 2 H), 4.32 (s, 10 H), 4.43 (t, $|J_{H-H}| = 2.4$ Hz, 2 H), 4.66 (dd, $J_{H-H} = 2.4$ and 1.4 Hz, 2 H), 7.2–7.5 (m, 16 H), 7.8–7.9 (m, 4 H); ^{13}C NMR (50 MHz, $CDCl_3$) δ 20.38, 33.25 (t, $^1J_{P-C} + ^3J_{P-C} = 19.2$ Hz), 67.24, 68.36, 69.81 (Cp), 73.10, 86.22, 91.77 (t, $^2J_{P-C} + ^4J_{P-C} = 9.2$ Hz), 126.97 (t, $^3J_{P-C} + ^5J_{P-C} = 10.1$ Hz, meta), 127.13 (t, $^3J_{P-C} + ^5J_{P-C} = 9.1$ Hz, meta), 127.83 (t, $^1J_{P-C} + ^3J_{P-C} = 39.4$ Hz, ipso), 129.25 (para), 130.58 (para),

132.35 (t, $^1J_{P-C} + ^3J_{P-C} = 43.3$ Hz, ipso), 133.40 (t, $^2J_{P-C} + ^4J_{P-C} = 9.6$ Hz, ortho), 137.55 (t, $^2J_{P-C} + ^4J_{P-C} = 11.4$ Hz, ortho); ^{31}P NMR (81 MHz, $CDCl_3$) δ 29.92. Anal. Calcd for $C_{48}H_{44}Br_2Fe_2P_2Pd$: C, 54.35; H, 4.18. Found: C, 54.27; H, 4.03.

trans-[PdCl₂]{(R,R)-(S,S)-PhTRAP} (8). To a suspension of $[PdCl_2](CH_3CN)_2$ (8.0 mg, 0.031 mmol) in CH_2Cl_2 (0.5 mL) was added a solution of (R,R)-(S,S)-**1a** (24.4 mg, 0.031 mmol) in CH_2Cl_2 (0.5 mL) at room temperature. The orange solution was stirred for 30 min. The product was purified by silica gel chromatography ($CH_2Cl_2/EtOAc = 20/1$): yield, 27.3 mg (92%); orange crystals; mp 230–235 °C (decomp); [α] $^{20}_D$ -726 (c 0.55, $CHCl_3$); 1H NMR (200 MHz, $CDCl_3$) δ 1.66 (td, $^3J_{P-H} + ^5J_{P-H} = 12.0$ and $|J_{H-H}| = 7.2$ Hz, 6 H), 3.72 (dd, $J = 2.5$ and 1.4 Hz, 2 H), 4.08 (tq, $^2J_{P-H} + ^4J_{P-H} = 6.8$ and $|J_{H-H}| = 7.2$ Hz, 2 H), 4.31 (s, 10 H), 4.42 (t, $J = 2.5$ Hz, 2 H), 4.67 (dd, $J = 2.5$ and 1.4 Hz, 2 H), 7.2–7.4 (m, 16 H), 7.9–8.0 (m, 4 H); ^{13}C NMR (50 MHz, $CDCl_3$) δ 19.88, 30.90 (t, $^1J_{P-C} + ^3J_{P-C} = 18.3$ Hz), 67.61, 68.06, 70.14 (Cp), 72.74, 86.68, 91.71 (t, $^2J_{P-C} + ^4J_{P-C} = 9.6$ Hz), 127.08 (t, $^3J_{P-C} + ^5J_{P-C} = 9.7$ Hz, meta), 127.23 (t, $^3J_{P-C} + ^5J_{P-C} = 9.0$ Hz, meta), 127.93 (t, $^1J_{P-C} + ^3J_{P-C} = 38.5$ Hz, ipso), 129.12 (para), 130.59 (para), 130.94 (t, $^1J_{P-C} + ^3J_{P-C} = 43.6$ Hz, ipso), 133.46 (t, $^2J_{P-C} + ^4J_{P-C} = 9.0$ Hz, ortho), 137.80 (t, $^2J_{P-C} + ^4J_{P-C} = 10.6$ Hz, ortho); ^{31}P NMR (81 MHz, $CDCl_3$) δ 25.11. Anal. Calcd for $C_{48}H_{44}Cl_2Fe_2P_2Pd$: C, 59.32; H, 4.56. Found: C, 59.10; H, 4.54.

trans-[PdI₂]{(R,R)-(S,S)-PhTRAP} (9). To a suspension of PdI_2 (1.64 g, 4.55 mmol) in CH_2Cl_2 (20 mL) was added a solution of (R,R)-(S,S)-**1a** (3.52 g, 4.43 mmol) in CH_2Cl_2 (55 mL) at room temperature. The deep orange solution was stirred for 40 min. After the remaining PdI_2 was filtered off, the solvent was evaporated to give a crude product in quantitative yield. The product was purified by silica gel chromatography (CH_2Cl_2): orange crystals; mp 160–165 °C (decomp); [α] $^{25}_D$ -250 (c 0.10, $CHCl_3$); 1H NMR (200 MHz, $CDCl_3$) δ 1.58 (td, $^3J_{P-H} + ^5J_{P-H} = 12.4$ and $|J_{H-H}| = 7.3$ Hz, 6 H), 4.03 (tq, $^2J_{P-H} + ^4J_{P-H} = 6.6$ and $|J_{H-H}| = 7.3$ Hz, 2 H), 4.07 (dd, $J_{H-H} = 2.6$ and 1.4 Hz, 2 H), 4.31 (s, 10 H), 4.49 (t, $|J_{H-H}| = 2.6$ Hz, 2 H), 4.67 (dd, $J_{H-H} = 2.6$ and 1.4 Hz, 2 H), 7.2–7.5 (m, 16 H), 7.7–7.8 (m, 4 H); ^{13}C NMR (50 MHz, $CDCl_3$) δ 19.69, 36.35 (t, $^1J_{P-C} + ^3J_{P-C} = 19.3$ Hz), 67.31, 69.15, 69.95 (Cp), 74.00, 86.27, 91.64 (t, $^2J_{P-C} + ^4J_{P-C} = 8.6$ Hz), 126.81 (t, $^3J_{P-C} + ^5J_{P-C} = 10.0$ Hz, meta), 127.23 (t, $^3J_{P-C} + ^5J_{P-C} = 9.5$ Hz, meta), 129.29 (t, $^1J_{P-C} + ^3J_{P-C} = 40.2$ Hz, ipso), 129.51 (para), 130.62 (para), 133.43 (t, $^2J_{P-C} + ^4J_{P-C} = 9.9$ Hz, ortho), 135.45 (t, $^1J_{P-C} + ^3J_{P-C} = 44.1$ Hz, ipso), 137.23 (t, $^2J_{P-C} + ^4J_{P-C} = 11.3$ Hz, ortho); ^{31}P NMR (81 MHz, $CDCl_3$) δ 27.82. Anal. Calcd for $C_{48}H_{44}Fe_2I_2P_2Pd$: C, 49.93; H, 3.84. Found: C, 49.90; H, 3.76.

trans-[PtCl₂]{(R,R)-(S,S)-PhTRAP} (trans-10). To a suspension of $[PtCl_2](CH_3CN)_2$ (17.3 mg, 0.050 mmol) in CH_2Cl_2 (3 mL) was added a solution of (R,R)-(S,S)-**1a** (39.8 mg, 0.050 mmol) in CH_2Cl_2 (2 mL) at room temperature. The orange solution was stirred at 40 °C for 30 min. The product was purified by silica gel chromatography (CH_2Cl_2) and recrystallized from $CH_2Cl_2/EtOH$: yield, 43.0 mg (82%); orange crystals; mp 240–245 °C (decomp); [α] $^{20}_D$ -571 (c 0.57, $CHCl_3$); 1H NMR (400 MHz, $CDCl_3$) δ 1.68 (td, $^3J_{P-H} + ^5J_{P-H} = 12.2$ and $|J_{H-H}| = 7.3$ Hz, 6 H), 3.75 (dd, $J = 2.4$ and 1.4 Hz, 2 H), 4.06 (tq, $^2J_{P-H} + ^4J_{P-H} = 7.3$ and $|J_{H-H}| = 7.3$ Hz, 2 H), 4.31 (s, 10 H), 4.39 (t, $J = 2.4$ Hz, 2 H), 4.64 (dd, $J = 2.4$ and 1.4 Hz, 2 H), 7.23–7.42 (m, 16 H), 7.83–7.90 (m, 4 H); ^{13}C NMR (100 MHz, $CDCl_3$) δ 19.99, 30.89 (t, $^1J_{P-C} + ^3J_{P-C} = 28.1$ Hz), 67.08, 67.82, 69.65 (Cp), 72.51, 86.57, 91.64 (t, $^2J_{P-C} + ^4J_{P-C} = 7.3$ Hz), 127.03 (t, $^1J_{P-C} + ^3J_{P-C} = 46.3$ Hz, ipso), 127.07 (t, $^3J_{P-C} + ^5J_{P-C} = 9.8$ Hz, meta), 127.26 (t, $^3J_{P-C} + ^5J_{P-C} = 10.7$ Hz, meta), 129.90 (para), 129.94 (t, $^1J_{P-C} + ^3J_{P-C} = 50.1$ Hz, ipso), 130.61 (para), 133.51 (t, $^2J_{P-C} + ^4J_{P-C} = 9.8$ Hz, ortho), 137.56 (t, $^2J_{P-C} + ^4J_{P-C} = 11.0$ Hz, ortho); ^{31}P NMR (81 MHz, $CDCl_3$) δ 21.41 (t, $J_{31P-31P} = 2612$ Hz). Anal. Calcd for $C_{48}H_{44}Cl_2Fe_2P_2Pt$: C, 54.36; H, 4.18. Found: C, 54.06; H, 4.04.

cis-[PtCl₂{(R,R)-(S,S)-PhTRAP}] (cis-10). After the *trans*-**10** was eluted by silica gel chromatography described above, *cis*-**10** was eluted with CH₂Cl₂/acetone (9/1): orange powder; ¹H NMR (200 MHz, CDCl₃) δ 0.7–0.9 (m, 6 H), 3.74 (m, 2 H), 3.88 (s, 10 H), 4.42 (m, 2 H), 4.87 (m, 2 H), 7.2–7.4 (m, 12 H), 7.5–7.6 (m, 4 H), 7.9–8.0 (m, 4 H); ³¹P NMR (81 MHz, CDCl₃) δ 16.12 (t, *J*_{Pt-31P} = 3668 Hz).

trans-[PtCl₂{(S,S)-(R,R)-1e}] (11). To a suspension of [PtCl₂(CH₃CN)₂] (10.4 mg, 0.0299 mmol) in CH₂Cl₂ (0.6 mL) was added unsymmetrical TRAP (S,S)-(R,R)-**1e** (24.7 mg, 0.0300 mmol) at room temperature. The orange solution was stirred at 35 °C for 30 min. The product was purified by silica gel chromatography (CH₂Cl₂) and recrystallized from CH₂Cl₂/EtOH in high yield: orange powder; mp 235–240 °C (decomp); [α]_D²⁰ +594 (c 0.56, CHCl₃); ¹H NMR (500 MHz, CDCl₃) δ 1.656 (dd, *J*_{P-H} = 12.2 and *J*_{H-H} = 7.5 Hz, 3 H), 1.665 (dd, *J*_{P-H} = 12.0 and *J*_{H-H} = 7.6 Hz, 3 H), 2.327 (s, 3 H), 2.333 (s, 3 H), 3.74 (dd, *J*_{H-H} = 2.5 and 1.5 Hz, 1 H), 3.76 (dd, *J*_{H-H} = 2.5 and 1.5 Hz, 1 H), 4.03 (m, 2 H, α-CH), 4.30 (s, 10 H), 4.37 (t, *J*_{H-H} = 2.5 Hz, 1 H), 4.38 (t, *J*_{H-H} = 2.5 Hz, 1 H), 4.62 (dd, *J*_{H-H} = 2.5 and 1.5 Hz, 1 H), 4.63 (dd, *J*_{H-H} = 2.5 and 1.5 Hz, 1 H), 7.06 (pseudo-d, 2 H), 7.11 (pseudo-d, 2 H), 7.18 (ddd, 2 H), 7.26 (pseudo-t, 2 H), 7.31 (m, 5 H), 7.39 (pseudo-t, 1 H), 7.74 (ddd, 2 H), 7.87 (m, 2 H); ¹³C NMR (125 MHz, CDCl₃) δ 19.95 (pseudo-d, ²*J*_{P-C} + ⁴*J*_{P-C} = 1.5 Hz), 19.98 (pseudo-d, ²*J*_{P-C} + ⁴*J*_{P-C} = 1.5 Hz), 21.40, 21.44, 30.84 (dd, ¹*J*_{P-C} + ³*J*_{P-C} = 26.9 Hz), 30.91 (t, ¹*J*_{P-C} + ³*J*_{P-C} = 26.9 Hz), 67.03, 67.08, 67.78 (t, ³*J*_{P-C} + ⁵*J*_{P-C} or ⁴*J*_{P-C} + ⁶*J*_{P-C} = 2.2 Hz), 67.90 (t, ³*J*_{P-C} + ⁵*J*_{P-C} or ⁴*J*_{P-C} + ⁶*J*_{P-C} = 2.5 Hz), 69.65 (Cp, 10 C), 72.42, 72.49, 86.58 (t, ³*J*_{P-C} + ⁵*J*_{P-C} = 1.5 Hz), 86.64 (t, ³*J*_{P-C} + ⁵*J*_{P-C} = 1.5 Hz), 91.69 (dd, ²*J*_{P-C} + ⁴*J*_{P-C} = 8.8 Hz), 91.86 (dd, ²*J*_{P-C} + ⁴*J*_{P-C} = 8.2 Hz), 123.54 (dd, ¹*J*_{P-C} + ³*J*_{P-C} = 49.1 Hz, ipso), 126.58 (dd, ¹*J*_{P-C} + ³*J*_{P-C} = 52.5 Hz, ipso), 127.02 (dd, ³*J*_{P-C} + ⁵*J*_{P-C} = 10.1 Hz, meta), 127.24 (dd, ¹*J*_{P-C} + ³*J*_{P-C} = 45.2 Hz, ipso), 127.23 (dd, ³*J*_{P-C} + ⁵*J*_{P-C} = 9.1 Hz, meta), 127.86 (dd, ³*J*_{P-C} + ⁵*J*_{P-C} = 10.4 Hz, meta), 128.07 (dd, ³*J*_{P-C} + ⁵*J*_{P-C} = 9.4 Hz, meta), 129.13 (para), 130.01 (dd, ¹*J*_{P-C} + ³*J*_{P-C} = 50.1 Hz, ipso), 130.54 (para), 133.45 (dd, ²*J*_{P-C} + ⁴*J*_{P-C} = 9.7 Hz, ortho), 133.53 (dd, ²*J*_{P-C} + ⁴*J*_{P-C} = 9.8 Hz, ortho), 137.48 (dd, ²*J*_{P-C} + ⁴*J*_{P-C} = 11.3 Hz, ortho), 137.60 (dd, ²*J*_{P-C} + ⁴*J*_{P-C} = 11.0 Hz, ortho); 139.16 (para), 140.78 (para); ³¹P NMR (202 MHz, CDCl₃) δ 20.68, 21.38 (main peaks, ABq, *J*_{31P-31P} = 490 Hz, 70/1 intensity; satellites, ABX spin system, *J*_{195Pt-31P} = 2550–2600 Hz and *J*_{195Pt-31P} = 2600–2650 Hz). Anal. Calcd for C₅₀H₄₈Cl₂Fe₂P₂Pt: C, 55.17; H, 4.44. Found: C, 55.11; H, 4.19.

trans-[IrCl(CO){(S,S)-(R,R)-PhTRAP}] (12). A solution of [IrCl(CO)₂(*p*-toluidine)] (78.1 mg, 0.200 mmol) and (S,S)-(R,R)-**1a** (160.5 mg, 0.202 mmol) in CH₂Cl₂ (10 mL) was stirred at 40 °C for 10 min. The solvent was concentrated, and the residue was recrystallized from CH₂Cl₂/EtOH to give 183.5 mg (88%) of *trans*-**12**: orange crystals; mp 230–235 °C (decomp); [α]_D²⁰ +598 (c 0.54, CHCl₃); ¹H NMR (400 MHz, CDCl₃) δ 1.55 (dd, *J*_{P-H} = 11.9 and *J*_{H-H} = 7.1 Hz, 3 H), 1.65 (dd, *J*_{P-H} = 11.7 and *J*_{H-H} = 7.2 Hz, 3 H), 3.40 (m, 1 H), 3.66 (m, 1 H), 3.89 (dq, *J*_{P-H} = 7.3 and *J*_{H-H} = 7.2 Hz, 1 H), 4.05 (dq, *J*_{P-H} = 7.3 and *J*_{H-H} = 7.1 Hz, 1 H), 4.26 (s, 5 H), 4.28 (s, 5 H), 4.34 (t, *J* = 2.6 Hz, 1 H), 4.45 (t, *J* = 2.6 Hz, 1 H), 4.54 (dd, *J* = 2.6 and 1.4 Hz, 1 H), 4.62 (dd, *J* = 2.6 and 1.6 Hz, 1 H), 7.25–7.45 (m, 16 H), 7.45–7.52 (m, 2 H), 7.98–8.03 (m, 2 H); ¹³C NMR (100 MHz, CDCl₃) δ 19.10 (dd, ²*J*_{P-C} = 3.7 and ⁴*J*_{P-C} = 1.8 Hz), 20.14 (dd, ²*J*_{P-C} = 3.7 and ⁴*J*_{P-C} = 1.8 Hz), 32.01 (d, ¹*J*_{P-C} = 30.5 Hz), 32.98 (d, ¹*J*_{P-C} = 30.0 Hz), 66.38, 67.02, 67.28 (d, ³*J*_{P-C} = 2.4 Hz), 67.72 (d, ³*J*_{P-C} = 2.5 Hz), 69.44 (Cp, 69.74 (Cp), 72.22, 72.33, 86.40 (d, ³*J*_{P-C} = 1.8 Hz), 87.02 (d, ³*J*_{P-C} = 1.9 Hz), 91.97 (d, ²*J*_{P-C} = 8.6 Hz), 92.33 (d, ²*J*_{P-C} = 8.6 Hz), 127.17 (d, ³*J*_{P-C} = 9.2 Hz, meta), 127.22 (d, ³*J*_{P-C} = 9.7 Hz, meta), 127.24 (d, ³*J*_{P-C} = 9.2 Hz, meta), 128.01 (d, ³*J*_{P-C} = 9.2 Hz, meta), 128.25 (dd, ¹*J*_{P-C} = 41.1 and ³*J*_{P-C} = 3.0 Hz, ipso), 128.98 (d, ⁴*J*_{P-C} = 2.1 Hz, para), 129.10 (dd, ¹*J*_{P-C} = 32.4 and ³*J*_{P-C} = 7.4 Hz, ipso), 129.15 (d, ⁴*J*_{P-C} = 2.5 Hz, para), 130.41 (dd, ¹*J*_{P-C} = 42.8 and ³*J*_{P-C} = 2.4 Hz, ipso), 130.45 (d, ⁴*J*_{P-C} =

2.4 Hz, para), 130.75 (d, ⁴*J*_{P-C} = 2.4 Hz, para), 131.44 (dd, ²*J*_{P-C} = 8.6 and ⁴*J*_{P-C} = 1.0 Hz, ortho), 133.62 (dd, ²*J*_{P-C} = 8.0 and ⁴*J*_{P-C} = 1.4 Hz, ortho), 135.56 (d, ¹*J*_{P-C} = 46.4 Hz, ipso), 136.74 (dd, ²*J*_{P-C} = 10.4 and ⁴*J*_{P-C} = 1.8 Hz, ortho), 137.49 (dd, ²*J*_{P-C} = 9.1 and ⁴*J*_{P-C} = 1.8 Hz, ortho), 172.74 (t, ²*J*_{P-C} = 10.7 Hz, CO); ³¹P NMR (81 MHz, CDCl₃) δ 21.00 (d, *J* = 343.9 Hz), 40.41 (d, *J* = 343.9 Hz); IR (KBr) 1960 cm⁻¹. Anal. Calcd for C₄₉H₄₄ClFe₂IrOP₂: C, 56.04; H, 4.22. Found: C, 55.88; H, 4.14.

trans-[RhCl(CO){(S,S)-(R,R)-PhTRAP}] (13). To a solution of [{Rh(CO)₂]₂(μ-Cl)₂] (48.3 mg, 0.124 mmol) in 5 mL of CH₂Cl₂ was added (S,S)-(R,R)-**1a** (202.3 mg, 0.255 mmol) at room temperature, and the mixture was stirred for 10 min. The solution was diluted with EtOH, and most of CH₂Cl₂ was evaporated. Orange crystals were collected and dried in vacuo to give 217.8 mg (92%) of *trans*-**13**: mp 230–235 °C (decomp); [α]_D²⁰ +700 (c 0.52, CHCl₃); ¹H NMR (400 MHz, CDCl₃) δ 1.59 (dd, *J*_{P-H} = 10.9 and *J*_{H-H} = 7.2 Hz, 3 H), 1.61 (dd, *J*_{P-H} = 10.9 and *J*_{H-H} = 7.2 Hz, 3 H), 3.39 (ddd, *J*_{P-H} = 1.4, *J*_{H-H} = 2.5, and *J*_{H-H} = 1.4 Hz, 1 H), 3.68 (ddd, *J*_{P-H} = 1.4, *J*_{H-H} = 2.5, and *J*_{H-H} = 1.4 Hz, 1 H), 3.85 (dq, *J*_{P-H} = 5.3 and *J*_{H-H} = 7.2 Hz, 1 H), 4.06 (dq, *J*_{P-H} = 6.7 and *J*_{H-H} = 7.2 Hz, 1 H), 4.26 (s, 5 H), 4.29 (s, 5 H), 4.33 (t, *J* = 2.5 Hz, 1 H), 4.38 (t, *J* = 2.5 Hz, 1 H), 4.58 (dd, *J* = 2.5 and 1.4 Hz, 1 H), 4.63 (dd, *J* = 2.5 and 1.4 Hz, 1 H), 7.23–7.46 (m, 16 H), 7.48–7.55 (m, 2 H), 7.96–8.03 (m, 2 H); ¹³C NMR (100 MHz, CDCl₃) δ 19.31 (d, ²*J*_{P-C} = 4.5 Hz), 19.55 (ddd, ²*J*_{P-C} = 4.3, ³*J*_{Rh-C} = 1.3 and ⁴*J*_{P-C} = 1.3 Hz), 32.05 (d, ¹*J*_{P-C} = 23.8 Hz), 32.06 (d, ¹*J*_{P-C} = 21.3 Hz), 66.55, 67.14 (d, ³*J*_{P-C} = 2.7 Hz), 67.17, 67.64 (d, ³*J*_{P-C} = 2.4 Hz), 69.50 (Cp), 69.76 (Cp), 71.96, 72.23, 86.15 (d, ³*J*_{P-C} = 1.9 Hz), 86.17 (d, ³*J*_{P-C} = 1.8 Hz), 92.07 (d, ²*J*_{P-C} = 10.3 Hz), 92.71 (d, ²*J*_{P-C} = 10.3 Hz), 127.10 (d, ³*J*_{P-C} = 8.5 Hz, meta), 127.19 (d, ³*J*_{P-C} = 9.2 Hz, meta), 127.27 (d, ³*J*_{P-C} = 9.1 Hz, meta), 128.18 (d, ³*J*_{P-C} = 8.0 Hz, meta), 128.72 (d, ⁴*J*_{P-C} = 1.8 Hz, para), 128.89 (d, ⁴*J*_{P-C} = 1.8 Hz, para), 129.02 (dd, ¹*J*_{P-C} = 24.4 and ³*J*_{P-C} = 7.9 Hz, ipso), 129.43 (ddd, ¹*J*_{P-C} = 32.4, ²*J*_{Rh-C} = 3.1, and ³*J*_{P-C} = 3.1 Hz, ipso), 130.29 (d, ⁴*J*_{P-C} = 2.4 Hz, para), 130.62 (d, ⁴*J*_{P-C} = 2.5 Hz, para), 131.49 (d, ²*J*_{P-C} = 9.1 Hz, ortho), 131.52 (dd, ¹*J*_{P-C} = 36.6 and ³*J*_{P-C} = 3.0 Hz, ipso), 133.35 (d, ²*J*_{P-C} = 7.9 Hz, ortho), 136.31 (dd, ¹*J*_{P-C} = 37.0 and ³*J*_{P-C} = 1.8 Hz, ipso), 136.85 (ddd, ²*J*_{P-C} = 11.6, ³*J*_{Rh-C} = 1.6, and ⁴*J*_{P-C} = 1.6 Hz, ortho), 137.46 (dd, ²*J*_{P-C} = 9.8 and ³*J*_{Rh-C} or ⁴*J*_{P-C} = 1.9 Hz, ortho), 187.83 (ddd, ¹*J*_{Rh-C} = 174.5, ²*J*_{P-C} = 17.1 and ²*J*_{P-C} = 13.4 Hz, CO); ³¹P NMR (81 MHz, CDCl₃) δ 26.25 (dd, ¹*J*_{Rh-P} = 129.4 and ²*J*_{P-P} = 354.8 Hz), 48.06 (dd, ¹*J*_{Rh-P} = 125.6 and ²*J*_{P-P} = 354.8 Hz); IR (KBr) 1972 cm⁻¹. Anal. Calcd for C₄₉H₄₄ClFe₂IrOP₂Rh: C, 61.25; H, 4.62. Found: C, 61.04; H, 4.65.

trans-[RhCl(CO){(S,S)-(R,R)-FurTRAP}] (14). [{Rh(CO)₂]₂(μ-Cl)₂] (16.8 mg, 0.043 mmol) and (S,S)-(R,R)-**1d** (65.2 mg, 0.086 mmol) were dissolved in 1 mL of CH₂Cl₂. After the evolution of carbon monoxide ceased, the solvent was evaporated. Recrystallization from CH₂Cl₂/EtOH gave **14** (85%) as orange crystals: mp 200–205 °C (decomp); [α]_D²⁰ +560 (c 0.25, CHCl₃); ¹H NMR (400 MHz, CDCl₃) δ 1.79 (dd, *J*_{P-H} = 11.8 and *J*_{H-H} = 7.1 Hz, 3 H), 1.88 (dd, *J*_{P-H} = 11.8 and *J*_{H-H} = 7.1 Hz, 3 H), 3.58 (m, 1 H), 3.67 (dq, *J*_{P-H} = 4.5 and *J*_{H-H} = 7.3 Hz, 1 H), 3.77 (dq, *J*_{P-H} = 5.7 and *J*_{H-H} = 7.3 Hz, 1 H), 3.84 (m, 1 H), 4.29 (s, 5 H), 4.32 (s, 5 H), 4.36 (m, 1 H), 4.51 (dd, *J*_{H-H} = 2.5 and 1.5 Hz, 1 H), 4.56 (dd, *J*_{H-H} = 2.5 and 1.5 Hz, 1 H), 6.38 (dt, *J* = 3.3 and 1.5 Hz, 1 H), 6.41 (ddd, *J* = 3.4 and 1.8 Hz, 1.0 Hz, 1 H), 6.45 (dt, *J* = 3.6 and 2.0 Hz, 1 H), 6.48 (ddd, *J* = 3.3, 1.5, and 1.3 Hz, 1 H), 6.52 (d, *J* = 3.4 Hz, 1 H), 6.86 (dt, *J* = 3.4 and 0.7 Hz, 1 H), 6.98 (ddd, *J* = 6.0, 1.8, and 0.7 Hz, 1 H), 7.60 (m, 1 H), 7.63 (m, 1 H), 7.68 (m, 1 H), 7.71 (m, 1 H), 7.83 (ddd, *J* = 6.0, 1.8, and 0.7 Hz, 1 H); ¹³C NMR (100 MHz, CDCl₃) δ 19.93 (dt, *J* = 5.6 and 1.0 Hz), 20.15 (ddd, *J* = 5.8, 1.7, and 0.8 Hz), 34.88 (d, *J* = 26.0 Hz), 36.12 (d, *J* = 25.9 Hz), 66.32 (d, *J* = 3.9 Hz), 67.13 (s), 67.38 (s), 67.52 (d, *J* = 3.0 Hz), 69.55 (s), 69.75 (s), 71.02 (s), 71.52 (s), 85.58 (d, *J* = 2.3 Hz), 86.04 (d, *J* = 2.3 Hz), 90.89 (d, *J* = 9.9 Hz), 92.40 (d, *J* = 10.7 Hz), 110.67 (d, *J* = 5.0 Hz), 110.74 (d, *J* = 3.5 Hz), 111.17 (s), 111.24 (s), 119.69 (d, *J* = 2.6 Hz), 122.43 (dd, *J* =

Table 4. Summary of Crystal Data and Details of Data Collection and Refinement Parameters for **7 and **14-CH₂Cl₂****

complex	7	14-CH₂Cl₂
formula	C ₄₈ H ₄₄ Br ₂ Fe ₂ P ₂ Pd	C ₄₂ H ₃₈ O ₅ Cl ₂ Fe ₂ P ₂ Rh
fw	1060.78	1005.67
cryst syst	monoclinic	triclinic
space group	P2 ₁ (No. 4)	P1 (No. 1)
<i>a</i> (Å)	12.778(6)	10.593(2)
<i>b</i> (Å)	9.917(7)	19.665(2)
<i>c</i> (Å)	17.458(4)	10.582(2)
α (deg)		102.86(1)
β (deg)	103.79(2)	107.51(1)
γ (deg)		81.36(1)
<i>V</i> (Å ³)	2148(1)	2041.2(6)
<i>Z</i>	2	2
<i>D</i> (calcd) (g/cm ³)	1.640	1.636
cryst size (mm ³)	0.30 × 0.20 × 0.15	0.50 × 0.25 × 0.20
μ(Mo Kα) (cm ⁻¹)	30.53	14.18
scan type	ω-2θ	ω-2θ
scan rate (deg/min)	8.0	8.0
scan width (deg)	1.15 + 0.30 tan θ	1.37 + 0.30 tan θ
2θ range (deg)	3-60	3-60
no. of measd reflns	6866	12489
no. of unique reflns	6603 (<i>R</i> _{int} = 3.80)	11890 (<i>R</i> _{int} = 0.018)
no. of obsd reflns	3441	10071
(<i>I</i> > 3.00σ(<i>I</i>))		
no. of variables	496	1062
<i>R</i>	0.047	0.032
<i>R</i> _w	0.061	0.036
<i>S</i>	1.99	1.55
max shift/error in final cycle	0.01	0.22
maximum peak in diff Fourier map (e/Å ³)	1.06	0.71
minimum peak in diff Fourier map (e/Å ³)	-0.75	-0.72

14.5 Hz, 1.6 Hz), 125.39 (d, *J* = 17.2 Hz), 129.19 (d, *J* = 20.6 Hz), 142.30 (ddd, *J* = 34.2, 13.7, and 1.4 Hz), 144.90 (dd, *J* = 52.3 and 7.3 Hz), 145.65 (ddd, *J* = 48.0, 6.6, and 3.5 Hz), 146.38 (d, *J* = 4.2 Hz), 146.71 (d, *J* = 4.6 Hz), 147.12 (d, *J* = 2.7 Hz), 147.49 (d, *J* = 3.8 Hz), 147.95 (ddd, *J* = 58.4, 2.5 and 1.7 Hz), 184.83 (ddd, *J* = 72.5, 18.2, and 14.9 Hz); ³¹P NMR (81 MHz, CDCl₃) δ 4.5 (dd, ¹*J*_{Rh-P} = 134.9 and ²*J*_{P-P} = 394.0 Hz), 12.3 (dd, ¹*J*_{Rh-P} = 133.3 and ²*J*_{P-P} = 394.0 Hz). Anal. Calcd for C₄₁H₃₆ClFe₂O₅P₂Rh·CH₂Cl₂: C, 50.16; H, 3.61. Found: C, 50.06; H, 3.65.

X-ray Crystal Structure Analysis of **7.** Suitable crystals for diffraction study were grown by slow diffusion of ethanol into a CH₂Cl₂ solution of **7** at 4 °C. The data were collected at 20 °C on a Rigaku AFC7R diffractometer with graphite-monochromated Mo Kα radiation. Cell constants and an orientation matrix for data collection were obtained from a least-squares refinement using the setting angles of 25 carefully centered reflections in the range of 24.45 < 2θ < 28.25°. The intensities of three standard reflections monitored every 150 reflections showed no serious decay. All data were corrected for Lorentz and polarization effects but not for

absorption. A correction for secondary extinction was applied (coefficient = 9.56834 × 10⁻⁷). A summary of cell parameters, data collection conditions, and refinement results is given in Table 4.

The initial positional parameters of palladium atoms were determined by the direct method (MITHRIL90). Subsequent difference Fourier synthesis located all non-hydrogen atoms (DIRDIF), which were refined anisotropically. All hydrogen atoms were located in calculated positions (*d*(C-H) = 0.95 Å), and their isotropic temperature factors were set equal to *B*_{eq} of the carbon atoms to which they were attached. All hydrogen atoms were included but not refined. All calculations were performed using the teXsan crystallographic software package.

X-ray Crystal Structure Analysis of **14-CH₂Cl₂.** Suitable crystals for diffraction study were grown by slow diffusion of ethanol into a CH₂Cl₂ solution of **14** at 4 °C. The data were collected at 20 °C on a Rigaku AFC7R diffractometer with graphite-monochromated Mo Kα radiation. Cell constants and an orientation matrix for data collection were obtained from a least-squares refinement using the setting angles of 25 carefully centered reflections in the range of 38.65 < 2θ < 39.57°. The intensities of three standard reflections monitored every 150 reflections showed no serious decay. All data were corrected for Lorentz and polarization effects but not for absorption. A summary of cell parameters, data collection condition, and refinement results is given in Table 4.

Cell parameters suggested that each unit cell contained a set of two independent molecules. The initial positional parameters of two rhodium atoms were determined by the direct method (SAPI91). Subsequent difference Fourier synthesis located all non-hydrogen atoms (DIRDIF), which were refined anisotropically. All hydrogen atoms were located in calculated positions (*d*(C-H) = 0.95 Å), and their isotropic temperature factors were set equal to *B*_{eq} of the carbon atoms to which they were attached. All hydrogen atoms were included in fixed positions, and their isotropic thermal parameters were refined. Two independent molecules have almost the same structure except for the positions of oxygen atoms in furyl groups on phosphorus atoms. All calculations were performed using the teXsan crystallographic software package.

Acknowledgment. We thank Mr. Tomohito Asai and Mr. Masaki Sudo for their efforts on the preparation of phosphine ligands and complexes.

Supporting Information Available: Details of full assignment of ¹H and ¹³C NMR spectra of **1a** with copies of 2D NMR spectra (¹³C-¹H HETCOR, ¹³C INADEQUATE, ¹³C-¹H HMBC), copies of ¹H and ¹³C{¹H} NMR spectra of **6b,e**; tables of atomic coordinates, *B*_{iso}/*B*_{eq}, anisotropic displacement parameters, and bond lengths and bond angles for **7** and **14**; ORTEP drawing of **14** (38 pages). This material is contained in libraries on microfiche, immediately follows this article in the microfilm version of the journal, and can be ordered from the ACS; see any current masthead page for ordering information.

OM950212I

Metallacycles with Stereogenic Metal Centers: Synthesis and Characterization of Diastereomeric Cycloruthenated Chiral Amines

Saeed Attar and John H. Nelson*

Department of Chemistry / 216, University of Nevada, Reno, Nevada 89557

Jean Fischer and André de Cian

Laboratoire de Cristallochimie (URA 424 du CNRS), Université Louis Pasteur, 4, rue Blaise Pascal, F-67070 Strasbourg Cedex, France

Jean-Pascal Sutter and Michel Pfeffer

Laboratoire de Synthèses Métallo-induites (URA 416 du CNRS), Université Louis Pasteur, 4, rue Blaise Pascal, F-67070 Strasbourg Cedex, France

Received May 31, 1995^o

The transmetalation reaction of enantiomerically pure (*R*)_C- or (*S*)_C-{ $\overline{\text{HgCl}}[\text{C}_6\text{H}_4\text{CH}(\text{Me})\text{NMe}_2]$ } with $[(\eta^6\text{-arene})\text{RuCl}_2]_2$ dimers, where $\eta^6\text{-arene} = \text{C}_6\text{H}_6$, (benzene **1**), $\text{C}_6\text{H}_5\text{CH}_3$ (toluene, **2**), and 1-Me-4-Prⁱ-C₆H₄ (cymene, **3**), in CH₃CN at ambient temperatures forms in each case a mixture of two diastereomeric ruthenacycles [*(R)*_C(*S*)_{Ru}-**a**, major, and (*R*)_C(*R*)_{Ru}-**a'**, minor, or (*S*)_C(*R*)_{Ru}-**b**, major, and (*S*)_C(*S*)_{Ru}-**b**, minor] of the type {($\eta^6\text{-arene})\overline{\text{RuCl}}[\text{C}_6\text{H}_4\text{CH}(\text{Me})\text{NMe}_2]$ } (**1a-a'**, **2a-a'**, **3a-a'** or **1b-b'**, **2b-b'**, **3b'-b**) in good chemical and optical yields. The diastereoselectivity of these reactions, which molecular mechanics calculations suggest to be under kinetic control, varies as a function of the nature of the arene ligand (de is the diastereomeric excess): benzene (90% de) > toluene (87% de) > cymene (67% de). These complexes are characterized in solution by a variety of spectroscopic techniques (¹H- and ¹³C-NMR, UV, CD) and in the solid-state by single-crystal X-ray crystallography and far-IR. X-ray crystallographic studies, carried out on **1b'**, **2b'**, and **3a**, establish the absolute configuration at the chiral Ru center in each. Both **1b'** and **2b'** crystallize in the orthorhombic space group *P*₂₁₂₁₂₁, *Z* = 4, but **3a** crystallizes in the monoclinic space group *P*₂₁, *Z* = 2. Unit cell parameters for: **1b'**: *a* = 12.886(3) Å, *b* = 17.254(5) Å, *c* = 6.726(2) Å, *V* = 1495.4 Å³. For **2b'**: *a* = 12.523(3) Å, *b* = 18.679(5) Å, *c* = 6.765(2) Å, *V* = 1582.6 Å³. For **3a**: *a* = 14.050(4) Å, *b* = 6.633(1) Å, *c* = 10.131(3) Å, *V* = 942.5 Å³. The latter data show that of the two possible diastereomeric envelope conformations of the five-membered chelate ring in each compound only the one with a minimum C-CH₃ ··· $\eta^6\text{-arene}$ interaction is formed. NMR (CDCl₃) studies show that the Ru-N bond is preserved in solution, leading to configurationally-stable (at Ru), optically-active species. Moreover, ¹H difference NOE spectroscopy reveals the existence of a dynamic equilibrium between the two limiting conformations of the five-membered chelate ring in each diastereomeric ruthenacycle.

Introduction

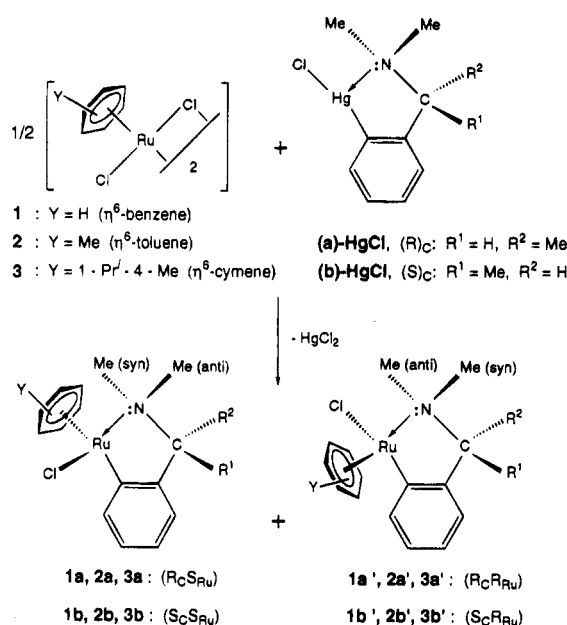
Stereoselective synthesis of organic compounds, promoted or catalyzed by optically-active transition-metal complexes, remains a very active area of research in organometallic chemistry.¹ In this respect, complexes containing either Ru(II) or Rh(I) have figured prominently.^{1c-e,2} In the case of ruthenium(II) complexes, much of the success achieved in recent years has been obtained using often expensive optically-active diphosphines such as BINAP [bis(diphenylphosphino)-1,1'-binaphthyl],^{2a-c} or aminophosphine phosphinite ligands.^{2d} The synthesis of a complex containing a chiral derivative of the *p*-cymene ligand has been reported recently.^{2e} Among the complexes of the latter group, those contain-

ing an arene ligand are especially effective, mainly due to special stability of the arene-metal bonds. Thus, in addition to classic hydrogenation of olefins, they are useful and specific catalyst precursors for C-H bond

(1) (a) Kolb, H. C.; van Nieuwenhze, M. S.; Sharpless, K. B. *Chem. Rev.* **1994**, *94*, 2483. (b) Kagan, H. B.; Riant, O. *Chem. Rev.* **1992**, *92*, 1007. (c) Noyori, R. *Chem. Soc. Rev.* **1989**, *18*, 187. (d) Brunner, H. *Top. Stereochem.* **1988**, *18*, 129. (e) Brunner, H. *Synthesis* **1988**, 645. (f) Brunner, H. *Acc. Chem. Res.* **1979**, *12*, 250. (g) Brookhart, M.; Timmers, D.; Tucker, J. R.; Williams, G. D.; Husk, G. R.; Brunner, H.; Hammer, B. *J. Am. Chem. Soc.* **1983**, *105*, 6721. (h) Sokolov, V. I. *Chirality and Optical Activity In Organometallic Compounds*; Gordon and Breach Science Publishers: New York, 1990. (i) Morrison, J. D., Ed. *Asymmetric Synthesis*; Academic Press: Orlando, 1985; Vol. 5 (Chiral Catalysis). (j) Bosnich, B., Ed. *Asymmetric Catalysis*; Martinus Nijhoff Publishers: Dordrecht, The Netherlands, 1986. (k) Davies, S. G. *Pure Appl. Chem.* **1988**, *60*, 40. (l) Davies, S. G. *Aldrichimica Acta* **1990**, *23*, 31. (m) Ito, Y.; Sawamura, M.; Hayashi, T. *J. Am. Chem. Soc.* **1986**, *108*, 6405. (n) Hayashi, T.; Uozumi, Y.; Yamasaki, A.; Sawamura, M.; Hamashima, H.; Ito, Y. *Tetrahedron Lett.* **1991**, *32*, 2799.

^o Abstract published in *Advance ACS Abstracts*, September 1, 1995.

Scheme 1



activation and activation of alkynes.^{2f} Furthermore, the ease and generality of their preparation and their thermodynamic stability have been additional factors in the recent rise of their use in catalytic studies.

We have embarked on a project to prepare a series of cyclometalated, diastereomeric complexes of Ru(II) of

the type $\{(\eta^6\text{-arene})\text{RuCl}[\text{C}_6\text{H}_4\text{CH}(\text{Me})\text{NMe}_2]\}$, **1a,a'**–

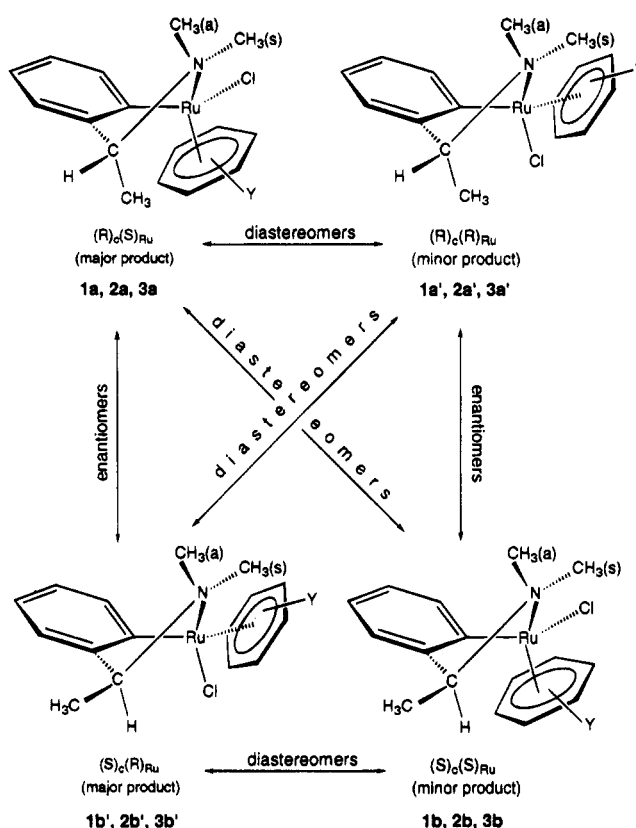
3b,b', where $\eta^6\text{-arene} = \text{C}_6\text{H}_6$ (benzene, **1**), $\text{C}_6\text{H}_5\text{Me}$ (toluene, **2**), or 1-Me-4-Prⁱ-C₆H₄ (cymene, **3**), and either of the two bidentate, chiral ligands (R)_C-(+)- or (S)_C-(–)- *N,N*-dimethyl-1-phenylethylamine, **a** or **b**, respectively (Schemes 1 and 2). The “prime” in the structural designations of each pair of diastereomers symbolizes the fact that the two members are identical in the absolute configuration of their benzylic carbon atom but are different in that of the ruthenium center.

Our interest in this project stems from the fact that the stability of the metal–arene bond in complexes containing this ligand often results in very interesting reactivity patterns and catalytic properties.^{2f} In addition, metallacycles with stereogenic metal centers have been used or implicated in a number of catalytically or stoichiometrically important asymmetric organic transformations.^{1d–m} It is generally believed that the chirality at the metal, in addition to that of the chiral ligand, plays an important role in such transformations. Nevertheless, the extent of such a role is not very well understood, mainly due to the lack of a large set of data on such complexes.^{1f,3g} A literature search³ reveals that there is only a handful of reports on resolved and well-characterized diastereomeric, monoarene ruthenacycles. Thus, further studies on these types of compounds are warranted.

Compounds **1a,a'**–**3b,b'**, which are obtained in high

(2) (a) Noyori, R.; Takaya, H. *Acc. Chem. Res.* **1990**, *23*, 345. (b) Wan, K.; Davis, M. E. *Tetrahedron: Asymmetry* **1993**, *4*, 2461. (c) Krasik, P.; Alper, H. *Tetrahedron: Asymmetry* **1992**, *3*, 1283. (d) Hapiot, F.; Agbossou, F.; Mortreux, A. *Tetrahedron: Asymmetry* **1994**, *5*, 515. (e) Petrici, P.; Pitzalis, E.; Marchetti, F.; Rosini, C.; Salvadori, P.; Bennett, M. A. *J. Organomet. Chem.* **1994**, *466*, 221. (f) Le Bozec, H.; Touchard, D.; Dixneuf, P. H. *Adv. Organomet. Chem.* **1989**, *29*, 163. (g) Faller, J. W.; Chase, K. *J. Organometallics* **1995**, *14*, 1592.

Scheme 2



chemical and optical yields, represent a novel series of stable and configurationally-rigid (under mild conditions) ruthenacycles with a stereogenic Ru(II) center. Furthermore, we have recently shown⁴ that internal alkynes insert into the Ru–C bonds of complexes of this type, leading to the formation of novel Ru(0) sandwich complexes with good chemo- and regioselectivities; the organic moiety is subsequently isolated by oxidative demetalation induced by CuBr₂. Thus, considering the well-defined geometry and configurational stability of these compounds (*vide infra*) in addition to their demonstrated reactivity,⁴ our long-term goals in undertaking this project are (i) to carry out studies on the stereochemical courses of simple reactions which they undergo and (ii) to utilize such information in asymmetric transformations of organic molecules. Herein we report the synthesis of ruthenacycles **1a,a'**–**3b,b'** and their characterization *via* a variety of spectroscopic methods (¹H- and ¹³C-NMR, IR, UV, CD). In addition, X-ray crystallographic characterization of three complexes (**1b'**, **2b'**, **3a**) has established the absolute configuration of the Ru(II) center in each compound. Finally, a possible explanation for the observed stereoselectivity in the reactions leading to the formation of these complexes is offered.

(3) (a) Brunner, H.; Oeschey, R.; Nuber, B. *Inorg. Chem.* **1995**, *34*, 3349. (b) Brunner, H.; Oeschey, R.; Nuber, B. *Angew. Chem., Int. Ed. Engl.* **1994**, *33*, 866. (c) Mandal, S. K.; Chakravarty, A. R. *Inorg. Chem.* **1993**, *32*, 3851. (d) Mandal, S. K.; Chakravarty, A. R. *J. Chem. Soc., Dalton Trans.* **1992**, 1627. (e) Mandal, S. K.; Chakravarty, A. R. *J. Organomet. Chem.* **1991**, *417*, C59. (f) Martin, G. C.; Boncella, J. M. *Organometallics* **1989**, *8*, 2863. (g) Consiglio, G.; Morandini, F. *Chem. Rev.* **1987**, *87*, 761. (h) Brunner, H. *Adv. Organomet. Chem.* **1980**, *18*, 151.

(4) (a) Abbenhuis, H. C. L.; Pfeffer, M.; Sutter, J.-P.; de Cian, A.; Fischer, J.; Ji, H. L.; Nelson, J. H. *Organometallics* **1993**, *12*, 4464. (b) Pfeffer, M. *Pure Appl. Chem.* **1992**, *64*, 335.

Results and Discussion

Ruthenacycles **1a,a'**–**3b,b'** are prepared by the transmetalation reaction of 1 equiv of either optically pure (*R*)_C - or (*S*)_C-[HgCl{C₆H₄CH(Me)NMe₂}]^{5a} **a**- or **b**-HgCl₂, respectively, with 0.5 equiv of each of the dimeric [(η^6 -arene)RuCl₂]₂ complexes,^{5b,c} where arene = η^6 -benzene (**1**), η^6 -toluene (**2**), or η^6 -cymene (**3**), in acetonitrile at ambient temperatures (Scheme 1). The latter dimers provide an ideal entryway into the synthesis of compounds of the type reported here due to their ease of preparation with a variety of arenes and also due to their remarkable air and moisture stability.^{5b,c} In addition, their transmetalation reactions with the Hg(II) derivatives of the chiral amine ligands are very clean and do not require extensive further workup. It should be noted here that attempts to prepare **1a,a'**–**3b,b'** via similar reactions with Zn(II) derivatives of the type L₂-Zn (L = **a** or **b**) met with failure mostly due to the air and moisture sensitivity of the latter which led to the formation of unidentified products and elemental ruthenium. The direct reaction of the ortholithiated derivatives of the two ligands **a** or **b** with the [(η^6 -arene)RuCl₂]₂ dimers also failed as elemental ruthenium was the major product.^{4a} It is noteworthy that these ruthenacycles can also be prepared via direct cyclo-metalation (intramolecular C–H bond activation) reaction starting from [(η^6 -arene)RuCl₂]₂ and one of the chiral amines **a** or **b**.^{4a} However, this reaction suffers from very poor chemical yields (~10%–20%) and from the fact that twice the amount of the often expensive chiral amine ligand is required. Performing the latter reaction in the presence of either Ag(C₂H₃O₂) or AgBF₄, following a report by Ryabov and Eldik^{5d} on the cycloplatination of an arylazide ligand, did not lead to any improvement of the previous results.

Each of the transmetalations (depicted in Scheme 1) leads to the formation of only two out of four possible diastereomers. The ruthenium atom becomes a chiral center during the course of this reaction, in addition to the existing chirality at the benzylic carbon atom of ligands **a** or **b**. The stereochemistry at the latter atom remains fixed as it is not a reaction center. Thus, each pair of diastereomers, e.g., **1a,a'**, differs only in the absolute configuration at their Ru center. The stereochemical relationships between the members of each diastereomeric pair, as well as those with the other two pairs, are illustrated in Scheme 2. Each pair is isolated from its crude reaction mixture as a homogeneous orange-red powder following removal of the formed HgCl₂ by filtration chromatography on alumina. The chemical yields are good, ranging from 50% to 55%. Each diastereomeric mixture can be further enriched in the major species by fractional crystallization from a CH₂Cl₂:(hexane–Et₂O, 1:1) mixture.

Since the members in each diastereomeric pair show well-separated signals in the (CDCl₃) ¹H-NMR spectra of their product mixture and are stable toward interconversion in solution (*vide infra*), the stereoselectivity or optical yield of each reaction can be assessed from

Table 1. Reaction Stereoselectivity for Ruthenacycles **1a,a'**–**3b,b'**

η^6 -arene	products		major:minor ratio	% de ^a
	major	minor		
benzene	1a	1a'	20:1	90.4
benzene	1b'	1b	20:1	90.4
toluene	2a	2a'	14:1	86.7
toluene	2b'	2b	14:1	86.7
cymene	3a	3a'	5:1	66.7
cymene	3b'	3b	5:1	66.7

^a Percentage of diastereomeric excess (de) = (% major – % minor), as determined from the ¹H-NMR spectra of the crude reaction products.

the ratio of their integrated intensities. The results are presented as percentages of diastereomeric excess (% de) in Table 1. As seen in this table, the major-to-minor ratio (hence, % de) remains constant with the changing chirality at the benzylic C atom, e.g., (**1a:1a'**) = (**1b':1b**) = 20. But, this ratio changes according to the nature of the arene ligand.

Each diastereomeric ratio corresponds to the reaction mixture obtained immediately after filtration chromatography to eliminate HgCl₂. The same ratio is obtained from the crude reaction mixture in each case; thus, the workup does not alter this ratio. In addition, the ¹H-NMR spectra obtained on CDCl₃, acetone-*d*₆, and CD₃-NO₂ solutions of these diastereomeric ruthenacycles are independent of time (days) and temperature (–20 to 50 °C), indicating their configurational stability.^{3a} Thus, each ratio reflects the difference in activation energies for the formation of two diastereomeric transition states from the same prochiral precursor, i.e., the [(η^6 -arene)-RuCl₂]₂ dimer, in the kinetically-controlled transmetalation reaction which leads to the formation of the two products (*vide infra*). It is noteworthy that, although optically-active organometallic compounds containing stereogenic metal centers were first reported more than a decade ago, there are not many clear examples of kinetic control of asymmetric induction in the formation of such compounds.^{1f,3} Furthermore, it has been possible to determine the optical yields of only a few of those reactions in which kinetic control has been indicated. This is mainly due to (i) interconversion of the two diastereomers caused by vigorous conditions often required to drive such reactions and (ii) the presence of paramagnetic species in crude reaction mixtures which prevents the obtainment of their ¹H-NMR spectra. Thus, the ruthenacycles reported here provide, in addition to their structural aspects, an opportunity to assess such stereoselectivities.

The solid-state and solution-phase structures of **1a,a'**–**3b,b'** were elucidated via a combination of X-ray crystallographic and NMR spectroscopic studies. We will first discuss the solid-state structures of three compounds as representatives: **1b'**, **2b'**, and **3a**. Suitable crystals were obtained by the slow diffusion of a 1:1 mixture of hexane–ether into a saturated CH₂Cl₂ solution of each compound. Crystallographic data and details of structure determination and refinement for the three compounds are presented in Table 2 and in the Experimental Section, respectively. The atomic coordinates and equivalent isotropic displacement parameters are given in Tables 3 (**1b'**), 4 (**2b'**), and 5 (**3a**). Table 6 presents a selected list of structural parameters for the three compounds. The molecular structures

(5) (a) Attar, S.; Nelson, J. H.; Fischer, J. *Organometallics*, in press. (b) Bennett, M. A.; Smith, A. K. *J. Chem. Soc., Dalton Trans.* **1974**, 233. (c) Zelonka, R. A.; Baird, M. C. *Can. J. Chem.* **1972**, *50*, 3063. (d) Ryabov, A. D.; van Eldik, R. *Angew. Chem., Int. Ed. Engl.* **1994**, *33*, 783.

Table 2. Crystallographic Data for Ruthenacycles 1b', 2b', and 3a

	1b'	2b'	3a
chem formula	C ₁₆ H ₂₀ NCIRu	C ₁₇ H ₂₂ NCIRu	C ₂₀ H ₂₈ NCIRu
fw	362.9	376.9	419.0
cryst syst	orthorhombic	orthorhombic	monoclinic
a (Å)	12.886(3)	12.523(3)	14.050(4)
b (Å)	17.254(5)	18.679(5)	6.633(1)
c (Å)	6.726(2)	6.765(2)	10.131(3)
β (deg)			93.42(2)
V (Å ³)	1495.4	1582.6	942.5
Z	4	4	2
space group	P2 ₁ 2 ₁ 2 ₁	P2 ₁ 2 ₁ 2 ₁	P2 ₁
λ (Å)	0.7107	0.7107	0.7107
ρ _{calcd} (g cm ⁻³)	1.612	1.582	1.476
μ (cm ⁻¹)	11.951	11.323	9.582
abs min / max	0.80 / 1.00	0.94 / 1.00	0.91 / 1.00
R(F) ^a	0.023	0.027	0.021
R _w (F) ^b	0.024	0.039	0.025

^a R(F) = Σ(|F_o| - |F_c|) / Σ(|F_o|). ^b R_w(F) = [Σw(|F_o| - |F_c|)² / Σw|F_c|²]^{1/2}; w = 1/σ²(F)² = σ²(counts) + (pI)².

Table 3. Atom Coordinates and Equivalent Isotropic Displacement Parameters^a for**(S)_C(R)_{Ru}-{(η⁶-C₆H₆)RuCl[C₆H₄CH(Me)NMe₂]}, 1b'**

atom	x	y	z	B (Å ²)
Ru	0.96653(2)	0.16695(1)	0.92541(4)	2.008(3)
Cl	0.83363(7)	0.15514(6)	1.1818(1)	3.20(2)
C1	1.0917(3)	0.2479(3)	0.8750(7)	4.10(9)
C2	1.0118(4)	0.2864(2)	0.9734(6)	4.4(1)
C3	0.9127(4)	0.2880(2)	0.8894(8)	4.5(1)
C4	0.8935(3)	0.2526(2)	0.7100(7)	4.42(9)
C5	0.9714(4)	0.2121(2)	0.6179(6)	4.46(9)
C6	1.0726(4)	0.2095(2)	0.6981(7)	3.98(8)
C7	1.0606(2)	0.1002(2)	1.1036(5)	2.33(6)
C8	1.1473(3)	0.1242(2)	1.2140(6)	2.88(7)
C9	1.0284(3)	0.0725(3)	1.3177(6)	3.53(8)
C10	1.1860(3)	-0.0055(3)	1.3154(6)	3.59(8)
C11	1.0997(3)	-0.0314(2)	1.2131(6)	3.33(8)
C12	1.0362(3)	0.0206(2)	1.1107(4)	2.31(6)
C13	0.9369(3)	-0.0023(2)	1.0088(5)	2.50(6)
C14	0.9235(4)	-0.0887(2)	0.9667(7)	3.76(9)
N	0.9264(2)	0.0494(2)	0.8280(4)	2.26(5)
C15	0.9975(3)	0.0220(2)	0.6695(6)	3.37(8)
C16	0.8182(3)	0.0473(2)	0.7506(7)	3.71(8)

^a Anisotropically refined atoms are given in the form of the isotropic equivalent displacement parameter defined as: (1/3)[a²β(1,1) + b²β(2,2) + c²β(3,3) + ab(cos γ)β(1,2) + ac(cos β)β(1,3) + bc(cos α)β(2,3)].

along with the adopted numbering schemes are shown as ORTEP drawings in Figures 1 (1b'), 2 (2b'), and 3 (3a).

For 1b' and 2b', the structure of each compound consists of four monomeric molecules arranged in an orthorhombic unit cell (space group P2₁2₁2₁). However, for 3a only two monomeric molecules crystallize in a monoclinic unit cell (space group P2₁). As seen in Figures 1–3, the geometry around the Ru atom in each structure is that of a "three-legged piano stool" in which the η⁶-coordinated arene ligand occupies the "stool" position while the C and N atoms of the arylamino ligand, in addition to the Cl atom, occupy the three "leg" positions. Thus, the Ru atom in each structure is in a pseudotetrahedral environment with four different groups attached to it, rendering it a chiral center. Since the chiral benzylic C atom of the arylamino group is not a reaction center in the course of formation of these diastereomers, its absolute configuration is unambiguously assigned according to that in the a- or b-HgCl starting material^{5a} (Scheme 1): (S)_C for 1b' and 2b' and

Table 4. Atom Coordinates and Equivalent Isotropic Displacement Parameters^a for (S)_C(R)_{Ru}-**{(η⁶-C₆H₅CH₃)RuCl[C₆H₄CH(Me)NMe₂]}, 2b'**

atom	x	y	z	B (Å ²)
Ru	0.96721(3)	0.16211(2)	0.85111(4)	2.043(4)
Cl	0.83242(9)	0.14822(6)	1.1090(2)	2.98(2)
C1	1.0955(5)	0.2369(3)	0.7976(9)	4.0(1)
C2	1.0713(6)	0.2041(3)	0.6198(8)	4.5(1)
C3	0.9680(7)	0.2068(3)	0.5489(8)	6.4(2)
C4	0.8890(6)	0.2441(4)	0.650(1)	7.6(2)
C5	0.9158(6)	0.2741(3)	0.834(1)	6.3(2)
C6	1.0196(6)	0.2727(2)	0.9067(8)	4.6(1)
C7	1.043(1)	0.3090(3)	1.100(1)	8.1(2)
C8	1.0650(3)	0.0944(2)	1.0238(6)	1.95(6)
C9	1.1535(3)	0.1212(2)	1.1325(7)	2.69(8)
C10	1.2164(4)	0.0726(3)	1.2396(7)	3.27(9)
C11	1.1904(4)	0.0011(3)	1.2401(7)	3.35(9)
C12	1.1023(4)	-0.0219(2)	1.1345(7)	2.75(7)
C13	1.0400(3)	0.0258(2)	1.0293(6)	2.23(6)
C14	0.9383(3)	0.0045(2)	0.9250(7)	2.18(7)
C15	0.9296(5)	-0.0758(3)	0.8766(9)	3.9(1)
N	0.9262(3)	0.0540(2)	0.7484(5)	2.30(6)
C16	0.8148(4)	0.0518(3)	0.6755(8)	3.63(9)
C17	0.9974(5)	0.0299(3)	0.5874(8)	3.6(1)

^a See footnote to Table 3.

Table 5. Atom Coordinates and Equivalent Isotropic Displacement Parameters^a for (R)_C(S)_{Ru}-**{(η⁶-1-Me-4-Prⁱ-C₆H₄)RuCl[C₆H₄CH(Me)NMe₂]}, 3a**

atom	x	y	z	B (Å ²)
Ru	0.22154(1)	0.794	0.91309(2)	1.997(3)
Cl	0.31402(6)	0.5226(1)	1.02009(8)	3.20(1)
C1	0.1669(2)	0.8836(6)	1.1140(3)	2.71(5)
C2	0.1111(2)	0.7300(5)	1.0480(3)	2.98(6)
C3	0.0685(2)	0.7580(6)	0.9192(3)	3.15(8)
C4	0.0866(2)	0.9374(6)	0.8480(3)	3.17(6)
C5	0.1463(2)	1.0818(6)	0.9113(3)	3.12(6)
C6	0.1837(2)	1.0585(6)	1.0447(3)	2.94(6)
C7	0.2066(2)	0.8451(6)	1.2546(3)	3.47(8)
C8	0.1389(3)	0.9289(9)	1.3526(4)	5.2(1)
C9	0.3069(3)	0.930(1)	1.2830(4)	5.4(1)
C10	0.0435(3)	0.9692(8)	0.7090(4)	4.84(9)
C11	0.2323(2)	0.6368(5)	0.7389(3)	2.77(6)
C12	0.1603(3)	0.5286(6)	0.6696(3)	3.38(7)
C13	0.1765(3)	0.4327(7)	0.5499(4)	4.49(8)
C14	0.2643(4)	0.4434(8)	0.4983(4)	5.2(1)
C15	0.3366(3)	0.5477(7)	0.5655(4)	4.36(8)
C16	0.3222(2)	0.6419(5)	0.6846(3)	2.99(6)
C17	0.4005(2)	0.7451(5)	0.7673(3)	3.15(7)
C18	0.4870(2)	0.807(1)	0.6918(4)	5.26(8)
N	0.3548(2)	0.9139(4)	0.8404(3)	2.69(5)
C19	0.3362(3)	1.0887(6)	0.7513(4)	3.90(7)
C20	0.4195(2)	0.9829(6)	0.9530(4)	3.90(8)

^a See footnote to Table 3.

(R)_C for 3a. The absolute configuration at ruthenium is then assigned assuming the following priority numbers:⁶ 1 (η⁶-arene ligand), 2 (Cl atom), 3 (N atom), and 4 (phenyl C atom). Thus, each of the structures 1b' and 2b' is designated as the (S)_C(R)_{Ru} diastereomer, while that of 3a is designated as the (R)_C(S)_{Ru} diastereomer. It is interesting to note that the ¹H-NMR spectra obtained on CDCl₃ solutions of the bulk samples from which the X-ray-quality crystals were isolated show the existence of two diastereomers in the same ratio as that observed before crystallization. Since the lack of any observable epimerization in these ruthenacycles in

(6) (a) Cahn, R. S.; Ingold, C.; Prelog, V. *Angew. Chem., Int. Ed. Engl.* 1966, 5, 385. (b) Stanley, K.; Baird, M. C. *J. Am. Chem. Soc.* 1975, 97, 6598. (c) Sloan, T. E. *Top. Stereochem.* 1981, 12, 1.

Table 6. Selected Structural Parameters for Ruthenacycles **1b'**, **2b'**, and **3a**

compound/ abs config	bond distances (Å)						bond angles (deg)			chelate ring puckering ^c
	Ru-C(arene) ^a	Ru-C(aryl)	Ru-N	Ru-Cl	C-C(arene) ^b	C-C(aryl) ^b	C(aryl)-Ru-N	C(aryl)-Ru-Cl	N-Ru-Cl	
1b' / [(S) _C (R) _{Ru}]	2.201(4)	2.057(3)	2.193(3)	2.439(1)	1.389(7)	1.391(5)	78.2(1)	87.43(9)	88.19(9)	18.9°
2b' / [(S) _C (R) _{Ru}]	2.202(6)	2.058(4)	2.196(4)	2.441(1)	1.389(4)	1.391(7)	78.2(2)	86.9(1)	88.1(1)	18.5°
3a / [(R) _C (S) _{Ru}]	2.225(4)	2.064(3)	2.201(3)	2.4373(8)	1.429(5)	1.389(6)	77.8(1)	86.69(9)	88.50(8)	18.4°
achiral ^d	2.18	2.08(1)	2.148(8)	2.430(2)	1.401(2)	1.372(3)	77.1(3)	86.0(3)	86.6(2)	18.2°

^a Mean value of the six Ru-C distances which range as follows: **1b'** [2.164(4)–2.274(4) Å], **2b'** [2.160(6)–2.272(7) Å], **3a** [2.169(3)–2.269(3) Å], achiral analog [2.13(2)–2.22(2) Å]. ^b Mean value of the six C-C distances. ^c The extent of this puckering is reflected in the value of the dihedral angle between the C(benzyl, chiral)-C(aryl) and C(aryl)-Ru-N planes. ^d Achiral analog of the benzene compound, $\{(\eta^6\text{-C}_6\text{H}_6)\text{RuCl}[\text{C}_6\text{H}_4\text{CH}_2\text{NMe}_2]\}$, from ref 4a.

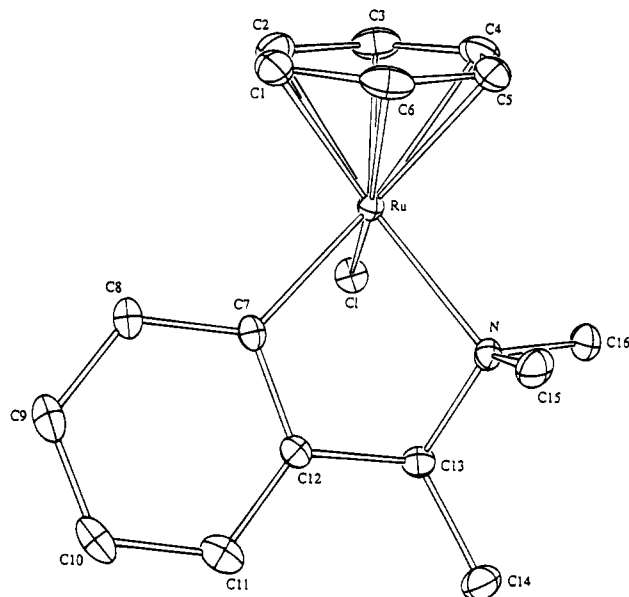


Figure 1. ORTEP drawing of $(S)_C(R)_{Ru}\{(\eta^6\text{-C}_6\text{H}_6)\text{RuCl}[\text{C}_6\text{H}_4\text{CH}(\text{Me})\text{NMe}_2]\}$, **1b'**, showing the atom-numbering scheme (50% probability ellipsoids); Hydrogen atoms have been omitted for clarity.

solution over a period of several days at ambient temperatures, hence, their configurational stability, has been established (*vide supra*), one has to assume that each bulk-crystallized sample is a solid mixture of the two diastereomers in a ratio equal to that observed in their solutions. Thus, we assign the crystal structures presented here to those of the major species in each diastereomeric mixture since it follows from the above discussion that the crystals of this species have a higher statistical chance of being isolated from a mixture. This argument is also supported by the reasonably high % de values obtained for these reactions, especially in the case of the **1a,a'** and **1b,b'** pairs (90% de). All attempts to separate the minor diastereomer by column chromatography and/or fractional crystallization have met with failure; the same solid mixture is obtained in every case.

As evident from the data in Table 6, the bond lengths and angles do not change significantly among the three structures. The effect of the additional steric requirement of the benzylic methyl group on the conformation of these structures becomes evident when one compares the structural parameters of these three compounds with those of the achiral analog of the η^6 -benzene compound, $\{(\eta^6\text{-C}_6\text{H}_6)\text{RuCl}[\text{C}_6\text{H}_4\text{CH}_2\text{NMe}_2]\}$.^{4a} One parameter which is clearly indicative of this effect is the Ru-N bond distance in the four complexes. It is shorter for the achiral analog [2.148(8) Å] than for the three

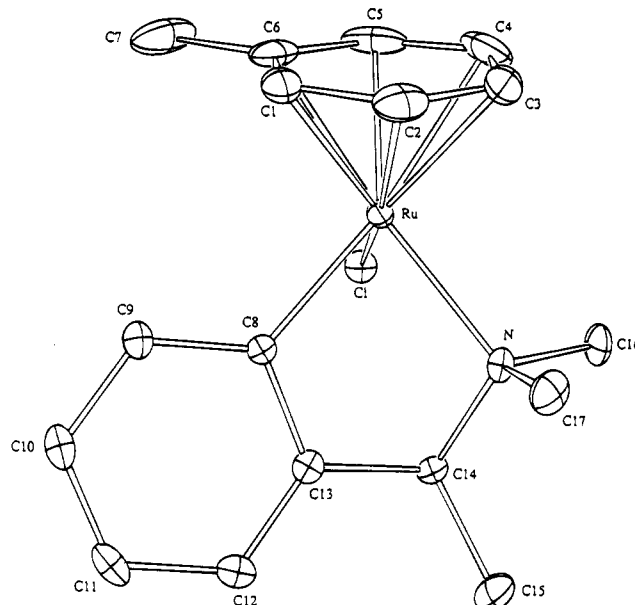


Figure 2. ORTEP drawing of $(S)_C(R)_{Ru}\{(\eta^6\text{-C}_6\text{H}_5\text{CH}_3)\text{-RuCl}[\text{C}_6\text{H}_4\text{CH}(\text{Me})\text{NMe}_2]\}$, **2b'**, showing the atom-numbering scheme (50% probability ellipsoids); hydrogen atoms have been omitted for clarity.

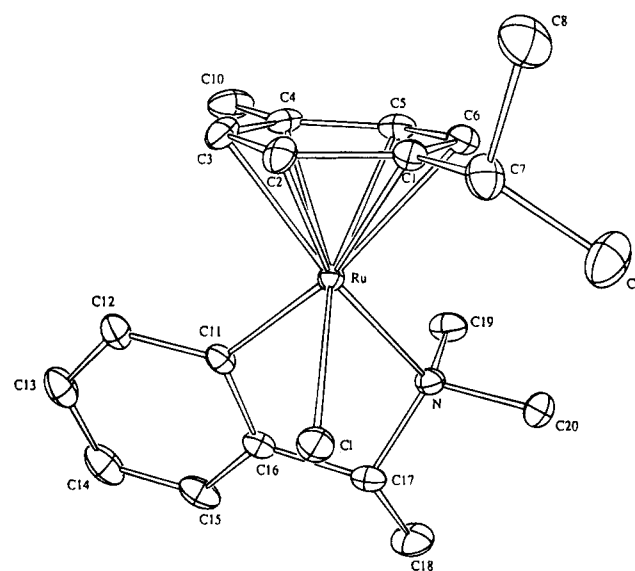
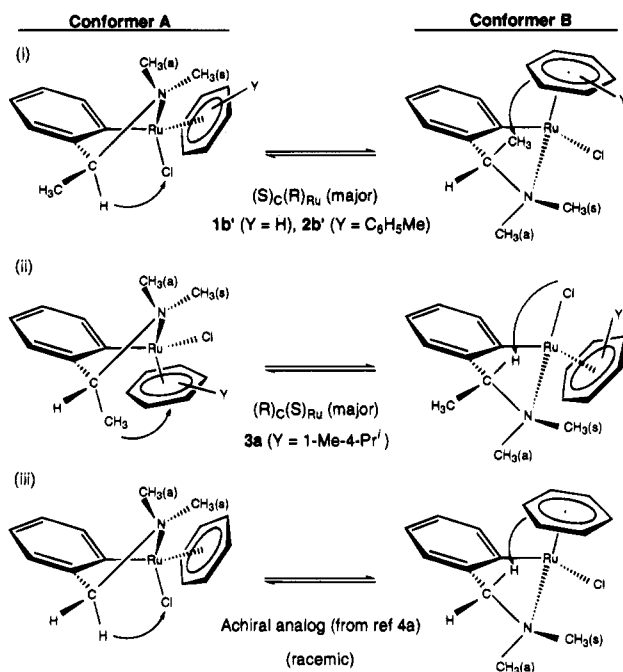


Figure 3. ORTEP drawing of $(R)_C(S)_{Ru}\{(\eta^6\text{-1-Me4-Pr-C}_6\text{H}_4)\text{RuCl}[\text{C}_6\text{H}_4\text{CH}(\text{Me})\text{NMe}_2]\}$, **3a**, showing the atom-numbering scheme (50% probability ellipsoids); Hydrogen atoms have been omitted for clarity.

chiral compounds [2.193(3) Å (**1b'**); 2.196(4) Å (**2b'**); 2.201(3) Å (**3a**)]. On the basis of a Ru covalent radius

Scheme 3



of 1.42 Å^{7a} and an N (sp^3) radius of 0.70 Å,^{7b} the estimated length of a Ru–N single bond is 2.12 Å. Thus, the Ru–N distances reported here are not significantly longer than the expected values. Factors such as residual strain in the chelate ring, the steric crowding of the axial groups, and the *trans* influence of the Cl group may contribute to such observed bond lengthening. The bite of the bidentate benzylamino ligand, represented by the C(aryl)–Ru–N angle, is remarkably similar ($\sim 78^\circ$) in the four complexes listed in Table 6.

The five-membered chelate ring in each compound is puckered at its Ru–N–C(benzyl) portion. The extent of this puckering is reflected in the value of the dihedral angle between the Ru–C(aryl)–C(aryl, ortho)–C(benzyl, chiral) and C(aryl)–Ru–N planes, and is listed in the last column in Table 6. The puckering of the chelate ring makes possible the existence of two limiting diastereomeric envelope conformations.^{8a} This is illustrated in Scheme 3 for the major diastereomer of each of the four complexes compared here.

As seen in Scheme 3, the 1,3-diaxial interaction is the most significant one in each of the two diastereomeric conformers **A** and **B**. The X-ray crystal structures presented in Figures 1–3 indicate that, in the solid-state, the 1,3-diaxial η^6 -arene $\cdots CH_3$ interaction in each compound is disfavored. Thus, for **1b'** and **2b'** only conformer **A**, and for **3a** only conformer **B**, are observed. This (η^6 -arene) \cdots (group) interaction is disfavored even when the group is H, as is the case in the structure of the achiral analog^{4a} (Scheme 3, reaction iii) which crystallizes only as conformer **A** and its enantiomer.

The solution structures of ruthenacycles **1a,a'**–**3b,b'** were elucidated by ¹H- and ¹³C{¹H}-NMR spectroscopic studies (Tables 7 and 8, respectively). Each spectrum shows two distinct sets of resonances for the arylamine

and arene protons which may be assigned to those of the major and minor diastereomeric pairs (Scheme 2) in varying ratios (Table 1). In our earlier report,^{4a} we had stated that, in the case of **1a,a'**, only one diastereomer could be detected in solution. Closer examination of the ¹H-NMR spectra of CDCl₃ solutions of both **1a–a'** and **1b'–b** pairs has revealed that both diastereomers are present in each solution in a ratio of 95%:5%, a ratio high enough to have permitted them to be overlooked earlier. Of particular aid in assigning the solution-phase structures is the observation of two N–CH₃ singlets (*syn* and *anti* to the η^6 -arene ring) for each of the major and minor species, which are indicative of their diastereotopic nature in these structures. This can be caused only if the pyramidal inversion at the N atom is blocked by its coordination to Ru, suggesting that the five-membered chelate ring found in the solid-state is also preserved in solution. The latter conclusion is also confirmed by our earlier report^{4a} on the structure of the achiral analog of the benzene compound, $\{(\eta^6-C_6H_6)-RuCl[C_6H_4CH_2NMe_2]\}$ where the CH₂–N group gives rise to two temperature-independent anisochronous signals (AX pattern; δ 4.32 and 2.82, $^2J_{HH} = 13$ Hz) in its ¹H-NMR (CDCl₃) spectrum. The preservation of the five-membered chelate structure in solution points toward the special configurational stability (at Ru) of these ruthenacycles, a feature which is unique among the comparable Ru(II) systems reported recently.^{3a–f} We will show in a subsequent publication that this chelate ring is not ruptured even by diphosphines.

The conformation of the chelate ring in solution was probed *via* ¹H difference NOE spectroscopy. It was found that irradiation of the arene protons results in enhancement of the signals for both the benzylic C–CH₃ and N–CH₃ (*syn*) groups. As seen in reactions i and ii of Scheme 3, the NOE results can only be explained in terms of a dynamic equilibrium between conformers **A** and **B** in solution. We have not been able to freeze out this equilibrium; however, such equilibria have been established for comparable systems. For example, the two possible conformations for the six-membered chelate ring of $\{[(5-MeO-8-N(Me)_2)CH_2]naphthyl\}MeRnSnBr$ (R = Me, Ph) can be frozen out on the NMR time scale below $-30^\circ C$.^{8b}

Configurationaly-rigid diastereomers such as **1a–1b'** (benzene), **2a–b'** (toluene), and **3a–b'** (cymene), which differ in the stereochemistry at their Ru centers, are expected to be optically active in solution and to give mirror-image CD spectra.^{1h,3h} Such spectra, along with the corresponding UV–vis data have been obtained on CH₂Cl₂ solutions of each compound (in the three pairs mentioned above) in the 300–600 nm region (see Experimental Section). The d–d electronic transitions of the metal chromophore dominate the spectra obtained in the visible and the near-UV regions, with the chiral center(s) in the ligand making only minor contributions to the chiroptical properties.^{1h} This latter statement is confirmed by the observation that the UV–vis and CD spectra of the Hg(II) salts of the chiral arylamino ligands **a** and **b** are transparent in this region.^{5a} With respect to the UV–vis spectra, each of the compounds **1a,b'** and **2a,b'** shows two strong absorption maxima at roughly similar wavelengths but with different molar absorptivities [λ_{max} , nm (ϵ , L mol⁻¹ cm⁻¹), for **1a,b'**, 366

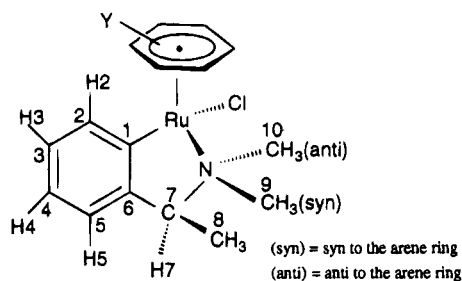
(7) (a) Howard, J.; Woodward, P. J. *J. Chem. Soc., Dalton Trans* **1975**, 59. (b) Bennett, M. J.; Mason, R. *Nature* **1965**, *205*, 760.

(8) (a) Hawkins, C. J. *Absolute Configuration of Metal Complexes*; Wiley: New York, 1971; Chapter 1. (b) van Koten, G.; Noltes, J. G. *J. Am. Chem. Soc.* **1976**, *98*, 5393.

Table 7. ^1H NMR Data for Ruthenacycles (1a,a')–(3b,b')^a

compd ^d / assgnmt ^e	δ (ppm) ^b /multiplicity ^c / J (Hz)					
	1a,1b' (major)	1a',b (minor)	2a,b' (major)	2a',b (minor)	3a,b' (major)	3a',b (minor)
H2	8.24/dd $^3J_{\text{H2H3}} = 7.5$ $^4J_{\text{H2H4}} = 1.5$	7.75/dd $^3J_{\text{H2H3}} = 7.5$ $^4J_{\text{H2H4}} = 1.5$	8.19/dd $^3J_{\text{H2H3}} = 7.5$ $^4J_{\text{H2H4}} = 1.0$	7.70/dd $^3J_{\text{H2H3}} = 7.5$ $^4J_{\text{H2H4}} = 1.0$	8.15/dd $^3J_{\text{H2H3}} = 7.5$ $^4J_{\text{H2H4}} = 1.0$	7.68/dd $^3J_{\text{H2H3}} = 7.5$ $^4J_{\text{H2H4}} = 1.0$
H3	7.08/tdd $^3J_{\text{H3H2}} = 7.5$ $^3J_{\text{H3H4}} = 7.5$ $^4J_{\text{H3H5}} = 1.5$ $^6J_{\text{H3H7}} = 1.0$	7.11/tdd $^3J_{\text{H3H2}} = 7.5$ $^3J_{\text{H3H4}} = 7.5$ $^4J_{\text{H3H5}} = 1.5$ $^6J_{\text{H3H7}} = (\text{n. r.})$	7.08/tt (app) $^3J_{\text{H3H2}} = 7.5$ $^3J_{\text{H3H4}} = 7.5$ $^4J_{\text{H3H5}} = \text{n. o.}^g$ $^6J_{\text{H3H7}} = 1.0$	7.11/tt (app) $^3J_{\text{H3H2}} = 7.5$ (n. r.) ^f $^3J_{\text{H3H4}} = 7.5$ (n. r.) ^f $^4J_{\text{H3H5}} = \text{n. o.}$ $^6J_{\text{H3H7}} = 1.0$ (n. r.)	7.09/t (app) $^3J_{\text{H3H2}} = 7.5$ $^3J_{\text{H3H4}} = 7.5$ $^4J_{\text{H3H5}} = \text{n. o.}$ $^6J_{\text{H3H7}} = \text{n. o.}$	7.08/t (app) $^3J_{\text{H3H2}} = 7.5$ $^3J_{\text{H3H4}} = 7.5$ $^4J_{\text{H3H5}} = \text{n. o.}$ $^6J_{\text{H3H7}} = \text{n. o.}$
H4	6.95/td $^3J_{\text{H4H3}} = 7.5$ $^3J_{\text{H4H5}} = 7.5$ $^4J_{\text{H4H2}} = 1.5$	6.94/td $^3J_{\text{H4H3}} = 7.5$ $^3J_{\text{H4H5}} = 7.5$ $^4J_{\text{H4H2}} = 1.5$	6.94/td (app) $^3J_{\text{H4H3}} = 7.5$ $^3J_{\text{H4H5}} = 7.5$ $^4J_{\text{H4H2}} = 1.0$	6.93/td (app) $^3J_{\text{H4H3}} = 7.5$ (n. r.) $^3J_{\text{H4H5}} = 7.5$ (n. r.) $^4J_{\text{H4H2}} = 1.0$ (n. r.)	6.92/td (app) $^3J_{\text{H4H3}} = 7.5$ $^3J_{\text{H4H5}} = 7.5$ $^4J_{\text{H4H2}} = 1.0$	6.90/td (app) $^3J_{\text{H4H3}} = 7.5$ $^3J_{\text{H4H5}} = 7.5$ $^4J_{\text{H4H2}} = 1.0$
H5	6.77/ddd $^3J_{\text{H5H4}} = 7.5$ $^4J_{\text{H5H3}} = 1.5$ $^5J_{\text{H5H2}} = 1.5$	6.74/ddd $^3J_{\text{H5H4}} = 7.5$ $^4J_{\text{H5H3}} = 1.5$ (n. r.) $^5J_{\text{H5H2}} = 1.5$ (n. r.)	6.76/d (app) $^3J_{\text{H5H4}} = 7.5$ $^4J_{\text{H5H3}} = 1.0$ (n. r.)	6.73/d (app) $^3J_{\text{H5H4}} = 7.5$ (n. r.) $^4J_{\text{H5H3}} = 1.0$ (n. r.)	6.72/d $^3J_{\text{H5H4}} = 7.5$	n. o.
H7	4.37/qd $^3J_{\text{H7H8}} = 7.0$ $^6J_{\text{H7H3}} = 1.0$ (n. r.)	3.83/qd $^3J_{\text{H7H8}} = 7.0$ $^6J_{\text{H7H3}} = 1.0$ (n. r.)	4.42/qd $^3J_{\text{H7H8}} = 7.0$ $^6J_{\text{H7H3}} = 1.0$ (n. r.)	3.85/qd $^3J_{\text{H7H8}} = 7.0$ $^6J_{\text{H7H3}} = 1.0$ (n. r.)	3.73/q $^3J_{\text{H7H8}} = 7.0$	3.41/q $^3J_{\text{H7H8}} = 7.0$
H8	1.18/d $^3J_{\text{H8H7}} = 7.0$	1.28/d $^3J_{\text{H8H7}} = 7.0$	1.18/d $^3J_{\text{H8H7}} = 7.0$	1.28/d $^3J_{\text{H8H7}} = 7.0$	1.17/d $^3J_{\text{H8H7}} = 7.0$	1.27/d $^3J_{\text{H8H7}} = 7.0$
H9 (syn)	2.47/s	1.96/s	2.44/s	3.06/s	2.41/s	1.94/s
H10 (anti)	3.38/s	3.36/s	3.33/s	3.16/s	3.30/s	3.30/s
η^6 -arene	5.34/s ^{e(i)}	5.29/s ^{e(i)}	e(ii), h	e(ii), h	e(iii), h	e(iii), h

^a Obtained at 500 MHz on CDCl_3 solutions (25 °C). ^b Referenced to TMS. ^c Multiplicity: (app) = apparent, d = doublet, dd = doublet of doublets, ddd = doublet of double-doublets; dt = doublet of triplets, q = quartet, qd = quartet of doublets, s = singlet, t = triplet, td = triplet of doublets, tdd = triplet of double-doublets, tt = triplet of triplets. ^d For structural designations see Schemes 1 and 2; for the major-to-minor ratios see Table 1. ^e Assignments are based on the following numbering scheme:



^f n. r. = not resolved due to partial obstruction of the resonance by those of other protons (mostly major). ^g n. o. = not observed due to total obstruction of the resonance by those of other protons (mostly major). ^h Assignments for the arene ring protons of toluene and cyclohexene are as follows (the assignments for the equivalent pairs of protons H12,H16 and H13,H15 are arbitrary): δ (multiplicity, J (Hz)) for **2a,b'** (major), H12, 5.42 (d, $^3J_{\text{H12H13}} = 5.5$); H13, 5.11 (t, $^3J_{\text{H13H12}} = ^3J_{\text{H13H14}} = 5.5$); H14, 4.88 (t, $^3J_{\text{H14H13}} = ^3J_{\text{H14H15}} = 5.5$); H15, 5.49 (t, $^3J_{\text{H15H14}} = ^3J_{\text{H15H16}} = 5.5$); H16, 4.88 (d, $^3J_{\text{H16H15}} = 5.5$); H17, 2.19 (s). For **2a',2b'** (minor), H12, 5.35 (d, $^3J_{\text{H12H13}} = 5.5$); H13, 5.17 (t, $^3J_{\text{H13H12}} = ^3J_{\text{H13H14}} = 5.5$); H14 (n. r.)^f; H15, 5.38 (t, $^3J_{\text{H15H14}} = ^3J_{\text{H15H16}} = 5.5$); H16, 4.59 (d, $^3J_{\text{H16H15}} = 5.5$); H17, 1.95 (s); For **3a,b'** (major), H12, 5.37 (d, $^3J_{\text{H12H13}} = 6.0$); H13, 4.39 (d, $^3J_{\text{H13H12}} = 6.0$); H15, 5.53 (d, $^3J_{\text{H15H16}} = 6.0$); H16, 4.50 (d, $^3J_{\text{H16H15}} = 6.0$); H17, 2.08 (s); H18, 2.96 (sep, $^3J_{\text{H18H19(p)}} = ^3J_{\text{H18H20(d)}} = 7.0$); H19(p), 1.31 (d, $^3J_{\text{H19(p)H18}} = 7.0$); H20(d), 1.09 (d, $^3J_{\text{H20(d)H18}} = 7.0$). For **3a',b'** (minor), H12 5.10 (d, $^3J_{\text{H12H13}} = 6.0$); H13, 4.58 (d, $^3J_{\text{H13H12}} = 6.0$); H15, 5.52 (d, $^3J_{\text{H15H16}} = 6.0$); H16, 4.51 (d, $^3J_{\text{H16H15}} = 6.0$); H17, 1.70 (s); H18, 2.87 (sep, $^3J_{\text{H18H19(p)}} = ^3J_{\text{H18H20(d)}} = 7.0$); H19(p), 1.30 (d, $^3J_{\text{H19(p)H18}} = 7.0$); H20(d), 1.18 (d, $^3J_{\text{H20(d)H18}} = 7.0$).

(1.4×10^3), 446 (1.5×10^3); for **2a,2b'**, 379, (6.0×10^2), 449, (8.0×10^2)]. However, **3a,b'** show only the absorption near 450 nm ($\epsilon = 7.2 \times 10^2$) very clearly, with the one near 370 nm having been reduced to an ill-defined shoulder. Nevertheless, the morphologies of the CD curves for these compounds are substantially similar. Figure 4 is a composite spectrum of two separate CD curves obtained for **1a** (top, dashed) and **1b'** (bottom, solid) and is representative of all three pairs. As seen in Figure 4, the CD spectra are defined by two intense Cotton effects, one at about 370 nm and another of opposite sign at about 450 nm.

Thus, there seems to be a clear correlation between the positions of the CD bands and UV-vis absorption maxima in these compounds. The amplitude ($\Delta\epsilon$) of

each Cotton effect varies with the % de in each mixture, being the highest for **1a** or **1b'** (90% de). The absolute configuration at Ru has been unambiguously determined by X-ray crystallography (*vide supra*) for one member in each of the above diastereomeric pairs: **1b'** [(*R*)_{Ru}], **2b'** [(*R*)_{Ru}], and **3a** [(*S*)_{Ru}]. As seen in Figure 4, the CD spectra of all three pairs show an almost enantiomeric (mirror-image) shape which must arise from the enantiomeric relationship between the Ru centers in each pair. Thus, we assign to the other member in each pair the opposite absolute configuration at Ru: **1a** [(*S*)_{Ru}], **2a** [(*S*)_{Ru}], and **3b'** [(*R*)_{Ru}]. By convention,⁹ the sign of a CD spectrum is determined by the sign of the Cotton effect at the longest wavelength where any such effect is observable. Thus, on the basis

Table 8. $^{13}\text{C}\{^1\text{H}\}$ NMR Data for Ruthenacycles (1a,a')–(3b,b')^a

compd ^e / assignmt ^d	δ (ppm) ^b					
	1a,b' (major)	1a',b (minor)	2a,b' (major)	2a',b (minor)	3a,b' (major)	3a',b (minor)
	Arylamino Ligand ^d					
C1 ^e	166.6	174.1	166.8	175.8	169.3	178.0
C2	137.3	139.3	137.3	139.2	149.8	146.8
C3	126.0	127.0	125.9	126.8	137.4	139.2
C4	123.4	122.5	123.2	122.2	126.1	126.8
C5	123.2	122.0	122.9	121.9	122.6	122.0
C6 ^e	149.5	148.0	149.7	147.7	110.6	113.5
C7	67.3	55.3	67.3	54.9	66.8	66.1
C8	9.3	10.4	9.3	10.3	21.1	22.2
C9 (syn)	49.5	31.9	49.3	30.9	49.2	44.0
C10 (anti)	52.3	44.3	52.0	44.3	52.2	54.6
	η^6 -Arene Ligand ^d					
C11	85.8 ^f	85.3 ^f	102.6	100.1	94.2	93.7
C12			86.2	86.7	87.6	83.7
C13			85.5	85.7	81.2	81.3
C14			81.2	82.0	77.2	79.6
C15			90.4	89.1	88.2	89.6
C16			78.5	75.8	78.2	75.4
C17			19.0	18.9	30.1	30.9
C18					17.7	20.7
C19 (p)					23.0	23.9
C20 (d)					9.3	10.3

^a Obtained at 125 MHz on CDCl₃ solutions (25 °C). ^b Referenced to TMS. ^c For structural designations see Schemes 1 and 2. ^d Assignments are based on the numbering scheme shown in footnote e to Table 7; in the toluene complexes (2a,b' and 2a',b) the assignments for C11–C16 are arbitrary; in the cymene complexes (3a,b' and 3a',b) the assignments for the equivalent C11, C16 and C12, C15 pairs are arbitrary. ^e Assignments of C1 and C6 were accomplished with the aid of APT spectra. ^f Value for the six equivalent C atoms (C11, C12, C13, C14, C15, and C16).

of the sign of the Cotton effect observed at 450 nm, we assign all the positive CD spectra to those complexes with an (*S*)_{Ru} absolute configuration (1–3a), and all the negative spectra to those with an (*R*)_{Ru} configuration (1–3b'). At this point, it is not clear which one of the two intense Cotton effects (450 or 370 nm) is a better indicator of the absolute configuration at the Ru center in these ruthenacycles.

Finally, we address the question of the observed stereoselectivity in the syntheses of these ruthenacycles. A logical corollary to the conclusion on the configurational stability of these compounds is that the transmetalation reactions leading to their formation are under kinetic, rather than thermodynamic, control. This is supported by the results of molecular mechanics calculations performed for the 12 possible diastereomers (1a,a'–3b,b') through the molecular-modeling program Spartan.^{10a} The utility and applicability of such programs for rapid calculation of conformational energy profiles and elucidation of subtle steric effects in structural organic^{10b–d} and organometallic^{10e,f} chemistry has already been established. Spartan, which incorporates such force fields as MM2, MM3, and SYBYL, deals with the problems associated with modeling π -bonded ligands in organotransition-metal chemistry. In our studies, a model of each diastereomeric molecule is built and its strain energy is calculated using the minimization routine in the program. It is found that, for each pair of diastereomers, the strain energy (E_{strain}) of the minor species is lower than that of the major, indicating that the former is thermodynamically more stable than the latter. This conclusion is in agreement with the kinetic control of this reaction since, according to Hammond's

postulate,¹¹ kinetically-controlled reactions proceed via early, reactant-like transition states, rendering product stability unimportant in determining the product ratio. Thus two "reactant-like" transition states for these transmetalation reactions may be visualized starting from the $[(\eta^6\text{-arene})\text{RuCl}_2]$ moiety (half of the starting dimer) and the chiral arylaminomercury(II) salt, a- or b-HgCl. The assumption that the former moiety is a reactant in this reaction is supported by reports^{5b,c} that $[(\eta^6\text{-arene})\text{Ru}(\text{CH}_3\text{CN})\text{Cl}_2]$ is the main species present in solutions of the corresponding dimeric compounds in CH₃CN (the solvent used in our preparations of these compounds). Moreover, halide-bridged bimetallic Hg(II) species have been implicated^{10a} and isolated^{10b} as intermediates in transmetalation reactions of the organic derivatives of this element. Thus, we propose that two diastereomeric, seven-membered chelated transition states are formed starting with a given stereochemistry at the benzylic C atom of either Hg(II) complex.

The labilization of the Ru–Cl bond *trans* to Hg (through the bridging Cl) in each transition state, and subsequent elimination of HgCl₂, results in the formation of the corresponding diastereomeric product. This proposal is supported by reports^{12c} that Hg(II) salts provide a metal-assisted pathway for the labilization of halide ions in kinetically-inert complexes (e.g., the Ru^{II} starting material). It seems that the (arylamino)-mercury(II) salt plays a dual role in this reaction, being a source of the chiral ligand as well as labilizing the *trans* Ru–Cl bond in the transition state. These ideas are schematically represented in Figure 5 for the (*S*)_C enantiomer, b–HgCl; the same results are obtained for the other enantiomer. Our calculations show that the two assumed transition states possess different strain energies, which indicates that they require different activation energies for their formation (ΔG_1^\ddagger and ΔG_2^\ddagger , kcal/mol). This explains the observed unequal concentration of the two diastereomers. In addition, and more importantly, it is noted that this difference in activation energies ($\Delta\Delta G^\ddagger$) decreases according to the nature of the η^6 -arene ligand benzene (26 kcal/mol) > toluene (24 kcal/mol) > cymene (18 kcal/mol). This trend in activation energy differences parallels that in decreasing stereoselectivity among the same series of compounds (Table 1) and is in agreement with Hammond's postulate, which states that the greater the transition-state (TS) energy differences, the higher the observed stereoselectivity would be. In each reaction then, the diastereomer with the lower activation energy is formed more quickly than the other, resulting in its higher concentration (major species). It is also noted that the magnitude of the transition-state $\Delta\Delta G^\ddagger$ value is much greater than that of the ground-state ΔE_{strain} , an observation which is in harmony with the conclusion on the kinetic control

(9) Djerassi, C.; Bunnenberg, E. *Proc. Chem. Soc., London* **1963**, 299.

(10) (a) Spartan is a UNIX-based molecular-modeling program which is available through Wavefunction, Inc. (Irvine, CA) and is supported by SiliconGraphics workstations. (b) Ripka, W. C.; Blaney, J. M. *Top. Stereochem.* **1991**, *20*, 1. (c) Lipkowitz, K. B.; Peterson, M. A. *Chem. Rev.* **1993**, *93*, 2463. (d) Eksterowicz, J. E.; Houk, K. N. *Chem. Rev.* **1993**, *93*, 2439. (e) Mackie, S. C.; Baird, M. S. *Organometallics* **1992**, *11*, 3712. (f) Hancock, R. D. *Prog. Inorg. Chem.* **1989**, *37*, 187.

(11) Hammond, G. S. *J. Am. Chem. Soc.* **1955**, *77*, 334.

(12) (a) Makarova, L. G. In *Organometallic Reactions*; Becker, E. I.; Tsutsui, M., Eds.; Wiley-Interscience: New York, 1970, Vol. 1, pp 190–193. (b) Constable, E. C.; Leese, T. A.; Tocher, D. A. *J. Chem. Soc., Chem. Commun.* **1989**, 570. (c) Twigg, M. V., Ed. *Mechanisms of Inorganic and Organometallic Reactions*; Plenum: New York, 1983–1991, Vols.1–7.

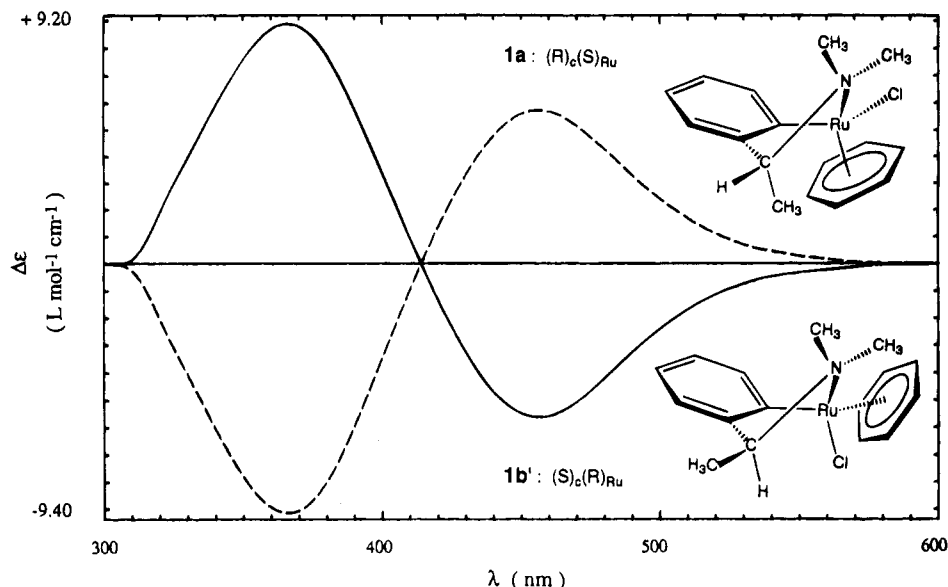


Figure 4. Circular dichroism (CD) curves obtained on CH_2Cl_2 solutions of $\{(\eta^6\text{-C}_6\text{H}_6)\text{RuCl}[\text{C}_6\text{H}_4\text{CH}(\text{Me})\text{NMe}_2]\}$ -containing as the major species: $(R)_C(S)_{\text{Ru}}$, **1a** (top, dashed), and $(S)_C(R)_{\text{Ru}}$, **1b'** (bottom, solid); the mirror-image relationship of these two diastereomers is illustrated very clearly.

of these reactions. The much lower $\Delta\Delta G^\ddagger$ value for the cymene transition states may be rationalized in terms of a more planar (less puckered) seven-membered chelate ring, brought about by a compromise between two opposing 1,3-diaxial interactions: the $\text{C}(\text{CH}_3)\cdots\text{Cl}$ interactions (minor TS) on the one hand and the $\text{C}(\text{CH}_3)\cdots\text{CH}(\text{CH}_3)_2$ interactions (major TS) on the other. The effect of the bulkiness of the cymene ligand substituents upon the puckering of the five-membered ring in the corresponding Ru(II) complex is evident from the slightly smaller value of its dihedral angle (reflecting this puckering) in **3a** (18.4°) as compared to those in **2a'** (18.5°) and **1a'** (18.9°) (Table 6). A more planar structure would have smaller angle and torsional strains, leading to an overall lower energy required for its formation.

At a reviewer's suggestion, an alternative mechanism for the formation of these complexes is illustrated in Scheme 4. The transition states in this scheme are analogous to the Wheland intermediates¹³ in electrophilic aromatic substitutions. An aronium ion with Pt and CH_3 substituents has been structurally characterized.¹⁴ The energy difference between the two diastereomeric transition states, though not calculated, would be expected to be larger than that between the diastereomeric transition states of Figure 5. The 1,3-diaxial interactions between the arene and $\text{C}(\text{CH}_3)$ moieties or the Cl and $\text{C}(\text{CH}_3)$ moieties in the five-membered chelate rings would be expected to be fairly substantial (compared to those in seven-membered chelate rings).^{8a} In this scheme, attack of Cl^- on the electrophilic Hg(II) center in each diastereomeric transition state and subsequent elimination of HgCl_2 would result in the formation of the corresponding diastereomeric products. If this mechanism were operative, it would not modify our conclusions concerning kinetic control of the diastereoselectivity.

(13) March, J. *Advanced Organic Chemistry*, 4th ed.; Wiley-Interscience: New York, 1992; pp 501–504.

(14) Terheijden, G.; van Koten, G.; Vinke, I. C.; Spek, A. L. *J. Am. Chem. Soc.* **1985**, *107*, 2891.

Experimental Section

A. Physical Measurements. NMR spectra were recorded on a Varian Unity Plus-500 FT-NMR spectrometer operating at 500 MHz for ^1H and at 125 MHz for ^{13}C . The chemical shifts for the latter nuclei were referenced to the residual solvent peaks in the observed spectra and are listed in Tables 7 and 8, respectively. FT-IR spectra were recorded on a Perkin-Elmer PE-1800 spectrometer for the far IR region (below 400 cm^{-1}) as a mineral oil mull on a polyethylene sheet (abbreviations: shp = sharp, sh = shoulder, st = strong, w = weak). UV-Visible spectra were recorded (at 25°C) on a Perkin-Elmer Lambda-11 UV-vis spectrophotometer, with a $1.0 \times 10^{-4}\text{ M}$ CH_2Cl_2 solution of each compound placed in a cuvette with a cell path-length (b) = 1.00 cm. CD spectra were recorded (at 25°C) on a JASCO J-600 spectropolarimeter, with a $2.0 \times 10^{-3}\text{ M}$ CH_2Cl_2 solution of each compound placed in a cell where $b = 1.00\text{ cm}$. Melting points were determined on a Mel-Temp apparatus; all complexes decomposed at temperatures above 180°C . Elemental analyses were performed by Galbraith Laboratories, Knoxville, TN.

B. Preparation of $\{(\eta^6\text{-arene})\text{RuCl}[\text{C}_6\text{H}_4\text{CH}(\text{Me})\text{NMe}_2]\}$

Ruthenacycles. The dimeric $\{(\eta^6\text{-arene})\text{RuCl}_2\}_2$ starting materials were prepared by established literature methods.^{5b,c} The enantiomerically-pure mercury(II) salts of the two chiral arylamino ligands were prepared according to our published method.^{5a} Acetonitrile (Aldrich Chemical Co., Milwaukee, WI) was dried over CaH_2 and distilled immediately before use. The diastereomerically-enriched mixtures of all six ruthenacycles (**1a,b'**, **2a,b'**, and **3a,b'**) were prepared *via* the same general route, i.e., the transmetalation reactions depicted in Scheme 1. The following procedure is representative:

(i) **Synthesis and Characterization of 1a** ($\eta^6\text{-arene}$ = benzene, major diastereomer $R_C S_{\text{Ru}}$) and **1b'** ($\eta^6\text{-arene}$ = benzene, major diastereomer = $S_C R_{\text{Ru}}$). Under a dry dinitrogen atmosphere, $\{(\eta^6\text{-C}_6\text{H}_6)\text{RuCl}_2\}_2$ (1, 1.04 g, 4.16 mmol) and either $(R)_C$ - or $(S)_C$ - $\{[\text{HgCl}[\text{C}_6\text{H}_4\text{CH}(\text{Me})\text{NMe}_2]\}$ (**a**- or **b**-**HgCl**, 1.64 g, 4.27 mmol) were suspended in CH_3CN ($\sim 100\text{ mL}$) and magnetically stirred at ambient temperatures. As the reaction proceeded, the original brick-red/brown color of the suspension gradually changed to a lighter orange-red (but still quite opaque) during the course of 8 h, after which time the solvent was removed *in vacuo*, forming a brown-green, solid residue. It is noteworthy

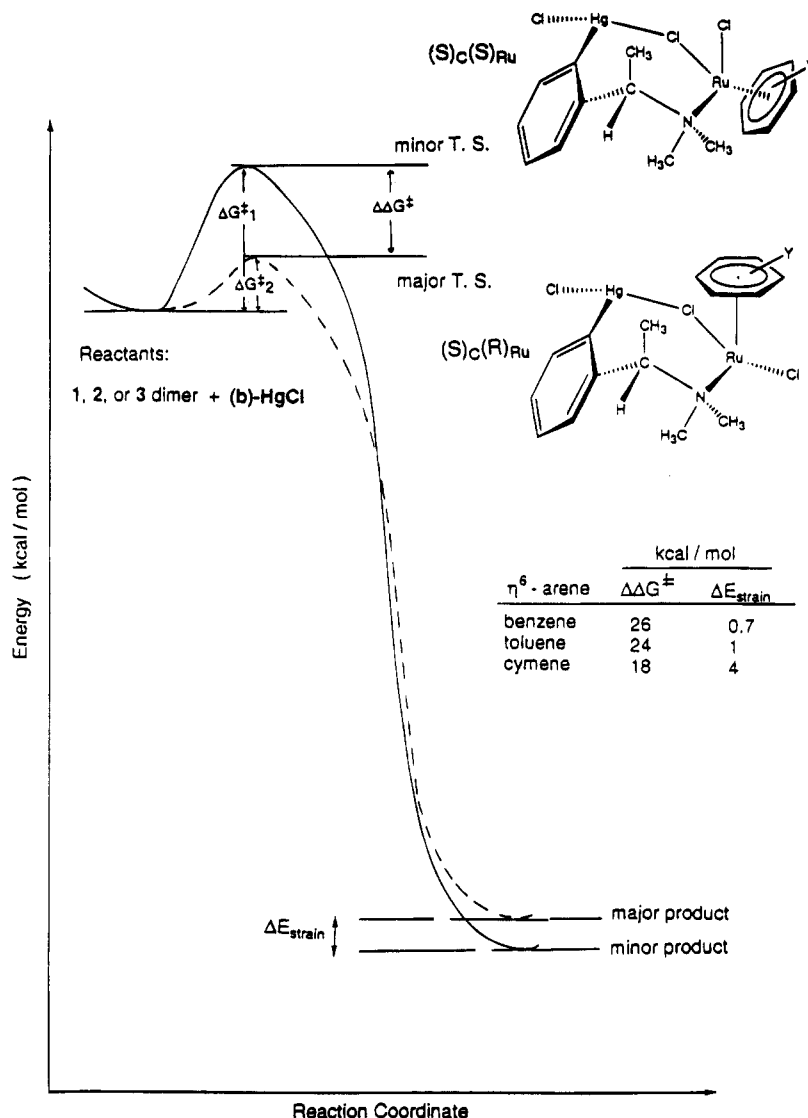


Figure 5. Schematic representation of the reaction coordinate for the transmetalations depicted in Scheme 1.

thy that increasing the reaction time to 72 h resulted in the formation of an almost transparent, orange solution. However, a similar brown-green residue was also formed upon evaporating the latter *in vacuo*. Further workup of this residue produced the product in chemical and optical yields similar to those described below. The addition of CH_2Cl_2 to the residue produced a mixture of a deep red-orange, transparent solution and a yellow-orange solid. This was left undisturbed for ~1 h, during which time a grayish-white powder (mostly HgCl_2) precipitated, which was removed by gravity filtration through Celite. The latter step seemed to facilitate the purification of the product mixture. The deep-red, transparent CH_2Cl_2 filtrate was subjected to filtration chromatography over a short ($\sim 5 \times 1 \text{ cm}^2$) column of alumina which had been packed with a mixture of hexane-ether (1:1) and was eluted with CH_2Cl_2 . A very dark green band (containing elemental Ru and organic impurities) moved very slowly as long as the solvent mixture contained a much greater excess of hexane-ether over CH_2Cl_2 . An orange-red band, which moved with the solvent front, was collected and evaporated *in vacuo*. The resulting orange-mustard powder was washed with several small portions of the hexane-ether mixture and filtered. Drying the resulting solid *in vacuo* gave the pure product as an orange-mustard, flaky solid: yield, 0.81 g (53.5%). Anal. Calcd for $\text{C}_{16}\text{H}_{20}\text{NRuCl}$: C, 52.95; H, 5.57; N, 3.86. Found for **1a,b'**: C, 52.86; H, 5.61; N, 3.92. IR Data $\nu_{(\text{Ru}-\text{Cl})}$ (cm^{-1}) for **1a,b'**, 266 (shp, st), 246 (shp, w). UV-vis Data λ_{max} , nm (ϵ , $\text{L mol}^{-1} \text{ cm}^{-1}$) for

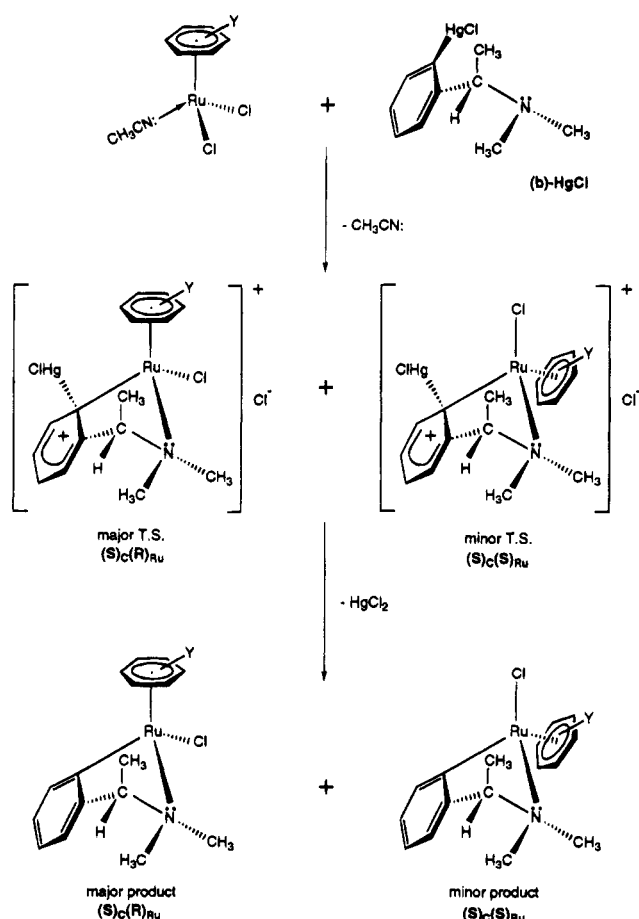
1a,b', 446 (1.5×10^3), 366 (1.4×10^3). CD Data λ_{max} , nm ($\Delta\epsilon$, $\text{L mol}^{-1} \text{ cm}^{-1}$) for **1a**, 457 (+6.2), 372 (-9.0); for **1b'**, 457 (-6.2), 372 (+9.0).

(ii) Characterization of **2a,b'** (η^6 -arene = toluene). Anal. Calcd for $\text{C}_{17}\text{H}_{22}\text{NRuCl}$: C, 54.17; H, 5.90; N, 3.72. Found for **2b'**: C, 54.01; H, 5.82; N, 3.56. IR data $\nu_{(\text{Ru}-\text{Cl})}$ (cm^{-1}) for **2a,b'**, 260 (shp, st), 248 (sh). UV-vis data λ_{max} , nm (ϵ , $\text{L mol}^{-1} \text{ cm}^{-1}$) for **2a,b'**, 449 (8.0×10^2), 379 (6.0×10^2). CD data λ_{max} , nm ($\Delta\epsilon$, $\text{L mol}^{-1} \text{ cm}^{-1}$) for **2a**, 455 (+5.7), 373 (-9.3); for **2b'**, 455 (-5.9), 373 (+8.7).

(iii) Characterization of **3a,b'** (η^6 -arene = cymene). Anal. Calcd for $\text{C}_{20}\text{H}_{26}\text{NRuCl}$: C, 57.33; H, 6.75; N, 3.34. Found for **3a**: C, 56.95; H, 6.67; N, 3.18. IR data $\nu_{(\text{Ru}-\text{Cl})}$ (cm^{-1}) for **3a,b'**, 288 (shp, st), 254 (shp, st). UV-vis data λ_{max} , nm (ϵ , $\text{L mol}^{-1} \text{ cm}^{-1}$) for **3a,b'**, 436 (7.2×10^2). CD data λ_{max} , nm ($\Delta\epsilon$, $\text{L mol}^{-1} \text{ cm}^{-1}$) for **3a**, 457 (+5.5), 378 (-7.7); for **3b'**, 457 (-5.1), 378 (+6.5).

C. X-ray Data Collection and Processing for 1b', 2b', and 3a. Deep red-orange needles of **1b'**, **2b'**, and **3a** were obtained by slow diffusion of a 1:1 mixture of hexane-ether into a saturated CH_2Cl_2 solution of each compound. Crystal data and details of data collection are given in Table 2. The samples were studied on an Enraf-Nonius CAD4F diffractometer with graphite-monochromated Mo $K\alpha$ radiation. Quantitative data were obtained at 293 K in the θ - 2θ mode. The resulting data sets were transferred to a VAX computer, and for all subsequent calculations the Enraf-Nonius SDP/VAX

Scheme 4



package¹⁵ was used. Three standard reflections measured every 1 h during the entire data collection period showed no significant trends. The raw data were converted to intensities and corrected for Lorentz, polarization, and absorption effects using ψ scans of four reflections. The structures were solved by the heavy-atom method. After refinement of the heavy atoms, difference-Fourier maps revealed maximas of residual electronic density close to the positions expected for hydrogen atoms. They were introduced in the structure calculations by their computed coordinates (CH = 0.95 Å) with isotropic temperature factors such as $B(\text{H}) = 1.38B_{\text{eq}}(\text{C}) \text{ \AA}^2$ but were not refined. Otherwise, solutions were obtained by full-matrix, least-squares refinements. The scattering factor coefficients and anomalous dispersion coefficients come respectively from parts a and b of ref 16.

Determination of the Absolute Configuration at Ru: The known absolute configuration at the benzylic carbon atom of each of the two starting arylamino-Hg(II) salts served as an internal reference in determining the absolute configuration at the Ru center of the corresponding diastereomer. In addition, the assignment of the Ru absolute configuration was confirmed by comparing $+x$, $+y$, $+z$ and $-x$, $-y$, $-z$ refinements. For **1b'** and **2b'**, the absolute configurations were confirmed using data sets collected with Cu K α radiation.

D. Molecular Mechanics Calculations. The calculations of strain energies for the two proposed transition states and the resulting diastereomeric products (Figure 5) were performed using the molecular-modeling program Spartan (Ver-

sion 3.1),^{10a} supported on a SiliconGraphics Indigo-2 workstation. The molecular mechanics (minimization) module within this program presently provides for the calculation of equilibrium geometries and strain energies on systems of 1000 or more atoms for the first 54 elements in the periodic table. In addition, this program can search the conformational space for both cyclic and acyclic molecules. The MM2 and MM3 force fields of Allinger and the SYBYL force field from Tripos, Inc., are supported (see the Spartan User's Guide for Version 3.1, Revision A, pp 1-13; Wavefunction, Inc., Irvine, CA, 1993 and 1994).

Each of the two structures was constructed using the "Expert Builder" input menu, and the strain energy was calculated by selecting the "Minimize+" option within this menu. Reproducibility of the calculated energies was generally within about 0.5 kcal/mol. The following is a representative description of the general procedure used: (1) The arylamino ligand, with either (*R*) or (*S*) configuration at the benzylic C atom, was first built and minimized. For each ligand, the conformer wherein the nitrogen lone pair of electrons was "syn" to the methyl group on the chiral C atom had a lower (more negative) strain energy; the rest of the final structure was built on this conformer in each case. (2) To the "free valency" on the 2-position of the arylamino phenyl ring thus built was added a tricoordinate Cd atom with a pyramidal geometry around it; the structure was then minimized. Cadmium was selected because the periodic table in this program does not presently provide parameters for any element beyond Xe (atomic no. 54). Since both Cd and Hg are in the same family of the periodic table and exhibit fairly similar chemical behaviors, it is assumed that the substitution of Cd for Hg in the transition states proposed here should have a minimal effect on the value of the difference in their energies ($\Delta\Delta G^\ddagger$). (3) To the remaining two free valencies of the Cd atom were added a monocoordinate Cl atom and a dicoordinate Cl atom, both with linear geometries; this structure was minimized as well. (4) To the free valency of the Cl atom in the latter structure was added a tetracoordinate Ru atom with tetrahedral geometry. The free valency on the Ru atom and that on the N atom (the lone pair) were connected, making a seven-membered ring; this structure was minimized. (5) Finally, to the two remaining free valencies in the Ru atom were added a monocoordinate Cl atom with linear geometry and a " η^6 -benzene" group from the "Ligands" option in this menu; the Ru atom is bonded to the centroid of the latter group. Depending on the desired configuration at Ru, the Cl atom or the benzene group was placed in the axial position of the seven-membered ring, "syn" to the axial methyl group on the chiral C atom. The resulting "transition-state" structure in each case was then minimized to yield its strain energy. For the η^6 -toluene and η^6 -cymene ligands, the average value for the energies of six and 18 conformations, respectively, was used.

Acknowledgment. We would like to thank Professor David A. Lightner for his generous permission to use the JASCO spectropolarimeter and also Dr. Stefan Boiadjev for helpful discussions on CD techniques and spectra. We are grateful to the donors of the Petroleum Research Fund (administered by the American Chemical Society) and NATO (Grant No. 0417/88) for financial support, to Johnson Mathey Aesar/Alfa for a generous loan of RuCl₃·3H₂O, and to the National Science Foundation (CHE-9214294) for funds to purchase the NMR spectrometer.

Supporting Information Available: For **1b'**, **2b'**, and **3a**, tables of X-ray crystallographic data including hydrogen atomic coordinates, anisotropic thermal parameters, and interatomic distances and angles (13 pages). Ordering information is given on any current masthead page.

OM950407G

(15) Frenz, B. A. In *The Enraf-Nonius CAD4-SDP in Computing in Crystallography*; Shenk, H., Olthof-Hazekamp, H., van Koningsfeld, H., Bassi, G. C., Eds.; Delft University Press: Delft, The Netherlands, 1978; pp 64-71.

(16) (a) Cromer, D. T.; Waber, J. T. *International Tables for X-ray Crystallography*; Kynoch: Birmingham, England, 1974; Vol. IV, Table 2.2b. (b) *Ibid.*, Table 2.3.1.

Selective Hydrosilylation of Alkynes Catalyzed by an Organoyttrium Complex

Gary A. Molander* and William H. Retsch

Department of Chemistry and Biochemistry, University of Colorado,
Boulder, Colorado 80309-0215

Received April 28, 1995[®]

The organoyttrium complex $\text{Cp}^*_2\text{YCH}_3\cdot\text{THF}$ ($\text{Cp}^* = \text{C}_5\text{Me}_5$) has been shown to be an effective precatalyst for the hydrosilylation of internal alkynes. The reaction with symmetrically substituted alkynes results in a single stereoisomer as the product of cis addition of phenylsilane to the alkyne. The reaction of various unsymmetrically substituted internal alkynes results in a regioselective hydrosilylation reaction that places the silane at the less hindered carbon of the alkyne. A variety of functional groups, e.g., halides, amines, protected alcohols, and trisubstituted olefins, are tolerated by the reaction conditions with no decrease in yield.

Introduction

The formation of alkenylsilanes by the catalytic hydrosilylation reactions of terminal alkynes has much precedent in the literature, but similar reactions with internal alkynes are significantly less common.¹ Symmetrical internal alkynes can be hydrosilylated to yield a single product,² but unsymmetrically substituted alkynes rarely react in a regioselective manner.³ The focus of the present research was to take advantage of the steric discrimination of an organoyttrium complex for the regioselective and stereoselective hydrosilylation of internal alkynes.

The organoyttrium species $\text{Cp}^*_2\text{YCH}(\text{TMS})_2$ ($\text{Cp}^* = \text{C}_5\text{Me}_5$) has been demonstrated to be an efficient precatalyst for the selective hydrosilylation of the less substituted olefin in a diene substrate.⁴ Similarly, the organoyttrium hydride catalyst derived from $\text{Cp}^*_2\text{YCH}_3\cdot\text{THF}$ has been shown to effect the hydrogenation of dienes in a selective manner.⁵ We now report that this latter complex also serves as an effective precatalyst for the regioselective hydrosilylation of internal unsymmetrical alkynes.

Results and Discussion

To be synthetically useful, a hydrosilylation procedure for internal alkynes would be expected to exhibit several distinguishing characteristics. First, the reaction must produce only one of two possible stereoisomers. Second, when the substrate is not symmetrically substituted, only one of two possible regioisomers should be formed. It would also be desirable if the process took place under relatively mild conditions at a reasonable rate, and tolerated a variety of functional groups as well. The

results outlined in Table 1 illustrate examples of the organoyttrium-catalyzed hydrosilylation of various alkynes and provide evidence that this procedure successfully fulfills these requirements.

The reaction of a symmetrical alkyne, 5-decyne, with 5 mol % of the precatalyst in the presence of phenylsilane cleanly produces the (*E*)-alkenylsilane as the sole product (entry 1). The stereochemistry of the double bond in the product was determined by an NOE difference experiment in which irradiation of the silane protons produced a 6% enhancement of the olefinic proton signal.

The reaction of unsymmetrical alkynes (entries 2–12) generated not only a single stereoisomer but also cleanly formed only one regioisomer in high yield. The regiochemistry, in most cases, was determined by the splitting pattern of the olefinic proton resonances. The examples depicted in entries 3, 4, and 9–12 demonstrate that a branching methyl group α to the alkyne provides sufficient steric differentiation to provide complete regioselectivity in the hydrosilylation reaction. The reaction of these substrates with phenylsilane is generally complete within 24 h at temperatures of 50 °C or less. The substrate depicted in entry 5, which contained a *tert*-butyl group on the alkyne, required longer reaction times and provided lower yields of the desired product because of competing side reactions. Presumably, the bulk of the *tert*-butyl group slows down the desired reaction enough to permit the dehydrogenative polymerization⁶ of phenylsilane to compete with hydrosilylation. Additionally, the silane polymerization forms hydrogen gas that hydrogenates the starting material to provide an olefinic byproduct, lowering the yield of the alkenylsilane.

Substrates with silyl ethers α to the alkyne (entries 6–8) required higher temperatures in order to react at a sufficient rate but still reacted with complete selectivity. Substrates depicted in entries 6 and 7 reacted cleanly and provided very good yields of the expected

[®] Abstract published in *Advance ACS Abstracts*, September 1, 1995.

(1) (a) Benkeser, R. A.; Burrows, M. L.; Nelson, L. E.; Swisher, J. V. *J. Am. Chem. Soc.* **1961**, *83*, 4385. (b) Chalk, A. J.; Harrod, J. F. *J. Am. Chem. Soc.* **1965**, *87*, 16. (c) Benkeser, R. A.; Ehler, D. F. *J. Organomet. Chem.* **1974**, *69*, 193. (d) Speier, J. L. *Adv. Organomet. Chem.* **1979**, *17*, 443–445. (e) Colvin, E. W. *Silicon in Organic Synthesis*; Butterworths: London, 1981; pp 45–48, 325–326.

(2) Ryan, J. W.; Speier, J. L. *J. Org. Chem.* **1966**, *31*, 2698.


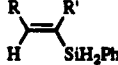
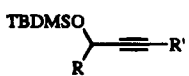
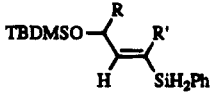
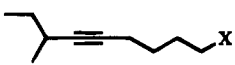
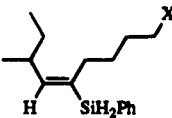
(3) Stork, G.; Jung, M. E.; Colvin, E.; Noel, Y. *J. Am. Chem. Soc.* **1974**, *96*, 3684.

(4) Molander, G. A.; Julius, M. *J. Org. Chem.* **1992**, *57*, 6347.

(5) Molander, G. A.; Hoberg, J. O. *J. Org. Chem.* **1992**, *57*, 3267.

(6) (a) Forsyth, C. M.; Nolan, S. P.; Marks, T. J. *Organometallics* **1991**, *10*, 2543. (b) Woo, H. G.; Walzer, J. F.; Tilley, T. D. *J. Am. Chem. Soc.* **1992**, *114*, 7047. (c) Radu, N. S.; Tilley, T. D.; Rheingold, A. L. *J. Am. Chem. Soc.* **1992**, *114*, 8293.

Table 1. Selective Hydrosilylation of Alkynes Catalyzed by $Cp^*_2YCH_3\cdot THF$

entry	substrate	product	reaction temperature (°C) ^a	% isolated yield ^b
				
1	1a R = <i>n</i> -butyl R' = <i>n</i> -butyl	2a	50	83 ^c
2	1b R = cyclohexyl R' = Me	2b	50	74
3	1c R = <i>sec</i> -butyl R' = Me	2c	50	74
4	1d R = <i>sec</i> -butyl R' = <i>n</i> -pentyl	2d	40	93
5	1e R = <i>tert</i> -butyl R' = <i>n</i> -decyl	2e	55	28 ^d
				
6	3a R = Me R' = Me	4a	90	82
7	3b R = Me R' = <i>n</i> -decyl	4b	90	89
8	3c R = H R' = Me	4c	90	23 ^d
				
9	5a X = Cl	6a	50	79
10	5b X = OTHP	6b	50	84
11	5c X = NMe ₂	6c	50	73 ^e
12	7	8	50	80

^a The reactions were run for 24 h at the specified temperature unless otherwise indicated. ^b Refers to the yields of purified materials. All products have been fully characterized spectroscopically (¹H, ¹³C NMR, IR), and elemental composition has been established by high-resolution mass spectrometry and/or combustion analysis. ^c Reaction time 12 h. ^d Reaction time 48 h. ^e Reaction time 17 h.

products, while the substrate in entry 8, differing only by the absence of a methyl group, reacted much more slowly and gave a lower yield. Alkynes **3**, **5**, and **7** (entries 6–12) demonstrate that the reaction is tolerant of a variety of functional groups. Even these oxygen- and nitrogen-containing functional groups do not appreciably affect the reactivity of the Lewis acidic metal complex.

Unsymmetrical alkynes that displayed less than complete selectivity in the hydrosilylation reaction are displayed in Table 2. The substrate in the first entry, 2-nonyne, affords two regioisomers under the reaction conditions. The ratio of products as determined by fused silica gas chromatographic analysis of the crude reaction mixture was 4.1:1. The olefinic proton resonances in

the ¹H NMR spectrum support this determination and provide evidence that **10a** is the major product. The olefinic proton resonance of the major product (**10a**) appears as a triplet of doublets,⁷ while the olefinic proton resonance of the minor product (**10b**) appears as a quartet. The other three entries are alkynes substituted in the β-position. Substrate **11** (entry 2) confirms that regioselectivity in methyl alkynes is reasonably high (7.3:1). The regioselectivity of the major product (**12a**) was determined by the ¹H NMR data in the same manner as that of **10a** described above. The alkyne in entry 3 is symmetrical, with the exception

(7) Appears as a triplet of doublets but is recognizable as a triplet of quartets in which the smaller peaks are not fully resolved.

Table 2. Hydrosilylation of Alkynes Yielding Mixtures of Products^a

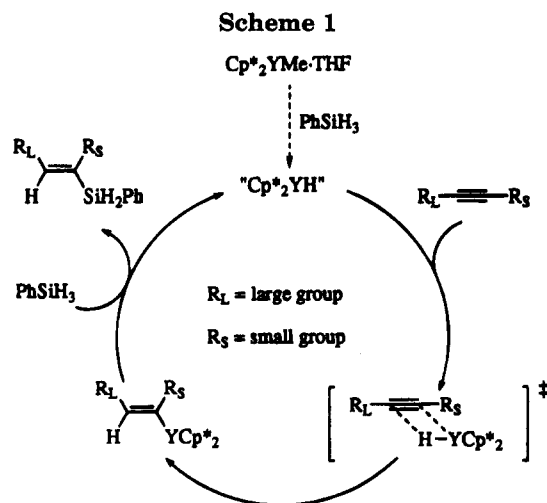
entry	substrate	products ^b		ratio major : minor
		major	minor	
1				4.1 : 1 7.2 : 1 ^d
2				7.3 : 1
3				1 : 1
4				2.5 : 1

^a The reactions were run for 24 h at 50 °C using the Cp*₂YCH₃(THF) precatalyst unless otherwise indicated. ^b All products have been characterized as mixtures by ¹H, ¹³C NMR, and IR, and elemental composition has been established by high-resolution mass spectrometry and/or combustion analysis. ^c Reaction temperature 40 °C. ^d The precatalyst Cp*₂YbCH(TMS)₂ was used.

of the β-methyl substituent. In this case, no selectivity was achieved and the product was a 1:1 mixture of regioisomers. When a bulkier substituent was used in the β-position (e.g., triphenylmethoxy, entry 4), the regioselectivity improved slightly to 2.5:1, as determined by integration of the olefinic protons in the ¹H NMR spectrum. The major product was determined by the diastereotopic protons on silicon in the ¹H NMR. The silane proton resonances of the major product (14a) appear as a singlet, and in the minor product (14b) they appear as an AB pattern owing to the proximity of the silicon to the stereocenter.

Some improvement in the regioselectivity was achieved when a precatalyst incorporating a lanthanide metal with a smaller ionic radius was used. Thus, Cp*₂YbCH(TMS)₂ was prepared and utilized in the hydrosilylation of substrates **9**, **11**, **13**, and **15** as outlined in Table 2. The regioselectivity for the reaction of phenylsilane with 2-nonyne (entry 1) using this precatalyst was improved from 4.1:1 to 7.2:1. This result can be attributed to the smaller ionic radius of ytterbium relative to that of yttrium. The smaller coordination sphere around the metal enhances the steric effects of the bulky organometallic complex, which improves the regioselectivity in the hydrosilylation reaction. Unfortunately, the selectivity of the reactions with alkynes substituted in the β-position was not enhanced by the use of the ytterbium complex.

A viable catalytic cycle, similar to the one proposed for the hydrosilylation of olefins,⁴ is outlined for the hydrosilylation of an unsymmetrical alkyne in Scheme 1. A σ-bond metathesis between Cp*₂YCH₃·THF and PhSiH₃ produces "Cp*₂YH", initiating the proposed catalytic cycle.^{4,6a,c,8} This reaction may occur through more than one pathway, but the end result is to produce a monomeric metal hydride species that serves as the active catalyst. Insertion of the alkyne into the metal-



hydride bond follows. The alkenylmetallic species produced by the insertion can react with PhSiH₃ through a σ-bond metathesis reaction to release the alkenylsilane and regenerate the active catalytic species. The alkyne insertion is both rapid and thermodynamically favorable,⁸ while the σ-bond metathesis step with phenylsilane appears to be the rate-limiting step. Attempts to use a bulkier silane in these reactions were unsuccessful. Thus, dimethylphenylsilane was unreactive with the alkynes under the reaction conditions.

In summary, the organoyttrium complex Cp*₂YCH₃·THF can be used to catalyze the hydrosilylation of simple and functionalized unsymmetrical internal alkynes. The reaction proceeds under fairly mild condi-

(8) (a) den Haan, K. H.; Wielstra, Y.; Teuben, J. H. *Organometallics* **1987**, *6*, 2053. (b) Nolan, S. P.; Porchia, M.; Marks, T. J. *Organometallics* **1991**, *10*, 1450. (c) Woo, H.-G.; Tilley, T. D. *J. Am. Chem. Soc.* **1989**, *111*, 8043. (d) Fu, P.-F.; Brard, L.; Marks, T. J. *Abstracts of Papers*, 207th National Meeting of the American Chemical Society, San Diego, CA, March 1994; American Chemical Society: Washington, DC, 1994; INOR 40.

tions to produce a single regioisomer in many cases. The resulting alkenylsilanes are stable compounds, easily purified by chromatography and distillation.

Experimental Section

All operations were performed with rigorous exclusion of oxygen and moisture in flamed Schlenk-type glassware on an argon line connected to a vacuum system (<0.04 mmHg) or in a nitrogen-filled Vacuum Atmospheres glovebox.

The cyclohexane for the reactions was distilled from Na/K alloy/benzophenone under argon and then stored in the glovebox. The alkynes 5-decyne, 1-cyclohexyl-1-propyne, and 2-butyne-1-ol were commercial samples dried over activated 4 Å molecular sieves, vacuum-transferred, and freeze/pump/thaw-degassed. The other alkynes were prepared from the alkylation of 3-methyl-1-pentyne, 3,3-dimethyl-1-butyne, or (\pm)-3-butyne-2-ol, using the appropriate alkyl halide.⁹ Protecting groups on the alcohols were installed according to published procedures.¹⁰ 8-(Dimethylamino)-3-methyl-4-nonyne (**13c**) was prepared from **13a** by alkylation of dimethylamine.¹¹ The products were dried over activated 4 Å molecular sieves and degassed as above or on the vacuum line depending on volatility. The phenylsilane was purchased from Aldrich and was freeze/pump/thaw-degassed before use. Anhydrous YCl_3 was purchased from Cerac. The complex $Cp^*_2YCH_3\cdot THF$ was prepared according to published procedures.¹² $Cp^*_2YbCH(TMS)_2$ was prepared similarly to the literature preparation of $Cp^*_2LnCH(TMS)_2$ ($Ln = La, Nd, Sm, Lu$).¹³ All compounds were stored in the glovebox after purification.

Procedure for Catalytic Hydrosilylation of 5-Decyne (1a). In the nitrogen atmosphere glovebox a solution of 0.009 g (0.024 mmol) of the precatalyst $Cp^*_2YCH_3\cdot THF$ in 1 mL of cyclohexane was added to a Teflon-valved Schlenk tube equipped with a magnetic stirbar. To this solution was added 0.072 g (0.52 mmol) of **1a** followed by 0.129 g (1.01 mmol) of phenylsilane. The reaction flask was sealed, removed from the glovebox, and placed in a magnetically stirred oil bath at 50 °C. After 12 h the reaction mixture was cooled to room temperature, diluted with 5 mL of hexanes, and filtered through a column of Florisil. The Florisil was rinsed two times with 5 mL portions of hexanes. The hexanes were combined and concentrated by rotary evaporation. Crude material was purified by flash chromatography in hexanes followed by Kugelrohr distillation to afford 83% (0.106 g, 0.43 mmol) of **2a**.

(E)-5-(Phenylsilyl)-5-decene (2a). Purification by flash chromatography and Kugelrohr distillation afforded 83% of the desired product: oven temperature (ot) 85 °C/0.30 mmHg; R_f 0.49 (hexanes); 1H NMR (400 MHz, $CDCl_3$) δ 0.84 (t, $J = 6.97$ Hz, 3H), 0.90 (t, $J = 6.97$ Hz, 3H), 1.22–1.38 (m, 8H), 2.11–2.19 (m, 4H), 4.52 (s, $^1J_{^{29}Si,H} = 194.0$ Hz, 2H), 6.00 (t, $J = 6.91$ Hz, 1H), 7.32–7.38 (m, 3H), 7.55–7.57 (m, 2H); ^{13}C NMR (100 MHz, $CDCl_3$) δ 13.92, 13.99, 22.46, 22.72, 28.53, 30.04, 31.53, 31.71, 127.90, 129.44, 132.76, 134.00, 135.54, 146.23; IR (neat)

2130 cm^{-1} ; HRMS calcd for $C_{16}H_{26}Si$ 246.1804, found 246.1805; LRMS (EI) m/z (relative intensity) 246 (4), 133 (22), 107 (100), 105 (57), 81 (29), 55 (40). Anal. Calcd for $C_{16}H_{26}Si$: C, 77.97; H, 10.63. Found: C, 77.85; H, 10.89.

(E)-1-Cyclohexyl-2-(phenylsilyl)-1-propene (2b). Purification by flash chromatography and Kugelrohr distillation afforded 74% of the desired product (97% pure by GC analysis): ot 75–80 °C/0.25 mmHg; R_f 0.46 (hexanes); 1H NMR (400 MHz, $CDCl_3$) δ 1.06–1.30 (m, 5H), 1.61–1.70 (m with overlapping doublet at 1.73, $J = 1.7$ Hz, 8H), 2.38–2.41 (m, 1H), 4.48 (s, $^1J_{^{29}Si,H} = 194.5$ Hz, 2H), 5.85–5.88 (m, 1H), 7.23–7.38 (m, 3H), 7.53–7.56 (m, 2H); ^{13}C NMR (100 MHz, $CDCl_3$) δ 15.57, 26.03, 26.20, 32.65, 37.89, 127.09, 128.72, 130.29, 133.15, 136.29, 152.76; IR (neat) 2924, 2850, 2130, 1448, 1428, 862, 836 cm^{-1} ; HRMS (EI) calcd for $C_{15}H_{22}Si$ 230.1491, found 230.1500; LRMS (EI) m/z (relative intensity) 230 (25), 188 (44), 152 (46), 147 (46), 123 (74), 107 (100), 81 (87.4), 67 (61), 55 (54), 41 (42).

(E)-4-Methyl-2-(phenylsilyl)-2-hexene (2c). Purification by flash chromatography and Kugelrohr distillation afforded 74% of the desired product (99% pure by GC analysis): ot 50–55 °C/0.15 mmHg; R_f 0.53 (hexanes); 1H NMR (400 MHz, $CDCl_3$) δ 0.87 (t, $J = 7.4$ Hz, 3H), 0.97 (d, $J = 6.7$ Hz, 3H), 1.24–1.41 (m, 2H), 1.75 (d, $J = 1.7$ Hz, 3H), 2.47–2.55 (m, 1H), 4.53 (s, $^1J_{^{29}Si,H} = 194.9$ Hz, 2H), 5.82 (dd, $J = 1.61, 9.3$ Hz, 1H), 7.34–7.42 (m, 3H), 7.56–7.59 (m, 2H); ^{13}C NMR (100 MHz, $CDCl_3$) δ 11.97, 15.63, 20.17, 29.88, 34.69, 126.94, 127.96, 129.51, 132.36, 135.46, 152.23; IR (neat) 2131 cm^{-1} ; HRMS calcd for $C_{13}H_{20}Si$ 204.1334, found 204.1322; LRMS (EI) m/z (relative intensity) 204 (25), 175 (12), 162 (77), 147 (76), 121 (91), 107 (100), 97 (77), 55 (67), 41 (29).

(E)-3-Methyl-5-(phenylsilyl)-4-decene (2d). Purification by flash chromatography and Kugelrohr distillation afforded 93% of the desired product (>99% pure by GC analysis): ot 80–86 °C/0.25 mmHg; R_f 0.64 (7% dichloromethane in hexanes); 1H NMR (400 MHz, $CDCl_3$) δ 0.83 (t, $J = 6.9$ Hz, 3H), 0.85 (t, $J = 7.5$ Hz, 3H), 0.94 (d, $J = 6.6$, 3H), 1.21–1.40 (m, 8H), 2.09–2.22 (m, 2H), 2.43–2.54 (m, 1H), 4.51 and 4.53 (AB system, $J_{AB} = 6.1$ Hz, $^1J_{^{29}Si,H} = 194.3$ Hz, 2H), 5.76 (d, $J = 9.5$ Hz, 1H), 7.32–7.40 (m, 3H), 7.55–7.57 (m, 2H); ^{13}C NMR (100 MHz, $CDCl_3$) δ 12.06, 13.98, 20.60, 22.46, 29.47, 29.98, 30.48, 31.88, 34.65, 127.90, 129.43, 132.46, 132.85, 135.50, 152.27; IR (neat) 2131.0 cm^{-1} ; HRMS calcd for $C_{17}H_{28}Si$ 260.1960, found 260.1972; LRMS (EI) m/z (relative intensity) 260 (6.2), 231 (6.6), 203 (29), 182 (36), 162 (27), 147 (20), 133 (18), 121 (35), 107 (100), 83 (57), 55 (31), 41 (23). Anal. Calcd for $C_{17}H_{28}Si$: C, 78.38; H, 10.83. Found: C, 78.44; H, 10.96.

(E)-2,2-Dimethyl-4-(phenylsilyl)-3-tetradecene (2e). Purification by flash chromatography and Kugelrohr distillation afforded 28% of the desired product (>99% pure by GC analysis): ot 85–90 °C/0.25 mmHg; R_f 0.64 (hexanes); 1H NMR (400 MHz, $CDCl_3$) δ 0.87 (t, $J = 6.8$ Hz, 3H), 1.13 (s, 9H), 1.22–1.37 (m, 16H), 2.28–2.31 (m, 2H), 4.49 (s, $^1J_{^{29}Si,H} = 194.5$ Hz, 2H), 5.99 (s, 1H), 7.31–7.39 (m, 3H), 7.54–7.56 (m, 2H); ^{13}C NMR (100 MHz, $CDCl_3$) δ 14.11, 22.68, 29.32, 29.41, 29.55, 29.58, 29.98, 30.06, 31.03, 31.10, 31.90, 55.21, 127.89, 129.42, 133.05, 133.96, 135.48, 154.76; IR (neat) 2130 cm^{-1} ; HRMS calcd for $C_{22}H_{38}Si$ 330.2743, found 330.2739; LRMS (EI) m/z (relative intensity) 330 (10), 315 (14), 287 (15), 273 (42), 189 (15), 175 (31), 161 (39), 121 (51), 107 (100), 97 (27), 83 (34), 69 (23), 57 (58), 43 (47). Anal. Calcd for $C_{22}H_{38}Si$: C, 79.92; H, 11.58. Found: C, 79.54; H, 11.77.

(E)-4-(tert-Butyldimethylsilyloxy)-2-phenylsilyl-2-pentene (4a). Purification by flash chromatography and Kugelrohr distillation afforded 82% of the desired product (>99% pure by GC analysis): ot 80–85 °C/0.25 mmHg; R_f 0.34 (7:1 hexanes/dichloromethane); 1H NMR (400 MHz, $CDCl_3$) δ 0.03 (s, 3H), 0.04 (s, 3H), 0.87 (s, 9H), 1.18 (d, $J = 6.3$ Hz, 3H), 1.72 (d, $J = 1.7$ Hz, 3H), 4.49 (s, $^1J_{^{29}Si,H} = 196.8$ Hz, 2H), 4.64–4.69 (m, 1H), 6.01 (dq, $J = 1.6, 7.6$ Hz, 1H), 7.33–7.41 (m, 3H), 7.53–7.55 (m, 2H); ^{13}C NMR (100 MHz, $CDCl_3$) δ -4.72, -4.58, 15.60, 18.23, 23.76, 25.86, 65.67, 126.73, 128.00,

(9) Typical alkylating procedure: 1.1 equiv of alkyne in THF was stirred at -78 °C. One equivalent of 1.6 M *n*-BuLi in hexanes was added, and the mixture was stirred for 0.5 h, followed by the addition of 1 equiv of the alkyl halide. The solution was warmed to room temperature followed by an aqueous workup. HMPA was added when the alkylation involved an alkyl halide other than MeI.

(10) (a) Corey, E. J.; Venkatesvarlu, A. *J. Am. Chem. Soc.* **1972**, *94*, 6190. (b) Corey, E. J.; Cho, H.; Rücker, C.; Hua, D. H. *Tetrahedron Lett.* **1981**, *22*, 3455. (c) Miyashita, M.; Yoshikoshi, A. *J. Org. Chem.* **1977**, *42*, 3772. (d) Colin-Messenger, C.; Girard, J.-P.; Rossi, J.-C. *Tetrahedron Lett.* **1992**, *33*, 2689.

(11) Chen, C.; Senanayake, C. H.; Bill, T. J.; Larsen, R. D.; Verhoeven, T. R.; Reider, P. *J. Org. Chem.* **1994**, *59*, 3738.

(12) (a) Threlkel, R. S.; Bercaw, J. E. *J. Organomet. Chem.* **1977**, *136*, 1. (b) Den Haan, K. H.; Teuben, J. H. *J. Organomet. Chem.* **1987**, *322*, 321. (c) Den Haan, K. H.; Wielstra, Y.; Eshuis, J. J. W.; Teuben, J. H. *J. Organomet. Chem.* **1987**, *323*, 181.

(13) Jeske, G.; Lauke, H.; Mauermann, H.; Swepston, P. N.; Schumann, H.; Marks, T. J. *J. Am. Chem. Soc.* **1985**, *107*, 8091.

129.66, 131.63, 135.50, 150.40; IR (neat) 2133 cm^{-1} ; HRMS calcd for $\text{C}_{17}\text{H}_{30}\text{OSi}_2$ 306.1835, found 306.1823; LRMS (EI) m/z (relative intensity) 306 (3), 249 (37), 207 (10), 193 (25), 181 (100), 171 (12), 145 (11), 135 (13), 121 (16), 107 (21), 75 (58), 57 (11), 41 (7). Anal. Calcd for $\text{C}_{17}\text{H}_{30}\text{OSi}_2$: C, 66.60; H, 9.86. Found: C, 66.39; H, 9.84.

(E)-2-((tert-Butyldimethylsilyloxy)-4-(phenylsilyl)-3-tetradecene (4b). Purification by flash chromatography and Kugelrohr distillation afforded 84% of the desired product (>99% pure by GC analysis): ot 100–120 $^\circ\text{C}/0.25$ mmHg; R_f 0.36 (7% dichloromethane in hexanes); ^1H NMR (400 MHz, CDCl_3) δ 0.02 (s, 3H), 0.03 (s, 3H), 0.86 (s, 9H), 0.87 (t, $J = 6.9$ Hz, 3H), 1.17–1.36 (m, 19H), 2.07–2.21 (m, 2H), 4.49 and 4.50 (AB system, $J_{\text{AB}} = 6.3$ Hz, $^1J_{\text{Si,H}} = 196.4$ Hz, 2H), 4.68 (dq, $J = 6.4, 7.5$ Hz, 1H), 5.98 (d, $J = 7.8$ Hz, 1H), 7.31–7.40 (m, 3H), 7.53–7.55 (m, 2H); ^{13}C NMR (100 MHz, CDCl_3) δ -4.61, -4.46, 14.11, 18.21, 22.69, 24.46, 25.87, 29.32, 29.39, 29.52, 29.55, 29.59, 29.74, 30.77, 31.91, 65.48, 127.96, 129.59, 132.12, 132.35, 135.56, 150.31; IR (neat) 2134.1 cm^{-1} ; HRMS calcd for $\text{C}_{26}\text{H}_{48}\text{OSi}_2$ 432.3244, found 432.3243; LRMS (EI) m/z (relative intensity) 432 (2.2), 375 (39), 300 (6.3), 181 (100), 121 (13), 107 (24), 75 (50), 57 (9), 41 (13).

(E)-1-((tert-Butyldimethylsilyloxy)-3-phenylsilyl-2-butene (4c). Purification by preparative thin-layer chromatography and Kugelrohr distillation afforded 23% of the desired product (>99% pure by GC analysis): ot 78–82 $^\circ\text{C}/0.10$ mmHg; R_f 0.60 (2:1 hexanes/dichloromethane); ^1H NMR (400 MHz, CDCl_3) δ 0.06 (s, 6H), 0.89 (s, 9H), 1.71 (s, 3H), 4.30 (d, $J = 5.2$ Hz, 2H), 4.50 (s, $^1J_{\text{Si,H}} = 197.0$ Hz, 2H), 6.10 (tq, $J = 1.7, 5.3$ Hz, 1H), 7.32–7.41 (m, 3H), 7.54–7.56 (m, 2H); ^{13}C NMR (100 MHz, CDCl_3) δ -5.15, 15.82, 18.37, 25.94, 60.69, 100.90, 128.00, 129.53, 129.70, 131.57, 145.27; IR (neat) 2133 cm^{-1} ; HRMS calcd for $\text{C}_{16}\text{H}_{28}\text{OSi}_2$ 292.1679, found 292.1690; LRMS (EI) m/z (relative intensity) 292 (12), 235 (41), 233 (20), 207 (12), 193 (38), 181 (100), 179 (63), 157 (19), 135 (19), 121 (13), 107 (21), 105 (27), 75 (77), 73 (42), 59 (14), 57 (12), 41 (10).

(E)-9-Chloro-3-methyl-5-(phenylsilyl)-4-nonene (6a). Purification by flash chromatography and Kugelrohr distillation afforded 79% of the desired product (98% pure by GC analysis): ot 60–70 $^\circ\text{C}/0.19$ mmHg; R_f 0.25 (hexanes); ^1H NMR (400 MHz, CDCl_3) δ 0.85 (t, $J = 7.4$ Hz, 3H), 0.95 (d, $J = 6.6$ Hz, 3H), 1.19–1.28 (m, 1H), 1.30–1.40 (m, 1H), 1.41–1.52 (m, 2H), 1.65–1.74 (m, 2H), 2.12–2.25 (m, 2H), 2.42–2.53 (m, 1H), 3.44 (t, $J = 6.7$ Hz, 2H), 4.52 and 4.54 (AB system, $J_{\text{AB}} = 7.3$ Hz, $^1J_{\text{Si,H}} = 195.5$ Hz, 2H), 5.80 (d, $J = 9.6$ Hz, 1H), 7.33–7.41 (m, 3H), 7.55–7.57 (m, 2H); ^{13}C NMR (100 MHz, CDCl_3) δ 12.06, 20.57, 26.90, 29.58, 29.90, 32.43, 34.72, 44.78, 127.97, 129.56, 131.57, 132.45, 135.46, 152.96; IR (neat) 2131.3 cm^{-1} ; HRMS calcd for $\text{C}_{16}\text{H}_{25}\text{SiCl}$ 279.1336 (M - H) $^+$, found 279.1325; LRMS (EI) m/z (relative intensity) 279 (30), 223 (27), 173 (39), 141 (97), 109 (100), 107 (83), 81 (90), 69 (55), 55 (68), 43 (14). Anal. Calcd for $\text{C}_{16}\text{H}_{25}\text{SiCl}$: C, 68.41; H, 8.97. Found: C, 68.01; H, 8.76.

(E)-3-Methyl-5-(phenylsilyl)-9-((tetrahydropyranyl)-oxy)-4-nonene (6b). Purification by flash chromatography and heating under high vacuum afforded 84% of the desired product (>99% pure by GC analysis): R_f 0.30 (7% ethyl acetate in hexanes); ^1H NMR (400 MHz, CDCl_3) δ 0.85 (t, $J = 7.4$ Hz, 3H), 0.94 (d, $J = 6.6$ Hz, 3H), 1.18–1.60 (m, 10H), 1.63–1.71 (m, 1H), 1.75–1.83 (m, 1H), 2.13–2.27 (m, 2H), 2.44–2.53 (m, 1H), 3.31 (dt, $J = 6.4, 9.6$ Hz, 1H), 3.44–3.49 (m, 1H), 3.67 (dt, $J = 6.6, 9.6$ Hz, 1H), 3.79–3.85 (m, 1H), 4.51–4.54 (m, $^1J_{\text{Si,H}} = 194.6$ Hz, 3H), 5.78 (d, $J = 9.6$ Hz, 1H), 7.31–7.40 (m, 3H), 7.54–7.56 (m, 2H); ^{13}C NMR (100 MHz, CDCl_3) δ 12.04, 19.52, 20.57, 25.49, 26.45, 29.69, 29.91, 30.26, 30.70, 34.64, 62.10, 67.21, 98.64, 127.90, 129.44, 132.09, 132.65, 135.45, 152.57; IR (neat) 2130.4 cm^{-1} ; HRMS calcd for $\text{C}_{21}\text{H}_{34}\text{O}_2\text{Si}$ 345.2250 (M - H) $^+$, found 345.2241; LRMS (EI) m/z (relative intensity) 346 (0.24), 261 (4.0), 232 (6.5), 203 (7.0), 177 (6.7), 123 (39), 107 (32), 85 (100), 67 (20), 55 (20), 41 (31).

(E)-9-(Dimethylamino)-3-methyl-5-(phenylsilyl)-4-nonene (6c). Purification by flash chromatography and Kugelrohr distillation afforded 73% of the desired product (>98% pure by GC analysis): ot 74–86 $^\circ\text{C}/0.16$ mmHg; R_f 0.26 (ethyl acetate on triethylamine-deactivated silica); ^1H NMR (400 MHz, CDCl_3) δ 0.84 (t, $J = 7.4$ Hz, 3H), 0.94 (d, $J = 6.6$ Hz, 3H), 1.19–1.43 (m, 6H), 2.11–2.44 (m with overlapping s at 2.16, 10H), 2.44–2.52 (m, 1H), 4.51 and 4.53 (AB system, $J_{\text{AB}} = 5.9$ Hz, $^1J_{\text{Si,H}} = 194.8$ Hz, 2H), 5.76 (d, $J = 4.9$ Hz, 1H), 7.31–7.39 (m, 3H), 7.54–7.56 (m, 2H); ^{13}C NMR (100 MHz, CDCl_3) δ 12.04, 20.55, 27.62, 27.83, 29.91, 30.40, 34.62, 45.48, 59.73, 127.90, 129.44, 132.07, 132.67, 135.46, 152.50; IR (neat) 2130.4 cm^{-1} ; HRMS calcd for $\text{C}_{15}\text{H}_{31}\text{NSi}$ 289.2226 (M - H) $^+$, found 289.2226; LRMS (EI) m/z (relative intensity) 289 (7.5), 274 (35), 232 (31), 182 (30), 107 (21), 105 (14), 58 (100), 45 (16), 44 (12), 42 (13), 30 (7.5), 29 (7.1). Anal. Calcd for $\text{C}_{15}\text{H}_{31}\text{NSi}$: C, 74.67; H, 10.79. Found: C, 74.63; H, 10.60.

(9E)-(6R,11R,S)-2,6,11-Trimethyl-9-(phenylsilyl)-2,9-tridecadiene (8). Purification by preparative thin-layer chromatography and heating under high vacuum at 60 $^\circ\text{C}$ for 3 h afforded 80% of the desired product (>99% pure by GC analysis): R_f 0.21 (hexanes); ^1H NMR (400 MHz, CDCl_3) δ 0.83 (t, $J = 6.7$ Hz, 3H), 0.85 (t, $J = 7.4$ Hz, 3H), 0.95 (d, $J = 6.6$ Hz, 3H), 1.04–1.40 (m, 7H), 1.58 (s, 3H), 1.67 (s, 3H), 1.83–1.95 (m, 2H), 2.06–2.24 (m, 2H), 2.43–2.54 (m, 1H), 4.52 and 4.54 (AB system, $J_{\text{AB}} = 7.0$ Hz, $^1J_{\text{Si,H}} = 194.6$ Hz, 2H), 5.07 (t, $J = 6.9$ Hz, 1H), 5.75 (d, $J = 9.6$ Hz, 1H), 7.32–7.40 (m, 3H), 7.55–7.58 (m, 2H); ^{13}C NMR (100 MHz, CDCl_3) δ 12.11, 17.62, 19.41, 19.50, 20.66, 25.50, 25.73, 27.93, 29.97, 32.53, 32.56, 34.67, 36.80, 36.88, 36.96, 124.94, 127.90, 129.44, 130.99, 132.53, 132.78, 135.51, 152.06; IR (neat) 2130.7 cm^{-1} ; HRMS calcd for $\text{C}_{22}\text{H}_{36}\text{Si}$ 328.2586, found 328.2576; LRMS (EI) m/z (relative intensity) 328 (1.4), 299 (14), 189 (17), 161 (29), 121 (50), 107 (100), 105 (43), 81 (38), 69 (90), 57 (11), 43 (14), 29 (18). Anal. Calcd for $\text{C}_{22}\text{H}_{36}\text{Si}$: C, 80.41; H, 11.04. Found: C, 80.35; H, 11.05.

(E)-2-(Phenylsilyl)-2-nonene (10a) and (E)-3-(Phenylsilyl)-2-nonene (10b). The product ratio in the crude reaction mixture was 4.1:1 by GC analysis. The major product was determined by the integration and splitting pattern of the olefinic resonances in the ^1H NMR. The products were inseparable by TLC and HPLC. Purification by preparative thin-layer chromatography and Kugelrohr distillation afforded an 81% yield of the product mixture (>98% overall purity by GC analysis): ot 50–58 $^\circ\text{C}/0.23$ mmHg; R_f 0.68 (hexanes); ^1H NMR (400 MHz, CDCl_3) δ 0.83–0.90 (m, 3H), 1.22–1.40 (m, 8H), 1.71–1.73 (m, 3H), 2.10–2.20 (m, 2H), 4.50 (s, $^1J_{\text{Si,H}} = 194.9$ Hz, 1.6H), 4.51 (s, $^1J_{\text{Si,H}} = 194.5$ Hz, 0.4H), 6.04 (td, $J = 6.9, 1.6$ Hz, 0.8H), 6.09 (q, $J = 6.5$ Hz, 0.2H), 7.33–7.41 (m, 3H), 7.54–7.60 (m, 2H); ^{13}C NMR (100 MHz, CDCl_3) δ 14.08, 14.64, 15.47, 22.60, 22.63, 28.87, 28.99, 29.05, 29.13, 29.28, 29.94, 31.68, 31.74, 127.92, 127.94, 128.46, 129.47, 129.52, 132.32, 132.67, 135.35, 135.48, 135.56, 139.89, 146.29; IR (neat) 2130.5 cm^{-1} ; HRMS calcd for $\text{C}_{15}\text{H}_{24}\text{Si}$ 232.1647, found 232.1639; LRMS (EI) m/z (relative intensity) 232 (5.3), 203 (5.8), 147 (24), 121 (39), 107 (100), 105 (80), 81 (26), 43 (27), 29 (31). Anal. Calcd for $\text{C}_{15}\text{H}_{24}\text{Si}$: C, 77.51; H, 10.41. Found: C, 77.50; H, 10.57.

(E)-5-Methyl-2-(phenylsilyl)-2-heptene (12a) and (E)-5-Methyl-3-(phenylsilyl)-2-heptene (12b). The product ratio in the crude reaction mixture was 7.3:1 by GC analysis. The major product was determined by the integration and splitting pattern of the olefinic resonances in the ^1H NMR. The products were inseparable by TLC. Purification by flash chromatography and Kugelrohr distillation afforded a 40% yield of the product mixture (>97% overall purity by GC analysis): ot 58–62 $^\circ\text{C}/0.28$ mmHg; R_f 0.53 (hexanes); ^1H NMR (400 MHz, CDCl_3) δ 0.79–0.89 (m, 6H), 1.10–1.19 (m, 1H), 1.31–1.47 (m, 2H), 1.70–1.72 (m, 3H), 1.94–2.01 (m, 1H), 2.09–2.16 (m, 1H), 4.50 (s, $^1J_{\text{Si,H}} = 194.8$ Hz, 2H), 6.05 (td, $J = 7.0, 1.6$ Hz, 0.88H), 6.15 (q, $J = 6.4$ Hz, 0.12H), 7.33–7.38 (m, 3H), 7.54–7.56 (m, 2H); ^{13}C NMR (100 MHz, CDCl_3) δ 11.56,

15.63, 19.13, 19.23, 29.34, 29.53, 34.66, 34.85, 35.78, 37.16, 127.91, 127.96, 129.19, 129.47, 129.52, 132.34, 135.47, 135.58, 140.69, 145.10; IR (neat) 2130.3 cm⁻¹; HRMS calcd for C₁₄H₂₂Si 218.1491, found 218.1497; LRMS (EI) *m/z* (relative intensity) 218 (13), 203 (5.6), 161 (33), 147 (43), 134 (43), 121 (60), 107 (100), 105 (74), 84 (22), 57 (24), 43 (18), 41 (29), 29 (31).

(E)-3-Methyl-6-(phenylsilyl)-5-decene (14a) and (E)-3-Methyl-5-(phenylsilyl)-5-decene (14b). The product ratio in the crude reaction mixture was 1:1 by GC analysis. The products were inseparable by TLC and HPLC. Purification by flash chromatography and Kugelrohr distillation afforded 73% of the product mixture (>99% overall purity by GC analysis): ot 84–98 °C/0.28 mmHg; *R_f* 0.55 (hexanes); ¹H NMR (400 MHz, CDCl₃) δ 0.78–0.92 (m, 9H), 1.01–1.52 (m, 7H), 1.94–2.04 (m, 1H), 2.11–2.19 (m, 3H), 4.50–4.54 (m, ¹*J*_{Si,H} = 194.5 Hz, 2H), 6.00–6.07 (m, 1H), 7.33–7.41 (m, 3H), 7.55–7.68 (m, 2H); ¹³C NMR (100 MHz, CDCl₃) δ 11.54, 11.56, 13.94, 14.00, 19.18, 19.26, 22.48, 22.75, 28.83, 29.37, 29.53, 30.14, 31.48, 31.63, 34.63, 34.96, 35.69, 37.60, 127.90, 129.43, 132.75, 132.78, 133.24, 134.71, 135.52, 135.54, 145.11, 147.07; IR (neat) 2130.3 cm⁻¹; HRMS calcd for C₁₇H₂₈Si 260.1960, found 260.1962; LRMS (EI) *m/z* (relative intensity) 260 (7.5), 203 (12), 161 (19), 147 (20), 121 (24), 107 (100), 105 (50), 97 (19), 81 (11), 55 (17), 29 (16). Anal. Calcd for C₁₇H₂₈Si: C, 78.38; H, 10.83. Found: C, 78.30; H, 10.72.

(E)-3-(Triphenylmethoxy)-6-(phenylsilyl)-5-decene (16a) and (E)-3-(Triphenylmethoxy)-5-(phenylsilyl)-5-decene (16b). The product ratio in the crude reaction mixture was

2.5:1 by ¹H NMR. The major product was determined by the diastereotopic protons on silicon in the ¹H NMR. The products were inseparable by TLC. Purification by flash chromatography and heating at 100 °C for 3 h at 0.12 mmHg afforded 64% of the product mixture (>95% overall purity by GC analysis): *R_f* 0.55 (hexanes); ¹H NMR (400 MHz, CDCl₃) δ 0.63–0.72 (m, 3H), 0.79–0.89 (m, 3H), 1.01–1.31 (m, 6H), 2.02–2.27 (m, 3.75H), 2.57 (dd, *J* = 15.0, 9.0 Hz, 0.25H), 3.38–3.43 (m, 0.71H), 3.52–3.57 (m, 0.29H), 4.29 and 4.31 (AB system, *J*_{AB} = 6.4 Hz, ¹*J*_{Si,H} = 199.2 Hz, 0.57H), 4.48 (s, ¹*J*_{Si,H} = 194.8 Hz, 1.43H), 5.88 (t, *J* = 6.6 Hz, 0.71H), 5.95 (t, *J* = 6.6 Hz, 0.29H), 7.21–7.51 (m, 20H); ¹³C NMR (100 MHz, CD₂-Cl₂) δ 8.59, 9.27, 14.07, 14.14, 22.80, 23.09, 25.46, 27.08, 29.41, 30.69, 31.71, 31.85, 33.13, 35.91, 73.86, 74.68, 86.83, 127.15, 127.23, 127.93, 127.97, 128.22, 128.26, 129.30, 129.35, 129.76, 129.84, 131.26, 132.88, 135.76, 135.80, 135.88, 142.64, 145.93, 148.88; IR (neat) 2129.9 cm⁻¹; HRMS calcd for C₃₅H₄₀OSi 503.2770 (M - H)⁺, found 503.2769; LRMS (EI) *m/z* (relative intensity) 503 (0.34), 243 (100), 165 (68), 107 (36), 105 (39), 91 (8.6), 77 (15), 41 (8.8), 29 (8.0). Anal. Calcd for C₃₅H₄₀OSi: C, 83.28; H, 7.99. Found: C, 83.01, H, 7.77.

Acknowledgment. We wish to thank the National Institutes of Health for their generous support of this research.

OM950311W

Analysis of Spectroscopic, Reactivity, and Structural Differences Originating Uniquely from Differing Modes of π -Facial Complexation. The Three Possible Stereoisomeric Bis(isodicyclopentadienyl)titanium Combinations

Florence Zaegel,[†] Judith C. Gallucci,[‡] Philippe Meunier,[†] Bernard Gautheron,^{*,‡} Eugene I. Bzowej,^{‡,1} and Leo A. Paquette^{*,‡}

Laboratoire de Synthèse et d'Electrosynthèse Organométalliques Associé au CNRS (URA 1685), Université de Bourgogne, BP 138, 21004 Dijon, Cédex, France, and the Evans Chemical Laboratories, The Ohio State University, Columbus, Ohio 43210

Received May 9, 1995[®]

The three diastereomeric (isodiCp)₂TiCl₂ complexes have been prepared in stereocontrolled fashion. The exo,exo isomer, on reaction with boron tribromide or with ethereal methyl-lithium, gives rise to the dibromo and dimethyl analogues which show reasonable stability. In contrast, the endo,endo and endo,exo dichlorides do not lead to stable products under analogous conditions. All three (isodiCp)₂TiCl₂ isomers do react well with pentafluorophenyllithium, leading to the air stable, crystalline (isodiCp)₂Ti(C₆F₅)Cl triad, whose members are readily distinguished by their NMR spectra. An analysis of the notable trends reflected in these spectra is reported. X-ray crystallographic analysis of the three diastereomers reveals the three pentafluorophenyl complexes to have in common a solid-state spatial arrangement which differs notably from that adopted by the exo,exo dichloride and dimethyl derivatives.

In recent years, considerable attention has been accorded to the complexation of cyclopentadienyl ligands endowed with diastereotopic faces to group 4 transition metals. An early example is the bis(η^5 -tricyclo[5.2.1.0^{2,6}]-deca-2,5-dienyl) or isodicyclopentadienyl anion (1).² A wide variety of optically active anions of this generic class has subsequently been developed.³⁻⁵ As a direct consequence of the inherent structural features of 1 and its congeners, the faces of these ligands feature distinctively different chemical environments. Their involvement in metalation reactions can lead to mixtures of metallocenes but often does not if proper controls are

exercised. The engagement of a single face is presently recognized to be subject to reasonable modulation by several factors, including nonbonded steric interactions,⁶ monomer-dimer preequilibrium complexation to lithium counterions,⁷ reaction temperature,⁸ and concentration.⁹

Since each ligand can in principle serve as precursor to three diastereomeric metallocenes, we have been led to investigate those features that distinguish such a subset of closely related complexes. To our knowledge, no investigation of this type has previously been undertaken. The one potential limitation of this study, ready access to the stereoisomerically pure diastereomers without the need to accomplish difficult separations, was lifted by our earlier discovery that structurally defined trimethylsilyl-substituted ligands undergo complexation exclusively via net inversion of configuration.¹⁰

Results and Discussion

Synthesis and Spectroscopic Analysis of the Diastereomeric (IsodiCp)₂TiCl₂ Complexes. The

[†] Université de Bourgogne.

[‡] The Ohio State University.

[®] Abstract published in *Advance ACS Abstracts*, September 1, 1995.

(1) NSERC (Canada) Postdoctoral Fellow, 1994-1995.

(2) Gallucci, J. C.; Gautheron, B.; Gugelchuk, M.; Meunier, P.; Paquette, L. A. *Organometallics* **1987**, *6*, 15.

(3) (a) McLaughlin, M. L.; McKinney, J. A.; Paquette, L. A. *Tetrahedron Lett.* **1986**, *27*, 5595. (b) Paquette, L. A.; McKinney, J. A.; McLaughlin, M. L.; Rheingold, A. L. *Tetrahedron Lett.* **1986**, *27*, 5599. (c) Paquette, L. A.; Gugelchuk, M.; McLaughlin, M. L. *J. Org. Chem.* **1987**, *52*, 4732. (d) Paquette, L. A.; McLaughlin, M. L. *Org. Synth.* **1989**, *68*, 220. (e) Paquette, L. A.; Moriarty, K. J.; McKinney, J. A.; Rogers, R. D. *Organometallics* **1989**, *8*, 1707. (f) Paquette, L. A.; Moriarty, K. J.; Rogers, R. D. *Organometallics* **1989**, *8*, 1506. (g) Moriarty, K. J.; Rogers, R. D.; Paquette, L. A. *Organometallics* **1989**, *8*, 1512.

(4) (a) Halterman, R. L.; Vollhardt, K. P. C. *Tetrahedron Lett.* **1986**, *27*, 1461. (b) Halterman, R. L.; Vollhardt, K. P. C. *Organometallics* **1988**, *7*, 883. (c) Chen, Z.; Halterman, R. L. *J. Am. Chem. Soc.* **1992**, *114*, 2276. (d) Halterman, R. L.; Ramsey, T. M. *Organometallics* **1993**, *12*, 2879. (e) Chen, Z.; Eriks, K.; Halterman, R. L. *Organometallics* **1991**, *10*, 3449.

(5) (a) Burger, P.; Hund, H.-U.; Evertz, K.; Brintzinger, H.-H. *J. Organomet. Chem.* **1989**, *378*, 153. (b) Bhaduri, D.; Nelson, J. H.; Wang, T.; Jacobson, R. A. *Organometallics* **1994**, *13*, 2291. (c) Burk, M. J.; Colletti, S. L.; Halterman, R. L. *Organometallics* **1991**, *10*, 2998. (d) Hollis, T. K.; Rheingold, A. L.; Robinson, N. P.; Whelan, J.; Bosnich, B. *Organometallics* **1992**, *11*, 2812. (e) Rheingold, A. L.; Robinson, N. P.; Whelan, J.; Bosnich, B. *Organometallics* **1992**, *11*, 1869. (f) Bandy, J. A.; Green, M. L. H.; Gardner, I. M.; Prout, K. *J. Chem. Soc., Dalton Trans.* **1991**, 2207.

(6) (a) Sivik, M. R.; Rogers, R. D.; Paquette, L. A. *J. Organomet. Chem.* **1990**, *397*, 177. (b) Rogers, R. D.; Sivik, M. R.; Paquette, L. A. *J. Organomet. Chem.* **1993**, *450*, 125.

(7) (a) Paquette, L. A.; Bauer, W.; Sivik, M. R.; Bühl, M.; Feigel, M.; Schleyer, P. von R. *J. Am. Chem. Soc.* **1990**, *112*, 8776. (b) Bauer, W.; O'Doherty, G. A.; Schleyer, P. von R.; Paquette, L. A. *J. Am. Chem. Soc.* **1991**, *113*, 7093. (c) Bauer, W.; Sivik, M. R.; Friedrich, D.; Schleyer, P. von R.; Paquette, L. A. *Organometallics* **1992**, *11*, 4178. (d) Zaegel, F.; Gallucci, J. C.; Meunier, P.; Gautheron, B.; Sivik, M. R.; Paquette, L. A. *J. Am. Chem. Soc.* **1994**, *116*, 6466.

(8) (a) Paquette, L. A.; Moriarty, K. J.; Meunier, P.; Gautheron, B.; Crocq, V. *Organometallics* **1988**, *7*, 1873. (b) Paquette, L. A.; Moriarty, K. J.; Meunier, P.; Gautheron, B.; Sornay, C.; Rogers, R. D.; Rheingold, A. L. *Organometallics* **1989**, *8*, 2159.

(9) Bhide, V. V.; Rinaldi, P. L.; Farona, M. F. *Organometallics* **1990**, *9*, 123 and the discussion in ref 11.

(10) Paquette, L. A.; Sivik, M. R. *Organometallics* **1992**, *11*, 3503.

Table 1. 400 MHz ^1H NMR Spectra of the (IsodiCp) $_2\text{TiCl}_2$ Diastereomers and Related Complexes^a

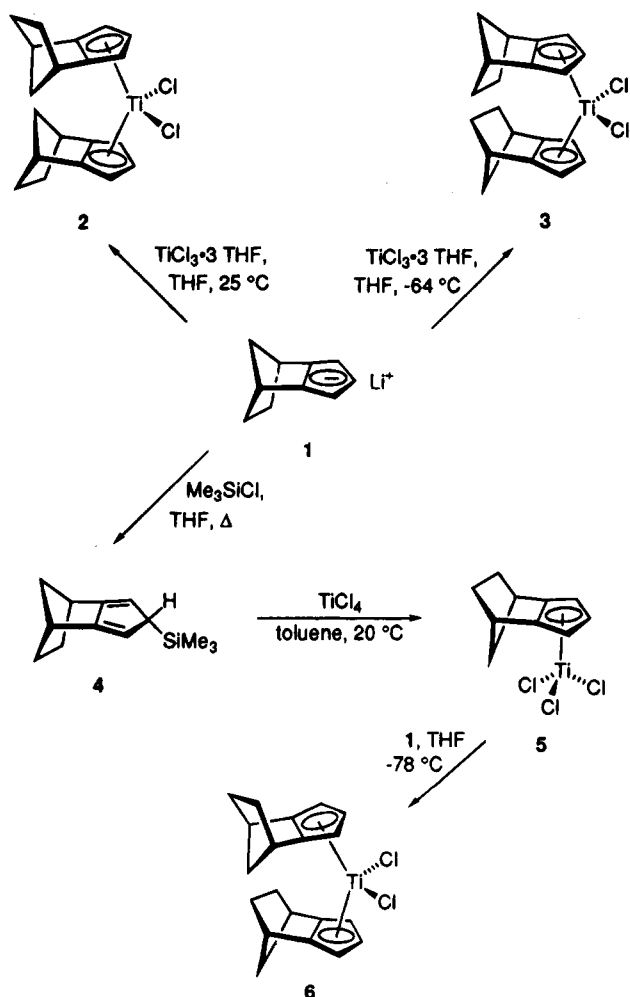
compd	cyclopentadienyl							methyl
	central	peripheral	bridgehead	exo ethano	endo ethano	syn methano	anti methano	
2 ^b	6.27 (t/2)	6.08 (d/4)	3.32 (s/4)	1.86 (d/4)	1.11 (d/4)	1.38 (d/2)	1.22 (d/2)	
3 ^b	5.84 (t/2)	6.33 (d/4)	3.34 (s/4)	1.85 (m/4)	1.73 (d/4)	1.91 (m/2)	1.85 (d/2)	
6 ^b	6.09 (t/1), exo	6.17 (d/2), exo	3.34 (s/2), endo	1.85 (m/4), exo	1.76 (d/2), endo	1.94 (m/1), endo	1.85 (d/1), endo	
	5.86 (t/1), endo	6.29 (d/2), endo	3.29 (s/2), exo	endo	1.09 (d/2), exo	1.32 (d/1), exo	1.18 (d/1), exo	
5 ^c	6.43 (t/1)	5.60 (d/2)	3.01 (s/2)	1.25 (d/2)	0.49 (dd/2)	1.94 (d/1)	1.02 (d/1)	
7 ^b	6.51 (t/2)	6.19 (d/4)	3.38 (s/4)	1.87 (d/4)	1.14 (d/4)	1.32 (d/2)	1.02 (d/2)	
8 ^c	6.07 (t/2)	5.58 (d/4)	2.75 (s/4)	1.53 (d/4)	1.22 (d/4)	0.85 (d/4)		0.25 (s/6)

^a Chemical shift in δ , multiplicity, relative integration. ^b In CDCl_3 solution. ^c In C_6D_6 as solvent.

Table 2. 50 MHz ^{13}C NMR Spectra of the (IsodiCp) $_2\text{TiCl}_2$ Diastereomers and Related Complexes^a

compd	cyclopentadienyl						
	central	peripheral	quaternary	ethano bridge	bridgehead	methano bridge	methyl
2 ^b	128.4	106.8	144.8	28.0	41.4	47.7	
3 ^b	121.3	111.6	154.3	27.2	42.8	59.1	
6 ^b	125.5	107.2	145.4	28.0	41.4	47.5	
	123.1	110.7	153.8	27.2	42.8	59.3	
5 ^c	125.8	113.7	149.8	28.6	42.3	50.2	
7 ^b	129.1	107.6	145.0	28.4	42.2	47.5	
8 ^c	118.8	103.7	136.1	29.4	40.6	47.1	46.1

^a Chemical shifts in δ . ^b In CDCl_3 solution. ^c In C_6D_6 as solvent.

Scheme 1

exo,exo-bis(isodicyclopentadienyl)titanium dichloride **2** was obtained stereoselectively by reacting **1** with $\text{TiCl}_3 \cdot 3\text{THF}$ in tetrahydrofuran solution at 25 °C followed by oxidation with HCl (Scheme 1).⁸ In contrast, admixing of **1** with $\text{TiCl}_3 \cdot 3\text{THF}$ in THF at -64 °C for 5 h followed by the introduction of cold CCl_4 prior to workup afforded **3** as an equally dark red crystalline solid (49%).¹¹ We attribute the resultant stereochemical

crossover to the high levels of dimeric lithium isodicyclopentadienide present in solution below -60 °C.^{7a,d} Arrival at *endo,exo* isomer **6** was accomplished somewhat less directly^{12,13} by treatment of the known silane **4**¹⁴ with TiCl_4 in toluene at 20 °C to produce initially *exo*-(isodiCp) TiCl_3 (**5**), followed by the dropwise introduction of **5** to 1 equiv of **1** also dissolved in THF at -78 °C. All three diastereomers are configurationally stable and exhibit no tendency to interconvert when heated in solution.

The fully assigned ^1H and ^{13}C NMR data for **2**, **3**, and **6** are compiled in Tables 1 and 2 along with those for **5** and two other derivatives to which attention will be drawn subsequently. A striking feature of these data is the very telltale response of the central and peripheral protons positioned on the cyclopentadienyl ring to the particular face being utilized for coordination to the titanium atom. Thus, *exo,exo* bonding as in **2** has the effect of deshielding the central proton (δ 6.27) while simultaneously shifting the peripheral protons somewhat to higher field (δ 6.08). In contrast, these same protons are strongly influenced in the opposite sense (δ 5.84, 6.33) when *endo,endo* complexation prevails as in **3**. A similar trend is apparent in the stereochemically mixed complex **6**, although the chemical shift differences exhibited by the *exo* ligand (δ 6.09, 6.17) reflect the actual state of affairs at a more accentuated level than those of the *endo* isodiCp component (δ 5.86, 6.29).

The electronegativity of the titanium center exerts an obvious influence on the norbornyl protons to which it is most closely positioned. In *exo* titanocenes, the anisochronous characteristics of the metal operate on the *syn* methano proton and shield it extensively (ca 0.6 ppm). On the other hand, an *endo* orientation positions the Ti proximal to the two magnetically

(11) Sornay, C.; Meunier, P.; Gautheron, B.; O'Doherty, G. A.; Paquette, L. A. *Organometallics* **1991**, *10*, 2082.

(12) Cardoso, A. M.; Clark, R. J. H.; Moorhouse, S. *J. Chem. Soc., Dalton Trans.* **1980**, 1156.

(13) For more recent examples of this chemistry, consult: (a) Llinas, G. H.; Mena, M.; Palacios, F.; Royo, P.; Serrano, R. *J. Organomet. Chem.* **1988**, *340*, 37. (b) Lund, E. C.; Livinghouse, T. *Organometallics* **1990**, *9*, 2426. (c) Winter, C. H.; Zhou, X.-X.; Dobbs, D. A.; Heeg, M. J. *Organometallics* **1991**, *10*, 210.

(14) Paquette, L. A.; Charumilind, P.; Gallucci, J. C. *J. Am. Chem. Soc.* **1983**, *105*, 7364.

Table 3. Ultraviolet Absorption Maxima of Representative Dichlorotitanium Complexes (CH₂Cl₂ Solution)

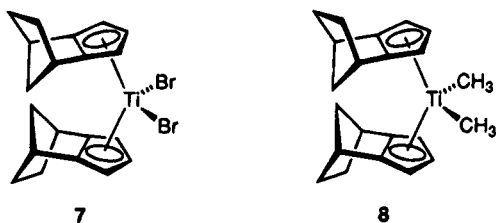
ligand 1	ligand 2	λ_{\max} (nm)
Cp	Cp	255.5
<i>t</i> -BuCp	<i>t</i> -BuCp	264
Cp	<i>exo</i> -isodiCp	257
Cp	<i>endo</i> -isodiCp	263
<i>t</i> -BuCp	<i>exo</i> -isodiCp	264
<i>t</i> -BuCp	<i>endo</i> -isodiCp	268
<i>exo</i> -isodiCp	<i>exo</i> -isodiCp	264
<i>exo</i> -isodiCp	<i>endo</i> -isodiCp	268
<i>endo</i> -isodiCp	<i>endo</i> -isodiCp	268

equivalent endo ethano hydrogens with closely comparable consequences (Table 1). The bridgehead norbornyl protons are not sensitive to stereochemistry, appear consistently at δ 3.3, and serve as a useful internal point of reference.^{14–16}

The ultraviolet absorption maxima of the (isodiCp)₂TiCl₂ isomers in CH₂Cl₂ solution have been compiled alongside those of simpler related systems in Table 3.

Consequences of Chlorine Substitution. The availability of the three possible stereoisomeric (isodiCp)₂TiCl₂ complexes has prompted an investigation of their effective involvement in representative transformations and a comparative analysis of product stability. Treatment of **2** with boron tribromide in dry dichloromethane at 20 °C for 2 h according to Druce et al.¹⁷ gave rise to the black, crystalline **7** in 86% yield after one recrystallization. Comparison of its ¹H NMR spectrum with that of **2** reveals a downward drift of those signals due to the central and peripheral cyclopentadienyl protons in addition to the anti methano hydrogen (Table 1). These effects are reasonable in light of the increased length of the Ti–Br bond, the change in electronegativity of the halogen, and the resultant response of Ti to these modifications. No loss of stereochemical integrity was seen.

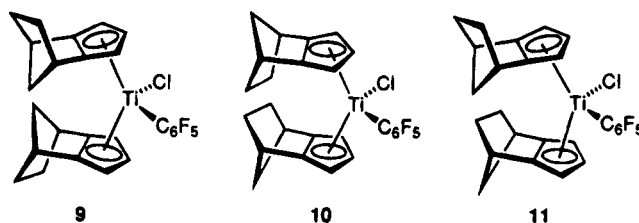
Comparable processing of **3** and **6** resulted in decomposition even at a temperature of –80 °C. Evidently, the highly reactive nature of BBr₃ suffices to destroy the diastereomers of **7**.



An analogous situation developed during the attempted preparation of the dimethyl derivatives. Whereas the *exo,exo* dichloride **2** reacted smoothly with >2 equiv of ethereal methyllithium^{18,19} to give the orange crystalline **8** (68%), the other two isomers proved to be very unstable and were not characterized. Although the spectral properties of **8** are in full agreement with its assigned structure, the replacement of elec-

tronegative chlorine atoms by methyl groups does have its consequences. Relative to **2**, all of the isodiCp protons are more shielded in **8** with the exception of the endo ethano protons located on the surface away from the metal. An exactly parallel trend is reflected in its ¹³C NMR spectrum (Table 2).

Success in engaging all three diastereomers in conversion to stable products was realized upon exposure of the dichlorides to pentafluorophenyllithium in ether solution at 0 °C.^{20,21} The resultant products **9–11** are



air-stable crystalline compounds differing in the color which they exhibit. As before, these diastereomeric complexes can readily be distinguished by their NMR spectra (Table 4). The trends in chemical shift are the same as those discussed above. However, the obvious reduction in symmetry causes several of the norbornyl proton pairs to be diastereotopic. This is most evident in the case of the peripheral cyclopentadienyl and bridgehead hydrogen atoms. Interestingly, the $\Delta\delta$ in chemical shift is most dramatic for the bridgehead protons. *Exo* bonding to the titanium as in **9** and the upper half of **11** gives rise to signals that are characteristically widely divergent (0.38 and 0.58 ppm, respectively). In contrast, *endo* complexation leads to less dramatic disparities (0.16 ppm for **10**, 0.15 for the lower half of **11**) as a consequence of the increased distance to the pentafluorophenyl substituent in this stereochemical arrangement.

The ¹³C NMR spectrum of **9** features a methano bridge carbon at 47.7 ppm and two well-separated quaternary cyclopentadienyl carbons at 149.3 and 142.7 ppm. In *endo,endo* isomer **10**, shielding of the methano bridge center by the metal no longer operates (now at 59.1 ppm) and the quaternary centers appear at 158.2 and 152.6 ppm, keeping with precedent.

X-ray Crystallographic Analyses of 8–11. The molecular structures of (isodiCp)₂TiMe₂ (**8**) and the three pentafluorophenyl derivatives **9–11** are shown in Figures 1–4, respectively. The numbering schemes used for **9–11** are identical, with the exception that **10** has additional letters (A and B) to distinguish between the two molecules in the asymmetric unit. A summary of crystallographic data is given in Table 5. Selected bond lengths and angles are listed in Tables 6–9. Final positional parameters appear in Tables 10–13. The data set for **10** was weak, and, with two molecules in the asymmetric unit, this structure is not as well determined as the other three. Nevertheless, it remains possible to compare various features for all four structures.

For all three diastereomers of (isodiCp)₂Ti(C₆F₅)Cl, the geometry about the Ti atom is pseudotetrahedral where the tetrahedron is defined by the chlorine atom,

(20) Chaudhari, M. A.; Treichel, P. M.; Stone, F. G. A. *J. Organomet. Chem.* **1964**, *2*, 206.

(21) (a) Moïse, C.; Leblanc, J. C.; Tirouflet, J. *J. Am. Chem. Soc.* **1975**, *97*, 6272. (b) Leblanc, J. C.; Moïse, C.; Tirouflet, J. *Nouv. J. Chim.* **1977**, *1*, 211.

(15) Gallucci, J. C.; Kravetz, T. M.; Green, K. E.; Paquette, L. A. *J. Am. Chem. Soc.* **1985**, *107*, 6592.

(16) Brown, F. K.; Houk, K. N. *J. Am. Chem. Soc.* **1985**, *107*, 1971 and relevant references cited therein.

(17) Druce, P. M.; Kingston, B. M.; Lappert, M. F.; Spalding, T. R.; Srivastava, R. C. *J. Chem. Soc. (A)* **1969**, 2106.

(18) Samuel, E.; Rausch, M. D. *J. Am. Chem. Soc.* **1973**, *95*, 6263.

(19) Mach, K.; Varga, V.; Hanus, V.; Sedmera, P. *J. Organomet. Chem.* **1991**, *415*, 87.

Table 4. 500 MHz ^1H , 125 MHz ^{13}C , and 188 MHz ^{19}F NMR Spectra of the Diastereomeric (IsodiCp) $_2\text{TiCl}(\text{C}_6\text{F}_5)$ Complexes^a

A. ^1H NMR Data

compd	cyclopentadienyl		bridgehead	exo ethano	endo ethano	syn methano	anti methano
	central	peripheral					
9	6.29 (t/2)	5.77 (m/2)	3.38 (d/2)	1.90 (m/2)	1.12 (m/4)	1.47 (m/2)	1.32 (m/2)
10	6.02 (t/2)	5.61 (m/2)	3.00 (d/2)	1.84 (m/2)	1.69 (m/4)	1.93 (m/2)	1.84 (m/2)
		5.75 (m/2)	3.41 (d/2)	1.93 (m/2)			
11	6.21 (t/1), exo	6.03 (m/1), endo	3.42 (d/1), endo	2.00 (m/1), endo	1.09 (m/2), exo	1.42 (m/1), exo	1.26 (m/1), exo
	6.10 (t/1), endo	5.72 (m/1), exo	3.40 (d/1), exo	1.89 (m/1), exo	1.81 (m/2), endo	2.00 (m/1), endo	1.89 (m/1), endo
		5.69 (m/1), endo	3.27 (d/1), endo	1.81 (m/1), exo	1.81 (m/1), endo		
		5.61 (m/1), exo	2.82 (d/1), exo				

B. ^{13}C NMR Data^a

compd	central	cyclopentadienyl		ethano bridge	bridgehead	methano bridge
		peripheral	quaternary			
9	119.9	105.0	149.3	28.9	41.8	47.7
		104.4	142.7	28.4	41.2	
10	113.6	108.2	158.2	27.6	43.4	59.1
		107.9	152.6	26.8	42.6	
11	117.4	109.8	158.9	29.0	43.4	59.9
		107.3	149.1	28.7	42.9	47.9
		106.8		28.5	42.3	
		103.1		27.6	41.3	

C. ^{19}F NMR Data

compd	ortho	para	meta
9	-105.54 (d/1), $J = 30.5$ Hz	-159.17 (t/1), $J = 20.8$ Hz	-161.45 (m/1)
	-114.26 (d/1), $J = 31.9$ Hz		-164.19 (m/1)
10	-105.54 (m/1)	-159.98 (t/1), $J = 19.9$ Hz	-161.47 (m/1)
	-114.49 (m/1)		-164.11 (m/1)
11	-105.48 (d/1), $J = 27.7$ Hz	-159.14 (t/1), $J = 19.4$ Hz	-161.38 (m/1)
	-114.51 (d/1), $J = 30.5$ Hz		-164.20 (m/1)

^a δ vs. Me_4Si or CFCl_3 , CDCl_3 solution. ^b The quaternary carbons of the C_6F_5 rings were not detectable because of extensive C/F coupling.

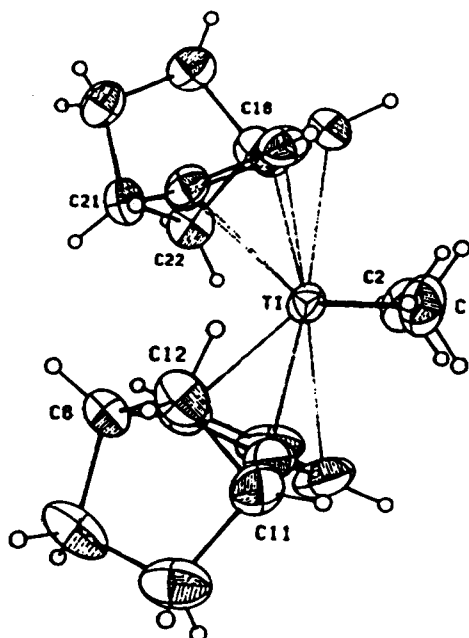


Figure 1. ORTEP representation of **8**; atoms drawn with 50% probability thermal ellipsoids. Hydrogen atoms are drawn with artificial radii.

$\text{C}(21)$ (the carbon atom of the C_6F_5 group bonded to Ti), and the ring centroids of the approximately planar five-membered rings of the isodiCp ligands. This pseudotetrahedral arrangement about the Ti atom is shared by the dimethyl derivative **8**.

When each of the pentafluorophenyl structures is viewed in projection onto the $\text{Cl-Ti-C}(21)$ plane, the

norbornane portion of one isodiCp ligand falls within the $\text{Cl-Ti-C}(21)$ angle. The norbornane portion of the second isodiCp ligand always lies on the opposite side of the Ti atom from the C_6F_5 group. For the *exo,exo* (**9**) and *endo,endo* (**10**) isomers, the *exo* and *endo* isodiCp subunits, respectively, project within the $\text{Cl-Ti-C}(21)$ angle. For the *exo,endo* isomer **11** (where there is a choice), the *exo* ligand projects within this angle. One of these projected views is shown in Figure 2 for structure **9**. These spatial arrangements contrast to that present in **8**, which, when viewed in projection onto the $\text{Ti}(\text{CH}_3)_2$ plane, shows the norbornane subunits oriented away from each other and projecting well outside of the $\text{CH}_3\text{-Ti-CH}_3$ angle. *exo,exo*-(IsodiCp) $_2\text{-TiCl}_2$ (**2**) shows the same structure in projection as **8**.²

For **9-11** the dihedral angle between the least-squares plane through the C_6F_5 group and the plane defined by $\text{Cl-Ti-C}(21)$ is rather small: 5.7° for **11**, 18.4° for **9**, 18.8° for **10B**, and 23.2° for **10A**. The fact that the C_6F_5 group lies almost in the plane defined by $\text{Cl-Ti-C}(21)$ is most likely the result of the aforementioned arrangement of the isodiCp ligands.

The Ti to Cp ring-carbon distances span a wide range, which is indicative of an asymmetric Ti-Cp ring interaction. These ranges are 2.379–2.446 Å for **8**, 2.354–2.440 Å for **9**, 2.316–2.573 Å for **10A**, 2.298–2.515 Å for **10B**, and 2.352–2.463 Å for **11**. The largest range is for the *endo,endo* isomer **10**. As seen in various $(\eta^5\text{-RCp})_2\text{MCl}_2$ structures,^{2,22} the metal-to-ring carbon distance is expected to be greatest for the carbon atom

(22) Howie, R. A.; McQuillan, G. P.; Thompson, D. W.; Lock, G. A. *J. Organomet. Chem.* **1986**, *303*, 213.

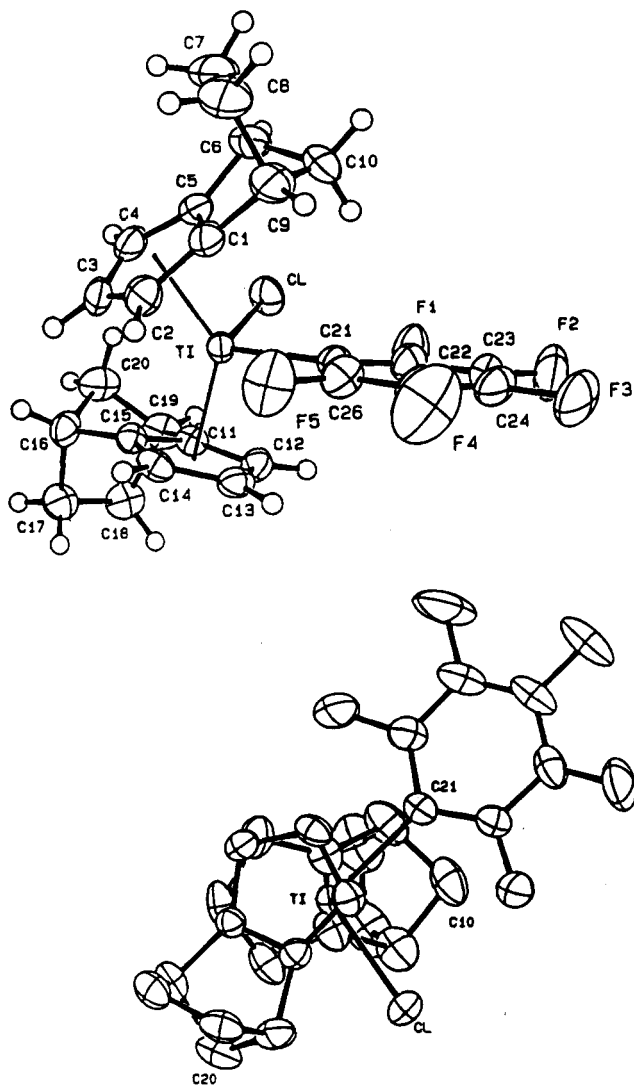


Figure 2. Two ORTEP representations of **9**; atoms drawn with 50% probability thermal ellipsoids. The labeling scheme on the upper drawing includes hydrogen atoms drawn with artificial radii. The view on the lower drawing is a projection of the structure onto the C1–Ti–C(21) plane with hydrogen atoms omitted for clarity.

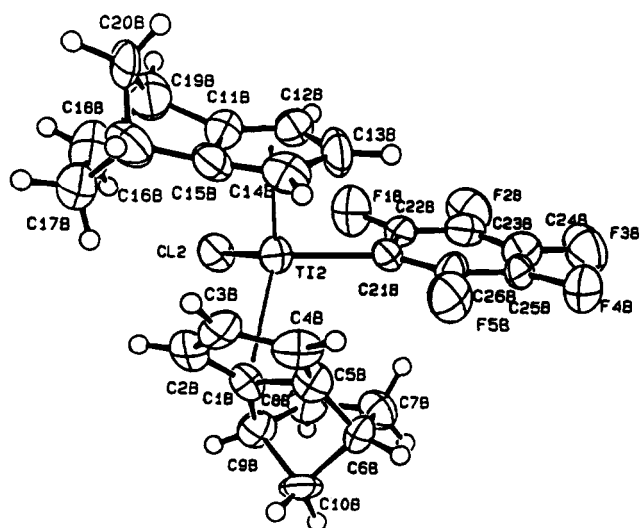


Figure 3. ORTEP representation of **10**; atoms drawn with 50% probability thermal ellipsoids. Hydrogen atoms are drawn with artificial radii.

bonded to a substituent group. In **9–11**, the carbon atoms C(1), C(5), C(11), and C(15) are bonded to a

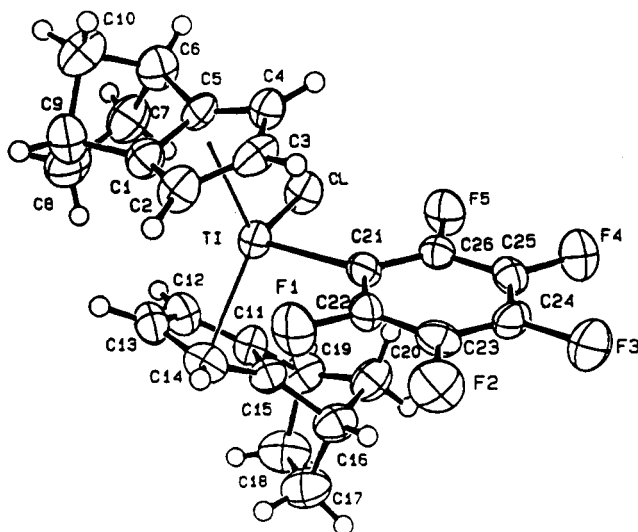


Figure 4. ORTEP representation of **11**; atoms drawn with 50% probability thermal ellipsoids. Hydrogen atoms drawn with artificial radii.

norbornyl fragment, and it is always one of these atoms out of each Cp which is the farthest distance from the Ti atom. In **8**, C(3) is farthest from the Ti atom for one Cp ring, while C(16) is farthest for the other ring.

For all four structures, the isodiCp ligands are bent about the bond common to the Cp ring and the norbornane fragment, and this bending is always in a direction away from the Ti atom. For example, in **9–11** the C(6) and C(9) atoms lie significantly out of the best plane through the five-membered ring C(1)–C(5) and are on the opposite side of this plane from the Ti atom. A measure of bending in these complexes is described by the dihedral angle between the least-squares planes through C(1)–C(2)–C(3)–C(4)–C(5) and C(6)–C(5)–C(1)–C(9) and, for the other isodiCp ligand, the dihedral angle between the C(11)–C(12)–C(13)–C(14)–C(15) best plane and the C(16)–C(15)–C(11)–C(19) best plane. The dihedral angles are identically identified for **8**. The dihedral angles for the endo-oriented isodiCp ligands are slightly larger than those for the exo ligands: 11.3 and 12.0° for **8**, 11.7 and 12.6° for **9**, 15.8 and 16.6° for **10A**, 15.7 and 16.4° for **10B**, and 16.8 (endo) and 12.4° (exo) for **11**. We again emphasize that coordination of the isodiCp ligand from the exo surface bends the Cp ring in the preferred endo direction.^{16,23} For the two structures reported here having coordination from the endo surface, the modestly exaggerated bending in the less preferred exo direction arises because the metal center and its substituents experience greater nonbonded steric compression when located on this π -surface.

The Cl–Ti–C(21) bond angle is slightly larger for **9–11** (at 102.0, 100.7, 97.6, and 100.9°) than the Cl–Ti–Cl angle observed for various $(\eta^5\text{-RCp})_2\text{MCl}_2$ structures (92.5–96.1°) and the CH₃–Ti–CH₃ angle of 92.4° in **8**. It is also larger than the C–Ti–Cl angle observed in Cp₂TiCl(μ - η^1 : η^6 -*o*-FC₆H₄)Cr(CO)₃ at 93.6(2)° and Cp₂TiCl(μ - η^1 : η^6 -*p*-CH₃C₆H₄)Cr(CO)₃ at 94.8(2)°.²⁴ These

(23) See the many references in: (a) Paquette, L. A.; Künzer, H.; Green, K. E.; DeLucchi, O.; Licini, G.; Pasquato, L.; Valle, G. *J. Am. Chem. Soc.* **1986**, *108*, 3453. (b) Paquette, L. A.; Shen, C.-C. *J. Am. Chem. Soc.* **1990**, *112*, 1159. (c) Irrgartinger, H.; Deuter, J.; Charumilind, P.; Paquette, L. A. *J. Am. Chem. Soc.* **1989**, *111*, 9236.

(24) van Rooyen, P. H.; Schindehutte, M.; Lotz, S. *Organometallics* **1992**, *11*, 1104.

Table 5. Experimental Crystallographic Data for 8–11

	8	9	10	11
formula	C ₂₂ H ₂₈ Ti	C ₂₆ H ₂₂ ClF ₅ Ti	C ₂₆ H ₂₂ ClF ₅ Ti	C ₂₆ H ₂₂ ClF ₅ Ti
space group	P2 ₁ 2 ₁ 2 ₁	P1	P2 ₁ /n	P2 ₁ /c
a, Å	7.792(2)	7.150(1)	14.826(3)	7.518(2)
b, Å	14.174(8)	12.187(1)	13.887(2)	18.064(3)
c, Å	16.012(4)	12.678(1)	21.572(3)	16.093(2)
α , deg		93.835(8)		
β , deg		90.187(8)	93.95(1)	90.93(2)
γ , deg		94.811(7)		
V, Å ³	1768	1098	4431	2185
Z	4	2	8	4
mol wt	340.35	512.80	512.80	512.80
D _{calcd} , g cm ⁻³	1.28	1.55	1.54	1.56
cryst size, mm ³	0.18 × 0.30 × 0.33	0.16 × 0.30 × 0.37	0.04 × 0.23 × 0.27	0.05 × 0.11 × 0.35
μ , cm ⁻¹	5.01	5.60	5.55	5.63
transmissn factors ^a		0.85–0.92		0.94–0.97
temp, °C	18	22	22	22
2 θ limits ^b	2 ≤ 2 θ ≤ 50°	4 ≤ 2 θ ≤ 55°	4 ≤ 2 θ ≤ 50°	4 ≤ 2 θ ≤ 50°
scan range, deg in ω	0.80 + 0.35 tan θ	1.30 + 0.35 tan θ	1.20	1.20
data colld	+h, +k, +l	+h, ±k, ±l	+h, +k, ±l	±h, +k, +l
scan type	ω -2 θ	ω -2 θ	ω	ω
no. of unique data	1814	5077	8214	4005
no. of obsd data ^c	1433	3993	2930	2004
final no. of variables	214	299	590	298
R(F) ^d	0.037	0.038	0.102	0.069
R _w (F) ^e	0.054	0.032	0.054	0.039
goodness-of-fit	0.44	1.96	1.50	1.35
max peak in final diff map, e/Å ³	0.3	0.29	0.68	0.41

^a An analytical absorption correction was applied to the data for 9 and 11. ^b Data were measured with a Rigaku AFC5S diffractometer using graphite-monochromated Mo K α radiation for 9–11 and with an Enraf-Nonius CAD-4 diffractometer with graphite-monochromated Mo K α radiation for 8. ^c Observed data used in the least-squares refinements are defined as $I \geq \sigma(I)$ for 9–11 and $F_o \geq 5\sigma(F_o)$ for 8. ^d $R(F) = \sum |F_o| - |F_c| / \sum |F_o|$. ^e $R_w(F) = [\sum w(|F_o| - |F_c|)^2 / \sum w|F_o|^2]^{1/2}$, with $w = 1/\sigma^2(F_o)$ for 9–11 and $w = 1/(\sigma^2(F_o) + 0.0042F_o^2)$ for 8.

Table 6. Selected Bond Distances (Å) and Angles (deg) for 8

Ti–C(1)	2.171(5)	Ti–C(2)	2.175(5)
Ti–C(3)	2.431(4)	Ti–C(4)	2.421(4)
Ti–C(5)	2.381(5)	Ti–C(6)	2.385(5)
Ti–C(7)	2.406(4)	Ti–C(13)	2.403(4)
Ti–C(14)	2.389(4)	Ti–C(15)	2.379(4)
Ti–C(16)	2.446(4)	Ti–C(17)	2.437(4)
Cent1–Ti	2.094	Cent2–Ti	2.086
C(1)–Ti–C(2)	92.4(2)	Cent1–Ti–Cent2	134.3
Cent1–Ti–C(1)	105.0	Cent1–Ti–C(2)	106.4
Cent2–Ti–C(1)	105.8	Cent2–Ti–C(2)	105.3

Table 7. Selected Bond Distances (Å) and Angles (deg) for 9

Ti–Cl	2.3453(7)	Ti–C(12)	2.402(2)
Ti–C(1)	2.429(2)	Ti–C(13)	2.372(2)
Ti–C(2)	2.378(2)	Ti–C(14)	2.370(2)
Ti–C(3)	2.354(2)	Ti–C(15)	2.383(2)
Ti–C(4)	2.403(2)	Ti–C(21)	2.273(2)
Ti–C(5)	2.440(2)	Ti–RC(1) ^a	2.082(2)
Ti–C(11)	2.427(2)	Ti–RC(2)	2.071(2)
Cl–Ti–C(21)	101.99(6)	C(21)–Ti–RC(1)	106.57(8)
Cl–Ti–RC(1)	104.28(7)	C(21)–Ti–RC(2)	101.52(8)
Cl–Ti–RC(2)	106.24(6)	RC(1)–Ti–RC(2)	132.6(1)

latter two structures both contain a small endocyclic C–C–C bond angle for the derivatized phenyl ring where the central carbon atom is σ bonded to the Ti atom. This small endocyclic C–C–C angle is also observed in each of the three pentafluorophenyl derivatives: 111.7(2)° for 9, 113(1) and 111(1)° for 10, and 111.5(6)° for 11.

Conclusion

The charge density of the carbon atoms in the cyclopentadienyl sector of the isodiCp ligand gives evidence of being quite sensitive to the π surface involved in complexation. These unique observations may possibly be the result of several factors, including differing

Table 8. Selected Bond Distances (Å) and Angles (deg) for 10

Ti(1)–Cl(1)	2.316(4)	Ti(2)–Cl(2)	2.333(4)
Ti(1)–C(1A)	2.453(12)	Ti(2)–C(1B)	2.512(14)
Ti(1)–C(2A)	2.378(13)	Ti(2)–C(2B)	2.419(13)
Ti(1)–C(3A)	2.340(13)	Ti(2)–C(3B)	2.298(13)
Ti(1)–C(4A)	2.418(13)	Ti(2)–C(4B)	2.370(13)
Ti(1)–C(5A)	2.492(14)	Ti(2)–C(5B)	2.515(14)
Ti(1)–C(11A)	2.508(13)	Ti(2)–C(11B)	2.498(15)
Ti(1)–C(12A)	2.358(12)	Ti(2)–C(12B)	2.385(14)
Ti(1)–C(13A)	2.316(12)	Ti(2)–C(13B)	2.336(15)
Ti(1)–C(14A)	2.415(13)	Ti(2)–C(14B)	2.367(13)
Ti(1)–C(15A)	2.573(14)	Ti(2)–C(15B)	2.451(15)
Ti(1)–C(21A)	2.260(13)	Ti(2)–C(21B)	2.245(13)
Ti(1)–RC(1A) ^a	2.102(13)	Ti(2)–RC(1B) ^c	2.109(14)
Ti(1)–RC(2A) ^a	2.124(14)	Ti(2)–RC(2B) ^d	2.100(15)

Cl(1)–Ti(1)–C(21A)	97.6(3)	Cl(2)–Ti(2)–C(21B)	100.7(4)
Cl(1)–Ti(1)–RC(1A)	108.4(4)	Cl(2)–Ti(2)–RC(1B)	103.2(4)
Cl(1)–Ti(1)–RC(2A)	104.8(4)	Cl(2)–Ti(2)–RC(2B)	108.5(5)
C(21A)–Ti(1)–RC(1A)	101.6(5)	C(21B)–Ti(2)–RC(1B)	107.1(5)
C(21A)–Ti(1)–RC(2A)	106.4(5)	C(21B)–Ti(2)–RC(2B)	100.1(5)
RC(1A)–Ti(1)–RC(2A)	132.6(6)	RC(1B)–Ti(2)–RC(2B)	133.0(6)

^a RC(1A) is the ring centroid for C(1A)–C(2A)–C(3A)–C(4A)–C(5A). ^b RC(2A) is the ring centroid for C(11A)–C(12A)–C(13A)–C(14A)–C(15A). ^c RC(1B) is the ring centroid for C(1B)–C(2B)–C(3B)–C(4B)–C(5B). ^d RC(2B) is the ring centroid for C(11B)–C(12B)–C(13B)–C(14B)–C(15B).

electronic contributions from the fused norbornyl subunit and nonbonded steric interactions, and additional studies to shed light on these issues are in progress. Recently, Doman, Hollis, and Bosnich have deduced on the strength of molecular mechanics force field calculations that the conformation adopted by bent metallocenes of the generic formula Cp₂MCl₂ in the crystal is not generally the most stable.²⁵ Although the importance of crystal-packing forces always needs to be reckoned with and the various possible conformations of 2, 3, 6, and 8–11 are quite probably close in energy, it is nonetheless remarkable that the three pentafluo-

Table 9. Selected Bond Distances (Å) and Angles (deg) for 11

Ti-Cl	2.336(2)	Ti-C(12)	2.412(7)
Ti-C(1)	2.452(7)	Ti-C(13)	2.359(7)
Ti-C(2)	2.381(6)	Ti-C(14)	2.372(7)
Ti-C(3)	2.352(7)	Ti-C(15)	2.419(7)
Ti-C(4)	2.389(7)	Ti-C(21)	2.264(6)
Ti-C(5)	2.463(6)	Ti-RC(1) ^a	2.092(7)
Ti-C(11)	2.447(7)	Ti-RC(2) ^b	2.085(7)
Cl-Ti-C(21)	100.9(2)	C(21)-Ti-RC(1)	102.5(3)
Cl-Ti-RC(1)	106.1(2)	C(21)-Ti-RC(2)	104.0(3)
Cl-Ti-RC(2)	106.0(2)	RC(1)-Ti-RC(2)	133.1(3)

^a RC(1) is the ring centroid for C(1)-C(2)-C(3)-C(4)-C(5).^b RC(2) is the ring centroid for C(11)-C(12)-C(13)-C(14)-C(15).**Table 10. Positional Parameters and B(eq) Values for 8**

atom	<i>x/a</i>	<i>y/b</i>	<i>z/c</i>	<i>B</i> (eq) ^a
Ti	-0.13069(9)	-0.94792(5)	-0.75728(4)	1.81
C(1)	0.0782(7)	-1.0491(3)	-0.7623(3)	3.22
C(2)	-0.3203(7)	-1.0542(4)	-0.7902(4)	3.32
C(3)	-0.0221(6)	-0.9432(4)	-0.6150(3)	2.51
C(4)	-0.1637(8)	-1.0028(4)	-0.6150(3)	3.48
C(5)	-0.3081(7)	-0.9472(5)	-0.6362(3)	3.53
C(6)	-0.2549(6)	-0.8532(4)	-0.6501(3)	2.81
C(7)	-0.0753(6)	-0.8521(3)	-0.6362(3)	2.13
C(8)	0.0726(6)	-0.7860(3)	-0.6189(3)	2.32
C(9)	0.0842(7)	-0.7826(5)	-0.5219(3)	3.49
C(10)	0.1475(7)	-0.8828(4)	-0.4984(3)	3.46
C(11)	0.1615(7)	-0.9342(3)	-0.5840(3)	2.76
C(12)	0.2228(6)	-0.8512(4)	-0.6381(3)	2.51
C(13)	-0.1979(5)	-0.8066(3)	-0.8336(2)	1.75
C(14)	-0.0190(5)	-0.8097(3)	-0.8231(3)	1.92
C(15)	0.0404(6)	-0.8893(3)	-0.8689(3)	2.27
C(16)	-0.0981(6)	-0.9320(3)	-0.9085(3)	2.45
C(17)	-0.2461(6)	-0.8818(3)	-0.8861(2)	1.93
C(18)	-0.4303(6)	-0.8637(3)	-0.9122(3)	2.37
C(19)	-0.4189(7)	-0.7779(4)	-0.9723(3)	2.77
C(20)	-0.3688(7)	-0.6950(3)	-0.9132(3)	2.68
C(21)	-0.3518(6)	-0.7427(3)	-0.8266(3)	2.32
C(22)	-0.4981(5)	-0.8148(4)	-0.8325(3)	2.67

^a $B(\text{eq}) = (8\pi^2/3)[a^2U_{11}(a^*)^2 + b^2U_{22}(b^*)^2 + c^2U_{33}(c^*)^2 + ab(\cos \gamma)U_{12}a^*b^* + ac(\cos \beta)U_{13}a^*c^* + bc(\cos \alpha)U_{23}b^*c^*]$.

rophenyl complexes preferentially adopt a three-dimensional arrangement in which one isodiCp ligand falls within the Cl-Ti-C(21) angle. (IsodiCp)(Cp)TiCl₂ and (isodiCp)(Me₅Cp)TiCl₂ have previously been recognized to have the exo portion of the isodiCp ligand similarly projected into the Cl-Ti-Cl angle.^{8b} Whatever the origins of this effect, they are not operational in **2** or in **8**, both of which have the norbornyl segments positioned as remotely from each other as possible. The space-filling nature of the C₆F₅ substituent and its electron-withdrawing capabilities are very likely responsible for the different geometric features. It remains to demonstrate that rotameric conformations adopted by Cp₂M-(C₆F₅)Cl complexes differ generically from those complexes lacking this particular aryl substituent.

Experimental Section

All manipulations were carried out under an argon atmosphere. The solvents were distilled from sodium benzophenone ketyl prior to use. The EI high-resolution mass spectra were recorded in the CSM at Dijon and at The Ohio State University Campus Chemical Instrumentation Center. Elemental analyses were performed by the "Service central de microanalyses du CNRS" (Lyon, France).

endo,endo-Bis(η⁵-isodicyclopentadienyl)titanium Dichloride (3). A solution of (isodicyclopentadienyl)lithium² (360 mg, 2.61 mmol) in dry THF (46 mL) was cooled to -64

Table 11. Positional Parameters and B(eq) Values for 9

atom	<i>x</i>	<i>y</i>	<i>z</i>	<i>B</i> (eq) ^a Å ²
Ti	0.22302(5)	0.28049(3)	0.31537(3)	2.18(1)
Cl	-0.06995(8)	0.30130(5)	0.39343(5)	3.71(3)
F(1)	-0.1695(2)	0.1577(1)	0.1955(1)	5.94(8)
F(2)	-0.2697(2)	0.0849(1)	0.0012(1)	6.44(9)
F(3)	-0.0215(3)	0.0957(1)	-0.1596(1)	6.48(9)
F(4)	0.3361(3)	0.1832(2)	-0.1186(1)	7.7(1)
F(5)	0.4421(2)	0.2560(1)	0.0742(1)	5.68(8)
C(1)	0.3015(3)	0.4417(2)	0.2164(2)	3.2(1)
C(2)	0.4686(3)	0.4049(2)	0.2563(2)	3.6(1)
C(3)	0.4606(3)	0.4194(2)	0.3671(2)	3.8(1)
C(4)	0.2908(4)	0.4636(2)	0.3960(2)	3.6(1)
C(5)	0.1939(3)	0.4772(2)	0.3020(2)	3.3(1)
C(6)	0.0359(4)	0.5355(2)	0.2597(2)	4.4(1)
C(7)	0.1325(5)	0.6462(2)	0.2254(2)	6.1(2)
C(8)	0.2554(5)	0.6098(2)	0.1313(2)	6.2(2)
C(9)	0.2128(4)	0.4817(2)	0.1194(2)	4.3(1)
C(10)	0.0051(4)	0.4726(2)	0.1506(2)	4.7(1)
C(11)	0.2194(3)	0.1461(2)	0.4484(2)	2.60(8)
C(12)	0.1726(3)	0.0892(2)	0.3510(2)	2.97(9)
C(13)	0.3316(3)	0.1025(2)	0.2862(2)	3.0(1)
C(14)	0.4733(3)	0.1690(2)	0.3411(2)	2.73(9)
C(15)	0.4020(3)	0.1973(2)	0.4424(2)	2.40(8)
C(16)	0.4625(3)	0.2368(2)	0.5539(2)	3.3(1)
C(17)	0.4870(4)	0.1289(2)	0.6098(2)	3.7(1)
C(18)	0.2849(4)	0.0744(2)	0.6162(2)	3.7(1)
C(19)	0.1645(3)	0.1555(2)	0.5632(2)	3.5(1)
C(20)	0.2728(4)	0.2660(2)	0.5997(2)	4.1(1)
C(21)	0.1402(3)	0.2184(2)	0.1473(2)	2.70(9)
C(22)	-0.0363(3)	0.1707(2)	0.1203(2)	3.3(1)
C(23)	-0.0946(4)	0.1305(2)	0.0194(2)	3.9(1)
C(24)	0.0314(4)	0.1356(2)	-0.0609(2)	4.2(1)
C(25)	0.2099(4)	0.1792(2)	-0.0402(2)	4.4(1)
C(26)	0.2596(3)	0.2181(2)	0.0613(2)	3.5(1)

^a The form of the equivalent isotropic displacement parameter is $B(\text{eq}) = (8\pi^2/3)\sum_i \sum_j U_{ij}a_i^*a_j^*$.

°C in a CHCl₃-liquid N₂ bath and added quickly to a solution of TiCl₃·3THF (550 mg, 1.35 mmol) in THF (40 mL) at the same temperature. The reaction mixture was stirred at -64 °C for 5 h. Freshly distilled and previously cooled CCl₄ (20 mL) was introduced, and the solution developed a dark red coloration. After 15 min of stirring, the reaction mixture was poured into 10 mL of concentrated hydrochloric acid and ice. The aqueous phase was extracted with CHCl₃, and the combined organic layers were washed with water, dried, and evaporated. Recrystallization of the residue from CH₂Cl₂-hexanes afforded **3** (243 mg, 49%) as a dark red solid, mp 208-210 °C; ¹H and ¹³C NMR (see Tables); MS *m/z* (relative intensity): 380 (M⁺, 13), 345 (M⁺ - Cl, 17), 249 (M⁺ - isodiCp, 46), 131 (C₁₀H₁₁, 84) 103 (C₈H₇, 100). Anal. Calcd for C₂₀H₂₂Cl₂Ti: C, 63.02; H, 5.77. Found: C, 62.93; H, 5.76.

exo-(η⁵-isodicyclopentadienyl)titanium Trichloride (5).

(Isodicyclopentadienyl)lithium (799 mg, 5.79 mmol) was dissolved in dry THF (30 mL), and freshly distilled trimethylsilyl chloride (7.5 mL, 59.1 mmol) was introduced dropwise. The reaction mixture was refluxed for 1 h, returned to room temperature, and stirred for an additional 2 h. Following solvent removal in vacuo, the product was extracted into pentane (3 × 8 mL), and the combined yellowish extracts were concentrated to leave the oily silane **4**,¹⁴ which was directly dissolved in toluene (2 mL). In a second flask, TiCl₄ (0.7 mL, 6.38 mmol) was diluted with dry toluene (5 mL). The solution of **4** was slowly transferred into the TiCl₄ solution via cannula, and the mixture was stirred at room temperature for 15 h. The solvent was removed in vacuo, and the dark green residue was triturated with pentane (3 × 10 mL). The pentane extracts were dried and concentrated to give **5** (1.337 g, 85%) as greenish crystals, mp 140-142 °C; ¹H and ¹³C NMR (see Tables). Anal. Calcd for C₁₀H₁₁Cl₃Ti: C, 42.08; H, 3.88. Found: C, 42.36; H, 4.00.

endo,exo-Bis(η⁵-isodicyclopentadienyl)titanium Dichloride (6). A solution of **5** (264 mg, 0.93 mmol) in dry THF (17 mL) at -78 °C was treated gradually with a solution of

Table 12. Positional Parameters for 10

atom	<i>x</i>	<i>y</i>	<i>z</i>	<i>B</i> (eq) ^a or <i>B</i> , Å ²
Ti(1)	0.7980(2)	0.2063(2)	0.7631(1)	2.7(1)
Cl(1)	0.8567(2)	0.3597(2)	0.7781(2)	3.8(2)
F(1A)	0.6657(5)	0.0497(5)	0.8406(4)	5.6(5)
F(2A)	0.5438(6)	0.0700(6)	0.9230(4)	6.6(5)
F(3A)	0.4839(6)	0.2458(6)	0.9542(4)	6.9(5)
F(4A)	0.5513(5)	0.4037(6)	0.8990(4)	6.4(5)
F(5A)	0.6767(5)	0.3905(5)	0.8200(4)	5.5(5)
C(1A)	0.790(1)	0.178(1)	0.6507(6)	3.2(7)
C(2A)	0.728(1)	0.115(1)	0.6797(6)	3.8(8)
C(3A)	0.6639(9)	0.174(1)	0.7030(6)	3.3(7)
C(4A)	0.6828(9)	0.272(1)	0.6903(6)	3.5(8)
C(5A)	0.759(1)	0.272(1)	0.6571(6)	3.1(7)
C(6A)	0.806(1)	0.330(1)	0.6100(7)	4.1(8)
C(7A)	0.907(1)	0.337(1)	0.6291(7)	5(1)
C(8A)	0.944(1)	0.234(1)	0.6224(7)	5(1)
C(9A)	0.858(1)	0.178(1)	0.6023(7)	5(1)
C(10A)	0.810(1)	0.253(1)	0.5571(6)	5(1)
C(11A)	0.8591(8)	0.105(1)	0.8525(6)	3.2(7)
C(12A)	0.8407(9)	0.0511(9)	0.7984(7)	3.4(7)
C(13A)	0.9024(9)	0.084(1)	0.7549(6)	3.3(7)
C(14A)	0.9534(9)	0.157(1)	0.7838(7)	3.7(8)
C(15A)	0.929(1)	0.171(1)	0.8445(7)	3.4(8)
C(16A)	0.964(1)	0.208(1)	0.9067(7)	4.9(9)
C(17A)	0.892(1)	0.268(1)	0.9337(7)	5(1)
C(18A)	0.820(1)	0.192(1)	0.9507(6)	4.6(8)
C(19A)	0.853(1)	0.097(1)	0.9239(6)	4.1(8)
C(20A)	0.958(1)	0.111(1)	0.9420(7)	6(1)
C(21A)	0.6858(9)	0.218(1)	0.8285(6)	2.7(7)
C(22A)	0.643(1)	0.141(1)	0.8546(7)	3.5(8)
C(23A)	0.579(1)	0.149(1)	0.8978(8)	5(1)
C(24A)	0.547(1)	0.237(1)	0.9120(7)	5(1)
C(25A)	0.5833(9)	0.315(1)	0.8862(7)	4.3(9)
C(26A)	0.649(1)	0.306(1)	0.8443(6)	3.5(8)
Ti(2)	0.2959(2)	0.0365(2)	0.7182(1)	3.2(1)
Cl(2)	0.2093(2)	0.1753(2)	0.7277(2)	4.2(2)
F(1B)	0.3733(6)	0.2540(5)	0.6769(4)	5.6(5)
F(2B)	0.4924(6)	0.3169(6)	0.6021(4)	6.3(6)
F(3B)	0.5901(6)	0.1939(7)	0.5361(4)	8.2(6)
F(4B)	0.5680(6)	0.0024(7)	0.5510(4)	7.2(6)
F(5B)	0.4450(5)	-0.0660(6)	0.6227(4)	5.8(5)
C(1B)	0.166(1)	0.003(1)	0.6401(7)	3.2(7)
C(2B)	0.146(1)	-0.031(1)	0.6986(7)	4.0(8)
C(3B)	0.212(1)	-0.103(1)	0.7132(6)	3.9(8)
C(4B)	0.269(1)	-0.110(1)	0.6641(7)	4.2(8)
C(5B)	0.242(1)	-0.044(1)	0.6179(7)	3.8(8)
C(6B)	0.239(1)	-0.023(1)	0.5493(6)	3.9(8)
C(7B)	0.255(1)	0.083(1)	0.5331(6)	4.5(8)
C(8B)	0.176(1)	0.136(1)	0.5625(7)	5.1(9)
C(9B)	0.120(1)	0.054(1)	0.5863(7)	4.2(8)
C(10B)	0.134(1)	-0.024(1)	0.5360(6)	4.7(8)
C(11B)	0.341(1)	0.072(1)	0.8294(7)	4(1)
C(12B)	0.406(1)	0.099(1)	0.7933(7)	5(1)
C(13B)	0.440(1)	0.013(1)	0.7668(7)	5(1)
C(14B)	0.389(1)	-0.061(1)	0.7862(7)	4.4(9)
C(15B)	0.323(1)	-0.027(1)	0.8238(7)	5(1)
C(16B)	0.267(1)	-0.058(1)	0.8766(8)	6(1)
C(17B)	0.173(1)	-0.010(2)	0.8680(7)	7(1)
C(18B)	0.190(1)	0.097(2)	0.8758(8)	8(1)
C(19B)	0.291(1)	0.105(1)	0.8853(9)	6(1)
C(20B)	0.311(1)	0.015(2)	0.9269(7)	7(1)
C(21B)	0.3977(9)	0.089(1)	0.6535(6)	3.2(7)
C(22B)	0.417(1)	0.186(1)	0.6465(7)	3.8(8)
C(23B)	0.481(1)	0.223(1)	0.6070(7)	4.4(9)
C(24B)	0.528(1)	0.161(1)	0.5743(7)	4.4(4) ^b
C(25B)	0.517(1)	0.064(1)	0.5805(7)	4.4(9)
C(26B)	0.454(1)	0.032(1)	0.6199(7)	4.3(9)

^a The form of the equivalent isotropic displacement parameter is $B(\text{eq}) = (8\pi^2/3)\sum_i U_{ij}a_i^*a_j^*$. ^b Refined isotropically.

(isodicyclopentadienyl)lithium (130 mg, 0.94 mmol) in THF (32 mL) at the same temperature. After 5 h of stirring at -78 °C, the reaction mixture was treated with concentrated HCl (5 mL) and ice, then extracted with CHCl₃ (20 mL and then 2 × 10 mL). The combined organic layers were washed with water, dried, and evaporated. The residue was recrystallized once from CH₂Cl₂-hexanes to give 194 mg (55%) of **6** as dark red crystals, mp 196–198 °C; ¹H and ¹³C NMR (see Tables); MS *m/z* (relative intensity): 380 (M⁺, 22), 345 (M⁺ - Cl, 29),

Table 13. Positional Parameters and *B*(eq) Values for 11

atom	<i>x</i>	<i>y</i>	<i>z</i>	<i>B</i> (eq), Å ²
Ti	0.2442(1)	0.44416(7)	0.71997(7)	2.92(6)
Cl	-0.0383(2)	0.4214(1)	0.6629(1)	4.2(1)
F(1)	0.4779(5)	0.5268(2)	0.8740(2)	4.6(2)
F(2)	0.4053(5)	0.6125(2)	1.0022(2)	5.1(2)
F(3)	0.0631(5)	0.6399(2)	1.0437(2)	5.3(2)
F(4)	-0.2046(5)	0.5785(2)	0.9532(2)	4.9(2)
F(5)	-0.1404(5)	0.4950(2)	0.8226(2)	4.5(2)
C(1)	0.4232(9)	0.3310(4)	0.7124(4)	3.6(4)
C(2)	0.4748(9)	0.3721(4)	0.7829(4)	4.0(4)
C(3)	0.3288(10)	0.3722(4)	0.8358(4)	3.9(4)
C(4)	0.1851(9)	0.3344(4)	0.7976(4)	3.8(4)
C(5)	0.2474(9)	0.3078(3)	0.7221(5)	3.4(3)
C(6)	0.2122(10)	0.2476(4)	0.6855(5)	4.6(4)
C(7)	0.2224(11)	0.2787(4)	0.5705(5)	5.5(5)
C(8)	0.4188(12)	0.2990(4)	0.5602(5)	5.9(5)
C(9)	0.5015(9)	0.2822(5)	0.6446(5)	5.0(4)
C(10)	0.3983(11)	0.2098(4)	0.6649(5)	5.3(5)
C(11)	0.2223(8)	0.5422(4)	0.6154(4)	3.4(4)
C(12)	0.3238(9)	0.4853(4)	0.5829(4)	4.1(4)
C(13)	0.4795(9)	0.4791(4)	0.6331(4)	3.9(4)
C(14)	0.4720(9)	0.5321(4)	0.6960(4)	3.8(4)
C(15)	0.3111(8)	0.5713(4)	0.6853(4)	3.3(3)
C(16)	0.2173(10)	0.6422(4)	0.7068(4)	4.2(4)
C(17)	0.2695(10)	0.6956(4)	0.6377(5)	5.5(5)
C(18)	0.1727(11)	0.6644(4)	0.5592(5)	5.7(5)
C(19)	0.0731(9)	0.5960(4)	0.5930(5)	4.6(4)
C(20)	0.0255(10)	0.6248(4)	0.6800(5)	5.0(4)
C(21)	0.1737(9)	0.5097(3)	0.8347(4)	2.9(3)
C(22)	0.3027(8)	0.5409(4)	0.8867(4)	3.0(3)
C(23)	0.2698(9)	0.5844(4)	0.9559(4)	3.3(4)
C(24)	0.1009(10)	0.5981(4)	0.9764(4)	3.4(4)
C(25)	-0.0351(8)	0.5679(4)	0.9312(4)	3.1(3)
C(26)	0.0044(9)	0.5241(3)	0.8626(4)	3.0(3)

^a The form of the equivalent isotropic displacement parameter is $B(\text{eq}) = (8\pi^2/3)\sum_i U_{ij}a_i^*a_j^*$.

249 (M⁺ - isodiCp, 18), 131 (C₁₀H₁₁, 58), 103 (C₈H₇, 100). Anal. Calcd for C₂₀H₂₂Cl₂Ti: C, 63.02; H, 5.77. Found: C, 62.73; H, 5.91.

exo,exo-Bis(η⁵-isodicyclopentadienyl)titanium Dibromide (7). Boron tribromide (465 mg, 1.84 mmol) was diluted with dry CH₂Cl₂ (3 mL) and slowly added to a solution of **2** (475 mg, 1.25 mmol) in CH₂Cl₂ (18 mL). The mixture was stirred at room temperature for 2 h before the volatiles were removed in vacuo. The residue was recrystallized from CH₂Cl₂-hexanes to furnish 506 mg (86%) of **7** as black crystals, mp 238–240 °C; ¹H and ¹³C NMR (see Tables); MS *m/z* (relative intensity): 470 (M⁺, 50), 389 (M⁺ - Br, 52), 339 (M⁺ - isodiCp, 31), 131 (isodiCp, 31). Anal. Calcd for C₂₀H₂₂Br₂Ti·1/2CH₂Cl₂: C, 48.04; H, 4.52. Found: C, 48.88; H, 4.60.

Dimethyl-exo,exo-bis(η⁵-isodicyclopentadienyl)titanium (8). A suspension of **2** (145 mg, 0.38 mmol) in dry ether (6 mL) was cooled to -80 °C, and methylolithium (0.45 mL of 2 M in ether, 0.90 mmol) was introduced dropwise. The reaction mixture was warmed to room temperature, stirred for 2 h, diluted with ether (6 mL), and filtered to remove the LiCl. The solid was rinsed with ether (2 × 5 mL), and the combined filtrates were evaporated. The residue was recrystallized from hexanes at -20 °C to afford **8** (87 mg, 68%) as very air-sensitive orange crystals, mp 140–150 °C decomp; ¹H and ¹³C NMR (see Tables); MS *m/z* (relative intensity): 340 (M⁺, 7), 325 (M⁺ - CH₃, 43), 310 (M⁺ - 2CH₃, 100). Anal. Calcd for C₂₂H₂₈Ti: C, 77.64; H, 8.23; Ti, 14.11. Found: C, 77.20; H, 8.43; Ti, 13.70.

General Procedure for Preparation of the Pentafluorophenyl Bis(η⁵-isodicyclopentadienyl)titanium Chlorides (9–11). Bromopentafluorobenzene (0.08 mL, 0.64 mmol, previously distilled under argon) was diluted with ether (3 mL) and cooled to -78 °C. *n*-Butyllithium (0.43 mL of 1.49 M in hexanes, 0.64 mmol) was added dropwise during 20 min. After 10 min of stirring at room temperature, the reaction mixture was recooled to 0 °C and a suspension of **2** (124 mg, 0.32 mmol)

in THF (5 mL) and ether (3 mL) was introduced via a cannula. The reaction mixture was stirred overnight at room temperature, filtered through Celite, and evaporated. Flash chromatography of the residue on silica gel (elution with hexanes-CH₂Cl₂, 7:3) afforded 64 mg (39%) of product. Analytically pure samples were obtained by crystallization from hexanes-CH₂Cl₂. Data for the exo,exo isomer **9**: orange-red crystals, mp 245–255 °C, decomp; MS *m/z* (*M*⁺) calcd 512.0810, obsd 512.0794. Anal. Calcd for C₂₆H₂₂ClF₅Ti: C, 60.90; H, 4.32. Found: C, 60.84; H, 4.16. For the endo,endo isomer **10**: dark red crystals, mp 182–192 °C, decomp; MS *m/z* (*M*⁺) calcd 512.0810, obsd 512.0762. Anal. Calcd for C₂₆H₂₂ClF₅Ti: C, 60.90; H, 4.32. Found: C, 60.65; H, 4.47. For the endo,exo isomer **11**: blood red crystals, mp 175–185 °C, decomp; MS *m/z* (*M*⁺) calcd 512.0810, obsd 512.0782. Anal. Calcd for C₂₆H₂₂ClF₅Ti: C, 60.90; H, 4.32. Found: C, 60.17; H, 4.40.

X-ray Crystallographic Analysis of 10. The data collection crystal was a red plate which was coated with epoxy as a precaution against air sensitivity. Examination of the diffraction pattern on a Rigaku AFC5S diffractometer indicated a monoclinic crystal system with systematic absences of $0k0$, $k = 2n + 1$, and $h0l$, $h + l = 2n + 1$. The space group is uniquely determined as *P*₂/n. Unit cell constants were obtained by a symmetry-restricted least-squares fit of the diffractometer setting angles for 25 reflections in the 2θ range 17–23° with Mo K α radiation ($\lambda(K\alpha_1) = 0.709\ 30\ \text{\AA}$).

Six standard reflections were measured after every 150 reflections during data collection and indicated a substantial amount of crystal decay had occurred. The average decrease in intensity was 18.7%. Data reduction included a linear decay correction and was done with the TEXSAN package.²⁶

The structure was solved with the direct methods procedure of SHELXS-86.²⁷ There are two molecules in the asymmetric unit, and they are labeled as "A" and "B". For the three structures **9–11**, full-matrix least-squares refinements were performed in TEXSAN;²⁶ the function minimized was $\sum w(|F_o| - |F_c|)^2$ with $w = 1/\sigma^2(F_o)$. It was not possible to refine atom C(24B) anisotropically, so it was kept isotropic. All of the other non-hydrogen atoms were refined anisotropically. Hydrogen atoms are included in the model as fixed contributions at calculated positions with C–H = 0.98 Å and $B_H = 1.2B_{eq}$ (attached carbon atom) for this structure and for **9** and **11**. The final refinement cycle was based on the 2930 intensities with $I > \sigma(I)$ and 590 variables and resulted in agreement indices of $R = 0.102$ and $R_w = 0.054$. A structure factor calculation for the 2003 intensities with $I > 3\sigma(I)$ gives an R value of 0.054. Scattering factors for all four structures are from the *International Tables for X-ray Crystallography* and include terms for anomalous dispersion.²⁸

X-ray Crystallographic Analysis of 9. Crystals of **9** are clear, orange-red rectangular rods. One rod was cleanly cut to a suitable size and used for data collection. Examination of the diffraction pattern on a Rigaku AFC5S diffractometer indicated a triclinic crystal system. Unit cell constants were obtained by a least-squares fit of the diffractometer setting angles for 25 reflections in the 2θ range 25–30° with Mo K α radiation ($\lambda(K\alpha_1) = 0.709\ 30\ \text{\AA}$).

Six standard reflections were measured after every 150

(26) TEXSAN, Single Crystal Structure Analysis Software, Version 5.0; Molecular Structure Corporation: The Woodlands, TX 77381, 1989.

(27) Sheldrick, G. M. *Acta Crystallogr.* **1990**, *A46*, 467.

(28) Scattering factors for the non-hydrogen atoms, including terms for anomalous dispersion, are from the *International Tables for X-ray Crystallography*; Kynoch Press: Birmingham, England, 1974; Vol. IV, pp 71 and 148. The scattering factor for the hydrogen atom is from the following: Stewart, R. F.; Davidson, E. R.; Simpson, W. T. *J. Chem. Phys.* **1965**, *42*, 3175.

reflections during data collection and indicated that the crystal was stable. Data reduction was done with the TEXSAN package.²⁶ An analytical absorption correction was applied to the data.²⁹

The structure was solved in *P* $\bar{1}$ by the Patterson method in SHELXS-86.²⁷ A secondary extinction parameter³⁰ refined to a final value of $9.7(11) \times 10^{-7}$. The final refinement cycle was based on the 3993 intensities with $I > \sigma(I)$ and 299 variables and resulted in agreement indices of $R = 0.038$ and $R_w = 0.032$.

X-ray Crystallographic Analysis for 11. Crystals of **11** are blood-red plates. Examination of the diffraction pattern on a Rigaku AFC5S diffractometer indicated a monoclinic crystal system with systematic absences of $h0l$, $l = 2n + 1$, and $0k0$, $k = 2n + 1$. The space group was uniquely determined as *P*₂*1*/*c*. Unit cell constants were obtained by a symmetry-restricted least-squares fit of the diffractometer setting angles for 25 reflections in the 2θ range 21–26° with Mo K α radiation ($\lambda(K\alpha_1) = 0.709\ 30\ \text{\AA}$).

Six standard reflections were measured after every 150 reflections during data collection and indicated a small amount of crystal decay. On average, the standards decreased in intensity by 1.6%. Data reduction included a linear decay correction which was done with the TEXSAN package.²⁶ An analytical absorption correction was also applied to the data.²⁹

The structure was solved by the direct methods procedure in SHELXS-86.²⁷ The final refinement cycle was based on the 2004 intensities with $I > \sigma(I)$ and 298 variables and resulted in agreement indices of $R = 0.069$ and $R_w = 0.039$.

X-ray Crystallographic Analysis for 8. A transparent single crystal of **8** was mounted in a thin-walled glass capillary under Ar and transferred to the goniometer. The space group was determined to be *P*₂*1**2*₁*2*₁ from the systematic absences. The structure of **8** has a pseudo 2-fold axis which bisects the CH₃–Ti–CH₃ angle. Because of the arrangement of the isodiCp ligands, the molecule is chiral in the solid state. Only one enantiomer has crystallized here in *P*₂*1**2*₁*2*₁.

Least-squares refinement with isotropic thermal parameters led to $R = 0.079$. The geometrically constrained hydrogen atoms were placed in calculated positions 0.95 Å from the bonded carbon atom and allowed to ride on that atom with B fixed at 5.5 Å². The methyl hydrogen atoms were included as a rigid group with rotational freedom at the bonded carbon atom (C–H = 0.95 Å, $B = 5.5\ \text{\AA}^2$).³¹ Refinement of non-hydrogen atoms with anisotropic temperature factors led to the final values of $R = 0.037$ and $R_w = 0.054$.

Acknowledgment. The Ohio State group thanks the National Science Foundation for their financial support of this research program and Prof. Robin Rogers for the X-ray crystallographic analysis of **8**. We are also grateful to Bruno Andrioletti and Dr. Bernard Boitrel (URA 1685, Dijon, France) for the 500 MHz NMR measurements.

Supporting Information Available: Tables of least-squares planes, bond lengths and angles, bond distances involving the hydrogen atoms, anisotropic displacement parameters, and calculated positional parameters for the hydrogen atoms of **8–11** (39 pages). Ordering information is given on any current masthead page.

OM950337N

(29) De Meulenaer, J.; Tompa, H. *Acta Crystallogr.* **1965**, *19*, 1014.

(30) Zachariasen, W. M. *Acta Crystallogr.* **1963**, *16*, 1139.

(31) Sheldrick, G. M. SHELX76, A system of computer programs for X-ray structure determination as locally modified, University of Cambridge: Cambridge, England, 1976.

Stereo- and Regioselectivity in Palladium-Catalyzed Allylic Etherification

Catherine Goux, Magali Massacret, Paul Lhoste, and Denis Sinou*

Laboratoire de Synthèse Asymétrique, associé au CNRS, CPE Lyon, Université Claude Bernard Lyon 1, 43 boulevard du 11 Novembre 1918, 69622 Villeurbanne Cedex, France

Received April 3, 1995[®]

The palladium(0)-catalyzed etherification of various allylic carbonates by phenols allows the easy preparation of various allylic aryl ethers. In the case of an unsymmetrical allylic carbonate, the regioselectivity of the process was temperature dependent. Under thermodynamic control, the less substituted allyl aryl ether was always obtained, while under kinetic control the stereoselectivity was influenced by steric and electronic factors. Phenols having meta or para substituents afford the allylic aryl ether with no selectivity using palladium(0)-dppb as the catalyst and with low chemical yields in the case of phenols bearing electron-withdrawing substituents. Ortho-substituted phenols gave predominantly the less substituted ethers. The phosphine ligand effect was very important on the regioselectivity, ortho-substituted phosphines giving the more substituted allyl aryl ether. The stereochemical course of the allylic etherification was found to be an overall retention of configuration.

Introduction

Palladium(0)-catalyzed nucleophilic substitution of allylic compounds is now a well-established methodology in organic synthesis.¹ The use of this reaction in synthetic strategies is mainly due to its high stereospecificity and chemoselectivity. However, although catalytic substitution using phosphine-palladium complexes and allylic acetates or carbonates is carried out routinely with carbon or nitrogen nucleophiles, oxygen nucleophiles and particularly aryloxides are not so popular in such processes and have proven to be somewhat capricious.²⁻⁹ In the case of O-arylation of

allylic acetates, the nucleophiles generally used are phenol,² sodium phenoxide,^{6c} stannyl phenoxide,^{7a} silyl phenoxide,^{7b} or phenol in the presence of KF on alumina;⁸ palladium-catalyzed nucleophilic opening of epoxides and oxetanes occurred in the presence of phenols.^{6a} Recently, by analogy with the work of Guibé and Saint-M'Leux,¹⁰ Larock and Lee¹¹ have shown that the palladium decarboxylation of allylic aryl carbonates was a valuable route to the allylic aryl ethers.

During the course of our studies on the formation of the carbon-oxygen bond *via* the O-alkylation of allylic carbonates in the presence of palladium(0) complexes,¹² we found that the use of phenols as the nucleophiles was a very simple and valuable synthetic route to these allylic aryl ethers. This result prompted us to study in some detail this reaction between a phenol and an allylic carbonate in order to understand the main factors affecting the regio- and stereocontrol of the reaction; this is important for practical synthetic applications and also for gaining more insight into the mechanism.

Results and Discussion

In order to determine the scope and limitations of the synthesis of allylic ethers via the O-alkylation of allylic carbonates with phenols we carried out the reaction of several carbonates 1-6 with various phenols in the presence of palladium(0)-dppb as the catalyst (Scheme 1).

The results collected in Table 1 show that the O-alkylation of allyl methyl carbonate (1) worked well with phenols containing electron-donating groups (entries 1-5), giving generally quite high yields of the corresponding allylic aryl ethers. Using phenols containing electron-withdrawing groups gave lower chemical yields

[®] Abstract published in *Advance ACS Abstracts*, September 1, 1995.

(1) (a) Trost, B. M.; Verhoeven, T. R. In *Comprehensive Organometallic Chemistry*; Wilkinson, G., Stone, F. G. A., Abel, E. W., Eds.; Pergamon Press: New York, 1982; Vol. 8, p 799. (b) Trost, B. M. *Acc. Chem. Res.* **1980**, *13*, 385. (c) Trost, B. M. *Angew. Chem., Int. Ed. Engl.* **1989**, *28*, 1173. (d) Goldeski, S. A. In *Comprehensive Organic Synthesis*; Trost, B. M., Ed.; Pergamon Press: Oxford, 1991; Vol. 4, p 585. (e) Tsuji, J. *Organic Synthesis with Palladium Compounds*; Springer-Verlag: Berlin, 1980. (f) Tsuji, J.; Minami, I. *Acc. Chem. Res.* **1987**, *20*, 140. (g) Tsuji, J. *Tetrahedron* **1986**, *42*, 4361. (h) Heck, R. F. *Palladium Reagents in Organic Synthesis*; Academic Press: London, 1985. (i) Consiglio, G.; Waymouth, R. M. *Chem. Rev.* **1989**, *89*, 257. (j) Frost, C. G.; Howarth, J.; Williams, J. M. *Tetrahedron: Asymmetry* **1992**, *3*, 1089.

(2) Takahashi, K.; Miyake, A.; Hata, G. *Bull. Chem. Soc. Jpn.* **1972**, *45*, 230; **1973**, *46*, 1021.

(3) Stanton, S. A.; Felman, S. W.; Parkhurst, C. S.; Godleski, S. A. *J. Am. Chem. Soc.* **1983**, *105*, 1964.

(4) (a) Trost, B. M.; Verhoeven, T. R.; Fortunak, J. M. *Tetrahedron Lett.* **1979**, 2301. (b) Trost, B. M.; Tenaglia, A. *Tetrahedron Lett.* **1988**, *29*, 2927, 2931. (c) Trost, B. M.; Ito, N.; Greenspan, P. P. *Tetrahedron Lett.* **1993**, *34*, 1421.

(5) (a) Larock, R. C.; Harrison, L. W.; Hsu, M. H. *J. Org. Chem.* **1984**, *49*, 3662. (b) Larock, R. C.; Leuck, D. J.; Harrison, L. W. *Tetrahedron Lett.* **1989**, *30*, 3487. (c) Larock, R. C.; Berrios-Peña, N. G.; Narayanan, K. J. *Org. Chem.* **1990**, *55*, 3447. (d) Larock, R. C.; Berrios-Peña, N. G.; Fried, C. A. *J. Org. Chem.* **1991**, *56*, 2615.

(6) (a) Deardorff, D. R.; Myles, D. C.; MacFerrin, K. D. *Tetrahedron Lett.* **1985**, *26*, 5615. (b) Deardorff, D. R.; Sambayati, S.; Linde, R. G., II; Dunn, M. M. *J. Org. Chem.* **1988**, *53*, 189. (c) Deardorff, D. R.; Linde, R. G., II; Martin, A. M.; Shulman, M. J. *J. Org. Chem.* **1989**, *54*, 2759. (7) (a) Keinan, E.; Roth, Z. *J. Org. Chem.* **1983**, *48*, 1769. (b) Keinan, E.; Sahai, M.; Roth, Z.; Nudelman, A.; Herzig, J. *J. Org. Chem.* **1985**, *50*, 3558.

(8) Muzart, J.; Genêt, J. P.; Denis, A. *J. Organomet. Chem.* **1987**, *326*, C-23.

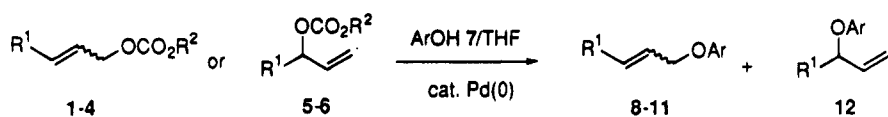
(9) Crilley, M. M. L.; Golding, B. T.; Pierpoint, C. *J. Chem. Soc., Perkin Trans. 1* **1988**, 2061.

(10) Guibé, F.; Saint-M'Leux, Y. *Tetrahedron Lett.* **1981**, *22*, 3591.

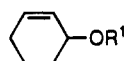
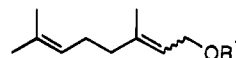
(11) Larock, R. C.; Lee, N. H. *Tetrahedron Lett.* **1991**, *32*, 6315.

(12) (a) Lakhmiri, R.; Lhoste, P.; Sinou, D. *Tetrahedron Lett.* **1989**, *30*, 4669. (b) Lakhmiri, R.; Lhoste, P.; Boullanger, P.; Sinou, D. *J. Chem. Res., Synop.* **1990**, 342; *J. Chem. Res., Miniprint* **1990**, 2301. (c) Lakhmiri, R.; Lhoste, P.; Sinou, D. *Synth. Commun.* **1990**, *20*, 1551. (d) Goux, C.; Lhoste, P.; Sinou, D. *Synlett* **1992**, 725.

Scheme 1



- | | | |
|---------------------------|----------------|----------------------------|
| 1 $R^1 = H$ | $R^2 = CH_3$ | 8 $R^1 = H$ |
| 2 $R^1 = C_6H_5$ | $R^2 = C_2H_5$ | 9 $R^1 = C_6H_5$ |
| 3 $R^1 = C_6H_5CH_2OCH_2$ | $R^2 = CH_3$ | 10 $R^1 = C_6H_5CH_2OCH_2$ |
| 4 $R^1 = n-C_3H_7$ | $R^2 = C_2H_5$ | 11 $R^1 = n-C_3H_7$ |
| 5 $R^1 = n-C_3H_7$ | $R^2 = C_2H_5$ | 12 $R^1 = n-C_3H_7$ |
| 6 $R^1 = n-C_3H_7$ | $R^2 = CH_3$ | |

13 $R^1 = CO_2CH_3$ 14 $R^1 = Ar$ 15 $R^1 = CO_2C_2H_5$ 16 $R^1 = Ar$

- a: Ar = C₆H₅; b: Ar = 4-CH₃C₆H₄; c: Ar = 3-CH₃C₆H₄; d: Ar = 2-CH₃C₆H₄; e: Ar = 2,6-diCH₃C₆H₃;
 f: Ar = 2-*t*-BuC₆H₄; g: Ar = 4-CH₃OC₆H₄; h: Ar = 2-CH₃OC₆H₄; i: Ar = 4-ClC₆H₄; j: Ar = 4-CNC₆H₄;
 k: Ar = 4-NO₂C₆H₄; l: Ar = 3-NO₂C₆H₄; m: Ar = 2-NO₂C₆H₄

Table 1. Palladium-Catalyzed Synthesis of Allylic Aryl Ethers^a

entry no.	carbonate	phenol	method ^b	T (°C)	product(s)	yield (%) ^c ratio (%) ^d
1	1	7a	A	60	8a	75
2		7a	B	60	8a	75
3		7e	B	60	8e	63
4		7g	B	60	8g	80
5		7h	B	60	8h	92
6		7i	B	60	8i	31
7		7i	B ^e	60	8i	64
8		7i	A	60	8i	56
9		7i	A ^e	60	8i	68
10		7k	A	60	8k	14
11		7k	B	60	8k	8
12		7k	B ^e	60	8k	16
13	(<i>E</i>)-2	7a	A	25	9a	80
14		7a	A	60	9a	89
15	(<i>Z</i>)-3	7a	A	25	10a	47
16		7a	A	60	10a	92
17	(<i>E</i>)-4	7a	A	25	11a + 12a	72
18		7a	A	60	11a + 12a	72
19	5	7a	A	25	11a + 12a	70
20		7a	A	60	11a + 12a	70
21	13	7a	A	60	14a	82
22		7e	A	60	14e	66
23	(<i>E</i>)-15	7a	A	60	16a	32

^a All reactions were carried out under a nitrogen atmosphere in the presence of 0.03 mmol of Pd₂(dba)₃ and 0.12 mmol of dppb in 5 mL of THF during 12 h. ^b Method A, [phenol]:[carbonate]:[Pd] = 50:25:1; Method B, [phenol]:[carbonate]:[Pd] = 25:32:1. ^c Isolated yield after purification and not optimized. ^d The 11/12 ratio was determined by GC. ^e Allyl *tert*-butyl carbonate was used. ^f The *E/Z* ratio was determined by ¹H NMR spectroscopy.

(entries 6–12). These differences in reactivity could be related to the nucleophilicity of the corresponding phenolate and its ability as a leaving group. However, increasing the amount of phenol or using a more sterically hindered carbonate as the π -allyl precursor

enhanced the chemical yield in the case of 4-chlorophenol (entries 6–9), but not in the case of 4-nitrophenol, for which the chemical yields were always low whatever the conditions used (entries 10–12); the poor yield observed in this case may arise from the nature of the 4-nitrophenolate group which is not only a weak nucleophile, but also an excellent leaving group.

In the reaction of (*E*)-cinnamyl ethyl carbonate (2) with phenol (7a), only the formation of (*E*)-cinnamyl phenyl ether (9a) in excellent chemical yield was observed, either at room temperature or at 60 °C (entries 13 and 14); this result is in agreement with the observations of Muzart et al.,⁸ but contrasts with those of Larock and Lee,¹¹ who obtained the two regioisomers. The reaction of (*Z*)-4-benzyloxy-1-(methoxycarbonyl)oxy-2-butene (3) with phenol (7a) (entries 15 and 16) gave regioselectively the linear allylic aryl ether 10a in a 90/10 *E/Z* ratio, as shown by ¹³C NMR spectroscopy; the C-1 and C-4 signals appeared respectively at δ 67.7 and 69.9 ppm for the *E*-isomer and at δ 63.9 and 65.8 ppm for the *Z*-isomer. The loss of the stereochemistry of the starting carbonate 3 is due to a rapid $\sigma \rightleftharpoons \eta^3 \rightleftharpoons \sigma$ interconversion of the π -allyl intermediate compared to the rate of O-arylation of this intermediate.

Cyclohexenyl methyl carbonate (13) reacted also with phenol (7a) or even with 2,6-dimethylphenol (7e), a sterically-hindered phenol, giving the corresponding cyclohexenyl aryl ethers 14a,e in quite good yields (entries 21 and 22), whereas geranyl ethyl carbonate (15) gave a mixture of geranyl and neryl phenyl ether (16a) (in a ratio 91/9) in 32% chemical yield only (entry 23).

The two regioisomeric carbonates 4 and 5 reacted with phenol to give identical mixtures of regio- and stereoisomeric ethers 11a and 12a, as expected from attack of the phenolate on the two allylic termini of the π -allylpalladium species, in a ratio depending of the reaction temperature. A more detailed study of the influence of the temperature on the regioselectivity of

Table 2. Palladium-Catalyzed Reaction between Phenol 7a and Carbonates 4–6. Temperature Effect on the Regioselectivity^a

entry no.	carbonate	T (°C)	t (h)	11a/12a (%) ^b	(E)/(Z) (%) ^b
1	4	25	0.2	44/56	88/12
			6	45/55	89/11
2	4	60	0.15	47/53	91/09
			1	54/46	90/10
3	5	25	0.2	44/56	88/12
			7	45/55	89/11
4	5	60	0.2	47/53	89/11
			1	54/46	89/11
5	6	25	0.2	45/55	91/09
			7	45/55	89/11

^a All reactions were carried out under a nitrogen atmosphere in the presence of 0.03 mmol of Pd₂(dba)₃, 0.12 mmol of dppb, 1.50 mmol of the carbonate, and 1.80 mmol of 7a in 5 mL of THF. The conversion was quantitative. ^b Determined by GC.

the O-arylation (Table 2) showed that at room temperature the two regioisomers 11a and 12a were obtained in a ratio 45/55 whatever the starting carbonate 4–6, and this ratio remained unchanged during the reaction course. Conversely, performing the reaction at 60 °C gave predominantly the more-substituted alkene 11 (70% vs. 30%) at equilibrium, the initial 11/12 ratio of 47/53 turning progressively into 70/30 no matter which carbonate was used. The treatment of the pure allyl phenyl ether 12a, prepared by a Mitsunobu reaction using 1-hexen-3-ol and phenol, at 60 °C in THF with a catalytic amount of palladium(0), gave exactly the same mixture of 11a/12a in a ratio of 70/30. The structures of compounds (E)-11a and 12a were determined by comparison of their ¹H and ¹³C spectra with authentic samples prepared by a Mitsunobu reaction. In the case of the linear ether 11a, the E- and Z-stereochemistries were determined on the basis of the NMR spectra of the mixture. The chemical shifts for the allylic carbons of the major isomer at δ 34.4 and 68.7 ppm are at lower field than those of the minor isomer (δ 29.8 and 63.9 ppm) and correspond to the E-isomer. This stereochemistry was confirmed by the coupling constant of the vinylic protons for this major isomer (³J = 15.4 Hz) being characteristic of E-stereochemistry. These results showed that at 25 °C, under kinetic control, the O-arylation was not regioselective, the phenolate attacking the two termini of the π-allyl intermediate. At 60 °C, the phenoxy group is a good leaving group in π-allylpalladium chemistry, and, in the presence of palladium(0) as the catalyst, compound 12a is transformed into the linear isomer 11a by formation of the π-allyl intermediate followed by attack of the phenolate on the less-substituted terminus of the π-allyl complex: that is, the reaction is under thermodynamic control. This behavior is drastically different from that observed in the S-alkylation of the carbonates 4 and 5 by thiolates,¹³ where the linear isomer, resulting from attack of the thiolate on the less substituted terminus of the π-allyl intermediate was predominantly formed even at low temperature. This could be due to the steric bulk of the thiolate compared to the phenolate. It is noteworthy that the E/Z ratio is always the same (90/10) whatever the conditions used.

A comparative study of different catalyst precursors in THF is reported in Table 3. Pd₂(dba)₃ in the presence

(13) Goux, C.; Lhoste, P.; Sinou, D. *Tetrahedron* **1994**, *50*, 103.

Table 3. Palladium-Catalyzed Reaction between Phenol 7a and Carbonate 5. Solvent and Catalyst Effects^a

entry no.	solvent	catalyst	t (h)	11a/12a (%) ^b	conv (%) ^c
1	THF	Pd ₂ (dba) ₃ + 2dppb	0.2	52/48	100
			3	49/51	
2	THF	Pd ₂ (dba) ₃ + 4dppb	0.2	44/56	100
			3	44/56	
3	THF	Pd ₂ (dba) ₃ + 8dppb	0.2	51/49	100
			3	51/49	
4	THF	Pd(OAc) ₂ + 4PPh ₃	0.2	51/49	30
			2	50/50	100
5	THF	Pd(acac) ₂ + 4PPh ₃	0.3	51/49	87
			4	50/50	100
6	THP	Pd ₂ (dba) ₃ + 4dppb	0.2	50/50	100
			2	50/50	
7	dioxane	Pd ₂ (dba) ₃ + 4dppb	0.3	50/50	100
			2.5	48/52	
8	diethoxyethane	Pd ₂ (dba) ₃ + 4dppb	0.2	50/50	77
			3	50/50	100
9	CH ₂ Cl ₂	Pd ₂ (dba) ₃ + 4dppb	0.2	60/40	31
			9	54/46	80

^a All reactions were carried out under a nitrogen atmosphere in the presence of 1.50 mmol of the carbonate 5, 1.80 mmol of 7a, and 0.06 mmol of palladium complex in 5 mL of THF. ^b Determined by GC. ^c Conversion of the carbonate 5 determined by GC.

of dppb is the most active catalyst, giving a quantitative conversion of the carbonate 5 after less than 10 min, no matter what the ratio of palladium to dppb. Among the solvents used, the cyclic ethers (THF, THP, and dioxane) gave the highest activities. We also noticed that the ratio of 11a/12a is always the same no matter what precatalyst or solvent is used.

The results reported in Table 4 concerning the O-arylation of carbonate 5 in the presence of Pd₂(dba)₃ and various ligands at 20 °C show that the 11a/12a ratio depends on the ligand used. Although it is difficult to rationalize these results, among the diphosphines used, dppb (1,4-bis(diphenylphosphino)butane), dpph (1,6-bis(diphenylphosphino)hexane), and dppd (1,10-bis(diphenylphosphino)decane) gave the best performances in terms of reaction rate (entries 5–7), the regioselectivity being unaffected by the ring size of the diphosphine with practically no selectivity in attack of the phenolate on the two termini of the π-allyl intermediate. From the results obtained with the monophosphines, it is obvious that steric and electronic effects direct the reaction to one or the other termini of the π-allyl complex. We observed that the 11a/12a ratio increased as the electron-withdrawing ability of the ligand increased; *i.e.*, 11a/12a increased in the order 43/57 [(4-CH₃OC₆H₄)₃P] < 46/54 [(4-CH₃C₆H₄)₃P] < 49/51 [(C₆H₅)₃P] < 53/47 [(4-FC₆H₄)₃P] < 64/36 [(4-ClC₆H₄)₃P] < 74/26 [(C₆H₅O)₃P] (entries 1, 9, 12–14, and 19). A strong π-acceptor ligand, which increases the positive charge character of the π-allyl complex, directs attack of the phenolate to the more substituted terminus.²⁰ A comparison of entries 9–11 shows that the use of a sterically-hindered

(14) Tolman, C. A. *Chem. Rev.* **1977**, *77*, 313.

(15) Rahman, Md. M.; Liu, M. Y.; Prock, A.; Giering, W. P. *Organometallics* **1987**, *6*, 650.

(16) Henderson, W. A., Jr.; Streuli, C. A. *J. Am. Chem. Soc.* **1960**, *82*, 5791.

(17) Allman, T.; Goel, R. G. *Can. J. Chem.* **1982**, *60*, 716.

(18) Jackson, R. A.; Kanluen, R.; Poe, A. *Inorg. Chem.* **1984**, *23*, 523.

(19) (a) Wada, M.; Higashizaki, S. *J. Chem. Soc., Chem. Commun.* **1984**, 482. (b) Wada, M.; Higashizaki, S. J.; Tsuboi, A. *J. Chem. Res., Synop.* **1985**, 38; *J. Chem. Res., Miniprint* **1985**, 467.

Table 4. Palladium-Catalyzed Reaction between Phenol 7a and Carbonate 5. Phosphine Ligand Effects^a

entry no.	ligand	Θ ^b	pK _a ^c	t (h)	11a/12a (%) ^d	conv (%) ^e
1	PPh ₃	145	2.73	0.2	49/51	100
				3	49/51	
2	dppm	121		0.5	48/52	27
				3	43/57	68
3	dppe	125		1	46/54	42
				5	43/57	100
4	dppp	127		1	42/58	57
				5	40/60	100
5	dppb		0.2	2	46/54	100
				3	45/55	
6	dpph		0.2	2	52/48	100
				2	52/48	
7	dppd		0.2	2	47/53	100
				3	48/52	
8	dppf		0.2	2	50/50	40
				2	43/57	100
9	(4-CH ₃ C ₆ H ₄) ₃ P	145	3.84	0.2	46/54	100
				4	48/52	
10	(3-CH ₃ C ₆ H ₄) ₃ P	165	3.30	0.2	45/55	100
				4	40/60	
11	(2-CH ₃ C ₆ H ₄) ₃ P	194	3.08	0.2	26/74	100
				5	28/72	
12	(4-ClC ₆ H ₄) ₃ P	145	1.03	0.2	64/36	18
				18	66/34	100
13	(4-FC ₆ H ₄) ₃ P	145	1.97	0.2	53/47	37
				7	50/50	100
14	(4-CH ₃ OC ₆ H ₄) ₃ P	145	4.59	0.2	43/57	60
				24	42/58	90
15	(2,6-di-CH ₃ OC ₆ H ₃) ₃ P		10.7 ^f	0.3	61/39	12
				22	60/40	40
16	(2,4,6-tri-CH ₃ OC ₆ H ₂) ₃ P		11.2 ^f	0.2	62/38	12
				22	57/43	19
17	(2-pyridyl)Ph ₂ P			0.2	69/31	100
				7	64/36	
18	(2-furyl) ₃ P			0.2	63/37	100
				2	63/37	
19	(C ₆ H ₅ O) ₃ P	128	-2	0.2	74/26	52
				22	81/19	100
20	[(CH ₃) ₃ C] ₃ P	182	11.4	22	no reaction	

^a All reactions were carried out under a nitrogen atmosphere in the presence of 0.03 mmol of Pd₂(dba)₃, 0.12 mmol of bidentate ligand or 0.24 mmol of monodentate ligand, 1.50 mmol of the carbonate 5, and 1.80 mmol of 7a in 5 mL of THF at 25 °C. ^b Cone angle data were taken from refs 14 and 15. ^c pK_a values were taken from refs 16–18. ^d Determined by GC. ^e Conversion of the carbonate 5 determined by GC. ^f Taken from ref 19.

phosphine having a high cone angle (entry 11) reverses the regioselectivity, the phenolate attacking in this case the more substituted terminus of the π-allyl complex to give predominantly the branched isomer 12a. One of the reasons for this reversed regioselectivity could be the coordination of only one sterically-demanding phosphine to the palladium, leading to a trigonal intermediate with the phosphine positioned near the less substituted terminus of the π-allyl complex; in this case,²⁰ the acceptor ligand induced a positive charge at the more substituted terminus of the π-allyl intermediate *trans* to it.

The use of basic phosphines as ligands (entries 15, 16, and 19) gave a catalyst having a lower reaction rate and a regioselectivity favoring the formation of the less substituted aryl allyl ether. A trialkylphosphine, such as tri-*tert*-butylphosphine, gave no reaction at all. In all cases, a small amount of the *Z*-isomer 11 was formed.

(20) (a) Akermark, B.; Hansson, S.; Krakenberger, B.; Vitagliano, A.; Zetterberg, K. *Organometallics* **1984**, *3*, 679. (b) Akermark, B.; Krakenberger, B.; Hansson, S.; Vitagliano, A. *Organometallics* **1987**, *6*, 620. (c) Sjögren, M. P. T.; Hansson, S.; Akermark, B.; Vitagliano, A. *Organometallics* **1994**, *13*, 1963.

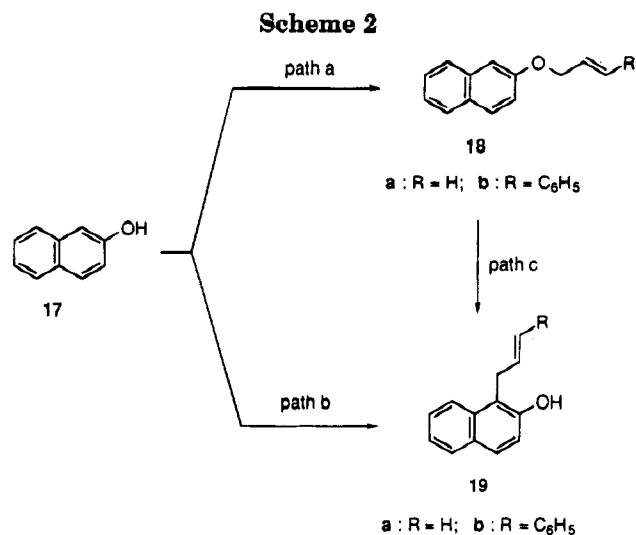
Table 5. Palladium-Catalyzed Reaction between Phenol 7 and Carbonate 5. Phenol Substituent Effect^a

entry no.	phenol	t (h)	11/12 ^b (% conv) ^c	% yield ^d (11 + 12)
1	7a	0.2	46/54 (100)	72
		3	45/55	
2	7b	0.2	44/56(100)	60
		2	43/57	
3	7c	0.33	48/52 (100)	70
		3	51/49	
4	7d	0.2	58/42 (100)	70
		3	57/42	
5	7e	0.2	72/28 (100)	73
		2	71/29	
6	7f	0.2	84/16 (100)	70
		2	83/17	
7	7g	0.2	44/56 (100)	72
		2	45/55	
8	7h	0.2	57/43 (100)	70
		4	56/44	
9	7i	0.2	46/54 (40)	63
		2	65/35 (100)	
10	7j	0.2	57/43 (10)	20
		2	60/40 (21)	
		5	61/39 (23)	
11	7k	0.2	61/39 (8)	10
		2	60/40 (12)	
12	7l	0.2	47/53 (29)	50
		4	45/55 (56)	
13	7m	0.2	58/42 (03)	15
		6	35/65 (18)	

^a All reactions were carried out under a nitrogen atmosphere in the presence of 0.03 mmol of Pd₂(dba)₃, 0.12 mmol of dppb, 1.50 mmol of the carbonate 5, and 1.80 mmol of 7 in 5 mL of THF at 25 °C. ^b Ratio 11/12 determined by GC. ^c Conversion of the carbonate 5 determined by GC. ^d Isolated yield after 12 h of reaction and purification, not optimized.

We also studied the influence of the substituent on phenol on the regioselectivity of the O-alkylation of carbonate 5. The results summarized in Table 5 showed that the nature of the substituent had the greatest influence on both the regioselectivity, the reaction rate and the product yield. The O-arylation of carbonate 5 occurred quantitatively in less than 10 min with phenols having electron-donating substituents (entries 1–8), and the corresponding allyl aryl ethers 11 and 12 are isolated in quite good yields. Conversely, phenols having electron-withdrawing substituents, such as cyano or nitro groups (entries 10–13), gave low yields of allyl aryl ethers. As postulated before, this could be related to the relative acidity of the corresponding phenol.²¹ Effectively, if the more acidic nitrophenol easily forms the nitrophenolate by an exchange process with the ethoxide, the nitrophenolate formed is probably less reactive in attack on the π-allyl complex than the methoxyphenolate, for example. Moreover, the nitrophenolate is also a very good leaving group and so the allyl aryl ether formed competes with the carbonate in formation of the π-allyl complex. The higher yield obtained with 3-nitrophenol compared to 2-nitrophenol and 4-nitrophenol is in agreement with this assumption (entries 11–13). Steric effects seem very important since phenols having substituents in the ortho position (entries 4–6 and 8) give predominantly the linear isomer 11 resulting from attack of the corresponding phenolate on the less substituted terminus of the π-allyl complex. While the reaction of 4-methylphenol on

(21) Fujio, M.; McIver, R. T.; Taft, R. W. *J. Am. Chem. Soc.* **1981**, *103*, 4017.



Path a: 1 + Pd₂(dba)₃/dppb, -20 °C (yield 41 %) or
2 + Pd₂(dba)₃/dppb, 25 °C (yield 34 %)

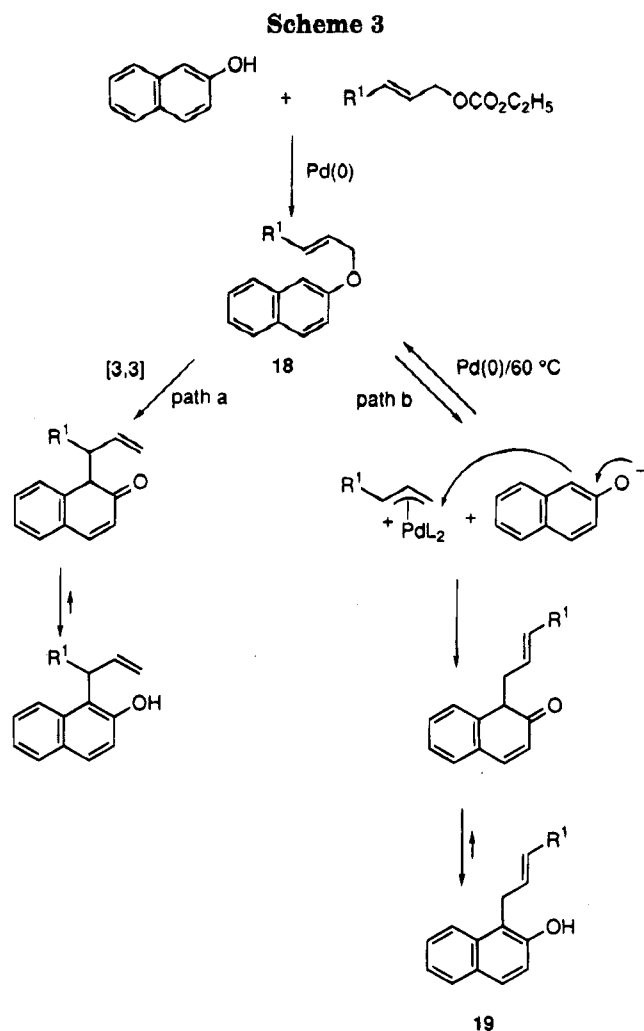
Path b: 1 + Pd₂(dba)₃/dppb, 20 °C (yield 48 %) or 60 °C (yield 54 %) or
2 + Pd₂(dba)₃/dppb, 60 °C (yield 40 %)

Path c: 18b + Pd₂(dba)₃/dppb, 60 °C (yield 40 %)

carbonate **5** gave the ethers **11b** and **12b** in a ratio 44/56 (entry 2), the use of 2-methylphenol reversed this **11d/12d** ratio to 58/42 (entry 4). Increasing the steric bulk of the ortho substituent from methyl to *tert*-butyl (entry 6) or introducing a second methyl group in the ortho position (entry 5) also modified this ratio to 84/16 for **11f/12f** and to 72/28 for **11e/12e**. Similar behavior was also found using 2-methoxyphenol (entry 8). Once again a very high stereoselectivity (up to 90%) in favor of the *E*-isomer was observed whatever phenol was used.

The structures of compounds **11** and **12** were unambiguously determined from the ¹H and ¹³C NMR spectra of the mixture. The ¹H NMR spectra of the linear isomer **11** was characterized by a doublet at approximately δ 4.5 ppm for the OCH₂ group and a doublet of triplets at δ 2.1 ppm for the other allylic proton, while the branched isomer **12** was mainly characterized by the signal of the allylic proton at approximately δ 4.5 ppm. The ¹³C NMR spectra of the mixture were characterized by the C-1 and C-4 signals at approximately δ 70 ppm and 34.4 ppm respectively for the linear isomer (*E*)-**11** and the C-3 signal at δ 79 ppm for the branched isomer **12**; we also noticed signals at δ 64 and 29.8 ppm for C-1 and C-4, respectively, corresponding to the isomer (*Z*)-**11**, the *E/Z* ratio being 90/10.

In the reaction of β-naphthol (**17**) with allyl methyl carbonate (**1**) or (*Z*)-cinnamyl ethyl carbonate (**2**) in the presence of palladium(0), two different products were obtained depending of the reaction temperature (Scheme 2). 2-(Allyloxy)naphthalene (**18a**) and 2-(*E*)-(cinnamyl-oxy)naphthalene (**18b**) were obtained when the reaction was performed at -20 and 25 °C respectively, whereas at 20 or 60 °C for **1** and at 60 °C for **2** only the *C*-allylated naphthols **19a,b** were formed. Treatment of the 2-(*E*)-(cinnamyl-oxy)naphthalene (**18b**) in the presence of palladium(0) as the catalyst at 65 °C in THF gave also the *C*-allylated compound **19b**. This last reaction indicated that at low temperature the allyloxy compound **18** is the kinetic product in the catalytic allylation of β-naphthol and that the *C*-allylated compound **19** is the thermodynamic product. The path for



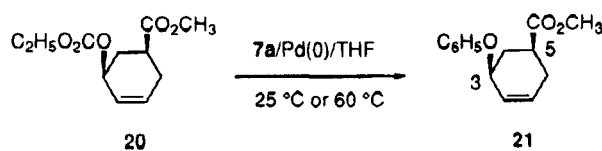
going from **18** to **19** could be (Scheme 3) *via* a Claisen rearrangement (path a) or *via* a π-allylpalladium complex (path b). The formation of the (*Z*)-1-cinnamyl-2-naphthol (**19b**) ruled out the possibility of a Claisen rearrangement and showed unambiguously that only path b is operating, since path a would lead to the branched isomer. The (allyloxy)naphthalene **18** reacted with palladium(0) to give the cationic complex and the enolate which can recombine leading to the starting allyl ether **18** or to the *C*-allylated product **19**; this last reaction is irreversible and complete conversion into the *C*-allylated compound is favored. Similar behavior has been observed by Balavoine et al.²² in the allylation of β-naphthol by allyl acetate in the presence of a platinum complex. Furthermore, the usual thermal Claisen rearrangement of allyl ethers takes place at higher temperatures.²³ The structures of compounds **18** and **19** were easily assigned by their ¹H NMR spectra with a doublet at δ 4.65 ppm (OCH₂ group) for compounds **18a,b** and at δ 3.82 ppm and 3.90 ppm (CH₂ group) for compounds **19a,b**. This assignment was also confirmed by ¹³C NMR spectroscopy by a signal at δ 68.8 ppm (OCH₂ group) for **18a,b** and at δ 29.4 and 28.5 ppm (CH₂ group) for **19a,b** respectively.

Finally, to examine the results of the stereochemical course of the *O*-alkylation of π-allyl complexes we chose the substrate **20**, which has been extensively employed

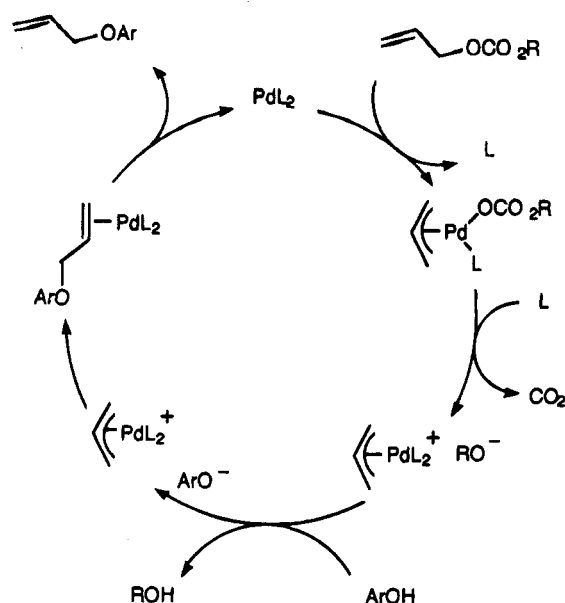
(22) Balavoine, G.; Bram, G.; Guibé, F. *Nouv. J. Chim.* **1978**, *2*, 207.

(23) Rhoads, S. J.; Raulins, N. R. *Organic Reactions* **1975**, *22*, 1.

Scheme 4



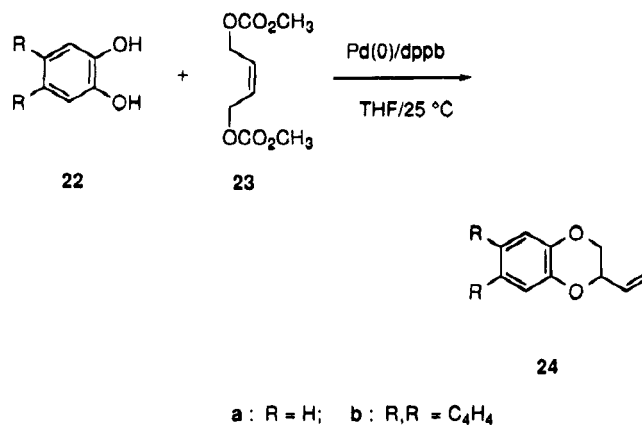
Scheme 5



for the characterization of nucleophiles.^{7,13,24,25} The reaction between the carbonate **20** and phenol (**7a**) in THF at 25 or 60 °C gave an unique compound **21** having *cis*-stereochemistry (Scheme 4). The assignment of stereochemistry was unambiguously done by NOE experiments; irradiation of the C-3 methine proton (δ 4.90 ppm) showed an enhancement of 13% in the C-5 methine proton signal at δ 2.75 ppm, and conversely irradiation of the C-5 methine proton signal at δ 2.75 ppm showed an enhancement of 10% of the C-3 methine signal at δ 4.90 ppm. This unambiguously showed that the two hydrogens H-3 and H-5 are in *cis*-positions. This observed *cis*-stereochemistry implied backside attack of the phenolate on the π -allyl intermediate; it is noteworthy that the observed stereospecificity contrasts with the poor stereoselectivity noticed in the same reaction using a tin phenolate as the nucleophile.⁷

All these results allowed us to propose a mechanism for the alkylation of allylic carbonates with phenol nucleophiles in the presence of a catalytic amount of palladium(0). The first step is the formation of the π -allylpalladium complex as a cationic species with inversion of configuration, leading to the formation of an alkoxide (Scheme 5). Exchange between the alkoxide and the phenol gives the nucleophile, which attacks the backside of the coordinated π -allyl giving the allyl aryl oxide with an overall retention of configuration. When the reaction was performed at 65 °C, the allyl aryl oxide could also react with the palladium(0) complex to give again the π -allylpalladium complex. In the case of phenols having electron-withdrawing substituents, the obtained allyl aryl ether competes strongly with the

Scheme 6



allylic carbonate in the oxidative addition to the palladium(0) complex, lowering the chemical yield of product.

One synthetic application of this O-alkylation of allylic carbonates involves the preparation of benzo-1,4-dioxanes (Scheme 6) starting from a 1,2-diphenol. The reaction of dicarbonate **23** with catechol (**22a**) or 2,3-dihydroxynaphthalene (**22b**) in the presence of palladium(0)-dppb as the catalyst gave the benzo-1,4-dioxanes **24a,b** in 60% and 67% chemical yields, respectively.

Conclusion

The results show that a palladium-based catalyst is excellent for producing aryl allyl ethers from allylic carbonates and phenols. Under kinetic control, the regioselectivity of the reaction is low, depending on steric and electronic factors of the ligand and the phenol used. Under thermodynamic control, the regioselectivity favors the less substituted allyl aryl ether. However, under these conditions, β -naphthol affords the *C*-allylated naphthol. The overall stereochemical course of the reaction is retention of configuration.

Experimental Section

All reactions that involved palladium complexes were carried out under a nitrogen atmosphere in Schlenk tubes. All solvents (tetrahydrofuran or THF, tetrahydropyran or THP, dioxane, dimethoxyethane, dichloroethane) were freshly distilled from the appropriate drying agent before use.²⁶ Column chromatography was performed on silica gel, Merck, grade 60 (230–400 mesh, 60 Å). GC analyses were carried out on a capillary column OV 101 (25 m \times 0.32 mm). All compounds were characterized through their 200-MHz ¹H and 50.3-MHz ¹³C NMR spectra, using CDCl₃ as the solvent and Me₄Si or chloroform-*d*₁ as an internal standard; carbon multiplicities were obtained from DEPT experiments. Elemental analyses were performed at the CNRS, Vernaison, France.

The following chemicals were bought from Aldrich and used as received: phenols **7a–m**, β -naphthol (**17**), catechol (**22a**), 2,3-dihydroxynaphthalene (**22b**), (*E*)-cinnamyl alcohol, (*Z*)-4-benzyloxy-2-buten-1-ol, 1-hexen-3-ol, (*E*)-2-hexen-1-ol, geraniol, 2-cyclohexen-1-ol, allyl methyl carbonate (**1**), Pd₂(dba)₃, Pd(OAc)₂, Pd(acac)₂, PPh₃, 1,1-bis(diphenylphosphino)methane (dppm), 1,2-bis(diphenylphosphino)ethane (dppe), 1,3-bis(diphenylphosphino)propane (dppp), 1,4-bis(diphenylphosphino)

(24) Trost, B. M.; Verhoeven, T. R. *J. Am. Chem. Soc.* **1980**, *102*, 4730.

(25) Bäckvall, J. E.; Granberg, K. L.; Heumann, A. *Isr. J. Chem.* **1991**, *31*, 17.

(26) Perrin, D. D.; Armarego, W. L. F.; Perrin, D. R. *Purification of Laboratory Chemicals*, 2nd ed.; Pergamon Press: New York, 1980.

no)butane (dppb), 1,6-bis(diphenylphosphino)hexane (dpph), 1,1'-bis(diphenylphosphino)ferrocene (dppf), (4-CH₃C₆H₄)₃P, (3-CH₃C₆H₄)₃P, (2-CH₃C₆H₄)₃P, (4-ClC₆H₄)₃P, (4-FC₆H₄)₃P, (4-CH₃OC₆H₄)₃P, (2,6-di-CH₃OC₆H₃)₃P, (2,4,6-tri-CH₃OC₆H₂)₃P, (2-pyridyl)Ph₂P, (2-furyl)₃P, (C₆H₅O)₃P, (Me₃C)₃P. 1,10-Bis(diphenylphosphino)decane (dppd) was prepared according to the literature procedure.²⁷ The alcohols were converted to the carbonates in good yields using standard procedures. Products **8e**,²⁸ **8g**,²⁹ **8h**,³⁰ **8i**,²⁹ **8k**,²⁹ **9a**,^{7b} **14a**,³¹ **14e**,¹¹ and **16a**,³² are known compounds.

Palladium-Mediated O-Allylation. General Procedure (Table 1, Entry 5). To a stirred solution of Pd₂(dba)₃ (27.0 mg, 0.03 mmol) and 1,4-bis(diphenylphosphino)butane (51.2 mg, 0.12 mmol) in tetrahydrofuran (3 mL) was added a degassed solution of the carbonate **1** (223 mg, 1.92 mmol) and the phenol **7h** (186 mg, 1.5 mmol) in 2 mL of tetrahydrofuran. The solution was stirred for 12 h at the desired temperature. Solvent evaporation followed by column chromatography through silica gel (hexane/ethyl acetate) afforded 226 mg of compound **8h** (yield 92%). The regio- and stereoisomers were not separated.

1-Phenoxy-2-hexene (11a). ¹H NMR: δ 0.91 (t, 3H, *J* = 7.3 Hz, H-6), 1.37–1.52 (m, 2H, H-5), 2.06 (dt, 2H, *J* = 7.3, 6.3 Hz, H-4), 4.46 (d, 2H, *J* = 5.6 Hz, H-1), 5.69 (dt, 1H, *J* = 15.4, 5.6 Hz, H-2), 5.84 (dt, 1H, *J* = 15.4, 6.3 Hz, H-3), 6.86–7.32 (m, 5H, C₆H₅). ¹³C{H} NMR: δ 13.7 (C-6), 22.2 (C-5), 34.4 (C-4), 68.7 (C-1), 125.0 (C-3), 135.4 (C-2), 114.8, 120.7, 129.4, and 158.8 (C₆H₅); *Z*-isomer, δ 13.7 (C-6), 22.6 (C-5), 29.8 (C-4), 63.9 (C-1), 125.0 (C-3), 134.1 (C-2), 114.8, 120.7, 129.4, and 158.8 (C₆H₅). Anal. Calcd for C₁₂H₁₆O (as a mixture of **11a** and **12a**): C, 81.77; H, 9.15. Found: C, 81.70; H, 9.28.

3-Phenoxy-1-hexene (12a). ¹H NMR: δ 0.93 (t, 3H, *J* = 7.3 Hz, H-6), 1.40–1.80 (m, 4H, H-4, H-5), 4.59 (dt, 1H, *J* = 6.1, 6.1 Hz, H-3), 5.17 (ddd, 1H, *J* = 10.4, 1.3, 1.3 Hz, H-1), 5.24 (ddd, 1H, *J* = 17.2, 1.3, 1.3 Hz, H-1), 5.84 (ddd, 1H, *J* = 17.2, 10.4, 6.1 Hz, H-2), 6.86–7.32 (m, 5H, C₆H₅). ¹³C{H} NMR: δ 14.0 (C-6), 18.6 (C-5), 37.8 (C-4), 78.7 (C-3), 116.2 (C-1), 138.3 (C-2), 116.0, 120.6, 129.3, and 158.5 (C₆H₅).

1-(4-Methylphenoxy)-2-hexene (11b). ¹H NMR: δ 0.91 (t, 3H, *J* = 7.4 Hz, H-6), 1.30–1.60 (m, 2H, H-5), 2.07 (dt, 2H, *J* = 7.2, 6.1 Hz, H-4), 2.26 (s, 3H, CH₃-C₆H₄), 4.41 (d, 2H, *J* = 5.1 Hz, H-1), 5.67 (dt, 1H, *J* = 15.4, 5.1 Hz, H-2), 5.83 (dt, 1H, *J* = 15.4, 6.1 Hz, H-3), 6.75–7.14 (m, 4H, C₆H₄). ¹³C{H} NMR: *E*-isomer, δ 13.7 (C-6), 20.4 (CH₃-C₆H₄), 22.2 (C-5), 34.4 (C-4), 68.8 (C-1), 125.2 (C-3), 135.1 (C-2), 116.0, 129.8, 138.4 and 156.7 (C₆H₄); *Z*-isomer, δ 13.7 (C-6), 20.4 (CH₃-C₆H₄), 22.6 (C-5), 29.8 (C-4), 64.0 (C-1), 125.2 (C-3), 133.9 (C-2), 116.0, 129.8, 138.4, and 156.7 (C₆H₄). Anal. Calcd for C₁₃H₁₈O (as a mixture of **11b** and **12b**): C, 82.06; H, 9.54. Found: C, 82.13; H, 9.53.

3-(4-Methylphenoxy)-1-hexene (12b). ¹H NMR: δ 0.93 (t, 3H, *J* = 7.4 Hz, H-6), 1.30–1.90 (m, 4H, H-4, H-5), 2.25 (s, 3H, CH₃-C₆H₄), 4.53 (dt, 1H, *J* = 7.9, 6.2 Hz, H-3), 5.15 (ddd, 1H, *J* = 10.4, 1.3, 1.3 Hz, H-1), 5.21 (ddd, 1H, *J* = 17.4, 1.3, 1.3 Hz, H-1), 5.83 (ddd, 1H, *J* = 17.4, 10.4, 6.1 Hz, H-2), 6.75–7.14 (m, 4H, C₆H₄). ¹³C{H} NMR: δ 14.0 (C-6), 18.6 (C-5), 20.4 (CH₃-C₆H₄), 37.8 (C-4), 78.9 (C-3), 116.1 (C-1), 138.4 (C-2), 114.6, 129.7, 138.4, and 156.4 (C₆H₄).

1-(3-Methylphenoxy)-2-hexene (11c). ¹H NMR: δ 0.93 (t, 3H, *J* = 7.4 Hz, H-6), 1.30–1.60 (m, 2H, H-5), 2.09 (dt, 2H, *J* = 7.2, 6.1 Hz, H-4), 2.24 (s, 3H, CH₃-C₆H₄), 4.42 (d, 2H, *J* = 5.5 Hz, H-1), 5.66 (dt, 1H, *J* = 15.5, 5.5 Hz, H-2), 5.81 (dt, 1H, *J* = 15.5, 6.1 Hz, H-3), 6.70–7.20 (m, 4H, C₆H₄). ¹³C{H}

NMR: *E*-isomer, δ 13.7 (C-6), 21.5 (CH₃-C₆H₄), 22.2 (C-5), 34.4 (C-4), 68.6 (C-1), 125.2 (C-3), 135.2 (C-2), 111.6, 115.5, 121.5, 129.1, 139.3, and 158.8 (C₆H₄); *Z*-isomer, δ 13.7 (C-6), 21.5 (CH₃-C₆H₄), 22.6 (C-5), 29.8 (C-4), 63.8 (C-1), 125.2 (C-3), 134.0 (C-2), 111.6, 115.5, 121.5, 129.1, 139.3, and 158.8 (C₆H₄). Anal. Calcd for C₁₃H₁₈O (as a mixture of **11c** and **12c**): C, 82.06; H, 9.54. Found: C, 82.34; H, 9.60.

3-(3-Methylphenoxy)-1-hexene (12c). ¹H NMR: δ 0.94 (t, 3H, *J* = 7.4 Hz, H-6), 1.30–1.90 (m, 4H, H-4, H-5), 2.25 (s, 3H, CH₃-C₆H₄), 4.57 (dt, 1H, *J* = 6.3, 6.1 Hz, H-3), 5.15 (ddd, 1H, *J* = 10.4, 1.3, 1.3 Hz, H-1), 5.23 (ddd, 1H, *J* = 17.3, 1.3, 1.3 Hz, H-1), 5.83 (ddd, 1H, *J* = 17.3, 10.4, 6.1 Hz, H-2), 6.70–7.20 (m, 4H, C₆H₄). ¹³C{H} NMR: δ 14.0 (C-6), 18.6 (C-5), 21.5 (CH₃-C₆H₄), 37.8 (C-4), 78.5 (C-3), 116.0 (C-1), 138.1 (C-2), 112.8, 116.9, 121.5, 129.0, 139.2, and 158.5 (C₆H₄).

1-(2-Methylphenoxy)-2-hexene (11d). ¹H NMR: δ 0.92 (t, 3H, *J* = 7.4 Hz, H-6), 1.30–1.60 (m, 2H, H-5), 2.08 (dt, 2H, *J* = 7.2, 6.2 Hz, H-4), 2.26 (s, 3H, CH₃-C₆H₄), 4.47 (d, 2H, *J* = 5.3 Hz, H-1), 5.69 (dt, 1H, *J* = 15.4, 5.3 Hz, H-2), 5.78 (dt, 1H, *J* = 15.4, 6.2 Hz, H-3), 6.70–7.20 (m, 4H, C₆H₄). ¹³C{H} NMR: *E*-isomer, δ 13.7 (C-6), 16.3 (CH₃-C₆H₄), 22.2 (C-5), 34.5 (C-4), 68.8 (C-1), 125.4 (C-3), 134.5 (C-2), 111.5–139.8, and 157.2 (C₆H₄); *Z*-isomer, δ 13.7 (C-6), 16.3 (CH₃-C₆H₄), 22.6 (C-5), 29.9 (C-4), 64.1 (C-1), 125.4 (C-3), 133.7 (C-2), 111.5–139.8, and 157.2 (C₆H₄). Anal. Calcd for C₁₃H₁₈O (as a mixture of **11d** and **12d**): C, 82.06; H, 9.54. Found: C, 81.81; H, 9.60.

3-(2-Methylphenoxy)-1-hexene (12d). ¹H NMR: δ 0.96 (t, 3H, *J* = 7.4 Hz, H-6), 1.30–1.90 (m, 4H, H-4, H-5), 2.26 (s, 3H, CH₃-C₆H₄), 4.60 (dt, 1H, *J* = 6.2, 6.0 Hz, H-3), 5.16 (ddd, 1H, *J* = 10.5, 1.3, 1.3 Hz, H-1), 5.22 (ddd, 1H, *J* = 17.4, 1.3, 1.3 Hz, H-1), 5.83 (ddd, 1H, *J* = 17.4, 10.5, 6.2 Hz, H-2), 6.70–7.20 (m, 4H, C₆H₄). ¹³C{H} NMR: δ 14.0 (C-6), 16.5 (CH₃-C₆H₄), 18.5 (C-5), 37.9 (C-4), 78.6 (C-3), 115.9 (C-1), 138.5 (C-2), 111.5–137.2, and 157.3 (C₆H₄).

1-(2,5-Dimethylphenoxy)-2-hexene (11e). ¹H NMR: δ 0.91 (t, 3H, *J* = 7.4 Hz, H-6), 1.30–1.50 (m, 2H, H-5), 1.90–2.10 (m, 2H, H-4), 2.27 (s, 3H, CH₃-C₆H₃), 2.29 (s, 3H, CH₃-C₆H₃), 4.23 (d, 2H, *J* = 4.4 Hz, H-1), 5.77 (t, 2H, *J* = 4.4, H-2, H-3), 6.80–7.00 (m, 4H, C₆H₃). ¹³C{H} NMR: *E*-isomer, δ 13.7 (C-6), 16.5 (CH₃-C₆H₃), 22.2 (C-5), 34.4 (C-4), 73.1 (C-1), 126.0 (C-3), 134.9 (C-2), 123.3, 128.7, 131.0, and 156.1 (C₆H₃); *Z*-isomer, δ 13.7 (C-6), 16.5 (CH₃-C₆H₃), 22.7 (C-5), 29.7 (C-4), 68.0 (C-1), 125.7 (C-3), 133.6 (C-2), 123.3, 128.7, 131.0, and 156.1 (C₆H₃). Anal. Calcd for C₁₄H₂₀O (as a mixture of **11e** and **12e**): C, 82.30; H, 9.87. Found: C, 82.26; H, 10.11.

3-(2,5-Dimethylphenoxy)-1-hexene (12e). ¹H NMR: δ 0.93 (t, 3H, *J* = 7.4 Hz, H-6), 1.30–1.58 (m, 4H, H-4, H-5), 2.27 (s, 3H, CH₃-C₆H₃), 2.29 (s, 3H, CH₃-C₆H₃), 4.24 (dt, 1H, *J* = 8.4, 8.4 Hz, H-3), 4.96 (ddd, 1H, *J* = 17.0, 1.6, 1.6 Hz, H-1), 5.03 (ddd, 1H, *J* = 10.1, 1.6, 1.6 Hz, H-1), 5.84 (ddd, 1H, *J* = 17.0, 10.1, 8.4 Hz, H-2), 6.80–7.00 (m, 4H, C₆H₃). ¹³C{H} NMR: δ 14.1 (C-6), 17.4 (CH₃-C₆H₃), 18.6 (C-5), 37.4 (C-4), 83.6 (C-3), 117.6 (C-1), 138.0 (C-2), 123.3, 128.7, 131.0, and 154.6 (C₆H₃).

1-(2-tert-Butylphenoxy)-2-hexene (11f). ¹H NMR: δ 0.92 (t, 3H, *J* = 7.4 Hz, H-6), 1.39 (s, 9H, *t*-Bu), 1.30–1.60 (m, 2H, H-5), 2.06 (dt, 2H, *J* = 7.2, 6.2 Hz, H-4), 4.48 (d, 2H, *J* = 4.9 Hz, H-1), 5.51 (dt, 1H, *J* = 15.5, 4.9 Hz, H-2), 5.83 (dt, 1H, *J* = 15.5, 6.2 Hz, H-3), 6.70–7.30 (m, 4H, C₆H₄). ¹³C{H} NMR: *E*-isomer, δ 13.6 (C-6), 22.2 (C-5), 29.8 (CMe₃), 34.8 (CMe₃), 34.4 (C-4), 68.7 (C-1), 126.5 (C-3), 134.3 (C-2), 111.2–138.3, and 157.6 (C₆H₄); *Z*-isomer, δ 13.6 (C-6), 22.6 (C-5), 29.8 (CMe₃), 34.8 (CMe₃), 29.8 (C-4), 64.0 (C-1), 125.4 (C-3), 133.7 (C-2), 111.2–138.3, and 157.6 (C₆H₄). Anal. Calcd for C₁₆H₂₄O (as a mixture of **11f** and **12f**): C, 82.00; H, 10.49. Found: C, 82.70; H, 10.41.

3-(2-tert-Butylphenoxy)-1-hexene (12f). ¹H NMR: δ 0.96 (t, 3H, *J* = 7.4 Hz, H-6), 1.41 (s, 9H, *t*-Bu), 1.30–1.90 (m, 4H, H-4, H-5), 4.75 (dt, 1H, *J* = 6.0, 6.0 Hz, H-3), 5.17 (ddd, 1H, *J* = 10.4, 1.3, 1.3 Hz, H-1), 5.20 (ddd, 1H, *J* = 17.4, 1.3, 1.3 Hz, H-1), 5.82 (ddd, 1H, *J* = 17.4, 10.4, 6.0 Hz, H-2), 6.70–7.30

(27) Hill, W. E.; MacAuliffe, C. A.; Niven, I. E.; Parish, R. V. *Inorg. Chim. Acta* **1979**, *38*, 273.

(28) Golborn, P.; Scheinmann, F. *J. Chem. Soc., Perkin Trans. 1* **1973**, 2870.

(29) White, W. N.; Gwyn, D.; Schlitt, R.; Girard, C.; Fife, W. *J. Am. Chem. Soc.* **1958**, *80*, 3271.

(30) Vowinkel, E. *Chem. Ber.* **1962**, *95*, 2997.

(31) Frater, G.; Schmid, H. *Helv. Chim. Acta* **1967**, *50*, 255.

(32) Hutchins, R. O.; Learn, K. *J. Org. Chem.* **1982**, *47*, 4380.

(m, 4H, C₆H₄). ¹³C{H} NMR: δ 14.1 (C-6), 18.6 (C-5), 29.8 (CMe₃), 34.8 (CMe₂), 37.8 (C-4), 77.4 (C-3), 116.4 (C-1), 138.0 (C-2), 113.1–133.0, and 156.0 (C₆H₄).

1-(4-Methoxyphenoxy)-2-hexene (11g). ¹H NMR: δ 0.90 (t, 3H, *J* = 7.3 Hz, H-6), 1.30–1.50 (m, 2H, H-5), 2.04 (dt, 2H, *J* = 6.4, 6.4 Hz, H-4), 3.71 (s, 3H, OCH₃), 4.40 (d, 2H, *J* = 5.1 Hz, H-1), 5.70 (dt, 1H, *J* = 15.4, 5.1 Hz, H-2), 5.80 (dt, 1H, *J* = 15.4, 6.4 Hz, H-3), 6.70–7.20 (m, 4H, C₆H₄). ¹³C{H} NMR: *E*-isomer, δ 13.6 (C-6), 21.1 (C-5), 34.4 (C-4), 55.5 (OCH₃), 69.4 (C-1), 125.3 (C-3), 135.0 (C-2), 113.4, 116.3, 151.9, and 152.8 (C₆H₄); *Z*-isomer, δ 13.6 (C-6), 22.6 (C-5), 29.8 (C-4), 55.5 (OCH₃), 64.5 (C-1), 125.3 (C-3), 133.8 (C-2), 113.4, 116.3, 151.9, and 152.8 (C₆H₄). Anal. Calcd for C₁₃H₁₈O₂ (as a mixture of **11g** and **12g**): C, 75.69; H, 8.80. Found: C, 75.69; H, 9.03.

3-(4-Methoxyphenoxy)-1-hexene (12g). ¹H NMR: δ 0.93 (t, 3H, *J* = 7.3 Hz, H-6), 1.30–1.80 (m, 4H, H-4, H-5), 3.70 (s, 3H, OCH₃), 4.48 (dt, 1H, *J* = 6.2, 5.6 Hz, H-3), 5.15 (ddd, 1H, *J* = 10.4, 1.3, 1.3 Hz, H-1), 5.21 (ddd, 1H, *J* = 17.3, 1.3, 1.3 Hz, H-1), 5.82 (ddd, 1H, *J* = 17.3, 10.4, 6.2 Hz, H-2), 6.70–7.20 (m, 4H, C₆H₄). ¹³C{H} NMR: δ 13.9 (C-6), 18.5 (C-5), 37.7 (C-4), 55.5 (OCH₃), 79.8 (C-3), 116.1 (C-1), 138.5 (C-2), 113.5, 114.7, 151.5, and 152.8 (C₆H₄).

1-(2-Methoxyphenoxy)-2-hexene (11h). ¹H NMR: δ 0.89 (t, 3H, *J* = 7.3 Hz, H-6), 1.30–1.50 (m, 2H, H-5), 2.03 (dt, 2H, *J* = 7.2, 6.2 Hz, H-4), 3.84 (s, 3H, OCH₃), 4.53 (d, 2H, *J* = 4.9 Hz, H-1), 5.72 (dt, 1H, *J* = 15.4, 4.9 Hz, H-2), 5.83 (dt, 1H, *J* = 15.4, 6.2 Hz, H-3), 6.70–7.30 (m, 4H, C₆H₄). ¹³C{H} NMR: *E*-isomer, δ 13.7 (C-6), 22.1 (C-5), 34.4 (C-4), 55.8 (OCH₃), 69.8 (C-1), 125.1 (C-3), 135.5 (C-2), 111.6–150.3 (C₆H₄); *Z*-isomer, δ 13.7 (C-6), 22.6 (C-5), 29.8 (C-4), 55.9 (OCH₃), 65.0 (C-1), 125.3 (C-3), 133.8 (C-2), 111.6–150.3 (C₆H₄). Anal. Calcd for C₁₃H₁₈O₂ (as a mixture of **11h** and **12h**): C, 75.69; H, 8.80. Found: C, 75.28; H, 8.88.

3-(2-Methoxyphenoxy)-1-hexene (12h). ¹H NMR: δ 0.95 (t, 3H, *J* = 7.3 Hz, H-6), 1.30–2.00 (m, 4H, H-4, H-5), 3.82 (s, 3H, OCH₃), 4.50–4.70 (m, 1H, H-3), 5.15 (ddd, 1H, *J* = 10.5, 1.3–1.3 Hz, H-1), 5.21 (ddd, 1H, *J* = 17.3, 1.3 and 1.3 Hz, H-1), 5.87 (ddd, 1H, *J* = 17.3, 10.5, 6.7 Hz, H-2), 6.70–7.30 (m, 4H, C₆H₄). ¹³C{H} NMR: δ 14.0 (C-6), 18.6 (C-5), 37.6 (C-4), 55.9 (OCH₃), 80.6 (C-3), 116.5 (C-1), 138.4 (C-2), 111.6–150.3 (C₆H₄).

1-(4-Chlorophenoxy)-2-hexene (11i). ¹H NMR: δ 0.90 (t, 3H, *J* = 7.3 Hz, H-6), 1.30–1.50 (m, 2H, H-5), 2.07 (dt, 2H, *J* = 6.8, 6.5 Hz, H-4), 4.41 (d, 2H, *J* = 5.9 Hz, H-1), 5.65 (dt, 1H, *J* = 15.4, 5.9 Hz, H-2), 5.82 (dt, 1H, *J* = 15.4, 6.5 Hz, H-3), 6.90–7.60 (m, 4H, C₆H₄). ¹³C{H} NMR: *E*-isomer, δ 13.7 (C-6), 22.1 (C-5), 34.4 (C-4), 69.1 (C-1), 124.6 (C-3), 135.7 (C-2), 116.0, 125.5, 129.3, and 157.4 (C₆H₄); *Z*-isomer, δ 13.7 (C-6), 22.6 (C-5), 29.8 (C-4), 64.3 (C-1), 124.6 (C-3), 134.5 (C-2), 116.0, 125.5, 129.3, and 157.4 (C₆H₄). Anal. Calcd for C₁₂H₁₅ClO (as a mixture of **11i** and **12i**): C, 68.41; H, 7.18. Found: C, 68.12; H, 7.38.

3-(4-Chlorophenoxy)-1-hexene (12i). ¹H NMR: δ 0.93 (t, 3H, *J* = 7.3 Hz, H-6), 1.30–1.80 (m, 4H, H-4, H-5), 4.52 (dt, 1H, *J* = 6.1, 6.1 Hz, H-3), 5.18 (ddd, 1H, *J* = 10.4, 1.1, 1.1 Hz, H-1), 5.20 (ddd, 1H, *J* = 17.4, 1.1, 1.1 Hz, H-1), 5.80 (ddd, 1H, *J* = 17.4, 10.4, 6.1 Hz, H-2), 6.90–7.60 (m, 4H, C₆H₄). ¹³C{H} NMR: δ 13.9 (C-6), 18.5 (C-5), 37.7 (C-4), 79.3 (C-3), 116.5 (C-1), 137.8 (C-2), 117.4, 125.5, 129.2, and 157.1 (C₆H₄).

1-(4-Cyanophenoxy)-2-hexene (11j). ¹H NMR: δ 0.95 (t, 3H, *J* = 7.3 Hz, H-6), 1.30–1.50 (m, 2H, H-5), 2.08 (dt, 2H, *J* = 7.2, 6.6 Hz, H-4), 4.52 (d, 2H, *J* = 5.4 Hz, H-1), 5.67 (dt, 1H, *J* = 15.4, 5.4 Hz, H-2), 5.83 (dt, 1H, *J* = 15.4, 6.6 Hz, H-3), 6.90–7.60 (m, 4H, C₆H₄). ¹³C{H} NMR: *E*-isomer, δ 13.7 (C-6), 21.1 (C-5), 34.4 (C-4), 69.1 (C-1), 119.3 (CN), 123.8 (C-3), 135.6 (C-2), 115.5, 133.8, and 162.0 (C₆H₄). Anal. Calcd for C₁₃H₁₅NO (as a mixture of **11j** and **12j**): C, 77.58; H, 7.51. Found: C, 77.13; H, 7.58.

3-(4-Cyanophenoxy)-1-hexene (12j). ¹H NMR: δ 0.95 (t, 3H, *J* = 7.3 Hz, H-6), 1.30–1.90 (m, 4H, H-4, H-5), 4.66 (dt, 1H, *J* = 6.1, 6.1 Hz, H-3), 5.24 (ddd, 1H, *J* = 10.6, 1.1, 1.1 Hz, H-1), 5.26 (ddd, 1H, *J* = 17.4, 1.1, 1.1 Hz, H-1), 5.82 (ddd, 1H,

J = 17.4, 10.6, 6.1 Hz, H-2), 6.90–7.60 (m, 4H, C₆H₄). ¹³C{H} NMR: δ 13.9 (C-6), 18.4 (C-5), 37.5 (C-4), 79.1 (C-3), 117.1 (C-1), 119.3 (CN), 136.9 (C-2), 116.4, 133.8, 133.9, and 161.8 (C₆H₄).

1-(4-Nitrophenoxy)-2-hexene (11k). ¹H NMR: δ 0.92 (t, 3H, *J* = 7.3 Hz, H-6), 1.30–1.50 (m, 2H, H-5), 2.09 (dt, 2H, *J* = 7.5, 6.5 Hz, H-4), 4.51 (d, 2H, *J* = 5.9 Hz, H-1), 5.67 (dt, 1H, *J* = 15.4, 5.9 Hz, H-2), 5.88 (dt, 1H, *J* = 15.4, 6.5 Hz, H-3), 6.90–8.20 (m, 4H, C₆H₄). ¹³C{H} NMR: *E*-isomer, δ 13.7 (C-6), 22.1 (C-5), 34.4 (C-4), 69.5 (C-1), 123.9 (C-3), 136.8 (C-2), 114.7, 125.9, 141.4, and 163.9 (C₆H₄). Anal. Calcd for C₁₂H₁₅NO₃ (as a mixture of **11k** and **12k**): C, 65.14; H, 6.83. Found: C, 65.11; H, 6.95.

3-(4-Nitrophenoxy)-1-hexene (12k). ¹H NMR: δ 0.96 (t, 3H, *J* = 7.3 Hz, H-6), 1.30–1.90 (m, 4H, H-4, H-5), 4.71 (dt, 1H, *J* = 6.3, 6.3 Hz, H-3), 5.26 (ddd, 1H, *J* = 10.6, 1.0, 1.0 Hz, H-1), 5.29 (ddd, 1H, *J* = 17.6, 1.0, 1.0 Hz, H-1), 5.83 (ddd, 1H, *J* = 17.6, 10.6, 6.3 Hz, H-2), 6.70–7.20 (m, 4H, C₆H₄). ¹³C{H} NMR: δ 13.6 (C-6), 18.4 (C-5), 37.5 (C-4), 79.6 (C-3), 117.2 (C-1), 136.7 (C-2), 115.6, 125.7, 141.2, and 163.6 (C₆H₄).

1-(3-Nitrophenoxy)-2-hexene (11l). ¹H NMR: δ 0.91 (t, 3H, *J* = 7.3 Hz, H-6), 1.30–1.60 (m, 2H, H-5), 2.08 (dt, 2H, *J* = 7.2, 6.6 Hz, H-4), 4.55 (d, 2H, *J* = 5.8 Hz, H-1), 5.68 (dt, 1H, *J* = 15.4, 5.8 Hz, H-2), 5.89 (dt, 1H, *J* = 15.4, 6.6 Hz, H-3), 7.20–7.80 (m, 4H, C₆H₄). ¹³C{H} NMR: *E*-isomer, δ 13.7 (C-6), 22.1 (C-5), 34.4 (C-4), 69.5 (C-1), 123.9 (C-3), 136.5 (C-2), 110.6, 122.0, 130.0, 149.1, and 159.3 (C₆H₄); *Z*-isomer, δ 13.7 (C-6), 22.6 (C-5), 29.9 (C-4), 64.7 (C-1), 123.8 (C-3), 135.3 (C-2), 110.6, 122.0, 130.0, 149.1, and 159.3 (C₆H₄). Anal. Calcd for C₁₂H₁₅NO₃ (as a mixture of **11l** and **12l**): C, 65.14; H, 6.83. Found: C, 65.02; H, 6.96.

3-(3-Nitrophenoxy)-1-hexene (12l). ¹H NMR: δ 0.96 (t, 3H, *J* = 7.3 Hz, H-6), 1.30–1.90 (m, 4H, H-4, H-5), 4.67 (dt, 1H, *J* = 6.2, 6.2 Hz, H-3), 5.24 (ddd, 1H, *J* = 10.5, 1.0, 1.0 Hz, H-1), 5.29 (ddd, 1H, *J* = 17.4, 1.0, 1.0 Hz, H-1), 5.83 (ddd, 1H, *J* = 17.4, 10.5, 6.2 Hz, H-2), 7.20–7.80 (m, 4H, C₆H₄). ¹³C{H} NMR: δ 13.6 (C-6), 18.5 (C-5), 37.6 (C-4), 79.6 (C-3), 117.3 (C-1), 137.0 (C-2), 109.3, 115.7, 122.8, 129.9, 149.1, and 159.0 (C₆H₄).

1-(2-Nitrophenoxy)-2-hexene (11m). ¹H NMR: δ 0.94 (t, 3H, *J* = 7.3 Hz, H-6), 1.30–1.50 (m, 2H, H-5), 2.10 (dt, 2H, *J* = 7.2, 6.5 Hz, H-4), 4.63 (d, 2H, *J* = 5.6 Hz, H-1), 5.67 (dt, 1H, *J* = 15.4, 5.6 Hz, H-2), 5.89 (dt, 1H, *J* = 15.4, 6.5 Hz, H-3), 6.90–7.80 (m, 4H, C₆H₄). ¹³C{H} NMR: *E*-isomer, δ 13.7 (C-6), 22.0 (C-5), 34.3 (C-4), 70.3 (C-1), 123.6 (C-3), 136.2 (C-2), 115.1, 120.3, 125.6, 133.9, 140.2, and 152.1 (C₆H₄); *Z*-isomer, δ 13.7 (C-6), 22.5 (C-5), 29.9 (C-4), 65.7 (C-1), 123.6 (C-3), 135.3 (C-2), 115.1, 120.3, 125.6, 133.9, 140.2, and 152.1 (C₆H₄). Anal. Calcd for C₁₂H₁₅NO₃ (as a mixture of **11m** and **12m**): C, 65.14; H, 6.83. Found: C, 64.90; H, 6.94.

3-(2-Nitrophenoxy)-1-hexene (12m). ¹H NMR: δ 0.94 (t, 3H, *J* = 7.3 Hz, H-6), 1.30–2.00 (m, 4H, H-4, H-5), 4.74 (dt, 1H, *J* = 6.3, 6.3 Hz, H-3), 5.24 (ddd, 1H, *J* = 10.5, 1.3, 1.3 Hz, H-1), 5.28 (ddd, 1H, *J* = 17.4, 1.3, 1.3 Hz, H-1), 5.86 (ddd, 1H, *J* = 17.4, 10.5, 6.2 Hz, H-2), 6.90–7.80 (m, 4H, C₆H₄). ¹³C{H} NMR: δ 13.8 (C-6), 18.2 (C-5), 37.5 (C-4), 80.8 (C-3), 117.3 (C-1), 136.8 (C-2), 116.5, 120.1, 125.3, 136.8, 140.7, and 151.5 (C₆H₄).

(E) and (Z)-4-Benzyloxy-1-phenoxy-2-butene (10a). Oil, yield: 92%. ¹H NMR: δ 4.00–4.05 (bm, 1.8H, H-4 of *E*-isomer), 4.10–4.12 (bm, 0.2H, H-4 of *Z*-isomer), 4.48–4.50 (bm, 4H, H-1, CH₂C₆H₅), 5.90–5.95 (m, 2H, H-2, H-3), 6.85–7.35 (m, 10H, C₆H₅). ¹³C{H} NMR δ 63.9 (C-1 of *Z*-isomer), 65.8 (C-4 of *Z*-isomer), 67.7 (C-1 of *E*-isomer), 69.9 (C-4 of *E*-isomer), 72.2 (CH₂C₆H₅ of *E*-isomer), 72.3 (CH₂C₆H₅ of *Z*-isomer), 114.7–158.5 (C-2, C-3, C₆H₅). Anal. Calcd for C₁₇H₁₈O₂: C, 81.28; H, 7.13. Found: C, 81.00; H, 7.20.

2-(Allyloxy)naphthalene (18a). Yield: 41% at –20 °C and 34% at 20 °C. ¹H NMR: δ 4.65 (ddd, 2H, *J* = 5.3, 1.5, 1.5 Hz, OCH₂), 5.32 (ddt, 1H, *J* = 10.4, 1.5, 1.5 Hz, =CH₂), 5.47 (ddt, 1H, *J* = 17.2, 1.5, 1.5 Hz, =CH₂), 6.13 (ddt, 1H, *J* = 17.2, 10.4, 5.3 Hz, –CH=), 7.13–7.78 (m, 7H, aromatics). ¹³C{H}

NMR: δ 68.7 (CH₂), 117.6 (=CH₂), 133.2 (-CH=), 107.0-134.5 (aromatics), in agreement with the literature.²²

1-Allyl-2-naphthol (19a). Yield: 54%. ¹H NMR: δ 3.82 (ddd, 2H, J = 5.7, 1.7, 1.7 Hz, CH₂), 5.04 (ddt, 1H, J = 10.5, 1.7, 1.7 Hz, =CH₂), 5.06 (ddt, 1H, J = 16.9, 1.7, 1.7 Hz, =CH₂), 5.10 (ddt, 1H, J = 16.9, 10.5, 5.7 Hz, -CH=), 5.20 (bs, 1H, OH), 7.00-7.80 (m, 6H, aromatics). ¹³C{H} NMR: δ 29.4 (CH₂), 116.1 (=CH₂), 133.4 (-CH=), 116.9-151.3 (aromatics), in agreement with the literature.²²

2-(E)-(Cinnamyl-oxo)naphthalene (18b). Yield: 34%. ¹H NMR: δ 4.67 (d, 2H, J = 5.5 Hz, OCH₂), 6.38 (dt, 1H, J = 15.9, 5.5 Hz, =CH-), 6.69 (d, 1H, J = 15.9 Hz, =CH-), 7.10-8.40 (m, 12H, aromatics). ¹³C{H} NMR: δ 68.8 (CH₂), 127.9 (-CH=), 133.0 (-CH=), 107.0-154.4 (aromatics), in agreement with the literature.³³

1-(E)-Cinnamyl-2-naphthol (19b). Yield: 40%. ¹H NMR: δ 3.93 (d, 2H, J = 2.9 Hz, OCH₂), 6.35 (dd, 1H, J = 15.5, 2.9 Hz, =CH-), 6.45 (d, 1H, J = 15.5 Hz, =CH-), 7.00-8.00 (m, 12H, aromatics). ¹³C{H} NMR: δ 28.5 (CH₂), 130.8 (-CH=), 133.4 (-CH=), 118.0-151.2 (aromatics). This compound was also obtained by treatment of 388 mg (1.5 mmol) of compound 18b in 5 mL of THF at 60 °C in the presence of Pd₂(dba)₃ (27 mg, 0.03 mmol) and dppb (51 mg, 0.12 mmol) for 24 h (yield: 40%).

cis-3-Phenoxy-5-(carbomethoxy)-1-cyclohexene (21). To a stirred solution of Pd₂(dba)₃ (27.0 mg, 0.03 mmol) and 1,4-bis(diphenylphosphino)butane (51.2 mg, 0.12 mmol) in tetrahydrofuran (3 mL) was added a degassed solution of the carbonate 20¹³ (342 mg, 1.92 mmol) and the phenol 7a (235 mg, 1.5 mmol) in 2 mL of tetrahydrofuran. The solution was stirred for 12 h at the desired temperature. Solvent evaporation followed by column chromatography through silica gel (hexane/ethyl acetate 6/1) afforded compound 21 (yield: 54% at 25 °C and 70% at 65 °C). ¹H NMR: δ 1.88 (ddd, 1H, J = 12.5, 12.5, 9.4 Hz, H-4_{ax}), 2.31-2.40 (m, 2H, H-6), 2.48 (dm, 1H, J = 12.5 Hz, H-4_e), 2.77 (ddm, 1H, J = 12.5 and 9.4 Hz,

H-5), 3.70 (s, 3H, OCH₃), 4.91-5.00 (m, 1H, H-3), 5.80-5.92 (m, 2H, H-1, H-2), 6.90-7.50 (m, 5H, aromatics) in agreement with the literature.⁷ ¹³C{H} NMR: δ 27.5 and 31.2 (C-4 and C-6), 38.1 (C-5), 51.9 (CH₃), 72.2 (C-3), 116.0, 121.0, 128.7, 129.0, 129.5, 157.5 (C-1, C-2, C₆H₅), 174.7 (CO₂).

Palladium-Mediated Synthesis of Benzo-1,4-dioxanes. To a stirred solution of Pd₂(dba)₃ (27.0 mg, 0.03 mmol) and 1,4-bis(diphenylphosphino)butane (51.2 mg, 0.12 mmol) in tetrahydrofuran (3 mL) was added a degassed solution of the dicarbonate 23 (223 mg, 1.50 mmol) and the diol 22 (2.20 mmol) in 3 mL of tetrahydrofuran. The solution was stirred for 24 h at room temperature. Solvent evaporation followed by column chromatography through silica gel (hexane/ethyl acetate 4/1) afforded the benzo-1,4-dioxane 24.

2-Vinylbenzo-1,4-dioxane (24a). Oil, yield: 60%. ¹H NMR: δ 3.85 (dd, 1H, J = 11.3, 7.9 Hz, H-3), 4.20 (dd, 1H, J = 11.3, 2.4 Hz, H-3), 4.56 (dddt, 1H, J = 7.9, 5.7, 2.4, 1.3 Hz, H-2), 5.32 (ddd, 1H, J = 10.3, 1.3, 1.3 Hz, =CH₂), 5.47 (ddd, 1H, J = 17.3, 1.3, 1.3 Hz, =CH₂), 5.87 (ddd, 1H, J = 17.3, 10.3, 5.7 Hz, -CH=), 6.70-7.00 (m, 4H, C₆H₄).³⁴ ¹³C{H} NMR: δ 65.5 (C-3), 74.0 (C-2), 119.0 (=CH₂), 133.0 (-CH=), 117.0, 122.0, and 143.0 (C₆H₄).

2-Vinylnaphtho[2,3]-1,4-dioxane (24b). Oil, yield: 67%. ¹H NMR: δ 4.02 (dd, 1H, J = 11.4, 7.9 Hz, H-3), 4.32 (dd, 1H, J = 11.4, 2.5 Hz, H-3), 4.75 (dddt, 1H, J = 7.9, 5.7, 2.5, 1.3 Hz, H-2), 5.40 (ddd, 1H, J = 10.5, 1.3, 1.3 Hz, =CH₂), 5.55 (ddd, 1H, J = 17.3, 1.3, 1.3 Hz, =CH₂), 5.95 (ddd, 1H, J = 17.3, 10.5, 5.7 Hz, -CH=), 7.20-7.80 (m, 6H, aromatics). ¹³C{H} NMR: δ 67.5 (C-3), 74.0 (C-2), 119.0 (=CH₂), 132.5 (-CH=), 112.5, 124.5, 126.0, and 129.5 (aromatics). Anal. Calcd for C₁₄H₁₂O₂: C, 79.22; H, 5.69. Found: C, 79.28; H, 5.70.

Acknowledgment. We thank the CNRS for financial support and the Ministry of Education for grants to C.G. and M.M.

OM9502446

(33) Glonti, G. Sh.; Revazishvili, T. N. *Soobshch. Akad. Nauk. Gruz. S.S.R.* 1985, 117, 525; *Chem. Abstr.* 1986, 104, 168080r.

(34) Rosnati, V.; Salimbeni, A. *Gazz. Chim. Ital.* 1977, 107, 271.

Catalytic Cyclooligomerization of Thietane by Tetraosmium and Tetraruthenium Tetrahydride Carbonyl Cluster Complexes

Richard D. Adams* and Stephen B. Falloon

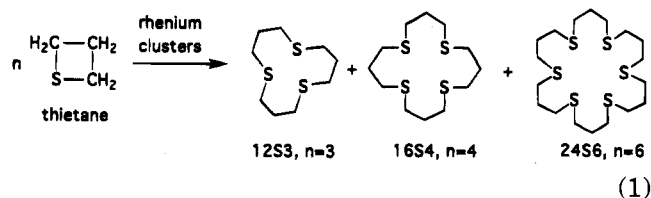
Department of Chemistry and Biochemistry, University of South Carolina,
Columbia, South Carolina 29208

Received May 4, 1995[®]

The new compounds $\text{Os}_4(\text{CO})_{11}(\text{SCH}_2\text{CH}_2\text{CH}_2)(\mu\text{-H})_4$, **3**, $\text{Os}_4(\text{CO})_{11}(12\text{S3})(\mu\text{-H})_4$, **4**, $\text{Ru}_4(\text{CO})_{11}(\text{SCH}_2\text{CH}_2\text{CH}_2)(\mu\text{-H})_4$, **5**, and $\text{Ru}_4(\text{CO})_{11}(12\text{S3})(\mu\text{-H})_4$, **6** (12S3 = 1,5,9-trithiacyclododecane) have been obtained from the reactions of $\text{Os}_4(\text{CO})_{11}(\text{NCMe})(\mu\text{-H})_4$ and $\text{Ru}_4(\text{CO})_{12}(\mu\text{-H})_4$ with thietane and 12S3, respectively. The molecular structure of **4** was established by a single-crystal X-ray diffraction analysis. The molecule contains a tetrahedral cluster of four osmium atoms with four bridging hydride ligands and a 12S3 ligand coordinated to one of the metal atoms through one of its three sulfur atoms. Compounds **3** and **4** were found to be efficient catalysts for the cyclooligomerization of thietane to 12S3 and 24S6 (24S6 = 1,5,9,13,17,21-hexathiacyclotetracosane) with a 6/1 preference for 12S3 after a 24 h reaction period. A kinetic study of the catalysis by **4** showed that the formation of 12S3 is first order in the concentration of **4**, which is consistent with the catalysis being produced by a tetranuclear cluster complex. Significant amounts of 12S3 and 24S6 were also obtained from thietane when **5** and **6** were used as catalyst precursors; however, the selectivity for 12S3 was significantly lower, and analysis after the reactions showed that most of the cluster complexes had decomposed. Crystal data for **4**: space group = $C2/c$, $a = 29.904(6)$ Å, $b = 11.815(2)$ Å, $c = 17.633(3)$ Å, $\beta = 91.28(2)^\circ$, $Z = 8$, 3384 reflections, $R = 0.058$.

Introduction

Polythioether macrocycles have attracted considerable interest for their potential to serve as ligands for the transition metals.¹ In the course of our recent studies of the ring opening reactions of the thietane ligands by nucleophiles,^{2,3} we have discovered the first examples of the formation of polythioether macrocycles by the catalytic cyclooligomerization of thietanes, eq 1.^{4,5} The



polythioether macrocycles 12S3 = 1,5,9-trithiacyclododecane, 16S4 = 1,5,9,13-hexathiacyclohexadecane, and 24S6 = 1,5,9,13,17,21-hexathiacyclotetracosane are

formed from thietane in the presence of $\text{Re}_3(\text{CO})_{10}[\mu\text{-}(\text{SCH}_2\text{CH}_2\text{CH}_2)(\mu\text{-H})_3]$,⁴ and 12S3 and 24S6 are formed in the presence of $\text{Re}_2(\text{CO})_9(\text{SCH}_2\text{CH}_2\text{CH}_2)$.⁵

In previous studies of the reactions of 3,3-dimethylthietane with $\text{Os}_3(\text{CO})_{10}(\text{NCMe})_2$, we observed ring-opening trimerization, but the cyclization step was preempted by reactions of the trimer at the metal atoms.⁶ We have now investigated the coordination and reactivity of thietane in the tetraosmium and tetraruthenium tetrahydride complexes, $\text{Os}_4(\text{CO})_{11}(\text{SCH}_2\text{CH}_2\text{CH}_2)(\mu\text{-H})_4$, **3**, and $\text{Ru}_4(\text{CO})_{11}(\text{SCH}_2\text{CH}_2\text{CH}_2)(\mu\text{-H})_4$, **5**. These complexes also produce appreciable amounts of 12S3 and 24S6 by catalytic cyclooligomerizations, but the ruthenium compound undergoes considerable decomposition and produces only small amounts of 12S3. The results of this study are reported here.

Experimental Section

General Data. Unless otherwise indicated all reactions were performed under a nitrogen atmosphere under normal room-lighting conditions. Reagent grade solvents were stored over 4-Å molecular sieves. $\text{Os}_4(\text{CO})_{12}(\mu\text{-H})_4$,⁷ **1**, and $\text{Ru}_4(\text{CO})_{12}(\mu\text{-H})_4$,⁸ were prepared according to the published procedures. Trimethylamine *N*-oxide dihydrate (Aldrich) was dehydrated by using a Dean-Stark apparatus with benzene as the solvent prior to use. 1,5,9-Trithiacyclododecane, 12S3, was prepared

[®] Abstract published in *Advance ACS Abstracts*, September 1, 1995.

(1) (1) (a) Cooper, S. R. In *Crown Compounds: Toward Future Applications*, Cooper, S. R., Ed.; VCH Publishers: New York, 1992, Chapter 15. (b) Cooper, S. R.; Rawley, S. C. *Struct. Bonding* **1990**, *72*, 1. (c) Blake, A. J.; Schröder, M. *Adv. Inorg. Chem.* **1990**, *35*, 1. (d) Cooper, S. R. *Acc. Chem. Res.* **1988**, *21*, 141.

(2) (a) Adams, R. D. *J. Cluster Sci.* **1992**, *3*, 263. (b) Adams, R. D.; Pompeo, M. P. *Organometallics* **1992**, *11*, 1460. (c) Adams, R. D.; Belinski, J. A.; Pompeo, M. P. *Organometallics* **1991**, *10*, 2539. (d) Adams, R. D.; Belinski, J. A.; Pompeo, M. P. *Organometallics* **1992**, *11*, 3129.

(3) Adams, R. D.; Cortopassi, J. E.; Falloon, S. B. *Organometallics* **1992**, *11*, 3794.

(4) Adams, R. D.; Falloon, S. B. *J. Am. Chem. Soc.* **1994**, *116*, 10540.

(5) Adams, R. D.; Cortopassi, J. E.; Falloon, S. B. *Organometallics* **1995**, *14*, 1748.

(6) Adams, R. D.; Pompeo, M. P. *J. Am. Chem. Soc.* **1991**, *113*, 1619.

(7) Johnson, B. F. G.; Lewis, J.; Raithby, P. R.; Sheldrick, G. M.; Wong, K. J. *Chem. Soc., Dalton Trans.* **1978**, 673.

(8) Knox, S. A. R.; Koepke, J. W.; Andrews, M. A.; Kaesz, H. D. *J. Am. Chem. Soc.* **1975**, *97*, 3943.

as described in our previous report.⁴ Thietane was purchased from Aldrich and was purified by vacuum distillation before use. All other reagents were purchased from Aldrich and were used as received. Infrared spectra were recorded on a Nicolet 5DXB FTIR spectrophotometer. ¹H NMR spectra were obtained on Bruker AM-300, WH-400, and AM-500 spectrometers operating at 300, 400, and 500 MHz, respectively. Separations were performed by TLC in air on Analtech 0.25-mm silica gel 60-Å F254 plates. Elemental analyses were performed by Oneida Research Services, Whitesboro, N.Y.

Preparation of Os₄(CO)₁₁(NCMe)(μ-H)₄, 2. A 102.6-mg amount of Os₄(CO)₁₂(μ-H)₄, **1** (0.093 mmol), was dissolved in 30 mL of methylene chloride and 20 mL of acetonitrile in a 100-mL three-neck round bottom flask equipped with a stir bar, a reflux condenser, a dropping funnel, and a nitrogen inlet. A 7.0-mg amount of Me₃NO (0.094 mmol) was added to 3 mL of CH₂Cl₂; this solution was then placed in the dropping funnel and was added over a 2-min period. The resulting solution was then allowed to stir at 25 °C for 1 h. The volatiles were removed under vacuum, and the product was separated by TLC using a hexane/methylene chloride 3/2 solvent mixture to yield 80.3 mg of Os₄(CO)₁₁(NCMe)(μ-H)₄, **2**, 78%. Spectra for **2**: IR (ν_{CO}, cm⁻¹, in hexane) 2094 (w), 2061 (vs), 2034 (m), 2023 (m), 2010 (m), 2004 (m), 1985 (m); ¹H NMR (δ, in CDCl₃) 2.48 (s, 3H), -18.26 (s, 2H), -18.58 (s, 2H).

Preparation of Os₄(CO)₁₁(SCH₂CH₂CH₂)(μ-H)₄, 3. A 30.6-mg amount of **2** (0.027 mmol) was dissolved in 20 mL of methylene chloride in a 25-mL three-neck round bottom flask equipped with a stir bar, a reflux condenser, and a nitrogen inlet. A 10-μL amount of thietane (0.14 mmol) was added, and the resulting solution was then stirred at reflux for 2 h. The volatiles were removed in vacuo, and the products were separated by TLC using a hexane/methylene chloride 2/1 solvent mixture to yield 22.3 mg of Os₄(CO)₁₁(SCH₂CH₂CH₂)(μ-H)₄, **3**, 90% yield, and 6.4 mg of unreacted **2**. Spectra for **3**: IR (ν_{CO}, cm⁻¹, in hexane) 2100 (w), 2076 (s), 2061 (vs), 2022 (vs), 2010 (s), 2000 (w); ¹H NMR (δ, in CDCl₃ at 25 °C) 3.81 (t, 4H, J_{H-H} = 8.0 Hz), 2.99 (quintet, br, 2H), -18.76 (s, br, 2H), -20.39 (s, br, 2H); ¹H NMR (δ, in CD₂Cl₂ at -55 °C) 3.88 (m, br), 3.58 (m, br), 3.08 (m, br), 2.96 (m, br), 2.64 (m, br); the hydride region can be interpreted in terms of three isomers: the major isomer [43% based on integration, -18.39 (s, br, 2H), -20.51 (s, br, 2H), minor isomer **A** [36%], -18.98 (s, 1H), -19.39 (s, 2H), -20.96 (s, 1H)], and minor isomer **B** [21%], -18.63 (s, br, 1H), -19.08 (s, br, 1H), -19.97 (s, br, 1H), -22.25 (s, br, 1H)]. The mass spectrum of **3** showed the parent ion at *m/e* = 1148 with an isotope distribution pattern consistent with the presence of four osmium atoms. An ion envelope at 1074 is attributed to M⁺ - thietane ligand. Additional ion envelopes at 1044, 1014, 986, 958, 930, 902, 874, 846, and 818 are attributed to the loss of thietane plus 1-9 CO ligands from the parent ion.

Preparation of Os₄(CO)₁₁(12S3)(μ-H)₄, 4. A 32-mg amount of **2** (0.029 mmol) was dissolved in 20 mL of methylene chloride in a 25-mL three-neck round bottom flask equipped with a stir bar, a reflux condenser, and a nitrogen inlet. A 6.0-mg amount of 12S3 (0.027 mmol) was added, and the resulting solution was then stirred at reflux for 2 h. The volatiles were removed under vacuum, and the products were separated by TLC using a hexane/acetone 3/2 solvent mixture to yield 16.2 mg of Os₄(CO)₁₁(12S3)(μ-H)₄, **4**, 91% yield, and 16.8 mg of **2**. Spectra for **4**: IR (ν_{CO}, cm⁻¹, in hexane) 2097 (w), 2081 (s), 2072 (vs), 2026 (vs), 2013 (s), 1956 (w); ¹H NMR (δ, in CDCl₃ at 25 °C): 3.20 (t, br, 4H), 2.74 (t, 4H, J_{H-H} = 6.2 Hz), 2.64 (t, 4H, J_{H-H} = 6.0 Hz), 2.02 (q, 4H, J_{H-H} = 6.2 Hz), 1.80 (q, 2H, J_{H-H} = 6.3 Hz), -18.83 (s, br, 2H), -20.47 (s, br, 2H); ¹H NMR (δ, in CD₂Cl₂ at -66 °C) 3.6-2.9 (m, br), 2.76 (m, br), 2.61 (m, br), 1.95 (m, br), 1.71 (m, br); the hydride region can be interpreted in terms of three isomers: the major isomer [66% of total based on integration, -18.60 (s, 2H), -20.45 (s, 2H)], minor isomer **A** [17%, -19.08 (s, 1H), -19.99 (s, 2H), -21.37 (s, 1H)], and

minor isomer **B** [17% -18.86 (s, br, 1H), -18.94 (s, br, 1H), -20.25 (s, br, 1H), -22.49 (s, br, 1H)]. Anal. Calcd for **4**: C, 18.54; H, 1.71. Found C, 18.60; H, 1.42. The mass spectrum of **4** showed the parent ion at *m/e* 1296 with an isotope distribution pattern consistent with the presence of four osmium atoms. An ion envelope at 1074 is attributed to M⁺ - 12S3 ligand. Additional ion envelopes at 1044, 1014, 986, 958, 930, 902, 874, 846, 818, 790, and 762 are attributed to the loss of 12S3 plus 1-11 CO ligands from the parent ion.

Preparation of Ru₄(CO)₁₁(SCH₂CH₂CH₂)(μ-H)₄, 5. A 50-mg amount of Ru₄(CO)₁₂(μ-H)₄ (0.067 mmol) was dissolved in 20 mL of methylene chloride in a 25-mL three-neck round bottom flask equipped with a stir bar, a reflux condenser, a dropping funnel, and a nitrogen inlet. A 5.0-μL amount of thietane (0.094 mmol) was added to the solution. A 5.0-mg amount of Me₃NO (0.094 mmol) was dissolved in 3 mL of CH₂Cl₂. This solution was then placed in a dropping funnel and added to the first solution over a 2-min period. The resulting solution was stirred at 25 °C for 1 h. The volatiles were then removed under vacuum, and the product was isolated by TLC using a hexane/methylene chloride 3/2 solvent mixture to yield

27.0 mg of Ru₄(CO)₁₁(SCH₂CH₂CH₂)(μ-H)₄, **5**, 54%. Spectra for **5**: IR (ν_{CO}, cm⁻¹, in hexane) 2097 (w), 2081 (vs), 2071 (vs), 2043 (vs), 2013 (s), 1960 (w); ¹H NMR (δ, in CDCl₃) 3.60 (t, 4H, J_{H-H} = 7.8 Hz), 3.00 (q, 2H, J_{H-H} = 7.8 Hz), -17.19 (s, 3H), -17.81 (s, 1H). Anal. Calcd for **5**: C, 21.26; H, 1.26. Found C, 21.64; H, 1.02.

Preparation of Ru₄(CO)₁₁(12S3)(μ-H)₄, 6. A 51.3-mg amount of Ru₄(CO)₁₂(μ-H)₄ (0.069 mmol) was dissolved in 20 mL of methylene chloride in a 25-mL three-neck round bottom flask equipped with a stir bar, a reflux condenser, a dropping funnel, and a nitrogen inlet. A 15.0-mg amount of 12S3 (0.068 mmol) was added to the solution. A 5.0-mg amount of Me₃NO (0.067 mmol) was dissolved 3 mL of CH₂Cl₂, and this solution was then added to the first solution over a 2-min period via the dropping funnel. The resulting solution was stirred at 25 °C for 1 h. The volatiles were then removed under vacuum, and the product was separated by TLC using a hexane/methylene chloride 1/1 solvent mixture. This was recrystallized from hexane/acetone 2/1 to yield 32.8 mg of Ru₄(CO)₁₁(12S3)(μ-H)₄, **6**, 55%. Spectra for **6**: IR (ν_{CO}, cm⁻¹, in hexane) 2097 (w), 2072 (vs), 2059 (vs), 2028 (vs), 2013 (s), 1958 (w); ¹H NMR (δ, in CDCl₃) 3.01 (t, 4H, J_{H-H} = 6.9 Hz), 2.67 (m, 8H), 2.02 (q, 4H, J_{H-H} = 6.5 Hz), 1.80 (q, 2H, J_{H-H} = 6.4 Hz), -17.16 (s, 1H), -17.21 (s, 3H). Anal. Calcd for **6**: C, 27.71; H, 2.81. Found C, 27.15; H, 2.44.

Catalytic Cyclooligomerizations. All catalytic reactions were performed under nitrogen in 25-mL three-neck round bottom flasks equipped with a stir bar, a reflux condenser, and a nitrogen inlet by using preweighed amounts of catalyst and thietane in the absence of an added solvent at the reflux temperature of the thietane (94 °C). Results of the experiments are listed in Table 1.

A typical procedure was as follows: a 6.0-mL amount of thietane (81 mmol) and a 14.0-mg amount (0.012 mmol) of **3** were added to the 25-mL three-neck round bottom flask. The reaction was heated to reflux and was stirred under nitrogen at this temperature for 24 h. After cooling, the excess thietane was removed in vacuo. The resulting residue weighed 402 mg. An ¹H NMR spectrum was taken of a portion of the residue and showed only two products: 1,5,9-trithiacyclododecane, 12S3⁹ [(δ, in CDCl₃) 2.67 (t, 12H, J_{H-H} = 6.7 Hz), 1.87 (q, 6H, J_{H-H} = 6.7 Hz)] and 1,5,9,13,17,21-hexathiacyclotetrasosane, 24S6¹⁰ [(δ, in CDCl₃) 2.60 (t, 24H, J_{H-H} = 7.2 Hz), 1.84 (q, 12H, J_{H-H} = 7.2 Hz)]. The mole ratio of 12S3/24S6 was 6/1, as determined by NMR integration of their resonances in the

(9) Rawle, S. C.; Admans, G. A.; Cooper, S. R. *J. Chem. Soc., Dalton Trans.* **1988**, 93.

(10) Ochrymowicz, L. A.; Mak, C.-P.; Michna, J. D. *J. Org. Chem.* **1974**, *14*, 2079.

Table 1. Results of the Catalytic Cyclooligomerizations of Thietane by Tetraosmium and Tetraruthenium Cluster Complexes

catalyst ^a	catalyst amount (mg)	reagent amount (mL)	wf of products ^b (mg)	ratio ^c of 12S3/24S6	rcn time (h)	TOF for 12S3 ^d
3	14.0	6.0	373	6/1	24	4.6
3	12.2	6.0	458	4/1	48	3.0
4	12.0	6.0	287	6/1	24	4.7
4^e	14.8	6.0	332	8/1	24	4.7
5^f	14.0	6.0	188	0.7/1	24	0.62
6^f	15.0	6.0	110	0.7/1	24	0.44
none		6.0	29 ^g	2/1	24	

^a All reactions were performed at the boiling point of thietane, 94 °C in the absence of solvent. ^b Only two products were formed, 12S3 and 24S6. This is the combined weight of both products. These weights were corrected for the noncatalyzed decomposition of thietane. ^c These are mole ratios. The NMR integration ratios are half these values, since the molecular weight of 24S6 is twice that of 12S3. ^d TOF = (moles of 12S3)/(moles of catalyst·hr). ^e This reaction was performed under irradiation from a tungsten lamp. ^f Substantial decomposition of the cluster complexes occurred during these reactions. ^g Contains a mixture of several products including 12S3 and 24S6.

reaction mixture. The products were separated by TLC (on AVICEL F microcrystalline cellulose) using a hexane/chloroform/ethyl acetate 2/1/1 solvent mixture as the eluent to give two bands. The first band contained the macrocycle 12S3,⁴ and the second band contained the macrocycle 24S6.⁵ In general, the nonvolatile residues are completely soluble in methylene chloride, which indicates the near absence of polymer formation. The results of these tests are listed in Table 1. The results are corrected for the noncatalytic decomposition of thietane, see below. Reactions performed with the rigorous exclusion of light or under irradiation by a 100-W tungsten lamp produced similar results, see below.

Catalytic Cyclooligomerization of Thietane by 3, "Long Term" Test. Under a nitrogen atmosphere was added 6.0 mL (81.0 mmol) of thietane to a 25-mL three-neck round bottom flask equipped with a stir bar, a reflux condenser, a nitrogen inlet, and 12.0 mg (0.010 mmol) of **3**. The thietane itself served as the solvent in this reaction. The solution was heated to reflux and was stirred under nitrogen at this temperature for 48 h. After the solution had been cooled, the unreacted thietane was removed in vacuo. The resulting residue weighed 516 mg. An ¹H NMR spectrum was taken of a portion of the residue. It showed the presence of only two organic products: the mole/mole ratio of 12S3/24S6 was 4/1 as determined by an NMR integration of the resonances.

Study of the Dependence of the Rate of Catalysis on the Concentration of 4. In a typical procedure a 6.0-mL amount of thietane (81 mmol) was added to a 25-mL three-neck round bottom flask equipped with a stir bar, a reflux condenser, and a nitrogen inlet. An appropriate amount of the catalyst **4** was added under nitrogen. All measurements were made at 93.0 ± 0.1 °C for a period of 1 h and were performed in duplicate. At the end of 1 h, the excess thietane was removed under vacuum, and the amount of product was then determined by weighing the resulting residue and subtracting the preweighed weight of the catalyst. At this short reaction time, the NMR spectra of the residues showed the presence of only one organic product, 12S3. An NMR spectrum recorded in the hydride region at -55 °C could be explained completely as a mixture of **4** (>97% total) and **3** (<3% total).

Catalytic Cyclooligomerization by 4 in the Presence of Light. A 6.0-mL amount of thietane (81 mmol) was added to a 25-mL three-neck round bottom flask equipped with a stir bar, a reflux condenser, a nitrogen inlet, and 14.8 mg (0.011 mmol) of **4**. The reaction was heated to reflux and was stirred under nitrogen at this temperature for 24 h with a 100-W tungsten lamp placed 6 in from the reaction flask. After the

Table 2. Crystallographic Data for Compound 4

compd	4
empirical formula	Os ₄ S ₃ O ₁₁ C ₂₀ H ₂₂
fw	1259.37
cryst syst	monoclinic
lattice param	
<i>a</i> , Å	29.904(6)
<i>b</i> , Å	11.815(2)
<i>c</i> , Å	17.633(3)
β, deg	91.28(2)
<i>V</i> , Å ³	2526(1)
space group	<i>C2/c</i> (No. 15)
<i>Z</i>	8
<i>ρ</i> _{calcd} g/cm ³	2.76
μ(Mo Kα), cm ⁻¹	165.1
temp, (°C)	20
2θ _{max} , (deg)	48.0
no. obsd used (<i>I</i> > 3σ(<i>I</i>))	3384
no. of variables	326
residuals: ^a <i>R</i> , <i>R</i> _w	0.058; 0.055
goodness of fit indicator	2.76
max shift in final cycle	0.00
largest peak in final diff map, e/Å ³	2.57
abs corr	empirical

$$^a R = \frac{\sum |F_{\text{obsd}}| - |F_{\text{calcd}}|}{\sum |F_{\text{obsd}}|}; R_w = \frac{[\sum |F_{\text{obsd}}| (|F_{\text{obsd}}| - |F_{\text{calcd}}|)^2]^{1/2}}{[\sum |F_{\text{obsd}}|^2]^{1/2}}; w = 1/\sigma^2(F_{\text{obsd}}); \text{GOF} = \frac{[\sum |F_{\text{obsd}}| (|F_{\text{obsd}}| - |F_{\text{calcd}}|) / \sigma(F_{\text{obsd}})]}{(n_{\text{data}} - n_{\text{vari}})}$$

solution had been cooled, the excess thietane was removed in vacuo. The resulting residue weighed 361 mg. A ¹H NMR spectrum was taken of a portion of the residue and showed that it consisted entirely of 12S3 and 24S6 in a mole ratio of 8/1.

Catalytic Cyclooligomerization of Thietane with 5 for 1 h. Under a nitrogen atmosphere was added 6.0 mL (81.0 mmol) of thietane to a 25-mL three-neck round bottom flask equipped with a stir bar, a reflux condenser, a nitrogen inlet, and 15.0 mg (0.019 mmol) of **5**. The thietane itself served as the solvent in this reaction. The solution was heated to reflux and was stirred under nitrogen at this temperature for 1 h. After cooling, the unreacted thietane was removed in vacuo. The resulting residue weighed 45 mg. An ¹H NMR spectrum was taken of the entire residue. The spectrum showed the presence of only two organic products, 12S3 and 24S6 in a mole ratio of 0.7/1 as determined by an NMR integration of the resonances. It was also noted that no hydride resonances remained, indicating that there were no hydride-containing clusters present in solution. The products of the reaction were separated by TLC using a hexane/methylene chloride 2/1 solvent mixture to yield 3.0 mg of **5**. No other carbonyl containing products could be identified.

Noncatalyzed Thermal Transformations of Thietane. A 6.0-mL amount of thietane (81 mmol) was added to a 25-mL round bottom flask equipped with a stir bar, a reflux condenser, and a nitrogen inlet. The liquid was brought to reflux and was maintained at this temperature with stirring for 24 h. After cooling, the volatiles were removed in vacuo at room temperature. The residue weighed 29 mg. A ¹H NMR spectrum of the residue exhibited the following resonances (δ, in CDCl₃): 5.79 (m, unknown), 5.10 (m, unknown), 3.66 (m, unknown), 3.08 (t, unknown), 2.64 (t, 12S3), 2.57 (t, 24S6), 1.84 (quintet, 12S3+24S6), 1.26 (m, unknown), 0.94 (t, unknown), and 0.02 (s, silicone grease). The mole ratio of 12S3/24S6 was 2/1 as determined by NMR integration. The products were separated by TLC using hexane/CH₂Cl₂ 2/1 solvent mixture as the eluent to give three bands: the first band contained silicone grease (4.8 mg) from the joints of the reaction equipment, the second band contained the macrocycle 12S3 (4 mg), and the third band (9 mg) consisted of a mixture 24S6 and some of the unidentifiable organic products.

Crystallographic Analyses. Light yellow crystals of **4** suitable for X-ray diffraction analysis were grown from solution in a 2/1 CH₂Cl₂/hexane solvent mixture by slow evaporation

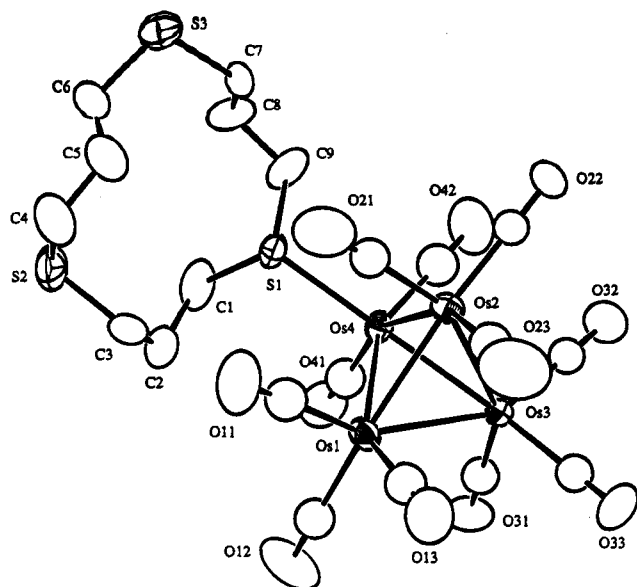


Figure 1. ORTEP diagram of $\text{Os}_4(\text{CO})_{11}(12\text{S3})(\mu\text{-H})_4$, **4**, showing 50% probability thermal ellipsoids.

of solvent at 25 °C. The crystal used in intensity measurements was mounted in a thin-walled glass capillary. Diffraction measurements were made on a Rigaku AFC6S fully automated four-circle diffractometer using graphite-monochromated Mo K α radiation. The unit cells were determined and refined from 15 randomly selected reflections obtained by using the AFC6S automatic search, center, index, and least-squares routines. Crystal data, data collection parameters, and results of these analyses are listed in Table 2. All data processing was performed on a Digital Equipment Corp. VAXstation 3520 computer by using the TEXSAN structure-solving program library obtained from the Molecular Structure Corp., The Woodlands, TX. Neutral atom scattering factors were calculated by the standard procedures.^{11a} Anomalous dispersion corrections were applied to all non-hydrogen atoms.^{11b} Lorentz-polarization (Lp) and absorption corrections were applied in each analysis. Full matrix least-squares refinements minimized the function: $\sum_{hkl} w(|F_o| - |F_c|)^2$, where $w = 1/\sigma(F)^2$, $\sigma(F) = \sigma(F_o^2)/2F_o$, and $\sigma(F_c^2) = [\sigma(I_{\text{raw}})^2 + (0.02(I_{\text{net}})^2)^{1/2}/Lp]$.

Compound **4** crystallized in the monoclinic crystal system. The space group $P2_1/n$ was established on the basis of the patterns of systematic absences observed during the collection of data. The structure was solved by a combination of direct methods (MITHRIL) and difference Fourier syntheses. All atoms heavier than carbon were refined with anisotropic thermal parameters. The carbon atoms in the 12S3 ring were also refined anisotropically. The positions of the hydrogen atoms on the 12S3 ligand were calculated by assuming idealized geometries and C-H = 0.95 Å. Their contributions were added to the structure factor calculations, but their positions were not refined. The hydride ligands were not located in the analysis and were ignored.

Results

Treatment of the compound $\text{Os}_4(\text{CO})_{11}(\text{NCMe})(\mu\text{-H})_4$ with thietane and 12S3 produced the compounds $\text{Os}_4(\text{CO})_{11}(\text{SCH}_2\text{CH}_2\text{CH}_2)(\mu\text{-H})_4$, **3**, and $\text{Os}_4(\text{CO})_{11}(12\text{S3})(\mu\text{-H})_4$, **4**, in the yields 90% and 91%, respectively. Both compounds were characterized by a combination of IR and ¹H NMR spectroscopy. Compound **4** was also characterized by a single-crystal X-ray diffraction analy-

Table 3. Positional Parameters and $B(\text{eq})$ Values (Å^2) for **4**

atom	x	y	z	$B(\text{eq})$
Os(1)	0.68705(4)	0.07705(7)	0.20287(5)	3.23(4)
Os(2)	0.65259(4)	-0.04221(7)	0.07589(5)	3.01(4)
Os(3)	0.62431(3)	-0.11109(6)	0.22866(4)	2.62(4)
Os(4)	0.58932(3)	0.08826(7)	0.16731(4)	2.61(4)
S(1)	0.5791(2)	0.2569(4)	0.0911(3)	3.8(3)
S(2)	0.6302(4)	0.5849(5)	0.0789(4)	6.9(5)
S(3)	0.5552(3)	0.4370(6)	-0.1490(3)	6.7(5)
O(11)	0.729(1)	0.259(2)	0.108(1)	10(2)
O(12)	0.699(1)	0.192(2)	0.356(1)	15(2)
O(13)	0.7756(7)	-0.055(2)	0.210(1)	9(1)
O(21)	0.6814(9)	0.139(2)	-0.038(1)	11(2)
O(22)	0.5967(9)	-0.183(1)	-0.036(1)	9(1)
O(23)	0.737(1)	-0.176(2)	0.062(1)	15(2)
O(31)	0.5928(6)	-0.052(1)	0.3861(8)	5(1)
O(32)	0.5430(7)	-0.250(1)	0.190(1)	7(1)
O(33)	0.6815(7)	-0.316(1)	0.278(1)	7(1)
O(41)	0.5485(8)	0.192(2)	0.3076(9)	7(1)
O(42)	0.5037(7)	-0.027(2)	0.120(1)	9(1)
C(1)	0.568(1)	0.380(2)	0.150(1)	5(1)
C(2)	0.612(1)	0.421(2)	0.186(1)	7(2)
C(3)	0.650(1)	0.459(2)	0.130(1)	6(2)
C(4)	0.659(1)	0.568(2)	-0.010(1)	6(2)
C(5)	0.633(1)	0.495(2)	-0.065(1)	5(1)
C(6)	0.587(1)	0.534(2)	-0.090(1)	7(2)
C(7)	0.547(1)	0.317(2)	-0.086(1)	4(1)
C(8)	0.522(1)	0.340(2)	-0.019(1)	5(1)
C(9)	0.528(1)	0.251(2)	0.038(1)	5(1)
C(11)	0.713(1)	0.191(2)	0.142(1)	5.7(6)
C(12)	0.694(1)	0.154(2)	0.303(1)	5.1(6)
C(13)	0.741(1)	-0.006(2)	0.207(1)	5.4(6)
C(21)	0.669(1)	0.072(2)	0.003(1)	4.9(6)
C(22)	0.6164(9)	-0.130(2)	0.007(1)	3.8(5)
C(23)	0.706(1)	-0.128(2)	0.064(1)	5.7(6)
C(31)	0.6041(9)	-0.074(2)	0.327(1)	4.2(5)
C(32)	0.5735(9)	-0.199(2)	0.204(1)	3.9(5)
C(33)	0.658(1)	-0.240(2)	0.263(1)	4.2(5)
C(41)	0.567(1)	0.150(2)	0.255(1)	4.8(6)
C(42)	0.536(1)	0.015(2)	0.139(1)	5.4(6)

Table 4. Intramolecular Distances for **4**^a

Os(1)-Os(2)	2.821(1)	Os(4)-C(41)	1.84(2)
Os(1)-Os(3)	2.951(1)	Os(4)-C(42)	1.88(3)
Os(1)-Os(4)	2.978(1)	S(1)-C(1)	1.82(2)
Os(1)-C(11)	1.89(3)	S(1)-C(9)	1.78(3)
Os(1)-C(12)	2.00(2)	S(2)-C(3)	1.82(3)
Os(1)-C(13)	1.89(3)	S(2)-C(4)	1.81(3)
Os(2)-Os(3)	2.956(1)	S(3)-C(6)	1.80(3)
Os(2)-Os(4)	2.948(1)	S(3)-C(7)	1.81(2)
Os(2)-C(21)	1.94(2)	O-C(av)	1.14(3)
Os(2)-C(22)	1.92(2)	C(1)-C(2)	1.54(5)
Os(2)-C(23)	1.90(3)	C(2)-C(3)	1.57(4)
Os(3)-Os(4)	1.786(1)	C(4)-C(5)	1.51(4)
Os(3)-C(31)	1.90(2)	C(5)-C(6)	1.50(4)
Os(3)-C(32)	1.88(2)	C(7)-C(8)	1.44(3)
Os(3)-C(33)	1.92(2)	C(8)-C(9)	1.47(3)
Os(4)-S(1)	2.419(5)		

^a Distances are in angstroms. Estimated standard deviations in the least significant figure are given in parentheses.

sis. An ORTEP diagram of the molecular structure of **3** is shown in Figure 1. Final atomic positional parameters are listed in Table 3. Selected intramolecular distances and angles are listed in Tables 4 and 5, respectively. The molecule is structurally similar to the compound $\text{Os}_4(\text{CO})_{11}[\text{P}(\text{OMe})_3](\mu\text{-H})_4$, **7**, which has been characterized structurally both by X-ray and neutron diffraction analysis.¹² Both compounds contain closed tetrahedral clusters of four osmium atoms. In **7** the hydride ligands were structurally located and refined. In **4** the hydride ligands were not located, but four of

(11) (a) *International Tables for X-ray Crystallography*; Kynoch Press: Birmingham, England, 1975; Vol. IV, Table 2.2B, pp 99-101. (b) *Ibid.*, Table 2.3.1, pp 149-150.

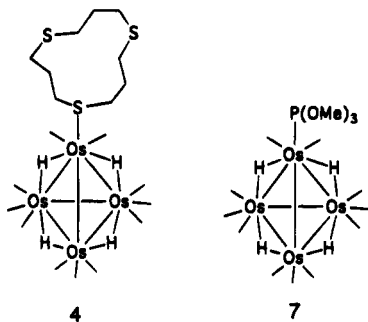
(12) Wei, C.-Y.; Garlaschelli, L.; Bau, R. *J. Organomet. Chem.* **1981**, *213*, 63.

Table 5. Intramolecular Bond Angles for 4^a

Os(2)–Os(1)–Os(3)	61.56(3)	S(1)–Os(4)–C(42)	97.9(8)
Os(2)–Os(1)–Os(4)	61.04(4)	Os(4)–S(1)–C(1)	111.1(8)
Os(3)–Os(1)–Os(4)	56.06(3)	Os(4)–S(1)–C(9)	110.7(8)
Os(1)–Os(2)–Os(3)	61.38(3)	C(1)–S(1)–C(9)	100(1)
Os(1)–Os(2)–Os(4)	62.12(4)	C(3)–S(2)–C(4)	101(2)
Os(3)–Os(2)–Os(4)	56.32(3)	C(6)–S(3)–C(7)	103(1)
Os(1)–Os(3)–Os(2)	57.06(3)	S(1)–C(1)–C(2)	109(2)
Os(1)–Os(3)–Os(4)	62.48(4)	C(1)–C(2)–C(3)	117(2)
Os(2)–Os(3)–Os(4)	61.71(3)	S(2)–C(3)–C(2)	109(2)
Os(1)–Os(4)–Os(2)	56.84(3)	S(2)–C(4)–C(5)	112(2)
Os(1)–Os(4)–Os(3)	61.47(3)	C(4)–C(5)–C(6)	118(3)
Os(1)–Os(4)–S(1)	105.3(2)	S(3)–C(6)–C(5)	116(2)
Os(2)–Os(4)–Os(3)	61.98(3)	S(3)–C(7)–C(8)	116(2)
Os(2)–Os(4)–S(1)	101.6(2)	C(7)–C(8)–C(9)	112(2)
Os(3)–Os(4)–S(1)	162.5(2)	S(1)–C(9)–C(8)	115(2)
S(1)–Os(4)–C(41)	95.7(8)	Os–C–O(av)	175(2)

^a Angles are in degrees. Estimated standard deviations in the least significant figure are given in parentheses.

the osmium–osmium bonds are significantly longer than the other two: Os(1)–Os(3) = 2.951(1) Å, Os(1)–Os(4) = 2.978(1) Å, Os(2)–Os(3) = 2.956(1) Å, and Os(2)–Os(4) = 2.948(1) Å versus Os(1)–Os(2) = 2.821(1) Å and Os(3)–Os(4) = 2.786(1) Å. These long bonds exhibit the same disposition as the hydride-bridged metal–metal bonds in **7** which are also similarly elongated.¹² Accordingly, it is assumed that the hydride ligands in **4** bridge the four long metal–metal bonds.



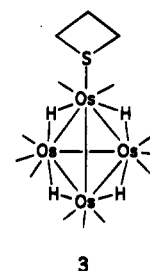
The 12S3 ligand is coordinated to only one metal atom of the cluster using only one of its three sulfur atoms, S(1), Os(4)–S(1) = 2.419(5) Å. The conformation of the 12S3 ligand is similar to that observed for the free molecule⁹ and other complexes in which only one of the sulfur atoms serves as a site for metal binding.^{5,9,13}

At 25 °C the ¹H NMR spectrum of **4** exhibits two very broad strongly shielded resonances at δ = –18.83 (s, 2H) and δ = –20.47 (s, 2H) due to the hydride ligands. This is consistent with the solid state structure. The resonances displayed by the 12S3 ligand are also consistent with the solid state structure: 3.20 (t, br, 4H), 2.74 (t, 4H, $J_{\text{H-H}}$ = 6.2 Hz), 2.64 (t, 4H, $J_{\text{H-H}}$ = 6.0 Hz), 2.02 (q, 4H, $J_{\text{H-H}}$ = 6.2 Hz), 1.80 (q, 2H, $J_{\text{H-H}}$ = 6.3 Hz). Interestingly, when the temperature is lowered, the hydride resonances broaden and then resolve into a new pattern, which indicates that the molecule exists in solution as a mixture of at least three isomers. For example, the spectrum of **4** at –66 °C exhibits nine resonances in the hydride region. The major isomer (66% of total based on integration) exhibits two resonances, –18.60 and –20.45 ppm, of equal intensity and

(13) (a) Edwards, A. J.; Johnson, B. F. G.; Khan, F. K.; Lewis, J.; Raithby, P. R. *J. Organomet. Chem.* **1992**, *426*, C44. (b) Blower, P. J.; Clarkson, J. A.; Rawle, S. C.; Hartman, J. R.; Wolf, R. E.; Yagbasan, R.; Bott, S. G.; Cooper, S. R. *J. Chem. Soc., Dalton Trans.* **1989**, *23*, 4040.

is attributed to the isomer as observed in the solid state. There are minor isomers **A** (17% of total), which exhibits three resonances [–19.08 (1H), –19.99 (2H), –21.37 (1H)], and **B** (17% of total), which exhibits four resonances [–18.86 (s, br, 1H), –18.94 (s, br, 1H), –20.25 (s, br, 1H), –22.49 (s, br, 1H)]. Without additional data it is not possible to identify these isomers uniquely, but it is believed that they are formed by different arrangements hydride ligands about the six metal–metal bonds. These isomers are dynamically averaged at room temperature as a result of rapid hydride ligand shifts between the different metal–metal bonds. Facile hydride ligand shifts in related tetraruthenium tetrahydride carbonyl cluster complexes have been observed previously.¹⁴

The IR spectrum and ¹H NMR spectrum of **3** in the hydride ligand region are very similar to those of **4**. Accordingly, it is proposed that the structure of **3** is



analogous to that of **4** with the substitution of a thietane ligand in the position of the 12S3 ligand. Compound **3** also exists in solution as a mixture of isomers similar to those found for **4**. This was confirmed by examining the ¹H NMR at –55 °C, which indicated three isomers: the major isomer 43%, with resonances at –18.39 and –20.51 ppm] and two lesser isomers, **A** 36%, [–18.98 (1H), –19.39 (2H), and –20.96 (1H) ppm] and **B** [(21%, –18.63 (1H), –19.08 (1H), –19.97 (1H), –22.25 (1H) ppm].

The reaction of Ru₄(CO)₁₂(μ-H)₄ with thietane and 12S3 in the presence of Me₃NO to assist in decarbonylation provided the new compounds Ru₄(CO)₁₁(S(CH₂–CH₂CH₂)(μ-H)₄, **5**, 54%, and Ru₄(CO)₁₁(12S3)(μ-H)₄, **6**, 55%, respectively. On the basis of the strong similarities of the IR spectra of these compounds to the osmium compounds **3** and **4** and to known monophosphine- and monophosphite-substituted derivatives of Ru₄(CO)₁₂(μ-H)₄,¹⁶ it can be safely concluded that all of these compounds have structures about the clusters that are analogous to that of **4**.

Catalytic Cyclooligomerization of Thietane.

When solutions of **3** or **4** were dissolved in thietane in the absence of solvent and then heated to reflux, the macrocycles 12S3 and 24S6 were formed catalytically. No other cyclooligomers were formed. The results are

(14) (a) Churchill, M. R.; Lashewycz, R. A.; Shapley, J. R.; Richter, S. I. *Inorg. Chem.* **1980**, *19*, 1277. (b) Shapley, J. R.; Richter, S. I.; Churchill, M. R.; Lashewycz, R. A. *J. Am. Chem. Soc.* **1977**, *99*, 7384. (c) Knox, S. A. R.; Kaesz, H. D. *J. Am. Chem. Soc.* **1971**, *93*, 4594.

(15) Laine, R. M. *J. Mol. Catal.* **1982**, *14*, 137. (b) Hilal, H. S.; Jondi, W.; Khalaf, S.; Abu-Halawa, R. *J. Organomet. Chem.* **1993**, *452*, 161. (c) Hilal, H. S.; Khalaf, S.; Jondi, W. *J. Organomet. Chem.* **1993**, *452*, 167.

(16) Bruce, M. I. *Comprehensive Organometallic Chemistry*; Wilkinson, G., Stone, F. G. A., Abel, E., Eds.; Pergamon, Oxford, 1982; Chapter 32.6, Table 2, p 894.

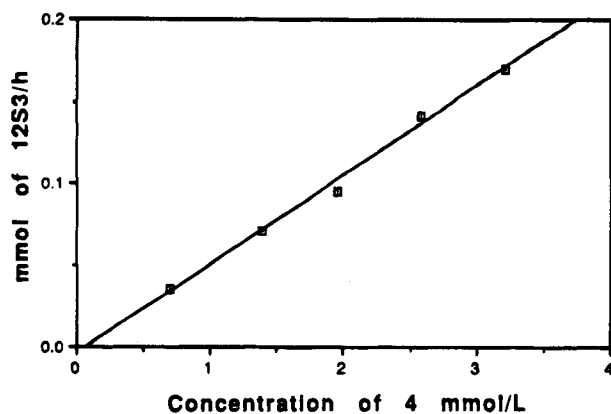


Figure 2. Plot of the rate of formation of 12S3 as a function of the concentration of **2**. Rates were determined after the first 1 h of reaction time.

listed in Table 1. After a period of 1 h, only 12S3 was observed. After a period of 24 h, both 12S3 and 24S6 were observed, but the amount of 12S3 was greater than six times the amount of 24S6. After a period of 48 h, the mole ratio 12S3/24S6 was about 4/1; thus, it appears that the amount of 24S6 does increase relative to that of the 12S3 as the reaction progresses. The catalytic activity and selectivity for 12S3 and 24S6 formation are virtually the same for **3** and **4**. The average turnover frequency (TOF) for the formation of 12S3 is about 4.7/h in the 24-h reaction period. A study of the rate of reaction as a function of the concentration of **4** showed a linear dependence in the concentration range $(0.7-3.2) \times 10^{-3}$ M, see Figure 2. This is consistent with the catalyst being a tetranuclear species and argues against a process involving cluster fragmentation.¹⁵ After one of the 1 h tests, the thietane solvent was removed under vacuum and an ¹H NMR spectrum of the residue was recorded in the hydride region at -55 °C. All of the observed resonances could be explained in terms of the presence of two compounds: **3** (<3% of total) and **4** (>97% of total).

The catalytic activity of **5** and **6** for 12S3 and 24S6 formation was examined under similar conditions. These compounds also produce the two macrocycles 12S3 and 24S6 catalytically, but the activity is considerably lower and the formation of 12S3 is much lower relative to that of 24S6, 0.7/1 over a 24-h period.

For completeness, the noncatalyzed thermal decomposition of thietane at its boiling point was also investigated. Indeed, some 12S3 and 24S6 is produced in the absence of added catalysts, but the level of production (≈ 4 mg of each over a 24-h period) is so low as to be almost insignificant. Nevertheless, the results listed in Table 1 have been corrected for this noncatalytic "background" production of 12S3 and 24S6. Small amounts of a few additional compounds that have not yet been fully characterized were also observed in the noncatalyzed decomposition.

A proposed mechanism for the catalytic cyclotrimerization of thietane by **3** and **4** is shown in Scheme 1. The reaction is believed to begin by a ring-opening addition of the sulfur atom of an uncoordinated molecule of thietane to one of the methylene groups attached to sulfur of the coordinated thietane ligand in **3**, step A. The thietane ligand in **3** could be activated toward this nucleophilic addition by removal of some of the electron density from the sulfur atom by the osmium atom to

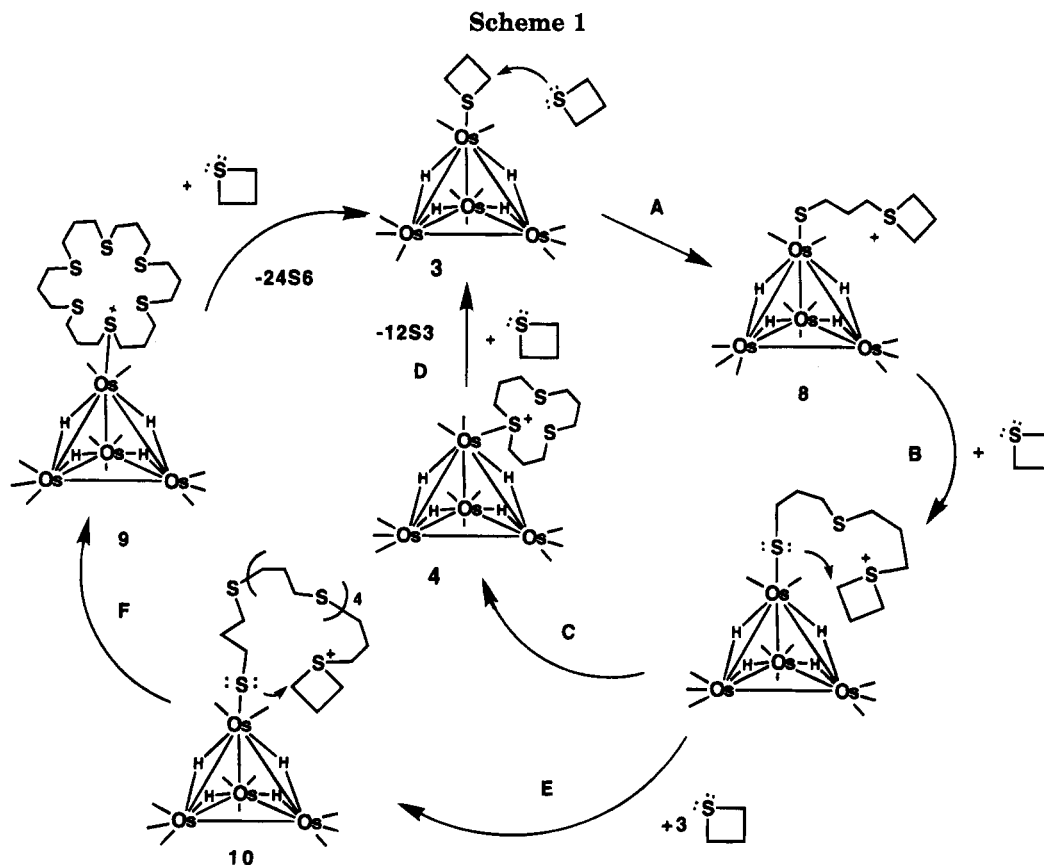
which it is coordinated. This would lead to the formation of a partial positive charge at the sulfur atom and also to a lesser extent at the neighboring carbon atoms. This is apparently sufficient to allow this nucleophilic addition step to proceed and would yield a zwitterionic intermediate, such as **8**. The negatively charged terminally coordinated thiolate sulfur atom is linked to a positively charged thietanium ring via a trimethylene chain. Similar nucleophilic ring-opening reactions have been observed for thietane ligands in bridging coordination modes.²⁻⁴ The dangling thietanium group should be sufficiently reactive to react spontaneously with additional uncoordinated thietane molecules by ring-opening additions, step B. The cationic ring-opening polymerization of thietanes by this mechanism is well known.¹⁷ Polymerization could ensue, but we have found that cyclization reactions occur instead. These may occur in the following way. After the addition of a second free molecule of thietane, cyclization occurs by addition of the coordinated thiolato sulfur atom to one of the α -carbon atoms in the thietanium ring, step C, and leads to the 12S3 complex **4**. The tendency toward cyclization in these complexes is probably enhanced by the zwitterionic nature of the intermediates, which should tend to keep the head and tail of the growing chain proximate to one another. The catalyst **3** can be regenerated from **4** by the simple substitution of the 12S3 ligand by thietane, step D. The catalysis observed by **4** is explained by this same catalytic cycle since **4** is a species in the cycle, and indeed the catalytic activity of **4** is not significantly different from that of **3**, as expected. This mechanism is similar to that proposed

for the cyclooligomerization of thietane by $\text{Re}_2(\text{CO})_9(\text{SCH}_2\text{CH}_2\text{CH}_2)_2$ but differs from that of $\text{Re}_3(\text{CO})_{10}[\mu\text{-SCH}_2\text{CH}_2\text{CH}_2(\mu\text{-H})_3]^4$ where the cyclization occurred at a thioether sulfur site and not at the thiolato sulfur atom. In the latter case the thiolato sulfur atom bridged two metal atoms and was evidently not sufficiently nucleophilic nor as available for the ring-closing cyclization step as it is for the terminally coordinated thiolato species involved in the mechanisms of **3** and $\text{Re}_2(\text{CO})_9(\text{SCH}_2\text{CH}_2\text{CH}_2)$. In one of our tests a sample of the reaction mixture was analyzed by ¹H NMR spectroscopy. Interestingly, all the resonances observed in the hydride region of the spectrum could be explained as a mixture of **3** and **4**. This indicates these catalytic reactions are very clean.

The formation of 24S6 could be explained by a mechanism similar to that shown for 12S3 by allowing the addition of 4 equiv of thietane to the intermediate, a combination of steps B and E, prior to the cyclization, step F, which would lead to 24S6 osmium cluster complex **9**, which has not yet been observed (see Scheme 1). We have not yet been able to determine why the formation of 24S6 is increased relative to that of 12S3 as the length of the reaction period is increased. In our study of the cyclooligomerization of thietane by

$\text{Re}_2(\text{CO})_9(\text{SCH}_2\text{CH}_2\text{CH}_2)$, we found that light appeared to promote the formation of 24S6,⁵ however, for the

(17) (a) Goethals, E. J. *Makromol. Chem., Macromol. Symp.* **1991**, 42/43, 51. (b) Goethals, E. J.; Drijvers, W.; van Ooteghem, D.; Buyle, A. M. *J. Macromol. Sci.-Chem.* **1973**, A7, 1375. (c) Goethals, E. J.; Florquin, S. M. *Makromol. Chem.* **1981**, 182, 3371.



osmium compounds, we found that light did not promote the formation of 24S6. One possible explanation for the increase in 24S6 as the reaction progresses would be that the 12S3 ligand in complex 4 could also undergo a ring-opening addition of thietane which could lead to an intermediate such as 10 in Scheme 1 and then to 24S6 by a subsequent cyclization.

The catalysis by 5 and 6 can be explained by a similar mechanism involving tetraosmium clusters. However, after a 24-h period of catalysis, only 3.0 mg of 5 from a starting quantity of 15.0 mg could be recovered. The lower activity and lower selectivity of the ruthenium complexes for cyclooligomerization may thus be attributed to degradation of the cluster. Much of the cyclooligomerization activity from the solutions of 5 could be occurring from cluster fragments that have not yet been identified.

It is notable that these tetraosmium clusters produce the macrocycles catalytically whereas Os₃(CO)₁₀[μ-SCH₂-CMe₂CH₂] did not.⁶ The lack of macrocycle formation by Os₃(CO)₁₀[μ-SCH₂CMe₂CH₂] can be attributed to reactions of the growing polymer at the metal atoms with the involvement of metal-metal bond cleavage processes. Such reactions may be inhibited by the

bridging hydride ligands in 3 and 4. It is believed that ability of the rhenium cluster, Re₃(CO)₁₀(μ-SCH₂CH₂-CH₂)(μ-H)₃, to produce catalytic cyclooligomerization of thietane without cluster fragmentation is due in part to the protection of the metal-metal bonds in this complex by the bridging hydride ligands.⁴

Finally, it should be noted that, although the catalytic activity of the complexes appears to involve intact cluster complexes at all stages of the process, in fact, all of the transformations appear to occur at the site of a single metal atom. Thus, it seems reasonable to expect that some mononuclear metal complexes should also be capable of performing this catalysis by a similar mechanism.

Acknowledgment. These studies were supported by the Division of Chemical Sciences of the Office of Basic Energy Sciences of the U.S. Department of Energy.

Supporting Information Available: Tables of interatomic distances and angles and anisotropic thermal parameters for the structure analysis (8 pages). Ordering information is given on any current masthead page.

OM950324+

Synthesis and Reactions of an (Aryloxy)titanium(IV) Hydride

Heinrich Nöth* and Martin Schmidt

*Institute of Inorganic Chemistry, University of Munich, Meiserstrasse 1,
D-80333 München, Germany*

Received April 14, 1995[®]

Attempts to prepare $(\text{ArO})_2\text{Ti}(\text{BH}_4)_2$, **6** (Ar = 2,6-diisopropylphenyl), from $(\text{ArO})_2\text{TiCl}_2$, **4**, and LiBH_4 failed due to its decomposition by ligand exchange and reduction into $(\text{ArO})_3\text{Ti}(\mu_3\text{-BH}_4)$, **7**, and $[(\text{ArO})\text{Ti}(\mu_3\text{-}(\text{BH}_4)_2)]_2$, **8**. Reaction of **8** with trimethylphosphine gives monomeric $(\text{ArO})\text{Ti}(\mu_2\text{-}(\text{BH}_4)_2)\cdot 2\text{PMe}_3$, **9**. Trimethylphosphine removes a BH_3 group from **7** with formation of the hydride $(\text{ArO})_3\text{TiH}\cdot\text{PMe}_3$, **10**. This adduct releases PMe_3 readily in solution, forming an equilibrium with $(\text{ArO})_3\text{TiH}$ which is attained at high rate. In spite of the weakly bonded PMe_3 the unsupported hydride $(\text{ArO})_3\text{TiH}$ could not be obtained from its PMe_3 adduct nor by olefin elimination from $(\text{ArO})_3\text{TiCMe}_3$, **12**. Hydrotitanation of alkynes to vinyltitanium compounds $(\text{ArO})_3\text{TiCH}=\text{CHR}$ proceeds readily and regioselectively if polar alkynes such as $\text{PhC}\equiv\text{CEMe}_3$ (E = Si, Sn) are used. The molecular structures of **7**–**10** and **12** were determined by X-ray crystallography.

Introduction

Compounds of titanium(IV) play an important role in organic synthesis. They are used as reagents as well as catalysts. Outstanding examples are the McMurry reaction¹ for the formation of C=C double bonds from ketones, or the epoxidation of olefinic bonds according to Sharpless,² or, as a more recent example, the Seebach reaction,³ which allows an enantioselective nucleophilic addition to carbonyl groups. It is the Sharpless reaction in particular which demonstrates the possibility to fix chiral alkoxides at the titanium atom in such a manner that the metal atom still remains the reactive center which influences the course of the reactions.

In addition, it is well-known that hydroborations can be mediated by titanium compounds,⁴ and this suggests that titanium hydroborates may be the reactive species. For this reason we investigated ways to make such compounds readily available as reducing reagents with specific properties. Moreover, it is also a challenge to prepare mononuclear and polynuclear titanium hydrides unsupported by Cp or Cp* ligands.⁵ One possible way of doing so is to use amido or RO substituents, and the present work describes some of our efforts to prepare titanium(IV) hydrides of the type $(\text{RO})_3\text{TiH}$ which might be enantioselective reducing reagents if chiral substituents R are part of the RO group.

To our knowledge there exist only a few representatives of titanium(IV) tetrahydroborates which are also characterized by X-ray methods. One of those is the bis-

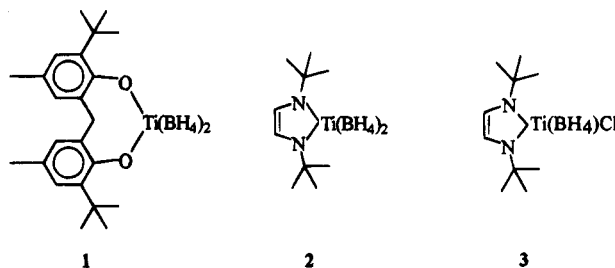


Figure 1.

(aryloxy)titanium(IV) bis(tetrahydroborate) **1**,⁶ and others are the bis(amido)titanium(IV) bis(tetrahydroborate) **2** and the bis(amido)titanium(IV) chlorotetrahydroborate **3**⁷ (Figure 1). The common feature of these compounds is that the titanium(IV) atom is part of a ring system.

Results

(Aryloxy)titanium(IV) tetrahydroborates. An obvious route to (aryloxy)titanium(IV) tetrahydroborates is the metathesis of (aryloxy)titanium(IV) chlorides with an alkali metal tetrahydroborate. The titanium chlorides are readily prepared from TiCl_4 and a phenol,⁸ and we synthesized $(2,6\text{-}i\text{-Pr}_2\text{C}_6\text{H}_3\text{O})_2\text{TiCl}_2$, **4**, by this route in boiling benzene. Reaction of **4** with LiBH_4 in ether leads in the first step to the titanium(IV) chloride tetrahydroborate, **5**, which can be readily recognized in an ^{11}B NMR spectrum at $\delta -9.9$. Further reaction of **5** with LiBH_4 is expected to form $(\text{ArO})_2\text{Ti}(\text{BH}_4)_2$, **6**. As the reaction according to eq 2 proceeds a new ^{11}B NMR signal at $\delta -15.6$ appears, replacing the signal at -9.9 ppm. In addition, diborane can be

(6) Corazza, F.; Floriani, C.; Chiesi-Villa, A.; Guastini, C. *Inorg. Chem.* **1991**, *30*, 145–148.

(7) Herrmann, W. A.; Denk, M.; Scherer, W.; Klingan, F. R. *J. Organomet. Chem.* **1993**, *444*, C21–C24.

(8) Shah, A.; Singh, A.; Mehrotra, R. C. *Indian J. Chem.* **1993**, *32A*, 632. Malhotra, K. C.; Sharma, N.; Bhatt, S. S.; Chaudhry, S. C. *Polyhedron* **1992**, *11*, 2065–2068. Duff, A. W.; Kamarudin, R. A.; Lappert, M. F.; Norton, R. T. *J. Chem. Soc., Dalton. Trans.* **1986**, 489–498.

[®] Abstract published in *Advance ACS Abstracts*, July 15, 1995.

(1) Mc Murry, J. E.; Fleming, M. P. *J. Am. Chem. Soc.* **1974**, *96*, 4708. Betschard, C.; Seebach, D. *Chimia* **1989**, *43*, 39–49.

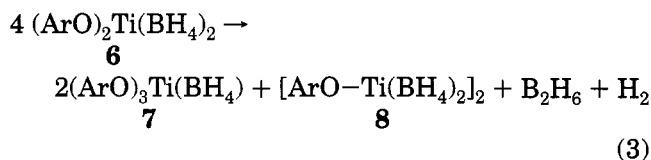
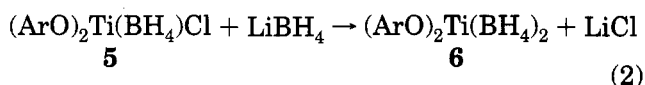
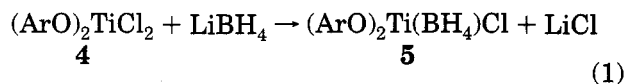
(2) Katsuki, T.; Sharpless, K. B. *J. Am. Chem. Soc.* **1980**, *102*, 5974–5976.

(3) Seebach, D.; Behrend, L.; Felix, D. *Angew. Chem.* **1991**, *103*, 1383–1385. *Angew. Chem., Int. Ed. Engl.* **1991**, *30*, 1008.

(4) Burgess, K.; van der Donk, W. A. *Organometallics* **1994**, *13*, 3616–3620.

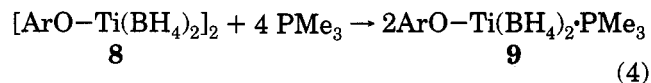
(5) (a) Troyanov, S. I.; Antropiusova, H.; Mach, K. *J. Organomet. Chem.* **1992**, *427*, 49–55. (b) Bercaw, J. E.; Marvich, R. H.; Bell, L. G.; Brintzinger, H. H. *J. Am. Chem. Soc.* **1972**, *94*, 1219–1234.

detected in the solution ($\delta(^{11}\text{B}) + 17$ ppm). Two compounds crystallize from the brown solution at -18 °C. The first and less soluble compound proved to be $(2,6\text{-}^i\text{Pr}_2\text{C}_6\text{H}_3\text{O})_3\text{TiBH}_4$, **7**; the second, more soluble compound is the turquoise-colored $(2,6\text{-}^i\text{Pr}_2\text{C}_6\text{H}_3\text{O})\text{Ti}(\text{BH}_4)_2$, **8**. Therefore, ligand exchange and reduction set in during the course of the reaction. These processes begin after the formation of compound **5**, and it is feasible that this starts with the formation of $(2,6\text{-}^i\text{Pr}_2\text{C}_6\text{H}_3\text{O})_2\text{Ti}(\text{BH}_4)_2$, **6**, as depicted in eqs 1–3. This would comply with previous findings that reduction of Ti(IV) to Ti(III) sets in after formation of titanium(IV) bis(tetrahydroborates) in reactions of titanium(IV) alkoxides with diborane in THF.⁹



The fact that a ^{11}B NMR signal can be detected for compound **8** points to the conclusion that this is not a monomeric but most likely a dimeric species of type $[\text{ROTi}(\text{BH}_4)_2]_2$ with bridging RO groups. However, no BH coupling can be observed, most likely due to residual paramagnetism.¹⁰ Analysis of the IR bands in the region of the BH stretching modes reveals that the BH_4 groups are μ_3 -bonded (via three hydrogen bridges) to the metal atom, both in compound **7** and in **8**.

Treatment of compound **8** with trimethylphosphine according to eq 4 yields the adduct **9** for which no ^{11}B



NMR signal could be recorded. This is in consonance with a mononuclear Ti(III) tetrahydroborate like $\text{Ti}(\text{BH}_4)_3 \cdot 2\text{PMe}_3$.¹¹

An X-ray structure determination of **8** confirmed the dimeric nature of this compound. Figure 2 depicts the molecular unit which has a crystallographically imposed C_i symmetry. There are two significant features of this structure. The first one is the planar four-membered Ti_2O_2 ring with an O–Ti–O bond angle of 81.29° . The analogous values for a dimeric Ti(IV) compound with a Ti_2O_2 core $[\text{Me}_2(^t\text{Bu}_3\text{CO})\text{Ti}^{\text{IV}}\mu(\text{OMe})]_2$ amount to 70.6° with a titanium to titanium distance of $3.290(3)$ Å.¹² This is most likely a consequence of the (partial) spin pairing of the d^1 electrons in the dimeric Ti(III) compound, **8**, and results in a distance between the two Ti atoms of $3.041(1)$ Å. These data fit very well with those

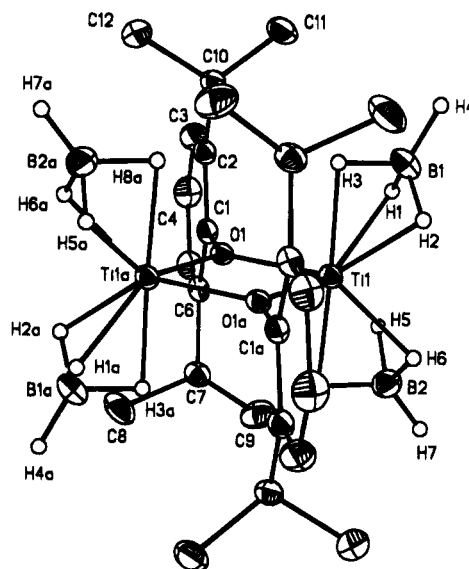


Figure 2. View of the molecular structure of **8** with selected bond lengths (Å) and angles (deg): Ti1–O1, 2.005(2); Ti1a–O1, 2.003(2); O1–C1, 1.407(3); Ti1–B1, 2.166(4); Ti1–B2, 2.162(4); Ti1–Ti1a, 3.041(1); Ti1–O1–Ti1a, 98.71(8); O1–Ti1–O1a, 81.29(8); B1–Ti1–B2, 118.1(2); O1–Ti1–B1, 113.00(13); O1–Ti1–B2, 113.02.

Table 1. Atomic Coordinates ($\times 10^4$) and Equivalent Isotropic Displacement Parameters ($\text{Å}^2 \times 10$) for **8**

atom	<i>x</i>	<i>y</i>	<i>z</i>	<i>U</i> (eq) ^a
Ti(1)	5457(5)	1278(5)	583(3)	29(2)
O(1)	4421(2)	1008(2)	−508(10)	28(4)
B(1)	4223(4)	2013(5)	1392(2)	49(9)
B(2)	7358(4)	2412(5)	630(3)	48(9)
C(1)	3823(3)	2139(3)	−1037(15)	30(6)
C(2)	2499(3)	2571(3)	−1046(2)	34(6)
C(3)	1962(3)	3738(4)	−1555(2)	46(8)
C(4)	2701(4)	4454(4)	−2029(2)	50(8)
C(5)	3997(4)	4000(4)	−2013(2)	44(8)
C(6)	4599(3)	2828(3)	−1524(15)	34(6)
C(7)	6012(3)	2348(4)	−1561(2)	39(7)
C(8)	6083(5)	1641(5)	−2357(3)	65(11)
C(9)	6994(4)	3689(4)	−1379(3)	59(10)
C(10)	1620(3)	1838(4)	−533(2)	37(7)
C(11)	1131(4)	3036(5)	−11(2)	53(9)
C(12)	446(4)	984(5)	−1025(2)	51(8)

^a *U*(eq) is defined as one-third of the trace of the orthogonalized U_{ij} tensor.

found for the Ti_2O_2 core of dimeric tris(2,6-dimethylphenoxy)titanium(III), which shows a remarkably low value for its magnetic moment.¹⁰ The second feature is the presence of μ_3 -bonded BH_4 groups, confirming the analysis of the IR data. In contrast to the acute O–Ti–O bond angle we note a rather wide B–Ti–B bond angle of $118.1(2)^\circ$. Thus, the Ti centers are present in a fairly distorted tetrahedral environment. Finally, one can note that the 2,6-diisopropylphenyl groups stand perpendicular to the Ti_2O_2 ring plane (see Table 1).

The X-ray structure of the adduct **8**·2PMe₃ (**9**) reveals the presence of a mononuclear species in the solid state. Figure 3 depicts its molecular structure. Interestingly, the trimethylphosphine ligands occupy the apical positions of a distorted trigonal bipyramid, while the two boron atoms and the oxygen atom are part of the trigonal plane (if we neglect the bridging hydrogen atoms). The point group symmetry of **9** is C_s , and this symmetry is imposed by a crystallographic mirror plane

(9) Thomann, M. Ph.D. Thesis, University of Munich, Munich, Germany, 1992; pp 65–93.

(10) Minhas, R.; Duchateau, R.; Gambarotta, S.; Bensimon, C. *Inorg. Chem.* **1992**, *31*, 4933–4938.

(11) Jensen, J. A.; Wilson, S. R.; Girolami, G. S. *J. Am. Chem. Soc.* **1988**, *110*, 4977–4982.

(12) Lubben, T. V.; Wolczanski, P. T. *J. Am. Chem. Soc.* **1987**, *109*, 424–455.

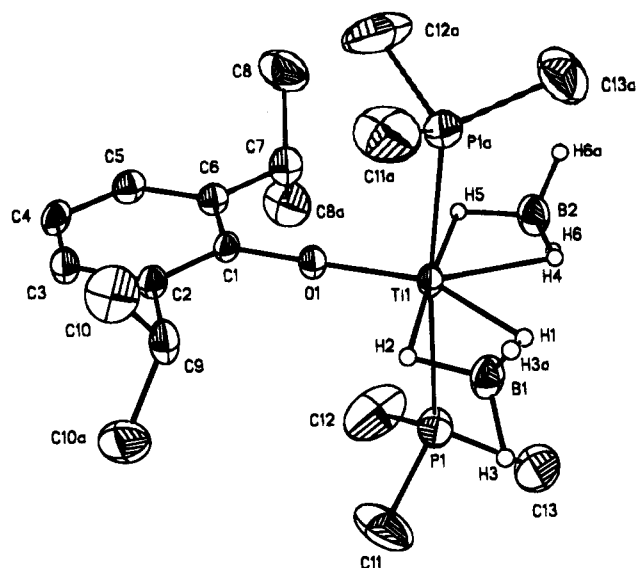


Figure 3. View of the molecular structure of **9** with selected bond lengths (Å) and angles (deg): Ti1–B1, 2.457(6); Ti1–B2, 2.444(6); Ti1–P(1,2), 2.590(2); Ti1–O1, 1.804(3); O1–C1, 1.361(5); B1–Ti1–B2, 121.1(2); B1–Ti1–O1, 122.4(2); B2–Ti1–O1, 116.5(2); O1–Ti1–P1, 93.49(3); O1–Ti1–P2, 93.49(3); Ti1–O1–C1, 177.7(3); P1–Ti1–P2, 171.86(6).

which passes through the atoms O1, Ti1 B1, B2, the phenyl group, and the tertiary carbon atoms of the isopropyl groups. A P1–Ti1–P1a bond angle of 171.8(1)° reveals a significant distortion from the ideal 180°, and this is most likely due to a repulsive interaction of the PMe₃ ligands with the isopropyl groups. A similar, although much less severe deviation from the ideal geometry is indicated by the B1–Ti1–B2 bond angle of 121.1(2)°. Another interesting feature is the almost linear C1–O1–Ti1 bond angle (177.7(4)°), and this is coupled with a very short Ti1–O1 bond length (1.804(4) Å) while the C1–O1 atom distance (1.368(6) Å) is typical of phenols.¹³ The Ti–O bond, therefore, suggests a strong interaction between both atoms (see Table 2). This point will be discussed later.

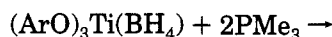
More important is the observation that the BH₄ groups are bonded in a μ_2 -fashion to the Ti center. This discerns complex **9** from complex **8**. If we consider a BH₄ group as a ligand similar to a halide, then we can classify compound **8** as a coordinative compound possessing a tetracoordinated Ti atom and complex **9** as being pentacoordinated. Consequently, there is more space available at a tetracoordinated center than on a pentacoordinated atom, and this obviously determines in a first approximation whether the BH₄ groups function as μ_2 - or μ_3 -ligands. This geometry is also reflected in the Ti–B bond lengths, which are 2.457(6) and 2.444(6) Å in **9** and 2.162(4) and 2.166(4) Å in **8**, and this difference of 0.29 Å fits with observations by Edelstein et al.¹⁴ who first pointed out this relationship which is useful if the hydrogen positions cannot be determined unambiguously or not at all. Moreover, these Ti–B bond lengths fit well with those found for the μ_2 -BH₄ group in bis(trimethylsilyl)benzamidinatotitanium(III) tetrahydroborate.¹⁵

Table 2. Atomic Coordinates ($\times 10^4$) and Equivalent Isotropic Displacement Parameters ($\text{Å}^2 \times 10$) for **9**

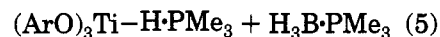
atom	x	y	z	$U(\text{eq})^a$
Ti(1)	1527(4)	2500	1219(8)	38(3)
O(1)	632(14)	2500	598(3)	42(7)
B(1)	1818(3)	2500	3694(6)	58(2)
B(2)	2452(3)	2500	-538(7)	63(2)
P(1)	1589(5)	675(7)	1366(11)	66(4)
C(1)	-33(2)	2500	76(4)	37(10)
C(2)	-602(2)	2500	986(4)	42(11)
C(3)	-1279(2)	2500	439(5)	51(12)
C(4)	-1390(2)	2500	-969(5)	52(12)
C(5)	-824(2)	2500	-1857(5)	52(12)
C(6)	-135(2)	2500	-1368(4)	45(11)
C(7)	479(3)	2500	-2363(5)	64(14)
C(8)	491(3)	3371(3)	-3270(5)	111(2)
C(9)	-499(2)	2500	2551(5)	57(13)
C(10)	-819(3)	3376(3)	3205(4)	93(15)
C(11)	1119(3)	159(3)	2804(7)	134(2)
C(12)	1156(4)	143(4)	-101(7)	163(3)
C(13)	2428(3)	113(3)	1451(6)	120(2)

^a $U(\text{eq})$ is defined as one-third of the trace of the orthogonalized U_{ij} tensor.

(Aryloxy)titanium(IV) hydride, (ArO)₃TiH·PMe₃. Treatment of (ArO)₃Ti(BH₄), **7**, with trimethylphosphine according to eq 5 leads to the formation of the hydride



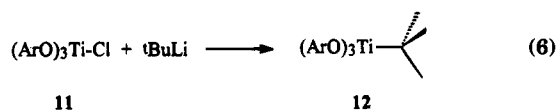
6



10

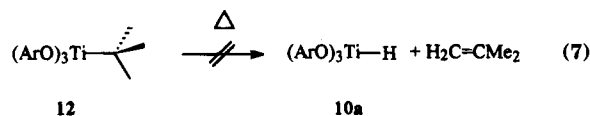
10. Removal of the BH₃ group from the tetrahydroborate without addition of PMe₃ could not be achieved. The orange-colored **10** dissolves freely in hexane or toluene, but the hydride decomposes in solution at temperature above 30 °C. Moreover, the solutions turn green on prolonged exposure to sunlight with formation of Ti(III) species.

So far we have not been able to remove the coordinated phosphine in **10**. For this reason an approach that would probably lead to a phosphine-free aryloxy-group-supported titanium(IV) hydride was considered, and the dehydrotitanation of an (aryloxy)titanium(IV) alkyl seemed to be a good choice. For this reason tris-(2,6-diisopropylphenoxy)titanium chloride, **11**, was reacted with *tert*-butyllithium according to eq 6. At 0 °C



a black oil was formed, from which tris(2,6-diisopropylphenoxy)-*tert*-butyltitanium, **12**, was isolated in 30% yield as amber-colored, cube-shaped crystals.

Under mass spectrometric conditions **12** loses isobutene. However, we were unable to achieve olefin elimination from **12** as shown in eq 7. A reaction sets



in at about 70 °C, but the hydride obviously decomposes already at this temperature, and it could not be trapped in the presence of a scavenger like phenylacetylene.

(13) Brown, C. J. *Acta Crystallogr.* **1951**, *4*, 100–103. Powell, H. M. *Acta Crystallogr.* **1953**, *6*, 256–259. Skinner, J. M.; Speakmann, J. C. *J. Chem. Soc.* **1951**, 185–191.

(14) Edelstein, N. *Inorg. Chem.* **1982**, *20*, 297–299.

Table 3. Selected $^{13}\text{C}/^1\text{H}$ NMR Data for the (Aryloxy)alkenyltitanium Compounds $(\text{ArO})_3\text{Ti}[-\text{C}^{\alpha}\text{R}^1=\text{C}^{\beta}\text{HR}^2]$, 13a,b, 14a,b, 15, and 16, and the Alkenylzirconocene Complexes 18 $\text{Cp}_2\text{ZrX}[-\text{CR}^1=\text{CHR}^2]$, 17–19 a .

compd	R ¹	R ²	$-\text{C}^{\alpha}\text{R}^1=$	$=\text{C}^{\beta}\text{HR}^2$
13a	H	Ph	187.2 8.97	143.81 7.87
13b	Ph	H	207.3	122.77 6.12/6.20
14a	SiMe ₃	H	223.05	135.32 [155.6 Hz] 6.72/ca. 7.0
14b	H	SiMe ₃	203.44 [127 Hz] 8.48	not assigned 7.15
15	SiMe ₃	Ph	221.38	148.45 [143 Hz] 9.09
16	SnMe ₃	Ph	223.37	152.05 [148 Hz] 9.11
17	SiMe ₃	Ph	204.5	109.4 [120 Hz] 8.41
X = Br				
18	H	SiMe ₃	202.7 [128 Hz] 8.03	143.3 [136 Hz] 6.63
X = Cl				
19	H	Ph	177.7 [122 Hz] 7.67	140.5 [153 Hz] 6.70
X = Cl				

^a Data given in the following order: ^{13}C chemical shift in ppm; $^1J(^{13}\text{C},^1\text{H})$ coupling constant is given in brackets followed by the ^1H NMR shift. ^b In benzene-*d*₆; 17 in CD₂Cl₂.

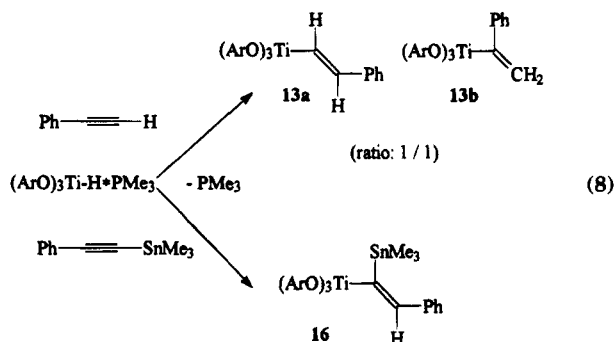
compounds 7 and 12 were determined by X-ray crystallography. They are depicted in Figures 5 and 6, their atomic coordinates and equivalent isotropic displacement parameters are shown in Tables 4 and 5, and several of their structural parameters are summarized in Table 6.

The average Ti–O and C–O bond distances can be considered as equal in both compounds, the main difference in the TiO₃ skeleton is found for the Ti–O–C bond angles. These are significantly larger in the tetrahydroborate than in the *tert*-butyl compound. This points to the conclusion that the steric influence of the tetrahydroborate group exceeds that of the *tert*-butyl group, and this can only be due to the bridging hydrogen atoms which are, of course, close to the titanium atom. Moreover, the Ti–B atom distance (2.204(2) Å) is in accord with a μ_3 -bonded tetrahydroborate group.

Figure 7 presents the molecular structure of the hydride 10. It shows a distorted trigonal bipyramidal arrangement of the ligand atoms around the Ti center. The equatorial positions are occupied by two oxygen atoms and the hydrogen atom, while the phosphorus atom and an oxygen atom are found at the apices of the trigonal bipyramid. (See Table 7:) The Ti–H bond length in compound 10 is 1.60(3) Å. The two equatorial H–Ti–O bond angles are significantly different (89.5(11) and 109.2(11)°), and this is due to the different orientation of the diisopropylphenoxy groups. More importantly, the Ti–O–C bond angle at O2 is 170.5(2)°, approaching linearity, while the Ti–O3–C25 bond angle is only 143.4(2)° and thus significantly more bent. However, the Ti–O1–C2 bond angle of the apical oxygen atom is 176.7(2)° and is much closer to 180° than the angle at atom O2. One may also note that the Ti–O bond lengths become shorter as the bond angle opens. We find Ti–O bond lengths of 1.800(3) Å at atom O2 and 1.848(3) Å at atom O3. The longer Ti–O1 atom distance of 1.811(3) Å is in accord with the general and well-known fact that bond lengths to apical atoms are longer than those within the trigonal plane. This holds at least for covalent compounds, and, therefore, com-

For this reason our studies exploring the chemistry of aryloxy-supported titanium(IV) hydrides had to be conducted with the PMe₃ adduct 10. This compound reacts with phenylacetylene. The addition of the Ti–H bond to the CC triple bond of this alkyne does not occur stereospecifically. Two vinyltitanium complexes, 13a,b, are formed in a 1:1 ratio and are characterized by the typical ^{13}C resonance at 187.2 ppm for 13a and 207.3 ppm for 13b. Moreover, the olefinic protons are also strongly deshielded with resonances at 7.83 and 8.92 ppm [$^3J(\text{H},\text{H})_{\text{trans}} = 18.3$ Hz] for 13a. Hydrolysis of 13a,b yields styrene in addition to the phenol, and deuteriolysis produces styrene with deuterium atoms in the α - and β -positions, respectively.

Much better selectivity for hydrotitanation with 10 is achieved by using silyl- or stannyl-substituted alkynes. Thus, the ratio of the Markovnikov to anti-Markovnikov addition, which leads to 14a,b, respectively, is 3:1 for Me₃Si–C≡C–H. Stereospecificity results by using the alkynes Me₃Si–C≡C–Ph or Me₃Sn–C≡C–Ph as shown in eq 8.



Proof for the *trans* orientation of the Ti and Sn substituents comes from the ^{119}Sn NMR spectrum. The signal at -36.3 ppm shows the typical pattern due to $^{119}\text{Sn},^1\text{H}$ coupling ($^3J = 177$ Hz), which is incompatible with *cis* or *geminal* geometry. For these cases coupling constants of the order of 120 (*cis*) and 10 Hz, respectively, are to be expected.¹⁶

Additional information on the structure of the vinyltitanium compounds are obtained from a comparison with alkenylzirconium complexes $\text{Cp}_2\text{Zr}(\text{X})-\text{CR}=\text{C}(\text{H})\text{R}'$, 17–19.¹⁷ With certain substituents R and R', e.g., SiMe₃ and Ph, an agostic interaction of the β H atom with the Zr atom can be detected. This results in a pronounced shielding of the β carbon atom from 150 to 110 ppm. Moreover, the coupling constant $^1J(^{13}\text{C},^1\text{H})$ is reduced to about 120 Hz in the presence of an agostic interaction. The data, summarized in Table 3, clearly demonstrate that there is no agostic interaction in the (aryloxy)-titanium(IV) alkenyls 13–16, which is probably due to the steric crowding at the Ti center, and this is most likely also the reason that the vinyltitanium complexes contain no more PMe₃ (Figure 4).

Molecular Structures of the Tris(2,6-diisopropylphenoxy)titanium Compounds, 7 and 12, and of Tris(2,6-diisopropylphenoxy)titanium hydride trimethylphosphine, 10. The molecular structures of

(15) Dick, D. G.; Duchateau, R. D.; Edema, J. J. H.; Gambarotta, S. *Inorg. Chem.* **1993**, *32*, 1959–1963.

(16) Wrackmeyer, B. *Annu. Rep. NMR Spectrosc.* **1985**, *16*, 73–186.

(17) Hyla-Kryspin, I.; Gleiter, R.; Krüger, C.; Zwtetler, R.; Erker, G. *Organometallics* **1990**, *9*, 517–523.

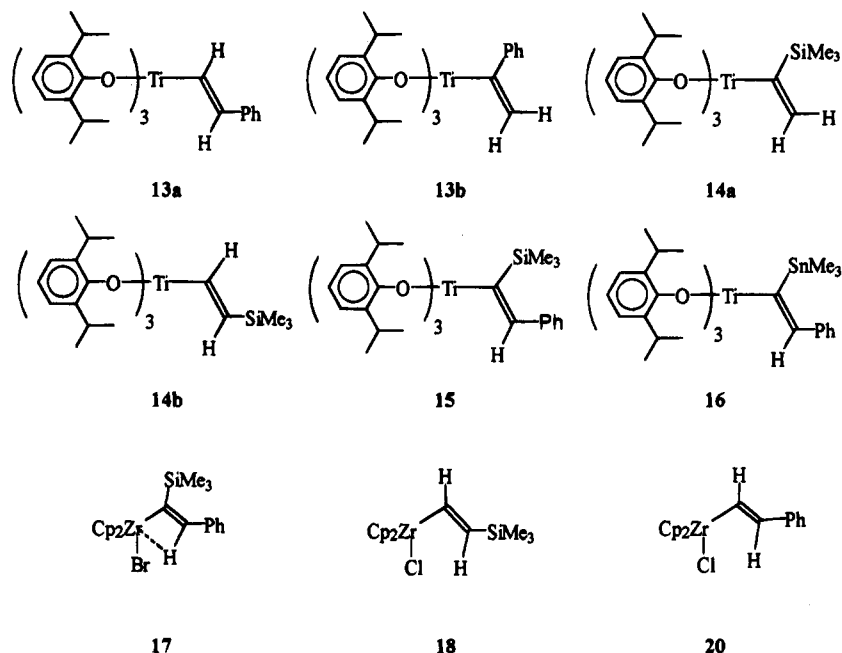


Figure 4.

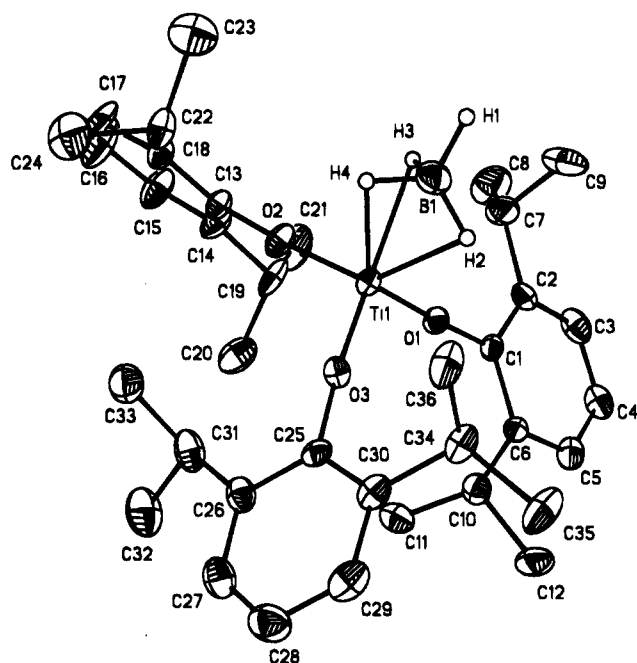


Figure 5. View of the molecular structure of **7** with selected bond lengths (Å) and angles (deg): Ti1–O1, 1.774(6); Ti1–O2, 1.781(6); Ti1–O3, 1.781(6); Ti1–B1, 2.207(13); C1–O1–Ti1, 173.3(6); C13–O2–Ti1, 172.2(5); C25–O3–Ti1, 171.8(5); B1–Ti1–O1, 110.1(4); B1–Ti1–O2, 110.2(4); B1–Ti1–O3, 111.9(4).

pound **10** seems to fall into this category. If this is so, then the Ti–O bonds should exhibit a polar covalent character involving sp-hybridized oxygen atoms O1 and O2.

The more acute Ti–O3–C25 bond angle has a consequence: it brings a hydrogen atom at C31 closer to the Ti atom (Ti–H distance, 2.75 Å) than would be the case if the bond angle were be 180°. From this point of view one may even assume that the Ti center approaches hexacoordination, and the geometrical consequence of this orientation of the H atom is reflected in the wide H–Ti–O3 bond angle of 126.0(12)°.

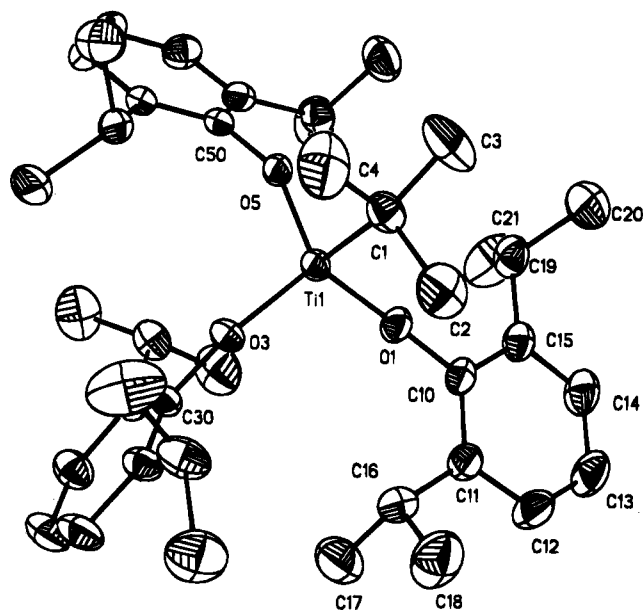


Figure 6. View of the molecular structure of **12** with selected bond lengths (Å) and angles (deg): Ti1–O1, 1.786(2); Ti1–O3, 1.799(2); Ti1–O5, 1.803(2); C10–O1–Ti1, 167.0(2); C30–O3–Ti1, 152.7(2); C50–O5–Ti1, 154.6(2); C1–Ti1–O1, 101.33(13); C1–Ti1–O3, 108.81(11); C1–Ti1–O5, 102.91(12); C2–C1–Ti1, 108.33(3).

In solution, the structure of **10** is more symmetrical since there is only one set of signals in the NMR spectra for the isopropyl and phenyl groups as well as for the PMe₃ ligand. At ambient temperature, the ¹H NMR signal for the Ti–H proton can be detected at δ 8.5. Compared with many other metal hydrides this signal indicates a strongly deshielded proton, very similar to that of the tricyclic triamidotitanium(IV) hydride **20** (δ 8.29),¹⁸ (Figure 8) and this is not unexpected for a metal atom with empty or fully occupied d-orbitals.¹⁹ A typical example is tris(2,6-diisopropylphenolato)tantalum di-

(18) Cummins, C. C.; Schrock, R. R.; Davies, W. M. *Organometallics* **1992**, *11*, 1452–1545.

(19) Buckingham, D.; Stevens, P. J. *J. Chem. Soc.* **1964**, 2747–2759.

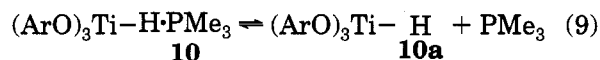
Table 4. Atomic Coordinates ($\times 10^4$) and Equivalent Isotropic Displacement Parameters ($\text{\AA}^2 \times 10$) for 7

atom	x	y	z	$U(\text{eq})^a$
Ti(1)	483(7)	1472(12)	1(8)	32(4)
O(1)	56(3)	1600(5)	889(3)	38(13)
O(2)	1312(3)	2161(5)	76(4)	46(14)
O(3)	578(3)	-168(5)	-186(3)	36(14)
B(1)	-114(7)	2429(13)	-896(8)	55(3)
C(1)	-344(4)	1680(8)	1527(5)	34(2)
C(2)	-520(4)	2850(8)	1817(6)	43(2)
C(3)	-918(6)	2891(11)	2479(6)	59(3)
C(4)	-1158(5)	1786(10)	2811(5)	52(3)
C(5)	-997(5)	624(11)	2495(5)	51(2)
C(6)	-589(4)	537(8)	1853(4)	33(2)
C(7)	-289(7)	4062(10)	1442(8)	71(3)
C(8)	-56(8)	5059(14)	2019(9)	99(5)
C(9)	-862(8)	4525(11)	935(8)	88(4)
C(10)	-375(5)	-726(9)	1507(6)	47(2)
C(11)	324(6)	-1118(10)	1789(6)	57(3)
C(12)	-911(6)	-1748(9)	1630(7)	66(3)
C(13)	1926(4)	2788(7)	142(5)	37(2)
C(14)	2154(5)	3108(10)	883(6)	51(3)
C(15)	2773(6)	3747(13)	923(6)	74(4)
C(16)	3163(7)	3964(17)	288(7)	97(5)
C(17)	2928(6)	3655(14)	-432(6)	77(4)
C(18)	2298(4)	3029(10)	-524(5)	43(2)
C(19)	1743(6)	2793(12)	1594(5)	62(3)
C(20)	2041(8)	1595(13)	1939(7)	87(4)
C(21)	1763(9)	3852(15)	2172(8)	100(5)
C(22)	2059(5)	2695(11)	-1307(6)	52(3)
C(23)	1812(8)	3867(13)	-1738(7)	84(4)
C(24)	2613(8)	2061(13)	-1782(7)	84(4)
C(25)	626(4)	-1459(8)	-222(4)	36(2)
C(26)	1245(4)	-2006(9)	39(6)	47(2)
C(27)	1282(5)	-3301(9)	-9(8)	61(2)
C(28)	756(7)	-4034(11)	-283(7)	72(3)
C(29)	155(6)	-3458(10)	-498(6)	59(3)
C(30)	71(5)	-2142(9)	-475(5)	43(2)
C(31)	1822(5)	-1200(11)	331(6)	61(3)
C(32)	2283(6)	-1870(14)	898(8)	88(4)
C(33)	2246(6)	-650(12)	-324(6)	70(3)
C(34)	-584(5)	-1502(10)	-707(5)	47(2)
C(35)	-1230(5)	-2322(12)	-619(7)	72(3)
C(36)	-542(5)	-953(14)	-1517(6)	62(3)

^a $U(\text{eq})$ is defined as one-third of the trace of the orthogonalized U_{ij} tensor.

hydride **21**,²⁰ with $\delta(^1\text{H})$ 14.86 presenting even more strongly deshielded Ta-bonded hydrogens, while the chemical shifts for zirconium-bonded hydrogen atoms are observed in the range 4–6 ppm.²¹

The facts that no $^2J(^{31}\text{P}, ^1\text{H})$ coupling can be observed for the TiH protons and that only a single ^{31}P signal is found for the phosphine at ambient temperature points to the conclusion that the equivalence of the OR groups is *not* due to Berry pseudorotation but rather to an equilibrium (eq 9).



Indeed, coupling can be observed at -60°C ($^2J(^{31}\text{P}, ^1\text{H}) = 76\text{ Hz}$), and coalescence occurs at -45°C as shown in Figure 9. Consequently, the chemical shift ($\delta = -37$) observed in the ^{31}P NMR spectrum of **10** at ambient temperature represents a time-averaged shielding, while

(20) Visciglio, V. M.; Fanwick, P. E.; Rothwell, I. P. *J. Chem. Soc., Chem. Commun.* **1992**, 1505–1507.

(21) James, B. D.; Nanda, R. K.; Wallbridge, M. G. H. *Inorg. Chem.* **1967**, *6*, 1979. Manriquez, J.; Mc Alister, D. R.; Sanner, R. D.; Bercaw, J. E. *J. Am. Chem. Soc.* **1978**, *100*, 2716–2725. Gozum, J. E.; Girolami, G. S. *J. Am. Chem. Soc.* **1991**, *113*, 3829–3837. Gozum, J. E.; Wilson, S. R.; Girolami, G. S. *J. Am. Chem. Soc.* **1992**, *114*, 9483–9492.

Table 5. Atomic Coordinates ($\times 10^4$) and Equivalent Isotropic Displacement Parameters ($\text{\AA}^2 \times 10$) for 12

atom	x	y	z	$U(\text{eq})^a$
Ti(1)	2747(5)	8776(5)	7503(3)	46(2)
C(1)	955(3)	7907(3)	7662(2)	67(9)
C(2)	-117(4)	8809(5)	7348(3)	105(15)
C(3)	1140(4)	6667(4)	7260(3)	122(2)
C(4)	622(5)	7611(6)	8427(3)	136(2)
O(1)	2702(2)	9280(2)	6594(10)	61(6)
C(10)	2379(3)	9766(3)	5939(2)	59(8)
C(11)	1741(4)	11010(3)	5871(2)	67(9)
C(12)	1401(4)	11443(4)	5198(2)	92(13)
C(13)	1689(5)	10689(5)	4626(2)	103(15)
C(14)	2324(4)	9482(5)	4713(2)	89(12)
C(15)	2696(4)	8985(4)	5363(2)	68(9)
C(16)	1427(4)	11871(4)	6488(2)	78(11)
C(17)	2379(6)	12933(5)	6491(3)	123(2)
C(18)	10(5)	12432(6)	6530(3)	134(2)
C(19)	3441(4)	7668(4)	5433(2)	83(11)
C(20)	2673(7)	6605(5)	5162(3)	152(2)
C(21)	4795(5)	7681(6)	5075(3)	149(2)
O(3)	2723(2)	10133(2)	8064(10)	52(5)
C(30)	3166(3)	11281(3)	8254(14)	49(7)
C(31)	4512(3)	11487(3)	8151(2)	56(8)
C(32)	4904(4)	12675(3)	8330(2)	76(10)
C(33)	4023(5)	13612(3)	8605(2)	86(12)
C(34)	2719(5)	13385(3)	8713(2)	81(11)
C(35)	2252(3)	12212(3)	8541(2)	61(9)
C(36)	5503(3)	10456(4)	7866(2)	71(10)
C(37)	6790(4)	10333(5)	8249(3)	121(2)
C(38)	5758(5)	10636(5)	7084(2)	116(2)
C(39)	818(4)	11928(4)	8670(2)	85(12)
C(40)	-166(5)	13107(5)	8622(3)	120(2)
C(41)	621(5)	11211(5)	9361(3)	144(2)
O(5)	3947(2)	7483(2)	7745(10)	52(5)
C(50)	5017(3)	6948(3)	8089(2)	49(7)
C(51)	6053(3)	6332(3)	7688(2)	56(8)
C(52)	7132(4)	5793(3)	8048(2)	74(10)
C(53)	7176(4)	5869(4)	8770(2)	81(11)
C(54)	6142(4)	6472(3)	9144(2)	70(10)
C(55)	5030(3)	7024(3)	8822(2)	55(8)
C(56)	5975(3)	6220(3)	6903(2)	64(9)
C(57)	7306(4)	6117(5)	6492(2)	111(2)
C(58)	5169(5)	5120(4)	6739(2)	106(15)
C(59)	3878(4)	7637(3)	9261(2)	66(9)
C(60)	3268(4)	6646(4)	9767(2)	91(13)
C(61)	4266(5)	8770(4)	9667(2)	99(14)

^a $U(\text{eq})$ is defined as one-third of the trace of the orthogonalized U_{ij} tensor.

Table 6. Comparison of Several Structural Parameters of (2,6- $^i\text{Pr}_2\text{H}_3\text{C}_6\text{O}$) $_3\text{Ti}(\text{BH}_4^t\text{Bu})$, **7 and **12**, in \AA and deg°**

	Ti–O (av)	O–C (av)	Ti–C	Ti–B	Ti–O–C (av)	O–Ti–O (av)
7	1.778(6)	1.372(10)		2.204(12)	173.4(5)	108.1(3)
12	1.796(2)	1.370(3)	2.095(3)		158.1(2)	114.11(9)

^a "av" denotes the average value for chemically equivalent bonds.

the signal moves at -60°C to -21 ppm . Addition of PMe_3 to the solution of **10** shifts the resonance to higher field. No triplet for the hydride resonance due to the formation of a compound of type $(\text{ArO})_3\text{TiH}\cdot 2\text{PMe}_3$, which should originate by an associative exchange with an excess of PMe_3 , was observed. This proves not only that an equilibrium is operative but also that the equilibrium is achieved at high rate. Thus, the phosphine is not strongly bonded to the Ti atom.

Consequently, this ligand can be replaced by a base exchange reaction with pyridine. However, $(\text{ArO})_3\text{TiH}\cdot\text{py}$ could not be isolated due to its ready decomposition, nor was it possible to remove PMe_3 in a high vacuum. This

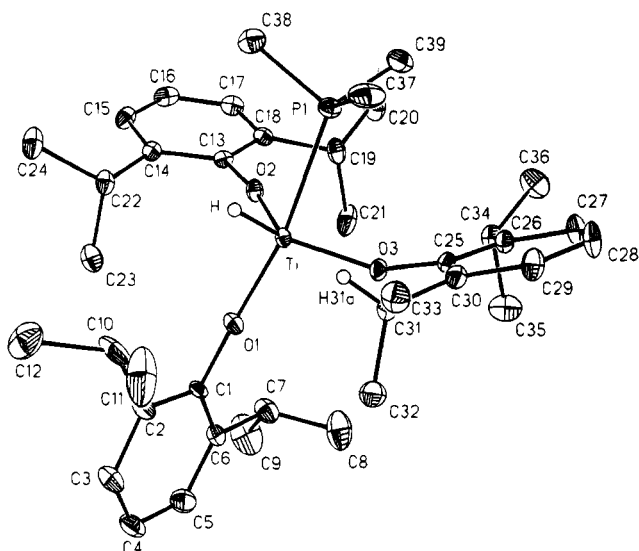


Figure 7. View of the molecular structure of **10** with selected bond lengths (Å) and angles (deg): Ti1–H1, 1.61(3); Ti1–O1, 1.810(3); Ti1–O2, 1.801(2); Ti1–O3, 1.850(2); Ti1–P1, 2.613(1); C1–O1–Ti1, 176.7(2); C13–O2–Ti1, 170.2(2); C25–O3–Ti1, 143.3(2); P1–Ti1–H1, 67.7(11); H–Ti1–O1, 89.5(11); H–Ti1–O2, 109.2(11).

would be the best way to arrive at the unsupported hydride, $(\text{ArO})_3\text{TiH}$, an aim that we could not yet achieve.

In contrast to the ready detection of the Ti-bonded hydrogen atom in the molecular structure as determined by X-ray and NMR methods, it was only with difficulty that the TiH unit was detected by IR spectroscopy. A band of medium to weak intensity at 1562 cm^{-1} was assigned to the Ti–H stretching vibration. This band is covered under bands due to CH deformation vibrations. However, if **10** was allowed to react with air, this band disappeared in difference spectra. Moreover, the assignment is further ascertained by comparing its frequency with those found for the Ti–H stretching vibrations of Cp_2TiH , $\text{Cp}_2\text{Ti}(\text{H})\text{N}_2$, or $\text{Cp}_2\text{Ti}(\text{H})\text{CO}$ ($1497\text{--}1561\text{ cm}^{-1}$).²² Crystal data and data collection parameters for **7–10** and **12** are shown in Table 8.

Discussion

The thermal stability of titanium(IV) tetrahydridoborates is rather limited and has so far only been demonstrated by the synthesis of compounds **1–3**,^{6,7} as well as by **5** and **7** in the present study. These examples indicate that compounds of type $\text{X}_2\text{Ti}(\text{BH}_4)_2$ are sufficiently stable against reduction to $\text{X}_2\text{Ti}(\text{BH}_4)$ if X_2 is a chelating ligand. However, if the extra stability due to chelation is missing, compounds of type $(\text{RO})_2\text{Ti}(\text{BH}_4)_2$ either tend to be reduced readily or are stabilized as $(\text{RO})_3\text{TiBH}_4$ by ligand exchange. This is further supported by the ease of formation of compounds of type $(\text{R}_2\text{N})_3\text{TiBH}_4$ ²³ or $(\text{RO})_3\text{Ti}(\text{BH}_4)$ ($\text{R} = \text{Bu}$, $t\text{Bu}$).⁹ These latter Ti(IV) tetrahydridoborates are accessible by allowing BH_3THF to react with $\text{Ti}(\text{OR})_4$.⁹ According to the electron pair donor–acceptor concept, developed extensively by V. Gutmann, a stability order $(\text{R}_2\text{N})_3\text{TiBH}_4 > (\text{RO})_3\text{TiBH}_4 \gg \text{Hal}_3\text{TiBH}_4$ ($\text{Hal} = \text{Cl}, \text{Br}, \text{I}$) is

Table 7. Atomic Coordinates ($\times 10^4$) and Equivalent Isotropic Displacement Parameters ($\text{\AA}^2 \times 10$) for **10**

atom	x	y	z	$U(\text{eq})^a$
Ti	7076(5)	362(3)	7215(3)	21(2)
P(1)	5062(8)	518(6)	6516(5)	30(3)
O(1)	8167(2)	–52(13)	7863(13)	29(6)
O(2)	7558(2)	310(13)	6326(13)	28(6)
O(3)	6932(2)	1318(13)	7611(13)	28(6)
C(1)	8956(3)	–349(2)	8383(2)	23(8)
C(2)	8736(3)	–1023(2)	8743(2)	35(10)
C(3)	9549(4)	–1275(2)	9292(2)	45(11)
C(4)	10545(4)	–895(3)	9468(3)	49(12)
C(5)	10749(3)	–255(3)	9082(2)	46(12)
C(6)	9968(3)	37(2)	8532(2)	31(9)
C(7)	10193(3)	739(2)	8092(3)	46(12)
C(8)	9845(5)	1451(3)	8446(3)	76(2)
C(9)	11401(4)	799(3)	7937(4)	89(2)
C(10)	7672(4)	–1484(3)	8535(3)	60(2)
C(11)	6920(5)	–1437(3)	9141(4)	105(3)
C(12)	7909(5)	–2307(3)	8369(3)	74(2)
C(13)	7948(3)	141(2)	5678(2)	23(9)
C(14)	8187(3)	–621(2)	5529(2)	26(9)
C(15)	8552(3)	–774(2)	4858(2)	35(10)
C(16)	8694(3)	–198(3)	4361(2)	38(11)
C(17)	8463(3)	544(2)	4527(2)	35(10)
C(18)	8088(3)	732(2)	5187(2)	27(9)
C(19)	7900(3)	1551(2)	5402(2)	37(10)
C(20)	7597(6)	2081(3)	4751(3)	83(2)
C(21)	8938(4)	1849(2)	5886(3)	58(14)
C(22)	8119(3)	–1230(2)	6105(2)	33(10)
C(23)	9202(3)	–1248(2)	6630(2)	43(11)
C(24)	7858(4)	–2022(2)	5785(3)	51(12)
C(25)	6175(3)	1821(2)	7823(2)	26(9)
C(26)	6112(3)	2551(2)	7512(2)	30(9)
C(27)	5287(3)	3041(2)	7711(2)	42(11)
C(28)	4583(4)	2820(2)	8205(3)	48(12)
C(29)	4696(3)	2113(2)	8531(2)	40(11)
C(30)	5497(3)	1591(2)	8353(2)	31(9)
C(31)	5659(3)	820(2)	8718(2)	32(10)
C(32)	6715(4)	825(2)	9273(2)	45(11)
C(33)	4655(4)	543(2)	9075(2)	44(11)
C(34)	6953(3)	2808(2)	7012(2)	37(10)
C(35)	7966(4)	3162(3)	7478(3)	59(14)
C(36)	6495(4)	3351(3)	6412(3)	59(14)
C(37)	3883(3)	496(3)	7039(2)	52(13)
C(38)	4774(4)	–280(2)	5900(2)	43(11)
C(39)	4735(4)	1343(2)	5931(2)	47(12)

^a $U(\text{eq})$ is defined as one-third of the trace of the orthogonalized U_{ij} tensor.

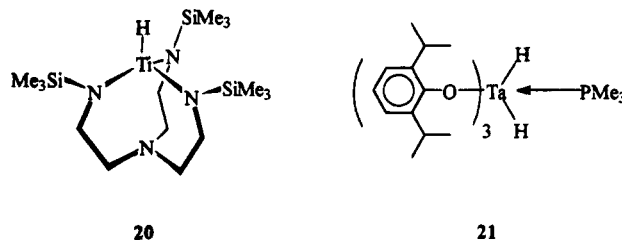
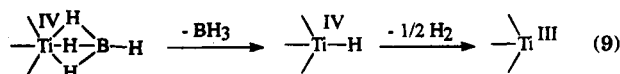


Figure 8.

to be expected, and indeed no $\text{Hal}_3\text{TiBH}_4$ have yet been reported.

The mechanism by which the Ti(IV) tetrahydridoborates decompose with concomitant reduction is still not unveiled. The most likely alternative is by loss of BH_3 , formation of the hydride and elimination of hydrogen as schematically depicted in eq 10.



The loss of BH_3 should be favored if the Lewis acidity of the Ti(IV) center increases. This would weaken the

(22) Tacke, M.; Teuben, J. v. Private communication.

(23) Mack, H. Ph.D. Thesis, University of Munich, Munich, Germany, 1995.

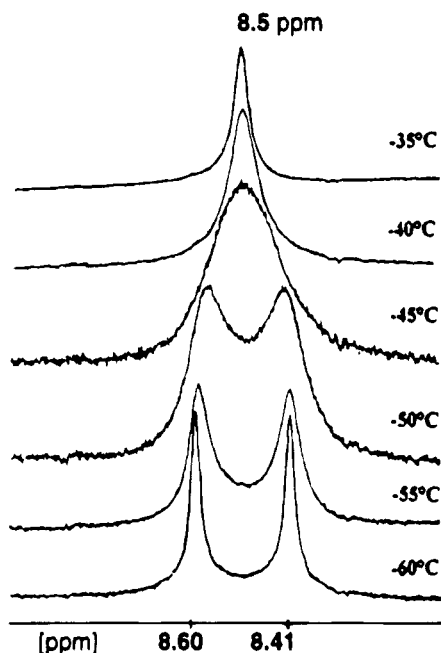


Figure 9. Temperature dependent ^1H NMR spectra of the hydride resonance in **10**.

H–B bridging bonds and would favor the release of BH_3 . While this step is feasible, the mechanism of the decomposition of the postulated Ti(IV) hydride remains unanswered. The release of BH_3 from the Ti(IV) tetrahydridoborates can be supported by a base such as pyridine or PMe_3 and others. PMe_3 is particularly helpful and led to the clean formation of **10**. In contrast, PMe_3 did not remove BH_3 groups from **8** but opened Ti–O bridging bonds of $[\text{ArOTi}(\text{BH}_4)_2]_2$ with formation of **9**. One can speculate that this may be due to BH_4 groups in **8** bonding to the Ti(III) center in a more polar fashion as compared with **6**. Removal of BH_3 units from metal tetrahydridoborates would then be controlled by kinetics. From this point of view the fairly high thermal stability of aminotitanium(IV) tetrahydridoborates is surprising because the basic amino groups could readily attack at the covalently bonded BH_4 groups with removal of BH_3 . This happens indeed, but only at temperatures exceeding 80°C .²³

Compounds of X_3TiBH_4 feature μ_3 -bonded BH_4 groups. Bond angles subtending at the Ti center, particularly the O–Ti–O bond angles, suggest tetracoordination with the boron atom as the fourth ligand center. This holds, in a first approximation, also for compound **8**, although the coordination numbers are, of course, 8 for **8** and 6 for **7**. The titanium(III) compound **9** is hepta-coordinated by O, P, and H atoms and features μ_2 -bonded BH_4 groups. On the other hand, the B–Ti–B bond angle as well as the P–Ti–P bond angles suggests a trigonal-bipyramidal structure. Thus the results of the molecular structures as determined by X-ray methods are in accord with a static model. However, in solution, the BH_4 group is fluxional as demonstrated by the quintuplet structure of its ^{11}B NMR signal. This chameleon type of behavior is typical for the BH_4 group as a ligand.

So far we have been unable to prepare $(\text{ArO})_3\text{TiH}$ unsupported by additional ligands such as PMe_3 . Nevertheless, compound **10** is the first fully characterized titanium(IV) hydride in addition to $\text{Ti}^{\text{III}}\text{Cp}_2$ and $\text{Ti}^{\text{II}}\text{Cp}^*$ hydrides.

The rather short Ti–H bond length (1.60(3) Å) seems to be considerably shorter than for the hydrogen atoms in a $\text{Cp}^*\text{Ti}(\text{H})$ derivative²⁴ or Ti–H–Ti bridge bonds, e.g., in $(\mu\text{-}\eta^5\text{-}\eta^5\text{-fulvalene})\text{bis}(\mu\text{-hydrido})\text{bis}(\eta^5\text{-cyclopentadienyltitanium})$.^{5a} In addition, a Ti–H bond length of 1.71 Å was calculated for $\text{Cp}_2\text{Ti}(\text{H})\text{SiMe}_3$ ²⁵ in a theoretical study. The short Ti–H bond found for **10** may be a result of the electronegativity of the RO groups and the oxidation state of Ti implying a small atomic radius. A more accurate determination of the Ti–H bond lengths by neutron diffraction would be welcome, since these bond lengths cannot be determined accurately enough by X-ray methods.

Nevertheless, the hydride **10**, which has been fully characterized, gives evidence that even a compound X_3TiH unsupported by an additional ligand may be synthesized, and taking Ti–H groups on the surface of a SiO_2 support, an $(\text{RO})_3\text{TiH}$ molecular hydride may finally become available.

Experimental Section

All reactions were performed under rigorous exclusion of moisture under dinitrogen or in vacuo. Glassware was flame-dried in vacuo. LiBH_4 and $^t\text{BuLi}$ were used as supplied (Chemmetall GmbH), 2,6-diisopropylphenol (Aldrich) was used after distillation, and TiCl_4 (Fluka) was used without further purification. NMR: JEOL 270 (^1H , ^{11}B , ^{31}P , ^{29}Si , ^{119}Sn), JEOL 400 (^1H , ^{13}C), and Bruker AC200 (^{11}B , ^{31}P). ESR: Bruker ESP 300. Mass spectra were recorded with a CH7-Varian MAT (70 eV). X-ray: Siemens P4 four-circle diffractometer with low-temperature attachment. Samples were mounted in glass capillaries by using perfluoropolyether oil (Fluka), and Mo K α radiation with a graphite monochromator was used. All calculations were performed by using the SHELXL PLUS PC package, and in the final refinement the SHELXL 93 program was employed.

Synthesis of Bis(2,6-diisopropylphenolato)titanium(IV) Dichloride, 4. To a solution of TiCl_4 (10.64 g, 54 mmol) in 10 mL of CCl_4 was added slowly a solution of diisopropylphenol (19.24 g, 108 mmol) in 25 mL of CCl_4 . The mixture was heated at reflux for 3.5 h until HCl evolution ceased. After the solvent was removed under reduced pressure, **4** was left as a dark red oil (25 g, 99%), soluble in benzene, toluene, hexane, and pentane. Compound **4** was used without further purification. Anal. Found for $\text{C}_{24}\text{H}_{34}\text{Cl}_2\text{O}_2\text{Ti}$ (M, 473.32 g/mol): Cl, 16.2. Calcd: 14.98. ^1H NMR ($\text{CDCl}_3/\text{CCl}_4$): δ 1.26 [d, $^3J(\text{H,H}) = 6.83$ Hz, 24H, $(\text{CH}_3)_2\text{CH}-$]; 3.50 [sept, 4H, $(\text{CH}_3)_2\text{CH}-$]; 7.12 (m, 6H, aromatic H). ^{13}C NMR (CDCl_3): δ 23.1 [$(\text{CH}_3)_2\text{CH}-$]; 27.5 [$(\text{CH}_3)_2\text{CH}-$]; 123.3 [$(\text{CH}_3)_2\text{CH}-\text{C}-\text{CH}-\text{CH}$]; 125.3 [$(\text{CH}_3)_2\text{CH}-\text{C}-\text{CH}$]; 138.1 [$(\text{CH}_3)_2\text{CH}-\text{C}$]; 165.8 (C–O–).

Reaction of Bis(2,6-diisopropylphenolato)titanium(IV) Dichloride, 4, with LiBH_4 . Bis(2,6-diisopropylphenolato)titanium(IV) dichloride (8.74 g, 18.5 mmol) was dissolved in 40 mL of hexane and cooled with an ice bath, and 57 mL of a 0.64 M solution of LiBH_4 in diethyl ether was added slowly with stirring. Stirring was continued for 2 h, and the precipitated LiCl was removed by centrifugation. The solvent was stripped off, and the black green solid was redissolved in 50 mL of hexane. Some insoluble material was removed by filtration, and the solution was reduced in vacuo to 30 mL and subsequently cooled to -18°C . After 18 h 10 mg of a dark red substance was isolated by filtration. We assume, that this is the etherate **6**·2 Et_2O on the basis of the ^1H NMR signal intensities. ^{11}B NMR ($\text{Et}_2\text{O}/\text{hexane}$): δ -15.6 . ^1H NMR

(24) You, Y.; Wilson, S. R.; Girolami, G. S. *Organometallics* **1994**, 13, 4655–4657.

(25) Harrod, J. F.; Ziegler, T.; Tschinke, V. *Organometallics* **1990**, 9, 897–902.

Table 8. Crystal Data and Data Collection Parameters

compd	7	8	9	10	12
formula	C ₃₆ H ₅₅ BO ₃ Ti	C ₂₄ H ₅₀ B ₄ O ₂ Ti	C ₁₈ H ₄₃ B ₂ OP ₂ Ti	C ₃₉ H ₆₁ O ₃ PTi	C ₄₀ H ₆₀ O ₃ Ti
fw	594.52	510.31	406.99	656.77	636.79
cryst dimens, mm ³	0.41 × 0.4 × 0.4	0.65 × 0.45 × 0.4	0.4 × 0.4 × 0.3	0.6 × 0.5 × 0.4	0.45 × 0.33 × 0.28
cryst syst	orthorhombic	monoclinic	orthorhombic	monoclinic	triclinic
space group	<i>Pna</i> 2 ₁	<i>P</i> 2 ₁ / <i>n</i>	<i>Pnma</i>	<i>P</i> 2 ₁ / <i>c</i>	<i>P</i> 1
<i>a</i> , Å	19.532(30)	10.196(3)	19.003(7)	12.072(4)	10.175(2)
<i>b</i> , Å	10.611(16)	8.719(2)	14.153(6)	17.588(7)	10.340(1)
<i>c</i> , Å	17.555(25)	17.484(4)	9.671(6)	18.327(7)	19.024(2)
α , deg	90	90	90	90	87.48(1)
β , deg	90	101.33(3)	90	97.38(2)	86.91(1)
γ , deg	90	90	90	90	85.64(2)
<i>V</i> , Å ³	3638.3(94)	1524.0(7)	2601.0(22)	3859.0(25)	1991.2(5)
ρ (calcd), g cm ⁻³	1.085	1.093	1.039	1.130	1.062
<i>Z</i>	4	2	4	4	2
temp, K	223	213	213	173	293
no. of reflns colld	6680	2663	3922	5762	6789
no. of unique reflns	3161	2344	1892	4938	6178
no. of obsd	2591	1876	1330	3970	4205
σ test	2	4	4	2	4
no of params	370	220	146	419	412
weighting scheme, ^a <i>x/y</i>	0.0871/3.3771	0.0842/0	0.0553/1.3813	0.0634/3.4425	0.0588/0.6973
final R (4 σ)	0.0724	0.0460	0.0437	0.0475	0.0531
final wR2	0.1826	0.1162	0.1066	0.1099	0.1228

$$^a w^{-1} = \sigma^2 F_o^2 + (xP)^2 + yP; P = (F_o^2 + 2F_c^2)/3.$$

(C₆D₆): δ 1.16 [t, 12H, H₃C-CH₂O]; 1.20 [d, ³J(H,H) = 5.67 Hz, 24H, (H₃C)₂CH-]; 1.4 (b, BH₄); 3.31 (quart, 8H, CH₂-O), 3.77 [sept, ³J(H,H) = 6.75 Hz, 4H, (H₃C)₂CH-]; 6.9-7.2 (m, 6H, aromatic H).

The brown solution was then kept for 3 days at -18 °C. After this period orange crystals of **7** had separated and were isolated by filtration. Yield: 0.9 g (16%), mp: 99-104 °C. Anal. Found for C₃₆H₅₅BO₃Ti (M, 594.52 g/mol): C, 72.22; H, 7.60. Calcd: C, 72.73; H, 9.32. ¹¹B NMR (Et₂O/hexane): δ -14.6 [quint, ¹J(B,H) = 88 Hz]. ¹H NMR (CDCl₃): δ 1.11 [d, ³J(H,H) = 6.87 Hz, 36H, (CH₃)₂CH-]; 2.0 (b, BH₄); 3.50 [sept, ³J(H,H) = 6.84 Hz, 6H, (CH₃)₂CH-]; 6.97-7.05 (m, 9H, aromatic H). ¹³C NMR (CDCl₃): δ 23.24 [(CH₃)₂CH-]; 26.99 [(CH₃)₂CH-]; 123.09, 123.16, 138.1, 165.8 (aromatic C). IR (Nujol, cm⁻¹): ν 2528.0 (B-H^b); 2207.4, 2195.6, 2139.9 (B-H^b).

Finally **8** precipitated after 10 days at -18 °C from the filtrate in green, well-shaped crystals. They were isolated by filtration. Yield: 0.4 g (17%). Mp: 161-165 °C (decomp). Anal. Found for C₂₄H₅₀B₄O₂Ti (M, 510.31 g/mol): C, 55.72; H, 9.38. Calcd: C, 56.56; H, 9.98. ¹¹B NMR (C₆D₆): δ -16.9 (b, *h*_{1/2} = 500 Hz). ¹H NMR (C₆D₆): δ 1.30 [s, 12H, (CH₃)₂CH-]; 3.67 [s, 2H, (CH₃)₂CH-]; 6.64-6.94 (aromatic H). IR (Nujol, cm⁻¹): ν 2569, 2560 (B-H^b); 2214, 2139, 2097, 2068 (B-H^b).

Synthesis of 2,6-Diisopropylphenoxytitanium Bis(tetrahydridoborate)bis(trimethylphosphine), 9. Bis[(2,6-diisopropylphenolato)titanium(III) bis(tetrahydridoborate)], **8** (0.1 g, 0.2 mmol), was dissolved in 2 mL of toluene, and 0.1 mL of PMe₃ (1 mmol) was added slowly with stirring. During a few minutes the color of the solution changed from green to brown. The mixture was kept at -30 °C for 4 weeks. Then the solution was reduced to 1 mL. After 2 days of being cooled at -30 °C crystals had separated, and these were isolated by decantation. Yield: 0.01 g (6%) of **9** as well-crystallized blackgreen needles; mp: 135-140 °C (decomp). Anal. Found for C₁₈H₄₃B₂OTiP₂ (M, 406.99 g/mol): C, 52.43; H, 10.18. Calcd: C, 53.12; H, 10.65. No ¹H, ¹³C, or ¹¹B NMR signals detectible. ESR: *g* = 1.7 (t; hyperfine coupling constant, *g* = 0.0022 cm⁻¹); IR (Nujol, cm⁻¹): ν 2412, 2401, 2377, 2368 (B-H^b); 2164, 2130 (B-H^b).

Synthesis of Tris(2,6-diisopropylphenoxy)titanium Chloride, 11. To a solution of 2,6-diisopropylphenol (7.4 mL, 40 mmol) in 20 mL of benzene was added a solution of TiCl₄ (1.4 mL, 13.3 mmol) in 30 mL of benzene. The mixture was then heated at reflux for 8 h until the HCl evolution had ceased. The solvent was then removed by distillation, and the

orange red solid residue was dried under reduced pressure to yield 7.2 g of **11** (90%); mp: 115-120 °C. Anal. Found for C₃₆H₅₁ClO₃Ti (M, 615.13 g/mol): C, 69.75; H, 7.60. Calcd: C, 70.29; H, 8.36. ¹H NMR (CDCl₃): δ 1.13 [d, ³J(H,H) = 6.84 Hz, 36H, (CH₃)₂CH-]; 3.43 [sept, ³J(H,H) = 6.84 Hz, 6H, (CH₃)₂CH-]; 6.98-7.07 (m, 9H, aromatic H). ¹³C NMR (CDCl₃): δ 23.06 [(CH₃)₂CH-]; 27.52 [(CH₃)₂CH-]; 123.01, 123.76, 137.42, 163.06 (aromatic C).

Synthesis of Tris(2,6-diisopropylphenoxy)titanium-(IV) Hydride Trimethylphosphine, 10. Tris(2,6-diisopropylphenoxy)titanium chloride (1.29 g, 2.1 mmol) was dissolved in 30 mL of Et₂O. Then LiBH₄ powder (0.5 g, 23 mmol) was added. After 2 h of stirring at ambient temperature, the solvent was removed and 60 mL of hexane were added to the residue. Insoluble material was then removed by filtration, and the filtrate was reduced to 20 mL. A 1 mL aliquot of PMe₃ was then added at -30 °C to the clear, orange-colored solution which changed suddenly to dark red. This solution was allowed to attain ambient temperature within 20 min. After this period the color had changed again to brown yellow. Compound **10** precipitated after 2 days from the solution at -30 °C in well-formed orange-brown crystals. These were isolated by filtration to yield 0.3 g of **10** (25%); mp: 105-110 °C (decomp). Anal. Found for C₃₉H₆₁O₃PTi (M, 656.77 g/mol): C, 71.81; H, 9.20. Calcd: C, 71.32; H, 9.36. ¹H NMR (*d*₈-toluene, +20 °C): δ 0.77 [s, 9H, P(CH₃)₂]; 1.26 [d; ³J(H,H) = 6.9 Hz, 36H, -CH(CH₃)₂]; 3.72 [sept, ³J(H,H) = 6.8 Hz, 6H, -CH(CH₃)₂]; 6.85-7.05 (m, aromatic H); 8.5 (s, 1H, Ti-H). ¹³C NMR (C₆D₆): δ 12.37 [d, ¹J(P,C) = 38 Hz, P(CH₃)₂]; 23.57 [-CH(CH₃)₂]; 27.59 [-CH(CH₃)₂]; 121.94, 123.23, 136.75, 163.56 (aromatic C). ³¹P (*d*₈-toluene, -60 °C): δ -21. ³¹P (*d*₈-toluene, +20 °C): δ -37. IR (Nujol, cm⁻¹): ν 1562 (Ti-H).

Synthesis of Tris(2,6-diisopropylphenolato)-tert-butyltitanium(IV), 12. Tris(2,6-diisopropylphenolato)titanium chloride (2.19 g, 3.57 mmol) was dissolved in 30 mL of pentane. A 2.55 mL aliquot of a ^tBuLi solution in pentane (1.4 M, 3.6 mmol) was added slowly while stirring. During this process the reaction mixture turned black. After 1 h of stirring the insoluble material was removed by filtration. The solvent was then distilled from the filtrate under reduced pressure, and the black residue was treated with 2 mL of diethyl ether. During storage of the solution at -18 °C, **12** separated in brown yellow crystals, which were isolated by filtration and washed with 2 mL of cold Et₂O. Yield: 0.7 g of **12** (30%). Anal. Found for C₄₀H₆₀O₃Ti (M, 636.79 g/mol): C, 74.45; H, 10.24. Calcd: C, 75.45; H, 9.50. M/z: 637 u. Mp: 106-110 °C. ¹H NMR (CDCl₃): δ 1.06 [d, ³J(H,H) = 6.86 Hz, 36H, (CH₃)₂CH-

]; 1.57 [s, 9H, $-\text{C}(\text{CH}_3)_3$]; 3.45 [sept, $^3J(\text{H,H}) = 6.82$ Hz, 6H, $(\text{CH}_3)_2\text{CH}-$]; 6.91–7.02 (m, aromatic H). ^{13}C NMR (CDCl_3): δ 22.68 [$-\text{C}(\text{CH}_3)_3$]; 23.73 [$(\text{CH}_3)_2\text{CH}-\text{Ar}$]; 26.98 [$(\text{CH}_3)_2\text{CH}-$]; 30.48 [$-\text{C}(\text{CH}_3)_3$]; 122.18, 123.20, 137.63, 160.03 (aromatic C).

NMR Spectroscopic Characterization of Tris(2,6-diisopropylphenolato)(2-phenylethenyl)titanium, 13a, and Tris(2,6-diisopropylphenolato)(1-phenylethenyl)titanium, 13b. One drop of phenylacetylene was added to a solution of the hydride (0.1 g of **10**) in 0.3 mL of C_6D_6 . The NMR spectra showed two products in the ratio 1/1.

13a: ^1H NMR (C_6D_6): δ 1.19 [d, $^3J(\text{H,H}) = 6.84$ Hz, 36H, $-\text{CH}(\text{CH}_3)_2$]; 3.75 [sept, $^3J(\text{H,H}) = 6.84$ Hz, 6H, $(\text{CH}_3)_2\text{CH}-\text{Ar}$]; 6.99–7.36 (m, 14H, aromatic H); 8.97, 7.87 (d, $^3J(\text{H,H})_{\text{trans}} = 18.1$ Hz, 2H, $-\text{C}(\text{H})=\text{C}(\text{Ph})\text{H}$). ^{13}C NMR (C_6D_6): δ 23.57 [$(\text{CH}_3)_2\text{CH}-$]; 27.81 [$(\text{CH}_3)_2\text{CH}-$]; 123.34, 123.45, 137.64, 161.5 (aromatic C); 187.2 [$\text{Ti}-\text{C}(\text{H})=\text{C}(\text{Ph})\text{H}$]; 143.81 [$\text{Ti}-\text{C}(\text{H})=\text{C}(\text{Ph})\text{H}$].

13b: ^1H NMR (C_6D_6): δ 1.11 [d, $^3J(\text{H,H}) = 6.83$ Hz, 36H, $-\text{CH}(\text{CH}_3)_2$]; 3.61 [sept, $^3J(\text{H,H}) = 6.83$ Hz, 6H, $(\text{CH}_3)_2\text{CH}-$]; 6.12, 6.20 [s, 2H, $=\text{CH}_2$, $^2J(\text{H,H})$ coupling constant not resolved]; 6.99–7.36 (m, 14H, aromatic H). ^{13}C NMR (C_6D_6): δ 23.74 [$(\text{CH}_3)_2\text{CH}-$]; 27.56 [$(\text{CH}_3)_2\text{CH}-\text{Ar}$]; 123.34, 123.52, 137.87, 161.5 (aromatic C); 122.77 [$\text{Ti}-\text{C}(\text{Ph})=\text{CH}_2$]; 207.3 [$\text{Ti}-\text{C}(\text{Ph})=\text{CH}_2$].

Deuterolysis of 13a,b: To the NMR sample containing **13a,b** was added two drops of D_2O , and the sample was shaken vigorously for 1 min. Insoluble solids were removed before the ^1H NMR spectrum was measured. ^1H NMR ($\text{C}_6\text{D}_6/\text{D}_2\text{O}$) of the olefinic protons of *E*-2-deuteriostyrene:²⁶ δ 5.57 [d, $^3J(\text{H,H})_{\text{trans}} = 17.6$ Hz, 1H, $\text{Ph}-\text{C}(\text{H})=\text{C}(\text{D})\text{H}$]; 6.55 [dt, $^3J(\text{H,H})_{\text{trans}} = 17.6$ Hz, $^3J(\text{H,D})_{\text{cis}} \approx 1.5$ Hz, 1H, $\text{Ph}-\text{C}(\text{H})=\text{C}(\text{D})\text{H}$]. For 1-deuteriostyrene: δ 5.06 [dt, $^2J(\text{H,H})_{\text{gem}} \approx 0.8$ Hz, $^3J(\text{H,D})_{\text{cis}} = 1.6$ Hz, 1H, $\text{Ph}-\text{C}(\text{D})=\text{CH}_2$]; 5.57 [dt, $^2J(\text{H,H})_{\text{gem}} \approx 0.8$ Hz, $^3J(\text{H,D})_{\text{trans}} = 2.7$ Hz, 1H, $\text{Ph}-\text{C}(\text{D})=\text{CH}_2$].

NMR Characterization of Tris(2,6-diisopropylphenolato)(1-(trimethylsilyl)ethenyl)titanium, 14a, and Tris(2,6-diisopropylphenolato)(2-(trimethylsilyl)ethenyl)titanium, 14b. To a solution of 0.1 g of the hydride **10** in 0.3 mL C_6D_6 was added one drop of (trimethylsilyl)acetylene. The NMR spectra showed two products, **14a** and **14b**, in the ratio 3/1.

14a: ^1H NMR (C_6D_6): δ 0.09 [s, 9H, $-\text{Si}(\text{CH}_3)_3$]; 1.19 [d, $^3J(\text{H,H}) = 6.83$ Hz, 36H, $-\text{CH}(\text{CH}_3)_2$]; 3.71 [sept, $^3J(\text{H,H}) = 6.84$ Hz, 6H, $(\text{CH}_3)_2\text{CH}-$]; 6.88–7.18 (m, 9H, aromatic H); 6.72 (s, 2H, $>\text{C}=\text{CH}_2$, the second signal of the CH_2 proton is hidden under the aromatic protons). ^{13}C NMR (C_6D_6): δ -0.32 [$-\text{Si}(\text{CH}_3)_3$]; 24.02 [$(\text{CH}_3)_2\text{CH}-$]; 27.50 [$(\text{CH}_3)_2\text{CH}-$]; 123.20, 123.58, 137.72, 161.27 (aromatic C); 135.32 [t, $^1J(\text{C,H}) = 155.6$ Hz, $>\text{C}=\text{CH}_2$]; 223.05 ($>\text{C}=\text{CH}_2$).

14b: ^1H NMR (C_6D_6): δ 0.06 [s, 9H, $-\text{Si}(\text{CH}_3)_3$]; 1.19 [d, $^3J(\text{H,H}) = 6.83$ Hz, 36H, $-\text{CH}(\text{CH}_3)_2$]; 3.71 [sept, $^3J(\text{H,H}) =$

6.84 Hz, 6H, $(\text{CH}_3)_2\text{CH}-\text{Ar}$]; 6.88–7.18 (m, 9H, aromatic H); 8.48 [d, $^3J(\text{H,H})_{\text{trans}} = 20.5$ Hz, 1H, $\text{Ti}-\text{C}(\text{H})=\text{C}(\text{SiMe}_3)\text{H}$]; 7.14 [d, $^3J(\text{H,H})_{\text{trans}} = 20.5$ Hz, 1H, $\text{Ti}-\text{C}(\text{H})=\text{C}(\text{SiMe}_3)$]. ^{13}C NMR (C_6D_6): δ -1.37 [$-\text{Si}(\text{CH}_3)_3$]; 24.02 [$(\text{CH}_3)_2\text{CH}-$]; 27.50 [$(\text{CH}_3)_2\text{CH}-$]; 123.20, 123.58, 137.72, 161.27 (aromatic C); 203.44 [d, $^1J(\text{C,H}) = 127$ Hz, $\text{Ti}(\text{H})\text{C}=\text{C}(\text{H})\text{SiMe}_3$]; the signal for the β vinyl carbon of $\text{Ti}-\text{C}(\text{H})=\text{C}(\text{H})\text{SiMe}_3$ could not be unambiguously assigned.

NMR Characterization of Tris(2,6-diisopropylphenolato)(*cis*-1-(trimethylsilyl)-2-phenylethenyl)titanium, 15.

To a solution of 1-(trimethylsilyl)-2-phenylethyne in 0.3 mL of C_6D_6 compound **10** was added until the ^{29}Si NMR signal of the trimethylsilyl group of 1-(trimethylsilyl)-2-phenylethyne at -17.9 ppm had disappeared. ^1H NMR (C_6D_6): δ 0.22 (s, 9H, $-\text{Si}(\text{CH}_3)_3$), 0.80 [d, $^2J(\text{P,H}) = 2.45$ Hz, 9H, $\text{P}(\text{CH}_3)_3$]; 1.19 [d, $^3J(\text{H,H}) = 6.84$ Hz, 32H, $-\text{CH}(\text{CH}_3)_2$]; 3.73 [sept, $^3J(\text{H,H}) = 6.84$ Hz, 6H, $-\text{CH}(\text{CH}_3)_2$]; 6.8–7.4 (m, 14H, aromatic H); 9.09 [s, 1H, $\text{Ti}(\text{Me}_3\text{Si})\text{C}=\text{C}(\text{Ph})\text{H}$]. ^{13}C NMR (C_6D_6): δ 1.35 [$-\text{Si}(\text{CH}_3)_3$]; 24.03 [$-\text{CH}(\text{CH}_3)_2$]; 27.52 [$-\text{CH}(\text{CH}_3)_2$]; 123.26, 123.56, 137.67, 161.80 (aromatic C/2,6-diisopropylphenolato); 148.45 [d, $^1J(\text{C,H}) = 143.4$ Hz, $\text{Ti}(\text{Me}_3\text{Si})\text{C}=\text{C}(\text{Ph})\text{H}$]; 221.38 [$\text{Ti}(\text{Me}_3\text{Si})\text{C}=\text{C}(\text{Ph})\text{H}$]. ^{29}Si NMR: δ -9.42. 2D NMR ($^1\text{H}/^{13}\text{C}$): crosspeaks at δ -9.09 (^1H) and 148.45 (^{13}C).

NMR Characterization of Tris(2,6-diisopropylphenolato)(*cis*-1-(trimethylstannyl)-2-phenylethenyl)titanium, 16.

To a solution of 1-(trimethylstannyl)-2-phenylethyne in C_6D_6 was added the hydride **10** until the ^{119}Sn NMR signal of the alkyne at -67.15 ppm had disappeared. The new signals that emerged were fully compatible with the formation of **16**. ^1H NMR (C_6D_6): δ 0.20 [s, 9H, $-\text{Sn}(\text{CH}_3)_3$]; 0.8 [d, $^2J(\text{P,H}) = 2.44$ Hz, 9H, $\text{P}(\text{CH}_3)_3$]; 1.19 [d, $^3J(\text{H,H}) = 6.84$ Hz, 36H, $-\text{CH}(\text{CH}_3)_2$]; 3.74 [sept, $^3J(\text{H,H}) = 6.84$ Hz, 6H, $-\text{CH}(\text{CH}_3)_2$]; 6.93–7.53 (m, 9H, aromatic H); 9.11 [s, $^3J(^{119}\text{Sn,H}) = 176.27$ Hz, $^3J(^{117}\text{Sn,H}) = 168.46$ Hz, 1H, $\text{Ti}(\text{Me}_3\text{Sn})\text{C}=\text{C}(\text{Ph})\text{H}$]. ^{13}C NMR (C_6D_6): δ -5.6 [$-\text{Sn}(\text{CH}_3)_3$]; 23.9 [$-\text{CH}(\text{CH}_3)_2$]; 27.52 [$-\text{CH}(\text{CH}_3)_2$]; 123.25, 123.54, 137.56, 161.52 (aromatic C/2,6-diisopropylphenoxy); 152.05 [d, $^1J(\text{C,H}) = 148$ Hz, $\text{Ti}(\text{Me}_3\text{Sn})\text{C}=\text{C}(\text{Ph})\text{H}$]; 223.37 [$\text{Ti}(\text{Me}_3\text{Sn})\text{C}=\text{C}(\text{Ph})\text{H}$]. ^{119}Sn NMR: δ -36.30 [ddec, $^2J(^{119}\text{Sn,H}) = 53.4$ Hz, $^3J(^{119}\text{Sn,H}_{\text{trans}}) = 177$ Hz].

Acknowledgment. We are grateful to Chemetall GmbH and BASF Aktiengesellschaft for additional support of our research efforts. We also thank Mr. S. Huber and Mr. P. Meyer for recording many NMR spectra.

Supporting Information Available: Tables giving crystal data and data collection and structure refinement details, bond distances and angles, and positional and thermal parameters and figures giving additional views of the structures and packing diagrams for **7–10** and **12** (49 pages). Ordering information is given on any current masthead page.

OM950271W

(26) Yoshino, T.; Manabe, Y.; Kikuchi, Y. *J. Am. Chem. Soc.* **1964**, *86*, 4670–4673.

Enthalpies of Reaction of ((*p*-cymene)RuCl₂)₂ with Monodentate Tertiary Phosphine Ligands. Importance of both Steric and Electronic Ligand Factors in a Ruthenium(II) System

Scaffold A. Serron and Steven P. Nolan*

Department of Chemistry, University of New Orleans, New Orleans, Louisiana 70148

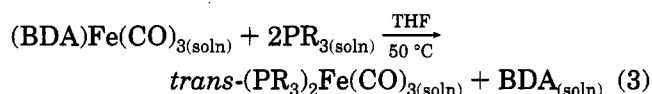
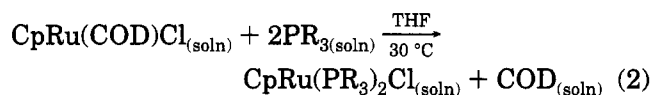
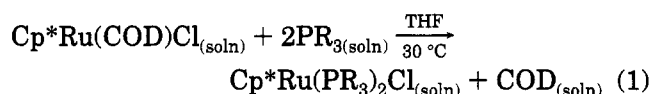
Received April 28, 1995*

The enthalpies of reaction of ((*p*-cymene)RuCl₂)₂ (*p*-cymene = (CH₃)₂CHC₆H₄CH₃) with a series of tertiary phosphine ligands, leading to the formation of (*p*-cymene)RuCl₂(PR₃) complexes (PR₃ = tertiary phosphine) have been measured by solution calorimetry in CH₂-Cl₂ at 30 °C. The range of reaction enthalpies spans some 22 kcal/mol. The overall relative order of stability established is as follows (PR₃; -Δ*H*, kcal/mol): P(*p*-CF₃C₆H₄)₃ < PCy₃ < PCy₂Ph < P(*p*-ClC₆H₄)₃ < P(OPh)₃ < P^{*i*}Pr₃ < PPh₃ < P(*p*-FC₆H₄)₃ < P(*p*-CH₃C₆H₄)₃ < PCyPh₂ < P(*p*-CH₃OC₆H₄)₃ < P^{*i*}Bu₃ < PBz₃ < PPh₂Et < PPh₂Me < P(OMe)₃ < PET₃ < PPhMe₂ < PMe₃. A quantitative analysis of ligand effect of the present data helps clarify the exact steric versus electronic ligand contributions to the enthalpy of reaction in this system. Both steric and electronic factors appear to play an important role in dictating the magnitude of the enthalpy of reaction.

Introduction

The importance of tertiary phosphine ligands in organometallic chemistry and catalysis is undeniable.^{1,2} Kinetic, catalytic, and structural studies have been conducted on organometallic complexes bearing this ancillary ligand type.³ In spite of the vast amount of information focusing on PR₃-transition metal complexes, few thermodynamic data regarding heats of binding of these ligands to metal centers exist.^{4–8} Interesting catalytic developments involving organoruthenium complexes would surely benefit from a better

understanding of ligand-binding affinity/thermochemical studies. We have most recently focused our thermochemical research efforts toward quantitatively addressing the relative importance of stereoelectronic factors as they effect enthalpies of ligand substitution reactions present in organo-group 8 metal centers^{9,10} (see eqs 1–3):



Cp = C₅H₅; Cp* = C₅Me₅; BDA = PhCH=CHCOMe; PR₃ = tertiary phosphine

We recently extended this work to emphasize the importance of electronic factors in a series of para-substituted triphenyl phosphine ligands with this (L)₂Fe(CO)₃ system.^{10c}

(8) (a) Nolan, S. P.; Hoff, C. D. *J. Organomet. Chem.* **1985**, *290*, 365–373. (b) Mukerjee, S. L.; Nolan, S. P.; Hoff, C. D.; de la Vega, R. *Inorg. Chem.* **1988**, *27*, 81–85.

(9) For organoruthenium systems, see: (a) Nolan, S. P.; Martin, K. L.; Stevens, E. D.; Fagan, P. J. *Organometallics* **1992**, *11*, 3947–3953. (b) Luo, L.; Fagan, P. J.; Nolan, S. P. *Organometallics* **1993**, *12*, 3405–3411. (c) Luo, L.; Zhu, N.; Zhu, N.-J.; Stevens, E. D.; Nolan, S. P.; Fagan, P. J. *Organometallics* **1994**, *13*, 669–675. (d) Li, C.; Cucullu, M. E.; McIntyre, R. A.; Stevens, E. D.; Nolan, S. P. *Organometallics* **1994**, *13*, 3621–3627. (e) Luo, L.; Li, C.; Cucullu, M. E.; Nolan, S. P. *Organometallics* **1995**, *14*, 1333–1338.

(10) For organoiron systems, see: (a) Luo, L.; Nolan, S. P. *Organometallics* **1992**, *11*, 3483–3486. (b) Luo, L.; Nolan, S. P. *Inorg. Chem.* **1993**, *32*, 2410–2415. (c) Li, C.; Nolan, S. P. *Organometallics* **1995**, *14*, 1327–1332.

* Abstract published in *Advance ACS Abstracts*, September 1, 1995.

(1) Collman, J. P.; Hegedus, L. S.; Norton, J. R.; Finke, R. G. *Principles and Applications of Organotransition Metal Chemistry*; 2nd ed.; University Science: Mill Valley, CA, 1987.

(2) Pignolet, L. H., Ed. *Homogeneous Catalysis with Metal Phosphine Complexes*; Plenum: New York, 1983.

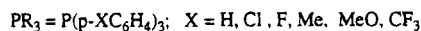
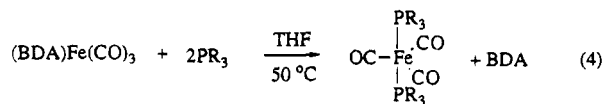
(3) (a) Noyori, R. *Asymmetric Catalysis in Organic Synthesis*; Wiley and Sons, Inc.: New York, 1994, and references cited therein. (b) Burk, M. J.; Harper, G. P.; Kalberg, C. S. *J. Am. Chem. Soc.* **1995**, *117*, 4423–4424 and references cited.

(4) For leading references in this area, see: (a) Nolan, S. P. *Bonding Energetics of Organometallic Compounds*. In *Encyclopedia of Inorganic Chemistry*; J. Wiley and Sons: New York, 1994. (b) Hoff, C. D. *Prog. Inorg. Chem.* **1992**, *40*, 503–561. (c) Martinho Simões, J. A.; Beauchamp, J. L. *Chem. Rev.* **1990**, *90*, 629–688. (d) Marks, T. J., Ed. *Bonding Energetics in Organometallic Compounds*; ACS Symposium Series 428; American Chemical Society: Washington, DC, 1990. (e) Marks, T. J., Ed. *Metal-Ligand Bonding Energetics in Organotransition Metal Compounds*; Polyhedron Symposium-in-Print 7; Pergamon: New York, 1988. (f) Skinner, H. A.; Connor, J. A. In *Molecular Structure and Energetics*; Liebman, J. F., Greenberg, A., Eds; VCH: New York, 1987; Vol. 2, Chapter 6. (g) Skinner, H. A.; Connor, J. A. *Pure Appl. Chem.* **1985**, *57*, 79–88. (h) Pearson, R. G. *Chem. Rev.* **1985**, *85*, 41–59. (i) Mondal, J. U.; Blake, D. M. *Coord. Chem. Rev.* **1983**, *47*, 204–238. (j) Mansson, M. *Pure Appl. Chem.* **1983**, *55*, 417–426. (k) Pilcher, G.; Skinner, H. A. In *The Chemistry of the Metal–Carbon Bond*; Hartley, F. R.; Patai, S., Eds.; Wiley: New York, 1982; pp 43–90. (l) Connor, J. A. *Top. Curr. Chem.* **1977**, *71*, 71–110.

(5) For a recent review of energetics of phosphorus(III) ligands to transition metal centers, see: Dias, P. B.; Minas de Piedade, M. E.; Martinho Simões, J. A. *Coord. Chem. Rev.* **1994**, *135/136*, 737–807.

(6) Nolan, S. P.; Lopez de la Vega, R.; Hoff, C. D. *Organometallics* **1986**, *5*, 2529–2537.

(7) (a) Manzer, L. E.; Tolman, C. A. *J. Am. Chem. Soc.* **1975**, *97*, 1955–1986. (b) Tolman, C. A.; Reutter, D. W.; Seidel, W. C. *J. Organomet. Chem.* **1976**, *117*, C30–C33.



In the present contribution, a ruthenium(II) arene system is investigated by solution calorimetry in order to gauge the relative importance of stereoelectronic phosphine factors on the enthalpy of ligand substitution. These results allow for a comparison with previously investigated thermochemical results of organo-group 8 systems.

Experimental Section

General Considerations. All manipulations involving organoruthenium complexes were performed under inert atmospheres of argon or nitrogen using standard high-vacuum or Schlenk tube techniques, or in a Vacuum/Atmospheres glovebox containing less than 1 ppm oxygen and water. Ligands were purchased from Strem Chemicals or Organometallics, Inc., and were used as received. Methylene chloride was distilled from P_2O_5 into flame-dried glassware prior to use. Only materials of high purity as indicated by NMR spectroscopy were used in the calorimetric experiments. NMR spectra were recorded using a Varian Gemini 300 MHz spectrometer. Calorimetric measurements were performed using a Calvet calorimeter (Setaram C-80) which was periodically calibrated using the TRIS reaction¹¹ or the enthalpy of solution of KCl in water.¹² The experimentally determined enthalpies for these two standard calibration reactions are the same within experimental error to literature values. This calorimeter has been previously described,¹³ and typical procedures are described below. Experimental enthalpy data are reported with 95% confidence limits.

¹H NMR Titrations. Prior to every set of calorimetric experiments involving a new ligand, an accurately weighed amount (± 0.1 mg) of the organoruthenium complex was placed in a Wilmad screw-capped NMR tube fitted with a septum, and CD_2Cl_2 was subsequently added. The solution was titrated with a solution of the ligand of interest by injecting the latter in aliquots through the septum with a microsyringe followed by vigorous shaking. The reactions were monitored by ¹H NMR spectroscopy, and the reactions were found to be rapid, clean, and quantitative under experimental calorimetric conditions. These conditions are necessary for accurate and meaningful calorimetric results and were satisfied for all organoruthenium reactions investigated. Only reactants and products were observed in the course of the NMR titration.

Calorimetric Measurement for Reaction between (*p*-cymene) RuCl_2 and Trimethylphosphine. The mixing vessels of the Setaram C-80 were cleaned, dried in an oven maintained at 120 °C, and then taken into the glovebox. A 20–30 mg sample of **1** was accurately weighed into the lower vessel, which was closed and sealed with 1.5 mL of mercury. A 4 mL aliquot of a 25% stock solution of diphos (1 g of PMe_3 in 25 mL of CH_2Cl_2) was added, and the remainder of the cell was assembled, removed from the glovebox, and inserted in the calorimeter. The reference vessel was loaded in an identical fashion with the exception that no organoruthenium complex was added to the lower vessel. After the calorimeter had reached thermal equilibrium at 30.0 °C (about 2 h), the vessels were removed from the calorimeter, taken into the glovebox, opened, and analyzed using ¹H NMR spectroscopy.

Conversion to (*p*-cymene) $\text{RuCl}_2(\text{PMe}_3)$ was found to be quantitative under these reaction conditions. The enthalpy of reaction, -50.2 ± 0.1 kcal/mol, represents the average of five individual calorimetric determinations. The enthalpy of solution of **1** was then added to this value to obtain a value of -55.3 ± 0.2 kcal/mol for all species in solution.

Calorimetric Measurement of Enthalpy of Solution of (*p*-cymene) RuCl_2 in CH_2Cl_2 . In order to consider all species in solution, the enthalpies of solution of **1** had to be directly measured. This was performed by using a procedure similar to the one described above with the exception that no ligand was added to the reaction cell. This enthalpy of solution represents the average of five individual determinations and is worth 5.1 ± 0.1 kcal/mol.

Synthesis. The compound $[\text{RuCl}_2(p\text{-cymene})]_2$ (**1**) was synthesized according to the literature procedure.¹⁴ Other organoruthenium complexes, (*p*-cymene) $\text{RuCl}_2(\text{PPh}_3)$, (*p*-cymene) $\text{RuCl}_2(\text{PCy}_3)$, (*p*-cymene) $\text{RuCl}_2(\text{P}(p\text{-MeC}_6\text{H}_4)_3)$, (*p*-cymene) $\text{RuCl}_2(\text{PPh}_2\text{Me})$, (*p*-cymene) $\text{RuCl}_2(\text{PPhMe}_2)$, and (*p*-cymene) $\text{RuCl}_2(\text{P}(\text{OPh})_3)$, have previously been reported.¹⁵ Experimental synthetic procedures, leading to isolation of previously unreported complexes, are described below.

(*p*-cymene) $\text{RuCl}_2(\text{PBz}_3)$ (2**).** A 50 mL flask was charged with 60 mg (0.20 mmol) of PBz_3 (tribenzyl phosphine), 61 mg (0.10 mmol) of $[\text{RuCl}_2(p\text{-cymene})]_2$, and 15 mL of CH_2Cl_2 . The clear wine red solution was stirred at room temperature for 15 min, after which the solvent was removed under vacuum. The residue was washed with 50 mL of hexane, filtered, and dried under vacuum, which afforded 67 mg of the product (yield: 66%). ¹H-NMR (300 MHz, CDCl_3): 1.18 (d, 6H, 2 CH_3), 1.67 (s, 3H, $-\text{CH}_3$), 2.65 (m, 1H, $-\text{CH}$), 3.36 (d, 6H, P- CH_2), 4.57 (d, 2H, $-\text{C}_6\text{H}_4$), 5.06 (d, 2H, $-\text{C}_6\text{H}_4$), 7.20 (m, 15H, Ph). Calcd for $\text{C}_{31}\text{H}_{35}\text{RuCl}_2\text{P}$: C, 60.97; H, 5.78. Found: C, 60.77; H, 5.75.

(*p*-cymene) $\text{RuCl}_2(\text{PCyPh}_2)$ (3**).** A 50 mL flask was charged with 103 mg (0.38 mmol) of PCyPh_2 (cyclohexyldiphenylphosphine), 98 mg (0.16 mmol) of $[\text{RuCl}_2(p\text{-cymene})]_2$, and 15 mL of CH_2Cl_2 . The clear wine red solution was stirred at room temperature for 15 min, after which the solvent was removed under vacuum. The residue was washed with 50 mL of hexane, filtered, and dried under vacuum, which afforded 116 mg of the product (yield: 63%). ¹H-NMR (300 MHz, CDCl_3): 0.5, 0.9 (m, 2H, P- C_6H_{11}), 1.00 (d, 6H, 2 CH_3), 1.23 (m, 2H, P- C_6H_{11}), 1.55 (m, 2H, P- C_6H_{11}), 1.79 (s, 6H, $-\text{CH}_3$), 2.15 (m, 2H, P- C_6H_{11}), 2.65 (m, 1H, $-\text{CH}$), 3.05 (m, 1H, P- C_6H_{11}), 4.77 (d, 2H, $-\text{C}_6\text{H}_4$), 4.95 (d, 2H, $-\text{C}_6\text{H}_4$), 7.45 (m, 8H, P-Ph), 7.92 (m, 2H, P-Ph). Calcd for $\text{C}_{28}\text{H}_{35}\text{RuCl}_2\text{P}$: C, 58.53; H, 6.14. Found: C, 58.38; H, 6.21.

(*p*-cymene) $\text{RuCl}_2(\text{P}^i\text{Pr}_3)$ (4**).** A 50 mL flask was charged with 70 mL (0.36 mmol) of P^iPr_3 (triisopropylphosphine), 100 mg (0.16 mmol) of $[\text{RuCl}_2(p\text{-cymene})]_2$, and 15 mL of CH_2Cl_2 . The clear wine red solution was stirred at room temperature for 15 min, after which the solvent was removed under vacuum. The residue was washed with 50 mL of hexane, filtered, and dried under vacuum, which afforded 113 mg of the product (yield: 74%). ¹H-NMR (300 MHz, CDCl_3): 1.30 (d, 6H, 2 CH_3), 1.33 (d, 18H, CH_3), 2.08 (s, 3H, $-\text{CH}$), 2.74 (m, 1H, $-\text{CH}$), 5.57 (q, 4H, $-\text{C}_6\text{H}_4$). Calcd for $\text{C}_{19}\text{H}_{35}\text{RuCl}_2\text{P}$: C, 48.92; H, 7.57. Found: C, 48.38; H, 7.21.

(*p*-cymene) $\text{RuCl}_2(\text{PMe}_3)$ (5**).** A 50 mL flask was charged with 45 mL (0.44 mmol) of PMe_3 (trimethylphosphine), 115 mg (0.19 mmol) of $[\text{RuCl}_2(p\text{-cymene})]_2$, and 15 mL of CH_2Cl_2 . The clear wine red solution was stirred at room temperature for 15 min, after which the solvent was removed under vacuum. The residue was washed with 50 mL of hexane, filtered, and dried under vacuum, which afforded 98 mg of the

(14) Bennett, M. A.; Huang, T.-N.; Matheson, T. W.; Smith, A. K. *Inorg. Synth.* **1982**, *21*, 74–79.

(15) (a) Demonceau, A.; Noels, A. F.; Saive, E.; Hubert, A. *J. Mol. Cat.* **1992**, *76*, 123–132. (b) Zelonka, R. A.; Baird, M. C. *Can. J. Chem.* **1972**, *50*, 3063–3072. (c) Petrici, P.; Bertozzi, S.; Lazzaroni, R.; Vitulli, G.; Bennett, M. A. *J. Organomet. Chem.* **1988**, *354*, 117–121.

(11) Ojelund, G.; Wadsö, I. *Acta Chem. Scand.* **1968**, *22*, 1691–1699.

(12) Kilday, M. V. *J. Res. Natl. Bur. Stand. (U.S.)* **1980**, *85*, 467–481.

(13) Nolan, S. P.; Hoff, C. D. *J. Organomet. Chem.* **1985**, *282*, 357–362.

product (yield: 68%). ¹H-NMR (300 MHz, CDCl₃): 1.16 (d, 6H, 2CH₃), 1.57 (d, 9H, P-CH₃), 2.02 (s, 3H, -CH₃), 2.80 (m, 1H, -CH), 5.38 (s, 4H, -C₆H₄). Calcd for C₁₃H₂₃RuCl₂P: C, 40.84; H, 6.07. Found: C, 40.75; H, 6.01.

(*p*-cymene)RuCl₂(PET₃) (6). A 50 mL flask was charged with 70 mL (0.48 mmol) of PET₃ (triethylphosphine), 110 mg (0.18 mmol) of [RuCl₂(*p*-cymene)]₂, and 15 mL of CH₂Cl₂. The clear wine red solution was stirred at room temperature for 15 min, after which the solvent was removed under vacuum. The residue was washed with 50 mL of hexane, filtered, and dried under vacuum, which afforded 110 mg of the product (yield: 72%). ¹H-NMR (300 MHz, CDCl₃): 1.11 (p, 9H, P-CH₂-CH₃), 1.21 (d, 6H, 2CH₃), 2.02 (p, 6H, PCH₂CH), 2.07 (s, 3H, -CH₃), 2.85 (m, 1H, -CH), 5.39 (q, 4H, -C₆H₄). Calcd for C₁₆H₂₉RuCl₂P: C, 45.28; H, 6.89. Found: C, 44.90; H, 6.76.

(*p*-cymene)RuCl₂(P(OMe)₃) (7). A 50 mL flask was charged with 43 mL (0.35 mmol) of P(OMe)₃ (trimethylphosphite), 110 mg (0.18 mmol) of [RuCl₂(*p*-cymene)]₂, and 15 mL of CH₂Cl₂. The clear wine red solution was stirred at room temperature for 15 min, after which the solvent was removed under vacuum. The residue was washed with ca. 50 mL of hexane, filtered, and dried under vacuum, which afforded 98 mg of the product (yield: 63%). ¹H-NMR (300 MHz, CDCl₃): 1.20 (d, 6H, 2CH₃), 2.14 (s, 3H, -CH₃), 2.88 (m, 1H, -CH), 3.75 (d, 9H, POCH₃), 5.37 (d, 2H, -C₆H₄), 5.53 (d, 2H, -C₆H₄). Calcd for C₁₃H₂₃RuCl₂PO₃: C, 36.28; H, 5.39. Found: C, 36.58; H, 5.10.

(*p*-cymene)RuCl₂(PCy₂Ph) (8). A 50 mL flask was charged with 120 mg (0.44 mmol) of PCy₂Ph (dicyclohexylphenylphosphine), 110 mg (0.18 mmol) of [RuCl₂(*p*-cymene)]₂, and 15 mL of CH₂Cl₂. The clear wine red solution was stirred at room temperature for 15 min, after which the solvent was removed under vacuum. The residue was washed with 50 mL of hexane, filtered, and dried under vacuum, which afforded 135 mg of the product (yield: 65%). ¹H-NMR (300 MHz, CDCl₃): 1.07 (d, 6H, 2CH₃), 1.24 (m, P(C₆H₁₁)₂), 1.40 (m, P(C₆H₁₁)₂), 1.71 (s, 3H, -CH₃), 1.80 (m, P(C₆H₁₁)₂), 2.50 (m, 1H, -CH), 2.65 (m, P(C₆H₁₁)₂), 2.80 (q, P(C₆H₁₁)₂), 4.95 (dd, 4H, -C₆H₄), 7.35 (m, 3H, PPh), 7.72 (m, 2H, PPh). Calcd for C₂₈H₄₁RuCl₂P: C, 57.93; H, 7.12. Found: C, 57.59; H, 7.14.

(*p*-cymene)RuCl₂(P^{*i*}Bu₃) (9). A 50 mL flask was charged with 74 mL (0.37 mmol) of P^{*i*}Bu₃ (triisobutylphosphine), 110 mg (0.18 mmol) of [RuCl₂(*p*-cymene)]₂, and 15 mL of CH₂Cl₂. The clear wine red solution was stirred at room temperature for 15 min, after which the solvent was removed under vacuum. The residue was triturated with 50 mL of hexane, filtered, and dried under vacuum, which afforded 125 mg of the product (yield: 68%). ¹H-NMR (300 MHz, CDCl₃): 1.02 (d, 18H, 6CH₃), 1.26 (d, 6H, 2CH₃), 2.00 (m, 3H, PCH(CH₃)₂), 2.08 (s, 3H, -CH₃), 2.85 (m, 1H, -CH), 5.28 (d, 2H, -C₆H₄), 5.42 (d, 2H, -C₆H₄). Calcd for C₂₂H₄₁RuCl₂P: C, 51.95; H, 8.13. Found: C, 51.55; H, 8.20.

(*p*-cymene)RuCl₂(PEtPh₂) (10). A 50 mL flask was charged with 74 mL (0.35 mmol) of PEtPh₂ (ethylidiphenylphosphine), 110 mg (0.18 mmol) of [RuCl₂(*p*-cymene)]₂, and 15 mL of CH₂Cl₂. The clear wine red solution was stirred at room temperature for 15 min, after which time the solvent was removed under vacuum. The residue was triturated with 50 mL of hexane, filtered, and dried under vacuum, which afforded 131 mg of the product (yield: 70%). ¹H-NMR (300 MHz, CDCl₃): 0.67 (q, 3H, CH₃), 0.77 (d, 6H, 2CH₃), 1.86 (s, 3H, -CH₃), 2.55 (m, 1H, -CH), 2.55 (q, 2H, P-CH₂CH₃), 5.05 (d, 2H, -C₆H₄), 5.24 (d, 2H, -C₆H₄), 7.44 (t, 6H, PPh), 7.85 (t, 4H, PPh). Calcd for C₂₄H₂₉RuCl₂P: C, 55.38; H, 5.62. Found: C, 54.85; H, 5.26.

(*p*-cymene)RuCl₂(P(*p*-ClC₆H₄)₃) (11). A 50 mL flask was charged with 123 mg (0.34 mmol) of P(*p*-ClC₆H₄)₃ (tris(*p*-chlorophenyl)phosphine), 100 mg (0.16 mmol) of [RuCl₂(*p*-cymene)]₂, and 15 mL of CH₂Cl₂. The clear wine red solution was stirred at room temperature for 15 min, after which the solvent was removed under vacuum. The residue was washed with 50 mL of hexane, filtered, and dried under vacuum, which

afforded 122 mg of the product (yield: 56%). ¹H-NMR (300 MHz, CDCl₃): 1.10 (d, 6H, 2CH₃), 1.83 (s, 3H, -CH₃), 2.85 (m, 1H, -CH), 4.94 (d, 2H, -C₆H₄), 5.23 (d, 2H, -C₆H₄), 7.32 (d, 6H, PPh), 7.70 (t, 6H, PPh). Calcd for C₂₈H₂₆RuCl₂P: C, 50.15; H, 3.91. Found: C, 49.73; H, 3.73.

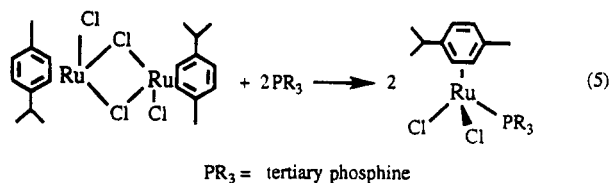
(*p*-cymene)RuCl₂(P(*p*-CH₃OC₆H₄)₃) (12). A 50 mL flask was charged with 120 mg (0.34 mmol) of P(*p*-CH₃OC₆H₄)₃ (tris(*p*-methoxyphenyl)phosphine), 100 mg (0.16 mmol) of [RuCl₂(*p*-cymene)]₂, and 15 mL of CH₂Cl₂. The clear wine red solution was stirred at room temperature for 15 min, after which the solvent was removed under vacuum. The residue was washed with ca. 50 mL of hexane, filtered, and dried under vacuum, which afforded 133 mg of the product (yield: 62%). ¹H-NMR (300 MHz, CDCl₃): 1.10 (d, 6H, 2CH₃), 1.83 (s, 3H, -CH₃), 2.85 (m, 1H, -CH), 3.78 (s, 3H, OCH₃), 4.91 (d, 2H, -C₆H₄), 5.21 (d, 2H, -C₆H₄), 6.83 (d, 6H, PPh), 7.71 (t, 6H, PPh). Calcd for C₃₁H₃₅RuCl₂PO₃: C, 56.53; H, 5.36. Found: C, 56.34; H, 5.01.

(*p*-cymene)RuCl₂(P(*p*-CF₃C₆H₄)₃) (13). A 50 mL flask was charged with 152 mg (0.32 mmol) of P(*p*-CF₃C₆H₄)₃ [tris(*p*-trifluoromethylphenyl)phosphine], 99 mg (0.16 mmol) of [RuCl₂(*p*-cymene)]₂, and 15 mL of CH₂Cl₂. The clear wine red solution was stirred at room temperature for 15 min, after which the solvent was removed under vacuum. The residue was washed with ca. 50 mL of hexane, filtered, and dried under vacuum, which afforded 180 mg of the product (yield: 72%). ¹H-NMR (300 MHz, CDCl₃): 1.05 (d, 6H, 2CH₃), 1.87 (s, -CH₃), 2.80 (m, 1H, -CH), 5.02 (d, 2H, -C₆H₄), 5.22 (d, 2H, -C₆H₄), 7.63 (d, 6H, PPh), 7.95 (t, 6H, PPh). Calcd for C₃₁H₂₆RuCl₂PF₉: C, 48.19; H, 3.39. Found: C, 47.89; H, 3.24.

(*p*-cymene)RuCl₂(P(*p*-FC₆H₄)₃) (14). A 50 mL flask was charged with 114 mg (0.36 mmol) of P(*p*-FC₆H₄)₃ [tris(*p*-fluorophenyl)phosphine], 110 mg (0.18 mmol) of [RuCl₂(*p*-cymene)]₂, and 15 mL of CH₂Cl₂. The clear wine red solution was stirred at room temperature for 15 min, after which the solvent was removed under vacuum. The residue was washed with ca. 50 mL of hexane, filtered, and dried under vacuum, which afforded 140 mg of the product (yield: 63%). ¹H-NMR (300 MHz, CDCl₃): 1.11 (d, 6H, -CH₃), 1.83 (s, 3H, -CH₃), 2.85 (m, 1H, -CH), 4.93 (d, 2H, -C₆H₄), 5.24 (d, 2H, -C₆H₄), 7.05 (t, 6H, PPh), 7.77 (m, 6H, PPh). Calcd for C₂₈H₂₆RuCl₂PF₃: C, 54.02; H, 4.21. Found: C, 53.76; H, 4.01.

Results

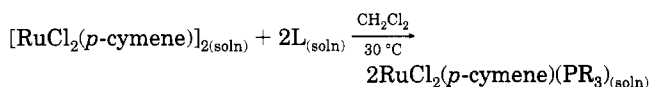
A facile entryway into the thermochemistry of (*p*-cymene)Ru(PR₃)Cl₂ complexes is made possible by the rapid and quantitative reaction of [(*p*-cymene)RuCl₂]₂ (1) with a variety of phosphine ligands (see eq 5). This



type of phosphine-binding reaction appears general and was found to be rapid and quantitative for all ligands calorimetrically investigated at 30.0 °C in methylene chloride. A compilation of phosphine and phosphite ligands along with their respective enthalpies of reaction where all species are in solution is listed in Table 1.

Discussion

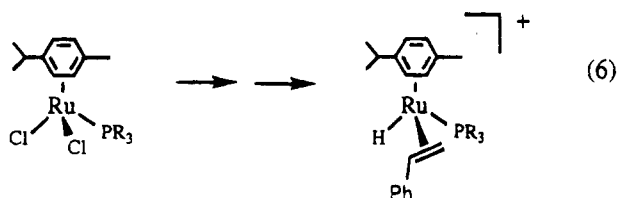
The complex [(*p*-cymene)RuCl₂] (1) and some of its phosphine derivatives have been demonstrated as efficient catalyst/catalyst precursors. Démonceau and co-workers have, for example, shown 1 and some of its phosphine derivatives to be efficient precursors for the

Table 1. Enthalpies of Substitution (kcal/mol) in the Reaction

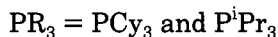
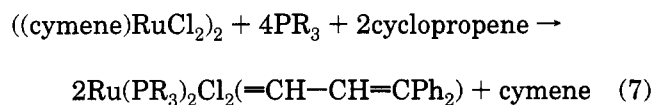
L	complex	$-\Delta H_{\text{rxn}}^a$
P(<i>p</i> -CF ₃ C ₆ H ₄) ₃	RuCl ₂ (<i>p</i> -cymene)(P(<i>p</i> -CF ₃ C ₆ H ₄) ₃)	33.4 ± 0.1
PCy ₃	RuCl ₂ (<i>p</i> -cymene)(PCy ₃)	34.4 ± 0.2
PCy ₂ Ph	RuCl ₂ (<i>p</i> -cymene)(PCy ₂ Ph)	34.6 ± 0.2
P(<i>p</i> -ClC ₆ H ₄) ₃	RuCl ₂ (<i>p</i> -cymene)(P(<i>p</i> -ClC ₆ H ₄) ₃)	34.8 ± 0.2
P(OPh) ₃	RuCl ₂ (<i>p</i> -cymene)(P(OPh) ₃)	35.5 ± 0.3
P ⁱ Pr ₃	RuCl ₂ (<i>p</i> -cymene)(P ⁱ Pr ₃)	35.6 ± 0.2
PPh ₃	RuCl ₂ (<i>p</i> -cymene)(PPh ₃)	36.3 ± 0.1
P(<i>p</i> -FC ₆ H ₄) ₃	RuCl ₂ (<i>p</i> -cymene)(P(<i>p</i> -FC ₆ H ₄) ₃)	36.5 ± 0.3
P(<i>p</i> -MeC ₆ H ₄) ₃	RuCl ₂ (<i>p</i> -cymene)(P(<i>p</i> -MeC ₆ H ₄) ₃)	37.6 ± 0.3
PCyPh ₂	RuCl ₂ (<i>p</i> -cymene)(PCyPh ₂)	38.8 ± 0.4
P(<i>p</i> -MeOC ₆ H ₄) ₃	RuCl ₂ (<i>p</i> -cymene)(P(<i>p</i> -MeOC ₆ H ₄) ₃)	39.0 ± 0.5
P ⁱ Bu ₃	RuCl ₂ (<i>p</i> -cymene)(P ⁱ Bu ₃)	39.6 ± 0.1
PBz ₃	RuCl ₂ (<i>p</i> -cymene)(PBz ₃)	40.7 ± 0.3
PEtPh ₂	RuCl ₂ (<i>p</i> -cymene)(PEtPh ₂)	45.2 ± 0.2
PPh ₂ Me	RuCl ₂ (<i>p</i> -cymene)(PPh ₂ Me)	45.6 ± 0.3
P(OMe) ₃	RuCl ₂ (<i>p</i> -cymene)(P(OMe) ₃)	45.9 ± 0.4
PEt ₃	RuCl ₂ (<i>p</i> -cymene)(PEt ₃)	51.3 ± 0.3
PPhMe ₂	RuCl ₂ (<i>p</i> -cymene)(PPhMe ₂)	52.5 ± 0.3
PMe ₃	RuCl ₂ (<i>p</i> -cymene)(PMe ₃)	55.3 ± 0.2

^a Enthalpy values are reported with 95% confidence limits.

ring-opening metathesis polymerization of olefins.¹⁵ Faller and Chase have recently reported on the utilization of phosphine derivatives of **1** as synthetic precursors leading to the facile isolation of stable ruthenium-olefin-hydride complexes (eq 6).¹⁶ Grubbs and Nguyen,



in synthetic studies related to their investigations on ring-opening and ring-closing metathesis reactions,¹⁷ have recently employed **1** as a synthon, leading to the isolation of catalytically active ruthenium-carbene complexes, (PR₃)₂Cl₂Ru(CH=CH=CPh₂) (eq 7).¹⁸ On



the basis of these recent observations concerning the reactivity of (**1**), thermochemical studies were undertaken in order to quantify the enthalpic driving forces behind the fragmentation and ligand binding observed for this dimeric complex. Enthalpies of reaction associated with phosphine coordination to the (*p*-cymene)-RuCl₂ fragment are presented and discussed in this contribution.

(16) Faller, J.; Chase, K. J. *Organometallics* **1995**, *14*, 1592–1600.
 (17) (a) Nguyen, S. T.; Johnson, L. K.; Grubbs, R. H.; Ziller, J. W. *J. Am. Chem. Soc.* **1992**, *114*, 3974–3975. (b) Fu, G. C.; Nguyen, S. T.; Grubbs, R. H. *J. Am. Chem. Soc.* **1993**, *115*, 9856–9857. (c) Nguyen, S. T.; Grubbs, R. H.; Ziller, J. W. *J. Am. Chem. Soc.* **1993**, *115*, 9858–9859.

(18) Nguyen, S. T.; Grubbs, R. H. Personal communication.

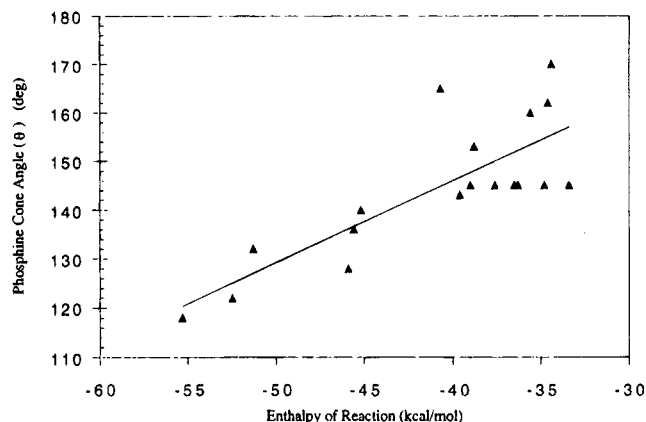


Figure 1. Enthalpy of reaction (kcal/mol) versus the phosphine cone angle (deg); slope = 1.674, $R = 0.80$.

Relative Importance of Steric/Electronic Ligand Factors. The thermodynamic entryway into this system is made possible by the rapid and quantitative nature of reaction 5 with a series of tertiary phosphine ligands. The enthalpy of reaction data found in Table 1 allow for an interpretation of the factors influencing the strength of the Ru-PR₃ bond in (*p*-cymene)RuCl₂(PR₃) complexes. The enthalpy values presented in the Table 1 are based on a molar amount of the dimer and span some 22 kcal/mol. This represents a variation of the single Ru-PR₃ bond disruption enthalpy of some 11 kcal/mol as a function of varied tertiary phosphine ligand. It can readily be seen from these reaction enthalpy data that the most sterically demanding phosphines are the weakest binders, this resulting from a possible combination of steric and electronic factors. In order to quantify the relative role of sterics vs. electronics in this phosphine system, a relationship first proposed by Tolman¹⁹ in which enthalpies of reaction are correlated to steric (θ , cone angle) and electronic (ν , A₁ carbonyl stretching frequency in Ni(CO)₃L, L = tertiary phosphine) factors was used (eq 8). Treatment

$$-\Delta H = A_0 + A_1\theta + A_2\nu \quad (8)$$

of the data in Table 1 according to eq 8 affords the following parameters: $A_0 = -1057.1$; $A_1 = 0.4542$; $A_2 = 0.4600$; $R = 0.88$. These results can be compared to earlier studies where the A_1/A_2 ratio was taken as a gauge of the relative importance of the steric vs. electronic factor. In the diaxial (L)₂Fe(CO)₃, this ratio was found to be 0.008, indicating an overwhelming influence of the electronic component.^{10a} This makes chemical sense since both PR₃ ligands occupy mutually trans coordination sites in the iron system. In a more closely related organoruthenium(II) system, Cp^{*}Ru(L)₂Cl, the ratio was calculated as 2.31, showing a slightly larger influence of the steric parameter.^{9b} In the present system, there does not appear to be an obvious dominant factor, and the A_1/A_2 ratio is 1.0. Graphically, this is illustrated in Figure 1, where a single component relationship does not yield a good correlation. It should also be stated that a similar relationship with the electronic parameter does not lead to a linear relationship ($R = 0.10$).

A number of other groups have been interested in discriminating between steric and electronic ligand

(19) Tolman, C. A. *Chem. Rev.* **1977**, *77*, 313–348.

factors.^{20,21} Giering and co-workers have applied a related but more quantitative test of kinetic and thermodynamic data to this question of stereoelectronic contributions.²² Results of this treatment are presented in eq 9, where ΔH is the enthalpy of reaction (kcal/

$$-\Delta H = -0.698 \pm 0.189\chi - 0.536 \pm 0.040\theta - 0.302 \pm 0.770E_{ar} + 125.55 \pm 6.34 \quad (9)$$

mol), χ is the electronic parameter associated with a given phosphine ligand, θ represents the phosphine steric factor, λ is a switching function that turns the steric effect when the size of the ligand exceeds the steric threshold (that is, $\lambda = 0$ when θ is less than the steric threshold angle and $\lambda = 1$ when θ is greater than the threshold angle value), and E_{ar} is the phosphine aryl substituent contribution. All phosphine parameter values (with the exception of the enthalpy data) utilized in the treatment have previously been reported by Giering and Prock.²² The correlation coefficient depicts the excellent fit of the data to this model. This treatment was performed for 15 ligands²³ and yields $R^2 = 0.960$ as a representation of the goodness of the fit. Here, no clear-cut conclusion can be drawn about the relative overwhelming importance of one factor over the other. The steric and electronic factors both appear to contribute in a relatively equal fashion to the enthalpy of reaction in the (*p*-cymene)RuCl₂(PR₃) system.

The relatively poor correlation obtained for the electronic vs. enthalpy data might point toward a small enthalpic contribution from the electronic parameter. We tested this hypothesis by considering a series of isosteric tertiary phosphine ligands. Here, as can be seen in Figure 2, a fair correlation is obtained when the electronic contribution is considered. The electronic factor does have a contribution since a lack of such an effect would have been reflected by a poor or nonexistent correlation in the Hammett relationship. The Hammett σ factors are considered as a good indication of electron donating contribution of the para phenyl group. This lack of an effect has been observed for enthalpy data of a series of isosteric phosphines in the Cp'Ru(PR₃)₂Cl (Cp' = C₅H₅ and C₅Me₅) system where steric factors have been determined to play a major role and has been

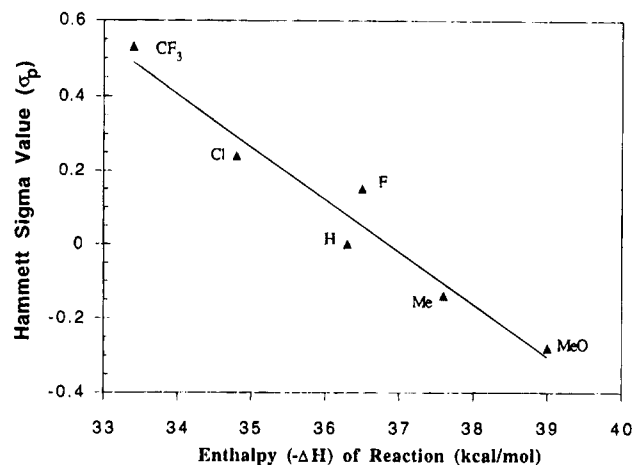


Figure 2. Enthalpy of reaction (kcal/mol) versus para substituent Hammett σ -parameter; slope = -0.14 , $R = 0.97$.

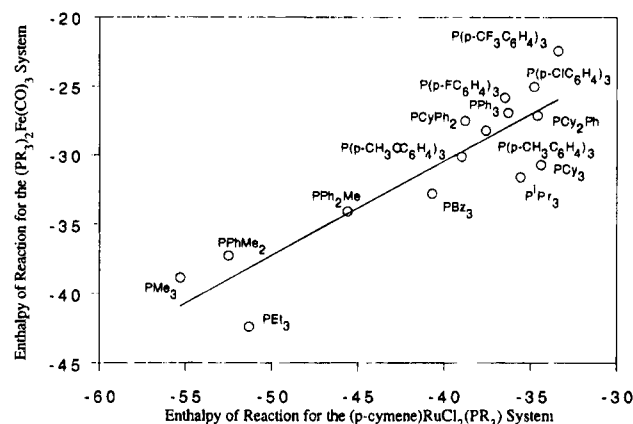
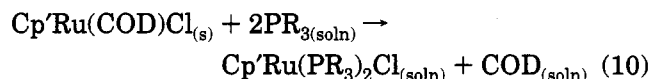


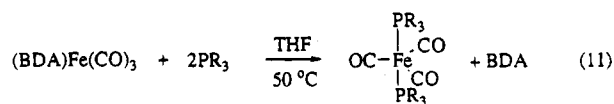
Figure 3. Enthalpies of reaction (kcal/mol) of (*p*-cymene)-RuCl₂(PR₃) versus (PR₃)₂Fe(CO)₃ (kcal/mol); slope = 0.686 , $R = 0.89$.

identified as the principal contributor to the enthalpy of reaction (see eq 10).²⁴



$$R = p\text{-XC}_6\text{H}_4; X = \text{Cl, F, Me, OMe, CF}_3, \text{ and H}$$

Comparison with Related Organometallic Systems. Most relevant systems are those revolving around group 8 metal centers. We have been involved in mapping out the thermochemical surfaces of iron and ruthenium complexes. The iron system most closely related to the present ruthenium system involves substitution of similar ligand types¹⁰ (eq 11). Direct



PR₃ = tertiary phosphine

comparison of relative bond enthalpy terms can be performed and is conveyed in Figure 3. It is quite surprising that, in spite of a different ancillary ligation and oxidation state, the iron thermochemical data

(24) Serron, S. A.; Li, C.; Luo, L.; Cucullu, M. E.; Nolan, S. P. Manuscript in preparation.

(20) (a) Rahman, M. M.; Liu, H.-Y.; Eriks, K.; Prock, A.; Giering, W. P. *Organometallics* **1989**, *8*, 1-7. (b) Liu, H.-Y.; Eriks, K.; Prock, A.; Giering, W. P. *Inorg. Chem.* **1989**, *28*, 1759-1763. (c) Poe, A. J. *Pure Appl. Chem.* **1988**, *60*, 1209-1216 and references cited therein. (d) Gao, Y.-C.; Shi, Q.-Z.; Kersher, D. L.; Basolo, F. *Inorg. Chem.* **1988**, *27*, 188-191. (e) Baker, R. T.; Calabrese, J. C.; Krusic, P. J.; Therien, M. J.; Trogler, W. C. *J. Am. Chem. Soc.* **1988**, *110*, 8392-8412. (f) Rahman, M. M.; Liu, H.-Y.; Prock, A.; Giering, W. P. *Organometallics* **1987**, *6*, 650-658.

(21) (a) Huynh, M. H. V.; Bessel, C. A.; Takeuchi, K. J. *Abstracts of Papers*, 208th National Meeting of the American Chemical Society, Washington, DC, Fall 1994; American Chemical Society: Washington, DC, 1994; INOR 165. (b) Perez, W. J.; Bessel, C. A.; See, R. F.; Lake, C. H.; Churchill, M. R.; Takeuchi, K. J. *Abstracts of Papers*, 208th National Meeting of the American Chemical Society, Washington, DC, Fall 1994; American Chemical Society: Washington, DC, 1994; INOR 166. (c) Ching, S.; Shriver, D. F. *J. Am. Chem. Soc.* **1989**, *111*, 3238-3243. (d) Lee, K.-W.; Brown, T. L. *Inorg. Chem.* **1987**, *26*, 1852-1856.

(22) (a) Fernandez, A. L.; Prock, A.; Giering, W. P. *Organometallics* **1994**, *13*, 2767-2772 and references cited. (b) Liu, H.-Y.; Eriks, K.; Prock, A.; Giering, W. P. *Organometallics* **1990**, *9*, 1758-1766. (c) Lorschach, B. A.; Prock, A.; Giering, W. P. *Organometallics* **1995**, *14*, 1694-1699.

(23) Four ligands have been omitted in the analysis (P(OPh)₃, P(OMe)₃, PBz₃, and P'Bu₃); these characteristically display deviations from this treatment and have for this reason been omitted. The phosphites have been excluded since they are considered to be a different ligand class.

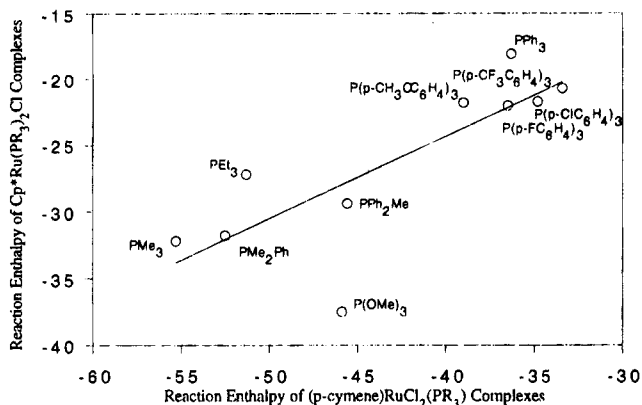


Figure 4. Enthalpies of reaction (kcal/mol) of (*p*-cymene)- $\text{RuCl}_2(\text{PR}_3)_2$ versus $\text{Cp}^*\text{Ru}(\text{PR}_3)_2\text{Cl}$ (kcal/mol); slope = 0.621, $R = 0.79$.

correlates to the present ruthenium enthalpies of reaction. This might be interpreted according to the argument that the ligand steric factor might play a more important role than denoted by the Tolman or Giering relationships, since the principal factor dictating the enthalpy of reaction in the iron system is steric. A good correlation between the two systems might point toward similar effects contributing in a similar fashion to the enthalpy of reaction. The relationship is noted as interesting, yet absolute conclusions concerning the relative importance of steric/electronic ligand effects cannot (we propose) be based on a system with such dissimilar characteristics.

There is no doubt that systems most closely related to the (*p*-cymene) $\text{RuCl}_2(\text{PR}_3)_2$ and deserving closer scrutiny are the $\text{Cp}'\text{Ru}(\text{PR}_3)_2\text{Cl}$ ($\text{Cp}' = \text{C}_5\text{H}_5$ (Cp) and C_5Me_5 (Cp^*)) systems. The available thermochemical information for the $\text{Cp}^*\text{Ru}(\text{PR}_3)_2\text{Cl}$ system⁹ is graphically presented and compared with the present (*p*-cymene) $\text{RuCl}_2(\text{PR}_3)_2$ system in Figure 4. In the Cp^* system, phosphine steric factors play a more important role than electronic considerations. Since the two systems presented show important similarities (oxidation state, ancillary ligands), one might expect a linear correlation to exist between the two systems, and the straightforward relationship of the related enthalpies of reaction illustrates this point.

A better relationship is obtained for the Cp system (Figure 5), since, as previously reported,⁹ steric factors appear to play a less important role in the Cp than in the Cp^* system. This would be in line with more even steric and electronic contributions in the present (*p*-cymene)ruthenium system as compared to the preva-

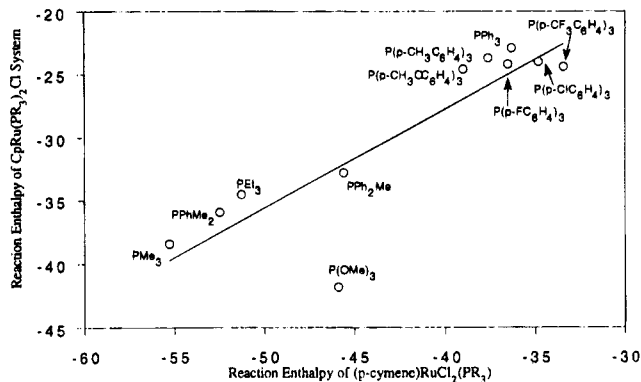


Figure 5. Enthalpies of reaction (kcal/mol) of (*p*-cymene)- $\text{RuCl}_2(\text{PR}_3)_2$ versus $\text{CpRu}(\text{PR}_3)_2\text{Cl}$ (kcal/mol); slope = 0.782, $R = 0.87$.

lence of one factor over the other in previously examined systems.

Conclusion

The labile nature of the chloride bridge in [*p*-cymene) RuCl_2] (1) was used to gain entry into the thermochemistry of ligand binding for monodentate phosphine/phosphite ligands. The enthalpy trend can be explained in terms of electronic and steric contribution to the enthalpy of reaction, with the both constituents playing important roles. A quantitative relationship is established between stereoelectronic and thermodynamic parameters and displays linear correlation. Reactions of monodentate ligands with 1 also show this reaction to be of synthetic use for isolation of complexes of formulation (*p*-cymene) $\text{Ru}(\text{PR}_3)_2\text{Cl}$. Further thermochemical, kinetic, mechanistic, and catalytic investigations focusing on this and related systems are presently underway.²⁵

Acknowledgment. The Board of Regents of the Louisiana Education Quality Support Fund (LEQSF-(RF/1993-96)-RD-A-47) and the National Science Foundation (Grant No. CHE-9305492) are gratefully acknowledged for support of this research. The authors are indebted to Johnson-Matthey/Aesar for the generous loan of ruthenium salts. The authors are also indebted to Professors Warren P. Giering and Russell Drago for helpful discussions.

OM950308C

(25) It has been suggested by one reviewer that structural differences might be present in this system when smaller cone angle phosphines are compared with more sterically demanding ones and that this factor might be correlated to the enthalpy data. We are presently exploring this avenue and thank the reviewer for this suggestion.

Toward One-Component Group 4 Homogeneous Ziegler–Natta Olefin Polymerization Catalysts: Hydroboration of Zirconium Bisalkyls with Pendant 2-Propenyl Groups Using $[(C_6F_5)_2BH]_2$

Rupert E. v. H. Spence and Warren E. Piers*,¹

Guelph-Waterloo Centre for Graduate Work in Chemistry, Guelph Campus, Department of Chemistry and Biochemistry, University of Guelph, Guelph, Ontario, Canada N1G 2W1

Received May 25, 1995[®]

Alkylation of bis[η^5 -(2-propenyl)cyclopentadienyl]zirconium dichloride, **2**, with CH_3Li , $KCH_2C_6H_5$, or $LiCH_2SiMe_3$ led to the bisalkyl derivatives **3a–c** ($R = CH_3$, **a**; $CH_2C_6H_5$, **b**; CH_2SiMe_3 , **c**), which were isolated as >95% pure yellow oils. The new ligand [2-(2-propenyl)cyclopentadienyl](*tert*-butylamino)dimethylsilane ($Cp^{allyl}SiNR$) was synthesized in a one-pot procedure and attached to zirconium via reaction of its dilithio salt with $ZrCl_4 \cdot 2THF$, producing $(Cp^{allyl}SiNR)ZrCl_2$, **4**, in 84% yield. Alkylation with the above reagents yielded alkyl derivatives **5a–c** ($R = CH_3$, **a**; $CH_2C_6H_5$, **b**; CH_2SiMe_3 , **c**) again as >95% pure yellow oils. Reactions of dichlorides **2** and **4** with the electrophilic borane $[(C_6F_5)_2BH]_n$, **1**, proceeded smoothly to the expected products in which the pendant double bond(s) was hydroborated, giving $[\eta^5-C_5H_4CH_2CH_2CH_2B(C_6F_5)_2]_2ZrCl_2$, **6**, and $[t-C_4H_9NSiMe_2-\eta^5-C_5H_3CH_2CH_2CH_2B(C_6F_5)_2]ZrCl_2$, **7**. Attempts to alkylate these compounds met with failure. Similarly, hydroborations of most of the alkyl derivatives **3a–c** and **5a–c** were not clean by virtue of the availability of alternate reaction pathways from hydroboration. Bisbenzyl complex **5b**, however, reacted cleanly with **1** to yield a complex, **8**, whose structure was elucidated using multinuclear and two-dimensional NMR techniques. In this complex, both benzyl groups on zirconium were observed to transfer to boron, giving a cationic zirconium compound stabilized by a coordinated benzyl group from the counterion $[(C_6H_5CH_2)B(C_6F_5)_2]$.

Introduction

Group 4 based “bent” metallocene dihalides are important catalyst precursors for a variety of oligomerization and polymerization processes, of which homogeneous Ziegler–Natta α -olefin polymerization² is arguably the most important. In commercial catalyst systems, the active species, believed to be a cationic metallocene alkyl, $[Cp_2MR]^+$,³ is generated from a Cp_2MX_2 precursor when it is treated with a Lewis acid cocatalyst such as methylaluminoxane (MAO)⁴ or $B(C_6F_5)_3$.⁵ The latter coactivator is advantageous because it is required only in stoichiometric quantities to generate active catalysts, allowing for direct study of these elusive species.⁶

Ligand modifications have played a key role in the development of new catalyst systems in which a remarkable degree of control over such polymer properties

as tacticity,⁷ block structure,⁸ and the level of incorporation of a comonomer⁹ may be realized. Given the impact of ligand structure (both steric and electronic) on the microstructure of the polymer produced, catalyst design remains an extremely active and important facet of research in this area. One of the principle targets in catalyst design has been a single-component catalyst with the activities of the commonly employed two-component systems but without the need for cocatalysts. Neutral, group 3, or lanthanide-based catalysts, which are isoelectronic to the cationic group 4 species, have been developed in this regard¹⁰ but thus far do not exhibit the required activities for commercial use. Another approach to this problem involves covalent attachment of the counteranion in cationic group 4 catalysts, forming a zwitterionic species.¹¹ In theory, such a catalyst could be a self-activating single-

(7) (a) Kaminsky, W.; K lper, K.; Brintzinger, H. H.; Wild, F. R. P. *Angew. Chem., Int. Ed. Engl.* **1985**, *24*, 507. (b) Ewen, J. A. *J. Am. Chem. Soc.* **1984**, *106*, 6355.

(8) Coates, G. W.; Waymouth, R. M. *Science* **1995**, *267*, 217.

(9) (a) Stevens, J. C.; Timmers, F. J.; Wilson, D. R.; Schmidt, G. F.; Nickias, P. N.; Rosen, R. K.; Knight, G. W.; Lai, S. Y. (DOW) European Patent EP-416-815-A2, March 13, 1991.

(10) (a) Burger, B. J.; Thompson, M. E.; Cotter, W. D.; Bercaw, J. E. *J. Am. Chem. Soc.* **1990**, *112*, 1566. (b) Shapiro, P. J.; Cotter, W. D.; Schaefer, W. P.; Labinger, J. A.; Bercaw, J. E. *J. Am. Chem. Soc.* **1994**, *116*, 4623. (c) Watson, P. L. *J. Am. Chem. Soc.* **1982**, *104*, 337. (d) Jeske, G.; Lauke, H.; Mauermann, H.; Swepston, P. N.; Schumann, H.; Marks, T. J. *J. Am. Chem. Soc.* **1985**, *107*, 8091.

(11) Hlatky, G. G.; Turner, H. W.; Eckman, R. R. *J. Am. Chem. Soc.* **1989**, *111*, 2728.

[®] Abstract published in *Advance ACS Abstracts*, September 1, 1995.

(1) Present address: Department of Chemistry, University of Calgary, 2500 University Drive N.W., Calgary, Alberta, T2N 1N4, Canada. E-mail: wpiers@acs.ucalgary.ca.

(2) Horton, A. D. *Trends Polym. Sci.* **1994**, *2*, 158.

(3) Jordan, R. F. *Adv. Organomet. Chem.* **1991**, *32*, 325.

(4) Sinn, H.; Kaminsky, W.; Vollmer, H. J. *Woldt, R. Angew. Chem., Int. Ed. Engl.* **1980**, *19*, 390.

(5) (a) Yang, X.; Stern, C. L.; Marks, T. J. *J. Am. Chem. Soc.* **1991**, *113*, 3623. (b) Yang, X.; Stern, C. L.; Marks, T. J. *Angew. Chem., Int. Ed. Engl.* **1992**, *31*, 1375.

(6) Yang, X.; Stern, C. L.; Marks, T. J. *J. Am. Chem. Soc.* **1994**, *116*, 10015.

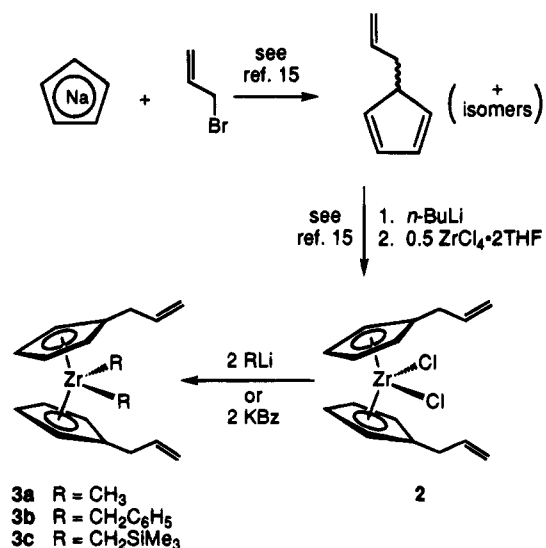
component system that lies dormant as a zwitterion in the absence of monomer. Another potential advantage of catalyst designs of this type would be control over cation/anion interactions; covalent attachment of the anion to some location in the ligand structure may restrict ion pairing and lead to more active catalysts.¹²

Covalent attachment of a Lewis acid coactivator to the ancillary ligand framework is one strategy for generating zwitterionic, self-activating catalysts, and, while attempts have been made,¹³ successful incorporation of a Lewis acid activator of sufficient potency into an ancillary ligand framework remains a significant synthetic challenge. Given the reactive nature of a Lewis acid strong enough to abstract alkyls from a group 4 metal, it would be synthetically prudent to incorporate it into the catalyst in the last step of its synthesis. One possible means of carrying out this plan would be hydroboration of a pendant olefin functionality as the means of grafting a Lewis acidic boron center into a defined location in the supporting ligand. In light of the work of Marks *et al.*, a logical borane reagent to employ would be $[(C_6F_5)_2BH]_n$, **1**, the synthesis of which we have recently reported.¹⁴ Borane **1** has proven to be an exceptional hydroboration reagent, as might be expected from its high electrophilicity. In this paper, we describe this reagent's reactivity toward several biscyclopentadienyl and cyclopentadienyl(amido)zirconium dichlorides and bisalkyl derivatives with 2-propenyl groups dangling from the cyclopentadienyl donors.

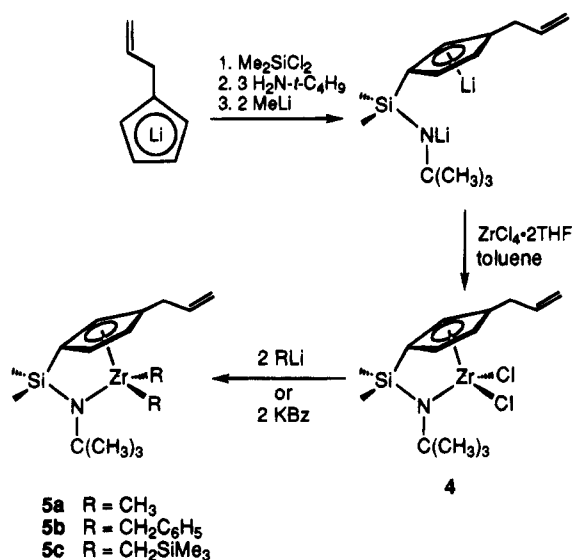
Results and Discussion

The prevailing ancillary ligand arrays employed in homogeneous Ziegler–Natta catalysts are based on either a biscyclopentadienyl donor set or a chelating cyclopentadienyl–amido arrangement. We therefore chose to examine the hydroboration of catalyst precursors containing 2-propenyl groups attached to the cyclopentadienyl rings of these two families of compounds. The syntheses of biscyclopentadienyl type zirconium dichloride and bisalkyl precursors for reaction with borane **1** were straightforwardly accomplished using commonly employed metathetical routes as outlined in Scheme 1. The complex bis[η^5 -(2-propenyl)cyclopentadienyl]zirconium dichloride, **2**, was synthesized using a procedure disclosed by Erker and Aul¹⁵ and was subsequently alkylated using alkyl lithium reagents or benzyl potassium. The bisalkyl derivatives **3a–c** were obtained as >95% pure (by ¹H NMR spectroscopy) viscous yellow or orange oils. Proton and ¹³C NMR data for all new compounds reported herein are summarized in Table 1. On standing or cooling, bisalkyls **3a–b** solidified into waxy solids which could be manipulated more conveniently, but attempts to purify these compounds via sublimation led to substantial decomposition. Crystals isolated from cooled solutions tended to liquify upon isolation and warming to room temperature. In practice, therefore, these compounds were employed in further reactions as the crude products.

Scheme 1



Scheme 2



A cyclopentadienyl–amido type ligand with a dangling 2-propenyl functionality, $H_2Cp^{allyl}SiNR$ ($R = t-C_4H_9$) was obtained as a mixture of isomers in 90% yield after distillation from a one-pot procedure in which 2-propenylcyclopentadienyllithium was treated with Me_2SiCl_2 followed by an excess of *tert*-butylamine (Scheme 2). Attachment of this ligand to zirconium was accomplished through reaction of its dilithio salt with $ZrCl_4 \cdot 2THF$ in toluene. Although the success of this methodology tends to be somewhat variable for these types of ligands, necessitating other approaches to ligand incorporation,¹⁶ we find $Li_2Cp^{allyl}SiNR$ to be conveniently and reproducibly bound in this manner to form **4** in excellent yield.

Alkylation of **4** with the same reagents employed for **2** again proceeded with no unusual observations to report. Like **3a–c**, the bisalkyl derivatives **5a–c** were either oils or gummy solids which defied purification and isolation by normal means. However, the com-

(12) Deck, P. A.; Marks, T. J. *J. Am. Chem. Soc.* **1995**, *117*, 6128.

(13) Larkin, S. A.; Shapiro, P. J. *Abstracts of Papers*, 209th Meeting of the American Chemical Society, Anaheim, CA, April 2–6, 1995; American Chemical Society, Washington, DC, 1995; INOR23.

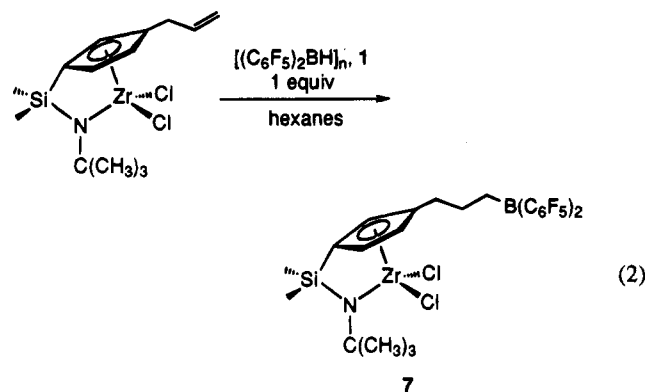
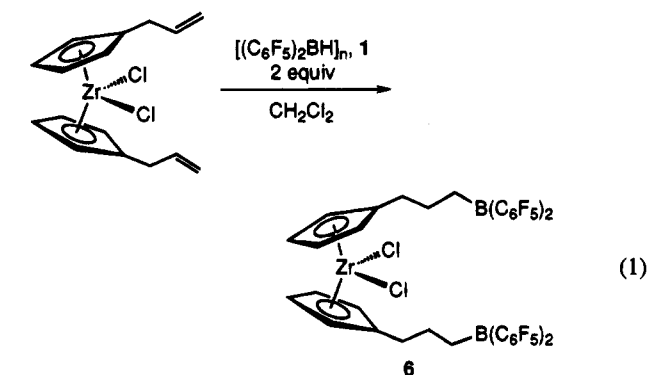
(14) Parks, D. J.; Spence, R. E. v H.; Piers, W. E. *Angew. Chem., Int. Ed. Engl.* **1995**, *34*, 809; *Angew. Chem.* **1995**, *107*, 895.

(15) Erker, G.; Aul, R. *Chem. Ber.* **1991**, *124*, 1301.

(16) Alternate routes are available: (a) Hughes, A. K.; Meetsma, A.; Teuben, J. H. *Organometallics* **1993**, *12*, 1936. (b) Piers, W. E.; Mu, Y.; MacGillivray, L. R.; Zaworotko, M. J. *Polyhedron* **1995**, *14*, 1.

pounds were seen to be >95% clean by ^1H and $^{13}\text{C}\{^1\text{H}\}$ NMR spectroscopy (Table 1) and were used as the crude oils. As can be seen from inspection of this data, the planar chirality imparted by the 1,3-substituted cyclopentadienyl ligand renders all protons with the same connectivity diastereotopic. To our knowledge the effect of an asymmetric ligand environment of this type on polymer microstructure has not been investigated.

Hydroboration of the dichloride derivatives **2** and **4** proceeded smoothly upon treatment with 2 and 1 equiv, respectively, of the borane reagent **1**, yielding the compounds **6** and **7** as shown in eq 1 and 2. Like



hydroboration of other olefinic substrates with **1**, the reactions were extremely rapid and proceeded to completion essentially upon mixing of the reagents as indicated by the immediate disappearance of characteristic olefinic resonances of the 2-propenyl group in the ^1H NMR and complete dissolution of the normally insoluble, dimeric borane **1**.¹⁴ In contrast, hydroboration of **2** with 9-BBN took several hours to reach conclusion.¹⁵ Within the detection limits of ^1H NMR spectroscopy, these hydroborations were highly regioselective, producing exclusively the 1,2 addition products shown.

Both **6** and **7** are prone to pick up 1 or 2 equiv of any Lewis base present in the system, and so donor solvents are to be avoided when handling these compounds. Complex **6**, for example, may be viewed as a chelating Lewis acid, and consistent with this notion is its propensity toward binding 1 equiv of diethyl ether or THF when exposed to these solvents. In the absence of donors, there does not appear to be any association between the Lewis acidic boron centers and the chloride ligands on zirconium. This is most convincingly demonstrated by the ^{11}B NMR chemical shifts found for **6**

and **7**, which are at 73.9 and 73.0 ppm, respectively. These resonances are in the chemical shift range typical of neutral, three-coordinate boron centers.¹⁷

Attempts to cleanly alkylate these compounds with a variety of alkylating agents (MeLi , $\text{KCH}_2\text{C}_6\text{H}_5$, AlMe_3 , ZnMe_2) met with failure, producing complex mixtures of products. Similar results were found regardless of the reaction conditions employed. These observations were not completely unanticipated in light of the high electrophilicity of the boron centers in these molecules and confirm the notion that incorporation of these Lewis acid activators into the molecular structure of the catalyst is best left as the ultimate step in the synthesis.

We therefore prepared the bisalkyl derivatives as described above and treated them with the borane **1** in the appropriate equivalency. The compounds **3a–c** and **5a–c** were all found to react immediately with the borane, but only the reaction between **1** and the $(\text{Cp}^{\text{allyl}}\text{SiNR})\text{ZrBz}_2$ derivative **5b** led to a stable, isolable product (*vide infra*). The outcomes of the other reactions were highly dependent on the size of the alkyl groups. For example, the reactions involving the two dimethyl compounds **3a** and **5a** were more complex than the reactions involving the bisalkyls incorporating larger (trimethylsilyl)methyl or benzyl groups. In addition to the desired hydroboration of the pendant olefin functionality, the borane also reacted with the zirconium carbon bonds as evidenced by the presence of both CH_4 and $\text{CH}_3\text{B}(\text{C}_6\text{F}_5)_2$ in the reaction product mixtures.¹⁸ In a separate study, **1** was found to be highly reactive toward the parent zirconocene bisalkyls; we have reported details of the reactions of $\text{Cp}_2\text{Zr}(\text{CH}_3)_2$ with **1** elsewhere.¹⁹

Reactions of the bis(trimethylsilyl)methyl derivatives **3c** and **5c** with **1** proceeded more selectively to give hydroborated products, as evidenced by the complete disappearance of olefinic signals in the ^1H NMR spectrum. Although spectra taken soon after mixing the reagents showed the reactions to be quite clean, the products were unstable in solution; decomposition to several products was observed within 30 min. In both cases, one of the compounds in the final mixture was identified as $\text{TMSCH}_2\text{B}(\text{C}_6\text{F}_5)_2$.²⁰

Unlike the above described chemistry, reaction between **1** and the dibenzyl complex **5b**, when carried out

(17) Kidd, R. G. In *NMR of Newly Accessible Nuclei*; Laszlo, P., Ed. Academic Press: New York, 1983; Vol. 2.

(18) In addition to sharp signals for molecular species in the product mixtures of the reactions of dimethyl derivatives **3a** and **5a** with **1**, broad, featureless resonances associated with a viscous oil were observed in the ^1H NMR spectrum. We speculate that this component of the product mixture results from the oligomerization of the pendant α -olefin functionality by active catalysts formed early in the reaction upon successful hydroboration and methyl abstraction. (This demonstrates another potential synthetic pitfall to be circumvented in the generation of these types of catalysts). Aside from the broad ^1H NMR spectra, we note in support of this notion that only sharp signals were observed in the ^1H NMR when a complex analogous to **5a** but with a 2-methyl-2-propenyl group dangling from the Cp ring was reacted with **1** (Spence, R. E. v H.; Piers, W. E. Unpublished results), presumably because the *gem*-disubstituted olefin cannot be oligomerized with catalysts of this type. However, this reaction was also extremely complex due to the variety of reaction pathways possible and the production of several diastereomers in each pathway.

(19) Spence, R. E. v H.; Parks, D. J.; Piers, W. E.; MacDonald, M. A.; Zaworotko, M. J.; Rettig, S. J. *Angew. Chem., Int. Ed. Engl.* **1995**, *34*, 1230; *Angew. Chem.* **1995**, *107*, 1337.

(20) ^1H NMR, C_6D_6 : 2.01, CH_2 (m, 2H, $^2J_{\text{HB}} = 1.5$ Hz); -0.075, CH_3 (s, 9H). This compound was independently generated from $\text{Cp}_2\text{Zr}(\text{CH}_2\text{TMS})_2$ and $\text{ClB}(\text{C}_6\text{F}_5)_2$.

Table 1. ^1H and $^{13}\text{C}\{^1\text{H}\}$ NMR Data for Isolated New Compounds^a

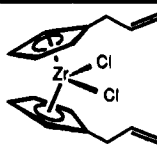
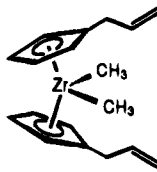
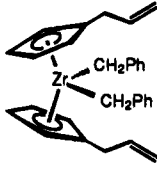
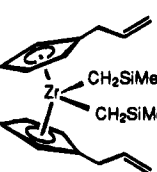
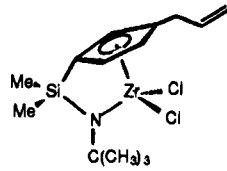
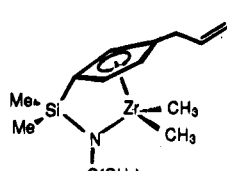
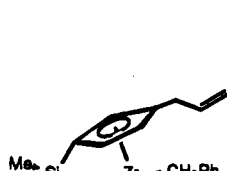
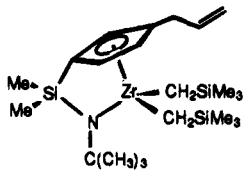
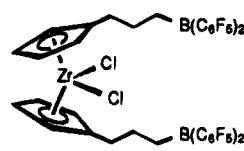
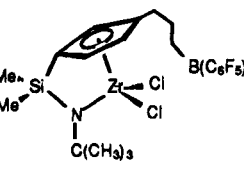
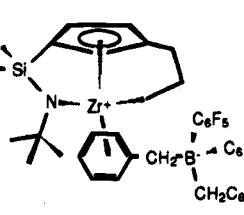
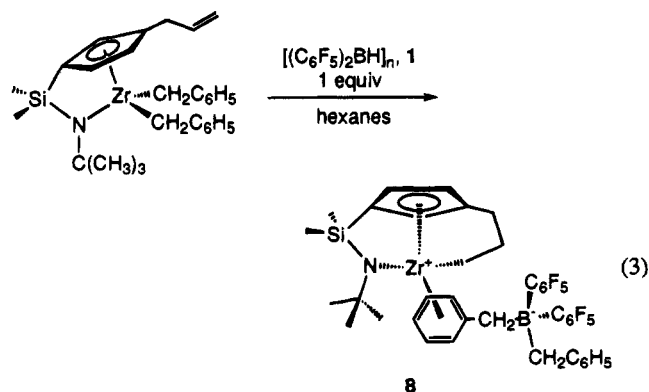
Compound	#	^1H NMR Data			$^{13}\text{C}\{^1\text{H}\}$ NMR Data	
		δ (ppm)	Assignment	J(Hz)	δ (ppm)	Assignment
	2b	5.88, 5.72 (m, 8H)	CpH		136.5	=CH
		5.84 (m, 2H)	=CH CH ₂		132.5	C _{ipso}
		4.97 (m, 2H)	=CHH	16.0, 1.6	116.5	=CH ₂
		4.96 (m, 2H)	=CHH	11.0	116.7, 112.3	CpCH
		3.36 (d, 4H)	CH ₂	6.8	34.6	CH ₂
	3a	5.84 (m, 2H)	=CH CH ₂		137.6	=CH
		5.69, 5.50 (m, 8H)	CpH		125.6	C _{ipso}
		5.02 (m, 2H)	=CHH	17.0, 1.5	115.7	=CH ₂
		4.98 (m, 1H)	=CHH	10.0	111.2, 108.1	CpCH
		3.11 (d, 4H)	CH ₂	6.4	34.5	CH ₂
		-0.21 (s, 6H)	ZrCH ₃		30.7	ZrCH ₃
	3b	7.22 (d, 4H)	CH _{ortho}	7.2	152.5	C _{ipso} (Ph)
		6.90 (m, 6H)	CH _{meta, para}		137.2	=CH
		5.67 (m, 2H)	=CH CH ₂		128.5, 126.1, 121.3	PhCH
		5.57, 5.48 (m, 8H)	CpH		125.7	C _{ipso} (Cp)
		4.91 (m, 2H)	=CH H	17.0, 1.4	115.8	=CH ₂
		4.92 (m, 2H)	=CHH	10.5	113.5, 111.6	CpCH
		2.77 (d, 4H)	CH ₂	6.4	61.7	ZrCH ₂
		1.83 (s, 4H)	ZrCH ₂		34.0	CH ₂
	3c	6.03, 5.50 (m, 8H)	CpH		137.5	=CH
		5.91 (m, 2H)	=CH CH ₂		124.7	C _{ipso}
		5.03 (m, 2H)	=CH H	17.1, 1.8	115.8	=CH ₂
		5.00 (m, 2H)	=CHH	10.1	112.1, 106.8	CpCH
		3.18 (d, 4H)	CH ₂	6.8	43.5	CH ₂
		0.13 (s, 18H)	SiCH ₃		34.9	ZrCH ₂
		0.04 (s, 4H)	ZrCH ₂		3.8	SiCH ₃
	4	6.41, 6.10, 5.98 (m, 3H)	CpH		138.6	C _{ipso}
		5.86 (m, 1H)	=CHCH ₂		135.8	=CH
		4.99 (m, 1H)	=CHH	17.0, 1.8	122.5, 121.8, 120.3	CpCH
		4.96 (m, 1H)	=CHH	10.0	117.1	=CH ₂
		3.30 (d, 2H)	=CCH ₂	6.8	109.0	CpC-Si
		1.29 (s, 9H)	NC(CH ₃) ₃		57.7, 32.7	NC(CH ₃) ₃
		0.25 (s, 6H)	SiCH ₃		34.1	CH ₂
					0.78, 0.63	SiCH ₃
	5a	6.38, 6.00, 5.82 (m, 3H)	CpH		136.9	=CH
		5.85 (m, 1H)	=CH CH ₂		132.7	C _{ipso}
		5.06 (m, 1H)	=CHH	17.2	120.1, 119.0, 116.8	CpCH
		4.98 (m, 1H)	=CHH	10.2	116.2	=CH ₂
		3.24 (m, 2H)	=CCH ₂	6.7	102.9	CpC-Si
		1.34 (s, 9H)	NC(CH ₃) ₃		55.5, 34.3	NC(CH ₃) ₃
		0.30 (s, 6H)	SiCH ₃		36.4	CH ₂
		0.11, 0.04 (s, 6H)	ZrCH ₃		34.0 ^d	ZrCH ₃
					1.59, 1.54	SiCH ₃
	5b	7.11, 7.05 (m, 4H)	CH _{meta}		147.3, 142.5	C _{ipso} (Ph)
		6.95, 6.90 (m, 2H)	CH _{para}	7.3, 7.4	137.4	=CH
		6.80, 6.60 (d, 4H)	CH _{ortho}	7.7, 7.1	132.1	C _{ipso} (Cp)
		6.04, 5.84, 5.76 (m, 3H)	CpH		130.4, 129.2, 127.5,	
		5.76 (m, 1H)	=CH CH ₂		127.1, 123.2, 122.1	PhCH
		4.97 (m, 2H)	=CH ₂		119.8, 119.3, 118.3	CpCH
		3.16 (dd, 1H)	=CCHH	15.8, 6.2	115.7	=CH ₂
		2.95 (dd, 1H)	=CCHH	15.8, 6.6	105.7	CpC-Si
		2.17, 1.63 (d, 2H)	ZrCH ₂	9.5	57.3, 33.9	NC(CH ₃) ₃
		1.56, 1.21 (d, 2H)	ZrCH ₂	10.6	55.5, 52.9	ZrCH ₂
		1.19 (s, 9H)	NC(CH ₃) ₃		33.9	CH ₂
0.33, 0.28 (s, 6H)	SiCH ₃		1.7, 1.2	SiCH ₃		

Table 1 (Continued)

Compound	#	^1H NMR Data			$^{13}\text{C}\{^1\text{H}\}$ NMR Data			
		δ (ppm)	Assignment	J(Hz)	δ (ppm)	Assignment		
	5c	6.59, 6.14, 6.07 (m, 3H)	CpH		137.1	=CH		
		5.93 (m, 1H)	=CH CH ₂		132.7	C _{ipso} (Cp)		
		5.08 (m, 1H)	=CHH	16.8	119.9, 119.0, 116.7	CpCH		
		5.02 (m, 1H)	=CHH	10.1, 1.7	116.1	=CH ₂		
		3.41 (dd, 1H)	=CCHH	15.3, 6.4	103.4	CpC-Si		
		3.32 (dd, 1H)	=CCHH	15.3, 6.6	56.0, 34.3	NC(CH ₃) ₃		
		1.36 (s, 9H)	NC(CH ₃) ₃		52.6, 52.6	ZrCH ₂		
		0.87, 0.20 (d, 2H)	ZrCH ₂	11.2	34.4	CH ₂		
		0.63, 0.05 (d, 2H)	ZrCH ₂	11.6	3.8, 3.3	Si(CH ₃) ₃		
		0.37, 0.35 (s, 6H)	SiCH ₃		1.9, 1.7	SiCH ₃		
		0.17, 0.16 (s, 18H)	SiCH ₃					
			6	5.89, 5.57 (m, 4H)	CpH		133.4	C _{ipso} (Cp)
2.75 (t, 4H)	CCH ₂			6.5	117.7, 110.8	CpCH		
1.90 (br t, 4H)	BCH ₂			7.5	32.7	CCH ₂		
1.76 (m, 4H)	CH ₂				32.0 (br)	CH ₂ B		
					26.2	CH ₂		
	7	6.41, 6.12, 5.99 (m, 3H)	CpH		139.9	C _{ipso} (Cp)		
		2.78 (m, 1H)	CCHH		122.7, 121.5, 120.1	CpCH		
		2.60 (m, 1H)	CCHH		109.5	CpC-Si		
		1.86 (br t, 2H)	BCH ₂		58.0, 32.6	NC(CH ₃) ₃		
		1.77 (m, 2H)	CH ₂		32.4	CCH ₂		
		1.29 (s, 9H)	CCH ₃		32.0	CH ₂ B		
		0.27 (s, 6H)	SiCH ₃		26.5	CH ₂		
					0.6, 0.5	SiCH ₃		
			8e	7.18 (m, 3H)	CH _{ortho,para}		159.7, 151.1, 147.7	C _{ipso} (Ph, Cp)
				7.05 (m, 2H)	CH _{meta}		129.1, 127.8, 123.8	PhCH
6.94, 6.66 (d, 2H)	η -CH _{ortho}			7.0, 6.8	128.7, 127.4	η -PhCH _{ortho}		
6.07, 6.81 (m, 2H)	η -CH _{meta}				128.6, 128.2	η -PhCH _{meta}		
5.82, 5.41, 4.96 (m, 3H)	CpH				127.3, 115.1, 112.7	CpCH		
5.76 (m, 1H)	η -CH _{para}			6.6	121.9	η -PhCH _{para}		
2.97 (br s, 2H)	BCH ₂ C ₆ H ₅				113.6	CpC-Si		
2.93, 2.83 (d, 2H)	BCH ₂ η -C ₆ H ₅			9.6	59.0, 34.3	NC(CH ₃) ₃		
2.24, 1.12 (m, 2H)	CH ₂				50.3	ZrCH ₂		
2.11 (m, 2H)	CCH ₂				40.5	CH ₂		
0.89, 0.31 (m, 2H)	ZrCH ₂				37.9, 33.3	BCH ₂ C ₆ H ₅		
0.77 (s, 9H)	CCH ₃		27.2	CCH ₂				
0.24, 0.05 (s, 6H)	SiCH ₃		5.0, 0.46	SiCH ₃				

^a ^1H NMR spectra were recorded in C₆D₆ at room temperature at 400 MHz except where noted. $^{13}\text{C}\{^1\text{H}\}$ NMR spectra were obtained in C₆D₆ at room temperature at 100 MHz except where noted. Spectra were referenced to solvent peaks. ^b NMR data for compound 2 in CDCl₃ were reported in reference 15. ^c ^1H and $^{13}\text{C}\{^1\text{H}\}$ spectra recorded at 200 and 50 MHz, respectively. ^d The resonance for the other diastereotopic ZrCH₃ group was obscured by the signal for the *t*-butyl group. ^e ^1H spectrum recorded in C₇D₈ at -20°C.

in hexanes, led to a product, **8**, in 61% yield as a yellow powder that precipitated from solution (eq 3). The



precise structure of this compound is unknown due to our inability to obtain single crystals for X-ray analysis; the compound tends to oil out of the aliphatic solvent systems employed and decomposes in chlorinated or donor solvents. Microanalytical data are consistent with an empirical formula comprising the components of the reaction, **5b** and **1**. Several lines of spectroscopic evidence led us to propose the structure depicted in eq 3 in which an exchange of both benzyl groups from zirconium to boron has taken place and in which the propyl side chain on the ring is tethered to the zirconium center.

Immediately evident from ^1H , ^{19}F , and $^{11}\text{B}\{^1\text{H}\}$ NMR data was the fact that hydroboration and alkyl abstraction by the boron center had taken place. Olefinic resonances from the 2-propenyl group were no longer

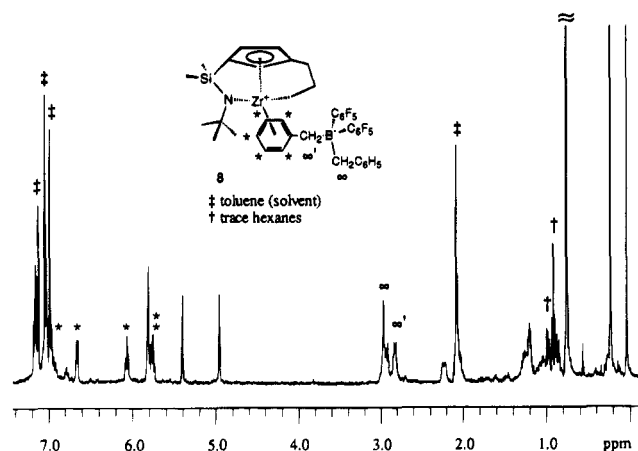


Figure 1. 400 MHz ^1H NMR spectrum of **8** (C_7D_8 , -20°C).

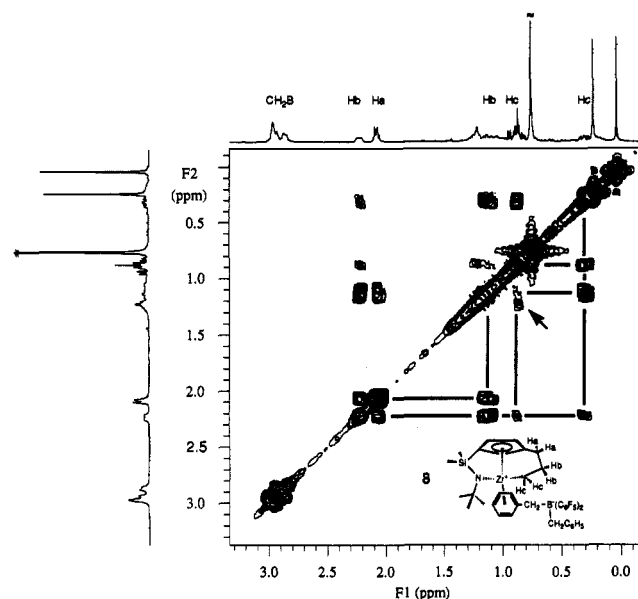


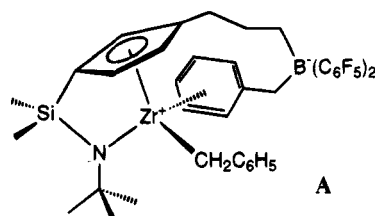
Figure 2. COSY45 plot of the 0–3.3 ppm region of the ^1H NMR spectrum of **8**. The cross-peak indicated by the arrow is due to the hexane present in the sample.

present. Furthermore, the chemical shift of the ^{11}B resonance (-9.1 ppm) indicated a four-coordinate, *anionic* boron center. The pattern of resonances in the ^{19}F NMR spectrum (-132.9 , *ortho*; -164.1 , *para*; -167.3 , *meta*) in which the resonance for the *para* fluorine atom was shifted upfield by about 15 ppm in comparison to that in neutral, three-coordinate compounds, was also typical of such a boron environment.⁶ Finally, in the $^{13}\text{C}\{^1\text{H}\}$ NMR spectrum, two broad resonances attributable to carbons bonded to boron were detected at 33.3 and 37.9 ppm. Only one such resonance would be expected if the reaction had stopped at simply hydroborating the pendant double bond.

The proton NMR spectrum of **8**, accumulated at -20°C , is shown in Figure 1. In the aromatic region of the ^1H NMR spectrum, in addition to a normal pattern of resonances for a typical benzyl group, five separate resonances were observed for the phenyl protons of the other benzyl moiety. The upfield shift of these resonances from their usual positions is indicative of coordination of the arene ring to the zirconium center. Similar features were evident in the $^{13}\text{C}\{^1\text{H}\}$ NMR spectrum (Table 1). This sort of behavior has been observed in other instances where benzyl groups have

been removed from organozirconium compounds using the Lewis acid abstractor $\text{B}(\text{C}_6\text{F}_5)_3$.^{6,21} In the absence of stronger bases, the cationic zirconium center obtains electrons from the π -system of the nonfluorinated arene ring of the benzyl group. Because of the asymmetric coordination environment about zirconium in **8** all five phenyl protons of the coordinated ring are inequivalent; a COSY experiment allowed the *ortho*, *meta*, and *para* protons to be assigned as given in Table 1.

The data discussed to this point do not distinguish between the structure proposed for **8** in eq 3 and one akin to that shown in **A** which would have resulted if



the reaction between **5b** and **1** had stopped at hydroboration and benzyl abstraction. Although a more complex reaction sequence must take place to arrive at **8**, structure **A** was rejected as a result of a heteronuclear multiple quantum coherence (HMQC) experiment²² which clearly showed that the two broad resonances in the $^{13}\text{C}\{^1\text{H}\}$ NMR spectrum assigned to carbons bonded to boron correlated to the broad resonance at 2.97 ppm and to the doublets at 2.93 and 2.83 in the ^1H NMR spectrum which we ascribed to the benzyl methylene groups. If the assignment of the benzyl protons is correct, this result implies that both benzyl groups have been transferred to boron. In support of this assignment, the COSY experiment showed that the resonances around 2.9 ppm do not correlate to any other peaks in the spectrum (Figure 2 shows the COSY plot for the 0–3.5 ppm region of the spectrum). Also, a separate NOESY experiment on the sample showed that these benzyl resonances correlate only with *ortho* protons on the phenyl rings, as would be expected on the basis of their physical proximity.

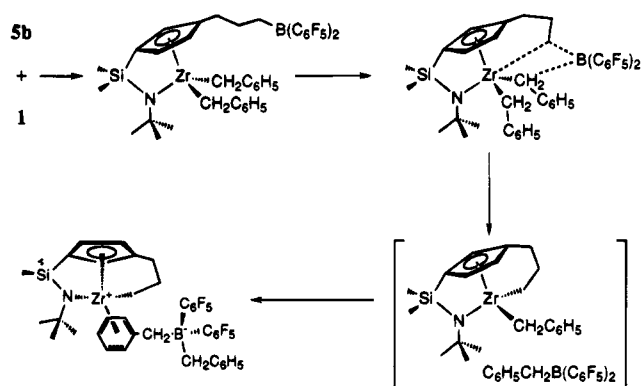
The HMQC and COSY experiments also aided in assignment of the six inequivalent protons and carbon resonances for the three methylenes of the propyl chain connecting the Cp ring to zirconium. Of particular interest were the two proton resonances at 0.31 and 0.89 ppm which were correlated to the carbon resonance at 50.3 ppm. The COSY plot shown in Figure 2 clearly establishes the connectivity of the protons in the $\text{CCH}_2\text{-CH}_2\text{CH}_2\text{X}$ ($\text{X} = \text{B}$ or Zr) and shows that these two protons and the carbon are due to the methylene unit bonded to X. The low-field position of the carbon peak is characteristic of carbons bonded to cationic zirconium centers; protons on such carbons typically also have rather high-field proton resonances.²³ Although carbon atoms bonded to the $\text{B}(\text{C}_6\text{F}_5)_2$ fragments typically resonate near 50 ppm, $\text{RCH}_2\text{B}(\text{C}_6\text{F}_5)_2$ protons typically

(21) (a) Pellachia, C.; Immirzi, A.; Grassi, A.; Zambelli, A. *Organometallics* **1993**, *12*, 4473. (b) Pellachia, C.; Immirzi, A.; Grassi, A. *J. Am. Chem. Soc.* **1993**, *115*, 1160. (c) Bochmann, M.; Lancaster, S. J.; Hursthouse, M. B.; Abdul Malik, K. M. *Organometallics* **1994**, *13*, 2235. (d) van der Linden, A.; Schaverien, C. J.; Meijboom, N.; Ganter, C.; Orpen, A. G. *J. Am. Chem. Soc.* **1995**, *117*, 3008.

(22) Bax, A.; Subramanian, S. *J. Magn. Reson.* **1986**, *67*, 565.

(23) Jordan, R. F.; LaPointe, R. E.; Bradley, P. K.; Baenziger, N. *Organometallics* **1989**, *12*, 2892.

Scheme 3



resonate in between 2 and 3.5 ppm.¹⁴ This data also favors **8** over the alternate structure **A**.

Other observations compatible with our assignment were the observed temperature dependence of the ¹H and ¹⁹F NMR spectra. Consistent with the presence of a loosely coordinated arene ring, exchange of substituents on boron was observed to be facile. In the ¹⁹F spectrum of **8** at room temperature, only one set of sharp signals for the diastereotopic C₆F₅ groups was observed. Upon being cooled, each resonance broadened, the signal due to the *ortho* fluorines most severely. At around -50 °C coalescence was observed, the signals emerging as four peaks at -129.9, -131.7, -134.4, and -135.3 ppm (average = -132.8 ppm) due to four diastereotopic *ortho* fluorines in the slow exchange regime. Chemical shift dispersion in the *meta* and *para* fluorines was not as extensive, but significant broadening was observed in these resonances also. In the ¹H NMR spectrum, the slow exchange spectrum was observed at -20 °C (Figure 1). Upon warming, the resonances assigned to the benzyl methylene protons broadened and coalesced into one broad resonance at 2.88 ppm; similarly *all* of the resonance for the phenyl protons coalesced into a broad peak centered around 6.89 ppm. Other resonances in the spectrum, most notably the signals for the diastereotopic methyl groups on silicon, remained sharp. These observations may be rationalized on the basis of an exchange process involving dissociation of the coordinated arene^{22a} and recoordination of the phenyl ring of the other benzyl group.

The details of how **8** forms are unknown, but the steps which must take place are depicted in Scheme 3. Likely hydroboration takes place first; subsequently an exchange between one of the benzyl groups (presumably the one closest to the dangling boron center) and the boron propyl moiety occurs. Whether this is a concerted process as shown in Scheme 3 or a stepwise sequence is unknown. The intermediacy of the neutral products is also in question; no evidence for production of C₆H₅-CH₂B(C₆F₅)₂ was observed, but, as mentioned above, in the hydroboration of **5c** some TMSCH₂B(C₆F₅)₂ was identified in the mixture of products. If produced, abstraction of the remaining benzyl group by C₆H₅-CH₂B(C₆F₅)₂ would lead to **8** as shown; alternatively, the exchanges necessary could be concerted in nature.

Summary and Concluding Remarks

Although we have not yet arrived at an internally activated catalyst system, our results show that such a goal is a realistic one. The strategy of using hydro-

boration to incorporate Lewis acidic boron centers into the ancillary ligand structure appears to be viable, but several observations herein provide guidance as to the conditions under which such chemistry may successfully produce a catalyst with the desired features. For example, since borane reagent **1** is also reactive toward metal–carbon bonds, alkyl groups or pendant functionalities must be chosen to bias the reagent toward hydroboration, which must be irreversible. It also appears from this study that the three-carbon tether is too long to avoid the exchange shown in Scheme 3 which leads to a complex such as **8**. Close inspection of the ¹H NMR spectrum of **8** shown in Figure 1 indicates that another species is present in minor amounts as evidenced by small ligand signals in the baseline. This is perhaps indicative of a species related to the desired structure **A** in which such an exchange has not taken place. This exchange is likely entropically favored in this particular system but may be enthalpically disfavored in related complexes with two- or one-carbon chains linking the boron to the cyclopentadienyl donor. We are currently exploring these and other strategies to circumvent the problems exposed in this work.

Experimental Section

General Procedures. All manipulations were performed either in a Braun MB-150 inert atmosphere glovebox or on greaseless vacuum lines equipped with Teflon needle valves (Kontes) using swivel frit-type glassware. Solvents were purified by distillation from an appropriate drying agent and stored in evacuated pots over either "titanocene"²⁴ (aliphatic solvents), sodium benzophenone ketyl (diethyl ether, THF), or CaH₂ (chlorinated solvents). *d*₆-Benzene was dried sequentially over activated 3 Å sieves and "titanocene" and was stored in the glovebox; other NMR solvents were dried analogously to the perprotio solvents.

The following reagents were synthesized using literature procedures: [η^5 -C₅H₄CH₂CH=CH₂]₂ZrCl₂,¹⁵ [(C₆F₅)₂BH]₂,¹⁴ and KCH₂C₆H₅.²⁵ All other materials were obtained from Aldrich and either used as received or dried and distilled prior to use.

Samples were analyzed by NMR spectroscopy on Varian Gemini 200 MHz and Unity 400 MHz instruments. ¹H spectra were referenced to residual protons in the deuterated solvent medium. ¹³C{¹H} NMR were referenced to solvent signals; signals broadened severely due to bonding to quadrupolar boron nuclei were detected using the HMQC pulse sequence. ¹⁹F NMR spectra were recorded at 376.2 MHz and referenced to CFCl₃. ¹¹B{¹H} NMR spectra were recorded at 128.3 MHz and referenced to BF₃·Et₂O at 0.0 ppm. Microanalyses were performed by Oneida Research Services, Inc., One Halsey Rd., Whitesboro, NY 13492.

Preparation of [η^5 -C₅H₄CH₂CH=CH₂]₂Zr(CH₃)₂, **3a. To a slurry of bis[η^5 -(2-propenyl)cyclopentadienyl]zirconium dichloride (300 mg, 0.81 mmol) in diethyl ether at -78 °C was added a 1.4 M diethyl ether solution of methyl lithium (1.15 mL, 1.61 mmol). The cooling bath was removed, and the reaction was stirred at room temperature for 15 min. The diethyl ether was removed *in vacuo*, hexanes were added, and the reaction was filtered. Removal of the hexanes gave a >95% pure (by NMR) yellow oil that could not be further purified.**

Preparation of [η^5 -C₅H₄CH₂CH=CH₂]₂Zr(CH₂C₆H₅)₂, **3b. THF (10 mL) was condensed into an evacuated flask containing bis[η^5 -(2-propenyl)cyclopentadienyl]zirconium dichloride (624 mg, 1.68 mmol) and benzylpotassium (436 mg, 3.35**

(24) Marvich, R. H.; Brintzinger, H. H. *J. Am. Chem. Soc.* **1971**, *93*, 2046.

(25) Schlosser, M.; Hartmann, J. *Angew. Chem., Int. Ed. Engl.* **1973**, *12*, 508.

mmol) at $-78\text{ }^{\circ}\text{C}$. The reaction was warmed to room temperature, at which point it became very dark in color. The THF was removed *in vacuo*, and hexanes (20 mL) were added. Filtration of the reaction mixture gave an orange solution that yielded a $>95\%$ pure (by NMR) oil on solvent removal.

Preparation of $[\eta^5\text{-C}_5\text{H}_4\text{CH}_2\text{CH}=\text{CH}_2]_2\text{Zr}(\text{CH}_2\text{SiMe}_3)_2$, 3c. To a slurry of bis $[\eta^5\text{-(2-propenyl)cyclopentadienyl}]$ zirconium dichloride (588 mg, 1.58 mmol) in diethyl ether (15 mL) at room temperature was added a 1 M pentane solution of [(trimethylsilyl)methyl]lithium (3.16 mL, 3.16 mmol). The reaction was stirred for 15 min before the volatiles were removed *in vacuo*. Hexanes (10 mL) were added, the reaction was filtered, and the hexanes were removed to give a $>95\%$ pure (by NMR) oil that solidified on standing: yield, 688 mg, 92%.

Preparation of [2-(2-propenyl)cyclopentadienyl](*tert*-butylamino)dimethylsilane, $\text{H}_2\text{Cp}^{\text{allyl}}\text{SiNR}$. To a solution of [(2-propenyl)cyclopentadienyl]lithium (8.0 g, 71.4 mmol) in THF (200 mL) at $-78\text{ }^{\circ}\text{C}$ was rapidly added Me_2SiCl_2 (9.21 g, 71.4 mmol) via syringe. The reaction was warmed to room temperature and was stirred for 15 h. To this reaction was added *tert*-butylamine (20 mL, 190 mmol), and a precipitate immediately formed. After the solution had been stirred for 2 days, the THF was removed *in vacuo* and hexanes (200 mL) were added. After filtration, the hexanes were removed from the orange solution and the resulting oil was distilled. The product was obtained as a mixture of isomers: yield, 15.1 g, 64.3 mmol, 90%; bp $49\text{ }^{\circ}\text{C}$, 10^{-3} Torr. ^1H NMR (CDCl_3 , ppm): 6.72, 6.45, 6.21, 6.11, CpH; 5.92, 5.18, 4.98, $\text{CH}=\text{CH}_2$; 3.39, NH; 3.17, CCH_2 ; 3.03, 2.96, CpH; 1.20, 1.11, NCH_3 ; 0.20, 0.19, $-\text{OCH}_3$, SiCH_3 .

Preparation of $\text{Li}_2\text{Cp}^{\text{allyl}}\text{SiNR}$. To a solution of [2-(2-propenyl)cyclopentadienyl](*tert*-butylamino)dimethylsilane (6.7 g, 28.5 mmol) in diethyl ether (150 mL) was added a 1.4 M diethyl ether solution of methylolithium (45 mL, 63 mmol). Addition was completed over 10 min and led to an orange solution. After a few hours a voluminous white precipitate started to form, and the reaction was stirred for a total of 15 h. The product was isolated by filtration and washed with a little diethyl ether: yield, 5.22 g, 21.1 mmol, 74%.

Preparation of $\text{Cp}^{\text{allyl}}\text{SiNRZrCl}_2$, 4. Toluene (50 mL) was condensed into an evacuated flask containing $\text{Li}_2\text{Cp}^{\text{allyl}}\text{SiNR}$ (2.118 g, 8.58 mmol) and $\text{ZrCl}_4(\text{THF})_2$ (3.236 g, 8.58 mmol) at $-78\text{ }^{\circ}\text{C}$. The reaction was warmed to room temperature and was stirred for 40 h. The toluene was removed *in vacuo*, and hexanes (50 mL) were added to the residues. After heating the hexanes to reflux, the reaction was filtered to leave an orange solution. The solvent volume was reduced to approximately 30 mL, the solution was cooled to $-78\text{ }^{\circ}\text{C}$, and the resulting white crystals were isolated by filtration: yield, 2.86 g, 7.23 mmol, 84%. Anal. Calcd: C, 42.51; H, 5.86; N, 3.54. Found: C, 43.29; H, 5.81; N, 3.50.

Preparation of $\text{Cp}^{\text{allyl}}\text{SiNRZr}(\text{CH}_3)_2$, 5a. To a solution of $\text{Cp}^{\text{allyl}}\text{SiNRZrCl}_2$ (554 mg, 1.4 mmol) in diethyl ether (15 mL) at room temperature was added a 1.4 M diethyl ether solution of methylolithium (2 mL, 2.8 mmol). After the solution had been stirred for 10 min, the diethyl ether was removed *in vacuo* and hexanes (10 mL) were added. The reaction was filtered, and the hexanes were removed to give the product as a pale yellow oil that was pure by ^1H NMR spectroscopy.

Preparation of $\text{Cp}^{\text{allyl}}\text{SiNRZr}(\text{CH}_2\text{C}_6\text{H}_5)_2$, 5b. THF (30 mL) was condensed into an evacuated flask containing $\text{Cp}^{\text{allyl}}\text{SiNRZrCl}_2$ (1.05 g, 2.65 mmol) and benzylpotassium (0.716 g, 5.5 mmol) at $-78\text{ }^{\circ}\text{C}$. The reaction was warmed to room temperature, at which point the red color of the benzylpotassium was observed to disappear. The volatiles were removed *in vacuo*, hexanes (25 mL) were added, and the reaction was taken to reflux and filtered. Removal of the hexanes gave a $>95\%$ pure yellow oil, which solidified to a gummy solid on standing: yield, 1.209 g, 2.39 mmol, 90%.

Preparation of $\text{Cp}^{\text{allyl}}\text{SiNRZr}(\text{CH}_2\text{SiMe}_3)_2$, 5c. To a solution of $\text{Cp}^{\text{allyl}}\text{SiNRZrCl}_2$ (198 mg, 0.5 mmol) in diethyl ether (15 mL) at $0\text{ }^{\circ}\text{C}$ was added a 1.0 M solution of [(trimethylsilyl)methyl]lithium in pentane (1.0 mL, 1.0 mmol). The reaction was warmed to room temperature, and the volatiles were removed *in vacuo*. Hexanes (10 mL) were added, and the reaction was filtered, leaving a $>95\%$ pure oil upon removal of the solvent.

Preparation of $[\eta^5\text{-C}_5\text{H}_4\text{CH}_2\text{CH}_2\text{CH}_2\text{B}(\text{C}_6\text{F}_5)_2]_2\text{ZrCl}_2$, 6. Bis(pentafluorophenyl)borane, 1 (279 mg, 0.81 mmol), and bis $[\eta^5\text{-(2-propenyl)cyclopentadienyl}]$ zirconium dichloride (150 mg, 0.40 mmol) were combined in a flask, and ≈ 10 mL of CH_2Cl_2 was vacuum transferred into the flask at $-78\text{ }^{\circ}\text{C}$. The reaction was stirred while being warmed to room temperature. The solvent was removed *in vacuo*, and the resulting gummy solid was triturated with hexanes. The white solid was isolated by filtration and washed with hexanes: yield, 329 mg (77%). ^{19}F NMR (C_6D_6): -132.0 (*ortho*, 2F), -149.0 (*para*, 1F), -162.7 (*meta*, 2F). $^{11}\text{B}\{^1\text{H}\}$ NMR (C_6D_6): 73.9.

Preparation of $[t\text{-C}_4\text{H}_9\text{NSiMe}_2\text{-}\eta^5\text{-C}_5\text{H}_3\text{CH}_2\text{CH}_2\text{B}(\text{C}_6\text{F}_5)_2]_2\text{ZrCl}_2$, 7. Hexane (20 mL) was condensed into an evacuated flask containing [(*tert*-butylamino)dimethyl(2-allylcyclopentadienyl)silane]zirconium dichloride (229 mg, 0.578 mmol) and bis(pentafluorophenyl)borane (200 mg, 0.578 mmol) at $-78\text{ }^{\circ}\text{C}$. The reaction was warmed to $35\text{ }^{\circ}\text{C}$ until all the reagents went into solution. The solvent volume was reduced by half, and the reaction was cooled to $-78\text{ }^{\circ}\text{C}$. The white solid that precipitated was isolated by filtration: yield, 288 mg, 67%. Anal. Calcd: C, 42.12; H, 3.26; N, 1.89. Found: C, 42.56; H, 3.00; N, 1.76. ^{19}F NMR (C_6D_6): -131.8 (*ortho*, 2F), -148.7 (*para*, 1F), -162.5 (*meta*, 2F). ^{11}B NMR (C_6D_6): 73.0.

Synthesis of 8. To a stirred suspension of bis(pentafluorophenyl)borane (823 mg, 2.39 mmol) in hexanes (5 mL) was added a solution of $\text{Cp}^{\text{allyl}}\text{SiNRZr}(\text{CH}_2\text{C}_6\text{H}_5)_2$ (1.209 g, 2.39 mmol) in hexanes (10 mL). As the reaction proceeded a yellow precipitate formed. After 2 h, the reaction was cooled to $-78\text{ }^{\circ}\text{C}$ and filtered: yield, 1.247 g, 1.46 mmol, 61%. C, 56.33; H, 4.49; N, 1.64. Found: C, 56.65; H, 4.96; N, 1.68. ^{19}F NMR (C_6D_6): -132.9 (*ortho*, 2F), -164.1 (*para*, 1F), -167.3 (*meta*, 2F). $^{11}\text{B}\{^1\text{H}\}$ NMR (C_6D_6): -9.1 .

Acknowledgment. Funding for this work was provided by the Novacor Research and Technology Center of Calgary, Alberta, and is gratefully acknowledged.

OM9503858

**Photochemically Activated Phosphorus–Carbon Bond
Cleavage in the Binuclear Ruthenium Complex
Ru₂(CO)₆(bpcd). Redox Reactivity, Molecular Orbital
Properties, and X-ray Diffraction Structures of
Ru₂(CO)₆(bpcd) and
Ru₂(CO)₆[μ -C=C(PPh₂)C(O)CH₂C(O)](μ -PPh₂)**

Huafeng Shen, Simon G. Bott,* and Michael G. Richmond*

*Department of Chemistry, Center for Organometallic Research and Education,
University of North Texas, Denton, Texas 76203*

Received April 26, 1995[⊗]

The reaction between the redox-active diphosphine ligand 4,5-bis(diphenylphosphino)-4-cyclopenten-1,3-dione (bpcd) and Ru₃(CO)₁₂ has been examined under a variety of conditions. Thermolysis of Ru₃(CO)₁₂ with bpcd affords the binuclear compounds Ru₂(CO)₆(bpcd) (**2**) and Ru₂(CO)₆[μ -C=C(PPh₂)C(O)CH₂C(O)](μ -PPh₂) (**3**) as the major and minor products, respectively. The disubstituted cluster Ru₃(CO)₁₀(bpcd) (**1**) has been synthesized and shown to contain a chelating bpcd ligand, on the basis of IR and ³¹P NMR data. The cluster Ru₃(CO)₁₀(bpcd) (chelating isomer) undergoes cluster fragmentation at ambient temperatures in the dark to give the binuclear compound Ru₂(CO)₆(bpcd) and Ru₃(CO)₁₂, with no evidence for the formation of **3**. Both **2** and **3** have been isolated and fully characterized in solution by IR and NMR spectroscopy, and the solid-state structure of each new binuclear compound has been established by X-ray diffraction analysis. The bpcd ligand in **2** bridges adjacent Ru(CO)₃ centers via the PPh₂ groups and the alkene bond of the dione moiety, and this gives rise to a formal dative Ru–Ru bond where the phosphine-substituted ruthenium center acts as the two-electron-donor ligand and the alkene-substituted ruthenium center as the acceptor site. P–C(dione) bond cleavage and π bond decoordination highlight the key structural features of **3**. Independent experiments reveal that binuclear **2** is converted to **3** by 366 nm light with a quantum efficiency of 0.035. Comparative photochemical experiments with the known binuclear compound Ru₂(CO)₆[(Z)-Ph₂-PCH=CHPPh₂] (**4**) provide no evidence for P–C bond cleavage, underscoring the overall importance of the nature of the ancillary diphosphine in controlling the course of reactivity in this genre of compound. The redox properties of **1**–**4** were explored by cyclic voltammetry, which revealed the presence of an irreversible oxidation process (metal based) for each of these compounds. Whereas **2** and **4** do not exhibit any reductive electrochemistry in CH₂-Cl₂, compounds **1** and **3**, with their available dione π^* acceptor orbital, undergo a reversible one-electron reduction at relatively low potential. The orbital composition of the HOMO and LUMO levels in **1**–**4** has been examined by carrying out extended Hückel MO calculations on the model compounds Ru₃(CO)₁₀(H₄-bpcd), Ru₂(CO)₆(H₄-bpcd), Ru₂(CO)₆[μ -C=C(PH₂)C(O)CH₂C(O)](μ -PH₂), and Ru₂(CO)₆[(Z)-H₂PCH=CHPH₂], and the results are discussed relative to the observed electrochemistry. The P–C bond cleavage that accompanies the conversion **2** → **3** is proposed to occur at one of the resulting biradical ruthenium centers, which are formed by the photochemically induced homolysis of the donor–acceptor ruthenium–ruthenium bond in **2**.

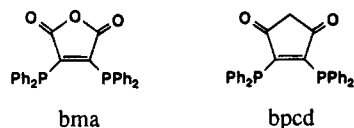
Introduction

The thermal and catalyst-mediated substitution chemistry of Ru₃(CO)₁₂ with phosphines has been extensively explored over the last several years.^{1–3} In several cases novel products derived from C–H and P–C bond activation have been isolated and structurally characterized.⁴ For example, one of the very first reports dealing with the degradation of a tertiary phosphine ligand at a triru-

thenium cluster involved the controlled pyrolysis of Ru₃(CO)₉(PR₃)₃ derivatives. Here several ortho-metalated phenyl-, phosphido-, and benzyne-containing clusters were isolated and characterized by solution methods.⁵ In fact, the controlled degradation of a wide variety of cluster-bound ligands has proved to be a convenient method into the mechanistic study of bond-breaking and bond-making processes at polynuclear ensembles.⁶ Continued research in this area of metal cluster chemistry is critical if new hybrid catalysts are to be exploited for their synthetic potential.

[⊗] Abstract published in *Advance ACS Abstracts*, September 1, 1995.

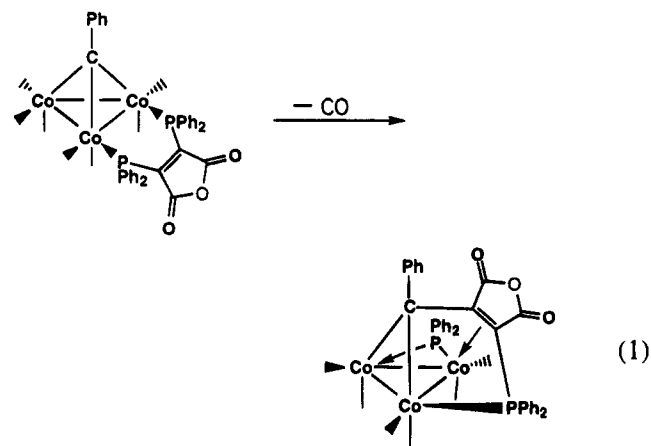
We have recently embarked on a program designed to study the reactivity of polynuclear clusters with redox-active phosphines in an effort to prepare new ligand/cluster redox systems. It is our hope that such compounds will display superior electron reservoir capabilities, as a result of the cooperative mixing of ligand and cluster orbitals. The two redox-active diphosphine ligands that we have concentrated on are 2,3-bis(diphenylphosphino)maleic anhydride (bma) and 4,5-bis(diphenylphosphino)-4-cyclopenten-1,3-dione (bpcd).



These two particular diphosphines, which were first prepared by Becher and Fenske,⁷ have been used as ligands in the synthesis and redox investigation of sundry mononuclear compounds by the same groups, with the bma ligand receiving the most attention.⁸ Extensive studies pertaining to the EPR properties and the enhanced substitutional reactivity of the 18 + δ complex $\text{Co}(\text{CO})_3(\text{bma})$ have been published by Tyler and Rieger,^{9,10} and with the exception of our recent report on the redox pair of $[\text{fac-ReBr}(\text{CO})_3(\text{bma})]^{0-}$, which dealt with the structural aspects of electron

accession on going from neutral $\text{fac-ReBr}(\text{CO})_3(\text{bma})$ to the corresponding 18 + δ complex $[\text{fac-ReBr}(\text{CO})_3(\text{bma})]^{-}$,¹¹ no other reactivity studies with these unique ligands exist, to our knowledge.

Given the complete absence of polynuclear reactivity with the ligands bma and bpcd, our first study involved the reaction using the tricobalt cluster $\text{PhCCO}_3(\text{CO})_9$, which initially proceeds to give the expected bma-substituted cluster $\text{PhCCO}_3(\text{CO})_7(\text{bma})$. This latter cluster was subsequently shown to exhibit exceptional lability with respect to P-C(maleic anhydride) bond scission, coupled with C-C bond reductive elimination to give $\text{Co}_3(\text{CO})_6[\mu_2-\eta^2:\eta^1-\text{C}(\text{Ph})\text{C}=\text{C}(\text{PPh}_2)\text{C}(\text{O})\text{OC}(\text{O})]-(\mu_2-\text{PPh}_2)$, as shown in eq 1.^{12,13}



- (1) (a) Karel, K. J.; Norton, J. R. *J. Am. Chem. Soc.* **1974**, *96*, 6812. (b) Shen, J.-K.; Shi, Y.-L.; Gao, Y.-C.; Shi, Q.-Z.; Basolo, F. *J. Am. Chem. Soc.* **1988**, *110*, 2414. (c) Poë, A. *J. Pure Appl. Chem.* **1988**, *60*, 1209. (d) Brodie, N. M. J.; Poë, A. *J. Organomet. Chem.* **1990**, *383*, 531. (e) Chin-Choy, T.; Keder, N. L.; Stucky, G. D.; Ford, P. C. *J. Organomet. Chem.* **1988**, *346*, 225. (f) Bruce, M. I.; Liddell, M. J.; Hughes, C. A.; Skelton, B. W.; White, A. H. *J. Organomet. Chem.* **1988**, *347*, 157. (g) Corrigan, J. F.; Doherty, S.; Taylor, N. J.; Carty, A. J.; Boroni, E.; Tiripicchio, A. *J. Organomet. Chem.* **1993**, *462*, C24.
- (2) (a) Lavigne, G.; Kaesz, H. D. *J. Am. Chem. Soc.* **1984**, *106*, 4647. (b) Lavigne, G.; Lukan, N.; Bonnet, J.-J. *Inorg. Chem.* **1987**, *26*, 2345. (c) Bruce, M. I.; Kehoe, D. C.; Mattinson, J. G.; Nicholson, B. K.; Rieger, P. H.; Williams, M. L. *J. Chem. Soc., Chem. Commun.* **1982**, 442. (d) Bruce, M. I.; Hambley, T. W.; Nicholson, B. K.; Snow, M. R. *J. Organomet. Chem.* **1982**, *235*, 83.
- (3) For other examples of $\text{Ru}_3(\text{CO})_{12}$ activation by catalyst mediation, see: (a) Darenbourg, D. J.; Gray, R. L.; Pala, M. *Organometallics* **1984**, *3*, 1928. (b) Day, M. W.; Hajela, S.; Kabir, S. E.; Irving, M.; McPhillips, T.; Wolf, E.; Hardcastle, K. I.; Rosenberg, E.; Milone, L.; Gobetto, R.; Osella, D. *Organometallics* **1991**, *10*, 2743. (c) Rivomanana, S.; Lavigne, G.; Lukan, N.; Bonnet, J.-J.; Yanez, R.; Mathieu, R. *J. Am. Chem. Soc.* **1989**, *111*, 8959.
- (4) (a) Lukan, N.; Lavigne, G.; Bonnet, J.-J. *Inorg. Chem.* **1987**, *26*, 585. (b) Deeming, A. J.; Smith, M. B. *J. Chem. Soc., Dalton Trans.* **1993**, 2041. (c) Lukan, N.; Bonnet, J.-J.; Ibers, J. A. *J. Am. Chem. Soc.* **1985**, *107*, 4484. (d) Nucciarone, D.; MacLaughlin, S. A.; Taylor, N. J.; Carty, A. *J. Organometallics* **1988**, *7*, 106. (e) Knox, S. A. R.; Lloyd, B. R.; Morton, D. A. V.; Nicholls, S. M.; Orpen, A. G.; Viñas, J. M.; Weber, M.; Williams, G. K. *J. Organomet. Chem.* **1990**, *394*, 385. (f) Manojlović-Muir, L.; Brandes, D. A.; Puddephatt, R. J. *J. Organomet. Chem.* **1987**, *332*, 201. (g) Bruce, M. I.; Williams, M. L.; Patrick, J. M.; Skelton, B. W.; White, A. H. *J. Chem. Soc., Dalton Trans.* **1986**, 2557.
- (5) Bruce, M. I.; Shaw, G.; Stone, F. G. A. *J. Chem. Soc., Dalton Trans.* **1972**, 2094.
- (6) (a) Lavigne, G. In *The Chemistry of Metal Cluster Complexes*; Shriver, D. F.; Kaesz, H. D.; Adams, R. D., Eds.; VCH: New York, 1990; Chapter 5. (b) Deeming, A. J. In *Transition Metal Clusters* Johnson, B. F. G., Ed.; Wiley: New York, 1980; Chapter 6.
- (7) (a) Fenske, D.; Becher, H. *J. Chem. Ber.* **1974**, *107*, 117. (b) Fenske, D. *Chem. Ber.* **1979**, *112*, 363.
- (8) (a) Becher, H. J.; Bensmann, W.; Fenske, D. *Chem. Ber.* **1977**, *110*, 315. (b) Fenske, D. *Angew. Chem., Int. Ed. Engl.* **1976**, *15*, 381. (c) Bensmann, W.; Fenske, D. *Angew. Chem., Int. Ed. Engl.* **1978**, *17*, 462; **1979**, *18*, 677. (d) Fenske, D.; Christidis, A. *Angew. Chem., Int. Ed. Engl.* **1981**, *20*, 129.
- (9) (a) Mao, F.; Tyler, D. R.; Keszler, D. *J. Am. Chem. Soc.* **1989**, *111*, 130. (b) Mao, F.; Philbin, C. E.; Weakley, T. J. R.; Tyler, D. R. *Organometallics* **1990**, *9*, 1510. (c) Fei, M.; Sur, S. K.; Tyler, D. R. *Organometallics* **1991**, *10*, 419.
- (10) (a) Mao, F.; Tyler, D. R.; Rieger, A. L.; Rieger, P. H. *J. Chem. Soc., Faraday Trans.* **1991**, *87*, 3113. (b) Mao, F.; Tyler, D. R.; Bruce, M. R.; Bruce, A. E.; Rieger, A. L.; Rieger, P. H. *J. Am. Chem. Soc.* **1992**, *114*, 6418.

The full scope of the reactivity of these and related ligands with other cluster compounds is under consideration by our groups,^{14,15} and for this reason we decided to investigate the substitution reaction between $\text{Ru}_3(\text{CO})_{12}$ and bpcd. Herein we report our data on the synthesis and reactivity studies of $\text{Ru}_3(\text{CO})_{10}(\text{bpcd})$, $\text{Ru}_2(\text{CO})_6(\text{bpcd})$, and $\text{Ru}_2(\text{CO})_6[\mu-\text{C}=\text{C}(\text{PPh}_2)\text{C}(\text{O})\text{CH}_2\text{C}(\text{O})]-(\mu_2-\text{PPh}_2)$, in addition to the X-ray diffraction structures of the last two binuclear compounds. Included are the cyclic voltammetry data and extended Hückel MO calculations on these new compounds. The importance of the bpcd ligand in promoting the observed P-C(dione) bond cleavage is discussed relative to the parent binuclear compound $\text{Ru}_2(\text{CO})_6[(Z)\text{-Ph}_2\text{PCH}=\text{CHPPh}_2]$.

Results and Discussion

I. Synthesis and Characterization of Compounds 1–3. The reaction between $\text{Ru}_3(\text{CO})_{12}$ and bpcd was explored under different conditions as a route to the bpcd-substituted cluster $\text{Ru}_3(\text{CO})_{10}(\text{bpcd})$. Refluxing $\text{Ru}_3(\text{CO})_{12}$ with bpcd in either 1,2-dichloroethane or toluene led only to the isolation of the binuclear complexes $\text{Ru}_2(\text{CO})_6(\text{bpcd})$ (**2**) and $\text{Ru}_2(\text{CO})_6[\mu-\text{C}=\text{C}(\text{PPh}_2)\text{C}(\text{O})\text{CH}_2\text{C}(\text{O})]-(\mu_2-\text{PPh}_2)$ (**3**), with the former com-

(11) Yang, K.; Bott, S. G.; Richmond, M. G. *Organometallics* **1995**, *14*, 2387.

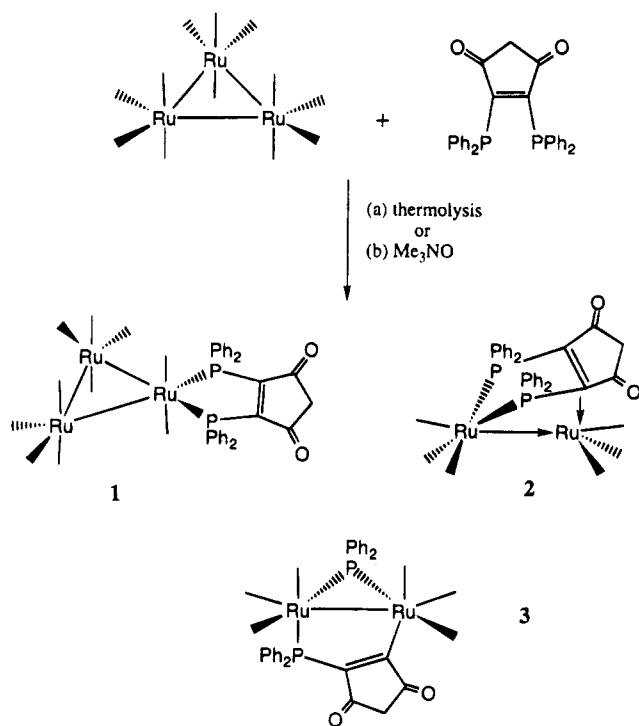
(12) Yang, K.; Smith, J. M.; Bott, S. G.; Richmond, M. G. *Organometallics* **1993**, *12*, 4779.

(13) Reaction of $\text{PhCCO}_3(\text{CO})_9$ with bpcd proceeds in an analogous fashion: Shen, H.; Bott, S. G.; Richmond, M. G. Unpublished results.

(14) Xia, C.-G.; Bott, S. G.; Richmond, M. G. *Inorg. Chim. Acta* **1995**, *230*, 45.

(15) Shen, H.; Williams, T. J.; Bott, S. G.; Richmond, M. G. *J. Organomet. Chem.*, in press.

Scheme 1



found always predominating. When the thermolysis reactions were monitored by IR spectroscopy, traces of the desired cluster were observed, but the facile fragmentation of **1** to **2** and Ru₃(CO)₁₂ precluded any possible isolation of **1**. Analogous cluster fragmentation behavior has already been noted in other phosphine-substituted triruthenium clusters.¹⁶ Activation of Ru₃(CO)₁₂ in MeCN/CH₂Cl₂ using the oxidative-decarbonylation reagent Me₃NO (2 equiv)¹⁷ in the presence of bpcd (1 equiv) led to cluster **1** in low yield (<25%), via the intermediacy of the solvated cluster Ru₃(CO)₁₀(MeCN)₂.¹⁸ As with the thermolysis reaction, **2** and **3** always accompanied the formation of **1**, as depicted by Scheme 1. These three compounds may be isolated by chromatography over silica gel with the appropriate solvent system.

A high-yield route to **1** was subsequently found by using the labile halide-bound cluster [Ru₃(CO)₁₁Cl]-[PPN].¹⁹ Here the desired cluster could be isolated as the sole observable product in fair yield, provided that the workup was not extensively delayed. Cluster **1** undergoes a slow decomposition in solution (*t*_{1/2} ≈ 6 h) at room temperature to afford only **2** and Ru₃(CO)₁₂. No sign of **3** was observed in the thermal decomposition of cluster **1**.²⁰ Stirring cluster **1** under CO (100 psi in the dark) slowed down the fragmentation of **1** (*t*_{1/2} ≈ 24 h), which suggests that dissociative CO loss from **1** may be important as the initial step in the decomposition of

Chart 1

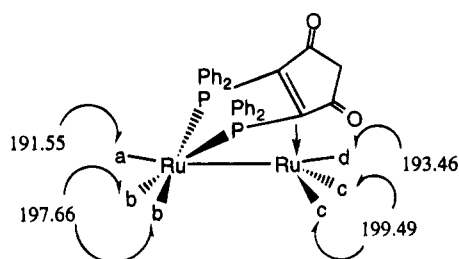


Table 1. X-Ray Crystallographic and Data Processing Parameters for Ru₂(CO)₆(bpcd) (**2**) and Ru₂(CO)₆[μ-C=C(PPh₂)C(O)CH₂C(O)](μ₂-PPh₂)-C₇H₁₆ (**3**)

	2	3
space group	monoclinic, P2 ₁ /c	monoclinic, P2 ₁ /n
cell const		
<i>a</i> , Å	11.8030(6)	13.6622(8)
<i>b</i> , Å	14.7830(8)	16.9995(9)
<i>c</i> , Å	19.582(1)	16.755(1)
β, deg	106.270(3)	110.066(6)
<i>V</i> , Å ³	3279.9(3)	3655.2(4)
mol formula	C ₃₅ H ₂₂ O ₈ P ₂ Ru ₂	C ₄₂ H ₃₈ O ₈ P ₂ Ru ₂
fw	834.65	934.85
formula units/cell (<i>Z</i>)	4	4
ρ, g cm ⁻³	1.690	1.699
cryst size, mm ³	0.06 × 0.11 × 0.24	0.11 × 0.16 × 0.44
abs coeff (μ _z), cm ⁻¹	10.49	9.51
λ (radiatn), Å	0.710 73	0.710 73
data collcn method	θ/2θ	θ/2θ
collcn range, deg	2.0 ≤ 2θ ≤ 44.0	2.0 ≤ 2θ ≤ 44.0
tot. no. of data collcd	4419	4866
no. of indep. data, <i>I</i> > 3σ(<i>I</i>)	3402	3684
tot. no. of variables	424	328
<i>R</i>	0.0216	0.0349
<i>R</i> _w	0.0258	0.0392
weights	[0.04 <i>F</i> ² + (σ <i>F</i>) ²] ⁻¹	[0.04 <i>F</i> ² + (σ <i>F</i>) ²] ⁻¹

1. The major products were Ru(CO)₅, identified by IR spectroscopy, and **2**, in addition to a small amount of Ru₃(CO)₁₂. While the mechanism for the fragmentation of **1** to **2** and Ru₃(CO)₁₂ is unknown at this point, we have determined that **2** does not afford compound **3** under comparable reaction conditions. Independent experiments (*vide infra*) have established that **2** is thermally stable in refluxing xylene and may be converted into **3** by near-UV light.

The infrared spectrum of **1** in CH₂Cl₂ exhibits terminal ν(CO) bands at 2085 (s), 2037 (s), 2005 (vs), and 1930 (w) cm⁻¹, in excellent agreement with the cluster Ru₃(CO)₁₀[(*Z*)-Ph₂PCH=CHPPh₂], which possesses an equatorially bound, chelating diphosphine ligand.²¹ The ν(CO) bands at 1749 (w) and 1718 (m) cm⁻¹ are assigned to the dione moiety associated with the bpcd ligand, on the basis of the similarity to frequencies for cyclopenten-3,5-dione and 4,5-dichloro-4-cyclopenten-1,3-dione.²² The ¹H NMR spectrum of **1** displayed a singlet at δ 3.61 (2H) and multiple resonances from δ 7.45 to 7.60 (20H) assignable to the bpcd methylene and phenyl groups, respectively. A single, sharp ³¹P resonance at δ 50.76 in the ³¹P{¹H} spectrum is indicative of chelated bpcd ligand that lies in the plane defined by the triruthenium frame.²³

(16) (a) Malik, S. K.; Poš, A. *Inorg. Chem.* **1978**, *17*, 1484; **1979**, *18*, 1241. (b) Bruce, M. I.; Williams, M. L.; Skelton, B. W.; White, A. H. *J. Organomet. Chem.* **1986**, *306*, 115.

(17) (a) Koelle, U. *J. Organomet. Chem.* **1977**, *133*, 53. (b) Albers, M. O.; Coville, N. J. *Coord. Chem. Rev.* **1984**, *53*, 227.

(18) Foulds, G. A.; Johnson, B. F. G.; Lewis, J. *J. Organomet. Chem.* **1985**, *296*, 147.

(19) (a) Han, S.-H.; Geoffroy, G. L.; Dombek, B. D.; Rheingold, A. L. *Inorg. Chem.* **1988**, *27*, 4355. (b) Rivomanana, S.; Lavigne, G.; Lugan, N.; Bonnet, J.-J. *Organometallics* **1991**, *10*, 2285. (c) Chin-Choy, T.; Harrison, W. T. A.; Stucky, G. D.; Keder, N.; Ford, P. C. *Inorg. Chem.* **1989**, *28*, 2028.

(20) The possibility of a bridged isomer of Ru₃(CO)₁₀(bpcd) giving compound **3** cannot be ruled out. However, such a species has not been observed.

(21) Shiu, K.-B.; Peng, S.-M.; Cheng, M.-C. *J. Organomet. Chem.* **1993**, *453*, 133.

(22) Dolphin, D.; Wick, A. *Tabulation of Infrared Spectral Data*; Wiley-Interscience: New York, 1977.

(23) Richmond, M. G.; Kochi, J. K. *Organometallics* **1987**, *6*, 254.

Table 2. Positional Parameters for the Non-Hydrogen Atoms of Ru₂(CO)₆(bpcd) (2) and Ru₂(CO)₆[μ-C=C(PPh₂)C(O)CH₂C(O)](μ₂-PPh₂)-C₇H₁₆ (3) with Estimated Standard Deviations in Parentheses^a

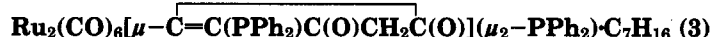
atom	x	y	z	B, Å ²	atom	x	y	z	B, Å ²
Ru ₂ (CO) ₆ (bpcd) (2)									
Ru(1)	0.22997(3)	0.13738(2)	0.00325(2)	2.246(7)	C(112)	0.5865(4)	0.1278(3)	0.2115(3)	3.7(1)
Ru(2)	0.11821(3)	0.22813(2)	0.09771(2)	2.205(7)	C(113)	0.7081(4)	0.1308(4)	0.2295(3)	5.3(1)
P(1)	0.35815(9)	0.13742(8)	0.12026(5)	2.35(2)	C(114)	0.7630(4)	0.1471(4)	0.1784(3)	5.8(2)
P(2)	0.27662(9)	0.29390(7)	0.01029(5)	2.10(2)	C(115)	0.7002(4)	0.1597(4)	0.1091(3)	5.6(1)
O(1)	0.1411(3)	-0.0520(2)	0.0268(2)	4.87(9)	C(116)	0.5768(4)	0.1566(3)	0.0900(3)	4.0(1)
O(2)	0.0065(3)	0.1585(3)	-0.1224(2)	5.49(9)	C(117)	0.3386(3)	0.0406(3)	0.1731(2)	2.73(9)
O(3)	0.3873(4)	0.0753(3)	-0.0871(2)	7.7(1)	C(118)	0.3768(4)	-0.0427(3)	0.1548(3)	3.8(1)
O(4)	0.0282(3)	0.3204(3)	0.2111(2)	5.96(9)	C(119)	0.3601(5)	-0.1206(3)	0.1898(3)	4.9(1)
O(5)	0.0092(3)	0.0510(2)	0.1283(2)	4.38(8)	C(120)	0.3046(5)	-0.1165(4)	0.2424(3)	5.4(1)
O(6)	-0.0989(3)	0.2832(3)	-0.0223(2)	6.1(1)	C(121)	0.2667(5)	-0.0361(4)	0.2607(3)	5.0(1)
O(12)	0.3831(3)	0.2367(2)	0.2783(2)	4.66(9)	C(122)	0.2842(4)	0.0428(3)	0.2271(2)	3.6(1)
O(14)	0.2574(3)	0.4768(2)	0.1167(2)	3.50(7)	C(211)	0.1732(3)	0.3629(3)	-0.0565(2)	2.26(9)
C(1)	0.1744(4)	0.0182(3)	0.0187(2)	3.1(1)	C(212)	0.1512(4)	0.3369(3)	-0.1268(2)	3.1(1)
C(2)	0.0898(4)	0.1525(3)	-0.0769(2)	3.4(1)	C(213)	0.0729(4)	0.3855(3)	-0.1807(2)	3.7(1)
C(3)	0.3310(4)	0.0985(3)	-0.0525(2)	3.8(1)	C(214)	0.0167(4)	0.4595(3)	-0.1642(3)	4.0(1)
C(4)	0.0646(4)	0.2889(3)	0.1680(2)	3.3(1)	C(215)	0.0397(4)	0.4865(3)	-0.0948(3)	3.9(1)
C(5)	0.0520(4)	0.1156(3)	0.1162(2)	3.0(1)	C(216)	0.1171(4)	0.4388(3)	-0.0414(2)	3.1(1)
C(6)	-0.0180(4)	0.2620(3)	0.0208(2)	3.6(1)	C(217)	0.4196(3)	0.3336(3)	0.0029(2)	2.24(8)
C(11)	0.3063(3)	0.2392(3)	0.1507(2)	2.26(8)	C(218)	0.4966(4)	0.3817(3)	0.0562(2)	3.4(1)
C(12)	0.3404(4)	0.2772(3)	0.2234(2)	3.1(1)	C(219)	0.6033(4)	0.4106(4)	0.0485(3)	4.5(1)
C(13)	0.3179(4)	0.3782(3)	0.2181(2)	3.4(1)	C(220)	0.6343(4)	0.3913(4)	-0.0118(3)	4.6(1)
C(14)	0.2764(3)	0.4006(3)	0.1392(2)	2.44(9)	C(221)	0.5595(4)	0.3435(4)	-0.0651(2)	4.5(1)
C(15)	0.2675(3)	0.3148(3)	0.0989(2)	2.11(8)	C(222)	0.4524(4)	0.3147(4)	-0.0579(2)	3.6(1)
C(111)	0.5200(4)	0.1408(3)	0.1415(2)	3.0(1)					
Ru ₂ (CO) ₆ [μ-C=C(PPh ₂)C(O)CH ₂ C(O)](μ ₂ -PPh ₂)-C ₇ H ₁₆ (3)									
Ru(1)	0.07479(4)	0.13173(3)	0.35481(3)	2.57(1)	C(115)	-0.0560(6)	-0.0560(6)	0.3280(5)	5.2(2)*
Ru(2)	-0.01860(4)	0.24230(3)	0.22102(3)	2.77(1)	C(116)	-0.0316(5)	-0.0788(4)	0.3129(4)	3.8(1)*
P(1)	0.0611(1)	0.0372(1)	0.24533(9)	2.71(3)	C(117)	0.1848(4)	0.0284(4)	0.2279(4)	3.0(1)*
P(2)	-0.1018(1)	0.17052(9)	0.29772(9)	2.64(3)	C(118)	0.2048(5)	0.0689(4)	0.1637(4)	4.0(1)*
O(1)	0.1031(4)	0.2492(3)	0.4985(3)	5.1(1)	C(119)	0.3060(6)	0.0306(5)	0.1612(5)	5.3(2)*
O(2)	0.1232(5)	0.0077(3)	0.4936(3)	6.8(2)	C(120)	0.3842(6)	0.0321(5)	0.2221(5)	5.5(2)*
O(3)	0.2852(3)	0.1837(3)	0.3445(3)	5.5(1)	C(121)	0.3654(6)	-0.0096(5)	0.2839(5)	5.1(2)*
O(4)	0.1609(4)	0.2764(4)	0.1547(4)	7.1(2)	C(122)	0.2659(5)	-0.0119(4)	0.2880(4)	4.0(1)*
O(5)	0.0497(4)	0.3719(3)	0.3563(3)	5.8(1)	C(211)	-0.1564(4)	0.2217(4)	0.3693(4)	3.1(1)*
O(6)	-0.1935(4)	0.3490(3)	0.1144(3)	5.5(1)	C(212)	-0.1472(5)	0.1909(4)	0.4473(4)	4.6(2)*
O(12)	-0.0617(4)	-0.0460(3)	0.0580(3)	4.8(1)	C(213)	-0.1982(6)	0.2277(5)	0.4976(5)	6.0(2)*
O(14)	-0.1600(4)	0.2175(3)	0.0073(3)	6.0(1)	C(214)	-0.2549(6)	0.2936(5)	0.4682(5)	5.9(2)*
C(1)	0.0905(5)	0.2067(4)	0.4428(4)	3.3(1)	C(215)	-0.2626(7)	0.3935(5)	0.3935(5)	6.2(2)*
C(2)	0.1033(5)	0.0518(4)	0.4394(4)	3.9(2)	C(216)	-0.2129(6)	0.2899(5)	0.3424(5)	4.8(2)*
C(3)	0.2088(5)	0.1626(4)	0.3488(4)	4.0(2)	C(217)	-0.2153(4)	0.1107(4)	0.2383(3)	2.7(1)*
C(4)	0.0951(5)	0.2642(4)	0.1792(4)	4.4(2)	C(218)	-0.2758(5)	0.1302(4)	0.1566(4)	3.5(1)*
C(5)	0.0244(5)	0.3235(4)	0.3064(4)	3.6(2)	C(219)	-0.3611(5)	0.0854(4)	0.1111(4)	4.3(1)*
C(6)	-0.1272(5)	0.3067(4)	0.1486(4)	3.7(2)	C(220)	-0.3868(6)	0.0203(5)	0.1475(5)	5.1(2)*
C(11)	-0.0288(4)	0.0715(4)	0.1450(3)	2.8(1)	C(221)	-0.3294(6)	0.0013(5)	0.2295(5)	5.0(2)*
C(12)	-0.0765(4)	0.0229(4)	0.0663(4)	3.3(1)	C(222)	-0.2442(5)	0.0460(4)	0.2757(4)	3.8(1)*
C(13)	-0.1435(5)	0.0781(4)	0.0007(4)	4.4(2)	C(1s)	0.4419(9)	0.0553(8)	0.5031(8)	3.6(3)*
C(14)	-0.1252(5)	0.1566(4)	0.0418(4)	3.7(2)	C(2s)	0.535(2)	0.053(1)	0.481(1)	8.5(5)*
C(15)	-0.0570(4)	0.1480(4)	0.1340(3)	3.0(1)	C(3s)	0.613(2)	0.040(1)	0.464(1)	7.9(5)*
C(111)	0.0283(5)	-0.0643(4)	0.2627(4)	3.2(1)*	C(1sa)	0.416(1)	0.014(1)	0.5184(9)	5.2(3)*
C(112)	0.0638(5)	-0.1279(4)	0.2278(4)	4.3(1)*	C(2sa)	0.482(2)	0.097(1)	0.488(1)	8.0(5)*
C(113)	0.0398(6)	-0.2041(5)	0.2437(5)	5.4(2)*	C(3sa)	0.562(2)	0.110(1)	0.460(1)	8.1(5)*
C(114)	-0.0194(6)	-0.2165(5)	0.2937(5)	5.8(2)*					

^a Anisotropically refined atoms are given in the form of the isotropic equivalent displacement parameter, defined as $(\frac{1}{3})[a^2B(1,1) + b^2B(2,2) + c^2B(3,3) + ab(\cos \gamma)B(1,2) + ac(\cos \beta)B(1,3) + bc(\cos \alpha)B(2,3)]$. Starred values represent atoms that were refined isotropically.

Binuclear **2** is best obtained from the direct thermolysis reaction between Ru₃(CO)₁₂ and bpcd. The IR spectrum of **2** in CH₂Cl₂ exhibits terminal ν(CO) bands at 2079 (vs), 2041 (vs), 2025 (s), 2001 (m), and 1978 (s) cm⁻¹, along with bpcd ν(CO) bands at 1701 (m) and 1674 (m) cm⁻¹. Coordination of the bpcd π bond leads to an AB quartet for the methylene protons centered at δ 3.76, as expected for diastereotopic protons. The calculated value of 0.13 for $J/\Delta\nu$ indicates that this spin system borders on the threshold of reverting to an AX spin system.²⁴ The ³¹P resonance at δ 25.21 has undergone a substantial upfield shift relative to cluster **1** as a result

of coordination of the bpcd π bond. A ¹³CO-enriched sample of **2** (ca. 20%) revealed terminal carbonyl resonances at δ 191.55 (*t*, $J_{P-C} = 7.53$ Hz), 193.46 (*s*), 197.66 (multiplet), and 199.49 (*s*), in an integral ratio of 1:1:2:2, respectively. The assignment of these resonances is shown in Chart 1. The second-order multiplet observed at δ 197.66 is derived from the pairwise equivalent CO groups at the phosphine-substituted Ru(CO)₃ center and their coupling with the two phosphine groups. This situation gives rise to an AA'XX' spin system. Due to the complex nature of this particular ¹³C resonance, no attempt was made to extract the various coupling constants that make up this spin system.²⁵ No evidence of dynamic behavior was found

(24) Bovey, F. A. *Nuclear Magnetic Resonance Spectroscopy*; Academic Press: New York, 1969.

Table 3. Selected Bond Distances (Å) and Angles (deg) in Ru₂(CO)₆(bpcd) (2) and

Ru ₂ (CO) ₆ (bpcd) (2)							
Bond Distances							
Ru(1)-Ru(2)	2.8859(5)	Ru(1)-P(1)	2.366(1)	O(2)-C(2)	1.130(5)	O(3)-C(3)	1.127(7)
Ru(1)-P(2)	2.373(1)	Ru(1)-C(1)	1.932(5)	O(4)-C(4)	1.147(6)	O(5)-C(5)	1.136(6)
Ru(1)-C(2)	1.949(4)	Ru(1)-C(3)	1.917(5)	O(6)-C(6)	1.127(5)	O(12)-C(12)	1.210(5)
Ru(2)-C(4)	1.895(5)	Ru(2)-C(5)	1.915(5)	O(14)-C(14)	1.208(5)	C(11)-C(12)	1.478(6)
Ru(2)-C(6)	1.936(4)	Ru(2)-C(11)	2.177(4)	C(11)-C(15)	1.492(5)	C(12)-C(13)	1.515(7)
Ru(2)-C(15)	2.173(4)	P(1)-C(11)	1.788(4)	C(13)-C(14)	1.520(6)	C(14)-C(15)	1.483(6)
P(2)-C(15)	1.795(4)	O(1)-C(1)	1.138(6)				
Bond Angles							
Ru(2)-Ru(1)-P(1)	70.26(3)	Ru(2)-Ru(1)-P(2)	69.50(3)	Ru(2)-C(11)-C(15)	69.8(2)	P(1)-C(11)-C(12)	127.9(3)
Ru(2)-Ru(1)-C(1)	95.0(1)	Ru(2)-Ru(1)-C(2)	91.4(2)	P(1)-C(11)-C(15)	118.2(3)	C(12)-C(11)-C(15)	108.6(3)
Ru(2)-Ru(1)-C(3)	166.8(1)	P(1)-Ru(1)-P(2)	82.44(4)	O(12)-C(12)-C(11)	126.9(4)	O(12)-C(12)-C(13)	124.8(4)
Ru(1)-Ru(2)-C(4)	172.6(1)	Ru(1)-Ru(2)-C(5)	90.1(1)	C(11)-C(12)-C(13)	108.3(3)	C(12)-C(13)-C(14)	106.5(3)
Ru(1)-Ru(2)-C(6)	92.9(2)	Ru(1)-Ru(2)-C(11)	75.7(1)	O(14)-C(14)-C(13)	123.2(4)	O(14)-C(14)-C(15)	128.8(4)
Ru(1)-Ru(2)-C(15)	76.5(1)	C(11)-Ru(2)-C(15)	40.1(1)	C(13)-C(14)-C(15)	108.0(3)	Ru(2)-C(15)-P(2)	99.0(2)
Ru(1)-P(1)-C(11)	97.9(1)	Ru(1)-P(2)-C(15)	98.5(1)	Ru(2)-C(15)-C(11)	70.1(2)	Ru(2)-C(15)-C(14)	116.5(3)
Ru(1)-C(1)-O(1)	179.0(4)	Ru(1)-C(2)-O(2)	177.3(4)	P(2)-C(15)-C(11)	116.0(3)	P(2)-C(15)-C(14)	130.4(3)
Ru(1)-C(3)-O(3)	177.8(4)	Ru(2)-C(4)-O(4)	175.3(4)	C(11)-C(15)-C(14)	108.4(3)		
Ru(2)-C(5)-O(5)	177.0(4)	Ru(2)-C(6)-O(6)	177.5(5)				
Ru ₂ (CO) ₆ [μ-C=C(PPh ₂)C(O)CH ₂ C(O)](μ ₂ -PPh ₂)-C ₇ H ₁₆ (3)							
Bond Distances							
Ru(1)-Ru(2)	2.8677(6)	Ru(1)-P(1)	2.397(2)	O(3)-C(3)	1.128(9)	O(4)-C(4)	1.13(1)
Ru(1)-P(2)	2.364(1)	Ru(1)-C(1)	1.905(6)	O(5)-C(5)	1.140(8)	O(6)-C(6)	1.145(8)
Ru(1)-C(2)	1.904(7)	Ru(1)-C(3)	1.941(7)	O(12)-C(12)	1.205(8)	O(14)-C(14)	1.202(8)
Ru(2)-P(2)	2.331(2)	Ru(2)-C(4)	1.947(8)	C(11)-C(12)	1.502(8)	C(11)-C(15)	1.350(9)
Ru(2)-C(5)	1.929(6)	Ru(2)-C(6)	1.907(6)	C(12)-C(13)	1.495(9)	C(13)-C(14)	1.48(1)
Ru(2)-C(15)	2.108(6)	P(1)-C(11)	1.805(5)	C(14)-C(15)	1.513(7)		
O(1)-C(1)	1.145(8)	O(2)-C(2)	1.137(8)				
Bond Angles							
Ru(2)-Ru(1)-P(1)	86.80(4)	Ru(2)-Ru(1)-P(2)	51.84(4)	Ru(1)-P(1)-C(11)	110.2(2)	Ru(1)-P(2)-Ru(2)	75.29(5)
Ru(2)-Ru(1)-C(1)	93.9(2)	Ru(2)-Ru(1)-C(2)	166.4(2)	P(1)-C(11)-C(12)	126.2(4)	P(1)-C(11)-C(15)	120.6(4)
Ru(2)-Ru(1)-C(3)	87.5(2)	Ru(1)-Ru(2)-P(2)	52.87(4)	C(12)-C(11)-C(15)	113.2(5)	O(12)-C(12)-C(11)	126.7(5)
Ru(1)-Ru(2)-C(4)	102.2(2)	Ru(1)-Ru(2)-C(5)	87.0(2)	O(12)-C(12)-C(13)	127.6(5)	C(11)-C(12)-C(13)	105.8(5)
Ru(1)-Ru(2)-C(6)	156.1(2)	Ru(1)-Ru(2)-C(15)	88.9(2)	C(12)-C(13)-C(14)	105.1(5)	O(14)-C(14)-C(13)	125.2(5)
Ru(1)-C(1)-O(1)	176.6(5)	Ru(1)-C(2)-O(2)	175.6(6)	O(14)-C(14)-C(15)	125.3(6)	C(13)-C(14)-C(15)	109.5(5)
Ru(1)-C(3)-O(3)	177.1(6)	Ru(2)-C(4)-O(4)	179.4(7)	Ru(2)-C(15)-C(11)	130.3(4)	Ru(2)-C(15)-C(14)	123.5(4)
Ru(2)-C(5)-O(5)	179.4(6)	Ru(2)-C(6)-O(6)	171.4(6)	C(11)-C(15)-C(14)	106.2(5)		

^a Numbers in parentheses are estimated standard deviations in the least significant digits.

for these CO groups, as the ¹³C NMR spectra were invariant over the temperature range -100 to +40 °C.

The phosphido-bridged compound **3** reveals ν(CO) bands assignable to the terminal carbonyl groups at 2078 (vs), 2045 (vs), 2018 (vs), 1996 (s), and 1980 (s) cm⁻¹, along with two bpcd ν(CO) bands at 1725 (w), and 1694 (s) cm⁻¹. The ¹H NMR spectrum of **3** shows a classical AB quartet centered at δ 2.79 with a J/Δν value of 1.5, consistent with the diastereotopic nature of these protons. The aromatic protons appear over the region δ 6.90-7.72. The two observed ³¹P resonances at δ 169.55 (J_{P-P} = 27.38 Hz) and δ 23.40 (J_{P-P} = 27.38 Hz) represent the μ₂-phosphido and phosphine moieties, respectively. Six carbonyl resonances were observed in a ¹³CO-enriched sample of **3** at δ 194.18 (d, J_{P-C} = 13.43 Hz), 195.50 (overlapping multiplet), 195.83 (dd, J_{P-C} = 10.69 Hz, J_{P-C} = 82.94 Hz), 200.13 (d, J_{P-C} = 55.74 Hz), and 201.84 (dd, J_{P-C} = 14.57 Hz, J_{P-C} = 48.89 Hz), in an integral ratio of 1:2:1:1:1, respectively, which are fully consistent with the structure of **3**. No attempt has been made to assign these resonances to specific CO groups. As with **2**, the CO groups in compound **3** did not exhibit any fluxional behavior.

(25) The complexity of the AA'XX' spin system is reduced to an AXX' spin system when the natural-abundance ¹³C{¹H} NMR spectrum of **2** is obtained. Spectral simulation under these conditions affords relative values of J_{A-X} = ±79.5 Hz, J_{A-X'} = ∓9.7 Hz, and |J_{X-X'}| = 31.2 Hz.

II. X-ray Diffraction Structures of Ru₂(CO)₆-

(bpcd) and Ru₂(CO)₆[μ-C=C(PPh₂)C(O)CH₂C(O)](μ₂-PPh₂). The molecular structures for **2** and **3** were established by X-ray diffraction analysis. Both clusters exist as discrete molecules in the unit cell with no unusually short inter- or intramolecular contacts. The X-ray data processing and collection parameters are listed in Table 1, and Tables 2 and 3 give the final fractional coordinates and selected bond distances and angles, respectively. The ORTEP diagram for each compound is shown in Figure 1.

The two Ru(CO)₃ centers in **2** are ligated by the bpcd ligand via the phosphine moieties at Ru(1) and the bpcd π bond at Ru(2). Each metal center in **2** is formally six-coordinate and exhibits a distorted-octahedral geometry, provided that the bpcd π bond that is coordinated to Ru(2) is treated as a two-coordinate ligand. The axial groups are defined by the Ru-Ru vector and the carbonyl groups C(3)O(3) and C(4)O(4). The Ru(1)-Ru(2) bond is best described as a dative or donor-acceptor bond, where the phosphine-substituted Ru(1) center acts as a two-electron donor to the Ru(2) acceptor center.²⁶ By this description, each ruthenium atom conforms to

(26) For examples of unbridged, dative M-M bonds, see: (a) Shipley, J. A.; Batchelor, R. J.; Einstein, F. W. B.; Pomeroy, R. K. *Organometallics* **1991**, *10*, 3620 and references therein. (b) Nakatsuji, H.; Hada, M.; Kawashima, A. *Inorg. Chem.* **1992**, *31*, 1740. (c) Sironi, A. *Inorg. Chem.* **1995**, *34*, 1342.

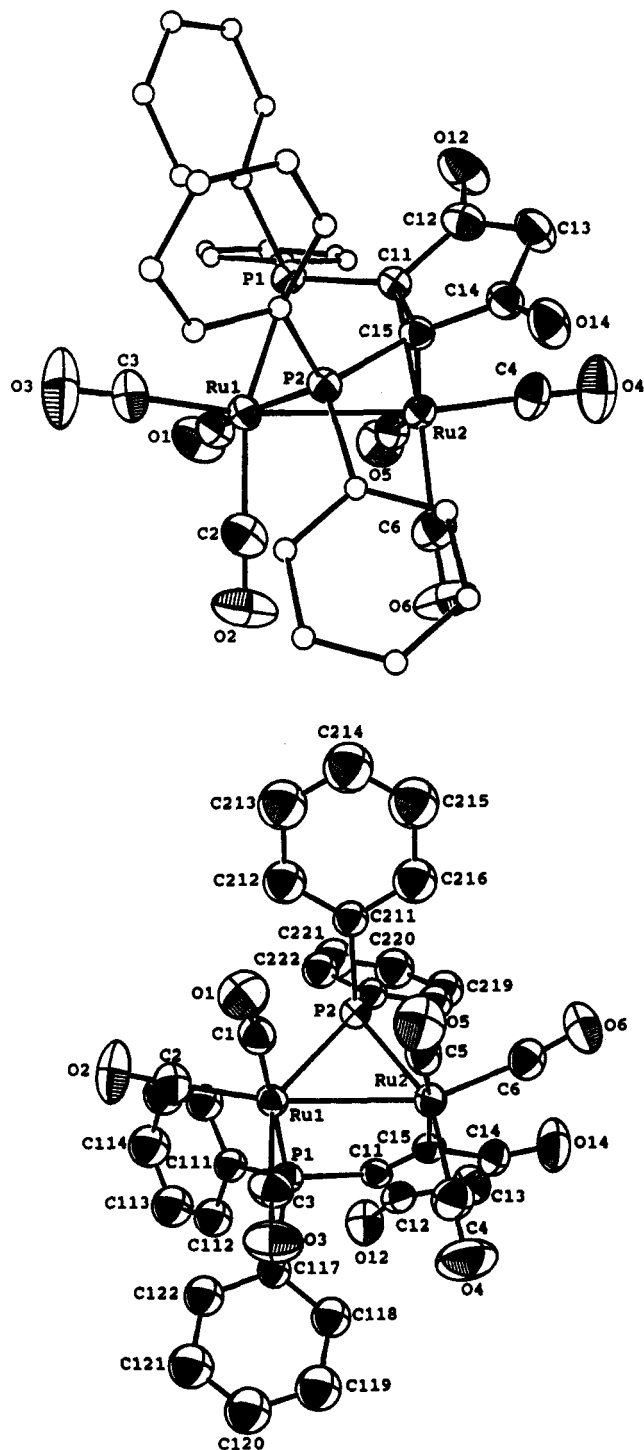


Figure 1. ORTEP drawings of the non-hydrogen atoms of (top) $\text{Ru}_2(\text{CO})_6(\text{bpcd})$ (**2**) and (bottom) $\text{Ru}_2(\text{CO})_6[\mu\text{-C-C-(PPh}_2\text{)C(O)CH}_2\text{C(O)}](\mu_2\text{-PPH}_2)\cdot\text{C}_7\text{H}_{16}$ (**3**). Thermal ellipsoids are drawn at the 50% probability level.

the EAN rule. The observed Ru(1)–Ru(2) distance of 2.8859(5) Å agrees well with the value reported for the related donor–acceptor compound $\text{Ru}_2(\text{CO})_6[(Z)\text{-Ph}_2\text{-PCH=CHPPH}_2]$ (**4**)^{16b} and other compounds possessing a Ru–Ru single bond.²⁷ The Ru–CO bond lengths range from 1.895(5) to 1.949(4) Å, with an average distance of 1.924 Å. The two axial CO groups are tipped slightly toward the bpcd ligand, given the observed bond angles of 166.8(1) and 172.6(1)° for Ru(2)–Ru(1)–C(3) and Ru(1)–Ru(2)–C(4), respectively. The C(11)–C(15) length of 1.492(5) Å is 0.142 Å longer than for bpcd

complexes that do not contain a coordinated π bond.^{14,15}

The oxidative addition of the P–C(dione) bond and decoordination of the bpcd π bond on going from **2** to **3** was ascertained by X-ray crystallography. The structure of **3** is similar to that of **2** insofar as it is formally six-coordinate and is based on a distorted-octahedral geometry. The Ru(1)–Ru(2) distance of 2.8677(6) Å agrees well with its single-bond designation, while the Ru(1)–P(2) and Ru(2)–P(2) phosphido bond lengths of 2.364(1) and 2.331(2) Å are similar to other reported phosphido-ruthenium bond distances.²⁸ Noticeable steric effects transmitted by one of the phenyl groups on P(1) and the C(14)–O(14) bond of the bpcd ligand are revealed by the bond angles of 166.4(2) and 156.1(2)° associated with the Ru(2)–Ru(1)–C(2) and Ru(1)–Ru(2)–C(6) linkages, respectively. Here the two CO groups in question are clearly tipped upward and away from the specified neighboring ligand.

III. Phosphorus–Carbon Bond Oxidative Addition in $\text{Ru}_2(\text{CO})_6(\text{bpcd})$. The reactivity of **2** was checked as it is a potential precursor to **3**. The thermal stability of **2** was established by its recovery from refluxing xylene solutions ($T \approx 140$ °C) with only minimal material loss (<5%). No evidence for the formation of **3** was found in any of the thermolysis reactions conducted, suggesting again that the formation of **3** from $\text{Ru}_3(\text{CO})_{12}/\text{bpcd}$ must derive from a path that does not involve the intermediacy of **2** (*vide supra*). Surprisingly, **2** is photosensitive and is converted to **3** by 366 nm light in CH_2Cl_2 with a quantum efficiency of 0.035. The nature of the solvent does not appear to be important, as reactions conducted in toluene and THF give identical quantum yields within experimental error. Near-UV irradiation of **2** is expected to lead to population of the $\sigma\sigma^*$ transition due to the strong absorption at 318 nm in **2**, which may be confidently assigned to the $\sigma\sigma^*$ manifold, on the basis of chemistry exhibited by other binuclear complexes.²⁹ Consistent with this mode of reactivity is that photolysis of **2** under CO (120 psi) gave $\phi_{\text{dis}} = 0.029$, which suggests that dissociative CO loss is an unimportant pathway en route to **3**.³⁰

In analogy to other σ -bonded dinuclear complexes, near-UV photolysis of **2** is expected to promote the homolysis of the Ru–Ru bond, coupled with the generation of a transient, bridged biradical species. However, unlike the neutral biradical species found in ligand-bridged compounds,³¹ homolysis of the dative Ru–Ru

(27) (a) Churchill, M. R.; Hollander, F. J.; Hutchinson, J. P. *Inorg. Chem.* **1977**, *16*, 2655. (b) Luga, N.; Lavigne, G.; Bonnet, J.-J.; Réau, R.; Neibecker, D.; Tkatchenko, I. *J. Am. Chem. Soc.* **1988**, *110*, 5369. (c) Blake, A. J.; Dyson, P. J.; Ingham, S. L.; Johnson, B. F. G.; Martin, C. M. *Organometallics* **1995**, *14*, 862. (d) Paw, W.; Keister, J. B.; Lake, C. H.; Churchill, M. R. *Organometallics* **1995**, *14*, 767.

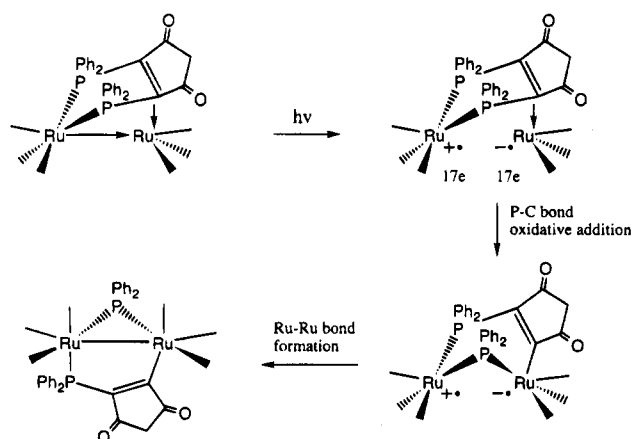
(28) (a) Deeming, A. J.; Doherty, S.; Powell, N. I. *Inorg. Chim. Acta* **1992**, *198*–200, 469. (b) Soucek, M. D.; Clubb, C. C.; Kyba, E. P.; Price, D. S.; Scheuler, V. G.; Aldaz-Palacios, H. O.; Davis, R. E. *Organometallics* **1994**, *13*, 1120. (c) Corrigan, J. F.; Dinardo, M.; Doherty, S.; Hogarth, G.; Sun, Y.; Taylor, N. J.; Carty, A. J. *Organometallics* **1994**, *13*, 3572.

(29) (a) Geoffroy, G. L.; Wrighton, M. S. *Organometallic Photochemistry*; Academic Press: New York, 1979. (b) Meyer, T. J.; Caspar, J. V. *Chem. Rev.* **1985**, *85*, 187. (c) Stiegman, A. E.; Tyler, D. R. *Acc. Chem. Res.* **1984**, *17*, 61.

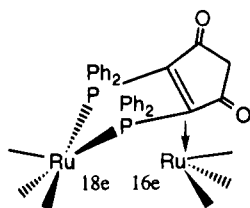
(30) Trapping experiments using CCl_4 as a solvent gave quantum yields unchanged relative to those with CH_2Cl_2 , THF, and toluene. This suggests that halogen atom abstraction by the proposed biradical intermediate is not competitive with ruthenium–ruthenium bond formation and P–C bond scission. The use of other trapping agents is planned, and the data will be reported upon project completion.

(31) (a) Lee, K.-W.; Hanckel, J. M.; Brown, T. L. *J. Am. Chem. Soc.* **1986**, *108*, 2266. (b) Lee, K.-W.; Brown, T. L. *Organometallics* **1985**, *4*, 1030.

Scheme 2



bond in **2** should afford a zwitterionic biradical intermediate, as shown in Scheme 2, and it is this species we believe controls the P-C(dione) bond cleavage observed in going from **2** to **3**.³² Loss of the Ru-Ru bond upon optical excitation to give a coordinatively unsaturated compound with 18e and 16e ruthenium centers can be



eliminated from consideration because ligand substitution occurs only at the phosphine-substituted ruthenium center.³³ Whether the oxidative addition step occurs while the bpcd π bond remains coordinated to Ru(2), followed by slippage of the π bond off the Ru(2) site, or by a concerted π slippage and P-C bond activation cannot be ascertained at this time. But what is clear is that (1) P-C bond cleavage takes place at the dione-substituted ruthenium atom and (2) the reaction occurs at an odd-electron ruthenium center. To our knowledge, no other reports exist dealing with the oxidative addition of a P-C bond at a paramagnetic metal center.³⁴ The nature of the alkene group plays a crucial role in this reaction. Photolysis of the alkene-bridged complex Ru₂(CO)₆[(Z)-Ph₂PCH=CHPh₂] (**4**)^{16b} did not show any signs of productive photochemistry, as only the unreacted **4** was recovered. These data underscore the importance of the electron-withdrawing properties of the ancillary substituents on the phosphine ligand in directing which of the P-C bonds is activated by the metal center.^{12,35}

IV. Electrochemical Studies. Cyclic voltammetry studies on clusters **1-4** were conducted at a platinum-disk electrode in CH₂Cl₂ solvent containing 0.25 M

(32) For a report on the photochemistry of an unbridged donor-acceptor compound, see: Male, J. L.; Davis, H. B.; Pomeroy, R. K.; Tyler, D. L. *J. Am. Chem. Soc.* **1994**, *116*, 9353.

(33) Irradiation of Ru₂(CO)₆(bpcd) in the presence of added PMe₃ or CNBu⁺ does not afford substitution products at the dione-substituted ruthenium center. This argues against the existence of a 16e center at this site. Shen, H.; Bott, S. G.; Richmond, M. G. Unpublished results.

(34) For reports of H and halogen atom abstraction reactions, see: (a) *Paramagnetic Organometallic Species in Activation/Selectivity, Catalysis*; Chanon, M., Julliard, M., Poite, J. C., Eds.; Kluwer: Boston, MA, 1989. (b) *Organometallic Radical Processes*; Troglor, W. C., Ed.; Elsevier: New York, 1990.

(35) (a) Dubois, R. A.; Garrou, P. E. *Organometallics* **1986**, *5*, 466. (b) Garrou, P. E. *Chem. Rev.* **1985**, *85*, 171.

Table 4. Cyclic Voltammetric Data for Compounds 1-4^a

compd	redox couple ^b			
	E_p^c	E_p^a	$E_{1/2}$	E_p^a
1	-0.73	-0.64	-0.69	0.63
2 ^{c,d}				1.20
3	-1.42	-1.30	-1.36	1.04
4 ^c				0.76
bpcd	-1.16	-1.08	-1.12	1.03

^a In ca. 10⁻³ M CH₂Cl₂ solutions containing 0.25 M TBAP at room temperature and a scan rate of 0.1 V s⁻¹. Potentials are in volts relative to a silver wire quasi-reference electrode, calibrated against ferrocene or decamethylferrocene. ^b E_p^c and E_p^a refer to the cathodic and anodic peak potentials of the CV waves. The half-wave potential $E_{1/2}$, which represents the chemically reversible redox couple, is defined as $(E_p^c + E_p^a)/2$. ^c An additional response at $E_p^a = 1.32$ V was also observed. ^d The presence of an irreversible reduction ($E_p^c = -1.90$ V) was recorded for **2** in MeCN/0.25 M TBAP.

tetra-n-butylammonium perchlorate (TBAP) as the supporting electrolyte. These data are summarized in Table 4. Both **1** and **3** exhibit a reversible one-electron reduction at $E_{1/2} = -0.69$ V and $E_{1/2} = -1.36$ V, respectively, on the basis of peak current (I_p^a/I_p^c) ratios of unity and the linear plots of the current function (I_p) as a function of the square root of the scan rate (v) over the scan rates of 0.05-1.0 V/s.³⁶ The ΔE_p value of 120 mV for the latter redox couple suggests that the reduction in **3** may be kinetically slow (i.e., k_{het} is slow) given that this value is greater than the 80 mV peak-to-peak separation observed for the one-electron standard ferrocene.³⁶ Only these two compounds that possess an uncomplexed 4-cyclopenten-1,3-dione ring exhibit a reversible one-electron reduction due to electron accession at the π^* system of the redox-active carbocyclic ring.^{15,37} In a majority of carbonyl clusters and binuclear compounds electron transfer leads to fragmentation of the starting compound because a metal-metal antibonding orbital is populated upon reduction.³⁸ However, no fragmentation of compounds **1** and **3** is seen during the time scale of these CV experiments, due to the redox-active 4-cyclopenten-1,3-dione ring, which provides an alternate ligand-based LUMO. Compounds **2** and **4**, which are similar in that they both contain a coordinated alkene bond from the diphosphine ligand, do not exhibit any reduction behavior in CH₂Cl₂ solvent. The room temperature CV of **3** is shown in Figure 2.

All four ruthenium compounds examined displayed an irreversible, metal-based oxidation (*vide supra*) that did not show any signs of reversibility at scan rates up to 2 V/s and temperatures down to -80 °C.

V. Extended Hückel Calculations. The composition of the HOMO and LUMO in compounds **1-4** was probed by carrying out extended Hückel molecular orbital calculations on the model compounds Ru₃(CO)₁₀-(H₄-bpcd), Ru₂(CO)₆(H₄-bpcd), Ru₂(CO)₆[μ -C=C(Ph₂)C-

(36) (a) Bard, A. J.; Faulkner, L. R. *Electrochemical Methods*; Wiley: New York, 1980. (b) Rieger, P. H. *Electrochemistry*; Chapman & Hall: New York, 1994.

(37) Yang, K.; Bott, S. G.; Richmond, M. G. *Organometallics* **1994**, *13*, 3788.

(38) For electrochemical studies on Ru₃(CO)₁₂, see: (a) Cyr, J. E.; Rieger, P. H. *Organometallics* **1991**, *10*, 2153. (b) Bond, A. M.; Dawson, P. A.; Peake, B. M.; Robinson, B. H.; Simpson, J. *Inorg. Chem.* **1977**, *16*, 2199. (c) Cyr, J. C.; DeGray, J. A.; Gosser, D. K.; Lee, E. S.; Rieger, P. H. *Organometallics* **1985**, *4*, 950. (d) Zanello, P.; Aime, S.; Osella, D. *Organometallics* **1984**, *3*, 1374.

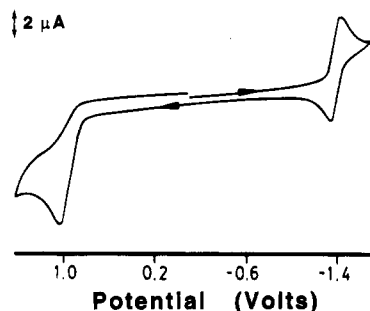


Figure 2. Cathodic scan cyclic voltammogram of $\text{Ru}_2(\text{CO})_6\text{-(}\mu\text{-C=C(PPh}_2\text{)C(O)CH}_2\text{C(O))}(\mu_2\text{-PPh}_2)$ (**3**) (ca. 10^{-3} M) at room temperature in CH_2Cl_2 containing 0.25 M TBAP and a scan rate of 0.1 V s^{-1} .

$(\text{O)CH}_2\text{C(O))}(\mu_2\text{-PPh}_2)$, and $\text{Ru}_2(\text{CO})_6[(\text{Z})\text{-H}_2\text{PCH=CPh}_2]$. Figure 3 shows the three-dimensional CACAO drawings of the HOMO and LUMO levels for bpcd-substituted compounds.³⁹

The HOMO in cluster **1** is found at -10.91 eV , and this orbital contains comparable contributions of Ru–Ru bonding (39%) with carbonyl π^* (36%) interactions. The essential features of this HOMO closely mimic the HOMO reported for the parent cluster $\text{Ru}_3(\text{CO})_{12}$.⁴⁰ The extended Hückel calculations indicate that the LUMO occurs at -10.21 eV and resides entirely on the bpcd ligand in a MO that is nodally similar to Ψ_4 of a six- π -electron system.⁴¹ This empty π^* acceptor orbital validates the premise made regarding the site for electron accession in the 0/1– redox couple of **1**. The prospect of producing relatively stable paramagnetic clusters that do not have fully occupied metal–metal antibonding orbitals provides, in part, the incentive for the future EPR and electron-transfer studies using this genre of compound.

Compound **2** may be viewed as arising from the union of the bpcd ligand with a $\text{Ru}_2(\text{CO})_6$ fragment. The HOMO in **2** has an energy of -10.93 eV and is represented by a bonding interaction between the $d_{x^2-y^2}$ orbital of each ruthenium center. Hybridization with ruthenium p_y and d_z^2 orbitals serves to further shape the HOMO for maximum bonding. Our HOMO corresponds to the $1a_1$ orbital interaction reported by Hoffmann for $\text{M}_2(\text{CO})_6$ fragments.⁴² The more interesting interactions occur between the b_1 (bonding d_{xz}) and a_2 (antibonding d_{xz}) orbitals of the $\text{Ru}_2(\text{CO})_6$ fragment and the π^* orbital belonging to the bpcd ligand. Here the bpcd π^* molecular orbital overlaps with the dimetal a_2 orbital via the alkene portion of the bpcd ligand. This overlap is bonding in nature and affords a MO immediately below the HOMO at -11.56 eV (not shown). The LUMO, which is found at -9.18 eV , may be described as an antibonding orbital between a hybridized d_{xz} orbital (14%) and the bpcd π^* system (32%). Not shown in the LUMO picture are the π^* contributions from the ruthenium CO groups (32%). The absence of

a noticeable ruthenium contribution at the phosphine-substituted ruthenium center (Ru(1)) in the LUMO stems from mixing of the b_1 and a_2 orbitals. Such an interaction is favorable because it leads to a reduction in antibonding interactions between the Ru(1)/CO and Ru(1)/Ru(2) groups.

The phosphido compound **3** displays a HOMO at -10.89 eV that is bonding in nature and is formed from the overlap of $d_{x^2-y^2}$ orbitals that have been hybridized with ruthenium p_x and p_y character. The ruthenium contribution accounts for 58% of the HOMO, with antibonding Ru/CO interactions (both σ and π^*) and a minor contribution from the dione ring making up the rest of the orbital composition. The LUMO is localized on the dione ring, and the nodal pattern of the LUMO has not been dramatically altered by P–C bond cleavage in comparison to the LUMO found for **1**. The energy level of the LUMO occurs at -10.24 eV .

The orbital properties of **4** were also explored by extended Hückel calculations. Except for the slightly higher energy found for the LUMO, compounds **2** and **4** were identical in every respect, requiring no additional comments.

Conclusions

The chelated cluster $\text{Ru}_3(\text{CO})_{10}(\text{bpcd})$ decomposes slowly in the absence of light in solution to give the donor-acceptor compound $\text{Ru}_2(\text{CO})_6(\text{bpcd})$ along with $\text{Ru}_3(\text{CO})_{12}$. The manner by which $\text{Ru}_2(\text{CO})_6[\mu\text{-C=C(PPh}_2\text{)C(O)CH}_2\text{C(O)}](\mu_2\text{-PPh}_2)$ forms from $\text{Ru}_3(\text{CO})_{12}/\text{bpcd}$ is not known at this time, but it has been ascertained that $\text{Ru}_2(\text{CO})_6(\text{bpcd})$ cannot be a direct precursor to this product. Near-UV irradiation of $\text{Ru}_2(\text{CO})_6(\text{bpcd})$ gives $\text{Ru}_2(\text{CO})_6[\mu\text{-C=C(PPh}_2\text{)C(O)CH}_2\text{C(O)}](\mu_2\text{-PPh}_2)$, as a result of P–C(dione) bond cleavage. The possibility of P–C bond oxidative addition at a biradical intermediate formed upon optical excitation seems likely. The electrochemical data reveal that both cluster **1** and binuclear **3** undergo a reversible one-electron reduction at a LUMO that is localized on the free 4-cyclopenten-1,3-dione ring present in each compound. Extended Hückel MO calculations have confirmed this scheme. The nodal pattern of the electron-withdrawing dione ring is disrupted upon complexation in **2**, and this effectively eliminates the availability of a low-potential, dione-based redox couple, leading to irreversible reductive electrochemistry.

Experimental Section

The starting $\text{Ru}_3(\text{CO})_{12}$ cluster was synthesized from $\text{RuCl}_3 \cdot n\text{H}_2\text{O}$ using the carbonylation procedure of Bruce,⁴³ while the ligand bpcd was prepared from 4,5-dichloro-4-cyclopenten-1,3-dione using the reported literature procedure.^{7,44} [PPN][Cl] was purchased from Aldrich Chemical Co. and used as received. The ^{13}C (>99%) used in the preparation of the ^{13}C -enriched $\text{Ru}_3(\text{CO})_{12}$ was obtained from Isotec, Inc. Toluene and THF were distilled from sodium/benzophenone, while CH_2Cl_2 and 1,2-dichloroethane were distilled from P_2O_5 under argon; all solvents were handled by using Schlenk techniques.⁴⁵ Purified solvents were stored in Schlenk storage

(39) Mealli, C.; Proserpio, D. M. *J. Chem. Ed.* **1990**, *67*, 399.

(40) (a) Delley, B.; Manning, M. C.; Ellis, D. E.; Berkowitz, J.; Trogler, W. C. *Inorg. Chem.* **1982**, *21*, 2247. (b) Schilling, B. E. R.; Hoffmann, R. *J. Am. Chem. Soc.* **1979**, *101*, 3456. (c) Green, J. C.; Mingos, D. M. P.; Seddon, E. A. *Inorg. Chem.* **1981**, *20*, 2595. (d) Tyler, D. R.; Levenson, R. A.; Gray, H. B. *J. Am. Chem. Soc.* **1978**, *100*, 7888.

(41) Albright, T. A.; Burdett, J. K.; Whangbo, M. H. *Orbital Interactions in Chemistry*; Wiley: New York, 1985.

(42) (a) Thorn, D. L.; Hoffmann, R. *Inorg. Chem.* **1978**, *17*, 126. (b) Hoffman, D. M.; Hoffmann, R.; Fisel, C. R. *J. Am. Chem. Soc.* **1982**, *104*, 3858.

(43) Bruce, M. I.; Jensen, C. M.; Jones, N. L. *Inorg. Synth.* **1989**, *26*, 259.

(44) Roedig, A.; Hörnig, L. *Chem. Ber.* **1955**, *88*, 2003.

(45) Shriver, D. F. *The Manipulation of Air-Sensitive Compounds*, McGraw-Hill: New York, 1969.

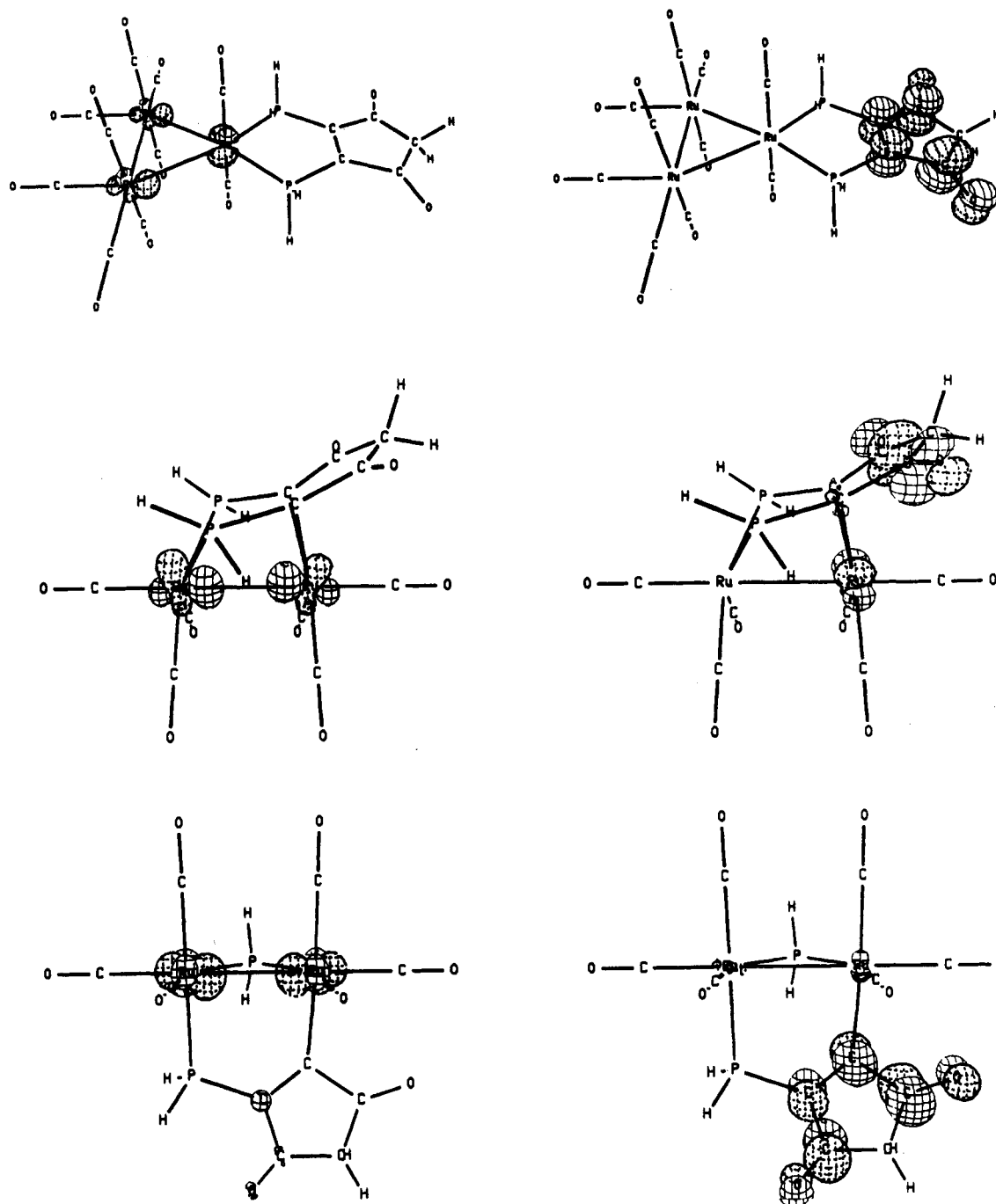


Figure 3. CACAO drawings of the HOMO (left) and the LUMO (right) for (top) Ru₃(CO)₁₀(H₄-bpcd) (chelating isomer), (middle) Ru₂(CO)₆(H₄-bpcd), and (bottom) Ru₂(CO)₆[μ-C=C(PH₂)C(O)CH₂C(O)](μ₂-PH₂).

vessels equipped with Teflon stopcocks. The TBAP (*Caution! strong oxidant*) used in the CV studies was obtained from Johnson Matthey Electronics and was recrystallized from ethyl acetate/petroleum ether, followed by drying for 2 days under vacuum. All C and H microanalyses were performed by Atlantic Microlab, Norcross, GA.

Infrared spectra were recorded on a Nicolet 20 SXB FT-IR spectrometer in 0.1 mm NaCl cells. UV-visible spectra were recorded on a Hewlett-Packard 8452A diode array spectrophotometer, using a 1.0 cm quartz UV-visible cell that was equipped with a Teflon stopcock. ¹H NMR spectra were recorded in CDCl₃ solvent at 200 MHz on a Varian Gemini-200 spectrometer, while the reported ¹³C and ³¹P NMR spectra were recorded at 75 and 121 MHz, respectively, and a Varian VXR-300 spectrometer. The reported ³¹P chemical shifts were referenced to external H₃PO₄ (85%), with positive chemical shifts to low field of the external standard.

All photochemical experiments were conducted at room temperature with Sylvania Blacklight bulbs, possessing a maximum output at 366 ± 20 nm. The light intensity was determined by ferrioxalate actinometry and was found to be on the order of ca. 1 × 10⁻⁷ einstein/min.⁴⁶ All quantum yields reported represent the average value for at least two separate reactions.

Synthesis of Ru₃(CO)₁₀(bpcd) (Chelating Isomer). To 0.20 g (0.31 mmol) of Ru₃(CO)₁₂ and 0.18 g (0.31 mmol) of [PPN][Cl] in a Schlenk tube was added 1.0 mL of CH₂Cl₂, followed by 20 mL of THF. The reaction solution was stirred at room temperature for ca. 10 min under argon and then examined by IR analysis, which revealed the quantitative formation of the anionic cluster [Ru₃(CO)₁₁Cl][PPN]. At this point, 0.15 g (0.33 mmol) of bpcd was added. The reaction

(46) (a) Calvert, J. G.; Pitts, J. N. *Photochemistry*; Wiley: New York, 1966. (b) Bowman, W. D.; Demas, J. N. *J. Phys. Chem.* **1976**, *80*, 2434.

mixture was stirred for ca. 1.0 h, with CO evolution being noticeable as the reaction leading to $\text{Ru}_3(\text{CO})_{10}(\text{bpcd})$ proceeded. After the solvents were removed under vacuum, the pure product was isolated by chromatography over silica gel using $\text{CH}_2\text{Cl}_2/\text{petroleum ether}$ (1:1) as the eluant. Due to the limited thermal stability of $\text{Ru}_3(\text{CO})_{10}(\text{bpcd})$, no combustion analysis was pursued. Yield: 0.11 g (32% based on $\text{Ru}_3(\text{CO})_{12}$ consumed). IR (CH_2Cl_2): $\nu(\text{CO})$ 2085 (s), 2037 (s), 2005 (vs), 1930 (w), 1749 (w, bpcd), 1718 (m, bpcd) cm^{-1} . ^1H NMR (CDCl_3): δ 3.61 (2H, s), aromatic multiplet 7.45–7.60 (20H). $^{31}\text{P}\{^1\text{H}\}$ NMR spectrum (CDCl_3): δ 50.76.

Synthesis of $\text{Ru}_2(\text{CO})_6(\text{bpcd})$ from $\text{Ru}_3(\text{CO})_{12}$. To 1.00 g (1.56 mmol) of $\text{Ru}_3(\text{CO})_{12}$ and 0.87 g (1.87 mmol) of bpcd in a 250 mL Schlenk flask was added 100 mL of toluene, followed by heating at ca. 100 °C overnight. When it was cooled, the reaction solution was examined by TLC analysis, which indicated the presence of two slow-moving products, in addition to a small amount of $\text{Ru}_3(\text{CO})_{12}$. Purification by column chromatography using petroleum ether as the eluant afforded the parent cluster $\text{Ru}_3(\text{CO})_{12}$ (0.22 g; 22% recovered), while a yellow fraction representing the phosphido-bridged compound **3** was obtained by employing a 1:1 mixture of $\text{CH}_2\text{Cl}_2/\text{petroleum ether}$ as the eluant (0.17 g; 17% based on $\text{Ru}_3(\text{CO})_{12}$ consumed). The title compound **2** was eluted from the column by using CH_2Cl_2 . Recrystallization of **2** from $\text{CH}_2\text{Cl}_2/\text{pentane}$ (1:1) afforded crystals of **2** suitable for microanalysis and X-ray diffraction analysis. Yield: 0.61 g (60% based on $\text{Ru}_3(\text{CO})_{12}$ consumed). IR (CH_2Cl_2): $\nu(\text{CO})$ 2079 (vs), 2041 (vs), 2025 (s), 2001 (m), 1978 (s), 1701 (m, bpcd), 1674 (m, bpcd) cm^{-1} . UV-vis (CH_2Cl_2): λ_{max} (nm) (ϵ , $\text{M}^{-1} \text{cm}^{-1}$) 246 ($\epsilon = 22\,596$), 318 ($\epsilon = 9368$). ^1H NMR (CDCl_3): δ 3.76 (2H, AB quartet, $J_{\text{H-H}} = 22.10$ Hz), aromatic resonances 6.95–8.10 (20H). $^{13}\text{C}\{^1\text{H}\}$ NMR spectrum (CH_2Cl_2): δ 191.55 (1C, t, $J_{\text{P-C}} = 7.53$ Hz), 193.46 (1C, s), 197.66 (2C, AAXX' spin system with ^{13}CO -enriched **2**), 199.49 (2C, s). $^{31}\text{P}\{^1\text{H}\}$ NMR spectrum (CDCl_3): δ 25.21. Anal. Calcd (found) for $\text{C}_{35}\text{H}_{22}\text{O}_8\text{P}_2\text{Ru}_2$: C, 50.37 (50.24); H, 2.66 (2.71).

Synthesis of $\text{Ru}_2(\text{CO})_6[\mu\text{-C}=\text{C}(\text{PPh}_2)\text{C}(\text{O})\text{CH}_2\text{C}(\text{O})](\mu_2\text{-PPh}_2)$ from Irradiation of $\text{Ru}_2(\text{CO})_6(\text{bpcd})$. To 25.0 mg of **2** in a 100 mL Schlenk tube was added 20 mL of CH_2Cl_2 , after which the vessel was irradiated overnight using two Sylvania Blacklight bulbs. The solvent was concentrated to a volume of 1.0 mL, and the product was then isolated by chromatography over silica gel using $\text{CH}_2\text{Cl}_2/\text{petroleum ether}$ (1:1) as the eluant. **3** was isolated as a light yellow solid and was recrystallized from $\text{CH}_2\text{Cl}_2/\text{pentane}$. Yield: 17.0 mg (68%). IR (CH_2Cl_2): $\nu(\text{CO})$ 2078 (vs), 2045 (vs), 2018 (vs), 1996 (s), 1980 (s), 1725 (w, bpcd), 1694 (s, bpcd) cm^{-1} . UV-vis (CH_2Cl_2): λ_{max} (nm) (ϵ , $\text{M}^{-1} \text{cm}^{-1}$) 246 ($\epsilon = 24\,257$), 302 (sh, $\epsilon = 9368$). ^1H NMR (CDCl_3): δ 2.79 (2H, AB quartet, $J_{\text{H-H}} = 20.84$ Hz), aromatic resonances 6.90–7.72 (20H). $^{13}\text{C}\{^1\text{H}\}$ NMR spectrum (CH_2Cl_2): δ 194.18 (1C, d, $J_{\text{P-C}} = 13.43$ Hz), 195.50 (2C, overlapping resonances), 195.83 (1C, dd, $J_{\text{P-C}} = 10.69$ Hz, $J_{\text{P-C}} = 82.94$ Hz), 200.13 (1C, d, $J_{\text{P-C}} = 55.74$ Hz), 201.84 (1C, dd, $J_{\text{P-C}} = 14.57$ Hz, $J_{\text{P-C}} = 48.89$ Hz). $^{31}\text{P}\{^1\text{H}\}$ NMR spectrum (CDCl_3): δ 169.55 ($\mu_2\text{-PPh}_2$; $J_{\text{P-P}} = 27.38$ Hz), 23.40 [PPh_2 - (dione); $J_{\text{P-P}} = 27.38$ Hz]. Anal. Calcd (found) for $\text{C}_{35}\text{H}_{22}\text{O}_8\text{P}_2\text{Ru}_2$: C, 50.37 (50.31); H, 2.66 (2.72).

X-ray Diffraction Structure of $\text{Ru}_2(\text{CO})_6(\text{bpcd})$. A golden crystal of dimensions $0.06 \times 0.11 \times 0.24 \text{ mm}^3$ was sealed inside a Lindemann capillary and then mounted on the goniometer of an Enraf-Nonius CAD-4 diffractometer. The radiation used was Mo K α monochromatized by a crystal of graphite. Cell constants were obtained from a least-squares refinement of 25 reflections with $2\theta > 35^\circ$. Intensity data in the range $2.0 \leq 2\theta \leq 44^\circ$ were collected at room temperature using the $\theta/2\theta$ scan technique in the variable-scan-speed mode and were corrected for Lorentz, polarization, and absorption (DIFABS). Three reflections (600, 080, 0010) were measured after every 3600 s of exposure time as a check of crystal stability (<2%). The structure was initially solved by using a Patterson map, and all of the non-hydrogen atoms were located with difference Fourier maps and refined by using full-matrix

least-squares methods. All non-hydrogen atoms were refined anisotropically. Refinement converged at $R = 0.0216$ and $R_w = 0.0258$ for 3402 unique reflections with $I > 3\sigma(I)$.

X-ray Diffraction Structure of $\text{Ru}_2(\text{CO})_6[\mu\text{-C}=\text{C}(\text{PPh}_2)\text{C}(\text{O})\text{CH}_2\text{C}(\text{O})](\mu_2\text{-PPh}_2)\text{-C}_7\text{H}_{16}$. Crystals of **3** suitable for X-ray crystallography were obtained from a CH_2Cl_2 solution containing **3** that had been layered with heptane. An orange crystal of dimensions $0.11 \times 0.16 \times 0.44 \text{ mm}^3$ was sealed inside a Lindemann capillary and then mounted on the goniometer of an Enraf-Nonius CAD-4 diffractometer. The radiation used was Mo K α monochromatized by a crystal of graphite. Cell constants were obtained from a least-squares refinement of 25 reflections with $2\theta > 30^\circ$. Intensity data in the range $2.0 \leq 2\theta \leq 44^\circ$ were collected at room temperature using the $\theta/2\theta$ -scan technique in the variable-scan speed mode and were corrected for Lorentz, polarization, and absorption (DIFABS). Three reflections (6 0 0, 0 -8 0, 0 0 8) were measured after every 3600 s of exposure time as a check of crystal stability (<1%). The structure was initially solved by using a Patterson map, and all of the non-hydrogen atoms were located with difference Fourier maps and refined by using full-matrix least-squares methods. A molecule of solvent, disordered over a center of inversion, was included in the model. With the exception of the phenyl and solvent carbons, all non-hydrogen atoms were refined anisotropically. Refinement converged at $R = 0.0349$ and $R_w = 0.0392$ for 3684 unique reflections with $I > 3\sigma(I)$.

Electrochemical Studies. Cyclic voltammetric experiments were carried out by using a PAR Model 273 potentiostat/galvanostat, equipped with positive feedback circuitry in order to compensate for iR drop. The three-electrode cell used in the CV studies was of homemade design, allowing for all CVs to be obtained under oxygen- and moisture-free conditions. All CV experiments employed a platinum disk (area 0.0079 cm^2) as the working and auxiliary electrode. All voltammograms utilized a silver-wire quasi-reference electrode, with the quoted potential data being referenced to the formal potential of either the $\text{Cp}_2\text{Fe}/\text{Cp}_2\text{Fe}^+$ or $\text{Cp}^*\text{Fe}/\text{Cp}^*\text{Fe}^+$ (internally added) redox couple, taken to have $E_{1/2} = 0.307 \text{ V}^{36}$ and $E_{1/2} = -0.200 \text{ V}$,⁴⁷ respectively.

Molecular Orbital Calculations. The extended Hückel calculations reported here were carried out with the original program developed by Hoffmann,⁴⁸ as modified by Mealli and Proserpio.³⁹ The input **Z** matrix for each compound examined was constructed by replacing the phenyl groups on the bpcd and (*Z*)- $\text{Ph}_2\text{PCH}=\text{CHPh}_2$ ligands with hydrogen groups. The P-H (1.42 Å) distances used in the extended Hückel calculations were taken from model compounds.⁴⁹

Acknowledgment. We wish to thank Prof. Carlo Mealli for providing us with a copy of his CACAO drawing program. Financial support from the Robert A. Welch Foundation (Grant Nos. B-1202-SGB and B-1039-MGR) and the UNT Faculty Research Program is gratefully appreciated.

Supporting Information Available: Textual presentations of the crystallographic experimental details and listings of bond distances, bond angles, and hydrogen positional and thermal parameters for compounds **2** and **3** (26 pages). Ordering information is given on any current masthead page.

OM9503048

(47) Ryan, M. F.; Richardson, D. E.; Lichtenberger, D. L.; Gruhn, N. E. *Organometallics* **1994**, *13*, 1190.

(48) (a) Hoffmann, R.; Lipscomb, W. N. *J. Chem. Phys.* **1962**, *36*, 2179. (b) Hoffmann, R. *J. Chem. Phys.* **1963**, *39*, 1397.

(49) *Handbook of Chemistry and Physics*, Weast, R. C., Ed.; 56th ed.; CRC: Cleveland, OH, 1975.

Migratory Insertion of a Phosphorus Ligand into a Transition Metal-Alkyl Bond

Hiroshi Nakazawa,^{*,†} Yoshitaka Yamaguchi,[†] Tsutomu Mizuta,[†]
Satoshi Ichimura,[‡] and Katsuhiko Miyoshi^{*,‡}

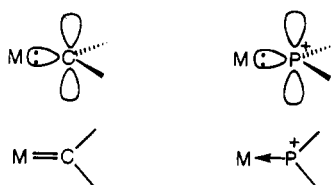
Coordination Chemistry Laboratories, Institute for Molecular Science, Myodaiji,
Okazaki 444, Japan, and Department of Chemistry, Faculty of Science, Hiroshima University,
Higashi-Hiroshima 739, Japan

Received June 5, 1995[⊙]

Treatment of $\text{Cp}(\text{CO})(\text{R}^1)\text{Fe}\{\text{PN}(\text{Me})\text{CH}_2\text{CH}_2\text{NMe}(\text{OR}^2)\}$ ($\text{R}^1 = \text{R}^2 = \text{Me}$, **1a**; $\text{R}^1 = \text{Me}$, $\text{R}^2 = \text{Et}$, **2a**; $\text{R}^1 = \text{CH}_2\text{Ph}$; $\text{R}^2 = \text{Me}$, **3a**) with $\text{BF}_3\cdot\text{OEt}_2$ and then with PPh_3 yields $[\text{Cp}(\text{CO})\text{-(PPh}_3)\text{Fe}\{\text{PN}(\text{Me})\text{CH}_2\text{CH}_2\text{NMe}(\text{R}^1)\}]^+$ ($\text{R}^1 = \text{Me}$, **1b**; $\text{R}^1 = \text{CH}_2\text{Ph}$, **3b**). The reaction proceeds via the formation of a cationic phosphonium complex, $[\text{Cp}(\text{CO})(\text{R}^1)\text{Fe}\{\text{PN}(\text{Me})\text{CH}_2\text{CH}_2\text{NMe}\}]^+$, by the abstraction of an OR group as an anion from a phosphorus atom, and then migratory insertion of the phosphonium ligand into the iron-alkyl bond takes place to give $[\text{Cp}(\text{CO})\text{-(BF}_2\text{OR}^2)\text{Fe}\{\text{PN}(\text{Me})\text{CH}_2\text{CH}_2\text{NMe}(\text{R}^1)\}]^+$, which is characterized by spectroscopic data. The cationic complex readily reacts with PPh_3 to give the final product. A $\eta^5\text{-C}_5\text{Me}_5$ derivative of **1a** and a monoamino-substituted phosphite complex $\text{Cp}(\text{CO})(\text{Me})\text{Fe}\{\text{PN}(\text{Me})\text{CH}_2\text{CH}_2\text{O}(\text{OMe})\}$ show the same reactivity. The reaction of silyl complexes $\text{Cp}(\text{CO})(\text{SiMe}_3)\text{Fe}\{\text{PN}(\text{Me})\text{CH}_2\text{CH}_2\text{NMe}(\text{OR})\}$ ($\text{R} = \text{Me}$, **Et**) with $\text{BE}_3\cdot\text{OEt}_2$ affords a phosphonium complex $[\text{Cp}(\text{CO})(\text{SiMe}_3)\text{Fe}\{\text{PN}(\text{Me})\text{CH}_2\text{CH}_2\text{NMe}\}]^+$, which does not show the migratory insertion into an iron-silyl bond. Iron complexes $\text{Cp}(\text{CO})(\text{CH}_2\text{OMe})\text{Fe}\{\text{PN}(\text{Me})\text{CH}_2\text{CH}_2\text{NMe}(\text{OR})\}$ ($\text{R} = \text{Me}$, **9a**; $\text{R} = \text{Et}$, **10a**) having an alkoxy group both on a carbon and on a phosphorus react with $\text{BF}_3\cdot\text{OEt}_2$ and then with PPh_3 to give $[\text{Cp}(\text{CO})(\text{CH}_2\text{PPh}_3)\text{Fe}\{\text{PN}(\text{Me})\text{CH}_2\text{CH}_2\text{NMe}(\text{OR})\}]^+$ ($\text{R} = \text{Me}$, **9e**; $\text{R} = \text{Et}$, **10e**). The results prove that the OMe in the CH_2OMe ligand is selectively abstracted to give the methylenide complex which is trapped with PPh_3 to give a phosphine ylide complex. Complexes **1b**· BF_4 and **10e**· BF_4 have been characterized by X-ray diffraction (crystal data for **1b**· BF_4 , monoclinic, $P2_1/n$, $a = 9.099(1)$ Å, $b = 13.727(2)$ Å, $c = 23.134(5)$ Å, $\beta = 91.48(1)^\circ$, $Z = 4$, $R = 0.063$; for **10e**· BF_4 , orthorhombic, $Pcab$, $a = 18.033(6)$ Å, $b = 24.619(6)$ Å, $c = 14.501(4)$ Å, $Z = 8$, $R = 0.059$).

Introduction

Phosphenium ions ($^+\text{PR}_2$) are unique ligands toward transition metals because they have both lone pair electrons and a vacant p orbital at the phosphorus.¹ Therefore, they can act as a σ -donor and also as a π -acceptor to a transition metal. In that sense, phosphenium complexes resemble singlet carbene complexes



(Customarily, a bond between M and C in a carbene complex is depicted as a double bond, whereas a bond between M and P in a phosphenium complex is described as a dative bond). Although some preparative

methods for transition metal phosphenium complexes have been reported,¹⁻⁵ their reactivities still remain to be exploited.

One of the most attracting reactions of carbene complexes is the so-called carbene migratory insertion into a transition metal-alkyl bond (perhaps more appropriately designated simply as a migration of an alkyl ligand to a carbene ligand or as a 1,2-rearrangement).⁶ The related phosphenium migratory insertion into a transition metal-alkyl bond has not been reported so far. In this paper, we report the unprec-

(2) (a) Day, V. W.; Tavanaiepour, I.; Abdel-Meguid, S. S.; Kirner, J. F.; Goh, L.-Y.; Muettterties, E. L. *Inorg. Chem.* **1982**, *21*, 657. (b) Choi, H. W.; Gavin, R. M.; Muettterties, E. L. *J. Chem. Soc., Chem. Commun.* **1979**, 1085. (c) Muettterties, E. L.; Kirner, J. F.; Evans, W. J.; Watson, P. L.; Abdel-Meguid, S. S.; Tavanaiepour, I.; Day, V. W. *Proc. Natl. Acad. Sci. U.S.A.* **1978**, *75*, 1056.

(3) (a) Cowley, A. H.; Kemp, R. A.; Ebsworth, E. A. V.; Rankin, D. W. H.; Walkinshaw, M. D. *J. Organomet. Chem.* **1984**, *265*, C19. (b) Cowley, A. H.; Kemp, R. A.; Wilburn, J. C. *Inorg. Chem.* **1981**, *20*, 4289. (4) Montemayor, R. G.; Sauer, D. T.; Fleming, S.; Bennett, D. W.; Thomas, M. G.; Parry, R. W. *J. Am. Chem. Soc.* **1978**, *100*, 2231.

(5) (a) Nakazawa, H.; Ohta, M.; Yoneda, H. *Inorg. Chem.* **1988**, *27*, 973. (b) Nakazawa, H.; Ohta, M.; Miyoshi, K.; Yoneda, H. *Organometallics* **1989**, *8*, 638. (c) Nakazawa, H.; Yamaguchi, Y.; Miyoshi, K. *J. Organomet. Chem.* **1994**, *465*, 193. (d) Nakazawa, H.; Yamaguchi, Y.; Mizuta, T.; Miyoshi, K. *Organometallics*, in press.

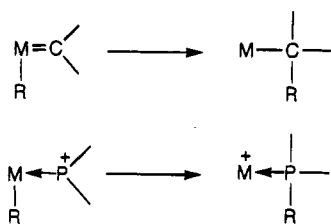
[†] Institute for Molecular Science.

[‡] Hiroshima University.

[⊙] Abstract published in *Advance ACS Abstracts*, September 1, 1995.

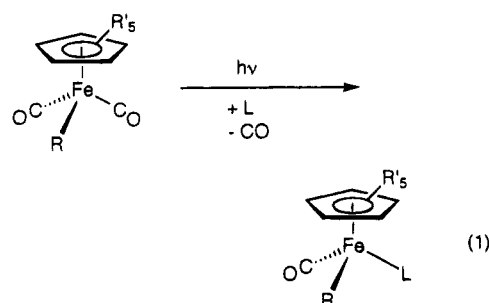
(1) Cowley, A. H.; Kemp, R. A. *Chem. Rev.* **1985**, *85*, 367.

edented example of a migratory insertion reaction of the phosphonium ligand into an iron-alkyl bond (in other words, an alkyl migration from a transition metal to a phosphonium ligand).



Results and Discussion

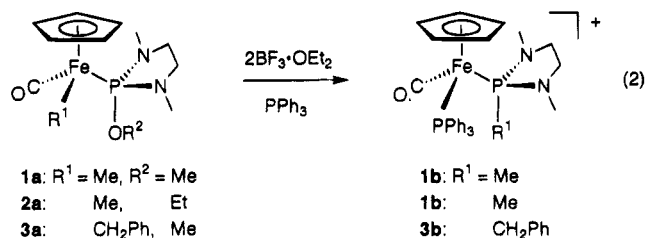
Migratory Insertion of Phosphonium Ligand into an Fe-C Bond. Iron complexes containing an alkyl group and (amino-substituted) phosphite (L) were synthesized from Cp(CO)₂FeMe and L by the photoreaction for the methyl complex (eq 1), and from Cp(CO)-



- 1a: R' = H, R = Me, L = PN(Me)CH₂CH₂NMe(OMe), (68 %)
 2a: R' = H, R = Me, L = PN(Me)CH₂CH₂NMe(OEt), (85 %)
 4a: R' = H, R = Me, L = PN(Me)CH₂CH₂O(OMe), (37 %)
 5a: R' = H, R = Me, L = P(OMe)₃, (65 %)
 6a: R' = Me, R = Me, L = PN(Me)CH₂CH₂NMe(OMe), (69 %)

IFeL, NaK_{2.8}, and ClCH₂Ph for the benzyl complex. The complexes were characterized by IR, ¹H, ¹³C, and ³¹P NMR spectra as well as elemental analyses. The two methyl groups and two methylene groups in an N(Me)-CH₂CH₂NMe substituent on a phosphorus ligand for 1a-3a and 6a were observed to be diastereotopic in the ¹H and ¹³C NMR spectra due to the chiral iron center. Complex 4a has two chiral centers (Fe and P), so the diastereomeric pair is expected to be obtained. In the photoreaction, both were formed in a similar ratio.

These complexes obtained thus far were subjected to the reaction with BF₃·OEt₂ and then PPh₃. Complex 1a was dissolved in CH₂Cl₂ and cooled at -78 °C. BF₃·OEt₂ and then PPh₃ were added to the solution to give a yellow powder. For the following reasons, we concluded that the complex obtained is formulated as [Cp(CO)(PPh₃)Fe{PN(Me)CH₂CH₂NMe(Me)}]BF₄ (1b·BF₄) (eq 2): (i) An IR absorption band due to ν_{CO}



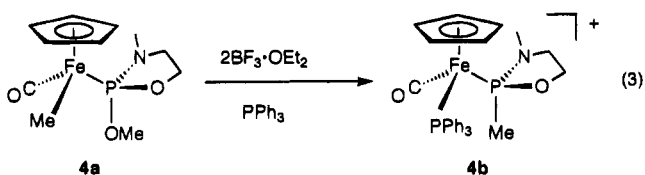
was observed 56 cm⁻¹ higher in frequency than that for the starting complex, indicating that the product is cationic. (ii) The ¹H and ¹³C NMR spectra showed that the amino-substituted phosphorus has no OMe group (no doublet at ca. 3.2 ppm in ¹H NMR or at ca. 52 ppm in ¹³C NMR) but has a Me group (a doublet at 1.53 ppm in ¹H NMR and at 23.46 ppm in ¹³C NMR). (iii) In the ³¹P NMR spectrum, two resonances were observed at 159.48 and 65.29 ppm as doublets with J_{PP} = 60.5 Hz,

indicating that PN(Me)CH₂CH₂NMe(Me) and PPh₃ are both coordinated to the same iron atom. For further confirmation of the structure of 1b·BF₄, the X-ray diffraction analysis was performed (vide infra).

In the above reaction, a Me group on the phosphorus in the product can be thought to come from the iron. The migration of an alkyl group from iron to phosphorus is proved by the reactions of 2a and 3a. Complex 2a has an OEt group in place of an OMe group on the P in 1a, and 3a has a CH₂Ph group in place of a Me group on the Fe in 1a. The products in the reactions of 2a and 3a with BF₃·OEt₂ and then PPh₃ were 1b·BF₄ and [Cp(CO)(PPh₃)Fe{PN(Me)CH₂CH₂NMe(CH₂Ph)}]BF₄ (3b·BF₄), respectively (eq 2). These results clearly show that an OR group on the phosphorus is eliminated and an alkyl group on the iron migrates to the phosphorus coordinating to the iron.

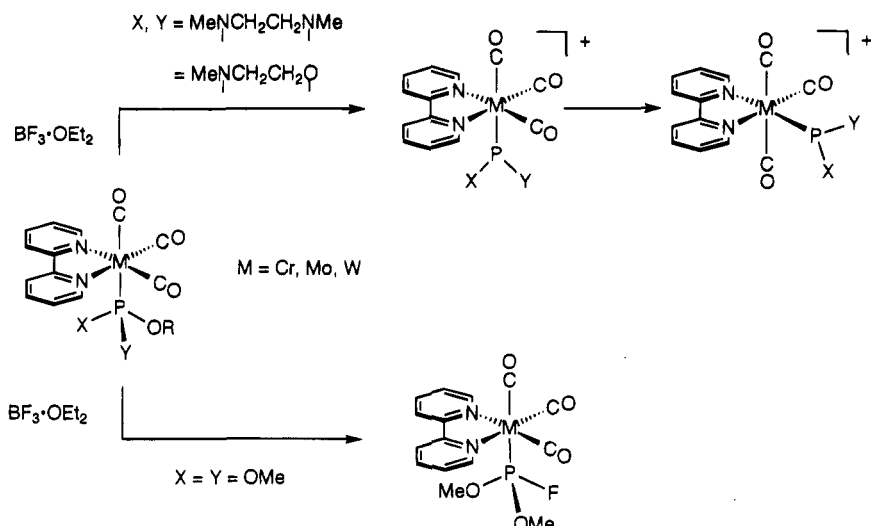
It has been reported that cationic phosphonium complexes of group 6 transition metals can be synthesized by the abstraction of an OR group on the coordinating phosphite as an anion by BF₃·OEt₂ (Scheme 1).⁵ The stability of the cationic phosphonium complexes is influenced by the substituents on the phosphorus. The stability decreases with decreasing number of amino substituents on a phosphonium phosphorus in the following order: diamino- > monoamino-monoalkoxy- >> dialkoxy-substituents. Diamino- and monoaminophosphonium complexes are stable in solution at room temperature for several days, whereas dialkoxyphosphonium complexes, which have not been detected even spectroscopically due to their high reactivity, pick up an F⁻ anion to become electrically neutral complexes with a P(OR)₂F ligand.

In the reaction of 1a-3a with BF₃·OEt₂, formation of a cationic iron phosphonium complex can be proposed. In order to examine the effect of a substituent on a phosphorus on the alkyl migration from Fe to P, we attempted the reactions of 4a having a monoamino-substituted phosphite and 5a having a typical phosphite. In the former reaction, the formation of an alkyl



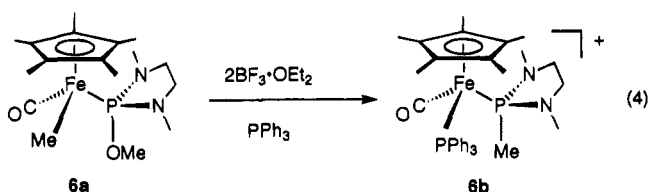
(6) For leading references see: (a) O'Connor, J. M.; Pu, L.; Woolard, S.; Chadha, R. K. *J. Am. Chem. Soc.* **1990**, *112*, 6731. (b) Hoover, J. F.; Stryker, J. M. *J. Am. Chem. Soc.* **1990**, *112*, 464. (c) Trace, R. L.; Sanchez, J.; Yang, J.; Yin, J.; Jones, W. M. *Organometallics* **1992**, *11*, 1440. (d) Adams, H.; Bailey, N. A.; Bentley, G. W.; Tattershall, C. E.; Taylor, B. F.; Winter, M. J. *J. Chem. Soc., Chem. Commun.* **1992**, 533. (e) Bergamini, P.; Costa, E. *Organometallics* **1994**, *13*, 1058.

Scheme 1



migration product was confirmed (eq 3). In contrast, the reaction of **5a** with $\text{BF}_3\cdot\text{OEt}_2$ and then PPh_3 yielded an unidentified product but no F-introduced products, for example $\text{Cp}(\text{CO})(\text{Me})\text{Fe}\{\text{P}(\text{OMe})_2\text{F}\}$, were detected even in the reaction mixture according to the ^{31}P NMR measurement. The details will be reported elsewhere.

The reaction of **6a** having $\eta^5\text{-C}_5\text{Me}_5$ in place of $\eta^5\text{-C}_5\text{H}_5$ in **1a** with $\text{BF}_3\cdot\text{OEt}_2$ then PPh_3 was also examined. The product was **6b** (eq 4), revealing that the modification of Cp to Cp* has no significant influence on the alkyl migration reaction from Fe to P.

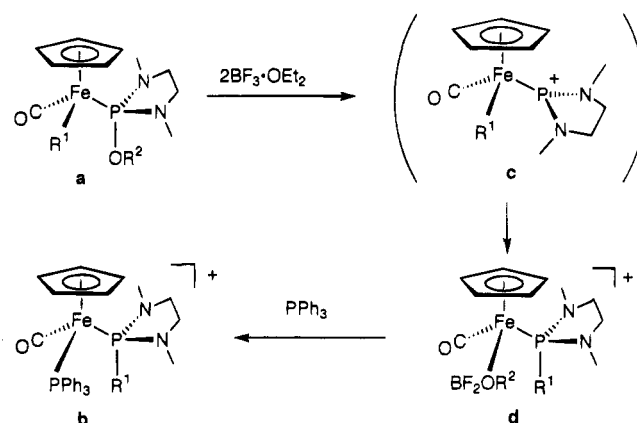


Consideration of a Reaction Intermediate. In the reaction of iron phosphite complexes with $\text{BF}_3\cdot\text{OEt}_2$, an OR group on a phosphorus is strongly suggested to be abstracted by $\text{BF}_3\cdot\text{OEt}_2$ as an anion to give a cationic iron phosphonium complex. Thus, we examined the reaction of **1a** in CH_2Cl_2 with $\text{BF}_3\cdot\text{OEt}_2$ only, in hopes of detecting an iron phosphonium complex, $[\text{Cp}(\text{CO})\text{(Me)Fe}\{\text{PN}(\text{Me})\text{CH}_2\text{CH}_2\text{NMe}\}]^+$, as an intermediate (**c** in Scheme 2). The isolation of the complex formed was unsuccessful, but the spectroscopic data of the reaction mixture gave information about the complex formed at this stage. The IR spectrum (in CH_2Cl_2) showed one absorption band at 1997 cm^{-1} in a ν_{CO} region which is 87 cm^{-1} higher than that for **1a**, indicating the formation of a cationic complex. The ^{31}P NMR spectrum (in CH_2Cl_2) showed a singlet at 214.58 ppm being 37.65 ppm lower in the magnetic field than that for **1a**. This suggests that the product may not be phosphonium

complex $[\text{Cp}(\text{CO})(\text{Me})\text{Fe}\{\text{PN}(\text{Me})\text{CH}_2\text{CH}_2\text{NMe}\}]^+$ because the ^{31}P NMR resonances of the phosphonium complexes shown in Scheme 1 were observed $104\text{--}137\text{ ppm}$ lower in magnetic field than those of the parent phosphite complexes.⁵ The ^{13}C NMR spectrum (in CH_2Cl_2) showed five resonances: $22.95\text{ (d, } J_{\text{PC}} = 12.2\text{ Hz, PCH}_3\text{)}$, $32.96\text{ (d, } J_{\text{PC}} = 12.2\text{ Hz, NCH}_3\text{)}$, $51.57\text{ (s, NCH}_2\text{)}$,

$83.00\text{ (s, C}_5\text{H}_5\text{)}$, $215.14\text{ (d, } J_{\text{PC}} = 29.3\text{ Hz, CO)}$. A doublet at 22.95 ppm with $J_{\text{PC}} = 12.2\text{ Hz}$ is assigned to a Me on a phosphorus, but no resonances due to an OMe on a phosphorus or due to a Me on an iron presented in the starting complex **1a** were observed. Therefore, the product is proposed to have a $[\text{Cp}(\text{CO})\text{Fe}\{\text{PN}(\text{Me})\text{CH}_2\text{CH}_2\text{NMe}(\text{Me})\}]^+$ moiety.

Scheme 2



$83.00\text{ (s, C}_5\text{H}_5\text{)}$, $215.14\text{ (d, } J_{\text{PC}} = 29.3\text{ Hz, CO)}$. A doublet at 22.95 ppm with $J_{\text{PC}} = 12.2\text{ Hz}$ is assigned to a Me on a phosphorus, but no resonances due to an OMe on a phosphorus or due to a Me on an iron presented in the starting complex **1a** were observed. Therefore, the product is proposed to have a $[\text{Cp}(\text{CO})\text{Fe}\{\text{PN}(\text{Me})\text{CH}_2\text{CH}_2\text{NMe}(\text{Me})\}]^+$ moiety.

The reaction mixture of **2a** with $\text{BF}_3\cdot\text{OEt}_2$ showed similar data (IR (ν_{CO}), 1994 cm^{-1} ; ^{31}P NMR (δ), 214.44 ppm) to those obtained in the corresponding reaction of **1a**. However, the small difference in the ^{31}P NMR chemical shifts was not due to the experimental error but was significant, because the two resonances were observed even when a mixture of **1a** and **2a** was treated with $\text{BF}_3\cdot\text{OEt}_2$.

We thus propose the reaction sequences in Scheme 2. In the reaction of **a** with $\text{BF}_3\cdot\text{OEt}_2$, an OR^2 group on a phosphorus atom is abstracted by BF_3 as an anion to give phosphonium complex **c** and $[\text{BF}_3\text{OR}^2]^-$, the latter of which may react with BF_3 to give BF_2OR^2 and BF_4^- serving as a counteranion of the final product **b**. Phosphonium complex **c** itself could not be detected, presumably due to its high reactivity. The R^1 group on an iron atom then migrates to the phosphonium phos-

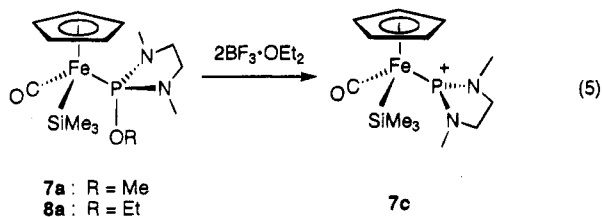
phorus to give $[\text{Cp}(\text{CO})\text{Fe}\{\text{PN}(\text{Me})\text{CH}_2\text{CH}_2\text{NMe}(\text{R}^1)\}]^+$, a 16-electron species, which is stabilized presumably by the coordination of BF_2OR^2 generated through the lone pair of the oxygen to give **d**. Therefore, an OR^2 group

exerts a small but not negligible effect on the ^{31}P NMR resonance of **d**. The BF_2OR^2 in **d** is readily replaced by a more strong base such as PPh_3 to give a stable complex **b**.

Alkyl migration to CO ligand to give an acyl ligand on a transition metal is well-known.⁷ Complex **c** has a terminal carbonyl ligand as well as a phosphonium ligand. It is thus notable that an alkyl group migrates exclusively to a phosphonium ligand in the present reaction.

Some examples⁸ and theoretical studies⁹ have been reported for the migration of an alkyl (or aryl) group from a coordinating phosphorus ligand to the transition metal to which it is coordinating. Our findings correspond to the reversed movement of an alkyl group (from a transition metal to a coordinating phosphorus), which is unprecedented.

Reaction of Iron Complexes Having a Silyl Group and Phosphite with $\text{BF}_3\cdot\text{OEt}_2$. The reaction of a silyl iron complex corresponding to the alkyl complex **1a** with $\text{BF}_3\cdot\text{OEt}_2$ showed very significant results from the mechanistic aspect. Silyl complexes **7a** and **8a** were prepared from $\text{Cp}(\text{CO})_2\text{Fe}(\text{SiMe}_3)$ and the corresponding phosphite by the photolysis. The reaction of **7a** with $\text{BF}_3\cdot\text{OEt}_2$ in CH_2Cl_2 gives a homogeneous solution, which shows very informative spectroscopic data about the product (**7c** in eq 5). The IR absorption



band due to ν_{CO} was observed 51 cm^{-1} higher in frequency than that for the starting complex **7a**. The ^{31}P NMR spectrum shows a singlet at 309.33 ppm. The very low chemical shift (132.69 ppm lower than that of the starting complex, 176.64 ppm) indicates the formation of a phosphonium complex (vide supra). In the ^{29}Si NMR spectrum, one doublet was observed at 37.42 ppm with $J_{\text{PSi}} = 37.6\text{ Hz}$. The chemical shift and coupling constant are similar to those for the starting complex **7a** ($\delta = 36.62\text{ ppm}$, $J_{\text{PSi}} = 43.0\text{ Hz}$), indicating that the SiMe_3 group in **7c** remains bound to the Fe. The ^{13}C NMR spectrum (in CH_2Cl_2) showed five resonances: 8.73 (s, $J_{\text{CSi}} = 48.8\text{ Hz}$, $\text{Si}(\text{CH}_3)_3$), 34.46 (d, $J_{\text{PC}} = 12.2\text{ Hz}$, NCH_3), 54.09 (s, NCH_2), 84.71 (s, C_5H_5), 214.06 (d, $J_{\text{PC}} = 28.1\text{ Hz}$, CO). A resonance due to POCH_3 was not detected, though it was observed at 51.04 ppm with $J_{\text{PC}} = 13.4\text{ Hz}$ for the starting complex, **7a**. It should be noted that two NMe carbons and two NCH_2 carbons for **7c** are not diastereotopic, though

those for **7a** are so, which is consistent with a planar geometry of the phosphorus atom in **7c**.

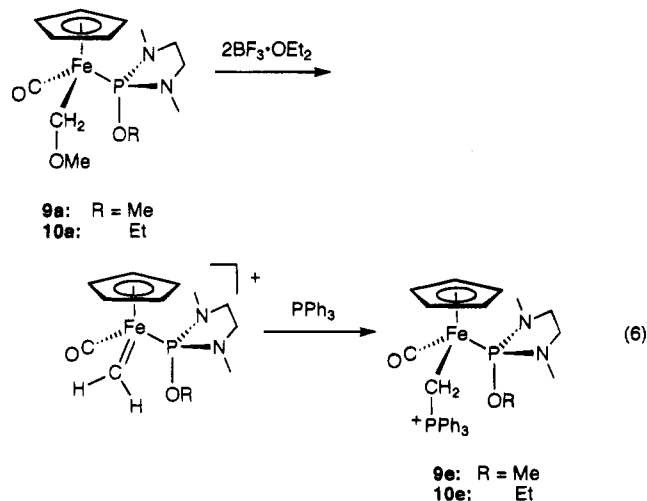
The reaction mixture of **8a** (having an OEt group in place of an OMe group in **7a**) with $\text{BF}_3\cdot\text{OEt}_2$ showed exactly the same spectroscopic data as those obtained from the reaction of **7a** with $\text{BF}_3\cdot\text{OEt}_2$. This observation strongly suggests the formation of **7c** and that the phosphonium phosphorus in **7c** has no contact with $\text{BF}_2\text{-OMe}$ or BF_2OEt generated.

Addition of PPh_3 to the solution containing **7c** caused no reaction. No silyl migration to the phosphonium phosphorus may be due to a stronger transition metal-silyl bond than -alkyl bond. Complex **7c** is stable in a solution at room temperature unless exposed to air. Although the isolation of **7c** has been unsuccessful so far, the detection of the phosphonium complex **7c** supports the reaction sequence proposed in Scheme 2 for the migratory insertion of a phosphonium ligand into an alkyl-iron bond.

Reaction of Iron Complexes Having both C-OR and P-OR Groups with $\text{BF}_3\cdot\text{OEt}_2$ and PPh_3 . Cationic iron carbene complexes have been prepared by the abstraction of an OR group as an anion from $(\text{C}_5\text{X}_5)_2\text{L}_2\text{-Fe}(\text{CY}_2\text{OR})$ ($\text{X} = \text{H, Me}$; $\text{L} = \text{CO}$, tertiary phosphine; $\text{Y} = \text{H, alkyl}$; $\text{R} = \text{alkyl, silyl}$).¹⁰ So we attempted the

reaction of $\text{Cp}(\text{CO})(\text{CH}_2\text{OMe})\text{Fe}\{\text{PN}(\text{Me})\text{CH}_2\text{CH}_2\text{NMe}(\text{OMe})\}$ (**9a**) with $\text{BF}_3\cdot\text{OEt}_2$ because it seemed interesting to examine which OMe group on the carbon or on the phosphorus is abstracted. If an OMe is abstracted from the carbon, a methyldene complex would be formed, whereas if abstraction from the phosphorus takes place, a phosphonium complex would be prepared.

Complex **9a** was prepared from $\text{Cp}(\text{CO})\text{IFe}\{\text{PN}(\text{Me})\text{CH}_2\text{CH}_2\text{NMe}(\text{OMe})\}$, $\text{NaK}_{2,8}$, and ClCH_2OMe . The treatment of **9a** with $\text{BF}_3\cdot\text{OEt}_2$ and then PPh_3 led to isolation of an orange complex. For the following reasons, we concluded that the product is a phosphine-stabilized methyldene complex formulated as $[\text{Cp}(\text{CO})(\text{CH}_2\text{PPh}_3)\text{Fe}\{\text{PN}(\text{Me})\text{CH}_2\text{CH}_2\text{NMe}(\text{OMe})\}]\text{BF}_4$ (**9e-BF₄**) (eq 6). (i)



(7) (a) Colquhoun, H. M.; Thompson, D. J.; Twigg, M. V. *Carbonylation: Direct Synthesis of Carbonyl Compounds*; Plenum Press: New York, 1991. (b) *Comprehensive Organometallic Chemistry*; Wilkinson, G., Ed.; Pergamon Press: Oxford, England, 1982; Vols. 4 and 8.

(8) For leading references see: (a) Garrou, P. E. *Chem. Rev.* **1985**, *85*, 171. (b) Chakravarty, A. R.; Cotton, F. A. *Inorg. Chem.* **1985**, *24*, 3584. (c) Dubois, R. A.; Garrou, P. E. *Organometallics* **1986**, *5*, 466. (d) Wang, W.-D.; Eisenberg, R. *J. Am. Chem. Soc.* **1990**, *112*, 1833. (e) Leeuwen, P. W. N. M.; Roobeek, C. F.; Orpen, A. G. *Organometallics* **1990**, *9*, 2179. (f) Grushin, V. V.; Vymenits, A. B.; Yanovsky, A. I.; Struchkov, Y. T.; Vol'pin, M. E. *Organometallics* **1991**, *10*, 48.

(9) Ortiz, J. V.; Havlas, Z.; Hoffmann, R. *Helv. Chim. Acta* **1984**, *67*, 1.

(10) For example see: (a) Brookhart, M.; Studabaker, W. B. *Chem. Rev.* **1987**, *87*, 411. (b) Davies, S. G.; Dordor-Hedgecock, I. M.; Sutton, K. H.; Whittaker, M. *J. Am. Chem. Soc.* **1987**, *109*, 5711. (c) Guerchais, V.; Astruc, D.; Nunn, C. M.; Cowley, A. H. *Organometallics* **1990**, *9*, 1036. (d) Vargas, R. M.; Theys, R. D.; Hossain, M. M. *J. Am. Chem. Soc.* **1992**, *114*, 777.

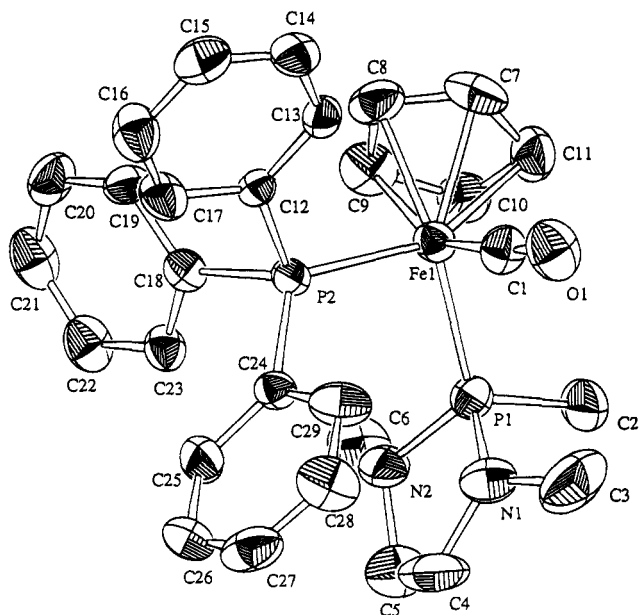


Figure 1. ORTEP drawing of $[\text{Cp}(\text{CO})(\text{PPh}_3)\text{Fe}\{\text{PN}(\text{Me})\text{CH}_2\text{CH}_2\text{NMe}(\text{Me})\}]^+$ (**1b**) with atom-labeling scheme (the BF_4^- counterion is omitted for clarity). The thermal ellipsoids are drawn at the 30% probability level.

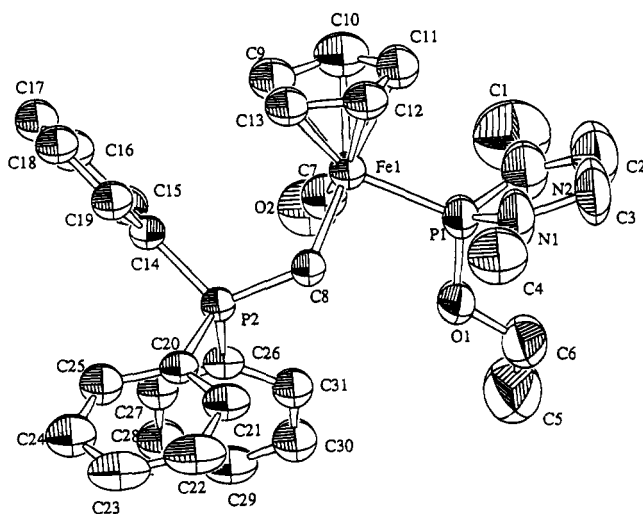


Figure 2. ORTEP drawing of $[\text{Cp}(\text{CO})(\text{CH}_2\text{PPh}_3)\text{Fe}\{\text{PN}(\text{Me})\text{CH}_2\text{CH}_2\text{NMe}(\text{OEt})\}]^+$ (**10e**) with atom-labeling scheme (the BF_4^- counterion is omitted for clarity). The thermal ellipsoids are drawn at the 30% probability level.

One ν_{CO} absorption band was observed in the IR spectrum, indicating the complex has a terminal CO ligand. (ii) In the ^{31}P NMR spectrum, two resonances were observed at 40.35 and 164.87 ppm, which were

assigned to PPh_3 and $\text{PN}(\text{Me})\text{CH}_2\text{CH}_2\text{NMe}(\text{OMe})$, respectively; they are not coupled with each other. (iii) In the ^1H NMR spectrum, two diastereotopic CH_2 protons were observed as an apparent triplet of doublets and a double double doublet due to the coupling to two kinds of phosphorus atoms and to the mutually geminal proton. (iv) The resonance due to $\text{P}-\text{OMe}$ was observed, but that due to $\text{C}-\text{OMe}$ was not.

The reaction may proceed as follows: the OMe abstraction on the carbon atom by BF_3 takes place to give a methyldene complex, which is then trapped by PPh_3 to give an ylide complex. However, another reaction pathway cannot be ruled out in which an OMe

Table 1. Summary of Crystal Data for **1b**· BF_4 and **10e**· BF_4

	1b · BF_4	10e · BF_4
formula	$\text{C}_{29}\text{H}_{33}\text{BF}_4\text{FeN}_2\text{OP}_2$	$\text{C}_{31}\text{H}_{37}\text{BF}_4\text{FeN}_2\text{O}_2\text{P}_2$
fw	630.19	674.20
cryst syst	monoclinic	orthorhombic
space group	$P2_1/n$	$Pcab$
cell constants		
a , Å	9.099(1)	18.003(6)
b , Å	13.727(2)	24.619(6)
c , Å	23.134(5)	14.501(4)
α , deg		
β , deg	91.48(1)	
γ , deg		
V , Å ³	2889(1)	6427(3)
Z	4	8
D_{calcd} , g cm ⁻³	1.45	1.39
μ , cm ⁻¹	6.85	5.68
cryst size, mm ³	0.32 × 0.12 × 0.10	0.45 × 0.40 × 0.30
radiation	Mo K α	Mo K α
	($\lambda = 0.71069$ Å)	($\lambda = 0.71069$ Å)
scan technique	$\omega-2\theta$	$\omega-2\theta$
scan range, deg	$3 < 2\theta < 55$	$3 < 2\theta < 50$
scan rate, deg min ⁻¹	5.1	6.0
no. of unique data	6972	5661
no. of unique data with $F_o > 3\sigma(F_o)$	2773	3788
R	0.063	0.059
R_w	0.054	0.064

group on the phosphorus is abstracted and then an OMe group on the carbon migrates to the phosphorus to give the methyldene complex. In order to elucidate the reaction pathway, complex **10a** was subjected to the reaction with $\text{BF}_3\cdot\text{OEt}_2$ then PPh_3 . The product was an

ylide complex, $[\text{Cp}(\text{CO})(\text{CH}_2\text{PPh}_3)\text{Fe}\{\text{PN}(\text{Me})\text{CH}_2\text{CH}_2\text{NMe}(\text{OEt})\}]\text{BF}_4$ (**10e**· BF_4) (eq 6), which was identified by an X-ray crystallographic study (vide infra) in addition to its spectroscopic data. Therefore, it was concluded that an OR group is abstracted selectively from the carbon but not from the phosphorus.

The reason for the selectivity may come from the difference in bond energy between C-O and P-O, or may come from the difference in overall stability between a methyldene complex and a phosphonium complex. Although the real reason for the selectivity is not clear now, our findings will give a clue when we compare transition-metal complexes with carbene and phosphonium as a ligand.

Crystal Structures of 1b· BF_4 and 10e· BF_4 . X-ray structure analyses of **1b**· BF_4 and **10e**· BF_4 were undertaken. The ORTEP drawings of **1b** and **10e** are displayed in Figures 1 and 2, respectively. The crystal data and the selected bond distances and angles are listed in Tables 1–3.

An X-ray crystal structure of **1b** shows a normal piano stool configuration. The iron has a cyclopentadienyl ligand in a η^5 fashion, a terminal CO ligand, a PPh_3 group, and a diamino-substituted tertiary phosphine,

$\text{PN}(\text{Me})\text{CH}_2\text{CH}_2\text{NMe}(\text{Me})$. Angles between three monodentate ligands are slightly greater than 90° : $\text{C1}-\text{Fe1}-\text{P1} = 90.6^\circ$, $\text{P1}-\text{Fe1}-\text{P2} = 95.8^\circ$, and $\text{P2}-\text{Fe1}-\text{C1} = 93.4^\circ$. P1 basically takes a tetrahedral geometry, though the $\text{N1}-\text{P1}-\text{N2}$ angle (93.4°) is smaller than the ideal angle due to the five-membered ring. N1 has a planar geometry (sum of the bond angles around N1 is 356.9°), whereas N2 is not planar (sum of the bond angles around N2 is 344.6°), presumably due to avoid-

Table 2. Selected Bond Distances (Å) and Angles (deg) for**[Cp(CO)(PPh₃)Fe{PN(Me)CH₂CH₂NMe(Me)}]⁺ (1b)**

Bond Distances			
Fe1-P1	2.201(2)	P2-C24	1.810(7)
Fe1-P2	2.237(2)	O1-C1	1.177(8)
Fe1-C1	1.727(7)	N1-C3	1.457(10)
P1-N1	1.651(6)	N1-C4	1.449(10)
P1-N2	1.676(6)	N2-C5	1.461(9)
P1-C2	1.800(8)	N2-C6	1.467(9)
P2-C12	1.833(7)	C4-C5	1.52(1)
P2-C18	1.842(7)		
Bond Angles			
P1-Fe1-P2	95.80(8)	C12-P2-C18	103.4(3)
P1-Fe1-C1	90.6(3)	C12-P2-C24	97.6(3)
P2-Fe1-C1	93.4(3)	C18-P2-C24	106.3(3)
Fe1-P1-N1	120.0(2)	P1-N1-C3	125.1(6)
Fe1-P1-N2	117.7(2)	P1-N1-C4	114.0(6)
Fe1-P1-C2	111.3(3)	C3-N1-C4	117.8(7)
N1-P1-N2	93.4(3)	P1-N2-C5	109.9(6)
N1-P1-C2	104.5(4)	P1-N2-C6	119.8(6)
N2-P1-C2	107.9(4)	C5-N2-C6	114.9(7)
Fe1-P2-C12	114.2(2)	Fe1-C1-O1	175.6(7)
Fe1-P2-C18	111.9(2)	N1-C4-C5	106.4(8)
Fe1-P2-C24	121.3(2)	N2-C5-C4	105.7(7)

Table 3. Selected Bond Distances (Å) and Angles (deg) for**[Cp(CO)(CH₂PPh₃)Fe{PN(Me)CH₂CH₂NMe(OEt)}]⁺ (10e)**

Bond Distances			
Fe1-P1	2.164(2)	P2-C26	1.817(4)
Fe1-C7	1.741(6)	O1-C6	1.440(7)
Fe1-C8	2.072(4)	O2-C7	1.158(7)
P1-O1	1.625(4)	N1-C3	1.446(10)
P1-N1	1.649(7)	N1-C4	1.45(1)
P1-N2	1.662(7)	N2-C1	1.41(1)
P2-C8	1.768(4)	N2-C2	1.45(1)
P2-C14	1.797(4)	C2-C3	1.45(2)
P2-C20	1.802(4)	C5-C6	1.41(1)
Bond Angles			
P1-Fe1-C7	92.9(2)	C20-P2-C26	104.7(2)
P1-Fe1-C8	92.1(1)	P1-O1-C6	120.7(3)
C7-Fe1-C8	97.3(2)	P1-N1-C3	115.2(7)
Fe1-P1-O1	109.7(1)	P1-N1-C4	124.6(5)
Fe1-P1-N1	119.9(2)	C3-N1-C4	119.5(8)
Fe1-P1-N2	119.3(2)	P1-N2-C1	125.4(6)
O1-P1-N1	107.9(3)	P1-N2-C2	113.6(8)
O1-P1-N2	105.9(3)	C1-N2-C2	119.7(9)
N1-P1-N2	92.4(3)	N2-C2-C3	109.9(9)
C8-P2-C14	113.7(2)	N1-C3-C2	107.6(9)
C8-P2-C20	113.0(2)	O1-C6-C5	112.3(6)
C8-P2-C26	111.5(2)	Fe1-C7-O2	174.1(5)
C14-P2-C20	104.4(2)	Fe1-C8-P2	119.1(2)
C14-P2-C26	108.9(2)		

ance of steric repulsion between the methyl group on N2 and the PPh₃ ligand.

The structure of **10e** is basically similar to that of **1b**. However, the iron has a methylene group to which PPh₃ bonds. The bond lengths of Fe1-C8 (2.072 Å) and C8-P2 (1.768 Å) and the bond angle Fe1-C8-P2 (119.1°) resemble those of the iron ylide complexes reported so far ([Cp*(CO)₂FeCH₂PPh₃]⁺,^{10c} Fe-C = 2.11 Å, C-P = 1.78 Å, ∠Fe-C-P = 118.1°, and (CO)₄FeCH₂PPh₃,¹¹ Fe-C = 2.122 Å, C-P = 1.755 Å, ∠Fe-C-P = 118.6°). The two nitrogen atoms on a phosphorus have planar geometries (the sum of the bond angles around N1 is 359.3°, and that around N2 is 358.7°).

Experimental Section

General Remarks. All reactions were carried out under an atmosphere of dry nitrogen by using Schlenk tube techniques. Column chromatography was done quickly in the air. Benzene, THF, hexane, and pentane were distilled from sodium metal, CH₂Cl₂ was distilled from P₂O₅, and these solvents were stored under nitrogen atmosphere. Acetone as an eluent was obtained from a common commercial source and was used without further purification. BF₃·OEt₂ was distilled prior to use.

IR spectra were recorded on a Shimadzu FTIR-8100A spectrometer. JEOL PMX-60, EX-270, and EX-400 instruments were used to obtain ¹H, ¹³C, ³¹P, and ²⁹Si NMR spectra. ¹H, ¹³C, and ²⁹Si NMR data were referenced to (CH₃)₄Si, and ³¹P NMR data were referenced to 85% H₃PO₄.

Preparation of Cp(CO)(Me)Fe{PN(Me)CH₂CH₂NMe(OMe)} (1a).

Cp(CO)₂FeMe (907 mg, 4.72 mmol), benzene (25 mL), and PN(Me)CH₂CH₂NMe(OMe) (0.65 mL, 656 mg, 4.43 mmol) were put in a Pyrex Schlenk tube, and the solution was irradiated with a 400 W medium-pressure mercury arc lamp at 0 °C for 1 h. After the solvent had been removed, the residue was loaded on an alumina column and eluted with CH₂Cl₂. The second eluted orange band was collected, and the solvent was removed in vacuo to give a yellow powder of **1a** (1011 mg, 3.24 mmol, yield 68%). Anal. Calcd for C₁₂H₂₁FeN₂O₂P: C, 46.18; H, 6.78; N, 8.97. Found: C, 46.35; H, 6.75; N, 8.88. IR (ν_{CO}, in CH₂Cl₂): 1910. ³¹P NMR (δ, in CH₂Cl₂): 176.93 (s). ¹H NMR (δ, in CDCl₃): -0.19 (d, J_{PH} = 5.0 Hz, 3H, FeCH₃), 2.72 (d, J_{PH} = 10.6 Hz, 3H, NCH₃), 2.74 (d, J_{PH} = 9.9 Hz, 3H, NCH₃), 3.10 (m, 2H, NCH₂), 3.23 (d, J_{PH} = 10.9 Hz, 3H, OCH₃), 3.45 (m, 2H, NCH₂), 4.38 (s, 5H, C₅H₅). ¹³C NMR (δ, in CDCl₃): -25.49 (d, J_{PC} = 30.5 Hz, FeCH₃), 33.23 (d, J_{PC} = 9.8 Hz, NCH₃), 33.44 (d, J_{PC} = 12.2 Hz, NCH₃), 51.42 (d, J_{PC} = 13.5 Hz, OCH₃), 51.61 (d, J_{PC} = 2.5 Hz, NCH₂), 51.73 (d, J_{PC} = 4.8 Hz, NCH₂), 82.64 (s, C₅H₅), 222.50 (d, J_{PC} = 47.6 Hz, CO).

Preparation of Cp(CO)(Me)Fe{PN(Me)CH₂CH₂NMe(OEt)} (2a).

Complex **2a** was prepared from Cp(CO)₂FeMe and PN(Me)CH₂CH₂NMe(OEt) in the same manner as that for **1a** (yield 85%). Anal. Calcd for C₁₃H₂₃FeN₂O₂P: C, 47.87; H, 7.11; N, 8.59. Found: C, 47.65; H, 6.96; N, 8.27. IR (ν_{CO}, in CH₂Cl₂): 1912. ³¹P NMR (δ, in CH₂Cl₂): 174.86 (s). ¹H NMR (δ, in CDCl₃): -0.18 (d, J_{PH} = 5.0 Hz, 3H, FeCH₃), 1.09 (t, J_{PH} = 7.1 Hz, 3H, OCH₂CH₃), 2.71 (d, J_{PH} = 10.6 Hz, 3H, NCH₃), 2.73 (d, J_{PH} = 10.2 Hz, 3H, NCH₃), 3.12 (m, 2H, NCH₂), 3.36 (m, 2H, NCH₂), 3.56 (m, 2H, OCH₂CH₃), 4.38 (s, 5H, C₅H₅). ¹³C NMR (δ, in CDCl₃): -25.11 (d, J_{PC} = 30.5 Hz, FeCH₃), 16.24 (d, J_{PC} = 6.1 Hz, OCH₂CH₃), 33.32 (d, J_{PC} = 9.8 Hz, NCH₃), 33.53 (d, J_{PC} = 12.2 Hz, NCH₃), 51.54 (d, J_{PC} = 2.4 Hz, NCH₂), 51.60 (d, J_{PC} = 6.1 Hz, NCH₂), 59.63 (d, J_{PC} = 13.4 Hz, OCH₂CH₃), 82.64 (s, C₅H₅), 222.55 (d, J_{PC} = 46.4 Hz, CO).

Preparation of Cp(CO)(CH₂Ph)Fe{PN(Me)CH₂CH₂NMe(OMe)} (3a).

Cp(CO)₂FeI (1526 mg, 5.02 mmol), benzene (60 mL), and PN(Me)CH₂CH₂NMe(OMe) (0.75 mL, 757 mg, 5.11 mmol) were put in a Pyrex Schlenk tube, and the solution was irradiated with a 400 W medium-pressure mercury arc lamp at 0 °C for 1.5 h. After filtration, the solvent was removed under reduced pressure, and the residue was loaded on an alumina column and eluted with CH₂Cl₂. The green band was collected, and the solvent was removed in vacuo to give a dark green powder of Cp(CO)IFe{PN(Me)CH₂CH₂NMe(OMe)} (1016 mg, 2.40 mmol, yield 48%). Anal. Calcd for C₁₁H₁₈FeIN₂O₂P: C, 31.16; H, 4.28; N, 6.61. Found: C, 31.40; H, 4.18; N, 6.63. IR (ν_{CO}, in CH₂Cl₂): 1950. ³¹P NMR (δ, in CH₂Cl₂): 165.88 (s). ¹H NMR (δ, in CDCl₃): 2.83 (d, J_{PH} = 10.9 Hz, 3H, NCH₃), 2.97 (d, J_{PH} = 9.9 Hz, 3H, NCH₃), 3.21 (m, 2H, NCH₂), 3.32

(11) Toupet, P. L.; Weinberger, B.; Abbayes, H. D.; Gross, U. *Acta Crystallogr.* **1984**, *C40*, 2056.

(d, $J_{\text{PH}} = 11.6$ Hz, 3H, OCH₃), 3.38 (m, 2H, NCH₂), 4.62 (d, $J_{\text{PH}} = 1.3$ Hz, 5H, C₅H₅). ¹³C NMR (δ , in CDCl₃): 33.45 (d, $J_{\text{PC}} = 11.0$ Hz, NCH₃), 34.36 (d, $J_{\text{PC}} = 9.8$ Hz, NCH₃), 51.77 (s, NCH₂), 51.81 (s, NCH₂), 52.18 (d, $J_{\text{PC}} = 12.2$ Hz, OCH₃), 81.35 (s, C₅H₅), 220.51 (d, $J_{\text{PC}} = 45.1$ Hz, CO).

NaK_{2.8} (0.9 mL, 756 mg, 5.71 mmol) was added to a solution of Cp(CO)IFe{PN(Me)CH₂CH₂NMe(OMe)} (961 mg, 2.27 mmol) of THF (50 mL), and the solution was stirred for about 30 min at room temperature, causing the color of the solution to change from green to brown. After filtration, the filtrate was added dropwise to a solution of ClCH₂Ph (0.27 mL, 297 mg, 2.35 mmol) of THF (20 mL), and the resulting solution was stirred overnight at room temperature. After insoluble materials had been removed by filtration, the solvent was removed from the filtrate under reduced pressure. The soluble product was extracted with pentane (20 mL \times 2) and removing the solvent under reduced pressure gave **3a** as a dark yellow oil (428 mg, 1.10 mmol, 49%). The complex was so unstable that the correct elemental analysis data could not be obtained, though satisfactory spectroscopic data were obtained. IR (ν_{CO} , in CH₂Cl₂): 1912. ³¹P NMR (δ , in CH₂Cl₂): 173.69 (s). ¹H NMR (δ , in CDCl₃): 1.89 (dd, $J_{\text{PH}} = 9.6$ Hz, $J_{\text{HH}} = 8.2$ Hz, 1H, FeCH₂), 2.60 (dd, $J_{\text{PH}} = 4.6$ Hz, $J_{\text{HH}} = 7.9$ Hz, 1H, FeCH₂), 2.77 (d, $J_{\text{PH}} = 9.9$ Hz, 3H, NCH₃), 2.80 (d, $J_{\text{PH}} = 9.6$ Hz, 3H, NCH₃), 3.16 (m, 2H, NCH₂), 3.29 (d, $J_{\text{PH}} = 10.9$ Hz, 3H, OCH₃), 3.37 (m, 2H, NCH₂), 4.21 (d, $J_{\text{PH}} = 1.0$ Hz, 5H, C₅H₅), 6.85 (t, $J_{\text{HH}} = 7.3$ Hz, 1H, *p*-C₆H₅), 7.90 (m, 4H, *o*- and *m*-C₆H₅). ¹³C NMR (δ , in CDCl₃): 3.39 (d, $J_{\text{PC}} = 25.6$ Hz, FeCH₂), 33.28 (d, $J_{\text{PC}} = 12.2$ Hz, NCH₃), 51.60 (d, $J_{\text{PC}} = 13.5$ Hz, OCH₃), 51.67 (d, $J_{\text{PC}} = 3.7$ Hz, NCH₂), 51.79 (d, $J_{\text{PC}} = 4.9$ Hz, NCH₂), 83.41 (s, C₅H₅), 121.20 (s, *p*-C₆H₅), 126.86 (s, *o*-C₆H₅), 127.51 (s, *m*-C₆H₅), 157.86 (d, $J_{\text{PC}} = 2.4$ Hz, ϵ -C₆H₅), 222.80 (d, $J_{\text{PC}} = 46.4$ Hz, CO).

Preparation of Cp(CO)(Me)Fe{PN(Me)CH₂CH₂O(OMe)} (**4a**). Complex **4a** was prepared from Cp(CO)₂FeMe and PN(Me)CH₂CH₂O(OMe) in the same manner as that for **1a**. In this case, the complexes eluted with CH₂Cl₂ from an alumina column were loaded again on a silica gel column and eluted with CH₂Cl₂. The orange band eluted after a yellow band containing Cp(CO)₂FeMe was collected and dried in vacuo to give **4a** as an orange oil (yield 37%). Anal. Calcd for C₁₁H₁₈FeNO₃P: C, 44.17; H, 6.07; N, 4.68. Found: C, 44.24; H, 6.04; N, 4.60. IR (ν_{CO} , in CH₂Cl₂): 1919. ³¹P NMR (δ , in CH₂Cl₂): 195.96 (s), 195.73 (s). ¹H NMR (δ , in CDCl₃): -0.28 (d, $J_{\text{PH}} = 5.6$ Hz, 1.5H, FeCH₃), -0.24 (d, $J_{\text{PH}} = 5.9$ Hz, 1.5H, FeCH₃), 2.73 (d, $J_{\text{PH}} = 9.9$ Hz, 1.5H, NCH₃), 2.79 (d, $J_{\text{PH}} = 10.6$ Hz, 1.5H, NCH₃), 3.17 (m, 1H, NCH₂), 3.33 (m, 1H, NCH₂), 3.42 (d, $J_{\text{PH}} = 11.2$ Hz, 1.5H, OCH₃), 3.44 (d, $J_{\text{PH}} = 10.9$ Hz, 1.5H, OCH₃), 4.21 (m, 1H, OCH₂), 4.33 (m, 1H, OCH₂), 4.49 (s, 5H, C₅H₅). ¹³C NMR (δ , in CDCl₃): -26.19 (d, $J_{\text{PC}} = 33.0$ Hz, FeCH₃), -25.63 (d, $J_{\text{PC}} = 32.9$ Hz, FeCH₃), 32.16 (d, $J_{\text{PC}} = 10.9$ Hz, NCH₃), 32.25 (d, $J_{\text{PC}} = 10.9$ Hz, NCH₃), 51.37 (s, NCH₂), 51.50 (s, NCH₂), 51.58 (d, $J_{\text{PC}} = 11.0$ Hz, OCH₃), 51.70 (d, $J_{\text{PC}} = 9.7$ Hz, OCH₃), 67.11 (d, $J_{\text{PC}} = 11.0$ Hz, OCH₂), 67.34 (d, $J_{\text{PC}} = 11.0$ Hz, OCH₂), 82.66 (s, C₅H₅), 83.04 (s, C₅H₅), 221.16 (d, $J_{\text{PC}} = 46.4$ Hz, CO), 221.46 (d, $J_{\text{PC}} = 45.1$ Hz, CO).

Preparation of Cp(CO)(Me)Fe{P(OMe)₃} (**5a**). The complex was prepared according to the literature method¹² (yield 65%). IR (ν_{CO} , in CH₂Cl₂): 1924. ³¹P NMR (δ , in CH₂Cl₂): 192.97 (s). ¹H NMR (δ , in CDCl₃): -0.17 (d, $J_{\text{PH}} = 4.6$ Hz, 3H, FeCH₃), 3.57 (d, $J_{\text{PH}} = 11.2$ Hz, 9H, OCH₃), 4.50 (s, 5H, C₅H₅). ¹³C NMR (δ , in CDCl₃): -26.15 (d, $J_{\text{PC}} = 32.9$ Hz, FeCH₃), 51.45 (d, $J_{\text{PC}} = 3.6$ Hz, OCH₃), 82.91 (s, C₅H₅), 220.82 (d, $J_{\text{PC}} = 46.4$ Hz, CO).

Preparation of Cp*(CO)(Me)Fe{PN(Me)CH₂CH₂NMe(OMe)} (**6a**). Complex **6a** was prepared from Cp*(CO)₂FeMe and PN(Me)CH₂CH₂NMe(OMe) by photolysis in the same

manner as that for **1a**. In this case, the reaction mixture was loaded on a silica gel column and eluted with CH₂Cl₂. The second eluted band was collected and loaded again on a new silica gel column. After the band that eluted with hexane was discarded, the orange band that eluted with CH₂Cl₂ was collected and the solvent was removed in vacuo to give **6a** as a dark yellow powder (yield 69%). Anal. Calcd for C₁₇H₃₁FeN₂O₂P: C, 53.42; H, 8.17; N, 7.33. Found: C, 53.54; H, 8.19; N, 6.90. IR (ν_{CO} , in CH₂Cl₂): 1894. ³¹P NMR (δ , in CH₂Cl₂): 175.02 (s). ¹H NMR (δ , in CDCl₃): -0.41 (d, $J_{\text{PH}} = 4.6$ Hz, 3H, FeCH₃), 1.61 (s, 15H, C₅(CH₃)₅), 2.62 (d, $J_{\text{PH}} = 9.6$ Hz, 3H, NCH₃), 2.73 (d, $J_{\text{PH}} = 9.9$ Hz, 3H, NCH₃), 3.18 (d, $J_{\text{PH}} = 10.6$ Hz, 3H, OCH₃), 3.35 (m, 4H, NCH₂). ¹³C NMR (δ , in CDCl₃): -14.74 (d, $J_{\text{PC}} = 30.5$ Hz, FeCH₃), 9.29 (s, C₅(CH₃)₅), 32.74 (d, $J_{\text{PC}} = 12.2$ Hz, NCH₃), 33.09 (d, $J_{\text{PC}} = 11.0$ Hz, NCH₃), 51.73 (d, $J_{\text{PC}} = 12.2$ Hz, OCH₃), 51.79 (d, $J_{\text{PC}} = 4.9$ Hz, NCH₂), 52.23 (d, $J_{\text{PC}} = 6.1$ Hz, NCH₂), 91.14 (s, C₅(CH₃)₅), 223.75 (d, $J_{\text{PC}} = 44.0$ Hz, CO).

Preparation of Cp(CO)(SiMe₃)Fe{PN(Me)CH₂CH₂NMe(OMe)} (**7a**). Cp(CO)₂Fe(SiMe₃) (1328 mg, 5.31 mmol), benzene (60 mL), and PN(Me)CH₂CH₂NMe(OMe) (1.16 mL, 1172 mg, 7.91 mmol) were put in a Pyrex Schlenk tube, and the solution was irradiated with a 400 W medium-pressure mercury arc lamp at 0 °C for 3.5 h. After some insoluble materials were removed by filtration, the filtrate was concentrated under reduced pressure and loaded on an alumina column. The yellow band that eluted with CH₂Cl₂ was collected, and the solvent was removed in vacuo. Pentane was added to the residue. After filtration to remove insoluble materials, the solvent was removed in vacuo to give **7a** as a yellow powder (1742 mg, 4.70 mmol, 89%). Anal. Calcd for C₁₄H₂₇FeN₂O₂PSi: C, 45.41; H, 7.35; N, 7.56. Found: C, 45.46; H, 7.12; N, 7.49. IR (ν_{CO} , in CH₂Cl₂): 1902. ³¹P NMR (δ , in CH₂Cl₂): 176.64 (s). ¹H NMR (δ , in CDCl₃): 0.26 (s, 9H, Si(CH₃)₃), 2.72 (d, $J_{\text{PH}} = 10.6$ Hz, 3H, NCH₃), 2.75 (d, $J_{\text{PH}} = 10.6$ Hz, 3H, NCH₃), 3.10 (m, 2H, NCH₂), 3.17 (d, $J_{\text{PH}} = 11.2$ Hz, 3H, OCH₃), 3.32 (m, 2H, NCH₂), 4.35 (d, $J_{\text{PH}} = 1.3$ Hz, 5H, C₅H₅). ¹³C NMR (δ , in CDCl₃): 8.80 (s, $J_{\text{CSi}} = 40.3$ Hz, Si(CH₃)₃), 33.50 (d, $J_{\text{PC}} = 11.0$ Hz, NCH₃), 33.58 (d, $J_{\text{PC}} = 12.2$ Hz, NCH₃), 51.04 (d, $J_{\text{PC}} = 13.4$ Hz, OCH₃), 51.37 (d, $J_{\text{PC}} = 2.4$ Hz, NCH₂), 51.71 (d, $J_{\text{PC}} = 3.7$ Hz, NCH₂), 81.13 (s, C₅H₅), 219.39 (d, $J_{\text{PC}} = 42.7$ Hz, CO). ²⁹Si NMR (δ , in CH₂Cl₂): 37.23 (d, $J_{\text{PSi}} = 41.7$ Hz).

Preparation of Cp(CO)(SiMe₃)Fe{PN(Me)CH₂CH₂NMe(OEt)} (**8a**). Complex **8a** was prepared from Cp(CO)₂Fe(SiMe₃) and PN(Me)CH₂CH₂NMe(OEt) in the same manner as that for **7a** (yellow powder, yield 85%). Anal. Calcd for C₁₅H₂₉FeN₂O₂PSi: C, 46.88; H, 7.61; N, 7.29. Found: C, 46.88; H, 7.36; N, 7.15. IR (ν_{CO} , in CH₂Cl₂): 1901. ³¹P NMR (δ , in CH₂Cl₂): 174.13 (s). ¹H NMR (δ , in CDCl₃): 0.28 (s, 9H, Si(CH₃)₃), 1.10 (t, $J_{\text{HH}} = 6.9$ Hz, 3H, OCH₂CH₃), 2.70 (d, $J_{\text{PH}} = 10.9$ Hz, 3H, NCH₃), 2.74 (d, $J_{\text{PH}} = 10.6$ Hz, 3H, NCH₃), 3.10 (m, 2H, NCH₂), 3.27 (m, 2H, NCH₂), 3.50 (m, 2H, OCH₂), 4.34 (s, 5H, C₅H₅). ¹³C NMR (δ , in CDCl₃): 8.93 (s, $J_{\text{CSi}} = 39.0$ Hz, Si(CH₃)₃), 16.16 (d, $J_{\text{PC}} = 6.1$ Hz, OCH₂CH₃), 33.44 (d, $J_{\text{PC}} = 12.2$ Hz, NCH₃), 33.65 (d, $J_{\text{PC}} = 11.0$ Hz, NCH₃), 51.30 (d, $J_{\text{PC}} = 2.4$ Hz, NCH₂), 51.59 (d, $J_{\text{PC}} = 4.9$ Hz, NCH₂), 59.76 (d, $J_{\text{PC}} = 13.5$ Hz, OCH₂), 81.11 (s, C₅H₅), 219.32 (d, $J_{\text{PC}} = 42.8$ Hz, CO). ²⁹Si NMR (δ , in CH₂Cl₂): 36.62 (d, $J_{\text{PSi}} = 43.0$ Hz).

Preparation of Cp(CO)(CH₂OMe)Fe{PN(Me)CH₂CH₂NMe(OMe)} (**9a**). NaK_{2.8} (0.95 mL, 798 mg, 6.02 mmol) was added to a solution of Cp(CO)IFe{PN(Me)CH₂CH₂NMe(OMe)} (987 mg, 2.33 mmol) in THF (50 mL), and the solution was stirred for about 30 min at room temperature, causing the color of the solution to change from green to brown. After filtration, the filtrate was added dropwise to a solution of ClCH₂OMe (0.18 mL, 191 mg, 2.37 mmol) in THF (20 mL) and stirred overnight at room temperature. After removing insoluble materials by filtration, the solvent was removed from the

(12) Alt, H. G.; Herberhold, M.; Rausch, M. D.; Edwards, B. H. Z. *Naturforsch.* **1979**, *34b*, 1070.

filtrate under reduced pressure. The soluble product was extracted with pentane (30 mL \times 2) and removing the solvent under reduced pressure gave **9a** as a yellow powder (353 mg, 1.03 mmol, 44%). Anal. Calcd for $C_{13}H_{23}FeN_2O_3P$: C, 45.63; H, 6.77; N, 8.19. Found: C, 45.72; H, 6.66; N, 8.15. IR (ν_{CO} , in CH_2Cl_2): 1911. ^{31}P NMR (δ , in CH_2Cl_2): 175.71 (s). 1H NMR (δ , in $CDCl_3$): 2.68 (d, $J_{PH} = 10.6$ Hz, 3H, NCH_3), 2.72 (d, $J_{PH} = 10.2$ Hz, 3H, NCH_3), 3.10 (m, 2H, NCH_2), 3.21 (d, $J_{PH} = 8.3$ Hz, 3H, $POCH_3$), 3.22 (s, 3H, CH_2OCH_3), 3.31 (m, 2H, NCH_2), 3.95 (t, $J = 5.3$ Hz, 1H, $FeCH_2$), 4.49 (s, 5H, C_5H_5), 5.32 (t, $J = 4.5$ Hz, 1H, $FeCH_2$). ^{13}C NMR (δ , in $CDCl_3$): 32.79 (d, $J_{PC} = 11.0$ Hz, NCH_3), 33.39 (d, $J_{PC} = 12.2$ Hz, NCH_3), 51.37 (d, $J_{PC} = 13.5$ Hz, $POCH_3$), 51.56 (s, NCH_2), 51.61 (s, NCH_2), 60.45 (s, CH_2OCH_3), 67.86 (d, $J_{PC} = 30.5$ Hz, $FeCH_2$), 83.27 (s, C_5H_5), 222.45 (d, $J_{PC} = 45.1$ Hz, CO).

Preparation of $Cp(CO)(CH_2OMe)Fe\{PN(Me)CH_2CH_2NMe(OEt)\}$ (10a**).** $Cp(CO)IFe\{PN(Me)CH_2CH_2NMe(OEt)\}$ was prepared from $Cp(CO)_2FeI$ and $PN(Me)CH_2CH_2NMe(OEt)$ by photolysis in the same manner as that for $Cp(CO)IFe\{PN(Me)CH_2CH_2NMe(OMe)\}$ (green powder, yield 31%). Anal. Calcd for $C_{12}H_{20}FeIN_2O_2P$: C, 32.90; H, 4.60; N, 6.40. Found: C, 32.93; H, 4.43; N, 6.43. IR (ν_{CO} , in CH_2Cl_2): 1953. ^{31}P NMR (δ , in CH_2Cl_2): 163.76 (s). 1H NMR (δ , in $CDCl_3$): 1.58 (t, $J_{HH} = 7.3$ Hz, 3H, CH_2CH_3), 2.83 (d, $J_{PH} = 10.9$ Hz, 3H, NCH_3), 2.94 (d, $J_{PH} = 10.2$ Hz, 3H, NCH_3), 3.25 (m, 4H, NCH_2), 3.66 (m, 2H, OCH_2), 4.61 (d, $J_{PH} = 1.3$ Hz, 5H, C_5H_5). ^{13}C NMR (δ , in $CDCl_3$): 16.15 (d, $J_{PC} = 4.9$ Hz, CH_2CH_3), 33.65 (d, $J_{PC} = 11.0$ Hz, NCH_3), 34.30 (d, $J_{PC} = 9.8$ Hz, NCH_3), 51.67 (d, $J_{PC} = 3.7$ Hz, NCH_2), 51.75 (d, $J_{PC} = 2.4$ Hz, NCH_2), 60.74 (d, $J_{PC} = 12.2$ Hz, OCH_2), 81.40 (s, C_5H_5), 220.71 (d, $J_{PC} = 44.0$ Hz, CO).

Complex **10a** was prepared from $Cp(CO)IFe\{PN(Me)CH_2CH_2NMe(OEt)\}$, $Nak_{2.8}$, and $ClCH_2OMe$ in the same manner as that for **9a** (greenish yellow oil, yield 49%). The complex was so unstable that the correct elemental analysis data could not be obtained, though satisfactory spectroscopic data were obtained. IR (ν_{CO} , in CH_2Cl_2): 1911. ^{31}P NMR (δ , in CH_2Cl_2): 173.43 (s). 1H NMR (δ , in $CDCl_3$): 1.09 (t, $J_{HH} = 6.9$ Hz, 3H, $POCH_2CH_3$), 2.67 (d, $J_{PH} = 10.6$ Hz, 3H, NCH_3), 2.71 (d, $J_{PH} = 10.6$ Hz, 3H, NCH_3), 3.08 (m, 2H, NCH_2), 3.23 (s, 3H, CH_2OCH_3), 3.25 (m, 2H, NCH_2), 3.53 (m, 2H, $POCH_2CH_3$), 3.95 (t, $J = 5.6$ Hz, 1H, $FeCH_2$), 4.48 (s, 5H, C_5H_5), 5.35 (t, $J = 4.6$ Hz, 1H, $FeCH_2$). ^{13}C NMR (δ , in $CDCl_3$): 16.16 (d, $J_{PC} = 4.9$ Hz, $POCH_2CH_3$), 32.88 (d, $J_{PC} = 11.0$ Hz, NCH_3), 33.46 (d, $J_{PC} = 12.2$ Hz, NCH_3), 51.45 (s, NCH_2), 51.50 (s, NCH_2), 59.65 (d, $J_{PC} = 13.4$ Hz, $POCH_2$), 60.40 (s, CH_2OCH_3), 68.40 (d, $J_{PC} = 30.5$ Hz, $FeCH_2$), 83.27 (s, C_5H_5), 222.51 (d, $J_{PC} = 45.2$ Hz, CO).

$[Cp(CO)(PPh_3)Fe\{PN(Me)CH_2CH_2NMe(Me)\}]BF_4$ (1b-BF₄**) from **1a**.** A solution of **1a** (275 mg, 0.88 mmol) of CH_2Cl_2 (20 mL) was cooled to $-78^\circ C$, and then $BF_3 \cdot OEt_2$ (0.22 mL, 248 mg, 1.75 mmol) was added. After the solution had been stirred for several minutes, PPh_3 (500 mg, 1.91 mmol) was added, and then the solution warmed to room temperature. After the solvent had been removed under reduced pressure, the residue was loaded on a silica gel column. After elution with CH_2Cl_2 , an orange complex that eluted with CH_2Cl_2 /acetone (8/1) was collected and dried in vacuo to give a yellowish orange powder of **1b-BF₄** (381 mg, 0.61 mmol, 68%). Anal. Calcd for $C_{29}H_{33}BF_4FeN_2OP_2$: C, 55.27; H, 5.28; N, 4.44. Found: C, 54.85; H, 5.21; N, 4.51. IR (ν_{CO} , in CH_2Cl_2): 1966. ^{31}P NMR (δ , in CH_2Cl_2): 65.29 (d, $J_{PP} = 60.5$ Hz, PPh_3), 159.48

(d, $J_{PP} = 60.5$ Hz, $PN(Me)CH_2CH_2NMe(Me)$). 1H NMR (δ , in $CDCl_3$): 1.59 (d, $J_{PH} = 5.9$ Hz, 3H, PCH_3), 2.12 (m, 2H, NCH_2), 2.41 (d, $J_{PH} = 10.9$ Hz, 3H, NCH_3), 2.63 (d, $J_{PH} = 11.9$ Hz, 3H, NCH_3), 2.94 (m, 2H, NCH_2), 4.80 (s, 5H, C_5H_5), 7.36–7.51 (m, 15H, C_6H_5). ^{13}C NMR (δ , in $CDCl_3$): 23.57 (d, $J_{PC} = 8.5$ Hz,

PCH_3), 33.72 (d, $J_{PC} = 6.1$ Hz, NCH_3), 33.82 (d, $J_{PC} = 7.3$ Hz, NCH_3), 50.78 (s, NCH_2), 51.48 (s, NCH_2), 85.93 (s, C_5H_5), 128.69 (d, $J_{PC} = 11.0$ Hz, $o-C_6H_5$), 130.91 (d, $J_{PC} = 2.4$ Hz, $p-C_6H_5$), 133.32 (d, $J_{PC} = 8.6$ Hz, $m-C_6H_5$), 134.18 (d, $J_{PC} = 47.6$ Hz, $\epsilon-C_6H_5$), 217.26 (dd, $J_{PC} = 28.1$, 35.4 Hz, CO).

$[Cp(CO)(PPh_3)Fe\{PN(Me)CH_2CH_2NMe(CH_2Ph)\}]BF_4$ (3b-BF₄**) from **3a**.** Complex **3b** was prepared from **3a**, $BF_3 \cdot OEt_2$, and PPh_3 in the same manner as that for **1b**. The crude product was purified by a silica gel column chromatography. After yellow and green bands that eluted with CH_2Cl_2 were discarded, an orange band that eluted with acetone was collected and the solvent was removed in vacuo. The resulting powder was washed with benzene (10 mL \times 2) and dried in vacuo to give an orange powder of **3b-BF₄** (yield 55%). Anal. Calcd for $C_{35}H_{37}BF_4FeN_2OP_2$: C, 59.52; H, 5.28; N, 3.97. Found: C, 59.31; H, 5.23; N, 4.21. IR (ν_{CO} , in CH_2Cl_2): 1963. ^{31}P NMR (δ , in CH_2Cl_2): 64.65 (d, $J_{PP} = 52.2$ Hz, PPh_3), 161.78

(d, $J_{PP} = 52.2$ Hz, $PN(Me)CH_2CH_2NMe(CH_2Ph)$). 1H NMR (δ , in CD_2Cl_2): 2.38 (m, 4H, NCH_2), 2.40 (d, $J_{PH} = 9.3$ Hz, 3H, NCH_3), 2.84 (d, $J_{PH} = 9.8$ Hz, 3H, NCH_3), 3.22 (d, $J_{PH} = 14.7$ Hz, 1H, PCH_2), 3.41 (d, $J_{PH} = 14.7$ Hz, 1H, PCH_2), 4.84 (s, 5H, C_5H_5), 7.05–7.48 (m, 20H, C_6H_5). ^{13}C NMR (δ , in CD_2Cl_2): 34.24 (d, $J_{PC} = 5.4$ Hz, NCH_3), 34.32 (d, $J_{PC} = 5.4$ Hz, NCH_3), 51.37 (s, NCH_2), 52.21 (s, NCH_2), 52.62 (d, $J_{PC} = 56.5$ Hz, PCH_2), 86.28 (s, C_5H_5), 127.45 (s, $C-p-C_6H_5$), 128.95 (s, $C-o-C_6H_5$), 129.05 (d, $J_{PC} = 10.7$ Hz, $P-o-C_6H_5$), 129.98 (s, $C-m-C_6H_5$), 131.40 (s, $P-p-C_6H_5$), 133.68 (d, $J_{PC} = 8.1$ Hz, $P-m-C_6H_5$), 134.61 (d, $J_{PC} = 10.8$ Hz, $C-\epsilon-C_6H_5$), 134.79 (d, $J_{PC} = 45.7$ Hz, $P-\epsilon-C_6H_5$), 218.05 (dd, $J_{PC} = 26.9$, 32.2 Hz, CO).

$[Cp(CO)(PPh_3)Fe\{PN(Me)CH_2CH_2O(Me)\}]BF_4$ (4b-BF₄**) from **4a**.** Complex **4b-BF₄** was prepared from **4a**, $BF_3 \cdot OEt_2$, and PPh_3 in the same manner as that for **1b-BF₄** (yield 19%). Anal. Calcd for $C_{28}H_{30}BF_4FeN_2OP_2$: C, 54.49; H, 4.90; N, 2.27. Found: C, 54.61; H, 5.09; N, 1.95. IR (ν_{CO} , in CH_2Cl_2): 1977. ^{31}P NMR (δ , in CH_2Cl_2): 65.33 (d, $J_{PP} = 64.4$ Hz, PPh_3), 66.74

(d, $J_{PP} = 71.7$ Hz, PPh_3), 203.51 (d, $J_{PP} = 71.7$ Hz, $PN(Me)CH_2CH_2O(Me)$), 203.95 (d, $J_{PP} = 64.4$ Hz, $PN(Me)CH_2CH_2O(Me)$). 1H NMR (δ , in $CDCl_3$): 1.06 (d, $J_{PH} = 6.3$ Hz, 1.5H, PCH_3), 1.69 (d, $J_{PH} = 6.3$ Hz, 1.5H, PCH_3), 2.71 (d, $J_{PH} = 11.9$ Hz, 1.5H, NCH_3), 2.77 (d, $J_{PH} = 11.9$ Hz, 1.5H, NCH_3), 3.01 (m, 1H, NCH_2), 3.31 (m, 1H, NCH_2), 3.51 (m, 1H, OCH_2), 3.98 (m, 0.5H, OCH_2), 4.16 (m, 0.5H, OCH_2), 4.80 (t, $J_{PH} = 1.7$ Hz, 2.5H, C_5H_5), 4.87 (t, $J_{PH} = 1.7$ Hz, 2.5H, C_5H_5), 7.39–7.63 (m, 15H, C_6H_5). ^{13}C NMR (δ , in $CDCl_3$): 22.68 (d, $J_{PC} = 17.1$ Hz, PCH_3), 25.34 (d, $J_{PC} = 17.1$ Hz, PCH_3), 31.93 (d, $J_{PC} = 4.9$ Hz, NCH_3), 32.01 (d, $J_{PC} = 6.1$ Hz, NCH_3), 49.54 (s, NCH_2), 49.63 (s, NCH_2), 67.27 (d, $J_{PC} = 11.0$ Hz, OCH_2), 67.96 (d, $J_{PC} = 9.8$ Hz, OCH_2), 86.29 (s, C_5H_5), 86.56 (s, C_5H_5), 128.77 (d, $J_{PC} = 9.7$ Hz, $o-C_6H_5$), 128.92 (d, $J_{PC} = 11.0$ Hz, $o-C_6H_5$), 130.98 (d, $J_{PC} = 2.4$ Hz, $p-C_6H_5$), 131.18 (d, $J_{PC} = 2.5$ Hz, $p-C_6H_5$), 133.08 (d, $J_{PC} = 9.8$ Hz, $m-C_6H_5$), 133.48 (d, $J_{PC} = 9.8$ Hz, $m-C_6H_5$), 133.81 (d, $J_{PC} = 54.9$ Hz, $\epsilon-C_6H_5$), 133.92 (d, $J_{PC} = 51.2$ Hz, $\epsilon-C_6H_5$), 214.94 (dd, $J_{PC} = 26.9$, 35.4 Hz, CO), 215.44 (dd, $J_{PC} = 26.9$, 33.0 Hz, CO).

$[Cp^*(CO)(PPh_3)Fe\{PN(Me)CH_2CH_2NMe(Me)\}]BF_4$ (6b-BF₄**) from **6a**.** Complex **6b-BF₄** was prepared from **6a**, $BF_3 \cdot OEt_2$, and PPh_3 in the same manner as that for **1b-BF₄** (yield 74%). Anal. Calcd for $C_{34}H_{43}BF_4FeN_2OP_2$: C, 58.31; H, 6.19; N, 4.00. Found: C, 58.04; H, 5.97; N, 3.59. IR (ν_{CO} , in CH_2Cl_2): 1939. ^{31}P NMR (δ , in CH_2Cl_2): 64.04 (d, $J_{PP} = 49.5$ Hz, PPh_3), 158.28 (d, $J_{PP} = 49.5$ Hz, $PN(Me)CH_2CH_2NMe(Me)$). 1H NMR (δ , in $CDCl_3$): 0.69 (d, $J_{PH} = 5.4$ Hz, 3H, PCH_3), 1.49 (s, 15H, C_6Me_5), 2.46 (d, $J_{PH} = 11.2$ Hz, 3H, NCH_3), 2.64 (d, $J_{PC} = 12.2$ Hz, 3H, NCH_3), 2.94 (m, 4H, NCH_2), 7.32–7.69 (m, 15H, C_6H_5). ^{13}C NMR (δ , in $CDCl_3$): 9.60 (s, $C_5(CH_3)_5$), 18.05 (d, $J_{PC} = 3.6$ Hz, PCH_3), 33.85 (d, $J_{PC} = 6.1$ Hz, NCH_3), 34.51 (d, $J_{PC} = 8.5$ Hz, NCH_3), 51.33 (d, $J_{PC} = 3.7$ Hz, NCH_2), 51.63 (d, $J_{PC} = 3.6$ Hz, NCH_2), 97.38 (s, $C_5(CH_3)_5$), 128.59 (d,

$J_{PC} = 9.7$ Hz, $o\text{-C}_6\text{H}_5$), 130.91 (s, $p\text{-C}_6\text{H}_5$), 133.31 (d, $J_{PC} = 41.5$ Hz, $\epsilon\text{-C}_6\text{H}_5$), 133.84 (d, $J_{PC} = 8.6$ Hz, $m\text{-C}_6\text{H}_5$), 221.45 (dd, $J_{PC} = 33.0, 25.7$ Hz, CO).

[Cp(CO)(SiMe₃)Fe{PN(Me)CH₂CH₂NMe}]⁺ (7c) from 7a. A solution of **7a** (195 mg, 0.53 mmol) in CH₂Cl₂ (4 mL) was cooled to -78 °C, and then BF₃·OEt₂ (0.14 mL, 158 mg, 1.11 mmol) was added. After the solution had warmed to room temperature, it was concentrated to about 0.5 mL under reduced pressure and then subjected to spectroscopic measurements. IR (ν_{CO} , in CH₂Cl₂): 1953. ³¹P NMR (δ , in CH₂Cl₂): 309.33 (s). ¹³C NMR (δ , in CH₂Cl₂): 8.73 (s, $J_{CSi} = 48.8$ Hz, Si(CH₃)₃), 34.46 (d, $J_{PC} = 12.2$ Hz, NCH₃), 54.09 (s, NCH₂), 84.71 (s, C₆H₅), 214.06 (d, $J_{PC} = 28.1$ Hz, CO). ²⁹Si NMR (δ , in CH₂Cl₂): 37.42 (d, $J_{PSi} = 37.6$ Hz).

[Cp(CO)(CH₂PPh₃)Fe{PN(Me)CH₂CH₂NMe(OMe)}]-BF₄ (9e-BF₄) from 9a. A solution of **9a** (1502 mg, 4.39 mmol) in CH₂Cl₂ (100 mL) was cooled to -78 °C, and then BF₃·OEt₂ (1.20 mL, 1355 mg, 9.55 mmol) was added. After the solution had been stirred for several minutes, PPh₃ (2300 mg, 8.79 mmol) was added, and then the solution was warmed to room temperature. After the solvent had been removed under reduced pressure, the residue was loaded on a silica gel column. After elution with CH₂Cl₂, an orange complex that eluted with CH₂Cl₂/acetone (8/1) was collected and dried in vacuo to give an orange powder of **9e-BF₄** (837 mg, 1.27 mmol, 29%). Anal. Calcd for C₃₃H₄₁BF₄FeN₂O₃P₂ (**9e-BF₄**·acetone): C, 55.25; H, 5.76; N, 3.91. Found: C, 55.48; H, 5.75; N, 3.72. IR (ν_{CO} , in CH₂Cl₂): 1939. ³¹P NMR (δ , in CH₂Cl₂): 40.35 (s, PPh₃), 164.87 (s, PN(Me)CH₂CH₂NMe(OMe)). ¹H NMR (δ , in acetone-*d*₆): 1.45 (ddd, $J = 23.1, 12.9, 10.2$ Hz, 1H, FeCH₂), 2.41 (td, $J = 13.2, 1.0$ Hz, 1H, FeCH₂), 2.76 (d, $J_{PH} = 10.6$ Hz, 3H, NCH₃), 3.04 (d, $J_{PH} = 10.6$ Hz, 3H, NCH₃), 3.42 (m, 3H, NCH₂), 3.55 (d, $J_{PH} = 11.2$ Hz, 3H, OCH₃), 3.61 (m, 1H, NCH₂), 4.20 (d, $J_{PH} = 1.3$ Hz, 5H, C₅H₅), 7.56–7.95 (m, 15H, C₆H₅). ¹³C NMR (δ , in acetone-*d*₆): -23.38 (dd, $J_{PC} = 29.3, 25.6$ Hz, FeCH₂), 32.89 (d, $J_{PC} = 11.0$ Hz, NCH₃), 33.29 (d, $J_{PC} = 10.9$ Hz, NCH₃), 52.42 (s, NCH₂), 52.44 (d, $J_{PC} = 3.7$ Hz, NCH₂), 52.66 (d, $J_{PC} = 13.4$ Hz, OCH₃), 84.04 (s, C₅H₅), 126.48 (d, $J_{PC} = 81.8$ Hz, $\epsilon\text{-C}_6\text{H}_5$), 130.21 (d, $J_{PC} = 11.0$ Hz, $m\text{-C}_6\text{H}_5$), 134.21 (d, $J_{PC} = 2.5$ Hz, $p\text{-C}_6\text{H}_5$), 134.42 (d, $J_{PC} = 8.5$ Hz, $o\text{-C}_6\text{H}_5$), 222.09 (dd, $J_{PC} = 46.4, 6.1$ Hz, CO).

[Cp(CO)(CH₂PPh₃)Fe{PN(Me)CH₂CH₂NMe(OEt)}]-BF₄ (10e-BF₄) from 10a. Complex **10e-BF₄** was prepared from **10a**, BF₃·OEt₂, and PPh₃ in the same manner as that for **9e-BF₄** (yield 19%). Anal. Calcd for C₃₁H₃₇BF₄FeN₂O₂P₂: C, 55.22; H, 5.53; N, 4.15. Found: C, 55.16; H, 5.53; N, 4.18. IR (ν_{CO} , in CH₂Cl₂): 1936. ³¹P NMR (δ , in CH₂Cl₂): 40.20 (s, PPh₃), 162.44 (s, PN(Me)CH₂CH₂NMe(OEt)). ¹H NMR (δ , in acetone-*d*₆): 1.34 (t, $J_{HH} = 7.1$ Hz, 3H, CH₃), 1.49 (dd, $J_{PH} = 13.7, 11.0$ Hz, 1H, FeCH₂), 2.43 (t, $J_{PH} = 12.9$ Hz, 1H, FeCH₂), 2.76 (d, $J_{PH} = 10.7$ Hz, 3H, NCH₃), 3.04 (d, $J_{PH} = 10.3$ Hz, 3H, NCH₃), 3.39 (m, 2H, NCH₂), 3.59 (br, 2H, OCH₂), 3.91 (m, 2H, NCH₂), 4.19 (s, 5H, C₅H₅), 7.69–7.95 (m, 15H, C₆H₅). ¹³C NMR (δ , in acetone-*d*₆): -23.17 (dd, $J_{PC} = 25.7, 29.3$ Hz, FeCH₂), 16.56 (d, $J_{PC} = 6.1$ Hz, OCH₂CH₃), 32.88 (d, $J_{PC} = 12.2$ Hz,

NCH₃), 33.24 (d, $J_{PC} = 11.0$ Hz, NCH₃), 52.31 (s, NCH₂), 61.65 (d, $J_{PC} = 12.2$ Hz, OCH₂), 84.04 (s, C₅H₅), 126.58 (d, $J_{PC} = 81.8$ Hz, $\epsilon\text{-C}_6\text{H}_5$), 130.19 (d, $J_{PC} = 11.0$ Hz, $m\text{-C}_6\text{H}_5$), 134.25 (d, $J_{PC} = 2.4$ Hz, $p\text{-C}_6\text{H}_5$), 134.45 (d, $J_{PC} = 9.8$ Hz, $o\text{-C}_6\text{H}_5$), 222.18 (dd, $J_{PC} = 6.1, 46.4$ Hz, CO).

X-ray Structure Determination for 1b-BF₄ and 10e-BF₄. Single crystals of **1b-BF₄** grown from CH₂Cl₂/hexane at room temperature and **10e-BF₄** grown from CH₂Cl₂/hexane in a refrigerator were individually mounted on an Enraf-Nonius CAD4 diffractometer and a Mac Science MXC3 diffractometer, respectively, and irradiated with graphite-monochromated Mo K α radiation ($\lambda = 0.71069$ Å). Cell constants and an orientation matrix for data collection, obtained from a least-squares refinement using the setting angles of 25 (for **1b-BF₄**) and 30 (for **10e-BF₄**) carefully centered reflections in the range $3^\circ < 2\theta < 55^\circ$ corresponded to a monoclinic cell with dimensions of $a = 9.099(1)$ Å, $b = 13.727(2)$ Å, $c = 23.134(5)$ Å, $\beta = 91.48(1)^\circ$, $Z = 4$, and $V = 2889(1)$ Å³ for **1b-BF₄** and corresponded to an orthorhombic cell with dimensions of $a = 18.003(6)$ Å, $b = 24.619(6)$ Å, $c = 14.501(4)$ Å, $Z = 8$, and $V = 6427(3)$ Å³ for **10e-BF₄**. $P2_1/n$ and $Pcab$ were selected as space groups for **1b-BF₄** and **10e-BF₄**, respectively, which led to successful refinements. The data were collected at temperature of 23 ± 1 °C using the ω - 2θ scan technique. The intensities of three representative reflections were measured after every 200 reflections. No decay correction was applied.

The structures were solved by a direct method with the DIRDIF program system¹³ for **1b-BF₄** and with the program Monte Carlo-Multan¹⁴ for **10e-BF₄**. The positions of all hydrogen atoms were calculated by assuming idealized geometries. Absorption and extinction corrections were then applied,^{15,16} and several cycles of a full-matrix least-squares refinement with anisotropic temperature factors for non-hydrogen atoms led to final R_w values of 0.054 and 0.064 for **1b-BF₄** and **10e-BF₄**, respectively. All calculations were performed using the program system teXsan¹⁷ for **1b-BF₄** and the program system Crystan-G¹⁴ for **10e-BF₄**.

Acknowledgment. This work was supported by the Grant-in-Aid for Scientific Research on Priority Area of Reactive Organometallics No. 06227250 from the Ministry of Education, Science and Culture, Japan.

Supporting Information Available: Additional structural data for complexes **1b-BF₄** and **10e-BF₄**, including tables of positional parameters and thermal parameters (10 pages). Ordering information is given on any current masthead page.

OM950424F

(13) Beurskens, P. T.; Admiraal, G.; Beurskens, G.; Bosman, W. P.; Garcia-Granda, S.; Gould, R. O.; Smits, J. M. M.; Smykalla, C. The DIRDIF program system. Technical Report of the Crystallography Laboratory, University of Nijmegen: University of Nijmegen: Nijmegen, The Netherlands, 1992.

(14) Furusaki, A. *Acta Crystallogr.* **1979**, *A35*, 220.

(15) Katayama, C. *Acta Crystallogr.* **1986**, *A42*, 19.

(16) Coppens, P.; Hamilton, W. C. *Acta Crystallogr.* **1970**, *A26*, 71.

(17) teXsan: Crystal Structure Analysis Package; Molecular Structure Corporation: The Woodlands, TX, 1985 and 1992.

β -Hydride Elimination and Regioselectivity in the Rhodium-Catalyzed Hydroformylation of Open Chain Unsaturated Ethers

Raffaello Lazzaroni,^{*,†} Roberta Settambolo,[‡] and Gloria Uccello-Barretta[†]

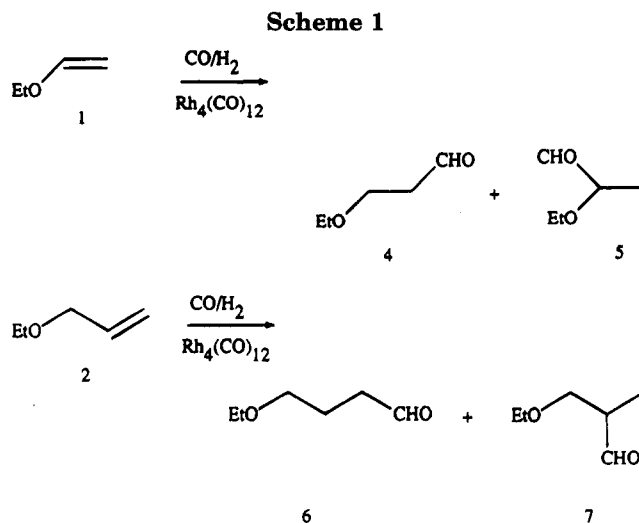
Centro di Studio del CNR per le Macromolecole Stereordinate ed Otticamente Attive, Dipartimento di Chimica e Chimica Industriale, via Risorgimento 35, Università di Pisa, 56126 Pisa, Italy, and Istituto di Chimica Quantistica ed Energetica Molecolare del CNR, via Risorgimento 35, Università di Pisa, 56126 Pisa, Italy

Received February 2, 1995[®]

The influence of the temperature on the regioselectivity in the rhodium-catalyzed hydroformylation of ethyl vinyl ether and ethyl allyl ether has been investigated in the range 20–120 °C. For both substrates, the amount of branched aldehyde decreases as the temperature increases, this effect being more pronounced for ethyl allyl ether than for ethyl vinyl ether. The ²H NMR investigation of the deuterioformylation products obtained at partial conversion, with particular attention to the unconverted substrates, points out the different behavior of the metal alkyl intermediates: at room temperature their formation is irreversible, at high temperature it becomes reversible for both isomers in the case of ethyl vinyl ether, but only for the branched one in the case of ethyl allyl ether. These results fully account for the observed influence of the temperature as well as the substrate structure on the regioselectivity.

Introduction

The influence of the reaction parameters and substrate structure on the regioselectivity of the hydroformylation of open chain oxygenated unsaturated compounds in the presence of rhodium-based catalytic precursors has been previously investigated.^{1,2} Nevertheless, no complete and satisfactory explanation of the observed phenomena has yet been provided. We are interested in the mechanistic aspects of this process and, in particular, the explanation of the observed¹ influence of the temperature on the distribution of the isomeric aldehydes (regioselectivity) in the Rh₄(CO)₁₂-catalyzed hydroformylation of two simple oxygenated olefins, i.e., ethyl vinyl ether (1) and ethyl allyl ether (2), containing the heteroatom in α or β position with respect to the vinyl group (Scheme 1, Figure 1). In accord with the generally accepted mechanism of the rhodium-catalyzed hydroformylation, linear and branched alkyl-metal complexes,^{3–6} arising from the insertion of olefin in the Rh–H bond, are assumed to be important intermediates (Scheme 2). The reverse process, i.e., the dissociation of the metal-alkyls via β -hydride elimination, can play an important role in the regioselectivity of the reaction, especially if it occurs with different rates for the two isomeric rhodium alkyls. As already shown in our



previous studies on simple olefins, such as 1-hexene⁷ and styrene,^{8,9} deuterioformylation experiments can be very useful in order to gain a deeper insight into this aspect.^{6,10,11} For this reason, we have studied the deuterioformylation of both 1 and 2 (Scheme 3) at two different temperatures (20 and 100 °C) and partial substrate conversion: the crude reaction mixtures obtained were directly investigated by ²H NMR spectroscopy, as previously done in the case of styrene,¹² in

* To whom correspondence should be addressed.

[†] Dipartimento di Chimica e Chimica Industriale.

[‡] Istituto di Chimica Quantistica ed Energetica Molecolare del CNR.

[®] Abstract published in *Advance ACS Abstracts*, August 1, 1995.

(1) Lazzaroni, R.; Bertozzi, S.; Poci, P.; Troiani, F.; Salvadori, P. *J. Organomet. Chem.* **1985**, *295*, 371.

(2) (a) Amer, I.; Alper, H. *J. Am. Chem. Soc.* **1990**, *112*, 3674. (b)

Doyle, M. P.; Shanklin, M. S.; Zlokazov, M. V. *Synlett.* **1994**, 615.

(3) Evans, J.; Schwartz, J.; Urquhart, P. W. *J. Organomet. Chem.* **1976**, *81*, C37.

(4) (a) Bennet, M. A.; Crisp, G. *Organometallics* **1986**, *5*, 1792. (b) *Ibid.* **1986**, *5*, 1800.

(5) (a) Ungvary, F.; Markò, L. *Organometallics* **1982**, *1*, 1125. (b) *Ibid.* **1986**, *5*, 2341.

(6) Pino, P. *J. Organomet. Chem.* **1980**, *200*, 223.

(7) Lazzaroni, R.; Uccello-Barretta, G.; Benetti, M. *Organometallics* **1989**, *8*, 2323.

(8) Lazzaroni, R.; Settambolo, R.; Raffaelli, A.; Pucci, S.; Vitulli, G. *J. Organomet. Chem.* **1988**, *339*, 357.

(9) Raffaelli, A.; Pucci, S.; Settambolo, R.; Uccello-Barretta, G.; Lazzaroni, R. *Organometallics* **1991**, *10*, 3892.

(10) Consiglio, G.; Morandini, F.; Haelg, R.; Pino, P. *J. Mol. Catal.* **1990**, *60*, 363.

(11) (a) Bianchi, M.; Piacenti, F.; Frediani, P.; Matteoli, U. *J. Organomet. Chem.* **1977**, *137*, 361. (b) von Bezard, D. A.; Consiglio, G.; Morandini, F.; Pino, P. *J. Mol. Catal.* **1980**, *7*, 431.

Scheme 2

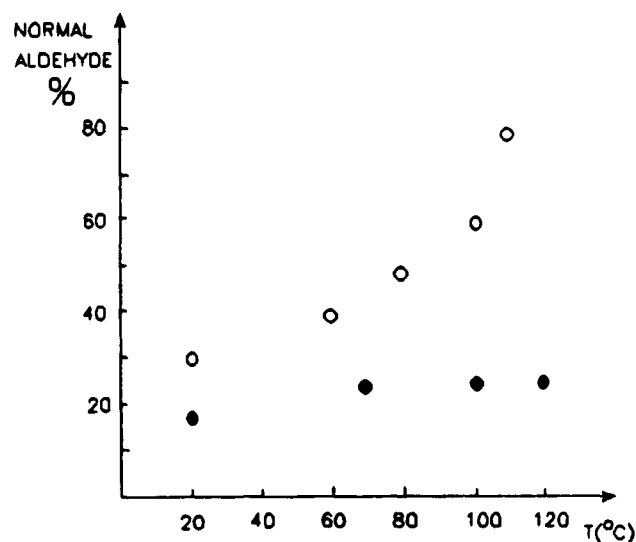
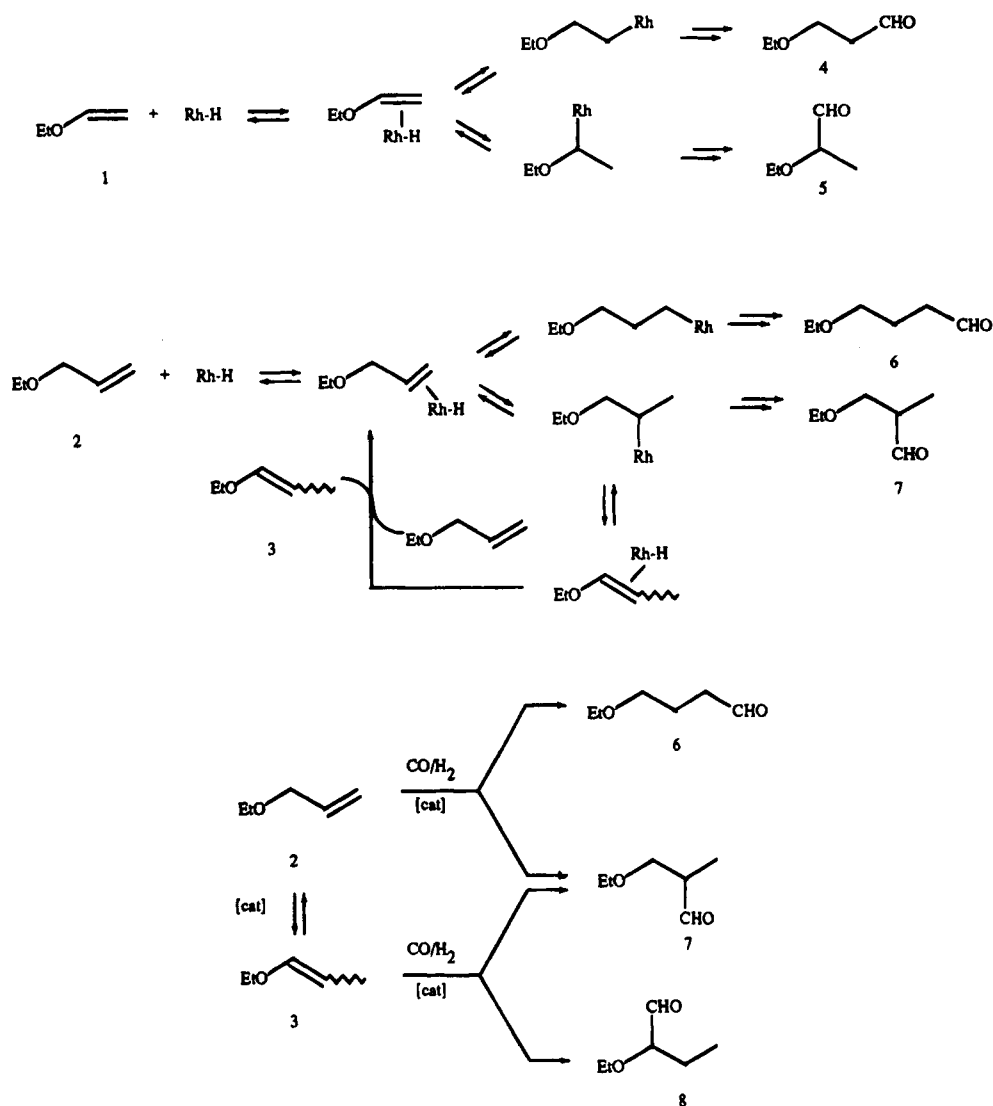


Figure 1. Hydroformylation (total pressure 100 atm, CO:H₂ 1:1) of the ethyl vinyl ether (●) and ethyl allyl ether (○) at partial conversion. Influence of the reaction temperature on the regioselectivity.

order to carefully observe the position of the deuterium atoms in the unconverted olefins.

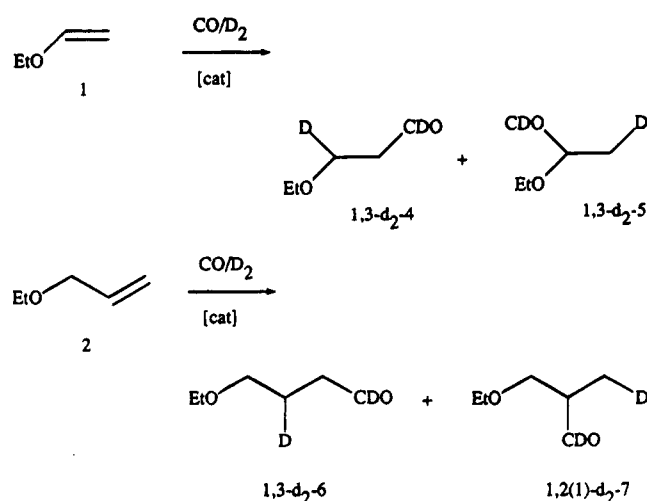
It is noteworthy that, in the case of the vinyl ether,

the presence of the oxygen atom directly bonded to the vinyl group eliminates the possibility of isomerization to internal olefin during the β-hydride elimination, and only two isomeric aldehydes (4 and 5) are obtained as products of the reaction (Scheme 2). By contrast, the allyl ether can isomerize to internal olefin 1-ethoxypropene (3) (Scheme 2). This process complicates the investigation of the influence of the temperature on the regioselectivity in the case of 2 because the aldehyde 8 (Scheme 2) could form in the reaction mixture. To avoid this problem we carried out our experiments at partial conversion of the substrate (30%), when an excess of terminal olefin was still present. Under these conditions no formation of aldehyde 8 was observed.

Results and Discussion

Hydroformylation Experiments. The hydroformylation of 2 was carried out with Rh₄(CO)₁₂ as catalytic precursor in the temperature range 20–120 °C and at a total pressure of 100 atm (CO:H₂, 1:1). Reactions were stopped after approximately the same drop of gas pressure, corresponding to a 30% substrate conversion

Scheme 3



into aldehydes. In this way correct values for the regioselectivity of the terminal double bond alone were obtained. The composition of reaction mixture was determined by GC analysis. Conversion of the oxygenated substrate to aldehydes was evaluated by GC analysis using toluene as internal standard. At 20 °C no isomerization of the substrate was observed: only the aldehydes **6** and **7** (Scheme 2) were formed; hence, in these conditions, the reaction is completely chemoselective. By contrast, at higher temperature the substrate does isomerize to some extent. In particular, at 100 °C, the chemoselectivity ((**6**+**7**)/**3**) is 57/43. As shown in Figure 1, the normal aldehyde content (and thus the regioselectivity) is particularly affected by the increase of the temperature. This value changes from 30% at 20 °C to 59% at 100 °C, the regioselectivity being in favor of the branched isomer (**7**/**6** = 70/30) at room temperature and in favor of the linear one (**7**/**6** = 41/59) at 100 °C. Polymeric compounds and hydrogenation products of olefins or aldehydes were not observed.

Hydroformylation of **1** was carried out under the same experimental conditions employed for **2**. As already reported,¹ the ratio of aldehydes **4** and **5** (Scheme 2) does not depend to any appreciable extent on the degree of conversion because **1** cannot isomerize. As shown in Figure 1, the linear isomer amount increases slightly with increase of the temperature, from 18% at 20 °C to 24% at 100 °C.

Deuterioformylation of Ethyl Allyl Ether (2). In order to elucidate the influence of the reaction temperature on the regioselectivity, deuterioformylation of **2** at partial substrate conversion (30%) has been investigated at 20 and 100 °C under CO and D₂ (1:1) constant pressure of 100 atm. Deuterioformylation and hydroformylation experiments give approximately the same regioselectivity when the reaction is carried out under identical conditions of temperature and pressure. The crude reaction mixtures were directly investigated by ²H NMR spectroscopy, allowing a rapid identification of the deuterated species, thanks to the similarity of the chemical shift ranges of ¹H and ²H nuclei. In Figure 2a the spectrum of the crude reaction mixture obtained by deuterioformylation at 20 °C shows only the signals of the two expected (Table 1) aldehydes, 1,3-dideuterio-4-ethoxybutanal (1,3-d₂-**6**) and 1-deuterio-2-(deuterio-methyl)-3-ethoxypropanal (1,2(1)-d₂-**7**), with no olefinic deuterium resonances being observed.

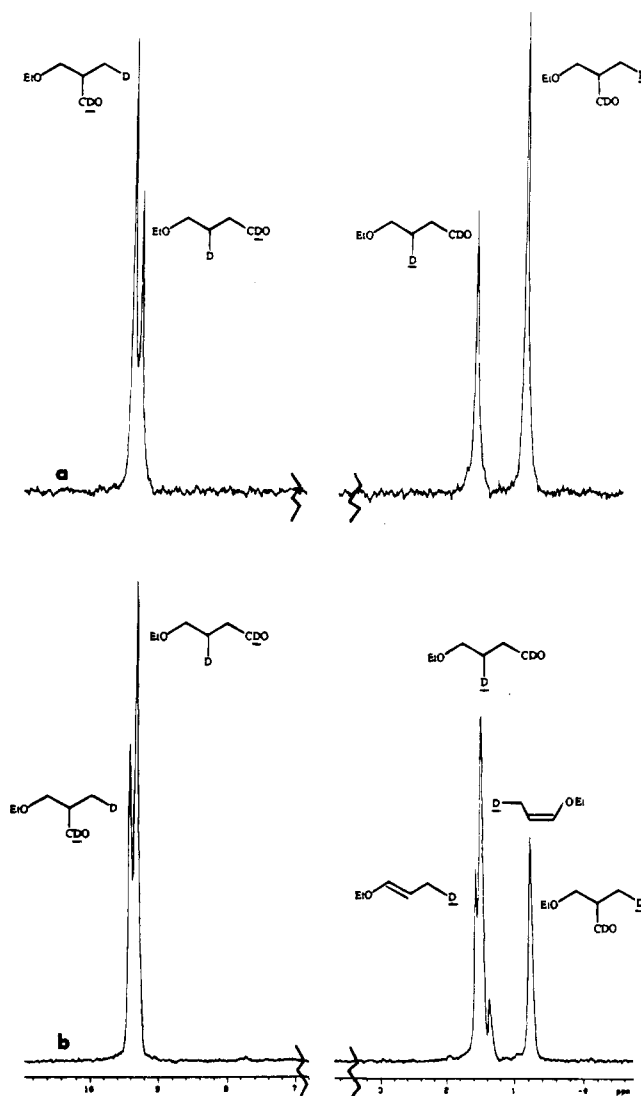


Figure 2. ²H NMR spectrum (46 MHz, 25 °C, C₆D₆ as external standard) of the crude reaction mixture in benzene, obtained by deuterioformylation of the ethyl allyl ether (**2**) at (a) 20 °C and at (b) 100 °C.

Table 1. ²H NMR Chemical Shifts^a of Mono- and Dideuterated Substrates^b Arising from the Deuterioformylation of Ethyl Allyl Ether (**2**) in the Presence of Rh₄(CO)₁₂

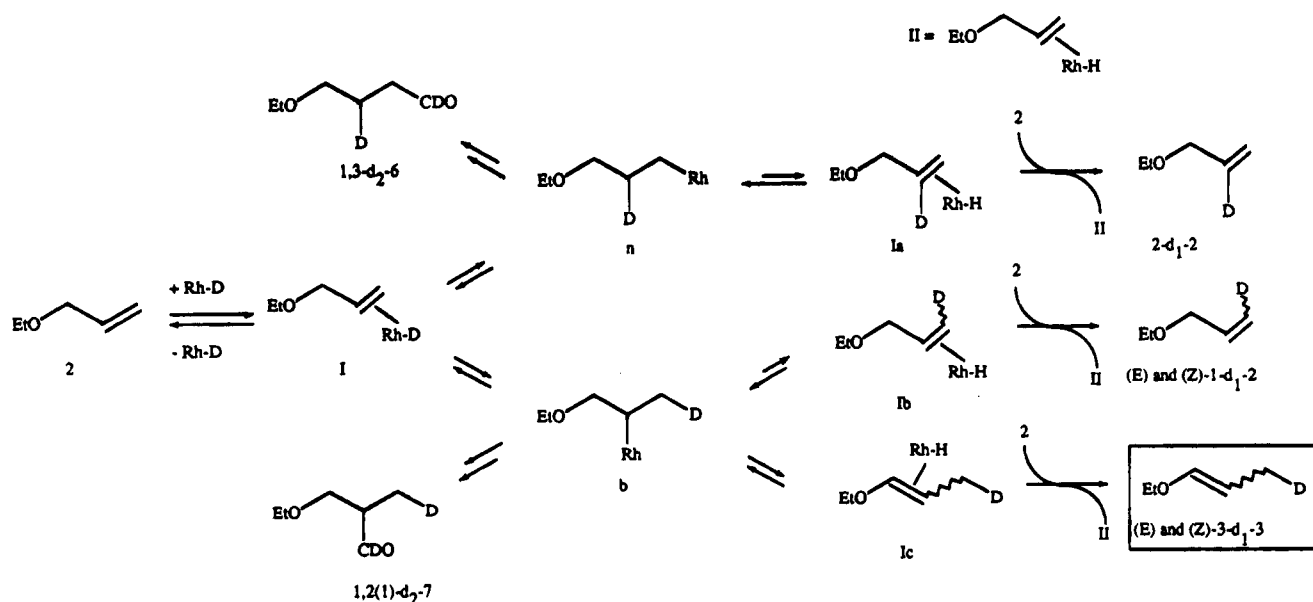
		δ, ppm
(<i>Z</i>)-3-d ₁ - 3	(<i>Z</i>)-EtO-CH=CH-CH ₂ D	1.38
(<i>E</i>)-3-d ₁ - 3	(<i>E</i>)-EtO-CH=CH-CH ₂ D	1.60
1,3-d ₂ - 6	EtO-CH ₂ -CHD-CH ₂ -CDO	9.35
1,2(1)-d ₂ - 7	EtO-CH ₂ -CH(CH ₂ D)-CDO	9.44
1,3-d ₂ - 6	EtO-CH ₂ -CHD-CH ₂ -CDO	1.53
1,2(1)-d ₂ - 7	EtO-CH ₂ -CH(CH ₂ D)-CDO	0.80

^a Referred to C₆D₆ as external standard; 46 MHz, C₆H₆, 25 °C.

^b **3** = 1-ethoxypropene, **6** = 4-ethoxybutanal, **7** = 2-methyl-3-ethoxypropanal.

In the ²H NMR spectrum of the crude reaction mixture obtained at 100 °C (Figure 2b) two resonances at 1.60 and 1.38 ppm are present in addition to the aldehyde signals. These signals can be ascribed to the two geometric isomers (*E*)-3-deuterio-1-ethoxypropene ((*E*)-3-d₁-**3**) and (*Z*)-3-deuterio-1-ethoxypropene ((*Z*)-3-d₁-**3**) arising from the presence of deuterium in the position 3 (EtO-CH=CH-CH₂D species). The forma-

Scheme 4



tion of *Z* and *E* monodeuterated 3 can be rationalized on the basis of the reaction sequence depicted in Scheme 4.

The π -complex I, formed by coordination of 2 to a rhodium deuteride species, gives rise to the isomeric alkylrhodium intermediates n and b. If this step is irreversible, the alkyl isomers will be converted into normal 1,3- d_2 -6 and branched 1,2(1)- d_2 -7 aldehydes, respectively. By contrast, if the formation of the rhodium alkyls is reversible, via a β -hydride elimination process, then the π -complexes rhodium hydride/monodeuterated 2 (Ia and Ib) and rhodium hydride/monodeuterated 3 (Ic) will form. Exchange of labeled olefins with unlabeled 2, present in excess at low conversion, could give the π -complex II (Rh-H/2 unlabeled), which originates the monodeuterated isomeric aldehydes, and the free deuterated olefins 2-deuterio-3-ethoxypropene (2- d_1 -2) (from the linear alkyl), (*E*)- and (*Z*)-1-deuterio-3-ethoxypropene (1- d_1 -2), and (*E*)- and (*Z*)-3- d_1 -3 (from the branched one). The ^2H NMR analysis (Figure 2) indicates that at room temperature the metal alkyls are formed irreversibly and are completely transformed into aldehydes (no resonances arising from olefinic deuterium atoms were present). In contrast, at high temperature only the formation of the branched alkyl is reversible, the linear alkyl intermediate giving the expected linear aldehyde. In particular only 3-deuterio-1-ethoxypropene was formed, the ^2H NMR signals at 1.60 and 1.38 ppm corresponding to the CH_2D groups of the two geometrical isomers (*E*) and (*Z*), respectively.

Deuterioformylation of Ethyl Vinyl Ether (1). Deuterioformylation of 1 was carried out under the same experimental conditions adopted for 2. Also in this case, deuterioformylation and hydroformylation experiments give approximately the same regioselectivity. In Figure 3a is reported the ^2H NMR spectrum of the crude reaction mixture obtained by deuterioformylation at 20 °C. Only the signals corresponding to the two expected aldehydes 1,3- d_2 -3-ethoxypropanal (1,3- d_2 -4) and 1,3- d_2 -2-ethoxypropanal (1,3- d_2 -5) (Table 2) are present.

In the ^2H NMR spectrum of the crude reaction mixture formed in the reaction at 100 °C (Figure 3b),

in addition to the signals of the isomeric aldehydes, four new resonances were observed. In particular the three resonances at 6.44, 4.16, and 3.97 ppm are due to deuterium nuclei on the vinyl moiety of 1. The signal at 6.44 ppm comes from the isotopic species $\text{EtO}-\text{CD}=\text{CH}_2$ (1- d_1 -1) having the deuterium at position 1 of the double bond. The two absorptions at 4.16 and 3.97 ppm come from the two geometrical isomers (*E*)-2-deuterio-1-ethoxyethene ((*E*)-2- d_1 -1) and (*Z*)-2-deuterio-1-ethoxyethene ((*Z*)-2- d_1 -1) arising from the presence of deuterium in position 2 ($\text{EtO}-\text{CH}=\text{CHD}$ species). The signal at 2.15 ppm can be ascribed to CHD α to the carbonyl group of the normal aldehyde 1,2-dideuterio-3-ethoxypropanal (1,2- d_2 -4).¹³ Analysis of the ^2H NMR data leads to important conclusions that can be summarized as follows: At low temperature deuterated 1 is not present in the reaction mixture. The two rhodium alkyl isomers n^I and b^I (Scheme 5) must, therefore, be formed irreversibly and be converted completely into the expected 1,3-dideuterated aldehydes. At high temperature the formation of both branched and normal alkyls is reversible; they undergo β -hydride elimination to give the two rhodium-hydride π -complexes IIIa and IIIb, in which 1- or 2- d_1 -1, respectively, is coordinated. When these complexes undergo intermolecular exchange with unlabeled 1, in addition to the complex IV (Rh-H/1 unlabeled), which gives the monodeuterated isomeric aldehydes, free (*E*)-2- d_1 -1, (*Z*)-2- d_1 -1, and 1- d_1 -1 are formed in solution. The three resonances in the range of vinylic protons found in the ^2H NMR spectrum at high temperature are in agreement with this interpretation. In addition, complex IIIb gives rise to the linear rhodium-alkyl intermediate n^{II}, from which the isomeric 1,2-dideuterated normal aldehyde can be formed, thus accounting for the signal at 2.15 ppm. A similar sequence for the complex IIIa would yield the aldehyde 1,2-dideuterio-2-ethoxypropanal (1,2- d_2 -5), via the branched alkyl-rhodium intermediate b^{II}, but no direct evidence for the presence of this species has been found

(13) GC-MS analysis of the crude reaction mixture recovered at 100 °C and 30% of conversion showed that the mono- and dideuterated species were present in both isomeric aldehydes, the trideuterated ones being present in very low amount (<4%) only in the branched isomer.

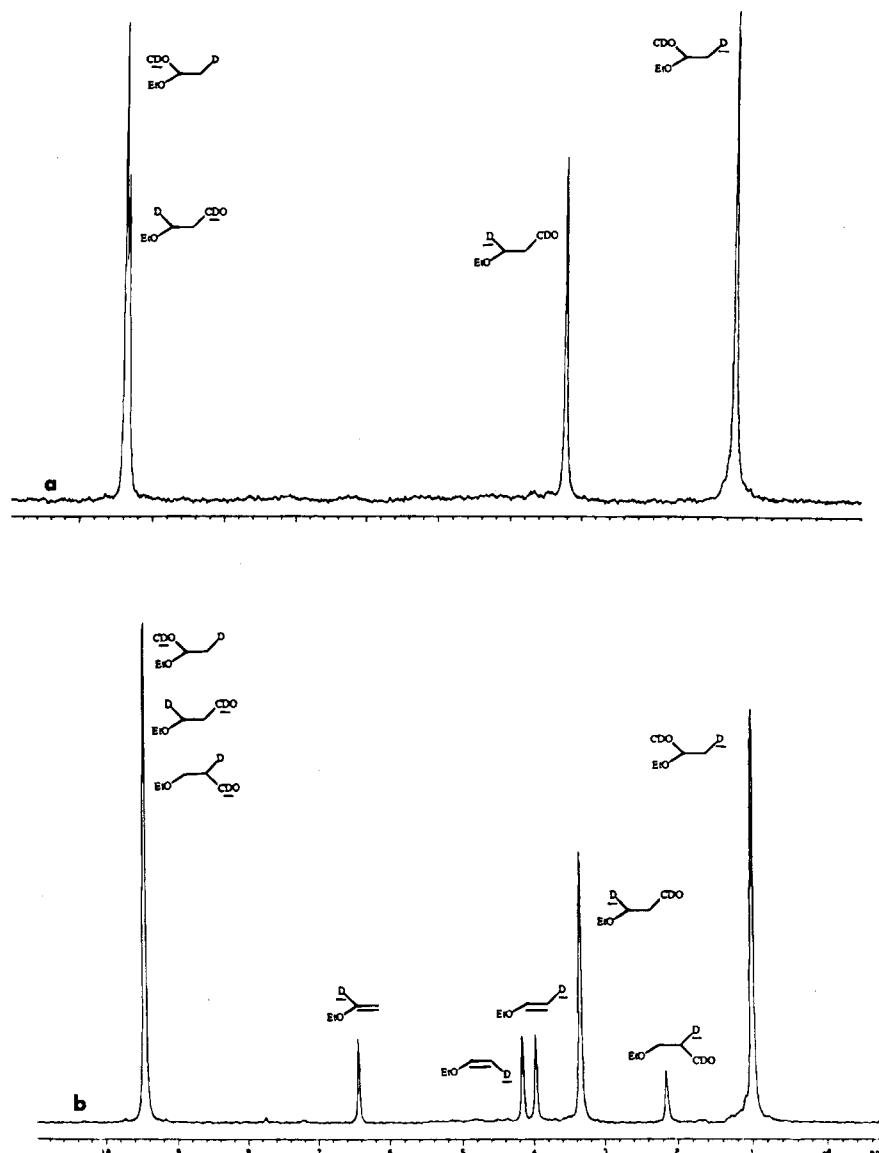


Figure 3. ^2H NMR spectrum (46 MHz, 25 °C, C_6D_6 as external standard) of the crude reaction mixture in benzene, obtained by deuterioformylation of the ethyl vinyl ether (**1**) at (a) 20 °C and at (b) 100 °C.

Table 2. ^2H NMR Chemical Shifts^a of Mono- and Dideuterated Substrates^b Arising from the Deuterioformylation of Ethyl Vinyl Ether (**1**) in the Presence of $\text{Rh}_4(\text{CO})_{12}$

		δ , ppm
1- <i>d</i> ₁ -1	$\text{EtO}-\text{CD}=\text{CH}_2$	6.44
(<i>E</i>)-2- <i>d</i> ₁ -1	(<i>E</i>)- $\text{EtO}-\text{CH}=\text{CHD}$	4.16
(<i>Z</i>)-2- <i>d</i> ₁ -1	(<i>Z</i>)- $\text{EtO}-\text{CH}=\text{CHD}$	3.97
	CDO	9.46
1,3- <i>d</i> ₂ -5	$\text{EtO}-\text{CH}(\text{CH}_2\text{D})-\text{CDO}$	0.99
1,2- <i>d</i> ₂ -5	$\text{EtO}-\text{CD}(\text{CDO})\text{CH}_3$	3.27
1,3- <i>d</i> ₂ -4	$\text{EtO}-\text{CHD}-\text{CH}_2-\text{CDO}$	3.34
1,2- <i>d</i> ₂ -4	$\text{EtO}-\text{CH}_2-\text{CHD}-\text{CDO}$	2.15

^a Referred to C_6D_6 as external standard; 46 MHz, C_6H_6 , 25 °C.
^b **5** = 2-ethoxypropanal, **4** = 3-ethoxypropanal.

in the ^2H NMR spectrum of the crude reaction mixture (Figure 3b). However, the ^2H NMR spectra of an isomerically omogeneous sample of the branched aldehyde (obtained by preparative GLC of the reaction mixture) shows a resonance at 3.27 ppm of very low intensity with respect to those of CH_2D and CDO, which must be assigned to the deuterium atom bound to the tertiary atom of 1,2-*d*₂-**5**. Therefore, when the reaction is carried out at 100 °C and low conversion, the 1,2-

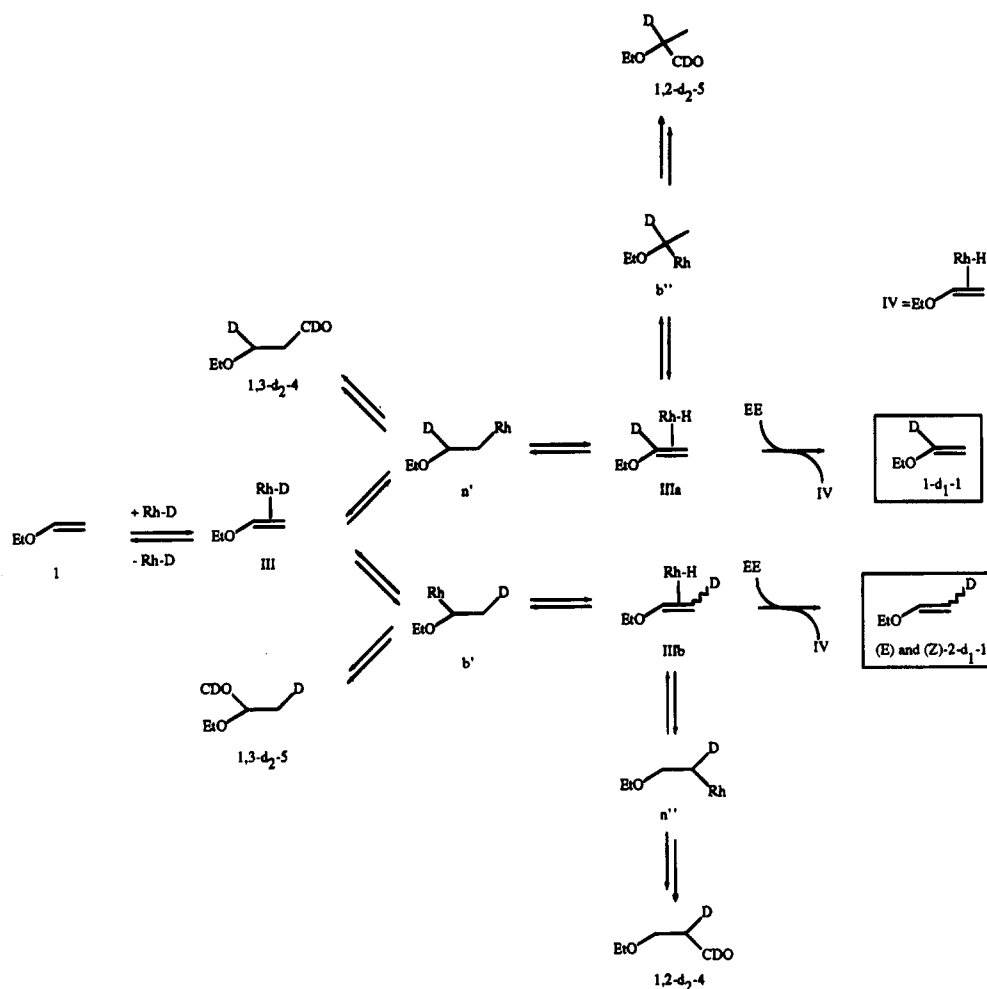
*d*₂-**5** species is obtained in very low amount and its characteristic resonance at 3.27 ppm is masked by the resonance at 3.34 ppm due to the linear isomer 1,3-*d*₂-**4**.¹⁴

Conclusions

The results of this investigation clearly show that the rearrangement of the isomeric metal-alkyl intermediates under hydroformylation conditions strongly depends on the reaction temperature and substrate structure and can be deduced by direct ^2H NMR observation of the crude deuterioformylation reaction mixtures. In the case of ethyl allyl ether **2**, at room temperature no isomerization to internal olefin **3** was observed in the unconverted substrate and no deuterium is present in

(14) It is noteworthy that the ^2H NMR spectrum of the crude reaction mixture arising from a deuterioformylation run of ethyl vinyl ether at 100 °C and 60% of conversion showed two partially superimposed resonances at 3.27 and 3.34 ppm due to the branched and linear aldehydes, respectively. In particular the signal at 3.27 ppm corresponds to the isotopic species $\text{EtO}-\text{CD}(\text{CDO})\text{CX}_3$ (X = H or D) arising from the branched alkyl-rhodium intermediate b'' (Scheme 5) or from deuterioformylation of 1-deuterio-1-ethoxyethene (1-*d*₁-1) formed, under hydroformylation condition, as described above.

Scheme 5



the residual **2**. Hence, the olefin addition to the metal hydride is not reversible under these conditions. At higher temperatures only 3-deuterio-1-ethoxypropene is formed as a consequence of the branched metal-alkyl intermediate rearrangement (Scheme 4). A similar behavior of the branched alkyls has been proposed in the rhodium-catalyzed hydroformylation of cyclic vinyl and allyl ethers.¹⁵ Thus, (i) at room temperature the regioselectivity of formation of the isomeric aldehydes reflects the regioselectivity of formation of the metal-alkyl intermediates, and (ii) the different behavior of *n* and *b* metal-alkyls toward the β -hydride elimination accounts for the decrease of the branched in favor of the normal one observed at high temperature. The linear alkyl is converted to linear aldehyde, while the branched one partially converts into branched aldehyde and partially regenerates a π -metal complex, the latter process becoming more significant as the temperature increases. In the case of ethyl vinyl ether, at room temperature no deuterium is present in the residual substrate. Hence, the olefin addition to the metal hydride is not reversible under these conditions. At higher temperatures (*E*)- and (*Z*)-1-deuterio-2-ethoxyethene, as well as 1-deuterio-1-ethoxyethene are formed (Scheme 5) as a consequence of rearrangement of both metal-alkyl intermediates. The above findings indicate that (i) at room temperature the regioselectivity of

formation of the isomeric aldehydes reflects the regioselectivity of formation of the metal-alkyl intermediates; (ii) the very similar behavior of branched *b* and linear *n* metal alkyls toward β -hydride elimination accounts for the slight influence of the temperature on the regioselectivity.

The apparent significant increase of the linear aldehyde with the increase of the temperature found in the case of the hydroformylation of ethyl allyl ether has been previously observed for the hydroformylation of styrene.¹⁶ For both substrates, at high temperatures the branched alkyl undergoes β -hydride elimination to a very large extent unlike the linear one in which this process occurs in very low amount. Different behavior has been observed for ethyl vinyl ether. In this case both rhodium-alkyl isomers give rearrangement at high temperature, therefore the regioselectivity is slightly influenced. In simple 1-alkenes such as 1-hexene¹⁷ the β -hydride elimination occurs for both rhodium-alkyl isomers at high temperature, but the rearrangement of the branched alkyl predominates over that of the linear one. As a consequence the regioselectivity changes from 52/48 at room temperature to 71/29 at 100 °C.

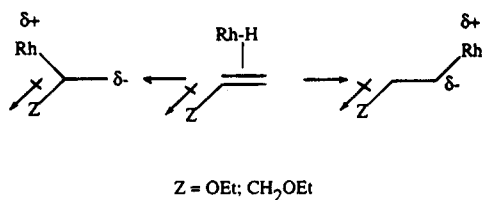
The very different behavior of ethyl vinyl ether with respect to styrene is unexpected: the linear rhodium-

(16) Lazzaroni, R.; Raffaelli, A.; Settambolo, R.; Bertozzi, S.; Vitulli, G. *J. Mol. Catal.* **1989**, *50*, 1.

(17) Lazzaroni, R.; Pertici, P.; Bertozzi, S.; Fabrizi, G. *J. Mol. Catal.* **1990**, *58*, 75.

(15) Polo, A.; Claver, C.; Castellón, S.; Ruiz, A. *Organometallics* **1992**, *11*, 3525.

Scheme 6



alkyl intermediate undergoes β -hydride elimination in the case of the ether, but not for the styrene, although both liberated olefins are stabilized, having the double bond conjugated with an ethereal oxygen or an aromatic ring.

It is noteworthy to point out the high regioselectivity in favor of the branched aldehyde observed for both ethers **1** and **2** at room temperature when there are no side reactions, such as β -hydride elimination. Under these conditions the regioselectivity reflects the relative rates of formation of the isomeric alkylrhodium intermediates. As already reported for styrene,¹⁶ the prevalence of the branched isomer must be related to the polarization required for the formation of a rhodium-carbon bond, having a partial negative charge on the carbon atom and a positive one on the rhodium atom. As shown in Scheme 6, the delocalization of the negative charge on the Z group due to the electron-withdrawing inductive effect of the oxygen atom is stronger in the intermediate leading to the branched isomer than the normal isomer. As a consequence the branched chain intermediate is stabilized and is preferred, resulting in regioselective formation of the branched aldehyde. This effect is especially significant in the case of the ethyl vinyl ether because the heteroatom is adjacent to the negative charge (regioselectivity in favor of the branched isomer, 82/18) rather than for ethyl allyl ether (regioselectivity, 70/30).

The above findings clearly point out the usefulness of the deuterioformylation reaction at partial substrate conversion in the investigation on the regioselectivity. In addition, these results also show that ²H NMR spectroscopy directly on the crude reaction mixtures is a valuable tool for mechanistic investigations in catalytic processes.

Experimental Section

Benzene was dried over molecular sieves and distilled under nitrogen. The starting vinyl and allyl ethers were commercially available. Rh₄(CO)₁₂ was prepared as reported in the literature.¹⁸ GC analyses of the reaction mixtures were performed on a Perkin-Elmer 8500 chromatograph equipped with a 12 m \times 0.22 mm BP1 capillary column, using helium as carrier gas. ²H NMR spectra of the crude products in benzene were recorded on a Varian VXR 300 spectrometer operating at 46 MHz for ²H. Chemical shifts were referred to C₆D₆ as external standard.

Hydroformylation or Deuterioformylation of Vinyl and Allyl Ethers: General Procedure. A solution of ether (10 mmol) and Rh₄(CO)₁₂ (5 mg; 6.7×10^{-3} mmol) in benzene (10 g) was introduced by suction into an evacuated stainless steel autoclave. Carbon monoxide was introduced, the autoclave was then rocked and heated to the reaction temperature, and hydrogen or deuterium was rapidly introduced up to the desired total pressure. When the gas absorption reached the value corresponding to the fixed conversion, the reaction mixture was siphoned out. The degree of conversion was measured by GLC, using toluene as an internal standard.

Acknowledgment. This work was supported by the research program Progetto Finalizzato per la Chimica Fine II.

OM950087A

(18) McCleverty, J.; Wilkinson, G. *Inorg. Synth.* **1966**, *8*, 211.

Investigation of the Formation of Ligated Dinitrogen from Rhenium-Bound Aryldiazene

Antonio Cusanelli and Derek Sutton*

Department of Chemistry, Simon Fraser University,
Burnaby, British Columbia, Canada V5A 1S6

Received May 5, 1995[⊗]

Chemical or electrochemical reduction of the cationic rhenium aryldiazene complexes $[\text{Cp}'\text{Re}(\text{L}_1)(\text{L}_2)(p\text{-N}_2\text{C}_6\text{H}_4\text{OMe})][\text{BF}_4]$ (**1b**–**7b**) generates the corresponding neutral dinitrogen complexes **1a**–**7a** of the type $\text{Cp}'\text{Re}(\text{L}_1)(\text{L}_2)(\text{N}_2)$ ((a) $\text{Cp}' = \text{Cp}$; $\text{L}_1 = \text{L}_2 = \text{CO}$ (**1a**); (b) $\text{Cp}' = \text{Cp}^*$, $\text{L}_1 = \text{CO}$, $\text{L}_2 = \text{PMe}_3$ (**3a**) or $\text{P}(\text{OMe})_3$ (**4a**); and (c) $\text{Cp}' = \text{Cp}^*$, $\text{L}_1 = \text{L}_2 = \text{CO}$ (**2a**), PMe_3 (**5a**), dmpe (**6a**), or $\text{P}(\text{OMe})_3$ (**7a**)). Evidence is presented in support of a proposed mechanism which involves one-electron reduction of the aryldiazene complex cation in **1b**–**7b** to the neutral 19-electron intermediate, followed by C–N bond homolysis to give **1a**–**7a** plus the *p*-methoxyphenyl radical that proceeds to form anisole by hydrogen atom abstraction from the solvent. The cathodic reduction peak potentials observed for **1b**–**7b** by cyclic voltammetry are increasingly negative in the sequence of coligands $(\text{PMe}_3)_2$ (**5b**, -1.89 V) > dmpe (**6b**, -1.74 V) > $[\text{P}(\text{OMe})_3]_2$ (**7b**, -1.41 V) > $(\text{CO})(\text{PMe}_3)$ (**3b**, -1.24 V) > $(\text{CO})[\text{P}(\text{OMe})_3]$ (**4b**, -0.98 V) > $(\text{CO})_2$ (**2b**, -0.62 V). The value for the dicarbonyl Cp^* complex **2b** is more negative than for the corresponding Cp complex **1b** (-0.46 V). These potentials are a good indication of the success of chemical reduction: all **1b**–**7b** are reduced to **1a**–**7a** by Na/Hg in THF, whereas Cp_2Co , which has a smaller reduction potential than Na/Hg, only reduces **1b**, **2b**, and **4b**. The reaction of **2b** with NaBH_4 is shown by full spectroscopic characterization to produce the aryldiazene complex $\text{Cp}^*\text{Re}(\text{CO})_2(p\text{-NHNC}_6\text{H}_4\text{OMe})$, which is thermally unstable and yields the dinitrogen complex **2a** and anisole.

Introduction

The first examples of rhenium dinitrogen complexes were reported in 1969 by Chatt et al.¹ These octahedral rhenium(I) dinitrogen complexes, *trans*- $\text{ReCl}(\text{N}_2)(\text{dppe})_2$, *trans*- $\text{ReCl}(\text{N}_2)(\text{PMe}_2\text{Ph})_4$, and *trans*- $\text{ReCl}(\text{N}_2)(\text{PPh}_3)_2(\text{PF}_3)_2$, were prepared by the degradation of the chelated benzyldiazene complex $\text{ReCl}_2(\text{PPh}_3)_2(\text{N}_2\text{COPh})$. The production of methyl benzoate in the reactions suggested that nucleophilic attack of methanol or methoxide ion on the carbonyl carbon atom may be involved in the production of the dinitrogen complexes.²

Since the initial discovery, numerous dinitrogen complexes of rhenium have been prepared by many different routes. For example, the rhenium hydrido dinitrogen complex $\text{ReH}(\text{N}_2)(\text{dppe})_2$ resulted from the reaction of the ammonium salt $[\text{NH}_4][\text{ReH}_9]$ with 2 equiv of dppe in 2-propanol under an atmosphere of dinitrogen.³ Furthermore, the half-sandwich rhenium dinitrogen complex $\text{CpRe}(\text{CO})_2(\text{N}_2)$ was synthesized by controlled oxidation of the corresponding hydrazine complex $\text{CpRe}(\text{CO})_2(\text{N}_2\text{H}_4)$ with H_2O_2 in the presence of copper(II) salts⁴ or by displacement of the labile THF ligand in $\text{CpRe}(\text{CO})_2(\text{THF})$ by dinitrogen under high pressure.⁵

Despite this, the original Chatt synthesis remained for more than a decade the only example in which an

organodiazene ligand was transformed into a dinitrogen ligand. However, it was observed several years ago in our laboratory that the aryldiazene ligand in the cationic manganese complex $[(\eta^5\text{-C}_5\text{H}_4\text{Me})\text{Mn}(\text{CO})_2(\text{N}_2\text{-Ar})][\text{BF}_4]$ was converted into ligated dinitrogen by I^- , Br^- , and Cl^- to yield the neutral complex $(\eta^5\text{-C}_5\text{H}_4\text{Me})\text{Mn}(\text{CO})_2(\text{N}_2)$;⁶ the only other product identified was the respective substituted arene, IAr , BrAr , or ClAr . The limited available experimental evidence obtained for these reactions was consistent with a nucleophilic displacement mechanism, though a radical process cannot be ruled out.

Interestingly, identical results were not obtained when these reactions were repeated with the analogous cationic aryldiazene complexes of rhenium, and products varied with the experimental conditions. For example, reaction of the rhenium aryldiazene complex $[\text{CpRe}(\text{CO})_2(p\text{-N}_2\text{C}_6\text{H}_4\text{OMe})][\text{BF}_4]$ with I^- gave not only the expected dinitrogen complex $\text{CpRe}(\text{CO})_2(\text{N}_2)$ but also the known⁷ diiodo complex $\text{CpRe}(\text{CO})_2\text{I}_2$. Treatment of the rhenium aryldiazene complex with Br^- yielded the dinitrogen complex, the corresponding dibromo complex $\text{CpRe}(\text{CO})_2\text{Br}_2$,⁸ and the carbonyl substitution complex $\text{CpReBr}(\text{CO})(p\text{-N}_2\text{C}_6\text{H}_4\text{OMe})$. GC–MS analysis of the reaction mixtures resulting from these halide ion additions showed in each case the presence of the respective iodo and bromo arene compounds ($\text{IC}_6\text{H}_4\text{OMe}$ or $\text{BrC}_6\text{H}_4\text{OMe}$) as well as the formation of anisole ($\text{C}_6\text{H}_5\text{-}$

[⊗] Abstract published in *Advance ACS Abstracts*, September 1, 1995.

(1) Chatt, J.; Dilworth, J. R.; Leigh, G. J. *J. Chem. Soc., Chem. Commun.* **1969**, 687.

(2) Chatt, J.; Dilworth, J. R.; Leigh, G. J. *J. Chem. Soc., Dalton Trans.* **1973**, 612.

(3) Tully, M. E.; Ginsberg, A. D. *J. Am. Chem. Soc.* **1973**, *95*, 2042.

(4) Sellmann, D. *J. Organomet. Chem.* **1972**, *36*, C27.

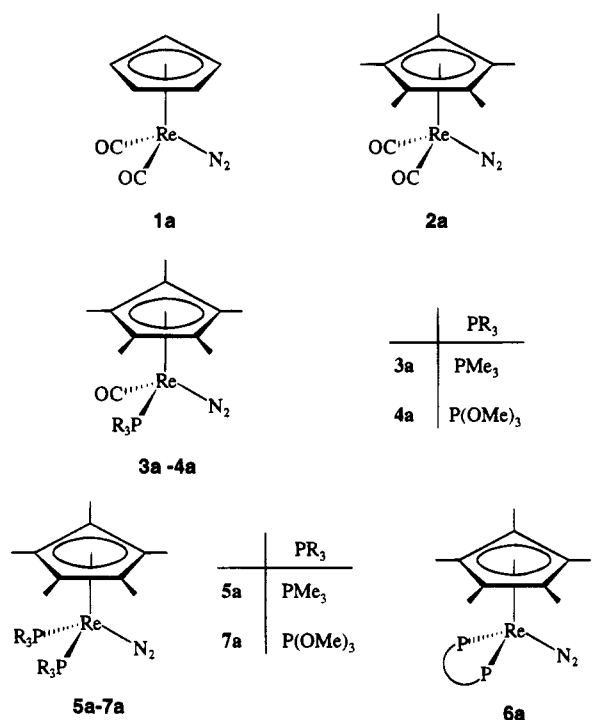
(5) Sellmann, D.; Kleinschmidt, E. Z. *Naturforsch., B: Anorg. Chem., Org. Chem.* **1977**, *32B*, 795.

(6) (a) Barrientos-Penna, C. F.; Einstein, F. W. B.; Sutton, D.; Willis, A. C. *Inorg. Chem.* **1980**, *19*, 2740. (b) Barrientos-Penna, C. F.; Sutton, D. *J. Chem. Soc., Chem. Commun.* **1980**, 111.

(7) Dong, D. F.; Hoyano, J. K.; Graham, W. A. G. *Can. J. Chem.* **1981**, *59*, 1455.

(8) Nesmeyanov, A. N.; Kolobova, N. E.; Makarov, Y. V.; Anisimov, K. N. *Bull. Acad. Sci. USSR., Div. Chem. Sci. (Engl. Trans.)* **1969**, 1687. King, R. B.; Reimann, R. H. *Inorg. Chem.* **1976**, *15*, 183.

Chart 1



OMe).⁹ Using Cl^- as the reagent produced only the carbonyl substitution complex $\text{CpReCl}(\text{CO})(p\text{-N}_2\text{C}_6\text{H}_4\text{OMe})$; the dichloro derivative $\text{CpRe}(\text{CO})_2\text{Cl}_2$ and the dinitrogen complex were not formed. Furthermore, the reaction of the halide ion X^- ($\text{X}^- = \text{I}^-, \text{Br}^-, \text{or Cl}^-$) with the pentamethylcyclopentadienyl analog $[\text{Cp}^*\text{Re}(\text{CO})_2(p\text{-N}_2\text{C}_6\text{H}_4\text{OMe})][\text{BF}_4]$ yielded in all cases exclusively the respective carbonyl substitution complex $\text{Cp}^*\text{ReX}(\text{CO})(p\text{-N}_2\text{C}_6\text{H}_4\text{OMe})$ with no production of the expected dinitrogen complex.⁹ These results, unlike those obtained for the related manganese complexes, could not be completely explained by a nucleophilic displacement mechanism but, instead, were suggestive of at least a competitive radical process.

It was clear from the synthetic results just presented that the chemistry associated with the conversion of the aryldiazenido ligand to the dinitrogen ligand, especially at a rhenium metal center, was complex and warranted further investigation. A general route to a wide variety of rhenium dinitrogen complexes has now been developed, the details of which are described in this paper. It is shown that chemical or electrochemical reduction of the cationic rhenium aryldiazenido complexes generates the corresponding neutral dinitrogen complexes of the type $\text{Cp}'\text{Re}(\text{L}_1)(\text{L}_2)(\text{N}_2)$ ((a) $\text{Cp}' = \text{Cp}$, $\text{L}_1 = \text{L}_2 = \text{CO}$ (**1a**);⁴⁻⁶ (b) $\text{Cp}' = \text{Cp}^*$, $\text{L}_1 = \text{CO}$, $\text{L}_2 = \text{PMe}_3$ (**3a**)¹⁰ or $\text{P}(\text{OMe})_3$ (**4a**);¹⁰ and (c) $\text{Cp}' = \text{Cp}^*$, $\text{L}_1 = \text{L}_2 = \text{CO}$ (**2a**),¹⁰ PMe_3 (**5a**), dmpe (**6a**), or $\text{P}(\text{OMe})_3$ (**7a**)) (Chart 1) cleanly, quickly, and in high yield. The mechanism of this conversion is discussed. While the dinitrogen complexes **1a-4a** have been described previously,^{6,10} some of the characterizing data obtained for these compounds when they have been synthesized by methods used in this study are included for authentication purposes and for a ready comparison with those dinitrogen compounds **5a-7a** that have been synthesized for the first time in this work.

Results

Synthesis and Characterization of Dinitrogen Complexes. (a) Reactions Involving Hydride Sources. The hydride sources LiAlH_4 and NaBH_4 were reacted with the cationic rhenium aryldiazenido complexes $[\text{Cp}^*\text{Re}(\text{CO})_2(p\text{-N}_2\text{C}_6\text{H}_4\text{OMe})][\text{BF}_4]$ (**2b**) and $[\text{Cp}^*\text{Re}(\text{PMe}_3)_2(p\text{-N}_2\text{C}_6\text{H}_4\text{OMe})][\text{BF}_4]$ (**5b**). Treatment of a solution of **5b** in methanol with either LiAlH_4 or NaBH_4 produced no reaction over several hours even after a large excess of the hydride source was added. By contrast, treatment of a solution of **2b** in methanol with excess solid LiAlH_4 afforded the known methoxy-carbonyl complex $\text{Cp}^*\text{Re}(\text{CO})(\text{COOMe})(p\text{-N}_2\text{C}_6\text{H}_4\text{OMe})$,⁹ which was characterized by IR and ^1H NMR spectroscopy. This was most likely formed as a result of methoxide being generated "in situ" from the reaction of LiAlH_4 with methanol, and the compound could be synthesized quantitatively by addition of NaOMe to a solution of **2b** in methanol, as reported previously.⁹ The dinitrogen complex **2a** was not formed in this reaction.

However, addition of excess NaBH_4 , as a solid, to a solution of **2b** in methanol at room temperature instead resulted in the initial formation of a deep red solution. The reaction then progressed further, with loss of the red color and formation of a yellow solution containing the dinitrogen complex **2a**. Similar results were obtained when this reaction was repeated using acetone as the solvent, in agreement with earlier studies.¹⁰⁻¹² GC analysis of the reaction mixture indicated that anisole ($\text{C}_6\text{H}_5\text{OMe}$) was also a product. An IR spectrum of the red solution which was formed immediately after the addition of NaBH_4 to a solution of **2b** in acetone at room temperature showed the complete disappearance of **2b** and the presence of two new strong absorptions of similar intensity at 1917 and 1852 cm^{-1} assigned to $\nu(\text{CO})$ of the intermediate species. IR spectra acquired every 5 min showed that the absorptions corresponding to the intermediate smoothly disappeared as the bands due to the dinitrogen complex **2a** gradually appeared, and **2a** was the final product.

The synthesis of the red solution was repeated at 195 K using acetone- d_6 as the solvent. A ^1H NMR spectrum of this solution acquired at 233 K demonstrated the disappearance of **2b** and the presence of resonances attributable to Cp^* and p -methoxyphenyl groups plus a broad singlet at δ 15.68 integrating to one proton. No signal upfield from TMS (in the hydride region) was observed. The intermediate species was reprepared at 195 K by adding NaBH_4 to an acetone- d_6 solution of the dicarbonyl aryldiazenido complex **2b**- $^{15}\text{N}_\alpha$, which was specifically ^{15}N -labeled at the rhenium-bound nitrogen atom (N_α). A ^1H NMR spectrum of this solution acquired at 233 K exhibited, in addition to the typical resonances expected for the Cp^* and the methoxyphenyl group, a doublet at δ 15.68 ($J_{\text{NH}} = 69$ Hz) integrating to one proton. A ^{15}N NMR spectrum of this solution obtained at this temperature also showed a doublet at δ -46.7 with the same coupling constant. The downfield doublet at δ 15.68 ($J_{\text{NH}} = 69$ Hz) observed in the low-temperature ^1H NMR spectrum and the doublet at

(10) Klahn, A. H.; Sutton, D. *Organometallics* **1989**, *8*, 198.

(11) Einstein, F. W. B.; Klahn-Oliva, A. H.; Sutton, D.; Tyers, K. G. *Organometallics* **1986**, *5*, 53.

(12) Klahn-Oliva, A. H. Ph.D. Thesis, Simon Fraser University, Burnaby, British Columbia, Canada, 1986.

δ -46.7 ($J_{\text{NH}} = 69$ Hz) detected in the low- δ -temperature ¹⁵N spectrum are confirmation of a one-bond ¹⁵N-H coupling. Therefore, since the ¹⁵N label was introduced at the rhenium-bound nitrogen atom (N_α) exclusively, the intermediate was unambiguously assigned as the aryldiazene complex Cp*Re(CO)₂(p-¹⁵NH¹⁴NC₆H₄OMe).

A ¹³C{¹H} NMR spectrum of this complex recorded at 233 K in acetone-*d*₆ exhibited, in addition to the typical resonances for the Cp* and aryldiazene groups, a single resonance in the carbonyl region at δ 208.32 indicative of two symmetry-equivalent CO ligands. To verify that a second resonance was not hidden under the solvent resonance, the ¹³C{¹H} NMR spectrum was reacquired at 233 K in methanol-*d*₄; the resulting spectrum was identical to that obtained previously using acetone-*d*₆.

(b) Reactions Involving the Triphenylmethyl Radical (Ph₃C•). Addition of excess Ph₃C, formed from the reduction of Ph₃CCl with zinc dust in THF, to a solution of the cationic dicarbonyl aryldiazene complexes **1b** or **2b** in CH₂Cl₂ at room temperature afforded the corresponding neutral dinitrogen complexes **1a** and **2a**, respectively, in moderate yield. In both cases the production of the dinitrogen complex was accompanied by the formation of a white precipitate that was identified by melting point, ¹H NMR spectroscopy, and elemental analysis as Ph₃COOCPh₃, formed by oxidation of the Ph₃C radical. Using freshly distilled and scrupulously degassed solvents and high-purity Ar as the inert atmosphere prevented the formation of this peroxide.

A gas chromatogram of the volatiles, which were removed under vacuum prior to the purification of the dinitrogen complexes, indicated the presence of anisole. Notably, no evidence to support the formation of the radical combination products Ph₃CC₆H₄OMe or Ph₃CCPh₃ was obtained. However, ¹H NMR spectroscopy and elemental analysis confirmed the presence of [Ph₃C]-[BF₄].

Interestingly, the addition of even a large excess of the triphenylmethyl radical to a solution of the aryldiazene complexes **3b-7b** in CH₂Cl₂ did not yield the dinitrogen complexes **3a-7a**. The starting aryldiazene complexes were recovered quantitatively even after the mixtures were stirred for 24 h.

(c) Reactions Involving Cobaltocene or Sodium. Addition of excess cobaltocene (Cp₂Co) to a solution of the dicarbonyl aryldiazene complexes **1b** and **2b** in acetone at room temperature gave the corresponding neutral dinitrogen complexes **1a** and **2a** in excellent yield. Unlike the triphenylmethyl radical chemistry mentioned above, Cp₂Co was also effective in reducing the cationic carbonyl trimethylphosphite aryldiazene complex **4b** to the dinitrogen complex **4a** in good yield. Again, anisole, confirmed by gas chromatography, was also formed in each of these reactions. The salt [Cp₂Co][BF₄] was also detected as a byproduct by ¹H NMR spectroscopy.

Notably, when this procedure was repeated for the remaining carbonyl trimethylphosphine or bis(phosphorus ligand) aryldiazene complexes **3b** or **5b-7b**, the corresponding dinitrogen complexes were not produced.

Treatment of a solution of **2b** in liquid ammonia/THF with sodium metal did not give the dinitrogen complex **2a** but instead the known⁹ neutral carbamoyl complex

Table 1. Cyclic Voltammetric Cathodic Peak Potentials for Complexes 1b-7b^a

complex	E_p^c (V)
[CpRe(CO) ₂ (p-N ₂ C ₆ H ₄ OMe)][BF ₄] (1b)	-0.46
[Cp*Re(CO) ₂ (p-N ₂ C ₆ H ₄ OMe)][BF ₄] (2b)	-0.62
[Cp*Re(CO)(PMe ₃)(p-N ₂ C ₆ H ₄ OMe)][BF ₄] (3b)	-1.24
[Cp*Re(CO){P(OMe) ₃ }(p-N ₂ C ₆ H ₄ OMe)][BF ₄] (4b)	-0.98
[Cp*Re(PMe ₃) ₂ (p-N ₂ C ₆ H ₄ OMe)][BF ₄] (5b)	-1.89
[Cp*Re(dmpe)(p-N ₂ C ₆ H ₄ OMe)][BF ₄] (6b)	-1.74
[Cp*Re{P(OMe) ₃ } ₂ (p-N ₂ C ₆ H ₄ OMe)][BF ₄] (7b)	-1.41

^a Recorded for 1.0 mM solutions of the complexes in acetonitrile at a Pt electrode with 0.2 M TEAP as the supporting electrolyte; scan rate 0.2 V/s; potentials are vs. SCE.

Cp*Re(CO)(CONH₂)(p-N₂C₆H₄OMe) was produced, identified by IR and ¹H NMR spectroscopy. This complex was confirmed to result when **2b** was added as a solid to liquid NH₃ in the absence of Na, as reported previously.⁹ Ammonia is therefore a poor choice of solvent for the sodium reactions because it reacts with **2b** quickly and completely to form the carbamoyl complex before the addition of Na, and no further reaction ensues. Repeating the Na/NH₃ reduction with **5b** did not yield the dinitrogen complex **5a** either; instead, the dihydride complex *trans*-Cp*Re(PMe₃)₂H₂ was produced and characterized by ¹H and ³¹P{¹H} NMR spectroscopy.^{13a} Sonication of a mixture of sodium metal and **2b** in THF afforded the dinitrogen complex **2a** in poor yield. However, addition of a solution of **2b** in THF to sodium amalgam at room temperature gave exclusively the dinitrogen complex **2a** in excellent yield. More importantly, treatment of any of the aryldiazene complexes **1b** or **3b-7b** with Na/Hg afforded the neutral dinitrogen complexes **1a** or **3a-7a**, respectively, in good yield. Once again, anisole was determined by gas chromatography to accompany the production of the dinitrogen complexes.

(d) Electrochemical Reduction. The cyclic voltammograms of **1b-7b** in MeCN, recorded at a scan rate of 0.2 V/s, displayed in each case a single cathodic wave between -0.46 and -1.89 V vs. SCE but no observable return anodic wave, indicating a chemically irreversible process (Table 1).

The cyclic voltammograms of the cationic dicarbonyl aryldiazene complexes **1b** and **2b** (Figure 1(a)) showed no signs of approaching electrochemical reversibility as the scan rate was increased to 1.0 V/s. However, at this scan rate a return anodic wave was clearly resolved for the cationic carbonyl phosphine and phosphite complexes **3b** and **4b** (Figure 1(b)). Unfortunately, it was not possible with the limited scan rates available with the electrochemical equipment at SFU to employ scan rates faster than 1.0 V/s to see whether a well-defined reversible wave form could be achieved for **3b**, **4b**, or any of the other cationic complexes. However, Richards and Bard successfully employed fast scan rate cyclic voltammetry and scanning electrochemical microscopy (SECM) to examine in more detail the electrochemical behavior of [Cp*Re(CO)₂(p-N₂C₆H₄OMe)][BF₄] (**2b**).^{13b} The cyclic voltammogram of **2b** exhibited a reversible wave with a cathodic peak potential of -0.66 V with respect to a silver quasireference electrode at a scan rate of 10 V/s. The anodic wave was first resolved at this

(13) (a) Herrmann, W. A.; Theiler, H. G.; Hertdweck, E.; Kiprof, P. *J. Organomet. Chem.* **1989**, *367*, 291. (b) Richards, T. C.; Bard, A. J.; Cusanelli, A.; Sutton, D. *Organometallics* **1994**, *13*, 757.

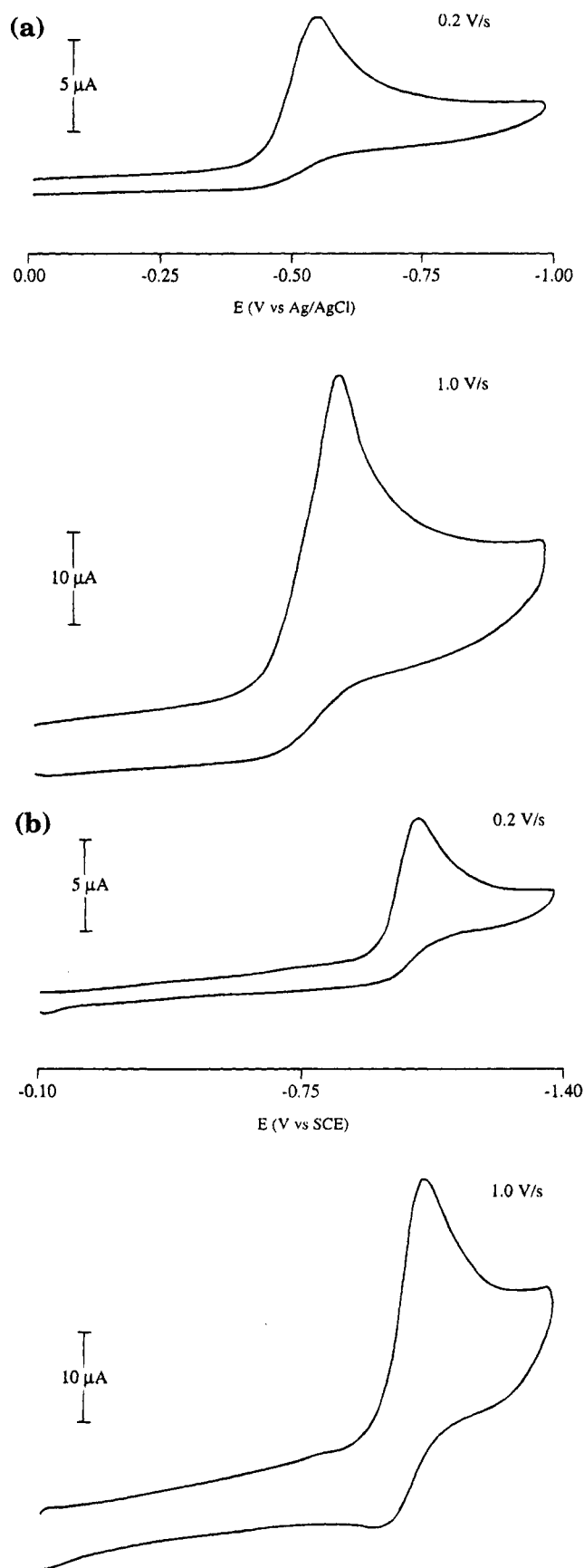


Figure 1. Cyclic voltammograms of (a) **2b** and (b) **3b** (1.0 mM MeCN solution; 0.2 M TEAP; Pt working electrode). scan rate and became well-defined at 50 V/s. Digital simulation of these cyclic voltammograms assuming an electrochemical E_rC_i mechanism afforded a rate constant $k_c = 145 \pm 10 \text{ s}^{-1}$ for the decomposition of the

reduced species to products. The validity of this rate constant was substantiated by SECM which also produced a value of 145 s^{-1} for k_c .^{13b}

The controlled potential electrolysis (CPE) of solutions of the cationic aryldiazenido complexes **1b–3b** and **5b** in acetonitrile (5 mM) was performed at a large Pt gauze electrode with tetraethylammonium perchlorate (TEAP, 0.2 M) as the supporting electrolyte. When the amount of charge consumed at the end of the CPE experiment was monitored, a value for the number of electrons involved in the overall reduction reaction was determined for **1b–3b**.^{13b} Exhaustive CPE of **1b–3b** (60 min) at a potential sufficiently more negative than their respective cathodic peak potentials vs. SCE (Table 1) indicated the consumption of 1 equiv of electrons in all cases. Monitoring the progress of the electrolysis of **1b–3b** by IR spectroscopy^{13b} showed the clean production of the corresponding neutral dinitrogen complexes **1a–3a**, respectively, in good yield and complete disappearance of **1b–3b**. Upon completion of the electrolysis, solvent and volatiles were removed by vacuum, and a gas chromatogram of the condensate confirmed the presence of anisole. The results from the CPE studies of the cationic bis(trimethylphosphine) aryldiazenido complex **5b** were inconclusive, since **5b** proved to be very air-sensitive and was easily oxidized to the known trioxo complex Cp^*ReO_3 ¹⁴ prior to or during the CPE measurements, despite all efforts to maintain an inert atmosphere in the CPE cell.

Discussion

Synthesis and Characterization of Dinitrogen Complexes. In this study, a wide variety of Cp and Cp^* rhenium aryldiazenido complexes has been converted to the corresponding dinitrogen complexes of general formula $\text{Cp}'\text{Re}(\text{L}_1)(\text{L}_2)(\text{N}_2)$ ((a) $\text{Cp}' = \text{Cp}$, $\text{L}_1 = \text{L}_2 = \text{CO}$ (**1a**);^{4–6} (b) $\text{Cp}' = \text{Cp}^*$, $\text{L}_1 = \text{CO}$, $\text{L}_2 = \text{PMe}_3$ (**3a**)¹⁰ or $\text{P}(\text{OMe})_3$ (**4a**);¹⁰ and (c) $\text{Cp}' = \text{Cp}^*$, $\text{L}_1 = \text{L}_2 = \text{CO}$ (**2a**),¹⁰ PMe_3 (**5a**), dmpe (**6a**), or $\text{P}(\text{OMe})_3$ (**7a**)) (Chart 1) by the use of NaBH_4 , Ph_3C , Cp_2Co , Na/Hg , or electrochemical reduction. Some of these compounds have been made from aryldiazenido complexes previously by employing reagents that included, among others, NaBH_4 , Bu^nLi , or iodide^{6,10–12} but reagents used here, such as Na/Hg or Cp_2Co , are superior in terms of yield, mild conditions, or ease of workup. Individual reagents are discussed separately below. In addition, we did attempt to synthesize **3a–7a** by oxidative removal of a carbonyl ligand in **2a** with PhIO or Me_3NO in a coordinating solvent such as MeCN, followed by subsequent substitution of the ligated solvent by phosphine or phosphite, but this was not successful.

The dinitrogen complexes **1a–7a** were obtained as analytically and spectroscopically pure pale yellow solids that are very soluble in the majority of organic solvents. As solids, complexes **1a–4a** can be exposed to air for short periods of time without appreciable deterioration and can be stored indefinitely at 263 K under an atmosphere of N_2 ; solutions are more air-sensitive.¹⁰ The bis(phosphorus ligand) dinitrogen complexes **5a** and **7a** and the bidentate phosphine dinitrogen complex **6a**, either in solution or as solids, are very air-sensitive, and

(14) (a) Klahn-Oliva, A. H.; Sutton, D. *Organometallics* **1984**, *3*, 1313. (b) Herrmann, W. A.; Serrano, R.; Bock, H. *Angew. Chem., Int. Ed. Engl.* **1984**, *23*, 383.

Table 2. IR, ¹H, ³¹P{¹H}, and ¹³C{¹H} NMR Data for the Dinitrogen Complexes 1a–7a

complex	IR (cm ⁻¹) ^a	¹ H NMR δ(Cp*) ^b	³¹ P{ ¹ H} NMR ^c	¹³ C{ ¹ H} NMR δ(CO) ^b
1a	2145 ν(NN); 1973, 1919 ν(CO)	5.23 s		195.79 s
1a- ¹⁵ N _α	2110 ν(NN); 1973, 1919 ν(CO)			
2a	2125 ν(NN); 1954, 1902 ν(CO)	2.09 s		200.09 s
2a- ¹⁵ N _α	2092 ν(NN); 1954, 1902 ν(CO)			
3a	2044 ν(NN); 1865 ν(CO)	2.00 d (J = 0.7)	-29.86	207.18 d (J = 7)
3a- ¹⁵ N _α	2011 ν(NN); 1865 ν(CO)			
4a	2078, 2066 ν(NN); 1877 ν(CO)	2.04 d (J = 0.8)	139.12	204.96 d (J = 12)
4a- ¹⁵ N _α	2045, 2033 ν(NN); 1877 ν(CO)			
5a	1975 ν(NN)	1.88 t (J = 0.7)	-35.31	
5a- ¹⁵ N _α	1943 ν(NN)			
5a- ¹⁵ N _β	1943 ν(NN)			
6a	1977 ν(NN)	1.92 s	-16.88	
7a	2014 ν(NN)	1.87 t (J = 0.8)	138.80	

^a In hexane. ^b In CDCl₃ for 1a–4a and in acetone-*d*₆ for 5a–7a; referenced to TMS; J given in Hz; δ given in ppm. ^c In CDCl₃ for 1a–4a and in acetone-*d*₆ for 5a–7a; referenced to 85% H₃PO₄; δ given in ppm.

exposure to air for even short periods of time results in the oxidation of these complexes to the known trioxo complex Cp*ReO₃.¹⁴ The trioxo complex was confirmed by bubbling O₂ (g) through a solution of the dinitrogen complexes 5a–7a in hexane for 5 min and then analyzing the product formed by ¹H NMR and mass spectroscopy. The mechanism for this conversion is not known, and is currently under investigation in our laboratory.

From the IR spectra of the dinitrogen complexes 1a–7a, recorded in hexane, ν(NN) was observed as a strong absorption in the 2145–1975 cm⁻¹ region (Table 2). The assignment of ν(NN) was confirmed by ¹⁵N isotopic substitution at the rhenium-bound nitrogen atom (N_α) in 1a–5a. In all cases an isotopic shift to lower wavenumber, by ca. 33 cm⁻¹, was observed for ν(NN). Data obtained in this study agree well with previously obtained values for 1a–4a.^{6,10} The two resolved ν(NN) absorptions reported¹⁰ for the carbonyl trimethylphosphite dinitrogen complex 4a and accounted for by the presence of conformational isomers brought about by the specific orientation of the Me group of the P(OMe)₃ ligand were observed for the material synthesized in this work by different procedures. In contrast to this result, the bis(trimethylphosphite) dinitrogen complex 7a exhibited only a single IR absorption for ν(NN).

For complexes 1a–7a the relative electronic properties of the Cp, Cp*, or phosphorus ligands are borne out by changes in ν(CO) or, more dramatically, by changes in ν(NN) (Table 2). The greater the σ-donor (or poorer the π-acceptor) ability of these ligands, the higher the degree of charge delocalization into the carbonyl or dinitrogen antibonding orbitals and the lower ν(CO) or ν(NN). Values for ν(NN) and, where applicable, for ν(CO), follow the order Cp > Cp* in comparable compounds, in agreement with the general view that Cp* is a better electron-donating ligand than Cp, and these findings are similar to those reported for the chromium dicarbonyl dinitrogen complexes (η-aryl)Cr(CO)₂(N₂) (aryl = C₆H₆, C₆H₃Me₃, or C₆Me₆).^{15a} Furthermore, the values follow the order of the coligands (CO)[P(OMe)₃] (4a) > (CO)(PMe₃) (3a) > [P(OMe)₃]₂ (7a) > dmpe (6a) ≈ (PMe₃)₂ (5a), which correlates with increasing σ-donor ability (or decreasing π-acceptor ability) of the phosphorus ligand. Taken together, these results conform to the view that PMe₃ is a significantly better electron-donating ligand [Δν(NN) = 81 cm⁻¹ on going from 2a

to 3a] than P(OMe)₃ [Δν(NN) = ca. 53 cm⁻¹ on going from 2a to 4a].

The ¹H NMR spectra for complexes 1a–4a exhibited the typical resonances expected for the Cp, Cp*, and phosphorus groups. The only observation of note was that the Cp* resonance in the carbonyl phosphine and phosphite complexes 3a and 4a was, as reported previously,¹⁰ split into a doublet with J_{H-P} couplings of 0.7 and 0.8 Hz, respectively, which supports the presence of a single phosphorus ligand in these complexes (Table 2). For complexes 5a–7a, the ¹H NMR spectra showed some notable features. The Cp* resonance for both the bis(trimethylphosphine) dinitrogen complex 5a and for the bis(trimethylphosphite) dinitrogen complex 7a appeared as a triplet, indicating that the Cp* methyls were observably coupled to two equivalent phosphorus ligands. Interestingly, for the bidentate phosphine dinitrogen complex 6a only a singlet Cp* resonance was observed. In 5a the resonance at δ 1.48 assigned to the PMe₃ protons was observed to be a virtual doublet integrating to 18H. The apparent coupling constant (²J_{H-P} + ⁴J_{H-P}), given by the separation between the two outside peaks, was 7.4 Hz. In 7a the resonance at δ 3.45 assigned to the P(OMe)₃ protons was also observed to be a virtual doublet, integrating to 18H with a coupling constant (³J_{H-P} + ⁵J_{H-P}) of 11.5 Hz.

The ³¹P{¹H} NMR spectra of complexes 3a–7a, in each case, displayed a single resonance in the normal region for a coordinated phosphine or phosphite (Table 2), which also indicates that in the bis(phosphorus ligand) complexes 5a–7a the phosphorus ligands are equivalent by symmetry. The ¹³C{¹H} NMR spectra of complexes 1a–4a showed a carbonyl carbon resonance in the region 195.79–207.18 ppm; a singlet was observed for 1a and 2a and a doublet for the phosphorus ligand complexes 3a and 4a with J_{C-P} = 7 and 12 Hz, respectively. The single resonance observed for δ(CO) for the dicarbonyl dinitrogen complexes 1a and 2a indicates that these two CO ligands are also symmetry equivalent. As has been indicated earlier,¹⁰ the ¹⁵N NMR spectra of some of these dinitrogen complexes, such as 1a and 2a, when labeled with ¹⁵N at the α position show that the label is scrambled into the β position. The data provided here are for the pure ¹⁵N_α isotopomer synthesized and quickly isolated below ambient temperature; full details of the isomerization study will be included in a separate paper.^{15b} Further characterization of the dinitrogen complexes 1a–7a was provided by mass spectroscopy. In all cases the molec-

(15) (a) Sellmann, D.; Maisel, G. Z. *Naturforsch.*, B: *Anorg. Chem., Org. Chem.* **1972**, *27*, 465. (b) For a preliminary account see: Cusanelli, A.; Sutton, D. J. *Chem. Soc., Chem. Commun.* **1989**, 1719.

ular ion M^+ was observed as a weak peak and was always accompanied by a fragment corresponding to loss of the dinitrogen ligand.

Reactions Using $NaBH_4$. Several years ago, the reaction of the aryldiazenido complexes $[CpRe(CO)_2(p-N_2C_6H_4R)][BF_4]$ ($R = Me, OMe, NEt_2$) and $[CpRe(CO)_2\{N_2C_6H_3(3,5-Me_2)\}][BF_4]$ with $NaBH_4$ was reported from this laboratory.¹⁶ The product in each case was the highly colored corresponding aryldiazene ($NH=NAr$) complex formed by nucleophilic attack of hydride at the metal-bound nitrogen N_α and was unambiguously identified as such by the NH resonance in the complex with $R = NEt_2$ which occurred as a doublet in the $^{15}N_\alpha$ -labeled isotopomer. The aryldiazene complex was thermally unstable resulting in the production of the dinitrogen complex $CpRe(CO)_2(N_2)$ (**1a**) and the corresponding arene. When a Cp^* analogue, namely $[Cp^*Re(CO)_2(p-N_2C_6H_4OMe)][BF_4]$ (**2b**) was reacted with $NaBH_4$ the transient red product formed en route to the dinitrogen compound **2a** was considered by analogy to be the aryldiazene complex $Cp^*Re(CO)_2(p-NHNC_6H_4OMe)$.^{11,12} It was not, however, characterized except for the IR spectrum ($\nu(CO) = 1914, 1850\text{ cm}^{-1}$ in acetone). Now, this compound has been completely characterized as part of this study.

The IR spectrum of the aryldiazene complex formed in situ from the addition of $NaBH_4$ to **2b** in acetone at low temperature showed two $\nu(CO)$ absorptions (1917 and 1852 cm^{-1} in acetone), which were lowered substantially from the corresponding positions in the aryldiazenido complex **2b** (2054 and 1995 cm^{-1} in acetone). The $\nu(NN)$ band for the aryldiazene complex was not observed in solution spectra, nor was the $\nu(NH)$ absorption. Notably, even ^{15}N isotopic substitution of the rhenium-bound nitrogen atom (N_α) in the aryldiazene complex $Cp^*Re(CO)_2(p-^{15}NH^{14}NC_6H_4OMe)$ did not lead to observable absorptions assignable to $\nu(NN)$ or $\nu(NH)$ in the solution spectra.

The 1H NMR spectrum readily demonstrated the presence of the aryldiazene ligand. The NH resonance occurs well downfield ($\delta 15.68$) and is at the lower end of the range (*ca.* $\delta 11-15$) observed for many other aryldiazenes,¹⁷⁻¹⁹ and the resonance was split into a sharp doublet ($J_{^{15}NH} = 69\text{ Hz}$) in the spectrum of the $^{15}N_\alpha$ derivative $Cp^*Re(CO)_2(p-^{15}NH^{14}NC_6H_4OMe)$. This coupling constant is in agreement with $J_{^{15}NH}$ values reported for other aryldiazene complexes, such as $[PtCl_2(PEt_3)_2(p-^{15}NH^{14}NC_6H_4F)][BF_4]$ ($J = 77\text{ Hz}$),¹⁷ $[RuCl_2(^{15}NH^{14}NPh)(CO)_2(PPh_3)_2][ClO_4]$ ($J = 65\text{ Hz}$),¹⁸ and $[W(CO)_2(NO)(PPh_3)_2(^{15}NH^{14}NPh)][PF_6]$ ($J = 63\text{ Hz}$),¹⁹ and is appropriate for metal-bound sp^2 -hybridized nitrogen.

The actual bonding mode of the ligand (i.e., end-on (η^1) or side-on (η^2) bonded) cannot be unambiguously deduced. The observed single resonance at $\delta 208.32$ in the carbonyl region in the $^{13}C\{^1H\}$ NMR spectrum at 233 K is not consistent with a η^2 -aryldiazene with the NN axis parallel to the Cp^* plane but would be consistent if the aryldiazene lies perpendicular to the Cp^* plane and in a plane equating the two CO ligands,

or is rotating. A η^1 -aryldiazene ligand freely rotating about the $Re-N$ bond would also result in equivalent carbonyl groups. Since the $\delta(NH)$ 1H NMR resonance is observed in the region where $\delta(NH)$ for crystallographically-determined η^1 -aryldiazene complexes resonates, it is likely that the aryldiazene is η^1 in this complex.¹⁸ To date, all previously reported aryldiazene complexes have been shown or are believed to be η^1 -bonded to the metal. It should be noted, however, that the closely related diphenyldiazene complex $CpRe(CO)_2(N_2Ph_2)$ is η^2 -bonded in the crystal structure, and undergoes rapid $\eta^1-\eta^2$ interconversion in solution.²⁰

It has been previously observed that reaction of the carbonyl trimethylphosphine complex $[Cp^*Re(CO)(PMe_3)(p-N_2C_6H_4OMe)][BF_4]$ (**3b**) with $NaBH_4$ resulted in no formation of an aryldiazene ligand; instead, there was substitution of PMe_3 to yield the hydrido complex $Cp^*ReH(CO)(p-N_2C_6H_4OMe)$.¹⁰ Here, we find that replacement of *both* CO ligands by PMe_3 appears to render the complex inert to hydride attack, as neither the corresponding aryldiazene, dinitrogen or hydrido complex was observed. Treatment of the bis(trimethylphosphine) complex **5b** with $NaBH_4$ resulted in no reaction. It is reasoned that an increase in the electron-donating ability of the ligand, as each CO group is replaced by PMe_3 , causes an increase of electron density at the metal center which in turn leads to greater metal $d-\pi^*$ ($NNAr$) back-bonding (reflected in the trend in $\nu(NN)$ values). The result is that the rhenium center and the rhenium-bound nitrogen atom in **5b** are made less susceptible to nucleophilic attack by hydride.

Reactions Using Triphenylmethyl or Cobaltocene. The cationic dicarbonyl aryldiazenido complexes $[Cp^*Re(CO)_2(p-N_2C_6H_4OMe)][BF_4]$ ($Cp' = Cp$ (**1b**) or Cp^* (**2b**)) were converted to the corresponding neutral dinitrogen complexes **1a** and **2a** at room temperature by reaction with a THF solution containing an excess of the triphenylmethyl radical. However, this reagent was completely ineffective when reacted with the phosphorus-substituted aryldiazenido complexes **3b-7b**. Reactions with Cp_2Co also resulted in the instantaneous formation of the dinitrogen complexes **1a** and **2a** in excellent yield, and this reagent was also effective in the case of the trimethylphosphite complex **4b**. However, it was not capable of reducing the remaining aryldiazenido complexes **3b** or **5b-7b** to the dinitrogen complexes.

The formation of anisole and $[Ph_3C][BF_4]$ or $[Cp_2Co][BF_4]$, respectively, in the reactions with Ph_3C or Cp_2Co is consistent with an electron transfer mechanism, resulting in the formation of a 19-electron neutral aryldiazenido complex intermediate $Cp^*Re(CO)(L)(N_2Ar)$ ($L = CO$ or $P(OMe)_3$). This is then visualized to decompose by CN bond homolysis to give the dinitrogen complex and an aryl radical which rapidly abstracts a hydrogen atom from the solvent to give anisole. No quantitative determination of the yields of anisole, $[Ph_3C][BF_4]$, or $[Cp_2Co][BF_4]$ was carried out. An attempt to observe by ESR the intermediate 19-electron radical in solution in the reaction of Ph_3C with the

(16) Barrientos-Penna, C. F.; Einstein, F. W. B.; Jones, T.; Sutton, D. *Inorg. Chem.* **1982**, *21*, 2578.

(17) Parshall, G. W. *J. Am. Chem. Soc.* **1967**, *89*, 1822.

(18) Haymore, B. L.; Ibers, J. A. *J. Am. Chem. Soc.* **1975**, *97*, 5369.

(19) Smith, M. R.; Hillhouse, G. L. *J. Am. Chem. Soc.* **1988**, *110*, 4066.

(20) Einstein, F. W. B.; Sutton, D.; Tyers, K. G. *Inorg. Chem.* **1987**, *26*, 111.

aryldiazenido complex **2b** was unsuccessful at room temperature and at 195 K.

Reactions Using Sodium Amalgam. The results with Ph₃C and Cp₂Co suggested that the inability to reduce the majority of the phosphine-substituted complexes such as **5b–7b** resulted from the complexes having reduction potentials for the reduction to the neutral aryldiazenido complex intermediate that are considerably more negative than are accessible with these reagents. Therefore, the use of the more powerful reductant sodium was examined. In agreement, sodium amalgam in THF was effective in reducing all of the aryldiazenido complexes **1b–7b** to the dinitrogen complexes **1a–7a**. We now consider this to be the most convenient and preferred reagent for production of all these rhenium dinitrogen complexes from the aryldiazenido complexes in excellent yield.

Electrochemical Methods. The suggestion that a one-electron chemical reduction was responsible for the conversion of the cationic aryldiazenido ligand to the neutral dinitrogen moiety was quantitatively corroborated by electrochemical measurements conducted on the complexes **1b–7b**. The cyclic voltammograms of these complexes displayed in each case a single irreversible cathodic wave, which was an indication of the relative reduction potential required to convert **1b–7b** to the corresponding neutral aryldiazenido complexes (Table 1).

The values of the cathodic peak potential reflect the expected electronic properties of the Cp, Cp*, or phosphorus ligands. For example, the Cp dicarbonyl complex **1b** has a smaller negative value for the potential (−0.46 V) than the Cp* analogue **2b** (−0.62 V). Furthermore, the potentials for the remaining aryldiazenido complexes follow the order of the coligands (PMe₃)₂ (**5b**, −1.89 V) > dmpe (**6b**, −1.74 V) > [P(OMe)₃]₂ (**7b**, −1.41 V) > (CO)(PMe₃) (**3b**, −1.24 V) > (CO)[P(OMe)₃] (**4b**, −0.98 V). Taken together, these results suggest that an increase in the σ-donor ability (or decrease in the π-acceptor ability) of an ancillary ligand leads to an increasingly negative value for the potential. These results satisfactorily account for the ability of sodium amalgam to reduce all of the aryldiazenido complexes and for Cp₂Co and Ph₃C to reduce only selected ones. The reduction potential of Cp₂Co is reported to be only *ca.* −0.9 V vs. SCE in CH₂Cl₂,²¹ whereas the reduction potential of sodium is *ca.* −3.0 V vs. SCE.²² The reduction potential of Ph₃C, to the best of our knowledge, has not been reported in the literature. The fact that Ph₃C was capable of reducing only the dicarbonyl complexes **1b** and **2b** suggests that the reduction capacity of Ph₃C is of the order of the potential determined for the Cp* dicarbonyl aryldiazenido complex **2b** (*ca.* −0.62 V).

Further evidence to support an electron transfer mechanism for the observed transformation of the aryldiazenido moiety to the respective dinitrogen derivative is provided by the results of fast scan rate cyclic voltammetry (CV) and scanning electrochemical microscopy (SECM) conducted by Richards and Bard and reported elsewhere.^{13b} These measurements provide a

first-order rate constant of $k_c = 145 \text{ s}^{-1}$ for the decomposition of the 19-electron intermediate in the case of Cp*Re(CO)₂(*p*-N₂C₆H₄OMe). The CPE study lends further support to an electrochemical E_rC₁ mechanism. Exhaustive controlled potential electrolysis of **2b** (60 min) at −0.62 V versus SCE indicated the consumption of 1 equiv of electrons. This result is clearly consistent with the production of the neutral 19-electron complex and its subsequent decomposition. In addition, exhaustive CPE of the Cp dicarbonyl complex **1b** and the Cp* carbonyl trimethylphosphine complex **3b** also established these reactions to be clean one-electron processes, and in all three cases IR monitoring showed the conversion of the aryldiazenido complex to the dinitrogen complex and GC analysis revealed anisole as a product, demonstrating the similarity of the chemical and electrochemical processes.

Conclusion

We have shown that chemical or electrochemical reduction of the cationic rhenium aryldiazenido complexes [Cp'Re(L₁)(L₂)(*p*-N₂C₆H₄OMe)][BF₄] (**1b–7b**) generates the corresponding neutral dinitrogen complexes **1a–7a** of the type Cp'Re(L₁)(L₂)(N₂) ((a) Cp' = Cp, L₁ = L₂ = CO (**1a**); (b) Cp' = Cp*, L₁ = CO, L₂ = PMe₃ (**3a**) or P(OMe)₃ (**4a**); and (c) Cp' = Cp*, L₁ = L₂ = CO (**2a**), PMe₃ (**5a**), dmpe (**6a**), or P(OMe)₃ (**7a**)). Evidence has been presented in support of a proposed mechanism that involves one-electron reduction of the aryldiazenido complex cation in **1b–7b** to the neutral 19-electron intermediate Cp'Re(L₁)(L₂)(*p*-N₂C₆H₄OMe), followed by C–N bond homolysis to give **1a–7a** plus the *p*-methoxyphenyl radical that, in turn, yields anisole by hydrogen atom abstraction from the solvent. The measured cathodic wave peak potentials of **1b–7b** have been found to be a good indication of whether chemical reduction by the various reductants studied is successful in producing **1a–7a**. The mechanism of NaBH₄ reduction of **2b** has been shown to be different from the one-electron reduction. The intermediate aryldiazene complex Cp*Re(CO)₂(*p*-NHNC₆H₄OMe) is formed first and is thermally unstable, yielding the dinitrogen complex **2a** and anisole. This is not a general reaction for all of the aryldiazenido complexes studied, however. For example, no reaction occurs between NaBH₄ and the bis PMe₃ complex **5b**.

Experimental Section

General Methods. All manipulations were performed under nitrogen or argon by using standard Schlenk, drybox, or vacuum line techniques unless stated otherwise. Drybox manipulations were carried out in a nitrogen-filled Vacuum Atmospheres HE-493 Dri-Lab with attached Dri-Train.

All NMR data were recorded on a Bruker AMX 400 instrument at operating frequencies of 400.1, 162.0, 100.6, 40.5, and 28.9 MHz for ¹H, ³¹P, ¹³C, ¹⁵N, and ¹⁴N nuclei, respectively. ¹H and ¹³C NMR chemical shifts are reported in ppm downfield (positive) of tetramethylsilane. ³¹P NMR chemical shifts are referenced to 85% H₃PO₄. ¹⁴N and ¹⁵N NMR chemical shifts are referenced to external nitromethane (MeNO₂). Acetone-*d*₆ and methanol-*d*₄ were used as solvents for all the low-temperature NMR work. The term "virtual doublet" refers to

(21) Herrmann, W. A.; Albach, R. W.; Behm, J. J. *Chem. Soc., Chem. Commun.* **1991**, 367.

(22) Bard, A. J.; Fan, F.-R. F.; Mirkin, M. V. In *Electroanalytical Chemistry*; Bard, A. J., Ed.; Marcel Dekker: New York, 1993; Vol. 18, p 243.

the non-first-order multiplet (filled-in doublet)²³ which is seen in some of the ¹H NMR spectra; the apparent coupling constant is given by the separation between the two outside peaks. Electron spin resonance (ESR) spectra were recorded both at room temperature and at low temperature on a Varian E-4 instrument. Gas chromatography of the solutions after chemical and electrochemical reductions were complete was performed on a Hewlett-Packard 5890 A Series gas chromatograph containing a DB-1 capillary column and equipped with a Hewlett-Packard 3392 A integrator. Identification of the chromatographic peak for anisole was made by comparison with that of the authentic compound.

The details for the preparation and purification of the cationic rhenium aryldiazenido complexes have been provided elsewhere.^{10,24} Methanol and acetone were distilled from calcium sulfate under nitrogen and used immediately. Hexamethylphosphoramide (HMPA) (Aldrich Chemical Co.) was distilled from calcium hydride and stored over 4 Å molecular sieves, which had been activated by drying under vacuum at 573 K for several days. Anisole (Fisher Scientific Co.) was used as received. Sodium metal (BDH Chemicals Ltd.) was washed with hexane prior to use and was freshly cut. Mercury (Aldrich) was cleaned by filtration through fine filter paper and distilled under vacuum. Ammonia gas (Linde Union Carbide) was used as purchased. Sodium borohydride (BDH) and lithium aluminum hydride (Alfa Products, Ventron Division) were used as purchased and were stored under nitrogen. The triphenylmethyl radical (Ph₃C[•]) was synthesized by zinc reduction of triphenylchloromethane (Ph₃CCl)²⁵ which was prepared by reaction of triphenylmethanol (Ph₃COH) (Aldrich) with acetyl chloride.²⁶ Cobaltocene (Cp₂Co) was prepared by reaction of anhydrous cobalt(II) chloride (Alfa) with sodium cyclopentadienide prepared from sodium and dicyclopentadiene (Aldrich)²⁷ and was sublimed under vacuum onto a dry ice-cooled cold finger before use.

Preparation of CpRe(CO)₂(N₂) (1a) and 1a-¹⁵N_α. A 5-fold stoichiometric excess of Cp₂Co was dissolved in a minimum amount of acetone (5 mL) and then added *via* syringe to a solution of the cationic dicarbonyl complex **1b** or **1b-¹⁵N_α** (100 mg, 0.189 mmol) in acetone (10 mL) at room temperature. The IR spectrum of this mixture recorded immediately after the cobaltocene addition showed the total disappearance of the cationic complex and only the presence of absorptions due to the dinitrogen complex **1a** or **1a-¹⁵N_α**. Diethyl ether (20 mL) was added to precipitate [Cp₂Co][BF₄], and the mixture was stirred for 30 min. The solution was filtered through a short column of Celite, and the solvent was removed under vacuum to give a pale brown oil. The oil was absorbed by a small amount of neutral alumina and dried under vacuum, and the mixture was chromatographed on alumina. Elution with hexane afforded **1a** or **1a-¹⁵N_α** as a pale yellow colored microcrystalline solid in 87% yield (55 mg, 0.16 mmol). IR (hexane): 2145 cm⁻¹ ν(NN) (2110 cm⁻¹ for ¹⁵N_α-labeled complex); 1973, 1919 cm⁻¹ ν(CO). ¹H NMR (CDCl₃): δ 5.23 (s, 5H, Cp). ¹³C{¹H} NMR (CDCl₃): δ 93.72 (s, Cp), 195.79 (s, CO). ¹⁵N NMR (acetone-*d*₆): δ -120.9 (s, ¹⁵N_α). ¹⁴N NMR (acetone-*d*₆): δ -120 (s, ¹⁴N_α), -26 (s, ¹⁴N_β). MS (EI): *m/z* 336 (337 in **1a-¹⁵N_α**) (M⁺), 308 (M⁺ - N₂). Anal. Calcd: C, 25.06; H, 1.49; N, 8.35. Found: C, 24.97; H, 1.71; N, 8.43.

Preparation of Cp*Re(CO)₂(N₂) (2a) and 2a-¹⁵N_α. A 5-fold stoichiometric excess of Cp₂Co was dissolved in a minimum amount of acetone (5 mL) and then added *via* syringe to a solution of the cationic dicarbonyl complex **2b** or

2b-¹⁵N_α (100 mg, 0.167 mmol) in acetone (10 mL) at room temperature. The IR spectrum of this mixture recorded immediately after the cobaltocene addition showed the total disappearance of the cationic complex and only the presence of absorptions corresponding to the dinitrogen complex **2a** or **2a-¹⁵N_α**. Purification following the procedure used for complex **1a** gave **2a** or **2a-¹⁵N_α** as a pale yellow colored microcrystalline solid in 89% yield (60 mg, 0.15 mmol). IR (hexane): 2125 cm⁻¹ ν(NN) (2092 cm⁻¹ for ¹⁵N_α-labeled complex); 1954, 1902 cm⁻¹ ν(CO). ¹H NMR (CDCl₃): δ 2.09 (s, 15H, Cp*). ¹³C{¹H} NMR (CDCl₃): δ 10.38 (s, C₅Me₅), 96.27 (s, C₅Me₅), 200.09 (s, CO). ¹⁵N NMR (acetone-*d*₆): δ -110.8 (s, ¹⁵N_α). ¹⁴N NMR (acetone-*d*₆): δ -110 (s, ¹⁴N_α), -26 (s, ¹⁴N_β). MS (EI): *m/z* 406 (407 in **2a-¹⁵N_α**) (M⁺), 378 (M⁺ - N₂). Anal. Calcd: C, 35.55; H, 3.70; N, 6.91. Found: C, 35.52; H, 3.74; N, 6.98.

Preparation of Cp*Re(CO)(PMe₃)(N₂) (3a) and 3a-¹⁵N_α. A sodium amalgam was prepared by adding small freshly cut pieces of sodium metal (5-fold stoichiometric excess) to a pool of mercury (5 mL) under argon with gentle stirring. The orange-brown solution of the cationic carbonyl phosphine complex **3b** or **3b-¹⁵N_α** (100 mg, 0.155 mmol) in THF (10 mL) was then added *via* syringe to the sodium amalgam at room temperature, and the mixture was vigorously stirred for 30 min. An IR spectrum of the resulting yellow-brown solution recorded at this time showed the total disappearance of the cationic complex and only the presence of absorptions corresponding to the dinitrogen complex **3a** or **3a-¹⁵N_α**. The solution was filtered through a short column of Celite, and the solvent was removed under vacuum to give a pale brown oil. The oil was absorbed by a small amount of neutral alumina and dried under vacuum, and the mixture was chromatographed on alumina. Elution with hexane afforded **3a** or **3a-¹⁵N_α** as a pale yellow colored microcrystalline solid in 82% yield (58 mg, 0.13 mmol). IR (hexane): 2044 cm⁻¹ ν(NN) (2011 cm⁻¹ for ¹⁵N_α-labeled complex); 1865 cm⁻¹ ν(CO). ¹H NMR (CDCl₃): δ 1.57 (d, 9H, PMe₃, J_{H-P} = 8.7 Hz), 2.00 (d, 15H, Cp*, J_{H-P} = 0.7 Hz). ¹³C{¹H} NMR (CDCl₃): δ 10.76 (s, C₅Me₅), 20.67 (d, PMe₃, J_{C-P} = 33 Hz), 93.29 (s, C₅Me₅), 207.18 (d, CO, J_{C-P} = 7 Hz). ³¹P{¹H} NMR (CDCl₃): δ -29.86 (s, PMe₃). ¹⁵N NMR (acetone-*d*₆): δ -91.3 (s, ¹⁵N_α). ¹⁵N NMR (CD₃CN): δ -93.2 (s, ¹⁵N_α). ¹⁴N NMR (acetone-*d*₆): δ -91 (s, ¹⁴N_α), -30 (s, ¹⁴N_β). MS (EI): *m/z* 454 (M⁺), 426 (M⁺ - N₂). Anal. Calcd: C, 37.08; H, 5.30; N, 6.16. Found: C, 36.92; H, 5.42; N, 6.28.

Preparation of Cp*Re(CO){P(OMe)₃}(N₂) (4a) and 4a-¹⁵N_α. A procedure similar to that described for the preparation of **2a** was used. The carbonyl phosphite dinitrogen complex **4a** or **4a-¹⁵N_α** was obtained in 79% yield as a pale yellow microcrystalline solid (57 mg, 0.11 mmol). IR (hexane): 2078, 2066 cm⁻¹ ν(NN) (2045, 2033 cm⁻¹ for ¹⁵N_α-labeled complex); 1877 cm⁻¹ ν(CO). ¹H NMR (CDCl₃): δ 2.04 (d, 15H, Cp*, J_{H-P} = 0.8 Hz), 3.52 (d, 9H, P(OMe)₃, J_{H-P} = 12.1 Hz). ¹³C{¹H} NMR (CDCl₃): δ 10.31 (s, C₅Me₅), 51.27 (s, P(OMe)₃), 94.15 (s, C₅Me₅), 204.96 (d, CO, J_{C-P} = 12 Hz). ³¹P{¹H} NMR (CDCl₃): δ 139.12 (s, P(OMe)₃). ¹⁵N NMR (acetone-*d*₆): δ -99.4 (s, ¹⁵N_α). ¹⁵N NMR (CD₃CN): δ -100.8 (s, ¹⁵N_α). ¹⁴N NMR (acetone-*d*₆): δ -99 (s, ¹⁴N_α), -29 (s, ¹⁴N_β). MS (EI): *m/z* 502 (M⁺), 474 (M⁺ - N₂). Anal. Calcd: C, 33.46; H, 4.78; N, 5.57. Found: C, 33.37; H, 4.89; N, 5.69.

Preparation of Cp*Re(PMe₃)₂(N₂) (5a), 5a-¹⁵N_α, and 5a-¹⁵N_β. A procedure similar to that described for the preparation of **3a** was used. The bis(trimethylphosphine) dinitrogen complex, **5a**, **5a-¹⁵N_α**, or **5a-¹⁵N_β** (synthesized from [Cp*Re(PMe₃)₂(*p*-¹⁵NC₆H₅)] [BF₄]), was obtained in 74% yield as a pale yellow microcrystalline solid (53 mg, 0.11 mmol). IR (hexane): 1975 cm⁻¹ ν(NN) (1943 cm⁻¹ for ¹⁵N_α- or ¹⁵N_β-labeled complex). ¹H NMR (acetone-*d*₆): δ 1.48 (virtual doublet, 18H, PMe₃, J_{app} = 7.4 Hz), 1.88 (t, 15H, Cp*, J_{H-P} = 0.7 Hz). ³¹P{¹H} NMR (acetone-*d*₆): δ -35.31 (s, PMe₃). ¹⁵N NMR (acetone-*d*₆): δ -82.1 (s, ¹⁵N_α), -51.7 (s, ¹⁵N_β). ¹⁴N NMR (acetone-*d*₆): δ -82 (s, ¹⁴N_α), -49 (s, ¹⁴N_β). MS (EI): *m/z* 502 (M⁺), 474 (M⁺ - N₂). Anal. Calcd: C, 38.31; H, 6.58; N, 5.59. Found: C, 38.01; H, 6.92; N, 5.87.

(23) (a) Wenzel, T. T.; Bergman, R. G. *J. Am. Chem. Soc.* **1986**, *108*, 4856. (b) Tilley, D. T.; Grubbs, R. H.; Bercaw, J. E. *Organometallics* **1984**, *3*, 274.

(24) Cusanelli, A.; Batchelor, R. J.; Einstein, F. W. B.; Sutton, D. *Organometallics* **1994**, *13*, 5096.

(25) Sabacky, M. J.; Johnson, C. S.; Smith, R. G.; Gutowsky, H. S.; Martin, J. C. *J. Am. Chem. Soc.* **1967**, *89*, 2054.

(26) Bachmann, W. E. *Org. Syntheses* **1943**, *23*, 100.

(27) Wilkinson, G.; Cotton, F. A.; Birmingham, J. M. *J. Inorg. Nucl. Chem.* **1956**, *2*, 95.

Preparation of Cp*Re(dmpe)(N₂) (6a). A procedure similar to that described for the preparation of **3a** was used. The bidentate phosphine dinitrogen complex **6a** was obtained in 79% yield as a pale yellow microcrystalline solid (57 mg, 0.11 mmol). IR (hexane): 1977 cm⁻¹ ν(NN). ¹H NMR (acetone-*d*₆): δ 1.33 (d, 6H, PMe₂CH₂CH₂Me₂P, J_{H-P} = 7.9 Hz), 1.35 (m, 4H, PMe₂CH₂CH₂Me₂P), 1.42 (d, 6H, PMe₂CH₂CH₂Me₂P, J_{H-P} = 7.8 Hz), 1.92 (s, 15H, Cp*). ³¹P{¹H} NMR (acetone-*d*₆): δ -16.88 (s, dmpe). MS (EI): *m/z* 500 (M⁺), 472 (M⁺ - N₂). Anal. Calcd: C, 38.46; H, 6.21; N, 5.61. Found: C, 38.22; H, 6.37; N, 5.81.

Preparation of Cp*Re(P(OMe)₃)₂(N₂) (7a). A procedure similar to that described for the preparation of **3a** was used. The bis(trimethylphosphite) dinitrogen complex **7a** was obtained in 71% yield as a pale yellow microcrystalline solid (54 mg, 0.090 mmol). IR (hexane): 2014 cm⁻¹ ν(NN). ¹H NMR (acetone-*d*₆): δ 1.87 (t, 15H, Cp*, J_{H-P} = 0.8 Hz), 3.45 (virtual doublet, 18H, P(OMe)₃, J_{app} = 11.5 Hz). ³¹P{¹H} NMR (acetone-*d*₆): δ 138.80 (s, P(OMe)₃). MS (EI): *m/z* 598 (M⁺), 570 (M⁺ - N₂). Anal. Calcd: C, 32.15; H, 5.53; N, 4.69. Found: C, 31.79; H, 5.78; N, 4.93.

Reaction of [Cp*Re(CO)₂(*p*-N₂C₆H₄OMe)][BF₄] (2b) with LiAlH₄. A 2-fold stoichiometric excess of LiAlH₄ was added as a solid to a solution of the cationic dicarbonyl complex **2b** (50 mg, 0.083 mmol) in methanol (10 mL) at room temperature. Upon addition, an immediate reaction occurred, with considerable gas evolution, and the color of the solution changed from red-brown to yellow. The solution was then filtered through a short column of Celite. Removal of the solvent under vacuum and subsequent extraction with hexane (3 × 20 mL) gave the methoxycarbonyl complex Cp*Re(CO)(COOMe)(*p*-N₂C₆H₄OMe) as a yellow solid in 89% yield (40 mg, 0.074 mmol). The dinitrogen complex **2a** was not formed in this reaction. IR (MeOH): 1937 cm⁻¹ ν(CO); 1632 cm⁻¹ ν(NN); 1614 ν(COOMe). ¹H NMR (CDCl₃): δ 2.10 (s, 15H, Cp*), 3.66 (s, 3H, COOMe), 3.82 (s, 3H, OMe), 6.93 (d, 2H, C₆H₄), 7.45 (d, 2H, C₆H₄).

Reaction of [Cp*Re(CO)₂(*p*-N₂C₆H₄OMe)][BF₄] (2b) with NaBH₄. A 2-fold stoichiometric excess of NaBH₄ was added as a solid to a solution of the cationic dicarbonyl complex **2b** (50 mg, 0.083 mmol) in acetone (10 mL) at room temperature. An instantaneous reaction took place, and the color of the solution changed from red-brown to deep red. An IR spectrum of this solution demonstrated the total disappearance of **2b** and the presence of minor absorptions corresponding to the dinitrogen complex **2a** which were also accompanied by major absorptions at 1917 and 1852 cm⁻¹. The solution was stirred for 1 h, during which time the color of the solution changed from red to yellow. An IR spectrum then obtained showed only the presence of **2a**. The solvent was removed under vacuum to give a yellow oil. The oil was then absorbed by a small amount of neutral alumina and dried under vacuum, and the mixture was then chromatographed on alumina. Elution with hexane afforded **2a** in 47% yield (16 mg, 0.039 mmol).

Low-Temperature ¹H, ¹³C{¹H}, and ¹⁵N NMR Experiments: Reaction of [Cp*Re(CO)₂(*p*-N₂C₆H₄OMe)][BF₄] (2b) or 2b-¹⁵N_α with NaBH₄. A solution of the cationic dicarbonyl complex **2b** or **2b-¹⁵N_α** in acetone-*d*₆ was transferred into an NMR tube (5 mm tube for ¹H and ¹³C{¹H}); 10 mm tube for ¹⁵N) which was kept in a Schlenk tube under a positive pressure of argon. The Schlenk tube containing the NMR solution was then cooled to 195 K in a dry ice-acetone bath. With a strong purge of argon, addition of a 2-fold stoichiometric excess of solid NaBH₄ directly to the NMR tube lead to the formation of a deep red solution. The NMR tube was quickly removed from the cold temperature bath and placed into the Bruker AMX 400 spectrometer whose cooling unit had been previously set to 233 K. The NMR sample was equilibrated for 30 min at this temperature before spectral acquisition. An identical procedure was used for obtaining spectra for each of the NMR active nuclei. The species responsible for the red solution was assigned as the neutral aryldiazene complex Cp*Re(CO)₂(*p*-NHNC₆H₄OMe). IR (acetone): 1917, 1852 cm⁻¹

ν(CO). ¹H NMR (acetone-*d*₆, 233 K): δ 2.02 (s, 15H, Cp*), 3.83 (s, 3H, OMe), 6.97 (d, 2H, C₆H₄), 7.60 (d, 2H, C₆H₄), 15.68 (broad singlet, 1H, NH) (d, 1H, ¹⁵N_αH, J_{H-N} = 69 Hz). ¹³C-{¹H} NMR (acetone-*d*₆, 233 K): δ 10.15 (s, C₅Me₅), 55.58 (s, OMe), 99.35 (s, C₅Me₅), 115.13, 120.99, 149.80, 160.03 (s, C₆H₄), 208.32 (s, CO). ¹³C{¹H} NMR (methanol-*d*₄, 233 K): δ 10.19 (s, C₅Me₅), 55.61 (s, OMe), 99.41 (s, C₅Me₅), 115.32, 121.22, 149.97, 160.65 (s, C₆H₄), 208.79 (s, CO). ¹⁵N NMR (acetone-*d*₆, 233 K): δ -46.7 (d, ¹⁵N_αH, J_{N-H} = 69 Hz).

Reaction of [Cp*Re(CO)₂(*p*-N₂C₆H₄OMe)][BF₄] (2b) with HMPA. The cationic dicarbonyl complex **2b** (50 mg, 0.083 mmol) was added directly to neat hexamethylphosphoramide (HMPA) (10 mL) at room temperature. An IR spectrum recorded immediately after the addition showed the presence of absorptions corresponding to the starting material **2b** as well as the newly formed dinitrogen complex **2a**. The solution was stirred for 24 h. No apparent color change was noted. An IR spectrum obtained at this time displayed the complete disappearance of the cationic complex and only the presence of absorptions due to **2a**. The dinitrogen complex was extracted with diethyl ether (2 × 20 mL), and the extractions were filtered through a column of Celite. The solvent was removed under vacuum to give a pale brown oil. The oil was then absorbed by a small amount of neutral alumina and dried under vacuum, and the mixture was chromatographed on alumina. Elution with hexane afforded **2a** in 35% yield (12 mg, 0.029 mmol).

Reaction of [Cp*Re(CO)₂(*p*-N₂C₆H₄OMe)][BF₄] (2b) with PMe₃. A 10-fold stoichiometric excess of neat PMe₃ was added *via* syringe to a solution of the cationic dicarbonyl complex **2b** (50 mg, 0.083 mmol) in acetone (10 mL) at room temperature. The solution was stirred for 30 min. No apparent color change was noted after this time. An IR spectrum of this solution showed the total disappearance of the cationic complex and only the presence of absorptions corresponding to the dinitrogen complex **2a**. The solvent was then removed under vacuum, and the remaining pale brown oil was extracted with diethyl ether (2 × 20 mL). The ether extractions were concentrated to ca. 2 mL under vacuum and chromatographed on a neutral alumina column. Elution with hexane produced **2a** in 42% yield (14 mg, 0.035 mmol).

Reaction of [CpRe(CO)₂(*p*-N₂C₆H₄OMe)][BF₄] (1b) with Ph₃C. A solution of the triphenylmethyl (trityl) radical (Ph₃C) was prepared by reduction of the corresponding chloride Ph₃CCl with zinc dust in THF. A 10-fold stoichiometric excess of the yellow triphenylmethyl radical solution was then added by cannula to an orange-brown solution of the cationic dicarbonyl complex **1b** (50 mg, 0.095 mmol) in CH₂Cl₂ (10 mL) at room temperature. The resulting orange solution was stirred for 30 min. An IR spectrum measured at this time showed the total disappearance of **1b** and the presence of absorptions corresponding exclusively to the dinitrogen complex **1a**. The solvent was then removed under vacuum, and the remaining pale brown oil was extracted with diethyl ether (2 × 20 mL). The ether extractions were concentrated to ca. 2 mL under vacuum and chromatographed on a neutral alumina column. Elution with hexane yielded **1a** in 58% yield (18 mg, 0.055 mmol).

Reaction of [Cp*Re(CO)₂(*p*-N₂C₆H₄OMe)][BF₄] (2b) with Ph₃C. A procedure identical to that described for the Cp analog **1b** was used. The dinitrogen complex **2a** was obtained in 63% yield (21 mg, 0.052 mmol).

Reaction of [Cp*Re(CO)₂(*p*-N₂C₆H₄OMe)][BF₄] (2b) with Na/THF. A stoichiometric amount of sodium metal was added in small pieces to a solution of the cationic dicarbonyl complex **2b** (50 mg, 0.083 mmol) in THF (10 mL) at room temperature. The solution was then sonicated for 60 min. During this time the red-brown solution of **2b** became yellow-brown. An IR spectrum of this solution showed the complete disappearance of **2b** and the presence of minor absorptions corresponding to the dinitrogen complex **2a**. Major absorptions at 1929 and 1615 cm⁻¹ were present as well. Attempts to isolate this

unknown neutral species were not successful due to its low stability to silica gel or neutral alumina columns. A partially purified sample obtained by extraction with hexane gave unsatisfactory ^1H NMR and mass spectra. Column chromatography using hexane as the elutant gave **2a** in 17% yield (6 mg, 0.014 mmol).

Reaction of $[\text{Cp}^*\text{Re}(\text{CO})_2(p\text{-N}_2\text{C}_6\text{H}_4\text{OMe})][\text{BF}_4]$ (2b**) with Na/NH_3 .** A two-necked flask was equipped with a dry ice condenser containing a dry ice-acetone mixture. The flask was also fitted with an ammonia gas line, so as to provide the solvent for the reaction by condensation, and a gas line to maintain a nitrogen atmosphere. The cationic dicarbonyl complex **2b** (50 mg, 0.083 mmol) was then added to the colorless liquid ammonia (100 mL). To this solution was added a minimum amount of THF (10 mL) to completely solubilize **2b**. A stoichiometric amount of sodium metal, as monitored by the color of the mixture (blue color indicates excess sodium), was then added in small pieces to the reaction flask. The mixture was stirred for 30 min. The ammonia was then allowed to escape, and the remaining THF solution was filtered through a short column of Celite. Removal of the solvent under vacuum and subsequent extraction with hexane (3 \times 20 mL) gave the neutral carbamoyl complex $\text{Cp}^*\text{Re}(\text{CO})_2(\text{CONH}_2)(p\text{-N}_2\text{C}_6\text{H}_4\text{OMe})$ as a yellow solid in 78% yield (34 mg, 0.065 mmol). The dinitrogen complex **2a** was not formed in this reaction. IR (CH_2Cl_2): 1931 cm^{-1} $\nu(\text{CO})$; 1625 cm^{-1} $\nu(\text{NN})$; 1586 cm^{-1} $\nu(\text{CONH}_2)$. ^1H NMR (CDCl_3): δ 2.12 (s, 15H, Cp^*), 3.83 (s, 3H, OMe), 6.95 (d, 2H, C_6H_4), 7.29 (d, 2H, C_6H_4); $\delta_{\text{N-H}}$ was not observed.

Reaction of $[\text{Cp}^*\text{Re}(\text{PMe}_3)_2(p\text{-N}_2\text{C}_6\text{H}_4\text{OMe})][\text{BF}_4]$ (5b**) with Na/NH_3 .** The bis(trimethylphosphine) complex **5b** (50 mg, 0.072 mmol) was taken up in THF (10 mL) and then added to liquid ammonia (100 mL) as described above for **2b**. A stoichiometric amount of sodium metal, as monitored by the color of the mixture, was added in small pieces to the reaction flask. The mixture was stirred for 30 min. The ammonia was then allowed to escape, and the remaining THF solution was filtered through a short column of Celite. The solvent was removed under vacuum, and the remaining yellow-brown oil was extracted with diethyl ether (2 \times 20 mL). The ether extractions were concentrated to ca. 2 mL under vacuum and chromatographed on a neutral alumina column. Elution with hexane gave *p*-anisidine ($\text{NH}_2\text{C}_6\text{H}_4\text{OMe}$). This was verified by GC-MS and by comparison of its ^1H NMR spectrum to that of an authentic sample. Using diethyl ether as the elutant afforded the dihydrido complex *trans*- $\text{Cp}^*\text{Re}(\text{PMe}_3)_2\text{H}_2$ ^{13a} as a yellow solid in 58% yield (20 mg, 0.042 mmol). (The dinitrogen complex **2a** was not formed in this reaction). ^1H NMR (benzene-*d*₆): δ 2.04 (s, 15H, Cp^*), 1.50 (virtual doublet, 18H, PMe_3 , $J_{\text{app}} = 7.5$ Hz), -11.89 (t, 2H, ReH , $J_{\text{H-P}} = 43.5$ Hz). $^{31}\text{P}\{^1\text{H}\}$ NMR (benzene-*d*₆): δ -37.57 (s, PMe_3).

Electrochemical Methods. Acetonitrile was distilled from calcium hydride under a nitrogen atmosphere and used immediately. The supporting electrolyte was electrometric grade tetraethylammonium perchlorate (TEAP) (Anachemia Science Inc.), which was purified by recrystallization from distilled water (2 times) and then dried under vacuum for 2 days.

Cyclic Voltammetry. Experiments were performed in a single-compartment cell. The working electrode was a stationary, mirror-polished, platinum (Pt) disk which measured 1 mm in diameter (Pine Instrument Co.). The Pt disk was surrounded by a cylindrical Teflon collar of 2.5 mm thickness. Before each experiment, the electrode was dipped sequentially in concentrated HNO_3 , then in saturated FeSO_4 in 2 M H_2SO_4 , and finally rinsed thoroughly with distilled water; this procedure provided a consistent electrode surface. A Pt wire was used as the counter electrode. The reference electrode was either a silver wire in a saturated solution of silver chloride (Ag/AgCl) or a standard calomel electrode (SCE). Results are reported with respect to SCE.

The sample solutions were thoroughly deaerated with oxygen-free N_2 , and an N_2 atmosphere was maintained through-

out the voltammetric measurements. All experiments were carried out at room temperature and used solutions of 0.2 M TEAP (as the supporting electrolyte) in MeCN. Concentrations of analytes were 1.0 mM for all experiments. The scan rate was 0.2 V/s unless stated otherwise. The CV apparatus consisted of a Princeton Applied Research EG&G 175 programmer and an EG&G 170 potentiostat. Electrical responses were recorded on a Hewlett-Packard 7046A X-Y recorder. CV measurements were carried out as follows. An acetonitrile solution containing the electrolyte was placed in the cell and then deaerated with a continuous stream of nitrogen gas until a cyclic voltammogram of the solution showed no fluctuations in the current. A solution of the particular cationic rhenium aryldiazenido complex in a minimum amount of degassed acetonitrile was injected into the cell. A cyclic voltammogram of the solution using a potential range of +2.0 to -2.0 V was then recorded.

Controlled Potential Electrolysis. A two-compartment cell was used. A sintered-glass disk of fine porosity separated the counter and working compartments. The working electrode was a Pt gauze. A Pt counter electrode was positioned above the working electrode to obtain a uniform potential distribution. An Ag/AgCl or SCE reference electrode was positioned close to the working electrode. The CPE apparatus consisted of a Princeton Applied Research EG&G 175 programmer, an EG&G 170 potentiostat, and a EG&G 179 coulometer. CPE measurements and analysis of the products were carried out as follows. The electrolyte solution was placed in the working electrode compartment of the cell. A small amount of the same solution was added to the counter electrode compartment until the solution levels were equalized. The solution in the working compartment was then deaerated with nitrogen gas while being stirred continuously. Pre-electrolysis was carried out until the background current became negligible. A 0.5 mL sample of the electrolyte solution was extracted by syringe, and an IR spectrum was collected. The spectrum would serve as a background for subsequent IR spectra. A solution of the particular cationic rhenium aryldiazenido complex in a minimum amount of degassed acetonitrile was then injected into the working compartment. A sample of the electrolysis solution was withdrawn, and an IR spectrum was recorded. The spectrum was then corrected by subtracting the background spectrum and was used as a reference from which to monitor the electrolysis. The electrolysis then proceeded at a given potential. At specific time intervals aliquots of the solution were withdrawn and analyzed by IR spectroscopy.

Preparation of the Dinitrogen Complexes 1a-3a by CPE. Controlled potential electrolysis (CPE) was carried out on the cationic rhenium aryldiazenido complexes **1b** (53 mg, 0.10 mmol), **2b** (60 mg, 0.10 mmol), and **3b** (65 mg, 0.10 mmol) using the procedure just described at the appropriate reduction potential (as determined by CV). An IR spectrum recorded after the bulk electrolysis was complete showed the total disappearance of the cationic complex and only the presence of absorptions corresponding to the respective dinitrogen complexes **1a-3a**. For **1a**: IR (MeCN containing TEAP) 2141 cm^{-1} $\nu(\text{NN})$; 1956, 1894 cm^{-1} $\nu(\text{CO})$. For **2a**: IR (MeCN containing TEAP) 2121 cm^{-1} $\nu(\text{NN})$; 1939, 1879 cm^{-1} $\nu(\text{CO})$. For **3a**: IR (MeCN containing TEAP) 2027 cm^{-1} $\nu(\text{NN})$; 1834 cm^{-1} $\nu(\text{CO})$. The solvent was removed under vacuum and the remaining solid was extracted with diethyl ether (3 \times 20 mL). The ether extractions were concentrated to ca. 2 mL under vacuum, and chromatographed on a neutral alumina column. Elution with hexane yielded **1a** in 73% yield (24 mg, 0.073 mmol), **2a** in 78% yield (32 mg, 0.078 mmol), and **3a** in 74% yield (34 mg, 0.074 mmol).

Acknowledgment. This work was supported by the Natural Sciences and Research Council of Canada. We thank Dr. S. Holdcroft for the use of electrochemical equipment and Dr. N. D. Lowe for help with cyclic voltammetry measurements.

Organotransition-Metal Metallocarboranes. 40. Regiospecific Halogenation of Transition-Metal Small Carborane Complexes^{1,2}

Kenneth E. Stockman, Dawn L. Garrett,[†] and Russell N. Grimes*

Department of Chemistry, University of Virginia, Charlottesville, Virginia 22901

Received May 12, 1995[⊙]

Methods for efficient, controlled direct halogenation of C₂B₃ and C₂B₄ carborane ligands in neutral *nido*- and *closo*-metallocarborane sandwich complexes are described. In an extension of our earlier work in this area, reactions of *nido*-Cp'Co(2,3-Et₂C₂B₃H₅) (Cp' = Cp*, Cp; Cp* = η⁵-C₅Me₅) with *N*-halosuccinimides placed Cl, Br, or I substituents on B(4) and/or B(6) but not on the middle boron (B(5)). In contrast, similar treatment of *closo*-LM-(2,3-Et₂C₂B₄H₄) species in which LM is Cp'Co, Cp*FeH, (η⁶-C₈H₁₀)Fe, or (η⁶-MeC₆H₄CHMe₂)-Ru gave *only* B(5)-monohalogen products. However, the triple-decker sandwich complex CpCo(2,3-Et₂C₂B₃H₅)CoCp was readily tribrominated by *N*-bromosuccinimide. Reactions of Cp'Co(Et₂C₂B₄H₄) with Cl₂ rapidly formed the respective B(5)-Cl derivatives, which in turn were converted to the B(4,5,6)-Cl₃ species; analogous reactions with Br₂ and I₂ were much slower and gave essentially only B(5)-monosubstituted products. The Cp'Co(Et₂C₂B₄H₃-5-X) derivatives (X = Cl, Br, I) were decapitated with TMEDA to give the corresponding *nido*-Cp'Co(Et₂C₂B₃H₄-5-X) products. The reaction of Cp*Fe^{II}H(Et₂C₂B₄H₄) with TMEDA was found to both deprotonate and decapitate the complex, affording respectively Cp*Fe^{III}-(Et₂C₂B₄H₄) and the previously unknown *nido*-Cp*Fe^{III}(Et₂C₂B₃H₅) complex. The new compounds were isolated via column chromatography and obtained in most cases as air-stable colored crystalline solids, characterized via multinuclear NMR, FTIR and mass spectroscopy.

Introduction

Recent papers in this series have described the synthesis of a variety of linked-cage and multidecker sandwich complexes from MC₂B₃ or MC₂B₄ small metallocarborane synthons where M is a transition metal.^{1,3} In the course of this work our group has developed several different synthetic approaches, in all of which substituents on the carborane ligand(s) play a major role. The introduction of appropriate functional groups allows one to tune the electronic properties of the metallocarborane substrate, as in the construction via metal stacking reactions of C₂B₃-bridged sandwiches having 2–6 rings and linked-sandwich systems having up to 17 metal centers.^{1a,3} As we have demonstrated, these reactions are promoted by the presence of Cl, acetyl, or other electron-withdrawing units on the carborane ligands, while certain other groups—e.g., ethyl—inhibit or block the stacking process. In other synthetically useful reactions, the substituents are directly involved; for example B-halogenated MC₂B_n clusters can be directly linked via Wurtz-type reactions

with sodium.⁴ Similarly, attachment of organic groups to the cage may permit the assembly of chain oligomers, polymers, or macrocycles via standard polymerization routes.

The importance of derivatization in this area has led us to devote considerable effort to the development of reliable, regiospecific routes to B- and C-functionalized small metallocarborane species.⁵ Methods for controlled halogenation are of particular significance, since halo-

(4) Wang, X.; Sabat, M.; Grimes, R. N. *Organometallics* 1995, 14, 4668.

(5) (a) Davis, J. H., Jr.; Attwood, M. D.; Grimes, R. N. *Organometallics* 1990, 9, 1171. (b) Piepgrass, K. W.; Grimes, R. N. *Organometallics* 1992, 11, 2397. (c) Piepgrass, K. W.; Stockman, K. E.; Sabat, M.; Grimes, R. N. *Organometallics* 1992, 11, 2404. (d) Benvenuto, M. A.; Grimes, R. N. *Inorg. Chem.* 1992, 31, 3897. (e) Benvenuto, M. A.; Sabat, M.; Grimes, R. N. *Inorg. Chem.* 1992, 31, 3904.

(6) Leading references: (a) Onak, T. P. In *Advances in Boron and the Boranes*; Liebman, J. F., Greenberg, A., Williams, R. E., Eds; Mol. Struct. Energ. 5; VCH: New York, 1988; pp 125–150. (b) Tomita, H.; Luu, H.; Onak, T. *Inorg. Chem.* 1991, 30, 812. (c) Nam, W.; Onak, T. *Inorg. Chem.* 1987, 26, 48. (d) Nam, W.; Onak, T. *Inorg. Chem.* 1987, 26, 1581. (e) Abdou, Z. J.; Abdou, G.; Onak, T.; Lee, S. *Inorg. Chem.* 1988, 25, 2678. (f) Ng, B.; Onak, T. *J. Fluorine Chem.* 1985, 27, 119. (g) Abdou, Z.; Soltis, M.; Oh, B.; Siwap, G.; Banuelos, T.; Nam, W.; Onak, T. *Inorg. Chem.* 1985, 24, 2363. (h) Ng, B.; Onak, T.; Banuelos, T.; Gomez, F.; Distefano, E. W. *Inorg. Chem.* 1985, 24, 4091. (i) Ng, B.; Onak, T.; Fuller, K. *Inorg. Chem.* 1985, 24, 4371. (j) Takimoto, C.; Siwapinyoyos, G.; Fuller, K.; Fung, A. P.; Liauw, L.; Jarvis, W.; Millhauser, G.; Onak, T. *Inorg. Chem.* 1980, 19, 107. (k) Dobbie, R. C.; Distefano, E. W.; Black, M.; Leach, J. B.; Onak, T. *J. Organomet. Chem.* 1976, 114, 233. (l) Maraschin, N. J.; Lagow, R. J. *Inorg. Chem.* 1975, 14, 1855. (m) Savory, C. G.; Wallbridge, M. G. H. *J. Chem. Soc., Dalton Trans.* 1974, 880. (n) Reilly, T. J.; Burg, A. B. *Inorg. Chem.* 1973, 12, 1450. (o) McAvoy, J. S.; Savory, C. G.; Wallbridge, M. G. H. *J. Chem. Soc. A* 1971, 3038. (p) Olsen, R. R.; Grimes, R. N. *Inorg. Chem.* 1971, 10, 1103. (q) Olsen, R. R.; Grimes, R. N. *J. Am. Chem. Soc.* 1970, 92, 5072. (r) Warren, R.; Paquin, D.; Onak, T.; Dunks, G.; Spielman, J. R. *Inorg. Chem.* 1970, 9, 2285. (s) Spielman, J. R.; Dunks, G. B.; Warren, R. *Inorg. Chem.* 1969, 8, 2172.

[†] Summer 1994 undergraduate research student from King College, Bristol, TN.

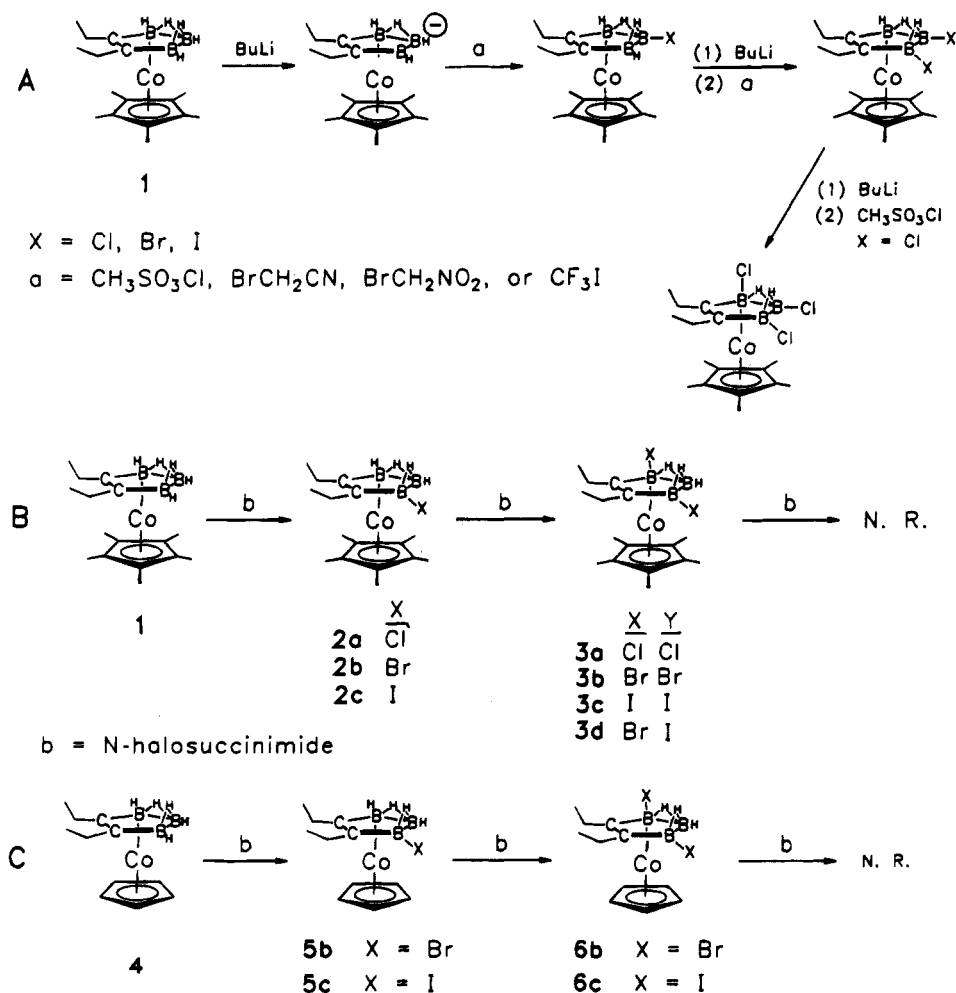
[⊙] Abstract published in *Advance ACS Abstracts*, September 1, 1995.

(1) (a) Part 39: Greiwe, P.; Sabat, M.; Grimes, R. N. *Organometallics* 1995, 14, 3683. (b) Part 38: Stockman, K. E.; Houseknecht, K. L.; Boring, E. A.; Sabat, M.; Finn, M. G.; Grimes, R. N. *Organometallics* 1995, 14, 3014. (c) Part 37: Stephan, M.; Müller, P.; Zenneck, U.; Pritzkow, H.; Siebert, W.; Grimes, R. N. *Inorg. Chem.* 1995, 34, 2058.

(2) Based in part on the Ph.D. thesis of K.E.S., University of Virginia, 1995.

(3) (a) Grimes, R. N. *Chem. Rev.* 1992, 92, 251. (b) Piepgrass, K. W.; Hölscher, M.; Meng, X.; Sabat, M.; Grimes, R. N. *Inorg. Chem.* 1992, 31, 5202. (c) Wang, X.; Sabat, M.; Grimes, R. N. *J. Am. Chem. Soc.* 1994, 116, 2687. (d) Meng, X.; Sabat, M.; Grimes, R. N. *J. Am. Chem. Soc.* 1993, 115, 6143.

Scheme 1



generated species play a multifaceted role in the synthesis of extended polymetallic cluster and sandwich systems.^{3d} Extensive studies on the halogenation of small carboranes⁶ (especially those of Onak and co-workers) have generated considerable insight into the substitution chemistry of those non-metal systems, which are structurally related but electronically distinct from the metal sandwich complexes of interest here. In an earlier publication^{5c} we described efficient regiospecific routes to mono-, di-, and tri-B-halo derivatives of *nido*-Cp*Co-(2,3-Et₂C₂B₃H₅) (1) where Cp* = η^5 -C₅Me₅, as shown in Scheme 1A,B.

In method A, reaction of the bridge-deprotonated cobaltacarborane monoanion with 1 equiv of an organohalogen reagent gives the B(5)-substituted product exclusively;^{5c} repetition of this sequence affords the dihalo and trihalo derivatives as shown. In contrast, treatment of *neutral* 1 with *N*-halosuccinimides (method B) effects substitution only at the B(4) and B(6) locations adjacent to the ring carbons, even when an excess of halogenating agent is employed.^{5c} Thus, the two approaches are complementary and permit the synthesis of a wide variety of B-halogenated species. Here we report the extension of this chemistry to a broad range of *nido*- and *closo*-metallacarborane substrates, including CpCo, Cp*Co, organoiron, and organoruthenium clusters and sandwich complexes, with emphasis on the synthetic rather than mechanistic aspects.

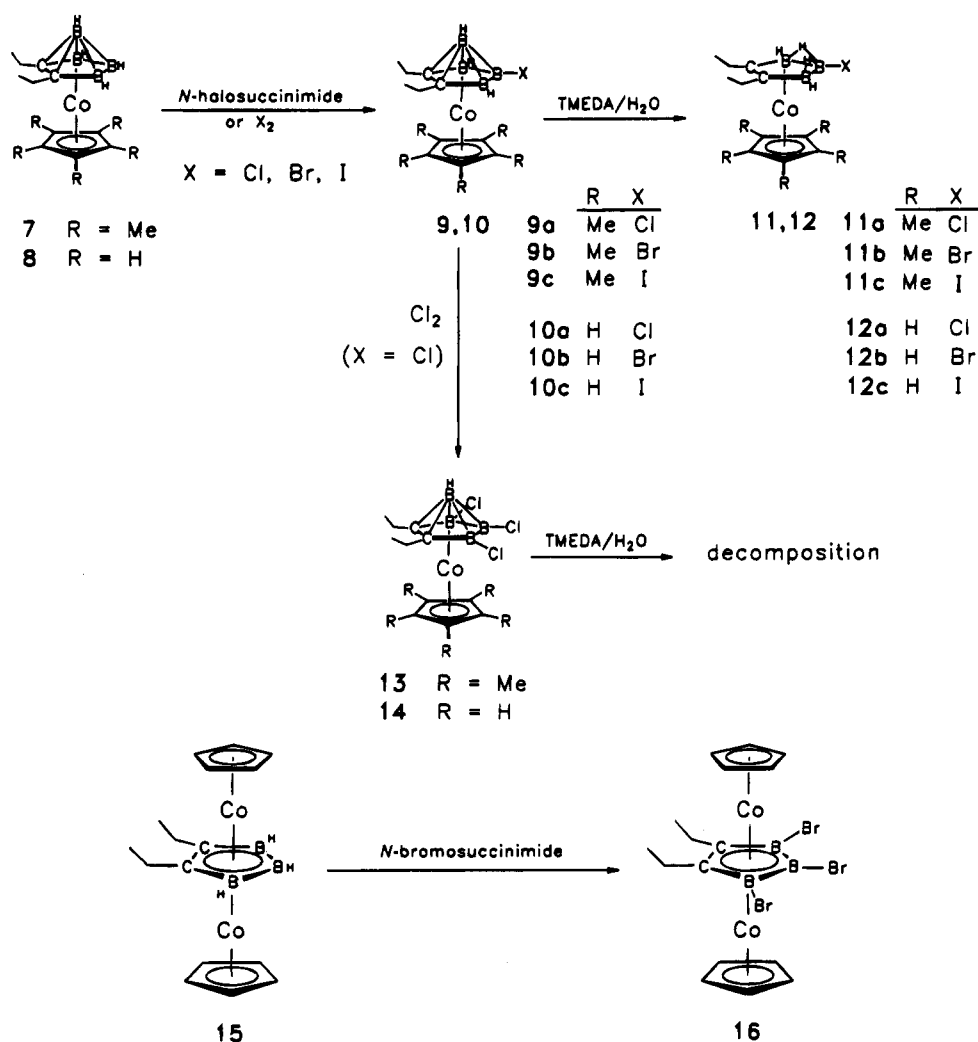
Results and Discussion

Halogenation of *nido*-Cp*Co(Et₂C₂B₃H₅) (Cp* = Cp*, Cp). The versatility of *N*-halosuccinimide reactions as a method for direct, regiospecific B(4)/B(6) substitution on neutral complexes, as in the synthesis of 2a-c and 3a-c from 1,^{5c} was extended to the preparation of the bromo iodo derivative 3d from 2c (Scheme 1B). Similar treatment of the CpCo complex 4 gave the bromo and iodo species 5b,c and 6b,c (Scheme 1C), which were isolated via chromatography on silica as air-stable crystalline solids and characterized from their ¹H, ¹¹B, and ¹³C NMR spectra and mass spectra. The proton resonances of the BHB bridging protons are, as noted earlier,^{3b} quite sensitive to electronic perturbation induced by substitution on the C₂B₃ ring. Thus, in the B(5)-X monohalo derivatives (Scheme 1A), the BHB signal is shifted substantially downfield ($\Delta\delta$ 1.98, 1.73 and 1.39 ppm for X = Cl, Br, and I, respectively) from its value in the unsubstituted complex (δ -5.96).^{3b,7}

In the B(4/6)-monohalo derivatives (2a-c), the pattern is more complex. In these asymmetric species there are two widely separated BHB resonances, one appearing at δ -3.84 to -3.89 and the other between δ -5.43 and -5.77; for the latter signal, the largest downfield shift occurs in the iodo species and the smallest in the

(7) Remeasurement of these spectra for the present study yielded slightly revised values (± 0.03 ppm) compared to those given in ref 3b.

Scheme 2



chloro compound, opposite to the case seen in the B(5)-X compounds. This trend is also found in the dihalo compounds **3a-d**, which exhibit single BHB resonances ranging from δ -3.66 for the dichloro down to -3.28 for the diiodo complex. In the bromo iodo compound **3d**, the BHB signal is found at δ -3.38, midway between those observed for the dibromo and diiodo species. A basically analogous pattern is seen in the CpCo series **5b,c** and **6b,c**, where again the deshielding is largest in the diiodo derivative whose BHB resonance is shifted nearly 3 ppm to lower field of that of the parent compound (δ -6.01).⁸ These empirical correlations between the pattern of substitution and bridging proton shifts have not yet received quantitative theoretical analysis, but they furnish a useful diagnostic tool for monitoring the electronic character of the carborane ring that has been exploited in multidecker sandwich synthesis.³

Halogenation of closo-Cobaltacarboranes. The reactivity of seven-vertex *closo*-CoC₂B₄ clusters toward radical halide sources is of interest in several respects: first, it addresses the mechanistic question of whether such reactions can proceed in the absence of BHB bridges; second, monohalogenated *closo* clusters are useful in preparing B-B-linked systems;⁴ third, "de-

capitation" (apex BH removal) of such clusters may provide an alternative synthetic route to halogenated *nido*-CoC₂B₃ species. Accordingly, the parent complex Cp*Co(Et₂C₂B₄H₄) (**7**)⁸ and its Cp analogue **8** were treated with *N*-halosuccinimides in THF or dichloromethane, producing the B(5)-monosubstituted species **9a-c** and **10a-c** in nearly quantitative yield (Scheme 2). The compounds were easily purified via flash chromatography and obtained as orange crystalline solids.

The bromination and iodination proceeded rapidly, but chlorination was slow, requiring 12-14 h for completion. In all cases, further halogen addition was not observed even when excess reagent was employed. The NMR spectra of these compounds show mirror symmetry, which is consistent with substitution at either the central equatorial boron (B(5)) or the apex (B(7)). This ambiguity was resolved by decapitation with TMEDA to generate in >90% yield the *nido* compounds **11a-c** and **12a-c** as shown, each of which retained its halo substituent and mirror symmetry; hence, the halogenation of **7** and **8** clearly occurs at B(5) and not at the apex position. Compounds **11a-c** are known species whose spectra data match those of the products obtained earlier^{5c} via deprotonation of the *nido* complex **1**; the CpCo complexes **12a-c** have not previously been reported.

(8) Davis, J. H., Jr.; Sinn, E.; Grimes, R. N. *J. Am. Chem. Soc.* **1989**, *111*, 4776.

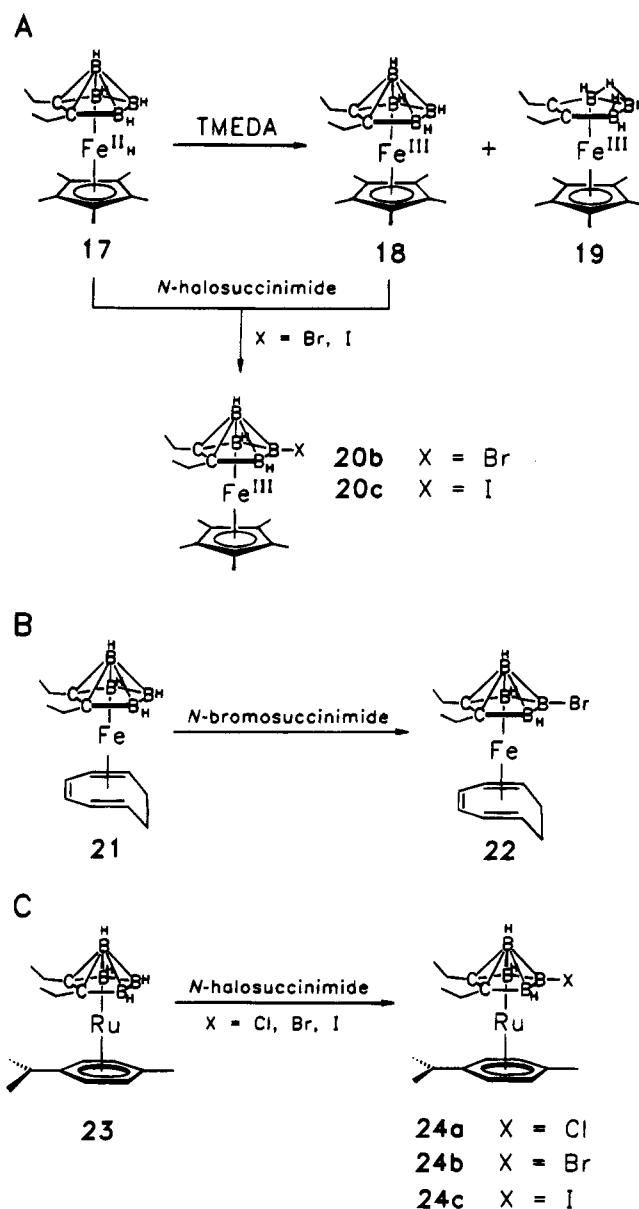
In an effort to achieve further substitution on the cage, we investigated reactions with elemental halogens. Treatment of **7** with Cl₂ in dichloromethane gave **9a** cleanly in less than 30 min; allowing the reaction to proceed overnight gave the trichloro derivative **13** as the sole isolated product (Scheme 2). Reaction of **7** with Br₂ was slower, requiring 4 h to give the monobromo species **9b**, and extended treatment afforded only a very small yield of a dibromo product that was identified from its mass spectrum. Iodination of **7** with elemental iodine was even slower, giving only the monoiodo compound **9c** and not reaching completion even in 24 h. The reaction of the CpCo complex **8** with elemental chlorine proceeded similarly to that of **7**, giving first the monochloro species **10a** and subsequently, in an overnight run, the trichloro compound **14**; the latter complex, obtained in 66% yield, was the only product detected. Attempted decapitation of **13** and **14** with wet TMEDA was unsuccessful, producing only uncharacterizable insoluble solids.

The general application of radical halide addition to cobaltacarboranes was extended to the dicobalt triple-decker sandwich **15**, in which both faces of the Et₂C₂B₃H₃ ring are coordinated to metal ions. Treatment of this complex with excess *N*-bromosuccinimide for 4 h in THF gave in 95% yield the dark red crystalline B(4,5,6)-tribromo species **16** (Scheme 2, bottom). Identification of this compound was straightforward from its mass spectrum (parent *m/z* 603) and multinuclear NMR spectra, which are consistent with a symmetric structure as shown.

Halogenation of Ferracarboranes and Ruthenacarboranes. Double-decker *closo*-LMC₂B₄ complexes of iron and ruthenium in which L is a cyclic hydrocarbon are useful synthons in multidecker and linked-cluster chemistry^{3a,5a,8,9} and also serve as model compounds for probing electronic properties.^{9e,10} As the controlled introduction of halogens or other substituents on the carborane ligand in these complexes has not previously been reported, we extended the current study to include several representative Fe and Ru complexes. In recent work^{10c} it was reported that the reaction of diamagnetic **17** with wet TMEDA removes the metal-bound proton, generating paramagnetic **18** instead of the expected decapitated species **19** (Scheme 3). However, in the present investigation we found that this treatment produces not only **18** (82%) but also the previously unknown nido complex **19**, isolated in 18% yield as a purple oil via flash chromatography on silica. The fact that **19** elutes as a faintly colored band very close to the solvent is probably the reason it was overlooked in the earlier study.

As depicted in Scheme 3a, **17** reacted with *N*-bromo- or *N*-iodosuccinimide to form both **18** and the respective

Scheme 3



B(5)-halo complexes **20b,c**; halogenated derivatives of diamagnetic **17** were not found. It is clear from these findings that the *N*-halosuccinimide reagent first deprotonates **17** to give **18** and then halogenates the latter species. On similar treatment of **18** directly, **20b,c** were obtained in high yield as purplish black crystals and characterized via proton NMR, IR, mass spectrometry, and elemental analysis. Despite their paramagnetism, assignment of the simple ¹H NMR spectra of these compounds is relatively straightforward (see Experimental Section) and supports the symmetrical B(5)-substituted structures.

Bromination of the (η^6 -cyclooctatriene)iron complex^{9a} **21** was accomplished in a similar manner (Scheme 3B), forming orange crystalline **22** in high yield as the only detectable product. The ability to regioselectively halogenate **21** is important for future synthetic operations, since **21** and other (η^6 -C₈H₁₀)Fe(carborane) complexes are versatile precursors to (arene)Fe(carborane) sandwich complexes via facile displacement of the cyclooctatriene ligand by arenes.^{9e}

The application of this chemistry to ruthenacarboranes was demonstrated by allowing the (cymene)Ru-

(9) (a) Davis, J. H., Jr.; Sinn, E.; Grimes, R. N. *J. Am. Chem. Soc.* **1989**, *111*, 4784. (b) Attwood, M. D.; Davis, J. H., Jr.; Grimes, R. N. *Organometallics* **1990**, *9*, 1177. (c) Davis, J. H., Jr.; Benvenuto, M.; Grimes, R. N. *Inorg. Chem.* **1991**, *30*, 1765. (d) Chase, K. J.; Grimes, R. N. *Inorg. Chem.* **1991**, *30*, 3957. (e) Fessenbecker, A.; Stephan, M.; Grimes, R. N.; Pritzkow, H.; Zenneck, U.; Siebert, W. *J. Am. Chem. Soc.* **1991**, *113*, 3061 and references therein.

(10) (a) Merkert, J. M.; Geiger, W. E.; Davis, J. H., Jr.; Attwood, M. D.; Grimes, R. N. *Organometallics* **1989**, *8*, 1580. (b) Merkert, J. M.; Geiger, W. E.; Attwood, M. D.; Grimes, R. N. *Organometallics* **1991**, *10*, 3545. (c) Stephan, M.; Davis, J. H., Jr.; Meng, X.; Chase, K. P.; Hauss, J.; Zenneck, U.; Pritzkow, H.; Siebert, W.; Grimes, R. N. *J. Am. Chem. Soc.* **1992**, *114*, 5214. (d) Merkert, J.; Davis, J. H., Jr.; Geiger, W.; Grimes, R. N. *J. Am. Chem. Soc.* **1992**, *114*, 9846.

(carborane) complex **23**⁸ to react with *N*-bromo- and *N*-iodosuccinimides (cymene = *p*-isopropyltoluene). In both instances, a single product was isolated via column chromatography in 89–92% yield as a pale yellow oil and characterized as the B(5)-halo derivative **24b,c** (Scheme 3C). The analogous synthesis of the B(5)-chloro species **24a** from *N*-chlorosuccinimide is reported elsewhere.^{1a} As in the case of compounds **9a–c** and **10a–c** discussed above, the NMR spectra of **24a–c** show mirror symmetry but cannot distinguish between B(5) (equatorial) and B(7) (apex) substitution. Again, however, the latter possibility may be discarded since decapitation of **24a** with TMEDA yields only *nido*-(cymene)Ru(2,3-Et₂C₂B₃H₄-5-Cl), proving that halogenation takes place at B(5) on the closo cage.^{1a}

Summary

Together with earlier findings,^{5c} this work establishes a general method for regiospecific halogenation of small neutral *nido*- and *closo*-metallocarborane complexes of Co, Fe, and Ru. The seven-vertex closo species are invariably halogenated at B(5) initially, with significant further substitution occurring only in reactions with Cl₂. In sharp contrast, the *nido* complexes are halogenated only at the outer borons (B(4,6)), with no observable substitution at B(5) even on treatment with excess halogenating reagent. The order of reactivity with *N*-halosuccinimides is I ≈ Br >> Cl, as iodination and bromination proceed readily (less than 5 min) while chlorination is usually much slower (hours). Reactions with *N*-halosuccinimides are generally very clean, proceeding sequentially (i.e., giving only monosubstituted products in 1:1 reactions). With elemental halogens the order of reactivity is reversed, proceeding most rapidly with Cl₂, and the reactions are less clean in that a mixture of products is generated.

These halogenations, conducted with neutral substrates, are assumed to involve radical mechanisms. In its application to *nido*-MC₂B₃ species, the fact that this approach results in substitution only at the B(4,6) positions complements with earlier method^{5c} employing reactions of anionic *nido* complexes with RX reagents, which afford specifically B(5)-substituted products. In combination, these two routes provide a versatile tool for designed synthesis that further illustrates the robust nature of small metallocarborane complexes and the ease with which they can be modified.

Experimental Section

Instrumentation. ¹H (300 and 500 MHz), ¹¹B (115.8 MHz), and ¹³C (75.5 and 125.3 MHz) NMR spectra were acquired on Nicolet NT-360, GE QE-300, or GE Omega-500 spectrometers. Unless otherwise indicated, ¹H and ¹³C NMR spectra were obtained in CDCl₃ solution and ¹¹B NMR spectra were recorded in CH₂Cl₂. In the proton NMR spectra of new compounds, all ethyl CH₂ signals were observed as doublets of quartets with coupling constants *J* = 7.5 and 15 Hz, and ethyl CH₃ resonances appeared as triplets with *J* = 7.5 Hz, unless otherwise stated. Unit-resolution mass spectra were obtained on a Finnegan MAT 4600 GC/MS spectrometer using perfluorotributylamine (FC43) as a calibration standard. In all cases, strong parent envelopes were observed, and the observed and calculated unit-resolution spectral patterns were in close agreement. Elemental composition and sample purity were established via elemental analysis on a Perkin-Elmer 2400 CHN Analyzer using (2,4-dinitrophenyl)hydrazone as a stan-

dard and/or by combination of multinuclear and mass spectral data. Infrared spectra were recorded as thin films on a Mattson Cygnus FTIR spectrometer.

Materials and Procedures. The starting compounds Cp*Co(Et₂C₂B₃H₄),^{8,11} Cp*Co(Et₂C₂B₃H₅),^{8,11} CpCo(Et₂C₂B₄H₄),⁸ CpCo(Et₂C₂B₃H₅),⁸ Cp*FeH(Et₂C₂B₃H₄),^{10c} Cp*Fe(Et₂C₂B₄H₄),^{10c} (cymene)Ru(Et₂C₂B₃H₄),⁸ and (C₈H₁₀)Fe(Et₂C₂B₄H₄)¹² were prepared by literature methods. Li(Et₃BH), *N*-halosuccinimides, chlorine, bromine, and iodine were purchased from commercial sources and used without further purification. Ruthenium(III) chloride monohydrate was acquired on loan from Johnson Matthey Corp. Petroleum ether was used as received, and methylene chloride was distilled from CaH₂. THF was distilled from Na/K alloy–benzophenone immediately prior to use. Column chromatography was performed on silica gel 60 (Merck). All reactions were conducted under an inert atmosphere unless otherwise indicated. Workup of products was generally carried out in air using benchtop procedures.

Syntheses. Cp*Co(2,3-Et₂C₂B₃H₃-4-Br-6-I) (3d). A 100 mg (0.25 mmol) sample of **2b** was dissolved in 15 mL of THF, and 115 mg (0.50 mmol) of *N*-iodosuccinimide was added, causing an immediate color change from orange to brown. After 15 min of stirring, the solution was evaporated and the residue was flash-chromatographed in hexane through 3 cm of silica to afford **3d** as a yellow-orange solid (129 mg, 0.25 mmol, quantitative yield). ¹H NMR (δ): 2.20 (CH₂, m, 4H), 1.78 (C₅Me₅, s, 15H), 1.09 (CH₃, t, 6H), -3.4 (BHB, vbr s, 1H). ¹³C NMR (δ): 105.3 (C₂B₃, br), 94.9 (C*Me₅), 21.1 (CH₂), 15.9 (CH₃), 9.9 (C₅Me*₅). ¹¹B NMR (δ): 9.4 (1B, s), 4.8 (1B, d, *J* = 154 Hz), -2.1 (1B, s). FTIR (cm⁻¹): 2967 m, 2932 m, 2871 w, 2554 m, 2380 w, 2342 w, 1645 s. MS: *m/z* 518 (molecular ion envelope).

CpCo(2,3-Et₂C₂B₃H₄-4(6)-Br) (5b) and CpCo(2,3-Et₂C₂B₃H₃-4,6-Br₂) (6b). A 105 mg (0.43 mmol) sample of **4** was dissolved in 50 mL of THF, and 72 mg (0.43 mmol) of *N*-bromosuccinimide was added, causing an immediate color change from yellow to brownish orange. The reaction was monitored by ¹¹B NMR spectroscopy and reached completion in 1 h. The solvent was removed via rotary evaporation, the residue was dissolved in hexane, and the solution was eluted on silica to give 140 mg (0.43 mmol, 98%) of yellow-orange crystalline **5b**. Further bromination of **5b** (140 mg, 0.43 mmol) with 1.5 equiv of *N*-bromosuccinimide produced a color change from orange to dark orange-brown. The reaction was complete within 1 h, and workup as above gave 119 mg (0.29 mmol, 67%) of orange-yellow crystalline **6b**. ¹H NMR for **5b** (δ): 4.77 (C₅H₅, s, 5H), 2.51 (CH₂, dq, 1H), 2.32 (CH₂, dq, 2H), 2.15 (CH₂, dq, 1H), 1.15 (CH₃, t, 6H), 1.09 (CH₃, t, 6H), -4.0 (BHB, vbr s, 1H), -5.4 (BHB, vbr s, 1H). ¹³C NMR (δ): 84.5 (C₅H₅), 26.7 (CH₂), 24.6 (CH₂), 16.5 (CH₃), 15.7 (CH₃). ¹¹B NMR (δ): 9.8 (1B, d, *J* = 145 Hz), 3.5 (1B, d, *J* = 139 Hz), 0.8 (1B, s). MS: *m/z* 323 (molecular ion envelope), 244 (-Br). ¹H NMR for **6b** (δ): 4.78 (C₅H₅, s, 5H), 2.50 (CH₂, dq, 2H), 2.28 (CH₂, dq, 2H), 1.13 (CH₃, t, 6H), -3.3 (BHB, vbr s, 1H). ¹³C NMR (δ): 84.5 (C₅H₅), 24.3 (CH₂), 14.4 (CH₃). ¹¹B NMR (δ): 6.4 (1B, d, *J* = 138 Hz), -2.1 (2B, s). MS: *m/z* 404 (molecular ion envelope), 322 (-Br).

CpCo(2,3-Et₂C₂B₃H₄-4(6)-I) (5c) and CpCo(2,3-Et₂C₂B₃H₃-4,6-I₂) (6c). The preceding procedure was followed using 104 mg (0.43 mmol) of **4** and 98 mg (0.43 mmol) of *N*-iodosuccinimide, producing an immediate color change from yellow to brownish orange. The reaction was complete in less than 1 h, giving on workup 142 mg (0.38 mmol, 90%) of orange crystalline **5c**. Further iodination of **5c** (100 mg, 0.27 mmol) with 1.5 equiv of *N*-iodosuccinimide produced a color change from orange to dark orange-brown. The reaction was complete within 1 h, and workup as above afforded 122 mg (0.24 mmol,

(11) An improved large-scale synthesis of these compounds that employs Schlenk instead of high-vacuum techniques has been developed: Stockman, K. E.; Müller, P. M.; Curtis, M. A.; Grimes, R. N., manuscript in preparation for *Inorg. Synth.*

(12) Swisher, R. G.; Grimes, R. N. *Organomet. Synth.* 1986, 3, 104.

90%) of orange crystalline **6c**. The latter compound was also obtained quantitatively on treatment of **4** with 2.5 equiv of *N*-iodosuccinimide. ^1H NMR for **5c** (δ): 4.77 (C_5H_5 , s, 5H), 2.52 (CH_2 , dq, 3H), 2.28 (CH_2 , dq, 1H), 2.12 (CH_2 , dq, 1H), 1.15 (CH_3 , t, 3H), 1.09 (CH_3 , t, 3H), -4.1 (BHB, vbr s, 1H), -5.4 (BHB, vbr s, 1H). ^{13}C NMR (δ): 85.2 (C_5H_5), 26.6 (CH_2), 25.6 (CH_2), 16.5 (CH_3), 15.6 (CH_3). ^{11}B NMR (δ): 4.8 (1B, d, $J = 103$ Hz), 0.4 (1B, d, $J = 141$ Hz), -4.0 (1B, s). MS: m/z 370 (molecular ion envelope), 244 (-I). ^1H NMR for **6c** (δ): 4.77 (C_5H_5 , s, 5H), 2.24-2.01 (CH_2 , m, 4H), 1.15 (CH_3 , t, 6H), -3.1 (BHB, vbr s, 1H). ^{13}C NMR (δ): 101.2 (C_2B_3), 83.4 (C_5H_5), 25.0 (CH_2), 15.1 (CH_3). ^{11}B NMR (δ): 6.4 (1B, d, $J = 138$ Hz), -2.1 (2B, s). MS: m/z 496 (molecular ion envelope), 369 (-I).

Cp*Co(2,3-Et₂C₂B₄H₃-5-Cl) (9a). A 200 mg (0.62 mmol) sample of Cp*Co(2,3-Et₂C₂B₄H₄) (**7**) was placed in a scintillation vial and dissolved in 5 mL of CH_2Cl_2 . The vial was fitted with a septum and the solution saturated with Cl_2 gas, after which the solution was allowed to stand for 2 h. The solvent was evaporated, yielding an orange solid from which starting material was removed by preparative thin-layer chromatography on silica (4:1 petroleum ether- CH_2Cl_2) to yield analytically pure **9a** (215 mg, 0.60 mmol, 97%). ^1H NMR (δ): 2.54 (CH_2 , dq, 2H), 2.30 (CH_2 , dq, 2H), 1.80 (C_5Me_5 , s, 15H), 1.21 (CH_3 , t, 6H). ^{13}C NMR (δ): 91.2 (C^*_5Me_5), 22.3 (CH_2), 15.4 (CH_3), 10.5 (C_5Me^*_5). ^{11}B NMR (δ): 18.8 (1B, s), 2.7 (3B, unresolved), 1.1 (1B, d, $J = 157$ Hz). MS: m/z (molecular ion envelope). Anal. Calcd for $\text{ClCoC}_{16}\text{B}_4\text{H}_{28}$: C, 53.68; H, 7.88. Found: C, 53.91; H, 7.84.

Cp*Co(2,3-Et₂C₂B₄H₃-5-Br) (9b). The procedure described above for preparing **5b** was employed using 200 mg (0.62 mmol) of **7** and 165 mg (0.93 mmol) of *N*-bromosuccinimide. After 1 h, the solvent was removed and flash chromatographed through 3 cm of silica gel in CH_2Cl_2 to give one orange band. Removal of solvent gave orange **9b** (245 mg, 0.61 mmol, 98%). ^1H NMR (δ): 2.47 (CH_2 , dq, 2H), 2.29 (CH_2 , dq, 2H), 1.80 (C_5Me_5 , s, 15H), 1.16 (CH_3 , t, 6H). ^{13}C NMR (δ): 95.9 (C_2B_4 , br), 91.4 (C^*_5Me_5), 21.4 (CH_2), 14.9 (CH_3), 9.4 (C_5Me^*_5). ^{11}B NMR (δ): 18.8 (1B, s), 2.7 (3B, unresolved). MS: m/z 402 (molecular ion envelope). Anal. Calcd for $\text{BrCoC}_{16}\text{B}_4\text{H}_{28}$: C, 47.75; H, 7.01. Found: C, 47.85; H, 7.40.

Cp*Co(2,3-Et₂C₂B₄H₃-5-I) (9c). The above procedure was employed using 200 mg (0.62 mmol) of **7** and 211 mg (0.93 mmol) of *N*-iodosuccinimide. After 1 h, the solvent was removed and the residue worked up as above to give orange **9c** (273 mg, 0.61 mmol, 98%). ^1H NMR (δ): 2.50 (CH_2 , dq, 2H), 2.30 (CH_2 , dq, 2H), 1.77 (C_5Me_5 , s, 15H), 1.16 (CH_3 , t, 6H). ^{13}C NMR (δ): 94.8 (C_2B_4 , br), 92.1 (C^*_5Me_5), 21.8 (CH_2), 15.5 (CH_3), 10.0 (C_5Me^*_5). ^{11}B NMR (δ): 17.3 (1B, s), 1.7 (2B, d, $J = 154$ Hz), 0.2 (1B, d, $J = 160$ Hz). MS: m/z 450 (molecular ion envelope). Anal. Calcd for $\text{ICoC}_{16}\text{B}_4\text{H}_{28}$: C, 42.76; H, 6.28. Found: C, 43.03; H, 5.98.

CpCo(2,3-Et₂C₂B₄H₃-5-Cl) (10a). The procedure used for **9a** was employed with 150 mg (0.59 mmol) of CpCo(2,3-Et₂C₂B₄H₄) (**8**) in 5 mL of THF, which was saturated with chlorine. After 4 h the solvent was evaporated and the solvent removed via chromatography in 4:1 petroleum ether- CH_2Cl_2 to afford pure **10a** (164 mg, 0.57 mmol, 97%). ^1H NMR (δ): 4.87 (C_5H_5 , s, 5H), 2.62 (CH_2 , dq, 2H), 2.39 (CH_2 , dq, 2H), 1.28 (CH_3 , t, 6H). ^{13}C NMR (δ): 92.4 (C_2B_4 , br), 83.8 (C_5H_5), 22.1 (CH_2), 15.1 (CH_3). ^{11}B NMR (δ): 23.7 (1B, s), 7.1 (1B, d, $J = 161$ Hz), -1.7 (2B, d, $J = 153$ Hz). MS: m/z 288 (molecular ion envelope). Anal. Calcd for $\text{ClCoC}_{11}\text{B}_4\text{H}_{18}$: C, 45.89; H, 6.30. Found: C, 46.27; H, 6.78.

CpCo(2,3-Et₂C₂B₄H₃-5-Br) (10b). The procedure employed for **9b** was followed using 50 mg (0.20 mmol) of **8** and 36 mg (0.20 mmol) of *N*-bromosuccinimide. After 1 h the solution was worked up as before to give one orange band of **10b** (66 mg, 0.20 mmol, 98%). ^1H NMR (δ): 4.87 (C_5H_5 , s, 5H), 2.62 (CH_2 , dq, 1H), 2.39 (CH_2 , dq, 2H), 1.28 (CH_3 , t, 6H). ^{13}C NMR (δ): 98.9 (C_2B_4 , br), 81.4 (C_5H_5), 24.6 (CH_2), 15.1 (CH_3). ^{11}B NMR (δ): 26.9 (2B, d, $J = 162$ Hz), 20.1 (1B, s), 1.9 (1B, d, $J = 169$ Hz). MS: m/z 333 (molecular ion envelope).

Anal. Calcd for $\text{BrCoC}_{11}\text{B}_4\text{H}_{18}$: C, 39.75; H, 5.46. Found: C, 39.34; H, 6.48.

CpCo(2,3-Et₂C₂B₄H₃-5-I) (10c). The procedure employed for **9c** was followed using 50 mg (0.20 mmol) of **8** and 45 mg (0.20 mmol) of *N*-iodosuccinimide. After 1 h the solution was worked up as before to give one orange band of **10c** (71 mg, 0.19 mmol, 95%). ^1H NMR (δ): 4.83 (C_5H_5 , s, 5H), 2.64 (CH_2 , dq, 1H), 2.39 (CH_2 , dq, 2H), 1.29 (CH_3 , t, 6H). ^{13}C NMR (δ): 99.2 (C_2B_4 , Br), 81.9 (C_5H_5), 24.7 (CH_2), 15.2 (CH_3). ^{11}B NMR (δ): 6.4 (1B, d, $J = 176$ Hz), 3.6 (2B, d, $J = 160$ Hz), 0.8 (1B, s). MS: m/z 380 (molecular ion envelope). Anal. Calcd for $\text{ICoC}_{11}\text{B}_4\text{H}_{18}$: C, 34.83; H, 4.78. Found: C, 35.23; H, 4.91.

CpCo(2,3-Et₂C₂B₃H₄-5-X) (12a, X = Br; 12c, X = I). A 100 mg sample of **10a**, **10b**, or **10c** was dissolved in 2 mL of TMEDA in a 50 mL flask, 2 drops of water were added, and the reaction mixture was stirred for 1 h and evaporated to dryness. The residue was flash-chromatographed in hexane through 3 cm of silica gel to give the respective product **12a-c** as a yellow solid. ^1H NMR (δ) for **12a**: 4.90 (C_5H_5 , s, 5H), 2.16 (CH_2 , dq, 2H), 2.06 (CH_2 , dq, 2H), 1.10 (CH_3 , t, 6H), -4.0 (BHB, vbr s, 2H). ^{13}C NMR for **12a** (δ): 84.6 (C_5H_5), 25.7 (CH_2), 16.0 (CH_3). ^{11}B NMR for **12a** (δ): 17.6 (1B, s), -2.8 (2B, d, $J = 136$ Hz). MS for **12a**: m/z 278 (molecular ion envelope). ^1H NMR (δ) for **12b**: 4.81 (C_5H_5 , s, 5H), 2.26-2.03 (CH_2 , m, 4H), 1.14 (CH_3 , t, 6H), -4.32 (BHB, vbr s, 2H). ^{13}C NMR for **12b** (δ): 81.1 (C_5H_5), 26.4 (CH_2), 16.4 (CH_3). MS for **12b**: m/z 323 (molecular ion envelope). ^1H NMR (δ) for **12c**: 4.87 (C_5H_5 , s, 5H), 2.61 (CH_2 , dq, 2H), 2.37 (CH_2 , dq, 2H), 1.11 (CH_3 , t, 6H), -3.06 (BHB, vbr s, 2H). ^{13}C NMR for **12c** (δ): 82.3 (C_5H_5), 27.5 (CH_2), 17.6 (CH_3). MS for **12c**: m/z 370 (molecular ion envelope).

Cp*Co(2,3-Et₂C₂B₄H-4,5,6-Cl₃) (13). A 200 mg (0.62 mmol) sample of Cp*Co(2,3-Et₂C₂B₄H₄) (**7**) was placed in a scintillation vial and dissolved in 10 mL of THF. The vial was capped with a septum and the solution saturated with Cl_2 gas, after which the solution was allowed to stand for 24 h. The solvent was evaporated, giving an orange solid which was flash-chromatographed in CH_2Cl_2 on 3 cm of silica to yield orange **13** (195 mg, 0.46 mmol, 75%). ^1H NMR (δ): 2.71 (CH_2 , dq, 1H), 2.27 (CH_2 , dq, 2H), 1.78 (C_5Me_5 , s, 15H), 1.07 (CH_3 , t, 6H). ^{13}C NMR (δ): 91.1 (C_2B_4 , br), 90.3 (C^*_5Me_5), 21.4 (CH_2), 14.5 (CH_3), 9.6 (C_5Me^*_5). ^{11}B NMR (δ): 7.2 (1B, d, 137 Hz), 4.0 (3B, s, unresolved). MS: m/z 427 (molecular ion envelope), 357 (-2 Cl). Anal. Calcd for $\text{Cl}_3\text{CoC}_{16}\text{B}_4\text{H}_{26}$: C, 45.02; H, 6.14. Found: C, 45.11, H, 6.12.

CpCo(2,3-Et₂C₂B₄H-4,5,6-Cl₃) (14). The procedure described for **13** was followed using 100 mg (0.39 mmol) of CpCo(2,3-Et₂C₂B₄H₄) (**8**). Workup as before gave 92 mg (0.39 mmol, 66%) of orange **14**. ^1H NMR (δ): 4.96 (C_5H_5 , s, 5H), 2.76 (CH_2 , dq, 1H), 2.55 (CH_2 , dq, 2H), 1.17 (CH_3 , t, 6H). ^{13}C NMR (δ): 98.5 (C_2B_4 , br), 79.8 (C_5H_5), 25.0 (CH_2), 15.1 (CH_3). MS: m/z 357 (molecular ion envelope). Anal. Calcd for $\text{Cl}_3\text{CoC}_{11}\text{B}_4\text{H}_{16}$: C, 37.03; H, 4.52. Found: C, 36.88; H, 4.42.

CpCo(2,3-Et₂C₂B₄H-4,5,6-Br₃)CoCp (16). The procedure described for **5b** was followed using 50 mg (0.14 mmol) of CpCo(2,3-Et₂C₂B₃H₃)CoCp (**15**) and 100 mg (0.55 mmol) of *N*-bromosuccinimide. The solution was stirred for 4 h with no apparent color change. The solvent was removed and the residue chromatographed in CH_2Cl_2 to yield dark red **16** (80 mg, 0.13 mmol, 95%). ^1H NMR (δ): 4.54 (C_5H_5 , s, 5H), 3.03 (CH_2 , q, 4H), 1.55 (CH_3 , t, 3H). ^{13}C NMR (δ): 82.9 (C_5H_5), 25.8 (CH_2), 19.2 (CH_3). ^{11}B NMR (δ): 54.7 (1B, s), 8.4 (2B, s). MS: m/z 603 (molecular ion envelope).

nido-Cp*Fe(2,3-Et₂C₂B₃H₅) (19). A 500 mg (1.55 mmol) sample of Cp*FeH(2,3-Et₂C₂B₄H₄) (**17**)^{10c} was treated with 3 mL of TMEDA and 2-3 drops of water and stirred for 4 h. After removal of solvent, the residue was column-chromatographed to give faint pink paramagnetic **19** (86 mg, 0.27 mmol, 18%) as the first band off the column and green-brown paramagnetic **18**^{10c} (400 mg, 1.27 mmol, 82%) as the second band. ^1H NMR for **19** (δ): 73.5 (CH_2 , s br, 1H), 41.5 (CH_2 , s br, 2H), -3.75 (CH_3 , s br, 3H), -7.76 (C_5Me_5 , s br, 15H). FTIR

for **19** (cm^{-1}): 2987 m, 2955 m, 2918 m, 2877 w, 2564 s, 2344 w, 2323 w. MS for **19**: m/z 311 (molecular ion envelope). Anal. Calcd for $\text{FeC}_{16}\text{B}_3\text{H}_{30}$: C, 61.85; H, 9.73. Found: C, 61.69; H, 10.01.

Cp*Fe(2,3-Et₂C₂B₄H₃-5-Br) (20b). The procedure described for **5b** was followed using 200 mg (0.62 mmol) of $\text{Cp}^*\text{FeH}(2,3\text{-Et}_2\text{C}_2\text{B}_4\text{H}_4)$ and 1 equiv of *N*-bromosuccinimide. The solution was stirred for 4 h, the solvent was removed, and the residue was flash-chromatographed in CH_2Cl_2 through 3 cm of silica gel to yield one purple band, characterized as metallic purple **20b** (240 mg, 0.60 mmol, 97%). ¹H NMR (δ): 16.2 (CH_2 , s br, 1H), 13.1 (CH_2 , s br, 2H), -1.1 (CH_3 , s br, 3H), -20.3 (C_5Me_5 , s br, 15H). FTIR (cm^{-1}): 2970 m, 2934 m, 2914 m, 2876 w, 2571 s, 2361 w, 2341 w. MS: m/z 400 (molecular ion envelope). Anal. Calcd for $\text{BrFeC}_{16}\text{B}_4\text{H}_{28}$: C, 48.12; H, 7.07. Found: C, 49.65; H, 6.72.

Cp*Fe(2,3-Et₂C₂B₄H₃-5-I) (20c). The above procedure was followed using 200 mg (0.62 mmol) of $\text{Cp}^*\text{FeH}(2,3\text{-Et}_2\text{C}_2\text{B}_4\text{H}_4)$ and 1 equiv of *N*-iodosuccinimide. Workup as before gave metallic purple **20c** (263 mg, 0.58 mmol, 95%). ¹H NMR (δ): 17.2 (CH_2 , s br, 1H), 10.4 (CH_2 , s br, 2H), -0.9 (CH_3 , s br, 3H), -21.6 (C_5Me_5 , s br, 15H). MS: m/z 446 (molecular ion envelope). Anal. Calcd for $\text{IFeC}_{16}\text{B}_4\text{H}_{28}$: C, 43.05; H, 6.32. Found: C, 43.85; H, 7.08.

($\eta^6\text{-C}_8\text{H}_{10}$)Fe(2,3-Et₂C₂B₄H₃-5-Br) (22). The procedure described for **5b** was followed using 100 mg (0.34 mmol) of $(\eta^6\text{-C}_8\text{H}_{10})\text{Fe}(2,3\text{-Et}_2\text{C}_2\text{B}_4\text{H}_4)$ (**21**)¹² and 91 mg (0.51 mmol) of *N*-bromosuccinimide. The solution was stirred for 2 h, the solvent was removed, and the residue was dissolved in CH_2Cl_2 and flash-chromatographed on 3 cm of silica gel to afford 107 mg (0.29 mmol, 85%) of **22** as orange crystals. ¹H NMR (δ): 5.88 (d, 2H), 5.78–5.74 (m, 2H), 5.17–5.13 (m, 1H), 2.30–

1.94 (m, 6H), 1.08 (CH_3 , t, 6H), 0.20–0.11 (m, 2H). ¹³C NMR (δ): 99.7 (C_8H_{10}), 92.3 (C_8H_{10}), 91.4 (C_8H_{10}), 32.5 (C_8H_{10}), 22.3 (CH_2), 14.5 (CH_3). ¹¹B NMR (δ): 19.7 (1B, s), 6.2 (2B, d, J = 165 Hz), 3.4 (1B, d, J = 142 Hz). MS: m/z 372 (molecular ion envelope).

($\eta^6\text{-MeC}_6\text{H}_4\text{CHMe}_2$)Ru(2,3-Et₂C₂B₄H₃-5-X) (24b, X = Br; 24c, X = I). The procedure described for the preceding synthesis was followed using 100 mg (0.54 mmol) of $(\eta^6\text{-MeC}_6\text{H}_4\text{CHMe}_2)\text{Ru}(2,3\text{-Et}_2\text{C}_2\text{B}_4\text{H}_4)$ (**23**)⁸ and 1 equiv of *N*-bromo- or *N*-iodosuccinimide. The solution was stirred for 8 h, the solvent was removed, and the residue was worked up as above to give in each case one pale yellow band, which was **24b** (213 mg (0.48 mmol, 89%) or **24c** (245 mg, 0.50 mmol, 92%). ¹H NMR for **24b** (δ): 5.32 (d, 2H), 5.28 (d, 2H), 2.66 (Me^*_2CH , m, 1H), 2.45–2.21 (CH_2 , m, 4H), 2.15 (CH_3 , s, 3H), 1.25 (*i*Pr CH_3 , d, 6H), 1.18 (CH_3 , t, 6H). ¹³C NMR for **24b** (δ): 118.2 (C_5H_5), 24.1 (CH_2), 13.2 (CH_3). ¹¹B NMR for **24b** (δ): 17.5 (1B, s), 7.1 (1B, d, J = 146 Hz), 1.5 (2B, d, J = 162 Hz). MS for **24b**: m/z 444 (molecular ion envelope). ¹H NMR for **24c** (δ): 5.53–5.24 (m, 4H), 2.72–2.60 (Me_2CH^* , m, 1H), 2.41–2.24 (CH_2 , m, 4H), 2.15 (CH_3 , s, 3H), 1.25 (*i*Pr CH_3 , d, 6H), 1.18 (CH_3 , t, 6H). ¹¹B NMR for **24c** (δ): 14.3 (1B, s), 7.2 (1B, d, J = 118 Hz), -0.1 (2B, d, J = 117 Hz). MS for **24c**: m/z 491 (molecular ion envelope). Anal. Calcd for $\text{IRuC}_{16}\text{B}_4\text{H}_{27}$: C, 39.17; H, 5.55. Found: C, 38.36; H, 5.98.

Acknowledgment. This work was supported in part by the National Science Foundation, Grant No. CHE 9322490, and the U.S. Army Research Office.

OM950346W

Organotransition-Metal Metallacarboranes. 41. Synthesis and Structure of B–B- and Cp*–Cp*-Linked Cobaltacarborane Clusters^{1,2}

Xiaotai Wang, Michal Sabat, and Russell N. Grimes*

Department of Chemistry, University of Virginia, Charlottesville, Virginia 22901

Received May 12, 1995[®]

In an application of Wurtz-type coupling reactions to metallacarborane chemistry, treatment of the B(5)-halogenated closo complexes Cp*Co(2,3-Et₂C₂B₄H₃-5-X) (X = Cl, Br, I; Cp* = η⁵-C₅Me₅) with sodium metal in THF gave a single red-orange, air-stable product in 20–34% isolated yield. This species was characterized via NMR, UV–visible, and mass spectroscopy and X-ray crystallography as a B–B-linked dimer, 5,5′-[Cp*Co(Et₂C₂B₄H₃)₂] (2). Reactions of the same halogenated monomers, as well as the parent complex (X = H), with alkyllithium reagents in THF generated in 28–56% yield the orange, air-stable dimeric products [(-CH₂C₅Me₄)Co(Et₂C₂B₄H₃-5-X)]₂ (3a–d; X = H, Cl, Br, I), which are linked via Cp*–Cp* connections. This geometry, apparently novel to metallacarborane chemistry, was established by an X-ray diffraction study on 3c and supported by spectroscopic data for the four species. Decapitation of these dimers in wet TMEDA gave in high yield the corresponding *nido* complexes [(-CH₂C₅Me₄)Co(Et₂C₂B₃H₄-5-X)]₂ (4a–d; X = H, Cl, Br, I) as air-stable yellow solids. In contrast, 2 was unaffected by similar treatment. The reaction of *nido*-Cp*Co(Et₂C₂B₃H₄-5-Cl) with sodium in THF gave the yellow air-stable dimeric species [Cp*Co(Et₂C₂B₃H₄)₂] (8) together with the unsubstituted monomer Cp*Co(Et₂C₂B₃H₅), a previously characterized complex. An X-ray crystal structure determination on 8 disclosed that the two CoC₂B₃ units are connected via a B–B–B three-center bond such that the two C₂B₃ rings are almost mutually perpendicular.

Introduction

Organometallic complexes containing two or more transition-metal centers command widespread interest for a variety of reasons, among which are their potential for effecting cooperative multinuclear catalytic action,³ their synthetic utility as building blocks in constructing electroactive or magnetoactive polymeric materials,⁴ and their value in studies of metal–metal electronic communication.^{3–5} For all such purposes, it is essential that the complexes be reasonably robust (preferably air-stable) and *not fragment into monometallic species in solution*, be soluble in common organic solvents, and be synthetically accessible. These conditions are satisfied by most metallacarboranes, and when one also takes into account the enormous variety of such complexes,⁶ it is clear that polymetal-centered carborane complexes

offer a particularly fertile area of investigation. Many examples of dimetallic or polymetallic metallacarborane clusters of 6–14 vertices have been reported,⁶ some of which were obtained by serendipitous means and others by directed syntheses. In the small metallacarborane category, methods for assembling and tailoring C₂B₃-bridged multidecker sandwich complexes via stacking of small building-block units have been developed in our laboratory.⁷ In species of this class (Chart 1A), the metal centers are in close proximity to each other (typically ca. 3.2 Å) and unpaired electrons are often (although not always⁸) extensively delocalized.^{5b,c,7b}

Other classes of polymetallic small metallacarboranes consist of linked clusters such as those depicted in Chart 1B, in which the metals reside in discrete polyhedral units that are linked via ligand–ligand, multicenter B–B–B, or other bonding modes.⁹ One can also combine the stacking and linked-cluster motifs in the same system, as in the type C species¹⁰ in Chart 1. Although

[®] Abstract published in *Advance ACS Abstracts*, September 1, 1995.

(1) (a) Part 40: Stockman K.; Garrett, D.; Grimes, R. N. *Organometallics* **1995**, *14*, 4661. (b) Part 39: Greiwe, P.; Sabat, M.; Grimes, R. N. *Organometallics* **1995**, *14*, 3683.

(2) Based in part on the Ph.D. dissertation of X.W., University of Virginia, 1995. Presented in part at the Third Boron U.S.A. Workshop, Washington State University, Pullman, WA, July 1992; Abstract 52.

(3) (a) Marks, T. J. *Acc. Chem. Res.* **1992**, *25*, 57. (b) Süß-Fink, G.; Meister, G. *Adv. Organomet. Chem.* **1993**, *35*, 41 and references therein.

(4) Recent examples: (a) Foxman, B. M.; Rosenbloom, M.; Sokolov, V.; Khrushchova, N. *Organometallics* **1993**, *12*, 4805. (b) Atzkern, H.; Bergerat, P.; Beruda, H.; Fritz, M.; Hiermeier, J.; Hudeczek, P.; Kahn, O.; Köhler, F. H.; Paul, M.; Weber, B. *J. Am. Chem. Soc.* **1995**, *117*, 997.

(5) Recent examples: (a) Tilsted, M.; Vollhardt, K. P. C.; Boese, R. *Organometallics* **1994**, *13*, 3146. (b) Pipal, J. R.; Grimes, R. N. *Organometallics* **1993**, *12*, 4452, 4459. (c) Merkert, J.; Davis, J. H., Jr.; Geiger, W.; Grimes, R. N. *J. Am. Chem. Soc.* **1992**, *114*, 9846. (d) Chin, T. T.; Lovelace, S. R.; Geiger, W. E.; Davis, C. M.; Grimes, R. N. *J. Am. Chem. Soc.* **1994**, *116*, 9359.

(6) Grimes, R. N. In *Comprehensive Organometallic Chemistry II*; Abel, E., Stone, F. G. A., Wilkinson, G., Eds.; Pergamon Press: Oxford, England, 1995; Vol. 1, Chapter 9, and references therein.

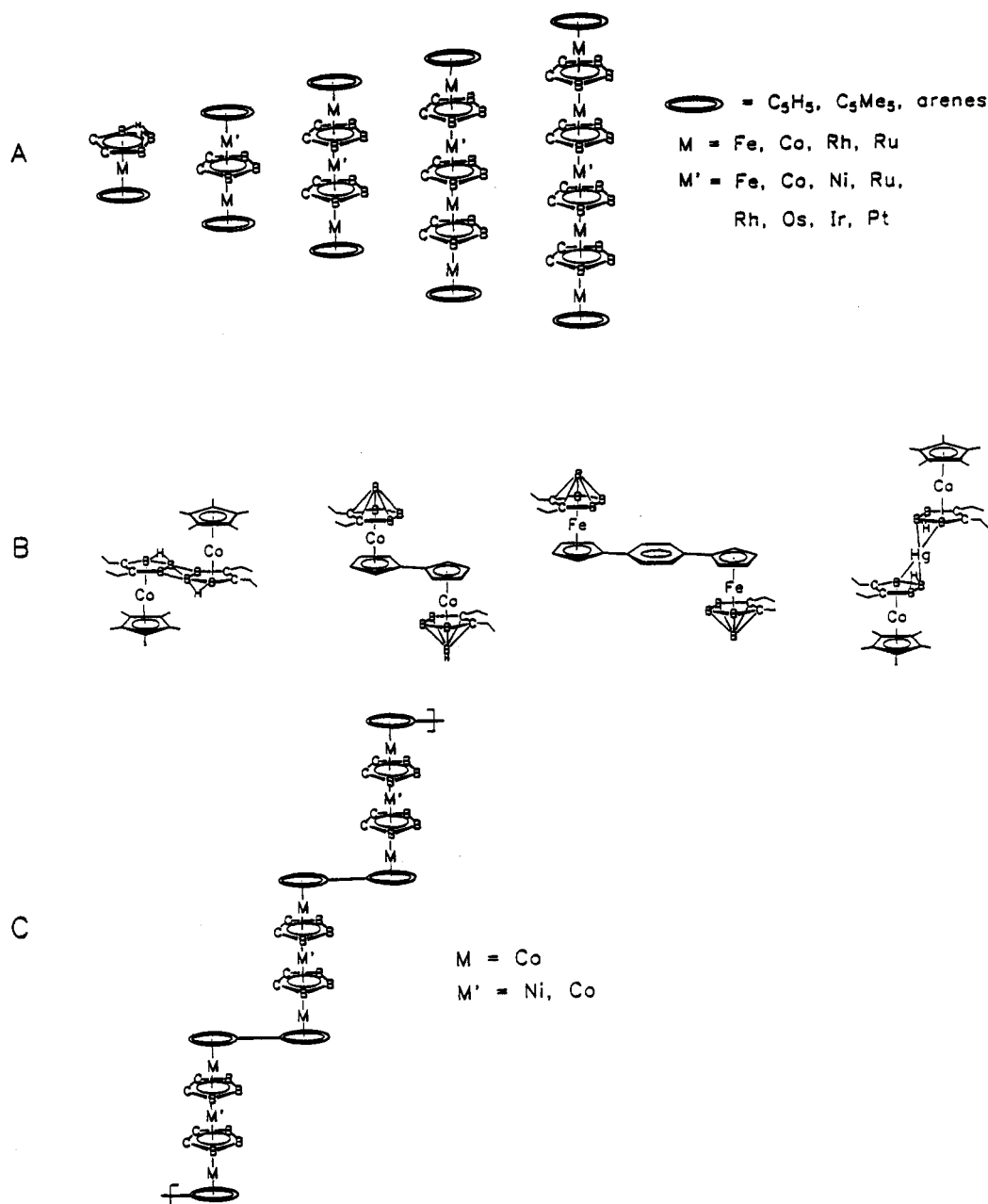
(7) (a) Grimes, R. N. *Chem. Rev.* **1992**, *92*, 251. (b) Piepgrass, K. W.; Meng, X.; Hölscher, M.; Sabat, M.; Grimes, R. N. *Inorg. Chem.* **1992**, *31*, 5202. (c) Wang, X.; Sabat, M.; Grimes, R. N. *J. Am. Chem. Soc.* **1994**, *116*, 2687. (d) Benvenuto, M. A.; Sabat, M.; Grimes, R. N. *Inorg. Chem.* **1992**, *31*, 3904.

(8) Stephan, M.; Müller, P.; Zenneck, U.; Pritzkow, H.; Siebert, W.; Grimes, R. N. *Inorg. Chem.* **1995**, *34*, 2058.

(9) (a) Piepgrass, K. W.; Curtis, M. A.; Wang, X.; Meng, X.; Sabat, M.; Grimes, R. N. *Inorg. Chem.* **1993**, *32*, 2156. (b) Stephan, M.; Davis, J. H., Jr.; Meng, X.; Chase, K. P.; Hauss, J.; Zenneck, U.; Pritzkow, H.; Siebert, W.; Grimes, R. N. *J. Am. Chem. Soc.* **1992**, *114*, 5214. (c) Finster, D. C.; Grimes, R. N. *Inorg. Chem.* **1981**, *20*, 863.

(10) Meng, X.; Sabat, M.; Grimes, R. N. *J. Am. Chem. Soc.* **1993**, *115*, 6143.

Chart 1



we have unexpectedly isolated and characterized several boron-linked dimers in the course of attempted metal stacking reactions (see below),^{9a} we sought in the present study to develop systematic routes to linked cobaltacarborane clusters via Wurtz reactions and similar approaches drawn from organic chemistry.

Results and Discussion

Synthesis and Characterization of Linked *Closo*-Cobaltacarborane Dimers. The halogenated complexes $\text{Cp}^*\text{Co}(\text{2,3-Et}_2\text{C}_2\text{B}_4\text{H}_3\text{-5-X})$ (**1b-d**), in which X = Cl, Br, I and $\text{Cp}^* = \eta^5\text{-C}_5\text{Me}_5$, were readily obtained in high-yield, regiospecific reactions via treatment of the parent complex¹¹ **1a** with *N*-halosuccinimides.^{1a} As shown in Scheme 1, each of these halo derivatives reacted with sodium in THF to afford the linked product $5,5'\text{-}[\text{Cp}^*\text{Co}(\text{Et}_2\text{C}_2\text{B}_4\text{H}_3)]_2$ (**2**) in isolated yields of 20, 42,

and 34% for X = Cl, Br, I, respectively. To our knowledge, these are the first applications of Wurtz-type reactions to the directed syntheses of B-B-linked metallaboron cluster dimers. Pretreatment of the sodium with methanol was found to increase both the rate of formation and the yields of the products, probably owing to activation of the sodium surface as well as to the formation of sodium methoxide which may promote heterolytic cleavage of the B-X bond.

Orange air-stable crystals of **2** were isolated following column chromatography on silica in air, and the compound was characterized by ¹H and ¹¹B NMR, UV-visible, and mass spectroscopy and elemental analysis. High symmetry is apparent in both the ¹H and ¹¹B NMR spectra (Table 1); in the boron spectrum, only two signals in a 3:1 area ratio are observed, owing to the superposition of area 1 and area 2 peaks (as is also the case in the unsubstituted monomer¹¹ $\text{CpCo}(\text{Et}_2\text{C}_2\text{B}_4\text{H}_4)$, although the spectrum of $\text{Cp}^*\text{Co}(\text{Et}_2\text{C}_2\text{B}_4\text{H}_4)$ exhibits a resolved 1:2:1 pattern¹¹). Since these data do not con-

(11) Davis, J. H., Jr.; Sinn, E.; Grimes, R. N. *J. Am. Chem. Soc.* **1989**, *111*, 4776.

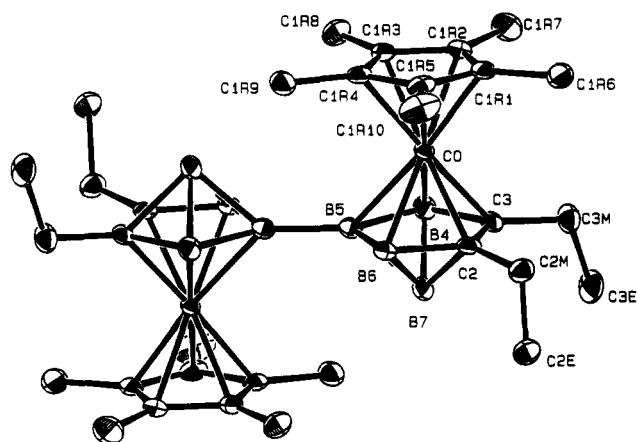
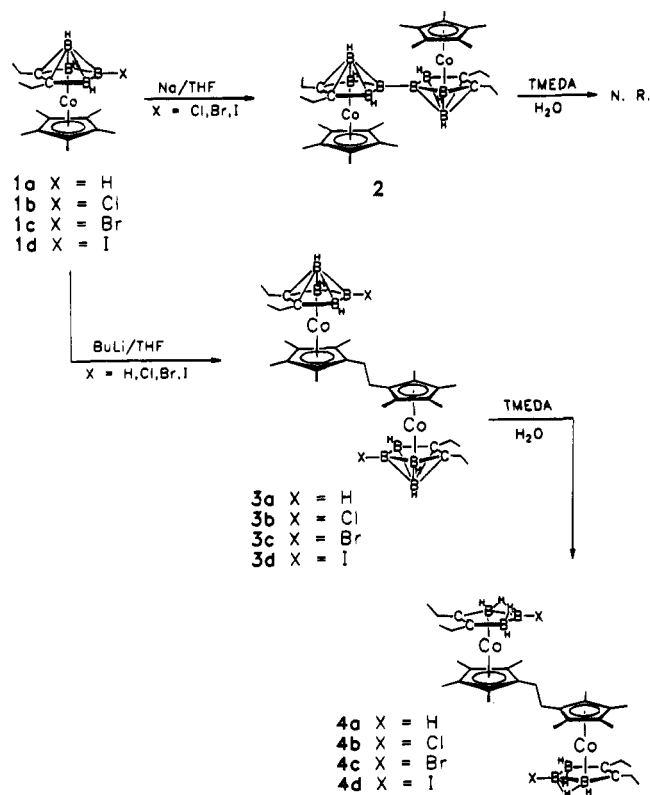


Figure 1. Molecular structure of 5,5'-[Cp*Co(Et₂C₂B₄H₃)₂] (2) with hydrogen atoms omitted.

Scheme 1



clusively distinguish between the B(5)–B(5')-linked and B(7)–B(7') (apically) linked isomers, an X-ray crystal structure determination was conducted on **2**. Tables 2 and 3 list the crystallographic parameters and bond distances and angles, respectively.

As depicted in Figure 1, **2** was identified as the B(5)–B(5') isomer with a centrosymmetric transoid conformation in the solid state. The two C₂B₃ rings are constrained by the inversion center to be mutually coplanar in the crystal, and the Co atoms are nearly centered over their respective carborane rings, the Co–C distances being slightly shorter than the Co–B bonds. The intercluster B–B distance in **2** is virtually identical with the neighboring B(5)–B(4) and B(5)–B(6) bonds (all ca. 1.69 Å) and is in the range observed in other boron-coupled species, e.g., 1,1'-(B₅H₈)₂,¹² (1.74(6) Å), 1,2'-

(B₅H₈)₂¹³ (1.660(8) Å), and C₂B₈H₁₁–C₂B₁₀H₁₁¹⁴ (1.681(2) Å). A strong covalent link between the polyhedral units in **2** is thereby indicated, probably involving some transfer of bonding electron density from the two cage frameworks to the intercluster bond as the hydrogens on B(5) and B(5') are replaced by a B–B interaction. This may account for the very slight deshielding of the proton NMR resonances one observes in **2** relative to the monomer **1a**. A related observation is that **2** appears unreactive toward wet tetramethylethylenediamine (TMEDA), in contrast to **1a**, which readily undergoes decapitation (loss of the apical BH) with this reagent.¹¹

As part of an exploration of possible alternative routes to cobaltacarborane dimers, the closo complexes **1a–d** were treated with alkyllithium reagents in THF. Other than *nido*-Cp*Co(Et₂C₂B₃H₅) (a "decapitation" byproduct of the reaction of **1a** (X = H)) the only isolated products, obtained in 28–56% yield on treatment with *n*-butyllithium or methyllithium, were the dimers **3a–d**, whose Cp*–Cp* linkages represent a geometry not previously encountered in metallocarborane chemistry (Scheme 1). The spectroscopic characterization of these orange air-stable species was straightforward, and the geometry shown was established via an X-ray diffraction study on **3c**. Although the mechanistic details of these reactions are unclear, it is probable that the initial step is deprotonation of the Cp* ligand by the alkyllithium reagent. Such reactions are relatively rare, as the Cp* hydrogens in η⁵-Cp* metal complexes are usually inert to bases; in contrast, methyl groups on η⁶-arenes are easily alkylated.^{15,16} Precedents for Cp* activation are apparently limited to the studies on Cp*IrL_n species by Maitlis et al.¹⁵ and a report by Gloaguen and Astruc on the polyalkylation of Cp*CoCp⁺ by *t*-BuOK and MeI.¹⁶ In our work, we infer that the strongly electron-withdrawing (Et₂C₂B₄H₃X)²⁻ ligands, which stabilize high metal oxidation states, enhance the polarity of the Cp* C–H bonds and hence promote their acidity. In contrast, carborane B–H bonds in general are far less polar and are not susceptible to base attack,¹⁷ so that the Cp* ligand is the preferred (and very likely the only possible) site for such reactions in **1a–d**.

The molecular structure of the B(5),B(5')-dibromo derivative **3c** is presented in Figure 2, with crystallographic information listed in Table 2 and bond distances and angles in Table 4. As in **2**, the molecule is centrosymmetric in the solid state, and the CoC₂B₄ cluster units exhibit normal seven-vertex closo geometry with typical bond lengths and bond angles. The cobalt lies approximately above the centroid of the C₂B₃ ring, although slightly closer to the cluster carbons than to the boron atoms. The central C–C (C(1R8)–C(1R8')) distance of 1.546(7) Å and the C(1R3)–C(1R8)–C(1R8')

(13) Briguglio, J. J.; Carroll, P. J.; Corcoran, E. J., Jr.; Sneddon, L. G. *Inorg. Chem.* **1986**, *25*, 4618. Single-bond B–B distances for other related structures are also cited in this paper.

(14) Subrtova, V.; Linek, A.; Hasek, J. *Acta Crystallogr.* **1982**, *B38*, 3147.

(15) (a) Miguel-Garcia, J. A.; Adams, H.; Bailey, N. A.; Maitlis, P. M. *J. Organomet. Chem.* **1991**, *413*, 427. (b) Miguel-Garcia, J. A.; Adams, H.; Bailey, N. A.; Maitlis, P. M. *J. Chem. Soc., Dalton Trans.* **1992**, 131.

(16) Gloaguen, B.; Astruc, D. *J. Am. Chem. Soc.* **1990**, *112*, 4607.

(17) For example, deprotonation of the icosahedral (C₂B₁₀H₁₂) carboranes via organolithium reagents takes place exclusively at the CH groups. See: Grimes, R. N. *Carboranes*; Academic Press: New York, 1970, and references therein.

(12) Grimes, R.; Wang, F. E.; Lewin, R.; Lipscomb, W. N. *Proc. Natl. Acad. Sci. U.S.A.* **1961**, *47*, 996.

Table 1. ^{11}B and ^1H FT NMR Data

115.8 MHz ^{11}B NMR Data		
compd	$\delta^{a,b}$	rel areas
$\text{Cp}^*\text{Co}(\text{2,3-Et}_2\text{C}_2\text{B}_4\text{H}_4)$ (1a) ^{c,d}	12.1 (134), 4.3 (162), 2.6 (185)	1:2:1
$\text{Cp}^*\text{Co}(\text{2,3-Et}_2\text{C}_2\text{B}_4\text{H}_3\text{-5-Cl})$ (1b) ^e	18.8, 2.7, 1.1 (157)	1:2:1
$\text{Cp}^*\text{Co}(\text{2,3-Et}_2\text{C}_2\text{B}_4\text{H}_3\text{-5-Br})$ (1c) ^e	18.8, 2.7	1:3 ^f
$\text{Cp}^*\text{Co}(\text{2,3-Et}_2\text{C}_2\text{H}_4\text{-5-I})$ (1d) ^e	17.3, 1.7 (154), 0.2 (160)	1:2:1
$5,5'-[\text{Cp}^*\text{Co}(\text{2,3-Et}_2\text{C}_2\text{B}_4\text{H}_3)]_2$ (2)	20.2, 4.2	1:3 ^f
$[(-\text{CH}_2\text{C}_5\text{Me}_4)\text{Co}(\text{2,3-Et}_2\text{C}_2\text{B}_4\text{H}_4)]_2$ (3a)	2.6, -6.2	1:3 ^f
$[(-\text{CH}_2\text{C}_5\text{Me}_4)\text{Co}(\text{2,3-Et}_2\text{C}_2\text{B}_4\text{H}_3\text{-5-Cl})]_2$ (3b)	23.0, 0.8	1:3 ^f
$[(-\text{CH}_2\text{C}_5\text{Me}_4)\text{Co}(\text{2,3-Et}_2\text{C}_2\text{B}_4\text{H}_3\text{-5-Br})]_2$ (3c)	18.5, 2.9	1:3 ^f
$[(-\text{CH}_2\text{C}_5\text{Me}_4)\text{Co}(\text{2,3-Et}_2\text{C}_2\text{B}_4\text{H}_3\text{-5-I})]_2$ (3d)	3.5	f
$[(-\text{CH}_2\text{C}_5\text{Me}_4)\text{Co}(\text{2,3-Et}_2\text{C}_2\text{B}_3\text{H}_5)]_2$ (4a)	8.0, 4.7	1:2
$[(-\text{CH}_2\text{C}_5\text{Me}_4)\text{Co}(\text{2,3-Et}_2\text{C}_2\text{B}_3\text{H}_4\text{-5-Cl})]_2$ (4b)	9.4, -12.0	1:2
$[(-\text{CH}_2\text{C}_5\text{Me}_4)\text{Co}(\text{2,3-Et}_2\text{C}_2\text{B}_3\text{H}_4\text{-5-Br})]_2$ (4c)	12.0, -0.6	1:2
$[(-\text{CH}_2\text{C}_5\text{Me}_4)\text{Co}(\text{2,3-Et}_2\text{C}_2\text{B}_3\text{H}_4\text{-5-I})]_2$ (4d)	-7.4, -12.8	1:2
$[\text{Cp}^*\text{Co}(\text{2,3-Et}_2\text{C}_2\text{B}_3\text{H}_4)]_2$ (8)	10.0, 6.7, 4.5, 1.2	f
<i>nido</i> - $\text{Cp}^*\text{Co}(\text{2,3-Et}_2\text{C}_2\text{B}_3\text{H}_5)$ (9) ^d	7.5 (146), 3.9 (134)	1:2

300 MHz ^1H NMR Data	
compd	$\delta^{g,h}$
1a ^d	2.51 m (ethyl CH ₂), 2.28 m (ethyl CH ₂), 1.77 s (C ₅ Me ₅), 1.19 t (ethyl CH ₃)
1b ^e	2.54 dq (ethyl CH ₂), 2.30 dq (ethyl CH ₂), 1.80 s (C ₅ Me ₅), 1.21 t (ethyl CH ₃)
1c ^e	2.47 dq (ethyl CH ₂), 2.29 dq (ethyl CH ₂), 1.80 s (C ₅ Me ₅), 1.16 t (ethyl CH ₃)
1d ^e	2.50 dq (ethyl CH ₂), 2.30 dq (ethyl CH ₂), 1.77 s (C ₅ Me ₅), 1.16 t (ethyl CH ₃)
2 ^e	2.57 dq (ethyl CH ₂), 2.39 dq (ethyl CH ₂), 1.80 s (C ₅ Me ₅), 1.20 t (ethyl CH ₃)
3a	2.45 m (ethyl CH ₂), 2.29 s (CH ₂ CH ₂), 2.24 m (ethyl CH ₂), 1.75 s (C ₅ Me ₅), 1.66 s (C ₅ Me ₅), 1.15 t (ethyl CH ₃)
3b	2.43 m (ethyl CH ₂), 2.36 s (CH ₂ CH ₂), 2.26 m (ethyl CH ₂), 1.78 s (C ₅ Me ₅), 1.73 s (C ₅ Me ₅), 1.13 t (ethyl CH ₃)
3c	2.43 m (ethyl CH ₂), 2.36 s (CH ₂ CH ₂), 2.27 m (ethyl CH ₂), 1.77 s (C ₅ Me ₅), 1.73 s (C ₅ Me ₅), 1.13 t (ethyl CH ₃)
3d	2.46 m (ethyl CH ₂), 2.33 s (CH ₂ CH ₂), 2.28 m (ethyl CH ₂), 1.76 s (C ₅ Me ₅), 1.73 s (C ₅ Me ₅), 1.13 t (ethyl CH ₃)
4a	2.25 s (CH ₂ CH ₂), 2.02 m (ethyl CH ₂), 1.83 m (ethyl CH ₂), 1.74 s (C ₅ Me ₅), 1.64 s (C ₅ Me ₅), 1.06 t (ethyl CH ₃), -6.0 br (BHB)
4b	2.28 s (CH ₂ CH ₂), 2.06 m (ethyl CH ₂), 1.80 m (ethyl CH ₂), 1.74 s (C ₅ Me ₅), 1.65 s (C ₅ Me ₅), 1.05 t (ethyl CH ₃), -4.0 br (BHB)
4c	2.30 s (CH ₂ CH ₂), 2.08 m (ethyl CH ₂), 1.82 m (ethyl CH ₂), 1.74 s (C ₅ Me ₅), 1.65 s (C ₅ Me ₅), 1.05 t (ethyl CH ₃), -4.3 br (BHB)
4d	2.30 s (CH ₂ CH ₂), 2.11 m (ethyl CH ₂), 1.84 m (ethyl CH ₂), 1.73 s (C ₅ Me ₅), 1.65 s (C ₅ Me ₅), 1.06 t (ethyl CH ₃), -4.6 br (BHB)
8	2.15 m (ethyl CH ₂), 2.00 m (ethyl CH ₂), 1.90 m (ethyl CH ₂), 1.81 s (C ₅ Me ₅), 1.64 s (C ₅ Me ₅), 1.24 t (ethyl CH ₃), 1.16 t (ethyl CH ₃), 1.01 t (ethyl CH ₃), 0.87 t (ethyl CH ₃), -5.1 br (BHB), -6.5 br (BHB)
9 ^d	2.09 m (ethyl CH ₂), 1.89 m (ethyl CH ₂), 1.76 s (C ₅ Me ₅), 1.10 t (ethyl CH ₃), -5.5 br (BHB)

^a Shifts relative to $\text{BF}_3\cdot\text{OEt}_2$, positive values downfield. H-B coupling (in Hz) is given in parentheses when resolved. ^b Dichloromethane solution except where otherwise indicated. ^c *n*-Hexane solution. ^d Reference 11. ^e Reference 1a. ^f Overlapped/superimposed peaks. ^g CDCl_3 solution; shifts relative to $(\text{CH}_3)_4\text{Si}$. Integrated peak areas in all cases are consistent with the assignments given. Legend: m = multiplet, s = singlet, sb = broad singlet, d = doublet, t = triplet, q = quartet. ^h B-H_{terminal} resonances are broad quartets and are mostly obscured by other signals.

Table 2. Experimental X-ray Diffraction Parameters and Crystal Data

	2	3c	8
empirical formula	$\text{Co}_2\text{C}_{32}\text{B}_5\text{H}_{56}$	$\text{Co}_2\text{Br}_2\text{C}_{32}\text{B}_5\text{H}_{54}$	$\text{Co}_2\text{C}_{32}\text{B}_5\text{H}_{58}$
fw	645.1	802.9	625.5
cryst color, habit	red plate	orange plate	red prism
cryst dimens, mm	0.41 × 0.37 × 0.14	0.46 × 0.33 × 0.21	0.48 × 0.42 × 0.28
space group	$P\bar{1}$	$P\bar{1}$	$P2_1/n$
<i>a</i> , Å	8.998(3)	8.892(3)	8.678(2)
<i>b</i> , Å	12.277(5)	13.346(2)	32.560(4)
<i>c</i> , Å	8.925(3)	8.367(4)	12.604(3)
α , deg	105.14(3)	94.48(3)	
β , deg	116.32(3)	111.88(2)	103.34(1)
γ , deg	85.81(3)	86.35(2)	
<i>V</i> , Å ³	852	918	3465
<i>Z</i>	1	1	4
$\mu(\text{Mo K}\alpha)$, cm ⁻¹	9.92	30.80	9.75
transmission factors	0.80–1.00	0.84–1.00	0.94–1.00
<i>D</i> (calcd), g cm ⁻³	1.257	1.452	1.199
$2\theta_{\text{max}}$, deg	50.0	50.0	50.0
no. of reflns measd	3227	2858	6661
no. of reflns obsd	3016	2630	6231
(<i>I</i> > 3 σ (<i>I</i>))			
<i>R</i>	0.030	0.028	0.031
<i>R</i> _w	0.041	0.039	0.054
largest peak in final diff map, e/Å ³	0.33	0.31	0.29

angle of 109.2° describe a normal $-\text{CH}_2\text{CH}_2-$ bridge linking the Cp^* units.

One expects that the chemistry of **3a–d** will closely parallel that of the corresponding monomers, and the proton NMR data for these complexes are very similar

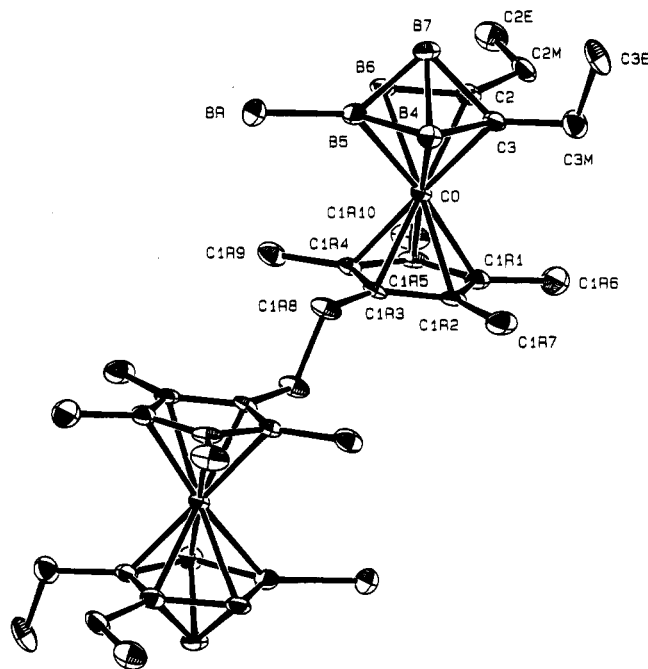


Figure 2. Molecular structure of $[(-\text{CH}_2\text{C}_5\text{Me}_4)\text{Co}(\text{Et}_2\text{C}_2\text{B}_4\text{H}_3\text{-5-Br})]_2$ (**3c**).

to those of the monomers^{1a,11} except for the complexity introduced by replacing C_5Me_5 with $\text{C}_5\text{Me}_4\text{CH}_2$ ligands. The ^{11}B NMR spectra of the dimers exhibit unusually

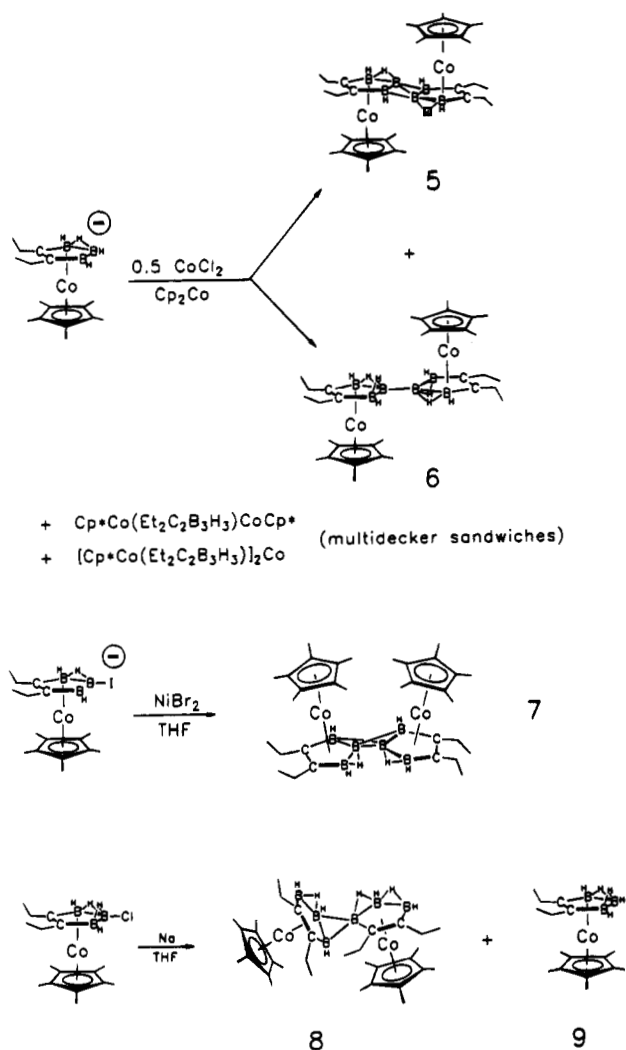
Table 3. Bond Distances and Selected Bond Angles for 5,5'-[Cp*Co(Et₂C₂B₄H₃)₂] (2)

Bond Distances (Å)			
Co-C(2)	2.011(3)	C(3)-B(7)	1.777(4)
Co-C(3)	2.014(3)	C(1R1)-C(1R2)	1.425(4)
Co-C(1R1)	2.062(3)	C(1R1)-C(1R5)	1.422(4)
Co-C(1R2)	2.057(3)	C(1R1)-C(1R6)	1.503(4)
Co-C(1R3)	2.039(3)	C(1R2)-C(1R3)	1.426(4)
Co-C(1R4)	2.039(3)	C(1R2)-C(1R7)	1.499(4)
Co-C(1R5)	2.047(3)	C(1R3)-C(1R4)	1.432(4)
Co-B(4)	2.100(3)	C(1R3)-C(1R8)	1.496(4)
Co-B(5)	2.184(3)	C(1R4)-C(1R5)	1.427(4)
Co-B(6)	2.092(3)	C(1R4)-C(1R9)	1.491(4)
C(2)-C(2M)	1.505(4)	C(1R5)-C(1R10)	1.500(4)
C(2)-C(3)	1.472(4)	B(4)-B(5)	1.695(4)
C(2)-B(6)	1.570(4)	B(4)-B(7)	1.778(4)
C(2)-B(7)	1.771(4)	B(5)-B(5')	1.690(6)
C(2M)-C(2E)	1.519(4)	B(5)-B(6)	1.695(4)
C(3M)-C(3)	1.508(4)	B(5)-B(7)	1.762(4)
C(3M)-C(3E)	1.523(4)	B(6)-B(7)	1.770(4)
C(3)-B(4)	1.571(4)		
Bond angles (deg)			
Co-C(2)-C(2M)	134.4(2)	B(5')-B(5)-B(7)	137.9(3)
C(2M)-C(2)-C(3)	123.3(2)	Co-C(3)-C(3M)	134.3(2)
C(2M)-C(2)-B(6)	124.3(2)	C(2)-C(3)-C(3M)	123.3(2)
C(2M)-C(2)-B(7)	134.4(2)	C(2)-C(3)-B(4)	112.0(2)
C(3)-C(2)-B(6)	112.0(2)	C(3M)-C(3)-B(4)	124.3(2)
C(3)-B(4)-B(5)	106.6(2)	C(3M)-C(3)-B(7)	134.7(2)
B(4)-B(5)-B(5)	128.8(3)	C(2)-B(6)-B(5)	106.6(2)
B(4)-B(5)-B(6)	102.7(2)	C(2)-C(2M)-C(2E)	113.0(2)
Co-B(5)-B(5')	136.1(2)	C(3)-C(3M)-C(3E)	112.4(2)
B(5')-B(5)-B(6)	128.5(3)		

Table 4. Bond Distances and Selected Bond Angles for [(-CH₂C₅Me₄)Co(Et₂C₂B₄H₃-5-Br)]₂ (3c)

Bond Distances (Å)			
Br-B(5)	1.963(5)	C(3)-B(4)	1.562(6)
Co-C(2)	2.037(4)	C(3)-B(7)	1.770(5)
Co-C(3)	2.033(4)	C(1R1)-C(1R2)	1.437(5)
Co-C(1R1)	2.072(4)	C(1R1)-C(1R5)	1.423(6)
Co-C(1R2)	2.045(4)	C(1R1)-C(1R6)	1.496(6)
Co-C(1R3)	2.016(3)	C(1R2)-C(1R3)	1.425(5)
Co-C(1R4)	2.036(4)	C(1R2)-C(1R7)	1.494(5)
Co-C(1R5)	2.059(4)	C(1R3)-C(1R4)	1.434(5)
Co-B(4)	2.099(4)	C(1R3)-C(1R8)	1.508(5)
Co-B(5)	2.107(4)	C(1R4)-C(1R5)	1.435(5)
Co-B(6)	2.110(4)	C(1R4)-C(1R9)	1.492(5)
C(2M)-C(2)	1.518(5)	C(1R5)-C(1R10)	1.503(5)
C(2M)-C(2E)	1.520(6)	C(1R8)-C(1R8')	1.546(7)
C(2)-C(3)	1.470(5)	B(4)-B(5)	1.667(6)
C(2)-B(6)	1.558(6)	B(4)-B(7)	1.802(6)
C(2)-B(7)	1.776(6)	B(5)-B(6)	1.671(6)
C(3M)-C(3)	1.509(5)	B(5)-B(7)	1.748(6)
C(3M)-C(3E)	1.537(6)	B(6)-B(7)	1.792(6)
Bond Angles (deg)			
Co-C(2)-C(2M)	134.7(3)	Co-C(3)-C(3M)	135.3(3)
C(2M)-C(2)-C(3)	120.1(3)	C(2)-C(3)-C(3M)	123.2(3)
C(2M)-C(2)-B(6)	127.0(3)	C(2)-C(3)-B(4)	112.9(3)
C(2M)-C(2)-B(7)	133.5(3)	C(3M)-C(3)-B(4)	123.5(3)
C(3)-C(2)-B(6)	112.4(3)	C(3M)-C(3)-B(7)	132.8(3)
C(3)-B(4)-B(5)	103.9(3)	C(3)-C(3M)-C(3E)	111.8(3)
Br-B(5)-Co	135.6(2)	C(2)-C(2M)-C(2E)	115.8(3)
Br-B(5)-B(4)	125.5(3)	Co-C(1R3)-C(1R8)	128.0(2)
Br-B(5)-B(6)	127.9(3)	C(1R3)-C(1R8)-C(1R8')	109.2(4)
Br-B(5)-B(7)	134.3(3)	C(1R2)-C(1R3)-C(1R8)	126.4(3)
B(4)-B(5)-B(6)	106.4(3)	C(1R4)-C(1R3)-C(1R8)	125.0(3)
C(2)-B(6)-B(5)	104.3(3)		

broad, overlapping signals that obscure the anticipated 1:2:1 pattern (which is clearly present in the spectra of the monomers **1a**,¹¹ **1b**,^{1a} and **1d**,^{1a} though not in **1c**^{1a}). The ¹¹B shifts of **3a** and **3d** differ significantly from those of their monomeric counterparts **1a,d** (Table 1), demonstrating that the replacement of a Cp* hydrogen atom with a -(CH₂C₅Me₄)CoEt₂C₂B₄H₄ unit has measurable electronic consequences. Whether this will lead

Scheme 2

to major differences in reactivity remains to be seen, but in at least one important respect these dimers are similar to the monomers: unlike the B-B-linked complex **2**, they are readily decapitated in wet TMEDA, generating the linked *nido*-cobaltacarborane species **4a-d** as yellow air-stable solids (Scheme 1). These double open-ended complexes furnish a new family of synthons that in principle can be used to construct oligomeric or polymeric -[(CH₂C₅Me₄)Co(Et₂C₂B₃H₂X)M(Et₂C₂B₃H₂X)-Co(C₅Me₄CH₂)]_n linked-quadruple-decker chains via deprotonation of the B-H-B bridges and face-coordination to M^{q+} metal ions.¹⁰

Synthesis and Characterization of Linked *nido*-Cobaltacarborane Dimers. Metallacarborane substrates having open C₂B₃ faces are highly versatile, reactive species and can be bound together in a variety of modes, including two-center B-B or three-center B-B-B interactions or combinations thereof. Additionally, in the presence of metal ions, they can form triple- or quadruple-decker sandwich complexes.⁷ In recent work^{9a} we isolated the dimers [Cp*Co(Et₂C₂B₃H₃)₂] (**5**, **7**) and [Cp*Co(Et₂C₂B₃H₄)₂] (**6**) as shown in Scheme 2. Compounds **5** and **7** were structurally characterized via X-ray crystallography and are isomers whose CoC₂B₃ units in both cases are joined via a pair of B-B-B three-center bonds (Chart 2A); in **6**, which has two more hydrogens than **5** and **7**, the linkage is a two-electron B-B single bond.

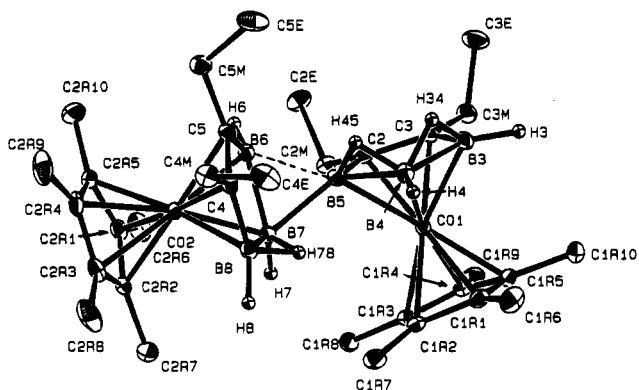
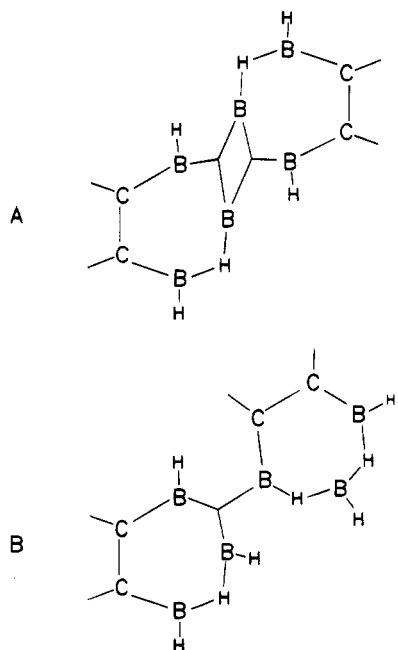


Figure 3. Molecular structure of $[\text{Cp}^*\text{Co}(\text{Et}_2\text{C}_2\text{B}_3\text{H}_4)]_2$ (**8**).

Chart 2



In the present study, our synthesis of **2** via Wurtz-type reactions of halogenated closo clusters, described above, led us to attempt an analogous linkage of *nido*-cobaltacarborane units, recognizing that the B–H–B bridging protons on the open face could lead to more complex interactions. This is in fact the case: as depicted in Scheme 2 (bottom), the treatment of neutral $\text{Cp}^*\text{Co}(\text{Et}_2\text{C}_2\text{B}_3\text{H}_4-5\text{-Cl})$ with sodium in THF afforded two major products that were identified as the dimeric species $[\text{Cp}^*\text{Co}(\text{Et}_2\text{C}_2\text{B}_3\text{H}_4)]_2$ (**8**), isolated as yellow crystals, and the unsubstituted *nido* monomer **9**¹¹ in yields of 15 and 42%, respectively. Since **9** can be quantitatively converted to the B(5)–chloro starting material, the net conversion of the latter species to **8** is ca. 25%.

From its ¹H and ¹¹B NMR spectra (Table 1) it is evident that **8** is asymmetric, and an X-ray diffraction analysis revealed yet another mode of intercage binding that differs from those found in **5**–**7**. The molecular structure of **8** is presented in Figure 3, while Tables 2 and 5 present the relevant crystal structure information, bond distances, and selected bond angles. This structure is “dimeric” only in a general sense, consisting of two dissimilar $\text{Cp}^*\text{Co}(\text{Et}_2\text{C}_2\text{B}_3\text{H}_4)$ units, one of which contains two B–H–B and two terminal hydrogens while the other has one B–H–B bridge and three terminal H atoms. The C_2B_3 ring planes are almost exactly per-

Table 5. Bond Distances and Selected Bond Angles for $[\text{Cp}^*\text{Co}(\text{Et}_2\text{C}_2\text{B}_3\text{H}_4)]_2$ (**8**)

Bond Distances (Å)			
Co(1)–C(2)	2.070(2)	B(4)–H(4)	1.15(3)
Co(1)–C(3)	2.075(2)	C(3)–B(3)	1.522(4)
Co(1)–C(1R1)	2.048(2)	C(4)–C(4M)	1.513(4)
Co(1)–C(1R2)	2.081(2)	C(4)–C(5)	1.431(4)
Co(1)–C(1R3)	2.093(2)	C(4)–B(8)	1.519(4)
Co(1)–C(1R4)	2.086(2)	C(4M)–C(4E)	1.528(4)
Co(1)–C(1R5)	2.074(2)	C(5)–C(5M)	1.512(4)
Co(1)–B(3)	2.053(3)	C(5)–B(6)	1.542(4)
Co(1)–B(4)	2.034(3)	C(5M)–C(5E)	1.521(4)
Co(1)–B(5)	2.113(3)	C(1R1)–C(1R2)	1.432(4)
Co(2)–C(4)	2.065(2)	C(1R1)–C(1R5)	1.426(4)
Co(2)–C(5)	2.058(2)	C(1R1)–C(1R6)	1.499(4)
Co(2)–C(2R1)	2.043(2)	C(1R2)–C(1R3)	1.427(3)
Co(2)–C(2R2)	2.047(2)	C(1R2)–C(1R7)	1.492(4)
Co(2)–C(2R3)	2.071(3)	C(1R3)–C(1R4)	1.426(3)
Co(2)–C(2R4)	2.075(3)	C(1R3)–C(1R8)	1.500(3)
Co(2)–C(2R5)	2.073(3)	C(1R4)–C(1R5)	1.422(3)
Co(2)–B(6)	2.041(3)	C(1R4)–C(1R9)	1.493(4)
Co(2)–B(7)	2.071(3)	C(1R5)–C(1R10)	1.493(4)
Co(2)–B(8)	2.030(3)	C(2R1)–C(2R2)	1.430(4)
C(2M)–C(2)	1.501(3)	C(2R1)–C(2R5)	1.414(4)
C(2M)–C(2E)	1.530(3)	C(2R1)–C(2R6)	1.499(4)
C(2)–C(3)	1.433(3)	C(2R2)–C(2R3)	1.419(4)
C(2)–B(5)	1.539(4)	C(2R2)–C(2R7)	1.504(4)
C(3M)–C(3)	1.517(4)	C(2R3)–C(2R4)	1.426(4)
C(3M)–C(3E)	1.523(4)	C(2R3)–C(2R8)	1.504(4)
C(2R4)–C(2R9)	1.501(4)	C(2R4)–C(2R5)	1.432(4)
C(2R5)–C(2R10)	1.496(4)	B(4)–H(34)	1.25(4)
B(3)–B(4)	1.805(4)	B(4)–H(45)	1.22(3)
B(4)–B(5)	1.836(4)	B(5)–H(45)	1.27(3)
B(5)–B(6)	1.937(4)	B(6)–H(6)	1.11(2)
B(5)–B(7)	1.873(4)	B(7)–H(7)	1.09(3)
B(6)–B(7)	1.751(4)	B(7)–H(78)	1.27(3)
B(7)–B(8)	1.842(4)	B(8)–H(8)	1.18(3)
B(3)–H(3)	1.14(3)	B(8)–H(78)	1.27(3)
B(3)–H(34)	1.23(4)		
Bond Angles (deg)			
C(2M)–C(2)–C(3)	122.7(2)	C(5M)–C(5)–B(6)	122.0(2)
C(2M)–C(2)–B(5)	121.3(2)	C(5)–C(5M)–C(5E)	111.6(2)
C(3)–C(2)–B(5)	115.6(2)	B(4)–B(5)–B(6)	128.6(2)
Co(1)–C(2)–C(2M)	124.2(2)	B(4)–B(5)–B(7)	119.6(2)
C(2)–C(2M)–C(2E)	113.8(2)	B(6)–B(5)–B(7)	54.7(1)
C(2)–C(3)–C(3M)	122.9(2)	Co(1)–B(5)–B(6)	165.6(2)
C(2)–C(3)–B(3)	115.7(2)	Co(1)–B(5)–B(7)	112.5(2)
C(3M)–C(3)–B(3)	121.1(2)	C(2)–B(5)–B(4)	104.3(2)
Co(1)–C(3)–C(3M)	128.2(2)	C(2)–B(5)–B(6)	114.7(2)
C(3)–C(3M)–C(3E)	111.0(2)	C(2)–B(5)–B(7)	129.6(2)
C(3)–B(3)–B(4)	105.8(2)	Co(2)–B(6)–B(5)	125.5(2)
C(4M)–C(4)–C(5)	123.1(2)	C(5)–B(6)–B(5)	117.7(2)
C(4M)–C(4)–B(8)	121.2(2)	C(5)–B(6)–B(7)	106.7(2)
Co(2)–C(4)–C(4M)	128.4(2)	B(5)–B(6)–B(7)	60.8(1)
C(5)–C(4)–B(8)	115.4(2)	Co(2)–B(7)–B(5)	127.4(2)
C(4)–C(4M)–C(4E)	110.1(2)	B(5)–B(7)–B(6)	64.5(1)
Co(2)–C(5)–C(5M)	127.0(2)	B(5)–B(7)–B(8)	117.0(2)
C(4)–C(5)–C(5M)	123.1(2)	B(6)–B(7)–B(8)	98.5(2)
C(4)–C(5)–B(6)	114.6(2)	C(4)–B(8)–B(7)	104.7(2)

pendicular, with a dihedral angle of 90.6°. The intercluster binding is unusual, with B(5) on one C_2B_3 ring coordinated to B(7) and B(6) on the other ring, at distances of 1.873(4) and 1.937(4) Å, respectively. Together with the intracage B(6)–B(7) interaction (1.751(4) Å), this triangular array suggests a three-center B–B–B bond as depicted in Chart 2B; in effect, B(5) can be viewed as replacing the “missing” bridge hydrogen on the other $\text{Et}_2\text{C}_2\text{B}_3\text{H}_4$ ring. While relatively long, the B(5)–B(6) and B(5)–B(7) distances are within bonding range and are similar to those found in a cobaltacarborane–carborane-coupled species isolated earlier by Sneddon et al.¹⁸

Compound **8** probably forms from an initially produced symmetrical B(5),B(5')-coupled isomer that undergoes a rearrangement whose net effect is the replacement of one of the original B-H-B bridging hydrogens (that involving B(6) and B(7)) with a B-B-B linkage. However, the accompanying formation of neutral **9** in substantial yield indicates that the sodium-promoted disproportionation of the chloro complex is a major competitive process in this reaction.

Electronic Spectra. The visible-ultraviolet absorption bands of the dimeric complexes (Experimental Section) appear at nearly the same wavelengths as their monomeric counterparts, and their molar extinction coefficients are approximately twice those of the monomers (reflecting, of course, the doubled molar concentration of metallacarborane cluster units in solutions of the dimers). For example, λ_{max} values (nm) for **1a** and the B-B-linked species **2** are respectively 300 ($\epsilon = 11\,718\text{ M}^{-1}\text{ cm}^{-1}$) and 294 ($\epsilon = 24\,469\text{ M}^{-1}\text{ cm}^{-1}$), while the corresponding values for the nido monomer Cp*Co(Et₂C₂B₃H₄Cl) and its Cp*-Cp*-linked dimer **4b** are 286 ($\epsilon = 20\,332\text{ M}^{-1}\text{ cm}^{-1}$) and 292 ($\epsilon = 37\,526\text{ M}^{-1}\text{ cm}^{-1}$). From these observations, it appears that the metal-ligand interactions in the B-B-linked and Cp*-Cp*-linked clusters are not greatly different from those in the corresponding monomeric complexes. The high extinction coefficients in both monomers and dimers are strongly suggestive of charge-transfer excitations, probably involving filled bonding MOs on the carborane ligands and empty antibonding MOs on the metal centers. Similar electronic behavior is seen in related metallacarborane complexes, e.g., in a number of our recently reported triple- and quadruple-decker sandwiches.^{7b}

Summary

It is apparent from this work and our earlier studies on coupling of small metallacarboranes^{9a} that reactions of closo derivatives such as **1a-d** can be synthetically useful, allowing the preparation of specific target dimers in good yield with minimal side reactions as in Scheme 1. On the other hand, nido complexes such as those depicted in Scheme 2 generate a much richer and less easily controlled chemistry that leads to structurally varied dimers featuring a range of intercalce binding modes. Of the new products reported here, the dimethylene-linked species **4a-d**, prepared via a reasonably efficient route, are potentially useful building blocks in the construction of polysandwich systems as noted earlier. If conditions can be found for decapitation of **2** to generate **6** directly, this would provide an additional synthetic tool that may permit the controlled assembly of directly B-B-coupled multidecker sandwich complexes. While **2** itself appears inert to TMEDA attack, as reported above, it may be possible to decap suitably tailored (e.g., halogenated) derivatives of **2**, and this strategy is among those to be explored in future studies.

Experimental Section

General operations, procedures, and instrumentation were as described in the accompanying paper.^{1a} Visible-ultraviolet spectra were recorded on a Hewlett-Packard 8452A diode array with a HP Vectra computer interface.

Synthesis of 5,5'-[Cp*Co(Et₂C₂B₃H₃)]₂ (2**).** THF (30 mL) was distilled under vacuum into a two-neck round-bottom flask

charged with 170 mg (0.42 mmol) of **1c**^{1a} to give an orange solution. An excess of pretreated sodium metal¹⁹ was added from an attached side tube at room temperature. The mixture was stirred for 1.5 h, during which time the solution turned deep red, and the flask was opened to the air. The solution was transferred via pipet to a flask, and the unreacted sodium was destroyed with 2-propanol. The solution was evaporated to dryness and flash-chromatographed in CH₂Cl₂ through 2 cm of silica gel. The solvent was removed via rotary evaporation to afford a red solid, which was dissolved in a minimum volume of CH₂Cl₂ and hexane, placed on a silica column, and eluted with 3:1 hexane-CH₂Cl₂. Two major orange bands were collected, the first of which was **2** (30 mg, 0.046 mmol, 42% based on **1c** consumed) and the second was recovered **1c** (80 mg, 0.20 mmol). MS: *m/z* 646 (molecular ion envelope). UV-visible absorptions (nm): 294 (100%; $\epsilon = 24\,469\text{ M}^{-1}\text{ cm}^{-1}$), 354 (64%), 466 (10%). Anal. Calcd for Co₂C₃₂B₈H₅₆: C, 59.58; H, 8.75. Found: C, 59.86; H, 9.22.

Compound **2** was also prepared from **1b,d** via an identical procedure, except that the reaction times employed were 6 h and 40 min, respectively. The isolated yields of **2** were 20% (from **1b**) and 34% (from **1d**).

Synthesis of [(-CH₂C₅Me₄)Co(Et₂C₂B₄H₄)]₂ (3a**).** By the above procedure, a solution of 410 mg (1.26 mmol) of **1a**¹¹ in 30 mL of THF was prepared and the solution was cooled in a dry ice-ethanol bath. *n*-Butyllithium (0.79 mL of 1.6 M solution in hexanes) was added via syringe, producing a color change from yellow-orange to red. Following 3 h of stirring at room temperature, the deep red solution was opened to the air and the solvent was removed to give a red solid that was worked up as in the synthesis of **2**. Elution from a silica column using hexane gave one yellow band, which was *nido*-Cp*Co(Et₂C₂B₃H₅)¹¹ (54 mg, 0.17 mmol). The eluent was switched to 2:1 hexane-CH₂Cl₂, producing two major orange bands, the first of which was **1a** (127 mg, 0.40 mmol) and the second was **3a** (80 mg, 0.12 mmol, 28%). MS: *m/z* 646 (molecular ion envelope). UV-visible absorptions (nm): 306 (100%), 426 (4%). Anal. Calcd for Co₂C₃₂B₈H₅₆: C, 59.58; H, 8.75. Found: C, 58.92; H, 8.62.

Synthesis of [(-CH₂C₅Me₄)Co(Et₂C₂B₄H₃-5-Cl)]₂ (3b**).** An identical procedure was followed employing 80 mg (0.22 mmol) of **1b**.^{1a} Column chromatography on silica in hexane-CH₂Cl₂ with a ratio ranging from 2:1 to 1:1 gave two major orange bands that were identified as **1b** (37 mg, 0.10 mmol) and **3b** (24 mg, 0.034 mmol, 56%). MS: *m/z* 716 (molecular ion envelope). UV-visible absorption (nm): 300. Anal. Calcd for Co₂Cl₂C₃₂B₈H₅₄: C, 53.83; H, 7.62. Found: C, 53.95; H, 8.26.

Synthesis of [(-CH₂C₅Me₄)Co(Et₂C₂B₄H₃-5-Br)]₂ (3c**).** The preceding synthesis and workup were repeated employing 110 mg (0.27 mmol) of **1c**,^{1a} of which 27 mg (0.067 mmol) was recovered, affording 30 mg (0.037 mmol, 36%) or orange solid **3c**. MS: *m/z* 804 (molecular ion envelope), 646 (-2Br). UV-visible absorption (nm): 232 (27%), 298 (100%). Anal. Calcd for Co₂Br₂C₃₂B₈H₅₄: C, 47.87; H, 6.78. Found: C, 47.59; H, 6.79.

Synthesis of [(-CH₂C₅Me₄)Co(Et₂C₂B₄H₃-5-I)]₂ (3d**).** The preceding synthesis and workup were repeated employing 135 mg (0.30 mmol) of **1d**,^{1a} of which 82 mg (0.18 mmol) was recovered, affording 23 mg (0.026 mmol, 43%) of orange solid **3c**. MS: *m/z* 898 (molecular ion envelope), 771 (-I). UV-visible absorption (nm): 306. Anal. Calcd for Co₂I₂C₃₂B₈H₅₄: C, 42.85; H, 6.07. Found: C, 42.40; H, 6.58.

Synthesis of [(-CH₂C₅Me₄)Co(Et₂C₂B₃H₅)]₂ (4a**).** A two-neck round-bottom flask was charged with 25 mg (0.039 mmol) of **3a** and 4 mL of TMEDA, and 3 drops of water were added. THF was added via pipet until all of the solid was dissolved, and the solution was stirred for 3 h under a flow of N₂.

(19) Sodium pieces were allowed to react with absolute methanol for several seconds under a flow of N₂. The methanol was syringed out and the metal was washed with dry THF and stored under vacuum in a side tube on the reaction flask.

Volatiles were removed by evaporation on a Schlenk line, giving a red solid which was dissolved in a minimum volume of CH_2Cl_2 and hexane and placed on a silica column. Elution with hexane gave one yellow band, which was **4a** (10 mg, 41%). MS: m/z 626 (molecular ion envelope). UV-visible absorptions (nm): 290 (100%), 386 (8%). Anal. Calcd for $\text{Co}_2\text{C}_{32}\text{B}_6\text{H}_{58}$: C, 61.44; H, 9.35. Found: C, 62.41; H, 9.53.

Synthesis of $[(-\text{CH}_2\text{C}_5\text{Me}_4)\text{Co}(\text{Et}_2\text{C}_2\text{B}_3\text{H}_4\text{-5-Cl})_2]$ (4b**).**

The preceding procedure was employed using 50 mg of **3b** and 4:1 hexane- CH_2Cl_2 as the eluting solvent, which afforded 40 mg (ca. 100%) of **4b**. Further elution of the column with 2:1 hexane- CH_2Cl_2 gave 8 mg of recovered **3b**. MS: m/z 696 (molecular ion envelope). UV-visible absorptions (nm): 232 (44%), 248 (38%), 292 (100%, $\epsilon = 37\,526\text{ M}^{-1}\text{ cm}^{-1}$), 390 (5%). Anal. Calcd for $\text{Co}_2\text{Cl}_2\text{C}_{32}\text{B}_6\text{H}_{56}$: C, 55.35; H, 8.13. Found: C, 54.23; H, 8.65.

Synthesis of $[(-\text{CH}_2\text{C}_5\text{Me}_4)\text{Co}(\text{Et}_2\text{C}_2\text{B}_3\text{H}_4\text{-5-Br})_2]$ (4c**).**

The procedure described for **4a** was employed using 50 mg of **3c**, which gave 39 mg (80%) of **4c** as the only major band. MS: m/z 784 (molecular ion envelope), 704 (-Br). UV-visible absorptions (nm): 292 (100%), 392 (5%). Anal. Calc for $\text{Co}_2\text{Br}_2\text{C}_{32}\text{B}_6\text{H}_{56}$: C, 49.07; H, 7.21. Found: C, 49.83; H, 7.58.

Synthesis of $[(-\text{CH}_2\text{C}_5\text{Me}_4)\text{Co}(\text{Et}_2\text{C}_2\text{B}_3\text{H}_4\text{-5-I})_2]$ (4d**).**

The procedure described for **4a** was employed using 250 mg of **3d**, except that the reaction time was 12 h and a 4:1 hexane- CH_2Cl_2 mixture was employed to elute the product. A total of 150 mg (61%) of **4d** was obtained. MS: m/z 878 (molecular ion envelope). UV-visible absorptions (nm): 234 (48%), 294 (100%), 388 (5%). Anal. Calcd for $\text{Co}_2\text{I}_2\text{C}_{32}\text{B}_6\text{H}_{56}$: C, 43.81; H, 6.43. Found: C, 43.42; H, 7.15.

Synthesis of $[\text{Cp}^*\text{Co}(\text{Et}_2\text{C}_2\text{B}_3\text{H}_4)]_2$ (8**).** THF (30 mL) was distilled under vacuum into a two-neck round-bottom flask charged with 636 mg (1.83 mmol) of $\text{Cp}^*\text{Co}(\text{Et}_2\text{C}_2\text{B}_3\text{H}_4\text{-5-Cl})$. An excess of sodium was added under a flow of nitrogen, and the flask was attached to a condenser and heated until the THF commenced boiling. Reflux with stirring was maintained for 3 h, during which time the solution turned deep red-black. The solution was opened to the air, evaporated to dryness, and flash-chromatographed in hexane through 2 cm of silica gel to give a red solution, from which the volatiles were removed to leave a red oily solid. The solid residue was dissolved in pentane and eluted in that solvent on a silica column, affording

yellow-orange **9**¹¹ (242 mg, 0.77 mmol) and yellow crystalline **8** (83 mg, 0.13 mmol). Allowing for quantitative conversion of recovered **9** to the starting material $\text{Cp}^*\text{Co}(\text{Et}_2\text{C}_2\text{B}_3\text{H}_4\text{-5-Cl})$, the net yield of **8** was 25%. MS: m/z 626 (molecular ion envelope), 324 ($\text{Cp}^*\text{CoEt}_2\text{C}_2\text{B}_4\text{H}_4^+$). UV-visible absorptions (nm): 300 (100%), 422 (26%). Anal. Calcd for $\text{Co}_2\text{C}_{32}\text{B}_6\text{H}_{58}$: C, 61.44; H, 9.35. Found: C, 62.11; H, 9.85.

X-ray Structure Determinations. Diffraction data were collected on a Rigaku AFC6S diffractometer at $-120\text{ }^\circ\text{C}$ using Mo K α radiation. Details of the data collections and structure determinations are listed in Table 1. For each crystal, the intensities of three standard reflections were monitored, showing no significant variation. Empirical absorption corrections were applied following ψ scanning of several reflections (transmission factors are reported in Table 1). All calculations were performed on a VAXstation 3520 computer employing the TEXSAN 5.0 crystallographic software package.²⁰ The structures were solved by direct methods in SIR88.²¹ Full-matrix least-squares refinement with anisotropic thermal displacement parameters was carried out for each structure, with the results summarized in Table 2. The final difference Fourier maps were featureless.

Acknowledgment. This work was supported by the U.S. Army Research Office and the National Science Foundation (Grant No. CHE 9322490). We thank Professor John Gladysz for helpful discussions on the activation of Cp^* ligands.

Supporting Information Available: Tables of atomic coordinates (including observed and calculated hydrogen atom positions for **8**), isotropic and anisotropic displacement parameters, and calculated mean planes for **2**, **3c**, and **8** (8 pages). Ordering information is given on any current masthead page.

OM950344B

(20) TEXSAN 5.0: Single Crystal Structure Analysis Software (1989), Molecular Structure Corp., The Woodlands, TX 77381.

(21) SIR88: Burla, M. C.; Camalli, M.; Cascarano, G.; Giacovazzo, C.; Polidori, G.; Spagna, R.; Viterbo, D. *J. Appl. Crystallogr.* **1989**, *22*, 389.

Structure of 2-Methyl-1-(phenylethynyl)cyclopentanol and of Its $\text{Co}_2(\text{CO})_6$ and $(\text{C}_5\text{H}_5)_2\text{Mo}_2(\text{CO})_4$ Cluster Complexes: $\text{Co}_2(\text{CO})_6$ as a Conformational Switch

Krisztina L. Malisza, Luc Girard, Donald W. Hughes, James F. Britten, and Michael J. McGlinchey*

Department of Chemistry, McMaster University, Hamilton, Ontario L8S 4M1, Canada

Received March 13, 1995[®]

Treatment of 2-methylcyclopentanone with $\text{PhC}\equiv\text{CMgBr}$ yields 2-methyl-1-(phenylethynyl)cyclopentanol (**6'**), in which the alkynyl group is axial and *cis* to the methyl substituent. Reaction with $\text{Co}_2(\text{CO})_6$ gives the cluster complex **9**, in which the (alkynyl) $\text{Co}_2(\text{CO})_6$ group adopts an equatorial position and the hydroxyl and methyl groups are now axial. In contrast, $(\text{C}_5\text{H}_5)_2\text{Mo}_2(\text{CO})_4$ reacts with **6'** to produce (2-methyl-1-(phenylethynyl)cyclopentene) $\text{Mo}_2(\text{CO})_4(\text{C}_5\text{H}_5)_2$, (**19**). The alkyne, **6'** and also the cobalt and molybdenum complexes, **9** and **19** have all been characterized by X-ray crystallography. The observed preference for the bulky $(\text{RC}\equiv\text{C})\text{Co}_2(\text{CO})_6$ substituent to occupy an equatorial site in cycloalkanes may be used to rationalize the stereospecificity of the Friedel-Crafts cyclization of cobalt-stabilized propargyl cations onto suitably activated aromatic rings.

Introduction

The generation and stabilization of carbocations in the vicinity of transition-metal centers continue to attract much interest.¹ These studies are directed not merely toward gaining an appreciation of the factors involved in delocalizing charge onto a neighboring metal; they also allow the development of novel synthetic strategies. Indeed, such intermediates now play a burgeoning role in organic synthesis.²

Our own recent efforts have been focused on the synthesis, characterization and molecular dynamics of carbocations stabilized by mono-, di- and trimetallic fragments, as in the molecules **1-3**.³⁻⁵ In particular, the

markers for the estradiol receptor site.⁶ Moreover, the steroidal clusters **4** and **5** are themselves of considerable current interest, not only because they are close analogues of widely used contraceptives or abortifacients but also because they hold considerable promise of providing a method of assaying hormonal receptor sites while avoiding the inconveniences associated with radiolabeling techniques.^{7,8}

In **4** and **5**, where the dimetallatetrahedrane is bonded to the cyclopentanol D ring of the hormone, the molecular conformation is dictated primarily by the demands of the polycyclic skeleton. Consequently, we chose to synthesize the $\text{Co}_2(\text{CO})_6$ and $(\text{C}_5\text{H}_5)_2\text{Mo}_2(\text{CO})_4$ complexes of 2-methyl-1-(phenylethynyl)cyclopentanol (**6**) to study the conformational influence exerted by an M_2C_2 cluster moiety on a cycloalkane.

Results and Discussion

Conformations of 2-Methyl-1-(phenylethynyl)cyclopentanol and of Its $\text{Co}_2(\text{CO})_6$ Complex. The

(2) (a) Harrington, P. J. *Transition Metals in Total Synthesis*; Wiley: New York, 1990; Chapters 4 and 8. (b) Marshall, J. A.; Gung, W. Y. *Tetrahedron Lett.* **1989**, 30, 309. (c) Montana, A. M.; Nicholas, K. M. *J. Org. Chem.* **1990**, 55, 1569. (d) Magnus, P.; Annoura, H.; Harding, J. *J. Org. Chem.* **1990**, 55, 1709. (e) Magnus, O.; Pitterna, T. *J. Chem. Soc., Chem. Commun.* **1991**, 541. (f) Magnus, O.; Fortt, S. M. *J. Chem. Soc., Chem. Commun.* **1991**, 544. (g) Mukai, C.; Kataoka, O.; Hanaoka, M. *J. Org. Chem.* **1993**, 58, 2946.

(3) (a) Downton, P. A.; Sayer, B. G.; McGlinchey, M. J. *Organometallics* **1992**, 11, 3281. (b) Malisza, K. L.; Chao, L. C. F.; Britten, J. F.; Sayer, B. G.; Jaouen, G.; Top, S.; Decken, A.; McGlinchey, M. J. *Organometallics* **1993**, 12, 2462. (c) Holmes, J. D.; Jones, D. A. K.; Pettit, R. J. *Organomet. Chem.* **1965**, 4, 324. (d) Acampora, M.; Ceccon, A.; Dal Farra, M.; Giacometti, G.; Rigatti, G. *J. Chem. Soc., Perkin Trans. 2* **1977**, 483.

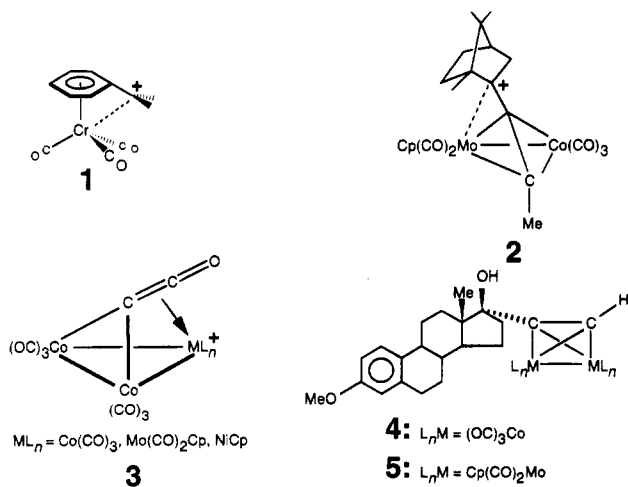
(4) (a) Gruselle, M.; El Hafa, H.; Nikolski, M.; Jaouen, G.; Vaissermann, J.; Li, L.; McGlinchey, M. J. *Organometallics* **1993**, 12, 4917. (b) Kondratenko, M.; El Hafa, H.; Gruselle, M.; Vaissermann, J.; Jaouen, G.; McGlinchey, M. J. *J. Am. Chem. Soc.* **1995**, 117, 6907.

(5) D'Agostino, M. F.; Mlekuz, M.; McGlinchey, M. J. *J. Organomet. Chem.* **1988**, 345, 371.

(6) Vessières, A.; Top, S.; Osella, D.; Mornon, J.-P.; Jaouen, G. *Angew. Chem., Int. Ed. Engl.* **1992**, 31, 753.

(7) Vessières, A.; Jaouen, G.; Gruselle, M.; Rossignol, J. L.; Savignac, M.; Top, S.; Greenfield, S. *J. Steroid Biochem.* **1988**, 29, 229.

(8) Jaouen, G.; Vessières, A.; Butler, I. S. *Acc. Chem. Res.* **1993**, 26, 361.

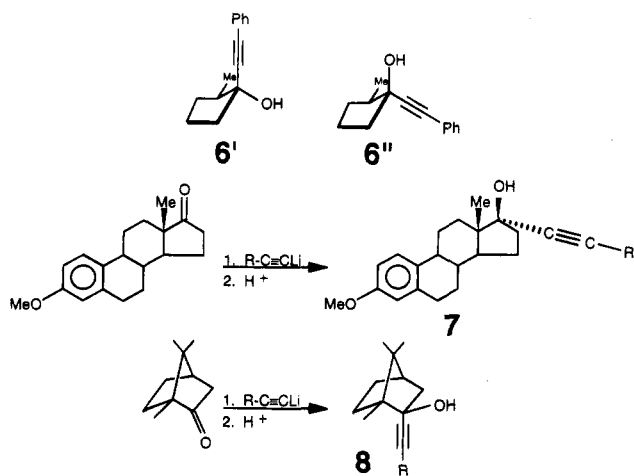


cations obtained by protonation of the steroidal complexes **4** and **5** have been studied as potential affinity

[®] Abstract published in *Advance ACS Abstracts*, September 1, 1995.

(1) 1. (a) In the field of metal-stabilized cations, many of the ideas currently espoused date back to a seminal review written almost 20 years ago: Pettit, R.; Haynes, L. W. In *Carbonium Ions*; Olah, G. A., Schleyer, P. v. R., Eds.; Wiley: New York, 1976; Vol. 5, pp 2049-2133. (b) McGlinchey, M. J.; Girard, L.; Ruffolo, R. *Coord. Chem. Rev.*, in press. (c) Caffyn, A. J. M.; Nicholas, K. M. In *Comprehensive Organometallic Chemistry II*; Wilkinson, G., Stone, F. G. A., Abel, E. W., Eds.; Pergamon Press: Oxford, U.K., 1995; Vol. 12, in press.

conversion of 3-methoxyestrone to the 17-alkynyl derivative **7** proceeds via nucleophilic attack exclusively on the α -face of the estrone presumably so as to avoid steric interactions with the β -methyl group bonded to C(13) of the steroidal skeleton. Subsequent treatment with the appropriate organometallic precursor leads to the tetrahedral cluster **4** or **5**.⁹ Analogous behavior has been reported for the attack of alkynyl anions on camphor; the product, **8**, again arises via attack on the less hindered face of the ketone, as shown by X-ray crystallographic studies on a series of metal clusters.¹⁰



In the course of their pioneering studies on alkynes, Cadiot and Chodkiewicz *et al.* found that the ratio of *cis* to *trans* attack by Grignard reagents or organolithiums on alkyl-substituted cyclopentanones and cyclohexanones did not simply follow Cram's rule¹¹ but that it varied with ring size, solvent, counterion, temperature, and, of course, identity of the nucleophile.¹² Thus, bulky alkyl or aryl Grignards or lithium reagents attacked predominantly (80–95%) on the face opposite to that occupied by the substituent already present. In contrast, alkynyl nucleophiles preferentially entered *cis* to the substituent. Moreover, in the presence of base, equilibration of the isomeric 2-methyl-1-(phenylethynyl)cyclopentanols led to the thermodynamically controlled ratio whereby the product in which the methyl and hydroxyl groups are *trans* is favored by a factor of 55:45. In that study, the assignment of stereochemistry was based on the assumption that the protons of a methyl group *cis* to the neighboring hydroxyl substituent would be shielded relative to the resonance position of the corresponding *trans* isomer. These assignments were buttressed by NMR data on related diphenylphosphine oxide derivatives of the analogous allenyl systems.^{12c} Subsequent work by Felkin¹³ and by Nguyễn Trong Anh and Eisenstein¹⁴ showed that the direction

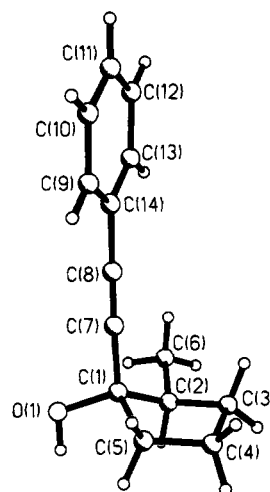


Figure 1. View of 2-methyl-1-(phenylethynyl)cyclopentanol (**6'**) showing the atomic numbering scheme.

of attack by a nucleophile on a cyclic ketone is influenced not only by the steric bulk of the incoming reagent but also by the torsion angle strain imposed on the system as the sp^2 carbon is transformed into an sp^3 center. However, some aspects of the Felkin–Anh model continue to attract comment and are still controversial.¹⁵

In seeking a simple model for the D-ring in the cobalt complex **4**, we decided to prepare the $Co_2(CO)_6$ complex of 2-methyl-1-(phenylethynyl)cyclopentanol. In our hands, slow addition of 2-methylcyclopentanone to (phenylethynyl)magnesium bromide at 0 °C yielded a 91:9 mixture of cyclopentanols. The surprising complexity of the 500 MHz 1H NMR spectrum of the major isomer of **6** belies the apparent simplicity of the molecule and, in order to resolve the overlapping methylene resonances, the spectra were recorded in $CDCl_3$, CD_2Cl_2 , C_6D_6 , and $DMSO-d_6$. The chemical shift difference between the protons at C(4) is small, but they are strongly coupled; this gives rise to severe second-order effects in the multiplets attributable to the neighboring methylenes at C(3) and C(5). The preliminary 1H and ^{13}C assignments were made from the 1H – 1H COSY and 1H – ^{13}C shift-correlated NMR spectra, and a series of spin-decoupling experiments yielded a set of J values.¹⁶ The relative orientations of the methyl and hydroxyl groups were obtained by a series of NOE difference experiments. For example, irradiation of the hydroxyl proton (in DMSO) produced clear NOE enhancements of the pseudoaxial hydrogens at C(2) and C(5). These data suggested a structure **6'** in which the phenylethynyl fragment occupies an axial position while the methyl is sited equatorially. That is, the major product obtained was not the one required to model the D-ring of the 17 α -ethynyl steroid complexes **4** and **5**.

These NMR assignments were corroborated by an X-ray crystallographic study of **6'**, which yielded the structure shown in Figure 1. Although the quality of

(9) Savignac, M.; Jaouen, G.; Rodger, C. A.; Perrier, R. E.; Sayer, B. G.; McGlinchey, M. J. *J. Org. Chem.* **1986**, *51*, 2328.

(10) (a) D'Agostino, M. F.; Frampton, C. S.; McGlinchey, M. J. *Organometallics* **1990**, *9*, 2972. (b) D'Agostino, M. F.; Frampton, C. S.; McGlinchey, M. J. *J. Organomet. Chem.* **1990**, *394*, 145.

(11) Cram, D. J.; Abd Elhazef, F. A. *J. Am. Chem. Soc.* **1952**, *74*, 5828.

(12) (a) Battioni, J.-P.; Chodkiewicz, W.; Cadiot, P. C. *R. Seances Acad. Sci. Ser. C* **1967**, *264*, 991. (b) Battioni, J.-P.; Capmau, M.-L.; Chodkiewicz, W. *Bull. Soc. Chim. Fr.* **1969**, 976. (c) Battioni, J.-P.; Chodkiewicz, W. *Bull. Soc. Chim. Fr.* **1969**, 981.

(13) (a) Cherest, M.; Felkin, H.; Prudent, N. *Tetrahedron Lett.* **1968**, 2201. (b) Cherest, M.; Felkin, H. *Tetrahedron Lett.* **1968**, 2205.

(14) (a) Nguyễn Trong Anh; Eisenstein, O. *Nouv. J. Chim.* **1977**, *1*, 61. (b) Nguyễn Trong Anh. *Top. Curr. Chem.* **1980**, *88*, 145.

(15) (a) Wu, Y.-D.; Tucker, J. A.; Houk, K. N. *J. Am. Chem. Soc.* **1991**, *113*, 5018. (b) Frenking, G.; Köhler, K. F.; Reetz, M. T. *Angew. Chem., Int. Ed. Engl.* **1991**, *30*, 1146. (c) Wu, Y.-D.; Houk, K. N.; Paddon-Row, M. N. *Angew. Chem., Int. Ed. Engl.* **1992**, *31*, 1019.

(16) It is noteworthy that the authors in refs 12 correctly identified the major product of this reaction as arising from alkynyl anion attack *cis* to the methyl group; however, they assigned the methyl to an axial site. Of course, a major problem with conformational analysis of cyclopentane rings is the phenomenon of pseudorotation which, if rapid on the NMR time scale, leads to time-averaged coupling constants.

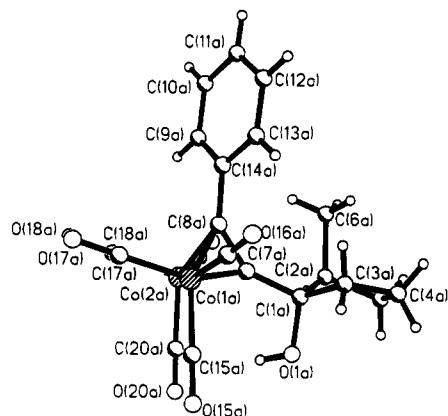
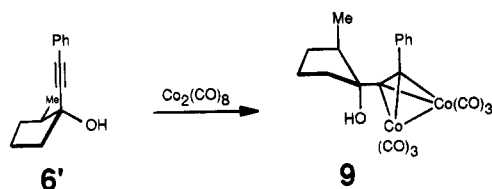


Figure 2. View of one of the independent molecules of (2-methyl-1-(phenylethynyl)cyclopentanol) $\text{Co}_2(\text{CO})_6$ (**9**) showing the atomic numbering scheme. Salient bond lengths (\AA): $\text{Co}(1\text{A})\text{--Co}(2\text{A})$, 2.466(3); $\text{Co}(1\text{A})\text{--C}(7\text{A})$, 1.984(13); $\text{Co}(1\text{A})\text{--C}(8\text{A})$, 1.992(13); $\text{Co}(2\text{A})\text{--C}(7\text{A})$, 1.964(14); $\text{Co}(2\text{A})\text{--C}(8\text{A})$, 1.973(16); $\text{C}(7\text{A})\text{--C}(8\text{A})$, 1.336(17); $\text{C}(1\text{A})\text{--C}(7\text{A})$, 1.497(17). Salient bond angles (deg): $\text{C}(1\text{A})\text{--C}(7\text{A})\text{--C}(8\text{A})$, 146.4(13); $\text{C}(7\text{A})\text{--C}(8\text{A})\text{--C}(14\text{A})$, 145.3(12); $\text{C}(6\text{A})\text{--C}(2\text{A})\text{--C}(1\text{A})\text{--O}(1\text{A})$, 170.6(12).

the available crystals did not allow us to refine the structure below an R value of $\sim 9\%$, and we prefer not to claim accurate bond parameters, the overall structure is readily apparent. The molecule adopts an envelope conformation, but the relatively large thermal parameters for the C(3), C(4), and C(5) atoms again reflect the ease of pseudorotation in such rings. Nevertheless, the positioning of the phenylethynyl moiety in the axial position at C(1) is evident, and the hydroxyl and methyl substituents occupy the equatorial sites at C(1) and C(2), respectively.

The alkyne **6'**, when treated with dicobalt octacarbonyl, yielded purple-black crystals of the cluster **9** in which the relative orientations of the methyl and hydroxyl groups must, of course, be maintained. This



assumption was verified by X-ray crystallography, but, as shown in Figure 2, we see that the envelope is now folded such that the very bulky dicobalt cluster occupies an equatorial site. This has the consequence of moving both the methyl and hydroxyl groups into axial positions. There are two independent molecules of **9** in the asymmetric unit, but their geometries differ only marginally. The cobalt–cobalt bond distance (average 2.468 \AA) and the cobalt–carbon bond lengths within the tetrahedron (average 1.985 \AA) are within the normal range for such systems.¹⁷ As is typical for such alkyne-derived clusters, the $\text{RC}\equiv\text{CR}$ linkage is no longer linear and in **9** the substituents are bent back by $34 \pm 2^\circ$.

It has been well-established by Nicholas that clusters such as **9**, in which a hydroxy group is located α to a

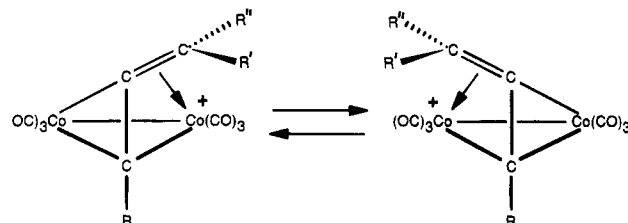


Figure 3. Antarafacial shift of a CR_2^+ group between cobalt centers.

cluster, upon protonation yield stable cations which undergo facile reactions with a variety of nucleophiles.¹⁸ It has also been unequivocally demonstrated that these carbocationic species owe their stability to the fact that the α -carbon leans over so as to interact with a metal vertex.¹⁹ Moreover, analogous to the behavior of the comprehensively studied trimetallic species $[\text{Co}_3(\text{CO})_9\text{C-CR}_2]^+$,²⁰ the alkylidene capping moiety migrates from one metal vertex to the other via an antarafacial shift process,²¹ as shown in Figure 3. Moreover, it has been established²² that a second fluxional process corresponding to suprafacial migration between metal centers has a slightly higher barrier than does the antarafacial shift mechanism. These fluxional phenomena have been extensively investigated, not only for clusters containing $\text{Co}(\text{CO})_3$ vertices but also for their $(\text{C}_5\text{H}_5)\text{-Mo}(\text{CO})_2$ analogues, and have been fully discussed elsewhere.^{1b}

Schreiber²² has turned these observations to synthetic advantage by changing the size of the R, R', and R'' groups so as to favor one of the diastereomers; this in turn leads to product selectivity because the attacking nucleophile must approach from the nonhindered face. Since these cations are strongly stabilized via a direct interaction with a metal, one can readily envisage that the initially formed cation would be one in which the metal can provide anchimeric assistance to the developing trigonal center.²³ In the case of **9**, we see that protonation would be expected to generate initially what may appear to be the sterically disfavored isomer **10'**, in which the methyl group is *proximal* to a $\text{Co}(\text{CO})_3$ vertex. However, the antarafacial migration process could change the molecule into the apparently less hindered isomer **10''**, in which the methyl group is now *distal* with respect to the metal vertex.

This whole process can be conveniently monitored by use of ^{13}C NMR spectroscopy. In particular, we note that in **9** the carbinol carbon, *i.e.* C(1), resonates at 87 ppm and the carbonyl ligands bonded to cobalt appear at 200 ppm. In the cation **10** these absorptions are found at 168 and 193 ppm, respectively; these last two values are typical of a metal-complexed carbocationic

(18) Nicholas, K. M. *Acc. Chem. Res.* **1987**, *20*, 207 and references therein.

(19) Osella, D.; Dutto, G.; Jaouen, G.; Vessièrès, A.; Raithby, P. R.; De Benedetto, L.; McGlinchey, M. J. *Organometallics* **1993**, *12*, 4545 and references therein.

(20) (a) Seyferth, D. *Adv. Organomet. Chem.* **1976**, *14*, 97. (b) Edidin, R. T.; Norton, J. R.; Mislów, K. *Organometallics* **1982**, *1*, 561.

(21) (a) Schilling, B. E. R.; Hoffmann, R. *J. Am. Chem. Soc.* **1979**, *101*, 3456. (b) D'Agostino, M. F.; Mlekuz, M.; Kolis, J. W.; Sayer, B. G.; Rodger, C. A.; Halet, J.-F.; Saillard, J.-Y.; McGlinchey, M. J. *Organometallics* **1986**, *5*, 2345.

(22) Schreiber, S. L.; Klimas, M. T.; Sammakia, S. *J. Am. Chem. Soc.* **1987**, *109*, 5749.

(23) El Hafa, H.; Cordier, C.; Gruselle, M.; Vaissermann, J.; Jaouen, G.; McGlinchey, M. J. *Organometallics* **1994**, *13*, 5149.

(17) (a) Kemmitt, R. D. W.; Russell, D. R. In *Comprehensive Organometallic Chemistry*; Wilkinson, G., Stone, F. G. A., Abel, E. W., Eds.; Pergamon Press: Oxford, U. K., 1982; Vol. 5, Chapter 34, p 195. (b) Dickson, R. S.; Fraser, P. J. *Adv. Organomet. Chem.* **1974**, *12*, 323.

Table 1. ^{13}C NMR Data for Methylcyclopentanols and Related Metal Complexes (in CD_2Cl_2)

molecule	C-1	C-2	C-3	C-4	C-5	Me	alkyne	CO's
<i>trans</i> -2-methylcyclopentanol ^a	81.0	43.4	35.1	22.7	33.0	19.5		
<i>cis</i> -2-methyl-cyclopentanol ^a	76.4	41.0	35.7	23.3	32.2	14.9		
2-methyl-1-cyclopentene ^{a,b}	c	46.7	31.2	21.9	42.3	12.9		
<i>trans</i> -2-methyl-1-(phenylethynyl)cyclopentanol (6')	79.0	46.4	31.5	21.1	41.3	16.9	92.6, 86.8	
<i>cis</i> -2-methyl-1-(phenylethynyl)cyclopentanol (6'')	c	46.7	31.2	21.9	42.3	12.9	c	
(<i>cis</i> -2-methyl-1-phenylethynyl)cyclopentanol) $Co_2(CO)_6$ (9)	87.0	48.5	32.2	21.2	41.5	18.9	92.9, 104.3	200.1
[(1-(2-methylcyclopentyl)-2-phenylethynyl) $Co_2(CO)_6$] ⁺ (10')	168.2	51.1	34.9	25.1	43.0	21.0	100.2, 104.2	193.1
(2-methyl-1-(phenylethynyl)-1-cyclopentene) $Co_2(CO)_6$, (11)	139.5 ^d	142.1 ^d	40.8	22.4	39.8	17.0	94.0, 104.2	200.5
(2-methyl-1-(phenylethynyl)cyclopentene) $Mo_2(CO)_4Cp_2$, (19) ^e	134.8 ^d	137.2 ^d	40.2	22.7	34.0	16.4	c	233

^aData from ref 39. ^bUnconventional numbering for ease of comparison of chemical shifts. ^cSignal not observed. ^dAssignments may be interchanged. ^eCyclopentadienyl resonance at 93.0 ppm.

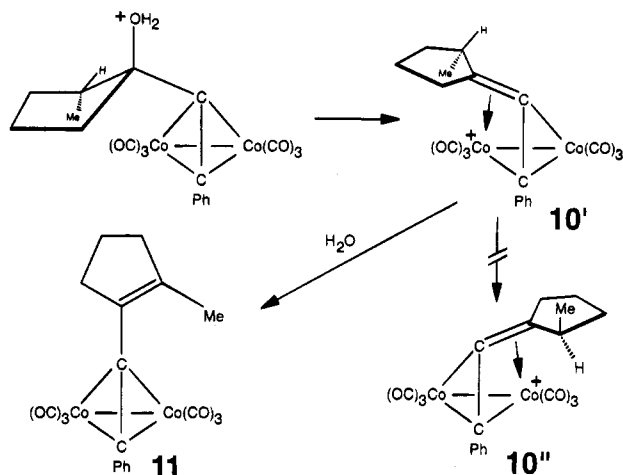


Figure 4. Protonation of **9** at low temperature yields a single cation which subsequently eliminates to form the corresponding cyclopentene.

center.^{10,24} When the cluster **9** is protonated at low temperature (-40 °C), only a single cation is detected by NMR. As the temperature is raised, there is a gradual diminution of the resonances attributable to the cation **10** and formation of the cyclopentene complex **11**. Likewise, treatment of the cation **10** with water also brings about elimination to give the cyclopentene complex **11**. The NMR data for these and other related molecules are collected in Table 1. The observation of a single cationic species at low temperature and its tendency toward ready loss of a proton suggest that the cation has the structure **10'**, in which the 2-methyl group is *proximal* to the $Co(CO)_3$ moiety and the *distal* methine proton is well-positioned for abstraction to yield the cyclopentene complex **11**. That is, as indicated in Figure 4, the sole cationic product is the one generated by cobalt-assisted elimination of water. In accord with the observations of Nicholas on a series of relatively bulky cations,²⁵ we assign the structure as the *anti* isomer, in which steric interactions between the groups bonded to the sp^2 center and the alkynyl substituent are minimized.

These results must be placed in the context of other reports on metal-stabilized propargyl cations. We note initially that Nicholas and Siegel have protonated **4**, the dicobalt hexacarbonyl complex of mestranol, and also (*epi*-mestranol) $Co_2(CO)_6$ (**12**). It was found (see Figure 5) that sodium borohydride treatment of the protonated product yielded in each case only the 17β -ethynyl isomer

(24) Padmanabhan, S.; Nicholas, K. M. *J. Organomet. Chem.* **1983**, *268*, C23.

(25) Bradley, D. H.; Khan, M. A.; Nicholas, K. M. *Organometallics* **1992**, *11*, 2598.

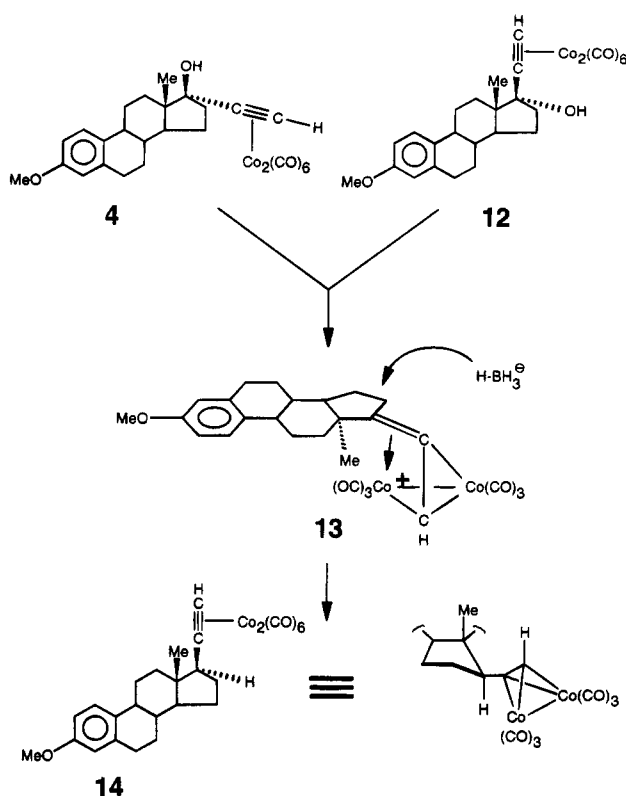


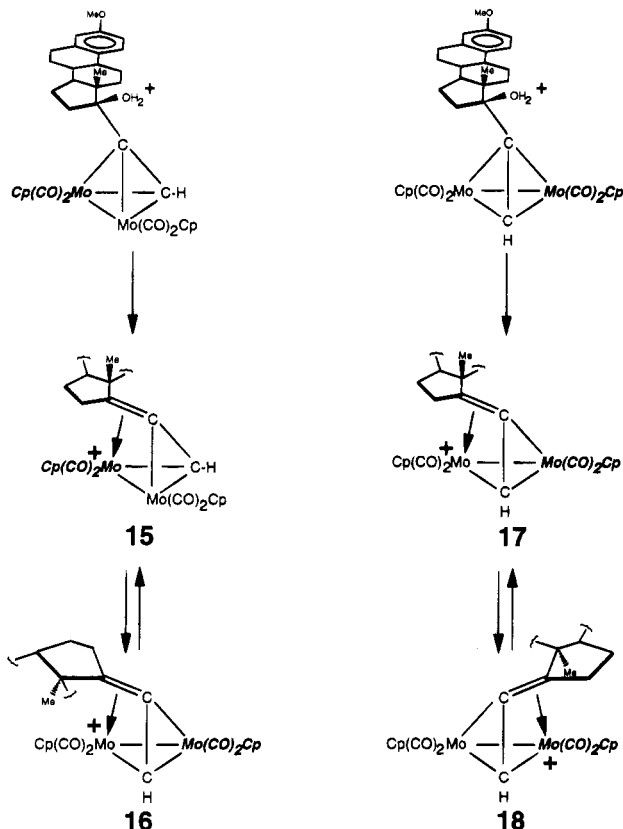
Figure 5. Protonation of (mestranol) $Co_2(CO)_6$ or of (*epi*-mestranol) $Co_2(CO)_6$, yielding a single product.

14. The authors proposed that the reaction proceeded via a common cationic intermediate, **13**, which underwent nucleophilic attack on the less hindered α face.²⁶ We should remind ourselves that protonation of the mestranol complex **4** should yield initially the cation with the cluster on the α -face of the steroid, since this allows anchimeric assistance from a cobalt center to alleviate the developing positive charge;²³ however, the antarafacial shift process provides ready access to diastereomer **13**. We are in complete accord with Nicholas and Siegel's suggestion of a common cationic intermediate, but one might raise the possibility that the stereochemistry of the product is not controlled solely by the propensity for nucleophilic attack on the α face. We note that the final product of borohydride attack on the metal-stabilized cation **13** allows the bulky dimetallatetrahedrane to occupy the pseudoequatorial position at C(17); the β -methyl group attached to C(13) must, of course, remain axial in the fused-ring steroidal skeleton. This situation parallels exactly the structure

(26) Nicholas, K. M.; Siegel, J. S. *J. Am. Chem. Soc.* **1985**, *107*, 4999.

found by X-ray crystallography for (2-methyl-1-(phenylethynyl)cyclopentanol)Co₂(CO)₆ (**9**).

It is relevant to recall the X-ray crystal structure of the closely analogous cationic dimolybdenum cluster **16**, in which the β -face of the steroid leans toward one of the molybdenum vertices.²⁷ In this structure, C(17) lies



only 2.74 Å from the molybdenum atom. However, variable-temperature NMR data reveal that **16** is in equilibrium with **15**, in which the α face of the steroid interacts with the other molybdenum center.²⁸ The barrier to interconversion of these two isomers is ~ 17 kcal mol⁻¹.^{29,30} We note that the two molybdenum clusters **15** and **16** are precisely those which would arise if the developing cationic center receives anchimeric assistance from the metal vertex. Cation **15** can form directly from **5** via protonation and elimination of water in an *anti-periplanar* fashion, while **16** results from the antarafacial migration of the steroidal vinylidene capping group. We note that such a process leaves the bond C(16)–C(15) as the *endo* edge in the transition state. In contrast, if the cationic center were to be generated at the other molybdenum vertex (and so produce diastereomer **17**), its interconversion to **18** would require that the antarafacial migration proceed via a sterically unfavorable transition state which places the steroidal C ring in the *endo* position.

(27) Gruselle, M.; Cordier, C.; Salmain, M.; El Amouri, H.; Guérin, C.; Vaissermann, J.; Jaouen, G. *Organometallics* **1990**, *9*, 2993.

(28) Cordier, C.; Gruselle, M.; Jaouen, G.; Bakhmutov, V. I.; Galakhov, M. V.; Troitskaya, L. L.; Sokolov, V. I. *Organometallics* **1991**, *10*, 2303.

(29) (a) Meyer, A.; McCabe, D. J.; Curtis, M. D. *Organometallics* **1987**, *6*, 1491. (b) Sokolov, V. I.; Barinov, I. V.; Reutov, O. A. *Izv. Akad. Nauk SSSR, Ser. Khim.* **1982**, 1922. (c) Galakhov, M. V.; Bakhmutov, V. I.; Barinov, I. V.; Reutov, O. A. *J. Organomet. Chem.* **1991**, *421*, 65. (d) Galakhov, M. V.; Bakhmutov, V. I.; Barinov, I. V. *Magn. Reson. Chem.* **1991**, *29*, 506.

(30) Girard, L.; Lock, P. E.; El Amouri, H.; McGlinchey, M. J. *J. Organomet. Chem.* **1994**, *478*, 189.

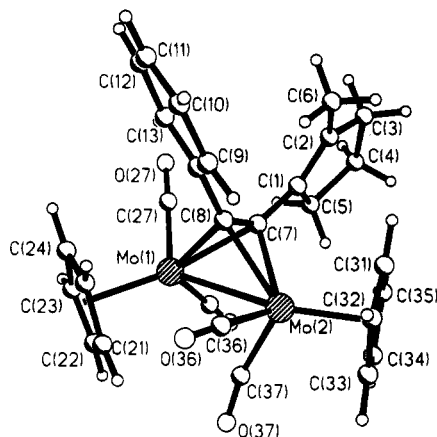
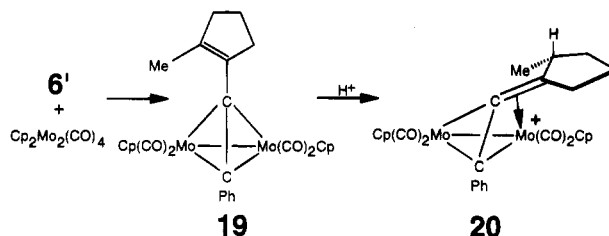


Figure 6. View of (2-methyl-1-(phenylethynyl)cyclopentene)Mo₂(CO)₄(C₅H₅)₂ (**19**) showing the atomic numbering scheme. Salient bond lengths (Å): Mo(1)–Mo(2), 2.947(3); Mo(1)–C(7), 2.227(12); Mo(1)–C(8), 2.227(12); Mo(2)–C(7), 2.184(15); Mo(2)–C(8), 2.184(14); C(7)–C(8), 1.345 (18); C(1)–C(7), 1.451(17); C(1)–C(2), 1.313(20). Salient bond angles (deg): C(1)–C(7)–C(8), 138.3(14); C(7)–C(8)–C(14), 136.2(13).

(2-Methyl-1-(phenylethynyl)cyclopentene)Mo₂(CO)₄(C₅H₅)₂. Treatment of 2-methyl-1-(phenylethynyl)cyclopentanol (**6**) with (C₅H₅)₂Mo₂(CO)₄ yields directly the molybdenum-complexed alkynylcyclopentene (**19**) as dark red crystalline plates. As is commonly the



case with molybdenum clusters,^{10b} it is the dehydration product, rather than the alcohol, that is isolated. The molybdenum complex was characterized by its NMR and mass spectra, by generation of the cation **20**, and finally by single-crystal X-ray diffraction. Figure 6 gives a view of the molecule. An examination of the Mo₂C₂ cluster fragment reveals a Mo–Mo bond of 2.947(3) Å and Mo–C distances within the tetrahedron which average 2.206(13) Å; the original alkyne linkage is no longer linear, and the phenyl and cyclopentenyl substituents are bent back by $\sim 43^\circ$. A common feature of (C₅H₅)₂Mo₂(CO)₄(RC≡CR) tetrahedral clusters is the presence of three terminal carbonyls while the fourth CO ligand adopts a semibridging posture.³¹ This pattern occurs in **19**, whereby the Mo–C=O angles are 177.2, 176.8, 177.3, and 167.2°. The torsion angle Cp(centroid)–Mo(1)–Mo(2)–Cp(centroid) is 159°.

Conformational Control of Metal-Mediated Cyclizations. The observation that a cobalt-complexed alkyne will preferentially occupy an equatorial site in a cycloalkane may provide a rationale for the stereochemical outcome of two recently reported cyclization

(31) (a) Bailey, W. I., Jr.; Chisholm, M. H.; Cotton, F. A.; Rankel, L. A. *J. Am. Chem. Soc.* **1978**, *100*, 5764. (b) Tondou, S.; Jaouen, G.; D'Agostino, M. F.; Maliszka, K. L.; McGlinchey, M. J. *Can. J. Chem.* **1992**, *70*, 1743 and references therein.

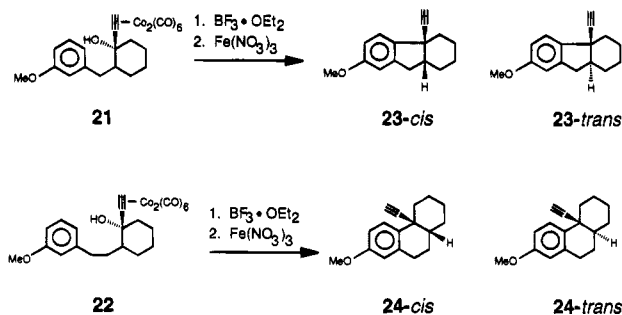
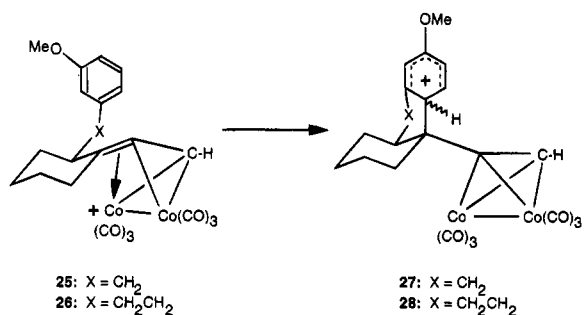


Figure 7. Cyclization of cobalt-stabilized cations, yielding only *cis*-products.

reactions.^{32,33} In each case, as shown in an elegant series of examples reported by Grove and co-workers, generation of the propargyl cation from **21** or **22** is facilitated by the presence of the $Co_2(CO)_6$ fragment. As depicted in Figure 7, Friedel–Crafts cyclization onto a suitably activated aromatic ring can yield a tricyclic final product, **23** or **24**, in which the alkyne is, in principle, either *cis* or *trans* to its C–H neighbor. Experimentally, the *cis* isomer is the exclusive product.^{32,33}

One can propose that, since the (relatively electron-rich) aromatic ring must attack the carbocationic center from the face opposite to the site of attachment of the cobalt, the favored trajectory of approach should be pseudo-axial so as to produce a final conformation in which the cluster can occupy the equatorial position. If this is indeed the case, then the benzyl substituent in the cationic intermediate **25** (or the phenylethyl substituent in **26**) should be located equatorially, and one could envisage formation of the five- and six-membered rings through transition states **27** and **28**, respectively.³⁴



The relative orientations of the benzyl (or phenylethyl) and the hydroxy functionalities in the starting material are irrelevant since the intermediate cobalt-stabilized cation can simply undergo an antarafacial migration from one cobalt to the other to generate the required conformation for cyclization.

It is clearly relevant to note that Melikyan and Nicholas have very recently offered a similar rationale

for their elegant $Mn(OAc)_3$ -mediated oxidative cycloaddition reactions of β -dicarbonyl compounds with $Co_2(CO)_6$ -complexed 1-alken-3-yne.³⁵ There is evidence to suggest that these manganese-promoted cyclizations involve oxidation of the intermediate radicals to cations prior to ring closure. It was also proposed that such ring closures could occur through a transition state in which the bulky (alkyne) $Co_2(CO)_6$ group is disposed pseudoequatorially with the incoming nucleophile attacking the carbocationic center from the pseudoaxial direction. Another indication of the preference for these cobalt clusters to adopt an equatorial site is Isobe's report of the facile epimerization of alkynyl sugars when they are complexed to a $Co_2(CO)_6$ moiety.³⁶

To conclude, we report that, in the cyclopentanol series, complexation of an axial alkynyl substituent by a $Co_2(CO)_6$ unit causes a conformational change such that the bulky M_2C_2 cluster fragment occupies an equatorial position. This effect can be invoked to rationalize the stereospecific cyclizations mediated by cobalt-complexed propargyl cations. Other crystallographically characterized molecules which illustrate the generality of this phenomenon will be the subject of future reports.³⁷

Experimental Section

All manipulations were carried out under an inert atmosphere, using freshly dried solvents. Fast atom bombardment (FAB) mass spectra were obtained on a VG ZAB-E spectrometer. 3-Nitrobenzyl alcohol was used as the sample matrix, and xenon was the bombarding species (8 kV). Microanalytical data are from Guelph Chemical Laboratories, Guelph, Ontario, Canada

¹H and ¹³C NMR spectra of **6** were recorded on a Bruker AM-500 spectrometer equipped with a 5 mm dual-frequency ¹H–¹³C probe, operating at 500.138 and 125.759 MHz, respectively; the sample was maintained at 30 °C by a Bruker BVT-1000 variable-temperature unit. ¹H spectra were obtained in 16K data points over a 5000 KHz spectral width and zero-filled to 32K before Fourier transformation. The ¹H FID's were processed with either Gaussian multiplication (for resolution enhancement) or exponential multiplication (line broadening 0.3 Hz). ¹H–¹H NOE difference spectra were acquired by subtraction of a control FID from an on-resonance FID. ¹³C spectra were acquired over a 29.411 KHz spectral width in 16K data points. Edited spectra were acquired with the DEPT pulse sequence. The ¹³C FID's were processed using exponential multiplication (line broadening 4.0 Hz) and zero-filled to 32K before Fourier transformation. The ¹³C–¹H 2-D chemical shift correlation spectra were acquired using the standard pulse sequence incorporating the BIRD pulse during the evolution period for ¹H–¹H decoupling in F1.³⁸ The ¹³C–¹H 2-D chemical shift correlation spectra via long-range couplings were acquired using the standard pulse sequence with the fixed delays optimized for a 10.4 Hz long-range coupling.^{38d} The compounds used in this study were dissolved in DMSO-*d*₆ or CD₂Cl₂ (Isotec, Inc.) to a concentration of approximately

(32) Grove, D. D.; Miskevich, F.; Smith, C. C.; Corte, J. R. *Tetrahedron Lett.* **1990**, 6277.

(33) Grove, D. D.; Corte, J. R.; Spencer, R. P.; Pauly, M. E.; Rath, N. P. *J. Chem. Soc., Chem. Commun.* **1994**, 49.

(34) It is not mandatory to invoke axial attack to produce *cis*-fused ring systems; several such cyclizations have been reported for systems in which no metal stabilization is involved: (a) Spencer, T. A.; Neel, H. S.; Ward, D. C.; Williamson, K. L. *J. Org. Chem.* **1966**, *31*, 434. (b) Hajos, Z. G.; Parrish, D. R. *J. Org. Chem.* **1974**, *39*, 1612. (c) Jackson, A. C.; Goldman, B. E.; Snider, B. B. *J. Org. Chem.* **1984**, *49*, 3988. (d) Barrow, C. J.; Bright, S. T.; Coxon, J. M.; Steel, P. J. *J. Org. Chem.* **1989**, *54*, 2542. (e) Bright, S. T.; Coxon, J. M.; Steel, P. J. *J. Org. Chem.* **1990**, *55*, 1338.

(35) Melikyan, G. G.; Vostrowsky, O.; Bauer, W.; Bestmann, H. J.; Khan, M.; Nicholas, K. M. *J. Org. Chem.* **1994**, *59*, 222.

(36) (a) Tanaka, S.; Tsukiyama, T.; Isobe, M. *Tetrahedron Lett.* **1993**, *34*, 5757. (b) Tanaka, S.; Isobe, M. *Tetrahedron* **1994**, *50*, 5633.

(37) Very recently, a comprehensive survey of crystallographically determined chair, half-chair, and boat cyclohexyl rings has appeared. The differing conformations were rationalized in terms of bond angles and torsional constraints: Sieburth, S. M. *J. Chem. Soc., Chem. Commun.* **1994**, 1663.

(38) (a) Bax, A. *J. Magn. Reson.* **1983**, *53*, 517. (b) Rutar, V. *J. Magn. Reson.* **1984**, *58*, 306. (c) Wilde, J. A.; Bolton, P. H. *J. Magn. Reson.* **1984**, *59*, 343. (d) Martin, G. E.; Zektzer, A. S. *J. Magn. Reson. Chem.* **1988**, *26*, 631.

Table 2. Crystallographic Data for 6, 9, and 19

	6	9	19
Crystal Data			
empirical formula	C ₁₄ H ₁₆ O	C ₂₀ H ₁₆ Co ₂ O ₇	C ₂₈ H ₂₄ Mo ₂ O ₄
color	colorless	purple	red
habit	chip	plate	plate
cryst size, mm ³	0.11 × 0.20 × 0.40	0.06 × 0.08 × 0.30	0.10 × 0.19 × 0.02
cryst syst	orthorhombic	monoclinic	monoclinic
space group	Pbcn	P2 ₁ /c	P2 ₁ /n
a, Å	23.493(4)	17.198(3)	14.070(10)
b, Å	11.357(4)	16.224(3)	11.176(6)
c, Å	8.816(2)	16.182(3)	16.018(9)
β, deg		110.89(2)	106.01(4)
V, Å ³	2352.2(12)	4218.3(13)	2421.1(12)
Z	8	8	4
fw	200.3	485.2	616.4
d(calcd), Mg/m ³	1.131	1.528	1.691
μ, cm ⁻¹	5.35	16.10	10.68
F(000)	864	1960	1232
Data Collection			
diffractometer	Rigaku AFC6R	Siemens P4	Siemens P4
radiation	Cu Kα (λ = 1.541 78 Å)	Mo Kα (λ = 0.710 73 Å)	Mo Kα
T, K	296	295	297
monochromator	graphite	graphite	graphite
2θ range, deg	7.0–45.0	5.0–45.0	7.0–45.0
scan type	ω	2θ–θ	ω
std rfln	3 std/97 rflns	3 std/97 rflns	3 std/97 rflns
index ranges	0 ≤ h ≤ 24, 0 ≤ k ≤ 12, –9 ≤ l ≤ 0	–18 ≤ h ≤ 17, –17 ≤ k ≤ 0, 0 ≤ l ≤ 17	0 ≤ h ≤ 15, 0 ≤ k ≤ 12, –17 ≤ l ≤ 16
no. of rflns collected	1791	6015	4437
no. of indep rflns	1791	5538	3372
no. of obsd rflns	1006 (F > 6.0σ(F))	2326 (F > 2.0σ(F))	1868 (F > 4.0σ(F))
abs cor	DIFABS	ψ scan	DIFABS
Solution and Refinement			
weighting scheme	w ⁻¹ = σ ² (F) + 0.0007F ²	w ⁻¹ = σ ² (F) + 0.0009F ²	w ⁻¹ = σ ² (F) + 0.0001F ²
no. of params refined	136	446	307
R, %	8.77	6.29	5.59
R _w , %	11.76	15.52	11.12
GOF	3.18	0.84	1.46
Δσ(max)	0.244	0.199	0.462
Δσ(mean)	0.019	0.015	0.017
N _v /N _v	7.4/1	5.3/1	6.1/1
Δσ _{max} , e/Å ³	0.66	0.74	0.58
Δσ _{min} , e/Å ³	–0.30	–0.41	–0.65

Table 3. Atomic Coordinates (×10⁴) and Equivalent Isotropic Displacement Coefficients (Å² × 10³) for 2-Methyl-1-(phenylethynyl)-cyclopentanol (6)

	x	y	z	U(eq) ^a
C(1)	4301(3)	3609(6)	540(6)	66(2)
C(2)	4481(3)	2793(7)	–669(8)	89(3)
C(3)	3998(4)	2468(7)	–1577(8)	90(3)
C(4)	3640(4)	3685(9)	–1650(11)	112(4)
C(5)	3840(3)	4408(7)	–459(9)	83(3)
C(6)	4810(4)	1790(8)	–25(10)	131(4)
C(7)	4001(2)	3028(5)	1776(6)	48(2)
C(8)	3739(2)	2571(5)	2764(6)	44(2)
C(9)	2984(3)	2606(5)	4699(6)	53(2)
C(10)	2675(3)	2057(7)	–1577(8)	72(3)
C(11)	2784(3)	914(7)	–1650(11)	75(3)
C(12)	3221(3)	290(5)	–1577(8)	73(3)
C(13)	3533(3)	851(5)	4373(7)	57(2)
C(14)	3418(2)	2012(4)	3970(6)	40(2)
O(1)	4722(2)	4362(3)	1145(4)	59(1)

^a Equivalent isotropic U, defined as one-third of the trace of the orthogonalized U_{ij} tensor.

25 mg/mL. Chemical shifts are reported in ppm relative to TMS using the residual solvent signals at 2.49 and 39.5 ppm (DMSO-) or 5.32 and 53.8 ppm (CD₂Cl₂) as internal references for the ¹H and ¹³C spectra, respectively.

2-Methyl-1-(phenylethynyl)cyclopentanol (6). To magnesium (2.8 g, 115 mmol) in ether (65 mL) was added bromoethane (13.6 g, 125 mmol). A solution of phenylethyne (8.89 g, 87 mmol) in ether (40 mL) was added dropwise, and

the mixture was stirred at room temperature for 1 h. The solution was cooled in ice, and 2-methylcyclopentanone (11.287 g, 115 mmol) in ether (45 mL) was then added dropwise over 1.5 h. The solution was heated to reflux for 30 min and then cooled to room temperature before addition of a saturated solution of ammonium chloride (200 mL). After ether extraction, drying over sodium sulfate, and removal of solvent, the residue was recrystallized from petroleum ether to give colorless needles of 6' (6.43 g, 32 mmol; 37%), mp 71 °C. ¹H NMR (500 MHz, DMSO-d₆): 6', δ 7.37 (5H, m, phenyl H's), 5.359 (α-OH), 1.992 (H-5β); 1.953 (H-2α), 1.902 (H-3β), 1.841 (H-5α), 1.655 (H-4α), 1.646 (H-4β), 1.286 (H-3α), 1.025 (β-Me). ²J values: H-3α–H-3β, –12.3 Hz; H-4α–H-4β, –12 Hz (estimated); H-5α–H-5β, –12.3 Hz. ³J values: β-Me–H-2α, 6.8 Hz; H-2α–H-3α, 6.8 Hz; H-2α–H-3β, 6.8 Hz; H-3α–H-4α, 6.8 Hz; H-3α–H-4β, 8.7 Hz; H-3β–H-4α, 12.1 Hz; H-3β–H-4β, 1.7 Hz; H-4α–H-5α, 6.4 Hz; H-4α–H-5β, 8.7 Hz; H-4β–H-5α, 8.0 Hz; H-4β–H-5β, 7.3 Hz. Since the pseudoaxial or pseudoequatorial character of the ring hydrogens is not always self-evident, the protons are designated according to their position on the α or β face of the molecule. ¹³C NMR (125 MHz, DMSO-d₆): 6', δ 131.1 (ortho C's), 128.6 (meta C's), 128.1 (para C), 122.8 (ipso C), 92.7 (C≡C–Ph), 84.0 (C≡C–Ph), 76.9 (C-1), 45.3 (C-2), 40.4 (C-5), 30.7 (C-3), 20.3 (C-4), 16.5 (Me). The alkyne carbons were assigned on the basis of long-range carbon–hydrogen couplings and are in accord with those reported for PhC≡CH.³⁹

(39) Kalinowski, H. O.; Berger, S.; Braun, S. *Carbon-13 NMR Spectroscopy*; Wiley: Salisbury, U.K., 1988; p 264.

Table 4. Atomic Coordinates ($\times 10^4$) and Equivalent Isotropic Displacement Coefficients ($\text{\AA}^2 \times 10^3$) for (2-Methyl-1-(phenylethynyl)-cyclopentanol) $\text{Co}_2(\text{CO})_6$ (9)

	x	y	z	$U(\text{eq})^a$
Co(1A)	8890(1)	1421(1)	474(1)	54(1)
Co(2A)	9381(1)	2071(1)	-629(1)	47(1)
O(1A)	10885(6)	2395(6)	1437(6)	79(5)
O(15A)	10308(8)	364(8)	1351(8)	124(7)
O(16A)	8134(10)	1562(10)	1810(8)	149(9)
O(17A)	7595(7)	371(7)	-742(7)	98(6)
O(18A)	8213(7)	1312(7)	-2235(7)	90(6)
O(19A)	9713(8)	3581(7)	-1451(7)	94(6)
O(20A)	10991(7)	1215(8)	-163(8)	114(7)
C(1A)	10170(9)	2914(9)	1233(8)	48(6)
C(2A)	10377(9)	3761(9)	1009(9)	65(7)
C(3A)	10976(10)	4099(9)	1889(11)	95(9)
C(4A)	10570(11)	3753(12)	2551(11)	116(11)
C(5A)	9974(9)	3080(10)	2068(8)	75(8)
C(6A)	9563(10)	4337(9)	626(9)	91(9)
C(7A)	9461(9)	2495(8)	536(8)	43(6)
C(8A)	8675(8)	2556(8)	-26(8)	45(6)
C(9A)	7622(7)	3386(7)	-1177(6)	102(6)
C(10A)	6943	3922	-1429	130(7)
C(11A)	6570	4140	-823	107(6)
C(12A)	6877	3824	34	116(6)
C(13A)	7556	3288	286	92(5)
C(14A)	7929	3070	-320	51(4)
C(15A)	9760(10)	784(10)	1006(10)	76(9)
C(16A)	8460(12)	1495(11)	1309(11)	91(10)
C(17A)	8102(10)	779(10)	-277(10)	63(8)
C(18A)	8680(9)	1604(10)	-1612(10)	64(8)
C(19A)	9611(10)	2976(11)	-1125(10)	67(8)
C(20A)	10373(10)	1525(10)	-338(9)	67(8)
Co(1B)	4496(1)	2036(1)	-988(1)	61(1)
Co(2B)	3799(1)	1498(1)	-3(1)	68(1)
O(1B)	2380(5)	2446(6)	-1950(6)	73(4)
O(15B)	3666(8)	941(8)	-2511(7)	122(7)
O(16B)	4815(8)	3387(9)	-2007(8)	101(7)
O(17B)	6176(7)	1382(9)	-122(9)	153(8)
O(18B)	5141(10)	416(9)	1100(10)	173(10)
O(19B)	2956(11)	1756(14)	1256(11)	158(11)
O(20B)	2593(9)	370(8)	-1224(9)	131(8)
C(1B)	2818(8)	2987(9)	-1210(8)	52(7)
C(2B)	2205(8)	3212(9)	-755(10)	68(8)
C(3B)	1612(9)	3829(11)	-1448(12)	104(10)
C(4B)	2144(11)	4273(10)	-1867(12)	105(10)
C(5B)	2977(9)	3821(9)	-1581(9)	69(7)
C(6B)	2622(9)	3630(10)	149(10)	99(9)
C(7B)	3593(9)	2559(8)	-653(8)	51(7)
C(8B)	4331(9)	2592(8)	41(8)	55(7)
C(9B)	5457(6)	2738(5)	1489(7)	86(5)
C(10B)	5982	3226	2168	113(6)
C(11B)	5934	4084	2099	90(6)
C(12B)	5361	4452	1350	91(5)
C(13B)	4835	3963	670	75(5)
C(14B)	4883	3106	740	53(4)
C(15B)	3993(9)	1351(11)	-1927(10)	75(8)
C(16B)	4728(10)	2856(11)	-1578(12)	78(10)
C(17B)	5505(11)	1630(11)	-468(10)	96(9)
C(18B)	4574(13)	830(12)	662(12)	101(11)
C(19B)	3280(13)	1648(16)	788(15)	105(13)
C(20B)	3076(12)	798(10)	-749(11)	88(10)

^a Equivalent isotropic U defined as one-third of the trace of the orthogonalized U_{ij} tensor.

(2-Methyl-1-(phenylethynyl)cyclopentanol) $\text{Co}_2(\text{CO})_6$ (9).

Dicobalt octacarbonyl (0.885 g, 2.50 mmol) and **6'** (0.50 g, 2.50 mmol) in THF (30 mL) were stirred at room temperature for 2 h. After removal of solvent, the residue was flash chromatographed on silica gel (particle size 20–45 μm); elution with hexane/ether (90/10) yielded purple crystals of **9** (1.03 g, 2.07 mmol; 84%), mp 49–50 °C. IR (CH_2Cl_2): ν_{CO} at 2090, 2052, 2025 cm^{-1} . ^1H NMR (200 MHz, CDCl_3): δ 7.4 (5H, m, phenyl H's), 2.2 (2H, m), 1.93 (4H, m), 1.52 (1H, m), 0.95 (3H, d, Me). Mass spectrum (FAB; m/z (%)): 486 (5) ($[\text{M}]^+$), 458 (40) ($[\text{M} - \text{CO}]^+$), 430 (80) ($[\text{M} - 2\text{CO}]^+$), 402 (85) ($[\text{M} - 3\text{CO}]^+$), 374

Table 5. Atomic Coordinates ($\times 10^4$) and Equivalent Isotropic Displacement Coefficients ($\text{\AA}^2 \times 10^3$) for (2-Methyl-1-(phenylethynyl)-cyclopentene) $\text{Mo}_2(\text{CO})_4\text{Cp}_2$ (19)

	x	y	z	$U(\text{eq})^a$
Mo(1)	6361(1)	2250(1)	3697(1)	34(1)
Mo(2)	4193(1)	2472(1)	3058(1)	44(1)
C(1)	5392(9)	4913(11)	2789(9)	37(5)
C(2)	5127(10)	5587(11)	2092(11)	47(6)
C(3)	5232(12)	6903(11)	2295(11)	57(7)
C(4)	5482(14)	6955(13)	3240(13)	88(10)
C(5)	5672(12)	5703(11)	3593(10)	59(7)
C(6)	4791(12)	5197(13)	1209(10)	68(7)
C(7)	5380(11)	3623(10)	2885(9)	41(6)
C(8)	5347(8)	2643(10)	2391(9)	44(5)
C(9)	4897(12)	1801(11)	909(10)	51(6)
C(10)	5159(16)	1578(12)	128(11)	68(8)
C(11)	6030(19)	1942(17)	51(14)	91(11)
C(12)	6670(13)	2513(16)	646(10)	80(8)
C(13)	6460(10)	2715(12)	1426(9)	55(6)
C(14)	5566(9)	2360(10)	1562(8)	41(5)
C(21)	6282(12)	163(12)	3926(12)	61(9)
C(22)	6995(15)	670(14)	4623(11)	66(8)
C(23)	7753(14)	1111(14)	4346(14)	69(9)
C(24)	7521(13)	920(12)	3449(14)	59(9)
C(25)	6632(13)	352(11)	3188(11)	58(8)
C(26)	6324(12)	3211(13)	4705(10)	57(7)
O(26)	6343(11)	3777(10)	5327(8)	95(7)
C(27)	7259(11)	3470(11)	3537(9)	39(6)
O(27)	7827(8)	4192(9)	3480(7)	61(5)
C(31)	3007(12)	3808(16)	2228(12)	68(8)
C(32)	2557(12)	2662(18)	2265(15)	95(10)
C(33)	2570(11)	2511(16)	3140(16)	90(10)
C(34)	3063(12)	3478(16)	3635(13)	73(8)
C(35)	3324(11)	4268(14)	3077(14)	67(8)
C(36)	4213(11)	869(14)	2595(12)	67(8)
O(36)	4185(9)	-98(10)	2308(9)	99(7)
C(37)	4645(13)	1799(12)	4205(13)	68(9)
O(37)	4733(11)	1380(10)	4897(9)	105(8)

^a Equivalent isotropic U , defined as one-third of the trace of the orthogonalized U_{ij} tensor.

(53) ($[\text{M} - 4\text{CO}]^+$), 346 (100) ($[\text{M} - 5\text{CO}]^+$), 318 (35) ($[\text{M} - 6\text{CO}]^+$). Anal. Calcd for $\text{C}_{20}\text{H}_{16}\text{Co}_2\text{O}_7$: C, 49.30; H, 3.52. Found: C, 49.79; H, 3.55.

(2-Methyl-1-(phenylethynyl)cyclopentene) $\text{Co}_2(\text{CO})_6$ (11).

A solution of **9** (50 mg, 0.103 mmol) in CD_2Cl_2 (2 mL) in an NMR tube was cooled in a dry-ice/acetone bath, and 4 drops of HBF_4 in ether were added. The sample was placed in a spectrometer probe that was already cooled to -40 °C, and the ^{13}C NMR spectrum of the cation was recorded. Upon quenching with water, the alkene **11** was produced and identified by its ^{13}C NMR spectrum. Mass spectrum of **11** (FAB; m/z (%)): 468 (7) ($[\text{M}]^+$), 440 (15) ($[\text{M} - \text{CO}]^+$), 412 (100) ($[\text{M} - 2\text{CO}]^+$), 384 (53) ($[\text{M} - 3\text{CO}]^+$), 356 (45) ($[\text{M} - 4\text{CO}]^+$), 328 (22) ($[\text{M} - 5\text{CO}]^+$), 300 (35) ($[\text{M} - 6\text{CO}]^+$).

(2-Methyl-1-(phenylethynyl)cyclopentene) $\text{Mo}_2(\text{CO})_4$ -

(C_5H_5) $_2$ (19). A mixture of $(\text{C}_5\text{H}_5)_2\text{Mo}_2(\text{CO})_6$ (1.20 g, 2.6 mmol), toluene (90 mL), and THF (10 mL) was heated to reflux for 2 days while dry N_2 was bubbled through the solution. After the mixture was cooled, **6** (0.52 g, 2.6 mmol) was added and the mixture heated under reflux for a further 2 days. After cooling, filtration, and removal of solvent, the residue was flash-chromatographed using hexane/ CH_2Cl_2 (90:10) as eluent to give red crystals of **19** (1.05 g, 1.7 mmol; 67%), 144–145 °C. ^1H NMR (200 MHz, CDCl_3): δ 7.3 (5H, m, phenyl H's), 5.25 (10H, s, Cp H's), 2.53 (2H, m), 2.4 (2H, m), 1.85 (2H, m), 1.38 (3H, s, Me). ^{13}C NMR data are collected in Table 1. Anal. Calcd for $\text{C}_{28}\text{H}_{25}\text{Mo}_2\text{O}_4$: C, 54.56; H, 3.92. Found: C, 54.26; H, 3.93.

X-ray Crystallography. The molecules **6'**, **9**, and **19** were characterized by single-crystal X-ray diffraction measurements. Numbers related to data collection appear in Table 2; profile analysis and empirical absorption corrections were made with the use of SHELXTL-PLUS.⁴⁰ All structures were

solved by direct methods. Atom coordinates are listed in Tables 3–5.

Acknowledgment. Financial support from the Natural Sciences and Engineering Research Council of Canada, and also from the donors of the Petroleum Research Fund, administered by the American Chemical Society, is gratefully acknowledged. K.L.M. thanks the Province of Ontario and the NSERC for graduate scholarships. Mass spectra were obtained courtesy of

(40) Sheldrick, G. M. SHELXTL PC (1990), Release 4.1; Siemens Crystallographic Research Systems, Madison, WI 53719.

Dr. Richard Smith of the McMaster Regional Centre for Mass Spectrometry. We thank Professor Gérard Jaouen and Dr. Michel Gruselle (Ecole Nationale Supérieure de Chimie, Paris) for helpful discussions and the reviewers for their perceptive comments.

Supporting Information Available: Tables of thermal parameters, bond lengths and angles, and H atom coordinates for **9** and **19** and a table of thermal parameters for **6'** (12 pages). Ordering information is given on any current mast-head page.

OM9501891

Selective Protonation of the Styryl Ligand of $\text{Ru}(\text{CH}_3)\{(\text{E})\text{-CH=CHPh}\}(\text{CO})_2(\text{P}^i\text{Pr}_3)_2$ and Migratory CO Insertion in the Methyl Group of $[\text{Ru}(\text{CH}_3)(\text{CO})_2(\text{P}^i\text{Pr}_3)_2]\text{BF}_4$

Cristina Bohanna, Miguel A. Esteruelas,* Fernando J. Lahoz, Enrique Oñate, and Luis A. Oro

Departamento de Química Inorgánica, Instituto de Ciencia de Materiales de Aragón, Universidad de Zaragoza-Consejo Superior de Investigaciones Científicas, 50009 Zaragoza, Spain

Received April 20, 1995[®]

Complex $\text{RuCl}\{(\text{E})\text{-CH=CHPh}\}(\text{CO})_2(\text{P}^i\text{Pr}_3)_2$ (**1**) reacts with CH_3Li in toluene at room temperature to give $\text{Ru}(\text{CH}_3)\{(\text{E})\text{-CH=CHPh}\}(\text{CO})_2(\text{P}^i\text{Pr}_3)_2$ (**2**). The structure of **2** was determined by an X-ray investigation. The coordination geometry around the ruthenium atom is octahedral with the phosphine ligands occupying *trans* positions. The perpendicular plane is formed by the methyl and styryl ligands mutually *cis* disposed and by two additional carbonyl groups. The reaction of **2** with $\text{HBF}_4\cdot\text{OEt}_2$ leads to styrene and the cationic five-coordinate complex $[\text{Ru}(\text{CH}_3)(\text{CO})_2(\text{P}^i\text{Pr}_3)_2]\text{BF}_4$ (**3**), which adds carbon monoxide to give the corresponding derivative $[\text{Ru}(\text{CH}_3)(\text{CO})_3(\text{P}^i\text{Pr}_3)_2]\text{BF}_4$ (**5**). The related styryl complex $[\text{Ru}\{(\text{E})\text{-CH=CHPh}\}(\text{CO})_3(\text{P}^i\text{Pr}_3)_2]\text{BF}_4$ (**6**) can be prepared by reaction of **1** with AgBF_4 under a carbon monoxide atmosphere. Complex **3** also reacts with NaCl , NaI , LiOPh , and $\text{LiC}\equiv\text{CPh}$. The reaction with NaCl leads to the η^1 -acyl carbonyl $\text{Ru}\{\text{C}(\text{O})\text{CH}_3\}\text{Cl}(\text{CO})(\text{P}^i\text{Pr}_3)_2$ (**7**). The structure of **7** was also determined by an X-ray investigation. The geometry of **7** can be rationalized as a square pyramid with the acyl ligand located at the apex. The reaction of **3** with NaI gives a mixture of the methyl dicarbonyl $\text{Ru}(\text{CH}_3)\text{I}(\text{CO})_2(\text{P}^i\text{Pr}_3)_2$ (**8**) and the η^1 -acyl-carbonyl $\text{Ru}\{\text{C}(\text{O})\text{CH}_3\}\text{I}(\text{CO})(\text{P}^i\text{Pr}_3)_2$ (**9**). Similarly, the treatment of **3** with LiOPh results in a rapidly established equilibrium mixture of the methyl dicarbonyl $\text{Ru}(\text{CH}_3)(\text{OPh})(\text{CO})_2(\text{P}^i\text{Pr}_3)_2$ (**12**) and the η^1 -acyl carbonyl $\text{Ru}\{\text{C}(\text{O})\text{CH}_3\}(\text{OPh})(\text{CO})(\text{P}^i\text{Pr}_3)_2$ (**13**), while the reaction of **3** with $\text{LiC}\equiv\text{CPh}$ affords $\text{Ru}(\text{CH}_3)(\text{C}\equiv\text{CPh})(\text{CO})_2(\text{P}^i\text{Pr}_3)_2$ (**14**). Under a CO atmosphere **14** is quantitatively converted into $\text{Ru}\{\text{C}(\text{O})\text{CH}_3\}(\text{C}\equiv\text{CPh})(\text{CO})_2(\text{P}^i\text{Pr}_3)_2$ (**15**). Under a CO atmosphere, **2** is in equilibrium with $\text{Ru}\{\text{C}(\text{O})\text{CH}_3\}\{(\text{E})\text{-CH=CHPh}\}(\text{CO})_2(\text{P}^i\text{Pr}_3)_2$ (**17**).

Introduction

A homogeneous catalyst must, in general, have free coordination sites, different potential coordination numbers for a given oxidation state, and different oxidation states which are readily accessible. The key to the processes is the creation of an open coordination site, which permits substrate binding and its subsequent activation.¹ In most cases, therefore, the creation of a coordination vacancy in saturated transition-metal complexes is by itself an objective. This may be achieved by thermal or photoinduced dissociation of Lewis bases, reductive elimination, intramolecular insertion of unsaturated ligands into M–H and M–C bonds,² hydrogenation in coordinating solvents of diene compounds,³ halide abstraction with silver or thallium salts,⁴ proto-

nation of polyhydrido complexes,⁵ and electrophilic attack at the α -carbon atom of a coordinated alkyl group.^{4,6}

The creation of an open coordination site by electrophilic attack at the α -carbon atom of η^1 -carbon unsaturated ligands, such as alkynyl and vinyl, is difficult. Electronic structures and reactivities of these fragments change, often dramatically, when they coordinate to late transition metals to form organometallic complexes. Coordination of $[\text{RC}\equiv\text{C}]^-$ and $[\text{RCH}=\text{CH}]^-$ to a metal center transfers the nucleophilicity from the α -carbon atom to the β -carbon atom. Thus, the addition of electrophiles to the electron-rich C_β of metal alkynyl derivatives has been described on many occasions and is the

[®] Abstract published in *Advance ACS Abstracts*, August 15, 1995.

(1) (a) Parshall, G. W.; Ittel, S. D. *Homogeneous Catalysis*, 2nd ed.; Wiley: New York, 1992. (b) Masters, C. *Homogeneous Transition-metal Catalysis*; Chapman and Hall: London, 1981. (c) Chaloner, P. A.; Esteruelas, M. A.; Joó, F.; Oro, L. A. *Homogeneous Hydrogenation*; Kluwer Academic: Boston, MA, 1994.

(2) Crabtree, R. H. *The Organometallic Chemistry of the Transition Metals*; Wiley: New York, 1988.

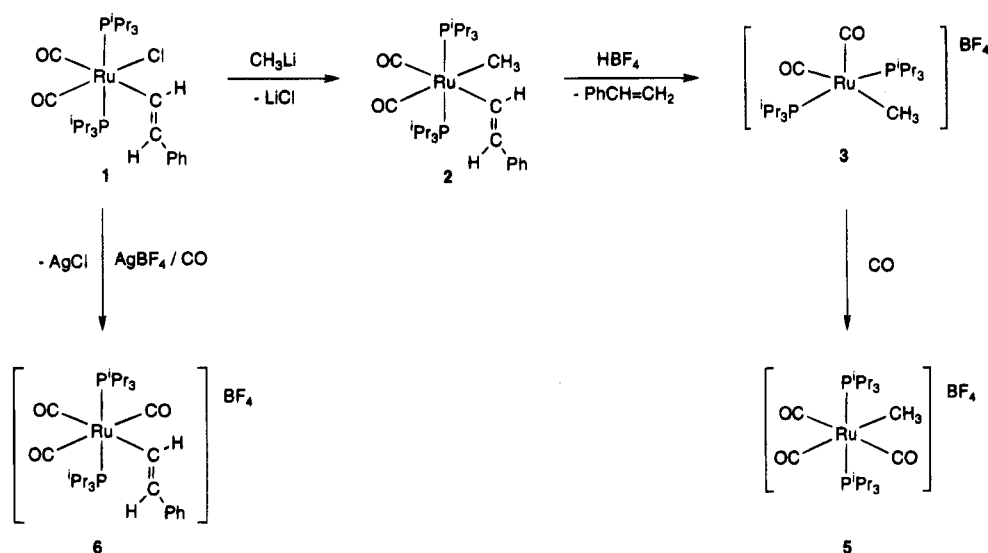
(3) (a) Schrock, R. R.; Osborn, J. A. *J. Am. Chem. Soc.* **1976**, *98*, 2134. (b) Crabtree, R. H.; Demou, P. C.; Eden, D.; Mihelcic, J. M.; Parnell, C. A.; Quirk, J. M.; Morris, G. E. *J. Am. Chem. Soc.* **1982**, *104*, 6994. (c) Crabtree, R. H.; Davis, M. W.; Mellea, M. F.; Mihelcic, J. M. *Inorg. Chim. Acta* **1983**, *72*, 223.

(4) Beck, W.; Sünkel, K. *Chem. Rev.* **1988**, *88*, 1405.

(5) (a) Chatt, J.; Coffey, R. S. *J. Chem. Soc. A* **1969**, 1963. (b) Empsall, H. D.; Heyde, E. M.; Mentzer, E.; Shaw, B. L.; Uttley, M. F. *J. Chem. Soc., Dalton Trans.* **1976**, 2069. (c) Olgemoller, B.; Bauer, H.; Beck, W. *J. Organomet. Chem.* **1980**, *213*, C57. (d) Rhodes, L. F.; Zubkowsky, J. D.; Foltling, K.; Huffman, J. C.; Caulton, K. G. *Inorg. Chem.* **1982**, *21*, 4185. (e) Allison, J. D.; Walton, R. A. *J. Chem. Soc., Chem. Commun.* **1983**, 401. (f) Crabtree, R. H.; Hlatky, G. G. *J. Am. Chem. Soc.* **1983**, *105*, 7302. (g) Crabtree, R. H.; Hlatky, G. G.; Parnell, C. P.; Segmüller, B. E.; Uriarte, R. J. *Inorg. Chem.* **1984**, *23*, 354. (h) Johnson, T. J.; Huffman, J. C.; Caulton, K. G.; Jackson, S. A.; Eisenstein, O. *Organometallics* **1989**, *8*, 2073. (i) Marinelli, G.; Rachidi, I.; Streib, W. E.; Eisenstein, O.; Caulton, K. G. *J. Am. Chem. Soc.* **1989**, *111*, 2396.

(6) (a) Lundquist, E. G.; Foltling, K.; Huffman, J. C.; Caulton, K. G. *Organometallics* **1990**, *9*, 2254. (b) Esteruelas, M. A.; Lahoz, F. J.; López, J. A.; Oro, L. A.; Schlünken, C.; Valero, C.; Werner, H. *Organometallics* **1992**, *11*, 2034.

Scheme 1



best known entry into the synthesis of vinylidene compounds.⁷ Similarly, the vinyl ligands of electron-rich metals are nucleophilic at the β -carbon atom and their reactions with electrophiles lead to carbene complexes.⁸

The η^1 -carbon unsaturated ligands do not always react with electrophiles by attack at the β -carbon atom. We have recently reported overwhelming evidence proving that the direction of H^+ addition to alkynyl and vinylacetato complexes of ruthenium and osmium is determined by the electronic nature of the metallic center, by the electronic properties of the ancillary ligands of the complexes, and also by the source of the electrophile.⁹ Continuing with our work in this field, we have now carried out the protonation of the methyl styryl derivative $[Ru(CH_3)\{(E)-CH=CHPh\}(CO)_2(P^iPr_3)_2]$. The reaction affords $[Ru(CH_3)(CO)_2(P^iPr_3)_2]^+$ and styrene. This result is of interest not only because the reaction has no precedent but also because the five-coordinate methyl complex is an entry to new acyl compounds.

The migratory insertion of carbon monoxide into metal-alkyl bonds is a reaction of fundamental importance in organometallic chemistry¹⁰ and has extensive application in catalysis, involving the hydroformylation process, the carbonylation of methanol, and the chain propagation steps in the Fischer-Tropsch reaction, which converts coal-derived synthesis gas to liquid hydrocarbons.^{1a,b}

In this paper, we report the synthesis of $[Ru(CH_3)(CO)_2(P^iPr_3)_2]^+$ by protonation of $Ru(CH_3)\{(E)-CH=CHPh\}(CO)_2(P^iPr_3)_2$ and the migratory CO insertion in the methyl group of $[Ru(CH_3)(CO)_2(P^iPr_3)_2]^+$.

Results and Discussion

1. Synthesis of $[Ru(CH_3)(CO)_2(P^iPr_3)_2]BF_4$ by Protonation of $Ru(CH_3)\{(E)-CH=CHPh\}(CO)_2$

- (7) Bruce, M. I. *Chem. Rev.* **1991**, *91*, 197.
 (8) (a) Davison, A.; Selegue, J. P. *J. Am. Chem. Soc.* **1978**, *100*, 7763.
 (b) Davison, A.; Selegue, J. P. *J. Am. Chem. Soc.* **1980**, *102*, 2455. (c) Casey, C. P.; Miles, W. H.; Tukkoda, H.; O'Connor, J. M. *J. Am. Chem. Soc.* **1982**, *104*, 3761. (d) Kremer, K. A.; Kuo, G.; O'Connor, E. I.; Helquist, P.; Kerber, R. C. *J. Am. Chem. Soc.* **1982**, *104*, 6119. (e) Bodner, G. S.; Smith, D. E.; Hatton, W. G.; Heah, P. G.; Georgion, S.; Rheingold, A. L.; Geib, S. J.; Hutchinson, J. P.; Gladysz, J. A. *J. Am. Chem. Soc.* **1987**, *109*, 7688.
 (9) Esteruelas, M. A.; Lahoz, F. J.; López, A. M.; Oñate, E.; Oro, L. A. *Organometallics* **1994**, *13*, 1669.

$(P^iPr_3)_2$. The latter compound was prepared by reaction of $RuCl\{(E)-CH=CHPh\}(CO)_2(P^iPr_3)_2$ (**1**) with CH_3Li in toluene at room temperature (Scheme 1).

$Ru(CH_3)\{(E)-CH=CHPh\}(CO)_2(P^iPr_3)_2$ (**2**) was isolated as a white solid in 72% yield and characterized by elemental analysis, by IR and 1H , $^{13}C\{^1H\}$, and $^{31}P\{^1H\}$ NMR spectroscopy, and by X-ray diffraction. Figure 1 shows a representation of the molecule. Selected bond distances and angles are listed in Table 1.

The coordination geometry around the ruthenium atom can be rationalized as a slightly distorted octahedron with the two phosphorus atoms of the trisopropylphosphine ligands occupying *trans* positions ($P(1)-Ru-P(2) = 175.77(4)^\circ$). The perpendicular plane is formed by the atoms C(1) and C(9) of the styryl and methyl ligands, mutually *cis* disposed ($C(1)-Ru-C(9) = 87.2(1)^\circ$), and the two carbonyl groups also *cis* disposed ($C(10)-Ru-C(11) = 93.1(2)^\circ$).

The methyl group is coordinated to the ruthenium center with a bond length of 2.205(4) Å. This value is comparable to the $Ru-Me$ bond lengths reported for $Ru(CH_3)I(\eta^4-NBD)(dad)$ (NBD = norbornadiene, dad = glyoxalbis(isopropylimine); 2.222(13) Å),¹¹ (+)- $[Ru(CH_3)(CO)(CNBu-t)(triphos)]^+$ (2.209(5) Å),¹² and $[cis-Ru(CH_3)(PMe_3)_4]_2Hg$ (2.21(1) Å).¹³ However, it is between

- (10) (a) Berke, H.; Hoffmann, R. *J. Am. Chem. Soc.* **1978**, *100*, 7224.
 (b) Monti, D.; Bassetti, M.; Sunley, G. J.; Ellis, P.; Maitlis, P. *Organometallics* **1991**, *10*, 4015. (c) García-Alonso, F. J.; Llamazares, A.; Riera, V.; Vivanco, M.; Díaz, M. R.; García-Granda, S. *J. Chem. Soc., Chem. Commun.* **1991**, 1058. (d) Carmona, E.; Contreras, L.; Poveda, M. L.; Sánchez, L. J.; Atwood, J. L.; Rogers, R. D. *Organometallics* **1991**, *10*, 61. (e) Carmona, E.; Contreras, L.; Gutiérrez-Puebla, E.; Monge, A.; Sánchez, J. L. *Organometallics* **1991**, *10*, 71. (f) Contreras, L.; Monge, A.; Pizzano, A.; Ruiz, C.; Sánchez, L.; Carmona, E. *Organometallics* **1992**, *11*, 3971. (g) Skagestad, V.; Tilset, M. *Organometallics* **1992**, *11*, 3293. (h) Jablonski, C. *Organometallics* **1992**, *11*, 658. (i) Bellachioma, G.; Cardaci, G.; Macchioni, A.; Reichenbach, G. *Inorg. Chem.* **1992**, *31*, 3018. (j) Kraakman, M. J. A.; de Klerk-Engels, B.; de Lange, P. P. M.; Vrieze, K.; Smeets, W. J. J.; Spek, A. L. *Organometallics* **1992**, *11*, 3774. (k) Dryden, N. H.; Legzdins, P.; Lundmark, P. J.; Riesen, A.; Einstein, F. W. B. *Organometallics* **1993**, *12*, 2085. (l) Debad, J. D.; Legzdins, P.; Batchelor, R. J.; Einstein, F. W. B. *Organometallics* **1993**, *12*, 2094. (m) Bellachioma, G.; Cardaci, G.; Jablonski, C.; Macchioni, A.; Reichenbach, G. *Inorg. Chem.* **1993**, *32*, 2404. (n) Bellachioma, G.; Cardaci, G.; Macchioni, A.; Madami, A. *Inorg. Chem.* **1993**, *32*, 554. (o) de Klerk-Engels, B.; Groen, J. H.; Kraakman, M. J. A.; Ernsting, J. M.; Vrieze, K.; Goubitz, K.; Fraanje, J. *Organometallics* **1994**, *13*, 3279. (p) Skagestad, V.; Tilset, M. *Organometallics* **1994**, *13*, 3134. (q) Bassetti, M.; Mannina, L.; Monti, D. *Organometallics* **1994**, *13*, 3293.

- (11) Rohde, W.; tom Dieck, H. *J. Organomet. Chem.* **1990**, *385*, 101.

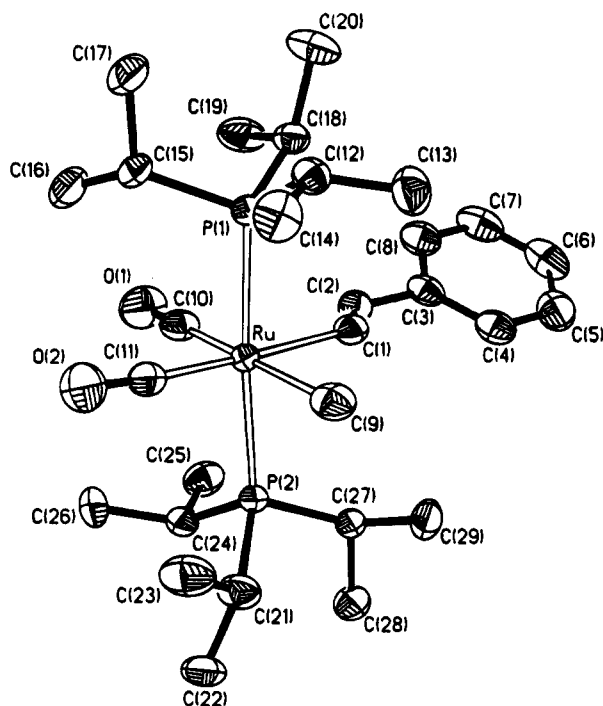


Figure 1. Molecular diagram of complex **2**. Thermal ellipsoids are shown at 50% probability.

Table 1. Selected Bond Distances (Å) and Angles (deg) for the Complex $\text{Ru}(\text{CH}_3)_2\{\text{(E)-CH=CHPh}\}(\text{CO})_2(\text{P}^i\text{Pr}_3)_2$ (**2**)

Ru-P(1)	2.4376(9)	Ru-C(11)	1.912(4)
Ru-P(2)	2.4265(9)	C(1)-C(2)	1.311(6)
Ru-C(1)	2.141(3)	C(2)-C(3)	1.497(5)
Ru-C(9)	2.205(4)	C(10)-O(1)	1.130(5)
Ru-C(10)	1.891(4)	C(11)-O(2)	1.145(5)
P(1)-Ru-P(2)	175.77(4)	C(1)-Ru-C(10)	89.8(2)
P(1)-Ru-C(1)	87.6(1)	C(1)-Ru-C(11)	175.5(2)
P(1)-Ru-C(9)	92.3(1)	C(9)-Ru-C(10)	176.4(2)
P(1)-Ru-C(10)	89.6(1)	C(9)-Ru-C(11)	90.0(2)
P(1)-Ru-C(11)	89.0(1)	C(10)-Ru-C(11)	93.1(2)
P(2)-Ru-C(1)	89.34(9)	Ru-C(1)-C(2)	130.6(3)
P(2)-Ru-C(9)	84.7(1)	C(1)-C(2)-C(3)	127.2(3)
P(2)-Ru-C(10)	93.3(1)	Ru-C(10)-O(1)	179.6(4)
P(2)-Ru-C(11)	93.9(1)	Ru-C(11)-O(2)	175.6(3)
C(1)-Ru-C(9)	87.2(1)		

0.05 and 0.1 Å longer than those found in $\text{Ru}\{\eta^5\text{-C}_5\text{H}_4\text{(neomenthyl)}\}(\text{CH}_3)(\text{CO})(\text{PPh}_3)$ (2.165(16) Å),¹⁴ $\text{R}_{\text{Ru}}\text{C-Ru}(\eta^5\text{-C}_5\text{H}_5)(\text{CH}_3)\{\text{Ph}_2\text{PCH}_2\text{CH}(\text{CH}_3)\text{PPh}_2\}$ (2.169(6) Å),¹⁵ $\text{Ru}(\text{CH}_3)(\text{SnCl}_3)(\eta^6\text{-C}_6\text{H}_6)\{\text{Ph}_2\text{PNHCH}(\text{CH}_3)\text{Ph}\}$ (2.155(9) Å),¹⁶ $\text{Ru}(\text{CH}_3)\text{I}(\text{CO})_2(\text{P}^i\text{Pr}=\text{CHCH}=\text{N}^i\text{Pr})$ (2.122(9) Å),^{10j} and $\text{Ru}_2(\text{CH}_3)\text{I}(\text{CO})_4(\text{P}^i\text{Pr-DAB})$ (2.115(5) Å).¹⁷

The alkenyl ligand shows a *trans* disposition for the two substituents, C_6H_5 and $\text{Ru}(\text{CH}_3)(\text{CO})_2(\text{P}^i\text{Pr}_3)_2$, at the C=C double bond. The Ru-C(1) distance (2.141(3) Å) is longer than the Ru-C distances found in the alkenylruthenium(II) derivatives $\text{Ru}\{\text{(E)-CH=CHPh}\}(\eta^2\text{-O}_2\text{CCH}_3)(\text{CO})(\text{PPh}_3)_2$ (2.030(15) Å),¹⁸ $\text{Ru}\{\text{(E)-CH=CH-C}_3\text{H}_7\}\text{Cl}(\text{CO})(\text{Me}_2\text{Hpz})(\text{PPh}_3)_2$ (2.05(1) Å),¹⁹ $\text{Ru}\{\text{(E)-}$

$\text{CH=CHCMe}_3\}\text{Cl}(\text{CO})(\text{Me}_2\text{Hpz})(\text{PPh}_3)_2$ (2.063(7) Å),²⁰ $\text{Ru}\{\text{(E)-CH=CHPh}\}(\eta^2\text{-O}_2\text{CH})(\text{CO})(\text{PPh}_3)_2$ (2.036(8) Å),²¹ and $[\text{Ru}\{\text{(E)-CH=CHCMe}_3\}(\text{CO})\{\text{NH}=\text{C}(\text{Me})(\text{Me}_2\text{pz})\}(\text{PPh}_3)_2]\text{PF}_6$ (2.067(8) Å),²² but it is comparable to that reported for $\text{Ru}\{\text{C}(\text{CO}_2\text{Me})=\text{C}(\text{CO}_2\text{Me})\text{Cl}\}\text{Cl}(\text{CO})_2(\text{PPh}_3)_2$ (2.16(2) Å).²³ The C(1)-C(2) bond length (1.311(6) Å) is similar to those found in the above-mentioned compounds.

The Ru-C(10) distance (1.891(4) Å) is statistically identical with the Ru-C(11) bond length (1.912(4) Å). Both C-O distances in the carbonyl group are also statistically identical. This suggests that the *trans* influences of the methyl and styryl ligands are similar. The Ru-P distances are clearly in the range expected and deserve no further comments.

In agreement with the mutually *cis* disposition of the two carbonyl ligands, the IR spectrum in Nujol shows two $\nu(\text{CO})$ absorptions at 1985 and 1922 cm^{-1} . In the ^1H NMR spectrum in benzene- d_6 , the methyl group gives, at 0.26 ppm, a triplet with a P-H coupling constant of 6.6 Hz. The vinyl protons of the styryl ligand appear at 8.16 (H_α) and 7.08 (H_β) with a H-H coupling constant of 18.4 Hz and P-H coupling constants of 2.5 and 1.9 Hz, respectively. The value of the H-H coupling constant is similar to that previously reported for the starting complex **1**²⁴ and agrees well with the *trans* stereochemistry of the two hydrogen atoms at the C=C double bond of the alkenyl ligand. In the $^{13}\text{C}\{^1\text{H}\}$ NMR spectrum, the C_α and C_β carbon atoms of the styryl ligand display triplets at 162.43 ($J_{\text{P-C}} = 15.2$ Hz) and 141.35 ($J_{\text{P-C}} = 4.1$ Hz) ppm, respectively. The methyl group appears as a triplet with a P-C coupling constant of 11.0 Hz. The $^{31}\text{P}\{^1\text{H}\}$ NMR spectrum shows a singlet at 38.1 ppm, in accordance with the mutually *trans* disposition of the phosphine ligands.

At first glance, complex **2** has three nucleophilic centers, the metal, the methyl group, and the β -carbon atom of the styryl ligand, and one electrophilic center, the α -carbon atom of the styryl group. Interestingly, the reaction of **2** with $\text{HBF}_4\cdot\text{OEt}_2$ gives styrene and the five-coordinate methyl compound **3** (Scheme 1). Formally, the proton of the acid attacks at the α -carbon atom of this ligand. Direct addition of the proton at the α -carbon atom of the styryl ligand does not seem likely in view of the electrophilicity of this atom and the expected strong nucleophilicity of the methyl group. Hence, it could be proposed that the proton initially attacks the metallic center to give the intermediate $[\text{RuH}(\text{CH}_3)\{\text{(E)-CH=CHPh}\}(\text{CO})_2(\text{P}^i\text{Pr}_3)_2]^+$ (**4**), which subsequently evolves by reductive elimination of styrene into **3** (eq 1).

The elimination of styrene from **4** merits further consideration. The order of bond strengths based upon recent results with several metal complexes that are

(18) Torres, M. R.; Perales, A.; Loumrhari, H.; Ros, J. *J. Organomet. Chem.* **1990**, *385*, 379.

(19) Torres, M. R.; Santos, A.; Perales, A.; Ros, J. *J. Organomet. Chem.* **1988**, *353*, 221.

(20) Romero, A.; Santos, A.; Vegas, A. *Organometallics* **1988**, *7*, 1988.

(21) Loumrhari, H.; Matas, L.; Ros, J.; Torres, M. R.; Perales, A. *J. Organomet. Chem.* **1991**, *403*, 373.

(22) López, J.; Santos, A.; Romero, A.; Echavarren, A. M. *J. Organomet. Chem.* **1993**, *443*, 221.

(23) Holland, P. R.; Howard, B.; Mawby, R. J. *J. Chem. Soc., Dalton Trans.* **1983**, 231.

(24) Werner, H.; Esteruelas, M. A.; Otto, H. *Organometallics* **1986**, *5*, 2295.

(12) Hommeltoft, S. I.; Cameron, A. D.; Shackleton, T. A.; Fraser, M. E.; Fortier, S.; Baird, M. C. *Organometallics* **1986**, *5*, 1380.

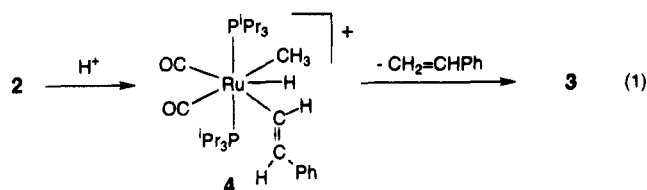
(13) Statler, J. A.; Wilkinson, G.; Thornton-Pett, M.; Hursthouse, M. B. *J. Chem. Soc., Dalton Trans.* **1984**, 1731.

(14) Lindsay, C.; Cesarotti, E.; Adams, H.; Bailey, N. A.; White, C. *Organometallics* **1990**, *9*, 2594.

(15) Consiglio, G.; Morandini, F.; Ciani, G.; Sironi, A. *Angew. Chem., Int. Ed. Engl.* **1983**, *22*, 333.

(16) Korp, J. D.; Bernal, I. *Inorg. Chem.* **1981**, *20*, 4065.

(17) Kraakman, M. J. A.; Vrieze, K.; Kooijman, H.; Spek, A. L. *Organometallics* **1992**, *11*, 3760.



active in C–H bond activation is H–vinyl > H–CH₃ and M–vinyl ≫ M–CH₃.²⁵ Thus, from a thermodynamic point of view, it seems to be the H–C bond strengths which determine the direction of the elimination, not the M–C bond strengths. The contrary situation has been proposed for the C–H activation. Jones and Feher²⁵ have suggested that it is the product's bond strengths (M–C) which determine the position of the hydrocarbon activation equilibria.

Kinetic arguments can also be used, in order to rationalize the elimination of styrene from 4. Low and Goddard²⁶ have proposed that the increased s character of the sp² hybrids causes this orbital to be less directional than the sp³ hybrids and, therefore, the sp² hybrids can have more multicentered bonding at the transition state, leading to lower activation energies for elimination. In accordance with this, it has been observed, for example, that (i) the reductive elimination of *cis*-Ni(CH₃)(C₆H₅)L₂ is faster than that from *cis*-Ni(CH₃)₂L₂,²⁷ (ii) the reaction of PhLi with PdCl₂(DIPHOS) yields biphenyl directly, whereas MeLi reacts with PdCl₂(DIPHOS) to afford PdMe₂(DIPHOS), which eliminates ethane slowly,²⁸ and (iii) platinum diphenylbis(phosphine) complexes can eliminate biphenyl,^{29ab} while platinum dimethylbis(phosphine) complexes are very stable.^{29c}

The reaction of 2 with HBF₄·OEt₂ was carried out at room temperature in acetone. Complex 3 was isolated as an air-sensitive white solid in 67% yield, which is stable for up to 1 month if kept at -20 °C under an argon atmosphere. In solution it rapidly decomposes to unidentified products. For this reason, complex 3 can be only characterized by elemental analysis and IR and ¹H and ³¹P{¹H} NMR spectroscopy. In the IR spectrum in Nujol, the most distinctive absorptions are two ν(CO) bands at 2030 and 1955 cm⁻¹ and an absorption due to the [BF₄]⁻ anion with T_d symmetry, at about 1100 cm⁻¹, indicating that this anion is not coordinated to the metallic center of 3. The basal site of the methyl group is strongly supported by the intensity ratio of the ν(CO) absorptions, which suggests an angle between the carbonyl ligands of 88.9°. The ¹H NMR spectrum contains, at 0.07 ppm, a triplet with a P–H coupling constant of 5.4 Hz, which was assigned to the protons of the methyl group. The ³¹P{¹H} NMR spectrum has a singlet at 47.0 ppm.

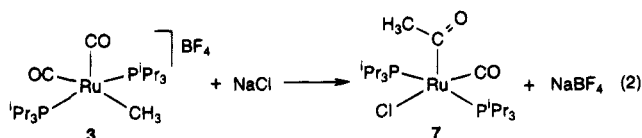
Under a carbon monoxide atmosphere, complex 3 affords the six-coordinate methyl derivative 5 (Scheme 1). The related styryl complex 6 can be obtained by

reaction of 1 with AgBF₄ under a carbon monoxide atmosphere.

Complex 5 was isolated as a white solid in 90% yield. The presence of three carbonyl ligands in a *mer* disposition was inferred from its IR and ¹³C{¹H} NMR spectra. The IR spectrum contains three ν(CO) bands at 2090 (m), 2010 (s), and 1990 (s) cm⁻¹ along with an absorption due to the [BF₄]⁻ anion with T_d symmetry. The ¹³C{¹H} NMR spectrum shows two carbonyl signals at 198.71 (t, J_{P–C} = 11.8 Hz) and 190.62 (t, J_{P–C} = 9.3 Hz) ppm in a 2:1 intensity ratio. The methyl group appears at -20.75 ppm as a triplet with a P–C coupling constant of 6.1 Hz. In the ¹H NMR spectrum of 5, the methyl protons give rise to a triplet at -0.03 ppm with a P–H coupling constant of 5.4 Hz. The ³¹P{¹H} NMR spectrum shows a singlet at 45.8 ppm.

The styryl derivative 6 was isolated also as a white solid in 80% yield. Similarly to 5, the presence of three carbonyl ligands in a *mer* disposition was inferred from its IR and ¹³C{¹H} NMR spectra. The IR spectrum of 6 in Nujol contains an absorption due to the [BF₄]⁻ anion with T_d symmetry and three ν(CO) bands in the terminal carbonyl region at 2100 (m), 2050 (s), and 2020 (s) cm⁻¹. As for 5, the ¹³C{¹H} NMR spectrum of 6 shows two carbonyl signals at 198.10 (t, J_{P–C} = 11.5 Hz) and 192.27 (t, J_{P–C} = 8.4 Hz) ppm in a 2:1 intensity ratio. The α-carbon atom of the styryl ligand appears at 130.00 ppm as a triplet with a P–C coupling constant of 10.9 Hz, while the β-carbon atom also appears as a triplet at 144.81 ppm and has a P–C coupling constant of 3.2 Hz. In the ¹H NMR spectrum, the most noticeable resonances are those corresponding to the styryl ligand. The α-proton appears at 7.28 ppm, while the β-proton lies at 6.78 ppm. The ³¹P{¹H} NMR spectrum shows a singlet at 45.6 ppm.

2. Migratory CO Insertion in the Methyl Group of 3. Treatment of a toluene suspension of 3 with NaCl in a 1:10 molar ratio at room temperature yields after 5 h a yellow solution, from which the acyl complex Ru{η¹-C(O)CH₃}Cl(CO)(PⁱPr₃) (7) can be isolated, by addition of methanol, as a yellow solid in 80% yield (eq 2).



Complex 7 was characterized by elemental analysis, IR and ¹H, ¹³C{¹H}, and ³¹P{¹H} NMR spectroscopy and X-ray diffraction. A view of the molecular geometry of this compound is shown in Figure 2. Selected bond distances and angles are listed in Table 2.

The geometry can be rationalized as a square pyramid with the acyl ligand located at the apex. The four atoms P, P', Cl, and C(1), forming the base, are approximately in one plane, whereas the ruthenium atom is located 0.2825(5) Å above this plane toward the apical position.

The acyl, chloride, and carbonyl groups are disposed in a T shape. This is in agreement with previous results obtained by Caulton and co-workers on the related RuHX(CO)(P^tBu₂Me)₂ systems, where the high stability of the *trans* Cl, CO disposition seems to be the result of a push–pull mechanism between the π-donor X and the π-acceptor CO groups. Furthermore, they have argued

(25) Jones, W. D.; Feher, F. J. *Acc. Chem. Res.* **1989**, *22*, 91.

(26) Low, J. J.; Goddard, W. A., III. *J. Am. Chem. Soc.* **1986**, *108*, 6115.

(27) Komiga, S.; Abe, Y.; Yamamoto, A.; Yamamoto, T. *Organometallics* **1983**, *2*, 1466.

(28) Gillie, A.; Stille, J. K. *J. Am. Chem. Soc.* **1980**, *102*, 4933.

(29) (a) Braterman, P. S.; Cross, R. J.; Young, G. B. *J. Chem. Soc., Dalton Trans.* **1976**, 1310. (b) Braterman, P. S.; Cross, R. J.; Young, G. B. *J. Chem. Soc., Dalton Trans.* **1977**, 1892. (c) Chatt, J.; Shaw, B. L. *J. Chem. Soc.* **1959**, 705.

(30) $[I(\text{higher } \nu)]/[I(\text{lower } \nu)] = \tan^2(\theta/2)$.

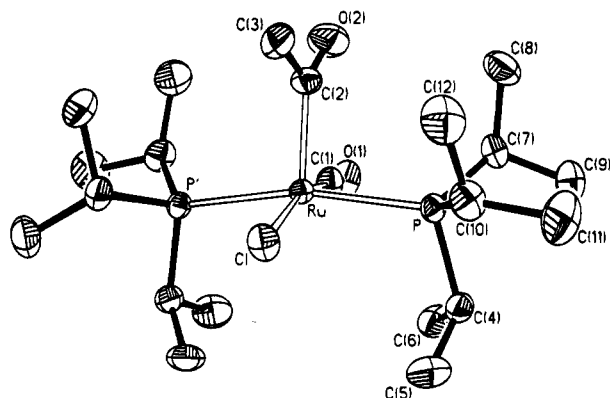


Figure 2. Molecular diagram of complex **7**. Thermal ellipsoids are shown at 50% probability.

Table 2. Selected Bond Distances (Å) and Angles (deg) for the Complex Ru{C(O)CH₃}Cl(CO)(PⁱPr₃)₂ (7**)**

Ru-P	2.4135(9)	C(1)-O(1)	1.166(10)
Ru-Cl	2.447(3)	C(2)-O(2)	1.215(8)
Ru-C(1)	1.776(8)	C(2)-C(3)	1.534(9)
Ru-C(2)	1.957(6)		
P-Ru-P ^a	166.54(4)	Cl-Ru-C(1)	165.0(3)
P-Ru-Cl	87.70(8)	Cl-Ru-C(2)	107.5(2)
P-Ru-C(1)	88.9(3)	C(1)-Ru-C(2)	87.3(3)
P-Ru-C(2)	93.5(2)	Ru-C(1)-O(1)	178.6(8)
P'-Ru-Cl	91.21(8)	Ru-C(2)-O(2)	128.8(5)
P'-Ru-C(1)	88.7(3)	Ru-C(2)-C(3)	113.7(4)
P'-Ru-C(2)	99.6(2)	O(2)-C(2)-C(3)	117.5(6)

^a P' is related to the independent P atom by the symmetry 2-fold axis.

that the X-Ru π donation makes these molecules not truly 16-valence electron species.³¹ We note that the stereo diagram shown in Figure 3 illustrates that also in the sixth (formally unoccupied) position of the octahedron the ruthenium atom is well-shielded. Four of the 12 methyl groups of the phosphine ligands surround the metal like an umbrella. The shielding effect of the methyl groups is certainly supported by the bending of the phosphorus-ruthenium-phosphorus axis, resulting in a P'-Ru-P angle of 166.54(4)°. A similar situation has been observed in the complexes Os{(E)-CH=CHPh}Cl(CO)(PⁱPr₃)₂ (P-Os-P = 167.4(1)°)²⁴ and [RuCl(=CHCH=CPh₂)(CO)(PⁱPr₃)₂][BF₄] (P-Ru-P = 163.36(3)°).³²

The acyl group is coordinated to the ruthenium center in a η^1 -acyl fashion with a Ru-C(2) bond length of 1.957(6) Å, which is about 0.1 Å longer than the values of 2.099(12) and 2.078(8) Å observed for [PPN][Ru₆C(CO)₁₆{C(O)Me}]³³ and Ru{C(O)Me}I(CO)₂(ⁱPrDAB),^{10j} respectively. The Ru-C(2)-O(2) and Ru-C(2)-C(3) angles are 128.8(5) and 113.7(4)°, and the C(2)-O(2) bond length is 1.215(8) Å, as expected for a C=O double bond of an η^1 -acyl ligand.³⁴ We note that the acyl ligands in the related complexes Ru{C(O)-*p*-tolyl}I(CO)-

(31) (a) Poulton, J. T.; Folting, K.; Streib, W. E.; Caulton, K. G. *Inorg. Chem.* **1992**, *31*, 3190. (b) Poulton, J. T.; Sigalas, M. P.; Eisenstein, O.; Caulton, K. G. *Inorg. Chem.* **1993**, *32*, 5490. (c) Heyn, R. H.; Huffman, J. C.; Caulton, K. G. *New J. Chem.* **1993**, *17*, 797. (d) Poulton, J. T.; Sigalas, M. P.; Folting, K.; Streib, W. E.; Eisenstein, O.; Caulton, K. G. *Inorg. Chem.* **1994**, *33*, 1476.

(32) Esteruelas, M. A.; Lahoz, F. J.; Oñate, E.; Oro, L. A.; Zeier, B. *Organometallics* **1994**, *13*, 4258.

(33) Chihara, T.; Aolei, K.; Yamazaki, H. *J. Organomet. Chem.* **1990**, *383*, 367.

(34) Allen, F. H.; Kennard, O.; Watson, D. G.; Brammer, L.; Orpen, A. G.; Taylor, R. *J. Chem. Soc., Perkin Trans. 2* **1987**, S1.

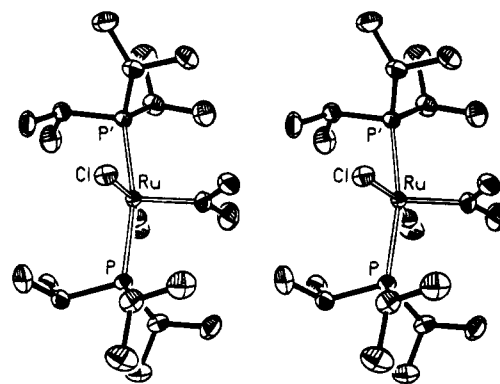
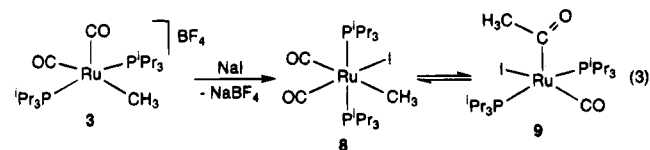


Figure 3. Stereoview of the molecule Ru{C(O)CH₃}Cl(CO)(CO)(PⁱPr₃)₂ (**7**).

(PPh₃)₂ and Ru{C(O)Me}I(CO)(PPh₃)₂ are coordinated in a η^2 fashion.³⁵ This again seems to suggest that the triisopropylphosphine ligands play a major role in the stabilization of the five-coordination for **7**.

In agreement with the presence of a terminal carbonyl ligand and an η^1 -acyl group in **7**, the IR spectrum in Nujol of this compound shows two ν (CO) bands at 1924 and 1630 cm⁻¹. The ¹H and ³¹P{¹H} NMR spectra of **7** in toluene-*d*₈ are temperature dependent. At room temperature, the ¹H NMR spectrum only contains the expected resonances for the triisopropylphosphine ligands. At -40 °C a new broad signal assigned to the methyl group of the acyl ligand appears at about 3 ppm ($\omega_{1/2}$ = 19 Hz). This signal is broad even at -75 °C ($\omega_{1/2}$ = 13 Hz). At 0 °C the ³¹P{¹H} NMR spectrum shows a broad signal at 45.8 ppm ($\omega_{1/2}$ = 55.8 Hz), while at -80 °C this signal is observed as a broad singlet ($\omega_{1/2}$ = 6.2 Hz). At the same temperature the ¹³C{¹H} NMR spectrum contains broad resonances at 237.13, 202.67, and 43.34 ppm, which were assigned to the carbonyl group of the acyl ligand, to the terminal carbonyl ligand, and the methyl group of the acyl ligand, respectively. The behavior of **7** in solution suggests that this compound has a rigid structure only at a temperature lower than -80 °C.

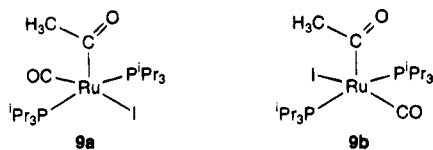
Treatment of **3** with NaI, under the same conditions as those previously described for the formation of **7**, leads to a yellow solid in 81% yield. According to the ¹H, ¹³C{¹H}, and ³¹P{¹H} NMR spectra of the solid, it is a mixture of the complexes Ru(CH₃)I(CO)₂(PⁱPr₃)₂ (**8**) and Ru{C(O)CH₃}I(CO)₂(PⁱPr₃)₂ (**9**), which are in a dynamic equilibrium in solution (eq 3).



At 57 °C the ¹H NMR spectrum of the solid in toluene-*d*₈ shows the expected resonances for the phosphine ligands along with a triplet at 2.16 (J_{P-H} = 2.4 Hz) ppm. At 17 °C the triplet is masked by the -CH- resonance of the isopropyl groups. When the temperature is lowered to -63 °C, a very broad signal between 3.2 and 2.5 ppm is observed. At -83 °C, this resonance splits into two singlets at 3.00 and 2.67 ppm and a triplet at

(35) Roper, W. R.; Taylor, G. E.; Waters, J. M.; Wright, L. J. *J. Organomet. Chem.* **1979**, *182*, C46.

0.67 ($J_{P-H} = 6$ Hz) ppm. This spectrum is consistent with an approximately 1:1:1 mixture of the conformers **9a** and **9b** and the methyl complex **8**.



The presence of the conformers **9a** and **9b** is also supported by the $^{13}C\{^1H\}$ NMR spectrum at -80 °C, which contains six resonances due to the acyl complex at 241.21 and 237.32 (C=O), 205.93 and 202.54 (C≡O), and 40.02 and 38.95 ($-CH_3$) ppm along with the resonances due to **8** at 200.85 and 196.16 (C≡O) and -14.50 (Ru- CH_3) ppm. The mutually *cis* disposition of the carbonyl ligands in **8** is supported by the presence of two resonances due to two inequivalent carbonyl groups.

The $^{31}P\{^1H\}$ NMR spectrum is also temperature dependent and totally consistent with the dynamic equilibrium shown in eq 3. Thus, at 0 °C, it shows a broad resonance, which splits into two singlets at 42.7 and 38.2 ppm as the temperature is lowered to -80 °C. The singlet at 42.7 ppm was assigned to the mixture of the conformers **9a** and **9b**, and the singlet at 38.2 ppm was assigned to the complex **8**.

In the solid state the acyl ligand is coordinated in a η^1 fashion. This is strongly supported by the IR spectrum in Nujol of the yellow solid, which shows a

Scheme 2

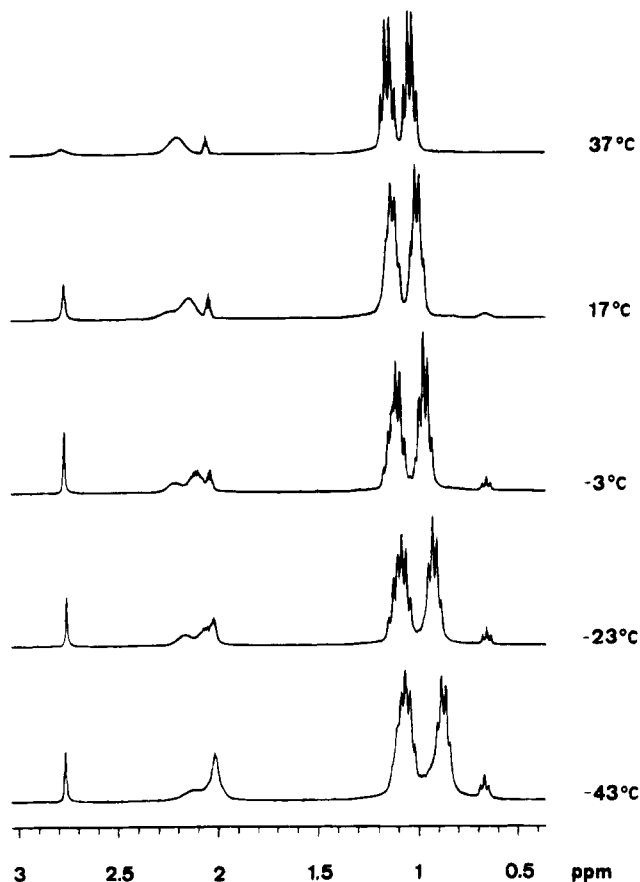
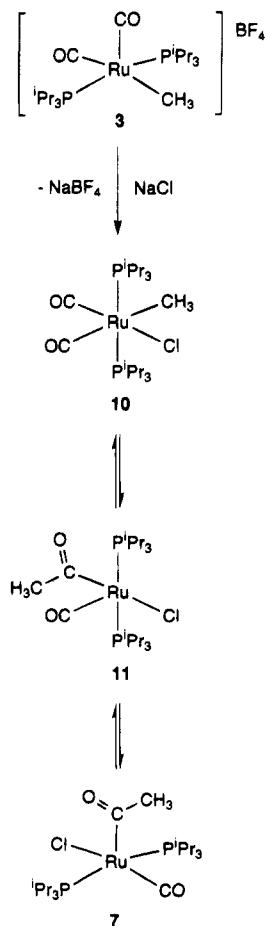
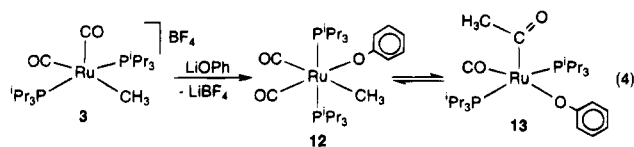


Figure 4. Variable-temperature 1H NMR spectra of $Ru(CH_3)(OPh)(CO)_2(P^iPr_3)_2$ (**12**) and $Ru\{C(O)CH_3\}(OPh)(CO)(P^iPr_3)_2$ (**13**) in C_7D_8 .

strong $\nu(CO)$ absorption at 1620 cm^{-1} . In the terminal carbonyl region the spectrum contains two $\nu(CO)$ bands at 1930 and 1917 cm^{-1} .

The fluxional behavior of **7** in solution can be rationalized in terms of an equilibrium similar to that shown in eq 3. Thus, the formation of **7** could involve the coordination of a chloride anion to the metallic center of **3** to give the six-coordinate methyl intermediate **10** (Scheme 2), followed by the 1,2-migration of the methyl group to the *cis*-disposed carbonyl ligand. The subsequent isomerization of **11** could yield **7**.

Under experimental conditions similar to those previously described for the preparation of **7**, complex **3** also reacts with $LiOPh$ and $LiC\equiv CPh$. The reaction of **3** with $LiOPh$ results in a rapidly established equilibrium mixture of the methyl-dicarbonyl $Ru(CH_3)(OPh)(CO)_2(P^iPr_3)_2$ (**12**) and the acyl carbonyl $Ru\{C(O)CH_3\}(OPh)(CO)(P^iPr_3)_2$ (**13**) (eq 4).



Figures 4 and 5 show the 1H and $^{31}P\{^1H\}$ NMR spectra, respectively, of the equilibrium mixture as a function of the temperature. At 17 °C, the 1H NMR spectrum shows two broad resonances at 2.77 and 0.68 ppm, which were assigned to the methyl group of the acyl ligand of **13** and the methyl ligand of **12**, respectively. When the temperature is lowered to -43 °C, the

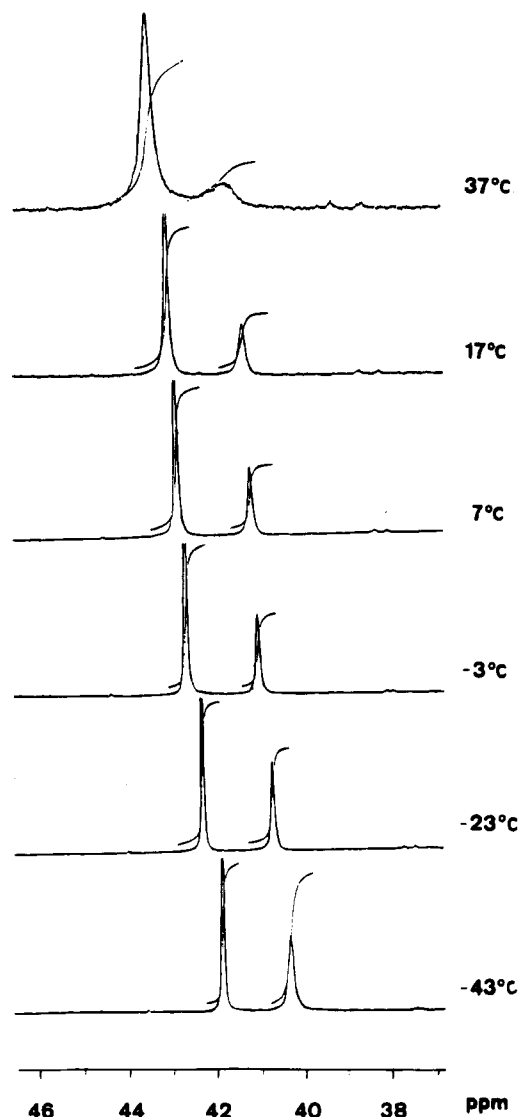


Figure 5. Variable-temperature $^{31}\text{P}\{^1\text{H}\}$ NMR spectra of $\text{Ru}(\text{CH}_3)(\text{OPh})(\text{CO})_2(\text{P}^i\text{Pr}_3)_2$ (**12**) and $\text{Ru}\{\text{C}(\text{O})\text{CH}_3\}(\text{OPh})(\text{CO})(\text{P}^i\text{Pr}_3)_2$ (**13**) in C_7D_8 .

Table 3. Calculated Values for K ($K = [\text{13}]/[\text{12}]$)

temp (K)	K	temp (K)	K
230	1.002	260	1.728
240	1.212	270	2.066
250	1.419	290	2.857

resonance at 2.77 ppm is converted into a singlet, while the resonance at 0.68 ppm gives rise to a triplet with a P–H coupling constant of 6.2 Hz. For each temperature the constant of the equilibrium shown in eq 4 was calculated (Table 3) by integration of the above-mentioned resonances. Linear least-squares analysis of $\ln K$ versus $1/T$ (Figure 6) provides values for ΔH and ΔS of 2.31 ± 0.07 kcal mol $^{-1}$ and 10.04 ± 0.28 cal K $^{-1}$ mol $^{-1}$, respectively. From Figure 5, the values calculated for ΔH and ΔS are 2.14 ± 0.09 kcal mol $^{-1}$ and 9.35 ± 0.33 cal K $^{-1}$ mol $^{-1}$.

This value of ΔS is in agreement with the higher number of molecular degrees of freedom in the five-coordinate acyl carbonyl compound **13** than in the six-coordinate methyl dicarbonyl derivative **12**. Furthermore, the values of ΔH and ΔS together indicate that the factors that underlie the migration are the higher number of molecular degrees of freedom in **13** and,

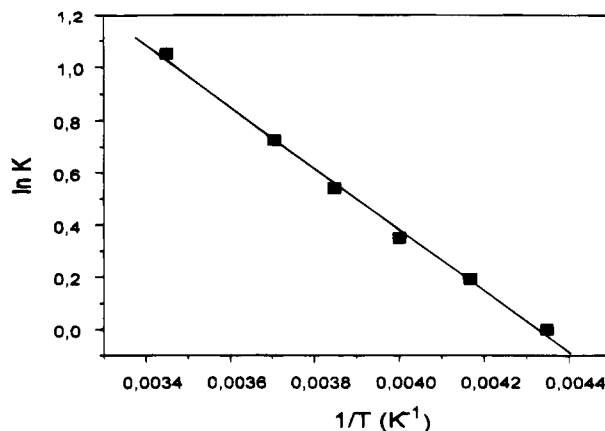


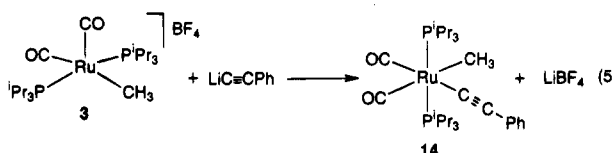
Figure 6. Plot of $\ln K$ versus $1/T$ for the equilibrium shown in eq 4.

therefore, the formation of **13** is favored when the temperature is increased.

In the $^{13}\text{C}\{^1\text{H}\}$ NMR spectrum at -33 °C, the most noticeable resonances of the acyl carbonyl complex **13** are two triplets at 245.15 ($J_{\text{P-C}} = 7.2$ Hz) and 206.53 ($J_{\text{P-C}} = 13.6$ Hz) ppm, which were assigned to the carbonyl group of the acyl ligand and the terminal carbonyl ligand, and a singlet at 44.56 ppm corresponding to the methyl group of the acyl ligand. Characteristic resonances of **12** are two triplets at 203.56 ($J_{\text{P-C}} = 10.8$ Hz) and 198.79 ($J_{\text{P-C}} = 10.1$ Hz) ppm due to two inequivalent terminal carbonyl ligands and a triplet at -0.35 ($J_{\text{P-C}} = 10.5$ Hz) ppm corresponding to the methyl ligand.

In the solid state the acyl ligand of **13** is coordinated in a η^1 fashion. This is supported by the IR spectrum in Nujol, which shows a $\nu(\text{CO})$ band at 1610 cm $^{-1}$.

The reaction of **3** with $\text{LiC}\equiv\text{CPh}$ leads to the six-coordinate methyl alkynyl derivative $\text{Ru}(\text{CH}_3)(\text{C}_2\text{Ph})(\text{CO})_2(\text{P}^i\text{Pr}_3)_2$ (**14**) (eq 5), which was isolated as a white solid in 77% yield.



The mutually *cis* disposition of the carbonyl ligands is strongly supported by the IR spectrum in Nujol, which contains in the terminal carbonyl region two $\nu(\text{CO})$ absorptions at 1995 and 1935 cm $^{-1}$. The alkynyl $\nu(\text{C}\equiv\text{C})$ vibration appears at 2094 cm $^{-1}$. In the ^1H NMR spectrum in benzene- d_6 at room temperature the most noticeable resonance is a triplet at 0.26 ($J_{\text{P-H}} = 6.0$ Hz) ppm, assigned to the methyl ligand. In the $^{13}\text{C}\{^1\text{H}\}$ NMR spectrum three triplets at 118.70 ($J_{\text{P-C}} = 20.2$ Hz), 113.72 ($J_{\text{P-C}} = 2.3$ Hz), and -13.80 ($J_{\text{P-C}} = 13.3$ Hz) ppm were assigned to the carbon atoms $\text{Ru}-\text{C}\equiv$, $\equiv\text{CPh}$, and $\text{Ru}-\text{CH}_3$, respectively. The $^{31}\text{P}\{^1\text{H}\}$ NMR spectrum contains a singlet at 41.9 ppm, indicating that the phosphine ligands are equivalent and are mutually *trans* disposed.

Under atmospheric pressure of carbon monoxide, complex **14** is quantitatively converted into the acyl derivative $\text{Ru}\{\text{C}(\text{O})\text{CH}_3\}(\text{C}_2\text{Ph})(\text{CO})_2(\text{P}^i\text{Pr}_3)_2$ (**15**) (eq 6). Figure 7 reflects the conversion of the methyl group to an acyl ligand. Thus, the triplet at 0.26 ppm in the ^1H

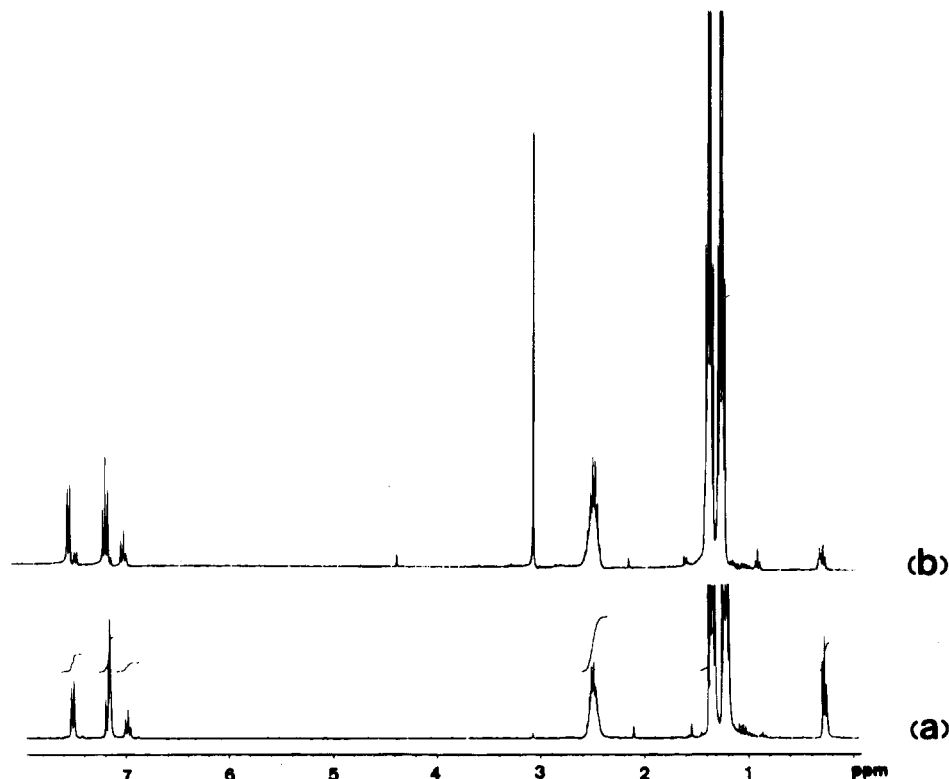
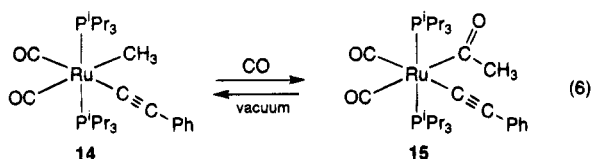


Figure 7. ^1H NMR spectra of the compounds $\text{Ru}(\text{CH}_3)(\text{C}\equiv\text{CPh})(\text{CO})_2(\text{P}^i\text{Pr}_3)_2$ (**14**) (a) and $\text{Ru}\{\text{C}(\text{O})\text{CH}_3\}(\text{C}\equiv\text{CPh})(\text{CO})_2(\text{P}^i\text{Pr}_3)_2$ (**15**) (b) at 20°C in C_6D_6 .

NMR spectrum of **14** (Figure 7a) appears as a singlet at 3.02 ppm in the ^1H NMR spectrum of **15** (Figure 7b).

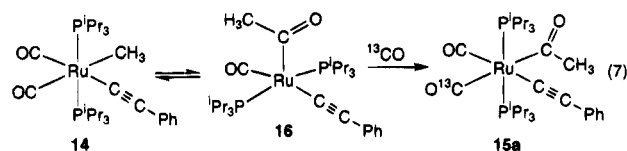


The mutually *cis* disposition of the terminal carbonyl ligands is strongly supported by the $^{13}\text{C}\{^1\text{H}\}$ NMR spectrum of **15**, which contains two triplets at 201.15 ($J_{\text{P-C}} = 9.1$ Hz) and 200.13 ($J_{\text{P-C}} = 11.0$ Hz) ppm due to inequivalent carbonyl ligands. The acyl group gives rise to a triplet at 266.42 ($J_{\text{P-C}} = 10.1$ Hz, $\text{Ru}-\text{C}(\text{O})-$) ppm and a singlet at 49.18 ($-\text{C}(\text{O})-\text{CH}_3$) ppm, whereas the most noticeable resonances of the alkynyl ligand are two triplets at 119.51 ($J_{\text{P-C}} = 17.5$ Hz) and 113.30 ($J_{\text{P-C}} = 1.8$ Hz) ppm, which were assigned to the C_α and C_β carbon atoms, respectively. The $^{31}\text{P}\{^1\text{H}\}$ NMR spectrum shows a singlet at 39.8 ppm.

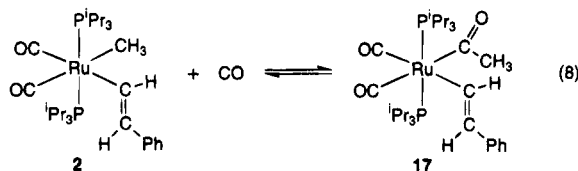
The reaction shown in eq 6 is completely reversible under vacuum at room temperature. This suggests that, in solution, the methyl dicarbonyl complex **14** is in equilibrium with a spectroscopically undetectable amount of the acyl carbonyl derivative $\text{Ru}\{\text{C}(\text{O})\text{CH}_3\}(\text{C}_2\text{-Ph})(\text{CO})(\text{P}^i\text{Pr}_3)_2$ (**16**). This compound, as for complexes **7**, **9**, and **13**, should have a square-pyramidal structure with the acyl ligand in the apical position. In agreement with this, we have observed that **14** reacts with ^{13}CO to give **15a** (eq 7).

The *trans* position of the acyl and ^{13}CO ligands was inferred from the signal due to the carbonyl group of the acyl ligand in the $^{13}\text{C}\{^1\text{H}\}$ NMR spectrum of **15a**, which appears as a doublet of triplets with a strong

(26 Hz) C–C coupling constant, typical for a *trans* arrangement.^{6a}



Under atmospheric pressure of carbon monoxide, the methyl styryl complex **2** is also in equilibrium with the styryl acyl derivative $\text{Ru}\{\text{C}(\text{O})\text{CH}_3\}\{(\text{E})-\text{CH}=\text{CHPh}\}(\text{CO})_2(\text{P}^i\text{Pr}_3)_2$ (**17**) (eq 8). At room temperature in ben-



zene- d_6 the **2**:**17** molar ratio is 1:1. Characteristic signals for **17** in the ^1H NMR spectrum are a singlet at 2.87 ppm and two doublets of triplets at 7.09 and 9.02 ppm, with a H–H coupling constant of 18.7 Hz and P–H coupling constants of 2.5 and 2.9 Hz, respectively. The singlet was assigned to the methyl group of the acyl ligand and the doublets of triplets to the H_β and H_α protons of the styryl group. In the $^{13}\text{C}\{^1\text{H}\}$ NMR spectrum the acyl ligand gives rise to a triplet at 261.62 ($J_{\text{P-C}} = 11.3$ Hz) ppm, assigned to the carbonyl group, and a singlet at 52.86 ppm due to the methyl group. The C_α carbon atom of the styryl ligand appears at 164.32 ppm and the C_β carbon atom at 140.51 ppm, both as triplets with P–C coupling constants of 15.1 and 4.5 Hz, respectively. The spectrum also contains two triplets at 205.15 ($J_{\text{P-C}} = 9.8$ Hz) and 202.85 ($J_{\text{P-C}} =$

9.0 Hz) ppm, which were assigned to two chemically inequivalent carbonyl ligands, in agreement with the structure proposed in eq 8. A singlet at 36.5 ppm in the $^{31}\text{P}\{^1\text{H}\}$ NMR spectrum is also consistent with the proposed structure of **17** (eq 8).

Concluding Remarks

This study has revealed that the reaction of the methyl styryl complex $\text{Ru}(\text{CH}_3)\{(\text{E})\text{-CH=CHPh}\}(\text{CO})_2(\text{P}^i\text{Pr}_3)_2$ with $\text{HBF}_4\cdot\text{OEt}_2$ leads selectively to styrene and the five-coordinate derivative $[\text{Ru}(\text{CH}_3)(\text{CO})_2(\text{P}^i\text{Pr}_3)_2]\text{-BF}_4$. The reactions of this complex with anionic monodentate nucleophilic reagents afford six-coordinate methyl dicarbonyl compounds of the type $\text{Ru}(\text{CH}_3)\text{X}(\text{CO})_2(\text{P}^i\text{Pr}_3)_2$, in equilibrium with the corresponding acyl derivatives $\text{Ru}\{\text{C}(\text{O})\text{CH}_3\}\text{X}(\text{CO})(\text{P}^i\text{Pr}_3)_2$ (X = Cl, I, OPh, C=CPh). The position of the equilibrium is markedly dependent upon X, increasing the tendency toward the migration in the sequence C=CPh < OPh < I < Cl. For X = OPh, the values of ΔH and ΔS have been calculated, and they suggest that the factors underlying the migration are the higher number of molecular degrees of freedom in the acyl carbonyl complex than in the methyl dicarbonyl derivative. The acyl compounds coordinate the acyl ligand in a η^1 fashion, in contrast to that observed by Roper *et al.* for related complexes containing triphenylphosphine as ligands.³⁵ The study of the structure of $\text{Ru}\{\text{C}(\text{O})\text{CH}_3\}\text{Cl}(\text{CO})(\text{P}^i\text{Pr}_3)_2$, determined by X-ray investigations, suggests that the steric demands of the trisopropylphosphine ligands play a main role in the stabilization of five-coordination for these compounds. Thus, 4 of the 12 methyl groups of the phosphine ligands surround the metal like an umbrella.

Experimental Section

General Considerations. All reactions were carried out with rigorous exclusion of air by using Schlenk-tube techniques. Solvents were dried by known procedures and distilled under argon prior to use. ^{13}C (99.74% in ^{13}C) was used as purchased. $\text{RuCl}\{(\text{E})\text{-CH=CHPh}\}(\text{CO})_2(\text{P}^i\text{Pr}_3)_2$ (**1**)²⁴ was prepared by published methods.

Physical Measurements. Infrared spectra were recorded as Nujol mulls on polyethylene sheets using a Perkin-Elmer 883 or a Nicolet 550 spectrometer. NMR spectra were recorded on a Varian UNITY 300 or on a Bruker 300 AXR. ^1H and $^{13}\text{C}\{^1\text{H}\}$ chemical shifts were measured relative to partially deuterated solvent peaks but are reported relative to tetramethylsilane. $^{31}\text{P}\{^1\text{H}\}$ chemical shifts are reported relative to H_3PO_4 (85%). The coupling constants J and N ($N = J(\text{HP}) + J(\text{HP}')$ for ^1H , and $N = J(\text{CP}) + J(\text{CP}')$ for ^{13}C) are given in hertz. C, H and N analyses were carried out with a Perkin-Elmer 2400 CHNS/O analyzer.

Preparation of $\text{Ru}(\text{CH}_3)\{(\text{E})\text{-CH=CHPh}\}(\text{CO})_2(\text{P}^i\text{Pr}_3)_2$ (2**).** A solution of $\text{RuCl}\{(\text{E})\text{-CH=CHPh}\}(\text{CO})_2(\text{P}^i\text{Pr}_3)_2$ (**1**; 140 mg, 0.23 mmol) in toluene (7 mL) was treated with a 1:2 excess of CH_3Li (0.30 mL, 1.6 M in hexane). After it was stirred for 30 min at room temperature, the dark suspension was filtered through Kieselguhr and evaporated to dryness. Addition of MeOH precipitated a white solid, which was washed several times with MeOH and dried in vacuo. Yield: 102.7 mg (75%). Anal. Calcd for $\text{C}_{29}\text{H}_{52}\text{O}_2\text{P}_2\text{Ru}$: C, 58.47; H, 8.80. Found: C, 58.12; H, 8.51. IR (Nujol, cm^{-1}): $\nu(\text{CO})$ 1985 (s), 1922 (s); $\nu(\text{C}=\text{C})$ 1600 (m). ^1H NMR (C_6D_6 , 20 °C): δ 8.16 (dt, 1H, $J_{\text{H-H}} = 18.4$ Hz, $J_{\text{P-H}} = 2.5$ Hz, $-\text{CH}=\text{CHPh}$), 7.48 (d, 2H, $J_{\text{H-H}} = 7.4$ Hz, $\text{H}_{\text{O-Ph}}$), 7.26 (t, 2H, $J_{\text{H-H}} = 7.4$ Hz, $\text{H}_{\text{m-Ph}}$), 7.08 (dt, 1H, $J_{\text{H-H}} = 18.4$ Hz, $J_{\text{P-H}} = 1.9$ Hz, $-\text{CH}=\text{CHPh}$), 7.00 (t, 1H, $J_{\text{H-H}} = 7.4$ Hz, $\text{H}_{\text{p-Ph}}$), 2.36 (m, 6H, $\text{PCH}(\text{CH}_3)_2$), 1.20 (dvt, 18H, N

= 12.2 Hz, $J_{\text{H-H}} = 6.9$ Hz, $\text{PCH}(\text{CH}_3)_2$), 1.07 (dvt, 18H, $N = 12.6$ Hz, $J_{\text{H-H}} = 6.9$ Hz, $\text{PCH}(\text{CH}_3)_2$), 0.26 (t, 3H, $J_{\text{H-P}} = 6.6$ Hz, $-\text{CH}_3$). $^{31}\text{P}\{^1\text{H}\}$ NMR (C_6D_6 , 20 °C): δ 38.1 (s). $^{13}\text{C}\{^1\text{H}\}$ NMR (C_6D_6 , 20 °C): δ 204.71 (t, $J_{\text{C-P}} = 11.1$ Hz, CO), 201.62 (t, $J_{\text{C-P}} = 9.6$ Hz, CO), 162.43 (t, $J_{\text{C-P}} = 15.2$ Hz, $-\text{CH}=\text{CHPh}$), 142.54 (t, $J_{\text{C-P}} = 2.3$ Hz, C_{ipsoPh}), 141.35 (t, $J_{\text{C-P}} = 4.1$ Hz, $-\text{CH}=\text{CHPh}$), 128.86, 124.77 (both s, C_6H_5 , together with another resonance masked by the signal of the solvent, C_6D_6), 25.48 (vt, $N = 20.3$ Hz, $\text{PCH}(\text{CH}_3)_2$), 19.99, 19.20 (both s, $\text{PCH}(\text{CH}_3)_2$), -9.81 (t, $J_{\text{C-P}} = 11.0$ Hz, CH_3).

Preparation of $[\text{Ru}(\text{CH}_3)(\text{CO})_2(\text{P}^i\text{Pr}_3)_2]\text{BF}_4$ (3**).** To a solution of $\text{Ru}(\text{CH}_3)\{(\text{E})\text{-CH=CHPh}\}(\text{CO})_2(\text{P}^i\text{Pr}_3)_2$ (**2**; 80 mg, 0.13 mmol) in acetone (8 mL) was added a stoichiometric amount of $\text{HBF}_4\cdot\text{OEt}_2$ (17.8 μL , 54% in OEt_2). The colorless solution became yellow immediately on addition of the reagent and was concentrated to ca. 1 mL. Addition of diethyl ether caused the precipitation of a white solid, which was washed with diethyl ether and dried in vacuo. Yield: 50.5 mg (67%). Anal. Calcd for $\text{C}_{21}\text{H}_{45}\text{BF}_4\text{O}_2\text{P}_2\text{Ru}$: C, 43.53; H, 7.83. Found: C, 43.66; H, 7.85. IR (Nujol, cm^{-1}): $\nu(\text{CO})$ 2030 (s), 1955 (s); $\nu(\text{BF}_4)$ 1050 (s). ^1H NMR ($\text{C}_3\text{D}_8\text{O}$, 20 °C): δ 2.85 (m, 6H, $\text{PCH}(\text{CH}_3)_2$), 1.51 (dvt, 36H, $N = 14.7$ Hz, $J_{\text{H-H}} = 8.0$ Hz, $\text{PCH}(\text{CH}_3)_2$), 0.07 (t, 3H, $J_{\text{H-P}} = 5.4$ Hz, $-\text{CH}_3$). $^{31}\text{P}\{^1\text{H}\}$ NMR ($\text{C}_3\text{D}_8\text{O}$, 20 °C): δ 47.0 (s).

Preparation of $[\text{Ru}(\text{CH}_3)(\text{CO})_3(\text{P}^i\text{Pr}_3)_2]\text{BF}_4$ (5**).** A slow stream of CO was bubbled through a solution of $[\text{Ru}(\text{CH}_3)(\text{CO})_2(\text{P}^i\text{Pr}_3)_2]\text{BF}_4$ (**3**; 75 mg, 0.12 mmol) in CH_2Cl_2 (5 mL) for 20 min. Concentration to ca. 1 mL followed by the addition of diethyl ether precipitated a white solid, which was washed with diethyl ether and dried in vacuo. Yield: 66 mg (90%). Anal. Calcd for $\text{C}_{22}\text{H}_{45}\text{BF}_4\text{NO}_3\text{P}_2\text{Ru}$: C, 43.50; H, 7.47. Found: C, 43.79; H, 7.26. IR (Nujol, cm^{-1}): $\nu(\text{CO})$ 2090 (m), 2010 (s), 1990 (s); $\nu(\text{BF}_4)$ 1100–1000 (s). ^1H NMR (CDCl_3 , 20 °C): δ 2.59 (m, 6H, $\text{PCH}(\text{CH}_3)_2$), 1.40 (dvt, 36H, $N = 14.7$ Hz, $J_{\text{H-H}} = 7.2$ Hz, $\text{PCH}(\text{CH}_3)_2$), -0.03 (t, 3H, $J_{\text{H-P}} = 5.4$ Hz, $-\text{CH}_3$). $^{31}\text{P}\{^1\text{H}\}$ NMR (CDCl_3 , 20 °C): δ 45.8 (s). $^{13}\text{C}\{^1\text{H}\}$ NMR (C_6D_6 , 20 °C): δ 198.71 (t, $J_{\text{C-P}} = 11.8$ Hz, CO), 190.62 (t, $J_{\text{C-P}} = 9.3$ Hz, CO), 26.23 (vt, $N = 23.2$ Hz, $\text{PCH}(\text{CH}_3)_2$), 19.34 (s, $\text{PCH}(\text{CH}_3)_2$), -20.75 (t, $J_{\text{C-P}} = 6.1$ Hz, $-\text{CH}_3$). MS (m/z): 521, M^+ ; 493, $\text{M}^+ - \text{CO}$; 465, $\text{M}^+ - 2\text{CO}$; 450, $\text{M}^+ - 2\text{CO} - \text{CH}_3$.

Preparation of $[\text{Ru}\{(\text{E})\text{-CH=CHPh}\}(\text{CO})_3(\text{P}^i\text{Pr}_3)_2]\text{BF}_4$ (6**).** A solution of **1** (100 mg, 0.16 mmol) in acetone (10 mL) was treated with the stoichiometric amount of AgBF_4 (31.6 mg, 0.16 mmol). After it was stirred for 2 h in the dark, at room temperature, the suspension was filtered through Kieselguhr. A clear, colorless solution was obtained. A slow stream of CO was bubbled through this solution for 15 min. Concentration to ca. 1 mL, followed by the addition of diethyl ether precipitated a white solid, which was washed with diethyl ether, and dried in vacuo. Yield: 89 mg (80%). Anal. Calcd for $\text{C}_{29}\text{H}_{49}\text{BF}_4\text{O}_3\text{P}_2\text{Ru}$: C, 50.08; H, 7.09. Found: C, 49.60; H, 6.83. IR (Nujol, cm^{-1}): $\nu(\text{CO})$ 2100 (m), 2050 (s), 2020 (s); $\nu(\text{C}=\text{C})$ 1620 (\bar{w}); $\nu(\text{BF}_4)$ 1100–1050. ^1H NMR (CDCl_3 , 20 °C): δ 7.36 (d, 2H, $J_{\text{H-H}} = 7.7$ Hz, $\text{H}_{\text{O-Ph}}$), 7.31 (t, 2H, $J_{\text{H-H}} = 7.7$ Hz, $\text{H}_{\text{m-Ph}}$), 7.28 (d, 1H, $J_{\text{H-H}} = 18.1$ Hz, $-\text{CH}=\text{CHPh}$), 7.22 (t, 1H, $J_{\text{H-H}} = 7.7$ Hz, $\text{H}_{\text{p-Ph}}$), 6.78 (d, 1H, $J_{\text{H-H}} = 18.1$ Hz, $-\text{CH}=\text{CHPh}$), 2.68 (m, 6H, $\text{PCH}(\text{CH}_3)_2$), 1.44 (dvt, 36H, $N = 15.1$ Hz, $J_{\text{H-H}} = 7.1$ Hz, $\text{PCH}(\text{CH}_3)_2$). $^{31}\text{P}\{^1\text{H}\}$ NMR (CDCl_3 , 20 °C): δ 45.6 (s). $^{13}\text{C}\{^1\text{H}\}$ NMR ($\text{C}_3\text{D}_8\text{O}$, 20 °C): δ 198.10 (t, $J_{\text{C-P}} = 11.5$ Hz, CO), 192.27 (t, $J_{\text{C-P}} = 8.4$ Hz, CO), 144.81 (t, $J_{\text{C-P}} = 3.2$ Hz, $-\text{CH}=\text{CHPh}$), 140.79 (t, $J_{\text{P-C}} = 1.9$ Hz, C_{ipsoPh}), 130.00 (t, $J_{\text{C-P}} = 10.9$ Hz, $-\text{CH}=\text{CHPh}$), 129.26, 127.11, 125.51 (all s, $-\text{C}_6\text{H}_5$), 27.45 (vt, $N = 23.5$ Hz, $\text{PCH}(\text{CH}_3)_2$), 19.50 (s, $\text{PCH}(\text{CH}_3)_2$). MS (m/z): 609, M^+ ; 581, $\text{M}^+ - \text{CO}$; 553, $\text{M}^+ - 2\text{CO}$; 451, $\text{M}^+ - 2\text{CO} - (\text{CH}=\text{CHPh})$.

Reaction of $[\text{Ru}(\text{CH}_3)(\text{CO})_2(\text{P}^i\text{Pr}_3)_2]\text{BF}_4$ (3**) with NaCl. Preparation of $[\text{Ru}\{\text{C}(\text{O})\text{CH}_3\}\text{Cl}(\text{CO})(\text{P}^i\text{Pr}_3)_2]$ (**7**).** A suspension of $[\text{Ru}(\text{CH}_3)(\text{CO})_2(\text{P}^i\text{Pr}_3)_2]\text{BF}_4$ (**3**; 150 mg, 0.25 mmol) in toluene (6 mL) was treated with a 1:10 excess of NaCl (146 mg, 2.5 mmol) and was stirred for 5 h at room temperature. The suspension was filtered through Kieselguhr, and the

yellow solution was concentrated to ca. 1 mL. Addition of MeOH precipitated a yellow solid, which was washed with MeOH and dried in vacuo. Yield: 105 mg (80%). Anal. Calcd for $C_{21}H_{45}ClO_2P_2Ru$: C, 47.77; H, 8.59. Found: C, 48.07; H, 8.69. IR (Nujol, cm^{-1}): $\nu(CO)$ 1924 (s); $\nu(C=O)$ 1630 (s). 1H NMR (C_6D_6 , 20 °C): δ 2.60 (m, 6H, $PCH(CH_3)_2$), 1.20 (dvt, 36H, $N = 13.4$ Hz, $J_{H-H} = 6.3$ Hz, $PCH(CH_3)_2$). 1H NMR (C_7D_8 , 10 °C): δ 2.64 (br, $COCH_3$), 2.55 (m, 6H, $PCH(CH_3)_2$), 1.15 (dvt, 36H, $N = 13.5$ Hz, $J_{H-H} = 6.6$ Hz, $PCH(CH_3)_2$). 1H NMR (C_7D_8 , -40 °C): δ 3.02 (br, $COCH_3$), 2.55 (br, $PCH(CH_3)_2$), 1.18 (br, $PCH(CH_3)_2$). 1H NMR (C_7D_8 , -75 °C): δ 3.06 (br, $COCH_3$), 2.60 (br, $PCH(CH_3)_2$), 1.20 (br, $PCH(CH_3)_2$). $^{31}P\{^1H\}$ NMR (C_6D_6 , 20 °C): δ 41.0 (br). $^{31}P\{^1H\}$ NMR (C_7D_8 , 10 °C): δ 46.0 (br). $^{31}P\{^1H\}$ NMR (C_7D_8 , 0 °C): δ 45.8 (br). $^{31}P\{^1H\}$ NMR (C_7D_8 , -40 °C): δ 45.6 (br). $^{31}P\{^1H\}$ NMR (C_7D_8 , -80 °C): δ 45.2 (br). $^{13}C\{^1H\}$ NMR (C_7D_8 , -80 °C): δ 237.13 (br, $COCH_3$), 202.67 (br, CO), 43.34 (br, $COCH_3$), 24.77 (br, $PCH(CH_3)_2$), 19.80, 19.41 (both s, $PCH(CH_3)_2$).

Reaction of $[Ru(CH_3)(CO)_2(P^iPr_3)_2]BF_4$ (3) with NaI.

The reaction was as for the preparation of 7, but with 3 (100 mg, 0.17 mmol) and NaI (254 mg, 1.7 mmol) as starting materials. A yellow solid was obtained. Yield: 85 mg (81%). Anal. Calcd for $C_{21}H_{45}IO_2P_2Ru$: C, 40.71; H, 7.32. Found: C, 40.81; H, 7.30. IR (Nujol, cm^{-1}): $\nu(CO)$ 1930 (s), 1917 (s); $\nu(C=O)$ 1620 (s). 1H NMR (C_7D_8 , 57 °C): δ 2.22 (m, 6H, $PCH(CH_3)_2$), 2.16 (t, 3H, $J_{P-H} = 2.4$ Hz), 1.32 (dvt, 36H, $N = 13.9$ Hz, $J_{H-H} = 7.3$ Hz, $PCH(CH_3)_2$). 1H NMR (C_7D_8 , 17 °C): δ 2.70 (m, 6H, $PCH(CH_3)_2$) (the resonance due to the acyl protons, $-COCH_3$, is masked by the signal of the solvent, C_7D_8), 1.13 (dvt, 36H, $N = 14.0$ Hz, $J_{H-H} = 7.7$ Hz, $PCH(CH_3)_2$). 1H NMR (C_7D_8 , -63 °C): δ 3.2-2.5 (br, $COCH_3$), 2.42 (br, $PCH(CH_3)_2$), 1.11 (br, $PCH(CH_3)_2$). 1H NMR (C_7D_8 , -83 °C): δ 3.00 (br, $COCH_3$, 9), 2.67 (br, $COCH_3$, 9), 2.32 (br, $PCH(CH_3)_2$, 8, 9), 0.91 (br, $PCH(CH_3)_2$, 8, 9), 0.67 (br t, $J_{P-H} = 6$ Hz, $-CH_3$, 8). $^{31}P\{^1H\}$ NMR (C_7D_8 , 17 °C): δ 41.4 (br). $^{31}P\{^1H\}$ NMR (C_7D_8 , -40 °C): δ 43.0 (br) (9), 37.7 (br) (8). $^{31}P\{^1H\}$ NMR (C_7D_8 , -80 °C): δ 42.7 (br) (9), 38.2 (br) (8). $^{13}C\{^1H\}$ NMR (C_7D_8 , -80 °C): δ 241.21 (br, $COCH_3$, 9), 237.32 (br, $COCH_3$, 9), 205.93 (br, CO, 9), 202.54 (br, CO, 9), 200.85 (br, CO, 8), 196.16 (br, CO, 8), 40.02 (s, $COCH_3$, 9), 38.95 (s, $COCH_3$, 9), 27.93 (br, $PCH(CH_3)_2$, 9), 26.85 (br, $PCH(CH_3)_2$, 8), 25.61 (br, $PCH(CH_3)_2$, 9) (the signals due to the $-CH_3$ of the P^iPr_3 ligands of 8 and 9 are masked by the resonance of the solvent, C_7D_8), -14.50 (br, $-CH_3$, 8).

Reaction of $[Ru(CH_3)(CO)_2(P^iPr_3)_2]BF_4$ (3) with PhOLi.

The reaction was as for the preparation of 7, but with 3 (100 mg, 0.17 mmol) and a 1:3 excess of PhOLi (51 mg, 0.51 mmol) as starting materials. A yellow solid was obtained. Yield: 79.6 mg (80%). Anal. Calcd for $C_{27}H_{50}O_3P_2Ru$: C, 55.37; H, 8.60. Found: C, 55.56; H, 8.77. IR (Nujol, cm^{-1}): $\nu(CO)$ 1895 (s); $\nu(C=O)$ 1610 (s). 1H NMR (C_7D_8 , 17 °C): δ 7.36 (t, 2H, $J_{H-H} = 6.3$ Hz, H_{m-Ph} , 12, 13), 7.10 (d, 2H, $J_{H-H} = 6.3$ Hz, H_{o-Ph} , 12, 13), 6.71 (t, 1H, $J_{H-H} = 6.3$ Hz, H_{p-Ph} , 12, 13), 2.77 (br, $COCH_3$, 13), 2.22 (m, 6H, $PCH(CH_3)_2$, 12, 13), 1.16 (br dvt, 18H, $N = 13.2$ Hz, $J_{H-H} = 6.6$ Hz, $PCH(CH_3)_2$, 12, 13), 1.05 (dvt, 18H, $N = 12.9$ Hz, $J_{H-H} = 6.9$ Hz, $PCH(CH_3)_2$, 12, 13), 0.68 (br, $-CH_3$, 12). 1H NMR (C_7D_8 , -43 °C): δ 7.40 (t, 2H, $J_{H-H} = 6.3$ Hz, H_{m-Ph} , 12), 7.36 (t, 2H, $J_{H-H} = 6.3$ Hz, H_{m-Ph} , 13), 7.10 (d, 2H, $J_{H-H} = 6.3$ Hz, H_{o-Ph} , 13), 7.01 (d, 2H, $J_{H-H} = 6.3$ Hz, H_{o-Ph} , 12), 6.71 (t, 1H, $J_{H-H} = 6.3$ Hz, H_{p-Ph} , 13), 6.69 (t, 1H, $J_{H-H} = 6.3$ Hz, H_{p-Ph} , 12), 2.84 (s, $COCH_3$, 13), 2.22 (m, 6H, $PCH(CH_3)_2$, 12, 13), 1.16 (dvt, 18H, $N = 13.2$ Hz, $J_{H-H} = 6.6$ Hz, $PCH(CH_3)_2$, 12, 13), 1.00 (dvt, 18H, $N = 12.9$ Hz, $J_{H-H} = 6.9$ Hz, $PCH(CH_3)_2$, 12, 13), 0.73 (t, 3H, $J_{P-H} = 6.2$ Hz, $-CH_3$, 12). $^{31}P\{^1H\}$ NMR (C_6D_6 , 17 °C): δ 43.1 (br) (13), 41.4 (br) (12). $^{31}P\{^1H\}$ NMR (C_7D_8 , -43 °C): δ 41.8 (s) (13), 40.3 (s) (12). $^{13}C\{^1H\}$ NMR (C_7D_8 , -33 °C): δ 245.15 (t, $J_{C-P} = 7.2$ Hz, $COCH_3$, 13), 206.53 (t, $J_{P-C} = 13.6$ Hz, CO, 13), 203.56 (t, $J_{C-P} = 10.8$ Hz, CO, 12), 198.79 (t, $J_{P-C} = 10.1$ Hz, CO, 12), 168.48 (s, $C_{ipso-Ph}$, 12), 168.20 (s, $C_{ipso-Ph}$, 13) (the signal due to $C_{ortho-Ph}$ of 12 is masked by the resonance of the solvent), 128.32 (s, $C_{ortho-Ph}$, 13), 119.85 (s, $C_{meta-Ph}$, 12), 118.26 (s, $C_{meta-Ph}$, 13),

114.00 (s, $C_{para-Ph}$, 12), 112.09 (s, $C_{para-Ph}$, 13), 44.56 (s, $COCH_3$, 13), 24.33 (vt, $N = 19.3$ Hz, $PCH(CH_3)_2$, 13), 23.92 (vt, $N = 18.8$ Hz, $PCH(CH_3)_2$, 12), 20.08 (s, $PCH(CH_3)_2$, 12), 19.75 (s, $PCH(CH_3)_2$, 13), 19.14 (s, $PCH(CH_3)_2$, 13), 19.08 (s, $PCH(CH_3)_2$, 12), -0.35 (t, $J_{P-C} = 10.5$ Hz, $-CH_3$, 12).

Preparation of $Ru(CH_3)(C\equiv CPh)(CO)_2(P^iPr_3)_2$ (14). A suspension of $[Ru(CH_3)(CO)_2(P^iPr_3)_2]BF_4$ (3; 150 mg, 0.25 mmol) in toluene (7 mL) was treated with the stoichiometric amount of $PhC\equiv CLi$ (27.4 mg, 0.25 mmol). After it was stirred for 1 h at room temperature, the suspension was filtered through Kieselguhr and the solution concentrated to ca. 1 mL. Addition of MeOH precipitated a white solid, which was washed with MeOH and dried in vacuo. Yield: 116 mg (77%). Anal. Calcd for $C_{29}H_{50}O_2P_2Ru$: C, 58.66; H, 8.49. Found: C, 58.46; H, 8.23. IR (Nujol, cm^{-1}): $\nu(C\equiv C)$ 2094 (m); $\nu(CO)$ 1995 (s), 1935 (s). 1H NMR (C_6D_6 , 20 °C): δ 7.50 (d, 2H, $J_{H-H} = 8.0$ Hz, H_{o-Ph}), 7.17 (t, 2H, $J_{H-H} = 8.0$ Hz, H_{m-Ph}), 6.96 (t, 1H, $J_{H-H} = 8.0$ Hz, H_{p-Ph}), 2.40 (m, 6H, $PCH(CH_3)_2$), 1.34 (dvt, 18H, $N = 13.4$ Hz, $J_{H-H} = 6.9$ Hz, $PCH(CH_3)_2$), 1.21 (dvt, 18H, $N = 12.9$ Hz, $J_{H-H} = 6.9$ Hz, $PCH(CH_3)_2$), 0.26 (t, 3H, $J_{H-P} = 6.0$ Hz, $-CH_3$). $^{31}P\{^1H\}$ NMR (C_6D_6 , 20 °C): δ 41.9 (s). $^{13}C\{^1H\}$ NMR (C_6D_6 , 20 °C): δ 205.10 (t, $J_{C-P} = 10.1$ Hz, CO), 198.20 (t, $J_{C-P} = 10.1$ Hz, CO), 130.60 (t, $J_{C-P} = 1.3$ Hz, $C_{ortho-Ph}$), 130.20 (t, $J_{C-P} = 1.9$ Hz, $C_{ipso-Ph}$), 124.70 (s, C_6H_5 , together with another resonance masked by the signal of C_6D_6), 118.70 (t, $J_{C-P} = 20.2$ Hz, $-C\equiv CPh$), 113.72 (t, $J_{C-P} = 2.3$ Hz, $-C\equiv CPh$), 25.30 (vt, $N = 20.2$ Hz, $PCH(CH_3)_2$), 20.20, 19.60 (both s, $PCH(CH_3)_2$), -13.80 (t, $J_{C-P} = 13.3$ Hz, $-CH_3$).

Reaction of $Ru(CH_3)(C\equiv CPh)(CO)_2(P^iPr_3)_2$ (14) with CO. Preparation of $Ru\{C(O)CH_3\}(C\equiv CPh)(CO)_2(P^iPr_3)_2$ (15).

A slow stream of CO was bubbled through a sample of $Ru(CH_3)(C\equiv CPh)(CO)_2(P^iPr_3)_2$ in benzene- d_6 (0.6 mL), in an NMR tube for 15 min. The 1H and $^{31}P\{^1H\}$ NMR spectra of the sample indicated 100% conversion to the acyl complex. Under an argon atmosphere, 15 loses CO, regenerating the starting material $Ru(CH_3)(C\equiv CPh)(CO)_2(P^iPr_3)_2$ (14) as shown by the 1H and $^{31}P\{^1H\}$ NMR spectra. 1H NMR (C_6D_6 , 20 °C): δ 7.55 (d, 2H, $J_{H-H} = 7.5$ Hz, H_{o-Ph}), 7.18 (t, 2H, $J_{H-H} = 7.5$ Hz, H_{m-Ph}), 7.00 (t, 1H, $J_{H-H} = 7.5$ Hz, H_{p-Ph}), 3.02 (s, 3H, $COCH_3$), 2.41 (m, 6H, $PCH(CH_3)_2$), 1.33 (dvt, 18H, $N = 13.5$ Hz, $J_{H-H} = 7.2$ Hz, $PCH(CH_3)_2$), 1.20 (dvt, 18H, $N = 13.5$ Hz, $J_{H-H} = 7.2$ Hz, $PCH(CH_3)_2$). $^{31}P\{^1H\}$ NMR (C_6D_6 , 20 °C): δ 39.8 (s). $^{13}C\{^1H\}$ NMR (C_6D_6 , 20 °C): δ 266.42 (t, $J_{C-P} = 10.1$ Hz, $COCH_3$), 201.15 (t, $J_{C-P} = 9.1$ Hz, CO), 200.13 (t, $J_{C-P} = 11.0$ Hz, CO), 130.64 (t, $J_{C-P} = 0.9$ Hz, $C_{ortho-Ph}$), 129.93 (t, $J_{C-P} = 1.4$ Hz, $C_{ipso-Ph}$), 128.62 (s, $C_{meta-Ph}$), 125.02 (s, $C_{para-Ph}$), 119.51 (t, $J_{C-P} = 17.5$ Hz, $-C\equiv CPh$), 113.30 (t, $J_{C-P} = 1.8$ Hz, $-C\equiv CPh$), 49.18 (s, $COCH_3$), 27.08 (vt, $N = 21.1$ Hz, $PCH(CH_3)_2$), 20.04, 19.54 (both s, $PCH(CH_3)_2$).

Reaction of $Ru(CH_3)(C\equiv CPh)(CO)_2(P^iPr_3)_2$ (14) with ^{13}CO . Preparation of $Ru\{C(O)CH_3\}(C\equiv CPh)(CO)_2(P^iPr_3)_2$ (15a). A sample of $Ru(CH_3)(C\equiv CPh)(CO)_2(P^iPr_3)_2$ in benzene- d_6 (0.6 mL), was placed under a ^{13}CO (99.74%) atmosphere in a NMR tube. After 15 min, the 1H and $^{31}P\{^1H\}$ NMR spectra were recorded, revealing the formation of 15a. Under an argon atmosphere, the complex loses ^{13}CO , regenerating the starting material $Ru(CH_3)(C\equiv CPh)(CO)_2(P^iPr_3)_2$ (14) as shown by the 1H and $^{31}P\{^1H\}$ NMR spectra. 1H NMR (C_6D_6 , 20 °C): δ 7.55 (d, 2H, $J_{H-H} = 7.5$ Hz, H_{o-Ph}), 7.18 (t, 2H, $J_{H-H} = 7.5$ Hz, H_{m-Ph}), 7.00 (t, 1H, $J_{H-H} = 7.5$ Hz, H_{p-Ph}), 3.02 (s, 3H, $COCH_3$), 2.41 (m, 6H, $PCH(CH_3)_2$), 1.33 (dvt, 18H, $N = 13.5$ Hz, $J_{H-H} = 7.2$ Hz, $PCH(CH_3)_2$), 1.20 (dvt, 18H, $N = 13.5$ Hz, $J_{H-H} = 7.2$ Hz, $PCH(CH_3)_2$). $^{31}P\{^1H\}$ NMR (C_6D_6 , 20 °C): δ 39.8 (d, $J_{P-C} = 9.7$ Hz). $^{13}C\{^1H\}$ NMR (C_6D_6 , 20 °C): δ 266.42 (dt, $J_{C-P} = 10.1$ Hz, $J_{C-C} = 26.0$ Hz, $COCH_3$), 201.15 (t, $J_{C-P} = 9.1$ Hz, ^{13}CO), 200.13 (dt, $J_{C-P} = 11.0$ Hz, $J_{C-C} = 2.5$ Hz, CO), 130.64 (t, $J_{C-P} = 0.9$ Hz, $C_{ortho-Ph}$), 129.93 (t, $J_{C-P} = 1.4$ Hz, $C_{ipso-Ph}$), 128.62 (s, $C_{meta-Ph}$), 125.02 (s, $C_{para-Ph}$), 119.51 (dt, $J_{C-P} = 17.5$ Hz, $J_{C-C} = 6.0$ Hz, $-C\equiv CPh$), 113.30 (t, $J_{C-P} = 1.8$ Hz, $-C\equiv CPh$), 49.18 (d, $J_{C-C} = 7.8$ Hz, $COCH_3$), 27.08 (vt, $N = 21.1$ Hz, $PCH(CH_3)_2$), 20.04, 19.54 (both s, $PCH(CH_3)_2$).

Table 4. Atomic Coordinates ($\times 10^4$; $\times 10^5$ for Ru and P Atoms) and Equivalent Isotropic Displacement Coefficients ($\text{\AA}^2 \times 10^3$; $\text{\AA}^2 \times 10^4$ for Ru and P Atoms) for the Compound $\text{Ru}(\text{CH}_3)_3\{(\text{E})\text{-CH=CHPh}\}(\text{CO})_2(\text{P}^i\text{Pr}_3)_2$ (2)

atom	<i>x/a</i>	<i>y/b</i>	<i>z/c</i>	U_{eq}^a
Ru	25106(3)	23428(2)	24793(2)	222(1)
P(1)	36582(9)	5122(7)	24296(6)	257(2)
P(2)	15001(9)	42281(7)	26298(6)	243(2)
O(1)	-264(3)	1127(3)	2435(2)	61(1)
O(2)	2282(4)	1844(3)	173(2)	72(1)
C(1)	2825(4)	2590(3)	4094(2)	32(1)
C(2)	2003(4)	2346(3)	4723(3)	36(1)
C(3)	2310(4)	2546(3)	5851(3)	35(1)
C(4)	3155(4)	3461(3)	6425(3)	41(1)
C(5)	3375(5)	3623(4)	7475(3)	53(1)
C(6)	2776(5)	2883(4)	7962(3)	54(1)
C(7)	1935(4)	1967(4)	7400(3)	51(1)
C(8)	1701(4)	1802(3)	6357(3)	44(1)
C(9)	4511(4)	3304(3)	2605(3)	42(1)
C(10)	776(4)	1578(3)	2449(3)	36(1)
C(11)	2375(4)	2077(3)	1037(3)	39(1)
C(12)	5587(3)	485(3)	2455(3)	33(1)
C(13)	6374(4)	1163(4)	3453(3)	48(1)
C(14)	6110(4)	822(4)	1538(3)	49(1)
C(15)	3116(4)	-528(3)	1199(3)	36(1)
C(16)	1567(4)	-732(3)	901(3)	52(1)
C(17)	3838(4)	-1671(3)	1057(3)	51(1)
C(18)	3431(4)	-201(3)	3508(3)	33(1)
C(19)	1940(4)	-594(3)	3533(3)	49(1)
C(20)	4380(5)	-1198(4)	3643(3)	53(1)
C(21)	2092(4)	5209(3)	1813(3)	40(1)
C(22)	1014(4)	6070(3)	1539(3)	46(1)
C(23)	2669(5)	4627(4)	859(3)	54(1)
C(24)	-426(4)	4220(3)	2374(3)	34(1)
C(25)	-1151(4)	3850(3)	3200(3)	44(1)
C(26)	-976(4)	3504(4)	1322(3)	51(1)
C(27)	1827(4)	5159(3)	3919(2)	30(1)
C(28)	1046(4)	6287(3)	4069(3)	43(1)
C(29)	3360(4)	5442(3)	4304(3)	47(1)

^a Equivalent isotropic U , defined as one-third of the trace of the orthogonalized U_{ij} tensor.

Reaction of $\text{Ru}(\text{CH}_3)_3\{(\text{E})\text{-CH=CHPh}\}(\text{CO})_2(\text{P}^i\text{Pr}_3)_2$ (2) with CO. Preparation of $\text{Ru}\{\text{C}(\text{O})\text{CH}_3\}\{(\text{E})\text{-CH=CHPh}\}(\text{CO})_2(\text{P}^i\text{Pr}_3)_2$ (17). A slow stream of CO was bubbled through a sample of $\text{Ru}(\text{CH}_3)_3\{(\text{E})\text{-CH=CHPh}\}(\text{CO})_2(\text{P}^i\text{Pr}_3)_2$ in benzene- d_6 (0.6 mL), in an NMR tube for 15 min. The ^1H and $^{31}\text{P}\{^1\text{H}\}$ NMR spectra of the sample revealed 50% conversion to the acyl complex. Under an argon atmosphere, 17 loses CO, regenerating the starting material $\text{Ru}(\text{CH}_3)_3\{(\text{E})\text{-CH=CHPh}\}(\text{CO})_2(\text{P}^i\text{Pr}_3)_2$ (2), as shown by the ^1H and $^{31}\text{P}\{^1\text{H}\}$ NMR spectra. ^1H NMR (C_6D_6 , 20 °C): δ 9.02 (dt, 1H, $J_{\text{H-H}} = 18.7$ Hz, $J_{\text{H-P}} = 2.9$ Hz, $-\text{CH}=\text{CHPh}$), 7.62 (d, 2H, $J_{\text{H-H}} = 7.3$, $H_{\text{o-Ph}}$), 7.27 (t, 2H, $J_{\text{H-H}} = 7.3$ Hz, $H_{\text{m-Ph}}$), 7.09 (dt, 1H, $J_{\text{H-H}} = 18.7$ Hz, $J_{\text{H-P}} = 2.5$ Hz, $-\text{CH}=\text{CHPh}$), 7.01 (t, 1H, $J_{\text{H-H}} = 7.3$ Hz, $H_{\text{p-Ph}}$), 2.87 (s, 3H, COCH_3), 2.30 (m, 6H, $\text{PCH}(\text{CH}_3)_2$), 1.10 (dvt, 36H, $N = 11.2$ Hz, $J_{\text{H-H}} = 5.9$ Hz, $\text{PCH}(\text{CH}_3)_2$). $^{31}\text{P}\{^1\text{H}\}$ NMR (C_6D_6 , 20 °C): δ 36.5 (s). $^{13}\text{C}\{^1\text{H}\}$ NMR (C_6D_6 , 20 °C): δ 261.62 (t, $J_{\text{C-P}} = 11.3$ Hz, COCH_3), 205.15 (t, $J_{\text{C-P}} = 9.8$ Hz, CO), 202.85 (t, $J_{\text{C-P}} = 9.0$ Hz, CO), 164.32 (t, $J_{\text{C-P}} = 15.1$ Hz, $-\text{CH}=\text{CHPh}$), 142.45 (t, $J_{\text{C-P}} = 2.4$ Hz, $\text{C}_{\text{ipso-Ph}}$), 140.51 (t, $J_{\text{C-P}} = 4.5$ Hz, $-\text{CH}=\text{CHPh}$), 128.81, 124.93 (both s, C_6H_5), together with another resonance masked by the signal of C_6D_6 , 52.86 (s, COCH_3), 27.04 (vt, $N = 20.8$ Hz, $\text{PCH}(\text{CH}_3)_2$), 19.72, 19.65 (both s, $\text{PCH}(\text{CH}_3)_2$).

X-ray Structure Analysis of $\text{Ru}(\text{CH}_3)_3\{(\text{E})\text{-CH=CHPh}\}(\text{CO})_2(\text{P}^i\text{Pr}_3)_2$ (2). Crystals suitable for an X-ray diffraction experiment were obtained by slow diffusion of methanol into a concentrated solution of 2 in toluene. Selected atomic coordinates and U_{eq} values are listed in Table 4. A summary of crystal data, intensity collection procedures, and refinement data is reported in Table 6. The crystal studied was glued on a glass fiber and mounted on a Siemens-STOE AED-2 diffractometer. Cell constants were obtained from the least-squares

Table 5. Atomic Coordinates ($\times 10^4$; $\times 10^5$ for Ru and P Atoms) and Equivalent Isotropic Displacement Coefficients ($\text{\AA}^2 \times 10^3$; $\text{\AA}^2 \times 10^4$ for Ru and P Atoms) for the Compound $\text{Ru}\{\text{C}(\text{O})\text{CH}_3\}\text{Cl}(\text{CO})(\text{P}^i\text{Pr}_3)_2$ (7)

atom	<i>x/a</i>	<i>y/b</i>	<i>z/c</i>	U_{eq}^a
Ru	50000	24111(3)	75000	194(1)
P	39826(3)	20882(8)	77008(5)	229(2)
Cl	4204(1)	2185(3)	5713(2)	32(1)
O(1)	5916(4)	1790(9)	9626(5)	41(2)
O(2)	5379(3)	5182(7)	8645(4)	54(1)
C(1)	5549(4)	2050(9)	8786(6)	32(2)
C(2)	5094(3)	4584(7)	7832(4)	32(1)
C(3)	4740(4)	5635(8)	6925(6)	45(2)
C(4)	3827(1)	8(3)	7744(2)	31(1)
C(5)	3544(2)	-796(4)	6751(3)	50(1)
C(6)	4491(2)	-788(4)	8530(2)	43(1)
C(7)	4106(1)	2818(3)	8902(2)	31(1)
C(8)	4004(2)	4541(4)	8880(2)	47(1)
C(9)	3700(2)	2042(5)	9338(2)	47(1)
C(10)	3113(1)	2736(4)	6668(2)	36(1)
C(11)	2491(2)	2405(4)	6834(3)	56(1)
C(12)	3084(2)	4365(4)	6334(3)	51(1)

^a Equivalent isotropic U , defined as one-third of the trace of the orthogonalized U_{ij} tensor.

Table 6. Crystal Data and Data Collection and Refinement for $\text{Ru}(\text{CH}_3)_3\{(\text{E})\text{-CH=CHPh}\}(\text{CO})_2(\text{P}^i\text{Pr}_3)_2$ (2) and $\text{Ru}\{\text{C}(\text{O})\text{CH}_3\}\text{Cl}(\text{CO})(\text{P}^i\text{Pr}_3)_2$ (7)

	2	7
	Crystal Data	
formula	$\text{C}_{29}\text{H}_{52}\text{O}_2\text{P}_2\text{Ru}$	$\text{C}_{21}\text{H}_{45}\text{O}_2\text{P}_2\text{ClRu}$
mol wt	595.75	528.06
color, habit	colorless, laminar crystals	Orange, irregular prism
cryst size, mm	0.68 × 0.49 × 0.04	0.88 × 0.29 × 0.40
space group	triclinic, $P\bar{1}$ (No. 2)	monoclinic, $C2/c$ (No. 15)
<i>a</i> , Å	9.677(2)	21.873(5)
<i>b</i> , Å	11.833(1)	8.759(3)
<i>c</i> , Å	13.619(2)	15.579(7)
α , deg	101.65(1)	90
β , deg	97.21(1)	119.94(1)
γ , deg	90.62(1)	90
V , Å ³	1514.2(4)	2586(2)
<i>Z</i>	2	4
$D(\text{calcd})$, g cm ⁻³	1.307	1.356
	Data Collection and Refinement	
diffractometer	4-circle Siemens-STOE AED	
$\lambda(\text{Mo K}\alpha)$, Å; technique	0.710 73; bisecting geometry	
monochromator	graphite oriented	
μ , mm ⁻¹	0.633	0.833
scan type	$\omega/2\theta$	$\omega/2\theta$
2θ range, deg	$3 \leq 2\theta \leq 50$	$3 \leq 2\theta \leq 52$
temp, K	233	173
no. of data collected	7044	5749
no. of unique data	5345 ($R_{\text{int}} = 0.0285$)	2539 ($R_{\text{int}} = 0.0349$)
no. of params refined	308	151
R^a ($F_o \geq 4.0\sigma(F_o)$)	0.0351	0.0299
R_w^b (all data)	0.0841	0.0821
S^c	1.033	1.230

^a $R(F) = \sum |F_o| - |F_c| / \sum |F_o|$. ^b $R_w(F^2) = [\sum [w(F_o^2 - F_c^2)^2] / \sum [w(F_o^2)^2]]^{1/2}$; $w^{-1} = [\sigma^2(F_o^2) + (aP)^2 + bP]$, where $P = [\max(F_o^2, 0) + 2F_c^2] / 3$ ($a = 0.0380$, $b = 0.59$; 7 , $a = 0.0327$, $b = 3.15$). ^c $S = [\sum [w(F_o^2 - F_c^2)^2] / (n - p)]^{1/2}$, where n is the number of reflections and p the number of parameters.

fit of the setting angles of 66 reflections in the range $20 \leq 2\theta \leq 45^\circ$. The 7044 recorded reflections were corrected for Lorentz and polarization effects. Three orientation and intensity standards were monitored every 55 min of measuring time; no variation was observed. Reflections were also corrected for absorption by a semiempirical method.³⁶

The structure was solved by Patterson (Ru atom) and conventional Fourier techniques. Refinement was carried out by full-matrix least squares with initial isotropic thermal parameters. Anisotropic thermal parameters were used in the last cycles of refinement for all non-hydrogen atoms. Hydrogen atoms were observed or calculated ($C-H = 0.97 \text{ \AA}$) and included in the refinement riding on carbon atoms with a common isotropic thermal parameter. Final $R(F, F \geq 4\sigma(F))$ and $R_w(F^2, \text{all reflections})$ values were 0.0351 and 0.0841.

X-ray Structure Analysis of $Ru\{C(O)CH_3\}Cl(CO)(P^iPr_3)_2$ (7). Suitable crystals were obtained by slow diffusion of methanol into a concentrated solution of **7** in toluene at -20°C . Selected atomic coordinates and U_{eq} values are listed in Table 5. Crystal analysis and data collection was performed as described previously for **2** (Table 6).

The analysis of the systematic absences for **7** led us to carry out the structural determination using two alternative space groups, Cc and $C2/c$. The symmetry of the proposed molecule—without a binary axis—together with the estimated value of Z from the cell volume ($Z = 4$) made the noncentrosymmetric alternative, Cc , more reasonable. The structure was initially solved in this space group by direct methods and conventional Fourier techniques. When all the non-hydrogen atoms of the molecule were positioned and isotropically refined, the difference Fourier map showed significant residual peaks in the plane of the acyl, carbonyl, and chloride ligands, indicating the existence of ligand disorder or a symmetry problem. The presence of additional evidence such as the correlation parameters between related atoms of both phosphines, the anomalous bond distances refined for these ligands, and the facile interpretation of the electronic residuals (two identical models related by a binary axis; 0.5 refined occupancy factor) directed us to consider the analysis of the structure in the centrosymmetric space group $C2/c$.

(36) North, A. C. T.; Phillips, D. C.; Mathews, F. S. *Acta Crystallogr., Sect. A* **1968**, *24*, 351.

The refinement of the molecule performed in the $C2/c$ group eliminated all the above problems. Final stages of the refinement were carried out by full-matrix least squares with anisotropic thermal parameters for all non-hydrogen atoms. Hydrogen atoms were observed or calculated ($C-H = 0.97 \text{ \AA}$) and included in the refinement riding on carbon atoms with a common isotropic thermal parameter. Final $R(F, F \geq 4\sigma(F))$ and $R_w(F^2, \text{all reflections})$ values were 0.0299 and 0.0821, for both molecules, **2** and **7**. All calculations were performed by use of the SHELXTL-Plus³⁷ and SHELXL-93³⁸ system of computer programs. Atomic scattering factors, corrected for anomalous dispersion for Ru, were taken from ref 39.

Acknowledgment. We thank the DGICYT (Project PB 92-0092, Programa de Promoción General del Conocimiento) and EU (Project: Selective Processes and Catalysis Involving Small Molecules) for financial support. E.O. thanks the Diputación General de Aragón (DGA) for a grant.

Supporting Information Available: Tables of anisotropic thermal parameters, atomic coordinates for hydrogen atoms, experimental details of the X-ray study, bond distances and angles, selected least-squares planes, and interatomic distances for **2** and **7** (20 pages). Ordering information is given on any current masthead page.

OM950288E

(37) Sheldrick, G. M. SHELXTL-PLUS, Siemens Analytical X-Ray Instruments, Madison, WI, 1990.

(38) Sheldrick, G. M. *J. Appl. Crystallogr.*, manuscript in preparation.

(39) *International Tables for Crystallography*; Kluwer Academic: Dordrecht, The Netherlands, 1992; Vol. C.

BF₃·Et₂O-Promoted Allylation Reactions of Allyl(cyclopentadienyl)iron(II) Dicarboxyl Complexes with Carbonyl Compounds

Songchun Jiang, Gregory E. Agoston, Ti Chen, Maria-Paz Cabal, and Edward Turos*

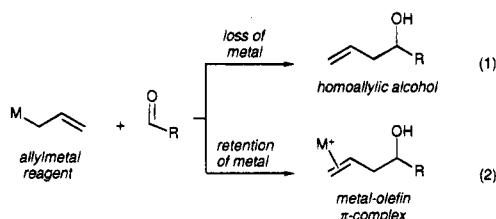
Department of Chemistry, State University of New York at Buffalo, Amherst, New York 14260

Received October 26, 1994[®]

The Lewis-acid-promoted reaction of allyl(cyclopentadienyl)iron dicarbonyl complexes with aldehydes, ketones, imines, and acetals has been investigated. These additions take place under mild conditions using BF₃·Et₂O to afford zwitterionic iron-alkene π -complexes as isolable yellow precipitates. The structures of the π -adducts derived from aldehydes have been characterized fully by proton, carbon, and fluorine NMR spectroscopy, infrared spectroscopy, and fast atom bombardment (FAB) mass spectrometry. Treatment of these iron-olefin salts with CH₃CN or NaI in acetone gives the demetalated homoallylic alcohols, amines, or ethers, respectively. The additions of 3-substituted allyliron complexes to aldehydes favor the formation of the 1,2-syn adduct regardless of the *E* or *Z* geometry of the starting reagent. Thus, the diastereofacial selectivity for these allylations is analogous to that of other allylmetal reagents (allylsilanes, allylstannanes) whose additions have been postulated to proceed through an open (extended) transition state.

Introduction

The nucleophilic addition of an allylmetal reagent to a carbonyl compound has become one of the most commonly used and thoroughly studied carbon-carbon bond-forming methods developed to date.¹ Over two dozen allylmetal reagents have been utilized thus far as nucleophilic partners in this procedure, and numerous studies have been carried out to delineate the regiochemical, stereochemical, and mechanistic features of the reaction. Yet, one of the more prominent aspects of the reaction that has not received much attention concerns the role of the metal group M during and after the addition process. For nearly all reported cases, the metal moiety is consumed during the course of the reaction or upon hydrolytic workup, providing the homoallylic alcohol as the isolated product (eq 1).



Recently, we introduced an alternative allylation procedure based on the reaction of allyl(cyclopentadienyl)iron dicarbonyl (M=Fe(CO)₂Cp)² with aldehydes³ or ketones⁴ in which the metal moiety is retained within

the adduct in the form of an isolable metal-olefin π -complex (eq 2). By virtue of their highly electrophilic nature, these iron-olefin π -adducts allow additional functionality to be introduced directly onto the double bond by a nucleophilic addition process.⁵⁻⁷ In this paper, we give a detailed account of our studies on the scope, limitations, and stereochemical features of the allylation reaction between allyliron complexes and aldehydes, ketones, acetals, and imines, and present data for the characterization of the resulting metal-olefin π -complexes.

Allyl(cyclopentadienyl)iron dicarbonyl (1), the parent reagent used in our studies, was first prepared by Green and Nagy in 1963 by metalation of allyl chloride with sodium [(cyclopentadienyl)iron(II) dicarbonyl].² Over the past three decades, extensive studies have been carried out in the laboratories of Rosenblum,⁸ Wojcicki,⁹ Baker,¹⁰ and Green² on the reaction of 1 (and its derivatives) with inorganic and organic electrophiles. Interestingly, activated double bond compounds X=Y generally react with allyliron complexes 1 to give [3+2]-

(5) Jiang, S.; Turos, E. *Organometallics* **1993**, *12*, 4280.

(6) Chen, T.; Jiang, S.; Turos, E. *Tetrahedron Lett.* **1994**, *35*, 8325.

(7) Jiang, S.; Turos, E. *Tetrahedron Lett.* **1994**, *35*, 7889.

(8) For accounts of the chemistry of organoiron carbonyl compounds, see: (a) Fatiadi, A. J. *J. Res. Natl. Inst. Stand. Technol.* **1991**, *96*, 1. (b) Rosenblum, M. J. *Organomet. Chem.* **1986**, *300*, 191. (c) Rosenblum, M. *Acc. Chem. Res.* **1974**, *122*. (d) Astruc, D. *Use of Organoiron Compounds in Organic Synthesis. In The Chemistry of the Carbon-Metal Bond*; Hartley, F. R., Ed.; Wiley: New York, **1987**; Vol. 4, Chapter 7, pp 625-731.

(9) (a) Bibler, J. P.; Wojcicki, A. *J. Am. Chem. Soc.* **1966**, *88*, 4862. (b) Hartman, F. A.; Pollick, P. J.; Downs, R. L.; Wojcicki, A. *J. Am. Chem. Soc.* **1967**, *89*, 2493. (c) Hartman, F. A.; Wojcicki, A. *Inorg. Chim. Acta* **1968**, *2*, 289. (d) Robinson, P. W.; Wojcicki, A. *J. Chem. Soc., Chem. Commun.* **1970**, 951. (e) Wojcicki, A. *Acc. Chem. Res.* **1971**, *4*, 344. (f) Su, S. R.; Wojcicki, A. *J. Organomet. Chem.* **1971**, *31*, C34. (g) Jacobson, S. E.; Wojcicki, A. *J. Am. Chem. Soc.* **1971**, *93*, 2535. (h) Lichtenberg, D. W.; Wojcicki, A. *J. Organomet. Chem.* **1971**, *33*, C77. (i) Thomasson, J. E.; Robinson, P. W.; Ross, D. A.; Wojcicki, A. *Inorg. Chem.* **1971**, *10*, 2130. (j) Yamamoto, Y.; Wojcicki, A. *Inorg. Chem.* **1973**, *12*, 1779. (k) Su, S. R.; Wojcicki, A. *Inorg. Chim. Acta* **1974**, *8*, 55.

[®] Abstract published in *Advance ACS Abstracts*, August 15, 1995.

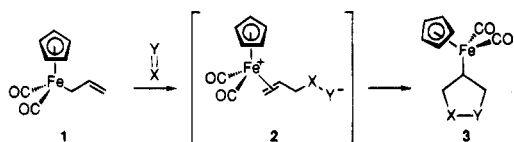
(1) (a) Yamamoto, Y.; Asao, N. *Chem. Rev.* **1993**, *93*, 2207. (b) Yamamoto, Y. *Acc. Chem. Res.* **1987**, *20*, 243. (c) Yamamoto, Y.; Maruyama, K. *Heterocycles* **1982**, *18*, 357. (d) Hoffmann, R. W. *Angew. Chem., Int. Ed. Engl.* **1982**, *21*, 555.

(2) Green, M. L. H.; Nagy, P. L. *J. Chem. Soc.* **1963**, 189.

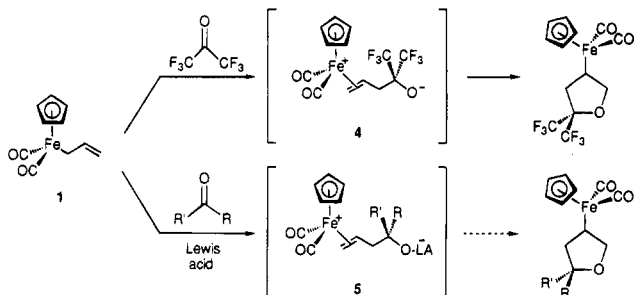
(3) Agoston, G. E.; Cabal, M. P.; Turos, E. *Tetrahedron Lett.* **1991**, *32*, 3001.

(4) Jiang, S.; Turos, E. *Tetrahedron Lett.* **1991**, *32*, 4639.

cycloadducts **3** through what is believed to be a stepwise formation and subsequent ring closure of dipolar inter-



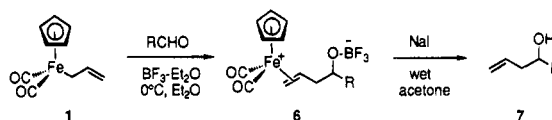
mediate **2**.¹¹ Various types of double-bond compounds take part in these allyliron cycloaddition reactions, including those where X=Y is C=C, C=N, C=S, S=O, and S=N. Despite this diversity of electrophilic functionality, perfluoroacetone was the only example of a compound reported to react with **1** at the carbonyl functionality (i.e., X=Y is C=O).¹² On occasion, Lewis acids have been used to catalyze the addition of **1** to otherwise unreactive π -systems (e.g., cyclohexenone).¹³ Thus, to expand upon the synthetic utility of this chemistry, we decided to explore the reaction of **1** with unactivated aldehydes and ketones under Lewis acid conditions to promote the formation of dipolar adducts **5**, structures which we anticipated would find utility as intermediates for synthesis.



BF₃-Promoted Reactions of Allyliron Complexes With Aldehydes.

To begin our studies, we first examined the reaction of complex **1** with aromatic and aliphatic aldehydes in the presence of BF₃·Et₂O.³ These reactions were carried out at 0 °C by adding complex **1** to a stirred solution of the aldehyde and BF₃·Et₂O in Et₂O; upon warming of the mixture to room temperature, iron-olefin π -complexes **6** are obtained as powdery yellow precipitates that could be easily filtered off and stored in the freezer without noticeable decomposition. These π -adducts were invariably found to contain small amounts of a coprecipitate¹⁴ that proved to be difficult to remove, thereby thwarting our attempts to obtain **6** in analytically pure form. To more accurately assess

the efficiency of these allylations, adducts **6** were treated with NaI in acetone¹⁵ to give the demetalated homoallylic alcohols **7**, which could be purified to homogeneity



Isolated yields of homoallylic alcohols 7	
a R=Ph (76%)	e R=4-CH ₃ OPh (56%)
b R=3-NO ₂ Ph (84%)	f R=cyclohexyl (55%)
c R=4-NO ₂ Ph (67%)	g R=(CH ₂) ₅ CH ₃ (50%)
d R=3-CH ₃ OPh (74%)	

by flash chromatography on silica gel. The ¹H NMR spectra of these products are identical to those of authentic samples. Overall yields of **7** are between 50% and 84%. Higher yields are typically observed for the reactions involving aromatic aldehydes while those of aliphatic aldehydes generally are less efficient. Electron-rich aryl aldehydes (e.g., 4-*N,N*-dimethylaminobenzaldehyde, 4-hydroxybenzaldehyde) do not react with **1** under these conditions and are recovered unchanged. Of the Lewis acids examined (BF₃·Et₂O, TiCl₄, SnCl₄, BBr₃, AlBr₃, AlMe₃, TMS triflate), BF₃·Et₂O is the most effective at promoting the allylation step. The allylations also proceed cleanly at -78 °C, although longer reaction times are generally required, and in most aprotic solvents (CH₂Cl₂, THF, Et₂O); however, diethyl ether is preferable due to the insolubility of the iron-olefin adducts which makes the salts more convenient to isolate by filtration or decantation.

The structures of iron-olefin π -adducts **6** were characterized on the basis of their twin CO stretching bands at 2075 and 2035 cm⁻¹ in the infrared spectrum (CH₂-Cl₂) and a sharp Cp-H resonance at 5.9 ppm in the proton NMR spectrum (acetone-*d*₆), signals which are characteristic for η^2 -cationic CpFe(CO)₂ π -complexes of terminal olefins.¹⁶ The ¹³C NMR spectra for **6a,b** display the expected CO resonances between 208 and 211 ppm as well as Cp resonances at 89.7 ppm.¹⁷ The absence of a hydroxyl signal in the infrared spectrum that supports the assignment of an alkoxide-BF₃ complex is further corroborated by the ¹⁹F NMR spectra of **6a** and of **6b**, which each show a signal at 151.2 ppm upfield from CFCl₃ for the RO-BF₃ species.¹⁸ Furthermore, the fast atom bombardment (FAB) mass spectra of **6** show the expected (M + 1 - BF₃) signal. Thus, zwitterionic structure **6** would appear to be the best representation for these adducts. Since the infrared absorption frequency for the CO ligands and the ¹H chemical shifts of the Cp ring and vinyl protons in **6** agree closely with those reported for simple cationic

(10) (a) Abram, T. S.; Baker, R.; Exon, C. M.; Rao, V. B. *J. Chem. Soc., Perkin Trans. 1* **1982**, 285. (b) Baker, R.; Exon, C. M.; Rao, V. B.; Turner, R. W. *J. Chem. Soc., Perkin Trans. 1* **1982**, 295. (c) Abram, T. S.; Baker, R.; Exon, C. M.; Rao, V. B.; Turner, R. W. *J. Chem. Soc., Perkin Trans. 1* **1982**, 301.

(11) Giering, W. P.; Rosenblum, M. *J. Am. Chem. Soc.* **1971**, 93, 5299. For a recent review on [3+2]-cycloadditions of allyliron complexes, see: Welker, M. E. *Chem. Rev.* **1992**, 92, 97.

(12) Lichtenberg, D. W.; Wojcicki, A. *Inorg. Chem.* **1975**, 14, 1295.

(13) (a) Giering, W. P.; Rosenblum, M.; Tancrede, J. *J. Am. Chem. Soc.* **1972**, 94, 7170. (b) Burcheister, A.; Klemarczyk, P.; Rosenblum, M. *Organometallics* **1982**, 1, 1679.

(14) We attribute the formation of this coadduct to the reaction of complex **1** with residual HF present in commercial BF₃·Et₂O, on the basis of the spectroscopic analysis of the salt: ¹H NMR (400 MHz, acetone-*d*₆) δ 5.87 (s, 5H, Cp protons), 5.35 (m, 1H), 4.06 (d, *J* = 7.8 Hz, 1H), 3.65 (d, *J* = 14.4 Hz, 1H), 1.91 (d, *J* = 5.7 Hz, 3H); ¹³C NMR (100 MHz, acetone-*d*₆) δ 210.8, 208.9, 89.6, 85.6, 55.7, 21.3; ¹⁹F NMR (376 MHz, acetone-*d*₆) δ -152.1; IR (CH₂Cl₂) 2070, 2030 cm⁻¹. These data match those obtained for a sample of Fe(CO)₂Cp(CH₂=CHC(H₃)⁺BF₄⁻ salt prepared by treatment of **1** with HBF₄/Ac₂O.

(15) Lennon, P. J.; Rosan, A.; Rosenblum, M.; Tancrede, J.; Waterman, P. *J. Am. Chem. Soc.* **1980**, 102, 7033.

(16) (a) Chang, T. C. T.; Coolbaugh, T. S.; Foxman, B. M.; Rosenblum, M.; Simms, N.; Stockman, C. *Organometallics* **1987**, 6, 2394. (b) Cutler, A.; Ehntholt, D.; Lennon, P.; Nicholas, K.; Marten, D. F.; Madhavarao, M.; Raghu, S.; Rosan, A.; Rosenblum, M. *J. Am. Chem. Soc.* **1975**, 97, 3149.

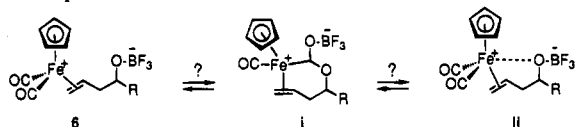
(17) For ¹³C NMR spectroscopic studies of cationic Fe(CO)₂Cp-olefin complexes, see: Laycock, D. E.; Baird, M. C. *Inorg. Chim. Acta* **1980**, 42, 263.

(18) This value is in close agreement with those reported for related BF₃ complexes. (a) Gillespie, R. J.; Hartman, J. S. *Can. J. Chem.* **1968**, 46, 2147. (b) Brownstein, S.; Eastham, A. M.; Latremouille, G. A. *J. Phys. Chem.* **1963**, 67, 1028.

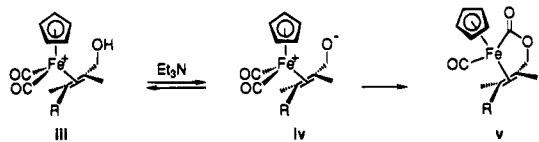
CpFe(CO)₂-olefin π -complexes, there is probably little if any through-space interaction between the alkoxide-BF₃ moiety and the iron center or its carbonyl ligands.¹⁹ The iron moiety appears to be bound nonselectively to either diastereomeric face of the alkene, since several of the signals in the proton and carbon NMR spectra of **6** appear as doublets. Consequently, attempts to grow crystals of **6** suitable for X-ray analysis have been unsuccessful. Upon prolonged exposure to the atmosphere, the yellow salts darken in appearance and eventually become viscous brown oils. The infrared spectra of these oils show the presence of a free hydroxyl group as well as CO stretching bands at 2075 and 2035 cm⁻¹, suggesting that the O-BF₃ moiety of the complex has strong propensity to hydrolyze without disruption of the iron-olefin π -complex.

Diastereoselectivity of BF₃·Et₂O-Promoted Additions of 3-Substituted Allyliron Complexes to Aldehydes. The stereochemistry of the products arising from reactions between allylic metal reagents and carbonyl compounds is an important mechanistic indicator of whether the reaction proceeds through an open (extended) or closed (cyclic) transition state.²⁰ Lewis acid-assisted additions of allylsilanes or allylstannanes to aldehydes generally favor the formation of the syn-addition product, an outcome that is largely insensitive to the *E* or *Z* geometry of the allylmetal reagent. This has been rationalized on the basis of an open transition state structure for the allylation process.²¹ On the other hand, nucleophilic reagents capable of forming a chelate to the carbonyl oxygen may react via a closed transition state model. For allyliron complexes **1**, either scenario can be envisioned if one considers that the CO ligands on Fe(CO)₂Cp may be able to coordinate to or preassociate with the Lewis acid-aldehyde complex.²² To address this question, we first examined the stereo-

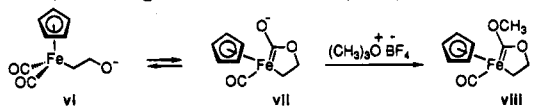
(19) Before this spectral information was obtained a question remained regarding whether complex **6** could exist in equilibrium with a variety of alternative structures such as **i** (from intramolecular addition of the alkoxide anion to a CO ligand) or **ii** (having Coulombic interaction of the alkoxide anion with the cationic metal center), which if present would alter the position of the CO signals in the NMR or infrared spectrum.



For instance, Rosenblum has shown that allylic alcohol complex **iii** is converted to lactone complex **v** upon treatment with Et₃N. Acidification of **v** with fluoroboric acid re-establishes complex **iii** (see ref 16b as well as the following: Begum, M. K.; Chu, K.-H.; Coolbaugh, T. S.; Rosenblum, M.; Zhu, X.-Y. *J. Am. Chem. Soc.* **1989**, *111*, 5252).

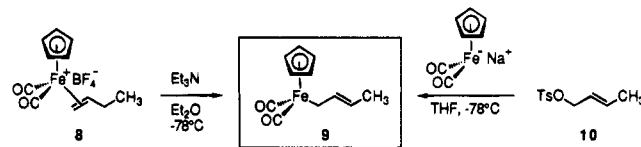


A similar type of alkoxide addition to the CO ligand has been observed for η^3 - β -oxidoethyliron complex **vi** (generated by attack of Fe(CO)₂Cp anion on ethylene oxide) which reacts with trimethylloxonium ion through its tautomer **vii** to give cycloadduct **viii**. See: (a) Klemarczyk, P.; Price, T.; Priester, W.; Rosenblum, M. *J. Organomet. Chem.* **1977**, *C25*, 139. (b) Lennon, P.; Priester, W.; Rosan, A. M.; Madhavarao, M.; Rosenblum, M. *J. Organomet. Chem.* **1977**, *C29*, 139.

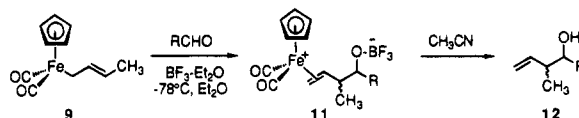


(20) Yamamoto, Y. *Aldrichimica Acta* **1987**, *20*, 45.

chemistry of BF₃-promoted additions to aldehydes using *E*-crotyliron reagent **9**.² Rosenblum has reported that **9** can be prepared as a 3:1 mixture of *E* and *Z* isomers by deprotonation of fluoroborate salt **8** at 0 °C using Et₃N.²³ Our attempts to improve the *E*:*Z* ratio of this procedure by conducting the deprotonation at lower temperature (-78 °C) were unsuccessful. However, we found that **9** can be prepared in isomerically pure *E* form (as judged from its ¹H NMR spectrum) by low-temperature metalation of *E*-tosylate **10**.²⁴



The reactions of **9** with aryl and aliphatic aldehydes were carried out at -78 °C in several different solvent systems (toluene, Et₂O, THF, CH₂Cl₂, hexane). Iron-alkene π -complexes **11**, which are formed as inseparable mixtures²⁵ of diastereomers, were converted directly to their homoallylic alcohols with CH₃CN^{8b} to more easily measure the syn/anti ratios for the mixtures of alcohols **12**. Yields and diastereomeric ratios of **12** are given below.²⁶ The structures of products **12a** from the



Isolated yields, syn:anti ratios of 12	
a R=Ph (70%, 6:1)	e R=4-CH ₃ OPh (51%, 4:1)
b R=3-NO ₂ Ph (85%, 6:1)	f R=cyclohexyl (41%, 14:1)
c R=4-NO ₂ Ph (73%, 6:1)	g R=(CH ₂) ₅ CH ₃ (29%, 7:1)
d R=3-CH ₃ OPh (75%, 7:1)	

additions to benzaldehyde were assigned by comparison of their ¹H NMR spectra to those reported by Yamamoto²⁷ for the syn- and anti-homoallylic alcohols, in which the major product was determined to have the syn stereochemistry. For the remaining homoallylic

(21) For stereochemical studies involving crotylsilanes and -stannanes, see: (a) Denmark, S. E.; Weber, E. J. *J. Am. Chem. Soc.* **1984**, *106*, 7970. (b) Denmark, S. E.; Weber, E. J. *J. Helv. Chim. Acta.* **1983**, *66*, 1655. (c) Hayashi, T.; Kabeta, K.; Hamaachi, I.; Kumada, M. *Tetrahedron Lett.* **1983**, *24*, 2865. (d) Yamamoto, Y.; Yatagai, H.; Ishikawa, Y.; Maeda, N.; Maruyama, K. *Tetrahedron* **1984**, *40*, 2239. (e) Yamamoto, Y.; Yatagai, H.; Naruta, Y.; Maruyama, K. *J. Am. Chem. Soc.* **1980**, *102*, 7107. (f) Sakurai, H. *Pure Appl. Chem.* **1982**, *54*, 1. (g) Hoffmann, R. W. *Angew. Chem., Int. Ed. Engl.* **1982**, *21*, 555. (h) Hosomi, A.; Sakurai, H. *Tetrahedron Lett.* **1976**, *17*, 1295. (i) Keck, G. E.; Abbott, D. E.; Boden, E. P.; Ehnolm, E. J. *Tetrahedron Lett.* **1984**, *25*, 3927. (j) Roush, W. R.; Ando, K.; Powers, D. B.; Palkowitz, A. D.; Halterman, R. L. *J. Am. Chem. Soc.* **1990**, *112*, 6339 and references cited therein.

(22) Complex **1** has been reported to react with high stereoselectivity toward substituted Fe(CO)₂Cp-olefin cationic complexes via a synclinal (gauche) or antiperiplanar (anti) orientation. See ref 15.

(23) Cutler, A.; Ehntholt, D.; Lennon, P.; Nicholas, K.; Marten, D. F.; Madhavarao, M.; Raghu, S.; Rosan, A.; Rosenblum, M. *J. Am. Chem. Soc.* **1975**, *97*, 3149.

(24) Kurth, M. J.; Decker, O. H. W. *J. Org. Chem.* **1985**, *50*, 5769.

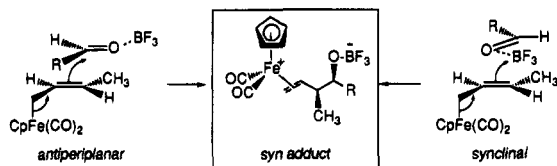
(25) These π -adducts are formed as inseparable mixtures of diastereomers and give complex NMR spectra. Therefore, no attempt was made to assign the structures of these complexes.

(26) Yields are based on the isolated amount of demetalated products which had been purified to homogeneity by flash chromatography. Diastereomeric ratios refer to the 1,2-syn/anti mixture of the demetalated products as determined by integration of nonoverlapping signals in the 400 MHz ¹H NMR spectrum.

(27) Yamamoto, Y.; Yatagai, H.; Maruyama, K. *J. Am. Chem. Soc.* **1981**, *103*, 1969.

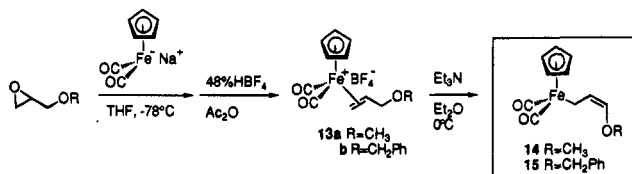
alcohols **12b–g**, the major product in each case was also determined to be the syn isomer on the basis that the homoallylic proton for the major (syn) isomer characteristically appears 0.1–0.3 ppm *downfield* in the ^1H NMR spectrum relative to that of the anti isomer. Integration of the nonoverlapping signals in the spectra of these product mixtures give syn:anti diastereomeric ratios between 4:1 and 14:1.

The syn selectivity suggests that these additions proceed through an open transition state with the iron reagent approaching the aldehyde– BF_3 complex in an antiperiplanar or synclinal orientation, in direct analogy



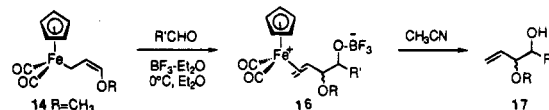
to what has been postulated for crotylsilane or crotylstannane additions to aldehydes.²¹ This “open” transition state model is intuitively most reasonable since a closed transition state would require that one of the CO ligands on iron coordinate to the BF_3 –carbonyl complex, which does not appear likely. While it would have been insightful to study in parallel the stereochemistry for reactions of the *Z*-crotyliron reagent, we were unfortunately not able to prepare the *Z* complex in its isomeric pure form.

Consequently, we opted to examine the stereochemistry for the corresponding reactions of *Z*-3-alkoxyallyliron reagents **14**²³ and **15**. These complexes were



prepared according to the procedure described by Rosenblum via metalation of the epoxides, acidification with HBF_4 to provide π -complexes **13**, and subsequent deprotonation with Et_3N , a process which has been shown to give exclusively the *Z* geometric isomer.²³ Indeed, the ^1H NMR spectra for **14** and **15** each show a single geometric isomer whose data are consistent with that reported for **14**.

The additions of **14** and **15** to aldehydes were conducted at 0 °C in Et_2O using 3 molar equiv of both the iron complex and $\text{BF}_3\cdot\text{Et}_2\text{O}$. As above, the crude metal-olefin salts **16** were converted to their homoallylic alcohols **17** whose syn/anti ratios were determined spectroscopically. The ^1H NMR spectra for the major and minor products for **17a** from the reaction of benzaldehyde with **14** match those reported²⁸ for the known syn and anti compounds, respectively. The assignment of syn/anti structures for **17b–e** and **17g–m** were based on the observation that the chemical shift of the homoallylic proton for the major (syn) product is consistently about 0.1–0.2 ppm *upfield* from that for the anti compound. The fact that *E*-**9**, *Z*-**14**, and *Z*-**15** each give the syn adduct as the predominant product supports the



Isolated yields, syn:anti ratios of 17	
a R=CH ₃ ; R'=Ph (60%, 4:1)	h R=CH ₂ Ph; R'=Ph (80%, 4:1)
b R'=3-NO ₂ Ph (80%, 2:1)	i R'=3-NO ₂ Ph (85%, 3:1)
c R'=4-NO ₂ Ph (80%, 3:1)	j R'=4-NO ₂ Ph (83%, 3:1)
d R'=3-CH ₃ OPh (77%, 3:1)	k R'=3-CH ₃ OPh (85%, 4:1)
e R'=4-CH ₃ OPh (60%, 2:1)	l R'=4-CH ₃ OPh (75%, 3:1)
f R'=cyclohexyl (45%, undetermined)	m R'=cyclohexyl (72%, 6:1)
g R'=(CH ₂) ₅ CH ₃ (35%, 7:1)	n R'=(CH ₂) ₅ CH ₃ (57%, undetermined)

argument that the allylation occurs through an open, nonchelated transition state.

Attempts To Alter the Regiochemistry of the Allylation Process by Photolysis. Allyliron complexes are known to undergo rapid 1,3-transposition²⁹ of the iron group by a radical-initiated mechanism.³⁰ Since this isomerization process could conceivably alter the regiochemistry of the allylation for additions involving 3-substituted allyliron reagents, we decided to repeat the above reactions of complexes **9** and **14** with aldehydes at 0 °C under strong light in the presence of 5 mol % of added $[\text{Fe}(\text{CO})_2\text{Cp}]_2$. The expectation was that $\text{Fe}(\text{CO})_2\text{Cp}$ radical generated under these conditions would promote the isomerization of **9** or **14** to its α -substituted regioisomer, which upon addition to the aldehyde would lead to the formation of the regioisomeric adduct. However, we did not observe any differences in the regiochemical outcome of these allylations, suggesting that allylic rearrangement of the iron complex does not interfere with the addition process.

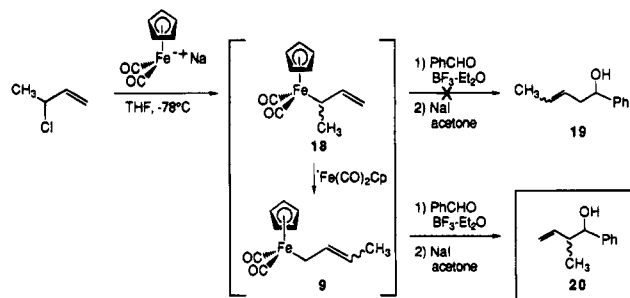
To further demonstrate this, similar experiments were carried out for the reactions of α -methylcrotyl iron complex **18**³¹ with benzaldehyde. Reagent **18** was prepared at low temperature from α -methylallyl chloride and reacted with benzaldehyde, either at –78 °C in the absence of light or at 0 °C in the presence of 5 mol % of $[\text{Fe}(\text{CO})_2\text{Cp}]_2$. We speculated that the reaction at low temperature in the absence of light would favor the formation of alcohol **19**, while the reaction under strong light would produce regioisomers **20** by *in situ* isomerization of **18** to crotyliron complex **9** in the presence of $\text{Fe}(\text{CO})_2\text{Cp}$ radical. However, the predominant adduct under both conditions was regioadduct **20**. This indicates that the 1,3-isomerization of **18** to crotyl complex **9** proceeds much more rapidly than the addition to the aldehyde, supporting a conclusion made earlier by Rosenblum that α -methyl complex **18** undergoes rapid²⁴ and irreversible rearrangement to **9**.³¹ Thus, it would seem that altering the α -regioselectivity of these crotyliron additions would not be easily achieved.

(29) (a) Fish, R. W.; Giering, W. P.; Marten, D.; Rosenblum, M. *J. Organomet. Chem.* **1976**, *105*, 101. (b) Klemarczyk, P.; Rosenblum, M. *J. Org. Chem.* **1978**, *43*, 3488. (c) Rosenblum, M.; Waterman, P. *J. Organomet. Chem.* **1981**, *206*, 197. (d) Fabian, B. D.; Labinger, J. A. *Organometallics* **1983**, *2*, 659. (e) Fabian, B. D.; Labinger, J. A. *J. Am. Chem. Soc.* **1979**, *101*, 2239. (f) Merour, J. Y.; Cadot, P. *C. R. Seances Acad. Sci., Ser. C* **1970**, *271*, 83.

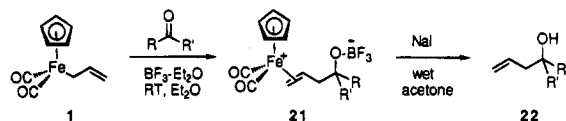
(30) Giering has measured the rate of $^{\text{C}}\text{Cl}_3$ addition to allyliron reagent **1** as being on the order of 10^{-5} s^{-1} : Lee, M.-T.; Waterman, P. S.; Magnuson, R. H.; Meirowitz, R. E.; Prock, A.; Giering, W. P. *Organometallics* **1988**, *7*, 2146.

(31) Cutler, A.; Ehntholt, D.; Giering, W. P.; Lennon, P.; Raghu, S.; Rosan, A.; Rosenblum, M. Tancrede, J.; Wells, D. *J. Am. Chem. Soc.* **1976**, *98*, 3495.

(28) Hoffmann, R. W.; Kemper, B. *Tetrahedron Lett.* **1981**, *22*, 5263.

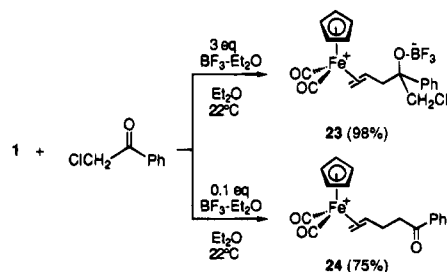


BF₃·Et₂O-Promoted Additions to Ketones. In comparison to aldehydes, ketones are generally regarded to have lower reactivity toward nucleophilic reagents. It is therefore not surprising that the reactions of **1** with aliphatic and aromatic ketones proceed more sluggishly than those of the corresponding aldehydes, and require three molar equivalents of both the Lewis acid and **1** at room temperature to reach completion.⁴ Produced in these reactions are iron-olefin complexes **21**, which can be stored in an anhydrous



Isolated yields of tertiary alcohols 22	
a R=CH ₃ , R'=(CH ₂) ₄ CH ₃	(77%)
b R=CH ₃ , R'=(CH ₂) ₂ (4-HOPh)	(60% + 38% recovered ketone)
c R=CH ₃ , R'=Ph	(84%)
d R=CH ₂ Cl, R'=Ph	(98%)
e R=R'=CH ₂ Ph	(61% + 30% recovered ketone)
f R=R'=(CH ₂) ₆	(77%)
g R=(CH ₂) ₅	(59%)
h R=CH ₂ CH(CH ₃)(CH ₂) ₃	(70%, 7:1:1 mixture of diastereomers)

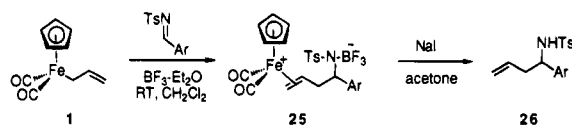
environment without decomposition. The infrared stretching bands at 2075 and 2035 cm⁻¹ and the proton resonance at 5.87 ppm (acetone-*d*₆) confirm the identity of these iron-olefin π -adducts. Upon demetalation with NaI, homoallylic tertiary alcohols **22** are obtained in good to excellent overall yield. As observed for the aldehyde allylations, electron-rich aromatic systems (e.g., benzophenone, 4-hydroxyphenyl ketones, 4-methoxyphenyl ketones) are completely inert under these conditions. In the case of α -chloroacetophenone, the addition of **1** occurs either at the carbonyl center (addition) or at the halide center (S_N2 displacement) depending on the reaction conditions.³²



BF₃·Et₂O-Promoted Additions to *N*-Tosylimines. Aromatic imines also serve as substrates in these

(32) Yields are for the demetalated products after flash chromatography.

allyliron additions to provide iron-alkene complexes **25**.^{6,33,34} Due to the low solubility of the imine-BF₃ complex in Et₂O, however, these reactions are best done in CH₂Cl₂ at room temperature. If desired, π -complexes **25** can be precipitated from solution upon completion



Isolated yields of homoallylic amines 26	
a Ar=Ph (70%)	c Ar=4-NO ₂ Ph (20%)
b Ar=3-CH ₃ OPh (50%)	d Ar=3-NO ₂ Ph (88%)

of the reaction by dilution with Et₂O and isolated by filtration through a glass frit. Demetalation of **25** affords homoallylic amines **26** in 20%–88% yield. A strong electron-withdrawing group on the imine nitrogen appears essential for the addition to work, since the reaction of **1** with the *N*-phenylimine of benzaldehyde gives a much lower yield of the π -complex (23%) than the *N*-tosylimine (70%), while the corresponding *N*-benzylimine and *N*-butylimine fail to react with **1**.³⁵

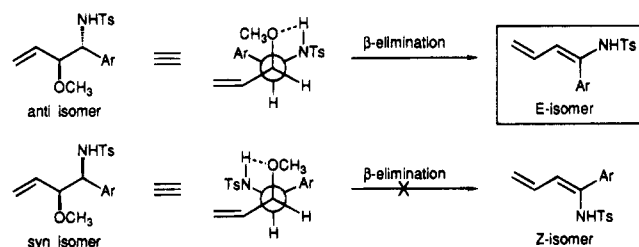
Under similar conditions, 3-methoxyallyliron complex **14** adds to *N*-tosylimines to give after demetalation with NaI a mixture of 1,2-syn homoallylic amine **27** and *E*-1-amino-1,3-diene **29**, each as single diastereomers. The diene product undoubtedly arises from the initial anti-addition product **28**, which presumably is formed in the allylation reaction but suffers elimination during the workup. The syn isomer **27**, however, is resistant to elimination and can be recovered without change even after prolonged exposure to the workup and purification conditions. We believe that the difference in suscepti-

(33) For articles on imine allylation reactions, refer to the following: (a) Emling, B. L.; Horvath, R. J.; Saraceno, A. J.; Ellermeyer, E. F.; Haile, L.; Hudac, L. D. *J. Org. Chem.* **1959**, *24*, 657. (b) Wuts, P. G. M.; Jung, Y.-W. *J. Org. Chem.* **1991**, *56*, 365. (c) Mauze, B.; Miginiac, L. *Bull. Chem. Soc. Fr.* **1973**, 1832. (d) Mauze, B.; Miginiac, L. *Bull. Chem. Soc. Fr.* **1973**, 1832, 1838. (e) Mauze, B.; Miginiac, L. *Bull. Chem. Soc. Fr.* **1973**, 1838. (f) Keck, G. E.; Enholm, E. J. *J. Org. Chem.* **1985**, *50*, 146. (g) Tanaka, H.; Yamashita, S.; Ikamoto, Y.; Torii, S. *Chem. Lett.* **1987**, 673. (h) Tanaka, H.; Nakahara, T.; Dhimane, H.; Torii, S. *Tetrahedron Lett.* **1989**, *30*, 1989. (i) Tanaka, H.; Inoue, K.; Pokorski, U.; Taniguchi, M.; Torii, S. *Tetrahedron Lett.* **1990**, *31*, 3023. (j) Bocoum, S.; Boga, C.; Savoia, D.; Umami-Ronchi, A. *Tetrahedron Lett.* **1991**, *32*, 1367. (k) Neumann, W. L.; Rogic, M. M.; Dunn, T. J. *Tetrahedron Lett.* **1991**, *32*, 5865. (l) Beuchet, P.; Le Marrec, N.; Mosset, P. *Tetrahedron Lett.* **1992**, *33*, 5959. (m) Keck, G. E.; Palani, A. *Tetrahedron Lett.* **1993**, *34*, 3223. (n) Giammaruco, M.; Taddei, M.; Ulivi, P. *Tetrahedron Lett.* **1993**, *34*, 3635. (o) Mokhalalati, M. K.; Wu, M.-J.; Pridgen, L. N. *Tetrahedron Lett.* **1993**, *34*, 47. (p) Sain, B.; Prajapati, D.; Sandhy, J. S. *Tetrahedron Lett.* **1992**, *33*, 4795. (q) Kira, M.; Hino, T.; Sakurai, H. *Chem. Lett.* **1991**, 277. (r) Ralbovsky, J. L.; Kinsella, M. A.; Sisko, J.; Weinreb, S. M. *Synth. Commun.* **1990**, *20*, 573. (s) Ciufolini, M. A.; Spencer, G. O. *J. Org. Chem.* **1989**, *54*, 4739.

(34) For related chemistry, refer to the following: (a) Larson, S. D.; Grieco, P. A.; Fobare, W. F. *J. Am. Chem. Soc.* **1986**, *108*, 3512. (b) Fujimoto, K.; Iwano, Y.; Hirai, K. *Bull. Chem. Soc. Jpn.* **1986**, *59*, 1363. (c) Fliiri, H.; Mak, C.-P. *J. Org. Chem.* **1985**, *50*, 3438. (d) Overman, L. E.; Malone, T. C.; Meier, G. P. *J. Am. Chem. Soc.* **1983**, *105*, 6993. (e) Prasad, K.; Adlgasser, K.; Sharma, R.; Stutz, P. *Heterocycles* **1982**, *19*, 2099. (f) Reider, P. J.; Rayford, R.; Grabowski, E. J. *J. Tetrahedron Lett.* **1982**, *23*, 379. (g) Kraus, G. A.; Neuenschwander, K. *J. Chem. Soc., Chem. Commun.* **1982**, 134. (h) Karady, S.; Amato, J. S.; Reamer, R. A.; Weinstock, L. M. *J. Am. Chem. Soc.* **1981**, *103*, 6765. (i) Yamamoto, Y.; Komatsu, T.; Maruyama, K. *J. Org. Chem.* **1985**, *50*, 3115. (j) Keck, G. E.; Enholm, E. J. *J. Org. Chem.* **1985**, *50*, 146. (k) Yamamoto, Y.; Nishii, S.; Maruyama, K.; Komatsu, T.; Ito, W. *J. Am. Chem. Soc.* **1986**, *108*, 7778.

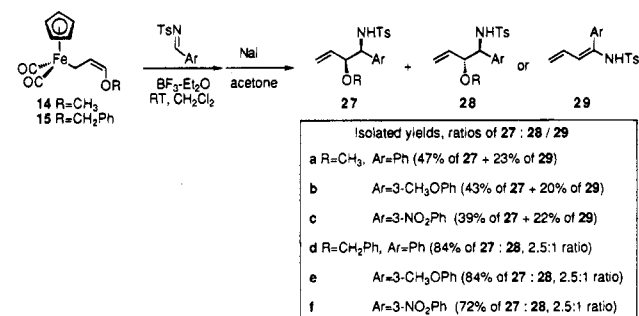
(35) Attempts to add the allyliron complexes to *in situ*-generated *N*-tosylimines of aryl or aliphatic aldehydes using the method of Weinreb (Melnick, M. J.; Freyer, A. J.; Weinreb, S. M. *Tetrahedron Lett.* **1988**, *29*, 3891) or Panek (Panek, J. S.; Jain, N. F. *J. Org. Chem.* **1994**, *59*, 2674) failed to produce the desired allylation adduct.

bility of the syn and anti isomers toward elimination arises from their different conformational stabilities. Elimination from the anti-homoallylic amine must occur such that the adjacent proton and methoxy groups are in an anti-periplanar orientation, a conformation which may be stabilized by hydrogen bonding between the methoxy and amino groups:



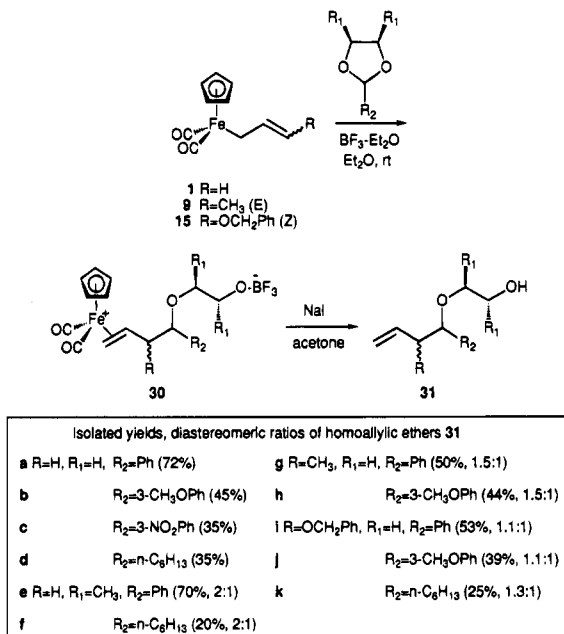
For the syn isomer, however, the anti-conformation required for the elimination would necessarily place the NHTs group gauche to both the OCH₃ and vinyl moieties, which may be conformationally disfavored.

In view of this argument, we expected that the elimination pathway could be avoided by using 3-benzyloxyallyliron complex **15**, whose larger alkoxy substituent would effectively block diene formation. This turns out to be the case, since the reaction of **15** with aryl tosylimines produces mixtures of syn- and anti-allylation products **27** and **28** without diene products being detected.³⁶



BF₃·Et₂O-Promoted Additions to Acetals. To further examine the scope of this allylation methodology, we extended the above studies to additions to acetals.³⁷ Reagent **1** adds to cyclic acetals of aromatic or alkyl aldehydes using BF₃·Et₂O to produce the expected ring-opened π -complexes **30**, which after demetalation provide homoallylic ethers **31** in yields of 35%–72%. Thus, like their carbonyl counterparts, cyclic acetals participate in these addition reactions, demonstrating for the first time the use of an allyl-transition metal complex as a nucleophilic partner in reactions with acetals. Contrary to what was observed for the allylations of aldehydes and ketones, electron-rich acetals (R₂ = 4-CH₃OPh) react *more rapidly* than electron-deficient systems (R₂ = 4-NO₂Ph), which is consistent with the view³⁸ that nucleophilic openings of cyclic

(36) Yamamoto has shown that Lewis acid-assisted addition of crotylmetal reagents to *N*-alkylimines gives the syn stereoisomer predominantly regardless of the organometallic reagent (see ref 34i). Precomplexation equilibria involving the Lewis acid and imine, however, can play a role in controlling the syn/anti stereoselectivity. Keck has reported that the syn/anti stereochemistry for Lewis acid-promoted crotylstannane additions to *N*-benzylimines is nearly independent of the Lewis acid but is highly dependent on the reaction conditions during the formation of the imine–Lewis acid complex (see ref 34j). For stereoselective allylation reactions of imines, see ref 34k.



acetals under Lewis acid conditions may proceed via an ionization-type displacement mechanism.³⁹ Reactions of acetals⁴⁰ derived from *meso*-2,3-butanediol with **1** give 2:1 mixtures of diastereomeric products (see **31e,f**). The 3-substituted complexes **9** and **15** also add to these acetals, although in lower yield and with poor diastereoselectivity (see **31g–k**).

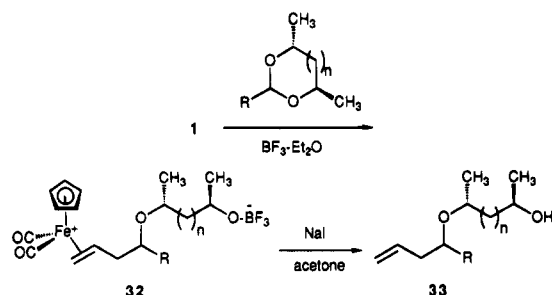
Reactions of **1** with C₂-symmetric acetals give diastereomeric mixtures⁴¹ of π -adducts **32**, which give ethers **33** upon demetalation.⁴² The structures of the major and minor homoallylic ethers **33** were established

(37) For other reports of allylmetal additions to acetals, see: (a) Hosomi, A.; Endo, M.; Sakurai, H. *Chem. Lett.* **1976**, 941. (b) Hosomi, A.; Sakurai, H. *Chem. Lett.* **1976**, 1295. (c) Hosomi, A.; Iguchi, H.; Endo, M.; Sakurai, H. *Chem. Lett.* **1979**, 977. (d) Sakurai, H.; Sasaki, K.; Hosomi, A. *Tetrahedron Lett.* **1981**, 22, 745. (e) Hosomi, A.; Ando, M.; Sakurai, H. *Chem. Lett.* **1986**, 365. (f) Tsunoda, T.; Suzuki, M.; Noyori, R. *Tetrahedron Lett.* **1980**, 21, 71. (g) Mukaiyama, T.; Nagaoka, H.; Murakami, M.; Ohshima, M. *Chem. Lett.* **1975**, 977. (h) Johnson, W. S.; Harbert, C. A.; Stipanovic, R. D.; *J. Am. Chem. Soc.* **1968**, 90, 5279. (i) Yamada, J.-i.; Asano, T.; Kadota, I.; Yamamoto, Y. *J. Org. Chem.* **1990**, 55, 6066. (j) Denmark, S. E.; Almstead, N. G. *J. Org. Chem.* **1991**, 56, 6458. (k) Denmark, S. E.; Almstead, N. G. *J. Org. Chem.* **1991**, 56, 6485. (l) Denmark, S. E.; Almstead, N. G. *J. Am. Chem. Soc.* **1991**, 113, 8089. (m) Lewis, M. D.; Cha, J. K.; Kishi, Y. *J. Am. Chem. Soc.* **1982**, 104, 4976. (n) McNamara, J. M.; Kishi, Y. *J. Am. Chem. Soc.* **1982**, 104, 7371. (o) Sekizaki, H.; Jung, M.; McNamara, J. M.; Kishi, Y. *J. Am. Chem. Soc.* **1982**, 104, 7372.

(38) There has been ongoing debate about the mechanism of acetal opening by nucleophilic reagents under Lewis acid conditions. For detailed studies and discussions on this topic, refer to refs 37 and 42 and the following papers: (a) Yamamoto, Y.; Nishii, S.; Yamada, J.-i. *J. Am. Chem. Soc.* **1986**, 108, 7116. (b) Samakia, T.; Smith, R. S. *J. Am. Chem. Soc.* **1992**, 114, 10998. (c) Samakia, T.; Smith, R. S. *J. Org. Chem.* **1992**, 57, 2997. (d) Choi, V. M. F.; Elliott, J. D.; Johnson, W. S. *Tetrahedron Lett.* **1984**, 25, 591. (e) Mori, A.; Fujiwara, J.; Maruoka, K.; Yamamoto, H. *J. Organomet. Chem.* **1985**, 285, 83. (f) Maruoka, K.; Yamamoto, H. *Angew. Chem., Int. Ed. Engl.* **1985**, 24, 668. (g) Silverman, R.; Edington, C.; Elliott, J. D.; Johnson, W. S. *J. Org. Chem.* **1987**, 52, 180. (h) Murata, S.; Suzuki, M.; Noyori, R. *Tetrahedron* **1988**, 44, 4259. (i) Schreiber, S. L.; Wang, Z. *Tetrahedron Lett.* **1988**, 29, 4085. (j) Denmark, S. E.; Willson, T. M. *J. Am. Chem. Soc.* **1989**, 111, 3475. (k) Denmark, S. E.; Willson, T. M.; Almstead, N. G. *J. Am. Chem. Soc.* **1989**, 111, 9258. (l) Johnson, W. S.; Crackett, P. H.; Elliot, J. D.; Jagodzinski, J. J.; Lindel, S. D.; Natarajan, S. *Tetrahedron Lett.* **1984**, 25, 3951.

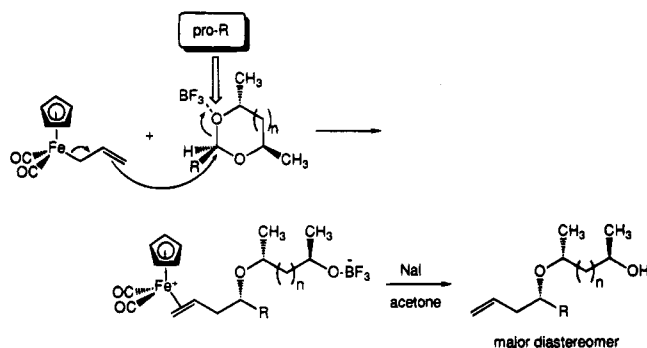
(39) In the case of the acetal where Ar = 4-NO₂Ph, the starting material is recovered quantitatively from the reaction mixture after NaI workup. For reactions involving the acetals of aliphatic aldehydes, substantial amounts of unreacted acetal or the aldehyde (from hydrolysis) can usually be recovered after workup.

(40) These acetals are formed as a 2:1 mixture of diastereomers, which was used in the allylation reactions without separation.



Isolated yields, diastereomeric ratios of 33			
a	n=0, R=Ph (50%, 2:1)	d	n=1, R=Ph (45%, 3:1)
b	R=3-CH ₃ OPh (40%, 3:1)	e	R=3-CH ₃ OPh (35%, 4:1)
c	R=n-C ₆ H ₁₃ (25%, 3:1)	f	R=n-C ₆ H ₁₃ (20%, 5:1)

by GC analysis⁴³ of their *tert*-butyldimethylsilyl ethers (tBuMe₂SiCl, pyr, DMAP, CH₂Cl₂) by comparison to authentic samples prepared using the procedure of Bartlett and Johnson.^{42a} In each case, the predominant allylation product arises from displacement of the pro-R acetal oxygen by the iron reagent. Acetals derived from (*R,R*)-2,4-pentanediol (*n* = 1) give slightly better stereoselectivity (3–5:1 syn:anti ratios) than those of the (*R,R*)-2,3-butanediol series (*n* = 0, 2–3:1 syn:anti ratios), a trend which had been noted previously by Bartlett and Johnson in their studies on allylsilane additions to chiral acetals.^{42a}



In summary, allylic (cyclopentadienyl)iron dicarboxyl complexes have been shown to react with a range of common organic functionality including aldehydes, ketones, *N*-tosylimines, and acetals in the presence of BF₃·Et₂O. The products formed in these reactions are zwitterionic iron–olefin π -complexes, which yield the homoallylic derivative upon demetalation. The stereochemical and reactivity patterns displayed by the iron complexes in these allylation reactions are closely

(41) Since these adducts are formed as inseparable mixtures of diastereomeric salts, no attempt was made to characterize the π -complexes by ¹H NMR spectra or to measure their optical rotations. Rosenblum has reported the synthesis and properties of optically-active iron–alkene π -complexes. See: (a) Begum, M. K.; Chu, K.-H.; Coolbaugh, T. S.; Rosenblum, M.; Zhu, X.-Y. *J. Am. Chem. Soc.* **1989**, *111*, 5252. (b) Turnbull, M. M.; Foxman, B. M.; Rosenblum, M. *Organometallics* **1988**, *7*, 200.

(42) Allylation reactions of chiral acetals: (a) Bartlett, P. A.; Johnson, W. S.; Elliott, J. D. *J. Am. Chem. Soc.* **1983**, *105*, 2088. (b) Andrew, R. G.; Conrow, R. E.; Elliott, J. D.; Johnson, W. S.; Ramezani, S. *Tetrahedron Lett.* **1987**, *28*, 6535. (c) Mori, A.; Ishihara, K.; Arai, I.; Yamamoto, H. *Tetrahedron* **1987**, *43*, 755. (d) Seebach, D.; Imwinkler, R.; Stucky, G. *Helv. Chim. Acta* **1987**, *70*, 448.

(43) Diastereomeric ratios of the homoallylic ethers and their *tert*-butyldimethylsilyl ethers were measured by gas chromatography using a 15 m methyl silicone capillary column at 175 °C and 10 psi of He, and their retention times were compared to those of standards prepared as described in ref 42a.

analogous to those reported for allyltrialkylsilanes and allyltrialkylstannanes. In the following paper, additional studies are presented which focus on the intermolecular and intramolecular addition of alkoxides to the iron–olefin π -adducts, and the development of a general [3+2]-cycloaddition route to furans and pyrrolidines using this organoiron methodology.

Experimental Section

All reactions were performed under an argon atmosphere using glassware and syringes that were predried overnight in an oven at 120 °C and assembled while still hot. TLC was carried out using EM Reagents plates with fluorescence indicator (SiO₂-60, F-254). Flash chromatography was performed using J. T. Baker flash chromatography silica gel (40 μ m). ¹H NMR spectra were recorded using a Varian 400 NMR instrument at 400 MHz in either CDCl₃ or acetone-*d*₆ as indicated. ¹³C NMR spectra were recorded using a Varian Gemini 300 NMR spectrometer at 75 MHz in CDCl₃ or acetone-*d*₆ as specified. ¹⁹F NMR spectra were measured at 376 MHz in CDCl₃ with PhCF₃ (δ –63.7) as an internal standard, and chemical shifts are reported upfield from CCl₃F. IR spectra for the zwitterionic π -complexes were measured in CH₂Cl₂ solution, and all others were obtained as thin films on NaCl plates using a Perkin Elmer 1310 spectrophotometer. Mass spectra were measured by electron impact (EI), chemical ionization (CI), or fast atom bombardment (FAB). The aldehydes and ketones were purchased (Aldrich Chemical Co.) and used without further purification. Acetals were synthesized from the aldehyde or ketone by reaction with the diol in benzene containing a catalytic amount of *p*-toluenesulfonic acid. *N*-Tosylimines were prepared by reacting the aldehyde with *N*-toluenesulfonamide in refluxing benzene or toluene in the presence of a catalytic amount of *p*-toluenesulfonic acid. The allylic cyclopentadienyliron(II) dicarboxyl complexes **1**, **9**, and **14** were prepared as described in refs 2 and 23, except that the final purification step (alumina column chromatography) was omitted. THF and Et₂O were distilled immediately prior to use from Na/benzophenone under argon, and CH₂Cl₂, benzene, toluene, and hexane were freshly distilled from CaH₂ under N₂. Combustion analyses were carried out by Atlantic Microlabs (Atlanta, GA).

Preparation of 13b from 3-(Benzyloxy)-1,2-epoxypropane. Olefin π -complex **13b** was prepared according to Rosenblum's procedure²³ for complex **13a** except that the recrystallization from CH₂Cl₂–Et₂O was omitted. From reaction with 9.60 g (58.5 mmol) of 3-benzyloxy-1,2-epoxypropane was obtained 17.98 g (75%, 43.6 mmol) of **13b**: ¹H NMR (400 MHz, acetone-*d*₆) δ 7.30–7.38 (m, 6H), 5.91 (s, 5H), 5.40–5.49 (m, 1H), 4.56 (s, 2H), 4.18–4.26 (m, 2H), 4.11–4.15 (m, 1H), 3.72 (d, *J* = 14.7 Hz, 1H); ¹³C NMR (100 MHz, acetone-*d*₆) δ 210.1, 209.1, 137.8, 128.6, 128.1, 127.7, 89.9, 86.9, 73.0, 69.0, 50.9; IR (CH₂Cl₂) 2075, 2035 cm⁻¹; FAB-MS 325.1 (M – BF₄), 269.1, 177.0.

Preparation of (3-(Benzyloxy)allyl)iron Complex 15 from π -Complex 13b. Triethylamine (4.0 mL, 28.7 mmol) was added dropwise to a suspension of 9.97 g (24.2 mmol) of **13b** in 120 mL of CH₂Cl₂ at 0 °C. The mixture was stirred for 1 h, and the solvent was removed *in vacuo* to give a reddish solid. The solid was washed with Et₂O (50 mL) and filtered through Celite, and the pad was washed with Et₂O (3 \times 10 mL) under argon in a septa-capped glass frit. The solvent was removed *in vacuo* to give 4.92 g (15.1 mmol, 62%) of **15** as a red oil: ¹H NMR (400 MHz, acetone-*d*₆) δ 7.28–7.42 (m, 5H), 5.9 d, *J* = 5.9 Hz, 1H), 4.92 (s, 5H), 4.78 (s, 2H), 4.63–4.72 (m, 1H), 2.17 (d, *J* = 8.8 Hz, 2H); IR (neat) 3120, 2860, 1996, 1944 cm⁻¹.

Representative Procedure for the BF₃·Et₂O-Promoted Allylation of Aldehydes using Allyliron Complex 1. A freshly prepared solution of **1** (0.709 g, 3.25 mmol) in Et₂O

(20 mL) was added dropwise to a stirred solution of benzaldehyde (1.024 g, 8.82 mmol) and $\text{BF}_3 \cdot \text{Et}_2\text{O}$ (0.41 mL, 3.25 mmol) in Et_2O (20 mL) at 0 °C under argon. The mixture was stirred at 0 °C for 4 h, and the yellow precipitate was collected by filtration through a fine-pore glass frit under argon, washed with anhydrous Et_2O (75 mL), and dried *in vacuo* to give 1.0 g (2.56 mmol, 80%, 1:1 mixture of facial isomers) of iron-olefin complex **6a**: ^1H NMR (400 MHz, acetone- d_6) δ 7.21–7.47 (m, 5H), 5.91 (s, 5H), 5.20–5.31 (m, 1H), 4.90–4.95 (m, isomer 1) and 4.79–4.83 (m, isomer 2) (total 1H), 4.12 (d, J = 8.7 Hz, isomer 1) and 4.09 (d, J = 7.8 Hz, isomer 2) (total 1H), 3.63 (d, J = 14.7 Hz, isomer 1) and 3.61 (d, J = 14.7 Hz, isomer 2) (total 1H), 2.84–2.95 (m, 1H), 1.77–1.95 (m, 1H); ^{13}C NMR (100 MHz, acetone- d_6) δ 211.9, 210.2, 128.5 (isomer 1) and 128.2 (isomer 2), 127.1 (isomer 1) and 127.6 (isomer 2), 126.1 (isomer 1) and 126.2 (isomer 2), 116.4, 89.7 (isomer 1) and 89.8 (isomer 2), 86.9 (isomer 1) and 85.6 (isomer 2), 73.5 (broad), 56.7 (isomer 1) and 56.2 (isomer 2), 44.3 (isomer 1) and 46.2 (isomer 2); ^{19}F NMR (376 MHz, CD_2Cl_2) δ -151.23; IR (CH_2Cl_2) 2075, 2035 cm^{-1} ; FAB-MS 325.1 ($\text{M} + \text{H} - \text{BF}_3$), 269.1, 177.0.

6b: 80% (1.14 g, 2.56 mmol, 1:1 mixture of facial isomers); ^1H NMR (400 MHz, acetone- d_6) δ 8.27 (s, 1H), 7.87 (t, J = 5.9 Hz, 1H), 5.64–5.68 (m, 1H), 5.93 (s, 5H), 5.03–5.39 (overlapping m, 2H), 4.13 (t, J = 7.8 Hz, 1H), 3.74 (d, J = 14.7 Hz, isomer 1) and 3.62 (d, J = 14.7 Hz, isomer 2) (total 1H), 3.08–3.11 (m, 1H), 1.89–1.97 (m, 1H); ^{13}C NMR (100 MHz, acetone- d_6) δ 210.7 (isomer 1) and 210.2 (isomer 2), 208.6 (isomer 1) and 208.5 (isomer 2), 148.7, 147.3 (isomer 1) and 147.3 (isomer 2), 135.2 (isomer 1) and 134.9 (isomer 2), 129.9 (isomer 1) and 129.9 (isomer 2), 122.4 (isomer 1) and 122.3 (isomer 2), 120.9 (isomer 1) and 120.9 (isomer 2), 89.8 (isomer 1) and 89.7 (isomer 2), 86.9 (isomer 1) and 85.7 (isomer 2), 74.1 (isomer 1) and 72.3 (isomer 2), 57.2 (isomer 2) and 55.5 (isomer 2), 45.9 (isomer 1) and 43.9 (isomer 2); IR (CH_2Cl_2) 2075, 2035 cm^{-1} ; FAB-MS 370.1 ($\text{M} + \text{H} - \text{BF}_3$), 314.1, 177.0.

6c: 70% (0.95 g, 2.2 mmol, 1:1 mixture of facial isomers); ^1H NMR (400 MHz, acetone- d_6) δ 8.21 (d, J = 7.8 Hz) and 7.7 (d, J = 7.8 Hz) (total 4H), 4.92 (s, 5H), 5.01–5.32 (overlapping m) (total 2H), 4.14 (d, J = 3.9 Hz, isomer 1), 4.12 (d, J = 3.9 Hz, isomer 2) (total 1H), 3.7 (d, J = 14.7 Hz, isomer 1) and 3.59 (d, J = 14.7 Hz, isomer 2) (total 1H), 2.95–3.08 (m, 1H), 1.86–2.00 (m, 1H); ^{13}C NMR (100 MHz, acetone- d_6) δ 210.8 (isomer 1) and 210.7 (isomer 2), 208.6 (isomer 1) and 208.4 (isomer 2), 152.5 (isomer 1) and 152.5 (isomer 2), 147.6 (isomer 1) and 147.6 (isomer 2), 127.5 (isomer 1) and 127.4 (isomer 2), 123.6 (isomer 1) and 123.5 (isomer 2), 89.8 (isomer 1) and 89.8 (isomer 2), 86.9 (isomer 1) and 83.2 (isomer 2), 74.6 (isomer 1) and 72.6 (isomer 2), 57.1 (isomer 1) and 56.6 (isomer 2), 45.9 (isomer 1) and 45.7 (isomer 2); IR (CH_2Cl_2) 2075, 2035 cm^{-1} ; FAB-MS 370.0 ($\text{M} + \text{H} - \text{BF}_3$), 314.1, 177.0.

6d: 80% (1.1 g, 2.6 mmol, 1:1 mixture of facial isomers); ^1H NMR (400 MHz, acetone- d_6) δ 7.24 (apparent dd, J = 6.8, 7.8 Hz, 1H), 6.93–6.95 (m, 2H), 6.82 (d, J = 7.8 Hz, 1H), 5.92 (s, 5H), 5.19–5.27 (m, 1H), 4.89–4.92 (m, isomer 1) and 4.77–4.80 (m, isomer 2) (total 1H), 4.11 (apparent dd, J = 7.8, 8.8 Hz, 1H), 3.78 (s, 3H), 3.68 (d, J = 14.7 Hz, isomer 1) and 3.63 (d, J = 14.7 Hz, isomer 2) (total 1H), 2.88–2.93 (m, 1H), 1.77–1.92 (m, 1H); ^{13}C NMR (100 MHz, acetone- d_6) δ 210.8, 208.7, 116.1 (isomer 1) and 160.2 (isomer 2), 146.4 (isomer 1) and 146.5 (isomer 2), 129.5 (isomer 1) and 129.5 (isomer 2), 118.3 (isomer 1) and 118.4 (isomer 2), 112.9 (isomer 1) and 113.0 (isomer 2), 11.8 (isomer 1) and 111.8 (isomer 2), 89.7 (isomer 1) and 89.8 (isomer 2), 84.4 (isomer 1) and 86.9 (isomer 2), 73.3 (isomer 1) and 75.6 (isomer 2), 56.2 (isomer 1) and 56.7 (isomer 2), 54.9 (broad), 44.3 (isomer 1) and 46.2 (isomer 2); ^{19}F NMR (376 MHz, CD_2Cl_2) δ -151.23; IR (CH_2Cl_2) 2075, 2035 cm^{-1} ; FAB-MS 355.1 ($\text{M} + \text{H} - \text{BF}_3$), 299.1, 177.0.

6e: 70% (0.96 g, 2.27 mmol, 1:1 mixture of facial isomers); ^1H NMR (400 MHz, acetone- d_6) δ 7.29 (d, J = 6.8 Hz) and 6.89 (d, J = 6.8 Hz) (total 4H), 5.92 (s, 5H), 5.18–5.30 (m, 1H), 4.80–4.89 (m, isomer 1) and 4.70–4.77 (m, isomer 2) (total

1H), 4.12 (d, J = 8.8 Hz, isomer 1) and 4.08 (d, J = 7.8 Hz, isomer 2) (total 1H), 3.78 (s, 3H), 3.65 (d, J = 4.8 Hz, isomer 1) and 3.62 (d, J = 3.9 Hz, isomer 2) (total 1H), 2.8–2.94 (m, 1H), 1.75–1.98 (m, 1H); ^{13}C NMR (100 MHz, acetone- d_6) δ 211.5, 208.3, 161.4, 131.9 (isomer 1) and 129.3 (isomer 2), 127.3 (isomer 1) and 125.6 (isomer 2), 114.6 (isomer 1) and 113.9 (isomer 2), 89.8 (isomer 1) and 89.7 (isomer 2), 89.4 (isomer 1) and 86.9 (isomer 2), 73.0, 56.7 (isomer 1) and 55.5 (isomer 2), 55.2 (isomer 1) and 55.0 (isomer 2), 48.8 (isomer 1) and 46.3 (isomer 2); IR (CH_2Cl_2) 2075, 2035 cm^{-1} ; FAB-MS 355.1 ($\text{M} + \text{H} - \text{BF}_3$), 337.1, 299.1, 281.1, 177.0.

6f: 65% (0.84 g, 2.11 mmol, 1:1 mixture of facial isomers); ^1H NMR (400 MHz, acetone- d_6) δ 5.91 (s, 5H), 5.27–5.40 (m, 1H), 3.94 (d, J = 4.9 Hz, isomer 1) and 3.89 (d, J = 5.9 Hz, isomer 2) (total 1H), 3.77 (d, J = 14.7 Hz, isomer 1) and 3.69 (d, J = 14.7 Hz, isomer 2) (total 1H), 3.5–3.60 (m, isomer 1) and 3.38–3.48 (m, isomer 2) (total 1H), 2.55–2.80 (m, 1H), 1–2 (m, 12H); ^{13}C NMR (100 MHz, acetone- d_6) δ 211.5, 208.3, 161.4, 131.9 (isomer 1) and 129.3 (isomer 2), 127.3 (isomer 1) and 125.6 (isomer 2), 114.6 (isomer 1) and 113.9 (isomer 2), 89.8 (isomer 1) and 89.7 (isomer 2), 89.4 (isomer 1) and 86.9 (isomer 2), 73.0, 56.7 (isomer 1) and 55.5 (isomer 2), 55.2 (isomer 1) and 55.0 (isomer 2), 48.8 (isomer 1) and 46.3 (isomer 2), 44.4 (isomer 1) and 44.3 (isomer 2), aliphatic signals overlapped with solvent peak at 29 and other signals at 26.3 and 26.2; IR (CH_2Cl_2) 2075, 2035 cm^{-1} ; FAB-MS 331.1 ($\text{M} + \text{H} - \text{BF}_3$), 275.1, 177.0.

6g: 60% (0.77 g, 1.94 mmol, 1:1 mixture of facial isomers); ^1H NMR (400 MHz, acetone- d_6) δ 5.90 (s, 5H), 5.19–5.39 (m, 1H), 4.06–4.14 (overlapping m), 3.90–3.95 (m) and 3.66–3.77 (m) (total 3H), 2.80 (s, 3H), 2.58–2.73 (m, 1H), 1.10–1.67 (m, 11H), 0.83–0.90 (m, 3H); ^{13}C NMR (100 MHz, acetone- d_6) δ 211.0, 208.8, 89.7 (isomer 1) and 89.6 (isomer 2), 86.9 (isomer 1) and 85.7 (isomer 2), 72.4, 56.4 (isomer 1) and 55.7 (isomer 2), 44.0 (isomer 1) and 43.9 (isomer 2), 32.1 (isomer 1) and 32.0 (isomer 2), signal overlapped with solvent at 26.0, 25.7 (isomer 1) and 25.6 (isomer 2), 22.8 (isomer 1) and 22.6 (isomer 2), 21.3, 13.8 (isomer 1) and 13.7 (isomer 2); IR (CH_2Cl_2) 2065, 2025 cm^{-1} ; FAB-MS 333.1 ($\text{M} + \text{H} - \text{BF}_3$), 277.2, 177.0.

Representative Procedure for the $\text{BF}_3 \cdot \text{Et}_2\text{O}$ -Promoted Addition of Complex 1 to Aldehydes with Demetalation.

A solution of freshly prepared complex **1** (0.262 g, 1.2 mmol) in Et_2O (5 mL) was added dropwise to a stirred solution of benzaldehyde (0.106 g, 1 mmol) and $\text{BF}_3 \cdot \text{Et}_2\text{O}$ (1.5 mmol, 0.19 mL) in Et_2O at 0 °C under argon. The mixture was stirred overnight while being warmed to room temperature, and the solvent was removed *in vacuo*. The solid residue was dissolved in acetone (20 mL), and a solution of NaI (0.200 g, 1.3 mmol) in acetone (20 mL) was added. The solution rapidly turned black, indicating formation of FpI. The solvent was evaporated *in vacuo*, and the residue was dissolved in Et_2O (50 mL) and filtered through a pad of Celite. The pad was washed with Et_2O (50 mL), and the solvent was evaporated. Purification of the black oil *via* flash chromatography (first CH_2Cl_2 and then 5:1 hexanes:EtOAc) gave 0.113 g (0.76 mmol, 76%) of **7a**:^{21h} ^1H NMR (300 MHz, CDCl_3) δ 7.21–7.34 (m, 5H), 5.72–5.86 (m, 1H), 5.10–5.20 (AB multiplet, 2H), 4.69–4.74 (m, 1H), 2.43–2.54 (m, 2H), 2.0 (d, J = 3.2 Hz, 1H); ^{13}C NMR (75 MHz, CDCl_3) δ 144.6, 135.2, 129.0, 128.1, 136.5, 118.7, 73.8, 44.0.

7b: 84% (0.162 g, 0.84 mmol); ^1H NMR (300 MHz, CDCl_3) δ 8.22 (s, 1H), 8.11 (d, J = 8.2 Hz, 1H), 7.69 (d, J = 7.7 Hz, 1H), 7.52 (t, J = 4.3 Hz, 1H), 5.68–5.85 (m, 1H), 5.10–5.20 (AB multiplet, 2H), 4.78–4.90 (m, 1H), 2.35–2.60 (m, 2H), 2.18 (s, 1H); ^{13}C NMR (75 MHz, CDCl_3) δ 148.9, 146.7, 133.9, 132.6, 129.9, 122.9, 121.4, 119.9, 72.5, 44.1.

7c:^{21d} 67% (0.129 g, 0.67 mmol); ^1H NMR (300 MHz, CDCl_3) δ 8.19 (d, J = 8.6 Hz) and 7.52 (d, J = 8.6 Hz) (total 4H), 5.65–5.85 (m, 1H), 5.10–5.20 (AB multiplet, 2H), 4.75–4.90 (m, 1H), 2.30–2.65 (m, 2H), 2.17 (d, J = 3.3 Hz, 1H); ^{13}C NMR (75 MHz, CDCl_3) δ 152.0, 147.8, 133.9, 127.2, 124.1, 119.9, 72.6, 44.0.

7d:⁴⁴ 74% (0.131 g, 0.74 mmol); ^1H NMR (300 MHz, CDCl_3) δ 7.21–7.27 (m, 1H), 6.90–7.00 (m, 2H), 6.75–6.90 (m, 1H),

5.7–5.90 (m, 1H), 5.12–5.17 (AB multiplet, 2H), 4.69 (m, 1H), 3.78 (s, 3H), 2.47 (m, 2H), 1.99 (d, $J = 3.0$ Hz, 1H); ^{13}C NMR (75 MHz, CDCl_3) δ 160.4, 146.4, 135.1, 130.0, 118.8, 118.6, 113.5, 112.0, 73.7, 55.5, 43.5.

7e:^{21d} 56% (0.100 g, 0.56 mmol); ^1H NMR (300 MHz, CDCl_3) δ 7.26 (d, $J = 8.7$ Hz) and 6.87 (d, $J = 8.7$ Hz) (total 4H), 5.65–5.90 (m, 1H), 5.09–5.17 (AB multiplet, 2H), 4.66 (m, 1H), 3.77 (s, 3H), 2.46 (apparent dd, $J = 6.6, 7.1$ Hz, 2H), 1.93 (d, $J = 1.9$ Hz, 1H); ^{13}C NMR (75 MHz, CDCl_3) δ 159.7, 136.8, 135.3, 127.7, 118.6, 114.3, 73.4, 55.6, 44.0.

7f:⁴⁵ 55% (0.0847 mg, 0.55 mmol); ^1H NMR (300 MHz, CDCl_3) δ 5.81 (m, 1H), 5.08–5.13 (AB multiplet, 2H), 3.35 (m, 1H), 2.33–2.27 (m, 1H), 2.04–2.14 (m, 1H), 1.50–1.75 (m, 6H), 0.91–1.39 (m, 6H); ^{13}C NMR (75 MHz, CDCl_3) δ 136.1, 118.3, 75.1, 43.4, 39.1, 29.3, 28.3, 26.7, 26.5, 26.3.

7g:^{21h} 50% (0.078 mg, 0.5 mmol); ^1H NMR (300 MHz, CDCl_3) δ 5.70–5.90 (m, 1H), 5.09–5.14 (AB multiplet, 2H), 3.60 (m, 1H), 2.24–2.30 (m, 1H), 2.05–2.15 (m, 1H), 1.15–1.6 (m, 11H), 0.85 (m, 3H); ^{13}C NMR (75 MHz, CDCl_3) δ 135.5, 118.4, 71.1, 42.2, 37.1, 32.0, 29.5, 25.8, 22.8, 14.2.

Representative Procedure for $\text{BF}_3\cdot\text{Et}_2\text{O}$ -Promoted Addition of Crotyliron Complex **E-9 to Aldehydes.** A 3 equiv amount (0.696 g, 3 mmol) of freshly prepared complex **E-9** (from equimolar amounts of *trans*-crotyl tosylate²⁴ and $\text{NaFe}(\text{CO})_2\text{Cp}$) in Et_2O (5 mL) was added dropwise to a stirred solution of benzaldehyde (0.106 g, 1 mmol) and $\text{BF}_3\cdot\text{Et}_2\text{O}$ (0.38 mL, 3 mmol) in Et_2O (20 mL) at -78°C under argon. The mixture was stirred for 24 h, and the solvent was evaporated. To the residue was added acetonitrile (20 mL), and the mixture was warmed to room temperature and stirred for several more hours. The solvent was removed *in vacuo*, and the residue was dissolved in CH_2Cl_2 (50 mL) and filtered through Celite. The pad was washed with CH_2Cl_2 (50 mL), and the filtrate was concentrated *in vacuo*. The crude product was purified by flash chromatography (CH_2Cl_2) to give 0.113 g (0.7 mmol, 70%, 6:1 syn:anti ratio) of **12a**:^{21d,i,46} ^1H NMR (400 MHz, CDCl_3) δ 7.20–7.30 (m, 5H), 5.61–5.82 (m, 1H), 5.17–5.23 (AB multiplet, anti) and 5.04–5.07 (AB multiplet, syn) (total 2H), 4.61 (d, $J = 4.9$ Hz, syn), and 4.36 (d, $J = 7.8$ Hz, anti) and 5.04–5.07 (AB multiplet, syn) (total 2H), 4.61 (d, $J = 4.9$ Hz, syn), and 4.36 (d, $J = 7.8$ Hz, anti) (total 1H), 2.55–2.65 (m, syn) and 2.45–2.50 (m, anti) (total 1H), 2.15 (br s, anti) and 1.87 (br s, syn) (total 1H), 1.0 (d, $J = 5.9$ Hz, syn) and 0.87 (d, $J = 6.8$ Hz, anti) (total 1H); ^{13}C NMR (75 MHz, CDCl_3) δ 143.5 (syn) and 143.2 (anti), 141.3 (anti) and 141.0 (syn), 128.8 (anti) and 128.6 (syn), 127.9 (syn) and 127.4 (anti), 127.3 (anti) and 127.1 (syn), 117.2 (anti) and 116.0 (syn), 78.0 (anti) and 77.7 (syn), 46.5 (anti) and 44.9 (syn), 16.7 (anti) and 14.3 (syn). Anal. Calcd for $\text{C}_{11}\text{H}_{14}\text{O}^{1/3}\text{H}_2\text{O}$: C, 78.56; H, 8.79. Found: C, 78.29; H, 8.98.

12b: 85% (0.176 g, 0.85 mmol, 6:1 syn:anti ratio); ^1H NMR (400 MHz, CDCl_3) δ 8.19 (s, 1H), 8.13 (d, $J = 7.8$ Hz, 1H), 7.66 (d, $J = 7.8$ Hz, 1H), 7.65 (t, $J = 7.8$ Hz, 1H), 5.70–5.82 (m, 1H), 5.19–5.27 (AB multiplet, anti) and 5.06–5.14 (AB multiplet, syn) (total 2H), 4.76 (d, $J = 4.9$ Hz, syn) and 4.50 (d, $J = 6.8$ Hz, anti), (total 1H), 2.57–2.63 (m, syn) and 2.40–2.48 (m, anti), (total 1H), 2.25 (d, $J = 2.0$ Hz, anti) and 2.08 (s, syn), (total 1H), 0.98 (d, $J = 6.8$ Hz, syn) and 0.92 (d, $J = 6.8$ Hz, anti) (total 3H); ^{13}C NMR (75 MHz, CDCl_3) δ 148.8 (anti) and 148.7 (syn), 145.6 (syn) and 145.4 (anti), 140.1 (syn) and 139.9 (anti), 133.6 (anti) and 133.3 (syn), 129.6 (anti) and 129.5 (syn), 122.7 (syn) and 122.7 (anti), 122.2 (anti) and 122.0 (syn), 118.1 (anti) and 116.8 (syn), 77.1 (anti) and 76.5 (syn), 46.4 (anti) and 44.9 (syn), 16.4 (anti) and 13.9 (syn); MS (CI, isobutane) m/z 208.1 (M + H, 91), 190.1 (16), 152.0 (100), 144.1 (29); HRMS (CI, isobutane) calcd for $\text{C}_{11}\text{H}_{14}\text{NO}_3$ (M + H) 208.0974, found 208.0962.

12c:⁴⁷ 73% (0.151 g, 0.73 mmol, 6:1 syn:anti ratio); ^1H NMR (400 MHz, CDCl_3) δ 8.20 (d, $J = 8.8$ Hz) and 7.50 (d, $J = 8.8$

Hz) (total 4H), 5.69–5.82 (m, 1H), 5.17–5.23 (overlapping AB multiplet, anti) and 5.07–5.15 (overlapping AB multiplet, syn) (total 2H), 4.78 (apparent dd, $J = 3.9, 4.9$ Hz, syn) and 4.50 (d, $J = 4.9$ Hz, anti) (total 1H), 2.58–2.62 (m, syn) and 2.40–2.50 (m, anti) (total 1H), 2.27 (d, $J = 2.0$ Hz, anti) and 2.05 (s, syn) (total 1H), 0.97 (d, $J = 6.8$ Hz, syn) and 0.93 (d, $J = 6.8$ Hz, anti); ^{13}C NMR (75 MHz, CDCl_3) δ 150.8 (syn) and 150.7 (anti), 147.8, 140.1 (syn) and 139.8 (anti), 128.2 (anti) and 127.9 (syn), 123.9 (anti) and 123.8 (syn), 118.2 (anti) and 116.9 (syn), 77.2 (anti) and 76.5 (syn), 46.4 (anti) and 44.9 (syn), 16.4 (anti) and 13.7 (syn); MS (CI, isobutane) m/z 208.1 (M + H, 100), 190.1 (8), 152.0 (22), 144.1 (14); HRMS (CI, isobutane) calcd for $\text{C}_{11}\text{H}_{14}\text{NO}_3$ (M + H) 208.0974, found 208.0958.

12d: 75% (0.132 g, 0.75 mmol, 7:1 syn:anti ratio); ^1H NMR (400 MHz, CDCl_3) δ 7.23–7.27 (m, 1H), 6.87–6.89 (m, 2H), 6.80–6.82 (m, 1H), 5.73–5.81 (m, 1H), 5.12–5.19 (AB multiplet, anti) and 5.04–5.08 (AB multiplet, syn) (total 2H), 4.60 (d, $J = 4.9$ Hz, syn) and 4.30 (d, $J = 7.8$ Hz, anti) (total 1H), 3.80 (s, 3H), 2.55–2.62 (m, syn) and 2.40–2.50 (m, anti) (total 1H), 2.12 (br s, anti) and 1.90 (br s, syn) (total 1H), 1.0 (d, $J = 6.8$ Hz, syn) and 0.88 (d, $J = 6.8$ Hz, anti) (total 3H); ^{13}C NMR (75 MHz, CDCl_3) δ 160.3 (anti) and 160.2 (syn), 145.1 (syn) and 144.9 (anti), 141.3 (anti) and 141.1 (syn), 129.7 (anti) and 129.6 (syn), 119.9 (anti) and 119.5 (syn), 117.1 (anti) and 115.9 (syn), 113.6 (anti) and 113.2 (syn), 112.8 (anti) and 112.7 (syn), 78.2 (anti) and 77.6 (syn), 55.5, 46.3 (anti) and 44.9 (syn), 16.7 (anti) and 14.3 (syn); MS (CI, isobutane) m/z 193.1 (M + H, 11), 175.1 (100), 137.0 (76); HRMS (CI, isobutane) calcd for $\text{C}_{12}\text{H}_{17}\text{O}_2$ (M + H) 193.1229, found 193.1208.

12e:⁴⁷ 51% (0.090 g, 0.51 mmol, 4:1 syn:anti ratio); ^1H NMR (400 MHz, CDCl_3) δ 7.22 (d, $J = 6.9$ Hz) and 6.87 (d, $J = 6.9$ Hz) (total 4H), 5.68–5.81 (overlapping m, 1H), 5.16–5.23 (AB multiplet, anti) and 5.02–5.05 (AB multiplet, syn) (total 2H), 4.55 (d, $J = 5.9$ Hz, syn) and 4.30 (d, $J = 7.8$ Hz, anti) (total 1H), 3.80 (s, 3H), 2.53–2.58 (m, syn) and 2.44–2.46 (m, anti) (total 1H), 2.09 (br s, anti) and 1.86 (br s, syn), 1.01 (d, $J = 6.8$ Hz, syn) and 0.84 (d, $J = 6.8$ Hz, syn) (total 3H); ^{13}C NMR (75 MHz, CDCl_3) δ 159.8 (anti) and 159.6 (syn), 141.6 (anti) and 141.1 (syn), 135.5 (syn) and 135.3 (anti), 128.6 (anti) and 128.3 (syn), 115.8 (syn) and 114.2 (anti), 114.0 (syn) and 113.4 (anti), 77.5 (overlapped with solvent), 55.5 (syn) and 55.4 (anti), 46.6 (anti) and 45.0 (syn), 16.7 (anti) and 14.6 (syn); MS (CI, isobutane) m/z 175.1 (M + H - H_2O , 100), 137.1 (11); HRMS (CI, isobutane) calcd for $\text{C}_{12}\text{H}_{16}\text{O}$ (M + H - H_2O) 175.1123, found 175.1127.

12f:^{21i,j,46} 41% (0.069 g, 0.41 mmol, 14:1 syn:anti ratio); ^1H NMR (400 MHz, CDCl_3) δ 5.77–5.85 (m, 1H), 5.06–5.10 (AB multiplet, 2H), 3.20 (m, syn) and 3.09 (m, anti) (total 1H), 2.40 (m, 1H), 0.8–2.0 (m, total 12H), 1.00 (d, $J = 6.8$ Hz, 3H); ^{13}C NMR (75 MHz, CDCl_3) δ 142.7 (syn) and 141.0 (anti), 116.6 (anti) and 115.1 (syn), 79.3 (anti) and 79.1 (syn), 40.8 (anti), 40.7 (anti), 40.6 (syn), 40.0 (syn), 30.3 (anti) and 30.0 (syn), 28.2, 27.3, 26.7, 26.5, 26.3, 26.2, 17.2 (anti) and 13.4 (syn). Anal. Calcd for $\text{C}_{11}\text{H}_{20}\text{O}$: C, 78.51; H, 11.98. Found: C, 78.22; H, 11.87.

12g:^{21j,46} 29% (0.0493 g, 0.29 mmol, 7:1 syn:anti ratio); ^1H NMR (400 MHz, CDCl_3) δ 5.75–5.84 (m, 1H), 5.06–5.12 (AB multiplet, 2H), 3.40–3.55 (m, syn) and 3.30–3.42 (m, anti) (total 1H), 2.40–2.50 (overlapping m, syn) and 2.23–2.32 (overlapping m, anti) (total 1H), 1.10–1.60 (m, 11H), 1.01 (d, $J = 6.8$ Hz, 3H), 0.87 (m, 3H); ^{13}C NMR (75 MHz, CDCl_3) δ 141.8 (anti) and 141.0 (syn), 116.8 (syn) and 115.8 (anti), 75.1, 44.4 (anti) and 43.7 (syn), 34.5 (anti) and 34.3 (syn), 32.1, 29.7, 26.4 (syn) and 25.9 (anti), 22.8, 16.4 (anti) and 14.2 (syn). Anal. Calcd for $\text{C}_{11}\text{H}_{22}\text{O}^{1/10}\text{H}_2\text{O}$: C, 76.77; H, 13.00. Found: C, 76.96; H, 12.61.

Representative Procedure for the $\text{BF}_3\cdot\text{Et}_2\text{O}$ -Promoted Addition of Complex **14 to Aldehydes.** A 3 equiv amount (0.744 g, 3 mmol) of freshly prepared complex **14** in Et_2O (5 mL) was added dropwise to a stirred solution of benzaldehyde

(44) Radcliffe, M. M.; Weber, W. P. *J. Org. Chem.* **1977**, *42*, 297.

(45) Peruzzo, V.; Tagliavini, G. *J. Organomet. Chem.* **1978**, *162*, 37.

(46) Wilson, S. R.; Guazzaroni, M. E. *J. Org. Chem.* **1989**, *54*, 3087.

(47) Widler, L.; Seebach, D. *Helv. Chim. Acta.* **1982**, *65*, 1085.

(0.106 g, 0.102 mL, 1 mmol) and $\text{BF}_3 \cdot \text{Et}_2\text{O}$ (0.38 mL, 3 mmol) in Et_2O (20 mL) at 0°C under argon. The mixture was stirred for 24 h, and the solvent was evaporated. To the residue was added acetonitrile (5 mL), and the mixture was stirred for several more hours. The solvent was removed *in vacuo*, and the residue was taken up in CH_2Cl_2 (50 mL) and filtered through Celite. The pad was washed with CH_2Cl_2 (50 mL), and the filtrate was concentrated *in vacuo*. The product was purified by flash chromatography (5:1 hexanes: EtOAc) to give 0.107 g (0.6 mmol, 60%; syn:anti ratio 4:1) of **17a**.⁴⁸ ^1H NMR (400 MHz, CDCl_3) δ 7.23–7.34 (m, 5H), 5.59–5.70 (m, anti) and 5.46–5.58 (m, syn) (total 1H), 5.18–5.28 (overlapping AB multiplet, anti) and 5.04–5.20 (overlapping AB multiplet, syn) (total 2H), 4.83 (t, $J = 3.9$ Hz, anti) and 4.50 (dd, $J = 2.0, 7.8$ Hz, syn) (total 1H), 3.77 (dd, $J = 3.9, 7.9$ Hz, anti) and 3.61 (apparent dd, $J = 6.8, 7.8$ Hz, syn) (total 1H), 3.37 (s, syn) and 3.33 (s, anti) (total 3H), 3.24 (broad s, syn) and 2.56 (d, $J = 3.9$ Hz, anti) (total 1H); ^{13}C NMR (75 MHz, CDCl_3) δ 140.4, 134.7 (syn) and 134.3 (anti), 128.7 (syn) and 128.6 (anti), 128.5 (syn) and 128.1 (anti), 128.0 (syn) and 127.3 (anti), 120.6 (anti) and 120.2 (syn), 88.0 (syn) and 87.1 (anti), 77.3 (syn) and 75.7 (anti), 57.1 (syn) and 57.0 (anti); MS (CI, isobutane) m/z 161.1 (M + H_2O , 51), 147.1 (15), 129.1 (100); HRMS (CI, isobutane) calcd for $\text{C}_{11}\text{H}_{13}\text{O}$ (M + H - H_2O) 161.0966, found 161.0954. Anal. Calcd for $\text{C}_{11}\text{H}_{14}\text{O}_2^{1/2}\text{H}_2\text{O}$: C, 72.66; H, 7.98. Found: C, 72.90; H, 8.36.

17b: 80% (0.178 g, 0.8 mmol, 2:1 syn:anti ratio); ^1H NMR (400 MHz, CDCl_3) δ 8.23 (s, 1H), 8.14 (d, $J = 7.8$ Hz, 1H), 7.67 (d, $J = 7.8$ Hz, 1H), 7.49 (t, $J = 7.8$ Hz, 1H), 5.52–5.65 (m, 1H), 5.02–5.35 (overlapping AB multiplets, 2H), 4.90 (apparent dd, $J = 2.9, 3.9$ Hz, anti) and 4.62 (d, $J = 7.8$ Hz, syn) (total 1H), 3.77 (dd, $J = 3.9, 7.6$ Hz, anti) and 3.58 (apparent dd, $J = 6.8, 7.8$ Hz, syn) (total 1H), 3.36 (s, syn) and 3.31 (s, anti) (total 3.5H) (overlapped with syn OH proton), 2.81 (d, $J = 2.9$ Hz, 0.5H, anti); ^{13}C NMR (75 MHz, CDCl_3) δ 148.7, 143.2 (anti) and 142.8 (syn), 134.2, 134.0, 133.7, 129.5 (syn) and 129.4 (anti), 123.3 (syn) and 123.0 (anti), 122.8 (syn) and 122.4 (anti), 121.6 (anti) and 121.4 (syn), 87.6 (syn) and 86.8 (anti), 76.0 (syn) and 74.8 (anti), 57.1 (syn) and 57.0 (anti); MS (CI, isobutane) m/z 206.1 (M + H - H_2O , 100), 192.1 (23), 176.1 (47), 162.1 (25), 122 (72); HRMS (CI, isobutane) calcd for $\text{C}_{11}\text{H}_{12}\text{NO}_3$ (M + H - H_2O) 206.0817, found 206.0803. Anal. Calcd for $\text{C}_{11}\text{H}_{13}\text{NO}_4$: C, 59.19; H, 5.87; N, 6.28. Found: C, 59.29; H, 5.88; N, 6.21.

17c: 80% (0.178 g, 0.8 mmol, 3:1 syn:anti ratio); ^1H NMR (400 MHz, CDCl_3) δ 8.18 (d, $J = 8.8$ Hz) and 7.52 (d, $J = 8.8$ Hz) (total 4H), 5.63–5.52 (m, 1H), 5.15–5.30 (overlapping AB multiplet, anti) and 5.05–5.26 (overlapping AB multiplet, syn) (total 2H), 4.91 (t, $J = 3.9$ Hz, anti) and 4.63 (d, $J = 7.8$ Hz, syn) (total 1H), 3.76 (apparent dd, $J = 3.9, 4.9$ Hz, anti), 3.55 (t, $J = 7.8$ Hz, syn) (total 1H), 3.36 (s, syn) and 3.32 (s, anti) (total 3H), 3.34 (s, overlapping signal, syn) and 2.76 (d, $J = 3.9$ Hz, anti) (total 1H); ^{13}C NMR (75 MHz, CDCl_3) δ 148.4 (anti) and 148.2 (syn), 148.0, 134.0 (syn) and 133.6 (anti), 128.7 (syn) and 128.2 (anti), 123.7, 121.6 (anti) and 121.4 (syn), 87.6 (syn) and 86.7 (anti), 76.2 (syn) and 75.0 (anti), 57.1 (syn) and 57.0 (anti); MS (CI, isobutane) m/z 224.1 (M + H - H_2O , 100), 206.1 (39), 192.1 (6), 176.1 (9), 162.0 (16); HRMS (CI, isobutane) calcd for $\text{C}_{11}\text{H}_{14}\text{NO}_4$ (M + H) 224.0923, found 224.0909. Anal. Calcd for $\text{C}_{11}\text{H}_{15}\text{NO}_4$: C, 59.19; H, 5.87; N, 6.28. Found: C, 59.39; H, 5.96; N, 6.14.

17d: 77% (0.160 g, 0.77 mmol, 3:1 syn:anti ratio); ^1H NMR (400 MHz, CDCl_3) δ 7.20–7.25 (m, 1H), 6.91 (s, 2H), 6.81–6.83 (m, 1H), 5.61–5.68 (m, anti) and 5.49–5.60 (m, syn) (total 1H), 5.18–5.29 (overlapping AB multiplet, anti) and 5.07–5.20 (overlapping AB multiplet, syn) (total 2H), 4.75 (t, $J = 3.9$ Hz, anti) and 4.47 (d, $J = 7.8$ Hz, syn) (total 1H), 3.81 (s, 3H), 3.75–3.79 (m, anti) and 3.59 (apparent dd, $J = 6.8, 7.8$ Hz, syn) (total 1H), 3.37 (s, syn) and 3.33 (s, anti) (total 3H), 3.22

(broad s, syn) and 2.55 (d, $J = 3.8$ Hz, anti) (total 1H); ^{13}C NMR (75 MHz, CDCl_3) δ 160.2, 142.6 (anti) and 142.1 (syn), 134.7 (syn) and 134.2 (anti), 129.6 (syn) and 129.4 (anti), 120.4, 120.1 (syn) and 119.7 (anti), 114.0 (syn) and 113.5 (anti), 113.3 (syn) and 112.9 (anti), 87.8 (syn) and 87.0 (anti), 76.7 (anti) and 75.6 (syn), 57.1 (syn) and 55.5 (anti); MS (CI, isobutane) m/z 209.1 (M + H, 11), 191.1 (100), 177.1 (20), 159.1 (83), 137.1 (18); HRMS (CI, isobutane) calcd for $\text{C}_{12}\text{H}_{15}\text{O}_3$ (M + H) 209.1178, found 209.1185. Anal. Calcd for $\text{C}_{12}\text{H}_{16}\text{O}_3$: C, 69.21; H, 7.74. Found: C, 69.11; H, 7.77.

17e: 60% (0.125 g, 0.60 mmol, 2:1 syn:anti ratio); ^1H NMR (400 MHz, CDCl_3) δ 7.25 (d, $J = 7.8$ Hz) and 6.85 (d, $J = 7.8$ Hz) (total 4H), 5.67–5.62 (m, anti) and 5.45–5.54 (m, syn) (total 1H), 5.19–5.29 (overlapping AB multiplet, anti) and 5.04–5.20 (overlapping AB multiplet, syn) (total 2H), 4.75 (t, $J = 3.9$ Hz, anti) and 4.44 (d, $J = 7.8$ Hz, syn) (total 1H), 3.79 (s, 3H), 3.73–3.78 (m, anti) and 3.60 (t, $J = 7.8$ Hz, syn) (total 1H), 3.37 (s, syn) and 3.31 (s, anti) (total 3H), 3.21 (s, syn) and 2.5 (d, $J = 2.9$ Hz, anti) (total 1H); ^{13}C NMR (75 MHz, CDCl_3) δ 160.0 (syn) and 159.7 (anti), 134.8 (syn) and 134.6 (anti), 133.1 (anti) and 132.5 (syn), 129.1 (syn) and 128.6 (anti), 120.5 (anti) and 120.0 (syn), 114.1 (syn) and 114.0 (anti), 88.0 (syn) and 87.2 (anti), 76.8 (syn) and 75.4 (anti), 57.1 (syn) and 57.0 (anti), 55.5; MS (CI, isobutane) m/z 191.1 (M + H - H_2O , 50), 177.1 (100), 159.1 (50), 137.1 (14); HRMS (CI, isobutane) calcd for $\text{C}_{12}\text{H}_{14}\text{O}_2$ (M + H - H_2O) 209.1178, found 209.1172. Anal. Calcd for $\text{C}_{12}\text{H}_{16}\text{O}_3$: C, 69.21; H, 7.74. Found: C, 69.15; H, 7.76.

17f:⁴⁸ 45% (0.082 g, 0.45 mmol, syn:anti ratio undetermined); ^1H NMR (400 MHz, CDCl_3) δ 5.60–5.69 (m, 1H), 5.20–5.40 (AB multiplet, 2H), 3.45–3.54 (m, 1H), 3.29 (br s, 4H), 2.48 (br s, 1H), 1.57–1.73 (overlapping m, 6H), 1.12–1.50 (overlapping m, 5H); ^{13}C NMR (75 MHz, CDCl_3) δ 153.8, 119.9, 84.6, 78.0, 56.6, 39.6, 30.5, 26.8, 26.64, 26.60, 26.4. Anal. Calcd for $\text{C}_{17}\text{H}_{24}\text{O}_2^{1/2}\text{H}_2\text{O}$: C, 77.65; H, 9.30. Found: C, 77.64; H, 9.08.

17g: 35% (0.065 g, 0.35 mmol, 7:1 syn:anti ratio); ^1H NMR (400 MHz, CDCl_3) δ 5.56–5.65 (m, 1H), 5.26–5.34 (AB multiplet, 2H), 3.66–3.72 (m, anti) and 3.40–3.50 (m, syn) (total 1H), 3.4–3.5 (br s, 4H), 2.66 (br s, 1H), 1.2–1.67 (m, 10H), 0.85–0.87 (m, 3H); ^{13}C NMR (75 MHz, CDCl_3) δ 135.7 (syn) and 134.9 (anti), 120.5, 87.4 (syn) and 86.5 (anti), 73.8 (syn) and 73.5 (anti), 56.7, 32.7, 32.0, 29.6, 25.7, 22.8, 14.2. Anal. Calcd for $\text{C}_{17}\text{H}_{26}\text{O}_2$: C, 70.92; H, 11.90. Found: C, 70.75; H, 11.81.

The same procedure using allyliron complex **15** afforded the following compounds (**17h–n**).

17h:⁴⁸ 80% yield (0.203 g, 0.8 mmol, 4:1 syn:anti ratio); ^1H NMR (400 MHz, CDCl_3) δ 7.20–7.40 (m, 10H), 5.70–5.81 (m, anti) and 5.60–5.69 (m, syn) (total 1H), 5.20–5.35 (overlapping AB multiplet, anti) and 5.10–5.26 (overlapping AB multiplet, syn) (total 2H), 4.82–4.88 (m, anti) and 4.58 (d, $J = 7.8$ Hz, syn) (total 1H), 4.68 (d, $J = 11.7$ Hz, syn) and 4.63 (d, $J = 11.7$ Hz, anti) and 4.39 (d, $J = 11.7$ Hz, syn) and 4.38 (d, $J = 11.7$ Hz, anti) (total 2H), 3.88 (apparent dd, $J = 6.8, 7.8$ Hz, syn) and 3.69 (d, $J = 4.9$ Hz, anti), 3.24 (s, syn) and 2.56 (d, $J = 3.9$ Hz, anti) (total 1H); ^{13}C NMR (75 MHz, CDCl_3) δ 141.1 (anti) and 140.5 (syn), 138.8 (anti) and 138.6 (syn), 135.1 (syn) and 134.7 (anti), 129.1 (syn) and 129.0 (anti), 128.7, 128.6, 128.54, 128.50, 128.4, 128.3, 128.2, 128.0, 127.5, 120.8 (anti) and 120.3 (syn), 85.7 (syn) and 84.7 (anti), 77.2 (syn) and 76.0 (anti), 71.2 (syn) and 70.9 (anti). Anal. Calcd for $\text{C}_{17}\text{H}_{18}\text{O}_2^{1/2}\text{H}_2\text{O}$: C, 79.35; H, 7.18. Found: C, 79.44; H, 7.25.

17i: 85% (0.254 g, 0.85 mmol, 3:1 syn:anti ratio); ^1H NMR (400 MHz, CDCl_3) δ 8.21 (s, 1H), 8.13 (d, $J = 7.8$ Hz, 1H), 7.66 (d, $J = 7.8$ Hz, 1H), 7.48 (t, $J = 7.8$ Hz, 1H), 7.19–7.38 (m, 5H), 5.65–5.78 (m, 1H), 5.20–5.40 (overlapping AB multiplet, anti) and 5.12–5.32 (overlapping AB multiplet, syn) (total 2H), 4.90 (d, $J = 4.9$ Hz, anti) and 4.67–4.71 (overlapping m) and 4.37 (d, $J = 11.7$ Hz, syn) and 4.36 (d, $J = 11.7$ Hz, anti) (total 3H), 3.93 (m, anti) and 3.83 (apparent dd, $J = 6.8, 7.8$ Hz, syn) (total 1H), 3.30 (br s, syn) and 2.70 (br s, anti)

(48) (a) Takai, K.; Nitta, K.; Utimoto, K. *Tetrahedron Lett.* **1988**, 29, 5263. (b) Koreeda, M.; Tanaka, Y. *Tetrahedron Lett.* **1987**, 28, 143.

(total 1H); ^{13}C NMR (75 MHz, CDCl_3) δ 148.7, 143.4 (anti) and 143.0 (syn), 138.3 (anti) and 138.1 (syn), 134.5 (syn) and 134.3 (anti), 129.5 (syn) and 129.4 (anti), 129.1, 129.0, 128.6, 128.4, 128.1, 127.5, 123.3 (syn) and 123.0 (anti), 122.8 (syn) and 122.6 (anti), 121.8 (anti) and 121.5 (syn), 84.9 (syn) and 84.3 (anti), 76.0 (syn) and 75.0 (anti), 71.1 (syn) and 70.9 (anti); HRMS (CI, isobutane) calcd for $\text{C}_{17}\text{H}_{18}\text{NO}_3$ (M + H - H_2O) 128.113, found 282.1144. Anal. Calcd for $\text{C}_{17}\text{H}_{17}\text{NO}_4$: C, 68.22; H, 5.73; N, 4.68. Found: C, 68.06; H, 5.79; N, 4.57.

17j: 83% (0.284 g, 0.85 mmol, 3:1 syn:anti ratio); ^1H NMR (400 MHz, CDCl_3) δ 8.17 (d, $J = 7.8$ Hz) and 7.49 (d, $J = 7.8$ Hz) (total 4H), 7.20–7.40 (m, 5H), 5.60–5.75 (m, 1H), 5.18–5.38 (overlapping AB multiplet, anti) and 5.12–5.31 (overlapping AB multiplet, syn) (total 2H), 4.90–4.94 (m, anti) and 4.61–4.70 (overlapping m), and 4.37 (d, $J = 11.7$ Hz) (total 3H), 3.90–3.98 (AB multiplet, anti) and 3.81 (apparent, $J = 6.8, 7.8$ Hz, syn) (total 1H), 3.29 (s, syn) and 2.73 (d, $J = 2.0$ Hz, anti) (total 1H); ^{13}C NMR (75 MHz, CDCl_3) δ 148.5 (anti) and 148.2 (syn), 148.1 (syn) and 148.0 (anti), 138.3 (anti) and 138.1 (syn), 134.4 (syn) and 134.1 (anti), 129.1 (syn) and 129.0 (anti), 128.7, 128.6, 128.4, 128.3, 128.1, 127.5, 123.74 (syn) and 123.68 (anti), 121.7 (anti) and 121.4 (syn), 85.0 (syn) and 84.3 (anti), 76.1 (syn) and 75.2 (anti), 71.1 (syn) and 70.9 (anti); MS (CI, isobutane) calcd for $\text{C}_{17}\text{H}_{18}\text{NO}_4$ (M + H) 300.1230, found 300.1233. Anal. Calcd for $\text{C}_{17}\text{H}_{17}\text{NO}_4$: C, 68.22; H, 5.73; N, 4.68. Found: C, 67.97; H, 5.80; N, 4.53.

17k: 85% (0.241 g, 0.85 mmol, 4:1 syn:anti ratio); ^1H NMR (400 MHz, CDCl_3) δ 7.20–7.40 (m, 7H), 6.91 (s, 2H), 6.82 (d, $J = 7.8$ Hz, 1H), 5.70–5.81 (m, anti) and 5.60–5.70 (m, syn) (total 1H), 5.20–5.38 (overlapping AB multiplet, anti) and 5.04–5.28 (overlapping AB multiplet, syn) (total 2H), 4.80–4.86 (m, anti) and 4.55 (d, $J = 7.8$ Hz, syn) (total 1H), 4.68 (d, $J = 11.7$ Hz, syn) and 4.63 (d, $J = 11.7$ Hz, anti) and 4.39 (d, $J = 11.7$ Hz, syn) and 4.38 (d, $J = 11.7$ Hz, anti) (total 2H), 3.92–3.98 (m, anti) and 3.85–3.89 (apparent dd, $J = 6.8, 7.8$ Hz, syn) (total 1H), 3.80 (s, 3H), 3.21 (s, syn) and 2.54 (d, $J = 2.9$ Hz, anti) (total 1H); ^{13}C NMR (75 MHz, CDCl_3) δ 160.2, 142.9 (anti) and 142.2 (syn), 138.8 (anti) and 138.6 (syn), 135.1 (syn) and 134.8 (anti), 129.7 (syn) and 129.6 (anti), 129.1 (syn) and 129.0 (anti), 128.5, 128.4, 128.4, 128.2, 120.7 (syn) and 120.4 (anti), 120.2 (syn) and 119.9 (anti), 114.1 (syn) and 113.8 (anti), 113.8 (anti), 113.4 (syn) and 112.9 (anti), 85.5 (syn) and 84.6 (anti), 77.1 (syn) and 75.9 (anti), 71.2 (syn) and 70.9 (anti), 55.5; MS (CI, isobutane) m/z 267.1 (M + H - H_2O , 100), 177.1 (92), 159.1 (54), 147.1 (49); HRMS (CI, isobutane) calcd for $\text{C}_{18}\text{H}_{20}\text{O}_2$ (M + H - H_2O) 267.1385, found 267.1367. Anal. Calcd for $\text{C}_{18}\text{H}_{20}\text{O}_3^{1/5}\text{H}_2\text{O}$: C, 75.08; H, 7.41. Found: C, 75.29; H, 7.15.

17l: 72% (0.187 g, 0.72 mmol, 3:1 syn:anti ratio); ^1H NMR (400 MHz, CDCl_3) δ 7.20–7.40 (m, 7H), 6.85 (d, $J = 8.8$ Hz, 2H), 5.73–6.83 (m, anti) and 5.57–5.67 (m, syn) (total 1H), 5.21–5.35 (overlapping AB multiplet, anti) and 5.09–5.23 (overlapping AB multiplet, syn) (total 2H), 4.78–4.80 (m, anti) and 4.52 (d, $J = 7.8$ Hz, syn) (total 1H), 4.68 (d, $J = 11.7$ Hz, syn) and 4.62 (d, $J = 12.7$ Hz, anti) and 4.43–4.56 (overlapping d), (total 2H), 3.91–3.95 (m, anti) 3.80 (apparent dd, $J = 6.8, 7.8$ Hz, syn) (total 1H), 3.80 (s, 3H), 3.21 (s, 1H), 2.45 (br s, 1H); ^{13}C NMR (75 MHz, CDCl_3) δ 160.0 (syn) and 159.8 (anti), 138.8 (anti) and 138.6 (syn), 135.1 (syn) and 135.0 (anti), 133.3 (anti) and 132.6 (syn), 129.2 (anti) and 129.1 (syn), 129.0, 128.7, 128.5, 128.4, 128.3, 128.2, 120.7 (anti) and 120.2 (syn), 114.1 (syn) and 114.0 (anti), 85.8 (syn) and 84.8 (anti), 76.8 (syn) and 75.6 (anti), 71.2 (syn) and 70.9 (anti), 55.6; MS (CI, isobutane) m/z 267.1 (M + H - H_2O , 21), 177.1 (100), 159.1 (28), 147.1 (36), 137.1 (39), 107.0 (6); HRMS (CI, isobutane) calcd for $\text{C}_{18}\text{H}_{19}\text{O}_2$ (M + H - H_2O) 267.1385, found 267.1356. Anal. Calcd for $\text{C}_{18}\text{H}_{20}\text{O}_3$: C, 76.03; H, 7.09. Found: C, 75.79; H, 7.13.

17m:⁴⁸ 72% (0.187 g, 0.72 mmol, 6:1 syn:anti ratio); ^1H NMR (400 MHz, CDCl_3) δ 7.20–7.40 (m, 5H), 5.73–5.83 (m, 1H), 5.30–5.37 (AB multiplet, 2H), 4.64 (d, $J = 11.7$ Hz) and 4.33 (d, $J = 11.7$ Hz) (total 2H), 4.20–4.50 (m, anti) and 3.80

(apparent dd, $J = 6.8, 7.8$ Hz) (total 1H), 3.49–3.52 (m, anti) and 3.29 (apparent dd, $J = 4.9, 5.9$ Hz, syn) (total 1H), 2.45 (br s, 1H), 1.40–1.80 (overlapping m, 6H), 1.10–1.36 (overlapping m, 5H); ^{13}C NMR (75 MHz, CDCl_3) δ 138.3, 136.7 (syn) and 135.2 (anti), 128.9, 128.8, 128.5, 128.3, 119.4 (syn) and 117.9 (anti), 82.0 (syn) and 81.7 (anti), 78.2 (syn) and 77.6 (anti), 70.6 (syn) and 70.4 (anti), 39.7 (syn) and 38.9 (anti), 30.4, 26.9, 26.8, 26.7, 26.4. Anal. Calcd for $\text{C}_{17}\text{H}_{24}\text{O}_2^{1/7}\text{H}_2\text{O}$: C, 77.65; H, 9.30. Found: C, 77.64; H, 9.08.

17n: 57% (0.149 g, 0.57 mmol, syn:anti ratio undetermined); ^1H NMR (400 MHz, CDCl_3) δ 7.20–7.40 (m, 5H), 5.70–5.90 (m, 1H), 5.25–5.40 (AB multiplet, 2H), 4.65 (d, $J = 11.7$) and 4.35 (d, $J = 11.7$) (total 2H), 3.72–3.78 (minor isomer, m), 3.53–3.61 (overlapping m) (total 2H), 2.55–2.80 (br s, 1H), 1.27–1.64 (overlapping m, 10H), 0.85–0.88 (m, 3H); ^{13}C NMR (75 MHz, CDCl_3) δ 138.9 (anti) and 138.8 (syn), 136.0 and 135.2, 129.1, 129.0, 128.9, 128.5, 128.4, 128.8, 128.2, 120.8 (syn) and 120.5 (anti), 85.5 (syn) and 84.0 (anti), 73.8 (syn) and 73.6 (anti), 70.7 (syn) and 70.6 (anti), 32.8 (syn) and 32.4 (anti), 32.0, 29.5, 25.9 (anti) and 25.7 (syn), 22.8, 14.2. Anal. Calcd for $\text{C}_{17}\text{H}_{26}\text{O}_2^{1/7}\text{H}_2\text{O}$: C, 77.11; H, 10.00. Found: C, 77.15; H, 9.86.

Representative Procedure for the BF_3 -Promoted Addition of Allyliron Complex 1 to Ketones. To a solution of 2-heptanone (0.114 g, 1.0 mmol) and $\text{BF}_3\cdot\text{Et}_2\text{O}$ (0.50 mL, 4.0 mmol) in anhydrous Et_2O (10 mL) was added a freshly-prepared solution of **1** (5 mL, 0.8 M, 4.0 mmol) in Et_2O under an argon atmosphere. The mixture was stirred at room temperature for 20 h. Filtration of the resulting yellow suspension through a fine-pore glass frit under argon provided the iron-olefin π -complex as a powdery yellow salt. Addition of moist acetone (20 mL) and NaI (0.9 g, 6 mmol) to this salt produced an immediate formation of FpI, as evidenced by the black coloration. After 2 h at room temperature, the solvent was removed *in vacuo*, and the black residue was taken up in CH_2Cl_2 (25 mL) and filtered through a Celite pad. The pad was washed with CH_2Cl_2 (25 mL), and the solvent was removed *in vacuo*. Purification of the residue by successive flash chromatography columns (CH_2Cl_2 and then 25% EtOAc : hexane) afforded 0.119 g (77%) of homoallylic alcohol **22a**⁴⁹ as a colorless oil: ^1H NMR (400 MHz, CDCl_3) δ 5.85 (m, 1H), 5.12 (m, 2H), 2.22 (d, $J = 7.2$ Hz, 2H), 1.44 (m, 3H), 1.39–1.20 (m, 6H), 1.15 (s, 3H), 0.88 (t, $J = 6.8$ Hz, 3H); IR (neat film) 3400, 3090, 2970, 2950, 2880, 1640, 1460, 1375, 1140, 982, 913 cm^{-1} .

Homoallylic Alcohol 22b: 60% yield (0.124 g, 0.60 mmol) plus 38% (0.063 g, 0.38 mmol) of recovered ketone; ^1H NMR (400 MHz, CDCl_3) δ 7.05 (d, $J = 7.6$ Hz, 2H), 6.75 (d, $J = 7.6$ Hz, 2H), 5.88 (m, 1H), 5.16 (m, 2H), 4.92 (s, 1H), 2.63 (m, 2H), 2.29 (d, $J = 6.8$ Hz, 2H), 1.74 (m, 2H), 1.52 (s, 1H), 1.25 (s, 3H); IR (neat film) 3360, 2980, 2948, 1623, 1510, 1445, 1371, 1230, 1170, 912, 824 cm^{-1} ; MS (CI, isobutane) m/z 189.1 (M + 1 - H_2O , 14), 165.1 (10), 149.1 (19), 147.1 (39), 108.1 (10), 147.0 (100); HRMS (CI, isobutane) calcd for $\text{C}_{13}\text{H}_{17}\text{O}$ (M + 1 - H_2O) 189.1279, found 189.1270. Anal. Calcd for $\text{C}_{13}\text{H}_{18}\text{O}_2$: C, 75.69; H, 8.80. Found: C, 75.41; H, 8.89.

Homoallylic Alcohol 22c:⁵⁰ 84% yield (0.140 g, 0.86 mmol); ^1H NMR (400 MHz, CDCl_3) δ 7.45–7.22 (m, 5H), 5.61 (m, 1H), 5.14 (m, 2H), 2.69 (dd, $J = 5.9, 13.7$ Hz, 1H), 2.50 (dd, $J = 8.8, 13.7$ Hz, 1H), 2.05 (s, 1H), 1.55 (s, 3H); IR (neat film) 3445, 3080, 3040, 2990, 2945, 1639, 1492, 1443, 1373, 1343, 1063, 1024, 993, 911, 760, 723, 696 cm^{-1} .

Homoallylic Alcohol 22d:⁵¹ 98% yield (0.192 g, 0.98 mmol); ^1H NMR (400 MHz, CDCl_3) δ 7.45–7.28 (m, 5H), 5.60 (m, 1H), 5.11 (m, 2H), 3.84 (m, 2H), 2.72 (d, $J = 6.8$ Hz, 2H), 2.60 (s, 1H); IR (neat film) 3570, 3080, 3040, 2967, 1636, 1490, 1442, 1330, 1255, 1170, 1060, 990, 908, 764, 720, 692 cm^{-1} .

(49) Okude, Y.; Hirano, S.; Hiyama, T.; Nozaki, H. *J. Am. Chem. Soc.* **1977**, *99*, 3179.

(50) Jadhav, P. K.; Bhat, K. S.; Perumal, P. T.; Brown, H. C. *J. Org. Chem.* **1986**, *51*, 432.

(51) Barluenga, J.; Florez, J.; Yus, M. *J. Chem. Soc., Perkin Trans. 1* **1983**, 3019.

Homoallylic Alcohol 22e: 61% yield (0.154 g, 0.61 mmol) plus 30% (64 mg, 0.30 mmol) of recovered ketone; $^1\text{H NMR}$ (400 MHz, CDCl_3) δ 7.29 (m, 10H), 5.95 (m, 1H), 5.16 (m, 2H), 2.81 (s, 4H), 2.16 (d, $J = 8.0$ Hz, 2H), 1.56 (s, 1H); IR (neat film) 3460, 3090, 3070, 3040, 2990, 2935, 1638, 1602, 1493, 1444, 1363, 1264, 1082, 1027, 992, 912, 728, 697 cm^{-1} . MS (CI, isobutane) m/z 235.1 ($M + 1 - \text{H}_2\text{O}$, 57), 211.1 (21), 162.0 (26), 161.1 (67), 160.1 (24), 157.1 (62), 143.1 (88), 133.1 (51), 131.1 (83), 119.1 (68), 117.1 (30), 105.1 (31). HRMS (CI, isobutane) calcd for $\text{C}_{18}\text{H}_{19}$ ($M + 1 - \text{H}_2\text{O}$) 235.1487, found 235.1485. Anal. Calcd for $\text{C}_{18}\text{H}_{20}\text{O}$: C, 85.67; H, 7.99. Found: C, 85.54; H, 8.06.

Homoallylic Alcohol 22f:⁵² 77% yield (0.119 g, 0.77 mmol); $^1\text{H NMR}$ (400 MHz, CDCl_3) δ 5.89 (m, 1H), 5.14 (m, 2H), 2.23 (d, $J = 8.0$ Hz, 2H), 1.68–1.36 (m, 13H); IR (neat film) 3410, 3084, 2930, 2865, 1636, 1455, 1440, 1344, 1274, 1233, 1183, 1120, 1040, 1019, 990, 965, 910 cm^{-1} .

Homoallylic Alcohol 22g:⁵³ 59% yield (0.083 g, 0.59 mmol); $^1\text{H NMR}$ (400 MHz, CDCl_3) δ 5.88 (m, 1H), 5.13 (m, 2H), 2.21 (d, $J = 6.8$ Hz, 2H), 1.64–1.25 (m, 11H); IR (neat film) 3520, 3090, 2990, 2950, 2870, 1640, 1445, 1350, 1262, 1163, 1138, 1034, 995, 975, 885 cm^{-1} .

Homoallylic Alcohol 22h:⁵⁴ 70% yield (0.106 g, 0.69 mmol, 7.1:1 mixture of diastereomers); $^1\text{H NMR}$ (400 MHz, CDCl_3) major isomer δ 5.89 (m, 1H), 5.15–5.07 (m, 2H), 2.18 (d, $J = 6.8$ Hz, 2H), 1.79–1.54 (m, 6H), 1.33 (s, 1H), 1.24 (m, 1H), 0.95 (t, $J = 12.8$ Hz, 1H), 0.88 (s) and 0.86 (s) (total 3H), 0.79 (m, 1H); minor isomer δ 5.88 (m, 1H), 5.18–5.11 (m, 2H), 2.30 (d, $J = 6.8$ Hz, 2H), 1.73–1.40 (m, 6H), 1.39–1.20 (m, 2H), 1.02 (t, $J = 12.6$ Hz, 1H), 0.90 (d, $J = 6.8$ Hz, 3H), 0.83 (m, 1H); IR (neat film) 3420, 3090, 2935, 2880, 2850, 1638, 1445, 1375, 1262, 1153, 989, 952, 913 cm^{-1} .

Representative Procedure for the $\text{BF}_3\cdot\text{Et}_2\text{O}$ -Promoted Additions of Complex 1 to *N*-Tosylimines. To a stirred solution of benzaldehyde *N*-tosylimine (0.259 g, 1.0 mmol) and $\text{BF}_3\cdot\text{Et}_2\text{O}$ (370 μL , 3.0 mmol) in CH_2Cl_2 (5 mL) at 0 $^\circ\text{C}$ under an argon atmosphere was added dropwise a freshly prepared solution of allyliron complex 1 (3.0 mmol) in CH_2Cl_2 (5 mL). The mixture was stirred for 12 h, and a solution of NaI (0.75 g, 5 mmol) in wet acetone (10 mL) was added. The reaction mixture was stirred for 4 h and evaporated. The residue was taken up in CH_2Cl_2 (25 mL) and filtered through a Celite pad. Evaporation and flash chromatography of the residue afforded 0.211 g (70%) of homoallylic amine 26a^{33r} as a colorless-to-pale yellow oil: $^1\text{H NMR}$ (400 MHz, CDCl_3) δ 7.44 (d, $J = 8.0$ Hz, 2H), 7.19–7.06 (m, 7H), 5.56–5.46 (m, 1H), 5.08–5.03 (m, 2H), 4.77 (d, $J = 6.0$ Hz, 1H), 4.37 (q, $J = 6.0$ Hz, 1H), 2.48–2.43 (m, 2H), 2.38 (s, 3H).

Homoallylic Amine 26b: 50% yield (0.166 g, 0.50 mmol); $^1\text{H NMR}$ (400 MHz, CDCl_3) δ 7.55 (d, $J = 8.0$ Hz, 2H), 7.14 (d, $J = 8.0$ Hz, 2H), 6.98 (d, $J = 8.0$ Hz, 2H), 6.70 (d, $J = 8.0$ Hz, 2H), 5.57–5.45 (m, 1H), 5.06–5.03 (m, 2H), 4.73 (d, $J = 6.0$ Hz, 1H), 4.32 (q, $J = 6.0$ Hz, 1H), 3.87 (s, 3H), 2.47–2.42 (m, 2H), 2.37 (s, 3H).

Homoallylic Amine 26c: 20% yield (0.067 g, 0.20 mmol); $^1\text{H NMR}$ (400 MHz, CDCl_3) δ 8.02 (d, $J = 8.0$ Hz, 1H), 7.84 (s, 1H), 7.51 (t, $J = 7.2$ Hz, 3H), 7.41 (t, $J = 8.0$ Hz, 1H), 7.13 (d, $J = 8.0$ Hz, 2H), 5.55–5.42 (m, 1H), 5.17–5.10 (m, 2H), 4.85 (d, $J = 6.0$ Hz, 1H), 4.51–4.46 (m, 1H), 2.44–2.40 (m, 2H), 2.33 (s, 3H).

Homoallylic Amine 26d: 88% yield (0.304 g, 0.88 mmol); $^1\text{H NMR}$ (400 MHz, CDCl_3) δ 8.02 (d, $J = 8.0$ Hz, 1H), 7.84 (s, 1H), 7.52 (t, $J = 7.2$ Hz, 3H), 7.41 (t, $J = 8.0$ Hz, 1H), 7.14 (d, $J = 8.0$ Hz, 2H), 5.53–5.44 (m, 1H), 5.18–5.11 (m, 2H), 4.88 (d, $J = 6.0$ Hz, 1H), 4.49 (q, $J = 6.0$ Hz, 1H), 2.49–2.40 (m, 2H), 2.35 (s, 3H).

Through a similar procedure, homoallylic amines 27a–c and dienes 29a–c were prepared from complex 14, and homoallylic amines 27/28d–f were obtained from complex 15.

Homoallylic Amine 27a: 47% yield (0.156 g, 0.47 mmol); $^1\text{H NMR}$ (400 MHz, CDCl_3) δ 7.55 (d, $J = 8.0$ Hz, 2H), 7.14–7.07 (m, 7H), 5.54–5.45 (m, 2H), 5.20–5.04 (m, 2H), 4.22 (t, $J = 5.4$ Hz, 1H), 3.60 (t, $J = 6.8$ Hz, 1H), 3.20 (s, 3H), 2.34 (s, 3H).

1,3-Diene 29a: 23% yield (0.069 g, 0.23 mmol); $^1\text{H NMR}$ (400 MHz, CDCl_3) δ 7.49 (d, $J = 8.0$ Hz, 2H), 7.26–7.23 (m, 5H), 7.18 (d, $J = 8.0$ Hz, 2H), 5.79 (d, $J = 4.8$ Hz, 1H), 5.65 (d, $J = 3.6$ Hz, 1H), 5.52 (d, $J = 3.2$ Hz, 1H), 4.36–4.23 (m, 2H), 2.38 (s, 3H).

Homoallylic Amine 27b: 43% yield (0.155 g, 0.43 mmol); $^1\text{H NMR}$ (400 MHz, CDCl_3) δ 7.45 (d, $J = 8.0$ Hz, 2H), 7.09 (d, $J = 8.0$ Hz, 2H), 6.98 (d, $J = 8.0$ Hz, 2H), 6.70 (d, $J = 8.0$ Hz, 2H), 5.53–5.44 (m, 2H), 5.17–5.04 (m, 2H), 4.17 (t, $J = 6.0$ Hz, 1H), 3.74 (s, 3H), 3.58 (t, $J = 6.8$ Hz, 1H), 3.22 (s, 3H), 2.34 (s, 3H).

1,3-Diene 29b: 20% yield (0.066 g, 0.20 mmol); $^1\text{H NMR}$ (400 MHz, CDCl_3) δ 7.50 (d, $J = 8.0$ Hz, 2H), 7.28–7.15 (m, 4H), 6.82 (d, $J = 8.0$ Hz, 2H), 5.77 (d, $J = 6.0$ Hz, 1H), 5.62 (d, $J = 4.2$ Hz, 1H), 5.52 (d, $J = 3.2$ Hz, 1H), 4.33–4.20 (m, 2H), 3.79 (s, 3H), 2.38 (s, 3H).

Homoallylic Amine 27c: 39% yield (0.145 g, 0.39 mmol); $^1\text{H NMR}$ (400 MHz, CDCl_3) δ 8.00 (d, $J = 8.0$ Hz, 1H), 7.83 (s, 1H), 7.54–7.30 (m, 4H), 7.09–7.03 (m, 2H), 5.57–5.47 (m, 2H), 5.30–5.03 (m, 2H), 4.37 (t, $J = 5.4$ Hz, 1H), 3.61 (t, $J = 6.8$ Hz, 1H), 3.21 (s, 3H), 2.33 (s, 3H).

1,3-Diene 29c: 22% yield (0.069 g, 0.22 mmol); $^1\text{H NMR}$ (400 MHz, CDCl_3) δ 8.11 (d, $J = 8.0$ Hz, 2H), 7.98 (s, 1H), 7.68 (d, $J = 8.0$ Hz, 1H), 7.58–7.47 (m, 2H), 7.23 (d, $J = 8.0$ Hz, 2H), 5.87 (d, $J = 5.0$ Hz, 1H), 5.64 (d, $J = 4.0$ Hz, 1H), 5.57 (d, $J = 3.2$ Hz, 1H), 4.36 (s, 2H), 2.38 (s, 3H).

Homoallylic Amine 27/28d: 84% yield (0.342 g, 0.84 mmol); $^1\text{H NMR}$ (400 MHz, CDCl_3) δ 7.52–7.04 (m, 14H), 5.78–5.12 (m, 4H), 4.53–3.92 (m, 4H), 2.39 (s, minor) and 2.34 (s, major) (total 3H).

Homoallylic Amine 27/28e: 84% yield (0.367 g, 0.84 mmol); $^1\text{H NMR}$ (400 MHz, CDCl_3) δ 7.52–6.65 (m, 13H), 5.65–5.10 (m, 4H), 4.54–4.20 (m, 4H), 3.80 (s, minor) and 3.75 (s, major) (total 3H), 2.38 (s, minor) and 2.34 (s, major) (total 3H).

Homoallylic Amine 27/28f: 72% yield (0.325 g, 0.72 mmol); $^1\text{H NMR}$ (400 MHz, CDCl_3) δ 8.01 (d, $J = 8.0$ Hz, 1H), 7.83 (s, 1H), 7.50–7.03 (m, 11H), 5.70–5.17 (m, 4H), 4.57–3.83 (m, 4H), 2.40 (s, minor) and 2.33 (s, major) (total 3H).

Representative Procedure for the $\text{BF}_3\cdot\text{Et}_2\text{O}$ -Promoted Addition of Complex 1 to Acetals. To a stirred solution of benzaldehyde dioxolane acetal (0.150 g, 1.0 mmol) and $\text{BF}_3\cdot\text{Et}_2\text{O}$ (370 μL , 3.0 mmol) in Et_2O (5 mL) at 0 $^\circ\text{C}$ under an argon atmosphere was added a solution of freshly-prepared allyliron complex 1 (3.0 mmol) in Et_2O (5 mL). The mixture was stirred at room temperature for 12 h, and a solution of NaI (0.75 g, 5 mmol) in wet acetone (10 mL) was added to the yellow suspension of the π -complex. The reaction mixture was stirred for 4 h and was evaporated. The residue was suspended in CH_2Cl_2 and filtered through a Celite pad. The filtrate was evaporated *in vacuo*, and the residue was purified by flash chromatography on silica gel to afford 0.138 g (72%) of homoallylic amine 31a as a pale yellow oil: $^1\text{H NMR}$ (400 MHz, CDCl_3) δ 7.37–7.26 (m, 5H), 5.84–5.73 (m, 1H), 5.10–5.03 (m, 2H), 4.31 (dd, $J = 7.8$, 5.8 Hz, 1H), 3.69 (dd, $J = 9.2$, 5.6 Hz, 2H), 3.48–3.44 (m, 1H), 3.42–3.37 (m, 1H), 2.63–2.55 (m, 1H), 2.46–2.39 (m, 1H), 2.24 (t, $J = 6.0$ Hz, 1H); MS (CI) m/z 193.2 ($M + 1$).

Homoallylic Ether 31b: 45% yield (0.100 g, 0.45 mmol); $^1\text{H NMR}$ (400 MHz, CDCl_3) δ 7.26–7.21 (m, 1H), 6.86–6.78 (m, 3H), 5.82–5.65 (m, 1H), 5.08–5.00 (m, 2H), 4.25 (dd, $J = 7.8$, 5.6 Hz), 3.78 (s, 3H), 3.67 (dd, $J = 9.5$, 5.0 Hz, 2H), 3.49–

(52) Rao, M. S. C.; Rao, G. S. K. *Indian J. Chem., Sect. B* 1988, 27B, 660.

(53) Katzenellenbogen, J. A.; Lenox, R. S. *J. Org. Chem.* 1973, 38, 326.

(54) Reetz, M. T. *Chem. Ber.* 1985, 118, 1441.

3.43 (m, 1H), 3.40–3.33 (m, 1H), 2.59–2.49 (m, 1H), 2.42–2.34 (m, 1H), 2.20 (t, $J = 6.0$ Hz, 1H); MS (CI) m/z 223.2 (M + 1).

Homoallylic Ether 31c: 35% yield (0.082 g, 0.35 mmol); ^1H NMR (400 MHz, CDCl_3) δ 8.17–8.13 (m, 2H), 7.66–7.63 (m, 1H), 7.56–7.52 (m, 1H), 5.81–5.71 (m, 1H), 5.09–5.03 (m, 2H), 4.46–4.43 (m, 1H), 3.74 (d, $J = 5.6$ Hz, 2H), 3.46 (d, $J = 5.6$ Hz, 2H), 2.65–2.58 (m, 1H), 2.49–2.41 (m, 1H), 2.03 (s, 1H).

Homoallylic Ether 31d: 35% yield (0.070 g, 0.35 mmol); ^1H NMR (400 MHz, CDCl_3) δ 5.88–5.78 (m, 1H), 5.11–5.06 (m, 2H), 3.70 (t, $J = 4.4$ Hz, 2H), 3.58–3.55 (m, 2H), 3.37–3.33 (m, 1H), 2.27 (t, $J = 6.4$ Hz, 2H), 1.51–1.47 (m, 2H), 1.31–1.27 (m, 8H), 0.88 (t, $J = 6.2$ Hz, 3H).

Homoallylic Ether 31e: 70% yield (0.154 g, 0.70 mmol); ^1H NMR (400 MHz, CDCl_3) δ 7.36–7.26 (m, 5H), 5.90–5.71 (m, 1H), 5.14–5.00 (m, 2H), 4.45–4.38 (m, 1H), 3.98–3.93 (m, minor) and 3.76–3.70 (m, major) (total 1H), 3.38–3.26 (m, 1H), 2.58–2.46 (m, 1H), 2.40–2.30 (m, 1H), 2.07 (s, 1H), 1.10 (d, $J = 6.0$ Hz, 3H), 1.04 (d, $J = 6.0$ Hz, 3H).

Homoallylic Ether 31f: 20% yield (0.046 g, 0.20 mmol); ^1H NMR (400 MHz, CDCl_3) δ 5.88–5.77 (m, 1H), 5.12–4.84 (m, 2H), 3.90–3.80 (m, 2H), 3.45–3.38 (m, 1H), 2.35–2.30 (m, 2H), 1.90–0.85 (m, 19H).

Analogously, homoallylic ethers **31g,h** were prepared from complex **9**, and homoallylic ethers **31i–k** were synthesized from complex **15**.

Homoallylic Ether 31g: 50% yield (0.103 g, 0.50 mmol); ^1H NMR (400 MHz, CDCl_3) δ 7.35–7.23 (m, 5H), 5.94–5.85 (m, minor) and 5.74–5.65 (m, major) (total 1H), 5.09–5.04 (m, minor) and 4.95–4.91 (m, major) (total 2H), 4.12 (d, $J = 6.8$ Hz, major) and 4.01 (d, $J = 7.7$ Hz, minor) (total 1H), 3.72–3.65 (m, 2H), 3.50–3.32 (m, 2H), 2.57–2.50 (m, 2H), 2.09 (t, $J = 6.4$ Hz, minor) and 1.99 (t, $J = 6.4$ Hz, major) (total 1H), 1.07 (d, $J = 6.8$ Hz, major) and 0.82 (d, $J = 6.8$ Hz, minor) (total 3H).

Homoallylic Ether 31h: 44% yield (0.104 g, 0.44 mmol); ^1H NMR (400 MHz, CDCl_3) δ 7.27–7.22 (m, 2H), 6.85–6.80 (m, 2H), 5.95–5.85 (m, minor) and 5.75–5.65 (m, major) (total 1H), 5.09–5.05 (m, minor) and 4.97–4.93 (m, major) (total 2H), 4.09 (d, $J = 6.8$ Hz, major) and 3.98 (d, $J = 8.8$ Hz, minor) (total 1H), 3.81 (s, minor) and 3.80 (s, major) (total 3H), 3.71–3.65 (m, 2H), 3.52–3.43 (m, 1H), 3.40–3.33 (m, 1H), 2.56–2.49 (m, 2H), 2.07 (t, $J = 6.4$ Hz, minor) and 1.98 (t, $J = 6.0$ Hz, major) (total 1H), 1.08 (d, $J = 6.8$ Hz, major) and 0.83 (d, $J = 6.8$ Hz, minor) (total 3H).

Homoallylic Ether 31i: 53% yield (0.158 g, 0.53 mmol); ^1H NMR (400 MHz, CDCl_3) δ 7.38–7.26 (m, 10H), 5.94–5.85 (m, minor) and 5.63–5.54 (m, major) (total 1H), 5.33 (d, $J = 10.0$ Hz, minor), 5.20–5.12 (m, major) (total 2H), 4.71 (d, $J = 6.0$ Hz, 1H), 4.68–3.42 (m, 6H), 2.70 (t, $J = 5.6$ Hz, major) and 2.54 (t, $J = 5.6$ Hz, minor) (total 1H), 1.70 (t, $J = 6.0$ Hz, 1H).

Homoallylic Ether 31j: 39% yield (0.128 g, 0.39 mmol); ^1H NMR (400 MHz, CDCl_3) δ 7.38–7.35 (m, 2H), 7.34–7.22 (m, 5H), 6.90–6.83 (m, 2H), 5.94–5.84 (m, minor) and 5.64–5.55 (m, major) (total 1H), 5.32 (d, $J = 10.0$ Hz, minor) and 5.22–5.14 (m, major) (total 2H), 4.71 (d, $J = 6.0$ Hz, 1H), 4.67–3.42 (m, 9H), 2.66 (t, $J = 5.6$ Hz, major) and 2.53 (t, $J = 5.6$ Hz, minor) (total 1H), 1.66 (t, $J = 5.8$ Hz, 1H).

Homoallylic Ether 31k: 25% yield (0.076 g, 0.25 mmol); ^1H NMR (400 MHz, CDCl_3) δ 7.38–7.26 (m, 5H), 5.93–5.84

(m, minor) and 5.79–5.70 (m, major) (total 1H), 5.39–5.24 (m, 2H), 4.71 (d, $J = 5.6$ Hz, 1H), 4.67–3.47 (m, 6H), 2.99–2.95 (m, 1H), 1.67 (t, $J = 6.0$ Hz, 1H), 1.38–1.26 (m, 8H), 0.88 (t, $J = 5.6$ Hz, 3H).

Homoallylic Ether 33a: 50% yield (0.110 g, 0.50 mmol); ^1H NMR (400 MHz, CDCl_3) δ 7.34–7.23 (m, 5H), 5.85–5.65 (m, 1H), 5.19–5.00 (m, 2H), 4.77–4.73 (m, minor) and 4.42–4.37 (m, major) (total 1H), 3.62–3.50 (m, 1H), 3.28–3.21 (m, minor) and 3.13–3.07 (m, major) (total 1H), 2.62–2.51 (m, 1H), 2.45–2.38 (m, 1H), 1.07 (d, $J = 6.0$ Hz, 3H), 1.01 (d, $J = 6.3$ Hz, 3H).

Homoallylic Ether 33b: 40% yield (0.100 g, 0.40 mmol); ^1H NMR (400 MHz, CDCl_3) δ 7.26–7.23 (m, 1H), 6.92–6.80 (m, 3H), 5.90–5.70 (m, 1H), 5.19–5.00 (m, 2H), 4.38–4.35 (m, 1H), 3.82 (s, minor) and 3.81 (s, major) (total 3H), 3.62–3.50 (m, 1H), 3.28–3.22 (m, minor) and 3.15–3.09 (m, major) (total 1H), 2.61–2.51 (m, 1H), 2.44–2.37 (m, 1H), 1.09 (d, $J = 6.0$ Hz, 3H), 1.04 (d, $J = 6.3$ Hz, 3H).

Homoallylic Ether 33c: 25% yield (0.057 g, 0.25 mmol); ^1H NMR (400 MHz, CDCl_3) δ 5.88–5.77 (m, 1H), 5.14–5.03 (m, 2H), 3.55–3.49 (m, 1H), 3.42–3.39 (m, 1H), 3.25–3.18 (m, 1H), 2.29–2.21 (m, 2H), 1.50–0.93 (m, 19H).

Homoallylic Ether 33d: 45% yield (0.105 g, 0.45 mmol); ^1H NMR (400 MHz, CDCl_3) δ 7.38–7.26 (m, 5H), 5.86–5.70 (m, 1H), 5.19–5.01 (m, 2H), 4.76–4.74 (m, minor) and 4.46–4.39 (m, major) (total 1H), 4.11–4.05 (m, 1H), 3.63–3.59 (m, 1H), 2.58–2.51 (m, 1H), 2.44–2.37 (m, 1H), 1.59–1.46 (m, 2H), 1.19 (d, $J = 6.0$ Hz, 3H), 1.12 (d, $J = 6.3$ Hz, 3H).

Homoallylic Ether 33e: 35% yield (0.092 g, 0.35 mmol); ^1H NMR (400 MHz, CDCl_3) δ 7.26–7.22 (m, 1H), 6.93–6.80 (m, 3H), 5.90–5.70 (m, 1H), 5.09–5.01 (m, 2H), 4.43–4.37 (m, 1H), 4.20–4.08 (m, 1H), 3.82 (s, 3H), 3.66–3.61 (m, minor) and 3.26–3.21 (m, major) (total 1H), 2.65–2.48 (m, 1H), 2.43–2.36 (m, 1H), 1.59–1.46 (m, 2H), 1.19 (d, $J = 6.0$ Hz, 3H), 1.12 (d, $J = 6.3$ Hz, 3H).

Homoallylic Ether 33f: 20% yield (0.048 g, 0.20 mmol); ^1H NMR (400 MHz, CDCl_3) δ 5.88–5.77 (m, 1H), 5.14–5.03 (m, 2H), 4.33–3.38 (m, 3H), 2.29–2.16 (m, 2H), 1.88–1.78 (m, 2H), 1.70–0.83 (m, 19H).

Acknowledgment. The donors of the Petroleum Research Fund, administered by the ACS, and the Wendy Will Case Cancer Fund are gratefully acknowledged for financial support of this research. We also thank Dr. Rosario Gonzalez for some initial studies on the reactions of **1** with imines and Dr. Dinesh Sukumaran for assistance in obtaining ^{19}F NMR spectra.

Registry No. (Supplied by Author): **7a**, [936-58-3]; **7b**, [71787-52-5]; **7c**, [14506-32-2]; **7d**, [24165-65-9]; **7e**, [24165-60-4]; **7f**, [69036-26-6]; **7g**, [36971-14-9]; **12a**, [25201-44-9]; **12c**, [83173-79-9]; **12e**, [83173-78-8] (syn isomer) and [84118-89-8] (anti isomer); **12f**, [106651-03-0] (syn isomer) and [106650-99-1] (anti isomer); **12g**, [114954-48-2]; **17a**, [81656-05-5] (syn isomer) and [81850-16-0] (anti isomer); **17f**, [110388-26-6] (syn isomer) and [110388-27-7] (anti isomer); **17h**, [120190-78-5] (syn isomer) and [120190-77-4] (anti isomer); **17m**, [120190-84-3] (syn isomer) and [120190-83-2] (anti isomer); **22a**, [40674-50-8]; **22c**, [4743-74-2]; **22d**, [79786-73-5]; **22f**, [49564-90-1]; **22g**, [1123-34-8]; **22h**, [114221-91-9] (syn isomer) and [114221-90-8] (anti isomer).

OM940818R

New Methodology for the Synthesis of Furans, Pyrrolidines, and 1,3-Polyols Using Allyl(cyclopentadienyl)iron(II) Dicarbonyl Complexes

Songchun Jiang, Ti Chen, and Edward Turos*

Department of Chemistry, State University of New York at Buffalo, Amherst, New York 14260

Received October 26, 1994[®]

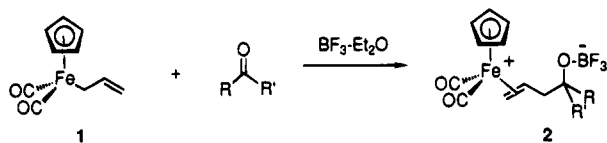
Synthetic methodology is reported for the preparation of 1,3-polyols, tetrahydrofurans, and pyrrolidines based on the Lewis acid-promoted reaction of allyl(cyclopentadienyl)iron dicarbonyl with aldehydes, ketones, and imines. The initial products of these additions are zwitterionic iron-olefin π -complexes, which can be further utilized for the construction of either acyclic (polyol) or heterocyclic (furan, pyrrolidine) structures. Methoxide and primary alkoxides add to the internal alkene center of the π -complex in a regiospecific manner to give (β -alkoxyalkyl)iron complexes, which upon stirring in methanolic ceric ammonium nitrate solution and subsequent reduction with lithium borohydride give 1,3,5-triol derivatives. Alternatively, treatment of the zwitterionic π -complex with potassium *tert*-butoxide in CH_2Cl_2 leads to formation of the furan cycloadduct by intramolecular addition of the homoallylic alkoxide to the cationic π -complex. The [3 + 2]-cycloaddition reaction of the allyliron complex with the carbonyl compound can also be executed, without isolation of the intermediate iron-olefin π -complex, using a Lewis acid catalyst. Similarly, *N*-tosylimines can be employed in the [3 + 2]-process for the synthesis of pyrrolidine esters. Of the catalysts examined, ZnCl_2 gives the best results for [3 + 2]-reactions involving aldehydes or *N*-tosylimines, while TiCl_4 is preferred for the ketone cycloadditions. The allyliron-carbonyl [3 + 2]-annulations can be effected in intramolecular fashion to provide multicyclic fused furan rings in a single synthetic operation.

Introduction

In the preceding article,¹ a new allylation procedure was described based on the BF_3 -promoted reaction of allylic (cyclopentadienyl)iron dicarbonyl complexes² with aldehydes,³ ketones,⁴ imines,⁵ and acetals.⁶ The unusual feature of this methodology is the fact that the product of the reaction retains the metal moiety in the form of a zwitterionic iron-olefin π -complex (structure 2). These investigations have explored the scope and

limitations of this reaction and provided detailed structural information about the π -adducts produced in the allylation. In this paper, we present our studies on the intermolecular and intramolecular reactions of these π -complexes with primary alkoxides and the extension of this methodology to the [3 + 2]-cycloadditions of allyliron complexes with carbonyl compounds and imines.

As a consequence of strong electron-withdrawal by the electropositive metal center, the alkene centers of cationic olefin- $\text{Fe}(\text{CO})_2\text{Cp}$ complexes 3 are rendered highly



[®] Abstract published in *Advance ACS Abstracts*, August 15, 1995.
(1) Jiang, S.; Agoston, G. E.; Chen, T.; Cabal, M.-P.; Turos, E. *Organometallics* **1995**, *14*, 4697.

(2) Green, M. L. H.; Nagy, P. L. I. *J. Chem. Soc.* **1963**, 189.

(3) Agoston, G. E.; Cabal, M. P.; Turos, E. *Tetrahedron Lett.* **1991**, *32*, 3001. This procedure provides the zwitterionic π -complex which is often contaminated with variable amounts of a co-adduct that is difficult to remove and which diminishes the efficiency of the cyclization step. This complex appears to be $\text{Fe}(\text{CO})_2\text{Cp}(\text{CH}_2=\text{CHCH}_3)^+\text{BF}_4^-$ from comparison of its ^1H -, ^{13}C -, and ^{19}F -NMR data to that of an authentic sample (ref 14, preceding paper). To minimize the formation of this impurity, an excess of the aldehyde or ketone is typically used in the allylation reaction.

(4) Jiang, S.; Turos, E. *Tetrahedron Lett.* **1991**, *32*, 4639.

(5) Chen, T.; Jiang, S.; Turos, E. *Tetrahedron Lett.* **1994**, *35*, 8325.

(6) For accounts of the chemistry of organoiron carbonyl compounds: (a) Fatiadi, A. J. *J. Res. Nat. Inst. Stand. Technol.* **1991**, *96*, 1. (b) Rosenblum, M. *J. Organomet. Chem.* **1986**, *300*, 191. (c) Rosenblum, M. *Acc. Chem. Res.* **1974**, *7*, 122. (d) Astruc, D. Use of Organoiron Compounds in Organic Synthesis. In *The Chemistry of the Carbon-Metal Bond*; Hartley, F. R., Ed.; Wiley: New York, 1987; Vol 4, Chapter 7, pp 625-731.

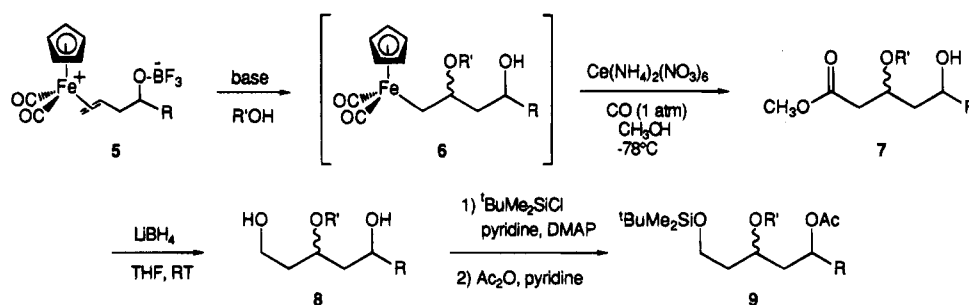
susceptible toward nucleophilic attack.⁷ Rosenblum⁸ and Busetto⁹ have independently examined the addition of heteronucleophiles and carbon nucleophiles to cationic

(7) For reviews, see: (a) Pearson, A. J. Transition Metal-Stabilized Carbocations in Organic Synthesis. In *The Chemistry of the Carbon-Metal Bond*; Hartley, F. R., Ed.; Wiley: New York, 1987; Vol. 4, Chapter 10, pp 889-980. (b) Davies, S. G.; Green, M. L. H.; Mingos, D. M. P. *Tetrahedron* **1978**, *34*, 3047.

(8) (a) Rosan, A. M.; Rosenblum, M.; Tancrede, J. *J. Am. Chem. Soc.* **1973**, *95*, 3062. (b) Lennon, P.; Madhavarao, M.; Rosan, A.; Rosenblum, M. *J. Organomet. Chem.* **1976**, *108*, 93. (c) Klemarczyk, P.; Price, T.; Priester, W.; Rosenblum, M. *J. Organomet. Chem.* **1977**, *C25*, 139. (d) Lennon, P.; Priester, W.; Rosan, A. M.; Madhavarao, M.; Rosenblum, M. *J. Organomet. Chem.* **1977**, *C29*, 139. (e) Turnbull, M. M.; Foxman, B. M.; Rosenblum, M. *Organometallics* **1988**, *7*, 200. (f) Begum, M. K.; Chu, K.-H.; Coolbaugh, T. S.; Rosenblum, M.; Zhu, X.-Y. *J. Am. Chem. Soc.* **1989**, *111*, 5252.

(9) Busetto, L.; Palazzi, A.; Ros, R.; Belluco, U. *J. Organomet. Chem.* **1970**, *25*, 207.

Scheme 1



	Isolated yields, diastereomeric ratios	
	(8)	(9)
a R = Ph; R' = CH ₃	(55%, 1.1:1)	(65% + 24% bis-silylated product)
b R = 3-NO ₂ -Ph; R' = CH ₃	(53%, 1.2:1)	(83%)
c R = 4-NO ₂ -Ph; R' = CH ₃	(47%, 1.1:1)	(77% + 2% bis-silylated product + 3% recovered alcohol)
d R = (CH ₂) ₅ CH ₃ ; R' = CH ₃	(30%, 1.1:1)	(70%)
e R = 4-NO ₂ -Ph; R' = CH ₂ Ph	(22%, 1.3:1)	(70%)
f R = 4-NO ₂ -Ph; R' = CH ₂ CH=CH ₂	(20%, 1.1:1)	(64%)

iron-olefin π -complexes and showed that the nucleophile attacks the olefin from the face opposite the metal group to afford β -substituted allyliron complexes **4**. While these additions generally work well for complexes of ethylene, propylene, or enol ethers, reactions involving more highly functionalized olefin complexes are often plagued by competitive processes such as allylic deprotonation, electron transfer, or attack of the nucleophile on the metal center. Concerned about this, we therefore set out to study the efficiency and regiochemical selectivity for the nucleophilic addition of alkoxides to zwitterionic π -complexes **5**.

Our initial attempts to add methoxide ion to π -complexes **5**³ using the published protocols^{8b,9} gave demetalated material as the only discernible product. Eventually, satisfactory conditions were found for adding methoxide (R' = CH₃) and primary alkoxides (R' = CH₂-Ph, CH₂CH=CH₂) to **5** to give (β -alkoxyalkyl)iron complexes **6** (Scheme 1). Because of their apparent instability, these crude σ -complexes **6** were treated immediately with methanolic Ce(NH₄)₂(NO₃)₆ at low temperature¹⁰ under an atmosphere of CO¹¹ to transform the iron group to a methyl ester.¹² Evaporation and flash chromatography of the crude residue gave a separable mixture of hydroxy esters **7** and their δ -lactones, which upon reduction with LiBH₄ in THF¹³ afforded diols **8**. Overall yields (from the aldehyde used to prepare **5**) and diastereomeric ratios of diols **8** are shown in Scheme 1.¹⁴ Diols **8** can be converted to triol derivatives **9** by monosilylation (TBSCl, DMAP) of the primary alcohol

followed by acetylation (Ac₂O, neat pyr) of the secondary hydroxyl group. The combined yields for these two steps are also listed in Scheme 1. The lack of diastereoselectivity of these transformations can be traced back to complex **5**, which is formed in the BF₃-promoted allylation reaction of complex **1** and aldehyde as a nearly equal mixture of facial isomers.¹ For characterization purposes, the individual diastereomers of **9e,9f** were separated by flash chromatography, but no attempt was made to assign their syn/anti stereochemistry.

The complete *regiochemical selectivity* observed for these alkoxide additions to **5** agrees with Rosenblum's earlier findings that oxygen nucleophiles add to cationic Fe(CO)₂Cp π -complexes of terminal olefins exclusively at the *internal* carbon center, apparently due to thermodynamic considerations.^{8b} We also find it noteworthy that the oxidative carboxylation of allyliron complexes **6** produces esters **7** cleanly despite the opportunity for **6** to undergo facile, acid-catalyzed β -elimination.¹⁵

During the course of these studies, we discovered that π -complexes **2** can be converted to tetrahydrofurans by treatment with KO^tBu in an *aprotic* solvent such as CH₂Cl₂ (Scheme 2). The progress of the cyclization can be monitored spectroscopically¹⁶ by observing the disappearance of the CO infrared stretching bands at 2075 and 2035 cm⁻¹ (for π -complex **2**) and the appearance of new signals at 2000 and 1945 cm⁻¹ (for σ -complex **10**). Iron furans **10** were converted directly to furan esters **11** with methanolic ceric ammonium nitrate. Overall yields of **11** from **2** are about 45% for complexes derived from aldehydes (**11a-c**), and around 20% for those prepared from ketones (**11d,e**). Roughly equal amounts of diastereomeric cycloadducts **11** are obtained in these

(10) When the oxidative CO insertion reaction is conducted at room temperature, only the demetalated homoallylic alcohol is obtained. It appears that lower temperatures disfavor the demetalation pathway and allow the esterification procedure to occur more cleanly. Reger and Mintz have observed a similar phenomenon for Ce(IV)-promoted oxidative CO insertion (Reger, D. L.; Mintz, E. *Organometallics* **1984**, *3*, 1759).

(11) (a) Nicholas, K. M.; Rosenblum, M. *J. Am. Chem. Soc.* **1973**, *95*, 4449. (b) Anderson, S. N.; Fong, C. W.; Johnson, M. D. *J. Chem. Soc., Chem. Commun.* **1973**, 163. (c) Bock, P. L.; Boschetto, D. J.; Rasmussen, J. R.; Demers, J. P.; Whitesides, G. M. *J. Am. Chem. Soc.* **1974**, *96*, 2814.

(12) Other common oxidants such as CuCl₂, Br₂, and O₂ were also tried without success, with the homoallylic alcohol being obtained in each case.

(13) The use of LiAlH₄ results in reduction of the nitro group for the nitrophenyl substrates.

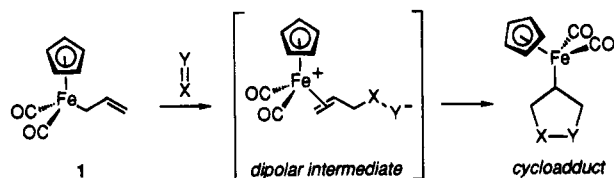
(14) If the esterification reaction is allowed to proceed for several days, dimethyl ether adducts are formed as a result of acid-catalyzed etherification of the benzylic alcohol in **7**. These compounds have been characterized on the basis of their ¹H NMR spectra, which show two methoxy ether signals near δ 3.3 and a singlet at δ 3.7 for the methyl ester. Each signal is a doublet, which indicates that the two diastereomers are formed in equal amounts.

(15) Erlacher, H. A.; Turnbull, M. M.; Chu, K.-H.; Rosenblum, M. *J. Org. Chem.* **1989**, *54*, 3012.

(16) η^1 -Allyliron dicarbonyl reagents show CO absorbances around 2010 and 1950 cm⁻¹, whereas η^2 -iron-olefin complexes characteristically absorb near 2070 and 2030 cm⁻¹.

base-promoted cyclization reactions, which is expected since π -complexes **2** are utilized as equimolar mixtures of facial isomers.¹

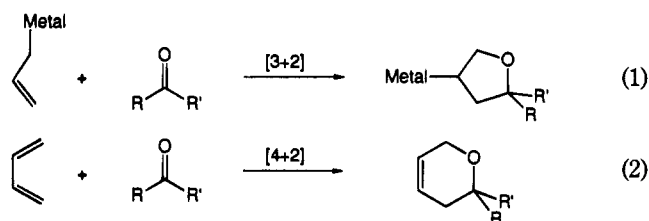
These intramolecular alkoxide additions to the cationic $\text{Fe}(\text{CO})_2\text{Cp}$ -olefin complexes offer ready access to tetrahydrofurans from carbonyl precursors. Thus, this allylation-cyclization procedure is analogous to those previously observed in reactions of **1** with activated



double bond compounds $\text{X}=\text{Y}$,⁶ which are thought to proceed through the intermediacy of a dipolar intermediate. However, only one example of such a process involving a carbonyl substrate has been reported.

To summarize, alkoxides add to the zwitterionic π -complexes **5** in a regioselective manner to afford (β -alkoxyalkyl)iron complexes. Depending on whether a protic or aprotic solvent is employed, these additions can be directed to occur through either an intermolecular or intramolecular mode to provide acyclic (polyol) or cyclic (furan) derivatives, respectively (Scheme 3).

Lewis Acid-Catalyzed [3 + 2]-Reactions. Despite the fact that furans are important structural subunits within numerous natural products and pharmaceutical agents, few methods have been reported for the direct formation of five-membered oxygen rings via the [3 + 2]-coupling of a 1,3-carbon dipole with a carbonyl compound (eq 1).¹⁷ In contrast, the analogous [4+2]-



hetero-Diels-Alder reaction^{18,19} of 1,3-dienes has found widespread popularity for the synthesis of six-membered ring heterocycles (eq 2).²⁰ With the goal of developing a general [3 + 2]-approach to furans and related heterocycles, we hoped to demonstrate the capability of Lewis acids to catalyze the allylation-cyclization procedure described above in a single operation.²¹

(17) (a) Panek, J. S.; Yang, M. *J. Am. Chem. Soc.* **1991**, *113*, 9868. (b) Danheiser, R. L.; Stoner, R. L.; Koyama, H.; Yamashita, D. S.; Klade, C. A. *J. Am. Chem. Soc.* **1989**, *111*, 4407. (c) van der Heide, T. A. J.; van der Baan, J. L.; de Kimpe, V.; Bickelhaupt, F.; Klumpp, G. W. *Tetrahedron Lett.* **1993**, *34*, 3309. (d) van der Louw, J.; van der Baan, J. L.; Stichter, H.; Out, G. J. J.; Bickelhaupt, F.; Klumpp, G. W. *Tetrahedron Lett.* **1988**, *29*, 3579. (e) Trost, B. M. *Angew. Chem., Int. Ed. Engl.* **1986**, *25*, 1.

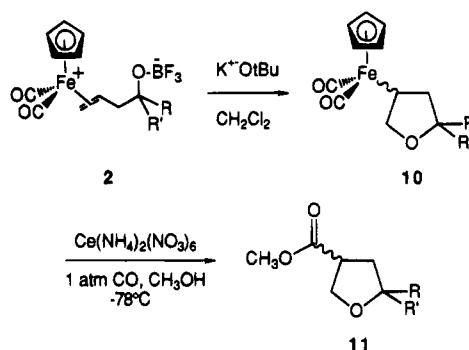
(18) (a) Danishefsky, S. J.; Pearson, W. H.; Harvey, D. F.; Maring, C. J.; Springer, J. P. *J. Am. Chem. Soc.* **1985**, *107*, 1256. (b) Danishefsky, S.; Bednarski, M. *Tetrahedron Lett.* **1985**, *26*, 2507. (c) Danishefsky, S. J.; Kerwin, J. F.; Kobayashi, S. *J. Am. Chem. Soc.* **1984**, *104*, 355. (d) Danishefsky, S. J.; Larson, E. R.; Askin, D. *J. Am. Chem. Soc.* **1982**, *104*, 6457. (e) Barluenga, J.; Aznar, F.; Cabal, M. P.; Valdes, C. *Tetrahedron Lett.* **1989**, *30*, 5923.

(19) Kerwin, J. F.; Danishefsky, S. *Tetrahedron Lett.* **1982**, *23*, 3739.

(20) *Hetero Diels-Alder Methodologies in Organic Synthesis*; Boger, D. L., Weinreb, S. M., Eds.; Academic Press: New York, 1987; Vol. 47, Chapter 4.

(21) Jiang, S.; Turos, E. *Tetrahedron Lett.* **1994**, *35*, 7889.

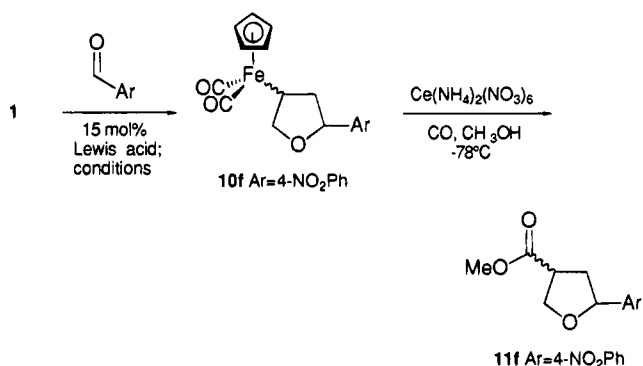
Scheme 2



Yields, trans:cis ratio of furans **11**

- | | |
|---|--|
| a | R=H, R'=Ph (45%, 1.5:1) |
| b | R=H, R'=3-NO ₂ Ph (43%, 1.2:1) |
| c | R=H, R'=3-CH ₃ OPh (45%, 1.2:1) |
| d | R=R'=(CH ₂) ₆ (19%) |
| e | R=CH ₃ , R'=Ph (20%, 1.5:1) |

To test this possibility, we first examined the reaction of 4-nitrobenzaldehyde with allyliron reagent **1** under



a variety of conditions using 15 mol % of catalyst. As above, the iron furan cycloadduct was converted directly to the methyl ester **11f** (R = H, R' = 4-NO₂Ph) using methanolic ceric ammonium nitrate. Of the Lewis acids probed to catalyze the [3 + 2]-reaction (Table 1), ZnCl_2 gives the highest yield and stereoselectivity. It is also evident that although BF_3 -etherate is the best Lewis acid for the allylation reaction,¹ it proves to be the least effective catalyst for the cycloaddition process.

We also surveyed a range of solvents and temperatures to find the best conditions for the [3 + 2]-reaction, using 4-nitrobenzaldehyde as substrate and 15 mol % ZnCl_2 as catalyst. The best yields and stereoselectivities for the formation of **11f** are obtained when the annulation is done in CH_2Cl_2 at room temperature (Table 2).

Applying this protocol to other carbonyl substrates, we determined that for reactions of aldehydes the best results are consistently obtained using 15 mol % ZnCl_2 in CH_2Cl_2 at room temperature (Table 3). While the diastereoselectivity²² of these [3 + 2]-reactions appears to be slightly better at lower temperature, the yields of furans are noticeably lower. For ketones, however, ZnCl_2 is completely ineffective at catalyzing the [3 + 2]-cycloaddition, and TiCl_4 appears to be the preferred catalyst. In a few cases, the cycloaddition was found to take place in the absence of Lewis acid, but these reactions are restricted to highly activated aromatic systems (e.g., Ar = 3-NO₂Ph or 4-NO₂Ph). Operation-

Scheme 3

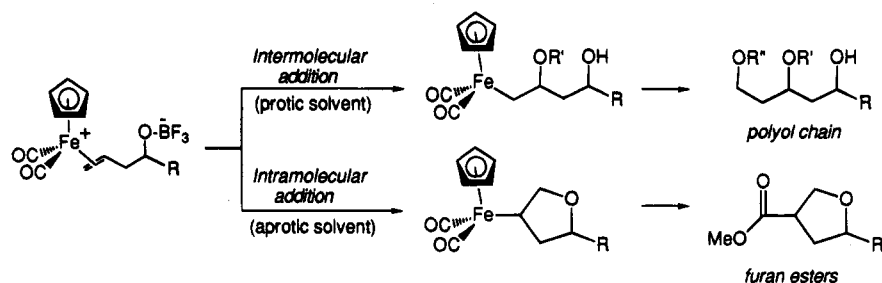


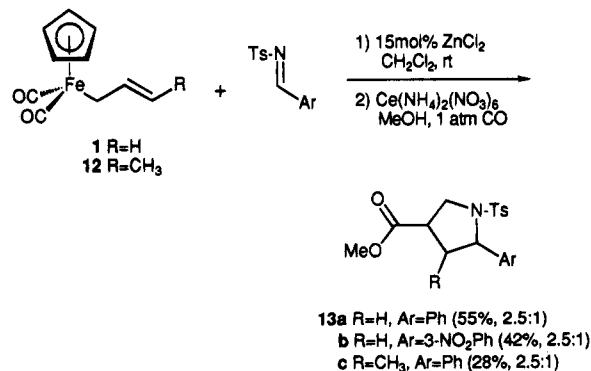
Table 1. Survey of Lewis Acid Catalysts for the [3 + 2]-Reaction of 1 With 4-Nitrobenzaldehyde (15 mol % in CH₂Cl₂ at 22 °C)

Lewis acid	time, h	% isolated yield, ^a ratio ^b
ZnCl ₂	14	71, 3.1:1
MgBr ₂	14	61, 1.6:1
SnCl ₄	15	58, 1.8:1
TiCl ₄	14	55, 2.0:1
AlBr ₃	12	45, 1.5:1
Ti(OPr) ₄	15	33, 1.9:1
BBr ₃	27	29, 1.6:1
BF ₃	28	18, 1.9:1

^a Isolated yields of furan esters after silica gel flash chromatography. ^b The trans:cis ratios were determined by integration of nonoverlapping signals in the ¹H NMR spectrum of the mixture.

ally, this catalytic Lewis acid method not only offers a more convenient procedure for effecting the [3 + 2]-annulation, since the intermediate π -complex does not have to be isolated, but, more importantly, avoids the necessity of having to use an external base to effect the final ring closure of the π -complex. This latter feature is particularly beneficial, since the efficiency of the cyclization step is highly dependent on the purity of the intermediate π -complex formed in the initial allylation reaction. Considering that this catalytic Lewis acid procedure utilizes the carbonyl compound as the limiting reagent, the relative yields of cycloadducts are considerably improved compared to those obtained from the stepwise method employing BF₃-etherate.³

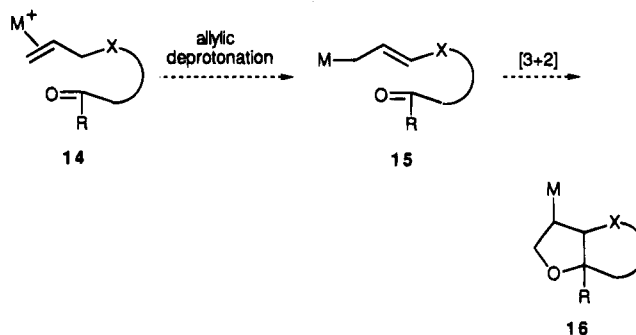
Lewis Acid-Catalyzed [3 + 2]-Reactions of Imines. This Lewis acid-catalyzed cycloaddition procedure can also be applied to *N*-tosylimines for the preparation of pyrrolidine derivatives **13**.^{23,24} Initial experiments



using **1** and the *N*-tosylimine of benzaldehyde (Ar = Ph) carried out in Et₂O gave only low yields of the cycloadduct, which we attribute to the low solubility and reactivity of the imine-Lewis acid complex in this solvent. However, these cycloadditions take place smoothly in CH₂Cl₂ solution at room temperature using 15 mol % ZnCl₂. Curiously, for the cycloaddition of

crotyliron complex **12**,² only two diastereomeric pyrrolidine esters **13** are isolated (stereochemistry not assigned).²⁵

Intramolecular [3 + 2]-Cycloadditions. The intramolecular addition of an allylmetal to a carbonyl center is a well-precedented method for constructing 1,2-vinylcycloalkanol.²⁶ Generally, the reaction takes place under Lewis acid conditions and provides the cycloadduct in high yield. We envisioned that application of our [3 + 2]-cycloaddition methodology to intramolecular systems would provide a conceptually attractive approach to the synthesis of fused furan rings **16** shown as follows:



The salient features of the approach are the ready availability of allylmetal complex **15** by allylic deprotonation²⁷ of cationic π -complex **14**, followed by the [3 + 2]-furan annulation.

To demonstrate the feasibility of this tandem cycloaddition approach, π -complex **18** was prepared by metalation²⁸ of the epoxide precursor **17**²⁹ (Scheme 4). Thus, reaction of epoxyketone **17**³⁰ with sodium (cyclopentadienyl)iron dicarboxylate in THF at 0 °C, followed by acidification with 48% fluoboric acid-acetic anhydride

(22) Semi-empirical (Spartan AM1) calculations indicate that the trans isomer of **11a** is approximately 0.3 kcal/mol more stable than the cis compound, based on their calculated heats of formation. Nuclear Overhauser enhancement (NOE) NMR studies on **11a** reveal that the major and minor products are the trans and cis stereoisomers, respectively, which show the ¹H NMR and NOE data indicated in Chart 1. For the remaining mixtures of stereoisomers **11b-e**, the major product in each case was likewise assigned to be the trans adduct on the basis of the fact that proton H_d at the carboxyl-substituted center of the ring for each of the major (trans) isomers is shifted downfield compared to the minor (cis) isomers. Thus, these cycloadducts appear to be formed as thermodynamic mixtures under these catalytic Lewis acid conditions. Additional studies are underway to determine at what stage equilibration may be taking place and how the stereochemical selectivities might be better controlled.

(23) For examples of [3 + 2]-cycloaddition reactions of imines, see: (a) Panek, J. S.; Jain, N. F. *J. Org. Chem.* **1994**, *59*, 2674. (b) Trost, B. M.; Marrs, C. M. *J. Am. Chem. Soc.* **1993**, *115*, 6636. (c) Trost, B. M.; Bonk, P. J. *J. Am. Chem. Soc.* **1985**, *107*, 1778. (d) References 13c,d.

(24) Pyrrolidines have also been prepared by BF₃-etherate-catalyzed addition of allyltrimethylsilane to α -amino aldehyde derivatives (Kiyooka, S.-i.; Shiomi, Y.; Kira, H.; Kaneko, Y.; Tanimori, S. *J. Org. Chem.* **1994**, *59*, 1958) and allyltrimethylsilane addition to an *N*-acyliminium-type species (Stahl, A.; Steckhan, E.; Nieger, M. *Tetrahedron Lett.* **1994**, *35*, 7371).

Table 2. Effect of Solvent and Temperature on the ZnCl₂-Catalyzed [3 + 2]-Reaction of 1 with 4-Nitrobenzaldehyde

solvent	temp, °C	time, h	% isolated yield, ^a ratio ^b
CH ₂ Cl ₂	22	14	71, 3.1:1
	-20	24	41, 3.5:1
	-78	37	25, 3.4:1
THF	22	14	40, 2.5:1
	-20	22	2, 1.9:1
hexane	22	14	34, 1.8:1
	-20	21	21, 2.3:1
Et ₂ O	22	13	29, 2.0:1
	-20	20	8, 1.9:1
benzene	22	14	22, 2.0:1
toluene	-20	23	3, 1.5:1

^a Isolated yields of furan esters after flash chromatography on silica gel. ^b The trans:cis ratios were determined by integration of nonoverlapping signals in the ¹H NMR spectrum of the mixture.

and dilution with Et₂O, provided π -complex **18** as a yellow precipitate in 70% yield.³¹ Treatment of π -complex **18** with a slight molar excess of Et₃N at 0 °C in CH₂Cl₂ gives allyliron complex **19** in 73% yield, which upon isolation by evaporation was treated with 15 mol % ZnCl₂ in CH₂Cl₂ at -20 °C to effect the cyclization. After 24 h, the crude mixture containing the iron furan was then added to a methanolic solution of ceric ammonium nitrate (5 equiv) at -78 °C under an atmosphere of CO. After evaporation and flash chromatography of the crude material, tricyclic furan esters **20** were obtained as a 2.3:1 mixture of epimers in 42% combined yield (30% combined overall yield from π -adduct **18**).³² Efforts are now underway to utilize this tandem cyclization strategy for the synthesis of multi-

cyclic fused ring systems having different ring sizes and heteronuclei within the skeleton.

To summarize our results, we have found that primary alkoxides add regiospecifically to the internal alkene center of iron-olefin π -complexes **2** to afford 1,3,5-triol derivatives. By carrying out these additions in an aprotic solvent, the zwitterionic salts can be cyclized to a furan adduct using a mild base to cleave the O-BF₃ linkage. The [3 + 2]-cycloaddition of allyliron complexes with carbonyl compounds and imines may be carried out in the presence of an appropriate Lewis acid catalyst. Intramolecular allyliron-ketone cycloadditions can be effected to construct multicyclic furan frameworks in a single step. Ongoing investigations in our laboratory are focusing on applications of this [3 + 2]-methodology to the synthesis of selected heterocyclic structures common to those in naturally occurring compounds.

Experimental Section

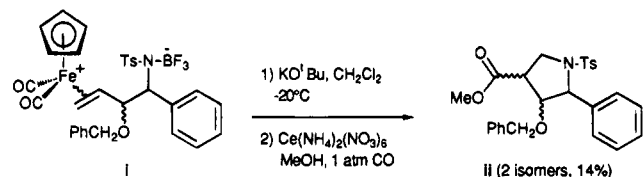
All reactions were performed under an argon atmosphere using glassware and syringes that were predried overnight in an oven at 120 °C and assembled while still hot. The aldehydes and ketones were purchased (Aldrich Chemical Co.) and used without further purification. *N*-Tosylimines were prepared by refluxing the aldehyde with *N*-toluenesulfonamide in benzene or toluene in the presence of a catalytic amount of *p*-toluenesulfonic acid. Benzyl alcohol and allyl alcohol were vacuum distilled immediately prior to use. Potassium *tert*-butoxide was sublimed under vacuum. The allylic (cyclopentadienyl)iron(II) dicarbonyl complexes **1** and **12** were prepared as described² by Green and Nagy, except that the final purification step (alumina column chromatography) was omitted. THF and Et₂O were distilled immediately prior to use from Na/benzophenone under argon. CH₂Cl₂, benzene, toluene, and hexane were freshly distilled from CaH₂ under N₂, and CH₃OH was distilled from Mg⁰ under argon. Flash chromatography was performed using J. T. Baker flash chromatography silica gel (40 μ m). TLC was carried out using EM Reagents plates with fluorescence indicator (SiO₂-60, F-254). ¹H NMR spectra were recorded using a Varian 400 NMR instrument at 400 MHz in CDCl₃. ¹³C NMR spectra were recorded using a Varian Gemini 300 NMR spectrometer at 75 MHz in CDCl₃. IR spectra were measured on a Perkin-Elmer 1310 spectrophotometer as a thin film on NaCl plates. Mass spectra were run using chemical ionization (CI) or fast-atom bombardment (FAB) ionization. Combustion analyses were performed by Atlantic Microlabs (Atlanta, GA).

Representative Procedure for the Preparation of Diols 8a-d. To a solution of 3-nitrobenzaldehyde (151 mg, 1.0 mmol) and BF₃-etherate (0.250 mL, 2 mmol) in anhydrous Et₂O (10 mL) at rt (rt = room temperature) is added a freshly prepared solution of **1** (5 mL, 0.5 M, 2.5 mmol) in anhydrous Et₂O. The mixture is stirred at rt for 3 h and evaporated *in vacuo*. The residue is dissolved in CH₃OH (10 mL), and anhydrous K₂CO₃ (207 mg, 1.5 mmol) is added at 0 °C. The

(31) Iron-olefin π -complex **18** gave the following spectral data: the ¹H NMR spectrum shows a singlet at 5.90 ppm for the Cp protons and signals at 5.28, 4.05, and 3.63 ppm for the vinyl protons; the ¹³C NMR spectrum gives resonances at δ 217.1 (ketone), 210.2 and 208.8 (C=O), and 89.5 (Cp); twin metal C=O stretching bands are observed at 2070 and 2030 cm⁻¹ and a C=O ketone stretch appears at 1695 cm⁻¹ in the infrared spectrum; the FAB mass spectrum shows signals of M-BF₄ (357.0) and Fp⁺ (177.0).

(32) We have assigned these products to be epimeric esters each having the cis-cis fused ring skeleton, which molecular modeling calculations (Spartan AM1 semi-empirical, gas phase) predict is favored over the cis-trans [5.5.7]-fused system by approximately 1.5 kcal/mol. Of the two epimeric structures shown in Chart 2, the major isomer is about 2 kcal/mol more stable according to the calculated gas phase heats of formation. ¹H-decoupling NMR and ¹H NOE difference data that support these assignments are also shown in Chart 2.

(25) A similar outcome was observed for the cyclization of zwitterionic π -adducts **i** prepared from complex **15** using the BF₃-etherate procedure.



Thus, treatment of the diastereomeric mixture of π -complexes with potassium *tert*-butoxide in CH₂Cl₂, followed by esterification with methanolic ceric ammonium nitrate, gave only two cycloadducts **ii** in 14% combined yield (stereochemistry undetermined). We believe that two of the diastereomeric π -complexes can cyclize without difficulty, while the other two isomeric forms may have severe steric interactions within the transition state that prevent cyclization.

(26) (a) Denmark, S. E.; Weber, E. J. *Helv. Chim. Acta* **1983**, *66*, 1655. (b) Denmark, S. E.; Weber, E. J. *J. Am. Chem. Soc.* **1984**, *106*, 7970. (c) Denmark, S. E.; Henke, B. R.; Weber, E. J. *J. Am. Chem. Soc.* **1987**, *109*, 2512. (d) Lee, T. V.; Roden, F. S.; Yeoh, H. T.-L. *Tetrahedron Lett.* **1990**, *31*, 2063. (e) Lee, T. V.; Roden, F. S. *Tetrahedron Lett.* **1990**, *31*, 2067. (f) Nishitani, K.; Yamakawa, K. *Tetrahedron Lett.* **1991**, *32*, 387. (g) Marshall, J. A.; DeHoff, B. S.; Crooks, S. L. *Tetrahedron Lett.* **1987**, *28*, 527. (h) Marshall, J. A.; Gung, W. Y. *Tetrahedron Lett.* **1988**, *29*, 1657. (i) Marshall, J. A.; Markwalder, J. A. *Tetrahedron Lett.* **1988**, *29*, 4811. (j) Marshall, J. A.; Gung, W. Y. *Tetrahedron Lett.* **1989**, *30*, 2183. (k) Marshall, J. A.; Welmaker, G. S.; Gung, B. W. *J. Am. Chem. Soc.* **1991**, *113*, 647. (l) Asao, K.; Iio, H.; Tokoroyama, T. *Tetrahedron Lett.* **1989**, *30*, 6397. (m) Gevorgyan, V.; Kadota, I.; Yamamoto, Y. *Tetrahedron Lett.* **1993**, *34*, 1313.

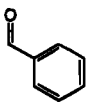
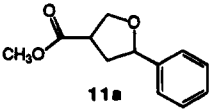
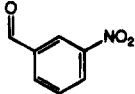
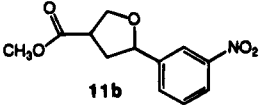
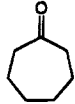
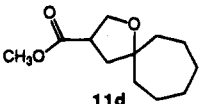
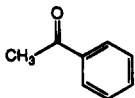
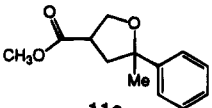
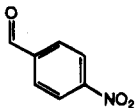
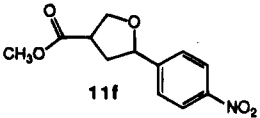
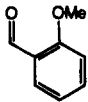
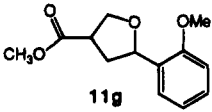
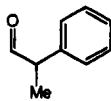
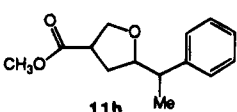
(27) Cutler, A.; Ehntholt, D.; Lennon, P.; Nicholas, K.; Marten, D. F.; Madhavarao, M.; Raghun, S.; Rosan, A.; Rosenblum, M. *J. Am. Chem. Soc.* **1975**, *97*, 3149.

(28) Giering, W. P.; Rosenblum, M.; Tancrede, J. *J. Am. Chem. Soc.* **1972**, *94*, 7170.

(29) Alternatively, π -complex **18** can be obtained by refluxing a solution of Fe(CO)₂Cp-isobutylene fluoborate with the olefin in CH₂Cl₂.

(30) Epoxy ketone **17** was prepared from cycloheptanone in three steps: (1) cyclohexylamine, PhH, pTsOH, reflux (90%); (2) LDA, THF, -78 °C, and then HMPA and 5-bromopent-1-ene (83%); (3) mCPBA, CH₂Cl₂ (83%).

Table 3. [3 + 2]-Cycloaddition Reactions of Iron Complex 1 and Carbonyl Compounds

Carbonyl Compound	Product	Reaction conditions	% yield ^a , ratio ^b
		ZnCl ₂ (15 mol%), CH ₂ Cl ₂ , RT	36% (2.1:1)
		ZnCl ₂ (100 mol%), CH ₂ Cl ₂ , RT	40% (1.1:1)
		no Lewis acid, CH ₂ Cl ₂ , RT	8% (1.8:1)
		ZnCl ₂ (15 mol%), CH ₂ Cl ₂ , RT	62% (2.7:1)
		no Lewis acid, CH ₂ Cl ₂ , RT	45% (1.9:1)
		ZnCl ₂ (100 mol%), CH ₂ Cl ₂ , RT	0%
		TiCl ₄ (200 mol%), CH ₂ Cl ₂ , -78°C	37%
		ZnCl ₂ (100 mol%), CH ₂ Cl ₂ , RT	0%
		TiCl ₄ (200 mol%), CH ₂ Cl ₂ , -78°C	15% (1.0:1)
		ZnCl ₂ (15 mol%), CH ₂ Cl ₂ , RT	71% (3.1:1)
		ZnCl ₂ (100 mol%), CH ₂ Cl ₂ , RT	50% (1.1:1)
		no Lewis acid, CH ₂ Cl ₂ , RT	60% (1.9:1)
		ZnCl ₂ (15 mol%), CH ₂ Cl ₂ , RT	31% (2.0:1)
		ZnCl ₂ (100 mol%), CH ₂ Cl ₂ , RT	28% (1.2:1)
		ZnCl ₂ (100 mol%), CH ₂ Cl ₂ , RT	16% ^c
		TiCl ₄ (200 mol%), CH ₂ Cl ₂ , -78°C	15% ^c

^a Isolated yields after flash chromatography on silica gel.

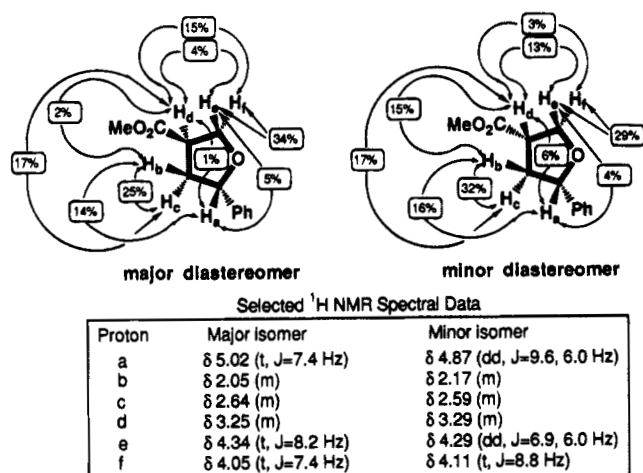
^b Ratios determined by integration of non-overlapping signals in the ¹H NMR spectrum.

^c Ratios not determined due to overlapping signals in the ¹H NMR spectrum.

mixture is stirred vigorously at 0 °C for 1 h. The progress of the reaction is followed by periodically removing a small aliquot and observing the disappearance of the twin CO infrared stretching bands at 2075 and 2035 cm⁻¹ for the π -complex and the appearance of new signals at 2000 and 1945 cm⁻¹ for the σ -complex. The reaction typically reaches completion within 1 h, at which time the reaction mixture is transferred dropwise over a 30 min period to a solution of ceric ammonium nitrate (4.1 g, 7.5 mmol) in CH₃OH (20 mL) at -78 °C under a CO atmosphere. After the solution is stirred at -78 °C for an additional 30 min, the solvent is warmed to rt and allowed to stir for an additional 30 min and then evaporated *in vacuo*. The residue is dissolved in H₂O (15 mL) and extracted with Et₂O (5 \times 15 mL). The combined ethereal layers are washed with brine (15 mL) and saturated NaHCO₃, dried over anhydrous MgSO₄, and evaporated. The crude product is dissolved in THF (10 mL) and treated with LiBH₄ (109 mg, 5 mmol) at rt for 12 h. The reaction is quenched by the addition of H₂O (10 mL), and the mixture is adjusted to pH 4 using 1 N HCl and extracted with CH₂Cl₂ (5 \times 20 mL). The organic layer is washed with brine (15 mL), dried over

anhydrous MgSO₄, and evaporated. Flash chromatography (acetone/CH₂Cl₂) of the mixture gives 136 mg (53%, 1.2:1 mixture of diastereomers) of diol **8b**. ¹H NMR (400 MHz, CDCl₃): isomer 1, δ 8.27 (s, 1H), 8.13 (d, J = 7.8 Hz, 1H), 7.71 (d, J = 7.8 Hz, 1H), 7.52 (t, J = 7.8 Hz, 1H), 5.14 (d, J = 7.8 Hz, 1H), 3.81 (m, 2H), 3.71 (m, 1H and OH), 3.45 (s, 3H), 2.09–2.00 (m, 1H), 2.00–1.83 (m, 3H and OH); isomer 2, δ 8.25 (s, 1H), 8.13 (d, J = 8.8 Hz, 1H), 7.73 (d, J = 7.8 Hz, 1H), 7.52 (dd, J = 7.8, 8.8 Hz, 1H), 5.01 (dd, J = 2.0, 9.8 Hz, 1H), 4.10 (s, OH), 3.81 (m, 2H), 3.75 (m, 1H), 3.47 (s, 3H), 2.05–1.80 (m, 4H), 1.77 (br s, OH). ¹³C NMR (75 MHz, CDCl₃) (mixture of diastereomers): δ 149.0, 149.0, 147.8, 147.5, 132.5, 132.3, 129.9, 122.9, 122.7, 121.3, 121.1, 79.9, 72.9, 70.8, 59.9, 59.5, 57.4, 56.7, 43.4, 42.2, 35.3, 35.4. IR (neat film) (mixture of diastereomers): 3420 (br), 3064, 2944, 1530, 1350, 1263, 1067, 728, 698 cm⁻¹. MS (CI, isobutane) (mixture of diastereomers): m/z 238 (M + 1 - H₂O, 33), 207 (12), 206 (100), 194 (26), 190 (11), 188 (23), 169 (11), 162 (12), 152 (28), 150 (61), 149 (17), 136 (11). HRMS (CI, isobutane) (mixture of diastereomers): calculated for C₁₂H₁₆NO₄ (M + 1 - H₂O), 238.1079; found 238.1053.

Chart 1



Diol 8a: 55% yield (115 mg, 0.55 mmol, 1.1:1). ¹H NMR (400 MHz, CDCl₃): isomer 1, δ 7.39–7.27 (m, 5H), 4.98 (dd, *J* = 3.6, 6.8 Hz, 1H), 3.85–3.71 (m, 2H), 3.68 (m, 1H), 3.43 (s, 3H), 3.08 (br s, OH), 2.02–1.90 (m, 2H), 1.87 (m, 2H), 1.60 (br s, OH); isomer 2, δ 7.39–7.27 (m, 5H), 4.87 (dd, *J* = 3.6, 9.2 Hz, 1H), 3.81 (m, 1H), 3.76–3.67 (m, 2H), 3.43 (s, 3H), 2.12–1.74 (m, 4H and 2OH). ¹³C NMR (75 MHz, CDCl₃) (mixture of diastereomers): δ 145.4, 145.2, 129.0, 128.1, 127.9, 126.3, 126.1, 80.0, 78.2, 73.5, 71.7, 60.2, 60.0, 57.3, 56.7, 43.3, 42.5, 35.8, 35.5. IR (neat film) (mixture of diastereomers): 3380 (br), 2950, 1450, 1370, 1060, 750, 695 cm⁻¹. MS (CI, isobutane) (mixture of diastereomers): *m/z* 193 (*M* + 1 – H₂O, 18), 178 (20), 177 (9), 163 (14), 162 (18), 161 (100), 160 (52), 159 (20), 149 (57), 147 (13), 145 (45), 143 (19), 133 (12), 131 (24), 129 (15), 117 (47), 115 (18), 107 (43), 105 (47), 104 (35). HRMS (CI, isobutane) (mixture of diastereomers): calcd for C₁₂H₁₇O₂ (*M* + 1 – H₂O), 193.1229; found, 193.1236.

Diol 8c: 47% yield (120 mg, 0.47 mmol, 1.1:1). ¹H NMR (400 MHz, CDCl₃): isomer 1, δ 8.21 (d, *J* = 8.8 Hz, 2H), 7.55 (d, *J* = 8.8 Hz, 2H), 5.01 (dd, *J* = 2.0, 9.6 Hz, 1H), 4.11 (s, OH), 3.85–3.69 (m, 3H), 3.47 (s, 3H), 2.01–1.80 (m, 4H), 1.77 (s, OH); isomer 2, δ 8.21 (d, *J* = 8.8 Hz, 2H), 7.54 (d, *J* = 8.8 Hz, 2H), 5.13 (d, *J* = 8.8 Hz, 1H), 3.79 (m, 2H), 3.72 (s, OH), 3.68 (m, 1H), 3.43 (s, 3H), 2.07–1.82 (m, 4H and OH). ¹³C NMR (75 MHz, CDCl₃) (mixture of diastereomers): δ 153.0, 152.7, 147.8, 147.8, 127.0, 126.9, 124.2, 80.0, 77.9, 73.0, 71.0, 59.9, 59.6, 57.3, 56.7, 43.4, 42.2, 35.4. IR (neat film) (mixture of diastereomers): 3380 (br), 2940, 1515, 1344, 1067, 851 cm⁻¹. MS (CI, isobutane) (mixture of diastereomers): *m/z* 256 (*M* + 1, 2), 238 (*M* + 1 – H₂O, 33), 208 (43), 207 (25), 206 (100), 194 (22), 176 (26), 152 (16), 150 (36), 122 (17), 120 (11), 115 (12), 106 (16). HRMS (CI, isobutane) (mixture of diastereomers): calcd for C₁₂H₁₆NO₄ (*M* + 1 – H₂O), 238.1079; found, 238.1072.

Diol 8d: 30% yield (66 mg, 0.30 mmol, 1.1:1). ¹H NMR (400 MHz, CDCl₃) (mixture of diastereomers): δ 3.9–3.62 (m, 4H), 3.42 (s) and 3.41 (s) (total 3H), 2.55 (br, OH), 2.15 (br, OH), 1.95–1.20 (m, 14H), 0.88 (t, *J* = 6.0 Hz, 3H). ¹³C NMR (75 MHz, CDCl₃) (mixture of diastereomers): δ 80.3, 78.3, 71.1, 69.2, 60.2, 59.9, 57.2, 56.7, 40.9, 40.1, 38.2, 38.2, 36.0, 35.7, 32.0, 29.5, 25.8, 25.6, 22.8, 14.2. IR (neat film) (mixture of diastereomers): 3360 (br), 2940, 1865, 1460, 1374, 1185, 1075 cm⁻¹. MS (CI, isobutane) (mixture of diastereomers): *m/z* 219 (*M* + 1, 40), 202 (6), 201 (47), 199 (6), 175 (9), 171 (14), 170 (12), 169 (100), 158 (10), 157 (88), 151 (18), 149 (14), 139 (5), 131 (11), 115 (11), 109 (6). HRMS (CI, isobutane) (mixture of diastereomers): calcd for C₁₂H₂₇O₃ (*M* + 1), 219.1960; found, 219.1908.

Representative Procedure for the Preparation of Diols 8e–f. To a solution of 4-nitrobenzaldehyde (151 mg, 1.0 mmol) and BF₃-etherate (0.250 mL, 2 mmol) in anhydrous Et₂O (10 mL) at rt is added a 0.5 M solution of **1** (5 mL, 2.5 mmol) in anhydrous Et₂O. The mixture is stirred at rt for 3 h and evaporated *in vacuo*. The residue is dissolved in benzyl

alcohol (20 mL) (or allyl alcohol), and a mixture of NaH (80 mg, 60% in mineral oil, 2 mmol) in benzyl alcohol (5 mL) (or allyl alcohol) is added dropwise to the solution at 0 °C over 10 min. After being stirred vigorously at 0 °C for 1 h, the mixture is transferred dropwise over a 30 min period to a solution of ceric ammonium nitrate (4.1 g, 7.5 mmol) in CH₃OH (20 mL) at –78 °C under a CO atmosphere. The mixture is stirred at –78 °C for 30 min and at rt for an additional 30 min. The solvent is concentrated *in vacuo* to half-volume, mixed with water (15 mL), and extracted with Et₂O (5 × 15 mL). The combined ethereal layers are washed with brine (15 mL) and saturated NaHCO₃ (2 × 10 mL), dried over anhydrous MgSO₄, and concentrated to remove the ether. The remaining liquid is diluted with THF (10 mL) and treated with LiBH₄ (109 mg, 5 mmol) at rt for 12 h. The reaction is quenched by the addition of H₂O (15 mL), and the mixture is adjusted to pH 4 using 1 N HCl and extracted with CH₂Cl₂ (5 × 15 mL). The organic layer is washed with brine (15 mL), dried over anhydrous MgSO₄, and evaporated *in vacuo* (maintaining the pot temperature below 85 °C). Purification of the crude product by successive flash chromatography (acetone/CH₂Cl₂) gives 73 mg (22%, 1.3:1 mixture of diastereomers) of diol **8e**. ¹H NMR (400 MHz, CDCl₃) (mixture of diastereomers): δ 8.18 (overlapping d, *J* = 8.8 Hz, 2H), 7.50 (overlapping d, *J* = 8.8 Hz, 2H), 7.37 (m, 5H), 5.09 (dd, *J* = 2.9, 5.8 Hz) and 4.98 (dd, *J* = 2.0, 8.8 Hz) (total 1H), 4.74–4.53 (m, 2H), 4.06–3.90 (m, 1H), 3.85–3.70 (m, 2H), 4.02 (s) and 3.40 (d, *J* = 3.0 Hz) (total 1H, OH), 2.06–1.84 (m, 4H), 1.17 (m, OH). ¹³C NMR (75 MHz, CDCl₃) (mixture of diastereomers): δ 153.0, 152.7, 147.8, 147.7, 138.4, 138.1, 129.2, 128.7, 128.6, 127.1, 126.9, 124.2, 75.3, 72.8, 72.0, 71.5, 70.8, 59.8, 59.5, 43.7, 42.8, 36.1, 36.0. IR (neat film) (mixture of diastereomers): 3400 (br), 2958, 2886, 1661, 1517, 1345, 1263, 1060, 850, 730, 692 cm⁻¹. MS (CI, isobutane) (mixture of diastereomers): *m/z* 314 (*M* + 1 – H₂O, 10), 296 (25), 284 (39), 268 (10), 224 (33), 223 (10), 222 (23), 210 (19), 208 (17), 207 (12), 206 (51), 204 (27), 196 (20), 193 (10), 192 (25), 190 (29), 189 (18), 188 (19), 184 (11), 178 (47), 177 (16), 176 (50), 176 (26), 175 (15), 174 (58), 165 (14), 160 (47), 159 (20), 158 (18), 152 (17), 150 (44), 146 (29), 145 (14), 144 (10), 138 (11), 132 (11), 129 (12), 122 (21), 120 (20), 108 (15), 108 (17), 107 (100), 106 (27). HRMS (CI, isobutane) (mixture of diastereomers): calcd for C₁₈H₂₀NO₄ (*M* + 1 – H₂O), 314.1392; found, 314.1375.

Diol 8f: 20% yield (57 mg, 0.20 mmol, 1.1:1). ¹H NMR (400 MHz, CDCl₃) (mixture of diastereomers): δ 8.21 (overlapping d, *J* = 8.8 Hz, 2H), 7.55 (d, *J* = 8.0 Hz, 2H), 5.95 (m, 1H), 5.36–5.23 (m, 2H), 5.15–5.01 (m, 1H), 4.23–3.92 (m, 3H), 3.90–3.70 (m, 2H), 3.63 (s, OH), 2.04–1.84 (m, 4H), 1.79 (s) and 1.74 (s) (total 1H, OH). ¹³C NMR (75 MHz, CDCl₃) (mixture of diastereomers): δ 152.9, 152.6, 147.9, 147.8, 134.8, 134.6, 127.0, 126.9, 124.2, 118.5, 118.2, 78.1, 75.9, 73.2, 70.9, 70.9, 70.3, 60.0, 59.6, 43.7, 42.4, 36.0, 35.9. IR (neat film) (mixture of diastereomers): 3400 (br), 2930, 2880, 1602, 1516, 1420, 1345, 1070, 920, 852, 723, 694 cm⁻¹. MS (CI, isobutane) (mixture of diastereomers): *m/z* 282 (*M* + 1, 2), 264 (*M* + 1 – H₂O, 13), 234 (8), 224 (5), 212 (42), 208 (17), 207 (5), 206 (28), 194 (11). HRMS (CI, isobutane) (mixture of diastereomers): calcd for C₁₄H₁₈NO₄ (*M* + 1 – H₂O), 264.1236; found, 264.1368.

Representative Procedure for the Silylation and Acetylation of Diols 8. A solution of diol **8b** (128 mg, 0.5 mmol) in CH₂Cl₂ is treated with ^tBuMe₂SiCl (226 mg, 1.5 mmol), pyridine (240 μL, 3.0 mmol), and DMAP (6 mg, 0.05 mmol) and is allowed to stir for 24 h and then evaporated *in vacuo*. The crude product is dissolved in a mixture of pyridine (10 mL) and Ac₂O (2.4 mL, 25 mmol), stirred for 12 h, and evaporated *in vacuo*. The residue is taken up in Et₂O (30 mL) and washed with 10% CuSO₄ (2 × 5 mL) and brine (10 mL), dried over MgSO₄, and evaporated. Flash chromatography (acetone/CH₂Cl₂) of the impure oil gives 170 mg of triol derivative **9b** (83% from the diol, 1.3:1 mixture of diastereomers). ¹H NMR (400 MHz, CDCl₃) (mixture of diastereomers): δ 8.23 (s) and 8.21 (s) (total 1H), 8.15 (overlapping d, *J* = 7.8 Hz, 1H), 7.67 (overlapping d, *J* = 6.8 Hz, 1H),

Scheme 4

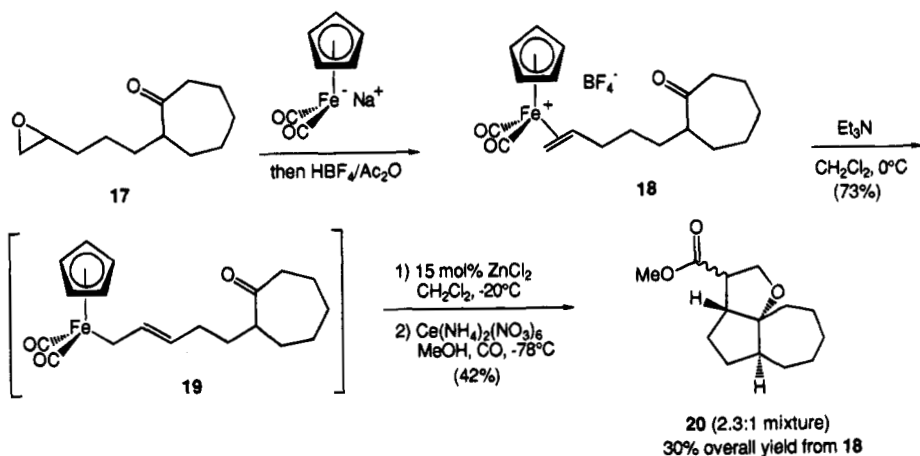
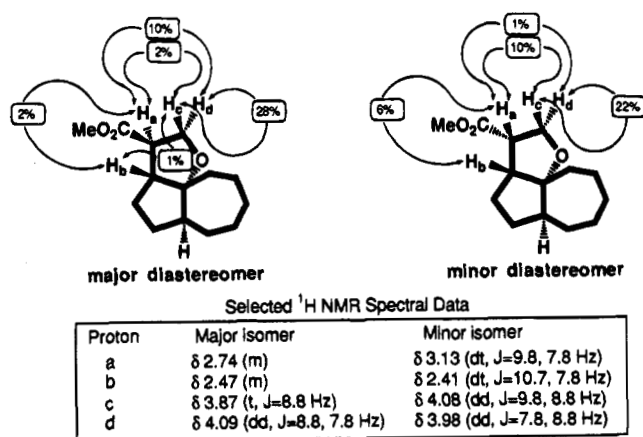


Chart 2



7.51 (m, 1H), 6.01 (dd, $J = 2.9, 10.6$ Hz) and 5.96 (t, $J = 7.3$ Hz) (total 1H), 3.73–3.58 (m, 2H), 3.47 (m) and 3.19 (m) (total 1H), 3.34 (s) and 3.26 (s) (total 3H), 2.22 (m) and 1.93 (m) (total 1H), 2.11 (s) and 2.08 (s) (total 3H), 1.79 (m, 2H), 1.64 (m, 1H), 0.88 (s) and 0.81 (s) (total 9H), 0.05 to -0.02 (m, 6H). ^{13}C NMR (75 MHz, CDCl_3) (mixture of diastereomers): δ 170.7, 170.6, 149.1, 144.2, 143.5, 133.6, 133.2, 130.1, 130.0, 123.4, 123.3, 122.1, 121.6, 75.0, 74.8, 73.1, 72.3, 59.5, 59.4, 57.6, 56.2, 42.4, 40.7, 37.1, 36.4, 26.0, 26.0, 21.2, 21.2, 18.3, 18.3, -5.3 , -5.4 . IR (neat film) (mixture of diastereomers): 2940, 2864, 1745, 1633, 1532, 1464, 1349, 1230, 1088, 1019, 832, 803, 773 cm^{-1} . MS (CI, isobutane) (mixture of diastereomers): m/z 412 ($M + 1$, 1), 322 (19), 291 (14), 290 (65), 264 (10), 232 (17), 203 (29), 190 (16), 160 (18), 159 (10), 158 (46), 146 (15), 145 (20), 133 (22), 132 (100), 120 (13), 119 (11). HRMS (CI, isobutane) (mixture of diastereomers): calcd for $\text{C}_{20}\text{H}_{34}\text{NO}_6\text{Si}$ ($M + 1$), 412.2155; found, 412.2163. Anal. Calcd for $\text{C}_{20}\text{H}_{33}\text{NO}_6\text{Si}$: C, 58.37; H, 8.08; N, 3.40. Found: C, 58.50; H, 8.16; N, 3.41.

Triol Derivative 9a: 65% yield (120 mg, 0.33 mmol). ^1H NMR (400 MHz, CDCl_3) (mixture of diastereomers): δ 7.36–7.32 (m, 5H), 5.94 (dd, $J = 4.0, 10.8$ Hz) and 5.88 (t, $J = 7.4$ Hz) (total 1H), 3.74–3.58 (m, 2H), 3.42 (m) and 3.20 (m) (total 1H), 3.33 (s) and 3.26 (s) (total 3H), 2.20 (m) and 1.92–1.60 (m) (total 4H), 2.07 (s) and 2.04 (s) (total 3H), 0.89 (s) and 0.84 (s) (total 9H), 0.05 to -0.01 (m, 6H). ^{13}C NMR (75 MHz, CDCl_3) (mixture of diastereomers): δ 170.9, 170.8, 141.8, 141.1, 129.1, 128.5, 128.4, 127.4, 126.9, 75.2, 75.1, 74.2, 73.3, 59.6, 59.5, 57.6, 56.4, 42.2, 40.9, 37.4, 36.9, 26.1, 21.5, 21.4, 18.4, 18.4, -5.3 , -5.3 . IR (neat film) (mixture of diastereomers): 2935, 2864, 1740, 1633, 1460, 1365, 1234, 1085, 1014, 831, 770 cm^{-1} . MS (CI, isobutane) (mixture of diastereomers): m/z 307 ($M + 1 - \text{CH}_3\text{CO}_2\text{H}$, 5), 276 (21), 275 (91), 203 (41), 191 (24), 149 (26), 145 (16), 143 (17), 118 (11), 117 (100), 115 (10). HRMS (CI, isobutane) (mixture of dia-

stereomers): calcd for $\text{C}_{18}\text{H}_{31}\text{O}_2\text{Si}$ ($M + 1 - \text{CH}_3\text{CO}_2\text{H}$), 307.2093; found, 307.2062.

Triol Derivative 9c: 77% yield (158 mg, 0.38 mmol). ^1H NMR (400 MHz, CDCl_3) (mixture of diastereomers): δ 8.20 (overlapping d, $J = 8.8$ Hz, 2H), 7.50 (overlapping d, $J = 8.8$ Hz, 2H), 5.99 (dd, $J = 2.8, 10.6$ Hz) and 5.94 (t, $J = 6.8$ Hz) (total 1H), 3.74–3.58 (m, 2H), 3.47 (m) and 3.19 (m) (total 1H), 3.34 (s) and 3.25 (s) (total 3H), 2.21 (m) and 1.91 (m) (total 1H), 2.11 (s) and 2.07 (s) (total 3H), 1.86–1.70 (m, 2H), 1.63 (m, 1H), 0.88 (s) and 0.82 (s) (total 9H), 0.05 to -0.02 (m, 6H). ^{13}C NMR (75 MHz, CDCl_3) (mixture of diastereomers): δ 170.7, 170.6, 149.3, 148.6, 148.2, 148.1, 128.1, 127.5, 124.4, 124.3, 74.9, 74.8, 73.1, 72.4, 59.5, 59.4, 57.6, 56.2, 42.3, 40.6, 37.0, 36.4, 26.0, 26.0, 21.2, 21.1, 18.3, 18.3, -5.3 , -5.4 . IR (neat film) (mixture of diastereomers): 2935, 2864, 1744, 1607, 1524, 1463, 1345, 1229, 1090, 832, 772 cm^{-1} . MS (CI, isobutane) (mixture of diastereomers): m/z 412 ($M + 1$, 5), 352 (16), 322 (14), 320 (16), 292 (12), 291 (26), 290 (100), 264 (19), 204 (12), 203 (62), 188 (11), 176 (10), 160 (15), 159 (11), 158 (19), 150 (15), 146 (16), 145 (44), 133 (31), 132 (13), 119 (28), 106 (24). HRMS (CI, isobutane) (mixture of diastereomers): calcd for $\text{C}_{20}\text{H}_{34}\text{NO}_6\text{Si}$ ($M + 1$), 412.2155; found, 412.2139.

Triol Derivative 9d: 70% yield (75 mg, 0.20 mmol). ^1H NMR (400 MHz, CDCl_3) (mixture of diastereomers): δ 5.12–4.94 (m, 1H), 3.68 (m, 2H), 3.42–3.24 (m, 1H), 3.31 (s) and 3.30 (s) (total 3H), 2.04 (s) and 2.02 (s) (total 3H), 1.88–1.50 (m, 6H), 1.27 (m, 8H), 0.89 (s, 12H), -0.05 (s, 6H). ^{13}C NMR (75 MHz, CDCl_3) (mixture of diastereomers): δ 171.4, 171.3, 75.6, 75.3, 72.2, 71.9, 59.7, 59.6, 57.5, 56.5, 39.8, 38.4, 37.6, 37.1, 35.2, 34.7, 31.9, 29.4, 26.1, 25.3, 22.7, 21.4, 18.4, 18.4, 14.2, -5.3 , -5.3 . IR (neat film) (mixture of diastereomers): 2940, 2870, 1740, 1460, 1522, 1368, 1240, 1090, 1015, 833, 771 cm^{-1} . MS (CI, isobutane) (mixture of diastereomers): m/z 375 ($M + 1$, 91), 345 (9), 344 (33), 343 (100), 317 (20), 316 (14), 315 (70), 284 (9), 283 (53), 257 (10), 203 (19), 152 (6), 151 (64), 145 (12), 135 (6), 133 (7), 129 (12), 119 (9), 117 (9), 109 (9), 107 (9), 101 (5). HRMS (CI, isobutane) (mixture of diastereomers): calcd for $\text{C}_{20}\text{H}_{43}\text{O}_4\text{Si}$ ($M + 1$), 375.2931; found, 375.2890.

Triol Derivative 9e: 70% yield (72 mg, 0.15 mmol). ^1H NMR (400 MHz, CDCl_3): isomer 1, δ 8.17 (d, $J = 8.0$ Hz, 2H), 7.45 (d, $J = 8.0$ Hz, 2H), 7.33 (m, 5H), 5.97 (dd, $J = 2.9, 10.0$ Hz, 1H), 4.58 (d, $J = 11.2$ Hz, 1H), 4.41 (d, $J = 11.2$ Hz, 1H), 3.79–3.64 (m, 3H), 2.08 (m, 1H), 2.00 (s, 3H), 1.95–1.83 (m, 2H), 1.70 (m, 1H), 0.88 (s, 9H), 0.05 (s, 6H); isomer 2, δ 8.13 (d, $J = 8.8$ Hz, 2H), 7.36–7.28 (m, 7H), 5.90 (t, $J = 7.0$ Hz, 1H), 4.53 (d, $J = 11.2$ Hz, 1H), 4.31 (d, $J = 11.2$ Hz, 1H), 3.70–3.60 (m, 2H), 3.45 (m, 1H), 2.27 (m, 1H), 2.03 (s, 3H), 1.99 (m, 1H), 1.85 (m, 1H), 1.72 (m, 1H), 0.82 (s, 9H), -0.02 (s, 6H). ^{13}C NMR (75 MHz, CDCl_3) (mixture of diastereomers): δ 170.6, 170.5, 149.4, 148.5, 148.2, 148.1, 139.0, 138.8, 129.0, 128.7, 128.4, 128.4, 128.3, 128.1, 127.5, 124.4, 124.3, 73.1, 73.0, 72.5, 72.5, 71.8, 70.9, 59.6, 59.5, 42.5, 41.0, 37.2, 37.0, 26.1, 26.0,

21.2, 21.1, 18.4, 18.3, -5.3, -5.4. IR (neat film) (mixture of diastereomers): 2962, 2940, 2864, 1744, 1604, 1520, 1460, 1345, 1225, 1090, 832, 770, 730, 690 cm^{-1} . MS (CI, isobutane) (mixture of diastereomers): m/z 488 ($M + 1$, 3), 291 (15), 290 (16), 290 (62), 279 (12), 189 (48), 188 (11), 187 (22), 150 (35), 145 (21), 133 (23), 131 (12), 131 (54), 108 (14), 107 (100). HRMS (CI, isobutane) (mixture of diastereomers): calcd for $\text{C}_{26}\text{H}_{38}\text{NO}_6\text{Si}$ ($M + 1$), 488.2468; found, 488.2454.

Triol Derivative 9f: 64% yield (79 mg, 0.18 mmol). ^1H NMR (400 MHz, CDCl_3): isomer 1, δ 8.19 (d, $J = 8.8$ Hz, 2H), 7.50 (d, $J = 8.8$ Hz, 2H), 5.94 (t, $J = 6.8$ Hz, 1H), 5.87 (m, 1H), 5.28–5.14 (m, 2H), 3.97 (m, 1H), 3.78 (m, 1H), 3.69–3.58 (m, 2H), 3.36 (m, 1H), 2.23 (m, 1H), 2.06 (s, 3H), 1.95 (m, 1H), 1.76 (m, 1H), 1.66 (m, 1H), 0.81 (s, 9H), -0.01 (d, $J = 4.0$ Hz, 6H); isomer 2, δ 8.20 (d, $J = 8.8$ Hz, 2H), 7.49 (d, $J = 8.8$ Hz, 2H), 5.98 (dd, $J = 4.0, 10.8$ Hz, 1H), 5.89 (m, 1H), 5.27–5.15 (m, 2H), 4.05 (m, 1H), 3.90 (m, 1H), 3.74–3.60 (m, 3H), 2.09 (s, 3H), 1.87–1.76 (m, 2H), 1.68–1.60 (m, 2H), 0.88 (s, 9H), 0.05 (s, 6H). ^{13}C NMR (75 MHz, CDCl_3) (mixture of diastereomers): δ 170.6, 170.5, 149.3, 148.6, 148.2, 148.1, 135.6, 135.5, 128.1, 127.5, 124.3, 124.3, 117.6, 117.1, 73.2, 73.1, 72.7, 72.4, 71.1, 69.9, 59.5, 59.4, 42.5, 40.9, 37.6, 37.0, 26.0, 26.0, 21.2, 21.1, 18.3, 18.3, -5.3, -5.4. IR (neat film) (mixture of diastereomers): 2960, 2940, 2864, 1744, 1605, 1523, 1463, 1367, 1345, 1230, 1090, 930, 832, 770 cm^{-1} . MS (CI, isobutane) (mixture of diastereomers): m/z 378 ($M + 1 - \text{CH}_3\text{CO}_2\text{H}$, 1), 291 (14), 290 (51), 290 (11), 229 (37), 220 (11), 190 (13), 188 (15), 187 (13), 176 (14), 173 (13), 162 (12), 160 (28), 158 (11), 150 (23), 147 (13), 146 (20), 145 (72), 145 (23), 133 (13), 132 (14), 131 (25), 129 (46), 129 (15), 120 (17), 119 (16), 117 (13), 115 (16), 115 (12), 113 (10), 108 (26), 107 (12), 106 (59), 101 (10). HRMS (CI, isobutane) (mixture of diastereomers): calcd for $\text{C}_{20}\text{H}_{32}\text{NO}_4\text{Si}$ ($M + 1 - \text{CH}_3\text{CO}_2\text{H}$), 378.2101; found, 378.2057.

Representative Procedure for [3 + 2]-Cycloadditions via Cyclization-CO Insertion Reactions of Iron-Olefin π -Complexes. Preparation of Iron-Olefin π -Complexes. A freshly-prepared solution of allyl(cyclopentadienyl)iron(II) dicarbonyl (1, 14 mmol) in 50 mL of anhydrous Et_2O is added to a stirred mixture of benzaldehyde (3.78 g, 42 mmol) and BF_3 -etherate (1.72 mL, 14 mmol) in anhydrous Et_2O (100 mL) at 0 $^\circ\text{C}$. The mixture is stirred at 0 $^\circ\text{C}$ for 3 h, and the yellow precipitate is collected by filtration under an argon atmosphere, washed with anhydrous Et_2O (150 mL), and dried *in vacuo* to afford 4.21 g (80%) of iron-olefin π -complex **2a**.

A similar procedure gives **2b** (4.89 g, 80%), **2c** (4.43 g, 75%), **2d** (2.17 g, 45%), and **2e** (2.45 g, 50%).

Cyclization-CO Insertion Reactions of Iron-Olefin π -Complexes. To a solution of iron-olefin π -complex (188 mg, 0.50 mmol) in CH_2Cl_2 is added KO^tBu (62 mg, 0.55 mmol) at -20 $^\circ\text{C}$, followed by the addition of acetone (1 mL). The mixture is allowed to stir at -20 $^\circ\text{C}$ for 12 h. After being warmed to rt, the mixture is added dropwise over a 30 min period to a solution of ceric ammonium nitrate (1.37 g, 2.5 mmol) in methanol (10 mL) at -78 $^\circ\text{C}$ under a CO atmosphere. After the mixture is stirred at -78 $^\circ\text{C}$ for an additional 30 min, the solvent is warmed to rt and allowed to stir for an additional 30 min and then evaporated *in vacuo*. The residue is triturated several times with small portions of CH_2Cl_2 until the washings are colorless, and the washings are transferred to a SiO_2 flash column and eluted with CH_2Cl_2 and then 2% acetone in CH_2Cl_2 . After further purification by a second flash column, 46 mg of tetrahydrofuran ester **11a** (45%) is obtained as a colorless oil. ^1H NMR (400 MHz, CDCl_3) (mixture of diastereomers): δ 7.41–7.22 (m, 5H), 5.02 (t, $J = 7.4$ Hz) and 4.87 (dd, $J = 6.0, 9.6$ Hz) (total 1H), 4.34 (t, $J = 8.2$ Hz) and 4.29 (dd, $J = 6.0, 8.8$ Hz) (total 1H), 4.11 (t, $J = 8.8$ Hz) and 4.05 (t, $J = 7.4$ Hz) (total 1H), 3.74 (s) and 3.71 (s) (total 3H), 3.27 (m, 1H), 2.68–2.55 (m, 1H), 2.20–2.02 (m, 1H). ^{13}C NMR (75 MHz, CDCl_3) (mixture of diastereomers): δ 174.9, 174.5, 142.6, 142.0, 129.0, 128.9, 128.2, 128.1, 126.5, 126.2, 82.0, 81.1, 70.9, 70.6, 52.4, 44.9, 44.1, 38.4, 38.0. IR (neat film): 2970, 2890, 1735, 1635, 1435, 1367, 1273, 1197, 1172, 1060, 1020,

748, 695 cm^{-1} . MS (CI, isobutane) (mixture of diastereomers): m/z 207 ($M + 1$, 51), 205 (26), 189 (12), 175 (12), 163 (28), 162 (62), 145 (14), 137 (11), 133 (16), 131 (26), 129 (14), 125 (15), 123 (23), 119 (11), 117 (16), 113 (100), 112 (22), 111 (34), 109 (26), 103 (11), 101 (13). HRMS (CI, isobutane): calcd for $\text{C}_{12}\text{H}_{15}\text{O}_3$ ($M + 1$), 207.1021; found, 207.1052.

Tetrahydrofuran Ester 11b: 43% yield (54 mg, 0.22 mmol, 1.2:1). ^1H NMR (400 MHz, CDCl_3) (mixture of diastereomers): δ 8.22 (s) and 8.21 (s) (total 1H), 8.13 (d, $J = 7.6$ Hz, 1H), 7.70 (d, $J = 8.0$ Hz) and 7.65 (d, $J = 7.6$ Hz) (total 1H), 7.51 (m, 1H), 5.10 (t, $J = 7.2$ Hz) and 4.97 (dd, $J = 7.2, 8.8$ Hz) (total 1H), 4.37 (t, $J = 8.4$ Hz) and 4.31 (dd, $J = 6.8, 8.8$ Hz) (total 1H), 4.11 (m, 1H), 3.75 (s) and 3.70 (s) (total 3H), 3.36–3.22 (m, 1H), 2.77–2.63 (m, 1H), 2.19–1.97 (m, 1H). ^{13}C NMR (75 MHz, CDCl_3) (mixture of diastereomers): δ 174.4, 174.1, 149.1, 149.1, 145.0, 144.6, 132.5, 132.3, 130.0, 123.1, 123.0, 121.5, 121.1, 80.7, 79.9, 71.1, 70.9, 52.5, 44.8, 44.1, 38.1, 38.1. IR (neat film) (mixture of diastereomers): 2970, 2892, 1735, 1527, 1435, 1349, 1270, 1198, 1171, 1065, 1018, 805, 730 cm^{-1} . MS (CI, isobutane) (mixture of diastereomers): m/z 252 ($M + 1$, 100), 250 (3), 236 (3), 235 (3), 234 (10), 222 (7), 220 (3). HRMS (CI, isobutane): calcd for $\text{C}_{12}\text{H}_{14}\text{O}_5$ ($M + 1$), 252.0872; found, 252.0854.

Tetrahydrofuran Ester 11c: 45% yield (53 mg, 0.23 mmol, 1.2:1). ^1H NMR (400 MHz, CDCl_3) (mixture of diastereomers): δ 7.26 (m, 2H), 6.94–6.80 (m, 2H), 5.00 (t, $J = 7.2$ Hz) and 4.86 (dd, $J = 6.8, 9.6$ Hz) (total 1H), 4.33 (t, $J = 8.2$ Hz) and 4.28 (dd, $J = 6.8, 8.8$ Hz) (total 1H), 4.10 (t, $J = 8.4$ Hz) and 4.04 (dd, $J = 6.8, 8.8$ Hz) (total 1H), 3.81 (s, 3H), 3.74 (s) and 3.70 (s) (total 3H), 3.26 (m, 1H), 2.67–2.55 (m, 1H), 2.19–2.01 (m, 1H). ^{13}C NMR (75 MHz, CDCl_3) (mixture of diastereomers): δ 174.8, 174.5, 160.5, 144.3, 143.7, 130.1, 130.0, 118.8, 118.4, 113.8, 113.5, 111.8, 111.6, 81.8, 80.9, 70.9, 70.6, 55.5, 52.4, 52.3, 44.8, 44.1, 38.3, 38.0. IR (neat film) (mixture of diastereomers): 2960, 1735, 1602, 1435, 1360, 1260, 1195, 1168, 1042, 855, 778, 692 cm^{-1} . MS (CI, isobutane) (mixture of diastereomers): m/z 237 ($M + 1$, 100), 236 (22), 235 (13), 230 (6), 219 (21), 205 (6), 175 (7), 159 (7), 135 (8), 129 (12), 113 (9). HRMS (CI, isobutane): calcd for $\text{C}_{13}\text{H}_{17}\text{O}_4$ ($M + 1$), 237.1127; found, 237.1077.

Tetrahydrofuran Ester 11d: 19% yield (20 mg, 0.094 mmol, 1.5:1). ^1H NMR (400 MHz, CDCl_3): δ 4.04–3.90 (m, 2H), 3.69 (s, 3H), 3.13 (m, 1H), 2.06–1.94 (m, 2H), 1.84 (m, 1H), 1.74–1.26 (m, 11H). ^{13}C NMR (75 MHz, CDCl_3) (mixture of diastereomers): δ 174.8, 87.3, 68.5, 52.1, 44.3, 41.9, 40.5, 40.0, 29.4, 29.3, 23.0, 22.9. IR (neat film): 2930, 2862, 1738, 1435, 1263, 1195, 1172, 1053 cm^{-1} . MS (CI, isobutane) (mixture of diastereomers): m/z 213 ($M + 1$, 100), 212 (23), 191 (13), 181 (30), 163 (19), 162 (42), 131 (23), 129 (12), 113 (84), 112 (18), 111 (31), 109 (94), 101 (16). HRMS (CI, isobutane): calcd for $\text{C}_{12}\text{H}_{21}\text{O}_3$ ($M + 1$), 213.1491; found, 213.1475.

Tetrahydrofuran Ester 11e: 20% yield (22 mg, 0.10 mmol, 1.5:1). ^1H NMR (400 MHz, CDCl_3) (mixture of diastereomers): δ 7.40–7.20 (m, 5H), 4.26–4.03 (m, 2H), 3.69 (s) and 3.57 (s) (total 3H), 3.31 (m) and 3.00 (m) (total 1H), 2.61–2.52 (m, 1H), 2.42–2.29 (m, 1H), 1.58 (s) and 1.51 (s) (total 3H). ^{13}C NMR (75 MHz, CDCl_3) (mixture of diastereomers): δ 174.6, 173.9, 147.9, 147.3, 128.9, 128.8, 127.3, 127.2, 125.2, 125.1, 85.8, 85.3, 69.4, 69.3, 52.3, 52.1, 44.8, 44.3, 43.0, 42.8, 29.9, 29.9. IR (neat film) (mixture of diastereomers): 3070, 2990, 2964, 2940, 1735, 1685, 1639, 1440, 1265, 1198, 729, 699 cm^{-1} . MS (CI, isobutane) (mixture of diastereomers): m/z 221 ($M + 1$, 100), 205 (24), 203 (14), 189 (7), 151 (9), 143 (16), 133 (9), 119 (11), 117 (7). HRMS (CI, isobutane): calcd for $\text{C}_{13}\text{H}_{17}\text{O}_3$ ($M + 1$), 221.1178; found, 221.1189.

Representative Procedure for ZnCl_2 -Catalyzed [3 + 2]-Cycloadditions. To a solution of 4-nitrobenzaldehyde (151 mg, 1.0 mmol) and ZnCl_2 (0.15 mL, 1 M in CH_2Cl_2 , 0.15 mmol) in CH_2Cl_2 (5 mL) is added a freshly-prepared solution of **1** (5 mL, 0.5 M, 2.5 mmol) under an argon atmosphere. The reaction is stirred at rt for 14 h and then added dropwise over a 30 min period to a solution of ceric ammonium nitrate (4.1

g, 7.5 mmol) in CH₃OH (20 mL) at -78 °C under a CO atmosphere. After the solution is stirred at -78 °C for an additional 30 min, the solvent is warmed to rt and allowed to stir for an additional 30 min and then evaporated *in vacuo*. The residue is triturated several times with small portions of CH₂Cl₂ until the washings are colorless, and the washings are transferred to a SiO₂ flash column and eluted with CH₂Cl₂ and then 2% acetone in CH₂Cl₂. Purification by a second flash column affords 178 mg of tetrahydrofuran ester **11f** (71%, 3.1:1 mixture of diastereomers) as a pale yellow oil. ¹H NMR (400 MHz, CDCl₃): major isomer, δ 8.21 (d, *J* = 8.8 Hz, 2H), 7.50 (d, *J* = 8.8 Hz, 2H), 5.11 (t, *J* = 7.8 Hz, 1H), 4.36 (t, *J* = 8.3 Hz, 1H), 4.10 (dd, *J* = 5.9, 8.8 Hz, 1H), 3.75 (s, 3H), 3.25 (m, 1H), 2.74 (m, 1H), 1.98 (dt, *J* = 12.7, 8.8 Hz, 1H); minor isomer, δ 8.21 (d, *J* = 8.8 Hz, 2H), 7.52 (d, *J* = 8.8 Hz, 2H), 4.98 (dd, *J* = 6.8, 8.8 Hz, 1H), 4.31 (dd, *J* = 5.9, 8.8 Hz, 1H), 4.14 (t, *J* = 8.8 Hz, 1H), 3.69 (s, 3H), 3.31 (m, 1H), 2.66 (m, 1H), 2.13 (dt, *J* = 14.7, 8.8 Hz, 1H). ¹³C NMR (75 MHz, CDCl₃) (mixture of diastereomers): δ 174.4, 174.1, 150.3, 150.0, 147.9, 127.1, 126.8, 124.2, 80.7, 80.0, 78.0, 71.1, 71.0, 52.5, 44.6, 44.0, 38.1, 38.0. IR (neat film) (mixture of diastereomers): 2960, 1735, 1605, 1520, 1436, 1348, 1273, 1200, 1173, 1072, 1009, 912, 853, 726 cm⁻¹. MS (CI, isobutane) (mixture of diastereomers): *m/z* 252 (M + 1, 100), 251 (3), 236 (3), 234 (3), 222 (8), 129 (5). HRMS (CI, isobutane): calcd for C₁₂H₁₄O₅N (M + 1), 252.0872; found, 252.0895. Anal. Calcd for C₁₂H₁₃O₅N: C, 57.37; H, 5.22. Found: C, 57.38; H, 5.27.

Tetrahydrofuran Ester 11a: 36% yield (75 mg, 0.36 mmol, 2.1:1 mixture of diastereomers).

Tetrahydrofuran Ester 11b: 62% yield (156 mg, 0.62 mmol, 2.7:1 mixture of diastereomers).

Tetrahydrofuran Ester 11g: 31% yield (73 mg, 0.31 mmol, 2.0:1 mixture of diastereomers). ¹H NMR (400 MHz, CDCl₃) (mixture of diastereomers): δ 7.48 (d, *J* = 7.6 Hz) and 7.39 (d, *J* = 6.8 Hz) (total 1H), 7.24 (m, 1H), 6.95 (m, 1H), 6.86 (d, *J* = 7.6 Hz, 1H), 5.28 (t, *J* = 6.8 Hz) and 5.16 (dd, *J* = 6.8, 8.8 Hz) (total 1H), 4.34 (t, *J* = 7.8 Hz) and 4.27 (dd, *J* = 6.8, 8.8 Hz) (total 1H), 4.10 (t, *J* = 8.4 Hz) and 4.04 (t, *J* = 7.8 Hz) (total 1H), 3.82 (s) and 3.82 (s) (total 3H), 3.73 (s) and 3.68 (s) (total 3H), 3.31–3.14 (m, 1H), 2.70 (m, 1H), 2.04–1.97 (m, 1H). ¹³C NMR (75 MHz, CDCl₃) (mixture of diastereomers): δ 174.8, 174.6, 156.9, 156.8, 131.5, 130.9, 128.8, 126.3, 126.1, 121.2, 121.0, 110.7, 110.7, 76.7, 70.7, 70.2, 55.6, 52.3, 44.9, 44.1, 37.0, 36.7. IR (neat film) (mixture of diastereomers): 2960, 1735, 1600, 1490, 1460, 1436, 1365, 1280, 1240, 1196, 1173, 1065, 1020, 927, 750 cm⁻¹. MS (CI, isobutane) (mixture of diastereomers): *m/z* 237 (M + 1, 7), 236 (12), 235 (11), 219 (48), 205 (M + 1 - CH₃OH, 19), 187 (55), 177 (39), 176 (21), 175 (31), 162 (15), 159 (41), 150 (30), 145 (11), 135 (24), 130 (24), 129 (100), 109 (11). HRMS (CI, isobutane): calcd for C₁₂H₁₃O₃ (M + 1 - CH₃OH), 205.0865; found, 205.0865.

General Procedure for ZnCl₂-Promoted [3 + 2]-Cycloadditions. This procedure is the same as that above except 1 molar equiv of ZnCl₂ is employed.

Tetrahydrofuran Ester 11a: 40% yield (82 mg, 0.40 mmol, 1.1:1 mixture of diastereomers).

Tetrahydrofuran Ester 11f: 50% yield (125 mg, 0.50 mmol, 1.1:1 mixture of diastereomers).

Tetrahydrofuran Ester 11g: 28% yield (57 mg, 0.28 mmol, 1.2:1 mixture of diastereomers).

Tetrahydrofuran Ester 11h: 16% yield (38 mg, 0.16 mmol, ratio not determined due to overlapping signals in the ¹H NMR spectrum). ¹H NMR (400 MHz, CDCl₃) (mixture of diastereomers): δ 7.25 (m, 5H), 4.12–3.76 (m, 3H), 3.68 (s), 3.68 (s), 3.67 (s), and 3.65 (s) (total 3H), 3.14–2.70 (m, 2H), 2.33–1.67 (m, 2H), 1.36 (overlapping d, *J* = 7.0 Hz) and 1.27 (overlapping d, *J* = 7.0 Hz) (total 3H). ¹³C NMR (75 MHz, CDCl₃) (mixture of diastereomers): δ 175.0, 175.0, 174.8, 174.7, 144.8, 144.5, 129.1, 128.9, 128.9, 128.4, 128.3, 128.3, 128.2, 127.1, 127.0, 127.0, 85.4, 84.9, 84.4, 84.0, 70.6, 70.5, 70.3, 70.2, 52.3, 52.2, 45.4, 45.3, 44.8, 44.6, 44.4, 44.0, 34.6, 33.8, 33.7, 33.4, 19.1, 18.8, 18.3, 17.9. IR (neat film) (mixture of

diastereomers): 2970, 2884, 1735, 1448, 1370, 1266, 1197, 1170, 1065, 1015, 925, 755, 696 cm⁻¹. MS (CI, isobutane) (mixture of diastereomers): *m/z* 235 (M + 1, 22), 223 (25), 217 (11), 203 (59), 185 (12), 157 (73), 131 (12), 129 (22). HRMS (CI, isobutane): calcd for C₁₄H₁₉O₃ (M + 1), 235.1334; found, 235.1327.

Representative Procedure for TiCl₄-Catalyzed [3 + 2]-Cycloadditions. To a solution of TiCl₄ (2.0 mL, 1 M solution in CH₂Cl₂, 2 mmol) in CH₂Cl₂ (5 mL) is added cycloheptanone (112 mg, 1.0 mmol) via a syringe at -78 °C, followed by slow addition (10 min) of a freshly-prepared solution of **1** (5 mL, 0.5 M, 2.5 mmol) under an argon atmosphere. The reaction is warmed to rt, anhydrous CH₃-OH (2 mL) is added to dissolve the viscous residue, and the dark red solution is added dropwise over a 30 min period to a solution of ceric ammonium nitrate (4.1 g, 7.5 mmol) in CH₃-OH (20 mL) at -78 °C under a CO atmosphere. After the mixture is stirred at -78 °C for an additional 30 min, the solvent is warmed to rt and allowed to stir for an additional 30 min and then evaporated *in vacuo*. The residue is triturated several times with small portions of CH₂Cl₂ until the washing is colorless, and the washings are transferred to a SiO₂ flash column and eluted with CH₂Cl₂ and then 2% acetone in CH₂Cl₂. Purification by a second flash column affords 79 mg of tetrahydrofuran ester **11d** (37%) as a colorless oil.

Tetrahydrofuran Ester 11e: 15% yield (33 mg, 0.15 mmol, 1.0:1 mixture of diastereomers).

Tetrahydrofuran Ester 11h: 15% yield (35 mg, 0.15 mmol).

Representative Procedure for Uncatalyzed [3 + 2]-Cycloadditions. To a solution of 4-nitrobenzaldehyde (151 mg, 1.0 mmol) in CH₂Cl₂ (5 mL) is added a freshly-prepared solution of **1** (5 mL, 0.5 M, 2.5 mmol) under an argon atmosphere. The reaction is stirred at rt for 43 h and then added dropwise over a 30 min period to a solution of ceric ammonium nitrate (4.1 g, 7.5 mmol) in CH₃OH (20 mL) at -78 °C under a CO atmosphere. After the mixture is stirred at -78 °C for an additional 30 min, the solvent is warmed to rt and allowed to stir for an additional 30 min and then evaporated *in vacuo*. The residue is triturated several times with small portions of CH₂Cl₂ until the washings are colorless, and the washings are transferred to a SiO₂ flash column and eluted with CH₂Cl₂ and then 2% acetone in CH₂Cl₂. Purification by a second flash column affords 150 mg of the tetrahydrofuran ester **11f** (60%, 1.9:1 mixture of diastereomers) as a pale yellow oil.

Tetrahydrofuran Ester 11a: 8% yield (17 mg, 0.08 mmol, 1.8:1 mixture of diastereomers).

Tetrahydrofuran Ester 11b: 45% yield (113 mg, 0.45 mmol, 1.9:1 mixture of diastereomers).

Representative Procedure for [3 + 2]-Reactions of *N*-Tosylimines. To a stirred solution of benzaldehyde *N*-tosylimine (259 mg, 1.0 mmol) and ZnCl₂ (0.15 mL, 1 M Et₂O, 0.15 mmol) in CH₂Cl₂ (5 mL) is added a 0.5 M solution of freshly-prepared **1** (5 mL, 2.5 mmol) under an argon atmosphere. The mixture is stirred at rt for 24 h and then added dropwise over a 30 min period to a methanolic solution (15 mL) of ceric ammonium nitrate (3.0 g, 5.5 mmol) at -78 °C under a CO atmosphere. After the mixture is stirred at -78 °C for an additional 30 min, the solution is warmed to rt and allowed to stir for an additional 30 min and then evaporated *in vacuo*. The residue is triturated several times with CH₂-Cl₂ (5 mL), and then the washings are transferred to a SiO₂ flash column and elute with CH₂Cl₂ and then 5% acetone in CH₂Cl₂. Additional purification by a second flash column affords 197 mg (55%) of pyrrolidine ester **13a** as a 2.5:1 mixture of diastereomers. ¹H NMR (400 MHz, CDCl₃): δ 7.69 (d, *J* = 8.8 Hz, 2H), 7.34–7.28 (m, 7H), 4.88 (m, major) and 4.75 (t, *J* = 8.0 Hz, minor) (total 1H), 3.89 (m, 1H), 3.75 (m, minor) and 3.58 (buried, major) (total 1H), 3.59 (s, minor) and 3.58 (s, major) (total 3H), 3.10 (pent, *J* = 8.0 Hz, major) and 2.85 (pent, *J* = 8.0 Hz, minor) (total 1H), 2.44 (buried, minor)

and 2.06 (m, major) (total 1H), 2.44 (s, major) and 2.43 (s, minor) (total 3H), 2.15 (m, 1H).

Pyrrolidine Ester 13b: 42% yield (170 mg, 0.42 mmol). ^1H NMR (400 MHz, CDCl_3): δ 8.14–8.06 (m, 2H), 7.75–7.50 (m, 4H), 7.34–7.30 (m, 2H), 4.91 (dd, $J = 8.0, 4.0$ Hz, major) and 4.80 (t, $J = 8.0$ Hz, minor) (total 1H), 3.96 (m, 1H), 3.82 (m, minor) and 3.63 (buried, major) (total 1H), 3.61 (s, minor) and 3.58 (s, major) (total 3H), 3.09 (pent, $J = 8.0$ Hz, major) and 2.79 (pent, $J = 8.0$ Hz, minor) (total 1H), 2.56 (m, minor) and 2.35 (m, major) (total 1H), 2.44 (s, major) and 2.43 (s, minor) (total 3H), 2.17 (m, minor) and 2.06 (m, major) (total 1H).

Similarly, pyrrolidine esters **13c** were prepared from crotyliron complex **12**.

Pyrrolidine Ester 13c: 28% yield (117 mg, 0.28 mmol). ^1H NMR (400 MHz, CDCl_3): δ 8.14–8.06 (m, 2H), 7.75–7.49 (m, 4H), 7.30–7.23 (m, 2H), 4.85 (m, 1H), 4.15 (m, minor) and 4.01 (m, major) (total 1H), 3.82 (m, minor) and 3.55 (m, major) (total 1H), 3.69 (s, minor) and 3.67 (s, major) (total 3H), 2.80 (m, 1H), 2.46 (m, 1H), 2.42 (s, major) and 2.40 (s, minor) (total 3H), 0.99 (d, $J = 6.8$ Hz, minor) and 0.60 (d, $J = 6.8$ Hz, major) (total 3H).

Preparation of Epoxyketone 17. To a solution of diisopropylamine (4.6 mL, 35 mmol) in THF (30 mL) is added slowly a solution of $^t\text{BuLi}$ (18.0 mL, 1.6 M in hexane, 28.8 mmol) at 0 °C, followed by the addition of cycloheptanone cyclohexylimine (4.257 g, 22 mmol) in THF (10 mL) over 15 min. The yellow solution is stirred at 0 °C for 30 min. HMPA (5 mL, 29 mmol) is added, followed by the slow addition of 5-bromopentene (4.33 g, 29 mmol) in THF (10 mL). After being stirred for 1 h at 0 °C, the reaction is quenched with Et_2O (100 mL). The mixture is washed with saturated NH_4Cl solution (3 \times 25 mL), and dried over MgSO_4 . Solvent is evaporated *in vacuo* and purified by flash chromatography (silica gel, 50% pentane: CH_2Cl_2) to afford 3.29 g (83%) of 2-(4'-pentenyl)cycloheptanone as a light yellow oil. ^1H NMR (400 MHz, CDCl_3): δ 5.78 (m, 1H), 4.95 (m, 2H), 2.47 (m, 3H), 2.03 (m, 2H), 1.85 (m, 4H), 1.70–1.52 (m, 2H), 1.34 (m, 6H). ^{13}C NMR (75 MHz, CDCl_3): δ 217.0, 139.1, 115.0, 52.4, 42.9, 33.9, 32.0, 31.5, 29.7, 28.6, 26.7, 24.7. IR (neat film): 3090, 2940, 2870, 1703, 1640, 1449, 1343, 1163, 987, 933, 909 cm^{-1} .

To the above ketone (2.48 g, 13.76 mmol) in CH_2Cl_2 (60 mL) at 0 °C is added mCPBA (4.15 g, 24.1 mmol) portionwise. The mixture is stirred at rt for 16.5 h and quenched with H_2O (10 mL) and saturated NaHCO_3 solution (25 mL). The aqueous layer is separated and washed with CH_2Cl_2 (25 mL). The organic layers are combined, washed with brine (25 mL), and dried over MgSO_4 . Evaporation and purification by flash chromatography gives 2.24 g (83%) of epoxyketone **17** as a colorless oil. ^1H NMR (400 MHz, CDCl_3) (mixture of diastereomers): δ 2.89 (m, 1H), 2.74 (t, $J = 4.4$ Hz, 1H), 2.65–2.40 (m, 4H), 1.85 (m, 4H), 1.71 (m, 1H), 1.61–1.25 (m, 9H). ^{13}C NMR (75 MHz, CDCl_3): δ 216.7, 52.4, 52.3, 52.2, 47.1, 47.1, 42.9, 42.9, 32.7, 32.5, 32.2, 32.1, 31.5, 31.4, 29.6, 29.6, 28.6, 24.6, 24.6, 23.9, 23.7. IR (neat film): 2940, 2865, 1697, 1447, 930, 825 cm^{-1} . MS (CI, isobutane): m/z 197 ($M + 1$, 100), 181 (23), 180 (21), 179 (99), 162 (14), 161 (77), 151 (26), 149 (18), 137 (16), 135 (20), 133 (20), 125 (18), 123 (33), 121 (18), 119 (16), 113 (19), 112 (15), 112 (71), 111 (29), 111 (16), 110 (11), 109 (73), 107 (36), 105 (20). HRMS (CI, isobutane): calcd for $\text{C}_{12}\text{H}_{21}\text{O}_2$ ($M + 1$), 197.1542; found, 197.1534.

Preparation of Iron–Olefin π -Complex 18. To a freshly-prepared solution of sodium (cyclopentadienyl)iron(II) dicarbonyl in THF (16 mL, 0.5 M, 8.0 mmol) is added slowly epoxyketone **17** (1.57 g, 8.0 mmol) in THF (10 mL) at 0 °C.

After being stirred for 1 h at 0 °C, a solution of HBF_4 (2.9 mL, 21.5 mmol) and Ac_2O (4.5 mL) is added dropwise to the mixture at 0 °C. The yellow solid is precipitated by addition of Et_2O (100 mL). Complex **18** (2.49 g, 70%) is collected by vacuum filtration, washed with Et_2O , and dried under vacuum. ^1H NMR (400 MHz, acetone- d_6): δ 5.90 (s, 5H), 5.28 (m, 1H), 4.05 (dd, $J = 2.5, 8.8$ Hz, 1H), 3.63 (dd, $J = 2.5, 14.6$ Hz, 1H), 2.51 (m, 2H), 2.41 (m, 2H), 1.90–1.20 (m, 13H). ^{13}C NMR (75 MHz, CDCl_3): δ 217.1, 210.2, 208.8, 89.5, 88.7, 54.8, 54.7, 52.0, 43.2, 43.2, 37.1, 31.8, 31.8, 31.6, 30.4, 30.3, 29.6, 29.6, 28.8, 28.7, 24.6, 24.5. IR (CH_2Cl_2): 3125, 3065, 2940, 2870, 2070, 2030, 1695, 1050 (br) cm^{-1} . MS (FAB, glycerol): m/z 357.0 (26) ($M - \text{BF}_4^-$), 181.1 (2) ($M + 1 - \text{Fp}^+ - \text{BF}_4^-$), 177.0 (Fp^+).

Preparation of Tricyclic Furan Ester 20. To a suspension of yellow complex **18** (444 mg, 1.0 mmol) in CH_2Cl_2 (10 mL) is added Et_3N (0.2 mL, 1.4 mmol) at 0 °C. The mixture is stirred at 0 °C for 30 min and then at rt for an additional 30 min. After solvent is removed *in vacuo*, the residue is triturated with Et_2O (3 \times 10 mL). The ethereal layers are combined and evaporated *in vacuo* to afford σ -complex **19** (263 mg, 73%) as a dark brown oil. ZnCl_2 (0.15 mL, 1 M in CH_2Cl_2 , 0.15 mmol) is added to σ -complex **19** in CH_2Cl_2 (10 mL) at –20 °C. A yellow precipitate is formed immediately. After 42 h at –20 °C, the mixture is stirred at rt for an additional 1.5 h. The brown solution is transferred to a solution of ceric ammonium nitrate (2.75 g, 5 mmol) in CH_3OH (15 mL) via a syringe pump at –78 °C under a CO atmosphere over 30 min. The mixture is stirred at –78 °C for 30 min and at rt for an additional 30 min. After evaporation *in vacuo*, the residue is triturated with small portions of CH_2Cl_2 and transferred to a flash column. Purification by flash chromatography (silica gel, CH_2Cl_2) affords tricyclic furan ester **20** (71 mg, 30% from iron–olefin π -complex **18**, 2.3:1 mixture of diastereomers) as a colorless oil. Data for the major isomer are as follows. ^1H NMR (400 MHz, CDCl_3): δ 4.09 (dd, $J = 7.8, 8.8$ Hz, 1H), 3.87 (t, $J = 8.8$ Hz, 1H), 3.69 (s, 3H), 2.74 (m, 1H), 2.47 (m, 1H), 2.02–1.86 (m, 4H), 1.86–1.72 (m, 2H), 1.60–1.52 (m, 3H), 1.50–1.40 (m, 2H), 1.38–1.20 (m, 4H). ^{13}C NMR (100 MHz, CDCl_3): δ 174.0, 98.1, 68.4, 54.8, 51.8, 51.6, 51.3, 35.9, 34.2, 32.4, 31.6, 31.4, 29.4, 24.1; IR (neat film) 2940, 2870, 1735, 1636, 1435, 1375, 1325, 1269, 1197, 1168, 1055, 1010, 849, 730 cm^{-1} . MS (CI, isobutane): m/z 239.2 ($M + 1$, 44), 221.2 (10), 162.0 (15), 135.1 (13), 129.1 (12). HRMS (CI, isobutane): calcd for $\text{C}_{14}\text{H}_{23}\text{O}_3$ ($M + 1$), 239.1647; found, 239.1628. Data for the minor isomer are as follows. ^1H NMR (400 MHz, CDCl_3): δ 4.08 (dd, $J = 8.8, 9.8$ Hz, 1H), 3.98 (dd, $J = 7.8, 8.8$ Hz, 1H), 3.67 (s, 3H), 3.13 (dt, $J = 9.8, 7.8$ Hz, 1H), 2.41 (dt, $J = 10.7, 7.8$ Hz, 1H), 2.00 (m, 1H), 1.90–1.52 (m, 7H), 1.52–1.30 (m, 7H). ^{13}C NMR (100 MHz, CDCl_3): δ 172.4, 96.8, 66.5, 53.6, 51.9, 51.5, 46.7, 36.8, 34.6, 32.7, 31.6, 27.7, 27.0, 23.6. IR (neat film): 2935, 2865, 1738, 1635, 1435, 1370, 1319, 1273, 1197, 1170, 1054, 1030 cm^{-1} . MS (CI, isobutane): m/z 239.2 ($M + 1$, 28), 221.2 (7), 162.0 (13), 135.1 (5), 113 (8). HRMS (CI, isobutane): calcd for $\text{C}_{14}\text{H}_{23}\text{O}_3$ ($M + 1$), 239.1647; found, 239.1631.

Acknowledgment. The donors of the Petroleum Research Fund, administered by the American Chemical Society, and the Wendy Will Case Cancer Fund are gratefully acknowledged for financial support of this research. We also thank Dr. Alicia Regueiro for carrying out some informative experiments on the preparation of cycloheptanone π -complex **18**.

OM940819J

Characteristic Physical and Chemical Properties of the 17-Valence-Electron Alkyl Complexes CpCr(NO)(L)R

Peter Legzdins* and Michael J. Shaw

Department of Chemistry, The University of British Columbia, Vancouver,
British Columbia, Canada V6T 1Z1

Raymond J. Batchelor and Frederick W. B. Einstein*

Department of Chemistry, Simon Fraser University, Burnaby,
British Columbia, Canada V5A 1S6

Received April 5, 1995[⊙]

CpCr(NO)(L)R 17-valence-electron complexes (L = Lewis base, R = hydrocarbyl) are preparable from their iodo precursors by metathesis reactions. Their ESR spectra vary greatly in appearance, ranging from featureless singlets to more complicated spectra which reveal varying degrees of delocalization of the unpaired electron. For instance, the X-band ESR spectrum of the prototypal complex CpCr(NO)(PPh₃)(CH₂SiMe₃) in hexanes exhibits signals which indicate that the unpaired electron density is delocalized virtually over the entire molecule. Consistently, the solid-state molecular structure of CpCr(NO)(PPh₃)(CH₂-SiMe₃) contains no unusual bond distances or angles, the intramolecular dimensions being comparable to those exhibited by related 18-electron CpCr(NO)-containing complexes. The redox properties of selected CpCr(NO)(L)R compounds have been established by cyclic voltammetry, and they reveal that these chromium species are difficult to reduce but relatively easy to oxidize. Neither the oxidation nor the reduction features display reversible behavior on the time scales of the cyclic voltammetry experiments, thereby indicating that these compounds decompose upon conversion to 16-electron cations or 18-electron anions and that the 17-valence-electron configuration is preferred. The chemical properties of the CpCr(NO)(L)R complexes reveal a degree of selective substitutional lability. Thus, CpCr(NO)(PPh₃)(CH₂SiMe₃) is inert to CO, H₂, and C₂H₄, but it does react with NO to produce the known CpCr(NO)₂(CH₂SiMe₃) and with [NO]PF₆ to form [CpCr(NO)₂(PPh₃)]PF₆, a previously inaccessible salt. Furthermore, treatment of CpCr(NO)(PPh₃)(CH₂SiMe₃) with 2 equiv of HSnPh₃ results in the loss of the alkyl group as Me₄Si and subsequent addition of an Sn-H bond to the Cr center to produce CpCr(NO)(PPh₃)(H)(SnPh₃). In solutions, the spectroscopic properties of the latter complex are consistent with it being a stannyl hydrido species. However, its solid-state ¹H NMR spectrum and molecular structure suggest that as a solid it is best viewed as tending toward the η²-stannane complex CpCr(NO)(PPh₃)(η²-HSnPh₃). Other CpCr(NO)(L)R complexes which are less sterically congested at the metal center than CpCr(NO)(PPh₃)(CH₂SiMe₃) react readily with CO to form CpCr(NO)(CO)₂ and CpCr(NO)(L)(CO).

Introduction

Paramagnetic organometallic complexes of the transition metals have in recent years been the focus of considerable attention.¹ This interest is due both to the recognition that organometallic radicals play key roles in many stoichiometric and catalytic processes and to the fact that unpaired electrons associated with these

complexes generally facilitate modes of reactivity which are unavailable to related diamagnetic compounds.¹ In particular, 17-valence-electron compounds have been studied extensively, and these studies have demonstrated that these species are generally highly reactive.² For instance, 17-electron complexes can function as potent hydrogen and halogen atom abstraction reagents,^{2a,b} and they are often unstable with respect to dimerization via formation of metal-metal or ligand-based carbon-carbon bonds.^{2b,c} In addition, they are usually quite substitutionally labile, a feature that

[⊙] Abstract published in *Advance ACS Abstracts*, September 1, 1995.
(1) (a) Noh, K. H.; Sendlinger, S. C.; Janiak, C.; Theopold, K. H. *J. Am. Chem. Soc.* **1989**, *111*, 9127. (b) Thomas, B. J.; Noh, S. K.; Schulte, G. K.; Sendlinger, S. C.; Theopold, K. H. *J. Am. Chem. Soc.* **1991**, *113*, 893. (c) Theopold, K. H. *Acc. Chem. Res.* **1990**, *23*, 263 and references cited therein. (d) Aase, T.; Tilset, M.; Parker, V. D. *J. Am. Chem. Soc.* **1990**, *112*, 4974. (e) Crocker, L. S.; Mattson, B. M.; Heinekey, D. M. *Organometallics* **1990**, *9*, 1011. (f) Astruc, D. *Acc. Chem. Res.* **1991**, *24*, 36. (g) Fortier, S.; Baird, M. C.; Preston, K. F.; Morton, J. R.; Zeigler, T.; Jaeger, T. J.; Watkins, W. C.; MacNeil, J. H.; Watson, K. A.; Hensel, K.; Le Page, Y.; Charlande, J. P.; Williams, A. J. *J. Am. Chem. Soc.* **1991**, *113*, 542. (h) Poli, R.; Owens, B. E.; Linck, R. G. *J. Am. Chem. Soc.* **1992**, *114*, 1302. (i) Luinstra, G. A.; ten Cate, L. C.; Heeres, H. J.; Pattiasina, J. W.; Meetsma, A.; Teuben, J. *Organometallics* **1991**, *10*, 3227. (j) Fei, M.; Sur, S. P.; Tyler, D. R. *Organometallics* **1991**, *10*, 419.

(2) (a) Brown, T. L. In *Organometallic Radical Processes*; Trogler, W. C., Ed.; Elsevier: New York, 1990; Chapter 3. (b) Tyler, D. R. *Prog. Inorg. Chem.* **1988**, *36*, 125. (c) Baird, M. C. *Chem. Rev.* **1988**, *88*, 1217. (d) Kowaleski, R. M.; Basolo, F.; Trogler, W. C.; Gedridge, R. W.; Newbound, T. D.; Ernst, R. D. *J. Am. Chem. Soc.* **1987**, *109*, 4860 and references cited therein. (e) Trogler, W. C. In *Organometallic Radical Processes*; Trogler, W. C., Ed.; Elsevier: New York, 1990; Chapter 9. (f) Coville, N. J. In *Organometallic Radical Processes*; Trogler, W. C., Ed.; Elsevier: New York, 1990; Chapter 4. (g) Kochi, J. K. In *Organometallic Radical Processes*; Trogler, W. C., Ed.; Elsevier: New York, 1990; Chapter 7. (h) Kochi, J. K. *J. Organomet. Chem.* **1988**, *300*, 139.

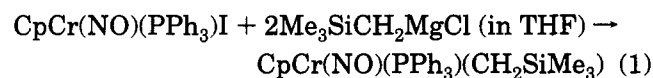
Table 1. Mass Spectral, Infrared, ESR, and Electrochemical Data

complex	MS (FAB; <i>m/z</i>)	IR ν_{NO} (THF; cm^{-1})	ESR		electrochemistry	
			<i>g</i> value (THF)	coupling const (G)	$E_{\text{p,a}}$ (V vs SCE)	$E_{\text{p,c}}$ (V vs SCE)
CpCr(NO)(PPh ₃)(CH ₂ SiMe ₃)	496 [P ⁺]	1624	1.998	$a_{\text{Cr}} = 5.3$ $a_{\text{CHH}} = 1.0$ $a_{\text{CHH}} = 12.0$ $a_{\text{P}} = 26.0$ $a_{\text{Cp}} = 0.6$ $a_{\text{N}} = 5.0$	0.43 ^b (NCMe)	-1.94 ^b
CpCr(NO)(py)(CH ₂ SiMe ₃)	313 [P ⁺]	1624	1.991	$a_{\text{Cr}} = 8$	0.29 ^b (THF)	-2.38 ^b
CpCr(NO)(pip)(CH ₂ SiMe ₃)	319 [P ⁺]	1606 ^a	1.990	$a_{\text{Cr}} = 15.7$ $a_{\text{CH}} \approx 8$ $a_{\text{N}} \approx 8$		
CpCr(NO)(pip)(CH ₂ Ph)	323 [P ⁺]	1585 ^a	1.976	$a_{\text{Cr}} = 17$	0.19 ^c (THF)	-2.09 ^c
CpCr(NO)(NH ₂ CMe ₃)(CH ₂ Ph)	307 [P ⁺]	1601 ^a	1.975	$a_{\text{Cr}} = 15$		
CpCr(NO)(THF)(CH ₂ SiMe ₃)		1631	1.994	$a_{\text{Cr}} = 15.5$ $a_{\text{CHH}} = 1.0$ $a_{\text{CHH}} = 10.5$ $a_{\text{N}} = 3.5$ $a_{\text{Cp}} = 3.5$ $a_{\text{THF}} = 0.4$		
CpCr(NO)(THF)(CH ₂ Ph)		1624	1.984	$a_{\text{Cr}} = 16$		
CpCr(NO)(THF)(<i>p</i> -tolyl)		1641	1.977	$a_{\text{Cr}} = 21$		
CpCr(NO)(THF)Me		1635	1.982	$a_{\text{Cr}} = 22$ $a_{\text{CH}} \approx 5$ $a_{\text{N}} \approx 5$		

^a Nujol mull. ^b Scan rate 0.30 V/s. ^c Scan rate 0.40 V/s.

permits them to be utilized as intermediates in electron-transfer-induced catalytic cycles.^{2c-h}

Two broad classes of 17-valence-electron complexes of chromium that we have been investigating recently are the cationic [Cp'Cr(NO)L₂]⁺ complexes³ and the neutral Cp'Cr(NO)(L)X (Cp' = Cp (η^5 -C₅H₅), Cp* (η^5 -C₅Me₅); L = Lewis base; X = halide or alkyl (R)) nitrosyl species.⁴ Although some halide-containing members of the latter class have been known for more than 25 years, the characteristic chemical properties of these compounds had remained largely unexplored. Consequently, we decided some time ago to undertake a wide-ranging investigation of these complexes. We first carried out studies dealing with the synthesis, characterization, and redox properties of representative 17-electron halide complexes.⁴ We next discovered the apparently simple iodide-for-alkyl metathesis reaction summarized in eq 1, in which 2 equiv of the Grignard



reagent is required to completely consume the CpCr(NO)(PPh₃)I reactant. Of some concern to us initially was the fact that similar reactions could not be utilized to prepare a range of related CpCr(NO)(L)(CH₂SiMe₃) complexes. A subsequent detailed study of conversion 1 established that it proceeds via initial loss of PPh₃ from the chromium's coordination sphere and permitted us to develop a general synthetic route to the desired CpCr(NO)(L)R (R = alkyl) complexes.⁵ In this paper we present the complete results of our studies concerning the characterization and reactivity of representative examples of these 17-valence-electron alkyl complexes. A portion of this work has been communicated previously.⁶

(3) Legzdins, P.; McNeil, W. S.; Batchelor, R. J.; Einstein, F. W. B. *J. Am. Chem. Soc.* **1994**, *116*, 6021.

(4) Legzdins, P.; McNeil, W. S.; Shaw, M. J. *Organometallics* **1994**, *13*, 562 and references cited therein.

(5) Legzdins, P.; Shaw, M. J. *J. Am. Chem. Soc.* **1994**, *116*, 7700.

Experimental Section

General procedures routinely employed in these laboratories have been described previously.⁷ All reagents were purchased from commercial suppliers or were prepared according to literature methods. Thus, CpCr(NO)(PPh₃)(CH₂SiMe₃),⁵ CpCr(NO)(L)R (L = piperidine (pip), NH₂CMe₃; R = CH₂SiMe₃, CH₂Ph),⁵ [CpCr(NO)I]₂,⁸ [CpCr(NO)(NCMe)₂PF₆],⁹ CpCr(NO)(CO)₂,¹⁰ HSnPh₃,¹¹ and [Cp₂Fe]PF₆¹² were prepared by published procedures. The CpCr(NO)(THF)R complexes (R = CH₂SiMe₃, CH₂Ph, *p*-tolyl, CH₃) were generated in situ by treatment of [CpCr(NO)I]₂ in THF with the appropriate Grignard reagent, RMgCl.⁵ The 400 MHz solid-state ¹H NMR spectrum was recorded by Ms. Patricia Aroca and Dr. Colin Fyfe of this department. The mass spectral, IR, ESR, and electrochemical data for the CpCr(NO)(L)R complexes investigated during this work are collected in Table 1.

Gas Chromatography. Gas chromatography was performed using a Shimadzu GC-14A gas chromatograph equipped with an OV-17 capillary column. The injector temperature and the detector temperature were normally set at 190 and 270 °C, respectively. The column temperature was kept at 40 °C for a period of 1 min after injection of the sample, whereupon it was raised 10 °C/min until a temperature of 250 °C was reached. The normal sample volume used was 0.1 μ L for liquid samples and 10 μ L for samples of the atmosphere above reaction mixtures. Compounds were identified by comparison of their retention times with those of authentic samples.

Electrochemical Measurements. The detailed methodology employed for cyclic voltammetry (CV) studies in these laboratories has been previously described.¹³ All potentials listed in Table 1 are reported versus the aqueous saturated calomel electrode (SCE).

ESR Measurements. Ambient-temperature X-band ESR spectra of $\sim 10^{-3}$ M solutions were recorded using a Varian

(6) Herring, F. G.; Legzdins, P.; McNeil, W. S.; Shaw, M. J.; Batchelor, R. J.; Einstein, F. W. B. *J. Am. Chem. Soc.* **1991**, *113*, 7049.

(7) Dryden, N. H.; Legzdins, P.; Rettig, S. J.; Veltheer, J. E. *Organometallics* **1992**, *11*, 2583.

(8) Legzdins, P.; Nurse, C. R. *Inorg. Chem.* **1985**, *24*, 327.

(9) Chin, T. T.; Legzdins, P.; Trotter, J.; Yee, V. C. *Organometallics* **1992**, *11*, 913.

(10) Chin, T. T.; Hoyano, J. K.; Legzdins, P.; Malito, J. T. *Inorg. Synth.* **1990**, *28*, 196.

(11) Eisch, J. J. *Organomet. Synth.* **1981**, *2*, 173.

(12) Smart, J. C.; Pinsky, B. L. *J. Am. Chem. Soc.* **1980**, *102*, 1009.

E-3 spectrometer or were recorded by Dr. F. G. Herring with the spectrometer and interfaced computer system described by Phillips and Herring.¹⁴ Computer simulations were performed to verify the splitting patterns observed in the various ESR spectra.

Synthesis of CpCr(NO)(py)(CH₂SiMe₃). Dark green CpCr(NO)(py)I (0.35 g, 1.00 mmol) was dissolved in THF (15 mL), and Me₃SiCH₂MgCl (2.00 mL, 1.0 M in Et₂O, 2.00 mmol) was added. Upon addition of the Grignard reagent, the solution changed from green to red-brown. The solution was stirred overnight, during which time a white solid precipitated and the solution became green-brown. The solvent was removed from the final mixture under reduced pressure, and the residue was extracted with Et₂O (3 × 20 mL). The extracts were combined and filtered through a column of alumina (1.5 × 3 cm). The column was washed with Et₂O until the washings were colorless and only a brown band remained at the top of the column. The Et₂O was removed in vacuo from the bright green filtrate. Pentane (5 mL) was added to the green oily residue, and the resulting solution was cooled to -78 °C. A bright green precipitate formed, was isolated at -78 °C by cannulation, and was washed with cold pentane (2 × 5 mL). This solid was dried in vacuo at -78 °C, but when it was warmed to room temperature, it melted and formed an olive green oil.

Anal. Calcd for C₁₄H₂₁N₂O₂SiCr: C, 53.65; H, 6.75; N, 8.94. Found: C, 52.42; H, 6.64; N, 9.20.

Reaction of CpCr(NO)(PPh₃)(CH₂SiMe₃) with [Cp₂Fe]PF₆. To a green solution of CpCr(NO)(PPh₃)(CH₂SiMe₃) (0.25 g, 0.50 mmol) in MeCN (10 mL) was added blue [Cp₂Fe]PF₆ (0.16 g, 0.50 mmol). The solution immediately turned dark blue, but after being stirred for 18 h, it changed back to green. The final solution was filtered through a plug of Celite (2 × 3 cm) supported on a glass frit and was then cooled to -30 °C overnight. This treatment resulted in the deposition of orange crystals, which were isolated by cannulating the supernatant solution into another vessel. The orange crystals were identified as ferrocene (0.10 g) by comparison of their characteristic IR spectrum with that of an authentic sample. The green mother liquor was concentrated under reduced pressure to a volume of 5 mL, and then Et₂O (5 mL) was added. The solution was cooled to 8 °C for 18 h to induce the formation of a mixture of orange and green crystals. The green crystals were identified as [CpCr(NO)(NCMe)₂]PF₆ by comparisons of its IR and FAB-MS spectra to those exhibited by an authentic sample.⁹

Reaction of CpCr(NO)(PPh₃)(CH₂SiMe₃) with NO. CpCr(NO)(PPh₃)(CH₂SiMe₃) (0.20 g, 0.40 mmol) was dissolved in Et₂O (10 mL), and NO was bubbled through the solution for 5 min. The solution was stirred for 1 h, whereupon a white precipitate formed. The final mixture was filtered through alumina (2 × 3 cm) supported on a glass frit, and the column was washed with Et₂O (3 × 10 mL). The solvent was removed from the combined filtrates, resulting in the isolation of CpCr(NO)₂(CH₂SiMe₃) (0.05 g, 47% yield) as a dark green oil.¹⁵ This oil was dried under vacuum overnight.

IR (Nujol): ν_{NO} 1778, 1676 cm⁻¹. IR (Et₂O): ν_{NO} 1778, 1674 cm⁻¹. ¹H NMR (CDCl₃): δ 5.39 (s, 5H, C₅H₅), 0.23 (s, 2H, CH₂), -0.03 (s, 9H, CH₃). ¹³C NMR (CDCl₃): δ 99.6 (C₅H₅), 4.70 (CH₂), 1.98 (CH₃). EIMS (probe temperature 120 °C): *m/z* 264 [P⁺], 249 [P⁺ - Me].

Reaction of CpCr(NO)(PPh₃)(CH₂SiMe₃) with [NO]PF₆. CpCr(NO)(PPh₃)(CH₂SiMe₃) (0.55 g, 1.1 mmol) was added to a stirred suspension of [NO]PF₆ (0.19 g, 1.1 mmol)

in CH₂Cl₂ (10 mL). Within 2 min, the ν_{NO} band at 1616 cm⁻¹ in the IR spectrum of the supernatant solution was replaced by bands at 1831 and 1738 cm⁻¹ and a broad band at 1669 cm⁻¹. The solvent was removed under reduced pressure, and then CH₂Cl₂ (1 mL) was reintroduced into the flask to obtain a green solution. A silica gel column (1 × 10 cm, Fisher, 60–80 mesh) was prepared using a CH₂Cl₂/Et₂O (97:3) solvent mixture. The green solution was applied to the top of the column and was eluted with the solvent mixture under a slight pressure of dinitrogen. Two pale brown bands followed by a dark green band were eluted and collected. The IR spectrum of the first eluate exhibited a broad ν_{NO} band at 1668 cm⁻¹, and that of the second displayed a broad ν_{NO} absorption at 1655 cm⁻¹. These solutions were concentrated in vacuo to incipient precipitation and cooled to -30 °C; however, no tractable products were isolable. The IR spectrum of the dark green band displayed two sharp ν_{NO} bands at 1831 and 1738 cm⁻¹. The dark green eluate was concentrated under reduced pressure and cooled to -30 °C overnight to induce the deposition of [CpCr(NO)₂(PPh₃)₂]PF₆ (0.38 g, 59% yield) as dark green microcrystals.

Anal. Calcd for C₂₃H₂₀N₂O₂F₆P₂Cr: C, 47.27; H, 3.44; N, 4.79. Found: C, 47.11; H, 3.47; N, 4.70. IR (Nujol): ν_{NO} 1826, 1730 cm⁻¹. IR (CH₂Cl₂): ν_{NO} 1831, 1738 cm⁻¹. 200 MHz ¹H NMR (CD₂Cl₂): δ 7.99–7.05 (m, 15H, P(C₆H₅)₃), 5.70 (s, 5H, C₅H₅). 50 MHz ¹³C{¹H} NMR (CD₂Cl₂): δ 153.97, 153.75, 153.60, 153.54, 153.14, 152.93, 150.93, 150.73, 149.76 (aromatic ring carbons), 122.90 (C₅H₅). 81 MHz ³¹P{¹H} NMR (CD₂Cl₂): δ 68.46 (PPh₃), -31.07 (septet, ¹J_{PF} = 710.62 Hz, PF₆⁻). 188 MHz ¹⁹F NMR (CD₂Cl₂): δ 4.30 (d, ¹J_{PF} = 710.68 Hz, PF₆⁻). FAB-MS *m/z* 439 [P⁺ - PF₆⁻].

Reaction of CpCr(NO)(PPh₃)(CH₂SiMe₃) with HSnPh₃. An emerald green solution of CpCr(NO)(PPh₃)(CH₂SiMe₃) (0.49 g, 1.0 mmol) in THF (20 mL) was treated with HSnPh₃ (0.50 mL, 2.0 mmol). The resulting mixture was refluxed for 2 h, after which time the ν_{NO} band in the IR spectrum of the solution had shifted from 1624 to 1639 cm⁻¹. The THF was removed from the green solution in vacuo, and the residue was extracted with Et₂O (50 mL). The Et₂O extracts were filter-cannulated into another vessel and then cooled to 8 °C for 2 days. This treatment resulted in the formation of 0.32 g of a green microcrystalline solid. This solid was placed in the thimble of a Soxhlet extractor and was extracted continuously with pentane for 7 days. This procedure resulted in the formation of large X-ray-quality single crystals of analytically pure CpCr(NO)(PPh₃)(H)(SnPh₃) (0.10 g, 13% yield).

Anal. Calcd for C₄₁H₃₆NOPSnCr: C, 64.76; H, 4.77; N, 1.84. Found: C, 64.90; H, 4.82; N, 1.90. IR (THF): ν_{NO} 1639 cm⁻¹. IR (Nujol): ν_{NO} 1621 cm⁻¹. 400 MHz ¹H NMR (C₆D₆): δ 8.09–7.43 (m, 15H, Sn(C₆H₅)₃), 7.40–6.80 (m, 15H, P(C₆H₅)₃), 4.56 (d, ²J_{PH} = 3.0 Hz, 5H, C₅H₅), -2.47 (d, ²J_{PH} = 90.3 Hz, ²J_{SnH} = 23.7 Hz, 1H, Cr-H). 50 MHz: ¹³C{¹H} NMR (C₆D₆): δ 147.05, 137.84, 137.61, 133.58, 133.46, 129.88, 129.15, 128.52, 128.48 (aromatic rings), 92.07 (C₅H₅). 81 MHz ³¹P NMR: δ 87.94 (²J_{SnP} = 38.6 Hz, PPh₃). FAB-MS: *m/z* 760 [P⁺ - H].

Reaction of CpCr(NO)(pip)(CH₂Ph) with CO. Bright green CpCr(NO)(pip)(CH₂Ph) (0.10 g, 0.3 mmol) was dissolved in THF (10 mL). The solution was stirred under an atmosphere of CO for 12 h, whereupon it underwent a gradual color change from green to orange. The solvent was vacuum-transferred into another vessel, and the resulting clear solution was analyzed by GC. Only one peak other than solvent was detected in the GC trace, and this was identified as toluene by comparison to an authentic sample. A water-cooled sublimation probe was attached to the flask containing the organometallic residue. The flask was evacuated and warmed with a hot water bath. Within 2 h, small bright orange crystals formed on the probe. These were identified as CpCr(NO)(CO)₂ by IR and EIMS comparisons to authentic samples.¹⁰ The remaining residue was recrystallized from Et₂O to obtain 0.01 g of a red solid, which was tentatively identified as CpCr(NO)(pip)(CO) on the basis of its spectroscopic properties (i.e.

(13) (a) Herring, F. G.; Legzdins, P.; Richter-Addo, G. B. *Organometallics* **1989**, *8*, 1485. (b) Legzdins, P.; Wassink, B. *Organometallics* **1984**, *3*, 1811. (c) Legzdins, P.; Lundmark, P. J.; Phillips, E. C.; Rettig, S. J.; Veltheer, J. E. *Organometallics* **1992**, *11*, 2991 and references cited therein.

(14) Phillips, P. S.; Herring, F. G. *J. Magn. Reson.* **1984**, *57*, 43.

(15) Legzdins, P.; Richter-Addo, G. B.; Wassink, B.; Einstein, F. W. B.; Jones, R. H. *J. Am. Chem. Soc.* **1989**, *111*, 2097.

IR (Nujol) ν_{NO} 1635 cm^{-1} , ν_{CO} 1905 cm^{-1} ; FAB-MS m/z 260 [P⁺], 232 [P⁺ - CO], 202 [P⁺ - CO - NO].

Reaction of CpCr(NO)(THF)(CH₂SiMe₃) with CO. A solution of [CpCr(NO)]₂ (0.27 g, 0.50 mmol) in THF (15 mL) was treated with Me₃SiCH₂MgCl (2.0 mL, 1.0 M in Et₂O, 2.0 mmol). The resulting dark red solution was stirred overnight and was then filtered through Celite to remove the white precipitate (presumably Mg salts) which had formed. The filtrate was placed under an atmosphere of CO and was stirred for a further 18 h, whereupon it turned light orange. The solution displayed intense IR bands at 2016, 1957, and 1701 cm^{-1} . The solvent was removed in vacuo, and the residue was sublimed onto a water-cooled probe to obtain 0.05 g (24% yield) of orange CpCr(NO)(CO)₂, identified by IR and EIMS comparisons to authentic samples.¹⁰

X-ray Crystallographic Analysis of CpCr(NO)(PPh₃)(CH₂SiMe₃). Crystals of the complex suitable for an X-ray crystallographic analysis were grown from a saturated solution in pentane maintained at 8 °C for a period of 1 week. A dark green block of CpCr(NO)(PPh₃)(CH₂SiMe₃) was mounted in a Lindemann capillary tube under argon. Intensity data (Mo K α /graphite monochromator) were collected at 200 K with an Enraf-Nonius CAD-4F diffractometer equipped with an extensively in-house-modified low-temperature attachment. The unit cell was determined from 25 well-centered reflections ($31^\circ \leq 2\theta \leq 40^\circ$). Two intensity standards were measured every 1 h of acquisition time and showed small periodic fluctuations ($\pm 1.5\%$) during the course of data acquisition. The data were corrected analytically for absorption by the Gaussian integration method.¹⁶ Data reduction included Lorentz and polarization corrections.

Peaks corresponding to all the hydrogen atoms but four (on the phenyl rings) were observed in an electron-density difference map after isotropic refinement of all the non-hydrogen atoms ($R = 0.075$). The methyl groups were all observed to have staggered orientations about the Si-C bonds. Subsequently, all hydrogen atoms were placed in calculated positions (C-H = 0.95 Å) and were assigned isotropic thermal parameters initially 10% larger than those for the corresponding carbon atoms. During refinement, the hydrogen atom coordinate shifts were linked with those of the carbon atoms to which they were bonded. A single parameter was refined for the isotropic thermal motion of the hydrogen atoms of each of the following types: methylene, methyl, phenyl, and cyclopentadienyl. The final full-matrix, least-squares refinement of 293 parameters for 2128 observed data included anisotropic thermal parameters for all non-hydrogen atoms. A weighting scheme based on counting statistics was applied such that $\langle w(|F_o| - |F_c|)^2 \rangle$ was nearly constant as a function of both $|F_o|$ and $(\sin \theta)/\lambda$.

Complex scattering factors for neutral atoms¹⁷ were used in the calculation of structure factors. The programs used for data reduction, structure solution, and initial refinement were from the NRCVAX Crystal Structure System.¹⁸ The program suite CRYSTALS¹⁹ was employed in the final refinement. All computations were carried out on a MicroVAX-II computer. Crystallographic data are summarized in Table 2. The final positional and equivalent isotropic thermal parameters for the non-hydrogen atoms are given in Table 3, and selected bond lengths and angles are provided in Table 4. A view of the solid-state molecular structure of CpCr(NO)(PPh₃)(CH₂SiMe₃) is shown in Figure 1. Additional experimental details, coordinates, and temperature factors for the hydrogen atoms, as well

Table 2. Crystallographic Data for the Complexes CpCr(NO)(PPh₃)(CH₂SiMe₃) and CpCr(NO)(PPh₃)(H)(SnPh₃)

compd	CpCr(NO)(PPh ₃)- (CH ₂ SiMe ₃)	CpCr(NO)(PPh ₃)- (H)(SnPh ₃)
formula	CrPONC ₂₇ H ₃₁	SnCrPONC ₄₁ H ₃₆
fw	496.60	760.40
cryst syst	monoclinic	triclinic
space group	<i>P</i> 2 ₁ / <i>c</i>	<i>P</i> $\bar{1}$
<i>a</i> , Å	7.962(3)	11.582(2)
<i>b</i> , Å	15.440(4)	11.961(2)
<i>c</i> , Å	20.883(6)	14.174(4)
α , deg		84.84(2)
β , deg	90.31 (3)	68.45(2)
γ , deg		67.89(2)
<i>V</i> , Å ³	2567.0	1689.3
<i>Z</i>	4	2
ρ_{calcd} , g/cm ³	1.285	1.495
λ (Mo K α), Å	0.709 30 (K α_1)	0.709 30 (K α_1)
μ (Mo K α), cm ⁻¹	5.6	11.3
temp, K	200	200
transmissn factors	0.876–0.930	0.769–0.813
min–max 2 θ , deg	4–46	4–50
no. of rflns with $I \geq 2.5\sigma(I)$	2128	5011
no. of variables	293	419
R_F^a	0.048	0.024
$R_w F^b$	0.052 ^c	0.033 ^d

^a $R_F = \sum(|F_o| - |F_c|)/\sum|F_o|$. ^b $R_w F = [\sum(w(|F_o| - |F_c|)^2)/\sum(wF_o^2)]^{1/2}$. ^c $w = [\sigma(F_o)^2 + 0.0006F_o^2]^{-1}$. ^d $w = [\sigma(F_o)^2 + 0.0002F_o^2]^{-1}$.

Table 3. Atomic Coordinates ($\times 10^4$) and Equivalent Isotropic Temperature Factors ($\text{Å}^2 \times 10^4$) for the Non-Hydrogen Atoms of CpCr(NO)(PPh₃)(CH₂SiMe₃) at 200 K

atom	<i>x/a</i>	<i>y/b</i>	<i>z/c</i>	U_{eq}^a
Cr	6510(1)	3208.7(6)	1186.5(4)	271
P	5149(2)	1945.7(9)	1589.8(7)	252
Si	6981(2)	3206(1)	-436.5(7)	348
N	4656(6)	3659(3)	994(2)	325
O	3339(6)	4039(3)	904(2)	459
C(1)	7026(7)	2584(4)	318(2)	338
C(2)	4962(8)	3787(4)	-571(3)	503
C(3)	8724(8)	4008(4)	-492(3)	447
C(4)	7214(9)	2418(4)	-1121(3)	494
C(11)	3674(7)	2114(4)	2245(3)	277
C(12)	2460(7)	1504(4)	2392(3)	343
C(13)	1445(7)	1602(4)	2914(3)	386
C(14)	1620(8)	2322(4)	3297(3)	395
C(15)	2768(8)	2953(4)	3153(3)	433
C(16)	3785(7)	2847(4)	2622(3)	354
C(21)	3868(7)	1363(4)	1001(3)	274
C(22)	2722(7)	1831(5)	638(3)	415
C(23)	1794(9)	1428(6)	166(3)	517
C(24)	1974(10)	552(6)	53(3)	503
C(25)	3042(9)	86(5)	420(4)	548
C(26)	4026(8)	487(4)	885(3)	460
C(31)	6584(7)	1119(3)	1894(3)	259
C(32)	7927(7)	873(4)	1508(3)	328
C(33)	9035(8)	248(4)	1708(3)	429
C(34)	8860(8)	-140(4)	2306(3)	427
C(35)	7559(8)	112(4)	2695(3)	370
C(36)	6435(7)	738(4)	2500(3)	316
C(51)	9085(7)	3097(4)	1643(3)	380
C(52)	9142(8)	3747(4)	1179(3)	342
C(54)	7271(8)	4150(4)	1930(3)	352
C(53)	8025(8)	4392(4)	1351(3)	385
C(55)	7949(7)	3350(4)	2109(3)	348

^a U_{eq} is the cube root of the product of the principal axes of the thermal ellipsoid.

as the anisotropic temperature factors and selected bond torsion angles, are given as supporting information.

X-ray Crystallographic Analysis of CpCr(NO)(PPh₃)(H)(SnPh₃). A green crystal of the complex was mounted on a glass filament with epoxy adhesive. Data were recorded at 200 K in a manner similar to that described in the preceding

(16) Busing, W. R.; Levy, H. A. *Acta Crystallogr.* **1957**, *10*, 180.

(17) *International Tables for X-ray Crystallography*; Kynoch Press: Birmingham, England, 1975; Vol. IV, p 99.

(18) Gabe, E. J.; LePage, Y.; Charland, J.-P.; Lee, F. L.; White, P. S. NRCVAX-An Interactive Program System for Structure Analysis. *J. Appl. Crystallogr.* **1989**, *22*, 384.

(19) Watkin, D. J.; Carruthers, J. R.; Betteridge, P. W. CRYSTALS; Chemical Crystallography Laboratory, University of Oxford: Oxford, England, 1984.

Table 4. Selected Bond Distances (Å) and Angles (deg) for CpCr(NO)(PPh₃)(CH₂SiMe₃) at 200 K

Cr-P	2.386(2)	Cr-Cp ^a	1.898
Cr-N	1.678(5)	P-C(11)	1.827(5)
Cr-C(1)	2.096(5)	P-C(21)	1.830(5)
Cr-C(51)	2.264(6)	P-C(31)	1.825(6)
Cr-C(52)	2.255(6)	Si-C(1)	1.845(5)
Cr-C(53)	2.215(6)	Si-C(2)	1.862(6)
Cr-C(54)	2.209(6)	Si-C(3)	1.864(6)
Cr-C(55)	2.247(5)	Si-C(4)	1.888(6)
C(11)-C(12)	1.385(8)	N-O	1.216(6)
C(11)-C(16)	1.381(7)	C(13)-C(14)	1.377(8)
C(12)-C(13)	1.368(8)	C(14)-C(15)	1.371(8)
C(21)-C(22)	1.385(8)	C(15)-C(16)	1.386(8)
C(21)-C(26)	1.380(8)	C(23)-C(24)	1.380(11)
C(22)-C(23)	1.377(8)	C(24)-C(25)	1.351(10)
C(31)-C(32)	1.395(7)	C(25)-C(26)	1.392(8)
C(31)-C(36)	1.402(7)	C(33)-C(34)	1.393(9)
C(32)-C(33)	1.372(8)	C(34)-C(35)	1.376(9)
C(51)-C(52)	1.396(8)	C(35)-C(36)	1.377(8)
C(51)-C(55)	1.388(8)	C(54)-C(53)	1.404(8)
C(52)-C(53)	1.385(9)	C(54)-C(55)	1.398(8)
Cp-Cr-P	121.4	Cp-Cr-N	126.4
C(1)-Cr-P	91.2(2)	C(2)-Si-C(1)	113.1(3)
C(1)-Cr-N	99.2(2)	C(3)-Si-C(1)	112.8(3)
C(11)-P-Cr	116.3(2)	C(3)-Si-C(2)	108.3(3)
C(21)-P-Cr	114.6(2)	C(4)-Si-C(1)	108.1(3)
C(31)-P-Cr	114.2(2)	C(4)-Si-C(2)	106.5(3)
C(21)-P-C(11)	102.4(2)	C(4)-Si-C(3)	107.7(3)
C(31)-P-C(11)	104.0(2)	Si-C(1)-Cr	119.8(3)
C(31)-P-C(21)	103.6(3)	O-N-Cr	173.6(4)
C(12)-C(11)-P	121.4(4)	C(22)-C(21)-P	118.3(5)
C(16)-C(11)-P	120.2(4)	C(26)-C(21)-P	123.2(5)
C(16)-C(11)-C(12)	118.3(5)	C(26)-C(21)-C(22)	118.4(6)
C(13)-C(12)-C(11)	121.1(6)	C(23)-C(22)-C(21)	120.4(7)
C(14)-C(13)-C(12)	119.6(6)	C(24)-C(23)-C(22)	120.6(7)
C(15)-C(14)-C(13)	120.7(6)	C(25)-C(24)-C(23)	119.4(7)
C(16)-C(15)-C(14)	119.0(6)	C(26)-C(25)-C(24)	120.7(7)
C(15)-C(16)-C(11)	121.1(6)	C(25)-C(26)-C(21)	120.4(7)
C(32)-C(31)-P	118.0(4)	C(36)-C(35)-C(34)	121.0(6)
C(36)-C(31)-P	123.5(4)	C(35)-C(36)-C(31)	120.2(6)
C(36)-C(31)-C(32)	118.4(5)	C(55)-C(51)-C(52)	108.0(6)
C(33)-C(32)-C(31)	120.6(6)	C(53)-C(52)-C(51)	108.3(6)
C(34)-C(33)-C(32)	120.6(6)	C(55)-C(54)-C(53)	107.4(6)
C(35)-C(34)-C(33)	119.1(6)	C(54)-C(53)-C(52)	108.0(6)
		C(54)-C(55)-C(51)	108.3(5)

^a Cp represents the center of mass of the cyclopentadiene ring.

section with the same instrument. Two standard reflections which were measured every 1 h of exposure time declined systematically in intensity by 10% during the course of the measurements. The data were corrected for absorption by the Gaussian integration method,¹⁶ and corrections were carefully checked against measured ψ scans. Data reduction included corrections for intensity-scale variation and for Lorentz and polarization effects.

Coordinates and anisotropic thermal parameters for all non-hydrogen atoms were refined. Positions of all hydrogen atoms of the phenyl and cyclopentadienyl groups were then clearly revealed in an electron-density difference map. These hydrogen atoms were, nonetheless, placed in calculated positions 0.95 Å from their respective carbon atoms and were assigned isotropic temperature factors initially proportionate to the equivalent isotropic temperature factors of the corresponding carbon atoms. NMR results along with the bond angles about the tin and chromium atoms indicated the presence of a hydrogen atom bridging Sn and Cr. Such a hydrogen atom (H(10)) was placed in a calculated position²⁰ with arbitrarily assigned Cr-H (1.65 Å) and Sn-H (1.92 Å) distances and an isotropic temperature factor of 0.04 Å². This position lay within a broad region of positive residual electron density, as indicated by the difference map. In subsequent cycles of

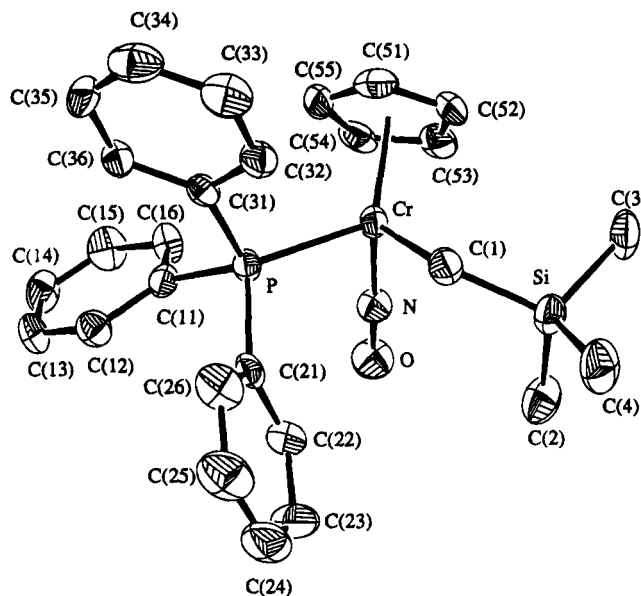


Figure 1. Solid-state molecular structure of CpCr(NO)-(PPh₃)(CH₂SiMe₃) at 200 K. The 50% probability displacement ellipsoids or spheres are shown for the non-hydrogen atoms.

refinement, the coordinate shifts for the hydrogen atoms of the phenyl and cyclopentadienyl groups were linked with those for their respectively bound carbon atoms. A mean isotropic temperature factor for all hydrogen atoms was refined, and the shifts were applied to the individual values.

A weighting scheme based on counting statistics was applied such that $\langle w(|F_o| - |F_c|)^2 \rangle$ was nearly constant as a function of both $|F_o|$ and $(\sin \theta)/\lambda$. Final full-matrix least-squares refinement of 419 parameters for 5011 data ($I_o \geq 2.5\sigma(I_o)$) converged at $R_F = 0.024$. The coordinates for H(10) were included in this refinement (0.144(3), 0.232(3), 0.204(3) after the last cycle). The absolute value of the final maximum shift/error was 0.25 for the z coordinate of H(10), but for all other variables it was 0.01 or less. Computations were carried out on MicroVAX-II and 80486 computers utilizing the programs specified in the previous section. Crystallographic details are summarized in Table 2. Final fractional atomic coordinates for the non-hydrogen atoms are listed in Table 5, and selected bond lengths and angles are summarized in Table 6. A view of the solid-state molecular structure of CpCr(NO)(PPh₃)(H)-(SnPh₃) is shown in Figure 2. Tables of additional crystallographic data, the coordinates for the hydrogen atoms, and the anisotropic temperature factors for CpCr(NO)(PPh₃)(H)-(SnPh₃) are given as supporting information.

Results and Discussion

Synthesis of CpCr(NO)(L)R Complexes. As we have described previously,⁵ the general synthetic route to the 17-valence-electron CpCr(NO)(L)R complexes involves (a) effecting the conversion from CpCr(NO)-(THF)I to CpCr(NO)(THF)R by treatment with 2 equiv of the appropriate Grignard reagent, RMgCl, in THF, (b) destroying any excess organomagnesium species remaining with MeI, and (c) introducing L to displace THF from the coordination sphere of the CpCr(NO)-(THF)R intermediate complex (eq 2).

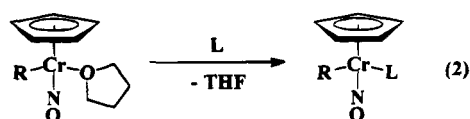


Table 5. Fractional Atomic Coordinates ($\times 10^4$) and Equivalent Isotropic Temperature Factors ($\text{\AA}^2 \times 10^4$) for the Non-Hydrogen Atoms of CpCr(NO)(PPh₃)(H)(SnPh₃) at 200 K

atom	x	y	z	U_{eq}^a
Sn	3032.7(2)	2338.0(1)	1999.7(1)	270
Cr	1243.0(4)	1282.1(3)	2730.9(3)	266
P	-844.7(6)	2797.9(5)	2867.8(5)	217
O	979(2)	1615(2)	4798(2)	483
N	1088(2)	1534(2)	3923(2)	333
C(1)	593(3)	34(2)	2170(2)	357
C(2)	1208(3)	-557(2)	2863(2)	382
C(3)	2551(3)	-654(2)	2453(2)	377
C(4)	2770(3)	-133(2)	1505(2)	329
C(5)	1559(3)	298(2)	1330(2)	329
C(11)	-1186(2)	4343(2)	3250(2)	240
C(12)	-1031(2)	4527(2)	4150(2)	297
C(13)	-1344(3)	5683(2)	4503(2)	334
C(14)	-1802(2)	6669(2)	3963(2)	329
C(15)	-1954(3)	6493(2)	3077(2)	330
C(16)	-1661(2)	5340(2)	2721(2)	292
C(21)	-2268(2)	2535(2)	3847(2)	247
C(22)	-2065(2)	1489(2)	4387(2)	287
C(23)	-3137(3)	1317(2)	5156(2)	319
C(24)	-4407(2)	2183(2)	5401(2)	315
C(25)	-4618(2)	3224(2)	4872(2)	335
C(26)	-3551(2)	3398(2)	4102(2)	311
C(31)	-1150(3)	2951(2)	1679(2)	298
C(32)	-258(3)	3271(3)	837(2)	428
C(33)	-416(4)	3375(3)	-91(3)	564
C(34)	-1449(5)	3144(4)	-191(3)	629
C(35)	-2319(5)	2823(4)	625(3)	628
C(36)	-2185(3)	2725(3)	1566(2)	438
C(41)	2780(2)	4037(2)	2626(2)	251
C(42)	3671(3)	4117(2)	3037(2)	295
C(43)	3542(3)	5215(2)	3395(2)	341
C(44)	2520(3)	6262(2)	3347(2)	332
C(45)	1632(3)	6205(2)	2937(2)	355
C(46)	1759(3)	5111(2)	2579(2)	337
C(51)	3683(2)	2677(2)	392(2)	290
C(52)	3541(3)	2087(2)	-327(2)	313
C(53)	3931(3)	2349(3)	-1342(2)	361
C(54)	4463(3)	3229(3)	-1657(2)	373
C(55)	4637(4)	3813(3)	-965(2)	487
C(56)	4250(4)	3546(3)	49(2)	448
C(61)	4846(3)	1149(2)	2243(2)	290
C(62)	4803(3)	824(2)	3222(2)	365
C(63)	5947(3)	122(3)	3410(2)	404
C(64)	7168(3)	-284(2)	2621(2)	379
C(65)	7234(3)	12(3)	1648(2)	419
C(66)	6088(3)	719(2)	1462(2)	351

^a U_{eq} is the cube root of the product of the principal axes of the thermal ellipsoid.

In some cases, the desired CpCr(NO)(L)R complexes may be obtained directly by treatment of CpCr(NO)(L)I with 2 equiv of RMgCl, but these latter conversions probably also proceed via the CpCr(NO)(THF)R intermediates. The isolable product compounds are bright to dark green solids which, though generally stable in air for short periods of time, are best stored under an atmosphere of dinitrogen. The physical and spectroscopic properties of these complexes are given in Table 1. In THF solution these compounds display ESR signals at g values less than 2.00 and ν_{NO} bands in their IR spectra at approximately 1625 cm^{-1} . Table 1 also contains the IR and ESR spectroscopic data for the CpCr(NO)(THF)R intermediate complexes in which R = Me, CH₂Ph, CH₂SiMe₃, and *p*-tolyl, although none of these THF complexes have yet proven to be isolable.

ESR Spectroscopy of the CpCr(NO)(L)R Complexes. The ESR spectra of these 17-electron alkyl-containing complexes (Table 1) vary greatly in appearance. Some of the complexes display featureless singlets

Table 6. Selected Intramolecular Distances (\AA) and Angles (deg) for CpCr(NO)(PPh₃)(H)(SnPh₃) at 200 K

Sn-Cr	2.6690(7)	Cr-N	1.676(2)
Sn-C(41)	2.166(2)	Cr-C(1)	2.220(3)
Sn-C(51)	2.174(3)	Cr-C(2)	2.205(3)
Sn-C(61)	2.179(3)	Cr-C(3)	2.213(3)
Sn-H(10)	1.84	Cr-C(4)	2.243(3)
Cr-H(10)	1.55	Cr-C(5)	2.241(3)
Cr-P	2.364(1)	Cr-Cp ^a	1.875
P-C(11)	1.827(2)	P-C(31)	1.825(3)
P-C(21)	1.836(2)	O-N	1.208(3)
C(41)-Sn-Cr	123.45(6)	C(61)-Sn-C(51)	105.0(1)
C(51)-Sn-Cr	118.75(7)	H(10)-Sn-Cr	34
C(51)-Sn-C(41)	99.54(9)	H(10)-Sn-C(41)	112
C(61)-Sn-Cr	107.22(7)	H(10)-Sn-C(51)	94
C(61)-Sn-C(41)	100.24(9)	H(10)-Sn-C(61)	140
P-Cr-Sn	105.98(3)	Cp-Cr-N	127.9
N-Cr-Sn	90.94(8)	H(10)-Cr-Sn	42
N-Cr-P	94.66(8)	H(10)-Cr-P	69
Cp-Cr-Sn	114.46	H(10)-Cr-N	113
Cp-Cr-P	118.03	Cp-Cr-H(10)	116
O-N-Cr	174.3(2)	Cr-H(10)-Sn	104
C(11)-P-Cr	118.66(8)	C(31)-P-Cr	112.50(9)
C(21)-P-Cr	113.30(8)	C(31)-P-C(11)	104.0(1)
C(21)-P-C(11)	100.2(1)	C(31)-P-C(21)	106.9(1)

^a See footnote a of Table 4.

in their ESR spectra. However, in several cases, the CpCr(NO)(L)R compounds exhibit more complicated spectra which reveal varying degrees of delocalization of the unpaired electron. For instance, the prototypal complex CpCr(NO)(PPh₃)(CH₂SiMe₃) was the first of this class of compounds that we discovered to display evidence of significant delocalization of its unpaired electron. The X-band ESR spectrum of this compound in hexanes at 25 °C is shown in Figure 3. This remarkable spectrum reveals hyperfine coupling of the signal to the metal and to atoms in all of the ligands in the metal's coordination sphere, thereby indicating that the unpaired electron density is delocalized virtually over the entire molecule. Such extensive delocalization of unpaired electron density has never been previously observed in an organometallic system.²¹ It has been noted, however, that the unpaired electrons in the bimetallic {[HB(Me₂pz)₃]Mo(NO)Cl}₂(3,3'-bpy) complex (Me₂pz = 3,5-dimethylpyrazolyl; 3,3'-bpy = 3,3'-bipyridine) are strongly coupled through the 3,3'-bpy ligand.²²

Other isolable CpCr(NO)(L)R complexes also display evidence of delocalization of the unpaired electron density. From the ESR spectra of CpCr(NO)(py)(CH₂-SiMe₃) CpCr(NO)(pip)(CH₂SiMe₃), and CpCr(NO)(pip)(CH₂Ph) it is clear that the unpaired electron interacts with the ligands even though these spectra possess broader line widths. For example, the ESR spectrum of CpCr(NO)(pip)(CH₂SiMe₃) exhibits coupling of the unpaired electron to two nonequivalent ¹⁴N nuclei and to a ¹H nucleus, the latter probably being on the methylene group. The magnitude of the ⁵³Cr coupling constant reveals that the unpaired electron interacts to a similar extent with the metal center in this complex as it does in CpCr(NO)(PPh₃)(CH₂SiMe₃). Other hy-

(21) The related diamagnetic CpRe(NO)(PPh₃)Cl complex displays some evidence of delocalization of the HOMO over the entire molecule. See: Lichtenberger, D. L.; Rai-Chaudhuri, A.; Seidel, M. J.; Gladysz, J. A.; Agbossou, S. K.; Igau, A.; Winter, C. H. *Organometallics* **1991**, *10*, 1355.

(22) McWhinnie, S. L. W.; Jones, C. J.; McCleverty, J. A.; Collison, D.; Mabbs, F. E. *J. Chem. Soc., Chem. Commun.* **1990**, 940.

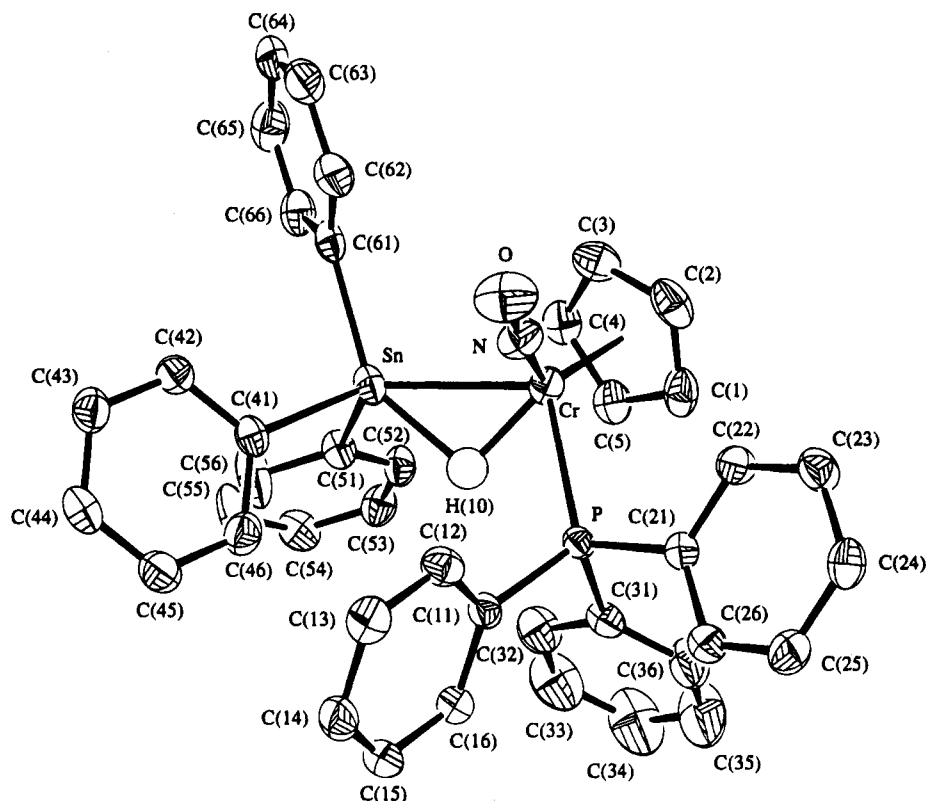


Figure 2. Solid-state molecular structure of $\text{CpCr}(\text{NO})(\text{PPh}_3)(\text{H})(\text{SnPh}_3)$ at 200 K. The 50% probability displacement ellipsoids are shown for the non-hydrogen atoms.

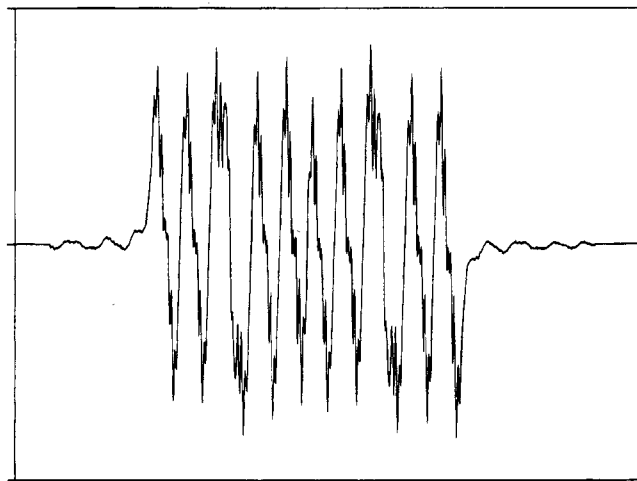


Figure 3. X-Band ESR spectrum of $\text{CpCr}(\text{NO})(\text{PPh}_3)(\text{CH}_2\text{SiMe}_3)$ in hexanes at 25 °C.

perfine couplings, if present, are not evident in this ESR spectrum since they are obscured by the width of the lines.

Some of the in situ generated $\text{CpCr}(\text{NO})(\text{THF})\text{R}$ complexes also appear to possess extensive delocalization of the unpaired electron density throughout the molecule. For example, the ESR signal of $\text{CpCr}(\text{NO})(\text{THF})(\text{CH}_2\text{SiMe}_3)$ species in THF solution appears as a pattern of 11 main lines, as shown in Figure 5. The overall pattern is the result of hyperfine coupling to the five equivalent protons on the Cp ring, the nitrosyl ^{14}N nucleus, and one of the diastereotopic protons on the methylene group. The coupling constant to the Cp protons is about the same as that observed for the ^{14}N nucleus, but both are only one-third as large as that found for the methylene proton. The fine structure

evident in each signal appears to result from an overlapping doublet of 1:2:1 triplets. This pattern may be attributed to coupling of the unpaired electron to the second diastereotopic methylene proton and also to two equivalent protons on the THF ligand. Which pair of THF protons interacts with the unpaired electron density would be governed by the orientation of the THF ligand with respect to the metal center. Nevertheless, the interaction with the THF ligand and the magnitude of the coupling to the Cp protons suggests that the unpaired electron in this system is even more delocalized than it is in the $\text{CpCr}(\text{NO})(\text{PPh}_3)(\text{CH}_2\text{SiMe}_3)$ complex (vide supra).

Solid-State Molecular Structure of $\text{CpCr}(\text{NO})(\text{PPh}_3)(\text{CH}_2\text{SiMe}_3)$. Among the relatively few 17-electron organometallic radical complexes to have been structurally characterized in the solid state, distortions in coordination geometry are common.^{2c,23} In contrast, in the solid-state molecular structure of $\text{CpCr}(\text{NO})(\text{PPh}_3)(\text{CH}_2\text{SiMe}_3)$, shown in Figure 1, all bond lengths and bond angles (Table 4) are normal and are comparable to those exhibited by related 18-electron cyclopentadienylchromium complexes which possess undistorted molecular geometries.²⁴ A few bond-torsion angles which describe the conformational features of the $\text{CpCr}(\text{NO})(\text{PPh}_3)(\text{CH}_2\text{SiMe}_3)$ molecule are as follows: $\text{Cr}-\text{C}(1)-\text{Si}-\text{C}(4) = -172.6(4)^\circ$, $\text{Si}-\text{C}(1)-\text{Cr}-\text{P} = 144.8(3)^\circ$, $\text{N}-\text{Cr}-\text{P}-\text{C}(31) = 179.4(3)^\circ$, $\text{Cr}-\text{P}-\text{C}(11)-$

(23) Baird, M. C. In *Organometallic Radical Processes*; Trogler, W. C., Ed.; Elsevier: New York, 1990; Chapter 2.

(24) (a) Greenhough, T. J.; Kolthammer, B. W. S.; Legzdins, P.; Trotter, J. *Acta Crystallogr., Sect. B* **1980**, *B36*, 795. (b) Ball, R. G.; Hames, B. W.; Legzdins, P.; Trotter, J. *Inorg. Chem.* **1980**, *19*, 3626. (c) Hermes, A. R.; Morris, R. J.; Girolami, G. S. *Organometallics* **1988**, *7*, 2372. (d) Daly, J. J.; Sanz, F.; Sneedon, R. P. A.; Zeiss, H. H. *J. Chem. Soc., Dalton Trans.* **1973**, 1497. (e) Herrmann, W. A.; Hubbard, J. L.; Bernal, I.; Korp, J. D.; Haymore, B. L.; Hillhouse, G. L. *Inorg. Chem.* **1984**, *23*, 2978.

C(16) = $-21.6(3)^\circ$, Cr–P–C(21)–C(22) = -49.7° , and Cr–P–C(31)–C(32) = -49.3° .

Even though the ESR spectrum of CpCr(NO)-(PPh₃)(CH₂SiMe₃) reveals that the unpaired electron has an unusually large coupling to one of the hydrogen atoms on the methylene group (vide supra), there is no structural evidence for any agostic interactions involving the methylene α -protons which were found during the structure determination.²⁵ The large difference between the hyperfine coupling constants to the two diastereotopic protons on the methylene group may thus be attributed to their different torsional relationships to the groups on Cr about the Cr–C(1) bond. Finally, it may also be noted that since the CpCr(NO)(PPh₃)(CH₂SiMe₃) molecule is asymmetric and contains strong crystal-field ligands, it is not subjected to a Jahn–Teller distortion of the type observed for CpCr(CO)₂(L) (L = PPh₃, PMe₃) systems in which the ligands forming the "legs" of the piano-stool structure are drawn toward each other.^{1g,2c,23,26}

Redox Properties of CpCr(NO)(L)R Complexes.

We have investigated the redox properties of selected CpCr(NO)(L)R complexes by cyclic voltammetry, and the results of these studies are collected in Table 1. These properties of these compounds differ in two important aspects from those displayed by their analogous halide complexes. First, the reduction potentials are much more negative for the alkyl complexes than for the halide species (Table 1).⁴ The shifts in reduction potentials are typical of those observed previously for the replacement of a halide ligand with an alkyl group in an organometallic complex.²⁷ The actual values of E'_{red} for the CpCr(NO)(L)R complexes investigated range from -1.9 to -2.3 V vs SCE, a feature which makes this series of compounds about as difficult to reduce as [Cp(η^6 -C₆Me₆)Fe]⁺ salts.²⁸ An important difference between these two systems, however, is that while the 18-electron Fe salts are reduced to 19-electron radicals, the 17-electron Cr complexes are ostensibly reduced to diamagnetic 18-electron species. The second difference is that the CpCr(NO)(L)R species display oxidation waves at fairly low positive potentials, in contrast to the CpCr(NO)(L)I complexes which do not display any oxidation features in THF. The end result, therefore, is that the CpCr(NO)(L)R complexes are difficult to reduce and are easy to oxidize. Interestingly, neither the oxidation nor the reduction features display reversible behavior on the time scales of the cyclic voltammetry experiments, thereby revealing that these electronically stable 17-electron compounds decompose upon conversion to 16-electron cations or 18-electron anions. This increase in reactivity upon formation of a complex with an even number of valence electrons is opposite to the usual trend observed between 17-electron and related 18-electron compounds.^{1h,4}

A cyclic voltammogram of CpCr(NO)(PPh₃)(CH₂SiMe₃) in MeCN is shown in Figure 4. After initial oxidation of the complex, features appear at negative potentials due to reduction of the oxidation products.

(25) The related Cp₂TiCH₂R (R = alkyl) systems are known to possess significant agostic interactions.¹¹

(26) MacConnachie, C. A.; Nelson, J. M.; Baird, M. C. *Organometallics* **1992**, *11*, 2522.

(27) Connely, N. G.; Geiger, W. E. *Adv. Organomet. Chem.* **1984**, *23*, 1.

(28) Astruc, D. *Chem. Rev.* **1988**, *88*, 1189.

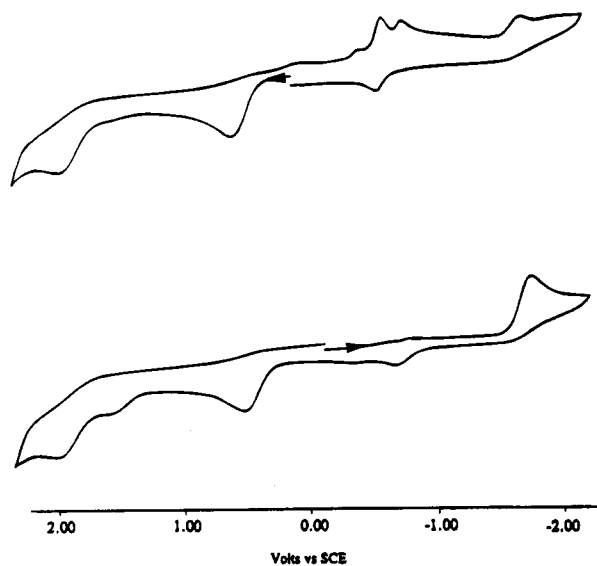


Figure 4. Cyclic voltammograms of CpCr(NO)(PPh₃)(CH₂SiMe₃) in MeCN at 25 °C.

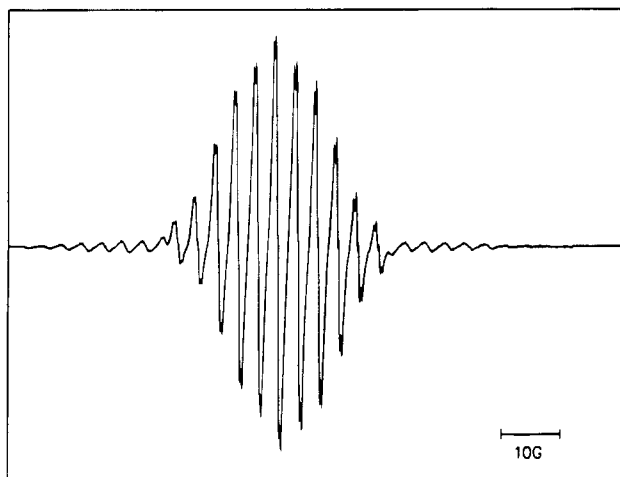
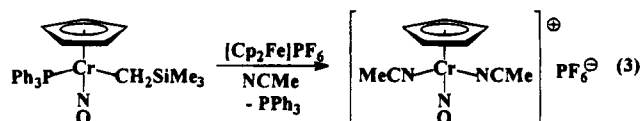


Figure 5. X-Band ESR spectrum of CpCr(NO)(THF)(CH₂SiMe₃) in THF at 25 °C.

These new features occur at potentials similar to those observed for the reduction of [CpCr(NO)(MeCN)₂]PF₆ (Table 1). Upon oxidation of CpCr(NO)(PPh₃)(CH₂SiMe₃), and probably the other CpCr(NO)(L)R complexes as well, it thus appears that the Cr–C σ -bond to the alkyl ligand is broken and the CH₂SiMe₃ radical is lost. Chemically, this oxidation process can be effected by treating CpCr(NO)(PPh₃)(CH₂SiMe₃) with [Cp₂Fe]PF₆ as summarized in eq 3.



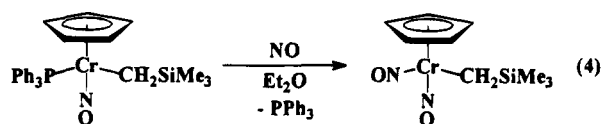
The loss of both the PPh₃ ligand and the alkyl group and subsequent formation of the known 17-electron radical cation complex [CpCr(NO)(MeCN)₂]PF₆⁹ is further evidence for the increased substitutional lability imparted by electron transfer from these CpCr(NO)(L)R complexes.

Reactivity of CpCr(NO)(PPh₃)(CH₂SiMe₃). The CpCr(NO)(PPh₃)(CH₂SiMe₃) complex is a fairly sterically hindered molecule, as has been established by

X-ray crystallography (vide supra). The steric protection of the metal center provided by the phosphine and the alkyl ligands results in this compound being less sensitive to air and moisture than the other complexes in its class. Indeed, $\text{CpCr}(\text{NO})(\text{PPh}_3)(\text{CH}_2\text{SiMe}_3)$ appears to be stable in air as a solid for several weeks. Furthermore, its reactivity with small neutral diamagnetic molecules is very limited. For instance, this complex does not react with carbon monoxide even when exposed to 600 psig of CO for 48 h in THF. Dihydrogen and ethylene do not react with the Cr complex under conditions similar to those used for CO.

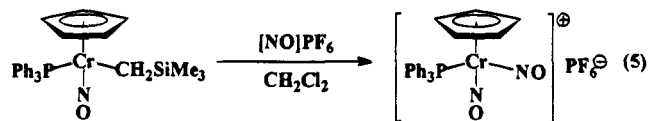
To delineate the characteristic reactivity of this interesting complex, we have treated $\text{CpCr}(\text{NO})(\text{PPh}_3)(\text{CH}_2\text{SiMe}_3)$ with several different reagents. We did not, however, investigate its reduction chemistry, given its relatively high E°_{red} value. The paramagnetic alkyl compound has been reacted with the small paramagnetic molecule NO, the electrophilic reagent $[\text{NO}]\text{-PF}_6$, and a potential source of a hydrogen atom, HSnPh_3 . The outcomes of these reactions are considered in the following sections.

(a) **With NO.** Solutions of $\text{CpCr}(\text{NO})(\text{PPh}_3)(\text{CH}_2\text{SiMe}_3)$ in Et_2O react with NO as summarized in eq 4.



This transformation results in the formation of the stable 18-valence-electron dinitrosyl species through substitution of the 2-electron phosphine ligand by the 3-electron nitrosyl ligand. The yield for this reaction appears to be quantitative by IR spectroscopy, which clearly reveals the conversion of the mononitrosyl starting material into the well-known dinitrosyl-containing product $\text{CpCr}(\text{NO})_2(\text{CH}_2\text{SiMe}_3)$.¹⁵

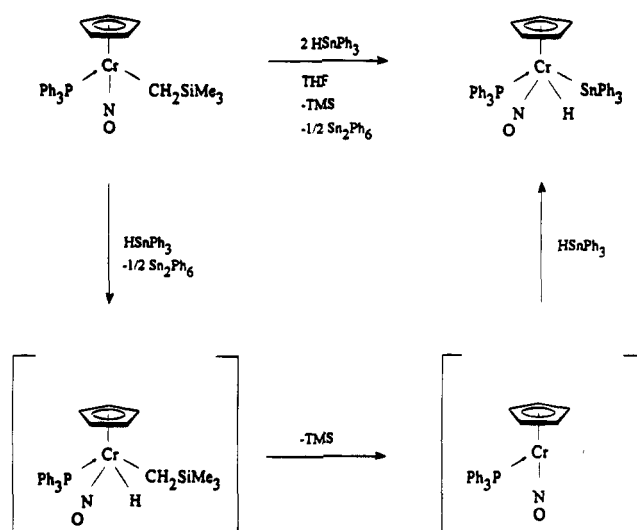
(b) **With $[\text{NO}]\text{PF}_6$.** Treatment of $\text{CpCr}(\text{NO})(\text{PPh}_3)(\text{CH}_2\text{SiMe}_3)$ in CH_2Cl_2 with the NO^+ electrophile results in Cr-C σ -bond cleavage rather than insertion, as occurs with $\text{CpCr}(\text{NO})_2\text{R}$ systems.²⁹ The reaction which occurs (eq 5) also results in the loss of the alkyl group from the metal center.



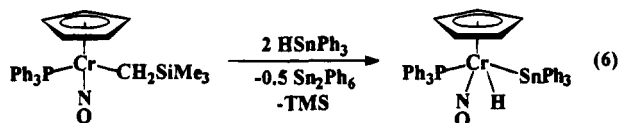
The CH_2SiMe_3 group is presumably lost as a radical during the reaction and is detected as a peak due to Me_4Si observed in the GC trace of the atmosphere above the final reaction mixture. The organometallic product of reaction 5 is interesting because it cannot be synthesized by treatment of the known $[\text{CpCr}(\text{NO})_2]^+$ cationic species with PPh_3 .³⁰ Nevertheless, $[\text{CpCr}(\text{NO})_2(\text{PPh}_3)]\text{-PF}_6$ can be purified by chromatography on silica gel and is air-stable once isolated.

(c) **With HSnPh_3 .** The reactivity of $\text{CpCr}(\text{NO})(\text{PPh}_3)(\text{CH}_2\text{SiMe}_3)$ with HSnPh_3 has also been investigated with a view to utilizing the tin reagent as a hydrogen atom source.^{2c} However, rather than produc-

Scheme 1



ing the expected 18-valence-electron $\text{CpCr}(\text{NO})(\text{PPh}_3)(\text{H})(\text{CH}_2\text{SiMe}_3)$ complex (for which a W analogue is known, from a different route),³¹ this reaction (eq 6) produces the novel $\text{CpCr}(\text{NO})(\text{PPh}_3)(\text{H})(\text{SnPh}_3)$ compound.



The conversion is effected in refluxing THF, and 2 equiv of HSnPh_3 is required to completely consume the organometallic reactant. The organometallic product of conversion 6 was the first chromium nitrosyl hydride ever isolated,⁶ and it is obtained as a green, air-stable, diamagnetic solid.³² A possible mechanistic pathway for its formation is outlined in Scheme 1. Under the experimental conditions necessary to effect this transformation, the Cr reactant could abstract a hydrogen atom from the stannane. The resulting alkyl hydride could then undergo reductive elimination, thereby forming a 16-electron, coordinatively unsaturated $[\text{CpCr}(\text{NO})(\text{PPh}_3)]$ fragment. This fragment could next oxidatively add another 1 equiv of stannane to form the final organometallic product. Support for these mechanistic ideas is provided by the detection of Me_4Si in the atmosphere above the final reaction mixture by gas chromatography. Furthermore, the production of the hexaphenyldistannane byproduct during reaction 6 can also be confirmed by IR spectroscopic and EIMS comparisons of the isolated material with authentic samples of Sn_2Ph_6 .

The physical properties of the $\text{CpCr}(\text{NO})(\text{PPh}_3)(\text{H})(\text{SnPh}_3)$ product merit some discussion. The solution ^1H NMR data for $\text{CpCr}(\text{NO})(\text{PPh}_3)(\text{H})(\text{SnPh}_3)$ in C_6D_6 indicate that there is little interaction between the

(31) Legzdins, P.; Martin, J. T.; Einstein, F. W. B.; Jones, R. H. *Organometallics* **1987**, *6*, 1826.

(32) The existence of $\text{HCr}(\text{CO})_4(\text{NO})$ at -40°C was reported prior to our work (Mantell, D. R.; Gladfelter, W. L. *J. Organomet. Chem.* **1988**, *347*, 333), and several *trans,trans*- $\text{Cr}(\text{H})(\text{CO})_2(\text{NO})(\text{PR}_3)_2$ complexes have been isolated subsequently (see: van der Zeijden, A. H.; Bürgi, T.; Berke, H. *Inorg. Chim. Acta* **1992**, *201*, 131; Peters, J. C.; Hillhouse, G. L.; Rheingold, A. L. *Polyhedron* **1994**, *13*, 1741).

(29) Legzdins, P.; Wassink, B.; Einstein, F. W. B.; Willis, A. C. *J. Am. Chem. Soc.* **1986**, *108*, 317.

(30) Regina, F. J.; Wojcicki, A. *Inorg. Chem.* **1980**, *19*, 3803.

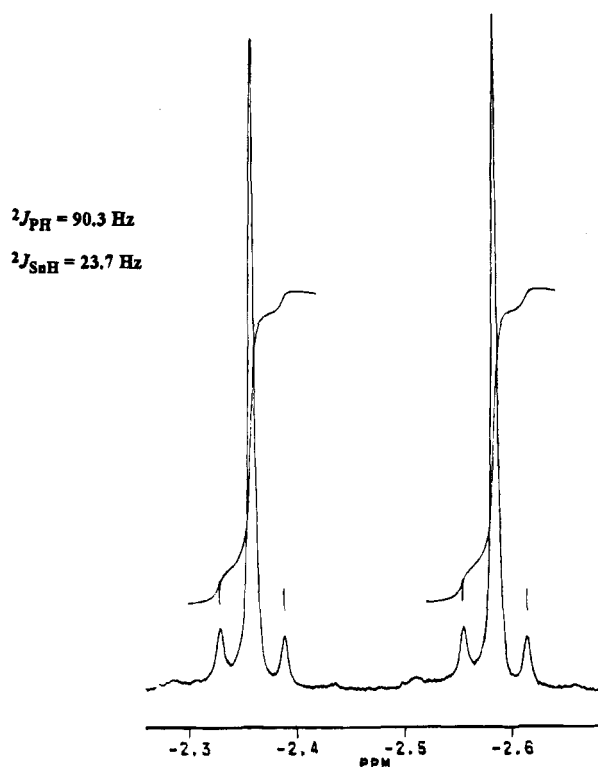


Figure 6. Hydride region of the ^1H NMR spectrum of $\text{CpCr}(\text{NO})(\text{PPh}_3)(\text{H})(\text{SnPh}_3)$ in C_6D_6 at ambient temperature.

hydride and the tin atoms and that the complex is correctly formulated as a stannyl hydrido species. Thus, the signal for the hydride at $\delta -2.47$ ppm (Figure 6) exhibits coupling to both phosphorus ($^2J_{\text{PH}} = 90.3$ Hz) and tin ($^2J_{\text{SnH}} = 23.7$ Hz). From the work of Schubert and co-workers on a series of similar complexes such as $\text{Cp}'\text{Mn}(\text{CO})_2(\text{H})(\text{SnPh}_3)$ ($\text{Cp}' = \eta^5\text{-C}_5\text{H}_4\text{Me}$), it is known that the magnitude of the Sn–H coupling constant is a direct measure of the amount of direct Sn–H bonding extant in the complex.^{33,34} In complexes where there is an agostic interaction between the transition metal and the Sn–H bond, the value of $^1J_{\text{SnH}}$ ranges from 1500 to 1800 Hz. Since the value of J_{SnH} evident in the ^1H NMR spectrum of $\text{CpCr}(\text{NO})(\text{PPh}_3)(\text{H})(\text{SnPh}_3)$ is less than 2% of the minimum value expected for an agostic interaction, it indicates that in solution there is no bond between the H and the Sn atoms in this complex.

$\text{CpCr}(\text{NO})(\text{PPh}_3)(\text{H})(\text{SnPh}_3)$ has also been subjected to an X-ray crystallographic analysis, and the solid-state molecular structure established by this analysis is shown in Figure 2. This 18-valence-electron complex effectively possesses a three-legged piano-stool structure, and its intramolecular metrical parameters (Table 6) are comparable to those exhibited by related cyclopentadienylmetal nitrosyl complexes.^{24,33} Evidently, the steric effects of the PPh_3 and SnPh_3 ligands are sufficiently large and that of the H ligand sufficiently small to force this molecular geometry on the complex rather than the expected four-legged piano-stool-type arrangement. Interestingly, the solid-state molecular structure of this complex indicates the possibility of an interaction between the Sn and H atoms; i.e., it may be viewed as

approaching an η^2 -stannane complex in the solid state. While the hydridic atom H(10) was poorly defined by this diffraction study, the bond angles at both the tin and chromium atoms (Table 6) corroborate its approximate location. The approximate hydride position and the arrangement of the other groups on both Sn and Cr atoms are consistent with the existence of some three-center, two-electron SnH–Cr bonding analogous to that invoked for $\text{Cp}'\text{Mn}(\text{CO})_2(\text{H})(\text{SnPh}_3)$.³³ Unfortunately, the solid-state ^1H NMR spectrum of $\text{CpCr}(\text{NO})(\text{PPh}_3)(\text{H})(\text{SnPh}_3)$ does not provide a definitive answer as to the electronic structure of the molecule. Most of the signal intensity in this spectrum appears as a very broad featureless singlet made up of the signals for the aromatic and cyclopentadienyl protons, but there is an unusually sharp signal at $\delta +2.50$ ppm which is attributable to the hydride resonance.

Reactivity of Other $\text{CpCr}(\text{NO})(\text{L})\text{R}$ Complexes with CO. As noted earlier in this report, $\text{CpCr}(\text{NO})(\text{PPh}_3)(\text{CH}_2\text{SiMe}_3)$ is inert to carbon monoxide even when exposed to high pressures of CO. However, less sterically congested $\text{CpCr}(\text{NO})(\text{L})\text{R}$ complexes react readily with CO. Thus, exposure of a THF solution of $\text{CpCr}(\text{NO})(\text{pip})(\text{CH}_2\text{Ph})$ to an atmosphere of CO results in the formation of $\text{CpCr}(\text{NO})(\text{CO})_2$ and $\text{CpCr}(\text{NO})(\text{pip})(\text{CO})$. It is unlikely that this reaction proceeds by reduction of the organometallic reactant by CO, since the amine complexes are more difficult to reduce than $\text{CpCr}(\text{NO})(\text{PPh}_3)(\text{CH}_2\text{SiMe}_3)$. It is more likely that the carbonyl product complexes are formed via initial CO coordination to the paramagnetic metal center, thereby forming $\text{CpCr}(\text{NO})(\text{pip})(\text{CO})(\text{CH}_2\text{Ph})$ as a 19-electron intermediate. This intermediate can then lose benzyl radicals prior to forming the very stable 18-electron products isolated.³⁵ These benzyl radicals then probably abstract H atoms from the solvent, thereby forming the toluene which is detectable by GC in the final reaction mixture. In a similar manner, exposure of in situ generated $\text{CpCr}(\text{NO})(\text{THF})(\text{CH}_2\text{SiMe}_3)$ to CO results in the formation of $\text{CpCr}(\text{NO})(\text{CO})_2$.

Interestingly, there is no evidence that insertion-type reactions occur with any of these complexes upon their being exposed to CO. This fact is in contrast to the facile CO-insertion processes undergone by the corresponding 16-electron dialkyl systems $\text{Cp}'\text{M}(\text{NO})\text{R}_2$ ($\text{M} = \text{Mo}, \text{W}$).^{36,37} Nevertheless, the facility of ligand substitutions in these $\text{CpCr}(\text{NO})(\text{L})\text{R}$ complexes is typical of the reactivity of 17-electron metal-centered radicals in general.² The unusual feature about the reactions of the $\text{CpCr}(\text{NO})(\text{L})\text{R}$ systems with CO is that the electron count at the metal center increases by 1 as a result of the substitution of a 1-electron-donor ligand for a two-electron ligand.

Summary

This work has established that the 17-valence-electron $\text{CpCr}(\text{NO})(\text{L})\text{R}$ compounds are unusual in that

(35) A similar loss of benzyl radicals has been invoked to occur during substitution reactions of the paramagnetic benzylchromium complexes $\text{Cp}'\text{Cr}(\text{L})(\text{CH}_2\text{Ph})_2$; see: Bhandari, G.; Kim, Y.; McFarland, J. M.; Rheingold, A. L.; Theopold, K. H. *Organometallics* **1995**, *14*, 738.

(36) (a) Dryden, N. H.; Legzdins, P.; Lundmark, P. J.; Riesen, A.; Einstein, F. W. B. *Organometallics* **1993**, *12*, 2085. (b) Debad, J. D.; Legzdins, P.; Batchelor, R. J.; Einstein, F. W. B. *Organometallics* **1993**, *12*, 2094.

(37) Richter-Addo, G. B.; Legzdins, P. *Metal Nitrosyls*; Oxford University Press: New York, 1992; Chapter 4.

(33) Schubert, U.; Kunz, E.; Harkers, B.; Willnecker, J.; Meyer, J. *J. Am. Chem. Soc.* **1989**, *111*, 2572.

(34) Schubert, U. *Adv. Organomet. Chem.* **1990**, *30*, 151.

in some cases the unpaired electrons are extensively delocalized throughout the metal's coordination sphere. These alkyl-containing complexes are easier to oxidize than are their iodo analogues, but they are harder to reduce. The reactivity that they display toward small molecules is somewhat dependent upon the steric congestion at the metal center. The ligand substitution reactions of the $\text{CpCr}(\text{NO})(\text{L})\text{R}$ complexes are dominated by their ability to lose ligands selectively to achieve an 18-valence-electron configuration in the final products. In particular, the loss of alkyl radicals occurs frequently during these latter transformations.

Acknowledgment. We are grateful to the Natural Sciences and Engineering Research Council of Canada

for support of this work in the form of grants to P.L. and F.W.B.E. We also thank Mr. K. M. Smith for helpful discussions and technical assistance and Professor F. G. Herring for assistance with the measurement and interpretation of some of the ESR spectra.

Supporting Information Available: Tables of supplementary crystallographic data, coordinates for the hydrogen atoms, anisotropic thermal parameters, and selected intramolecular torsion angles for the complexes $\text{CpCr}(\text{NO})(\text{PPh}_3)(\text{CH}_2\text{SiMe}_3)$ and $\text{CpCr}(\text{NO})(\text{PPh}_3)(\text{H})(\text{SnPh}_3)$ and tables giving additional bond distances and angles and least-squares planes for $\text{CpCr}(\text{NO})(\text{PPh}_3)(\text{H})(\text{SnPh}_3)$ (19 pages). Ordering information is given on any current masthead page.

OM950245Y

Gas-Phase Characterization by Photoelectron Spectroscopy of Unstabilized α -Unsaturated Arsines: Ethylidene- and Ethylidynarsines¹

V. Métail,[†] A. Senio,[†] L. Lassalle,[‡] J.-C. Guillemin,[‡] and G. Pfister-Guillouzo^{*,†}

Laboratoire de Physicochimie Moléculaire, URA CNRS 474, 64000 Pau, France, and
Laboratoire de Synthèses et Activations de Biomolécules, URA CNRS 1467,
35700 Rennes, France

Received May 18, 1995[®]

Primary unsaturated arsines, vinylarsine (**1**), prop-1-enylarsine (**2**), and ethynylarsine (**3**), prepared by a chemoselective reduction of the corresponding dichloroarsines, have been characterized in the gas phase by their photoelectron (PE) spectra. Their base-induced rearrangements on solid K_2CO_3 , in vacuum gas–solid reactions (VGSR) conditions, led, respectively, to ethylidenearsine (**4**), propylidenearsine (**5**), and ethylidynarsine (**6**). For the first time, electronic structures of primary α -unsaturated arsines and low-coordinate arsenic compounds are evidenced and the coherence with phosphorus analogues is confirmed. In particular, six narrow and well-resolved bands at 9.6, 10.6, 11.9, 12.7, 14.0, and 15.4 eV are observed in the PE spectra of **1**, and the spectrum of **3** exhibits three ionizations at 9.9, 10.6, and 11.6 eV. The spectra attributed to **4** and **5** display a broad band with a shoulder at 9.6 and 10.3 eV and at 9.5 and 10.2 eV, respectively. Two well-resolved bands at 9.6 and 12.1 eV are observed for **6**.

Introduction

Primary heterocompounds with double or triple bonds such as $CH_2=CHOH$, $HC\equiv COH$, $CH_2=CHNH_2$, and $HC\equiv CNH_2$ are well-known for their ability to isomerize into the corresponding heteroalkenes, -allenes, and -alkynes. This property depends mainly on the acidity of the hydrogen(s) bonded to heteroatom. The acid properties are related with the stability of the anionic species and the neutral molecule, the last one depending on the interactions between the $\pi_{C=C}$ system and the heteroatom lone pair. Experimental characterization of these molecules has been performed either in a matrix² or in the gas phase by mass spectrometry or photoelectron spectroscopy (PES).³ This last technique has proved to be particularly suitable for direct observation of compounds in which this type of interaction occurs. In this area, primary α -unsaturated phosphorus derivatives and the corresponding carbon–phosphorus multiple-bonded derivatives^{4–8} have been investigated

both from the experimental and theoretical points of view. Recent publications devoted to the preparation of the first primary α -unsaturated arsines⁹ and unstabilized arsaalkynes^{9b} prompted us to study alkenyl- and alkynylarsines and their rearrangement reactions with the aim to observe low-coordinate arsenic derivatives by photoelectron spectroscopy.

Experimental Section

Photoelectron spectra were recorded with a Helectros 0078 photoelectron spectrometer equipped with an 127° cylindrical analyzer using 21.21 eV He I and 40.81 eV He II radiation as the photon source and monitored by a microcomputer supplemented with a digital analog converter. Helium ionization at 4.98 eV and nitrogen ionization at 15.59 eV were used as references.

Arsines 1–3. The vinyl- and ethynyldichloroarsines were synthesized as previously reported.⁹ The corresponding primary arsines, vinylarsine (**1**), prop-1-enylarsine (**2**), and ethynylarsine (**3**) were prepared by chemoselective reduction of the dichloroarsines with tributylstannane or dichloroalane in tetraglyme⁹ (Scheme 1). To record the photoelectron spectra, two cold traps were fitted on a vacuum line (*ca.* 10^{-3} mbar)

[†] Laboratoire de Physicochimie.

[‡] Laboratoire de Synthèses et Activations de Biomolécules.

[®] Abstract published in *Advance ACS Abstracts*, September 15, 1995.

(1) Application of Photoelectron Spectroscopy to Molecular Properties. Part 49. Part 48: Chuburu, F.; Lacombe, S.; Pfister-Guillouzo, G.; Wentrup, C. *New J. Chem.* **1994**, *18*, 879–888.

(2) (a) Ethenol: Holmes, J. L.; Lossing, F. P. *J. Am. Chem. Soc.* **1982**, *104*, 2648–2649. Rodler, M.; Bauder, A. *J. Am. Chem. Soc.* **1984**, *106*, 4025–4028. Hawkins, M.; Andrews, L. *J. Am. Chem. Soc.* **1983**, *105*, 2523–2530. Ripoll, J. L. *New J. Chem.* **1979**, *3*, 195–198. Capon, B.; Rycroft, D. S.; Watson, T. W.; Zucco, C. *J. Am. Chem. Soc.* **1981**, *103*, 1761–1765. (b) Ethynamine: Lasne, M. C.; Ripoll, J. L. *Bull. Soc. Chim. Fr.* **1986**, 766–770.

(3) (a) Ethenol: Matti, G. Y.; Osman, O. I.; Upham, J. F.; Suffolk, R. J.; Kroto, H. W. *J. Electron. Spectrosc. Relat. Phenom.* **1989**, *49*, 195–201. (b) Ethenamine: Lafon, C.; Gonbeau, D.; Pfister-Guillouzo, G.; Lasne, M. C.; Ripoll, J. L.; Denis, J. M. *Nouv. J. Chim.* **1986**, *10*, 69–72. (c) Ethynol: Von Baar, B.; Weiske, T.; Terlouw, J. K.; Schwarz, H. *Angew. Chem., Int. Ed. Engl.* **1986**, *25*, 282–284. (d) Ethynamine: Wentrup, C.; Briehl, H.; Lorenca, P.; Vogelbacher, U. J.; Winter, H. W.; Maquestiau, A.; Flammang, R. *J. Am. Chem. Soc.* **1988**, *110*, 1337–1343. Von Baar, B.; Koch, W.; Lebrilla, C.; Terlouw, J.; Weiske, T.; Schwarz, H. *Angew. Chem., Int. Ed. Engl.* **1986**, *25*, 827–828.

(4) (a) Gonbeau, D.; Lacombe, S.; Lasnes, M. C.; Ripoll, J. L.; Pfister-Guillouzo, G. *J. Am. Chem. Soc.* **1988**, *110*, 2730–2735. (b) Lacombe, S.; Dong, W.; Pfister-Guillouzo, G.; Guillemin, C.; Denis, J. M. *Inorg. Chem.* **1992**, *31*, 4425–4427.

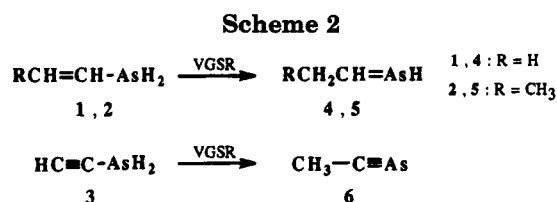
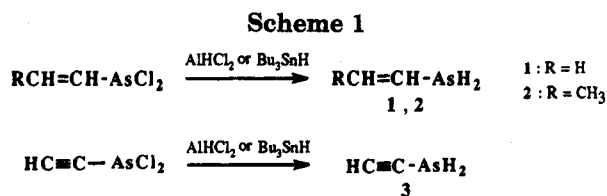
(5) (a) Lacombe, S.; Gonbeau, D.; Cabioch, J. L.; Pellerin, B.; Denis, J. M.; Pfister-Guillouzo, G. *J. Am. Chem. Soc.* **1988**, *110*, 6964–6967. (b) Dong, W.; Lacombe, S.; Gonbeau, D.; Pfister-Guillouzo, G. *New J. Chem.* **1994**, *18*, 629–641.

(6) Guillemin, J. C.; Janati, T.; Denis, J. M. *J. Chem. Soc., Chem. Commun.* **1992**, 415–416.

(7) Bock, H. *Phosphorus, Sulfur Silicon Relat. Elem.* **1990**, *49/50*, 3–53.

(8) (a) Bock, H.; Bankman, M. *Angew. Chem., Int. Ed. Engl.* **1986**, *25*, 265–266. (b) Bock, H.; Bankman, M. *Angew. Chem., Int. Ed. Engl.* **1989**, *28*, 911–912.

(9) (a) Alkenylarsines: Guillemin, J. C.; Lassalle, L. *Organometallics* **1994**, *13*, 1525–1527. (b) Alkynylarsines: Guillemin, J. C.; Lassalle, L.; Dréan, P.; Wlodarczak, G.; Demaison, J. *J. Am. Chem. Soc.* **1994**, *116*, 8930–8936 and references therein for other gas–solid reaction experiments.



and the last one was connected to the PES inlet. The dichloroarsine (5 mmol) was then added slowly (10 min) by syringe through a septum to the reducing agent solution cooled at 273 K. Due to their instability, volatile arsines 1–3 were continuously distilled *in vacuo* from the reaction mixture during and after the addition of dichloroarsine. The first cold trap (213 K) removed selectively the less volatile products, and compounds 1–3 were condensed in the second cold trap (liquid nitrogen bath, 77 K). At the end of the reaction, this cold trap was warmed to 183 K to remove traces of AsH_3 . After subsequent heating of the trap to the suitable temperature (1, 163 K; 2, 173 K; 3, 193 K), the analysis of the arsines 1–3 was completed by recording the photoelectron spectra of the gaseous flow.

Base-Induced Rearrangement of Arsines 1–3. The base-induced rearrangement of 1–3 was performed by contacting the gaseous α -unsaturated arsines with solid potassium carbonate at 373 K in vacuum gas–solid reactions (VGSR) conditions^{9b} (Scheme 2). Powdered and dried potassium carbonate (15 g) was introduced into a VGSR reactor ($l = 30$ cm, i.d. = 3.5 cm, Pyrex tube) and then horizontally distributed between two pads of glass wool 20 cm distant from each other. This reactor was fitted in an oven onto a vacuum line connected to the PES inlet. Arsines 1–3 (3.0 mmol) were prepared as reported above, and each was vaporized slowly *in vacuo* through the reactor. In addition, the purity of arsines 1–3 before their reaction on solid K_2CO_3 heated to 373 K was directly checked by PES (due to the parallel connection). The products were analyzed in the gas phase by photoelectron spectroscopy without further purification.

Results and Discussion

Only three primary and one secondary vinylarsines^{9a} and the alk-1-ynylarsine parent compound^{9b} have been described in the literature. Such compounds exhibit a half-life of about 30 min at room temperature in a solvent. Thus, their stability ranges between these of the corresponding phosphines^{5,6} and amines.^{3b,d} The decomposition of the arsenic derivatives leads to an insoluble brown oligomeric material and not to the corresponding carbon–arsenic multiple-bonded compounds.

Several arsaalkenes^{10–13} and three arsaalkynes^{9b,14} have been described. Due to the high reactivity of the $\text{C}=\text{As}$ double bond, its stabilization can be achieved only be aromatic conjugation (benzazarsole¹⁰ and 1,3-aza-

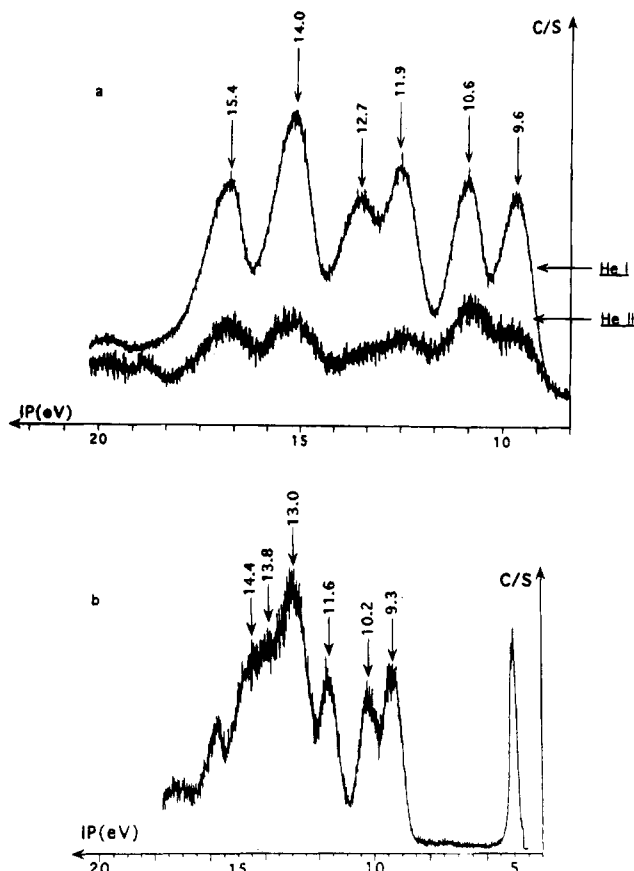


Figure 1. Photoelectron spectra of (a) vinylarsine (1) and (b) 1-propenylarsine (2).

arsinine¹¹), by steric hindrance ($\text{MeAs}=\text{C}(\text{OSiMe}_3)\text{-Bu}^t$),¹² or by coordination to transition metal fragments ($\text{PhAs}=\text{CH}_2$) RhCp^*).¹³ The kinetically stabilized 2-(2,4,6-tri-*tert*-butylphenyl)-1-arsaethyne^{14a} has been isolated in form of pale yellow crystals. *In situ* generation then complexing of $\text{R}-\text{C}\equiv\text{As}$ ($\text{R} = \text{H}, \text{CH}_3, \text{C}_6\text{H}_5, \text{SiMe}_3$)^{14b} or the chemical trapping of *tert*-butylarsaalkyne ($t\text{-BuC}\equiv\text{As}$)¹⁵ have also been described, but all attempts to characterize these derivatives spectroscopically failed. Moreover, even the isolated compounds cannot be vaporized. The base-induced rearrangement of ethynylarsine 3 in the gaseous phase is the first approach to a volatile and unstabilized arsaalkyne.^{9b} We used this facile rearrangement to prepare and to characterize by PES the ethynylarsine 6 and then to study the rearrangement products of the vinylarsines 1 and 2.

Vinyl-(1,2) and Ethynylarsine (3). Vinylarsines (1, 2) and ethynylarsines (3) are cleanly produced by a chemoselective reduction of the corresponding dichloroarsines.⁹ The reaction is performed in a vacuum line directly connected, via a cryogenic trap, to the PES inlet, and the gas flow is directly analyzed. The spectra of vinylarsine (1), prop-1-enylarsine (2), and ethynylarsine (3) are displayed in Figures 1a,b and 2, respectively. The He II spectrum of compound 1 is shown in Figure 1a. In the ethynylarsine 1 spectrum, six narrow and well-resolved bands are observed at 9.6, 10.6, 11.9, 12.7, 14.0, and 15.4 eV. With the He II radiation, the intensities of the first, third, and fourth bands decrease. For the prop-1-enylarsine (2), three well-resolved ionizations at 9.3, 10.2, and 11.6 eV and a broad band at 13.0 eV with marked shoulders at 13.8 and 14.4 eV have been

(10) Richter, R.; Sieler, J.; Richter, A.; Heinicke, J.; Tzschach, A.; Lindqvist, O. *Z. Anorg. Allg. Chem.* **1983**, *501*, 146–152.

(11) Märkl, G.; Dietl, S.; Ziegler, M. L.; Nuber, B. *Angew. Chem., Int. Ed. Engl.* **1988**, *27*, 709–710.

(12) Becker, G.; Gutekunst, G. *Z. Anorg. Allg. Chem.* **1980**, *470*, 157–166.

(13) Werner, H.; Paul, W.; Zolk, R. *Angew. Chem., Int. Ed. Engl.* **1984**, *23*, 626–627.

(14) (a) Märkl, G.; Sejpká, H. *Angew. Chem., Int. Ed. Engl.* **1986**, *25*, 264. (b) Seyferth, D.; Merola, J. S.; Henderson, R. S. *Organometallics* **1982**, *1*, 859–866.

(15) Hitchcock, P. B.; Johnson, J. A.; Nixon, J. F. *Angew. Chem., Int. Ed. Engl.* **1993**, *32*, 103–104.

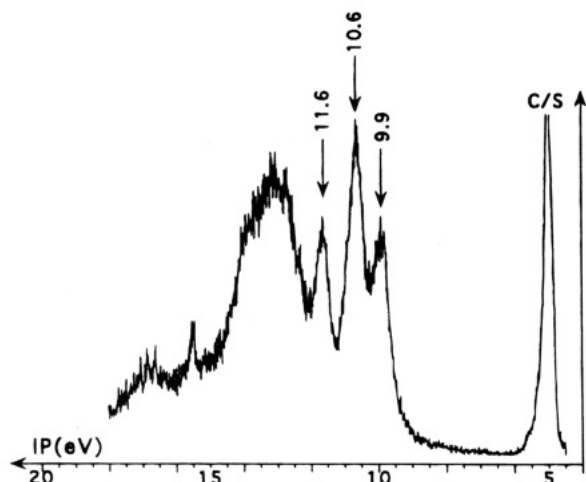


Figure 2. Photoelectron spectrum of ethynylarsine (3).

observed. The ethynylarsine **3** spectrum exhibits three ionizations at 9.9, 10.6, and 11.6 eV.

The PE spectrum of vinylphosphine has been analyzed on the basis of free rotation of the phosphino moiety, in contrast to ethenol and ethenamine for which the rotamer with the lone pair eclipsing the π system was characterized in the gas phase.⁵ The stabilizing interaction $n_X-\pi^*_{C=C}$ is weaker for ethynylphosphine due to the less pronounced directional character of the lone pair (*s*-character increasing). In fact, the He I photoelectron spectra of the series XH_3 and XMe_3 ($X = N, P, As, Sb$)¹⁶ show that the first ionization potentials assigned to the n_X lone pair are constant for all heteroatoms. Since this result is not in agreement with other atomic and molecular properties, such as basicity, atomic ionization potentials, and electronegativity, the anomalous constancy of the first IP values of XH_3 and XMe_3 was interpreted in terms of increasing in *s*-character of the lone pair on going from N to Sb.

Experimentally, with He II radiation, we observed for **1** a greater decrease in the first band intensity than for the second one, associated to greater participation of lone pair in the ionization. Compound **2**, which is methylated on the double bond, shows a similar shift to lower potentials for the first two bands (attributed to the ejection of one electron from the molecular orbitals resulting from interactions between the $C=C$ system and the arsenic lone pair). Thus, not only can the existence of the unique rotamer with the lone pair eclipsing the σ_{C-C} bond be ruled out, but the presence of a large population of rotamers with considerable arsenic lone pair- $\pi_{C=C}$ interactions can be supposed.

In addition, compounds **1** and **2** exhibit between the two first bands an energy gap of 0.95–1.0 eV (compared with 1.25 eV for vinylphosphine) resulting from weak $n_{As}-\pi_{C=C}$ interactions which are directly related to a greater C-As bond length and a more pronounced pyramidal configuration of the arsenic atom.

These observations suggest a free rotation of arsino group as previously observed for phosphino-analogue. Counterbalance between stabilizing ($n-\pi^*$, $n-\sigma^*$) and destabilizing ($n-\pi$, $n-\sigma$) interactions induces rotation tendency of heteroelement group around the σ_{C-X} bond.

For vinylarsine (**1**), the proposed free rotation of an arsino moiety around the C-As bond was checked by a theoretical study (3-21G basis set including d polariza-

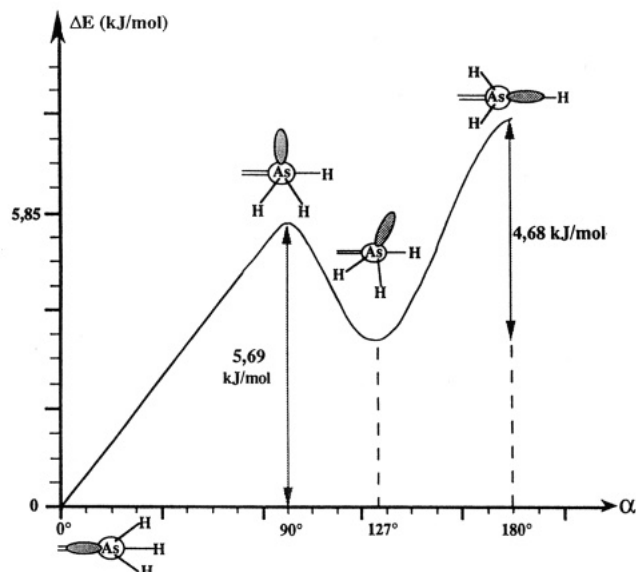


Figure 3. Rotation of the AsH_2 group about the As-C bond. Relative energies as a function of the dihedral angle between the arsenic lone pair and the C-C-As plane.

tion orbitals on the arsenic atom, geometrical parameters of different stationary points optimized after a second-order Moller-Plesset perturbation method). The curve of the potential energy hypersurface shows the existence of two minima at 0 and 127° (dihedral angle between arsenic lone pair and C-C-As plane) and two saddle points at 90 and 180°. The heights of rotation barriers are very low (5.68 and 4.68 kJ mol^{-1} , respectively). The same order of magnitude was observed for vinylphosphine (8–10 kJ mol^{-1}). The more energetically stable rotamer is assigned the geometrical structure with the arsenic lone pair eclipsing the σ_{C-C} bond (Figure 3).

This first characterization of vinylarsine by photoelectron spectroscopy emphasizes electronic structure similar to that of vinylphosphine (analogous profile of potential hypersurfaces curves with same energetically favored conformation, ionic state energies closed).

An electronic similarity occurs as well between ethynylphosphine and ethynylarsine **3**.⁶ For these systems, owing to the local cylindrical symmetry of acetylenic triple bond, all rotamers have the same energy and orbital energies are identical. It is worth noticing that for two rotamers, the heteroatom lone pair of which interacts strongly with only one of the acetylenic π orbitals, the first and third observed ionization potentials are described as a linear combination of the acetylenic π orbital and the arsenic lone pair. We observed a lower gap for **3** (1.7 eV), compared with its phosphorus analogues (2.06 eV), revealing weak interactions. The ionization potential of the other unperturbed π orbital is 10.6 eV and can be compared with 11.40 eV for acetylene. Thus, the destabilizing inductive effect of the arsino group is large.

Base-Induced Rearrangement of Vinyl- and Ethynylarsines. Vinylarsines (**1**, **2**) and ethynylarsine (**3**) have been vaporized over solid K_2CO_3 heated to 373 K. The gaseous flow was directly analyzed by photoelectron spectroscopy without further purification. As observed for the corresponding phosphorus derivatives,⁴ the expected arsaalkenes, ethylidenearsine (**4**), and propylidenearsine (**5**), are very unstable compounds. The ethylidenearsine (**6**), formed in the base-induced re-

(16) Elbel, S.; Bergman, H.; Enblin, W. *J. Chem. Soc., Faraday Trans. 2* 1974, 70, 555–559.

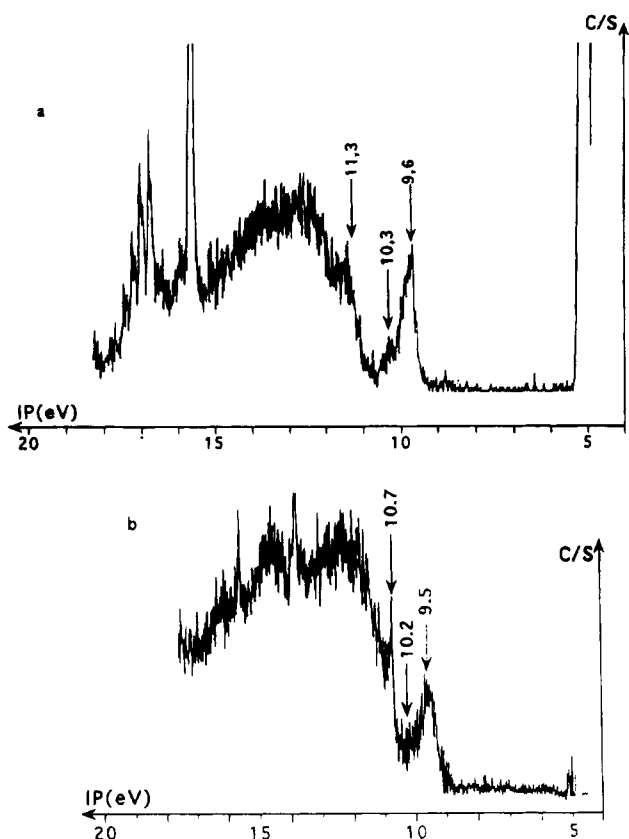


Figure 4. Photoelectron spectra of the gaseous products of reaction (a) of **1** and (b) of **2** over K_2CO_3 .

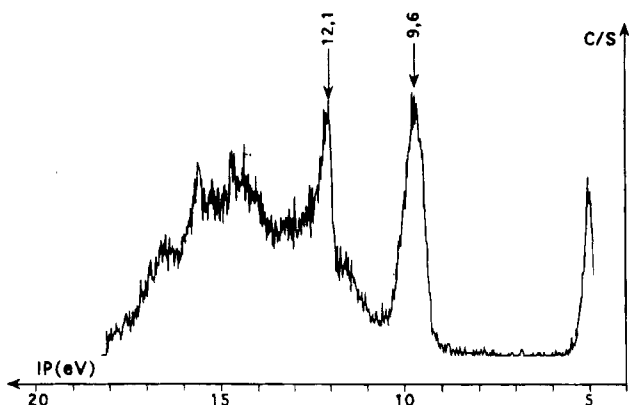


Figure 5. Photoelectron spectrum of the gaseous product of reaction of **3** over K_2CO_3 .

arrangement of the arsine **3**, is sufficiently stable to be condensed, revaporized, and analyzed.^{9b} A good purity is obtained as shown by the low-temperature 1H and ^{13}C NMR spectra. Thus, we can conclude that we obtained a PE spectrum of a quite pure product. The PE spectra of the vinylarsine (**1**) and propenylarsine (**2**) rearrangements and of the ethylidenearsine (**6**) are shown Figures 4a,b and 5, respectively.

Ethylidenearsine (4) and Propylidenearsine (5). The spectrum shown in Figure 4a presents a broad band at 9.6 eV with a shoulder at 10.3 eV followed by a second ionization at 11.3 eV. For 1-propenylarsine (**2**), the reaction is always partial. The spectrum obtained by digital subtraction of the spectrum of the starting compound is slightly shifted toward lower energy: it displays a broad signal at 9.5 eV with a shoulder and a second ionization at 10.7 eV. This spectrum shows numerous similarities with that of ethylidenephosphine.⁴ Thus, the first band at 9.75 eV was assigned

to the ionization of the $\pi_{C=P}$ orbital and the second band at 10.35 eV resulted from the ejection of one electron from the phosphorus lone pair.⁴ These assignments are supported only by experimental results because really sophisticated calculations, even with an extended basis set, cannot provide a satisfactory interpretation of the ionic states of these molecules (see ref 17 for phosphorus analogues).

Taking our experimental observations into account, it is reasonable to associate these two photoelectron spectra to ethylidenearsine (**4**) and propylidenearsine (**5**), respectively. The ionization at 9.6 eV for **4** (9.5 eV for **5**) is associated with the ejection of an electron of the $\pi_{C=As}$ orbital. Weak intensity ionizations at 10.3 eV for **4** (10.2 eV for **5**) are due to the ejection of an electron of the lone pair of arsenic atom (n_{As}). We observed a similar value in the spectrum of the corresponding phosphorus derivative.

Thus, for the first time, a carbon–arsenic double bond has been characterized in the gas phase by its photoelectron spectrum. Quantum mechanical calculations confirm the thermodynamic stability of this entity; $CH_3CH=AsH$ ($E_T = -2302.08858$ au) is 12.1 kJ mol⁻¹ more stable than $CH_2=CH-AsH_2$ ($E_T = -2302.08397$ au) (3-21G**MP2).

Ethylidenearsine. In the PE spectrum displayed in Figure 5, two well-resolved bands observed at 9.6 eV (a strong one) and 12.1 eV (a narrow band) characterize, without ambiguity, ethylidenearsine (**6**). The first band is assigned to ionization of the $\pi_{C=As}$ orbital, and the second one is assigned to ionization of the orbital localized on the arsenic sp lone pair. The shift of the first band to lower energy relative to ethylidenephosphine (9.77 eV) corresponds to a slightly more diffuse effect of the carbon–arsenic bond. Ionization of the arsenic lone pair appears at the same energy in the phosphorus case. In addition, according to quantum calculations $CH_3C=As$ ($E_T = -2300.92354$ au) is 93.3 kJ mol⁻¹ more stable than the starting compound $HC=CA_sH_2$ ($E_t = -2300.88797$ au). This energy difference probably explains the quantitative yield of triple-bond isomerization product and the partial double-bond rearrangement.

Thus, this photoelectron spectroscopy study led to the characterization in the gas phase of the carbon–arsenic triple bond and supports the results obtained by microwave spectroscopy.^{9b}

Conclusion

Primary alkenyl- and alkynylarsines have been characterized in the gas phase by their photoelectron spectra. The base-catalyzed isomerization of these compounds proves unambiguously the existence of low-coordinate arsenic derivatives, such as ethylidenearsine, propylidenearsine, and ethylidenearsine in the gas phase. Quantum mechanical calculations of the electronic structure of these systems are presently being undertaken with the aim of understanding the influence of hydrogen's strength of acid on isomerization reactions.

OM950359+

1,12-Dimethyl[1.1]ferrocenophane, an Organometallic Cyclohexane Analogue with Extraordinary Flexibility. Molecular Structure of a Third Isomer, *exo,endo,syn*-1,12-Dimethyl[1.1]ferrocenophane

Jan-Martin Löwendahl^{*,†}

Department of Organic Chemistry, Göteborg University, S-412 96 Göteborg, Sweden

Mikael Håkansson^{*,‡}

Department of Inorganic Chemistry, Chalmers University of Technology, S-412 96 Göteborg, Sweden

Received January 23, 1995[®]

A third isomer of 1,12-dimethyl[1.1]ferrocenophane (DMFCP), i.e. *exo,endo,syn*-1,12-dimethyl[1.1]ferrocenophane (**1c**), has been isolated and structurally characterized by X-ray diffraction. The conformational properties of **1c** and other [1.1]ferrocenophanes are discussed and compared with those of cyclohexanes.

Introduction

The conformational properties of the [1.1]ferrocenophanes have been discussed ever since 1,12-dimethyl[1.1]ferrocenophane (DMFCP) (Figure 1) was synthesized in 1966.¹ One of the original issues was if DMFCP preferred the "flexible" *syn* conformation (e.g. **1a**, Figure 2) or the "rigid" *anti* conformation (e.g. **1b**, Figure 2), and for a long time the *anti* conformation was ruled out due to the alleged inability to relieve internal steric strain.²⁻⁶ This led Mueller-Westerhoff and co-workers to assign an *exo,endo,syn*-DMFCP structure to the second isomer to be isolated from the synthesis of DMFCP.⁷ The set of NMR signals shown by this orange-red powder in a CDCl₃ solution is compliant with a *syn-syn* interconverting *exo,endo,syn*-DMFCP as well as with a C_{2h} type *exo,exo,anti*-DMFCP.⁸ Recently we were able to crystallize and structurally characterize an *anti* conformer of DMFCP, from a hexane solution of this orange-red powder. This structure demonstrated that there are ways of relieving steric strain in *anti* conformers as well.⁹ We now report the X-ray structure of crystals obtained from a THF solution of the orange-red powder which shows that these crystals consists of a third isomer of DMFCP, i.e. *exo,endo,syn*-1,12-dimethyl[1.1]ferrocenophane (**1c**). At present it is not clear which conformational isomer is the dominant species in solution. For a diagrammatical representation of

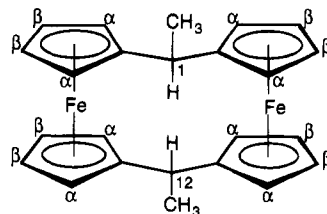


Figure 1. 1,12-Dimethyl[1.1]ferrocenophane (DMFCP) consists of two ferrocene units connected with two carbon bridges, i.e. C1 and C12. The ring protons next to the carbon bridges are named α -protons, and the other ring protons are named β -protons.

1a-c and the parent compound [1.1]ferrocenophane (**2**) see Figure 2.

The parent compound [1.1]ferrocenophane (**2**) shows unusual flexibility, and a complex degenerate interconversion was proposed to explain the simple NMR spectrum (only three signals) of **2**.⁶ We have proven that **2** indeed goes through a degenerate internal rearrangement and determined the free energy of activation to be 28 ± 4 kJ mol⁻¹.¹⁰ The most likely mechanism for this interconversion is a pseudorotation of the same type that can be seen in the cyclohexane system. In order to clarify some of the conformational properties of the [1.1]ferrocenophane molecules, we now introduce a comparison between the cyclohexane and [1.1]ferrocenophane systems.

Experimental Section

General Data. All operations were carried out under nitrogen. Tetrahydrofuran (THF) and hexane were distilled from sodium/benzophenone shortly prior to use.

Preparation of *exo,endo,syn*-1,12-Dimethyl[1.1]ferrocenophane (1c**).** A mixture of the 1,12-dimethyl[1.1]ferrocenophane isomers was prepared according to the literature method.⁷ This isomer mixture (9 g) was dissolved in 800 mL of hexane by gentle warming, whereafter the temperature was lowered to approximately 4 °C, which resulted in the crystal-

(10) Löwendahl, M.; Davidsson, Ö.; Ahlberg, P. *J. Chem. Res., Symp.* **1993**, 1, 40-41.

[†] E-mail address: jml@oc.chalmers.se.

[‡] E-mail address: hson@inoc.chalmers.se.

[®] Abstract published in *Advance ACS Abstracts*, September 1, 1995.

(1) Watts, W. E. *J. Am. Chem. Soc.* **1966**, *88*, 855-856.

(2) Mueller-Westerhoff, U. T.; Nazzal, A.; Proessdorf, W. *J. Am. Chem. Soc.* **1981**, *103*, 7678-7681.

(3) Kansal, V. K.; Watts, W. E.; Mueller-Westerhoff, U. T.; Nazzal, A. *J. Organomet. Chem.* **1983**, *243*, 443-449.

(4) Barr, T. H.; Lentzner, H. L.; Watts, W. E. *Tetrahedron* **1969**, *25*, 6001-6013.

(5) McKechnie, J. S.; Berstedt, B.; Paul, I. C.; Watts, W. E. *J. Organomet. Chem.* **1967**, *8*, 29-31.

(6) Watts, W. E. *J. Organomet. Chem.* **1967**, *10*, 191-192.

(7) Cassens, A.; Eilbracht, P.; Nazzal, A.; Proessdorf, W.; Mueller-Westerhoff, U. T. *J. Am. Chem. Soc.* **1981**, *103*, 6367-6372.

(8) Löwendahl, M. Thesis, Göteborg University, 1995.

(9) Löwendahl, M.; Davidsson, Ö.; Ahlberg, P.; Håkansson, M. *Organometallics* **1993**, *12*, 2417-2419.

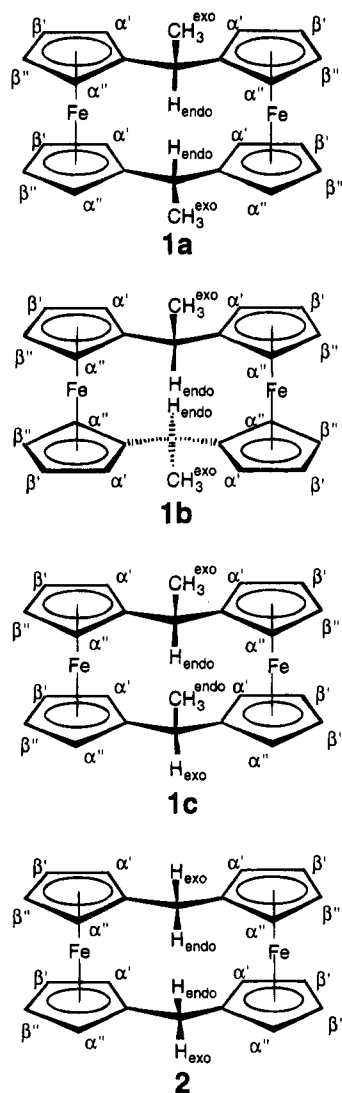


Figure 2. Diagrammatic representation of compounds **1a–c**, and **2**.

lization of mainly **1a** (3 g) after a few days. The solution was decanted and evaporated to dryness, yielding an orange-red powder (6 g). A portion of this orange-red powder (100 mg) was then dissolved in 5.0 mL of THF at ambient temperature. The crystallization of large red needles (64 mg) of **1c** was achieved by cooling the solution to 4 °C for a few days.

NMR Spectroscopy. All NMR spectra were recorded using a Varian Unity 500 spectrometer. The measuring frequency was 500 MHz (^1H). THF- d_8 was used as a solvent. Typically 5 mg of the compound was dissolved in 1 mL of the solvent.

Proton NMR: one doublet at 1.23 ($J = 7.1$ Hz) ppm for the methyl groups; one quartet at 3.60 ppm ($J = 7.1$ Hz) for the methine protons; four multiplets for the ring protons, with β -protons at 4.24 and 4.27 ppm and α -protons at 4.12 and 4.16 ppm ($J < 1.5$ Hz). The THF signal at 3.58 ppm was taken as the reference signal.

X-ray Crystallography. Crystal and experimental data for $[\text{C}_{24}\text{H}_{24}\text{Fe}_2]$ (**1c**) are summarized in Table 1. Data were collected at 200 K with a Rigaku AFC6R diffractometer, using a red irregular-shaped crystal with the dimensions $0.30 \times 0.30 \times 0.30$ mm, which was mounted in a Lindemann capillary. Diffracted intensities were measured using graphite-monochromated Mo $K\alpha$ ($\lambda = 0.71073$ Å) radiation from an RU200 rotating anode source operated at 9 kW (50 kV, 180 mA). The $\omega/2\theta$ scan mode was employed, and stationary background counts were recorded on each side of the reflection, the ratio of peak counting time and background counting time being

Table 1. Crystallographic Data for *exo,endo,syn*-1,12-Dimethyl[1.1]ferrocenophane (1c**)**

formula	$\text{C}_{24}\text{H}_{24}\text{Fe}_2$	β , deg	90
fw	424.15	γ , deg	90
color	red	V , Å ³	3592(4)
cryst syst	orthorhombic	Z	8
space group	$Pbca$ (No. 61)	d_{calc} , g/cm ³	1.569
a , Å	14.949(8)	μ , cm ⁻¹	16.19
b , Å	18.745(5)	T , K	200
c , Å	12.819(5)	R	0.035
α , deg	90	R_w	0.045

2:1. Data were measured for $5 < 2\theta < 50^\circ$, using an ω scan rate of $8.0^\circ/\text{min}$ and a scan width of $(1.26 + 0.30 \tan \theta)^\circ$. Weak reflections ($I < 10.0\sigma(I)$) were rescanned up to three times and counts accumulated to improve counting statistics. The intensities of three reflections monitored regularly after measurement of 150 reflections confirmed the crystal stability during data collection. Correction was made for Lorentz and polarization effects. No correction was made for the effects of absorption, owing to failure to obtain a more satisfactory structural model from empirically corrected data (by means of azimuthal scans, yielding a transmission factor range of 0.76–1.00 with an average value of 0.94). Cell constants were obtained by least-squares refinement from the setting angles of 20 reflections in the range $15 < 2\theta < 30^\circ$.

The structure was solved by direct methods (MITHRIL),¹¹ and the hydrogens were located from difference maps. Full-matrix least-squares refinement, including anisotropic thermal parameters for the iron and carbon atoms, with positional parameters (the isotropic thermal parameters were fixed) for the hydrogen atoms, gave a final $R = 0.035$ ($R_w = 0.045$) for 307 parameters and 2238 observed reflections. The maximum and minimum values in the final difference map were 0.61 and -0.56 e/Å³, respectively. Fractional coordinates and thermal parameters are given in Table 2, and selected intramolecular distances and angles are listed in Table 3. The crystallographic numbering is shown in Figure 3. All calculations were carried out with the TEXSAN¹² program package. Atomic scattering factors and anomalous dispersion correction factors were taken from ref 13. Figure 3 has been drawn with ORTEP.¹⁴

Results and Discussion

When considering the conformational space of the [1.1]ferrocenophane system, it is rewarding to use an analogy with the well-investigated cyclohexane system.^{15–21} First, when one looks at the boat conformer of cyclohexane and the *syn* conformer of [1.1]ferrocenophane, it becomes apparent that the bow and stern carbon atoms in cyclohexane (atoms 1 and 4 in Figure

(11) Gilmore, C. J. *J. Appl. Crystallogr.* **1984**, *17*, 42.

(12) TEXSAN-TEXRAY Structure Analysis Package, Molecular Structure Corp., The Woodlands, TX, 1989.

(13) *International Tables for X-ray Crystallography*; Kynoch Press: Birmingham, England, 1974; Vol. IV.

(14) Johnson, C. K. ORTEP. Report ORNL-3794; Oak Ridge National Laboratory, Oak Ridge, TN, 1965.

(15) Anet, F. A. L.; Bourn, A. J. R. *J. Am. Chem. Soc.* **1967**, *89*, 760–768.

(16) Burkert, U.; Allinger, N. L. *Molecular Mechanics*; American Chemical Society: Washington, DC, 1982.

(17) Cremer, D.; Szabo, K. J. In *Conformational Behavior of Six-Membered Rings: Analysis, Dynamics and Stereoelectronic Effects*; Juaristi, E., Ed.; VCH: Weinheim, Germany, in press. We thank Prof. D. Cremer and Ph. D. K. Szabo for making their manuscript available to us prior to publication.

(18) Eliel, E. L.; Wilen, S. H.; Mander, L. N. *Stereochemistry of Organic Compounds*; Wiley: New York, 1993; pp 13–14, 49–51, 686–726.

(19) March, J. *Advanced Organic Chemistry: Reactions, Mechanisms, and Structure*, 4th ed.; Wiley-Interscience: New York, 1992; pp 143–146.

(20) Sachse, H. *Ber. Bunsen-Ges. Phys. Chem.* **1890**, *23*, 1363.

(21) Sachse, H. *Z. Phys. Chem.* **1892**, *10*, 203.

Table 2. Positional Parameters and $B(\text{eq})$ or B Values (\AA^2) for *exo,endo,syn*-1,12-Dimethyl-[1.1]ferrocenophane (1c**)**

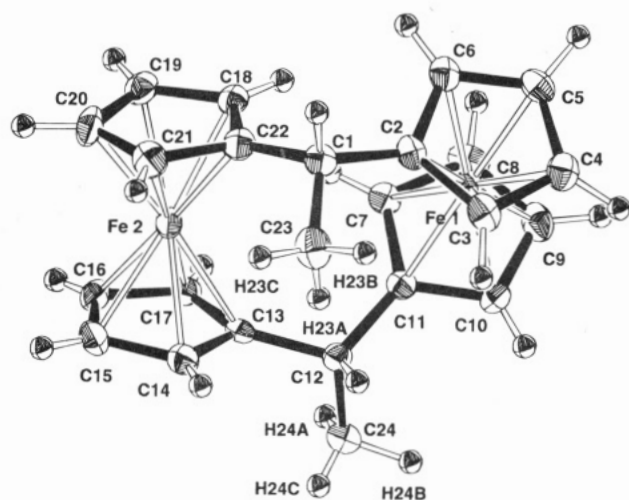
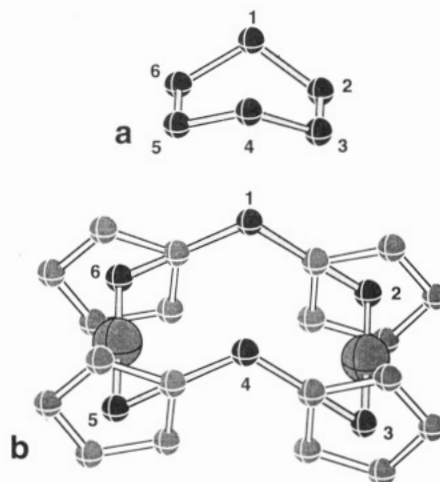
atom	x	y	z	$B(\text{eq})/B$
Fe(1)	0.40120(4)	0.15095(3)	0.67568(5)	1.51(3)
Fe(2)	0.15840(4)	0.09322(3)	0.48136(5)	1.62(3)
C(1)	0.3715(3)	0.0473(2)	0.4625(3)	1.8(2)
C(2)	0.4232(3)	0.0785(2)	0.5541(3)	1.7(2)
C(3)	0.4844(3)	0.1359(3)	0.5499(4)	2.0(2)
C(4)	0.5341(3)	0.1384(3)	0.6450(4)	2.2(2)
C(5)	0.5027(3)	0.0820(2)	0.7089(4)	2.0(2)
C(6)	0.4346(3)	0.0449(3)	0.6532(4)	1.8(2)
C(7)	0.2702(3)	0.1697(2)	0.7231(3)	1.7(2)
C(8)	0.3304(3)	0.1717(3)	0.8092(3)	1.9(2)
C(9)	0.3945(3)	0.2262(3)	0.7906(4)	2.4(2)
C(10)	0.3740(3)	0.2566(3)	0.6927(4)	2.0(2)
C(11)	0.2981(3)	0.2226(2)	0.6493(3)	1.5(2)
C(12)	0.2550(3)	0.2468(2)	0.5487(3)	1.6(2)
C(13)	0.1805(3)	0.2011(2)	0.5054(3)	1.6(2)
C(14)	0.1679(3)	0.1859(3)	0.3977(4)	2.0(2)
C(15)	0.0831(3)	0.1547(3)	0.3842(4)	2.4(2)
C(16)	0.0419(3)	0.1498(3)	0.4831(4)	2.1(2)
C(17)	0.1025(3)	0.1785(2)	0.5575(4)	1.8(2)
C(18)	0.2272(3)	0.0225(2)	0.5756(3)	1.6(2)
C(19)	0.1389(3)	-0.0029(2)	0.5548(4)	2.1(2)
C(20)	0.1303(3)	-0.0098(3)	0.4453(4)	2.5(2)
C(21)	0.2135(3)	0.0102(3)	0.3990(4)	2.3(2)
C(22)	0.2738(3)	0.0310(2)	0.4800(3)	1.9(2)
C(23)	0.3855(4)	0.0916(3)	0.3652(4)	2.6(2)
C(24)	0.2184(4)	0.3229(3)	0.5646(4)	2.4(2)
H(1)	0.396(3)	0.001(2)	0.448(3)	2.2
H(3)	0.485(3)	0.176(2)	0.499(4)	2.4
H(4)	0.573(3)	0.180(2)	0.662(3)	2.6
H(5)	0.524(3)	0.067(2)	0.785(4)	2.4
H(6)	0.397(3)	0.006(2)	0.676(3)	2.2
H(7)	0.218(3)	0.141(2)	0.723(3)	2.0
H(8)	0.326(3)	0.142(2)	0.871(3)	2.3
H(9)	0.444(3)	0.240(2)	0.833(3)	2.9
H(10)	0.402(3)	0.293(2)	0.667(3)	2.4
H(12)	0.300(2)	0.253(2)	0.496(3)	1.9
H(14)	0.208(3)	0.194(2)	0.347(3)	2.4
H(15)	0.057(3)	0.138(2)	0.321(4)	2.9
H(16)	-0.004(3)	0.136(3)	0.496(4)	2.5
H(17)	0.092(3)	0.179(2)	0.621(4)	2.2
H(18)	0.252(3)	0.031(2)	0.641(3)	1.9
H(19)	0.088(3)	-0.014(2)	0.606(4)	2.5
H(20)	0.077(3)	-0.028(2)	0.408(4)	3.0
H(21)	0.229(3)	0.014(2)	0.325(4)	2.8
H(23A)	0.364(3)	0.139(3)	0.376(4)	3.1
H(23B)	0.456(3)	0.094(3)	0.343(4)	3.1
H(23C)	0.358(3)	0.075(3)	0.303(4)	3.1
H(24A)	0.176(3)	0.319(3)	0.616(4)	2.9
H(24B)	0.270(3)	0.357(3)	0.589(3)	2.9
H(24C)	0.202(3)	0.345(3)	0.510(4)	2.9

4a) are analogous to the bridge methylene carbon atoms in [1.1]ferrocenophane (atoms 1 and 4 in Figure 4b). Second, the other carbon atoms in the cyclohexane ring (atoms 2, 3, 5, and 6 in Figure 4a) are then analogous to the dummy atoms which are placed at the center of gravity of the cyclopentadienyl moieties (atoms 2, 3, 5, and 6 in Figure 4b).

The extent of this analogy is especially clear from Figure 5, where a comparison is made between 1,12-dimethyl[1.1]ferrocenophane (DMFCP) and 1,4-dimethylcyclohexane. Consider, for example, *exo,exo,syn*-DMFCP (*syn* = boat), which is analogous to boat-1(e),4(e)-dimethylcyclohexane (e = equatorial). It is well-known that boat-1(e),4(e)-dimethylcyclohexane can interconvert into boat-1(a),4(a)-dimethylcyclohexane (a = axial) *via* pseudorotation (or ring inversion), and the same mechanistic pathways are also open to *exo,exo,syn*-DMFCP, whereby it becomes *endo,endo,syn*-DMFCP. Consequently, there are eight structures of

Table 3. Selected Intramolecular Distances (\AA) and Angles (deg) for $[\text{C}_{24}\text{H}_{24}\text{Fe}_2]$ (1c**)**

Fe(1)-C(2)	2.093(4)	Fe(1)-C(3)	2.056(4)
Fe(1)-C(4)	2.039(5)	Fe(1)-C(5)	2.039(5)
Fe(1)-C(6)	2.070(5)	Fe(1)-C(7)	2.081(5)
Fe(1)-C(8)	2.050(4)	Fe(1)-C(9)	2.042(5)
Fe(1)-C(10)	2.033(5)	Fe(1)-C(11)	2.072(4)
Fe(2)-C(13)	2.073(5)	Fe(2)-C(14)	2.047(5)
Fe(2)-C(15)	2.036(5)	Fe(2)-C(16)	2.040(5)
Fe(2)-C(17)	2.051(5)	Fe(2)-C(18)	2.068(5)
Fe(2)-C(19)	2.054(5)	Fe(2)-C(20)	2.029(5)
Fe(2)-C(21)	2.053(5)	Fe(2)-C(22)	2.082(4)
C(1)-C(2)	1.523(6)	C(1)-C(22)	1.500(5)
C(11)-C(12)	1.511(6)	C(12)-C(13)	1.500(5)
C(1)-C(23)	1.514(7)	C(12)-C(24)	1.500(5)
C(2)-C(3)	1.413(6)	C(3)-C(4)	1.427(6)
C(4)-C(5)	1.418(7)	C(5)-C(6)	1.425(6)
C(6)-C(2)	1.428(6)	C(7)-C(8)	1.424(6)
C(8)-C(9)	1.421(7)	C(9)-C(10)	1.412(7)
C(10)-C(11)	1.416(6)	C(7)-C(11)	1.432(6)
C(2)-C(1)-C(22)	117.0(4)	C(2)-C(1)-H(1)	108(3)
C(2)-C(1)-C(23)	110.7(4)	C(11)-C(12)-C(13)	117.3(4)
C(11)-C(12)-H(12)	110(2)	C(11)-C(12)-C(24)	108.4(4)
C(1)-C(2)-C(3)	126.3(4)	C(1)-C(2)-C(6)	125.2(4)
C(2)-C(3)-C(4)	109.3(4)	C(12)-C(13)-C(14)	124.6(4)
C(12)-C(13)-C(17)	127.3(4)	C(13)-C(14)-C(15)	108.8(4)

**Figure 3.** ORTEP drawing showing the crystallographic numbering in **1c**.**Figure 4.** Structure elements that are common to both cyclohexane and [1.1]ferrocenophane.

DMFCP, with respect to the positions of the bridges (*syn* or *anti*) and to the positions of the methyl groups (*exo* or *endo*). However, of these eight structures, there are two pairs with identical structures, two *exo,endo,anti*-DMFCP isomers (Figure 6A), and two *exo,endo,syn*-

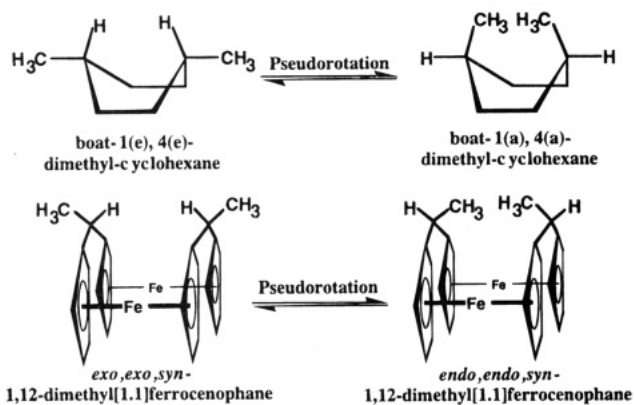


Figure 5. Example of the common conformational properties of cyclohexane and [1.1]ferrocenophane.

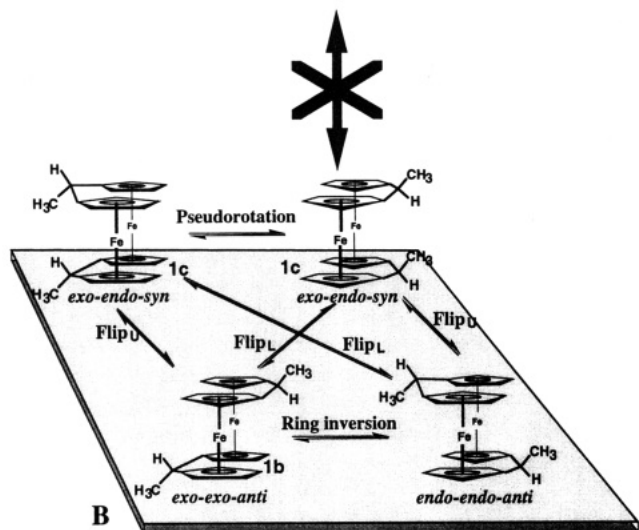
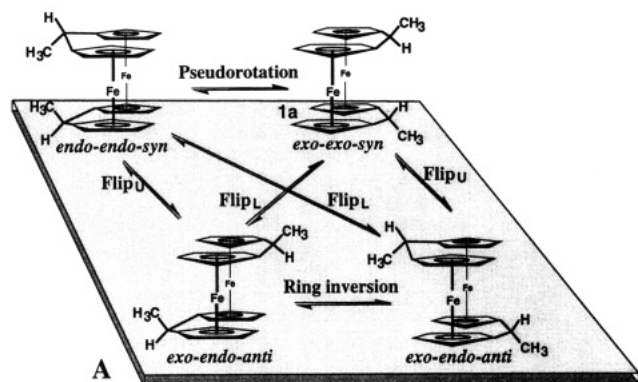


Figure 6. The six diastereoisomers of 1,12-dimethyl[1.1]ferrocenophane and their interconversion pathways. Flip_U and Flip_L means a flip of the upper and lower bridges, respectively.

DMFCP isomers (**1c**, Figure 6B), which are connected *via* ring inversion and pseudorotation, respectively. This leaves six possible diastereoisomers¹⁸ of DMFCP. Figure 6 depicts these diastereoisomers as well as their interconversion pathways. For simplicity the comparison is always made between boat and *syn* structures and chair and *anti* structures and not, in some cases, the more energetically stable twist forms (see Table 4). Furthermore, if a twist is introduced in the diastereoisomers the complexity increases since there will be enantiomeric pairs of each structure. The optical activity depends on whether the twist is clockwise or anti-clockwise relative to the eclipsed starting point.

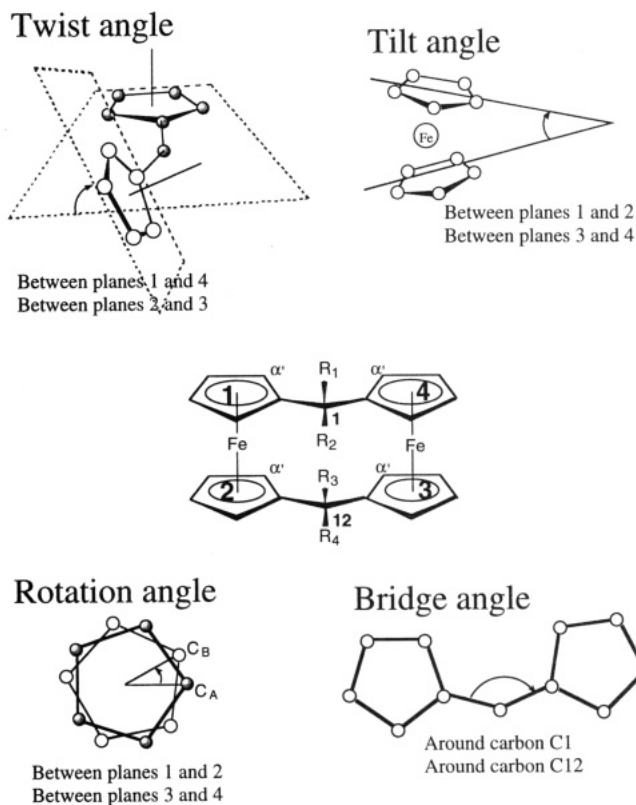


Figure 7. Description of the four essential angles in a [1.1]ferrocenophane molecule.

Figure 6A shows *exo,exo,syn*-DMFCP (**1a**), *endo,endo,syn*-DMFCP, and *exo,endo,anti*-DMFCP which all are conformational isomers¹⁸ i.e. they can interconvert without breaking any bonds. Figure 6B shows *exo,exo,anti*-DMFCP (**1b**), *endo,endo,anti*-DMFCP, and *exo,endo,syn*-DMFCP (**1c**), which also are conformational isomers. The conformers within parts A and B of Figure 6 belong to different configurational isomers;¹⁸ i.e., they cannot interconvert unless there is a bond broken (or inversion at a carbon). In Figure 6, the term "flip" means a flip of one of the bridge carbons from one side to the other, which is the mechanistic equivalent of half a ring inversion. Out of the six diastereoisomers, three have been crystallized so far. The first isomer to be structurally characterized by X-ray diffraction was *exo,exo,syn*-DMFCP^{5,22} (**1a**), and the second isomer was *exo,exo,anti*-DMFCP⁹ (**1b**). The crystal structure of the third isomer, *exo,endo,syn*-DMFCP (**1c**), is reported in this work.

The relatively large variation in the Fe–C bond distances (Table 3) can be rationalized in terms of the twist and tilt experienced by **1c**. Still, the carbons in each cyclopentadienyl ring are essentially coplanar. The Fe1···Fe2 intramolecular distance of 4.533(2) Å does not suggest any metal–metal interaction. We have previously suggested that the main structural features of a [1.1]ferrocenophane molecule is given by four essential angles: the *twist*, the *rotation*, the *tilt*, and the *bridge* angle (see Figure 7).⁹ The twist angle is defined as the dihedral angle between the best planes of the cyclopentadienyl rings of the *same* organic ligand. The rotation angle is defined by the [C_A–(center of gravity of ring

(22) McKechnie, J. S.; Maier, C. A.; Bersted, B.; Paul, I. C. *J. Chem. Soc., Perkin Trans. 2* **1973**, 138–143.

Table 4. The Four Essential Angles (deg) in Different Isomers of 1,12-Dimethyl[1.1]ferrocenophane Together with Two Different Forms of [1.1]Ferrocenophane

isomer	twist angle	rotation angle	tilt angle	bridge angle
1a (<i>exo,exo,syn</i>) ²²	30.2	21.5	3.1	115.8
	31.5	23.9	3.0	117.5
1b (<i>exo,exo,anti</i>) ⁷	36.1	3.4	4.1	116.9
	34.0	53.9 ^a	22.7	118.1
1c (<i>exo,endo,syn</i>) (this work)	39.4	32.0	7.3	117.0
	38.2	31.4	6.2	117.3
2a (<i>syn</i>) ²³	13.8	~10	2.4	121.3
	12.7	~10	1.4	121.7
2b (<i>syn</i>) ²⁴	1.6	0.5	3.6	121.8
	3.2	0.6	1.0	122.5

^a A rotation angle of 53.9° is reasonable only with reference to a [1.1]ferrocenophane molecule, but for a comparison with ferrocene derivatives a value of 18.1° (72–53.9) is the adequate rotation angle. This angle is close to an ideal midpoint (18.0°) between an eclipsed and a staggered conformation.

A)–(center of gravity of ring B)–C_B] torsion angle, where rings A and B are the cyclopentadienyl rings of one “ferrocene unit”. The tilt angle can then be defined as the dihedral angle between the two rings (i.e. from different organic ligands) of such a ferrocene unit. Finally, the bridge angle is defined as the bond angle around the bridging carbon with respect to the two quaternary ring carbons in the same organic ligand. In Table 4, these angles are listed for **1a–c** and for the two known phases of the unsubstituted parent [1.1]ferrocenophane (**2**).^{23,24}

From the data in Table 4, some general relationships involving the essential angles can be established (there are a few special exceptions).

1. The bridge angle seems not to be coupled to any other angle.
2. The twist and rotation angles are directly linked as components of a “pure” pseudorotation.
3. The tilt angle automatically induces a change in the twist angle which usually, but not always, leads to a change in the rotation angle.
4. The tilt angle is instrumental in the ring inversion mechanism.

Furthermore, the data in Table 4 indicate three different mechanisms to relieve internal steric strain in [1.1]ferrocenophane molecules, bearing in mind that packing effects—i.e. intermolecular contacts—also will be of significance for the solid-state conformation. There are several intermolecular H···H distances in **1c** in the order of 2.3–2.7 Å, which can be compared with several intramolecular contacts that lie in the same range. The first mechanism involves an opening of the bridge angle in order to reduce H···H intramolecular repulsive interactions of the α' protons. This mechanism is utilized by all the [1.1]ferrocenophanes but is especially visible in **2b**, which exhibits a bridge angle of 122°. The second mechanism increases the twist and rotation angles, i.e. starts a movement along a pseudo-rotational path, which initially results in an increase of the distances between the α' protons in the same organic ligand. In this mechanism, both the twist angles and

the rotation angles change in a coupled manner, and it is used by all [1.1]ferrocenophanes with the exception of **2b** (**1b** comprises a special case, *vide infra*). In the third mechanism, the tilt angle is altered, which seems to be the mechanism with the steepest energy potential. The effect of tilting is divided into two parts. First, as in the case of **1b** (*exo,exo,anti*), where the *anti* conformation of the carbon bridges makes a pseudorotation impossible, the asymmetric tilt (tilting of only one ferrocene unit) induces a twist. This tilt-induced twist has the same effect as in a *syn* conformer. Second, a symmetric tilt (tilting both the ferrocene units to the same degree and in the same direction respectively, e.g. outwards) has the effect of making the carbon bridges come apart. This reduces the steric interaction between the *endo* methine protons in e.g. **1a** (*exo,exo,syn*) and is especially important in **1c** (*exo,endo,syn*) in order to reduce the steric tension between the *endo* methyl protons (e.g. H23A) and the *endo* methine proton (e.g. H12), referring to Figure 3.

The phenomena which are hardest to rationalize with a cyclohexane analogy are the conformational properties of the ferrocene units. However, the effects of movements in the “organometallic ball bearing”, which is how ferrocene can be considered, may be explained in terms of bond rotation and bond angle bending. First, consider the cyclopentadienyl moieties as two carbon rings floating on the “iron ball”, i.e. Fe²⁺. When they are parallel to each other, the Gibbs free energy of activation for their rotation, relative to each other, is 0.9 kcal/mol,²⁵ which is much less than 2.9 kcal/mol, the Gibbs free energy of activation for the C–C bond rotation in ethane.¹⁹ The movement of cyclopentadienyl moieties toward each other on the surface of the “iron ball” represents a tilt in the ferrocene unit, or a bending over the iron atom. This would mean a bending of, for example, the bond angle defined by atoms 1, 2, and 3 in Figure 4a, which is the prerequisite for a ring inversion mechanism. One difference with regard to the cyclohexane system is that in [1.1]ferrocenophane the 2–3 distance has to become shorter with an opening of the 1–2–3 angle (see Figure 4b) and that the 2–3–4 angle has to be equal to the 1–2–3 angle. To somehow put the energetic requirements for bending in ferrocene in perspective, the MM2 type bending force constants of ferrocene in a ferrocenophane and a C–C–C bond angle have been set to 0.500 mdyn/deg (73.2 kcal/deg)^{26,27} and 0.450 mdyn/deg (65.9 kcal/deg),¹⁶ respectively, where the natural bond angles are set to 111.01 and 109.5°, respectively.

The NMR spectrum of **1c** in THF indicates a degenerate interconversion (or accidental chemical shift equivalence), since only six signals can be recorded,⁷ e.g. only one doublet for the methyl protons at 1.23 ppm. However, whether this interconversion occurs *via* a pseudorotation, or *via* ring inversion with **1b** as an intermediate, is not possible to deduce. Computational chemistry may be able to model the [1.1]ferrocenophane system well enough to give us the answers in the future,

(25) Haaland, A. *Acc. Chem. Res.* **1979**, *12*, 415–422.

(26) The units have been corrected relative to the original paper after personal communication with Dr. Rudzinski.

(27) Rudzinski, J. M.; Ōsawa, E. *J. Phys.-Org. Chem.* **1992**, *5*, 382–394.

(23) Rheingold, A. L.; Mueller-Westerhoff, U. T.; Swiegers, G. F.; Haas, T. J. *Organometallics* **1992**, *11*, 3411–3417.

(24) Håkansson, M.; Löwendahl, M.; Davidsson, Ö.; Ahlberg, P. *Organometallics* **1993**, *12*, 2841–2844.

although a number of problems are currently encountered, such as the lack of well-developed molecular-mechanics parametrization, the size (220 electrons), and the notorious difficulties in *ab initio* calculations on ferrocene itself.²⁸ One might, however, hope that the experimental data gathered so far in the [1.1]ferrocenophane system and the parallels that can be drawn with the cyclohexane system will be an incentive to advance the computational methods sufficiently in order to handle this kind of system.

Acknowledgment. We thank Professor Per Ahlberg for fruitful discussions and the Swedish Natural Science Research Council (NFR) for financial support.

Supporting Information Available: Tables of anisotropic thermal parameters for the non-hydrogen atoms, all bond distances and angles, intermolecular contacts, and least-squares planes for **1c** (20 pages). Ordering information is given on any current masthead page. A QUICKTIME film illustrating the pseudorotation of [1.1]ferrocenophane has been produced. Contact J.-M.L. for information on how to retrieve it.

(28) Park, C.; Almlöf, J. *J. Chem. Phys.* **1991**, *95*, 1829–1833.

OM950051I

Synthesis and Structure of Novel Group 6 Complexes of Dibenzofulvalenes

Robert C. Kerber* and Brian Waldbaum

Department of Chemistry, SUNY at Stony Brook, Long Island, New York 11794-3400

Received May 15, 1995^o

The complexes ($\mu, \eta^5: \eta^5$ -dibenzo[*a,d*]fulvalene) $M_2(CO)_6$ (**1a**, $M = Cr$; **1b**, $M = Mo$; **4**, $M = Mo$, [*a,f*] isomer; **1c**, $M = W$) were prepared in the cases of Cr and Mo by a one-pot double-deprotonation, migration, and oxidation sequence starting with ($\mu, \eta^5: \eta^5$ -3,3'-biindenyl) $M_2(CO)_6$ (**3a,b**) and in the case of W directly from 1,1'-biindenyl and $W(CO)_3(py)_3$. The dianion of **1a** reacted with Diazald to give ($\mu, \eta^5: \eta^5$ -dibenzo[*a,d*]fulvalene) $Cr_2(CO)_4(NO)_2$, **15**. Crystal structures were determined for **3a**, **4**, and the trimethyl phosphite substitution product of **1b** (**11**). The solid state conformation of **3a** apparently results from a compromise between the tendency of the tricarbonylchromium moieties to point in opposite directions and the preference for an *s-trans* configuration of the organic ligand. The Mo-Mo bond length in **4** is 3.286(4) Å, compared with 3.371(1) Å found in (fulvalene)dimolybdenum hexacarbonyl; both structures exhibit comparable degrees of pyramidalization, although the annulated analogue is significantly more twisted. The Mo-Mo bond of **11** was also shorter (3.317 Å) than that of the fulvalene analogue. The degree of twisting found in **11** is intermediate between **4** and (fulvalene)dimolybdenum hexacarbonyl.

Bimetallic compounds have attracted a great deal of attention in recent years on the basis of the idea that the concerted effects of two metals in close proximity should result in novel reactions useful in stoichiometric synthesis and in catalysis.¹ Fulvalene (bicyclopentadienylidene) has provided the foundation for many bimetallic complexes² in part because of the strong bonding of its cyclopentadienyl rings to early and middle transition metals. In contrast to the well-studied cyclopentadienylmetal carbonyl dimers, the fulvalene-bridged analogues are expected to show, and have shown in several cases, enhanced reactivity. This is due, in part, to the ability of the fulvalene ligand to allow for metal-metal bond cleavage while inhibiting fragmentation to mononuclear complexes; the potential for metal-metal cooperativity is maintained thru relative proximity and possibly by communication through the π -bond system of the fulvalene ligand.³ Unique chemistry is also expected as a result of the distortion of the fulvalene ligand seen in several structures of metal-metal bonded bimetallic derivatives. The ring centroids of a planar fulvalene are separated by 4 Å,⁴ while most M-M bonds are less than 3.5 Å long. Consequently, the fulvalene ligand acquires a pyramidalized structure to accommodate M-M bond lengths of 2.8–3.5 Å: still longer, and

possibly more reactive, than those in the analogous cyclopentadienyl dimers.⁵

Nonetheless, there are shortcomings to fulvalene as a bridging ligand. Cyclopentadienyl rings almost invariably bond to transition metals in an η^5 manner. This results in strong bonding, but the η^5 -Cp ring occupies three coordination sites of the metal, leaving little room for additional ligands in the case of late transition metals, and it tends to disfavor associative reactions which require reduction in hapticity.⁶ In contrast, (η^5 -indenyl)metal compounds often display enhanced reactivity in ligand substitution reactions. This phenomenon, termed the "indenyl effect,"⁷ is attributed to the ease of slippage from a nominally 18-electron η^5 structure to a 16-electron η^3 structure, assisted by restoration of full aromaticity to the benzene ring. The "indenyl effect" may be expected to enhance the reactivity of dibenzofulvalene complexes relative to those of fulvalene. We herein report the synthesis of novel group 6 bimetallic complexes **1a–c** and offer a preliminary comparison of their reactivity with that of the analogous fulvalene compounds.

The route to complexes **1** is shown in Scheme 1. Starting material **2**, 1,1'-biindenyl,⁸ is used as a mixture of the *d,l* and *meso* forms; it is available in high yield from the $CuCl_2$ -mediated oxidative coupling of indenide anions⁹ and is significantly more stable than dihydrofulvalene, the starting material used in the synthesis of the fulvalene analogues.¹⁰ Treatment of **2** with either

^o Abstract published in *Advance ACS Abstracts*, September 15, 1995.

(1) Review articles include: Muettterties, E. L.; Krause, M. J. *Angew. Chem., Int. Ed. Engl.* **1983**, *22*, 147–204. Roberts, D. A.; Geoffroy, G. L. *Comprehensive Organometallic Chemistry*; Wilkinson, G.; Stone, F. G. A., Abel, E. W., Eds.; Pergamon Press: Oxford, U.K., 1982; Vol. 6, chapter 40, pp 763–877. Gladfelter, W. L.; Geoffroy, G. L. *Adv. Organomet. Chem.* **1980**, *18*, 207–73. Beck, W.; Niemer, B.; Wieser, M. *Angew. Chem., Int. Ed. Engl.* **1993**, *32*, 923–49.

(2) (a) Tilset, M.; Vollhardt, K. P. C.; Boese, R. *Organometallics* **1994**, *13*, 3146–69 and previous papers, cited therein, from the Vollhardt group. (b) El Amouri, H.; Besace, Y.; Vaissermann, J.; Jaouen, G.; McGlinchey, M. J. *Organometallics* **1994**, *13*, 4426–30. (c) Delville, M. -H.; Lacoste, M.; Astruc, D. *J. Am. Chem. Soc.* **1992**, *114*, 8310–1.

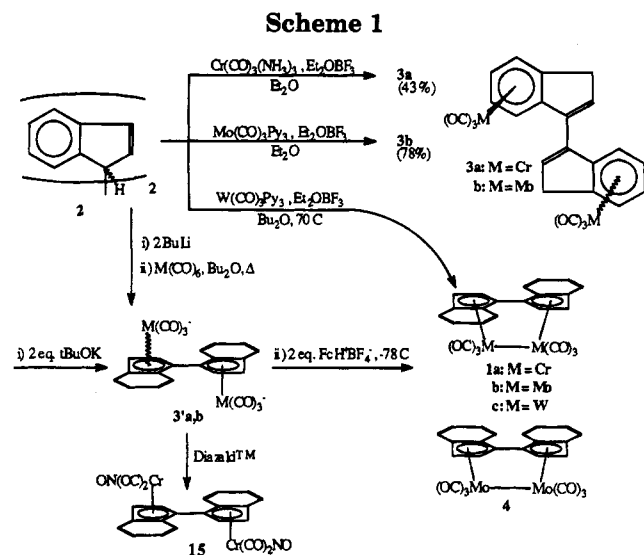
(3) Desbois, M.-H.; Astruc, D.; Guillin, J.; Maiot, J. P.; Varret, F. *J. Am. Chem. Soc.* **1985**, *107*, 5280.

(4) Churchill, M. R.; Wormald, J. *Inorg. Chem.* **1969**, *8*, 1970.

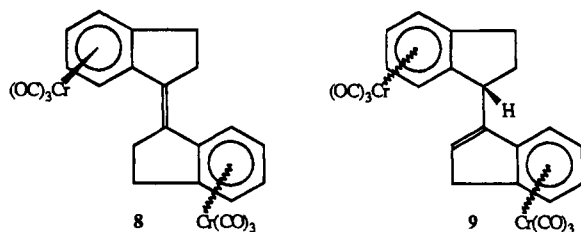
(5) McGovern, P. A.; Vollhardt, K. P. C. *Synlett* **1990**, 493–500.

(6) Cotton, F. A. *Disc. Faraday Soc.* **1969**, *47*, 79–83. Crabtree, R. H. *The Organometallic Chemistry of the Transition Metals*; J. Wiley & Sons, Inc.: New York, 1988; pp 104–5.

(7) Review: O'Connor, J. M.; Casey, C. P. *Chem. Rev.* **1987**, *87*, 307–18. More recent examples cited by: Poë, A. J. *Mechanisms of Inorganic and Organometallic Reactions*; Twigg, M. V., Ed.; Plenum Press: New York, 1991; chapter 10, pp 239–41. Szajek, L. P.; Lawson, R. J.; Shapley, J. R. *Organometallics* **1991**, *10*, 357–61. Frankcom, J. C.; Green, J. C.; Nagy, A.; Kakkar, A. K.; Marder, T. B. *Organometallics* **1993**, *8*, 3688–97. Ceccon, A.; Gambaro, A.; Saverio, S.; Valle, G.; Vanzo, A. *J. Chem. Soc., Chem. Commun.* **1989**, 51–2. Habib, A.; Tanke, R. S.; Holt, E. M.; Crabtree, R. H. *Organometallics* **1989**, *8*, 1225–31. Merola, J. S.; Kacmarcik, R. T. *Organometallics* **1989**, *8*, 778–84.

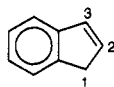


$\text{Cr}(\text{CO})_3(\text{NH}_3)_3$ ¹¹ or $\text{Mo}(\text{CO})_3(\text{py})_3$ ¹² (3 equiv) in the presence of $\text{Et}_2\text{O}\cdot\text{BF}_3$ in Et_2O forms either **3a** (43%) or **3b** (78%), respectively. In both cases, the double bonds of the organic ligand migrate during complexation to give exclusively the 3,3'-biindenyl complexes. (η^6 -3,3'-Biindenyl) $\text{Cr}(\text{CO})_3$, **10**, as well as reduced compounds **8** and **9**, form as side products in the synthesis of **3a**, with NH_3 conceivably serving as the proton source. Analogous products are not detected in the case of **3b**.



The ability of the tricarbonylmetal moieties to point either in the same or opposite direction, combined with that of the organic ligand to assume either an *s-cis* or *s-trans* conformation, generates four idealized diastereomeric possibilities. Complexes of the type (arene)- $(\text{Cr}(\text{CO})_3)_2$ in which the arene is a rigid, fused polycyclic system usually occur as the *anti* isomer.¹³ In the case of (μ , η^6 : η^6 -biphenyl) $(\text{Cr}(\text{CO})_3)_2$ where the phenyl groups can rotate freely, the benzene rings assume a nearly coplanar conformation, and the tricarbonylchromium moieties are *anti*.¹⁴ Introduction of *ortho* substituents causes the molecule to twist away from an idealized *anti* planar arrangement; in cases where an *ortho* substitu-

(8) The position of substituents on the five-membered ring of indene are indicated as shown.



(9) Nicolet, P.; Sanchez, J.-Y.; Benaboura, A.; Abadie, M. J. M. *Synthesis* **1987**, 202-3.

(10) Vollhardt, K. P. C.; Weidman, T. W. *Organometallics* **1984**, 3, 82-6.

(11) Peitz, D. J.; Palmer, R. T.; Radonovich, L. J.; Woolsey, N. F. *Organometallics* **1993**, 12, 4580-4.

(12) Nesmeyanov, A. N.; Krivykh, V. V.; Kaganovich, V. S.; Rybinskaya, M. I. *J. Organomet. Chem.* **1975**, 102, 185-93.

(13) See ref 11. An exception is *cis*-(μ , η^6 : η^6 -9,9-dimethyl-9-silafluorene) $(\text{Cr}(\text{CO})_3)_2$: Kirillova, N. I.; Gusev, A. I.; Afanasova, O. B. *Metalloorg. Khim.* **1988**, 1, 1278.

(14) Allegra, G.; Natta, G. *Atti. Accad. Naz. Lincei* **1961**, 31, 399.

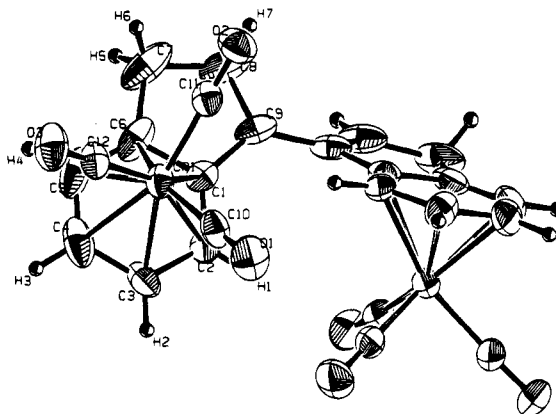


Figure 1. ORTEP drawing of **3a** showing the labeling scheme. Atoms are represented by thermal ellipsoids at the 30% level.

Table 1. Positional Parameters for Compound **3a**

atom	x	y	z
Cr(1)	0.71179(9)	0.12815(8)	0.2110(1)
O(1)	0.5697(5)	-0.0224(3)	0.1347(6)
O(2)	0.5944(4)	0.2050(4)	-0.0457(5)
O(3)	0.8853(4)	0.0578(4)	0.1014(6)
C(1)	0.6435(6)	0.2289(5)	0.3082(6)
C(2)	0.6358(6)	0.1548(5)	0.3706(7)
C(3)	0.7322(7)	0.1059(5)	0.4192(7)
C(4)	0.8354(7)	0.1320(8)	0.4063(8)
C(5)	0.8426(9)	0.2056(9)	0.344(1)
C(6)	0.7482(8)	0.2543(7)	0.2949(8)
C(7)	0.733(1)	0.3370(7)	0.230(1)
C(8)	0.610(1)	0.3545(5)	0.2085(8)
C(9)	0.5595(6)	0.2930(5)	0.2525(7)
C(10)	0.6245(6)	0.0350(5)	0.1648(8)
C(11)	0.6400(6)	0.1736(6)	0.0521(8)
C(12)	0.8162(6)	0.0837(5)	0.1420(7)
H(1)	0.5636	0.1347	0.3812
H(2)	0.7265	0.0524	0.4630
H(3)	0.9021	0.0942	0.4422
H(4)	0.9165	0.2214	0.3357
H(5)	0.7803	0.3800	0.2822
H(6)	0.7506	0.3370	0.1471
H(7)	0.5707	0.4058	0.1677

ent is present on both rings, the arene tricarbonylchromium moieties are nearly perpendicular.¹⁵ Only one diastereomer of **3a** could be detected (NMR, IR) even in initial reaction mixtures. The crystal structure (Figure 1 and Tables 1 and 2) showed this to be the (*d,l*) isomer (i.e., $\text{M}(\text{CO})_3$ groups *cis* as shown in Scheme 1). Conformationally, the organic ligand is twisted away from an idealized (*anti*, *s-cis*) conformation, the torsion angle defined by $\text{C}(8)-\text{C}(9)-\text{C}(9')-\text{C}(8)'$ being $-51(2)^\circ$. MM3¹⁶ force field calculations on the free ligand (3,3'-biindenyl) favor a nearly *s-trans* minimum, the torsion angle mentioned above being -145° . The solid state conformation of **3a** apparently results from a compromise between the tendency of the tricarbonylchromium moieties to point in opposite directions and the preference for an *s-trans* configuration of the organic ligand. The two halves of the molecule are related by a crystallographic C_2 axis through $\text{C}(9)-\text{C}(9)'$. Note that the $\text{Cr}(\text{CO})_3$ moieties assume a staggered conformation with respect to the benzene rings.

(15) Rose-Munch, F.; Bellot, O.; Mignon, L.; Semra, A.; Robert, F.; Jeannin, Y. *J. Organomet. Chem.* **1991**, 402, 1-16. Halwax, E.; Vollenkle, H. *Monatsh. Chem.* **1983**, 114, 687.

(16) Force field calculations were performed on a Silicon Graphics Indy workstation running MacroModel 3D version 4.0 implementing Allinger's MM3 force field (Allinger, N. C. *J. Am. Chem. Soc.* **1989**, 111, 8552) with a parameter set from the 1991 version.

Table 2. Selected Bond Distances and Angles in 3a

Intramolecular Distances ^a			
Cr(1)–C(1)	2.236(7)	Cr(1)–C(11)	1.827(8)
Cr(1)–C(2)	2.233(7)	Cr(1)–C(12)	1.824(8)
Cr(1)–C(3)	2.203(7)	O(1)–C(10)	1.142(7)
Cr(1)–C(4)	2.199(8)	O(2)–C(11)	1.153(7)
Cr(1)–C(5)	2.205(9)	O(3)–C(12)	1.154(7)
Cr(1)–C(6)	2.22(1)	C(9)–C'(9)	1.47(1)
Cr(1)–C(10)	1.838(8)		
Intramolecular Bond Angles ^a			
C(1)–Cr(1)–C(10)	116.6(3)	C(5)–Cr(1)–C(10)	154.6(5)
C(1)–Cr(1)–C(11)	89.7(3)	C(5)–Cr(1)–C(11)	115.8(4)
C(1)–Cr(1)–C(12)	153.2(3)	C(5)–Cr(1)–C(12)	90.5(4)
C(2)–Cr(1)–C(10)	90.8(3)	C(6)–Cr(1)–C(10)	153.6(3)
C(2)–Cr(1)–C(11)	116.0(3)	C(6)–Cr(1)–C(11)	89.5(4)
C(2)–Cr(1)–C(12)	154.7(3)	C(6)–Cr(1)–C(12)	116.3(3)
C(3)–Cr(1)–C(10)	91.1(3)	C(10)–Cr(1)–C(11)	89.7(3)
C(3)–Cr(1)–C(11)	152.8(3)	C(10)–Cr(1)–C(12)	90.1(3)
C(3)–Cr(1)–C(12)	117.9(3)	C(11)–Cr(1)–C(12)	89.3(3)
C(4)–Cr(1)–C(10)	118.0(5)	Cr(1)–C(10)–O(1)	179.2(7)
C(4)–Cr(1)–C(11)	152.4(5)	Cr(1)–C(11)–O(2)	177.3(7)
C(4)–Cr(1)–C(12)	91.1(3)	Cr(1)–C(12)–O(3)	177.3(7)
Torsion or Conformation Angles ^b			
(1)(2)(3)(4)	angle	(1)(2)(3)(4)	angle
C(1)C(9)C'(9)C'(1)	–55(1)	C(4)C(5)C(6)C(7)	176.5(8)
C(1)C(9)C'(9)C(8)	126.9(5)	C(8)C(9)C'(9)C'(8)	–51(2)

^a Distances are in angstroms, and angles are in degrees. Estimated standard deviations in the least significant figure are given in parentheses. ^b The sign is positive if when looking from atom 2 to atom 3 a clockwise motion of atom 1 would superimpose it on atom 4.

NMR spectroscopy on **3b** was not feasible as it is highly insoluble (as is **3a**) in most common solvents and, to the extent that it does dissolve, decomposes very quickly to give 3,3'-biindenyl. This greater lability of (arene)Mo(CO)₃ versus (arene)Cr(CO)₃ is highly precedented.¹⁷

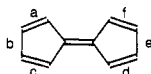
Double deprotonation of either **3a** or **3b** results in migration¹⁸ of both tricarbonylmetal moieties to the five-membered rings (based on IR and ¹H NMR) to give the bis-η⁵-dianions **3'a** and **3'b**. The ¹H NMR for **3'b** shows two diastereomers, presumably arising from two diastereomers present in samples of **3b**. Subsequent low-temperature treatment with ferrocenium fluoroborate converts **3'b** to both **1b** (54%) and **4** (ca. 5%). This provides additional evidence that **3b** occurs as a mixture of diastereomers, in contrast to **3a** which gives exclusively **1a** (ca. 49%). Compound **4** is of particular interest when viewed as a transition metal complex of the enigmatic dibenzo[*a,f*]fulvalene.¹⁹

Dibenzo[*a,f*]fulvalene was first claimed by Anastassiou²⁰ in 1966, but the accompanying spectroscopic data

(17) Davis, R.; Kane-Maguire, L. A. P. Molybdenum Compounds with η²–η⁸ Carbons Ligands. In *Comprehensive Organometallic Chemistry*; ed. Wilkinson, G., Stone, F. G. A., Abel, E. A., Eds.; Pergamon: Oxford, U.K., 1982; Vol. 3, pp 1212, 1215.

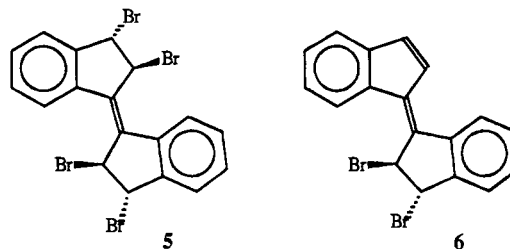
(18) (a) Novikova, L. N.; Ustynyuk, N. A.; Zvorykin, V. E.; Dneprovskaya, L. S.; Ustynyuk, Yu. A. *J. Organomet. Chem.* **1985**, *292*, 237–43. (b) Nesmeyanov, A. N.; Ustynyuk, N. A.; Novikova, L. N.; Rybina, T. N.; Ustynyuk, Yu. A.; Oprunenko, Yu. F.; Trifonova, O. I. *J. Organomet. Chem.* **1980**, *184*, 63–75. (c) Nesmeyanov, A. N.; Ustynyuk, N. A.; Makarova, L. G.; Andre, S.; Ustynyuk, Yu. A.; Novikova, L. N.; Luzikov, Yu. N. *J. Organomet. Chem.* **1978**, *154*, 45–63. (d) Nicholas, K. M.; Kerber, R. C.; Stiefel, E. I. *Inorg. Chem.* **1971**, *10*, 1519.

(19) The bonds in the parent fulvalene are labelled as shown. Dibenzo[*a,f*]fulvalenes are named according to which bonds are benzanulated.



better fit the [*a,d*] isomer, and the mechanism given for its formation by base-induced decomposition of dibromotruaxane did not preclude the formation of the [*a,d*] isomer. In a subsequent paper,²¹ Anastassiou referred to the product without comment as the [*a,d*] isomer. The [*a,f*] isomer was next mentioned²² in 1987 as having been formed along with the [*a,d*] isomer by deprotonation and oxidation of a dihydro precursor, but no data were given.

In our hands, at least 10 trials following the literature preparation²³ of dibenzo[*a,d*]fulvalene—double deprotonation of **2** in THF followed by oxidation at –78 °C with either CuCl₂ or AgBF₄—failed to produce anything except low yields of 1,3'- or 3,3'-biindenyl and substantial red tarry material that would not elute from a column. In contrast, reaction of 1 equiv of bromine with the doubly-deprotonated hydrocarbon results in formation of **5** and **6** (ca. 1.7:1). The structure of **5** was



determined by ¹H and ¹³C NMR and MS, and confirmed by a low-quality crystal structure (two carbons were non-positive-definite) which showed it to be the *S,S,S,S*-isomer, as pictured (we assume the molecule occurs as a racemic mixture along with the *R,R,R,R*-isomer). The structure of **6** was inferred from its ¹H NMR spectrum, as it was never obtained totally pure. The stereochemistry of **6** has not been definitively determined, but we infer that the bromines are *trans* from the lack of coupling of the associated protons and by comparison to **5**. Additional runs employing either 1 or 2 equiv of bromine yielded inconsistent results, forming **5** and **6** in variable yields and ratios. Use of 3 equiv or more, with quick addition of the bromine, consistently produces fairly pure **5** (ca. 67%) by trapping the dibenzo[*a,d*]fulvalene as it forms and so protecting it from polymerization. Treatment of **5** with NaI in acetone at room temperature consistently gives the [*a,d*] isomer after column chromatography but in variable yields (22 to 68%). We have found that the [*a,d*] isomer can be synthesized directly from doubly-deprotonated **2** at –78 °C by employing 1 equiv of dibromine as oxidizing agent if diethyl ether is substituted for THF as solvent. Again, variable yields (36–51%) result. Care must be taken during workup of the crude product as dibenzo[*a,d*]fulvalene has shown itself to be exquisitely acid sensitive, a fact hitherto unmentioned in the literature (see Experimental Section).

It turns out that a small amount of the [*a,f*] isomer (<4%) is formed in the above mentioned syntheses. In addition, we have found that both [*a,f*] and [*a,d*] isomers form, in varying ratios, as side products from various

(20) Anastassiou, A. G.; Setliff, F. L.; Griffin, G. W. *J. Org. Chem.* **1966**, *31*, 2705–8.

(21) Anastassiou, A. G.; Griffin, G. W. *J. Org. Chem.* **1968**, *33*, 3441–8.

(22) Escher, A.; Rutsch, W.; Neuenschwander, M. *Helv. Chim. Acta* **1987**, *70*, 1623–37.

(23) Escher, A.; Rutsch, W.; Neuenschwander, M. *Helv. Chim. Acta* **1986**, *69*, 1644–54.

Table 3. Positional Parameters for Compound 4

atom	x	y	z
Mo(1)	0.0960(1)	0.7833(1)	0.1592(1)
Mo(2)	0.1848(1)	0.6359(1)	0.1721(1)
O(1)	0.0936(9)	0.700(1)	0.352(1)
O(2)	0.275(1)	0.8426(9)	0.330(1)
O(3)	0.3014(8)	0.7399(8)	0.179(1)
O(4)	0.333(1)	0.535(1)	0.315(2)
O(5)	0.2602(9)	0.6522(8)	0.455(1)
O(6)	0.089(1)	0.908(1)	0.296(2)
C(1)	0.048(1)	0.785(1)	-0.052(1)
C(2)	0.021(1)	0.719(2)	-0.037(1)
C(3)	-0.033(1)	0.741(1)	-0.012(2)
C(4)	-0.036(1)	0.817(1)	-0.009(2)
C(5)	0.011(1)	0.848(1)	-0.040(2)
C(6)	0.021(2)	0.916(1)	-0.057(2)
C(7)	0.072(2)	0.930(1)	-0.085(2)
C(8)	0.116(1)	0.873(1)	-0.090(2)
C(9)	0.107(1)	0.804(1)	-0.070(2)
C(10)	0.052(1)	0.651(1)	-0.013(1)
C(11)	0.051(1)	0.598(1)	0.062(2)
C(12)	0.097(1)	0.539(1)	0.077(2)
C(13)	0.122(1)	0.546(1)	0.004(2)
C(14)	0.094(1)	0.6155(9)	-0.055(1)
C(15)	0.107(1)	0.637(1)	-0.142(2)
C(16)	0.145(1)	0.589(1)	-0.164(2)
C(17)	0.177(2)	0.525(2)	-0.100(2)
C(18)	0.164(2)	0.501(1)	-0.020(2)
C(19)	0.100(1)	0.731(1)	0.287(2)
C(20)	0.214(1)	0.816(1)	0.270(2)
C(21)	0.258(1)	0.704(1)	0.184(1)
C(22)	0.278(1)	0.570(1)	0.261(2)
C(23)	0.229(1)	0.652(1)	0.349(2)
C(24)	0.091(2)	0.862(2)	0.246(2)
H(1)	-0.0624	0.7077	0.0013
H(2)	-0.0655	0.8432	0.0108
H(3)	-0.0015	0.9576	-0.0469
H(4)	0.0804	0.9789	-0.1073
H(5)	0.1529	0.8825	-0.1075
H(6)	0.1407	0.7658	-0.0667
H(7)	0.0226	0.6030	0.0967
H(8)	0.1081	0.4978	0.1316
H(9)	0.0882	0.6856	-0.1840
H(10)	0.1504	0.6012	-0.2272
H(11)	0.2088	0.4955	-0.1155
H(12)	0.1852	0.4537	0.0193

thermal and photochemical reactions of **1b** (which is uncontaminated by **4**). In CDCl₃ at 250 MHz the [*a,f*] isomer exhibits the following: δ 6.90 (d, 5.9 Hz, 2H), δ 6.94 (d, 5.5 Hz, 2H), δ 7.25 (m, 6H), δ 8.36 (d, 6.8 Hz, 2H). Corroborating this assignment, an ¹H NMR sample initially containing an equimolar mixture of the [*a,f*] and [*a,d*] isomers (based on integral ratios) which was stored for 2 days in the dark at 0 °C as a semisolid (it tenaciously retained solvent) later showed a 2.3:1 enrichment of the more stable [*a,d*] isomer; allowing the sample to sit in solution at room temperature in the dark an additional 16 h increased the preponderance of the [*a,d*] form to 3:1. This ratio did not change further after the sample was allowed to sit in solution at room temperature in the light for several more days. MM3¹⁶ calculations place the [*a,f*] isomer at 12.79 kJ/mol higher energy than the [*a,d*] form.

That **4** is a complex of dibenzo[*a,f*]fulvalene was proven by an X-ray structure (Tables 3 and 4); an

Table 4. Selected Bond Distances and Angles in 4

Intramolecular Distances ^a			
Mo(1)–Mo(2)	3.286(4)	Mo(2)–C(13)	2.44(2)
Mo(1)–C(1)	2.37(2)	Mo(2)–C(14)	2.41(2)
Mo(1)–C(2)	2.38(2)	Mo(2)–C(21)	1.95(2)
Mo(1)–C(3)	2.33(2)	Mo(2)–C(22)	1.96(2)
Mo(1)–C(4)	2.30(2)	Mo(2)–C(23)	1.97(2)
Mo(1)–C(5)	2.41(2)	Mo(2)–Cp2	2.020(2)
Mo(1)–C(19)	1.95(3)	O(1)–C(19)	1.15(4)
Mo(1)–C(20)	2.03(2)	O(2)–C(20)	1.12(3)
Mo(1)–C(24)	1.95(3)	O(3)–C(21)	1.18(3)
Mo(1)–Cp1	2.013(2)	O(4)–C(22)	1.11(3)
Mo(2)–C(10)	2.31(1)	O(5)–C(23)	1.14(3)
Mo(2)–C(11)	2.33(2)	O(6)–C(24)	1.12(4)
Mo(2)–C(12)	2.31(2)		
Intramolecular Bond Angles ^a			
C(19)–Mo(1)–C(20)	99.4(9)	Mo(1)–C(20)–O(2)	171(2)
C(19)–Mo(1)–C(24)	80(1)	Mo(2)–C(21)–O(3)	171(2)
C(20)–Mo(1)–C(24)	81(1)	Mo(2)–C(22)–O(4)	177(2)
C(21)–Mo(2)–C(22)	85(1)	Mo(2)–C(23)–O(5)	171(2)
C(21)–Mo(2)–C(23)	94.5(9)	Mo(1)–C(24)–O(6)	179(3)
C(22)–Mo(2)–C(23)	81(1)	C(2)–C(10)–Cp2	176(1)
Mo(1)–C(19)–O(1)	172(2)	C(10)–C(2)–Cp1	166(2)
Torsion or Conformation Angles ^b			
(1)(2)(3)(4)	angle	(1)(2)(3)(4)	angle
Mo(1)Mo(2)C(10)C(2)	17(2)	C(19)Mo(1)Mo(2)C(21)	-132.6(7)
Mo(2)Mo(1)C(2)C(10)	16(2)	C(19)Mo(1)Mo(2)C(23)	-35.8(9)
C(3)C(2)C(10)C(11)	-14(2)	C(20)Mo(1)Mo(2)C(21)	-31.1(9)
C(3)C(2)C(10)C(14)	167(1)	C(20)Mo(1)Mo(2)C(23)	66(1)
C(1)C(2)C(10)C(14)	-33(3)	Cp1Mo(1)Mo(2)Cp2	-25.9(1)
C(1)C(2)C(10)C(11)	146(2)		

^a See footnote *a* of Table 2. ^b See footnote *b* of Table 2.

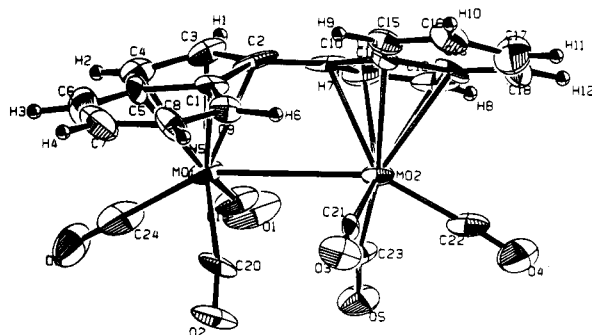


Figure 2. ORTEP drawing of **4** showing the labeling scheme. Atoms are represented by thermal ellipsoids at the 30% level.

ORTEP diagram is presented in Figure 2. The Mo–Mo bond length is 3.286(4) Å compared to 3.371(1) Å found in (fulvalene)dimolybdenum hexacarbonyl, FvMo₂(CO)₆.²⁴ Both five-membered rings are nearly planar with a dihedral angle θ between them of 28.2°, compared to 15.3° found in FvMo₂(CO)₆. The difference is due to greater twisting in **4**. As a measure of pyramidalization, Vollhardt's dihedral angle²⁴ θ , defined as the angle between the planes defined by the five-membered rings, proves descriptive only for untwisted structures; large twist angles result in anomalously large values of the dihedral angle θ . We have found the average of the angles C(4)–C(5)–Cp(2) and C(5)–C(4)–Cp(1) (where

(24) Drage, J. S.; Vollhardt, P. C. *Organometallics* **1986**, *5*, 280–297.

(25) Abrahamson, H. B.; Heeg, M. J. *Inorg. Chem.* **1984**, *23*, 2281–6.

(26) Kretschmar, S. A.; Cass, M. E.; Turowski, P. N. *Acta Crystallogr.* **1987**, *C43*, 435–7.

(27) Begley, M. J.; Puntambekar, S. G.; Wright, A. H. *J. Chem. Soc., Chem. Commun.* **1987**, 1251–2.

(28) Kerber, R. C.; Miran, M. J.; Waldbaum, B.; Rheingold, A. L. *Organometallics* **1995**, *14*, 2002–8.

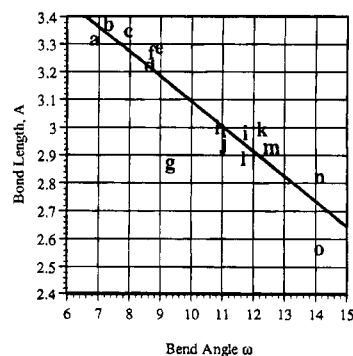
(29) Seyferth, D.; Anderson, L. L.; Davis, W. B.; Cowie, M. *Organometallics* **1992**, *11*, 3736–44.

(30) Girard, L.; Decken, A.; Blecking, A.; McGlinchey, M. J. *J. Am. Chem. Soc.* **1994**, *116*, 6427–8.

(31) Kahn, A. P.; Boese, R.; Blümel, J.; Vollhardt, K. P. C. *J. Organomet. Chem.* **1994**, *472*, 149–162.

(32) Weidman, T. W.; Vollhardt, K. P. C. *J. Am. Chem. Soc.* **1983**, *105*, 1676–7.

(33) Song, J.-S.; Han, S.-H.; Nguyen, S. T.; Geoffroy, G. L.; Rheingold, A. L. *Organometallics* **1990**, *9*, 2386–95.



- a. **11**, this work.
 b. $\text{FvMo}_2(\text{CO})_6$, ref. 24.
 c. $\text{FvW}_2(\text{CO})_6$, ref. 25.
 d. $\text{FvMo}_2(\text{CO})_4(\text{PMe}_3)_2$, ref. 26.
 e. **4**, this work.
 f. (1-Oxacyclopent-2-ylidene) $\text{FvMo}_2(\text{CO})_5$, ref. 24.
 g. $(\mu, \eta^3: \eta^3\text{-anthracene})\text{Fe}_2(\text{CO})_6$, ref. 27.
 h. $(\mu, \eta^3: \eta^3\text{-biallylene})\text{Fe}_2(\text{CO})_5\text{PPh}_3$, ref. 28.
 i. *cis*- $(\mu, \eta^3: \eta^3\text{-2,2'-bi(3-phenylthioallyl)})\text{Fe}_2(\text{CO})_6$, ref. 29.
 j. (1,2,4,5-tetramethylenebenzene) $\text{Fe}_3(\text{CO})_9$, ref. 30.
 k. $\text{Fv}(\text{OC})_3\text{WRh}(\text{CO})\text{C}(\text{O})\text{Me}$, ref. 31.
 l. $(\mu, \eta^5: \eta^5\text{-dibenzo[a,d]fulvalene})\text{Mo}_2(\text{CO})_4(\text{PhC}\equiv\text{CPh})$, unpublished results.
 m. $(\mu, \eta^3: \eta^3\text{-biallylene})\text{Fe}_2(\text{CO})_6$, ref. 28.
 n. $\text{FvRu}_2(\text{CO})_4$, ref. 32.
 o. $(\mu_2, \eta^3: \eta^3\text{-2,2'-biallyl})\text{-}(\mu_3\text{-phenylimido})\text{Fe}_3(\text{CO})_7$, ref. 33.

Figure 3. Correlation of bend angle ω with metal–metal bond length.

the Cp's are the five-membered ring centroids), the bend angle ω , to be a better measure of intrinsic pyramidalization: A plot (Figure 3) of metal–metal bond lengths versus bend angle ω for a series of 15 bimetallic fulvalene and biallylene compounds gives a linear correlation coefficient of -0.893 . When the dihedral angle is used instead, the correlation drops to -0.498 . The bend angles for **4** and $\text{FvMo}_2(\text{CO})_6$ are 9 and 7.3° , respectively, indicating comparable degrees of pyramidalization. In **4**, the two five-membered rings are twisted about the C(4)–C(5) bond by approximately 24° , the average of the torsion angles C(14)–C(10)–C(2)–

C(1) and C(11)–C(10)–C(2)–C(3). MM3¹⁶ calculations on uncomplexed dibenzo[*a,f*]fulvalene find an energy minimum at 18° . The analogous twist angle in $\text{Fv-Mo}_2(\text{CO})_6$ is 4.3° .

Compounds **1a,b** and **4** are also accessible by direct reaction of doubly deprotonated **2** with $\text{M}(\text{CO})_6$ ($\text{M} = \text{Cr}, \text{Mo}$) in refluxing Bu_2O ³⁴ followed by addition of ferrocenium fluoroborate at -78°C .

Compound **1c** forms directly in 14% yield from **2**, $\text{W}(\text{CO})_3(\text{py})_3$, and $\text{Et}_2\text{O}\cdot\text{BF}_3$ at 70°C , no bis- η^6 intermediate being detected. The reaction of indene under similar conditions gives $(\eta^5\text{-C}_9\text{H}_7)\text{WH}$.^{18a} It is plausible that **1c** is formed via an analogous dihydride which subsequently loses H_2 during heating.

Compounds **1a–c** are exceptionally insoluble in common solvents; attempts to recrystallize **1b** resulted in microcrystals not suitable for X-ray diffraction. To the extent that it does dissolve, **1a** quickly decomposes to dibenzo[*a,d*]fulvalene as evidenced by ¹H and ¹³C NMR spectroscopy. Compound **1b** is indefinitely stable in solution (under N_2) except in DMSO in which it slowly decomposes to dibenzo[*a,d*]fulvalene. No signs of decomposition of **1c** in DMSO were witnessed. The increased lability of **1a** may be due, in part, to the relative weakness of the Cr–Cr bond as compared with Mo and W.³⁵ In addition, Nesmeyanov and co-workers found that the stabilities of η^5 -indenyl and -fluorenyl complexes increase on going from Cr to Mo to W.^{18c} A more stable bis- η^5 derivative, **15**, was synthesized by treating **3'a** with Diazald at -78°C in Et_2O to give $(\mu, \eta^5: \eta^5\text{-dibenzo[a,d]fulvalene})[\text{Cr}(\text{CO})_2\text{NO}]_2$ in 16% yield.

Photolysis of **1b** in THF at 300 nm in the presence of excess $\text{P}(\text{OCH}_3)_3$ for 3 days gives the monosubstitution product, **11**, in 29% yield. In contrast, $\text{FvMo}_2(\text{CO})_6$ was reported to be inert to PPh_3 and $\text{P}(\text{OCH}_3)_3$ under similar photolytic conditions.²⁴ An ORTEP diagram for **11** (Tables 5 and 6) is presented in Figure 4. The $\text{P}(\text{OCH}_3)_3$ ligand occupies a pseudo-axial position in the "sawhorse" structure. The Mo–Mo bond length is 3.3172(8) Å, still

Table 5. Positional Parameters for Compound 11

atom	x	y	z	atom	x	y	z
Mo(1)	0.63526(2)	0.42576(3)	0.65646(4)	O(3)	0.5276(2)	0.6576(4)	0.9979(4)
Mo(2)	0.55543(2)	0.54844(4)	0.78684(4)	C(23)	0.7478(3)	0.2168(5)	0.7846(7)
P(1)	0.69955(5)	0.3255(1)	0.6528(2)	C(21)	0.5372(2)	0.6152(5)	0.9214(6)
C(14)	0.6249(2)	0.5476(4)	0.5206(5)	C(22)	0.7715(2)	0.4363(6)	0.6476(7)
C(5)	0.5419(2)	0.5288(4)	0.5982(5)	O(7)	0.6915(2)	0.5029(4)	0.8576(4)
C(13)	0.5323(2)	0.6229(4)	0.6254(5)	O(8)	0.6990(1)	0.2381(3)	0.5718(4)
C(6)	0.5064(2)	0.4739(4)	0.6520(5)	C(25)	0.6696(2)	0.4767(4)	0.7850(6)
C(10)	0.4384(2)	0.5029(5)	0.7705(6)	C(26)	0.6615(3)	0.1749(6)	0.5689(8)
C(4)	0.5820(2)	0.4959(4)	0.5386(5)	H(1)	0.4197	0.5460	0.8120
C(3)	0.5895(2)	0.4048(4)	0.4990(5)	H(2)	0.7245	0.4735	0.4141
C(12)	0.4956(2)	0.6267(4)	0.7002(6)	H(3)	0.4475	0.2856	0.6999
C(18)	0.7020(2)	0.5152(5)	0.4457(6)	H(4)	0.7443	0.6275	0.4435
C(11)	0.4777(2)	0.5361(4)	0.7133(5)	H(5)	0.5141	0.3341	0.6160
C(1)	0.6574(2)	0.4846(4)	0.4751(5)	H(6)	0.3992	0.3904	0.7993
C(8)	0.4554(2)	0.3499(5)	0.7051(6)	H(7)	0.6167	0.6853	0.5665
C(17)	0.7134(2)	0.6048(6)	0.4631(6)	H(8)	0.6904	0.7300	0.5204
C(20)	0.6094(2)	0.6271(5)	0.8077(5)	H(9)	0.7517	0.1978	0.8586
C(7)	0.4943(2)	0.3781(4)	0.6523(6)	H(10)	0.7424	0.1631	0.7390
C(19)	0.5701(2)	0.4523(5)	0.8980(6)	H(11)	0.7770	0.2428	0.7590
C(9)	0.4269(2)	0.4125(6)	0.7636(6)	H(12)	0.7773	0.4280	0.7258
C(15)	0.6381(2)	0.6404(4)	0.5370(6)	H(13)	0.7998	0.4465	0.6111
C(2)	0.6356(2)	0.3964(4)	0.4660(5)	H(14)	0.7525	0.4903	0.6400
C(16)	0.6817(3)	0.6666(5)	0.5087(6)	H(15)	0.6328	0.2044	0.5508
O(5)	0.7113(1)	0.2838(3)	0.7713(4)	H(16)	0.6660	0.1253	0.5175
O(4)	0.7482(1)	0.3584(3)	0.6031(4)	H(17)	0.6568	0.1461	0.6418
O(6)	0.5926(2)	0.2606(3)	0.7798(5)	H(18)	0.5486	0.6764	0.5986
O(2)	0.6383(2)	0.6801(3)	0.8189(5)	H(19)	0.5667	0.3570	0.4971
C(24)	0.6085(2)	0.3248(4)	0.7366(5)	H(20)	0.4842	0.6813	0.7367
O(1)	0.5749(2)	0.3993(4)	0.9668(5)	H(21)	0.6503	0.3387	0.4415

Scheme 2

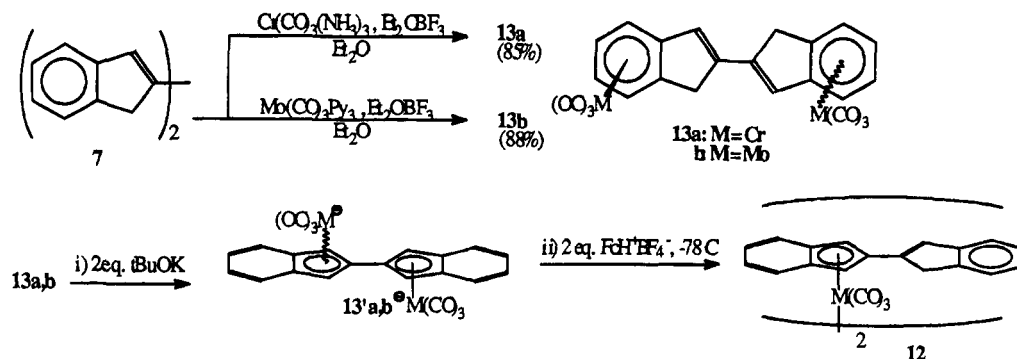


Table 6. Selected Bond Distances and Angles in 11

Intramolecular Distances ^a			
Mo(1)–Mo(2)	3.3172(8)	Mo(2)–C(20)	1.953(6)
Mo(1)–P(1)	2.367(2)	Mo(2)–C(19)	1.981(7)
Mo(1)–C(14)	2.428(6)	Mo(2)–C(21)	1.962(7)
Mo(1)–C(4)	2.332(6)	Mo(2)–Cp2	2.029(7)
Mo(1)–C(3)	2.337(6)	P(1)–O(5)	1.587(5)
Mo(1)–C(1)	2.433(6)	P(1)–O(4)	1.607(5)
Mo(1)–C(2)	2.335(6)	P(1)–O(8)	1.600(5)
Mo(1)–C(24)	1.919(6)	C(20)–O(2)	1.147(8)
Mo(1)–C(25)	1.984(7)	C(19)–O(1)	1.14(1)
Mo(1)–Cp1	2.039(6)	O(5)–C(23)	1.448(9)
Mo(2)–C(5)	2.325(6)	O(4)–C(22)	1.42(1)
Mo(2)–C(13)	2.324(6)	O(6)–C(24)	1.160(8)
Mo(2)–C(6)	2.417(6)	O(3)–C(21)	1.14(1)
Mo(2)–C(12)	2.322(6)	O(7)–C(25)	1.146(8)
Mo(2)–C(11)	2.430(6)	O(8)–C(26)	1.42(1)
Intramolecular Bond Angles ^a			
P(1)–Mo(1)–C(24)	81.9(2)	O(4)–P(1)–O(8)	90.9(2)
P(1)–Mo(1)–C(25)	81.2(2)	C(4)–C(5)–Cp2	173.5(6)
C(24)–Mo(1)–C(25)	95.4(3)	C(5)–C(4)–Cp1	172.8(6)
C(20)–Mo(2)–C(19)	98.7(3)	Mo(2)–C(20)–O(2)	173.7(6)
C(20)–Mo(2)–C(21)	79.7(3)	Mo(2)–C(19)–O(1)	173.7(6)
C(19)–Mo(2)–C(21)	81.1(3)	P(1)–O(5)–C(23)	120.8(5)
Mo(1)–P(1)–O(5)	112.7(2)	P(1)–O(4)–C(22)	120.9(4)
Mo(1)–P(1)–O(4)	121.1(2)	Mo(1)–C(24)–O(6)	176.1(6)
Mo(1)–P(1)–O(8)	119.4(2)	Mo(2)–C(21)–O(3)	176.8(7)
O(5)–P(1)–O(4)	105.1(2)	P(1)–O(8)–C(26)	122.1(5)
O(5)–P(1)–O(8)	104.5(2)	Mo(1)–C(25)–O(7)	176.0(5)
Torsion or Conformation Angles ^b			
(1)(2)(3)(4)	angle	(1)(2)(3)(4)	angle
Mo(1)Mo(2)C(5)C(4)	-14.6(3)	C(20)Mo(2)Mo(1)C(24)	134.5(3)
Mo(2)Mo(1)C(4)C(5)	-14.4(3)	C(20)Mo(2)Mo(1)C(25)	37.5(3)
C(14)C(4)C(5)C(13)	16.7(9)	C(19)Mo(2)Mo(1)C(24)	33.1(3)
C(14)C(4)C(5)C(6)	-156.3(6)	C(19)Mo(2)Mo(1)C(25)	-63.9(3)
C(13)C(5)C(4)C(3)	-171.7(6)	Cp2Mo(2)Mo(1)Cp1	24.2(3)
C(6)C(5)C(4)C(3)	15.3(9)		

^a See footnote *a* of Table 2. ^b See footnote *b* of Table 2.

shorter than that found in $\text{FvMo}_2(\text{CO})_6$ even though substitution of a phosphine ligand for a carbonyl tends to increase metal–metal bond lengths. The dihedral angle θ between the two five-membered rings is 21.1° , while the bend angle ω is 7° . The two rings are twisted relative to each other about the C(4)–C(5) bond by 16° (the average of the torsional angles C(3)–C(4)–C(5)–C(6) and C(14)–C(4)–C(5)–C(13)). The indenyl ring bound to Mo(2) exhibits an angle of 5.0° between the five- and six-membered rings and an angle of 9.2° between the plane defined by C(5)–C(13)–C(12) and the six-membered ring; the other indenyl unit is more nearly planar with corresponding angles of 2.1 and 5.7° . Both metals are distorted toward an η^3 bonding mode; this tends to slightly decrease the metal–metal bond length compared to the fulvalene analogue.

If 2,2'-biindenyl, **7**,³⁶ is substituted for **2** as in Scheme 2, then the first step can be carried out successfully to

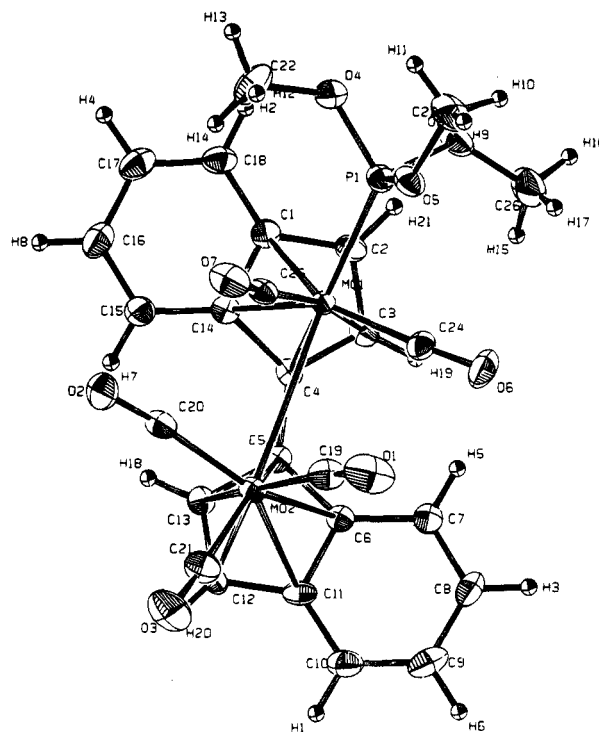
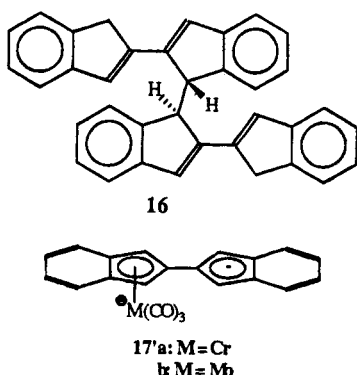


Figure 4. ORTEP drawing of **11** showing the labeling scheme. Atoms are represented by thermal ellipsoids at the 30% level.

give the analogous $(\text{arene})\text{M}_2(\text{CO})_6$ ($\text{M} = \text{Cr}, \text{Mo}$) complexes, **13a** (85%) and **13b** (88%), both high-melting, highly insoluble compounds. In the case of **13a**, in contrast to **3a**, both diastereomers form in approximately equal amounts, as evidenced by ^1H NMR spectroscopy in $\text{DMSO}-d_6$. A similar analysis of **13b** proved infeasible due to its extreme lability in DMSO . Both **13a** and **13b** can be doubly deprotonated with corresponding migration of the $\text{M}(\text{CO})_3$ units to the five-membered rings giving **13'a** and **13'b**, as evidenced by ^1H NMR spectroscopy; however, attempts to convert the dianions to the corresponding neutral metal–metal bonded species (analogues of **1a,b**) by treatment with various oxidizing agents failed. In particular, treatment of **13'a** with either CuCl_2 or Br_2 in THF at -78°C resulted in recovery of **7**. Treatment of **13'a** with either 1,2-dibromoethane or I_2 in Et_2O at -78°C resulted in **7** and the monochromium compound ($\eta^6\text{-7}$) $\text{Cr}(\text{CO})_3$, **14**. With I_2 , (*d,l*)-1,1'-bi(2,2'-biindenyl),³⁷ **16**, formed as well. Note that **16** formally results from oxidative coupling of monodeprotonated **7**. Treatment of **13'b** with ferrocenium tetrafluoroborate as in Scheme 2 resulted in **12** in 9% yield. Treatment of **13'a** under similar conditions gave a crude product which proved

too labile to purify but whose IR and ^1H NMR spectra closely resemble those of **12**. The ^1H NMR of this product, presumably the analogous chromium dimer, was significantly broadened, possibly due to partial homolytic cleavage of the relatively weak Cr–Cr bond. In benzonitrile solution, $[\text{CpCr}(\text{CO})_3]_2$ is in rapid equilibrium with its monomeric subunits, the latter existing in about 1% abundance as shown by ESR spectroscopy.³⁵ Treatment of **13b** with 2 equiv of CF_3COOH resulted in **7**. In contrast, protonation of $\text{Li}_2[\text{FvMo}_2(\text{CO})_6]$ at 20 °C resulted in the neutral metal dihydride complex which decomposed quantitatively to $\text{FvMo}_2(\text{CO})_6$ over a period of 24 h.²⁴ Reaction of **13a** with Diazald gave (η^5 -2-(2'-indenyl)indenyl) $\text{Cr}(\text{CO})_2\text{NO}$ (ca. 8%). No evidence of a dichromium compound was seen.

Efforts to synthesize hetero bimetallic complexes of dibenzo[*b,e*]fulvalene have so far failed. Double deprotonation of **14** to give **17a** followed by addition of $\text{Fe}(\text{CO})_4\text{I}_2$ at -78 °C gives **7** and **16**; the analogous molybdenum dianion **17b**, formed from $\text{Mo}(\text{CO})_6$ and doubly deprotonated **7** in refluxing Bu_2O , reacts similarly.



Failure of **13a,b** to form bimetallic complexes analogous to **1a,b** is puzzling. In contrast to **3a,b**, treatment with oxidizing agents results predominantly in partial or complete demetalation.

In conclusion, we have reported the synthesis of novel dibenzo[*a,d*]- and [*a,f*]fulvalene metal–metal bonded complexes and have compared their structural features with their fulvalene analogues. The benzo rings convey some synthetic advantages arising from the stability of **2** and their role as sites of transient complexation in **3**. The molybdenum complex, **1b**, has shown reactivity differences from its fulvalene analogue consistent with operation of the indenyl effect. More extensive reactivity studies are underway, and the results will be reported in a future paper.

Experimental Section

General Procedures. All reactions were performed in flame-dried glassware under an atmosphere of dinitrogen using double manifold and Schlenk techniques. Carbon tetrachloride was distilled and stored in a tightly sealed bottle.

(34) This procedure is a variation of that found in: Birdwhistell, R.; Hackett, P.; Manning, A. R. *J. Organomet. Chem.* **1978**, *157*, 239–41.

(35) Davis, R.; Kane-Maguire, L. A. P. Chromium Compounds with η^2 – η^5 Carbon Ligands. In *Comprehensive Organometallic Chemistry* Wilkinson, G., Stone, F. G. A., Abel, E. A., Eds.; Pergamon: Oxford, U.K., 1982; Vol. 3, p 961.

(36) Synthesis and spectroscopic data: Baierweck, P.; Simmross, U.; Müllen, K. *Chem. Ber.* **1988**, *121*, 2195–2200. We prefer a synthesis based on Ni^0 -induced coupling of 2-bromoindene.

(37) Simmross, U.; Müllen, K. *Chem. Ber.* **1993**, *126*, 969–73.

Trifluoroacetic acid was distilled immediately before use. Diethyl ether and tetrahydrofuran were distilled over Na under dinitrogen immediately before use. Dibutyl ether was distilled *in vacuo* and stored under dinitrogen. 1-Methyl-2-pyrrolidinone was anhydrous, 99+% grade purchased from Aldrich in a Sure/Seal bottle. Acetone was HPLC grade and was sparged with dinitrogen for 10 min before use. CuCl_2 was dried at 110 °C for 24 h before use. ^1H NMR data were referenced to the residual solvent proton resonance unless otherwise indicated. Microanalyses were performed by Galbraith Laboratories, Inc. Indene and boron trifluoride etherate were distilled and stored at -20 °C. $\text{Mo}(\text{CO})_3(\text{py})_3$,³⁸ $\text{W}(\text{CO})_5(\text{py})_3$,³⁸ and $\text{Cr}(\text{CO})_3(\text{NH}_3)_3$ ³⁹ were synthesized according to published procedures and stored under dinitrogen at -20 °C. 1,1'-Biindenyl⁴⁰ and ferrocenium tetrafluoroborate⁴¹ were synthesized according to published procedures.

2,2'-Biindenyl (7). 2-Bromo-1-indanol was synthesized according to ref 42 in 81% yield (lit. 78%). The bromohydrin was then dehydrated to 2-bromoindene by an improved version of the procedure found in ref 43: A 1 L round bottom flask was charged with 300 mL of CCl_4 and 12.64 g (89.0 mmol) of P_2O_5 . On the neck was fitted a Soxhlet extraction apparatus, the sintered glass thimble of which was charged with 18.94 g (89.0 mmol) of the bromohydrin. The CCl_4 was brought to reflux, and heating was continued for 21 h. The mixture was then cooled to room temperature and the product filtered through Celite. To the filtrate was added Na_2CO_3 with stirring, followed by anhydrous MgSO_4 to dry, and the mixture filtered again. The filtrate was roto-evaporated to give 14.79 g of crude 2-bromoindene which was distilled *in vacuo* (0.05 atm), collecting the fraction boiling at 87–112 °C to give 11.02 g (64%) of spectroscopically pure (^1H NMR) product.

The 2-bromoindene was then homocoupled using the procedure of ref 44: To a 500 mL three-neck round bottom flask equipped with a mechanical stirrer was added 8.87 g (135.7 mmol) of Zn powder, 7.04 g (54.3 mmol) of anhydrous NiCl_2 , 45.06 g (271.4 mmol) of KI, and 250 mL of 1-methyl-2-pyrrolidinone. The mixture was stirred at 60–65 °C for 1 h after which time 26.45 g (135.6 mmol) of 2-bromoindene was added in one portion. Heating was continued for 3 days, after which time the reaction mixture was cooled to room temperature. Approximately 10 mL of 6 N HCl was cautiously added with stirring. After gas evolution ceased, 150 mL of distilled H_2O was added and the mixture transferred to a separatory funnel, to which was added approximately 200 mL of CH_2Cl_2 . The organic layer was drawn off and filtered through Celite. The precipitate contained undissolved product and had to be washed 10 times more with CH_2Cl_2 . The combined light-yellow filtrate was roto-evaporated, and 500 mL MeOH was added to the pot residue to precipitate the product which was isolated by a final filtration to give 13.38 g (86%) of microcrystalline, spectroscopically pure **7**. Spectral data agreed with those in ref 36.

5 and 6. Into a stirring solution of **2** (0.620 g, 2.69 mmol) in 25 mL of THF at room temperature was syringed 2.2 mL (5.5 mmol) of a 2.5 M solution of *n*-BuLi in hexanes; the color of the solution immediately became dark brown. The solution was promptly cooled to -78 °C with a dry ice bath, and Br_2 (0.14 mL, 2.73 mmol) was quickly added by syringe resulting in gas evolution and a dark red-brown solution. The dry ice was allowed to sublime overnight after which the reaction was quenched with ~10 mL of distilled water and the resulting

(38) Hieber, W.; Mühlbauer, F. *Z. Anorg. Allg. Chem.* **1935**, *221*, 337.

(39) Razuvaev, G. A.; Artemov, A. N.; Aladjin, A. A.; Sirotkin, N. I. *J. Organomet. Chem.* **1976**, *111*, 131–5.

(40) Nicolet, P.; Sanchez, J. -Y.; Benaboura, A.; Abadie, M. J. M. *Synthesis* **1987**, 202–3.

(41) Hendrickson, D. N.; Sohn, Y. S.; Gray, H. B. *Inorg. Chem.* **1971**, *10*, 1559.

(42) Lindley, W. A.; MacDowell, D. W. H. *J. Org. Chem.* **1982**, *47*, 705–9.

(43) Porter, H. D.; Suter, C. M. *J. Am. Chem. Soc.* **1935**, *57*, 2024.

(44) Takagi, K.; Mimura, H.; Inokawa, S. *Bull. Chem. Soc. Jpn.* **1984**, *57*, 3517–22.

mixture extracted with ~50 mL of CH₂Cl₂. The red organic layer was dried with MgSO₄, filtered, and roto-evaporated. The residue was chromatographed on a 15 cm high, 4 cm diameter bed of hexane-packed silica gel (40–140 mesh). The column was eluted consecutively with 200 mL batches of 0, 5, 10, 20, and 50% Et₂O/hexane and EtOAc. The set of fractions eluting in the 0–5% regime contained predominantly **5** and **6** in ~1:1 ratio, while the fractions eluting in the 10–20% regime contained predominantly **5**; later fractions were complex mixtures. The fractions eluting in the 10% regime were, after roto-evaporation, crystallized from hexane/CHCl₃, and the resulting crop was recrystallized by slow diffusion of hexane into a saturated CHCl₃/EtOAc solution. The overall yields of **5** and **6**, determined by integral ratios, were 17% and 18%, respectively. **5**: ¹H NMR (300 MHz, CD₂Cl₂) δ 5.64 (s, 2H), δ 5.73 (s, 2H), δ 7.49 (d of t; 1.0 Hz, 7.5 Hz; 2H), δ 7.58 (d of t; 1.3 Hz, 7.6 Hz; 2H), δ 7.63 (d, 7.8 Hz, 2H), δ 7.96 (d, 7.8 Hz, 2H); ¹³C NMR (62.9 MHz, CD₂Cl₂) δ 53.9, 56.0, 126.9, 127.0, 130.6, 131.1, 137.6, 137.8, 143.6; MS (EI), *m/z* (based on ⁷⁹Br) 386 (2) (M – 2Br)⁺, 307 (20) (M – 3Br)⁺, 228 (100) (C₁₈H₁₂)⁺; dec 180 °C. Anal. Calcd for C₁₈H₁₂Br₄: C, 39.46; H, 2.21. Found: C, 38.17; H, 2.70. **6**: ¹H NMR (250 MHz, CDCl₃) δ 5.63 (s, 1H), δ 5.86 (s, 1H), δ 6.93 (d, 5.6 Hz, 1H), δ 7.08 (d, 5.7 Hz, 1H), δ 7.3–7.95 (multiplet, 8H). Compound **5** can be consistently synthesized relatively free of **6** and in respectable yield as follows: **2** (0.506 g, 2.20 mmol), *n*-BuLi (1.8 mL, 4.5 mmol), Br₂ (0.45 mL, 8.8 mmol), and 25 mL of Et₂O as solvent are brought to reaction as above except that the reaction is stopped 5.5 h after the addition of Br₂, the dry ice having sublimed by then. The crude mixture is roto-evaporated and the residue washed with distilled H₂O (1 × 100 mL) and MeOH (2 × 50 mL), and dried with suction to give 0.803 g (67%) of reasonably pure **5**.

Synthesis of Dibenzofulvalene. Method 1. Starting with 2.02 g (8.77 mmol) of **2** in 100 mL of Et₂O, **5** was synthesized as above. The crude product was obtained by roto-evaporation, and 100 mL of distilled H₂O was added to the residue. The aqueous layer was extracted with 200 mL of CH₂Cl₂, and the organic layer was dried with anhydrous MgSO₄, filtered, and rotoevaporated. The residue was transferred to a 250 mL round bottom flask equipped with a sidearm and magnetic stirrer; the flask was subsequently degassed with a stream of dinitrogen for 5 min. With the dinitrogen still flowing, 100 mL of acetone was quickly added along with ca. 0.1 g of anhydrous Na₂CO₃. The mixture was stirred for 5 min, and then NaI (5.26 g, 35.1 mmol) was quickly added under a stream of dinitrogen. Stirring was continued for 3 h, after which time the reaction mixture was filtered. The flask and funnel were washed with an additional 200 mL of CHCl₃, and the combined organic layers were extracted with 10% aqueous thiosulfate (1 × 150 mL) and distilled H₂O (1 × 100 mL). The organic layer was dried with anhydrous MgSO₄, filtered, and roto-evaporated over anhydrous Na₂CO₃. The residue was chromatographed on a 15 cm high, 4 cm diameter bed of hexane-packed, degassed Florisil (60–100 mesh) to give 0.474 g (24%) of reasonably pure [*a,d*] isomer.

Method 2. A 100 mL round bottom flask with sidearm was soaked in base-bath (1 liter of 95% EtOH, 120 mL of H₂O, 120 g of NaOH) for several min, washed with copious amounts of distilled water, and flame-dried under a stream of dinitrogen. To this flask was added, under a stream of dinitrogen, 1.00 g (4.35 mmol) of **2**, 50 mL of Et₂O, and a Teflon-coated stir bar. To the stirring solution was added by syringe 3.6 mL (9.0 mmol) of a 2.5 M solution of *n*-BuLi in hexanes. The reaction mixture was cooled to –78 °C with a dry ice bath, and Br₂ (0.23 mL, 4.49 mmol) was quickly added by syringe. The dry ice was allowed to sublime, and the reaction mixture was stirred an additional 2 h at room temperature. An additional 100 mL of Et₂O was added, and the organic layer was washed with 10% aqueous sodium thiosulfate (150 mL) and distilled H₂O (100 mL). The organic layer was dried with MgSO₄, filtered, and roto-evaporated over anhydrous Na₂CO₃. The residue was chromatographed on a 15 cm high, 4 cm diameter

bed of hexane-packed silica gel (40–140 mesh, pH = 7) to give 0.506 g (51%) of reasonably pure dibenzo[*a,d*]fulvalene. Under similar conditions except with THF as solvent, use of 1 equiv of I₂ (calculated on **2**) as the oxidizing agent gave an intractable dark greenish-brown crude product whose ¹H NMR was very complex.

($\mu, \eta^6: \eta^5$ -**6,3,3'-Biindenyl**)Cr₂(CO)₆ (**3a**). The procedure followed is that of ref 45. Into a stirring, room-temperature mixture of 1,1'-biindenyl (0.755 g, 3.28 mmol) and Cr(CO)₃(NH₃)₃ (1.85 g, 9.88 mmol) in Et₂O (75 mL) was syringed Et₂O·BF₃ (6 mL, 49 mmol). Stirring was continued for 6 days, during which time the initially yellow reaction mixture was seen to darken with the formation of an orange-brown precipitate and a burgundy solution. The reaction mixture was filtered with suction. The reaction vessel and precipitate from the filtration were washed twice with Et₂O and the washings also filtered. The resultant brown precipitate was washed with 1 M HCl (2×), distilled H₂O (1×), and MeOH (1×). The washed precipitate, green in color, was first suction dried (~5 min) and then dried *in vacuo* (~5 min) to give 0.705 g (43%) of **3a**. The product at this stage was fairly pure by ¹H NMR and was used without further purification. It can be crystallized by pentane diffusion into an EtOAc solution: ¹H NMR (250 MHz, DMSO-*d*₆) δ 3.56 (d, 24.9 Hz, 2H), δ 3.84 (d, 24.4 Hz, 2H), δ 5.61 (quasi-triplet, 5.8 Hz, 2H), δ 5.73 (quasi-triplet, 6.1 Hz, 2H), δ 6.20 (d, 6.1 Hz, 2H), δ 6.31 (d, 5.7 Hz, 2H), δ 6.82 (s, 2H); ¹³C NMR (62.9 MHz, DMSO-*d*₆) δ 38.7, 89.4, 92.0, 92.2, 93.2, 114.5, 115.3, 133.3, 135.5, 234.2; MS (EI), *m/z* 502 (9) (M)⁺, 418 (38) (M – 3CO)⁺, 390 (24) (M – 4CO)⁺, 362 (22) (M – 5CO)⁺, 334 (100) (M – 6CO)⁺, 282 (100) (M – 6CO-Cr)⁺, 228 (20) (C₁₈H₁₂)⁺; IR (KBr) 1959 (s), 1870 (s), 663 (w), 631 (w) cm⁻¹; mp 187.5–190 °C. Anal. Calcd for Cr₂C₂₄H₁₄O₆: Cr, 20.70. Found: Cr, 20.95.

($\mu, \eta^6: \eta^5$ -**6,3,3'-Biindenyl**)Mo₂(CO)₆ (**3b**). 1,1'-Biindenyl (0.518 g, 2.25 mmol) and Mo(CO)₃(py)₃ (2.83 g, 6.77 mmol) in Et₂O (50 mL) were treated with Et₂O·BF₃ (4.1 mL, 33.3 mmol) as in the preparation of **3a**. A color change to a green precipitate and red solution occurred within less than 1 h, but stirring was continued for 6 days. The resultant precipitate was worked up as in the preparation of **3a** to give green colored **3b** (1.03 g, 78%). An ¹H NMR of the filtrate obtained by filtering the crude reaction mixture showed 3,3'-biindenyl with no sign of η^6 -complexed products. If the reaction is run at reflux instead of room temperature, then it may be worked up after only 3 days to give 80% yield: MS (EI), *m/z* (based on ⁹⁶Mo) 412 (2) (M – Mo(CO)₃)⁺, 328 (8) (M – Mo(CO)₆)⁺, 266 (2) (Mo(CO)₆)⁺, 230 (76) (C₁₈H₁₄)⁺, 115 (100) (C₉H₇)⁺; IR (KBr) 1962 (sh), 1948 (s), 1867 (s), 1844 (s) cm⁻¹; dec >144 °C.

[($\mu, \eta^5: \eta^5$ -Dibenzo[*a,d*]fulvalene)Cr₂(CO)₆]²⁻ (**3'a**). **3a** (0.04 g, 0.0796 mmol) was dissolved in 1 mL of DMSO-*d*₆. While the solution stirred, 0.32 mL (0.32 mmol) of a 1 M THF solution of *t*-BuOK was introduced by syringe. The color became dark, and stirring was continued for 5 min. In the meantime, an NMR tube was placed inside a 1 L round bottom flask supplied with a vacuum adapter. The setup was evacuated and refilled with dinitrogen. The DMSO-*d*₆ solution was then transferred with a syringe to the NMR tube through a rubber septum in the vacuum adapter. The adapter was removed and the NMR tube quickly capped with a rubber septum. A proton NMR was taken within 5 min. The same sample was afterward transferred with a syringe to a degassed IR NaCl cell and an IR taken: ¹H NMR (250 MHz, DMSO-*d*₆) δ 4.75 (br s, 2H), δ 5.27 (br s, 2H), δ 6.59 (br s, 4H), δ 7.27 (m, 4H); IR (DMSO-*d*₆) 1886 (s), 1784 (s), 1755 (sh) cm⁻¹.

[($\mu, \eta^5: \eta^5$ -Dibenzo[*a,d*]fulvalene)Mo₂(CO)₆]²⁻ (**3'b**). **3b** (0.086 g, 0.146 mmol) was suspended in 5 mL of Et₂O. While the solution stirred, 0.58 mL (0.58 mmol) of a 1 M THF solution of *t*-BuOK was introduced by syringe. The color changed instantly from a light green to a darker brownish-green.

Stirring was continued for 10 min after which time 1 mL of DMSO- d_6 was added; the color immediately became greenish-black. The Et₂O was then removed *in vacuo*. The remaining DMSO- d_6 solution was then treated as in the procedure for **3a**. ¹H NMR (250 MHz, DMSO- d_6): δ 5.32 (d, 1.9 Hz, 2H), δ 5.76 (d, 1.9 Hz, 2H), δ 6.70 (m, 4H), δ 7.31 (d, 7.8 Hz, 2H), δ 7.63 (d, 7.5 Hz, 2H); these represent the most intense signals. For each such signal there was a corresponding signal slightly upfield one-tenth as intense and similar in overall appearance. These signals are assigned to the dianion of **4**: δ 5.23 (br s, 2H), δ 5.68 (br s, 2H), δ 6.25 (m, 4H), δ 7.08 (d, 7.4 Hz, 2H), δ 7.44 (d, 7.0 Hz, 2H); IR (DMSO- d_6) 1889, 1777 cm⁻¹.

($\mu,\eta^5:\eta^5$ -Dibenzo[*a,d*]fulvalene)Cr₂(CO)₆ (1a). Method 1. Into a stirring suspension of **3a** (0.105 g, 0.209 mmol) in 10 mL of Et₂O was syringed 0.44 mL (0.44 mmol) of a 1 M THF solution of *t*-BuOK without immediate color change. Stirring was continued for 35 min still without change, at which point reflux was begun. Reflux was continued for 45 min after which time the heating mantle was removed and the reaction mixture cooled to -78 °C in a dry ice bath. Ferrocenium tetrafluoroborate (0.114 g, 0.418 mmol) was added quickly and stirring allowed to continue for an additional 7 h while the dry ice slowly sublimed away. The reaction mixture was roto-evaporated, the residue was washed with CHCl₃ (3 \times), and the washings were discarded. The precipitate was then washed with distilled H₂O (1 \times) and MeOH (2 \times) and dried with suction. The IR of the green precipitate (0.067 g) indicated a mixture of **3a** and **1a**. Compound **1a** was obtained in purer form by a direct thermal route, method 2.

Method 2. The procedure is like that given in ref 34. Into a stirring solution of 1,1'-biindenyl (0.496 g, 2.15 mmol) in 25 mL of Bu₂O was syringed 1.81 mL (4.53 mmol) of a 2.5 M solution of *n*-BuLi in hexanes causing the reaction mixture to become a cloudy yellow. Cr(CO)₆ (1.00 g, 4.55 mmol) was quickly added, and the reaction mixture was subsequently brought to reflux. After 18 min at reflux, the color had become deep green. Cr(CO)₆ that sublimed into the condenser was intermittently returned to the flask with 1 mL of washings of Bu₂O quickly introduced at the top of the condenser under a flow of dinitrogen. The system was kept at reflux for a total of 70 min after which time the heat was removed. The system was allowed to cool to room temperature and then cooled to -78 °C with a dry ice bath. Ferrocenium tetrafluoroborate (1.17 g, 4.30 mmol) was quickly added and the reaction mixture stirred for 7 h as the dry ice slowly sublimed. The Bu₂O was removed *in vacuo* (the distillate was yellow with ferrocene and also contained some unreacted Cr(CO)₆) leaving a pot residue that was dark brown in color. The crude product was dry-loaded onto a 15 cm high, 4 cm diameter bed of hexane-packed, degassed silica gel (40–140 mesh) and the column eluted consecutively with 200 mL batches of 0, 10, and 20% Et₂O/hexane, 10% EtOAc/Et₂O, EtOAc, 10% CH₃CN/Et₂O, and MeOH. A forerun of ferrocene, dibenzo[*a,d*]fulvalene, 3,3'-biindenyl, and (1-indanylidene)-1-indene eluted in the 10–20% Et₂O/hexane regime. The later fractions were combined and roto-evaporated. The residue was washed with CHCl₃ (3 \times). The washings, which were deep red, were shown to contain mainly dibenzo[*a,d*]fulvalene by IR. The green precipitate was washed (to remove a contaminant giving a strong, broad peak in the IR at 1084 cm⁻¹) with distilled H₂O (1 \times), MeOH (2 \times), and CHCl₃ (1 \times), the CHCl₃ washing again being deep red. Washing the precipitate, now more brownish-green in color, with either toluene or acetone also gave deep red filtrates, the red color not diminishing in intensity after repeated washings; only hexane gave a colorless filtrate. Presumably, the red color was due to dibenzofulvalenes which formed as **1a** decomposed upon dissolution. An NMR of the precipitate in DMSO- d_6 showed only dibenzo[*a,d*]fulvalene. IR (KBr): 1997 (s), 1937 (s), 1919 (sh), 1892 (s), 747 (w), 604 (w), 574 (w), 552 (w) cm⁻¹. Crude yield: 49% (0.053 g).

($\mu,\eta^5:\eta^5$ -Dibenzo[*a,d*]fulvalene)Mo₂(CO)₆ (1b). Method 1. Into a stirring suspension of **3b** (0.729 g, 1.24 mmol) in 50

mL of Et₂O was syringed 2.6 mL (2.6 mmol) of a 1 M THF solution of *t*-BuOK with immediate color change to deeper green. After being stirred for 30 min, the reaction mixture was cooled to -78 °C with a dry ice bath. Ferrocenium tetrafluoroborate (0.677 g, 2.48 mmol) was quickly added, and stirring was continued for 5 h. The reaction mixture, consisting of a dark brown solution and green precipitate, was then warmed to room temperature and roto-evaporated. The residue was washed with hexane (2 \times) and CHCl₃ (3 \times), and the dark red washings were discarded. The remaining precipitate was washed with distilled H₂O (2 \times), MeOH (1 \times) and Et₂O (1 \times) and dried *in vacuo* to give spectroscopically pure dark bluish-green **1b** (0.389 g, 53.5%): ¹H NMR (300 MHz, CDCl₃) δ 5.31 (d, 3.3 Hz, 2H), δ 6.50 (d, 3.2 Hz, 2H), δ 6.80 (d, 8.7 Hz, 2H), δ 6.91 (quasi t, 2H), δ 7.10 (quasi t, 2H), δ 7.67 (d, 8.4 Hz, 2H); ¹³C NMR (62.9 MHz, DMSO- d_6) δ 82.7, 85.2, 87.0, 106.7, 107.0, 122.5, 124.6, 125.8, 127.4; MS (EI), *m/z* (based on ⁹⁶Mo) 560 (9) (M - CO)⁺, 532 (5) (M - 2CO)⁺, 504 (13) (M - 3CO)⁺, 476 (39) (M - 4CO)⁺, 448 (20) (M - 5CO)⁺, 420 (66) (M - 6CO)⁺, 228 (31) (C₁₈H₁₂)⁺, 226 (100) (C₁₈H₁₀)⁺, 192 (88) (Mo₂)⁺; IR (KBr) 2002 (s), 1968 (m), 1949 (m), 1930 (m), 1899 (s), 1872 (w); dec >278.5 °C. Anal. Calcd for C₂₄H₁₂O₆Mo₂: C, 49.00; H, 2.06; Mo, 32.62. Found: C, 48.28; H, 2.05; Mo, 39.65.

Method 2. 1,1'-Biindenyl (1.309 g, 5.68 mmol), 4.8 mL (12.0 mmol) of a 2.5 M solution of *n*-BuLi in hexanes, Mo(CO)₆ (3.013 g, 11.4 mmol), and 60 mL of Bu₂O were brought to reaction as in the thermal route for **1a**, except that the system was refluxed for only 30 min, and after the addition of ferrocenium tetrafluoroborate (3.12 g, 11.4 mmol), stirring was continued for 21 h. THF was added to the residue from the Bu₂O removal and the mixture filtered. The filtrate was roto-evaporated. The precipitate was washed with hexane (2 \times), toluene (2 \times), distilled H₂O (2 \times), and MeOH (2 \times). The hexane filtrate was shown by ¹H NMR to contain predominantly ferrocene and 3,3'-biindenyl with only traces of **4** and **1b**; likewise, the MeOH filtrate was mostly ferrocene. The MeOH-washed precipitate was spectroscopically pure **1b** (0.764 g). The toluene filtrate (0.865 g after removal of solvent) contained significant amounts of **4** and **1b** (~1.7:1) and was chromatographed on a 15 cm high, 4 cm diameter bed of hexane-packed, degassed silica gel (40–140 mesh). The column was eluted consecutively with 200 mL batches of 0, 10, 20, and 50% Et₂O/hexane, and 10% EtOAc/Et₂O. A forerun of 3,3'-biindenyl and ferrocene eluted in the 0–20% Et₂O/hexane regime. Two more sets of fractions followed: the first contained purely **4** and **1b** (~2.1:1), and the second contained **1b** and an unknown compound that exhibited a pair of doublets at δ 5.34 and 6.45 ppm with a coupling constant of 3.5 Hz; only a trace of **4** was seen in the baseline. The first set of fractions was rechromatographed on silica with 200 mL batches of 10, 20, 30, and 50% Et₂O/hexane and 50% EtOAc/hexane. The set of fractions eluting in the 20–50% Et₂O/hexane regime were combined; they were shown to contain **4** and **1b** in a 3.3:1 ratio. Three recrystallizations from EtOAc by slow diffusion of pentane yielded crystals suitable for X-ray diffraction. The final yield of **4** before recrystallizations was determined by integral ratios to be 0.16 g (5%); that of **1b** was 0.84 g (25%).

($\mu,\eta^5:\eta^5$ -Dibenzo[*a,d*]fulvalene)W₂(CO)₆ (1c). The procedure described is modeled after that given in ref 18a. A three-neck flask equipped with a magnetic stirrer was charged with 1,1'-biindenyl (0.300 g, 1.30 mmol), W(CO)₃(py)₃ (1.97 g, 3.90 mmol), and Bu₂O (25 mL). Et₂O-BF₃ (2.4 mL, 19.5 mmol) was syringed into the stirring reaction mixture; no immediate change was noticed. With an oil bath, the temperature was gradually increased to 65 °C over a 15 min period by which time the color had become brownish-orange. The temperature was maintained between 65 and 75 °C for 2 h more. The Bu₂O was removed *in vacuo*. EtOAc was added to the pot residue and the mixture filtered. The precipitate was washed with 1 M HCl, distilled H₂O, and MeOH and dried *in vacuo* to give spectroscopically pure **1c** (0.094 g). The filtrate was washed, in turn, with 1 M HCl and distilled H₂O. The organic layer

was dried with anhydrous MgSO_4 , filtered, and roto-evaporated. The pot residue was dry-loaded onto a 15 cm high, 4 cm diameter bed of hexane-packed, degassed silica gel (40–140 mesh). The column was eluted consecutively with 200 mL portions of 0, 5, 10, 20, 50, and 100% EtOAc/heptane and finally 200 mL of CH_3CN . The fractions eluting from 50% onward were combined and rotoevaporated. The residue was washed with Et_2O (2 \times) and CH_2Cl_2 (2 \times) and the precipitate collected to give spectroscopically pure dark blue-green **1c** (0.048 g). The combined yield was 14%. $^1\text{H NMR}$ (300 MHz, $\text{DMSO}-d_6$) δ 6.05 (d, 3.2 Hz, 2H), δ 6.94 (d, 3.2 Hz, 2H), δ 6.98 (t, 7.8 Hz, 2H), δ 7.17 (quasi-triplet, 2H), δ 7.26 (d, 8.8 Hz, 2H), δ 7.81 (d, 8.5 Hz, 2H); $^{13}\text{C NMR}$ (62.9 MHz, $\text{DMSO}-d_6$) δ 78.7, 81.7, 85.7, 104.1, 104.7, 122.9, 124.8, 126.1, 128.0; FAB MS m/z 764 (1.2), 736 (1.0), 708 (1.1) due to $\text{M}^+ - (0, 1, 2 \text{ CO})$, based on ^{184}W ; IR (KBr) 2000 (s), 1946 (s), 1909 (s), 1887 (s) cm^{-1} ; dec >292 °C.

($\mu, \eta^5: \eta^5$ -Dibenzo[*a,f*]fulvalene) $\text{Mo}_2(\text{CO})_6$ (**4**). See preparation of **1b**, method 2. Note that **4** forms also via method 1 (ca. 4:1, **1b** to **4**) but was not isolated and purified from those runs. $^1\text{H NMR}$ (300 MHz, CDCl_3) δ 4.17 (d, 3.3 Hz, 2H), δ 5.83 (d, 3.3 Hz, 2H), δ 7.14 (t, 7.8 Hz, 2H), δ 7.28 (quasi t; 6.8 Hz, 7.6 Hz; 2H), δ 7.61 (d, 8.8 Hz, 2H), δ 7.74 (d, 8.5 Hz, 2H); $^{13}\text{C NMR}$ (75.5 Hz, CDCl_3) δ 76.6, 77.0, 77.4, 79.0, 83.7, 86.3, 104.4, 109.4, 124.2, 124.4, 125.2, 127.6, 221.4, 226.7, 231.1; MS (EI), m/z (based on ^{96}Mo) 560 (17) ($\text{M} - \text{CO}$) $^+$, 532 (10) ($\text{M} - 2\text{CO}$) $^+$, 504 (7) ($\text{M} - 3\text{CO}$) $^+$, 476 (45) ($\text{M} - 4\text{CO}$) $^+$, 448 (55) ($\text{M} - 5\text{CO}$) $^+$, 420 (99) ($\text{M} - 6\text{CO}$) $^+$, 226 (100) ($\text{C}_{18}\text{H}_{10}$) $^+$, 192 (76) (Mo_2) $^+$; IR (KBr) 2006, 1958, 1908 cm^{-1} ; dec > 239 °C. Anal. Calcd for $\text{C}_{24}\text{H}_{12}\text{O}_6\text{Mo}_2$: C, 49.00; H, 2.06; Mo, 32.62. Found: C, 48.86; H, 2.23; Mo, 34.50.

($\mu, \eta^5: \eta^5$ -Dibenzo[*a,d*]fulvalene) $\text{Cr}_2(\text{CO})_4(\text{NO})_2$ (**15**). Into a stirring suspension of **3a** (0.397 g, 0.790 mmol) in 25 mL of Et_2O cooled with an ice/MeOH bath was syringed 1.6 mL (1.6 mmol) of a 1 M THF solution of t-BuOK. Stirring was continued for a 0.5 h after which time the reaction mixture was cooled with a dry ice bath. Diazald (0.346 g, 1.62 mmol) was quickly added, and stirring was continued for 24 h as the dry ice slowly sublimed. The bluish-purple reaction mixture was then roto-evaporated, and the residue was chromatographed on a 15 cm high, 4 cm diameter bed of hexane-packed, degassed silica gel (40–140 mesh). The column was eluted with 200 mL batches of 0, 5, 10, 20, 50, and 100% Et_2O /hexane. The fractions eluting in the 0 to 20% regime were combined to give, after removal of solvent, 0.063 g (16%) of fairly pure ($^1\text{H NMR}$), red colored **15** which was recrystallized at -20 °C from toluene/hexane. $^1\text{H NMR}$ (300 MHz, CDCl_3) δ 5.54 (d, 2.5 Hz, 2H), δ 6.00 (d, 2.8 Hz, 2H), δ 7.1 (m, 4H), δ 7.5 (m, 4H); $^{13}\text{C NMR}$ (62.9 MHz, acetone- d_6) δ 78.9, 93.5, 99.8, 110.5, 112.0, 123.6, 126.8, 127.1, 127.9, 237.3, 238.3; MS (EI), m/z 476 (2) ($\text{M} - \text{CO}$) $^+$, 448 (13) ($\text{M} - 2\text{CO}$) $^+$, 420 (14) ($\text{M} - 3\text{CO}$) $^+$, 392 (3) ($\text{M} - 4\text{CO}$) $^+$, 362 (100) ($\text{M} - 4\text{CO}-\text{NO}$) $^+$, 332 (2) ($\text{M} - 4\text{CO}-2\text{NO}$) $^+$, 280 (10) ($\text{C}_{18}\text{H}_{12}\text{Cr}$) $^+$, 228 (14) ($\text{C}_{18}\text{H}_{12}$) $^+$, 52 (95) (Cr) $^+$; IR(KBr) 2014 (s), 1935 (s), 1698 (s), 748 (m), 624 (m), 464 (w) cm^{-1} ; dec >203 °C.

($\mu, \eta^6: \eta^6$ -2,2'-Biindenyl) $\text{Cr}_2(\text{CO})_6$ (**13a**). 2,2'-Biindenyl, **7** (0.538 g, 2.34 mmol), and $\text{Cr}(\text{CO})_3(\text{NH}_3)_3$ (1.30 g, 6.96 mmol) were treated with $\text{Et}_2\text{O}\cdot\text{BF}_3$ (4.3 mL, 35.0 mmol) in Et_2O (50 mL) as with **3a**. A color change to a red suspension was apparent within 1 h. Stirring was continued for 2 days, and the resultant orange precipitate was worked up as above (including additional washings with CH_2Cl_2 (2 \times) to eliminate **7** and **14** side products) to give (1.00 g, 85%) **13a**. The $^1\text{H NMR}$ of the product showed two isomers of **13a** as well as minor contamination from **7** and **14**, making the region between δ 3.6 and 4.0 ppm rather complicated. Intentional synthesis of **14** using 1 equiv of $\text{Cr}(\text{CO})_3(\text{py})_3$ produced **13a** as a side product which was eluted from a silica column with EtOAc, enriched in one isomer and with less **7** contamination. The $^1\text{H NMR}$ of the principal isomer (300 MHz, acetone- d_6 , reference TMS) showed δ 3.82 (d, 22.5 Hz, 2H), δ 3.97 (d, 22.2 Hz, 2H), δ 5.51 (q, 6.6 Hz, 2H), δ 5.61 (q, 5.9 Hz, 2H), δ 6.11 (m, 4H), δ 6.84 (s, 2H); MS (EI), m/z 502 (0.2) (M) $^+$, 446 (0.4) ($\text{M} - 2\text{CO}$) $^+$,

418 (0.6) ($\text{M} - 3\text{CO}$) $^+$, 362 (0.4) ($\text{M} - 5\text{CO}$) $^+$, 334 (2) ($\text{M} - 6\text{CO}$) $^+$, 282 (4) ($\text{M} - 6\text{CO}-\text{Cr}$) $^+$, 230 (3) ($\text{C}_{18}\text{H}_{14}$) $^+$, 52 (100) (Cr) $^+$; IR (KBr) 1960 (s), 1889 (s), 1847 (s), 839 (w), 668 (m), 629 (m), 521 (w) cm^{-1} ; dec >274 °C. Only the AB patterns for the CH_2 groups are resolvable in the $^1\text{H NMR}$ of a sample containing both isomers in comparable amounts: $^1\text{H NMR}$ (250 MHz, $\text{DMSO}-d_6$) δ 3.65 (d, 22.9, 2H), δ 3.70 (d, 22.5 Hz, 2H), δ 3.91 (d, 25 Hz, 2H), δ 3.97 (d, 22.4 Hz, 2H).

($\mu, \eta^6: \eta^6$ -2,2'-Biindenyl) $\text{Mo}_2(\text{CO})_6$ (**13b**). **7** (0.507 g, 2.20 mmol) and $\text{Mo}(\text{CO})_3(\text{py})_3$ (2.80 g, 6.70 mmol) were treated with $\text{Et}_2\text{O}\cdot\text{BF}_3$ (4 mL, 32.5 mmol) in Et_2O (50 mL) as with **3a**. Stirring was continued for 2 h, and the resultant orange precipitate worked up as above to give (1.15 g, 88%) **13b**: IR (KBr) 1954 (s), 1846 (s), 836 (w), 619 (w), 587 (w), 495 (w) cm^{-1} ; dec >170 °C.

($\mu, \eta^5: \eta^5$ -Dibenzo[*b,e*]fulvalene) $\text{Cr}_2(\text{CO})_6$ (**13'a**). About 20 mg of **13a** was dissolved in 1.5 mL of $\text{DMSO}-d_6$ under dinitrogen. While the solution stirred, an excess of solid t-BuOK was quickly added resulting in a rapid color change to dark brown. The solution was stirred for 5 min before being transferred by syringe to an evacuated NMR tube equipped with a 24/40 joint; the bottom portion of the tube was immersed in liquid dinitrogen during the transfer. The tube was sealed with a torch, and the NMR was taken 10 min after the transfer. $^1\text{H NMR}$ (300 MHz, $\text{DMSO}-d_6$): δ 5.07 (s, 4H), δ 6.5 (m, 4H), δ 7.2 (m, 4H). An IR sample was prepared as follows: To a stirring suspension of **13a** (0.206 g, 0.410 mmol) in 20 mL of THF was quickly added solid t-BuOK (0.098 g, 0.873 mmol) with no immediate color change. The reaction mixture was warmed to ~ 40 °C for 26 min during which time the color became yellow. A 1 mL aliquot was removed by syringe and injected into a degassed NaCl IR cell: IR (THF) 1961, 1895, 1794, 1754 cm^{-1} .

($\mu, \eta^6: \eta^6$ -Dibenzo[*b,e*]fulvalene) $\text{Mo}_2(\text{CO})_6$ (**13'b**). Into a stirring suspension of **13b** (0.05 g, 0.0847 mmol) in 10 mL of Et_2O was syringed 0.17 mL (0.17 mmol) of a 1 M THF solution of t-BuOK. Within 20 min at room temperature, the color had become yellow. $\text{DMSO}-d_6$ (1 mL) was then added by syringe, and the Et_2O was removed *in vacuo*. The residual solution was then transferred to an NMR tube as in the procedure for **3'a**: $^1\text{H NMR}$ (250 MHz, $\text{DMSO}-d_6$) δ 5.68 (s, 4H), δ 6.58 (dd; 2.8 Hz, 6.3 Hz; 4H), δ 7.26 (dd; 2.6 Hz, 6.2 Hz; 4H).

(η^5 -2-(2'-Indenyl)indenyl) $\text{Mo}(\text{CO})_3$ (**12**). Into a stirring suspension of **13b** (0.219 g, 0.371 mmol) in 25 mL of Et_2O was syringed 0.77 mL (0.77 mmol) of a 1 M THF solution of t-BuOK. Within 25 min, a color change to yellow had occurred, and the reaction mixture was cooled to -78 °C in a dry ice bath. Ferrocenium tetrafluoroborate (0.202 g, 0.740 mmol) was added quickly, and 5 min afterward the dry ice was removed, at which point the reaction mixture was green in color. Within 25 min, the color had become brown, and the reaction vessel was covered in aluminum foil. Three hours later, the color was blackish-purple; 2 h thereafter, the reaction mixture was roto-evaporated. The residue was dry-loaded onto a 15 cm high, 4 cm diameter bed of hexane-packed, degassed alumina (80–200 mesh) which had been dried at 100 °C *in vacuo* overnight. The column was eluted with 200 mL portions of 0, 10, 50, and 100% CH_2Cl_2 /hexane. A forerun of ferrocene eluted in the 50% regime followed by **12** (0.014 g, 9%) in the 100% regime: $^1\text{H NMR}$ (250 MHz, CDCl_3) δ 3.72 (s, 4H), δ 5.17 (s, 4H), δ 6.91 (s, 2H), δ 7.05 (m, 4H), δ 7.15 (d of t; 1.3 Hz, 7.3 Hz; 2H), δ 7.22 (m, 6H), δ 7.34 (d, 7.5 Hz, 2H), δ 7.42 (d, 7.3 Hz, 2H); $^{13}\text{C NMR}$ (75.5 MHz, CDCl_3) δ 38.7, 77.6, 93.7, 106.3, 120.9, 123.7, 124.6, 125.0, 126.4, 126.7, 128.0, 143.0, 143.5, 145.4, 229.8; IR (KBr) 1996, 1950, 1921, 1896 (with shoulder on left) cm^{-1} ; dec >230 °C.

8–10. **2** (0.608 g, 2.64 mmol), $\text{Cr}(\text{CO})_3(\text{NH}_3)_3$ (1.48 g, 8.01 mmol), $\text{Et}_2\text{O}\cdot\text{BF}_3$ (4.8 mL, 39.0 mmol), and 50 mL of Et_2O were brought to reaction as above to give 0.462 g (35%) of **3a**. The filtrate that resulted from filtering the crude reaction mixture was washed with 1 M HCl(aq) and distilled H_2O , dried with anhydrous MgSO_4 , filtered, and roto-evaporated. The residue

was chromatographed on a 15 cm high, 4 cm diameter bed of hexane-packed, degassed florisil (60–100 mesh) using 200 mL batches of 0, 5, 10, 20, and 50% Et₂O/hexane, 10% EtOAc/Et₂O, and EtOAc. The fractions eluting in the 0–20% regime contained predominantly 3,3'-biindenyl. The fractions eluting in the 20–50% regime contained predominantly **10**: ¹H NMR (250 MHz, acetone-*d*₆) δ 3.60 (s, 2H), δ 3.64 (d, 24.4 Hz, 1H), δ 3.87 (d, 24.4 Hz, 1H), δ 5.55 (t, 6.3 Hz, 6.2 Hz, 1H), δ 5.67 (t, 6.5 Hz, 1H), δ 6.16 (d, 6.3 Hz, 1H), δ 6.24 (d, 6.2 Hz, 1H), δ 6.87 (s, 1H), δ 6.88 (s, 1H), δ 7.27 (t, 7.3 Hz, 1H), δ 7.34 (quasi t, 1H), δ 7.57 (d, 7.2 Hz, 1H), δ 7.62 (d, 7.1 Hz, 1H); IR (KBr) 1957 (s), 1875 (s), 665 (w), 630 (w) cm⁻¹. The fractions eluting in the 50% Et₂O to 10% EtOAc regime contained a mixture of **10** and **8** in a 3:1 ratio. The yields of **10** and **8** as determined by integral ratios were 0.065 g (6.8%) and 0.019 g (1.4%). **8**: ¹H NMR (250 MHz, acetone-*d*₆) δ 2.9 (m, 8H), δ 5.64 (t, 6.3 Hz, 2H), δ 5.85 (d, 6.4 Hz, 2H), δ 6.39 (d, 6.6 Hz, 2H); other resonance buried under signals for **10** between 5.4 and 5.6 ppm. The fractions eluting in the 10% EtOAc regime contained predominantly **3a** (0.202 g). The last set of fractions contained predominantly **9**: These fractions, after roto-evaporation, were recrystallized by slow diffusion of pentane into a saturated EtOAc solution to give 0.032 g (2.4%) of **9**. ¹H NMR (300 MHz, CDCl₃) δ 2.6–3.0 (m, 5H), δ 3.65 (d of d; 1 Hz, 6.8 Hz; 2H), δ 5.24 (m, 2H), δ 5.34 (quasi t, 1H), δ 5.43 (m, 2H), δ 5.85 (quasi t, 2H), δ 6.35 (d, 6.6 Hz, 1H), δ 6.69 (s, 1H); ¹³C NMR (62.9 MHz, CDCl₃) (unprotonated and carbonyl carbons not seen) δ 29.3, 30.5, 33.4, 38.7, 87.4, 88.7, 88.9, 89.7, 90.1, 90.2, 90.8, 92.5, 135.0; IR (KBr) 1947 (s), 1860 (s), 667 (w), 628 (w) cm⁻¹.

(μ, η^5 : η^5 -Dibenzo[*a,d*]fulvalene)Mo₂(CO)₅P(OCH₃)₃ (**11**). A stirring, degassed solution of **1b** (0.093 g, 0.158 mmol) and P(OCH₃)₃ (0.075 mL, 0.636 mmol) in 50 mL of THF was irradiated at 300 nm in a Rayonet photochemical reactor for 3 days. The reaction mixture was then roto-evaporated, and the residue was chromatographed on a 15 cm high, 4 cm diameter bed of hexane-packed, degassed silica gel (40–140 mesh). The column was eluted with 200 mL portions of 0, 5, 10, and 20% EtOAc/hexane. A forerun of dibenzo[*a,d*]fulvalene and P(OCH₃)₃ eluted in the 0–10% regime. This was followed by two more sets of fractions, the first set composed of **11** and **1b** in approximately 2.7:1 ratio while the second set contained **11** and **1b** in approximately 9:1 ratio. The overall yield of **11** determined by integral ratios was 29% (0.031 g). The product from the second set of fractions was recrystallized by diffusion of pentane into a saturated THF solution: ¹H NMR (300 MHz, CDCl₃) δ 3.59 (d, 11.4 Hz, 9H), δ 5.20 (d, 3.4 Hz, 1H), δ 5.35 (d, 3.3 Hz, 1H), δ 6.23 (d of d; 3.5 Hz, 6.6 Hz; 1H), δ 6.42 (d, 3.2 Hz, 1H), δ 6.8–7.1 (m, 6H), δ 7.55 (d, 8.4 Hz, 1H), δ 7.65 (d, 8.4 Hz, 1H); MS (EI), *m/z* (based on ⁹⁶Mo) 656 (7) (M - CO)⁺, 600 (9) (M - 3CO)⁺, 572 (4) (M - 4CO)⁺, 544 (19) (M - 5CO)⁺, 529 (17) (M - 5CO - CH₃)⁺, 482 (13) (M - 5CO - 2OCH₃)⁺, 451 (17) (M - 5CO - 3OCH₃)⁺, 420 (14) (C₁₈H₁₂Mo₂)⁺, 228 (49) (C₁₈H₁₂)⁺, 192 (15) (Mo₂)⁺, 93 (100) (P(OCH₃)₂)⁺; IR (KBr) 1977 (s), 1924 (s), 1895 (s), 1875 (s), 1828 (m), 1020 (m), 741 (m), 540 (w) cm⁻¹; dec 237.5 °C.

(η^6 -7)Cr(CO)₃ (**14**). **7** (0.518 g, 2.25 mmol) and Cr(CO)₃(NH₃)₃ (0.508 g, 2.71 mmol) were treated with Et₂O·BF₃ (2.1 mL, 17.1 mmol) in Et₂O (50 mL) as with **3a**. Stirring was continued for 2 days after which time CH₂Cl₂ was added. The reaction mixture was washed, in turn, with 1 M HCl and distilled H₂O. The orange organic layer was dried with MgSO₄, filtered, and roto-evaporated. The crude product was dry-loaded onto a 15 cm high, 4 cm diameter bed of hexane-packed, degassed silica gel (40–140 mesh) which had been dried at 100 °C *in vacuo* overnight. After elution of a forerun of **7**, the product, orange in color, began to elute with 200 mL of 20% Et₂O/hexane. After an additional 200 mL of 50% Et₂O/hexane followed by 200 mL of 10% EtOAc/Et₂O, it had completely eluted. As it could not be gotten entirely free of **7**, a yield of 0.39 g (48%) was determined by integral ratios: ¹H NMR (250 MHz, acetone-*d*₆) δ 3.71 (s, 2H), δ 3.83 (d, 22.0 Hz, 1H), δ 4.01 (d, 22.5 Hz, 1H), δ 5.49 (d of t; 1 Hz, 6.4 Hz; 1H),

δ 5.57 (d of t; 1.1 Hz, 6.4 Hz; 1H); δ 6.05 (d, 6.0 Hz, 1H), δ 6.12 (d, 6.8 Hz, 1H), δ 6.74 (s, 1H), δ 7.08 (s, 1H), δ 7.21 (m, 2H) (here, overlap with the signals for **7** prevented more detailed analysis of the pattern), δ 7.39 (d, 6.8 Hz, 1H), δ 7.44 (d, 6.8 Hz, 1H); MS (EI), *m/z* 310 (2) (M - 2CO)⁺, 282 (19) (M - 3CO)⁺, 230 (8) (C₁₈H₁₄)⁺, 52 (100) (Cr)⁺; IR (NaCl) 1950, 1865 cm⁻¹; dec >175 °C.

Reaction of 13'a with Diazald. **13a** (0.412 g, 0.820 mmol), *t*-BuOK (1.6 mL, 1.6 mmol), Diazald (0.356 g, 1.66 mmol), and 25 mL of Et₂O were combined as above except (a) an ice/MeOH bath was not used during deprotonation, (b) the reaction mixture was stirred for 1.5 h after addition of *t*-BuOK, and (c) the reaction mixture was stirred for 7 h after the addition of Diazald. The reaction mixture was roto-evaporated and the residue chromatographed on a 15 cm high, 4 cm diameter bed of hexane-packed, degassed silica gel (40–140 mesh). The column was eluted with 200 mL batches of 0, 5, 10, 20, 50, and 100% EtOAc/cyclohexane, and the first eleven fractions (28 mL each) were combined and roto-evaporated. An ¹H NMR of the residue indicated a mixture of **7** and (η^5 -2-(2'-indenyl)indenyl)Cr(CO)₂NO (singlets at δ 3.55 and 5.8 ppm in a 1:1 ratio were attributed to the -CH₂ group and the complexed five-membered ring protons of the latter, respectively) as well as some other minor unidentified contaminants. The MS and IR of the residue are reported: MS (EI), *m/z* 367 (6) (M)⁺, 339 (34) (M - CO)⁺, 311 (73) (M - 2CO)⁺, 281 (100) (M - 2CO - NO)⁺, 230 (100) (C₁₈H₁₄)⁺, 229 (60) (M - 2CO - NO - Cr)⁺, 52 (100) (Cr)⁺; IR (KBr) 2016 (s), 1945 (s), 1686 (s), 751 (w), 627 (w) cm⁻¹.

Reaction of 13'a with CuCl₂. To a stirring, room temperature suspension of **13a** (0.206 g, 0.410 mmol) in 20 mL of THF was quickly added under a stream of dinitrogen solid *t*-BuOK (0.098 g, 0.873 mmol). Stirring was continued for 7 min after which time the reaction mixture was heated to ~40 °C with an oil bath. Within 20 min, the color of the mixture had become yellow-orange. One and one half hours thereafter, anhydrous CuCl₂ (0.116 g, 0.863 mmol) was added quickly under a stream of dinitrogen. Stirring was continued for 20 min after which time the reaction mixture was cooled to room temperature and roto-evaporated. An IR (KBr) of the residue indicated the presence of **7**; in addition, weak signals at 1979, 1958, 1926, and 1880 cm⁻¹ were seen. CH₂Cl₂ was added to the crude, and the organic layer was washed with distilled H₂O. The H₂O layer was colorless while the organic layer consisted of an orange solution with a suspended red material; the suspended material quickly became green in the separatory funnel. The organic layer was drawn off, the green material filtered, and the filtrate dried over anhydrous MgSO₄. The filtrate was roto-evaporated, and an IR (KBr) was taken of the residue as well as of the green precipitate. That of the green precipitate showed the presence of mostly H₂O along with a medium-intensity signal at 513 cm⁻¹; that of the residue showed the presence of **7** as well as medium-intensity signals at 1958 and 1879 cm⁻¹. The ¹H NMR of the residue showed mainly **7**.

Reaction of 13'a with Br₂. To a stirring, room-temperature suspension of **13a** (0.194 g, 0.386 mmol) in 20 mL of THF was quickly added under a stream of dinitrogen solid *t*-BuOK (0.087 g, 0.775 mmol). The reaction mixture was warmed to ~40 °C, and stirring was continued for 35 min, after which time the color had become light orange. The reaction flask was then covered in aluminum foil and cooled to -78 °C with a dry ice bath. Br₂ (0.020 mL, 0.390 mmol) was added via syringe. The dry ice was removed, and stirring was continued for 2 h and 40 min. The reaction mixture was then roto-evaporated, and an IR (KBr) were taken of the residue. The IR showed the presence of **7** as well as weak signals at 1979, 1958, 1926, and 1880 cm⁻¹. CH₂Cl₂ was added to the residue, resulting in a brown solution with a green precipitate. The precipitate was filtered off and dried with suction to give 0.145 g. An IR (KBr) of the precipitate showed the presence of H₂O along with medium-intensity signals at 1475 and 512 cm⁻¹. The CH₂Cl₂ filtrate was washed with distilled H₂O, dried with

anhydrous MgSO_4 , filtered, and roto-evaporated. The residue was chromatographed on a 15 cm high, 4 cm diameter bed of hexane-packed, degassed silica gel (40–140 mesh). The column was eluted with 200 mL batches of 10% and 100% Et_2O /hexane. The first three fractions eluting in the 10% regime were combined and roto-evaporated to give a residue weighing 0.013 g; an ^1H NMR showed it to be fairly pure **7**. The latter four fractions in the same regime were combined and roto-evaporated to give a residue weighing 0.029 g. It gave an ^1H NMR characteristic of a complex mixture; however, the presence of **7** and 1-hydroxy-2-(2'-indenyl)indene in a 5:1 ratio was confirmed by MS. The origin of the 1-hydroxy-2-(2'-indenyl)indene is unclear. It has also been isolated from the reaction of doubly-deprotonated **7** with $\text{FeCl}_2\cdot 3/2\text{THF}$, as well as from the reaction of **13b** with iodine. 1-Hydroxy-2-(2'-indenyl)indene: ^1H NMR (250 MHz, CDCl_3) δ 3.63 (d, 22.5 Hz, 1H), δ 3.75 (d, 21.5 Hz, 1H), δ 5.39 (s, 1H), δ 6.75 (s, 1H), δ 7.17–7.44 (m, 8H), δ 7.53 (d, 6.3 Hz, 1H); MS (EI), m/z 246 (79) (M^+), 229 (56) ($\text{M} - \text{OH}^+$), 228 (53) ($\text{M} - \text{H}_2\text{O}^+$), 215 (40), 202 (33), 131 (47) ($\text{C}_9\text{H}_7\text{O}^+$), 115 (100) (C_9H_7^+); IR (KBr) 1461 (m), 1390 (m), 844 (m), 750 (s, with shoulder at lower frequency), 717 (m) cm^{-1} . Mp: sample darkened at 160.5 °C and liquefied with further darkening at 186–191 °C. Lack of material prevented further analysis. The last two fractions in the 100% regime gave, after roto-evaporation, a residue weighing 0.015 g. The ^1H NMR was characteristic of a complex mixture, but 1-hydroxy-2-(2'-indenyl)indene could again be identified.

Reaction of 13a with 1,2-Dibromoethane. To a stirring suspension of **13a** (0.202 g, 0.402 mmol) in 20 mL of Et_2O was quickly added under a stream of dinitrogen solid *t*-BuOK (0.101g, 0.900 mmol). The mixture was then heated at reflux 40 min, after which time the reaction flask was wrapped in aluminum foil and the temperature lowered to -78 °C with a dry ice bath. 1,2-Dibromoethane (35 μL , 0.406 mmol) was then added via syringe, and stirring was continued for 18 h. The reaction mixture was roto-evaporated, and the residue was chromatographed on a 15 cm high, 4 cm diameter bed of hexane-packed, degassed alumina (80–200 mesh). The column was eluted with 200 mL batches of 0, 20, 40, and 100% dichloroethane/hexane, and EtOAc. The fractions eluting in the 40% regime consisted of 0.028 g (30%) of fairly pure **7**. The fractions eluting with 100% dichloroethane contained mainly **14** (0.035 g, 24%). The last set of fractions contained 0.011 g of less pure **14**.

Reaction of 13a with I_2 . Into a stirring suspension of **3a** (0.277 g, 0.551 mmol) in 20 mL of Et_2O was syringed 1.2 mL (1.2 mmol) of a 1 M THF solution of *t*-BuOK. The reaction mixture was heated at reflux for 20 min, after which time the reaction flask was wrapped in aluminum foil, and the temperature was lowered to -78 °C with a dry ice bath. Over a 5 min period, a solution of I_2 (0.142 g, 0.559 mmol) in 20 mL of Et_2O was added with a dropping funnel. The reaction mixture was stirred for 15 min at -78 °C. The dry ice was then removed and stirring continued until the reaction mixture reached ambient temperature. The dark purple mixture was roto-evaporated, and the residue was chromatographed on a 15 cm high, 4 cm diameter bed of hexane-packed, degassed silica gel (40–140 mesh). The column was eluted with 200 mL batches of 0, 20, and 50% Et_2O /hexane and 10% EtOAc/ Et_2O . The residue from roto-evaporating the fractions eluting in the 0–20% regime was of negligible weight and was shown by ^1H NMR to consist of **7** and **16** in a 7:2 ratio. The residue (0.003 g) from roto-evaporating the fractions eluting in the 20–50% regime also showed ^1H NMR signals for **7** and **14** in a complex mixture. An MS of these fractions confirmed the presence of **7**, **16**, and **14**. In addition, a peak at mass 510 amu was tentatively assigned to one or more complexes of the type $(\eta^6\text{-16})\text{Cr}(\text{CO})_3$. The residue (0.006 g) from roto-evaporating a later set of fractions eluting in the 50% regime gave an ^1H NMR complicated by line broadening possibly due to paramagnetic impurities. A MS showed the presence of **7**, **14**, and 1-hydroxy-2-(2'-indenyl)indene. The residue (0.048 g) from

roto-evaporating the last set of fractions gave an ^1H NMR that was severely distorted by line-broadening. An MS showed the presence of **7**, **14**, 1-hydroxy-2-(2'-indenyl)indene, and **16**.

Reaction of 13a with Ferrocenium Fluoroborate. Into a stirring suspension of **3a** (0.238 g, 0.474 mmol) in 25 mL of THF was syringed 0.98 mL (0.98 mmol) of a 1 M THF solution of *t*-BuOK. The reaction mixture was heated at reflux for 40 min after which time the reaction flask was wrapped in aluminum foil and the temperature lowered to -78 °C with a dry ice bath. Ferrocenium fluoroborate (0.266 g, 0.975 mmol) was quickly added under a stream of dinitrogen, and stirring was continued for 19 h as the dry ice sublimed. The dark red reaction mixture was roto-evaporated, and an ^1H NMR and IR of the residue were taken. ^1H NMR (250 MHz, CDCl_3) (all signals very broad): δ 3.8 (br s), δ 4.2 (br s, ferrocene), δ 5.1 (br s), 7.0 (br s), 7.1–7.6 (br m). The singlet at 3.8 ppm was presumably due to both the chromium dimer (analogue of **12**) and **7**, so an integral was not meaningful. IR (KBr): 1993 (s), 1943 (s), 1918 (s), 1909 (s), 1898 (sh), 1872 (m), 1106 (m), 1084 (s), 861 (w), 816 (m), 739 (m), 578 (m) cm^{-1} (the 1106 and 1084 cm^{-1} are presumably due to BF_4^-). The residue was chromatographed on a 15 cm high, 4 cm diameter bed of hexane-packed, degassed alumina (80–200 mesh). The column was eluted with 200 mL batches of 0, 50, and 100% CH_2Cl_2 /hexane. All fractions eluting in the 0–50% regime consisted of **7** and ferrocene. The last three fractions consisted of 1-hydroxy-2-(2'-indenyl)indene (0.007 g, 6%).

Reaction of 13b with CF_3COOH . To a stirring suspension of **13b** (0.226 g, 0.383 mmol) in 25 mL of Et_2O was syringed 0.8 mL (0.8 mmol) of a 1 M THF solution of *t*-BuOK. Stirring was continued for 35 min until the color had become light yellowish-orange. The temperature was lowered to -78 °C with a dry ice bath, and CF_3COOH (62 μL , 0.80 mmol) was added by syringe. After 15 min, the dry ice was removed, and the reaction flask was wrapped in aluminum foil. When it had reached ambient temperature, the brownish-yellow reaction mixture was roto-evaporated, and an IR was taken of the residue; it showed the presence of **7** along with very weak signals at 1979 and 1954 cm^{-1} . An ^1H NMR showed essentially pure **7**. The crude reaction mixture was washed with CH_2Cl_2 (3 \times) to remove **7** (0.086 g, 98%). The remaining dark brown precipitate (0.12 g), which was insoluble in acetone, MeOH, and H_2O , gave the following IR (KBr): 1709 (s), 1420 (m), 1365 (s), 1205 (s), 1138 (m), 967 (w), 838 (w), 804 (w), 723 (w), 534 (w) cm^{-1} .

Reaction of $[(\eta^5\text{-C}_9\text{H}_6\text{-C}_9\text{H}_8)\text{Cr}(\text{CO})_3]^{2-}$ (17'a**) and $\text{Fe}(\text{CO})_4\text{I}_2$.** To a stirring solution of **14** (0.440 g, 1.20 mmol) in 40 mL of THF was syringed 2.5 mL (2.5 mmol) of a 1 M THF solution of *t*-BuOK, resulting in immediate color change to dark brown. The reaction mixture was heated at ~ 40 °C for 40 min with an oil bath, after which time the temperature was lowered to -78 °C with a dry ice bath. With a dropping funnel, a solution of $\text{Fe}(\text{CO})_4\text{I}_2$ (0.508 g, 1.20 mmol) in 15 mL THF was added over a 4 min period. After the addition was complete, the reaction mixture was held at -78 °C for 5 min, and then the dry ice was removed. When the dark maroon reaction mixture had reached ambient temperature, distilled H_2O (100 mL) followed by CH_2Cl_2 (100 mL) was added. This resulted in an emulsion which gradually broke over 30 min to give a very light green aqueous layer and a brownish-green organic layer. The organic layer was separated, dried over anhydrous MgSO_4 , filtered, and roto-evaporated. An IR of the residue showed very weak 2033, 1939, and 1878 cm^{-1} signals. The residue was chromatographed on a 15 cm high, 4 cm diameter bed of hexane-packed, degassed silica gel (40–140 mesh). The column was eluted with 200 mL batches of 0, 5, 10, and 100% Et_2O /hexane. The residue from roto-evaporating the set of fractions eluting in the 5–10% regime weighed 0.131 g and contained **7** and **16** in a 2.1:1 ratio. The residue from roto-evaporating the set of fractions eluting in the 10–100% regime weighed 0.010 g and exhibited a more complex ^1H NMR that was distorted by line-broadening; however, **7** and **16** in a 0.8:1 ratio could be identified. The residue from roto-evaporat-

Table 7. Crystallographic Data for Compounds 3a, 4, 5, and 11

formula	C ₂₄ H ₁₄ Cr ₂ O ₆ , 3a	C ₂₄ H ₁₂ Mo ₂ O ₆ , 4	C ₁₈ H ₁₂ Br ₄ , 5	C ₂₆ H ₂₁ Mo ₂ O ₈ P, 11
cryst color/habit	yellow-orange	brown	brown	dark green
cryst size, mm	not recorded	0.2 × 0.2 × 0.4	0.075 × 0.4 × 0.4	0.2 × 0.2 × 0.8
space group	C2/c	C2/c	P2 ₁ /n	Pbca
a, Å	12.438(3)	21.40(2)	9.003(3)	29.028(3)
b, Å	16.186(2)	18.69(2)	17.881(2)	14.502(2)
c, Å	10.732(2)	13.71(1)	10.857(3)	12.052(1)
α, deg	90	90	90	90
β, deg	107.49(1)	130.11(3)	93.18(1)	90
γ, deg	90	90	90	90
V, Å ³	2060.6(8)	4194(12)	1744.8(8)	5073.5(19)
Z	4	8	4	8
D(calc), g cm ⁻³	1.617	1.863	2.0856	1.7916
diffractometer	Enraf-Nonius CAD-4	Enraf-Nonius CAD-4	Enraf-Nonius CAD-4	Enraf-Nonius CAD-4
radiation (graphite monochromator)	Mo Kα (λ = 0.710 73)	Mo Kα (λ = 0.710 73)	Mo Kα (λ = 0.710 73)	Mo Kα (λ = 0.710 73)
temp	ambient	ambient	ambient	ambient
μ, cm ⁻¹	10.656	12.055	91.315	10.744
2θ range, deg	0 < 2θ < 50	0 < 2θ < 52	0 < 2θ < 54	0 < 2θ < 56
abs corr	DIFABS	DIFABS	DIFABS	DIFABS
reflens colld	1615	4495	3018	6770
indept reflens	1500	4270	2775	6767
obsd reflens	681	2020	1536	3035
min, max abs	0.9183, 1.0722	0.7574, 1.1504	.8142, 1.0706	0.9058, 1.0386
R(F), R _w (F), %	3.6, 3.6	7.9, 8.4	6.1, 6.8	3.74, 3.60

ing the last set of fractions in the 100% regime weighed 0.040 g; it gave an ¹H NMR that was severely distorted by line-broadening, but **16** could tentatively be identified. The IR spectra of all three sets of fractions showed medium to weak 2028 and 1983 cm⁻¹ consistent with the presence of a trace of η⁵-Cr(CO)₃I type product(s).

Reaction of [(η⁵-C₉H₆-C₉H₆)Mo(CO)₃]²⁻ (17b**) with Fe(CO)₄I₂.** Into a stirring suspension of **7** (0.500 g, 2.17 mmol) and Mo(CO)₆ (0.574 g, 2.17 mmol) in 25 mL of Bu₂O was syringed 1.75 mL (4.38 mmol) of a 2.5 M solution of n-BuLi in hexanes. The reaction mixture was heated at reflux for 40 min, after which time it was cooled to -78 °C with a dry ice bath. Fe(CO)₄I₂ (0.926 g, 2.20 mmol) was added quickly under a stream of dinitrogen, and the reaction mixture was allowed to stir for 14 h as the dry ice sublimed. The Bu₂O was removed *in vacuo*, and the residue was chromatographed on a 15 cm high, 4 cm diameter bed of hexane-packed, degassed silica gel (40–140 mesh). The column was eluted with 200 mL batches of 0, 5, 10, 20, and 100% EtOAc/hexane. The residue from roto-evaporating the fractions eluting in the 10% regime weighed 0.114 g and contained predominantly **7** and **16** in a 1.7:1 ratio. The residue resulting from roto-evaporating the fractions eluting in the 20 to 100% regime weighed 0.194 g and gave an ¹H NMR characteristic of a complex mixture; however, the presence of **7** was confirmed by IR. In addition, the IR exhibited strong peaks at 2028 and 1949 cm⁻¹, consistent with the presence of η⁵-Mo(CO)₃I type product(s). Recrystallization efforts afforded **7**. The residue from roto-evaporating the last set of fractions weighed 0.073 g and gave an ¹H NMR that was distorted by line-broadening. The IR showed medium-intensity peaks at 2030 and 1964 cm⁻¹.

X-ray Diffraction Analysis of 3a, 4, 5, and 11. Data collection for all four structures began with a random search at low θ to yield 25 reflections which were indexed to give an initial unit cell. An accurate cell was obtained using higher angle (θ = 10–12°) reflections. For **3a**, **4**, and **11**, initial direct methods solution (either MITHRIL or SHELXS) revealed the metals and most of the other heavy atoms. A difference Fourier map then yielded the remaining heavy atoms. After partial refinement, hydrogen atom positions were calculated, and the structure was subjected to full anisotropic refinement

of the heavy atoms using full-matrix least squares. A DIFABS absorption correction was applied, and the structure was refined with five more cycles of least squares.

In the case of **5**, initial SHELXS solution revealed some of the carbon skeleton. A difference Fourier map revealed the four bromines. The structure was then subjected to least-squares refinement after which the remainder of the carbon skeleton was located, followed by another three cycles of least squares. The atoms were then flagged anisotropic, three cycles of least squares were performed, a DIFABS correction was applied, another three cycles of least squares were performed, the hydrogen positions were calculated, and finally, five cycles of least squares were performed, after which two carbons remained non-positive-definite

Acknowledgment. We thank Mr. David Nellis for mounting the crystals and acquiring the data sets. We are also grateful to Prof. K. P. C. Vollhardt for supplying us with crystallographic coordinates for (μ,η⁵:η⁵-fulvalene)W(CO)₃Rh(CO)C(O)CH₃ for use in the correlation. B.W. is a recipient of a GAANN fellowship.

Note added in proof: (Dibenzo[*b,e*]fulvalene)Mo₂(CO)₆ does form in reaction of **13b** and FcH⁺. The spectroscopic data reported herein for **12** are due to an equimolar mixture of **7** and the dibenzofulvalene complex.

Supporting Information Available: ORTEP structures, packing diagrams, and tables of least-squares planes, important intermolecular contacts, complete positional and isotropic and anisotropic thermal parameters, and bond lengths and angles for compounds **3a**, **4**, and **11** (65 pages). This material is contained in many libraries on microfiche, immediately follows this article in the microfilm version of the journal, can be ordered from the ACS, and can be downloaded from the Internet; see any current masthead page for ordering information and Internet access instructions.

OM950348G

Syntheses and Characterization of Hybrid Bi- and Multidentate Tellurium Ligands Derived from *N,N*-Dimethylbenzylamine: Coordination Behavior of Bis[2-((dimethylamino)methyl)phenyl] Telluride with Chromium Pentacarbonyl

Rupinder Kaur,[†] Harkesh B. Singh,^{*,†} and Ray J. Butcher[‡]

Departments of Chemistry, Indian Institute of Technology, Powai, Bombay 400 076, India, and Howard University, Washington, DC, 20059

Received April 26, 1995[⊗]

A range of bi- and multidentate tellurium ligands containing both Te and N donor atoms have been synthesized and characterized by multinuclear NMR (¹H, ¹³C, ¹²⁵Te), MS, and single-crystal X-ray diffraction studies. Bidentate ligand 2-NMe₂CH₂C₆H₄TeMe (**4**) was obtained from the reaction of 2-NMe₂CH₂C₆H₄TeLi (**3**) with MeI. The reaction, in addition to the expected telluride **4**, afforded the novel 2-NMe₂CH₂C₆H₄TeI (**5**) and the tridentate ligand (2-NMe₂CH₂C₆H₄)₂Te (**6**) in poor yields. The compound is monomeric with weak intermolecular contacts between the Te and iodine atoms from adjacent molecules. Alternatively, ligand **6** has been obtained by the reaction of 2-NMe₂CH₂C₆H₄Li (**2**) and TeI₂, and its bonding capabilities have been evaluated. Ligand **6** displaces the THF ligand in Cr(CO)₅THF to give the complex Cr(CO)₅(2-NMe₂CH₂C₆H₄)₂Te (**13**) in which the ligand is bonded only through Te. Reaction of **6** with Cr(CH₃CN)₃(CO)₃ also gives the same complex **13**. Structures of the free ligand and its complex have been determined. Ligand **6** crystallizes in monoclinic space group *P*2₁/*n* with *a* = 10.2310(10) Å, *b* = 5.6110(10) Å, *c* = 32.010(3) Å, β = 97.13°(1), *V* = 1823.4(4) Å³, *Z* = 4, *D*_c = 1.443 mg/m³ (Mo Kα radiation at 293(2) K). The Te atom is pyramidal, and the Cr-Te distance of 2.6665 (9) Å is the shortest known. The bidentate ligand 2-NMe₂CH₂C₆H₄TePh (**7**) has been similarly obtained from **2** by reaction with PhTeBr. Oxidative workup of **3** afforded the ditelluride (2-NMe₂CH₂C₆H₄)₂Te₂ (**8**). Reaction of **8** with diazomethane gave the telluroether ligand (2-NMe₂CH₂C₆H₄Te)₂CH₂ (**9**). Other multidentate ligands of the type (2-NMe₂CH₂C₆H₄Te)₂E (**10-12**) (E = (CH₂)₃, S, Se) were obtained by the reaction of Br(CH₂)₃Br, S, and Se with **3**, respectively.

1. Introduction

Organotellurium compounds have become increasingly important as versatile reagents in modern organic synthesis.¹ A well-established method of obtaining a range of otherwise reactive and unstable organotellurium compounds is intramolecular coordination.^{2,3} Intramolecular coordination also provides a very useful method for the synthesis of "hybrid" bi- and multidentate ligands containing "hard" donor atoms such as nitrogen or oxygen in addition to "soft" tellurium. Hybrid organotellurium ligands are important as they offer the prospect of coordination to both hard and soft transition metal centers, giving rise to complexes possessing novel structures and reactivities. In addition they are suitable for the synthesis of heterobimetallic complexes which have applications in homogeneous catalysis.⁴

Nitrogen donor complexes have a very important role to play in organic synthesis.⁵ Tellurium ligands incorporating nitrogen donor atoms are well-known.¹ Although several examples of hybrid tellurium ligands incorporating sp² nitrogen atoms, e.g., azobenzenes,⁶ azomethines,⁷ and substituted pyridines,⁸ are available in the literature, far fewer examples of organotellurium ligands having sp³ nitrogen are known. Di(*o*-aminophenyl)ditelluride was one of the first examples of this kind to be synthesized.⁶ Levason *et al.*⁹ have reported methyl *o*-(dimethylamino)phenyl telluride and related hybrid ligands. Gysling *et al.*¹⁰ have described the preparation of the aryl analog, phenyl *o*-(diphenylamino)phenyl telluride. Recently Khandelwal *et al.* have reported telluroamine, bis[(2-aryltelluro)ethyl]amine,

(4) Hope, E. G.; Levason, W. *Coord. Chem. Rev.* **1993**, *122*, 109.

(5) Togni, A.; Vananzi, L. M. *Angew. Chem., Int. Ed. Engl.* **1994**, *33*, 497.

(6) (a) Cobbeldick, R. E.; Einstein, F. W. B.; McWhinnie, W. R.; Musa, F. H. *J. Chem. Res.* **1979**, 901(M); **1979**, 145(S).

(7) (a) Al-Salim, N.; Hamor, T. A.; McWhinnie, W. R. *J. Chem. Soc., Chem. Commun.* **1986**, 453. (b) Minkin, V. I.; Sadekov, I. D.; Maksimenko, A. A.; Kompan, O. E.; Struchkov, Yu. T. *J. Organomet. Chem.* **1991**, *402*, 331. (c) Wu, Y. J.; Ding, K. L.; Wang, Y.; Zhu, Z.; Yang, L. *J. Organomet. Chem.* **1994**, *468*, 13.

(8) (a) Hamor, T. A.; Al-Salim, N.; West, A. A.; McWhinnie, W. R. *J. Organomet. Chem.* **1986**, *310*, C5. (b) Al-Salim, N.; West, A. A.; McWhinnie, W. R.; Hamor, T. A. *J. Chem. Soc., Dalton Trans.* **1988**, 2363.

(9) Kemmitt, T.; Levason, W. *Organometallics* **1989**, *8*, 1303.

(10) Gysling, H. J.; Luss, H. R. *Organometallics* **1984**, *3*, 596.

[†] Indian Institute of Technology.

[‡] Howard University.

[⊗] Abstract published in *Advance ACS Abstracts*, September 1, 1995.

(1) (a) Engman, L. *Acc. Chem. Res.* **1985**, *18*, 274. (b) Petraghani, N.; Comasseto, J. V. *Synthesis* **1986**, *1*, 791, 897. (c) *The Chemistry of Organic Selenium and Tellurium Compounds*; Patai, S., Rappoport, Z., Eds.; Wiley: New York, 1986 and 1987; Vols. 1 and 2. (d) Irgolic, K. J. In *Methods of Organic Chemistry*; Klamann, D., Ed.; Georg Thieme Verlag: Stuttgart, 1990; Vol. E12b.

(2) Sudha, N.; Singh, H. B. *Coord. Chem. Rev.* **1994**, *135/136*, 469.

(3) McWhinnie, W. R. *Phosphorous, Sulfur Silicon Relat. Elem.* **1992**, *67*, 107.

and 2-(2-(aryltelluro)ethyl)pyridine types of ligands.¹¹ Examples of organotellurium compounds containing an *ortho*-amino group¹² and a tetradentate tripodal Te,N ligand are also known.¹³ All the examples mentioned above include ligands which are capable of forming five-membered rings upon chelation with metals. Very few examples of ligands capable of forming six-membered chelates are known.^{14–17} This paper discusses the syntheses of a series of bi- and multidentate Te,N ligands capable of forming six-membered rings upon chelation.

2. Experimental Section

General Procedures. All reactions were carried out under the exclusion of air and moisture, under an atmosphere of dinitrogen. Reactions were monitored using TLC techniques. Solvents and Hg were purified by standard techniques.¹⁵ All chemicals were of reagent grade and were used as received. The following starting materials were prepared according to literature methods: diphenyl ditelluride,¹⁹ TeI₂,²⁰ Cr(CO)₅-THF,²¹ and Cr(CO)₃(CH₃CN)₃.²² Melting points were recorded in capillary tubes and are uncorrected. Elemental analyses were performed on a Carbo-Erba model 1106 elemental analyzer. IR spectra were recorded on a Nicolet Impact 400 FT-IR spectrometer. Magnetic resonance spectra, ¹H (299.94 MHz), ¹³C (75.42 MHz), and ¹²⁵Te (94.75 MHz), were recorded on a Varian VXR 300S spectrometer at the indicated frequencies. Chemical shifts are cited with respect to SiMe₄ as the internal standard (¹H and ¹³C) and to a 0.3 M solution of Te(S₂CNET₂)₂ in CDCl₃ as the external standard (¹²⁵Te).²³ Positive chemical shifts are downfield from Te(S₂CNET₂)₂. The assignment of carbons in the ¹³C NMR spectra are in accordance with the figure.²⁴ ¹²⁵Te NMR spectra were obtained from ca. 20% w/v solutions in CDCl₃ at 25 °C. Satisfactory spectra were obtained after ca. 100–10000 transients. Values quoted are using the high-frequency positive convention. Mass spectra were obtained on a Jeol D-300(EI/CI) spectrometer and are reported as *m/e* (ion percent relative intensity). In case of an isotopic pattern, the value given is for the most intense peak.

(11) (a) Singh, A. K.; Srivastava, V.; Khandelwal, B. L. *Polyhedron* **1990**, *9*, 495. (b) Singh, A. K.; Srivastava, V.; Khandelwal, B. L. *Polyhedron* **1990**, *9*, 851. (c) Khalid, A.; Khandelwal, B. L.; Singh, A. K.; Singh, T. P.; Padmanabhan, B. *J. Coord. Chem.* **1994**, *31*, 19.

(12) Al-Rubaie, A. Z.; Al-Salim, N. I.; Al-Jadaan, A. N. *J. Organomet. Chem.* **1993**, *443*, 67.

(13) Singh, A. K.; Srivastava, V. *J. Coord. Chem.* **1990**, *21*, 39.

(14) (a) Christiaens, L.; Luxen, A.; Evers, M.; Thiabaut, Ph.; Mbuyi, M.; Welter, A. *Chem. Scr.* **1984**, *24*, 178. (b) Gornitzka, H.; Besser, S.; Herbst-Irmer, R.; Kilimann, U.; Edelmann, F. T. *J. Organomet. Chem.* **1992**, *437*, 299. (c) Detty, M. R.; Friedman, A. E.; McMillan, M. *Organometallics* **1995**, *14*, 1442.

(15) Maslokov, A. G.; McWhinnie, W. R.; Perry, M. C.; Shaikh, N.; McWhinnie, S. L. W.; Hamor, T. A. *J. Chem. Soc., Dalton Trans.* **1993**, 619.

(16) Engman, L.; Stern, D.; Pelcman, M.; Andersson, C. M. *J. Org. Chem.* **1994**, *59*, 1973.

(17) Singh, H. B.; Sudha, N.; West, A. A.; Hamor, T. A. *J. Chem. Soc., Dalton Trans.* **1990**, 907.

(18) Perrin, D. D.; Armarego, W. L. F.; Perrin, D. R. *Purification of Laboratory Chemicals*, 2nd ed.; Pergamon Press: New York, 1980.

(19) Haller, W. S.; Irgolic, K. J. *J. Organomet. Chem.* **1972**, *38*, 97.

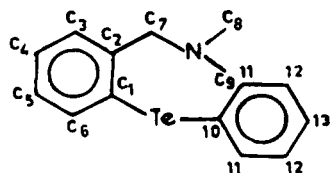
(20) Brauer, G. *Handbook of Preparative Inorganic Chemistry*, 3rd ed.; Academic Press: New York, 1975.

(21) Werner, H.; Prinz, R. *Chem. Ber.* **1967**, *100*, 265.

(22) Tate, D. P.; Knipple, W. R.; Augl, J. M. *Inorg. Chem.* **1962**, *1*, 433.

(23) Zumbulyadis, N.; Gysling, H. J. *J. Organomet. Chem.* **1980**, *192*, 183.

(24)



Synthesis of 2-NMe₂CH₂C₆H₄TeMe (4).^{14a} A stirred solution of *N,N*-dimethylbenzylamine **1** (1.53 mL, 1.37 g, 10.2 mmol) in dry ether (50 mL) was treated dropwise with a 1.6 M solution of *n*-butyllithium in hexane (7.5 mL, 12.0 mmol) under N₂. On being stirred for 24 h at room temperature, a white slurry of the lithiated product **2** was obtained. Tellurium powder (1.3 g, 10.2 mmol) was added to this under a brisk flow of N₂ gas, and stirring continued for additional 3 h until all the tellurium dissolved to give the lithium arenetelluroate **3**.¹⁷ The reaction mixture was cooled to 0 °C, after which iodomethane (0.64 mL, 1.448 g, 10.2 mmol) was syringed in; stirring continued for 0.5 h, following which the reaction was quenched with water and the aqueous phase was extracted with ether. The ether extracts were dried over anhydrous sodium sulfate, filtered, and concentrated to give a crude reddish-yellow oil. Separation by flash chromatography (SiO₂, 100–200 mesh, ethyl acetate) gave four fractions. The first fraction obtained as a yellow oil after evaporation of the solvent *in vacuo* corresponded to the desired ligand, **4** (1.15 g, 41%). Anal. Calcd for C₁₀H₁₅NTe: C, 43.39; H, 5.43; N, 5.06. Found: C, 42.32; H, 4.60; N, 5.74. ¹H NMR (CDCl₃): δ 7.50–7.47 (m, 1H, Ar–H), 7.12–7.06 (m, 3H, Ar–H), 3.44 (s, 2H, CH₂), 2.18 (s, 6H, NMe₂), 1.83 (s, 3H, TeMe). ¹³C NMR (CDCl₃): δ 119.3 (C₁), 140.4 (C₂), 126.8 (C₃), 127.6 (C₄), 124.5 (C₅), 132.2 (C₆), 65.5 (C₇), 42.7 (C₈, C₉) –17.0 (TeCH₃). MS: *m/e* 279 (M⁺, 28), 264 (M⁺ – CH₃, 44), 220 (C₆H₄CH₂NTe, 12), 134 (C₆H₄CH₂NMe₂, 100), 91 (220 – Te, 49), 77 (C₆H₅, 5), 58 (CH₂NMe₂, 9).

Synthesis of 2-NMe₂CH₂C₆H₄TeI (5). This compound was obtained as a minor product (second fraction after column chromatography) in the preparation of ligand **4** (0.34 g, 8%, mp 162 °C). Anal. Calcd for C₉H₁₂NTeI: C, 27.78; H, 3.12; N, 3.60. Found: C, 27.80; H, 3.18; N, 3.56. ¹H NMR (CDCl₃): δ 8.12–8.08 (m, 1H, Ar–H), 7.26–7.20 (m, 2H, Ar–H), 7.08–7.05 (m, 1H, Ar–H), 3.89 (s, 2H, CH₂), 2.75 (s, 6H, NMe₂). ¹³C NMR (CDCl₃): δ 117.1 (C₁), 138.3 (C₂), 129.2 (C₃), 129.3 (C₄), 126.3 (C₅), 138.4 (C₆), 67.4 (C₇), 46.8 (C₈, C₉). MS: *m/e* 390 (M⁺, 11), 263 (M⁺ – CH₃, 63), 220 (C₆H₄CH₂NTe, 8), 134 (C₆H₄CH₂NMe₂, 100), 91 (220 – Te, 95).

Synthesis of (2-NMe₂CH₂C₆H₄)₂Te (6).¹⁶ **Method A.** The desired ligand **6** was obtained as a minor product in the preparation of **4** as already described. Separation of the crude oil obtained after reaction, by flash chromatography, gave, after removal of the solvent (from the last fraction), light yellow crystals of **6** (0.120 g, 3%, mp 98 °C). Anal. Calcd for C₁₈H₂₄N₂Te: C, 54.60; H, 6.07; N, 7.08. Found: C, 54.53; H, 6.24; N, 7.24. ¹H NMR data was in full accordance with reported¹⁶ values. ¹³C NMR (CDCl₃): δ 126.1 (C₁), 143.2 (C₂), 127.6 (C₃), 128.7 (C₄), 126.5 (C₅), 138.6 (C₆), 67.3 (C₇), 44.3 (C₈, C₉). MS: *m/e* 396 (M⁺, 5), 218 (C₇H₆Te, 8), 179 (8), 134 (NMe₂CH₂C₆H₄, 100), 91 (C₇H₇, 11), 58 (CH₂NMe₂, 2).

Method B. To a cooled stirred solution of **2** at 0 °C was added TeI₂ (1.95 g, 5.1 mmol) in the powdered form. The reaction was stirred at this temperature for 0.5 h. The TeI₂ was found to be consumed completely. Usual workup gave, on removal of solvent *in vacuo*, yellow crystals of **6**. The compound was recrystallized from pentane (1.30 g, 65%). Other analyses are as above.

Synthesis of 2-NMe₂CH₂C₆H₄TePh (7). Ligand **7** was prepared by the reaction of **2** with PhTeBr.¹⁰ A solution of PhTeBr was prepared *in situ* by the addition of Br₂ (0.82 g, 0.26 mL, 5.1 mmol) in 12 mL of benzene to a –78 °C solution of Ph₂Te₂ (2.09 g, 5.1 mmol) in 125 mL of dry ether. The solution was stirred for 15 min in an ice bath, and the resulting suspension of the dark-red PhTeBr was transferred *via* a cannula to **2** at –78 °C. The solution was then stirred in an ice bath for 1 h and at room temperature for 0.5 h. The usual workup afforded a pale yellow oil, which crystallized upon cooling to give white crystals of **7**. The compound was recrystallized from *n*-pentane (1.44 g, 42%, mp 77 °C). Anal. Calcd for C₁₅H₁₇NTe: C, 53.16; H, 5.02; N, 4.13. Found: C, 53.21; H, 5.08; N, 4.13. ¹H NMR (CDCl₃): δ 7.90–7.87 (m,

2H, Ar-H), 7.37–6.88 (m, 7H, Ar-H), 3.52 (s, 2H, CH₂), 2.24 (s, 6H, NMe₂). ¹³C NMR (CDCl₃): δ 122.7 (C₁), 140.6 (C₂), 128.5 (C₃), 129.1 (C₄), 125.7 (C₅), 134.5 (C₆), 66.2 (C₇), 43.7 (C₈, C₉), 120.9 (C₁₀), 140.3 (C₁₁), 127.8 (C₁₂), 129.1 (C₁₃). MS: *m/e* 341 (M⁺, 63), 279 (28), 196 (15), 129 (C₇H₆N, 20), 105 (C₇H₆N, 34), 86 (C₇H₂, 100), 55 (C₃H₅N, 40).

Synthesis of (2-NMe₂CH₂C₆H₄Te)₂ (8). Telluroate (3) was poured into a beaker, and oxygen was passed through at a moderate rate for 10 min, after which time water (100 mL) was added into the beaker and oxygen was passed through for additional 0.5 h. The organic phase was extracted with ether and washed several times with water. Usual workup gave a yellow oil, which was flash-chromatographed using diethyl ether as the eluant. The yellow fraction obtained was concentrated and cooled at -20 °C to give yellow crystals of 8. These were filtered, rinsed with ether, and dried under nitrogen (1.33 g, 50%, mp 87 °C). Anal. Calcd for C₁₈H₂₄N₂Te₂: C, 41.28; H, 4.59; N, 5.35. Found: C, 41.36; H, 4.45; N, 5.36. ¹H NMR (CDCl₃): δ 8.01–7.98 (d, 2H, Ar-H), 7.15–6.98 (m, 6H, Ar-H), 3.55 (s, 4H, CH₂), 2.30 (s, 12H, NMe₂). ¹³C NMR (CDCl₃): δ 113.0 (C₁), 140.8 (C₂), 128.0 (C₃), 127.7 (C₄), 126.1 (C₅), 138.9 (C₆), 66.3 (C₇), 43.8 (C₈, C₉). MS: *m/e* 524 (M⁺, 5), 262 (C₆H₄CH₂NMe₂Te, 91), 220 (C₆H₄CH₂Te, 28), 179 (15), 134 (C₆H₄CH₂NMe₂, 100), 91 (220 - Te, 50), 77 (C₇H₇, 4), 58 (CH₂NMe₂, 8).

Synthesis of (2-NMe₂CH₂C₆H₄Te)₂(CH₂)₃ (9). To a solution of 8 (0.26 g, 0.5 mmol) in dry ether 0 °C was added an excess of diazomethane in ether while a brisk flow of nitrogen passed through the reaction flask. The reaction was stirred at this temperature for 3 h. Excess diazomethane was removed by bubbling nitrogen through the solution, and finally the ether was removed under *vacuo*. The resulting yellow oil was the desired ligand, 9 (0.26 g, 100%). ¹H NMR (CDCl₃): δ 7.71–7.68 (d, 2H, Ar-H), 7.17–7.03 (m, 6H, Ar-H), 3.46 (s, 4H, CH₂), 3.29 (s, 2H, TeCH₂), 2.18 (s, 12H, NMe₂). ¹³C NMR (CDCl₃): δ 124.1 (C₁), 140.7 (C₂), 128.1 (C₃), 127.8 (C₄), 125.2 (C₅), 132.5 (C₆), 65.8 (C₇), 44.3 (C₈, C₉). MS: *m/e* 538 (M⁺, 2), 394 (C₁₈H₂₄N₂Te, 2), 258 (5), 220 (C₆H₄CH₂Te, 8), 179 (18), 134 (C₆H₄CH₂NMe₂, 100), 91 (220 - Te, 68), 58 (CH₂NMe₂, 35).

Synthesis of (2-NMe₂CH₂C₆H₄Te)₂(CH₂)₃ (10). Addition of 1,3-dichloropropane (4.80 mL, 5.76 g, 5.1 mmol) at -196 °C to 3 followed by usual workup gave yellow oil of the ditelluro-ether ligand 10 (1.38 g, 48%). Anal. Calcd for C₂₁H₃₀N₂Te₂: C, 44.52; H, 5.30; N, 5.04. Found: C, 43.42; H, 4.98; N, 4.01. ¹H NMR (CDCl₃): δ 7.55–7.51 (d, 2H, Ar-H), 7.25–7.01 (m, 6H, Ar-H), 3.69, 3.61 (t, 4H, TeCH₂), 3.40, 3.42 (s, 4H, CH₂), 2.73–2.65 (m, 2H, CCH₂C), 2.15, 2.16 (s, 12H, NMe₂). ¹³C NMR (CDCl₃): δ 119.1, 119.6 (C₁), 138.1, 141.5 (C₂), 127.6, 127.7 (C₃), 128.8, 128.9 (C₄), 125.7, 125.8 (C₅), 133.5, 133.8 (C₆), 65.5, 66.7 (C₇), 43.6, 43.7 (C₈, C₉), 32.59, 33.9 (CCH₂C), 10.0, 3.2 (TeCH₂).

Synthesis of (2-NMe₂CH₂C₆H₄Te)₂S (11). Dissolution of 3 in THF (150 mL) after removal of ether gave a red-colored solution, which was filtered under nitrogen to remove unreacted tellurium (if any). The filtered solution was collected in a two-necked flask, one end of which was connected to an N₂ gas supply. The reaction mixture was frozen to -78 °C, and sulfur powder was added (0.16 g, 5.1 mmol). All the sulfur was found to react as the reaction mixture slowly attained room temperature to give a yellow solution. Usual workup gave, on removal of the solvent, a yellow solid of 11. The compound was recrystallized from ether (1.27 g, 45%, mp 122 °C). Anal. Calcd for C₁₈H₂₄N₂Te₂S: C, 38.90; H, 4.32; N, 5.04. Found: C, 38.89; H, 4.76; N, 4.88. ¹H NMR (CDCl₃): δ 8.23–8.20 (d, 2H, Ar-H), 7.23–7.02 (m, 6H, Ar-H), 3.63 (s, 4H, CH₂), 2.36 (s, 12H, NMe₂). ¹³C NMR (CDCl₃): δ 123.6 (C₁), 139.5 (C₂), 127.0 (C₃), 128.0 (C₄), 125.8 (C₅), 133.5 (C₆), 65.8 (C₇), 44.6 (C₈, C₉). MS: *m/e* 552 (M⁺, 5), 526 (M⁺ - S, 5), 264 (C₆H₄CH₂NMe₂Te, 20), 220 (C₆H₄CH₂Te, 10), 134 (C₆H₄CH₂NMe₂, 100), 91 (220 - Te, 22).

Synthesis of (2-NMe₂CH₂C₆H₄Te)₂Se (12). Ligand 12 was obtained by an analogous method to that of 11 by addition of selenium (0.40 g, 5.1 mmol) to 3 (1.6 g, 72%, mp 114 °C). Anal. Calcd for C₁₈H₂₄N₂Te₂Se: C, 35.87; H, 3.98; N, 4.65. Found: C, 36.18; H, 4.40; N, 4.60. ¹H NMR (CDCl₃): δ 8.21–8.18 (d, 2H, Ar-H), 7.15–6.97 (m, 6H, Ar-H), 3.55 (s, 4H, CH₂), 2.31 (s, 12H, NMe₂). ¹³C NMR (CDCl₃): δ 119.9 (C₁), 139.6 (C₂), 126.9 (C₃), 127.8 (C₄), 125.8 (C₅), 135.5 (C₆), 65.6 (C₇), 44.3 (C₈, C₉). MS: *m/e* 601 (M⁺, 3), 523 (M⁺ - Se, 16), 389 (19), 263 (C₆H₄CH₂NMe₂Te, 60), 133 (C₆H₄CH₂NMe₂, 93), 90 (C₇H₆, 100).

Synthesis of Cr(CO)₅(2-NMe₂CH₂C₆H₄)₂Te (13). Method A. A solution of Cr(CO)₅THF²¹ obtained after photolysis of Cr(CO)₆ (0.096 g, 0.44 mmol) in THF (75 mL) was treated with a solution of 6 (0.17 g, 0.44 mmol) in THF (10 mL) at room temperature. The reaction was stirred at room temperature for 0.5 h, after which insoluble green products were separated by filtration over a pad of Celite. The resulting yellow solution obtained was concentrated. Hexane (5 mL) was added to the filtrate, and it was cooled to 5 °C to give a yellow powder. The product was recrystallized from hexane to give 13 as pale yellow crystals (0.20 g, 78%, mp 97 °C). Anal. Calcd for C₂₃H₂₄N₂CrO₅Te: C, 46.97; H, 4.11; N, 4.76. Found: C, 46.78; H, 3.81; N, 4.38. ¹H NMR (CDCl₃): δ 7.94–7.91 (d, 2H, Ar-H), 7.31–7.12 (m, 6H, Ar-H), 3.70, 3.15 (dd, AB system, 4H, CH₂, ²J_{HH} = 15 Hz), 2.14 (s, 12H, NMe₂). ¹³C NMR (CDCl₃): δ 223.7, 217.4 (CO-C), 121.4 (C₁), 142.6 (C₂), 128.9 (C₃), 129.3 (C₄), 128.4 (C₅), 137.5 (C₆), 66.5 (C₇), 44.6 (C₈, C₉). IR (hexane) ν(CO) = 2058 (m), 1946 (s), 1935 cm⁻¹.

Method B. A yellow solid of Cr(CO)₅(CH₃CN)₃²² obtained after thermolysis of Cr(CO)₆ (0.192 g, 0.88 mmol) in CH₃CN (100 mL) and removal of the solvent *in vacuo* was refluxed for a period of 0.5 h with a solution of 6 (0.34 g, 0.88 mmol) in THF (50 mL). The pale yellow solution obtained was filtered over Celite, concentrated, and cooled to 5 °C after addition of hexane (5 mL) to give 13 (0.10 g, 20%). Other analyses are as described above.

X-ray Structure Determinations of 5, 6, and 13. Compound 5 was obtained as brick red hexagonal plates from dichloromethane–hexane after 1 day at -20 °C. Pale yellow needles of ligand 6 were obtained from hexane after 2 days by slow evaporation at 5 °C. Yellow parallelepiped of complex 13 were obtained similarly from hexane after several weeks at -20 °C. All diffraction measurements were performed on an Enraf-Nonius CAD4 diffractometer using graphite-monochromated Mo Kα radiation (λ = 0.710 73 Å). The unit cell was determined from 25 randomly selected reflections using the automatic search index and the least-squares routine. During data collection, the intensities of four monitor reflections showed no decay effects. The structures were solved by direct methods. The analytical scattering factors of Cromer and Waber²⁵ were used; real and imaginary components of anomalous scattering for the atoms were included in the calculations. All computational work was carried out using Siemens programs SHELTLX PLUS,²⁶ PLUTO,²⁷ and ORTEP.²⁸ Crystal data and numerical details of measurement of intensity details are given in Table 1.

3. Results and Discussion

Ligand Synthesis and Characterization. Synthesis of the desired ligands 4 and 6–12 was accomplished in yields ranging from 40%–75% by the organolithium route (Scheme 1). Orthometalation was

(25) Cromer, D. T.; Waber, T. *International Tables for X-ray Crystallography*; Kynoch Press: Birmingham, England, 1974; Vol. IV.

(26) SHELTLX PLUS. X-ray Instruments Group, Nicolet Instruments Corp.: Madison, WI 53711, 1983.

(27) PLUTO-78. Motherwell, S.; Clegg, W. Programme for Plotting Molecular and Crystal Structures; University of Cambridge: Cambridge, England, 1978.

(28) ORTEP-II. Johnson, L. K. Report ORNL-5138; Oak Ridge National Laboratory: Oak Ridge, TN, 1976.

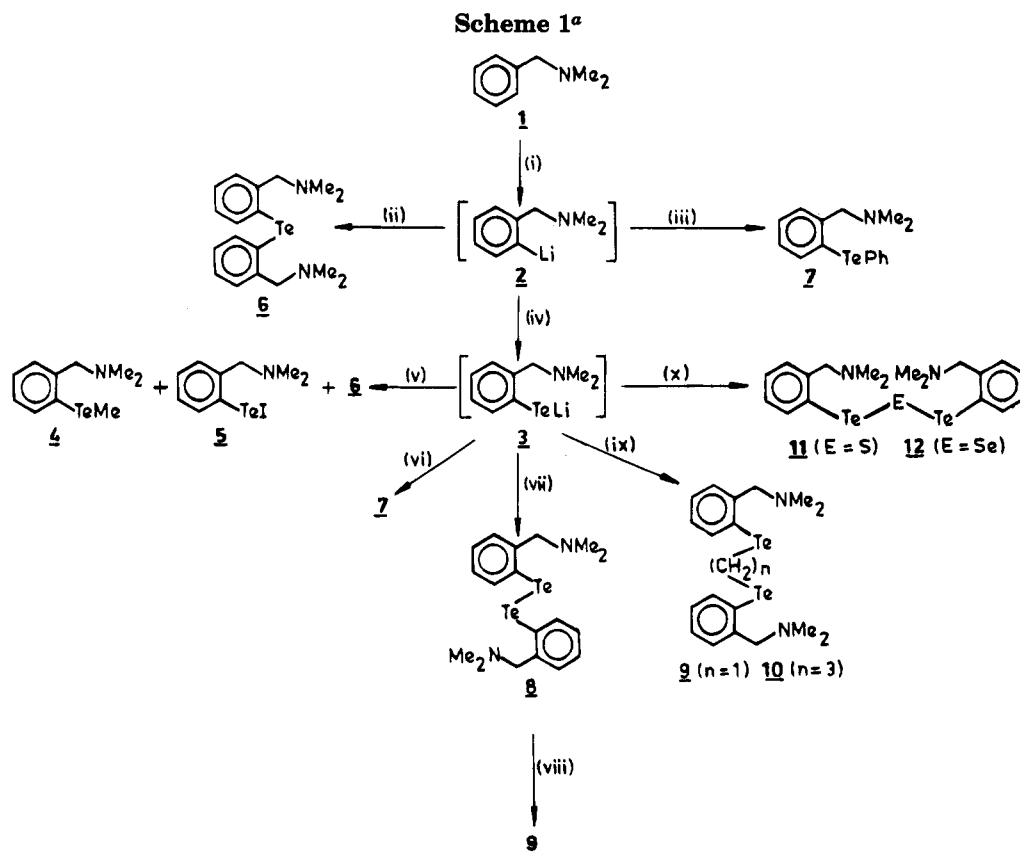
Table 1. Crystallographic Data and Measurements for 2-NMe₂CH₂C₆H₄TeI (5), (2-NMe₂CH₂C₆H₄)₂Te (6), and Cr(CO)₅(2-NMe₂CH₂C₆H₄)₂Te (13)

	Crystal Data		
	C ₉ H ₁₂ NTeI	C ₁₈ H ₂₄ N ₂ Te	C ₂₃ H ₂₄ CrN ₂ O ₅ Te
empirical formula	C ₉ H ₁₂ NTeI	C ₁₈ H ₂₄ N ₂ Te	C ₂₃ H ₂₄ CrN ₂ O ₅ Te
fw	388.7	395.99	588.04
cryst color and habit	red plates	pale yellow needles	yellow parallelopipeds
cryst size (mm ³)	0.53 × 0.45 × 0.15	0.37 × 0.35 × 0.08	0.65 × 0.55 × 0.15
cryst syst	orthorhombic	monoclinic	orthorhombic
space group	<i>Pbca</i>	<i>P2₁/n</i>	<i>Cmc2₁</i>
unit cell dimens			
<i>a</i> (Å)	8.6610(10)	10.2310(10)	18.930(4)
<i>b</i> (Å)	11.1420(10)	5.6110(10)	9.135(12)
<i>c</i> (Å)	23.5780(10)	32.010(3)	14.181(3)
α (deg)	90	90	90
β (deg)	90	97.13(1)	90
γ (deg)	90	90	90
volume (Å ³)	2275.3(3)	1823.4(4)	2452.3(9)
<i>Z</i>	8	4	4
density (Mg/mm ³) (calcd)	2.269	1.443	1.593
abs coeff (mm ⁻¹)	5.281	1.628	1.667
<i>F</i> (000)	1424	792	1168
	Measurement of Intensity Data		
temp (K)	293(2)	293(2)	203(2)
θ range for data collen	3.66–30.00°	2.03–25.00°	2.15–32.48°
index ranges	0 ≤ <i>h</i> ≤ 12 –15 ≤ <i>k</i> ≤ 0 –33 ≤ <i>l</i> ≤ 0	–12 ≤ <i>h</i> ≤ 12 0 ≤ <i>k</i> ≤ 6 –1 ≤ <i>l</i> ≤ 38	0 ≤ <i>h</i> ≤ 28 0 ≤ <i>k</i> ≤ 13 21 ≤ <i>l</i> ≤ 0
no of reflns colled	5104	3019	2357
no. of indpt reflns (<i>R</i> _{int})	3290	2364	2357
	0.1380	0.0175	0.0000
abs cor	semiempirical from ψ-scans	semiempirical from ψ-scans	NA
max and min transm	1.000 and 0.364	0.967 and 0.711	NA
refinement method	full-matrix least-squares on <i>F</i> ²	full-matrix least-squares on <i>F</i> ²	full-matrix least-squares on <i>F</i> ²
no. of data/restraints/params	3290/0/112	2845/0/195	2357/0/159
goodness-of-fit on <i>F</i> ²	0.961	1.034	1.105
final <i>R</i> indices [<i>I</i> > 2σ(<i>I</i>)]	<i>R</i> 1 = 0.0339 w <i>R</i> 2 = 0.0874	<i>R</i> 1 = 0.0344 w <i>R</i> 2 = 0.0530	<i>R</i> 1 = 0.0340 w <i>R</i> 2 = 0.0847
<i>R</i> indices (all data)	<i>R</i> 1 = 0.0483 w <i>R</i> 2 = 0.0911	<i>R</i> 1 = 0.0621 w <i>R</i> 2 = 0.0871	<i>R</i> 1 = 0.0348 w <i>R</i> 2 = 0.0854
abs structure param			0.00
extinction coeff	0.0064(4)	0.0004(2)	0.0027(4)
largest diff peak and hole (e Å ⁻³)	1.270 and –0.888	0.303 and –0.286	4.003 and –1.651

readily accomplished according to the procedure of Klein and Hauser²⁹ to give a solution of aryllithium **2**, which was further reacted with finely ground tellurium powder to give lithium arenetelluroate **3**. Syntheses of hybrid bidentate ligand **4** was achieved by the reaction of **3** with MeI. Preliminary workup afforded an impure yellow oil, which was purified by column chromatography. Four fractions obtained after column chromatography corresponded to the desired ligand **4** in 41% yield as an air sensitive yellow liquid, a red solid (8%, which was identified to be **5**), unreacted amine, and the known telluride ligand¹⁶ **6** (3% yield). The reaction was repeated several times to check its reproducibility. The unexpected formation of **5** can be rationalized by the existence of elemental iodine in solution, which upon reaction with **3** affords **5**. In a related study 2-[(phenylamino)carbonyl]benzenetellurenyl iodide was obtained by the addition of iodine to the tellurium-containing benzanilide-derived lithium dianion.³⁰ Isolation of **5** is determined by the strong stabilization of the N–Te–I system to 10–Te–3 tellurane with intramolecular Te··N links (where N–X–L classification is used).³¹ The intramolecular coordination was confirmed by the single-crystal X-ray structure of **5** (*vide infra*). Reaction of **5** with RLi probably leads to the formation of **6** in minor yield.

Ligand **7** was obtained by two routes, first by the treatment of **3** with C₆H₅Br. A yellow viscous semisolid was obtained in moderate yield (37%). However, separation of the unreacted amine posed a major problem. Hence, alternatively, ligand **7** was prepared by reaction of **2** with PhTeBr by nucleophilic substitution on tellurium by a carbon nucleophile. The yield in this case was higher (42%) and afforded a crystalline white product. The telluride ligand **6** was obtained in low yields in the preparation of **4**. Alternatively, reaction of **2** with TeI₂ was carried out in the ratio 2:1 to yield **6** in excellent yields. This two-step reaction is a direct method and gives better yields compared to the recent literature method.¹⁶ The synthesis of **8**, though conceptually simple, proved to be a difficult task in practice. Isolation of the product and its subsequent crystallization depend on the ratio of product and the unreacted amine. It has been observed that less than 10% of unreacted amine favors crystallization. The complete workup procedure, including chromatography using diethyl ether as the solvent, gave, on cooling, a yellow solid of **8** in 50% yield. It is important to use peroxide-free ether for both reaction and purification. While attempts to grow the good quality crystals from various solvents were unsuccessful, slow evaporation of an ethereal solution gave after several days of standing parallelopipeds of **8** from the mother liquor. A method involving the reaction of **3** with excess CH₂Cl₂³² was attempted for **9** (52%); however, the purity was low.

(29) Klein, K. P.; Hauser, C. R. *J. Org. Chem.* **1967**, *32*, 1479.(30) Engman, L.; Hallberg, A. *J. Org. Chem.* **1989**, *54*, 2264.(31) Perkins, C. W.; Martin, J. S. *J. Am. Chem. Soc.* **1980**, *102*, 1155.



^a Legend: (i) *n*-BuLi, (ii) TeI₂, (iii) PhTeBr, (iv) Te⁰, (v) MeI, (vi) PhBr, (vii) [O], (viii) CH₂N₂, (ix) X(CH₂)_nX, X = Cl, Br, (x) E = S, Te.

Alternatively, **9** was prepared by the reaction of **8** with diazomethane³³ in 100% yield (based on **8**). Although the second method involves the preparation of ditelluride and its subsequent reaction with diazomethane, the purity of the product in this case is high. The reaction of **3** with Cl(CH₂)₃Cl gave **10** as a yellow liquid in 48% yield. Minor amounts of R₂Te and R₂Te₂ were also formed (responsible for slightly lower elemental analysis than expected). Insertion of S and Se into the Te–Te bond was achieved by the reaction of **3** with elemental S and Se to give **11** and **12** in good yields (45% and 72%, respectively).³⁴

The ¹H and ¹³C chemical shifts for the tellurium ligands observe a trend that is indicative of M···N coordination. The NMe₂ resonances (¹H NMR) in particular are sensitive to the electronegativity of the group attached directly to tellurium. In the ¹³C spectra the effect of the M···N coordination is experienced most by the *ortho* and *ipso* carbons. The *ipso* (C₁) carbon resonances span the range 113–126 ppm, and the *ortho* carbon resonances (C₂) were in the range (138.3–141.9 ppm) and are the most deshielded.

¹²⁵Te NMR. The tellurium ligands and derivative **5** show relatively narrow line widths (<2 Hz). The chemical shifts are given in Table 2. The ¹²⁵Te chemical shifts range 920 ppm, with the signals being both shielded and deshielded with respect to Te(S₂CNEt₂)₂. The signals are deshielded in all cases, however, with

Table 2. ¹²⁵Te Chemical Shifts for Organotellurium Ligands

entry no.	tellurium ligand	¹²⁵ Te (ppm)	² J _{Te-H} (Hz)
1	2-NMe ₂ CH ₂ C ₆ H ₄ TeMe (4)	-561	29
2	2-NMe ₂ CH ₂ C ₆ H ₄ TeI (5)	358	
3	(2-NMe ₂ CH ₂ C ₆ H ₄) ₂ Te (6)	-289	
4	2-NMe ₂ CH ₂ C ₆ H ₄ TePh (7)	-198	
5	(2-NMe ₂ CH ₂ C ₆ H ₄ Te) ₂ (8)	-479	
6	(2-NMe ₂ CH ₂ C ₆ H ₄ Te) ₂ CH ₂ (9)	not recorded	
7	(2-NMe ₂ CH ₂ C ₆ H ₄ Te) ₂ (CH ₂) ₃ (10)	-435, -439	33, 28
8	(2-NMe ₂ CH ₂ C ₆ H ₄ Te) ₂ S (11)	194	
9	(2-NMe ₂ CH ₂ C ₆ H ₄ Te) ₂ Se (12)	96	

respect to TeMe₂. The resonance position is very sensitive to the electron-withdrawing effect of the substituent group. Thus a decrease in chemical shift is observed in going from R = Me to I, with R = Me being most shielded (-561 ppm) and R = I being most deshielded (358 ppm). The proton-coupled spectra for **4** show the presence of a quartet with ²J_{Te-H} = 29 Hz, which agrees well with the literature value of a related compound.⁹ In **10** a set of triplets occurs at -435 and -439 ppm with ²J_{Te-H} of 33 and 28 Hz, respectively. This agrees with similar observations made by ¹H and ¹³C NMR, indicating, probably, the presence of two distinct isomeric species. Decomposition of **10** occurs slowly in CDCl₃ solution, giving peaks for both **6** and **8**. For **5**, **11**, and **12** downfield shifts are observed due to deshielding of Te by more electronegative atoms like I, S, and Se. For **11** minor amounts of polysulfides (<1%) such as RTe(S)₂₋₄TeR are detected by ¹²⁵Te NMR. These appear even more downfield with respect to **11** (¹²⁵Te = 273, 288, and 298 ppm). Similarly for **12** a minor amount of polyselenide RTe(Se)₂TeR is detected (¹²⁵Te = 145 ppm). There is no indication of an

(32) Hope, E. G.; Kemmitt, T.; Levason, W. *Organometallics* **1988**, *7*, 78.

(33) Jones, C. H. W.; Sharma, R. D. *Organometallics* **1996**, *5*, 805.

(34) Kollemann, C.; Obendorf, D.; Sladky, F. *Phosphorous Sulfur Relat. Elem.* **1988**, *38*, 69. (b) Kollemann, C.; Sladky, F. *Organometallics* **1991**, *10*, 2101.

"exchange equilibrium phenomenon" as observed for related compound PhTeSeTePh^{34b} (giving rise to PhTeTePh and PhTeSeSeTeR) as no peaks for the ditelluride were detected by ^{125}Te NMR. This indicates the stability of compound **12** as a result of intramolecular coordination.

Complexation Reactions. Attempts to displace ligating carbonyls in $\text{Cr}(\text{CO})_6$ by the bidentate ligand **4** in THF in a thermal reaction led only to decomposition of the ligand and reprecipitation of Te even under mild conditions ($<65^\circ\text{C}$). Stirring an equimolar solution of the tridentate ligand **6** with the monoactivated species $\text{Cr}(\text{CO})_5\text{THF}$ at room temperature gave a yellow solid which was stable in air at room temperature. Elemental analysis recorded on the crude product matched exactly with $\text{Cr}(\text{CO})_5$ (**6**). The IR spectrum of the complex (**13**) shows three high-frequency bands at $\nu = 2058$ (m), 1946 (s), and 1935 (s) cm^{-1} (compared to $\text{Cr}(\text{CO})_5\text{THF}$), suggesting a local point symmetry C_{4v} . These observations are indicative of the incorporation of a ligand with good π -acceptor characteristics, which induces a stronger donation of electrons from the chromium center toward Te. Complex **13** is readily soluble in both nonpolar and slightly polar solvents like chloroform. It shows, however, slow decomposition in solution to give a green precipitate. This is evidenced clearly in the ^1H NMR spectra of the compounds, which gives, in addition to the compound peaks, impurity peaks corresponding to free ligand arising presumably from decomposition of the complex in solution and regeneration of the ligand. The ^1H NMR for **13** indicates a dynamic coordination of the internal base NMe_2 in the complex. The CH_2 protons form an AB pattern (δ 3.15, 3.70 ppm, $^2J_{\text{HH}} = 15$ Hz) at ambient temperature in contrast to a singlet observed for the free ligand **6**. At low temperature ($+15^\circ\text{C}$) the peaks become sharper. This is the result of hindered rotation of the phenyl substituents with simultaneous fixation of the NMe_2 groups in the sense of an alternating, dynamic coordination of the N donor at a time to the Te center. These findings were supplemented by the single-crystal X-ray structure analysis of **13** (*vide infra*). This type of behavior was first observed and excellently interpreted for the related (2- $\text{NMe}_2\text{CH}_2\text{C}_6\text{H}_4$) $_{2\text{Si}}=\text{Cr}(\text{CO})_5$ complex.³⁵ In the ^{13}C NMR spectra the most interesting features are the upfield shift (5 ppm) of the *ipso* carbon resonance compared to free ligand and the downfield shift of the of CO resonances (δ 217.4 and 223.7 ppm). The presence of low-intensity resonances of the uncoordinated ligand **6** again indicates a partial decomposition of **13** in solution. At low temperature, however, the complex crystallizes in the pure form. When the reaction of the same ligand, **6**, was carried out with another carbonyl precursor, $[\text{Cr}(\text{CO})_3(\text{CH}_3\text{CN})_3]$, the maximum hapticity of which matched that of the ligand in THF at room temperature, the identical product **13** was obtained. This is perhaps the most interesting feature of this reaction. This type of carbonyl redistribution for reactions starting from metal tetra- or tricarbonyl precursor has been reported.³⁶ Two possible reasons which could explain the formation of the mono-coordinated complex are, first, the preference for the

(35) Probst, R.; Leis, C.; Gampers, S.; Herdtweck, E.; Zybilla, C.; Auner, N. *Angew. Chem., Int. Ed. Engl.* **1991**, *30*, 1132.

(36) Bates, C. M.; Morley, C. P.; Di Vaira, M. *J. Chem. Soc., Chem. Commun.* **1994**, 2621.

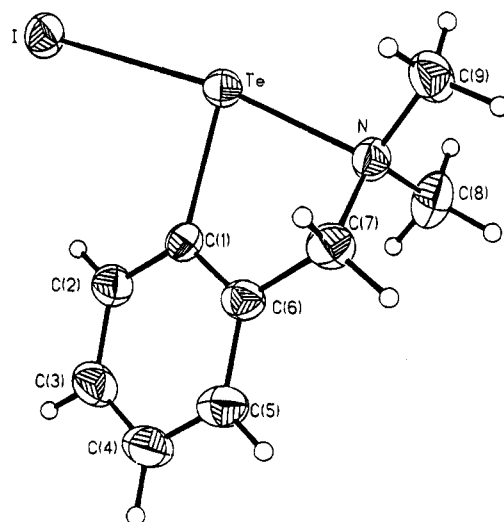


Figure 1. Molecular structure of 2- $\text{NMe}_2\text{CH}_2\text{C}_6\text{H}_4\text{TeI}$ (**5**).

Table 3. Atomic Coordinates ($\times 10^4$) and Equivalent Isotropic Displacement Parameters ($\text{\AA}^2 \times 10^3$) for **5**

atom	x	y	z	$U(\text{eq})^a$
I	-2383(1)	4306(1)	925(1)	52(1)
Te	49(1)	6071(1)	796(1)	35(1)
N	2058(4)	7509(3)	828(1)	40(1)
C(1)	557(4)	6215(4)	1676(2)	36(1)
C(2)	144(5)	5379(5)	2080(2)	46(1)
C(3)	566(6)	5565(5)	2642(2)	57(1)
C(4)	1386(6)	6580(5)	2799(2)	56(1)
C(5)	1786(6)	7403(4)	2396(2)	50(1)
C(6)	1386(5)	7231(4)	1825(2)	40(1)
C(7)	1784(6)	8136(4)	1372(2)	45(1)
C(8)	3556(5)	6908(5)	828(2)	60(1)
C(9)	1911(6)	8323(4)	343(2)	53(1)

^a $U(\text{eq})$ is defined as one-third of the trace of the orthogonalized U_{ij} tensor.

formation of the more stable five-membered chelate ring involving the N, Te, and C atoms rather than the six-membered ring involving N, Te, Cr, and C atoms which would have been formed if the ligand were to bind in a tridentate fashion and, secondly, a conversion of the $\text{Cr}(\text{CO})_3(\text{MeCN})_3$ precursor in THF to give $\text{Cr}(\text{CO})_5\text{THF}$, which reacts further to give **13**.

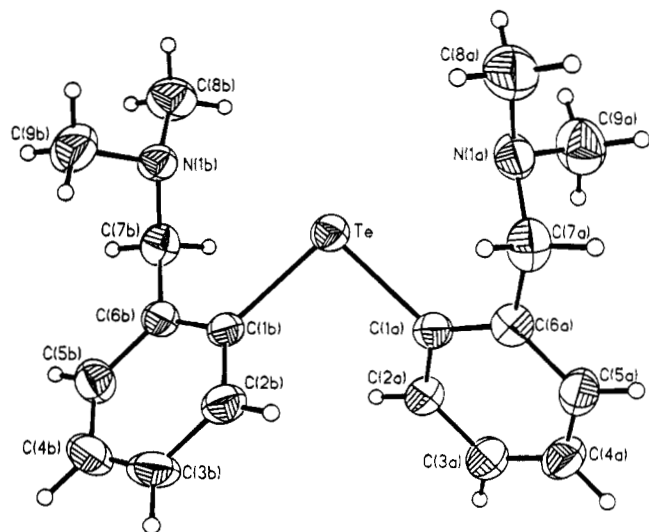
X-ray Structure of 5. The molecular structure of **5** with atom numbering is shown in Figure 1. Table 3 gives the atomic coordinates with equivalent isotropic displacement parameters, and Table 4 gives the selected bond lengths and angles. Very few examples of structurally characterized Te(II) RTeI compounds have been reported,³⁷ although several examples of RTeBr and RTeCl compounds are known.² A typical 10-Te-3 tellurane, with T-shaped geometry around Te, is found with strong nonvalent $\text{Te} \cdots \text{N}$ interaction. The three-coordinate Te is bonded to a carbon atom and to an iodine atom and shows a $\text{N} \cdots \text{Te}$ separation of 2.366(4) \AA , well within the sum of van der Waals radii (3.7 \AA) for N and Te ($N = 1.5$ and $\text{Te} = 2.20$ \AA) as reported by Pauling.³⁸ This distance is comparable to the $\text{Te} \cdots \text{N}$

(37) (a) Vicentine, G.; Geisbrecht, E. *Chem. Ber.* **1959**, *92*, 40. (b) Sadekov, I. D.; Ladatko, A. A.; Nivorozhkin, V. L.; Kompan, O. E.; Struchkov, Yu. T.; Minkin, V. I. *Zh. Obshch. Khim.* **1990**, *60*, 2764. (c) Maksimenko, A. A.; Maslakov, A. G.; Mehrotra, G. K.; Abarkarov, G. M.; Sadekov, I. D.; Minkin, V. I. *Zh. Obshch. Khim.* **1988**, *58*, 1176. (d) Maksimenko, A. A.; Sadekov, I. D.; Maslakov, A. G.; Mehrotra, G. K.; Kompan, O. E.; Struchkov, Yu. T.; Lindeman, S. V.; Minkin, V. I. *Metallorg. Khim.* **1988**, *2*, 1151.

Table 4. Bond Lengths (Å) and Angles (deg) for 5^a

I-Te	2.8982(4)	Te-C(1)	2.127(4)
Te-N	2.366(4)	N-C(8)	1.460(6)
N-C(9)	1.467(6)	N-C(7)	1.480(5)
C(1)-C(2)	1.379(6)	C(1)-C(6)	1.387(5)
C(2)-C(3)	1.389(6)	C(3)-C(4)	1.387(7)
C(4)-C(5)	1.365(6)	C(5)-C(6)	1.403(5)
C(6)-C(7)	1.508(6)		
C(1)-Te-N	76.43(13)	C(1)-Te-I	95.65(11)
N-Te-I	172.08(8)	C(8)-N-C(9)	111.1(4)
C(8)-N-C(7)	111.1(3)	C(9)-N-C(7)	111.8(3)
C(8)-N-Te	110.1(3)	C(9)-N-Te	109.2(3)
C(7)-N-Te	103.3(2)	C(2)-C(1)-C(6)	120.7(4)
C(2)-C(1)-Te	124.7(3)	C(6)-C(1)-Te	114.6(3)
C(1)-C(2)-C(3)	119.3(5)	C(4)-C(3)-C(2)	120.7(4)
C(5)-C(4)-C(3)	119.5(4)	C(4)-C(5)-C(6)	120.9(4)
C(1)-C(6)-C(5)	118.9(4)	C(1)-C(6)-C(7)	119.0(3)
C(5)-C(6)-C(7)	122.1(4)	N-C(7)-C(6)	109.5(3)

^a Symmetry transformations were used to generate equivalent atoms.

**Figure 2.** Molecular structure of (2-NMe₂CH₂C₆H₄)₂Te (**6**).

distance reported for related structure *viz.* 2-(bromotelluro)-*N*-(*p*-tolyl)benzylamine [Te··N = 2.375 Å]¹⁵ but is longer than the average Te··N reported for 2-(chlorotellurenyl)-4-methylbenzalaniline [Te··N = 2.223 Å].^{37c} The increased distance is probably due to the lower electronegativity of X situated in the *trans* position relative to N in the X-Te··N fragment. The N and I occupy axial positions, and the N-Te-I angle is 172.08° (slightly distorted). Two unshared lone pairs and C(1) occupy the equatorial plane. The Te-C(1) distance [2.127(4) Å] is unexceptional, the phenyl ring is planar, and the bonds and angles are unexceptional. The Te-I distances [2.899(4) Å] are longer compared to the sum of single-bond covalent radii for the Te and I (2.7 Å) (Te = 1.37 and I = 1.33 Å) but are significantly shorter than the sum of van der Waals radii (4.35 Å) (Te = 2.20 and I = 2.15 Å). Weak intermolecular interactions of I and Te of the neighboring molecule observed in the packing diagram ($-1/2 - x, -1/2 + y, z$) explain the relatively long Te-I distance. Similar observations³⁹ have also been made for the C₄H₈OTeI₂, C₄H₈STeI₂, and C₆H₁₆OSiTeI₂ compounds.

(38) Pauling, L. *The Nature of the Chemical Bond*, 3rd ed.; Cornell University Press: Ithaca, NY, 1960; pp 224, 260.

(39) (a) Hope, H.; Knobler, C.; McCullough, J. D. *Inorg. Chem.* **1973**, *12*, 2665. (b) Knobler, C.; McCullough, J. D.; Hope, H. *Inorg. Chem.* **1970**, *9*, 797. (d) Al-Rubaie, A. Z.; Uemura, S.; Masuda, H. *J. Organomet. Chem.* **1991**, *410*, 309.

Table 5. Atomic Coordinates (×10⁴) and Equivalent Isotropic Displacement Parameters (Å² × 10³) for 6

atom	x	y	z	U(eq) ^a
Te	1312(1)	1782(1)	1074(1)	47(1)
N(1A)	3806(3)	4367(8)	897(1)	56(1)
N(1B)	-1026(3)	-1064(7)	573(1)	49(1)
C(1A)	2672(4)	2290(9)	1628(1)	44(1)
C(1B)	-315(4)	1251(8)	1425(1)	42(1)
C(2A)	2639(4)	759(10)	1963(1)	55(1)
C(2B)	-515(4)	2823(10)	1743(1)	57(1)
C(3A)	3518(4)	975(10)	2328(2)	63(2)
C(3B)	-1578(5)	2544(12)	1973(2)	72(2)
C(4A)	4437(4)	2768(11)	2353(2)	65(2)
C(4B)	-2439(5)	675(12)	1878(2)	70(2)
C(5A)	4500(4)	4287(10)	2020(2)	60(1)
C(5B)	-2253(4)	-856(10)	1563(2)	64(2)
C(6A)	3626(4)	4064(9)	1652(2)	47(1)
C(6B)	-1199(4)	-592(9)	1326(1)	48(1)
C(7A)	3715(4)	5687(9)	1288(2)	60(1)
C(7B)	-1047(4)	-2283(9)	972(1)	55(1)
C(8A)	3629(5)	5884(11)	530(2)	89(2)
C(8B)	-645(5)	-2706(10)	259(2)	77(2)
C(9A)	5034(5)	3001(11)	918(2)	83(2)
C(9B)	-2282(4)	76(12)	430(2)	83(2)

^a U(eq) is defined as one-third of the trace of the orthogonalized U_{ij} tensor.

Table 6. Bond Lengths (Å) and Angles (deg) for 6^a

Te-C(1A)	2.133(4)	Te-C(1B)	2.142(4)
N(1A)-C(8A)	1.444(6)	N(1A)-C(9A)	1.466(6)
N(1A)-C(7A)	1.467(6)	N(1B)-C(8B)	1.451(5)
N(1B)-C(7B)	1.453(5)	N(1B)-C(9B)	1.458(5)
C(1A)-C(2A)	1.377(6)	C(1A)-C(6A)	1.389(6)
C(1B)-C(2B)	1.381(6)	C(1B)-C(6B)	1.384(6)
C(2A)-C(3A)	1.390(6)	C(2B)-C(3B)	1.395(6)
C(3A)-C(4A)	1.372(7)	C(3B)-C(4B)	1.379(7)
C(4A)-C(5A)	1.373(7)	C(4B)-C(5B)	1.357(7)
C(5A)-C(6A)	1.395(6)	C(5B)-C(6B)	1.401(6)
C(6A)-C(7A)	1.489(6)	C(6B)-C(7B)	1.501(6)

C(1A)-Te-C(1B)	92.9(2)	C(8A)-N(1A)-C(9A)	111.4(4)
C(8A)-N(1A)-C(7A)	112.5(4)	C(9A)-N(1A)-C(7A)	111.7(4)
C(8B)-N(1B)-C(7B)	110.2(4)	C(8B)-N(1B)-C(9B)	111.4(4)
C(7B)-N(1B)-C(9B)	111.9(4)	C(2A)-C(1A)-C(6A)	119.3(4)
C(2A)-C(1A)-Te	119.2(3)	C(6A)-C(1A)-Te	121.5(3)
C(2B)-C(1B)-C(6B)	119.6(4)	C(2B)-C(1B)-Te	119.6(3)
C(6B)-C(1B)-Te	120.8(3)	C(1A)-C(2A)-C(3A)	121.7(5)
C(1B)-C(2B)-C(3B)	120.9(5)	C(4A)-C(3A)-C(2A)	118.7(5)
C(4B)-C(3B)-C(2B)	119.3(5)	C(3A)-C(4A)-C(5A)	120.5(5)
C(5B)-C(4B)-C(3B)	119.9(5)	C(4A)-C(5A)-C(6A)	121.0(5)
C(4B)-C(5B)-C(6B)	121.6(5)	C(1A)-C(6A)-C(5A)	118.9(5)
C(1A)-C(6A)-C(7A)	120.4(4)	C(5A)-C(6A)-C(7A)	120.7(4)
C(1B)-C(6B)-C(5B)	118.7(5)	C(1B)-C(6B)-C(7B)	121.3(4)
C(5B)-C(6B)-C(7B)	120.0(5)	N(1A)-C(7A)-C(6A)	112.0(4)
N(1B)-C(7B)-C(6B)	112.4(4)		

^a Symmetry transformations were used to generate equivalent atoms.

X-ray Structure of 6. An ORTEP view of **6** is shown in Figure 2. The atomic coordinates with equivalent isotropic displacement parameters are provided in Table 5, and the selected bond distances and angles are given in Table 6. The structure shows **6** as a discrete monomer with four molecules per unit cell. The bond configuration about Te atom is V-shaped, and the C(1A)-Te-C(1B) angle is 92.9(2)°. Owing to the presence of two monodentate N-donor atoms and to the possibility of intramolecular coordination with the Te atom, it is possible that either one or both Te··N coordination bonds may be formed. In the former case the structure would correspond to 10-Te-3 tellurane and in the latter case to 12-Te-4 tellurane. A look at the structure shows that the Te··N interaction cannot be completely ruled out as the N(1A) as the N(1B) atoms

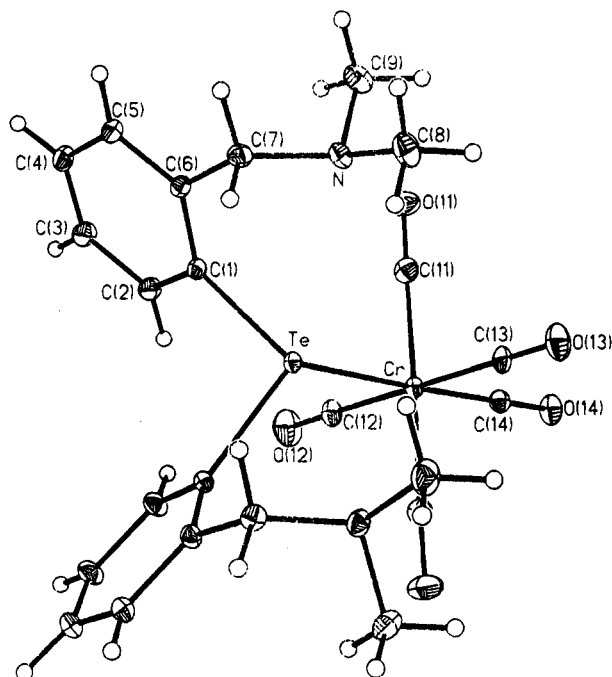


Figure 3. Molecular structure of $\text{Cr}(\text{CO})_5(2\text{-NMe}_2\text{CH}_2\text{C}_6\text{H}_4)_2\text{Te}$ (13).

form the characteristic envelope over the Te atom which would result in the formation of the five-membered ring (*cis*-conformation). The structure is not symmetrical as the two chemically equivalent $2\text{-Me}_2\text{NCH}_2\text{C}_6\text{H}_4$ fragments are differently positioned about the Te [Te–C(1A), (2.133)(4) Å; Te–C(1B), (2.142)(4) Å; C(6A)–C(7A), (1.489)(6) Å; C(6B)–C(7B), (1.501)(6) Å]. These Te–C(1) distances are intermediate between the sum of Pauling's single-bond covalent radii³⁸ for Te (1.37 Å) and sp^2 -hybridized carbon (0.74 Å) and the Te–C (aromatic) of (2.166 Å) as given by Allen *et al.*⁴⁰ The Te··N(1A) distance of 3.048 Å is significantly different from the Te··N(1B) distance of 3.145 Å. This indicates a more pronounced interaction of one N with Te. In addition, the average Te··N distances of 3.0965 Å are longer compared to the average Te··N distances in related Te,N telluride structures *viz.* bis[2-(isopropyl-imino)methyl]phenyl telluride [Te··N = 2.720(3) Å]^{7b} and 1,6-bis(2-butyltelluro)phenyl-2,5-diazahexa-1,5-diene [Te··N = 2.773 Å].^{7a} These longer distances (which may be attributed to the sp^3 hybridization state of N) are nevertheless well within the van der Waals radii of Te and N (3.61 Å) and probably represent a weak but significant interaction. Due to absence of data on related telluride ligands with sp^3 -hybridized N, a direct comparison was not possible. The closest comparison is to the halide derivative *viz.* 2-(bromotelluro)-*N*-(*p*-tolyl)benzylamine [Te··N = 2.375 Å]¹⁵ and [2-(dimethylamino)methyl]phenyltellurium(II) iodide [Te··N = 2.366 Å] (*vide supra*) in which the distances are shorter.

X-ray Structure of 13. An ORTEP view of 13 is shown in Figure 3. Table 7 gives the atomic coordinates with equivalent isotropic displacement parameters, and Table 8 gives the selected bond lengths and bond angles. Few structurally characterized compounds containing Cr–Te bonds are reported in literature.^{41–45} Structure 13 contains four molecules per unit cell. In this

Table 7. Atomic Coordinates ($\times 10^4$) and Equivalent Isotropic Displacement Parameters ($\text{Å}^2 \times 10^3$) for 13

atom	x	y	z	$U(\text{eq})^a$
Te	0	1139(1)	0	14(1)
Cr	0	2316(1)	–1721(1)	15(1)
O(11)	1601(2)	2529(5)	–1783(3)	40(1)
O(12)	0	5485(6)	–1067(5)	46(1)
O(13)	0	–876(6)	–2364(4)	36(1)
O(14)	0	3336(4)	–3740(3)	27(1)
N	1397(2)	–609(3)	–145(2)	22(1)
C(1)	845(2)	2123(4)	767(3)	16(1)
C(2)	882(2)	3612(4)	961(3)	22(1)
C(3)	1391(2)	4156(4)	1582(3)	26(1)
C(4)	1873(2)	3216(4)	1990(3)	25(1)
C(5)	1865(2)	1735(4)	1749(3)	22(1)
C(6)	1357(2)	1177(3)	1139(3)	18(1)
C(7)	1359(2)	–426(4)	883(3)	20(1)
C(8)	1208(2)	–2100(5)	–419(4)	33(1)
C(9)	2107(2)	–243(5)	–487(3)	31(1)
C(11)	1001(2)	2398(4)	–1734(3)	24(1)
C(12)	0	4282(7)	–1290(4)	25(1)
C(13)	0	314(6)	–2123(3)	22(1)
C(14)	0	2948(5)	–2960(4)	20(1)

^a $U(\text{eq})$ is defined as one-third of the trace of the orthogonalized U_{ij} tensor.

Table 8. Bond Lengths (Å) and Angles (deg) for 13^a

Te–C(1)'	2.133(3)	Te–C(1)	2.133(3)
Te–Cr	2.6665(9)	Cr–C(14)	1.849(6)
Cr–C(11)	1.896(4)	Cr–C(11)'	1.896(4)
Cr–C(12)	1.897(6)	Cr–C(13)	1.915(5)
O(11)–C(11)	1.144(5)	O(12)–C(12)	1.143(7)
O(13)–C(13)	1.140(7)	O(14)–C(14)	1.162(7)
N–C(8)	1.461(5)	N–C(9)	1.468(5)
N–C(7)	1.469(5)	C(1)–C(2)	1.390(5)
C(1)–C(6)	1.401(5)	C(2)–C(3)	1.397(5)
C(3)–C(4)	1.379(6)	C(4)–C(5)	1.395(5)
C(5)–C(6)	1.389(5)	C(6)–C(7)	1.509(5)
C(1)'–Te–C(1)	97.2(2)	C(1)'–Te–Cr	107.25(10)
C(1)–Te–Cr	107.25(10)	C(14)–Cr–C(11)	88.76(12)
C(14)–Cr–C(11)'	88.76(12)	C(11)–Cr–C(11)'	175.3(2)
C(14)–Cr–C(12)	90.6(2)	C(11)–Cr–C(12)	88.04(12)
C(11)'–Cr–C(12)	88.04(12)	C(14)–Cr–C(13)	90.9(2)
C(11)–Cr–C(13)	91.99(12)	C(11)'–Cr–C(13)	91.99(12)
C(12)–Cr–C(13)	178.5(2)	C(14)–Cr–Te	174.4(2)
C(11)–Cr–Te	91.42(12)	C(11)'–Cr–Te	91.42(12)
C(12)–Cr–Te	95.0(2)	C(13)–Cr–Te	83.5(2)
C(8)–N–C(9)	110.4(3)	C(8)–N–C(7)	111.0(3)
C(9)–N–C(7)	110.3(3)	C(2)–C(1)–C(6)	119.6(3)
C(2)–C(1)–Te	123.4(2)	C(6)–C(1)–Te	116.8(2)
C(1)–C(2)–C(3)	120.5(4)	C(4)–C(3)–C(2)	119.9(4)
C(3)–C(4)–C(5)	119.6(3)	C(6)–C(5)–C(4)	121.0(3)
C(5)–C(6)–C(1)	119.1(3)	C(5)–C(6)–C(7)	120.3(3)
C(1)–C(6)–C(7)	120.6(3)	N–C(7)–C(6)	110.5(3)
O(11)–C(11)–Cr	175.3(4)	O(12)–C(12)–Cr	177.2(6)
O(13)–C(13)–Cr	179.9(5)	O(14)–C(14)–Cr	179.6(4)

^a Symmetry transformations were used to generate equivalent atoms: prime, $-x, y, z$.

compound an equalization of bond lengths C(1)–Te, C(6)–C(7), and C(7)–N occurs (2.133(3), 1.509(5), and 1.469(5) Å, respectively), giving rise to a symmetric disposition of the $2\text{-NMe}_2\text{CH}_2\text{C}_6\text{H}_4$ fragments about Te. These values are comparable to the corresponding average values for C(1)–Te [2.138(4) Å], C(6)–C(7)

(41) Flomer, W. A.; O'Neal, S. C.; Kolis, J. W.; Jeter, D.; Cordes, A. W. *Inorg. Chem.* **1988**, *27*, 969.

(42) Hermann, W. A.; Rohrmann, J.; Ziegler, M.; Zahr, T. *J. Organomet. Chem.* **1984**, *273*, 221.

(43) Lappert, M. F.; Martin, T. R.; McLaughlin, G. M. *J. Chem. Soc., Chem. Commun.* **1980**, 635.

(44) Shen, J.; Gao, Y.; Shi, Q.; Rheingold, A. L.; Basolo, F. *Inorg. Chem.* **1991**, *30*, 1868.

(45) Goh, L. Y.; Tay, M. S.; Wei, C. *Organometallics* **1994**, *13*, 1813.

(40) Allen, F. H.; Watson, D. G.; Brammer, L.; Orpen, A. G.; Taylor, R. *J. Chem. Soc., Perkin Trans. 2* **1987**, S1.

[1.495(6) Å], and C(7)–N [1.460(6)] observed in the free ligand (*vide supra*). The C(1)–Te–C(1) angle increases to 97.2° compared to 92.9° in **6**. The Te··N distance of 3.096 Å is intermediate between the Te–N(1A) [3.048 Å] and Te–N(1B) [3.145 Å] distances observed in **6**. This also indicates a more pronounced interaction of one N with Te in **6**. The Te atom is pyramidal, and the sum of angles at Te is 311.3°. The coordination geometry at Cr is only slightly distorted from a regular octahedral, the largest distortion [C(14)–Cr–Te, 174.4°] likely results from a steric interaction with the overlying phenyl rings. The compound is monomeric; however, it is linked to neighboring molecules by weak H··O–C intermolecular contacts between the H α proton (α to Te on the benzene ring) and –CO of the next molecule. Such interactions have not been reported for the other related compounds.^{41–45} This is perhaps the most interesting feature of the molecule. Also, the Cr–Te distance of 2.6665(9) Å in **13** is significantly shorter than the sum of single-bond radii of Cr (1.48 Å)⁴⁶ and Te (1.37 Å).³⁸ The highest reported value for Cr–Te is 2.814(1) Å in [CpCr(CO)₃]₂Te,⁴¹ and the lowest value is 2.6844(1) Å in Cr(CO)₅Te(*p*-CH₃OC₆H₄)₂.⁴⁴ Hence, this is the shortest Cr–Te distance value reported so far.

Summary and Conclusions

Several bi-, tri-, and multidentate Te(II) ligands derived from *N,N*-dimethylbenzylamine have been prepared and isolated by the “organolithium” route, starting either from RLi or RTeLi (R = 2-NMe₂CH₂C₆H₄). Unexpected products RTeI (**5**) and R₂Te (**6**) have been obtained in the preparation of the bidentate ligand

RTeMe (**4**). A mechanism for the formation has been proposed. The molecular structure of a representative intramolecularly stabilized Te(II) ligand **6** containing an sp³-hybridized nitrogen has been determined for the first time. In contrast to ¹H NMR observations showing the two 2-NMe₂CH₂C₆H₄ fragments to be equivalent at room temperature, an unsymmetrical disposition of the two 2-NMe₂CH₂C₆H₄ fragments about Te is observed by X-ray crystallography. The Te–N(1A) [3.048 Å] and Te–N(1B) [3.145 Å] distances are nonequivalent. Complexation reactions of **6** with chromium carbonyl precursor ligands gave **13**, in which a monodentate mode of coordination *via* Te was observed. The results described in the paper demonstrate a carbonyl redistribution to give the more stable monocoordinated complex. In contrast to the free ligand **6**, an equivalence of the 2-NMe₂CH₂C₆H₄ fragments is observed in the complex **13** [Te–N = 3.096 Å]. In the iodide derivative **5** is observed a strong intramolecular Te··N [Te–N = 2.366(4) Å].

Acknowledgment. We are very grateful to the RSIC, IIT, Bombay, India, for the 300 MHz NMR facility, Dr. C. V. V. Satyanarayan for recording multinuclear NMR, and the RSIC, Lucknow, India, for recording mass spectra. H.B.S. is grateful to the BRNS, Department of Energy, Bombay, India, and the CSIR, New Delhi, India, for funding this work. R.K. thanks the CSIR, New Delhi, India, for a Senior Research Fellowship.

Supporting Information Available: Tables of anisotropic thermal parameters and hydrogen coordinates and representative figures (8 pages). Ordering information is given on any current masthead page.

OM950301V

(46) Cotton, F. A.; Richardson, D. C. *Inorg. Chem.* **1966**, *5*, 1851.

Oxidation of Substrates by an Iridium Dioxygen Complex: Intramolecular Oxidation of Carbon Monoxide and Activation of a Carbonyl Group by Attack of a Heterocyclic Nitrogen

Miguel A. Ciriano,* José A. López, Luis A. Oro,* and Jesús J. Pérez-Torrente

Departamento de Química Inorgánica, Instituto de Ciencia de Materiales de Aragón, Universidad de Zaragoza-CSIC, E-50009 Zaragoza, Spain

Maurizio Lanfranchi, Antonio Tiripicchio, and Marisa Tiripicchio Camellini

Dipartimento di Chimica Generale ed Inorganica, Chimica Analitica, Chimica Fisica, Centro di Studio per la Strutturistica Diffraattometrica del CNR, Università di Parma, Viale delle Scienze 78, I-43100 Parma, Italy

Received April 24, 1995[®]

The square-planar complex $[\text{Ir}(\text{C}_7\text{H}_4\text{NS}_2)(\text{CO})(\text{PPh}_3)_2]$ (**1**) is obtained in high yield from the reaction of lithium benzothiazole-2-thiolate ($\text{LiC}_7\text{H}_4\text{NS}_2$) with Vaska's complex, $[\text{IrCl}(\text{CO})(\text{PPh}_3)_2]$. Coordination of the new ligand in **1** and in the homologous rhodium complex should occur through the sulfur atom, as shown by their protonation reactions with HBF_4 , which give the hydrido-iridium(III) complex $[\text{IrH}(\text{C}_7\text{H}_4\text{NS}_2)(\text{CO})(\text{PPh}_3)_2]\text{BF}_4$ and the rhodium(I) compound $[\text{Rh}(\text{CO})(\text{PPh}_3)_2(\text{C}_7\text{H}_5\text{NS}_2)]\text{BF}_4$, respectively. The neutral ligand $\text{C}_7\text{H}_5\text{NS}_2$ reacts with **1** to give $[\text{IrH}(\text{C}_7\text{H}_4\text{NS}_2)_2(\text{CO})(\text{PPh}_3)_2]$ (**4**). Complex **1** adds dihydrogen, methyl iodide, and dioxygen. The dioxygen complex $[\text{Ir}(\text{C}_7\text{H}_4\text{NS}_2)(\text{O}_2)(\text{CO})(\text{PPh}_3)_2]$ (**7**) undergoes an intramolecular oxidation of the carbonyl ligand, catalyzed by water, to yield the carbonate complex $[\text{Ir}(\text{C}_7\text{H}_4\text{NS}_2)(\text{CO}_3)(\text{PPh}_3)_2]$ (**8**). Labeling studies show that the reaction is multistep and oxygen from water is incorporated into the carbonate ligand. Sulfur dioxide is oxidized by complex **7**, but in addition, activation of the carbonyl group occurs by attack of the heterocyclic nitrogen of the benzothiazole-2-thiolate ligand to give $[\text{Ir}\{\text{C}(\text{O})\text{NC}(\text{S})\text{SC}_6\text{H}_4\}(\text{SO}_4)(\text{PPh}_3)_2]$ (**11**). In **8** both benzothiazole-2-thiolate and carbonate anions act as N,S- and O,O-chelating ligands. The structure of **11** shows a C,S-chelating ligand, obtained by an unprecedented incorporation of the carbonyl group of **7** into the benzothiazole-2-thiolate through the heterocyclic nitrogen, in addition to a chelating sulfato ligand.

Introduction

The activation of dioxygen by coordination to a transition metal¹ has attracted considerable attention in recent years owing to its importance in biological systems² and in the oxidation of organic³ and inorganic molecules.⁴ Fundamental in these studies is the controlled transfer of oxygen to a molecule of substrate. The most common (radical chain) pathway for oxygen transfer involves transition-metal-promoted autoxidation. More controlled oxidations may be achieved if the metal

center serves for the coordination of both substrate and dioxygen where bond breaking and re-forming steps occur at the metal center. A recent model of this template synthesis is the oxidation of alcohols to carboxylic acids by an iridium dioxygen complex.⁵ In addition, a rare example of a clean O-O bond rupture concurrent with carbon-oxygen bond formation has been reported by Bercaw,⁶ but an understanding of the intimate mechanism of the oxygen atom transfer is still required.

[®] Abstract published in *Advance ACS Abstracts*, August 15, 1995.

(1) (a) Klotz, M.; Kurtz, D. M., Jr. *Chem. Rev.* **1994**, *94*, 567. (b) *Oxygen Complexes and Oxygen Activation by Transition Metals*; Martell, A. E., Sawyer, D. T., Eds.; Plenum Press: New York, 1988. (c) Mimoun, H. In *Comprehensive Coordination Chemistry*; Wilkinson, G., Gillard, R. D., McCleverty, J. A., Eds.; Pergamon Press: Oxford, U.K., 1987; Vol. 6, p 317. (d) Gubelmann, M. H.; Williams, A. F. *Struct. Bonding (Berlin)* **1983**, *55*, 1.

(2) Sheu, C.; Sawyer, D. T. *J. Am. Chem. Soc.* **1990**, *112*, 8212. Tyeklar, Z.; Karhin, K. D. *Acc. Chem. Res.* **1989**, *22*, 241. Niederhoffer, E. C.; Timmons, J. H.; Martell, A. E. *Chem. Rev.* **1984**, *84*, 137. Ingraham, L. L.; Meyer, D. L. In *Biochemistry of Dioxygen*; Biochemistry of the Elements 4; Fieden, E., Ed.; Plenum Press: New York, 1985. Momeuteau, M.; Reed, C. A. *Chem. Rev.* **1994**, *94*, 659. Springer, B. A.; Sligar, S. G.; Olson, J. S.; Phillips, G. N., Jr. *Chem. Rev.* **1994**, *94*, 699. Stenkamp, R. E. *Chem. Rev.* **1994**, *94*, 715. Magnus, K. A.; Ton-That, H.; Carpenter, J. E. *Chem. Rev.* **1994**, *94*, 727. Kitajima, N.; Moro-Oka, Y. *Chem. Rev.* **1994**, *94*, 737. Feig, A. L.; Lippard, S. J. *Chem. Rev.* **1994**, *94*, 759. Pecoraro, V. L.; Baldwin, M. J.; Gelasco, A. *Chem. Rev.* **1994**, *94*, 807.

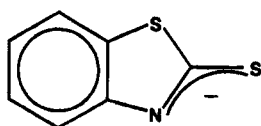
(3) Sheldon, R. A.; Kochi, J. K. *Metal-Catalyzed Oxidations of Organic Compounds*; Academic Press: New York, 1981. Jorgensen, K. A. *Chem. Rev.* **1989**, *89*, 431. Day, V. W.; Kemplerer, W. G.; Lockledge, S. P.; Main, D. J. *J. Am. Chem. Soc.* **1990**, *112*, 2031. Chambers, R. C.; Hill, C. L. *Inorg. Chem.* **1989**, *28*, 2509. Lee, J. S.; Oyama, S. T. *Catal. Rev.—Sci. Eng.* **1988**, *30*, 249. Sheu, C.; Sawyer, D. T. *J. Am. Chem. Soc.* **1990**, *112*, 8212. Weber, L.; Haufe, G.; Rehorek, D.; Henning, H. *J. Chem. Soc., Chem. Commun.* **1991**, 502. Kitajima, N.; Ito, M.; Fukui, H.; Moro-Oka, Y. *J. Chem. Soc., Chem. Commun.* **1991**, 102. Bilgrien, C.; Davis, S.; Drago, R. S. *J. Am. Chem. Soc.* **1987**, *109*, 3786. Ali, B. E.; Brégeault, J.-M.; Mercier, J.; Martin, J.; Martin, C.; Convert, O. *J. Chem. Soc., Chem. Commun.* **1989**, 825. Drago, R. S. *Coord. Chem. Rev.* **1992**, *117*, 185.

(4) (a) Lawson, H. J.; Atwood, J. D. *J. Am. Chem. Soc.* **1988**, *110*, 3680. (b) Lawson, H. J.; Atwood, J. D. *J. Am. Chem. Soc.* **1989**, *111*, 6223. (c) Fettingner, J. C.; Churchill, M. R.; Bernard, K. A.; Atwood, J. D. *J. Organomet. Chem.* **1988**, *349*, 377. (d) Wakatsuki, Y.; Maniwa, M.; Yamazaki, H. *Inorg. Chem.* **1990**, *29*, 4204.

(5) Bianchini, C.; Meli, A.; Peruzzini, M.; Vizza, F. *J. Am. Chem. Soc.* **1990**, *112*, 6726.

(6) Van Asselt, A.; Trimmer, M. S.; Henling, L. M.; Bercaw, J. E. *J. Am. Chem. Soc.* **1988**, *110*, 8254.

Chart 1



benzothiazole-2-thiolate

Oxidation of carbon monoxide by a transition metal dioxygen complex has been observed for platinum, iridium, and rhodium compounds,^{4a,b,7} and oxidation of a carbonyl ligand by O₂ in a dinuclear complex has been recently reported.⁸ The kinetics studies^{4b} of the oxidation of carbon monoxide by the dioxygen adduct of [IrR(CO)(PR'₃)₂] (R = alkyl, alkoxy) reveal a reversible cleavage of one of the two Ir-O bonds followed by attack at this oxygen atom by free CO. Furthermore, the presence of the R group gives rise to a chemistry different from that of their halide analogs.^{4c,9} In view of this feature, we have prepared the Vaska type complex [Ir(C₇H₄NS₂)(CO)(PPh₃)₂], which contains an anionic (S or N donor atom) and potentially binucleating or chelating ligand, expecting new chemical properties relative to the above-mentioned systems. In this paper we describe some reactions of this complex and, in particular, those of its dioxygen derivative that lead to the intramolecular oxidation of the carbonyl ligand to carbonate and to the activation of the carbonyl ligand by attack of the heterocyclic nitrogen of the ligand in the oxidation of sulfur dioxide. Part of these results have been previously communicated.¹⁰

Results and Discussion

Synthesis, Structure, and Protonation Reactions of [Ir(C₇H₄NS₂)(CO)(PPh₃)₂] (1). The complex [IrCl(CO)(PPh₃)₂] reacts with the lithium salt of benzothiazole-2-thiolate (LiC₇H₄NS₂) in refluxing tetrahydrofuran to give the yellow complex [Ir(C₇H₄NS₂)(CO)(PPh₃)₂] (1) in high yield. The reaction stops at the mononuclear complex 1 even if the refluxing is maintained for long periods, as occurs in the reactions of Vaska's complex with alkaline salts of thiolates¹¹ and disubstituted pyrazolates.¹² Thus, elimination of triphenylphosphine in this reaction to give the dinuclear complex [{Ir(μ-C₇H₄NS₂)(CO)(PPh₃)₂}] does not take place, in contrast with the syntheses of the pyrazolate (pz)¹³ and phosphide¹⁴ complexes of iridium [{Ir(μ-X)(CO)(PPh₃)₂}] (X = pz, PPh₂) by the same method.

Compound 1 is square-planar, like its homologous rhodium complex¹⁵ [Rh(C₇H₄NS₂)(CO)(PPh₃)₂]. The phosphine ligands are in a trans disposition, in accord

with their equivalency in their ³¹P{¹H} NMR spectrum, and the coordination mode of the benzothiazole-2-thiolate ligand is monodentate. Although this ligand can act as a bidentate group chelating through the sulfur and nitrogen atoms, the positions of ν(CO) at 1966 cm⁻¹ in 1 and 1982 cm⁻¹ for the homologous rhodium complex are the usual ones for tetracoordinated complexes of iridium and rhodium of this type;¹⁵ they should be at lower frequency for pentacoordinated structures.^{7b} Coordination of benzothiazole-2-thiolate in these complexes is through the S atom, as evidenced by their protonation reactions, which show in addition differences in the reactivities of these compounds (see Scheme 1).

Protonation of the rhodium complex with HBF₄ takes place on the nitrogen in the free arm of the ligand to give the rhodium(I) complex [Rh(CO)(PPh₃)₂(C₇H₅NS₂)]-BF₄ (2) quantitatively.¹⁶ In contrast, protonation of the iridium complex occurs on the metal, giving the iridium(III) hydrido complex [IrH(C₇H₄NS₂)(CO)(PPh₃)₂]-BF₄ (3) as a yellow solid in good yield. Oxidation of the iridium center upon reaction is detected by the increase in ν(CO) (at 2060 cm⁻¹ in 3). In addition, benzothiazole-2-thiolate should change its coordination mode to act as a bidentate and chelating ligand through the S and N atoms. Complex 3 is octahedral with equivalent *trans* phosphine ligands, and the hydrido ligand is *cis* to both phosphorus atoms, which gives rise to a triplet in the ¹H NMR spectrum (¹J_{HP} = 10.5 Hz). The chemical shift of the hydride resonance in bis(phosphine)iridium complexes¹⁷ is sensitive to the donor atom *trans* to it, in such a way that electronegative atoms shift this resonance to higher fields. The position found in complex 3 (δ -14.5 ppm) is similar to that found in complexes with hydride *trans* to a thiolate group (δ ~-15 ppm), suggesting that it is *trans* to the sulfur atom.

The final result of this reaction could lead one to think that the iridium center is more basic than the uncoordinated nitrogen of the ligand benzothiazole-2-thiolate (pK_a of C₇H₅NS₂ 6.9).¹⁸ If so, the direct protonation of the metal would leave the hydrido ligand *trans* to a vacant coordination site, which should then be occupied by the free nitrogen atom of the ligand. Then the hydride would be *trans* to the nitrogen atom, which is not the case. Hence, the result should be due to a different reaction course. Most probably the reaction starts with the protonation of the nitrogen atom, as occurs for its homologous rhodium complex, followed by the oxidative addition of the N-H bond to the metal center to give the complex where the hydrido ligand is *trans* to the sulfur atom, as found in 3. Oxidative-addition reactions of N-H bonds to iridium complexes have been reported recently.¹⁹ Further support for this rationalization is the reaction of 2-mercaptobenzothiazole (the neutral form of the ligand) with complex 1 to give the iridium(III) hydrido complex [IrH(C₇H₄NS₂)₂]-

(7) (a) Hayward, P. J.; Blake, D. M.; Wilkinson, G.; Nyman, C. J. *J. Am. Chem. Soc.* **1970**, *92*, 5873. (b) Siegl, W. O.; Lapporte, S. J.; Collman, J. P. *Inorg. Chem.* **1971**, *10*, 2158.

(8) Antonelli, D. M.; Cowie, M. *Organometallics* **1991**, *10*, 2173.

(9) Thompson, J. S.; Atwood, J. D. *Organometallics* **1991**, *10*, 3525. McFarland, J. M.; Churchill, M. R.; See, R. F.; Lake, C. H.; Atwood, J. D. *Organometallics* **1991**, *10*, 3530.

(10) Ciriano, M. A.; Lanfranchi, M.; Oro, L. A.; Pérez-Torrente, J. J.; Tiripicchio, A.; Tiripicchio-Camellini, M. *J. Organomet. Chem.* **1994**, *4689*, C31.

(11) Gaines, T.; Roundhill, D. M. *Inorg. Chem.* **1974**, *13*, 2521.

(12) Bandini, A. L.; Banditelli, G.; Bonati, F.; Minghetti, G.; Demartin, F.; Manassero, M. *J. Organomet. Chem.* **1984**, *269*, 91.

(13) Beveridge, K. A.; Buschnell, G. W.; Dixon, K. R.; Eadie, D. T.; Stobart, S. R.; Zaworotko, M. J. *J. Am. Chem. Soc.* **1982**, *104*, 920.

(14) Kreter, P.; Meek, D. W. *Inorg. Chem.* **1983**, *22*, 319.

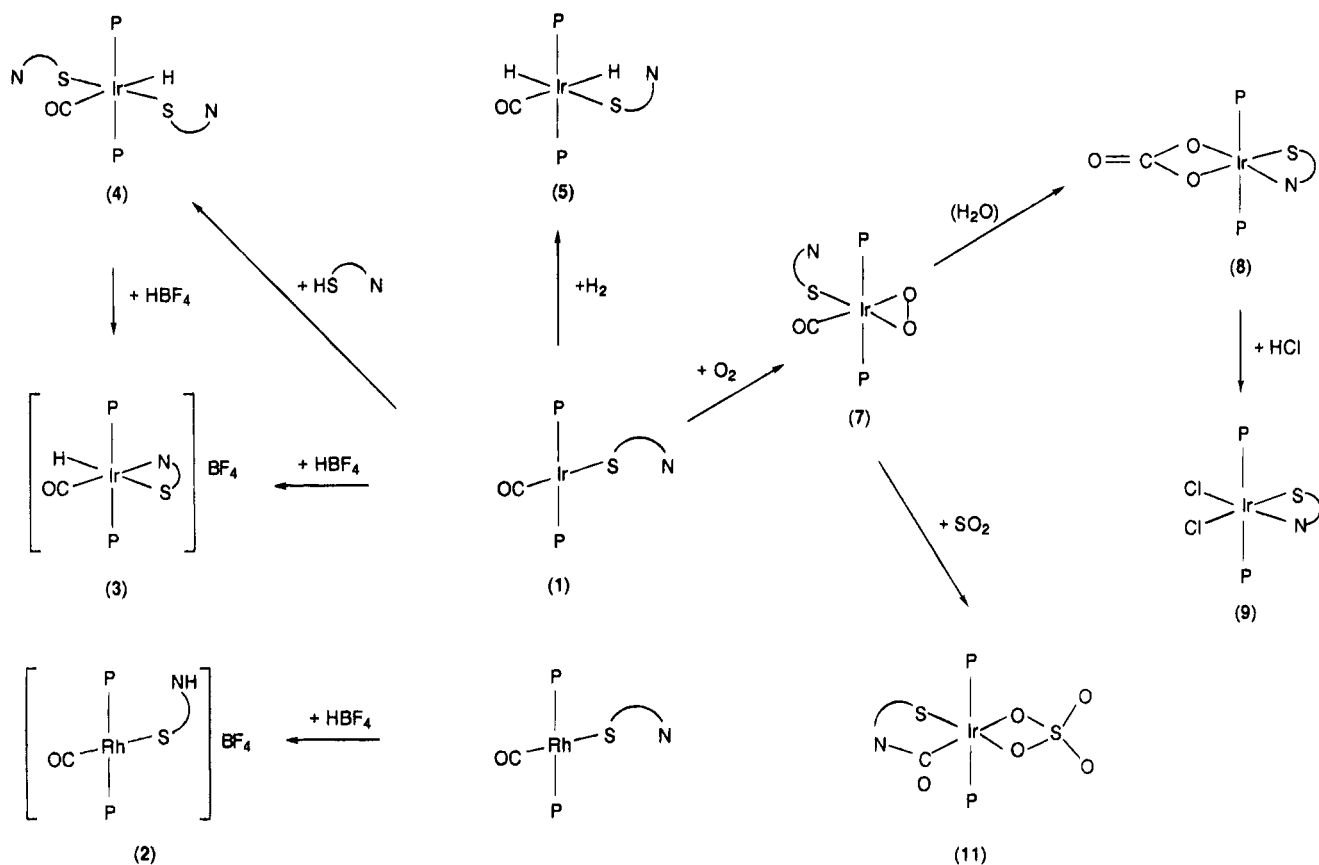
(15) Thompson, J. S.; Randall, S. L.; Atwood, J. D. *Organometallics* **1991**, *10*, 3906. Rappoli, B. J.; Janik, T. S.; Churchill, M. R.; Thompson, J. S.; Atwood, J. D. *Organometallics* **1988**, *7*, 1939. Bernard, K. A.; Churchill, M. R.; Janik, T. S.; Atwood, J. D. *Organometallics* **1990**, *9*, 12.

(16) Ciriano, M. A.; Pérez-Torrente, J. J.; Lahoz, F. J.; Oro, L. A. *J. Organomet. Chem.* **1993**, *455*, 225.

(17) Olgemoller, B.; Beck, W. *Inorg. Chem.* **1983**, *22*, 997.

(18) Narratel, O.; Liska, J. *Collect. Czech. Chem. Commun.* **1968**, *33*, 987 (taken from: Raper, E. S. *Coord. Chem. Rev.* **1985**, *61*, 115).

(19) Schaad, D. R.; Landis, C. R. *Organometallics* **1992**, *11*, 2024 and references therein.

Scheme 1^a

^a Abbreviations: P = PPh₃; N⁺S⁻ = benzothiazole-2-thiolate.

(CO)(PPh₃)₂] (4). In complex 4 the hydrido ligand is *trans* to the carbonyl group, as evidenced by its chemical shift in the ¹H NMR spectrum; both phosphine ligands are equivalent, mutually *trans*, and are *cis* to the hydrido group. As the protonation of the coordinated ligand by the free molecule is unlikely, a concerted oxidative addition of either the N–H or S–H bond of one of the tautomeric forms of the ligand to the metal should occur. In this way, the oxidative addition of 2-mercaptobenzothiazole to 1 gives a complex where the carbonyl and hydrido ligands are mutually *trans*. Complex 4 was reacted with tetrafluoroboric acid to investigate whether the benzothiazole-2-thiolate ligands are coordinated to the iridium through the N or the S atom, as described above. The protonation of one ligand indeed occurs, but whether it takes place at the N or at the S atom is unknown, since this ligand is released as free 2-mercaptobenzothiazole; the other benzothiazole-2-thiolate ligand remaining in the complex becomes chelating, and thus, complex 3 is produced quantitatively in this reaction.

Oxidative-Addition Reactions of [Ir(C₇H₄NS₂)(CO)(PPh₃)₂] (1). Complex 1 differs from Vaska's complex because it contains a potentially binucleating or chelating ligand having an uncoordinated donor atom. The electronic environment on the metal created by benzothiazole-2-thiolate can be compared with that of Vaska's complex through oxidative-addition reactions as shown below, and besides, the possible coordination of the free end of the ligand in these reactions may produce unpredictable consequences.

Methyl iodide reacts with complex 1, giving the already known complex [IrI₂(Me)(CO)(PPh₃)₂], which

does not contain the benzothiazole-2-thiolate ligand. The reaction should be multistep; the first oxidative addition should take place as for Vaska's complex to give [Ir(Me)I(C₇H₄NS₂)(CO)(PPh₃)₂], which is followed by a reductive elimination of 2-(methylthio)benzothiazole. A further oxidative addition of methyl iodide to the intermediate [IrI(CO)(PPh₃)₂] affords the final product. Hydrogen reacts with complex 1 to give the complex [IrH₂(C₇H₄NS₂)(CO)(PPh₃)₂] (5) as a white solid in good yield. Complex 5 is isolated as a single isomer having two equivalent phosphine ligands *trans* to each other and two hydrido ligands mutually *cis*. One of the hydride ligands is *trans* to the carbonyl group and the other *trans* to the sulfur, in accord with their chemical shifts in the ¹H NMR spectrum. The structure of complex 5, in which the nitrogen atom is uncoordinated, is shown in Scheme 1. Thus, the addition of hydrogen is a concerted process that occurs parallel to the S–Ir–CO axis of the complex. The related *cis*-dihydrido complex [IrH₂(C₇H₄NS₂)(PPh₃)₂] (6) is obtained by reaction of the solvated species [IrH₂(PPh₃)₂S₂]⁺ (S = acetone) with LiC₇H₄NS₂. A single isomer having the phosphine ligands in *trans* positions results from this reaction. Interestingly, the chemical shifts of the hydrido ligands in 6, *trans* to the N and S atoms, are largely shifted to higher field relative to those in the related complexes 3–5.

Oxygen reacts irreversibly with complex 2 in tetrahydrofuran or dichloromethane, giving an orange solution extremely sensitive to traces of water. In these solutions there is a single compound, as observed by ³¹P NMR spectroscopy, characterized as the dioxygen complex [Ir(C₇H₄NS₂)(O₂)(CO)(PPh₃)₂] (7). Attempts to

isolate this compound gave slightly impure off-white solids due to its high reactivity. In **7** both phosphine ligands are equivalent and are therefore in a *trans* disposition. Oxidation of the iridium center is detected by an increase in $\nu(\text{CO})$ at 2015 cm^{-1} and a new IR band at 885 cm^{-1} ($\nu(\text{O}-\text{O})$) characteristic of peroxo or η^2 -bonded dioxygen complexes of iridium. The structure of this dioxygen complex is then octahedral, with the dioxygen, carbonyl, and benzothiazole-2-thiolate ligands in the equatorial plane, the last ligand being monodentate and presumably bonded to the metal by the sulfur atom.

Oxidations with $[\text{Ir}(\text{C}_7\text{H}_4\text{NS}_2)(\text{O}_2)(\text{CO})(\text{PPh}_3)_2]$ (7**).** Addition of water discolors the solutions of complex **7**, from which yellow crystals analyzed as $[\text{Ir}(\text{C}_7\text{H}_4\text{NS}_2)(\text{CO}_3)(\text{PPh}_3)_2]$ (**8**) are obtained. Characterization of **8** as a carbonate complex in solution and in the solid state relies on spectroscopic evidence and on an X-ray diffraction study. This yellow compound does not have a carbonyl group but has a strong $\nu(\text{C}=\text{O})$ band at 1683 cm^{-1} in its IR spectrum. This and a resonance at δ 167 ppm in the $^{13}\text{C}\{^1\text{H}\}$ NMR spectrum of **8**, which has no attached protons in the ^{13}C APT spectrum, are characteristic of carbonate complexes. Although oxidation of carbon monoxide by dioxygen complexes is known,^{4a,b,7} confirmation of this type of reaction by the presence of the carbonate group and the structure of the complex **8** in the solid state required an X-ray diffraction study (see below). A chemical confirmation of the presence of the carbonate ligand comes from the reaction of complex **8** with strong acids, but the product depends on the anion. Acids such as HCl, having a coordinating anion, protonate the carbonate ligand in complex **8** to give carbon dioxide; the vacant coordination positions are occupied by the anion of the acid, giving $[\text{Ir}(\text{C}_7\text{H}_4\text{NS}_2)(\text{Cl})_2(\text{PPh}_3)_2]$ (**9**). On the other hand, acids which have poorly coordinating anions such as HBF₄ reacts with complex **8** in a similar fashion but the coordination positions left are occupied by water molecules to give $[\text{Ir}(\text{C}_7\text{H}_4\text{NS}_2)(\text{H}_2\text{O})_2(\text{PPh}_3)_2](\text{BF}_4)_2$ (**10**).

X-ray Crystal Structure of the Carbonato Complex **8.** A view of $[\text{Ir}(\text{C}_7\text{H}_4\text{NS}_2)(\text{CO}_3)(\text{PPh}_3)_2]$ (**8**) is shown in Figure 1 together with the atom-numbering scheme. Selected bond distances and angles are given in Table 1. The Ir atom displays an octahedral coordination with the two apical positions occupied by P atoms from PPh₃ ligands (Ir–P = 2.370(3) and 2.354(3) Å), two *cis*-equatorial sites occupied by O atoms from the chelating carbonate ligand (Ir–O(1) = 2.068(6) Å and Ir–O(2) = 2.071(6) Å), and the remaining two equatorial sites occupied by the N and S(1) atoms from the chelating benzothiazole-2-thiolate (Ir–S(1) = 2.425(3) Å and Ir–N = 2.061(7) Å). To the best of our knowledge, this is the first structurally characterized iridium complex in which the carbonate anion acts as a chelating ligand. In the dinuclear complex $[\text{Ir}_2(\text{CO})_2(\mu\text{-CO}_3)(\mu\text{-dppm})_2]$ the carbonate ligand bridges two Ir atoms through two oxygen atoms with Ir–O bond distances of 2.08(1) and 2.09(1) Å.²⁰ The four-membered O(1)C(8)O(2)Ir and NC(1)S(1)Ir chelating rings are planar and are characterized by very narrow bite angles (N–Ir–S(1) = 66.9(2)° and O(1)–Ir–O(2) = 64.1(3)°). The complex as a whole has an approximate C_s sym-

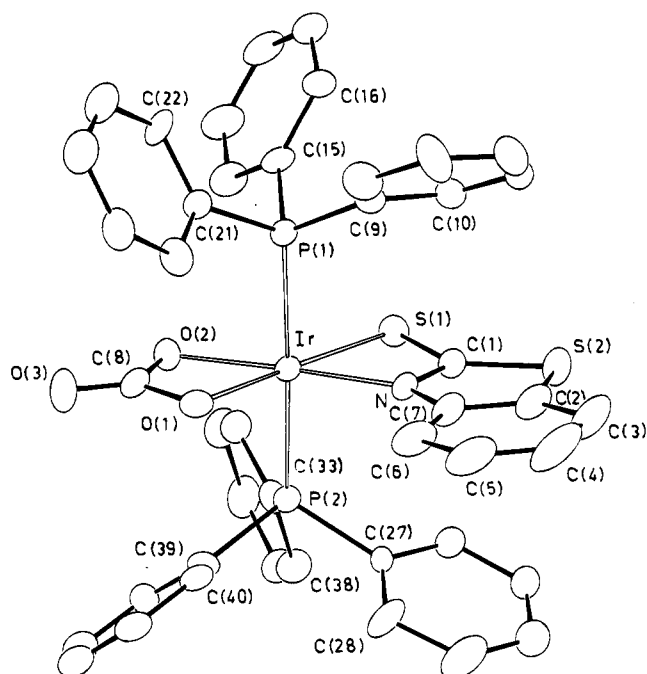


Figure 1. View of the molecular structure of the complex $[\text{Ir}(\text{C}_7\text{H}_4\text{NS}_2)(\text{CO}_3)(\text{PPh}_3)_2]$ (**8**) with the atom-numbering scheme. The thermal ellipsoids are drawn at the 30% probability level.

Table 1. Selected Bond Distances (Å) and Angles (deg) for Complex **8**

Ir–S(1)	2.425(3)	Ir–N	2.061(7)
Ir–P(1)	2.370(3)	Ir–P(2)	2.354(3)
Ir–O(1)	2.068(6)	Ir–O(2)	2.071(6)
P(1)–C(9)	1.80(1)	P(2)–C(27)	1.84(1)
P(1)–C(15)	1.83(1)	P(2)–C(33)	1.81(1)
P(1)–C(21)	1.82(1)	P(2)–C(39)	1.83(1)
S(1)–C(1)	1.70(1)	O(1)–C(8)	1.34(1)
S(2)–C(1)	1.74(1)	O(2)–C(8)	1.35(1)
S(2)–C(2)	1.76(1)	O(3)–C(8)	1.21(1)
N–C(1)	1.32(1)	C(3)–C(4)	1.40(2)
N–C(7)	1.39(1)	C(4)–C(5)	1.40(2)
C(2)–C(3)	1.39(2)	C(5)–C(6)	1.43(2)
C(2)–C(7)	1.39(2)	C(6)–C(7)	1.39(2)
O(1)–Ir–O(2)	64.1(3)	O(1)–Ir–N	113.2(3)
P(1)–Ir–N	92.1(2)	P(2)–Ir–N	91.6(2)
P(1)–Ir–O(2)	88.7(2)	P(2)–Ir–O(2)	87.7(2)
P(1)–Ir–O(1)	91.6(2)	P(2)–Ir–O(1)	91.0(2)
S(1)–Ir–N	66.9(2)	S(1)–Ir–O(2)	115.9(2)
S(1)–Ir–P(1)	90.0(1)	S(1)–Ir–P(2)	87.5(1)
Ir–S(1)–C(1)	79.3(3)	C(1)–S(2)–C(2)	89.3(5)
Ir–O(1)–C(8)	93.5(6)	Ir–O(2)–C(8)	93.2(6)
Ir–N–C(7)	142.9(6)	Ir–N–C(1)	103.2(6)
C(1)–N–C(7)	113.9(8)	C(4)–C(5)–C(6)	119.5(13)
S(2)–C(1)–N	113.7(7)	C(5)–C(6)–C(7)	116.4(11)
S(1)–C(1)–N	110.6(7)	N–C(7)–C(6)	126.1(10)
S(1)–C(1)–S(2)	135.4(6)	N–C(7)–C(2)	112.5(9)
S(2)–C(2)–C(7)	110.5(8)	O(2)–C(8)–O(3)	126.0(10)
S(2)–C(2)–C(3)	125.4(9)	O(1)–C(8)–O(3)	124.8(10)
C(2)–C(3)–C(4)	113.9(13)	O(1)–C(8)–O(2)	109.2(8)
C(3)–C(4)–C(5)	124.5(15)		

metry, with the carbonate and benzothiazole-2-thiolate ligands lying on the mirror plane. In the tetranuclear complex $\text{Ir}_4(\mu\text{-C}_7\text{H}_4\text{NS}_2)_4\text{I}_2(\text{CO})_8$ two benzothiazole-2-thiolates have been found bridging two Ir atoms through the same S and N atoms with slightly shorter Ir–S bond distances (2.382(7) and 2.408(6) Å) and slightly longer Ir–N bond distances (2.09(2) and 2.11(2) Å) than in **8**.²¹ Also, in the dinuclear complex $\text{Ir}_2(\mu\text{-C}_5\text{H}_4\text{NS})\text{I}(\text{CO})_4(\text{CH}_2\text{I})$, in which two pyridine-2-thiolates form chelating rings comparable to those formed by benzothiazole-2-

(20) Reinking, M. K.; Ni, J.; Fanwick, P. E.; Kubiak, C. P. *J. Am. Chem. Soc.* **1989**, *111*, 6459.

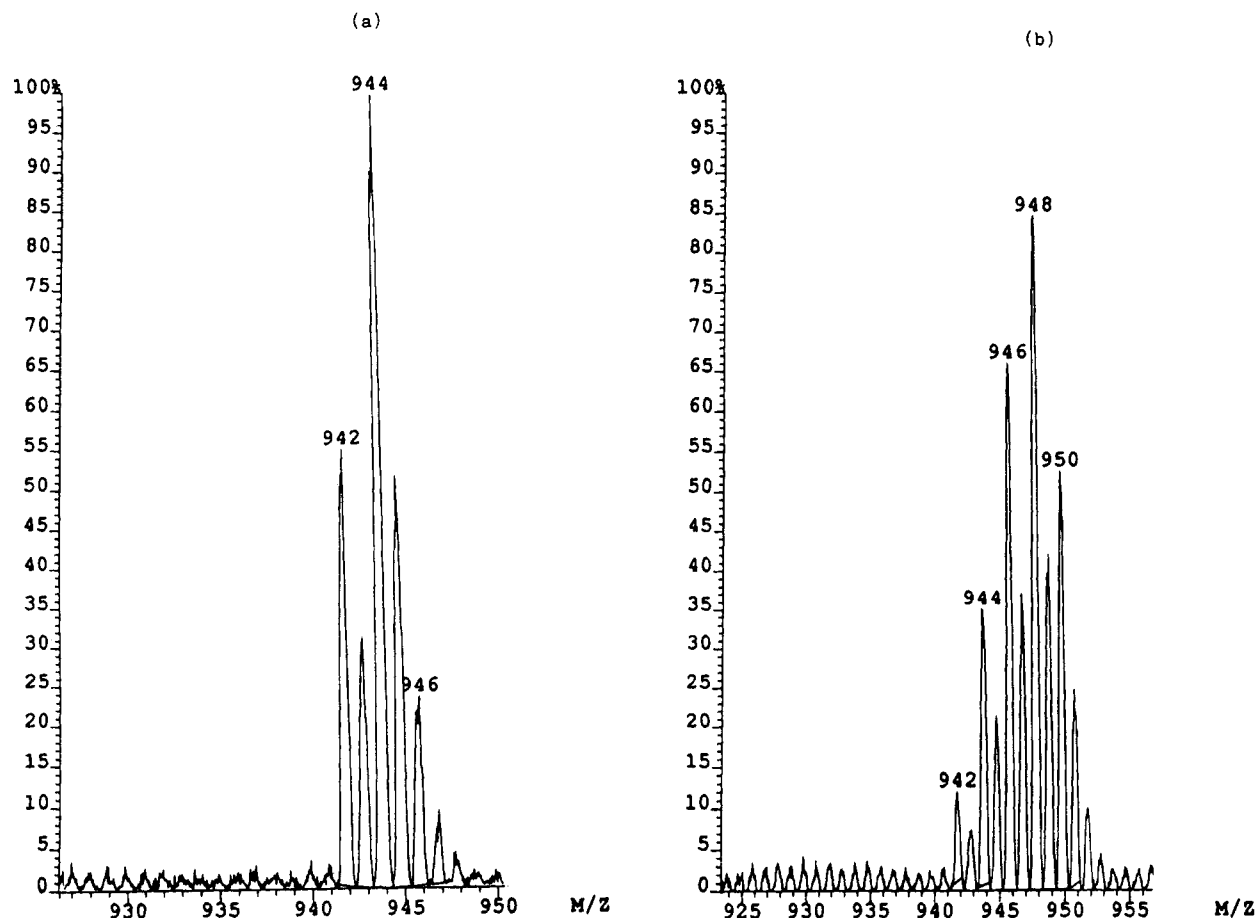


Figure 2. Fine structure of the molecular ion in the mass spectra of the carbonate complex **8** obtained (a) with labeled H_2^{18}O and (b) with unlabeled H_2O .

thiolate, the Ir–S and Ir–N bond distances show the same trend (Ir–S = 2.360(4) and 2.361(4) Å, Ir–N = 2.112(12) and 2.109(11) Å).²²

The action of water is essential to accomplish the oxidation of the carbonyl ligand in the dioxygen complex **7**. In fact, the elements for building up the carbonate ligand, i.e., the atoms of oxygen and carbon, are already coordinated as ligands in complex **7** but the reaction does not take place under anhydrous conditions. The need for water is one differential feature in the oxidation of the carbonyl ligand or carbon monoxide in comparison with other systems; the second is that in previous reports one of the reacting molecules, either CO or O_2 , is not coordinated to the metal. In view of this novelty, we decided to investigate the reaction further. Chemical evidence for the mechanism and the action of the water were obtained using both labeled water (H_2^{18}O) and protonation reactions of complex **7**.

Incorporation of oxygen from water into the carbonate ligand is revealed by the mass spectrum of the carbonate complex **8** obtained from the reaction of complex **7** with labeled water. The fine structure of the molecular ion is made by overlapping the fine structures of the isotopomers containing from zero up to three ^{18}O atoms. Figure 2 shows the fine structures of the molecular ions of the normal and labeled carbonate complexes for

comparative purposes. The analysis of this structure gives the following proportions of the isotopomers: C^{16}O_3 , 17%; $\text{C}^{18}\text{O}^{16}\text{O}_2$, 17%; $\text{C}^{18}\text{O}_2^{16}\text{O}$, 53%; C^{18}O_3 , 13%.

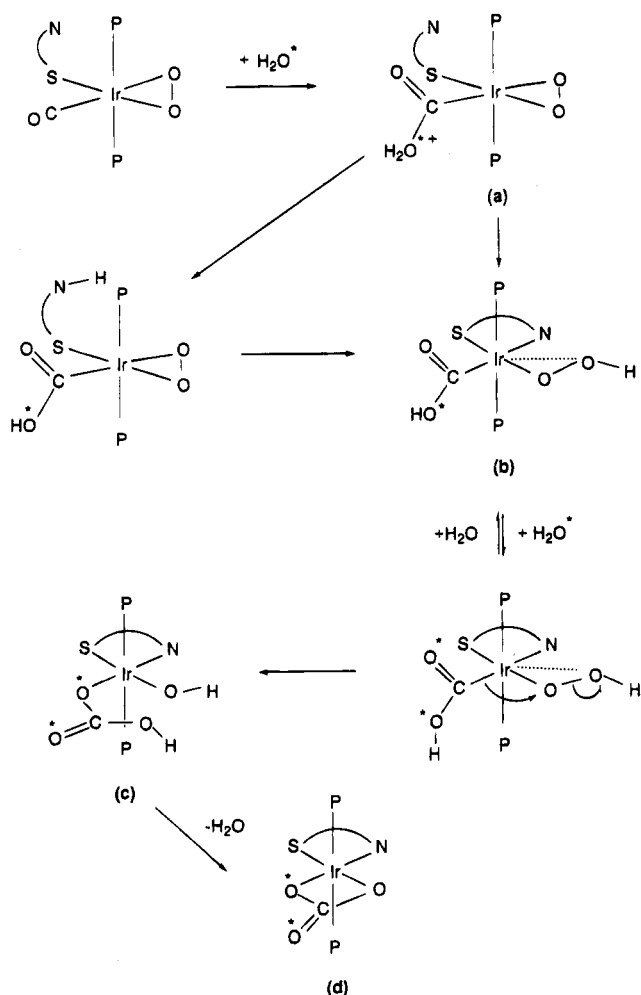
As the carbonate complex **8** does not interchange oxygen with labeled water after 3 days, it is evident that water reacts with complex **7** at the carbonyl ligand. Furthermore, the presence of the isotopomer containing three ^{18}O atoms in the carbonate shows that the mechanism is multistep and one of the intermediates interchanges oxygen with water. A possible mechanism to account for some of these results, outlined in Scheme 2, starts with a nucleophilic attack of water at the carbonyl ligand. The ability of the carbonyl group to carry out such a nucleophilic attack is increased upon oxidation, as revealed by the $\nu(\text{CO})$ frequency of complex **7** relative to that of the iridium(I) complex **1**, and it is a well-documented reaction for the late transition metals.²³ This would give an iridium(III) complex containing a protonated hydrocarbonyl ligand (a), which easily transfers the proton to a close basic center in the molecule, either to the nitrogen or to the dioxygen ligand. In the first instance a further transfer of the proton to the dioxygen ligand occurs which would open the metallacycle to give species b, as observed for the reactions of dioxygen complexes with electrophiles.²⁴ Then benzothiazole-2-thiolate should become a chelating ligand. The attack by an electrophile at the dioxygen ligand enhances the heterolysis of the O–O bond, as pointed out by Bercau.⁶ In this way, a hydroxy-

(21) Ciriano, M. A.; Sebastián, S.; Oro, L. A.; Tiripicchio, A.; Tiripicchio Camellini, M.; Lahoz, F. J. *Angew. Chem., Int. Ed. Engl.* **1988**, *27*, 402.

(22) Ciriano, M. A.; Viguri, F.; Oro, L. A.; Tiripicchio, A.; Tiripicchio Camellini, M.; Lahoz, F. J. *Angew. Chem., Int. Ed. Engl.* **1987**, *26*, 444.

(23) Ford, P. C.; Rokicki, A. *Adv. Organomet. Chem.* **1988**, *28*, 140

(24) Tatsuno, Y.; Otsuka, S. *J. Am. Chem. Soc.* **1981**, *103*, 5832.

Scheme 2. Proposed Mechanism for the Reaction of [Ir(C₇H₄NS₂)(O₂)(CO)(PPh₃)₂] (7) with Water^a


^a The asterisk denotes labeled ¹⁸O.

(hydrogencarbonate)iridium(III) complex results (c), and the reaction ends up with the formation of the carbonate group (d) and elimination of water. The water then acts as a catalyst for the reaction, but unlabeled water results from it. The mechanism relies on the following observations.

Protonation of the dioxygen complex is required for the formation of the carbonate ligand. Thus, addition of an ethereal solution of HBF₄ to the dioxygen complex 7 in the molar ratio 0.25:1 gives the carbonate complex, as observed by ³¹P{¹H} NMR. The other two phosphorus-containing species in solution are triphenylphosphine oxide and complex 10, the product from the reaction of the carbonate complex with HBF₄. The protonation occurs at the dioxygen ligand but not at the nitrogen, since two new singlets at δ 5.78 and 5.58 ppm observed in the ¹H NMR spectrum of the reaction mixture should be attributed to hydroxo species, the hydroperoxo ligand²⁵ among them, but resonances at low field due to acidic N-H are not detected. These two resonances disappear when the reaction is completed to give a broad band centered at 5.5 ppm. Besides, an IR band at 860 cm⁻¹ observed in the IR spectrum of this mixture evidences the presence of the peroxy group. The action of the acid

is catalytic for the formation of the carbonate complex, but part of it reacts with the product. In fact, complex 10 crystallizes out from this mixture if an excess of acid is used.

Other nucleophiles react similarly to water. Thus, ammonia gas reacts with the dioxygen complex 7, giving the carbonate complex 8. Presumably, an intermediate complex in this reaction contains an amidocarbonate ligand, which should undergo hydrolysis by the water formed in the reaction to give the carbonate complex. On the other hand, methanol reacts with complex 7, giving the dihydride complex 6 in low yield, but the carbonate complex 8 does not result from this reaction.

Aqueous hydrogen peroxide reacts with complex 1 to give triphenylphosphine oxide and some of the carbonate complex. Oxidation of the phosphine ligands is not observed in the reaction of the dioxygen complex 7 with water, which rules out that hydrogen peroxide participates in the reaction.

This simple mechanism explains the presence of the isotopomers C¹⁶O₃ and CO₂¹⁸O; the former is due to the formation of normal water in the reaction, but it does not justify the presence of the most abundant isotopomer, containing two ¹⁸O atoms. For that, an exchange of oxygen between labeled water and the hydroxycarbonyl ligand is the most reasonable proposal, as observed in carboxylic acids.²⁶ Furthermore, a fast exchange of both oxygen atoms of the hydroxycarbonyl ligand in [Ru(bpy)₂(CO){C(O)OH}]⁺ with labeled H₂¹⁸O has been reported recently,²⁷ in accord with our proposal. A further exchange of oxygen between an intermediate, for example the hydrogencarbonate ligand (c in Scheme 2), and labeled water should occur to give the isotopomer containing three ¹⁸O atoms in the carbonate ligand.

Sulfur dioxide reacts with the dioxygen complex 7 in tetrahydrofuran at atmospheric pressure to give the sulfate complex 11. The sulfato ligand is coordinated in complex 11 in a bidentate and chelating mode, as deduced from the positions of the fundamental modes of this ligand.²⁸ Oxidation of SO₂ is a common reaction of metal dioxygen complexes. More surprising is that complex 11 does not have a terminal carbonyl ligand but has a ν(CO) band at 1680 cm⁻¹. Furthermore, the molecular ion in the mass spectrum of 11 corresponds to the formula [Ir(C₇H₄NS₂)(SO₄)(CO)(PPh₃)₂], which shows that an unusual reaction has taken place on the carbonyl group. The X-ray diffraction study of 11 has revealed that the carbonyl group inserts formally into the metal-nitrogen bond. In this way, a new bidentate ligand is formed on incorporation of the carbonyl group into benzothiazole-2-thiolate between the heterocyclic nitrogen and the metal. Complex 11 should be then reformulated as [Ir{C(O)NC(S)SC₆H₄}(SO₄)(PPh₃)₂].

X-ray Crystal Structure of the Sulfato Complex 11. In the crystals of 11 two crystallographically independent, but very similar, [Ir{C(O)NC(S)SC₆H₄}-

(26) Patai, S., Ed. *The Chemistry of Carboxylic Acids and Esters*; Interscience: New York, 1969; Chapter 3, p 393, and Chapter 10, p 484.

(27) Tanaka, H.; Tzeng, B. C.; Nagao, H.; Peng, S. M.; Tanaka, K. *Inorg. Chem.* **1993**, *32*, 1508.

(28) Nakamoto, K. *Infrared and Raman Spectra of Inorganic and Coordination Compounds*, 3rd ed.; Wiley-Interscience: New York, 1978.

(25) Morvillo, A.; Bressan, M. *J. Organomet. Chem.* **1987**, *332*, 337. Sukuzi, H.; Matsura, S.; Moro-Oka, Y.; Ikawa, T. *J. Organomet. Chem.* **1985**, *286*, 247.

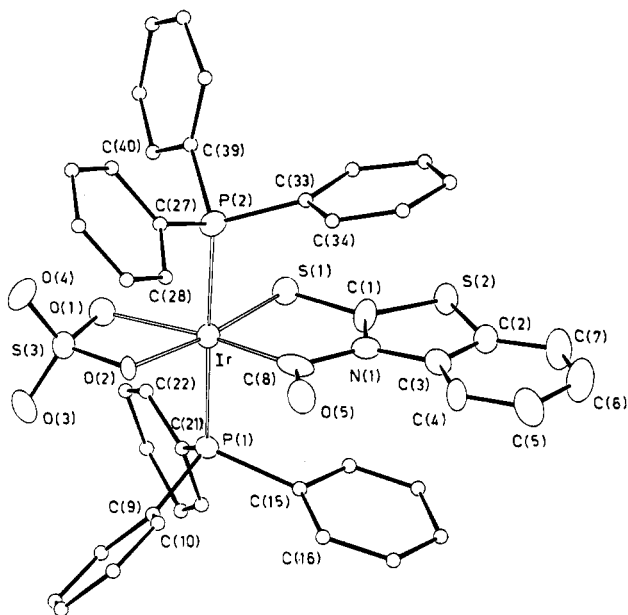


Figure 3. View of the molecular structure of one of the two independent complexes $[\text{Ir}\{\text{C}(\text{O})\text{NC}(\text{S})\text{SC}_6\text{H}_4\}(\text{SO}_4)(\text{PPh}_3)_2]$ (**11**) with the atom-numbering scheme. The thermal ellipsoids are drawn at the 30% probability level.

$(\text{SO}_4)(\text{PPh}_3)_2]$ complexes are present. The structure of one of them is shown in Figure 3 together with the atom-numbering scheme. Selected bond distances and angles are given in Table 2. In the octahedral coordination around the Ir atom the two axial positions are occupied by P atoms from PPh_3 groups, whereas two *cis*-equatorial sites are occupied by O atoms from the chelating sulfato ligand and the remaining two by the C(8) and S(1) atoms of the new chelating ligand, obtained by an unprecedented incorporation of the carbonyl group of **7** into benzothiazole-2-thiolate through the heterocyclic nitrogen. The Ir–P bond distances, 2.368(4) and 2.386(5) Å [2.376(4) and 2.367(4) Å; hereafter the values in brackets refer to the second independent complex] are comparable to those found in **8**. The two Ir–O bond distances, 2.154(9) and 2.067(8) Å [2.187(9) and 2.123(8) Å], are significantly different, probably because of the different trans effects of the S and C atoms. The O(1)S(3)O(2)Ir four-membered chelating ring is planar, with a bite angle of 66.4(4)° [65.2(4)°]. The Ir–S(1) and Ir–C(8) bond distances are 2.323(4) Å [2.293(4) Å] and 1.96(1) Å [1.93(1) Å], respectively. Also, the S(1)C(1)N(1)C(8)Ir five-membered chelating ring, with a bite angle of 86.1(5)° [87.3(4)°], is planar with the O(5) atom lying in the same plane. The new ligand has preserved its planarity after insertion of the adjacent CO ligand. The values of the N(1)–C(8) (1.51(2) Å [1.49(2) Å]) and C(8)–O(5) (1.20(2) Å [1.21(2) Å]) bond distances are in accordance with a slight delocalization of the double bond, as shown by the resonance structures in Scheme 3. The weakness of the N–C bond is revealed also by the mass spectrum of **11**, which shows the sequential loss of the sulfato and then the carbonyl group from the molecular ion. In contrast, the carbonyl group is not observed in the fragmentation of formamides. Furthermore, this bond should be similar to that in *N*-acyl derivatives of pyridine, which are proposed intermediates in acylation reactions of organic substrates where 4-(dimethylamino)pyridine is added to promote the reaction.⁴ The *N*-acyl derivative easily transfers the

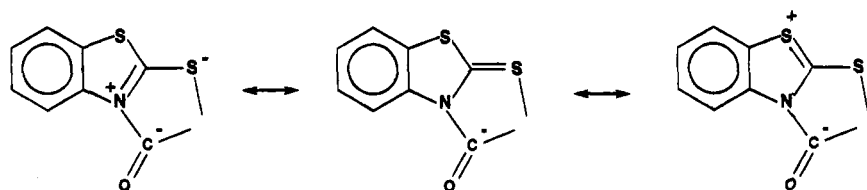
Table 2. Selected Bond Distances (Å) and Angles (deg) for Complex **11**

	complex 1	complex 2
Ir–S(1)	2.323(4)	2.292(4)
Ir–P(1)	2.368(4)	2.376(4)
Ir–P(2)	2.386(5)	2.367(4)
Ir–O(1)	2.154(9)	2.187(9)
Ir–O(2)	2.067(8)	2.123(8)
Ir–C(8)	1.96(1)	1.93(1)
S(1)–C(1)	1.71(1)	1.67(1)
S(2)–C(1)	1.69(2)	1.73(2)
S(2)–C(2)	1.71(1)	1.79(2)
S(3)–O(1)	1.51(1)	1.53(1)
S(3)–O(2)	1.53(1)	1.50(1)
S(3)–O(3)	1.44(1)	1.43(1)
S(3)–O(4)	1.44(1)	1.45(1)
P(1)–C(9)	1.78(2)	1.85(2)
P(1)–C(15)	1.89(2)	1.82(2)
P(1)–C(21)	1.82(1)	1.83(2)
P(2)–C(27)	1.86(2)	1.85(2)
P(2)–C(33)	1.86(2)	1.79(2)
P(2)–C(39)	1.82(2)	1.84(2)
O(5)–C(8)	1.20(2)	1.21(2)
N(1)–C(1)	1.33(2)	1.35(2)
N(1)–C(3)	1.44(2)	1.42(2)
N(1)–C(8)	1.51(2)	1.49(2)
C(2)–C(3)	1.38(2)	1.40(2)
C(2)–C(7)	1.41(2)	1.36(2)
C(3)–C(4)	1.36(2)	1.40(2)
C(4)–C(5)	1.40(2)	1.38(2)
C(5)–C(6)	1.40(3)	1.40(2)
C(6)–C(7)	1.35(2)	1.38(2)
O(2)–Ir–C(8)	102.0(5)	101.8(5)
O(1)–Ir–O(2)	66.4(4)	65.2(4)
P(2)–Ir–C(8)	89.6(5)	87.7(5)
P(2)–Ir–O(2)	89.8(3)	89.1(3)
P(2)–Ir–O(1)	90.1(3)	94.3(3)
P(1)–Ir–C(8)	89.3(5)	90.3(5)
P(1)–Ir–O(2)	91.2(3)	92.1(3)
P(1)–Ir–O(1)	91.1(3)	87.8(3)
S(1)–Ir–C(8)	86.1(5)	87.3(4)
S(1)–Ir–O(1)	105.4(3)	105.7(3)
S(1)–Ir–P(2)	89.0(2)	90.0(2)
S(1)–Ir–P(1)	90.1(1)	89.1(2)
Ir–S(1)–C(1)	98.2(5)	97.1(6)
C(1)–S(2)–C(2)	90.1(8)	90.9(8)
O(3)–S(3)–O(4)	114.9(7)	112.0(7)
O(2)–S(3)–O(4)	109.4(6)	112.8(7)
O(2)–S(3)–O(3)	110.4(6)	108.8(6)
O(1)–S(3)–O(4)	112.6(7)	112.3(7)
O(1)–S(3)–O(3)	109.5(6)	110.1(7)
O(1)–S(3)–O(2)	98.9(5)	100.2(5)
Ir–O(1)–S(3)	95.7(6)	95.4(5)
Ir–O(2)–S(3)	98.9(4)	98.9(4)
C(3)–N(1)–C(8)	129.6(12)	129.7(11)
C(1)–N(1)–C(8)	118.9(12)	117.1(12)
C(1)–N(1)–C(3)	111.5(12)	113.2(13)
O(5)–C(8)–N(1)	114.1(13)	113.6(12)
Ir–C(8)–N(1)	116.0(10)	116.1(9)
Ir–C(8)–O(5)	129.9(13)	130.2(11)

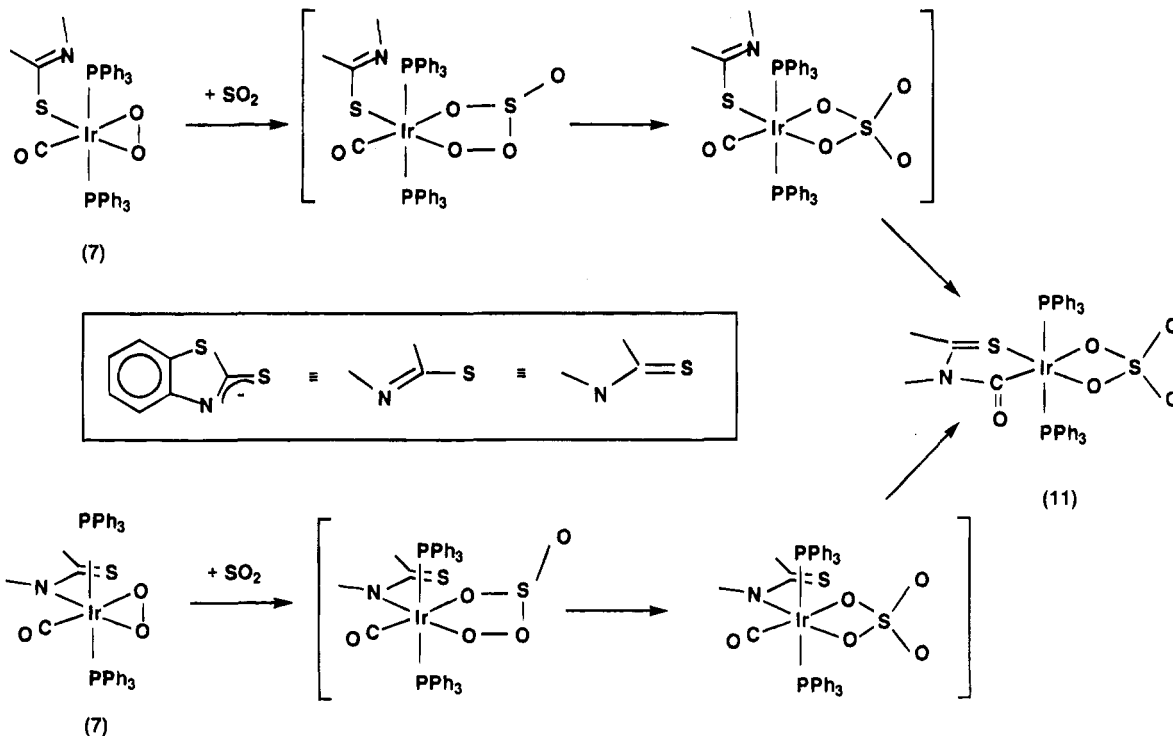
acyl group because of the instability associated with the weak N–C(O) bond.

The reactions described here involve the dioxygen ligand as a central place of reactivity of complex **7**. In fact, all require an electrophile (H^+ and SO_2 respectively) to start a further reaction. This electrophile is directly added or generated in the reaction and then selectively attacks at the dioxygen ligand, opening the dioxo metallacycle. In other words, the Lewis acids bind to a dipolar intermediate ($\text{M}^+ - \text{O} - \text{O}^-$) through the free oxygen atom as the first step in these reactions. The second step involves the breaking of the O–O bond to give the hydrogencarbonate or the sulfate ligand. A further reaction takes place then in the formation of complex **11**. As benzothiazole-2-thiolate still has a free

Scheme 3



Scheme 4. Possible Pathways Leading to the Formation of Complex 11



arm, there are two different but indistinguishable possibilities depending on the donor atom (S or N) bonded to the iridium atom (Scheme 4). The first alternative implies that the carbonyl group inserts into the N-Ir bond while the sulfur atom covers the vacant coordination position. In the second case, the uncoordinated nitrogen adds to the carbonyl group to straightforwardly give the new organic ligand. Both possibilities have been proposed in the reactions of carbon monoxide with amido and imido complexes of rhodium.²⁹ Molecular models suggest that the S-coordination of benzothiazole-2-thiolate is preferred for steric reasons and that the second alternative is the most probable. Then the carbonyl group simply undergoes a nucleophilic attack by the aromatic nitrogen of benzothiazole-2-thiolate. On the other hand, this reaction is quite uncommon for tertiary amines and heterocyclic compounds due to their reluctance to give formyl derivatives. In fact, homogeneous catalysis of the water-gas shift reaction and related reactions in organic basic solvents, in which nucleophilic attack at carbonyl groups is involved, is carried out in pyridine and tertiary amines to avoid side reactions.²³ In this case, the reaction involves the unprecedented attack of a heterocycle at coordinated carbon monoxide, resulting in the carbonylation of the nitrogen to give a new organic ligand without loss of the aromaticity of this ring.

Experimental Section

General Considerations. All reactions were carried out under a dry nitrogen atmosphere using Schlenk techniques, but isolations of most of the compounds were performed in air. Solvents were dried by refluxing over Na/benzophenone ketyl or CaH₂ and distilled under nitrogen immediately before use. ¹H, ³¹P{¹H}, and ¹³C{¹H} NMR spectra were recorded on a Varian XL-200 operating at 200.057, 80.984, and 50.309 MHz respectively; chemical shifts are reported relative to tetramethylsilane and phosphoric acid as external references. IR spectra (range 4000–200 cm⁻¹) were recorded on a Perkin-Elmer 783 spectrometer as Nujol mulls between polyethylene sheets or in solution in NaCl windows. Elemental analyses were carried out with a Perkin-Elmer 240-B microanalyzer. Molecular weights were determined with a Knauer osmometer using chloroform solutions of the complexes. Mass spectra were recorded with a VG Autospec apparatus using the FAB method. O₂ and H₂ were used as received. SO₂ was prepared according to a reported method and dried through H₂SO₄. H₂¹⁸O (99%) was purchased from Aldrich and used as received, and HBF₄·OEt₂ (54% solution in diethyl ether) was purchased from Merck. [IrCl(CO)(PPh₃)₂]³⁰ and [IrH₂(Me₂CO)₂(PPh₃)₂][PF₆]³¹ were prepared by literature procedures.

Preparation of the Compounds. [Ir(C₇H₄NS₂)(CO)(PPh₃)₂] (1). A solution of 2-mercaptobenzothiazole (0.033 g, 0.20 mmol) in tetrahydrofuran (10 mL) was added to a solution of *n*-butyllithium (0.12 mL, 1.64 mol L⁻¹, 0.20 mmol) in hexane.

(30) Vrieze, K.; Collman, J. P.; Sears, C. P., Jr.; Kubota, M. *Inorg. Synth.* **1978**, *11*, 101.

(31) Shapley, J. R.; Schrock, R. R.; Osborn, J. A. *J. Am. Chem. Soc.* **1969**, *91*, 2816.

(29) Ge, Y. W.; Sharp, P. R. *Organometallics* **1988**, *7*, 2234; *Inorg. Chem.* **1992**, *31*, 379.

After the mixture was stirred for 10 min, solid $[\text{IrCl}(\text{CO})\text{(PPh}_3)_2]$ (0.156 g, 0.20 mmol) was added and the mixture refluxed for 1 h to give a bright red solution. Concentration of this solution to ca. 1 mL and slow addition of diethyl ether rendered complex **1** as a yellow microcrystalline solid which was filtered, washed with methanol, and dried under vacuum (yield 0.154 g, 85%). Anal. Calcd for $\text{C}_{44}\text{H}_{34}\text{IrNOP}_2\text{S}_2$: C, 58.00; H, 3.76; N, 1.53. Found: C, 57.76; H, 4.01; N, 1.40. Molecular weight: calcd, 911; found, 738. IR (cm^{-1} , CH_2Cl_2): $\nu(\text{CO})$ 1966 s. $^{31}\text{P}\{^1\text{H}\}$ NMR (δ , CDCl_3 , 293 K): 26.6 (s).

[IrH(C₇H₄NS₂)₂(CO)(PPh₃)₂]BF₄ (3). Tetrafluoroboric acid in diethyl ether (17 μL , 0.12 mmol) was added to a solution of the complex $[\text{Ir}(\text{C}_7\text{H}_4\text{NS}_2)(\text{CO})(\text{PPh}_3)_2]$ (**1**; 0.12 mmol) in a mixture of tetrahydrofuran and diethyl ether (1:5; 10 mL). The yellow solid immediately formed was filtered, washed with diethyl ether, and vacuum dried (yield 90%). Anal. Calcd for $\text{C}_{44}\text{H}_{36}\text{BF}_4\text{IrNOP}_2\text{S}_2$: C, 52.90; H, 3.53; N, 1.40. Found: C, 52.45; H, 3.72; N, 1.37. Molar conductivity, Λ_{M} ($\text{S cm}^2 \text{mol}^{-1}$, acetone): 128. IR (cm^{-1}): $\nu(\text{Ir-H})$ (Nujol) 2185 m; $\nu(\text{CO})$ (CH_2Cl_2) 2060 s. ^1H NMR (δ , CDCl_3 , 293 K): 7.44–7.29 (m, 32H, PPh₃ and $\text{C}_7\text{H}_4\text{NS}_2$); 7.00 (dd, 1H, $\text{C}_7\text{H}_4\text{NS}_2$); 6.78 (d, 1H, $\text{C}_7\text{H}_4\text{NS}_2$); -14.51 (t, $J_{\text{H-P}} = 10$ Hz, 1H, Ir-H). $^{31}\text{P}\{^1\text{H}\}$ NMR (δ , CDCl_3 , 293 K): 10.5 (s).

[IrH(C₇H₄NS₂)₂(CO)(PPh₃)₂] (4). Solid 2-mercaptobenzothiazole (0.019 g, 0.11 mmol) was added to a solution of the complex **1** (0.100 g, 0.11 mmol) in tetrahydrofuran (10 mL). The mixture was refluxed for 2 h to give a colorless solution. Evaporation under vacuum to 1 mL and slow addition of diethyl ether gave white crystals of the complex, which were filtered, washed with diethyl ether, and dried under vacuum (yield 0.093 g, 65%). Anal. Calcd for $\text{C}_{51}\text{H}_{39}\text{IrN}_2\text{OP}_2\text{S}_4$: C, 56.81; H, 3.64; N, 2.59. Found: C, 56.45; H, 4.05; N, 2.17. IR (cm^{-1}): $\nu(\text{Ir-H})$ (Nujol) 2165 m; $\nu(\text{CO})$ (CH_2Cl_2) 2030 s. ^1H NMR (δ , CDCl_3 , 293 K): 7.64 (m, 16H) and 7.10 (m, 22H) PPh₃ and $\text{C}_7\text{H}_4\text{NS}_2$ ligand; -11.67 (t, $J_{\text{H-P}} = 11$ Hz, 1H, Ir-H). $^{31}\text{P}\{^1\text{H}\}$ NMR (δ , CDCl_3 , 293 K): 1.8 (s).

Reaction of [IrH(C₇H₄NS₂)₂(CO)(PPh₃)₂] (4) with HBF₄·EtO₂. Tetrafluoroboric acid in diethyl ether (7.6 μL , 0.05 mmol) was added to a stirred solution of the complex **4** (0.060 g, 0.05 mmol) in dichloromethane (3 mL). The mixture was stirred for 30 min, and then diethyl ether (15 mL) was added. A yellow microcrystalline solid was immediately formed, which was filtered, washed with diethyl ether, and vacuum-dried. The compound was identified as the complex **3** (0.050 g, 90%) by comparison of its spectroscopic properties.

[IrH₂(C₇H₄NS₂)₂(CO)(PPh₃)₂] (5). Hydrogen was bubbled through a solution of complex **1** (0.091 g, 0.10 mmol) in tetrahydrofuran (5 mL) for 10 min, and then the solution was stirred under a hydrogen atmosphere for 4 h. Concentration of the resulting yellow solution to ca. 1 mL and addition of diethyl ether gave the complex as a white microcrystalline solid which was isolated by filtration (yield 0.073 g, 80%). Anal. Calcd for $\text{C}_{44}\text{H}_{36}\text{IrNOP}_2\text{S}_2$: C, 57.88; H, 3.97; N, 1.53. Found: C, 58.38; H, 4.85; N, 1.44. Molecular weight: calcd, 913; found, 931. IR (cm^{-1} , Nujol): $\nu(\text{Ir-H}) + \nu(\text{CO})$ 2120, 2090, 1988. ^1H NMR (δ , CDCl_3 , 293 K): 7.44 (m, 12H, PPh₃); 7.40 (m, 1H, $\text{C}_7\text{H}_4\text{NS}_2); 7.25 (m, 1H, $\text{C}_7\text{H}_4\text{NS}_2); 7.16 (m, 18H, PPh₃); 7.10 (m, 1H), 7.00 (m, 1H) ($\text{C}_7\text{H}_4\text{NS}_2); -9.25 (td, $J_{\text{H-P}} = 18$ Hz, $J_{\text{H-H}} = 4$ Hz, 1H, Ir-H); -14.77 (td, $J_{\text{H-P}} = 15$ Hz, $J_{\text{H-H}} = 4$ Hz, 1H, Ir-H). $^{31}\text{P}\{^1\text{H}\}$ NMR (δ , CDCl_3 , 293 K): 11.0 (s).$$$

[IrH₂(C₇H₄NS₂)₂(PPh₃)₂] (6). Solid $[\text{IrH}_2(\text{Me}_2\text{CO})_2(\text{PPh}_3)_2]\text{-PF}_6$ (0.150 g, 0.15 mmol) was added to a solution of $\text{LiC}_7\text{H}_4\text{NS}_2$ in tetrahydrofuran (10 mL) prepared by reaction of 2-mercaptobenzothiazole (0.025 g, 0.15 mmol) with butyllithium (0.10 mL, 1.54 mol L^{-1} , 0.15 mmol) in hexane. The mixture was reacted for 30 min to give a yellow solution, which was concentrated to ca. 1 mL under vacuum. Addition of methanol to the concentrate gave the complex as a white solid which was separated by filtration, washed with methanol, and vacuum-dried (yield 0.088 g, 65%). Anal. Calcd for $\text{C}_{43}\text{H}_{36}\text{IrNP}_2\text{S}_2$: C, 58.31; H, 4.06; N, 1.58. Found: C, 58.67; H, 4.52; N, 1.58. Molecular weight: calcd, 884; found, 874.

Table 3. Experimental Data for the X-ray Diffraction Studies of Compounds 8 and 11

	8	11
formula	$\text{C}_{44}\text{H}_{34}\text{IrNO}_3\text{P}_2\text{S}_2$	$\text{C}_{44}\text{H}_{34}\text{IrNO}_5\text{P}_2\text{S}_3$
mol wt	943.04	1007.10
cryst syst	monoclinic	monoclinic
space group	$P2_1/n$	$P2_1$
radiation (λ , Å)	graphite monochromated (Mo K α , 0.710 73)	nickel filtered (Cu K α , 1.541 78)
a , Å	15.626(6)	14.414(8)
b , Å	20.568(8)	20.220(6)
c , Å	11.996(5)	14.800(5)
β , deg	93.52(2)	107.41(2)
V , Å ³	3848(3)	4116(3)
Z	4	4
D_{calcd} , g cm^{-3}	1.628	1.625
$F(000)$	1872	2000
cryst size, mm	0.15 \times 0.24 \times 0.35	0.10 \times 0.22 \times 0.30
μ , cm^{-1}	36.82 (Mo K α)	86.92 (Cu K α)
diffractometer	Philips PW 1100	Siemens AED
scan type	$\theta/2\theta$	$\theta/2\theta$
scan speed, deg/min	3–12	3–12
θ range, deg	3–23	3–70
std rfln	one measd after	100 reflctns
rflns measd	hkl	hkl
no. of unique data total	5520	8374
no. of unique data obsd ($I > 2\sigma(I)$)	3643	5324
R^a	0.0344	0.0423
R_w^b	0.0441	0.0526

$$^a R = \sum ||F_o| - |F_c|| / \sum |F_o|. \quad ^b R_w = [\sum w(|F_o| - |F_c|)^2 / \sum w(F_o)^2]^{1/2}.$$

IR (cm^{-1} , Nujol): $\nu(\text{Ir-H})$ 2150 m, 2110 m. ^1H NMR (δ , CDCl_3 , 293 K): 7.65 (m, 12H, PPh₃); 7.52 (m, 1H, $\text{C}_7\text{H}_4\text{NS}_2$); 7.13 (m, 18H, PPh₃); 7.07 (m, 1H), 6.78 (t, 1H), 6.75 (d, 1H) ($\text{C}_7\text{H}_4\text{NS}_2$); -21.23 (td, $J_{\text{H-P}} = 16$ Hz, $J_{\text{H-H}} = 7$ Hz, 1H, Ir-H); -22.68 (td, $J_{\text{H-P}} = 16$ Hz, $J_{\text{H-H}} = 7$ Hz, 1H, Ir-H). $^{31}\text{P}\{^1\text{H}\}$ NMR (δ , CDCl_3 , 293 K): 22.8 (s).

[Ir(C₇H₄NS₂)(O₂)(CO)(PPh₃)₂] (7). Oxygen was bubbled through a solution of complex **1** (0.100 g, 0.11 mmol) in dichloromethane (5 mL) for 10 min. The solution was stirred under an oxygen atmosphere for 30 min and then concentrated under vacuum to ca. 1 mL. Addition of hexane gave the complex as an off-white solid, which was washed several times with hexane and then vacuum-dried (yield 0.077 g, 75%). Anal. Calcd for $\text{C}_{44}\text{H}_{34}\text{IrNO}_3\text{P}_2\text{S}_2$: C, 56.04; H, 3.63; N, 1.48. Found: C, 54.98; H, 3.52; N, 1.38. IR (cm^{-1}): $\nu(\text{CO})$ (CH_2Cl_2) 2015 s; $\nu(\text{O-O})$ (Nujol) 885 s. $^{31}\text{P}\{^1\text{H}\}$ NMR (δ , CDCl_3 , 293 K): 6.1 (s).

[Ir(C₇H₄NS₂)(CO)₃(PPh₃)₂] (8). An orange solution of the complex **1** (0.150 g, 0.16 mmol) in tetrahydrofuran (15 mL) and distilled water (3 mL) was stirred under an oxygen atmosphere for 2 h to give a yellow solution. The solvents were removed under vacuum, and the residue was extracted with dichloromethane. The extract was dried over MgSO_4 and concentrated to ca. 1 mL. Addition of diethyl ether gave yellow crystals of complex **8**, which were filtered, washed with diethyl ether, and vacuum-dried (yield 0.120 g, 78%). Anal. Calcd for $\text{C}_{44}\text{H}_{34}\text{IrNO}_3\text{P}_2\text{S}_2$: C, 56.04; H, 3.63; N, 1.48. Found: C, 55.90; H, 3.86; N, 1.35. Molecular weight: calcd, 943; found, 966. IR (cm^{-1} , Nujol): $\nu(\text{CO})$ 1683 s. $^{13}\text{C}\{^1\text{H}\}$ NMR (δ , CDCl_3 , 293 K): 181.6 (CS), 125.2, 122.3, 119.5, 114.5 (CH), 145.1, and 128.9 ($\text{C}_7\text{H}_4\text{NS}_2$ ligand); 133, 129.3, 127.0, 126.2 (PPh₃ ligands); 167.1 (CO_3). $^{31}\text{P}\{^1\text{H}\}$ NMR (δ , CDCl_3 , 293 K): -3.8 (s). MS (FAB): m/e 944($\text{M}^+ + \text{H}$, 45%), 882($\text{M}^+ - \text{HCO}_3$, 100%). Good quality crystals suitable for X-ray diffraction were obtained by slow diffusion of diethyl ether into a concentrated solution of the complex in dichloromethane.

[Ir(C₇H₄NS₂)Cl₂(PPh₃)₂] (9). A solution of HCl (0.8 mL, 0.21 mol L^{-1} , 0.17 mmol) in acetone was added to a solution of complex **8** (0.080 g, 0.08 mmol) in dichloromethane (10 mL)

Table 4. Atomic Coordinates ($\times 10^4$) and Equivalent^a Isotropic Thermal Parameters ($\text{\AA}^2 \times 10^4$) for the Non-Hydrogen Atoms of Complex 8

atom	<i>x/a</i>	<i>y/b</i>	<i>z/c</i>	<i>U</i> _{eq}	atom	<i>x/a</i>	<i>y/b</i>	<i>z/c</i>	<i>U</i> _{eq}
Ir	2570.6(2)	667.4(2)	754.8(3)	312(1)	C(19)	4322(8)	1752(6)	3827(9)	663(48)
S(1)	4083(2)	397(1)	819(2)	405(8)	C(20)	3655(7)	1448(5)	3191(8)	540(39)
S(2)	4029(2)	-1107(1)	209(2)	544(10)	C(21)	1595(6)	682(5)	3387(7)	374(31)
P(1)	2539(2)	425(1)	2683(2)	338(8)	C(22)	1676(7)	943(5)	4479(8)	546(39)
P(2)	2699(2)	994(1)	-1109(2)	358(8)	C(23)	937(9)	1044(6)	5048(9)	694(49)
O(1)	1282(4)	906(4)	656(5)	440(24)	C(24)	125(9)	900(6)	4589(11)	718(51)
O(2)	2282(4)	1624(3)	1117(5)	415(22)	C(25)	36(7)	640(6)	3494(10)	640(43)
O(3)	778(5)	1933(4)	1044(7)	658(30)	C(26)	788(6)	545(5)	2868(9)	522(39)
N	2798(5)	-290(4)	360(6)	355(27)	C(27)	2929(6)	330(5)	-2081(7)	377(32)
C(1)	3642(6)	-329(5)	433(7)	399(33)	C(28)	2264(7)	43(6)	-2730(9)	666(45)
C(2)	2967(7)	-1387(5)	3(8)	560(41)	C(29)	2479(9)	-507(7)	-3379(11)	861(58)
C(3)	2725(10)	-2030(6)	-193(10)	804(55)	C(30)	3316(8)	-741(6)	-3384(9)	614(44)
C(4)	1842(12)	-2119(8)	-362(12)	1035(69)	C(31)	3956(7)	-434(6)	-2769(8)	579(41)
C(5)	1231(9)	-1626(8)	-267(10)	822(56)	C(32)	3766(7)	99(5)	-2107(8)	484(37)
C(6)	1509(7)	-973(6)	-49(9)	618(43)	C(33)	3551(6)	1577(5)	-1285(8)	426(34)
C(7)	2390(7)	-877(5)	107(8)	498(39)	C(34)	3853(7)	1957(5)	-354(8)	496(37)
C(8)	1428(7)	1527(5)	959(8)	453(39)	C(35)	4477(7)	2427(5)	-522(9)	597(43)
C(9)	2613(7)	-422(5)	3065(7)	439(35)	C(36)	4805(7)	2530(5)	-1537(9)	580(43)
C(10)	3393(7)	-774(5)	2893(8)	505(39)	C(37)	4482(7)	2161(5)	-2496(8)	523(39)
C(11)	3436(8)	-1436(5)	3109(8)	579(43)	C(38)	3871(7)	1684(5)	-2352(8)	556(40)
C(12)	2753(9)	-1762(5)	3550(10)	688(51)	C(39)	1730(6)	1385(5)	-1715(7)	460(37)
C(13)	2008(8)	-1429(5)	3759(11)	751(52)	C(40)	945(7)	1055(6)	-1692(7)	537(41)
C(14)	1930(7)	-751(6)	3510(10)	620(44)	C(41)	179(7)	1340(7)	-2127(8)	674(49)
C(15)	3425(6)	822(5)	3486(7)	417(35)	C(42)	229(9)	1985(8)	-2578(9)	810(59)
C(16)	3845(7)	509(5)	4415(8)	521(39)	C(43)	983(10)	2320(7)	-2587(9)	836(57)
C(17)	4507(7)	848(7)	5016(9)	647(47)	C(44)	1765(7)	2032(6)	-2152(8)	602(43)
C(18)	4750(7)	1459(6)	4712(9)	596(44)					

^a Equivalent isotropic *U*, defined as one-third of the trace of the orthogonalized *U*_{ij} tensor.

slowly to give a yellow-green solution in 10 min. This solution was dried over MgSO₄ and then filtered. Concentration of the filtrate to ca. 1 mL and addition of diethyl ether rendered yellow crystals of the complex, which were isolated by filtration, washed with diethyl ether, and vacuum-dried (yield 0.056 g, 70%). Anal. Calcd for C₄₃H₃₄Cl₂IrNP₂S₂: C, 54.14; H, 3.95; N, 1.46. Found: C, 53.84; H, 4.34; N, 1.37. Molecular weight: calcd, 954; found, 990. ³¹P{¹H} NMR (δ , CDCl₃, 293 K): -9.8 (s).

Reaction of [Ir(C₇H₄NS₂)(O₂)(CO)(PPh₃)₂] (7) with NH₃. A solution of the dioxygen complex 7 (prepared as described above; 0.16 mmol) in dichloromethane (10 mL) was stirred under an NH₃ atmosphere for 48 h. Concentration of the orange solution to 2 mL and addition of diethyl ether gave a yellow solid, which was filtered, washed with diethyl ether, and vacuum-dried. The compound was identified as the carbonate complex 8 (yield 0.120 g, 80%) by comparison of the IR and NMR spectra with those obtained from a pure sample. When the reaction time is reduced to 12 h and the mixture worked up as above, pale yellow solids containing mixtures of the carbonate complex and the starting material are obtained.

Reaction of [Ir(C₇H₄NS₂)(O₂)(CO)(PPh₃)₂] (7) with HBF₄·EtO₂. Method A. NMR-Monitored Experiment. A 5 mm NMR tube was charged with 0.5 mL of a CDCl₃ solution (0.06 mol L⁻¹) of the dioxygen complex 7 (0.03 mmol) and HBF₄·EtO₂ (7 μ L, 0.05 mmol) to give a yellow solution. The reaction was periodically monitored by ¹H NMR spectroscopy. After 30 min a yellow microcrystalline solid precipitated off.

Method B. Preparative-Scale Experiment. HBF₄·EtO₂ (42 μ L, 0.30 mmol) was added to a solution of the dioxygen complex 7 (0.15 mmol) in dichloromethane (10 mL; prepared as described above). The color of the solution changed from red to orange-yellow, and a pale yellow solid precipitated off. The suspension was stirred for 2 h and then concentrated to 2 mL. Addition of diethyl ether (15 mL) gave [Ir(C₇H₄NS₂)(H₂O)₂(PPh₃)₂](BF₄)₂ (10) as a yellow solid, which was recrystallized from acetone/diethyl ether (yield 0.125 g, 76%). Anal. Calcd for C₄₃H₃₈B₂F₈IrNO₂P₂S₂: C, 47.26; H, 3.50; N, 1.28. Found: C, 47.01; H, 3.47; N, 1.15. IR (cm⁻¹, Nujol): 3350, 1650 (H₂O); 1080 (BF₄).

[Ir{C(O)NC(S)SC₆H₄}(SO₄)(PPh₃)₂] (11). Oxygen was bubbled through a solution of complex 1 (0.170 g, 0.18 mmol) in tetrahydrofuran (10 mL) for 30 min to give a solution of complex 7. Then, SO₂ was bubbled for 10 min to give a pale yellow solution which was stirred under a SO₂ atmosphere for 2 h to render a yellow solid, which was filtered, washed with tetrahydrofuran, and vacuum-dried (yield 0.125 g, 68%). Anal. Calcd for C₄₃H₃₄IrNO₄P₂S₃: C, 52.76; H, 3.50; N, 1.43. Found: C, 52.79; H, 3.71; N, 1.25. IR (cm⁻¹, Nujol): 1680 ν (C=O); 1257, 1155, 927, 890, 690, 650 (SO₄). MS (FAB): *m/e* 1007 (M⁺ - H, 45%), 911 (M⁺ - SO₄, 28%), 882 (M⁺ - HSO₄ - CO, 100%). ³¹P{¹H} NMR (δ , CDCl₃, 293 K): -6.0 (s). Good quality crystals suitable for X-ray diffraction were obtained by slow diffusion of diethyl ether into a concentrated solution of the complex in dichloromethane.

X-ray Data Collection, Structure Determination, and Refinement for Compounds 8 and 11. The crystallographic data for both compounds are summarized in Table 3. Data were collected at room temperature (22 °C) on a Philips PW 1100 (8) and on a Siemens AED diffractometer (11), using graphite-monochromated Mo K α (8) and nickel-filtered Cu K α radiation (11) and the $\theta/2\theta$ scan type. The reflections were collected with a variable scan speed of 3–12° min⁻¹ for both compounds and a scan width (deg) of 1.30 + 0.346 tan θ (8) and 1.30 + 0.142 tan θ (11). One standard reflection was monitored every 75 measurements; no significant decay was noticed over the time of data collection. The individual profiles have been analyzed by following the method of Lehmann and Larsen.³² Intensities were corrected for Lorentz and polarization effects. A correction for absorption was applied (maximum and minimum values for the transmission factors were 1.09 and 0.94 (8), 1.174 and 0.889 (11)).³³ Only the observed reflections were used in the structure solutions and refinements.

The structures were solved by Patterson and Fourier methods and refined by full-matrix least squares, first with isotropic thermal parameters and then with anisotropic ther-

(32) Lehmann, M. S.; Larsen, F. K. *Acta Crystallogr., Sect. A* 1974, 30, 580.

(33) Walker, N.; Stuart, D. *Acta Crystallogr., Sect. A* 1983, 39, 158. Ugozzoli, F. *Comput. Chem.* 1987, 11, 109.

Table 5. Atomic Coordinates ($\times 10^4$) and Equivalent^a Isotropic Thermal Parameters ($\text{\AA}^2 \times 10^4$) for the Non-Hydrogen Atoms of Complex 11

atom	<i>x/a</i>	<i>y/b</i>	<i>z/c</i>	<i>U</i>	atom	<i>x/a</i>	<i>y/b</i>	<i>z/c</i>	<i>U</i>
Ir(1)	81.7(5)	2500	4627.8(5)	347(2) ^a	Ir(2)	5418.9(5)	1986.1(4)	-56.0(5)	368(2) ^a
S(11)	-99(3)	3624(2)	4300(3)	408(14) ^a	S(12)	5633(3)	873(2)	224(3)	480(14) ^a
S(21)	1138(3)	4708(2)	5428(3)	449(14) ^a	S(22)	4390(3)	-201(2)	-936(3)	574(16) ^a
S(31)	-802(3)	1328(2)	3896(3)	401(13) ^a	S(32)	6255(3)	3171(2)	746(3)	436(14) ^a
P(11)	-939(2)	2590(2)	5614(2)	310(11) ^a	P(12)	6456(3)	1925(2)	-1036(2)	418(13) ^a
P(21)	1133(3)	2431(3)	3655(3)	419(13) ^a	P(22)	4344(2)	2022(2)	879(2)	342(11) ^a
O(11)	-1060(6)	2026(6)	3538(6)	437(34) ^a	O(12)	6614(7)	2466(6)	1012(6)	474(34) ^a
O(21)	92(7)	1481(4)	4735(6)	225(30) ^a	O(22)	5398(6)	3036(4)	-104(6)	209(25) ^a
O(31)	-1573(7)	1061(5)	4225(8)	496(43) ^a	O(32)	5913(8)	3453(6)	1474(8)	555(44) ^a
O(41)	-519(8)	918(6)	3225(7)	567(46) ^a	O(42)	6984(8)	3582(6)	528(9)	589(48) ^a
O(51)	1732(7)	2410(6)	6300(8)	551(45) ^a	O(52)	3777(7)	2117(5)	-1706(8)	542(43) ^a
N(11)	1416(8)	3479(6)	5828(8)	380(45) ^a	N(12)	4109(9)	1045(6)	-1291(8)	410(45) ^a
C(11)	842(11)	3902(7)	5223(12)	432(59) ^a	C(12)	4698(11)	620(9)	-684(11)	512(61) ^a
C(21)	2078(11)	4495(8)	6397(10)	435(59) ^a	C(22)	3377(11)	34(8)	-1918(12)	491(61) ^a
C(31)	2175(10)	3818(7)	6538(10)	362(50) ^a	C(32)	3358(11)	727(7)	-2000(10)	425(52) ^a
C(41)	2876(10)	3524(8)	7255(10)	448(59) ^a	C(42)	2622(10)	1029(9)	-2715(10)	464(58) ^a
C(51)	3522(11)	3939(9)	7904(14)	622(72) ^a	C(52)	1955(12)	613(7)	-3314(12)	508(61) ^a
C(61)	3492(15)	4623(11)	7750(13)	722(85) ^a	C(62)	1991(13)	-74(9)	-3199(14)	663(75) ^a
C(71)	2774(11)	4891(9)	7037(13)	663(77) ^a	C(72)	2720(12)	-379(9)	-2497(12)	603(69) ^a
C(81)	1197(11)	2749(8)	5708(12)	465(62) ^a	C(82)	4315(11)	1764(6)	-1120(10)	357(52) ^a
C(91)	-1144(10)	1841(7)	6151(10)	418(37)	C(92)	3266(11)	1488(8)	416(11)	464(37)
C(101)	-347(13)	1436(10)	6558(12)	590(48)	C(102)	3358(13)	820(9)	612(13)	594(46)
C(111)	-467(14)	823(10)	6924(13)	668(52)	C(112)	2591(15)	389(11)	180(15)	779(59)
C(121)	-1408(13)	601(9)	6852(13)	646(49)	C(122)	1750(16)	657(12)	-445(16)	860(65)
C(131)	-2201(14)	986(10)	6454(13)	667(52)	C(132)	1666(15)	1303(11)	-668(15)	764(57)
C(141)	-2055(12)	1606(8)	6096(12)	578(45)	C(142)	2414(13)	1734(10)	-253(13)	650(51)
C(151)	-410(11)	3170(8)	6640(11)	427(37)	C(152)	4820(12)	1760(8)	2087(12)	528(42)
C(161)	178(11)	2928(8)	7515(11)	484(40)	C(162)	5786(12)	1715(8)	2534(13)	597(45)
C(171)	633(13)	3372(10)	8213(14)	649(51)	C(172)	6181(14)	1499(9)	3470(13)	600(48)
C(181)	532(12)	4043(9)	8065(12)	542(43)	C(182)	5519(15)	1349(11)	3934(16)	853(61)
C(191)	-48(13)	4284(10)	7198(13)	642(52)	C(192)	4488(15)	1360(11)	3541(15)	801(62)
C(201)	-510(11)	3857(8)	6507(12)	507(40)	C(202)	4164(16)	1598(10)	2603(15)	803(62)
C(211)	-2143(10)	2951(7)	5105(10)	372(33)	C(212)	3819(11)	2844(8)	951(11)	502(39)
C(221)	-2554(11)	2993(8)	4133(11)	504(42)	C(222)	3453(12)	3209(9)	121(13)	595(48)
C(231)	-3467(12)	3255(9)	3727(12)	568(45)	C(232)	3048(15)	3856(11)	143(15)	770(58)
C(241)	-3941(13)	3515(10)	4333(13)	648(52)	C(242)	3001(15)	4096(12)	983(15)	864(65)
C(251)	-3580(14)	3458(10)	5337(14)	784(58)	C(252)	3386(15)	3756(11)	1799(15)	822(59)
C(261)	-2641(13)	3211(9)	5675(14)	667(52)	C(262)	3778(14)	3104(11)	1816(15)	769(57)
C(271)	1620(12)	1583(9)	3639(13)	561(45)	C(272)	5942(11)	1422(8)	-2114(11)	469(38)
C(281)	1989(12)	1239(9)	4438(12)	511(44)	C(282)	5411(14)	1735(11)	-2945(14)	809(59)
C(291)	2358(14)	605(11)	4461(16)	773(60)	C(292)	4964(13)	1325(11)	-3739(15)	678(53)
C(301)	2256(15)	337(12)	3591(16)	940(69)	C(302)	4961(15)	670(11)	-3666(15)	803(58)
C(311)	1935(14)	649(10)	2776(15)	791(60)	C(312)	5472(11)	373(9)	-2838(12)	566(42)
C(321)	1557(12)	1299(10)	2759(13)	627(49)	C(322)	5950(14)	770(10)	-2065(14)	651(50)
C(331)	2223(11)	2966(8)	4099(11)	466(39)	C(332)	7612(12)	1526(9)	-471(12)	536(42)
C(341)	3055(11)	2732(9)	4744(11)	552(44)	C(342)	7972(12)	1473(9)	508(12)	548(42)
C(351)	3801(15)	3155(11)	5144(15)	794(60)	C(352)	8883(15)	1159(11)	885(16)	822(62)
C(361)	3728(13)	3828(9)	4948(12)	575(47)	C(362)	9398(18)	902(13)	359(18)	920(75)
C(371)	2894(12)	4074(10)	4307(12)	601(48)	C(372)	9054(18)	961(12)	-642(18)	945(74)
C(381)	2175(13)	3624(9)	3881(12)	549(44)	C(382)	8188(13)	1288(10)	-1040(15)	695(53)
C(391)	667(11)	2736(8)	2444(11)	471(41)	C(392)	6711(11)	2734(8)	-1458(11)	487(38)
C(401)	-339(13)	2827(9)	2039(13)	660(50)	C(402)	7676(14)	2936(10)	-1385(14)	691(53)
C(411)	-684(17)	3088(12)	1148(16)	995(71)	C(412)	7734(16)	3594(11)	-1753(15)	849(64)
C(421)	-35(18)	3162(14)	584(19)	1134(84)	C(422)	6983(16)	3979(12)	-2069(15)	876(67)
C(431)	932(15)	3014(11)	963(15)	844(65)	C(432)	6058(18)	3812(12)	-2175(17)	876(72)
C(441)	1263(12)	2839(8)	1901(12)	558(43)	C(442)	5919(14)	3157(10)	-1864(13)	614(50)

^a Equivalent isotropic *U*, defined as one-third of the trace of the orthogonalized U_{ij} tensor.

mal parameters for the non-hydrogen atoms, except for the carbon atoms of the phenyl rings of **11**. Since the space group *P2*₁ leads to a chiral configuration in the structure of **11**, a refinement of the non-hydrogen atoms with anisotropic thermal parameters was carried out using the coordinates $-x$, $-y$, $-z$; a slight decrease in the *R* and *R_w* values was obtained ($R(x,y,z) = 0.0462$, $R_w(x,y,z) = 0.0555$; $R(-x,-y,-z) = 0.0449$, $R_w(-x,-y,-z) = 0.0538$). The latter model was selected, and the reported data refer to this model. All hydrogen atoms were placed at their geometrically calculated positions and refined "riding" on the corresponding carbon atoms (with isotropic thermal parameters). The final cycles of refinement were carried out on the basis of 512 (**8**) and 665 (**11**) variables; after the last cycles, no parameters shifted by more than 0.81 (**8**) and 0.97 (**11**) esd. The highest remaining peak in the final difference map was equivalent to about 0.94 (**8**) and 0.98 (**11**)

$e/\text{\AA}^3$. In the final cycles of refinement the weighting scheme $w = K[\sigma^2(F_o) + gF_o^2]^{-1}$ was used; at convergence the *K* and *g* values were 0.570 and 0.0047 (**8**) and 0.643 and 0.0029 (**11**), respectively. The analytical scattering factors, corrected for the real and imaginary parts of anomalous dispersion, were taken from ref 34. All calculations were carried out on the Gould Powernode 6040 and Encore 91 computers of the "Centro di Studio per la Strutturistica Diffraattometrica" del CNR, Parma, Italy, using the SHELX-76 and SHELXS-86 systems of crystallographic computer programs.³⁵ The final atomic coordinates for the non-hydrogen atoms are given in Tables 4 (**8**) and 5 (**11**). The atomic coordinates of the hydrogen atoms are given in Tables SI (**8**) and SII (**11**) and

(34) *International Tables for X-Ray Crystallography*; Kynoch Press: Birmingham, England, 1974; Vol. IV.

the thermal parameters in Tables SIII (8) and SIV (11) (supporting information).

Acknowledgment. We thank Prof. Dr. C. Bianchini for fruitful discussions and the Dirección General de Investigación Científica y Técnica (DGICYT, Project

(35) Sheldrick, G. M. SHELX-76 Program for crystal structure determination, University of Cambridge: Cambridge, England, 1976. Sheldrick, G. M. SHELXS-86 Program for the Solution of Crystal Structures; University of Göttingen: Göttingen, Germany, 1986.

PB88-0056) and the Consiglio Nazionale delle Ricerche (Rome) for financial support.

Supporting Information Available: Atomic coordinates of the hydrogen atoms (Tables SI (8) and SII (11)), thermal parameters (Tables SIII (8) and SIV (11)), and all bond distances and angles (Tables SV (8) and SVI (11)) (18 pages). Ordering information is given on any current masthead page.

OM9502953

Crystal Structures of Chiral Halo{2-[1-(S)-(dimethylamino)ethyl]phenyl-C¹,N}mercury(II) Complexes

Saeed Attar and John H. Nelson*

Department of Chemistry, University of Nevada, Reno, Nevada 89557-0020

Jean Fischer

Cristallochimie et de Chimie Structurale (URA424 CNRS), Université Louis Pasteur, F-67070 Strasbourg Cedex, France

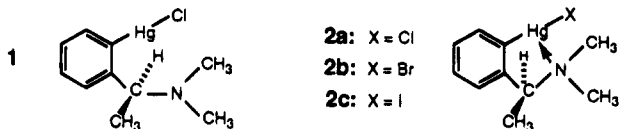
Received January 11, 1995[®]

The reaction of HgCl₂ with enantiomerically pure o-lithio-(S)-(-)-dimethyl(1-phenylethyl)amine, (S)-ArLi, results in good yields of (S)-{HgCl[C₆H₄CH(Me)NMe₂]}, **2a**. The bromide (**2b**) and iodide (**2c**) analogs were prepared by metathetic reactions of **2a** with NaBr and NaI, respectively. Single-crystal X-ray crystallographic data on all three complexes show that the Hg atom in each is nonplanar with three different groups bonded to it, making it a stereocenter. Thus, with the chiral benzylic carbon of the chelating amine ligand having the (S) absolute configuration, these complexes form as only the (S)_C(R)_{Hg} diastereomers.

Introduction

Organomercury(II) compounds of the type RHgX or R₂Hg (R = alkyl or aryl; X = halide) have received a lot of attention for the past two decades, and a large number of them are known.¹ Among the reasons for this attention are the continuing search for pharmacologically active drugs and simple preparations of organomercury compounds, the latter being related to their remarkable stability to air and water which in turn engenders them with utility as versatile synthetic agents.

We have utilized the mercury(II) chloride complex **2a**, designated (S)-ArHgCl, as a very convenient starting material in the syntheses of chiral ruthenium half-sandwich compounds.² Van Koten and co-workers³ proposed structures **1** and **2a** for CDCl₃ solutions of this



compound at room temperature and -70 °C, respectively. Compounds **2a-c** are among the few examples of three-coordinate Hg in organometallic complexes. In this note, we raise the possibility, for the first time, that Hg may be considered a stereocenter in the solid state

on the basis of the X-ray crystallographic evidence presented below.

Results and Discussion

Complex **2a** was obtained in 81% yield *via* a slight modification of the procedure reported by Osman et al.^{4a} for the preparation of R₂M and RMCl compounds (R = *N,N*-dimethylbenzylamine; M = Zn, Cd). We have consistently obtained yields of 75%–81% in our preparations of **2a** and its (*R*)-(+)-analog. By way of comparison, van Koten and co-workers report³ that treatment of (S)-ArLi with HgCl₂ gave metallic mercury, but pure **2a** was obtained from the reaction of HgCl₂ with (S)-ArCu. It should be noted that attempts to prepare **2a** *via* the reaction of (S)-(-)-dimethyl(1-phenylethyl)amine with mercury(II) acetate in the presence of LiCl, as reported by Huo et al.,^{5c,d} yielded only trace amounts of **2a**. The bromide (**2b**) and iodide (**2c**) analogs were prepared in similar yields (≥80%) by metathetic reactions of **2a** with NaBr and NaI, respectively.

X-ray crystal structures of the three halide complexes **2a-c** show similar features (Tables 1 and 2). The structure of the chloride analog **2a** (Figure 1) is repre-

(4) (a) Osman, A.; Steevensz, R. G.; Tuck, D. G.; Meinema, H. A.; Noltes, J. G. *Can. J. Chem.* **1984**, *62*, 1698. (b) (S)-(-)-Dimethyl(1-phenylethyl)amine, (S)-ArH, was obtained *via* the Eschweiler-Clarke^{4c,d} methylation of the commercially available (S)-(-)-1-phenylethylamine. (c) Cope, C. A.; Ciganek, E.; Fleckenstein, L. J.; Meisinger, M. A. P. *J. Am. Chem. Soc.* **1960**, *82*, 4651. (d) Clarke, H. T.; Gillespie, H. B.; Weisshaus, S. Z. *J. Am. Chem. Soc.* **1933**, *55*, 4571.

(5) (a) Huheey, J. E. *Inorganic Chemistry*, 3rd ed.; Harper & Row: New York, 1983; pp 258–259. (b) Pakhomov, V. I. *J. Struct. Chem. (Engl. Transl.)* **1963**, *4*, 540. (c) Huo, S. Q.; Wu, Y. J.; Zhu, Y.; Yang, L. *J. Organomet. Chem.* **1994**, *470*, 17. (d) *Ibid.* **1994**, *481*, 235. (e) Hawkins, C. J. *Absolute Configuration of Metal Complexes*; Wiley: New York, 1971; Chapter 1. (f) For pertinent discussions see: van der Schaaf, P. A.; Boersma, J.; Kooijman, H.; Spek, A. L.; van Koten, G. *Organometallics* **1993**, *12*, 4334. Jiang, Q.; Rügger, H.; Venanzi, L. M. *J. Organomet. Chem.* **1995**, *488*, 233. (g) Atwood, J. L.; Berry, D. E.; Stobart, S. R.; Zaworotko, M. J. *Inorg. Chem.* **1983**, *22*, 3480. (h) Canty, A. J.; Deacon, G. B. *Inorg. Chim. Acta.* **1980**, *45*, L225. (i) Canty, A. J.; Gatehouse, B. M. *J. Chem. Soc., Dalton Trans.* **1976**, 2018. (j) Canty, A. J.; Marker, A.; Barron, P.; Healy, P. C. *J. Organomet. Chem.* **1978**, *144*, 371.

[®] Abstract published in *Advance ACS Abstracts*, September 15, 1995.

(1) (a) Brodersen, K.; Hummel, H.-U. In *Comprehensive Coordination Chemistry*; Wilkinson, G., Gillard, R., McCleverty, J. A., Eds.; Pergamon Press: Oxford, 1987; Vol. 5, pp 1047–1097. (b) Wardell, J. L. In *Comprehensive Organometallic Chemistry*; Wilkinson, G., Stone, F. G. A., Abel, E. W., Eds.; Pergamon Press: Oxford, 1982; Vol. 2, pp 863–978. (c) Wardell, J. L., Ed. *Organometallic Compounds of Zinc, Cadmium and Mercury*; Chapman and Hall: New York, 1985; pp 11–130. (d) Eller, P. G.; Bradley, D. C.; Hursthouse, M. B.; Meek, D. W. *Coord. Chem. Rev.* **1977**, *24*, 1. (e) Greenwood, N. N.; Earnshaw, A. *Chemistry of the Elements*; Pergamon Press: Oxford, 1984; p 1408.

(2) Abbenhuis, H. C. L.; Pfeffer, M.; Sutter, J.-P.; de Cian, A.; Fischer, J.; Ji, H.-L.; Nelson, J. H. *Organometallics* **1993**, *12*, 4464.

(3) Van der Ploeg, A. F. M. J.; van der Kolk, C. E. M.; van Koten, G. *J. Organomet. Chem.* **1981**, *212*, 283.

Table 1. Crystallographic Data for [(S)-ArHgX] Complexes 2a-c

	X = Cl (2a)	X = Br (2b)	X = I (2c)
formula	C ₁₀ H ₁₄ NClHg	C ₁₀ H ₁₄ NBrHg	C ₁₀ H ₁₄ NIHg
fw	384.29	428.74	475.74
cryst syst	orthorhombic	orthorhombic	orthorhombic
a (Å)	5.880(1)	5.892(1)	5.937(1)
b (Å)	13.344(4)	13.318(4)	13.410(4)
c (Å)	14.716(4)	14.905(4)	15.209(4)
V (Å ³)	1154.6	1169.5	1210.9
Z	4	4	4
space group	P2 ₁ 2 ₁ 2 ₁	P2 ₁ 2 ₁ 2 ₁	P2 ₁ 2 ₁ 2 ₁
λ (Å)	0.7107	0.7107	0.7107
ρ _{calcd} (g cm ⁻³)	2.210	2.435	2.609
μ (cm ⁻¹)	135.2	165.0	151.95
abs min/max	0.48/1.00	0.63/1.00	0.49/0.99
R(F) ^a	0.028	0.036	0.033
R _w (F) ^b	0.042	0.051	0.049

^a $R(F) = \sum(|F_o| - |F_c|) / \sum|F_o|$. ^b $R_w(F) = [\sum w(|F_o| - |F_c|)^2] / \sum w|F_o|^2$; $w = 1/\sigma^2(F)^2 = \sigma^2(\text{counts}) + (pI)^2$.

representative. For **2a-c**, four molecules are packed in an orthorhombic unit cell, in the noncentrosymmetric space group P2₁2₁2₁. The intermolecular interactions in the lattice are those of Hg···X between two adjacent molecules at 3.1 (X = Cl), 3.4 (X = Br), and 3.8 Å (X = I). These distances are not significantly different from the sum of the van der Waals radii^{5a} for Hg (1.50 Å) and that for each of the three halide atoms: Cl (1.70–1.90 Å), Br (1.80–2.00 Å), and I (1.95–2.12 Å). Thus, no intermolecular Hg···X bonding interaction may be constituted here. The intermolecular Hg···X distances obtained in our work compare well with those calculated for the three PhHgX complexes from their powder diffraction patterns:^{5b} 3.4 (X = Cl), 3.5 (X = Br), and 3.6 Å (X = I).

Selected structural parameters for the three complexes are presented in Table 2. A literature search¹ reveals that the structures of **2a-c** represent the first examples of diastereomeric Hg(II) complexes (*vide infra*). The coordination geometry around Hg is best described as T-shaped, the preferred geometry in almost all cases where such three-coordination has been observed.^{1d} The five-membered chelate ring consisting of atoms Hg–N–C7–C6–C1 has the expected envelope (puckered) conformation.^{5e} Of the two enantiomeric envelope conformations that arise from the folding along the Hg···C7 line for molecules such as these, only the one that minimizes the interactions between the two N-methyl groups and the C-methyl group is observed. For the three compounds, the dihedral angles between the Hg–C1–C6–C7 and Hg–N–C7 planes are 137.0(6) (**2a**), 138.2(9) (**2b**), and 134.2(9)° (**2c**). In all three compounds the α-methyl group is located equatorially nearly in the plane of the phenyl ring. This methyl group orientation has been observed for about half the compounds containing the {M-*o*-aryl-CH(Me)NMe₂} fragment found in the Cambridge Structural Data Base.^{5f} The Hg–Cl distance of 2.323(3) Å in **2a** is comparable to others reported, e.g., 2.25 Å in HgCl₂,^{1e} 2.364 Å in dichloronicotinomercury(II),^{1a} and 2.296 and 2.390 Å for the recently reported mercury(II) chloride complexes of ferrocenylimines {(C₅H₅)Fe[C₅H₄C(R)=NArHgCl]} (R = H, Ar = *o*-C₆H₄OCH₃^{5c} and R = Me, Ar = *o*-C₆H₄Cl^{5d}), respectively. The Hg–Cl distance in PhHgCl has not been reported, as the authors faced difficulty growing crystals.^{5b} The Hg–Br distance of 2.451(2) Å in **2b** compares well with those reported for PhHgBr (2.43 Å)^{5b}

and HgBr₂ (2.48 Å).^{1e} The Hg–I distance of 2.622(1) Å in **2c** may be compared with that reported for HgI₂ (2.78 Å),^{1e} although the latter distance corresponds to six-coordinate Hg(II); this distance has not been reported for PhHgI.^{5b} The ν_{Hg-X} values for **2a-c** (322, 234, and 170 cm⁻¹, respectively) are comparable to those reported for the PhHgX complexes (320, 259, and 170 cm⁻¹, respectively,⁶ indicating similar Hg–X bond strengths in the two series. The Hg–Cl distances in **2a-c** are similar [2.04(1), 2.07(1), and 2.02(1) Å, respectively], are all slightly shorter than the normal range for a mercury–carbon bond (2.05–2.10 Å),^{1a} and may be compared to those reported for {[PhCH₂NMe₂]-C₁N₂Hg} (2.10(2) Å)^{5g} and for the (ferrocenylimine)mercury(II) chloride complexes mentioned above (2.016 Å for R = H^{5c} and 2.037 Å for R = CH₃^{5d}). The Hg–Cl distance in **2b** [2.07(1) Å] may be compared with that reported for PhHgBr (2.08 Å).^{5b} The similar Hg–N distances in **2a-c** [2.65(1), 2.64(2), and 2.63(1) Å, respectively] are considerably shorter than the sum of the van der Waals radii for Hg (1.50 Å)^{5a,g,h} and N (1.55 Å)^{5a,i} and may be compared to such values as 2.89 Å reported for {[PhCH₂NMe₂]-C₁N₂Hg}^{5g} and 2.897 Å (R = H)^{5c} and 2.766 Å (R = CH₃)^{5d} for the ferrocenylimine compounds. According to the criteria suggested by Canty et al.,^{5h,i} the Hg–N distances in **2a-c** certainly constitute bonding (albeit weak) interactions.

The lability of the Hg–N bond is indicated by the temperature dependence of the NMe₂ resonances in the ¹H- and ¹³C-NMR spectra of (CD₃)₂CO solutions of **2a-c**. At 25 °C, only one resonance is observed for the C (δ 42.6) and H (δ 2.29) nuclei of the NMe₂ group which is possible only if the Hg–N bond is cleaved (structure 1) in solution at ambient temperatures so that the two Me groups become equivalent through rotation about the N–C7 bond, leading to pyramidal inversion of the N atom. However, at temperatures below –70 °C, two equally intense resonances are observed for both nuclei (¹³C δ 40.9, 44.5; ¹H δ 2.16, 2.53), indicating the nonequivalence of the two N-methyl groups due to blocked inversion of the N atom which results from its coordination to Hg.³ The ¹⁹⁹Hg δ values (neat Me₂Hg ref) for **2a-c** are –948.9, –1058.7, and –1246.6 ppm, respectively. The increased shielding of this signal (**2a** < **2b** < **2c**) may be explained in terms of decreased electronegativity of the halide (Cl > Br > I), making the Hg–X bond more covalent. In the variable temperature (VT) ¹⁹⁹Hg NMR spectra of compound **2a** (in acetone-*d*₆) only a single, broad resonance is observed, which progressively shifts upfield with decreasing temperature (from –948.9 ppm at 25 °C to –1009.5 ppm at –90 °C). This result is in agreement with a previous observation^{5j} that for unidentate and bidentate ligands for similar basicity (e.g., pyridine and bipyridine), chelation with bidentate ligands to give three-coordinate Hg results in upfield shifts of ¹⁹⁹Hg δ relative to those of linear complexes, indicating increased shielding of the Hg center. The broadness of the ¹⁹⁹Hg resonances (Δν_{1/2} = 100 Hz) may, however, be indicative of a very low-energy dynamic process attributable to the pyramidal inversion of the Hg atom as a stereocenter in **2a-c**. It should be noted, however, that it is difficult to draw definite conclusions since ¹⁹⁹Hg chemical shifts are

(6) (a) Barraclough, C. G.; Berkovic, G. E.; Deacon, G. B. *Aust. J. Chem.* **1977**, *30*, 1905. (b) Green, J. H. S. *Spectrochim. Acta* **1968**, *24A*, 863. (c) Goggin, P. L.; McEwan, D. M. *J. Chem. Res., Synop.* **1978**, 171.

Table 2. Selected Structural Parameters for Complexes 2a-c

X	bond lengths (Å)			bond angles (deg)			sum of angles around Hg (deg)	distance of Hg from the Cl-N-X plane (Å)
	Hg-X	Hg-Cl	Hg-N	X-Hg-Cl	X-Hg-N	Cl-Hg-N		
Cl	2.323(3)	2.04(1)	2.65(1)	174.2(3)	106.0(3)	74.5(4)	354.7	0.1087(4)
Br	2.451(2)	2.07(1)	2.64(2)	173.8(4)	104.9(3)	74.9(5)	353.6	0.1209(5)
I	2.622(1)	2.02(1)	2.63(1)	174.0(3)	104.1(3)	74.9(5)	353.0	0.1190(5)
av		2.04(2)	2.64(2)	174.0(4)	105.0(3)	74.8(4)	353.8	0.1162(5)

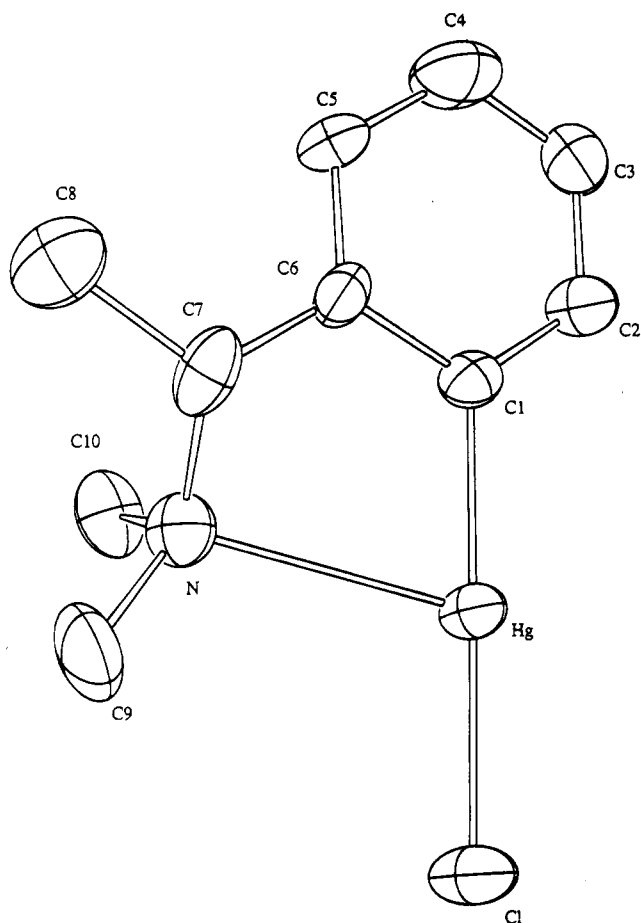


Figure 1. ORTEP drawing of [(*S*)-ArHgCl] (**2a**), showing the atom-numbering scheme (50% probability ellipsoids).

highly temperature and medium dependent, even for compounds that are inert toward coordination by donor molecules.

The optical activities of **2a-c** were determined by obtaining their room-temperature UV-vis and CD spectra (in EtOH) in the 200–300 nm region, which corresponds to $\pi-\pi^*$ transitions of the aryl (benzene) chromophore.^{7a} With respect to UV-vis spectra, all three complexes show absorption maxima with comparable λ_{max} values but different ϵ values; compared to the ϵ values of the free ligand (*S*)-ArH, those of **2a-c** are much greater. Compounds **2a-c** show CD spectra with the same rotational sense, i.e., positive Cotton effects are observed at the longest wavelength (by convention)^{7b} where any such effect is detectable (~ 273 nm). However, the positions of the absorption maxima and their corresponding values of molecular ellipticity $[\theta]_l$ are different for each compound. The CD spectrum of **2a** (Figure 2, curve 3) is representative; the $[\theta]_l$ values for all three compounds are summarized in the Experimental Section. For comparison, the CD spectra of the free

ligand (*S*)-ArH (curve 1), its enantiomer (*R*)-ArH (curve 2), and the enantiomer of complex **2a**, i.e., (*R*)-ArHgCl (curve 4), have also been included in Figure 2. Both the free ligands and their corresponding complexes show CD spectra with the same rotational sense, e.g., the CD spectra of both (*S*)-ArH (curve 1) and (*S*)-ArHgCl (curve 3) are positive at ~ 270 nm. However, from about 240 down to 200 nm, the curves corresponding to the two enantiomeric complexes (curves 3 and 4) are much enhanced and are of opposite rotational sense of those of their corresponding free ligands (curve 1 and 2, respectively). Since the lack of N-coordination at room temperature is established for these complexes (*vide supra*), the substantial changes in both the value and the sense of each CD curve can be accounted for only by the asymmetric perturbation in the electronic transitions of the aryl chromophore caused by Hg coordination to the ring carbon.

Finally, we raise the question of whether Hg can be considered a stereocenter in compounds **2a-c**. Our rationale is as follows. In the solid-state structures of **2a-c** (Table 2), the Hg atom deviates by an average of 0.12 Å from the mean plane defined by the X (= Cl, Br, I), N, and C1 atoms. The average value for the sum of the three angles around Hg [$353.7(5)^\circ$] is less than 360° (the value expected for a planar structure). Thus, the molecules are pyramidal, with Hg located at the apex of each pyramid and connected to three different groups. This is a situation similar to that in chiral tertiary amines or phosphines. The absolute configuration of the chiral benzylic carbon in **2a-c**, i.e., (*S*),^{7a,8a} is not affected by coordination of Hg to the aryl ring. Thus, we propose that the title compounds **2a-c**, and their (*R*)_C enantiomers, be considered diastereomeric complexes as they each contain two stereocenters in the solid state. The absolute configuration at Hg in each of the **2a-c** complexes is (*R*) assuming the following priority numbers:⁸ 1 (X = Cl, Br, I), 2 (N), 3 (Cl), and 4 (the apex of the pyramid). Therefore, one may designate **2a-c** as the (*S*)_C(*R*)_{Hg} diastereomers. This is another demonstration of how a single stereogenic center (i.e., the benzylic C atom) can determine the absolute configuration of a metal center (i.e., the Hg atom) in a cyclometalated chelate ring.^{9a} The single, broad resonance in the ¹⁹⁹Hg NMR spectrum of **2a** may be an average signal of two species, (*S*)_C(*R*)_{Hg} and (*S*)_C(*S*)_{Hg}, rapidly equilibrating through a pyramidal-like inversion at Hg with an activation barrier so low that the exchange can not be stopped (even at -90°C). A similar dynamic process, reported^{9b} for the mercury(II) chloride complex of *N,N,N',N'*-tetramethylethylenediamine (where the Hg atom is part of a five-membered ring), has a barrier of about 5–7 kcal/mol.

(8) (a) Cahn, R. S.; Ingold, C.; Prelog, V. *Angew. Chem., Int. Ed. Engl.* **1966**, *5*, 385. (b) Stanley, K.; Baird, M. C. *J. Am. Chem. Soc.* **1975**, *97*, 6598. (c) Sloan, T. E. *Top. Stereochem.* **1981**, *12*, 1.

(9) (a) Jastrzebski, J. T. B. H.; van Koten, G. *Adv. Organomet. Chem.* **1993**, *35*, 241. (b) Caulton, K. G. *Inorg. Nucl. Chem. Lett.* **1973**, *9*, 533.

(7) (a) Cymerman, C. J.; Chan, R. P. K.; Roy, S. K. *Tetrahedron* **1987**, *23*, 3573. (b) Djerassi, C.; Bunnenberg, E. *Proc. Chem. Soc.* **1963**, 299.

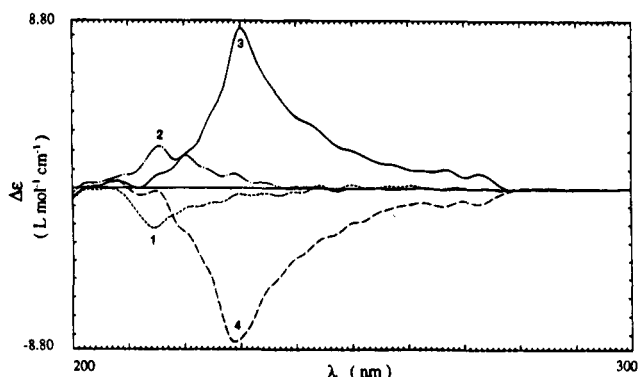


Figure 2. Circular dichroism (CD) curves of EtOH solutions of (S)-(-)-dimethyl(1-phenylethyl)amine, (S)-ArH (1, ---), its enantiomer (R)-ArH (2, - · - · -), the (S)-ArHgCl complex **2a** (3, —), and its enantiomer (R)-ArHgCl (4, - - -).

Experimental Section

A. Physical Measurements. NMR spectra were recorded on a Varian Unity Plus-500 spectrometer operating at 500 MHz for ^1H , 125 MHz for ^{13}C , and 89.4 MHz for ^{199}Hg . Infrared spectra were recorded on a Perkin-Elmer PE-1800 FT spectrometer for the far IR region (below 400 cm^{-1}) and a Perkin-Elmer Paragon 1000 PC FT spectrometer for the region $400\text{--}4000\text{ cm}^{-1}$. UV-visible spectra were recorded on a Perkin-Elmer Lambda-11 UV/VIS spectrophotometer. CD spectra were recorded on JASCO J-600 and/or J-40 spectropolarimeters.

B. Preparation of *o*-Lithio-(S)-(-)-dimethyl(1-phenylethyl)amine, (S)-ArLi.¹⁰ Under a dry dinitrogen atmosphere and utilizing standard Schlenk techniques, *tert*-butyllithium (125 mL of 1.7 M solution in pentane, 212 mmol) was added slowly *via* an addition funnel to (S)-(-)-dimethyl(1-phenylethyl)amine, (S)-ArH^{4b} (32 mL, 28.8 g, 193 mmol) in freshly-distilled hexane (40 mL), all at room temperature. A white solid was formed within 1 h. The reaction mixture was stirred for at least 15 h, after which the (S)-ArLi product was collected on a filter stick under high vacuum. It was then washed with several portions of freshly-distilled hexane to remove unreacted *t*-BuLi (until the pink filtrate became colorless), dried under vacuum, and transferred to a glovebox for further preparative work: yield 25.2 g (84.1%).

C. Preparation of (S)-ArHgCl, **2a.** Powdered HgCl_2 (43.2 g, 159 mmol) was slowly added over 1 h to a cooled ($-77\text{ }^\circ\text{C}$) suspension of (S)-ArLi (25.2 g, 162 mmol) in anhydrous Et_2O (250 mL) under a dry dinitrogen atmosphere. After the addition of HgCl_2 was complete, the mixture was gradually warmed up to room temperature and was stirred for an additional 5 h. The removal of LiCl by filtration through Celite and reduction of the colorless Et_2O filtrate under reduced pressure afforded the white microcrystalline product; this was recrystallized by rapid cooling of its hot hexane solution: yield 49.3 g (80.6%); mp $77\text{--}78\text{ }^\circ\text{C}$ (lit.³ $70\text{ }^\circ\text{C}$). NMR data: all spectra were obtained on acetone- d_6 solutions; ^1H (25 $^\circ\text{C}$, TMS ref) δ 1.33 (d, $^3J_{\text{HH}} = 6.5\text{ Hz}$, 3H, C- CH_3), 2.29 [s, 6H, $\text{N}(\text{CH}_3)_2$], 3.53 (q, $^3J_{\text{HH}} = 6.5\text{ Hz}$, 1H, C-H), 7.1-7.7 (m, 4H, C_6H_5); ^1H ($-77\text{ }^\circ\text{C}$) (spectrum similar to that at $25\text{ }^\circ\text{C}$ except that the singlet at δ 2.29 due to NMe_2 is split into two singlets at δ 2.16 and 2.53 (3H each)); ^{13}C ($25\text{ }^\circ\text{C}$, TMS ref) (numbering of C atoms follows that in the X-ray crystal structure, Figure 1a) δ 21.5 (C8), 42.6 (C9, C10 av), 66.6 (C7, $^3J_{\text{Hg-C}} = 93\text{ Hz}$), 127.7 (C3, $^3J_{\text{Hg-C}} = 213\text{ Hz}$), 129.1 (C5, $^3J_{\text{Hg-C}} = 169\text{ Hz}$), 129.2 (C4, $^4J_{\text{Hg-C}} = 33\text{ Hz}$), 138.3 (C2, $^2J_{\text{Hg-C}} = 136\text{ Hz}$), 148.7 (C1, $^1J_{\text{Hg-C}} = 2541\text{ Hz}$), 151.6 (C6, $^2J_{\text{Hg-C}} = 52\text{ Hz}$); ^{13}C ($-77\text{ }^\circ\text{C}$) (spectrum similar to that at $25\text{ }^\circ\text{C}$ except for two singlets at δ 40.9 and 44.5 (C9 and C10) due to splitting of the NMe_2 singlet

at δ 42.6); VT ^{199}Hg (neat Me_2Hg ref) δ -948.9 ($25\text{ }^\circ\text{C}$, $\Delta\nu_{1/2} = 100\text{ Hz}$), -952.4 ($0\text{ }^\circ\text{C}$), -955.6 ($-15\text{ }^\circ\text{C}$), -957.7 ($-40\text{ }^\circ\text{C}$), -1009.5 ($-70\text{ }^\circ\text{C}$) and constant at this value from -70 to $-90\text{ }^\circ\text{C}$. IR Data: $\nu_{\text{Hg-Cl}}$ 322 cm^{-1} (strong and very sharp) with a shoulder at 307 cm^{-1} due to the $\text{Hg-}^{37}\text{Cl}$ stretch (Nujol mull on polyethylene sheet); $\nu_{\text{Hg-N}}$ 491 cm^{-1} (weak; Nujol mull between NaCl plates). UV-vis data: for the free ligand (S)-ArH ($c = 1.1 \times 10^{-4}\text{ M}$ in EtOH, $25\text{ }^\circ\text{C}$) λ_{max} (nm)/ ϵ ($\text{L mol}^{-1}\text{ cm}^{-1}$), 272/0.80, 267/2.4, 264/3.2, 258/6.3, 252/7.9, 207/1.3 $\times 10^3$; for **2a** ($c = 8.1 \times 10^{-6}\text{ M}$ in EtOH, $25\text{ }^\circ\text{C}$) λ_{max} (nm)/ ϵ ($\text{L mol}^{-1}\text{ cm}^{-1}$), 273/2.4 $\times 10^3$, 257/5.0 $\times 10^3$, 246/7.6 $\times 10^3$, 229/1.7 $\times 10^4$, 201/7.8 $\times 10^5$. CD data: since CD curves of enantiomeric pairs agreed to within 5% (Figure 2), only that of the (S)-enantiomer of the ligand [(S)-ArH] and its corresponding complex [(S)-ArHgCl], **2a**, are described here as molecular ellipticity $[\theta]_\lambda$ (in units of $\text{deg cm}^2/\text{dmol}$), where $[\theta]_\lambda = 3300 \times (\Delta\epsilon)_\lambda$ and $(\Delta\epsilon)_\lambda$ is the measured CD quantity (in units of $\text{L mol}^{-1}\text{ cm}^{-1}$) at a given wavelength; $c = 0.011\text{ M}$ in EtOH at $25\text{ }^\circ\text{C}$ for both (S)-ArH and (S)-ArHgCl. For (S)-ArH: $[\theta]_{290} = 0$, $[\theta]_{285} = +254$, $[\theta]_{279} = -190$, $[\theta]_{273} = 0$, $[\theta]_{268} = +508$, $[\theta]_{261} = +762$, $[\theta]_{256} = +635$, $[\theta]_{250} = +888$, $[\theta]_{244} = +698$, $[\theta]_{241} = -825$, $[\theta]_{237} = -1320$, $[\theta]_{230} = -1206$, $[\theta]_{226} = -2665$, $[\theta]_{223} = -3427$, $[\theta]_{216} = -7260$. For (S)-ArHgCl (**2a**), $[\theta]_{290} = 0$, $[\theta]_{273} = +2723$, $[\theta]_{268} = +3960$, $[\theta]_{258} = +4208$, $[\theta]_{250} = +6930$, $[\theta]_{241} = +11\,138$, $[\theta]_{230} = +27\,638$, $[\theta]_{226} = +14\,438$, $[\theta]_{223} = +7343$, $[\theta]_{216} = +2723$.

D. Preparation of (S)-ArHgX Compounds **2b,c.** (i) Synthesis and Characterization of **2b** (X = Br). To a stirred solution of **2a** (1.0 g, 2.6 mmol) in 95% EtOH (100 mL) was added solid NaBr (2.68 g, 26 mmol), and the resulting cloudy, white mixture was stirred for 1 h at room temperature. The mixture was then taken to dryness under reduced pressure, and the product was extracted with CH_2Cl_2 . Volume reduction of this extract afforded **2b** as a white microcrystalline solid: yield 0.95 g (85.6%); mp $89\text{--}90\text{ }^\circ\text{C}$. NMR data: all spectra were obtained on acetone- d_6 solutions; ^1H (25 and $-70\text{ }^\circ\text{C}$) (these spectra were identical in shape and δ values to those described for **2a** above); ^{13}C ($25\text{ }^\circ\text{C}$) (numbering of C atom follows that in the X-ray crystal structure for **2a**, Figure 1a) δ 21.6 (C8), 42.6 (C9, C10 av), 66.9 (C7, $^3J_{\text{Hg-C}} = 92\text{ Hz}$), 127.8 (C3, $^3J_{\text{Hg-C}} = 211\text{ Hz}$), 129.1 (C5, $^3J_{\text{Hg-C}} = 168\text{ Hz}$), 129.2 (C4, $^4J_{\text{Hg-C}} = 31\text{ Hz}$), 138.2 (C2, $^2J_{\text{Hg-C}} = 138\text{ Hz}$), 152.5 (C1, $^1J_{\text{Hg-C}} = 2462\text{ Hz}$), 151.9 (C6, $^2J_{\text{Hg-C}} = 52\text{ Hz}$); ^{13}C ($-77\text{ }^\circ\text{C}$) (spectrum similar to that of **2a** at this temp); VT ^{199}Hg δ -1058.7 ($25\text{ }^\circ\text{C}$), similar behavior to that of **2a** from 25 to $-90\text{ }^\circ\text{C}$. IR data: $\nu_{\text{Hg-Br}}$ 234 cm^{-1} (strong and sharp; Nujol mull on polyethylene sheet); $\nu_{\text{Hg-N}}$ 490 cm^{-1} (weak; Nujol mull between NaCl plates). UV-vis data ($c = 8.1 \times 10^{-6}\text{ M}$ in EtOH, $25\text{ }^\circ\text{C}$) λ_{max} (nm)/ ϵ ($\text{L mol}^{-1}\text{ cm}^{-1}$): 230/8.1 $\times 10^3$, 201/1.3 $\times 10^5$. CD data ($c = 8.1 \times 10^{-3}\text{ M}$ in EtOH, $25\text{ }^\circ\text{C}$) $[\theta]_\lambda$ (in units of $\text{deg cm}^2/\text{dmol}$), $[\theta]_{290} = 0$, $[\theta]_{273} = +2000$, $[\theta]_{266} = +3000$, $[\theta]_{246} = +7250$, $[\theta]_{236} = +16\,250$, $[\theta]_{232} = +15\,500$, $[\theta]_{229} = +16\,500$, $[\theta]_{228} = +13\,500$, $[\theta]_{227} = +12\,250$, $[\theta]_{222} = -1000$, $[\theta]_{221} = -3000$, $[\theta]_{218} = +4500$, $[\theta]_{214} = +1500$, $[\theta]_{212} = +1250$, $[\theta]_{211} = 0$, $[\theta]_{208} = +3750$, $[\theta]_{204} = +5000$, $[\theta]_{202} = +750$.

(ii) Synthesis and Characterization of **2c** (X = I). A procedure similar to that for the preparation of **2b** was followed, except that NaBr was replaced with NaI. Compound **2c** was obtained as a beige microcrystalline solid: yield 0.97 g (78.3%); mp $81\text{--}83\text{ }^\circ\text{C}$. NMR Data: all spectra were obtained on acetone- d_6 solutions; ^1H (25 and $-70\text{ }^\circ\text{C}$) (these spectra were identical in shape and δ values to those described for both **2a** and **2b** above); ^{13}C ($25\text{ }^\circ\text{C}$) (numbering of C atoms follows that in the X-ray crystal structure for **2a**, Figure 1a) δ 21.8 (C8), 42.6 (C9, C10 av), 66.7 (C7, $^3J_{\text{Hg-C}} = 88\text{ Hz}$), 127.7 (C3, $^3J_{\text{Hg-C}} = 204\text{ Hz}$), 129.1 (C5, $^3J_{\text{Hg-C}} = 161\text{ Hz}$), 129.1 (C4, $^4J_{\text{Hg-C}} = 29\text{ Hz}$), 138.1 (C2, $^2J_{\text{Hg-C}} = 137\text{ Hz}$), 159.2 (C1, $^1J_{\text{Hg-C}} = 2347\text{ Hz}$), 152.3 (C6, $^2J_{\text{Hg-C}} = 50\text{ Hz}$); ^{13}C ($-77\text{ }^\circ\text{C}$) (not obtainable due to precipitation of **2c** at temperatures below $0\text{ }^\circ\text{C}$); ^{199}Hg ($25\text{ }^\circ\text{C}$) δ -1246.6 . IR data: $\nu_{\text{Hg-I}}$ 170 cm^{-1} (weak; Nujol mull on polyethylene sheet); $\nu_{\text{Hg-N}}$ 489 cm^{-1} (weak; Nujol mull between NaCl plates). UV-vis Data: ($c = 8.1 \times 10^{-6}\text{ M}$

(10) Van Koten, G.; Jastrzebski, J. T. B. H. *Tetrahedron* **1989**, *45*, 569.

in EtOH, 25 °C), λ_{\max} (nm)/ ϵ (L mol⁻¹ cm⁻¹): 233/1.6 \times 10⁴, 201/1.3 \times 10⁵. CD data: ($c = 8.1 \times 10^{-3}$ M in EtOH, 25 °C), $[\theta]_{\lambda}$ (in units of deg cm²/dmol) $[\theta]_{290} = 0$, $[\theta]_{273} = +4000$, $[\theta]_{267} = +5000$, $[\theta]_{255} = +6000$, $[\theta]_{252} = +10\ 000$, $[\theta]_{247} = +11\ 000$, $[\theta]_{246} = +13\ 000$, $[\theta]_{242} = 0$, $[\theta]_{238} = -4000$, $[\theta]_{234} = -5250$, $[\theta]_{231} = -6000$, $[\theta]_{228} = -3500$, $[\theta]_{225} = -2000$, $[\theta]_{224} = +3000$, $[\theta]_{222} = +9000$, $[\theta]_{218} = +13\ 500$, $[\theta]_{213} = +15\ 000$, $[\theta]_{209} = -18\ 500$, $[\theta]_{208} = +12\ 000$, $[\theta]_{206} = +6500$, $[\theta]_{204} = +3000$, $[\theta]_{201} = -10\ 000$.

E. X-ray Data Collection and Processing. Colorless needles of **2a–c** were obtained by slow evaporation of hexane solutions of each. Crystal data and details of data collection are given in Table 1. The samples were studied on an Enraf-Nonius CAD4F diffractometer with graphite-monochromated Mo K α radiation. Quantitative data were obtained at 293 K in the θ - 2θ mode. The resulting data sets were transferred to a VAX computer, and for all subsequent calculations the Enraf-Nonius SDP/VAX package¹¹ was used. Three standard reflections measured every 1 h during the entire data collection period showed no significant trends. The raw data were converted to intensities and corrected for Lorentz, polarization, and absorption effects using ψ scans of four reflections ($14 < \theta < 16^\circ$). The structures were solved by the heavy-atom method. After refinement of the heavy atoms, difference-

Fourier maps revealed maximas of residual electronic density close to the positions expected for hydrogen atoms. They were introduced in the structure calculations by their computed coordinates (C–H = 0.95 Å) with isotropic temperature factors such as $B(\text{H}) = 1.38B_{\text{eq}}(\text{C})$ Å² but not refined. The atomic positional and thermal parameters and the extinction parameters were refined by full-matrix least-squares methods. The scattering factor coefficients and anomalous dispersion coefficients come, respectively, from parts a and b of ref 12.

Acknowledgment. We would like to thank Prof. David A. Lightner for his generous permission to use the JASCO spectropolarimeters and also Dr. Stefan Boiadjiev for helpful discussions on CD techniques and spectra. The financial support of the Petroleum Research Fund, administered by the American Chemical Society, is gratefully acknowledged.

Supporting Information Available: Tables of X-ray crystallographic data, including atomic coordinates, interatomic distances and angles, and anisotropic thermal parameters for compounds **2a–c** (12 pages). Ordering information is given on any current masthead page.

OM950021F

(11) Frenz, B. A. *The Enraf-Nonius CAD4-SPD in Computing in Crystallography*; Shenk, H., Olthof-Hazekamp, H., van Koningsveld, H., Bassi, G. C., Eds.; Delft University Press: Delft, The Netherlands, 1978; pp 64–71.

(12) (a) Cromer, D. T.; Waber, J. T. *International Tables for X-ray Crystallography*; Kynoch Press: Birmingham, England, 1974; Vol. IV, Table 2.2b; (b) Table 2.3.1.

1,3-Dipolar Cycloaddition Reactions to the C=X-M Fragment. 15. Reaction of Ru(CO)₃(*i*-Pr-DAB) with the Electron-Deficient Alkenes Dimethyl Maleate and Dimethyl Fumarate. CO Substitution versus 1,3-Dipolar Cycloaddition

Maarten van Wijnkoop, Paul P. M. de Lange, Hans-Werner Frühauf,* and Kees Vrieze

Laboratorium voor Anorganische Chemie, J. H. van 't Hoff Instituut, Universiteit van Amsterdam, Nieuwe Achtergracht 166, 1018 WV Amsterdam, The Netherlands

Wilberth J. J. Smeets and Anthony L. Spek

Bijvoet Center for Biomolecular Research, Vakgroep Kristal- en Structuurchemie, Universiteit Utrecht, Padualaan 8, 3584 CH Utrecht, The Netherlands

Received May 22, 1995[⊙]

In situ prepared Ru(CO)₃(*i*-Pr-DAB) reacts with dimethyl maleate at ca. -30 °C. When the reaction mixture is warmed up to room temperature under an atmosphere of CO (1.1 bar), the ruthenabicyclo[2.2.2] complex **10a** is obtained in ≤90% yield. Complex **10a** has been characterized both spectroscopically (IR, ¹H and ¹³C NMR) and by X-ray structure determination; **10a** has a [2.2.2]bicyclic structure in which the bridgehead positions are occupied by the ruthenium atom and the C-C-coupled former imine carbon atom. If the reaction is performed in the absence of CO as an additional ligand, a small amount (up to 10%) of the CO-substitution product Ru(CO)₂(η²-dimethyl maleate)(*i*-Pr-DAB) (**12a**) is formed. The reaction of Ru(CO)₃(*i*-Pr-DAB) with dimethyl fumarate at -50 °C with consequent warming to ambient temperatures gives rise to a complex product mixture from which the bicyclo[2.2.2]Ru(CO)₂ complex **9b** (50%–60% yield) and Ru(CO)₂(η²-dimethyl fumarate)(*i*-Pr-DAB) (**12b**, 15%–20% yield) can be isolated. Complexes **9b** and **12b** have been characterized spectroscopically (IR, ¹H and ¹³C NMR) and by elemental analyses. The molecular structure of **12b** has been determined by single-crystal X-ray diffraction. The coordination geometry around the central ruthenium atom in **12b** is distorted trigonal bipyramidal, with the two imine N-donor atoms occupying an equatorial and an axial position and the alkene in the equatorial plane. In solution complex **12b** shows a dynamic behavior, which is interpreted in terms of a coupled alkene rotation–Berry pseudorotation.

Introduction

Over the past years, the reactivity of R-DAB¹-containing transition metal complexes toward unsaturated substrates, especially with respect to C–C and C–N bond formation, has been studied extensively in our laboratory.² The current research has focused on the reactions of mononuclear M(CO)_{3-n}(CNR)_n(R-DAB) (M = Fe, Ru; n = 0, 1) complexes with the activated

alkynes, dimethyl acetylenedicarboxylate (DMADC) and methylpropynoate (MP), which are depicted in Scheme 1.³ The initial step in these reactions is described as an oxidative 1,3-dipolar [3+2] cycloaddition of the activated alkyne (the dipolarophile) to the M–N=C fragment (the 1,3-dipole), which results in formation of the bicyclo[2.2.1] intermediate (**2**). The subsequent reaction of intermediate **2** proceeds either inter- or intramolecularly, depending on the metal, on L, and on the other reactants present in solution (cf. Scheme 1).

For the Fe(CO)₃(R-DAB) complexes the 1,3-dipolar reactivity is restricted to activated alkynes such as

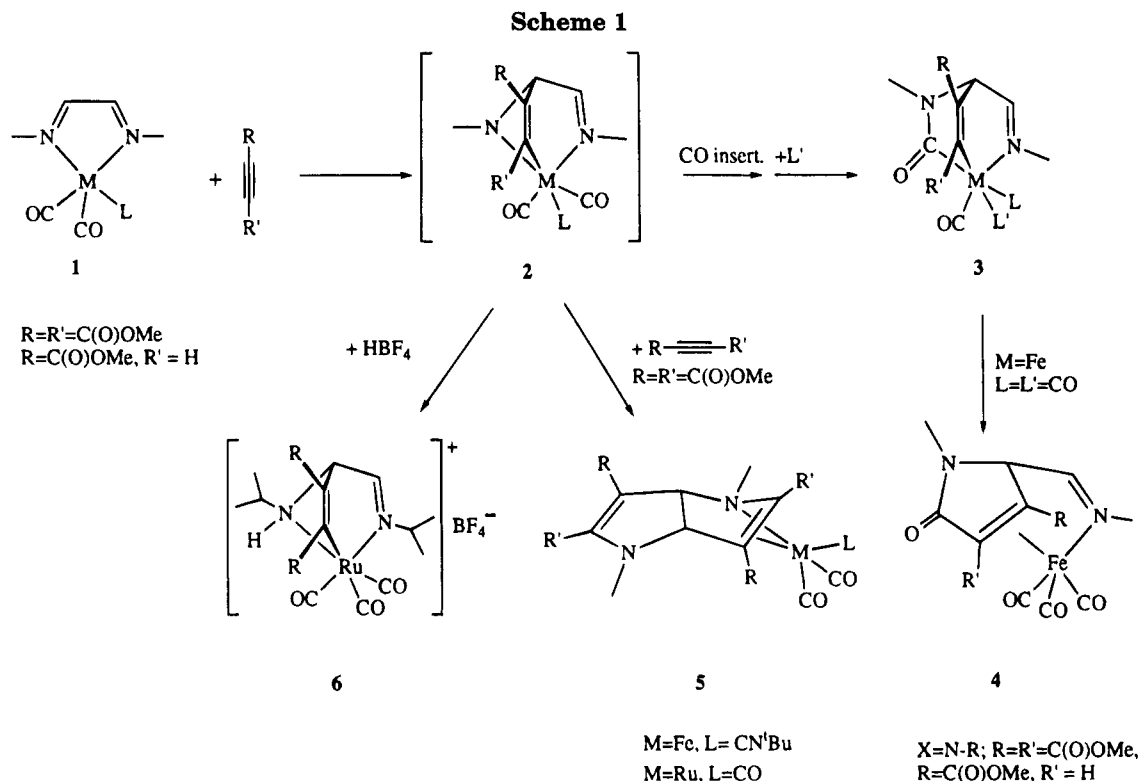
* To whom correspondence should be addressed.

[⊙] Abstract published in *Advance ACS Abstracts*, September 1, 1995.

(1) The abbreviations used throughout this text are as follows. The 1,4-diaza-1,3-butadienes of formula RN=C(H)–C(H)=NR are abbreviated as R-DAB. R-ADA stands for 1,6-di-R-1,6-diazahexa-1,5-diene-3,4-di-R-aminato, RN=C(H)(H)C(NR)(H)C(NR)C(H)=NR, the reductively C–C-coupled formally dianionic dimer of R-DAB ligated to two metal atoms. THPP stands for 1,4,3a,6a-tetrahydropyrrolo[3,2-*b*]pyrrole (Hantzsch–Widman nomenclature). Dimethyl acetylene dicarboxylate and methyl propynoate are abbreviated as DMADC and MP, respectively.

(2) (a) Keijsper, J.; Polm, L. H.; van Koten, G.; Vrieze, K.; Stam, C. H.; Schagen, J.-D. *Inorg. Chim. Acta* **1985**, *103*, 137. (b) Staal, L. H.; Polm, L. H.; Balk, R. W.; van Koten, G.; Vrieze, K.; Brouwers, A. M. F. *Inorg. Chem.* **1980**, *19*, 3343. (c) Keijsper, J.; Polm, L. H.; van Koten, G.; Vrieze, K.; Abbel, G.; Stam, C. H. *Inorg. Chem.* **1984**, *23*, 2142. (d) Staal, L. H.; van Koten, G.; Vrieze, K.; van Santen, B.; Stam, C. H. *Inorg. Chem.* **1981**, *20*, 3598. (e) Muller, F.; Dijkhuis, D. I. P.; van Koten, G.; Vrieze, K.; Heijdenrijk, D.; Rotteveel, M. A.; Stam, C. H.; Zoutberg, M. C. *Organometallics* **1989**, *8*, 992.

(3) (a) Part 6: de Lange, P. P. M.; Frühauf, H.-W.; van Wijnkoop, M.; Vrieze, K.; Wang, Y.; Heijdenrijk, D.; Stam, C. H. *Organometallics* **1990**, *9*, 1691. (b) Part 7: van Wijnkoop, M.; de Lange, P. P. M.; Frühauf, H.-W.; Wang, Y.; Goubitz, K.; Stam, C. H. *Organometallics* **1992**, *11*, 3607. (c) Part 8: de Lange, P. P. M.; Frühauf, H.-W.; van Wijnkoop, M.; Kraakman, M. J. A.; Kranenburg, M.; Groot, H. J. P.; Vrieze, K.; Fraanje, J.; Wang, Y.; Numan, M. *Organometallics* **1993**, *12*, 417. (d) Part 10: de Lange, P. P. M.; van Wijnkoop, M.; Frühauf, H.-W.; Vrieze, K.; Goubitz, K. *Organometallics* **1993**, *12*, 428. (e) Part 11: de Lange, P. P. M.; de Boer, R. P.; van Wijnkoop, M.; Ernsting, J. M.; Frühauf, H.-W.; Vrieze, K.; Smeets, W. J. J.; Spek, A. L.; Goubitz, K. *Organometallics* **1993**, *12*, 440. de Boer, R. P.; de Lange, P. P. M.; Frühauf, H.-W.; Vrieze, K. *J. Chem. Soc., Chem. Commun.* **1992**, 580. (f) Part 12: de Lange, P. P. M.; Alberts, E.; van Wijnkoop, M.; Frühauf, H.-W.; Vrieze, K.; Kooijman, H.; Spek, A. L. *J. Organomet. Chem.* **1994**, *465*, 241.



DMADC and MP. With alkenes such as dimethyl maleate and dimethyl fumarate, two well-known electrophilic dipolarophiles, no cycloaddition reaction is observed. Irradiation of $\text{Fe}(\text{CO})_3(\text{R-DAB})$ in the presence of the latter alkenes on the other hand results in formation of the CO-substitution products $\text{Fe}(\text{CO})_2(\eta^2\text{-alkene})(\text{R-DAB})$.⁴

As has been shown previously⁵ the M-N=C fragment can be characterized as a nucleophilic or type I dipole.⁶ Cycloaddition reactions of a nucleophilic 1,3-dipole are HOMO controlled, i.e., the interaction of the dipole HOMO with the dipolarophile LUMO is predominant. Consequently the reactivity will be enhanced by an increase of the dipole HOMO. We found that this could be achieved in two ways: (i) in the case of $M = \text{Fe}$ by increasing the electron density on the dipole by introducing one or more better σ -donating coligands (CNR instead of CO)^{3a,c-f} and (ii) by exchanging the central metal atom Fe for Ru.⁷ The increased reactivity of $\text{Ru}(\text{CO})_3(i\text{-Pr-DAB})$ ^{3b} is expressed by a significantly lower activation energy for the cycloaddition reaction with DMADC. Furthermore, in the reaction of $\text{Ru}(\text{CO})_3(i\text{-Pr-DAB})$ with excess DMADC, the intact $\text{Ru}(\text{II})\text{-N=C}$ unit of intermediate **2** is evidently activated enough to undergo a second cycloaddition reaction, which finally

results in formation of compound **5**. This reaction is also encountered for the activated $\text{Fe}(\text{CO})_2(\text{CNR})(i\text{-Pr-DAB})$ complexes.^{3a,c} The increased reactivity toward alkynes prompted us to investigate the reactivity of $\text{Ru}(\text{CO})_3(i\text{-Pr-DAB})$ toward the alkenes dimethyl maleate and dimethyl fumarate. De Lange et al. reported on the reactions of highly activated $\text{Fe}(\text{CNR})_3(i\text{-Pr-DAB})$ with dimethyl maleate.^{3e} When an aromatic isocyanide is used, a cycloaddition reaction occurs, resulting in the formation of a bicyclo[2.2.2] $\text{Fe}(\text{CNR})_3$ complex (see Figure 1). This complex however is thermally unstable and reacts at elevated temperature back to its starting components by means of an unprecedented isocyanide deinsertion and a cycloreversion reaction.

The present article describes the reactions of $\text{Ru}(\text{CO})_3(i\text{-Pr-DAB})$ with dimethyl maleate and dimethyl fumarate. In these reactions two different pathways are followed. The main reaction is a 1,3-dipolar cycloaddition, which gives rise to formation of ruthenabicyclo[2.2.2] complexes (**9** and **10**). This reaction is accompanied by a side reaction, in which a terminal carbonyl ligand is substituted by the alkene, resulting in the formation of $\text{Ru}(\text{CO})_2(\eta^2\text{-alkene})(i\text{-Pr-DAB})$ (**12**). The X-ray crystal structures of both types of complexes will be discussed.

Experimental Section

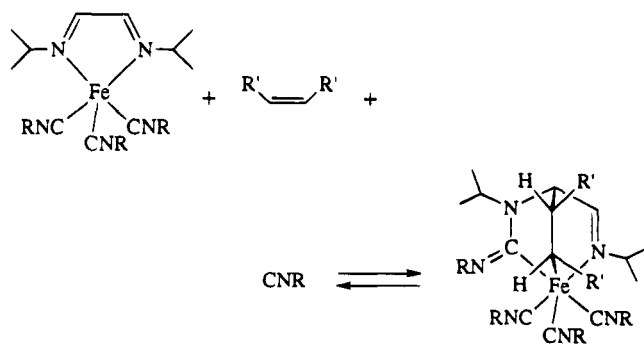
Materials and Apparatus. ¹H and ¹³C NMR spectra were obtained on a Bruker AMX 300 spectrometer. IR spectra were recorded with a Perkin-Elmer 283 instrument, using matched NaCl cells. Elemental analyses were carried out by Dornis u. Kolbe, Microanalytisches Laboratorium, Mülheim a. d. Ruhr, Germany. The solvents were carefully dried and distilled under nitrogen prior to use. All preparations were carried out under an atmosphere of dry nitrogen by conventional Schlenk techniques. Silica gel for column chromatography (Kieselgel 60, 70–230 mesh, E. Merck, Darmstadt, Germany) was dried and activated prior to use. $\text{Ru}_3(\text{CO})_{12}$ (Strem Chemicals, Inc.),

(4) Frühauf, H.-W.; Pein, I.; Seils, F. *Organometallics* **1987**, *6*, 1613.

(5) This is based on the following: (i) the finding that the reactivity is restricted to electron-deficient alkynes and (ii) preliminary CAS-SCF calculations,²⁹ which show comparably high-lying HOMO and LUMO levels for both the $d^8\text{-ML}_4$ M-N=C dipole and the isolobally related organic azomethine ylide. See refs 3b,c,e.

(6) Application of the frontier molecular orbital theory to 1,3-dipolar cycloadditions by Sustmann provides a semiquantitative classification of these cycloadditions into three types depending on the relative disposition of the 1,3-dipole and the dipolarophile frontier orbitals. (a) Sustmann, R. *Tetrahedron Lett.* **1971**, 2717. (b) Sustmann, R.; Trill, H. *Angew. Chem., Int. Ed. Engl.* **1972**, *11*, 838. (c) Sustmann, R. *Pure Appl. Chem.* **1974**, *40*, 569.

(7) Whether this is solely a consequence of an increase in the dipole HOMO level or also the result of other (steric) contributions is not completely clear. A more detailed discussion is presented in this article in the section on complex formation.



R = 2,6-xylyl, R' = C(O)OMe

Figure 1. Reversible cycloaddition of $\text{Fe}(\text{CNR})_3(i\text{-Pr-DAB})$ with DMM (after ref 3e).

dimethyl maleate (Janssen), and dimethyl fumarate were purchased commercially and used without purification. $\text{Ru}_2(\text{CO})_5(i\text{-Pr-ADA})$ was prepared from $\text{Ru}_3(\text{CO})_{12}$ and $i\text{-Pr-DAB}$ by published procedures.⁸ For the preparation of $\text{Ru}(\text{CO})_3(i\text{-Pr-DAB})$ the following procedure was used.⁹ A suspension of 0.47 g (0.75 mmol) $\text{Ru}_2(\text{CO})_5(i\text{-Pr-ADA})$ in 120 mL of toluene was stirred under an atmosphere of CO (1.1 bar) for 15 min at 95 °C. During the reaction the color of the solution turned from orange to intense red, and IR spectroscopy revealed an almost quantitative conversion of the starting compound to $\text{Ru}(\text{CO})_3(i\text{-Pr-DAB})$ (>95%). Since on removal of the solvent under reduced pressure CO is split off and $\text{Ru}_2(\text{CO})_5(i\text{-Pr-ADA})$ is reformed, the reactions of $\text{Ru}(\text{CO})_3(i\text{-Pr-DAB})$ with the alkenes were carried out without isolation of the mononuclear complex.

Synthesis of Bicyclo[2.2.2] $\text{Ru}(\text{CO})_2$ (9b) and $\text{Ru}(\text{CO})_2$ (η^2 -dimethyl fumarate)($i\text{-Pr-DAB}$) (12b). A freshly prepared solution of 1.5 mmol $\text{Ru}(\text{CO})_3(i\text{-Pr-DAB})$ in 120 mL of toluene (*vide supra*) was cooled to ca. -50 °C, and a solution of 216 mg (1.5 mmol) of dimethyl fumarate in 10 mL of toluene was added dropwise during 30 min. The red reaction mixture was warmed up to room temperature and stirred for an additional 3 h. After the solvent was evaporated to dryness, the product mixture was redissolved in 1–2 mL of CH_2Cl_2 and separated by column chromatography on silica gel. Elution with diethyl ether afforded a red fraction containing **12b**. After removal of the solvent, **12b** was obtained as red powder in a 15%–20% yield. Subsequent elution with CH_2Cl_2 gave a light brown fraction containing **9b**. After removal of the solvent, the residue was washed twice with 10 mL of diethyl ether and dried in vacuo. Complex **9b** was obtained as off-white powder in 50%–60% yield.

Crystals of **12b**, suitable for X-ray diffraction, were obtained from a saturated solution of the complex in diethyl ether/pentane (1:1) at -30 °C. Anal. Found (calcd) for $\text{C}_{17}\text{H}_{24}\text{N}_2\text{O}_7\text{Ru}$, **9b**: C, 43.42 (43.49); H, 5.21 (5.16); N, 5.95 (5.97). Anal. Found (calcd) for $\text{C}_{16}\text{H}_{24}\text{N}_2\text{O}_6\text{Ru}$, **12b**: C, 43.61 (43.53); H, 5.55 (5.48); N, 6.40 (6.35).

Synthesis of Bicyclo[2.2.2] $\text{Ru}(\text{CO})_3$ (10a). A freshly prepared solution of 1.5 mmol $\text{Ru}(\text{CO})_3(i\text{-Pr-DAB})$ in 120 mL of toluene (*vide supra*) was cooled to -30 °C, and a solution of 186 μL (1.5 mmol) of dimethyl maleate in 10 mL of toluene was added dropwise during 30 min. The light brown reaction mixture was warmed up to room temperature under an atmosphere of CO (1.1 bar) and stirred for an additional 3 h. After the solvent was evaporated to dryness, the residue was redissolved in 1–2 mL of CH_2Cl_2 and purified by column chromatography on silica gel. Elution with CH_2Cl_2 /diethyl ether (1:1) afforded a colorless fraction that contained the

Table 1. Crystallographic Data and Details of Data Collection and Refinement for Complexes **10a** and **12b**

	10a	12b
(a) Crystal Data		
formula	$\text{C}_{18}\text{H}_{24}\text{N}_2\text{O}_8\text{Ru}$	$\text{C}_{16}\text{H}_{24}\text{N}_2\text{O}_6\text{Ru}$
M_w	497.47	441.45
cryst syst	monoclinic	monoclinic
space group	$C2/c$	$P2_1/n$
a, b, c (Å)	24.440(2), 11.286(1), 18.286(1)	12.701(1), 9.361(1), 16.426(1)
β (deg)	115.92(1)	99.44(1)
V (Å ³)	4536.4(7)	1926.5(3)
Z	8	4
D_{calcd} (g/cm ³)	1.457	1.522
$F(000)$	2032	904
μ (cm ⁻¹)	7.2	8.3
cryst size (mm ³)	0.53 × 0.20 × 0.10	0.12 × 0.22 × 0.50
(b) Data Collection		
temp (K)	295	100
$\theta_{\text{min}}, \theta_{\text{max}}$	1.24, 27.50	1.26, 27.50
radiation	Mo K α	Mo K α (Zr-filtered), 0.710 73 Å
scan type	$\omega/2\theta$	$\omega/2\theta$
$\Delta\omega$ (deg)	0.56 + 0.35 tan θ	0.93 + 0.35 tan θ
horiz and vert aperture (mm)	5.2, 4.0	3.0, 5.0
cryst to detector dist (mm)	173	173
ref reflns	-6 -2 5; -5 1 7; -8 2 7	-2 0 6; 3 2 -2; -3 2 2
data set	h -32:29; k -14:14; l -24:23	h -16:16; k 0:12; l -21:21
tot. no. of data	15607	5274
tot. no. of unique data	5199	4419
no. of obsd data ($I > 2.5\sigma(I)$)	4045	3729
(c) Refinement		
no. of refined params	281	246
weighting scheme	$w = 1/\sigma^2(F)$	$w = 1/\sigma^2(F)$
final R, R_w, S	0.0273, 0.0237, 1.67	0.030, 0.034, 1.40
$(\Delta/\sigma)_{\text{av}}$ in final cycle	0.03	0.01
res density (min, max) e Å ⁻³	-0.28, 0.28	-1.03, 1.49

product. After removal of the solvent, complex **10a** was obtained as white powder in 85%–90% yield. Crystals suitable for X-ray diffraction were obtained from a saturated solution of **10a** in CH_2Cl_2 /diethyl ether (1:1) or CH_2Cl_2 /pentane (3:1) at -20 °C. Anal. Found (calcd) for $\text{C}_{18}\text{H}_{24}\text{N}_2\text{O}_8\text{Ru}$, **10a**: C, 43.55 (43.46); H, 4.92 (4.87); N, 5.69 (5.63).

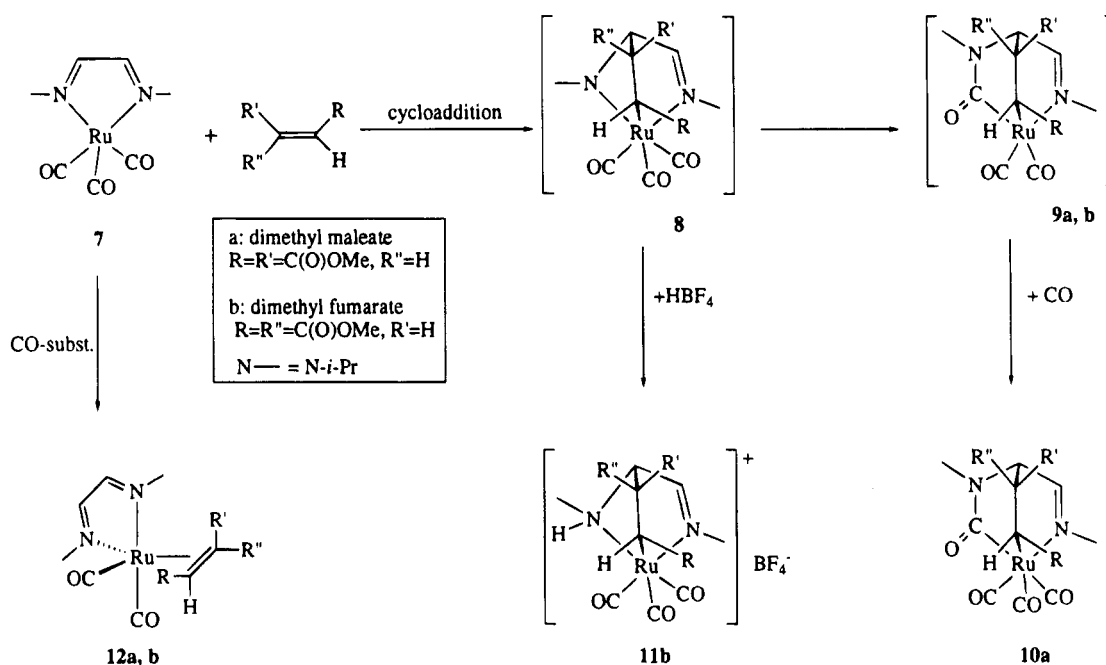
Synthesis of Bicyclo[2.2.1] $\text{Ru}(\text{CO})_3]^+\text{BF}_4^-$ (11b). A freshly prepared solution of 1.5 mmol $\text{Ru}(\text{CO})_3(i\text{-Pr-DAB})$ in 120 mL of toluene (*vide supra*) was cooled to -50 °C, and a solution of 216 mg (1.5 mmol) of dimethyl fumarate in 10 mL of toluene was added. Upon subsequent addition of 0.3 mL of a solution of HBF_4 in diethyl ether (54%) to the reaction mixture a yellow precipitate was formed. After this mixture was warmed to room temperature, the solvent was decanted and the precipitate was washed twice with 20 mL of diethyl ether. The residue was redissolved in 2–3 mL of CH_2Cl_2 and was again precipitated with 20 mL of diethyl ether. After removal of the supernatant, the precipitate was dried in vacuo yielding 70%–75% of yellowish-white **11b**. Further purification by recrystallization from CH_2Cl_2 /diethyl ether (1:3) at -30 °C afforded **11b** as an off-white microcrystalline powder. Anal. Found (calcd) for $\text{C}_{17}\text{H}_{25}\text{N}_2\text{O}_7\text{BF}_4\text{Ru}$, **11b**: C, 36.48 (36.64); H, 4.58 (4.53); N, 5.01 (5.03).

Crystal Structure Determination of 10a. Crystal data and numerical details of the structure determination are given in Table 1. A yellowish plate-shaped crystal was mounted on top of a glass-fiber and transferred to an Enraf-Nonius CAD4T diffractometer (rotating anode, 50 kV, 200 mA) for data

(8) (a) Staal, L. H.; Polm, L. H.; Vrieze, K.; Ploeger, F.; Stam, C. H. *Inorg. Chem.* **1981**, *20*, 3590. (b) Staal, L. H.; Polm, L. H.; Balk, R. W.; van Koten, G.; Vrieze, K.; Brouwers, A. M. F. *Inorg. Chem.* **1980**, *19*, 3343.

(9) Mul, W. P.; Elsevier, C. J.; Frühräuf, H.-W.; Vrieze, K.; Pein, I.; Zoutberg, M. C.; Stam, C. H. *Inorg. Chem.* **1990**, *29*, 2336.

Scheme 2



collection. Unit cell parameters were determined from a least-squares treatment of the SET4 setting angles of 25 reflections with $11.4 < \theta < 14.0^\circ$. Unit cell parameters were checked for the presence of higher lattice symmetry.¹⁰ Data were corrected for Lp, for a small linear decay (2.2%) of the intensity control reflections during the 99 h of X-ray exposure time, but not for absorption. The structure was solved with direct methods (SHELXS86)¹¹ and a series of subsequent difference Fourier analyses. Refinement on F was carried out by full-matrix least-squares techniques. H atoms were introduced on calculated positions (C–H = 0.98 Å) and included in the refinement riding on their carrier atoms. All non-hydrogen atoms were refined with anisotropic thermal parameters, H atoms with one common isotropic thermal parameter [$U = 0.098(2) \text{ \AA}^2$]. Weights were introduced in the final refinement cycles, convergence was reached at $R = 0.0273$, $R_w = 0.0237$, $w = 1/\sigma^2(F)$. Neutral atom scattering factors were taken from Cromer and Mann¹² and corrected for anomalous dispersion.¹³ All calculations were performed with SHELX76¹⁴ and PLATON¹⁵ (geometrical calculations and illustration) on a DEC-5000.

Crystal Structure Determination of 12b. Pertinent data on the structure determination have been collected in Table 1. A red crystal was mounted on top of a glass-fiber and transferred to an Enraf-Nonius CAD4 diffractometer for data collection at 100 K. Unit cell parameters were determined from a least-squares treatment of the SET4 setting angles of 25 reflections in the range $14 < \theta < 20^\circ$. Data were corrected for Lp and absorption (DIFABS¹⁶ correction range 0.91:1.07). The structure was solved with direct methods (SHELXS86)¹¹ and refined by full-matrix least-squares on F (SHELX76)¹⁴ to $R = 0.030$ ($R_w = 0.034$) for 3726 reflections with $I > 2.5\sigma(I)$. Hydrogen atoms were introduced on calculated positions (C–H = 1.08 Å) and included in the refinement riding on their carrier atoms. Neutral atom scattering factors were taken from Cromer and Mann¹² and corrected for anomalous dispersion.¹³ All calculations were performed on a microvax-II cluster.

Geometrical calculations and the thermal ellipsoid plot were done with the program PLATON.¹⁵

Results and Discussion

Reaction of Ru(CO)₃(*i*-Pr-DAB) with Dimethyl Maleate. In situ prepared Ru(CO)₃(*i*-Pr-DAB) reacts readily at -30°C in toluene with dimethyl maleate. When the reaction mixture is warmed up to room temperature under an atmosphere of CO (1.1 bar), the ruthenabicyclo[2.2.2] complex **10a** is obtained as the single product in a high yield (cf. Scheme 2). White, air-stable **10a** can be isolated from the crude reaction mixture by chromatography on silica gel, employing CH₂Cl₂/diethyl ether (1:1) as the eluent. It has been characterized by IR, ¹H and ¹³C NMR, and elemental analysis. The X-ray molecular structure of **10a** is in agreement with the spectroscopic data in solution. The complex consists of a bicyclo[2.2.2] structure in which the former imine carbon atom and the central ruthenium atom occupy the bridgehead positions. It should be noted that **10a** may exist in two diastereomeric configurations, depending on which face of the alkene reacts with the Ru–N=C dipole. Both the NMR data and the X-ray crystal structure show only one diastereomer, which, when combined with the high yield of **10a**, suggests that the reaction is highly diastereoselective. In view of the exceptionally long Ru–C (former alkene) bond, complex **10a** possesses an unexpected thermal stability. It does not show any indication of a rearrangement reaction *via* reductive elimination, comparable to the one observed for bicyclo[2.2.2]Fe(CO)₃ complexes (**3** → **4** in Scheme 1), nor does it show a reverse reaction like that reported for the bicyclo[2.2.2]-Fe(CNR)₃ complex^{3e} (Figure 1). The proposed mechanism of formation of **10a**, which is analogous to the one reported for the reaction of Ru(CO)₃(*i*-Pr-DAB) with the activated alkyne DMADC (cf. Scheme 1), will be discussed in more detail in the section on complex formation.

If the reaction is performed without CO present as an additional ligand, a significant amount of a red

(10) Spek, A. L. *J. Appl. Crystallogr.* **1988**, *21*, 578.

(11) Sheldrick, G. M. *SHELXS86, Program for Crystal Structure Determination*; University of Göttingen: Göttingen, Germany, 1986.

(12) Cromer, D. T.; Mann, J. B. *Acta Crystallogr.* **1968**, *A24*, 321.

(13) Cromer, D. T.; Liberman, D. *J. Chem. Phys.* **1970**, *53*, 1891.

(14) Sheldrick, G. M. *SHELX76, Crystal Structure Analysis Package*; University of Cambridge: Cambridge, England, 1976.

(15) Spek, A. L. *Acta Crystallogr.* **1990**, *A46*, C34.

(16) Walker, N.; Stuart, D. *Acta Crystallogr.* **1983**, *A39*, 158.

compound is formed in combination with complex **10a**. The IR data of this byproduct ($\nu(\text{CO})$: 1997, 1935 cm^{-1}) obtained from the crude reaction mixture suggest that it is probably $\text{Ru}(\text{CO})_2(\eta^2\text{-dimethyl maleate})(i\text{-Pr-DAB})$ (**12a**). However the purification of this complex by chromatography on silica gel proved to be impossible because, firstly, a large part of the complex decomposes during chromatography and because, second, the remaining red fraction that can be obtained apparently contains **12b** instead of **12a**. This is evident from the marked resemblance of both the ^1H and ^{13}C NMR data of the latter fraction with those of **12b**. Furthermore, the temperature dependent ^1H NMR also points to a dynamic behavior similar to that of **12b** (*vide infra*). For **12a** a different behavior would be expected on account of its symmetry properties, i.e., the total C_s symmetry of the square pyramidal transient in the coupled alkene rotation-Berry pseudorotation (structure **a**, Figure 6) should give rise to simultaneous equilibration of the inequivalent alkene and DAB halves. Although we have not been able to unambiguously establish that the dimethyl maleate complex is still intact in the crude reaction mixture,¹⁷ we assume that the *cis/trans* isomerization occurs during the chromatographic workup procedure. This is supported by the observation that hardly any decomposition occurs during chromatography of the dimethyl fumarate complex **12b**. Isomerizations of this type are not unprecedented; Kruczynski et al.¹⁸ reported that $\text{Ru}(\text{CO})_4(\eta^2\text{-diethyl maleate})$ undergoes a facile thermal conversion (50 °C) to the corresponding fumarate complex.

Reaction of $\text{Ru}(\text{CO})_3(i\text{-Pr-DAB})$ with Dimethyl Fumarate. The reaction of $\text{Ru}(\text{CO})_3(i\text{-Pr-DAB})$ with dimethyl fumarate shows several marked differences with respect to the reaction with the *cis*-substituted alkene. Apart from the slightly lower temperature (-50 °C) for the initial reaction, the reaction is apparently less straightforward. After the reaction mixture is warmed to room temperature, the IR and NMR data reveal a complex product mixture, which contains complexes **9b** and **12b** as the main components (cf. Scheme 2). Both these complexes can be separated from the crude reaction mixture by column chromatography on silica gel. Performance of the reaction under an atmosphere of CO does not alter the product distribution, e.g., complex **9b** does not react further to a tricarbonyl species isostructural to the dimethyl maleate complex **10a**, and the CO-substitution product **12b** also remains intact. As already indicated, the crude reaction mixture also contains small amounts of at least one other, probably bicyclic, complex, which we were not able to purify or characterize. Since **9b** can also exist in two diastereomeric configurations (cf. Figure 2), a small amount of the second diastereomer may be present.

Complex **9b** is stable at ambient temperatures and has been characterized by IR, ^1H and ^{13}C NMR spectroscopy, and elemental analysis. This implies that **9b**,

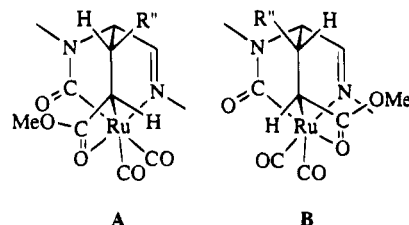


Figure 2. Two possible diastereomeric configurations of complex **9b** with the proposed intramolecular stabilization.

depicted in Scheme 2 as coordinatively unsaturated, must be stabilized by an additional intra- or intermolecular interaction. On the basis of both the IR data, which indicate a dicarbonyl species and an $\text{Ru}-\text{O}=\text{C}$ interaction, and the ^{13}C NMR data, which show a large downfield shift for one of the ester carbonyls, it is assumed that the oxygen atom of an ester carbonyl occupies the vacant coordination site. Figure 2 represents two diastereomeric configurations of **9b** stabilized by an intramolecular O-coordination. Although this involves the formation of a four-membered ring, this possibility is in our opinion the most likely. The alternative, stabilization by an intermolecular interaction with one of the ester carbonyl O atoms on one Ru atom coordinated to a second Ru unit and vice versa, cannot be excluded.^{19,20b} It appears, however, less likely since the presence of only one set of resonances in the ^1H and ^{13}C NMR would require a complete symmetry of this dinuclear complex. The exact configuration of complex **9b** (A or B) could not be determined from the available spectroscopic data. Unfortunately, we were not able to obtain crystals suitable for an X-ray structure determination.

Complex **12b** is stable at room temperature and soluble in all commonly used organic solvents. Surprisingly, for an $\text{Ru}(0)$ complex, **12b** is even relatively air-stable. The complex has been characterized by IR, ^1H and ^{13}C NMR spectroscopy, and elemental analysis. The X-ray molecular structure of **12b** reveals a distorted trigonal bipyramidal coordination geometry, in which the two imine N-donor atoms occupy equatorial and axial positions, and the alkene is situated in the equatorial plane. In solution, complex **12b** shows a dynamic behavior that will be discussed in the section on NMR spectroscopy. At slightly elevated temperatures (40–50 °C) the complex readily decomposes with liberation of the alkene.

When HBF_4 is added to the reaction mixture immediately after the cycloaddition reaction with dimethyl fumarate, complex **11b** is obtained. In **11b**, the amido nitrogen is protonated, which prevents the CO insertion and, hence, conserves the original bicyclo[2.2.1] structure. The ^1H NMR of the crude product shows a second set of resonances (ca. 10% in intensity), which is slightly shifted relative to the main set of resonances. This is probably due to the presence of a small amount of

(19) In the reaction of $\text{Ru}(\text{CO})_3(i\text{-Pr-DAB})$ with DMADC it was also possible to characterize a comparable unsaturated complex.^{3b} In that case we preferred an intermolecular O-coordination. An intramolecular O-coordination would involve a highly strained four-membered ring since the former alkyne carbon atom in the ring is sp^2 -hybridized.

(20) (a) Torres, M. R.; Santos, A.; Ros, J.; Solans, X. *Organometallics* **1987**, *6*, 1091. (b) Lindner, E.; Jansen, R.-M.; Mayer, H. A.; Hiller, W.; Fawzi, R. *Organometallics* **1989**, *8*, 2355. (c) Guilbert, B.; Demerseman, B.; Dixneuf, P. H.; Mealli, C. *J. Chem. Soc., Chem. Commun.* **1989**, 1035. (d) Blackmore, T.; Bruce, M. I.; Stone, F. G. A. *J. Chem. Soc., Dalton Trans.* **1974**, 106.

(17) The IR data of the red complex, obtained from the crude reaction mixture, are apparently different from those of **12b**; however, the ^1H NMR data of the crude reaction mixture did not allow for an unambiguous assignment of the resonances expected for **12a**. Attempts to purify the red compound by an alternative workup procedure, i.e., extracting it with pentane/diethyl ether (2:1) from the crude residue obtained after removal of the solvent, did not have the desired result.

(18) Kruczynski, L.; Martin, J. L.; Takats, J. *J. Organomet. Chem.* **1974**, *80*, C9.

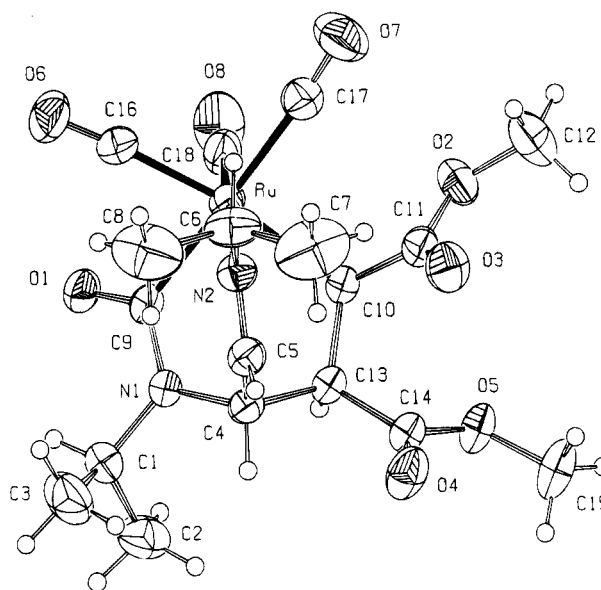


Figure 3. ORTEP drawing of complex 10a (50% probability) with the adopted atom labeling.

Table 2. Fractional Coordinates of the Non-Hydrogen Atoms and Equivalent Isotropic Thermal Parameters of Complex 10a

atom	x	y	z	$U_{eq}^a \text{ \AA}^2$
Ru	0.32416(1)	-0.16951(2)	0.33920(1)	0.0396(1)
O(1)	0.29451(7)	0.07996(14)	0.28981(10)	0.0549(6)
O(2)	0.43018(9)	-0.30329(15)	0.52455(11)	0.0656(7)
O(3)	0.46332(8)	-0.34345(15)	0.43063(11)	0.0659(7)
O(4)	0.53866(8)	-0.17948(18)	0.36952(10)	0.0676(7)
O(5)	0.55447(7)	-0.15336(15)	0.49815(9)	0.0539(6)
O(6)	0.19501(9)	-0.14048(17)	0.20475(13)	0.0805(8)
O(7)	0.30359(11)	-0.41926(19)	0.39746(13)	0.0916(9)
O(8)	0.28691(10)	-0.0547(2)	0.45952(12)	0.0919(10)
N(1)	0.38060(8)	0.02213(16)	0.28479(11)	0.0428(6)
N(2)	0.36068(8)	-0.23335(17)	0.26087(11)	0.0437(6)
C(1)	0.38464(12)	0.1308(2)	0.24354(15)	0.0544(9)
C(2)	0.43965(14)	0.2047(2)	0.29580(19)	0.0747(11)
C(3)	0.38208(16)	0.1034(3)	0.16067(17)	0.0867(13)
C(4)	0.42848(9)	-0.06656(19)	0.30467(12)	0.0403(7)
C(5)	0.40465(10)	-0.1786(2)	0.25733(12)	0.0437(7)
C(6)	0.33608(13)	-0.3402(3)	0.20806(15)	0.0632(10)
C(7)	0.38477(17)	-0.4305(3)	0.2225(2)	0.1146(19)
C(8)	0.30438(19)	-0.3011(3)	0.12068(18)	0.117(2)
C(9)	0.33245(10)	0.0011(2)	0.30139(13)	0.0424(7)
C(10)	0.42077(9)	-0.15332(19)	0.43174(12)	0.0386(7)
C(11)	0.44097(11)	-0.2749(2)	0.46010(15)	0.0489(8)
C(12)	0.44647(17)	-0.4212(3)	0.5556(2)	0.1015(17)
C(13)	0.46016(9)	-0.08984(19)	0.39717(12)	0.0386(7)
C(14)	0.52094(10)	-0.1478(2)	0.41769(13)	0.0447(8)
C(15)	0.61264(12)	-0.2115(3)	0.52462(17)	0.0751(10)
C(16)	0.24260(11)	-0.1587(2)	0.25342(15)	0.0537(8)
C(17)	0.31309(11)	-0.3335(3)	0.37460(15)	0.0556(8)
C(18)	0.30046(11)	-0.0995(2)	0.41432(16)	0.0559(9)

^a $U_{eq} = 1/3$ of the trace of the orthogonalized U tensor.

another diastereomer. After recrystallization, the major diastereomer is obtained in a pure form.

Molecular Structure of the Ruthenabicyclo[2.2.2] Complex 10a. An ORTEP drawing with the atomic numbering scheme of the bicyclo[2.2.2]Ru(CO)₃ complex 10a is shown in Figure 3, and the fractional coordinates and bond distances and angles are given in Tables 2 and 3, respectively. Complex 10a has a [2.2.2]-bicyclic structure in which the bridgehead positions are occupied by the ruthenium atom and the C-C-coupled former imine carbon atom. The coordination geometry around the central ruthenium atom is slightly distorted octahedral. The mutual trans positions in the octahe-

Table 3. Selected Bond Distances (Å) and Angles (deg) of the Non-Hydrogen Atoms of 10a (Esd's in Parentheses)

Bond Distances			
Ru-N(2)	2.118(2)	O(6)-C(16)	1.132(4)
Ru-C(9)	2.085(2)	O(7)-C(17)	1.118(4)
Ru-C(10)	2.231(2)	O(8)-C(18)	1.135(4)
Ru-C(16)	1.927(3)	N(1)-C(1)	1.466(3)
Ru-C(17)	2.018(3)	N(1)-C(4)	1.460(3)
Ru-C(18)	1.882(3)	N(1)-C(9)	1.359(3)
N(2)-C(5)	1.266(3)	C(4)-C(5)	1.499(3)
C(4)-C(13)	1.544(3)	C(6)-C(7)	1.500(5)
C(6)-C(8)	1.505(4)	C(10)-C(13)	1.540(3)
Bond Angles			
N(2)-Ru-C(9)	87.66(9)	Ru-N(2)-C(5)	119.13(15)
N(2)-Ru-C(10)	85.51(8)	Ru-N(2)-C(6)	122.77(18)
N(2)-Ru-C(16)	93.60(10)	C(5)-N(2)-C(6)	118.1(2)
N(2)-Ru-C(17)	93.45(10)	N(1)-C(4)-C(5)	111.58(19)
N(2)-Ru-C(18)	172.57(10)	N(1)-C(4)-C(13)	110.67(18)
C(9)-Ru-C(10)	87.24(9)	C(5)-C(4)-C(13)	111.79(17)
C(9)-Ru-C(16)	83.54(10)	N(2)-C(5)-C(4)	120.4(2)
C(9)-Ru-C(17)	178.04(11)	Ru-C(9)-O(1)	123.22(19)
C(9)-Ru-C(18)	87.70(10)	Ru-C(9)-N(1)	177.04(16)
C(10)-Ru-C(16)	170.77(9)	O(1)-C(9)-N(1)	119.6(2)
C(10)-Ru-C(17)	94.45(10)	Ru-C(10)-C(11)	105.74(16)
C(10)-Ru-C(18)	88.47(10)	Ru-C(10)-C(13)	111.77(13)
C(16)-Ru-C(17)	94.77(11)	C(11)-C(10)-C(13)	113.8(2)
C(16)-Ru-C(18)	91.64(10)	C(4)-C(13)-C(10)	115.13(18)
C(17)-Ru-C(18)	91.36(11)	C(4)-C(13)-C(14)	108.25(18)
C(1)-N(1)-C(4)	118.4(2)	C(10)-C(13)-C(14)	114.79(18)
C(1)-N(1)-C(9)	121.4(2)	Ru-C(16)-O(6)	173.1(2)
C(4)-N(1)-C(9)	120.19(18)	Ru-C(17)-O(7)	173.1(3)
		Ru-C(18)-O(8)	178.2(2)

dron are occupied by the former alkene carbon C(10) and the carbonyl carbon C(16), by the inserted carbonyl carbon C(9) and the carbonyl carbon C(17), and by the imine nitrogen N(2) and the third carbonyl carbon C(18). This arrangement is clearly responsible for the variations in the bond lengths of the terminal carbonyls to ruthenium. The Ru-C(18) bond length of 1.882(3) Å is significantly shorter than the Ru-C(16) and Ru-C(17) bond lengths of 1.927(3) and 2.018(3) Å, respectively, which is the result of the trans position of the former carbonyl to the σ -donor N(2). The Ru-N(2) bond length of 2.118(2) Å is within the range normally found for Ru-N (imine) σ -bonds (2.10–2.15 Å).²¹ Likewise, the Ru-C(9) bond length of 2.085(2) Å is in agreement with the distances commonly observed for Ru-C(=O) bonds.²² On the other hand, the exceptionally long Ru-C(10) bond length of 2.231(2) Å suggests that the former alkene carbon atom is only weakly bonded to the ruthenium atom. As a consequence of the cycloaddition reaction, the central C(10)-C(13) bond of the former alkene is reduced to a single bond, which is reflected in the bond length of 1.540(3) Å. Furthermore, the average bond angles around C(10) and C(13) indicate that both the carbon atoms are sp³ hybridized. The dihedral angles between the ester substituents (15.3(3)°) and the alkene C-H bonds (12.5(3)°) imply that their mutual cis positions in the starting alkene are retained in the complex after the cycloaddition reaction. Only one diastereomeric configuration, with the ester substituents on the side of the intact imine fragment, is observed crystallographically. Both the reduced imine bond

(21) (a) Polm, L. H.; Mul, W. P.; Elsevier, C. J.; Vrieze, K.; Christophersen, M. J. N.; Stam, C. H. *Organometallics* **1988**, *7*, 423. (b) Muller, F.; Dijkhuis, D. I. P.; van Koten, G.; Vrieze, K.; Heijdenrijk, D.; Rotteveel, M. A.; Stam, C. H.; Zoutberg, M. C. *Organometallics* **1989**, *8*, 992. (c) Mul, W. P.; Elsevier, C. J.; Frühauf, H.-W.; Vrieze, K.; Pein, I.; Zoutberg, M. C.; Stam, C. H. *Inorg. Chem.* **1990**, *29*, 2336.

(22) (a) Wagner, H.; Jungbauer, A.; Thiele, G.; Behrens, H. Z. *Naturforsch.* **1979**, *34B*, 1487. (b) Kraakman, M. J. A.; de Klerk-Engels, B.; de Lange, P. P. M.; Vrieze, K.; Smeets, W. J. J.; Spek, A. L. *Organometallics* **1992**, *11*, 3774.

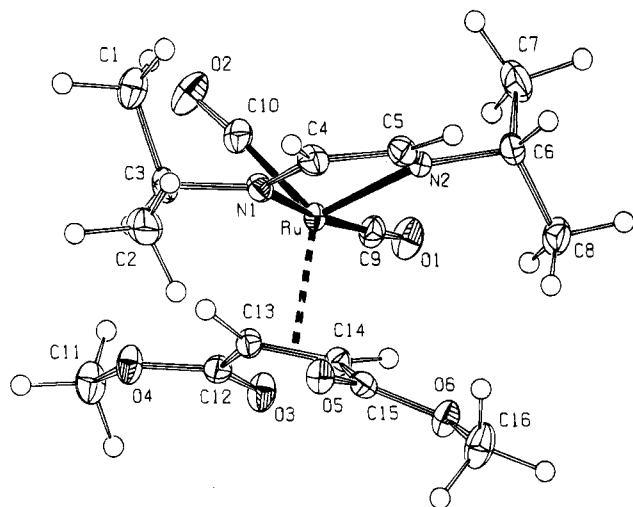


Figure 4. ORTEP drawing of complex 12b (50% probability) with the adopted atom labeling.

Table 4. Fractional Coordinates of the Non-Hydrogen Atoms and Equivalent Isotropic Thermal Parameters of Complex 12b

atom	x	y	z	$U_{eq}, \text{\AA}^2$
Ru	0.77875(2)	0.65007(2)	0.51181(1)	0.0152(1)
O(1)	0.64021(17)	0.4637(2)	0.38795(13)	0.0285(7)
O(2)	0.95060(17)	0.6046(3)	0.40548(14)	0.0342(7)
O(3)	0.60865(16)	0.7958(2)	0.33316(12)	0.0265(6)
O(4)	0.74613(16)	0.9505(2)	0.34625(12)	0.0248(6)
O(5)	0.68379(16)	0.9144(2)	0.64145(12)	0.0218(6)
O(6)	0.53581(16)	0.7775(2)	0.61837(12)	0.0240(6)
N(1)	0.88272(18)	0.7561(3)	0.60453(14)	0.0189(7)
N(2)	0.77621(18)	0.5231(3)	0.61865(15)	0.0197(7)
C(1)	1.0686(2)	0.8060(4)	0.5912(2)	0.0306(10)
C(2)	0.9623(3)	0.9905(3)	0.6549(2)	0.0345(10)
C(3)	0.9584(2)	0.8717(3)	0.59133(19)	0.0248(9)
C(4)	0.8888(2)	0.7039(3)	0.67804(18)	0.0234(8)
C(5)	0.8263(2)	0.5796(3)	0.68627(18)	0.0226(8)
C(6)	0.7177(2)	0.3892(3)	0.62902(19)	0.0236(8)
C(7)	0.7542(3)	0.2714(3)	0.5761(2)	0.0357(11)
C(8)	0.5985(2)	0.4158(4)	0.6094(2)	0.0294(10)
C(9)	0.6917(2)	0.5367(3)	0.43506(17)	0.0209(8)
C(10)	0.8906(2)	0.6184(3)	0.45026(18)	0.0227(8)
C(11)	0.7309(3)	0.9613(4)	0.25753(17)	0.0297(10)
C(12)	0.6803(2)	0.8589(3)	0.37701(17)	0.0198(8)
C(13)	0.7094(2)	0.8505(3)	0.46712(16)	0.0185(7)
C(14)	0.6366(2)	0.7842(3)	0.51416(16)	0.0181(8)
C(15)	0.6251(2)	0.8347(3)	0.59645(16)	0.0184(8)
C(16)	0.5134(3)	0.8181(4)	0.6979(2)	0.0331(10)

$^a U_{eq} = 1/3$ of the trace of the orthogonalized U tensor.

N(1)–C(4) (1.460(3) Å) and the newly formed C(4)–C(13) bond (1.544(3) Å) are normal single bonds. The relatively short N(1)–C(9) distance of 1.359(3) Å points to a partial double-bond character commonly found for amide functions.²³

Molecular Structure of Ru(CO)₂(dimethyl fumarate)(*i*-Pr-DAB) (12b). An ORTEP drawing with the atomic numbering scheme of Ru(CO)₂(η^2 -dimethyl fumarate)(*i*-Pr-DAB) (12b) is shown in Figure 4, and the fractional coordinates and bond distances and angles are given in Tables 4 and 5, respectively. The coordination geometry around the central ruthenium atom is distorted trigonal bipyramidal with the two imine N-donor atoms occupying equatorial and axial positions. The plane through the five-membered heterometallic cycle Ru–N(1)–C(4)–C(5)–N(2) is almost perpendicular

Table 5. Selected Bond Distances (Å) and Angles (deg) of the Non-Hydrogen Atoms of 12b (Esd's in Parentheses)

Bond Distances			
Ru–N(1)	2.095(2)	O(3)–C(12)	1.217(3)
Ru–N(2)	2.124(3)	N(1)–C(4)	1.293(4)
Ru–C(9)	1.866(3)	N(2)–C(5)	1.299(4)
Ru–C(10)	1.897(3)	C(4)–C(5)	1.427(4)
Ru–C(13)	2.150(3)	C(12)–C(13)	1.468(4)
Ru–C(14)	2.205(3)	C(13)–C(14)	1.439(4)
O(1)–C(9)	1.152(3)	C(14)–C(15)	1.462(4)
O(2)–C(10)	1.150(4)		
Bond Angles			
N(1)–Ru–N(2)	75.97(10)	Ru–N(2)–C(5)	114.0(2)
N(1)–Ru–C(9)	173.60(11)	Ru–N(2)–C(6)	130.12(19)
N(1)–Ru–C(10)	91.36(11)	C(5)–N(2)–C(6)	115.5(2)
N(2)–Ru–C(9)	98.76(11)	N(1)–C(4)–C(5)	116.6(3)
N(2)–Ru–C(10)	117.85(11)	N(2)–C(5)–C(4)	116.9(3)
C(9)–Ru–C(10)	87.91(12)	Ru–C(9)–O(1)	178.0(2)
C(13)–Ru–C(14)	38.57(10)	Ru–C(10)–O(2)	172.4(3)
Ru–N(1)–C(3)	125.76(18)	C(12)–C(13)–C(14)	119.1(2)
Ru–N(1)–C(4)	115.7(2)	C(13)–C(14)–C(15)	121.8(2)
C(3)–N(1)–C(4)	118.0(2)		

(83.04(18)°) to the plane defined by Ru–C(13)–C(14), which implies that the coordinated alkene lies in the equatorial plane. This is in accordance with the theoretical calculations by Albright et al., which demonstrate that this orientation is energetically more favorable than the one perpendicular to the equatorial plane.²⁴ The largest deviations from the *tbp* geometry are observed for the N(1)–Ru–N(2) (75.97(10)°) and the N(2)–Ru–C(9) (98.76(11)°) angles, indicating that the N(2) atom is slightly bent out of the equatorial plane, toward N(1). This is clearly the consequence of the limited bite angle of the chelating DAB ligand (ca. 75–80°). The Ru–N(1) and Ru–N(2) distances of 2.095(2) and 2.124(3) Å, respectively, are in agreement with values generally observed for Ru–N (imine) σ -bonds.²¹ The small mutual difference in these bond distances is probably a result of their respective axial and equatorial positions. The N(1)–C(4) and N(2)–C(5) bond lengths of 1.293(4) and 1.299(4) Å, respectively, are normal for σ -N-donating imine fragments. The Ru–C(13) (2.150(3) Å) and Ru–C(14) (2.205(3) Å) bonds differ significantly, pointing to a slightly asymmetrical coordination of the alkene ligand. This feature is probably related to their relative positions with respect to the σ -donating nitrogen atom N(2) and the carbonyl carbon atom C(10). The Ru–C(alkene) bond lengths are comparable to those in $[(\eta^5\text{-C}_5\text{Me}_5)\text{Ru}(\text{bipyridine})(\text{diethyl maleate})]^+\text{PF}_6^-$, recently reported by Balavoine et al.²⁵ The central C(13)–C(14) bond length (1.439(4) Å) of the coordinated alkene indicates a substantial reduction of the C–C bond order, due to back-donation by the electron-rich ruthenium atom into the antibonding alkene π^* -orbital. This is also expressed by the NMR spectroscopic data (*vide infra*). As expected for an η^2 -coordinated alkene,²⁴ the ester substituents are bent away from the metal as evident from the torsion angle C(12)–C(13)–C(14)–C(15) of $-145.5(3)^\circ$, thus deviating $35.5(3)^\circ$ from 180° .

IR Spectroscopy. The IR data of the complexes discussed in this section are listed in Table 6. The ν -(CO) absorptions of the bicyclic products 9b, 10a, and 11b show characteristic differences reflecting the changes

(24) Albright, T. A.; Hoffmann, R.; Thibeault, J. C.; Thorn, D. L. *J. Am. Chem. Soc.* **1979**, *101*, 3801 and references therein.

(25) Balavoine, G. G. A.; Boyer, T.; Livage, C. *Organometallics* **1992**, *11*, 456.

(23) *Handbook of Chemistry and Physics*, 56th ed.; CRC Press: Cleveland, OH, 1975.

Table 6. IR Data of the Ruthenabicyclo Complexes 9b, 10a, and 11b and the Ru(CO)₂(η^2 -Dimethyl Fumarate)(*i*-Pr-DAB) Complex 12b

compd	$\nu(\text{CO})$, ^a in cm ⁻¹
9b	2032 (s), 1961 (s), 1720 (m), 1617 (m)
10a	2090 (s), 2027 (s br), 1725 (m br), 1685 (m)
11b^b	2121(s), 2064 (s), 2043 (s), 1725 (m), 1700 (m)
12b	2002 (s), 1938 (s), 1685 (s)

^a Measured in CH₂Cl₂, s = strong, m = medium, br = broad.

^b The N–H stretching band is observed at 3200 cm⁻¹.

in the amount of π -back-donation to the terminal CO ligands associated with the electron density on the central ruthenium atom. For complex **10a** one sharp absorption band and one broad absorption band are observed at relatively high frequency, which confirms that it contains three terminal CO ligands. The high wavenumbers are evidently the result of the poor π -back-donation by the central Ru(II) atom. The band positions are similar to those reported for the alkyne derived bicyclo[2.2.2]Ru(CO)₃ complex **3**. Three absorptions of equal intensity are observed for the terminal CO ligands in **11b**. They are found at extremely high frequencies, which is consistent with the cationic nature of this complex, and are comparable to those reported for the DMADC-derived ruthenabicyclo[2.2.1] complex **6**. The N–H bond in **11b** gives rise to an absorption in the $\nu(\text{N-H})$ region at ca. 3200 cm⁻¹, which again corresponds to complex **6**. As expected, the ester carbonyls of **10a** and **11b** give rise to absorptions between 1680 and 1725 cm⁻¹. The IR data of complex **9b** differ significantly from those of **10a** and **11b**. The $\nu(\text{CO})$ region of complex **9b** shows only two absorptions of equal intensity at relatively low frequency, which indicates that this compound is a dicarbonyl species. Besides, in the organic $\nu(\text{C=O})$ region of **9b**, one of the ester carbonyl stretching bands is observed at a much lower wavenumber (1617 cm⁻¹). As was shown in an earlier part of this series,^{3b} such a frequency shift is indicative for an Ru–O=C interaction. Several examples of complexes containing an Ru–O=C fragment, that show a similar feature have been reported in the literature.²⁰ Finally it should be noted that an intermediate **9a**, comparable to **9b**, is observed in the reaction **7** → **10a** ($\nu(\text{CO}) = 2030, 1962$ cm⁻¹ in toluene); however, this species could not be isolated.

For complex **12b** two carbonyl stretching bands are observed at 1935 and 2002 cm⁻¹, which are slightly higher than those reported for Fe(CO)₂(η^2 -dimethyl fumarate)(*i*-Pr-DAB) ($\nu(\text{CO}) = 1991.5, 1937.5$ cm⁻¹). This is attributed to a small decrease in π -back-donation commonly observed in going from Fe to Ru.^{26,27} Both ester carbonyls of **12b** give rise to one broad absorption at 1685 cm⁻¹.

NMR Spectroscopy. Complexes 9b, 10a, and 11b. The ¹H and ¹³C NMR spectroscopic data of the complexes **9b**, **10a**, and **11b** are listed in Tables 7 and 8, respectively. For all three complexes only one set of resonances is observed, which indicates that only one diastereomer is present. The NMR data of complex **10a**

are consistent with the molecular structure in the solid state (*vide supra*). Because the NMR data of the complexes show close resemblance to those reported for the DMADC-derived ruthenabicyclocomplexes **3** and **6** (cf. Scheme 1) they will be frequently compared.

¹H NMR. In compounds **9b**, **10a**, and **11b**, the former imine protons are shifted ca. 3.5 ppm upfield in comparison to the intact imine protons that resonate at approximately 8.5 ppm. This reflects the change in hybridization (sp² → sp³) of the former imine carbon atom resulting from the cycloaddition reaction. In both **9b** and **10a**, the ³J coupling between these protons is ca. 5 Hz, which is in agreement with the DMADC-derived complex **3**. In **11b**, like in **6**, this coupling constant is significantly smaller (2 Hz), indicating a larger dihedral angle between the C–H bonds as a consequence of the distorted bicyclo[2.2.1] geometry. The proton on the former imine carbon atom in **10a** furthermore couples with the former alkene proton (³J = 2.3 Hz). In **11b** the resonance of the former imine proton is observed as a broad singlet due to an additional small coupling with the N–H proton, whereas in **9b** it coincides with an *i*-Pr methine proton septet. The resonance of the former alkene proton in **9b** and **11b** indicates a slightly larger coupling (³J ≈ 3.5 Hz) with the former imine proton relative to **10a**. The significant differences in the positions of the Ru–C–H proton resonances in **9b**, **10a**, and **11b** are probably caused by the changes in the electron density of the metal atom. The large ³J coupling of 10.6 Hz between the alkene protons in **10a** indicates that their C–H bonds are almost coplanar, which is consistent with the structure in the solid state (*vide infra*). Unexpectedly, the alkene protons in **9b** and **11b** also show a relatively large mutual coupling (8.1 and 9.5 Hz, respectively), which suggests a torsion of the former alkene C–C bond. The N–H proton of **11b** resonates at 5.25 ppm, comparable to the N–H in **6**, and shows a large coupling (10.1 Hz) with the *i*-Pr methine proton. The remaining ¹H resonances of the DAB ligand and those of the methoxy protons of all three complexes are found at their expected positions.

¹³C NMR. All three complexes show the characteristic upfield shift ($\Delta\delta \approx 110$ ppm), due to the rehybridization, of the former imine carbon atom C(4) relative to the intact imine carbon atom C(5)). The positions of the remaining ¹³C resonances of complex **10a** are similar to those reported for the DMADC-derived ruthenabicyclo[2.2.2] complex **6**, except of course for the resonances of the former alkene carbon atoms. The C–C-coupled carbon atom (C(13)) resonates at 49.0 ppm, a normal value for an sp³-hybridized ester-substituted carbon nucleus. The resonance of the other former alkene carbon atom (C(14)), σ -bonded to ruthenium, is observed at 17.9 ppm. This upfield position is probably the consequence of diamagnetic shielding by the ruthenium atom. The assignment of the resonances is based on a heteronuclear 2D-correlated (¹H–¹³C) measurement. In the ¹³C NMR of **9b** three resonances are observed between 189–194 ppm, which are assigned to C(16) and C(17) of the two terminal CO ligands and to the inserted carbonyl carbon atom (C(9)). A substantial downfield shift ($\Delta\delta \approx 20$ ppm) is observed for the resonance of the ester carbonyl carbon atom C(11), which is indicative for an Ru–O=C interaction.^{20c} The

(26) Grevels, F.-W.; Reuvers, J. G. A.; Takats J. *J. Am. Chem. Soc.* **1981**, *103*, 4069.

(27) (a) Mul, W. P.; Elsevier, C. J.; Frühauf, H.-W.; Vrieze, K.; Pein, I.; Zoutberg, M. C.; Stam, C. H. *Inorg. Chem.* **1990**, *29*, 2336. (b) van Dijk, H. K.; Stufkens, D. J.; Oskam, A. *J. Am. Chem. Soc.* **1989**, *111*, 541. (c) Muller, F. Ph.D. Thesis, University of Amsterdam, Amsterdam, The Netherlands, 1988.

Table 7. ^1H NMR Data of the Ruthenabicyclo Complexes **9b**, **10a**, and **11b** and the $\text{Ru}(\text{CO})_2(\eta^2\text{-Dimethyl Fumarate})(i\text{-Pr-DAB})$ Complexes **12b^{a,b}**

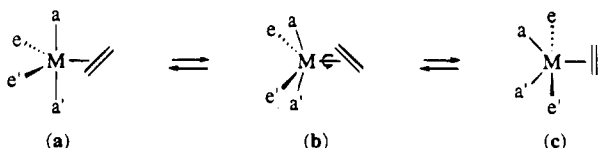
compd	δ , ppm
9b	8.58 (1H, d, 5.0 Hz, N=CH); 4.96 (1H, sept, 6.8 Hz, <i>i</i> -Pr CH); 4.71 (2H, m, NCH and <i>i</i> -Pr CH); ^c 3.73, 3.69 (2 \times 3H, 2xs, OMe); 3.32 (1H, dd, 8.1 Hz, 3.2 Hz, Ru-CH-CH); 2.13 (1H, d, 8.1 Hz, Ru-CH-CH); 1.34 (6H, d, 6.7 Hz, <i>i</i> -Pr Me); 1.10, 1.01 (2 \times 3H, 2 \times d, 6.8 Hz, <i>i</i> -Pr Me)
10a	8.55 (1H, d, 5.4 Hz, N=CH); 4.95 (1H, sept, 6.8 Hz, <i>i</i> -Pr CH); 4.85 (1H, dd, 5.4 Hz, 2.3 Hz, N-CH); 3.86 (1H, sept, 6.6 Hz, <i>i</i> -Pr CH); 3.63, 3.53 (2 \times 3H, 2 \times s, OMe); 3.16 (1H, d, 10.6 Hz, Ru-CH-CH); 2.77 (1H, dd, 10.6 Hz, 2.3 Hz, Ru-CH-CH); 1.36, 1.27 (2 \times 3H, 2 \times d, 6.6 Hz, <i>i</i> -Pr Me); 1.08, 0.98 (2 \times 3H, 2 \times d, 6.8 Hz, <i>i</i> -Pr Me)
11b	8.41 (1H, d, 2.0 Hz, N=CH); 5.25 (1H, br d, 10.1 Hz, N-H); 4.65 (1H, br s, N-CH); 4.11 (1H, sept, 6.5 Hz, <i>i</i> -Pr CH); 3.95 (1H, dd, 9.5 Hz, 3.7 Hz, Ru-CH-CH); 3.77, 3.71 (2 \times 3H, 2 \times s, OMe); 3.37 (1H, dsept, 10.1 Hz, 6.2 Hz, <i>i</i> -Pr CH); 2.68 (1H, d, 9.5 Hz, Ru-CH-CH); 1.49, 1.39 (2 \times 3H, 2 \times d, 6.5 Hz, <i>i</i> -Pr Me); 1.38, 1.34 (2 \times 3H, 2 \times d, 6.2 Hz, <i>i</i> -Pr Me)
12b^d	8.11, 7.93 (2 \times 1H, 2 \times s, N=CH); 4.53, 4.24 (2 \times 1H, 2 \times sept, 6.4 Hz, <i>i</i> -Pr CH); 3.68, 3.36 (2 \times 3H, 2 \times s, OMe); 3.45, 3.18 (2 \times 1H, 2 \times d, 9.3 Hz, HC=CH); 1.53, 1.49, 1.46, 1.40 (4 \times 3H, 4 \times d, 6.4 Hz, <i>i</i> -Pr Me)

^a The δ values (in ppm, relative to TMS) have been measured in CDCl_3 solution at 293 K and 300.13 MHz. ^b s = singlet, d = doublet, dd = double doublet, sept = septet, dsept = double septet, m = multiplet. ^c Individualized assignment is not possible due to partial overlap. ^d Measured at the slow exchange limit (243 K) in CDCl_3 and 300.13 MHz.

Table 8. ^{13}C NMR Data of the Ruthenabicyclo Complexes **9b**, **10a**, and **11b** and the $\text{Ru}(\text{CO})_2(\eta^2\text{-Dimethyl Fumarate})(i\text{-Pr-DAB})$ Complexes **12b**

compd	δ , ^a ppm
9b^b	193.8, 193.1, 189.6 (C(9), C(16), C(17)); 201.5, 176.6 (C(11), C(14)); 171.2 (C(5)); 58.6 (C(6)); 55.4 (C(4)); 52.9, 52.8 (C(12), C(15)); 48.0 (C(13)), 43.8 (C(1)); 34.2 (C(10)); 24.4, 23.3, 22.7, 21.4 (C(2), C(3), C(7), C(8))
10a^b	199.7, 195.1, 190.6 (C(16), C(17), C(18)); 189.6 (C(9)); 183.4, 175.4 (C(11), C(14)); 172.4 (C(5)); 68.2 (C(6)); 55.6 (C(4)); 52.7, 50.9 (C(12), C(15)); 49.0 (C(13)); 42.4 (C(1)); 24.2, 23.1, 22.3, 21.1 (C(2), C(3), C(7), C(8)); 17.9 (C(10))
11b^b	193.3, 190.9, 183.6 (C(16), C(17), C(18)); 180.3, 173.5 (C(11), C(14)); 176.5 (C(5)); 66.7 (C(6)); 65.6 (C(4)); 53.8 (C(13)); 53.7, 52.5 (C(12), C(15)); 44.6 (C(1)); 34.0 (C(10)); 24.7 (2x), 24.1, 19.2 (C(2), C(3), C(7), C(8))
12b^c	203.5, 201.0 (C(9), C(10)); 178.4, 173.6 (C(12), C(15)); 153.5, 152.3 (C(4), C(5)); 68.0, 60.4 (C(3), C(6)); 52.0, 50.8 (C(11), C(16)); 40.0, 38.8 (C(13), C(14)); 27.0, 25.7, 25.6, 22.2 (C(1), C(2), C(7), C(8))

^a The δ values (in ppm, relative to TMS) have been measured in CDCl_3 solution at 243 K and 75.47 MHz. ^b Atomic numbering according to Figure 4. ^c Atomic numbering according to Figure 5.

**Figure 5.** Schematic representation of an alkene rotation coupled with a Berry pseudorotation (after ref 24).

σ -Ru-bonded carbon atom C(14) resonates at 34.2 ppm, slightly downfield in comparison to **10a**. The ^{13}C NMR data of **11b** are analogous to those reported for the DMADC-derived ruthenabicyclo[2.2.1] complex **6**. The ^{13}C resonances of the CO ligands are found at relatively high field (183.6–193.3 ppm) reflecting a decrease in π -back-donation, consistent with the cationic nature of **11b**. The former alkene carbon atoms C(13) and C(14) resonate at 53.8 and 34.0 ppm, respectively.

$\text{Ru}(\text{CO})_2(\eta^2\text{-dimethyl fumarate})(i\text{-Pr-DAB})$ (12b**).** The ^1H and ^{13}C NMR data of complex **12b**, listed in Tables 7 and 8, respectively, are comparable to those reported by Frühauf et al. for the isostructural complex $\text{Fe}(\text{CO})_2(\eta^2\text{-dimethyl fumarate})(i\text{-Pr-DAB})$.⁴ Like the latter compound, complex **12b** shows temperature dependent NMR spectra due to intramolecular exchange processes, which will be discussed below.

NMR Data at the Limit of Slow Exchange. In the limit of slow exchange the ^1H and ^{13}C NMR spectra of complex **12b** show double sets of resonances for both the alkene and the DAB ligand. This is in agreement with structure **a** in Figure 5, wherein the positions **e** and **a** are occupied by the R-DAB nitrogen atoms and **e'** and **a'** are occupied by the carbonyl ligands. This is supported by the X-ray molecular structure of **12b**, which also shows a trigonal bipyramidal (tbp) coordination geometry (*vide supra*). As expected, the alkene protons show a substantial upfield coordination shift ($\Delta\delta \approx 3$ ppm), which is attributed to the increase in electron

density due to π -back-bonding, or, which reflects a considerable degree of rehybridization ($sp^2 \rightarrow sp^3$) of the alkene C atoms. The ^{13}C resonances of the coordinated alkene carbon atoms (39–40 ppm) are likewise shifted upfield relative to the free alkene (130 ppm). Their positions agree nicely with those reported by Grevels et al. for $\text{Ru}(\text{CO})_4(\eta^2\text{-dimethyl fumarate})$.²⁶ The coordination shifts of the alkene resonances are slightly larger than those reported for the corresponding $\text{Fe}(\text{CO})_2(\eta^2\text{-alkene})(\text{R-DAB})$ complexes.⁴ The carbonyl carbon atoms give rise to signals at 201.0 and 203.5 ppm, which are slightly downfield compared to those reported for $\text{Ru}(\text{CO})_4(\eta^2\text{-dimethyl fumarate})$ (ca. 192 ppm). This is evidently the result of the substitution of two π -accepting carbonyl ligands for two σ -donating N atoms, which enhances π -back-donation to the remaining carbonyls. The ^1H and ^{13}C resonances of the DAB ligand are observed at normal positions.

Dynamic Behavior. The dynamic process of **12b** involves a rotation of the alkene ligand around the bond axis to the central metal atom. The calculated activation barriers for pure alkene rotation in an otherwise rigid tbp complex exceed the normally observed experimental values by a factor of 2–3.²⁴ The reason is that the rotation actually occurs in the apical position of an intermediate square-pyramidal (sqp) geometry, reached by distortion during a Berry pseudorotation (structure **b** in Figure 5). This implies that the symmetry properties of the intermediate sqp arrangement, shown in Figure 6b for complex **12b**, should provide an adequate explanation for the observed spectral changes upon raising the temperature from the slow exchange limit. Since the coordinated alkene (C_2) and the complex fragment (C_s) do not possess a common symmetry element, the total symmetry of complex **12b** remains C_1 even in the transient sqp geometry (cf. Figure 6b). Fast rotation of the alkene is therefore expected to

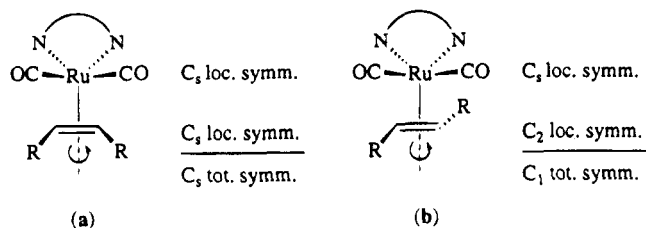


Figure 6. Symmetry considerations for alkene rotation in thermally excited square pyramidal geometries of complexes **12**: (a) dimethyl maleate and (b) dimethyl fumarate.

average its two halves, whereas the nuclei related by local C_s symmetry in the ligands of the ML_4 fragment should remain nonisochronous. This behavior is indeed observed for **12b**. Upon raising the temperature from the slow exchange limit, the resonances assigned to the alkene and methoxy protons coalesce, whereas those assigned to the DAB nuclei remain unchanged. In the fast exchange the alkene and methoxy protons each give rise to one resonance at 3.38 and 3.52 ppm, respectively. Because the alkene and methoxy proton signals show partial overlap in the intermediate exchange, it was not possible to accurately determine the coalescence temperature. For the methoxy protons coalescence occurs between 275 and 281 K. Combined with the $\Delta\nu = 96.45$ Hz for these resonances in the slow exchange, this gives a ΔG_c^\ddagger (alkene) of roughly 54.5–57 kJ/mol. Although some caution must be exercised on account of the large margin of error, this value appears to be somewhat higher than the one reported for $Fe(CO)_2(\eta^2\text{-dimethyl fumarate})(i\text{-Pr-DAB})$ (52.9 ± 1.1 kJ/mol). A similar trend is observed for the coupled alkene rotation–Berry pseudorotation in $M(CO)_4(\eta^2\text{-dimethyl fumarate})$ ²⁶ and $M(CO)_4(\eta^2\text{-diethyl fumarate})$ ¹⁸ ($M = Fe, Ru$). The slightly higher activation barriers for the Ru compounds are consistent with an increase in the metal to π^* (alkene)-back-bonding, which is supported by the somewhat larger coordination shift of the alkene resonances for ruthenium as compared with iron (*vide supra*). At 303 K the resonances assigned to the DAB ligand in **12b** show some broadening, which points to a second dynamic process causing equilibration of the two DAB halves. This behavior, also observed for the isostructural iron complex,⁴ is interpreted in terms of a reversible dissociation of the alkene. In that case the local C_s symmetry of the unsaturated $M(CO)_2(R\text{-DAB})$ ($M = Fe, Ru$) intermediate determines the overall symmetry. Unfortunately this dynamic process could not be studied in detail because **12b** readily decomposes at these temperatures.

Complex Formation. The product formation in the reactions of $Ru(CO)_3(i\text{-Pr-DAB})$ with the activated alkenes dimethyl maleate and dimethyl fumarate can be explained by employing the two independent reaction routes depicted in Scheme 2. Although these pathways are apparently competitive, they are also independent, i.e., the chemical properties and behavior of the $Ru(CO)_2(\eta^2\text{-alkene})(i\text{-Pr-DAB})$ complexes (*vide supra*) indicate that they are certainly not intermediates in the cycloaddition reaction. In the following both pathways will therefore be discussed separately.

The initial step in the main reaction route consists of an oxidative 1,3-dipolar [3+2] cycloaddition of the activated alkene across the $Ru-N=C$ fragment, which results in the formation of the bicyclo[2.2.1] intermedi-

ate **8**. This is supported by the isolation of the N-protonated complex **11b**, in which this initial bicyclo[2.2.1] geometry is retained. The observation that the cis position of the alkene protons and ester substituents of dimethyl maleate is maintained in the organometallic complex indicates that the cycloaddition reaction is presumably a concerted process. Furthermore, in the case of dimethyl maleate, the cycloaddition reaction apparently proceeds with very high diastereoselectivity. The preference for an approach of the alkene with its ester groups away from the 1,3-dipole may be accounted for by a lower steric hinderance of the alkene protons, relative to the ester moieties, with the *i*-Pr substituent on the dipole nitrogen atom during the alkene approach. The experimental and spectroscopic data obtained from the reaction of $Ru(CO)_3(i\text{-Pr-DAB})$ with dimethyl fumarate point to a less pronounced diastereoselectivity.

Comparison of electron-deficient alkenes with the corresponding alkynes shows that the former are less reactive toward nucleophiles, which implies that their LUMO orbitals are somewhat higher in energy.²⁸ The finding that $Ru(CO)_3(i\text{-Pr-DAB})$, in contrast to $Fe(CO)_3(i\text{-Pr-DAB})$, does show 1,3-dipolar reactivity toward activated alkenes consequently indicates that the $Ru-N=C$ dipole possesses a higher HOMO level. This is also expressed by its enhanced reactivity toward DMADC.^{3b} It should be mentioned that CAS–SCF calculations on the model systems $M(CO)_3(HN=C(H)-C(H)=NH)$ ($M = Fe, Ru$) show comparable HOMO levels for both dipoles.²⁹ It should be born in mind, however, that these are model systems, whereas in practice even small changes in the relative energetic disposition of the interacting HOMO and LUMO may have a profound effect on the 1,3-dipolar reactivity. Another explanation may be that the more diffuse orbitals on the Ru dipole (4d in origin vs. 3d at $Fe-N=C$) allow for an earlier interaction with the approaching dipolarophile and therefore lower the activation energy. In view of the previous remarks we note that steric influences may also contribute to the increased reactivity since the approach of the activated alkene is probably facilitated on the ruthenium complex. Finally the small increase in the reactivity of $Ru(CO)_3(i\text{-Pr-DAB})$ toward dimethyl fumarate (*vide supra*) suggests that the LUMO level of this alkene is slightly lower in energy. We have not been able to obtain unambiguous confirmation for this observation in the literature. Generally, comparable to slightly higher LUMO levels are assumed for the trans ester-substituted alkenes.^{26,30}

The bicyclo[2.2.1] intermediate **8** subsequently undergoes an intramolecular CO insertion in the $Ru-N$ (amido) bond which results in the formation of the coordinatively unsaturated bicyclo[2.2.2] intermediate **9**. However, in the presence of HBf_4 the amido nitrogen is protonated, which prevents the CO insertion and hence conserves the bicyclo[2.2.1] structure (**8b** → **11b**). Surprisingly intermediate **9** shows a marked difference

(28) (a) Houk, K. N.; Sims, J.; Duke, R. E.; Strozier, R. W.; George, J. K. *J. Am. Chem. Soc.* **1973**, *95*, 7287. (b) Houk, K. N.; Sims, J.; Watts, C. R.; Luskus, L. J. *J. Am. Chem. Soc.* **1973**, *95*, 7301.

(29) Dedieu, A.; Liddel, M. J. Unpublished results.

(30) Dekker, G. P. C. M.; Elsevier, C. J.; Vrieze, K.; van Leeuwen, P. W. N. M.; Roobeek, C. F. *J. Organomet. Chem.* **1992**, *430*, 357. For a more detailed discussion see Dekker, G. P. C. M. Ph.D. Thesis, University of Amsterdam, Amsterdam, The Netherlands, 1991; Chapter 3.

in reactivity depending on the alkene. In the case of dimethyl maleate, the 16-electron complex **9a** shows the expected behavior, i.e., it readily reacts with CO to give the ruthenabicyclo[2.2.2] complex **10a**. In contrast, complex **9b** remains intact under these conditions; even being stirred at ambient temperatures under CO for a longer period of time does not result in any formation of the corresponding **10b**. On the basis of the available data we cannot provide a straightforward explanation for the increased stability of **9b** relative to **9a**. It may be related to the diastereomeric configuration of **9b**, but this can only be confirmed by an X-ray crystal structure of **9b**, which, despite several attempts, could not be obtained.

With respect to the CO-substitution reaction (**7** → **12**) the following remarks can be made. Although the product distribution indicates that this reaction is apparently less favorable than the cycloaddition reaction, it does proceed with relative ease at comparatively low temperatures, whereas in the isostructural $\text{Fe}(\text{CO})_3(\text{R-DAB})$ CO substitution can only be achieved photochemically. This agrees with the finding that Ru-CO bonds are generally weaker than Fe-CO bonds, which, in the case of $\text{M}(\text{CO})_3(\text{R-DAB})$, is evident from the decrease in π -back-donation found for ruthenium (IR, ^{13}C NMR) and the finding that $\text{Ru}(\text{CO})_3(i\text{-Pr-DAB})$ readily loses CO under reduced pressure to give $\text{Ru}_2(\text{CO})_5(i\text{-Pr-ADA})$ (see Experimental Section). The CO substitution furthermore shows a dependence on the alkene. If the reaction of $\text{Ru}(\text{CO})_3(\text{R-DAB})$ with dimeth-

yl maleate is performed under an atmosphere of CO, no substitution product is formed (*vide supra*). Whether this results from blocking the substitution pathway or from a back-reaction of the substitution product (**12a** → **7**) could not be distinguished. In contrast, the fumarate complex **12b** is readily formed and stable under similar conditions, which implies a stronger ruthenium to alkene bond. This again tends to indicate a slightly increased π -acidity (lower LUMO level) of dimethyl fumarate, resulting in increased ruthenium → π^* (alkene)-back-bonding.

Acknowledgment. We thank M. J. A. Kraakman for helpful discussions and J. M. Ernsting for his advice on recording the 300.13 MHz heteronuclear 2D-correlated NMR spectra. The investigation was supported in part (W.J.J.S. and A.L.S.) by the Netherlands Foundation for Chemical Research (SON) with financial aid from the Netherlands Organization for Scientific Research (NWO). The X-ray data of **12b** were kindly collected by A. J. M. Duisenberg.

Supporting Information Available: Tables of fractional coordinates and isotropic thermal parameters of the hydrogen atoms, anisotropic thermal parameters, and complete lists of bond distances and angles of both the hydrogen and non-hydrogen atoms of complexes **10a** and **12b** (9 pages). Ordering information is given on any current masthead page.

OM950367Q

Is π -Back-Bonding Important for σ -Bound Aldehyde and Ketone Complexes? Synthesis and Structural Characterization of Aromatic Aldehyde Complexes of the $[\text{CpFe}(\text{CO})_2]^+$ Cation

Ronald L. Cicero and John D. Protasiewicz*

Department of Chemistry, Case Western Reserve University, Cleveland, Ohio 44106-7078

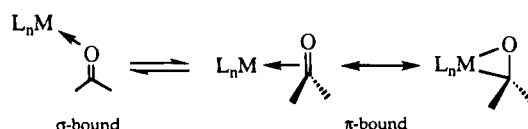
Received May 30, 1995*

The synthesis and characterization of a series of organometallic complexes, $[\text{CpFe}(\text{CO})_2(\text{O}=\text{C}(\text{H})\text{Ar})]\text{PF}_6$ (Ar = Ph (1), *p*-MeC₆H₄ (2), *p*-NMe₂C₆H₄ (3), *p*-OMeC₆H₄ (4), *p*-CF₃C₆H₄ (5), *p*-ClC₆H₄ (6), *p*-(dimethylamino)cinnamaldehyde (7); Cp = η^5 -cyclopentadienyl) are presented. Oxidation of $[\text{CpFe}(\text{CO})_2]_2$ with AgPF₆ or $[\text{Cp}_2\text{Fe}]\text{PF}_6$ in the presence of a 5-fold excess of aromatic aldehyde led to the formation of 1-7 in good to excellent yields (especially with the latter oxidant). Compounds 1-7 were analyzed by a combination of ¹H NMR (solution) and FTIR spectroscopic (solid and solution state) methods. Single-crystal X-ray diffraction studies on 6 and $[\text{CpFe}(\text{CO})_2(\text{O}=\text{C}(\text{H})\text{-}i\text{-OMeC}_6\text{H}_4)]\text{SbF}_6$ (8) were also performed. Binding of these aldehydes to $[\text{CpFe}(\text{CO})_2]^+$ in solution and the solid state occurs exclusively through oxygen σ -donor interactions. Structural evidence for π -back-bonding in σ -bound aldehyde complexes is presented. These solid-state effects, however, do not manifest themselves in the solution equilibrium binding constants for this class of substrates.

Introduction

Addition reactions promoted by the binding of an organic carbonyl group to a transition-metal complex are central to many catalytic and stoichiometric reactions.¹⁻⁵ A particularly attractive class of substrates for nucleophilic activation are ketones and aldehydes.^{6,7} Chiral organometallic Lewis acids such as $[\text{CpRe}(\text{NO})(\text{PPh}_3)]^+$, $[\text{Cp}^*\text{Re}(\text{NO})(\text{PPh}_3)]^+$, and $[\text{Tp}^*\text{W}(\text{CO})(\text{Ph-C}\equiv\text{CMe})]^+$ (Tp' = hydrotris(3,5-dimethylpyrazolyl)borate) can promote enantioselective nucleophile additions to aldehydes⁸⁻¹¹ and ketones.¹²⁻¹⁸ Nucleophile addition to these substrates can potentially be greatly affected

by the binding mode of the ketone or aldehyde to the metal center. Adducts of $[\text{CpRe}(\text{NO})(\text{PPh}_3)]^+$ with aromatic aldehydes contain equilibrium mixtures of σ -bound (η^1) and π -bound (η^2) isomers:



The σ to π ratios correlate with the electron-donating or -withdrawing ability of the substituents on the aromatic nucleus, hence the presence of electron-withdrawing groups results in an increase of the π -bound isomer, while electron-donating groups shift the equilibrium to favor the σ -bound isomers.¹⁹⁻²¹ One aspect of the reactivity studies that intrigued us was the proposition that the σ -bound aldehydes are more reactive toward nucleophile addition than their π -bound counterparts.²² Reduction can promote an isomerization from σ - to π -bound complexation of aldehydes and ketones in $[\text{Os}(\text{NH}_3)_5(\text{O}=\text{CR}^1\text{R}^2)]^{3+}$.²³ An investigation of the electronic factors governing this equilibrium has suggested that aldehyde complexes of the organometallic Lewis acid $[\text{CpFe}(\text{CO})_2]^+$ should exist exclusively as σ -bound isomers.²⁴ The synthesis of $[\text{CpFe}(\text{CO})_2(\sigma\text{-isobutyraldehyde})]\text{PF}_6$ and $[\text{CpFe}(\text{CO})_2(\sigma\text{-benzaldehyde})]\text{PF}_6$ have been reported, and the latter has been structurally characterized.^{1,25} Benzaldehyde and cin-

* Abstract published in *Advance ACS Abstracts*, September 15, 1995.

(1) Shambayati, S.; Schreiber, S. L. In *Comprehensive Organic Synthesis*; Trost, B. M., Ed.; Pergamon Press: New York, 1991; Vol. 1, p 283.

(2) Yamaguchi, M. In *Comprehensive Organic Synthesis*; Trost, B. M., Ed.; Pergamon Press: New York, 1991; Vol. 1, p 325.

(3) Rosenblum, M. *Acc. Chem. Res.* **1974**, *7*, 122.

(4) Reger, D. L. *Acc. Chem. Res.* **1988**, *21*, 229.

(5) Fatiadi, A. J. *J. Res. Natl. Inst. Stand. Technol.* **1991**, *96*, 1.

(6) Huang, Y.-H.; Gladysz, J. A. *J. Chem. Educ.* **1988**, *65*, 298.

(7) Faller, J. W.; Gunderson, L.-L. *Tetrahedron Lett.* **1993**, *34*, 2275.

(8) Fernández, J. M.; Emerson, K.; Larsen, R. H.; Gladysz, J. A. *J. Am. Chem. Soc.* **1986**, *108*, 8268.

(9) Garner, C. M.; Fernández, J. M.; Gladysz, J. A. *Tetrahedron Lett.* **1989**, *30*, 3931.

(10) Garner, C. M.; Méndez, N. Q.; Kowalczyk, J. J.; Fernández, J. M.; Emerson, K.; Larsen, R. D.; Gladysz, J. A. *J. Am. Chem. Soc.* **1990**, *112*, 5146.

(11) Agbossou, F.; Ramsden, J. A.; Huang, Y.-H.; Arif, A. M.; Gladysz, J. A. *Organometallics* **1992**, *11*, 693.

(12) Fernández, J. M.; Emerson, K.; Larsen, R. D.; Gladysz, J. A. *J. Chem. Soc., Chem. Commun.* **1988**, 37.

(13) Dalton, D. M.; Gladysz, J. A. *J. Organomet. Chem.* **1989**, *370*, C17.

(14) Dalton, D. M.; Gladysz, J. A. *J. Chem. Soc., Dalton Trans.* **1991**, 2741.

(15) Dalton, D. M.; Fernández, J. M.; Emerson, K.; Larsen, R. D.; Arif, A. M.; Gladysz, J. A. *J. Am. Chem. Soc.* **1990**, *112*, 9198.

(16) Dalton, D. M.; Garner, C. M.; Fernández, J. M.; Gladysz, J. A. *J. Org. Chem.* **1991**, *56*, 6823.

(17) Klein, D. P.; Dalton, D. M.; Méndez, N. Q.; Arif, A. M.; Gladysz, J. A. *J. Organomet. Chem.* **1991**, *412*, C7.

(18) Caldarelli, J. L.; Wagner, L. E.; White, P. S.; Templeton, J. L. *J. Am. Chem. Soc.* **1994**, *116*, 2878.

(19) Méndez, N. Q.; Arif, A. M.; Gladysz, J. A. *Angew. Chem., Int. Ed. Engl.* **1990**, *29*, 1473.

(20) Méndez, N. Q.; Mayne, C. L.; Gladysz, J. A. *Angew. Chem., Int. Ed. Engl.* **1990**, *29*, 1475.

(21) Méndez, N. Q.; Seyler, J. W.; Arif, A. M.; Gladysz, J. A. *J. Am. Chem. Soc.* **1993**, *115*, 2323.

(22) Klein, D. P.; Gladysz, J. A. *J. Am. Chem. Soc.* **1992**, *114*, 8710.

(23) Harman, W. D.; Sekine, M.; Taube, H. *J. Am. Chem. Soc.* **1988**, *110*, 2439.

(24) Delbecq, F.; Sautet, P. *J. Am. Chem. Soc.* **1992**, *114*, 2446.

(25) Foxman, B. M.; Klemarczyk, P. T.; Liptrot, R. E.; Rosenblum, M. *J. Organomet. Chem.* **1980**, *187*, 253.

namaldehyde complexes of $[\text{CpRu}(\text{PPh}_3)(\text{CO})]^+$ have been prepared and shown to exist as σ -adducts.²⁶ On the other hand, benzaldehyde binds to $[\text{Fe}(\text{PEt}_3)_2(\text{CO})_2]$ in a π -mode.²⁷

Lewis acid catalysis of reactions by $[\text{CpFeLL}']^+$ is becoming increasingly important, and an understanding of the factors which dictate the binding of organic carbonyl functionalities to these iron centers will be required for the rational design of new and enantioselective systems.²⁸⁻³² We have thus undertaken the synthesis of a wide range of aromatic aldehyde complexes of the form $[\text{CpFe}(\text{CO})_2(\text{O}=\text{C}(\text{H})\text{Ar})]^+$, in order to ascertain whether or not such species might display the "amphichelic" behavior observed for aromatic aldehyde complexes of $[\text{CpRe}(\text{NO})(\text{PPh}_3)]^+$ and to begin explorations of their reactivity.^{1,33} Previous work has established that preparation of the ketone and aliphatic aldehyde complexes $[\text{CpFe}(\text{CO})_2(\text{O}=\text{CR}^1\text{R}^2)]^+$ could be effected by oxidation of $[\text{CpFe}(\text{CO})_2]_2$ by Ag^+ in the presence of $\text{O}=\text{CR}^1\text{R}^2$.^{25,34} We have found that this simple route, by modification of the oxidant utilized and the method used for product isolation, provides a general route to analogous aromatic aldehyde complexes. We furthermore provide detailed evidence that these aromatic aldehyde complexes exist entirely as σ -bound isomers in both the solid and solution phases and supply evidence for the importance of π -backbonding in σ -bound aldehydes.

Experimental Section

General Methods. All reactions and manipulations were carried out under a nitrogen atmosphere by using standard Schlenk techniques or a Vacuum Atmospheres drybox. Solvents were distilled under nitrogen from sodium benzophenone ketyl. Deuterated solvents were dried by passage over a column of alumina and stored under nitrogen. Benzaldehyde, *p*-tolualdehyde, *p*-anisaldehyde, and *p*-(trifluoromethyl)benzaldehyde were purchased from Aldrich Chemical Co. and were used as purchased after degassing. $[\text{CpFe}(\text{CO})_2]_2$, silver hexafluorophosphate, *p*-(dimethylamino)benzaldehyde, *p*-chlorobenzaldehyde, and *p*-(dimethylamino)cinnamaldehyde were also purchased from Aldrich Chemical Co. and were dried under vacuum. Ferrocenium hexafluorophosphate was prepared by reported methods.³⁵ Proton chemical shifts were referenced to residual solvent peaks. ^1H NMR spectra were recorded on Varian XL200 and Varian Gemini 300 instruments using CD_2Cl_2 as the solvent. Both liquid and solid-state IR spectra were recorded on a Midac PRS FTIR spectrometer using freshly distilled dichloromethane as the solvent for IR samples and Nujol mulls for solid-state samples. Elemental analysis was performed by Oneida Research Services Inc., Whitesboro, NY.

$[\text{CpFe}(\text{CO})_2(\text{O}=\text{C}(\text{H})\text{C}_6\text{H}_5)]\text{PF}_6$ (1). **Method A.** To a Schlenk flask charged with 13 mL of CH_2Cl_2 were added 0.500

g of $[\text{CpFe}(\text{CO})_2]_2$ (1.4 mmol) and 1.502 g of benzaldehyde (14.2 mmol). The mixture was stirred for 10 min, after which time 0.924 g of Cp_2FePF_6 (2.8 mmol) was rapidly added. The initial dark red mixture turned dark red-brown after 5 min and was stirred for an additional 2 h. The resulting solution was filtered. To the red solution was added 20 mL of diethyl ether in 0.5 mL increments over the course of 45 min, effecting precipitation of red crystals. The red solid was collected by filtration, washed with three 2 mL portions of diethyl ether, and dried under vacuum for 1 h, yielding 0.941 g (77.8%) of dark red microcrystalline 1.

Method B. In this method, 0.262 g of $[\text{CpFe}(\text{CO})_2]_2$ (0.7 mmol) and 0.617 g of benzaldehyde (5.8 mmol) were added to a Schlenk flask charged with 6 mL of CH_2Cl_2 . The resulting mixture was stirred and chilled in an ice bath for 10 min. To the vigorously stirred chilled solution was rapidly added 0.359 g of AgPF_6 (1.4 mmol), effecting an immediate color change from red to black with a noticeable precipitate forming. The resulting solution was stirred at 0 °C for 20 min, after which time the mixture was warmed to room temperature. The mixture was filtered, and the filtrate was worked up as in method A using 10 mL of diethyl ether. This method yielded 0.195 g (30.7%) of red 1. FTIR (Nujol, cm^{-1}): 3121 (w), 2072 (s, ν_{CO}), 2036 (s, ν_{CO}), 2021 (s, ν_{CO}), 1634 (s, $\nu_{\text{O}=\text{CHR}}$), 1599 (m), 1579 (m), 1321 (w), 1225 (w), 1177 (w), 838 (s), 760 (w), 722 (w), 684 (w). FTIR (CH_2Cl_2 , cm^{-1}): 2076 and 2031 (ν_{CO}), 1626 ($\nu_{\text{O}=\text{CHR}}$). ^1H NMR: δ 9.48 (1 H, s), 7.79 (2 H, m), 7.56 (2 H, m), 5.43 (5 H, s). Anal. Calcd for $\text{C}_{14}\text{H}_{11}\text{O}_3\text{FePF}_6$: C, 39.28; H, 2.59. Found: C, 39.19; H, 2.41.

$[\text{CpFe}(\text{CO})_2(\text{O}=\text{C}(\text{H})\text{-}p\text{-C}_6\text{H}_4\text{CH}_3)]\text{PF}_6$ (2). **Method A.** A 0.501 g amount of $[\text{CpFe}(\text{CO})_2]_2$ (1.4 mmol), 1.704 g of *p*-tolualdehyde (14.2 mmol), and 0.939 g of Cp_2FePF_6 (2.8 mmol) yielded 1.008 g (80.5%) of dark red microcrystalline 2.

Method B. A 0.255 g amount of $[\text{CpFe}(\text{CO})_2]_2$ (0.7 mmol), 0.282 g of *p*-tolualdehyde (2.3 mmol), and 0.355 g of AgPF_6 (1.4 mmol) yielded 0.262 g (41.1%) of the red powder 2. FTIR (Nujol, cm^{-1}): 3123 (m), 2070 (s, ν_{CO}), 2012 (s, ν_{CO}), 1637 (m), 1620 (m), 1599 (s), 1568 (s), 1395 (m), 1317 (w), 1235 (w), 1178 (s), 1125 (w), 1019 (w), 878 (s), 844 (s), 825 (s), 772 (m), 740 (w), 722 (w), 703 (w). FTIR (CH_2Cl_2 , cm^{-1}): 2075 and 2030 (ν_{CO}), 1596 ($\nu_{\text{O}=\text{CHR}}$). ^1H NMR: δ 9.35 (1 H, s), 7.69 (2 H, d ($J = 8.2$ Hz)), 7.36 (2 H, d ($J = 8.2$ Hz)), 5.41 (5 H, s), 2.46 (3 H, s). Anal. Calcd for $\text{C}_{15}\text{H}_{13}\text{O}_3\text{FePF}_6$: C, 40.75; H, 2.96. Found: C, 40.61; H, 2.76.

$[\text{CpFe}(\text{CO})_2(\text{O}=\text{C}(\text{H})\text{-}p\text{-C}_6\text{H}_4\text{N}(\text{CH}_3)_2)]\text{PF}_6$ (3). **Method A.** A 0.502 g amount of $[\text{CpFe}(\text{CO})_2]_2$ (1.4 mmol), 1.796 g of *p*-(dimethylamino)benzaldehyde (12.0 mmol), and 0.940 g of Cp_2FePF_6 (2.8 mmol) yielded 1.216 g (90.8%) of dark red microcrystalline 3.

Method B. A 0.251 g amount of $[\text{CpFe}(\text{CO})_2]_2$ (0.7 mmol), 0.327 g of *p*-(dimethylamino)benzaldehyde (2.2 mmol), and 0.357 g of AgPF_6 (1.4 mmol) yielded 0.526 g (79.0%) of red 3. FTIR (Nujol, cm^{-1}): 3118 (w), 2067 (s, ν_{CO}), 2008 (s, ν_{CO}), 1621 (w), 1572 (s), 1533 (s), 1327 (w), 1270 (w), 1183 (s), 843 (s), 737 (w), 722 (w). FTIR (CH_2Cl_2 , cm^{-1}): 2070 and 2024 (ν_{CO}), 1619 ($\nu_{\text{O}=\text{CHR}}$). ^1H NMR: δ 8.58 (1 H, s), 7.55 (2 H, d ($J = 9.2$ Hz)), 6.67 (2 H, d ($J = 9.2$ Hz)), 5.34 (5 H, s), 3.16 (6 H, s). Anal. Calcd for $\text{C}_{16}\text{H}_{16}\text{O}_3\text{FeNPF}_6$: C, 40.79; H, 3.42; N, 2.97. Found: C, 40.88; H, 3.22; N, 3.05.

$[\text{CpFe}(\text{CO})_2(\text{O}=\text{C}(\text{H})\text{-}p\text{-C}_6\text{H}_4\text{OCH}_3)]\text{PF}_6$ (4). **Method A.** A 0.503 g amount of $[\text{CpFe}(\text{CO})_2]_2$ (1.4 mmol), 1.907 g of *p*-anisaldehyde (14.0 mmol), and 0.942 g of Cp_2FePF_6 (2.8 mmol) yielded 1.112 g (85.4%) of red microcrystalline 4.

Method B. A 0.251 g amount of $[\text{CpFe}(\text{CO})_2]_2$ (0.7 mmol), 0.966 g of *p*-anisaldehyde (7.1 mmol), and 0.356 g of AgPF_6 (1.4 mmol) yielded 0.349 g (53.7%) of red microcrystalline 4. FTIR (Nujol, cm^{-1}): 3123 (w), 2062 (s, ν_{CO}), 2022 (s, ν_{CO}), 1629 (w), 1599 (m), 1568 (m), 1514 (w), 1339 (w), 1307 (w), 1267 (m), 1246 (w), 1167 (m), 1022 (w), 842 (s), 722 (w). FTIR (CH_2Cl_2 , cm^{-1}): 2074 and 2029 (ν_{CO}), 1594, 1586 (sh) ($\nu_{\text{O}=\text{CHR}}$). ^1H NMR: δ 9.15 (1 H, s), 7.77 (2 H, d ($J = 8.9$ Hz)), 7.00 (2 H, d ($J = 8.9$ Hz)), 5.39 (5 H, s), 3.92 (3 H, s). Anal. Calcd for $\text{C}_{15}\text{H}_{13}\text{O}_4\text{FePF}_6$: C, 39.33; H, 2.86. Found: C, 39.20; H, 2.67.

(26) Faller, J. W.; Ma, Y.; Smart, C. J.; DiVerdi, M. J. *J. Organomet. Chem.* **1991**, *420*, 237.

(27) Birk, R.; Berke, H.; Hund, H.-U.; Evertz, K.; Huttner, G.; Zsolnai, L. *J. Organomet. Chem.* **1988**, *342*, 67.

(28) Kündig, E. P.; Bourdin, B.; Bernardinelli, G. *Angew. Chem., Int. Ed. Engl.* **1994**, *33*, 1856.

(29) Bonnesen, P. V.; Puckett, C. L.; Honeychuck, R. V.; Hersh, W. H. *J. Am. Chem. Soc.* **1989**, *111*, 6070.

(30) Bach, T.; Fox, D. N. A.; Reetz, M. T. *J. Chem. Soc., Chem. Commun.* **1992**, 1634.

(31) Colombo, L.; Ulgheri, F.; Prati, L. *Tetrahedron Lett.* **1989**, *30*, 6435.

(32) Olson, A. S.; Seitz, W. J.; Hossain, M. M. *Tetrahedron Lett.* **1991**, *32*, 5299.

(33) Shambayati, S.; Crowe, W. E.; Schreiber, S. L. *Angew. Chem., Int. Ed. Engl.* **1990**, *29*, 256.

(34) Boudjouk, P.; Woell, J. B.; Radonovich, L. J.; Eyring, M. W. *Organometallics* **1982**, *1*, 582.

(35) Duggan, D. M.; Hendrickson, D. N. *Inorg. Chem.* **1975**, *14*, 955.

Table 1. Infrared Data for [CpFe(CO)₂(aldehyde)]PF₆

compd	aldehyde	FTIR (Nujol)		FTIR (CH ₂ Cl ₂)	
		$\nu_{\text{C=O}}$	$\nu_{\text{O=CHR}}$	$\nu_{\text{C=O}}$	$\nu_{\text{O=CHR}}$
1	benzaldehyde	2072, 2021	1634	2075, 2031	1626
2	<i>p</i> -tolualdehyde	2070, 2012	1637	2075, 2030	1596
3	<i>p</i> -(dimethylamino)benzaldehyde	2067, 2008	1621	2070, 2024	1619
4	<i>p</i> -anisaldehyde	2062, 2022	1629	2074, 2029	1594, 1586 (sh)
5	<i>p</i> -(trifluoromethyl)benzaldehyde	2077, 2026	1650	2077, 2033	1637
6	<i>p</i> -chlorobenzaldehyde	2072, 2015	1631	2075, 2031	1626
7	<i>p</i> -(dimethylamino)cinnamaldehyde	2066, 2030	1563	2070, 2024	1546

[CpFe(CO)₂(O=C(H)-*p*-C₆H₄CF₃)]PF₆ (5). **Method A.** A 0.500 g amount of [CpFe(CO)₂]₂ (1.4 mmol), 2.457 g of *p*-(trifluoromethyl)benzaldehyde (14.0 mmol), and 0.944 g of Cp₂FePF₆ (2.8 mmol) yielded 0.296 g (21.1%) of the red powder 5.

Method B. A 0.510 g amount of [CpFe(CO)₂]₂ (1.4 mmol), 2.413 g of *p*-(trifluoromethyl)benzaldehyde (13.8 mmol), and 0.712 g of AgPF₆ (2.8 mmol) yielded 0.487 g of (68.1%) of bright red crystalline 5. FTIR (Nujol, cm⁻¹): 2077 (s, ν_{CO}), 2026 (s, ν_{CO}), 1650 (m, $\nu_{\text{O=CHR}}$), 1582 (w), 1514 (w), 1324 (s), 1314 (s), 1221 (w), 1176 (m), 1133 (m), 1113 (w), 1065 (m), 1017 (w), 829 (s), 722 (w). FTIR (CH₂Cl₂, cm⁻¹): 2077 and 2033 (ν_{CO}), 1637 ($\nu_{\text{O=CHR}}$). ¹H NMR: 9.67 (1 H, s), 7.96 (2 H, d ($J = 8.2$ Hz)), 7.81 (2 H, d ($J = 8.2$ Hz)), 5.44 (5 H, s). Anal. Calcd for C₁₅H₁₀O₃F₃FePF₆: C, 36.32; H, 2.03. Found: C, 36.30; H, 1.83.

[CpFe(CO)₂(O=C(H)-*p*-C₆H₄Cl)]PF₆ (6). **Method A.** A 0.500 g amount of [CpFe(CO)₂]₂ (1.4 mmol), 2.102 g of *p*-chlorobenzaldehyde (15.0 mmol), and 0.944 g of Cp₂FePF₆ (2.8 mmol) yielded 0.605 g (46.3%) of red microcrystalline 6.

Method B. A 0.250 g amount of [CpFe(CO)₂]₂ (0.7 mmol), 1.013 g of *p*-chlorobenzaldehyde (7.2 mmol), and 0.357 g of AgPF₆ (1.4 mmol) yielded 0.240 g (36.7%) of the red powder 6. FTIR (Nujol, cm⁻¹): 3125 (w), 2072 (s, ν_{CO}), 2015 (s, ν_{CO}), 1631 (s, $\nu_{\text{O=CHR}}$), 1594 (m), 1567 (m), 1416 (w), 1305 (w), 1228 (w), 1172 (w), 1088 (w), 1016 (w), 875 (m), 847 (s), 823 (s), 721 (w). FTIR (CH₂Cl₂, cm⁻¹): 2076 and 2031 (ν_{CO}), 1626 ($\nu_{\text{O=CHR}}$). ¹H NMR: δ 9.48 (1 H, s), 7.77 (2 H, d ($J = 8.6$ Hz)), 7.54 (2 H, d ($J = 8.6$ Hz)), 5.42 (5 H, s). Anal. Calcd for C₁₄H₁₀O₃ClFePF₆: C, 36.36; H, 2.18. Found: C, 36.47; H, 1.92.

[CpFe(CO)₂(*p*-dimethylamino)cinnamaldehyde)]PF₆ (7). **Method A.** A 0.501 g amount of [CpFe(CO)₂]₂ (1.4 mmol), 2.100 g of *p*-(dimethylamino)cinnamaldehyde (12.0 mmol), and 0.944 g of Cp₂FePF₆ (2.8 mmol) yielded 0.690 g (49.0%) of orange microcrystalline 7. FTIR (Nujol, cm⁻¹): 3124 (w), 2066 (s, ν_{CO}), 2030 (s, ν_{CO}), 1563 (s, $\nu_{\text{O=CHR}}$), 1338 (m), 1168 (s), 1067 (w), 1025 (w), 974 (w), 943 (w), 842 (s), 728 (m). FTIR (CH₂Cl₂, cm⁻¹): 2070 and 2024 (ν_{CO}), 1546 ($\nu_{\text{O=CHR}}$). ¹H NMR: δ 8.56 (1 H, d ($J = 8.9$ Hz)), 7.61 (1 H, d ($J = 14.9$ Hz)), 7.54 (2 H, d ($J = 9.0$ Hz)), 6.72 (2 H, d ($J = 9.0$ Hz)), 6.47 (1 H, dd ($J = 14.9$ Hz, $J = 8.9$ Hz)), 5.32 (5 H, s), 3.13 (6 H, s). Anal. Calcd for C₁₈H₁₈O₃FeNPF₆: C, 43.49; H, 3.65; N, 2.82. Found: C, 43.59; H, 3.48; N, 2.72.

X-ray Crystallography for [CpFe(CO)₂(O=C(H)-*p*-C₆H₄Cl)]PF₆ (6). Data Collection and Reduction. Data were collected with a Siemens P4 instrument (Mo K α radiation ($\lambda = 0.71073$ Å)). An irregularly shaped red crystal of dimensions 0.12 × 0.36 × 0.48 mm, grown by vapor diffusion of Et₂O into a concentrated solution of 6 in CH₂Cl₂, was glued onto the tip of a glass fiber. The crystal was judged to be acceptable on the basis of ω scans and rotation photography. A random search located reflections to generate the reduced primitive cell, cell lengths being corroborated by axial photography. Additional reflections with 2θ values between 24.8 and 25° were appended to the reflection array and yielded the refined cell constants. A monoclinic cell was confirmed by examination on the diffractometer. The final cell constants obtained are presented in Table 2. Data were collected as presented in Table 2 and were corrected for absorption (empirical ψ scan).

Determination and Refinement of the Structure. The crystal was found to have 2/m Laue symmetry, and the systematic absences were in agreement with the space group P2₁/c. Direct methods (Siemens SHELXTL PLUS, PC Version

Table 2. Crystal Data and Structure Refinement Details for 6 and 8

	C ₁₄ H ₁₀ ClF ₆ FeO ₃ P	C ₁₅ H ₁₀ O ₄ FeSbF ₆
Empirical formula	C ₁₄ H ₁₀ ClF ₆ FeO ₃ P	C ₁₅ H ₁₀ O ₄ FeSbF ₆
fw	462.49	548.85
temp K	298(2)	298(2)
wavelength (Å)	0.71073	0.71073
cryst syst	monoclinic	orthorhombic
space group	P2 ₁ /c	P2 ₁ 2 ₁ 2 ₁
unit cell dimens		
<i>a</i> (Å)	7.0509(6)	7.8844(4)
<i>b</i> (Å)	15.065(2)	12.5920(5)
<i>c</i> (Å)	16.7850(13)	18.8630(12)
β (deg)	100.907(7)	
<i>V</i> (Å ³)	1750.7(3)	1872.7(2)
<i>Z</i>	4	4
density (calcd)	1.755	1.947
abs coeff (mm ⁻¹)	1.177	2.292
<i>F</i> (000)	920	1064
cryst size (mm)	0.12 × 0.36 × 0.48	0.08 × 0.08 × 0.20
θ range for data collection (deg)	2.47–25.00	1.94–24.00
index ranges	$-1 < h < 8, -1 < k < 17, -19 < l < 19$	$-1 < h < 9, -1 < k < 14, -1 < l < 21$
no. of rflns collected	4179	2280
no. of indep rflns	3071 ($R_{\text{int}} = 0.0253$)	2104 ($R_{\text{int}} = 0.0237$)
refinement method	full-matrix least-squares on F^2	full-matrix least-squares on F^2
no. of data/restraints/params	3070/0/236	2103/0/245
goodness of fit on F^2	1.291	1.000
Final <i>R</i> indices [$I > 2\sigma(I)$]	$R1 = 0.0484, wR2 = 0.1268$	$R1 = 0.0449, wR2 = 0.1064$
<i>R</i> indices (all data)	$R1 = 0.0727, wR2 = 0.1425$	$R1 = 0.0625, wR2 = 0.1183$
extinction coeff absolute	0.0016(8)	0.0000(4)
structure param	NA	0.04(7)
largest diff peak and hole (e/Å ³)	0.580 and -0.448	0.776 and -0.591

5.01 β) revealed all of the non-hydrogen atoms. All non-hydrogen atoms were refined anisotropically. Hydrogen atoms were generated at idealized positions with common isotropic thermal parameters. The final least-squares refinement converged at the *R* factors reported in Table 2. Atomic coordinates and isotropic displacements are given in Table 3. Table 4 provides selected bond lengths and bond angles.

X-ray Crystallography for [CpFe(CO)₂(O=C(H)-*p*-OMeC₆H₄)]SbF₆ (8). Data Collection and Reduction. A small red needle-shaped crystal (dimensions 0.08 × 0.08 × 0.20 mm) was cut from a longer specimen (grown by vapor diffusion of Et₂O into a concentrated solution of 8 in CH₂Cl₂; FTIR (Nujol, cm⁻¹) ν_{CO} 2075, 2029) and glued onto the tip of a glass fiber. Data were collected as described for 6 and in Table 2.

Determination and Refinement of the Structure. The crystal was found to have *mmm* Laue symmetry, and the systematic absences were in agreement with P2₁2₁2₁. Direct methods (Siemens SHELXTL PLUS, PC Version 5.01 β) revealed all of the non-hydrogen atoms. All non-hydrogen atoms were refined anisotropically. Hydrogen atoms were generated at idealized positions with common isotropic thermal parameters. The final least-squares refinement converged at the *R* factors reported in Table 2. Atomic coordinates and isotropic dis-

Table 3. Atomic Coordinates ($\times 10^4$) and Equivalent Isotropic Displacement Parameters ($\text{\AA}^2 \times 10^3$) for 6^a

	<i>x</i>	<i>y</i>	<i>z</i>	<i>U</i> (eq)
Fe	1287(1)	6393(1)	3860(1)	43(1)
Cl	2684(2)	11986(1)	4925(1)	89(1)
P	4717(2)	6589(1)	7024(1)	58(1)
O(1)	5283(5)	5862(3)	4457(2)	90(1)
O(2)	-290(5)	5988(2)	5314(2)	69(1)
O(3)	1717(4)	7662(2)	4079(2)	52(1)
C(1)	3756(7)	6074(3)	4256(3)	60(1)
C(2)	353(6)	6157(3)	4775(3)	51(1)
C(3)	2160(6)	8065(3)	4719(3)	50(1)
C(4)	2337(5)	9027(2)	4760(2)	44(1)
C(5)	2651(7)	9444(3)	5501(3)	60(1)
C(6)	2742(7)	10355(3)	5555(3)	62(1)
C(7)	2560(6)	10836(3)	4868(3)	53(1)
C(8)	2275(7)	10445(3)	4116(3)	64(1)
C(9)	2155(7)	9531(3)	4053(3)	57(1)
C(10)	1586(8)	6099(4)	2679(3)	80(2)
C(11)	858(8)	5349(3)	3052(3)	71(1)
C(12)	-900(7)	5585(3)	3232(3)	62(1)
C(13)	-1282(7)	6463(3)	3005(3)	65(1)
C(14)	235(9)	6771(3)	2650(3)	75(2)
F(1)	4547(7)	7580(2)	6744(2)	129(2)
F(2)	6901(5)	6626(3)	7080(4)	155(2)
F(3)	2502(5)	6516(3)	7031(3)	135(2)
F(4)	4339(9)	6227(3)	6146(2)	158(2)
F(5)	4976(7)	6954(3)	7916(2)	130(2)

^a *U*(eq) is defined as one-third of the trace of the orthogonalized U_j tensor.

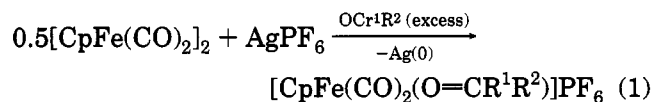
Table 4. Selected Bond Lengths (\AA) and Angles (deg) for 6

Bond Lengths			
Fe-C(1)	1.807(5)	Fe-C(2)	1.818(5)
Fe-O(3)	1.960(3)	O(1)-C(1)	1.112(5)
O(2)-C(2)	1.115(5)	O(3)-C(3)	1.221(5)
Fe-C(11)	2.062(4)	Fe-C(10)	2.080(4)
Fe-C(12)	2.087(4)	Fe-C(13)	2.090(4)
Fe-C(14)	2.104(4)	Cl-C(7)	1.737(4)
Bond Angles			
C(1)-Fe-C(2)	96.6(2)	C(1)-Fe-O(3)	94.9(2)
C(2)-Fe-O(3)	95.7(2)	C(3)-O(3)-Fe	130.9(3)
O(1)-C(1)-Fe	176.0(4)	O(2)-C(2)-Fe	176.6(4)
O(3)-C(3)-C(4)	122.8(4)		

placements are given in Table 5. Table 6 lists selected bond lengths and bond angles.

Results and Discussion

Ketone complexes of $[\text{CpFe}(\text{CO})_2]^+$ have been described. The first such complex prepared, $[\text{CpFe}(\text{CO})_2(\text{acetone})]\text{ClO}_4$, was obtained by reaction of $[\text{CpFe}(\text{CO})_2]_2$ with ferric perchlorate in acetone.³⁶ Since then, several general synthetic routes have been developed.^{25,34,37} Employing AgPF_6 in place of ferric perchlorate as the oxidant allowed isolation of a wider range of ketone adducts (acetone, cyclohexanone, cyclohexanone, 3-methylcyclohexanone; eq 1).^{3,37} For some substrates, better



yields were obtained if $[\text{CpFe}(\text{CO})_2\text{X}]$ ($\text{X} = \text{Br}, \text{I}$) replaced $[\text{CpFe}(\text{CO})_2]_2$ (isobutyraldehyde, methyl isopropyl ketone, diisopropyl ketone, 7-norbornanone, acrolein, and crotonaldehyde; eq 2).^{29,34} If the ketone is

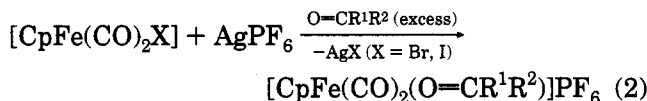
Table 5. Atomic Coordinates ($\times 10^4$) and Equivalent Isotropic Displacement Parameters ($\text{\AA}^2 \times 10^3$) for 8^a

	<i>x</i>	<i>y</i>	<i>z</i>	<i>U</i> (eq)
Fe	-4301(2)	3088(1)	1199(1)	42(1)
O(1)	-652(13)	3379(8)	1030(6)	86(3)
O(2)	-4136(16)	2573(9)	2715(5)	89(3)
O(3)	-4246(11)	1623(5)	821(4)	51(2)
O(4)	-3241(14)	-3217(6)	-67(4)	69(3)
C(1)	-2078(18)	3254(10)	1102(7)	53(3)
C(2)	-4167(20)	2746(10)	2132(6)	61(3)
C(3)	-3871(14)	805(9)	1124(6)	49(3)
C(4)	-3758(15)	-223(8)	795(6)	43(3)
C(5)	-3309(19)	-1108(9)	1205(7)	62(4)
C(6)	-3108(21)	-2098(10)	886(7)	66(4)
C(7)	-3418(17)	-2212(9)	176(6)	55(3)
C(8)	-3889(20)	-1360(8)	-240(6)	57(4)
C(9)	-4051(20)	-383(9)	66(6)	56(3)
C(10)	-3338(24)	-3413(13)	-828(8)	94(5)
C(11)	-5291(18)	3815(12)	292(7)	69(4)
C(12)	-4634(19)	4582(11)	766(8)	69(4)
C(13)	-5507(18)	4532(11)	1399(8)	70(4)
C(14)	-6741(18)	3727(11)	1337(8)	65(4)
C(15)	-6618(17)	3314(12)	669(8)	65(4)
Sb	920(1)	804(1)	2384(1)	54(1)
F(1)	-1289(14)	937(17)	2630(9)	232(9)
F(2)	3116(15)	675(15)	2172(7)	193(7)
F(3)	1236(23)	2217(7)	2500(6)	189(8)
F(4)	637(22)	-612(7)	2279(5)	172(6)
F(5)	445(20)	994(8)	1447(4)	163(6)
F(6)	1429(14)	621(8)	3337(4)	110(3)

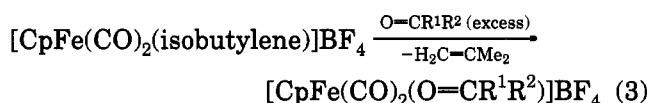
^a *U*(eq) is defined as one-third of the trace of the orthogonalized U_j tensor.

Table 6. Selected Bond Lengths (\AA) and Angles (deg) for 8

Bond Lengths			
Fe-C(1)	1.774(14)	Fe-C(2)	1.815(13)
Fe-O(3)	1.978(7)	O(1)-C(1)	1.14(2)
O(2)-C(2)	1.121(13)	O(3)-C(3)	1.214(13)
Fe-C(13)	2.086(13)	Fe-C(14)	2.102(14)
Fe-C(11)	2.091(13)	Fe-C(12)	2.067(12)
Fe-C(15)	2.102(13)	O(4)-C(7)	1.352(13)
Bond Angles			
C(1)-Fe-C(2)	94.0(7)	C(1)-Fe-O(3)	92.9(5)
O(2)-Fe-O(3)	97.2(5)	C(3)-O(3)-Fe	128.9(7)
O(1)-C(1)-Fe	178.5(12)	O(2)-C(2)-Fe	176.6(14)
O(3)-C(3)-C(4)	125.1(10)		



basic enough, displacement of isobutylene from $[\text{CpFe}(\text{CO})_2(\text{isobutylene})]^+$ yields ketone complexes (diphenylcyclopropenone and phenalene; eq 3).³⁴

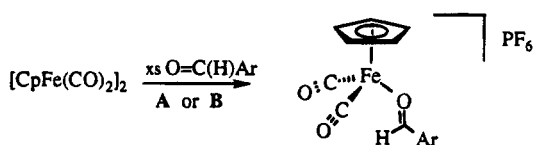


The first method (eq 1) was developed for the synthesis of aromatic aldehyde complexes, as this method potentially offered a simple one-pot procedure. Reaction of $[\text{CpFe}(\text{CO})_2]_2$ with AgPF_6 in CH_2Cl_2 at 0°C in the presence of excess benzaldehyde led immediately to a deep red solution and a gray precipitate. Removal of the precipitate of $\text{Ag}(0)$ followed by addition of excess Et_2O to precipitate the product as previously described afforded red oils which could not be purified further.²⁵ The red sticky solids which could be obtained in some cases displayed some of the desired infrared spectral properties.

(36) Johnson, E. C.; Meyer, T. J.; Winterton, N. *Inorg. Chem.* **1971**, *10*, 1673.

(37) Williams, W. E.; Lalor, F. J. *J. Chem. Soc., Dalton Trans.* **1973**, 1329.

Scheme 1



Compound	Ar	Yield (%)	
		B AgPF ₆	A [Cp ₂ Fe]PF ₆
1	H-	30.7	77.8
2	Me-	41.1	80.5
3	Me ₂ N-	79.0	90.8
4	MeO-	54.7	85.4
5	F ₃ C-	21.1	68.1
6	Cl-	36.7	46.3
7	Me ₂ N-	-	49.0

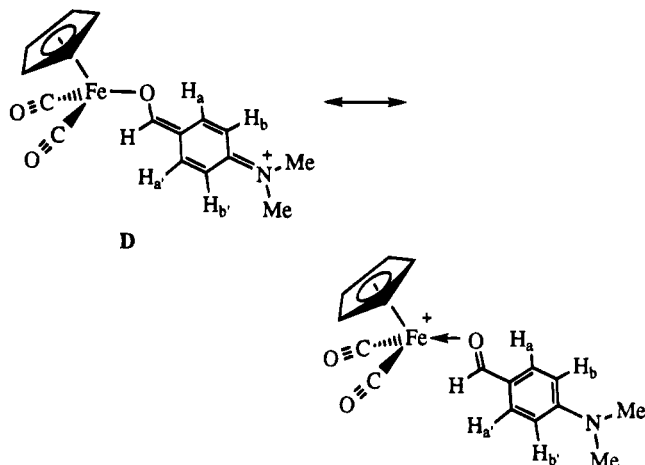
Slow addition of excess Et₂O (over a 1/2 h period) to CH₂Cl₂ solutions containing [CpFe(CO)₂(O=C(H)Ph)]PF₆ (1), however, produced crystalline 1 in good yield (30.7%) and in analytical purity after washing with Et₂O and drying under vacuum. In this manner we were successful in obtaining a series of aromatic aldehyde complexes (Scheme 1, method B). Compounds 1–7 are all highly crystalline red solids and are air stable in the solid state. These complexes have limited solubility in CH₂Cl₂ solution and show signs of decomposition over time in this solvent.

Although a ready method, the yields were not optimal. Variation of the reaction conditions (temperature and concentrations) did not substantially alter the yields for 1. Reactions conducted in chlorobenzene also did not improve yields. A dramatic improvement in the yield was realized (77.8%), however, when AgPF₆ was replaced by [Cp₂Fe]PF₆ as the oxidant (Scheme 1; method A). This substitution not only resulted in substantially higher yields for 1–7, but also resulted in easier workups, as the byproduct ferrocene is soluble in Et₂O and stays in solution; only a small amount of unreacted [Cp₂Fe]PF₆ need be removed prior to crystallization of the product with Et₂O.

Yields of isolated aldehyde complexes obtained by both methods varied as a function of the basic nature of the aldehyde; hence, the highest isolated yields (method A) were realized for *p*-(dimethylamino)benzaldehyde (90.8%) and *p*-anisaldehyde (85.4%), while the lowest yield was obtained for *p*-chlorobenzaldehyde (46.3%). Attempts at isolation of adducts of [CpFe(CO)₂]⁺ with either *p*-nitrobenzaldehyde or pentafluorobenzaldehyde failed, presumably owing to the exceedingly weak donor ability of the carbonyl groups in these electron-deficient aldehydes.

¹H NMR (CD₂Cl₂) spectral characterization of 1, 2, and 4–7 reveals a single set of resonances for each species, consistent with a single isomer existing in solution or rapid equilibration of isomeric complexes. A resonance for the aldehyde proton in each complex is observed in the region 8.5–9.7 ppm, consistent with the

presence of a σ -bound aldehyde.²¹ Compound 3, however, displayed broad resonances for protons of the aromatic ring. Variable-temperature ¹H NMR studies of 3 revealed the signals (protons H_a, H_{a'} and H_b, H_{b'}) to undergo a decolascence phenomenon upon cooling (while all other signals remain sharp down to –80 °C), suggesting that rotation about the aryl-formyl bond is hindered owing to contributions from resonance form D. The spectra are reminiscent of that reported for the



p-anisaldehyde adduct of [HC(py)₃M(NO)₂]²⁺ (M = Mo, W).³⁸ Binding of anisaldehyde to the molybdenum and tungsten Lewis acids resulted in an increase of about 4 kcal/mol in $\Delta G^{\ddagger}_{298}$ for rotation about the aryl-formyl bond. The [CpFe(CO)₂]⁺ cation has been shown to be a weaker Lewis acid than [HC(py)₃M(NO)₂]²⁺,²⁹ thus, this effect is not observed for 4 but becomes apparent in 3 owing to the presence of the more donating NMe₂ versus the OMe group. A value of $\Delta G^{\ddagger}_{298} = 15$ kcal/mol for 3 was obtained, which is 4.5 kcal/mol greater than for free *p*-(dimethylamino)benzaldehyde.³⁷ This is in contrast with the observed reduced activation barrier for rotation about the aryl-formyl bond determined for [Cr(CO)₃(η^6 -*p*-(dimethylamino)benzaldehyde)].³⁹

The carbonyl stretching frequencies for the [CpFe(CO)₂]⁺ fragment in 1–7 (Table 1) are somewhat invariant except for the solid-state spectrum of 4, perhaps for reasons indicated above. Only one set of $\nu_{C=O}$ signals in the FTIR spectra of 1–7 was observed in both solid-state measurements (Nujol mull) and solution-phase studies (CH₂Cl₂). The carbonyl stretch for the aldehyde species was identified in the region of 1550–1650 cm⁻¹, consistent with a σ -ligating mode for these aldehydes and paralleling previously characterized aldehyde and ketone adducts of [CpFe(CO)₂]⁺. The carbonyl stretching frequency of 1555 cm⁻¹ (CH₂Cl₂) for [CpRe(NO)(PPh₃)(σ -*p*-anisaldehyde)]PF₆ is somewhat lower than the values of 1594 and 1586 (sh) cm⁻¹ obtained for 4, consistent with the expected higher Lewis acidity for the rhenium species. The presence of two $\nu_{C=O}$ in the solution FTIR spectrum of 4 might arise from the existence of two isomers with differing orientations of the OMe group with respect to the formyl group.

Complete establishment of the solid-state structure of 6 was achieved through a single-crystal X-ray diffraction study (Figure 1). Table 3 lists atomic coordinates and isotropic displacement parameters. Table 4 lists selected bond distances and angles. As indicated by the infrared studies, the aldehyde is bound to the

(38) Faller, J. W.; Ma, Y. *J. Am. Chem. Soc.* **1991**, *113*, 1579.(39) Roques, B. P. *J. Organomet. Chem.* **1977**, *136*, 33.

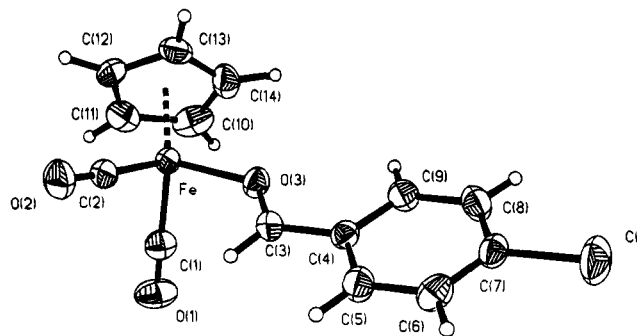


Figure 1. ORTEP diagram of the cation of $[\text{CpFe}(\text{CO})_2(p\text{-chlorobenzaldehyde})]\text{PF}_6$ (**6**).

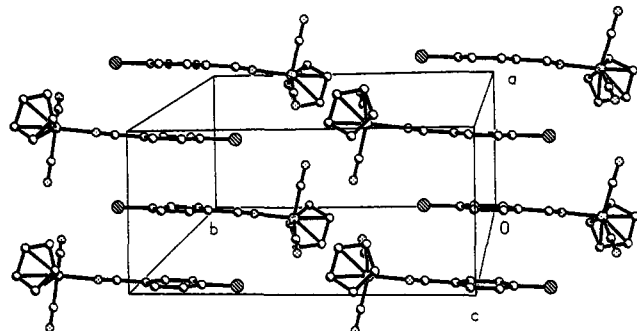


Figure 2. Packing diagram of the cations in $[\text{CpFe}(\text{CO})_2(p\text{-chlorobenzaldehyde})]\text{PF}_6$ (**6**).

Table 7. Important Structural Features of Ketone and Aldehyde Complexes of $[\text{CpFe}(\text{CO})_2]^+$

ketone or aldehyde	Fe—O (Å)	O=C (Å)	Fe—O—C (deg)	ref
<i>p</i> -chlorobenzaldehyde	1.960(3)	1.221(5)	130.9(3)	47
<i>p</i> -anisaldehyde	1.978(7)	1.214(13)	128.9(7)	47
4-methoxy-3-butenolate	1.962		133.9	40
3-methylcyclohexenone	1.980(6)	1.256(10)	133.4(5)	25
tropone	1.983(5)	1.238(8)	136.9(4)	34

organometallic Lewis acid solely through the oxygen atom of the carbonyl group. Four complexes of $[\text{CpFe}(\text{CO})_2]^+$ with ketones have been crystallographically characterized to date: $[\text{CpFe}(\text{CO})_2(\text{tropone})]\text{PF}_6$,³⁴ $[\text{CpFe}(\text{CO})_2(3\text{-methylcyclohexenone})]\text{PF}_6$,²⁵ $[\text{CpFe}(\text{CO})_2(4\text{-methoxy-3-butenolate})]\text{PF}_6$,^{33,40} and $[\text{CpFe}(\text{CO})_2(\text{cinnamaldehyde})]\text{PF}_6$.^{33,40} These structures compare favorably with the structure of the aldehyde complex **6**, as can be seen in Table 7. The most notable difference between **6** and the other structures is the decreased Fe—O bond length of 1.960(3) Å. A shorter C=O bond length can be expected on the basis of the greater inductive effect of the *p*-chlorophenyl group.⁴¹ A shorter Fe—O bond is somewhat counterintuitive, however, as aldehydes are known to bind more weakly than ketones.²⁵ Analysis of the packing of the cations in **6** reveals extensive π -stacking of the aromatic residues in the crystal lattice (Figure 2). It is not clear if such effects would increase, rather than decrease, the iron—oxygen distances.

To pursue this point further, we have conducted crystallographic studies of $[\text{CpFe}(\text{CO})_2(p\text{-anisaldehyde})]\text{PF}_6$ (**4**) and $[\text{CpFe}(\text{CO})_2(\text{benzaldehyde})]\text{PF}_6$ (**1**).⁴² These studies clearly revealed the σ -binding mode for each aldehyde (and a reasonable Fe—O bond length of 1.965-

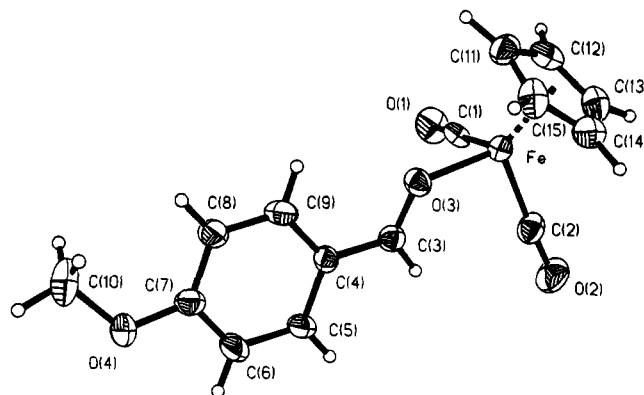


Figure 3. ORTEP diagram of the cation of $[\text{CpFe}(\text{CO})_2(p\text{-anisaldehyde})]\text{SbF}_6$ (**8**).

(10) Å for **1**), but unfortunately the crystals in each case were of insufficient quality and suffered from disorder problems, thus preventing high-quality structural details. For this reason we prepared $[\text{CpFe}(\text{CO})_2(p\text{-anisaldehyde})]\text{SbF}_6$ (**8**) by replacing AgPF_6 with AgSbF_6 (eq 1) as an oxidant to introduce the SbF_6^- anion. Figure 3 shows the resulting ORTEP diagram of the cation of **8**. Table 5 lists atomic coordinates and isotropic displacement parameters. Table 6 lists selected bond distances and angles. The more electron-rich anisaldehyde complex contains a Fe—O distance of 1.987(7) Å, which is significantly longer than the corresponding distance in **6** but shorter than that in all but one of the other structurally characterized ketone complexes listed in Table 7. No stacking of the aromatic residues of **8** is observed in the crystal lattice. The *p*-anisaldehyde ligand is essentially coplanar in the structures of **8**, $[\text{CpRe}(\text{NO})(\text{PPh}_3)(p\text{-anisaldehyde})]\text{PF}_6$, and $[\text{Zn}(\text{SeC}_6\text{H}_2\text{tBu}_3)_2(p\text{-anisaldehyde})]_2$.⁴³ The corresponding C=O distances are 1.214(13), 1.271(8), and 1.242(10) Å respectively.

Shortened Fe—O bond lengths for **6** and **8** might be justified if there exists a significant π -back-bonding component to the bonding in the Fe—O bond, especially in light of the shorter Fe—O bond length for **6** relative to **8**. Such effects are clearly manifested in the Re—O and Re—C distances for π -bound aldehydes of $[\text{CpRe}(\text{NO})(\text{PPh}_3)]^+$.⁴⁴ Structurally characterized σ -bound aldehyde and ketone complexes of $[\text{CpRe}(\text{NO})(\text{PPh}_3)]^+$ suggest a similar trend (albeit smaller).²¹ Thus, $[\text{CpRe}(\text{NO})(\text{PPh}_3)(p\text{-anisaldehyde})]\text{PF}_6$, $[\text{CpRe}(\text{NO})(\text{PPh}_3)(\text{acetophenone})]\text{PF}_6$, and $[\text{CpRe}(\text{NO})(\text{PPh}_3)(\text{acetone})]\text{PF}_6$ display Re—O bond distances of 2.080(5), 2.080(5), and 2.099(5) Å, respectively. Observation of an elongated C=O bond length (1.271(8) Å) for $[\text{CpRe}(\text{NO})(\text{PPh}_3)(p\text{-anisaldehyde})]\text{PF}_6$ and comparisons to other σ -bound aldehyde complexes led Gladysz and co-workers to first point out the structural consequences of π -back-bonding in these complexes. Arguments for π -back-bonding in $[\text{CpFe}(\text{CO})_2(\text{acrolein})]\text{PF}_6$ have also been forwarded to explain the reduced lability of the Fe—O bond relative to stronger organometallic Lewis acids used for catalysis of the Diels—Alder reaction between acrolein and isoprene.²⁹ Yields for compounds **1**–**7**, however, do not reflect the added stability which should occur for the electron-deficient aldehydes.

(40) Shambayati, S.; Schreiber, S. L. Personal communication.

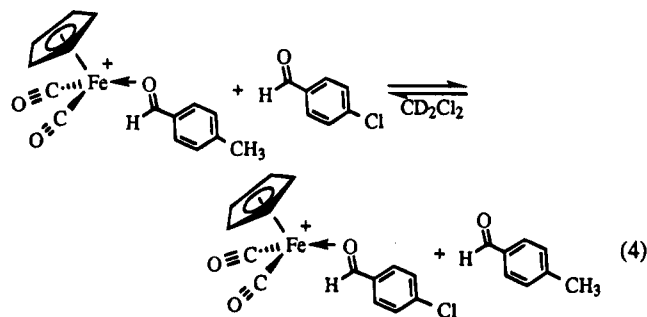
(41) Berthier, G.; Serre, J. In *The Chemistry of the Functional Groups*; Patai, S., Ed.; Interscience: New York, 1966; Vol. 1, p 1.

(42) The unpublished structure of $[\text{CpFe}(\text{CO})_2(\eta^1\text{-benzaldehyde})]\text{SbF}_6$ is mentioned in ref 26.

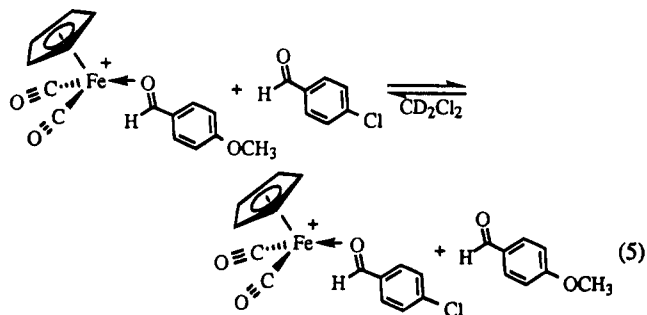
(43) Bochmann, M.; Webb, K. J.; Hursthouse, M. B.; Mazid, M. J. *Chem. Soc., Chem. Commun.* **1991**, 1735.

(44) Boone, B. J.; Klein, D. P.; Méndez, N. Q.; Seyler, J. W.; Arif, A. M.; Gladysz, J. A. *J. Chem. Soc., Chem. Commun.* **1995**, 279.

We thus decided to determine if the existence of π -back-bonding in these complexes would necessarily result in increased stability in the resultant aldehyde complex. The competitive binding of several of the aldehydes to the organometallic Lewis acid $[\text{CpFe}(\text{CO})_2]^+$ was investigated by ^1H NMR. Addition of *p*-chlorobenzaldehyde to a CD_2Cl_2 solution of $[\text{CpFe}(\text{CO})_2(p\text{-tolualdehyde})]\text{PF}_6$ leads to partial formation of $[\text{CpFe}(\text{CO})_2(p\text{-chlorobenzaldehyde})]\text{PF}_6$ and free *p*-tolualdehyde. The equilibrium (eq 4) was rapidly established,



and NMR integration of the characteristic aldehyde protons revealed the relative amounts of the species present. Addition of *p*-tolualdehyde to a CD_2Cl_2 solution of $[\text{CpFe}(\text{CO})_2(p\text{-chlorobenzaldehyde})]\text{PF}_6$ (the complementary experiment) leads to the same equilibrium distribution of products, and an average K_{eq} value of 0.26 was obtained. This value corresponds to a difference in bond strengths (if differential solvation effects are ignored) of about 1 kcal/mol. We have also determined $K_{\text{eq}} = 0.075$ for the corresponding set of competition experiments between *p*-chlorobenzaldehyde and *p*-anisaldehyde (eq 5). Both of these values are consis-



tent with expectations that the more electron-rich carbonyls should serve as better ligands for the organometallic Lewis acid.

Recently the commonly held belief that shorter bonds always reflect stronger bonds has been challenged.⁴⁵ Ernst and co-workers have discovered that PX_3 ($\text{X} = \text{Me}, \text{OMe}, \text{F}$) adducts of the open titanocene $\text{Ti}(2,4\text{-C}_7\text{H}_{11})$ ($\text{C}_7\text{H}_{11} = \text{dimethylpentadienyl}$) display titanium-phosphorus bond lengths that decrease across this series, while at the same time the titanium-phosphorus bond strengths decrease. π -Back-bonding would be expected to lead to shorter bonds, but for these complexes the differing electronegativities of the ligand substituents apparently lead to differing orbital contributions or extensions for the $\text{Ti}-\text{P}$ bond. The data in Table 7 clearly indicate that the more strongly held ketones have the longer $\text{Fe}-\text{O}$ bonds, while the weaker

aldehyde adducts have the shorter $\text{Fe}-\text{O}$ bond lengths. Thus, binding of aldehydes and ketones to $[\text{CpFe}(\text{CO})_2]^+$ follows the same behavior as PR_3 adducts of $[\text{Ti}(2,4\text{-C}_7\text{H}_{11})]$.

A possible explanation for the counterintuitive $\text{Fe}-\text{O}$ bond lengths may lie in repulsive ($2c-4e$) interactions between the Fp -centered HOMO and the filled π -orbital of the carbonyl group. Fenske-Hall calculations on the isoelectronic $[\text{CpFe}(\text{PH}_3)_2(\text{vinyl})]$ system have shown that such repulsive interactions are more important than attractive π -backbonding interactions.⁴⁶ The current complexes may be even more sensitive to such interactions, owing to the lower energy of the $[\text{CpFe}(\text{CO})_2]^+$ HOMO's compared to HOMO's of $[\text{CpFe}(\text{PH}_3)_2]^+$ and to the polarization of the carbonyl π -bond (causing it to be O-centered). The longer $\text{Fe}-\text{O}$ bonds observed for the Fp^+ ketone (and *p*-anisaldehyde) adducts compared to those for the *p*-chlorobenzaldehyde complex could be justified by an increase in the energy of the π -orbital of the carbonyl group and increased repulsive interactions. We cannot conclude at this time, however, how the presence of shortened bond lengths or π -backbonding effects may influence the rates of substitution in $[\text{CpFe}(\text{CO})_2(\text{aldehyde})]\text{PF}_6$ or how the reactivity of the bound aldehydes in such complexes may be influenced. These effects may be most important for comparisons among different Lewis acids.²⁹

Conclusions

Syntheses of a series of aromatic aldehyde complexes of the organometallic Lewis acid $[\text{CpFe}(\text{CO})_2]^+$ have revealed that even with π -acidic aromatic aldehydes the organic carbonyl groups display only σ -binding modes. No evidence for the alternative side-bound, or π -bound, isomers was detected by ^1H NMR and FTIR studies. We have further obtained the single-crystal X-ray structures of two of these species, $[\text{CpFe}(\text{CO})_2(p\text{-chlorobenzaldehyde})]\text{PF}_6$ and $[\text{CpFe}(\text{CO})_2(p\text{-anisaldehyde})]\text{SbF}_6$, which clearly demonstrate that binding occurs exclusively through the oxygen atom of the carbonyl group. These structures reveal shortened $\text{Fe}-\text{O}$ bond distances that could be rationalized by the presence of π -backbonding between the iron complex and the aldehydes. Shortened $\text{Fe}-\text{O}$ bond distances in these complexes do not appear to result in increased $\text{Fe}-\text{O}$ bond strengths, however, and suggest that repulsive ($2c-4e$) interactions between the filled iron-centered HOMO and the π -orbital of the carbonyl group may be equally or more influential than π -backbonding in dictating $\text{Fe}-\text{O}$ distances.

Acknowledgment. We gratefully acknowledge support for this work by a CWRU Research Initiation Grant, crystallographic assistance by Rebecca Zaniewski, and an insightful reviewer for bringing ref 46 to our attention.

Supporting Information Available: Structural diagrams and tables of all bond distances and angles, anisotropic thermal parameters, and H atom positional parameters for **6** and **8** (10 pages). Ordering information is given on any current masthead page.

OM9503959

(45) Ernst, R. D.; Freeman, J. W.; Stahl, L.; Wilson, D. R.; Arif, A. M.; Nuber, B.; Ziegler, M. L. *J. Am. Chem. Soc.* **1995**, *117*, 5075.

(46) Kostic, N. M.; Fenske, R. F. *Organometallics* **1982**, *1*, 974.

(47) This work.

Synthesis and Structure of Zirconium–Group 13 Heterobimetallic Compounds

Francis M. G. de Rege, William M. Davis, and Stephen L. Buchwald*

Department of Chemistry, Massachusetts Institute of Technology,
Cambridge, Massachusetts 02139

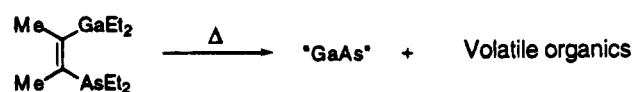
Received April 18, 1995[®]

The reaction of main-group (B, Al, and Ga) alkoxides with zirconocene complexes of benzyne was used to prepare novel zirconium–group 13 heterobimetallic compounds [R₂E-(μ-OR')(μ-1,2-aryl)Zr(η⁵-C₅H₅)₂] [E = B, R = Et, R' = Me, aryl = phenyl (**1**); E = B, R = Me, R' = Et, aryl = phenyl (**2**); E = B, R = Et, R' = Me, aryl = 3-methoxyphenyl (**3**); E = Al, R = Et, R' = Et, aryl = phenyl (**5**); E = Ga, R = Me, R' = Me, aryl = 3-methoxyphenyl (**6**)] and [(EtO)₂B(μ-1,2-naphthyl)Zr(η⁵-C₅H₅)₂(OEt)] (**4**). Complexes **3** and **4** have been characterized by X-ray crystallography. Compound **3** contains a dative bond from an oxygen lone pair of the methoxy ligand on the zirconium to an acceptor p-orbital on the boron atom (¹¹B NMR; δ 8.26 ppm). In contrast, the weakly Lewis acidic boron center in **4** (¹¹B NMR; δ 29.7 ppm) does not show a bonding interaction between the alkoxy ligand on the zirconocene fragment and the boron center.

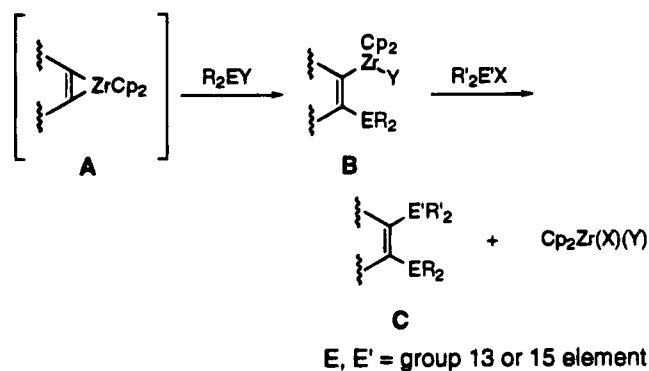
Introduction

Much of the current interest in main-group heterobimetallic complexes is due to their potential use as single source precursors for electronic, optical, or refractory materials.¹ Vicinally disubstituted olefins or arenes with two main-group fragments would be interesting to study as possible precursors to ceramic materials (Scheme 1), but few of these compounds are known.² Since we have been interested in the synthesis of novel main-group compounds *via* zirconocene-mediated routes for several years,³ the synthesis of such main-group complexes is an attractive goal. Scheme 2 shows how this could be achieved, possibly as a one-pot procedure, in two transmetalation steps from a zirconocene complex of an alkyne or aryne. In the first step, as described by Erker,⁴ a main-group compound would react with a zirconocene aryne or alkyne complex **A** giving a heterobimetallic complex **B**. In the second step, the transmetalation from zirconium to a main-group species^{3,5} would then lead to the desired compounds **C**.

Scheme 1.



Scheme 2



We recently reported a procedure for the preparation of zirconium–boron heterobimetallic complexes by the reaction of borates and borinates with zirconocene complexes of arynes. The most interesting aspect of these reactions was that the combination of (EtO)₃B with zirconocene benzyne complexes led to a product which contained the boron fragment *ortho* to the substituent on the benzene ring. In contrast, when Et₂BOMe was used, the product observed had the boron fragment *meta* to the substituent on the benzene ring.

[®] Abstract published in *Advance ACS Abstracts*, September 1, 1995.

(1) (a) Cowley, A. H.; King, C. S.; Deeken, A. *Organometallics* **1995**, *14*, 20. (b) Cleaver, W. M.; Späth, M.; Hnyk, D.; McMurdo, G.; Power, M. B.; Stuke, M.; Rankin, D. W. H.; Barron, A. R. *Organometallics* **1995**, *14*, 690. (c) Wells, R. L. *Coord. Chem. Rev.* **1992**, *112*, 273. (d) Jones, A. C. *J. Cryst. Growth* **1993**, *129*, 728. (e) Cowley, A. H.; Jones, R. A. *Polyhedron* **1994**, *13*, 1149. (f) Petrie, M. A.; Power, P. P. *Organometallics* **1993**, *12*, 1592. (g) Wells, R. L.; McPhail, A. T.; Self, M. F.; Laske, J. A. *Organometallics* **1993**, *12*, 3333. (h) Beachley, O. T., Jr.; Royster, T. L., Jr.; Arhar, J. R.; Rheingold, A. L. *Organometallics* **1993**, *12*, 1976.

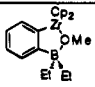
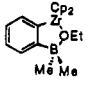
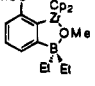
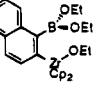
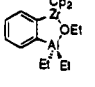

(2) (a) Wrackmeyer, B.; Guldner, G.; Abu-Orabi, S. T. *Tetrahedron* **1989**, *45*, 1119. (b) Wang, K. K.; Chu, K. H.; Lin, Y.; Chen, J. H. *Tetrahedron* **1989**, *45*, 1105. (c) Schacht, W.; Kaufmann, D. *J. Organomet. Chem.* **1987**, *331*, 139. (d) Kaufmann, D. *Chem. Ber.* **1987**, *120*, 901. (e) Kersch, S.; Wrackmeyer, B. *J. Chem. Soc., Chem. Commun.* **1985**, 1199. (f) Schewchuk, E.; Wild, S. B. *J. Organomet. Chem.* **1977**, *128*, 115. (g) Binger, P.; Köster, R. *J. Organomet. Chem.* **1974**, *73*, 205.

(3) (a) Buchwald, S. L.; Fisher, R. A.; Foxman, B. M. *Angew. Chem., Int. Ed. Engl.* **1990**, *29*, 771. (b) Fisher, R. A.; Nielsen, R. B.; Davis, W. M.; Buchwald, S. L. *J. Am. Chem. Soc.* **1991**, *113*, 165. (c) Spence, R. E. v. H.; Hsu, D. P.; Buchwald, S. L. *Organometallics* **1992**, *11*, 3492. (d) Hsu, D. P.; Warner, B. P.; Fisher, R. A.; Davis, W. M. *Organometallics* **1994**, *13*, 5160. (e) Buchwald, S. L.; Fisher, R. A.; Davis, W. M. *Organometallics* **1989**, *8*, 2082.

(4) (a) Albrecht, M.; Erker, G.; Nolte, M.; Krüger, C. *J. Organomet. Chem.* **1992**, *427*, C21. (b) Erker, G.; Albrecht, M. *Organometallics* **1992**, *11*, 3517. (c) Erker, G.; Albrecht, M.; Krüger, C.; Werner, S. *J. Am. Chem. Soc.* **1992**, *114*, 8531. (d) Erker, G.; Noe, R.; Wingbermühle, D. *Chem. Ber.* **1994**, *127*, 805. (e) Erker, G.; Noe, R.; Wingbermühle, D. *Angew. Chem., Int. Ed. Engl.* **1993**, *32*, 1213.

(5) (a) Fagan, P. J.; Nugent, W. A.; Calabrese, J. C. *J. Am. Chem. Soc.* **1994**, *116*, 1880. (b) Fryzuk, M. D. *Chemica Scripta* **1989**, *29*, 427. (c) Cole, T. E.; Quintanilla, R. *J. Org. Chem.* **1992**, *57*, 7366. (d) Deloux, L.; Skrzypczak-Jankun, E.; Cheesman, B. V.; Srebniak, M. *J. Am. Chem. Soc.* **1994**, *116*, 10302. (e) Negishi, E.; Takahashi, T. *Synthesis* **1988**, 1. (f) Zablocka, M.; Igau, A.; Majoral, J. P.; Pietrusiewicz, K. M. *Organometallics* **1993**, *12*, 603. (g) Boutonnet, F.; Dufour, N.; Straw, T.; Igau, A.; Majoral, J. P. *Organometallics* **1991**, *10*, 3939.

Table 1. Results for the Synthesis of Zirconium–Main-Group Aromatic Compounds

Compound	Structure	Isolated Yield
1		78%
2		54%
3		52%
4		55%
5		44%
6		52% ^a

^a Isolated as an inseparable mixture of **6a** and **6b** in a ratio of 65:35.

Thus, the regioselectivity could be manipulated by the choice of boron reagent used. It was shown that these intermediate complexes could be converted, without isolation, to the corresponding halophenols, resulting in an overall regioselective synthesis of halophenols.⁶

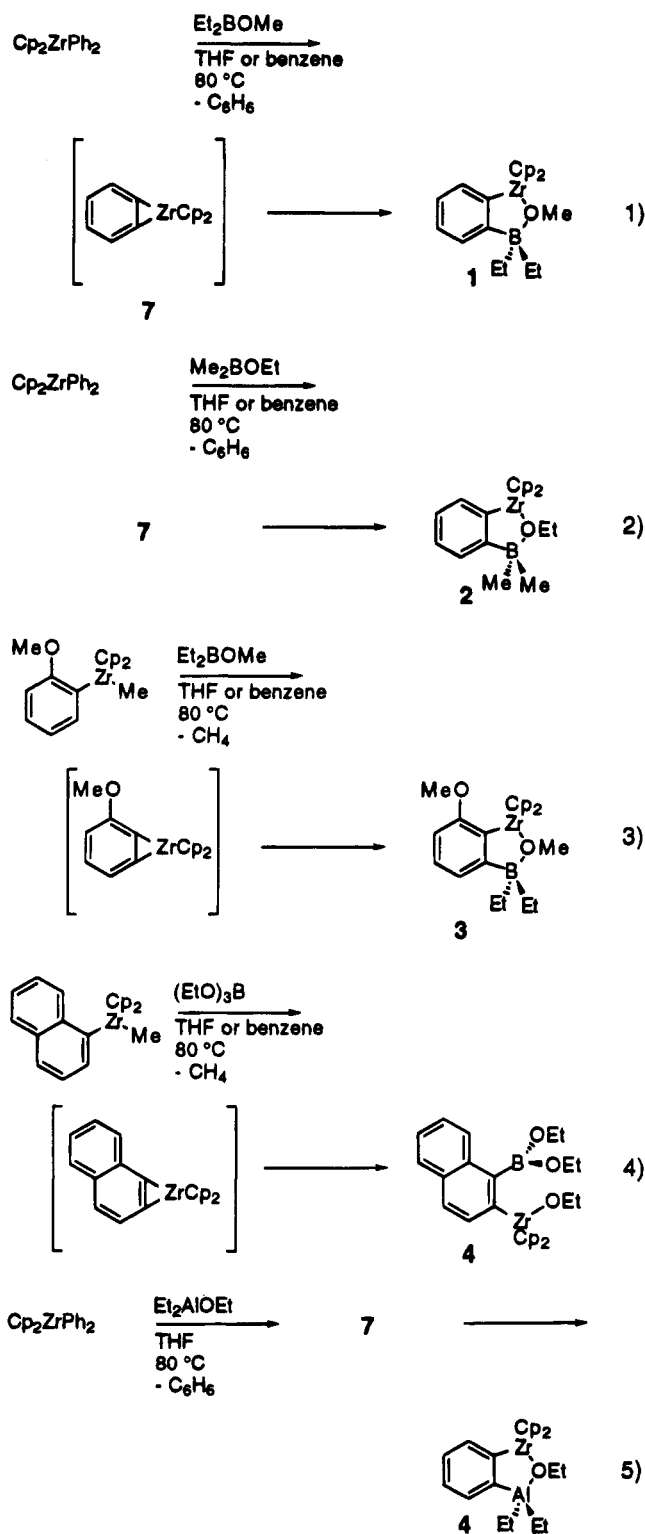
Herein we report, for the first time, the isolation and characterization of several of the complexes (**1–4**, Table 1) which were intermediates in our procedure for the synthesis of halophenols. The structures of **3** and **4**, as determined by X-ray crystallography, are also reported. In addition, we have isolated the aluminum (**5**) analogue of **1** and gallium (**6**) analogue of **3**.

Results and Discussion

The zirconium–group 13 heterobimetallic compounds that were prepared are listed in Table 1. These were all made by treating a group 13 alkoxide with an appropriate zirconocene complex of an aryne.⁷ The products were obtained in 80–90% yield (¹H NMR) and were isolated in yields of 44–78% (based on Cp₂ZrPh₂ for **1**, **2**, and **5** and based on Cp₂Zr(Me)Cl for **3**, **4**, and **6**).

Treatment of **7**, generated *in situ* from diphenylzirconocene, with either Et₂BOMe or Me₂BOEt in THF or benzene leads, respectively, to the isolation of **1** (78%) or **2** (54%) (eqs 1 and 2). Similarly, **3** (52%) and **4** (55%) were prepared from zirconocene–aryne complexes and Et₂BOMe or (EtO)₃B (eqs 3 and 4). It was not possible to isolate the benzene analog of **4** in pure form (it was ~80% pure as estimated by ¹H NMR).

While the reactions of borates and borinates with **7** proceeded in benzene, the reaction of Et₂AlOEt and **7** needs a more coordinating solvent and was carried out in THF (eq 5). We attribute this to the strong heteroatom mediated bridging that occurs in aluminum com-



plexes.⁸ These highly bridged structures would make the aluminum–oxygen bond less likely to react with the zirconium–carbon bond of **7** based on steric and electronic grounds. In a coordinating solvent such as THF, the oligomers are broken up by the interaction of THF with the aluminum center.

When we performed the reaction of Me₂GaOMe with **7**, we found that ligand exchange occurs between the phenyl ligands on Cp₂ZrPh₂ and the methoxy ligands

(6) de Rege, F. M. G.; Buchwald, S. L. *Tetrahedron* **1995**, *51*, 4291.
(7) Broene, R. D.; Buchwald, S. L. *Science* **1993**, *261*, 1696.

(8) (a) Eisch, J. J. In *Comprehensive Organometallic Chemistry*, Wilkinson, G., Ed.; Pergamon: New York, 1982; Vol. 1; pp 555–682.
(b) Odom, J. D. In *Comprehensive Organometallic Chemistry*, Wilkinson, G., Ed.; Pergamon: New York, 1982; pp 253–310.

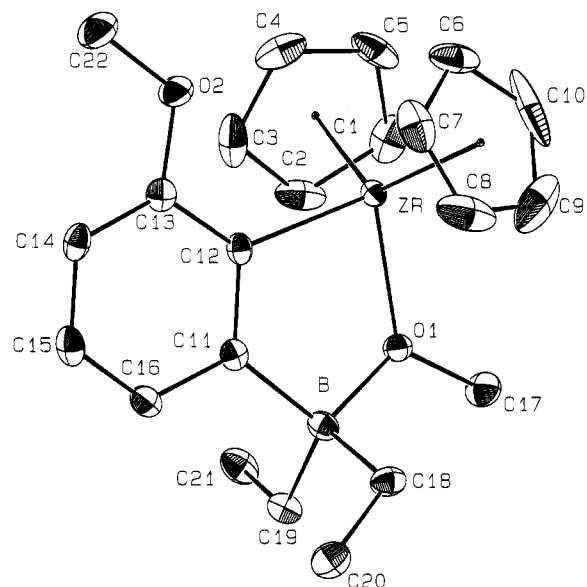
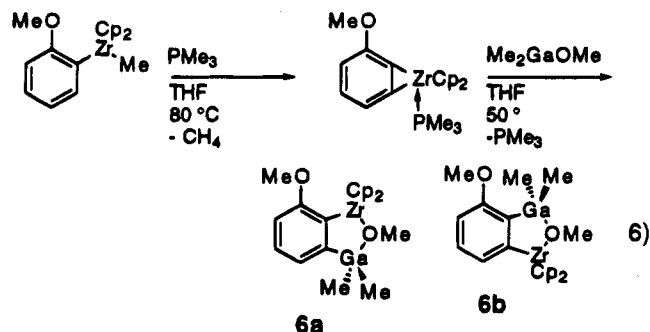


Figure 1. ORTEP drawing of **3** (thermal ellipsoids at 35% probability).

on Me_2GaOMe . We therefore generated the PMe_3 adduct of the zirconocene-benzyne complex, 7-PMe_3 , which was then treated with Me_2GaOMe (eq 6). Unlike the reaction with boron reagents, the reaction was not very regioselective, giving a 52% isolated yield of **6** as a 65:35 mixture of isomers **a** and **b**.⁹



Single crystals of **3**, suitable for X-ray structure determination, were obtained by the slow diffusion of pentane into a saturated solution of **3** in toluene. An ORTEP diagram of **3** is shown in Figure 1, and selected bond lengths and bond angles of **3** are given in Table 2.

For comparison to **3**, the structure of **4** was also determined by X-ray crystallography. Single crystals of **4** were obtained by the diffusion of pentane into a saturated solution of **4** in toluene at -40°C over a 2 week period. There are two fragments in the unit cell of **4** where one fragment (fragment 2) has some disorder. An ORTEP diagram of **4** is shown in Figure 2, while Table 3 lists some important bond lengths and angles of **4** taken from fragment 1. The corresponding values for fragment 2 do not vary from these values significantly.

Figure 3 highlights some of the structural features of **3** and **4**. The $\text{B}-\text{O}(1)$ bond length in **3** of $1.622(5)\text{ \AA}$ is slightly longer than the sum of covalent radii (1.54

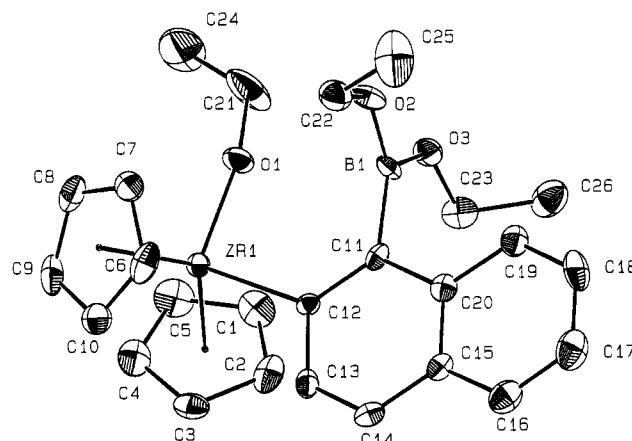


Figure 2. ORTEP drawing of **4** (thermal ellipsoids at 35% probability).

Table 2. Selected Bond Lengths and Angles for **3**

atoms	length (\AA)	atoms	angle (deg)
Zr-O(1)	2.104(2)	O(1)-Zr-C(12)	83.2(1)
Zr-C(12)	2.231(4)	Zr-C(12)-C(13)	130.2(3)
B-O(1)	1.622(5)	O(1)-B-C(11)	104.5(3)
B-C(18)	1.635(6)	O(1)-B-C(18)	107.4(3)
B-C(19)	1.627(6)	O(1)-B-C(19)	107.9(3)
B-C(11)	1.629(6)	C(11)-B-C(18)	112.4(3)
O(1)-C(17)	1.432(5)	C(11)-B-C(19)	113.8(3)
O(2)-C(22)	1.423(5)	C(18)-B-C(19)	110.3(3)
C(11)-C(12)	1.412(5)	C(11)-C(12)-C(13)	120.0(3)
C(12)-C(13)	1.406(5)	C(12)-C(13)-C(14)	122.2(4)
C(13)-C(14)	1.381(6)	C(13)-C(14)-C(15)	118.0(4)
C(14)-C(15)	1.388(6)	C(14)-C(15)-C(16)	121.3(4)
C(15)-C(16)	1.377(6)	C(11)-C(16)-C(15)	121.9(4)
C(16)-C(11)	1.420(6)	Zr-O(1)-B	116.8(2)
		Zr-O(1)-C(17)	124.9(2)
		B-O(1)-C(17)	117.5(3)

Table 3. Selected Bond Lengths and Angles for **4**, Fragment 1

atoms	length (\AA)	atoms	angle (deg)
Zr-O(1)	1.916(5)	O(1)-Zr-C(12)	97.9(2)
Zr-C(12)	2.302(6)	Zr-C(12)-C(13)	118.4(9)
B-O(1)	2.84	Zr-O(1)-C(21)	160.2(6)
B-O(2)	1.357(9)	O(2)-B-C(11)	124.0(7)
B-O(3)	1.353(9)	O(3)-B-C(11)	123.5(7)
B-C(11)	1.60(1)	O(2)-B-O(3)	112.2(6)
O(1)-C(21)	1.36(1)	C(20)-C(11)-B	116.6(6)
O(2)-C(22)	1.417(9)	C(11)-C(12)-C(13)	117.3(6)
C(3)-C(23)	1.416(9)	C(12)-C(13)-C(14)	123.8(6)
C(11)-C(12)	1.391(9)	C(13)-C(14)-C(15)	119.7(6)
C(12)-C(13)	1.423(9)	C(14)-C(15)-C(16)	121.4(7)
C(13)-C(14)	1.368(9)	C(15)-C(16)-C(17)	120.7(7)
C(14)-C(15)	1.409(9)	C(16)-C(17)-C(18)	120.7(7)
C(15)-C(20)	1.407(9)	C(17)-C(18)-C(19)	119.8(7)
C(15)-C(16)	1.411(9)	C(18)-C(19)-C(20)	121.5(7)
C(16)-C(17)	1.35(1)	C(11)-C(20)-C(15)	120.6(6)
C(17)-C(18)	1.40(1)	C(11)-C(20)-C(19)	121.9(6)
C(18)-C(19)	1.37(1)	C(15)-C(20)-C(19)	117.5(6)
C(19)-C(20)	1.423(9)		
C(20)-C(11)	1.450(9)		

\AA),¹⁰ consistent with a dative interaction. In contrast, the $\text{B}-\text{O}(1)$ distance in **4** is greater than 2.8 \AA , implying that there is no bond. In **3**, the coordination environment of boron is almost tetrahedral where the average bond distance from boron to the carbon atoms bonded to it is $1.630(6)\text{ \AA}$, a characteristic value for tetracoor-

(9) A difference NOE experiment supported the assignment of isomers. A 1.8% NOE was found in compound **6a** between the methyl groups on the gallium atom and the ortho proton on the aromatic ring. A 1.0% NOE was found in compound **6b** between the methyl groups on the gallium and the ortho methoxy group.

(10) (a) Pelter, A.; Smith, K. In *Comprehensive Organic Chemistry*, Jones, D. N., Ed.; Pergamon: New York, 1979; Vol. 3, pp 915-924. (b) Nöth, H.; Staude, S.; Thomann, M.; Kroner, J.; Paine, R. T. *Chem. Ber.* **1994**, *127*, 1923. (c) Rettig, S. J.; Trotter, J.; Kliegel, W.; Nanninga, D. *Can. J. Chem.* **1978**, *56*, 1676.

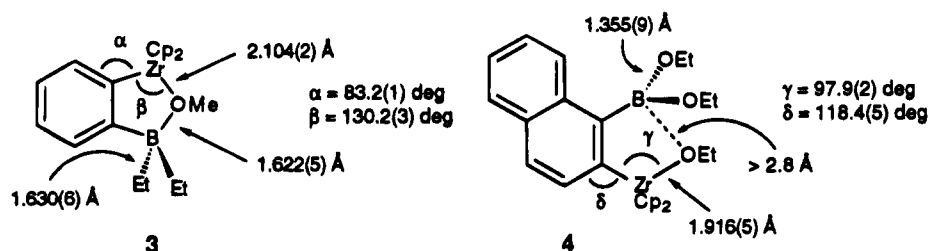
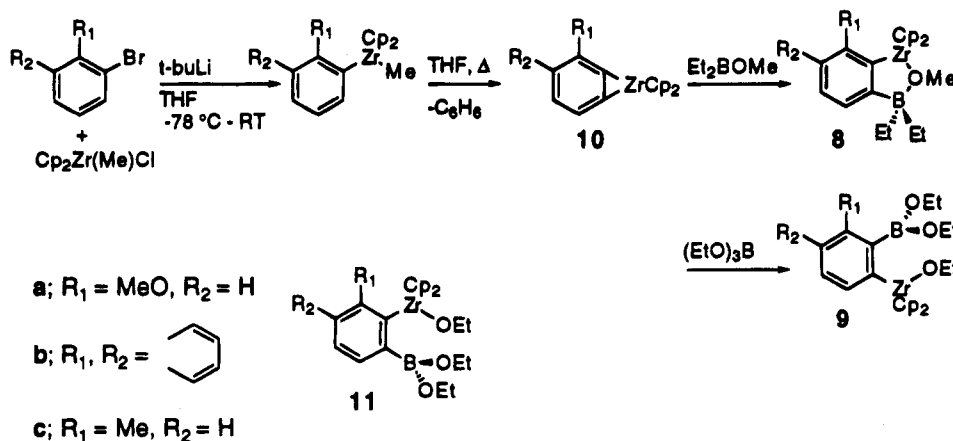


Figure 3.

Scheme 3



dinate boron compounds (typically 1.62–1.65 Å).^{8b} The average boron–oxygen (ethoxy ligands) bond distance in **4** is 1.355(9) Å, which is a typical value for a tricoordinated alkoxy boron compound (1.38 Å for (EtO)₃B). The geometry of **3**, where the aryl ring, boron, zirconium, and oxygen are nearly coplanar,¹¹ does not allow for zirconium–oxygen multiple bonding to occur, and therefore, the Zr–O(1) bond length of 2.104(2) Å is close to that expected for a zirconium–oxygen single bond (~2.0 Å).¹² In comparison, **4** has a Zr–O(1) bond length of 1.916(5) Å implying that there may be some multiple bond character in the zirconium–oxygen bond due to π -donation from an oxygen lone pair to an empty orbital on zirconium. The C(12)–Zr–O(1) bond angle (γ , Scheme 3) in **4** of 97.9(2)^o is in the range expected for a d^0 Cp₂ZrR₂ complex,¹³ while the corresponding angle in **3** (β , Scheme 3) of 83.2(1)^o is smaller than theoretically expected but close to that seen for other oxazirconacycles.¹⁴

The solution structures of compounds **1–4** were probed by ¹¹B NMR. The chemical shifts indicated that the boron atoms in **1–3** are tetracoordinate while in **4** the boron center is tricoordinate. For comparison, the chemical shifts of these zirconium–boron complexes and some other known boron compounds are listed (Table 4). The chemical shift of compounds **1–3** are those of a fairly electron-rich boron center, such as a borate. This is consistent with a bridging alkoxide between the boron and zirconium in **1–3**. The ¹H NMR spectra of **1** and **3**

Table 4. Representative ¹¹B Chemical Shifts

borane	δ (ppm, $\delta(\text{BF}_3\cdot\text{Et}_2\text{O}) = 0$)
Li[B(Ph) ₄] ^a	-16.6
Li[B(OMe) ₄] ^a	2.7
PhB(OMe) ₂ ^b	28.7
1	7.13
2	1.14
3	8.29
4	29.65

^a See ref 15. ^b See ref 10a.

show that the methylene protons are diastereotopic, also consistent with a bridging structure. In contrast, the ¹¹B NMR chemical shift for **4** suggests a boron center that is moderately electron rich, such as a borinate. For example, the chemical shift of **4** is very similar to that of PhB(OMe)₂.^{10a} From this, and the solid state structure, it is reasonable to assume that there is no bridging alkoxy group between the boron and the zirconium of **4** in solution.

The different structures seen in **1–3** vs **4** can be explained by the electronic nature of the boron center. In **4**, π -donation from an oxygen lone pair partially fills the empty p-orbital on the boron and decreases its tendency to bridge. Since no π -donation is available for **1–3**, the electrophilic boron center takes on an additional ligand in the form of a bridging methoxy group.

The reaction of Et₂BOMe and (EtO)₃B with zirconocene complexes of substituted benzynes proceeded to give zirconium–boron complexes **8** and **9**, respectively (Scheme 3). We previously have shown that these insertion reactions are highly regioselective and that the regioisomer obtained could in most cases be controlled by the boron reagent used.⁶ For the reactions of compounds containing unsaturated functional groups with **10**, the insertion reaction is also highly regioselective, but only insertion from the less hindered side of **10** occurs leading to the kinetic product.^{7,16} Similarly, the reaction of Et₂BOMe with **10** gives the expected

(11) For the plane containing the aromatic ring, Zr, O(1), and B, the mean deviation from the plane is 0.0683 Å.

(12) Howard, W. A.; Parkin, G. *J. Am. Chem. Soc.* **1994**, *116*, 606.

(13) Lauher, J. W.; Hoffmann, R. *J. Am. Chem. Soc.* **1976**, *98*, 1729.

(14) (a) Seyferth, D.; Wang, T.; Davis, W. M. *Organometallics* **1994**, *13*, 4134. (b) Mashima, K.; Yamakawa, M.; Takaya, H. *J. Chem. Soc., Dalton Trans.* **1991**, 2851. (c) Tikkanen, W. R.; Petersen, J. L. *Organometallics* **1984**, *3*, 1651. (d) Erker, G.; Engel, K.; Atwood, J. L.; Hunter, W. E. *Angew. Chem., Int. Ed. Engl.* **1983**, *22*, 494.

(15) Nöth, H.; Vahrenkamp, H. *Chem. Ber.* **1966**, 1049.

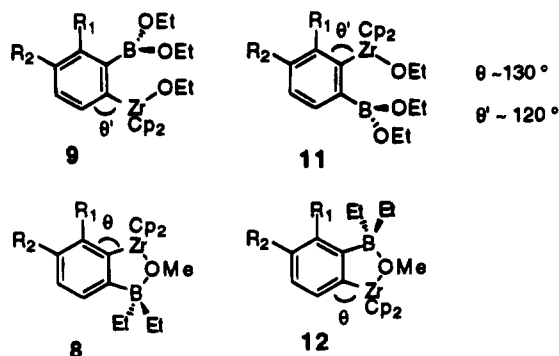


Figure 4.

Table 5. Effect of Temperature on the Product Distribution in the Reaction of 10a with (EtO)₃B

temp (°C)	reacn	ratio of isomers	
		11a	9a
25	10a·PMe ₃ + (EtO) ₃ B	95	5
80	10a + (EtO) ₃ B	50	50
110	10a + (EtO) ₃ B	21	79

kinetic product **8**. In contrast, the reaction of (EtO)₃B with **10b** or **10c** gives **9b** or **9c**, where the boron reagent ultimately approaches from the more congested side of **10**. In the reaction of (EtO)₃B with **10a**, both **9a** and **11a** were obtained.

As shown in Table 5, the ratio of **9a** to **11a** depended on the temperature at which the reaction was carried out. At room temperature the reaction of **10a**·PMe₃ with (EtO)₃B gave mostly **11a** (**a** to **b**, 95:5). At 110 °C the ratio is reversed (**a** to **b**, 21:79). At the intermediate temperature of 80 °C, equilibration is slow and the ratio after 1 week is 50:50. Thus the product mixture at room temperature is the kinetic one while that formed at 110 °C represents the thermodynamic distribution.

The reason that **9** and related compounds are more stable than their corresponding regioisomers (e.g., **11**) is probably steric in nature. In **11** the substituent on the aromatic ring (R₁) is close to the large zirconocene fragment, while in **9** the same substituent is positioned next to the relatively small B(OEt)₂ fragment (Figure 4). One might expect that the same arguments should apply in comparing the relative stabilities of **8** and **12** (Figure 4). As previously noted, however, only **8**¹⁷ is observed when **7** is generated in the presence of Et₂BOMe. This may be due to the methoxy group which bridges between the zirconium and boron in **8**, pulling the zirconium away from the substituent R₁, leading to a lessening of the steric interaction between R₁ and the zirconocene fragment in **8**. The boron-centered group in **12** is also effectively larger than that in **9**, since it is sp³ hybridized, exacerbating the interaction of R₁ with the BEt₂ fragment in **12** relative to that of R₁ with the B(OEt)₂ fragment in **9**.

In the case of the reaction between Me₂GaOMe and **10a**·PMe₃ it is not clear why two isomers (**6a**, **b**) are observed. We suspected that **6a** might be favored kinetically while **6b** would predominate under thermodynamic conditions. We noticed that heating the mixture **6a**, **b** to higher temperatures led to a change in

the ratios of **6a** to **6b** (65:35 for **a** to **b** at 50 °C, 32:68 for **a** to **b** at 110 °C) but significant decomposition to unknown products also occurred, diminishing the relevance of this observation. The structure of **6** may be important in understanding the observed isomeric distribution; unfortunately, attempts to grow single crystals of **6** or an analog suitable for X-ray crystallographic analysis have, to date, been unsuccessful.

In summary we have prepared a series of zirconium-group 13 heterobimetallic compounds by the reaction of zirconocene-aryne complexes and main-group complexes containing alkoxy ligands. The crystal structures of zirconium-boron heterobimetallic complexes **3** and **4** as well as ¹¹B NMR have shown these to have very different structures both in the solid state and in solution. The most important difference in the structures of **3** and **4** is that **3** contains a methoxy ligand bonded to boron and zirconium while **4** has no bridging alkoxide. We believe that this structural difference causes different intermolecular steric interactions in **3** and **4**, accounting, at least in part, for the different regiochemistry observed in the reactions to form these complexes.

Experimental Section

General Considerations. All reactions were carried out under an atmosphere of purified argon or nitrogen using standard Schlenk techniques. Transfer and storage of air-sensitive, moisture-sensitive, or hygroscopic materials were performed in a Vacuum Atmospheres Co. drybox under an atmosphere of nitrogen. Nuclear magnetic resonance (NMR) spectra were recorded on a Varian Unity-300 or a Varian XL-300 Fourier transform spectrometer. Melting points were determined with a Haake Buchler melting point apparatus and are uncorrected. Gas chromatography (GC) analyses were performed on a Hewlett-Packard Model 5890 gas chromatograph with a flame ionization detector and a Model 3392A integrator using a 25 m capillary column with polymethylsiloxane (Hewlett-Packard) as a stationary phase. Combustion analysis was performed by E&R Microanalytical Laboratory, Corona, NY.

Tetrahydrofuran (THF), toluene, and pentane were dried and deoxygenated by refluxing and distilling from sodium/benzophenone ketyl under an argon atmosphere. Diphenylzirconocene was prepared by the reaction of zirconocene dichloride with phenylmagnesium bromide.¹⁸ Zirconocene methyl chloride¹⁹ and Me₂GaOMe²⁰ were prepared by the published procedures. All other reagents were commercially available and used without further purification.

Preparation of Et₂B(μ-OMe)(μ-1,2-phenyl)ZrCp₂ (1). A dry sealable Schlenk tube with a stirring bar was charged with diphenylzirconocene (0.376 g, 1 mmol) in a glovebox. The flask was removed from the glovebox and attached to a Schlenk line, and THF (10 mL) was added. Et₂BOMe (0.26 mL, 2 mmol) was added *via* syringe. The flask was sealed and heated in an oil bath at 80 °C for 18 h. After the reaction mixture was allowed to cool to room temperature, the volatiles were removed *in vacuo*. The crude boron-zirconium complex was redissolved in toluene (5 mL), and pure product was precipitated from the solution upon slow addition of pentane (20 mL) and cooling in an ice bath. The solvents were decanted from

(16) Buchwald, S. L.; Watson, B. T.; Lum, R. T.; Nugent, W. A. *J. Am. Chem. Soc.* **1987**, *109*, 7137.

(17) Compound **8c** was heated at 110 °C in THF-*d*₈ for 2 days, and only decomposition vs mesitylene internal standard was seen. Nothing attributable to **12** was observed.

(18) (a) Erker, G. *J. Organomet. Chem.* **1977**, *134*, 189. (b) Samuel, E.; Rausch, M. E. *J. Am. Chem. Soc.* **1973**, *95*, 6263.

(19) Wales, P. C.; Weigold, H.; Bell, P. *J. Organomet. Chem.* **1971**, *33*, 181.

(20) Coats, G. E.; Hayter, R. G. *J. Am. Chem. Soc.* **1953**, 2519.

the solids *via* cannula filtration, and the product was washed twice with cold pentane (10 mL). Residual solvents were removed *in vacuo* to give **1**, 0.310 g (78%), as a bright yellow powder: ^1H NMR (300 MHz, CD_2Cl_2) δ 0.53 (m, 4H), 0.71 (t, $J = 7.2$ Hz, 6H), 3.16 (s, 3), 6.30 (s, 10H), 6.91 (m, 3H), 7.15 (d, $J = 6.3$ Hz, 1H); ^{13}C NMR (300 MHz, THF- d_6) δ 11.66, 15.33 (broad), 52.71, 114.85, 124.09, 125.14, 133.75, 135.69, 193.80; ^{11}B NMR (300 MHz, C_6D_6 , $\text{BF}_3\text{-OEt}_2$ ext. ref.) δ 7.13; mp 118–124 °C. Anal. Calcd for $\text{C}_{21}\text{H}_{27}\text{OZrB}$: C, 63.46; H, 6.85. Found: C, 63.30; H, 6.63.

Preparation of $\text{Me}_2\text{B}(\mu\text{-OEt})(\mu\text{-1,2-phenyl})\text{ZrCp}_2$ (2**).** Compound **2** was made in a similar fashion as **1** except that Me_2BOEt (0.28 g, 2 mmol) was used instead of Et_2BOME . The yield for **2** was 0.207 g (54%) of a bright yellow powder: ^1H NMR (300 MHz, CD_2Cl_2) δ -0.11 (s, 6H), 1.24 (t, $J = 7.0$ Hz, 3H), 3.83 (q, $J = 7.2$ Hz, 2H), 6.16 (s, 10H), 6.88 (dd, $J = 7.2$ Hz, 1H), 6.93 (dd, $J = 7.2$ Hz, 1H), 7.16 (d, $J = 6.9$ Hz, 1H), 7.20 (d, $J = 6.6$ Hz, 1H); ^{13}C NMR (300 MHz, THF- d_6) δ 11.05 (broad), 18.40, 64.86, 113.43, 124.65, 125.84, 134.75, 136.02, 192.73; ^{11}B NMR (300 MHz, C_6D_6 , $\text{BF}_3\text{-OEt}_2$ ext. ref.) δ 1.14; mp 146–147 °C. Anal. Calcd for $\text{C}_{20}\text{H}_{25}\text{OZrB}$: C, 62.62; H, 6.57. Found: C, 62.30; H, 6.35.

Preparation of $\text{Et}_2\text{B}(\mu\text{-OMe})(\mu\text{-1,2-(3-methoxyphenyl)})\text{ZrCp}_2$ (3**).** A dry sealable Schlenk tube was charged with zirconocene (methyl) chloride (1.088 g, 4 mmol) in a glovebox. The flask was removed from the glovebox and attached to a Schlenk line, and THF (20 mL) was added. The flask was then charged with 2-bromoanisole (0.50 mL, 4 mmol) and cooled to -78 °C. Using a gastight syringe, *tert*-butyllithium (3.6 mL, 1.7 M in pentane, 6 mmol) was added. After 15 min, the flask was removed from the -78 °C bath and allowed to warm to room temperature. Et_2BOME (1.05 mL, 8 mmol) was added *via* syringe, and the flask was sealed and then heated in an oil bath for 18 h at 80 °C. After the reaction mixture was allowed to cool to room temperature, the volatiles were removed *in vacuo*. Residual THF was removed from the crude product by adding toluene (10 mL) and removing this under vacuum. The product was dissolved in toluene (10 mL) and the resulting solution cannula filtered from the solid impurities to a round bottom Schlenk flask. The toluene was removed *in vacuo* to give a solid which was dissolved in a minimal quantity of toluene (~5 mL). Product precipitated out of the solution upon slow addition of pentane (20 mL) and cooling in an ice bath. The solvents were decanted using a cannula filter, and the remaining solid was washed twice with cold pentane (5 mL). Residual solvents were removed *in vacuo* to give 0.889 g (52%) of yellow product: ^1H NMR (300 MHz, C_6D_6) δ 0.94 (m, 4H), 1.20 (t, $J = 7.6$ Hz, 6H), 2.65 (s, 3H), 3.40 (s, 3H), 5.98 (s, 10H), 6.43 (d, $J = 7.1$ Hz, 1H), 7.28 (m, 2H); ^{13}C NMR (300 MHz, THF- d_6) δ 11.72, 15.26, 52.21, 54.56, 104.75, 114.65, 126.03, 127.37, 162.74, 178.04; ^{11}B NMR (300 MHz, C_6D_6 , $\text{BF}_3\text{-OEt}_2$ ext. ref.) δ 8.29; mp 149–154 °C. Anal. Calcd for $\text{C}_{22}\text{H}_{30}\text{BO}_2\text{Zr}$: C, 61.67; H, 7.06. Found: C, 61.62; H, 6.96.

Preparation of $(\text{EtO})_2\text{B}(\mu\text{-1,2-naphthyl})\text{ZrCp}_2(\text{OEt})$ (4**).** A dry sealable Schlenk tube was charged with zirconocene (methyl) chloride (0.544 g, 2 mmol) in a glovebox. The flask was removed from the glovebox and attached to a Schlenk line, and THF (20 mL) was added. The flask was then charged with 1-bromonaphthalene (0.28 mL, 2 mmol) and cooled to -78 °C. Using a gastight syringe, *tert*-butyllithium (1.8 mL, 1.7 M in pentane, 3 mmol) was added. After 15 min, the flask was removed from the -78 °C bath and allowed to warm to 0 °C over 20 min. $(\text{EtO})_2\text{B}$ (0.68 mL, 4 mmol) was added *via* syringe. The flask was sealed and was then heated in an oil bath for 5 h at 50 °C. After the reaction mixture was allowed to cool to room temperature, the volatiles were removed *in vacuo*. Residual THF was removed from the crude product by the addition of toluene (10 mL) and removing this *in vacuo*. The product was dissolved in toluene (10 mL) and the resulting solution cannula filtered from the insoluble materials to a round bottom Schlenk flask where the filtrate was concentrated *in vacuo*. Crystals and powdered product were obtained

from the crude product by diffusion of pentane into a concentrated solution of the product in toluene at -40 °C over 2 weeks. The solids were isolated and residual solvents were removed *in vacuo*, to yield 0.543 g (55%) of a mixture of yellow powder and crystals: ^1H NMR (300 MHz, C_6D_6) δ 1.03 (t, $J = 7.1$ Hz, 3H), 1.17 (t, $J = 7.1$ Hz, 6H), 3.96 (m, 4H), 4.00 (q, $J = 7.0$ Hz, 2H), 5.92 (s, 10H), 7.40 (m, 3H), 7.63 (d, $J = 8.1$ Hz, 1H), 7.81 (d, $J = 8.1$ Hz, 1H), 7.98 (d, $J = 8.1$ Hz, 1H); ^{13}C NMR (300 MHz, THF- d_6) δ 17.88, 20.79, 60.37, 69.81, 112.23, 123.48, 124.56, 125.23, 127.87, 129.15, 132.13, 136.73, 136.88, 180.68; ^{11}B NMR (300 MHz, C_6D_6 , $\text{BF}_3\text{-OEt}_2$ ext. ref.) δ 29.65; mp 115–120 °C. Anal. Calcd for $\text{C}_{26}\text{H}_{31}\text{O}_3\text{ZrB}$: C, 63.27; H, 6.33. Found: C, 63.26; H, 6.58.

Preparation of $\text{Et}_2\text{Al}(\mu\text{-OEt})(\mu\text{-1,2-phenyl})\text{ZrCp}_2$ (5**).** A dry sealable Schlenk tube with a stirring bar was charged with diphenylzirconocene (0.376 g, 1 mmol) in a glovebox. The flask was removed from the glovebox and attached to a Schlenk line, and THF (10 mL) was added. Et_2AlOEt (0.63 mL, 1.6 M in toluene, 1 mmol) was added *via* syringe. The flask was sealed, and the solution was heated in an oil bath for 18 h at 80 °C. After the reaction mixture was allowed to cool to room temperature, the volatiles were removed *in vacuo*. Residual THF was removed from the crude product by addition of toluene (10 mL) and removing the solvent mixture under vacuum. Pentane (10 mL) was added to the crude aluminum-zirconium complex, and the flask was sonicated for 30 min leading to a brown suspension in an orange solution. The solution was cannula filtered into a round bottom Schlenk flask, and the solvents were removed under vacuum until approximately 2 mL of solution remained as well as an orange precipitate. The flask was cooled in an ice bath while the solvents were decanted from the solids. Residual solvents were removed *in vacuo* leaving 0.188 g (44%) of a light orange-brown powder: ^1H NMR (300 MHz, C_6D_6) δ 0.27 (m, 4H), 1.15 (t, $J = 6.9$ Hz, 3H), 1.35 (t, $J = 8.0$ Hz, 6H), 3.34 (q, $J = 6.9$ Hz, 2H), 5.54 (s, 10H), 7.21 (m, 2H), 7.56 (m, 1H), 7.98 (m, 1H); ^{13}C NMR (300 MHz, THF- d_6) δ 1.46 (broad), 10.36, 18.47, 67.27, 109.98, 126.55, 127.66, 133.70, 139.25, 201.81; mp 96–98 °C. Anal. Calcd for $\text{C}_{22}\text{H}_{29}\text{OZrAl}$: C, 61.79; H, 6.83. Found: C, 61.73; H, 6.90.

Preparation of $\text{Me}_2\text{Ga}(\mu\text{-OMe})(\mu\text{-1,2-(3-methoxyphenyl)})\text{ZrCp}_2$ (6a,b**).** A dry sealable Schlenk tube was charged with zirconocene (methyl) chloride (0.544 g, 2 mmol) in a glovebox. The flask was removed from the glovebox and attached to a Schlenk line, and THF (20 mL) was added. The flask was then charged with 2-bromoanisole (0.25 mL, 2 mmol) and cooled to -78 °C. Using a gastight syringe, *tert*-butyllithium (1.8 mL, 1.7 M in pentane, 3 mmol) was added. After 15 min, the flask was removed from the -78 °C bath and allowed to warm to room temperature. PMe_3 (1 mL, 10 mmol) was added to the solution *via* syringe. The flask was sealed and was then heated in an oil bath for 18 h at 80 °C. After the reaction mixture was allowed to cool to room temperature, the volatiles were removed *in vacuo*. THF (20 mL) was added to dissolve the solids, and Me_2GaOMe (0.288 g, 2.2 mmol) was added to the solution. The flask was again sealed and was heated in an oil bath at 50 °C for 6 h. The flask was removed from the oil bath, and after cooling of the solution to room temperature, the solvents were removed *in vacuo*. Residual THF was removed from the crude product by addition of toluene (10 mL) and removing this under vacuum. Pentane (50 mL) was added to the product, and the flask was sonicated for 1 h. The solution was cannula filtered from the solids and concentrated to approximately 3 mL. The solution was cooled in an ice bath and decanted from the precipitates that had formed. Residual solvent was removed *in vacuo* leaving 0.477 g (52%) of an off-white powder which was a mixture of the two isomers **6a,b** in the ratio of 65:35,⁹ respectively. When the reaction was run at approximately 110 °C,²¹ a yield of 0.266 g (29%) was obtained where the ratio of **6a** to **6b** was 32:68. **6a**: ^1H NMR (300 MHz, C_6D_6) δ 0.01 (s, 6H), 3.09 (s, 3H), 3.49 (s, 3H), 5.78 (s, 10H), 6.38 (dd, $J = 6.0, 3.0$ Hz, 2H), 7.23 (d, J

Table 6. Crystal Data for 3 and 4

	compd	
	3	4
mol formula	C ₂₂ H ₂₉ BO ₂ Zr	C ₂₆ H ₃₁ BO ₃ Zr
mol wt	428.51	493.56
cryst color	orange	orange
cryst habit	prismatic	prismatic
cryst dimens, mm	0.380 × 0.320 × 0.430	0.280 × 0.410 × 0.320
cell constns		
<i>a</i> , Å	9.4805(8)	8.242(1)
<i>b</i> , Å	14.300(1)	16.628(1)
<i>c</i> , Å	15.204(1)	17.700(1)
<i>α</i> , Å		89.92(3)
<i>β</i> , deg	101.84(2)	90.63(2)
<i>γ</i> , deg		90.36(3)
<i>V</i> , Å ³	2017.4(6)	2425.5(6)
space group	<i>P</i> 2 ₁ / <i>c</i>	<i>P</i> 1
<i>Z</i>	4	4
<i>D</i> _{calc} , g/cm ³	1.411	1.352
diffractometer	Enraf-Nonius CAD-4	Enraf-Nonius CAD-4
radiation	Mo Kα (0.710 69 Å)	Mo Kα (0.710 69 Å)
temp, °C	86	86
attenuator	Zr foil (factor = 17.9)	Zr foil (factor = 17.9)
take off angle, deg	2.8	2.8
scan rate, deg/min	1.9–16.5 (in <i>ω</i>)	1.9–16.5 (in <i>ω</i>)
scan width	0.80 + 0.35 tan <i>θ</i>	0.80 + 0.35 tan <i>θ</i>
2 <i>θ</i> _{max} , deg	49.9	45.1
reflcs measd	3934	7041
unique reflcs	3700	607
corrs		
Lorenz–polarization	0.87–1.19	0.94–1.05
abs	(transm factors)	(transm factors)
secondary extinctn	0.95402 × 10 ⁻⁷ (coeff)	0.26846 × 10 ⁻⁶ (coeff)
obsd reflcs	2791 (<i>I</i> > 3.00σ(<i>I</i>))	4543 (<i>I</i> > 3.00σ(<i>I</i>))
no. variables	236	569
<i>R</i>	0.039	0.049
<i>R</i> _w	0.041	0.052
mas/min in final diff map, e/Å ³	0.41, -0.58	0.48, -0.67
GOF	3.64	1.43

= 3.0 Hz, 1H), 7.24 (d, *J* = 6.0 Hz, 1H); ¹³C NMR (300 MHz, THF-*d*₈) δ 7.32, 54.99, 58.29, 107.64, 128.60, 130.15, 163.10, 199.38. **6b**: ¹H NMR (300 MHz, C₆D₆) δ 0.08 (s, 6H), 3.15 (s, 3H), 3.43 (s, 3H), 5.66 (s, 10H), 6.42 (d, *J* = 7.8 Hz, 1H), 7.10 (d, *J* = 6.9 Hz, 1H), 7.28 (dd, *J* = 7.5 Hz, 2H); ¹³C NMR (300 MHz, THF-*d*₈) δ 6.78, 55.22, 57.83, 106.77, 112.21, 128.43, 129.59, 166.26, 199.38. Anal. Calcd for C₂₀H₂₅O₂ZrGa: C, 52.41; H, 5.50. Found: C, 52.23; H, 5.57.

Preparation of (EtO)₂B(μ-1,2-(3-methoxyphenyl))ZrCp₂(OEt) (9a, 11a). The procedure used is the same as that for **3** except that (1) (EtO)₃B (0.34 mL, 2 mmol) was used instead of Et₂BOMe, (2) three different reaction temperatures were used leading to different ratios of **9a** to **11a**, and (3) the product could not be isolated cleanly and so its structure was deduced by conversion to methoxyphenol. Integration of ¹H NMR cyclopentadiene resonances of **9a** (δ 5.81) and **11a** (δ 6.00) was used for determination of the isomeric ratios listed in Table 5.

Temperature Dependence of the Product Ratio. These experiments were done in toluene-*d*₈²² with mesitylene as an internal standard. The room-temperature reaction was done using **8a**·PMe₃ as in the synthesis of **6**, and the ratio of **9a** to **11a** observed was 5:95. The reaction run at 80 °C gave a ratio of **9a** to **11a** of 50:50 after heating for 1 week. At 110 °C, the product ratio of **9a** and **11a** was 79:21 after 18 h.

Derivatization. The reaction to synthesize **9a** and **11a** was done at 110 °C in THF.²¹ The solvents were removed from the crude **9a** and **11a** products, and this was redissolved in

THF. An aqueous solution of HCl (2 mL, 10%) was added *via* syringe. The reaction flask was cooled in an ice bath, and NaOH (5 mL, 3 M) was added dropwise followed by the dropwise addition of H₂O₂ (3 mL, 30%). This was allowed to stir for 15 min at 0 °C and then allowed to warm up to room temperature. Excess sodium thiosulfate was used to quench the reaction, and the crude product was extracted in ether (3 × 50 mL). The product was dried over magnesium sulfate and concentrated *in vacuo*. The GC and ¹H NMR showed two main products of >95% purity in a ratio of 7:3. Comparison with purchased materials showed 2-methoxyphenol (70%) and 3-methoxyphenol (30%).

X-ray Data Collection, Structure Determination, and Refinement. General Comments. A summary of the data collection parameters is given in Table 6. The crystals were mounted on a glass fiber. All measurements were made on an Enraf-Nonius CAD-4 diffractometer with graphite monochromated Mo Kα radiation. Cell constants, listed in Table 6, and an orientation matrix for data collection were obtained from a least-squares refinement using the setting angles of 25 carefully centered reflections in the range of 14.00 < 2*θ* < 22.00°.

The data were collected at -86 °C using the *ω*-2*θ* scan technique. Moving crystal moving counter background measurements were made by scanning an additional 25% above and below the scan range. The counter aperture consisted of a variable horizontal slit with a width ranging from 2.0 to 2.5 mm and a vertical slit set to 2.0 mm. The diameter of the incident beam collimator was 0.7 mm, and the crystal to detector distance was 21 cm. For intense reflections an attenuator was automatically inserted in front of the detector.

An empirical absorption correction, using the program DIFABS,²³ was applied which resulted in the transmission factors listed in Table 6. The intensities were corrected for

(21) To measure the temperature, a thermometer was placed inside a sealable Schlenk tube (200 mL, 20 cm from the bottom to the seal) with 10 mL of THF. It was found that when the tube was immersed up to the level of the solvent in an oil bath set at 150 °C, the temperature of the THF was 110 °C.

(22) These experiments were also done in THF, and approximately the same ratios were observed.

Table 7. Atomic Coordinates and B Values (\AA^2) for 3

atom	x	y	z	B(eq)
Zr	0.23690(4)	0.24212(2)	-0.00152(2)	1.54(1)
O(1)	0.4603(3)	0.2206(2)	0.0146(2)	1.8(1)
O(2)	0.0284(3)	0.3792(2)	-0.1646(2)	2.7(1)
C(1)	0.2416(6)	0.2876(3)	0.1588(3)	3.4(2)
C(2)	0.3100(5)	0.3604(4)	0.1224(3)	3.3(2)
C(3)	0.2053(7)	0.4036(3)	0.0566(3)	3.7(2)
C(4)	0.0759(5)	0.3574(4)	0.0535(3)	3.7(2)
C(5)	0.0981(5)	0.2876(4)	0.1157(3)	3.6(2)
C(6)	0.0154(5)	0.1469(4)	-0.0520(4)	3.9(2)
C(7)	0.0741(6)	0.1552(4)	-0.1271(3)	3.7(2)
C(8)	0.1988(7)	0.1086(5)	-0.1135(5)	5.3(3)
C(9)	0.2216(7)	0.0696(4)	-0.0311(7)	7.0(4)
C(10)	0.109(1)	0.0932(5)	0.0090(4)	6.3(3)
C(11)	0.4154(4)	0.3320(3)	-0.1209(2)	1.7(1)
C(12)	0.2679(4)	0.3306(3)	-0.1169(2)	1.7(1)
C(13)	0.1695(4)	0.3877(3)	-0.1749(3)	2.0(1)
C(14)	0.2119(5)	0.4467(3)	-0.2366(3)	2.2(2)
C(15)	0.3572(5)	0.4498(3)	-0.2394(3)	2.4(2)
C(16)	0.4564(4)	0.3947(3)	-0.1836(3)	2.2(2)
C(17)	0.5439(5)	0.1587(3)	0.0790(3)	2.7(2)
C(18)	0.5791(4)	0.1765(3)	-0.1213(3)	2.3(2)
C(19)	0.6820(4)	0.3186(3)	-0.0122(3)	2.3(2)
C(20)	0.6560(5)	0.2037(3)	-0.1959(3)	2.9(2)
C(21)	0.6635(5)	0.3905(3)	0.0586(3)	2.7(2)
C(22)	-0.0762(5)	0.4381(4)	-0.2181(4)	3.6(2)
B	0.5372(4)	0.2639(3)	-0.0623(3)	1.9(2)

Lorentz and polarization effects. A correction for secondary extinction was also applied. No decay corrections were required since the crystals displayed crystal and electronic stability.

The structure was solved using direct methods.²⁴ The non-hydrogen atoms were refined anisotropically.

Neutral atom scattering factors were taken from Cromer and Waber.²⁵ Anomalous dispersion effects were included in F_c ; the values for $\Delta f'$ and $\Delta f''$ were those of Cromer.²⁶ All calculations were performed using the TEXSAN²⁷ crystallographic software package of Molecular Structure Corp.

X-ray Data Collection, Structure Determination, and Refinement for 3. On the basis of the systematic absences of $h0l$, $l \neq 2n$, and $0k0$; $k \neq 2n$, and the successful solution and refinement of the structure, the space group was determined to be $P2_1/c$.

The final cycle of full-matrix least-squares refinement was based on 2791 observed reflections ($I > 3.00\sigma(I)$) and 236 variable parameters and converged (largest parameter shift was 0.00 times its esd) with $R = 0.039$ and $R_w = 0.041$.

The standard deviation of an observation of unit weight was 3.64. The weighting Scheme was based on counting statistics and included a factor ($p = 0.02$) to downweight the intense reflections. Plots of $\sum w(|F_o| - |F_c|)^2$ vs $|F_o|$, reflection order in data collection, $(\sin \theta)/\lambda$, and various classes of indices showed no unusual trends. The maximum and minimum peaks on the final difference Fourier map corresponded to 0.41 and -0.58 e/\AA^3 , respectively.

The final values for refined coordinates of **3** are given in Table 7.

X-ray Data Collection, Structure Determination, and Refinement for 4. On the basis of systematic absences of

Table 8. Atomic Coordinates and B Values (\AA^2) for 4

atom	x	y	z	B(eq)
Zr(1)	0.22144(8)	0.02010(4)	0.79061(4)	1.95(3)
O(1)	-0.0045(5)	0.0392(3)	0.8068(3)	3.2(3)
O(2)	-0.2068(5)	-0.0096(3)	0.6626(3)	2.7(2)
O(3)	-0.2144(5)	-0.1064(3)	0.7513(3)	2.8(2)
C(1)	0.190(1)	-0.0750(5)	0.9021(5)	3.9(4)
C(2)	0.301(1)	-0.1104(4)	0.8553(4)	3.5(4)
C(3)	0.442(1)	-0.0616(5)	0.8544(4)	3.3(4)
C(4)	0.410(1)	0.0028(5)	0.9031(5)	3.8(4)
C(5)	0.256(1)	-0.0047(5)	0.9310(4)	4.0(5)
C(6)	0.319(1)	0.0902(4)	0.6715(4)	3.5(4)
C(7)	0.200(1)	0.1389(4)	0.6996(5)	3.2(4)
C(8)	0.253(1)	0.1698(4)	0.7680(5)	3.6(4)
C(9)	0.407(1)	0.1403(5)	0.7832(5)	3.9(4)
C(10)	0.449(1)	0.0912(4)	0.7235(5)	3.6(4)
C(11)	0.0457(8)	-0.1035(4)	0.6693(4)	2.0(3)
C(12)	0.1938(8)	-0.0758(4)	0.6975(4)	1.7(3)
C(13)	0.3367(8)	-0.1109(4)	0.6681(4)	2.4(3)
C(14)	0.3358(9)	-0.1693(4)	0.6137(4)	2.5(3)
C(15)	0.1869(9)	-0.1982(4)	0.5844(4)	2.3(3)
C(16)	0.181(1)	-0.2587(5)	0.5286(4)	3.5(4)
C(17)	0.037(1)	-0.2848(5)	0.5000(5)	4.1(5)
C(18)	-0.109(1)	-0.2513(5)	0.5240(4)	3.8(4)
C(19)	-0.1064(9)	-0.1937(4)	0.5791(4)	2.9(4)
C(20)	0.0419(9)	-0.1649(4)	0.6112(4)	2.3(3)
C(21)	-0.144(1)	0.0607(8)	0.8419(7)	9.9(8)
C(22)	-0.150(1)	0.0325(5)	0.5982(5)	3.6(4)
C(23)	-0.164(1)	-0.1747(5)	0.7930(4)	3.4(4)
C(24)	-0.149(1)	0.1292(7)	0.8855(7)	8.0(7)
C(25)	-0.254(1)	0.0149(6)	0.5312(5)	6.2(6)
C(26)	-0.286(1)	-0.2412(5)	0.7822(5)	4.6(5)
B(1)	-0.126(1)	-0.0707(5)	0.6966(4)	2.1(4)
Zr(2)	0.22912(8)	0.51940(4)	0.71978(4)	1.82(3)
O(4)	0.4527(5)	0.5354(3)	0.6976(3)	2.5(2)
O(5)	0.6703(5)	0.4813(3)	0.8378(2)	2.2(2)
O(6)	0.6509(5)	0.3822(3)	0.7513(3)	2.7(2)
C(27)	0.134(1)	0.5889(4)	0.8392(4)	3.0(4)
C(28)	0.266(1)	0.6342(4)	0.8140(4)	3.1(4)
C(29)	0.224(1)	0.6693(4)	0.7444(5)	3.3(4)
C(30)	0.066(1)	0.6456(4)	0.7271(4)	3.0(4)
C(31)	0.0095(9)	0.5961(4)	0.7854(4)	2.9(4)
C(32)	0.172(1)	0.4948(5)	0.5809(4)	3.4(4)
C(33)	0.243(1)	0.4241(5)	0.6081(4)	3.3(4)
C(34)	0.137(1)	0.3884(4)	0.6595(4)	3.3(4)
C(35)	-0.0018(9)	0.4376(5)	0.6639(4)	3.0(4)
C(36)	0.021(1)	0.5014(4)	0.6141(4)	3.1(4)
C(37)	0.4052(8)	0.3938(4)	0.8410(4)	1.8(3)
C(38)	0.2577(8)	0.4238(4)	0.8143(4)	1.8(3)
C(39)	0.1124(8)	0.3922(4)	0.8467(4)	2.1(3)
C(40)	0.1144(8)	0.3364(4)	0.9024(4)	2.5(3)
C(41)	0.2615(8)	0.3051(4)	0.9306(4)	2.1(3)
C(42)	0.265(1)	0.2470(5)	0.9888(4)	3.4(4)
C(43)	0.409(1)	0.2187(5)	1.0164(5)	4.2(5)
C(44)	0.555(1)	0.2466(5)	0.9869(4)	3.8(4)
C(45)	0.5549(9)	0.3028(4)	0.9300(4)	2.9(4)
C(46)	0.4068(8)	0.3343(4)	0.9000(4)	2.0(3)
C(47)	0.597(1)	0.5564(6)	0.6627(5)	5.8(5)
C(48)	0.6320(9)	0.5255(4)	0.9035(4)	3.3(4)
C(49)	0.576(1)	0.3135(5)	0.7156(5)	4.3(5)
C(50)	0.588(1)	0.5980(7)	0.5942(6)	7.6(7)
C(51)	0.747(1)	0.5044(5)	0.9658(4)	4.0(4)
C(52)	0.644(3)	0.292(2)	0.648(1)	7(2)
C(52*)	0.715(3)	0.261(1)	0.694(2)	6(1)
B(2)	0.575(1)	0.4214(5)	0.8080(4)	1.9(4)

$h0l$, $l \neq 2n$, and $0k0$, $k \neq 2n$, and the successful solution and refinement of the structure, the space group was determined to be $P2_1/c$.

The final cycle of full-matrix least-squares refinement was based on 4543 observed reflections ($I > 3.00\sigma(I)$) and 569 variable parameters and converged (largest parameter shift was 0.00 times its esd) with $R = 0.049$ and $R_w = 0.052$.

The standard deviation of an observation of unit weight was 1.43. The weighting Scheme was based on counting statistics and included a factor ($p = 0.02$) to downweight the intense reflections. Plots of $\sum w(|F_o| - |F_c|)^2$ vs $|F_o|$, reflection order in

(23) Walker, N.; Stuart, D. *Acta Crystallogr.* **1983**, A39, 158.

(24) (a) Gilmore, C. J. *J. Appl. Crystallogr.* **1984**, 17, 42. (b) Beurskens, P. T. Direct Methods for Difference Structures—an automatic procedure for phase extension and refinement of difference structure factors, Crystallography Laboratory, Nijmegen, The Netherlands, 1984.

(25) Cromer, D. T.; Waber, J. T. *International Tables for X-Ray Crystallography*; The Kynoch Press: Birmingham, England, 1974; Vol. IV, Table 2.2.A.

(26) Cromer, D. T. *International Tables for X-Ray Crystallography*; The Kynoch Press: Birmingham, England, 1974; Vol. IV, Table 2.3.1.

(27) TEXSAN-TEXRAY Structure Analysis Package, Molecular Structure Corp., The Woodlands, TX.

data collection, $(\sin \theta)/\lambda$, and various classes of indices showed no unusual trends. The maximum and minimum peaks on the final difference Fourier map corresponded to 0.48 and $-0.67 e/\text{\AA}^3$, respectively. Atomic Coordinates for **4** are found in Table 8.

Acknowledgment. This work was supported, in part, by a grant from the Office of Naval Research, who we gratefully acknowledge. We thank Dr. Daniel M.

Giaquinta for help with the refinement of the crystal structure of **4**.

Supporting Information Available: Text describing crystallographic procedures and Tables of X-ray parameters, complete atom positional and thermal parameters, bond distances and angles, and torsion angles (56 pages). Ordering information is given on any current masthead page.

OM950278D

Synthesis and Characterization of Unsymmetric Ferrocene-Terminated Phenylethynyl Oligomers $\text{Cp}_2\text{Fe}-[\text{C}\equiv\text{C}-\text{C}_6\text{H}_4]_n-\text{X}$ ($\text{X} = \text{SH}, \text{SMe}, \text{SOMe}, \text{and SO}_2\text{Me}$)

Richard P. Hsung,[†] Christopher E. D. Chidsey,[‡] and Lawrence R. Sita*,[†]

Searle Chemistry Laboratory, Department of Chemistry, The University of Chicago, Chicago, Illinois 60637, and Department of Chemistry, Stanford University, Stanford, California 94305

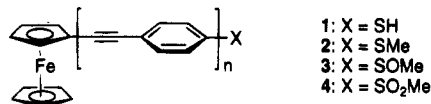
Received May 25, 1995[⊗]

The syntheses and full characterization of the titled compounds are described for $\text{X} = \text{SH}$ and $n = 1-3$ (**1a-c**), $\text{X} = \text{SMe}$ and $n = 1-4$ (**2a-d**), $\text{X} = \text{SOMe}$ and $n = 1$ and 2 (**3a,b**), and $\text{X} = \text{SO}_2\text{Me}$ and $n = 1-3$ (**4a-c**). In addition, the molecular structure of **2b** has been determined by crystallographic analysis. Single crystals of **2b** are (at 23 °C) monoclinic, space group $P2_1/c$, with $a = 6.031(2)$ Å, $b = 33.457(12)$, $c = 10.364(4)$ Å, $\beta = 90.90(3)^\circ$, $V = 2091.2(13)$ Å³, and $Z = 4$ ($D_{\text{calcd}} = 1.373$ mg m⁻³; $\mu(\text{Mo K}\alpha) = 0.831$ mm⁻¹). The availability of compounds **1a-c** should prove useful for investigating the factors which govern the rate of electron transfer across interfacial barriers such as those presented by self-assembled monolayer (SAM) structures.

Introduction

Self-assembled monolayer (SAM) structures¹ composed of *n*-alkanethiol derivatives chemisorbed onto gold surfaces and bearing varying amounts of pendant electroactive ferrocene groups have proven to be excellent systems in which factors governing the rate of electron transfer across interfacial barriers can be investigated.² Accordingly, a natural extension of these studies is to systematically modify the nature of the interfacial barrier and obtain structure-property relationships that can then be used to provide a clearer picture of how structural effects can mediate the electron transfer process. In this regard, we have recently focused our attention on the fabrication, characterization, and investigation of new classes of SAM structures derived from ferrocene-terminated conjugated arenethiol derivatives of varying conjugation length and, in particular, those derived from the family of ferrocene-terminated phenylethynyl oligomers represented by **1** (see Chart 1). At the outset, however, it was recognized that efficient, high-yielding routes to these arylthiol derivatives posed several synthetic challenges, not the least of which was the identification of protocols that would be compatible with the various sites of reactivity in these compounds. Herein we now report a general synthetic scheme that has been successfully employed to provide members of **1** for $n = 1-3$. In addition, since it was of interest to investigate the redox properties of

Chart 1



these new molecular systems, the synthesis and complete characterization of several members of the families of ferrocene-terminated phenylethynyl oligomers represented by **2-4**, which possess both the electron-donating methyl sulfide and the electron-withdrawing methyl sulfoxide and methyl sulfone moieties, respectively, are also reported. These latter compounds are of potential interest since a number of ferrocene-terminated conjugated oligomeric systems are known to display interesting nonlinear optical properties.³

Results and Discussion

(a) Synthesis. The family of oligomers represented by **2** provided a convenient target toward which various synthetic strategies for the construction of the conjugated phenylethynyl backbones of **1-4** could be explored. In this regard, it was decided that, in addition to a stepwise iterative approach, a more efficient convergent scheme would be considered for the syntheses of the longer oligomers (i.e., for $n \geq 3$). As Scheme 1 shows, the synthesis of **2a** ($n = 1$) could be achieved in a straightforward manner through the palladium-catalyzed Heck coupling reaction of ferrocenylacetylene (**5**)⁴ with 4-iodophenyl methyl sulfide (**6**) to provide **2a** in a 91% yield.⁵⁻⁷ For the synthesis of **2b** ($n = 2$), the (trimethylsilyl)(4-iodophenyl)acetylene derivative **8** was

(3) Long, N. J. *Angew. Chem., Int. Ed. Engl.* **1995**, *34*, 21 and references cited therein.

(4) Rosenblum, M.; Brawn, N.; Papenmeier, J.; Applebaum, M. *J. Organomet. Chem.* **1966**, *6*, 173.

(5) For recent reviews of the Heck reaction, see: (a) Heck, R. F. In *Comprehensive Organic Synthesis*; Trost, B. M., Fleming, I., Eds.; Pergamon Press: New York, 1991; Vol. 4, pp 833-863. (b) Hegedus, L. S. *Tetrahedron* **1984**, *40*, 2415. (c) Heck, R. F. *Org. React.* **1982**, *27*, 345.

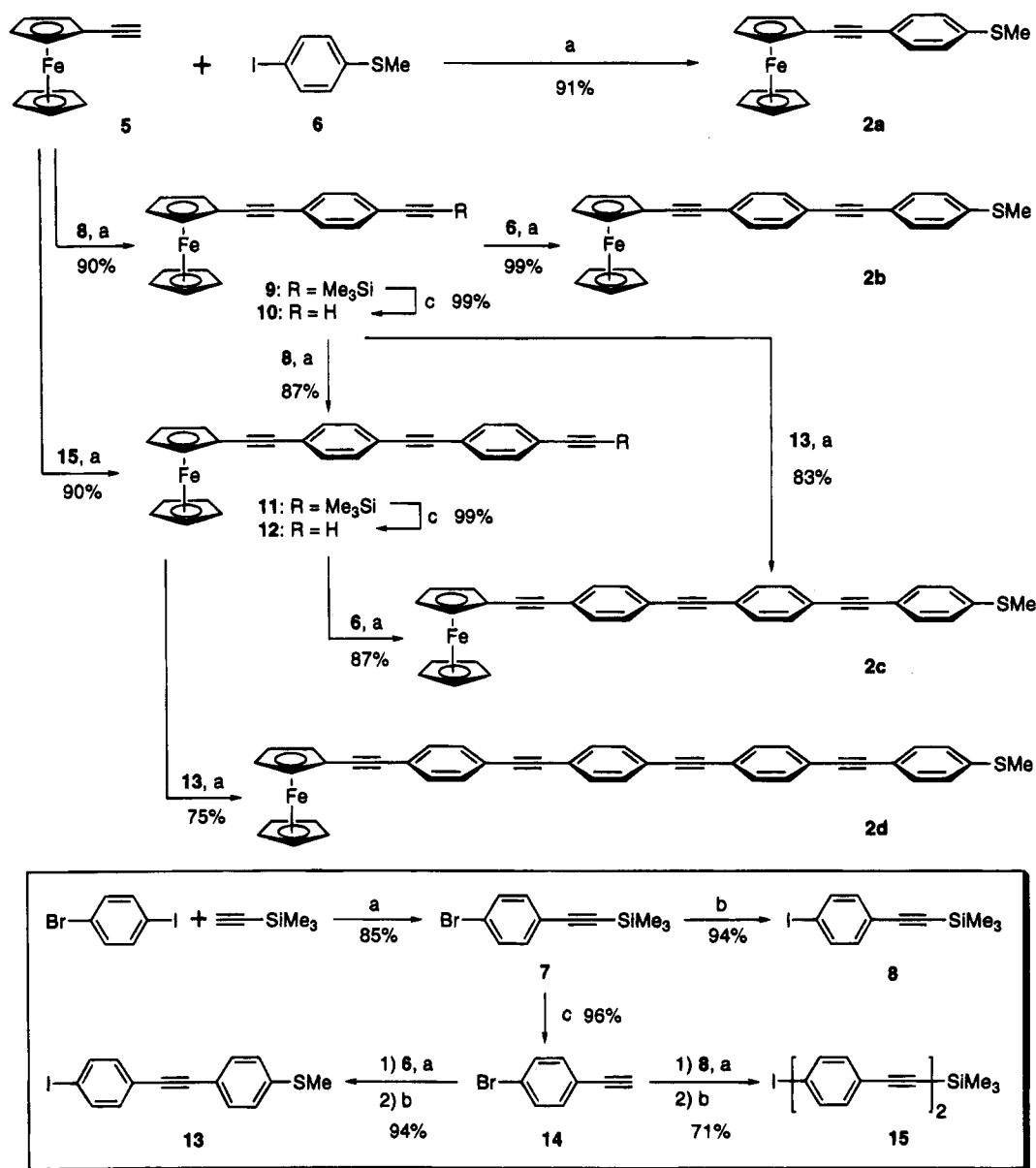
[†] The University of Chicago.

[‡] Stanford University.

[⊗] Abstract published in *Advance ACS Abstracts*, September 1, 1995.

(1) For general reviews of self-assembled monolayers, see: (a) Salen, J. D.; Allara, D. L.; Andrade, J. D.; Chandross, E. A.; Garoff, S.; Israelachvili, J.; McCarthy, T. J.; Murray, R. F.; Rabolt, J. F.; Wynne, K. J.; Yu, H. *Langmuir* **1987**, *3*, 932. (b) Ulman, A. *An Introduction to Ultrathin Organic Films from Langmuir-Blodgett to Self-Assembly*; Academic Press, Inc.: New York, 1991.

(2) For representative papers, see: (a) Chidsey, C. E. D.; Bertozzi, C. R.; Putvinski, T. M.; Mujisce, A. M. *J. Am. Chem. Soc.* **1990**, *112*, 4301. (b) Chidsey, C. E. D. *Science* **1991**, *251*, 919. (c) Finklea, H. O.; Hanshew, D. D. *J. Am. Chem. Soc.* **1992**, *114*, 3137. (d) Rowe, G. K.; Creager, S. E. *J. Phys. Am. Chem.* **1994**, *98*, 5500. (e) Herr, B. R.; Mirkin, C. A. *J. Am. Chem. Soc.* **1994**, *116*, 1157. (f) Carter, M. T.; Rowe, G. K.; Richardson, J. N.; Tender, L. M.; Terrill, R. H.; Murray, R. W. *J. Am. Chem. Soc.* **1995**, *117*, 2896.

Scheme 1^a

^a Legend: (a) Pd(PPh₃)₂Cl₂ (1.8 mol %), CuI (5.5 mol %), Et₂NH, 50 °C, 15–24 h. (b) (i) t-BuLi (2 equiv), Et₂O, –78 °C. (ii) I₂, –78 to 0 °C, 20 min. (c) TBAF, CH₂Cl₂, room temperature, 1.5 h.

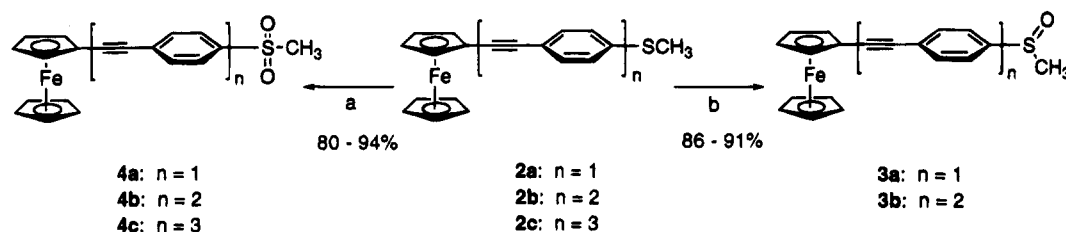
first prepared in two steps through the coupling of commercially available 1-bromo-4-iodobenzene with (trimethylsilyl)acetylene to provide the intermediate aryl bromide 7,⁸ which was then subjected to halogen exchange (80% overall yield of 8) (see box in Scheme 1). Coupling of 8 with 5 provided the ferrocene derivative 9, which was then treated with tetrabutylammonium fluoride (TBAF) to remove the trimethylsilyl group and to generate 10 (Scheme 1). Satisfactorily, the subsequent coupling of 10 with the aryl iodide 6 proceeded in a high yield (99%) to provide the extended ferrocene-terminated oligomer 2b.

(6) For the use of the Heck reaction to prepare a variety of phenylethyne oligomers, see: (a) Zhang, J.; Pesak, D. J.; Ludwick, J. L.; Moore, J. S. *J. Am. Chem. Soc.* **1994**, *116*, 4227. (b) Schumm, J. S.; Pearson, D. L.; Tour, J. M. *Angew. Chem., Int. Ed. Engl.* **1994**, *33*, 1360.

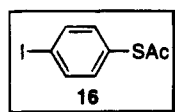
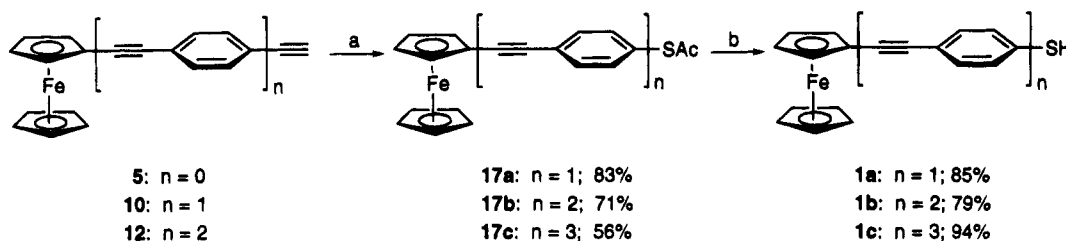
(7) It has recently been determined that a variety of thiophenol protecting groups (i.e., *S*-methyl, *S*-benzyl, *S*-trityl, and *S*-acetyl) are compatible with the Heck reaction, see: Hsung, R. P.; Babcock, J. R.; Chidsey, C. E. D.; Sita, L. R. *Tetrahedron Lett.* **1995**, *36*, 4525.

(8) Steinmetz, M. G.; Yu, C.; Li, L. *J. Am. Chem. Soc.* **1994**, *116*, 932.

Through a repetition of the general scheme used to construct compound 2b, longer oligomers of 2 could be produced in a stepwise fashion. Thus, coupling of 10 with the key building block 8 was carried out to provide 11, which was further backbone extended to obtain 2c (*n* = 3) through the “end-capping” of the intermediate 12 via coupling with 6 (Scheme 1). However, due to anticipated solubility limitations imposed by the longer oligomers, a convergent strategy was conceived to provide rapid access to these extended systems. Accordingly, as shown in Scheme 1, another key building block represented by compound 13 was prepared in three steps from 7 (90% overall yield), and coupling of this compound with the ferrocene derivative 12 then directly provided 2d (*n* = 4) in high yield. Finally, an even shorter route to longer oligomers of 2 was explored that utilizes the building block 15 which can easily be prepared in two steps from 7 (68% overall yield; see box in Scheme 1). Some appreciation of the advantages represented by these latter two convergent approaches for the synthesis of oligomers of 2 can be obtained by

Scheme 2^a

^a Legend: (a) 2.1 equiv of MCPBA, CH_2Cl_2 , -50 to -30 °C, 30 min to 20 h. (b) 1.04 equiv of MCPBA, CH_2Cl_2 , -50 to -30 °C, 30 min to 20 h.

Scheme 3^a

^a Legend: (a) **16**, $\text{Pd}(\text{PPh}_3)_2\text{Cl}_2$ (1.8 mol %), CuI (5.5 mol %), $\text{THF}/\text{Hunig's base}$ (1:1), 50 °C, 20–40 h. (b) (i) Et_2NH or $n\text{-BuNH}_2$ (2–5 equiv), CHCl_3 , 50 °C, 15–24 h; (ii) Zn , HOAc , CH_2Cl_2 , room temperature, 5–35 min.

comparing the overall yield of **2c** that is derived from **5** by the following approaches: (1) the stepwise approach utilizing **8** and **6** (5 steps, 66%), (2) the convergent approach utilizing **8** and **13** (3 steps, 74%), and (3) the convergent approach utilizing **15** and **6** (2 steps, 78%).

Compounds **2a–c** could be selectively oxidized to provide several members of the families of sulfoxide and sulfone oligomers represented by **3** and **4**, respectively. Hence, as Scheme 2 shows, reaction of **2a** with 1.04 equiv of *m*-chloroperbenzoic acid (MCPBA) in dichloromethane (CH_2Cl_2) at -50 °C cleanly provided the sulfoxide derivative **3a** in high yield. Correspondingly, the same reaction of **2a** performed with 2.1 equiv of MCPBA generated the sulfone **4a** in high yield (93%) and with virtually no side products being detected. Given the anticipated reactivity of the triple bonds, it was somewhat surprising to find that these oxidation reactions proceeded equally well for the longer oligomers of **2**. Thus, **2b** could be converted to both **3b** and **4b** (91% and 94% yield, respectively), and compound **2c** could be smoothly oxidized to the sulfone derivative **4c**.⁹

For the synthesis of the primary target compounds represented by **1**, it was necessary to identify a thiophenol protecting group that was both compatible with the Heck reaction and which subsequently could be selectively removed to provide the desired ferrocene arene-thiols in high yield. During the course of the present investigations, it was determined that the *S*-acetyl moiety could adequately meet both of these requirements.^{7,10} Accordingly, couplings of **5**, **10**, and **12** with *S*-acetyl-4-iodobenzene (**16**) proceeded in high yields to provide the respective *S*-acetylated intermediates

(9) Due to solubility limitations, oxidation of **2d** to the corresponding compounds, **3d** and **4d**, was not attempted.

(10) Recently, Tour and co-workers have also proposed using the *S*-acetyl group for the synthesis of arene-thiols, see: Tour, J. M. *Trends Polym. Sci.* **1994**, *2*, 332 reference 26.

Table 1. Selected Properties of 2–4

n	λ_{max} (nm) ^a			E^f (mV) ^b	
	2	3	4	2	4
a	312	307	308	267	314
b	331	330	330	283	299
c	345		336	287	c
d	357				c

^a Anhydrous tetrahydrofuran (THF) used as the solvent. ^b Cyclic voltammetry was performed using 1 mM of substrate in THF (0.1 M $(n\text{-Bu})_4\text{N}^+\text{PF}_6^-$) at a glassy carbon working electrode, a Pt counter electrode, and a Ag/Ag^+ reference electrode ($T = 298$ K, scan rate = 20 mV/s). The ferrocene/ferrocenium redox couple was observed at 125 mV under identical conditions. ^c Not measured.

17a–c which were then deprotected to generate the corresponding compounds **1a–c** according to Scheme 3.

(b) **Properties.** All the oligomers of **1–4** that were prepared were found to be crystalline or waxy solids that could be purified to homogeneity by conventional column chromatography, and analytic and spectroscopic analyses support their structural formulations as shown. Here it can be mentioned that, although these compounds are all fairly robust, solutions of the arene-thiols **1a–c** are all prone to oxidize to the corresponding disulfides unless deoxygenated solvents are employed.

From the full spectroscopic characterization of the oligomers of **1–4** shown in Schemes 1–3, several interesting structure–property relationships could be derived. For instance, as Table 1 reveals, the lowest energy transition for the oligomers of **2** was found to increasingly red-shift with increasing chain length. Thus, while compound **2a** ($n = 1$) exhibits a λ_{max} at 312 nm, this value progressively shifts to longer wavelengths in going to **2b** ($\lambda_{\text{max}} = 331$; $n = 2$) to **2c** ($\lambda_{\text{max}} = 345$; $n = 3$) and finally to **2d** ($\lambda_{\text{max}} = 357$; $n = 4$). Similar trends are observed for the oligomers of **3** and **4** as well as for other families of phenylethynyl oligomers.^{6b}

Table 2. Fractional Coordinates of the Non-Hydrogen Atoms ($\times 10^4$) and Equivalent Isotropic Thermal Parameters ($\times 10^3$) for **2b^a**

atom ^b	x	y	z	$B_{\text{eq}}, \text{\AA}^2$
Fe	945(4)	3072(1)	578(3)	49(1)
S	-16341(9)	-691(2)	-3610(6)	92(3)
C1	512(26)	2490(5)	1074(16)	45(5)
C2	211(30)	2748(5)	2176(17)	57(5)
C3	2125(28)	2966(5)	2404(18)	64(6)
C4	3674(31)	2846(5)	1489(18)	63(6)
C5	2737(26)	2551(5)	657(16)	50(5)
C6	-1351(32)	3221(5)	-803(18)	70(6)
C7	-1550(30)	3478(5)	228(18)	65(6)
C8	485(29)	3673(5)	373(18)	65(6)
C9	1974(32)	3530(5)	-569(18)	68(6)
C10	779(30)	3240(6)	-1281(20)	76(7)
C11	-1006(28)	2196(5)	581(16)	45(5)
C12	-2202(26)	1932(6)	252(16)	53(5)
C13	-3722(25)	1622(5)	-123(16)	41(5)
C14	-3206(29)	1395(5)	-1208(17)	60(6)
C15	-4691(30)	1100(6)	-1622(18)	72(6)
C16	-6629(27)	1020(5)	-963(16)	46(5)
C17	-7074(29)	1244(5)	103(17)	57(5)
C18	-5649(26)	1549(5)	560(17)	48(5)
C19	-8193(30)	720(6)	-1401(17)	57(5)
C20	-9557(32)	488(6)	-1738(18)	61(6)
C21	-11117(30)	204(5)	-2147(19)	57(5)
C22	-12549(32)	12(6)	-1277(21)	78(7)
C23	-14138(31)	-263(6)	-1717(19)	71(6)
C24	-14369(30)	-349(5)	-2986(19)	60(6)
C25	-12961(34)	-165(6)	-3826(24)	94(7)
C26	-11342(36)	110(6)	-3425(21)	88(7)
C27	-18067(32)	-806(6)	-2278(18)	85(7)

^a The numbers in parentheses are the estimated standard deviations in the last significant digit. ^b Atoms are labeled in agreement with Figure 1.

Table 3. Bond Lengths (\AA) for **2b^{a,b}**

Fe-C1	2.030(17)	C6-C7	1.378(26)
Fe-C2	2.033(18)	C6-C10	1.386(27)
Fe-C3	2.042(18)	C7-C8	1.395(25)
Fe-C4	2.031(19)	C8-C9	1.420(26)
Fe-C5	2.052(16)	C9-C10	1.410(27)
Fe-C6	2.039(19)	C11-C12	1.188(25)
Fe-C7	2.056(18)	C12-C13	1.433(24)
Fe-C8	2.039(18)	C13-C14	1.396(24)
Fe-C9	2.042(19)	C13-C18	1.392(23)
Fe-C10	2.009(21)	C14-C15	1.395(26)
Fe-Cnt(1) ^c	1.644	C15-C16	1.389(25)
Fe-Cnt(2) ^c	1.654	C16-C17	1.366(24)
S-C24	1.767(19)	C16-C19	1.446(25)
S-C27	1.784(20)	C17-C18	1.412(24)
C1-C2	1.445(24)	C19-C20	1.179(27)
C1-C5	1.431(22)	C20-C21	1.398(26)
C1-C11	1.433(23)	C21-C22	1.412(28)
C2-C3	1.382(24)	C21-C26	1.366(29)
C3-C4	1.400(26)	C22-C23	1.400(27)
C4-C5	1.422(24)	C23-C24	1.351(28)

^a The numbers in parentheses are the estimated standard deviations in the last significant digit. ^b Atoms are labeled in agreement with Figure 1. ^c Cnt(1) is the centroid of the C1-C5 ring, Cnt(2) is the centroid of the C6-C10 ring.

Finally, for each of the series, **2-4**, the λ_{max} values were observed to be insensitive to solvent polarity.

Of primary interest to the planned investigation of electroactive SAMs prepared from **1** are the values of the formal redox potentials, E^f , for the ferrocene moieties of **2a-d**. As shown in Table 1, the E^f values for the observed reversible one-electron oxidations of **2a-c** are all shifted to higher oxidation potentials relative to that of ferrocene itself.¹¹ Thus, an E^f value of 267 mV is obtained for **2a** which can be compared to the value

Table 4. Bond Angles (deg) for **2b^{a,b}**

Cnt(1)-Fe-Cnt(2) ^c	179.2	C(13)-C(14)-C(15)	118.8(16)
C(24)-S-C(27)	104.7(9)	C(14)-C(15)-C(16)	121.8(17)
C(2)-C(1)-C(5)	106.5(14)	C(15)-C(16)-C(17)	117.9(16)
C(2)-C(1)-C(11)	127.1(15)	C(15)-C(16)-C(19)	122.0(16)
C(5)-C(1)-C(11)	125.9(15)	C(17)-C(16)-C(19)	120.0(16)
C(1)-C(2)-C(3)	109.5(15)	C(16)-C(17)-C(18)	122.9(16)
C(2)-C(3)-C(4)	107.3(16)	C(13)-C(18)-C(17)	117.7(15)
C(3)-C(4)-C(5)	110.3(16)	C(16)-C(19)-C(20)	176.5(21)
C(1)-C(5)-C(4)	106.3(15)	C(19)-C(20)-C(21)	178.1(20)
C(7)-C(6)-C(10)	109.9(17)	C(20)-C(21)-C(22)	122.0(18)
C(6)-C(7)-C(8)	106.7(16)	C(20)-C(21)-C(26)	120.4(18)
C(7)-C(8)-C(9)	109.5(16)	C(22)-C(21)-C(26)	117.5(18)
C(8)-C(9)-C(10)	105.5(16)	C(21)-C(22)-C(23)	120.9(19)
C(6)-C(10)-C(9)	108.3(17)	C(22)-C(23)-C(24)	121.1(18)
C(1)-C(11)-C(12)	174.6(19)	S(1)-C(24)-C(23)	123.6(15)
C(11)-C(12)-C(13)	177.5(19)	S(1)-C(24)-C(25)	118.5(16)
C(12)-C(13)-C(14)	117.5(15)	C(23)-C(24)-C(25)	117.9(18)
C(12)-C(13)-C(18)	121.6(15)	C(24)-C(25)-C(26)	122.8(21)
C(14)-C(13)-C(18)	120.9(15)	C(21)-C(26)-C(25)	119.8(20)

^a The numbers in parentheses are the estimated standard deviations in the last significant digit. ^b Atoms are labeled in agreement with Figure 1. ^c Cnt(1) is the centroid of the C(1)-C(5) ring, and Cnt(2) is the centroid of the C(6)-C(10) ring.

of 125 mV recorded for the ferrocene-ferrocenium couple under identical conditions. Interestingly, on going from **2a** to the oligomer **2b**, one observes an additional 16 mV shift to higher oxidation potential. However, in going from **2b** to **2c**, there appears to be virtually no change in this parameter and it can be anticipated that 287 mV is very close to the limit expected for longer oligomers of **2**. As a final note, the E^f values obtained for the oligomers of **2** can be compared to those observed for the corresponding oligomers of **4** which possess the electron-withdrawing methyl sulfone moiety instead of the methyl sulfide functional group. In this regard, as expected, both **4a,b** have E^f values which are shifted to higher oxidation potentials relative to those of **2a,b**, respectively (see Table 1). However, it is interesting to observe that in going from **4a** to **4b** there is a reduction in oxidation potential ($\Delta E^f = -15$ mV) which tends to suggest that the inductive effect of the sulfone moiety is attenuated fairly quickly as the length of the conjugated phenylethynyl backbone in these oligomers increases.

(c) Crystallographic Analysis of **2b.** In order to obtain structural parameters that might aid in the planned investigations of SAMs derived from **1**, the crystallographic analysis of **2b** was conducted. Fractional coordinates of non-hydrogen atoms are given in Table 2; bond lengths and bond angles are given in Tables 3 and 4, respectively. As shown by this data and Figure 1, the solid-state structure obtained for **2b** reveals few bond length or bond angle distortions. The average C-C bond length within the cyclopentadienyl rings of the ferrocene moiety is 1.407 \AA , and those of each of the aromatic rings are 1.391 (C13-C18) and 1.384 \AA (C21-C26), respectively. The lengths of the carbon-carbon triple bonds involved in connecting these three fragments together are 1.188(25) and 1.179(27) \AA . The two cyclopentadienyl rings are nearly parallel to one another with the Cnt(1)-Fe-Cnt(2) angle being 179.2° [Cnt(1) is the centroid of the C1-C5 ring, and Cnt(2) is the centroid of the C6-C10 ring]. Furthermore, as shown in Figure 2, the aromatic ring defined by C13-C18 is nearly coplanar with the cyclopentadienyl ring described by C1-C5, but not with the aromatic ring defined by C21-C26. Finally, the overall length

(11) The cyclic voltammetry of **2d** was not performed due to solubility limitations.

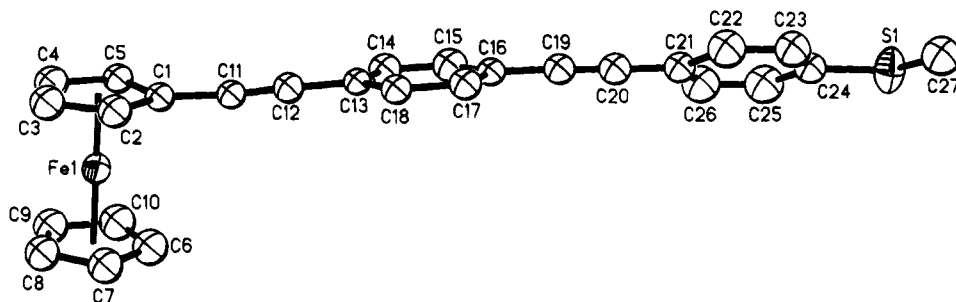


Figure 1. Molecular structure of **2b** with hydrogen atoms omitted for the purpose of clarity.

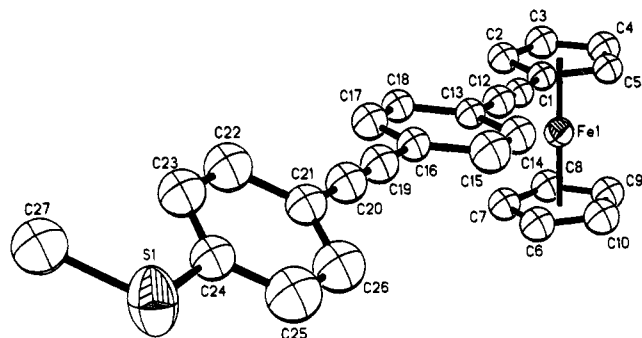


Figure 2. Different perspective of the molecular structure of **2b**.

of a single molecule of **2b** is approximately 18 Å as calculated from the midpoint of the C3–C4 bond to the S atom.

Experimental Section

All reactions were carried out under an atmosphere of nitrogen, and all reagents were obtained from commercial suppliers and used without further purification unless otherwise indicated. Tetrahydrofuran (THF) and diethyl ether (Et₂O) were distilled from Na–benzophenone under nitrogen. Methylene chloride and benzene were distilled from calcium hydride under nitrogen. Methanol was dried over activated 4 Å molecular sieves prior to use. Thin-layer chromatography (TLC) analysis was performed using EM Science silica gel 60 (F254) plates (0.25 mm), and the eluted plates were observed under a UV detector and/or stained with either an aqueous solution of potassium permanganate (KMnO₄) or an ethanolic solution of phosphomolybdic acid (PMA) followed by heating. Chromatographic purifications were performed by flash chromatography¹² on EM Science silica gel (230–400 mesh). ¹H NMR spectra were obtained at either 300 or 500 MHz using chloroform-*d*₁ as the solvent and tetramethylsilane as an internal reference. ¹³C NMR spectra were recorded at 75 MHz using chloroform-*d*₁ as the solvent. Infrared spectra (cm⁻¹) were recorded either neat or as Nujol mulls, and absorptions are described qualitatively as follows: s, strong; m, medium; w, weak. Low-resolution mass spectra were recorded on a Finnigan 1015 mass spectrometer; high-resolution mass spectra were recorded on a VG 70-250 instrument.

Preparation of 4-Iodophenyl Methyl Sulfide (6). To a solution of 2.03 g (10.0 mmol) of 4-bromophenyl methyl sulfide in 30 mL of Et₂O, cooled to –78 °C was slowly added 11 mL of a solution of *tert*-butyllithium (1.7 M in pentane, 20.0 mmol) dropwise. After the addition was complete, the reaction mixture was stirred for 35–45 min at –78 °C, after which time a solution of 3.05 g (12.0 mmol) of iodine in 75 mL of Et₂O, precooled to –78 °C, was added dropwise via a cannula. The mixture was then stirred at –78 °C for 10 min and at 0 °C for 25 min, whereupon it was poured into 150 mL of saturated aqueous sodium thiosulfite overlaid with 150 mL of Et₂O. The

ether layer was washed with 2 × 150 mL of saturated aqueous sodium thiosulfite and 2 × 150 mL of saturated aqueous sodium chloride, dried with anhydrous sodium sulfate, and filtered, and the solvents were removed *in vacuo* to provide 2.78 g of a solid material. The crude product was purified via filtration through a short silica gel column in a 60-μ frit funnel (4 × 5 cm; eluent, 9:1 hexane/CH₂Cl₂ solvent mixture) to provide 2.50 g of the desired aryl iodide **6** as a colorless solid (99% yield) which rapidly discolors in air. Analytically pure material in the form of white needles was obtained by recrystallization from hexane. Data for **6**: mp 37.0–38.0 °C; *R*_f = 0.30 (9:1 hexane/CH₂Cl₂); ¹H NMR δ 2.44 (s, 3H), 6.94 (d, 2H, *J* = 8.3 Hz), 7.52 (d, 2H, *J* = 8.3 Hz); ¹³C NMR δ 15.6, 89.1, 128.1, 137.6, 138.5; IR (neat) 3037 w, 2970 w, 2955 w, 2912 s, 2852 w, 1471 m, 1425 m, 1383 s, 1116 m, 1093 m, 976 m, 965 m, 803 s; MS (EI) *m/e* (relative intensity) 250 (100) M⁺, 235 (16), 217 (2), 204 (2), 123 (5), 108 (13).

General Procedure for Palladium-Catalyzed Coupling Reactions of Alkynes with Aryl Iodides in the Presence of Protected Thiols.⁷ The appropriate ferrocenyl arylalkyne (0.05–1.7 mmol scale), aryl iodide, Pd(PPh₃)₂Cl₂ (1.8 mol %), and CuI (5.5 mol %) were dissolved in diethylamine in a Kontes Schlenk flask. The reaction mixture was deoxygenated using the freeze–pump–thaw method (three cycles), and, at the end of the last cycle, the reaction mixture was backfilled with nitrogen and the flask was sealed. The mixture was then stirred at 50 °C for 15–24 h with the progress of the reaction being carefully monitored by TLC analysis (1:1 CH₂Cl₂/hexane). When the reaction was complete, the solvents were removed *in vacuo* and the desired product was isolated by column chromatography.

Preparation of 2a. Compound **5** (104.9 mg, 0.50 mmol) was coupled with 131.2 mg (0.51 mmol) of the aryl iodide **6** according to the general procedure to provide 150.6 mg (91% yield) of the aryl sulfide **2a** as an orange-red crystalline material. Data for **2a**: mp 149.0–151.0 °C; *R*_f = 0.56 (1:1 CH₂Cl₂/hexane); ¹H NMR δ 2.48 (s, 3H), 4.21 (brs, 7H), 4.46 (t, 2H, *J* = 1.6 Hz), 7.14 (d, 2H, *J* = 8.1 Hz), 7.34 (d, 2H, *J* = 8.1 Hz); ¹³C NMR δ 15.5, 68.8, 69.9, 70.1, 71.3, 85.4, 87.1, 120.3, 125.9, 126.9, 131.7; IR (neat) 3101 w, 2922 m, 1651 w, 1585 w, 1496 m, 1438 w, 1399 s, 1105 s, 1090 m, 1027 m; UV (THF) (ε) λ_{max} 312 nm (27 130); MS (EI) *m/e* (relative intensity) 332 (100) M⁺, 317 (2), 251 (4), 227 (3), 195 (4), 166 (9), 152 (4), 121 (6); HRMS *m/e* for C₁₉H₁₆FeS, calcd 332.0322, found 332.0313.

Preparation of 1-(4-Iodophenyl)-2-(trimethylsilyl)ethyne (8). 1-(4-Bromophenyl)-2-(trimethylsilyl)ethyne (**7**)⁸ (1.27 g, 5.0 mmol) was transhalogenated according to the same procedure as that used for the preparation of the aryl iodide **6** to provide 1.47 g (94% yield) of the aryl iodide **8** as a pale yellow solid. Data for **8**: mp 56.0–58.0 °C; *R*_f = 0.43 (1:1 CH₂Cl₂/hexane); ¹H NMR δ 0.24 (s, 9H), 71.3 (d, 2H, *J* = 7.9 Hz), 7.58 (d, 2H, *J* = 7.9 Hz); ¹³C NMR δ –0.2, 94.4, 95.8, 103.9, 122.6, 133.4, 137.3; IR (neat) 2959 m, 2898 w, 2159 s, 1482 s, 1389 w, 1249 s, 1217 w, 1055 w, 1006 m, 864 s, 843 s, 819 s, 760 m; MS (EI) *m/e* (relative intensity) 300 (100) M⁺, 286 (100), 271 (8), 255 (10), 173 (13), 154 (84), 143 (54), 128 (20), 117 (16).

Preparation of 9. Compound **5** (351.7 mg, 1.68 mmol) was coupled with 504.3 mg (1.68 mmol) of **8** according to the general procedure to provide 577.8 mg (90% yield) of **9** as an

(12) Still, W. C.; Kahn, M.; Mitra, A. *J. Org. Chem.* **1978**, *43*, 2923.

orange-red crystalline material. Data for **9**: mp 169.0–170.0 °C; $R_f = 0.09$ (1:9 CH₂Cl₂/hexane); ¹H NMR δ 0.25 (s, 9H), 4.21 (brs, 5H), 4.22 (t, 2H, $J = 1.8$ Hz), 4.46 (t, 2H, $J = 1.8$ Hz), 7.35 (brs, 4H); ¹³C NMR δ -0.1, 64.8, 68.9, 70.0, 71.4, 85.4, 90.5, 95.9, 104.8, 122.1, 124.1, 131.3, 131.8; IR (neat) 3179 w, 3161 w, 3086 w, 2954 w, 1600 m, 1559 w, 1501 w, 1247 s, 844 s; MS (EI) m/e (relative intensity) 382 (100) M⁺, 367 (3), 337 (2), 285 (3), 246 (3), 210 (3), 184 (16), 159 (2); HRMS m/e for C₂₃H₂₂FeSi, calcd 382.0840, found 382.0829.

Preparation of 10. To a solution of 524.6 mg (1.37 mmol) of **9** in 50 mL of CH₂Cl₂ was slowly added 1.51 mL of a solution of TBAF (1 M in THF) dropwise. The reaction mixture was stirred at room temperature for 1.5 h, after which time the solvents were removed *in vacuo*. The resulting crude material was then purified via column chromatography (1:9 CH₂Cl₂/hexane) to provide 424.0 mg (99% yield) of the desired product as an orange-red crystalline material. Data for **10**: mp 140.0–141.0 °C; $R_f = 0.67$ (1:1 CH₂Cl₂/hexane); ¹H NMR δ 3.14 (s, 1H), 4.22 (brs, 5H), 4.23 (t, 2H, $J = 1.4$ Hz), 4.47 (t, 2H, $J = 1.4$ Hz), 7.38 (brs, 4H); ¹³C NMR δ 64.8, 69.0, 70.0, 71.5, 78.6, 83.4, 85.3, 90.7, 121.1, 124.5, 131.2, 132.0; IR (neat) 3271 s, 3005 w, 2968 w, 2917 w, 2842 w, 1619 m, 1518 m, 1381 w, 1040 w; MS (EI) m/e (relative intensity) 310 (100) M⁺ + H, 310 (67) M⁺, 253 (6), 227 (2), 190 (9), 163 (3), 156 (6), 152 (3), 121 (17); HRMS m/e for C₂₀H₁₄Fe, calcd 310.0445, found 310.0453.

Preparation of 2b. Compound **10** (31.0 mg, 0.10 mmol) was coupled with 25.0 mg (0.10 mmol) of **6** according to the general procedure to provide 43.1 mg (99% yield) of **2b** as an orange-red crystalline material. Data for **2b**: mp 172.0–174.0 °C; $R_f = 0.56$ (1:1 CH₂Cl₂/hexane); ¹H NMR δ 2.49 (s, 3H), 4.22 (brs, 5H), 4.23 (t, 2H, $J = 1.6$ Hz), 4.48 (t, 2H, $J = 1.6$ Hz), 7.16 (d, 2H, $J = 8.3$ Hz), 7.39 (d, 2H, $J = 8.3$ Hz), 7.40 (brs, 4H); ¹³C NMR δ 15.2, 66.8, 68.9, 70.0, 71.4, 85.5, 89.3, 90.5, 90.8, 119.3, 122.4, 123.7, 125.8, 131.3, 131.4, 131.8, 132.4; IR (neat) 2958 w, 2921 m, 2872 w, 2858 w, 2362 m, 2344 w, 1513 s, 1164 w, 1104 w, 1088 m, 835 s, 818 s; UV (THF) (ε): λ_{max} 331 nm (10 480); MS (EI) m/e (relative intensity) 432 (100) M⁺, 417 (23), 310 (8), 250 (38), 216 (19), 193 (8), 121 (8); HRMS m/e for C₂₇H₂₀FS, calcd 432.0635, found 432.0631.

Preparation of 11. Compound **10** (185.0 mg, 0.60 mmol) was coupled with 196.8 mg (0.66 mmol) of **8** according to the general procedure to provide 249.7 mg (87% yield) of **11** as an orange-red crystalline material. Data for **11**: mp 191.0–192.0 °C; $R_f = 0.67$ (1:1 CH₂Cl₂/hexane); ¹H NMR δ 0.26 (s, 9H), 4.22 (s, 5H), 4.23 (t, 2H, $J = 1.6$ Hz), 4.47 (t, 2H, $J = 1.6$ Hz), 7.40 (d, 4H, $J = 1.4$ Hz), 7.41 (brs, 4H); ¹³C NMR δ -0.1, 64.8, 69.0, 70.0, 71.4, 85.5, 90.6, 90.7, 91.2, 96.4, 104.6, 122.0, 123.0, 123.1, 124.1, 131.3, 131.4, 131.5, 131.9; IR (neat) 2955 m, 2927 w, 2202 m, 2155 m, 1517 m, 1252 m, 866 s, 837 s; MS (EI) m/e (relative intensity) 482 (100) M⁺, 467 (3), 410 (2), 346 (2), 316 (2), 234 (23), 185 (2); HRMS m/e for C₃₁H₂₆FeSi, calcd 482.1153, found 482.1158.

Preparation of 12. Compound **11** (240.5 mg, 0.50 mmol) was desilylated in the same manner as described for the preparation of **10** to provide 204.3 mg (99% yield) of desired product as an orange red solid. Data for **12**: mp 198.0–199.0 °C; $R_f = 0.26$ (1:1 CH₂Cl₂/hexane); ¹H NMR δ 3.16 (s, 1H), 4.22 (brs, 5H), 4.23 (t, 2H, $J = 1.8$ Hz), 4.48 (t, 2H, $J = 1.8$ Hz), 7.41 (d, 4H, $J = 2.0$ Hz), 7.42 (brs, 4H); ¹³C NMR δ 64.8, 69.0, 70.0, 71.5, 79.0, 83.2, 85.5, 90.4, 90.8, 91.3, 121.9, 122.0, 123.6, 124.1, 131.3, 131.4, 131.5, 132.1; IR (neat) 3265 s, 2985 w, 2201 m, 1594 w, 1518 s, 1359 w, 1255 w, 1106 w, 844 s, 821 m; MS (EI) m/e (relative intensity) 410 (100) M⁺, 352 (7), 289 (23), 205 (19), 121 (36); HRMS m/e for C₂₈H₁₈Fe, calcd 410.0758, found 410.0749.

Preparation of 2c from the Arylalkyne 12. Compound **12** (41.0 mg, 0.10 mmol) was coupled with 25.0 mg (0.10 mmol) of **6** according to the general procedure to provide 46.3 mg (87% yield) of the aryl sulfide **2c** as an orange-red solid. Data for **2c**: mp 227.0–229.0 °C; $R_f = 0.55$ (1:1 CH₂Cl₂/hexane); ¹H NMR δ 2.49 (s, 3H), 4.23 (brs, 5H), 4.24 (t, 2H, $J = 1.6$ Hz), 4.48 (t, 2H, $J = 1.6$ Hz), 7.22 (d, 2H, $J = 8.3$ Hz), 7.39 (d, 2H,

$J = 8.3$ Hz), 7.42 (d, 4H, $J = 2.7$ Hz), 7.45 (brs, 4H); ¹³C NMR δ 15.1, 64.6, 69.0, 69.9, 71.4, 82.2, 82.6, 83.5, 90.6, 90.7, 91.0, 120.7, 122.9, 123.2, 124.1, 125.7, 131.2, 131.4, 131.5, 131.6, 131.8, 134.3, 137.4; IR (neat) 2923 m, 2211 m, 1536 s, 1443 m, 1164 w, 1104 m, 1086 w, 1027 w, 837 s, 821 s; UV (THF) (ε): λ_{max} 345 nm (67 039); MS (EI) m/e (relative intensity) 532 (100) M⁺, 517 (8), 308 (19), 262 (100), 183 (56), 128 (69); HRMS m/e for C₃₅H₂₄FeS, calcd 532.0948, found 532.0966.

Preparation of 14. Compound **7** (506.0 mg, 2.0 mmol) was desilylated in the same manner as described for the preparation of **10** to provide 347.2 mg (96% yield) of **14** as a white crystalline material. Data for **14**: mp 56.0–58.0 °C; $R_f = 0.45$ (1:9 CH₂Cl₂/hexane); ¹H NMR δ 3.10 (s, 1H), 7.30 (d, 2H, $J = 8.4$ Hz), 7.41 (d, 2H, $J = 8.4$ Hz); ¹³C NMR δ 78.3, 82.6, 121.0, 123.1, 131.6, 133.5; IR (neat) 3267 s, 2924 w, 1584 m, 1484 s, 1468 m, 1396 m, 1267 w, 1068 m, 1010 m, 821 s; MS (EI) m/e (relative intensity) 182 (98) M⁺ + 2, 180 (100) M⁺, 101 (50), 75 (29).

Preparation of 13. Compound **14** (210.0 mg, 1.2 mmol) was coupled with 290.1 mg (1.2 mmol) of **6** according to the general procedure to afford 306.1 mg (95% yield) of the aryl bromide intermediate as a white solid [mp 148.0–149.0 °C; $R_f = 0.37$ (1:9 CH₂Cl₂/hexane); ¹H NMR δ 2.48 (s, 3H), 7.15 (d, 2H, $J = 8.4$ Hz), 7.32 (d, 2H, $J = 8.4$ Hz), 7.37 (d, 2H, $J = 8.4$ Hz), 7.42 (d, 2H, $J = 8.4$ Hz); ¹³C NMR δ 15.3, 88.4, 90.3, 122.3, 122.4, 125.8, 131.6, 131.8, 132.9, 138.6, 139.7; IR (neat) 2975 w, 2919 m, 2445 m, 1594 m, 1497 m, 1318 s, 821 s; MS (EI) m/e (relative intensity) 304 (100) M⁺ + 2, 302 (100) M⁺, 289 (31), 287 (31), 208 (12), 152 (12); HRMS m/e for C₁₅H₁₁⁷⁹BrS, calcd 301.9765, found 301.9767; m/e for C₁₅H₁₁⁸¹BrS, calcd 303.9744, found 303.9761]. This compound (246.0 mg, 0.81 mmol) was then transhalogenated according to the same procedure as that used for the preparation of the aryl iodide **6** to provide 278.0 mg (99% yield) of the desired product **13** as a white solid. Data for **13**: mp 164.0–166.0 °C; $R_f = 0.70$ (1:1 CH₂Cl₂/hexane); ¹H NMR δ 2.48 (s, 3H), 7.15 (d, 2H, $J = 8.4$ Hz), 7.18 (d, 2H, $J = 8.0$ Hz), 7.37 (d, 2H, $J = 8.0$ Hz), 7.63 (d, 2H, $J = 8.4$ Hz); ¹³C NMR δ 15.3, 88.5, 94.0, 119.1, 125.8, 128.2, 128.3, 131.8, 133.0, 137.5, 139.7; IR (neat) 2985 w, 2976 w, 2888 w, 1653 m, 1590 m, 1495 m, 1389 m, 819 s; MS (EI) m/e (relative intensity) 350 (100) M⁺, 335 (23), 208 (12), 175 (12), 112 (8).

Preparation of 2c from the Arylalkyne 10. Compound **10** (15.5 mg, 0.050 mmol) was coupled with 17.5 mg (0.050 mmol) of **13** according to the general procedure to provide 22.1 mg (83% yield) of **2c**.

Preparation of 15. Compound **14** (166.7 mg, 0.92 mmol) was coupled with 276.0 mg (0.92 mmol) of **8** according to the general procedure to afford 305.6 mg (94% yield) of the aryl bromide intermediate as a white solid [mp 138.0–139.0 °C; $R_f = 0.17$ (hexane); ¹H NMR δ 0.25 (s, 9H), 7.32 (d, 2H, $J = 8.4$ Hz), 7.39 (brs, 4H), 7.43 (d, 2H, $J = 8.4$ Hz); ¹³C NMR δ -0.1, 82.1, 90.1, 96.5, 104.5, 122.6, 122.7, 122.9, 123.2, 131.3, 131.7, 131.9, 133.0; IR (neat) 2959 w, 2157 w, 1500 m, 1254 s, 1244 m, 867 m, 837 s, 821 s, 760 m; MS (EI) m/e (relative intensity) 354 (33) M⁺ + 2, 352 (32) M⁺, 339 (36), 337 (35), 223 (8), 170 (8), 168 (8), 149 (49), 94 (47), 79 (100)]. This compound (52.5 mg, 0.15 mmol) was then transhalogenated according to the same procedure as that used for the preparation of the aryl iodide **6** to provide 60.1 mg of a crude material consisting of 75% of the desired product **15** and 25% of the dehalogenated side product that could be used without purification for subsequent palladium-catalyzed coupling reactions. Analytically pure **15** was obtained by preparative TLC. Data for **15**: mp 148.0–150.0 °C; $R_f = 0.17$ (hexane); ¹H NMR δ 0.25 (s, 9H), 7.18 (d, 2H, $J = 8.0$ Hz), 7.39 (brs, 4H), 7.65 (d, 2H, $J = 8.0$ Hz); ¹³C NMR δ -0.1, 89.0, 90.4, 91.3, 96.2, 104.6, 115.5, 122.7, 122.9, 131.2, 131.4, 133.1, 137.6; IR (neat) 2963 w, 2959 w, 2935 w, 1509 w, 1501 w, 1390 w, 1252 m, 1244 m, 868 w, 837 s, 821 m, 756 w; MS (EI) m/e (relative intensity) 400 (18) M⁺, 385 (17), 274 (100), 259 (100), 229 (21), 130 (63); HRMS m/e for C₁₉H₁₇ISi, calcd 400.0144, found 400.0140.

Preparation of the Arylalkyne 11 from 5. Compound

5 (6.6 mg, 0.032 mmol) was coupled with 12.6 mg of **15** (0.032 mmol) according to the general procedure to provide 13.7 mg (90% yield) of **11** as an orange-red solid.

Preparation of 2d. Compound **12** (19 mg, 0.046 mmol) was coupled with 19.3 mg (0.046 mmol) of **13** according to the general procedure to provide 21.8 mg (75% yield) of **2d** as an orange-red solid. Data for **2d**: mp 225.0–230 °C (decomp); $R_f = 0.56$ (1:1 CH₂Cl₂/hexane); ¹H NMR δ 2.49 (s, 3H), 4.23 (brs, 5H), 4.24 (t, 2H, $J = 1.2$ Hz), 4.48 (t, 2H, $J = 1.2$ Hz), 7.17 (d, 2H, $J = 8.5$ Hz), 7.39 (d, 2H, $J = 8.5$ Hz), 7.42 (d, 4H, $J = 2.4$ Hz), 7.45 (brs, 4H), 7.46 (brs, 4H); IR (neat) 2982 s, 2870 s, 2203 w, 1725 m, 1519 m, 1066 w, 1056 m, 837 s; UV (THF) (ε): λ_{max} 357 nm (18 101); MS (EI) m/e (relative intensity) 632 (2) M⁺, 547 (2), 520 (3), 506 (16), 454 (29), 430 (18), 418 (100), 410 (6), 379 (42), 370 (8).

Preparation of 3a. To a solution of 88.6 mg (0.27 mmol) of **2a** in 80 mL of CH₂Cl₂ cooled to –40 °C was added 46.0 mg (0.27 mmol) of MCPBA. The reaction mixture was stirred at –40 °C for 24 h while the progress of the reaction was monitored closely by TLC analysis (Et₂O). After the reaction was complete, the solvents were removed *in vacuo* to provide a crude product, which was purified by column chromatography to yield 79.7 mg (86% yield) of **3a** as an orange-red crystalline material. Data for **3a**: mp 156.5–157.5 °C; $R_f = 0.12$ (Et₂O); ¹H NMR δ 2.74 (s, 3H), 4.25 (brs, 5H), 4.28 (t, 2H, $J = 1.7$ Hz), 4.52 (t, 2H, $J = 1.7$ Hz), 7.61 (brd, 4H, $J = 1.8$ Hz); ¹³C NMR δ 42.9, 66.6, 69.1, 70.0, 71.8, 88.1, 92.8, 123.4, 132.0, 132.2, 141.1; IR (neat) 2929 m, 2922 m, 2884 w, 1590 m, 1414 m, 1054 s, 1050 s, 1000 s, 822 m; UV (THF) (ε): λ_{max} 272 nm (28 744), 307 nm (33 688); MS (EI) m/e (relative intensity) 348 (26) M⁺, 332 (100), 317 (28), 285 (9), 251 (6), 226 (6), 211 (3), 195 (8); HRMS m/e for C₁₉H₁₆FeOS, calcd 348.0271, found 348.0251.

Preparation of 4a. Compound **2a** (16.6 mg, 0.050 mmol) was treated with 2.0 equiv of MCPBA in the same manner as described above for the preparation of **3a** to provide 16.9 mg (93% yield) of **4a** as an orange-red solid. Data for **4a**: mp 142.0–144.0 °C; $R_f = 0.23$ (Et₂O); ¹H NMR δ 3.07 (s, 3H), 4.26 (brs, 5H), 4.32 (t, 2H, $J = 1.7$ Hz), 4.54 (t, 2H, $J = 1.7$ Hz), 7.64 (d, 2H, $J = 8.4$ Hz), 7.89 (d, 2H, $J = 8.4$ Hz); ¹³C NMR δ 44.5, 63.7, 69.4, 70.1, 71.7, 84.3, 93.6, 127.3, 131.9, 133.8, 138.7; IR (neat) 3029 w, 2923 w, 2206 m, 1608 w, 1591 m, 1310 s, 1146 s, 1087 w, 761 m; UV (THF) (ε): λ_{max} 266 nm (14 231), 308 nm (12 046); MS (EI) m/e (relative intensity) 364 (100) M⁺, 332 (4), 301 (3), 285 (30), 229 (9), 202 (4), 189 (2), 163 (7), 121 (10); HRMS m/e for C₁₉H₁₆FeO₂S, calcd 364.0220, found 364.0234.

Preparation of 3b. Compound **2b** (43.2 mg, 0.10 mmol) was treated with 1.0 equiv of MCPBA in the same manner as described above for the preparation of **3a** to provide 40.9 mg (91% yield) of **3b** as an orange-red solid. Data for **3b**: mp 179.0–180.0 °C; $R_f = 0.14$ (Et₂O); ¹H NMR δ 2.75 (s, 3H), 4.26 (brs, 5H), 4.27 (t, 2H, $J = 1.7$ Hz), 4.52 (t, 2H, $J = 1.7$ Hz), 7.48 (brs, 4H), 7.66 (dd, 4H, $J = 5.3, 8.5$ Hz); ¹³C NMR δ 43.9, 64.7, 69.1, 70.0, 71.5, 85.4, 89.6, 91.0, 91.4, 121.6, 123.6, 124.4, 126.1, 131.3, 131.6, 132.3, 145.6; IR (neat) 3115 w, 3089 w, 2972 m, 2935 m, 2381 w, 2352, 2251, 2234 w, 1774 m, 1544 m, 1540 m, 1530 m, 1112 m, 1066 s, 856 s, 823 s; UV (THF) (ε): λ_{max} 330 nm (41 574); MS (EI) m/e (relative intensity) 448 (29) M⁺, 432 (100), 417 (19), 385 (6), 329 (6), 295 (6), 263 (4), 216 (11), 184 (10); HRMS m/e for C₂₇H₂₀FeOS, calcd 448.0584, found 448.0562.

Preparation of 4b. Compound **3b** (35.7 mg, 0.080 mmol) was treated with 2.0 equiv of MCPBA in the same manner as described above for the preparation of **3a** to provide 34.7 mg (94% yield) of **4b** as an orange-red solid. Data for **4b**: mp 168.0–170.0 °C (decomp); $R_f = 0.14$ (Et₂O); ¹H NMR δ 3.08 (s, 3H), 4.26 (brs, 5H), 4.27 (t, 2H, $J = 1.9$ Hz), 4.52 (t, 2H, $J = 1.9$ Hz), 7.50 (d, 4H, $J = 1.0$ Hz), 7.71 (d, 2H, $J = 8.4$ Hz), 7.93 (d, 2H, $J = 8.4$ Hz); ¹³C NMR δ 44.5, 64.7, 69.1, 70.0, 71.5, 85.3, 89.0, 91.3, 93.3, 121.1, 124.8, 127.4, 129.0, 131.4, 131.7, 132.2, 139.6; IR (neat) 2924 w, 1697 w, 1590 w, 1426 m, 1308 s, 1151 s, 1131 s, 840 m, 763 m; UV (THF) (ε): λ_{max}

330 nm (33 363); MS (EI) m/e (relative intensity) 464 (73) M⁺, 448 (33), 432 (100), 417 (19), 385 (22), 329 (16), 263 (11), 216 (16), 121 (23); HRMS m/e for C₂₇H₂₀FeO₂S, calcd 464.0588, found 464.0540.

Preparation of 4c. Compound **2c** (29.0 mg, 0.055 mmol) was treated with 2.0 equiv of MCPBA in the same manner as described above for the preparation of **3a** to provide 24.6 mg (80% yield) of **4c** as an orange-red solid. Data for **4c**: mp 153.0–155.0 °C (decomp); $R_f = 0.08$ (Et₂O); ¹H NMR δ 3.08 (s, 3H), 4.26 (brs, 5H), 4.27 (t, 2H, $J = 1.7$ Hz), 4.52 (t, 2H, $J = 1.7$ Hz), 7.48 (d, 4H, $J = 1.0$ Hz), 7.54 (brs, 4H), 7.71 (d, 2H, $J = 8.3$ Hz), 7.94 (d, 2H, $J = 8.3$ Hz); ¹³C NMR δ 44.5, 66.8, 69.0, 70.0, 71.5, 89.3, 89.5, 90.4, 90.9, 91.7, 93.0, 122.0, 123.9, 127.4, 128.9, 130.3, 131.3, 131.5, 131.6, 131.8, 132.3, 133.9, 139.7; IR (neat) 2924 w, 1702 m, 1565 m, 1426 m, 1399 s, 1314 s, 1263 m, 1155 s, 837 s; UV (THF) (ε): λ_{max} 336 nm (21 151); MS (EI) m/e (relative intensity) 564 (100) M⁺, 485 (20), 429 (20), 376 (11), 364 (11), 318 (15), 218 (26); HRMS m/e for C₃₅H₂₄FeO₂S, calcd 564.0846, found 564.0820.

Preparation of 4-Iodobenzenethiol. To a suspension of 3.02 g (10.0 mmol) of pipsyl chloride in 70 mL of H₂O cooled in an ice-bath was cautiously added 12 mL of concentrated sulfuric acid followed by 4.14 g (63 mmol) of zinc dust. The mixture was stirred for 30 min and then refluxed for 6 h. After cooling, the reaction mixture was poured into a mixture of 50 mL of H₂O and 50 mL of saturated aqueous ammonium chloride overlaid with 250 mL of Et₂O. The aqueous layer was extracted with 2 × 250 mL of Et₂O, and the combined organic layers were washed with an equal volume of saturated aqueous sodium chloride, dried with anhydrous sodium sulfate, and then filtered through a pad of silica gel. Upon removal of the solvents *in vacuo*, 1.03 g (44% yield) of the desired material was obtained as a white solid [mp 73.0–74.0 °C; $R_f = 0.59$ (1:1 CH₂Cl₂/hexane); ¹H NMR δ 3.43 (s, 1H), 7.01 (d, 2H, $J = 8.3$ Hz), 7.54 (d, 2H, $J = 8.3$ Hz); ¹³C NMR δ 93.1, 129.9, 132.1, 139.0; IR (neat) 3190 w, 2922 w, 2382 s, 2336 s, 1468 m, 1384 m, 1099 m, 1005 m, 806 s; MS (EI) m/e (relative intensity) 236 (100) M⁺, 109 (71), 65 (24)].

Preparation of S-Acetyl-4-iodothiophenol (16). To a solution of 730.0 mg (3.1 mmol) of 4-iodobenzenethiol in 50 mL of CH₂Cl₂ were added 528.9 mg (7.73 mmol) of imidazole and 408.2 μL (4.3 mmol) of acetic anhydride sequentially. The mixture was stirred at room temperature for 15 h, and then the solvents were removed *in vacuo*. The crude product was purified by column chromatography to provide 701.2 mg (82% yield) of **16** as a white solid material. Data for **16**: mp 54.0–55.0 °C; $R_f = 0.30$ (1:1 CH₂Cl₂/hexane); ¹H NMR δ 2.43 (s, 3H), 7.13 (d, 2H, $J = 8.4$ Hz), 7.74 (d, 2H, $J = 8.4$ Hz); ¹³C NMR δ 30.2, 95.9, 127.7, 135.9, 138.3, 193.2; IR (neat) 2929 m, 2903 w, 2851 w, 1696 s, 1466 m, 1382 w, 1120 w, 1116 w, 1006 s, 812 m; MS (EI) m/e (relative intensity) 278 (100) M⁺, 236 (100), 191 (3), 127 (9), 109 (100), 82 (28), 69 (48).

Preparation of 17a. Compound **5** (62.9 mg, 0.30 mmol) was coupled with 83.4 mg (0.30 mmol) of **16** (1.0 equiv) according to the general procedure except that 10 mL of a 1:1 of THF/diisopropylethylamine (Hunig's base) solvent mixture was used instead of diethylamine⁷ to provide 89.7 mg (83% yield) of **17a** as an orange-red crystalline material. Data for **17a**: mp 96.0–98.0 °C; $R_f = 0.22$ (1:1 CH₂Cl₂/hexane); ¹H NMR δ 2.43 (s, 3H), 4.24 (brs, 5H), 4.26 (t, 2H, $J = 1.6$ Hz), 4.51 (t, 2H, $J = 1.6$ Hz), 7.36 (d, 2H, $J = 8.2$ Hz), 7.50 (d, 2H, $J = 8.2$ Hz); ¹³C NMR δ 30.2, 64.7, 69.0, 70.0, 71.5, 85.1, 90.4, 125.3, 127.1, 131.9, 134.2, 193.7; IR (neat) 2922 m, 2917 w, 1704 s, 1590 s, 1121 m, 1116 m, 1105 m, 1000 w, 945 w, 822 m, 818 m; MS (EI) m/e (relative intensity) 360 (100) M⁺, 318 (57), 251 (6), 195 (8), 121 (12); HRMS m/e for C₂₀H₁₆FeOS, calcd 360.0271, found 360.0276.

Preparation of 1a. To a solution of 66.5 mg (0.185 mmol) of **17a** in 2 mL of chloroform was added 6 mL of diethylamine. The mixture was then stirred at room temperature for 30 min, at which time the solvents were removed *in vacuo*. The resulting crude material was then purified by column chromatography to provide 38.5 mg (65% yield) of the disulfide of

Table 5. Crystal, Data Collection, and Refinement Parameters for 2b

formula	C ₂₇ H ₂₀ FeS
fw	432.3
color; habit	orange prism
size (mm ³)	0.037 × 0.065 × 0.170
cryst syst	monoclinic
space group	P2 ₁ /c
a, Å	6.031(2)
b, Å	33.457(12)
c, Å	10.364(4)
β, deg	90.90(3)
volume, Å ³	2091.2(13)
Z	4
D _{calcd} , mg m ⁻³	1.373
temp, °C	23
radiation	Mo Kα (graphite-monochromated)
scan technique	ω
μ, mm ⁻¹	0.831
2θ _{max} , deg	45
no. of data	3109
no. of data in refinement	935
R	0.083
criteria	I > 4σ(I)

1a as an orange-red solid [mp 173.0–175.0 °C; $R_f = 0.58$ (1:1 CH₂Cl₂/hexane); ¹H NMR δ 4.23 (brs, 10H), 4.25 (t, 4H, $J = 1.8$ Hz), 4.51 (t, 4H, $J = 1.8$ Hz), 7.42 (dd, 8H, $J = 8.8, 10.8$ Hz); IR (neat) 2924 m, 2917 w, 2363 m, 2335 w, 2330 w, 1494 s, 1395 m, 1162 w, 1105 m, 1025 m, 823 s, 813 s; MS (EI) m/e (relative intensity) 634 (2) M⁺, 382 (2), 318 (100), 286 (8), 228 (6), 121 (14); HRMS m/e for C₃₆H₂₈Fe₂S₂ calcd 634.0175, found 634.0140]. To a solution of this disulfide in 4 mL of CH₂Cl₂ were added 2–4 drops of glacial acetic acid and ca. 100 mg of zinc dust. The heterogeneous mixture was then stirred at room temperature for 5 min, after which time the mixture was passed through a pipette-sized silica gel column to provide 37.5 mg (99% yield) of **1a** as an orange-red solid. Data for **1a**: mp 114.0–115.0 °C; $R_f = 0.52$ (1:1 CH₂Cl₂/hexane); ¹H NMR δ 3.49 (s, 1H), 4.24 (brs, 7H), 4.49 (t, 2H, $J = 1.8$ Hz), 7.21 (d, 2H, $J = 8.3$ Hz), 7.34 (d, 2H, $J = 8.3$ Hz); ¹³C NMR δ 64.2, 68.8, 69.9, 71.3, 84.8, 88.7, 121.2, 129.0, 131.9, 136.1; IR (neat) 2928 m, 2924 m, 2919 w, 2557 w, 2547 w, 2358 w, 2362 w, 2219 w, 2206 w, 1592 s, 1497 s, 1399 m, 1100 s, 1093 m, 817 s; MS (EI) m/e (relative intensity) 318 (100) M⁺, 286 (35), 267 (19), 228 (8), 186 (8), 165 (15), 149 (23); HRMS m/e for C₁₈H₁₄FeS, calcd 318.0166, found 318.0170.

Preparation of 17b. Compound **10** (93.1 mg, 0.30 mmol) was coupled with 83.4 mg (0.30 mmol) of **16** according to the procedure used to prepare **17a** to provide 98.7 mg (71% yield) of **17b** as an orange-red solid. Data for **17b**: mp 183–185 °C; $R_f = 0.18$ (1:1 CH₂Cl₂/hexane); ¹H NMR δ 2.44 (s, 3H), 4.26 (brs, 5H), 4.27 (t, 2H, $J = 1.6$ Hz), 4.51 (t, 2H, $J = 1.6$ Hz), 7.40 (d, 2H, $J = 8.2$ Hz), 7.47 (brs, 4H), 7.56 (d, 2H, $J = 8.2$ Hz); ¹³C NMR δ 30.3, 64.8, 69.0, 70.0, 71.5, 84.6, 85.5, 86.7, 91.0, 121.6, 127.4, 131.3, 131.6, 132.0, 132.4, 134.2, 135.1, 198.8; IR (neat) 3268 w, 3093 w, 3076 w, 2922 w, 1697 s, 1514 m, 1484 s, 1397 w, 1118 w, 1105 m, 828 s; MS (EI) m/e (relative intensity) 460 (100) M⁺, 418 (44), 386 (10), 295 (7), 209 (6), 121 (10); HRMS m/e for C₂₈H₂₀FeOS, calcd 460.0584, found 460.0575.

Preparation of 1b. Compound **17b** (20.3 mg, 0.044 mmol) was treated according to the procedure used to prepare **1a** to provide 14.7 mg of an orange-red solid, which is the disulfide (79% yield) [$R_f = 0.48$ (1:1 CH₂Cl₂/hexane); ¹H NMR δ 4.25 (brs, 14H), 4.50 (t, 4H, $J = 1.7$ Hz), 7.45 (brs, 8H), 7.47 (brs, 8H); IR (neat) 2923 m, 2916 w, 2363 m, 2335 w, 2331 m, 1490 s, 1390 m, 1160 s, 1105 m, 1025 w, 823 s, 813 s; MS (EI) m/e (relative intensity) 834 (1) M⁺, 693 (1), 490 (16), 466 (100), 432 (100), 417 (42), 385 (16), 295 (16), 265 (37), 216 (26), 149 (11), 121 (26)]. This disulfide was then treated with acetic acid and zinc dust according to general procedure to provide 14.6 mg (99% yield) of **1b** as an orange-red solid. Data for **1b**: mp 141.5–143.5 °C; $R_f = 0.42$ (1:1 CH₂Cl₂/hexane); ¹H NMR δ 3.54 (brs, 1H), 4.25 (brs, 5H), 4.27 (t, 2H, $J = 1.7$ Hz),

4.51 (t, 2H, $J = 1.7$ Hz), 7.21 (d, 2H, $J = 8.2$ Hz), 7.31 (d, 2H, $J = 8.2$ Hz), 7.45 (brs, 4H); ¹³C NMR δ 64.9, 69.0, 70.0, 71.5, 85.5, 89.7, 90.4, 90.6, 122.2, 123.9, 127.2, 128.9, 131.3, 131.4, 132.1, 136.1; IR (neat) 2920 s, 2851 m, 2558 m, 2490 w, 2202 m, 1598 m, 1515 s, 1105 s, 835 s, 821 s; MS (EI) m/e (relative intensity) 418 (100) M⁺, 386 (2), 328 (2), 295 (3), 263 (3), 209 (12), 121 (8); m/e for C₂₆H₁₈FeS, calcd 418.0479, found 418.0487.

Preparation of 17c. Compound **12** (41.0 mg, 0.10 mmol) was coupled with 27.8 mg (0.10 mmol) of **16** according to the procedure used to prepare **17a** to provide 31.2 mg (56% yield) of **17c** as an orange-red solid. Data for **17c**: mp 193.0–195.0 °C; $R_f = 0.39$ (1:1 CH₂Cl₂/hexane); ¹H NMR δ 2.42 (s, 3H), 4.22 (brs, 5H), 4.23 (s, 2H), 4.48 (brt, 2H, $J = 1.7$ Hz), 7.36 (d, 2H, $J = 8.0$ Hz), 7.42 (dd, 4H, $J = 3.0, 9.3$ Hz), 7.46 (brs, 4H), 7.50 (d, 2H, $J = 8.0$ Hz); ¹³C NMR δ 30.3, 66.8, 69.0, 70.0, 71.5, 85.5, 90.5, 90.6, 90.7, 90.8, 91.3, 122.0, 122.8, 123.3, 124.1, 124.3, 128.3, 131.0, 131.3, 131.5, 131.6, 132.2, 134.2, 193.4; IR (neat) 2957 m, 2925 s, 2870 w, 2854 w, 1708 s, 1679 w, 1608 w, 1589 m, 836 s; MS (EI) m/e (relative intensity) 560 (100) M⁺, 518 (39), 517 (31), 259 (19), 128 (16); HRMS m/e for C₃₆H₂₄FeOS, calcd 560.0897, found, 560.0920.

Preparation of 1c. Compound **17c** (7 mg, 0.013 mmol) was treated according to the procedure used to prepare **1a** to provide 6.8 mg (79% yield) of the disulfide as an orange-red solid [$R_f = 0.52$ (1:1 CH₂Cl₂/hexane); ¹H NMR δ 4.22 (brs, 5H), 4.23 (s, 2H), 4.48 (brt, 2H, $J = 1.7$ Hz), 7.39 (brs, 4H), 7.42 (brs, 4H), 7.46 (brs, 4H)]. This disulfide was then treated with acetic acid and zinc dust according to general procedure to provide 6.1 mg (94% yield) of **1c** as an orange-red solid. Data for **1c**: mp 191.0–194.0 °C (decomp); $R_f = 0.42$ (1:1 CH₂Cl₂/hexane); ¹H NMR δ 3.50 (s, 1H), 4.22 (brs, 5H), 4.23 (brs, 2H), 4.48 (brt, 2H, $J = 1.7$ Hz), 7.19 (d, 2H, $J = 8.0$ Hz), 7.34 (d, 2H, $J = 8.0$ Hz), 7.42 (dd, 4H, $J = 1.9, 10.7$ Hz), 7.44 (brs, 4H); IR (neat) 2956 m, 2923 s, 2855 m, 2362 m, 2337 m, 1652 w, 1541 w, 1458 w, 1122 m, 1106 s, 837 m; MS (EI) m/e (relative intensity) 518 (100) M⁺, 486 (2), 365 (3), 279 (4), 259 (16), 128 (16); m/e for C₃₄H₂₂FeS, calcd 518.0782, found 518.0806.

Crystal Data for Compound 2b. Crystals suitable for X-ray analysis were obtained from CH₂Cl₂/hexane at 4 °C. Crystallographic data are summarized in Table 5. Single crystals are (at 296 K) monoclinic, space group P2₁/c, with $a = 6.031(2)$ Å, $b = 33.457(12)$ Å, $c = 10.364(4)$ Å, $\beta = 90.90(3)^\circ$, $V = 2091.2(13)$ Å³, and $Z = 4$ ($D_{\text{calcd}} = 1.373$ mg m⁻³; $\mu(\text{Mo K}\alpha) = 0.831$ mm⁻¹). A total of 3109 symmetry-independent reflections having $2\theta(\text{Mo K}\alpha) < 45^\circ$ were collected using full ω scans on a Siemens P4 rotating anode diffractometer using graphite-monochromated Mo K α radiation. The structure was solved by “direct methods” techniques with the SHELXTL PLUS (PC Version) software package. The resulting structural parameters were refined to convergence R (unweighted, based on F) = 0.083 for 935 independent absorption-corrected reflections having $2\theta(\text{Mo K}\alpha) < 45^\circ$ and $I > 4\sigma(I)$ with use of full-matrix least-squares refinement and a structural model that incorporated anisotropic thermal parameters for all non-hydrogen atoms and isotropic thermal parameters for all hydrogen atoms. Hydrogen atoms were included using a riding model with $d(\text{C-H}) = 0.96$ Å and $U(\text{iso}) = 0.8$ Å².

Acknowledgment. We thank the National Science Foundation (IBN-9319656) for support of this work and Dr. Joseph W. Ziller, University of California, Irvine, CA, for the crystallographic analysis of **2b**. L.R.S. is a Camille and Henry Dreyfus Teacher-Scholar and a Beckman Young Investigator.

Supporting Information Available: Tables of positional parameters of hydrogen atoms and anisotropic displacement coefficients for **2b** and NMR spectra of products **1–4**, **6**, and **8–17** (26 pages). Ordering information is given on any current masthead page.

OM9503914

Bifunctional Carriers of Organometallic Functionalities: Alkali-Metal–Zirconium–Hydrido, –Alkyl, and –Allyl Derivatives of *meso*-Octaethylporphyrinogen and Their Reaction with Isocyanides

Denis Jacoby, Sylviane Isoz, and Carlo Floriani*

Institut de Chimie Minérale et Analytique, BCH, Université de Lausanne, CH-1015 Lausanne, Switzerland

Kurt Schenk

Institut de Physique, Université de Lausanne, CH-1015 Lausanne, Switzerland

Angiola Chiesi-Villa and Corrado Rizzoli

Dipartimento di Chimica, Università di Parma, I-43100 Parma, Italy

Received May 10, 1995[⊗]

The reaction of alkali-metal organometallics with the *meso*-octaethylporphyrinogen-zirconium complex $[(\eta^5\text{-}\eta^1\text{-}\eta^5\text{-}\eta^1\text{-Et}_8\text{N}_4)\text{Zr}(\text{THF})]$ (**1**), acting as a bifunctional carrier, led to the formation of bimetallic K-Zr and Li-Zr organometallics. Such compounds formed from the addition of the nucleophilic fragment to zirconium, while the alkali-metal cation remained bonded to the electron-rich periphery of the porphyrinogen moiety. The addition of KH to **1** in a 1:1 molar ratio led to the formation of the dinuclear complex $[(\eta^5\text{-}\eta^1\text{-}\eta^5\text{-}\eta^1\text{-Et}_8\text{N}_4)\text{Zr}]_2\text{-}\{\mu\text{-KH}\}_2$ (**2**), while with a large excess of KH under controlled conditions we obtained a tetranuclear polyhydride species, $[(\eta^5\text{-}\eta^1\text{-}\eta^1\text{-}\eta^1\text{-Et}_8\text{N}_4)\text{Zr}]_4\{\text{KH}\}_8(\text{THF})_{10}$, (**3**), having the $[\text{Zr}_4\text{K}_4\text{H}_8]$ skeleton containing both μ_2 - and μ_3 -hydrides. In toluene-THF, the addition of LiR to **1** gave the monomeric dimetallic lithium-zirconium alkyls $[(\eta^5\text{-}\eta^1\text{-}\eta^1\text{-}\eta^1\text{-Et}_8\text{N}_4)\text{Zr-R}]\{\text{Li}(\text{THF})_2\}$ (R = Me, **4**; R = Bu^t, **5**). The reaction of **1** with potassium allyl gave a structurally complex, bimetallic, polynuclear compound where the allyl fragment interacts in both an η^1 and η^2 fashion, with zirconium and potassium, respectively, to give complex **6**, $[(\eta^5\text{-}\eta^1\text{-}\eta^1\text{-}\eta^1\text{-Et}_8\text{N}_4)\text{Zr}(\mu\text{-}\eta^3\text{-C}_3\text{H}_5)\text{K}]_n$. Other potassium-zirconium alkyl derivatives are accessible *via*: (i) the hydrozirconation of olefins using complex **2** (the reaction of **2** with ethylene gave $[(\eta^5\text{-}\eta^1\text{-}\eta^1\text{-}\eta^1\text{-Et}_8\text{N}_4)\text{Zr-CH}_2\text{CH}_3]_2(\mu\text{-K})_2$ (**7**)) and (ii) the exchange of the alkali-metal cation (the reaction of **4** with KH led to the corresponding KMe derivative supported by **1**, $[(\eta^5\text{-}\eta^1\text{-}\eta^1\text{-}\eta^1\text{-Et}_8\text{N}_4)\text{Zr-Me}]\{\text{K}(\text{THF})\}_2$ (**8**)). The bimetallic K-Zr alkyl and hydrido derivatives are very reactive in insertion reactions. The reaction of **2** and **4** with Bu^tNC led respectively, to the corresponding η^2 -iminoformyl $[(\eta^5\text{-}\eta^1\text{-}\eta^1\text{-}\eta^1\text{-Et}_8\text{N}_4)\text{Zr}(\eta^2\text{-CH=NBu}^t)]_2(\mu\text{-K})_2$ (**9**), and η^2 -iminoacetyl $[(\eta^5\text{-}\eta^1\text{-}\eta^1\text{-}\eta^1\text{-Et}_8\text{N}_4)\text{Zr}(\eta^2\text{-C(Me)=NBu}^t)]\{\text{Li}(\text{THF})\}$ (**10**), complexes. As such, **9** and **10** should be considered as polar alkali-metal iminoformyl and iminoacetyl derivatives bonded to the bifunctional complex **1**.

Introduction

The Zr-H and Zr-C functionalities have played a primary role in the development of organometallic

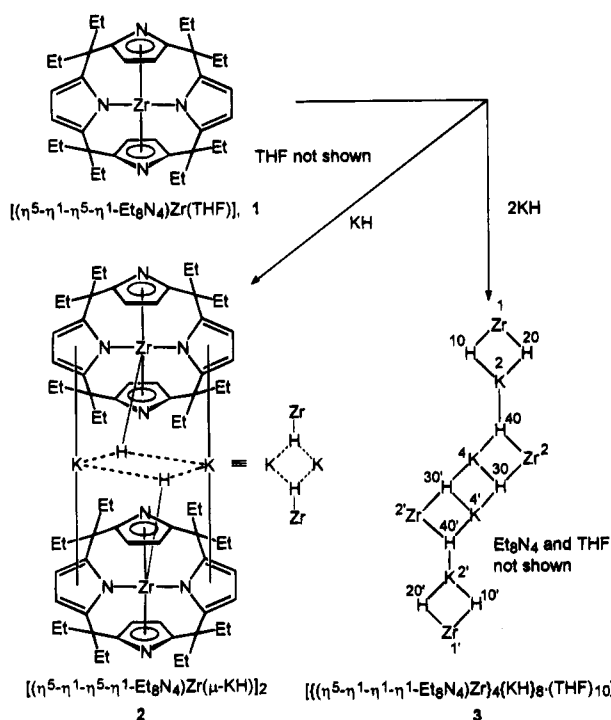
chemistry and in the application of organometallic methodologies to organic synthesis and catalysis.¹ In addition, an equally important role has been played by the alkali-metal organometallics.² We introduced recently the use of *meso*-octaalkylporphyrinogen complexes as carriers for polar organometallics,³ to combine the advantages of both approaches and eventually to move to the use of such complexes as catalysts. The carrier properties of polar organometallics have been largely developed only in case of the MR_n^{m-} metalate forms,⁴ which include the widely used cuprate deriva-

[⊗] Abstract published in *Advance ACS Abstracts*, September 1, 1995.
 (1) (a) Wailes, P. C.; Courts, R. P.; Weigold, H. *Organometallic Chemistry of Titanium, Zirconium and Hafnium*; Academic: New York, 1974. (b) Cardin, D. J.; Lappert, M. F.; Raston, C. L. *Chemistry of Organozirconium and Hafnium Compounds*; Wiley: New York, 1986. (c) Buchwald, S. L.; Nielsen, R. B. *Chem. Rev.* **1988**, *88*, 1047. (d) Negishi, E.-I. In *Comprehensive Organic Synthesis*; Paquette, L. A., Ed.; Pergamon: Oxford, U.K., 1991; Vol. 5, p 1163. (e) Grossman, R. B.; Buchwald, S. L. *J. Org. Chem.* **1992**, *57*, 5803 and references therein. (f) Negishi, E.-I.; Takahashi, T. *Acc. Chem. Res.* **1994**, *27*, 124 and references therein. (g) Schore, N. E. In *Comprehensive Organic Synthesis*; Paquette, L. A., Ed.; Pergamon: Oxford, U.K., 1991; Vol. 5, p 1037. (h) Erker, G.; Krüger, C.; Müller, G. *Adv. Organomet. Chem.* **1985**, *24*, 1 and references therein. (i) Swanson, D. R.; Negishi, E. *Organometallics* **1991**, *10*, 825. (j) Erker, G.; Pfaff, R.; Krüger, C.; Werner, S. *Organometallics* **1993**, *12*, 3559. (k) Erker, G.; Noe, R.; Krüger, C.; Werner, S. *Organometallics* **1992**, *11*, 4174. (l) Erker, G.; Pfaff, R. *Organometallics* **1993**, *12*, 1921. (m) Jordan, R. F. *Adv. Organomet. Chem.* **1991**, *32*, 325.

(2) (a) Schlosser, M. *Organoalkali Reagents In Organometallics in Synthesis*; Schlosser, M., Ed.; Wiley: New York, 1994; Chapter 1. (b) As a general reference to organoalkali-metal complexes: Weiss, E. *Angew. Chem., Int. Ed. Engl.* **1993**, *32*, 1501.

(3) (a) Jacoby, D.; Isoz, S.; Floriani, C.; Chiesi-Villa, A.; Rizzoli, C. *J. Am. Chem. Soc.* **1995**, *117*, 2805 and references therein. (b) *Ibid.* **1995**, *117*, 2793 and references therein. (c) Jacoby, D.; Floriani, C.; Chiesi-Villa, A.; Rizzoli, C. *J. Am. Chem. Soc.* **1993**, *115*, 3595 and references therein.

Scheme 1



tives.⁵ We report here a number of examples of polar organometallics, especially for potassium, carried by the zirconium-*meso*-octaethylporphyrinogen^{3c} complex. These potassium derivatives can add as such or can be formed directly on the carrier *via* a hydrozirconation reaction or metathesis from another alkali-metal derivative. The latter approach has made available some nearly inaccessible potassium-organometallic derivatives² by a very smooth route. The reactions of the Zr-H and Zr-C bonds with BuⁿCN leading to η^2 -iminoformyl and η^2 -iminoacyl groups are reported.

Results and Discussion

The bifunctional nature of complex 1 allows its use for carrying polar, ion-pair, and ionic species. The metal site behaves as a Lewis acid center, while the electron-rich periphery, i.e. the σ -bonded pyrrolyl anions, is available for binding metal ions. This behavior of 1 is exemplified by its reactivity with MH [M = Li, Na, K], which is particularly complex, and depends on (i) the nature of the alkali-metal ion, (ii) the reaction conditions, and (iii) the MH:Zr stoichiometric ratio. In general, such a reaction leads either to a 1:1 dimeric adduct (see 2)^{3c,6} or to the metalation of the *meso*-ethyl groups.^{3a} We report here the full details of the reaction of 1 with KH, leading to an unprecedented polynuclear hydride. The reaction of 1 with KH in a 1:1 KH:Zr ratio led to the dinuclear complex 2, the detailed synthesis

of which is reported here. The use of a 2:1 MH:Zr ratio under rigorous reaction conditions (see Experimental Section) led to the formation of the polynuclear species 3. An excess of KH and drastic reaction conditions led, instead, to the mono- and bis-metalation of the *meso*-ethyl chains.^{3a}

In the case of 2, each zirconium atom is $\eta^5\text{:}\eta^1\text{:}\eta^5\text{:}\eta^1$ -bonded to the porphyrinogen anion, while each potassium cation is η^5 -bonded to two pyrrolyl anions to form a bent bis(cyclopentadienyl)-type sandwich.⁶ In the case of 3, due to the complexity of the structure we show only the potassium-zirconium-hydride skeleton, using the same numbering scheme shown in Figure 1A. The structure consists of the centrosymmetric tetramer $\text{K}_4\text{-Zr}_4\text{H}_8$.⁷ Only four K ions participate in the metal-hydride skeleton, while the other four are bonded to the porphyrinogen periphery (K1, K1', K3, K3'). In the asymmetric unit, we have two independent zirconium ions, Zr1 and Zr2, each one being $\eta^1\text{:}\eta^1\text{:}\eta^1\text{:}\eta^5$ -bonded to the porphyrinogen. Selected interatomic distances are listed in Table 1, while conformational parameters are shown in Table 2. The coordination environments for the four independent K ions are shown in Figure 1B. K1, K2, and K3 show a bent-sandwich type of bonding to two pyrrolyl anions with a dihedral angle between the ring planes varying from 78.9(2) to 55.4(2) to 34.4(3)°, respectively, around the metal ion. The K- η^5 -pyrrolyl anion centroid distances range from 2.928(7) to 3.233(3) Å, the longest one being observed for K1. We should emphasize that the K-C distances for this case fall in a rather wide range (~0.5 Å). Nevertheless, the geometry of these interactions, the relevant deformations they exert on the conformation of the [Zr(Et₂N₄)] moieties, and their continuous variations suggest η^5 -pyrrole-alkali-metal interactions. In a single case, we observe one pyrrolyl anion η^5 -bonded to two potassium cations (K3, K4') on both faces (Figure 1A). In the structure there are two kinds of hydrides: the doubly bridging H10 and H20 and the triply bridging H30 and H40, with the Zr-H and K-H distances being significantly shorter for the μ_2 than for the μ_3 mode (Table 1).⁸ We were unable to identify the bridging hydride ligands in the NMR spectrum. The only structural information we can draw from the NMR spectrum is the $\eta^1\text{:}\eta^1\text{:}\eta^1\text{:}\eta^5$ bonding mode of the porphyrinogen around the zirconium ions in solution, as we found for the structure in the solid state.

Equation 1 shows an interesting extension of the use of 1 to bind polar organometallics. The reactions shown in (1) were carried out in a mixture of toluene and THF and complexes 4 and 5 were obtained as light yellow crystalline solids upon addition of *n*-hexane.

The structure displayed for 4 and 5 is based on the X-ray analysis results obtained for 5 (*vide infra*). The

(4) (a) Reetz, M. T. In *Organotitanium Reagents in Organic Synthesis*; Springer: Berlin, Germany, 1986. (b) Reetz, M. T.; Steinbach, R.; Westermann, J.; Peter, R.; Wenderoth, B. *Chem. Ber.* **1985**, *118*, 1441. (c) Reetz, M. T.; Wenderoth, B. *Tetrahedron Lett.* **1982**, *23*, 5259. (d) Morris, R. J.; Girolami, G. S. *Organometallics* **1991**, *10*, 792. (e) Quan, R. W.; Bazan, G. C.; Kiely, A. F.; Schaefer, W. P.; Bercaw, J. E. *J. Am. Chem. Soc.* **1994**, *116*, 4489.

(5) (a) Lipshutz, B. H.; Sengupta, S. in *Organic Reactions*; Paquette, L. A., Ed.; Wiley: New York, 1992; Vol. 41, Chapter 2. (b) Lipshutz, B. H. In *Organometallics in Synthesis, a Manual*; Schlosser, M., Ed.; Wiley: New York, 1994; Chapter 4.

(6) Jacoby, D.; Floriani, C.; Chiesi-Villa, A.; Rizzoli, C. *J. Am. Chem. Soc.* **1993**, *115*, 7025.

(7) (a) For a survey of group IV and V hydrides, see: Toogood, G. E.; Wallbridge, M. G. H. *Adv. Inorg. Chem. Radiochem.* **1982**, *25*, 267. (b) Carlin, D. J.; Lappert, M. F.; Raston, C. L. *Chemistry of Organozirconium and -Hafnium Compounds*; Ellis Horwood: Chichester, U.K., 1986. (c) Cardin, D. J.; Lappert, M. F.; Raston, C. L. In *Comprehensive Organometallic Chemistry*; Wilkinson, G.; Stone, F. G. A.; Abel, E. W., Eds.; Pergamon: Oxford, U.K., 1981; Vol. 3, Chapter 23.2, p 45. (d) Schwartz, J. *Pure Appl. Chem.* **1980**, *52*, 733. Wolczanski, P. T.; Bercaw, J. E. *Acc. Chem. Res.* **1980**, *13*, 121. (e) Labinger, J. A. *Transition Metal Hydrides*; Dedieu, A., Ed.; VCH: Weinheim, Germany, 1992. Buchwald, S. L.; La Maire, S. J.; Nielsen, R. B.; Watson, B. T.; King, S. M. *Tetrahedron Lett.* **1987**, *28*, 3895.

(8) (a) Evans, W. J.; Meadows, H. J.; Hanusa, P. T. *J. Am. Chem. Soc.* **1984**, *106*, 4454. (b) Wailes, P. C.; Weigold, H.; Bell, A. P. *J. Organomet. Chem.* **1972**, *43*, C29.

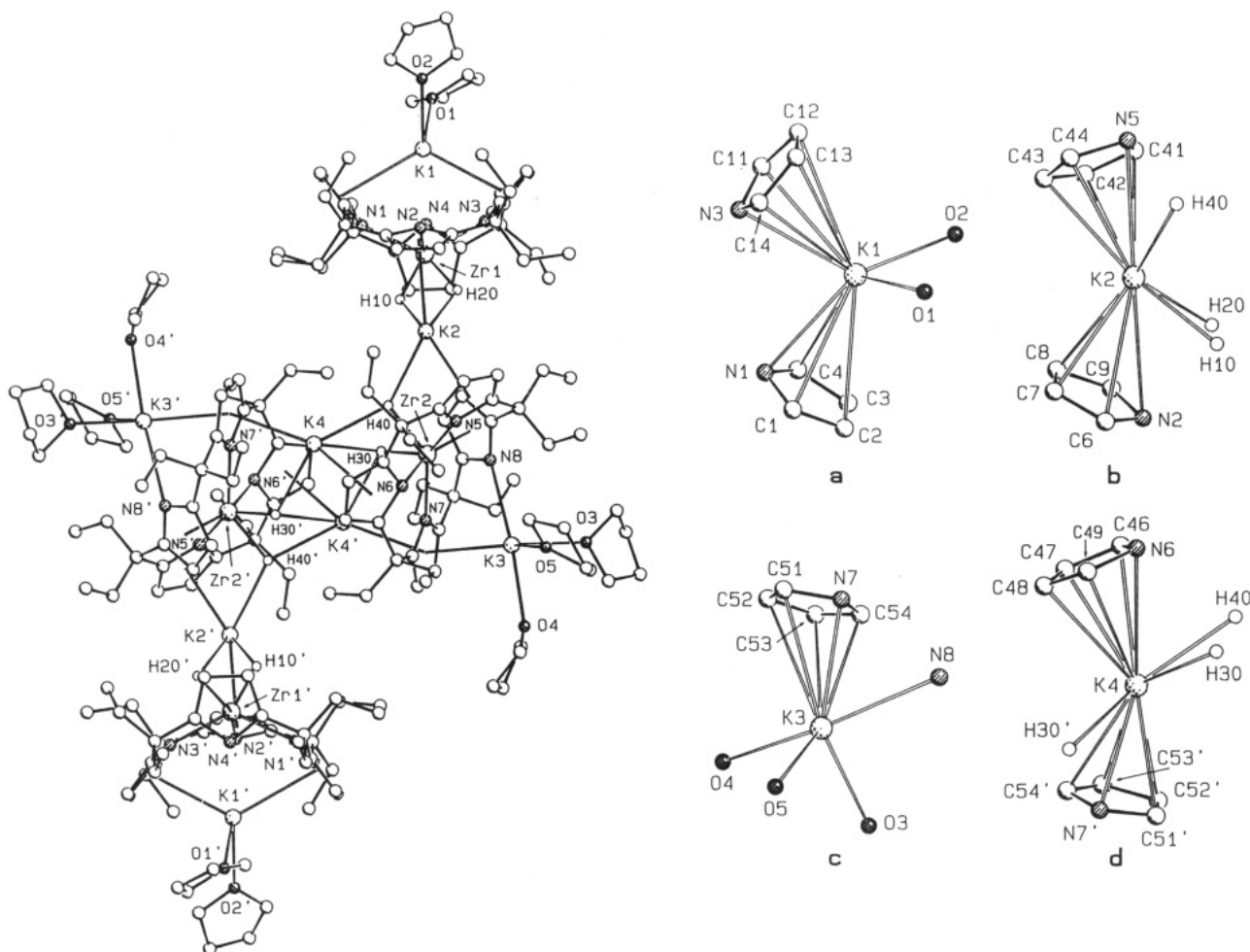
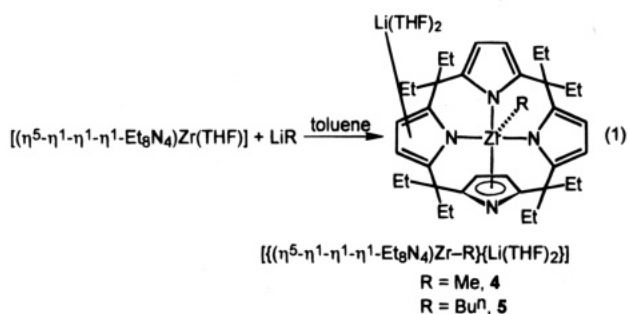


Figure 1. (A, left) SCHAKAL drawing of the asymmetric unit in complex **3**. The prime denotes a transformation of $-x$, $-y$, $1 - z$. The disorder is omitted for clarity. (B, right) SCHAKAL drawings showing the coordination environments of the potassium atoms in complex **3**. The prime denotes a transformation of $-x$, $-y$, $1 - z$.



complexation of the polar LiR unit occurs with the separation of the ion pairs, with the nucleophilic alkyl group adding to zirconium, while the lithium cation is complexed by the porphyrinogen periphery. The bonding mode of the porphyrinogen, as discussed in detail in a previous report, changes from $\eta^5\text{:}\eta^1\text{:}\eta^5\text{:}\eta^1$ to $\eta^5\text{:}\eta^1\text{:}\eta^1\text{:}\eta^1$ as a consequence of a change in the electronic demands of the metal and, to some degree, for steric reasons.^{3c,9} A major question is whether such a bonding mode remains unchanged in solution, or what kind of relationship may exist between the structure in the solid state and that in solution. The ¹H NMR spectrum at room temperature is in agreement with two kinds of pyrroles, namely two η^5 and two η^1 types. When the

temperature raised to 330 K, a singlet for the pyrrolic 3,4-protons was observed, apparently consistent with a fluxional behavior for the pyrrole fragments exchanging their position from η^5 to η^1 to η^5 . However, when the temperature was lowered, no change was observed in the NMR spectrum. We observed two triplets for the methyl groups of the eight *meso*-ethyl groups, and a single quartet for the methylenes,³ indicating that the major geometrical differentiation occurs for the methyl group rather than for the methylene moiety. This is due to some rigid conformational effects of the ethyl groups, four of them protecting the metal and four outside of the metal coordination sphere.¹⁰

The structure of **5** is reported in Figure 2, and relevant bond distances and angles are listed in Table 3. The four nitrogen atoms lie in a plane from which Zr is displaced by 0.819(1) Å toward the butyl ligand. The molecule maintains a saddle-shaped conformation, though small differences are observed in the dihedral angles (Table 2). The porphyrinogen ligand shows the $\eta^5\text{:}\eta^1\text{:}\eta^1\text{:}\eta^1$ -bonding mode with the η^5 -bonded pyrrole ring nearly perpendicular to the N₄ core. The [Li(THF)₂]⁺ cation is linked to N4 (2.109(7) Å) and to C1 (albeit by a rather long distance, 2.642(10) Å). The Zr–C(Buⁿ)

(10) De Angelis, S.; Solari, E.; Floriani, C.; Chiesi-Villa, A.; Rizzoli, C. *J. Am. Chem. Soc.* **1994**, *116*, 5691, 5702. Jacoby, D.; Floriani, C.; Chiesi-Villa, A.; Rizzoli, C. *J. Chem. Soc., Chem. Commun.* **1991**, 220. Jubb, J.; Jacoby, D.; Floriani, C.; Chiesi-Villa, A.; Rizzoli, C. *Inorg. Chem.* **1992**, *31*, 1306.

(9) (a) Jacoby, D.; Floriani, C.; Chiesi-Villa, A.; Rizzoli, C. *J. Chem. Soc., Chem. Commun.* **1991**, 790. (b) Rosa, A.; Ricciardi, M.; Sgamellotti, A.; Floriani, C. *J. Chem. Soc., Dalton Trans.* **1993**, 3759.

Table 1. Selected Bond Distances (Å) and Angles (deg) for Complex 3^a

Zr1-N1	2.306(5)	Zr1-C17	2.614(5)	Zr2-N5	2.251(4)	Zr2-C57	2.651(5)
Zr1-N2	2.286(4)	Zr1-C18	2.601(5)	Zr2-N6	2.246(4)	Zr2-C58	2.603(5)
Zr1-N3	2.292(5)	Zr1-C19	2.509(6)	Zr2-N7	2.325(4)	Zr2-C59	2.481(6)
Zr1-N4	2.384(4)	Zr1-Cp4	2.231(5)	Zr2-N8	2.408(5)	Zr2-Cp8	2.235(6)
Zr1-C16	2.505(5)			Zr2-C56	2.493(5)		
Zr1-H10	1.78	K2-H20	2.51	Zr2-H30	1.80	K4-H40	2.79
Zr1-H20	1.79	K2-H40	2.90	Zr2-H40	2.08	K4-H30'	2.90
K2-H10	2.51			K4-H30	2.66		
K1-O1	2.724(6)	K1-O2	2.702(6)	K1-N1	3.261(4)	K1-N4	3.380(4)
K1-N1	3.250(4)	K1-C3	3.531(8)	K1-N3	3.148(5)	K1-C13	3.598(8)
K1-C1	3.471(6)	K1-C4	3.350(7)	K1-C11	3.317(7)	K1-C14	3.372(7)
K1-C2	3.622(9)	K1-Cp1	3.233(3)	K1-C12	3.593(7)	K1-Cp3	3.201(7)
K2-N2	3.438(4)	K2-C8	3.168(5)	K2-N5	3.171(5)	K2-C43	3.140(8)
K2-C6	3.411(6)	K2-C9	3.304(6)	K2-C41	3.172(7)	K2-C44	3.147(6)
K2-C7	3.221(6)	K2-Cp2	3.090(6)	K2-C42	3.153(8)	K2-Cp5	2.928(7)
K3-N7	3.010(5)	K3-C53	3.428(7)	K3-O3	2.712(8)	K3-N8	3.011(4)
K3-C51	3.314(7)	K3-C54	3.076(7)	K3-O4	2.716(4)		
K3-C52	3.540(9)	K3-Cp7	3.063(7)	K3-O5	2.723(6)		
K4-N6	3.458(6)	K4-C48	3.325(8)	K4-N7'	3.020(5)	K4-C53'	3.438(9)
K4-C46	3.253(8)	K4-C49	3.531(7)	K4-C51'	3.119(7)	K4-C54'	3.201(8)
K4-C47	3.135(8)	K4-Cp6	3.123(7)	K4-C52'	3.358(8)	K4-Cp7'	3.009(8)
N1-C1	1.401(7)	N3-C11	1.352(6)	N5-C41	1.392(8)	N7-C51	1.367(7)
N1-C4	1.399(7)	N3-C14	1.388(7)	N5-C44	1.400(8)	N7-C54	1.393(8)
N2-C6	1.411(8)	N4-C16	1.380(8)	N6-C46	1.395(8)	N8-C56	1.353(10)
N2-C9	1.366(8)	N4-C19	1.354(7)	N6-C49	1.435(7)	N8-C59	1.369(7)
C18-Zr1-C19	31.3(2)	Cp4-Zr1-N2	162.3(2)	C58-Zr2-C59	32.1(2)	Cp8-Zr2-N6	162.5(2)
C17-Zr1-C18	31.8(2)	Cp4-Zr1-N1	94.6(2)	C57-Zr2-C58	31.1(2)	Cp8-Zr2-N5	95.5(2)
C16-Zr1-C17	31.4(2)	N2-Zr1-N3	77.4(1)	C56-Zr2-C57	31.7(2)	N6-Zr2-N7	81.5(2)
N4-Zr1-C19	32.0(2)	N1-Zr1-N3	127.0(1)	N8-Zr2-C59	32.5(2)	N5-Zr2-N7	138.0(1)
N4-Zr1-C16	32.7(2)	N1-Zr1-N2	77.7(1)	N8-Zr2-C56	32.0(2)	N5-Zr2-N6	76.9(2)
Cp4-Zr1-N3	95.3(2)			Cp8-Zr2-N7	94.5(2)		
O1-K1-O2	83.2(2)						
N5-K2-C44	25.6(1)	C42-K2-C43	26.0(2)	N2-K2-C6	23.8(1)	C7-K2-C8	25.6(2)
N5-K2-C41	25.3(1)	C41-K2-C42	25.0(2)	N2-K2-C9	23.3(1)	C8-K2-C9	24.9(2)
C43-K2-C44	25.1(2)			C6-K2-C7	23.8(2)		
O5-K3-N8	113.5(2)	O3-K3-N8	92.3(2)	N7-K3-C54	26.4(1)	C52-K3-C53	23.2(2)
O4-K3-N8	164.5(2)	O3-K3-O5	92.1(2)	N7-K3-C51	24.2(1)	C53-K3-C54	23.7(2)
O4-K3-O5	81.9(2)	O3-K3-O4	86.0(2)	C51-K3-C52	22.6(2)		
N6-K4-C49	23.7(1)	C47-K4-C48	25.2(2)	N7'-K4-C51'	25.7(1)	C52'-K4-C53'	23.8(2)
N6-K4-C46	23.8(1)	C48-K4-C49	23.1(2)	N7'-K4-C54'	25.7(1)	C53'-K4-C54'	23.6(2)
C46-K4-C47	25.0(2)			C51'-K4-C52'	23.9(2)		

^a Cp1, Cp2, Cp3, Cp4, Cp5, Cp6, Cp7, and Cp8 refer to the centroids of the pyrrole rings containing N1, N2, N3, N4, N5, N6, N7, and N8 respectively. The prime denotes a transformation of $-x, -y, 1-z$.

Table 2. Comparison of Structural Parameters for Compounds 3, 5, 6, and 10

	3 ^a	5	6	10 ^a
dist of atoms from N ₄ core, Å				
N1	-0.044(4) [-0.034(4)]	-0.004(2)	-0.016(6)	-0.095(2)
N2	0.046(4) [0.064(5)]	0.005(2)	0.012(5)	0.097(2)
N3	-0.044(4) [-0.037(4)]	-0.004(2)	-0.011(5)	-0.084(2)
N4	0.042(4) [0.052(5)]	0.004(2)	0.010(5)	0.082(2)
Zr	0.977(1) [0.848(1)]	0.819(1)	0.864(1)	0.910(1)
dist of Zr from A, Å ^b	1.066(1) [0.457(1)]	0.880(1)	1.002(1)	0.432(1)
dist of Zr from B, Å	1.511(1) [1.328(1)]	1.775(1)	1.735(1)	1.145(1)
dist of Zr from C, Å	0.849(1) [0.023(1)]	0.806(1)	0.929(1)	0.217(1)
dist of Zr from D, Å	2.214(1) [2.219(1)]	2.273(1)	2.215(1)	2.261(1)
dihedral angles between the N ₄ core and the A-D rings, deg				
A	126.5(2) [166.8(2)]	134.7(1)	130.8(2)	137.0(1)
B	163.0(2) [162.0(2)]	147.9(1)	152.3(2)	158.3(1)
C	132.1(2) [151.6(2)]	136.9(1)	132.3(2)	156.7(1)
D	90.1(2) [90.2(2)]	92.1(1)	92.1(2)	94.8(1)

^a Molecule B in brackets. ^b A-D refer to the pyrrole and pyridine rings containing N1, N2, N3, and N4, respectively.

bond distance is like that of the cyclopentadienyl derivatives.^{1b}

Equation 2 shows a further example of the use of 1 to bind polar organometallics. The reaction of 1 with potassium allyl gave 6 as a yellow crystalline solid. Its

¹H NMR spectrum at 298 K is not informative on the allyl bonding mode, while it shows two singlets for the pyrrolic 3,4-protons of the same intensity, indicating the presence of two η^5 - and two η^1 -pyrrolyl anions in solution. However, the solid-state structure, as shown

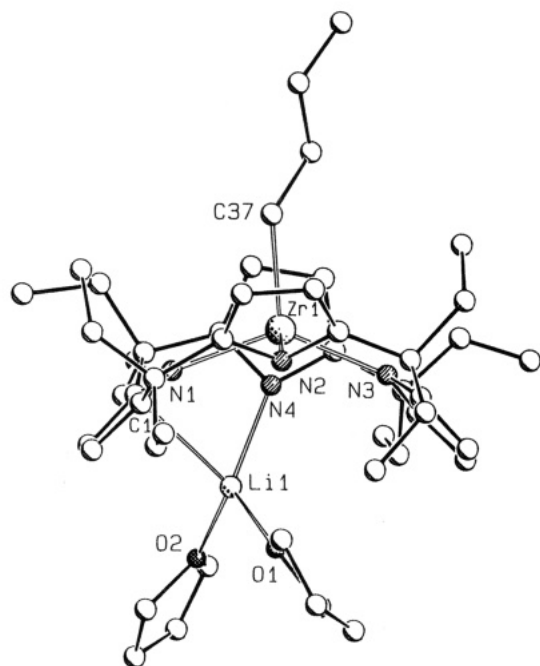
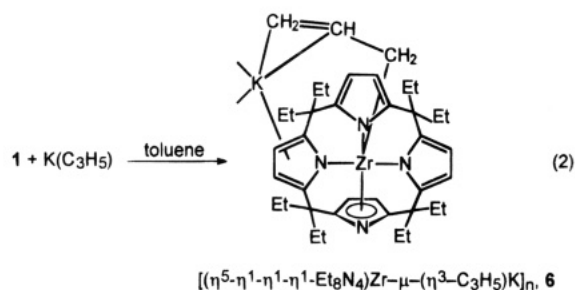


Figure 2. SCHAKAL perspective view of complex 5.

Table 3. Selected Bond Distances (Å) and Angles (deg) for Complex 5^a

Zr1-N1	2.227(3)	N2-C9	1.402(4)
Zr1-N2	2.203(2)	N3-C11	1.393(5)
Zr1-N3	2.218(3)	N3-C14	1.390(4)
Zr1-N4	2.435(2)	N4-C16	1.383(4)
Zr1-C16	2.552(3)	N4-C19	1.393(5)
Zr1-C17	2.682(3)	C1-C2	1.364(4)
Zr1-C18	2.685(4)	C2-C3	1.406(5)
Zr1-C19	2.553(4)	C3-C4	1.371(4)
Zr1-Cp4	2.296(3)	C6-C7	1.380(5)
Zr1-C37	2.248(3)	C7-C8	1.390(6)
Li1-C1	2.642(10)	C8-C9	1.375(5)
Li1-O1	1.892(9)	C11-C12	1.370(6)
Li1-O2	1.969(8)	C12-C13	1.402(5)
Li1-N4	2.112(6)	C13-C14	1.364(6)
N1-C1	1.396(4)	C16-C17	1.388(5)
N1-C4	1.380(4)	C17-C18	1.403(6)
N2-C6	1.386(5)	C18-C19	1.391(4)
C37-Zr1-Cp4	100.1(1)	C1-N1-C4	106.0(3)
N3-Zr1-Cp4	95.3(1)	Zr1-N2-C9	110.9(2)
N2-Zr1-Cp4	167.7(1)	Zr1-N2-C6	113.2(2)
N2-Zr1-C37	92.2(1)	C6-N2-C9	106.3(3)
N2-Zr1-N3	80.0(1)	Zr1-N3-C14	122.4(2)
N1-Zr1-Cp4	95.1(1)	Zr1-N3-C11	126.8(2)
N1-Zr1-C37	104.4(1)	C11-N3-C14	105.6(3)
N1-Zr1-N3	136.4(1)	Zr1-N4-C19	78.5(2)
N1-Zr1-N2	81.0(1)	Zr1-N4-C16	78.6(2)
Zr1-N1-C4	127.4(2)	C16-N4-C19	105.8(3)
Zr1-N1-C1	121.3(2)	Zr1-C37-C38	128.8(3)

^a Cp4 refers to the centroid of the pyrrolic ring N4, C16, C17, C18, C19.



in Figure 3, is significantly different from that observed in solution. Complex 6, which crystallizes with one THF

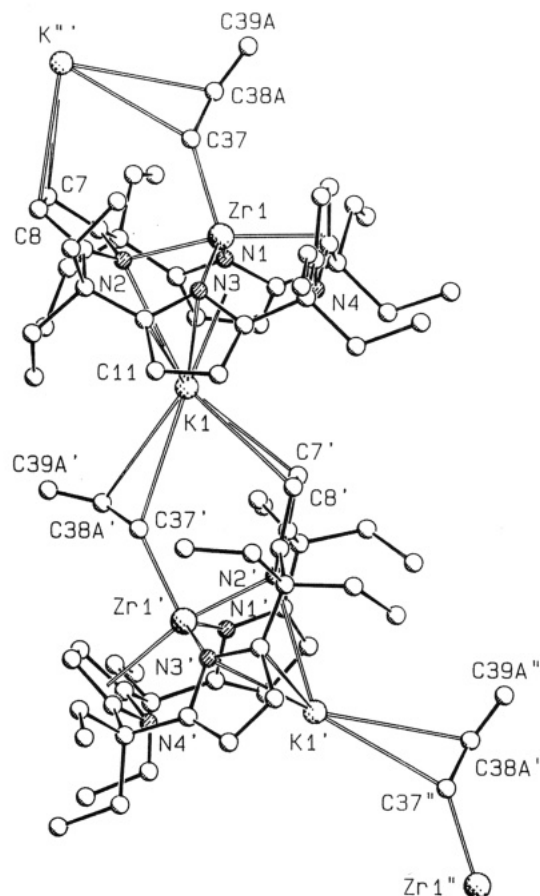


Figure 3. SCHAKAL perspective view of complex 6 showing the polymeric chain. Primes refer to the following transformations: (') $x, -y, 0.5 + z$; (") $x, y, 1 - z$; (""') $x, -y, -0.5 + z$.

molecule for every two complex molecules, has a polymeric chain structure running parallel to the crystallographic [001] axis (Figure 3), where the porphyrinogen units are bridged by potassium cations (Table 4). The porphyrinogen unit shows an $\eta^1:\eta^1:\eta^1:\eta^5$ bonding mode to zirconium with a conformation close to that reported for 5 (see Table 2). The four nitrogen atoms lie in a plane which is nearly perpendicular to the η^5 -bonded pyrrole. The potassium cation bridges two adjacent porphyrinogens related by a C glide. Potassium is η^5 -bonded to the pyrrolyl anion containing N1 η^3 -bonded to that containing N3 and C11, η^1 -bonded to N2, and linked to an adjacent porphyrinogen unit *via* an η^2 -interaction with the allyl group (C37 and C38) and a pyrrolyl anion (C7 and C8) (Figure 3). Although the disorder affecting C37 and C38 from the allyl group does not allow discussion of the C-C bond distances, the data in Table 4 support the σ -bonding mode of the allyl to zirconium (Zr-C37, 2.271(8) Å; Zr-C38A, 3.22(2) Å; Zr-C38B, 3.31(3) Å). C38 and C39 of the allylic group were found to be disordered over two positions (A and B).

It is well-known that the alkali-metal ion plays a crucial role in the chemistry of polar organometallics.² We expect that the same would be true for the case of these polar organometallics bonded to an appropriate carrier. We should admit that potassium organometallics are not as numerous and as easily available as the corresponding lithium derivatives.² In order to overcome such difficulties, we have in our case two possibili-

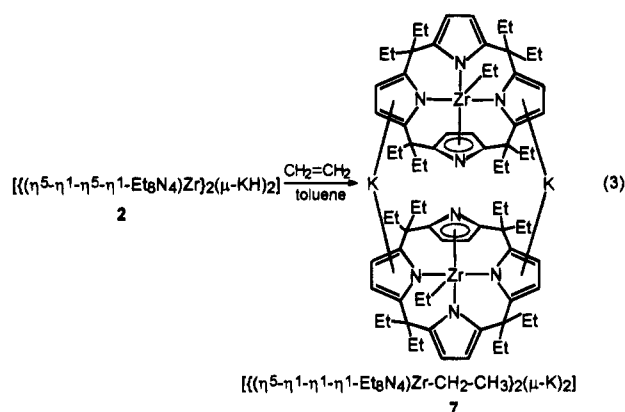
Table 4. Selected Bond Distances (Å) and Angles (deg) for Complex 6^a

Zr1-N1	2.236(5)	N1-C4	1.388(8)
Zr1-N2	2.259(5)	N2-C6	1.399(11)
Zr1-N3	2.211(6)	N2-C9	1.419(8)
Zr1-N4	2.383(5)	N3-C11	1.389(9)
Zr1-C16	2.500(8)	N3-C14	1.405(9)
Zr1-C17	2.620(7)	N4-C16	1.395(7)
Zr1-C18	2.616(7)	N4-C19	1.367(9)
Zr1-C19	2.523(6)	C1-C2	1.392(9)
Zr1-Cp4	2.237(7)	C2-C3	1.409(11)
Zr1-C37	2.271(8)	C3-C4	1.385(9)
K1-N1	3.246(7)	C6-C7	1.377(10)
K1-N2	3.152(6)	C7-C8	1.410(13)
K1-N3	3.392(5)	C8-C9	1.381(12)
K1-C1	3.535(7)	C11-C12	1.357(13)
K1-C2	3.651(9)	C12-C13	1.406(11)
K1-C3	3.498(9)	C13-C14	1.362(12)
K1-C4	3.275(10)	C16-C17	1.402(11)
K1-C11	3.438(6)	C17-C18	1.404(11)
K1-C7'	3.207(8)	C18-C19	1.383(9)
K1-C8'	3.286(10)	C37-C38A	1.38(2)
K1-C37'	3.325(8)	C37-C38B	1.37(3)
K1-C38A'	3.460(18)	C38A-C39A	1.29(3)
K1-C38B'	3.65(3)	C38B-C39B	1.29(4)
N1-C1	1.407(8)		
C37-Zr1-Cp4	104.9(2)	K1-N2-C6	120.0(4)
N3-Zr1-Cp4	96.9(3)	Zr1-N2-C9	114.0(4)
N3-Zr1-C37	108.4(2)	Zr1-N2-C6	113.4(4)
N2-Zr1-Cp4	166.7(2)	C6-N2-C9	106.3(5)
N2-Zr1-C37	88.4(2)	Zr1-N3-C14	120.5(4)
N2-Zr1-N3	78.9(2)	Zr1-N3-C11	128.6(5)
N1-Zr1-Cp4	95.2(2)	C11-N3-C14	105.1(5)
N1-Zr1-C37	111.7(3)	Zr1-N4-C19	79.5(3)
N1-Zr1-N3	133.2(2)	Zr1-N4-C16	78.1(3)
N1-Zr1-N2	79.2(2)	C16-N4-C19	105.6(5)
Zr1-N1-C4	127.0(4)	Zr1-C37-C38B	130.6(12)
Zr1-N1-C1	121.0(4)	Zr1-C37-C38A	122.6(8)
C1-N1-C4	105.2(5)	C37-C38A-C39A	135.7(19)
Zr1-N2-K1	78.7(1)	C37-C38B-C39B	137.9(26)
K1-N2-C9	122.0(4)		

^a Cp4 refers to the centroid of the pyrrolic ring N4,C16,C17,C18,C19. The prime denotes a transformation of $x, -y, 0.5 + z$.

ties: (i) the hydrozirconation reaction¹¹ of olefins and acetylenes using **2**, and (ii) the alkali-metal ion exchange.

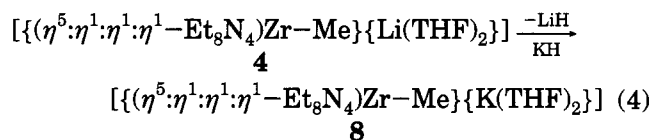
The hydrozirconation of ethylene is shown in reaction 3.



Reaction 3 occurs under relatively mild conditions and gives good yields of the corresponding potassium-alkyl derivative. Complex **7** has spectroscopic data very similar to those of $[(\eta^5\text{-}\eta^1\text{-}\eta^1\text{-}\eta^1\text{-Et}_8\text{N}_4)\text{Zr-CH}_2\text{CH}_3]_2(\mu\text{-Na})_2$,^{3c} the dimeric structure of which was established with an X-ray analysis. Such dimeric structures are

usually broken into the monomeric species by good coordinating solvents such as THF.^{3c}

An alkali-metal ion exchange has been carried out according to reaction 4. A THF solution of **4** reacts smoothly with an equimolar amount of KH, leading to **8**.



The solid-state structure we propose for **8** is close to that of **4** and to that of the sodium analogue, $[(\eta^5\text{-}\eta^1\text{-}\eta^1\text{-}\eta^1\text{-Et}_8\text{N}_4)\text{Zr-Et}]_2\{\text{Na}(\text{THF})_2\}$.^{3c} We should emphasize that the occurrence of the alkali-metal-zirconium alkyl derivative as a monomer or as a dimer depends exclusively on the solvent; the dimeric form is isolated from toluene, while the monomeric form is obtained from THF solvating the alkali-metal cation.^{3c} Another common characteristic of the alkyl derivatives of zirconium porphyrinogen thus far reported is the difference between the bonding mode of the porphyrinogen to the metal, being $\eta^5\text{-}\eta^1\text{-}\eta^1\text{-}\eta^1$ in the solid state and $\eta^1\text{-}\eta^5\text{-}\eta^1\text{-}\eta^5$ in solution, as revealed by the NMR spectrum at room temperature.

The reactions reported so far including those discussed above, led to the formation of Zr-H and Zr-C bonds *via* the addition of a polar organometallic to the bifunctional complex **1**. They have involved migratory insertion reactions, which have significant precedence in cyclopentadienyl- and alkoxy-zirconium chemistry.^{7e,12} The reactions of **2**, **5**, and **6** with BuⁿCN parallel the known behavior of the cyclopentadienyl and alkoxy derivatives,^{7e,12,13} even though in this case we are dealing with metalate forms. However, a striking

(11) Schwartz, J.; Labinger, J. A. *Angew. Chem., Int. Ed. Engl.* **1976**, *15*, 333. Carr, D. B.; Yoshifujii, M.; Shoer, L. I.; Gell, K. I.; Schwartz, J. *Ann. N.Y. Acad. Sci.* **1977**, *295*, 127. Hart, D. W.; Blackburn, T. F.; Schwartz, J. *J. Am. Chem. Soc.* **1975**, *97*, 679. Hart, D. W.; Schwartz, J. *J. Am. Chem. Soc.* **1974**, *96*, 8115. Gibson, T. *Tetrahedron Lett.* **1982**, *23*, 157. Bock, P. L.; Boschetto, D. J.; Rasmussen, J. R.; Demers, J. P.; Whitesides, G. M. *J. Am. Chem. Soc.* **1974**, *96*, 2814. Labinger, J. A.; Hart, D. W.; Seibert, W. E.; Schwartz, J. *J. Am. Chem. Soc.* **1975**, *97*, 3851. Bertelo, C. A.; Schwartz, J. *J. Am. Chem. Soc.* **1976**, *98*, 262; **1975**, *97*, 228. Blackburn, T. F.; Labinger, J. A.; Schwartz, J. *Tetrahedron Lett.* **1975**, *16*, 3041. Neghishi, E.; Yoshida, T. *Tetrahedron Lett.* **1980**, *21*, 1501. Neghishi, E.; Takahashi, T. *Aldrichim. Acta* **1985**, *18*, 31. Neghishi, E.; Miller, J. A.; Yoshida, T. *Tetrahedron Lett.* **1984**, *25*, 3407. Jordan, R. F.; Lapointe, R. E.; Bradley, P. K.; Baenzinger, N. *Organometallics* **1989**, *8*, 2892 and references therein. For a survey of group IV and V hydrides, see: Toogood, G. E.; Wallbridge, M. G. H. *Adv. Inorg. Chem. Radiochem.* **1982**, *25*, 267. Cardin, D. J.; Lappert, M. F.; Raston, C. L. In *Comprehensive Organometallic Chemistry*; Wilkinson, G.; Stone, F. G. A., Eds.; Pergamon: Oxford, U.K., 1981; Vol. 3, Chapter 23.2, p 45. Schwartz, J. *Pure Appl. Chem.* **1980**, *52*, 733. Buchwald, S. L.; La Maire, S. J.; Nielsen, R. B.; Watson, B. T.; King, S. M. *Tetrahedron Lett.* **1987**, *28*, 3895.

(12) (a) Durfee, L. D.; Rothwell, I. P. *Chem. Rev.* **1988**, *88*, 1059. (b) Wolczanski, P. T.; Bercaw, J. E. *Acc. Chem. Res.* **1980**, *13*, 121. (c) Headford, C. E. L.; Roper, W. R. In *Reactions of Coordinated Ligands*; Braterman, P. S., Ed.; Plenum: New York, 1986, Vol. 1, Chapter 8.

(13) Singleton, E.; Ossthizen, H. E. *Adv. Organomet. Chem.* **1983**, *22*, 209. Otsuka, S.; Nakamura, A.; Yoshida, T.; Naruto, M.; Ataba, K. *J. Am. Chem. Soc.* **1973**, *95*, 3180. Yamamoto, Y.; Yamazaki, H. *Inorg. Chem.* **1974**, *13*, 438. Aoki, K.; Yamamoto, Y. *Inorg. Chem.* **1976**, *15*, 48. Bellachio, G.; Cardaci, G.; Zanazzi, P. *Inorg. Chem.* **1987**, *26*, 84. Maitlis, P. M.; Espinet, P.; Russell, M. J. H. In *Comprehensive Organometallic Chemistry*; Wilkinson, G.; Stone, F. G. A., Eds.; Pergamon: London, 1982; Vol. 8, Chapter 38.4. Crociani, B. In *Reactions of Coordinated Ligands*; Braterman, P. S., Ed.; Plenum: New York, 1986; Chapter 9. Ruiz, J.; Vivanco, M.; Floriani, C.; Chiesi-Villa, A.; Rizzoli, C. *Organometallics* **1993**, *12*, 1811. Klöse, A.; Solari, E.; Ferguson, R.; Chiesi-Villa, A.; Rizzoli, C. *Organometallics* **1993**, *12*, 2414.

Experimental Section

General Procedure. All reactions were carried out under an atmosphere of purified nitrogen. Solvents were dried and distilled before use by standard methods. The synthesis of complex **1** has been carried out as reported.^{3c} The synthesis of potassium allyl has been carried out following the Schlosser procedure.¹⁶ Infrared spectra were recorded with a Perkin-Elmer 883 spectrophotometer; ¹H NMR spectra were measured on 200-AC and 400-DPX Bruker instruments.

Synthesis of 2. KH (1.10 g, 27.50 mmol) was added to a toluene solution of **1** (19.30 g, 27.5 mmol). The suspension was heated to 100 °C for 2 days and then cooled to room temperature. The resulting complex **2** is a white microcrystalline solid, which was removed by filtration, washed with toluene, and collected (88%). Crystals suitable for X-ray analysis were obtained from a diluted solution in toluene. The insolubility of the complex prevented NMR characterization. Anal. Calcd for C₇₂H₉₈K₂N₈Zr₂: C, 64.84; H, 7.41; N, 8.41. Found: C, 65.03; H, 7.32; N, 8.18.

Synthesis of 3. A THF (300 mL) solution of **1** (22.04 g, 31.48 mmol) was reacted with KH (2.61 g, 65.1 mmol). The suspension was heated to 40 °C for 30 h. A very small amount of undissolved solid was removed by filtration, and the solvent was evaporated to dryness. The solid was collected using toluene (150 mL), where the complex is only slightly soluble. The yellow powder was then filtered and dried in vacuo (63%). Crystallization from THF/hexane gave a crystalline yellow solid, suitable for X-ray analysis. Anal. Calcd for C₁₈₄H₂₈₀K₈N₁₆O₁₀Zr₄: C, 62.17; H, 7.96; N, 6.31. Found: C, 62.14; H, 7.39; N, 6.65. ¹H NMR (THF-*d*₈, room temperature): δ 0.42 (t, Me, 12 H), 0.47 (t, Me, 12 H), 1.80 (q, CH₂, 16 H), 5.10 (s, C₄H₂N, 2 H), 5.80 (s, C₄H₂N, 6 H).

Synthesis of 4. MeLi (5.0 mL, 1.6 M in Et₂O, 8.00 mmol) was added in a dropwise fashion to a toluene (100 mL) and THF (5 mL) solution of **1** (4.92 g, 7.10 mmol). The mixture was stirred at room temperature for 2 h and then evaporated to dryness. The resulting light-yellow solid was dissolved with *n*-hexane (50 mL), and then the solution was filtered (72%). Recrystallization of the solid was carried out from an *n*-hexane/toluene mixture. Anal. Calcd for C₄₅H₆₇LiN₄O₂Zr: C, 67.97; H, 8.75; N, 7.05. Found: C, 67.60; H, 8.78; N, 6.90. ¹H NMR (C₆D₆): δ 0.09 (s, Me-Zr, 3 H), 0.82 (t, CH₃, 12 H), 0.89 (t, CH₃, 12 H), 1.24 (m, THF, 8 H), 2.00 (m, CH₂, 16 H), 3.07 (m, THF, 8 H), 6.09 (s, C₄H₂N, 4 H), 6.67 (s, C₄H₂N, 4 H).

Synthesis of 5. BuⁿLi (2.0 mL, 1.6 M, 3.20 mmol) was added to a toluene/THF (100 mL/5 mL) solution of **1** (2.25 g, 3.20 mmol). The mixture was stirred at 50 °C for 2 h, after which time a very small amount of solid was removed by filtration and the filtrate was evaporated to dryness. The residue was dissolved in warm *n*-hexane (80 mL). The *n*-hexane solution gave light yellow crystals upon standing and cooling (80%). Anal. Calcd for C₄₈H₇₃LiN₄O₂Zr: C, 68.94; H, 8.80; N, 6.70. Found: C, 68.90; H, 8.77; N, 6.68. ¹H NMR (C₆D₆): δ 0.29 (m, Buⁿ-Zr, 2 H), 0.81 (t, CH₃, 12 H), 0.89 (t, CH₃, 12 H), 0.97 (t, Buⁿ-Zr, 3 H), 1.21 (m, THF, 8 H), 1.27 (m, Buⁿ-Zr, 2 H), 1.98 (m, CH₂, 16 H), 3.06 (m, THF, 8 H), 6.07 (s, C₄H₂N, 4 H), 6.72 (s, C₄H₂N, 4 H).

Synthesis of 6. Solid potassium allyl (0.93 g, 13.00 mmol) was added to a toluene (150 mL) solution of **1** (7.78 g, 12.00 mmol). The mixture was stirred at room temperature for 1 h, after which time the solid formed was solubilized by heating to 50 °C. A very small amount of solid was filtered from the warm solution. When this solution was cooled followed by addition of *n*-hexane, the filtrate gave yellow crystals of **6**, which were dried in vacuo (75%). Anal. Calcd for C₃₉H₅₃KN₄Zr: C, 66.14; H, 7.54; N, 7.91. Found: C, 66.13; H, 7.71; N, 7.46. IR: ν(C=C) 1603 cm⁻¹. ¹H NMR (C₆D₆, 298 K, 400

MHz): δ 0.84 (t, CH₃, 12 H, *J* = 7.4 Hz), 0.66 (t, CH₃, 12 H, *J* = 7.4 Hz), 1.88 (q, CH₂, 12 H), 2.07 (q, CH₂, 4 H), 3.00 (d, allyl CH₂, 4 H, *J* = 11.4 Hz), 5.74 (quint, allyl CH, 1 H, *J* = 11.4 Hz), 5.93 (s, C₄H₂N, 4 H), 6.31 (s, C₄H₂N, 4 H). The crystals used for the X-ray analysis contain one THF molecule for every two Zr complexes.

Synthesis of 7. A suspension of **2** (5.55 g, 8.30 mmol) in toluene (150 mL) was heated to 70 °C under an atmosphere of ethylene. The solid dissolved to give a yellow solution. The solution was concentrated to ca. 50 mL, and *n*-hexane (100 mL) was added. Complex **7** formed as a crystalline solid (72%) from this solution. Anal. Calcd for C₃₈H₅₃KN₄Zr: C, 65.68; H, 7.69; N, 8.07. Found: C, 65.92; N, 7.89; H, 8.19. ¹H NMR (C₆D₆): δ 0.20 (q, CH₂-Zr, 2 H, *J* = 7.6 Hz), 0.73 (t, CH₃, 12 H), 0.84 (t, CH₃, 12 H), 1.43 (t, CH₃CH₂-Zr, 3 H, *J* = 7.6 Hz), 1.90 (q, CH₂, 16 H), 5.93 (s, C₄H₂N, 4 H), 6.64 (s, C₄H₂N, 4 H).

Synthesis of 8. KH (0.09 g, 2.19 mmol) was added to a THF (50 mL) solution of **4** (1.70 g, 2.14 mmol). The yellow color turned progressively green, and the small amount of black precipitate which formed was removed by filtration. The solution was concentrated to dryness and the solid collected using *n*-hexane (40 mL). The yellow-green solid was then dried in vacuo (74%). Anal. Calcd for C₄₁H₅₉KN₄OZr: C, 65.28; H, 7.90; N, 7.43. Found: C, 65.32; N, 7.86; H, 7.29. ¹H NMR (C₆D₆, room temperature): δ 0.40 (s, Me-Zr, 3 H), 0.75 (t, Me, 12 H), 0.84 (t, Me, 12 H), 1.27 (m, THF, 2 H), 1.8-2.3 (m, CH₂, 16 H), 3.30 (m, THF, 2 H), 5.97 (s, C₄H₂N, 4 H), 6.61 (s, C₄H₂N, 4 H).

Synthesis of 9. Bu^tNC (0.20 mL, 1.80 mmol) was added to a toluene (50 mL) suspension of **2** (1.15 g, 1.80 mmol). The suspension was stirred for 15 h to give a solution. The solvent was reduced to half of its volume, and the solution gave **9** as a microcrystalline solid containing toluene of crystallization (60%) when left to stand in the freezer. Anal. Calcd for C₄₈H₆₆KN₆Zr: C, 68.40; H, 7.83; N, 8.31. Found: C, 68.29; H, 7.85; N, 8.33. IR (Nujol): ν(C=N) 1552 cm⁻¹. ¹H NMR (C₆D₆): δ 0.66 (t, CH₃, 12 H), 0.69 (t, CH₃, 12 H), 1.07 (s, Bu^t, 9 H), 2.06 (q, CH₂, 16 H), 2.11 (s, C₇H₈, 3 H), 6.03 (s, C₄H₂N, 8 H), 7.16 (m, C₇H₈, 5 H), 10.16 (s, CH=N-Bu^t, 1 H).

Synthesis of 10. Bu^tNC (0.30 mL, 2.70 mmol) was added to a toluene (100 mL) solution of **4** (2.00 g, 2.50 mmol), and the mixture was stirred for 5 h at room temperature. The solvent was reduced to two-thirds of its volume and upon addition of *n*-hexane (50 mL), followed by standing, gave yellow crystals of **10** (53%). Anal. Calcd for C₄₆H₆₈LiN₅OZrC₇H₈, C₅₃H₇₈LiN₅OZr: C, 70.78; H, 8.74; N, 7.79. Found: C, 69.79; H, 8.43; N, 7.83. IR (Nujol): ν(C=N) 1607 cm⁻¹. ¹H NMR (C₆D₆): δ 0.75 (t, CH₃, 12 H), 1.03 (s, Bu^t, 9 H), 1.08 (t, CH₃, 12 H), 1.16 (m, THF, 4 H), 1.93 (m, CH₂, 16 H), 2.19 (s, Me-C=N, 3 H), 3.25 (m, THF, 4 H), 6.25 (s, C₄H₂N, 8 H). The crystals used for the X-ray analysis contain C₇H₈ in a 1:1 molar ratio.

X-ray Crystallography for Complexes 3, 5, 6, and 10. Suitable crystals were mounted in glass capillaries and sealed under nitrogen. The reduced cells were obtained with the use of TRACER.¹⁷ Crystal data and details associated with data collection are given in Tables 6 and S1. Data were collected at room temperature (295 K) on a single-crystal diffractometer (Enraf-Nonius CAD4 for **3**, **5**, and **10** and Philips PW1100 for **6**). For intensities and background individual reflection profiles were analyzed.¹⁸ The structure amplitudes were obtained after the usual Lorentz and polarization corrections,¹⁹ and the absolute scale was established by the Wilson method.²⁰ The crystal quality was tested by ψ scans, which showed that

(17) Lawton, S. L.; Jacobson, R. A. TRACER (a cell reduction program); Ames Laboratory, Iowa State University of Science and Technology; Ames, IA, 1965.

(18) Lehmann, M. S.; Larsen, F. K. *Acta Crystallogr., Sect. A: Cryst. Phys., Diff., Theor. Gen. Crystallogr.* **1974**, *A30*, 580-584.

(19) Data reduction was carried out on an IBM AT personal computer equipped with an INMOS T800 transputer.

(20) Wilson, A. J. C. *Nature* **1942**, *150*, 151.

(16) Schlosser, M. J. *Organomet. Chem.* **1967**, *8*, 9. Desponds, O. Thesis Dissertation, University of Lausanne, Lausanne, Switzerland, **1991**. Schlosser, M.; Desponds, O.; Lehmann, R.; Moret, E.; Rauchschwalbe, G. *Tetrahedron* **1993**, *49*, 10175.

Table 6. Experimental Data for the X-ray Diffraction Studies on Crystalline Compounds 3, 5, 6, and 10

	3	5	6	10
formula	C ₁₈₄ H ₂₈₀ K ₈ N ₁₆ O ₁₀ Zr ₄	C ₄₈ H ₇₃ LiN ₄ O ₂ Zr	C ₃₉ H ₅₃ KN ₄ Zr·0.5C ₄ H ₈ O	C ₄₆ H ₆₈ LiN ₅ OZr·C ₇ H ₈
a (Å)	13.240(3)	11.451(3)	28.412(4)	21.535(2)
b (Å)	19.815(9)	11.692(3)	22.334(3)	12.294(2)
c (Å)	19.876(4)	18.726(6)	15.419(2)	19.154(3)
α (deg)	74.49(2)	72.66(2)	90	90
β (deg)	83.43(2)	79.78(2)	110.66(2)	96.34(1)
γ (deg)	79.29(3)	78.12(2)	90	90
V (Å ³)	4926(3)	2323.8(12)	9155.0(25)	5040.0(12)
Z	1	2	8	4
fw	3554.0	836.3	744.3	897.4
space group	P $\bar{1}$ (No. 2)	P $\bar{1}$ (No. 2)	C2/c (No. 15)	P2 ₁ /c (No. 14)
t (°C)	22	22	22	22
λ (Å)	0.710 69	0.710 69	0.710 69	0.710 69
ρ _{calcd} (g cm ⁻³)	1.198	1.195	1.080	1.164
μ (cm ⁻¹)	4.30	2.70	3.54	2.51
transmission coeff	0.831–1.000	0.813–1.000	0.889–1.000	0.924–1.000
R ^a	0.044	0.046	0.056	0.037
wR2 ^b	0.122	0.111	0.135	0.086
GOF ^c	0.468	0.926	1.066	0.848

^a R1 = $\Sigma|\Delta F|/\Sigma|F_o|$. ^b wR2 = $[\Sigma(w(\Delta F^2)^2)/\Sigma(wF_o^2)^2]^{1/2}$. ^c GOF = $[\Sigma w|\Delta F|^2/(\text{NO} - \text{NV})]^{1/2}$.

crystal absorption effects could not be neglected. The data were corrected for absorption using a semiempirical method²¹ for complex **6** and ABSORB²² for **3**, **5**, and **10**. The function minimized during the least-squares refinement was $\Sigma w(\Delta F^2)^2$. Weights were applied according to the scheme $w = 1/[\sigma^2(F_o)^2 + (aP)^2]$ ($P = (F_o^2 + 2F_c^2)/3$) with $a = 0.0000, 0.0436, 0.0648, 0.0243$ for complexes **3**, **5**, **6**, and **10**, respectively. Anomalous scattering corrections were included in all structure factor calculations.^{23b} Scattering factors for neutral atoms were taken from ref 23a for nonhydrogen atoms and from ref 24 for H. Among the low-angle reflections no correction for secondary extinction was deemed necessary.

All calculations were carried out on an IBM PS/2/80 personal computer and on an ENCORE 91 computer. The structures were solved by the heavy-atom method starting from three-dimensional Patterson maps using the observed reflections. Structure refinements were based on the unique observed data for **5**, **6**, and **10** and on the total data for **3** using SHELX92.²⁵

Refinement was first done isotropically and then anisotropically for all non-H atoms, except for some of the disordered atoms. The structures of complexes **5** and **10** were refined straightforwardly. In complex **3**, the C61 and C62 carbons of an ethyl group were found to be statistically distributed over two positions (A, B) with a site occupation factor of 0.5. Four of the five THF molecules (O1–C80··C83, O2–C84··C87, O3–C88··C91, O5–C96··C99) were found to be heavily affected by conformational disorder. The best fit was obtained by splitting the C81, C82, C85, C86, C88, C89, C90, C91, C96, C97, and C98 carbons over two positions (A, B) with a site occupation factor of 0.5. The C81B, C96A, C96B, C97A, C97B, C98A, C98B, and C99 positions were isotropically refined,

since the anisotropic refinement did not lead to convergence. The C–O and C–C bond distances of the disordered THF molecules were constrained to be 1.48(1) and 1.54(1) Å, respectively. In complex **6**, the C38 and C39 carbon atoms of the allyl anion were found to be disordered over two positions (A, B) and isotropically refined with the site occupation factors given in Table S4 (supporting information). Moreover, the THF solvent molecule of crystallization was found to be disordered over two positions related by an inversion center and was isotropically refined with a site occupation factor of 0.5 with constraints imposed on the C–C and C–O bond distances.

For all complexes the hydrogen atoms, except those related to disordered carbon atoms, which were ignored, were located from difference Fourier maps. They were introduced in the subsequent refinements as fixed atom contributions with U 's kept at 0.10 for **3**, **5**, and **6** and 0.08 Å² for **10**. The final difference maps showed no unusual features, with no significant peak above the general background. Final atomic coordinates are listed in Tables S2–S5 for non-H atoms and in Tables S6–S9 for hydrogens. Thermal parameters are given in Tables S10–S13, bond distances and angles in Tables S14–S17.²⁶

Acknowledgment. We thank the "Fonds National Suisse de la Recherche Scientifique" (Grant No. 20-40268.94) and Ciba-Geigy SA (Basel, Switzerland) for financial support.

Supporting Information Available: Tables of experimental details associated with data collection and structure refinement, final atomic coordinates for non-H atoms, hydrogen atom coordinates, thermal parameters, and bond distances and angles and ORTEP drawings for **3**, **5**, **6**, and **10** (38 pages). Ordering information is given on any current masthead page.

OM9503398

(21) North, A. C. T.; Phillips, D. C.; Mathews, F. S. *Acta Crystallogr., Sect. A: Cryst. Phys., Diff., Theor. Gen. Crystallogr.* **1968**, *A24*, 351.

(22) Uguzzoli, F. ABSORB, a Program for F_o Absorption Correction. In *Comput. Chem.* **1987**, *11*, 109.

(23) (a) *International Tables for X-ray Crystallography*; Kynoch Press: Birmingham, U.K., 1974; Vol. IV, p 99. (b) *Ibid.*, p 149.

(24) Stewart, R. F.; Davidson, E. R.; Simpson, W. T. *J. Chem. Phys.* **1965**, *42*, 3175.

(25) Sheldrick, G. M. SHELXL92 Gamma Test: Program for Crystal Structure Refinement; University of Göttingen, Göttingen, Germany, 1992.

(26) See paragraph at the end regarding supporting information.

Synthesis of New Butadiene–Osmium(0) and –Ruthenium(0) Complexes by Reductive Carbon–Carbon Coupling of Two Alkenyl Fragments

Cristina Bohanna, Miguel A. Esteruelas,* Fernando J. Lahoz, Enrique Oñate, Luis A. Oro, and Eduardo Sola

Departamento de Química Inorgánica, Instituto de Ciencia de Materiales de Aragón, Universidad de Zaragoza-Consejo Superior de Investigaciones Científicas, 50009 Zaragoza, Spain

Received May 10, 1995[®]

The five-coordinate complexes $\text{Os}\{(\text{E})\text{-CH=CHR}\}\text{Cl}(\text{CO})(\text{PiPr}_3)_2$ ($\text{R} = \text{Ph}$ (**3**), H (**6**)) react with $\text{CH}_2=\text{CHMgBr}$ to give the osmium(0) derivatives $\text{Os}(\eta^4\text{-C}_4\text{H}_5\text{R})(\text{CO})(\text{PiPr}_3)_2$ ($\text{R} = \text{Ph}$ (**5**), H (**7**)). The molecular structure of **5** has been determined by X-ray crystallography. The coordination around the osmium atom can be described as a distorted square pyramid with a triisopropylphosphine ligand located at the apex. The base is formed by the carbonyl group and the other triisopropylphosphine ligand mutually *cis* disposed and by the midpoints of both terminal carbon–carbon bonds of the diene. The reaction of the chloro–styryl–ruthenium(II) complex $\text{Ru}\{(\text{E})\text{-CH=CHPh}\}\text{Cl}(\text{CO})(\text{PiPr}_3)_2$ (**4**) with $\text{CH}_2=\text{CHMgBr}$ leads to $\text{Ru}\{(\text{E})\text{-CH=CHPh}\}(\text{CH=CH}_2)(\text{CO})(\text{PiPr}_3)_2$ (**10**), which affords $\text{Ru}(\eta^4\text{-C}_4\text{H}_5\text{Ph})(\text{CO})(\text{PiPr}_3)_2$ (**11**) by stirring in hexane at 50 °C. **10** reacts with carbon monoxide to give $\text{Ru}\{(\text{E})\text{-CH=CHPh}\}(\text{CH=CH}_2)(\text{CO})_2(\text{PiPr}_3)_2$ (**12**), which can be also prepared by reaction of $\text{Ru}\{(\text{E})\text{-CH=CHPh}\}\text{Cl}(\text{CO})_2(\text{PiPr}_3)_2$ (**13**) with $\text{CH}_2=\text{CHMgBr}$.

Introduction

The reactions of alkynes with transition-metal hydrido complexes generally lead to vinyl derivatives.¹ The five-coordinate complexes $\text{MHCl}(\text{CO})(\text{PiPr}_3)_2$ ($\text{M} = \text{Os}$ (**1**), Ru (**2**)) follow this trend. Thus, the reactions of **1** and **2** with phenylacetylene afford the corresponding styryl derivatives $\text{M}\{(\text{E})\text{-CH=CHPh}\}\text{Cl}(\text{CO})(\text{PiPr}_3)_2$ ($\text{M} = \text{Os}$ (**3**), Ru (**4**)).² The most remarkable features of the structure of these compounds are, first, the square pyramidal coordination of the metal with the styryl ligand in the apical position and, second, the *trans* position of the two substituents—the phenyl group and the metallic fragment—at the carbon–carbon double bond. From a catalytic point of view, it has been proved that **3** is a key intermediate in the selective hydrogenation of phenylacetylene,³ and **3** and **4** are side products in the catalytic hydrosilylation of phenylacetylene with triethylsilane.⁴

Continuing with our study on the chemical properties of **3** and **4**, we have now investigated the reactivity of **3** and **4** toward $\text{CH}_2=\text{CHMgBr}$. During this research, we have found that the reactions of **3** and **4** with $\text{CH}_2=\text{CHMgBr}$ lead to π -(phenyl)butadiene complexes. Transition-metal butadiene complexes previously reported have been generally prepared by reducing a metal halide or halo complex in the presence of butadiene,⁵ by thermal or photolytic ligand displacement,⁶

by metal atom evaporation techniques,⁷ and by reaction of halo complexes with butadienylmagnesium derivatives.⁸ The reductive coupling of two vinyl fragments to give a π -butadiene complex is rare, and previously, it has been only observed on zirconium.⁹

The formation of carbon–carbon bonds at transition-metal centers has received a great deal of attention in recent years.^{9–22} Catalytic systems involving transition metal complexes often form a carbon–carbon bond

(5) (a) Hoberg, H.; Jenni, K.; Raabe, E.; Krüger, C.; Schroth, G. *J. Organomet. Chem.* **1987**, *320*, 325. (b) Diamond, G. M.; Green, M. L. H.; Walker, N. M.; Howard, J. A. K.; Mason, S. A. *J. Chem. Soc., Dalton Trans.* **1992**, 2641.

(6) (a) Ashworth, T. V.; Singleton, E.; Laing, M.; Pope, L. *J. Chem. Soc., Dalton Trans.* **1978**, 1032. (b) Erker, G.; Wicher, J.; Engel, K.; Rosenfeldt, F.; Dietrich, W.; Krüger, C. *J. Am. Chem. Soc.* **1980**, *102*, 6344. (c) Kotzian, M.; Kreiter, C. G.; Michael, G.; Özkar, S. *Chem. Ber.* **1983**, *116*, 3637. (d) Büch, H. M.; Binger, P.; Goddard, R.; Krüger, C. *J. Chem. Soc., Chem. Commun.* **1983**, 648. (e) Kreiter, C. G.; Kotzian, M. *J. Organomet. Chem.* **1985**, *289*, 295. (f) Kreiter, C. G.; Wendt, G.; Sheldrick, W. S. *J. Organomet. Chem.* **1987**, *333*, 47. (g) Green, M. L. H.; Hare, P. M.; Bandy, J. A. *J. Organomet. Chem.* **1987**, *330*, 61. (h) Fryzuk, M. D.; Joshi, K.; Rettig, S. *J. Polyhedron*, **1989**, *8*, 2291. (i) Kreiter, C. G.; Kern, U. *J. Organomet. Chem.* **1993**, *459*, 199. (j) Blake, A. J.; Halcrow, M. A.; Schröder, M. *J. Chem. Soc., Dalton Trans.* **1994**, 1631.

(7) Brown, P. R.; Green, M. L. H.; Hare, P. M.; Bandy, J. A. *Polyhedron* **1988**, *7*, 1819.

(8) (a) Oro, L. A. *Inorg. Chim. Acta* **1977**, *21*, L6. (b) Wreford, S. S.; Whitney, J. F. *Inorg. Chem.* **1981**, *20*, 3918. (c) Yasuda, H.; Tatsumi, K.; Okamoto, T.; Mashima, K.; Lee, K.; Nakamura, A.; Kai, Y.; Kanehisa, N.; Kasai, N. *J. Am. Chem. Soc.* **1985**, *107*, 2410. (d) Müller, J.; Qiao, K.; Siewing, M.; Westphal, B. *J. Organomet. Chem.* **1993**, *458*, 219.

(9) (a) Beckhaus, R.; Thiele, K.-H. *J. Organomet. Chem.* **1984**, *268*, C7. (b) Czisch, P.; Erker, G.; Korth, H.-G.; Sustmann, R. *Organometallics* **1984**, *3*, 945.

(10) (a) Kurosawa, H.; Emoto, M.; Ohnishi, H.; Miki, K.; Kasai, N.; Tatsumi, K.; Nakamura, A. *J. Am. Chem. Soc.* **1987**, *109*, 6333. (b) Kurosawa, H.; Ohnishi, H.; Emoto, M.; Kawasaki, Y.; Murai, S. *J. Am. Chem. Soc.* **1988**, *110*, 6272. (c) Bianchini, C.; Graziani, M.; Kaspar, J.; Meli, A.; Vizza, F. *Organometallics* **1994**, *13*, 1165.

(11) Negishi, E.; Takahashi, T.; Baba, S.; Van Horn, D. E.; Okukado, N. *J. Am. Chem. Soc.* **1987**, *109*, 2393.

(12) Brady, C.; Pettit, R. *J. Am. Chem. Soc.* **1980**, *102*, 6181.

(13) Amatore, C.; Jutand, A. *Organometallics* **1988**, *7*, 2203.

[®] Abstract published in *Advance ACS Abstracts*, September 15, 1995.

(1) Crabtree, R. H. *The Organometallic Chemistry of the Transition Metals*; J. Wiley and Sons: New York, 1988; pp 147–162.

(2) Werner, H.; Esteruelas, M. A.; Otto, H. *Organometallics* **1986**, *5*, 2295.

(3) Andriollo, A.; Esteruelas, M. A.; Meyer, U.; Oro, L. A.; Sánchez-Delgado, R.; Sola, E.; Valero, C.; Werner, H. *J. Am. Chem. Soc.* **1989**, *111*, 7431.

(4) (a) Esteruelas, M. A.; Oro, L. A.; Valero, C. *Organometallics* **1991**, *10*, 462. (b) Esteruelas, M. A.; Herrero, J.; Oro, L. A. *Organometallics* **1993**, *12*, 2377.

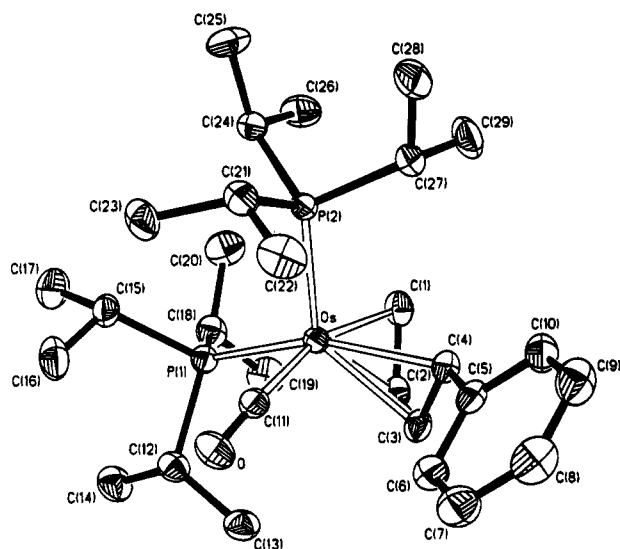


Figure 1. ORTEP view of the molecular structure of $\text{Os}(\eta^4\text{-C}_4\text{H}_5\text{Ph})(\text{CO})(\text{PiPr}_3)_2$ (**5**).

through alkyl-acyl conversions with carbon monoxide.¹⁴ There exist also increasing examples of carbon-carbon bond formation through reductive-elimination reactions.¹⁵ In addition, the desire to develop new methods for carbon-carbon bond formation of use in organic synthesis has spurred many such investigations. In this respect, numerous examples of the migratory insertion

(14) (a) Parshall, G. W. *Homogeneous Catalysis*; J. Wiley and Sons: New York, 1980. (b) Masters, C. *Homogeneous Transition Metal Catalysis*; Chapman and Hall: London, 1981. (c) Atwood, J. D. *Inorganic and Organometallic Reaction Mechanisms*; Brooks/Cole: Mill Valley, CA, 1985.

(15) (a) Thorn, D. L.; Tulip, T. H. *Organometallics* **1982**, *1*, 1580. (b) Thorn, D. L. *Organometallics* **1985**, *4*, 192. (c) Komiya, S.; Shibue, A. *Organometallics* **1985**, *4*, 684. (d) Komiya, S.; Ishikawa, M.; Ozaki, S. *Organometallics* **1988**, *7*, 2238. (e) Himmel, S. E.; Young, G. B. *Organometallics* **1988**, *7*, 2440. (f) Thaler, E. G.; Folting, K.; Caulton, K. G. *J. Am. Chem. Soc.* **1990**, *112*, 2664. (g) Thompson, J. S.; Atwood, J. D. *Organometallics* **1991**, *10*, 3525. (h) Goldberg, K. I.; Yang, J. Y.; Winter, E. L. *J. Am. Chem. Soc.* **1994**, *116*, 1573.

(16) Selna, H. E.; Merola, J. S. *J. Am. Chem. Soc.* **1991**, *113*, 4008.

(17) (a) Dobson, A.; Moore, D. S.; Robinson, S. D.; Hursthouse, M. B.; New, L. *Polyhedron* **1985**, *4*, 1119. (b) Jia, G.; Reingold, A. L.; Meek, D. W. *Organometallics* **1989**, *8*, 1378. (c) Field, L.; George, A. V.; Hambley, T. W. *Inorg. Chem.* **1990**, *29*, 4565. (d) Bianchini, C.; Peruzzini, M.; Zanobini, F.; Frediani, P.; Albinati, A. *J. Am. Chem. Soc.* **1991**, *113*, 5453. (e) Wakatsuki, Y.; Yamazaki, H.; Kumegawa, N.; Satoh, T.; Satoh, J. Y. *J. Am. Chem. Soc.* **1991**, *113*, 9604. (f) Jia, G.; Gallucci, J. C.; Rheingold, A. L.; Haggerthy, B. S.; Meek, D. W. *Organometallics* **1991**, *10*, 3459. (g) Jia, G.; Meek, D. W. *Organometallics* **1991**, *10*, 1444. (h) Field, L. D.; George, A. V.; Malouf, E. Y.; Slip, I. H. M.; Hambley, T. W. *Organometallics* **1991**, *10*, 3842. (i) McMullen, A. K.; Selege, J. P.; Wang, J. G. *Organometallics* **1991**, *10*, 3421. (j) Bianchini, C.; Bohanna, C.; Esteruelas, M. A.; Frediani, P.; Meli, A.; Oro, L. A.; Peruzzini, M. *Organometallics* **1992**, *11*, 3837. (k) Albertin, G.; Antoniutti, S.; Del Ministro, E.; Bordignon, E. *J. Chem. Soc., Dalton Trans.* **1992**, 3203. (l) Field, L. D.; George, A. V.; Purches, G. R.; Slip, I. H. M. *Organometallics* **1992**, *11*, 3019. (m) Santos, A.; López, J.; Matas, L.; Ros, J.; Galan, A.; Echavarren, A. M. *Organometallics* **1993**, *12*, 4215. (n) Hughes, D. L.; Jiménez-Tenorio, M.; Leigh, G. J.; Rowley, A. T. *J. Chem. Soc., Dalton Trans.* **1993**, 3151. (o) Schäfer, M.; Mahr, N.; Wolf, J.; Werner, H. *Angew. Chem., Int. Ed. Engl.* **1993**, *32*, 1315. (p) Wiedeman, R.; Steinert, P.; Schäfer, M.; Werner, H. *J. Am. Chem. Soc.* **1993**, *115*, 9864. (q) Barbaro, C.; Bianchini, C.; Frediani, P.; Peruzzini, M.; Polo, A.; Zanobini, F. *Inorg. Chim. Acta* **1994**, *220*, 5.

(18) (a) Brookhart, M.; Volpe, A. F., Jr.; Yoon, J. *Comprehensive Organic Synthesis*; Trost, B. M., Fleming, I., Ed.; Pergamon Press: London, 1991; Vol. 4, Section 3.5. (b) Chang, S.; Yoon, J.; Brookhart, M. *J. Am. Chem. Soc.* **1994**, *116*, 1869.

(19) Carnahan, E. M.; Protasiewicz, R. D.; Lippard, S. J. *Acc. Chem. Res.* **1993**, *26*, 90.

(20) Liebeskind, L. S.; Chidambaram, R. *J. Am. Chem. Soc.* **1987**, *109*, 5025.

(21) O'Connor, J. M.; Pu, L.; Rheingold, A. L. *J. Am. Chem. Soc.* **1990**, *112*, 6232.

(22) Thorn, D. L.; Tulip, T. H. *J. Am. Chem. Soc.* **1981**, *103*, 5984.

Table 1. Selected Bond Lengths (Å) and Angles (deg) for the Complex $\text{Os}(\eta^4\text{-C}_4\text{H}_5\text{Ph})(\text{CO})(\text{PiPr}_3)_2$ (**5**)^a

Os-P(1)	2.3806(8)	Os-C(11)	1.861(3)
Os-P(2)	2.3768(9)	C(1)-C(2)	1.453(5)
Os-C(1)	2.246(3)	C(2)-C(3)	1.411(4)
Os-C(2)	2.193(3)	C(3)-C(4)	1.441(5)
Os-C(3)	2.184(3)	C(11)-O	1.167(4)
Os-C(4)	2.259(3)		
P(1)-Os-P(2)	108.75(3)	M(1)-Os-M(2)	59.3(1)
P(1)-Os-M(1)	94.41(9)	M(1)-Os-C(11)	142.8(1)
P(1)-Os-M(2)	137.83(9)	M(2)-Os-C(11)	97.0(1)
P(1)-Os-C(11)	85.4(1)	C(1)-C(2)-C(3)	117.2(3)
P(2)-Os-M(1)	118.4(1)	C(2)-C(3)-C(4)	117.5(3)
P(2)-Os-M(2)	112.73(9)	C(3)-C(4)-C(5)	120.2(3)
P(2)-Os-C(11)	96.4(1)	Os-C(11)-O	175.8(3)

^a M(1) and M(2) represent the midpoints of the C(1)-C(2) and C(3)-C(4) olefin double bonds, respectively.

of vinylidene groups into metal-vinyl¹⁶ and metal-alkynyl¹⁷ bonds and the implications that such reactions may have for the catalytic alkyne oligomerization have been studied. Other pathways leading to carbon-carbon bond formation which should be mentioned are the alkylation of (η^3 -allyl)iron compounds,¹⁸ the reductive-coupling of two isocyanide ligands to form a bis-(alkylamino)acetylene group,¹⁹ the reaction of terminal alkynes with cobaltacyclopentenedione compounds to provide 5-alkylidene cyclopenten-2-ene-1,4-dienes,²⁰ the intramolecular coupling of two carbene ligands to afford olefins,²¹ and the alkyl migration from a metal atom to the carbon atom of a coordinated carbene ligand.²²

In this paper, we describe the synthesis and characterization of new π -butadiene-osmium(0) and -ruthenium(0) compounds, which have been formed by the unusual coupling of two alkenyl fragments at the metallic center.

Results and Discussion

Treatment of **3** with $\text{CH}_2=\text{CHMgBr}$ in toluene gives a colorless solution from which compound **5** is separated as a white solid in 85% yield (eq 1). Complex **5** was fully characterized by elemental analysis, IR and ¹H, ³¹P{¹H}, and ¹³C{¹H} NMR spectroscopies, and X-ray diffraction.

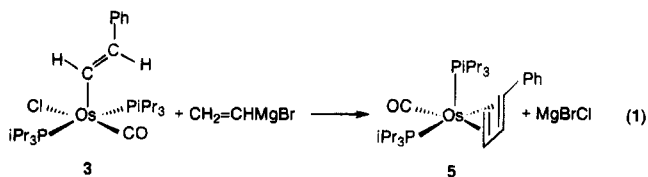
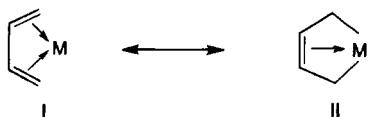


Figure 1 shows an ORTEP drawing of the molecule of **5**. Selected bond distances and angles are listed in Table 1. The geometry of this compound can be described as a square pyramid with a triisopropylphosphine ligand located at the apex. The atoms C(11) and P(1) and the midpoints of the bonds C(1)-C(2) and C(3)-C(4) form the base and are approximately in one plane (maximum deviation 0.098(3) Å), whereas the osmium atom is located 0.6832(5) Å above this plane toward the apical position.

The most conspicuous features of the solid state structure are those related to the $\text{Os}(\eta^4\text{-C}_4\text{H}_5\text{Ph})$ unit. The osmium-carbon (terminal) distances ($\text{Os}-\text{C}(1)$, 2.246(3) Å; $\text{Os}-\text{C}(4)$ = 2.259(3) Å) are significantly longer

Scheme 1



than the osmium-carbon(central) distances (Os-C(2), 2.193(3) Å; Os-C(3), 2.184(3) Å). Both carbon(terminal)-carbon(central) distances (C(1)-C(2), 1.453(5) Å; C(3)-C(4), 1.441(5) Å) are also longer than the carbon(central)-carbon(central) distance (C(2)-C(3), 1.411(4) Å).

The type of bonding of *cis*-butadiene ligands to transition metals can be described in terms of resonance hybrids of the forms **I** ($\eta^4-\pi$) and **II** ($\sigma^2-\pi$) (Scheme 1).

In our complex the geometric data commented above generate some ambiguity: while all the separations observed between osmium and the carbon atoms are in the usual range for Os-olefin complexes, and also agree well with a structure of type **I**, on the other side, the C-C bond distances show a long-short-long pattern more adequate for a type **II** structure. In order to determine the relative contribution of the resonance forms **I** and **II** in a structure of this type of compound, the parameters θ , Δd and Δl have been defined.²³ For a diene ligand labeled as the phenylbutadiene of **5**, the parameter θ is the dihedral angle between the C(1)-M-C(4) and C(1)-C(2)-C(3)-C(4) planes, while the parameters Δd and Δl can be calculated from the eqs 2 and 3, respectively.

$$\Delta d = \{d[M-C(1)] + d[M-C(4)]\}/2 - \{d[M-C(2)] + d[M-C(3)]\}/2 \quad (2)$$

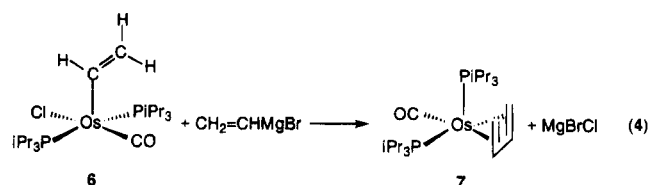
$$\Delta l = \{l[C(1)-C(2)] + l[C(3)-C(4)]\}/2 - l[C(2)-C(3)] \quad (3)$$

For the vast majority of middle and late transition metal diene complexes, which generally were assumed to adopt the $\eta^4-\pi$ structure, the dihedral angle θ is in the range 75–90°, Δd is between -0.1 and 0.1 Å, and Δl lies between -0.1 and 0 Å. On the other hand, for the complexes of the early transition metals, which show a $\sigma^2-\pi$ structure, the corresponding dihedral angles always exceed 90°, with a corresponding change in Δd of -0.4 to 0 Å. Δl falls in the range 0–0.2 Å.²³ The values obtained for complex **5** are $\theta = 83.0(1)^\circ$, $\Delta d = 0.064(3)$ Å, and $\Delta l = 0.036(5)$ Å. On the basis of the above mentioned criteria, **5** appears to be approaching the crossover between **I** and **II** assignments, suggesting a structure involving predominantly $\eta^4-\pi$ coordination but with significant $\sigma^2-\pi$ contribution.

The ^1H , $^{13}\text{C}\{^1\text{H}\}$, and $^{31}\text{P}\{^1\text{H}\}$ NMR spectra are in agreement with the structure shown in Figure 1. The protons of the diene ligand give rise to five signals at 5.16, 5.03, 1.94, 1.32, and -0.22 ppm (Figure 2), which were assigned to the protons **d**, **c**, **b**, **e**, and **a**, respectively. The values of $J_{ab} = 3.9$ and $J_{ac} = J_{bc} = 6.9$ Hz are consistent with a significant contribution of the resonance form **II** to the real structure of **5**.²⁴ In the $^{13}\text{C}\{^1\text{H}\}$ NMR spectrum the carbon atoms of the diene

display four double doublets at 75.48 ($J_{P-C} = 3.7$ and 2.3 Hz), 71.98 ($J_{P-C} = 3.7$ and 0.9 Hz), 44.80 ($J_{P-C} = 26.7$ and 4.6 Hz), and 21.22 ($J_{P-C} = 5.6$ and 3.2 Hz), which were assigned to the carbon atoms C(3), C(2), C(4), and C(1), respectively. In agreement with the mutually *cis* disposition of the triisopropylphosphine ligands the $^{31}\text{P}\{^1\text{H}\}$ NMR spectrum contains two doublets at 13.8 and 3.2 ppm, with a P-P coupling constant of 10.7 Hz.

In a similar manner to the chloro-styryl complex **3**, the related chloro-vinyl compound Os(CH=CH₂)Cl(CO)(PiPr₃)₂ (**6**) reacts with CH₂=CHMgBr to give the π -butadiene-osmium(0) derivative Os(η^4 -C₄H₆)(CO)-(PiPr₃)₂ (**7**) (eq 4), which was isolated as a white solid in 80% yield.



The structure of **7** is proposed on the basis of its ^1H , $^{13}\text{C}\{^1\text{H}\}$, and $^{31}\text{P}\{^1\text{H}\}$ NMR spectra. Figure 3 shows the ^1H COSY NMR spectrum. The diene protons display six resonances at 5.05, 4.56, 1.71, 1.64, -0.77, and -1.07 ppm. The resonances at low field (5.05 and 4.56 ppm) were assigned to the internal protons **i** and **h**, respectively. The signals at 1.71 and 1.64 ppm were assigned to the *syn*-CH₂ protons **g** and **j**, and the resonances at higher field (-0.77 and -1.07) to the *anti*-CH₂ protons **f** and **k**. The chemical shifts of butadiene protons agree well with those previously reported for the complex Os(η^4 -C₄H₆)(CO)₃.²⁵ In addition, it should be mentioned that the values of $J_{fg} = 2.6$, $J_{jk} = 3.6$, $J_{ik} = J_{ij} = 6.8$, and $J_{hf} = J_{hg} = 6.7$ Hz are similar to those of **5**, suggesting that there is also a significant contribution of the resonance form **II** to the structure of **7**. In the $^{13}\text{C}\{^1\text{H}\}$ NMR spectrum the carbon atoms of the diolefin give rise to four doublet of doublets. The carbon atoms of the carbon-carbon bond disposed *trans* to the triisopropylphosphine ligand appear at 76.68 (CH; $J_{P-C} = 3.9$ and 1.0 Hz) and 24.40 (CH₂; $J_{P-C} = 28.7$ and 5.7 Hz), while the carbon atoms of the carbon-carbon bond disposed *trans* to the carbonyl group appear at 71.01 (CH; both $J_{P-C} = 2.4$ Hz) and 23.11 (CH₂; both $J_{P-C} = 3.2$ Hz) ppm. The values of $Q_{trans-P} = 1.52$ and $Q_{trans-CO} = 1.40$ ²⁶ agree well with that previously reported for Os(η^4 -C₄H₆)(CO)₃ ($Q = 1.60$).²⁷ The $^{31}\text{P}\{^1\text{H}\}$ NMR spectrum shows two doublets at 18.9 and 6.2 ppm, with a P-P coupling constant of 9.5 Hz.

The reactions of the chloro-styryl (**3**) and chloro-vinyl (**6**) complexes with CH₂=CHMgBr most probably involve the replacement of the Cl⁻ anion by the vinyl group to give styryl-vinyl (**8**) or bis(vinyl) (**9**) intermediates that by reductive carbon-carbon coupling yield the butadiene derivatives **5** and **7** respectively (eq 5).

(25) Zobl-Ruh, S.; von Philipsborn, W. *Helv. Chim. Acta* **1980**, *63*, 773.

(26) $Q = \Delta\delta C_1/\Delta\delta C_2$, where $\Delta\delta C = \delta C_{coord} - \delta C_{free}$.



(27) Jolly, P. W.; Mynott, R. *Adv. Organomet. Chem.* **1981**, *19*, 257.

(23) Yasuda, H.; Nakamura, A. *Angew. Chem., Int. Ed. Engl.* **1987**, *26*, 723.

(24) (a) Benn, R.; Schroth, G. *J. Organomet. Chem.* **1982**, *228*, 71. (b) Brookhart, M.; Cox, K.; Cloke, F. G. N.; Green, J. C.; Green, M. L. H.; Hare, P. M.; Bashkin, J.; Derome, A. E.; Grebenik, P. D. *J. Chem. Soc., Dalton Trans.* **1985**, 423.

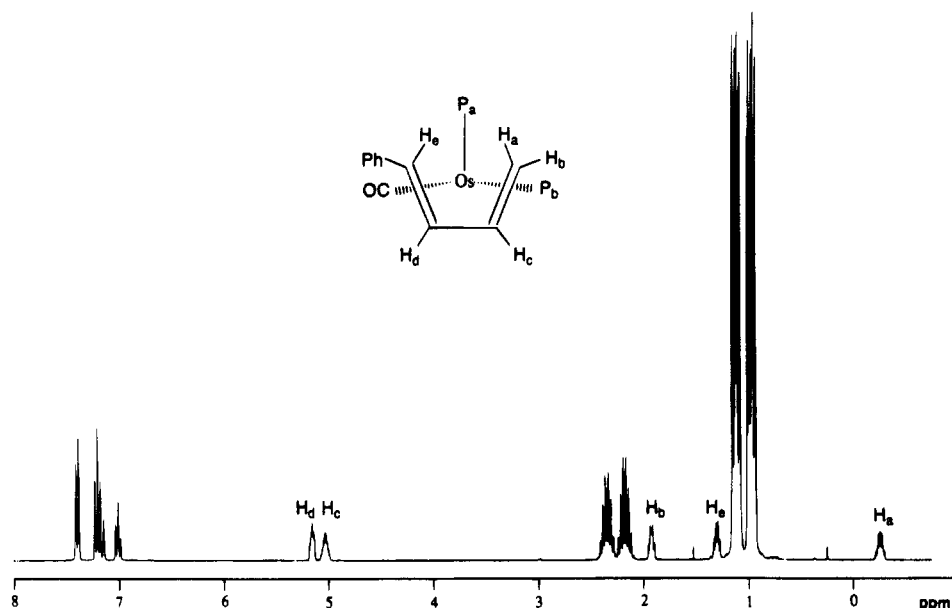


Figure 2. ^1H NMR spectrum of complex $\text{Os}(\eta^4\text{-C}_4\text{H}_5\text{Ph})(\text{CO})(\text{PiPr}_3)_2$ (**5**) in C_6D_6 at 20°C .

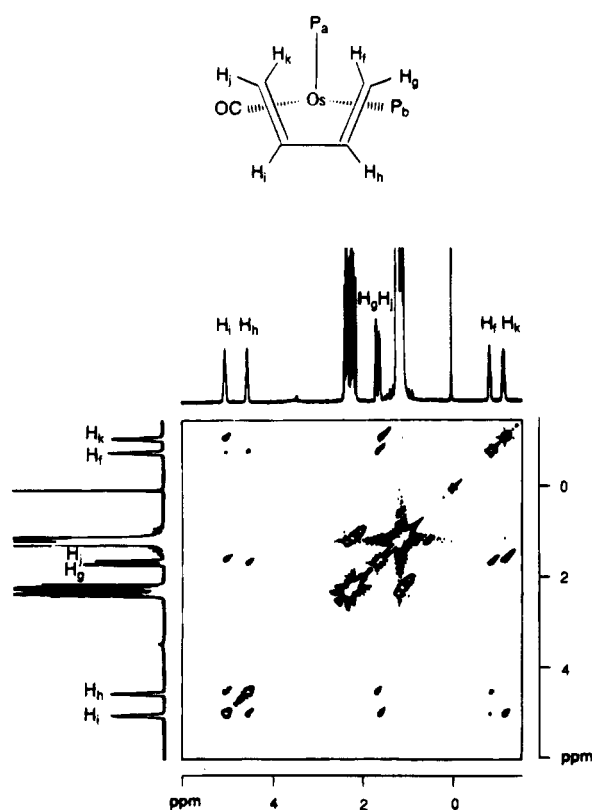
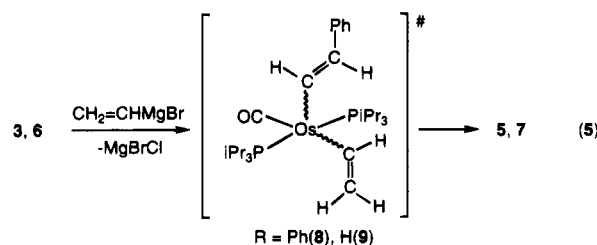
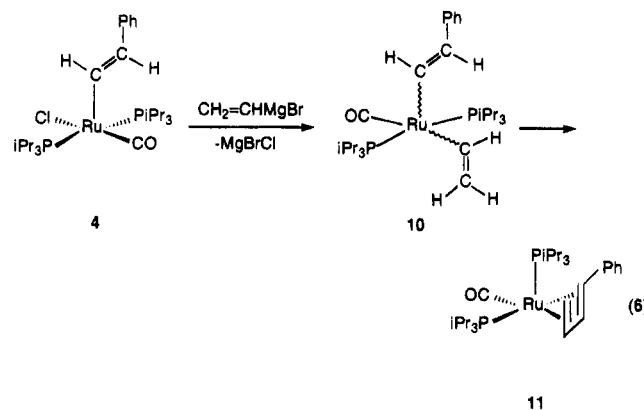


Figure 3. ^1H COSY NMR of the complex $\text{Os}(\eta^4\text{-C}_4\text{H}_6)(\text{CO})(\text{PiPr}_3)_2$ (**7**) in CDCl_3 at 20°C .



Attempts to detect these intermediates have been unsuccessful. However, in favor of this mechanistic proposal, we have observed that the chloro-styryl-

ruthenium(II) complex $\text{Ru}\{\text{(E)-CH=CHPh}\}\text{Cl}(\text{CO})(\text{PiPr}_3)_2$ (**4**) reacts with $\text{CH}_2=\text{CHMgBr}$ to give the styryl-vinyl intermediate $\text{Ru}\{\text{(E)-CH=CHPh}\}(\text{CH}=\text{CH}_2)(\text{CO})(\text{PiPr}_3)_2$ (**10**), which leads to the π -(phenyl)butadiene $\text{Ru}(\eta^4\text{-C}_4\text{H}_5\text{Ph})(\text{CO})(\text{PiPr}_3)_2$ (**11**) (eq 6), after 15 h stirring in hexane at 50°C .



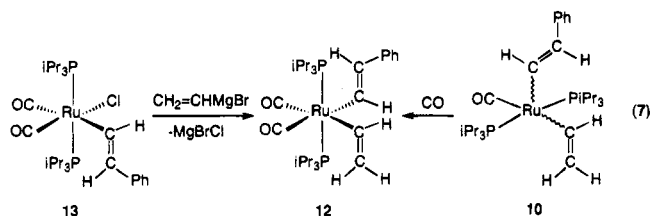
Complex **10** was isolated as red crystals in 72% yield and characterized by ^1H , $^{13}\text{C}\{^1\text{H}\}$, and $^{31}\text{P}\{^1\text{H}\}$ NMR spectroscopies. In the ^1H NMR spectrum, the most noticeable signals are the resonances due to the styryl and vinyl ligands. The protons of the styryl ligand give rise to two doublet of triplets at 8.78 and 6.88 ppm. The *trans* stereochemistry at the carbon-carbon double bond is strongly supported by the proton-proton coupling constant of 17.4 Hz which is a typical value for this arrangement.²⁸ The protons of the vinyl ligand display a doublet of doublets at 7.99 ppm and two doublet of triplets at 5.80 and 5.45 ppm. In the $^{13}\text{C}\{^1\text{H}\}$ NMR spectrum the α -carbon atom of the styryl ligand appears at 165.83 ppm as a triplet with a P-C coupling constant of 13.7 Hz and the β -carbon atom at 141.78 ppm, also as a triplet, with a P-C coupling constant of 2.4 Hz. The α -carbon atom of the vinyl ligand gives rise to a triplet at 172.65 ppm with a P-C coupling constant of

(28) Esteruelas, M. A.; García, M. P.; Martín, M.; Nürnberg, O.; Oro, L. A.; Werner, H. J. *Organomet. Chem.* **1994**, *466*, 249.

14.6 Hz, while the β -carbon atom appears as a broad singlet at 135.51 ppm. The $^{31}\text{P}\{^1\text{H}\}$ NMR spectrum shows a singlet at 39.5 ppm.

Complex **11** was isolated as a yellow solid in 75% yield and characterized by elemental analysis and IR and ^1H , $^{13}\text{C}\{^1\text{H}\}$, and $^{31}\text{P}\{^1\text{H}\}$ NMR spectroscopies. As for complex **5**, the ^1H spectrum in benzene- d_6 shows five signals for the diene protons at 5.30, 5.20, 1.90, 1.40, and 0.07 ppm. The resonances at low field (5.30 and 5.20 ppm) were assigned to the internal protons, the resonance at 1.90 ppm was assigned to the *syn*-CH₂ proton, and the resonances at 1.40 and 0.07 ppm were assigned to the *anti*-terminal protons. The H-H coupling constants are similar to those observed for **5** and therefore are consistent for a significant contribution of the metallacycle resonance form to the structure of **11**. The carbon atoms of the diene in the $^{13}\text{C}\{^1\text{H}\}$ NMR spectrum display two virtual triplets at 79.76 ($J_{\text{P-C}} = 2.9$ Hz) and 29.93 ($J_{\text{P-C}} = 3.4$ Hz) ppm, a double doublet at 52.03 ($J_{\text{P-C}} = 27.9$ and 3.8 Hz) ppm, and a doublet at 78.62 ($J_{\text{P-C}} = 2.9$ Hz). The signals at 79.76 and 52.03 ppm were assigned to the carbon atoms disposed *trans* to the triisopropylphosphine ligand, while the resonances at 78.62 and 29.93 ppm were assigned to the carbon atoms disposed *trans* to the carbonyl group. The $^{31}\text{P}\{^1\text{H}\}$ NMR spectrum contains two broad singlets at 53.9 and 48.0 ppm.

The coordination number 6 for **10** can be achieved by reaction with carbon monoxide. By passage of a slow stream of this gas through a hexane suspension of **10**, the dicarbonyl complex $\text{Ru}\{(\text{E})\text{-CH=CHPh}\}(\text{CH=CH}_2)(\text{CO})_2(\text{PiPr}_3)_2$ (**12**) is obtained as a white solid in 90% yield. Complex **12** can be also prepared by reaction of $\text{Ru}\{(\text{E})\text{-CH=CHPh}\}\text{Cl}(\text{CO})_2(\text{PiPr}_3)_2$ (**13**) with $\text{CH}_2=\text{CH-MgBr}$ (eq 7) in 82% yield.



In agreement with the *cis* disposition of the two carbonyl ligands of **12**, the IR spectrum of this compound in Nujol shows two $\nu(\text{CO})$ absorptions at 1990 and 1935 cm^{-1} , and the $^{13}\text{C}\{^1\text{H}\}$ NMR spectrum in benzene- d_6 shows two triplets at 204.00 and 203.96 ppm with P-C coupling constants of 9.6 and 10.6 Hz, respectively. Furthermore, the spectrum contains four triplets due to carbon atoms of the styryl and vinyl ligands at 167.80, 161.90, 142.42, and 141.41 ppm with P-C coupling constants of 14.3, 15.2, 2.3, and 4.6 Hz, respectively. In the ^1H NMR spectrum the protons of the styryl ligand give rise to two double triplets at 8.29 and 7.09 ppm with a H-H coupling constant of 18.4 Hz and P-H coupling constants of 2.5 and 2.2 Hz, while the protons of the vinyl ligand display three resonances at 7.91, 6.60, and 6.03 ppm. The $^{31}\text{P}\{^1\text{H}\}$ NMR spectrum shows a singlet at 36.2 ppm.

In contrast to the behavior of **10**, reductive carbon-carbon coupling between the styryl and vinyl fragments of the saturated complex **12** is not observed, suggesting that the unsaturated ligand environment around of the

metallic center is a determinant factor for the coupling. This is in good agreement with that previously observed for the coordinatively saturated platinum(IV) complex $\text{Pt}(\text{CH}_3)_3\text{I}(\text{dppe})$ ($\text{dppe} = \text{bis}(1,2\text{-diphenylphosphino})\text{-ethane}$), where the dissociation of the I^- anion is necessary for the reductive elimination of ethane.^{15h} In our case a bulky phosphine as triisopropylphosphine favors the formation of unsaturated five-coordinate species and therefore, most probably, the coupling process.

Concluding Remarks

The reactions of the complexes $\text{M}\{(\text{E})\text{-CH=CHR}\}\text{Cl}(\text{CO})(\text{PiPr}_3)_2$ ($\text{M} = \text{Os}, \text{R} = \text{Ph}, \text{H}; \text{M} = \text{Ru}, \text{R} = \text{Ph}$) with $\text{CH}_2=\text{CHMgBr}$ lead to the corresponding π -butadiene complexes $\text{M}(\eta^4\text{-C}_4\text{H}_5\text{R})(\text{CO})(\text{PiPr}_3)_2$. These transformations involve the replacement of the Cl^- anion by the vinyl group to give styryl-vinyl or bis(vinyl) intermediates that by reductive carbon-carbon coupling afford the butadiene derivatives.

Reductive carbon-carbon coupling between the alk- enyl fragments of the saturated compound $\text{Ru}\{(\text{E})\text{-CH=CHR}\}(\text{CH=CH}_2)(\text{CO})_2(\text{PiPr}_3)_2$ is not observed. This seems to suggest that the presence of a coordination vacancy in the starting compound could be a determinant factor for this type of coupling.

Experimental Section

General Considerations. All reactions were carried out with rigorous exclusion of air by using Schlenk-tube techniques. Solvents were dried by known procedures and distilled under argon prior to use. $\text{Os}\{(\text{E})\text{-CH=CHPh}\}\text{Cl}(\text{CO})(\text{PiPr}_3)_2$ (**3**), $\text{Ru}\{(\text{E})\text{-CH=CHPh}\}\text{Cl}(\text{CO})(\text{PiPr}_3)_2$ (**4**), $\text{Os}(\text{CH=CH}_2)\text{Cl}(\text{CO})(\text{PiPr}_3)_2$ (**6**), and $\text{Ru}\{(\text{E})\text{-CH=CHPh}\}\text{Cl}(\text{CO})_2(\text{PiPr}_3)_2$ (**12**), were prepared by published methods.²

Physical Measurements. Infrared spectra were recorded as Nujol mulls on polyethylene sheets using a Perkin-Elmer 883 or a Nicolet 550 spectrometer. NMR spectra were recorded on a Varian Unity 300 or on a Bruker 300 AXR. ^1H and $^{13}\text{C}\{^1\text{H}\}$ chemical shifts were measured relative to partially deuterated solvent peaks but are reported relative to tetramethylsilane. $^{31}\text{P}\{^1\text{H}\}$ chemical shifts are reported relative to H_3PO_4 (85%). Coupling constants J and N ($N = J(\text{HP}) + J(\text{HP}')$ for ^1H , and $N = J(\text{CP}) + J(\text{CP}')$ for ^{13}C) are given in hertz. C, H, and N analyses were carried out in a Perkin-Elmer 2400 CHNS/O analyzer.

Preparation of $\text{Os}(\eta^4\text{-C}_4\text{H}_5\text{Ph})(\text{CO})(\text{PiPr}_3)_2$ (5**).** A suspension of $\text{Os}\{(\text{E})\text{-CH=CHPh}\}\text{Cl}(\text{CO})(\text{PiPr}_3)_2$ (**3**) (100 mg, 0.15 mmol) in 5 mL of toluene was treated with 0.20 mL of $\text{CH}_2=\text{CHMgBr}$ (1.0 M solution in THF) and stirred during ca. 5 min at room temperature. The resulting suspension was filtered through kieselguhr, and the solvent was removed. Addition of methanol lead to the precipitation of a white solid. The solution was decanted, and the solid was washed with methanol and dried in vacuo. Yield: 85.3 mg (85%). Anal. Calcd for $\text{C}_{25}\text{H}_{52}\text{O}_2\text{OsP}_2$: C, 52.08; H, 7.84. Found: C, 51.94; H, 7.53. IR (Nujol, cm^{-1}): $\nu(\text{CO})$ 1867 (s). ^1H NMR (C_6D_6 , 20 $^\circ\text{C}$, labeling scheme in Figure 2): δ 7.40 (d, $J_{\text{H-H}} = 7.5$ Hz, 2H, $\text{H}_{\text{ortho-Ph}}$), 7.21 (t, $J_{\text{H-H}} = 7.5$ Hz, 2H, $\text{H}_{\text{meta-Ph}}$), 7.01 (t, $J_{\text{H-H}} = 7.5$ Hz, 1H, $\text{H}_{\text{para-Ph}}$), 5.16 (m, 1H, H_d), 5.03 (m, 1H, H_c), 2.36 (m, 3H, $\text{PCH}(\text{CH}_3)_2$), 2.20 (m, 3H, $\text{PCH}(\text{CH}_3)_2$), 1.94 (m, $J_{\text{H}_b\text{-H}_c} = 6.9$ Hz, $J_{\text{H}_b\text{-H}_a} = J_{\text{H}_b\text{-P}_b} = 3.9$ Hz, $J_{\text{H}_b\text{-P}_a} = 1$ Hz, 1H, H_b), 1.32 (m, 1H, H_e), 1.16 (dd, $J_{\text{H-P}} = 12.3$ Hz, $J_{\text{H-H}} = 7.2$ Hz, 9H, $\text{PCH}(\text{CH}_3)_2$), 1.12 (dd, $J_{\text{H-P}} = 12.6$ Hz, $J_{\text{H-H}} = 7.2$ Hz, 9H, $\text{PCH}(\text{CH}_3)_2$), 1.00 (dd, $J_{\text{H-P}} = 12.9$ Hz, $J_{\text{H-H}} = 6.9$ Hz, 9H, $\text{PCH}(\text{CH}_3)_2$), 0.99 (dd, $J_{\text{H-P}} = 12.0$ Hz, $J_{\text{H-H}} = 6.9$ Hz, 9H, $\text{PCH}(\text{CH}_3)_2$), -0.22 (m, $J_{\text{H}_a\text{-H}_c} = 6.9$ Hz, $J_{\text{H}_a\text{-H}_b} = J_{\text{H}_a\text{-P}_a} = J_{\text{H}_a\text{-P}_b} = 3.9$ Hz, 1H, H_a). $^{13}\text{C}\{^1\text{H}\}$ NMR (C_6D_6 , 20 $^\circ\text{C}$): δ 192.42 (dd,

$J_{C-P} = 11.5$ Hz, $J_{C-P} = 2.8$ Hz, CO), 147.21 (d, $J_{C-P} = 2.3$ Hz, $C_{ipso-Ph}$), 128.43 (d, $J_{C-P} = 0.9$ Hz, $C_{ortho-Ph}$), 126.36 (d, $J_{C-P} = 1.9$ Hz, $C_{meta-Ph}$), 123.50 (d, $J_{C-P} = 1.0$ Hz, $C_{para-Ph}$), 75.48 (dd, $J_{C-P} = 3.7$ Hz, $J_{C-P} = 2.3$ Hz, $CH_2=CHCH=CHPh$), 71.98 (dd, $J_{C-P} = 3.7$ Hz, $J_{C-P} = 0.9$ Hz, $CH_2=CHCH=CHPh$), 44.80 (dd, $J_{C-P} = 26.7$ Hz, $J_{C-P} = 4.6$ Hz, $CH_2=CHCH=CHPh$), 31.68 (d, $J_{C-P} = 22.6$ Hz, $PCH(CH_3)_2$), 30.25 (d, $J_{C-P} = 19.8$ Hz, $PCH(CH_3)_2$), 21.22 (dd, $J_{C-P} = 5.6$ Hz, $J_{C-P} = 3.2$ Hz, $CH_2=CHCH=CHPh$), 20.64 (s, $PCH(CH_3)_2$), 20.32 (s, $PCH(CH_3)_2$), 19.87 (s, $PCH(CH_3)_2$). $^{31}P\{^1H\}$ NMR (C_6D_6 , 20 °C): δ 13.8 (d, $J_{P-P} = 10.7$ Hz), 3.2 (d, $J_{P-P} = 10.7$ Hz).

Preparation of Os($\eta^4-C_4H_8$)(CO)(PiPr₃)₂ (7). A suspension of Os(CH=CH₂)Cl(CO)(PiPr₃)₂ (**6**) (100 mg, 0.18 mmol) in 5 mL of toluene was treated with 0.24 mL of CH₂=CHMgBr (1.0 M solution in THF) and stirred during ca. 5 min at room temperature. The resulting suspension was filtered through kieselguhr, and the solvent was removed. Addition of methanol caused the precipitation of a white solid. The solution was decanted, and the solid was washed with methanol and dried in vacuo. Yield: 85.4 mg (80%). Anal. Calcd for C₂₃H₄₈O₂OsP₂: C, 46.60; H, 8.16. Found: C, 46.71; H, 8.35. IR (Nujol, cm⁻¹): $\nu(CO)$ 1870 (s). 1H NMR (CDCl₃, 20 °C, labeling scheme in Figure 3): δ 5.05 (m, $J_{H_1-H_2} = J_{H_1-H_3} = 6.8$ Hz, $J_{H_1-H_4} = 3.9$ Hz, $J_{H_1-P_a} = 3.7$ Hz, $J_{H_1-P_b} = 3.2$ Hz, 1H, H₁), 4.56 (m, $J_{H_2-H_3} = J_{H_2-H_4} = 6.7$ Hz, $J_{H_2-H_5} = 3.9$ Hz, $J_{H_2-P_a} < 1$ Hz, 1H, H₂), 2.38 (m, 3H, $PCH(CH_3)_2$), 2.25 (m, 3H, $PCH(CH_3)_2$), 1.71 (ddd, $J_{H_3-H_4} = 6.7$ Hz, $J_{H_3-H_5} = 2.6$ Hz, $J_{H_3-P_b} = 3.2$ Hz, 1H, H₃), 1.64 (m, $J_{H_4-H_5} = 6.8$ Hz, $J_{H_4-H_6} = 3.6$ Hz, $J_{H_4-P_b} = 2.9$ Hz, $J_{H_4-P_a} = 1$ Hz, 1H, H₄), 1.25 (dd, $J_{H_5-P} = 12.9$ Hz, $J_{H_5-H} = 7.2$ Hz, 18H, $PCH(CH_3)_2$), 1.16 (dd, $J_{H_6-P} = 11.3$ Hz, $J_{H_6-H} = 7.5$ Hz, 18H, $PCH(CH_3)_2$), -0.77 (m, $J_{H_7-H_8} = 6.7$ Hz, $J_{H_7-P_b} = 3.5$ Hz, $J_{H_7-P_a} = 3.2$ Hz, $J_{H_7-H_9} = 2.6$ Hz, 1H, H₇), -1.07 (m, $J_{H_8-H_9} = 6.8$ Hz, $J_{H_8-H_2} = J_{H_8-P_a} = J_{H_8-P_b} = 3.6$ Hz, 1H, H₈). $^{13}C\{^1H\}$ NMR (CDCl₃, 20 °C): δ 191.25 (dd, $J_{C-P} = 11.1$ Hz, $J_{C-P} = 2.5$ Hz, CO), 76.68 (dd, $J_{C-P} = 3.9$ Hz, $J_{C-P} = 1.0$ Hz, $CH_2=CH-CH=CH_2$), 71.01 (vt, $J_{C-P} = J_{C-P} = 2.4$ Hz, $CH_2=CHCH=CH_2$), 30.19 (d, $J_{C-P} = 22.9$ Hz, $PCH(CH_3)_2$), 29.11 (d, $J_{C-P} = 19.8$ Hz, $PCH(CH_3)_2$), 24.40 (dd, $J_{C-P} = 28.7$ Hz, $J_{C-P} = 5.7$ Hz, $CH_2=CHCH=CH_2$), 23.11 (vt, $J_{C-P} = J_{C-P} = 3.2$ Hz, $CH_2=CHCH=CH_2$), 21.11 (s, $PCH(CH_3)_2$), 20.81 (d, $J_{C-P} = 1.5$ Hz, $PCH(CH_3)_2$), 19.78 (d, $J_{C-P} = 2.8$ Hz, $PCH(CH_3)_2$), 19.74 (s, $PCH(CH_3)_2$). $^{31}P\{^1H\}$ NMR (CDCl₃, 20 °C): δ 18.9 (d, $J_{P-P} = 9.5$ Hz), 6.2 (d, $J_{P-P} = 9.5$ Hz).

Preparation of Ru{(E)-CH=CHPh}(CH=CH₂)(CO)-(PiPr₃)₂ (10). A suspension of Ru{(E)-CH=CHPh}Cl(CO)-(PiPr₃)₂ (**4**) (201.5 mg, 0.34 mmol) in 10 mL of hexane was treated with 0.44 mL of CH₂=CHMgBr (1.0 M solution in THF) and stirred during ca. 10 min at room temperature. The resulting suspension was filtered through kieselguhr, and the obtained orange solution concentrated to ca. 2 mL and cooled at -78 °C. The red crystals obtained were decanted and washed with cool hexane. Yield: 142 mg (72%). 1H NMR (C_6D_6 , 20 °C): δ 8.78 (dt, $J_{H-H} = 17.4$ Hz, $J_{H-P} = 2.1$ Hz, 1H, RuCH=CHPh), 7.99 (dd, $J_{H-H} = 15.6$ Hz, $J_{H-H} = 8.7$ Hz, 1H, RuCH=CH₂), 7.51 (d, $J_{H-H} = 7.8$ Hz, 2H, H_{ortho-Ph}), 7.29 (dd, $J_{H-H} = 7.8$ Hz, $J_{H-H} = 6.6$ Hz, 2H, H_{meta-Ph}), 6.98 (t, $J_{H-H} = 6.6$ Hz, 1H, H_{para-Ph}), 6.88 (dt, $J_{H-H} = 17.4$ Hz, $J_{H-P} = 2.4$ Hz, 1H, RuCH=CHPh), 5.80 (dt, $J_{H-H} = 8.7$ Hz, $J_{H-P} = 3.0$ Hz, 1H, RuCH=CH₂), 5.45 (dt, $J_{H-H} = 15.6$ Hz, $J_{H-P} = 1.8$ Hz, 1H, RuCH=CH₂), 2.44 (m, 6H, $PCH(CH_3)_2$), 1.08 (dvt, N = 12.9 Hz, $J_{H-H} = 6.0$ Hz, 36H, $PCH(CH_3)_2$). $^{13}C\{^1H\}$ NMR (C_6D_6 , 20 °C): δ 205.65 (t, $J_{H-P} = 11.3$ Hz, CO), 172.65 (t, $J_{C-P} = 14.6$ Hz, RuCH=CH₂), 165.83 (t, $J_{C-P} = 13.7$ Hz, RuCH=CHPh), 141.78 (t, $J_{C-P} = 2.4$ Hz, RuCH=CHPh), 135.51 (s, RuCH=CH₂), 128.91 (s, $C_{ortho-Ph}$), 124.61 (s, $C_{meta-Ph}$), 124.35 (s, $C_{para-Ph}$), 25.86 (vt, N = 19.2 Hz, $PCH(CH_3)_2$), 19.82 (s, $PCH(CH_3)_2$). $^{31}P\{^1H\}$ NMR (C_6D_6 , 20 °C): δ : 39.5 (s).

Preparation of Ru($\eta^4-C_4H_8$ Ph)(CO)(PiPr₃)₂ (11). A solution of Ru{(E)-CH=CHPh}(CH=CH₂)(CO)(PiPr₃)₂ (**10**) (215 mg, 0.37 mmol) in 10 mL of hexane was left to stir for 15 h at 50 °C. The solution was then filtered through kieselguhr and concentrated to dryness. Addition of MeOH caused the

precipitation of a yellow solid which was washed several times with MeOH and dried in vacuo. Yield: 161 mg (75%). Anal. Calcd for C₂₅H₅₂O₂P₂Ru: C, 60.08; H, 9.04. Found: C, 59.48; H, 8.32. IR (Nujol, cm⁻¹): $\nu(CO)$ 1887 (s). 1H NMR (C_6D_6 , 20 °C, labeling scheme in Figure 2): δ 7.40 (d, $J_{H-H} = 7.5$ Hz, 2H, H_{ortho-Ph}), 7.21 (t, $J_{H-H} = 7.5$ Hz, 2H, H_{meta-Ph}), 7.01 (t, $J_{H-H} = 7.5$ Hz, 1H, H_{para-Ph}), 5.30 (dd, $J_{H_2-H_3} = 7.4$ Hz, $J_{H_2-H_4} = 4.6$ Hz, 1H, H₂), 5.20 (m, $J_{H_3-H_4} = J_{H_3-P_b} = 7.9$ Hz, $J_{H_3-H_5} = 7.0$ Hz, $J_{H_3-H_6} = 4.6$ Hz, 1H, H₃), 2.27 (m, 3H, $PCH(CH_3)_2$), 2.04 (m, 3H, $PCH(CH_3)_2$), 1.90 (m, $J_{H_4-H_5} = 7.0$ Hz, $J_{H_4-P_b} = 4.1$ Hz, $J_{H_4-H_6} = 2.6$ Hz, $J_{H_4-H_7} = 0.2$ Hz, 1H, H₄), 1.40 (m, $J_{H_5-H_6} = 7.4$ Hz, $J_{H_5-P_a} = J_{H_5-P_b} = 6.3$ Hz, 1H, H₅), 1.10 (m, 36H, $PCH(CH_3)_2$), 0.07 (m, $J_{H_6-H_7} = 7.9$ Hz, $J_{H_6-P_a} = 7.8$ Hz, $J_{H_6-P_b} = 4.9$ Hz, $J_{H_6-H_8} = 2.6$ Hz, 1H, H₆). $^{13}C\{^1H\}$ NMR (C_6D_6 , 20 °C): δ 210.78 (dd, $J_{C-P} = 15.8$ Hz, $J_{C-P} = 7.5$ Hz, CO), 146.48 (d, $J_{C-P} = 3.0$ Hz, $C_{ipso-Ph}$), 128.40 (s, $C_{ortho-Ph}$), 126.45 (d, $J_{C-P} = 1.5$ Hz, $C_{meta-Ph}$), 123.60 (s, $C_{para-Ph}$), 79.76 (vt, $J_{C-P} = 2.9$ Hz, $CH_2=CHCH=CHPh$), 78.62 (d, $J_{C-P} = 2.9$ Hz, $CH_2=CHCH=CHPh$), 52.03 (dd, $J_{C-P} = 27.9$ Hz, $J_{C-P} = 3.8$ Hz, $CH_2=CHCH=CHPh$), 30.48 (d, $J_{C-P} = 13.0$ Hz, $PCH(CH_3)_2$), 29.93 (vt, $J_{C-P} = 3.4$ Hz, $CH_2=CHCH=CHPh$), 29.08 (d, $J_{C-P} = 14.1$ Hz, $PCH(CH_3)_2$), 20.45 (d, $J_{C-P} = 15.4$ Hz, $PCH(CH_3)_2$), 19.89 (d, $J_{C-P} = 14.8$ Hz, $PCH(CH_3)_2$). $^{31}P\{^1H\}$ NMR (C_6D_6 , 20 °C): δ 53.9 (s), 48.0 (s).

Preparation of Ru{(E)-CH=CHPh}(CH=CH₂)(CO)-(PiPr₃)₂ (12). Route a. A slow stream of carbon monoxide was bubbled for 5 min through a solution of Ru{(E)-CH=CHPh}(CH=CH₂)(CO)(PiPr₃)₂ (**10**) (170 mg, 0.29 mmol) in 8 mL of hexane. The deep purple solution becomes colorless instantaneously. After concentration to ca. 2 mL white crystals were obtained. The product was washed several times with hexane and dried in vacuo. Yield: 160 mg (90%).

Route b. A suspension of Ru{(E)-CH=CHPh}Cl(CO)-(PiPr₃)₂ (**13**) (180.0 mg, 0.29 mmol) in 10 mL of hexane was treated with 0.38 mL of CH₂=CHMgBr (1.0 M solution in THF) and stirred during ca. 30 min at room temperature. The resulting suspension was dried, and the residue was treated with 7 mL of toluene and filtered through kieselguhr. The obtained solution was dried and treated with hexane to give a white solid which was decanted and washed with hexane. Yield: 144 mg (82%).

Anal. Calcd for C₃₀H₅₂O₂P₂Ru: C, 59.29; H, 8.62. Found: C, 58.93; H, 8.31. IR (Nujol, cm⁻¹): $\nu(CO)$ 1990 (s), 1935 (s). 1H NMR (C_6D_6 , 20 °C): δ 8.29 (dt, $J_{H-H} = 18.4$ Hz, $J_{H-P} = 2.5$ Hz, 1H, RuCH=CHPh), 7.91 (ddt, $J_{H-H} = 19.5$ Hz, $J_{H-H} = 12.4$ Hz, $J_{H-P} = 2.0$ Hz, 1H, RuCH=CH₂), 7.50 (d, $J_{H-H} = 7.6$ Hz, 2H, H_{ortho-Ph}), 7.28 (t, $J_{H-H} = 7.6$ Hz, 2H, H_{meta-Ph}), 7.09 (dt, $J_{H-H} = 18.4$ Hz, $J_{H-P} = 2.2$ Hz, 1H, RuCH=CHPh), 7.01 (t, $J_{H-H} = 7.6$ Hz, 1H, H_{para-Ph}), 6.60 (ddt, $J_{H-H} = 12.4$ Hz, $J_{H-H} = 3.0$ Hz, $J_{H-P} = 3.0$ Hz, 1H, RuCH=CH₂), 6.03 (ddt, $J_{H-H} = 19.5$ Hz, $J_{H-H} = 3.0$ Hz, $J_{H-P} = 2.0$ Hz, 1H, RuCH=CH₂), 2.43 (m, 6H, $PCH(CH_3)_2$), 1.07 (dvt, N = 12.9 Hz, $J_{H-H} = 6.0$ Hz, 36H, $PCH(CH_3)_2$). $^{13}C\{^1H\}$ NMR (C_6D_6 , 20 °C): δ 204.00 (t, $J_{C-P} = 9.6$ Hz, CO), 203.96 (t, $J_{C-P} = 10.6$ Hz, CO), 167.80 (t, $J_{C-P} = 14.3$ Hz, RuCH=CH₂), 161.90 (t, $J_{C-P} = 15.2$ Hz, RuCH=CHPh), 142.42 (t, $J_{C-P} = 2.3$ Hz, RuCH=CHPh), 141.41 (t, $J_{C-P} = 4.6$ Hz, RuCH=CH₂), 128.91 (s, $C_{ortho-Ph}$), 124.90 (s, $C_{para-Ph}$), 124.70 (s, $C_{meta-Ph}$), 26.06 (vt, N = 24.2 Hz, $PCH(CH_3)_2$), 19.57 (s, $PCH(CH_3)_2$), 19.60 (s, $PCH(CH_3)_2$). $^{31}P\{^1H\}$ NMR (C_6D_6 , 20 °C): δ 36.2 (s).

X-ray Structure Analysis of Os($\eta^4-C_4H_8$ Ph)(CO)(PiPr₃)₂ (5). Crystals suitable for an X-ray diffraction experiment were obtained from a saturated solution of **5** in acetone at -20 °C. Atomic coordinates and U_{eq} values are listed in Table 2. A summary of crystal data, intensity collection procedure, and refinement is reported in Table 3. The colorless prismatic crystal studied was glued on a glass fiber and mounted on a Siemens AED-2 diffractometer. Cell constants were obtained from the least-squares fit of the setting angles of 63 reflections in the range $20 \leq 2\theta \leq 50^\circ$. The recorded reflections (7116) were corrected for Lorentz and polarization effects. Three

Table 2. Atomic Coordinates ($\text{\AA} \times 10^4$; $\times 10^5$ for Os and P Atoms) and Equivalent Isotropic Displacement Coefficients ($\text{\AA}^2 \times 10^3$; $\times 10^4$ for Os and P Atoms) for the Compound $\text{Os}(\eta^4\text{-C}_4\text{H}_5\text{Ph})(\text{CO})(\text{PiPr}_3)_2$ (5**)**

atom	<i>x/a</i>	<i>y/b</i>	<i>z/c</i>	U_{eq}^a
Os	22888(1)	16019(1)	29402(1)	182(1)
P(1)	23099(8)	36195(7)	22382(5)	220(2)
P(2)	10229(8)	8202(7)	20098(5)	197(2)
O	5433(2)	807(2)	1976(2)	35(1)
C(1)	434(3)	2191(3)	4048(2)	28(1)
C(2)	1901(4)	2086(3)	4340(2)	28(1)
C(3)	3007(4)	943(3)	4338(2)	26(1)
C(4)	2579(3)	-35(3)	4073(2)	23(1)
C(5)	3701(3)	-1247(3)	4029(2)	26(1)
C(6)	5245(4)	-1387(3)	3785(2)	30(1)
C(7)	6261(4)	-2540(3)	3759(3)	38(1)
C(8)	5763(4)	-3591(3)	3997(3)	39(1)
C(9)	4259(4)	-3465(3)	4249(3)	38(1)
C(10)	3237(4)	-2305(3)	4264(2)	31(1)
C(11)	4199(3)	1104(3)	2320(2)	25(1)
C(12)	4112(3)	3925(3)	2417(2)	28(1)
C(13)	4639(4)	3470(3)	3386(3)	34(1)
C(14)	4172(4)	5259(3)	2096(3)	39(1)
C(15)	2329(4)	3956(3)	929(2)	31(1)
C(16)	3902(4)	3464(3)	439(2)	40(1)
C(17)	1640(5)	5276(3)	467(3)	46(1)
C(18)	822(4)	5001(3)	2568(2)	33(1)
C(19)	781(4)	5243(3)	3559(3)	40(1)
C(20)	-755(4)	5022(3)	2358(3)	43(1)
C(21)	2202(3)	8(3)	1068(2)	28(1)
C(22)	3481(4)	-1092(3)	1429(3)	41(1)
C(23)	2821(4)	857(4)	294(2)	37(1)
C(24)	-557(3)	1939(3)	1375(2)	26(1)
C(25)	-1175(4)	1499(3)	642(3)	40(1)
C(26)	-1867(4)	2540(3)	2041(3)	38(1)
C(27)	282(4)	-460(3)	2671(2)	28(1)
C(28)	-112(5)	-1312(3)	2109(3)	42(1)
C(29)	-1050(4)	-75(4)	3390(3)	43(1)

^a Equivalent isotropic *U* defined as one-third of the trace of the orthogonalized U_{ij} tensor.

orientation and intensity standards were monitored every 55 min of measuring time; no variation was observed. Reflections were also corrected for absorption by an semiempirical (ψ -scan) method.²⁹

The structure was solved by Patterson (Os atom) and conventional Fourier techniques. Refinement was carried out by full-matrix least squares with initial isotropic thermal parameters. Anisotropic thermal parameters were used in the last cycles of refinement for all non-hydrogen atoms. Hydrogen atoms were observed and included in the refinement riding on carbon atoms with a common isotropic thermal parameter. Atomic scattering factors, corrected for anomalous dispersion for Os and P, were taken from ref 30. The function minimized was $\sum w([F_o] - [F_c])^2$, with the weight defined as $w^{-1} = \sigma^2[F_o]$

(29) North, A. C. T.; Phillips, D. C.; Mathews, F. S. *Acta Crystallogr.* **1968**, A24, 351.

Table 3. Crystal Data and Data Collection and Refinement for $\text{Os}(\eta^4\text{-C}_4\text{H}_5\text{Ph})(\text{CO})(\text{PiPr}_3)_2$ (5**)**

Crystal Data	
formula	$\text{C}_{29}\text{H}_{52}\text{O}_2\text{OsP}_2$
mol wt	668.88
color and habit	colorless, transparent prism
crystal size, mm	$0.37 \times 0.29 \times 0.34$
crystal syst	triclinic
space group	$P\bar{1}$ (No. 2)
<i>a</i> , \AA	9.320(1)
<i>b</i> , \AA	11.590(1)
<i>c</i> , \AA	14.749(2)
α , deg	79.34(1)
β , deg	82.10(1)
γ , deg	72.34(1)
<i>V</i> , \AA^3	1486.3(3)
<i>Z</i>	2
<i>D</i> (calcd), g cm^{-3}	1.495
Data Collection and Refinement ^a	
diffractometer	4-circle Siemens-STOE AED
λ (Mo K α) \AA ; technique	0.710 73, bisecting geometry
monochromator	graphite oriented
μ , mm^{-1}	4.42
scan type	$\omega/2\theta$
2θ range, deg	$3 \leq 2\theta \leq 50$
temp (K)	200
no. of data collec	7116
no. of unique data	6779 ($R_{\text{int}} = 0.025$)
unique obsd data	6357 ($F_o \geq 4.0\sigma(F_o)$)
no. of params refined	300
<i>R</i> , <i>R_w</i>	0.0230, 0.0245

^a $R = (\sum [|F_o| - |F_c|]) / \sum F_o$; $R_w = (\sum (|F_o| - |F_c|)w^{1/2}) / \sum (|F_o|w^{1/2})$, $w^{-1} = \sigma^2(F_o) + 0.000292(F_o)^2$.

+ 0.000292 $[F_o]^2$. Final *R* and *R_w* values were 0.0230 and 0.0245. All calculations were performed by the use of the SHELXTL-PLUS system of computer program.³¹

Acknowledgment. We thank the DGICYT (Project PB 92-0092, Programa de Promoción General del Conocimiento) and EU (Project Selective Processes and Catalysis Involving Small Molecules) for financial support. E.O. thanks the Diputación General de Aragón (DGA) for a grant.

Supporting Information Available: Tables of anisotropic thermal parameters, atomic coordinates and *U* values for hydrogen atoms, experimental details of the X-ray study, bond distances and angles, and selected least squares planes for **5** (12 pages). Ordering information is given on any current masthead page.

OM9503407

(30) *International Tables for X-Ray Crystallography*; Kynoch Press: Birmingham, England, 1974; Vol. IV.

(31) Sheldrick, G. M. *SHELXTL PLUS*; Siemens Analytical X-ray Instruments, Inc.: Madison, WI, 1990.

Synthesis and Crystal Structures of Lithium Complexes from the Metalation of 2-Picoline Derivatives

Wing-Por Leung,* Ling-Hong Weng, Ru-Ji Wang, and Thomas C. W. Mak

Department of Chemistry, The Chinese University of Hong Kong, Shatin, NT, Hong Kong

Received May 22, 1995[®]

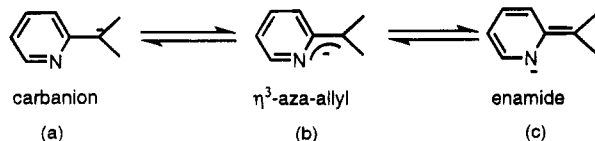
Metalation of the 2-picoline derivatives 2-R'R''CHC₅H₄N (R' = Ph, SiBu^tMe₂; R'' = SiMe₃, H) with BuⁿLi/tmeda (tmeda = Me₂NCH₂CH₂NMe₂) in hexane affords the organolithium complexes [2-(Me₃Si)PhC(C₅H₄N)Li(tmeda)] (1), [2-(Bu^tMe₂Si)HC(C₅H₄N)Li(tmeda)]₂ (2), and [2-Ph(H)C(C₅H₄N)Li(tmeda)]₂ (3). X-ray analysis has shown that the deprotonated species [2-R'R''CC₅H₄N]⁻ acts as an amide rather than an alkyl ligand. The Li atoms are bonded more strongly to the pyridyl nitrogen than to the α-carbon, as shown by the long Li-C_α bond distances. The relatively short C_α-C_{py} distances of 1.382, 1.385, and 1.37 Å in 1-3, respectively, suggest that they have substantial double-bond character. The C-C distances within the pyridine ring are significantly different and are consistent with a nonaromatic moiety having the charge localized at nitrogen, befitting the description of 1-3 as "enamido" types of lithium complexes.

Introduction

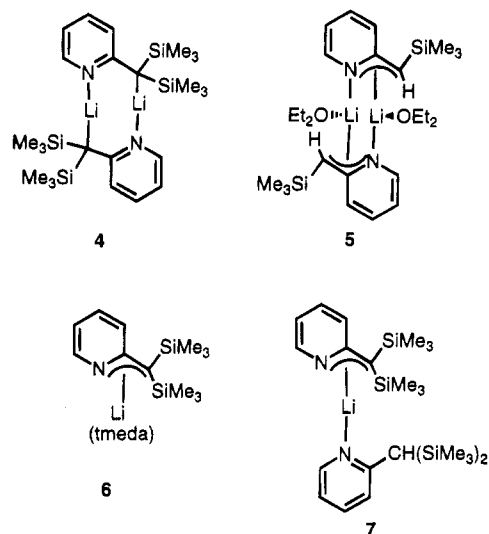
Organolithium compounds are commonly used as transfer reagents in organometallic chemistry of the anionic fragment and also as a source of base or nucleophile for organic synthesis. In recent years there has been broad interest in structural studies dealing with organolithium compounds,¹ which provide a rationale of their reactivity based on their degree of aggregation and the extent and nature of their solvation.

Metalation of 2-picoline using various lithium reagents to yield 2-picolyllithium compounds was reported as early as 1974.² Lithium compounds derived from metalation of 2,6-dimethylpyridine³ and bis(pyridyl)methyl⁴ have also been reported. The structures of lithium compounds derived from 2-R_{3-n}CH_nC₅H₄N (R = SiMe₃, Ph; n = 1, 2), prepared from their reactions with BuⁿLi, were described recently.⁵ The versatility of these lithium compounds as transfer reagents has been demonstrated in the synthesis of a variety of metal complexes.⁶

In principle, three resonance structures are possible for such a picolyl anion: (a) C-centered carbanion, (b) delocalized aza-allyl ion, and (c) N-centered enamide ion.



X-ray structural studies of such lithium compounds provide useful information for assigning the type of complex formed. The molecular geometries of the lithium complexes 4-7, derived from the metalation of



2-R_{3-n}CH_nC₅H₄N (R = SiMe₃; n = 1, 2), were shown to be influenced by solvents and the degree of substitution at the ipso carbon.⁵ The lithium atom in the centrosymmetrical dinuclear complex [2-(Me₃Si)₂C(Li)C₅H₄N]₂ (4) is bonded closely to C_α of one ligand and nitrogen of the other ligand, showing it to be a C-centered type of complex. In the presence of other coordinating ligands such as ether, tmeda (tetramethylethylenediamine), and the parent picoline, novel η³-azaallyl-type structures

(4) (a) Gornitzka, H.; Stalke, D. *Angew. Chem., Int. Ed. Engl.* **1994**, *33*, 693. (b) Gornitzka, H.; Stalke, D. *Organometallics* **1994**, *13*, 4398.

(5) (a) Papasergio, R. I.; Skelton, B. W.; Twiss, P.; Raston, C. L.; White, A. H.; *J. Chem. Soc. Dalton Trans.* **1990**, 1161. (b) Engelhardt, L. M.; Jacobsen, G. E.; Junk, P. C.; Raston, C. L.; White, A. H. *J. Chem. Soc., Dalton Trans.* **1988**, 1011.

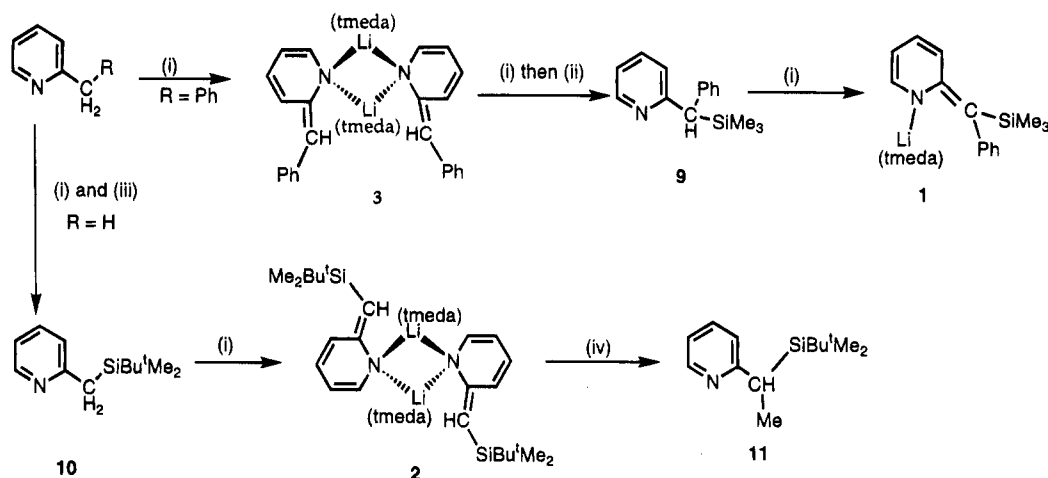
(6) (a) Colgan, D.; Papasergio, R. I.; Raston, C. L.; White, A. H. *J. Chem. Soc., Chem. Commun.* **1984**, 1708. (b) Papasergio, R. I.; Raston, C. L.; White, A. H. *J. Chem. Soc., Chem. Commun.* **1983**, 1419. (c) Papasergio, R. I.; Raston, C. L.; White, A. H. *J. Chem. Soc., Chem. Commun.* **1984**, 612. (d) Henderson, M. J.; Papasergio, R. I.; Raston, C. L.; White, A. H.; Lappert, M. F. *J. Chem. Soc., Chem. Commun.* **1986**, 672. (e) Engelhardt, L. M.; Jolly, B. S.; Lappert, M. F.; Raston, C. L.; White, A. H. *J. Chem. Soc., Chem. Commun.* **1988**, 336. (f) Jones, C.; Engelhardt, L. M.; Junk, P. C.; Hutchings, D. S.; Patalinghug, W. C.; Raston, C. L.; White, A. H. *J. Chem. Soc., Chem. Commun.* **1991**, 1560. (g) Engelhardt, L. M.; Kynast, U.; Raston, C. L.; White, A. H. *Angew. Chem., Int. Ed. Engl.* **1987**, *26*, 681.

[®] Abstract published in *Advance ACS Abstracts*, September 1, 1995.

(1) Setzer, W. N.; Schleyer, P. v. R. *Adv. Organometal. Chem.* **1985**, *24*, 352.

(2) Beumel, O. F.; Smith, W. N., Jr.; Rybalka, B. *Synthesis* **1974**, 43.

(3) (a) Hacker, H.; Schleyer, P. v. R.; Reber, G.; Müller, G.; Brandsma, L. *J. Organomet. Chem.* **1986**, *316*, C4. (b) Schleyer, P. v. R.; Hacker, H.; Dietrich, H.; and Mahdi, W. *J. Chem. Soc., Chem. Commun.* **1985**, 622.

Scheme 1^a

^a Reagents and conditions: (i) BuⁿLi, tmeda, hexane/ether; (ii) Me₃SiCl, hexane/ether; (iii) Bu^tMe₂SiCl, hexane/ether; (iv) MeI, hexane/ether.

5–7 were found. In 5 and 6, each lithium atom is approximately in the plane of the pyridine ring with appreciable π -bonding between.

Recently, structural studies on the diphenylpyridyl-methyl complexes [Ph₂CC₅H₄NLi₂·2OEt₂] (8a), [Ph₂CC₅H₄NNa·3THF] (THF = tetrahydrofuran) (8b), and [Ph₂CC₅H₄NK·pmdeta] (pmdeta = (Me₂NCH₂CH₂)₂NMe₂) (8c) showed that the alkali-metal atoms are bonded directly to the nitrogen and suggested that the negative charge on the ligand is almost totally localized at the nitrogen atom.⁷

In the present paper, we report the synthesis and structural results of the organolithium complexes 1–3, which are based on the picoline derivatives 2-R'R''CHC₅H₄N (R' = Ph or SiBu^tMe₂; R'' = H, SiMe₃). The influence of the degree of substitution and the role of different substituents at C_α are shown in the structures of these compounds. The charge delocalization and the coordination behavior of the anion are considered and compared with those in 4–7 and 8a.

Results and Discussion

Preparation of Compounds 1–3. The lithium complexes 1–3 and their derivatives were prepared by the reactions of BuⁿLi/tmeda and then SiMe₃Cl or MeI under different conditions, as shown in Scheme 1. BuⁿLi in conjunction with tmeda acts as an activating agent; this use has become a common practice in the metalation of organic substrates.⁸ It enhances the reactivity of the lithium reagent as well as increases the solubility of the compound in a low-polarity organic solvent by decreasing the degree of aggregation. Replacement of the acidic α -hydrogen of 2-picoline or 2-benzylpyridine with lithium, followed by quenching with the appropriate chlorosilane or MeI, gave the silylated derivatives 2-Ph(Me₃Si)CHC₅H₄N (9), 2-(Bu^tMe₂Si)CH₂C₅H₄N (10), and 2-(Bu^tMe₂Si)CH(Me)C₅H₄N (11), respectively. In the preparation of 10, no bis-silylated compound, *viz.* 2-(Bu^tMe₂Si)₂HCC₅H₄N, was obtained. It has been reported earlier that the conditions for the preparation of the monosilylated picoline derivative

2-(Me₃Si)CH₂C₅H₄N from the lithiated compound are rather critical.⁵ The conditions for the formation of the monosilylated compound as the major product versus a mixture of the mono- and bis-silylated compounds are dependent on the order of adding the SiMe₃Cl. This was explained by the relative acidities of the methyl groups in 2-methylpyridine and 2-(Me₃Si)CH₂C₅H₄N and the relative concentration of SiMe₃Cl and the lithiated species in the reaction mixture.⁹ In the present work, the possibility of forming the bis-silylated compound 2-(Bu^tMe₂Si)₂HCC₅H₄N is minimal, as the SiBu^tMe₂ group is comparatively more bulky than the SiMe₃ group, and hence incorporating a second SiBu^tMe₂ group would be sterically more unfavorable. The incorporation of different substituent groups (Ph, SiMe₃, and SiBu^tMe₂) can change the steric crowding around C_α and decreases the degree of aggregation. It also alters the lipophilicity and the solubility of the lithium compounds, significant for the isolation of crystalline compounds from a hydrocarbon solvent.

The lithium complexes were isolated as extremely air-sensitive crystalline solids and characterized by ¹H and ¹³C NMR spectroscopy and formation of derivatives by treatment with SiMe₃Cl and MeI. The ¹H NMR spectra of the lithium complexes show significant upfield shifts for the ring protons when compared with their signals in the conjugate acids. This is consistent with the data obtained for some deprotonated methyl-substituted pyridines which are due to the delocalization of charges.¹⁰ The methine proton signal at 2.75 ppm of the lithiated compound 2 shows a significant downfield shift when compared with the methylene proton signal at 2.33 ppm of its conjugate acid 10. This is due to the changing of the *ipso* carbon from sp³ to sp² hybridization, suggesting the existence of the "enamide" contribution in solution.

Crystal Structures of Compounds 1–3. The results of the single-crystal structure determinations of 1–3 have shown that all the anionic ligands [2-R'R''CHC₅H₄N]⁻ (R' = Ph, SiBu^tMe₂; R'' = SiMe₃, H) are bonded strongly to the lithium *via* the nitrogen and are consistent with the amide complexes being formed.

(7) Pieper, U.; Stalke, D. *Organometallics* **1993**, *12*, 1201.

(8) Wakefield, B. J. In *Comprehensive Organometallic Chemistry*; Wilkinson, G., Stone, F. G. A., Abel, E. W., Eds.; Pergamon Press: Oxford, U.K., 1982; Vol 7.

(9) Jones, C.; Kennard, C. H. L.; Raston, C. L.; Smith, G. J. *Organomet. Chem.* **1990**, *396*, C39.

(10) Konishi, K.; Takahashi, K. *Bull. Chem. Soc. Jpn.* **1977**, *50*, 2512; **1983**, *56*, 1612.

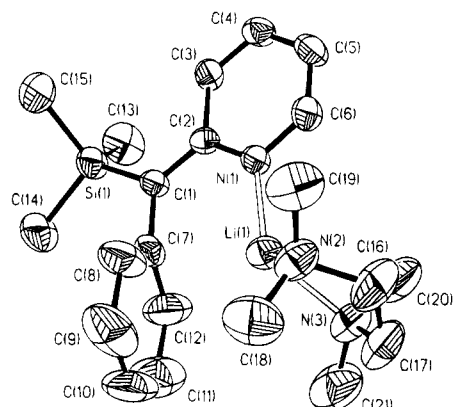


Figure 1. Perspective view of one of the two independent molecules in **1**. The thermal ellipsoids are drawn at the 35% probability level, and the interaction of the Li atom with the C(7)–C(8) bond is indicated by a broken bond.

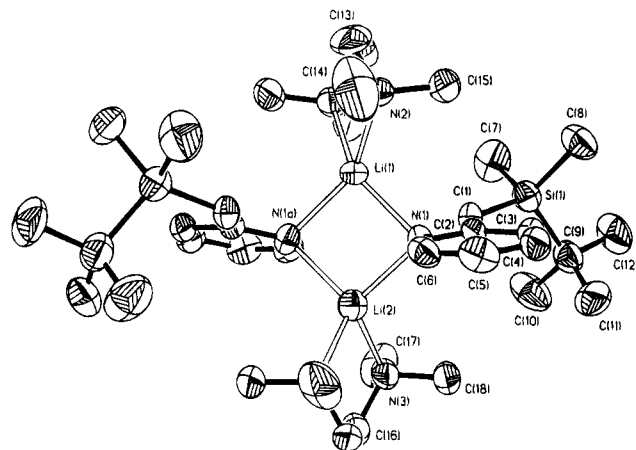


Figure 2. Perspective view of the C₂ dimeric molecule in **2**. The thermal ellipsoids are drawn at the 35% probability level.

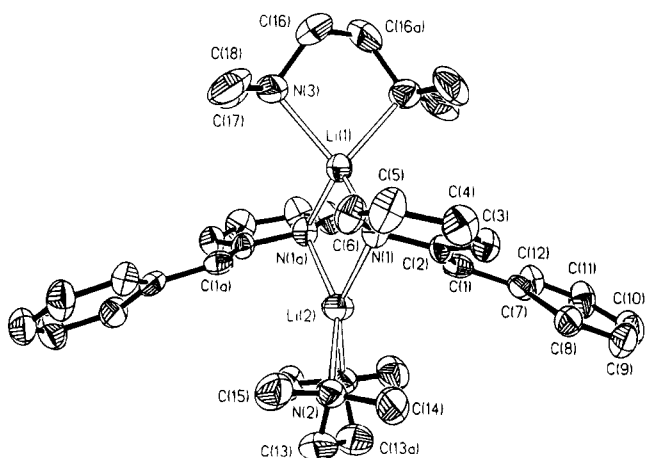


Figure 3. Perspective view of the C₂ dimer in **3**. The thermal ellipsoids are drawn at the 25% probability level.

Figure 1 shows the molecular structure of one of the two independent molecules of **1**; Figures 2 and 3 show the molecular structures of **2** and **3**, respectively. Selected intramolecular structural data are shown in Tables 1–3, respectively.

The comparative selected structural data for compounds having [2-R'R''CHC₅H₄N][−] (R' = Ph, SiBu^tMe₂; R'' = SiMe₃, H) ligands are compared in Table 4. From these data, it is possible to show the extent of charge delocalization in the anionic ligand, as depicted in

Table 1. Selected Intramolecular Distances (Å) and Angles (deg) with Estimated Standard Deviations (Esd's) in Parentheses for [2-(Me₃Si)PhC(C₅H₄N)]{Li(tmeda)} (**1**)

molecule I		molecule II	
Li(1)–N(1)	1.977(9)	Li(2)–N(4)	1.979(8)
Li(1)–N(2)	2.128(9)	Li(2)–N(5)	2.11(1)
Li(1)–N(3)	2.13(1)	Li(2)–N(6)	2.14(1)
Li(1)–C(1)	3.288(8)	Li(2)–C(31)	3.293(9)
Li(1)–C(7)	2.661(8)	Li(2)–C(37)	2.68(1)
Li(1)–C(8)	2.74(1)	Li(2)–C(38)	2.78(1)
N(1)–C(2)	1.379(5)	N(4)–C(32)	1.386(6)
N(1)–C(6)	1.347(6)	N(4)–C(36)	1.343(6)
C(1)–C(2)	1.382(6)	C(31)–C(32)	1.390(6)
C(1)–C(7)	1.489(7)	C(31)–C(37)	1.490(6)
C(2)–C(3)	1.443(7)	C(32)–C(33)	1.445(5)
C(3)–C(4)	1.350(7)	C(33)–C(34)	1.340(7)
C(4)–C(5)	1.394(6)	C(34)–C(35)	1.386(8)
C(5)–C(6)	1.356(8)	C(35)–C(36)	1.362(6)
C(7)–C(8)	1.38(1)	C(37)–C(38)	1.36(1)
C(7)–C(12)	1.36(1)	C(37)–C(42)	1.359(9)
C(8)–C(9)	1.42(1)	C(38)–C(39)	1.38(1)
C(9)–C(10)	1.35(2)	C(39)–C(40)	1.33(1)
C(10)–C(11)	1.28(2)	C(40)–C(41)	1.30(1)
C(11)–C(12)	1.42(2)	C(41)–C(42)	1.397(9)
N(1)–Li(1)–N(2)	118.8(5)	N(4)–Li(2)–N(5)	118.4(4)
N(1)–Li(1)–N(3)	121.8(5)	N(4)–Li(2)–N(6)	123.9(4)
N(2)–Li(1)–N(3)	86.5(3)	N(5)–Li(2)–N(6)	86.5(4)
N(1)–Li(1)–C(7)	72.8(3)	N(4)–Li(2)–N(37)	73.2(3)
N(2)–Li(1)–C(7)	135.5(5)	N(5)–Li(2)–N(37)	132.0(4)
N(3)–Li(1)–C(7)	125.8(4)	N(6)–Li(2)–N(37)	127.9(4)
Li(1)–N(1)–C(2)	126.5(4)	Li(2)–N(4)–N(32)	126.1(4)
Li(1)–N(1)–C(6)	115.7(3)	Li(2)–N(4)–N(36)	115.4(4)
Si(1)–C(1)–C(7)	116.7(3)	Si(2)–C(31)–C(32)	124.2(3)
Si(1)–C(1)–C(2)	124.5(3)	Si(2)–C(31)–C(37)	116.7(3)
C(2)–C(1)–C(7)	118.6(4)	C(32)–C(31)–C(37)	119.1(4)

Table 2. Selected Intramolecular Distances (Å) and Angles (deg) with Estimated Standard Deviations (Esd's) in Parentheses for [2-(Bu^tMe₂Si)HC(C₅H₄N)]{Li(tmeda)}₂ (**2**)

Li(1)–Li(2)	2.88(1)	Li(2)–C(2)	3.633
Li(1)–C(2)	3.202	Li(2)–N(1)	2.143(8)
Li(1)–N(1)	2.181(4)	Li(2)–N(3)	2.140(9)
Li(1)–N(2)	2.217(5)	N(1)–C(6)	1.354(7)
N(1)–C(2)	1.386(5)	C(1)–C(7)	1.489(7)
C(1)–C(2)	1.385(7)	C(3)–C(4)	1.333(8)
C(2)–C(3)	1.437(6)	C(5)–C(6)	1.358(8)
C(4)–C(5)	1.406(6)		
N(1)–Li(1)–N(2)	99.4(2)	N(1)–Li(2)–N(3)	113.2(1)
N(1)–Li(1)–N(1a)	95.4(2)	N(1)–Li(2)–N(1a)	97.6(5)
N(2)–Li(2)–N(1a)	146.3(1)	N(3)–Li(2)–N(1a)	125.2(2)
N(2)–Li(1)–N(2a)	84.7(3)	N(3)–Li(2)–N(3a)	85.2(5)
Si(1)–C(1)–C(2)	129.7(3)		

structures a–c above, by comparison of the Li–C_α, Li–N_{py}, and C_α–C_{py} distances in these complexes. The Li–C(1) (i.e. Li–C_α) distances of **1–3**, ranging from 2.70 to 3.42 Å, are too long to be considered bonding interactions, while other complexes have shorter distances such as 2.43 Å in the C-centered ligand in **4** and 2.36 Å in the η²-azaallyl-type ligand in **5**. The Li–N(1) (i.e. Li–N_{py}) distances in **1–3** are in good accord with those of typical lithium amides.¹¹ As a consequence of the charge being largely localized at the nitrogen, the C(1)–C(2) (i.e. C_α–C_{py}) distances of **1–3**, ranging from 1.37 to 1.38 Å, suggest more enhanced double-bond character than in compounds **4–7** and **8a**. The geometry at C(1) also indicates that the α-carbon is sp²-hybridized. The comparatively short C(3)–C(4) and C(5)–C(6) bond

(11) Gregory, K.; Schleyer, P. v. R. *Adv. Organomet. Chem.* **1991**, *37*, 67.

Table 3. Selected Intramolecular Distances (Å) and Angles (deg) with Estimated Standard Deviations (Esd's) in Parentheses for [$\{2\text{-Ph(H)C(C}_5\text{H}_4\text{N)}\}\{\text{Li(tmeda)}\}_2\}$ (3**)**

Li(1)–Li(2)	2.91(3)	Li(1)–N(1)	2.09(1)
Li(2)–N(1)	2.26(1)	Li(2)–C(1)	2.70(1)
Li(2)–N(2)	2.21(2)	N(1)–C(2)	1.40(1)
N(1)–C(6)	1.33(1)	C(1)–C(2)	1.37(1)
C(1)–C(7)	1.47(1)	C(2)–C(3)	1.43(1)
C(3)–C(4)	1.35(1)	C(4)–C(5)	1.41(1)
C(5)–C(6)	1.37(1)	C(7)–C(8)	1.39(1)
C(7)–C(12)	1.39(1)	C(8)–C(9)	1.37(1)
C(9)–C(10)	1.35(2)	C(10)–C(11)	1.37(1)
C(11)–C(12)	1.35(1)		
N(1)–Li(2)–C(1)	55.7(3)	N(1)–Li(2)–N(2)	96.7(2)
C(1)–Li(2)–N(2)	106.4(3)	N(1)–Li(2)–N(1a)	90.8(7)
C(1)–Li(2)–N(1a)	95.2(5)	N(2)–Li(2)–N(1a)	157.6(3)
C(1)–Li(2)–C(1a)	140.7(8)	N(2)–Li(2)–C(1a)	102.5(3)
N(2)–Li(2)–N(2a)	84.3(7)	Li(1)–N(1)–Li(2)	84.2(6)
C(2)–C(1)–C(7)	128.5(7)		

Table 4. Comparative Selected Structural Data for Compounds Having $[2\text{-R}'\text{R}''\text{CHC}_5\text{H}_4\text{N}]^-$ ($\text{R}' = \text{H, Ph, SiMe}_3$; $\text{R}'' = \text{SiBu}'\text{Me}_2, \text{H}$) Ligands

compd	R'	R''	Li–C(1) (Å)	Li–N (Å)	C(1)–C(2)
1	Ph	SiMe ₃	3.288(8)	1.977(9)	1.382(6)
2	H	SiMe ₂ Bu'	3.418(av)	2.181(4)	1.385(7)
3	H	Ph	2.70(1)	2.09(1)	1.37(1)
8a	Ph	Ph	3.26(4)	1.972	1.405(4)
4	SiMe ₃	SiMe ₃	2.43(2)	1.96(2)	
5	H	SiMe ₃	2.36(1)	2.19	

distances within the pyridine rings also suggest that they have substantial double-bond character and non-aromaticity in the pyridine ring due to charge redistribution. The crystal structures of **5–7** have been shown to have the azaallyl type of bonding, the lithium atom being bonded to both the α -carbon and the nitrogen, and hence are indicative of delocalization of charge along the CCN linkage. In compound **4**, the contact ion pair type of structure shows that the Li atom is bonded closely to the C _{α} atom.

X-ray structure determination shows that compound **1** is monomeric. There are two independent molecules in the asymmetric unit, which have the same configuration. The anion $[2\text{-Me}_3\text{Si(Ph)CC}_5\text{H}_4\text{N}]^-$ acts as an N-centered amide ligand bonded to the lithium *via* nitrogen at a distance of 1.977(9) Å, similar to that of 1.972(5) Å in **8a**. The Li–C(1) distance of 3.288(8) Å is long and hence nonbonding. The negative charge of the anion is localized at nitrogen rather than the deprotonated carbon. The C(1)–C(2) distance of 1.382(6) Å and the geometry at C(1) (sum of valence angles 359.8°) suggests the presence of an exocyclic double bond. The alternating C–C bond distances are consistent with nonaromaticity within the pyridine ring. The shortest Li–C distance in **1** (Li–C7 = 2.661(8) Å, Figure 1, Table 1) is too long to be considered a bonding interaction. The dihedral angles between the pyridyl and phenyl groups in each independent molecule of **1** are 79.1 and 90.2°.

Compound **2** is dimeric, with a crystallographic C₂ axis passing through the two lithium atoms and the centers of each ethylene group of the tmeda ligands. The lithium atoms are bridged by the pyridyl nitrogen atoms to form a (LiN)₂ four-membered ring. Each lithium atom in a distorted-tetrahedral environment is being surrounded by the nitrogen atoms from two substituted pyridyl ligands and the chelating tmeda. The Li···Li distance of 2.88(1) Å is longer than that in the dimeric species **4** (2.560(9) Å), which bears a smaller SiMe₃

group. The average Li–N_{py} distance of 2.162 Å is significantly longer than the similar distance in **1**, presumably due to repulsion between the lithium atoms, and is a consequence of the intermolecular amide bridge formation. The Si atom is almost in the plane of the pyridyl ring, a feature similar to that in $[\{2\text{-(Me}_3\text{Si)HC(C}_5\text{H}_4\text{N)Li(tmeda)}\}_2]$.⁵ The Si(1)–C(1)–C(2) angle of 129.7°, the C(1)–C(2) distance of 1.385(7) Å, and the C–C bond distance within the pyridyl ring suggest that the anion ligand behaves as an N-centered amide type ligand.

Compound **3** is also a dimer of C₂ symmetry similar to that in **2**, and the anionic ligand $[2\text{-Me}_3\text{Si(Ph)CC}_5\text{H}_4\text{N}]^-$ acts as a bridging amide for the lithium atoms, which are in different environments. Li(1) is coordinated by the tmeda ligand and the bridging pyridyl nitrogen atom in a distorted-tetrahedral geometry. The Li to *ipso* carbon distance of 2.70 Å is again too long to be considered a bonding interaction. The butterfly conformation is probably caused by the twist of the tmeda molecules relative to the anionic ligands. The Li···Li distance of 2.91(3) Å is the longest between the dimeric compound **2** and $[\{2\text{-(Me}_3\text{Si)HC(C}_5\text{H}_4\text{N)Li(tmeda)}\}_2]$. This is presumably due to the weak interaction of Li(2) with C(1), which pulls it further from the opposite Li atom of the (LiN)₂ four-membered ring. The two amide bridges are unsymmetrical, as shown by the different Li–N distances of 2.09 and 2.26 Å, respectively.

By comparison of the available structural results of the lithium complexes with the ligand $[2\text{-R}'\text{R}''\text{CHC}_5\text{H}_4\text{N}]^-$ in this work and those in the literature, it appears that the nature of lithium–ligand interactions, the electron density distribution within the ligand, and also the degree of aggregation of the complex depend on (i) the steric and electronic nature of the group at the *ipso* carbon, (ii) the degree of substitution at the *ipso* carbon, and (iii) the nature and the presence of an ancillary base ligand such as tmeda or Et₂O. The structural studies have clearly shown that the 2-picoline derivatives are capable of ligation in different ways due to delocalization of charge. Surprisingly, the N-centered amide type of coordination mode seems to be more predominant, although the metal complexes derived from these organolithium complexes are mainly metal alkyl complexes.

Experimental Section

All manipulations were carried out under an inert atmosphere of argon gas by standard Schlenk techniques or in a dinitrogen glovebox. Solvents were dried over and distilled from CaH₂ (hexane) and/or Na (Et₂O). 2-Picoline, 2-benzylpyridine, Bu^tMe₂SiCl, and Me₃SiCl were purchased from Aldrich and used without further purification. The ¹H and ¹³C NMR spectra were recorded at 250 and 62.90 MHz, respectively, using a Bruker WM-250 or ARX-500 instrument. All spectra were recorded in benzene-*d*₆, and the chemical shifts δ are relative to SiMe₄.

Preparation of 2-(Bu^tMe₂Si)CH₂C₅H₄N (10**), the Conjugate Acid of the Anion of **2**.** To a solution mixture of 2-picoline (5.70 g, 61.2 mmol) and tmeda (7.15 g, 61.5 mmol) in ether (70 mL) at 0 °C was slowly added a solution of Bu^tLi in hexane (39.0 mL, 1.6 M, 61.4 mmol). The solution changed from colorless to red. The red solution was added to a solution of Bu^tMe₂SiCl (8.90 g, 5.91 mmol) in ether (40 mL) at 0 °C. The resulting yellow slurry was stirred for 5 h at 25 °C; water

(20 mL) was added. The organic layer was separated, and the aqueous layer was extracted with 2 × 60 mL of ether. The ethereal extracts were combined with the organic layer and dried over anhydrous MgSO₄. The filtrate was concentrated, and the product distillate of bp 59–61 °C/10⁻² mmHg collected was collected, corresponding to **2H** (9.86 g, 80.5%). Anal. Found: C, 69.24; H, 10.21; N, 6.77. Calcd for C₁₂H₂₁NSi: C, 69.50; H, 10.21; N, 6.75. ¹H NMR (250 MHz, C₆D₆): δ -0.02 (s, 6H, SiMe₂), 0.88 (s, 9H, SiBu^t), 2.33 (s, 2H, SiCH₂), 6.57 (m, 1H, C₅H₄N), 6.65 (m, 1H, C₅H₄N), 7.04 (m, 1H, C₅H₄N), 8.42 (m, 1H, C₅H₄N). ¹³C NMR (62.90 MHz, C₆D₆): δ -5.93 (SiMe₂), 16.92 (SiCH₂), 26.60 (CMe, SiBu^t), 26.24 (C, SiBu^t), 119.08 (CH, C₅H₄N), 122.28 (CH, C₅H₄N), 135.34 (CH, C₅H₄N), 149 (C, C₅H₄N). Mass spectrum (*m/z*): 207 (P⁺).

Preparation of 2-(Me₃Si)CHPhC₅H₄N, the Conjugate Acid of the Anion of 1. To a solution of 2-benzylpyridine (5.00 g, 29.5 mmol) and tmeda (4.60 mL, 30.5 mmol) in ether (30 mL) at 0 °C was slowly added a solution of BuⁿLi in hexane (18.70 mL, 30.0 mmol). The resulting deep red solution was warmed to room temperature and was stirred for 4 h. The red solution was then added to a solution of Me₃SiCl (3.40 g, 31.3 mmol) in ether (20 mL) and was stirred at room temperature for a further 4 h. To the white suspension was added water (20 mL), and the organic layer was separated. The aqueous layer was extracted with ether (2 × 30 mL). The ethereal extracts were combined with the organic layer and dried over anhydrous MgSO₄. The filtrate was concentrated to a yellow viscous oil. After addition of MeOH (5 mL) and storage at -20 °C, a white crystalline solid was isolated, washed with cold MeOH, and dried under vacuum to give **1H** (4.40 g, 61.7%). Anal. Found: C, 74.27; H, 7.93; N, 5.63. Calcd for C₁₅H₁₉NSi: C, 74.63; H, 7.93; N, 5.80. ¹H NMR (250 MHz, C₆D₆): δ 0.13 (s, 9H, SiMe₃), 3.56 (s, 1H, CH), 6.55 (m, 1H), 6.76 (d, 1H, *J* = 7.4 Hz), 6.97 (t, 1H, *J* = 7.7 Hz), 7.03 (d, 1H, *J* = 9.53 Hz), 7.17 (m, 2H), 7.46 (d, 2H, *J* = 7.65 Hz), 8.46 (d, 1H, *J* = 3.75 Hz). ¹³C NMR (62.90 MHz, C₆D₆): δ -1.72 (SiMe₃), 48.71 (C-), 120.03, 123.67, 125.28, 128.75, 135.78, 142.25, 148.92, 163.82 (aromatic/C₅H₄N). Mass spectrum (*m/z*): 241 (P⁺).

Preparation of [{2-(Me₃Si)CPhC₅H₄N}{Li(tmeda)}] (1). To a solution of **1H** (3.72 g, 15.4 mmol) and tmeda (2.40 mL, 15.9 mmol) at 0 °C was added a solution of BuⁿLi in hexane (10.0 mL, 1.6 M, 16.0 mmol). The orange solution was set aside at -20 °C for 1 day, whereafter orange crystals of the title compound **1** (5.51 g, 98.3%) were collected and dried *in vacuo*. ¹H NMR (500 MHz, C₆D₆): δ 0.38 (s, 9H, SiMe₃), 1.23 (s, 4H, NCH₂), 1.41 (s, 12H, NMe₂), 5.69 (t, 1H, *J* = 5.5 Hz), 6.53 (t, 1H, *J* = 7.0 Hz), 6.68 (d, 1H, *J* = 9.0 Hz), 6.74 (t, 1H, *J* = 8.0 Hz), 6.88 (t, 2H, *J* = 7.5 Hz), 7.15 (s, 1H), 7.35 (d, 2H, *J* = 8.0 Hz). ¹³C NMR (62.90 MHz, C₆D₆): δ 2.45 (SiMe₃), 45.30 (C-)(NCH₂), 56.31 (NCH₂), 80.34 (NMe₂), 102.49, 117.55, 120.75, 125.25, 128.75, 129.14, 131.31, 133.02, 147.14, 150.22, 163.81 (aromatic/C₅H₄N).

Preparation of [{2-(Bu^tMe₂Si)CHC₅H₄N}{Li(tmeda)}] (2). To a solution of **2H** (2.29 g, 11.04 mmol) and tmeda (1.67 mL, 11.06 mmol) at 0 °C was added a solution of BuⁿLi in hexane (6.95 mL, 1.6 M, 11.12 mmol). The orange solution was set aside at -20 °C for 1 day; the orange crystals deposited were collected and dried *in vacuo* to give the title compound **2** (3.53 g, 97%). ¹H NMR (500 MHz, C₆D₆): δ 0.35 (s, 6H, SiMe₂), 1.22 (s, 9H, SiBu^t), 1.88 (s, 4H, NCH₂), 2.12 (s, 12H, NMe₂), 2.75 (s, 1H, SiCH), 5.51 (t, 1H, *J* = 5.8 Hz), 6.47 (d, 1H, *J* = 9.0 Hz), 6.55 (t, 1H, *J* = 7.5 Hz), 7.21 (d, 1H, *J* = 5.0 Hz) (C₅H₄N). ¹³C NMR (62.90 MHz, C₆D₆): δ -3.02, 19.89, 45.71, 57.21, 100.17, 118.24, 132.63, 147.92, 168.24.

Preparation of [{2-PhCH(C₅H₄N)}{Li(tmeda)}] (3). To a solution of 2-benzylpyridine (4.36 g, 25.8 mmol) and tmeda (4.5 mL, 30.1 mmol) at 0 °C was added a solution of BuⁿLi in hexane (16.5 mL, 1.6 M, 26.4 mmol). The deep red solution was set aside at 20 °C for 1 day; the resulting dark red crystals were collected and dried *in vacuo* to give the title compound **3**

Table 5. X-ray Crystallographic Data for 1–3

	1	2	3
space group	P2 ₁ /c (No.14)	C2 (No.5)	C2/c (No.15)
<i>a</i> (Å)	19.345(4)	14.009(3)	14.191(3)
<i>b</i> (Å)	11.918(2)	14.957(3)	19.153(4)
<i>c</i> (Å)	21.210(4)	11.113(2)	16.514(3)
β (deg)	103.04(3)	108.97(3)	100.00(3)
<i>V</i> (Å ³)	4764(2)	2202(1)	4420(2)
<i>Z</i>	8	2	4
density (g cm ⁻³)	1.014	0.994	0.963
μ (mm ⁻¹)	0.11	0.11	0.06
<i>F</i> (000)	1584	728	1396
2θ _{max} (deg)	44	48	48
no. of unique data measd	5726	2614	3437
no. of obsd data	3117	1672	1162
<i>R</i> _F	0.062	0.055	0.08
<i>R</i> _{wF}	0.061	0.054	0.079

(6.77 g, 98%). Crystals used for X-ray determination were obtained by recrystallization from ether.

Preparation of 2-(Bu^tMe₂Si)C(Me)HC₅H₄N (11) from 2. To a solution of **2** (1.35 g, 4.01 mmol) was added slowly a solution of MeI (0.58 g, 4.09 mmol) in ether at 0 °C. The whole reaction mixture was warmed to room temperature and stirred for 4 h. To the resulting yellow mixture was added 10 mL of water, and the organic layer was separated and dried with anhydrous MgSO₄. It was then filtered, and the solvent was removed under vacuum to give a pale yellow oily residue (99% yield). Anal. Found: C, 69.79; H, 10.46; N, 6.20. Calcd for C₁₃H₂₃NSi: C, 69.33; H, 10.47; N, 6.33. ¹H NMR (250 MHz, C₆D₆): δ -0.10 (s, 3H, SiMe), 0.08 (s, 3H, SiMe), 0.86 (s, 9, SiBu^t), 1.48 (d, 3H, *J* = 7.25 Hz, CMe), 2.52 (q, 1H, *J* = 7.38 Hz, CH), 6.56 (t, 1H, *J* = 5.86 Hz), 6.70 (d, 1H, *J* = 7.93 Hz), 7.04 (t, 1H, *J* = 7.65 Hz), 8.44 (d, 1H, *J* = 4.72 Hz) (C₅H₄N). ¹³C NMR (62.90 MHz, C₆D₆): δ -6.75, 7.05, 16.15, 17.69, 27.10, 30.45, 119.49, 121.70, 135.34, 149.25. Mass spectrum (*m/z*): 221 (P - 1)⁺.

X-ray Crystallography. The crystallographic data for 1–3 are shown in Table 5. Crystals of **1** and **2** were grown from hexane and those of **3** from ether. X-ray data were collected using single crystals sealed in capillaries under dinitrogen, and raw intensities were collected on a Siemens P4/PC four-circle diffractometer at 294 K. The structures were solved by direct phase determination, and all non-hydrogen atoms were subjected to anisotropic refinement. The hydrogen atoms were generated geometrically (C–H bonds fixed at 0.96 Å) and allowed to ride on their respective parent C atoms; they were assigned appropriate isotropic temperature factors and included in the structure factor calculations. In **3** there is free tmeda in the lattice cavities formed by the loose packing of the complex molecules, and its site occupancy factor was assigned to be 1/2 on account of its low electron density. Computations were performed using the SHELXTL PC program package¹² on a PC 486 computer. Analytic expressions of atomic scattering factors were employed, and anomalous dispersion corrections were incorporated.¹³

Acknowledgment. This work was supported by Hong Kong Research Grants Council Earmarked Grant CUHK 22/91.

Supporting Information Available: Tables of crystal data, bond distances and angles, atomic coordinates and equivalent isotropic temperature factors, anisotropic thermal parameters, and hydrogen atom coordinates and assigned isotropic temperature factors for 1–3 (20 pages). Ordering information is given on any current masthead page.

OM950373M

(12) Sheldrick, G. M. In *Crystallographic Computing 3*; Sheldrick, G. M., Krieger, C., Goddard, R., Eds.; Oxford University Press: New York, 1985; p 175.

(13) *International Tables for X-Ray Crystallography*; Kynoch Press: Birmingham, U.K., 1974.

Synthesis and Oxidation of Platinum(II) Ferrocenylacetylide Complexes, *trans*-[Pt(C≡Cfc)(Ar)(Ph₃P)₂]

Masaru Sato* and Emiko Mogi

Chemical Analysis Center, Saitama University, Urawa, Saitama 338, Japan

Motomi Katada

Tokyo Metropolitan University, Faculty of Science, Hachioji, Tokyo 260-11, Japan

Received April 3, 1995*

A number of *trans*-Pt(II) ferrocenylacetylide complexes were synthesized from the reaction of ferrocenylacetylene and *trans*-Ar(Ph₃P)₂PtI. The cyclic voltammograms showed on reversible wave near -0.15 V and one irreversible wave at +0.72-0.95 V. The latter anodic potentials correlate linearly with the Hammett σ_p^+ constant. The one-electron-oxidized species were isolated from the reaction of the *trans*-Pt(II) ferrocenylacetylide complexes with DDQ or FcHPF₆ as stable solids. The interaction parameter α^2 , calculated from the absorption maximum (ν_{\max}) of the intervalence transfer (IT) band observed at 1055-1075 nm, indicates the presence of a small degree of interaction between the two metals in the heteronuclear mixed-valence complexes. Also, the values of ν_{\max} correlate linearly with the Hammett σ_p^+ constants of the substituents on the aryl ligand. The structure of *trans*-[Pt(C≡Cfc)(C₆H₄CO₂Et-*p*)(Ph₃P)₂] was confirmed by a single-crystal X-ray determination.

Introduction

The chemistry of heterobinuclear complexes having an unsaturated hydrocarbon bridge has been actively investigated from a variety of viewpoints, e.g. structure, catalytic activity, development of functional material, etc.¹ In materials science chemistry, the importance of ferrocene-containing transition-metal complexes has also increased.^{2,3} Recent reports indicate the possibility of nonlinear optics in Ru(II)-, Os(II)-,⁴ and Mn(I)-ferrocenylacetylide complexes⁵ and the important role of the mixed-valence state in Ru(II)-ferrocenylacetylide complexes.⁶ In the latter, heterobinuclear organometallic compounds showing mixed-valence-like properties were synthesized in order to obtain more insight into the electronic structure of mixed-valence compounds and the factors affecting electron transfer between interacting sites, as well as the extent of delocalization of the valence electrons. Thus far, the oxidation reactions of several ferrocene derivatives involving a transition metal as another component have been investigated by electronic spectroscopy⁷⁻⁹ and cyclic voltammetry.⁷⁻¹³

We here report the systematic synthesis and oxidation of *trans*-Pt(II) ferrocenylacetylide complexes. There are several other reports of Pt(II) ferrocenylacetylides.¹⁴⁻¹⁶

Results and Discussion

The reaction of ferrocenylacetylene with *trans*-[PtI-(*p*-RC₆H₄)(Ph₃P)₂], which was prepared from oxidative addition of *p*-RC₆H₄I to Pt(Ph₃P)₄, in Et₂NH/CH₂Cl₂ in the presence of a catalytic amount of CuI gave *trans*-[Pt(C≡Cfc)(*p*-RC₆H₄)(Ph₃P)₂] (Fc = ferrocenyl; 1-6) in good yield. The structures of the products were assigned by the IR and ¹H, ¹³C, and ³¹P NMR spectra, which are summarized in Table 1. For example, the stretching vibration for the C≡C bond of 2 is observed at 2120 and 2104 cm⁻¹. Such splitting of the stretching vibration for the C≡C bond is rarely observed and may likely originate from a Fermi-resonance effect.¹⁷ The ¹³C NMR spectrum of 2 gave carbon signals for the acetylide group at δ 109.20 (t, ²J_{CP} = 16.0 Hz) and 111.70 (s). In the ¹H NMR spectrum of 2, the methyl and phenylene protons of the tolyl ligand resonate at δ 1.95 (s, 3H) and at δ 6.10 (d, 2H), and 6.45 (d, 2H), respectively, and the ferrocenyl ring protons at δ 3.33

* Abstract published in *Advance ACS Abstracts*, September 15, 1995.

(1) Beck, W.; Niemer, B.; Wieser, M. *Angew. Chem., Int. Ed. Engl.* **1993**, *32*, 923.

(2) Miller, J. S.; Epstein, A. J.; Reiff, W. M. *Chem. Rev.* **1988**, *88*, 201.

(3) Nalwa, H. S. *Appl. Organomet. Chem.* **1991**, *5*, 349.

(4) Colbert, M. C. B.; Ingham, S. L.; Lewis, J.; Long, N. J.; Raithby, P. R. *J. Chem. Soc., Dalton Trans.* **1994**, 2215.

(5) Colbert, M. C. B.; Edwards, A. J.; Lewis, J.; Long, N. J.; Page, N. A.; Parker, D. G.; Raithby, P. R. *J. Chem. Soc., Dalton Trans.* **1994**, 2589.

(6) Sato, M.; Shintate, H.; Kawata, Y.; Sekino, M.; Katada, M.; Kawate, S. *Organometallics* **1994**, *13*, 1956.

(7) (a) Dowling, N.; Henry, P. M.; Lewis, N. A.; Taube, H. *Inorg. Chem.* **1981**, *20*, 2345. (b) Dowling, N.; Henry, P. M. *Inorg. Chem.* **1982**, *21*, 4088.

(8) Colbran, S. B.; Robinson, B. H.; Simpson, J. *Organometallics* **1983**, *2*, 943, 952.

(9) Kotz, J. C.; Neyhart, G.; Vining, W. J.; Rausch, M. D. *Organometallics* **1983**, *2*, 79.

(10) Diaz, A. F.; Mueller-Westerhoff, U. T.; Nazzari, A.; Tanner, M. *J. Organomet. Chem.* **1982**, *236*, C45.

(11) Kotz, J.; Neyhart, G.; Vining, W. J.; Rausch, M. D. *Organometallics* **1983**, *2*, 79.

(12) Clemente, D. A.; Pilloni, G.; Corain, B.; Longato, B.; Tiripicchio-Camellini, M. *Inorg. Chim. Acta* **1986**, *115*, L9.

(13) (a) Schwarzhaus, K. E.; Shottenberger, H. *Z. Naturforsch.* **1983**, *38B*, 1493. (b) Obendorf, D.; Schottenberger, H.; Rieker, C. *Organometallics* **1991**, *10*, 1293.

(14) Chisholm, M. H.; Potkul, R. K. *Synth. React. Inorg. Met.-Org. Chem.* **1978**, *8*, 65.

(15) Weigand, W.; Robl, C. *Chem. Ber.* **1993**, *126*, 1807.

(16) Russo, M. V.; Furlani, A.; Licocchia, S.; Paolesse, R.; Villa, A. C.; Guastini, C. *J. Organomet. Chem.* **1994**, *469*, 245.

(17) Bellamy, L. J. *The Infrared Spectra of Complex Molecules*, 3rd ed.; Chapman and Hall: London, 1975; p 64.

Scheme 1

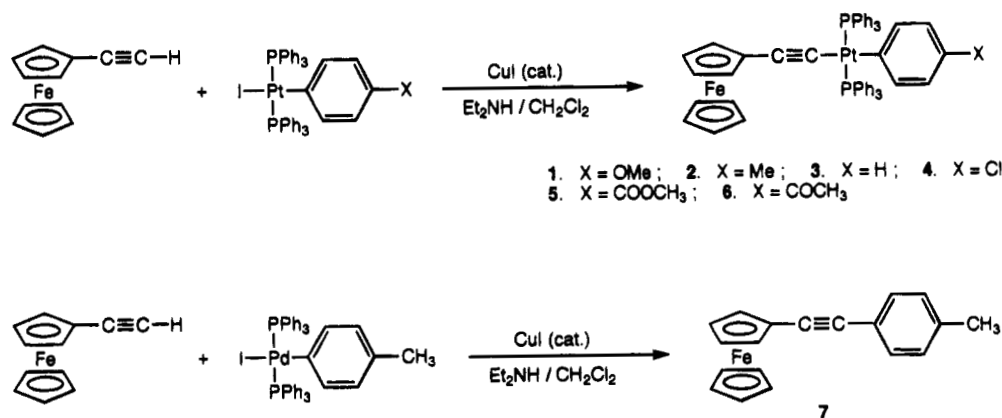


Table 1. NMR and IR Data for Complexes 1–6

com- plex	¹ H NMR (δ)	¹³ C NMR (ppm)	³¹ P NMR (ppm)	IR (cm ⁻¹)
1	3.53 (s, 3H, OCH ₃), 3.33 (t, <i>J</i> = 1.8 Hz, 2H, Cp β), 3.52 (bs, 2H, Cp α, Cp unsub), 5.96 (d, <i>J</i> = 8.5 Hz, 2H, C ₆ H ₄), 6.46 (d, <i>J</i> = 8.5 Hz, 2H, C ₆ H ₄), 7.22–7.62 (m, 30H, PPh ₃)	55.58 (s, OCH ₃), 66.25 (s, Cp β), 69.19 (s, Cp unsub), 69.97 (s, Cp α), 73.38 (s, Cp ipso), 108.50 (t, <i>J</i> = 15.6 Hz, C≡C), 111.20 (s, C≡C), 113.62 (s, C ₆ H ₄), 127.46 (t, <i>J</i> = 5.2 Hz, PPh ₃), 129.61 (s, PPh ₃), 131.73 (t, <i>J</i> = 28.2 Hz, PPh ₃), 134.90 (t, <i>J</i> = 6.1 Hz, PPh ₃), 139.05 (s, C ₆ H ₄), 146.96 (t, <i>J</i> = 10.1 Hz, C ₆ H ₄), 154.96 (s, C ₆ H ₄)	21.88 (<i>J</i> _{PtP} = 2987 Hz)	2120, 2104
2	1.95 (s, 3H, CH ₃), 3.32 (bs, 2H, Cp β), 3.71 (bs, 7H, Cp α, Cp unsub), 6.10 (d, <i>J</i> = 7.6 Hz, 2H, C ₆ H ₄), 6.45 (d, <i>J</i> = 7.6 Hz, 2H, C ₆ H ₄), 7.22–7.58 (m, 30H, PPh ₃)	20.45 (s, CH ₃), 66.23 (s, Cp β), 69.20 (s, Cp unsub), 69.98 (s, Cp α), 73.45 (s, Cp ipso), 109.14 (t, <i>J</i> = 15.9 Hz, C≡C), 111.14 (s, C≡C), 127.41 (t, <i>J</i> = 5.2 Hz, PPh ₃), 127.91 (s, C ₆ H ₄), 129.11 (s, C ₆ H ₄), 129.53 (s, PPh ₃), 131.79 (t, <i>J</i> = 28.2 Hz, PPh ₃), 134.92 (t, <i>J</i> = 6.2 Hz, PPh ₃), 139.09 (s, C ₆ H ₄), 151.73 (t, <i>J</i> = 9.9 Hz, C ₆ H ₄)	21.41 (<i>J</i> _{PtP} = 3009 Hz)	2120, 2104
3	3.32 (bs, 2H, Cp β), 3.72 (bs, 7H, Cp α, Cp unsub), 6.20–6.35 (m, 3H, C ₆ H ₅), 6.62 (d, <i>J</i> = 7.6 Hz, 2H, C ₆ H ₅), 7.21–7.61 (m, 30H, PPh ₃)	66.23 (s, Cp β), 69.19 (s, Cp unsub), 69.96 (s, Cp α), 73.30 (s, Cp ipso), 108.30 (t, <i>J</i> = 16.0 Hz, C≡C), 111.30 (s, C≡C), 120.27 (s, C ₆ H ₅), 126.86 (s, C ₆ H ₅), 127.47 (t, <i>J</i> = 5.0 Hz, PPh ₃), 129.61 (s, PPh ₃), 131.63 (t, <i>J</i> = 28.2 Hz, PPh ₃), 134.84 (t, <i>J</i> = 5.9 Hz, PPh ₃), 139.51 (s, C ₆ H ₅), 157.82 (t, <i>J</i> = 9.9 Hz, C ₆ H ₅)	21.85 (<i>J</i> _{PtP} = 2999 Hz)	2120, 2105
4	3.33 (bs, 2H, Cp β), 3.71 (bs, 7H, Cp α, Cp unsub), 6.22 (d, <i>J</i> = 8.1 Hz, 2H, C ₆ H ₄), 6.52 (d, <i>J</i> = 8.1 Hz, 2H, C ₆ H ₄), 7.25–7.56 (m, 30H, PPh ₃)	66.33 (s, Cp β), 69.19 (s, Cp unsub), 69.97 (s, Cp α), 73.03 (s, Cp ipso), 106.83 (t, <i>J</i> = 15.9 Hz, C≡C), 111.71 (s, C≡C), 126.57 (s, C ₆ H ₄), 127.57 (t, <i>J</i> = 5.0 Hz, PPh ₃), 129.82 (s, C ₆ H ₄), 130.00 (s, C ₆ H ₄), 131.35 (t, <i>J</i> = 28.7 Hz, PPh ₃), 134.83 (t, <i>J</i> = 6.5 Hz, PPh ₃), 154.96 (s, C ₆ H ₄), 146.96 (t, <i>J</i> = 10.1 Hz, C ₆ H ₄)	21.88 (<i>J</i> _{PtP} = 2987 Hz)	2121, 2104
5	1.30 (t, <i>J</i> = 7.1 Hz, 3H, CH ₃), 3.32 (t, <i>J</i> = 1.8 Hz, 2H, Cp β), 3.71 (bs, 7H, Cp α, Cp unsub), 4.23 (q, <i>J</i> = 7.1 Hz, 2H, CH ₂), 6.75 (d, <i>J</i> = 8.2 Hz, 2H, C ₆ H ₄), 6.88 (d, <i>J</i> = 8.2 Hz, 2H, C ₆ H ₄), 7.23–7.60 (m, 30H, PPh ₃)	14.43 (s, CH ₃), 59.70 (s, CH ₂), 66.33 (s, Cp β), 69.17 (s, Cp unsub), 69.96 (s, Cp α), 72.97 (s, Cp ipso), 106.36 (t, <i>J</i> = 15.2 Hz, C≡C), 112.09 (s, C≡C), 122.32 (s, C ₆ H ₄), 127.00 (C ₆ H ₄), 127.56 (t, <i>J</i> = 5.3 Hz, PPh ₃), 129.85 (s, PPh ₃), 131.22 (t, <i>J</i> = 28.5 Hz, PPh ₃), 134.76 (t, <i>J</i> = 6.1 Hz, PPh ₃), 139.11 (s, C ₆ H ₄), 168.46 (s, CO), 170.56 (t, <i>J</i> = 9.7 Hz, C ₆ H ₄)	21.53 (<i>J</i> _{PtP} = 2952 Hz)	2114, 2098
6	2.31 (s, 3H, COCH ₃), 3.33 (t, <i>J</i> = 1.8 Hz, 2H, Cp β), 3.71 (s, 5H, Cp unsub), 3.72 (t, <i>J</i> = 1.8 Hz, 2H, Cp α), 6.79 (bs, 4H, C ₆ H ₄), 7.23–7.61 (m, 30H, PPh ₃)	26.12 (s, COCH ₃), 66.40 (s, Cp β), 69.12 (s, Cp unsub), 70.00 (s, Cp α), 72.91 (s, Cp ipso), 105.93 (t, <i>J</i> = 16.1 Hz, C≡C), 112.34 (s, C≡C), 125.85 (s, C ₆ H ₄), 127.62 (t, <i>J</i> = 5.5 Hz, PPh ₃), 130.08 (s, PPh ₃), 130.20 (s, C ₆ H ₄), 131.23 (t, <i>J</i> = 28.7 Hz, PPh ₃), 134.81 (t, <i>J</i> = 6.0 Hz, PPh ₃), 139.28 (s, C ₆ H ₄), 172.75 (t, <i>J</i> = 9.6 Hz, C ₆ H ₄), 199.36 (s, CO)	21.58 (<i>J</i> _{PtP} = 2952 Hz)	2121, 2104

(t, 2H) and 3.71 (bs, 7H). Consistent with the *trans* configuration around the Pt(II) atom, a single resonance of the ³¹P nucleus with a ¹⁹⁵Pt satellite (*J*_{PtP} = 3009 Hz) is observed at 21.41 ppm. Under similar conditions, the reaction of ferrocenylacetylene with the Pd analog [PdI-(C₆H₄Me-*p*)(PPh₃)₂] gave no Pd complex, *trans*-[PdI-(C≡Cfc)(C₆H₄Me-*p*)(PPh₃)₂], but the coupling product, *p*-MeC₆H₄C≡Cfc (**7**), in good yield. The IR spectrum of **7** shows C≡C stretching vibrations at 2222 and 2207 cm⁻¹. In the ¹³C NMR spectrum of **7**, the acetylenic

carbons appear at δ 85.82 and 87.42 as singlets. The ¹H NMR spectrum of **7** exhibits only doublets at δ 7.12 and 7.38 in the phenyl proton region.

The structure of complex **5** was confirmed by a single-crystal X-ray diffraction. The crystallographic data and the positional parameters are listed in Tables 2 and 3, respectively. An ORTEP view of **5** is shown in Figure 1, along with selected numbering of the atoms. Selected bond distances and angles are summarized in Table 4. The Pt–P distances (2.296(2) and 2.305(2) Å) in **5** are

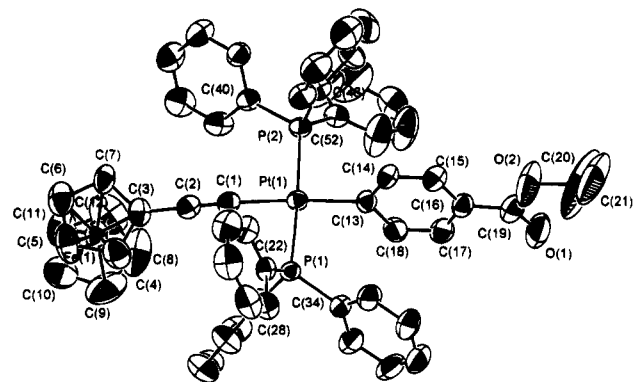


Figure 1. ORTEP drawing of 5.

Table 2. Crystal and Intensity Collection Data for 5

mol formula	C ₅₇ H ₄₈ O ₂ P ₂ FePt
mol wt	1077.90
cryst syst	monoclinic
space group	P2 ₁ /n (No. 14)
a, Å	12.338(4)
b, Å	22.865(3)
c, Å	16.991(4)
β, deg	100.64(2)
V, Å ³	4710.89
Z	4
D _{calcd} g cm ⁻³	1.52
cryst dimens, mm	0.22 × 0.20 × 0.18
linear abs coeff, cm ⁻¹	34.124
radiation (λ, Å)	Mo Kα (0.710 73)
rfln (hkl) limits	0 < h < 17, 0 < k < 24, -24 < l < 23
total no. of rflns measd	11 829
no. of unique rflns	11 550
no. of rflns used in least squares	8606
least squares	719
R	0.038
R _w	0.047
max peak in final Fourier map, e Å ⁻³	0.97
min peak in final Fourier map, e Å ⁻³	-1.69

similar to those of related Pt(II) ferrocenylacetylide complexes, e.g. 2.278(1) Å in *trans*-[PtH(C≡CFC)(PPh₃)₂]¹⁸ and 2.310(3) and 2.314(3) Å in *cis*-[Pt(C≡CFC)₂(PPh₃)₂]¹⁹. The Pt–C(1) distance (2.034(7) Å) is similar to those in *cis*-[Pt(C≡CFC)₂(PPh₃)₂] (1.991(10) and 2.010(11) Å) and is slightly shorter than that in *trans*-[PtH(C≡CFC)(PPh₃)₂] (2.137(10) Å). The longer Pt–C bond in the latter is probably due to the strong trans influence of the hydride ligand. The ferrocenylacetylene moiety is terminal, linearly bonded to the Pt(II) atom in the fashion usual for terminal alkynes, (Pt–C(1)–C(2), 172.4(6)°; C(1)–C(2)–C(3), 179.8(8)°). The bond parameters are not unexpected. The C(1)–C(2) (1.179(10) Å) and C(2)–C(3) distances (1.442(10) Å) fall in the range typical of metal acetylides. The angles around the Pt(II) atom are near 90° (P(1)–Pt–C(1), 84.2(2)°; P(2)–Pt–C(1), 92.7(2)°; P(1)–Pt–C(13), 91.5(2)°; P(2)–Pt–C(13), 91.4(2)°), and thus the Pt(II) atom adopts a slightly distorted square-planar configuration. The square plane containing the Pt(II) atom in 5 is nearly coplanar (7.60°) with the substituted cyclopentadienyl ring of the ferrocenyl part, in contrast to the case for *trans*-[PtH(C≡CFC)(PPh₃)₂]¹⁸ and *cis*-[Pt(C≡CFC)₂(PPh₃)₂]¹⁹ in which the planes are nearly perpendicular

Table 3. Functional Atomic Coordinates and U(iso) Values for 5

atom	x/a	y/b	z/c	U(iso) (Å ²)
Pt(1)	0.04820(2)	0.22186(1)	-0.25316(1)	0.037
Fe(1)	0.31407(9)	0.01018(5)	-0.33710(6)	0.054
P(1)	0.10887(13)	0.26117(7)	-0.36158(9)	0.038
P(2)	0.00135(13)	0.18138(8)	-0.13977(9)	0.039
O(1)	-0.3623(5)	0.4426(3)	-0.2974(4)	0.096
O(2)	-0.2476(7)	0.4758(3)	-0.1915(5)	0.122
C(1)	0.1623(5)	0.1588(3)	-0.2602(4)	0.043
C(2)	0.2354(6)	0.1272(3)	-0.2673(4)	0.047
C(3)	0.3245(6)	0.0884(3)	-0.2761(4)	0.050
C(4)	0.3848(8)	0.0912(4)	-0.3408(6)	0.077
C(5)	0.4672(8)	0.0450(4)	-0.3258(8)	0.085
C(6)	0.4587(7)	0.0162(5)	-0.2555(6)	0.078
C(7)	0.3691(7)	0.0408(3)	-0.2255(5)	0.060
C(8)	0.1552(10)	0.0015(6)	-0.3920(11)	0.115
C(9)	0.2272(14)	-0.0040(7)	-0.4487(7)	0.120
C(10)	0.2951(10)	-0.0533(6)	-0.4252(7)	0.102
C(11)	0.2709(9)	-0.0773(4)	-0.3562(7)	0.087
C(12)	0.1818(10)	-0.0449(6)	-0.3326(8)	0.107
C(13)	-0.0581(5)	0.2914(3)	-0.2494(4)	0.041
C(14)	-0.0369(5)	0.3355(3)	-0.1909(4)	0.045
C(15)	-0.1054(6)	0.3837(3)	-0.1894(4)	0.050
C(16)	-0.2001(5)	0.3895(3)	-0.2471(4)	0.047
C(17)	-0.2234(6)	0.3467(4)	-0.3067(4)	0.063
C(18)	-0.1534(6)	0.2996(4)	-0.3086(4)	0.056
C(19)	-0.2776(7)	0.4371(4)	-0.2495(5)	0.064
C(20)	-0.332(2)	0.523(1)	-0.190(2)	0.247
C(21)	-0.2924(19)	0.5654(9)	-0.1633(14)	0.194
C(22)	0.2479(5)	0.2913(3)	-0.3323(4)	0.042
C(23)	0.2937(6)	0.3286(3)	-0.3829(5)	0.060
C(24)	0.4003(7)	0.3516(4)	-0.3565(6)	0.075
C(25)	0.4590(7)	0.3358(4)	-0.2819(7)	0.081
C(26)	0.4141(7)	0.2995(4)	-0.2328(6)	0.076
C(27)	0.3090(6)	0.2778(3)	-0.2577(4)	0.054
C(28)	0.1106(6)	0.2060(3)	-0.4400(4)	0.045
C(29)	0.0273(7)	0.1660(3)	-0.4521(5)	0.060
C(30)	0.0180(9)	0.1262(4)	-0.5147(5)	0.080
C(31)	0.0935(10)	0.1264(5)	-0.5640(5)	0.087
C(32)	0.1778(10)	0.1656(5)	-0.5513(6)	0.094
C(33)	0.1868(7)	0.2055(4)	-0.4888(5)	0.071
C(34)	0.0326(6)	0.3215(3)	-0.4177(4)	0.050
C(35)	0.0422(7)	0.3775(4)	-0.3862(5)	0.065
C(36)	-0.0147(9)	0.4245(4)	-0.4279(6)	0.083
C(37)	-0.0846(8)	0.4142(5)	-0.5003(6)	0.084
C(38)	-0.0959(7)	0.3594(5)	-0.5307(6)	0.077
C(39)	-0.0370(6)	0.3126(4)	-0.4903(5)	0.061
C(40)	0.0651(5)	0.1131(3)	-0.1027(4)	0.043
C(41)	0.0677(7)	0.0671(3)	-0.1568(4)	0.059
C(42)	0.1068(8)	0.0129(4)	-0.1288(5)	0.074
C(43)	0.1434(7)	0.0032(4)	-0.0485(6)	0.070
C(44)	0.1407(7)	0.0477(4)	0.0046(5)	0.066
C(45)	0.1015(6)	0.1322(3)	-0.0220(4)	0.055
C(46)	0.0446(5)	0.2302(3)	-0.0550(3)	0.045
C(47)	-0.0201(7)	0.2435(4)	0.0007(5)	0.064
C(48)	0.0170(9)	0.2793(5)	0.0650(6)	0.095
C(49)	0.1199(10)	0.3049(4)	0.0727(6)	0.082
C(50)	0.1850(8)	0.2940(4)	0.0175(5)	0.075
C(51)	0.1478(6)	0.2566(3)	-0.0465(5)	0.058
C(52)	-0.1445(5)	0.1650(3)	-0.1420(4)	0.046
C(53)	-0.2248(8)	0.2024(5)	-0.1762(9)	0.114
C(54)	-0.3355(8)	0.1896(5)	-0.1806(9)	0.121
C(55)	-0.3698(7)	0.1413(5)	-0.1524(6)	0.077
C(56)	-0.2914(9)	0.1036(6)	-0.1165(9)	0.133
C(57)	-0.1793(7)	0.1153(6)	-0.1128(7)	0.117

to each other. Such a difference may be due to steric or packing effects rather than an electronic effect. The angle between the plane containing the Pt(II) atom and the plane of the aryl ligand is 18.80°.

The cyclic voltammograms of 1–6 and related compounds were measured in a solution of 0.1 M *n*-Bu₄NClO₄ in CH₂Cl₂ at a Pt electrode and a sweep rate of 0.1 V s⁻¹. The redox potentials vs FcH/FcH⁺ are summarized in Table 5. Complexes 1–6 show one reversible redox wave and one irreversible anodic wave,

(18) Russo, M. V.; Furlani, A.; Lococchia, S.; Paolesse, R.; Villa, A. C.; Guastini, C. *J. Organomet. Chem.* **1994**, *469*, 245.

(19) Weigand, W.; Robl, C. *Chem. Ber.* **1993**, *126*, 1807.

Table 4. Selected Bond Distances and Angles for 5

Bond Distances (Å)			
Pt(1)–P(1)	2.296(2)	Pt(1)–P(2)	2.305(2)
Pt(1)–C(1)	2.034(7)	Pt(1)–C(13)	2.070(7)
Fe(1)–C(3)	2.059(8)	Fe(1)–C(4)	2.054(10)
Fe(1)–C(5)	2.026(10)	Fe(1)–C(6)	2.052(10)
Fe(1)–C(7)	2.017(8)	Fe(1)–C(8)	2.019(13)
Fe(1)–C(9)	2.024(14)	Fe(1)–C(10)	2.068(13)
Fe(1)–C(11)	2.079(10)	Fe(1)–C(12)	2.074(13)
P(1)–C(22)	1.829(7)	P(1)–C(28)	1.837(7)
P(1)–C(34)	1.835(8)	P(2)–C(40)	1.808(7)
P(2)–C(46)	1.823(7)	P(2)–C(52)	1.832(7)
C(1)–C(2)	1.179(10)	C(2)–C(3)	1.442(10)

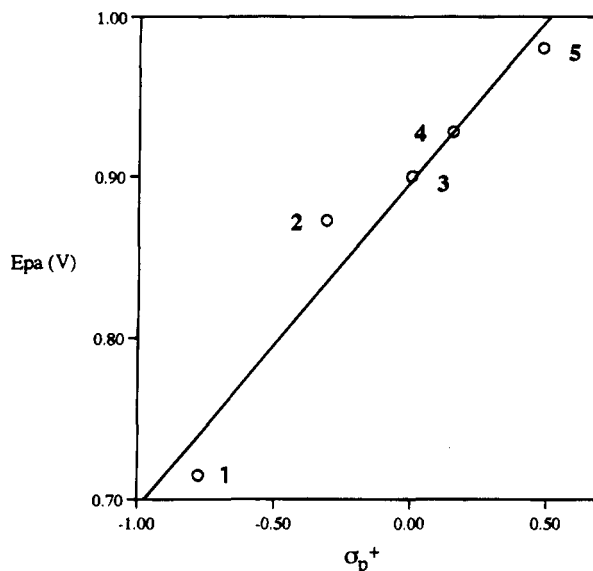
Bond Angles (deg)			
P(1)–Pt(1)–C(1)	84.2(2)	P(1)–Pt(1)–C(13)	91.5(2)
P(2)–Pt(1)–C(1)	92.7(2)	P(2)–Pt(1)–C(13)	91.4(2)
P(1)–Pt(1)–P(2)	175.6(1)	C(1)–Pt(1)–C(13)	174.7(3)
Pt(1)–C(1)–C(2)	172.4(6)	C(1)–C(2)–C(3)	179.8(8)
Pt(1)–P(1)–C(22)	110.9(3)	Pt(1)–P(1)–C(28)	111.3(3)
Pt(1)–P(1)–C(34)	120.0(3)	C(22)–P(1)–C(28)	108.6(3)
C(28)–P(1)–C(34)	102.2(3)	C(22)–P(1)–C(34)	102.9(3)
Pt(1)–P(2)–C(40)	118.5(3)	Pt(1)–P(2)–C(46)	109.4(3)
Pt(1)–P(2)–C(52)	117.5(3)	C(40)–P(2)–C(46)	102.1(3)
C(40)–P(2)–C(52)	101.1(3)	C(46)–P(2)–C(52)	106.6(3)

Table 5. Redox Potentials (vs FcH/FcH⁺) of Complexes 1–8 in 0.1 M Bu₄NClO₄ Solution in CH₂Cl₂ at 0.1 V s⁻¹

compd	<i>E</i> _{1/2} (V)	<i>E</i> _{p,a} (V)	compd	<i>E</i> _{1/2} (V)	<i>E</i> _{p,a} (V)
1	-0.16	+0.90	5	-0.14	+0.99
2	-0.13	+0.93	6	-0.14	+0.98
3	-0.13	+0.87	7	+0.12	
4	-0.16	+0.72	8		+0.61

which are assigned to the redox of the ferrocenyl and the Ar(Ph₃P)₂Pt⁻ moieties, respectively, because the reference compounds *p*-MeC₆H₄C≡Cfc (7) and *trans*-[Pt(C≡CPh)(C₆H₄Me-*p*)(Ph₃P)₂] (8) afford waves at +0.12 and +0.61 V, respectively. The first redox potential of complexes 1–6 is lower than that of the reference compound 7. This is probably because of the electron-donating ability of the Ar(Ph₃P)₂Pt⁻ part. On the other hand, the second anodic potential is higher than that of the reference complex 8. This is probably due to a result of charge effects arising from the proximity of the ferrocenium center in the molecule as well as to the stabilization of the one-electron-oxidation products of 1–6 by electron delocalization over the two metal sites. The anodic potentials of 1–5 correlate linearly with the Hammett σ_p^+ constants of the substituents of the aryl ligand on the Pt atom ($R = 0.955$; Figure 2), but the redox potentials in the ferrocenyl part remain unchanged irrespective of the substituent. This seems to indicate that the substituent on the aryl ligand conjugatively adjusts the electron density on the Pt(II) atom and increases the resistance for the two-electron oxidation according to the electron-attracting ability (σ_p^+) of the substituent, but such a substituent effect cannot be transferred through the acetylene bond to the ferrocenyl part in the neutral complexes 1–6.

Complexes 1–6 were oxidized with 2,3-dichloro-4,5-dicyanobenzoquinone (DDQ) in benzene/CH₂Cl₂ to give the one-electron-oxidized complexes 1a–6a in good yield. Similarly, oxidation of 3 with FcHPF₆ in CH₂Cl₂ afforded the PF₆⁻ salt of the one-electron-oxidized complex (3b). The structures of the complexes were determined by the IR spectra and elemental analyses. For example, complex 1a shows the C≡C stretching vibration at 2076 cm⁻¹ and absorptions of the DDQ anion at 2212 (C≡N) and 1574 cm⁻¹ (C=O). The

**Figure 2.** Plot of $E_{p,a}$ vs σ_p^+ for complexes 1–5 ($y = 0.203x + 0.898$; $r = 0.970$).

stretching vibration of the C≡C bond for 1a–6a is observed in a region slightly lower (2068–2076 cm⁻¹) than that of the corresponding neutral complexes, as shown in Table 6. This means that the unpaired electron is localized in the ferrocenyl part, as shown by the limited structure A, and the limited structure B is only a slight contributor to the structure of the one-electron-oxidized complexes 1a–6a. A similar small shift of the C≡C stretching vibration was also observed in the series Cp(CO)₂FeC≡Cfc, in which there was a small amount of electron delocalization between the metal atoms.²⁰ The Mössbauer spectrum of 2a shows one broad signal ($IS = 0.58$ mm s⁻¹) which is characteristic of the ferrocenium ions,²¹ indicating that the oxidized site in 2a is the ferrocenyl part and that there is little electron interaction between the two metals. The result is consistent with the IR spectral data described above.

Complexes 1a–6a show an absorption band in the near-infrared region, while the neutral complexes 1–6 show no absorption in that region. In the biferrrocene monocation system, a typical class II mixed-valence complex, the intervalence band appears in the near-infrared region and shows a linear correlation of λ_{max} with $1/n^2 - 1/D_s$ of the solvent used, where n and D_s are the optical and static dielectric constants of the solvent involved.²² As shown in Figure 3, the near-infrared band of 2a is also dependent on the solvent used and correlates linearly with $1/n^2 - 1/D_s$. This suggests that the near-infrared band observed in complexes 1a–6a is an intervalence transfer (IT) band. Hush proposed an expression for the interaction parameter α^2 which afforded an approximate measure of the degree of ground-state delocalization in a mixed-valence complex, where d is the distance between two metal centers:²³

$$\alpha^2 = [(4.2 \times 10^{-4})\epsilon_{max}\Delta\nu_{1/2}]/\nu_{max}d^2$$

By using the internuclear distance (6.06 Å) observed for

(20) Sato, M.; Hayashi, Y.; Shintate, H.; Katada, M.; Kawata, S. *J. Organomet. Chem.* **1994**, *471*, 179.

(21) Birchall, T.; Drummond, I. *Inorg. Chem.* **1971**, *10*, 399.

(22) Powers, M. J.; Meyer, T. J. *J. Am. Chem. Soc.* **1978**, *100*, 4393.

(23) Hush, N. S. *Prog. Inorg. Chem.* **1967**, *8*, 391.

Scheme 2

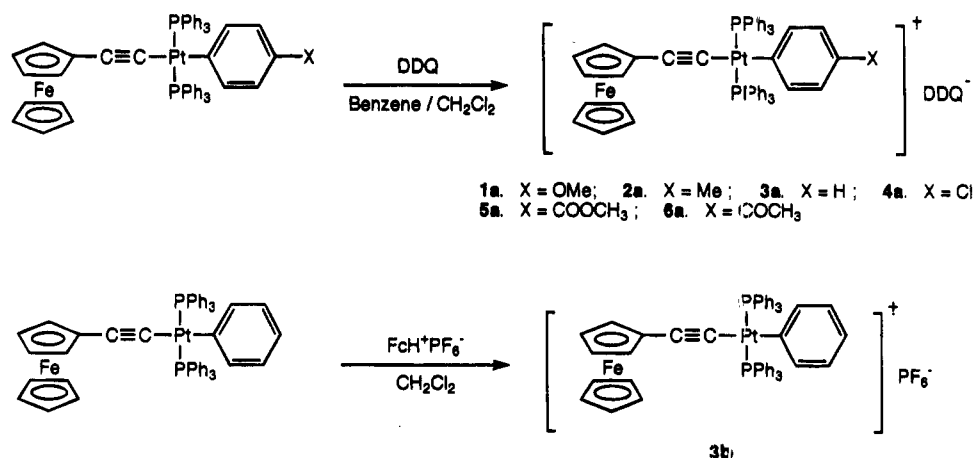
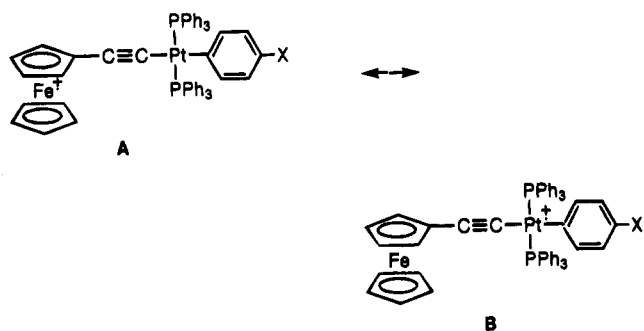


Table 6. IR and Near-IR Spectral Data for Oxidized Complexes 1a–6a and 1b

compd	IR (KBr) (ν_{CC} , cm^{-1})	solvent	λ_{max} (nm)	ν_{max} (cm^{-1})	ϵ_{max}	$10^3\alpha^2$
1a	2076	CH ₂ Cl ₂ acetone CH ₃ NO ₂ CH ₃ CN	1075	9302	1734	6.46
1b	2068	CH ₂ Cl ₂	1060	9434	928	3.85
2a	2072	CH ₂ Cl ₂	1065	9390	1728	5.99
3a	2076	CH ₂ Cl ₂	1080	9259	1893	6.49
4a	2068	CH ₂ Cl ₂	1095	9132	2054	7.36
5a						
6a	2068	CH ₂ Cl ₂	1055	9479	2016	7.19

Scheme 3



5 as the value of d , α^2 values were calculated for 1a–6a. These are summarized in Table 6, along with the values for λ_{max} , ν_{max} , and ϵ_{max} . The α^2 values calculated for 1a–6a are near those for several class II mixed-valence ions having a similar internuclear distance: $[\text{FcC}\equiv\text{CFc}]^+$ (2.4×10^{-3}),²² $[\text{FcC}\equiv\text{NRu}(\text{NH}_3)_5]^+$ (2.3×10^{-3}),⁷ and $[\text{FcC}\equiv\text{CFe}(\text{CO})_2\text{Cp}]^+$ (6.37×10^{-3}).²⁰

Solutions of complexes 1a–6a in CH₂Cl₂ are somewhat unstable, and the values of ϵ_{max} were not reproducible, so that the α^2 values showed no good correlation with the Hammett σ_p^+ constants. However, the values of ν_{max} correlate linearly with the Hammett σ_p^+ constants ($R = 0.900$; Figure 4). This means that the electron delocalization is promoted by the electron-donating ability of the substituent on the aryl ligand coordinated to the Pt(II) atom. It is noteworthy that the substituent effect is conjugatively, not inductively, transferred through the phenylene group to the Pt(II) atom. The $p\pi$ - $d\pi$ conjugation probably plays an important role in the electron transfer between the substituent and the Pt(II) atom. The trend that electron delocalization between the metal centers is enhanced

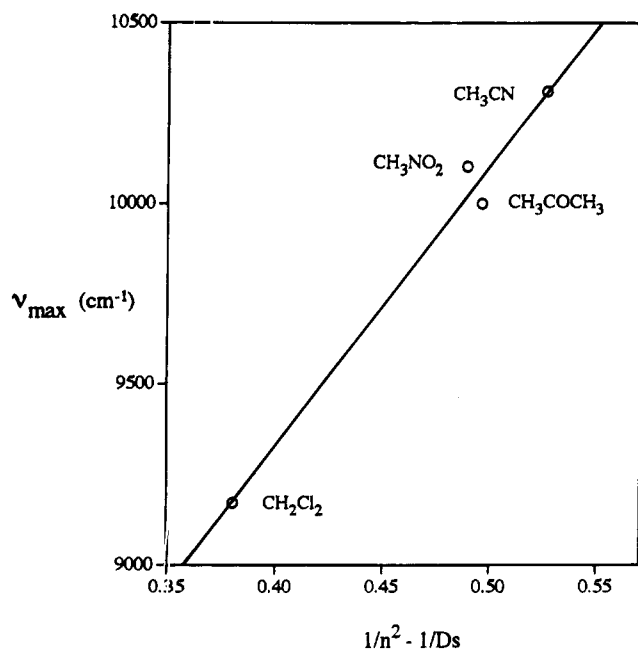


Figure 3. Plot of ν_{max} vs $1/n^2 - 1/D_s$ for 2a in various solvents ($y = 7735.762x + 6238.919$; $r = 0.992$).

by the increase of electron density in the total system is consistent with that found in the Cp(phosphine)₂-FeC≡CFc series.²⁴

In summary, novel heterobinuclear complexes, *trans*-(aryl)(PPh₃)₂PtC≡CFc, were prepared. The reaction of the complexes with DDQ gave stable one-electron-oxidized species, in which a small degree of electron delocalization is present between the two metal sites. Thus, these complexes would not be expected to be candidates for electron-conductive materials, because of poor electron delocalization in the molecules. It is noteworthy that electron delocalization in the oxidized species is enhanced by an electron-donating substituent on the aryl ligand coordinated to the Pt(II) atom.

Experimental Section

All reactions were carried out under a nitrogen atmosphere. Ferrocenylacetylene,²⁵ *trans*-(Ar)(PPh₃)₂PtI,²⁶ and FcHPF₆²⁷ were prepared by the methods given in the literature. All the

(24) Sato, M.; Hayashi, Y.; Katada, M.; Kawata, S. Submitted for publication in *Organometallics*.

(25) Rosenblum, M.; Brown, N.; Papenmeiner, J.; Applebaum, M. *J. Organomet. Chem.* **1966**, *6*, 173.

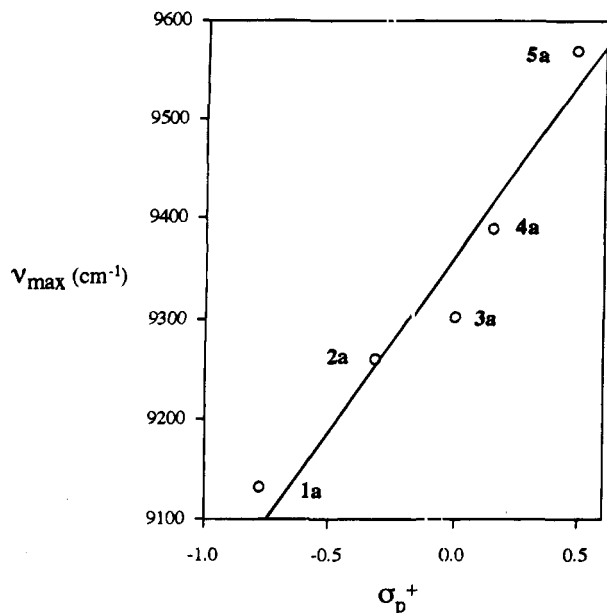


Figure 4. Plot of ν_{\max} vs σ_p^+ for complexes 1a–5a in CH_2Cl_2 ($y = 328.046x + 9360.728$; $r = 0.966$).

other chemicals are reagent grade and are commercially available. Solvents were dried by the standard procedures. IR spectra were recorded as KBr pellets on a Perkin-Elmer 1600 spectrometer. NMR spectra (in CDCl_3) were recorded on Bruker AM400 and ARX400 instruments, using TMS as an internal standard. ^{31}P and ^{195}Pt NMR signals were referred to external 85% H_3PO_4 and K_2PtCl_4 as the standard, respectively. Electrochemical measurements were by cyclic voltammetry in a solution of 0.1 M (*n*-Bu) $_4\text{NClO}_4$ in CH_2Cl_2 under nitrogen at 25 °C, using a standard three-electrode cell on a BAS CV-27 analyzer. All potentials were referenced to the ferrocene-ferrocenium couple, which had a potential of +0.19 V vs Ag/AgNO_3 in this medium. The scan rate was 100 mV s^{-1} . Mössbauer spectra were measured with a constant-acceleration-type spectrometer, and the velocity scale was calibrated on the spectrum of metallic iron at room temperature. Spectra were fitted with Lorentzian-line shapes by least squares. The isomer shift was reported with respect to α -Fe foil at room temperature. The error of the values of isomer shift and quadrupole splitting was estimated to be within $\pm 0.02 \text{ mm s}^{-1}$.

***trans*-[Pt(C≡CFC)(C₆H₄OCH₃-*p*)(PPh₃)₂] (1).** **General Procedure.** The Pt(II) ferrocenylacetylides complexes were prepared according to Sonogashira's method.²⁸ *trans*-[Pt(C₆H₄OCH₃-*p*)(PPh₃)₂] (381 mg, 0.4 mmol) was treated with ferrocenylacetylene (84 mg, 0.4 mmol) in CH_2Cl_2 (20 mL) and diethylamine (20 mL) in the presence of a catalytic amount of CuI at room temperature for 20 min. After evaporation of the solvent, the crude product obtained was chromatographed on an alumina column by using CH_2Cl_2 /hexane as the eluent. Recrystallization of the separated product from CH_2Cl_2 /hexane gave orange crystals (395 mg, 96%): mp 154 °C dec. Anal. Calcd for $\text{C}_{55}\text{H}_{46}\text{OP}_2\text{FePt} \cdot \frac{1}{2}\text{CH}_2\text{Cl}_2$: C, 61.81; H, 4.39. Found: C, 61.93; H, 4.41.

***trans*-[Pt(C≡CFC)(C₆H₄CH₃-*p*)(PPh₃)₂] (2):** orange crystals (67.6%); mp 174 °C dec. Anal. Calcd for $\text{C}_{53}\text{H}_{46}\text{P}_2\text{FePt}$: C, 64.78; H, 4.55. Found: C, 64.49; H, 4.56.

***trans*-[Pt(C≡CFC)(C₆H₅)(PPh₃)₂] (3):** orange crystals (72.6%); mp 179 °C dec. Anal. Calcd for $\text{C}_{54}\text{H}_{44}\text{P}_2\text{FePt}$: C, 64.48; H, 4.40. Found: C, 64.24; H, 4.44.

***trans*-[Pt(C≡CFC)(C₆H₄Cl-*p*)(PPh₃)₂] (4):** orange crystals (72.6%); mp 206 °C dec. Anal. Calcd for $\text{C}_{54}\text{H}_{43}\text{P}_2\text{ClFePt}$: C, 62.34; H, 4.16. Found: C, 62.09; H, 4.27.

***trans*-[Pt(C≡CFC)(C₆H₄CO₂Et-*p*)(PPh₃)₂] (5):** orange crystals (82.9%); mp 179 °C dec. IR (KBr): 1698 cm^{-1} (C=O). Anal. Calcd for $\text{C}_{57}\text{H}_{48}\text{O}_2\text{P}_2\text{FePt}$: C, 63.52; H, 4.49. Found: C, 63.29; H, 4.54.

***trans*-[Pt(C≡CFC)(C₆H₄COCH₃)(PPh₃)₂] (6):** orange crystals (59.0%); mp 177 °C dec; IR (KBr) 1668 cm^{-1} (CO). Anal. Calcd for $\text{C}_{56}\text{H}_{46}\text{OP}_2\text{FePt}$: C, 64.19; H, 4.43. Found: C, 64.00; H, 4.37.

Ferrocenyltolylacetylene (7). To a solution of ferrocenylacetylene (105 mg, 0.5 mmol), *trans*-[PdI(C₆H₄Me-*p*)(PPh₃)₂] (430 mg, 1.5 mmol) in CH_2Cl_2 (20 mL), and Et₂NH (20 mL) was added copper(I) iodide (0.1 equiv). The mixture was stirred for 20 min at room temperature. After evaporation, the residue was chromatographed on alumina by elution of CH_2Cl_2 /hexane to give **7** (122 mg, 81%) as red-orange crystals: mp 109–110 °C; IR (KBr) 2222 and 2207 cm^{-1} ; ^1H NMR (CDCl_3) δ 2.35 (s, 3H, Me), 4.24 (bs, 7H, Cp β + Cp unsub), 4.49 (t, $J = 1.9$ Hz, 2H, Cp α), 7.12 (d, $J = 8.2$ Hz, 2H, C₆H₄), and 7.38 (d, $J = 8.2$ Hz, 2H, C₆H₄); ^{13}C NMR (CDCl_3) δ 21.44 (Me), 65.60 (Cp ipso), 68.67 (Cp β), 69.92 (Cp unsub), 71.33 (Cp α), 85.82 (Fc C), 87.42 (Ar C), 120.89 (C₆H₄), 129.02 (C₆H₄), 131.29 (C₆H₄), and 137.68 (C₆H₄). Anal. Calcd for $\text{C}_{19}\text{H}_{16}\text{Fe}$: C, 76.02; H, 5.37. Found: C, 76.05; H, 5.37.

***trans*-[Pt(C≡CFC)(C₆H₄OCH₃-*p*)(PPh₃)₂][DDQ] (1a).** **General Procedure.** To a solution of complex **1** (31 mg, 0.03 mmol) in CH_2Cl_2 (0.5 mL) and benzene (3.5 mL) was slowly added a solution of DDQ (8 mg, 0.035 mmol), with use of an ice–water bath under nitrogen. After the mixture was stirred for 15 min, the resulting green crystals (37 mg, 98%) were filtered: mp 139 °C dec; IR (KBr) 2212 (C≡N), 2080 (C≡C), and 1574 cm^{-1} (C=O); vis–near-IR (CH_2Cl_2) 1096 (ϵ 2050), 584 (5370), 462 (9690), and 349 nm (10 500). Anal. Calcd for $\text{C}_{63}\text{H}_{46}\text{N}_2\text{O}_3\text{P}_2\text{Cl}_2\text{FePt}$: C, 59.90; H, 3.67; N, 2.22. Found: C, 59.90; H, 3.67; N, 2.15.

***trans*-[Pt(C≡CFC)(C₆H₄CH₃-*p*)(PPh₃)₂][DDQ] (2a):** green crystals (55%); mp 146 °C dec; IR (KBr) 2212 (C≡N), 2083 (C≡C), and 1574 cm^{-1} (C=O); vis–near-IR (CH_2Cl_2) 1080 (ϵ 1890), 585 (5490), 462 (10 100), and 349 nm (10 200). Anal. Calcd for $\text{C}_{63}\text{H}_{46}\text{N}_2\text{O}_2\text{P}_2\text{Cl}_2\text{FePt}$: C, 60.69; H, 3.72. Found: C, 60.97; H, 3.71.

***trans*-[Pt(C≡CFC)(C₆H₅)(PPh₃)₂][DDQ] (3a):** green crystals (60%); mp 136 °C dec; IR (KBr) 2212 (C≡N), 2082 (C≡C), and 1571 cm^{-1} (C=O); vis–near-IR (CH_2Cl_2) 1075 (ϵ 1730), 587 (5040), 461 (9710), and 350 nm (9640). Anal. Calcd for $\text{C}_{62}\text{H}_{44}\text{N}_2\text{O}_2\text{P}_2\text{Cl}_2\text{FePt}$: C, 60.41; H, 3.60; N, 2.27. Found: C, 60.67; H, 3.61; N, 2.25.

***trans*-[Pt(C≡CFC)(C₆H₄Cl-*p*)(PPh₃)₂][DDQ] (4a):** dark red crystals (80%); mp 152 °C dec; IR (KBr) 2211 (C≡N), 2089 (C≡C), and 1574 cm^{-1} (C=O); vis–near-IR (CH_2Cl_2) 1065 (ϵ 1730), 587 (5010), 461 (9510), and 350 nm (9620). Anal. Calcd for $\text{C}_{62}\text{H}_{43}\text{N}_2\text{O}_2\text{P}_2\text{Cl}_3\text{FePt}$: C, 58.76; H, 3.42; N, 2.21. Found: C, 58.81; H, 3.44; N, 2.14.

***trans*-[Pt(C≡CFC)(C₆H₄CO₂Et-*p*)(PPh₃)₂][DDQ] (5a):** green crystals (72%); mp 104 °C dec; IR (KBr) 2211 (C≡N), 2086 (C≡C), 1705 (C=O), and 1580 cm^{-1} (C=O); vis–near-IR (CH_2Cl_2) 1045 (ϵ 1820), 587 (5040), 461 (9710), and 350 nm (9640). Anal. Calcd for $\text{C}_{65}\text{H}_{48}\text{N}_2\text{O}_4\text{P}_2\text{Cl}_2\text{FePt}$: C, 59.83; H, 3.71; N, 2.15. Found: C, 60.36; H, 3.76; N, 2.02.

***trans*-[Pt(C≡CFC)(C₆H₄COCH₃-*p*)(PPh₃)₂] (6a):** green crystals (64%); mp 124 °C dec; IR (KBr) 2214 (C≡N), 2068 (C≡C), 1662 (C=O), and 1575 cm^{-1} (C=O); vis–near-IR (CH_2Cl_2) 1055 (ϵ 2020), 585 (4180), 461 (8090), and 349 nm (8430). Anal. Calcd for $\text{C}_{64}\text{H}_{46}\text{N}_2\text{O}_3\text{P}_2\text{Cl}_2\text{FePt}$: C, 60.30; H, 3.64; N, 2.20. Found: C, 60.58; H, 3.72; N, 2.37.

***trans*-[Pt(C≡CFC)(C₆H₅)(PPh₃)₂][PF₆] (3b).** To a solution of complex **3** (30 mg, 0.03 mmol) in CH_2Cl_2 (3 mL) was slowly added a solution of ferrocenium hexafluorophosphate (12 mg, 0.035 mmol) in CH_2Cl_2 (5 mL), with use of an ice–water bath under nitrogen. After the mixture was stirred for

(26) Sugita, N.; Minkiewicz, V. J.; Heck, R. F. *Inorg. Chem.* **1978**, *17*, 2809.

(27) (a) Hendrickson, D. N.; Sohn, Y. S.; Gray, H. B. *Inorg. Chem.* **1971**, *10*, 1559. (b) Duggan, D. M.; Hendrickson, D. N. *Inorg. Chem.* **1975**, *14*, 955.

(28) Sonogashira, K.; Yatabe, T.; Tohda, Y.; Takahashi, S.; Hagihara, N. *J. Chem. Soc., Chem. Commun.* **1977**, 291.

15 min, the solution was filtered and concentrated to ca. 1 mL under reduced pressure. Benzene was added in order to induce crystallization, and the resulting violet crystals (29 mg, 85%) were filtered; mp 182 °C dec; IR (KBr) 2078 (C=C) and 839 cm^{-1} (PF₆); vis-near-IR (CH₂Cl₂) 1060 (ϵ 930), 476 (440), and 376 nm (460). Anal. Calcd for C₅₄H₄₄F₆P₃FePt: C, 56.36; H, 3.85. Found: C, 56.42; H, 3.85.

Structure Determination. Crystal data for **5**: C₅₇H₄₈O₂P₂FePt, fw 1077.90, monoclinic, $P2_1/n$; $a = 12.338(4)$ Å, $b = 22.865(3)$ Å, $c = 16.991(4)$ Å; $\beta = 100.64(2)^\circ$; $V = 4710.89$ Å³; $Z = 4$; $D_{\text{calcd}} = 1.52$ g cm^{-3} ; $\mu(\text{Mo K}\alpha) = 34.124$ cm^{-1} ; $T = 298$ K; crystal size $0.20 \times 0.20 \times 0.18$ mm.

Data collection was performed at room temperature on a Mac Science MXC18K diffractometer with graphite-monochromated Mo K α radiation and an 18-kW rotating anode generator. Of 11 829 reflections collected, 11 550 reflections were

unique, of which 8606 reflections with $I > 3.00\sigma(I)$ were used for refinement. The structure was solved with the Dirdif-Patty method in Crystan GM (software package for structure determination) and refined finally by a full-matrix least-squares procedure. Absorption correction with the ψ -scan method and anisotropic refinement of non-hydrogen atoms were carried out. All hydrogen atoms, located from difference Fourier maps, were isotropically refined. $R = 0.038$, and $R_w = 0.047$.

Supporting Information Available: Tables of crystal data and data collection and refinement details, all positional and thermal parameters, bond distances and angles, torsion angles, and least-squares planes for **5** (57 pages). Ordering information is given on any current masthead page.

OM9502401

Skeletal Rearrangement and Acetylide Migration in the Butterfly Cluster Complexes with Formula $Cp^*WOS_3(CO)_{11}(C\equiv CCH_2OMe)$

Pei-Chiun Su,[†] Shun-Jean Chiang,[†] Lin-Lin Chang,[†] Yun Chi,^{*,†} Shie-Ming Peng,^{*,‡} and Gene-Hsiang Lee[‡]

Departments of Chemistry, National Tsing Hua University, Hsinchu 30043, Taiwan, Republic of China, and National Taiwan University, Taipei 10764, Taiwan, Republic of China

Received June 22, 1995[⊗]

Treatment of $Cp^*W(CO)_3(C\equiv CCH_2OMe)$ with $Os_3(CO)_{10}(NCMe)_2$ in refluxing toluene afforded two cluster compounds (**2a**, **2b**) with identical molecular formula $Cp^*WOS_3(CO)_{11}(C\equiv CCH_2OMe)$. Both compounds contain a butterfly skeletal arrangement and a multisite bound $\mu_4-\eta^2$ -acetylide ligand. Complex **2a** can be converted to **2b** by relocating the $Cp^*W(CO)_2$ fragment from the hinge site to a wingtip position. The acetylide migration in **2b** and the kinetic studies of the conversion between **2a** and **2b** are presented.

Introduction

The C_2 hydrocarbons hold a key position in the development of organometallic cluster chemistry, as they have been found to be important intermediates for catalytic CO hydrogenation reaction. Therefore, much activity has been focused on the synthesis and reactivity of complexes containing C_2 hydrocarbon ligands, namely, dicarbide, acetylene, and acetylide fragments.¹ Among these C_2 hydrocarbon derivatives, the chemistry of acetylide complexes has attracted considerable attention and become a flourishing subject in recent years.² For example, Carty and co-workers have reported the synthesis of ruthenium phosphido clusters containing various multisite bound acetylide ligands.³ Other independent investigations, such as the reactivity studies on triosmium acetylide clusters by Deeming⁴ and the preparation of heterometallic acetylide compounds using mononuclear acetylide precursors by Yamazaki,⁵ Vahrenkamp,⁶ and Akita,⁷ provided substantial knowledge about the bonding and reaction mechanism of acetylide ligands.

During our investigation of the heterometallic cluster chemistry, we have successfully synthesized butterfly acetylide clusters with formula $CpWOS_3(CO)_{11}(C\equiv CR)$,

$R = Ph$ and Bu^n ,⁸ and examined their chemical reactivities, in particular the cluster building and degradation reactions and the C-C bond formation with an additional C_2 fragment.⁹ Recently, we have extended the preparation of related derivatives by changing the ancillary ligand on tungsten atom and the substituent on acetylide ligand, which led to the isolation of two structural derivatives with identical molecular formula $Cp^*WOS_3(CO)_{11}(C\equiv CCH_2OMe)$. Although both isomers adopt a butterfly geometry, they possess a different arrangement of metal atoms and can be interconverted at elevated temperature by moving the $Cp^*W(CO)_2$ fragment from the hinge to the wingtip position. In this article, we address the details of this skeletal rearrangement and the migration of acetylide ligand on one of the WOS_3 butterfly coordination spheres. This skeletal rearrangement complements the framework isomerism observed in mixed tetrahedral cluster compounds $CpMFeCO_2(CO)_8(\mu_3-S)(AsMe_2)$ and $CpMFeCO_2(CO)_8(\mu_3-PMe)(AsMe_2)$, $M = Mo$ and W ,¹⁰ and the formation of spiked-triangular acetylide cluster compounds by metal exchange.¹¹

Experimental Section

General Information and Materials. Infrared spectra were recorded on a Perkin-Elmer 2000 FT-IR spectrometer.

[†] National Tsing Hua University.

[‡] National Taiwan University.

[⊗] Abstract published in *Advance ACS Abstracts*, September 15, 1995.

(1) (a) Raithby, P. R.; Rosales, M. J. *Adv. Inorg. Radiochem.* **1985**, *29*, 169. (b) Bruce, M. I.; Swincer, A. G. *Adv. Organomet. Chem.* **1983**, *22*, 59. (c) Kaesz, H. D.; Humphries, A. P. *Prog. Inorg. Chem.* **1979**, *25*, 146. (d) Aime, S.; Deeming, A. J. *J. Chem. Soc., Dalton Trans.* **1983**, 1807. (e) Rosenberg, E. *Polyhedron* **1989**, *8*, 383. (f) Nickias, P. N.; Selegue, J. P.; Young, B. A. *Organometallics* **1988**, *7*, 2248. (g) Afzal, D.; Lenhert, P. G.; Lukehart, C. M. *Organometallics* **1987**, *6*, 546. (h) Zhou, Y.; Seyler, J. W.; Weng, W.; Arif, A. M.; Gladysz, J. A. *J. Am. Chem. Soc.* **1993**, *115*, 8509. (i) Huang, T.-K.; Chi, Y.; Peng, S.-M.; Lee, G.-H.; Wang, S.-L.; Liao, F.-L. *Organometallics* **1995**, *14*, 2164.

(2) Nast, R. *Coord. Chem. Rev.* **1982**, *47*, 89.

(3) (a) Belnkiron, P.; Taylor, N. J.; Carty, A. J. *J. Chem. Soc., Chem. Commun.* **1995**, 327. (b) Corrigan, J. F.; Taylor, N. J.; Carty, A. J. *J. Chem. Soc., Chem. Commun.* **1994**, 1769. (c) Sun, Y.; Taylor, N. J.; Carty, A. J. *Organometallics* **1992**, *11*, 4293.

(4) (a) Boyar, E.; Deeming, A. J.; Felix, M. S. B.; Kabir, S. E.; Adatia, T.; Bhusate, R.; McPartlin, M.; Powell, H. R. *J. Chem. Soc., Dalton Trans.* **1989**, 5. (b) Deeming, A. J.; Felix, M. S. B.; Bates, P. A.; Hursthouse, M. B. *J. Chem. Soc., Chem. Commun.* **1987**, 461.

(5) Yasufuku, K.; Aoki, K.; Yamazaki, H. *Bull. Chem. Soc. Jpn.* **1975**, *48*, 1616.

(6) (a) Roland, E.; Vahrenkamp, H. *J. Mol. Catal.* **1983**, *21*, 233. (b) Albiez, T.; Powell, A. K.; Vahrenkamp, H. *Chem. Ber.* **1990**, *123*, 667.

(7) (a) Akita, M.; Moro-oka, Y. *Bull. Chem. Soc. Jpn.* **1995**, *68*, 420. (b) Akita, M.; Ishii, N.; Takabuchi, A.; Tanaka, M.; Moro-oka, Y. *Organometallics* **1994**, *13*, 258. (c) Akita, M.; Terada, M.; Moro-oka, Y. *Organometallics* **1992**, *11*, 1825.

(8) (a) Chi, Y.; Lee, G.-H.; Peng, S.-M.; Wu, C.-H. *Organometallics* **1989**, *8*, 1574. (b) Chi, Y.; Wu, C.-H.; Peng, S.-M.; Lee, G.-H. *Organometallics* **1990**, *9*, 2305.

(9) (a) Chi, Y.; Lee, G.-H.; Peng, S.-M.; Wu, C.-H. *Organometallics* **1989**, *8*, 1574. (b) Hwang, D.-K.; Chi, Y.; Peng, S.-M.; Lee, G.-H. *J. Organomet. Chem.* **1990**, *389*, C7. (c) Wu, C.-H.; Chi, Y.; Peng, S.-M.; Lee, G.-H. *J. Chem. Soc., Dalton Trans.* **1990**, 3025. (d) Chi, Y.; Hsu, S.-F.; Peng, S.-M.; Lee, G.-H. *J. Chem. Soc., Chem. Commun.* **1991**, 1019. (e) Chi, Y.; Wu, C.-H.; Peng, S.-M.; Lee, G.-H. *Organometallics* **1991**, *10*, 1676.

(10) Müller, M.; Schacht, H.-T.; Fischer, K.; Enslin, J.; Gütlisch, P.; Vahrenkamp, H. *Inorg. Chem.* **1986**, *25*, 4032.

(11) (a) Bernhardt, W.; Vahrenkamp, H. *J. Organomet. Chem.* **1988**, *355*, 427. (b) Roland, E.; Bernhardt, W.; Vahrenkamp, H. *Chem. Ber.* **1986**, *119*, 2566.

¹H and ¹³C NMR spectra were recorded on a Bruker AM-400 (400.13 MHz) or a Bruker AMX-300 (300.6 MHz) instrument. Mass spectra were obtained on a JEOL-HX110 instrument operating in fast atom bombardment modes (FAB). All reactions were performed under a nitrogen atmosphere using deoxygenated solvents dried with an appropriate reagent. The progress of reactions were monitored by analytical thin-layer chromatography (5735 Kieselgel 60 F₂₅₄, E. Merck), and the products were separated on commercially available preparative thin-layer chromatographic plates (Kieselgel 60 F₂₅₄, E. Merck). The acetylide complexes LW(CO)₃(C≡CCH₂OMe), L = Cp and Cp*, were prepared from the reactions of appropriate chloride complexes LW(CO)₃Cl with methyl propargyl ether (Aldrich) in Et₂NH solution and in the presence of catalytic amount of CuI. Elemental analyses were performed at the NSC Regional Instrumentation Center at National Cheng Kung University, Tainan, Taiwan.

Preparation of Cp*WO₃(CO)₁₁(C≡CCH₂OMe). Os₃(CO)₁₀(NCMe)₂ (206 mg, 0.215 mmol), CpW(CO)₃(C≡CCH₂OMe) (125 mg, 0.32 mmol), and toluene (45 mL) were added into a 100 mL reaction flask. The solution was then heated to reflux and continued heating for 30 min, during which time the color changed from yellow-orange to dark-brown. After cooling of the solution to room temperature, the solvent was removed under vacuum. The residue was separated by thin-layer chromatography (dichloromethane:hexane = 1:3), giving 51 mg of red Cp*WO₃(CO)₁₁(C≡CCH₂OMe) (**1a**, 0.042 mmol, 20%) as the only isolable cluster product.

Spectral data for **1a**: MS (FAB, ¹⁹²Os, ¹⁸⁴W), *m/z* 1202 (M⁺); IR (C₆H₁₂) ν(CO), 2084 (w), 2059 (vs), 2034 (m), 2012 (s), 1999 (m), 1985 (w), 1971 (m), 1961 (vw) cm⁻¹; ¹H NMR (CDCl₃, 294 K) δ 5.32 (s, 5H), 4.47 (d, 1H, *J*_{H-H} = 13.9 Hz), 4.25 (d, 1H, *J*_{H-H} = 13.9 Hz), 3.56 (s, 3H); ¹³C NMR (CDCl₃, 240 K) CO, δ 210.8 (W-CO, *J*_{W-C} = 141 Hz), 204.2 (W-CO, broad), 181.0 (3CO), 173.0 (1C), 171.5 (1C), 169.7 (1C); δ 180.2 (CCCH₂OMe), 156.8 (CCCH₂OMe), 88.8 (C₅H₅), 85.7 (CH₂OMe), 58.6 (OMe). Anal. Calcd for C₂₀H₁₀O₁₂Os₃W: C, 20.07; H, 0.84. Found: C, 20.15; H, 0.80.

Preparation of Cp*WO₃(CO)₁₁(C≡CCH₂OMe). In a typical reaction, Os₃(CO)₁₀(NCMe)₂ (200 mg, 0.215 mmol), Cp*W(CO)₃(C≡CCH₂OMe) (111 mg, 0.284 mmol), and toluene (50 mL) were added into a 100 mL reaction flask. The solution was then heated to reflux and continued heating for 25 min, during which time the color changed from yellow-orange to brown and finally to dark-brown. After the solution was allowed to cool to room temperature, the solvent was removed under vacuum. The residue was separated by thin-layer chromatography (dichloromethane:hexane = 1:4), giving 57 mg of dark-brown isomer of Cp*WO₃(CO)₁₁(C≡CCH₂OMe) (**2b**, 0.045 mmol, 21%) and 59 mg of red-orange isomer of Cp*WO₃(CO)₁₁(C≡CCH₂OMe) (**2a**, 0.046 mmol, 22%) according to the order of their elution. Crystals of **2b** suitable for X-ray diffraction study were obtained from a layered solution of dichloromethane-methanol at room temperature.

Spectral data for **2a**: MS (FAB, ¹⁹²Os, ¹⁸⁴W), *m/z* 1272 (M⁺); IR (C₆H₁₂) ν(CO), 2081 (m), 2056 (vs), 2032 (m), 2010 (s), 1993 (m), 1983 (w), 1969 (w), 1960 (w) cm⁻¹; ¹H NMR (CDCl₃, 294 K) δ 4.47 (d, 1H, *J*_{H-H} = 12.8 Hz), 4.41 (d, 1H, *J*_{H-H} = 12.8 Hz), 3.53 (s, 3H), 2.00 (s, 15H); ¹³C NMR (CD₂Cl₂, 294 K) CO, δ 215.1 (W-CO, *J*_{W-C} = 142 Hz), 209.8 (W-CO, *J*_{W-C} = 151 Hz), 180.7 (br), 177.8 (3CO, br), 175.8 (3CO, br), 172.8 (br), 170.7 (br); δ 190.0 (CCCH₂OMe), 154.2 (CCCH₂OMe), 103.5 (C₅Me₅), 83.7 (CH₂OMe), 57.9 (OMe), 11.1 (C₅Me₅). Anal. Calcd for C₂₅H₂₀O₁₂Os₃W: C, 23.70; H, 1.59. Found: C, 23.58; H, 1.64.

Spectral data for **2b**: MS (FAB, ¹⁹²Os, ¹⁸⁴W), *m/z* 1272 (M⁺); IR (C₆H₁₂) ν(CO), 2079 (m), 2043 (s), 2015 (s), 1999 (m, br), 1985 (m), 1948 (w, br), 1928 (w, br) cm⁻¹; ¹H NMR (CDCl₃, 294 K) δ 4.44 (s, 2H), 3.55 (s, 3H), 2.24 (s, 15H); ¹³C NMR (CD₂Cl₂, 294 K) CO, δ 207.8 (2W-CO, *J*_{W-C} = 165 Hz), 182.0, 179.5 (6CO, br), 170.9 (2CO, br); δ 218.5 (CCCH₂OMe), 156.4 (CCCH₂OMe), 101.8 (C₅Me₅), 87.1 (CH₂OMe), 58.2 (OMe), 11.1

Table 1. Experimental Data for the X-ray Diffraction Study on **2b**

formula: WO ₃ O ₁₂ C ₂₅ H ₂₀	<i>d</i> (calcd) = 2.844 g/cm ³
mol wt: 1266.86	<i>F</i> (000) = 4590
cryst system: orthorhombic	μ(Mo Kα) = 168.8 mm ⁻¹
space group: <i>Pbca</i>	transm factors: 0.287, 1.000
<i>a</i> = 17.107(7) Å	reflens with <i>I</i> > 2σ(<i>I</i>): 3993
<i>b</i> = 19.567(2) Å	<i>R</i> _F , <i>R</i> _w , GOF: 0.045, 0.040, 2.89
<i>c</i> = 17.676(3) Å	no. of atoms and refined params:
<i>V</i> = 5917(3) Å ³	61; 371 (3993 out of 5187 reflens)
<i>Z</i> = 8	minimize function: Σ(<i>w</i> <i>F</i> _o - <i>F</i> _c ²)
λ(Mo Kα) = 0.709 30 Å	max Δ/σ ratio: 0.0338
<i>hkl</i> ranges: 0-20, 0-23, 0-20	resid electron (max/min):
cryst size: 0.20 × 0.30 × 0.60 mm	-2.090/3.340 e/Å ³
no. of unique reflens: 5187	weights scheme: <i>w</i> ⁻¹ = σ ² (<i>F</i> _o)

(C₅Me₅). Anal. Calcd for C₂₅H₂₀O₁₂Os₃W: C, 23.70; H, 1.59. Found: C, 23.60; H, 1.62.

Thermolysis of **2a.** A toluene solution (15 mL) of **2a** (8.8 mg, 0.0069 mmol) was heated at reflux temperature for 15 min under N₂ atmosphere, during which time the color changed from red to red-brown. After the solvent was removed under vacuum, the residue was separated by thin-layer chromatography (dichloromethane:hexane = 1:4), giving 3.3 mg of **2b** (0.0026 mmol, 38%) and 2.7 mg of **2a** (0.0021 mmol, 31%) approximately. Trace amount of Cp*WO₃(CO)₈(C≡CCH₂OMe) (**3**) was noted on the TLC plate, but no isolation was attempted. Thermolysis of **2b** gave an identical distribution of products.

Reaction of **2a with CO.** A toluene solution (35 mL) of **2a** (32 mg, 0.025 mmol) was heated to reflux and continued heating for 6 h under CO atmosphere (1 atm), during which time the color changed from red to orange. After the solvent was removed in vacuo, the residue was separated by thin-layer chromatography (dichloromethane:hexane = 1:4), giving 7 mg of **2b** (22%), another 7 mg of **2a** (22%), and 12 mg of yellow Cp*WO₃(CO)₈(C≡CCH₂OMe) (**3**, 0.012 mmol, 48%). Replacement of **2a** with **2b** afforded 30% of **2a**, 20% of **2b**, and 32% of **3** under a similar reaction condition.

Spectral data for **3**: MS (FAB, ¹⁹²Os, ¹⁸⁴W), *m/z* 996 (M⁺); IR (C₆H₁₂) ν(CO), 2072 (s), 2037 (s), 1999 (vs), 1992 (m), 1957 (m), 1911 (w, br) cm⁻¹; ¹H NMR (CDCl₃, 294 K) δ 4.86 (d, 1H, *J*_{H-H} = 12.0 Hz), 4.76 (d, 1H, *J*_{H-H} = 12.0 Hz), 3.44 (s, 3H), 2.13 (s, 15H); ¹³C NMR (CDCl₃, 294 K) CO, δ 211.0 (W-CO, *J*_{W-C} = 164 Hz), 208.8 (W-CO, *J*_{W-C} = 160 Hz), 180.0 (br), 179.1 (3CO), 177.5 (br), 171.2 (br); δ 140.3 (CCCH₂OMe), 101.0 (C₅Me₅), 73.0 (CCCH₂OMe), 72.1 (CH₂OMe), 58.3 (OMe), 11.7 (C₅Me₅). Anal. Calcd for C₂₂H₂₀O₉Os₂W: C, 26.62; H, 2.03. Found: C, 26.47; H, 2.03.

X-ray Crystallography. For complex **2b**, diffraction measurements were carried out on a Nonius CAD-4 diffractometer with crystal dimensions 0.05 × 0.25 × 0.50 mm. Lattice parameters were determined from 25 randomly selected reflections, with 2θ angle in the range 18.94-27.86°. Intensities were corrected for Lorentz, polarization, and absorption effects (*ψ* scans). Three standard reflections were monitored every 3600 s with intensity variation <2%, 4σ. Of the 9090 unique reflections collected, 6143 reflections with *I* > 2σ(*I*) were used for the refinement. The structure was solved by using the NRCC-SDP-VAX package and refined to *R*_F = 0.045, *R*_w = 0.040, and GOF = 2.46 for 753 parameters, weighting scheme *w*⁻¹ = σ²(*F*_o), and highest Δ/σ ratio 0.03. All non-hydrogen atoms were refined anisotropically. A difference map following convergence showed residual electron density within the range -2.09/3.34 e/Å³ (min/max). The data collection and refinement parameters and the atomic coordinates are given in Tables 1 and Table 2, respectively.

Kinetic Studies. In a typical reaction, 5-8 mg of **2a** or **2b** was dissolved in 0.45 mL of toluene-*d*₈ solvent, and the solution was loaded into a 5-mm NMR tube equipped with a Teflon PTFE valve. The NMR tube was immersed into a preheated oil bath controlled by a thermostat. The tube was withdrawn from the bath for periodic examination by ¹H NMR

Table 2. Atomic Coordinates and Equivalent Isotropic Displacement Coefficients for 2b

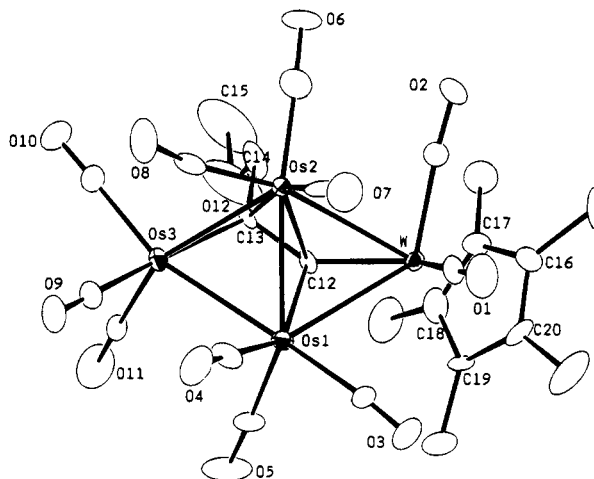
	x	y	z	B_{iso}
W	0.61085(4)	0.15744(5)	0.03027(4)	1.68(3)
Os(1)	0.68028(4)	0.17193(5)	0.18191(4)	2.05(3)
Os(2)	0.65595(4)	0.04078(5)	0.13064(4)	1.77(3)
Os(3)	0.80384(5)	0.07432(5)	0.19262(4)	2.29(3)
O(1)	0.4426(8)	0.1606(10)	0.1075(7)	5.4(9)
O(2)	0.5626(8)	0.0280(8)	-0.0597(7)	4.1(7)
O(3)	0.5479(9)	0.2768(9)	0.1860(7)	5.3(9)
O(4)	0.6446(9)	0.1390(9)	0.3458(7)	5.6(9)
O(5)	0.8069(11)	0.2796(10)	0.1998(11)	8.3(12)
O(6)	0.6492(9)	-0.0851(8)	0.0266(7)	5.1(8)
O(7)	0.4928(7)	0.0356(9)	0.2038(7)	4.8(9)
O(8)	0.6911(10)	-0.0579(9)	0.2610(9)	7.5(11)
O(9)	0.7969(8)	0.0635(9)	0.3669(7)	4.6(8)
O(10)	0.9062(10)	-0.0518(9)	0.1719(8)	6.2(10)
O(11)	0.9456(9)	0.1652(10)	0.1949(10)	7.3(11)
O(12)	0.8708(11)	0.0671(13)	-0.0087(9)	10.9(15)
C(1)	0.5069(11)	0.1576(12)	0.0816(8)	2.8(10)
C(2)	0.5800(10)	0.0740(11)	-0.0216(9)	2.6(10)
C(3)	0.5958(12)	0.2373(11)	0.1814(10)	3.0(10)
C(4)	0.6585(12)	0.1502(12)	0.2856(9)	3.6(11)
C(5)	0.7587(12)	0.2407(12)	0.1923(11)	3.9(11)
C(6)	0.6540(12)	-0.0356(13)	0.0627(10)	4.0(11)
C(7)	0.5511(13)	0.0362(11)	0.1771(9)	3.8(11)
C(8)	0.6873(13)	-0.0166(12)	0.2137(10)	3.7(11)
C(9)	0.8025(11)	0.0685(12)	0.3019(9)	2.8(10)
C(10)	0.8674(13)	-0.0082(13)	0.1803(11)	4.2(11)
C(11)	0.8948(11)	0.1321(11)	0.1950(10)	3.1(10)
C(12)	0.7105(10)	0.1286(11)	0.0799(7)	1.9(8)
C(13)	0.7732(10)	0.0787(11)	0.0803(8)	2.0(8)
C(14)	0.8063(10)	0.0441(13)	0.0094(9)	3.6(12)
C(15)	0.9074(16)	0.0283(23)	-0.0655(15)	11.8(26)
C(16)	0.5639(12)	0.2024(12)	-0.0805(10)	3.5(10)
C(17)	0.6437(11)	0.1835(11)	-0.0928(9)	2.6(9)
C(18)	0.6881(12)	0.2238(12)	-0.0493(9)	3.5(10)
C(19)	0.6378(12)	0.2704(10)	-0.0068(10)	2.9(9)
C(20)	0.5605(12)	0.2558(12)	-0.0275(10)	3.3(10)
C(21)	0.4929(12)	0.1769(14)	-0.1267(11)	4.8(12)
C(22)	0.6696(14)	0.1382(13)	-0.1558(10)	4.7(13)
C(23)	0.7732(12)	0.2319(16)	-0.0558(13)	5.9(15)
C(24)	0.6643(14)	0.3311(12)	0.0358(11)	4.7(13)
C(25)	0.4874(15)	0.2954(15)	-0.0060(14)	6.5(15)

spectroscopy. The concentration of reactant and product was monitored by integration of the methoxyl and the corresponding Cp* signals. The reaction rates were examined at 346, 357, 362, and 366 K. Two attempts were recorded at each temperature, one starting from **2a** and the second from **2b**. Equilibrium constants K_{eq} were determined from the ratio of **2a/2b** after at least 5 half-lives $t_{1/2}$. Plots of $\log([A]_t - [A]_{\text{eq}}/[A]_0 - [A]_{\text{eq}})$ vs reaction time were linear; $[A]_0$ = initial concentration, $[A]_{\text{eq}}$ = concentration at equilibrium, and $[A]_t$ = concentration measured at time t . The rate constants k_{obs} are the slopes of the lines as determined by least-squares fitting.

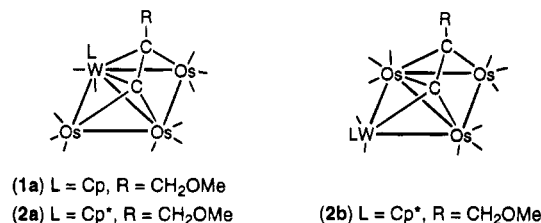
Results and Discussion

Synthesis and Characterization. Condensation of $\text{Os}_3(\text{CO})_{10}(\text{NCMe})_2$ with the acetylide complex $\text{CpW}(\text{CO})_3(\text{C}\equiv\text{CCH}_2\text{OMe})$ in refluxing toluene produced a red tetranuclear acetylide complex $\text{CpWOs}_3(\text{CO})_{11}(\text{C}\equiv\text{CCH}_2\text{OMe})$ (**1a**) in 20% yield. This acetylide complex was separated by using thin-layer chromatography on silica gel plates and recrystallization. Both the CO pattern of the IR spectrum and the ^{13}C NMR data confirmed that it is isostructural with the previously characterized acetylide derivatives $\text{CpWOs}_3(\text{CO})_{11}(\text{C}\equiv\text{CR})$, R = Ph and Bu^n ,⁶ which contains a butterfly cluster geometry with the W atom located at the hinge position (Scheme 1).

On the other hand, the reactions by using Cp* derivative $\text{Cp}^*\text{W}(\text{CO})_3(\text{C}\equiv\text{CCH}_2\text{OMe})$ afforded two but-

**Figure 1.** Molecular structure of **2b** and the atomic numbering scheme.

Scheme 1



terfly complexes (**2a,b**) in 20% and 21% yields, respectively. These acetylide complexes **2a,b** eluted very close to one another on the TLC plates and required repeated recrystallization to obtain both compounds in pure form. The NMR spectral data indicated that they share many important features with that of the Cp derivative **1a**. One is the observation of two acetylide signals in the ^{13}C NMR spectra, δ 190.0 and 154.2 for **2a** and δ 218.5 and 156.4 for **2b**, which are comparable with the chemical shift of the μ_4 - η^2 -acetylide ligand reported.¹² The red derivative **2a** can be easily identified to have a structure closely related to the Cp derivative **1a**, as it shows a similar IR $\nu(\text{CO})$ pattern. However, the second, dark-brown derivative **2b** which contains a hitherto unknown structure has never been observed in this acetylide cluster system. Therefore, we proceeded to carry out the X-ray diffraction analysis.

Crystal Structure of 2b. The ORTEP diagram and the scheme used for labeling the atoms are shown in Figure 1. Selected bond distances and angles are listed in Table 3. The molecule consists of a WOs_3 butterfly arrangement, with atoms W and Os(3) defining the wingtip positions, and atoms Os(1) and Os(2), the hinge positions. Each osmium atom associates with three CO ligands, and the tungsten, with two CO ligands and a Cp* ligand. Most CO ligands are linear with the M-CO angles in the narrow range 173(2)–178(2)°. The only exception is the semibridging CO ligand on Os(2) atom, which is leaning toward the Os(3) atom with distances Os(2)-C(8) = 1.93(2) Å and Os(3)-C(8) = 2.70(2) Å and angle $\angle\text{Os}(2)\text{-C}(8)\text{-O}(8) = 166(2)^\circ$. The dihedral angle between the triangular wings W-Os(1)-Os(2) and Os(1)-Os(2)-Os(3) is 131.41(4)°. This angle is almost identical to that (131.4(3)°) of the structurally charac-

(12) Carty, A. J.; Cherkas, A. A.; Randall, L. H. *Polyhedron* 1988, 7, 1045.

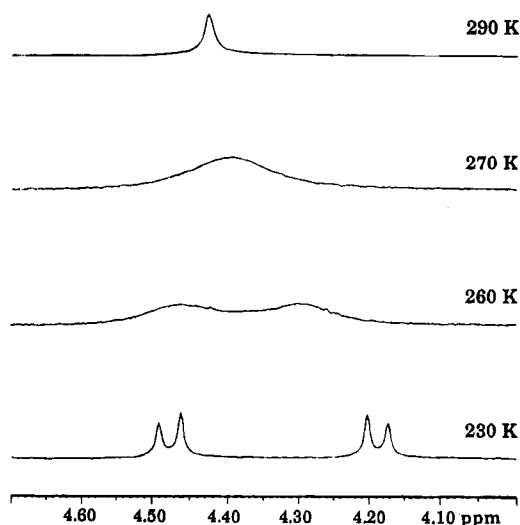
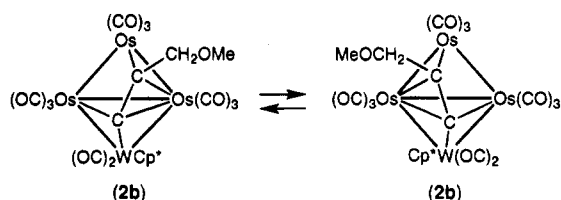
Table 3. Selected Bond Distances (Å) and Bond Angles (deg) of 2b (Esd's in Parentheses)

(A) Metal–Metal and Metal–Acetylide Distances			
W–Os(1)	2.946(1)	W–Os(2)	2.992(1)
Os(1)–Os(2)	2.753(1)	Os(1)–Os(3)	2.855(1)
Os(2)–Os(3)	2.834(1)	W–C(12)	2.00(2)
Os(1)–C(12)	2.06(2)	Os(2)–C(12)	2.15(2)
Os(2)–C(13)	2.32(2)	Os(3)–C(13)	2.06(1)
C(12)–C(13)	1.45(3)		
(B) Metal–Carbonyl and Cp* Ligand Distances			
W–C(1)	2.00(2)	W–C(2)	1.94(2)
Os(1)–C(3)	1.93(2)	Os(1)–C(4)	1.92(2)
Os(1)–C(5)	1.91(2)	Os(2)–C(6)	1.92(2)
Os(2)–C(7)	1.97(2)	Os(2)–C(8)	1.93(2)
Os(3)–C(8)	2.70(2)	Os(3)–C(9)	1.94(2)
Os(3)–C(10)	1.96(2)	Os(3)–C(11)	1.92(2)
W–C(16)	2.29(2)	W–C(17)	2.30(2)
W–C(18)	2.33(2)	W–C(19)	2.35(2)
W–C(20)	2.34(2)		
(C) Metal–Carbonyl Ligand Angles			
∠W–C(1)–O(1)	175(2)	∠W–C(2)–O(2)	173(2)
∠Os(1)–C(3)–O(3)	175(2)	∠Os(1)–C(4)–O(4)	178(2)
∠Os(1)–C(5)–O(5)	177(2)	∠Os(2)–C(6)–O(6)	174(2)
∠Os(2)–C(7)–O(7)	178(2)	∠Os(2)–C(8)–O(8)	166(2)
∠Os(3)–C(9)–O(9)	176(2)	∠Os(3)–C(10)–O(10)	176(2)
∠Os(3)–C(11)–O(11)	178(2)		

terized derivative of **2a**, CpW_{Os}(CO)₁₁(C≡CPh).⁶ In addition, formal electron counts at the individual metal atoms (neutral ligands and metals assumed) give 17e at Os(3), 18e at W and Os(1), and 19e at Os(2) atom. The electron deficiency at Os(3) is compensated by the formation of some bonding interaction with the CO ligands of the electron-rich Os(2) center.

The acetylide ligand is noteworthy, which occupies the open face of the butterfly framework, and is coordinated in multisite fashion with its α -carbon located at the center of the WOs₂ triangle with distances W–C(12) = 2.00(2) Å, Os(1)–C(12) = 2.06(2) Å, and Os(2)–C(12) = 2.15(2) Å and with the β -carbon atom linked to Os(2) and Os(3) atoms with bond distances Os(2)–C(13) = 2.32(2) Å and Os(3)–C(13) = 2.06(1) Å. The μ_4 - η^2 mode of bonding resembles that of polynuclear acetylide cluster complexes,¹³ in which the acetylide ligand can be considered as σ -bonded to one metal atom via its α -carbon and also interacting with the second metal triangle via a parallel ($2\sigma + \pi$) bonding mode of a typical μ_3 -alkyne ligand.¹⁴ The structural parameters of **2b** are compatible with this definition, as the distances to the hinge Os(2) atom, which bears the π -bonding, are much longer than other metal–carbon distances, W–C(12), Os(1)–C(12), and Os(3)–C(13).

Solution Fluxionality of 2b. In contrast to the ¹H NMR spectrum of the red isomer **2a**, which show a pair of doublets for the methylene hydrogens at all temperatures, the ¹H NMR spectrum of **2b** shows only one methylene signal at δ 4.44 at 297 K, in addition to the anticipated signals of methoxyl and Cp* ligands (Figure 2). This methylene signal broadens and collapses on lowering the temperature. At 230 K, it turns to two

**Figure 2.** Variable-temperature ¹H NMR spectra of **2b** in CD₂Cl₂ solution, showing the region of methylene resonances.**Scheme 2**

well-resolved doublets at δ 4.48 and 4.14 with coupling constant $^2J_{H-H} = 11.7$ Hz. This exchange of proton resonance signals is a consequence of the migration of acetylide ligand from one Os–Os edge to the other (Scheme 2), which averages the chemical environment of diastereotopic methylene hydrogens at elevated temperature. The barrier of acetylide migration, $\Delta G^\ddagger = 51$ kJ/mol, is obtained from the coalescence temperature 270 K and the chemical shift difference $\Delta\nu = 136$ Hz.

The migrational motion of acetylide ligand was further confirmed by variable-temperature ¹³C NMR studies; see Figure 1s of the Supporting Information. At 200 K, the ¹³C NMR spectrum shows two W–CO signals at δ 207.6 ($J_{W-C} = 150$ Hz) and 207.1 ($J_{W-C} = 180$ Hz) and seven Os–CO signals at δ 188.9 (br), 184.1 (br), 182.4, 176.7 (br), 175.0 (3CO, br), 172.1, and 168.7. Upon warming of the sample to 245 K, the broad Os–CO signals at δ 188.9, 184.1, and 176.7 merge into a broad signal at δ 184.0, showing the onset of tripodal Os(CO)₃ rotation. With further increase of the temperature to 260 K, one sharp W–CO resonance was observed at δ 207.2 and five Os–CO signals at δ 183.4, 182.1, 175.2, 172.3, and 169.1 in an intensity ratio 3:1:3:1:1. The sharp Os–CO signal at δ 182.1 and two broad Os–CO signals at δ 172.3 and 169.1 were assigned to the axial and the corresponding equatorial CO ligands on the unique Os atom at the wingtip position. The assignment was achieved according to their line-broadening behavior, since the rise of a time-averaged plane of mirror symmetry that bisects the hinge Os–Os bond and lies on both the wingtip metal atoms generates such an exchange pattern. Finally, the ¹³C NMR spectrum at 294 K exhibited three Os–CO resonances at δ 182.0, 179.5 (6CO, br) and 170.9 (2CO, br), which confirms the

(13) (a) Weatherell, C.; Taylor, N. J.; Carty, A. J.; Sappa, E.; Tiripicchio, A. *J. Organomet. Chem.* **1985**, *291*, C9. (b) Roland, E.; Vahrenkamp, H. *Organometallics* **1983**, *2*, 1048. (c) Carty, A. J.; MacLaughlin, S. A.; Taylor, N. J. *J. Am. Chem. Soc.* **1981**, *103*, 2456. (d) Lanfranchi, M.; Tiripicchio, A.; Sappa, E.; MacLaughlin, S. A.; Carty, A. J. *J. Chem. Soc., Chem. Commun.* **1982**, 538. (e) Bantel, H.; Hansert, B.; Powell, A. K.; Tasi, M.; Vahrenkamp, H. *Angew. Chem., Int. Ed. Engl.* **1989**, *28*, 1059.

(14) (a) Sappa, E.; Tiripicchio, A.; Braunstein, P. *Chem. Rev.* **1983**, *83*, 203. (b) Sappa, E.; Tiripicchio, A.; Carty, A. J.; Toogood, G. E. *Prog. Inorg. Chem.* **1987**, *35*, 437.

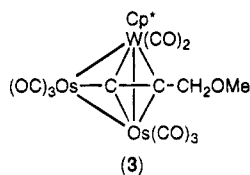
Table 4. Kinetic Parameters for the Isomerization between 2a and 2b (Esd's in Parentheses)^a

temp (K)	K_{eq}	k_{obs} (min ⁻¹)	k_1 (min ⁻¹)	k_{-1} (min ⁻¹)
366	0.86(5)	$4.4(3) \times 10^{-2}$	$2.0(2) \times 10^{-2}$	$2.4(2) \times 10^{-2}$
362	0.86(1)	$2.6(1) \times 10^{-2}$	$1.2(1) \times 10^{-2}$	$1.4(1) \times 10^{-2}$
357	0.82(1)	$1.5(1) \times 10^{-2}$	$6.8(4) \times 10^{-3}$	$8.3(4) \times 10^{-3}$
346	0.80(4)	$3.4(2) \times 10^{-3}$	$1.5(2) \times 10^{-3}$	$1.8(2) \times 10^{-3}$

^a k_1 = rate constants of the isomerization from **2a** to **2b**; k_{-1} = the reverse of k_1 . $K_{eq} = k_1/k_{-1}$; $k_{obs} = (k_1 + k_{-1})$.

formation of dynamic C_s symmetry on the butterfly cluster framework.

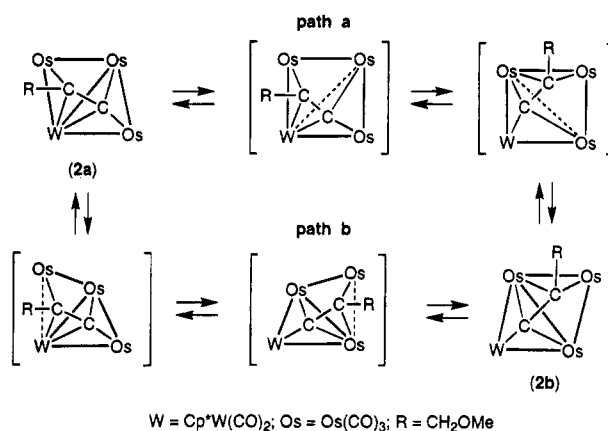
Isomerization between 2a and 2b. Thermolysis of either **2a** or **2b** in refluxing toluene clearly produced a mixture of both the acetylide complexes in an approximate 1:1 ratio. When the reaction was performed under CO atmosphere, we obtained similar 1:1 distribution of **2a,b**, along with the formation of the trinuclear complex $Cp^*WOs_2(CO)_8(C\equiv CCH_2OMe)$ (**3**) due to a frag-



mentation reaction via removal of an $Os(CO)_3$ unit. These observations indicate that, in addition to the acetylide migration discussed in the previous section, the metal skeleton undergoes some kind of reorganization to allow the W atom moving between the hinge and the wingtip position.

Kinetic studies were carried out to calculate the energy barrier of the skeletal rearrangement. The equilibrium constants K_{eq} and the rate constants k_{obs} , k_1 , and k_{-1} measured at the temperature range 346–366 K are summarized in Table 4. Linear regression analysis of these parameters gives a ΔH^\ddagger of 133(5) kJ/mol for the skeletal isomerization from **2a** to **2b** and a ΔH^\ddagger of 130(6) kJ/mol for the reverse process. These ΔH^\ddagger values are much larger than the barrier for acetylide migration observed in **2b** (51 kJ/mol) but are similar to that of the mean Os–Os bond enthalpy observed in the $Os_3(CO)_{12}$ molecule, 130 kJ/mol.¹⁵ Hence, this important finding suggests that the orientation of the acetylide ligand has little influence on the rates of skeletal rearrangement and that the isomerization probably passes through an unimolecular pathway with one metal–metal bond broken in the transition state.

On the basis of the above kinetic data, we propose a likely mechanism which involves a square metal framework, produced by concurrent lengthening of the hinge metal–metal bond and formation of partial interaction between wingtip metal atoms (Scheme 3). This transition state would have four metal atoms resided in an indistinguishable position. Following the acetylide migration on the square metal framework, the cleavage of the hinge W–Os bond and the subsequent formation of the Os–Os bond would produce the observed skeletal isomerization.

Scheme 3

W = $Cp^*W(CO)_2$; Os = $Os(CO)_3$; R = CH_2OMe

The isomerization may alternatively proceed through a spiked-triangular transition state, which is obtained by cleavage of a metal–metal bond between the hinge W atom and the adjacent Os atom at the wingtip position (path b of Scheme 3). This intermediate possesses a WOs_2 triangular framework with a pendent $Os(CO)_3$ unit. Subsequent formation of **2b** can be expected if the $Os(CO)_3$ fragment in the intermediate moves to the adjacent Os–Os edge to form a new bond with the Os atom at the opposite position. In this case as well the W atom exchanges its position on the butterfly core; thus it cannot be differentiated from the first proposed path a. We favor the second pathway, as the skeletal rearrangement was accompanied by the formation of trace amount of **3** upon thermolysis. It appears to us that the trinuclear complex **3** is produced through the identical intermediate by further addition of CO to the pendent $Os(CO)_3$ fragment, followed by cleavage of Os–Os bond and releasing of an $Os(CO)_4$ fragment to form $Os_3(CO)_{12}$.

Summary. $Cp^*W(CO)_3(C\equiv CCH_2OMe)$ reacts with $Os_3(CO)_{10}(NCMe)_2$ to afford butterfly cluster **1a** with the W atom occupying the hinge position. However, upon changing the ancillary ligand to Cp^* ligand, we obtained two derivatives **2a,b** in equal proportion. Complex **2a** is isostructural to the Cp derivative **1a**, while complex **2b** adopts a similar butterfly framework but with the W atom located at the wingtip position, which linked to the α -carbon of the acetylide ligand. It appears that formation of **2b** is caused by the substitution of the Cp^* ligand and CH_2OMe group, as the reaction of $Cp^*W(CO)_3(C\equiv CPh)$ and $Os_3(CO)_{10}(NCMe)_2$ have failed to generate the respective derivative of **2b**. In addition to the electronic effect of CH_2OMe on the acetylide ligand, the steric crowding of the Cp^* ligand seems to be an important factor in favoring the generation of **2b**, as the wingtip site is found to be less congested and can reduce the repulsion with nearby CO ligands if the W atom is placed at this location. However, as this steric effect are not very influential, isomer **2b** equilibrates with **2a** upon heating in solution. To our knowledge, this skeletal rearrangement between butterfly cluster framework is unprecedented, although there are a few examples that have been reported for the transformation of butterfly and tetrahedral clusters¹⁶ and the polyhedral isomerization in higher nuclearity clusters $Cp^*_2W_2Ru_4(CO)_{12}(\mu-PPH)_2$, $[Re_7IrC(CO)_{23}]^{2-}$, and $Os_6Pt(CO)_{17}(\mu_3-NCMe)(COD)$.¹⁷ As we have observed the generation of **3** in a trace amount through cluster

(15) (a) Connor, J. A. In *Transition Metal Clusters*; Johnson, B. F. G., Ed.; Wiley: New York, 1981; p 345. (b) Conner, J. A. *Top. Curr. Chem.* **1977**, *71*, 71.

fragmentation, it is likely that the transition state contains the spiked-triangular framework with a pendant Os(CO)₃ fragment. This postulation is consistent with the observation of Vahrenkamp that the acetylide clusters with related spiked-triangular metal frameworks can be generated by exchanging the position of transition-metal atoms.^{6,11}

In addition, the migration of acetylide in **2b** possesses a much lower barrier than that of the skeletal rearrangement. The former resembles that of the acetylide rotation on the triangular surface of heterometallic clusters LWRu₂(CO)₈(C≡CR) (L = Cp and Cp*; R = Ph and Bu^t)¹⁸ and triruthenium compound Ru₃(CO)₉(μ-H)(C≡CBu^t) and its phosphine derivatives.¹⁹ In contrast, the acetylide ligand in **2a** is static on the time scale of

NMR spectroscopy. This is apparently due to the much stronger π-bonding between the acetylide ligand and the wingtip W atom, which prohibits the acetylide ligand undergoing migration to the adjacent Os–Os edge to form the π-interaction with the Os atom at the opposite wingtip position.

Acknowledgment. We are grateful to the National Science Council of the Republic of China for financial support (Grant No. NSC 84-2113-M007-020).

Supporting Information Available: Variable-temperature ¹³C NMR spectra (Figure 1s) and tables of hydrogen atom coordinates and *B* values and anisotropic thermal parameters of **2b** (3 pages). Ordering information is given on any current masthead page.

OM9504821

(16) (a) Chi, Y.; Su, C.-J.; Farrugia, L. J.; Peng, S.-M.; Lee, G.-H. *Organometallics* **1994**, *13*, 4167. (b) Chi, Y.; Wu, F.-J.; Liu, B.-J.; Wang, C.-C.; Wang, S.-L. *J. Chem. Soc., Chem. Commun.* **1989**, 873. (c) Horwitz, C. P.; Shriver, D. F. *Organometallics* **1984**, *3*, 756. (d) Chi, Y.; Shu, H.-Y.; Peng, S.-M.; Lee, G.-H. *J. Chem. Soc., Chem. Commun.* **1991**, 1023.

(17) (a) Wang, J.-C.; Lin, R.-C.; Chi, Y.; Peng, S.-M.; Lee, G.-H. *Organometallics* **1993**, *12*, 4061. (b) Wang, J.-C.; Chi, Y.; Tu, F.-H.; Shyu, S.-G.; Peng, S.-M.; Lee, G.-H. *J. Organomet. Chem.* **1994**, *481*, 143. (c) Ma, L.; Wilson, S. R.; Shapley, J. R. *J. Am. Chem. Soc.* **1994**, *116*, 787. (d) Couture, C.; Farrar, D. H. *J. Chem. Soc., Dalton Trans.* **1987**, 2245.

(18) (a) Chi, Y. *J. Chin. Chem. Soc.* **1992**, *39*, 591. (b) Hwang, D.-K.; Chi, Y.; Peng, S.-M.; Lee, G.-H. *Organometallics* **1990**, *9*, 2709. (c) Chi, Y.; Lee, G.-H.; Peng, S.-M.; Liu, B.-J. *Polyhedron* **1989**, *8*, 2003.

(19) (a) Farrugia, L. J.; Shirley, E. R. *Organometallics* **1992**, *11*, 196. (b) Predieri, G.; Tiripicchio, A.; Vignali, C.; Sappa, E. *J. Organomet. Chem.* **1988**, *342*, C33. (c) Rosenberg, E.; Barner-Thorsen, C.; Milone, L.; Aime, S. *Inorg. Chem.* **1985**, *24*, 231.

Metal Activation of Dibenzo[*b,d*]thiophene. Reactivity of the C-S Insertion Product [MeC(CH₂PPh₂)₃]IrH(η²(C,S)-C₁₂H₈S)

Claudio Bianchini,^{*,1a} Juan A. Casares,^{1a} M. Victoria Jiménez,^{1a} Andrea Meli,^{1a} Simonetta Moneti,^{1a} Francesco Vizza,^{1a} Verónica Herrera,^{1b} and Roberto Sánchez-Delgado^{1b}

Istituto per lo Studio della Stereochimica ed Energetica dei Composti di Coordinazione, ISSECC-CNR, Via J. Nardi 39, 50132 Firenze, Italy, and Instituto Venezolano de Investigaciones Científicas, IVIC, Caracas 1020 A, Venezuela

Received May 22, 1995[®]

The reactivity of the Ir(III) complex (triphos)IrH(η²(C,S)-DBT) (**1**), obtained by insertion of the [(triphos)IrH] fragment into a C-S bond of DBT, has been studied in THF [triphos = MeC(CH₂PPh₂)₃; DBT = dibenzo[*b,d*]thiophene]. Compound **1** reacts with CO (5 atm, ≥ 50 °C) to give the 2-phenylthiophenolate complex (triphos)Ir(CO)(SC₁₂H₉) (**3**) and with MeI/NaBPh₄ to give the thioether complex [(triphos)IrH(MeSC₁₂H₈)]BPh₄ (**5**). Treatment of **1** with a strong protic acid results in the formation of the μ-thiolate dimer [(triphos)IrH(μ-SC₁₂H₉)₂HIr(triphos)](BPh₄)₂ (**8**). Deuterium labeling experiments exclude the proposition that the proton attacks the terminal hydride ligand in **1**. A mechanism is proposed which involves attack by H⁺ at the sulfur atom, followed by proton transfer to the metalated carbon atom. The dimer **8** reacts with CO to give either **4** (1 atm, 20 °C) or the dicarbonyl complex [(triphos)Ir(CO)₂]BPh₄ (**6**) plus free 2-phenylthiophenol (5 atm, ≥ 70 °C). 2-(Methylthio)biphenyl is obtained from either carbonylation (5 atm of CO, ≥ 60 °C) or hydrogenation (5 atm of H₂, ≥ 100 °C) of **5**. In the latter case, all the iridium is incorporated into the trihydride (triphos)IrH₃. All the carbonylation and hydrogenation reactions have been studied *in situ* by high-pressure NMR (HPNMR) spectroscopy in sapphire tubes. Some of the results herein presented provide mechanistic information on the heterogeneous hydrodesulfurization (HDS) of DBT.

Introduction

Crude oil contains a variety of organosulfur compounds, a large part of which is eliminated by treatment with high pressures of H₂ over a hot heterogeneous catalyst.² This process is commonly referred to as hydrodesulfurization (HDS).

After HDS treatment, residual sulfur in fuels is present mainly in thiophenic forms and predominantly as benzothiophene and dibenzothiophene derivatives.³ Indeed, dibenzothiophenes are the compounds which are particularly difficult to degrade. For this reason, a great deal of fundamental work is currently being carried out to try to understand the HDS mechanism of dibenzothiophenes. Among the various approaches which have been developed to give information on this process, the study of the coordination and reactivity of the model

substrate dibenzo[*b,d*]thiophene (DBT) with soluble metal complexes has emerged as a powerful mechanistic tool.⁴⁻¹⁹ A new impulse in this last homogeneous modeling approach has recently been provided by the appearance in the literature of some reports in which it is shown that metal-activated DBT can either be desulfurized to biphenyl and H₂S or be hydrogenated to 2-phenylthiophenol.^{4,5} Both reactions can be performed in either stoichiometric⁵ or catalytic⁴ fashion depending on the reacting metal system.

[®] Abstract published in *Advance ACS Abstracts*, September 15, 1995.

(1) (a) ISSECC, CNR, Firenze. (b) IVIC, Caracas.
(2) (a) Mitchell, P. C. H. *The Chemistry of Some Hydrodesulfurization Catalysts Containing Molybdenum*; Climax Molybdenum Co. Ltd.: London, 1967. (b) Schuman, S. C.; Shalit, H. *Catal. Rev.* **1970**, *4*, 245. (c) Weisser, O.; Landa, O. *Sulfide Catalysts. Their Properties and Applications*; Pergamon: Oxford, U.K., 1973. (d) Gates, B. C.; Katzer, J. R.; Schuit, G. C. A. *Chemistry of Catalytic Properties*; McGraw-Hill: New York, 1979. (e) Satterfield, C. N. *Heterogeneous Catalysis in Practice*; McGraw-Hill: New York, 1980. (f) *Geochemistry of Sulfur in Fossil Fuels*; Orr, W. L., White, C. M., Eds. ACS Symposium Series 429; American Chemical Society: Washington, DC, 1990. (g) McCulloch, D. C. In *Applied Industrial Catalysis*; Leach, B. E.; Ed.; Academic: New York, 1983; Vol. 1, p 69. (h) Lyapina, N. K. *Russ. Chem. Rev. (Engl. Transl.)* **1982**, *51*, 189. (i) Challenger, F. *Aspects of the Organic Chemistry of Sulfur*; Butterworths: London, 1959.

(3) Galpern, G. D. In *Thiophene and its Derivatives*; Gronowitz, S., Ed.; Wiley: New York, 1985; Part I.

(4) Bianchini, C.; Jiménez, M. V.; Meli, A.; Moneti, S.; Vizza, F.; Herrera, V.; Sánchez-Delgado, R. A. *Organometallics* **1995**, *14*, 2342.

(5) (a) Garcia, J. J.; Maitlis, P. M. *J. Am. Chem. Soc.* **1993**, *115*, 12200. (b) Garcia, J. J.; Mann, B. E.; Adams, H.; Bailey, N. A.; Maitlis, P. M. *J. Am. Chem. Soc.* **1995**, *117*, 2179.

(6) Jones, W. D.; Dong, L. *J. Am. Chem. Soc.* **1991**, *113*, 559.

(7) Jones, W. D.; Chin, R. M. *J. Am. Chem. Soc.* **1992**, *114*, 9851.

(8) Jones, W. D.; Chin, R. M. *J. Organomet. Chem.* **1994**, *472*, 311.

(9) Benson, J. W.; Angelici, R. J. *Organometallics* **1993**, *12*, 680.

(10) Sánchez-Delgado, R. A.; Herrera, V.; Bianchini, C.; Masi, D.; Mealli, C. *Inorg. Chem.* **1993**, *32*, 3766.

(11) Benson, J. W.; Angelici, R. J. *Organometallics* **1992**, *11*, 922.

(12) Rao, K. M.; Day, C. L.; Jacobson, R. A.; Angelici, R. J. *Inorg. Chem.* **1991**, *30*, 5046.

(13) Goodrich, J. D.; Nickias, P. N.; Selegue, J. P. *Inorg. Chem.* **1987**, *26*, 3424.

(14) Choi, M.-G.; Angelici, R. J. *Organometallics* **1991**, *10*, 2436.

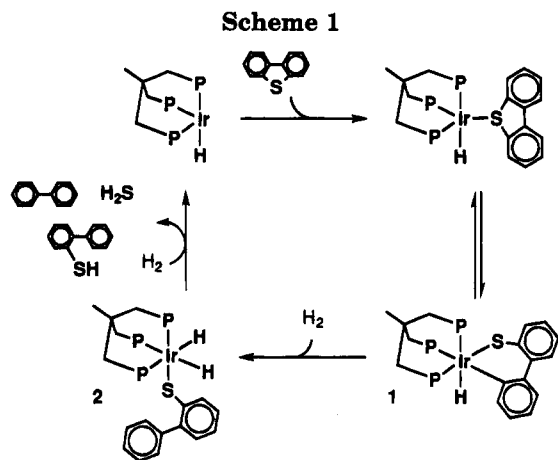
(15) Fischer, E. O.; Goodwin, H. A.; Kreiter, C. G.; Simmons, H. D., Jr.; Sonogashira, K.; Wild, S. B. *J. Organomet. Chem.* **1968**, *14*, 359.

(16) Lee, C. C.; Steele, B. R.; Sutherland, R. G. *J. Organomet. Chem.* **1980**, *186*, 265.

(17) Wang, C.-M. J.; Angelici, R. J. *Organometallics* **1990**, *9*, 1770.

(18) Chen, J.; Su, Y.; Jacobson, R. A.; Angelici, R. J. *J. Organomet. Chem.* **1992**, *428*, 415.

(19) (a) Polam, J. R.; Porter, L. C. *J. Organomet. Chem.* **1994**, *482*, 1. (b) Polam, J. R.; Porter, L. C. *Organometallics* **1993**, *12*, 3504.



The catalyst which brings about the conversion of DBT to a mixture of biphenyl, H_2S , and 2-phenylthiophenol is the 16-electron fragment [(triphos)IrH] [triphos = $\text{MeC}(\text{CH}_2\text{PPh}_2)_3$]. This unsaturated fragment is capable of cleaving DBT in tetrahydrofuran to give the C–S insertion product (triphos)IrH($\eta^2(\text{C},\text{S})$ -DBT) (**1**), which is hydrogenated (100 °C, 5 atm of H_2) to the 2-phenylthiophenolate dihydride (triphos)Ir(H) $_2$ (SC_{12}H_9) (**2**). Finally, the dihydride complex gives biphenyl, H_2S , and 2-phenylthiophenol upon treatment with 30 atm of H_2 at 170 °C (Scheme 1).⁴

A crucial compound in the transformation of DBT described above is the C–S insertion product **1**, which is unique in the relevant literature as it contains both a C–S cleaved DBT and the terminal hydride ligand necessary to initiate the hydrogenation reaction. On the other hand, the known metal complexes containing cleaved DBT number less than a handful (Chart 1) and their reactivity has scarcely been investigated.^{5–8}

In this paper, we report on the reactivity of **1**, particularly regarding the reductive coupling of the terminal hydride with the metalated carbon atom of the iridabenzothiabenzenes system.

Experimental Section

General Procedure. All reactions and manipulations were routinely performed under a nitrogen atmosphere by using standard Schlenk techniques unless otherwise stated. Tetrahydrofuran (THF) was distilled from LiAlH_4 , CH_2Cl_2 from CaH_2 , and *n*-heptane from sodium. The solvents were stored over 4-Å molecular sieves and purged with nitrogen before use. $\text{HBF}_4 \cdot \text{Et}_2\text{O}$ (85% solution in Et_2O), $\text{CF}_3\text{SO}_3\text{D}$ (98 atom % D), and LiHBEt_3 (1.0 M solution in THF) were purchased from Aldrich. All other chemicals were commercial products and were used as received without further purification. Literature methods were used for the preparation of (triphos)IrH($\eta^2(\text{C},\text{S})$ -DBT) (**1**),⁴ (triphos)Ir(H) $_2$ (SC_{12}H_9) (**2**),⁴ (triphos)IrH($\eta^2(\text{C},\text{S})$ -BT) (**10**),²⁰ and (triphos)Ir(η^3 - $\text{S}(\text{C}_6\text{H}_4)\text{CH}=\text{CH}_2$) (**11**).²⁰ All metal complexes were collected on sintered-glass frits and washed with appropriate solvents before being dried in a stream of nitrogen. Infrared spectra were recorded on a Perkin-Elmer 1600 Series FT-IR spectrophotometer using samples milled in Nujol between KBr plates. Deuterated solvents for NMR measurements were dried over molecular sieves. ^1H NMR spectra were obtained on a Bruker ACP 200 (200.13 MHz) spectrometer. ^1H NMR shifts are recorded relative to residual ^1H resonance in the deuterated solvent: CD_2Cl_2 , δ 5.32; CDCl_3 , δ 7.23. The $^{13}\text{C}\{^1\text{H}\}$ NMR spectra were recorded on the Bruker

ACP 200 instrument operating at 50.32 MHz. The $^{13}\text{C}\{^1\text{H}\}$ NMR shifts are given relative to the solvent resonance: CD_2Cl_2 , δ 54.2; CDCl_3 , δ 77.7. $^{31}\text{P}\{^1\text{H}\}$ NMR spectra were recorded either on a Varian VXR 300 or a Bruker ACP 200 spectrometer operating at 121.42 MHz and 81.01 MHz, respectively. Chemical shifts are relative to external 85% H_3PO_4 with downfield values reported as positive. Broad band and selective $^1\text{H}\{^{31}\text{P}\}$ NMR experiments were carried out on the Bruker ACP 200 instrument equipped with a 5-mm inverse probe and a BFX-5 amplifier device. ^{13}C DEPT, ^1H – ^{13}C 2D HETCOR, and ^1H – ^1H 2D COSY NMR experiments were conducted on the Bruker ACP 200 spectrometer. The high-pressure NMR (HPNMR) experiments were carried out in 10-mm sapphire tubes (Saphicon Inc., Milford, NH); for the design of the titanium pressure head see ref 21. Conductivities were measured with an Orion Model 990101 conductance cell connected to a Model 101 conductivity meter. The conductivity data were obtained at sample concentrations of ca. 10^{-3} M in nitroethane solutions at room temperature. GC analyses were performed on a Shimadzu GC-14 A gas chromatograph equipped with a flame ionization detector and a 30-m (0.25-mm i.d., 0.25- μm FT) SPB-1 Supelco fused silica capillary column. GC/MS analyses were performed on a Shimadzu QP-5000 apparatus equipped with a column identical to that used for GC analyses. Reactions at high temperature or under controlled pressure of carbon monoxide and hydrogen were performed with a Parr 4565 reactor equipped with a Parr 4842 temperature and pressure controller.

Reaction of (triphos)IrH($\eta^2(\text{C},\text{S})$ -DBT) (1**) with CO. A. Synthesis of (triphos)Ir(CO)(SC_{12}H_9) (**3**).** A solution of **1** (0.25 g, 0.25 mmol) in THF (30 mL) was pressurized with carbon monoxide to 5 atm at room temperature in a Parr reactor and then heated at 80 °C for 3 h. The bomb was then cooled to room temperature, and after being depressurized and vented under a nitrogen stream, the contents were transferred into a Schlenk-type flask. Addition of *n*-heptane (30 mL) led to the precipitation of **3** as pale yellow microcrystals. They were filtered off and washed with *n*-pentane; yield 100%. Anal. Calcd (found) for $\text{C}_{54}\text{H}_{48}\text{IrOP}_3\text{S}$: C, 62.96 (62.43); H, 4.70 (4.58); Ir, 18.66 (18.25); S, 3.11 (2.93). IR: $\nu(\text{CO})$ 1902 (vs) cm^{-1} .

B. Sapphire Tube HPNMR Experiment. A 10-mm sapphire HPNMR tube was charged with a THF- d_8 (2 mL) solution of **1** (0.05 g, 0.05 mmol) under nitrogen, pressurized with carbon monoxide to 5 atm at room temperature, and then placed into a NMR probe. The reaction was monitored by variable-temperature $^{31}\text{P}\{^1\text{H}\}$ NMR spectroscopy. The conversion of **1** to **3** started already at ca. 50 °C.

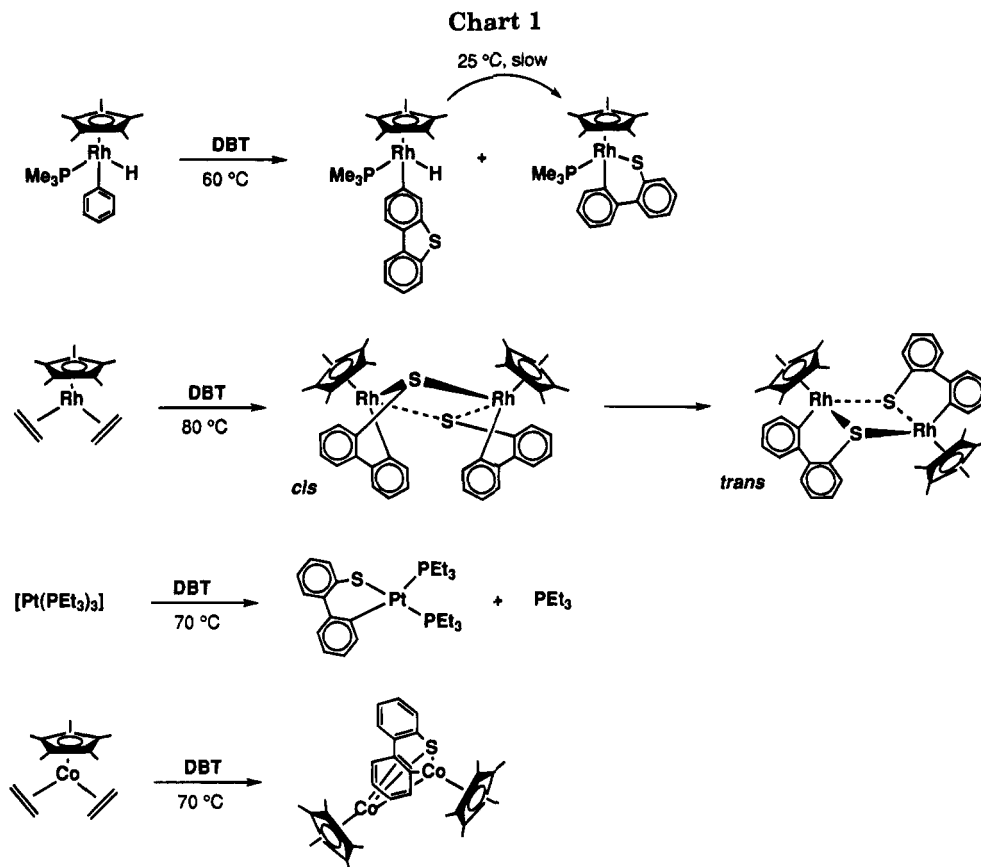
Synthesis of [(triphos)IrH(CO)(SC_{12}H_9)]BPh $_4$ (4**).** **Method A.** A solution of **3** (0.26 g, 0.25 mmol) in THF (30 mL) was treated with a slight excess of $\text{HBF}_4 \cdot \text{OEt}_2$ (54 μL , 0.27 mmol). After ca. 20 min, NaBPh_4 (0.85 g, 0.25 mmol) in ethanol (20 mL) was added to the reaction mixture. On partial evaporation of the solvents **4** precipitated as off-white microcrystals. They were filtered off and washed with *n*-pentane; yield 83%. Anal. Calcd (found) for $\text{C}_{78}\text{H}_{69}\text{BIrOP}_3\text{S}$: C, 69.38 (69.25); H, 5.15 (5.02); Ir, 14.23 (14.08); S, 2.37 (2.11). Δ_M : 54 Ω^{-1} cm^2 mol^{-1} . IR: $\nu(\text{Ir}-\text{H})$ 2120 (s) cm^{-1} ; $\nu(\text{CO})$ 2068 (vs) cm^{-1} . ^1H NMR (CD_2Cl_2 , 20 °C): δ -9.38, dt, $^2J(\text{HP}) = 128.2$, 8.7 Hz, Ir–H. $^{13}\text{C}\{^1\text{H}\}$ NMR (CD_2Cl_2 , 20 °C): δ 169.7, dt, $^2J(\text{CP}) = 116.3$, 5.6 Hz, IrCO.

Method B. Carbon monoxide was bubbled through a solution of **8** (0.21 g, 0.08 mmol) in CH_2Cl_2 (20 mL) at room temperature for 30 min. During this time the color of the solution turned from red orange to pale yellow. On addition of ethanol (20 mL) and partial evaporation of the solvent **4** precipitated in 85% yield.

Synthesis of [(triphos)IrH($\text{MeSC}_{12}\text{H}_9$)]BPh $_4$ (5**).** A 3-fold excess of neat MeI (48 μL) was syringed into a solution of **1** (0.25 g, 0.25 mmol) in THF (10 mL) at room temperature. After

(20) Bianchini, C.; Meli, A.; Peruzzini, M.; Vizza, F.; Moneti, S.; Herrera, V.; Sánchez-Delgado, R. A. *J. Am. Chem. Soc.* **1994**, *116*, 4370.

(21) Elsevier, C. J. *J. Mol. Catal.* **1994**, *92*, 285.



30 min, addition of NaBPh_4 (0.85 g, 0.25 mmol) in ethanol (30 mL) and partial evaporation of the solvents under a steady stream of nitrogen gave off-white crystals of **5**. They were filtered off and washed with ethanol and *n*-pentane; yield 88%. Anal. Calcd (found) for $\text{C}_{78}\text{H}_{71}\text{BP}_3\text{IrS}$: C, 70.10 (69.99); H, 5.35 (5.23); Ir, 14.38 (14.17); S, 2.40 (2.23). Δ_M : $50 \Omega^{-1} \text{cm}^2 \text{mol}^{-1}$. IR: $\nu(\text{Ir-H})$ 2104 (s) cm^{-1} . ^1H NMR (CD_2Cl_2 , 20 °C): δ -7.99, dt, $^2J(\text{HP}) = 140.3$, 11.7 Hz, Ir-H; 2.31, d, $^4J(\text{HP}) = 4.0$ Hz, SMe. $^{13}\text{C}\{^1\text{H}\}$ NMR (CD_2Cl_2 , 20 °C): δ 146.1, br s, IrC; 29.7, d, $^3J(\text{CP}) = 3.9$ Hz, SMe; the rest of the resonances of DBT were masked by those of the phenyl carbons of triphos ligand and the BPh_4^- counteranion (120–140 ppm).

Reaction of 5 with CO. A. Preparative Scale. A solution of **5** (0.27 g, 0.20 mmol) in THF (30 mL) was pressurized with carbon monoxide to 5 atm at room temperature in a Parr reactor and then heated at 100 °C for 3 h. The bomb was then cooled to room temperature, and after being depressurized and vented under a nitrogen stream, the contents were transferred into a Schlenk-type flask. The volatiles were then removed in vacuo at room temperature and a portion of the residue analyzed by ^1H and $^{31}\text{P}\{^1\text{H}\}$ NMR spectroscopy. The dicarbonyl [(triphos)Ir(CO) $_2$]BPh $_4$ (**6**)²² was the only iridium complex detected in solution. The rest of the residue was chromatographed over a silica column (a 5:1 mixture of *n*-pentane/ CH_2Cl_2 as eluent). The organic phase was then concentrated to dryness in vacuo, and the residue was characterized by ^1H and $^{13}\text{C}\{^1\text{H}\}$ NMR and GC/MS as 2-(methylthio)biphenyl.²³ ^1H NMR (CDCl_3 , 20 °C): δ 7.5–7.2, m, 9H, CH; 2.38, s, 3H, SMe. $^{13}\text{C}\{^1\text{H}\}$ NMR (CDCl_3 , 20 °C): δ 140.9, C; 140.5, C; 137.1, C; 129.9, CH; 129.3, CH; 129.3, CH; 128.0, CH; 128.0, CH; 127.9, CH; 127.5, CH; 125.2, CH; 124.7, CH; 16.0, Me. GC/MS (EIMS, 70 eV) [m/e (%): 200 (90) M^+ , 185 (100) $\text{M} - \text{Me}^+$, 184 (82), 152 (26) $\text{M} - \text{HSMe}^+$.

B. Sapphire Tube HPNMR Experiment. A 10-mm sapphire HPNMR tube was charged with a THF- d_8 (2 mL)

solution of **5** (0.07 g, 0.05 mmol) under nitrogen, pressurized with CO to 5 atm at room temperature, and then placed into a NMR probe. The reaction was monitored by variable-temperature $^{31}\text{P}\{^1\text{H}\}$ NMR spectroscopy. Appreciable conversion of **1** to **6** occurred already at ca. 60 °C.

Reaction of 5 with H $_2$. A. Preparative Scale. A solution of **5** (0.27 g, 0.20 mmol) in THF (30 mL) was pressurized with hydrogen to 5 atm at room temperature in the Parr reactor and then heated at 120 °C for 3 h. The bomb was then cooled to room temperature, and after being depressurized and vented under a nitrogen stream, the contents were transferred into a Schlenk-type flask. The volatiles were then removed in vacuo at room temperature. The residue was divided into three portions. One portion, analyzed by IR and multinuclear NMR spectroscopy, was shown to contain the trihydrido complex (triphos)IrH $_3$ (**7**)²⁴ as the only iridium complex. Triphenylboron was separated by the second portion by sublimation (70 °C, 0.5 Torr). The rest of the residue, chromatographed and analyzed as described above, was found to contain 2-(methylthio)biphenyl. There was no evidence for the formation of other hydrogenated species.

B. Sapphire Tube HPNMR Experiment. A 10-mm sapphire HPNMR tube was charged with a THF- d_8 (2 mL) solution of **5** (0.07 g, 0.05 mmol) under nitrogen, pressurized with hydrogen to 5 atm at room temperature, and then placed into a NMR probe. The reaction was monitored by variable-temperature $^{31}\text{P}\{^1\text{H}\}$ NMR spectroscopy. Appreciable conversion of **5** to **7** was observed to occur starting from ca. 100 °C.

Reaction of 1 with HBF $_4$ ·OEt $_2$. A. Preparative Scale. A slight excess of HBF $_4$ ·OEt $_2$ (54 μL , 0.27 mmol) was added to a solution of **1** (0.25 g, 0.25 mmol) in THF or CH_2Cl_2 (30 mL) at room temperature. There was an immediate color change from pale yellow to red orange. After ca. 20 min, NaBPh $_4$ (0.85 g, 0.25 mmol) in ethanol (20 mL) was added to the reaction mixture. On partial evaporation of the solvents

(22) Barbaro, P.; Bianchini, C.; Meli, A.; Peruzzini, M.; Vacca, A.; Vizza, F. *Organometallics* **1991**, *10*, 2227.

(23) Emrick, D. D.; Truce, W. E. *J. Org. Chem.* **1960**, *25*, 1103.

(24) Janser, P.; Venanzi, L. M.; Bachechi, F. *J. Organomet. Chem.* **1985**, *296*, 229.

under a brisk stream of nitrogen orange microcrystals of [(triphos)IrH(μ -SC₁₂H₈)₂HIr(triphos)](BPh₄)₂ (**8**) precipitated. They were filtered off and washed with *n*-pentane; yield 84%. Anal. Calcd (found) for C₁₅₄H₁₃₈B₂Ir₂P₆S₂: C, 69.94 (69.21); H, 5.26 (5.18); Ir, 14.54 (14.38); S, 2.42 (2.23). Λ_M : 98 Ω^{-1} cm² mol⁻¹. IR: ν (Ir-H) 2140 (s) cm⁻¹. ¹H NMR (CD₂Cl₂, -20 °C): δ -1.37, dt, ²*J*(HP) = 132.2, 10.2 Hz, IrH.

B. NMR Studies. Compound **1** (0.05 g, 0.05 mmol) in CD₂Cl₂ (0.7 mL) was treated with 1 equiv of CF₃SO₃D (ca. 45 μ L) in an NMR tube. ¹H and ³¹P{¹H} NMR spectra of the reaction mixture recorded at -20 °C showed the formation of a complex, **8-d**₁, displaying a ³¹P NMR spectrum identical with that of **8** (no coupling of the phosphorus nuclei with deuterium was observed). Most importantly, the ¹H NMR spectrum contains a hydride resonance with chemical shift and intensity (as compared to the signal of the CH₃ substituent of triphos) identical with those of pure **8**. This evidence, coupled with the mass spectrum of monodeuterated 2-phenylthiophenol which was produced from **8-d**₁ (preparative scale) by treatment with CO (*vide infra*), is unambiguously consistent with the incorporation of deuterium into the phenyl ring of the 2-phenylthiophenolate bridging ligand.

In a second NMR experiment, a 5-mm screw-cap NMR tube was charged with a THF-*d*₈ (0.7 mL) solution of **1** (0.05 g, 0.05 mmol) under nitrogen at -78 °C. A stoichiometric amount of HBF₄·OEt₂ (ca. 10 μ L) was syringed into the tube. Immediately there was a color change from colorless to red orange. The tube was positioned into the NMR probe pre-cooled at -80 °C, and ¹H and ³¹P{¹H} NMR spectra were recorded showing that the quantitative conversion of **1** to **8** occurs with no detectable intermediate at a temperature as low as -78 °C.

Reaction of 2 with HBF₄·OEt₂. A screw-cap 5-mm NMR tube was charged with a THF-*d*₈ (0.7 mL) solution of **2** (30 mg, 0.03 mmol) under nitrogen. A stoichiometric amount of HBF₄·OEt₂ (ca. 10 μ L) was syringed into the tube. Immediately there was a color change from pale yellow to red orange. ¹H and ³¹P{¹H} NMR spectra of this solution recorded at -20 °C showed the quantitative conversion of **2** to **8** and evolution of H₂ (¹H NMR: singlet at 4.7 ppm).

Reaction of 8 with LiHBEt₃. To a red orange solution of **8** (0.21 g, 0.08 mmol) in THF (30 mL) at room temperature was added a 4-fold excess of LiHBEt₃ (0.32 mL, 0.32 mmol). Immediately the solution became pale yellow in color. After ca. 20 min, ethanol (20 mL) was added to the reaction mixture. On slow concentration pale yellow crystals of **2** were obtained in 85% yield.

Reaction of 8 or 4 with CO. A. Preparative Scale. A solution of either **8** (0.21 g, 0.08 mmol) or **4** (0.20 g, 0.15 mmol) in THF (30 mL) was pressurized with carbon monoxide to 5 atm at room temperature in a Parr reactor and then heated at 120 °C for 3 h. The bomb was then cooled to room temperature, and after being depressurized and vented under a nitrogen stream, the contents were transferred into a Schlenk-type flask. The volatiles were then removed in vacuo at room temperature, and a portion of the residue analyzed by ¹H and ³¹P{¹H} NMR spectroscopy. The dicarbonyl **6** was the only iridium complex detected in solution. The rest of the residue was chromatographed over a silica column (a 5:1 mixture of *n*-pentane/CH₂Cl₂ as eluent). The organic phase was evaporated to dryness in vacuo, and the residue was authenticated as 2-phenylthiophenol²⁵ by ¹H NMR and GC/MS. ¹H NMR (CDCl₃, 20 °C): δ 7.5–7.1, m, 9H, CH; 3.36, s, 1H, SH. GC/MS (EIMS, 70 eV) [*m/e* (%): 186 (70) M⁺, 185 (100) M – H⁺, 152 (42) M – H₂S⁺].

B. Sapphire Tube HPNMR Experiment. A 10-mm sapphire HPNMR tube was charged with a THF-*d*₈ (2 mL) solution of **4** (0.04 g, 0.03 mmol) under nitrogen, pressurized with CO to 5 atm at room temperature, and then placed into

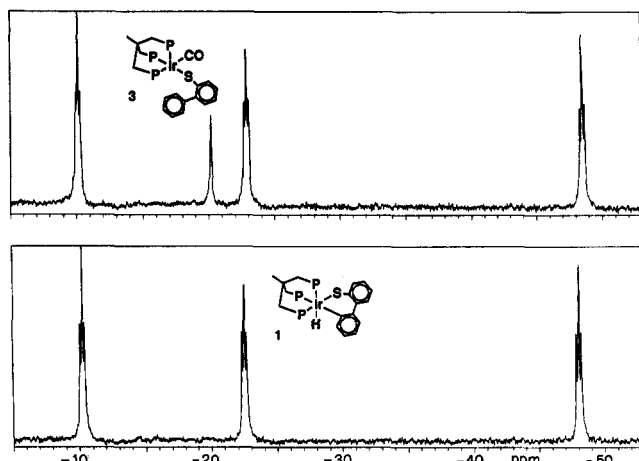


Figure 1. ³¹P{¹H} HPNMR study (sapphire tube, THF-*d*₈, 81.01 MHz) of the reaction of **1** with CO (5 atm): 20 °C (bottom); 50 °C after 20 min (top).

a NMR probe. The reaction was monitored by variable-temperature ³¹P{¹H} NMR spectroscopy. The conversion of **4** to **6** occurred already at ca. 70 °C.

Synthesis of [(triphos)IrH(MeSC₆H₄)]BPh₄ (12**).** A 3-fold excess of neat MeI (48 μ L) was syringed into a solution of (triphos)IrH(η^2 (C,S)-BT) (**10**) (0.24 g, 0.25 mmol) in THF (10 mL) at room temperature. After 30 min, addition of NaBPh₄ (0.85 g, 0.25 mmol) in ethanol (30 mL) and partial evaporation of the solvents under a steady stream of nitrogen gave off-white crystals of **12**. They were filtered off and washed with ethanol and *n*-pentane; yield 80%. Anal. Calcd (found) for C₇₄H₆₉BP₃IrS: C, 69.09 (68.65); H, 5.41 (5.37); Ir, 14.94 (14.54); S, 2.49 (2.25). Λ_M : 52 Ω^{-1} cm² mol⁻¹. IR: ν (IrH) 2110 (s), ν (C=C) 1550 (m) cm⁻¹. ¹H NMR (CD₂Cl₂, 20 °C): δ -10.44, dt, ²*J*(HP) = 132.1, 11.4 Hz, Ir-H; 3.12, d, ⁴*J*(HP) = 3.0 Hz, SMe. ¹³C{¹H} NMR (CD₂Cl₂, 20 °C): δ 35.3, d, ³*J*(CP) = 9.1 Hz, SMe; the resonances of BT were masked by those of the phenyl carbons of triphos ligand and BPh₄⁻ (120–140 ppm).

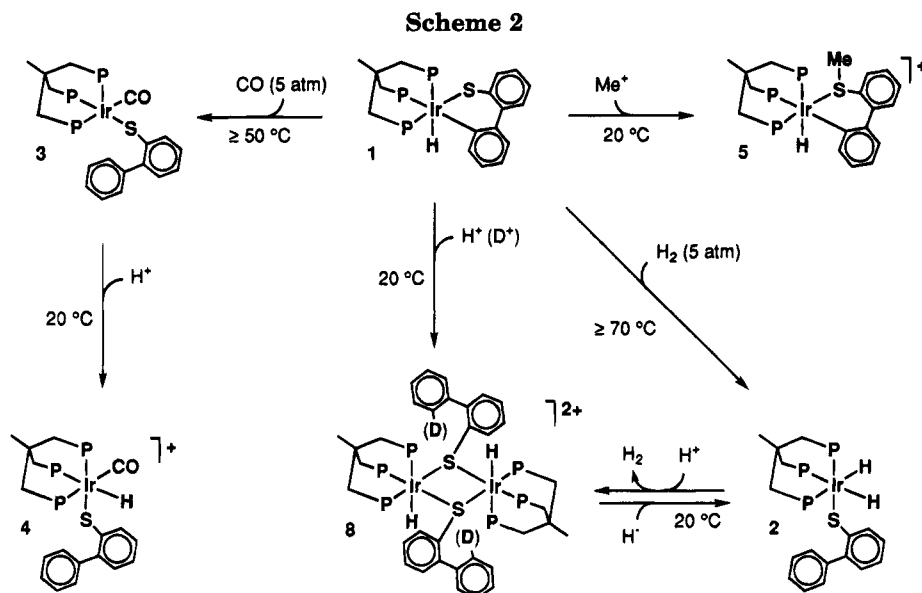
Synthesis of [(triphos)Ir(η^3 -MeS(C₆H₄)CH=CH₂)]BPh₄ (13**).** This complex was prepared in 90% yield analogously to **12** except for the substitution of **11** for **10**. Anal. Calcd (found) for C₇₄H₆₉BP₃IrS: C, 69.09 (68.79); H, 5.41 (5.33); Ir, 14.94 (14.70); S, 2.49 (2.29). Λ_M : 52 Ω^{-1} cm² mol⁻¹. ¹H NMR (CD₂Cl₂, 20 °C): δ 3.53, m, ³*J*(HH) = 8.1, 7.8 Hz, CH=CH₂; 2.10, m, ³*J*(HH) = 8.1 Hz, ²*J*(HH) = 3.9 Hz, CH=CHH'; 1.86, m, ³*J*(HH) = 7.8 Hz, ²*J*(HH) = 3.9 Hz, CH=CHH'; 1.82, dd, ⁴*J*(HP) = 3.6, 1.0 Hz, SCH₃. ¹³C{¹H} NMR (CD₂Cl₂, 20 °C): δ 43.8, ddd, ²*J*(CP) = 31.4, 7.3, 2.4 Hz, CH=CH₂; ca. 36, partially masked by the aliphatic carbons of triphos, CH=CH₂; 27.2, d, ³*J*(CP) = 8.9 Hz, SCH₃. The other resonances of BT were masked by those of the phenyl carbons of triphos ligand and BPh₄⁻ (120–140 ppm).

Thermal Isomerization of 12 to 13. A 5-mm NMR tube was charged with a THF-*d*₈ (0.7 mL) solution of **12** (0.04 g, 0.03 mmol) under nitrogen and then placed into a NMR probe. The reaction was monitored by variable-temperature ³¹P{¹H} NMR spectroscopy. The isomerization of **12** to **13** began to occur already at ca. 60 °C; complete conversion was achieved in 4 h at 90 °C.

Results

Reaction of (triphos)IrH(η^2 (C,S)-DBT) (1**) with CO.** The C–S insertion complex **1** is fully stable in THF at 170 °C in the presence of an excess of DBT. At this temperature, partial decomposition of the complex (10% in 3 h) occurs in pure THF to give free DBT (reversible ring closure) and several unidentified products due to

(25) Klemm, L. H.; Karchesy, J. J. *J. Heterocycl. Chem.* **1978**, *15*, 281.



interaction of the regenerated [(triphos)IrH] fragment with the solvent.⁴

The formal coupling of the terminal hydride ligand of **1** to the metalated carbon atom of the Ir- $\eta^2(C,S)$ -DBT ring to give the dihydride **2** has previously been observed upon reaction with H₂.⁴ We have now found that this coupling reaction occurs also by treatment of **1** in THF with CO (5 atm) and at a temperature ≥ 50 °C (Figure 1). At a temperature of 80 °C for 3 h, the complex (triphos)Ir(CO)(SC₁₂H₉) (**3**) is quantitatively formed (Scheme 2).

Compound **3** belongs to the numerous family of five-coordinate metal complexes with the triphos ligand. Like **3**, these are generally highly fluxional on the NMR time scale because of a fast non-bond-breaking interconversion between square-pyramidal and trigonal-bipyramidal structures.^{24,26,27} Which of the two structures is adopted in either the slow-exchange regime or the solid state ultimately depends on the nature of both the metal center and the coligands. In the case at hand, the complex may safely be assigned the square-pyramidal geometry in the slow-exchange regime as shown by the ³¹P{¹H} NMR spectrum in CD₂Cl₂ which consists of an A₃ pattern at room temperature and of an AMQ pattern at -90 °C (Table 1).

Treatment of **3** in THF with HBF₄·OEt₂, followed by metathetical reaction with NaBPh₄, gives the Ir(III) hydrido complex [(triphos)IrH(CO)(SC₁₂H₉)]BPh₄ (**4**) by selective attack of H⁺ at the electron-rich d⁸-metal center. As expected, **4** is stereochemically rigid in solution where it adopts an octahedral structure (³¹P{¹H} NMR AMQ spin system). In accord with the increased oxidation state of the metal center, $\nu(\text{CO})$ in **4** appears at higher energy (2068 cm⁻¹) as compared to the Ir(I) precursor **3** (1902 cm⁻¹).

Methylation of 1 and Subsequent Reactions of the Resulting Thioether Complex with CO or H₂. Treatment of **1** with MeI, followed by metathetical reaction with NaBPh₄, gives the thioether complex [(triphos)IrH($\eta^2(C,S)$ -MeSC₁₂H₈)]BPh₄ (**5**) as a result of

Table 1. ³¹P{¹H} NMR Spectral Data for the New Complexes^a

complex	pattern	chem shift, ppm ^b			coupling const, Hz		
		$\delta(\text{A})$	$\delta(\text{M})$	$\delta(\text{Q})$	$J(\text{AM})$	$J(\text{AQ})$	$J(\text{MQ})$
3	A ₃	-19.8					
	AMQ ^d	-4.1	-24.2	-28.8	21.5	21.5	61.4
4	AMQ	-15.3	-23.7	-44.7	25.8	14.0	25.3
5	AMQ	-10.7	-21.7	-41.2	17.6	17.6	17.6
8	AM ₂	2.3	8.8				
	AM ₂ ^c	2.9	9.2		9.5		
12	AMQ	-13.3	-24.5	-37.8	18.3	18.3	18.3
13	AMQ	-14.1	-21.3	-34.1	23.1	26.1	24.9

^a All spectra were recorded at 20 °C in CD₂Cl₂ solutions unless otherwise stated. ^b The chemical shifts (δ 's) are relative to 85% H₃PO₄; downfield values are assumed as positive. ^c At -20 °C. ^d At -90 °C.

selective delivery of Me⁺ to the sulfur atom of the iridathiacycle.

Compound **5** exhibits a stereochemically rigid octahedral structure in solution, similar to that of the thiolate precursor with which the thioether complex shares all of its relevant NMR and IR characteristics. In contrast, the formation of the S-Me bond apparently increases the thermal stability of the complex which, in fact, is more robust than **1** (no decomposition in THF up to 170 °C).

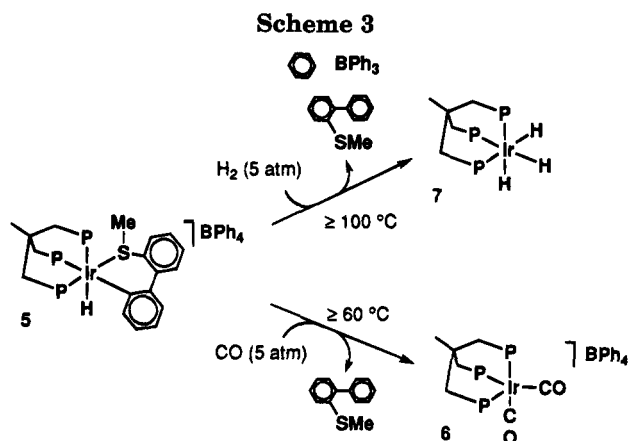
The slightly higher stability of the methylated product is clearly indicated by the reactions with H₂ and CO, which occur at higher temperatures (≥ 100 and 60 °C, respectively) than those of the thiolate precursor at identical pressures (Scheme 3).

The reaction of **5** with CO gives the known dicarbonyl [(triphos)Ir(CO)₂]BPh₄ (**6**)²² and free 2-(methylthio)-biphenyl.²³ The latter product is also obtained from the reaction with H₂ which leads to the incorporation of all of the iridium present into the trihydrido complex (triphos)IrH₃ (**7**).²⁴ The formation of the neutral trihydride **7** is not surprising in view of previous literature reports.²⁰ The extra hydride ligand comes from a heterolytic H₂ splitting step at the iridium center promoted by THF and BPh₄⁻. The latter counteranion is the ultimate target of the released proton which, in fact, cleaves a B-C bond to give benzene and triphenylboron (detected).²⁰

Reaction of 1 with Protic Acids. Compound **1** in

(26) (a) Bianchini, C.; Meli, A.; Peruzzini, M.; Vizza, F.; Frediani, P.; Ramirez, J. A. *Organometallics* **1990**, *9*, 226. (b) Bianchini, C.; Barbaro, P.; Meli, A.; Peruzzini, M.; Vacca, A.; Vizza, F. *Organometallics* **1993**, *12*, 2505.

(27) Dahlenburg, L.; Mirzaei, F. *Inorg. Chim. Acta* **1985**, *97*, L1.



THF is quantitatively converted to the dimer $[(\text{triphos})\text{IrH}(\mu\text{-SC}_{12}\text{H}_9)_2\text{H}(\text{triphos})](\text{BPh}_4)_2$ (**8**) by treatment with $\text{HBF}_4\cdot\text{OEt}_2$, followed by addition of NaBPh_4 in ethanol. In an independent experiment carried out with the use of $\text{CF}_3\text{SO}_3\text{D}$, it has been observed *via* NMR spectroscopy that deuterium is selectively incorporated into the phenyl ring of the bridging 2-phenylthiophenolate ligand to give $[(\text{triphos})\text{IrH}(\mu\text{-SC}_{12}\text{H}_8\text{D})_2\text{H}(\text{triphos})](\text{BPh}_4)_2$ (**8-d₁**) (Scheme 2). No intermediate species was seen (^{31}P NMR) during the conversion of **1** to **8** even when the reaction between **1** and H^+ was carried out at -80°C .

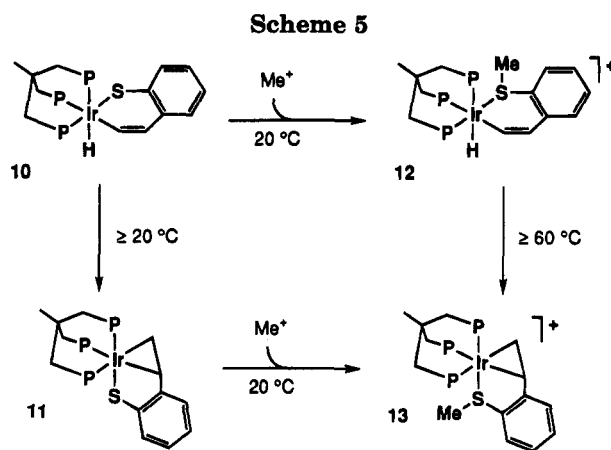
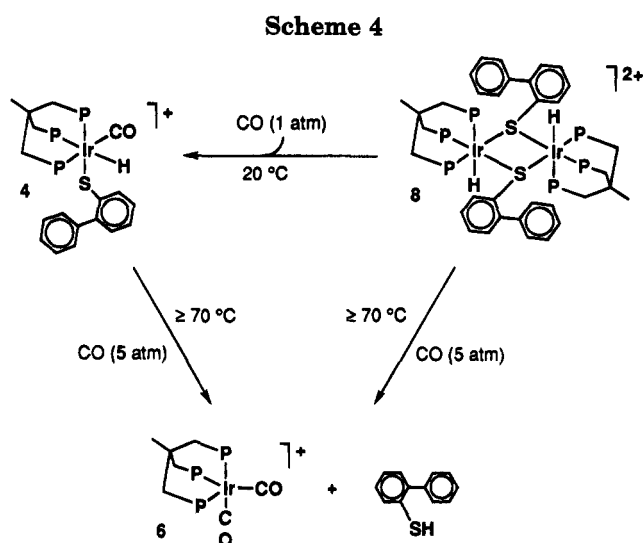
Compound **8** has a close precedent in the dimer $[(\text{triphos})\text{IrH}\{\mu\text{-}o\text{-S}(\text{C}_6\text{H}_4\text{C}_2\text{H}_5)_2\text{H}(\text{triphos})\}](\text{BF}_4)_2$ (**9**) prepared by cleavage and hydrogenation of benzo[*b*]thiophene (BT) at the $[(\text{triphos})\text{Ir}]^+$ fragment.²⁰ In particular, **8** and **9** can be similarly prepared by protonation of the corresponding thiolate dihydride complexes **2** and $(\text{triphos})\text{Ir}(\text{H})_2\{o\text{-S}(\text{C}_6\text{H}_4)\text{C}_2\text{H}_5\}$, respectively (Scheme 2).

Since **8** and **9** show comparable NMR and IR characteristics, a detailed description of the spectroscopic properties of the former compound is not given here.

The chemistry of **8** is quite interesting. The dimeric structure of the complex can be broken up by addition of either H^- to give **2** or CO (1 atm, 20°C) to give **4**. Quantitative elimination of 2-phenylthiophenol²⁵ from **8** can be achieved by reaction with a higher pressure of CO (5 atm) at a temperature $\geq 70^\circ\text{C}$. Under the same conditions, 2-phenylthiophenol is also eliminated from the carbonyl **4** (Scheme 4). The final iridium complex collected from both reactions is the dicarbonyl **6**.

Methylation of the BT C-S Insertion Product $(\text{triphos})\text{IrH}(\eta^2(\text{C,S})\text{-BT})$ (10**).** In order to see whether the increased thermal stability of the S-methylated product, particularly regarding the C-H coupling step, is a common feature in other metal-inserted thiophenes, we have reacted the BT-derived complex $(\text{triphos})\text{IrH}(\eta^2(\text{C,S})\text{-BT})$ ²⁰ (**10**) with MeI (Scheme 5).

Like **1**, alkylation selectively occurs at the sulfur atom to give the thioether complex $[(\text{triphos})\text{IrH}(\text{MeSC}_6\text{H}_5)]\text{-BPh}_4$ (**12**). Complex **12** thermally rearranges in THF to the *o*-(methylthio)styrene tautomer $[(\text{triphos})\text{Ir}(\eta^3\text{-MeS}(\text{C}_6\text{H}_4)\text{CH}=\text{CH}_2)]\text{BPh}_4$ (**13**) above 60°C , whereas the nonmethylated product **10** converts to the 2-vinylthiophenolate tautomer $(\text{triphos})\text{Ir}(\eta^3\text{-S}(\text{C}_6\text{H}_4)\text{CH}=\text{CH}_2)$ ²⁰ (**11**) already at 20°C . Compound **13** can independently be prepared by methylation of **11** under similar reaction conditions.

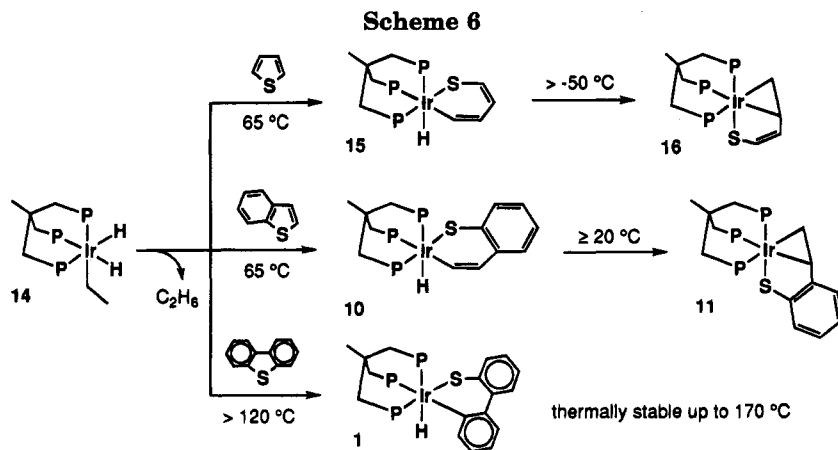


Identification of the novel complexes **12** and **13** was made by IR and NMR spectroscopies. The spectral data are fully comparable with those of the nonalkylated precursors **10** and **11**,²⁰ the only remarkable differences being given by the absorptions of the methyl group. Accordingly, both **12** and **13** are assigned an octahedral structure. In the former complex, the metal center is coordinated by a *fac*-triphos ligand, by a terminal hydride, and by the carbon and sulfur atoms of an *o*-(methylthio)styryl ligand. In **13**, the octahedral structure is given by a *fac*-triphos ligand and by an *o*-(methylthio)styrene ligand which uses the sulfur atom and the olefinic bond to bind iridium.

Discussion

Among the various thiophenic residues in fossil fuels, the dibenzothiophenes are the most difficult to desulfurize under heterogeneous HDS conditions.^{2,3} The question of the competitive reactivity of thiophene (T), BT, and DBT has been tackled by means of homogeneous modeling studies. The few reports on the subject are scarcely informative, particularly because they are all biased by the method of generation of the reactive metal system.^{5,6} The present work for the first time describes a case in which it is unequivocally demonstrated that the energy barrier to C-S insertion of DBT is higher than those of T and BT.

In the course of previous studies, we have found that the $[(\text{triphos})\text{IrH}]$ fragment in THF reacts with DBT to give the C-S insertion product **1** only above 120°C ,⁴



whereas the C-S bond scission of either T^{28,29} or BT²⁹ already occurs at the temperature (ca. 65°C) at which the reactive 16-electron fragment is thermally generated from the precursor (triphos)Ir(H)₂(C₂H₅) (14) (Scheme 6).

As is evident from the chemistry shown in Scheme 6, the kinetic products of the reactions between the [(triphos)IrH] fragment and T, BT, or DBT are hydride iridathiacycles. These C-S insertion products exhibit a dramatically different stability in solution. In fact, while 1 is thermally stable up to 170°C , the products of T^{28,29} and BT^{20,29} activation (15, 10) transform at much lower temperatures (-50 and 20°C , respectively) into the thermodynamically more stable butadiene-thiolate (16) and 2-vinylthiophenolate (11) products by hydride coupling to the metalated carbon atom of the thiacycle. Compound 10 can be isolated, although contaminated by its thermodynamic product, when the precursor to the [(triphos)IrH] fragment is reacted with BT in refluxing THF. In contrast, the C-S insertion product of T, 15, cannot be intercepted as the activation energy for the hydride migration step is very low (however, 15 can be prepared by an independent procedure).²⁸

Since the migration of the hydride to the metalated carbon atom of cleaved thiophenic molecules may be considered as the initial step of the subsequent hydrogenation reaction, it is thus possible that the refractory nature of DBT to HDS may also be a consequence of the difficulty with which the metal-SC₁₂H₉ ring adds a hydride species (which are numerous on the surface of HDS catalysts).³⁰

We have shown in this report that the coupling between the hydride and the metalated carbon atom in 1 is a feasible step that, however, requires the aid of a reagent (CO or H₂) to trap the unsaturated [(triphos)-Ir(SC₁₂H₉)] fragment. Alternatively, the formation of a C-H bond to give a 2-phenylthiophenolate ligand can be achieved by addition of a proton.

The capability of CO to promote reductive coupling steps *via* coordination to the metal center is rather common in organometallic chemistry and certainly does

not occur in the HDS process. In contrast, the reactions with either H⁺ or H₂ are much more interesting, especially in view of the evidence that H₂, adsorbed molecularly, may dissociate heterolytically on the HDS catalyst surface, which thus contains H⁻ and H⁺ probably in the form of sulfhydryl (SH) and hydryl (MH) moieties.³¹

The reaction between 1 and H⁺ is somewhat thought-provoking. In principle, a molecule such as 1 may contain three nucleophilic sites: the terminal hydride ligand, the sulfur atom, and the metalated carbon atom (we exclude a direct attack at the Ir(III) metal center). In the first case, a transient $\eta^2\text{-H}_2$ ligand would form,³² which is a common precursor to intramolecular proton transfer reactions.³³ In the second case, an S-H bond would form,^{33c,34} followed by proton transfer to the carbon atom.²⁸ The fact that the reaction between 1 and the deuterated acid gives selective incorporation of deuterium into the phenyl ring of the 2-phenylthiophenolate bridging ligand of 8 excludes the first hypothesis. In this case, we would have seen both deuterium and protium incorporation into the phenyl ring as well as the formation of an Ir-D bond, none of which, in fact, have been observed. Accordingly, the proton either adds directly to the metalated carbon atom or interacts with the sulfur, from which the proton moves to the carbon atom at a later stage (this should be a low-energy process as no intermediate species has spectroscopically been detected even at -80°C). The following formation of the dimer 8 is a trivial step in view of the unsaturated character of the [(triphos)Ir-(H)(SC₁₂H₉)]⁺ fragment.

Indirect support in favor of the initial attack by H⁺ at the sulfur atom of 1 (Scheme 7a) is provided by the reaction with Me⁺, which selectively results in the formation of an S-Me bond to give 5, as well as some

(31) (a) Neurock, M.; van Santen, R. A. *J. Am. Chem. Soc.* **1994**, *116*, 4427. (b) Topsøe, N.; Topsøe, H. *J. Catal.* **1993**, *139*, 641.

(32) (a) Chinn, M. S.; Heinekey, D. M. *J. Am. Chem. Soc.* **1987**, *109*, 5865. (b) Chinn, M. S.; Heinekey, D. M. *J. Am. Chem. Soc.* **1990**, *112*, 5166. (c) Collman, J. P.; Wagenknecht, P. S.; Hembre, R. T.; Lewis, N. S. *J. Am. Chem. Soc.* **1990**, *112*, 1294. (d) Bianchini, C.; Peruzzini, M.; Zanobini, F. *J. Organomet. Chem.* **1990**, *390*, C16. (e) Morris, R. H. *Inorg. Chem.* **1992**, *31*, 1471.

(33) (a) Jessop, P. G.; Morris, R. H. *Coord. Chem. Rev.* **1992**, *121*, 155. (b) Chinn, M. S.; Heinekey, D. M.; Payne, N. G.; Sofield, C. D. *Organometallics* **1989**, *8*, 1824. (c) Schlaf, M.; Morris, R. H. *J. Chem. Soc., Chem. Commun.* **1995**, 625. (d) Bianchini, C.; Meli, A.; Peruzzini, M.; Frediani, P.; Bohanna, C.; Esteruelas, M. A.; Oro, L. A. *Organometallics* **1992**, *11*, 138.

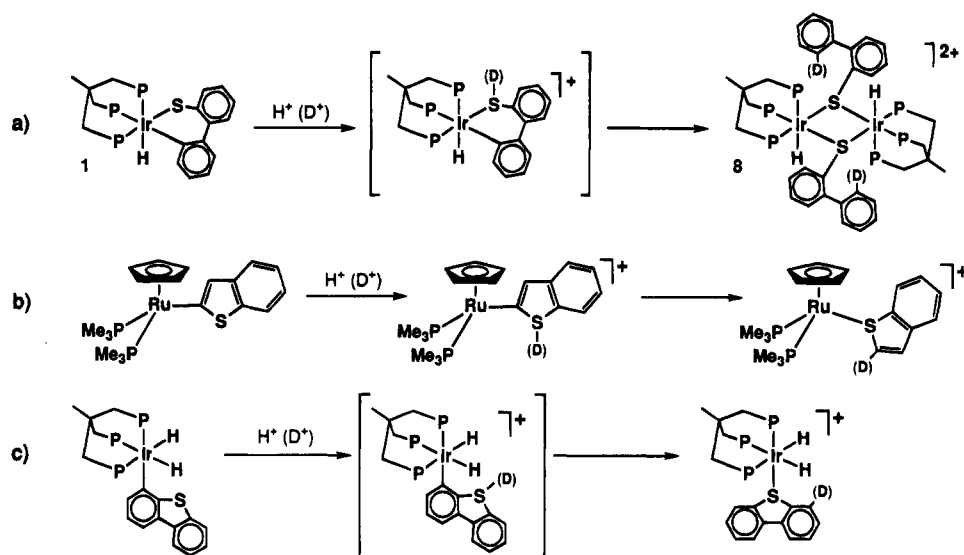
(34) Wander, S. A.; Reibenspies, J. H.; Kim, J. S.; Darensburg, M. Y. *Inorg. Chem.* **1994**, *33*, 1421.

(28) Bianchini, C.; Meli, A.; Peruzzini, M.; Vizza, F.; Frediani, P.; Herrera, V.; Sánchez-Delgado, R. A. *J. Am. Chem. Soc.* **1993**, *115*, 2731.

(29) Bianchini, C.; Jiménez, M. V.; Meli, A.; Moneti, S.; Vizza, F. *J. Organomet. Chem.* **1995**, in press.

(30) (a) Jobic, H.; Clugnet, G.; Lacroix, M.; Yuan, S.; Mirodatos, C.; Breyse, M. *J. Am. Chem. Soc.* **1993**, *115*, 3654. (b) Givens, K. E.; Dillard, J. G. *J. Catal.* **1984**, *86*, 108. (c) Wright, C. J.; Fraser, D.; Moyes, R. B.; Wells, P. B. *Appl. Catal.* **1981**, *1*, 49.

Scheme 7



related precedents in the literature. For example, the 2-benzothieryl complex $\text{Cp}(\text{PMe}_3)_2\text{Ru}(2\text{-BTyl})$ ³⁵ and the 4-dibenzothieryl complex $(\text{triphos})\text{Ir}(\text{H})_2(4\text{-DBTyl})$ ⁴ each react with H^+ to give the $\eta^1(\text{S})\text{-BT}$ (or DBT) complexes $[\text{Cp}(\text{PMe}_3)_2\text{Ru}(\eta^1(\text{S})\text{-BT})]^+$ and $[(\text{triphos})\text{Ir}(\text{H})_2(\eta^1(\text{S})\text{-DBT})]^+$, respectively (Scheme 7b,c). In both cases, evidence has been provided (deuterium labeling experiments) in favor of a mechanism involving straightforward attack by the proton at the sulfur atom followed by hydrogen migration to the metalated carbon atom.

A final aspect of the present work that is worthy of comment regards some chemical consequences of the methylation reaction of **1**.

As already observed for T^{28} and BT ,³⁶ the insertion of a metal center into a C–S bond of DBT increases the nucleophilicity of the sulfur atom, which can be alkylated under milder conditions as compared to free thiophenes.³⁷ Interestingly, the methylated product **5** is more stable to the reductive coupling between the hydride and the metalated carbon atom than **1**. The HPNMR studies show, in fact, that higher temperatures (at the same pressures of CO or H_2) are required to promote such a reductive elimination step in the methylated product **5** than in the nonmethylated compound **1**. A higher energy barrier to hydride migration for the methylated product is observed also in case of the BT-derived complex **12** (Scheme 5). The alkylation, decreasing the donor capability of the sulfur atom (thioether vs thiolate), should decrease the overall basicity of the metal center. Accordingly, one may argue that the thioether complexes should be less stable to reductive elimination than the thiolate ones. Since this is not experimentally observed, our conclusion is that the lesser propensity of the methylated products to undergo

the C–H reductive coupling step may be due to either an increase of the Ir–H and Ir–C bond strengths or the destabilization of the transition state for the following addition of CO , H_2 , or the double bond.

Conclusions

On the basis of a comparative study of the interaction of the 16-electron fragment $[(\text{triphos})\text{IrH}]$ with thiophene, benzo[*b*]thiophene, and dibenzo[*b,d*]thiophene, it is concluded that: (i) the C–S bond cleavage of DBT is the process with the highest activation energy and (ii) the DBT C–S insertion product is the most reluctant to undergo the coupling of a hydride ligand to the metalated carbon atom of the iridathiacycle. These results are consistent with the experimental observation that dibenzothiophenes are more difficult to desulfurize under HDS conditions than thiophenes and benzothiophenes.

The sulfur atom of DBT increases its nucleophilic character after C–S bond cleavage by a metal center. Upon methylation of the C–S insertion product, the resulting thioether complex exhibits a lower propensity to C–H reductive coupling as compared to the nonalkylated complex.

Electrophilic addition of H^+ to the C–S insertion product results in C–H bond formation to give a 2-phenylthiophenolate ligand. Deuterium labeling studies exclude the proposition that the proton attacks the terminal hydride ligand in the C–S insertion product and rather suggest a mechanism, already proposed for heterogeneous HDS, in which the sulfur atom mediates the transfer of the proton to the metalated carbon atom.

Acknowledgment. We thank the Progetto Strategico "Tecnologie Chimiche Innovative", CNR, Rome, Italy, for financial support. Postdoctoral grants to J.A.C. and M.V.J. from the Ministerio de Educación y Ciencia of Spain are gratefully acknowledged.

OM950372U

(35) Benson, J. W.; Angelici, R. J. *Inorg. Chem.* **1993**, *32*, 1871.

(36) Bianchini, C.; Frediani, P.; Herrera, V.; Jiménez, M. V.; Meli, A.; Rincón, L.; Sánchez-Delgado, R. A.; Vizza, F. *J. Am. Chem. Soc.* **1995**, *117*, 4333.

(37) (a) Acheson, R. M.; Harrison, D. R. *J. Chem. Soc. C* **1970**, 1764. (b) Green, T. K.; Whitley, P.; Wu, K.; Lloyd, W. G.; Gan, L. Z. *Energy Fuels* **1994**, *8*, 244.

Rhodium-Assisted Transformations of Substituted Thiophenes into Butadienyl Methyl Sulfides

Claudio Bianchini,* M. Victoria Jiménez, Andrea Meli, and Francesco Vizza

Istituto per lo Studio della Stereochimica ed Energetica dei Composti di Coordinazione, ISSECC-CNR, Via J. Nardi 39, 50132 Firenze, Italy

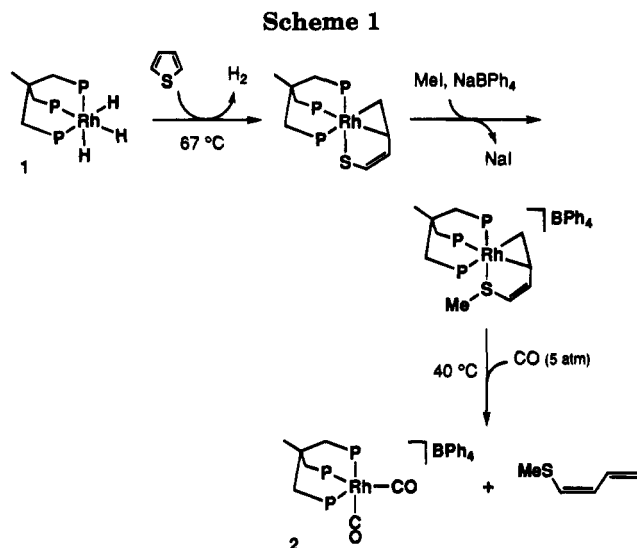
Received May 25, 1995[©]

The novel butadienethiolate complex (triphos)Rh(η^3 -SC(Tyl)=CHCH=CH₂) (Tyl = thienyl) has been prepared by reaction of (triphos)RhH₃ with 2,2'-bithiophene (2-TylT) in refluxing tetrahydrofuran (THF) (triphos = MeC(CH₂PPh₂)₃). Insertion of rhodium occurs exclusively at the C-S bond of a thienyl group of TylT distal to the other thienyl. Complexes of 1-(methylthio)buta-1,3-diene with the formula [(triphos)Rh(η^3 -MeSCR=CR'CH=CH₂)]BPh₄ have been prepared by treatment of the corresponding butadienethiolate complexes (triphos)-Rh(η^3 -SCR=CR'CH=CH₂) (R' = H, R = Me, COMe, CO₂Et, Tyl; R = H, R' = Me, COMe, OMe) with MeI, followed by a metathetical reaction with NaBPh₄. The Rh thioether complexes react with CO (5 atm, 70 °C) in THF to give free butadienyl methyl sulfides (Z)-MeSCR=CR'CH=CH₂ and, quantitatively, the dicarbonyl complex [(triphos)Rh(CO)₂]BPh₄. The butadienyl methyl sulfides have been purified by LC and characterized by their NMR and MS properties. *Inter alia*, the chemistry presented herein provides a novel entry into the synthesis of substituted-butadienyl methyl sulfides, for which a general methodology is still lacking.

Introduction

Thiophene (T) is a molecule of substantial interest for its extraordinarily wide range of chemical applications. Organic chemists largely use T as a precursor to a variety of products via electrophilic attack (nitration, halogenation, sulfonation, acylation, alkylation, etc.), often followed by desulfuration (e. g., synthesis of long-chain alkanes).¹ More recent and sophisticated applications span the use of T as a model compound to study the mechanism of the hydrodesulfurization (HDS) reaction of fossil fuels,² the preparation of new materials with unusual physical properties (electrical,³ magnetic,⁴ nonlinear optical⁵), and the synthesis of complex molecules of biological importance.⁶

We have recently shown that T can efficiently be used for the synthesis of conjugated organosulfur compounds via metal-promoted C-S bond cleavage, followed by electrophilic attack and carbonylation.⁷ Scheme 1 il-



lustrates the procedure for the preparation of butadienyl methyl sulfide.

The success of this method has inspired us to investigate alternative methods of synthesizing butadienyl methyl sulfides bearing various substituents in the butadienyl moiety. Such $\alpha,\beta,\gamma,\delta$ -unsaturated sulfides are, in fact, generally difficult to prepare using standard organic chemistry procedures,⁸ even though they are excellent starting materials for further structural elaborations (Diels-Alder additions, reductions, oxidation of either the sulfur or the double bond, polymerization^{8,9}) as well as molecules endowed with a specific activity (nonlinear optical, radicophilic^{5,10}).

The first step of our investigation was to determine whether the 16-electron fragment [(triphos)RhH], gen-

[©] Abstract published in *Advance ACS Abstracts*, September 15, 1995.

(1) March, J. *Advances Organic Chemistry*, 4th ed.; Wiley: New York, 1992.

(2) (a) Angelici, R. J. In *Encyclopedia of Inorganic Chemistry*; King, R. B., Ed.; Wiley: New York, 1994; Vol. 3, p 1433. (b) Sánchez-Delgado, R. A. *J. Mol. Catal.* **1994**, *86*, 287. (c) Wiegand, B. C.; Friend, C. M. *Chem. Rev.* **1992**, *92*, 491. (d) Girgis, M. J.; Gates, B. C. *Ind. Eng. Chem. Res.* **1991**, *30*, 2021. (e) Rauchfuss, T. B. *Prog. Inorg. Chem.* **1991**, *39*, 259. (f) Angelici, R. J. *Coord. Chem. Rev.* **1990**, *105*, 61. (g) Prins, R.; deBeer, V. H. J.; Somorjai, G. A. *Catal. Rev.—Sci. Eng.* **1989**, *31*, 1. (h) Friend, C. M.; Roberts, J. T. *Acc. Chem. Res.* **1988**, *21*, 394. (i) Angelici, R. J. *Acc. Chem. Res.* **1988**, *21*, 387.

(3) (a) Graf, D. D.; Day, N. C.; Mann, K. R. *Inorg. Chem.* **1995**, *34*, 1562. (b) Shaver, A.; Butler, I. S.; Gao, J. P. *Organometallics* **1989**, *8*, 2079. (c) Tour, J. M.; Wu, R.; Schumm, J. *J. Am. Chem. Soc.* **1991**, *113*, 7064.

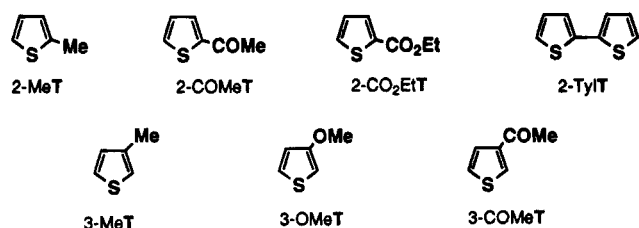
(4) Mitsumori, T.; Inoue, K.; Koga, N.; Iwamura, H. *J. Am. Chem. Soc.* **1995**, *117*, 2067.

(5) Long, N. J. *Angew. Chem., Int. Ed. Engl.* **1995**, *34*, 21.

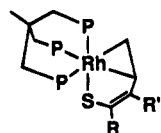
(6) (a) Jaouhari, R.; Guénot, P.; Dixneuf, P. H. *J. Chem. Soc., Chem. Commun.* **1986**, 1255. (b) Nicolau, K. C.; Renaud, J.; Nantermet, P. G.; Couladouros, E. A.; Guy, R. K.; Wrasidlo, W. *J. Am. Chem. Soc.* **1995**, *117*, 2409.

(7) Bianchini, C.; Frediani, P.; Herrera, V.; Jiménez, M. V.; Meli, A.; Rincón, L.; Sánchez-Delgado, R. A.; Vizza, F. *J. Am. Chem. Soc.* **1995**, *117*, 4333.

Chart 1



erated by thermolysis of the trihydride (triphos)RhH₃ (**1**; triphos = MeC(CH₂PPh₂)₃),¹¹ was capable of cleaving substituted thiophenes in a regioselective manner. Our attempt was successful, as the fragment [(triphos)RhH] does react with thiophenes substituted in either the 2- or the 3-position to give C–S insertion products of the formula (triphos)Rh(η³-SCR=CR'CH=CH₂) (**I**).¹² Most



R' = H, R = Me (**3**), COMe (**4**), CO₂Et (**5**)

R = H, R' = Me (**6**), COMe (**7**), OMe (**8**)

I

importantly, the insertions are regioselective, as they occur exclusively at the C–S bond distal to the substituent in the thiophene.

On the basis of these previous results, we herein describe the transformation of the substituted thiophenes shown in Chart 1 to their corresponding butadienyl methyl sulfides.

Experimental Section

General Information. All reactions and manipulations were routinely performed under a nitrogen atmosphere by using standard Schlenk techniques, unless otherwise stated. Tetrahydrofuran (THF) and diethyl ether were distilled from LiAlH₄, CH₂Cl₂ was distilled from CaH₂, and *n*-heptane was distilled from sodium. The solvents were stored over molecular sieves and purged with nitrogen prior to use. 2,2'-Bithiophene (2-TylT) was purchased from Aldrich. All other chemicals were commercial products and were used as received without further purification. The trihydride (triphos)RhH₃¹¹ (**1**) and the butadienethiolate complexes (triphos)Rh(η³-SCR=CR'CH=CH₂) (R' = H, R = Me (**3**), COMe (**4**), CO₂Et (**5**); R = H, R' = Me (**6**), COMe (**7**), OMe (**8**))¹² were prepared as previously described. All metal complexes were collected on sintered-glass frits and washed with appropriate solvents before being

(8) (a) Crumbie, R. L.; Ridley, D. D. *Aust. J. Chem.* **1981**, *34*, 1017. (b) Onishi, T. Jpn. Kokai Tokkyo Koho, 1991. (c) Tsuchihashi, G.; Ogura, K.; Yamamoto, S. Jpn. Kokai Tokkyo Koho, 1978. (d) Metzner, P.; Pham, T. N.; Vialle, J. *Tetrahedron* **1986**, *42*, 2025. (e) Masson, S.; Thuillier, A. *Tetrahedron Lett.* **1980**, *21*, 4085. (f) Michalik, M.; Peseke, K. *J. Prakt. Chem.* **1987**, *329*, 705. (g) Gupta, A. K.; Ila, H.; Jujappa, H. *Tetrahedron* **1989**, *45*, 1509. (h) Datta, A.; Ila, H.; Jujappa, H. *J. Org. Chem.* **1990**, *55*, 5589. (i) Hanko, R.; Hammond, M. D.; Fruchtmann, R.; Pfitzner, J.; Place, G. A. *J. Med. Chem.* **1990**, *33*, 1163. (j) Jones, G. D.; Doorenbos, H. E. *J. Macromol. Sci., Chem.* **1984**, *A21*, 155.

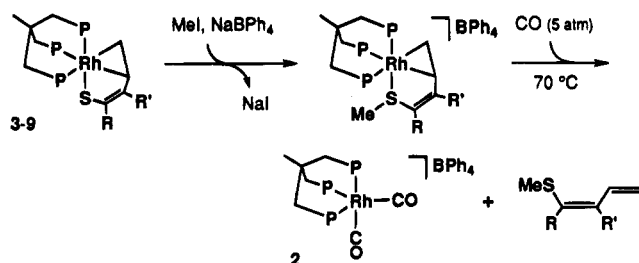
(9) (a) Gillard, M.; T'Kint, C.; Sonveaux, E.; Ghosez, L. *J. Am. Chem. Soc.* **1979**, *101*, 5837. (b) Huber, S.; Stamouli, P.; Jenny, T.; Neier, R. *Helv. Chim. Acta* **1986**, *69*, 1898. (c) Trost, B. M.; Vladuchick, W. C.; Bridges, A. J. *J. Am. Chem. Soc.* **1980**, *102*, 3548. (d) Evans, D. A.; Bryan, C. A.; Sims, C. L. *J. Am. Chem. Soc.* **1972**, *94*, 2891.

(10) Stévenart-De Mesmaeker, N.; Merényi, R.; Viehe, H. G. *Tetrahedron Lett.* **1987**, *28*, 2591.

(11) Ott, J.; Venanzi, L. M.; Ghilardi, C. A.; Midollini, S.; Orlandini, A. *J. Organomet. Chem.* **1985**, *291*, 89.

(12) Bianchini, C.; Jiménez, M. V.; Meli, A.; Vizza, F. *Organometallics* **1995**, *14*, 3196.

Scheme 2



R' = H, R = Me (**10**), COMe (**11**), CO₂Et (**12**), Tyl (**13**)

R = H, R' = Me (**14**), COMe (**15**), OMe (**16**)

dried under a stream of nitrogen. Infrared spectra were recorded on a Perkin-Elmer 1600 Series FT-IR spectrophotometer using samples mullied in Nujol between KBr plates. Deuterated solvents for NMR measurements were dried over molecular sieves. The ¹H NMR spectra were obtained on a Bruker ACP 200 (200.13 MHz) spectrometer, with shifts recorded relative to the residual ¹H resonance in the deuterated solvent: CD₂Cl₂, δ 5.32; CDCl₃, δ 7.23. The ¹³C{¹H} NMR spectra were recorded on a Bruker ACP 200 instrument operating at 50.32 MHz, with shifts given relative to the solvent resonance: CD₂Cl₂, δ 54.4; CDCl₃, δ 77.7. The ³¹P-{¹H} NMR spectra were recorded on a Bruker ACP 200 spectrometer operating at 81.01 MHz; chemical shifts here are relative to external 85% H₃PO₄, with downfield values reported as positive. Broad-band and selective ¹H{³¹P} NMR experiments were carried out on the Bruker ACP 200 instrument equipped with a 5-mm inverse probe and a BFX-5 amplifier device. Finally, ¹³C DEPT, ¹H-¹³C 2D HETCOR, and ¹H-¹H 2D COSY NMR experiments were conducted on the Bruker ACP 200 spectrometer. Conductivities were measured with an Orion Model 990101 conductance cell connected to a Model 101 conductivity meter. The conductivity data were obtained at sample concentrations of ca. 10⁻³ M in nitroethane solutions at room temperature. GC/MS analyses were performed on a Shimadzu QP-5000 apparatus equipped with a 30 m (0.25 mm i.d., 0.25 μm FT) SPB-1 Supelco fused silica capillary column. Reactions under controlled pressure of carbon monoxide were performed with a Parr 4565 reactor equipped with a Parr 4842 temperature and pressure controller.

Preparation of (triphos)Rh(η³-SC(Tyl)=CHCH=CH₂) (9**).** To a stirred suspension of **1** (0.50 g, 0.68 mmol) in THF (40 mL) was added a 10-fold excess of 2-TylT (1.13 g), and then the mixture was heated at reflux temperature. Within a few minutes the solid dissolved. After ca. 3 h, the resulting yellow-brown solution was concentrated to ca. 5 mL. Addition of *n*-heptane (20 mL) led to precipitation of **9** as orange microcrystals, which were collected by filtration and washed with *n*-pentane; yield 76%. Anal. Calcd (found) for C₄₉H₄₆P₃RhS₂: C, 65.77 (65.66); H, 5.18 (5.09); Rh, 11.50 (11.32); S, 7.17 (7.00). IR: ν(C=C) 1570 (m) cm⁻¹.

General Procedure for the Preparation of [(triphos)-Rh(η³-MeSCR=CR'CH=CH₂)]BPh₄ (R' = H, R = Me (10**), COMe (**11**), CO₂Et (**12**), Tyl (**13**); R = H, R' = Me (**14**), COMe (**15**), OMe (**16**)).** A 3-fold excess of neat MeI (48 μL) was syringed into a stirred solution of the appropriate butadienethiolate complex (triphos)Rh(η³-SCR=CR'CH=CH₂) (R' = H, R = Me (**3**), COMe (**4**), CO₂Et (**5**), Tyl (**9**); R = H, R' = Me (**6**), COMe (**7**), OMe (**8**); 0.25 mmol) in CH₂Cl₂ (30 mL) at room temperature. After ca. 30 min, NaBPh₄ (0.85 g, 0.25 mmol) in ethanol (30 mL) was added to the resulting solution. Partial evaporation of the solvents under a steady stream of nitrogen led to the precipitation of yellow-orange microcrystals of **10–16**, which were collected by filtration and washed with *n*-pentane; yield 85–90%. Selective methylation of the sulfur atoms of **3–9** can analogously be achieved by using other alkylating agents such as MeOSO₂CF₃ and Me₃OBF₄. However, MeI is the reagent of choice because it is the cheapest and the easiest to handle.

Table 1. $^{31}\text{P}\{^1\text{H}\}$ NMR Spectral Data for the New Complexes^a

complex	pattern	chem shift, ppm ^b			coupling const, Hz					
		$\delta(\text{A})$	$\delta(\text{M})$	$\delta(\text{Q})$	$J(\text{AM})$	$J(\text{AQ})$	$J(\text{MQ})$	$J(\text{ARh})$	$J(\text{MRh})$	$J(\text{QRh})$
9	AMQX	30.9	-1.2	-4.2	34.3	29.4	37.5	108.9	117.9	106.3
10	AMQX	28.9	1.8	-6.1	36.5	36.5	36.5	114.8	111.3	104.4
11	AMQX	28.5	7.9	-8.1	35.1	38.7	29.5	112.9	117.5	100.2
12	AMQX	28.8	6.9	-7.8	35.8	38.4	30.5	114.7	116.3	100.5
13	AMQX	29.1	3.8	-6.2	36.4	36.4	36.4	116.8	113.6	101.9
14	AMQX	30.2	5.0	-6.9	36.4	36.4	36.4	115.2	113.2	101.9
15	AMQX	30.9	6.2	-7.1	36.5	36.5	36.5	116.4	115.5	101.1
16	AMQX	29.0	5.8	-9.1	37.5	37.5	37.5	114.6	114.1	101.1

^a All spectra were recorded at 20 °C in CD_2Cl_2 solutions. ^b The chemical shifts (δ 's) are relative to 85% H_3PO_4 ; downfield values are assumed as positive.

[(triphos)Rh(η^3 -MeSC(Me)=CHCH=CH₂)]BPh₄ (10). Anal. Calcd (found) for C₇₁H₆₉BP₃RhS: C, 73.45 (73.05); H, 5.99 (5.78); Rh, 8.86 (8.92); S, 2.76 (2.69). Λ_{M} : 50 $\Omega^{-1}\text{cm}^2\text{mol}^{-1}$.

[(triphos)Rh(η^3 -MeSC(COMe)=CHCH=CH₂)]BPh₄ (11). Anal. Calcd (found) for C₇₂H₆₉BOP₃RhS: C, 72.73 (72.33); H, 5.85 (5.51); Rh, 8.65 (8.63); S, 2.69 (2.61). Λ_{M} : 52 $\Omega^{-1}\text{cm}^2\text{mol}^{-1}$. IR: $\nu(\text{C}=\text{O})$ 1678 (s) cm^{-1} .

[(triphos)Rh(η^3 -MeSC(CO₂Et)=CHCH=CH₂)]BPh₄ (12). Anal. Calcd (found) for C₇₃H₇₁BO₂P₃RhS: C, 71.92 (71.57); H, 5.87 (5.54); Rh, 8.44 (8.44); S, 2.63 (2.50). Λ_{M} : 52 $\Omega^{-1}\text{cm}^2\text{mol}^{-1}$. IR: $\nu(\text{C}=\text{O})$ 1709 (s) cm^{-1} .

[(triphos)Rh(η^3 -MeSC(Tyl)=CHCH=CH₂)]BPh₄ (13). Anal. Calcd (found) for C₇₄H₆₉BP₃RhS₂: C, 72.31 (71.99); H, 5.66 (5.39); Rh, 8.37 (8.32); S, 5.22 (5.23). Λ_{M} : 55 $\Omega^{-1}\text{cm}^2\text{mol}^{-1}$. IR: $\nu(\text{C}=\text{C})$ 1569 (m) cm^{-1} .

[(triphos)Rh(η^3 -MeSCH=C(Me)CH=CH₂)]BPh₄ (14). Anal. Calcd (found) for C₇₁H₆₉BP₃RhS: C, 73.45 (73.00); H, 5.99 (5.62); Rh, 8.86 (8.89); S, 2.76 (2.67). Λ_{M} : 54 $\Omega^{-1}\text{cm}^2\text{mol}^{-1}$.

[(triphos)Rh(η^3 -MeSCH=C(OMe)CH=CH₂)]BPh₄ (15). Anal. Calcd (found) for C₇₂H₆₉BOP₃RhS: C, 72.73 (72.49); H, 5.85 (5.55); Rh, 8.55 (8.69); S, 2.69 (2.68). Λ_{M} : 52 $\Omega^{-1}\text{cm}^2\text{mol}^{-1}$. IR: $\nu(\text{C}=\text{O})$ 1681 (s) cm^{-1} .

[(triphos)Rh(η^3 -MeSCH=C(OMe)CH=CH₂)]BPh₄ (16). Anal. Calcd (found) for C₇₁H₆₉BOP₃RhS: C, 72.45 (72.13); H, 5.91 (5.55); Rh, 8.74 (8.49); S, 2.72 (2.54). Λ_{M} : 54 $\Omega^{-1}\text{cm}^2\text{mol}^{-1}$. IR: $\nu(\text{C}=\text{O})$ 1156 (s) cm^{-1} .

Synthesis of the Butadienyl Methyl Sulfides 17–23.

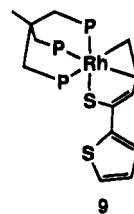
In a typical experiment, a THF (50 mL) solution of the appropriate methylbutadienethiolate complex [(triphos)Rh(η^3 -MeSCR=CR'CH=CH₂)]BPh₄ (10–16; ca. 0.3 mmol) was reacted with CO (5 atm) at 70 °C for 3 h in a Parr reactor. After the bomb was depressurized and vented under a nitrogen stream, the contents were transferred into a Schlenk-type flask. The volatiles were then removed in vacuo at room temperature and a portion of the residue was analyzed by ¹H and ³¹P{¹H} NMR spectroscopy. In all of the reactions, [(triphos)Rh(CO)₂]BPh₄¹¹ (2) was the only rhodium complex detected in solution. The rest of the residue was chromatographed on a silica column (diethyl ether as eluant) to eliminate the rhodium complex. The diethyl ether phase was then evaporated at atmospheric pressure and the residue, dissolved in CDCl₃, was appropriately characterized by ¹H and ¹³C{¹H} NMR and GC/MS spectroscopy. In all cases, the yields of the sulfides 17–23 exceeded 90% based on ¹H NMR integration with respect to *tert*-butyl methyl ether (δ 3.21, OMe; δ 1.20, CMe₃) as internal standard. Due to the limited preparative scale imposed by the cost of the rhodium precursors, no attempt was made to isolate pure samples of the organosulfur compounds.

Results and Discussion

The preparations and the principal reactions described in this article are illustrated in Scheme 2. Selected NMR spectral data for the metal complexes are collected in Table 1 (³¹P{¹H} NMR) and Table 2 (¹H, ¹³C-

¹H} NMR). Selected NMR and MS data for the organosulfur products are collected in Table 3 (¹H NMR) and Table 4 (¹³C{¹H} NMR, MS). ¹³C DEPT, ¹³C–¹H 2D HETCOR, ¹H–¹H 2D COSY, and selective-decoupling spectra allowed the total and unequivocal assignment of all hydrogen and carbon resonances for all metal complexes and organosulfur compounds as labeled in Tables 2 and 3, respectively.

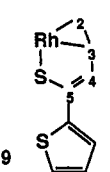
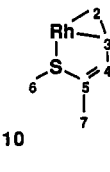
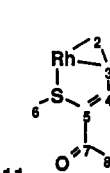
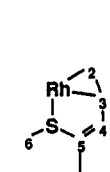
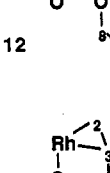
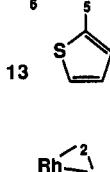
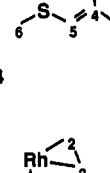
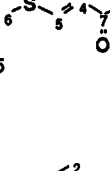
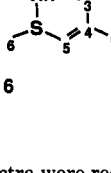
Reaction of the Trihydride (triphos)RhH₃ (1) with 2,2'-Bithiophene. The butadienethiolate complex (triphos)Rh(η^3 -SC(Tyl)=CHCH=CH₂) (9; Tyl = thienyl) was obtained as orange crystals by following the procedure used for the preparation of the congeners shown by I, e.g. stirring a THF solution of 1 with an excess of 2-TylT at reflux temperature. As previously observed for all of the substituted thiophenes shown in Chart 1, insertion is seen exclusively at the C–S bond distal to the thienyl substituent.¹² Mechanistically, the reaction proceeds through the intermediacy of a transient hydridorhodathiacycle complex, (triphos)Rh(H)(η^2 -(C,S)-SC(Tyl)=CHCH=CH), which rapidly undergoes hydride migration to the metalated carbon atom of the thio ligand.¹³



The NMR characteristics of 9 are comparable with those of the butadienethiolate congeners 3–8. Thus, 9 is analogously assigned an octahedral structure with the rhodium center coordinated by a *fac*-triphos ligand and by a 5-thienyl-substituted butadienethiolate ligand which uses the sulfur atom and the distal olefinic end to bind the metal. In line with previous observations, the Rh–C₂–C₃ ring exhibits a pronounced metallacyclopropane structure ($\delta(\text{C}_3)$ 63.1, $\delta(\text{C}_2)$ 40.2, $^2J(\text{C}_2,3\text{P}) \approx 32$ Hz).^{7,12}

(13) (a) Bianchini, C.; Meli, A.; Peruzzini, M.; Vizza, F.; Frediani, P.; Herrera, V.; Sánchez-Delgado, R. A. *J. Am. Chem. Soc.* **1993**, *115*, 2731. (b) Bianchini, C.; Meli, A.; Peruzzini, M.; Vizza, F.; Moneti, S.; Herrera, V.; Sánchez-Delgado, R. A. *J. Am. Chem. Soc.* **1994**, *116*, 4370. (c) Bianchini, C.; Jiménez, M. V.; Meli, A.; Moneti, S.; Vizza, F. *J. Organomet. Chem.*, in press.

Table 2. ^1H and $^{13}\text{C}\{^1\text{H}\}$ NMR Spectral Data for the New Complexes^a

complex	^1H NMR		$^{13}\text{C}\{^1\text{H}\}$ NMR	
	assignt	δ (multiplicity, J) ^{b,c}	assignt	δ (multiplicity, J) ^b
 9	H4	6.64 (t, $^3J(\text{H4Rh}) = 1.0$, $^3J(\text{H4H3}) = 4.9$)	C3	63.1 (dt, $^2J(\text{CP}) = 31.8$, 9.7)
	H2'	3.15 (m, $^2J(\text{H2}'\text{Rh}) = 2.0$, $^3J(\text{H2}'\text{H3}) = 9.1$)	C2	40.2 (br d, $^2J(\text{CP}) = 32.7$)
	H3	2.95 (m, $^2J(\text{H3Rh}) = 1.3$, $^3J(\text{H3H2}) = 7.6$)	C4	e
	H2	2.01 (m, $^2J(\text{H2Rh}) = 1.5$, $^2J(\text{H2H2}') = 0.5$)	C5	e
	HTyl	d	CTyl	e
 10	H4	6.95 ^f	C4	149.8 (br s)
	H3	3.20 (m, $^2J(\text{H3Rh}) = 1.3$, $^3J(\text{H3H4}) = 4.8$)	C3	58.4 (dd, $^2J(\text{CP}) = 22.2$, 10.2)
	H2'	2.58 (m, $^2J(\text{H2}'\text{Rh}) = 2.0$, $^3J(\text{H2}'\text{H3}) = 9.3$)	C2	47.8 (dd, $^2J(\text{CP}) = 23.4$, 11.2)
	H2	2.38 (m, $^2J(\text{H2Rh}) = 1.6$, $^2J(\text{H2H2}') = 2.2$, $^3J(\text{H2H3}) = 7.8$)	C6	22.3 (br s)
	H7	2.11 (s)	C7	18.5 (s)
 11	H6	1.74 (s)	C5	e
	H4	8.55 (t, $^3J(\text{H4H3}) = 5.8$)	C7	192.7 (s)
	H3	3.44 (m, $^2J(\text{H3Rh}) = 1.2$, $^3J(\text{H3H2}) = 8.7$)	C4	170.1 (br s)
	H2'	2.71 (m, $^2J(\text{H2}'\text{Rh}) = 2.2$, $^2J(\text{H2}'\text{H2}) = 2.2$, $^3J(\text{H2}'\text{H3}) = 8.9$)	C3	54.2 (m)
	H8	2.50 (s)	C2	51.5 (dm, $^2J(\text{CP}) = 35.6$)
 12	H2	2.21 ^g	C8	28.1 (s)
	H6	1.62 (br s)	C6	24.9 (d, $^3J(\text{CP}) = 5.5$)
	H4	8.64 (t, $^3J(\text{H4H3}) = 5.9$)	C5	e
	H8	4.31 (q, $^3J(\text{H8H9}) = 7.2$)	C4	169.4 (br s)
	H3	3.40 (m, $^2J(\text{H3Rh}) = 1.2$, $^3J(\text{H3H2}) = 8.5$)	C7	163.2 (s)
 13	H2'	2.74 (m, $^2J(\text{H2}'\text{Rh}) = 2.1$, $^2J(\text{H2}'\text{H2}) = 2.0$, $^3J(\text{H2}'\text{H3}) = 9.1$)	C8	62.6 (s)
	H2	2.23 ^g	C3	54.2 (m)
	H6	1.66 (s)	C2	51.0 (dm, $^2J(\text{CP}) = 34.8$)
	H9	1.39 (t)	C6	24.0 (d, $^3J(\text{CP}) = 5.1$)
	H4	7.52 ^f	C9	14.8 (s)
 14	H6	1.69 (s)	C5	e
	H4	5.44 (br s, $^4J(\text{H5H7}) = 1.4$)	C4	167.1 (br s)
	H3	3.37 (m, $^2J(\text{H3Rh}) = 1.2$, $^3J(\text{H3H2}) = 7.8$)	C5	110.0 (d, $^3J(\text{CP}) = 11.0$)
	H2'	2.48 (m, $^2J(\text{H2}'\text{Rh}) = 2.1$, $^3J(\text{H2}'\text{H3}) = 9.2$)	C3	62.2 (dd, $^2J(\text{CP}) = 22.0$, 11.0)
	H7	2.34 (d)	C2	49.8 (dd, $^2J(\text{CP}) = 22.6$, 11.6)
 15	H2	2.04 (m, $^2J(\text{H2Rh}) = 1.7$, $^2J(\text{H2H2}') = 2.1$)	C6	24.3 (d, $^3J(\text{CP}) = 6.1$)
	H6	1.41 (br s)	C7	22.9 (s)
	H5	6.44 (br s)	C7	195.1 (s)
	H3	4.05 (m, $^2J(\text{H3Rh}) = 1.4$, $^3J(\text{H3H2}') = 8.9$)	C4	165.0 (br s)
	H8	2.52 (s)	C5	124.2 (d, $^3J(\text{CP}) = 12.8$)
 16	H2'	2.31 ^g	C3	54.6 (dm, $^2J(\text{CP}) = 21.9$)
	H2	2.02 (m, $^2J(\text{H2Rh}) = 1.7$, $^2J(\text{H2H2}') = 2.0$, $^3J(\text{H2H3}) = 8.3$)	C2	50.4 (dm, $^2J(\text{CP}) = 23.2$)
	H6	1.43 (br s)	C8	28.6 (s)
	H5	4.73 (m, $^4J(\text{H5H3}) = 1.5$)	C6	23.6 (br s)
	H7	3.91 (s)	C4	168.2 (br s)
 16	H3	3.32 (m, $^2J(\text{H3Rh}) = 1.8$, $^3J(\text{H3H2}) = 8.0$)	C5	82.1 (d, $^3J(\text{CP}) = 7.8$)
	H2'	2.62 (m, $^2J(\text{H2}'\text{Rh}) = 2.2$, $^3J(\text{H2}'\text{H3}) = 9.0$)	C3	63.1 (dd, $^2J(\text{CP}) = 22.4$, 11.1)
	H2	1.96 (m, $^2J(\text{H2Rh}) = 1.2$, $^2J(\text{H2H2}') = 2.2$)	C7	59.8 (s)
	H2	1.33 (br s)	C2	48.8 (dd, $^2J(\text{CP}) = 22.1$, 10.9)
	H6	1.33 (br s)	C6	24.1 (d, $^3J(\text{CP}) = 6.4$)

^a All spectra were recorded at room temperature in CD_2Cl_2 solutions at 200.13 (^1H NMR) and 50.32 MHz ($^{13}\text{C}\{^1\text{H}\}$ NMR). ^b Chemical shifts are given in ppm and are relative to either the residual ^1H resonance in the deuterated solvent (^1H NMR) or the deuterated solvent resonance ($^{13}\text{C}\{^1\text{H}\}$ NMR). Key: s, singlet; d, doublet; t, triplet; q, quartet; m, multiplet; br, broad. Coupling constants (J) are in hertz. ^c The $J(\text{HH})$ values were determined on the basis of $^1\text{H}\{^31\text{P}\}$ NMR experiments. ^d Masked by the aromatic protons of the triphos ligand. ^e Masked by the phenyl carbons of the triphos ligand. ^f Masked by the aromatic protons of the triphos ligand. The chemical shift was determined from a $^1\text{H}-^1\text{H}$ 2D-COSY experiment. ^g Masked by the aliphatic protons of the triphos ligand. The chemical shift was determined from a $^1\text{H}-^1\text{H}$ 2D-COSY experiment.

Table 3. ^1H NMR Spectral Data for the Butadienyl Methyl Sulfides^a

Compound	δH , multiplicity ^b										$J\text{HH}^b$									
	1	2	3	4c	4t	5	6	7	8	9	13	14c	14t	16	23	24c	24t	34c	34t	4c4t
	-	6.12, brd	6.81, dt	5.07, dm	5.17, dm	2.33, s	2.12, m	-	-	-	-	-	-	-	10.6	0.8	0.8	10.3	16.9	2.0
	-	7.38, d	7.15, ddd	5.62, dd	5.73, dd	2.24, s	-	2.48, s	-	-	-	-	-	-	10.8	-	-	9.8	16.6	1.3
	-	7.43, brd	7.07, ddd	5.56, ddd	5.68, ddd	2.28, s	-	4.28, q	1.32, t	-	-	-	-	-	10.9	0.7	0.7	10.1	16.9	1.7
	-	6.76, brd	7.12, ddd	5.32, ddd	5.45, ddd	2.24, s	-	7.27, dd	7.04, dd	7.31, dd	-	-	-	-	10.5	0.7	0.7	10.1	16.9	1.8
	5.93, m	-	6.83, ddd	5.16, dt	5.27, ddd	2.31, s	1.98, d	-	-	-	0.7	1.5	0.6	1.5	-	-	-	10.8	17.3	1.4
	7.51, s	-	6.60, dd	5.55, dd	5.60, dd	2.34, s	-	2.51, s	-	-	-	-	-	-	-	-	-	11.7	17.9	1.1
	5.22, m	-	6.92, ddd	5.23, dt	5.66, ddd	2.21, s	3.68, s	-	-	-	0.6	1.7	0.6	-	-	-	-	11.2	17.2	1.9

^a All spectra were recorded at room temperature in CDCl_3 solutions at 200.13 MHz (^1H NMR). ^b Chemical shifts are given in ppm and are relative to the residual ^1H resonance in the deuterated solvent. Key: s, singlet; d, doublet; t, triplet; q, quartet; m, multiplet; br, broad. Coupling constants (J) are in hertz. ^c $0 < J(\text{H}_6\text{H}_{4t}), J(\text{H}_6\text{H}_{4c}), J(\text{H}_6\text{H}_3), J(\text{H}_6\text{H}_2) < 0.5$ Hz. ^d $J(\text{H}_7\text{H}_8) = 7.1$ Hz. ^e $J(\text{H}_6\text{H}_5) = 5.2$ Hz, $J(\text{H}_7\text{H}_9) = 1.2$ Hz, $J(\text{H}_8\text{H}_9) = 3.7$ Hz.

Although much less abundant than thiophenes, oligothiophenes such as 2-TylT are found in fossil fuels.¹⁴ On the other hand, oligothiophenes may form in the course of the HDS process from side reactions involving either thiophene C-H bond activation by metal centers^{6a,15} or pyrolysis of the thiophenes.¹⁶ It was thus surprising to us to find that no homogeneous modeling study of the reactivity of 2-TylT with transition-metal complexes has appeared in the HDS-relevant literature over the past 30 years. To the best of our knowledge, the only report is the one by Manuel and Meyer in 1964, which describes the insertion of iron from $\text{Fe}_3(\text{CO})_{12}$ into a C-S bond of 2-TylT.¹⁷ As we found for **9**, insertion is seen in the C-S bond distal to the thienyl substituent. The same iron complex, which is a thiaferrole of the formula $\text{Fe}_2(2,2'\text{-C}_4\text{H}_3\text{SC}_4\text{H}_3\text{S})(\text{CO})_6$, was later also ob-

tained by Rauchfuss by thermal decomposition of the thienyl complex $\text{CpFe}(\text{CO})_2(2\text{-C}_4\text{H}_3\text{S})$.¹⁸

Our idea to insert rhodium into a C-S bond of 2-TylT has been motivated not only by the interest to gain insight into the metal-assisted opening of oligothiophenes (as part of our modeling studies on HDS) but also by the purpose of linking a thienyl group to an $\alpha,\beta,\gamma,\delta$ -unsaturated hydrocarbon moiety, because of the interest in the resulting product for its potential nonlinear optical activity.⁵

Methylation of the Butadienethiolate Complexes. Selective methylation of the sulfur atom of the butadienethiolate complexes **3-9** was achieved in THF by treatment with MeI at room temperature.⁷ Metathetical reaction with NaBPh_4 gives tetraphenylborate salts of the formula $[(\text{triphos})\text{Rh}(\eta^3\text{-MeSCR}=\text{CR}'\text{CH}=\text{CH}_2)]\text{BPh}_4$ ($\text{R}' = \text{H}$, $\text{R} = \text{Me}$, (**10**), COMe (**11**), $\text{CO}_2\text{-Et}$ (**12**), Tyl (**13**); $\text{R} = \text{H}$, $\text{R}' = \text{Me}$ (**14**), COMe (**15**), OMe (**16**); Scheme 2).

(14) (a) *Geochemistry of Sulfur in Fossil Fuels*; Orr, W. L., White, C. M., Eds. ACS Symposium Series 429; American Chemical Society: Washington, DC, 1990. (b) Galpern, G. D. In *Thiophene and its Derivatives*; Gronowitz, S., Ed.; Wiley: New York, 1985; Part I.

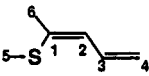
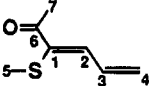
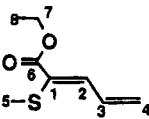
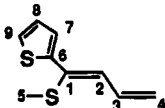
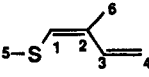
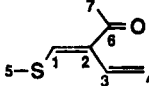
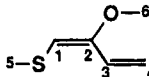
(15) Wang, D.-L.; Hwang, W.-S. *J. Organomet. Chem.* **1991**, *406*, C29.

(16) Katritzky, A. R.; Lagowski, J. M. In *The Principles of Heterocyclic Chemistry*; Methuen: London, 1967.

(17) Manuel, T. A.; Meyer, T. J. *Inorg. Chem.* **1964**, *3*, 1049.

(18) Ogilvy, A.; Draganjac, M.; Rauchfuss, T. B.; Wilson, S. R. *Organometallics* **1988**, *7*, 1171.

Table 4. $^{13}\text{C}\{^1\text{H}\}$ NMR and MS Data for the Butadienyl Methyl Sulfides

Compound	$^{13}\text{C}\{^1\text{H}\}$ NMR data in CDCl_3 (δ)									MS data (EI)	
	C1	C2	C3	C4	C5	C6	C7	C8	C9	ion	<i>m/e</i> (%)
	144.7	128.8	130.7	116.9	17.6	24.8	-	-	-	M M-Me	114 (37) 99 (100) 84 (20) 65 (80) 45 (52)
	149.6	134.4	144.7	126.8	19.8	197.5	27.7	-	-	M M-Me M-COMe	142 (18) 127 (38) 99 (9) 84 (27) 65 (34) 45 (26) 43 (100)
	148.6	134.0	144.6	126.4	19.6	165.9	62.1	14.7	-	M M-Me M-OEt M-CO ₂ Et	172 (62) 157 (78) 127 (27) 113 (17) 99 (41) 85 (100) 84 (63) 65 (47) 58 (53) 45 (71)
	146.9	128.0	134.9	120.5	18.9	134.3	126.3	126.4	128.3	M M-Me M-HSMe	182 (6) 167 (100) 134 (49) 91 (18) 69 (11) 45 (19)
	128.4	142.1	129.0	116.2	22.2	16.2	-	-	-	M M-Me	114 (62) 99 (100) 84 (20) 65 (79) 45 (65)
	147.4	141.1	144.2	122.4	19.6	195.7	27.2	-	-	M M-Me M-COMe	142 (36) 127 (59) 99 (19) 84 (26) 65 (44) 45 (73) 43 (100)
	98.6	143.8	124.7	116.4	23.2	55.6	-	-	-	M M-Me M-2Me	130 (38) 115 (100) 100 (7) 87 (12) 72 (16) 71 (16) 55 (27) 45 (76)

All compounds are isolated as yellow-orange crystals, which are fairly air-stable in both the solid state and solution.

Like the neutral butadienethiolate precursors,¹² the thioether compounds **10**–**16** exhibit, in solution, a rigid octahedral structure in which the thio ligand is still η^3 -anchored to rhodium *via* the C_2 – C_3 double bond and the sulfur atom. This bonding mode has been authenticated by an X-ray diffraction analysis on the iridium 1-(methylthio)butadiene complex [(triphos)Ir(η^3 -MeSCH=CH=CH=CH₂)]BPh₄.^{13a} A close analog to this system is the 1-(methylthio)butadiene complex [(triphos)-Rh(η^3 -MeSCH=CH=CH=CH₂)]BPh₄.⁷

The addition of a methyl group to the sulfur atom does not appreciably alter the ^1H NMR parameters of the vinyl moiety of the starting butadienethiolate ligands, unlike the chemical shifts of the H_5 hydrogen in the 4-substituted compounds and of the H_4 hydrogen in the 5-substituted compounds, which move upfield and downfield, respectively. This phenomenon may be explained by taking into account that alkylation of the sulfur atom actually reduces the electron density on both the metal and the thio ligand, thus causing a polarization of the

electrons in the double bond toward the metal center. The deshielding effect on the atoms in the 4-position is also evident from the $^{13}\text{C}\{^1\text{H}\}$ NMR spectra. As an example, we show in Figure 1 that C_4 in **12** resonates at ca. 170 ppm, while this signal in the corresponding butadienethiolate complex is masked by the phenyl carbons of triphos (120–140 ppm).

Carbonylation Reactions. The rhodium thioether complexes **10**–**16** were dissolved in THF and then subjected to a CO atmosphere (5 atm) in autoclaves. At 70 °C, all complexes quantitatively transform into the known dicarbonyl [(triphos)Rh(CO)₂]BPh₄¹¹ within 3 h, while the neutral 1-(methylthio)buta-1,3-dienes (**17**–**23**), substituted in either the 1- or 2-position, are liberated in solution (Scheme 2). These have been purified by LC and then characterized in CDCl_3 solution (Chart 2).

A single isomer is obtained for each product with retention of the *Z* structure adopted in the rhodium precursors, as shown by a comparison of the proton NMR spectra of some of the present 1-(methylthio)buta-1,3-dienes with those of similar compounds.^{8a-d,10}

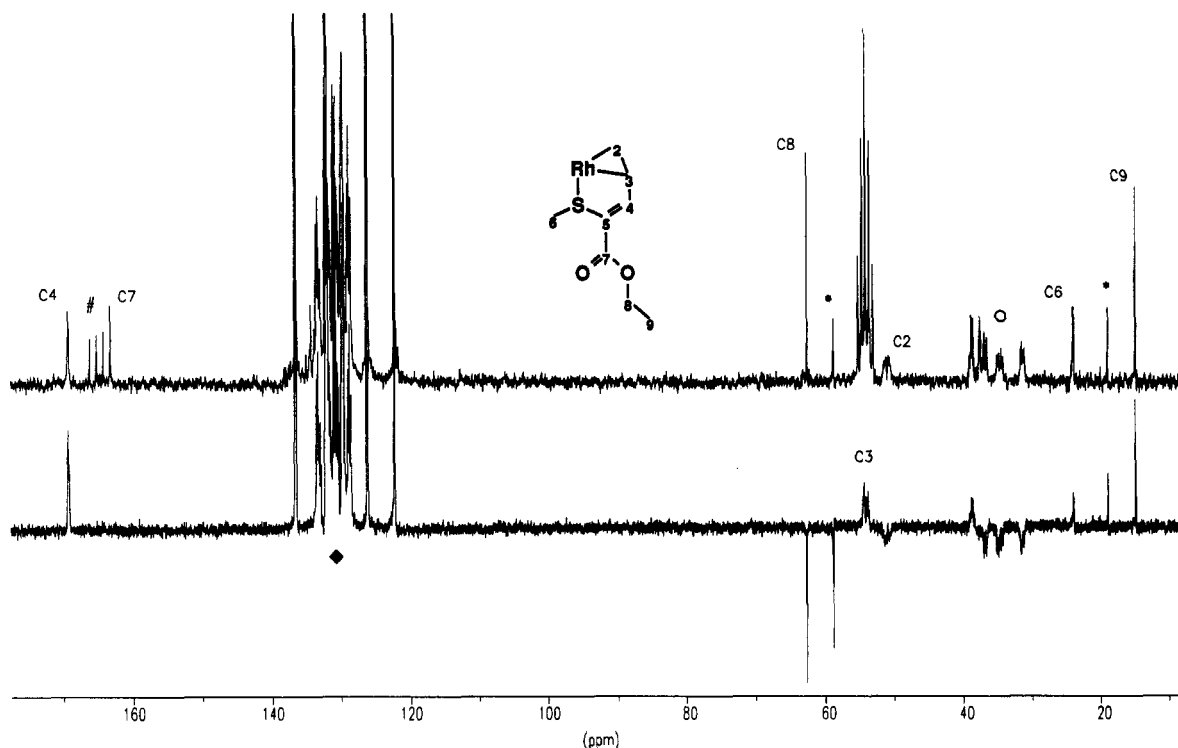
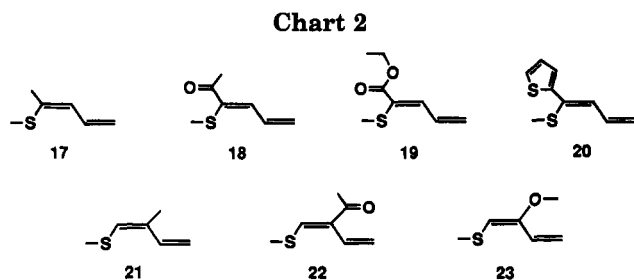


Figure 1. $^{13}\text{C}\{^1\text{H}\}$ NMR (upper) and ^{13}C DEPT (lower) spectra of **12** in CD_2Cl_2 at 20°C (50.32 MHz): (#) quaternary carbons of BPh_4^- ; (♦) phenyl carbons of triphos and BPh_4^- ; (*) carbons of the ethanol of crystallization; (O) aliphatic carbons of triphos.



Butadienes with sulfur substituents are difficult to prepare, and a general methodology for their preparation is lacking. The compound (*Z*)-1-(methylthio)-1-(carbomethoxy)buta-1,3-diene (similar to **19**) has been synthesized by a [3,2]-sigmatropic rearrangement of the corresponding sulfonium salt,¹⁰ while 1-(methylthio)-2-alkylbuta-1,3-dienes (similar to **21**) have been prepared by the reaction of α,β -unsaturated aldehydes with alkanethiols in the presence of acid catalysts.^{8b,c} Some 1-(alkylthio)buta-1,3-dienes, without substituents on the butadienyl moiety, have been synthesized by the base-assisted ring-opening reactions of 2,5-dihydrothiophene 1-oxide, 2,5-dihydrothiophene 1,1-dioxide, or 1-alkyl-2,5-dihydrothiophene salts.^{8a} In contrast, the synthesis of the substituted 1-(methylthio)buta-1,3-dienes described in this paper is a general methodology which offers several advantages over current organic chemistry procedures. These include the use of cheap, largely available thiophenic molecules, the generally excellent

yields, and the capability of easily varying either the sulfur substituent (by varying the initial electrophile) or the butadiene substituent(s) (by varying the starting thiophene). This last feature is perhaps the most exciting, as it provides access not only to tailored products of great utility as organic synthons^{8,9} but also to molecules with unusual specific properties. For example, 1-(methylthio)-1-acetylbuta-1,3-diene (**18**) and 1-(methylthio)-1-(carboethoxy)buta-1,3-diene (**19**) belong to the class of 1,1-captodative butadienes with application as radicophilic reagents,¹⁰ while the conjugated 1-(methylthio)buta-1,3-diene (**20**) has potential in the field of second- and third-order nonlinear optical activity.⁵

An obvious disadvantage of the present methodology is the need to use an expensive metal, rhodium, which, however, is able to be totally recovered at the end of the reaction. Current investigations center upon finding a less expensive metal for these reactions and in the development of a catalyst system for the process.

Acknowledgment. We thank the Progetto Strategico "Tecnologie Chimiche Innovative", CNR, Rome, Italy, and the European Community (Contract CHRX CT93-0147) for financial support. A postdoctoral grant to M.V.J. from the Ministerio de Educación y Ciencia of Spain is gratefully acknowledged.

OM9503860

Catalytic Enantioselective Hydrogenation of 1,1-Disubstituted Alkenes with Optically Active Titanocene and Zirconocene Complexes Containing either Identical or Different Ligands

Leo A. Paquette,* Mark R. Sivik,^{1a} Eugene I. Bzowej,^{1b} and Kenetha J. Stanton^{1c}

Evans Chemical Laboratories, The Ohio State University, Columbus, Ohio 43210

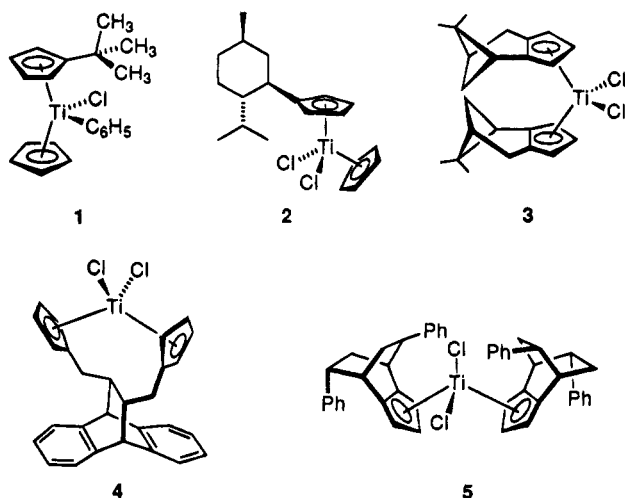
Received April 18, 1995[®]

The synthesis of a variety of nonbridged optically active C_2 - and C_1 -symmetric titanocenes and zirconocenes is reported together with a detailed investigation of the ability of these complexes to effect the catalytic asymmetric hydrogenation of 2-phenyl-1-butene and 2-(α -naphthyl)-1-butene. The respective dihydro products are shown to be produced with enantiomeric excesses ranging from 4% to 69%. The absolute configuration of these 2-arylbutanes was noted to be sensitive to the three-dimensional characteristics of the particular bicyclo-fused ligand involved. For a series of verbenone-related metallocenes, an increase in the size of a substituent positioned α and syn to the metal center was found to be unfavorable for stereoinduction. This phenomenon has been rationalized in transition state terms, with the alkene approaching laterally to engage in hydrogen atom transfer. The three-dimensional stereochemical model advanced in explanation of the observed catalytic selectivity underscores the development of steric biases during olefin coordination to the reactive metal hydride intermediate.

Optically active titanocene and zirconocene complexes are in increasing demand as a direct result of their ability to effect asymmetric homogeneous catalytic reactions of various types.^{2,3} The classical means for generating chirality in these systems involves the elaboration of a stereogenic metal center.^{4,5} However, the considerable difficulty associated with the preparation of nonracemic **1** and related molecules severely

cyclopentadienyl ligands may be chiral. The earliest members of this class were made available by attaching a single chiral auxiliary such as menthyl to one of the rings as in **2**.⁶ Subsequently, enantiomerically pure complexes derived by fusing cyclopentadiene rings to naturally occurring terpenes, e.g. **3**, made their appearance.^{7,8} In the past several years, these metallocenes have been joined by bridged bis(cyclopentadienyl) complexes typified by **4**⁹ and others constructed of C_2 -symmetric annulated cyclopentadienes such as **5**.¹⁰

Ellis et al. have itemized several of the possible complications associated with the preparation of belted metallocenes related to **4**.¹¹ These include predominant or exclusive formation of "meso" isomers with loss of chirality,¹² formation of diastereomeric complexes other than the desired C_2 -symmetric species,^{13,14} and related



reduces their serviceability. Alternatively, one or both

(6) Cesarotti, E.; Kagan, H. B.; Goddard, R.; Krüger, C. *J. Organomet. Chem.* **1978**, *162*, 297.

(7) (a) Halterman, R. L.; Vollhardt, K. P. C. *Tetrahedron Lett.* **1986**, *27*, 1461. (b) Halterman, R. L.; Vollhardt, K. P. C. *Organometallics* **1988**, *7*, 883.

(8) (a) McLaughlin, M. L.; McKinney, J. A.; Paquette, L. A. *Tetrahedron Lett.* **1986**, *27*, 5595. (b) Paquette, L. A.; McKinney, J. A.; McLaughlin, M. L.; Rheingold, A. L. *Tetrahedron Lett.* **1986**, *27*, 5599. (c) Paquette, L. A.; Moriarty, K. J.; McKinney, J. A.; Rogers, R. D. *Organometallics* **1989**, *8*, 1707. (d) Paquette, L. A.; Moriarty, K. J.; Rogers, R. D. *Organometallics* **1989**, *8*, 1506. (e) Moriarty, K. J.; Rogers, R. D.; Paquette, L. A. *Organometallics* **1989**, *8*, 1512. (f) Sivik, M. R.; Rogers, R. D.; Paquette, L. A. *J. Organomet. Chem.* **1990**, *397*, 177. (g) Rogers, R. D.; Sivik, M. R.; Paquette, L. A. *J. Organomet. Chem.* **1993**, *450*, 125.

(9) (a) Gibis, K.-L.; Helmchen, G.; Huttner, G.; Zsolnai, L. *J. Organomet. Chem.* **1993**, *445*, 181. (b) Chen, Z.; Halterman, R. L. *Synlett* **1990**, 103. (c) Chen, Z.; Eriks, K.; Halterman, R. L. *Organometallics* **1991**, *10*, 3449.

(10) Halterman, R. L.; Vollhardt, K. P. C.; Welker, M. E.; Bläser, D.; Boese, R. *J. Am. Chem. Soc.* **1987**, *109*, 8105.

(11) Ellis, W. W.; Hollis, T. K.; Odenkirk, W.; Whelan, J.; Ostrander, R.; Rheingold, A. L.; Bosnich, B. *Organometallics* **1993**, *12*, 4391.

(12) Bandy, J. A.; Green, M. L. H.; Gardiner, I. M.; Prout, K. *J. Chem. Soc., Dalton Trans.* **1991**, 2207.

(13) Burk, M. J.; Colletti, S. L.; Halterman, R. L. *Organometallics* **1991**, *10*, 2998.

[®] Abstract published in *Advance ACS Abstracts*, October 1, 1995.
(1) (a) National Needs Fellow, 1989-1990; Amoco Foundation Fellow, 1991. (b) NSERC (Canada) Postdoctoral Fellow, 1994-1995. (c) University Fellow, 1991-1992.

(2) Duthaler, R. O.; Hafner, A. *Chem. Rev.* **1992**, *92*, 807.

(3) Halterman, R. L. *Chem. Rev.* **1992**, *92*, 965.

(4) (a) Moise, C.; Leblanc, J.-C.; Tirouflet, J. *Tetrahedron Lett.* **1974**, 1723. (b) Moise, C.; Leblanc, J.-C.; Tirouflet, J. *J. Am. Chem. Soc.* **1975**, *97*, 6272.

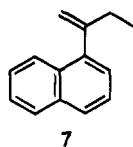
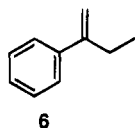
(5) (a) Brunner, H. *Acc. Chem. Res.* **1979**, *12*, 250. (b) Brunner, H. *Adv. Organomet. Chem.* **1980**, *18*, 151.

phenomena.¹⁵ Notwithstanding, chiral *ansa*-titanocenes and zirconocenes possessing a bridge at the 1- and 1'-positions¹⁶ are highly effective catalysts in enantioselective synthesis,^{17-19a} including stereoselective Ziegler-Natta polymerization.^{16,19b,20}

The utilization of C_2 -symmetric annulated cyclopentadienyl ligands has been highly touted because they are homotopic and metal complexation to either equivalent π -face affords only a single diastereomer, e.g., **5**.¹⁰ While this is true, C_1 -symmetric 1,2-disubstituted cyclopentadienyl ligands should not be downgraded. The diastereotopic nature of their two faces offers the possibility that diastereomeric mixtures of complexes will result. However, one face of the anion can often be engaged in reaction in advance of the other by virtue of steric control⁸ or by proper modulation of monomer-dimer equilibria involving lithium ions²¹ and reaction temperature.²² Furthermore, net inversion of π -facial selectivity can be readily achieved by silylation on the less hindered surface followed by electrophilic attack with inversion of configuration.²³ Accordingly, the number of chiral catalysts available from a C_1 -symmetric cyclopentadiene can be more than double that capable of being produced by C_2 -symmetric systems,^{22b} thus providing improved opportunity for assessing those transition states operational in asymmetric reactions and their stereodifferentiating relationship to the ligands involved.

Results

Selection of Olefinic Substrates. The pioneering studies of Cesarotti and Kagan²⁴ served to define the enantioselective hydrogenation of 2-phenyl-1-butene (**6**)²⁵ as the benchmark process for evaluating the



asymmetric inducing ability of cyclopentadienyl-derived metallocenes. The absolute configurations of both enan-

tiomers of 2-phenylbutane are consequently firmly established. The *S* isomer has been reported to exhibit a maximum optical rotation ($[\alpha]_D^{20}$) of +22.7 (c 1.0, ethanol),²⁶ and this value has served as a point of reference in the present study.

The higher naphthalene analogue **7** has also been examined in order to assess the extent to which a somewhat greater disparity in the relative size of the substituents flanking the double bond would impact on enantioselection. In addition to a larger steric differentiation between the geminal substituents, this substrate offers an additional aromatic ring for possible π -directing capabilities and greater hindrance to rotation about the σ bond connecting the naphthyl ring system to the olefinic center.²⁷ Acquisition of the nonracemic dihydro form of **7**, viz. 2-(α -naphthyl)butane (**8**), was originally reported by Menicagli and co-workers.²⁸ Beginning with optically active 2-(α -naphthyl)propionic acid, they were able to demonstrate that the + enantiomer has the *S* configuration. Enantiomeric purity was not achieved, and the optical rotation of the completely homogeneous antipode was projected to be $[\alpha]_D^{25}$ +25.4 (neat). Since the survey nature of this investigation was not projected to provide quantities of **8** adequate for optical assay in undiluted form, we initially set out to develop an enzymatic route to this hydrocarbon for the purpose of defining a broader range of usable $[\alpha]_D$ values.

The application of Kazlauskas' procedure²⁹ to racemic ester **12** provided alcohol **14** of only 24% ee as determined by Mosher ester analysis³⁰ (Scheme 1). Following reductive removal of the hydroxyl group, (-)-**8** was obtained. This sample exhibited $[\alpha]_D^{20}$ -6.6 (neat) or $[\alpha]_D^{20}$ -1.4 (c 2.3, ethanol). On this basis, the maximum rotation for neat and solution samples of **8** would be -27.2 and -5.7, respectively. These data were considered to be inconsistent with Menicagli's reports, the discrepancy perhaps arising because of the low optical purity of our sample and the large extrapolation involved.

An alternative means for producing **8** by enzymatic means was therefore pursued. In an adaptation of the method of Bloch,³¹ ester **16** was hydrolyzed at pH 7.3 with horse liver esterase (Scheme 2). After 30 h, optically active acid **17** was isolated in 32% yield, exhibited a rotation of -133.6 in CH_2Cl_2 , and was tentatively assigned the *R* configuration by analogy to

(14) Hollis, T. K.; Rheingold, A. L.; Robinson, N. P.; Whelan, J.; Bosnich, B. *Organometallics* **1992**, *11*, 2812.

(15) Rheingold, A. L.; Robinson, N. P.; Whelan, J.; Bosnich, B. *Organometallics* **1992**, *11*, 1869.

(16) Brintzinger, H. H. In *Transition Metals and Organometallics as Catalysts for Olefin Polymerization*; Kaminsky, W., Sinn, H., Eds.; Springer-Verlag: Berlin, Heidelberg, 1988.

(17) (a) Collins, S.; Kuntz, B. A.; Hong, Y. *J. Org. Chem.* **1989**, *54*, 4154. (b) Collins, S.; Hong, Y.; Taylor, N. *J. Organometallics* **1990**, *9*, 2695. (c) Collins, S.; Hong, Y.; Ramachandran, R.; Taylor, N. *J. Organometallics* **1991**, *10*, 2349.

(18) (a) Grossman, R. B.; Doyle, R. A.; Buchwald, S. L. *Organometallics* **1991**, *10*, 1501. (b) Grossman, R. B.; Davis, W. M.; Buchwald, S. L. *J. Am. Chem. Soc.* **1991**, *113*, 2321. (c) Willoughby, C. A.; Buchwald, S. L. *J. Am. Chem. Soc.* **1992**, *114*, 7562. (d) Broene, R. D.; Buchwald, S. L. *J. Am. Chem. Soc.* **1993**, *115*, 12569. (e) Lee, N. E.; Buchwald, S. L. *J. Am. Chem. Soc.* **1994**, *116*, 5985. (f) Willoughby, C. A.; Buchwald, S. L. *J. Am. Chem. Soc.* **1994**, *116*, 11703.

(19) (a) Waymouth, R.; Pino, P. *J. Am. Chem. Soc.* **1990**, *112*, 4911. (b) Coates, G. W.; Waymouth, R. M. *J. Am. Chem. Soc.* **1991**, *113*, 6270.

(20) For selected recent citations, see: (a) Ewen, J. A.; Jones, R. L.; Razavi, A.; Ferrara, J. D. *J. Am. Chem. Soc.* **1988**, *110*, 6255. (b) Collins, S.; Gauthier, W. J.; Holden, D. A.; Kuntz, B. A.; Taylor, N. J.; Ward, D. G. *Organometallics* **1991**, *10*, 2061.

(21) (a) Paquette, L. A.; Bauer, W.; Sivik, M. R.; Bühl, M.; Feigel, M.; Schleyer, P. v. R. *J. Am. Chem. Soc.* **1990**, *112*, 8776. (b) Bauer, W.; O'Doherty, G. A.; Schleyer, P. v. R.; Paquette, L. A. *J. Am. Chem. Soc.* **1991**, *113*, 7093. (c) Bauer, W.; Sivik, M. R.; Friedrich, D.; Schleyer, P. v. R.; Paquette, L. A. *Organometallics* **1992**, *11*, 4178. (d) Paquette, L. A.; Sivik, M. R.; Bauer, W.; Schleyer, P. v. R. *Organometallics* **1994**, *13*, 4919.

(22) (a) Paquette, L. A.; Moriarty, K. J.; Meunier, P.; Gautheron, B.; Sornay, C.; Rogers, R. D.; Rheingold, A. L. *Organometallics* **1989**, *8*, 2159. (b) Sornay, C.; Meunier, P.; Gautheron, B.; O'Doherty, G. A.; Paquette, L. A. *Organometallics* **1991**, *10*, 2082.

(23) Paquette, L. A.; Sivik, M. R. *Organometallics* **1992**, *11*, 3503.

(24) (a) Cesarotti, E.; Ugo, R.; Kagan, H. B. *Angew. Chem., Int. Ed. Engl.* **1979**, *18*, 779. (b) Cesarotti, E.; Ugo, R.; Vitiello, R. *J. Mol. Catal.* **1981**, *12*, 63.

(25) Lardicci, L.; Menicagli, R.; Salvadori, P. *Gazz. Chim. Ital.* **1968**, *98*, 738.

(26) Craig, J. C.; Pereira, W. E., Jr.; Halpern, B.; Westley, J. W. *Tetrahedron* **1971**, *27*, 1173.

(27) Anderson, J. E.; Hazelhurst, C. J. *J. Chem. Soc., Chem. Commun.* **1980**, 1188.

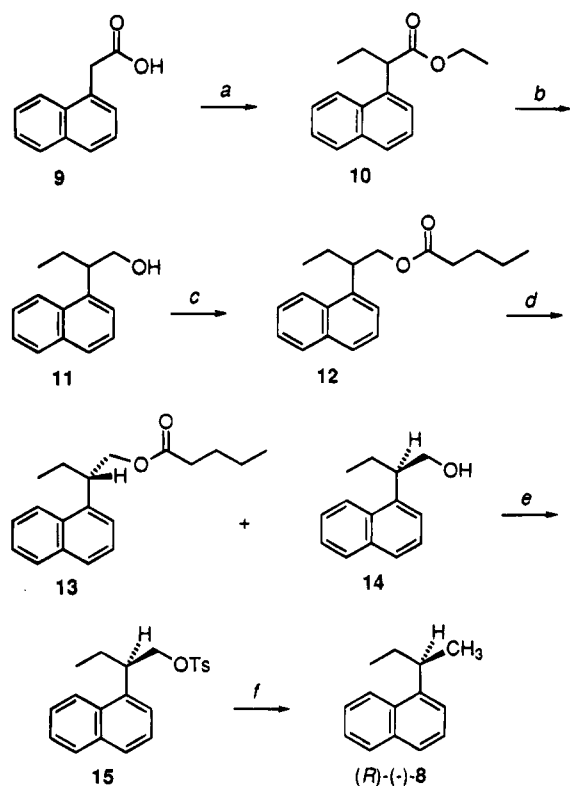
(28) (a) Menicagli, R.; Lardicci, L.; Botteghi, C. *Chem. Ind.* **1974**, 920. (b) Menicagli, R.; Piccolo, O.; Lardicci, L.; Wis, M. L. *Tetrahedron* **1979**, *35*, 1301. (c) Piccolo, O.; Menicagli, R.; Lardicci, L. *Tetrahedron* **1979**, *35*, 1751. (d) Menicagli, R.; Piccolo, O. *J. Org. Chem.* **1980**, *45*, 2581.

(29) Kazlauskas, R. *J. Org. Synth.* **1992**, *70*, 60.

(30) (a) Dale, J. A.; Dull, D. L.; Mosher, H. S. *J. Org. Chem.* **1969**, *34*, 2543. (b) Dale, J. A.; Mosher, H. S. *J. Am. Chem. Soc.* **1973**, *95*, 512.

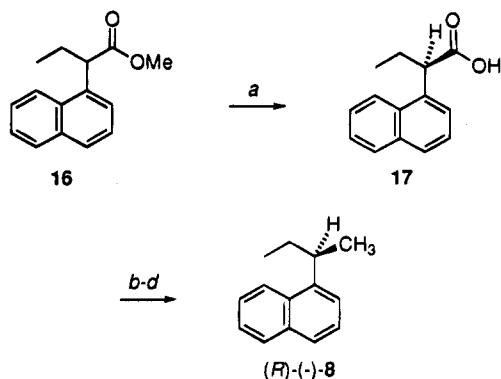
(31) Ahmar, M.; Girard, C.; Bloch, R. *Tetrahedron Lett.* **1989**, *30*, 7053.

Scheme 1



^a LDA (> 2 equiv), THF, HMPA, 0 °C; CH₃CH₂I. ^b LiAlH₄, THF, Δ. ^c CH₃(CH₂)₃C(O)Cl, Et₃N, ether, 0 °C. ^d Bovine pancreas acetone powder, pH 7 phosphate buffer, ether; 1 N NaOH dropwise to maintain pH 7.2. ^e TsCl, py, CH₂Cl₂, 0 °C. ^f Li(B(CH₂CH₃))H, THF.

Scheme 2

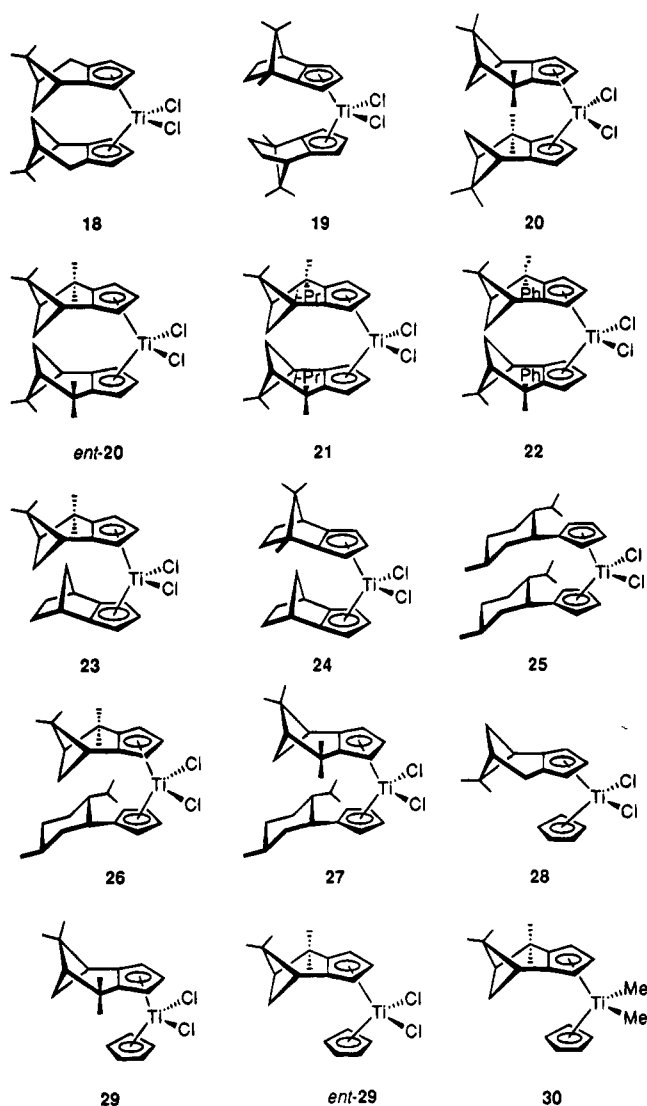


^a Horse liver esterase, pH 7 phosphate buffer, THF; 0.5 M NaOH dropwise to maintain pH 7.3. ^b LiAlH₄, THF, 0 °C. ^c TsCl, py, CH₂Cl₂, 0 °C → rt. ^d Li(B(CH₂CH₃))H, THF.

earlier results.³¹ Lithium aluminum hydride reduction of 17 produced an alcohol determined to have an optical purity of 87.3% after Mosher ester analysis.³⁰ The subsequent conversion to 8 gave material that displayed an $[\alpha]_D^{25}$ of -22.2° (neat) or -4.38 in ethanol solution. Correction for the existing level of enantiomeric excess increases these values to -25.4 (neat) and -5.01 (ethanol), thus confirming Menicagli's configurational assignment and maximum rotation.

The Choice of Chiral Complexes. The optically active titanocene complexes that were evaluated as asymmetric hydrogenation catalysts are compiled in Chart 1. The syntheses of 18,^{8d} 19,^{8c} 20,^{8e} *ent*-20,^{8f} 25,⁶ 28,^{8d} and 29^{8e} have been previously described. The

Chart 1

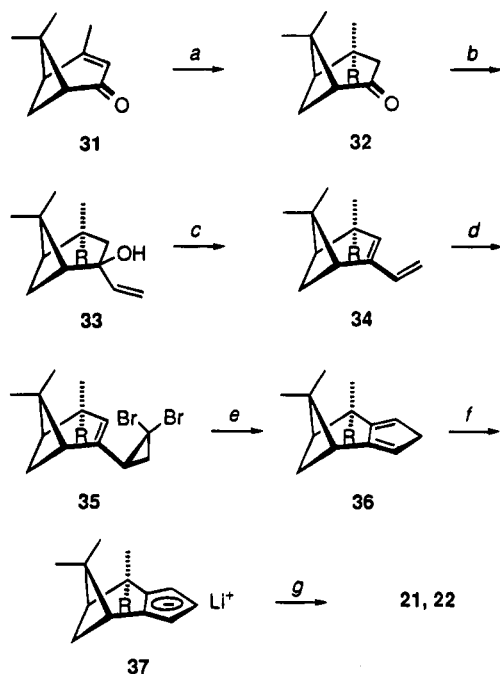


remainder are new, and the details of their preparation are provided in the Experimental Section. Note that dichlorides 26 and 27 are diastereomerically related. This feature is made possible because of the readiness with which unnatural (1*R*,5*R*)-(+)-verbenone (31) is available by the oxidation of (1*R*)-(+)- α -pinene.³² The series *ent*-20–22 was prepared in an effort to assess the consequences of increased steric bulk by the pair of "inside" substituents on hydrogenation enantioselectivity. The titanocenes 21 and 22 were accessed in a manner paralleling that developed for *ent*-20 (Scheme 3). Following addition of the appropriate homocuprate to 31, ketones 32 were individually treated with vinylmagnesium bromide at 0 °C. Addition occurred stereoselectively under steric control of the apical methyl group to give 33b,c exclusively. Following dehydration with activated basic alumina (activity I) and dibromocarbene addition under phase transfer conditions, recourse was made to the Skattebøl rearrangement³³ for the purpose of annulating the cyclopentadiene ring onto the pinane framework as in 36. The lithium cyclopentadienides 37 were smoothly transformed into

(32) Sivik, M. R.; Stanton, K. J.; Paquette, L. A. *Org. Synth.* **1995**, *72*, 57.

(33) (a) Skattebøl, L. *Tetrahedron* **1967**, *23*, 1107. (b) Butler, D. N.; Gupta, I. *Can. J. Chem.* **1978**, *56*, 80. (c) Charumilind, P.; Paquette, L. A. *J. Am. Chem. Soc.* **1984**, *106*, 8225.

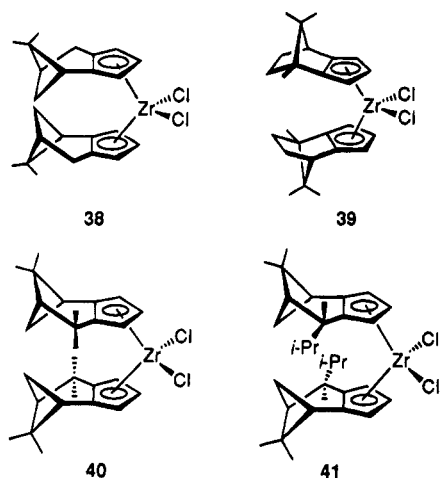
Scheme 3



a, R = CH₃; b, R = CH(CH₃)₂; c, R = C₆H₅

^a CH₃Li, CuI, Me₃SiCl or RMgCl, CuBr•SMe₂, HMAP or DMAP, THF, -78 °C. ^b CH₂=CHMgBr, THF, 0 °C. ^c Basic Al₂O₃, 150 °C, 0.5 Torr. ^d CHBr₃, 50% NaOH, TEBA, ethanol, CH₂Cl₂. ^e CH₃Li, ether, 0 °C. ^f *n*-BuLi, ether-hexanes, 0 °C. ^g TiCl₃, DME, -78 °C to reflux; conc HCl, air.

Chart 2



the stereochemically homogeneous titanocenes by conventional means.

The structural features of the catalysts span a substantial range: (a) symmetrical dimers in which both chiral ligands are constituted of bridged cyclopentadienyl units; (b) complexes which feature two chiral cyclopentadienyl units of different type; (c) titanocenes whose chirality is dictated by one ligand only, with the other being constituted of the parent Cp or of the isodicyclopentadiene unit with coordination to its exo face.

By comparison, a much smaller group of zirconocenes was examined (Chart 2). All are of the C₂-symmetric dimer type. The first two (**38**, **39**) have been described previously.^{3c-e}

Asymmetric Hydrogenation Studies. The first series of reductions to be investigated involved 2-phenyl-

Table 1. Enantioselective Hydrogenation of **6** with Titanocene Complexes^a

expt no.	complex	T, °C/cocatalyst	[α] _D ²⁰ (C ₂ H ₅ OH)	% ee
1	18	-20/ <i>n</i> -BuLi	-2.11	9
2	19	-20/ <i>n</i> -BuLi	-7.88	35
3	20	-20/ <i>n</i> -BuLi	-10.1	44
4	<i>ent</i> - 20	-20/ <i>n</i> -BuLi	+15.5	69
5	21	-20/ <i>n</i> -BuLi	+2.8	12
6	22	-20/ <i>n</i> -BuLi	+7.4	33
7	23	-20/ <i>n</i> -BuLi	+3.8	17
8	24	-20/ <i>n</i> -BuLi	-7.6	33
9	25	-20/ <i>n</i> -BuLi	-2.3	10
10	26	-20/ <i>n</i> -BuLi	+6.2	27
11	27	-20/ <i>n</i> -BuLi	+1.5	7
12	28	-20/ <i>n</i> -BuLi	-0.75	4
13	29	-20/ <i>n</i> -BuLi	-3.64	17
14	<i>ent</i> - 29	-20/ <i>n</i> -BuLi	+5.67	25

^a All reactions were performed in toluene under 20 psi of hydrogen according to method A. The chemical yields were quantitative.

1-butene (**6**) and the titanocene dichlorides depicted in Chart 1. Typically, the hydrogenations were carried out on 2–4 mmol of olefin substrate in the presence of 0.02–0.04 mmol of catalyst, and ~0.2–0.4 mmol of cocatalyst. The use of Red-Al for activation, in the manner originally reported by Cesarotti,²⁴ was briefly examined. However, the Brintzinger protocol³⁴ involving the use of an alkyl lithium proved to be more serviceable and was adopted throughout this investigation. The results are compiled in Table 1.

Several relevant conclusions can be drawn from these data. In general, complexes that are C₂-symmetric deliver 2-phenylbutane at higher levels of optical purity than do C₁-symmetric complexes. Experiments 2–4 and 6 are particularly noteworthy. Similar conclusions were arrived at by Vollhardt.¹⁰ Of additional interest is the fact that the chirality induced by these titanocenes, which are substituted with alkyl groups on the pair of carbon atoms directly linked to the cyclopentadienyl ligands, have the capacity for inducing a higher level of enantioselection than their counterparts with hydrogens in these positions. The comparisons of **18** versus *ent*-**20** and of **28** with **29** are exemplary. Within the pinane subfamily of catalysts, *ent*-**20** gave rise to the highest level of asymmetric induction observed (69%). The isopropyl (**21**) and phenyl homologs (**22**) seemingly have become too sterically congested and consequently limit facial discrimination as the alkene approaches. Although an upper limit of steric feasibility can be exceeded, advantages normally accrue to catalysts which carry structurally larger ligands. For example, C₁-symmetric complexes such as **23** and **24**, which feature an isodicyclopentadienyl component, produce 2-phenylbutane in a more optically enriched state than comparable structures, e.g., **28**, **29**, and *ent*-**29**, having only a cyclopentadienyl ring.

As expected,³⁵ the catalytic activity of the chiral zirconocenes **38**–**41** was considerably lower than the titanium compounds. While the experiments defined in Table 1 were standardized to a temperature of -20 °C, a reaction time of 48 h, and a hydrogen pressure of 20 psi in order to achieve complete reaction, **38**–**41** proved unreactive under these conditions. Reduction did occur slowly at +20 °C and 40 psi (Table 2).

(34) Smith, J. A.; Brintzinger, H. H. *J. Organomet. Chem.* **1981**, *218*, 159.

(35) Cuenca, T.; Flores, J. C.; Royo, P. *J. Organomet. Chem.* **1993**, *462*, 191.

Table 2. Asymmetric Hydrogenation of **6** with Zirconocene Complexes^a

expt no.	complex	reacn time, days	T, °C/cocatalyst	P, psi	% conversion	config of product	% ee ^b
15	38	7	20/ <i>n</i> -BuLi	40	>99	S	15
16	39	4	20/ <i>n</i> -BuLi	20	49	R	4
17	40	10	20/ <i>n</i> -BuLi	40	>99	R	53
18	41	32	20/CH ₃ Li	40	>99	R	4

^a Method D was followed. ^b The optical rotations were performed in 95% ethanol.

Table 3. Enantioselective Hydrogenation Results for **7** (Method B)

expt no.	complex	T, °C/cocatalyst ^b	P, psi	% conversion	config of product	% ee ^a
A. Titanocene Catalysts						
19	19	22/CH ₃ Li	29	96	R	16
20	<i>ent</i> - 20	-18/CH ₃ Li	28	>99	S	61
21	<i>ent</i> - 20	22/CH ₃ Li	28	100	S	53
22	<i>ent</i> - 20	22/CH ₃ Li ^c	1	98	S	50
23	<i>ent</i> - 20	22/ <i>n</i> -BuLi ^c	39.5	100	S	53
24	23	22/CH ₃ Li	26	100	S	28
25	23	-30 to -15/ <i>n</i> -BuLi	28	97	S	32
26	25	22/CH ₃ Li	20	>99	R	2
27	25	22/ <i>n</i> -BuLi	20	93	R	8
28	26	22/ <i>n</i> -BuLi ^c	29	100	S	61
29	26	22/ <i>n</i> -BuLi ^d	29	22	S	60
30	<i>ent</i> - 29	22/CH ₃ Li	27	100	S	17
31	<i>ent</i> - 29	22/ <i>n</i> -BuLi	26	100	S	25
32	30	-78/CH ₃ Li	28	100	S	15
33	30	22/CH ₃ Li ^e	28	100	S	13
34	30	22/ <i>n</i> -BuLi ^f	29	100	S	16
B. Zirconocene Catalysts (Method D)						
35	38	20/ <i>n</i> -BuLi	40	17	S	9
36	40	20/ <i>n</i> -BuLi	40	44	R	14

^a The optical rotations were determined either on neat samples or in 95% ethanol solution. ^b The reactions were performed in toluene solvent except where noted. ^c Hexane was the reaction medium; expt 23 required 96 h to go to completion. ^d The reaction time was 163 h. ^e Reduction was complete in 15 min. ^f Reduction was complete in 30 min.

Reaction times of 4–32 days were necessary. No parallel trend in enantioselection was seen relative to the titanocene analogues. While **38** (15% ee) was more effective than **18** (9% ee), **39** (4% ee) was substantially inferior to **19** (35% ee). Notwithstanding these differences, the higher reactivity of titanium catalysts provides greater utility for this class of compounds than the zirconocenes for enantioselective hydrogenation.

In general, enantioselectivity increases for the naphthyl olefin **7** relative to **6** in the examples studied (Table 3). A comparison of experiments 7 and 25 involving **23** as catalyst revealed that the level of chiral induction increases from 17% to 32% ee. The selectivity normally increased with decreasing temperature, although little effect was observed in a number of cases. A dependence on cocatalyst was also noted. In general, recourse to methyllithium increased the reactivity of the hydrogenation system relative to when *n*-butyllithium was present. A companion effect often observed was a decrease in asymmetric inducing ability with methyllithium. This phenomenon is clearly evident upon inspection inter alia of experiments 22/23, 26/27, 30/31, and 33/34.

The reactivity of dimethyltitanocene **30** was greatly elevated relative to the dichlorides. Quite unexpectedly, however,³⁵ the use of a cocatalyst was required to achieve reduction. Both alkylolithiums are effective, with *n*-butyllithium delivering product of modestly higher ee than that exhibited by methyllithium as usual.

Solvent effects were briefly examined with *ent*-**20** as the probe precatalyst. In this instance, the activity of the hydrogenation system was found to be significantly increased in hexane relative to toluene. In the first of these solvents, **7** was completely reduced in approximately 1 h at 22 °C (expt 22). An increase in the

reaction time to 40 h or more was necessary to reach the same point when toluene was the medium (expt 21). The percent ee in the naphthylbutane was very similar in the two cases (53 vs 50%). In our estimation, this solvent effect will prove to be a general phenomenon.

Discussion

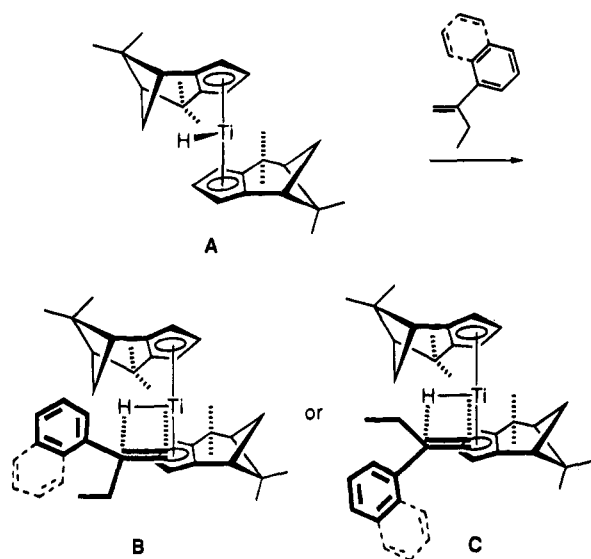
X-ray crystallographic analyses of several of the nonbridged metallocene systems utilized in this study have been detailed earlier. In the solid state, the C₂-symmetric titanocene *ent*-**20**^{8f} and zirconocene **39**^{8e} adopt three-dimensional characteristics featuring in common a significant out-of-plane tilting of the coordinating five-membered rings. However, they differ widely in the mutual orientation of their ligands. Their distinctive conformational arrangements, which range from synclinal for the Ti example to distal for the Zr complex, are not considered to be of fundamental significance since open metallocenes are recognized to possess low-energy torsional potentials such that rotation about the central metal in either direction is virtually unimpeded.³⁶ Crystal packing forces are likely responsible for the observed conformational features. Relevantly, the "freezing-out" of a bent metallocene rotamer in solution has only recently been observed in chiral nonbridged bis(indenyl) complexes of special design.³⁷

It has been postulated that reductions of the type examined here involving 2 equiv of *n*-butyllithium

(36) Doman, T. N.; Hollis, T. K.; Bosnich, B. *J. Am. Chem. Soc.* **1995**, *117*, 1352.

(37) Erker, G.; Aulbach, M.; Knickmeier, M.; Wingbermühle, D.; Krüger, C.; Nolte, M.; Werner, S. *J. Am. Chem. Soc.* **1993**, *115*, 4590.

Scheme 4



proceed with the conversion of a Ti(IV) to a Ti(III) intermediate via β -hydride elimination.^{38,39} The resulting titanocene hydride then assumedly serves as the catalytic species involved in the hydrogen transfer process. If this mechanistic profile holds for the present hydrogenation conditions, then the variations in asymmetric induction which accompany the change in aryl substitution in the alkene are not adequately accommodated if the complex adopts that conformation in which the ligands are distal (Scheme 4; the tilting of the ligands about the Ti is not accentuated).

Before an analysis is carried out, it must be recognized that the observed enantioselectivity may be a direct consequence of the kinetics of complexation of the alkene if the subsequent insertion step is facile. Alternatively, the distribution of dihydro enantiomers may be the product of a preequilibrium involving diastereomeric complexes if the insertion step is more energy demanding. All of this is further complicated if the insertion step itself is reversible. We have no information on any of these options.

Nonetheless, adaptation of the Lauher-Hoffmann theoretical analysis⁴⁰ for the maximization of metal hydride HOMO/olefin LUMO overlap, as pioneered by Buchwald for related complexes,^{1,39} to our transition state models has several implications. The spatial orientation of the valence orbitals at the metal are so directed that incorporation of the olefin very likely occurs laterally as shown in **B** and **C**. Once in the chiral cleft, the alkene becomes subject to hydride transfer from the metal. Reductive cleavage of the titanium-carbon bond ensues. The issue of the extent to which **B** and **C** may be formed is, of course, related directly to the steric factors present in the ligands and the bulk of those substituents present on the double bond. A reasonable sensitivity to spatial demands can be anticipated.

Transition state **B** is destined to lead to dihydro product of the *S* configuration, while passage via **C** will

give rise to the *R* enantiomer. The experimental facts are that **6** and **7** are converted by *ent*-**20** predominantly into the respective (*S*)-2-arylbutane. From among the C_2 -symmetric titanocenes, *ent*-**20** delivers reduction product in the highest percent enantiomeric excess (69% for **6**, 61% for **7**; expts 4, 20). Notably, the verbenone-derived ligand in *ent*-**20** projects only a methyl substituent in that direction syn to the metal center. The higher homologs **21** and **22**, which have isopropyl and phenyl groups located at the same interior sites, are clearly less effective asymmetric catalysts (expts 5, 6). Our working model must take account of these facts.

Other trends are evident. Although pinane derivative **18** lacks comparable substituents α to the Cp ring and is consequently less able to transfer chirality, sufficient recognition is achieved between the catalyst and olefin to induce product stereochemistry that is opposite to that realized in the preceding reductions (expt 1). Transition state **C** may gain greater kinetic importance when these methyl substituents are lacking. The C_1 -symmetric complexes **23**, **24**, and **27-30** are only modestly effective at enantioselective hydrogenation (expts 7, 8, 11-14, 24, 25, 30-34). The related complex **26** has proven generally more effective toward both alkenes (expts 10, 28, 29). The consequences of varying the alkene structure on substrate stereoselectivity are also reflected in the data compiled in Tables 1 and 3. For the titanocenes **19** and *ent*-**20**, a decrease in the observed enantiomeric excess materializes when progressing from **6** to **7**. For precatalysts **25** and *ent*-**29**, the percent ee's remained essentially constant for both olefins. In contrast, the behavior of **23** and **26** is distinguished by an increased ee for the α -naphthyl derivative.

The geometric features present in **B**, although in conformance with the requirement that *S* dihydro product be formed, are not fully accommodating of the experimental facts. If the assumption is made that the aryl substituent in the alkene assumes a local conformation which maintains conjugative overlap with the neighboring olefinic center until the hydrogen atom is transferred from the metal, then the α -naphthyl group would need to be positioned as in **B** and be energetically disadvantaged because of its enforced proximity to the ethyl substituent. This steric interaction need not develop in **C** because the α -naphthyl subunit is no longer oriented proximal to the verbenone ligands. In addition, the methano bridge experiences less steric compression in **C** due to its proximity to the ethyl group of the olefin as compared to **B** where a methano/aryl interaction operates. This balance of forces should facilitate preferred passage via **C**, a conclusion at odds with its role as precursor to *R* dihydro product.

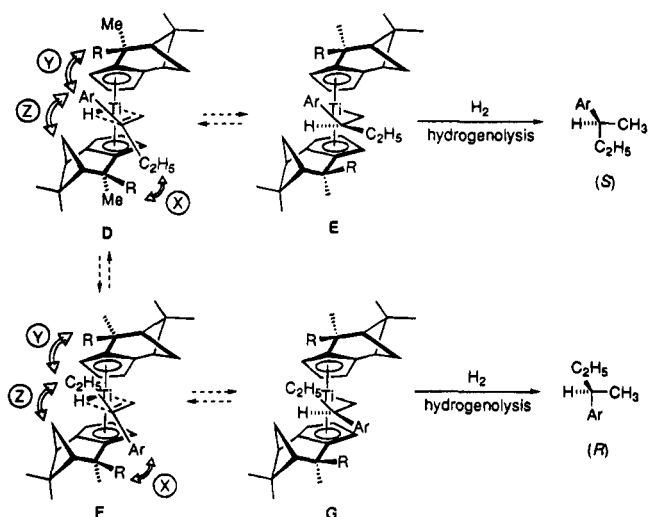
On the other hand, much of the close contact in **B** is skirted if the verbenone-derived ligands are oriented in a more gauchelike arrangement (Scheme 5). According to this model, the initial nonparallel approach of the olefin will be governed predominantly by those nonbonded interactions that develop in the region labeled as a circled X. As the complexation process advances and the olefin approaches even further, a second interaction designated as a circled Y gains importance. The Cp wedge must be at its widest point at this stage of reaction in order to assimilate the alkene properly. The degree of tilting becomes so substantial that mutual compression of the ligands must not become excessive.

(38) (a) Bercaw, J. E.; Brintzinger, H. H. *J. Am. Chem. Soc.* **1969**, *91*, 7301. (b) Bercaw, J. E.; Marvich, R. H.; Bell, L. G.; Brintzinger, H. H. *J. Am. Chem. Soc.* **1972**, *94*, 1219.

(39) Berk, S. C.; Kreutzler, K. A.; Buchwald, S. L. *J. Am. Chem. Soc.* **1991**, *113*, 5093.

(40) Lauher, J. W.; Hoffmann, R. *J. Am. Chem. Soc.* **1976**, *98*, 1729.

Scheme 5



The stacked arrangements proposed in **D** and **F** minimize complications of this type. Notwithstanding, the methano bridge closest to C-1 of the olefin could also exert an effect, indicated by a circled Z, the extent of which will depend, of course, upon the structural features of the complex.

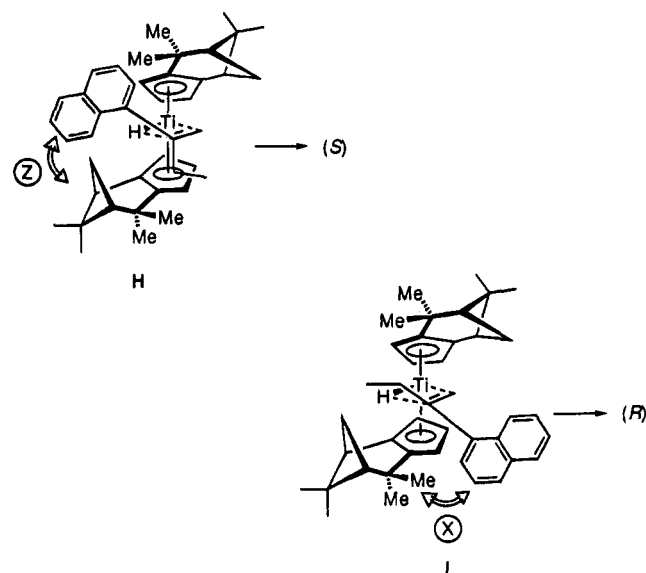
According to Scheme 5, the phenyl group in **6** should prefer to approach the titanocene hydride as in **D** since steric interaction circled X will be less when C₂H₅ is projected close to the R substituent. This compressional advantage will be somewhat offset as reaction progresses and steric compression in the circled Y corridor begins to exert itself. Evidently, however, when R is methyl, the reaction coordinate along **D** and **E** is significantly more favored and the *S* dihydro product dominates appreciably.

As the R group increases in size from methyl to phenyl and isopropyl, the relative differences in energy between diastereomeric transition states **D/F** and **E/G** are lessened because the steric bulk of R offsets the difference in size between the aryl and ethyl substituents of the alkene within the molecular cavity. Thus, the enantioselectivity decreases. This phenomenon would be expected to be particularly significant if a preequilibrium is established and olefin insertion becomes kinetically retarded as the cavity is more densely crowded.

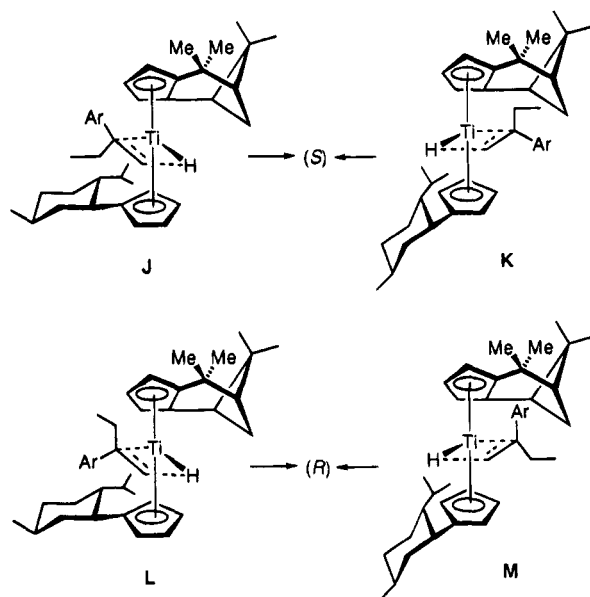
When this steric control element by an R group is not present as in the case in **18**, the dominant steric interaction may involve the methano bridge and be of type circled Z. In such a case, the involvement of **F** and **G** should be favored and formation of the *R* antipode would be anticipated. Indeed, this enantiomer is dominant in the product, although only to a modest level. The possibility remains open that **18** may actually prefer to be oriented as in **B** and **C** since repulsive interactions involving the R group are now minimal. Progression through **C** also leads to the *R* enantiomer.

The small dropoff in enantioselectivity that surfaces during the reduction of **7** as compared to **6** by *ent*-**20** may equally well stem from nonbonded interactions operational in the circled Z sector when the α -naphthyl group is involved. The necessity of maintaining conjugative overlap could be responsible for destabilization as in **H** and consequential greater involvement of **I**. This

possibility would lead to an erosion in the proportion of *S* enantiomer ultimately formed.



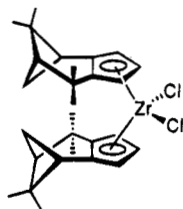
Titanocene **26** was among the most effective catalysts for the enantioselective hydrogenation of **7**. The demonstrated kinetic preference for formation of *S*-(+)-**8** conforms to operation of the transition state trajectories defined as **J** and/or **K**. When Ar is α -naphthyl, the



reduction in steric compression available in **J** and **K** significantly overshadows that attainable in either **L** or **M**. The reduced bulk of the phenyl group in **6** is sufficient to bring transition state models **L** and **M** into closely competitive operation versus **J** and **K**.

Although complete understanding of these phenomena must await further study, it is already clear that the orientation of the R groups in **D**–**G** relative to the H–Ti–H₂C=CRR' plane is critical to the energy differences separating the two diastereomeric complexes. Despite the longer bond lengths present in the zirconocenes, there exists a reasonable parallel with the titanocenes. For example, **40**, which has verbenone-like ligands enantiomeric to those present in *ent*-**20**, reduces **6** to (*R*)-2-phenylbutane with an enantioselectivity

closely approaching that exhibited by *ent*-**20** (expts 4, 17) but antipodal to it.



40

Experimental Section

General. All reactions were carried out under an inert atmosphere of argon unless otherwise indicated. Glassware was generally oven-dried or flame-dried in vacuo and purged well with argon. Dichloromethane was distilled from CaH₂ under nitrogen or argon prior to use. Benzene, hexanes, diethyl ether, toluene, and tetrahydrofuran were distilled from sodium/benzophenone prior to use. DMF, HMPA, and pyridine were distilled from CaH₂ and stored over molecular sieves under argon. Reactions were monitored by thin-layer chromatography (TLC) or gas chromatography. Flash column chromatography was performed using Kieselgel 60 (230–400 AST Mesh) silica gel or basic alumina (Brockmann 1, standard grade, Aldrich). ¹H and ¹³C NMR spectra were recorded predominantly on Bruker 80, 250, and/or Bruker 300 MHz instruments. The high-resolution mass spectra were obtained at The Ohio State University Campus Chemical Instrumentation Center. Elemental analyses were performed at the Scandinavian Microanalytical Laboratory, Herlev, Denmark.

(±)-2-(α-Naphthyl)butanol (11). *n*-Butyllithium (95.7 mL, 2.5 M in hexanes, 0.25 mol) was added to diisopropylamine (24.21 g, 0.24 mol) in 300 mL of THF at 0 °C. A solution of 1-α-naphthylacetic acid (**9**) (20.00 g, 0.11 mol) in 30 mL of THF was introduced followed by addition of HMPA (21.87 g, 0.122 mol). The red solution was stirred for 25 min before ethyl iodide (50.26 g, 0.32 mol) was introduced. The solution was warmed to rt (room temperature) and quenched with 10% HCl solution (200 mL) 30 min later. Extraction with petroleum ether (3 × 150 mL), washing with brine, and drying afforded 34.0 g of unpurified ester **10**.

The above material was dissolved in 100 mL of THF and added slowly to a slurry of lithium aluminum hydride (6.02 g, 0.16 mol) in 500 mL of THF at 0 °C. After addition was complete, the slurry was heated to reflux for 10 h, cooled to 0 °C, and quenched with saturated sodium potassium tartrate solution. Extraction with ether (3 × 200 mL) and drying afforded alcohol **11** as a colorless oil (12.26 g, 57% based on **11**): IR (neat, cm⁻¹) 3375, 1035, 795, 780; ¹H NMR (300 MHz, CDCl₃) δ 8.19 (d, *J* = 7.6 Hz, 1 H), 7.89 (dd, *J* = 7.4, 2.9 Hz, 1 H), 7.77 (d, *J* = 8.1 Hz, 1 H), 7.47–7.58 (m, 3 H), 7.40 (dd, *J* = 7.2, 1.1 Hz, 1 H), 3.90 (d, *J* = 3.2 Hz, 1 H), 3.88 (d, *J* = 3.2 Hz, 1 H), 3.68 (m, *J* = 8.0 Hz, 1 H), 1.91 (dm, *J* = 44.1, 7.9 Hz, 2 H), 1.65 (br s, 1 H), 0.92 (t, *J* = 7.4 Hz, 3 H); ¹³C NMR (75 MHz, CDCl₃) 138.4, 134.0, 132.7, 128.9, 126.9, 125.9, 125.4, 123.5, 123.1, 66.7, 43.6, 25.1, 11.9 ppm; HRMS *m/z* (M⁺) calcd for C₁₄H₁₆O 200.1201, obsd 200.1204. *Anal.* Calcd for C₁₄H₁₆O: C, 83.96; H, 8.05. Found: C, 83.86; H, 8.20.

2-(α-Naphthyl)butyl Pentanoate (12). Alcohol **11** (5.80 g, 29.0 mmol) was combined with ether (150 mL) and triethylamine (3.22 g, 31.9 mmol). The cooled (0 °C) solution was treated with valeryl chloride (3.85 g, 31.9 mmol). After being stirred for 1 h at 0 °C, the reaction mixture was warmed to rt and quenched after an additional 1 h with saturated NaHCO₃ solution (100 mL). Extraction with ether (3 × 100 mL), drying, and concentration afforded ester **12** (8.10 g, 98%): IR (neat, cm⁻¹) 1740, 1732, 1464, 1260, 1175, 778; ¹H NMR (300 MHz, CDCl₃) δ 8.19 (d, *J* = 8.4 Hz, 1 H), 7.88 (d, *J* = 9.4 Hz, 1 H), 7.76 (d, *J* = 8.0 Hz, 1 H), 7.40–7.57 (m, 4 H), 4.39 (m, *J* = 6.9 Hz, 2 H), 3.86 (m, *J* = 6.3 Hz, 1 H), 2.24 (t, *J* = 7.3 Hz, 2 H), 1.96 (dm, *J* = 34.9, 7.4 Hz, 2 H), 1.51 (m, 2 H), 1.24 (m, 2 H),

0.91 (t, *J* = 7.7 Hz, 3 H), 0.86 (t, *J* = 7.3 Hz, 3 H); ¹³C NMR (75 MHz, CDCl₃) 173.7, 137.8, 133.9, 132.5, 128.8, 127.0, 125.8, 125.30, 125.27, 123.5, 123.0, 67.8, 40.0, 33.9, 26.9, 25.3, 22.0, 13.5, 11.7 ppm; HRMS *m/z* (M⁺) calcd for C₁₉H₂₄O₂ 284.1776, obsd 284.1780.

Enzymatic Hydrolysis of 12. Ester **12** (8.80 g, 30.9 mmol), ether (100 mL), and pH 7.0 phosphate buffer solution (100 mL) were combined at rt. The pH was adjusted to 7.2 with a few drops of 1 N NaOH solution. Addition of bovine pancreas acetone powder (5.45 g, Sigma) followed by slow addition of 1.0 N NaOH solution (16.1 mL) by means of a syringe pump connected to a pH controller in order to maintain the pH at 7.2 ± 0.05 afforded a mixture of ester **13** and alcohol **14**. Separation afforded 3.87 g (91%) of **13** and 2.94 g (90%) of alcohol **14**; [α]_D²² = -9.7 (c 4.0, CHCl₃). Mosher ester analysis indicated this material to be of 24.1% ee.

(-)-(2S)-2-(α-Naphthyl)butyl *p*-Toluenesulfonate (15). Alcohol **14** (2.70 g, 13.5 mmol), CH₂Cl₂ (75 mL), and pyridine (50 mL) were combined in a flask. The solution was cooled to 0 °C, and *p*-toluenesulfonyl chloride (2.83 g, 14.8 mmol) was added. After 1 h at 0 °C, the mixture was stirred at rt for 10 h, poured into 200 mL of ether, and washed with 2 M H₂SO₄ until the aqueous phases were acidic. The organic layer was washed with saturated NaHCO₃ solution (100 mL), dried, filtered, and concentrated to afford a near colorless oil which solidified on standing. There was obtained 3.59 g (75%) of **15** as a white solid, mp 65–68 °C: IR (neat, cm⁻¹) 1355, 1188, 1174, 950, 775; ¹H NMR (300 MHz, CDCl₃) δ 7.95 (m, 1 H), 7.85 (m, 1 H), 7.73 (d, *J* = 8.1 Hz, 1 H), 7.60 (d, *J* = 8.3 Hz, 2 H), 7.47 (dd, *J* = 6.3, 3.3 Hz, 2 H), 7.39 (t, *J* = 7.5 Hz, 1 H), 7.25 (d, *J* = 6.9 Hz, 1 H), 7.18 (d, *J* = 8.1 Hz, 2 H), 4.25 (dm, *J* = 9.8, 7.3 Hz, 2 H), 3.77 (t, *J* = 8.1 Hz, 1 H), 2.39 (s, 3 H), 2.05 (dm, *J* = 8.5, 6.6 Hz, 1 H), 1.84 (dm, *J* = 7.2, 1.3 Hz, 1 H), 0.84 (t, *J* = 7.4 Hz, 3 H); ¹³C NMR (75 MHz, CDCl₃) 144.4, 135.9, 134.0, 132.8, 132.1, 129.6, 129.0, 127.7, 127.4, 126.1, 125.5, 125.3, 123.9, 122.6, 73.4, 40.4, 24.6, 21.5, 11.5 ppm; HRMS *m/z* (M⁺) calcd for C₂₁H₂₂O₃S 354.1290, obsd 354.1288; [α]_D²⁰ = -21.5 (c 4.0, ether).

(-)-(2R)-2-(α-Naphthyl)butane (8). A cooled (0 °C) solution of tosylate **15** (2.50 g, 7.03 mmol) and THF (50 mL) was treated with lithium triethylborohydride (10.6 mL, 1.0 M in THF, 10.6 mmol). The reaction mixture was stirred for 60 min at 0 °C and at rt for 10 h, at which point saturated NH₄-Cl solution (50 mL) was introduced. Extraction with ether (3 × 25 mL), drying, and concentration afforded **8** (0.63 g, 48%) after chromatography on silica gel (elution with pentane) as a colorless oil: ¹H NMR (300 MHz, CDCl₃) δ 8.27 (d, *J* = 8.1 Hz, 1 H), 7.98 (dd, *J* = 7.2, 1.9 Hz, 1 H), 7.83 (d, *J* = 8.0 Hz, 1 H), 7.49–7.66 (m, 4 H), 3.65 (m, *J* = 6.8 Hz, 1 H), 1.99 (dm, *J* = 7.3, 0.8 Hz, 1 H), 1.88 (m, *J* = 7.4 Hz, 1 H), 1.51 (d, *J* = 6.8 Hz, 3 H), 1.07 (t, *J* = 7.4 Hz, 3 H); ¹³C NMR (75 MHz, CDCl₃) 143.7, 134.0, 131.8, 128.9, 126.2, 125.6 (2 C), 125.2, 123.2, 122.4, 35.3, 30.6, 21.2, 12.2 ppm; [α]_D²⁰ = -6.55 (neat); [α]_D²⁰ = -1.37 (c 2.3, ethanol).

Methyl 2-(α-Naphthyl)butanoate (16). A flame-dried three-necked 250 mL flask was charged with distilled diisopropylamine (3.85 mL, 27.5 mmol) and THF (40 mL). To the cooled solution (-78 °C) was added dropwise *n*-butyllithium (21.2 mL, 27.5 mmol, 1.3 M). After 3 h, a solution of racemic methyl (α-naphthyl)acetate (5 g, 25 mmol) in THF (20 mL) was introduced *via* cannula followed 1.5 h later with HMPA (4.8 mL, 27.5 mmol) and 15 min later with ethyl iodide (2.5 mL, 31.3 mmol). The bright yellow solution, which was allowed to warm to ambient temperature overnight, was quenched by the addition of water and extracted with ether. Purification of the concentrate by chromatography on silica gel (elution with 10% ethyl acetate in hexanes) afforded **16** (5.25 g, 92%) as a colorless oil: ¹H NMR (80 MHz, CDCl₃) δ 8.06–8.20 (m, 1 H), 7.70–7.91 (m, 2 H), 7.40–7.56 (m, 4 H), 4.29 (dd, *J* = 8.0, 6.8 Hz, 1 H), 3.63 (s, 3 H), 1.76–2.60 (m, 2 H), 0.96 (t, *J* = 7.3 Hz, 3 H).

Enzymatic Hydrolysis of 16. A three-necked flask was charged with **16** (5.23 g, 22.91 mmol) and horse liver esterase

(4.6 g, Sigma; acetone powder). Water (200 mL) was added, and the mixture was mechanically stirred as 0.5 M NaOH (17.2 mL, 8.6 mmol, 0.38 eq) was added *via* syringe pump at such a rate as to maintain the pH at or below 7.3. After 30 h, all of the base had been consumed and the mixture was filtered through Celite. The Celite was washed well with water, and the aqueous filtrate was extracted with ether, acidified with 2 N HCl, and re-extracted with three portions of CH₂Cl₂ (75 mL). After drying and solvent evaporation *in vacuo*, the residue was purified by chromatography on silica gel (elution with 20% ethyl acetate in hexanes) to give **17** (650 mg, 35%) as a colorless oil: ¹H NMR (80 MHz, CDCl₃) δ 8.02–8.23 (m, 1 H), 7.69–7.98 (m, 2 H), 7.30–7.68 (m, 4 H), 4.31 (t, *J* = 4.7 Hz, 1 H), 1.75–2.52 (m, 2 H), 0.98 (t, *J* = 4.7 Hz, 3 H); [α]_D²² = -133.6 (c 3.3, CH₂Cl₂, unpurified).

(-)-(2*R*)-2-(α-Naphthyl)butane (**8**). A cooled (0 °C) solution of (-)-(2*R*)-**17** (607 mg, 2.83 mmol) in THF (25 mL) was treated with LiAlH₄ (320 mg, 8.5 mmol) with vigorous stirring overnight. After recoiling of the gray mixture to 0 °C and careful quenching with dilute HCl, the reaction mixture was extracted with ether (3 × 50 mL). The dried concentrate was purified by chromatography on silica gel (elution with 20% ethyl acetate in hexanes) yielding the *R* alcohol (525 mg, 92%) as a colorless oil. This material exhibited [α]_D²² = -39.1 (c 3.3, ethanol). Mosher ester analysis indicated the alcohol to be of 87.3% ee.

A solution of the above alcohol (959 mg, 4.79 mmol) in CH₂Cl₂ (30 mL) and pyridine (18 mL) was cooled to 0 °C. Freshly recrystallized *p*-toluenesulfonyl chloride (1.1 g, 5.75 mmol) was added, and the solution was stirred under an atmosphere of argon for 4 h at 0 °C and then at ambient temperature for an additional 36 h. The reaction mixture was poured into ether (200 mL) and washed with H₂SO₄ solution (1.8 M) until the washings were acidic. The organic layer was then washed with NaHCO₃ solution, dried, and evaporated to yield a near colorless oil, which was purified by filtration through silica gel (elution with 10% ethyl acetate in hexanes) to give the tosylate as a colorless oil (1.59 g, 94%) with spectral properties identical to those reported above. This compound exhibited an [α]_D²² = -82.2 (c 1.35, CHCl₃).

The tosylate (1.562 g, 4.41 mmol) was dissolved in THF (30 mL) in a dry flask under argon. To the ice-cooled solution was added lithium triethylborohydride (6.6 mL, 6.6 mmol, 1 M) dropwise with vigorous stirring. Stirring was maintained for 21 h, the reaction mixture was recooled to 0 °C, and saturated NH₄Cl solution was added slowly with stirring. Dilution with ether and twofold washing with saturated NH₄Cl solution, once with NaHCO₃ solution, and once with brine followed by drying and concentration *in vacuo* provided a light yellow oil, purification of which by chromatography on silica gel (elution with hexanes) provided **8** (724 mg, 89%) as a colorless oil: [α]_D²² = -22.2 (neat); [α]_D²⁴ = -4.38 (c 1.05, ethanol).

(-)-(η⁵-[*exo*-Isodicyclopentadienyl])(η⁵-[*exo*-(1*S*,8*S*)-7,7,9,9-tetramethyl-tricyclo[6.1.1.0^{2,6}]deca-3,5-dien-2-yl]-dichlorotitanium (**23**). Optically pure (-)-(1*S*,8*S*)-tetramethyltricyclo[6.1.1.0^{2,6}]deca-2,5-diene (**36a**) (3.00 g, 15.9 mmol) was placed in a 250 mL three-necked round-bottomed flask fitted with gas inlet, septum, and condenser, dissolved in 30 mL each of ether and hexane, cooled to 0 °C, and treated with *n*-butyllithium (13.3 mL, 1.2 M in hexane, 15.9 mmol) *via* syringe. A white solid formed as the mixture was warmed to 25 °C. The flask was fitted with an apparatus to filter air-sensitive solids 10 h later. The solid, collected under inert gas, was washed with hexane (15 mL) and vacuum dried to give 2.80 g (91%) of lithium salt **37a** as a moisture- and air-sensitive solid: ¹H NMR (400 MHz, 0.35 M, THF-*d*₆) δ 5.43 (dd, *J* = 2.6, 2.6 Hz, 1 H), 5.30 (dd, *J* = 2.6, 2.6 Hz, 1 H), 5.22 (dd, *J* = 2.6, 2.6 Hz, 1 H), 2.50 (ddd, *J* = 8.5, 5.6, 5.6 Hz, 1 H), 2.44 (dd, *J* = 5.6, 5.6 Hz, 1 H), 1.69 (dd, *J* = 5.6, 5.6 Hz, 1 H), 1.58 (d, *J* = 8.5 Hz, 1 H), 1.31 (s, 3 H), 1.18 (s, 6 H), 0.52 (s, 3 H); ⁶Li NMR (93 MHz, 0.35 M, THF-*d*₆) δ -7.74; ¹³C NMR (100 MHz, 0.35 M, THF-*d*₆) 124.5, 121.2, 98.7, 98.5, 98.0, 57.3, 46.1, 45.4, 38.2, 35.0, 34.3, 35.0, 29.8, 29.0, 26.0 ppm.

The above salt (315 mg, 1.62 mmol) was dissolved in 15 mL of THF and added to a cold (-78 °C) solution of (*exo*-isodicyclopentadienyl)trichlorotitanium (463 mg, 1.62 mmol) *via* cannula. The reaction mixture was maintained at -78 °C for 3 h and allowed to warm to room temperature. After 24 h, the solvent was removed *in vacuo* leaving a green-brown solid, which was recrystallized from toluene at -20 °C to afford **23** (483 mg, 68%), mp 240.0–241.4 °C (toluene): ¹H NMR (300 MHz, CDCl₃) δ 6.34 (t, *J* = 2.8 Hz, 1 H), 6.32 (d, *J* = 2.5 Hz, 2 H), 6.11 (br s, 1 H), 5.93 (t, *J* = 2.4 Hz, 2 H), 3.35 (br s, 2 H), 2.80 (t, *J* = 5.2 Hz, 1 H), 2.54 (ddd, *J* = 11.9, 10.5, 6.3 Hz, 1 H), 2.08 (d, *J* = 10.5 Hz, 1 H), 1.87 (dd, *J* = 10.4, 2.6 Hz, 2 H), 1.67 (t, *J* = 5.3 Hz, 1 H), 1.47 (br t, *J* = 9.4 Hz, 2 H), 1.42 (s, 3 H), 1.40 (s, 3 H), 1.28 (s, 3 H), 1.10 (dd, *J* = 7.6, 2.2 Hz, 2 H), 0.44 (s, 3 H); ¹³C NMR (75 MHz, CDCl₃) 149.9, 147.2, 145.7, 143.3, 126.6, 118.1, 117.8, 109.9, 107.1, 107.0, 54.3, 48.1, 45.3, 41.4, 41.3, 40.6, 30.9, 23.0, 28.1, 28.0, 27.6, 24.3 ppm; HRMS *m/z* (M⁺ - Cl) calcd for C₂₄H₃₀ClTi 401.1516, obsd 401.1525; [α]_D²⁰ -60.0 (c 0.05, CHCl₃). Anal. Calcd for C₂₄H₃₀Cl₂Ti: C, 65.92; H, 6.91. Found: C, 65.92; H, 7.01.

(-)-(η⁵-[*exo*-Isodicyclopentadienyl])(η⁵-(1*R*,7*R*)-1,10,10-trimethyltricyclo[5.2.1.0^{2,6}]deca-3,5-dien-2-yl)dichlorotitanium (**24**). (*exo*-Isodicyclopentadienyl)trichlorotitanium²³ (316 mg, 1.11 mmol) and 50 mL of THF were placed in a 100 mL round-bottomed flask equipped with a side arm. The solution was cooled to -78 °C, and to it was added camphor-cyclopentadienide lithium salt^{8c} (200 mg, 1.11 mmol) dissolved in THF (20 mL) *via* cannula. One hour later, the dry ice bath was removed and the mixture was stirred for 2 days, filtered through Celite, and concentrated to leave a red oil, which crystallized from toluene-pentane to give **24** (152 mg, 36%) as a red powder, mp 183–184 °C (toluene): ¹H NMR (300 MHz, CDCl₃) δ 6.36 (m, 2 H), 6.22 (m, 2 H), 6.14 (t, *J* = 2.8 Hz, 1 H), 5.99 (t, *J* = 2.8 Hz, 1 H), 3.31 (br s, 2 H), 2.76 (d, *J* = 4.3 Hz, 1 H), 2.05–1.50 (series of m, 8 H), 1.24 (s, 3 H), 1.10 (dd, *J* = 5.3, 2.7 Hz, 2 H), 0.92 (s, 3 H), 0.28 (s, 3 H); ¹³C NMR (75 MHz, CDCl₃) 125.5, 124.2, 112.8, 108.0, 107.6, 70.1, 54.2, 51.5, 47.7, 41.6, 41.5, 32.4, 28.2, 28.0, 25.5, 21.1, 19.9, 12.9 ppm; HRMS *m/z* (M⁺ - Cl) calcd for C₂₃H₂₈ClTi 387.1359, obsd 387.1365; [α]_D¹⁹ -175.4 (c 0.12, toluene).

(+)-(η⁵-Neomenthylcyclopentadienyl)(η⁵-[*exo*-(1*S*,8*S*)-7,7,9,9-tetramethyltricyclo[6.1.1.0^{2,6}]deca-3,5-dien-2-yl]-dichlorotitanium (**26**). An isomeric mixture of neomenthylcyclopentadienes (22.40 g, 0.110 mol) was placed in a three-necked 500 mL round-bottomed flask fitted with two septa, condenser, and gas inlet. The hydrocarbon mixture was degassed and dissolved in hexane (100 mL) and ether (150 mL) under argon. The solution was cooled to 0 °C while *n*-butyllithium (43.8 mL, 2.5 M in hexane, 0.110 mol) was added *via* syringe. A white precipitate formed as the mixture thickened. One hour later, the ice bath was removed and the flask swirled a few times. After 6 h at 25 °C, the mixture was filtered through a Schlenk filter stick under argon. Washing of the white solid twice with hexane (20 mL) and vacuum drying for 6 h afforded the lithium salt (13.62 g, 59%) as a moisture- and air-sensitive solid.

Neomenthylcyclopentadienyllithium (6.83 g, 32 mmol) was taken up in 50 mL of THF, and this solution was added dropwise *via* cannula to a solution of chlorotrimethylsilane (7.06 g, 65 mmol) in 350 mL of THF at 0 °C. The reaction mixture was stirred for 1 h, kept at 25 °C for 10 h, and poured into a mixture of saturated NaCl solution (100 mL) and ether (200 mL). The separated aqueous phase was extracted with ether (3 × 100 mL), and the ethereal layers were dried, filtered, and concentrated to leave a light yellow oil, which was redissolved in twice its volume of hexane and passed through a 2-in. pad of silica gel (elution with hexane) to give, after concentration, 8.00 g (89%) of the silane as a colorless oil: IR (neat, cm⁻¹) 2962, 2945, 2880, 2850, 1254, 989, 870, 840, 817; ¹H NMR (300 MHz, CDCl₃) δ 6.62 (br s, 1 H), 6.40 (br s, 1 H), 6.21 (d, *J* = 1.1 Hz, 1 H), 3.15 (br d, *J* = 4.2 Hz, 2 H), 1.82 (br s, 1 H), 1.78 (br d, *J* = 1.8 Hz, 2 H), 1.55 (br t, *J* = 13.0 Hz, 3 H), 1.24 (dt, *J* = 12.7, 5.0 Hz, 2 H), 1.06 (br m, 1 H), 0.92 (d,

$J = 6.5$ Hz, 6 H), 0.85 (d, $J = 6.2$ Hz, 3 H), -0.07 (s, 9 H); ^{13}C NMR (75 MHz, CDCl_3) 147.8, 134.9, 135.0, 129.4, 51.0, 48.1, 43.0, 38.3, 36.1, 30.5, 27.1, 27.1, 23.1, 21.5, 21.5, -1.9 ppm; HRMS m/z (M^+) calcd for $\text{C}_{15}\text{H}_{32}\text{Si}$ 276.2273, obsd 276.2272; $[\alpha]_{\text{D}}^{20} +19.3$ (c 4.5, hexane).

The silane mixture (8.00 g, 28.9 mmol) was degassed, dissolved in 35 mL of toluene, and added to a cold (-78 °C) solution of titanium tetrachloride (5.49 g, 28.9 mmol) and 150 mL of toluene. After 2 h at -78 °C, the mixture was warmed to rt and stirred for 10 h. The solvent was removed in vacuo leaving a green-brown oil, Kugelrohr distillation of which (110–130 °C, 4×10^{-3} Torr) yielded the complex as a yellow-orange syrup (4.96 g, 48%) which crystallized into a solid mass on standing, mp 53–55 °C: ^1H NMR (300 MHz, CDCl_3) δ 7.23 (q, $J = 2.2$ Hz, 1 H), 7.00 (dt, $J = 3.3, 2.2$ Hz, 1 H), 6.93 (q, $J = 2.2$ Hz, 1 H), 6.77 (q, $J = 3.2$ Hz, 1 H), 3.55 (br d, $J = 3.4$ Hz, 1 H), 2.12 (dq, $J = 16.2, 2.5$ Hz, 1 H), 1.90 (br m, 2 H), 1.69 (br m, 1 H), 1.19–1.41 (m, 4 H), 1.01 (d, $J = 6.2$ Hz, 3 H), 0.91 (d, $J = 6.2$ Hz, 3 H), 0.83 (dd, $J = 17.1, 6.2$ Hz, 1 H), 0.74 (d, $J = 6.2$ Hz, 3 H); ^{13}C NMR (75 MHz, CDCl_3) 148.4, 125.0, 123.6, 123.4, 122.7, 49.9, 39.9, 39.7, 35.2, 29.6, 28.2, 24.5, 22.6, 22.0, 20.6 ppm; HRMS m/z (M^+) calcd for $\text{C}_{15}\text{H}_{23}\text{Cl}_3\text{Ti}$ 323.062, obsd 323.0582; $[\alpha]_{\text{D}}^{20} +87.5$ (c 0.3, CHCl_3). Anal. Calcd for $\text{C}_{15}\text{H}_{23}\text{Cl}_3\text{Ti}$: C, 50.38; H, 6.48. Found: C, 50.83; H, 6.60.

Lithium *exo*-(1*S*,8*S*)-7,7,9,9-tetramethyltricyclo[6.1.1.0^{2,6}]-deca-3,5-dienide (**37a**) (217 mg, 1.12 mmol) was dissolved in 15 mL of THF and added dropwise via cannula to a cold (-78 °C) solution of (neomenthylcyclopentadienyl)trichlorotitanium (400 mg, 1.12 mmol) in 35 mL of THF. The brick red solution was stirred for 2 h at -78 °C and for 24 h at 25 °C prior to concentration to leave a green-brown solid. The solid was dissolved in toluene (5 mL) from which crystals of **26** formed at -20 °C (330 mg, 58%), mp 110–113 °C: ^1H NMR (300 MHz, CDCl_3) δ 6.73 (q, $J = 2.2$ Hz, 1 H), 6.31–6.38 (m, 4 H), 6.19 (q, $J = 2.3$ Hz, 1 H), 5.99 (t, $J = 2.3$ Hz, 1 H), 3.54 (br d, $J = 3.3$ Hz, 1 H), 2.84 (t, $J = 5.2$ Hz, 1 H), 2.55 (ddd, $J = 11.8, 10.6, 6.3$ Hz, 1 H), 2.17 (dt, $J = 13.7, 4.0$ Hz, 1 H), 2.02 (d, $J = 10.5$ Hz, 1 H), 1.91 (m, $J = 6.8$ Hz, 1 H), 1.81 (m, 1 H), 1.67 (t, $J = 1.1$ Hz, 1 H), 1.62 (br d, $J = 8.9$ Hz, 1 H), 1.41 (s, 6 H), 1.29 (s, 3 H), 1.26 (m, 3 H), 0.99 (d, $J = 6.4$ Hz, 3 H), 0.98 (m, 2 H), 0.88 (d, $J = 6.4$ Hz, 3 H), 0.72 (d, $J = 6.4$ Hz, 3 H), 0.45 (s, 3 H); ^{13}C NMR (75 MHz, CDCl_3) 149.7, 143.9, 141.0, 126.4, 121.0, 119.1, 117.4, 115.8, 112.9, 111.1, 54.4, 50.1, 45.3, 45.3, 40.6, 39.4, 38.2, 35.6, 31.0, 30.0, 29.9, 29.2, 28.4, 27.7, 24.7, 24.4, 22.8, 22.3, 20.8 ppm; HRMS m/z ($M^+ - \text{Cl}$) calcd for $\text{C}_{29}\text{H}_{42}\text{Cl}_4\text{Ti}$ 473.2455, obsd 473.2455; $[\alpha]_{\text{D}}^{20} -150$ (c 0.2, CHCl_3). Anal. Calcd for $\text{C}_{29}\text{H}_{42}\text{Cl}_4\text{Ti}$: C, 68.37; H, 8.31. Found: C, 68.36; H, 8.29.

(η^5 -Neomenthylcyclopentadienyl)(η^5 -[*exo*-(1*R*,8*R*)-7,7,9,9-tetramethyl-tricyclo[6.1.1.0^{2,6}]-deca-3,5-dien-2-yl]-dichlorotitanium (**27**). Copper iodide (28.53 g, 0.150 mmol, purified by complexation to potassium iodide)⁴¹ was placed in a 1000 mL flame-dried three-necked round-bottomed flask equipped with an addition funnel, gas inlet, septum, and stir bar. The near white solid was slurried in 300 mL of ether, and the flask was placed in an ice bath. Methyl lithium (200 mL, 1.5 M in ether, 0.30 mmol) was gradually introduced over 30 min. The mixture turned bright yellow and then became colorless at the equivalence point (2 equiv of CH_3Li to 1 equiv of CuI). Fifteen minutes later, a solution of (1*R*)-(+)-verbenone (22.50 g, 0.150 mol), chlorotrimethylsilane (32.54 g, 0.300 mmol), and 50 mL of ether was added over 30 min. The mixture was stirred for 2 h at 0 °C and monitored by TLC. After complete reaction, saturated NH_4Cl solution (150 mL) was gradually introduced. The ice bath was removed, and the mixture was stirred for 30 min at rt. Concentrated ammonium hydroxide solution (50 mL) was added, and the mixture was stirred until all of the copper salts dissolved. The blue mixture was poured into a separatory funnel, the separated aqueous layer was extracted with ether, and the combined organic phases were washed with water (100 mL) and brine (100 mL)

prior to drying and concentration. (+)-(1*R*,5*R*)-7,7,9,9-Tetramethylbicyclo[3.1.1]heptan-2-one (**32a**) was obtained as a light yellow oil, (24.22 g, 97%). The spectral data were identical to those of the enantiomer; $[\alpha]_{\text{D}}^{20} +49$ (c 0.7, ethanol).

In a 300 mL three-necked round-bottomed flask fitted with condenser, addition funnel, and gas inlet were placed magnesium turnings (1.46 g, 60.2 mmol) and 100 mL of tetrahydrofuran. In the addition funnel was placed vinyl bromide (8.37 g, 5.52 mL, 78.3 mmol) and 20 mL of THF. Carefully, a small amount of this solution was added to the magnesium while simultaneously heating the mixture to initiate the reaction. After a slight change in color, the heat was removed and the final portion of halide solution was added dropwise as the reaction mixture continued to reflux. Once addition was completed, the mixture was stirred until all of the magnesium metal was consumed (approximately 2 h), cooled to 0 °C, and treated with a solution of the above ketone (5.00 g, 30.1 mmol) in 20 mL of THF dropwise over 20 min. The reaction mixture was stirred at 0 °C for 1 h and at rt for 6 h. Saturated NH_4Cl solution (200 mL) was slowly added, the layers were separated, and the aqueous phase was extracted with ether (3×150 mL). The combined organic fractions were dried, filtered, and concentrated to give a light yellow oil, which was purified by chromatography (silica gel, elution with 10% ethyl acetate in petroleum ether) to give 4.90 g (84%) of (-)-(1*R*,2*S*,5*R*)-4,4,6,6-tetramethyl-2-vinylbicyclo[3.1.1]heptan-2-ol (**33a**) as colorless crystals, mp 62.5–63.5 °C (from ethyl acetate): IR (CHCl_3 , cm^{-1}) 3593, 1468, 995, 936; ^1H NMR (300 MHz, CDCl_3) δ 6.05 (dd, $J = 16.3, 10.6$ Hz, 1 H), 5.20 (dd, $J = 16.3, 1.0$ Hz, 1 H), 5.01 (dd, $J = 9.7, 1.0$ Hz, 1 H), 2.15 (dt, $J = 6.3, 1.5$ Hz, 1 H), 1.95 (dd, $J = 15.7, 5.3$ Hz, 2 H), 1.84 (t, $J = 4.9$ Hz, 1 H), 1.58 (t, $J = 5.1$ Hz, 1 H), 1.52 (s, 1 H), 1.30 (s, 3 H), 1.26 (s, 3 H), 1.20 (d, $J = 11.1$ Hz, 1 H), 1.09 (s, 3 H), 0.95 (s, 3 H); ^{13}C NMR (75 MHz, CDCl_3) 146.4, 111.1, 77.2, 53.4, 52.5, 45.8, 40.0, 33.7, 31.9, 30.7, 29.3, 27.0, 26.2 ppm; HRMS m/z (M^+) calcd for $\text{C}_{13}\text{H}_{22}\text{O}$ 194.1671, obsd 194.1671; $[\alpha]_{\text{D}}^{20} -1.3$ (c 3.9, CHCl_3). Anal. Calcd for $\text{C}_{13}\text{H}_{22}\text{O}$: C, 80.35; H, 11.41. Found: C, 80.58; H, 11.41.

This allylic alcohol (3.10 g, 16.0 mmol) and alumina (100 g, activity I) were combined in a one-necked round-bottomed flask. The alumina was evenly coated, and the solid mixture was allowed to stand for 3 h. The flask containing the solid mixture was connected to a receiver for bulb-to-bulb distillation and slowly heated under vacuum (0.5 mmHg). The product was collected in the receiver at -78 °C. After 1 h of heating at 150 °C, the distillation was stopped. The product was passed through a short column of silica gel (elution with 1% ether in pentane) to give (-)-(1*S*,5*R*)-4,4,6,6-tetramethyl-2-vinylbicyclo[3.1.1]hept-2-ene (**34a**) as a near colorless oil (1.16 g, 41%): IR (neat, cm^{-1}) 1625, 1474, 1383, 1367, 990, 894, 853; ^1H NMR (300 MHz, CDCl_3) δ 6.37 (dd, $J = 10.8, 6.6$ Hz, 1 H), 5.26 (s, 1 H), 5.09 (d, $J = 17.4$ Hz, 1 H), 4.91 (d, $J = 9.7$ Hz, 1 H), 2.54 (t, $J = 5.1$ Hz, 1 H), 2.26 (m, 1 H), 1.70 (dt, $J = 3.8, 2.0$ Hz, 1 H), 1.38 (d, $J = 9.2$ Hz, 1 H), 1.29 (s, 3 H), 1.04 (s, 3 H), 0.97 (s, 3 H), 0.96 (s, 3 H); ^{13}C NMR (75 MHz, CDCl_3) 144.3, 138.5, 139.0, 110.6, 54.0, 41.72, 41.70, 38.9, 31.2, 30.2, 27.9, 26.2, 24.6 ppm; HRMS m/z (M^+) calcd for $\text{C}_{13}\text{H}_{20}$ 176.1565, obsd 176.1569; $[\alpha]_{\text{D}}^{20} -19.5$ (c 7.5, hexane). Anal. Calcd for $\text{C}_{13}\text{H}_{20}$: C, 88.57; H, 11.43. Found: C, 88.57; H, 11.55.

To diene **34a** from above (7.40 g, 0.042 mol) in 100 mL of dichloromethane was added bromoform (15.91 g, 0.063 mol), benzyltriethylammonium chloride (0.25 g, 0.91 mmol), and 0.5 mL of ethanol. The mechanically stirred mixture was cooled in an ice bath and treated slowly with 21 mL of 50% sodium hydroxide solution. Once addition was complete, the two-phase system was stirred for 24 h at rt and poured into a separatory funnel. The separated aqueous layer was diluted with 100 mL of water and extracted with dichloromethane (3×200 mL). The combined organic fractions were dried, filtered, and concentrated to leave a brown oil, which was passed through a 2-in. pad of silica gel (elution with hexane) and concentrated at 25 °C to give **35a** as a light yellow oil.

(41) Kauffman, G. B.; Fang, L. Y. *Inorg. Synth.* **1983**, *22*, 101.

The material was placed in a 1000 mL round-bottomed flask equipped with a side arm and dissolved in 500 mL of anhydrous ether. The flask was cooled in an ice bath at which time methylolithium (115.0 mL, 1.5 M in ether, 0.172 mol) was slowly introduced via syringe. The light yellow-green solution was allowed to stir at rt for 24 h after addition was complete and added to 1000 mL of ice/salt water via cannula. The separated aqueous phase was extracted three times with ether (200 mL), and the combined organic layers were dried, filtered, and concentrated at rt to give a yellow-orange oil, purification of which on a short column of silica gel (elution with pentane) gave 5.01 g (62% based on recovered **34a**) of pure cyclopentadiene **36a** as a faint yellow oil. Spectral data are identical with those reported earlier for the enantiomer;^{8e} $[\alpha]_D^{20}$ -22.2 (c 8.0, hexane).

Lithium salt **37a** of this cyclopentadiene (217 mg, 1.12 mmol), prepared in the manner described above, was taken up in 20 mL of THF and added to a solution of (neomenthylcyclopentadienyl)trichlorotitanium (400 mg, 1.12 mmol) in 30 mL of THF at -78 °C via cannula. After 2 h, the dry ice bath was removed and the mixture was allowed to stir at 25 °C for 24 h, concentrated, and redissolved in dichloromethane (ca. 50 mL). This solution was filtered through a Celite pad, and the filtrate was concentrated. Sublimation (170–175 °C, 5 × 10⁻⁴ Torr) of a portion of the solid and crystallization of the remaining material from toluene at -20 °C afforded 353 mg (62%) of **27** as a fluffy green microcrystalline solid, mp 201–202 °C (toluene): ¹H NMR (300 MHz, CDCl₃) δ 6.77 (q, *J* = 2.1 Hz, 1 H), 6.56 (q, *J* = 3.0 Hz, 1 H), 6.41 (t, *J* = 2.3 Hz, 1 H), 6.31 (q, *J* = 2.8 Hz, 1 H), 6.08–6.12 (m, 3 H), 3.55 (br d, *J* = 3.0 Hz, 1 H), 2.85 (t, *J* = 5.2 Hz, 1 H), 2.53 (ddd, *J* = 11.8, 10.6, 6.3 Hz, 1 H), 2.15 (dd, *J* = 9.6, 4.1 Hz, 1 H), 2.03 (d, *J* = 10.6 Hz, 1 H), 1.93 (m, *J* = 4.2 Hz, 1 H), 1.82 (br m, 1 H), 1.63 (dd, *J* = 11.4, 6.1 Hz, 1 H), 1.56 (d, *J* = 24.2 Hz, 1 H), 1.40 (s, 3 H), 1.37 (s, 3 H), 1.30 (s, 3 H), 1.28 (m, 3 H), 0.98 (d, *J* = 6.1 Hz, 3 H), 0.97 (m, 2 H), 0.88 (d, *J* = 6.4 Hz, 3 H), 0.70 (d, *J* = 6.2 Hz, 3 H), 0.43 (s, 3 H); ¹³C NMR (75 MHz, CDCl₃) 152.0, 141.3, 141.0, 126.5, 120.9, 117.4, 117.0, 116.6, 113.5, 111.4, 54.5, 49.9, 45.4, 45.3, 40.2, 39.3, 38.4, 35.5, 30.8, 30.1, 29.9, 29.2, 28.5, 27.6, 24.6, 24.3, 22.8, 22.3, 20.7 ppm; HRMS *m/z* (*M*⁺ - Cl) calcd for C₂₉H₄₂³⁷Cl⁴⁶Ti 473.2471, obsd 473.2467; $[\alpha]_D^{20}$ +356.1 (c 0.1, CHCl₃). Anal. Calcd for C₂₉H₄₂Cl₂Ti: C, 68.37; H, 8.31. Found: C, 68.33; H, 8.33.

(-)-(η⁵-Cyclopentadienyl)(η⁵-[*exo*-(1*S*,8*S*)-7,7,9,9-tetramethyltricyclo-[6.1.1.0^{2,6}]deca-3,5-dien-2-yl])dichlorotitanium (*ent*-**29**). In the drybox, the lithium cyclopentadienide **37a** described earlier (300 mg, 1.55 mmol) was weighed into a round-bottomed flask equipped with a side arm. Another flask was charged with cyclopentadienyltitanium trichloride (339 mg, 1.55 mmol). After addition of 30 mL of tetrahydrofuran to the lithium salt, the flask was cooled to -78 °C. To this near colorless solution was added the titanium reagent in 15 mL of dry tetrahydrofuran via cannula dropwise over 20 min. Upon addition, the reaction mixture turned brick red. After addition was complete, the reaction mixture was stirred at -78 °C for 1 h, allowed to warm to rt, and stirred for an additional 10 h. The solvent was removed in vacuo leaving a brown-red residue, which was taken up in dichloromethane (30 mL) and filtered through a Celite pad. The red solution was again quickly concentrated to give a brown-red solid. This solid was dissolved in a small amount of dry toluene and cooled to -20 °C. After 6 h, crystals of *ent*-**29** formed and were collected as a brown fluffy microcrystalline solid, 243 mg (42%). Spectral data are identical to those reported for the enantiomer;^{8e} $[\alpha]_D^{20}$ -225 (c 0.14, toluene).

(+)-(1*R*,4*S*,5*R*)-4-Isopropyl-4,6,6-trimethyltricyclo[3.1.1]heptan-2-one (**32b**). In a flame-dried 1000 mL three-necked round-bottomed flask fitted with a gas inlet, addition funnel, and large stir bar was placed CuBr·DMS complex (1.03 g, 5.0 mmol). Tetrahydrofuran (200 mL) and 4-(dimethylamino)pyridine (24.40 g, 0.20 mol) were added, and the resulting slurry was cooled to -78 °C. Isopropylmagnesium chloride (60.0 mL, 2.0 M in ether, 0.20 mol) was added, causing the

gray-tan slurry to turn bright yellow-orange. After 15 min, a solution of **31** (15.0 g, 0.10 mol) and chlorotrimethylsilane (21.70 g, 0.20 mol) in 150 mL of tetrahydrofuran was added slowly over 1 h. The mixture was stirred at -78 °C for 4 h before it was allowed to warm to rt and then quenched by the slow addition of saturated NH₄Cl solution (200 mL) and, 2 h later, 75 mL of concentrated NH₄OH solution. The mixture was allowed to stir until the aqueous layer was blue. After separation and extraction of the aqueous phase with ether (4 × 200 mL), the combined organic layers were washed with 1 N HCl (3 × 100 mL), water (100 mL), and brine (100 mL), prior to drying and concentration to give a light yellow oil, purification of which on silica gel (elution with 10% ethyl acetate in petroleum ether) afforded 14.77 g (75%) of **32b** as a colorless oil: IR (neat, cm⁻¹) 1720, 1473, 1396, 1375, 1270; ¹H NMR (300 MHz, CDCl₃) δ 2.43 (m, 2 H), 2.33 (m, 1 H), 2.15 (d, *J* = 19.6 Hz, 1 H), 2.04 (t, *J* = 5.0 Hz, 1 H), 1.69 (m, *J* = 6.8 Hz, 1 H), 1.58 (d, *J* = 8.8 Hz, 1 H), 1.29 (s, 3 H), 0.93 (s, 3 H), 0.88 (s, 3 H), 0.79 (d, *J* = 6.8 Hz, 3 H), 0.66 (d, *J* = 6.8 Hz, 3 H); ¹³C NMR (62.5 MHz, CDCl₃) 214.0, 57.6, 50.7, 48.2, 40.5, 36.3, 27.4, 25.6, 23.3, 18.4, 17.3, 16.2 ppm; HRMS *m/z* (*M*⁺) calcd for C₁₃H₂₂O 194.1671, obsd 194.1669; $[\alpha]_D^{20}$ +25.7 (c 3.6, ethanol). Anal. Calcd for C₁₃H₂₂O: C, 80.36; H, 11.41. Found: C, 80.17; H, 11.41.

(+)-(1*R*,2*S*,4*S*,5*R*)-4-Isopropyl-4,6,6-trimethyl-2-vinyltricyclo[3.1.1]heptan-2-ol (**33b**). Magnesium turnings (3.65 g, 0.150 mol) were placed into a 1000 mL three-necked round-bottomed flask fitted with a condenser, gas inlet, addition funnel, and septum. THF (300 mL) was added, and the magnesium was activated by addition of a few drops of ethyl bromide. A solution of vinyl bromide (16.86 g, 0.158 mol) and THF (50 mL) was slowly introduced into the slurry. Once all of the magnesium had dissolved, the solution was cooled to 0 °C. Ketone **32b** (14.75 g, 0.075 mol) in 50 mL of THF was slowly added, and the mixture was stirred at 0 °C for 2 h and at rt for an additional 6 h before it was carefully neutralized with saturated NH₄Cl solution (200 mL). The layers were separated, and the aqueous phase was extracted with ether (4 × 125 mL). The combined organic layers were dried and concentrated to leave an orange oil. TLC analysis indicated the presence of two nearly superimposable compounds, with **33b** consisting of 52% (ca. 8.75 g) of the product mixture as determined by ¹H NMR. Data for **33b**: IR (neat, cm⁻¹) 3422, 1417, 1369, 993; ¹H NMR (300 MHz, CDCl₃) δ 6.04 (dd, *J* = 17.3, 10.4 Hz, 1 H), 5.19 (dd, *J* = 17.3, 1.2 Hz, 1 H), 4.99 (dd, *J* = 10.7, 1.1 Hz, 1 H), 2.19 (d, *J* = 16.0 Hz, 1 H), 2.08 (m, 1 H), 1.80 (m, *J* = 6.2 Hz, 1 H), 1.74 (d, *J* = 16.0 Hz, 2 H), 1.34 (s, 1 H), 1.31 (s, 3 H), 1.26 (s, 3 H), 1.22 (d, *J* = 10.2 Hz, 1 H), 0.98 (d, *J* = 5.6 Hz, 1 H), 0.86 (d, *J* = 6.8 Hz, 3 H), 0.84 (s, 3 H), 0.63 (d, *J* = 6.8 Hz, 3 H); ¹³C NMR (75 MHz, CDCl₃) 146.6, 111.0, 77.1, 51.6, 50.9, 43.7, 39.4, 37.8, 35.2, 29.6, 26.1, 24.9, 19.6, 17.8, 16.2 ppm; HRMS *m/z* (*M*⁺) calcd for C₁₅H₂₆O 222.1984, obsd 222.1956.

(+)-(1*S*,4*S*,5*R*)-4-Isopropyl-4,6,6-trimethyl-2-vinyltricyclo[3.1.1]hept-2-ene (**34b**). The mixture from above was adsorbed onto basic alumina (200 g, activity I, activated at 450 °C for 12 h) until the solid adsorbent was evenly coated, placed into a Kugelrohr apparatus after standing at rt for 4 h, and heated to 160 °C under 1.5 mmHg for 1 h. The oil was collected in a receiver cooled to -78 °C. The alumina mixture was eluted with several portions of ether until TLC analysis indicated no product in the washings. The eluents were combined, dried, and evaporated to leave a light yellow oil, purification of which by chromatography on silica gel (elution with 1% ether in petroleum ether) afforded 5.24 g (65%) of **34b**: IR (neat, cm⁻¹) 1498, 1450, 900, 769, 706; ¹H NMR (300 MHz, C₆D₆) δ 6.37 (dd, *J* = 17.4, 10.7 Hz, 1 H), 5.55 (br s, 1 H), 5.11 (d, *J* = 17.4 Hz, 1 H), 4.92 (d, *J* = 10.7 Hz, 1 H), 1.61 (t, *J* = 5.4 Hz, 1 H), 2.19 (m, 1 H), 1.97 (m, 1 H), 1.77 (m, *J* = 6.8 Hz, 1 H), 1.46 (d, *J* = 9.3 Hz, 1 H), 1.31 (s, 3 H), 0.99 (s, 3 H), 0.86 (s, 3 H), 0.85 (d, *J* = 6.9 Hz, 3 H), 0.67 (d, *J* = 6.9 Hz, 3 H); ¹³C NMR (75 MHz, C₆D₆) 144.2, 138.9, 133.4, 110.6, 51.5, 43.1, 41.8, 41.2, 35.3, 29.1, 28.0, 24.5, 17.6, 16.02, 15.99 ppm;

HRMS m/z (M^+) calcd for $C_{15}H_{24}$ 204.1878, obsd 204.1866; $[\alpha]_D^{20} -24$ (c 3.0, $CHCl_3$). Anal. Calcd for $C_{15}H_{24}$: C, 88.16; H, 11.84. Found: C, 88.11; H, 11.90.

Dibromocarbene Addition to 34b. In a 250 mL three-necked round-bottomed flask fitted with a mechanical stirrer and addition funnel was placed diene **34b** (2.20 g, 10.7 mmol), dichloromethane (75 mL), bromoform (4.04 g, 16.0 mmol), benzyltriethylammonium chloride (64 mg, 2.3×10^{-4} mmol), and ethanol (5 drops). The mixture was vigorously stirred at 0 °C while a 50% NaOH solution (5.3 mL) was slowly added to the flask and for an additional 24 h at rt before water (100 mL) was added. The aqueous layer was extracted with dichloromethane (3×40 mL), and the combined organic layers were dried, filtered, and concentrated to leave a brown oil which was taken up in 50 mL of hexane and passed through a 0.5-in. pad of silica gel (elution with several small portions of hexane). Solvent removal gave **35b** as a light yellow oil (2.93 g, 70%): IR (neat, cm^{-1}) 1472, 1370, 1109, 660; 1H NMR (300 MHz, $CDCl_3$) δ 5.49 (br s, 1 H), 2.12 (m, 2 H), 1.91 (dd, $J = 5.7, 1.6$ Hz, 2 H), 1.77 (m, $J = 6.8$ Hz, 1 H), 1.52 (d, $J = 9.2$ Hz, 1 H), 1.43 (dd, $J = 7.6, 4.4$ Hz, 1 H), 1.38 (dd, $J = 16.1, 8.6$ Hz, 1 H), 1.24 (s, 3 H), 1.00 (s, 3 H), 0.84 (s, 3 H), 0.82 (d, $J = 7.1$ Hz, 3 H), 0.66 (d, $J = 7.1$ Hz, 3 H); ^{13}C NMR (75 MHz, $CDCl_3$) 139.9, 132.5, 50.9, 45.5, 43.1, 42.2, 37.2, 35.5, 29.8, 28.9, 28.0, 26.5, 25.5, 17.6, 15.9, 15.8 ppm; HRMS m/z (M^+) calcd for $C_{16}H_{24}^{79}Br^{81}Br$ 376.0224, obsd 376.0226.

(+)-(1*S*,7*S*,8*S*)-7-Isopropyl-7,9,9-trimethyltricyclo[6.1.1.0^{2,6}]deca-2,5-diene (**36b**). Dibromide **35b** (2.90 g, 7.71 mmol) was dissolved in 300 mL of anhydrous ether. The solution was cooled to 0 °C, and methyllithium (22.0 mL, 1.4 M in ether, 30.8 mmol) was introduced via syringe. The solution was allowed to warm to rt and to stir for 24 h before it was added to 300 mL of ice water via cannula. The layers were separated and brine (100 mL) was added to the aqueous phase. Three extractions of the aqueous layer were completed using ether (75 mL). After the combined organic layers were dried, the solvent was removed to leave a light yellow oil, which was placed atop a short column of kieselghur and eluted with pentane to afford 1.31 g (78%) of a mixture of cyclopentadienes from which the lithium salt was prepared in the prescribed fashion. Reprotonation of **37b** provided **36b** in pure condition: IR (neat, cm^{-1}) 1388, 1379; 1H NMR (300 MHz, $CDCl_3$) δ 6.09 (t, $J = 1.2$ Hz, 1 H), 5.75 (q, $J = 1.6$ Hz, 1 H), 2.95 (dd, $J = 5.1, 3.5$ Hz, 2 H), 2.63 (t, $J = .1$ Hz, 1 H), 2.40 (ddd, $J = 10.0, 6.1, 4.3$ Hz, 1 H), 1.94 (t, $J = 5.6$ Hz, 1 H), 1.84 (m, $J = 4.9$ Hz, 1 H), 1.53 (d, $J = 10.1$ Hz, 1 H), 1.36 (s, 3 H), 1.06 (s, 3 H), 1.03 (d, $J = 6.8$ Hz, 3 H), 0.76 (d, $J = 6.8$ Hz, 3 H), 0.75 (s, 3 H); ^{13}C NMR (75 MHz, $CDCl_3$) 152.3, 151.9, 125.4, 119.4, 51.3, 43.7, 42.4, 40.3, 34.0, 28.0, 27.9, 27.8, 24.4, 18.6, 18.1, 16.8 ppm; HRMS m/z (M^+) calcd for $C_{16}H_{24}$ 216.1878, obsd 216.1876; $[\alpha]_D^{20} -6.9$ (c 1.0, hexane).

(-)-Bis[η^5 -(1*S*,7*S*,8*S*)-6-isopropyl-7,9,9-trimethyltricyclo[6.1.1.0^{2,6}]deca-2,5-dien-3-yl]dichlorotitanium (**21**). A solution of **37b** (1.33 g, 5.98 mmol) in dry 1,2-dimethoxyethane (30 mL) was cooled to -78 °C and transferred via cannula to an equally cold slurry of titanium(III) chloride (459 mg, 2.98 mmol) in the same solvent. After 1 h at this temperature, the mixture was heated at reflux for 48 h and processed as described below for **22**. There was obtained a 20% yield of **21** as purple crystals, mp 195–196 °C (from toluene): 1H NMR (300 MHz, $CDCl_3$) δ 6.39 (br s, 2 H), 6.29 (t, $J = 2.5$ Hz, 2 H), 5.91 (br s, 2 H), 2.76 (br m, 4 H), 2.43 (br m, 4 H), 1.97 (t, $J = 4.8$ Hz, 2 H), 1.40 (s, 6 H), 1.11 (d, $J = 6.5$ Hz, 6 H), 1.02 (s, 6 H), 0.74 (d, $J = 6.2$ Hz, 6 H), 0.42 (s, 6 H); ^{13}C NMR (75 MHz, $CDCl_3$) 150.2, 147.3, 122.1, 114.9, 111.4, 51.2, 46.6, 45.3, 44.8, 31.2, 28.0, 27.9, 24.5, 20.1, 19.6, 16.8 ppm; HRMS m/z calcd for $C_{32}H_{46}Cl_2Ti$ ($M^+ - Cl$) 513.2767, obsd 513.2782; $[\alpha]_D^{20} -250$ (c 0.07, $CHCl_3$).

(+)-(1*R*,4*R*,5*S*)-4-Phenyl-4,6,6-trimethyltricyclo[3.1.1]heptan-2-one (**32c**). In a flame-dried 1000 mL three-necked round-bottomed flask fitted with gas inlet, addition funnel, and large stir bar was placed copper(I) bromide dimethyl sulfide complex (0.5 g, 2.5 mmol). Tetrahydrofuran (200 mL) and

4-(dimethylamino)pyridine (21.14 g, 0.173 mol) were added, and the resulting slurry was cooled to -78 °C. Phenylmagnesium bromide (63.0 mL, 3.0 M in ether, 0.190 mol) was then introduced causing the gray-tan slurry to turn bright yellow-orange. After 15 min, a solution of **31** (13.0 g, 0.087 mol) and chlorotrimethylsilane (18.8 g, 0.173 mol) in 150 mL of tetrahydrofuran was added slowly over 60 min. After 4 h of stirring at -78 °C, the reaction mixture was allowed to warm to rt and quenched by the slow addition of a saturated NH_4Cl solution (200 mL) and, after 2 h, 75 mL of concentrated NH_4OH . The slurry was allowed to stir until the aqueous layer was blue. After separation and extraction with ether (4×200 mL), the combined organic layers were washed with 1 N HCl (3×100 mL), water (100 mL), and brine (100 mL), prior to drying, and concentrated to give a light yellow oil. Purification of this residue on silica gel (elution with 10% ethyl acetate in petroleum ether) afforded 16.0 g (81%) of **32c** as a white crystalline solid, mp 72 °C; IR (CCl_4 , cm^{-1}) 1715, 1495, 1445, 990, 710; 1H NMR (300 MHz, $CDCl_3$) δ 7.35–7.15 (m, 5 H), 3.20 (d, $J = 19.9$ Hz, 1 H), 2.81 (d, $J = 19.9$ Hz, 1 H), 2.66 (m, $J = 9.9$ Hz, 1 H), 2.60 (m, $J = 3.1$ Hz, 1 H), 2.57 (m, 1 H), 1.48 (s, 3 H), 1.47 (s, 3 H), 1.40 (dd, $J = 9.9, 3.1$ Hz, 1 H), 1.16 (s, 3 H); ^{13}C NMR (75 MHz, $CDCl_3$) 212.4, 151.5, 128.2, 125.5, 125.4, 56.5, 50.6, 48.4, 40.2, 39.7, 31.6, 27.4, 26.5, 25.4 ppm; HRMS m/z (M^+) calcd for $C_{18}H_{20}O$ 228.1514, obsd 228.1513; $[\alpha]_D^{20} +66.3$ (c 3.0, ethanol). Anal. Calcd for $C_{18}H_{20}O$: C, 84.16; H, 8.77. Found: C, 84.10; H, 8.81.

(+)-(1*S*,4*R*,5*S*)-4-Phenyl-4,6,6-trimethyl-2-vinyltricyclo[3.1.1]hept-2-ene (**34c**). Placed in a 1000 mL three-necked round-bottomed flask fitted with condenser, addition funnel, and gas inlet was 300 mL of dry THF. The flask was cooled to 0 °C, and vinylmagnesium bromide (113.9 mL, 1.0 M in THF, 0.114 mol) was added followed by the slow addition of **32c** (13.0 g, 0.057 mol) in 50 mL of THF over 30 min. The mixture was stirred at 0 °C for 1 h and at rt for 10 h, before being quenched at 0 °C with saturated NH_4Cl solution (200 mL). The layers were separated, and the aqueous layer was extracted with ether (4×150 mL). The combined organic layers were dried and concentrated. The remaining oil was purified by chromatography on silica gel (elution with 20% ethyl acetate in petroleum ether) to give an inseparable mixture of **33c** (major) and unreacted **32c**. This material was taken directly into the next step.

The mixture from above was evenly adsorbed onto basic alumina (25 g, activated at 450 °C for 24 h), placed into a Kugelrohr apparatus after standing at rt for 4 h, and heated to 160 °C under 1.5 mmHg for 1 h. The oil was collected in a receiver at -78 °C. The alumina mixture was eluted with several portions of ether until the eluate became clear. The eluates were combined, dried, and evaporated to leave an orange oil, purification of which by chromatography on kieselghur (elution with 1% ether in pentane) afforded **34c** as a colorless oil (2.67 g, 19% based on recovered **32c**): IR (neat, cm^{-1}) 1960, 1630, 1368, 1260; 1H NMR (300 MHz, C_6D_6) δ 7.16–7.23 (m, 4 H), 7.02–7.07 (m, 1 H), 6.50 (dd, $J = 17.4, 10.7$ Hz, 1 H), 5.70 (s, 1 H), 5.13 (d, $J = 17.4$ Hz, 1 H), 4.98 (d, $J = 10.8$ Hz, 1 H), 2.53 (t, $J = 5.4$ Hz, 1 H), 2.25 (dt, $J = 5.9, 2.1$ Hz, 1 H), 2.03 (dt, $J = 11.5, 5.7$ Hz, 1 H), 1.36 (s, 3 H), 1.29 (s, 3 H), 1.23 (d, $J = 9.4$ Hz, 1 H), 1.05 (s, 3 H); ^{13}C NMR (75 MHz, C_6D_6) 151.2, 145.4, 138.3, 130.9, 126.7, 125.8, 111.5, 53.5, 46.8, 42.1, 40.9, 30.6, 27.9, 26.7, 24.3 ppm (one C not observed); HRMS m/z (M^+) calcd for $C_{18}H_{22}$ 238.1724, obsd 238.1742; $[\alpha]_D^{20} +16.2$ (c 1.5, $CHCl_3$). Anal. Calcd for $C_{18}H_{22}$: C, 90.70; H, 9.30. Found: C, 90.33; H, 9.49.

Dibromocarbene Addition to Diene 34c. A 250 mL three-necked round-bottomed flask was fitted with a mechanical stirrer, addition funnel, and gas inlet. To the flask was added **34c** (2.20 g, 9.2 mmol), dichloromethane (100 mL), benzyltriethylammonium chloride (56 mg, 0.20 mmol), bromoform (3.50 g, 13.8 mmol), and ethanol (0.5 mL). The mixture was vigorously stirred at 0 °C while a 50% sodium hydroxide solution (4.6 mL) was added dropwise over 20 min and for an additional 24 h at rt before it was poured into a

separatory funnel and diluted with water (100 mL). The separated aqueous layer was extracted with dichloromethane (3 × 100 mL). The combined organic layers were dried and concentrated to leave a brown-red oil. The oil was diluted to twice its volume with ether and passed through a 1-in. pad of silica gel (elution with ether). Concentration of the eluent gave 3.50 g (92%) of **35c** as a yellow-orange oil: IR (CHCl₃, cm⁻¹) 1491, 1441, 1109, 1030, 761, 700, 657; ¹H NMR (300 MHz, CDCl₃) δ 7.18–7.26 (m, 4 H), 7.05 (dt, *J* = 6.6, 1.4 Hz, 1 H), 5.64 (t, *J* = 0.8 Hz, 1 H), 2.20 (br m, 3 H), 1.97 (dt, *J* = 9.0, 5.5 Hz, 1 H), 1.91 (dt, *J* = 4.5, 1.0 Hz, 1 H), 1.45 (d, *J* = 9.8 Hz, 1 H), 1.35 (s, 3 H), 1.22 (s, 3 H), 1.08 (d, *J* = 7.2 Hz, 1 H), 1.07 (s, 3 H); ¹³C NMR (75 MHz, CDCl₃) 151.1, 141.5, 130.1, 126.7, 126.6, 125.9, 53.0, 46.8, 45.2, 42.6, 37.0, 31.3, 28.0, 26.62, 26.57, 25.2 ppm (one C not observed); HRMS *m/z* (*M*⁺) calcd for C₁₉H₂₂Br₂ 410.0068, obsd 410.0032.

(+)-(1*S*,7*R*,8*S*)-7-Phenyl-7,9,9-trimethyltricyclo[6.1.1.0^{2,6}]-deca-2,5-diene (**36c**). The above oil (3.50 g, 8.53 mmol) was dissolved in anhydrous ether (500 mL) under an inert atmosphere. The flask was cooled to 0 °C, and methylolithium (22.7, 1.5 M in ether, 34.1 mmol) was added via syringe. After 2 h, the reaction mixture was warmed to rt and stirred for 24 h prior to its addition to ice water via cannula. The ethereal layer was separated, and the aqueous layer was extracted with ether (3 × 200 mL). After the combined organic layers were dried, the solvent was removed to give a yellow-brown oil, which was placed atop a short column of silica gel (elution with 1% ether in pentane) to give 1.56 g (73%) of **36c** as a colorless oil: IR (neat, cm⁻¹) 1494, 1446, 1387, 1375, 765, 704; ¹H NMR (300 MHz, C₆H₆) δ 7.38 (dd, *J* = 7.3, 1.4 Hz, 2 H), 7.18 (t, *J* = 7.3 Hz, 2 H), 7.06 (t, *J* = 7.3 Hz, 1 H), 6.13 (t, *J* = 1.2 Hz, 1 H), 5.86 (q, *J* = 1.7 Hz, 1 H), 3.03 (d, *J* = 0.8 Hz, 1 H), 2.98 (t, *J* = 1.6 Hz, 1 H), 2.27 (d, *J* = 5.7 Hz, 1 H), 2.20 (d, *J* = 5.0 Hz, 1 H), 2.16 (dt, *J* = 9.7, 5.7 Hz, 1 H), 1.63 (s, 3 H), 1.26 (s, 3 H), 1.13 (d, *J* = 6.4 Hz, 1 H), 0.93 (s, 3 H); ¹³C NMR (75 MHz, C₆H₆) 150.2, 149.6, 132.6, 129.5, 127.2, 125.9, 125.8, 120.4, 53.9, 46.7, 43.8, 42.4, 41.0, 30.9, 29.9, 27.8, 24.6 ppm; HRMS *m/z* (*M*⁺) calcd for C₁₉H₂₂ 250.1722, obsd 250.1712; [α]_D²⁰ +74.9 (*c* 1.8, hexane).

(-)-Bis(η⁵-[(1*S*,7*S*,8*S*)-7-phenyl-7,9,9-trimethyltricyclo[6.1.1.0^{2,6}]-deca-2,5-dien-3-yl]dichlorotitanium (**22**). Into a dry 250 mL three-necked round-bottomed flask was placed a solution of **36c** (1.56 g, 0.23 mmol) in 45 mL of hexane. Ether (20 mL) was added, the solution was cooled to 0 °C, and *n*-butyllithium (4.8 mL, 1.3 M in hexane, 6.3 mmol) was introduced over a few minutes as a white solid precipitated. The mixture was stirred at 0 °C for 1 h and at rt for 24 h. Concentration in vacuo left a white solid which was redissolved in 10 mL of ether and 50 mL of DME. In a drybox, titanium(III) chloride (481 mg, 3.12 mmol) was weighed into a flask equipped with a side arm. DME (50 mL) was added, the purple-blue slurry was cooled to -78 °C, and the anion solution was introduced via cannula over 20 min. After 1 h at -78 °C, the mixture was heated to reflux for 48 h, cooled to 0 °C, and treated with 50 mL of concentrated HCl in air for 5 min. The now red mixture was poured into a separatory funnel, the organic phase was washed with saturated CaCl₂ solution (50 mL), and the combined aqueous layers were extracted with 50 mL of dichloromethane. The combined organic fractions were dried, filtered, and concentrated to give a red-brown residue, which was dissolved in 5 mL of dry toluene and cooled to -20 °C. The resulting crystals were collected and washed with pentane to give 234 mg (12%) of **22** as a green microcrystalline solid, mp 195 °C (dec, toluene): ¹H NMR (300 MHz, CDCl₃) δ 7.47 (d, *J* = 7.4 Hz, 4 H), 7.33 (t, *J* = 5.3 Hz, 4 H), 7.19 (t, *J* = 7.4 Hz, 2 H), 6.83 (t, *J* = 2.2 Hz, 2 H), 5.84 (t, *J* = 2.1 Hz, 2 H), 5.56 (t, *J* = 2.9 Hz, 2 H), 2.65 (dt, *J* = 10.7, 5.6 Hz, 2 H), 2.59 (t, *J* = 5.2 Hz, 2 H), 2.43 (t, *J* = 5.3 Hz, 2 H), 2.15 (d, *J* = 10.2 Hz, 2 H), 1.55 (s, 6 H), 1.45 (s, 6 H), 0.45 (s, 6 H); ¹³C NMR (62.5 MHz, CDCl₃) 149.0, 147.4, 142.8, 127.9, 126.9, 126.1, 122.4, 115.1, 114.5, 50.8, 48.0, 45.2, 44.1, 32.5, 31.3, 27.8, 24.4 ppm; HRMS *m/z* calcd for C₃₈H₄₂Cl₂Ti (*M*⁺), C₃₈H₄₂ClTi (*M*⁺ - Cl), C₃₈H₄₂Ti (*M*⁺ - 2Cl) 616.25, 581.28,

546.31, obsd 616.37, 581.39, 582.39, 546.41; [α]_D²⁰ -2600 (*c* 0.02, CHCl₃).

(-)-(η⁵-Cyclopentadienyl)(η⁵-[*exo*-(1*S*,8*S*)-7,7,9,9-tetramethyltricyclo[6.1.1.0^{2,6}]-deca-3,5-dien-2-yl]dimethyltitanium (**30**). Dichloride *ent*-**29** (36 mg, 0.097 mmol) was dissolved in dry ether (3 mL) under argon. To the cooled (0 °C) violet solution was added methylolithium (135 μL, 0.2 mmol). A color change to orange ensued. After 20 min, the heterogeneous yellow mixture was quenched by the addition of water and extracted with ether (3 × 20 mL). The combined organic layers were washed with brine, dried, and evaporated to give **30** as a yellow-orange solid (29 mg, 87%) that was immediately dissolved in dry toluene (20 mL, 4.2 × 10⁻³ M) and stored at -10 °C until needed: ¹H NMR (300 MHz, C₆D₆) δ 5.87 (s, 5 H), 5.86–5.84 (m, 2 H), 5.48 (dd, *J* = 2.7, 2.3 Hz, 1 H), 2.32 (t, *J* = 5.3 Hz, 1 H), 2.15 (ddd, *J* = 12.0, 6.4, 5.6 Hz, 1 H), 1.43 (dd, *J* = 6.3, 5.2 Hz, 1 H), 1.25 (s, 3 H), 1.23 (s, 3 H), 0.87 (s, 3 H), 0.79 (d, *J* = 9.9 Hz, 1 H), 0.67 (s, 3 H), 0.21 (s, 3 H), 0.19 (s, 3 H); ¹³C NMR (75 MHz, C₆D₆) 135.5, 133.5, 115.3, 113.8, 111.9, 110.3, 55.2, 48.5, 47.0, 45.3, 44.2, 39.5, 32.1, 30.7, 30.3, 27.9, 24.9 ppm; HRMS *m/z* calcd for C₂₀H₂₇Ti (*M*⁺ - CH₃) 315.1592, obsd 315.1580; [α]_D²² -146.5 (*c* 1.63, CHCl₃).

(+)-Bis[η⁵-(1*R*,7*S*)-1,10,10-trimethyltricyclo[5.2.1.0^{2,6}]-deca-3,5-dien-2-yl]dichlorozirconium (**39**). In a drybox, zirconium tetrachloride (324 mg, 1.39 mmol) and camphorocyclopentadienyl lithium salt^{8c} (500 mg, 2.77 mmol) were placed in an oven-dried, side-arm flask equipped with a magnetic stirring bar and septum. The solids were cooled to -78 °C, and dry CH₂Cl₂ (10 mL) was slowly introduced. The slurry was allowed to stir overnight with slow warming to rt, filtered through Celite under argon, and concentrated in vacuo. The solid residue was sublimed at 140 °C and 3 × 10⁻³ Torr to give 210 mg (30%) of **39** as yellow crystals.^{8c}

(+)-Bis[η⁵-(1*R*,8*R*)-7,7,9,9-tetramethyltricyclo[6.1.1.0^{2,6}]-deca-2,5-dien-4-yl]dichlorozirconium (**40**). Zirconium tetrachloride (1.17 g, 5.02 mmol) was slurried in dry 1,2-dimethoxyethane (20 mL), cooled to -78 °C, and treated via cannula with a solution of *ent*-**37a** (2.00 g, 10.3 mol). After 1 h of stirring at -78 °C, the mixture was allowed to warm to rt, stirred overnight, refluxed for 2 days, cooled to rt, and freed of solvent in vacuo. The yellow residue was dissolved in dry CH₂Cl₂ (25 mL), cooled to 0 °C, treated with 4 N HCl (5 mL), and stirred at 0 °C for 15 min. The separated organic layer was washed with water (25 mL), and the combined aqueous phases were extracted with CH₂Cl₂ (3 × 30 mL). The organic solutions were combined, dried, and evaporated to leave a light brown residue, which was sublimed at 165 °C and 3 × 10⁻⁴ Torr. There was obtained 290 mg (11%) of **40** as yellow crystals;^{8e} [α]_D²⁰ +229 (*c* 0.76, CHCl₃).

(+)-Bis[η⁵-(1*R*,7*R*,8*R*)-7-isopropyl-7,9,9-trimethyltricyclo[6.1.1.0^{2,6}]-deca-2,5-dien-4-yl]dichlorozirconium (**41**). In a drybox, zirconium tetrachloride (262 mg, 1.12 mmol) and **37b** (500 mg, 2.25 mmol) were placed in an oven-dried, side-arm flask equipped with a stir bar and septum. The solids were cooled to -78 °C under argon, and dry CH₂Cl₂ (10 mL) was added very slowly via syringe with stirring. The slurry was allowed to stir for 1 h at -78 °C before being warmed to rt and stirred overnight. The reaction mixture was filtered through Celite under argon and concentrated *in vacuo*. The solid residue was sublimed at 150 °C and 2.5 × 10⁻³ Torr to give 0.18 g (27%) of **41** as yellow crystals, mp >190 °C, dec: ¹H NMR (300 MHz, CDCl₃) δ 6.25 (t, *J* = 2.5 Hz, 2 H), 6.21 (t, *J* = 3.0 Hz, 2 H), 5.87 (t, *J* = 2.5 Hz, 2 H), 2.75 (t, *J* = 5.1 Hz, 2 H), 2.62 (m, *J* = 6.7 Hz, 2 H), 2.51–2.43 (m, 2 H), 2.33 (d, *J* = 10.3 Hz, 2 H), 1.99 (t, *J* = 5.7 Hz, 2 H), 1.40 (s, 6 H), 1.07 (d, *J* = 6.6 Hz, 6 H), 1.00 (s, 6 H), 0.76 (d, *J* = 6.8 Hz, 6 H), 0.38 (s, 6 H); ¹³C NMR (75 MHz, CDCl₃) 142.9, 141.1, 116.5, 111.5, 109.4, 51.4, 45.7, 45.3, 43.9, 32.1, 28.4, 27.7, 24.4, 19.8, 19.3, 16.6 ppm; HRMS *m/z* (*M*⁺) calcd for C₃₂H₄₆Cl₂Zr 590.2020, obsd 590.2035; [α]_D²⁰ +115 (*c* 0.15, CHCl₃). Anal. Calcd for C₃₂H₄₆Cl₂Zr: C, 64.83; H, 7.82. Found: C, 64.75; H, 7.79.

Asymmetric Hydrogenation Procedure. A. Reduction of 2-Phenyl-1-butene with Optically Active Ti-

tanocenes. An optically active titanocene dichloride (0.02–0.04 mmol) and 2-phenyl-1-butene were placed in a dry Fischer–Porter bottle. The mixture was degassed briefly and dissolved in 5 mL of toluene. The red solution was subjected to three freeze–pump–thaw cycles before a hydrogen atmosphere was established. When the solution reached rt, *n*-butyllithium (0.20–0.40 mmol in hexane) was introduced via syringe. The typically gray-green solution was blanketed with 20 psi of hydrogen and placed in a thermostated bath. After 48 h, the reaction mixture was quenched with 6 N HCl, extracted with ether (2 × 2 mL), and dried. Yields were determined by capillary GC–MS. A portion of the product was purified by preparative gas chromatography using a column (5.5 ft × 0.25 in. diameter) packed with 5% SE 30 on Chromosorb W. Separation was achieved with an oven temperature of 80 °C, injector temperature at 180 °C, detector temperature at 180 °C, and a helium gas flow of 40 mL/min. The optical rotations measured in 95% ethanol at 20 °C were compared to $[\alpha]_D^{20} +22.7$ (*c* 1, 95% ethanol) reported for optically pure (*S*)-(+)-2-phenylbutane.²⁶

B. Reduction of 2-(α -Naphthyl)-1-butene under Medium Pressure. A Fischer–Porter thick-walled bottle was charged with **7** (1 equiv) and the catalyst (0.01–0.05 equiv). The container was attached to a medium pressure hydrogenation apparatus and evacuated for several hours. Freshly distilled toluene (from CaH₂) or hexanes was introduced via syringe, and the solution was subjected to three freeze-thaw cycles before a hydrogen atmosphere was reestablished. Butyllithium or methyllithium (0.1–0.2 equiv) was added at rt, and the pressure was raised to the appropriate level. Cooling was carried out if required. After reaction was deemed complete, 5% HCl was added and the mixture was extracted with ether as above. Purification through silica gel (hexane elution) gave a colorless oil with varying amounts of **7** and **8**. The unreacted **7** was removed as follows. The crude mixture containing **7** and **8** was dissolved in dry THF under an atmosphere of argon and cooled in an ice bath. BH₃·SMe₂ in THF (5 equiv based on unreacted **7**) was added, and the mixture was stirred for several hours. After the mixture was recooled to 0 °C, excess aqueous NaOH solution was slowly added followed by excess 30% H₂O₂ solution. After an additional 2 h, the mixture was diluted with ether, the layers were separated, and the organic layer was washed once with water, once with saturated brine, and dried. Purification of the concentrate by chromatography (silica gel, hexanes) yielded pure **8** as a colorless oil.

C. Reduction Studies Involving **30.** The solution of **7** (253 mg, 1.388 mmol) was prepared as in method B. A solution of **30** in toluene (6.6 mL, 0.2776 mmol) was added under an atmosphere of argon. The yellow solution was degassed by three freeze-thaw cycles before a hydrogen atmosphere was

established. The pressure was set to 29 psi, and the mixture was stirred overnight at rt. No reduction in pressure occurred; therefore, the solution was degassed once more as above and the pressure reset to 29 psi. Several hours later with no drop in pressure or color change methyllithium (0.035 mmol) was added at rt and the pressure was readjusted to 29 psi. A color change from yellow to gray-violet occurred immediately. After 15 min, the pressure gauge indicated 24.1 psi. After an additional 23.5 h, the pressure decreased only slightly and the reaction mixture was quenched as in method B. ¹H NMR analysis indicated that >97% hydrogenation had occurred. The level of enantioselectivity was determined to be 13% ee.

D. Prototypical Zirconocene Reduction. An optically active zirconocene dichloride (0.02 mmol) and **6** or **7** (2.00 mmol) were placed in a dry Fischer–Porter bottle containing a magnetic stir bar. The mixture was briefly degassed under vacuum and dissolved in dry toluene (5 mL) under a hydrogen atmosphere. This mixture was subjected to three freeze–pump–thaw cycles before reestablishing the hydrogen atmosphere. A solution of alkyllithium in hexane (0.20 mmol) was added via syringe at rt. The resulting mixture was then placed in a thermostated bath, and the hydrogen pressure was increased to 40 psi. After being stirred for the specified time period, the reaction mixture was quenched with 6 N HCl. The aqueous layer was extracted with ether (2 × 5 mL), and the combined organic layers were dried. In the case of **6**, the 2-phenylbutane was separated from residual olefin via preparative gas chromatography at an oven temperature of 80 °C, injector and detector temperatures of 180 °C, and a helium gas flow of 40 mL/min. For **7**, the concentrated mixture was dissolved in dry THF (2 mL) in an oven-dried, side-arm flask equipped with a stir bar and septum. The solution was cooled to 0 °C, and BH₃·THF (0.56 mL, 1.0 M in THF, 0.56 mmol) was added dropwise via syringe. The mixture was allowed to stir at rt overnight, followed by the addition of a 15% NaOH solution (0.5 mL, 2.00 mmol). A solution of 30% hydrogen peroxide (0.7 mL, 7.00 mmol) was added dropwise and the mixture allowed to stir 1 h before being poured into water (3 mL). The aqueous layer was extracted with ether (3 × 5 mL), and the combined organic layers were washed with brine (3 × 5 mL), dried, and concentrated to give a yellow oil, which was directly subjected to silica gel chromatography (elution with hexanes) to afford **8**.

Acknowledgment. This work has been supported by a grant from the National Science Foundation. M.R.S., E.I.B., and K.J.S. acknowledge with gratitude their receipt of the fellowship awards cited in ref 1.

OM950282P

Electrochemical Studies of Organometallic Complexes with Tetra-*n*-butylammonium Tetrakis[3,5-bis(trifluoromethyl)phenyl]borate as the Electrolyte. X-ray Crystal Structure of $[\text{C}_5(\text{CF}_3)(\text{CH}_3)_4\text{Fe}(\text{C}_5\text{H}_5)]$

Paul G. Gassman,[†] John R. Sowa, Jr.,^{*‡} Michael G. Hill,[‡] and Kent R. Mann^{*}

Department of Chemistry, University of Minnesota, Kolthoff Hall, Minneapolis, Minnesota 55455

Received May 30, 1995[⊙]

The tetra-*n*-butylammonium tetrakis[3,5-bis(trifluoromethyl)phenyl]borate ($\text{TBA}^+\text{TFPB}^-$) electrolyte/methylene chloride solvent system improves the electrochemical reversibility of pentamethylcyclopentadienyl (Cp^*) ruthenocenes, $\text{Cp}^*\text{RuCp}'$ ($\text{Cp}' = \text{fluorenyl, indenyl, cyclopentadienyl (Cp), acetylcyclopentadienyl, pentachlorocyclopentadienyl}$), as indicated by $i_{p,c}/i_{p,a}$ ratios of 0.79–1.0 as determined by cyclic voltammetry. The quasi-reversible potentials (E°) of the $\text{Cp}^*\text{RuCp}'$ complexes and the complete series of group 9 Cp_2M and Cp^*_2M complexes ($\text{M} = \text{Fe, Ru, Os}$) are also reported in $\text{TBA}^+\text{TFPB}^-/\text{CH}_2\text{Cl}_2$. In addition, a study of the E° values of group 9 complexes containing the (trifluoromethyl)tetramethylcyclopentadienyl (Cp^\ddagger) ligand indicate that the Cp^\ddagger complexes are slightly (0.06–0.08 V per Cp^\ddagger) more difficult to oxidize than the cyclopentadienyl (Cp) derivatives. The structure of $[\text{C}_5(\text{CF}_3)(\text{CH}_3)_4\text{Fe}(\text{C}_5\text{H}_5)]$ was determined at -101°C by a single-crystal X-ray diffraction study. The structure shows eclipsed Cp^\ddagger and Cp rings, and the iron to Cp^\ddagger centroid distance (1.643 Å) is slightly shorter than the iron to Cp centroid distance (1.651 Å); otherwise, no extreme differences in the coordination of the Cp^\ddagger and Cp rings are noted. An infrared spectroelectrochemistry study of *trans*- $[\text{Cp}^\ddagger\text{Fe}(\text{CO})_2]_2$ shows that it is electrochemically oxidized to *trans*- $[\text{Cp}^\ddagger\text{Fe}(\text{CO})_2]_2^+$ in $\text{TBA}^+\text{TFPB}^-/\text{CH}_2\text{Cl}_2$.

Introduction

Recently Mann and co-workers reported¹ quasi-reversible electrochemical potentials E° of ruthenocene (1) and osmocene (2) with use of tetra-*n*-butylammonium tetrakis[3,5-bis(trifluoromethyl)phenyl]borate ($\text{TBA}^+\text{TFPB}^-$) electrolyte in methylene chloride solvent. Previously, complexes 1 and 2 were previously known to give only irreversible oxidation processes. To explore the general utility of the $\text{TBA}^+\text{TFPB}^-/\text{CH}_2\text{Cl}_2$ electrolyte/solvent system, we have studied the electrochemistry of several pentamethylcyclopentadienyl (Cp^*) ruthenocene complexes ($\text{Cp}^*\text{RuCp}'$; $\text{Cp}' = \text{fluorenyl}$ (3), indenyl (4), cyclopentadienyl (Cp) (5), acetylcyclopentadienyl (6), pentachlorocyclopentadienyl (7), Cp^* (8) that, except for 8, were previously reported² to give irreversible electrochemical oxidations. We also report the E° values for the complete series of group 9 Cp_2M ($\text{M} = \text{Fe, Ru}$ (1), Os (2)) and Cp^*_2M ($\text{M} = \text{Fe, Ru}$ (8), Os (9)) complexes in $\text{TBA}^+\text{TFPB}^-/\text{CH}_2\text{Cl}_2$. In addition, we were interested in determining the electronic properties of the recently discovered³ (trifluoromethyl)tetramethylcyclopentadienyl (Cp^\ddagger) ligand by studying the electrochemistry of $\text{Cp}^\ddagger\text{FeCp}$ (10), $\text{Cp}^\ddagger_2\text{Ru}$ (11), and $\text{Cp}^\ddagger_2\text{Os}$ (12)

complexes. Previously, we demonstrated³ that the Cp^\ddagger ligand is electronically equivalent to the cyclopentadienyl (Cp) ligand and sterically equivalent to the pentamethylcyclopentadienyl ligand (Cp^*). Thus, Cp^\ddagger can be used to determine the importance of steric and electronic effects in Cp and Cp^* complexes. As one demonstration of the utility of Cp^\ddagger , we report an infrared spectroelectrochemical study of the oxidation of $[\text{Cp}^\ddagger\text{Fe}(\text{CO})_2]_2$ (13) and a comparison to the previously reported⁴ studies of $[\text{CpFe}(\text{CO})_2]_2$ (14) and $[\text{Cp}^*\text{Fe}(\text{CO})_2]_2$ (15) complexes.

Experimental Section

The following compounds were purchased from commercial sources (Aldrich or Strem) and, unless otherwise stated, were used as received: ruthenocene (1), osmocene (2) (recrystallized from anhydrous methanol under an atmosphere of argon), dicarbonylcyclopentadienyliron dimer (14), ferrocene (purified by sublimation, 50°C , 10^{-2} mm), and cobaltocene. The complexes (η^5 -fluorenyl)(η^5 -pentamethylcyclopentadienyl)ruthenium (3),² (η^5 -indenyl)(η^5 -pentamethylcyclopentadienyl)ruthenium (4),² (η^5 -cyclopentadienyl)(η^5 -pentamethylcyclopentadienyl)ruthenium (5),² (η^5 -acetylcyclopentadienyl)(η^5 -pentamethylcyclopentadienyl)ruthenium (6),² (η^5 -pentachlorocyclopentadienyl)(η^5 -pentamethylcyclopentadienyl)ruthenium (7),² bis(η^5 -pentamethylcyclopentadienyl)ruthenium (8),² bis(η^5 -pentamethylcyclopentadienyl)osmium (9),⁵ (η^5 -cyclopentadienyl)(η^5 -(trifluoromethyl)tetramethylcyclopentadienyl)iron (10),³ bis(η^5 -

(4) Bullock, J. P.; Palazotto, M. C.; Mann, K. R. *Inorg. Chem.* 1991, 30, 1284.

(5) Albers, M. O.; Liles, D. C.; Robinson, D. J.; Shaver, A.; Singleton, E.; Wiege, M. B.; Boeyens, J. C. A.; Levendis, D. C. *Organometallics* 1986, 5, 2321.

[†] Deceased April 21, 1993.

[‡] Current addresses: J.R.S., Department of Chemistry, Seton Hall University, South Orange, NJ 07079; M.G.H., Department of Chemistry, Occidental College, Los Angeles, CA 90041.

[⊙] Abstract published in *Advance ACS Abstracts*, September 15, 1995.

(1) Hill, M. G.; Lamanna, W. M.; Mann, K. R. *Inorg. Chem.* 1991, 30, 4687.

(2) Gassman, P. G.; Winter, C. H. *J. Am. Chem. Soc.* 1988, 110, 6130.

(3) Gassman, P. G.; Mickelson, J. W.; Sowa, J. R., Jr. *J. Am. Chem. Soc.* 1992, 114, 6942.

Table 1. Electrochemical Data for Organometallic Complexes in TBA⁺TFPB⁻/CH₂Cl₂^a and TBA⁺ClO₄⁻/CH₂Cl₂^b Electrolyte/Solvent Systems

compd	$E^{o'}$ (V) in TBA ⁺ TFPB ⁻ ^a	ΔE (V) ^{a,c}	$i_{p,c}/i_{p,a}$ ^{a,d}	$E_{1/2}$ (V) in TBA ⁺ ClO ₄ ⁻ ^b	$i_{p,c}/i_{p,a}$ ^{b,d,e}
Cp ₂ Ru (1)	1.03 ^f	0.089	0.94	0.97	0.60
Cp ₂ Os (2)	0.83 ^f	0.085	1.0		
Cp [*] Ru (fluorenyl) (3)	0.41	0.096 ^g	0.88 ^g	0.51	0.38
Cp [*] Ru (indenyl) (4)	0.51	0.084	1.0	0.60	0.68
Cp [*] RuCp (5)	0.69	0.099 ^h	0.81 ^h	0.71	0.55
Cp [*] Ru (acetylCp) (6)	0.93	0.075	0.86	0.91	0.42
Cp [*] Ru (C ₅ Cl ₅) (7)	1.41	0.083	0.79	1.47	0.29
Cp [*] ₂ Ru (8)	0.48	0.080	1.0	0.59	0.88
Cp [*] ₂ Os (9)	0.31	0.074	0.97		
Cp ⁺ FeCp (10)	0.53	0.090	1.0		
Cp ₂ Fe	0.47 ^f	0.090	1.0	0.48 ⁱ	
Cp [*] ₂ Fe	-0.12	0.079	0.99		
Cp [*] ₂ Ru (11)	1.15	0.097	0.92		
Cp [*] ₂ Os (12)	0.98	0.084	0.99		
[Cp ⁺ Fe(CO) ₂] ₂ (13)	0.70	0.10	0.90		
[CpFe(CO) ₂] ₂ (14)	0.64	0.085	1.0		
[Cp [*] Fe(CO) ₂] ₂ (15)	0.28	0.082	0.81		

^a Potentials ($E^{o'}$) vs aqueous AgCl/Ag in 1.0 M KCl calibrated using an $E^{o'}$ value of ferrocene of 0.47 V.¹ The electrolyte/solvent system is 0.10 M TBA⁺TFPB⁻/CH₂Cl₂, and ca. 0.5 mM solutions of the metal complexes were used. ^b Reference 2. Potentials ($E_{1/2}$) vs SCE were calculated using an $E^{o'}$ value for ferrocene of 0.48 V. The electrolyte/solvent system is 0.10 M TBA⁺ClO₄⁻/CH₂Cl₂. ^c Anodic potential ($E_{p,a}$) minus cathodic potential ($E_{p,c}$) determined by CV. The scan rate was 100 mM s⁻¹ unless otherwise indicated. ^d Ratio of cathodic current ($i_{p,c}$) to anodic current ($i_{p,a}$). ^e Calculated from the original data. ^f Reference 1. ^g Scan rate 500 mV s⁻¹. ^h Scan rate 250 mV s⁻¹. ⁱ Reference 11a.

(trifluoromethyl)tetramethylcyclopentadienyl)ruthenium (11),³ bis(η^5 -(trifluoromethyl)tetramethylcyclopentadienyl)osmium (12),³ dicarbonyl(pentamethylcyclopentadienyl)iron dimer (15),⁶ and decamethylferrocene⁶ were prepared as previously reported. Unless otherwise stated, all solvents were purified by distillation from standard drying agents⁷ under an atmosphere of argon. Compound characterization and purity were established by NMR (Varian VXR-300 MHz or Bruker NR/300) and FTIR (Mattson Polaris) spectroscopy.

Preparation of [(C₅(CF₃)(CH₃)₄)Fe(CO)₂]₂ (13). Previously³ the preparation of 13 from Cp⁺H and Fe(CO)₅ in refluxing octane gave an impurity (identified as [Cp⁺(CO)Fe(μ -CO)₂Fe(CO)Cp⁺]) which was detected in the cyclic voltammogram. As the Cp⁺H starting material does not contain Cp⁺H, the defluorination reaction apparently occurs as a side reaction during the reaction between Fe(CO)₅ and Cp⁺H. Pure 13 is obtained by the following procedure.

To a solution of impure 13 (1.1 g, ~1.8 mmol) in methylene chloride (100 mL) was added a solution of iodine (0.47 g, 1.9 mmol) in methylene chloride (50 mL) to give a mixture of Cp⁺Fe(CO)₂I and Cp⁺Fe(CO)₂I (1.6 g). After removal of the solvent on a rotary evaporator, the mixture was chromatographed in air on a column (25 × 3 cm) of neutral alumina (Brockman activity I). The first brown band was eluted with a mixture of 10% methylene chloride in hexanes, and the solution was evaporated to dryness on a rotary evaporator to give pure Cp⁺Fe(CO)₂I (1.0 g, 2.3 mmol). Further elution with a mixture of 20–50% methylene chloride in hexanes gave a second brown band of pure Cp⁺Fe(CO)₂I (0.17 g, 0.45 mmol).

To a solution of Cp⁺Fe(CO)₂I (1.0 g, 2.3 mmol) in tetrahydrofuran (50 mL) was added cobaltocene^{8a,b} (0.45 g, 2.5 mmol), and the reaction mixture was stirred under an atmosphere of argon for 30 min, after which time the infrared spectrum indicated that the reaction was complete. The solvent was removed under vacuum, and the residue was dissolved in methylene chloride (30 mL); diethyl ether (30 mL) was added to precipitate the Cp₂Co⁺I⁻, and the solution was filtered. After evaporation of the solvent under vacuum, the purple residue was dissolved in a minimum amount of warm methylene

chloride and the solution was filtered through a column (15 × 3 cm) of neutral alumina. Recrystallization from a mixture of 50% methylene chloride in hexanes at -15 °C overnight gave dark purple crystals of 13 (0.47 g, 0.78 mmol) in 67% yield based on Cp⁺Fe(CO)₂I. Complex 13 is sensitive to air in solution, but it is stable in air as a solid. Mp: 245 °C dec. Anal. Calcd for C₂₄H₂₄F₆Fe₂O₄ (M_r = 602.14): C, 47.87; H, 4.02. Found: C, 47.82; H, 4.07. ¹H NMR (CDCl₃): δ 1.84 (q, J_{HF} = 2 Hz, 2,5-CH₃), 1.59 (s, 3,4-CH₃). ¹³C NMR (CDCl₃): δ 240.8 (br s, CO), 124.9 (q, J_{CF} = 272 Hz, CF₃), 101.2 (s, 2,5-C-CH₃), 99.7 (s, 3,4-C-CH₃), 86.7 (q, J_{CF} = 36 Hz, C-CF₃), 9.5 (s, 2,5-CH₃), 8.0 (s, 3,4-CH₃). ¹⁹F NMR (CDCl₃): δ (vs CFC₃) -52.79. IR (CH₂Cl₂): ν (CO) 1952, 1776 cm⁻¹. MS: m/e calcd for C₂₄H₂₄F₆Fe₂O₄ 602.0278, found 602.0267.

Electrochemical Experiments. The electrochemical analyses were performed with use of a Bioanalytical Systems (BAS) Model 100 electrochemical analyzer or a Princeton Applied Research Model 273 potentiostat. Cyclic voltammetry (CV) and Osteryoung square wave voltammetry (OSWV) were performed at room temperature (~20 °C) with a normal three-electrode configuration consisting of a highly polished glassy-carbon-disk working electrode (A = 0.07 cm²), an AgCl/Ag reference electrode containing 1.0 M aqueous KCl, and a platinum-wire counter electrode. The working component of the electrochemical cell was separated from the reference compartment by a modified Luggin capillary. All three compartments contained a 0.10 M solution of TBA⁺TFPB⁻ electrolyte. Analyses were performed on 0.75–1.0 mL of 0.5 mM solutions of the organometallic complexes.

The methylene chloride solvent used for all electrochemical and spectroelectrochemical (*vide infra*) experiments was distilled from phosphorus pentoxide under an atmosphere of argon. Tetra-*n*-butylammonium tetrakis[3,5-bis(trifluoromethyl)phenyl]borate (TBA⁺TFPB⁻/CH₂Cl₂) was obtained as a gift from the 3M Co. Alternatively, the electrolyte was prepared by metathesis of TBA⁺Br⁻ (Aldrich) and Na⁺TFPB⁻ in a solution of methanol. Deionized water was added dropwise to precipitate the TBA⁺TFPB⁻, which was further purified by filtration through a column of neutral alumina in methylene chloride solvent. The electrolyte (mp 97 °C) was dried under vacuum at 90 °C. Immediately prior to use, the electrolyte solutions were passed through a short column of neutral alumina (80–200 mesh, Fisher Scientific) which was

(6) King, R. B.; Bisnette, M. B. *J. Organomet. Chem.* **1967**, *8*, 287.

(7) Perrin, D. D.; Armarego, W. L. F.; Perrin, D. R. *Purification of Laboratory Chemicals*, 2nd ed.; Pergamon: New York, 1980.

(8) For similar synthetic procedures see: (a) Connelly, N. G.; Manners, I. J. *J. Chem. Soc., Dalton Trans.* **1989**, 283. (b) Field, L. D.; Masters, A. F.; Gibson, M.; Latimer, D. R.; Hambley, T. W.; Buys, I. E. *Inorg. Chem.* **1993**, *32*, 211.

(9) Brookhart, M.; Grant, B.; Volpe, A. F., Jr. *Organometallics* **1992**, *11*, 3920.

Table 2. Crystallographic Data for $[\text{C}_5(\text{CF}_3)(\text{CH}_3)_4]\text{Fe}(\text{C}_5\text{H}_5)$ (10)

(a) Crystal Parameters	
empirical formula, wt	$\text{C}_{15}\text{H}_{17}\text{F}_3\text{Fe}$, 310.14
cryst color, habit	yellow, needle
cryst dimens	$0.550 \times 0.200 \times 0.150$ mm
cryst class	triclinic
no. rflns for unit cell (2θ range)	23 (30.1–49.1°)
θ scan fwhm	0.00
space group	$P\bar{1}$ (No. 2)
<i>a</i>	7.617(5) Å
<i>b</i>	8.346(4) Å
<i>c</i>	12.650(5) Å
α	70.19(3)°
β	81.52(3)°
γ	63.67(2)°
<i>V</i>	678(1) Å ³
<i>Z</i>	2
<i>d</i> _{calc}	1.519 g cm ⁻³
$\mu_{\text{Mo K}\alpha}$	11.27 cm ⁻¹
(b) Data Collection	
diffractometer	Enraf-Nonius CAD-4
monochromator	graphite
radiation	Mo K α ($\lambda = 0.71069$ Å)
temp	-101 °C
attenuator	Zr foil (factor 17.8)
takeoff angle	2.8°
scan type	ω
scan rate	2.1–8.2° min ⁻¹ (in ω)
scan width	($1.20 + 0.35 \tan \Theta$)°
$2\theta_{\text{max}}$	54.0°
no. of rflns collected	3094
no. of unique rflns	2885
(c) Solution and Refinement	
no. of observns ($I > 2.00\sigma(I)$) (N_o)	1362
no. of variables (N_v)	200
N_o/N_v	6.81
<i>R</i> , <i>R</i> _w	0.056, 0.067
goodness of fit	2.14
max peak in final diff map	0.67 Å ⁻³
min peak in final diff map	-0.91 Å ⁻³
max shift/error in final cycle	0.00

activated at 300 °C. Working solutions were prepared by recording background cyclic voltammograms of the electrolyte solution before addition of the organometallic compound. The working compartment of the cell was bubbled with solvent-saturated argon to deaerate the solution; however, in some cases, the entire cell and electrolyte solution were prepared in a nitrogen atmosphere glovebox (Braun).

Potentials were recorded vs aqueous AgCl/Ag and are not corrected for the junction potential.¹⁰ The redox potentials of the transition-metal complexes were calibrated with the ferrocenium/ferrocene (Fc⁺/Fc) couple¹¹ in TBA⁺TFPB⁻/CH₂Cl₂, which was defined at the previously reported¹ value of the Fc⁺/Fc couple (0.47 V) and was determined after each series of runs. The *E*^o, ΔE , and *i*_{p,c}/*i*_{p,a} values were determined by CV or OSWV and are reported as averaged values of three scans on the same solution; the maximum error in the reported *E*^o and ΔE values is ± 0.01 V, and the error in *i*_{p,c}/*i*_{p,a} values is estimated to be approximately 5%.

Spectroelectrochemical Experiments. Infrared changes accompanying the thin-layer bulk electrolysis of [Cp⁺Fe(CO)₂]₂ (13) were measured with use of a flow-through spectrochemical thin-layer cell as previously described.¹² The spectroelectrochemical cell, background (0.10 M TBA⁺TFPB⁻/CH₂Cl₂), and sample (3 mM of 13, 0.10 M TBA⁺TFPB⁻/CH₂Cl₂) solutions were prepared in a nitrogen atmosphere glovebox. Infrared

(10) Gagné, R. R.; Koval, C. A.; Lisensky, G. C. *Inorg. Chem.* **1980**, *19*, 2854.

(11) The ferrocenium/ferrocene couple is a recommended standard for electrochemical measurement of *E*^o values; see: (a) Geiger, W. E. In *Organometallic Radical Processes*; Troglor, W. C., Ed.; Journal of Organometallic Chemistry Library 22; Elsevier: New York, 1990; p 142. (b) Gritzner, G.; Kuta, J. *Pure Appl. Chem.* **1984**, *56*, 461.

(12) Bullock, J. P.; Mann, K. R. *Inorg. Chem.* **1989**, *28*, 4006.

Table 3. Atomic Coordinates and Equivalent Isotropic Thermal Parameters for the Non-Hydrogen Atoms in $[\text{C}_5(\text{CF}_3)(\text{CH}_3)_4]\text{Fe}(\text{C}_5\text{H}_5)$ (10)

atom	<i>x</i>	<i>y</i>	<i>z</i>	<i>B</i> (eq), Å ²
Fe	0.3168(1) ^b	-0.1363(1)	0.77108(7)	1.43(8)
F1	-0.0461(8)	0.3590(6)	0.6658(4)	5.4(5)
F2	-0.0850(7)	0.2351(5)	0.8371(3)	4.3(4)
F3	-0.2774(6)	0.2746(6)	0.7153(5)	5.3(5)
C1	0.415(1)	-0.0103(9)	0.8477(6)	2.3(6)
C2	0.434(1)	-0.1866(8)	0.9215(5)	2.0(6)
C3	0.558(1)	-0.3265(8)	0.8702(5)	2.1(6)
C4	0.6146(9)	-0.2344(9)	0.7639(5)	2.1(6)
C5	0.530(1)	-0.042(1)	0.7512(5)	2.3(6)
C11	0.0369(8)	0.0332(8)	0.7241(5)	1.5(5)
C12	0.0474(9)	-0.1390(8)	0.8040(5)	1.6(5)
C13	0.1716(9)	-0.2831(8)	0.7556(5)	1.8(5)
C14	0.235(1)	-0.2031(9)	0.6491(5)	2.0(6)
C15	0.1504(9)	-0.0052(8)	0.6275(5)	1.8(5)
C21	-0.090(1)	0.2217(9)	0.7357(5)	2.2(6)
C22	-0.054(1)	-0.166(1)	0.9154(5)	2.6(6)
C23	0.223(1)	-0.491(1)	0.8109(6)	3.0(7)
C24	0.363(1)	-0.307(1)	0.5700(6)	3.3(7)
C25	0.178(1)	0.131(1)	0.5203(5)	2.7(6)

^a Equivalent isotropic thermal parameter. ^b Standard deviations are given in parentheses.

Table 4. Selected Bond Lengths (Å) and Bond Angles (deg) for $[\text{C}_5(\text{CF}_3)(\text{CH}_3)_4]\text{Fe}(\text{C}_5\text{H}_5)$ (10)

Bond Lengths (Å)					
Fe–C(1)	2.051(9) ^a	C(1)–C(2)	1.407(9)	C(11)–C(21)	1.482(9)
Fe–C(2)	2.053(7)	C(1)–C(5)	1.424(9)	C(12)–C(22)	1.500(9)
Fe–C(3)	2.054(6)	C(2)–C(3)	1.426(9)	C(13)–C(23)	1.52(1)
Fe–C(4)	2.041(7)	C(3)–C(4)	1.416(9)	C(14)–C(24)	1.50(1)
Fe–C(5)	2.048(9)	C(4)–C(5)	1.40(1)	C(15)–C(25)	1.505(9)
Fe–C(11)	2.007(6)	C(11)–C(12)	1.425(8)	F(1)–C(21)	1.330(9)
Fe–C(12)	2.041(7)	C(11)–C(15)	1.432(8)	F(2)–C(21)	1.331(9)
Fe–C(13)	2.047(9)	C(12)–C(13)	1.426(9)	F(3)–C(21)	1.333(9)
Fe–C(14)	2.061(8)	C(13)–C(14)	1.408(8)		
Fe–C(15)	2.050(6)	C(14)–C(15)	1.421(9)		
Bond Angles (deg)					
C(1)–C(2)–C(3)	108.2(5)	C(12)–C(11)–C(15)	109.1(5)		
C(2)–C(1)–C(5)	107.1(6)	C(11)–C(12)–C(13)	106.0(5)		
C(2)–C(3)–C(4)	107.8(5)	C(12)–C(13)–C(14)	109.8(5)		
C(3)–C(4)–C(5)	107.7(6)	C(13)–C(14)–C(15)	107.8(5)		
C(1)–C(5)–C(4)	109.1(6)	C(11)–C(15)–C(14)	107.2(5)		

^a Standard deviations are given in parentheses.

data were collected on a Mattson Sirius 100 FTIR spectrophotometer. All spectra were corrected for a stray light error (13%) which originates from the inadvertent collection of light off the front of the CaF₂ plates of the spectroelectrochemical cell. Bulk electrolyses were performed with use of the BAS-100 thin-layer bulk electrolysis program.

Structure Determination of $[\text{C}_5(\text{CF}_3)(\text{CH}_3)_4]\text{Fe}(\text{C}_5\text{H}_5)$ (10). Yellow needles of 10 were grown from a mixture of ethanol and water in air at room temperature. Data were collected on an Enraf-Nonius CAD-4 diffractometer with graphite-monochromated Mo K α radiation. The structure was solved by direct methods, and the non-hydrogen atoms were refined anisotropically.¹³ All calculations were performed using the TEXSAN crystallographic software package.^{13c} The crystallographic data (Table 2), the atomic coordinates and isotropic thermal parameters of the non-hydrogen atoms (Table 3), and selected bond lengths and angles (Table 4) are listed in the respective tables in parentheses. Other crystallographic data are included in the supporting information.

(13) (a) Gilmore, C. J. *J. Appl. Crystallogr.* **1984**, *17*, 42. (b) Beurskens, P. T. D. *DIRDIF*; Technical Report 1984/1; Crystallographic Laboratory, Toernooiveld, 6525 Ed Nijmegen, The Netherlands. (c) TEXSAN-TEXRAY Structure Analysis Package, Molecular Structure Corp., College Station, TX, 1985. (d) Johnson, C. K. ORTEP; Report ORNL-5138; Oak Ridge National Laboratory, Oak Ridge, TN, 1976.

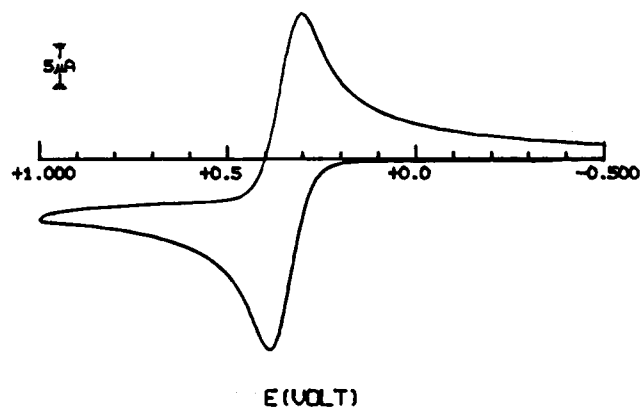


Figure 1. Cyclic voltammogram of Cp*Ru(indenyl) (**4**); $E^{\circ} = 0.51$ V and $i_{p,c}/i_{p,a} = 1.0$, in 0.10 M TBA⁺TFPB⁻/CH₂Cl₂.

Results and Discussion

Electrochemistry of Metallocene Complexes.

We were interested in determining the general utility of the TBA⁺TFPB⁻/CH₂Cl₂ electrolyte/solvent system for obtaining redox potentials (E°) of metallocene complexes. The E° values of substituted ruthenocene complexes **1** and **3–7**, which were previously reported² to undergo irreversible oxidation in TBA⁺ClO₄⁻/CH₂Cl₂, were redetermined in TBA⁺TFPB⁻/CH₂Cl₂ (Table 1). As previously shown, ruthenocene (**1**) gave a quasi-reversible redox potential ($E^{\circ} = 1.03$ V), indicated by the $i_{p,c}/i_{p,a}$ ratio of 1.0. The electrochemical reversibilities of complexes **3–7** are remarkably improved, as indicated by $i_{p,c}/i_{p,a}$ ratios which range from 0.79 for complex **7** to 1.0 for complex **4** (Figure 1). In contrast, the range of $i_{p,c}/i_{p,a}$ ratios of **1** and **3–7** previously determined² in TBA⁺ClO₄⁻/CH₂Cl₂ was 0.29–0.68 (Table 1). It was recently reported¹⁴ that addition of alumina to the electrochemical cell compartment improved the electrochemical reversibility of (η^6 -arene)Cr(CO)₃ complexes; however, this offered no improvement in the $i_{p,c}/i_{p,a}$ ratio of complex **7**. In addition to the improved $i_{p,c}/i_{p,a}$ ratios in TBA⁺TFPB⁻/CH₂Cl₂, the peak separation between the anodic and cathodic peaks ($\Delta E = E_{p,a} - E_{p,c}$) for **3–7** is small, as these values range from 0.075 V for complex **6** to 0.099 V for complex **5** (Table 1). Although we did not generally obtain completely reversible behavior for **3–7**, it is readily apparent that use of the TBA⁺TFPB⁻/CH₂Cl₂ electrolyte/solvent system results in a general improvement in the quality of the CV scans of these complexes which, except for Cp*₂Ru (**8**), were previously reported to be electrochemically irreversible. It is likely that the chemical inertness⁹ of the TFPB anion and hydrophobicity of TBA⁺TFPB⁻ contribute to the improved stability of the substituted ruthenocenium cations. Recently Gassman and Deck reported^{14b} that the use of TBA⁺TFPB⁻/CH₂Cl₂ resulted in major improvements in the reversibility of CV scans of (η^6 -arene)Cr(CO)₃ complexes with electron-withdrawing groups on the arene ligand.

The good agreement between the quasi-reversible values of the ruthenocene complexes reported here and the irreversible potentials previously reported indicates that the follow-up reactions which lead to irreversible

behavior are rapid and the rates are similar for this set of substituted ruthenocene cations.^{15,16} Nevertheless, for these complexes the E° values for the oxidation process are likely more reliable than the irreversible values (Table 1). Thus, the recently reported¹⁶ $E_{p,a}$ values (values in parentheses are reported vs SCE using E° of ferrocene in TBA⁺PF₆⁻/CH₂Cl₂ as 0.48 V¹) for **7** (1.59 V) and **8** (0.63 V) are 0.08 and 0.06 V, respectively, higher than the reversible potentials (E°) which are reported in the same paper. This suggests that the potentials ($E_{p,a}$) reported for Cp*Ru(C₅F₅) (1.52 V), Cp*Ru(C₅H₄NO₂) (1.18 V), and Cp*Ru(C₅(CF₃)₄H) (1.78 V) determined in TBA⁺PF₆⁻/CH₂Cl₂ are also shifted to slightly higher potential than the reversible potential. Although the E° value of Cp*Ru(C₅(CF₃)₄H) is likely too high in solutions containing the TBA⁺TFPB⁻ electrolyte,¹⁷ it would be interesting to determine the E° values of Cp*Ru(C₅F₅) and Cp*Ru(C₅H₄NO₂) in TBA⁺TFPB⁻/CH₂Cl₂.

In addition to the electrochemical evaluation of the effect of substituted cyclopentadienyl ligands on the electron density of the ruthenium metal in ruthenocenes,^{1,2,16} X-ray photoelectron spectroscopy (XPS)^{2,3,18} and Fourier transform ion cyclotron resonance mass spectroscopy methods¹⁹ have also been used. To compare electrochemical redox potentials for substituted ruthenocene compounds that have been reported by different researchers, we have found that it is best to consider a relative error of at least ± 0.1 V in the reported potential. Nevertheless, we find that there is a good correlation of relative ligand effects among the different methods of analysis, and we obtain the following trend listed in order of decreasing electron donation: fluorenyl > pentamethylcyclopentadienyl \approx indenyl > cyclopentadienyl \approx (trifluoromethyl)tetramethylcyclopentadienyl > acetylacetylcyclopentadienyl > nitrocyclopentadienyl > pentachlorocyclopentadienyl \approx pentafluorocyclopentadienyl > tetrakis(trifluoromethyl)cyclopentadienyl. The electronic equivalence of the cyclopentadienyl and (trifluoromethyl)tetramethylcyclopentadienyl ligands is discussed below.

A comparison of the effect of permethylation of the cyclopentadienyl ligand²⁰ on the quasi-reversible E° values of group 9 metallocenes indicates that the relative electron-donating effect of the Cp* ligand slightly decreases as one goes down the period from Fe (0.59 V) to Ru (0.55 V) to Os (0.52 V). As previously shown, the sequential replacement of Cp by Cp* in ferrocene derivatives is additive;²⁰ however, this is not a general trend, as the replacement of one Cp by one Cp* to give Cp*Ru(Cp) (**5**) results in a 0.34 V change in

(15) Kissinger, P. T. In *Laboratory Techniques in Electroanalytical Chemistry*; Kissinger, P. T., Heineman, W. R., Eds.; Dekker: New York, 1994; pp 29–39.

(16) (a) Richardson, D. E.; Ryan, M. F.; Geiger, W. E.; Chin, T. T.; Hughes, R. P.; Curnow, O. J. *Organometallics* **1993**, *12*, 613. (b) Hughes, R. P.; Zheng, X.; Ostrander, R. L.; Rheingold, A. L. *Organometallics* **1994**, *13*, 1567.

(17) The anodic limit of the electrolyte/solvent system starts at ca. 1.7 V.

(18) Gassman, P. G.; Macomber, D. W.; Hershberger, J. W. *Organometallics* **1983**, *2*, 1470.

(19) (a) Ryan, M. F.; Siedle, A. R.; Burk, M. J.; Richardson, D. E. *Organometallics* **1992**, *11*, 4231. (b) Richardson, D. E.; Ryan, M. F.; Khan, Md. N. I.; Maxwell, K. A. *J. Am. Chem. Soc.* **1992**, *114*, 10482.

(20) A similar study was recently published; however, the reported $E_{1/2}$ values for the oxidation of Cp₂Ru and Cp₂Os are likely irreversible: Denisovich, L. I.; Peterleitner, M. G.; Kravtsov, D. N.; Kreindlin, A. Z.; Fadeeva, S. S.; Rybinskaya, M. I. *Organomet. Chem. USSR (Engl. Transl.)* **1988**, *1*, 166; *Metalloorg. Khim.* **1988**, *1*, 301.

(14) (a) Hunter, A. D.; Mozol, V.; Tsai, S. D. *Organometallics* **1992**, *11*, 2251. (b) Gassman, P. G.; Deck, P. A. *Organometallics* **1994**, *13*, 1934.

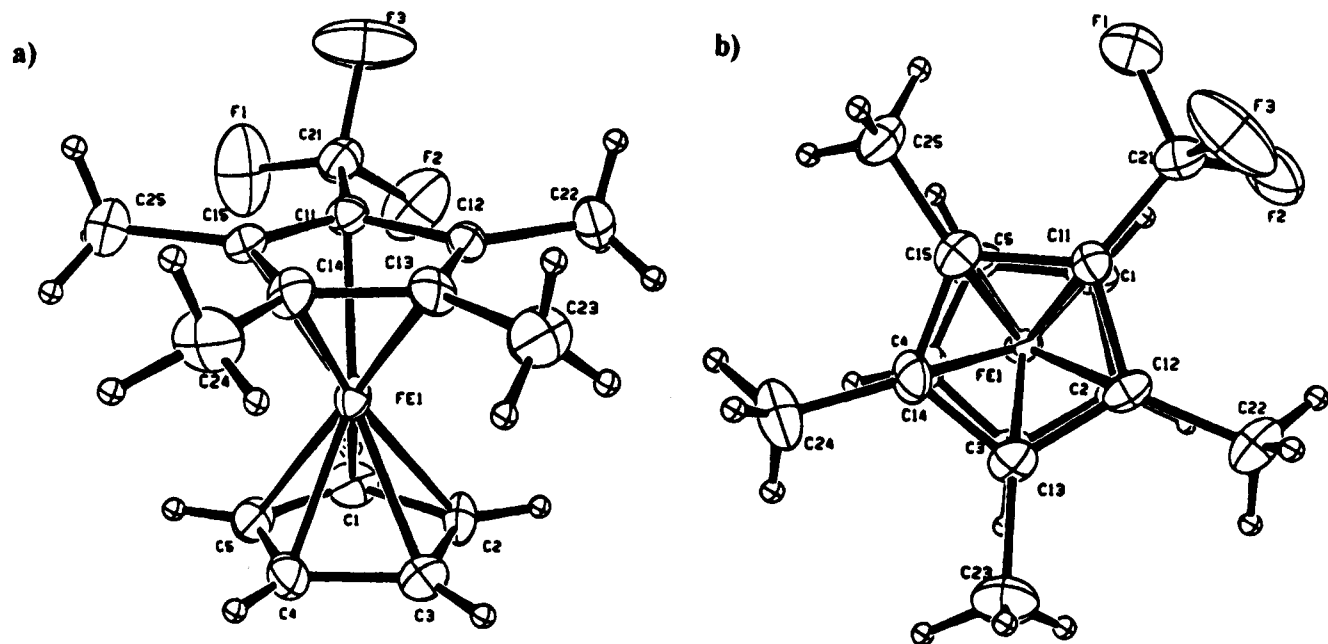


Figure 2. ORTEP drawings of Cp^+FeCp (**10**): (a) side view; (b) top view, which illustrates the eclipsed cyclopentadienyl rings and similar structures of the Cp^+ and Cp ligands except for differences in steric bulk.

the E° value but the second replacement, to give $\text{Cp}^*_2\text{-Ru}$ (**8**), only results in a 0.21 V change in the E° value.² Thus, the cause of the slight decrease in electron-donating ability of Cp^* as one goes from Fe to Ru to Os may be due to the weaker effect of the second Cp^* . However, it is not clear whether this is due to electronic or steric properties. We believe that this is the first complete comparison of the redox potentials of all of the group 9 Cp_2M and Cp^*_2M complexes where all of the potentials are quasi-reversible.²⁰

Electrochemistry of (Trifluoromethyl)cyclopentadienyl Complexes. Recently,³ we demonstrated the electronic equivalence of the cyclopentadienyl (Cp) and the (trifluoromethyl)tetramethylcyclopentadienyl (Cp^+) ligand as indicated by XPS. Thus, we were interested in comparing the reversible redox potentials of complexes of Cp^+ with those of Cp and Cp^* . Table 1 shows that the Cp^+ complexes **10–13** are slightly more difficult to oxidize by 0.06–0.08 V per Cp^+ ligand than the respective Cp complexes. Although the electrochemical data indicate a slight difference between Cp and Cp^+ complexes, this difference is small when a comparison is made with the Cp^* complexes, since relative to Cp^* , the Cp^+ derivatives are more difficult to oxidize by 0.3–0.4 V per Cp^+ ligand.

To understand more fully the nature of coordination of the Cp^+ ligand, we performed a single-crystal X-ray crystallographic study of $[\text{C}_5(\text{CF}_3)(\text{CH}_3)_4]\text{Fe}(\text{C}_5\text{H}_5)$ ($\text{Cp}^+\text{-FeCp}$).²¹ The ORTEP^{13d} drawing (Figure 2) clearly indicates that the Cp^+ and Cp rings are eclipsed. In contrast, the revised crystal structure of ferrocene reported by Seiler and Dunitz²² shows the Cp rings are staggered by 9° from the eclipsed geometry. In $\text{Cp}^+\text{-FeCp}$, the C11 ring carbon on which the CF_3 group is located has a shorter Fe–C(ring) bond distance (2.007-

6) Å) than that found for the C12–C15 (2.041–2.061 Å) ring carbons. However, the Cp and Cp^+ rings are essentially planar, as the dihedral angle between the least-squares planes is only 0.63° , which can be compared to that calculated (0.46°) for ferrocene. The intraring bond distances (1.408–1.432 Å) and bond angles (106.0 – 109.8°) within the Cp^+ ring are remarkably similar to the bond distances (1.40–1.426 Å) and bond angles (107.1 – 109.1°) in the unsubstituted Cp ring of Cp^+FeCp . Finally, the iron to Cp^+ -centroid distance (1.643 Å) is 0.016 Å shorter than the iron to unsubstituted Cp -centroid distance. Although crystal structures of ruthenocene complexes show shorter metal to centroid distances for more electron-withdrawing ligands,^{2,16b,23} which suggests that the Cp^+ ligand is slightly more electron withdrawing than Cp , steric effects may also account for the longer iron to unsubstituted Cp -centroid distance, as the iron to Cp^+ -centroid distance (1.643 Å) is similar to that in ferrocene (1.648 Å). In fact, the average iron to Cp^+ -centroid distance in Cp^+FeCp (1.651 Å) is, within experimental error, equivalent to that distance (1.648 Å) in ferrocene. Therefore, this crystallographic comparison of the Cp^+ and Cp ligands in the same molecule shows no extreme differences (e.g., ring slippage²⁴) between the coordination of these two ligands, and except for differences in steric bulk the structures of the two ligands are practically the same.

Electrochemical and Spectroelectrochemical Studies of $[\text{Cp}^+\text{Fe}(\text{CO})_2]_2$ (13**).** The quasi-reversible electrochemical potentials of $[\text{Cp}^+\text{Fe}(\text{CO})_2]_2$ complexes ($\text{Cp}^+ = \text{Cp}^+$ (**13**), Cp (**14**), Cp^* (**15**)) are readily deter-

(23) This may not be a general trend, as crystal structures of $\text{Cp}^*\text{-Ru}(\text{C}_5(\text{CF}_3)_4\text{H})^{23a}$ and $\text{CpRu}(\text{C}_5(\text{CO}_2\text{Me}))^{23b}$ show very similar Ru–Cp' (centroid) distances, within experimental error, in spite of large differences in electronic characteristics; see, for example: (a) Burk, M. J.; Arduengo, A. J., III; Calabrese, J. C.; Harlow, R. L. *J. Am. Chem. Soc.* **1989**, *111*, 8938. (b) Bruce, M. I.; Skelton, B. W.; Wallis, R. C.; Walton, J. K.; White, A. H.; Williams, M. L. *J. Chem. Soc., Chem. Commun.* **1981**, 428.

(24) (a) O'Connor, J. M.; Casey, C. P. *Chem. Rev.* **1987**, *87*, 307. (b) Byers, L. R.; Dahl, L. F. *Inorg. Chem.* **1980**, *19*, 277. (c) Yu, M.; Struchkov, Y. T.; Chernega, A. N.; Meidine, M. F.; Nixon, J. F. *J. Organomet. Chem.* **1992**, *436*, 79.

(21) The compounds Cp^*_2Ru and Cp^*_2Os both crystallize in isomorphous triclinic cells with $Z = 1$; however, the molecules appear to be orientationally disordered and we could not obtain accurate information about the light atoms in the molecules.

(22) Seiler, P.; Dunitz, J. D. *Acta Crystallogr., Sect. B* **1979**, *B35*, 1068.

Table 5. Infrared Carbonyl Stretching Frequencies of the Parent $[\text{Cp}^*\text{Fe}(\text{CO})_2]_2$ ($\text{Cp}^* = \text{Cp}, \text{Cp}^\ddagger, \text{Cp}^*$) and Radical-Cation $[\text{Cp}^*\text{Fe}(\text{CO})_2]_2^+$ Complexes^a

compd	parent $\nu(\text{CO}), \text{cm}^{-1}$	radical-cation $\nu(\text{CO}), \text{cm}^{-1}$
$[\text{Cp}^*\text{Fe}(\text{CO})_2]_2$ (13)	1952, 1776	2018, 1904
$[\text{Cp}\text{Fe}(\text{CO})_2]_2$ (14) ^b	1955, ^c 1995, ^d 1773	2023, ^c 2055, ^d 1934
$[\text{Cp}^*\text{Fe}(\text{CO})_2]_2$ (15) ^b	1922, 1747	1987, 1884

^a CH_2Cl_2 solvent. ^b Reference 4. ^c Trans isomer. ^d Cis isomer.

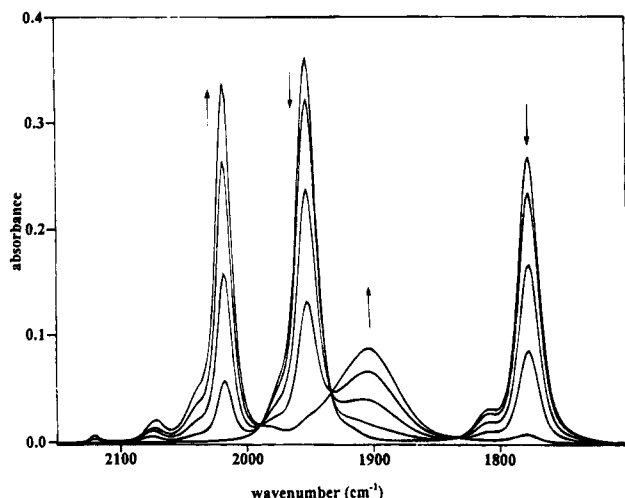
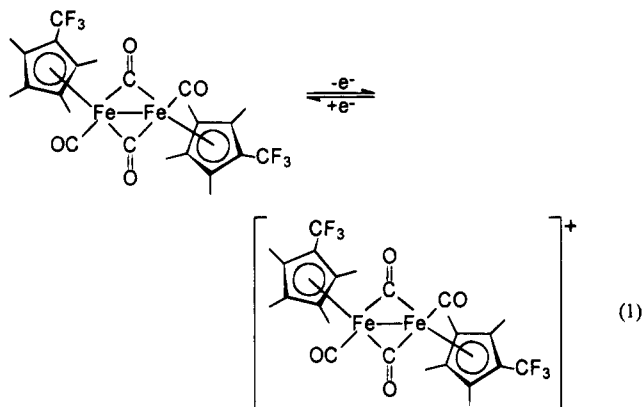


Figure 3. Infrared spectral changes upon oxidation of a solution of $[\text{Cp}^*\text{Fe}(\text{CO})_2]_2$ (**13**) in 0.10 M $\text{TBA}^+\text{TFPB}^-/\text{CH}_2\text{Cl}_2$ at ca. 1.0 V. The peaks due to the trans parent dimer ($\nu(\text{CO})$ 1952, 1776 cm^{-1}) decrease in intensity as the concentration of the trans radical-cation dimer, $[\text{Cp}^*\text{Fe}(\text{CO})_2]_2^+$ ($\nu(\text{CO})$ 2018, 1904 cm^{-1}), increases during oxidation.

mined in $\text{TBA}^+\text{TFPB}^-/\text{CH}_2\text{Cl}_2$ (Table 1). Thus, similar E° values are obtained for **13** (0.70 V) and **14** (0.64 V), compared to that of **15** (0.28 V). Since Cp^\ddagger and Cp are electronically similar ligands, this result indicates that the electrochemical potentials of complexes **13**–**15** are controlled by the electronic properties of the Cp' ligand as opposed to the steric properties.

An infrared spectroelectrochemistry study of $[\text{Cp}^*\text{Fe}(\text{CO})_2]_2$ (**13**) was performed in $\text{TBA}^+\text{TFPB}^-/\text{CH}_2\text{Cl}_2$ to determine the structure of the oxidation product and to compare the reactivity of the Cp^\ddagger complex to that of the Cp and Cp^* derivatives. The neutral starting material $[\text{Cp}^*\text{Fe}(\text{CO})_2]_2$ exists only as the trans isomer, as for $[\text{Cp}^*\text{Fe}(\text{CO})_2]_2$;²⁵ however, because of the similar electronic properties of Cp^\ddagger and Cp , the $\nu(\text{CO})$ values of **13** are similar to those of the trans isomer of $[\text{Cp}\text{Fe}(\text{CO})_2]_2$ (Table 5).⁴ As **13** is oxidized (Figure 3), the bands at 1952 and 1776 cm^{-1} decrease in intensity as two bands at 2018 and 1904 (br cm^{-1}) grow in isobestically. As previously observed for $\text{trans}-[\text{Cp}^*\text{Fe}(\text{CO})_2]_2^+\text{PF}_6^-$ (Table 5), the new bands indicate the presence of a single isomer;⁴ thus, these are assigned to the terminal and bridging bands of $\text{trans}-[\text{Cp}^*\text{Fe}(\text{CO})_2]_2^+\text{TFPB}^-$ (eq 1).



After complete formation of $\text{trans}-[\text{Cp}^*\text{Fe}(\text{CO})_2]_2^+\text{TFPB}^-$ was observed, bulk reduction of the solution cleanly regenerated the trans isomer of $[\text{Cp}^*\text{Fe}(\text{CO})_2]_2$ (eq 1). Previous spectroelectrochemical studies⁴ of $\text{cis}, \text{trans}-[\text{Cp}\text{Fe}(\text{CO})_2]_2$ indicated the formation of $\text{cis}, \text{trans}-[\text{Cp}\text{Fe}(\text{CO})_2]_2^+\text{PF}_6^-$. Since Cp^\ddagger and Cp are nearly electronically equivalent ligands,³ the steric bulk of the Cp^\ddagger ligand probably precludes the formation of $\text{cis}-[\text{Cp}^*\text{Fe}(\text{CO})_2]_2^+\text{TFPB}^-$.

The trans Cp and Cp^\ddagger complexes have similar $\nu(\text{CO})$ stretching frequencies (Table 5);³ thus, we can assign the small bands at 2122 and 2074 cm^{-1} (Figure 3) as due to trace byproducts which result from the disproportionation of $[\text{Cp}^*\text{Fe}(\text{CO})_2]_2^+\text{TFPB}^-$ by comparison with the byproducts formed in the oxidation of $[\text{Cp}\text{Fe}(\text{CO})_2]_2$.⁴ These two bands are assigned to the species $\text{Cp}^*\text{Fe}(\text{CO})_3^+\text{TFPB}^-$ in comparison to the bands of $\text{Cp}\text{Fe}(\text{CO})_3^+\text{PF}_6^-$ (2126, 2081 cm^{-1}).⁴ However, the slightly more intense 2074 cm^{-1} band overlaps with the band of another byproduct, which is likely $[\text{Cp}^*\text{Fe}(\text{CO})_2(\text{OH}_2)]^+\text{TFPB}^-$, as addition of water causes an increase in the intensity of this band. The remaining band from the latter byproduct is located under the 2018 cm^{-1} peak of $[\text{Cp}^*\text{Fe}(\text{CO})_2]_2^+\text{TFPB}^-$, as bulk reduction of the solution gave a band at 2023 cm^{-1} (cf. the $\nu(\text{CO})$ values⁴ of $\text{Cp}\text{Fe}(\text{CO})_2(\text{OH}_2)^+\text{PF}_6^-$ at 2076 and 2030 cm^{-1}). We also note that small shoulders occur on the high-energy side of the bridging $\nu(\text{CO})$ band of **13**. It is unlikely that this is due to the triply bridging $[\text{Cp}^*\text{Fe}(\mu\text{-CO})_3\text{FeCp}^\ddagger]$ complex, due to the high-intensity photolytic conditions required to generate the related Cp and Cp^* derivatives.²⁶ Previously, Manning²⁷ assigned the higher energy shoulder in $[\text{Cp}\text{Fe}(\text{CO})_2]_2$ to a weak symmetric stretch of the bridging CO groups in the cis isomer; however, as this band also occurs in the trans-only derivatives **13** and $[\text{Cp}^*\text{Fe}(\text{CO})_2]_2$,²⁸ it is likely that this band also results from a symmetric stretch of the CO groups in the trans isomers.

Conclusions

We have shown that cyclic voltammetry in tetra-*n*-butylammonium tetrakis[3,5-bis(trifluoromethyl)phenyl]borate electrolyte and methylene chloride solvent ($\text{TBA}^+\text{TFPB}^-/\text{CH}_2\text{Cl}_2$) improves the electrochemical reversibility of pentamethylcyclopentadienyl (Cp^*) ruthenocenes, $\text{Cp}^*\text{RuCp}'$ ($\text{Cp}' = \text{fluorenyl}, \text{indenyl}, \text{cyclopentadienyl}$ (Cp), acetylcyclopentadienyl, pentachlorocyclopentadienyl), as indicated by $i_{p,c}/i_{p,a}$ ratios of 0.79–1.0. Quasi-reversible electrochemical potentials of a total of 17 substituted cyclopentadienyl complexes were

(25) Teller, R. G.; Williams, J. M. *Inorg. Chem.* **1980**, *19*, 2770.

(26) (a) Blaha, J. P.; Bursten, B. E.; Dewan, J. C.; Frankel, R. B.; Randolph, C. L.; Wilson, B. A.; Wrighton, M. S. *J. Am. Chem. Soc.* **1985**, *107*, 4561. (b) Hooker, R. H.; Mahmoud, K. A.; Rest, A. J. *J. Chem. Soc., Chem. Commun.* **1983**, 1022.

(27) Manning, A. R. *J. Chem. Soc. A* **1968**, 1319.

(28) See the supplementary material in ref 4 for the spectroelectrochemically generated infrared spectra of $[\text{Cp}^*\text{Fe}(\text{CO})_2]_2$ and $[\text{Cp}^*\text{Fe}(\text{CO})_2]_2^+$.

determined in TBA⁺TFPB⁻/CH₂Cl₂, including complexes containing the (trifluoromethyl)tetramethylcyclopentadienyl (Cp[†]) ligand. Although the Cp[†] complexes are slightly more difficult to oxidize (0.06–0.08 V per Cp[†]) than the Cp derivatives, the redox potentials of the Cp[†] complexes are more similar to those of the Cp derivatives than to those of the Cp* derivatives. The crystal structure of [C₅(CF₃)(CH₃)₄]Fe(C₅H₅) indicates no extreme differences in the coordination of the Cp[†] and Cp rings except for differences in steric bulk. In addition, an infrared spectroelectrochemical study of [Cp[†]Fe(CO)₂]₂ illustrates two important characteristics of the Cp[†] ligand: (1) upon oxidation its steric properties cause structural changes in [Cp[†]Fe(CO)₂]₂ so that it behaves like the related Cp* derivative and (2) its electronic properties cause the *E*^o values and the *ν*(CO) values to be more similar to those of the Cp derivative.

Acknowledgment. The crystal structure of Cp[†]-FeCp was determined by Professor Doyle Britton. We thank Professor John Ellis for use of his FTIR spectrophotometer for the spectroelectrochemistry experiments, and we also thank Tim Wilson for his help with some of those experiments. We thank Dr. William Lamanna at the 3M Co. for a sample of TBA⁺TFPB⁻. Finally, we are grateful to the NSF for its support of this work.

Supporting Information Available: Crystal data for 10, including complete tables of atomic coordinates and thermal parameters for the hydrogen and non-hydrogen atoms, general temperature factor expressions (*U*), bond distances and angles, and least-squares planes (14 pages). Ordering information is given on any current masthead page.

OM950397T

Synthesis and Characterization of CO₂-Bridged Ruthenium-Zirconium and Rhenium-Zirconium Complexes

Dorothy H. Gibson,* Jayesh M. Mehta, Bradley A. Sleadd,
Mark S. Mashuta, and John F. Richardson

Department of Chemistry and Center for Chemical Catalysis, University of Louisville,
Louisville, Kentucky 40292

Received May 17, 1995[®]

The synthesis and characterization of the CO₂-bridged complexes Cp**Ru*(CO)₂(CO₂)/Zr(X)Cp₂ (**2a**, **3a**, **5a**; X = Cl, Me, SnPh₃), Cp**Re*(CO)(NO)(CO₂)/Zr(X)Cp₂ (**2b**, **3b**, **5b**; X = Cl, Me, SnPh₃), and Cp**Ru*(CO)₂(CO₂)/SnPh₃ (**4**) are described. Compounds **2a,b** have been structurally characterized. The geometry about the zirconium atom in **2a,b** is edge-capped tetrahedral. All compounds have been characterized by solid-state IR data; comparisons of these data with those from other symmetrical μ₂-η³-CO₂ compounds show that, although ν_{asym} for the CO₂ ligand varies slightly with the metallocarboxylate fragment, it is highly dependent upon the coordination geometry of the metal center which binds the two carboxyl oxygens.

Introduction

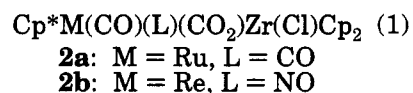
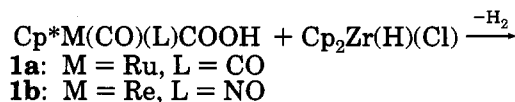
Bimetallic transition-metal complexes with bridging carbon dioxide ligands provide important homogeneous models for intermediates in the catalytic fixation of CO₂.¹ In previous work, we have identified three bonding types for compounds having CO₂ bridged between two metal centers;^{1*n,r,v*} such compounds have been suggested as necessary intermediates for the activation of CO₂.² The μ₂-η² complexes have the carboxyl carbon bound to one metal center and a single carboxyl oxygen bound to the second metal center. Compounds of the μ₂-η³ type, which have both carboxyl oxygens bound to the same metal center, are of two kinds: those which are highly symmetrical and demonstrate nearly

equivalent C–O bond lengths and nearly equivalent O–M bond lengths and those which are unsymmetrical, where these bond lengths are inequivalent, especially with regard to the O–M bonds. The two types are distinguishable by their IR ν_{OCO} bands.

Compounds having CO₂ bridged between a late transition metal and an early transition metal metallocene derivative have been reported previously,^{1*b,k,t*} but none have been structurally characterized. We report new synthetic methods leading to several such compounds and the structural characterizations of two of the compounds as well as new insights into relationships between the structural characteristics of the symmetrically bonded compounds and their IR ν_{OCO} bands.³ These relationships are expected to have particular importance in identifying the nature of active metal-bound CO₂-containing species in both homogeneous and heterogeneous catalytic processes.

Results and Discussion

Synthesis of the CO₂-Bridged Compounds. Reactions of the metallocarboxylic acids Cp**Ru*(CO)₂CO₂H⁴ (**1a**; Cp* = η⁵-C₅Me₅) and Cp**Re*(CO)(NO)COOH^{1*r*} (**1b**) with Cp₂Zr(Cl)(H) afforded the corresponding CO₂-bridged complexes in good yields: 63% for **2a** and 69% for **2b**. The procedure is outlined in eq 1. Both



compounds have been fully characterized through el-

(3) A preliminary account of this work was presented at the Third International Conference on Carbon Dioxide Utilization in Norman, OK, on May 1, 1995.

(4) Suzuki, H.; Omori, H.; Moro-oka, Y. *J. Organomet. Chem.* **1987**, 327, C49.

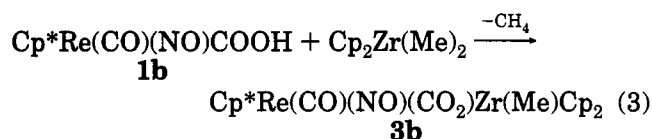
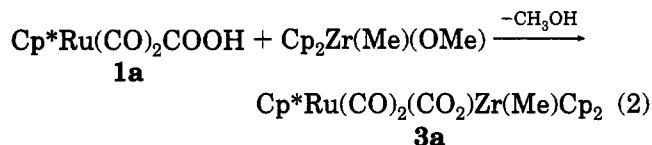
[®] Abstract published in *Advance ACS Abstracts*, September 1, 1995.

(1) (a) Audett, J. D.; Collins, T. J.; Santarsiero, B. D.; Spies, G. H. *J. Am. Chem. Soc.* **1982**, 104, 7352. (b) Tso, C. T.; Cutler, A. R. *J. Am. Chem. Soc.* **1986**, 108, 6069. (c) Gibson, D. H.; Ong, T.-S. *J. Am. Chem. Soc.* **1987**, 109, 7191. (d) Senn, D. R.; Gladysz, J. A.; Emerson, K.; Larsen, R. D. *Inorg. Chem.* **1987**, 26, 2737. (e) Bennett, M. A.; Robertson, G. B.; Rokicki, A.; Wickramasinghe, W. A. *J. Am. Chem. Soc.* **1988**, 110, 7098. (f) Pilato, R. S.; Geoffroy, G. L.; Rheingold, A. L. *J. Chem. Soc., Chem. Commun.* **1989**, 1287. (g) Pilato, R. S.; Housmekerides, C. E.; Jernakoff, P.; Rubin, D.; Geoffroy, G. L.; Rheingold, A. L. *Organometallics* **1990**, 9, 2333. (h) Field, J. S.; Haines, R. J.; Sundermeyer, J.; Woolam, S. F. *J. Chem. Soc., Chem. Commun.* **1990**, 985. (i) Gibson, D. H.; Richardson, J. F.; Ong, T.-S. *Acta Crystallogr.* **1991**, C47, 259. (j) Torreson, I.; Michelin, R. A.; Marsella, A.; Zanardo, A.; Pinna, F.; Strukul, G. *Organometallics* **1991**, 10, 623. (k) Vites, J. C.; Steffey, B. D.; Giuseppetti-Dery, M. E.; Cutler, A. R. *Organometallics* **1991**, 10, 2827. (l) Gibson, D. H.; Ong, T.-S.; Ye, M. *Organometallics* **1991**, 10, 1811. (m) Gibson, D. H.; Ye, M.; Richardson, J. F. *J. Am. Chem. Soc.* **1992**, 114, 9716. (n) Szalda, D. J.; Chou, M. H.; Fujita, E.; Creutz, C. *Inorg. Chem.* **1992**, 31, 4712. (o) Field, J. S.; Haines, R. J.; Sundermeyer, J.; Woolam, S. F. *J. Chem. Soc., Dalton Trans.* **1993**, 2735. (p) Gibson, D. H.; Richardson, J. F.; Mbadike, O. P. *Acta Crystallogr.* **1993**, B49, 784. (q) Pinkes, J. R.; Cutler, A. R. *Inorg. Chem.* **1994**, 33, 759. (r) Gibson, D. H.; Mehta, J. M.; Ye, M.; Richardson, J. F.; Mashuta, M. S. *Organometallics* **1994**, 13, 1070. (s) Yang, Y.-L.; Chen, J.-D.; Liu, Y.-C.; Cheng, M.-C.; Wang, Y. *J. Organomet. Chem.* **1994**, 467, C8. (t) Pinkes, J. R.; Steffey, B. D.; Vites, J. C.; Cutler, A. R. *Organometallics* **1994**, 13, 21. (u) Gibson, D. H.; Ye, M.; Richardson, J. F.; Mashuta, M. S. *Organometallics* **1994**, 13, 4559. (v) Gibson, D. H.; Ye, M.; Sleadd, B. A.; Mehta, J. M.; Mbadike, O. P.; Richardson, J. F.; Mashuta, M. S. *Organometallics* **1995**, 14, 1242.

(2) (a) Fachinetti, G.; Floriani, C.; Zanazzi, P. F. *J. Am. Chem. Soc.* **1978**, 100, 7405. (b) Gambarotta, S.; Arena, F.; Floriani, C.; Zanazzi, P. F. *J. Am. Chem. Soc.* **1982**, 104, 5082.

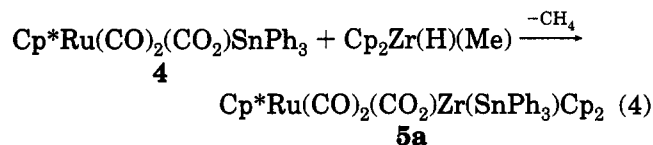
emental analyses, spectral properties, and X-ray structure determinations. Both have been identified as fully chelated $\mu_2\text{-}\eta^3\text{-CO}_2$ complexes with five-coordinate zirconium atoms (see below).

Compounds **3a,b** were obtained by similar procedures which again take advantage of the reactivity of the metallocarboxylic acids toward acid-sensitive functional groups on zirconocene derivatives. Reaction of **1a** with $\text{Cp}_2\text{Zr(OMe)(Me)}^5$ afforded **3a**, while reaction of **1b** with $\text{Cp}_2\text{Zr(Me)}_2^6$ gave **3b** in 67% and 85% yields, respectively. The methods are outlined in eqs 2 and 3. Both



compounds have been characterized through elemental analyses and spectral properties; on the basis of these characteristics (see below), both are formulated as $\mu_2\text{-}\eta^3\text{-CO}_2$ complexes.

The procedures which have been used for the preparation of the trimetallic compounds **5a,b** are quite distinct from the methods used for **2a,b** and **3a,b**. In these reactions, our starting materials were $\text{Cp}^*\text{Ru(CO)}_2(\text{CO}_2)\text{SnPh}_3$ (**4**;⁷ see Experimental Section) and the previously characterized $\text{Cp}^*\text{Re(CO)(NO)(CO}_2\text{)SnPh}_3$,^{1r} which were used in combination with $\text{Cp}_2\text{Zr(H)(Me)}^8$ as illustrated in eq 4 for **5a**. Compounds **5a,b** were



obtained in good yields (80% and 66%, respectively) and have been characterized by elemental analyses and spectral properties. On the basis of spectral comparisons with **2a,b** (see below and Experimental Section), **5a,b** have also been formulated as $\mu_2\text{-}\eta^3\text{-CO}_2$ complexes with zirconium bound to the carboxyl oxygens and with the triphenyltin group bound to zirconium also. Initially, we thought that compounds **3a,b** might be intermediates in these reactions, but control experiments between **3a** or **3b** and Ph_3SnH gave no evidence for the formation of **5a** or **5b**. Also, the reaction of **4** with $\text{Cp}_2\text{Zr(Cl)(Me)}^9$ afforded **2a** and MeSnPh_3 (see Experimental Section). Thus, we tentatively propose

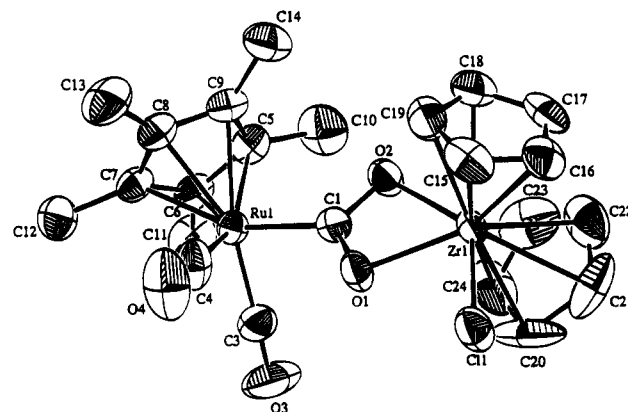


Figure 1. ORTEP drawing of **2a** with thermal ellipsoids shown at the 50% probability level.

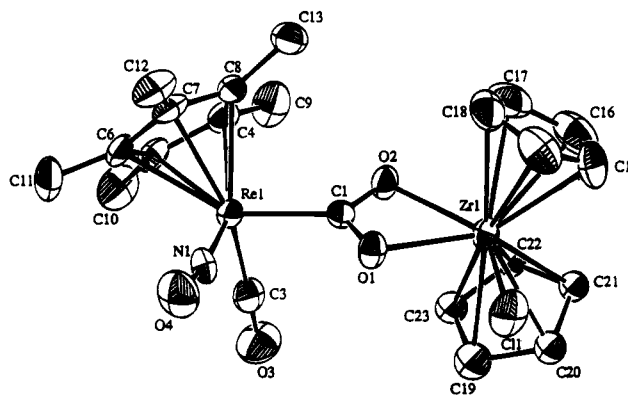
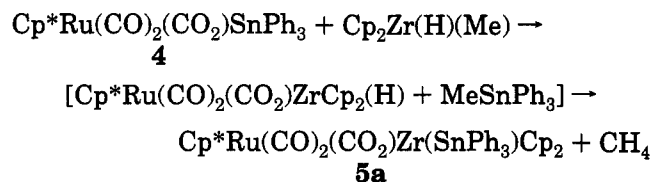


Figure 2. ORTEP drawing of **2b** with thermal ellipsoids shown at the 50% probability level.

the route shown in Scheme 1 for the formation of these two products, as illustrated for **5a**. This new synthetic methodology for a zirconium complex is based on a transmetalation reaction using the CO₂-bridged tin complex as transfer agents for the metallocarboxylate fragment. This method provides an important alternative for these systems, since *in situ* generation of a metallocarboxylate in aqueous media followed by trapping with a second metal to form the CO₂-bridged complex, as we have done with some other systems previously,^{1p,v} is not a viable option for the moisture-sensitive zirconium complexes.

Scheme 1



Structural Characterization of 2a,b. The solid-state structures of **2a,b** were established by X-ray crystallography and are the first CO₂-bridged compounds involving zirconium to be structurally characterized. The ORTEP diagram for **2a** is shown in Figure 1, and the diagram for **2b** is shown in Figure 2. The crystallographic data for both compounds are summarized in Table 1. Atomic positional parameters for **2a** are shown in Table 2; those for **2b** are shown in Table 4. Selected bond distances and angles are shown in Tables 3 and 5 for **2a,b**, respectively. Both compounds

(5) Wailes, P. C.; Weigold, H.; Bell, A. P. *J. Organomet. Chem.* **1972**, *34*, 155.

(6) Hunter, W. E.; Hrcncir, D. D.; Bynum, R. V.; Pentilla, R. A.; Atwood, J. L. *Organometallics* **1983**, *2*, 750.

(7) The solid-state structure of **4** has been established by X-ray crystallography: $\text{C}_{31}\text{H}_{30}\text{O}_4\text{SnRu}$, monoclinic, $P2_1/c$; $a = 12.250(3)$ Å, $b = 11.917(2)$ Å, $c = 19.872(4)$ Å, $\beta = 100.90(2)^\circ$; $R = 0.029$, $R_w = 0.030$. The compound is isostructural with $\text{Cp}^*\text{Fe(CO)}_2(\text{CO}_2)\text{SnPh}_3$,^{1v} showing unequal bonding of the carboxylate oxygens to Sn: O(1)–Sn, 2.100(3) Å; O(2)–Sn, 2.425(3) Å.

(8) Gell, K. I.; Posin, B.; Schwartz, J.; Williams, G. M. *J. Am. Chem. Soc.* **1982**, *104*, 1846.

(9) Wailes, P. C.; Weigold, H.; Bell, A. P. *J. Organomet. Chem.* **1971**, *33*, 181.

Table 1. Summary of Crystallographic Data for 2a,b

	2a	2b
formula	C ₃₀ H ₃₃ ClO ₄ RuZr	C ₂₃ H ₂₇ Cl ₃ NO ₄ ReZr
cryst syst	monoclinic	triclinic
space group	<i>P</i> 2 ₁ / <i>n</i>	<i>P</i> 1
<i>a</i> , Å	13.962(4)	10.753(3)
<i>b</i> , Å	13.239(5)	13.892(3)
<i>c</i> , Å	16.114(4)	10.296(4)
α, deg		107.50(2)
β, deg	90.56(2)	114.34(2)
γ, deg		77.07(2)
<i>V</i> , Å ³	2978(1)	1327.6(8)
<i>Z</i>	4	2
<i>D_c</i> , g/cm ³	1.53	1.91
cryst dimens, mm	0.56 × 0.50 × 0.45	0.50 × 0.35 × 0.35
cryst descriptn	colorless block	orange block
μ(Mo Kα), cm ⁻¹	9.78	52.79
abs cor	ψ scans	same
transmissn factors:	0.959/1.000	0.779/1.000
min/max		
radiation (λ, Å)	Mo Kα (0.710 73)	same
diffractometer	Enraf-Nonius CAD4	same
monochromator	graphite cryst	same
temp, °C	23(1)	23(1)
scan range	0.70 + 0.35 tan θ	0.75 + 0.35 tan θ
scan speed, deg/min	1–5	1–5
max 2θ, deg	54.0	50.0
no. of unique rflns collected	6787	4667
no. of rflns included (<i>I</i> _o > 3σ(<i>I</i> _o))	4871	4371
no. of params	315	285
computer hardware	Silicon Graphics Iris Indigo	same
computer software	teXsan (msc)	same
extinctn coeff	5.47 × 10 ⁻⁷	7.80 × 10 ⁻⁷
agreement factors ^a		
<i>R</i>	0.037	0.027
<i>R_w</i>	0.038	0.029
function minimized	Σw(<i>F</i> _o - <i>F</i> _c) ²	same
GOF	1.88	3.20
weighting scheme	[σ ² (<i>F</i> _o)] ⁻¹	same
high peak in final diff map, e/Å ³	0.66	1.31

$$^a R = \sum ||F_o| - |F_c|| / \sum (|F_o|); R_w = [\sum w(|F_o| - |F_c|)^2 / \sum w F_o^2]^{1/2}.$$

exhibit highly symmetrical $\mu_2\eta^3$ bonding of the bridging CO₂ ligand. The C–O bond lengths in **2a** are 1.281(5) and 1.285(5) Å, while those in **2b** are 1.271(7) and 1.296(8) Å. The O–Zr bond lengths in **2a** are 2.221(3) and 2.236(3) Å, while those in **2b** are 2.201(3) and 2.245(4) Å. Also, the carboxyl C–O bond lengths in **2b** are very near to those in Cp*Re(CO)(NO)(CO)₂Re(CO)₃(PPh₃)^{1r} reported earlier: 1.289(8) and 1.296(6) Å. The geometry around the zirconium atom in **2a,b** is similar to that in the chlorozirconium dithiocarbamate complexes characterized several years ago by Fay et al.¹⁰ This group defined the geometry about the zirconium atom by considering the centroids to the two cyclopentadienyl rings together with the bonds to three remaining ligands. Thus, the geometry around the zirconium atom was described as edge-capped tetrahedral with elongated Zr–Cl bonds, as are those in **2a,b** at 2.518(1) and 2.525(2) Å, respectively. This geometry, with regard to the metal atom which binds both carboxyl oxygens, is distinct from that of the late-transition-metal complexes which we have structurally characterized previously;^{1r,u} those have involved octahedral rhenium centers bound to the two oxygens.

Table 2. Atomic Positional Parameters for 2a

atom	<i>x</i>	<i>y</i>	<i>z</i>	<i>B</i> _{eq} , Å ²
Ru(1)	0.23464(2)	0.03295(3)	-0.04287(2)	2.999(8)
Zr(1)	0.22524(3)	0.14392(3)	0.23415(2)	3.059(9)
Cl(1)	0.1867(1)	-0.00768(9)	0.32219(7)	5.23(3)
O(1)	0.2083(2)	0.0227(2)	0.1399(2)	3.91(7)
O(2)	0.2353(2)	0.1736(2)	0.0979(2)	3.99(7)
O(3)	0.4026(3)	-0.0926(3)	0.0128(2)	8.0(1)
O(4)	0.0899(3)	-0.1300(3)	-0.0089(2)	8.5(1)
C(1)	0.2231(3)	0.0809(3)	0.0775(2)	3.3(1)
C(3)	0.3375(4)	-0.0456(4)	-0.0063(3)	4.7(1)
C(4)	0.1452(4)	-0.0680(4)	-0.0192(3)	4.9(1)
C(5)	0.2870(3)	0.1750(3)	-0.1031(3)	3.7(1)
C(6)	0.3139(3)	0.0932(3)	-0.1533(3)	3.7(1)
C(7)	0.2304(3)	0.0440(3)	-0.1831(2)	3.5(1)
C(8)	0.1497(3)	0.0969(4)	-0.1502(3)	3.8(1)
C(9)	0.1845(3)	0.1781(3)	-0.1023(3)	3.9(1)
C(10)	0.3522(4)	0.2533(4)	-0.0650(3)	5.9(1)
C(11)	0.4144(3)	0.0666(4)	-0.1781(3)	5.7(1)
C(12)	0.2239(4)	-0.0410(4)	-0.2438(3)	5.2(1)
C(13)	0.0473(3)	0.0768(5)	-0.1723(3)	6.2(2)
C(14)	0.1260(4)	0.2613(4)	-0.0644(3)	5.8(1)
C(15)	0.0538(3)	0.1701(4)	0.2768(4)	5.4(1)
C(16)	0.1097(4)	0.2290(4)	0.3300(3)	5.0(1)
C(17)	0.1489(3)	0.3069(3)	0.2836(3)	4.8(1)
C(18)	0.1213(4)	0.2943(4)	0.2019(3)	4.8(1)
C(19)	0.0613(3)	0.2097(4)	0.1982(3)	5.3(1)
C(20)	0.3890(4)	0.0875(4)	0.2813(7)	9.2(2)
C(21)	0.3583(4)	0.1682(7)	0.3370(3)	7.4(2)
C(22)	0.3568(4)	0.2533(5)	0.2914(5)	6.8(2)
C(23)	0.3804(4)	0.2344(6)	0.2161(5)	7.0(2)
C(24)	0.4020(4)	0.1376(6)	0.2063(5)	7.1(2)
C(25a)	0.8237(6)	0.3938(9)	0.0783(7)	8.7 ^b
C(25b)	0.7804(5)	0.3802(7)	0.0779(6)	7.3 ^b
C(26a)	0.7561(8)	0.4489(8)	0.0328(7)	7.4 ^b
C(26b)	0.7200(7)	0.4436(7)	0.0323(6)	4.5 ^b
C(27a)	0.6589(7)	0.4266(9)	0.0400(7)	9.1 ^b
C(27b)	0.6209(6)	0.4323(8)	0.0374(7)	10.9 ^b
C(28a)	0.6293(5)	0.3492(10)	0.0927(8)	10.2 ^b
C(28b)	0.5822(5)	0.3576(9)	0.0881(8)	9.7 ^b
C(29a)	0.6969(7)	0.2942(8)	0.1382(7)	8.6 ^b
C(29b)	0.6427(8)	0.2941(8)	0.1338(7)	9.6 ^b
C(30a)	0.7941(6)	0.3164(8)	0.1310(6)	5.9 ^b
C(30b)	0.7418(7)	0.3054(7)	0.1287(6)	6.6 ^b
C(31)	0.8938(9)	0.4063(9)	0.0722(6)	17.0(5)

^a $B_{eq} = \frac{8}{3} \pi^2 (U_{11}(aa^*)^2 + U_{22}(bb^*)^2 + U_{33}(cc^*)^2 + 2U_{12}aa^*bb^* \cos \gamma + 2U_{13}aa^*cc^* \cos \beta + 2U_{23}bb^*cc^* \cos \alpha)$. ^b The toluene solvate was refined as two rigid groups (a and b) with individual atomic thermal parameters.

Table 3. Selected Bond Distances (Å) and Bond Angles (deg) for 2a

Bond Distances			
C(1)–O(1)	1.285(5)	O(1)–Zr	2.221(3)
C(1)–O(2)	1.281(5)	O(2)–Zr	2.236(3)
Ru–C(1)	2.050(4)	Cl–Zr	2.518(1)
Bond Angles			
O(1)–C(1)–O(2)	113.4(3)	O(1)–Zr–Cl	77.72(8)
O(1)–Zr–O(2)	57.5(1)	O(2)–Zr–Cl	135.12(8)
Ru–C(1)–O(1)	124.7(3)		
Ru–C(1)–O(2)	121.9(3)		

IR Spectral Data. One of the few physical methods which organometallic chemists who are studying soluble metal complexes have in common with investigators in the area of heterogeneous catalysis is FTIR spectroscopy, particularly the DRIFTS¹¹ technique (diffuse reflectance infrared Fourier transform spectroscopy). With this in mind, we have developed a base of DRIFTS data over the past several years for the ν_{asym} and ν_{sym} CO₂ bands in a variety of CO₂-bridged complexes which has been correlated with our structural data on these

(10) Silver, M. E.; Eisenstein, O.; Fay, R. C. *Inorg. Chem.* **1983**, *22*, 759.

(11) Griffiths, P. W.; deHaseth, J. A. *Fourier Transform Infrared Spectroscopy*; Wiley: New York, 1986; Chapter 5.

Table 4. Atomic Positional Parameters for 2b

atom	x	y	z	B _{eq} , ^a Å ²
Re(1)	0.21757(2)	-0.18732(2)	0.13210(3)	2.317(6)
Zr(1)	0.67192(5)	-0.34841(4)	0.29417(6)	2.29(1)
Cl(1)	0.7490(2)	-0.3975(1)	0.0798(2)	4.64(4)
Cl(2)	0.5295(3)	0.1145(2)	0.0900(3)	9.72(9)
Cl(3)	0.4226(2)	0.2817(2)	0.2733(2)	6.69(6)
O(1)	0.4831(4)	-0.3086(3)	0.1154(4)	2.75(9)
O(2)	0.4732(4)	-0.2852(3)	0.3274(4)	2.73(9)
O(3)	0.3751(5)	-0.0011(3)	0.2679(6)	5.3(1)
O(4)	0.1640(5)	-0.2094(4)	-0.1795(5)	5.3(1)
N(1)	0.1969(5)	-0.1990(4)	-0.0514(6)	3.4(1)
C(1)	0.4115(5)	-0.2715(4)	0.1981(6)	2.3(1)
C(3)	0.3180(6)	-0.0717(5)	0.2150(7)	3.3(2)
C(4)	0.1513(6)	-0.1924(5)	0.3149(6)	3.0(1)
C(5)	0.0586(5)	-0.1164(4)	0.2418(6)	2.7(1)
C(6)	-0.0138(5)	-0.1648(4)	0.0947(7)	2.9(1)
C(7)	0.0355(6)	-0.2738(4)	0.0767(7)	2.8(1)
C(8)	0.1351(6)	-0.2877(4)	0.2128(7)	2.7(1)
C(9)	0.2367(7)	-0.1731(6)	0.4762(7)	4.9(2)
C(10)	0.0307(7)	-0.0060(5)	0.3097(8)	4.7(2)
C(11)	-0.1239(6)	-0.1173(5)	-0.0213(8)	4.6(2)
C(12)	-0.0184(6)	-0.3538(5)	-0.0611(7)	4.2(2)
C(13)	0.1983(7)	-0.3890(5)	0.2481(8)	4.1(2)
C(14)	0.6931(9)	-0.5406(5)	0.2201(8)	5.0(2)
C(15)	0.8057(7)	-0.5144(6)	0.344(1)	5.2(2)
C(16)	0.7642(9)	-0.4697(6)	0.4614(8)	5.6(2)
C(17)	0.6222(9)	-0.4656(5)	0.407(1)	5.2(2)
C(18)	0.5788(7)	-0.5093(5)	0.2569(9)	4.8(2)
C(19a)	0.738(2)	-0.173(1)	0.324(2)	3.5(3)
C(19b)	0.701(1)	-0.1600(7)	0.372(2)	2.7 ^b
C(20a)	0.867(2)	-0.242(1)	0.369(2)	2.8(2)
C(20b)	0.815(2)	-0.211(1)	0.336(1)	3.4 ^b
C(21a)	0.883(1)	-0.2722(9)	0.499(2)	2.3(2)
C(21b)	0.8943(9)	-0.2693(9)	0.438(2)	4.8 ^b
C(22a)	0.765(2)	-0.222(1)	0.537(1)	2.2(2)
C(22b)	0.829(2)	-0.255(1)	0.537(1)	5.4 ^b
C(23a)	0.681(1)	-0.160(1)	0.435(2)	2.6(2)
C(23b)	0.710(2)	-0.187(1)	0.496(2)	3.7 ^b
C(24)	0.5133(8)	0.2440(6)	0.1590(8)	5.5(2)

^a See footnote a in Table 2. ^b Atoms were refined as a rigid group with individual atomic thermal parameters.

Table 5. Selected Bond Distances (Å) and Bond Angles (deg) for 2b

Bond Distances			
C(1)-O(1)	1.296(8)	O(1)-Zr	2.201(3)
C(1)-O(2)	1.271(7)	O(2)-Zr	2.245(4)
Re-C(1)	2.097(5)	Cl-Zr	2.525(2)
Bond Angles			
O(1)-C(1)-O(2)	113.9(4)	O(1)-Zr-Cl	77.7(1)
O(1)-Zr-O(2)	57.9(2)	O(2)-Zr-Cl	135.5(1)

compounds.^{11,m,u,v} Thus, compounds having μ_2 - η^2 -CO₂ ligands show these bands near 1500 and 1140 cm⁻¹. The unsymmetrical μ_2 - η^3 complexes which have been characterized to date all have the carboxyl oxygens bound to a trigonal-bipyramidal tin center and show the ν_{asym} and ν_{sym} bands near 1430 and 1140 cm⁻¹, respectively. The symmetrical analogs have involved two late transition metals in each case, but the metal binding the carboxyl oxygens has always been an octahedral Re center. This group of compounds shows the higher frequency CO₂ band near 1435 cm⁻¹, while the position of the second band varies with the metalcarboxylate system: compounds derived from CpFe(CO)(PPh₃)-CO₂^{1m,u} show the band near 1250 cm⁻¹, whereas the one derived from Cp*Re(CO)(NO)CO₂^{1r} shows the band near 1280 cm⁻¹.

From a structural perspective, compound 2b is clearly of the symmetrical μ_2 - η^3 type. Also, in DRIFTS spectra, the ν_{sym} band for the CO₂ ligand in the compound is found at 1288 cm⁻¹ in agreement with other compounds

of the symmetrical type derived from the same rhenium metalcarboxylate; for example, Cp*Re(CO)(NO)(CO₂)-Re(CO)₃(PPh₃)^{1r} shows this band at 1282 cm⁻¹. However, compound 2b shows the ν_{asym} band at 1350 cm⁻¹, while the bis-rhenium complex shows this band at 1437 cm⁻¹ in the manner of other symmetrical complexes derived from two late transition metals. Additionally, the closely related zirconium (and titanium) complexes prepared by Cutler, for which isotopic labeling studies have been done to assist in making IR band assignments,^{1k} also show the ν_{asym} bands in the 1350 cm⁻¹ region. The corresponding DRIFTS spectra for 2a show analogous bands at 1339 and 1287 cm⁻¹. We were puzzled by the difference in the IR data from the two groups of symmetrical compounds until recently, when we prepared and structurally characterized another μ_2 - η^3 complex derived from the same rhenium metalcarboxylate, Cp*Re(CO)(NO)(CO₂)Mo(CO)₂Cp. This compound has highly symmetrical bonding of the CO₂ ligand but shows square-based-pyramidal geometry about the Mo atom.^{3,12} The latter compound shows the two characteristic stretching bands for the CO₂ ligand at 1319 and 1280 cm⁻¹. Thus, it is now clear that the position of the ν_{sym} band in the μ_2 - η^3 -CO₂ complexes is determined by the symmetrical or unsymmetrical nature of the bonding of the CO₂ ligand while the ν_{asym} band position depends, primarily, on the coordination geometry at the metal center binding the two oxygens. The reasons for the dependence of ν_{asym} on these structural parameters are not yet apparent.

Compounds 3a,b and 5a,b follow the same pattern for these CO₂ bands as the other zirconium complexes and are also formulated with symmetrical μ_2 - η^3 bonding of the CO₂ ligand in each case: 3a shows bands at 1341 and 1285 cm⁻¹ and 3b shows bands at 1340 and 1288 cm⁻¹, while the trimetallic compounds 5a,b show the bands at 1339 and 1265 cm⁻¹ and 1336 and 1275 cm⁻¹, respectively. The new tin complex 4 shows these CO₂ bands at 1464 and 1171 cm⁻¹, as is typical for unsymmetrical μ_2 - η^3 complexes having the two carboxyl oxygens bound to tin.^{1v}

Experimental Section

General Data. Reactions and manipulations were carried out under an atmosphere of prepurified nitrogen in Schlenkware or in a Vacuum Atmospheres glovebox (with Dri-train). All glassware was dried in the oven before use. The reagent grade solvents dichloromethane and chloroform were used as received. Benzene, toluene, and hexane were dried over concentrated sulfuric acid and fractionally distilled before use. Solvents used in the glovebox were distilled under nitrogen from the following drying agents: sodium benzophenone ketyl for tetrahydrofuran (THF) and ether; P₂O₅ for dichloromethane, pentane, hexane, benzene, and toluene. Triphenyltin chloride, triphenylstannane, Cp₂Zr(H)(Cl), and benzene-*d*₆ were obtained from Aldrich; dichloromethane-*d*₂ was obtained from Cambridge Isotope Laboratories or Aldrich. Cp*Re(CO)(NO)COOH,^{1r} Cp*Ru(CO)₃+BF₄⁻,¹³ Cp*Ru(CO)₂-COOH,⁴ Cp*Re(CO)(NO)(CO₂)SnPh₃,^{1r} Cp₂Zr(H)(Me),⁸ Cp₂Zr(Cl)(Me),⁹ Cp₂Zr(Me)₂,⁶ and Cp₂Zr(OMe)(Me)⁵ were prepared as described previously. Spectral data were obtained on the following instruments: FT-NMR, Bruker AMX-500; FT-IR, Mattson Galaxy series 5000. Diffuse reflectance FT-IR data were obtained on the Mattson instrument with a DRIFTS

(12) (a) Gibson, D. H.; Franco, J. O.; Mehta, J. M.; Mashuta, M. S.; Richardson, J. F. *Organometallics*, in press.

accessory (Spectra Tech, Inc., Barnes Analytical Division) as KCl dispersions and at 1 cm⁻¹ resolution. ¹H and ¹³C NMR chemical shifts were referenced to residual protons in the deuterated solvents. Melting points were obtained on a Thomas-Hoover capillary melting point apparatus and are uncorrected. Elemental analyses were performed by Midwest Microlab, Indianapolis, IN.

CpRu*(CO)₂(CO₂)Zr(Cl)Cp₂ (2a).** (a) In a Schlenk flask under N₂, Cp**Ru*(CO)₃⁺BF₄⁻ (1.00 g, 2.46 mmol) was dissolved in ca. 20 mL of CH₂Cl₂. To this vigorously stirred solution was added ca. 4–5 mL of a saturated aqueous solution of Na₂CO₃. The mixture was stirred until IR spectral monitoring indicated that the cation had been completely converted to Cp**Ru*(CO)₂COOH (ca. 1 h). The CH₂Cl₂ layer was then separated, and the aqueous layer was extracted with CH₂Cl₂ (3 × 5 mL). The combined CH₂Cl₂ fractions were dried over MgSO₄ and filtered. To this solution was added Cp₂Zr(H)(Cl) (0.6 g, 2.33 mmol), which was stirred for ca. 30 min. The solvent was removed under vacuum, and the residue was extracted with toluene, filtered, and concentrated. The product was precipitated from solution with hexane, affording 0.87 g (63% yield) of a white solid, mp 125 °C dec.

Anal. Calcd for C₂₃H₂₅ClO₄RuZr: C, 46.57; H, 4.25. Found: C, 46.84; H, 4.32. IR (DRIFTS): ν_{CO} 2020 (s), 1969 (s) cm⁻¹; ν_{OCO} 1339 (w), 1287 (m) cm⁻¹. ¹H NMR (C₆D₆): δ 6.10 (s, 10H), 1.61 (s, 15H). ¹³C NMR (C₆D₆): δ 220.41 (s, CO₂), 201.58 (s, CO), 114.15 (s), 101.48 (s), 9.90 (s).

(b) In a glovebox, Cp**Ru*(CO)₂(CO₂)SnPh₃ (1.38 g, 2.01 mmol) and Cp₂Zr(Cl)(Me) (0.55 g, 2.01 mmol) were dissolved in ca. 25 mL of toluene. The solution was stirred for 1 h and concentrated under vacuum. The product was precipitated from solution with hexane, affording 0.86 g (72% yield) of a white solid. Also formed was MeSnPh₃, which was identified by comparison of its ¹H and ¹³C NMR spectra with those of an authentic sample.¹⁴

CpRe*(CO)(NO)(CO₂)Zr(Cl)Cp₂ (2b).** Cp*(CO)(NO)-ReCOOH (0.20 g, 0.47 mmol) and Cp₂Zr(H)(Cl) (0.10 g, 0.39 mmol) were stirred in toluene (30 mL) at room temperature for 1 h. The resulting clear orange solution was then concentrated to 10 mL under vacuum. Pentane (40 mL) was added to induce precipitation of the product as a yellow solid. Recrystallization of this yellow solid with toluene–pentane (1:6, v/v) gave yellow crystals of the title compound (0.48 g, 69%), mp 146 °C.

Anal. Calcd for C₂₂H₂₅ClNO₄ReZr: C, 38.84; H, 3.70. Found: C, 38.69; H, 3.68. IR (DRIFTS): ν_{CO} 1969 (s); ν_{NO} 1707 (s); ν_{OCO} 1348 (w), 1288 (m) cm⁻¹. ¹H NMR (C₆D₆): δ 6.16 (s, 5H), 6.14 (s, 5H), 1.66 (s, 15H). ¹³C NMR (C₆D₆): δ 217.91 (s, CO₂), 207.67 (s, CO), 114.26 (s), 114.20 (s), 105.03 (s), 9.90 (s).

CpRu*(CO)₂(CO₂)Zr(Me)Cp₂ (3a).** In a Schlenk flask under N₂, Cp**Ru*(CO)₃⁺BF₄⁻ (0.31 g, 0.76 mmol) was dissolved in ca. 20 mL of CH₂Cl₂. To this vigorously stirred solution was added ca. 4–5 mL of a saturated aqueous solution of Na₂CO₃. The mixture was stirred until IR spectral monitoring indicated that the cation had been completely converted to Cp**Ru*(CO)₂COOH (ca. 1 h). The CH₂Cl₂ layer was then separated, and the aqueous layer was extracted with CH₂Cl₂ (3 × 5 mL). The combined CH₂Cl₂ fractions were dried over MgSO₄ and filtered. To this solution was added Cp₂Zr(Me)-(OMe) (0.20 g, 0.75 mmol), and the mixture was stirred for ca. 30 min. Solvent was removed under vacuum, and the residue was extracted with toluene and then filtered and concentrated. The product was precipitated from this solution with hexane, affording 0.29 g (67% yield) of a pale yellow solid, mp 128 °C dec.

Anal. Calcd for C₂₄H₂₈O₄RuZr: C, 50.32; H, 4.93. Found: C, 50.15; H, 4.91. IR (DRIFTS): ν_{CO} 2014 (s), 1956 (s) cm⁻¹; ν_{OCO} 1341 (w), 1285 (m) cm⁻¹. ¹H NMR (C₆D₆): δ 5.88 (s, 10H), 1.61 (s, 15H, Cp* Me), 0.39 (s, 3H, Zr–Me). ¹³C NMR (C₆D₆):

δ 218.04 (s, CO₂), 201.79 (s, CO), 110.71 (s), 101.04 (s), 30.09 (s, Zr–Me), 9.91 (s, Cp* Me).

CpRe*(CO)(NO)(CO₂)Zr(Me)Cp₂ (3b).** Cp*(CO)(NO)-ReCOOH (0.50 g, 1.18 mmol) and Cp₂Zr(Me)₂ (0.30 g, 1.18 mmol) were slurried in ether (30 mL). The mixture was stirred at room temperature for 2 h, during which time the solution became clear. The dark red solution was then concentrated to 10 mL under vacuum. Pentane (30 mL) was added to induce precipitation of Cp*(CO)(NO)ReCOOZr(Me)Cp₂ as a light orange solid. The solid was recrystallized from ether–pentane (1:3, v/v) to give an analytically pure, light yellow powder (0.65 g, 85% yield), mp 149 °C.

Anal. Calcd for C₂₃H₂₅NO₄ReZr: C, 41.86; H, 4.28. Found: C, 41.98; H, 4.35. IR (DRIFTS): ν_{CO} 1969 (s); ν_{NO} 1697 (s); ν_{OCO} 1340 (w), 1288 (m) cm⁻¹. ¹H NMR (C₆D₆): δ 5.94 (s, 5H), 5.92 (s, 5H), 1.66 (s, 15H, Cp* Me) and 0.40 (s, 3H, Zr–Me). ¹³C NMR (C₆D₆): δ 216.14 (s, CO₂), 208.67 (s, CO), 110.79 (s), 104.54 (s), 30.31 (s, Zr–Me), 9.89 (s, Cp* Me).

CpRu*(CO)₂(CO₂)SnPh₃ (4).** In a Schlenk flask under nitrogen, Cp**Ru*(CO)₃⁺BF₄⁻ (0.40 g, 0.98 mmol) and Ph₃SnCl (0.38 g, 1.00 mmol) were dissolved in ca. 20 mL of CH₂Cl₂. KOH (0.5 mL of a 4 M solution) was quickly added to the vigorously stirred solution. The mixture was stirred for another 15 min, and the CH₂Cl₂ layer was separated. The aqueous layer was extracted with CH₂Cl₂ (3 × 5 mL), and the combined CH₂Cl₂ fractions were dried over MgSO₄. The mixture was then filtered, and the solvent was removed on a rotary evaporator. The residue was extracted with toluene, which was then filtered and concentrated under vacuum. The product was precipitated from solution with hexane, affording 0.56 g (84% yield) of an off-white solid, mp 123 °C dec.

Anal. Calcd for C₃₁H₃₀O₄RuSn: C, 54.24; H, 4.41. Found: C, 53.94; H, 4.30. IR (DRIFTS): ν_{CO} 2025 (s), 1956 (s) cm⁻¹; ν_{OCO} 1464 (w), 1171 (m) cm⁻¹. ¹H NMR (C₆D₆): δ 7.59 (m, 15H), 1.54 (s, 15H). ¹³C NMR (CD₂Cl₂): δ 204.79 (s, CO₂), 201.31 (s, CO), 142.23 (s), 142.29 (d, J_{SnC} = 608.7 Hz), 142.18 (d, J_{SnC} = 610.5 Hz), 137.16 (s; d, J_{SnC} = 47.8 Hz), 129.52 (s), 128.76 (s; d, J_{SnC} = 60.4 Hz), 101.55 (s), 10.30 (s). With this compound the δ and J values for the two active isotopes of Sn are different for the ipso phenyl carbon.

CpRu*(CO)₂(CO₂)Zr(SnPh₃)Cp₂ (5a).** In a glovebox, Cp**Ru*(CO)₂(CO₂)SnPh₃ (0.32 g, 0.47 mmol) and Cp₂Zr(Me)-(H) (0.13 g, 0.55 mmol) were added to ca. 25 mL of toluene. The mixture was stirred for 3 h, filtered, and concentrated under vacuum. The product was precipitated by adding hexane, affording 0.34 g (80% yield) of a pale yellow solid, mp 170 °C dec.

Anal. Calcd for C₄₁H₄₀O₄RuSnZr: C, 54.25; H, 4.44. Found: C, 54.53; H, 4.46. IR (DRIFTS): ν_{CO} 2021 (s), 1981 (s) cm⁻¹; ν_{OCO} 1339 (w), 1265 (m) cm⁻¹. ¹H NMR (C₆D₆): δ 7.68 (m, 15H), 5.97 (s; d, J_{SnH} = 6.9 Hz; 10H), 1.46 (s, 15H). ¹³C NMR (CD₂Cl₂): δ 227.73 (s, CO₂), 201.11 (s, CO), 151.83 (s; d, J_{SnC} = 93.1 Hz), 138.10 (s; d, J_{SnC} = 30.1 Hz), 128.00 (s; d, J_{SnC} = 24.9 Hz), 127.00 (s), 108.23 (s, d, J_{SnC} = 100.2 Hz), 101.42 (s), 10.25 (s). Only one J_{SnC} value is observed in each case.

CpRe*(CO)(NO)(CO₂)Zr(SnPh₃)Cp₂ (5b).** In a glovebox, Cp₂Zr(H)(Me) (0.10 g, 0.46 mmol) was stirred vigorously in 30 mL of toluene, and the mixture was cooled to 10 °C. Then, Cp*(CO)(NO)ReCOOSnPh₃ (0.20 g, 0.26 mmol) dissolved in 10 mL of toluene was added over 20 min. Stirring was continued for 2 h at 10 °C and for 30 min at 23 °C. The mixture was then filtered and the filtrate concentrated until the solution became cloudy. A layer of hexane was added (10 mL) and the mixture cooled to –20 °C. The resulting precipitate was isolated by filtration and dried under vacuum (0.10 g); another 0.08 g was isolated after the filtrate was concentrated (total yield 70%): mp 180 °C dec.

Anal. Calcd for C₄₀H₄₀NO₄ReSnZr: C, 48.29; H, 4.05. Found: C, 47.96; H, 4.15. IR (DRIFTS): ν_{CO} 1982 (s); ν_{NO} 1724 (s); ν_{OCO} 1336 (w), 1275 (m) cm⁻¹. ¹H NMR (C₆D₆): δ 7.60 (m, 15H), 6.02 (s, 5H), 6.00 (s, 5H), 1.50 (s, 15H). ¹³C NMR (CD₂-

(13) Nelson, G. O. *Organometallics* **1983**, *2*, 1474.

(14) Al-Allaf, T. A. K. *J. Organomet. Chem.* **1986**, *306*, 337.

Cl₂): δ 224.13 (s; d, $J_{\text{SnC}} = 65.3$ Hz, CO₂), 207.16 (s, CO), 151.64 (s; d, $J_{\text{SnC}} = 89.8$ Hz), 138.11 (s; d, $J_{\text{SnC}} = 30.5$ Hz), 128.02 (s; d, $J_{\text{SnC}} = 25.4$ Hz), 127.02 (s), 108.39 (s), 108.36 (s), 105.18 (s), 10.29 (s). Only one J_{SnC} value is observed in each case.

Attempted Reaction of Cp*Ru(CO)₂(CO₂)Zr(Me)Cp₂ (3a) with Ph₃SnH. In a glovebox, **3a** (0.20 g, 0.35 mmol) and Ph₃SnH (0.13 g, 0.37 mmol) were dissolved in ca. 20 mL of toluene. The solution was allowed to stand for 2 h, and then the solvent was removed under vacuum. ¹H NMR analysis of the residue showed only unreacted starting materials.

Attempted Reaction of Cp*(CO)(NO)Re(CO₂)Zr(Me)-Cp₂ (3b) with Ph₃SnH. In a glovebox, Ph₃SnH (58 mg, 0.15 mmol) and **3b** (0.10 g, 0.15 mmol) were dissolved in toluene and the mixture was allowed to stand for 2 h. The solution was then evaporated to dryness and the residue taken up in benzene-*d*₆. Analysis of NMR spectral data indicated only the two starting materials.

X-ray Crystal Structure of 2a. A suitable crystal was grown by cooling a toluene solution of **2a** at -30 °C for 5 days. Data were collected on an Enraf-Nonius CAD4 diffractometer at 23 °C; the crystallographic data are outlined in Table 1. Selected bond distances and bond angles are shown in Table 3. Of 6787 unique reflections, 4871 were considered observed ($I > 3\sigma(I)$). The structure was solved using Patterson methods and refined with anisotropic thermal parameters for all non-hydrogen atoms except for the disordered toluene carbon atoms (see below). The calculated positions and thermal parameters for the H atoms were kept constant with temperature factors set to 1.2 times those of the carbon atoms to which they are bonded. The complex contains one molecule of toluene solvate. Its disorder was adequately modeled using two half-occupancy C₆H₅ phenyl groups and a common methyl carbon atom. Both aromatic fragments of the solvate, C(25a)–C(30a) and C(25b)–C(30b), were refined as rigid groups with individual isotropic thermal parameters. A final R index of 0.037 with $R_w = 0.039$ was obtained for 335 variables. All computations were performed using the teXsan¹⁵ package (Molecular Structure Corp.).

X-ray Crystal Structure of 2b. A suitable crystal was grown by layering a saturated CH₂Cl₂ solution of **2b** with hexane and then cooling the sample to -30 °C. Data were collected on an Enraf-Nonius CAD4 diffractometer; the data

are outlined in Table 1. Selected bond distances and bond angles are shown in Table 5. Of 4667 unique reflections, 4371 were considered observed ($I > 3\sigma(I)$). The structure was solved using Patterson methods and refined with anisotropic thermal parameters for all non-hydrogen atoms, except for the disordered Cp carbon atoms (see below), while the calculated positions and thermal parameters for the H atoms were kept constant. The temperature factors of the hydrogen atoms were set to 1.2 times the temperature factors of the carbon atoms to which they were bonded. The complex contains one molecule of methylene chloride solvate. One cyclopentadienyl ring bonded to the zirconium atom was found to be disordered. It was satisfactorily modeled with two half-occupancy cyclopentadienyl groups. The first group, C(19a)–C(23a), was refined as individual isotropic atoms while the second fragment, C(19b)–C(23b), was refined as a rigid group with individual isotropic thermal parameters. A final R index of 0.027 with $R_w = 0.029$ was obtained for 265 variables. All computations were performed using the teXsan package (Molecular Structure Corp.).¹⁵

Acknowledgment. Support of this work by the United States Department of Energy, Division of Chemical Sciences (Office of Basic Energy Sciences), is gratefully acknowledged. The X-ray equipment was purchased with assistance from the National Science Foundation (Grant No. CHE-9016978). Support of the Molecular Structure Laboratory through the NSF/KY EPSCoR program (Grant No. EHR-9108764) is also gratefully acknowledged. B.A.S. gratefully acknowledges support from a GAANN Fellowship from the United States Department of Education (Grant No. P200A10139). We thank Deborah Freedman for assistance in the structure determination of **4**.

Supporting Information Available: Tables of anisotropic thermal parameters, H atom positional parameters, bond distances, bond angles, and torsional angles for **2a,b** (13 pages). This material is contained in many libraries on microfiche, immediately follows this article in the microfilm version of the journal, and can be ordered from the ACS; ordering information is given on any current masthead page.

(15) teXsan: Single Crystal Structure Analysis Software, Version 1.6 (1993); Molecular Structure Corp., The Woodlands, TX 77381.

Synthesis and Characterization of Ru₃ and Ru₄ Clusters with Isopropenylbenzene and Diisopropenylbenzene Ligands

Dario Braga,* Janice J. Byrne, Fabrizia Grepioni, and Emilio Parisini

Dipartimento di Chimica G. Ciamician, Università di Bologna, Via Selmi 2, 40126 Bologna, Italy

Paul J. Dyson, Petra E. Gaede, Brian F. G. Johnson,* and David Reed

Department of Chemistry, The University of Edinburgh, West Mains Road, Edinburgh, EH9 3JJ, U.K.

Received May 9, 1995[⊗]

The four clusters Ru₃(CO)₇(μ₃-η²:η²:η²-C₆H₄-{η²-CCH₃CH₂})_{2-1,3}, **1**, Ru₄(CO)₉(μ₃-η²:η²:η²-C₆H₄-{η²-CCH₃CH₂})_{2-1,3}, **2**, Ru₃(CO)₈(μ₃-η²:η²:η²-C₆H₅-{η²-CCH₃CH₂}), **3**, and Ru₄(CO)₁₀(μ₃-η²:η²:η²-C₆H₅-{η²-CCH₃CH₂}), **4**, have been prepared and characterized both spectroscopically and by means of single-crystal X-ray diffraction. The presence of the propenyl substituent(s) on the aromatic ligands results in the observed preference of the rings toward a facial coordination mode, formally donating all their π-electrons to the metal cluster unit.

Introduction

Arene cluster chemistry has emerged as an important area of modern organometallic cluster chemistry. Clusters of nuclearity between three and eight are known in which one or more arene ligands are present,¹ and much of the current interest arises from the analogy between the interaction of arenes with polynuclear metal complexes and that with metal surfaces.² As a result of a detailed study of the interaction of arene ligands with ruthenium and osmium clusters, which has provided to date a large number of mono- and bis-substituted arene-cluster compounds, it has been established that, in general, aromatic rings show a preference toward the two basic bonding modes: the terminal (η⁶) or the face-capping (μ₃-η²:η²:η²) arrangement. Although the interconversion of these two bonding types has been observed in some cases as a consequence of changes in the experimental conditions, the factors influencing the choice of a specific bonding arrangement remain obscure. Extended-Hückel calculations have shown that in the cases of the isomeric pairs Ru₅C(CO)₁₂(η⁶-C₆H₆) and Ru₅C(CO)₁₂(μ₃-C₆H₆) and Ru₆C(CO)₁₁(η⁶-C₆H₆)₂ and Ru₆C(CO)₁₁(η⁶-C₆H₆)(μ₃-C₆H₆) the apical isomers are the more thermodynamically stable, although the benzene ruthenium interaction is stronger in the facial isomers.³ We are now expanding the chemistry of arene clusters by employing substituted arenes carrying unsaturated side chains such as isopropenyl groups.

At the time of our first report of the molecular structures of the tetrahedral cluster species Ru₄(CO)₉(μ₃-η²:η²:η²-C₆H₄-{η²-CCH₃CH₂})_{2-1,3}, **2**, and Ru₄(CO)₁₀

(μ₃-η²:η²:η²-C₆H₅-{η²-CCH₃CH₂}), **4**,⁴ no other examples of metal clusters bearing the 1,3-diisopropenylbenzene or isopropenylbenzene ligands were known. These two closely related structures were found to be the only examples of six-membered rings attached to a tetranuclear cluster in the facial coordination mode. Face-capping arenes have been previously introduced into clusters (or clusters assembled on the arene) in species with nuclearity of three (Ru,^{5a} Os,^{5b} Co,^{5c} and Rh^{5d}), five (Ru⁶), and six (Ru^{7a} and Os^{7b}).

In this paper we finish the series by reporting on the preparation and the structural characterization of the isopropenylbenzene and 1,3-diisopropenylbenzene face-capping derivatives based on the Ru₃ and Ru₄ cluster units. The π interaction of the side arm(s) with the nearest metal atom is thought to stabilize the facial with respect to the (hypothetical) terminal isomer. The large variety of structural analogies for all the reported compounds is taken as an indication of the major contribution of the unsaturated substituent on the ring to the observed bonding arrangement.

We are also interested in the investigation of the intermolecular interactions in crystalline clusters and complexes.⁸ In particular, we have recently found that carbonyl and arene ligands tend to form intermolecular hydrogen bond links of the C-H···O type. In arene clusters the donor atom is usually an arene carbon while

(4) Braga, D.; Grepioni, F.; Parisini, E.; Dyson, P. J.; Ingham, S. L.; Johnson, B. F. G.; Blake, A. *J. Chem. Soc., Chem. Commun.* **1995**, 537.

(5) (a) Braga, D.; Grepioni, F.; Johnson, B. F. G.; Lewis, J.; Housecroft, C. E.; Martinelli, M. *Organometallics* **1991**, *10*, 1260. (b) Gallop, M. A.; Gomez-Sal, M. P.; Housecroft, C. E.; Johnson, B. F. G.; Lewis, J.; Owen, S. M.; Raithby, P. R.; Wright, A. H. *J. Am. Chem. Soc.* **1992**, *114*, 2502. (c) Wadepohl H.; Büchner, K.; Herrmann, M.; Pritzkow, H. *Organometallics* **1991**, *10*, 861. (d) Müller, J.; Gaede, P. E.; Qiao, K. *Angew. Chem., Int. Ed. Engl.* **1993**, *32*, 1697.

(6) Braga, D.; Sabatino, P.; Dyson, P. J.; Blake, A. J.; Johnson, B. F. G. *J. Chem. Soc., Dalton Trans.* **1994**, 393.

(7) (a) Dyson, P. J.; Johnson, B. F. G.; Lewis, J.; Martinelli, M.; Braga, D.; Grepioni, F. *J. Am. Chem. Soc.* **1993**, *115*, 9062. (b) Lewis, J.; Li C.-K.; Raithby, P. R.; Wong, W.-T. *J. Chem. Soc., Dalton Trans.* **1993**, 999.

(8) Braga, D.; Grepioni, F. *Acc. Chem. Res.* **1994**, *27*, 51.

[⊗] Abstract published in *Advance ACS Abstracts*, September 1, 1995.

(1) Braga, D.; Dyson, P. J.; Grepioni, F.; Johnson, B. F. G. *Chem. Rev.* **1994**, *94*, 1585.

(2) Samorjai, G. A. *The Building of Catalysts: a Molecular Surface Science Approach*. In *Catalyst Design-Progress and Perspectives*; Hegedus, L. L., Ed.; John Wiley & Sons: New York, 1987.

(3) Braga, D.; Dyson, P. J.; Grepioni, F.; Johnson, B. F. G.; Calhorda, M. J. *Inorg. Chem.* **1994**, *33*, 3218.

Table 1. ¹H NMR Spectrum Assignment for Species 1

signal label	1	2	3	4
A	0.56	0.28	4.75	4.36
B	0.87	0.55	0.88	0.85
C	1.35	1.37	1.56	1.56
D	1.46	1.49		
E	1.52	1.72	1.64	1.15
F	1.85	1.87		
G	2.84	2.94		
H	3.07	3.33	2.94	3.05
J	5.59	5.22	4.85	4.74
K	6.19	5.47	4.99	4.76
L			5.21	5.23

the acceptor is the O-atom of the CO ligands with a clear-cut preference for ligands in bridging bonding modes.⁹ The crystal structures of the four species discussed in this paper offer an interesting opportunity to study the hydrogen bonding network in arene clusters.

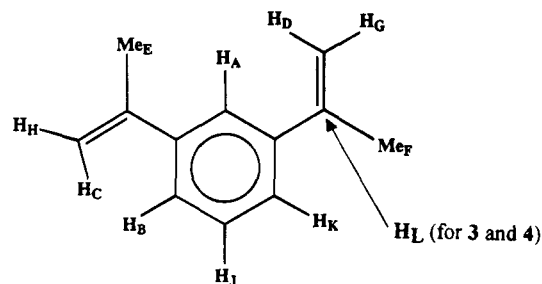
Results and Discussion

The reaction of Ru₃(CO)₁₂ with 1,3-diisopropenylbenzene in octane at reflux temperature for 1.5 h results in a dark brown solution. Separation of the products from this solution may be achieved by chromatography on silica, eluting with a solution of 20% dichloromethane-hexane. A variety of products may be isolated, the majority in very low yield. However, two compounds are obtained in reasonable yield, these being, in order of elution, a red and a red/brown compound with low *R_f* values and only just resolvable into separate bands. These were extracted into dichloromethane and subsequently characterized as Ru₃(CO)₇(μ₃-η²:η²:η²-C₆H₄-{η²-CCH₃CH₂})₂-1,3, **1**, and Ru₄(CO)₉(μ₃-η²:η²:η²-C₆H₄-{η²-CCH₃CH₂})₂-1,3, **2**, respectively.

The mass spectrum of **1** contains a parent ion at 659 (calc 658) amu and is followed by a series of peaks corresponding to the loss of carbonyl ligands which is typical for these types of clusters. A similar spectrum is obtained for **2**, with a parent peak observed at 815 (calc 815) amu.

The ¹H NMR spectra of compounds **1**-**4** were recorded in CDCl₃; the signals are listed in Table 1. Assignments of these spectra were made using decoupling and *n*Oe techniques. The ¹H NMR spectrum of compound **1** will be described in detail, while the precise assignments of compounds **2**-**4** can be appreciated from Table 1, which corresponds to Figure 1.

The ¹H NMR spectrum of **1** indicates that the diisopropenylbenzene ligand is asymmetrically bound to the cluster (see Figure 1) producing 10 signals labeled A-K. Decoupling at signal J affects K and B, with each losing a *ca.* 7 Hz coupling, and decoupling at signal K removes a 7 Hz coupling from J and couplings of *ca.* 1.5 Hz from each of A and B. Hence, A, B, J and K all arise from the "aromatic" protons, with J ascribable to H(91) and A to H(121) on the basis of the coupling constants to each. Integration shows that signals E and F arise from the protons of the methyl groups. The remaining signals (C, D, G, and H) derive from the alkenic protons,

**Figure 1.** Assignment of the ¹H NMR spectrum of **1**.

with decoupling experiments showing signals C and H arising from geminal protons as do signals D and G.

Irradiation at signal E resulted in the enhancement of signal A and signal H, whereas irradiation at F caused enhancement of G and K. Hence, as signal A arises from H(121), then E is due to Me(31) and signal H to the proton *cis* to the methyl group on C(11). Consequently, signal F arises from Me(61) with K being due to H(101) and G from the proton [H(41)] *cis* to Me(61). It is also worth commenting on the frequencies at which the aromatic resonances are observed. Two C-H resonances at δ 6.19 (K) and 5.59 (J) are higher than usual for C-H resonances of a μ_3 -bound ring [cf. Ru₃(CO)₉(μ₃-η²:η²:η²-C₆H₆), δ = 4.56 ppm].⁴ However, two C-H resonances occur at very low frequencies, these being δ 0.87 (B) and 0.56 (A). Comparing the C-H resonance of proton A with that observed in the free ligand, a change of about 7 ppm has taken place. This "additional" shielding must be due to not only metal-induced anisotropy but also the position of these protons in ring currents from the arene ring itself as well as from that of the double bond on the pendant-arm.

Isopropenylbenzene has been reacted with Ru₃(CO)₁₂ in an analogous manner to diisopropenylbenzene, and two compounds, **3** and **4**, closely related to **1** and **2** have been identified, *albeit* in lower yield. These compounds were characterized as Ru₃(CO)₈(μ₃-η²:η²:η²-C₆H₅-{η²-CCH₃CH₂})₂, **3**, and Ru₄(CO)₁₀(μ₃-η²:η²:η²-C₆H₅-{η²-CCH₃CH₂})₂, **4**. The mass spectrum of **3** and **4** exhibit parent peaks at 644 (calc 645) and 802 (calc 803) amu, respectively, together with peaks corresponding to the sequential loss of several carbonyl ligands. The ¹H NMR spectra of **3** and **4** were described above (see Table 1 and Figure 1).

Molecular Structures in the Solid State. The molecular structures of species **1**-**4** are shown in Figures 2a and 3-5, respectively. A simplified model of the disorder shown by **1** in its crystal (see below) is shown in Figure 2b. Relevant structural parameters for the four molecules are listed in Table 2-5.

The Ru-Ru bond distances in the triangular metal cluster of **3** range from 2.798(3) to 2.865(3) Å, and a comparable bond length distribution is found in the two different orientations of the trimetallic unit for the disordered crystalline form of **1** [2.769(6)-2.900(2) Å]. The metal-metal bond lengths in the tetrahedral arrangements of the four ruthenium atoms in compounds **2** and **4** fall in the ranges 2.662(2)-2.882(2) and 2.6829(12)-2.9082(12) Å, respectively. An enhanced similarity between the average intermetallic distances in the trinuclear and in the tetranuclear clusters may be obtained by considering only the metal atoms involved in the coordination of the ring systems, the

(9) (a) Braga, D.; Grepioni, F.; Biradha, R.; Pedireddi, V. R.; Desiraju, G. R.; *J. Am. Chem. Soc.* **1995**, *117*, 3156. (b) Braga, D.; Grepioni, F.; Wadepohl, H.; Gebert, S.; Calhorda, M. J.; Veiros, L. F. *Organometallics*, in press. (c) Braga, D.; Grepioni, F.; Calhorda, M. J.; Veiros, L. F. *Organometallics* **1995**, *14*, 121.

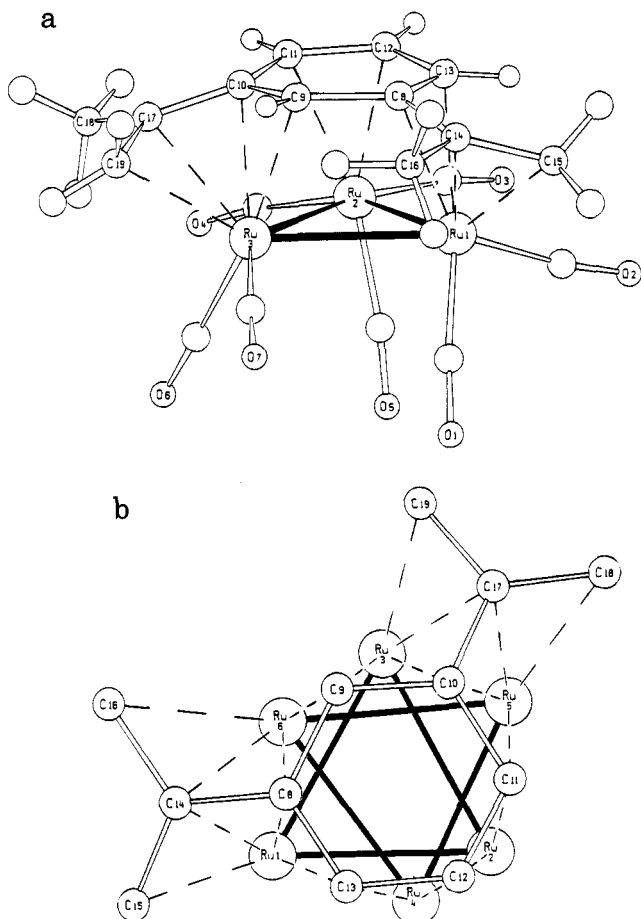


Figure 2. (a) Molecular structure of $\text{Ru}_3(\text{CO})_7(\mu_3\text{-}\eta^2\text{:}\eta^2\text{:}\eta^2\text{-C}_6\text{H}_4\text{-}\{\eta^2\text{-CCH}_3\text{CH}_2\}_2\text{-1,3})$, **1** (major image), in the solid state. The C atoms of the CO ligands bear the same numbering as the corresponding O atoms. (b) Simplified model of the disordered molecular structure of **1** in the solid state. The CO ligands are omitted for clarity. The atoms Ru(1), Ru(2), and Ru(3) belong to the major image, whereas Ru(4), Ru(5), and Ru(6) belong to the minor one.

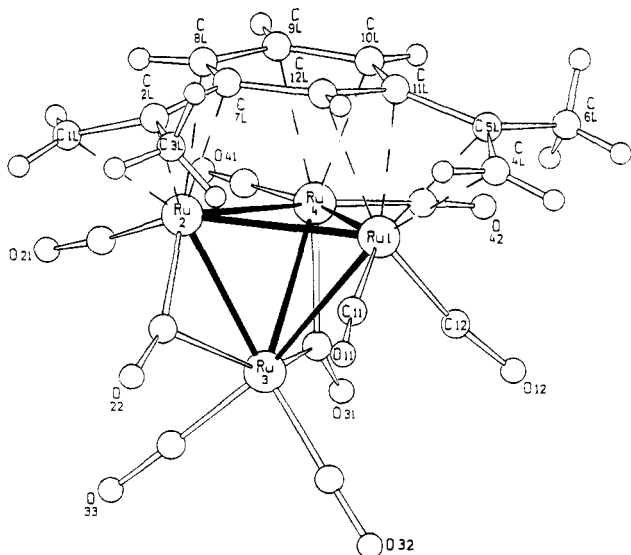


Figure 3. Molecular structure of $\text{Ru}_4(\text{CO})_9(\mu_3\text{-}\eta^2\text{:}\eta^2\text{:}\eta^2\text{-C}_6\text{H}_4\text{-}\{\eta^2\text{-CCH}_3\text{CH}_2\}_2\text{-1,3})$, **2**, in the solid state. The C atoms of the CO ligands bear the same numbering as the corresponding O atoms.

shortest Ru–Ru distances in the tetrahedral compounds **2** and **4** always being associated with the metal atom

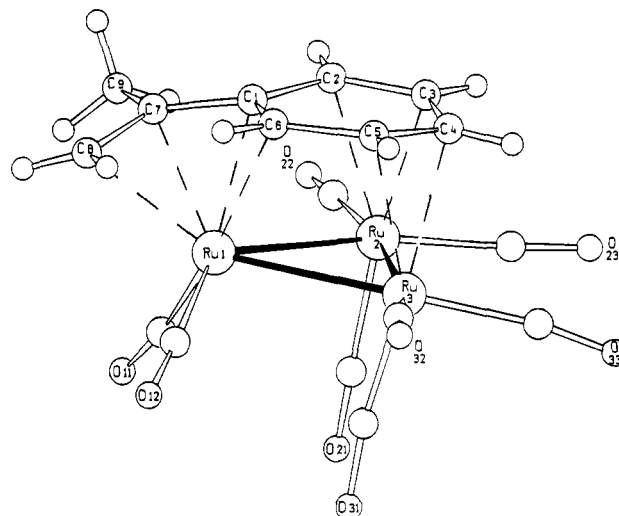


Figure 4. Molecular structure of $\text{Ru}_3(\text{CO})_8(\mu_3\text{-}\eta^2\text{:}\eta^2\text{:}\eta^2\text{-C}_6\text{H}_5\text{-}\{\eta^2\text{-CCH}_3\text{CH}_2\})$, **3**, in the solid state. The C atoms of the CO ligands bear the same numbering as the corresponding O atoms.

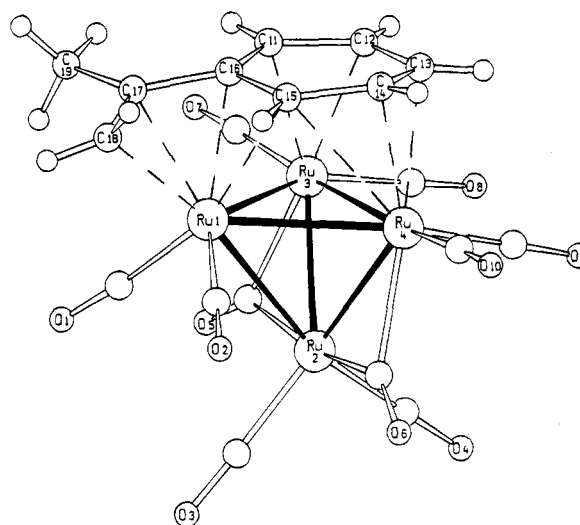


Figure 5. Molecular structure of $\text{Ru}_4(\text{CO})_{10}(\mu_3\text{-}\eta^2\text{:}\eta^2\text{:}\eta^2\text{-C}_6\text{H}_5\text{-}\{\eta^2\text{-CCH}_3\text{CH}_2\})$, **4**, in the solid state. The C atoms of the CO ligands bear the same numbering as the corresponding O atoms.

not interacting with the conjugated arene [Ru(2)–Ru(3) = 2.662(2) Å for species **2**, and Ru(2)–Ru(3) = 2.6933(12) Å and Ru(2)–Ru(4) = 2.6829(12) Å for species **4**]. In compounds **2** and **4** two Ru–Ru bonds are spanned by bridging CO's, while all the CO ligands are terminally bound in species **1** and **3**.

All the reported structures are related by the same type of interaction of the ring systems and of the unsaturated side arms with a trimetallic face. The diisopropenylbenzene and the isopropenylbenzene ligands formally contribute 10 and 8 electrons to the metal clusters through five and four η^2 -interactions, respectively. Thus, the total electron count for the tetrahedral and triangular species is 60 and 48, respectively, in keeping with the total number of valence electrons typically associated with tetranuclear and trinuclear cluster species.

The C=C fragment of the substituent group(s) formally replaces a carbonyl ligand on the cluster. Contrary to previous observations on other facially coordinated arene ligands,² no regular "long–short" alternation

Table 2. Selected Bond Lengths (Å) and Angles (deg) for 1a

Ru(1)–Ru(2)	2.780(2)	Ru(5)–C(17)	2.196(12)
Ru(1)–Ru(3)	2.900(2)	Ru(3)–C(19)	2.32(2)
Ru(2)–Ru(3)	2.847(2)	Ru(1)–C(14)	2.213(11)
Ru(4)–Ru(5)	2.769(6)	Ru(6)–C(14)	2.371(10)
Ru(4)–Ru(6)	2.829(5)	Ru(1)–C(15)	2.303(12)
Ru(5)–Ru(6)	2.891(5)	mean Ru–C(CO)	1.89(5)
Ru(1)–C(8)	2.221(10)	mean C–O(CO)	1.12(3)
Ru(6)–C(8)	2.199(9)	C(8)–C(13)	1.409(14)
Ru(6)–C(9)	2.181(9)	C(8)–C(14)	1.46(2)
Ru(3)–C(9)	2.216(9)	C(8)–C(9)	1.460(14)
Ru(3)–C(10)	2.212(10)	C(9)–C(10)	1.43(2)
Ru(5)–C(10)	2.203(10)	C(10)–C(17)	1.41(2)
Ru(5)–C(11)	2.406(11)	C(10)–C(11)	1.45(2)
Ru(2)–C(11)	2.355(11)	C(11)–C(12)	1.40(2)
Ru(2)–C(12)	2.291(10)	C(12)–C(13)	1.45(2)
Ru(4)–C(12)	2.376(11)	C(14)–C(15)	1.44(2)
Ru(4)–C(13)	2.338(10)	C(14)–C(16)	1.52(2)
Ru(1)–C(13)	2.330(10)	C(17)–C(19)	1.45(2)
Ru(3)–C(17)	2.292(12)	C(17)–C(18)	1.47(2)
Ru(2)–Ru(1)–Ru(3)	60.11(4)	C(14)–C(8)–C(9)	120.6(9)
Ru(1)–Ru(2)–Ru(3)	62.05(4)	C(10)–C(9)–C(8)	119.6(9)
Ru(2)–Ru(3)–Ru(1)	57.84(4)	C(17)–C(10)–C(9)	117.8(11)
Ru(5)–Ru(4)–Ru(6)	62.18(13)	C(17)–C(10)–C(11)	122.5(11)
Ru(4)–Ru(5)–Ru(6)	59.92(13)	C(9)–C(10)–C(11)	118.9(11)
Ru(4)–Ru(6)–Ru(5)	57.90(14)	C(12)–C(11)–C(10)	119.4(10)
mean O–C–Ru	167(4)	C(11)–C(12)–C(13)	122.4(10)
C(14)–C(8)–Ru(6)	78.0(6)	C(8)–C(13)–C(12)	118.2(11)
C(9)–C(8)–Ru(6)	69.8(5)	C(15)–C(14)–C(8)	120.3(11)
C(13)–C(8)–Ru(1)	76.2(6)	C(15)–C(14)–C(16)	120.0(12)
C(14)–C(8)–Ru(1)	70.6(6)	C(8)–C(14)–C(16)	119.6(11)
C(9)–C(8)–Ru(1)	111.4(6)	C(10)–C(17)–C(19)	116.4(12)
C(13)–C(8)–C(14)	117.6(10)	C(10)–C(17)–C(18)	123.9(14)
C(13)–C(8)–C(9)	120.3(10)	C(19)–C(17)–C(18)	118.8(14)

^a The atoms Ru(1), Ru(2), and Ru(3) belong to the major image, whereas Ru(4), Ru(5), and Ru(6) belong to the minor one. The Ru–C(CO) and C–O distances have been averaged on the full set of distances relative to the two molecular images.

is detected in the C–C bond distances within the rings. In fact, the amount of electron density on the metal coordinated to the aliphatic arm is greater than if the metal were interacting with a third carbonyl ligand, since this is a stronger π acceptor than the olefinic fragment. This results in a slight lengthening of the C-pairs involved in the coordination of the same metal with respect of the remaining ones.

In order to form a favorable bonding interaction with the cluster unit, two of the carbon atoms of the ring bend toward the metals. Due to the π interaction of the side arm(s) with the nearest metal, a slightly off-centered displacement of the ring with respect to eclipsing of the midpoints of the C=C double bonds over the metal atoms can be observed in all the structures. A small degree of rotation of the ligand about the coordination axis can be observed in both structures carrying the monosubstituted arene (**3** and **4**), whereas a much smaller rotational effect is associated with the diisopropenylbenzene ligand (Figure 6). The isopropenylbenzene and diisopropenylbenzene ligands are chiral at the α -C atom(s). Since all species crystallize in centrosymmetric space groups, both enantiomers are present in the crystal structures.

The disordered structure of **1** consists of two different orientations of the trimetallic unit [Ru(1)–Ru(3) and Ru(4)–Ru(6), respectively], forming a slightly shifted "star of David" in projection, together with the CO's and the facially coordinated diisopropenylbenzene ligand. The occupancy associated with the two images of the molecule is 0.70 and 0.30. The two superimposed

Table 3. Selected Bond Lengths (Å) and Angles (deg) for 2a

Ru(1)–Ru(2)	2.882(2)	Ru(3)–C(31)	1.949(12)
Ru(1)–Ru(3)	2.860(2)	Ru(4)–C(31)	2.109(12)
Ru(1)–Ru(4)	2.823(2)	C(31)–O(31)	1.21(2)
Ru(2)–Ru(3)	2.662(2)	Ru(1)–C(4L)	2.271(12)
Ru(2)–Ru(4)	2.830(2)	Ru(1)–C(5L)	2.214(12)
Ru(3)–Ru(4)	2.837(2)	Ru(1)–C(11L)	2.156(12)
Ru(1)–C(11)	1.902(12)	Ru(1)–C(12L)	2.278(11)
Ru(1)–C(12)	1.876(12)	Ru(2)–C(1L)	2.281(12)
Ru(2)–C(21)	1.865(13)	Ru(2)–C(2L)	2.212(12)
Ru(3)–C(32)	1.852(14)	Ru(2)–C(7L)	2.159(11)
Ru(3)–C(33)	1.830(13)	Ru(2)–C(8L)	2.264(11)
Ru(4)–C(41)	1.862(12)	Ru(4)–C(9L)	2.365(12)
Ru(4)–C(42)	1.876(11)	Ru(4)–C(10L)	2.344(11)
C(11)–O(11)	1.142(14)	C(1L)–C(2L)	1.41(2)
C(12)–O(12)	1.162(14)	C(2L)–C(3L)	1.50(2)
C(21)–O(21)	1.15(2)	C(2L)–C(7L)	1.46(2)
C(32)–O(32)	1.15(2)	C(7L)–C(8L)	1.43(2)
C(33)–O(33)	1.17(2)	C(8L)–C(9L)	1.45(2)
C(41)–O(41)	1.148(14)	C(9L)–C(10L)	1.37(2)
C(42)–O(42)	1.129(14)	C(10L)–C(11L)	1.46(2)
mean Ru–C(term CO)	1.866(13)	C(11L)–C(12L)	1.45(2)
mean C–O(term CO)	1.15(2)	C(12L)–C(7L)	1.41(2)
Ru(2)–C(22)	1.913(13)	C(11L)–C(5L)	1.46(2)
Ru(3)–C(22)	2.361(13)	C(5L)–C(4L)	1.39(2)
C(22)–O(22)	1.18(2)	C(5L)–C(6L)	1.49(2)
mean O–C–Ru(term CO)	175.5(11)	C(7L)–C(8L)–C(9L)	119.1(11)
Ru(2)–C(22)–O(22)	155.5(11)	C(8L)–C(9L)–C(10L)	121.7(11)
Ru(3)–C(22)–O(22)	128.2(10)	C(9L)–C(10L)–C(11L)	119.8(10)
Ru(3)–C(31)–O(31)	137.1(10)	C(10L)–C(11L)–C(12L)	118.5(10)
Ru(4)–C(31)–O(31)	134.3(9)	C(11L)–C(12L)–C(7L)	120.8(10)
C(1L)–C(2L)–C(3L)	120.2(11)	C(10L)–C(11L)–C(5L)	123.2(10)
C(1L)–C(2L)–C(7L)	117.1(11)	C(12L)–C(11L)–C(5L)	117.5(10)
C(3L)–C(2L)–C(7L)	122.3(11)	C(11L)–C(5L)–C(4L)	116.8(10)
C(2L)–C(7L)–C(8L)	116.7(10)	C(11L)–C(5L)–C(6L)	121.1(10)
C(2L)–C(7L)–C(12L)	121.3(10)	C(4L)–C(5L)–C(6L)	122.0(11)
C(12L)–C(7L)–C(8L)	119.5(10)		

^a term = terminal.

Table 4. Selected Bond Lengths (Å) and Angles (deg) for 3

Ru(1)–Ru(2)	2.865(3)	mean Ru–C(CO)	1.91(2)
Ru(1)–Ru(3)	2.824(3)	mean C–O(CO)	1.12(2)
Ru(2)–Ru(3)	2.798(3)	Ru(1)–C(1)	2.16(2)
Ru(1)–C(11)	1.90(2)	Ru(2)–C(2)	2.38(2)
Ru(1)–C(12)	1.89(2)	Ru(2)–C(3)	2.33(2)
Ru(2)–C(21)	1.91(2)	Ru(3)–C(4)	2.36(2)
Ru(2)–C(22)	1.96(2)	Ru(3)–C(5)	2.31(2)
Ru(2)–C(23)	1.90(2)	Ru(1)–C(6)	2.27(2)
Ru(3)–C(31)	1.88(2)	Ru(1)–C(7)	2.22(2)
Ru(3)–C(32)	1.94(2)	Ru(1)–C(8)	2.24(2)
Ru(3)–C(33)	1.90(2)	C(1)–C(2)	1.42(3)
C(11)–O(11)	1.11(2)	C(1)–C(6)	1.43(3)
C(12)–O(12)	1.12(2)	C(1)–C(7)	1.44(3)
C(21)–O(21)	1.12(2)	C(2)–C(3)	1.38(3)
C(22)–O(22)	1.12(2)	C(3)–C(4)	1.45(3)
C(23)–O(23)	1.11(2)	C(4)–C(5)	1.39(3)
C(31)–O(31)	1.17(3)	C(5)–C(6)	1.45(3)
C(32)–O(32)	1.11(2)	C(7)–C(8)	1.43(3)
C(33)–O(33)	1.12(2)	C(7)–C(9)	1.51(3)
Ru(3)–Ru(1)–Ru(2)	58.93(7)	C(2)–C(3)–C(4)	121(2)
Ru(3)–Ru(2)–Ru(1)	59.80(6)	C(5)–C(4)–C(3)	119(2)
Ru(2)–Ru(3)–Ru(1)	61.26(6)	C(4)–C(5)–C(6)	120(2)
mean O–C–Ru	175(2)	C(1)–C(6)–C(5)	119(2)
C(2)–C(1)–C(6)	119(2)	C(1)–C(7)–C(8)	117(2)
C(2)–C(1)–C(7)	124(2)	C(1)–C(7)–C(9)	125(2)
C(6)–C(1)–C(7)	117(2)	C(8)–C(7)–C(9)	118(2)
C(3)–C(2)–C(91)	121(2)		

structural models are related by the combination of a reflection in a mirror plane passing through Ru(1) and the midpoint of Ru(2)–Ru(3) followed by a rotation of 180° of the whole molecule about the arene coordination axis (see Figure 2b).

In a comparison of C–C distances it must be remembered that in **1** the distance results from the weighted

Table 5. Selected Bond Lengths (Å) and Angles (deg) for 4a

Ru(1)–Ru(2)	2.9647(12)	C(3)–O(3)	1.150(14)
Ru(1)–Ru(3)	2.8517(11)	C(4)–O(4)	1.12(2)
Ru(1)–Ru(4)	2.8795(12)	C(7)–O(7)	1.153(14)
Ru(2)–Ru(3)	2.6933(12)	C(8)–O(8)	1.137(14)
Ru(2)–Ru(4)	2.6829(12)	C(9)–O(9)	1.130(14)
Ru(3)–Ru(4)	2.9082(12)	C(10)–O(10)	1.10(2)
Ru(3)–C(11)	2.257(11)	mean Ru–C(term CO)	1.887(12)
Ru(3)–C(12)	2.283(11)	mean C–O(term CO)	1.130(15)
Ru(4)–C(13)	2.400(12)	Ru(2)–C(5)	2.088(11)
Ru(4)–C(14)	2.201(11)	Ru(3)–C(5)	2.128(12)
Ru(1)–C(15)	2.318(10)	C(5)–O(5)	1.142(13)
Ru(1)–C(16)	2.180(9)	Ru(2)–C(6)	2.009(13)
Ru(1)–C(17)	2.190(10)	Ru(4)–C(6)	2.183(13)
Ru(1)–C(18)	2.236(10)	C(6)–O(6)	1.160(14)
Ru(1)–C(1)	1.899(12)	C(11)–C(12)	1.41(2)
Ru(1)–C(2)	1.875(11)	C(11)–C(16)	1.42(2)
Ru(2)–C(3)	1.879(13)	C(12)–C(13)	1.42(2)
Ru(2)–C(4)	1.892(13)	C(13)–C(14)	1.39(2)
Ru(3)–C(7)	1.902(13)	C(14)–C(15)	1.40(2)
Ru(3)–C(8)	1.863(12)	C(15)–C(16)	1.428(14)
Ru(4)–C(9)	1.845(12)	C(16)–C(17)	1.45(2)
Ru(4)–C(10)	1.940(13)	C(17)–C(18)	1.41(2)
C(1)–O(1)	1.109(13)	C(17)–C(19)	1.50(2)
C(2)–O(2)	1.142(13)		
mean O–C–Ru(term CO)	176.6(12)	C(14)–C(15)–C(16)	118.6(10)
O(5)–C(5)–Ru(2)	141.4(10)	C(11)–C(16)–C(15)	119.3(10)
O(5)–C(5)–Ru(3)	139.2(9)	C(11)–C(16)–C(17)	123.6(10)
O(6)–C(6)–Ru(2)	144.1(11)	C(15)–C(16)–C(17)	116.5(9)
C(12)–C(11)–C(16)	120.3(10)	C(18)–C(17)–C(16)	116.2(10)
C(11)–C(12)–C(13)	119.6(11)	C(18)–C(17)–C(19)	122.4(11)
C(12)–C(13)–C(14)	119.1(11)	C(16)–C(17)–C(19)	121.3(10)
C(13)–C(14)–C(15)	122.1(11)		

average of the aliphatic C–C single bonds and of olefinic C=C double bonds. Therefore, in keeping with the 7:3 occupancy ratio of the disordered model, the C atoms pairs of the unsaturated side chains belonging to the major image show a greater double bond character than the ones bound to the minor image [1.43(2) vs 1.51(2) Å, on average, for the two side arms].

The packing diagrams for the species 2–4 are shown in Figures 7–9, respectively. In all three cases a high packing efficiency is achieved by means of a tight interlocking of carbonyl ligands and arene fragments belonging to adjacent molecules. A diffuse network of H-bonding interactions involving the oxygens of the CO's is also responsible for further stabilization of the crystal structure.

After having normalized all the C–H bond lengths to 1.08 Å, we calculated all the short H···O intermolecular contacts between the reference molecule and the surrounding ones.¹⁰ In order to consider all relevant contacts below the O–H van der Waals distance as possible intermolecular H···O interactions, a cut-off distance of 2.6 Å was applied. Close attention was also paid to the donor–acceptor C(CH) \cdots O distances. All the short C–H···O contacts observed are listed in Table 6. The short C–H···O separations are comparable to those usually found in systems carrying facial arene ligands.^{9c} Interestingly, only a few CO ligands participate in short interactions and of these three are involved in bifurcated and trifurcated interactions. Furthermore in 2, it is O(22) and O(3), both belonging to semibridging CO's, that participate in the H-bonding, in keeping with the higher basicity of bridging that of terminal CO ligands.¹¹

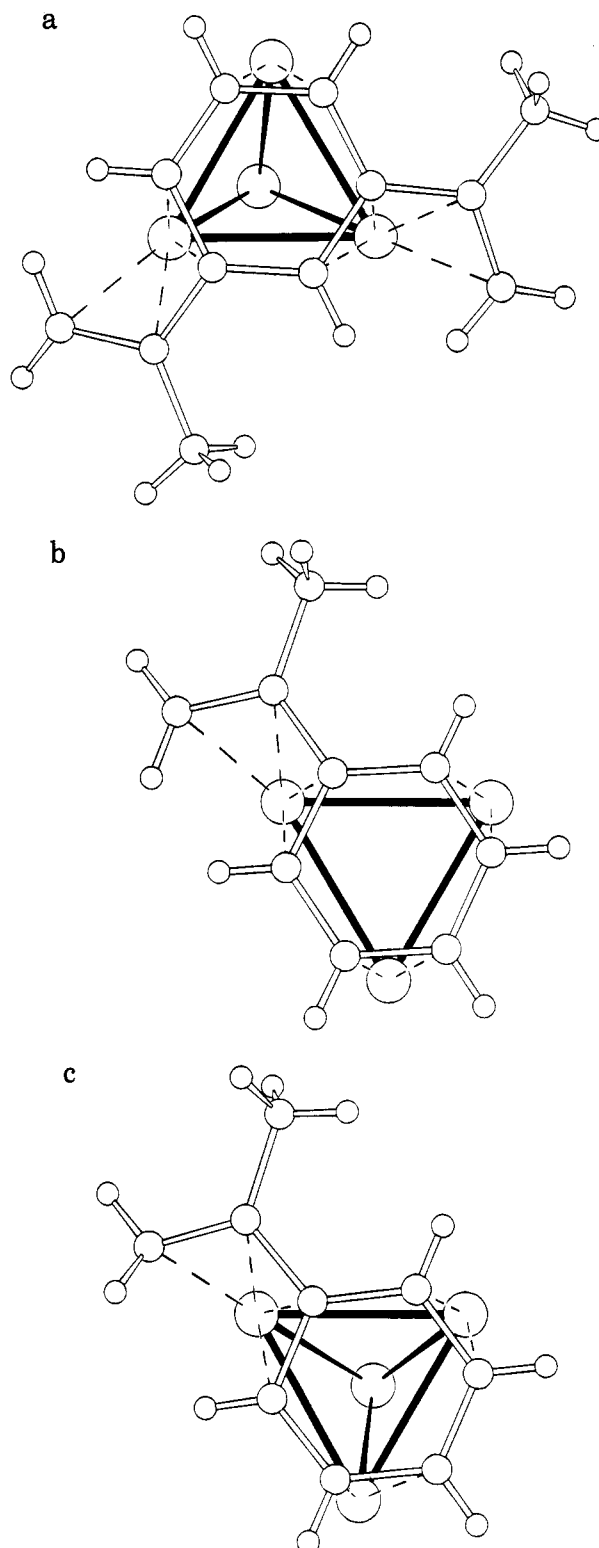


Figure 6. Comparative projection of the rings coordination planes in 2–4 (a–c, respectively) showing the slight off-centered displacement of the ring with respect to eclipsing of the midpoints of the C=C double bonds over the metal atoms in all the structures and the small rotation of the ligand about the coordination axis in both structures carrying the monosubstituted arene (3 and 4). The CO ligands have been omitted for clarity.

Concluding Comments

It is noteworthy that, using arenes with the isopropenyl functional group, the first tetrahedral cluster to bear a face-capping arene have been produced. This is

(10) Spek, A. L. PLATON. *Acta Crystallogr., Sect. A* 1990, 46, C31.

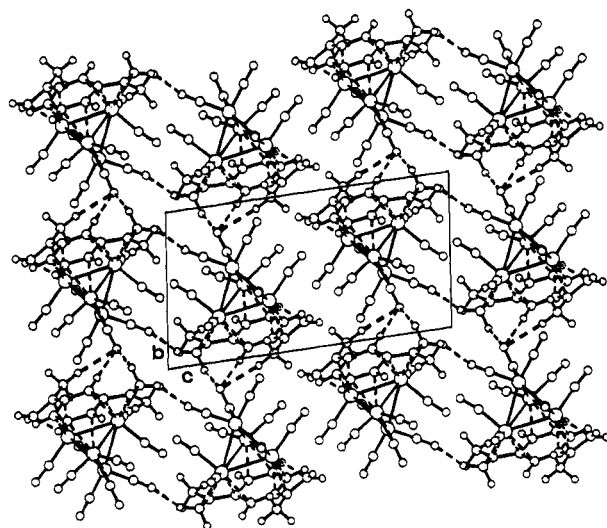


Figure 7. View down the *a* axis of the crystal structure of **2**. The blackened dashed lines represent the shortest C-H...O intermolecular interactions.

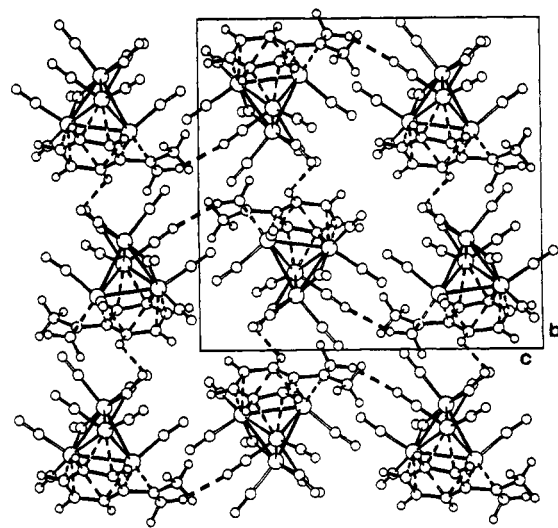


Figure 9. View down the *a* axis of the crystal structure of **4**. The blackened dashed lines represent the shortest C-H...O intermolecular interactions.

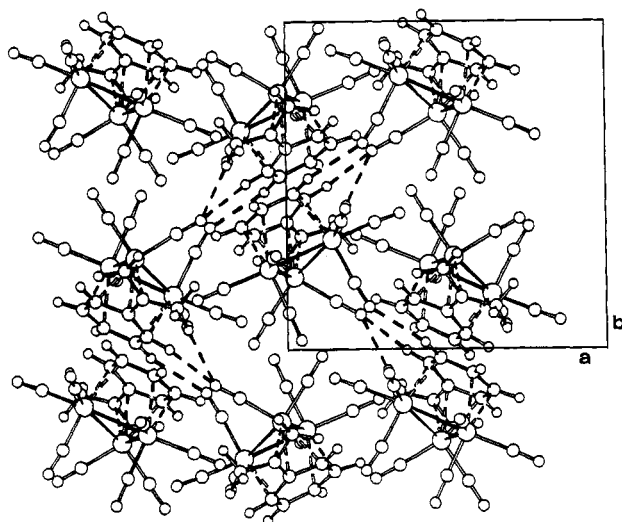


Figure 8. View down the *c* axis of the crystal structure of **3**. The blackened dashed lines represent the shortest C-H...O intermolecular interactions.

despite extensive studies of tetrahedral cobalt, ruthenium, and osmium clusters. In the case of ruthenium only butterfly clusters have been previously isolated.

The frequencies at which some of the C-H resonances occur are significantly different from that observed for the free ligand, with changes of up to δ 7 ppm. Clearly, this indicates that the chemistry of the ring system is markedly different, and while we have not as yet undertaken a detailed study of the organo moieties coordinated in the facial mode, preliminary experiments indicate a very different chemistry.

Experimental Section

General Procedures and Materials. Reactions were carried out using octane purchased from Aldrich Chemicals, and nitrogen gas was passed over the top of the condenser. Otherwise, precautions were not taken to exclude air and water from the system and the workup to the products was carried out using standard laboratory grade solvents. Infrared

(11) Horwitz, C. P.; Shriver, D. F. *Adv. Organomet. Chem.* **1984**, *23*, 218.

Table 6. Analysis of Potential Hydrogen Bonds (Distances in Å, Angles in deg, with All the C-H Distances Normalized to 1.08 Å)

	C...O	H...O	CH...O
Compound 2			
C(3)-H(3)...O(31)	3.439	2.419	156.9
C(4)-H(4)...O(31)	3.272	2.356	141.6
C(6)-H(6)...O(11)	3.363	2.392	148.9
C(8)-H(8)...O(41)	3.412	2.374	160.7
C(9)-H(9)...O(22)	3.206	2.465	124.8
C(12)-H(12)...O(31)	3.603	2.524	178.1
C(4)-H(4)...O(32)	3.338	2.478	135.7
Compound 3			
C(2)-H(2)...O(11)	3.420	2.347	172.1
C(3)-H(3)...O(21)	3.461	2.548	141.7
C(4)-H(4)...O(31)	3.398	2.502	139.6
C(5)-H(5)...O(23)	3.283	2.593	121.1
C(9)-H(9)...O(11)	3.646	2.571	173.3
Compound 4			
C(11)-H(11)...O(2)	3.300	2.457	134.1
C(15)-H(15)...O(3)	3.308	2.524	128.6
C(18)-H(18)...O(8)	3.462	2.436	158.2

spectra were recorded on a Perkin-Elmer 1710 Fourier-transform instrument. Mass spectra were obtained by positive fast atom bombardment on a Kratos MS50TC, calibrated with CsI. ¹H NMR spectra were recorded using a Bruker AM360 spectrometer referenced to internal TMS.

The cluster Ru₃(CO)₁₂ was prepared according to the literature method. Diisopropenylbenzene and isopropenylbenzene were purchased from Aldrich Chemicals and used without further purification.

Thermolysis of Ru₃(CO)₁₂ with Diisopropenylbenzene in Octane: Preparation of **1 and **2**.** A suspension of Ru₃(CO)₁₂ (100 mg) in octane (15 mL) containing an excess of diisopropenylbenzene (1 mL) was heated to reflux for 1.5 h. During this period the reaction was monitored by both IR spectroscopy and spot TLC, which indicated that majority of the starting material had been consumed and that several new materials were present. The reaction mixture was filtered and the solvent removed from the filtrate under reduced pressure. The products were separated by TLC, using a solution of dichloromethane-hexane (1:4, v/v) as eluent. The two main products with poorest elution rates were extracted into dichloromethane and characterized by spectroscopy as Ru₃(CO)₇(μ₃-η²:η²:η²-C₆H₄-{η²-CCH₃CH₂})₂-1,3, **1** (red, 32%), and Ru₄(CO)₉(μ₃-η²:η²:η²-C₆H₄-{η²-CCH₃CH₂})₂-1,3, **2** (red-brown, 27%).

Spectroscopic Data for **1.** IR ν_{CO} (CH₂Cl₂): 2043 (m), 2002 (vs), 1990 (s, sh), 1960 (w) cm⁻¹. Positive FAB mass

Table 7. Crystal Data and Details of Measurements for 1–4

	1	2	3	4
formula	C ₁₈ H ₁₄ O ₈ Ru ₃	C ₂₁ H ₁₄ O ₉ Ru ₄	C ₁₇ H ₁₀ O ₈ Ru ₃	C ₁₉ H ₁₀ O ₁₀ Ru ₄
mol wt	629.50	814.60	645.46	802.55
temp (°C)	293	150	150	293
system	monoclinic	triclinic	orthorhombic	monoclinic
space group	<i>P</i> 2 ₁ / <i>n</i>	<i>P</i> 1	<i>P</i> bca	<i>P</i> 2 ₁ / <i>n</i>
<i>a</i> (Å)	9.637(2)	8.835(4)	12.475(3)	9.057(5)
<i>b</i> (Å)	13.278(2)	8.899(4)	12.652(3)	15.140(1)
<i>c</i> (Å)	15.738(7)	15.422(8)	22.839(13)	15.846(7)
α (deg)	90.0	96.04(3)	90.0	90.0
β (deg)	94.54(3)	92.14(3)	90.0	93.36(4)
γ (deg)	90.0	111.36(3)	90.0	90.0
<i>V</i> (Å ³)	2007.5	1119.2	3605	2169
<i>Z</i>	4	2	8	4
<i>F</i> (000)	1208	776	2464	1520
λ(Mo Kα) (Å)	0.710 69	0.710 69	0.710 69	0.710 69
μ(Mo Kα) (mm ⁻¹)	2.258	2.699	2.526	2.786
θ-range (deg)	3–28	2.5–22.5	3–22.5	2.5–25
octants explored (<i>h</i> _{min} / <i>h</i> _{max} , <i>k</i> _{min} / <i>k</i> _{max} , <i>l</i> _{min} / <i>l</i> _{max})	–12/12, 0/17, 0/20	–9/9, –9/9, 0/16	0/13, 0/13, 0/24	–10/10, 0/17, 0/18
measd reflcns	4987	3517	2480	3943
unique reflcns	4822	2944	2354	3803
no. of refined params	355	157	169	298
GOF on <i>F</i> ²	1.140	1.122	1.003	1.045
<i>R</i> ₁ (on <i>F</i> , <i>I</i> > 2σ(<i>I</i>))	0.0727	0.0474	0.0701	0.0472
<i>wR</i> ₂ (on <i>F</i> ² , all data)	0.2009	0.2120	0.1602	0.1648

spectrum: 659 (calc 658) amu. ¹H NMR (CDCl₃): δ 6.19 (m, 1H), 5.59 (m, 1H), 3.07 (m, 1H), 2.84 (m, 1H), 1.85 (s, 3H), 1.52 (s, 3H), 1.46 (m, 1H), 1.35 (m, 1H), 0.87 (m, 1H), 0.56 (m, 1H) ppm.

Spectroscopic Data for 2. IR N_{CO} (CH₂Cl₂): 2060 (m), 2001 (vs), 1968 (w, br), 1924 (w, br), 1794 (w, vbr) cm⁻¹. Positive FAB mass spectrum: 815 (calc 815) amu. ¹H NMR (CDCl₃): δ 5.47 (m, 1H), 5.22 (m, 1H), 3.33 (m, 1H), 2.94 (m, 1H), 1.87 (m, 1H), 1.72 (m, 1H), 1.49 (s, 3H), 1.37 (s, 3H), 0.55 (m, 1H), 0.28 (m, 1H) ppm.

Thermolysis of Ru₃(CO)₁₂ with Isopropenylbenzene in Octane: Preparation of 3 and 4. A suspension of Ru₃(CO)₁₂ (150 mg) in octane (15 mL) containing a large excess of isopropenylbenzene (2 mL) was heated to reflux for 1.5 h. During this period the reaction was monitored by both IR spectroscopy and spot TLC, which indicated that the majority of the starting material had been consumed and that several new materials were present. The reaction mixture was filtered and the solvent removed from the filtrate under reduced pressure. The products were separated by TLC, using a solution of dichloromethane–hexane (1:4, v/v) as eluent. In order of elution, the two main bands were extracted into dichloromethane and characterized by spectroscopy as Ru₃(CO)₈(μ₃-η²:η²:η²-C₆H₅-{η²-CCH₃CH₂}), **3** (red-orange, 8%), and Ru₄(CO)₁₀(μ₃-η²:η²:η²-C₆H₄-{η²-CCH₃CH₂}), **4** (brown, 16%).

Spectroscopic Data for 3. IR N_{CO} (CH₂Cl₂): 2062 (vs), 2024 (vs), 2000 (s), 1988 (w), 1963 (w), 1936 (w) cm⁻¹. Positive FAB mass spectrum: 644 (calc 645) amu. ¹H NMR (CDCl₃): δ 5.21 (m, 1H), 4.99 (m, 1H), 4.85 (m, 1H), 4.75 (m, 1H), 2.94 (m, 1H), 1.64 (s, 3H), 1.56 (m, 1H), 0.88 (m, 1H) ppm.

Spectroscopic Data for 4. IR N_{CO} (CH₂Cl₂): 2089 (w), 2060 (m), 2029 (vs), 1967 (w), 1834 (w, br) cm⁻¹. Positive FAB mass spectrum: 802 (calc 803) amu. ¹H NMR (CDCl₃): δ 5.23 (m, 1H), 4.76 (m, 1H), 4.74 (m, 1H), 4.36 (m, 1H), 3.05 (m, 1H), 1.56 (m, 1H), 1.15 (s, 3H), 0.85 (m, 1H) ppm.

Crystal Structure Determination. Crystal data and details of measurements for all the compounds discussed

herein are summarized in Table 7. The diffraction intensities were collected at room temperature on a Enraf-Nonius CAD-4 diffractometer for the species **1** and **4** and at 150 K on a Stöe four-circle diffractometer for the species **2** and **3**, both equipped with a graphite monochromator (Mo Kα radiation, λ = 0.710 69 Å). The intensities were reduced to *F*_o², and the structures were solved by direct methods, followed by difference Fourier and subsequent full-matrix least-square refinements using the computer programs SHELX86 and SHELXL93.¹² Scattering factors for neutral atoms were taken from the appropriate tables.¹³ All non-H atoms were allowed to vibrate anisotropically. The H atoms in the species **2–4** were added in calculated positions and refined "riding" on their respective C atoms. Due to the presence of structural disorder, no hydrogens were added to the model of compound **1**.

Acknowledgment. We thank the University of Edinburgh and the SERC for financial assistance. D.B., F.G., and B.F.G.J. thank NATO for a travel grant. The Erasmus project "Crystallography" is acknowledged for financing J.J.B. at Bologna. We also thank Dr. A. J. Blake for collecting diffraction data for **2** and **3**.

Supporting Information Available: Tables of anisotropic thermal parameters and fractional atomic coordinates and *U* values for the non-hydrogen atoms, fractional atomic coordinates and *U* values for the hydrogen atoms, and complete bond lengths and angles and ORTEP drawings (23 pages). Ordering information is given on any current masthead page.

OM950331Y

(12) (a) Sheldrick, G. M. SHELX86, Program for the Solution of Crystal Structures, University of Göttingen, 1986. (b) Sheldrick, G. M. SHELX93, University of Göttingen, Germany, 1993.

(13) *International Tables for X-Ray Crystallography*; Kynoch Press: Birmingham, England, 1975; Vol. IV, pp 99–149.

Reactivity and Stereochemistry of β -Heteroatom Elimination. A Detailed Study through a Palladium-Catalyzed Cyclization Reaction Model

Guoxin Zhu and Xiyan Lu*

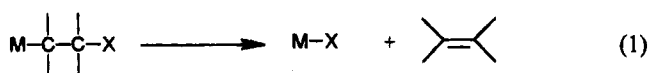
Shanghai Institute of Organic Chemistry, Chinese Academy of Sciences, 354 Fenglin Lu, Shanghai 200032, China

Received May 5, 1995[®]

The elimination of palladium and the β -leaving group of the organopalladium intermediate formed in a palladium(II)-catalyzed cyclization of 4'-heteroatom-2'-alkenyl 2-alkynoates leading to α -methylene- γ -butyrolactones is sensitive to the leaving-group ability of the substituents β to palladium. The reactivity order of β -elimination for different leaving groups was studied. The reaction of palladium chloride, palladium acetate, and palladium hydroxide elimination showed strict steric requirement requiring an antiperiplanar arrangement of palladium and the leaving group on the carbon β to palladium.

Introduction

β -Elimination, as one of the most important reactions of (σ -alkyl)metal compounds, involves interconversion of alkyl and olefin ligands.¹ Formally, β -elimination involves the cleavage of a bond on the carbon atom β to the metal in an organometallic species to produce an unsaturation, e.g.:



The most common examples of β -elimination are found in alkylmetals, where X = H, which have been explored extensively.² Although the elimination of a β -heteroatom with the metal is also apparently a general reaction, relatively fewer examples are known and the generality of this process is still limited.^{3–6} Recently, we reported a divalent palladium-catalyzed cyclization of 4'-heteroatom-2'-alkenyl 2-alkynoates stereoselectively affording α -methylene- γ -butyrolactone derivatives. In this reaction, in order to regenerate the catalytic species Pd(II), a heteroatom was introduced

[®] Abstract published in *Advance ACS Abstracts*, September 1, 1995.

(1) Collman, J. P.; Hegedus, L. S. *Principles and Applications of Organotransition Metal Chemistry*; University Science Books: Mill Valley, CA, 1987. Kochi, J. K. *Organometallic Mechanism and Catalysis*; Academic Press: New York, 1978. Yamamoto, A. *Organotransition Metal Chemistry; Fundamental Concepts and Applications*; John Wiley & Sons: New York, 1986. Heck, R. F. *Organotransition Metal Chemistry*; Academic Press: New York, 1974.

(2) Hegedus, L. S. In *The Chemistry of the Metal-Carbon Bond*; Hartley, F. R., Ed.; Wiley: Chichester, U.K., 1985; Vol. 2, p 401. Keinan, E.; Kumar, S.; Dangur, V.; Vaya, J. *J. Am. Chem. Soc.* **1994**, *116*, 11151 and references cited therein.

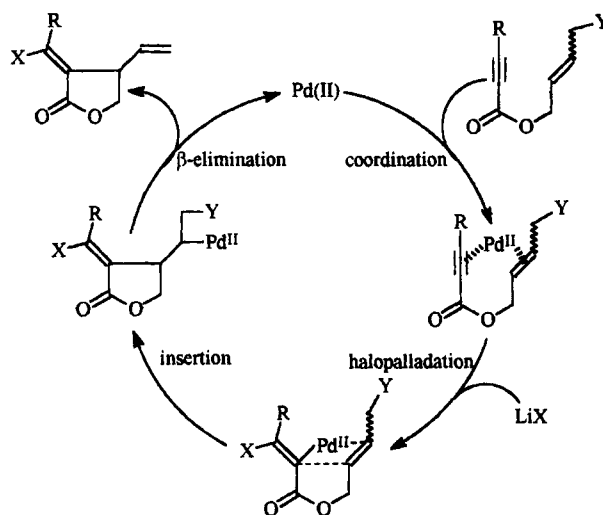
(3) Shiu, L.; Yu, C.; Wong, K.; Chen, B.; Cheng, W.; Yuan, T.; Luh, T. *Organometallics* **1993**, *12*, 1018 and references cited therein.

(4) Daves found that the acetoxy group was a good leaving group and the alkoxy group was a poor leaving group in their palladium-catalyzed reaction: Cheng, J. C.-Y.; Daves, G. D., Jr. *Organometallics* **1986**, *5*, 1753.

(5) For *syn* elimination of palladium and β -hydroxyl, see: Hacksell, V.; Daves, G. D., Jr. *Organometallics* **1983**, *2*, 772. Cheng, J. C.-Y.; Hacksell, V.; Daves, G. D., Jr. *J. Org. Chem.* **1986**, *51*, 3093. Bäckvall, J. E.; Åkermark, B.; Ljunggren, S. O. *J. Am. Chem. Soc.* **1979**, *101*, 2411. For anti-periplanar elimination of palladium and the β -acetoxy group, see: Daves, G. D., Jr. *Acc. Chem. Res.* **1990**, *23*, 201.

(6) For nonstereospecific elimination of palladium and chloride, see: Henry, P. M. *Acc. Chem. Res.* **1973**, *6*, 16.

Scheme 1



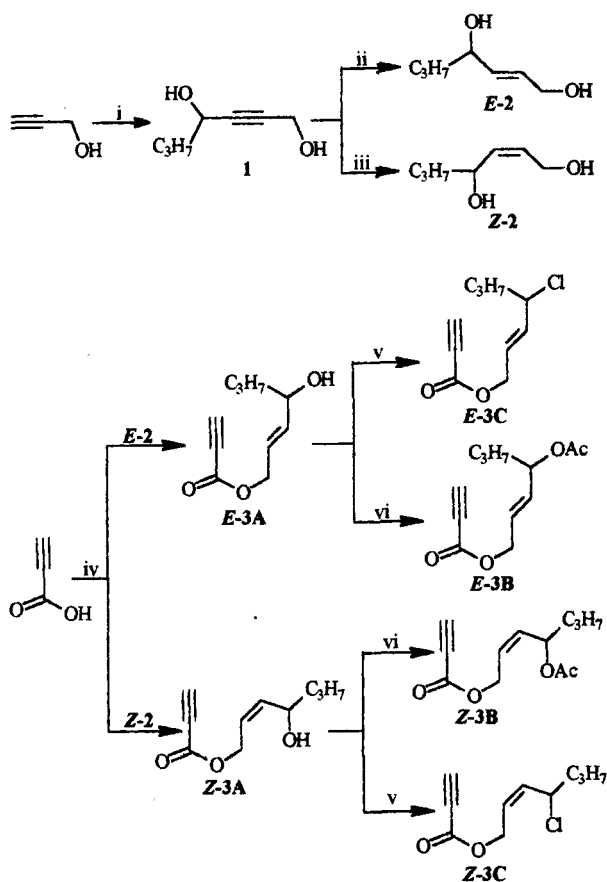
into the 4'-position of the substrate. In the resulting cyclic intermediate by intramolecular carbon-carbon double bond insertion into a vinyl-palladium bond formed by halopalladation of the carbon-carbon triple bond, the heteroatom is located at the β -position of the palladium. Thus, this heteroatom directed the β -elimination reaction to regenerate the catalytic species Pd(II) affording β -vinyl-substituted α -methylene- γ -butyrolactones (Scheme 1).⁷

In this paper, we wish to report the reactivity and stereochemistry of the elimination of palladium and the heteroatom β to palladium using the Pd(II)-catalyzed cyclization mentioned above as the model reaction.

Results and Discussion

Reactivity of Elimination of Palladium and Different Heteroatoms β to Palladium. In order to study the elimination of palladium and different leaving

(7) (a) Lu, X.; Ma, S.; Ji, J.; Zhu, G.; Jiang, H. *Pure Appl. Chem.* **1994**, *66*, 1501. (b) Ma, S.; Lu, X. *J. Chem. Soc., Chem. Commun.* **1990**, 733. Ma, S.; Lu, X. *J. Org. Chem.* **1991**, *56*, 5120. (c) Zhu, G.; Ma, S.; Lu, X. *J. Chem. Res. (S)* **1993**, 366. Zhu, G.; Ma, S.; Lu, X. *J. Chem. Res. (M)* **1993**, 2467. (d) Ma, S.; Lu, X. *J. Organomet. Chem.* **1993**, *447*, 305.

Scheme 2^a

^a Reagents and conditions: (i) (a) EtMgBr, THF, (b) *n*-PrCHO, (c) H₃O⁺, 60%; (ii) LiAlH₄, THF, reflux, 66%; (iii) P₂-Ni (catalyst), H₂ (1 atm), rt, 90%; (iv) DCC, DMAP (catalyst), Et₂O, -20 °C to rt, 52.5% for *E*-**3A**, 50% for *Z*-**3A**; (v) PCl₃, Et₂O, -20 to 0 °C; (vi) Ac₂O, MeCN, CoCl₂ (catalyst), 80 °C; 86% for *E*-**3B**; 63% for *Z*-**3B**.

groups in the above-mentioned cyclization reaction, the starting materials 4'-heteroatom-2'-(*Z*)- or (*E*)-heptenyl 2-propynoates (**3**) were prepared according to Scheme 2.

2-Heptyne-1,4-diol (**1**) was obtained by alkylation of butanal.⁸ Catalytic hydrogenation⁹ and LiAlH₄ reduction¹⁰ of compound **1** afforded (*Z*)- and (*E*)-2-heptene-1,4-diol (**2**) with high stereoselectivities, respectively. The selective mono-esterification of the primary hydroxyl group of the diols **2** in the presence of DCC catalyzed by DMAP in ether afforded the esters **3A**. 4'-Acetoxy-substituted substrates **3B** were obtained by subsequent acetylation of the hydroxyl group in compounds **3A**. Chlorination of compounds **3A** was realized by controlling the reaction temperature at -20 °C, which afforded 4'-chloro-substituted substrates **3C**. Compound *E*-**3D** was synthesized by methylation of 4'-hydroxyl-2'-(*E*)-butenyl 2-butynoate with MeI in the presence of NaH.

The cyclization of 4'-heteroatom-2'-heptenyl propynoates (**3**) occurred smoothly under the catalysis of palladium(II) in HOAc at room temperature. The results were shown in Table 1.

(8) Brandsma, L. *Preparative Acetylenic Chemistry*, 2nd ed.; Elsevier: Amsterdam, 1988; p 79.

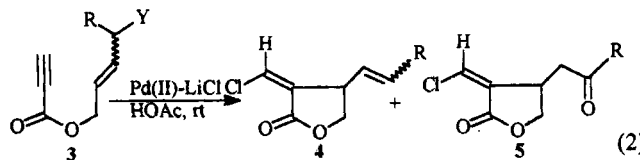
(9) Brown, C. A.; Ahuja, V. K. *J. Chem. Soc., Chem. Commun.* **1973**, 533.

(10) Cowie, J. S.; Lander, P. D.; Landor, S. R. *J. Chem. Soc., Perkin Trans. 1* **1973**, 720.

Table 1. Reactivity of Elimination of Palladium and Different Heteroatoms β to Palladium^a

entry	compd	R	L	config ^b	cat. ^c	time (h)	isolated yield (%)	
							4 (<i>Z:E</i>) ^d	5
1	3C	Pr	Cl	<i>Z</i>	A	8	80 (44:56)	
2	3C	Pr	Cl	<i>E</i>	A	8	80 (27:73)	
3	3B	Pr	OAc	<i>Z</i>	A	48	60 (63:37)	
4	3B	Pr	OAc	<i>E</i>	A	48	75 (45:55)	
5	3B	Pr	OAc	<i>Z</i>	B	48	65 (65:35)	
6	3B	Pr	OAc	<i>E</i>	B	48	75 (47:53)	
7	3A	Pr	OH	<i>Z</i>	B	72	35 (81:19)	19
8	3A	Pr	OH	<i>E</i>	B	72	50 (37:63)	19
9 ^e	3D	H	OMe	<i>E</i>	A	10	50 (4D) ^f	
10 ^e	3D	H	OMe	<i>E</i>	A ^g	12	60 (4D') ^h	

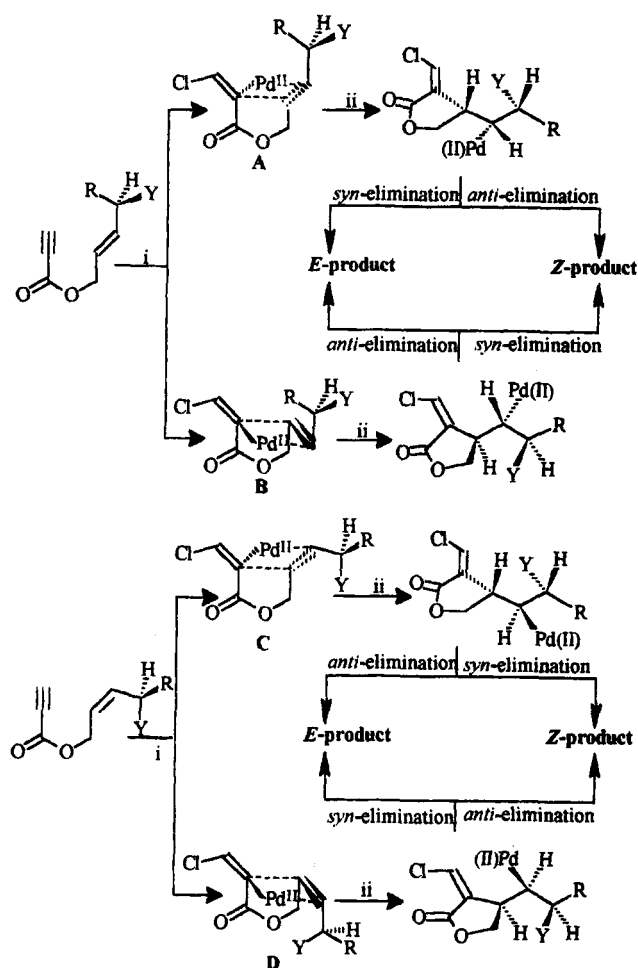
^a Reaction conditions: Alkynoates (**3**) (1.0 mmol), catalyst (0.05 mmol), LiX (4.0 mmol), and HOAc (5 mL) at rt. ^b Referring to the carbon-carbon double bond in the substrate (**3**). ^c A = Pd(OAc)₂, B = PdCl₂(PhCN)₂. ^d All exocyclic double bonds of **4** and **5** were in *Z*-form, the ratios (referring to the carbon-carbon double bond of alkenyl at the β-position of lactone rings) were determined by 300 MHz ¹H NMR. ^e The substrate **3D** was 4'-methoxyl-2'-(*E*)-butenyl 2-butynoate. ^f The product **4D** was (*Z*)-α-(chloroethylidene)-β-vinyl-γ-butyrolactone. ^g LiBr was used instead of LiCl in the reaction. ^h The product **4D'** was (*Z*)-α-(bromoethylidene)-β-vinyl-γ-butyrolactone.



When the leaving group in the substrates was a chloride (**3C**, Y = Cl), the cyclization proceeded quickly affording β-chloride elimination product as the sole cyclic product in good yield (entries 1 and 2, Table 1) without competitive β-hydride elimination. The exocyclic carbon-carbon double bond in the lactone product was believed to be in the *Z*-configuration by comparing the chemical shift of the vinylic protons of the exocyclic carbon-carbon double bond with its analogues.⁷ The configuration of the carbon-carbon double bond at the β-position of the lactone was determined by the ¹H NMR method. Irradiation of the signal at 2.09–2.02 ppm led to the observation of two doublets of two groups of vinylic protons with coupling constants of 10.6 and 15.3 Hz, implying that the product was a mixture of two geometrical isomers with respect to the carbon-carbon double bond at the β-position of lactone ring, the ratio of which was determined by ¹H NMR.

For the acetate substrates (**3B**, Y = OAc), the cyclization reaction also occurred smoothly affording the β-acetoxy elimination product as the sole cyclic product under similar conditions, but the reaction was slower than the corresponding chloro-substituted substrates (entries 3–6, Table 1). Much slower reaction was found in case of hydroxyl substrates (**3A**, Y = OH). Besides the low reaction rate for hydroxyl substrates, the reaction was also less selective and two cyclic products **4** and **5** were isolated (entries 7 and 8, Table 1). Compound **5** was formed by β-hydride elimination in the last step. This result indicates that the reactivities of the β-hydroxyl and β-hydride eliminations are comparable and the reaction gives rise to a mixture of products.

From the results shown in Table 1, we could find that the elimination of palladium and a good leaving group (e.g. chloride, acetoxy⁴) was easier and faster than

Scheme 3^a

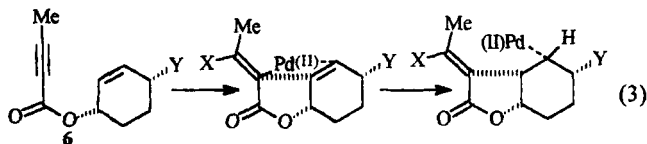
^a Legend: (i) chloropalladation; (ii) intramolecular insertion.

β -hydride elimination, while, for the hydroxyl group, its leaving-group ability was similar to that of a β -hydride. Thus, the ability of β -elimination of different leaving groups at the β position of palladium followed the order $\text{Cl} > \text{OAc} > \text{OH} \approx \text{H}$. Daves found that in their (glycal)-palladium system, alkoxy was a poor leaving group in palladium(II) β -elimination reactions.⁴ However, in our case, when the leaving group was changed to a methoxyl (entries 9 and 10, Table 1), the reaction also proceeded quickly to afford only one cyclic product through β -methoxyl elimination, indicating that methoxyl group was a better leaving group than hydride.

The results shown in Table 1 also imply that the configuration of the carbon-carbon double bond in substrates **3** had some influence on the cyclization, especially on the stereochemistry of β -elimination. Substrates with a *Z*-carbon-carbon double bond tended to give products with more *Z*-carbon-carbon double bond at the β -position of the lactone; however, substrates with an *E*-carbon-carbon double bond gave the corresponding β -*E*-olefin product predominantly. These results indicate that the configuration of the carbon-carbon double bond had some memory during the cyclization reaction. Such a memory effect increased when going from the chlorine substrates (**3C**) to the acetate substrates (**3B**) to the hydroxyl substrates (**3A**); that is, it increases with the covalency of the bond between palladium and the heteroatom ($\text{Cl} < \text{OAc} < \text{OH}$). On the other hand, both the *re*-face and *si*-face of

the carbon-carbon double bond in the substrate could coordinate with the palladium before the intramolecular double bond insertion into vinylpalladium formed by halopalladation of the carbon-carbon triple bond (Scheme 3). There is no significant energy difference between these two coordination complexes (A to D in Scheme 3), so this type of substrates would give different transition states and is not suitable to study the stereochemistry of β -elimination in the next step.

Stereochemistry of Elimination of Palladium and the Leaving Group β to Palladium. Although the fact that syn-periplanar arrangement of palladium and β -hydride is required for the β -hydride elimination reaction is well-known,^{1,2} the studies on the stereochemistry of elimination of palladium and a heteroatom on the carbon β to palladium are rare. Daves reported that palladium acetate elimination required an anti-periplanar arrangement of palladium and the oxygen substituent.⁵ Nonstereospecific elimination of palladium chloride was reported by Henry.⁶ On the basis of our previous studies, it occurs to us that our cyclization reaction⁷ may be used as a model reaction to study the stereochemistry of β -elimination. In the cyclization of 2-propynoates **3**, both the *re*-face and *si*-face of the carbon-carbon double bond in the substrate could coordinate to vinylpalladium, which made the intermediate formed by intramolecular insertion variable. If the allylic double bond was fixed in a cyclic substrate, such as compound **6**¹¹ (eq 3), after halopalladation of

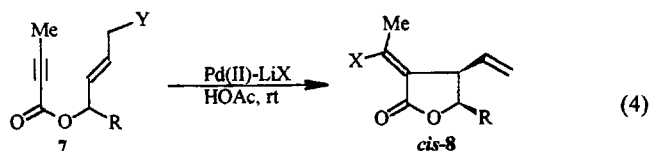


the carbon-carbon triple bond, the coordination of the carbon-carbon double bond with vinylpalladium species should only be in one direction due to the rigidity of the cyclohexenyl ring. Thus, a stereodefined new carbon-palladium bond generated by intramolecular carbon-carbon double bond insertion could be quenched by β -elimination reaction, and the stereochemistry of β -elimination could be deduced from the cyclic product formed in the reaction. Unfortunately, under the cyclization conditions, the reactions of both *cis*-**6** and *trans*-**6** (eq 3, $\text{Y} = \text{OAc}$ or OH) were very slow and resulted in a complex mixture. So we failed to obtain any useful information for the stereochemical study using *cis*-**6** and *trans*-**6**.

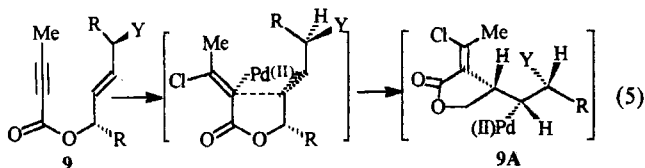
In our previous work,¹² we found that the diastereoselectivity in the intramolecular carbon-carbon double bond insertion step could be controlled by the substituents at the 3- and 1'-positions of the cyclization precursors. For 2-butynoates (**7**), the substituent R at the 1'-position could control the stereoselectivity in the step of the intramolecular insertion affording the *cis*-lactone (*cis*-**8**) (referring to β, γ -substituents) as the sole cyclic product (eq 4).

(11) Compounds **6** were prepared from 2-butynoic acid and the corresponding stereodefined cyclohexenols (Bäckvall, J. E.; Byström, S. E.; Nordberg, R. E. *J. Org. Chem.* **1984**, *49*, 4619) in the presence of DCC and DMAP.

(12) Ma, S.; Zhu, G.; Lu, X. *J. Org. Chem.* **1993**, *58*, 3692.

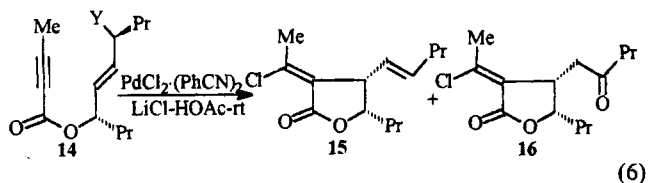


On the basis of such a stereoselectivity in the step of intramolecular carbon-carbon double bond insertion into the vinylpalladium bond, we chose stereodefined 2-butynoate **9** as the model compound to study the stereochemistry of β -heteroatom elimination. According to our previous results, halopalladation of the carbon-carbon triple bond followed by stereoselective intramolecular carbon-carbon double bond insertion would generate a stereodefined cyclic intermediate (**9A**) with a newly formed σ -carbon-palladium bond. Subsequent elimination of palladium and the leaving group would afford the lactone product with a *Z*- or *E*-double bond at the β -position of the lactone ring according to the steric requirement of the elimination (eq 5).

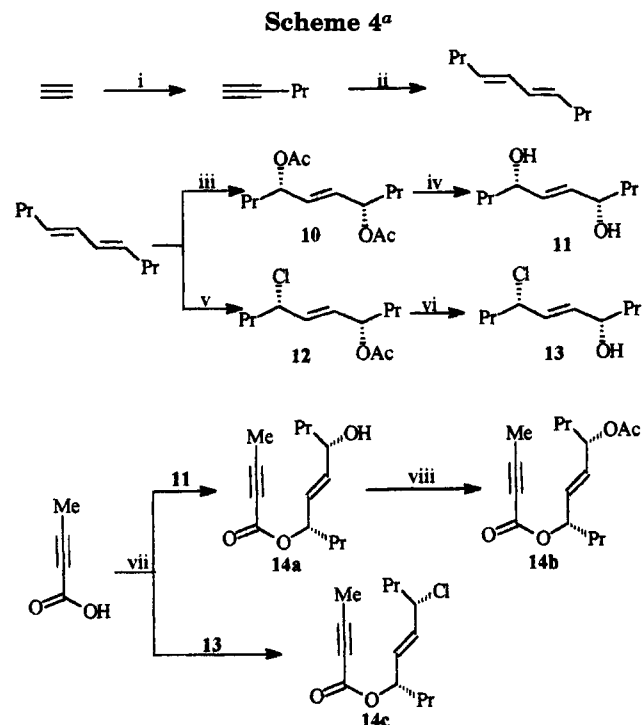


The stereodefined starting materials **14a–14c** were synthesized according to the route shown in Scheme 4.

E-(*R**,*R**)-4,7-Diacetoxy-5-decene (**10**)¹² and *E*-(*R**,*R**)-4-acetoxy-7-chloro-5-decene (**12**)¹³ were prepared by the methods reported by Bäckvall. Hydrolysis of **10** and **12** afforded the corresponding hydroxyl compounds **11** and **13**, which were directly esterified with 2-butynoic acid affording 2-butynoates **14a** and **14c** in the presence of DCC catalyzed by DMAP. The acetoxy substrate **14b** was prepared by acetylation of **14a** in the presence of a catalytic amount of CoCl_2 (eq 6).



The results of palladium(II)-catalyzed cyclization of **14** were shown in Table 2. Under the catalysis of $\text{PdCl}_2(\text{PhCN})_2$, cyclization of **14c** occurred quickly giving the lactone **15** as the sole product. The relative configuration of the substituents at the β, γ -positions was determined by comparing the ^1H NMR spectra with its analogs obtained in our previous work;^{7,12} the double bond of the alkenyl group at the β -position was believed to be in *E*-form based on the *J* value ($J = 15$ Hz) between the two vinylic protons. Under similar reaction conditions, the acetate substrate **14b** also afforded the lactone **15** with *E* double bond of the alkenyl group at the β -position as the sole product. Although the cyclization of hydroxyl substrate **14a** gave two cyclic products **15** and **16**, the double bond of alkenyl group at the β -position of the lactone product **15** was also in *E*-form. These results showed that the elimination of

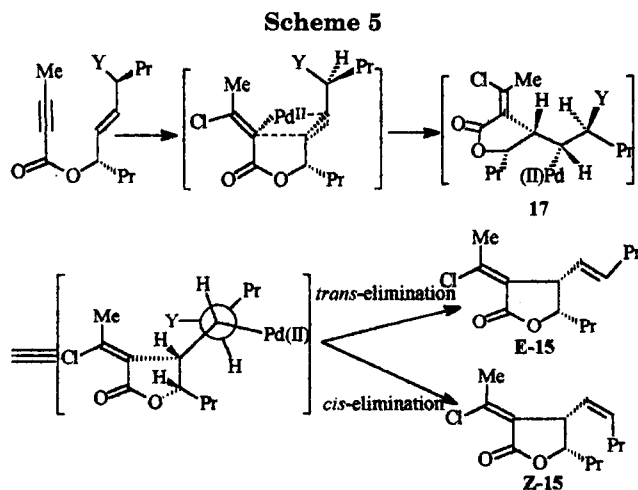


^a Reagents and conditions: (i) NaH, DMSO, *n*-PrBr; (ii) (a) DIBAL-H, hexane/THF, (b) CuCl; (iii) LiOAc·2H₂O, MnO₂, *p*-benzoquinone, HOAc-H₂O-hexane, Pd(OAc)₂ (catalyst); (iv) NaOH (2M), MeOH; (v) LiCl, LiOAc·2H₂O, *p*-benzoquinone, HOAc-hexane, Pd(OAc)₂ (catalyst); (vi) K₂CO₃, MeOH; (vii) DCC, DMAP, CH₂Cl₂, -20 °C to rt, 52% for **14a**, 77% for **14c**; (viii) Ac₂O, CoCl₂ (catalyst), MeCN, 80 °C, 88%.

Table 2. Stereochemistry of Elimination of Palladium and the Leaving Group β to Palladium^a

entry	substrate	leaving group (Y)	time (h)	isolated yield (%)	
				15 (<i>E:Z</i>) ^b	16
1	14a	OH	60	23 (>97:3)	51
2	14b	OAc	60	91 (>97:3)	
3	14c	Cl	3	85 (>97:3)	

^a Reaction conditions: Alkynoates (**14**) (1.0 mmol), catalyst (0.05 mmol), LiX (4.0 mmol), and HOAc (5 mL) at rt. ^b Determined by 300 MHz ^1H NMR spectra.



palladium and the leaving groups, such as chloride, acetoxy, and hydroxyl, all occurred in a highly stereoselective way. The stereochemistry of β -elimination can be deduced from the analysis based on Scheme 5.

As we have discussed, the intramolecular carbon-carbon double bond insertion into the vinylpalladium

(13) Bäckvall, J. E.; Schink, H. E.; Renko, Z. D. *J. Org. Chem.* **1990**, *55*, 826.

bond formed by halopalladation of the carbon-carbon triple bond would generate the cyclic intermediate **17** with a newly formed stereodefined carbon-palladium bond. The latter gave the final organic product through elimination of palladium(II) and the leaving group on the β -carbon of palladium. As illustrated in Scheme 5, *anti*-elimination of palladium and the leaving group would afford an *E*-carbon-carbon double bond of the alkenyl group at the β -position of the lactone, while a *Z*-carbon-carbon double bond which is stable under the cyclization condition^{7c} would result from *syn*-elimination. During our study, *E*-carbon-carbon double bond products were obtained as the sole products in all cases, implying that the elimination required the antiperiplanar arrangement for the palladium and the leaving group, such as chloride, acetoxy, and hydroxyl groups.

Conclusions

In summary, we have demonstrated the order of leaving-group ability and the stereochemistry of β -heteroatom elimination in the cyclization reaction of 4'-heteroatom-2'-alkenyl 2-alkynoates under the catalysis of palladium(II). When the substrate has a good leaving group (e.g. acetate, chlorine), an antiperiplanar arrangement for palladium and the leaving group is required and no competitive β -hydride elimination was observed; when the substituent at the 4'-position of the substrate is a poor leaving group (e.g. hydroxyl), both β -hydroxy and β -hydride eliminations occurred, but the β -hydroxy elimination also required an antiperiplanar arrangement.

Experimental Section

The starting materials 2-heptyne-1,4-diol,⁸ (*Z*)- and (*E*)-2-heptene-1,4-diols,^{9,10} 4,6-decadiene,¹³ *E*-(*R**,*R**)-4,7-diacetoxy-5-decene,¹¹ *E*-(*R**,*R**)-5-acetoxy-7-chloro-5-decene,¹³ *E*-(*R**,*R**)-4,7-dihydroxy-5-decene,¹¹ *E*-(*R**,*R**)-5-hydroxy-7-chloro-5-decene,¹¹ and 1-pentyne¹⁴ were synthesized according to the literature methods.

Synthesis of 4'-Hydroxy-2'-(*E*)-heptenyl 2-Propynoate (E-3A**).** To a solution of propynoic acid (2.20 g, 31.4 mmol) and 2-*E*-heptene-1,4-diol (4.08 g, 31.4 mmol) in ether (anhydrous, 20 mL) was added a solution of DCC (6.46 g, 31.4 mmol) and DMAP (0.19 g, 1.6 mmol) in ether (anhydrous, 28 mL) at -20 °C with stirring, and then the reaction was carried out at rt (room temperature) for 24 h. After filtering and removal of the solvent, the crude product was submitted to chromatography on silica gel (eluent: petroleum ether/ethyl acetate = 10:1.5) to afford **E-3A**: yield 3.0 g (55%) of oil; ¹H NMR (300 MHz, CDCl₃) 5.90–5.73 (m, 2H), 4.69 (d, *J* = 5.1 Hz, 2H), 4.16 (dt, *J*₁ = 6.4 Hz, *J*₂ = 5.7 Hz, 1H), 2.94 (s, 1H), 1.91 (br, 1H), 1.57–1.48 (m, 2H), 1.46–1.31 (m, 2H), 0.93 (t, *J* = 7.1 Hz, 3H); IR (neat) 3400, 3300, 2980, 2880, 2120, 1720, 1460, 1380, 1230, 970, 760 cm⁻¹; MS *m/e* 165 (M⁺ - OH, 1.80), 139 (0.91), 121 (1.24), 107 (1.08), 95 (13.16), 71 (37.80), 69 (100.00), 55 (12.15). HRMS: calcd for C₁₀H₁₃O₂ (M⁺ - OH), *m/e* 165.0916; found, *m/e* 165.0932.

4'-Hydroxy-2'-(*Z*)-heptenyl 2-propynoate (Z-3A**)** was synthesized similarly: oil; ¹H NMR (300 MHz, CDCl₃) 5.68–5.59 (m, 2H), 4.90 (ddd, *J*₁ = 6.8 Hz, *J*₂ = 1.0 Hz, *J*₃ = 12 Hz, 1H), 4.70 (ddd, *J*₁ = 5.1 Hz, *J*₂ = 1.2 Hz, *J*₃ = 12 Hz, 1H), 4.47 (m, 1H), 2.95 (s, 1H), 2.30 (br, 1H); IR (neat) 3400, 3260, 2920, 2880, 2100, 1705, 1460, 1220, 1050, 760 cm⁻¹; MS *m/e* 183 (M⁺ + 1, 0.64), 165 (M⁺ - OH, 24.63), 151 (0.50), 137 (0.23),

113 (4.26), 109 (2.15), 95 (100.00), 71 (39.81), 69 (77.61), 53 (36.65). HRMS: calcd for C₁₀H₁₄O₃, *m/e* 182.0943; found, *m/e* 182.0940.

1'-(*R)-Propyl-4'-(*R**)-hydroxyl-2'-(*E*)-heptenyl 2-butyrate (**14a**) and 1'-(*R**)-propyl-4'-(*R**)-chloro-2'-(*E*)-heptenyl 2-butyrate (**14c**)** were synthesized similarly but using CH₂Cl₂ instead of Et₂O as solvent.

1'-(*R)-Propyl-4'-(*R**)-hydroxyl-2'-(*E*)-heptenyl 2-Butynoate (**14a**):** oil; ¹H NMR (300 MHz, CDCl₃) 5.75 (dd, *J*₁ = 5.9 Hz, *J*₂ = 15 Hz, 1H), 5.61 (dd, *J*₁ = 6.8 Hz, *J*₂ = 15 Hz, 1H), 5.31 (q, *J* = 6.7 Hz, 1H), 4.11 (q, *J* = 6.0 Hz, 1H), 1.99 (s, 3H), 1.90 (br, 1H), 1.68–1.30 (m, 8H), 0.92 (t, *J* = 7.4 Hz, 6H); IR (neat) 3400, 2960, 2880, 2250, 1720, 1470, 1260, 1070, 970, 750 cm⁻¹; MS *m/e* 221 (M⁺ - OH, 2.40), 191 (1.61), 177 (4.36), 171 (0.28), 155 (8.95), 137 (15.55), 125 (13.38), 111 (63.38), 67 (100.00). HRMS: calcd for C₁₂H₁₅O₂ (M⁺ - Et - H₂O), *m/e* 191.1072; found, *m/e* 191.1054.

1'-(*R)-Propyl-4'-(*R**)-chloro-2'-(*E*)-heptenyl 2-Butynoate (**14c**):** oil; ¹H NMR (300 MHz, CDCl₃) 5.79 (dd, *J*₁ = 7.7 Hz, *J*₂ = 15.7 Hz, 1H), 5.67 (dd, *J*₁ = 6.2 Hz, *J*₂ = 15 Hz, 1H), 5.32 (q, *J* = 6.4 Hz, 1H), 4.34 (m, 1H), 1.99 (s, 3H), 1.80–1.57 (m, 4H), 1.44–1.33 (m, 4H), 0.93 (t, *J* = 7.4 Hz, 6H); IR (neat) 2960, 2860, 2240, 1715, 1465, 1250, 1065, 970, 750 cm⁻¹; MS *m/e* 221 (M⁺ - Cl, 18.35), 205 (0.38), 203 (0.70), 193 (0.35), 191 (1.16), 175 (0.84), 173 (1.144), 156 (0.74), 154 (3.51), 137 (12.24), 121 (1.73), 95 (13.25), 67 (100.00). HRMS: calcd for C₁₄H₂₁O₂, *m/e* 221.1542; found, *m/e* 221.1541.

Acetylation of Allylic Hydroxyl Group. This was carried out under the similar way reported in our previous paper.^{7c}

4'-Acetoxy-2'-(*Z*)-heptenyl 2-Propynoate (Z-3B**):** oil; ¹H NMR (300 MHz, CDCl₃) 5.71–5.65 (m, 1H), 5.59–5.53 (m, 1H), 5.49–5.46 (m, 1H), 4.91 (dd, *J*₁ = 1.5 Hz, *J*₂ = 6.6 Hz, 1H), 4.84 (dd, *J*₁ = 1.0 Hz, *J*₂ = 6.6 Hz, 1H), 2.92 (s, 1H), 2.04 (s, 3H), 1.75–1.20 (m, 4H), 0.93 (t, *J* = 7.2 Hz, 3H); IR (neat) 3250, 2940, 2880, 2100, 1740, 1450, 1370, 1230, 1020 cm⁻¹; MS *m/e* 207 (0.21), 181 (0.55), 165 (M⁺ - OAc, 2.96), 155 (3.83), 141 (9.71), 135 (2.83), 112 (48.79), 107 (8.28), 95 (16.44), 69 (34.00), 53 (33.99), 43 (100.00). HRMS: calcd for C₁₀H₁₂O₂ (M⁺ - HOAc), *m/e* 164.0837; found, *m/e* 164.0881.

4'-Acetoxy-2'-(*E*)-heptenyl 2-Propynoate (E-3B**):** ¹H NMR (300 MHz, CDCl₃) 5.79–5.76 (m, 2H), 5.31–5.25 (m, 1H), 4.68 (d, *J* = 4.2 Hz, 2H), 2.94 (s, 1H), 2.06 (s, 3H), 1.63–1.56 (m, 2H), 1.35–1.32 (m, 2H), 0.92 (t, *J* = 7.3 Hz, 3H); IR (neat) 3250, 2960, 2880, 2100, 1740, 1720, 1460, 1380, 1230, 970, 760 cm⁻¹; MS *m/e* 206 (0.68), 181 (0.69), 165 (100.00), 155 (20.98), 123 (1.18), 112 (17.64), 95 (94.15), 69 (6.44), 53 (12.48), 43 (23.61). HRMS: calcd for C₁₀H₁₂O₂ (M⁺ - HOAc): *m/e* 164.0837; found, *m/e* 164.0790.

1'-(*R)-Propyl-4'-(*R**)-acetoxy-2'-(*E*)-heptenyl 2-Butynoate (**14b**):** oil; ¹H NMR (300 MHz, CDCl₃) 5.64 (m, 2H), 5.32–5.24 (m, 2H), 2.06 (s, 3H), 2.00 (s, 3H), 1.66–1.54 (m, 4H), 1.38–1.27 (m, 4H), 0.91 (t, *J* = 7.8 Hz, 6H); IR (neat) 2920, 2850, 2210, 1730, 1460, 1360, 1240, 1060, 970, 750 cm⁻¹; MS *m/e* 237 (M⁺ - Ac, 0.40), 221 (M⁺ - OAc, 3.12), 205 (0.50), 197 (5.59), 177 (6.07), 155 (18.08), 141 (16.36), 137 (4.84), 125 (19.74), 111 (26.92), 67 (100.00). HRMS: calcd for C₁₄H₂₁O₂: *m/e* 221.1542; found, *m/e* 221.1552.

4'-Chloro-2'-heptenyl 2-propynoates (3C**)** were prepared by chlorination of corresponding hydroxyl compounds (**3A**) according to the literature method¹⁵ at -20 °C.

4'-Chloro-2'-(*Z*)-heptenyl 2-propynoate (Z-3C**):** oil; ¹H NMR (300 MHz, CDCl₃) 5.88–5.63 (m, 2H), 4.87–4.65 (m, 3H), 2.93 (s, 1H), 2.07–1.71 (m, 2H), 1.50–1.38 (m, 2H), 0.93 (t, *J* = 6.1 Hz, 3H); IR (neat) 3250, 2920, 2840, 2100, 1720, 1460, 1220, 750 cm⁻¹; MS *m/e* 203 (M⁺(³⁷Cl) + 1, 7.31), 202 (M⁺(³⁷Cl) - 1, 3.13), 201 (M⁺(³⁵Cl) + 1, 22.99), 172 (0.39), 165 (8.56), 149 (2.40), 131 (3.74), 121 (2.39), 112 (3.22), 95 (100.00), 89 (94.34), 69 (4.19). HRMS: calcd for C₁₀H₁₃O₂ (M⁺ - Cl): *m/e* 165.0916; found, *m/e* 165.0924.

4'-Chloro-2'-(E)-heptenyl 2-Propynoate (E-3C): oil, ^1H NMR (300 MHz, CDCl_3) 5.90–5.76 (m, 2H), 4.69 (m, 1H), 4.41–4.31 (m, 2H), 2.91 (s, 1H), 1.84–1.75 (m, 2H), 1.51–1.36 (m, 2H), 0.94 (t, $J = 7.5$ Hz, 3H); IR (neat) 3250, 2940, 2850, 2100, 1720, 1450, 1380, 1220, 970, 750 cm^{-1} ; MS m/e 203 (M^{+37}Cl) + 1, 3.73), 202 (M^{+37}Cl), 1.93), 201 (M^{+35}Cl) + 1, 12.33), 200 (M^{+35}Cl), 1.85), 172 (0.24), 165 (0.47), 130 (1.11), 112 (1.64), 95 (37.50), 91 (32.04), 89 (100.00), 69 (2.04), 53 (10.86), 43 (5.51). HRMS: calcd for $\text{C}_{10}\text{H}_{14}\text{O}_2\text{Cl}$ ($\text{M}^+ + 1$), m/e 201.0682 (^{35}Cl), 203.0653 (^{37}Cl); found, m/e 201.0698 (^{35}Cl), 203.0618 (^{37}Cl).

Palladium(II)-Catalyzed Cyclization of 4'-Heteroatom-2'-Alkenyl 2-Alkynoate. General Procedure. To a stirred solution of alkynoate (1.0 mmol) in HOAc (5 mL) and LiCl (170 mg, 4.0 mmol) was added palladium catalyst (0.05 mmol) at rt. The reaction was monitored by TLC on silica gel. After the reaction was complete, ethyl acetate (60 mL) was added. Then the mixture was washed with water (1 \times 5 mL) and brine (2 \times 5 mL). The organic layer was dried (Na_2SO_4). After removal of the solvent, flash column chromatography on silica gel afforded the pure lactone product.

α -(Z)-Chloromethylene- β -(1'-(E)-pentenyl)- γ -butyrolactone (4): oil, ^1H NMR (300 MHz, CDCl_3) {6.53 (d, $J = 2.8$ Hz) for *E*-isomer; 6.49 (d, $J = 3.2$ Hz) for *Z*-isomer; 1H}, 5.80–5.65 (m, 1H), 5.34–5.25 (m, 1H), 4.50–4.43 (m, 1H), {4.14 (dddd, $J_1 = 1.0$ Hz, $J_2 = 2.7$ Hz, $J_3 = 8.8$ Hz, $J_4 = 17$ Hz) for *Z*-isomer; 3.76 (ddd, $J_1 = 2.7$ Hz, $J_2 = 8.3$ Hz, $J_3 = 17$ Hz) for *E*-isomer, 1H}, 3.98–3.87 (m, 1H), 2.09–2.02 (m, 2H), 1.43 (sextet, $J = 7.5$ Hz, 2H), 0.95–0.89 (m, 3H) [irradiation of the signal at 2.09–2.02 ppm led to the observation of two doublets of two groups of vinylic protons: 5.75 (d, $J = 11$ Hz) and 5.70 (d, $J = 15$ Hz)]; IR (neat) 2920, 2850, 1765, 1640, 1460, 1375, 1170, 1020 cm^{-1} ; MS m/e 203 (M^{+37}Cl) + 1, 1.78), 202 (M^{+37}Cl), 5.31), 201 (38.07), 200 (2.53), 165 (2.53), 149 (37.91), 133 (6.03), 131 (5.41), 128 (100.00), 121 (25.08), 113 (21.69), 107 (50.23), 105 (15.92), 93 (19.63), 91 (38.05). HRMS: calcd for $\text{C}_{10}\text{H}_{13}\text{O}_2\text{Cl}$, m/e 200.0604; found, m/e 200.0621.

α -(Z)-(Chloromethylene)- β -(2'-oxopentyl)- γ -butyrolactone (5): oil, ^1H NMR (300 MHz, CDCl_3) 6.72 (d, $J = 2.1$ Hz, 1H), 4.54 (dd, $J_1 = 7.9$ Hz, $J_2 = 9.4$ Hz, 1H), 3.92 (dd, $J_1 = 4.5$ Hz, $J_2 = 9.3$ Hz, 1H), 3.66–3.61 (m, 1H), 2.89–2.69 (m, 2H), 2.42 (t, $J = 7.4$ Hz, 2H), 1.63 (sextet, $J = 7.4$ Hz, 2H), 0.93 (t, $J = 7.3$ Hz, 3H); IR (neat) 3050, 2950, 2850, 1760, 1715, 1630,

1460, 1410, 1380, 1180 cm^{-1} ; MS m/e 219 (M^{+37}Cl) + 1, 0.79), 217 (M^{+35}Cl) + 1, 2.11), 181 ($\text{M}^+ - \text{Cl}$, 6.04), 175 (M^{+37}Cl) + 1 - CO_2 , 1.40), 173 (M^{+35}Cl) + 1 - CO_2 , 3.78), 147 (M^{+37}Cl) - COPr , 2.93), 145 (M^{+37}Cl) - COPr , 7.71), 133 (M^{+37}Cl) - $\text{CH}_2\text{-COPr}$, 3.55), 131 (M^{+35}Cl) - CH_2COPr , 10.2), 105 (4.67), 103 (13.63), 86 (16.73), 71 (100.00). HRMS: calcd for $\text{C}_{10}\text{H}_{13}\text{O}_3$ ($\text{M}^+ - \text{Cl}$), m/e 181.0865; found, m/e 181.0872.

***cis*- γ -Propyl- β -(1'-(E)-pentenyl)- α -(Z)-(chloroethylidene)- γ -butyrolactone (15):** oil, ^1H NMR (300 MHz, CDCl_3) 5.54 (dt, $J_1 = 15$ Hz, $J_2 = 6.8$ Hz, 1H), 5.29 (dd, $J_1 = 15$ Hz, $J_2 = 8.8$ Hz, 1H), 4.37–4.31 (m, 1H), 3.62 (dt, $J_1 = 1.6$ Hz, $J_2 = 7.6$ Hz, 1H), 2.24 (s, 3H), 2.04 (q, $J = 7.1$ Hz, 2H), 1.64–1.36 (m, 6H), 0.94 (t, $J = 7.1$ Hz, 3H), 0.89 (t, $J = 7.4$ Hz, 3H); IR (neat) 2960, 2880, 1760, 1660, 1460, 1380, 1220, 1170, 1120, 980 cm^{-1} ; MS m/e 259 (M^{+37}Cl) + 1, 10.55), 258 (M^{+37}Cl), 5.17), 257 (M^{+35}Cl) + 1, 31.39), 221 ($\text{M}^+ - \text{Cl}$, 2.83), 198 (3.37), 196 (2.70), 186 (8.28), 184 (24.90), 157 (17.38), 155 (74.06), 149 (20.35), 144 (31.47), 142 (100.00), 121 (25.56), 105 (12.76), 71 (17.63), 55 (12.76). HRMS: calcd for $\text{C}_9\text{H}_{11}\text{O}_2\text{Cl}$ ($\text{M}^+ - \text{C}_5\text{H}_{10}$); m/e 186.0447; found, m/e 186.0472.

***cis*- γ -Propyl- β -(2'-oxopentyl)- α -(Z)-(chloroethylidene)- γ -butyrolactone (16):** oil, ^1H NMR (300 MHz, CDCl_3) 4.36 (m, 1H), 3.80 (m, 1H), 2.85 (dd, $J_1 = 8.7$ Hz, $J_2 = 19$ Hz, 1H), 2.43 (t, $J = 7.2$ Hz, 2H), 2.28 (s, 3H), 2.29 (dd, $J_1 = 4.4$ Hz, $J_2 = 18$ Hz, 1H), 1.65–1.33 (m, 6H), 0.93 (t, $J = 7.3$ Hz, 6H); IR (neat) 2950, 2880, 1760, 1715, 1660, 1470, 1380, 1240 cm^{-1} ; MS m/e 275 (M^{+37}Cl) + 1, 14.92), 274 (M^{+37}Cl), 7.84), 273 (M^{+35}Cl) + 1, 43.33), 272 (M^{+35}Cl), 3.46), 257 (4.84), 255 (13.97), 237 ($\text{M}^+ - \text{Cl}$, 11.03), 201 (3.62), 189 (5.65), 187 (13.79), 151 (22.22), 149 (19.55), 137 (15.46), 129 (38.18), 121 (11.86), 71 (100.00). HRMS: calcd for $\text{C}_{14}\text{H}_{21}\text{O}_3\text{Cl}$; m/e 272.1179 (^{35}Cl); found, m/e 272.1188.

Acknowledgment. We thank the National Natural Science Foundation of China and Chinese Academy of Sciences for financial support.

Supporting Information Available: ^1H NMR spectra of compounds *E*-3A, *Z*-3A, *E*-3B, *Z*-3B, *E*-3C, *Z*-3C, 4, 5, 14a–c, 15, and 16 (13 pages). Ordering information is given on any current masthead page.

OM9503252

Preparation of Bi- and Trimetallic Compounds via [(C₅H₅-η⁶-C₆H₅)Cr(CO)₃]

Y. K. Kang and Y. K. Chung*

Department of Chemistry and Center for Molecular Catalysis, College of Natural Sciences, Seoul National University, Seoul 151-742, Korea

Soon W. Lee¹

Department of Chemistry, Sung Kyun Kwan University, Suwon 440-746, Korea

Received March 27, 1995[©]

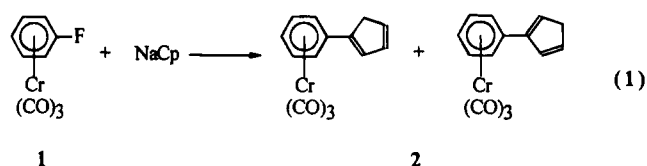
Tricarbonyl(cyclopentadienyl-η⁶-benzene)chromium (**2**) and its lithium (or potassium) salt (**3**), presumably [(C₅H₄-η⁶-C₆H₅Cr(CO)₃]⁻, have been used to make bi- and trimetallic compounds. Upon reaction with Fe₂(CO)₉, **2** yields CrFe(CO)₆(μ-η⁶:η⁴-C₁₁H₁₀) (**4**). The reaction of **3** with M(CO)₃(CH₃CN)₃ (M = Cr, W) and Diazald leads to CrM(CO)₅(NO)(μ-η⁶:η⁵-C₁₁H₉) (**7**, M = Cr; **8**, M = W). Reactions of **3** with Mn(CO)₅Br, CCl(PPh₃)₃, and FeCl₂ result in the formation of CrMn(CO)₆(μ-η⁶:η⁵-C₁₁H₉) (**9**), CoCr(CO)₃(η⁴-C₄Ph₄)(μ-η⁶:η⁵-C₁₁H₉) (**10**), and Cr₂-Fe(CO)₆(μ-η⁶:η⁵-C₁₁H₉)₂ (**11**), respectively. The molecular structure of **11** has been determined by X-ray crystallography.

Introduction

Chemical processes involving two or more organometallic units in combination with one another are becoming of increasing importance.² Especially heterobimetallic complexes that are resistant to fragmentation are attractive for studies. A common synthetic strategy involves the use of difunctional ligands, which are capable of coordinating to two different metal centers. ⁻C₅H₄PPh₂,³ ⁻C₅H₄-SiMe₂CH₂PR₂,⁴ ⁻OCH₂PPh₂,⁵ X(C₅H₄)²⁻ (X = CH₂, CHMe, C≡C, SiMe₂),⁶ ⁻C₅H₄(CH₂)₂PPh₂,⁷ fulvalene,⁸ biphenyl,⁹ and indenyl¹⁰ have been used to construct heterobimetallic compounds. However, the scope of synthetic application to heterometallic compounds is limited because general

approaches have not been elaborated. In an effort to find general approaches, we recently reported the use of the cyclopentadienyl ring in (C₅H₅-η⁶-C₆H₆)Mn(CO)₃ as a π-coordinating ligand to other organometallic reagents.^{11,12}

Cyclopentadienyl anions and arene rings are known to be excellent ligands. Thus, it seems likely that cyclopentadienyl and arene serve as valuable and important ligands for introduction into heterometallic complexes. We recently found that (C₅H₅-η⁶-C₆H₅)Cr(CO)₃ (**2**) was a good starting material for the synthesis of diaryl heterobimetallic compounds. The synthesis of **2** was reported by Gottardi et al. (eq 1).¹³



We have explored the utility of compound **2**. Herein we report the reactions of **2** or the lithium (or potassium) salt of **2** with organometallic reagents resulting in the

* Abstract published in *Advance ACS Abstracts*, September 1, 1995.
(1) X-ray analysis for **11**.

(2) Gladfelter, W. L.; Geoffroy, G. L. *Adv. Organomet. Chem.* **1980**, *18*, 2037. Demerseman, B.; Dixneuf, P. H.; Douglade, J.; Mercier, R. *Inorg. Chem.* **1982**, *21*, 3942. Albers, M. O.; Robinson, D. J.; Coville, N. *J. Coord. Chem. Rev.* **1986**, *69*, 127.

(3) Casey, C. P.; Bullock, R. M.; Fultz, W. C.; Rheingold, A. L. *Organometallics* **1982**, *1*, 1591. Casey, C. P.; Nief, F. *Organometallics* **1985**, *4*, 1218. Casey, C. P.; Bullock, R. M. *Acc. Chem. Res.* **1987**, *20*, 167.

(4) Schore, N. E. *J. Am. Chem. Soc.* **1979**, *101*, 7410. Schore, N. E.; Benner, L. S.; LaBelle, B. E. *Inorg. Chem.* **1981**, *20*, 3200. LeBlanc, J. C.; Moise, C.; Maisonnat, A.; Poilblanc, R.; Charrier, C.; Mathey, F. *J. Organomet. Chem.* **1982**, *231*, C43. Rausch, M. D.; Edwards, B. H.; Rogers, R. D.; Atwood, J. L. *J. Am. Chem. Soc.* **1983**, *105*, 3882.

(5) Ferguson, G. S.; Wolczanski, P. T. *Organometallics* **1985**, *4*, 1601. Ferguson, G. S.; Wolczanski, P. T. *J. Am. Chem. Soc.* **1986**, *108*, 8293. Ferguson, G. S.; Wolczanski, P. T.; Paranyi, L.; Zonneville, M. C. *Organometallics* **1988**, *7*, 1967.

(6) Cuenca, T.; Padilla, A.; Royo, P.; Parra-Hake, M.; Pellinelli, M. A.; Tiripicchio, A. *Organometallics* **1995**, *14*, 848. Gomez-Sal, P.; de Jesus, E.; Perez, A. I.; Royo, P. *Organometallics* **1993**, *12*, 4633. Plenio, H. *Chem. Ber.* **1991**, *124*, 2185. Ciruelos, S.; Cuenca, T.; Flores, J. C.; Gomez, R.; Gomez-Sal, P.; Royo, P. *Organometallics* **1993**, *12*, 944. Reddy, K. P.; Petersen, J. L. *Organometallics* **1989**, *8*, 2107. Levanda, C.; Bechgaard, K.; Cowan, D. O. *J. Org. Chem.* **1976**, *41*, 2700. Kramer, J. A.; Hendrickson, D. N. *Inorg. Chem.* **1980**, *19*, 3330.

(7) Lee, I.; Dahan, F.; Maisonnat, A.; Poilblanc, R. *Organometallics* **1994**, *13*, 2743.

(8) Ashworth, T. V.; Agreda, T. C.; Hertweck, E.; Hermann, W. A. *Angew. Chem., Int. Ed. Engl.* **1986**, *25*, 289. Gambarotta, S.; Chiang, M. Y. *Organometallics* **1987**, *6*, 897. Egan, J. W., Jr.; Petersen, J. L. *Organometallics* **1986**, *5*, 906. Lacoste, M.; Astruc, D.; Garland, M. T.; Varret, F. *Organometallics* **1988**, *7*, 2253. Vollhardt, K. P. C.; Weidman, T. W. *Organometallics* **1984**, *3*, 82.

(9) Geiger, W. E.; Van Order, N., Jr.; Pierce, T.; Bitterwolf, T. E.; Rheingold, A. L.; Chasteen, N. D. *Organometallics* **1991**, *10*, 2403. Elschenbroich, C.; Heck, J. J. *J. Am. Chem. Soc.* **1979**, *101*, 6773. Bitterwolf, T. E.; Raghuvver, K. S. *Inorg. Chim. Acta* **1990**, *172*, 59. Top, S.; Jaouen, G. *J. Organomet. Chem.* **1979**, *182*, 381. Bitterwolf, T. E. *J. Organomet. Chem.* **1980**, *252*, 305.

(10) Bonifaci, C.; Cecon, A.; Gambaro, A.; Ganis, P.; Santi, S.; Valle, G.; Venzo, A. *Organometallics* **1993**, *12*, 4211. Cecon, A.; Elsevier, C. J.; Ernsting, J. M.; Gambaro, A.; Santi, S.; Venzo, A. *Inorg. Chim. Acta* **1993**, *204*, 15. Cecon, A.; Gambaro, A.; Santi, S.; Venzo, A. *J. Mol. Catal.* **1991**, *69*, L1. Cecon, A.; Gambaro, A.; Santi, S.; Valle, G.; Venzo, A. *J. Chem. Soc., Chem. Commun.* **1989**, 51. Green, M. L. H.; Lowe, N. D.; O'Hare, D. *J. Chem. Soc., Chem. Commun.* **1986**, 1547. Bonifaci, C.; Cecon, A.; Gambaro, A.; Ganis, P.; Mantovani, L.; Santi, S.; Venzo, A. *J. Organomet. Chem.* **1994**, *475*, 267. Van Order, N., Jr.; Geiger, W. E.; Bitterwolf, T. E.; Rheingold, A. L. *J. Am. Chem. Soc.* **1987**, *109*, 5680. Bonifaci, C.; Cecon, A.; Gambaro, A.; Ganis, P.; Santi, S.; Venzo, A. *Organometallics* **1995**, *14*, 2430.

(11) Chung, T.-M.; Chung, Y. K. *Organometallics* **1992**, *11*, 2822.

(12) Kim, J.-A.; Chung, T.-M.; Chung, Y. K.; Lee, S. W. *J. Organomet. Chem.* **1995**, *486*, 211.

(13) Cecon, A.; Gambaro, A.; Gottardi, F.; Mannoli, F.; Venzo, A. *J. Organomet. Chem.* **1989**, *363*, 91.

formation of bi- and trimetallic compounds, and we also report the molecular structure of $[\text{Cr}_2\text{Fe}(\text{CO})_6(\mu\text{-}\eta^6\text{:}\eta^5\text{-C}_{11}\text{H}_9)_2]$. In the bi- and trimetallic complexes presented in this report, the metals are not linked by metal-metal bonds but are linked by a diaryl functional ligand in which one metal is bonded to a cyclopentadienyl ligand and the other metal is bonded to the arene ring.

Experimental Section

All reactions were conducted under nitrogen using standard Schlenk type flask and cannula techniques. Workup procedures were done in air.

Elemental analyses were done at the Korea Basic Science Center or at the Chemical Analytic Center, College of Engineering, Seoul National University. ^1H NMR spectra were obtained with a Varian XL-200 instrument. Infrared spectra were recorded on a Shimadzu IR-470 (spectra measured as films on NaCl by evaporation of solvent). Mass spectra were recorded with a VG ZAB-E double-focusing mass spectrometer.

Compounds $(\text{C}_6\text{H}_5\text{-}\eta\text{-C}_6\text{H}_5)\text{Cr}(\text{CO})_3$,¹³ $\text{M}(\text{CO})_3(\text{CH}_3\text{CN})_3$ ($\text{M} = \text{Cr}, \text{W}$),¹⁴ $\text{CoCl}(\text{PPh}_3)_3$ ¹⁵ and $\text{Mn}(\text{CO})_5\text{Br}$ ¹⁶ were synthesized according to the published procedures.

Synthesis of $\text{CrFe}(\text{CO})_6(\mu\text{-}\eta^6\text{:}\eta^4\text{-C}_{11}\text{H}_{10})$, 4. Compound 2 (0.30 g, 1.08 mmol) and 30 mL of benzene were placed in a Schlenk flask. $\text{Fe}_2(\text{CO})_9$ (1.1 g, 3.0 mmol) was added to the reaction flask while the flask was vigorously flushed with nitrogen gas. The mixture was refluxed for 6 h. The reaction mixture was cooled to room temperature. Silica gel (2 g) was added to the reaction mixture, and the solvent was removed by rotary evaporator. After column chromatography with hexane/ether (v/v, 10:1), the product was obtained in 54% yield (0.20 g). Mp 193 °C; IR $\nu(\text{CO})$ 2040, 1960, 1878 cm^{-1} ; ^1H NMR (CDCl_3) δ 5.85 (vs, 1 H), 5.68 (m, 1 H), 5.32 (m, 2 H), 5.18 (t, 6.2 Hz, 1 H), 5.11 (d, 6.8 Hz, 2 H), 3.25 (m, 1 H), 2.82 (vd, 11.6 Hz, 1 H), 2.52 (vd, 11.6 Hz, 1 H) ppm. Anal. Calcd for $\text{C}_{17}\text{H}_{10}\text{-CrFeO}_6$: C, 48.84; H, 2.41. Found: C, 48.74; H, 2.39.

Synthesis of $[(\mu\text{-}\eta^6\text{-C}_{11}\text{H}_9)\text{CrFe}(\text{CO})_6]\text{BF}_4$, 5. To 4 (177 mg, 0.42 mmol) dissolved in 20 mL of CH_3CN was slowly added Ph_3CBF_4 (210 mg, 0.63 mmol) in 5 mL of CH_3CN via cannula at 0 °C. The resulting solution was stirred for 30 min, and then any solids were filtered off. The filtrate was concentrated to ca. 5 mL, and precipitation was caused adding excess diethyl ether. The precipitates were washed with CH_2Cl_2 (10 mL \times 2). The yield was 195 mg (93%). IR $\nu(\text{CO})$ 2116, 2068, 1960, 1880 cm^{-1} ; ^1H NMR (d_6 -acetone) δ 6.15 (t, 1.71 Hz, 2 H), 6.04 (d, 6.59 Hz, 2 H), 5.91 (t, 1.71 Hz, 2 H), 5.87 (t, 6.10 Hz, 1 H), 5.71 (t, 6.47 Hz, 2 H) ppm. Anal. Calcd for $\text{C}_{17}\text{H}_9\text{BF}_4\text{CrFeO}_6$: C, 40.52; H, 1.80. Found: C, 40.43; H, 1.96.

Synthesis of $(\text{Ph-}\eta^5\text{-C}_5\text{H}_4)\text{Fe}(\text{CO})_3\text{BF}_4$, 6. NOBF_4 (0.05 g, 0.43 mmol) was added to the solution of 4 (0.10 g, 0.24 mmol) in 10 mL of CH_2Cl_2 at room temperature. After the resulting solution had been stirred for 1 h, 1 mL of CH_3NO_2 was added to the reaction mixture. The resulting solution was stirred for 10 min, and then any solids were filtered off. The filtrate was concentrated to ca. 5 mL. Excess diethyl ether was added to the filtrate to precipitate the product. The precipitates were washed with CH_2Cl_2 (10 mL \times 2). The yield was 92%. IR $\nu(\text{CO})$ 2112, 2056 cm^{-1} ; ^1H NMR (d_6 -acetone) δ 8.02 (d, 5.61 Hz, 2 H), 7.60 (m, 3 H), 6.75 (m, 2 H), 6.30 (m, 2 H) ppm. Anal. Calcd for $\text{C}_{14}\text{H}_9\text{BF}_4\text{FeO}_3$: C, 45.71; H, 2.46. Found: C, 46.09; H, 2.54.

Synthesis of $\text{Cr}_2(\text{CO})_5(\text{NO})(\mu\text{-}\eta^6\text{:}\eta^5\text{-C}_{11}\text{H}_9)$, 7. Compound 2 (0.278 g, 1 mmol) and 30 mL of THF were placed in a Schlenk flask. *n*-BuLi (1.25 mmol, 0.5 mL of a 2.5 M solution in

n-hexane) was added dropwise to the reaction flask at 0 °C. After the resulting solution had been stirred for 1 h, a THF solution of $\text{Cr}(\text{CO})_3(\text{CH}_3\text{CN})_3$ (2.27 mmol, generated in situ in 10 mL of THF) was transferred via cannula to the reaction mixture. The resulting mixture was refluxed for 12 h and then cooled to room temperature. Diazald (0.214 g, 1 mmol) was added to the resulting solution. The solution was stirred for 2 h, and the solvent was removed on a rotary evaporator. The resulting residue was extracted with diethyl ether. To the ether extracts was added silica gel (2 g) in hexane (10 mL). After evaporation of the solvent, flash column chromatography with a mixture of ether and hexane (v/v, 1:20) gave the product (0.397 g, 96%). Mp 185 °C (decomp); IR $\nu(\text{CO})$ 2008, 1966, 1938, 1879 cm^{-1} , $\nu(\text{NO})$ 1678 cm^{-1} ; ^1H NMR (CDCl_3) δ 4.57 (t, 2.44 Hz, 2 H), 4.48 (m, 4 H), 4.26 (m, 1 H), 4.19 (t, 2.44 Hz, 2 H) ppm. Anal. Calcd for $\text{C}_{18}\text{H}_9\text{Cr}_2\text{NO}_6$: C, 46.28; H, 2.18; N, 3.37. Found: C, 46.01; H, 2.06; N, 3.20.

Synthesis of $\text{CrW}(\text{CO})_5(\text{NO})(\mu\text{-}\eta^6\text{:}\eta^5\text{-C}_{11}\text{H}_9)$, 8. A typical procedure was almost the same as the synthesis of 5, except $\text{W}(\text{CO})_3(\text{CH}_3\text{CN})_3$ is used instead of $\text{Cr}(\text{CO})_3(\text{CH}_3\text{CN})_3$. Yield: 73%. IR $\nu(\text{CO})$ 2004, 1960, 1924, 1882 cm^{-1} , $\nu(\text{NO})$ 1648 cm^{-1} ; ^1H NMR (CDCl_3) δ 4.99 (t, 2.2 Hz, 2 H), 4.56 (t, 2.2 Hz, 2 H), 4.43 (m, 4 H), 4.21 (m, 1 H) ppm. Anal. Calcd for $\text{C}_{18}\text{H}_9\text{-CrNO}_6\text{W}$: C, 35.12; H, 1.66; N, 2.56. Found: C, 34.90; H, 1.51; N, 2.36. HRMS m/z , M^+ , calcd 546.9342, obsd 546.9357.

Synthesis of $\text{CrMn}(\text{CO})_6(\mu\text{-}\eta^6\text{:}\eta^5\text{-C}_{11}\text{H}_9)$, 9. Compound 2 (0.208 g, 0.75 mmol) and 40 mL of benzene were placed in a Schlenk flask. *n*-BuLi (1 mmol, 0.4 mL of a 2.5 M solution in *n*-hexane) was added dropwise to the flask at 10 °C. After the resultant solution had been stirred for 1 h, $\text{BrMn}(\text{CO})_5$ (0.30 g, 1.12 mmol) was added while the reaction flask was vigorously flushed with nitrogen gas. The mixture was refluxed for 12 h. The reaction mixture was cooled to room temperature. After evaporation of the solvent, the residue was extracted with ether. To the ether extracts was added silica gel (2 g) in hexane (10 mL). After evaporation of the solvent, flash column chromatography with a mixture of ether and hexane (v/v, 1:10) gave the product (0.123 g, 40%). IR $\nu(\text{CO})$ 2011, 1965, 1925, 1880 cm^{-1} ; ^1H NMR (CDCl_3) δ 4.50–4.35 (m, 4 H), 4.21 (m, 3 H), 3.87 (m, 2 H) ppm. Anal. Calcd for $\text{C}_{17}\text{H}_8\text{CrMnO}_6$: C, 49.0; H, 2.18. Found: C, 48.6; H, 1.84.

Synthesis of $\text{CoCr}(\text{CO})_5(\eta^4\text{-C}_4\text{Ph}_4)(\mu\text{-}\eta^6\text{:}\eta^5\text{-C}_{11}\text{H}_9)$, 10. A solution of 2 (0.278 g, 1 mmol) in 10 mL of THF was slowly transferred via cannula to a solution of KH (0.05 g, 1.25 mmol) in 10 mL of THF at 0 °C. The resulting solution was stirred for 1 h at 0 °C. $\text{CoCl}(\text{PPh}_3)_3$ (0.88 g, 1 mmol) and diphenylacetylene (0.40 g, 1.1 mmol) in 20 mL of toluene were added to the reaction flask while the reaction flask was vigorously flushed with nitrogen gas. The mixture was refluxed for 12 h. The reaction mixture was cooled to room temperature, and removal of the solvent gave yellow crude solids. After recrystallization in hexane, the product was obtained in 43% yield. Mp 206 °C; IR $\nu(\text{CO})$ 1959, 1880 cm^{-1} ; ^1H NMR (CDCl_3) δ 5.10 (m, 20 H), 5.01 (d, 6.6 Hz, 2 H), 4.90 (t, 1.95 Hz, 2 H), 4.75 (t, 1.95 Hz, 2 H) ppm. HRMS m/z $\text{M}^+ - \text{Cr}(\text{CO})_3$, calcd 556.1594, obsd 556.1601.

Synthesis of $\text{Cr}_2\text{Fe}(\text{CO})_6(\mu\text{-}\eta^6\text{:}\eta^5\text{-C}_{11}\text{H}_9)_2$, 11. Compound 2 (0.278 g, 1 mmol) and 30 mL of THF were placed in a Schlenk flask. *n*-BuLi (1.25 mmol, 0.5 mL of a 2.5 M solution in *n*-hexane) was added dropwise to the flask at 0 °C. After the solution had been stirred for 1 h, anhydrous FeCl_2 (0.06 g, 0.48 mmol) was added to the reaction flask while it was vigorously flushed with nitrogen gas. The reaction mixture was refluxed for 12 h, cooled to room temperature, and filtered. Removal of the solvent gave crude solids. The crude product was recrystallized by methylene chloride and ether. Yield: 76% (0.223 g). Mp 175 °C; IR $\nu(\text{CO})$ 1939, 1853 cm^{-1} ; ^1H NMR (CDCl_3) δ 5.45–5.25 (m, 10 H), 4.50 (t, 1.95 Hz, 4 H), 4.37 (t, 1.95 Hz, 4 H) ppm. Anal. Calcd for $\text{C}_{28}\text{H}_{18}\text{Cr}_2\text{FeO}_6$: C, 55.11; H, 2.97. Found: C, 54.62; H, 2.90.

X-ray Structure Determination of $\text{Cr}_2\text{Fe}(\text{CO})_6(\mu\text{-}\eta^6\text{:}\eta^5\text{-C}_{11}\text{H}_9)_2$, 11. All X-ray data were collected with use of an

(14) Quick, M. H.; Angelici, R. J. *Inorg. Synth.* 1979, 19, 160.

(15) Yamazaki, H.; Wakatsuki, Y. In *Organometallic Syntheses*; King, R. B., Eisch, J. J., Eds.; Academic Press: New York, 1988; Vol. 4, p 278.

(16) Tate, D. P.; Knippe, W. R.; Augl, J. M. *Inorg. Chem.* 1962, 1, 433.

Table 1. Crystal Data and Structure Refinement for 11

formula	C ₂₈ H ₁₈ Cr ₂ FeO ₆
fw	610.27
cryst syst	monoclinic
space group	Cc
a, Å	20.564(9)
b, Å	7.858(3)
c, Å	18.048(3)
β, deg	124.91(3)
V, Å ³	2391.6(14)
Z	4
d(calcd), Mg/m ³	1.695
cryst size, mm ³	0.2 × 0.3 × 0.3
λ/Å	0.710 73 (Mo Kα)
tot. no. of observns	4592
no. of unique data (I > 2σ(I))	1664
2θ range/deg	3–50
no. of params refined	334
R1 = (Σ F _o - F _c)/Σ F _o	0.0661
wR2 = {Σ[w(F _o ² - F _c ²) ²]/Σ[w(F _o ²)] ^{1/2}	0.1737
GOFF on F ²	1.065

Enraf-Nonius CAD4 automated diffractometer equipped with an Mo X-ray tube and a graphite crystal monochromator.

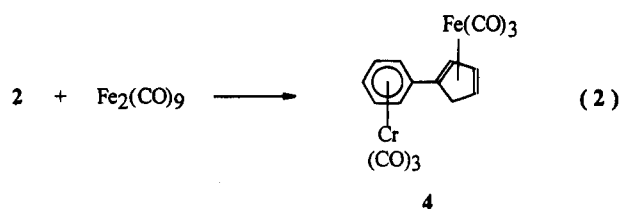
A red crystal of **11** having approximate dimensions 0.2 × 0.3 × 0.3 mm³, was used for crystal and intensity data collection. Details on crystal and intensity data are given in Table 1. The orientation matrix and unit cell parameters were determined from 25 machine-centered reflections with 12 < 2θ < 24°. Axial photographs were used to verify the unit cell choice. Intensities of three check reflections were monitored after every 1 h during data collection. Data were corrected for Lorentz and polarization effects. The intensity data were empirically corrected with ψ-scan data. All calculations were carried out on a personal computer with the SHELXS-86 and SHELXL-93 programs.

The unit cell parameters and systematic absences, *hkl* (*h* + *k* = 2*n* + 1), *h0l* (*h* or *l* = 2*n* + 1), and *0k0* (*k* = 2*n* + 1), indicated two possible space groups: *Cc* and *C2/c*. A statistical analysis of intensities suggested a noncentrosymmetric space group, and the structure converged only in the space group *Cc*. The structure was solved by direct methods. All non-hydrogen atoms were refined anisotropically. All hydrogen atoms were positioned geometrically and refined using a rigid model. Final atomic positional parameters for non-hydrogen atoms were shown in Table 2, and the selected bond distances and bond angles are shown in Table 3.

Results and Discussion

Recently activation of haloarene by the Cr(CO)₃ moiety has been attracting much attention in connection with the formation of bi- and polymetallic compounds via the nucleophilic substitution of halogen.¹⁷ Compound **2** was prepared by the formal nucleophilic substitution of fluoride by cyclopentadienide.¹³ Compound **2** is an isomeric mixture and is reacted further without isolation of regioisomers.^{11,13}

Treatment of **2** with Fe₂(CO)₉ in refluxing benzene led to the isolation of **4** in 54% yield (eq 2). At first we



expected a dimeric compound with bridging carbonyls [(C₅H₄-C₆H₅)Cr(CO)₃]-Fe(CO)₂ as a product. In-

Table 2. Atomic Coordinates (×10⁴) and Equivalent Isotropic Parameters (Å² × 10³) for 11

atom	x	y	z	U(eq) ^a
Fe	8965(1)	8754(2)	1762(1)	35(1)
Cr(1)	6189(1)	11852(3)	103(1)	38(1)
Cr(2)	7489(1)	5647(3)	3428(1)	38(1)
C(1)	6496(10)	9120(21)	43(12)	53(4)
C(2)	5818(10)	9200(22)	65(13)	51(4)
C(3)	5796(9)	10016(24)	692(11)	55(4)
C(4)	6462(11)	10855(20)	1378(12)	54(4)
C(5)	7157(9)	10785(19)	1448(9)	42(3)
C(6)	7162(8)	9966(17)	752(10)	41(3)
C(7)	7916(8)	9917(18)	814(9)	41(3)
C(8)	8120(10)	8605(19)	400(9)	43(3)
C(9)	8848(9)	9038(21)	567(11)	46(4)
C(10)	9122(8)	10570(21)	1084(12)	54(4)
C(11)	8545(11)	11096(20)	1232(12)	58(4)
C(12)	9097(9)	6428(17)	2315(9)	43(3)
C(13)	9802(10)	6922(19)	2449(13)	53(4)
C(14)	10044(8)	8442(21)	2948(11)	49(4)
C(15)	9481(10)	8884(22)	3133(9)	50(4)
C(16)	8873(7)	7583(17)	2719(8)	36(3)
C(17)	8181(8)	7578(17)	2755(9)	36(3)
C(18)	7477(9)	6665(17)	2104(11)	41(3)
C(19)	6817(10)	6655(21)	2141(12)	53(4)
C(20)	6848(9)	7481(23)	2831(11)	52(4)
C(21)	7551(12)	8315(22)	3523(11)	51(4)
C(22)	8182(10)	8377(18)	3445(10)	48(4)
C(30)	6836(9)	13518(22)	145(10)	46(4)
C(40)	5604(11)	11997(18)	-1133(12)	50(4)
C(50)	5607(10)	13549(25)	150(10)	50(4)
C(60)	8459(10)	3978(22)	3413(12)	51(4)
C(70)	8509(9)	5491(20)	4673(11)	46(4)
C(80)	7227(9)	3927(24)	3400(14)	57(4)
O(30)	7223(9)	14619(16)	167(10)	71(4)
O(40)	5244(8)	12117(16)	-1911(8)	60(3)
O(50)	5250(7)	14664(18)	194(8)	63(3)
O(60)	8812(8)	2908(17)	3346(10)	69(3)
O(70)	8925(7)	5388(16)	5435(7)	62(3)
O(80)	6820(8)	2877(19)	3337(10)	77(4)

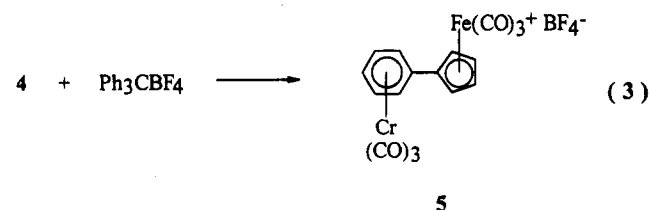
^a U(eq) is defined as one-third of the trace of the orthogonalized U_{ij} tensor.

Table 3. Selected Bond Distances (Å) and Bond Angles (deg)

Fe-C(10)	2.02(2)	Fe-C(7)	2.05(2)
Cr(1)-C(30)	1.84(2)	Cr(1)-C(1)	2.26(2)
Cr(1)-C(4)	2.18(2)	C(1)-C(6)	1.40(2)
C(6)-C(7)	1.49(2)	C(30)-O(30)	1.16(2)
C(10)-Fe-C(12)	155.9(6)	Cr(1)-C(50)-O(50)	176(2)
C(6)-C(1)-C(2)	115(2)	C(3)-C(4)-C(5)	121(2)
C(7)-C(8)-C(9)	107.7(13)	C(7)-C(11)-C(10)	109(2)

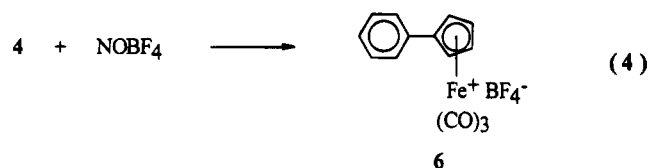
stead, we obtained **4** as the sole product. Compound **4** could be a mixture of two isomers as is the precursor **1**. However, according to the ¹H NMR spectrum of **4**, only one isomer was produced. This might be due to isomerization during the reaction.

Treatment of **4** with Ph₃CBF₄ in CH₃CN gave **5** in 93% yield (eq 3). Compound **5** is a reddish crystalline



compound. According to the carbonyl stretching frequencies of chromium carbonyls attached to the phenyl ring of **4** (1960, 1878 cm⁻¹) and of **5** (1960, 1880 cm⁻¹), the positive charge on **5** does not give an appreciable electronic effect to the chromium carbonyls.

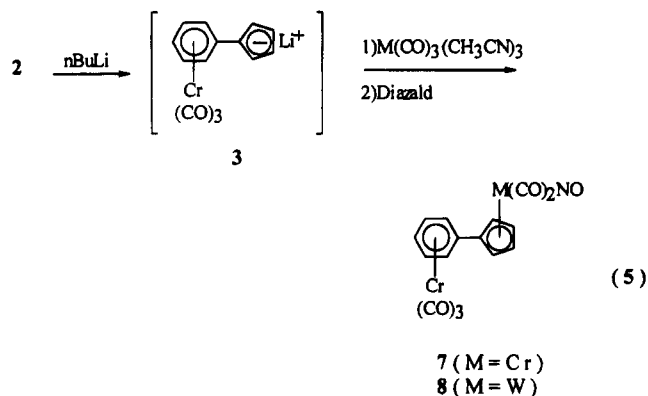
Treatment of **4** with 2 equiv of NOBF_4 in CH_2Cl_2 gave **6** in 92% yield (eq 4). When **4** was treated with 1 equiv



of NOBF_4 at -10°C , there was almost no reaction within 3 h. When the reaction temperature was warmed to room temperature for 6 h, we could see the formation of **6** by checking the IR spectrum. Thus, the reaction seemed to be rather sensitive to the reaction temperature. Compounds of (arene) $\text{Cr}(\text{CO})_2\text{NO}$ were known to be rather unstable;¹⁸ thus, we did not expect nitrosylation of chromium carbonyl. Instead we expected iron dicarbonyl nitrosyl complex. However, **6** was obtained. With deprotonation, the chromium tricarbonyl moiety was also removed.

Several years ago, Rausch et al.¹⁹ reported the use of phenylcyclopentadienylthallium (PhCpTl) to synthesize organometallic compounds. However, they did not report the synthesis of phenylcyclopentadienyliron derivatives. Instead they reported the formation of ruthenium derivatives, e.g., $[\text{PhCpRu}(\text{CO})_2]_2$ and $\text{PhCpRu}(\text{CO})_2\text{Cl}$. The yields (5%–8%) of the reaction were too low to use in synthetic work. Thus, **6** can be used as a good precursor to make phenyl-substituted cyclopentadienyliron complexes.

Compound **2** can be easily lithiated in high efficiency by treatment with $n\text{-BuLi}$. The lithiated compound, presumably **3**, was used without isolation. Treatment of **3** with $\text{Cr}(\text{CO})_3(\text{CH}_3\text{CN})_3$ and then with Diazald led to the isolation of **7** (96%) (eq 5). Single crystals of **7**



suitable for X-ray studies were grown in CH_2Cl_2 . However, according to the X-ray studies,²⁰ the crystallographically independent complexes are located in the two crystallographic inversion centers and the complex

(17) Ishii, Y.; Ishino, Y.; Aoki, T.; Hidai, M. *J. Am. Chem. Soc.* **1992**, *114*, 5429. Li, J.; Hunter, A. D.; McDonald, R.; Santarsiero, B. D.; Bott, S. G.; Atwood, J. L. *Organometallics* **1992**, *11*, 3050. Richter-Addo, G. B.; Hunter, A. D. *Inorg. Chem.* **1989**, *28*, 4063.

(18) Connelly, N. G.; Kelly, R. L. *J. Chem. Soc., Dalton Trans.* **1974**, 2334. Ball, D. E.; Connelly, N. G. *J. Organomet. Chem.* **1973**, *55*, C24.

(19) Singh, P.; Rausch, M. D.; Bitterwolf, T. E. *J. Organomet. Chem.* **1988**, *352*, 273.

(20) Crystal data for **7**: space group $P\bar{1}$; cell parameters $a = 10.590(4) \text{ \AA}$, $b = 10.840(2) \text{ \AA}$, $c = 7.138(3) \text{ \AA}$, $\alpha = 90.10(3)^\circ$, $\beta = 102.77(6)^\circ$, $\gamma = 89.94(2)^\circ$; $Z = 2$; $R = 7.64$; $wR = 20.21$. The crystal structure of **7** was solved by Prof. M. S. Lah (Han Yang University, Korea).

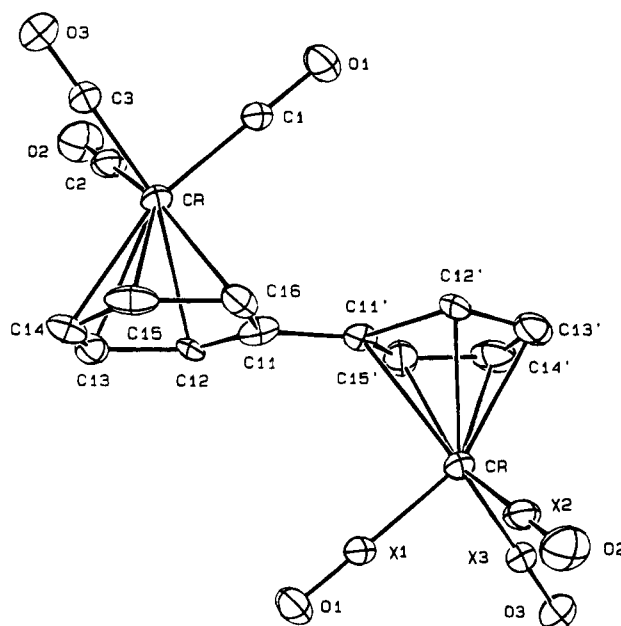
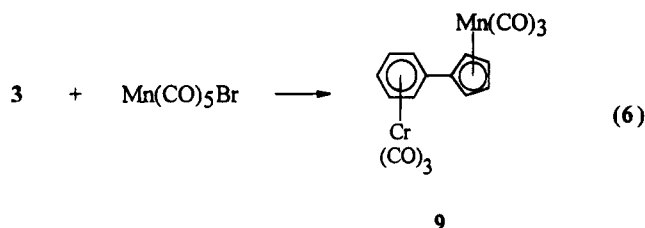


Figure 1. ORTEP drawing of compound **7**. One of the disordered configurations is shown.

with pseudoinversion symmetry is disordered in the crystallographic inversion center with half-occupancy of each orientation. Any discussions about geometry are not meaningful. Thus we only report the ORTEP drawing of **7** (Figure 1).

When **3** was treated with $\text{W}(\text{CO})_3(\text{CH}_3\text{CN})_3$ and then with Diazald, the expected compound **8** (73%) was obtained. Single crystals of **8** suitable for X-ray studies were grown in CH_2Cl_2 . However, we confronted almost the same problems as in **7**. The crystal **8** was disordered in the crystallographic inversion center with half-occupancy of each orientation. When the nitrosylation was performed by using NOBF_4 , the yield was rather low. The IR spectra of nitrosyl ligands in **7** and **8** display absorption frequencies at 1678 and 1648 cm^{-1} . As in the case of other cyclopentadienyl compounds, the stretching frequencies of nitrosyl ligands decrease as the central metals become heavier.²¹

Treatment of **3** with $\text{Mn}(\text{CO})_5\text{Br}$ in refluxing benzene produces the yellow compound **9** in 40% yield (eq 6). The

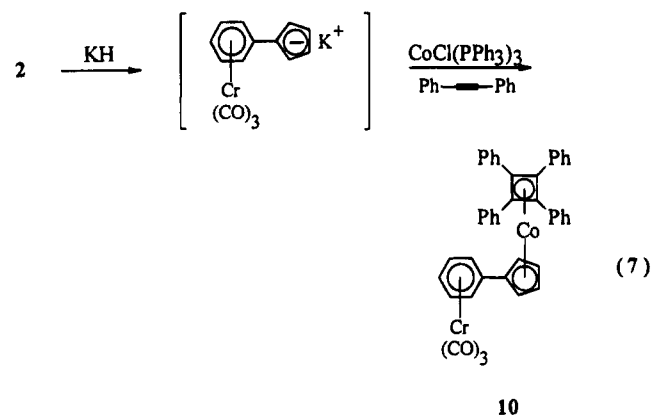


yellow solid is air-stable and soluble in organic solvents. The IR spectrum of **9** displays metal carbonyl frequencies at 2011, 1965, 1925, and 1880 cm^{-1} . On the basis of intensity and position, the bands at 2011 and 1925 cm^{-1} are assigned to the carbonyl ligands of (cyclopentadienyl) $\text{Mn}(\text{CO})_3$.²²

Treatment of the potassium salt of **3** with $\text{CoCl}(\text{PPh}_3)_3$ and diphenylacetylene in refluxing THF led to isolation

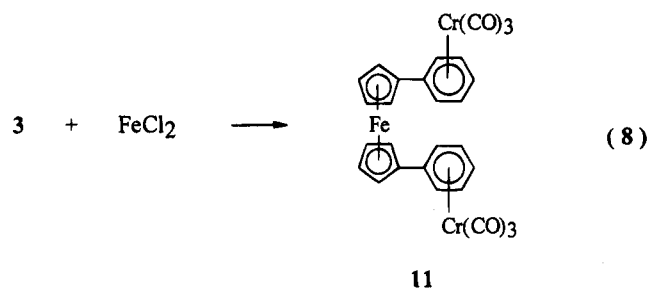
(21) Hoyano, J. K.; Legzdins, P.; Malito, J. T. *Inorg. Synth.* **1978**, *18*, 126. Malito, J. T.; Shakir, R.; Atwood, J. L. *J. Chem. Soc., Dalton Trans.* **1980**, 1253.

of compound **10** (eq 7). At first we wanted to prepare



the cobalt carbonyl compound via Co₂(CO)₈. However, the expected product was too unstable to isolate and characterize completely (IR ν(CO) 2016, 1954, and 1869 cm⁻¹). To increase the stability of cobalt derivative, we used diphenylacetylene as a ligand. During this reaction, diphenylacetylenes were dimerized to give tetraphenylcyclobutadienyl ligands.²³ Thus compound **10** was synthesized and characterized fully. Compared to the stability of cobalt dicarbonyl derivative, **10** is much more stable. However, during the purification, **10** slowly decomposed.

Treatment of **3** with FeCl₂ in THF led to the formation of ferrocene derivative **11** in 76% yield (eq 8). Compound



11 is slightly soluble in diethyl ether and chloroform and freely soluble in methylene chloride and acetone. Single crystals of **11** suitable for X-ray studies were grown in CH₂Cl₂. The geometry of **11** with the atomic numbering scheme used is depicted in Figure 2, and selected distances and angles are given in Table 3. Compound **11** adopts an eclipse conformation with the phenyl groups located in the same direction. This cofacial arrangement of the two phenyl rings seems to be less favorable.²⁴ Recently, Plenio reported^{24a} an eclipsed 1,1'-orientation of the two substituents of 1,1'-bis(3,4-dimethylcyclopenta-1,3-dienyl)ferrocene. For **11** and 1,1'-bis(3,4-dimethylcyclopenta-1,3-dienyl)ferrocene,

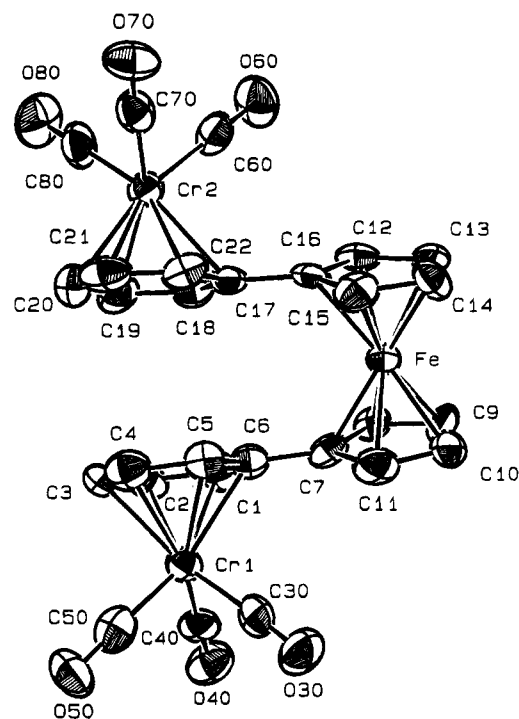


Figure 2. ORTEP drawing of compound **11**.

the stacking of the two π-systems seems to compensate for the sterically less favorable cofacial 1,1'-orientation of the substituents. The Cp rings are nearly perfect planes and are nearly parallel, the angle between the planes being 3(1)°. In the same way, the phenyl rings are nearly perfect planes and are nearly parallel with the dihedral angle being 5(1)°. The torsion angle between the cyclopentadienyl ring and the phenyl ring (25(1)°) is comparable to the twist angle (27.5°) of the phenyl rings in (biphenyl)[Cr(CO)₂](μ-P₂Me₄).²⁵

We have demonstrated that the cyclopentadiene ring of **2** can be coordinated to the second metal (Fe) by cyclopentadienyl or cyclopentadienyl fashions. The cyclopentadienyl ring of the lithiated compound **3** can be coordinated to the second metal (Cr, W, Mn, Fe, or Co), demonstrating incorporation of two different transition metals into a single molecule. Recently, bimetallic compounds containing two transition metal moieties joined to a diaryl ligand were considered as models for the study of the mixed valences.¹³ This study provides one of the potentially attractive methods of preparing diaryl dinuclear complexes with different electronic and structural requirements. Now we are continuing to study of the properties of the novel bi- and trimetallic compounds.

Acknowledgment. We are grateful to the Korea Science Engineering Foundation (Grant No. 93-05-00-02) for support of this research program.

Supporting Information Available: Tables of full bond distances and bond angles, anisotropic thermal parameters, and hydrogen atom coordinates for **11** (7 pages). This material is contained in many libraries on microfiche, immediately follows this article in the microfilm version of the journal, and can be ordered from ACS; see any current masthead page for ordering information.

OM950223B

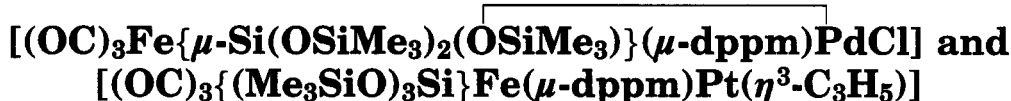
(22) Piper, T. S.; Cotton, F. A.; Wilkinson, G. J. *Inorg. Nucl. Chem.* **1955**, *1*, 165. Fischer, R. D. *Chem. Ber.* **1960**, *93*, 165. Brown, D. A.; Sloan, H. J. *J. Chem. Soc.* **1963**, 4389. Adams, D. M.; Squire, A. *J. Chem. Soc., Dalton Trans.* **1974**, 558.

(23) Efraty, A. *Chem. Rev.* **1977**, *77*, 692.

(24) (a) Plenio, H. *Organometallics* **1992**, *11*, 1856. (b) Grossel, M. C.; Goldspink, M. R.; Hriljac, J. A.; Weston, S. C. *Organometallics* **1991**, *10*, 851.

(25) Geiger, W. E.; Van Order, N., Jr.; Pierce, T.; Bitterwolf, T. E.; Rheingold, A. L.; Chasteen, N. D. *Organometallics* **1991**, *10*, 2403.

Novel CO-Induced Silyl Migration in Heterobimetallic Iron–Palladium Methyl Complexes Leading to μ -Siloxycarbene Complexes. Crystal Structures of the Metallasiloxanes



Michael Knorr*[†] and Pierre Braunstein*

Laboratoire de Chimie de Coordination, Associé au CNRS (URA 0416), Université Louis Pasteur, 4 rue Blaise Pascal, F-67070 Strasbourg Cedex, France

Antonio Tiripicchio and Franco Ugozzoli

Dipartimento di Chimica Generale ed Inorganica, Chimica Analitica, Chimica Fisica, Università di Parma, Centro di Studio per la Strutturistica Diffattometrica del CNR, Viale delle Scienze 78, I-43100 Parma, Italy

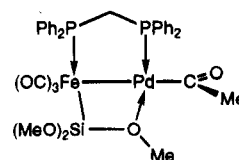
Received March 29, 1995[©]

The heterobimetallic alkyl, siloxyl complex $[(OC)_3Fe\{\mu-Si(OSiMe_3)_2(OSiMe_3)\}(\mu-dppm)Pd(Me)]$ (**2a**), which displays a $\mu-\eta^2$ -Si–O bridge, was prepared by alkylation of $[(OC)_3Fe\{\mu-Si(OSiMe_3)_2(OSiMe_3)\}(\mu-dppm)PdCl]$ (**1**) with MeLi. The analogous complex $[(OC)_3Fe\{\mu-Si(OSiMe_3)_2(OSiMe_3)\}(\mu-dppm)Pd(Me)]$ (**2b**) was obtained by reaction of $K[Fe\{SiMe(OSiMe_3)_2\}(CO)_3(\eta^1-dppm)]$ with a cold THF solution of $[Pd(Cl)(Me)(1,5-COD)]$. The dynamic behavior of the $Si(OSiMe_3)_3$ ligand in **2a** was investigated by variable-temperature ^{13}C -NMR spectroscopy and is consistent with rapid rotation of the siloxyl ligand about the Fe–Si bond at ambient temperature. Upon treatment of a hexane solution of **2a** with CO, the siloxycarbene-bridged complex $[(OC)_3Fe(\mu-C\{OSi(OSiMe_3)_3\}Me)(\mu-dppm)Pd(CO)]$ (**3a**) was formed quantitatively. Complex **2b** reacted in an analogous manner. This transformation results from CO insertion followed by a silyl migration and its mechanism is discussed. The allyl complex $[(OC)_3\{(Me_3SiO)_3Si\}Fe(\mu-dppm)Pt(\eta^3-C_3H_5)]$ (**5**) was prepared and addition of RNC (R = *t*-Bu, 2,6-dimethylphenyl) yielded the labile σ -allyl complexes $[(OC)_3\{(Me_3SiO)_3Si\}Fe(\mu-dppm)Pt(\eta^1-C_3H_5)(CNR)]$ (**6**) which are in equilibrium with **5** due to facile RNC dissociation. In the presence of an excess *t*-BuNC, complex $[(OC)_3\{(Me_3SiO)_3Si\}Fe(\mu-dppm)Pt(\eta^1-C_3H_5)(CNR)_2]$ (**7**) was formed which contains a pentacoordinated platinum center. The solid-state structures of complexes **1** and **5** have been determined by single-crystal X-ray diffraction.

Introduction

The insertion of carbon monoxide into the metal–carbon bond of mononuclear complexes plays a fundamental role in organometallic chemistry and homogeneous catalysis owing to the importance of C–C coupling reactions.^{1–3} As part of our studies on the reactivity of heterometallic, alkoxy-silyl complexes, we prepared a series of alkyl complexes of the type $[(OC)_3Fe\{\mu-Si(OMe)_2(OMe)\}(\mu-dppm)MR]$ (M = Pd, Pt; R = Me, Et, norbornyl) and investigated their ability to insert CO and isocyanides into the metal–alkyl bond.^{4–6} The acyl

complex $[(OC)_3Fe\{\mu-Si(OMe)_2(OMe)\}(\mu-dppm)Pd\{C(O)Me\}]$ was shown to insert olefins into the Pd–C σ -bond, thus allowing sequential CO/olefin incorporation.⁴



We were intrigued by the possibility that a siloxyl ligand in place of $Si(OMe)_3$ could induce a different reactivity toward small molecules. Both silicon ligands are characterized by a dynamic behavior associated with

[†] Present address: Universität des Saarlandes, Anorganische Chemie, D-66041 Saarbrücken, Germany.

[©] Abstract published in *Advance ACS Abstracts*, September 1, 1995.

(1) Garrou, P. E.; Heck, R. F. *J. Am. Chem. Soc.* **1976**, *98*, 4115.

(2) Anderson, G. K.; Cross, R. J. *Acc. Chem. Res.* **1984**, *17*, 67.

(3) Yamamoto, A. *Organotransition Metal Chemistry*; Wiley & Sons: New York, 1986.

(4) Braunstein, P.; Knorr, M.; Stährfeldt, T. *J. Chem. Soc., Chem. Commun.* **1994**, 1913.

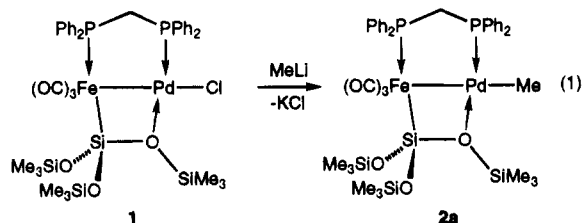
(5) Braunstein, P.; Faure, T.; Knorr, M.; Stährfeldt, T.; DeCian, A.; Fischer, J. *Gazz. Chim. Ital.* **1995**, *125*, 35.

(6) (a) Knorr, M.; Braunstein, P.; DeCian, A.; Fischer, J. *Organometallics* **1995**, *14*, 1302. (b) Braunstein, P.; Knorr, M. In *Metal-Ligand Interactions, Structure and Reactivity*; NATO ASI Series; Russo, N., Salahub, D. R., Eds.; Kluwer Academic Publishers: Dordrecht, The Netherlands, 1995, in press. (c) Braunstein, P.; Knorr, M. *J. Organomet. Chem.* **1995**, *500*, in press. (d) Braunstein, P.; Knorr, M. Unpublished results.

the labile, donor O→M interaction, which renders the three substituents at silicon equivalent on the NMR time scale. However, a slight change in lability could directly affect the coordination and insertion of small molecules.⁴ We report here on Fe–Pt–allyl and Fe–Pd–Me complexes which contain these ligands and present carbonylation studies which lead to bridging siloxycarbene complexes via a CO-induced silyl migration.

Results

We recently prepared the siloxyl complex $[(OC)_3Fe\{\mu-Si(OSiMe_3)_2(OSiMe_3)\}(\mu-dppm)PdCl]$ (**1**)⁷ which contains a $\mu-\eta^2$ -SiO interaction. This feature suggests possible modes of interaction between metal complexes or particles and the silica surface of heterogeneous catalysts. Although we had no direct proof for the occurrence of a dative bond between the oxygen of the siloxane chain and the Pd center, such an interaction was assumed by comparison between the spectroscopic data of **1** and those of the structurally characterized trialkoxysilyl analogous complex $[(OC)_3Fe\{\mu-Si(OMe)_2(OMe)\}(\mu-dppm)PdCl]$.⁸ This $\mu-\eta^2$ -SiO interaction has now been established by the crystal structure determination of **1**. Since this type of bonding was expected to play a crucial role in the reactivity of corresponding alkyl complexes (see below), as observed with $-Si(OMe)_3$ derivatives,^{4–6} we set out to prepare the methyl complex **2a** according to the reaction of eq 1.



Crystal Structure of $[(OC)_3Fe\{\mu-Si(OSiMe_3)_2(OSiMe_3)\}(\mu-dppm)PdCl]$ (**1**).

A view of the structure of **1** is shown in Figure 1; selected bond distances and angles are given in Table 1. The Fe atom is located in a distorted-octahedral environment involving the Pd, P(1), and Si(1) atoms and three carbon atoms from the carbonyl groups. The square planar geometry around the Pd atom is achieved by the coordination of the O(6) atom of the siloxane ligand, and by the Cl, P(2), and Fe atoms. This structure is closely related to that of

$[(OC)_3Fe\{\mu-Si(OMe)_2(OMe)\}(\mu-dppm)PdCl]$ ⁸ in which the Fe–Pd and Pd–Cl bond distances, 2.582(1) and 2.303(2) Å, differ slightly from those found in **1**, 2.544(2) and 2.384(2) Å, respectively, whereas the Fe–Si bond distances are almost identical, 2.275(2) and 2.277(3) Å, respectively. The most important feature of the structure of **1** is the coordination mode of the siloxane moiety forming a Si(1)–Fe–Pd–O(6) four-membered ring, in which the dative Pd–O(6) bond distance, 2.245(5) Å, is significantly longer than that found for the Si(OMe)₃ analogue, 2.100(4) Å. In addition to steric factors, the weaker electron donating ability of the oxygen atom in a Si–O–SiMe₃ chain compared to a Si–OMe group

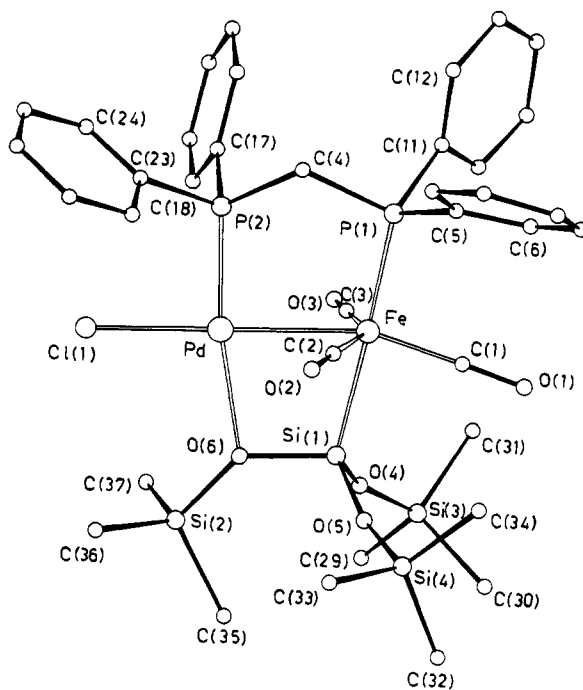


Figure 1. View of the structure of $[(OC)_3Fe\{\mu-Si(OSiMe_3)_2(OSiMe_3)\}(\mu-dppm)PdCl]$ (**1**) in the crystal.

Table 1. Selected Bond Distances (Å) and Angles (deg) of Complex **1**

Pd–Fe	2.544(2)	Pd–Cl	2.384(2)
Pd–P(2)	2.187(3)	Pd–O(6)	2.245(5)
Fe–P(1)	2.219(3)	Fe–Si(1)	2.277(3)
Fe–C(1)	1.749(6)	Fe–C(2)	1.766(8)
Fe–C(3)	1.782(7)	Si(1)–O(4)	1.603(4)
Si(1)–O(5)	1.607(7)	Si(1)–O(6)	1.668(4)
Si(2)–O(6)	1.670(5)	Si(3)–O(4)	1.624(4)
Si(4)–O(5)	1.612(7)	O(1)–C(1)	1.145(8)
O(2)–C(2)	1.157(9)	O(3)–C(3)	1.144(8)
Cl–Pd–O(6)	97.2(1)	Cl–Pd–P(2)	91.5(1)
Fe–Pd–O(6)	81.4(1)	Fe–Pd–P(2)	99.9(1)
Pd–Fe–C(3)	75.9(2)	Pd–Fe–C(2)	72.2(2)
Pd–Fe–Si(1)	76.2(1)	Pd–Fe–P(1)	101.6(1)
C(1)–Fe–C(3)	101.9(3)	C(1)–Fe–C(2)	107.6(3)
Si(1)–Fe–C(3)	86.1(2)	Si(1)–Fe–C(2)	84.8(2)
Si(1)–Fe–C(1)	84.8(2)	P(1)–Fe–C(3)	99.1(2)
P(1)–Fe–C(2)	89.0(2)	P(1)–Fe–C(1)	97.4(2)
Fe–Si(1)–O(6)	104.1(2)	Fe–Si(1)–O(5)	116.1(2)
Fe–Si(1)–O(4)	116.1(2)	O(5)–Si(1)–O(6)	106.4(3)
O(4)–Si(1)–O(6)	105.8(2)	O(4)–Si(1)–O(5)	107.5(2)
Si(1)–O(4)–Si(3)	156.3(3)	Si(1)–O(5)–Si(4)	165.3(4)
Si(1)–O(6)–Si(2)	131.1(3)	Pd–O(6)–Si(2)	127.4(2)
Pd–O(6)–Si(1)	98.2(2)	Fe–C(1)–O(1)	177.7(7)
Fe–C(2)–O(2)	178.6(6)	Fe–C(3)–O(3)	177.6(5)

probably contributes to the lengthening of the Pd–O distance in **1**. The four-membered ring is almost planar [maximum deviation 0.072(4) Å for the O(6) atom] and makes an angle of 5.1(1)° with the Pd, Fe, P(1), P(2), and C(4) mean plane. As observed with other molecules which contain a $\mu-\eta^2$ -Si–O bridge, the Si(1)–O(6) bond distance (1.668(4) Å) is longer than the Si(1)–O(4) and Si(1)–O(5) distances (1.603(4) and 1.607(7) Å).^{5, 8–14}

(9) Braunstein, P.; Knorr, M.; Piana, H.; Schubert, U. *Organometallics* **1991**, *10*, 828.

(10) Braunstein, P.; Knorr, M.; Villarroya, E.; DeCian, A.; Fischer, J. *Organometallics* **1991**, *10*, 3714.

(11) Balegronne, F.; Braunstein, P.; Douce, L.; Dusausoy, Y.; Grandjean, D.; Knorr, M.; Strampfer, M. *J. Cluster Sci.* **1992**, *3*, 275.

(12) Braunstein, P.; Faure, T.; Knorr, M.; Balegronne, F.; Grandjean, D. *J. Organomet. Chem.* **1993**, *462*, 271.

(13) Adams, R. D.; Cortopassi, J. E.; Pompeo, M. P. *Inorg. Chem.* **1992**, *31*, 2563.

(7) Knorr, M.; Braunstein, P. *Bull. Soc. Chim. Fr.* **1992**, *129*, 663.

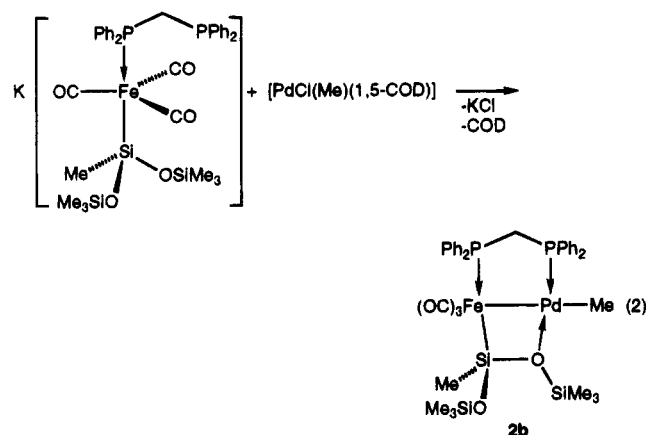
(8) Braunstein, P.; Knorr, M.; Tiripicchio, A.; Tiripicchio-Camellini, M. *Angew. Chem., Int. Ed. Engl.* **1989**, *28*, 1361.

A related dative interaction between the oxygen of a metallasiloxane and a zirconium center has recently been described in the mononuclear complex $[(\eta\text{-C}_5\text{Me}_5)\text{ZrCl}_2(\text{CH}_2\text{SiMe}_2\text{OSiMe}_3)]$.¹⁵ Despite the oxophilic character of zirconium, the Zr–OSiMe₃ distance (2.427(3) Å) in this four-membered cycle is considerably longer than in our case. The authors noted that such a lengthening compared to other Zr–O bonds may result from steric interactions and from the competition between the zirconium center and the empty 3d orbitals on Si for the oxygen lone pairs. (Note however that, in contrast to previous concepts,¹⁶ it is currently believed that when appropriate, back-bonding into silicon-element antibonding σ^* orbitals, rather than into silicon 3d orbitals, should be invoked.¹⁷)

Synthesis and Reactivity of Bimetallic Siloxyl Complexes. CO Insertion and Silyl Migration Reactions. Although alkylation of **1** with MeLi in Et₂O offers a satisfactory synthetic access to **2a**, this yellow, air-stable bimetallic complex was best prepared (85% yield) by the reaction of the metalate $\text{K}[\text{Fe}\{\text{Si}(\text{OSiMe}_3)_3\}(\text{CO})_3(\eta^1\text{-dppm})]^-$ with $[\text{PdCl}(\text{Me})(1,5\text{-COD})]$ ¹⁸ or $[\text{PdMe}(\text{SMe}_2)(\mu\text{-Cl})_2]$.¹⁹ Note that mononuclear iron–siloxyl complexes have recently been obtained by condensation of ferrosilanol, -diols, and -triols with chlorosilanes.²⁰

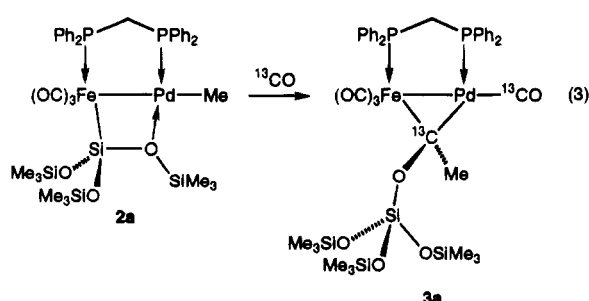
In order to establish whether rapid exchange of the –OSiMe₃ groups was taking place, as in the corresponding –Si(OMe)₃ complex, we undertook a variable-temperature ¹³C-NMR study. At 298 K two doublets are observed in a 2:1 ratio at δ 216.4 and 214.4, corresponding to the CO groups. The siloxyl moiety gives rise to a sharp singlet at δ 2.40, and the Pd-bound methyl group resonates at δ 1.58. Upon cooling of the CDCl₃ solution down to 253 K, the siloxyl resonance changes to a broad signal at δ 2.36, whereas the singlet of the methyl group at δ 1.84 remains sharp. At 223 K two distinct sharp singlets in a approximately 1:2 ratio are found at δ 3.42 and 2.15 together with a third singlet at δ 1.98 for the Pd-bound methyl group. These findings demonstrate that the siloxyl ligand displays in solution a labile and dynamic dative interaction with palladium via one of its oxygen atoms, as first demonstrated for the Si(OMe)₃ group.⁸ The dynamic process probably involves rotation of the siloxyl ligand about the Fe–Si bond and can be slowed down at low-temperatures to give a rigid structure on the NMR time scale which creates nonequivalent trimethylsiloxy groups. The high stability of **2a** associated with its interesting reactivity (see below) prompted us to attempt the synthesis of a Fe–Pd complex with an asymmetric siloxyl unit. Reaction of the metalate $\text{K}[\text{Fe}\{\text{SiMe}(\text{OSiMe}_3)_2\}(\text{CO})_3(\eta^1\text{-dppm})]^-$ with a cold THF solution of $[\text{PdCl}(\text{Me})(1,5\text{-COD})]$

afforded $[(\text{OC})_3\text{Fe}\{\mu\text{-SiMe}(\text{OSiMe}_3)(\text{OSiMe}_3)\}(\mu\text{-dppm})\text{Pd}(\text{Me})]$ **2b** in moderate yield (eq 2).



The stability of **2b** in solution appears somewhat reduced compared to that of **2a**. This may be explained by the fact that in **2b** the coordination sphere of the Pd center can be completed in the dynamic regime by only one of *two* exchanging OSiMe₃ groups. In the IR spectrum, the replacement of an electron-withdrawing OSiMe₃ substituent in **2a** by a more electron-donating methyl group in **2b** causes a slight shift of the $\nu(\text{CO})$ stretching frequencies to lower wavenumbers. It remains to be seen how the chiral nature of the Si atom in the rigid structure affects the stereochemical reactivity of this molecule.

Unexpectedly, the outcome of the carbonylation of complexes **2** differed markedly from that of the Si(OMe)₃ derivative. After purging of a solution of **2a** for 3 min with CO and removal of the solvent (CDCl₃ or hexane), a red, waxy solid was obtained in quantitative yield. Elemental analyses and spectroscopic data are in agreement with the formulation of the product as the heterobimetallic siloxycarbene-bridged complex $[(\text{OC})_3\text{Fe}\{\mu\text{-C}[\text{OSi}(\text{OSiMe}_3)_3]\text{Me}\}(\mu\text{-dppm})\text{Pd}(\text{CO})]$ (**3a**). The presence in **3a** of a terminal CO ligand on Pd was evidenced in the IR spectrum by a strong $\nu(\text{CO})$ band at 2035 cm⁻¹. The NMR data obtained when using ¹³C-enriched (99%) CO are consistent with incorporation of the labeled ¹³C-nuclei as outlined in eq 3. The ³¹P-NMR spectrum of



the ¹³C-enriched complex contains a doublet of doublets pattern centered at δ 65.1 for the Fe-bound P atom with a ²⁺³*J*(P–P) coupling of 139 Hz and a ²*J*(¹³C–P) coupling of 17 Hz and a second doublet of doublets at δ 15.2 for the Pd-bound P atom with a ²*J*(¹³C–P) coupling of 52 Hz. The ¹³C–P coupling between the P(Pd) nucleus and the Pd-bound terminal CO ligand is too small to be observed, probably because of their mutual cis arrange-

(14) Adams, R. D.; Cortopassi, J. E.; Yamamoto, J. H. *Organometallics* **1993**, *12*, 3036.

(15) Lyszak, E. L.; O'Brien, J. P.; Kort, D. A.; Hendges, S. K.; Redding, R. N.; Bush, T. L.; Hermen, M. S.; Renkema, K. B.; Silver, M. E.; Huffman, J. C. *Organometallics* **1993**, *12*, 338.

(16) Kwart, H.; King, K. *d-orbitals in the Chemistry of Silicon, Phosphorus and Sulfur*; Springer: New York, 1977.

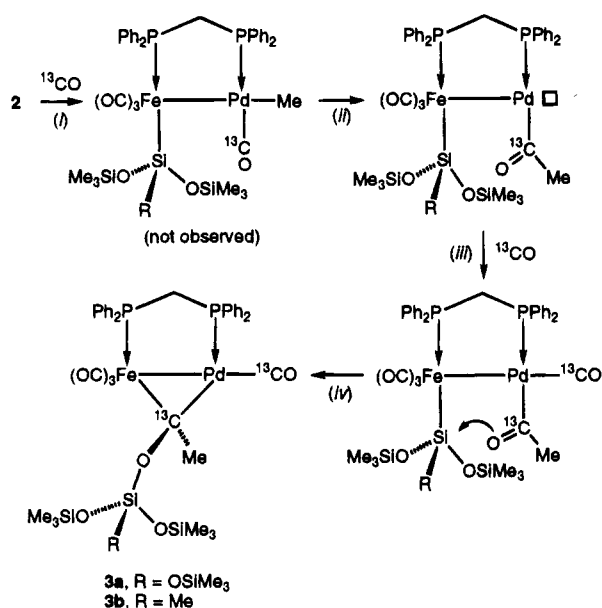
(17) (a) Janoschek, R. *Chem. Zeit.* **1988**, *22*, 128. (b) Bock, H. *Angew. Chem., Int. Ed. Engl.* **1989**, *28*, 1627.

(18) Lapido, F. T.; Anderson, G. K. *Organometallics* **1994**, *13*, 303.

(19) Byers, P. K.; Cauty, A. J.; Engelhardt, L. M.; White, A. H. *J. Chem. Soc., Dalton Trans.* **1986**, 1731.

(20) Malisch, W.; Schmitzer, S.; Kaupp, G.; Hindahl, K.; Käß, H.; Wachtler, U. In *Organosilicon Chemistry, From Molecules to Materials*; Auner, N., Weis, J., Eds.; VCH: Weinheim, Germany, 1994; p 185.

Scheme 1. Suggested Pathway for the Formation of Complexes 3



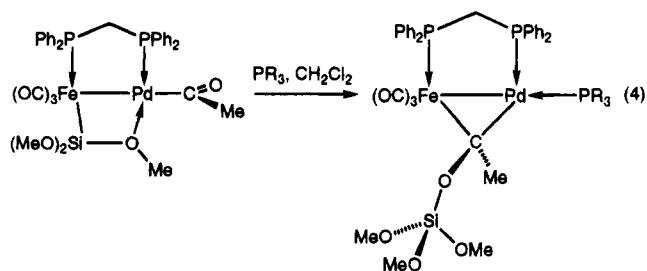
ment. The pattern observed for the μ -carbene resonance at δ 218.8, which is coupled with the P nuclei by 52 and 17 Hz, respectively, is consistent with this structure. A singlet at δ 187.1 is found for the Pd-bound CO ligand. The iron-bound CO's at δ 215.5 and 211.4 are enriched only to a very small extent (less than 10%) during the carbonylation reaction. Because of a $^1J(\text{C}-\text{C})$ coupling of 30 Hz the low-field signal for the migrated methyl group appears as a doublet at δ 47.1, a value consistent with those quoted for other bimetallic complexes containing a $\mu\text{-C}(\text{Me})(\text{OR})$ ligand.²¹ In the $^1\text{H-NMR}$ spectrum, the methyl protons are also shifted to low field and give rise to a doublet of doublets at δ 3.10 with $^4J(\text{P}-\text{H})$ couplings of 11.0 and 3.2 Hz. A further splitting occurs in the labeled complex due to a $^2J(^{13}\text{C}-\text{H})$ coupling of 3.2 Hz. Notwithstanding the asymmetry of the molecule induced by the stereogenic μ -carbenic carbon, the dppm protons appear as a triplet centered at δ 3.44. At 233 K this resonance is however transformed into a complex multiplet (AB pattern with additional phosphorus couplings) owing to the diastereotopic nature of these protons.

When CO was bubbled for 5 min through a solution of **2b**, a similar, quantitative rearrangement was observed. The spectroscopic data for $[(\text{OC})_3\text{Fe}\{\mu\text{-C}(\text{Me})\text{OSiMe}(\text{OSiMe}_3)_2\}(\mu\text{-dppm})\text{Pd}(\text{CO})]$ (**3b**) are very similar to those for **3a** and are given in the Experimental Section. Unfortunately, the stability of both **3a** and **3b** is somewhat limited. Even in the solid-state, insoluble materials are formed in considerable amounts after 1 day, so that elemental analyses have been carried out immediately after the preparation of the compounds.

The formation of complexes **3** can be tentatively rationalized as follows (Scheme 1): after (i) displacement of the donor Si-O-Pd bond by CO followed (ii)

by a cis migration of the methyl ligand and (iii) occupation of the free coordination site by another CO ligand, an intermediate would be formed which has the acyl ligand trans to the dppm phosphorus on Pd and syn to the migrating siloxyl moiety. A subsequent migration (iv) of the siloxyl ligand (perhaps facilitated by a cyclic transition state involving some dative interaction of the acyl oxygen with silicon) to the acyl oxygen to form a siloxy carbene would account for the final product. Accordingly, purging a solution of $[(\text{OC})_3\text{Fe}\{\mu\text{-Si}(\text{OSiMe}_3)_2(\text{OSiMe}_3)\}(\mu\text{-dppm})\text{PdCl}]$ (**1**) with CO for 15 min resulted in no change in the IR spectrum. As in the cases of the mononuclear acyl-silyl complexes *cis*- $[(\text{OC})_4\text{Fe}\{\text{C}(\text{O})\text{Me}\}\text{SiMe}_3]$ ²⁴ and $[(\text{OC})_3\text{HCo}\{\text{C}(\text{O})\text{Me}\}\text{SiR}_3]$ ²⁵ and of the phosphine-induced silyl shift observed in related Fe-Pt acyl complexes,⁶ the formation of a strong silicon-oxygen bond is assumed to be the driving force for this rearrangement. Remember that in the case of the $\text{Si}(\text{OMe})_3$ derivative $[(\text{OC})_3\text{Fe}\{\mu\text{-Si}(\text{OMe})_2(\text{OMe})\}(\mu\text{-dppm})\text{PdMe}]$, carbonylation led to a stable acyl complex, which showed no tendency to rearrange even under prolonged CO exposure.⁴ In contrast, no acyl intermediate could be trapped in the carbonylation of **2** (see Scheme 1).

This contrasting behavior between the $-\text{Si}(\text{OMe})_3$ and the $-\text{Si}(\text{OSiMe}_3)_3$ derivatives may be assigned to the more electropositive character of the central Si atom in the latter case since OSiMe_3 substituents are less electron donating than methoxy groups. Only in the presence of a donor ligand such as $\text{P}(\text{Et})_3$ or PPh_3 was formation of a carbene complex observed in the $\text{Si}(\text{OMe})_3$ case. Thus, addition of PPh_3 to the acyl complex $[(\text{OC})_3\text{Fe}\{\mu\text{-Si}(\text{OMe})_2(\text{OMe})\}(\mu\text{-dppm})\text{PdC}(\text{O})\text{Me}]$ afforded the corresponding siloxycarbene complex (eq 4). Full details on these carbene complexes will appear later.^{6b-d} A similar behavior was observed in related Fe-Pt complexes.^{6a}



Coordination of a phosphine to the palladium will increase the basicity of the acyl oxygen and increase the tendency for Si-O bond formation despite the less electropositive character of the Si center. As indicated above, the Fe-Si distances in **1** and $[(\text{OC})_3\text{Fe}\{\mu\text{-Si}(\text{OMe})_2(\text{OMe})\}(\mu\text{-dppm})\text{PdCl}]$ are almost identical. This is also likely to be the case for the methyl derivatives, and we therefore rule out that a different Fe-Si bond strength in the two derivatives could be responsible for their different reactivity.

Upon addition of PPh_3 to a CH_2Cl_2 solution of **3a** the CO ligand on Pd is readily substituted to afford the more stable $[(\text{OC})_3\text{Fe}\{\mu\text{-C}(\text{Me})\text{OSi}(\text{OSiMe}_3)_3\}(\mu\text{-dppm})\text{Pd}(\text{P}-$

(21) Awang, M. R.; Jeffery, J. C.; Stone, F. G. A. *J. Chem. Soc., Dalton Trans.* **1983**, 9, 2091.

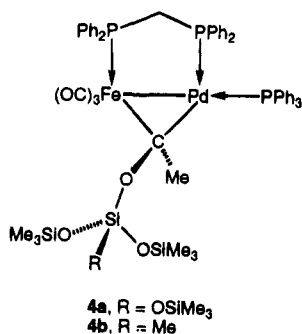
(22) (a) Akita, M.; Oku, T.; Moro-Oka, Y. *J. Chem. Soc., Chem. Commun.* **1992**, 1031. (b) Hanna, P. K.; Gregg, B. T.; Cutler, A. R. *Organometallics* **1991**, 10, 31.

(23) Mead, K. A.; Moore, I.; Stone, F. G. A.; Woodward, P. *J. Chem. Soc., Dalton Trans.* **1983**, 9, 2083.

(24) Brinkmann, K. C.; Blakeny, A. J.; Krone-Schmidt, W.; Gladysz, J. A. *Organometallics* **1984**, 3, 1325.

(25) Gregg, B. T.; Cutler, A. R. *Organometallics* **1992**, 11, 4276.

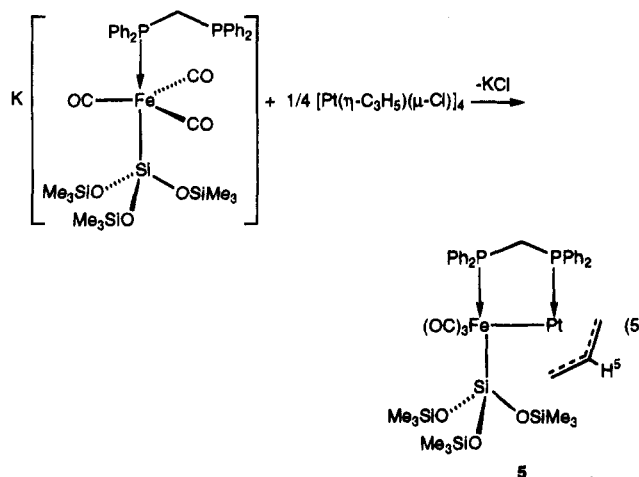
Ph₃)] (**4a**), which was fully characterized. The analogo-



gous complex **4b**, prepared in a similar manner, was identified spectroscopically by comparison with **4a**. Its ³¹P{¹H}-NMR spectrum consists of three resonances: the iron-bound phosphorus gives rise to a doublet of doublets at δ 65.5 with couplings of 131 and 4 Hz, the latter being due to the PPh₃ ligand, which resonates at δ 18.0. The doublet at δ 14.5 for the dppm phosphorus on Pd shows no resolved coupling with the PPh₃ ligand, owing to their mutual cis-orientation. In the ¹H-NMR spectrum, the dppm protons are now inequivalent even at ambient temperature and give rise to two multiplets centered at δ 3.38.

By analogy with the structure of the related Fe–Pt complex [(OC)₃Fe{μ-C(Et)OSi(OMe)₃}{μ-dppm}Pt(PPh₃)],⁶ we believe that the carbene ligand in **3** and **4** adopts a symmetrical bridging position with respect to the metal centers. No other bridging siloxycarbene complex appears to have been isolated, although such complexes have recently been invoked as intermediates in the hydrosilylation reaction of a bridging CO ligand in a dinuclear Ru complex.^{22a} A heterobimetallic 17-electron intermediate of the type [(OC)₄R(O)C}Mn{μ-CH(OSiR'₃)}FeCp(CO)₂] has been proposed by Cutler *et al.* in the manganese-catalyzed hydrosilylation of organoiron acyl complexes.^{22b} Dppm-bridged heterobimetallic W–Pt complexes with asymmetrically bonded μ-carbene ligands have however been described.^{21,23} Thus, by reaction of a mononuclear tungsten carbene complex with Pt(COD)₂, Stone *et al.* obtained [PtW{μ-C(OMe)Me}(CO)₅(COD)], which afforded after treatment with dppm the complex [PtW{μ-C(OMe)Me}(CO)₅(η¹-dppm)]. The latter compound isomerized in solution to yield [(OC)Pt(μ-dppm){μ-C(OMe)Me}W(CO)₄], in which the ligand arrangement is very similar to that in **3**.

Synthesis and Structure of a Fe–Pt Allyl Siloxyl Complex. We have recently described the Fe–Pd complex [(OC)₃{(Me₃SiO)₃Si}Fe(μ-dppm)Pd(η³-C₃H₅)] and investigated the rapid η³ → η¹ → η³ isomerization of the allyl ligand by variable-temperature NMR techniques.¹² In order to favor the η¹ structure and explore its reactivity toward CO, we turned our attention toward the analogous Fe–Pt complex since it was expected that the dative O→Pt interaction would be stronger (or less labile) than in the palladium case. This assumption was based on previous comparative studies of the dynamic behavior of [(OC)₃Fe{μ-Si(OMe)₂(OMe)}{μ-dppm}PdCl] and [(OC)₃Fe{μ-Si(OMe)₂(OMe)}{μ-dppm}PtCl].⁶ The ivory complex **5** was prepared according to eq 5 and characterized by analytical and spectroscopic methods as well as by X-ray diffraction (see below).



Since the allyl ligand occupies two coordination sites, it was expected that the siloxyl ligand would act as a terminal ligand, in contrast to the situation in **2a**. The singlet resonance observed in the ¹³C NMR spectrum for the OMe protons and the ²⁺³J(PP) coupling constants of 105 Hz observed in the ³¹P{¹H}-NMR spectrum are consistent with the structure drawn for **5** which also corresponds to the solid-state structure (see below). The allyl ligand is bonded to Pt in a η³-manner, as evidenced by NMR spectroscopy. Assignments of the ¹H-NMR resonances result from comparison between the spectra of **5** and the low temperature spectrum of its Pd analogue.¹² In contrast to its Pd counterpart, **5** shows no dynamic behavior in the temperature range 253–298 K, so that, in addition to the resonances for the inequivalent dppm protons, five distinct signals for the allylic protons are observed. The ¹³C NMR spectrum contains a singlet for the siloxane at δ 1.8. The allylic carbons appear as a singlet for C(1) at δ 62.0, a doublet with a J(P–C) coupling of 40 Hz for C(3), and a further doublet for C(2) at δ 105.8 (J(P–C) = 3 Hz).

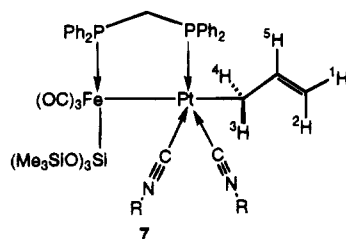
Crystal Structure of [(OC)₃{(Me₃SiO)₃Si}Fe(μ-dppm)Pt(η³-C₃H₅)] (5**).** A view of the structure of **5** is shown in Figure 2; selected bond distances and angles are given in Table 2. The Fe atom has an octahedral environment, more distorted than that of **1**, involving the Pt atom, the P(1) atom from the dppm bridging ligand, the Si(1) atom from the Si(OSiMe₃)₃ ligand, and three carbon atoms from the carbonyl groups. The coordination of the Pt atom involves the Fe atom, the P(2) atom from the dppm bridging ligand, and the carbon atoms of the allyl ligand interacting in the usual η³-fashion. The Fe–Pt distance, 2.675(3) Å, is indicative of a metal–metal bond. The geometry around the platinum atom is similar to that observed in mononuclear Pd– or Pt–allyl complexes, such as [Pt(η³-C₃H₅)(PR₃)Cl]^{26,27} or in related bimetallic complexes.^{5,9} The C(40) carbon deviates by 0.064(9) Å from the FePtP(2) plane, whereas the carbon atoms C(38) and C(39) are disposed above (0.172(9) Å), and below (0.481(9) Å) this plane. The FePtP(2) plane forms with the C(38)C(39)C(40) and PtC(38)C(40) planes dihedral angles of 112.8(3) and 4.3(2)°, respectively. The Pt–C(38) distance, 2.279(9) Å, is significantly longer than Pt–

(26) Del Pra, A.; Zanotti, G.; Carturan, G. *Inorg. Chim. Acta* **1979**, *33*, L137.

(27) Carturan, G.; Belluco, U.; Del Pra, A.; Zanotti, G. *Inorg. Chim. Acta* **1979**, *33*, 155.

doublet for the dppm phosphorus on iron at δ 63.7 with a ${}^{2+3}J(\text{P}-\text{P})$ coupling of 85 Hz and a second doublet at δ 18.4 for the platinum-bound phosphorus nucleus with a ${}^1J(\text{Pt}-\text{P})$ coupling of 3414 Hz. As in the case of **6a** the allylic resonances in the ${}^1\text{H}$ -NMR spectrum are very broad, thus precluding further information. From a very concentrated solution containing a slight excess of *t*-BuNC, we succeeded in isolating an off-white solid whose elemental analyses and IR spectrum ($\nu(\text{C}\equiv\text{N})$ at 2197 cm^{-1}) support the formation of **6b**. In the presence of at least 3 equiv of *t*-BuNC a complex formulated as $[(\text{OC})_3\{\text{Me}_3\text{OSi}\}_3\text{Fe}(\mu\text{-dppm})\text{Pt}(\eta^1\text{-C}_3\text{H}_5)(t\text{-BuNC})_2]$ (**7**) was formed in solution as the only species, according to the ${}^{31}\text{P}$ -NMR spectrum. It could not be isolated pure in the solid-state and was always contaminated with **6b**. It displays a doublet at δ 69.9 and a second doublet at δ 4.4, which correspond to P nuclei which are mutually coupled (${}^{2+3}J(\text{P}-\text{P}) = 50\text{ Hz}$). The ${}^1J(\text{Pt}-\text{P})$ coupling of 1594 Hz is drastically reduced compared with that of **6b** (3414 Hz) and **5** (4127 Hz), probably owing to the penta-coordination of the platinum center.

In contrast to the well-resolved and sharp resonances in the ${}^{31}\text{P}$ -NMR spectrum, the doublet observed in the ${}^{195}\text{Pt}$ NMR spectrum of **7** is very broad, probably owing



to isocyanide exchange on platinum. This resonance appears at δ -2894 whereas the tetracoordinated platinum nucleus in **5** resonates at δ = -3285 ppm and displays a well-resolved doublet of doublets pattern. Again the allylic and dppm resonances in the ${}^1\text{H}$ -NMR spectrum are broadened. A precise assignment of the allylic protons can be done by selective decoupling experiments and comparison of the data with those reported for the η^1 -allyl ligand in mononuclear Pd(II) and Pt(II) complexes.³⁰ The resonance of the equivalent allylic protons H(3) and H(4) is readily assigned: at 283 K these protons give rise to a relatively sharp triplet at δ 2.95 (${}^2J(\text{Pt}-\text{H}) = 92.5\text{ Hz}$), probably resulting from an accidentally similar coupling of 9 Hz with H(5) and the phosphorus nucleus. The H(5) proton appears at δ 6.20 as a very broad signal without any fine structure. The H(1) and H(2) protons give rise to two broad doublets at δ 4.42 and 4.76 due to a coupling of 11.4 and 15.1 Hz with H(5). The triplet at δ 3.90 is attributed to the dppm-methylene protons. Irradiation of the H(5) resonance simplifies the pattern of H(3) and H(4) to a doublet, whereas the protons H(1) and H(2) now appear as broad singlets with additional platinum satellites (${}^4J(\text{Pt}-\text{H}) = 22, 20\text{ Hz}$). As expected the dppm resonance is not affected by this selective decoupling experiment. Several signals are observed for the free and coordinated *t*-BuNC ligands in the 1.1–1.6 ppm region.

(30) (a) Fryzuk, M. D.; MacNeil, P. A.; Rettig, S. J.; Secco, A. S.; Trotter, J. *Organometallics* **1982**, *1*, 918. (b) Numata, S.; Okawara, R.; Kurosawa, H. *Inorg. Chem.* **1977**, *16*, 1737.

We found no evidence by IR and NMR monitoring for insertion of isocyanide into the Pt-carbon bond of **7**, even after prolonged reaction times and a 5-fold excess of *t*-BuNC. Only progressive fragmentation to mononuclear species occurred. We also investigated the reactivity of **5** toward phenylacetylene and $\text{MeO}_2\text{-CC}\equiv\text{CCO}_2\text{Me}$. Despite the large excess of alkyne used (5 equiv), the ${}^{31}\text{P}$ -NMR spectrum remained unchanged in both cases after 1 day.

Conclusion

Dppm-stabilized heterobimetallic Fe-M (M = Pd, Pt) siloxyl complexes have been prepared and characterized which contain a methyl or an allyl ligand bound to M. The Fe-Pt η^3 -allyl complex **5** reacted reversibly with isocyanide ligands to give complexes containing an η^1 -allyl ligand. Insertion of CO into the metal-CH₃ bond of **2a,b** was investigated and found to occur under mild conditions, leading to heterometallic complexes containing a bridging siloxycarbene. This new functionality results from a siloxyl migration reaction from Fe to the oxygen atom of the intermediately formed acyl ligand. We have previously shown that the corresponding migration of a trialkoxysilyl ligand requires the presence of a donor ligand, such as a phosphine or a phosphite, which renders the acyl oxygen more electron-rich and maintains the acyl ligand in a suitable syn position with respect to the migrating silyl moiety. These examples, together with the recently reported migrations of a silyl ligand between two metal centers,^{31–33} emphasize new reactivity patterns for the metal-silicon bond in a bimetallic environment and the unique properties it may confer to polymetallic complexes.

Experimental Section

All reactions were performed in Schlenk-tube flasks under purified nitrogen. Solvents were dried and distilled under nitrogen before use, tetrahydrofuran over sodium benzophenone-ketyl, toluene, benzene, and hexane over sodium, and dichloromethane from P_2O_5 . Nitrogen (Air liquide, R-grade) was passed through BASF R3-11 catalyst and molecular sieve columns to remove residual oxygen or water. Elemental C, H, and N analyses were performed by the Service Central de Microanalyses du CNRS. Infrared spectra were recorded in the $4000\text{--}400\text{ cm}^{-1}$ region on Bruker IFS 66 spectrometers. The ${}^1\text{H}$ -, ${}^{31}\text{P}\{^1\text{H}\}$ -, and ${}^{13}\text{C}\{^1\text{H}\}$ -NMR spectra were recorded at 300, 121.5, and 75.5 MHz, respectively, on a Bruker AC 300 instrument. Phosphorus chemical shifts were externally referenced to 85% H_3PO_4 in H_2O with the downfield chemical shift reported as positive. ${}^{195}\text{Pt}$ chemical shifts were measured on a Bruker ACP 200 instrument (42.79 MHz) and externally referenced to K_2PtCl_4 in water with downfield chemical shifts reported as positive. The reactions were generally monitored by IR in the $\nu(\text{CO})$ region. $[\text{Pt}(\eta^3\text{-C}_3\text{H}_5)(\mu\text{-Cl})_4]$ was prepared as described in the literature.³⁴

mer-[(OC)₃Fe{μ-Si(OSiMe₃)₂(OSiMe₃)₂}(μ-dppm)Pd(Me)] (2a). Method a. To a solution of complex **1** (0.48 g, 0.50 mmol) in Et_2O at 0 °C was added in slight excess a Et_2O solution of MeLi. After the solution was stirred for 0.5 h, a drop of MeOH was added (to destroy excess MeLi) and the

(31) Braunstein, P.; Knorr, M.; Hirle, B.; Reinhard, G.; Schubert, U. *Angew. Chem. Int. Ed. Engl.* **1992**, *31*, 1583.

(32) Akita, M.; Oku, T.; Hua, R.; Moro-Oka, Y. *J. Chem. Soc., Chem. Commun.* **1993**, 1670.

(33) Lin, W.; Wilson, S. R.; Girolami, G. S. *Organometallics* **1994**, *13*, 3022.

(34) Lukas, J. *Inorg. Synth.* **1974**, *15*, 79.

solvent was removed under vacuum. Extraction of the product with warm hexane (100 mL) and filtration gave a solution which was concentrated and placed at $-20\text{ }^{\circ}\text{C}$ overnight. A yellow powder was obtained and filtered (0.202 g, 42%). A higher yield method is detailed below.

Method b. A solution of $\text{K}[\text{Fe}\{\text{Si}(\text{OSiMe}_3)_3\}(\text{CO})_3(\eta^1\text{-dppm})]$ (0.860 g, 1 mmol) in THF (25 mL) was added to a suspension of $[\{\text{PdMe}(\text{SM}_2)(\mu\text{-Cl})\}_2]$ (0.219 g, 0.5 mmol) in cold THF (5 mL, $-30\text{ }^{\circ}\text{C}$). After the mixture was stirred for 5 min, all volatiles were removed under vacuo (formation of small amounts of elemental Pd) and the yellow-brown residue was extracted with Et_2O (25 mL) and with hexane (15 mL). This mixture was slowly concentrated under reduced pressure to induce precipitation of the spectroscopically pure yellow product. Yield: 0.800 g, 85%. (Anal. Found: C, 48.52 H, 5.86. Calc for $\text{C}_{38}\text{H}_{52}\text{FeO}_6\text{P}_2\text{PdSi}_4$ ($M = 941.39$): C, 48.48 H, 5.57.) IR (hexane): $\nu(\text{CO})$ 1961 s, 1899 s, 1864 vs cm^{-1} . $^1\text{H-NMR}$ (300 MHz, 298 K, C_6D_6): δ 0.55 (s, 27 H, SiMe_3), 0.86 (s, 3 H, Me), 3.43 (dd, 2 H, PCH_2P , $^2J(\text{P-H}) = 9.5, 11.4$), 6.82–7.69 (m, 20 H, C_6H_5). $^1\text{H-NMR}$ (300 MHz, 298 K, CDCl_3): δ 0.27 (s, 27 H, SiMe_3), 0.42 (s, 3H, Me), 3.63 (dd, 2 H, PCH_2P , $^2J(\text{P-H}) = 9.5, 11.4$), 7.14–7.79 (m, 20 H, C_6H_5). $^{31}\text{P}\{^1\text{H}\}\text{-NMR}$ (121.5 MHz, 298 K, CDCl_3): δ 43.5 (d, P(Pd), $^{2+3}J(\text{P-P}) = 54$ Hz), 63.0 (d, P(Fe), $^{2+3}J(\text{P-P}) = 54$ Hz). $^{13}\text{C}\{^1\text{H}\}\text{-NMR}$ (75.5 MHz, 298 K, CDCl_3): δ 1.58 (s, PdCH₃), 2.40 (s, SiCH₃), 48.18 (dd, PCH_2P , $^1J(\text{P-C}) = 18, 31.4$), 128.1–136.8 (m, C_6H_5), 214.4 (d, FeCO, $^2J(\text{P-C}) = 14$ Hz), 216.4 (d, FeCO, $^2J(\text{P-C}) = 18$ Hz).

mer-[(OC)₃Fe{μ-Si(Me)(OSiMe₃)(OSiMe₃)}(μ-dppm)Pd(Me)] (2b). This compound was prepared in a similar manner to **2a**, and the green-yellow product was isolated in 48% yield. (Anal. Found: C, 49.65; H, 5.57. Calc for $\text{C}_{36}\text{H}_{46}\text{FeO}_5\text{P}_2\text{PdSi}_3$ ($M = 867.23$): C, 49.86; H, 5.35.) IR (hexane): $\nu(\text{CO})$ 1957 s, 1895 s, 1862 vs cm^{-1} . $^1\text{H-NMR}$ (300 MHz, 298 K, C_6D_6): δ 0.48 (s, 18 H, SiMe_3), 0.81 (s, 3 H, PdMe), 1.16 (s, 3 H, SiCH_3), 3.39 (dd, 2 H, PCH_2P , $^2J(\text{P-H}) = 9.5, 11.4$), 6.84–7.68 (m, 20 H, C_6H_5); $^1\text{H-NMR}$ (300 MHz, 298 K, CDCl_3): δ 0.28 (s, 18 H, SiMe_3), 0.40 (s, 3 H, PdCH₃), 0.68 (s, 3 H, SiCH_3), 3.57 (dd, 2 H, PCH_2P , $^2J(\text{P-H}) = 9.5, 11.4$), 7.16–7.74 (m, 20 H, C_6H_5). $^{31}\text{P}\{^1\text{H}\}\text{-NMR}$ (121.5 MHz, 298 K, CDCl_3): δ 45.4 (d, P(Pd), $^{2+3}J(\text{P-P}) = 58$ Hz, 63.5 (d, P(Fe), $^{2+3}J(\text{P-P}) = 58$ Hz).

[(OC)₃Fe{μ-C[OSi(OSiMe₃)₃]Me}(μ-dppm)Pd(CO)] (3a). CO was bubbled for 3 min through a solution of **2a** (0.094 g, 0.1 mmol) in hexane (7 mL). After removal of all volatiles, spectroscopically pure **3a** was obtained in quantitative yield in form of a waxy red solid. (Anal. Found: C, 48.03; H, 5.30. Calc for $\text{C}_{40}\text{H}_{52}\text{FeO}_8\text{P}_2\text{PdSi}_4$ ($M = 997.41$): C, 48.17; H, 5.26.) IR (hexane): $\nu(\text{CO})$ 2035 s, 2004 m, 1947 vs, 1930 s cm^{-1} . $^1\text{H-NMR}$ (300 MHz, 298 K, CDCl_3): δ 0.10 (s, 27 H, SiMe_3), 3.09 (dd, 3 H, Me, $^4J(\text{P-H}) = 3.2, 11.0$), 3.44 (t, 2 H, PCH_2P , $^2J(\text{P-H}) = 9.6$ Hz), 7.15–7.74 (m, 20 H, C_6H_5). $^{31}\text{P}\{^1\text{H}\}\text{-NMR}$ (121.5 MHz, 298 K, CDCl_3): δ 15.2 (d, P(Pd), $^{2+3}J(\text{P-P}) = 139$), 65.1 (d, P(Fe), $^{2+3}J(\text{P-P}) = 139$ Hz). $^{13}\text{C}\{^1\text{H}\}\text{-NMR}$ (75.5 MHz, 298 K, CDCl_3 , ^{13}C -enriched sample): δ 1.66 (s, SiCH₃), 38.80 (t, PCH_2P , $^1J(\text{PC}) = 19$), 47.10 (d, $\mu\text{-CCH}_3$, $^1J(\text{C-C}) = 30$), 128.1–138.5 (m, C_6H_5), 187.1 (s, PdCO), 211.4 (d, FeCO, $^2J(\text{P-C}) = 13$), 215.2 (d, FeCO, $^2J(\text{P-C}) = 15$), 218.8 (dd, $\mu\text{-C}$, $^2J(\text{P-C}) = 17, 52$ Hz).

[(OC)₃Fe{μ-C[OSi(Me)(OSiMe₃)₂]Me}(μ-dppm)Pd(CO)] (3b). This complex was obtained quantitatively in a similar manner to **3a**. Removal of all volatiles gave a red-brown oily residue of the pure product. (Anal. Found: C, 49.41; H, 5.03. Calc for $\text{C}_{38}\text{H}_{46}\text{FeO}_7\text{P}_2\text{PdSi}_3$ ($M = 923.25$): C, 49.44; H, 5.64.) IR (hexane): $\nu(\text{CO})$ 2033 s, 2003 m, 1946 vs, 1928 s cm^{-1} . $^1\text{H-NMR}$ (300 MHz, 298 K, CDCl_3): δ 0.09 (s, 3H, SiMe), 0.12 (s, 18 H, SiMe_3), 3.08 (dd, 3 H, CH₃, $^4J(\text{PH}) = 2.9, 11.3$), 3.41 (t, 2 H, PCH_2P , $^2J(\text{PH}) = 9.6$), 7.15–7.72 (m, 20 H, C_6H_5). $^{31}\text{P}\{^1\text{H}\}\text{-NMR}$ (121.5 MHz, 298 K, CDCl_3): δ 15.3 (d, P(Pd), $^{2+3}J(\text{P-P}) = 140$), 65.0 (d, P(Fe), $^{2+3}J(\text{P-P}) = 140$ Hz).

[(OC)₃Fe{μ-C[OSi(OSiMe₃)₃]Me}(μ-dppm)Pd(PPh₃)] (4a). Solid PPh₃ (0.140 g) was added in slight excess to a sample of

Table 3. Summary of Crystallographic Data for Complexes 1 and 5

	1	5
mol formula	$\text{C}_{37}\text{H}_{49}\text{ClFeO}_6\text{P}_2\text{PdSi}_4$	$\text{C}_{40}\text{H}_{54}\text{FeO}_6\text{P}_2\text{PtSi}_4$
mol wt	961.78	1056.09
cryst system	monoclinic	monoclinic
space group	$P2_1/c$	$P2_1/n$
radiatn	graphite-monochromated	Nb-filtered
(Mo Kα)	($\lambda = 0.71073\text{ \AA}$)	($\lambda = 0.71073\text{ \AA}$)
a, Å	19.013(4)	10.472(4)
b, Å	14.026(5)	16.421(5)
c, Å	19.225(6)	27.654(7)
β, deg	113.77(2)	94.52(2)
V, Å ³	4692(3)	4741(3)
Z	4	4
D_{calcd} , g cm ⁻³	1.361	1.480
F(000)	1976	2128
cryst dimens, mm	0.20 × 0.24 × 0.30	0.25 × 0.28 × 0.35
μ(Mo Kα), cm ⁻¹	9.58	34.63
2θ range, deg	6–52	6–48
reflens measd	±h, k, l	±h, k, l
tot. no. of unique data	9580	7651
no. of unique obsd data	4017 [$I > 2\sigma(I)$]	4412 [$I > 3\sigma(I)$]
R^a	0.0326	0.0478
R_w^b	0.0422	0.0510

$$^a R = \sum |F_o| - |F_c| / \sum |F_o|. \quad ^b R_w = [\sum w(|F_o| - |F_c|)^2 / \sum w(F_o)^2]^{1/2}.$$

3a (0.50 mmol) (prepared *in situ* from 0.415 g, 0.50 mmol, of **2a**) in CH_2Cl_2 . Immediately after addition, a vigorous gas evolution was observed. IR monitoring indicated a quantitative conversion to **4a** within 15 min. After removal of all volatiles, $^{31}\text{P-NMR}$ examination of the crude residue revealed the presence of **4a** as the sole species together with traces of O=PPh_3 . Extraction of the residue with Et_2O /hexane (1:1, 10 mL) and subsequent concentration afforded pure **4a** as a brown yellow powder in 76% yield. (Anal. Found: C, 55.32; H, 5.52. Calc for $\text{C}_{57}\text{H}_{67}\text{FeO}_7\text{P}_3\text{PdSi}_4$ ($M = 1231.69$): C, 55.58; H, 5.48.) IR (CH_2Cl_2): $\nu(\text{CO})$ 1982 m, 1918 vs, 1894 s, sh cm^{-1} . $^1\text{H-NMR}$ (200 MHz, 298 K, CDCl_3): δ 0.14 (s, 27 H, SiMe_3), 2.45 (d, broad due to unresolved $^4J(\text{P-H})$ couplings, 3 H, CH₃, $^4J(\text{P-H}) = 11.2$), 3.30 (m, 1 H, PCH_2P), 3.47 (m, 1 H, PCH_2P), 7.15–7.92 (m, 35 H, C_6H_5). $^{31}\text{P}\{^1\text{H}\}\text{-NMR}$ (81.1 MHz, 298 K, CDCl_3): δ 14.1 (d, P(Pd), $^{2+3}J(\text{P-P}) = 131$), 17.2 (d, PPh₃, $^3J(\text{P-P}) = 4$), 65.0 (dd, P(Fe), $^{2+3}J(\text{P-P}) = 131$, $^3J(\text{P-P}) = 4$ Hz). $^{13}\text{C}\{^1\text{H}\}\text{-NMR}$ (50.3 MHz, 298 K, CDCl_3): δ 1.51 (s, SiCH₃), 40.91 (ddd, PCH_2P , $^1J(\text{PC}) = 17, 26, ^3J(\text{PC}) = 7$), 46.10 (s, $\mu\text{-CCH}_3$), 127.1–138.92 (m, C_6H_5), 206.83 (dd, $\mu\text{-C}$, $^2J(\text{P-C}) = 15, 71$ Hz), 216.94 (d, FeCO, $^2J(\text{P-C}) = 21$), 218.80 (d, FeCO, $^2J(\text{P-C}) = 6$), 221.10 (d, FeCO, $^2J(\text{P-C}) = 25$ Hz).

[(OC)₃Fe{μ-C[OSi(Me)(OSiMe₃)₂]Me}(μ-dppm)Pd(PPh₃)] (4b). Solid PPh₃ (0.006 g) was added in slight excess into a NMR tube containing a sample of **3b** (0.018 g, 0.02 mmol) in CDCl_3 . Immediately after addition, a gas evolution was observed. Subsequent NMR measurements showed a quantitative conversion to **4**. IR (CH_2Cl_2): $\nu(\text{CO})$ 1979 m, 1912 vs, 1898 s cm^{-1} . $^1\text{H-NMR}$ (300 MHz, 298 K, CDCl_3): δ 0.09 (s, 3 H, SiMe), 0.12 (s, 18 H, SiMe_3), 2.38 (dt, 3 H, CH₃, $^4J(\text{P-H}) = 3.2, 12.6$), 3.30 (m, 1 H, PCH_2P), 3.46 (m, 1 H, PCH_2P), 7.12–7.86 (m, 35 H, C_6H_5). $^{31}\text{P}\{^1\text{H}\}\text{-NMR}$ (121.5 MHz, 298 K, CDCl_3): δ 14.5 (d, P(Pd), $^{2+3}J(\text{P-P}) = 131$), 18.0 (d, PPh₃, $^3J(\text{P-P}) = 4$), 65.0 (dd, P(Fe), $^{2+3}J(\text{P-P}) = 131$, $^3J(\text{P-P}) = 4$ Hz).

[(OC)₃(Me₃SiO)₃Si}Fe(μ-dppm)Pt(η³-C₃H₅)] (5). A solution of $\text{K}[\text{Fe}\{\text{Si}(\text{OSiMe}_3)_3\}(\text{CO})_3(\eta^1\text{-dppm})]$ (0.860 g, 1.0 mmol) in THF (25 mL) was added to a slurry of $[\text{Pt}(\eta^3\text{-C}_3\text{H}_5)(\mu\text{-Cl})_4]$ (0.271 g, 0.25 mmol) in THF (5 mL). After completion of the reaction (15 min, IR monitoring of the disappearance of the $\nu(\text{CO})$ bands at 1928 w, 1840 vs, and 1808 s cm^{-1} due to the metalate), the yellow solution was filtered and evaporated to

Table 4. Fractional Atomic Coordinates ($\times 10^4$) and Equivalent Isotropic Thermal Parameters ($\text{\AA}^2 \times 10^4$) with Esd's in Parentheses for the Non-Hydrogen Atoms of Complex 1

	<i>x/a</i>	<i>y/b</i>	<i>z/c</i>	<i>U_{eq}^a</i>
Pd	1456(1)	982(1)	2231(1)	494(2)
Fe	2563(1)	18(1)	3175(1)	466(3)
Cl	454(1)	2047(1)	1497(1)	824(8)
P(1)	1948(1)	-1210(1)	3399(1)	477(6)
P(2)	636(1)	37(1)	2422(1)	503(6)
Si(1)	3156(1)	1212(1)	2815(1)	550(7)
Si(2)	2403(1)	2890(1)	1784(1)	851(9)
Si(3)	4295(1)	2376(2)	4226(1)	984(11)
Si(4)	4230(1)	290(2)	2077(2)	1161(15)
O(1)	4114(3)	-539(4)	4151(3)	1160(29)
O(2)	2231(3)	-753(3)	1663(3)	910(26)
O(3)	2269(3)	1463(3)	4123(3)	842(23)
O(4)	3610(2)	1980(3)	3457(2)	738(19)
O(5)	3718(3)	886(3)	2420(3)	927(27)
O(6)	2435(2)	1806(3)	2155(2)	556(16)
C(1)	3496(4)	-338(4)	3763(4)	696(30)
C(2)	2353(3)	-446(4)	2259(4)	631(29)
C(3)	2368(3)	893(4)	3746(3)	567(24)
C(4)	946(3)	-1195(4)	2686(3)	546(23)
C(5)	2318(3)	-2365(4)	3269(3)	545(24)
C(6)	2988(4)	-2652(5)	3792(5)	1357(45)
C(7)	3321(5)	-3500(6)	3706(6)	1528(56)
C(8)	2985(5)	-4060(5)	3111(5)	961(41)
C(9)	2280(5)	-3813(5)	2615(5)	1119(49)
C(10)	1935(4)	-2954(5)	2687(4)	866(35)
C(11)	1920(3)	-1410(4)	4316(3)	551(24)
C(12)	1498(4)	-2155(5)	4422(4)	714(31)
C(13)	1563(5)	-2415(6)	5127(5)	979(44)
C(14)	2051(6)	-1967(7)	5734(5)	1188(55)
C(15)	2474(6)	-1207(7)	5668(4)	1295(55)
C(16)	2415(4)	-923(5)	4948(4)	893(37)
C(17)	317(3)	475(5)	3132(3)	596(26)
C(18)	417(3)	1427(5)	3337(4)	703(30)
C(19)	181(4)	1773(6)	3871(4)	932(40)
C(20)	-167(5)	1185(9)	4203(5)	1118(50)
C(21)	-273(4)	242(8)	4000(4)	989(44)
C(22)	-33(4)	-107(6)	3470(4)	783(33)
C(23)	-221(3)	-147(4)	1555(3)	588(25)
C(24)	-939(4)	92(5)	1483(4)	884(33)
C(25)	-1559(4)	-26(7)	801(5)	1169(47)
C(26)	-1455(5)	-368(7)	193(5)	1122(47)
C(27)	-751(5)	-617(5)	239(4)	918(38)
C(28)	-116(4)	-495(5)	925(4)	720(30)
C(29)	4232(8)	3666(7)	4232(6)	2125(93)
C(30)	5228(4)	2003(10)	4188(5)	1808(72)
C(31)	4222(5)	1858(7)	5071(4)	1168(45)
C(32)	5112(6)	873(11)	2275(9)	2970(140)
C(33)	3706(7)	189(12)	1037(6)	2480(113)
C(34)	4409(7)	-910(8)	2453(7)	1943(90)
C(35)	3389(4)	3261(6)	1928(5)	1218(48)
C(36)	1789(5)	2867(7)	763(4)	1450(54)
C(37)	2033(5)	3686(5)	2325(6)	1490(60)

^a Equivalent Isotropic *U* defined as one-third of the trace of the orthogonalized *U_{ij}* tensor.

dryness. The residue was extracted with warm Et₂O (ca. 35 mL). After addition of hexane (15 mL) to the filtered solution and slow concentration in vacuo, an ochre powder precipitated, which was collected by filtration and dried in vacuo. Concentration of the mother liquor afforded a further crop of the air-stable product. Overall isolated yield: 0.866 g, 82%. (Anal. Found: C, 45.73; H, 5.32. Calc for C₄₀H₅₄FeO₆P₂PtSi₄ (*M* = 1056.09) C, 45.49; H, 5.15.) IR (CH₂Cl₂): $\nu(\text{CO})$ 1959 s, 1890 vs, 1862 s cm⁻¹. ¹H-NMR (300 MHz, CDCl₃, 298 K): δ 0.13 (s, 27 H, OSiCH₃), 1.98 (d, 1 H, ³J(H-H⁵) = 11.0, *J*(Pt-H) = 54, allyl H³), 2.85 (t, 1 H, ³J(H-H⁵) ~ ³J(P-H) = 10.5, *J*(Pt-H) = 36, allyl H²), 3.41 (s br, allyl H⁴), 3.83 (center of two multiplets, 2 H, PCH₂P), 4.68 (m, not resolved, 1 H, allyl H¹), 4.75 (m, partially obscured by H¹, 1 H, allyl H⁵), 6.95-7.51 (m, 20 H, C₆H₅). ³¹P{¹H}-NMR (81.02 MHz, CDCl₃): δ 21.9 (d, P(Pt), ²⁺³*J*(P-P) = 106, ¹*J*(P-Pt) = 4127), 67.7 (d, P(Fe), ²⁺³*J*(P-P) = 106, ²*J*(P-Pt) = 109 Hz). ¹⁹⁵Pt{¹H}-NMR (CH₂-

Table 5. Fractional Atomic Coordinates ($\times 10^4$) and Equivalent Isotropic Thermal Parameters ($\text{\AA}^2 \times 10^4$) with Esd's in Parentheses for the Non-Hydrogen Atoms of Complex 5

	<i>x/a</i>	<i>y/b</i>	<i>z/c</i>	<i>U_{eq}^a</i>
Pt	364(1)	7343(1)	2694(1)	447(2)
Fe	2547(1)	7595(1)	3243(1)	400(5)
P(1)	3498(2)	8113(2)	2614(1)	413(9)
P(2)	920(3)	8143(2)	2089(1)	438(9)
Si(1)	1788(3)	7370(2)	3999(1)	439(9)
Si(2)	-872(3)	7661(3)	4394(1)	718(14)
Si(3)	3049(4)	8666(3)	4747(2)	961(19)
Si(4)	2437(5)	5623(2)	4439(2)	933(19)
O(1)	5040(8)	7479(5)	3782(3)	894(40)
O(2)	1072(9)	9096(5)	3350(3)	782(36)
O(3)	2255(8)	5844(5)	3016(3)	776(37)
O(4)	2545(7)	7886(5)	4429(3)	698(31)
O(5)	1917(10)	6441(5)	4175(3)	915(41)
O(6)	295(7)	7592(5)	4043(3)	686(31)
C(1)	4010(11)	7540(6)	3573(4)	530(43)
C(2)	1659(10)	8513(7)	3311(4)	569(45)
C(3)	2306(10)	6551(8)	3084(4)	572(46)
C(4)	2361(9)	8746(6)	2227(4)	445(38)
C(5)	4807(10)	8816(6)	2787(4)	484(41)
C(6)	4598(12)	9480(7)	3092(5)	769(55)
C(7)	5564(13)	9969(8)	3280(5)	855(62)
C(8)	6773(13)	9828(8)	3165(5)	844(64)
C(9)	7032(12)	9199(9)	2870(5)	920(65)
C(10)	6050(12)	8685(8)	2677(5)	835(60)
C(11)	4237(9)	7465(6)	2173(3)	442(39)
C(12)	4559(10)	7743(7)	1722(4)	595(42)
C(13)	5114(11)	7265(9)	1411(4)	722(52)
C(14)	5329(12)	6450(8)	1517(4)	728(56)
C(15)	5099(11)	6156(8)	1967(5)	797(57)
C(16)	4512(11)	6651(7)	2287(4)	638(46)
C(17)	1267(9)	7585(6)	1549(4)	498(40)
C(18)	1313(10)	7956(7)	1102(4)	606(46)
C(19)	1636(12)	7515(9)	706(4)	795(60)
C(20)	1901(13)	6700(9)	749(5)	873(65)
C(21)	1850(11)	6323(7)	1185(5)	671(52)
C(22)	1545(11)	6749(7)	1589(4)	605(47)
C(23)	-312(10)	8873(6)	1854(4)	446(39)
C(24)	-1365(12)	8571(7)	1577(4)	669(50)
C(25)	-2361(12)	9077(9)	1418(5)	790(58)
C(26)	-2271(13)	9888(9)	1523(5)	799(60)
C(27)	-1254(14)	10183(8)	1785(5)	951(67)
C(28)	-265(11)	9682(7)	1953(5)	698(52)
C(29)	1877(19)	9507(10)	4651(8)	1846(128)
C(30)	4597(15)	8986(11)	4541(6)	1631(105)
C(31)	3227(15)	8347(12)	5401(5)	1399(92)
C(32)	2251(24)	5706(12)	5093(6)	2158(151)
C(33)	1340(16)	4756(9)	4170(7)	1546(105)
C(34)	4090(16)	5417(11)	4286(7)	1678(119)
C(35)	-223(13)	7670(10)	5036(4)	1172(76)
C(36)	-1785(14)	8587(9)	4230(6)	1308(86)
C(37)	-1967(14)	6791(9)	4314(5)	1201(81)
C(38)	-555(10)	6408(5)	3167(3)	820(40)
C(39)	-1452(5)	6873(6)	2878(4)	1626(73)
C(40)	-1492(5)	6939(6)	2369(3)	773(37)

^a Equivalent Isotropic *U* defined as one-third of the trace of the orthogonalized *U_{ij}* tensor.

Cl₂/CDCl₃): δ -3285 (dd, ¹*J*(Pt-P) = 4127, ²⁺³*J*(Pt-P) = 109 Hz). ¹³C{¹H}-NMR (100.6 MHz, CDCl₃): δ 1.8 (s, OSiC), 41.5 (dd, PCP, ¹*J*(P-C) = 17, 31), 62.0 (s, allyl C¹, *J*(Pt-C) = 120), 72.8 (d, allyl C³, *J*(P-C) = 40, *J*(Pt-C) = 153), 105.8 (d, allyl C², *J*(P-C) = 3, *J*(Pt-C) = 25 Hz), 127.8-137.9 (m, aromatic), 214.8 (br, CO).

[(OC)₃(Me₃OSi)₃Si]Fe(μ -dppm)Pt(C \equiv N^{*t*}Bu)(η ⁻¹-C₆H₅) (6b). To a solution of 5 (0.212 g, 0.2 mmol) in CH₂Cl₂ (5 cm³) was added ^{*t*}BuNC (0.017 g, 0.2 mmol). After addition of hexane (5 mL) to the clear yellow solution the mixture was concentrated under reduced pressure and kept at -25 °C. After 2 d, the off-white product was isolated: yield 0.124 g, 52%. Anal. Found: C, 46.82; H, 5.19; N, 1.14. C₄₅H₆₃FeNO₆P₂PtSi₄·0.5CH₂Cl₂ (*M* = 1139.22 + 48.47): C, 46.25; H, 5.46; N, 1.18. IR (KBr): $\nu(\text{CN})$ 2194 vs, $\nu(\text{CO})$ 1957 s, 1890s, 1860 vs,

$\nu(\text{C}=\text{C})$ 1610 cm^{-1} . $^{31}\text{P}\{^1\text{H}\}$ -NMR (81.02 MHz, CDCl_3): δ 21.9 (d, P(Pt), $^{2+3}J(\text{P}-\text{P}) = 106$, $^1J(\text{P}-\text{Pt}) = 4127$), 67.7 (d, P(Fe), $^{2+3}J(\text{P}-\text{P}) = 106$, $^2J(\text{P}-\text{Pt}) = 109$ Hz).

X-ray Crystal Structure Determinations. Suitable single crystals of **1** and **5** were grown from Et_2O /hexane and from heptane, respectively. The crystal data are summarized in Table 3. Data were collected at room temperature on a Enraf-Nonius CAD-4 (**1**) and a Siemens AED (**5**) diffractometers using the $\theta/2\theta$ scan type. The reflections were collected with variable scan speeds of 16.5 (**1**) and 3–12° (**5**) min^{-1} and scan widths of $(0.8 + 0.35 \tan \theta)^\circ$ (**1**) and of $(1.2 + 0.346 \tan \theta)^\circ$ (**5**). One standard reflection was monitored every 200 (**1**) and 100 (**5**) measurements; no significant decay was noticed over the data collection period. Intensities were corrected for Lorentz and polarization effects. A correction for absorption was applied to the data of **5** (maximum and minimum values for the transmission factors were 1.150 and 0.867).^{35,36}

The structures were solved by Patterson and Fourier methods and refined first by full-matrix least-squares with isotropic thermal parameters and then by full-matrix least-squares with anisotropic thermal parameters for all non-hydrogen atoms, excepting for the allyl carbon atoms of **5**. All hydrogen atoms (excepting those of the allyl ligand in **5**) were placed at their geometrically calculated positions and refined "riding" on the corresponding carbon atoms. In the final cycles of refinement a weighting scheme, $w = [\sigma^2(F_o) + gF_o^2]^{-1}$ was used; at convergence the g values were 0.006 (**1**) and 0.002 (**5**), respectively. The atomic scattering factors, corrected for the real and imaginary parts of anomalous dispersion, were taken from ref 37. The final cycles of refinement were carried

out on the basis of 471 (**1**) and 479 (**5**) variables. The largest remaining peak in the final difference map was equiv to about 0.43 (**1**) and 1.52 (**5**) $e/\text{\AA}^3$. All calculations were carried out on the Gould Povernode 6040 and Encore 91 computers of the "Centro di Studio per la Strutturistica Diffrattometrica" del CNR, Parma, Italy, using the SHELX-76 and SHELXS-86 systems of crystallographic computer programs.³⁸ The final atomic coordinates for the non-hydrogen atoms are given in Tables 4 (**1**) and 5 (**5**).

Acknowledgment. We thank the Centre National de la Recherche Scientifique and the the Commission of the European Communities (Contract CHRX-CT93-0277) for financial support, the Deutsche Forschungsgemeinschaft for a habilitation grant to M. K., and Johnson Matthey PLC for a generous loan of PdCl_2 .

Supporting Information Available: Tables of hydrogen atom coordinates and U values (Tables SI and SII), thermal parameters for the non-hydrogen atoms (Tables S-III and S-IV), and complete bond distances and angles (Tables S-V and S-VI) (12 pages). Ordering information is given on any current masthead page.

OM950231S

(37) *International Tables for X-Ray Crystallography*; Kynoch Press: Birmingham, England, 1974; Vol. IV.

(38) Sheldrick, G. M. SHELX-76. Program for crystal structure determination, University of Cambridge, England, 1976. Sheldrick, G. M. SHELXS-86 Program for the solution of crystal structures, University of Göttingen, 1986.

(35) Walker, N.; Stuart, D. *Acta Crystallogr., Sect. A* **1983**, *39*, 158.

(36) Ugozzoli, F. *Comp. Chem.* **1987**, *11*, 109.

Synthesis of Di- and Monosubstituted Allenylidene-Ruthenium [(Ph₂PCH₂PPh₂)₂ClRu=C=C=C(Y)R]PF₆ and Acetylide Complexes by Activation of Prop-2-yn-1-ols

Daniel Touchard, Nadine Pirio, and Pierre H. Dixneuf*

Laboratoire de Chimie de Coordination Organique, URA CNRS 415, Campus de Beaulieu, Université de Rennes, 35042 Rennes, France

Received March 23, 1995[®]

The reaction of *cis*-RuCl₂(dppm)₂, **1** (dppm = Ph₂PCH₂PPh₂), with HC≡C-C(OH)R₂ and NaPF₆ affords stable 3,3-disubstituted allenylidenes [(dppm)₂ClRu=C=C=CR₂]PF₆, **3a-e**. The activation of monosubstituted propargyl alcohols with **1** and NaPF₆ allows the general access to stable *secondary* allenylidenes [(dppm)₂ClRu=C=C=C(H)R]PF₆ **4f-i** (R = Ar), **5** (R = (*E*)-CH=CHPh) or that to (dppm)₂ClRu=C=CH-CH=CH₂]PF₆ **6**. Complex **1** reacts with HC≡C-C(=CH₂)CH₃, promotes the 1,4 migration of the (HC≡C) proton, and gives [(dppm)₂ClRu=C=C=CMe₂]PF₆, **3e**, which can be deprotonated at the C(4) carbon. Allenylidene **3a** (R = Ph) easily adds nucleophile at the C(3) carbon to give the acetylide (dppm)₂ClRu-C≡C-CPh₂(OMe), **9a**, with MeONa, and (dppm)₂ClRu-C≡C-CPh₂H, **12a**, with NaBH₄. By contrast, *secondary* allenylidenes **4f,g,i** with MeONa give mixed hydride acetylide complexes *trans*-(dppm)₂(H)Ru-C≡C-CH(OMe)R, **10**, and with NaBH₄ (dppm)₂(Cl)Ru-C≡C-CH₂R.

Introduction

Since the discovery of the first vinylidene metal complex,¹ the chemistry of metal-containing heteroallenes M=C=CR₂ has experienced important developments due to the discovery of general methods of access,² especially directly from terminal alkynes and ruthenium complexes,³⁻⁵ and due to their use for the preparation of a variety of carbenes^{2,6} or carbynes.⁷ The involvement of M=C=CHR species in selective catalytic transformations of terminal alkynes⁸ constitutes the most promising aspect of vinylidene-metal complexes. By contrast, the chemistry of their allenylidene homologues M=C=C=CR₂ is only beginning to be studied, even though the first allenylidene-metal complexes

were made by Fischer⁹ and Berke¹⁰ in 1976, and despite their potential in synthesis due to both their cumulene and M=C functionalities. Allenylidene-metal complexes have been prepared from Fischer type carbenes, which are α,β-unsaturated carbenes formed by heteroatom group elimination at the C(1) carbon with Lewis acids,⁹ and recently by addition of amine to alkynyl carbenes.¹¹ The addition of a (C)₃ skeleton also leads to allenylidene derivatives, such as by reaction of Li₂C₃-Ph₂ with TiCl₂Cp₂¹² or [C≡C-CR₂O]²⁻ dianion on addition to group 6 metal, manganese, and iron carbonyl complexes followed by oxygen elimination.^{10,13,14} There is no doubt that the most general route to allenylidene-metal complexes is based on the direct activation of *tertiary* propargyl alcohol derivatives directly with 16-electron metal species (eq 1). The process involves the

* Abstract published in *Advance ACS Abstracts*, July 15, 1995.

(1) King, R. B.; Saran, M. S. *Chem. Commun.* **1972**, 1052; *J. Am. Chem. Soc.* **1972**, *95*, 1817.

(2) (a) Bruce, M. I.; Swincer, A. G. *Adv. Organomet. Chem.* **1983**, *22*, 59. (b) Bruce, M. I. *Chem. Rev.* **1991**, *91*, 197. (c) Antonova, A. B.; Johansson, A. A. *Russ. Chem. Rev.* **1989**, *58*, 693.

(3) (a) Bruce, M. I.; Wallis, R. C. *J. Organomet. Chem.* **1978**, *161*, C1. (b) Bruce, M. I.; Wallis, R. C. *Aust. J. Chem.* **1979**, *32*, 1471. (c) Bruce, M. I.; Swincer, A. G.; Wallis, R. C. *J. Organomet. Chem.* **1979**, *171*, C5. (d) Bruce, M. I.; Koutsantonis, G. A. *Aust. J. Chem.* **1991**, *44*, 207. (e) Bullock, R. M. *J. Chem. Soc., Chem. Commun.* **1989**, *3*, 165. (f) Lompfrey, J. R.; Selegue, J. P. *J. Am. Chem. Soc.* **1992**, *114*, 5518. (g) Consiglio, G.; Morandini, F. *Inorg. Chim. Acta* **1987**, *127*, 79. (h) Consiglio, G.; Morandini, F.; Ciani, G. F.; Sironi, A. *Organometallics* **1986**, *5*, 1976. (i) Morandini, F.; Consiglio, G.; Sironi, A.; Moret, M. *J. Organomet. Chem.* **1988**, *356*, C79. (j) Werner, H.; Stark, A.; Shulz, M.; Wolf, J. *Organometallics* **1992**, *11*, 1126. (k) Gamasa, M. P.; Gimeno, J.; Martin-Vaca, B. M.; Borge, J.; Garcia-Granda, S.; Perez-Carreño, E. *Organometallics* **1994**, *13*, 4045.

(4) (a) Touchard, D.; Haquette, P.; Pirio, N.; Toupet, L.; Dixneuf, P. *H. Organometallics* **1993**, *12*, 3132. (b) Touchard, D.; Morice, C.; Cadierno, V.; Haquette, P.; Toupet, L.; Dixneuf, P. *H. J. Chem. Soc., Chem. Commun.* **1994**, 859. (c) Faulker, C. W.; Inghan, S. L.; Khan, M. S.; Lewis, J.; Long, N. J.; Raithby, P. R. *J. Organomet. Chem.* **1994**, *482*, 139.

(5) Le Lagadec, R.; Roman, E.; Toupet, L.; Müller, U.; Dixneuf, P. *H. Organometallics* **1994**, *13*, 5030 and references cited therein.

(6) Le Bozec, H.; Ouzzine, K.; Dixneuf, P. *H. Organometallics* **1991**, *10*, 2768.

(7) Kim, H. P.; Angelici, R. J. *Adv. Organomet. Chem.* **1987**, *27*, 51.

(8) (a) Landon, S. J.; Shulman, P. M.; Geoffroy, G. L. *J. Am. Chem. Soc.* **1985**, *107*, 6739. (b) Mahé, R.; Dixneuf, P. H.; Lécolier, S. *Tetrahedron Lett.* **1986**, *27*, 6333. (c) Mahé, R.; Sasaki, Y.; Bruneau, C.; Dixneuf, P. H. *J. Org. Chem.* **1989**, *54*, 1518. (d) Höfer, J.; Doucet, H.; Bruneau, C.; Dixneuf, P. H. *Tetrahedron Lett.* **1991**, *32*, 7409. (e) Wakatsuki, Y.; Yamazaki, H.; Kumegawa, N.; Satoh, T.; Satoh, J. Y. *J. Am. Chem. Soc.* **1991**, *113*, 9604. (f) Wakatsuki, Y.; Yamazaki, H.; Kumegawa, N.; Johar, P. S. *Bull. Chem. Soc. Jpn.* **1993**, *66*, 987. (g) Bianchini, C.; Peruzzini, M.; Frediani, P. *J. Am. Chem. Soc.* **1991**, *113*, 5453. (h) Trost, B. M.; Kottirsch, G. *J. Am. Chem. Soc.* **1990**, *112*, 2816. (i) Doucet, H.; Höfer, J.; Bruneau, C.; Dixneuf, P. H. *J. Chem. Soc., Chem. Commun.* **1993**, 850. (j) Trost, B. M.; Dyker, G.; Kulawiec, R. *J. Am. Chem. Soc.* **1990**, *112*, 7809. (k) Trost, B. M.; Kulawiec, R. *J. Am. Chem. Soc.* **1992**, *114*, 5579. (l) Trost, B. M.; Kulawiec, R. J.; Hammes, A. *Tetrahedron Lett.* **1993**, *34*, 587. (m) Trost, B. M.; Flygare, J. A. *J. Am. Chem. Soc.* **1992**, *114*, 5476. (n) Rappert, T.; Yamamoto, A. *Organometallics* **1994**, *13*, 4984. (o) Bianchini, C.; Frediani, P.; Masi, D.; Peruzzini, M.; Zanobini, F. *Organometallics* **1994**, *13*, 4616.

(9) Fischer, E. O.; Kalder, H.-J.; Franck, A.; Köhler, F. H.; Huttner, G. *Angew. Chem., Int. Ed. Engl.* **1976**, *15*, 623.

(10) Berke, H. *Angew. Chem., Int. Ed. Engl.* **1976**, *15*, 624.

(11) (a) Duetsch, M.; Stein, F.; Lackmann, R.; Pohl, E.; Herbst-Irmer, R.; de Meijere, A. *Chem. Ber.* **1992**, *125*, 2051. (b) Stein, F.; Duetsch, M.; Noltemeyer, M.; de Meijere, A. *Synlett* **1993**, 486. (c) Stein, F.; Duetsch, M.; Pohl, E.; Herbst-Irmer, R.; de Meijere, A. *Organometallics* **1993**, *12*, 2556. (d) Aumann, R. *Chem. Ber.* **1992**, *125*, 2773.

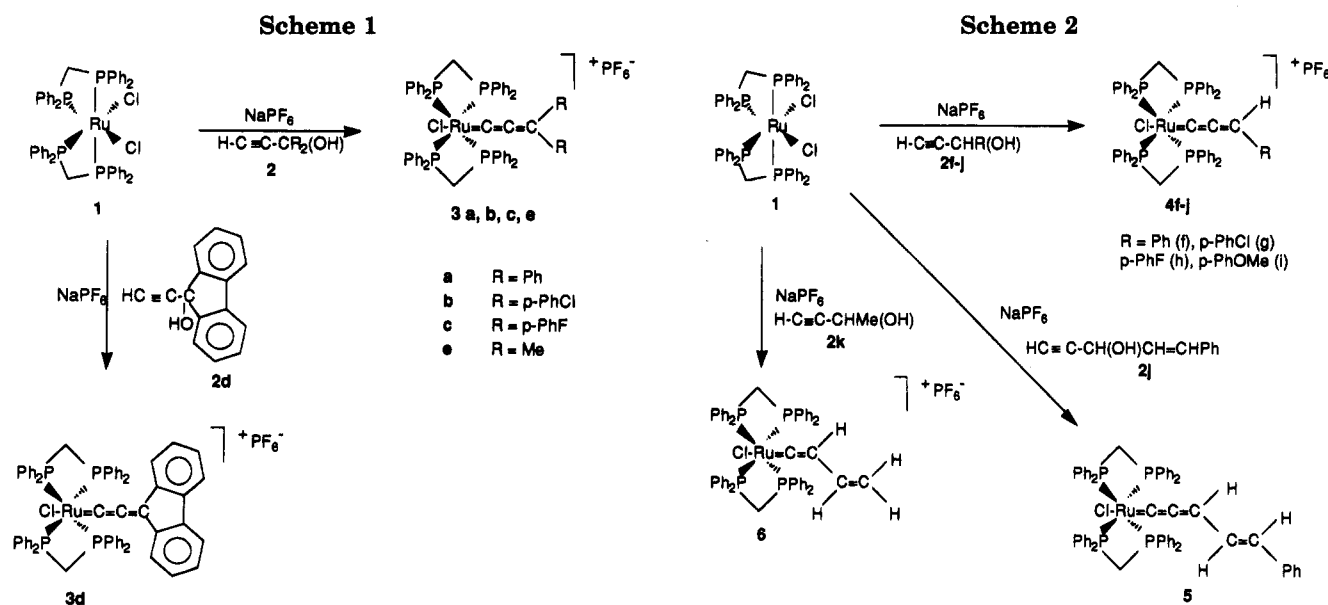
(12) Binger, P.; Müller, P.; Wenz, R.; Mynott, R. *Angew. Chem., Int. Ed. Engl.* **1990**, *29*, 1037.

Table 1. Selected NMR Data for Allenylidene Compounds^a

(a) [(Ph ₂ PCH ₂ PPh ₂) ₂ (Cl)Ru=C=C=CR ₂]PF ₆ (3)					
compd	δ(³¹ P) ppm	δ(¹³ C) ppm			
		Ru=C (² J _{PC} , Hz)	Ru=C=C (³ J _{PC} , Hz)	Ru=C=C=C (⁴ J _{PC} , Hz)	
3a	-14.83	306.72 (14.5)	208.94 (2.5)	161.88	
3b	-14.78	307.33 (14.3)	213.92	156.63	
3c	-14.33	304.64 (14.3)	208.51 (4.0)	157.22 (2.2)	
3d	-15.11	312.02 (14.9)	218.10 (2.7)	155.46 (1.8)	
3e	-14.45	322.69 (13.9)	199.85 (2.3)	173.33	

(b) [(Ph ₂ PCH ₂ PPh ₂) ₂ ClRu=C=C=C(H)(R)]PF ₆ (4 and 5)					
compd	δ (³¹ P) ppm	δ(¹³ C and ¹ H) ppm			
		Ru=C (² J _{PC} , ³ J _{CH} , Hz)	Ru=C=C (³ J _{PC} , Hz)	Ru=C=C=C (⁴ J _{PC} , ¹ J _{CH} , Hz)	=CH (⁵ J _{PH} , Hz)
4f	-14.91	323.10 (14.4, 6.6)	217.28	150.86 (165.1)	8.49 (2.7)
4g	-15.17	323.24 (14.4, 6.6)	220.24	148.84 (165.5)	8.47 (2.8)
4h	-14.88	321.27 (14.4, 6.6)	215.85	148.84 (165.5)	8.39 (2.8)
4i	-13.71	308.38 (14.3, 6.3)	200.78	149.92 (163.2)	8.03 (2.6)
5	-14.59	315.17 (14.3, 6.9)	220.36	149.85 (164.2)	8.06 (2.3)

^a All spectra in CD₂Cl₂ at 297 K.



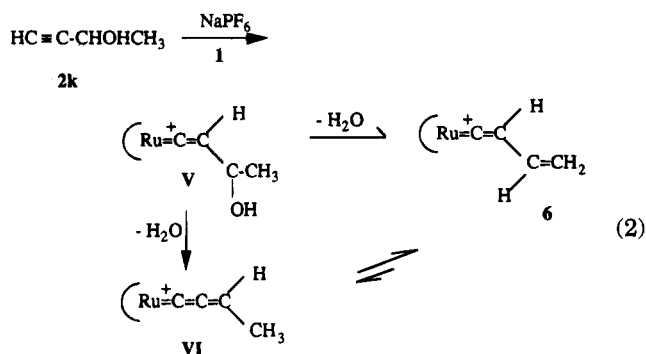
vinyliidene complexes from **1**.^{4a} It is supposed that the first step of the reaction consists in the dissociation, in the polar solvent, of one Ru–Cl bond, leading to the 16-electron species, [RuCl(dppm)₂]PF₆,^{4a} followed by addition and modification of the alkyne in the *trans* position to the chloride, likely to decrease steric interaction between the phenyl groups of both dppm ligands.

It is noteworthy that all allenylidenes **3a–e** are stable especially toward the addition of methanol at C(1) carbon, contrast to the similar reaction of RuCl₂(PR₃)₂arene derivatives¹⁷ leading to unsaturated carbenes of type **III** *via* reactive allenylidenes **II** (eq 1). This difference in behavior can be explained in terms of electron-releasing capability of the *trans*-(dppm)₂ClRu⁺ moiety with respect to the (arene)(PR₃)ClRu⁺ species. The oxidation potentials measured by cyclic voltammetry are *E*_{1/2} = 0.46 and 0.92 V (SCE)³² for *trans*-RuCl₂(dppm)₂ and RuCl₂(PPh₃)(C₆Me₆),^{17c} respectively. We can assume that a similar sequence of electron-releasing ability is found for the cationic species: *trans*-(dppm)₂ClRu⁺ > (C₆Me₆)(PPh₃)ClRu⁺ and thus the *trans*-(dppm)₂ClRu⁺ moiety is expected to decrease the electron deficiency of the [Ru=C=C=CR₂]⁺ group and especially that of the C(1) carbon atom. The inertness of the C(1) carbon may also be due to steric protection

for it was observed in the structure of *trans*-[(dppm)₂ClRu=C=CH₂]PF₆^{4a} that four phenyl groups, one on each phosphorus atom, sterically protect the C(1) carbon bonded to the ruthenium site. Indeed we shall show later that the addition of nucleophiles to complexes **3** takes place at the C(3) carbon atom.

Synthesis of Secondary Allenylidene [Ru=C=C=C(H)(R)] Complexes. All attempts to produce monosubstituted allenylidene–ruthenium by activation of secondary propargyl alcohols have failed. Especially RuCl₂(PR₃)₂arene derivatives readily reacted with 1-mono-substituted prop-2-yn-1-ols, NaPF₆, and methanol to produce a variety of α,β-unsaturated and polyenyl carbenes *via* reactive γ-monosubstituted allenylidenes,¹⁷ but the latter could never be isolated. The activation of secondary propargyl alcohols HC≡C–CHOHAr, **2f–i**, with the more electron-rich complex **1** has thus been studied. Complex **1** did react with alkynes **2f–i** in dichloromethane with a slight excess of NaPF₆, and stable red allenylidenes, containing one hydrogen atom at the C(3) carbon, **4f** (84%), **4g** (73%), **4h** (68%), and **4i** (70%) were isolated (Scheme 2). Analogously, the (*E*)-1-alkenylprop-2-yn-1-ol HC≡C–CHOH–CH=CH–Ph, **2j**, treated with complex **1** and NaPF₆ afforded the first γ-monosubstituted alkenyl allenylidene **5** (77%) which

retained the (*E*)-configuration of the CH=CH bond. However, the activation with **1** of the secondary alcohol containing a deprotonable methyl group HC≡C-CH(OH)CH₃, **2k**, led to a different process, and the brown unstable vinyl vinylidene-ruthenium complex **6** (63%) was obtained (Scheme 2). The latter likely results from the vinylidene (V) formation^{18a} (eq 2) followed by



dehydration directly into **6** or *via* the monosubstituted allenylidene (VI) which may contain a more basic C(4) carbon atom than the C(2) carbon of **6**. It was previously observed that complex **1** and unsubstituted propargyl alcohol HC≡CCH₂OH afforded vinylidene derivatives analogous to V, as simple terminal alkynes,^{4a} without further dehydration. The comparative activation of HC≡CCH₂OH, HC≡CCH(OH)CH₃, **2k**, and HC≡C-C(OH)(CH₃)₂, **2e**, by complex **1** shows the drastic influence of the introduction of one and two methyl groups at the C(1) carbon of propargyl alcohol. The activation of **2k** by **1** is in contrast with that of the more electron-releasing RuCl(PMe₂Ph)₂C₅Me₅ that led to vinylidene of type V.⁵

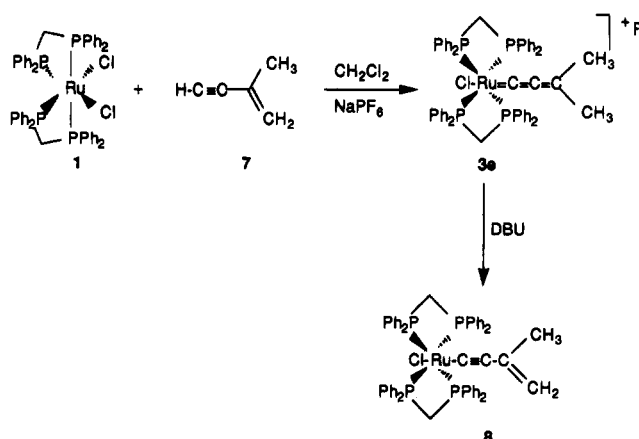
The secondary allenylidenes **4** display spectroscopic properties analogous to those of allenylidenes **3**, with some exceptions. The infrared absorption for the C=C=C group occurs at higher ν (cm⁻¹) for monosubstituted **4** than for disubstituted **3** allenylidene complexes [ν (C=C=C) = 1938 cm⁻¹ (**4a**) and 1928 cm⁻¹ (**3a**)]. The low-field (Ru=C) carbon nucleus δ ~320 ppm is coupled with four ³¹P phosphorus nuclei but also with the C(3)-H proton (³J_{CH} ~ 6 Hz), and the C(3)H carbon resonance gives evidence for its coupling with the proton (¹J_{CH} ~ 165 Hz). In ¹H NMR the C(3)-H proton is coupled with the four ³¹P nuclei (quintet, ⁵J_{PH} ~ 2-3 Hz) (Table 1). Although the new vinyl vinylidene complex **6**, ν (C=C) = 1636 cm⁻¹, is unstable and no ¹³C NMR spectrum could be recorded, its ¹H NMR spectrum clearly shows its C=CH-CH=CH₂ arrangement.

The activation of HC≡C-CH(OH)R, **2f-k**, with RuCl₂(dppm)₂ constitutes the most straightforward access to monosubstituted allenylidene M=C=C=C(H)R complexes. Recently, *primary* allenylidenes have been postulated in the activation of propargyl alcohol itself,³³ and *secondary* allenylidenes have been claimed to be formed by addition of an amine to a (trimethylsilyl)ethynyl carbene-chromium carbonyl derivative followed

(32) Oxidation potentials were measured using cyclic voltammetry (200 mV s⁻¹) with platinum and saturated calomel electrodes (SCE) in acetonitrile for RuCl₂(PR₃)(C₆Me₆)^{17c} and in dichloromethane for *cis*-(E_{1/2} = 0.84 V) and *trans*-(E_{1/2} = 0.46 V) RuCl₂(dppm)₂ complexes.

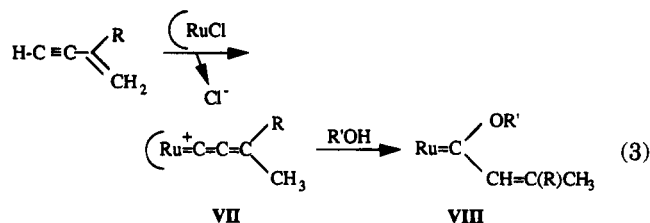
(33) In the substitution of the γ -hydroxy group in [C₅Me₅(PMe₂Ph)₂Ru=C-CHCH₂OH][PF₆]⁵ and in its trapping with PPh₃ to give (C₅H₅)(PPh₃)₂Ru-CC=C-CH₂PPh₃⁺, PF₆⁻.^{18c}

Scheme 3



by desilylation^{11a,34} and by dehydration of the γ -hydroxy vinylidene rhodium complex on alumina or by acid catalysis.^{27b}

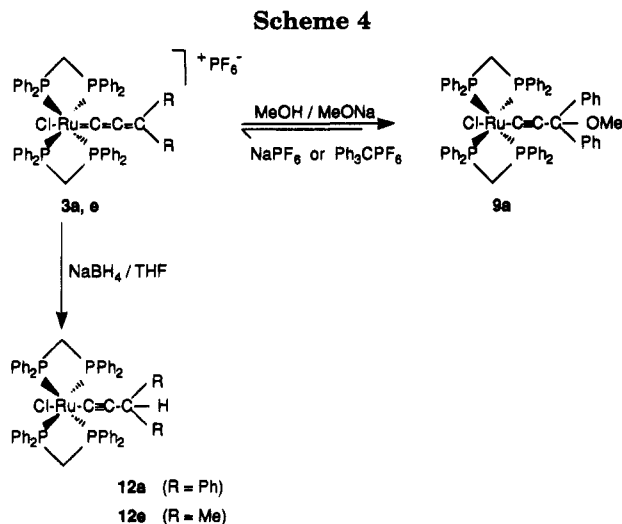
Activation of Isopropenylacetylene. The first attempt to activate vinyl acetylenes was undertaken with RuCl₂(L)arene derivatives (L = PR₃,²⁹ CNR,³⁰ carbene³⁰) for the synthesis of α,β -unsaturated carbenes. The reaction was understood in terms of the initial formation of allenylidenes (VII) *via* 1,4 migration of the terminal HC≡C proton to the C(4) carbon followed by addition of methanol to the C(1) carbon of the allenylidene intermediate to give the carbene VIII (eq 3).



As we have shown here that the (dppm)₂ClRu⁺ moiety can stabilize the allenylidene intermediate at a much greater extent than a (C₆Me₆)(L)ClRu⁺ species and as the complex **3e** obtained from **2e** was stable, the activation of isopropenylacetylene **7** with RuCl₂(dppm)₂, **1**, and NaPF₆ was attempted. It affords the γ,γ -dimethylallenylidene-ruthenium complex (39%) identical to **3e** obtained previously from **2e** (Scheme 3). The latter complex does not add alcohol to give carbene of type VIII, and the reaction, **1** + **7** → **3e**, clearly shows that the activation of isopropenyl acetylene takes place *via* 1,4 migration of the terminal alkyne proton to the C(4) carbon, likely *via* the vinylidene Ru⁺=C=CH-CMe=CH₂ intermediate. It is noteworthy that this intermediate is not stable with respect to the Ru⁺=C=CH-CH=CH₂ moiety in complex **6**. This comparison points out the first difference in behavior of mono- and disubstituted allenylidene metal complexes.

Transformation of Allenylidenes into Acetylide Metal Complexes. The complex **3e** is a rare example of stable allenylidene having hydrogen atoms at the C(4) carbon atom,^{16b,18} and thus its deprotonation could be anticipated. The treatment of **3e** with a base (DBU)

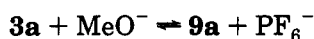
(34) The resulting complex (OC)₅Cr=C=C=C(NR₂)(SiMe₃) was desilylated and gave (OC)₅Cr=C=C=CH(NR₂).^{11a} However this result has been questioned: Rahm, A.; Wulff, W. D.; Rheingold, A. L. *Organometallics* **1993**, *12*, 597.



led to the deprotonation of the C(4) carbon and formation of a stable isopropenyl acetylide ruthenium complex **8**²¹ (Scheme 3). Another isopropenyl acetylide ruthenium complex was recently made by reaction of Cp(L)₂Ru(THF)⁺ with lithium isopropenylacetylene.^{18d}

The inhibition of allenylidenes **3** and **4** to react with alcohols to give unsaturated carbenes of type III (eq 1) by addition of alcohol at the C₁ carbon, as do RuCl₂(PR₃)₂(arene) derivatives, led us to consider the addition of the stronger nucleophile sodium methoxide. Complex **3a** reacts with MeONa in methanol to give the yellow acetylide derivative **9a** (55%) resulting from addition of the methoxide at carbon C(3) of the allenylidene ligand (Scheme 4). The addition at C(3) carbon rather than at C(1) carbon may be due to the protection of C(1) carbon by steric effect of four phenyl groups of the dppm ligands as observed by X-ray diffraction study of *trans*-[(dppm)₂ClRu=C=CH₂]PF₆.^{4a}

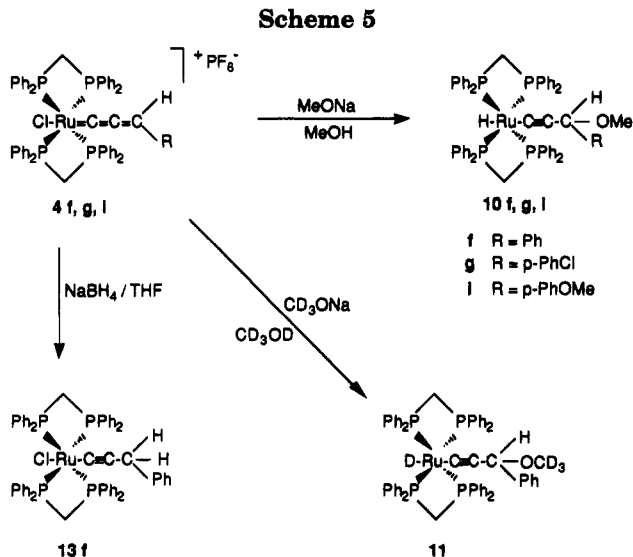
Complex **9a** readily gives back the stable allenylidene **3a**, as its treatment with an excess of Ph₃CPF₆ in dichloromethane afforded **3a**. The addition of the strong acid HBF₄ to **9a** eliminates methanol and gives back the allenylidene but with the BF₄⁻ anion *trans*-[(dppm)₂(Cl)Ru=C=C=CPh₂]BF₄, **3'a**. Such an elimination with an acid was already observed by reaction of (MeC₅H₄)-(OC)₂Mn-C≡C-CPh₂OMe.¹³ⁱ More surprising is the reaction of **9a** with only NaPF₆ in dichloromethane that immediately gives **3a** (55%), showing that the presence of the non coordinating salt in a polar medium orientates the equilibrium



toward the formation of the stable salt **3a** (Scheme 4).

The reaction of the *secondary* allenylidene **4f** with MeONa/MeOH by contrast afforded the yellow mixed hydride acetylide derivative **10f** (31%). Complex **10f** [IR (KBr): ν(C≡C), 2073; ν(Ru-H), 1813 cm⁻¹] gives a quintet in ¹H NMR at δ -7.19 ppm (²J_{PH} = 20 Hz) (Scheme 5). Analogously, by reaction of complexes **4g,i** with MeONa/MeOH the derivatives *trans*-H-Ru-C≡C-CH(OMe)Ar, **10g** (34%, δ(RuH) -7.16 ppm), and **10i** (36%, δ(RuH) -7.21 ppm) were isolated.

The reaction of **4f** with CD₃ONa in CD₃OD allowed the formation of the deuteriated complex **11** (29%) (Scheme 5). This reaction clearly shows that the hydride bonded to ruthenium in derivatives **10** and **11**



arises from the methoxide, likely *via* coordination of the methoxide and β-elimination, releasing formaldehyde as already observed in other systems.³⁵ The formation of hydrides **10** from **4**, under the same conditions as the transformation **3a** → **9a**, points out the specific influence of the C≡C-CH(OMe)Ph ligand, with respect to that of C≡C-CPh₂OMe, toward the substitution of the halide.

Because the methoxide adds to the C(3) carbon of allenylidenes **3** and **4**, the addition of hydride was also attempted. Complex **3a** was reacted with sodium borohydride in tetrahydrofuran and the yellow acetylide **12a** was isolated, in 40% yield, resulting also from addition of hydride to the C(3) carbon (Scheme 4). Complex **3e** also reacted with NaBH₄ to afford the analogous acetylide **12e**, but in very low yield (16%) due to its instability. If deprotonation with NaBH₄ had occurred, the stable isopropenylacetylide **8** would have been observed.

The secondary allenylidene **4f** on treatment with NaBH₄ afforded the product **13f** resulting from the hydride addition to the C(3) carbon (Scheme 5). In that case, the substitution of chloride by the hydride arising from BH₄⁻ does not take place. Thus, it appears that the substitution of the chloride takes place only under the influence of the *trans*-C≡C-CH(OMe)Ar ligand by methoxide.

Experimental Section

General Data. All reactions were performed under argon or nitrogen atmosphere with use of Schlenk techniques. The solvents were deoxygenated and dried by standard methods. Infrared spectra were recorded on a Nicolet 205 FT-IR spectrometer. ¹H (300.13 MHz), ³¹P (121.50 MHz), and ¹³C (75.47 MHz) NMR spectra were recorded on a Bruker AC 300 P spectrometer at 297 K and were referenced to TMS for ¹H and ¹³C and to 85% H₃PO₄ for ³¹P. Elemental analyses were performed by the Service Central de Microanalyse du CNRS at Vernaison, France.

The complex *cis*-RuCl₂(dppm)₂, **1** (dppm = Ph₂PCH₂PPh₂),³¹ propargyl alcohols **2a-d,f-k**,³⁶ and isopropenylacetylene **7**³⁶ were prepared by literature methods. The commercial (Janssen) dimethylpropargyl alcohol, **2e**, was used as received.

(35) Bruce, M. I.; Humphrey, M. G.; Swincer, A. G.; Wallis, R. C. *Aust. J. Chem.* **1984**, *37*, 1747.

(36) Brandsma, L. X. In *Preparative Acetylenic Chemistry*, 2nd ed.; Elsevier: New York, 1988.

Synthesis of Allenylidenes $trans$ -[(dppm)₂(Cl)Ru=C=C-CR¹R²]PF₆ (3a-j). A solution of an excess of propargyl alcohol **2** (1.1 mmol) in 60 mL of dichloromethane was added to **1** (0.5 mmol) and NaPF₆ (1.0 mmol). After being stirred for 4 h at room temperature, the solution was filtered through a filter-paper-tipped cannula, the solvent was removed under vacuum, and the precipitate was washed with diethyl ether. After dissolution in a minimum of dichloromethane and slow addition of hexane, in order to form a biphasic system, crystals of **3** were obtained.

$trans$ -[(dppm)₂(Cl)Ru=C=C-CPh₂]PF₆ (3a). (a) **Synthesis from 1.** From 470 mg of **1** (0.5 mmol), 168 mg of NaPF₆ (1.0 mmol), and 229 mg of H-C≡C-CPh₂OH, **2a** (1.1 mmol), was isolated 550 mg of dark red crystals of **3a** (89%). Anal. Calcd for C₆₅H₅₄ClF₆P₅Ru-CH₂Cl₂: C, 59.81; H, 4.26; Cl, 8.02; P, 11.68. Found: C, 59.94; H, 4.27; Cl, 7.78; P, 12.12. IR (cm⁻¹, KBr): 1928 (s, ν_{C=C}), 839 (s, ν_{PF}). ¹H NMR (300.13 MHz, CD₂Cl₂, 297 K, δ ppm): 7.60–6.55 (50 H, Ph), 5.31, 5.18 (ABX₂X', 4 H, PCH₂P, ²J_{HAHB} = 15.6 Hz, |²J_{PFA} + ⁴J_{PFA}| = 9 Hz, |²J_{PFB} + ⁴J_{PFB}| = 9.2 Hz). ¹³C{¹H} NMR (75.47 MHz, CD₂Cl₂, 297 K, δ ppm): 306.72 (quint, Ru=C, ²J_{PC} = 14.5 Hz), 208.94 (broad quint, Ru=C=C, ³J_{PC} = 2.5 Hz), 161.88 (broad s, Ru=C=C=C), 144.81 (s, Ph), 133.76–128.69 (Ph), 46.85 (quint, PCH₂P, |¹J_{PC} + ³J_{PC}| = 23.6 Hz). ¹³C NMR (75.47 MHz, CD₂Cl₂, 297 K, δ ppm): 144.81 (t, Ph, ³J_{CH} = 7.7 Hz), 46.88 (t quint, PCH₂P, ¹J_{CH} = 136.2 Hz, |¹J_{PC} + ³J_{PC}| = 23.4 Hz). ³¹P{¹H} NMR (121.50 MHz, CD₂Cl₂, 297 K, δ ppm): -14.83 (s, PPh₂), -143.92 (sept, PF₆, ¹J_{PF} = 711.4 Hz).

(b) **Synthesis from 9a with NaPF₆.** To a solution of **9a** in dichloromethane was added 10 equiv of NaPF₆. After being stirred for 1 h at room temperature, the solution was filtered through a filter-paper-tipped cannula, the solvent was removed under vacuum, and the precipitate was washed with diethyl ether. After dissolution in a minimum of dichloromethane, the slow addition of hexane allowed the formation of a biphasic system, affording crystals of **3a** (55%). IR (cm⁻¹, KBr): 1927 (s, ν_{C=C}), 833 (s, ν_{PF}). ³¹P{¹H} NMR (121.50 MHz, CD₂Cl₂, 297 K, δ ppm): -14.83 (s, PPh₂), -143.94 (sept, PF₆, ¹J_{PF} = 709.9 Hz).

(c) **Synthesis from 9a with Ph₃CPF₆.** To a solution of **9a** in dichloromethane was added 10 equiv of Ph₃CPF₆. After 30 min of being stirred at room temperature, the solution was filtered through a filter-paper-tipped cannula, the solvent was removed under vacuum, and the precipitate was washed with diethyl ether. After dissolution in a minimum of dichloromethane and slow addition of hexane, in order to form a biphasic system, crystals of **3a** were obtained (51%). Anal. Calcd for C₆₅H₅₄ClF₆P₅Ru-CH₂Cl₂: C, 59.81; H, 4.26. Found: C, 59.80; H, 4.31. IR (cm⁻¹, KBr): 1927 (s, ν_{C=C}), 837 (s, ν_{PF}). ³¹P{¹H} NMR (121.50 MHz, CD₂Cl₂, 297 K, δ ppm): -14.83 (s, PPh₂), -143.94 (sept, PF₆, ¹J_{PF} = 709.9 Hz).

$trans$ -[(dppm)₂(Cl)Ru=C=C-CPh₂]BF₄ (3'a). To a solution of **9a** in dichloromethane was added 10 equiv of HBF₄·Et₂O. After 30 min of being stirred at room temperature, the solution was filtered through a filter-paper-tipped cannula, the solvent was removed under vacuum, and the precipitate was washed with diethyl ether. After dissolution in a minimum of dichloromethane, the slow addition of hexane allowed the formation of a biphasic system, affording crystals of **3'a** (63%). Anal. Calcd for C₆₅H₅₄BClF₄P₄Ru-0.5CH₂Cl₂: C, 58.12; H, 4.26. Found: C, 58.30; H, 4.21. IR (cm⁻¹, KBr): 1924 (s, ν_{C=C}). ³¹P{¹H} NMR (121.50 MHz, CD₂Cl₂, 297 K, δ ppm): -14.83 (s, PPh₂).

$trans$ -[(dppm)₂(Cl)Ru=C=C-C(p-C₆H₄Cl)₂]PF₆ (3b). From 470 mg of **1** (0.5 mmol), 168 mg of NaPF₆ (1.0 mmol) and 305 mg of H-C≡C-C(p-C₆H₄Cl)₂(OH), **2b** (1.1 mmol), was isolated 580 mg of red crystals of **3b** (88%). Anal. Calcd for C₆₅H₅₂Cl₃F₆P₅Ru: C, 59.62; H, 4.00. Found: C, 59.74; H, 4.17. IR (cm⁻¹, KBr): 1921 (s, ν_{C=C}), 837 (s, ν_{PF}). ¹H NMR (300.13 MHz, CD₂Cl₂, 297 K, δ ppm): 7.46–6.37 (48 H, Ph), 5.33, 5.17 (ABX₂X', 4 H, PCH₂P, ²J_{HAHB} = 15.6 Hz, |²J_{PFA} + ⁴J_{PFA}| = 8.6 Hz, |²J_{PFB} + ⁴J_{PFB}| = 9.8 Hz). ¹H{³¹P} NMR (300.13 MHz,

CD₂Cl₂, 297 K, δ ppm): 5.34, 5.17 (AB, 4 H, PCH₂P, ²J_{HAHB} = 15.7 Hz). ¹³C{¹H} NMR (75.47 MHz, CD₂Cl₂, 297 K, δ ppm): 307.33 (quint, Ru=C, ²J_{PC} = 14.3 Hz), 213.92 (broad s, Ru=C=C), 156.63 (broad s, Ru=C=C=C), 142.95 (s, Ph), 138.43 (s, Ph), 133.91–127.27 (Ph), 45.98 (quint, PCH₂P, |¹J_{PC} + ³J_{PC}| = 23.8 Hz). ¹³C NMR (75.47 MHz, CD₂Cl₂, 297 K, δ ppm): 142.95 (t, Ph, ³J_{CH} = 7.6 Hz), 138.43 (tt, Ph, ³J_{HH} = 10.8 Hz, ⁴J_{HH} = 3.3 Hz), 45.99 (t quint, PCH₂P, ¹J_{CH} = 136.3 Hz, |¹J_{PC} + ³J_{PC}| = 11.9 Hz). ³¹P{¹H} NMR (121.50 MHz, CD₂Cl₂, 297 K, δ ppm): -14.78 (s, PPh₂), -143.41 (sept, PF₆, ¹J_{PF} = 710.6 Hz).

$trans$ -[(dppm)₂(Cl)Ru=C=C-C(p-C₆H₄F)₂]PF₆ (3c). From 470 mg of **1** (0.5 mmol), 168 mg of NaPF₆ (1.0 mmol) and 269 mg of H-C≡C-C(p-C₆H₄F)₂(OH), **2c** (1.1 mmol), was isolated 430 mg of violet crystals of **3c** (69%). Anal. Calcd for C₆₅H₅₂ClF₆P₅Ru: C, 61.16; H, 4.10; P, 12.13. Found: C, 61.42; H, 4.19; P, 12.25. IR (cm⁻¹, KBr): 1939 (s, ν_{C=C}), 844 (s, ν_{PF}). ¹H NMR (300.13 MHz, CD₂Cl₂, 297 K, δ ppm): 7.44–6.77 (48 H, Ph), 5.32, 5.15 (ABX₂X', 4 H, PCH₂P, ²J_{HAHB} = 15.6 Hz, |²J_{PFA} + ⁴J_{PFA}| = 8.6 Hz, |²J_{PFB} + ⁴J_{PFB}| = 9.4 Hz). ¹H{³¹P} NMR (300.13 MHz, CD₂Cl₂, 297 K, δ ppm): 5.32, 5.14 (AB, 4 H, PCH₂P, ²J_{HAHB} = 15.7 Hz). ¹³C{¹H} NMR (75.47 MHz, CD₂Cl₂, 297 K, δ ppm): 304.64 (quint, Ru=C, ²J_{PC} = 14.3 Hz), 208.51 (broad quint, Ru=C=C, ³J_{PC} = 4.0 Hz), 164.98 (d, Ph, ¹J_{CF} = 256.4 Hz), 157.22 (broad quint, Ru=C=C=C, ⁴J_{PC} = 2.2 Hz), 141.11 (s, Ph), 133.63–128.78 (Ph), 116.73 (s, Ph), 116.43 (s, Ph), 46.27 (quint, PCH₂P, |¹J_{PC} + ³J_{PC}| = 23.6 Hz). ¹³C NMR (75.47 MHz, CD₂Cl₂, 297 K, δ ppm): 164.98 (d m, Ph, ¹J_{CF} = 256.6 Hz), 141.10 (broad t, Ph), 116.60 (d, Ph, ¹J_{CH} = 147.9 Hz), 116.43 (d, Ph, ¹J_{CH} = 154.25 Hz), 46.27 (t quint, PCH₂P, ¹J_{CH} = 136.2 Hz, |¹J_{PC} + ³J_{PC}| = 23.8 Hz). ³¹P{¹H} NMR (121.50 MHz, CD₂Cl₂, 297 K, δ ppm): -14.33 (s, PPh₂), -143.44 (sept, PF₆, ¹J_{PF} = 710.6 Hz).

$trans$ -[(dppm)₂(Cl)Ru=C=C-C(o-C₆H₄-C₆H₄-o)]PF₆ (3d). From 470 mg of **1** (0.5 mmol), 168 mg of NaPF₆ (1.0 mmol), and 227 mg of H-C≡C-C(o-C₆H₄-C₆H₄-o)(OH), **2d** (1.1 mmol), was isolated 430 mg of violet crystals of **3d** (69%). Anal. Calcd for C₆₅H₅₂ClF₆P₅Ru-0.5CH₂Cl₂: C, 61.41; H, 4.17; P, 12.09. Found: C, 61.94; H, 4.27; P, 12.20. IR (cm⁻¹, KBr): 1939 (s, ν_{C=C}), 844 (s, ν_{PF}). ¹H NMR (300.13 MHz, CD₂Cl₂, 297 K, δ ppm): 7.66–5.37 (48 H, Ph), 5.43, 5.30 (ABX₂X', 4 H, PCH₂P, ²J_{HAHB} = 15.6 Hz, |²J_{PFA} + ⁴J_{PFA}| = 8.2 Hz, |²J_{PFB} + ⁴J_{PFB}| = 10.4 Hz). ¹H{³¹P} NMR (300.13 MHz, CD₂Cl₂, 297 K, δ ppm): 5.43, 5.30 (AB, 4 H, PCH₂P, ²J_{HAHB} = 15.6 Hz). ¹³C{¹H} NMR (75.47 MHz, CD₂Cl₂, 297 K, δ ppm): 312.02 (quint, Ru=C, ²J_{PC} = 14.9 Hz), 218.10 (broad quint, Ru=C=C, ³J_{PC} = 2.7 Hz), 155.46 (broad quint, Ru=C=C=C, ⁴J_{PC} = 1.8 Hz), 145.98 (s, Ph), 141.00 (s, Ph), 133.59–128.83 (Ph), 45.48 (quint, PCH₂P, |¹J_{PC} + ³J_{PC}| = 22.8 Hz). ¹³C NMR (75.47 MHz, CD₂Cl₂, 297 K, δ ppm): 145.97 (broad t, Ph), 145.97 (t, Ph, ³J_{CH} = 7.3 Hz), 45.36 (t quint, PCH₂P, ¹J_{CH} = 136.5 Hz, |¹J_{PC} + ³J_{PC}| = 24.2 Hz). ³¹P{¹H} NMR (121.50 MHz, CD₂Cl₂, 297 K, δ ppm): -15.11 (s, PPh₂), -143.41 (sept, PF₆, ¹J_{PF} = 710.6 Hz).

$trans$ -[(dppm)₂(Cl)Ru=C=C-CMe₂]PF₆ (3e). (a) **Synthesis from 1 and Dimethylpropargyl Alcohol 2e.** From 470 mg of **1** (0.5 mmol), 168 mg of NaPF₆ (1.0 mmol), and 107 μL of H-C≡C-CMe₂(OH), **2e** (1.1 mmol), was isolated 440 mg of green crystals of **3e** (79%). Anal. Calcd for C₅₅H₅₀-ClF₆P₅Ru-0.25CH₂Cl₂: C, 58.33; H, 4.47; Cl, 4.67; P, 13.60. Found: C, 58.30; H, 4.65; Cl, 5.24; P, 12.97. IR (cm⁻¹, KBr): 1964 (s, ν_{C=C}), 839 (s, ν_{PF}). ¹H NMR (300.13 MHz, CD₂Cl₂, 297 K, δ ppm): 7.42–7.19 (40 H, Ph), 5.21, 5.10 (ABX₂X', 4 H, PCH₂P, ²J_{HAHB} = 15.5 Hz, |²J_{PFA} + ⁴J_{PFA}| = 8.0 Hz, |²J_{PFB} + ⁴J_{PFB}| = 10.2 Hz); 0.78 (s, 3 H, Me). ¹H{³¹P} NMR (300.13 MHz, CD₂Cl₂, 297 K, δ ppm): 5.09, 5.21 (AB, 4 H, PCH₂P, ²J_{HAHB} = 15.6 Hz). ¹³C{¹H} NMR (75.47 MHz, CD₂Cl₂, 297 K, δ ppm): 322.69 (quint, Ru=C, ²J_{PC} = 13.9 Hz), 199.85 (broad quint, Ru=C=C, ³J_{PC} = 2.3 Hz), 173.33 (broad s, Ru=C=C=C), 133.66–128.84 (Ph), 46.79 (quint, PCH₂P, |¹J_{PC} + ³J_{PC}| = 23.6 Hz), 35.24 (s, Me). ¹³C NMR (δ ppm): 46.80 (t quint, PCH₂P, ¹J_{CH} = 136.4 Hz, |¹J_{PC} + ³J_{PC}| = 23.6 Hz), 35.24 (q, Me, ¹J_{CH}

= 129.6 Hz). $^{31}\text{P}\{^1\text{H}\}$ NMR (121.50 MHz, CD_2Cl_2 , 297 K, δ ppm): -14.00 (s, PPh_2), -143.46 (sept, PF_6 , $^1J_{\text{PF}} = 710.5$ Hz).

(b) Synthesis from 1 and Isopropenylacetylene 7. From 470 mg of **1** (0.5 mmol), 168 mg of NaPF_6 (1.0 mmol), and 73 mg of $\text{H}-\text{C}\equiv\text{C}-\text{C}(\text{Me})=\text{CH}_2$, **7** (1.1 mmol), was isolated 220 mg of green crystals of **3e** (39%) after 24 h of reaction. Anal. Calcd for $\text{C}_{55}\text{H}_{50}\text{ClF}_6\text{P}_5\text{Ru}$: C, 59.17; H, 4.51. Found: C, 59.19; H, 5.03. IR (cm^{-1} , KBr): 1964 (s, $\nu_{\text{C}=\text{C}}$), 840 (s, ν_{PF}). $^{31}\text{P}\{^1\text{H}\}$ NMR (121.50 MHz, CD_2Cl_2 , 297 K, δ ppm): -14.45 (s, PPh_2), -143.92 (sept, PF_6 , $^1J_{\text{PF}} = 711.0$ Hz).

trans-[(dppm)₂(Cl)Ru=C=C=CHPh]PF₆ (4f). From 470 mg of **1** (0.5 mmol), 168 mg of NaPF_6 (1.0 mmol), and 145 mg of $\text{H}-\text{C}\equiv\text{C}-\text{CHPh}(\text{OH})$, **2f** (1.1 mmol), was isolated 490 mg of red crystals of **4f** (84%). Anal. Calcd for $\text{C}_{59}\text{H}_{50}\text{ClF}_6\text{P}_5\text{Ru}$: C, 60.86; H, 4.33; Cl, 3.04; P, 13.30. Found: C, 60.88; H, 4.33; Cl, 3.66; P, 13.05. IR (cm^{-1} , KBr): 1938 (s, $\nu_{\text{C}=\text{C}}$), 839 (s, ν_{PF}). ^1H NMR (300.13 MHz, CD_2Cl_2 , 297 K, δ ppm): 8.49 (quint, 1 H, δ , $^5J_{\text{PH}} = 2.7$ Hz), 7.66–6.69 (45H, Ph), 5.32, 5.24 ($\text{ABX}_2\text{X}'_2$, 4 H, PCH_2P , $^2J_{\text{HAHB}} = 15.5$ Hz, $^2J_{\text{PHA}} + ^4J_{\text{PHA}} = 8.0$ Hz, $^2J_{\text{PHB}} + ^4J_{\text{PHB}} = 10.2$ Hz). $^1\text{H}\{^{31}\text{P}\}$ NMR (300.13 MHz, CD_2Cl_2 , 297 K, δ ppm): 8.49 (s, 1H, =CH), 5.32, 5.24 (AB, 4 H, PCH_2P , $^2J_{\text{HAHB}} = 15.6$ Hz). $^{13}\text{C}\{^1\text{H}\}$ NMR (75.47 MHz, CD_2Cl_2 , 297 K, δ ppm): 323.08 (quint, $\text{Ru}=\text{C}$, $^2J_{\text{PC}} = 14.4$ Hz), 217.31 (broad quint, $\text{Ru}=\text{C}=\text{C}$, $^3J_{\text{PC}} = 2.7$ Hz), 150.86 (broad s, $\text{Ru}=\text{C}=\text{C}$), 142.80 (s, Ph), 133.71–128.87 (Ph), 46.42 (quint, PCH_2P , $^1J_{\text{PC}} + ^3J_{\text{PC}} = 23.6$ Hz). ^{13}C NMR (δ ppm): 323.10 (d quint, $\text{Ru}=\text{C}$, $^3J_{\text{CH}} = 6.6$ Hz, $^2J_{\text{PC}} = 14.4$ Hz), 217.28 (m, $\text{Ru}=\text{C}=\text{C}$), 150.86 (d, $\text{Ru}=\text{C}=\text{C}=\text{C}$, $^1J_{\text{CH}} = 165.1$ Hz), 142.79 (t, =C–C, $^3J_{\text{CH}} = 7.6$ Hz), 46.42 (dd quint, PCH_2P , $^1J_{\text{CHA}} = 135.7$ Hz, $^1J_{\text{CHB}} = 137.4$ Hz, $^1J_{\text{PC}} + ^3J_{\text{PC}} = 23.6$ Hz). $^{31}\text{P}\{^1\text{H}\}$ NMR (121.50 MHz, CD_2Cl_2 , 297 K, δ ppm): -14.91 (s, PPh_2), -143.35 (sept, PF_6 , $^1J_{\text{PF}} = 710.8$ Hz).

trans-[(dppm)₂(Cl)Ru=C=C=CH(p-C₆H₄Cl)]PF₆ (4g). From 470 mg of **1** (0.5 mmol), 168 mg of NaPF_6 (1.0 mmol), and 183 mg of $\text{H}-\text{C}\equiv\text{C}-\text{CH}(p\text{-C}_6\text{H}_4\text{Cl})(\text{OH})$, **2g** (1.1 mmol), was isolated 440 mg of red crystals of **4g** (73%). Anal. Calcd for $\text{C}_{59}\text{H}_{49}\text{Cl}_2\text{F}_6\text{P}_5\text{Ru}$: C, 57.57; H, 4.06; Cl, 8.57; P, 12.47. Found: C, 57.58; H, 4.19; Cl, 8.40; P, 12.46. IR (cm^{-1} , KBr): 1950 (s, $\nu_{\text{C}=\text{C}}$), 840 (s, ν_{PF}). ^1H NMR (300.13 MHz, CD_2Cl_2 , 297 K, δ ppm): 8.47 (quint, 1H, =CH, $^5J_{\text{PH}} = 2.8$ Hz), 7.45–6.54 (44 H, Ph), 5.30, 5.21 ($\text{ABX}_2\text{X}'_2$, 4 H, PCH_2P , $^2J_{\text{HAHB}} = 15.5$ Hz, $^2J_{\text{PHA}} + ^4J_{\text{PHA}} = 8.0$ Hz, $^2J_{\text{PHB}} + ^4J_{\text{PHB}} = 10.4$ Hz). $^1\text{H}\{^{31}\text{P}\}$ NMR (300.13 MHz, CD_2Cl_2 , 297 K, δ ppm): 8.47 (s, 1 H, =CH), 5.30, 5.21 (AB, 4 H, PCH_2P , $^2J_{\text{HAHB}} = 15.7$ Hz). $^{13}\text{C}\{^1\text{H}\}$ NMR (75.47 MHz, CD_2Cl_2 , 297 K, δ ppm): 323.24 (quint, $\text{Ru}=\text{C}$, $^2J_{\text{PC}} = 14.5$ Hz), 220.27 (broad quint, $\text{Ru}=\text{C}=\text{C}$, $^3J_{\text{PC}} = 2.7$ Hz), 148.28 (broad quint, $\text{Ru}=\text{C}=\text{C}=\text{C}$, $^4J_{\text{PC}} = 2.2$ Hz), 141.21 (s, Ph), 139.68 (s, Ph); 133.66–128.79 (Ph), 46.03 (quint, PCH_2P , $^1J_{\text{PC}} + ^3J_{\text{PC}} = 23.4$ Hz). ^{13}C NMR (δ ppm): 323.26 (d quint, $\text{Ru}=\text{C}$, $^3J_{\text{CH}} = 6.6$ Hz, $^2J_{\text{PC}} = 14.4$ Hz), 220.24 (m, $\text{Ru}=\text{C}=\text{C}$), 148.26 (d, m, $\text{Ru}=\text{C}=\text{C}=\text{C}$, $^1J_{\text{CH}} = 162.8$ Hz), 141.20 (t, Ph, $^3J_{\text{CH}} = 7.9$ Hz), 139.68 (m, Ph), 46.03 (dd quint, PCH_2P , $^1J_{\text{CHA}} = 135.1$ Hz, $^1J_{\text{CHB}} = 137.7$ Hz, $^1J_{\text{PC}} + ^3J_{\text{PC}} = 22.6$ Hz). $^{31}\text{P}\{^1\text{H}\}$ NMR (121.50 MHz, CD_2Cl_2 , 297 K, δ ppm): -15.17 (s, PPh_2), -143.38 (sept, PF_6 , $^1J_{\text{PF}} = 710.7$ Hz).

trans-[(dppm)₂(Cl)Ru=C=C=CH(p-C₆H₄F)]PF₆ (4h). From 470 mg of **1** (0.5 mmol), 168 mg of NaPF_6 (1.0 mmol), and 165 mg of $\text{H}-\text{C}\equiv\text{C}-\text{CH}(p\text{-C}_6\text{H}_4\text{F})(\text{OH})$, **2h** (1.1 mmol), was isolated 400 mg of red crystals of **4h** (68%). Anal. Calcd for $\text{C}_{55}\text{H}_{49}\text{ClF}_7\text{P}_5\text{Ru}$: C, 58.34; H, 4.11; Cl, 5.79. Found: C, 58.90; H, 3.96; Cl, 5.23. IR (cm^{-1} , KBr): 1950 (s, $\nu_{\text{C}=\text{C}}$), 840 (s, ν_{PF}). ^1H NMR (300.13 MHz, CD_2Cl_2 , 297 K, δ ppm): 8.39 (quint, 1 H, =CH, $^5J_{\text{PH}} = 2.8$ Hz), 7.44–6.60 (44 H, Ph), 5.30, 5.20 ($\text{ABX}_2\text{X}'_2$, 4 H, PCH_2P , $^2J_{\text{HAHB}} = 15.5$ Hz, $^2J_{\text{PHA}} + ^4J_{\text{PHA}} = 8.0$ Hz, $^2J_{\text{PHB}} + ^4J_{\text{PHB}} = 10.4$ Hz). $^1\text{H}\{^{31}\text{P}\}$ NMR (300.13 MHz, CD_2Cl_2 , 297 K, δ ppm): 8.40 (s, 1 H, =CH), 5.30, 5.20 (AB, 4 H, PCH_2P , $^2J_{\text{HAHB}} = 15.6$ Hz). $^{13}\text{C}\{^1\text{H}\}$ NMR (75.47 MHz, CD_2Cl_2 , 297 K, δ ppm): 321.25 (quint, $\text{Ru}=\text{C}$, $^2J_{\text{PC}} = 14.4$ Hz), 215.88 (broad quint, $\text{Ru}=\text{C}=\text{C}$, $^3J_{\text{PC}} = 2.7$ Hz), 165.84 (d, Ph, $^1J_{\text{CF}} = 259.4$ Hz), 148.41 (broad s, $\text{Ru}=\text{C}=\text{C}=\text{C}$), 139.68 (s, Ph), 133.87–128.86 (Ph), 117.61 (s, Ph), 117.31 (s, Ph), 46.10 (quint, PCH_2P , $^1J_{\text{PC}} + ^3J_{\text{PC}} = 23.4$ Hz). ^{13}C NMR

(δ ppm): 321.27 (d quint, $\text{Ru}=\text{C}$, $^3J_{\text{CH}} = 6.6$ Hz, $^2J_{\text{PC}} = 14.4$ Hz), 215.85 (m, $\text{Ru}=\text{C}=\text{C}$), 165.84 (d m, Ph, $^1J_{\text{CF}} = 259.5$ Hz), 148.42 (d, $\text{Ru}=\text{C}=\text{C}=\text{C}$, $^1J_{\text{CH}} = 165.5$ Hz), 139.67 (t, Ph, $^3J_{\text{CH}} = 7.4$ Hz), 117.61 (dd, Ph, $^1J_{\text{CH}} = 166.4$ Hz, $^3J_{\text{CH}} = 3.9$ Hz), 117.32 (dd, Ph, $^1J_{\text{CH}} = 166.5$ Hz, $^3J_{\text{CH}} = 3.8$ Hz), 46.10 (dd quint, PCH_2P , $^1J_{\text{CHA}} = 135.3$ Hz, $^1J_{\text{CHB}} = 137.8$ Hz, $^1J_{\text{PC}} + ^3J_{\text{PC}} = 23.4$ Hz). $^{31}\text{P}\{^1\text{H}\}$ NMR (121.50 MHz, CD_2Cl_2 , 297 K, δ ppm): -14.88 (s, PPh_2), -143.38 (sept, PF_6 , $^1J_{\text{PF}} = 710.9$ Hz).

trans-[(dppm)₂(Cl)Ru=C=C=CH(p-C₆H₄OMe)]PF₆ (4i). From 470 mg of **1** (0.5 mmol), 168 mg of NaPF_6 (1.0 mmol), and 177 mg of $\text{H}-\text{C}\equiv\text{C}-\text{CH}(p\text{-C}_6\text{H}_4\text{OMe})(\text{OH})$, **2i** (1.1 mmol), was isolated 420 mg of red crystals of **4i** (70%). Anal. Calcd for $\text{C}_{60}\text{H}_{52}\text{ClF}_6\text{OP}_5\text{Ru}$: C, 60.33; H, 4.39; P, 12.97. Found: C, 60.38; H, 4.43; P, 12.45. IR (cm^{-1} , KBr): 1943 (s, $\nu_{\text{C}=\text{C}}$), 841 (s, ν_{PF}). ^1H NMR (300.13 MHz, CD_2Cl_2 , 297 K, δ ppm): 8.03 (quint, 1 H, =CH, $^5J_{\text{PH}} = 2.6$ Hz), 7.54–6.60 (44 H, Ph), 5.26, 5.17 ($\text{ABX}_2\text{X}'_2$, 4 H, PCH_2P , $^2J_{\text{HAHB}} = 15.6$ Hz, $^2J_{\text{PHA}} + ^4J_{\text{PHA}} = 8.2$ Hz, $^2J_{\text{PHB}} + ^4J_{\text{PHB}} = 10.2$ Hz), 3.86 (s, 3H, OMe). $^1\text{H}\{^{31}\text{P}\}$ NMR (300.13 MHz, CD_2Cl_2 , 297 K, δ ppm): 8.03 (s, 1H, =CH), 5.26, 5.17 (AB, 4 H, PCH_2P , $^2J_{\text{HAHB}} = 15.5$ Hz). $^{13}\text{C}\{^1\text{H}\}$ NMR (75.47 MHz, CD_2Cl_2 , 297 K, δ ppm): 308.37 (quint, $\text{Ru}=\text{C}$, $^2J_{\text{PC}} = 14.1$ Hz), 200.78 (broad quint, $\text{Ru}=\text{C}=\text{C}$, $^3J_{\text{PC}} = 2.6$ Hz), 165.33 (s, Ph), 149.92 (broad s, $\text{Ru}=\text{C}=\text{C}$), 137.38 (s, Ph), 134.75–128.77 (Ph), 115.88 (s, Ph), 56.50 (s, OMe), 46.84 (quint, PCH_2P , $^1J_{\text{PC}} + ^3J_{\text{PC}} = 23.6$ Hz). ^{13}C NMR (δ ppm): 308.38 (d quint, $\text{Ru}=\text{C}$, $^3J_{\text{CH}} = 6.3$ Hz, $^2J_{\text{PC}} = 14.3$ Hz), 200.78 (m, $\text{Ru}=\text{C}=\text{C}$), 165.34 (m, Ph), 149.92 (d, $\text{Ru}=\text{C}=\text{C}=\text{C}$, $^1J_{\text{CH}} = 163.2$ Hz), 137.38 (t, Ph, $^3J_{\text{CH}} = 7.2$ Hz), 115.88 (dd, Ph, $^1J_{\text{CH}} = 163.1$ Hz, $^3J_{\text{CH}} = 3.95$ Hz), 56.50 (q, OMe, $^1J_{\text{CH}} = 145.7$ Hz), 46.84 (dd quint, PCH_2P , $^1J_{\text{CHA}} = 135.3$ Hz, $^1J_{\text{CHB}} = 137.1$ Hz, $^1J_{\text{PC}} + ^3J_{\text{PC}} = 23.4$ Hz). $^{31}\text{P}\{^1\text{H}\}$ NMR (121.50 MHz, CD_2Cl_2 , 297 K, δ ppm): -13.71 (s, PPh_2), -143.40 (sept, PF_6 , $^1J_{\text{PF}} = 710.7$ Hz).

trans-[(dppm)₂(Cl)Ru=C=C=CH(CH=CHPh)]PF₆ (5). From 470 mg of **1** (0.5 mmol), 168 mg of NaPF_6 (1.0 mmol), and 174 mg of $\text{H}-\text{C}\equiv\text{C}-\text{CH}(\text{CH}=\text{CHPh})(\text{OH})$, **2j** (1.1 mmol), was isolated 460 mg of red crystals of **5** (77%). Anal. Calcd for $\text{C}_{61}\text{H}_{53}\text{ClF}_6\text{P}_5\text{Ru}$: C, 61.49; H, 4.48; Cl, 2.98; P, 13.01. Found: C, 61.75; H, 4.64; Cl, 2.51; P, 13.17. IR (cm^{-1} , KBr): 1947 (s, $\nu_{\text{C}=\text{C}}$), 1553 (m, $\nu_{\text{C}=\text{C}}$), 837 (s, ν_{PF}). ^1H NMR (300.13 MHz, CD_2Cl_2 , 297 K, δ ppm): 8.06 (d quint, 1 H, $\text{Ru}=\text{C}=\text{C}-\text{CH}$, $^5J_{\text{PH}} = 2.3$ Hz, $^3J_{\text{HH}} = 11.3$ Hz), 7.63–7.19 (40H, Ph and $\text{CH}=\text{CHPh}$ masked by signals of phenyls), 5.23, 5.15 ($\text{ABX}_2\text{X}'_2$, 4 H, PCH_2P , $^2J_{\text{HAHB}} = 15.6$ Hz, $^2J_{\text{PHA}} + ^4J_{\text{PHA}} = 8.0$ Hz, $^2J_{\text{PHB}} + ^4J_{\text{PHB}} = 10.6$ Hz) and $\text{CH}=\text{CHPh}$ masked by signal of PCH_2P group). $^1\text{H}\{^{31}\text{P}\}$ NMR (300.13 MHz, CD_2Cl_2 , 297 K, δ ppm): 8.07 (d, 1 H, $\text{Ru}=\text{C}=\text{C}-\text{CH}$, $^3J_{\text{HH}} = 11.4$ Hz), 5.23, 5.16 (AB, 4 H, PCH_2P , $^2J_{\text{HAHB}} = 15.6$ Hz), 5.21 (dd, $\text{CH}=\text{CHPh}$, $^3J_{\text{HH}} = 11.2$ Hz, $^3J_{\text{HH}} = 15.2$ Hz). $^1\text{H}\{^{31}\text{P}\}$ NMR with irradiation at δ 8.1 ppm (δ ppm): 5.21 (d, 1 H, $\text{CH}=\text{CHPh}$, $^3J_{\text{HH}} = 14.0$ Hz). $^{13}\text{C}\{^1\text{H}\}$ NMR (75.47 MHz, CD_2Cl_2 , 297 K, δ ppm): 315.15 (quint, $\text{Ru}=\text{C}$, $^2J_{\text{PC}} = 14.5$ Hz), 220.37 (broad quint, $\text{Ru}=\text{C}=\text{C}$, $^3J_{\text{PC}} = 2.7$ Hz), 152.56 (s, $\text{CH}=\text{CHPh}$), 149.85 (broad s, $\text{Ru}=\text{C}=\text{C}$), 137.03 (s, Ph), 136.53 (broad s, $\text{CH}=\text{CHPh}$), 133.75–128.70 (Ph), 46.69 (quint, PCH_2P , $^1J_{\text{PC}} + ^3J_{\text{PC}} = 23.2$ Hz). ^{13}C NMR (δ ppm): 315.17 (d quint, $\text{Ru}=\text{C}$, $^2J_{\text{PC}} = 14.35$ Hz, $^3J_{\text{CH}} = 6.9$ Hz), 220.36 (m, $\text{Ru}=\text{C}=\text{C}$), 152.58 (d m, $\text{CH}=\text{CHPh}$, $^1J_{\text{CH}} = 155.4$ Hz), 149.85 (d m, $\text{Ru}=\text{C}=\text{C}=\text{C}$, $^1J_{\text{CH}} = 164.2$ Hz), 137.06 (m, Ph), 136.53 (d, $\text{CH}=\text{CHPh}$, $^1J_{\text{CH}} = 159.8$ Hz), 46.69 (dd quint, PCH_2P , $^1J_{\text{CHA}} = 135.1$ Hz, $^1J_{\text{CHB}} = 137.8$ Hz, $^1J_{\text{PC}} + ^3J_{\text{PC}} = 23.2$ Hz). Heteronuclear $^{13}\text{C}-^1\text{H}$ correlation (CD_2Cl_2 , 297 K): the signal $\text{CH}=\text{CHPh}$ is found at 7.43 ppm as a doublet with coupling constant $^3J_{\text{HH}} = 15.4$ Hz. $^{31}\text{P}\{^1\text{H}\}$ NMR (121.50 MHz, CD_2Cl_2 , 297 K, δ ppm): -14.59 (s, PPh_2), -143.38 (sept, PF_6 , $^1J_{\text{PF}} = 710.7$ Hz).

Synthesis of Vinylidene trans-[(dppm)₂(Cl)Ru=C=CH¹-CH²=CH³]PF₆ (6). It was prepared by using the general procedure for synthesis of allenylidenes. From 470 mg of **1** (0.5 mmol), 168 mg of NaPF_6 (1.0 mmol), and 86 μL of $\text{H}-\text{C}\equiv\text{C}-\text{CHMe}(\text{OH})$, **2k** (1.1 mmol), was isolated 350 mg of brown crystals of **6** (63%) after 36 h of reaction. Complex **6**

was very sensitive, and no elemental analysis or ^{13}C NMR spectrum could be obtained. IR (cm^{-1} , KBr): 1636 (s, $\nu_{\text{C}=\text{C}}$), 838 (s, ν_{PF_6}). ^1H NMR (300.13 MHz, CD_2Cl_2 , 297 K, δ ppm): 7.52–7.06 (40 H, Ph), 5.17, 5.13 ($\text{ABX}_2\text{X}'_2$, 4 H, PCH_2P , $^2J_{\text{HAHB}} = 15.4$ Hz, $^2J_{\text{PHA}} + ^4J_{\text{PHA}} = 8.8$ Hz, $^2J_{\text{PHB}} + ^4J_{\text{PHB}} = 9.4$ Hz), 4.63 ddd, 1 H, $\text{CH}^2=\text{CH}_2$, $^3J_{\text{H}^1\text{H}^2} = 16.5$ Hz), 4.10 (dd, 1 H, $(\text{CH}=\text{CH}_2)\text{H}^3_{\text{trans}}$, $^3J_{\text{HHtrans}} = 16.5$ Hz, $^2J_{\text{HH}} = 0.7$ Hz), 3.78 (dd, 1 H, $(\text{CH}=\text{CH}_2)\text{H}^3_{\text{cis}}$, $^3J_{\text{HHcis}} = 10.0$ Hz, $^2J_{\text{HH}} = 1.5$ Hz), 3.30 (d quint, 1 H, $\text{Ru}=\text{C}=\text{CH}$, $^3J_{\text{H}^1\text{H}^2} = 9.4$ Hz, $^4J_{\text{PH}} = 3.0$ Hz). $^{31}\text{P}\{^1\text{H}\}$ NMR (121.50 MHz, CD_2Cl_2 , 297 K, δ ppm): -16.24 (s, PPh_2), -143.58 (sept, PF_6 , $^1J_{\text{PF}} = 710.8$ Hz).

Synthesis of the Acetylide *trans*-(dppm) $_2$ (Cl)Ru-C≡C-(Me)=CH $_2$ (8). To a solution of 335 mg of **3e** (0.3 mmol) in 30 mL of tetrahydrofuran was added 90 μL of 1,8-diazabicyclo[5.4.0]undec-7-ene (DBU) (0.6 mmol). The reaction mixture was stirred at room temperature for 30 min. The solvent was removed under vacuum. The crude product was filtered with dichloromethane through alumina using a chromatography column. Recrystallization from THF/*n*-pentane (40:80) afforded 70 mg of yellow crystals of **8** (24%). Anal. Calcd for $\text{C}_{55}\text{H}_{49}\text{ClP}_4\text{Ru}$: C, 68.07; H, 5.09; Cl, 3.65. Found: C, 68.68; H, 5.45; Cl, 3.91. IR (cm^{-1} , KBr): 2057 (m, $\nu_{\text{C}=\text{C}}$), 1590 (m, $\nu_{\text{C}=\text{C}}$). ^1H NMR (300.13 MHz, CD_2Cl_2 , 297 K, δ ppm): 7.49–7.10 (40 H, Ph), 4.89 (quint, 4 H, PCH_2P , $^2J_{\text{PH}} + ^4J_{\text{PH}} = 8.4$ Hz), 4.19 (m, 1 H, $\text{trans}=\text{CH}_2$), 3.77 (d, 1 H, $\text{cis}=\text{CH}_2$, $^2J_{\text{HH}} = 3.3$ Hz), 0.96 (s, 3 H, Me). $^{13}\text{C}\{^1\text{H}\}$ NMR (75.47 MHz, CD_2Cl_2 , 297 K, δ ppm): 135.95 (quint, Ph, $^1J_{\text{PC}} + ^3J_{\text{PC}} = 22.4$ Hz), 135.35 (quint, Ph, $^1J_{\text{PC}} + ^3J_{\text{PC}} = 20.4$ Hz), 133.84 (m, Ph), 132.61 (s, $\text{Ru}-\text{C}\equiv\text{C}$), 129.72 (s, Ph), 129.47 (s, Ph), 127.95 (s, Ph), 119.23 (quint, $\text{Ru}-\text{C}\equiv\text{C}$, $^2J_{\text{PC}} = 15.5$ Hz), 114.14 (s, $\text{Ru}-\text{C}\equiv\text{C}-\text{C}$), 110.33 (s, $=\text{CH}_2$), 50.28 (quint, PCH_2P , $^1J_{\text{PC}} + ^3J_{\text{PC}} = 20.6$ Hz), 24.53 (s, Me). ^{13}C NMR (δ ppm): 135.94 (m, Ph), 135.35 (m, Ph), 133.88 (d m, Ph, $^1J_{\text{CH}} = 163.0$ Hz), $\text{Ru}-\text{C}\equiv\text{C}$ masked by phenyl signals, 129.72 (d t, Ph, $^1J_{\text{CH}} = 160.8$ Hz, $^3J_{\text{CH}} = 7.3$ Hz), 129.47 (d t, Ph, $^1J_{\text{CH}} = 160.7$ Hz, $^3J_{\text{CH}} = 7.35$ Hz), 127.96 (d m, Ph, $^1J_{\text{CH}} = 161.3$ Hz), 119.23 (quint, $\text{Ru}-\text{C}\equiv\text{C}$, $^2J_{\text{PC}} = 15.6$ Hz), 114.14 (m, $\text{Ru}-\text{C}\equiv\text{C}-\text{C}$), 110.33 (t m, $=\text{CH}_2$, $^1J_{\text{CH}} = 155.9$ Hz), 50.28 (t quint, PCH_2P , $^1J_{\text{CH}} = 135.3$ Hz, $^1J_{\text{PC}} + ^3J_{\text{PC}} = 20.8$ Hz), 24.53 (q m, Me, $^1J_{\text{CH}} = 126.6$ Hz). $^{31}\text{P}\{^1\text{H}\}$ NMR (121.50 MHz, CD_2Cl_2 , 297 K, δ ppm): -5.67 (s, PPh_2).

Synthesis of Acetylides *trans*-(dppm) $_2$ (X)Ru-C≡C-(R 1)(R 2)(OMe) (X = Cl, H) (9 and 10). To a solution of allenylidenes **3** in methanol was added 10 equiv of MeONa. The reaction mixture was stirred at room temperature for 2 h. A rapid color change of the solution from red to yellow was observed with the formation of a yellow precipitate. After decantation of the remaining solution, the crude product was washed with methanol. Crystallization from THF/*n*-pentane mixtures afforded crystals of **9** and **10**.

***trans*-(dppm) $_2$ (Cl)Ru-C≡C-CPh $_2$ (OMe) (9a).** From 595 mg of **3a** (0.48 mmol) dissolved in 50 mL of methanol and 259 mg of MeONa (4.8 mmol), was isolated 300 mg of yellow crystals of **9a** (55%). Anal. Calcd for $\text{C}_{66}\text{H}_{57}\text{ClOP}_4\text{Ru}$: C, 70.36; H, 5.10. Found: C, 70.34; H, 5.38. IR (cm^{-1} , KBr): 2060 (m, $\nu_{\text{C}=\text{C}}$). ^1H NMR (300.13 MHz, CD_2Cl_2 , 297 K, δ ppm): 7.56–6.60 (50 H, Ph), 4.92, 4.62 ($\text{ABX}_2\text{X}'_2$, 4 H, PCH_2P , $^2J_{\text{HAHB}} = 14.1$ Hz, $^2J_{\text{PHA}} + ^4J_{\text{PHA}} = 8.6$ Hz, $^2J_{\text{PHB}} + ^4J_{\text{PHB}} = 9.0$ Hz), 2.19 (s, 3 H, OMe). $^{13}\text{C}\{^1\text{H}\}$ NMR (75.47 MHz, CD_2Cl_2 , 297 K, δ ppm): 147.26 (s, Ph), 136.79 (quint, Ph, $^1J_{\text{PC}} + ^3J_{\text{PC}} = 21.8$ Hz), 135.45 (quint, Ph, $^1J_{\text{PC}} + ^3J_{\text{PC}} = 21.2$ Hz), 133.82–125.94 (Ph), 109.33 (quint, $\text{Ru}-\text{C}\equiv\text{C}$, $^2J_{\text{PC}} = 14.9$ Hz), 107.75 (s, $\text{Ru}-\text{C}\equiv\text{C}$), 81.83 (s, $\text{Ru}-\text{C}\equiv\text{C}-\text{C}$), 51.07 (s, OMe), 49.51 (quint, PCH_2P , $^1J_{\text{PC}} + ^3J_{\text{PC}} = 20.8$ Hz). ^{13}C NMR (δ ppm): 147.26 (t, Ph, $^3J_{\text{CH}} = 6.9$ Hz), 136.79 (m, Ph), 135.50 (m, Ph), 51.06 (q, OMe, $^1J_{\text{CH}} = 138.1$ Hz), 49.51 (t quint, PCH_2P , $^1J_{\text{CH}} = 135.5$ Hz, $^1J_{\text{PC}} + ^3J_{\text{PC}} = 20.4$ Hz). $^{31}\text{P}\{^1\text{H}\}$ NMR (121.50 MHz, CD_2Cl_2 , 297 K, δ ppm): -4.30 (s, PPh_2).

***trans*-(dppm) $_2$ (H)Ru-C≡C-CHPh(OMe) (10f).** From 442 mg of **4f** (0.38 mmol) dissolved in 40 mL of methanol and 205 mg of MeONa (3.8 mmol), was isolated 120 mg of yellow crystals of **10f** (31%). Anal. Calcd for $\text{C}_{60}\text{H}_{54}\text{OP}_4\text{Ru}$: C, 70.93;

H, 5.36. Found: C, 70.35; H, 5.84. IR (cm^{-1} , KBr): 2073 (m, $\nu_{\text{C}=\text{C}}$), 1813 (m, $\nu_{\text{Ru}-\text{H}}$). ^1H NMR (300.13 MHz, CD_2Cl_2 , 297 K, δ ppm): 7.59–7.04 (45 H, Ph), 4.74 (s, 1 H, $\text{Ru}-\text{C}\equiv\text{C}-\text{CH}$), 4.78–4.53 ($\text{ABX}_2\text{X}'_2$, 4 H, PCH_2P , $^2J_{\text{HAHB}} = 14.4$ Hz, $^2J_{\text{PHA}} + ^4J_{\text{PHA}} = 7.0$ Hz) [the chemical shifts δ_A and δ_B and the coupling constant $^2J_{\text{PHA}} + ^4J_{\text{PHA}}$ could not be determined due to the presence of the CH signal], 2.71 (s, 3 H, OMe), -7.19 (quint, $\text{Ru}-\text{H}$, $^2J_{\text{PH}} = 20.0$ Hz). $^{13}\text{C}\{^1\text{H}\}$ NMR (75.47 MHz, CD_2Cl_2 , 297 K, δ ppm): 143.59 (s, Ph), 140.91 (m), 138.10 (m), 134.13–126.74 (Ph), 123.64 (quint, $\text{Ru}-\text{C}\equiv\text{C}$, $^2J_{\text{PC}} = 13.4$ Hz), 109.89 (s, $\text{Ru}-\text{C}\equiv\text{C}$), 75.71 (s, $\text{Ru}-\text{C}\equiv\text{C}-\text{C}$), 55.23 (quint, PCH_2P , $^1J_{\text{PC}} + ^3J_{\text{PC}} = 21.4$ Hz), 53.91 (s, OMe). ^{13}C NMR (δ ppm): 143.58 (m), 140.88 (m), 138.10 (m), 75.71 (d m, $\text{Ru}-\text{C}\equiv\text{C}-\text{C}$, $^1J_{\text{CH}} = 143.6$ Hz), 55.21 (t quint, PCH_2P , $^1J_{\text{CH}} = 145.6$ Hz, $^1J_{\text{PC}} + ^3J_{\text{PC}} = 21.8$ Hz), 53.91 (q d, OMe, $^1J_{\text{CH}} = 140.4$ Hz, $^3J_{\text{CH}} = 4.1$ Hz). $^{31}\text{P}\{^1\text{H}\}$ NMR (121.50 MHz, CD_2Cl_2 , 297 K, δ ppm): 3.08 (s, PPh_2).

***trans*-(dppm) $_2$ (H)Ru-C≡C-CH(p-C $_6$ H $_4$ Cl)(OMe) (10g).** From 300 mg of **4g** (0.25 mmol) dissolved in 30 mL of methanol and 135 mg of MeONa (2.5 mmol), was isolated 90 mg of yellow crystals of **10g** (34%). Anal. Calcd for $\text{C}_{60}\text{H}_{53}\text{ClOP}_4\text{Ru}$: C, 68.60; H, 5.09; Cl, 3.37; P, 11.79. Found: C, 68.53; H, 4.99; Cl, 3.78; P, 11.99. IR (cm^{-1} , KBr): 2073 (m, $\nu_{\text{C}=\text{C}}$), 1800 (m, $\nu_{\text{Ru}-\text{H}}$). ^1H NMR (300.13 MHz, CD_2Cl_2 , 297 K, δ ppm): 7.56–6.92 (44 H, Ph), 4.74 (s, 1 H, CH), 4.80–4.54 ($\text{ABX}_2\text{X}'_2$, 4 H, PCH_2P , $^2J_{\text{HAHB}} = 14.2$ Hz, $^2J_{\text{PHA}} + ^4J_{\text{PHA}} = 7.2$ Hz) [chemical shifts δ_A and δ_B and coupling constant $^2J_{\text{PHA}} + ^4J_{\text{PHA}}$ could not be determined due to the presence of CH signal], 2.72 (s, 3 H, OMe), -7.16 (quint, 1 H, $\text{Ru}-\text{H}$, $^2J_{\text{PH}} = 19.9$ Hz). $^{13}\text{C}\{^1\text{H}\}$ NMR (75.47 MHz, CD_2Cl_2 , 297 K, δ ppm): 142.30 (s, Ph), 140.8 (m), 138.05 (m), 133.98–127.48 (Ph), 124.96 (quint, $\text{Ru}-\text{C}\equiv\text{C}$, $^2J_{\text{PC}} = 13.4$ Hz), 109.23 (s, $\text{Ru}-\text{C}\equiv\text{C}$), 74.82 (s, CH), 55.29 (quint, PCH_2P , $^1J_{\text{PC}} + ^3J_{\text{PC}} = 21.6$ Hz), OMe masked by the solvent signal. ^{13}C NMR (δ ppm): 142.30 (m), 140.79 (m), 138.06 (m), 74.82 (d m, CH, $^1J_{\text{CH}} = 143.85$ Hz), 55.28 (t quint, PCH_2P , $^1J_{\text{CH}} = 134.9$ Hz, $^1J_{\text{PC}} + ^3J_{\text{PC}} = 21.4$ Hz), 53.94 (q d, OMe, $^1J_{\text{CH}} = 140.6$ Hz, $^3J_{\text{CH}} = 4.1$ Hz). $^{31}\text{P}\{^1\text{H}\}$ NMR (121.50 MHz, CD_2Cl_2 , 297 K, δ ppm): 3.04 (s, PPh_2).

***trans*-(dppm) $_2$ (H)Ru-C≡C-CH(p-C $_6$ H $_4$ OMe)(OMe) (10i).** From 406 mg of **4i** (0.34 mmol) dissolved in 40 mL of methanol and 184 mg of MeONa (3.4 mmol), was isolated 150 mg of yellow crystals of **10i** (36%). Anal. Calcd for $\text{C}_{61}\text{H}_{56}\text{O}_2\text{P}_4\text{Ru}$: C, 70.04; H, 5.40. Found: C, 69.49; H, 5.24. IR (cm^{-1} , KBr): 2081 (m, $\nu_{\text{C}=\text{C}}$), 1804 (m, $\nu_{\text{Ru}-\text{H}}$). ^1H NMR (300.13 MHz, CD_2Cl_2 , 297 K, δ ppm): 7.57–6.59 (44 H, Ph), 4.74 (s, 1 H, CH), 4.78–4.53 ($\text{ABX}_2\text{X}'_2$, 4 H, PCH_2P , $^2J_{\text{HAHB}} = 14.1$ Hz, $^2J_{\text{PHA}} + ^4J_{\text{PHA}} = 7.0$ Hz) [the chemical shifts δ_A and δ_B and the coupling constant $^2J_{\text{PHA}} + ^4J_{\text{PHA}}$ could not be determined because of the presence of the CH signal], 3.76 (s, 3 H, OMe), 2.68 (s, 3 H, OMe), -7.21 (quint, 1 H, $\text{Ru}-\text{H}$, $^2J_{\text{PH}} = 19.9$ Hz). $^{13}\text{C}\{^1\text{H}\}$ NMR (75.47 MHz, CD_2Cl_2 , 297 K, δ ppm): 158.79 (s), 140.98 (m), 138.16 (m), 136.06 (s), 134.12–125.73 (Ph), 123.12 (quint, $\text{Ru}-\text{C}\equiv\text{C}$, $^2J_{\text{PC}} = 13.4$ Hz), 113.25 (s, Ph), 110.14 (s, $\text{Ru}-\text{C}\equiv\text{C}$), 75.22 (s, CH), 55.63 (s, OMe), 55.30 (quint, PCH_2P , $^1J_{\text{PC}} + ^3J_{\text{PC}} = 21.4$ Hz), 53.73 (s, OMe). ^{13}C NMR (δ ppm): 158.76 (m), 141.01 (m), 138.14 (m), 136.05 (m), 113.24 (d m, Ph, $^1J_{\text{CH}} = 157.6$ Hz), 75.22 (d m, CH, $^1J_{\text{CH}} = 143.8$ Hz), 55.63 (q, OMe, $^1J_{\text{CH}} = 143.5$ Hz), 55.30 (t quint, PCH_2P , $^1J_{\text{CH}} = 133.9$ Hz, $^1J_{\text{PC}} + ^3J_{\text{PC}} = 20.8$ Hz), 53.74 (q d, OMe, $^1J_{\text{CH}} = 142.4$ Hz, $^3J_{\text{CH}} = 4.5$ Hz). $^{31}\text{P}\{^1\text{H}\}$ NMR (121.50 MHz, CD_2Cl_2 , 297 K, δ ppm): 3.00 (s, PPh_2).

***trans*-(dppm) $_2$ (D)Ru-C≡C-CHPh(OCD $_3$) (11).** To 150 mg of **4f** (0.13 mmol) dissolved in 10 mL of deuteriated methanol CD_3OD was added a solution of 30 mg of sodium (1.3 mmol) in 5 mL of CD_3OD . The formation of a yellow precipitate was observed after 2 h of reaction at room temperature. The yellow solid was washed with 5 mL of CD_3OD and dried. Crystallization in a THF/pentane mixture afforded 37 mg of **11** (29%). Anal. Calcd for $\text{C}_{60}\text{H}_{50}\text{D}_4\text{OP}_4\text{Ru}$: C, 70.65; H, 4.96. Found: C, 70.09; H, 5.03. IR (cm^{-1} , KBr): 2070 (m, $\nu_{\text{C}=\text{C}}$) ^1H NMR (300.13 MHz, CD_2Cl_2 , 297 K, δ ppm): 7.59–7.04 (45 H, Ph), 4.75 (s, 1 H, $\text{Ru}-\text{C}\equiv\text{C}-\text{CH}$), 4.78–4.53

(ABX₂X'₂, 4 H, PCH₂P, ²J_{HAHB} = 14.4 Hz, |²J_{P_{HB}} + ⁴J_{P_{HB}}| = 7.0 Hz). No signals for OCH₃ and Ru-H were observed. ³¹P NMR (121.50 Hz, CD₂Cl₂, 297 K, δ ppm): 3.15 (PPh₂).

Synthesis of Acetylides *trans*-(dppm)₂(Cl)Ru-C≡C-CH(R¹)(R²) (12 and 13). *trans*-(dppm)₂(Cl)Ru-C≡C-CHPh₂ (12a). To a solution of the allenylidene **3a-e** and **4f** in 30 mL of tetrahydrofuran was added a light excess of NaBH₄. After 1 h of being stirred at room temperature, the solution was filtered through a filter-paper-tipped cannula, the solvent was removed under vacuum, and the precipitate was dissolved in diethyl ether (3 × 40 mL). After filtration, the solution was concentrated under vacuum until the complex started to crystallize.

From 335 mg of **3a** (0.27 mmol) was isolated 120 mg of yellow crystals of **12a** (40%). Anal. Calcd for C₆₆H₅₅ClP₄Ru: C, 71.20; H, 5.06; Cl, 3.23; P, 11.30. Found: C, 71.18; H, 5.14; Cl, 3.24; P, 11.58. IR (cm⁻¹, KBr): 2081 (m, ν_{C≡C}). ¹H NMR (300.13 MHz, CD₂Cl₂, 297 K, δ ppm): 7.52–6.57 (50 H, Ph), 4.89, 4.78 (ABX₂X'₂, 4 H, PCH₂P, ²J_{HAHB} = 14.1 Hz, |²J_{P_{HA}} + ⁴J_{P_{HA}}| = 8.6 Hz, |²J_{P_{HB}} + ⁴J_{P_{HB}}| = 8.8 Hz), 4.26 (broad s, 1 H, CH). ¹³C{¹H} NMR (75.47 MHz, CD₂Cl₂, 297 K, δ ppm): 146.52 (s, Ph), 136.28 (quint, Ph, |¹J_{PC} + ³J_{PC}| = 22.6 Hz), 135.71 (quint, Ph, |¹J_{PC} + ³J_{PC}| = 10.2 Hz), 133.82–125.47 (Ph), 108.99 (s, Ru-C≡C), 103.13 (quint, Ru-C≡C, ²J_{PC} = 15.6 Hz), 49.93 (quint, PCH₂P, |¹J_{PC} + ³J_{PC}| = 20.6 Hz), 48.12 (s, CH). ¹³C NMR (δ ppm): 146.52 (m, Ph), 136.20 (m, Ph), 135.71 (m, Ph), 108.99 (d, Ru-C≡C, ²J_{CH} = 9.9 Hz), 103.13 (d quint, Ru-C≡C, ³J_{CH} = 3.2 Hz, ²J_{PC} = 15.6 Hz), 49.93 (t quint, PCH₂P, ¹J_{CH} = 135.4 Hz, |¹J_{PC} + ³J_{PC}| = 20.4 Hz), 48.11 (d m, CH, ¹J_{CH} = 129.5 Hz). ³¹P{¹H} NMR (121.50 MHz, CD₂Cl₂, 297 K, δ ppm): -5.26 (s, PPh₂).

trans-(dppm)₂(Cl)Ru-C≡C-CHMe₂ (12e). From 223

mg of **3e** (0.20 mmol) was isolated 30 mg of yellow crystals of **12e** (16%). This product was very sensitive, and either elemental analysis nor a ¹³C NMR spectrum could be obtained. IR (cm⁻¹, KBr): 2089 (m, ν_{C≡C}). ¹H NMR (300.13 MHz, CD₂Cl₂, 297 K, δ ppm): 7.53–7.08 (40 H, Ph), 4.90, 4.84 (ABX₂X'₂, 4 H, PCH₂P, ²J_{HAHB} = 14.1 Hz, |²J_{P_{HA}} + ⁴J_{P_{HA}}| = 8.6 Hz, |²J_{P_{HB}} + ⁴J_{P_{HB}}| = 8.2 Hz), 1.59 (sept, 1 H, CH, ³J_{HH} = 7.6 Hz), 0.28 (d, Me, ³J_{HH} = 6.8 Hz). ³¹P{¹H} NMR (121.50 MHz, CD₂Cl₂, 297 K, δ ppm): -5.65 (s, PPh₂).

trans-(dppm)₂(Cl)Ru-C≡C-CH₂Ph (13f). From 442 mg of **4f** (0.38 mmol) was isolated 180 mg of yellow crystals of **13f** (46%). Anal. Calcd for C₅₉H₅₁ClP₄Ru: C, 69.44; H, 5.04; Cl, 3.47. Found: C, 69.36; H, 5.23; Cl, 3.24. IR (cm⁻¹, KBr): 2103 (m, ν_{C≡C}). ¹H NMR (300.13 MHz, CD₂Cl₂, 297 K, δ ppm): 7.54–6.53 (45 H, Ph), 4.92, 4.82 (ABX₂X'₂, 4 H, PCH₂P, ²J_{HAHB} = 14.2 Hz, |²J_{P_H} + ⁴J_{P_H}| = 8.6 Hz), 2.75 (s, 2 H, CH₂). ¹³C{¹H} NMR (75.47 MHz, CD₂Cl₂, 297 K, δ ppm): 141.94 (s, Ph), 136.35–125.21 (Ph), 105.94 (s, Ru-C≡C), 101.44 (quint, Ru-C≡C, ²J_{PC} = 15.6 Hz), 50.37 (quint, PCH₂P, |¹J_{PC} + ³J_{PC}| = 20.4 Hz), 29.40 (s, CH₂). ¹³C NMR (δ ppm): 141.94 (m, Ph), 105.93 (t, Ru-C≡C, ²J_{CH} = 9.6 Hz), 101.44 (m, Ru-C≡C), 50.38 (t quint, PCH₂P, ¹J_{CH} = 135.1 Hz, |¹J_{PC} + ³J_{PC}| = 20.6 Hz), 29.36 (t m, CH₂, ¹J_{CH} = 127.7 Hz). ³¹P{¹H} NMR (121.50 MHz, CD₂Cl₂, 297 K, δ ppm): -5.47 (s, PPh₂).

Acknowledgment. We thank the "Ministère de la Recherche et de la Technologie" for the award of a thesis grant to N.P. and the European Union (HCM Programme CHRX-CT94-0501) for financial support.

OM950217F

Addition of Aldehydes and Acyl Chlorides to $[\text{Rh}(\text{P}^i\text{Pr}_3)_2\text{Cl}]_2$. Thermodynamics and Molecular and Crystal Structures of $\text{Rh}(\text{P}^i\text{Pr}_3)_2\text{ClX}[\text{C}(\text{O})\text{Ph}]$ ($\text{X} = \text{H}, \text{Cl}$)

Kun Wang, Thomas J. Emge, and Alan S. Goldman*

Department of Chemistry, Rutgers—The State University of New Jersey,
New Brunswick, New Jersey 08903

Chunbang Li and Steven P. Nolan*

Department of Chemistry, University of New Orleans, New Orleans, Louisiana 70148

Received June 5, 1995*

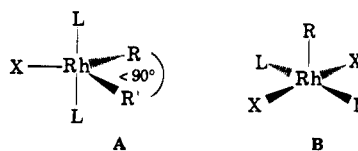
Addition of aldehyde (RCHO; R = *n*-octyl, Ph, *p*-Tol, *p*-MeOC₆H₄, *p*-CF₃C₆H₄) to $[\text{Rh}(\text{P}^i\text{Pr}_3)_2\text{Cl}]_2$ (**1**) results in rapid addition of the aldehyde C–H bond to yield $\text{Rh}(\text{P}^i\text{Pr}_3)_2\text{ClH}[\text{C}(\text{O})\text{R}]$ (**2-R**). **2-Ph** was isolated, and a single-crystal X-ray diffraction study reveals a trigonal-bipyramidal structure with a small H–Rh–C(acyl) angle of 85(4)°. Enthalpies of addition to **1** were measured by solution calorimetry (R, $\Delta H/(\text{kcal/mol})$): octyl, -15.2 ± 0.3 ; Ph, -10.8 ± 0.4 ; *p*-Tol, -10.6 ± 0.4 ; *p*-CF₃C₆H₄, -12.7 ± 0.4 ; *p*-MeOC₆H₄, -10.5 ± 0.3 . Electron-withdrawing para substituents on the aromatic aldehydes favor addition. Addition of nonanal is more favorable than addition of benzaldehydes, probably due to steric effects, particularly the close hydride–phenyl contact found in **2-Ph**. **1** reacts with acyl chlorides (RC(O)Cl, R = octyl, Ph) rapidly to give $\text{Rh}(\text{P}^i\text{Pr}_3)_2\text{Cl}_2[\text{C}(\text{O})\text{R}]$ (**3-R**). **3-Ph** possesses a square-pyramidal structure. The enthalpies of addition were also measured calorimetrically (R, $\Delta H/(\text{kcal/mol})$): octyl, -24.6 ± 0.3 ; Ph, -21.7 ± 0.3 . Relative to the addition of acyl chlorides, the exothermicity of aldehyde addition is greater than would be expected on the basis of thermodynamic data for related late-transition-metal complexes.

Complexes containing the RhL_2X moiety (where L is a tertiary phosphine and X[−] is most frequently chloride) promote a diverse array of organic transformations. The hydrogenation of olefins¹ and the decarbonylation of acyl chlorides and aldehydes² mediated by Wilkinson's catalyst and the photo- and thermochemical dehydrogenation of alkanes^{3–6} catalyzed by $\text{Rh}(\text{PMe}_3)_2(\text{CO})\text{Cl}$ are but a few such examples. Oxidative addition of RhL_2Cl to give five-coordinate Rh(III) complexes is known to be a key step in many of these reactions.⁷ Furthermore, even reactions which do not involve free three-coordinate Rh(I) may involve five-coordinate Rh(III) complexes; the thermodynamics of the latter species are thus of considerable interest.

In particular, the thermodynamics of addition of RhL_2X to R–R' species appear to be quite favorable, where R and R' are hydrocarbyl, silyl, H, or related groups. This is relevant, for example, in the context of olefin hydrogenation (which can involve the intermedi-

ates $\text{H}_2\text{RhL}_2\text{Cl}$ and (alkyl)HRhL₂Cl¹), hydrosilation,⁷ hydroformylation, aldehyde decarbonylation,² and alkane dehydrogenation.^{5,6}

The first structure of a complex of the form $\text{ML}_2\text{XRR}'$ was reported by Otsuka, that of $\text{Rh}(\text{P}^i\text{Bu}_3)_2\text{ClH}_2$.⁸ Subsequent examples include $\text{Ir}(\eta^3\text{-PNP})(\text{Me})(\text{neo-Pe})$ (neo-Pe = neopentyl, PNP = (Ph₂PCH₂Me₂Si)₂N),⁹ $\text{Ir}(\text{P}^i\text{Pr}_3)_2\text{Cl}(\text{Ph})\text{H}$,¹⁰ and $\text{Rh}(\text{P}^i\text{Pr}_3)_2\text{ClH}_2$.¹¹ All of these complexes may be considered as roughly trigonal bipyramidal (tbp) with axial phosphines (structure A); all reveal surprisingly small R–M–R' angles (65–83°). The



small R–M–R' angles have been explained by Eisenstein *et al.*,¹² on the basis of extended Hückel and later *ab initio* molecular orbital (MO) calculations of $\text{IrL}_2\text{H}_2\text{Cl}$. In simplest terms, the key to Eisenstein's explanation may be viewed as follows. If the M–Cl and M–P bonds define the *x* and *z* axes, respectively, then the hydride ligands (an out-of-phase combination) donate

(8) Yoshida, T.; Otsuka, S.; Matsumoto, M.; Nakatsu, K. *Inorg. Chim. Acta* **1978**, *29*, L257–L259.

(9) Fryzuk, M. D.; MacNeil, P. A.; Ball, R. G. *J. Am. Chem. Soc.* **1986**, *108*, 6414–6416.

(10) Werner, H.; Hohn, A.; Dziallas, M. *Angew. Chem., Int. Ed. Engl.* **1986**, *25*, 1090–1092.

(11) Harlow, R. L.; Thorn, D. L.; Baker, R. T.; Jones, N. L. *Inorg. Chem.* **1992**, *31*, 993–997.

(12) El-Idrissi, I.; Eisenstein, O.; Jean, Y. *New J. Chem.* **1990**, *14*, 671–677.

* Abstract published in *Advance ACS Abstracts*, October 1, 1995.

(1) Halpern, J. *Inorg. Chim. Acta* **1981**, *50*, 11–19 and references therein.

(2) Collman, J. P.; Hegedus, L. S.; Norton, J. R.; Finke, R. G. *Principles and Applications of Organotransition Metal Chemistry*; University Science Books: Mill Valley, CA, 1987; pp 768–775.

(3) Nomura, K.; Saito, Y. *J. Chem. Soc., Chem. Commun.* **1988**, 161.

(4) Sakakura, T.; Sodeyama, T.; Tokunaga, M.; Tanaka, M. *Chem. Lett.* **1988**, 263–264.

(5) (a) Maguire, J. A.; Boese, W. T.; Goldman, A. S. *J. Am. Chem. Soc.* **1989**, *111*, 7088–7093. (b) Maguire, J. A.; Boese, W. T.; Goldman, M. E.; Goldman, A. S. *Coord. Chem. Rev.* **1990**, *97*, 179–192.

(6) (a) Maguire, J. A.; Goldman, A. S. *J. Am. Chem. Soc.* **1991**, *113*, 6706–6708. (b) Maguire, J. A.; Petrillo, A.; Goldman, A. S. *J. Am. Chem. Soc.* **1992**, *114*, 9492–9498.

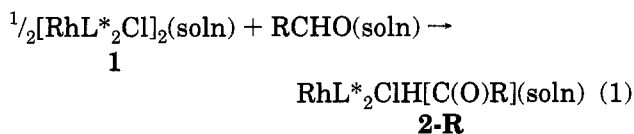
(7) Collman, J. P.; Hegedus, L. S.; Norton, J. R.; Finke, R. G. *Principles and Applications of Organotransition Metal Chemistry*; University Science Books: Mill Valley, CA, 1987; pp 523–576.

into the d_{xy} orbital while the chloride ligand can act as a π -donor into the same empty d orbital. Replacing one of the hydrides with a second chloride was calculated to greatly reduce the favorability of this structure, presumably due to the poorer σ -donating ability of chloride and also its π -donating ability which (for the second chloride) would result only in interaction with filled d orbitals.

In accord with this theory, Fryzuk found that $\text{Ir}(\eta^3\text{-PNP})\text{RI}$ complexes are square pyramidal (structure **B**), unlike the $\text{tbp Ir}(\eta^3\text{-PNP})\text{RR}'$ analogs (structure **A**).¹³ Likewise, Thorn *et al.* found that $(\text{P}^i\text{Pr}_3)_2\text{RhCl}_2\text{H}$ is square pyramidal (structure **B**, $\text{R} = \text{H}$) in contrast with $\text{tbp}(\text{P}^i\text{Pr}_3)_2\text{RhClH}_2$.¹¹ Herein we report analogous determinations for acyl-H and acyl-Cl adducts of RhL^*_2Cl ($\text{L}^* = \text{P}^i\text{Pr}_3$): these are found to possess structures **A** and **B**, respectively. The five-coordinate complexes are formed by the addition of aldehydes and acyl chlorides, respectively, to $[\text{RhL}^*_2\text{Cl}]_2$ (**1**). Calorimetric measurements reveal that the relative enthalpies of these addition reactions are different from values which would be expected on the basis of the relevant thermodynamics of related late-metal systems. These measurements serve to highlight the thermodynamic stability of the R-H adducts of structure **A**.

Results and Discussion

$\text{RhL}^*_2\text{ClH}[\text{C}(\text{O})\text{R}]$ (2**).** Addition of aldehyde RCHO ($\text{R} = n\text{-octyl, Ph, } p\text{-Tol, } p\text{-CF}_3\text{C}_6\text{H}_4, p\text{-MeOC}_6\text{H}_4$) to a solution of $[\text{RhL}^*_2\text{Cl}]_2$ (**1**) results in rapid C-H bond addition to give complexes **2**. To our knowledge, these



are the first directly observed or isolated examples of a class of unsaturated acyl hydrides which have been presumed to be intermediates in aldehyde decarbonylation.^{2,14} Accordingly, complexes **2-R** slowly decompose to give $\text{RhL}^*_2\text{Cl}(\text{CO})$ and RH ; the mechanism of these reactions is currently under study.

Spectroscopic data for **2-R** are all consistent with the proposed formulation (see Experimental Section). A single-crystal X-ray diffraction study of **2-Ph** showed it to possess structure **A** (Figure 1). Crystallographic details and selected bond distances and angles are listed in Tables 1 and 2. The position of the hydride was located and refined. The phenyl ring is almost coplanar (dihedral angle $7.6(6)^\circ$) with the equatorial plane defined by $\text{Rh}-\text{Cl}(1)-\text{C}(1)$. The most important aspect of this structure is the small $\text{C}(1)-\text{Rh}-\text{H}$ angle of $85(4)^\circ$. This is somewhat greater than (but within experimental error of) the $\text{R}-\text{Rh}-\text{R}'$ angle of the above-mentioned examples; this is not surprising, however, considering that there is a close contact between a phenyl ortho

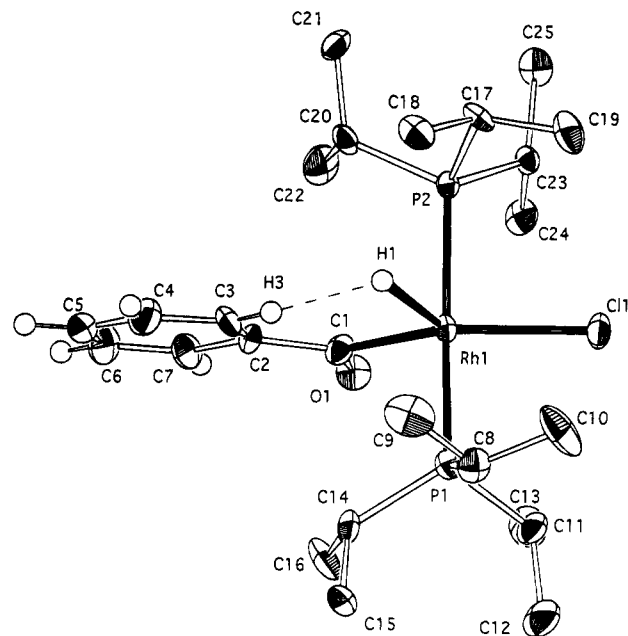
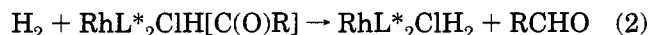


Figure 1. ORTEP diagram of $\text{Rh}(\text{P}^i\text{Pr}_3)_2\text{ClH}[\text{C}(\text{O})\text{Ph}]$ (**2-Ph**). The short $\text{H}(3)-\text{H}(1)$ contact is indicated by a dashed line.

hydrogen atom and the hydride ligand: $\text{H}(1)-\text{H}(3) = 1.85(14) \text{ \AA}$ (the van der Waals radius (Pauling) of H is 1.2 \AA). Presumably the $\text{C}(1)-\text{Rh}-\text{H}$ angle would be even smaller in the absence of this significant steric interaction.

Reaction 1 is complete within several minutes of mixing and is therefore suitable for calorimetric study. Decomposition of **2-R** (to give RH and $\text{RhL}^*_2(\text{CO})\text{Cl}$) also proceeds rapidly at ambient temperatures, but it was found that decomposition can be greatly inhibited by adding excess P^iPr_3 . Solution calorimetry was therefore carried out in the presence of added phosphine. Reaction enthalpies are shown in Table 3. For comparison we have included the previously determined value for addition of H_2 .¹⁵ While we are unaware of other examples in which both $\text{H}-\text{C}(\text{O})\text{R}$ and H_2 addition enthalpies have been determined, the moderately lower exothermicity of the aldehyde additions ($8\text{--}13 \text{ kcal/mol}$ less than H_2 addition) seems in accord with the present understanding of the thermodynamics of such reactions.¹⁶

The enthalpy of the hypothetical reaction of eq 2 (ΔH_2) is equal to the difference between ΔH_1 and the enthalpy of H_2 addition to **1** (-23.6 kcal/mol).¹⁵ Relative $\text{Rh}-\text{H}$



$$\Delta H_2 = -23.6 \text{ kcal/mol} - \Delta H_1$$

and $\text{Rh}-\text{acyl}$ bond dissociation energies (BDE's) can be calculated from eq 2 on the basis of the available $D_{\text{H}-\text{C}(\text{O})\text{R}}$ data. For $\text{R} = \text{Ph}$, $\Delta H_2 = -12.8 \text{ kcal/mol}$. Using 86.9 kcal/mol as the value of $D_{\text{H}-\text{C}(\text{O})\text{R}}$,¹⁷ it is calculated that the $\text{Rh}-\text{H}$ bond is 30 kcal/mol stronger than $D_{\text{Rh}-\text{C}(\text{O})\text{Ph}}$.

The bridge strength of **1** was previously determined to be at least 17.8 kcal/mol ; we believe the actual value is probably not much greater.^{15,18} Addition of half the

(13) Fryzuk, M. D.; MacNeil, P. A.; Rettig, S. J. *Organometallics* **1986**, *5*, 2469-2476.

(14) A cationic five-coordinate $\text{Rh}(\text{III})$ acyl hydrido complex, $[(\text{PPh}_3)_2\text{RhH}(\eta^2(\text{N},\text{C})\text{-acyl})]^+$, was isolated previously by treating $(\text{PPh}_3)_2\text{RhHCl}$ ($\eta^2(\text{N},\text{C})\text{-acyl}$) with AgBF_4 (the precursor was isolated from the reaction of the chelating aldehyde 8-quinolinecarboxaldehyde with Wilkinson's catalyst). Note that the five-membered chelate ring hindered decarbonylation at room temperature. Suggs, J. W. *J. Am. Chem. Soc.* **1978**, *100*, 640-641.

(15) Wang, K.; Rosini, G. P.; Nolan, S. P.; Goldman, A. S. *J. Am. Chem. Soc.* **1995**, *117*, 5082-5088.

Table 1. Crystallographic Details for Rh(PⁱPr₃)₂ClH[C(O)Ph] (2-Ph) and Rh(PⁱPr₃)₂Cl₂[C(O)Ph] (3-Ph)

complex	Rh(P ⁱ Pr ₃) ₂ ClH[C(O)Ph]	Rh(P ⁱ Pr ₃) ₂ Cl ₂ [C(O)Ph]
formula	C ₂₅ H ₄₈ ClOP ₂ Rh	C ₂₅ H ₄₇ Cl ₂ OP ₂ Rh
fw	564.93	599.38
cryst size, mm	0.25 × 0.15 × 0.10	0.20 × 0.16 × 0.10
cryst system	orthorhombic	orthorhombic
space group	P2 ₁ 2 ₁ 2 ₁ (No. 19)	P2 ₁ 2 ₁ 2 ₁ (No. 19)
a, Å	8.600(2)	10.545(2)
b, Å	15.227(4)	14.385(4)
c, Å	21.552(6)	18.829(6)
V, Å ³	2822.3(13)	2856.2(13)
no. of rflns; θ (range) for cell detn, deg	25; 12.3–15.7	25; 13.4–15.8
Z	4	4
d _{calc} , g/cm ³	1.330	1.394
temp, K	153(5)	153(5)
μ, cm ⁻¹	8.27	9.12
F(000)	1192	1256
θ range, deg	2 to 26	2 to 23
index ranges	0 ≤ h ≤ 10, 0 ≤ k ≤ 18, 0 ≤ l ≤ 26	0 ≤ h ≤ 11, 0 ≤ k ≤ 15, 0 ≤ l ≤ 20
no. of rflns collected	2912	2272
max, min transmissn	0.940, 0.905	0.917, 0.863
no. of indep rflns	2673	2190
no. of observed (I > 2σ(I)) rflns	2211	2064
no. of data/params	2669/274	2190/292
GOF on F ²	1.071	1.060
R(F), R _w (F ²) (I > 2σ(I))	0.048, 0.102	0.029, 0.063
R(F), R _w (F ²) (all data)	0.066, 0.116	0.033, 0.065
absolute structure param ^a	-0.07(8)	-0.07(5)
largest diff peak and hole, e/Å ³	1.3 and -0.5	0.6 and -0.4

^a Flack, H. D. *Acta Crystallogr.* **1983**, A39, 876–881.

Table 2. Selected Interatomic Distances (Å) and Angles (deg) for Rh(PⁱPr₃)₂ClH[C(O)Ph] (2-Ph)

Bond Lengths			
Rh(1)–C(1)	1.936(8)	Rh(1)–H(1)	1.77(13)
Rh(1)–P(2)	2.346(2)	Rh(1)–P(1)	2.348(3)
Rh(1)–Cl(1)	2.457(2)	O(1)–C(1)	1.226(13)
C(1)–C(2)	1.503(14)		
Bond Angles			
C(1)–Rh(1)–H(1)	85(4)	P(2)–Rh(1)–H(1)	75(4)
P(1)–Rh(1)–H(1)	98(4)	Cl(1)–Rh(1)–H(1)	128(4)
C(1)–Rh(1)–P(2)	94.0(3)	C(1)–Rh(1)–P(1)	92.7(3)
P(2)–Rh(1)–P(1)	169.35(8)	C(1)–Rh(1)–Cl(1)	147.0(4)
P(2)–Rh(1)–Cl(1)	89.47(9)	P(1)–Rh(1)–Cl(1)	89.41(9)

minimum bridge strength to $-\Delta H_1$ gives the corresponding lower limits for $-\Delta H$ of addition to monomeric RhL*₂Cl (Table 3).

The effects of electronic factors were probed by varying the para substituent on the phenyl group of the aromatic aldehydes. The exothermicity of reaction 1 is increased by electron-withdrawing substituents, consistent with the reaction being somewhat "oxidative" in nature. A plot of $-\Delta H_1$ values versus the Hammett σ_p constants¹⁹ yields a line ($r = 0.981$) with a slope of 2.8(4).

(16) As an initial approximation the relationship proposed by Bercaw and Bryndza, $D_{M-X} - D_{M-Y} = D_{R-X} - D_{R-Y}$,^{16a} would suggest that the additions would be comparably exothermic. However, C–H additions are generally much less exothermic than addition of H₂; the fact that M–H BDE's are "anomalously" high (i.e. deviate from this relationship) has been discussed in detail.^{16b} The difference in this case, however, should not be quite so great: aldehyde addition to low-valent metal centers appears to be more favorable than alkane or even arene C–H addition, probably due to the greater electronegativity of the acyl group and/or the possibility of M–acyl π -back-bonding. Thus, an enthalpy difference of ca. 10 kcal/mol between addition of H₂ and the aldehyde C–H bond seems reasonable. (a) Bryndza, H. E.; Fong, L. K.; Paciello, R. A.; Tam, W.; Bercaw, J. E. *J. Am. Chem. Soc.* **1987**, *109*, 1444–1456. (b) Labinger, J. A.; Bercaw, J. E. *Organometallics* **1988**, *7*, 926–928.

(17) *CRC Handbook of Chemistry and Physics*, 71st ed.; Lide, D. R., Ed.; CRC Press: Boca Raton, FL, 1990; pp 9–86–9–102.

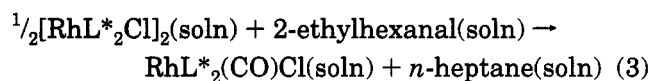
(18) (a) Pribula, A. J.; Drago, R. S. *J. Am. Chem. Soc.* **1976**, *98*, 2784–2788. (b) Drago, R. S.; Miller, J. G.; Hoselton, M. A.; Farris, R. D.; Desmond, M. J. *J. Am. Chem. Soc.* **1983**, *105*, 444–449.

(19) Gordon, A. J.; Ford, R. A. In *The Chemist's Companion*; Wiley-Interscience: New York, 1972; pp 429–437.

By comparison, addition of para-substituted benzoyl chlorides to Rh(PMe₃)₂(CO)Cl was investigated by equilibrium methods; a slope of 1.93(2) (albeit with only three data points) was found for a similar plot.²⁰ Addition to RhL*₂Cl is thus apparently more "oxidative"; this might be expected since Rh(PMe₃)₂(CO)Cl should be less electron-rich than RhL*₂Cl in view of its less-electron-rich phosphines and the presence of the electron-withdrawing CO ligand.

In spite of the trend toward increased exothermicity with increasing addendum electronegativity, oxidative addition of nonanal is seen to be significantly more exothermic than addition of the benzaldehydes. This is almost certainly attributable to steric factors; as noted above, there is significant crowding in the benzoyl complex manifested by the H–H nonbonding distance of 1.85(14) Å.

The decarbonylation of 2-ethylhexanal mediated by **1** was previously found to be 36.5 kcal/mol exothermic (eq 3).¹⁵



$$\Delta H_3 = -36.5 \text{ kcal/mol}$$

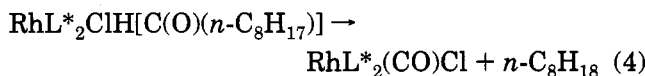
Reaction with nonanal in analogy with eq 3 would be ca. 1.2 kcal/mol more exothermic (based simply on heats of formation of the aldehydes²¹); $\Delta H = -37.7$ kcal/mol. When this is combined with the enthalpy of addition of nonanal to **1** (–15.2 kcal/mol), the enthalpy of reaction 4 can be estimated. Equation 4 represents the sum of the sequence of steps following nonanal C–H addition, leading to decarbonylation.

(20) Rosini, G. P.; Goldman, A. S. To be submitted for publication.

(21) Stull, D. R.; Westrum, E. F.; Sinke, G. C. *The Chemical Thermodynamics of Organic Compounds*; Robert E. Kreiger Publishing: Malabar, FL, 1987.

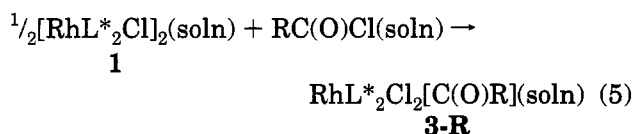
Table 3. Enthalpy of Addition of XY to 1 (ΔH_1) and the Hypothetical Monomer $\text{Rh}(\text{P}^i\text{Pr}_3)_2\text{Cl}$ ($-\Delta H_{\text{min}}$) in Solution (kcal/mol)

XY	ΔH_1 (eq 1)	$-\Delta H_{\text{min}}$
H_2^a	-23.6 ± 0.6	32.5
$\text{C}_8\text{H}_{17}\text{CHO}$	-15.2 ± 0.3	24.1
PhCHO	-10.8 ± 0.4	19.7
(<i>p</i> -Tol)CHO	-10.5 ± 0.4	19.4
(<i>p</i> - $\text{CF}_3\text{C}_6\text{H}_4$)CHO	-12.7 ± 0.4	21.6
(<i>p</i> - MeOC_6H_4)CHO	-10.5 ± 0.3	19.4
$\text{C}_8\text{H}_{17}\text{C}(\text{O})\text{Cl}$	-24.6 ± 0.3	33.5
PhC(O)Cl	-21.7 ± 0.3	30.6

^a From ref 15.

$$\Delta H_4(\text{calc}) = -22.5 \text{ kcal/mol}$$

$\text{RhL}^*_2\text{Cl}_2[\text{C}(\text{O})\text{R}]$ (3). In analogy with the addition of aldehydes, the reaction of acyl chlorides with 1 in benzene results in rapid formation of complexes 3.

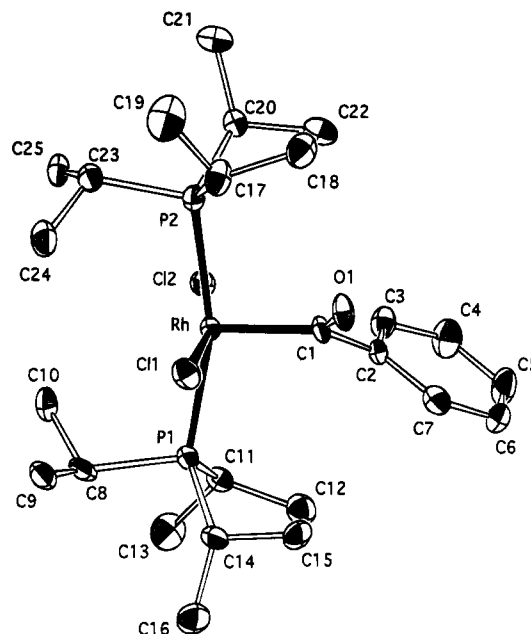


R = Ph, octyl

Formation of 3 was revealed by IR and ^1H - and ^{31}P NMR (see Experimental Section), as well as single crystal X-ray diffraction (R = Ph; Figure 2). Crystallographic details and selected bond distances and angles are listed in Tables 1 and 4. Most importantly, the C(1)–Rh–Cl(1) and C(1)–Rh–Cl(2) angles are $90.6(2)$ and $103.2(2)^\circ$, respectively; i.e., the geometry is approximately represented by structure B. The Cl(1)–Rh–Cl(2) and P(1)–Rh–P(2) angles are $166.24(6)$ and $163.45(7)^\circ$, respectively. There is no mirror plane, although Cl(1)–Rh–Cl(2)–C(1) and P(1)–Rh–P(2)–C(1) each define a plane. The phenyl ring is twisted out of the Cl(1)–Rh–Cl(2)–C(1) plane and is located between interstices of Cl and P. A similar structure was reported by Baird *et al.*²² for the closely related complex $\text{Rh}(\text{PPh}_3)_2\text{Cl}_2[\text{C}(\text{O})\text{CH}_2\text{CH}_2\text{Ph}]$. The C(1)–Rh–Cl(1) and C(1)–Rh–Cl(2) angles were reported to be $100(3)$ and $102(2)^\circ$, while the Cl(1)–Rh–Cl(2) and P(1)–Rh–P(2) angles were $168.7(5)$ and $174.5(5)^\circ$, respectively. Similarly, spectroscopic data indicate that **3-octyl** is isostructural with **3-Ph**.

The change of structure, from A to B upon replacing H with Cl, is in accord with the experimental and theoretical results discussed above.

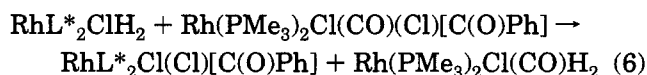
Consistent with Kampmeier's studies²³ on Wilkinson's catalyst, we found that complexes 3 slowly decompose to give $\text{RhL}^*_2\text{Cl}(\text{CO})$ and $\text{RhL}^*_2\text{Cl}_2\text{Ph}$ (not PhCl). Like that of hydride 2, decomposition of 3 was severely inhibited by the presence of excess P^iPr_3 ; solution calorimetry was carried out in its presence accordingly. However, P^iPr_3 was found to react slowly with benzoyl chloride under the reaction conditions (see Experimental Section). Individual calorimetry of the reaction between

**Figure 2.** ORTEP diagram of $\text{Rh}(\text{P}^i\text{Pr}_3)_2\text{Cl}_2[\text{C}(\text{O})\text{Ph}]$ (**3-Ph**).**Table 4. Selected Bond Lengths (Å) and Angles (deg) for $\text{Rh}(\text{P}^i\text{Pr}_3)_2\text{Cl}_2[\text{C}(\text{O})\text{Ph}]$ (**3-Ph**)**

Bond Lengths			
Rh–C(1)	1.985(6)	Rh–Cl(2)	2.334(2)
Rh–Cl(1)	2.343(2)	Rh–P(2)	2.385(2)
Rh–P(1)	2.408(2)	O(1)–C(1)	1.197(7)
C(1)–C(2)	1.499(8)		
Bond Angles			
C(1)–Rh–Cl(2)	103.2(2)	C(1)–Rh–Cl(1)	90.6(2)
Cl(2)–Rh–Cl(1)	166.24(6)	C(1)–Rh–P(2)	94.6(2)
Cl(2)–Rh–P(2)	87.89(6)	Cl(1)–Rh–P(2)	91.05(6)
C(1)–Rh–P(1)	101.9(2)	Cl(2)–Rh–P(1)	89.92(6)
Cl(1)–Rh–P(1)	87.20(6)	P(2)–Rh–P(1)	163.45(6)

benzoyl chloride and P^iPr_3 was therefore measured and the enthalpy subtracted from the observed enthalpy of reaction involving the organorhodium complexes. The enthalpy of reaction 5 was thus determined to be -21.7 ± 0.3 kcal/mol after the small correction (0.3 kcal/mol) for the P^iPr_3 /benzoyl chloride reaction.

The values for the exothermicity of acyl chloride addition (R = Ph, 21.7 kcal/mol; R = octyl, 24.6 kcal/mol) are unexpectedly low when compared with addition of either H_2 (23.6 kcal/mol) or the corresponding aldehydes (10.8 and 15.2 kcal/mol, respectively). For example, equilibrium studies reveal that the enthalpy of addition of benzoyl chloride to $\text{Rh}(\text{PMe}_3)_2(\text{CO})\text{Cl}$ is -13.3 kcal/mol, whereas the addition of H_2 is never observed, even under high H_2 pressures and at low temperature, and can be estimated as less negative than -6 kcal/mol.²⁰ Therefore, the hypothetical metathesis (6) must be endothermic by at least 9 kcal/mol.



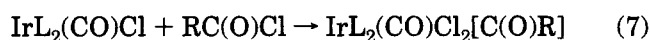
$$\Delta H_6(\text{calc}) \geq +9.2 \text{ kcal/mol}$$

As noted above, increased electron withdrawing by benzoyl para substituents favors aldehyde addition to RhL^*_2Cl more than acyl chloride addition to $\text{Rh}(\text{PMe}_3)_2(\text{CO})\text{Cl}$. Solely on the basis of that trend, i.e. increased electronegativity favoring addition to RhL^*_2Cl , it would

(22) Egglestone, D. L.; Baird, M. C.; Lock, C. J. L.; Turner, G. J. *Chem. Soc., Dalton Trans.* **1977**, 1576–1582.(23) Kampmeier, J. A.; Rodehorst, R. M.; Philip, J. B. *J. Am. Chem. Soc.* **1981**, *103*, 1847–1849.

be predicted that reaction 6 would be *exothermic*. In addition, the ability of chloride to act as a π -donor²⁴ would, *a priori*, be expected to further favor reaction 6 since the chloride-containing product is coordinatively unsaturated. It should be noted, however, that steric factors probably contribute to the endothermicity of reaction 6 since the larger addendum (benzoyl chloride vs H₂) is transferred to the species with bulkier phosphines (though this effect should be somewhat mitigated by the PMe₃ complex possessing an additional ligand, CO).

Similarly, addition of either aldehyde or H₂ can be compared with addition of acyl chlorides to the complexes IrL₂(CO)Cl. Blake has found that acyl chloride addition to these complexes is very exothermic (ca. 25 kcal/mol):²⁵



R	L	ΔH (kcal/mol)
Me	PMe ₃	-29
Me	P ^t BuPh ₂	-22
Me	P(CH ₂ Ph) ₃	-18
Me	PMe ₂ Ph	-29
Ph	PMe ₂ Ph	-26

As with Rh(PMe₃)₂(CO)Cl, H₂ addition is significantly less exothermic, for example (L, ΔH /(kcal/mol)): P^tBuPh₂, -11.5; PPh₃, -14.9; PEt₃, -13.3.²⁶ The case of L = P^tBuPh₂ provides perhaps the best comparison with the present work in view of the similar cone angles of P^tBuPh₂ (157°) and P^tPr₃ (160°); in that case H₂ addition is 10.5 kcal/mol less exothermic than CH₃C(O)-Cl addition, whereas in the present case, addition of H₂ is 1.0 kcal/mol less exothermic than addition of C₈H₁₇C(O)-Cl.

Consistent with the modest exothermicity of H₂ addition to the iridium complexes, the reaction of aldehyde, even with Ir(PMe₃)₂(CO)Cl, gives at most a minute concentration of adduct even after 14 days at 50 °C.²⁷ While it cannot be stated definitively that the failure to observe a significant concentration of aldehyde adduct results from thermodynamics, rather than kinetics, the former explanation seems more likely. For example, in the case of the analogous phenyl hydride L₂Ir(CO)ClPhH, elimination of benzene is thermodynamically favorable and the reaction proceeds at observable rates. Similarly, we find that elimination of aldehyde from the CO adducts of **2**, RhL₂(CO)H-[C(O)R], is kinetically facile (complete after 2 h at ambient temperature). Assuming aldehyde addition to (PMe₃)₂Ir(CO)Cl is in fact thermodynamically too unfavorable to yield a major product, we can estimate the reaction enthalpy as being less negative than ca. -6 kcal/mol. In that case, the difference between enthalpies of addition of aldehydes and acyl chlorides is

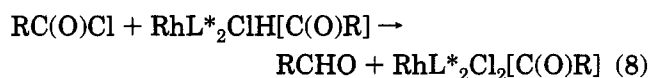
Table 5. $D_{\text{Rh-Cl}} - D_{\text{Rh-H}}$ for Complexes **2-R** and **3-R** (Values in kcal/mol)

R	ΔH_8 ($\Delta H_5 - \Delta H_1$)	$D_{\text{Cl-C(O)R}} - D_{\text{H-C(O)R}}^a$	$D_{\text{Rh-Cl}} - D_{\text{Rh-H}}$
Ph	-10.9	-7.2	3.7
alkyl	-9.4	-4.1	5.3

^a Values are obtained from eq 9 on the basis of ΔH_f° values given in ref 28.

greater than 23 kcal/mol for Ir(PMe₃)₂(CO)Cl, in comparison with a difference of only 9–11 kcal/mol in the case of RhL₂*Cl; i.e., $\Delta\Delta H > \text{ca. } 13 \text{ kcal}$. The possible significance of steric factors in this case is obviously less than in comparing addition of acyl chlorides vs H₂. It would seem very unlikely that *most* of the difference is due to an effect of the bulkier phosphines *specific to addition of acyl chlorides vs aldehydes*, particularly since the larger phosphines are present on the species with lower coordination number. (Note also that Ir-(P^tBuPh₂)₂(CO)Cl adds acetyl chloride only 7 kcal/mol less favorably than does the PMe₃ complex. Thus, since the *total* effect of sterics is apparently not so great, even if the bulkier phosphines disfavor acyl chloride addition more than aldehyde addition, the *difference* should be quite small.) Nevertheless, significant crowding is observed in the structures of **2** and **3**, and the steric difference between chloride and hydride may make *some* contribution to the value of $\Delta\Delta H$.

Thus, addition of H₂ or aldehyde C-H bonds to RhL₂*Cl is unusually exothermic relative to addition of acyl chlorides. This same point can be expressed in terms of M-H and M-Cl BDE's. For example, eq 8 can be obtained by subtracting eq 5 from eq 1, and it can be seen that $D_{\text{Rh-Cl}} - D_{\text{Rh-H}} = D_{\text{Cl-C(O)Ph}} - D_{\text{H-C(O)Ph}} - \Delta H_8$. The quantity $D_{\text{Cl-C(O)R}} - D_{\text{H-C(O)R}}$ is probably best



calculated on the basis of ΔH_f° values for the aldehyde and acyl chlorides, using eq 9.^{17,21,28-30} This approach



$$\Delta H_9 = D_{\text{Cl-C(O)R}} - D_{\text{H-C(O)R}} =$$

$$\Delta H_f(\text{RCHO}) + \Delta H_f(\text{Cl}^\bullet) - \Delta H_f(\text{RC}(\text{O})\text{Cl}) - \Delta H_f(\text{H}^\bullet)$$

eliminates errors due to uncertainty in the enthalpy of formation of the acyl radical. It yields, as might be expected, similar values of $D_{\text{Cl-C(O)R}} - D_{\text{H-C(O)R}}$ for R = Ph and R = alkyl: -7.2 and -4.1 kcal/mol, respectively (values for R = alkyl are obtained for R = Me and assumed to hold for *n*-alkyls; thermodynamic data are not available for the higher acyl chlorides). The Rh-Cl BDE's of **3-Ph** and **3-octyl** are thereby found to be 3.7 and 5.3 kcal/mol greater than the Rh-H BDE's of **2-Ph** and **2-octyl** (Table 5). Note that if literature values of $D_{\text{Cl-C(O)R}} - D_{\text{H-C(O)R}}$ are used, the values obtained for $D_{\text{Rh-Cl}} - D_{\text{Rh-H}}$ are even smaller, particu-

(28) The following ΔH_f° values (kcal/mol) were used: MeC(O)Cl(g), -58.30;²¹ MeCHO(g), -39.76;²¹ H[•](g), 52.10;¹⁷ Cl[•](g), 28.99;¹⁷ PhCHO(g), -8.77;²⁹ PhC(O)Cl(g), -24.67.³⁰ Values for $D_{\text{Cl-C(O)R}} - D_{\text{H-C(O)R}}$ thus obtained are therefore gas-phase values.

(29) Ingold, K. U.; Roberts, B. P. In *Landolt-Bornstein*; Fischer, H., Ed.; Springer-Verlag: Berlin, 1983; Vol. 13, part C.

(30) Pedley, J. B.; Naylor, R. D.; Kirby, S. P. *Thermochemical Data of Organic Compounds*; Chapman and Hall: London, 1986.

(24) (a) Hauger, B. E.; Gusev, D.; Caulton, K. G. *J. Am. Chem. Soc.* **1994**, *116*, 208–214. (b) Poulton, J. T.; Folting, K.; Streib, W. E.; Caulton, K. G. *Inorg. Chem.* **1992**, *31*, 3190–3191 and references therein.

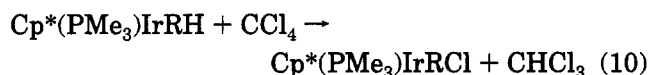
(25) Yoneda, G.; Lin, S.; Wang, L.; Blake, D. M. *J. Am. Chem. Soc.* **1981**, *103*, 5768–5771.

(26) Mondal, J. U.; Blake, D. M. *Coord. Chem. Rev.* **1982**, *47*, 205–238.

(27) After heating a sample of Ir(PMe₃)₂(CO)Cl at 50 °C in the presence of 0.7 M CH₃CHO, we observe a weak resonance, relatively constant in intensity after 1 day, possibly attributable to the C-H addition product. Assuming $\Delta S = \text{ca. } -25 \text{ eu}$, the calculated ΔH of addition is ca. -6 kcal/mol. Alternatively, if this resonance is *not* due to the C-H adduct, then ΔH is even less negative and/or the addition is kinetically difficult.

larly for the benzoyl complexes; for example $D_{\text{Cl}-\text{C}(\text{O})\text{R}} - D_{\text{H}-\text{C}(\text{O})\text{R}}$ is reportedly¹⁷ -12.9 ($\text{R} = \text{Ph}$)³¹ and -5 kcal/mol ($\text{R} = \text{Me}$), yielding respective values for $D_{\text{Rh}-\text{Cl}} - D_{\text{Rh}-\text{H}}$ of -2.0 and 4.4 kcal/mol.

In contrast, Bergman and Hoff *et al.*³² directly measured a series of reactions, which like eq 8, involve C-Cl/M-H metathesis:



It was found that $D_{\text{Ir}-\text{H}}$ is ca. 19 kcal/mol less than $D_{\text{Ir}-\text{Cl}}$. Likewise, in the example cited above,²⁵ $\text{Ir}(\text{PMe}_3)_2(\text{CO})\text{Cl}$ adds acetyl chloride >23 kcal/mol more exothermically than acetaldehyde; expressed in terms of BDE's, $D_{\text{Ir}-\text{Cl}}$ is greater than $D_{\text{Ir}-\text{H}}$ by $> \text{ca. } 18$ kcal/mol. It should be noted, however, that other reported systems reveal values of $D_{\text{M}-\text{Cl}} - D_{\text{M}-\text{H}}$ which are not as large, though they are greater than the values found in the present work. For example, Blake *et al.* reported that the average Ir-H BDE is ca. 11 kcal/mol weaker than the average Ir-Cl BDE for $\text{L}_2\text{Cl}(\text{CO})\text{IrX}_2$.^{33,34} Similarly, the average values of $D_{\text{M}-\text{Cl}} - D_{\text{M}-\text{H}}$ for Cp_2MX_2 ³⁵ are 12.5 kcal/mol ($\text{M} = \text{Mo}$) and 10.1 kcal/mol ($\text{M} = \text{W}$). However, these are differences in average bond strengths and, as has been noted,³³ the use of Cl_2 as a reagent in the iridium case introduces substantial experimental difficulties. Thus, we consider the above comparisons (i.e. those involving the systems of eqs 6-8 and 10) to be more meaningful. Nevertheless, at this point the value of $D_{\text{M}-\text{Cl}} - D_{\text{M}-\text{H}}$ for a "typical" system is unclear; therefore, the magnitude by which the present system deviates from "typical" must also be uncertain.

In conclusion, we report that aldehydes and acyl chlorides yield isolable adducts of RhL^*_2Cl that are structurally very different. In comparison with the enthalpy of addition of acyl chlorides, the addition of aldehydes and H_2 is more exothermic than would be expected on the basis of thermodynamic data for related late-transition-metal complexes. This is perhaps particularly surprising since RhL^*_2Cl is very electron rich, and the resulting adducts (**2** and **3**) are coordinatively unsaturated; both of these factors should, *a priori*, favor formation of the Rh-Cl bond in view of the electronegativity and π -basicity²⁴ of the Cl ligand. These results suggest that the unusual structure of **2** (i.e. structure **A**) confers unusual stability on complexes of the form $\text{RhL}_2\text{XRR}'$. This conclusion may help rationalize the remarkably wide range of reactions of nonpolar substrates that are mediated by rhodium(I) complexes.

Experimental Section

General Procedures. All manipulations were conducted under an argon atmosphere either in a Vacuum Atmospheres

(31) An alternative value for the C-Cl BDE of $\text{PhC}(\text{O})\text{Cl}$, 81.5 ± 2.6 kcal/mol, which is more consistent with the acetyl-chloride BDE of 81 kcal/mol,¹⁷ has been determined by photoacoustic calorimetry: Martinho Simões, J. A.; Griller, D. *Chem. Phys. Lett.* **1989**, *158*, 175-177.

(32) Nolan, S. P.; Hoff, C. D.; Stoutland, P. O.; Newman, L. J.; Buchanan, J. M.; Bergman, R. G.; Yang, G. K.; Peters, K. G. *J. Am. Chem. Soc.* **1987**, *109*, 3143-3145 and references therein.

(33) Burke, N. E.; Singhal, A.; Hintz, M. J.; Ley, J. A.; Hui, H.; Smith, L. R.; Blake, D. M. *J. Am. Chem. Soc.* **1979**, *101*, 74-79.

(34) Yoneda, G.; Blake, D. M. *Inorg. Chem.* **1981**, *20*, 67-71 and references therein.

(35) Calado, J. C. D.; Dias, A. R.; Simões, J. A. M.; Silva, M. A. V. R. D. *J. Organomet. Chem.* **1979**, *174*, 77-80.

Dry-Lab glovebox or by using standard Schlenk techniques. Aldehydes and benzoyl chloride were obtained from Aldrich and dried with molecular sieves before vacuum distillation. Trisopropyl phosphine (Strem Chemicals) was used as received. C_6D_6 (99.5% atom-*d*, Cambridge Isotope Laboratories) was dried over Na and vacuum-distilled prior to use. All other solvents were either distilled from dark purple solutions of benzophenone ketyl or dried over molecular sieves. $[\text{RhL}^*_2\text{Cl}]_2$ (**1**) was synthesized according to Werner.³⁶

NMR spectra were recorded on either a Varian VXR-200 or XL-400 spectrometer. ³¹P NMR chemical shift values are expressed in reference to 85% H_3PO_4 . IR spectra were recorded on a Mattson Cygnus 100 FTIR spectrometer.

Only materials of high purity as indicated by IR and NMR spectroscopy were used in the calorimetric experiments. Calorimetric measurements were performed using a Calvet calorimeter (Setaram C-80) which was periodically calibrated using the TRIS reaction³⁷ or the enthalpy of solution of KCl in water.³⁸ The experimental enthalpies for these two standard reactions compared very closely to literature values. This calorimeter and the experimental procedures used have been previously described.³⁹ Typical procedures are described below. Experimental enthalpy data are reported with 95% confidence limits.

Calorimetric Measurement of Reactions between $[\text{RhL}^*_2\text{Cl}]_2$ (1**) and Aldehydes in the Presence of Added P^iPr_3 .** The calorimetric measurements for the reaction of **1** with aldehydes are similar and are exemplified by that of the reaction between **1** and benzaldehyde.

The mixing vessels of the Setaram C-80 were cleaned, dried in an oven maintained at 120 °C, and then taken into the glovebox. A 30-40 mg sample of **1** was accurately weighed into the lower vessel; it was closed and sealed with 1.5 mL of mercury. Four milliliters of a stock solution of benzaldehyde was added (0.63 mL of benzaldehyde in 16 mL of freshly dried and distilled benzene, and 0.4 mL of P^iPr_3 which was found to retard decarbonylation of **2-Ph**). The remainder of the cell was assembled, removed from the glovebox, and inserted in the calorimeter. The reference vessel was loaded in an identical fashion, with the exception that no organorhodium complex was added to the lower vessel. After the calorimeter had reached thermal equilibrium at 30.0 °C (about 2 h), the calorimeter was inverted, thereby allowing the reactants to mix. After the reaction had reached completion and the calorimeter had once again reached thermal equilibrium (ca. 2 h), the vessels were removed from the calorimeter. Conversion to $\text{RhL}^*_2\text{ClH}[\text{C}(\text{O})\text{Ph}]$ was found to be quantitative under these reaction conditions. The enthalpy of reaction, -6.0 ± 0.2 kcal/mol, represents the average of five individual calorimetric determinations. The enthalpy of reaction with all species in solution, -10.8 ± 0.4 kcal/mol (Table 3), includes the previously reported¹⁵ enthalpy of solution of **1** in benzene.

Calorimetric Measurement of Reactions between $[\text{RhL}^*_2\text{Cl}]_2$ (1**) and Benzoyl Chloride in the Presence of Added P^iPr_3 .** The protocol used here was different from that of measuring the reaction of **1** with aldehydes. The calorimeter cell was assembled in a fashion similar to that previously mentioned, with the exception that a solution/solution configuration was used instead of the solid/solution standard protocol. This was used in order to impede the reaction of benzoyl chloride with P^iPr_3 during the equilibration stage of the experiment. Individual calorimetry of the reaction between benzoyl chloride and P^iPr_3 was measured and the enthalpy

(36) Werner, H.; Wolf, J.; Hohn, A. *J. Organomet. Chem.* **1985**, *287*, 395-407.

(37) Ojelund, G.; Wadsö, I. *Acta Chem. Scand.* **1968**, *22*, 1691-1699.

(38) Kilday, M. V. *J. Res. Natl. Bur. Stand. (U.S.)* **1980**, *85*, 467-481.

(39) Nolan, S. P.; Hoff, C. D.; Landrum, J. T. *J. Organomet. Chem.* **1985**, *282*, 357-362.

subtracted from the observed enthalpy of reaction involving the organorhodium complexes. A 30–40 mg sample of **1** was accurately weighed and dissolved in 2 mL of benzene. This solution was treated with P^iPr_3 for reasons similar to those above. This solution was then syringed into the outer compartment of the cell. Two milliliters of a stock solution of benzoyl chloride (0.47 mL in 10 mL of benzene) was syringed into the inner compartment of the cell. After the calorimeter had reached thermal equilibrium at 30.0 °C (about 2 h), the calorimeter was inverted, thereby allowing the reactants to mix. After the reaction had reached completion and the calorimeter had once again reached thermal equilibrium (ca. 2 h), the vessels were removed from the calorimeter. Conversion to $RhL^*_2Cl_2[C(O)Ph]$ was found to be quantitative under these reaction conditions. The enthalpy of reaction, -16.9 ± 0.2 kcal/mol, represents the average of five individual calorimetric determinations.

Reaction of $[RhL^*_2Cl]_2$ (1**) with Nonanal in the Presence of Added P^iPr_3 .** **1** (0.5 mL of a 13 mM solution) was mixed with 50 μ L of 1.0 M P^iPr_3 in C_6D_6 in an NMR tube, 34 μ L (16 equiv with respect to Rh) of nonanal was added, and the NMR tube was shaken before the ^{31}P NMR spectrum was taken. The acylhydrido complex **2** formed exclusively after ca. 10 min at 25 °C and negligible subsequent reactions (<3%) were observed after 2 h. $RhL^*_2ClH[C(O)C_8H_{17}]$: ^{31}P NMR (C_6D_6 , 162 MHz) δ 47.74 (dd, $J_{Rh-P} = 128.12$ Hz, $J_{H-P} = 10$ Hz); 1H NMR (C_6D_6 , 400 MHz, hydride region only): δ -15.1 (dt, $J_{Rh-H} = 24.1$ Hz); IR (C_6D_6) 1681.8 (m) cm^{-1} .

Reaction of $[RhL^*_2Cl]_2$ (1**) with Benzaldehyde in the Presence of Added P^iPr_3 .** **1** (0.5 mL of a 13 mM solution) was mixed with 50 μ L of 1.0 M P^iPr_3 in C_6D_6 in an NMR tube, 20 μ L (16 equiv with respect to Rh) of benzaldehyde was added, and the NMR tube was shaken before the ^{31}P NMR spectrum was taken. **2-Ph** formed exclusively after ca. 10 min at 25 °C, and negligible subsequent reactions (<3%) were observed after 2 h. For spectroscopic data, see the isolation of **2-Ph**.

Reaction of $[RhL^*_2Cl]_2$ (1**) with *p*-Tolualdehyde in the Presence of Added P^iPr_3 .** **1** (0.5 mL of a 13 mM solution) was mixed with 50 μ L of 1.0 M P^iPr_3 in C_6D_6 in an NMR tube, 24 μ L (16 equiv with respect to Rh) of *p*-tolualdehyde was added, and the NMR tube was shaken before the ^{31}P NMR spectrum was taken. **2-(p-Tol)** formed exclusively after ca. 10 min at 25 °C, and negligible subsequent reactions (<3%) were observed after 2 h. $RhL^*_2ClH[C(O)(p-Tol)]$: ^{31}P NMR (C_6D_6 , 162 MHz) δ 44.41 (dd, $J_{Rh-P} = 118.9$ Hz, $J_{H-P} = 10$ Hz); 1H NMR (C_6D_6 , 400 MHz, hydride region only): δ -19.14 (dt, $J_{Rh-H} = 34$ Hz); IR (C_6D_6) 1605.6 (m) cm^{-1} .

Reaction of $[RhL^*_2Cl]_2$ (1**) with α,α,α -Trifluoro-*p*-tolualdehyde in the Presence of Added P^iPr_3 .** **1** (0.5 mL of a 13 mM solution) was mixed with 50 μ L of 1.0 M P^iPr_3 in C_6D_6 in an NMR tube, 27 μ L (16 equiv with respect to Rh) of α,α,α -trifluoro-*p*-tolualdehyde was added, and the NMR tube was shaken before the ^{31}P NMR spectrum was taken. **2-(p-CF₃C₆H₄)** formed exclusively after ca. 10 min at 25 °C, and negligible subsequent reactions (<3%) were observed after 2 h. $RhL^*_2ClH[C(O)(p-CF_3C_6H_4)]$: ^{31}P NMR (C_6D_6 , 162 MHz) δ 44.8 (dd, $J_{Rh-P} = 119.2$ Hz, $J_{H-P} = 10$ Hz); 1H NMR (C_6D_6 , 400 MHz, hydride region only) δ -18.36 (dt, $J_{Rh-H} = 32.4$ Hz); IR (C_6D_6) 1674.1 (m) cm^{-1} .

Reaction of $[RhL^*_2Cl]_2$ (1**) with *p*-Anisaldehyde in the Presence of Added P^iPr_3 .** **1** (0.5 mL of a 13 mM solution in C_6D_6) was treated with 10 μ L of P^iPr_3 (4 equiv with respect to Rh) in an NMR tube, 25 μ L (16 equiv with respect to Rh) of *p*-anisaldehyde was added, and the NMR tube was shaken before the ^{31}P NMR spectrum was taken. The initial purple solution turned to orange-yellow gradually, and the acyl hydrido complex $Rh(P^iPr_3)_2Cl(H)[C(O)(p-MeOC_6H_4)]$ formed exclusively after ca. 10 min at room temperature; negligible decomposition was observed after 3 h. $Rh(P^iPr_3)_2Cl(H)[C(O)(p-MeOC_6H_4)]$: ^{31}P NMR (C_6D_6 , 81 MHz) δ 44.78 (d, $J_{Rh-P} =$

118.8 Hz); 1H NMR (C_6D_6 , 200 MHz, hydride region only) δ -19.3 (dt, $J_{Rh-H} = 35.5$ Hz, $J_{P-H} = 10$ Hz); IR (C_6D_6) 1579.6 (m) cm^{-1} .

Reaction of $[RhL^*_2Cl]_2$ (1**) with Benzoyl Chloride in the Presence of Added P^iPr_3 .** **1** (0.5 mL of 13 mM solution) was mixed with 50 μ L of 1.0 M P^iPr_3 in C_6D_6 in an NMR tube, 7.2 μ L (5 equiv with respect to Rh) of benzoyl chloride was added, and the NMR tube was shaken before the ^{31}P NMR spectrum was taken. The acyl chloro complex **3-Ph** formed exclusively after ca. 10 min at room temperature, and negligible subsequent reactions (<3%) were observed after 2 h. For spectroscopic data, see the isolation of **3-Ph**.

Reaction of $[RhL^*_2Cl]_2$ (1**) with Nonanoyl Chloride in the Absence of Added P^iPr_3 .** Nonanoyl chloride was found to react with P^iPr_3 rapidly; therefore, no phosphine was used in this experiment. **1** (0.5 mL of a 13 mM solution in C_6D_6) was treated with 15 μ L (8 equiv with respect to Rh) of nonanoyl chloride in an NMR tube with shaking. The initial purple solution turned to orange-yellow immediately. ^{31}P NMR indicated that the acyl chloro complex $RhL^*_2Cl_2[C(O)(CH_2)_7CH_3]$ formed exclusively, and negligible decomposition was observed after 180 min. $RhL^*_2Cl_2[C(O)(CH_2)_7CH_3]$: ^{31}P NMR (C_6D_6 , 81 MHz) δ 27.78 (d, $J_{Rh-P} = 102.4$ Hz); IR (C_6D_6) 1712.7 (m) cm^{-1} .

Isolation of $RhL^*_2ClH[C(O)Ph]$ (2-Ph**).** X-ray quality crystals of **2-Ph** were obtained by the following method. **1** (40 mg, 0.044 mmol) was mixed with 0.2 mL of toluene in a 20-mL scintillation vial, whereupon 40 μ L (0.39 mmol) of benzaldehyde was added. The vial was swirled for ca. 10 min to dissolve **1**, yielding an orange solution; 0.1 mL of P^iPr_3 was then added, and the vial was put into a -35 °C freezer immediately. ^{31}P NMR (C_6D_6 , 162 MHz): δ 45.3 (dd, $J_{Rh-P} = 119$ Hz, $J_{H-P} = 9.2$ Hz); 1H NMR (C_6D_6 , 400 MHz): δ 1.12 (dq, ($^3J_{P-H} + ^5J_{P-H}$)/2 = 6.7 Hz, 18 H, *Me*), 1.22 (dq, ($^3J_{P-H} + ^5J_{P-H}$)/2 = 6.5 Hz, 18 H, *Me*; two signals due to diastereotopy), 2.36 (m, 6 H, *PCHMe*), 7.10 (m, 3 H, *Ph*), 8.34 (m, 2 H, *Ph*), -18.91 (dt, $J_{Rh-H} = 36$ Hz, 1 H, hydride); IR (C_6D_6) 1638.4 (m) cm^{-1} .

Isolation of $RhL^*_2Cl_2[C(O)Ph]$ (3-Ph**).** X-ray quality crystals of **3-Ph** were obtained by the following method. **1** (40 mg, 0.044 mmol) was mixed with 0.2 mL of toluene in a 20-mL scintillation vial, whereupon 70 μ L (0.61 mmol) of benzoyl chloride was added. The vial was swirled to dissolve **1**, and an orange solution resulted. The vial was then put into a -35 °C freezer immediately. No P^iPr_3 was used, since it was found to react with benzoyl chloride. ^{31}P NMR (C_6D_6 , 162 MHz): δ 28.60 (d, $J_{Rh-P} = 100.6$ Hz). 1H NMR (C_6D_6 , 400 MHz): δ 1.19 (q, ($^3J_{P-H} + ^5J_{P-H}$)/2 = 6.5 Hz, 36 H, *Me*), 2.92 (m, 6 H, *PCHMe*), 7.76 (m, 2 H, *Ph*), 8.34 (m, 3 H, *Ph*); IR (C_6D_6): 1663 (m) cm^{-1} .

X-ray Crystallography. A crystal of **2-Ph** was immersed in oil and then placed in the low-temperature nitrogen stream on a CAD4 diffractometer (graphite-monochromatized Mo $K\alpha$ radiation, $\lambda = 0.71073$ Å) for the single-crystal X-ray data collection. Data were later collected for a crystal of **3-Ph**, which was handled in the same way as above. Three intensity standard reflections were checked every 1 h and showed less than 2% decay for either **2-Ph** or **3-Ph**. The total measured reflections (2912 for **2-Ph** and 2272 for **3-Ph**) were corrected for Lorentz effects, polarization, decay, and absorption, the last correction employing the numerical method found in SHELX76.⁴⁰ The structures of **2-Ph** and **3-Ph** were solved by direct methods (SHELXS86)⁴¹ and refined by least-squares and Fourier techniques based upon F^2 (SHELXL93).⁴² For **2-Ph** and **3-Ph**, all non-H atoms were refined with anisotropic

(40) Sheldrick, G. M. SHELX76. Program for Crystal Structure Determination; University of Cambridge, Cambridge, England, 1976.

(41) Sheldrick, G. M. SHELXS86. Program for the Solution of Crystal Structures; University of Gottingen, Gottingen, Germany, 1986.

(42) Sheldrick, G. M. SHELXL93. Program for Crystal Structure Refinement; University of Gottingen, Gottingen, Germany, 1993.

displacement parameters. For **2-Ph** and **3-Ph**, the H atoms were fixed to their calculated positions with isotropic displacement parameters equal to 1.2 times the isotropic equivalent displacement parameters of the C atoms to which they were bound, except for H(1) in **2-Ph**, whose coordinates were varied and whose isotropic displacement parameter was fixed at 0.08 Å². There were no indications of extinction in the X-ray data for **2-Ph** or **3-Ph**. The ORTEP diagrams in Figures 1 and 2 were drawn with ellipsoids at the 50% probability level. Crystal packing in either structure is composed of dispersive (e.g., van der Waals) interactions between phosphine ligands in adjacent molecules.

Acknowledgment. Support for this research by the National Science Foundation (Grants CHE-9121695 to

A.S.G. and CHE-9305492 to S.P.N.) and the Louisiana Education Quality Support Fund is gratefully acknowledged.

Supporting Information Available: Listings of intramolecular distances and angles, torsion angles, least-squares planes, anisotropic displacement parameters, and H atom parameters for **2-Ph** and **3-Ph** (17 pages). This material is contained in many libraries on microfiche, immediately follows this article in the microfilm version of the journal, can be ordered from the ACS, and can be downloaded from the Internet; see any current masthead page for ordering information and Internet access instructions.

OM9504213

Electrochemical Reduction of CO₂ Catalyzed by a Dinuclear Palladium Complex Containing a Bridging Hexaphosphine Ligand: Evidence for Cooperativity

Bryan D. Steffey, Calvin J. Curtis, and Daniel L. DuBois*

National Renewable Energy Laboratory, Golden, Colorado 80401

Received April 27, 1995[®]

The complexes [Pd₂(CH₃CN)₂(eHTP)](BF₄)₄ and [Pd₂(PEt₃)₂(eHTP)](BF₄)₄ (where eHTP is bis(bis((diethylphosphino)ethyl)phosphino)methane, (Et₂PCH₂CH₂)₂PCH₂P(CH₂CH₂PEt₂)₂) were prepared and characterized. [Pd₂(CH₃CN)₂(eHTP)](BF₄)₄ catalyzes the electrochemical reduction of CO₂ to CO in acidic dimethylformamide solutions. The rate of this reaction exhibits a biphasic dependence on acid, with a first-order dependence at low acid concentrations and zero-order dependence at acid concentrations greater than 0.06 M. At high acid concentrations the rate-limiting step is first order in catalyst and first order in CO₂. When compared to the kinetic properties of previously studied mononuclear complexes, these data suggest both palladium atoms are involved in CO₂ reduction. The closely related complex [Pd₂(PEt₃)₂(eHTP)](BF₄)₄ undergoes two reversible two-electron reductions. The mixed-valence intermediate resulting from the first two-electron reduction is unstable and undergoes rapid decomposition.

Introduction

Structural and spectroscopic studies have shown that CO₂ binding can be enhanced by cooperative effects between two metals and between a metal and its ligand.¹⁻¹⁰ The two metals involved may be a transition metal and an alkali metal, two transition metals, or a transition metal and a main group metal. Bimetallic activation has also been implicated in the electrocatalytic reduction of CO₂ to CO¹¹ and the coupling of CO₂ and alkynes.¹² In these catalytic reactions, a transition metal and a magnesium ion are involved, but only the transition metal is recycled in a catalytic fashion. The

magnesium ions act as stoichiometric reagents. Catalytic reactions observed for Ni(cyclam)⁺ (where cyclam is 1,4,8,11-tetraazacyclotetradecane) adsorbed on Hg may also proceed through bimetallic intermediates,^{13,14} but no direct evidence has been presented, and dinuclear complexes based on Ni(cyclam)²⁺ have shown no cooperative effects.¹⁵ Bimetallic copper complexes and trimetallic nickel clusters have been reported to catalyze the electrochemical reduction of CO₂.¹⁶ Mechanistic studies of these bimetallic complexes are consistent with a transition state containing one CO₂ per two copper sites which may indicate a possible cooperative interaction. Unfortunately, no analogous mononuclear complexes exhibiting catalytic activity are available for comparison with these dinuclear complexes. Recent examples of bimetallic activation of other substrates include C-H activation of methane,¹⁷ phosphonate and phosphate ester hydrolysis,¹⁸ and hydroformylation of olefins.¹⁹

Structural studies and van der Waals energy calculations carried out by Stanley and co-workers on dipalladium complexes of the bridging hexaphosphine ligand eHTP [(Et₂PCH₂CH₂)₂PCH₂P(CH₂CH₂PEt₂)₂] have shown that the preferred structure is a conformation with the palladium atoms nearly eclipsed as shown in

[®] Abstract published in *Advance ACS Abstracts*, September 15, 1995.

(1) (a) Pinkes, J. R.; Steffey, B. D.; Vites, J. C.; Cutler, A. R. *Organometallics* **1994**, *13*, 21. (b) Vites, J. C.; Steffey, B. D.; Giuseppetti-Dery, M. E.; Cutler, A. R. *Organometallics* **1991**, *10*, 2827. (c) Steffey, B. D.; Vites, J. C.; Cutler, A. R. *Organometallics* **1991**, *10*, 3432.

(2) (a) Gibson, D. H.; Ye, M.; Richardson, J. F. *J. Am. Chem. Soc.* **1992**, *114*, 9716. (b) Gibson, D. H.; Mehta, J. M.; Ye, M.; Richardson, J. F.; Mashuta, M. S. *Organometallics* **1994**, *13*, 1070.

(3) (a) Pilato, R. S.; Geoffroy, G. L.; Rheingold, A. L. *Organometallics* **1990**, *9*, 2333. (b) Housmekerides, C. E.; Ramage, D. L.; Kretz, C. M.; Shontz, J. T.; Pilato, R. S.; Geoffroy, B. L.; Rheingold, A. L.; Haggerty, B. S. *Inorg. Chem.* **1992**, *31*, 4453.

(4) (a) Fujita, E.; Creutz, C.; Sutin, N.; Brunshwig, B. S. *Inorg. Chem.* **1993**, *32*, 2657. (b) Szalda, D. J.; Chou, M. H.; Fujita, E.; Creutz, C. *Inorg. Chem.* **1992**, *31*, 4712. (c) Fujita, E.; Szalda, D.; Creutz, C.; Sutin, N. *J. Am. Chem. Soc.* **1988**, *110*, 4870.

(5) Tanaka, H.; Tzeng, B.-C.; Nagao, H.; Peng, S.-M.; Tanaka, K. *Inorg. Chem.* **1993**, *32*, 1508.

(6) (a) Gamborotta, S.; Arena, F.; Floriani, C.; Zanazzi, P. F. *J. Am. Chem. Soc.* **1982**, *104*, 5082. (b) Floriani, C.; *Pure Appl. Chem.* **1983**, *55*, 1.

(7) Bianchini, C.; Meli, A. *J. Am. Chem. Soc.* **1984**, *106*, 2698.

(8) Schmidt, M. H.; Miskelly, G. M.; Lewis, N. S. *J. Am. Chem. Soc.* **1990**, *112*, 3420.

(9) (a) Darensbourg, D. J.; Wiegrefe, H. P.; Wiegrefe, P. H. *J. Am. Chem. Soc.* **1990**, *112*, 9252. (b) Darensbourg, D. J.; Hanckel, R. K.; Banch, C. G.; Pala, M.; Simmons, D.; White, J. N. *J. Am. Chem. Soc.* **1985**, *107*, 7463. (c) Darensbourg, D. J.; Pala, M. *J. Am. Chem. Soc.* **1985**, *107*, 5687.

(10) (a) Henary, M.; Zink, J. I. *J. Am. Chem. Soc.* **1988**, *110*, 5582. (b) Lundquist, E. G.; Foltz, K.; Huffman, J. C.; Caulton, K. G. *Inorg. Chem.* **1987**, *26*, 205.

(11) Hammouche, M.; Lexa, D.; Momenteau, M.; Savéant, J.-M. *J. Am. Chem. Soc.* **1991**, *113*, 8455.

(12) (a) Dérien, S.; Duñach, E.; Périchou, J. *J. Am. Chem. Soc.*, **1991**, *113*, 8447. (b) Dérien, S.; Duñach, E.; Périchou, J. *J. Organomet. Chem.* **1990**, *385*, C43.

(13) Beley, M.; Collin, J.-P.; Ruppert, R.; Sauvage, J.-P. *J. Am. Chem. Soc.* **1986**, *108*, 7461.

(14) (a) Balazs, G. B.; Anson, F. C. *J. Electroanal. Chem.* **1992**, *322*, 325. (b) Fujihira, M.; Hirata, Y.; Suga, K. *Ibid.* **1990**, *292*, 199.

(15) Collin, J. P.; Jouaiti, A.; Sauvage, J.-P. *Inorg. Chem.* **1988**, *27*, 1986.

(16) (a) Haines, R. J.; Wittrig, R. E.; Kubiak, C. P. *Inorg. Chem.* **1994**, *33*, 4723. (b) Ratcliff, K. S.; Lentz, R. E.; Kubiak, C. P. *Organometallics*, **1992**, *11*, 1986.

(17) Zhang, X.-X.; Wayland, B. B. *J. Am. Chem. Soc.* **1994**, *116*, 7897.

(18) (a) Hance, D. H.; Czarnik, A. W. *J. Am. Chem. Soc.* **1993**, *115*, 12165. (b) Tsubouchi, A.; Bruce, T. C. *J. Am. Chem. Soc.* **1994**, *116*, 11614.

(19) Laneman, S. A.; Stanley, G. G. *Adv. Chem. Ser.* **1992**, No. 230, 349.

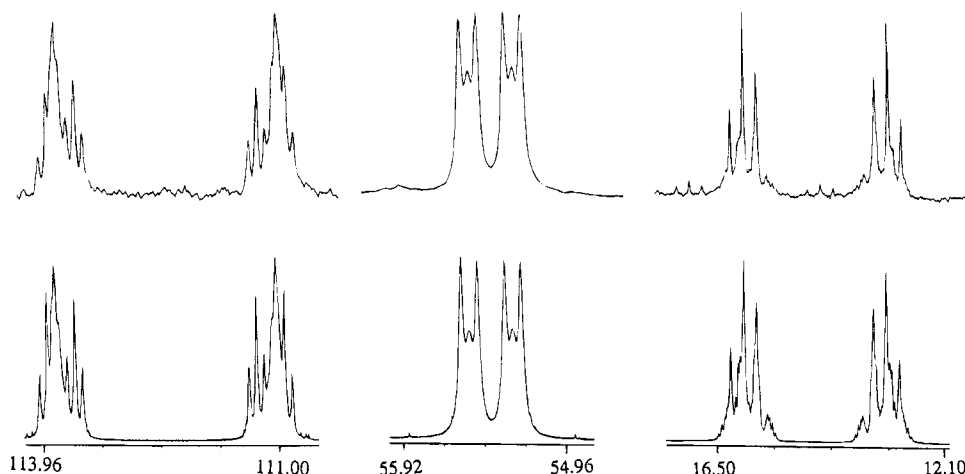
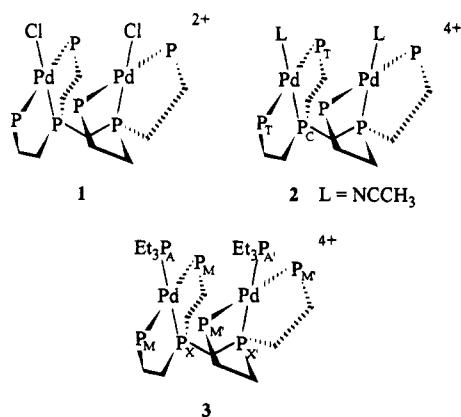


Figure 1. Calculated (bottom) and experimental (top) ^{31}P NMR spectra for $[\text{Pd}_2(\text{PEt}_3)_2\text{eHTP}](\text{BF}_4)_4$. Parameters used in the simulation are listed in the Experimental Section.

structure **1**.²⁰ Work from our laboratory has demon-



strated that the closely related $[\text{Pd}(\text{triphosphine})(\text{CH}_3\text{CN})](\text{BF}_4)_2$ complexes catalyze the electrochemical reduction of CO_2 to CO in acidic dimethylformamide or acetonitrile solutions.²¹ These catalysts exhibit second order rate constants as high as $300 \text{ M}^{-1} \text{ s}^{-1}$ and can be very selective with current efficiencies exceeding 95% for the production of CO . Our results and those of Stanley and co-workers suggested that the complex $[\text{Pd}_2(\text{CH}_3\text{CN})_2(\text{eHTP})](\text{BF}_4)_4$, **2**, in which the chloride ligands of **1** are replaced with acetonitrile, might exhibit cooperative effects for CO_2 reduction by forming intermediates containing a bridging CO_2 ligand. This paper describes studies of **2** as a catalyst for electrochemical CO_2 reduction.

Results

Synthesis and Characterization of Complexes.

The ligand eHTP was prepared as described in the literature.²² Reaction of 1 equiv of eHTP with 2 equivs of $[\text{Pd}(\text{CH}_3\text{CN})_4](\text{BF}_4)_2$ resulted in formation of $[\text{Pd}_2(\text{CH}_3\text{CN})_2(\text{eHTP})](\text{BF}_4)_4$, **2**. The ^{31}P NMR spectrum of **2**

consists of two singlets at 63.8 and 110.2 ppm assigned to the terminal, P_T , and central, P_C , phosphorus atoms, respectively, of the coordinated hexaphosphine ligand. These assignments are based on the relative intensities of these resonances and on the similarity of the chemical shifts to those observed for monomeric analogues.²¹ The presence of coordinated acetonitrile is indicated by CN stretching and combination bands at 2295 and 2323 cm^{-1} in the infrared spectrum.²³

The labile acetonitrile of **2** is readily replaced by triethylphosphine forming $[\text{Pd}_2(\text{PEt}_3)_2(\text{eHTP})](\text{BF}_4)_4$, **3**. The ^{31}P NMR spectrum of **3** is complex as shown by the top trace in Figure 1. This spectrum has been analyzed as an $\text{AA}'\text{XX}'\text{M}_2\text{M}_2'$ spin system using the parameters listed in the Experimental Section. This analysis indicates a 47 Hz coupling between the two central phosphorus atoms, P_X and P_X' , and a 9 Hz coupling between P_A and P_X . Similar four-bond coupling constants have been observed in phosphido-bridged dimers of Pd and Pt.²⁴ The other coupling constants and chemical shift values of **3** are close to those observed for other square planar $[\text{Pd}(\text{triphosphine})(\text{PEt}_3)](\text{BF}_4)_2$ complexes.²¹ On the basis of their spectroscopic data both **2** and **3** are assigned the bridged square-planar structures shown above.

Electrochemical Studies. Cyclic voltammograms of **2** under different conditions are shown in Figure 2. Cyclic voltammogram a is of the complex under a nitrogen atmosphere. With the exception of the cathodic peak observed at -1.94 V , only a featureless cathodic current is observed with an onset potential of approximately -1.1 V . These same features are observed for all scan rates between 0.05 and 100 V/s. A similar cyclic voltammogram is observed in the presence of CO_2 as shown by trace b. Under an atmosphere of CO , the current onset of the first wave and the cathodic peak at -1.95 V are shifted to more positive potentials. Controlled potential electrolysis of dimethylformamide solutions of **2** at -1.3 V under N_2 , CO_2 , and CO atmospheres resulted in the passage of 2.0 ± 0.2 Faradays/mol of **2** or 1.0 Faraday/mol of palladium. The product was the same in all cases. The ^{31}P NMR

(20) Saum, S. E.; Laneman, S. A.; Stanley, G. G. *Inorg. Chem.* **1990**, *29*, 5065.

(21) (a) DuBois, D. L.; Miedaner, A. *J. Am. Chem. Soc.* **1987**, *109*, 113. (b) DuBois, D. L.; Miedaner, A.; Haltiwanger, R. C. *J. Am. Chem. Soc.* **1991**, *113*, 8753. (c) Bernatis, P. R.; Miedaner, A.; Haltiwanger, R. C.; DuBois, D. L. *Organometallics* **1994**, *13*, 4835. (d) Miedaner, A.; Curtis, C. J.; Barkley, R. M.; DuBois, D. L. *Inorg. Chem.* **1994**, *33*, 5482.

(22) Askham, F. R.; Stanley, G. C.; Marques, E. C. *J. Am. Chem. Soc.* **1985**, *107*, 7423.

(23) Storkhoff, B. N.; Lewis, H. C., Jr. *Coord. Chem. Rev.* **1977**, *23*, 1.

(24) Glaser, R.; Kountz, D. J.; Waid, R. D.; Gallucci, J. C.; Meek, D. W. *J. Am. Chem. Soc.* **1984**, *106*, 6324.

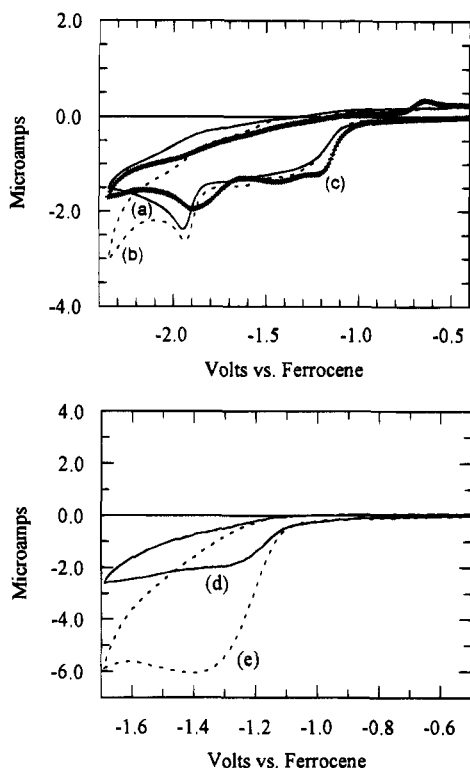
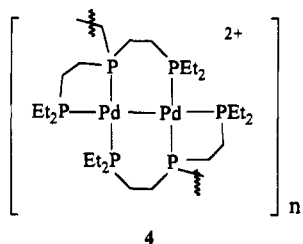


Figure 2. Cyclic voltammograms of a 1.3×10^{-3} M solution of $[\text{Pd}_2(\text{CH}_3\text{CN})_2\text{eHTP}](\text{BF}_4)_2$ in dimethylformamide: (a) under nitrogen (solid line), (b) saturated with CO_2 at 620 mmHg (dashed line), (c) saturated with CO at 620 mmHg (++++). Cyclic voltammograms of same solution containing 0.076 M HBF_4 (d) under nitrogen (solid line) and (e) saturated with CO_2 (dashed line). The supporting electrolyte was 0.3 M NEt_4BF_4 , all scan rates were 0.1 V/s, and the working electrode was glassy carbon.

spectrum of the product can be analyzed to a first approximation as an AA'BB'XX' spin system with additional small coupling. This pattern is similar to that observed for the Pd(I) dimer $[\text{Pd}(\text{etpE})]_2(\text{BF}_4)_2$ (where etpE is bis((diethylphosphinoethyl)phenylphosphine), $(\text{Et}_2\text{PCH}_2\text{CH}_2)_2\text{PPh}$) whose structure has been confirmed by an X-ray diffraction study.^{21b} Cyclic voltammograms of the reduction product of **2** in acetonitrile exhibit an irreversible cathodic wave at -1.95 V and an irreversible anodic wave at $+0.54$ V. The analogous complex $[\text{Pd}(\text{etpE})]_2(\text{BF}_4)_2$ has cathodic and anodic waves at -1.86 and $+0.58$ V. On the basis of the coulometric, spectroscopic, and cyclic voltammetric data, the cathodic waves at -1.94 V of cyclic voltammograms a and b of Figure 2 are assigned to the reduction of a Pd(I)–Pd(I) bond in a tetrameric ($n = 2$) or oligomeric species such as **4**. The observation that this peak persists at high scan rates indicates that this species forms very rapidly upon reduction of **2**.



Cyclic voltammograms d and e of Figure 2 are of **2** in the presence of 0.076 M HBF_4 under nitrogen and CO_2

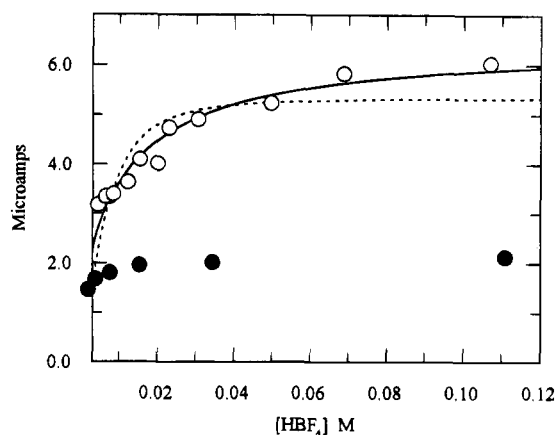


Figure 3. Peak current as a function of acid concentration for solutions saturated with CO_2 (open circles) and nitrogen (solid circles). The dashed line represents the best fit curve using eq 1 ($k_1 = 31 \text{ M}^{-1} \text{ s}^{-1}$ and $k_2 = 5.9 \times 10^4 \text{ M}^{-2} \text{ s}^{-1}$), and the solid line represents the best fit curve using eq 2 ($k_1 = 45 \text{ M}^{-1} \text{ s}^{-1}$ and $k_2 = 380 \text{ M}^{-1} \text{ s}^{-1}$). As discussed in the text, the values obtained for k_1 and k_2 should not be interpreted as true rate constants.

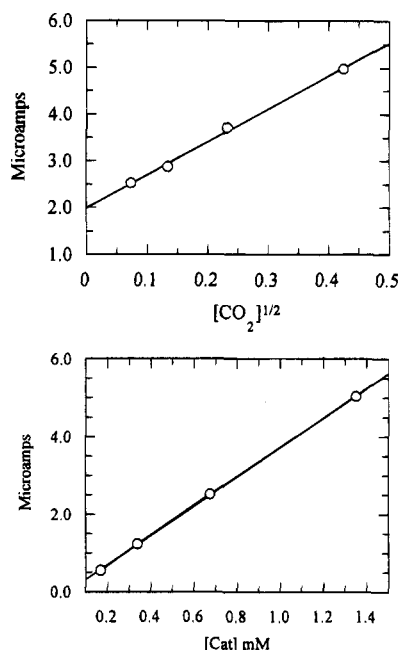


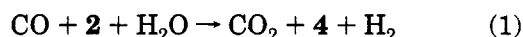
Figure 4. Plots showing the dependence of the catalytic current on CO_2 (top graph) and catalyst concentrations (bottom graph).

atmospheres, respectively. An increase in the cathodic current is observed in the presence of CO_2 compared to nitrogen. This increase is attributed to the reduction of CO_2 to CO . Electrolysis at -1.3 V of a dimethylformamide solution of **2** containing 0.1 M HBF_4 and 0.18 M CO_2 produced CO with a current efficiency of 85%. The other product formed during electrolysis is hydrogen, which accounts for the remaining charge consumed. A turnover number of 8 was calculated based on the moles of CO produced per mol of catalyst. The catalyst was considered deactivated when the current had decayed to 10% of its original value.

The dependence of the catalytic current on substrate and catalyst concentrations are shown in Figures 3 and 4. A plot of the catalytic current versus acid concentration (Figure 3, open circles) is biphasic. The catalytic current initially increases with acid concentration and

then becomes independent of it. As discussed in more detail later, this behavior is consistent with a first-order dependence of the catalytic rate on acid at low acid concentrations and a zero-order dependence at high acid concentrations. The solid circles in Figure 3 show the currents observed for solutions of different acid concentrations in the absence of CO₂. At all acid concentrations a significant current enhancement is observed for solutions purged with CO₂ compared to those purged with N₂. Plots of the catalytic current versus the square root of the CO₂ concentration and versus the catalyst concentration are shown in Figure 4. The square root dependence of the catalytic current on CO₂ concentration is consistent with a rate-determining step that is first order in CO₂.²⁵ The linear dependence of the current on catalyst concentration implies a first order dependence on the catalyst concentration as well.

The catalytic current was decreased by approximately 20% when the CO₂ pressure was held constant at 1 atm and the partial pressure of CO was increased to 0.5 atm (scan rate 0.1 V/s). This indicates that the product, CO, inhibits the reaction. Reaction of CO with **2** in undried dimethylformamide-*d*₇ produces H₂, CO, and **4** over a period of 1-2 days with no detectable intermediates as shown in eq 1. The production of **4** was monitored by



³¹P NMR spectroscopy, and the formation of H₂ and CO₂ was measured by gas chromatography. Reaction 1 is promoted by addition of water, and it is retarded in the presence of 0.07 M HBF₄. Although reaction 1 occurs in acidic DMF solutions under conditions identical to those for catalytic reactions, the rate is slow with less than 1 equiv of H₂ produced in 24 h. These results suggest that hydrogen produced during the electrochemical reduction does not arise from the water gas shift reaction and that the formation of **4** is competitive with hydrogen production.

Ideally the catalytic current should be independent of the scan rate.^{25a} However, the catalytic current exhibited a square root dependence on the scan rate for scan rates between 0.05 and 100 V/s at room temperature as shown in Figure 5. The catalytic current also remained scan rate dependent for solutions cooled to -50 °C.

Cyclic voltammograms of **3** at two different scan rates are shown in Figure 6. At 10 V/s (voltammogram a), two reversible two-electron reductions are observed at -1.12 and -1.44 V. These two waves are assigned to the two Pd(II/0) couples expected for **3**. Analogous [Pd-(triphosphine)(PEt₃)](BF₄)₂ complexes are known to undergo reversible two-electron reductions.²¹ The difference in the redox potentials of these two waves (0.32 V) indicates that there is a significant interaction between the two palladium sites. For comparison, Δ*E*_{1/2} is 0.11 V for a dinuclear palladium complex containing the bridging tetrakis(diphenylphosphino)benzene ligand.²⁶ On the basis of the difference in the redox potentials of these two couples, a comproportionation constant of 7 × 10¹⁰ can be calculated for formation of the mixed-valence complex from Pd(II)-Pd(II) and Pd(0)-Pd(0)

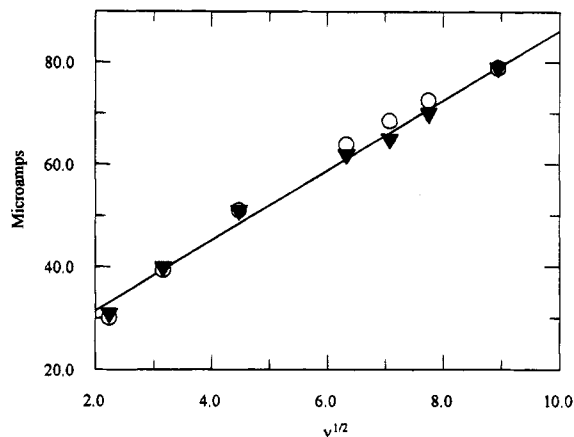


Figure 5. Plot of the catalytic current vs the square root of the scan rate. The solid triangles represent the experimentally observed data. The open circles represent the currents calculated assuming the catalytic and decomposition rates given in the text. The solid line represents the best linear fit of the experimental data.

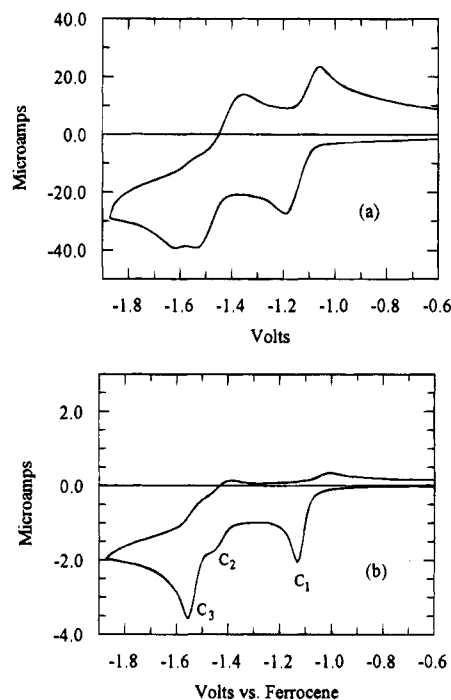


Figure 6. Cyclic voltammograms of 2.24×10^{-3} M solutions of [Pd₂(PEt₃)₂eHTP](BF₄)₂ in dimethylformamide under nitrogen at scan rates of 10 V/s (top graph) and 0.05 V/s (bottom graph).

dimers.²⁷ The mixed-valence complex [Pd(0)Pd(II)-(PEt₃)₂(eHTP)](BF₄)₂ is unstable with a lifetime of a few tenths of a second based on the scan rate dependence of cyclic voltammograms of **3**. Cyclic voltammogram b of Figure 6 was recorded at a scan rate of 0.05 V/s. The two reversible waves observed in voltammogram a have become irreversible, and wave c₃ has increased at the expense of c₂. On the basis of a linear plot of *i*_p versus the square root of the scan rate between 0.05 and 1.0 V/s, the first reduction wave, c₁, is diffusion controlled. Wave c₁ also has an *E*_p - *E*_{p/2} value of 29 mV at a scan rate of 50 mV/s. This value agrees well with the 25 mV value expected for a reversible two-electron reduction

(25) (a) Savéant, J. M.; Vianello, E. *Electrochimica Acta* **1965**, *10*, 905. (b) Savéant, J.-M.; Su, K. B. *J. Electroanal. Chem.* **1985**, *196*, 1.

(c) Nadjo, L.; Savéant, J.-M.; Su, K. B. *Ibid.* **1985**, *196*, 23.

(26) Wang, P.-W.; Fox, M. A. *Inorg. Chem.* **1984**, *33*, 2938.

(27) Heinze, J. *Angew. Chem., Int. Ed. Engl.* **1984**, *23*, 831.

followed by a fast chemical reaction.²⁸ Addition of excess triethylphosphine (0.5 M) does not change the cyclic voltammogram observed. This result excludes the possibility of a reversible loss of triethylphosphine being the rate determining step in the decomposition of the mixed-valence complex. Controlled potential electrolysis of complex **3** carried out at -1.3 V in acetonitrile resulted in the passage of 2.0 Faradays/mol which is consistent with a two-electron reduction of **3**.

Discussion

[Pd₂(CH₃CN)₂(eHTP)](BF₄)₂, **2**, is readily prepared from eHTP and [Pd(CH₃CN)₄](BF₄)₂. Substitution of the labile acetonitrile ligand of **2** with triethylphosphine produces [Pd₂(PET₃)₂(eHTP)](BF₄)₂, **3**. The coupling observed by ³¹P NMR between the two central phosphorus atoms of **3**, ²J_{P-P} = 43 Hz, and between the triethylphosphine ligand and the central phosphorus atom of the second square-planar unit, ⁴J_{P-P} = 9 Hz, suggests a significant interaction between the two square-planar units. The 300 mV difference between the two Pd(II/0) couples observed by cyclic voltammetry for **3** is also consistent with a strong interaction between the two palladium sites.

The increased current observed in the presence of CO₂ for acidic solutions of **2** suggested that **2** catalyzes the electrochemical reduction of CO₂ (Figure 2 trace e). This was confirmed by controlled potential electrolysis experiments carried out at -1.3 V and identification of CO as the major reduction product by gas chromatography. The dependence of the catalytic current on acid concentration (Figure 3) is consistent with two different rate-determining steps. For monomeric [Pd(triethylphosphine)(CH₃CN)](BF₄)₂ complexes, two rate determining steps were also observed.²¹ In that case, a linear dependence of the catalytic current on acid concentration was observed for solutions with low acid concentrations. Because of the square root dependence of the catalytic current on substrate concentration,²⁵ a linear dependence is consistent with a rate-determining step that is second order in acid, which implies a transition state involving two protons. The proposed rate-determining step at low acid concentrations is the cleavage of the C-O bond to form CO and water. At higher acid concentrations the current was independent of acid, first order in catalyst, and exhibited a square root dependence on the concentration of CO₂. This is consistent with a rate determining step that is first order in catalyst and CO₂. On the basis of this and other electrochemical data, the reaction of a Pd(I) species with CO₂ was proposed as the rate determining reaction at high acid concentrations. For the mononuclear complexes, the kinetic data were fit to eq 2, where *i*_c is the

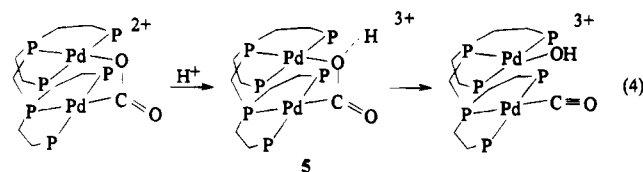
$$\frac{i_c}{i_d} = \frac{\sigma}{0.447} \sqrt{\frac{RT}{nFv}} \sqrt{\frac{k_1 k_2 [\text{CO}_2] [\text{H}^+]^2}{k_1 [\text{CO}_2] + k_2 [\text{H}^+]^2}} \quad (2)$$

catalytic current, *i*_d is the peak current due to reversible reduction of the catalyst, *v* is the scan rate, *n* is the number of electrons involved in catalyst reduction, *k*₁ and *k*₂ are rate constants for the two rate-determining

steps discussed above, and *σ* is a factor which depends on whether the second electron transfer to the catalyst occurs at the electrode surface or in solution. Using eq 2, the best fit curve to the data shown in Figure 3 is shown by the dashed line. The observed data do not fit this model well. A better fit is obtained using eq 3,

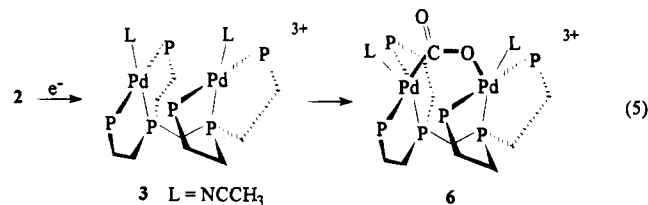
$$\frac{i_c}{i_d} = \frac{\sigma}{0.447} \sqrt{\frac{RT}{nFv}} \sqrt{\frac{k_1 k_2 [\text{CO}_2] [\text{H}^+]}{k_1 [\text{CO}_2] + k_2 [\text{H}^+]}} \quad (3)$$

which assumes a first-order dependence on acid at low acid concentrations. The solid line shown in Figure 3 is the best curve obtained assuming a first-order dependence on acid. The data are clearly much more consistent with this model. The presence of only one proton in the activated complex of the dimeric catalyst suggests the possibility of a transition state with a bridging CO₂ molecule as shown in eq 4. In structure



5, one proton of the mononuclear transition state has been replaced by the second palladium atom of the dimer. This would account for the biphasic dependence of catalytic current of **2** on acid concentration and also for the difference in the acid dependence observed for monomeric catalysts and **2**.

At high acid concentrations, the first-order dependence of the rate-limiting step on the concentrations of **2** and CO₂ is consistent with two palladium atoms and one CO₂ molecule in the transition state. This stoichiometry could reflect a cooperative binding as shown by structure **6** in eq 5, or it could simply be the result of



deactivation of the second palladium due to reduction of the first. To distinguish between these two possibilities, an effort was made to measure the rate of this reaction. Determination of catalytic rate constants using eq 3 requires a reliable value for the peak current under noncatalytic conditions. As can be seen from cyclic voltammogram a of Figure 2, determination of an appropriate peak current for **2** is difficult because no peaks are observed. Complex **3** was prepared to provide a good estimate of this value. In previous work, [Pd-(triethylphosphine)(PET₃)](BF₄)₂ complexes have exhibited reversible two-electron reductions, and two reversible two-electron reductions are observed for **3**. Dividing the peak currents observed for the two-electron reductions of **3** by 2.83²⁹ should provide a reasonably good estimate of the current expected for a reversible one electron

(28) Andrieux, C. P.; Savéant, J. M. In *Investigation of Rates and Mechanisms of Reactions*; Bernasconi, C. F., Ed.; Wiley: New York, 1986; Vol. 6, 41E, Part 2, 331.

(29) Bard, A. J.; Faulkner, L. R. *Electrochemical Methods*; Wiley: New York, 1980; p 218.

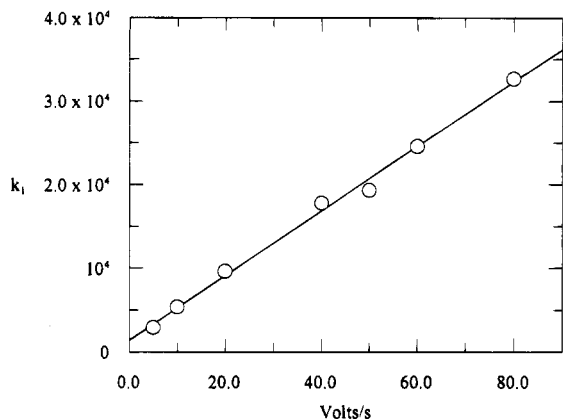


Figure 7. Plot of the rate constant k_1 , calculated according to eq 2, as a function of the scan rate.

reduction of **2**, because **2** and **3** are expected to have very similar diffusion coefficients. Using the value of i_d obtained in this manner, eq 2 can be used to fit the data shown in Figure 3. The solid curve shown is the fit obtained using values of 45 and 380 $\text{M}^{-1} \text{s}^{-1}$ for k_1 and k_2 . These values do not reflect true rate constants for this reaction because they are scan rate dependent. However, the dependence of the catalytic currents on substrate and catalyst concentrations is consistent with the proposed rate-determining steps.

Ideally the catalytic current should not depend on the scan rate. However, because of the square root dependence observed for the catalytic current (Figure 5), the apparent rate constants calculated using eq 3 exhibit a linear dependence on the scan rate as shown in Figure 7 for k_1 . This linear dependence could arise from (1) a slow catalytic reaction, (2) depletion of the substrates, (3) rapid decomposition of the catalyst, or (4) inhibition by the product CO. A slow catalytic reaction can be ruled out on the basis of the large catalytic currents observed and the fact that enhanced currents are observed in the presence of CO_2 even at scan rates as high as 100 V/s. A diffusion-controlled wave with small or no current enhancement in the presence of CO_2 is expected for a slow catalytic reaction at high scan rates. Depletion of substrates can be discounted because other monomeric catalysts show much larger currents that are scan rate independent under identical conditions. The third possibility, decomposition of the catalyst, is a reasonable possibility. Controlled potential electrolysis experiments indicate the turnover number for **2** is low, 8, and on the basis of ^{31}P NMR spectra of the spent reaction mixture, the major decomposition product is the tetrameric or oligomeric compound **4** discussed above. The formation of **4** must occur very rapidly, because the reduction wave assigned to this product is observed at scan rates as high as 100 V/s under CO_2 and N_2 atmospheres. Finally, the peak current of cyclic voltammograms simulated assuming a decomposition reaction with a rate competitive with the catalytic reaction has a square root dependence on scan rate as shown in Figure 5. The calculated peak currents are the results of simulations assuming a rate constant for k_1 (eq 2) of $1 \times 10^5 \text{ M}^{-1} \text{ s}^{-1}$ and a first-order rate constant for the decomposition of the catalyst of $3 \times 10^4 \text{ s}^{-1}$. These values are not unique in fitting the data but only serve to illustrate that the assumption of a competing decomposition reaction is consistent with the ob-

served behavior of the catalytic current on scan rate.³⁰ Carbon monoxide inhibits the catalytic current as discussed above. This product inhibition could also contribute to the nonideal behavior of the catalytic current. Although CO and H_2O react with **2** to form **4**, H_2 , and CO_2 , reaction 1 is slow and unlikely to contribute to the observed current inhibition. The reaction of reduced forms of **2** with CO appears to be more rapid as indicated by the shift in the first reduction wave of **2** to more positive potentials in the presence of CO as shown by trace c of Figure 2. It is therefore concluded that it is a reduced form of **2** which binds CO sufficiently rapidly to produce inhibition. However, any CO complexes which form are not stable since reduction of **2** in the presence of CO produces **4**.

Attempts to slow the decomposition reaction by lowering the temperature to -50°C and reducing the catalyst concentration were unsuccessful, because the catalytic current still exhibited a scan rate dependence under these conditions. In principle, at sufficiently high scan rates the decomposition of the catalyst should become insignificant and a true catalytic current could be measured. However, this does not occur for scan rates as high as 100 V/s as shown in Figure 7. Consequently a true rate constant cannot be determined, but a lower limit of at least $25 \times 10^3 \text{ M}^{-1} \text{ s}^{-1}$ can be inferred for k_1 from this data. This rate constant is 3 orders of magnitude larger than the $25 \text{ M}^{-1} \text{ s}^{-1}$ value expected for a mononuclear $[\text{Pd}(\text{triphosphine})(\text{CH}_3\text{CN})](\text{BF}_4)_2$ complex with a redox potential of -1.18 V . This result supports a cooperative effect between the two metal sites of **2** during the electrochemical reduction of CO_2 to CO.

Summary and Conclusions

Complex **2** catalyzes the reduction of CO_2 to CO in acidic DMF solutions. Three observations suggest a cooperative interaction between the two palladium sites and CO_2 during the catalytic cycle. (1) At low acid concentrations, the first-order dependence of the catalytic rate on acid concentration observed for **2** compared to a second-order dependence for mononuclear complexes is consistent with the second palladium atom of **2** binding to an oxygen atom of CO_2 as shown in structure **5**. (2) At high acid concentrations, the dependence of the catalytic current on the concentrations of CO_2 and catalyst is consistent with two palladium atoms per CO_2 . (3) The catalytic rate of CO_2 reduction for **2** is at least 3 orders of magnitude greater than that expected for a mononuclear $[\text{Pd}(\text{triphosphine})(\text{CH}_3\text{CN})](\text{BF}_4)_2$ complex having the same potential. These observations suggest that dinuclear complexes such as **2** can provide a useful approach for dramatically enhancing catalytic rates of CO_2 reduction. On the other hand, the very high rate of decomposition of these catalysts must be overcome before advantage can be taken of these higher catalytic rates. Research is in progress to address this issue.

Experimental Section

Materials and Physical Methods. Reagent-grade diethyl ether and toluene were purified by distillation from sodium

(30) Simulations of cyclic voltammograms under catalytic conditions were carried out using the program Digisim (Bioanalytical Systems, Inc.).

benzophenone ketyl. Acetonitrile was distilled from CaH₂ under nitrogen. Reagent-grade dimethylformamide from Burdick and Jackson was deoxygenated by purging with nitrogen and stored in an inert-atmosphere glovebox. Acetone-*d*₆ was dried over 4-Å molecular sieves, vacuum transferred, and stored in a glovebox. Triethylphosphine was obtained from Strem Chemicals, Inc. and used without further purification. The ligand eHTP and [Pd(CH₃CN)₄](BF₄)₂ were prepared by literature methods.^{22,31}

NMR spectra were obtained on a Varian Unity 300 MHz NMR spectrometer operating at 299.95, 121.42, and 75.43 MHz for ¹H, ³¹P, and ¹³C nuclei, respectively. Chemical shifts for ¹H NMR spectra are reported in ppm relative to tetramethylsilane using solvent peaks as secondary references. ³¹P NMR chemical shifts are referenced to external H₃PO₄. Infrared spectra were obtained using a Nicolet 510 P spectrometer on samples prepared as Nujol mulls or dichloromethane solutions. Coulometric measurements were carried out at 25–30 °C using a Princeton Applied Research Model 173 potentiostat equipped with a Model 179 digital coulometer and a Model 175 universal programmer. The working electrode was constructed from a reticulated vitreous carbon rod with a 1-cm diameter and length of 2.5 cm (100 pores/in., The Electrosynthesis Co., Inc.). The counter electrode was a glassy carbon rod, and a Pt wire immersed in a 50:50 mixture of permethylferrocene/permethylferrocenium was used as a reference electrode.³² The electrode compartments were separated by Vycor disks (7-mm diameter). Measurements of current efficiencies for gas production were carried out in a sealed flask (120 mL). In a typical experiment, a 1.0 × 10⁻³ M solution of **2** in dimethylformamide (10.0 mL) was saturated with CO₂ (0.18 M at 620 mmHg³³) by purging the solution for approximately 30 min. HBF₄ (50 μL of a 7.6 M aqueous solution) was added via syringe and the solution electrolyzed at -1.3 V. The electrolyses were considered complete when the current had decayed to approximately 5–10% of the initial value. During the course of the electrolysis, gas aliquots were withdrawn for gas chromatographic analysis. The gases were analyzed at 200 °C using a 1/8 in. × 15 ft stainless steel column packed with 60/80 carboxen 1000 support (Supelco). Cyclic voltam-

metry and chronoamperometry experiments were carried out using a Cypress Systems computer-aided electrolysis system. The working electrode was a glassy carbon disk of approximately 1-mm diameter. The counter electrode was a glassy carbon rod, and the reference electrode was a Pt wire immersed in a permethylferrocene/permethylferrocenium solution. Ferrocene was used as an internal standard, and all potentials are reported vs the ferrocene/ferrocenium couple.³⁴ All solutions for cyclic voltammetry and coulometric experiments were 0.3 N NEt₄BF₄ in dimethylformamide.

Synthesis. [Pd₂(CH₃CN)₂(eHTP)](BF₄)₄, **2.** A solution of eHTP (1.00 g, 1.84 mmol) in toluene (20 mL) was added to a solution of [Pd(CH₃CN)₄](BF₄)₂ (1.63 g, 3.68 mmol) in acetonitrile (50 mL), and the orange reaction mixture was stirred for 1 h. The solvent was removed with a vacuum to produce a yellow solid which was washed with ether and dried. The product was recrystallized from a mixture of acetonitrile and ether (yield 1.8 g, 83%). Anal. Calcd for C₂₉H₆₄B₄F₁₆N₂P₆Pd₂: C, 29.35; H, 5.44; N, 2.36; P, 15.66. Found: C, 29.76; H, 5.59; N, 2.07; P, 15.65. ¹H NMR (acetone-*d*₆): PCH₂P, 3.65 ppm (t); PCH₂CH₂P, 3.1 and 2.4 ppm (m); PCH₂CH₃, 2.4 ppm (m); CH₃CN, 1.98 ppm (s); PCH₂CH₃, 1.30 ppm (m). ³¹P NMR (acetone-*d*₆): P_C, 110.2 ppm (s); P_T, 63.8 ppm (s).

[Pd₂(PEt₃)₂(eHTP)](BF₄)₄, **3.** A solution of eHTP (0.25 g, 0.46 mmol) in toluene (5 mL) was added to a solution of [Pd(CH₃CN)₄](BF₄)₂ (0.41 g, 0.92 mmol) in acetonitrile (25 mL), and the orange reaction mixture was stirred for 1 h. Triethylphosphine (0.11g, 0.95 mmol) was added to the reaction mixture, which was stirred for an additional 2 h. The solvent was removed in a vacuum, and the orange solid which resulted was washed repeatedly with ether and dried (0.34 g, 55%). Anal. Calcd for C₄₂H₉₀B₄F₁₆P₈Pd₂: C, 35.96; H, 6.47; P, 17.66. Found: C, 37.11; H, 6.47; P, 16.74. ¹H NMR (acetone-*d*₆): PCH₂P, 3.63 ppm (t); PCH₂CH₂P and PCH₂CH₃, 3.4–2.0 ppm (m); PCH₂CH₃, 1.35 ppm (m). ³¹P NMR (acetone-*d*₆): P_A, 14.63 ppm; P_M, 55.4 ppm; P_X, 112.4 ppm; J_{AX}, 326 Hz; J_{AX}, 9 Hz; J_{AM}, 31 Hz; J_{MX}, 11.7 Hz; J_{XX}, 42.7 Hz.

Acknowledgment. This work was supported by the United States Department of Energy, Office of Basic Energy Sciences, Chemical Sciences Division.

OM950306S

(31) (a) Sen, A.; Ta-Wang, L. *J. Am. Chem. Soc.* **1981**, *103*, 4627. (b) Hathaway, B. J.; Holah, D. G.; Underhill, A. E. *J. Chem. Soc.* **1962**, 2444.

(32) Bashkin, J. K.; Kinlen, P. *Inorg. Chem.* **1990**, *29*, 4507.

(33) *Solubilities of Inorganic and Organic Compounds*; Stephen, H.; Stephen T., Eds.; Pergamon: New York, 1958; Vol. 1, p 1063.

(34) (a) Gagne, R. R.; Koval, C. A.; Lisensky, G. C. *Inorg. Chem.* **1980**, *19*, 2854. (b) Gritzner, G.; Kuta, J. *Pure Appl. Chem.* **1984**, *56*, 462.

Ferrocenylenegermane Polymers and Copolymers

Ramesh N. Kapoor,[†] Guy M. Crawford,[†] Jawad Mahmoud,[†]
Vyacheslav V. Dementiev,[†] My T. Nguyen,[‡] Arthur F. Diaz,[‡] and
Keith H. Pannell*

Department of Chemistry, University of Texas at El Paso, El Paso, Texas 79968-0513, and
IBM Almaden Research Center, 650 Harry Road, San Jose, California 95120

Received February 8, 1995[®]

Ferrocenylenegermane polymers and copolymers (**1**) have been prepared, in situ, by thermal treatment of the product from the reaction between dilithioferrocene and the corresponding R_2GeCl_2 , $R = \text{methyl (1a)}$, ethyl (**1b**), n -butyl (**1c**), or their mixtures, $Me_2GeCl_2 + n\text{-Bu}_2\text{-}GeCl_2$ (**1d**) and $Et_2GeCl_2 + n\text{-Bu}_2\text{-}GeCl_2$ (**1e**). Thin films of the polymers can exhibit both semicrystalline or amorphous morphology dependent upon the nature of the alkyl group and/or mode of casting. When cast from THF, **1c** was observed as an amorphous material; however, after time a crystalline form was obtained. Films of mixed polymer systems, **1b** + **1c**, cast from THF immediately resulted in crystalline forms for both polymers, i.e., a seeding of **1c** by **1b** occurred. The diethyl/di- n -butyl copolymer was amorphous and elastomeric as was the dimethyl/di- n -butyl analog. Cyclic voltammetry indicated the presence of two reversible redox couples in solution with potentials slightly higher than the Si analogs. The copolymers also exhibited distinctive electrochemistry and not a combination of the two individual components.

Introduction

The study of inorganic/organometallic compounds as new materials, or as prematerial systems, is developing rapidly in the hope that the metallic component can bring new and unusual properties to the resulting materials.¹ Electrical, optical, and high-temperature conversions are among the potential properties of interest in this class of chemicals. There has long been interest in the area of organometallic polymers containing ferrocene groups both as pendant and backbone units,² including silicon-based systems which have been shown to possess interesting electrochemical, thermal, conducting, and electrooptical properties.³⁻⁶ Foucher et al. recently reported the preparation of the related ferrocenylenegermane analogs, $[FCGeR_2]_n$, $FC = (\eta^5\text{-}C_5H_4)Fe(\eta^5\text{-}C_5H_4)$, $R = \text{Me, Et, Ph}$,⁷ which prompted us to report our own studies on such compounds including the di- n -butylgermyl polymer and a copolymer with dimethyl/di- n -butylgermane and diethyl/di- n -butylgermane units, a new type of ferrocenylene polymer. Wide-angle X-ray diffraction and cyclic voltammetric electrochemical studies are reported on the ferrocenylenegermane polymers for the first time.

Experimental Section

Organogermanium compounds were synthesized by published procedures⁸ or purchased from Gelest Inc. Wide-angle X-ray scattering and electrochemical properties were investigated using previously described experimental conditions and equipment.⁵ Analyses were performed by Galbraith Laboratories Inc.

Synthesis of Ferrocenylenediethylgermane Polymer, 1b. To a mixture of ferrocene (3.0 g, 16 mmol) and TMEDA (5 mL, 33 mmol) dissolved in hexane (60 mL) was added slowly a solution of n -butyllithium in hexanes (22 mL of a 1.6 M solution). After about 2 h, an orange precipitate formed, and the system was stirred for 12 h. The precipitate was washed with hexane until essentially colorless, and 50 mL of hexane was added. The resulting slurry was stirred and cooled to -78°C . To this stirred system was added Et_2GeCl_2 (3.23 g, 16 mmol in 5 mL hexane) over a 2 h period. The solution was warmed to room temperature and stirred overnight. The reaction mixture was filtered, and the solvent was removed under vacuum to leave red-orange crystals. ^{13}C NMR confirmed the presence of the ferrocenophane by observation of

(4) (a) Foucher, D. A.; Tang, B.-Z.; Manners, I. *J. Am. Chem. Soc.* **1992**, *114*, 6246. (b) Tang, B.-Z.; Foucher, D. A.; Lough, A.; Coombs, N.; Sodhi, R.; Manners, I. *J. Chem. Soc., Chem. Commun.* **1993**, 523. (c) Foucher, D. A.; Ziembinski, R.; Tang, B.-Z.; Macdonald, P. M.; Massey, J.; Jaeger, C. R.; Vancso, G. J.; Manners, I. *Macromolecules* **1993**, *26*, 2878. (d) Foucher, D. A.; Honeyman, C. H.; Nelson, J. M.; Tang, B.-Z.; Manners, I. *Angew. Chem., Int. Ed. Engl.* **1993**, *32*, 1709. (e) Foucher, D. A.; Ziembinski, R.; Peterson, R.; Pudelski, J.; Edwards, M.; Ni, Y.; Massey, J.; Jaeger, C. R.; Vancso, C. J.; Manners, I. *Macromolecules* **1994**, *27*, 3992. (f) Rulkens, R.; Lough, A. J.; Manners, I. *J. Am. Chem. Soc.* **1994**, *116*, 797.

(5) (a) Nguyen, M. T.; Diaz, A. F.; Dementiev, V. V.; Sharma, H. K.; Pannell, K. H. *Proc., SPIE-Int. Soc. Opt. Eng.* **1993**, *1910*, 230. (b) Nguyen, M. T.; Diaz, A. F.; Dementiev, V. V.; Pannell, K. H. *Chem. Mater.* **1993**, *5*, 1389. (c) Nguyen, M. T.; Diaz, A. F.; Dementiev, V. V.; Pannell, K. H. *Chem. Mater.* **1994**, *6*, 952. (d) Pannell, K. H.; Dementiev, V. V.; Li, H.; Cervantes-Lee, F.; Nguyen, M. T.; Diaz, A. F. *Organometallics* **1994**, *13*, 3644.

(6) Tanaka, M.; Hayashi, H. *Bull. Chem. Soc. Jpn.* **1993**, *66*, 334. (7) (a) Foucher, D. A.; Manners, I. *Makromol. Chem., Rapid Commun.* **1993**, *14*, 63. (b) Foucher, D. A.; Edwards, M.; Burrow, R. A.; Lough, A. J.; Manners, I. *Organometallics* **1994**, *13*, 4959.

(8) Lee, M. E.; Bobbitt, K. L.; Lei, D.; Gaspar, P. P. *Synth. React. Inorg. Met.-Org. Chem.* **1990**, *20*, 77.

[†] University of Texas at El Paso.

[‡] IBM Almaden Research Center.

[®] Abstract published in *Advance ACS Abstracts*, September 1, 1995.

(1) (a) *Inorganic and Organometallic Polymers*; Zeldin, M., Wynne, K. J., Allcock, H. R., Eds. ACS Symposium Series 360; American Chemical Society: Washington, DC, 1988. (b) Mark, J. E.; Allcock, H. R.; West, R. *Inorganic Polymers*; Prentice Hall Polymer Science and Engineering Series; Prentice Hall: Englewood Cliffs, NJ, 1992.

(2) (a) Gonsalves, K. E.; Rausch, M. D. In ref 1a, Chapter 36. (b) Hayes, G. F.; George, M. H. In *Organometallic Polymers*; Carraher, C. E., Sheats, J. E., Pittman, C. U., Eds.; Academic Press: New York, 1978; p 13.

(3) (a) Zuaodung, D.; Xiaoyao, W.; Jing, L. *Shandong Daxue Xuebao* **1987**, *22*, 115. (b) Pannell, K. H.; Rozell, J. M.; Zeigler, J. M. *Macromolecules* **1988**, *21*, 278. (c) Pannell, K. H.; Rozell, J. M.; Vincenti, S. In *Silicon-Based Polymer Science: A Comprehensive Resource*; Zeigler, J. M., Fearon, F. W. G., Eds.; Advances in Chemistry Series 224; American Chemical Society: Washington, DC, 1990; Chapter 20. (d) Diaz, A.; Seymour, M.; Pannell, K. H.; Rozell, J. M. *J. Electrochem. Soc.* **1990**, *137*, 503.

the *ipso*-C resonance at 31 ppm. No attempt was made to further purify this material, which was then dissolved in 20 mL of toluene and heated in a sealed tube to 105 °C for 10 day. The toluene was removed under vacuum, and the polymeric residue was dissolved in THF (10 mL), filtered, and precipitated by addition of methanol (300 mL) to form the polymer, **1b**, as a yellow solid (1.5 g, 4.7 mmol, 29%). Gel permeation chromatography using polystyrene standards gave molecular weights in the range 40 000–80 000 from different syntheses. All polymer products exhibited monomodal molecular weight distributions. Anal. for $C_{14}H_{18}FeGe$, calcd (found): C, 53.43 (52.82); H, 5.76 (5.81).

In a similar manner we produced the previously reported polyferrocenylenedimethylgermane (**1a**, 30%–40%) and the new dibutyl analog (**1c**, 40%–50%. Anal. for $C_{18}H_{26}FeGe$, calcd (found): C, 58.30 (57.48); H, 7.07 (7.16)). Polymerization by heating the crude ferrocenophane materials, or their mixtures, in a sealed tube for 3 h gave similar products. Spectral and other related data are listed in Table 1.

Preparation of Ferrocenylenediethylgermane-co-ferrocenylenedi-*n*-butylgermane. To a slurry of dilithioferrocene prepared as above from 3.0 g (16 mmol) of ferrocene was added at –78 °C an equimolar mixture of Et_2GeCl_2 (1.62 g, 8 mmol) and $n-Bu_2GeCl_2$ (2.06 g, 8 mmol), and the mixture was stirred for 1 h, warmed to room temperature, and stirred for 12 h. The solvent was removed under reduced pressure, and ^{13}C NMR spectroscopy indicated the presence of the two ferrocenophane complexes in the residue, with *ipso*-C at 29.6 ppm ($n-Bu_2Ge$) and at 31.0 ppm (Et_2Ge). The residue was placed in a sealed tube and heated to 140 °C for 3 h. Workup as above yielded 1.4 g (2.1 mmol, 26%) of polymer as a thick orange/red gum which was analyzed to yield the data in Table 1. Dissolution in THF and sequential precipitation by methanol produced six fractions, a–f. NMR data from the fractions could not be distinguished, nor could their WAXS data; all were amorphous materials with a very broad signal between 6.4–8.5 Å. Anal. for $C_{32}H_{44}Fe_2Ge_2$, calcd (found): C, 56.06 (54.86); H, 6.47 (5.71).

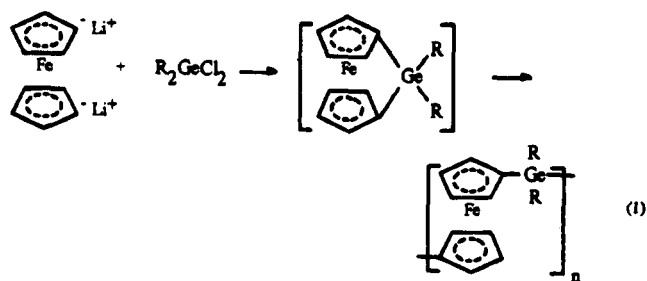
Wide-Angle Scattering X-ray Diffraction. The experiments were performed with thin films cast from toluene or THF solutions onto microscope glass slides using previously described equipment. The experiments were repeated under identical conditions after several hours and/or weeks to note changes.

Electrochemistry. The electrochemical measurements⁵ were carried out in a one-compartment cell equipped with a platinum disk working electrode (surface area = 0.2 cm², a gold wire counter electrode, and an Ag/AgCl (3.8 N KCl) double-junction reference electrode. The cyclic voltammograms were recorded using a EG&G PAR potentiostat/galvanostat (model 273) connected to an IBM *x-y-z* plotter (model 7424 MT). Dichloromethane solutions containing 0.1 M $n-Bu_4NBF_4$ were used for measurements.

Results and Discussion

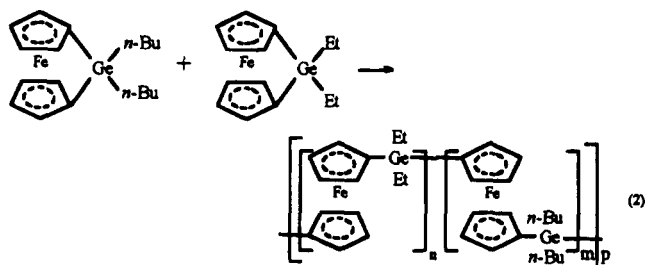
Synthesis. The homopolymers were readily synthesized by heating the hexane-extracted products of the reaction of dilithioferrocene and the corresponding dichlorogermane, without the isolation of the parent [1]germylferrocenophane, in overall good to moderate yields, eq 1. Molecular weights in the range 40 000–100 000 were obtained, permitting ready analysis of their polymer properties. This method is similar to that originally reported by Rosenberg for the formation of the ferrocenylenesilane polymers.⁹

Solution or melt polymerization did not produce polymers with significantly differing molecular weights



R = Me (**1a**), Et (**1b**), *n*-Bu (**1c**).

in these experiments. Indeed, the molecular weights from different experiments with the same technique, i.e., melt or solution, covered a range similar to that between the two techniques. The values presented here are typical, and all are lower than those reported by thermal treatment of pure isolated germylferrocenophanes. This is probably due to the presence of impurities during the thermal treatment; however, we feel that the nature of the polymers obtained is justification for the process used. If higher molecular weights are needed, then perhaps isolation of the intermediate ferrocenophanes would be appropriate; however, during this isolation process, which can involve sublimation, polymerization often occurs at the same time. Ferrocenylenegermane copolymers were obtained by heating the extracted product from the reaction of dilithioferrocene and 1 equiv of a 50:50 mixture of the two appropriate dichlorodialkylgermanes, eq 2.



In a similar fashion we obtained the dimethylgermane-co-di-*n*-butylgermane polymer (**1f**).

Structure. The spectroscopic properties of the polymers are in expectation with their proposed structures, and all data are presented in Table 1. The data for the dimethylgermane polymer are in agreement with those reported for the high molecular weight form, $M_w = 2 \times 10^5$ to 2×10^6 .⁷ There appears to be little change in the spectral properties of the polymers as a function of molecular weight. In the case of the copolymers we could distinguish the two components via 1H and ^{13}C NMR spectroscopy. In each case the germanium copolymers contained, within experimental error, the same relative amounts of the two starting components. All polymers exhibit a UV/visible spectrum with bands centered at 215 and 275 nm (sh) and at 450 nm, typical of the ferrocenyl group when recorded in THF.

To determine possible heterogeneity in the copolymers we performed a successive precipitation–fractionation of copolymer **1e** by slow titration of a THF solution with methanol, collecting six individual fractions, a–f. Each fraction was investigated with respect to its NMR, molecular weight, and wide-angle X-ray scattering, WAXS (*vide infra*), properties. For each fraction we were unable to detect any significant spectroscopic

(9) Rosenberg, H. U.S. Patent 3,426,053, Appl. August 1966, granted February 1969; *Chem. Abstr.* 1969, 70, 78551v.

Table 1. Analytical and Spectral Data and Some Properties for Poly(ferrocenylenegermanes):
[–FC–GeR₂–FC–GeR₂–]_n

compd no.	R'	R''	T _g ^a (°C)	yield (%)	mol wt ^b (×10 ³)		NMR (ppm)		UV/vis λ _{max} (nm) (ε)	cyclic voltammetry data (V)			
					M _w	M _n	¹ H	¹³ C		E _{pa1}	E _{pc1}	E _{pa2}	E _{pc2}
1a	Me	Me	37	36	82.7	74.0	0.68 (Me); 4.01; 4.13 (FC)		450 (140)	0.60	0.72	0.67	0.55
1b	Et	Et	21	29	45.0	39.0	1.10 (CH ₃); 1.30 (CH ₂); 4.15; 4.32 (FC)		451 (140)	0.42	0.28	0.69	0.62
1c	<i>n</i> -Bu	<i>n</i> -Bu	-23	37	47.8	43.9	1.04; 1.36; 1.51; 1.71 (<i>n</i> -Bu); 4.22; 4.36 (FC)		448 (130)	0.52	0.35	0.83	0.68
1d	Me	<i>n</i> -Bu	28	33	96.4	58.7	0.65 (Me); 0.88; 0.91; 0.96; 1.23 (<i>n</i> -Bu); 4.12; 4.18; 4.27; 4.31 (FC)		442 (380)	0.54	0.45	0.73	0.69
1e	Et	<i>n</i> -Bu	9	26	79.5	64.2	1.05; 1.08; 1.30; 1.50; 1.58; 1.71 (Et + <i>n</i> -Bu); 4.16; 4.32 (FC)		451 (380)	0.54	0.40	0.80	0.73

^a DSC: Perkin-Elmer DSC-7, 30 °C/min. ^b GPC: Styragel column, polystyrene standards, THF.

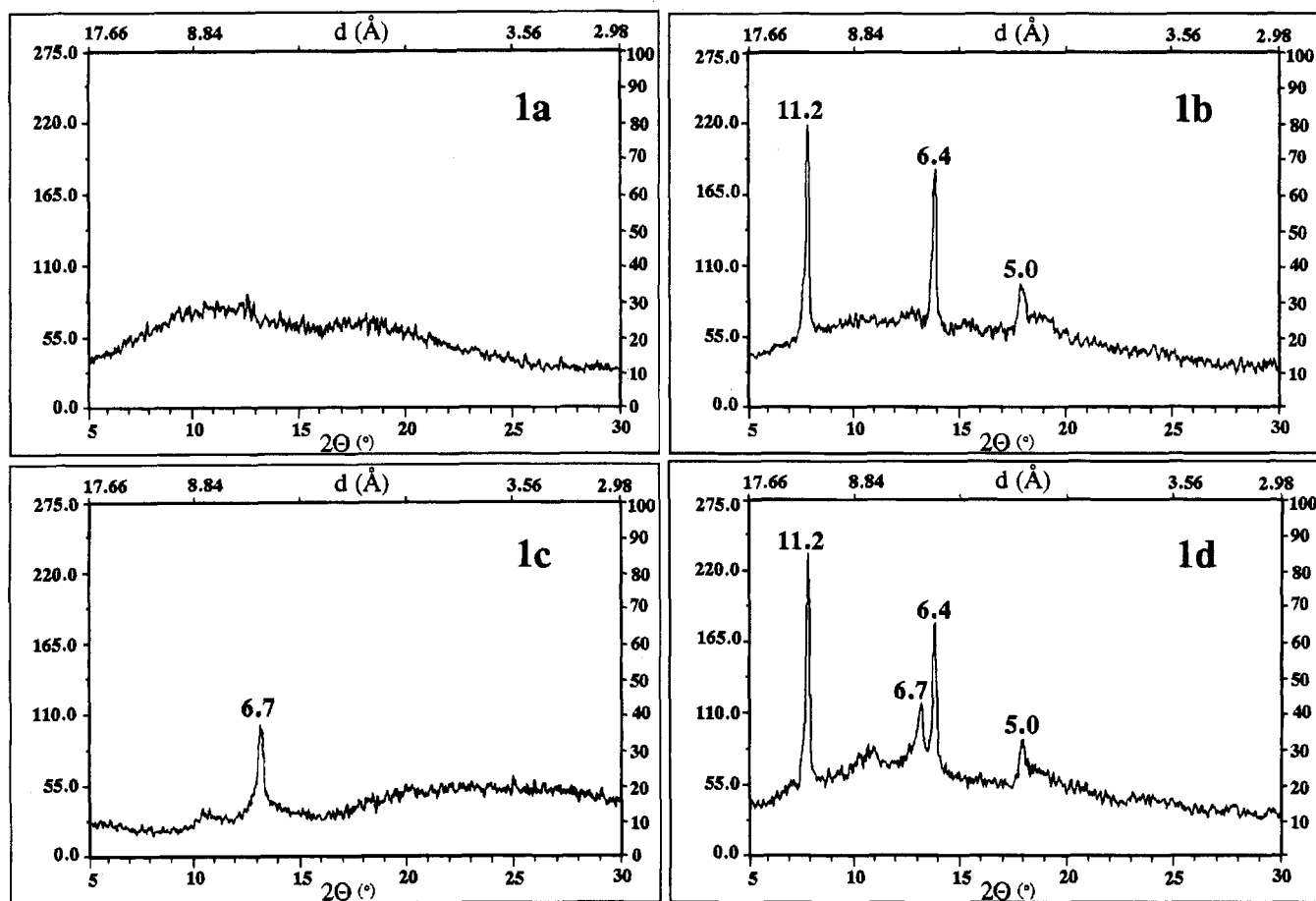


Figure 1. WAXS spectra of dialkylgermaneferrocylene polymers: (a) di-*n*-butyl, *t* = 0; (b) di-*n*-butyl, *t* = 7 days; (c) diethyl; (d) 50:50 mixture of di-*n*-butyl/diethyl, *t* = 0.

differences; the ¹H and ¹³C NMR data, chemical shifts, and approximate integrations were in accord with 1:1 monomer unit incorporation for all fractions, suggesting that we formed copolymers, the first example of the ferrocylene systems. The molecular weight distributions in fractions a–f changed regularly as would be expected. (*M*_w, *M*_n, polydispersity): (a) 95 000 (76 800), 1.24; (b) 60 000 (51 400), 1.35; (c) 50 000 (40 200) 1.21; (d) 35 000 (29 500) 1.21; (e) 20 000 (14 800) 1.36; (f) 15 000 (12 100) 1.30.

The polymers were investigated by WAXS. Each of the homopolymers, R = Me, Et, and *n*-Bu, possess a partial crystallinity, with different spacings noted for the three distinct alkyl groups, Figure 1. Immediate

WAXS examination of a film of the di-*n*-butylgermane homopolymer cast from THF revealed little crystalline character, Figure 1a; however, after several hours a crystalline form was observed, Figure 1b. In our hands the diethylgermane analog always produced a partially crystalline material upon film casting, Figure 1c. Casting a mixture of the ferrocenylenediethylgermane and -di-*n*-butylgermane homopolymers always produced a mixture of the two crystalline polymers, i.e., 1b seeded the crystallization of 1c, Figure 1d. This latter observation strongly suggests a similar crystalline form for the two polymers, and the slow recrystallization of the *n*-butyl analog reflects the ordering of the longer chain *n*-butyl group needed prior to crystallization. The

degree of crystallinity, to the extent that it can be measured by inspection of these diffraction patterns, increases the order Me < Et < *n*-Bu. Furthermore, the spacings observed are almost identical with those reported for the corresponding silicon analogs under identical conditions. The diethyl and di-*n*-butyl polymers exhibited strong sharp reflections at 6.7 and 6.4 Å, respectively. These distances are reminiscent of the Fe··Fe distance along the polymer chain obtained from oligomer structures and MMX calculations, which were shown to be dependent upon the conformation of the backbones.^{5d} The homo-di-*n*-butylgermane polymer also exhibited an extra, intense, well-defined peak at 11.2 Å. It is tempting to assign this to an interchain distance implying an ordering of the ferrocenylene chains. The reason for this extra ordering of the polymers containing the butyl chain (also noted for the silicon analog)^{5b} is unclear. However, interchain butyl–butyl group hydrophobic interactions could be responsible. For the shorter alkyl chains the interaction distance may not be close enough for significant ordering, whereas for the longer dihexyl-substituted polymer (only reported for the Si system) it is lost, probably due to entropic reasons.

The copolymers exhibited a predominantly noncrystalline character. Partial ordering was observed via a broad envelope of reflections in the general region between 6.1 and 8.0 Å. The WAXS spectrum of the copolymer involving both the Et and *n*-Bu groups, **1e**, lacked all traces of the previously well-resolved crystallinity of the related homopolymers. These data reinforce our assertion that we are dealing with true copolymers and not simple mixtures of the two homopolymers since, as noted above, mixtures of **1b,c** provided a crystalline material under all the conditions we employed.

We are unable to completely address the question as to whether **1d,e** are random or block copolymers. The ¹³C NMR of the copolymers are remarkably clean, which could signify that they could be very regular ABABAB systems; however, we think this unlikely. The physical properties of the copolymers are very distinctive. They tend to form considerably more elastic materials and tend to form gels in solution to a larger extent than the homopolymer analogs. This is particularly true for methyl-containing polymers which tend to form insoluble rubber materials after a time, whereas samples of the diethylgermane-*co*-di-*n*-butylgermane polymer have been stored in our laboratory for many months without noticeable change in properties. The *T_g* data for polymers **1d,e** (recorded in Table 1) exhibited a single *T_g*, supporting their designation as random copolymers and not block copolymers or blends.

Electrochemistry. Solutions of the homopolymers in CH₂Cl₂ were investigated using cyclic voltammetry. Two distinct oxidation processes were observed, the first, *E_{pa1}*, between 0.45 and 0.6 V, and the second, *E_{pa2}*,

between 0.55 and 0.83 V, and two corresponding reduction processes, *E_{pc1}* and *E_{pc2}*, Table 1. The behavior is similar to that observed for the polymeric and oligomeric silicon analogs and reflects the coulombic effect of the first oxidized FC cations upon the potential required to oxidize a neighboring ferrocenylene unit.^{4,5,10,11} The Ge polymers exhibit slightly higher oxidation potentials than the Si analogs. For both the Si and Ge polymers, the introduction of the *n*-butyl group onto the group 14 bridge significantly increases the difference between the first and second oxidation potentials. It seems that the increased hydrophobicity of the butyl groups effectively decreases solvation at the first oxidized site, thereby increasing its effective charge, which further translates into a greater coulombic effect upon the neighboring ferrocenyl unit. The shape of the cyclic voltammograms of the Ge polymers also differs from those of the Si polymers in that the initial oxidation appears as a much broader peak, reflecting slower electron exchange of the Ge polymer with the working electrode.

The copolymers exhibit similar electrochemical behavior. For polymer **1e** the oxidations at 0.54 and 0.80 V are close to those of the di-*n*-butyl polymer at 0.52 and 0.83 V. The first oxidation and reduction waves are significantly broader than those of the homopolymers, indicating the possibility of multiple peaks resulting from gross structural variations among those ferrocenylene units undergoing oxidation–reduction. The voltammograms of **1d,e** are distinctly different to those of the appropriate mixture of **1a–c** in which two sets of redox behavior may be observed representing each homopolymer.

Conclusions

We have used the simplified synthetic procedure of thermal treatment of nonisolated ferrocenophanes, first reported by Rosenberg for ferrocenylenesilane polymers,⁹ to form germanium analogs. The study concerned the following: (a) report and discussion of WAXS structural data and seeding of polymers, including the slow amorphous to crystal polymer transformation; (b) the first copolymerization of ferrocenophanes and characterization of copolymers which contrasted mixtures of homopolymers; (c) electrochemical study on the polymers; (d) the effect of the *n*-butyl group upon structure and electrochemistry of the polymers.

Acknowledgment. Support of this research by the NSF, Grant No. RII-88-02973, and the Robert A. Welch Foundation, Houston, TX, Grant No. AH-546, is gratefully acknowledged.

OM9501079

(10) Dementiev, V. V.; Cervantes-Lee, F.; Párkányi, L.; Sharma, H.; Pannell, K. H.; Nguyen, M. T.; Diaz, A. F. *Organometallics* **1993**, *12*, 1983.

(11) Brandt, P. F.; Rauchfuss, T. B. *J. Am. Chem. Soc.* **1992**, *114*, 1926.

Synthesis and Isomerism of Monofunctional Arylated Cyclotetrasilanes

Ulrich Pöschl and Karl Hassler*

Institute of Inorganic Chemistry, Graz University of Technology, Stremayrgasse 16,
A-8010 Graz, Austria

Received May 25, 1995[©]

By the introduction of the novel educt 1,2,3,4-tetraphenyl-1,2,3,4-tetra-*para*-tolylcyclotetrasilane (**2**), which shows significantly higher solubility and reactivity than octaphenylcyclotetrasilane, the first selective monofunctionalization of a perarylated cyclotetrasilane was achieved. Compound **2** was synthesized by ring closure of phenyl-*para*-tolylchlorosilane with lithium. The cyclotetrasilanes Si₄Ph₄-*p*-Tol₃X with X = OSO₂CF₃, F, Cl, Br, I, H or *t*-Bu were prepared by dearylation of **2** with trifluoromethanesulfonic acid and subsequent reaction with lithium or potassium halides, sodium boranate, and *tert*-butyllithium, respectively. The compounds were isolated in high yield and purity. They were characterized by ¹H, ¹³C, ¹⁹F, and ²⁹Si NMR spectroscopy.

Introduction

The perphenylated cyclosilanes Si₄Ph₈, Si₅Ph₁₀, and Si₆Ph₁₂ synthesized by Kipping in 1921 were the first cyclosilanes to be known.¹ Until a few years ago the reaction with hydrogen halides was the only way to functionalize perarylated cyclosilanes. Catalytic dearylation with gaseous HCl, HBr, or HI using the respective aluminum halides as catalysts allowed the preparation of the perhalogenated derivatives (Cl₂Si)_m,² (Br₂Si)_m,³ and (I₂Si)_m,⁴ with *m* = 4, 5, or 6. In liquid HBr and HI, Si₆Ph₆Br₆⁵ and Si₅Ph₅I₅,⁶ respectively, were formed. Selective mono- or disubstitution was not achieved by this kind of dearylation.

The first selective monofunctionalization of decaphenylcyclopentasilane was reported by Uhlig in 1989,⁷ i.e., the dearylation of Si₅Ph₁₀ by use of trifluoromethanesulfonic acid (CF₃SO₃H, abbreviated as TfOH, triflic acid). Matyjaszewski et al. studied the reaction of octaphenylcyclotetrasilane with triflic acid.⁸ They identified Si₄Ph_{8-n}(OTf)_n, with *n* = 1, 2, 3, or 4, and were able to synthesize the tri- and tetratriflates in high yield. However, they did not arrive at the selective formation of (trifluoromethanesulfonyl)oxyheptaphenylcyclotetrasilane, Si₄Ph₇OTf.

Our reasons for the synthesis and characterization of monofunctional arylated cyclosilanes are the following. The partially phenylated cyclosilanes can be used for the preparation of novel cyclosilanes such as Si₄I-*t*-Bu, Si₄Br₇H, or Si₄Cl₇F as well as for the synthesis of polycyclic silanes. Moreover, we are planning to use the synthesized compounds as targets for the study of

molecular dynamics (conformational changes such as the pseudorotation of cyclopentasilanes and the ring flip of cyclotetrasilanes). Our results concerning mono- and difunctional phenylated cyclopentasilanes have been reported in a previous paper.⁹

Results and Discussion

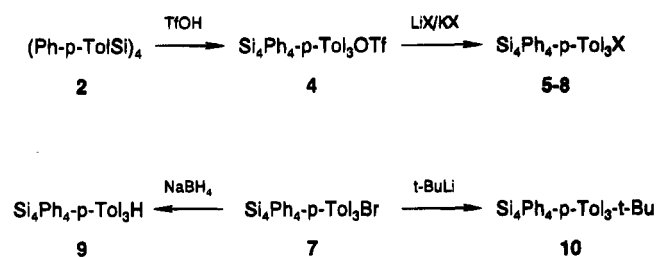
Despite manifold variations of the reaction conditions we could not achieve selective monofunctionalization of octaphenylcyclotetrasilane by dearylation with triflic acid (triflation). In agreement with Matyjaszewski et al. we ascribe this primarily to the very low solubility of the educt, which applies for every common solvent. The triflations were generally performed in toluene, which is known to be one of the best solvents for Si₄-Ph₈. The reaction mixtures consisted of three phases: triflic acid (liquid) and Si₄Ph₈ (solid) suspended in toluene, in which very little Si₄Ph₈ (3 mg/mL at 20 °C) and TfOH were dissolved. The monotriflate Si₄Ph₇OTf, which is formed in a first step of reaction, is very well soluble and therefore undergoes further triflation much faster than the suspended educt. The strong electron-withdrawing effect of the triflate group does inhibit further dearylation (ditriflation), but obviously this deactivation of the monotriflate does not compensate for the solubility, and the triflation of dissolved Si₄Ph₇OTf occurs faster than that of suspended Si₄Ph₈. In contrast, the five-membered cycle Si₅Ph₁₀ is soluble enough (28 mg/mL in toluene at 20 °C) to perform triflation at low temperatures in a reaction system, which is homogeneous except for suspended triflic acid. Triflation of Si₅Ph₁₀ dissolved in toluene at 0 °C selectively yields Si₅Ph₉OTf.^{7,10} In the absence of the multiphase effect described above, the deactivation arising from the first triflate substituent sufficiently reduces the rate of further dearylation to allow selective monotriflation.

To obtain a perarylated cyclotetrasilane with increased solubility we synthesized 1,2,3,4-tetraphenyl-1,2,3,4-tetra-*para*-tolylcyclotetrasilane (**2**) by the ring

[©] Abstract published in *Advance ACS Abstracts*, August 1, 1995.
(1) Kipping, F. S.; Sands, H. E. *J. Chem. Soc.* **1921**, 119, 830; 848.
(2) Hengge, E.; Kovar, D. *J. Organomet. Chem.* **1977**, 125, C29; *Z. Anorg. Allg. Chem.* **1979**, 458, 163.
(3) Hengge, E.; Bauer, G. *Angew. Chem.* **1973**, 85, 304; *Monatsh. Chem.* **1975**, 106, 503. Hengge, E.; Lunzer, F. *Monatsh. Chem.* **1976**, 107, 371. Kovar, D.; Utvary, K.; Hengge, E. *Monatsh. Chem.* **1979**, 110, 1295.
(4) Hengge, E.; Kovar, D. *Angew. Chem.* **1981**, 93, 698.
(5) Hengge, E.; Lunzer, F. *Monatsh. Chem.* **1976**, 107, 371.
(6) Hengge, E.; Marketz, H. *Monatsh. Chem.* **1976**, 107, 371.
(7) Uhlig, W.; Tzschach, A. *J. Organomet. Chem.* **1989**, 378, C1.
(8) Chrusciel, J.; Cypriak, M.; Fossum, E.; Matyjaszewski, K. *Organometallics* **1992**, 11, 3257.

(9) Pöschl, U.; Siegl, H.; Hassler, K. *J. Organomet. Chem.*, in press.
(10) Uhlig, T.; Tretner, C. *J. Organomet. Chem.* **1992**, 436, C1.
(11) Gilman, H.; Peterson, D. J.; Tomasi, R. A.; Harrell, R. L. *J. Organomet. Chem.* **1965**, 4, 167.

Scheme 1



X = F, Cl, Br, I

closure reaction of Ph-*p*-TolSiCl₂ (1) with lithium. Depending on the reaction conditions the ring closure yields a mixture of (Ph-*p*-TolSi)₄ (2) and (Ph-*p*-TolSi)₅ (3). In analogy to the perphenylated cyclosilanes, a thermodynamical preference for the formation of 3 is assumed due to the high ring strain of the four-membered cycle.¹¹

Since excess lithium causes ring cleavage, the influences of reaction temperature, solvent and monomer concentration were investigated using stoichiometric amounts of lithium. In accordance with the standard preparation of Si₄Ph₈,¹² 1 was diluted with THF and added to powdered lithium at a high rate. The heat of reaction caused reflux within a few minutes. After the mixture had been refluxed for several hours, the yield of 2 varied between 0% and 5%, depending primarily on the rate of monomer addition and eventual intermediate cooling. The percentages given for the yield of 2 refer to the educt 1. In general, only minor amounts of products other than 2 or 3 were observed. Addition of 1 to a suspension of Li in THF, which was refluxed already in advance, led to the formation of 3; under these conditions 2 was not observed at all. At 0 °C the desired product, 2, was obtained in 13% yield. Additional experiments in THF at temperatures down to -70 °C did not result in a significant increase of the yield.

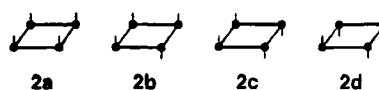
In toluene, even after several hours of reflux, no reaction of 1 with Li was observed. Experiments with various solvent mixtures of toluene and THF led to the reaction conditions given in the Experimental Section. The addition of THF to a mixture of lithium, toluene, and 1 at 0 °C yielded 24% of 2, which readily crystallizes and thus can be easily separated from 3, which is by far more soluble and could not yet be obtained in crystalline state.

Variation of the concentration of 1 in the range 0.5–0.05 g/mL did not cause a significant change of the product composition, regardless of reaction temperature and solvent. Higher dilution only caused an inconveniently strong decrease of the reaction rate.

The progress of reaction was observed by ²⁹Si NMR spectroscopy. In the beginning of the reaction the formation of 2 seemed to occur faster than the formation of 3. However, for complete conversion of the spectroscopically detected intermediates, the reaction mixture had to be stirred for several days, and finally the amount of 3 prevailed. Despite manifold variations of the reaction conditions the yield of 2 could not be raised above 24%.

(12) Jarvie, A. W. P.; Winkler, H. J. S.; Peterson, D. J.; Gilman, H. *J. Am. Chem. Soc.* **1961**, *83*, 1921.

Chart 1



On the whole the optimum conditions for the synthesis of 2 are in sharp contrast to the usual preparation of Si₄Ph₈. The highest yields of Si₄Ph₈ (about 30% relative to Ph₂SiCl₂) generally are obtained at high temperatures in THF. Presumably this difference is due to the low solubility of Si₄Ph₈, which precipitates from the THF suspension immediately after being formed and therefore is hardly affected by ring cleavage with suspended lithium. In the synthesis of 2 and 3 such cleavage probably plays a key role prohibiting higher yields of 2.

At present the possibilities for a more efficient, electrochemical synthesis of 2 are investigated. A first electrolysis of 1 using HMPT/ET₄NBF₄ solvent/electrolyte systems and aluminum sacrificial electrodes in an undivided cell yielded very promising results: 2 was formed without 3 being observed at all. Further electrochemical investigations are intended, and comprehensive results will be reported subsequently.

As expected, the solubility of (Ph-*p*-TolSi)₄ (2) is much higher than that of Si₄Ph₈. In toluene at 20 °C a solubility of about 25 mg/mL was measured for 2 (Si₄Ph₈, 3 mg/mL). Another important aspect concerning the dearylation by triflic acid are the different reactivities of phenyl and *para*-tolyl substituents. Compared to phenyl groups, the Si–C bond in *para*-tolyl-substituted silanes is known to be significantly more reactive toward protonic acids as dearylating reagents.¹³ Accordingly, by use of triflic acid *para*-tolyl groups can be selectively cleaved from silanes containing *para*-tolyl and phenyl substituents in parallel. A manuscript with the results concerning di- and trisilanes is in preparation.¹⁴ For *para*-anisyl- and naphthyl-substituted monosilanes Schmidbauer et al. found a similar gradation of reactivity toward triflic acid.¹⁵ The *para*-anisyl substituents can be selectively cleaved in the presence of naphthyl groups which in turn can be selectively cleaved in the presence of phenyl substituents. However, in contrast to phenyl- and *para*-tolyl-substituted chlorosilanes, neither anisyl- nor naphthyl-substituted monosilanes can be reductively coupled with alkali metals to obtain the corresponding oligosilanes we are interested in.

Dearylation of 2 with 1 equiv of triflic acid selectively yields Si₄Ph₄-*p*-Tol₃OTf (4). Further reaction of 4 with lithium or potassium halides leads to Si₄Ph₄-*p*-Tol₃F (5), Si₄Ph₄-*p*-Tol₃Cl (6), Si₄Ph₄-*p*-Tol₃Br (7), and Si₄Ph₄-*p*-Tol₃I (8) in high purity and 90%–95% yield. Si₄Ph₄-*p*-Tol₃H (9) and Si₄Ph₄-*p*-Tol₃-*t*-Bu (10) can be obtained by reaction of 7 with sodium boranate or *tert*-butyllithium, respectively (Scheme 1).

(Ph-*p*-TolSi)₄ is supposed to exist in four diastereomeric forms (Chart 1).¹⁶ Nevertheless, 2 crystallizes

(13) Eaborn, C. In *Organosilicon Chemistry 2*; IUPAC; Butterworths: London, 1969. Hengge, E.; Eberhardt, H. *Monatsh. Chem.* **1979**, *110*, 39.

(14) Köll, W.; Hassler, K. To be submitted.

(15) Schröck, R.; Angermaier, K.; Sladek, A.; Schmidbauer, H. *Organometallics* **1994**, *13*, 3399.

(16) In Charts 1 and 2 and in Scheme 2, the dots at the edges of the four-membered cycles stand for PhSi and *para*-tolyl groups are indicated by simple vertical lines.

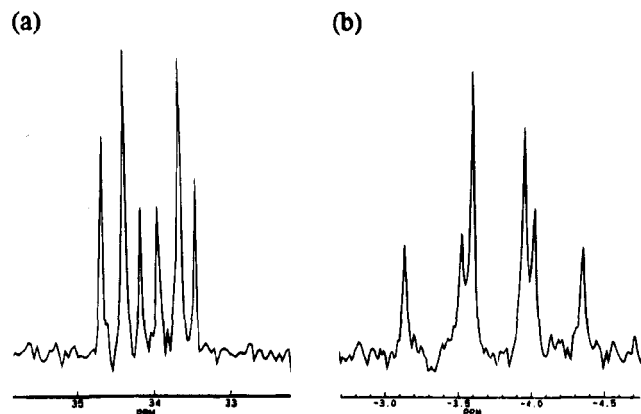


Figure 1. ²⁹Si NMR spectra (SiPhX region, ¹H decoupled) of (a) Si₄Ph₄-*p*-Tol₃OTf (4a-f) and (b) Si₄Ph₄-*p*-Tol₃-*t*-Bu (10a-f).

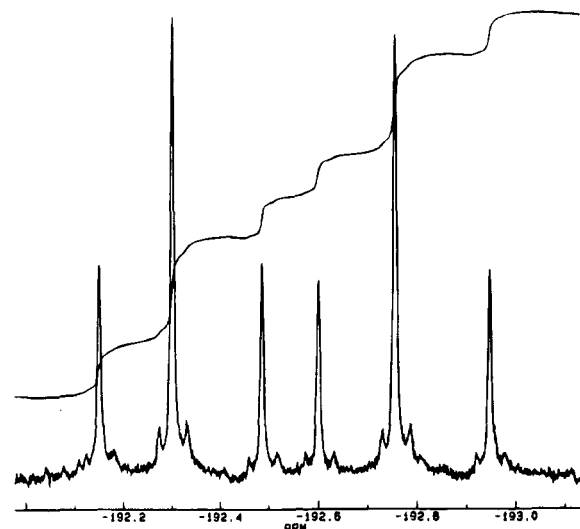
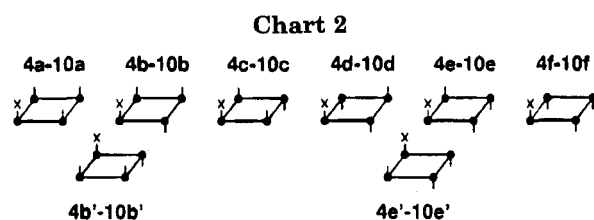


Figure 2. ¹⁹F NMR spectrum of Si₄Ph₄-*p*-Tol₃F (5a-f) with integral plot.



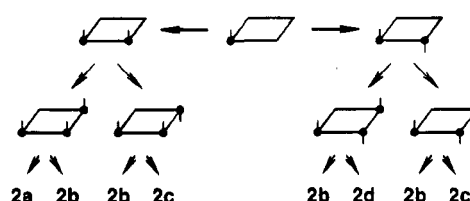
readily and its ²⁹Si NMR spectrum shows only one sharp line with a half-bandwidth of 3 Hz (¹H decoupled). ¹H and ¹³C and NMR spectra confirmed the existence of several isomers but did not provide definite information about their number and quantitative ratio. The ¹³C spectrum shows eight groups of aromatic carbon signals (two singlets and six multiplets with two to six lines) and a methyl signal split up in two lines. The ¹H spectrum consists of six multiplets: three of the aryl-H multiplets with intensities equivalent to 8 H each, one of them equivalent to 12 H, and the methyl-H multiplet equivalent to 12 H. However, the interpretation of the NMR spectra of the products 4-10 lead to a clear picture of the isomeric composition of 2.

Compounds 4-10 are supposed to consist of six diastereomers each, two of the diastereomers existing in two enantiomeric forms (Chart 2). Accordingly their NMR spectra show multiplet structures consisting of six

Table 1. ²⁹Si NMR Data (δ/ppm) for Si₄Ph₄-*p*-Tol₃X (4-10)

compd no.	X	Si(1)	Si(2,4)	Si(3)
4	OTf	34.39	-20.91	-29.88
		34.08	-20.98	-29.97
		33.86	-21.07	-30.03
		33.74	-21.19	-30.16
		33.42	-21.29	-30.28
		33.18	-21.41	-30.38
5	F	33.38 (d)	-20.64 (d)	-29.45 (m)
		33.22 (d)	-20.74 (d)	
6	Cl	10.93	-19.07	-23.99
		10.77	-19.12	-24.11
		10.66	-19.27	-24.23
		10.60	-19.37	-24.36
			-19.49	
			-19.55	
7	Br	2.61	-20.29	-23.56
		2.41	-20.43	-23.62
		2.35	-20.48	-23.70
		2.22	-20.55	-23.77
		2.13	-20.68	-23.85
8	I	-21.51	-21.94	-23.50
		-21.66	-22.12	-23.65
		-21.72	-22.31	-23.87
		-21.78		-24.05
			-24.18	
			-24.39	
9	H	-54.16	-22.14	-23.23
		-54.23	-22.24	-23.35
		-54.38	-22.40	
		-54.45	-22.55	
		-54.60		
		-54.67		
10	<i>t</i> -Bu	-3.13	-21.40	-23.01
		-3.52	-21.56	-23.16
		-3.59		
		-3.95		
		-4.02		
		-4.35		

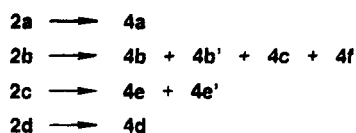
Scheme 2



lines. Partly the measured signals were overlapping, but all the multiplets which could be resolved showed characteristic patterns with intensity ratios such as 1:2:1:1:2:1 or 1:1:2:2:1:1 (see Table 1 and Figures 1 and 2). These are exactly the ratios expected stochastically. The assumption of a random controlled formation of 2a-d in the course of reductive coupling of 1 with lithium is illustrated in Scheme 2. Presuming equal probability for *cis* and *trans* positions, referring to the phenyl and *para*-tolyl substituents of the added Ph-*p*-TolSi group, a ratio of 1:4:2:1 is obtained for 2a:2b:2c:2d. Supposing equal reactivity of every *para*-tolyl group of 2 toward triflic acid, this educt composition fully explains the spectroscopically observed intensity ratios by the formation of eight stereoisomers of 4-10 in equimolar amounts.

As an example Scheme 3 elucidates the stereochemistry of triflation, leading from the quantitative ratio 1:4:2:1 for the isomers of 2 to the ratio 1:2:1:1:2:1 for 4a:4b:4c:4d:4e:4f. For simplicity, a mechanism of dearylation with configurational retention was assumed in this representation; i.e., the triflate group retains the

Scheme 3



position of the *para*-tolyl group it substitutes. But this is not a necessary precondition. A reaction mechanism involving either inversion or configurational equilibration (equal probability for retention and inversion) would cause different reaction pathways in detail but result in the same overall product composition.

Irrespective of the mechanism of subsequent exchange reactions, the quantitative ratio of the triflate isomers (4a–f) is preserved among the derivatives (5a–f to 10a–f).

The ^{29}Si NMR data of $\text{Si}_4\text{Ph}_4\text{-}p\text{-Tol}_3\text{X}$ (4–10) are given in Table 1. With increasing electronegativity of the halogen substituents, the signals arising from the SiPhX groups of 5–8 show the expected increase of δ (low-field shift).¹⁷

Experimental Section

General Comment. All operations with triflate or halogen compounds were carried out under nitrogen using Schlenk techniques; reductive coupling with lithium was performed under an argon atmosphere. The triflate- and iodine-substituted cyclotetrasilanes are highly sensitive to moisture. In contrast, the fluorine, chlorine, and bromine derivatives are stable for several hours when exposed to air. Solvents were distilled from potassium. Lithium and potassium halides were dried by heating for several hours in vacuo. Trifluoromethanesulfonic acid was used as received from Merck-Schuchardt (Art. 821166, 1.71 g cm^{-3} , 98%). The NMR measurements were performed on a Bruker 300 MSL spectrometer in C_6D_6 unless mentioned otherwise. ^{29}Si spectra were recorded at 59.6 MHz using INEPT pulse sequences with ^1H decoupling mostly. ^1H , ^{13}C , and ^{19}F spectra were recorded at 300.1, 75.5, and 282.4 MHz, respectively. Chemical shifts are reported relative to TMS and CFCl_3 , respectively.

Phenyl-*para*-tolyl-dichlorosilane, Ph-*p*-TolSiCl₂ (1). 4-Bromotoluene (1000 g, 5.85 mol) was dissolved in diethyl ether (1600 mL) and dropwise added to magnesium (145 g, 5.96 mol) suspended in diethyl ether (700 mL). The reaction was initiated by the addition of iodine, and after all the 4-bromotoluene had been added the resulting suspension was refluxed for another 16 h. The solution of *p*-TolMgBr was decanted from the excess magnesium. Within 4 h of vigorous stirring, the Grignard compound was dropwise added to PhSiCl_3 (1360 g, 6.43 mol), which was diluted with diethyl ether (300 mL) and cooled with ice. After 6 h of being stirred at room temperature, the suspension was refluxed for 14 h. Then the diethyl ether was removed by distillation and replaced by toluene (1000 mL). The salts were removed by filtration at approximately 50 °C and washed with toluene (6 × 400 mL). Subsequently the solvent was removed, and, after vacuum distillation using a 30 cm Vigreux column, 1 was obtained as a colorless liquid (978 g, 62.6% relative to 4-bromotoluene): 267.23 g mol^{-1} , bp 92–95 °C (0.01 mbar), ^{29}Si NMR (δ/ppm) 6.05, MS (m/z) 266 (M^+).

1,2,3,4-Tetraphenyl-1,2,3,4-tetra-*para*-tolylcyclotetrasilane (2). Compound 1 (108 g, 0.40 mol) was dissolved in toluene (100 mL) and added to powdered Li (5.90 g, 0.85 mol) suspended in toluene (50 mL). At 0 °C THF (20 mL) was added dropwise, and after being stirred for 4 h the reaction mixture was warmed to room temperature. For complete

conversion the suspension had to be stirred for 6 days. Then the solvent mixture was replaced by toluene (300 mL). The salts were removed by filtration and washed with toluene. Precipitation from toluene/heptane yielded 2 as a colorless crystalline solid (19 g, 24% relative to 1): 785.29 g mol^{-1} ; mp 228–234 °C. Anal. $\text{C}_{52}\text{H}_{48}\text{Si}_4$ (found/calcd): C, 79.54/79.53; H, 6.18/6.16. ^{29}Si NMR (δ/ppm) –22.09; ^{13}C NMR (δ/ppm , CDCl_3) 138.5, 137.6, 137.4, 135.6, 135.5, 135.3, 135.2, 135.1, 135.0, 130.8, 130.7, 129.8, 129.7, 129.1, 129.0, 128.9, 128.8, 128.7, 127.9, 127.8, 127.7, 127.6, 21.5, 21.4; ^1H NMR (δ/ppm , CDCl_3) 7.35 m (8H), 7.25 m (12H), 7.08 (8H), 6.94 m (8H), 2.32 m (12H). IR (<1000 cm^{-1}) 996 m, 973 m, b, 889 s, b, 797 vs, 734 vs, 721 w, 711 m, 697 vs, 686 sh, 667 vw, 639 w, 625 s, 615 m, 525 w, 493 vs, 478 vw, 467 s, b, 418 vw, 408 s, 365 m, 357 w, 341 m, b, 324 w, 314 w, 303 vw, 280 vw.

1,2,3,4,5-Pentaphenyl-1,2,3,4,5-penta-*para*-tolylcyclotetrasilane (3). Compound 1 (100 g, 0.37 mmol) was dissolved in THF (250 mL) and added to powdered Li (5.20 g, 0.75 mol) within 10 min (vigorous refluxing). The reaction mixture was refluxed for 20 h. THF was replaced by toluene, and the salts were removed by filtration. By the addition of heptane minor amounts of 2 were crystallized and removed by filtration. Then the solvents were removed, and 3 was precipitated from ethyl acetate/methanol. The precipitate was washed with methanol and dried in vacuo, yielding 3 as a colorless powder (61 g, 83% relative to 1): 981.62 g mol^{-1} ; mp 76–79 °C. Anal. $\text{C}_{65}\text{H}_{60}\text{Si}_5$ (found/calcd): C, 79.43/79.53; H, 6.36/6.16. ^{29}Si NMR (δ/ppm) –34.95. IR (<1000 cm^{-1}): 997 m, 965 vw, 945 m, b, 920 vw, 890 w, 847 m, b, 799 vs, 735 vs, 711 sh, 699 vs, 678 sh, 639 w, 622 s, 614 s, 549 m, b, 512 sh, 496 vs, 469 s, b, 404 m, b, 390 w, 366 m, 359 sh, 333 sh, 326 s, 311 sh, 286 sh, 280 w.

$\text{Si}_4\text{Ph}_4\text{-}p\text{-Tol}_3\text{X}$ with X = OTf, F, Cl, Br, I, H, or *t*-Bu (4–10). Compound 2 (4.25 g, 5.4 mmol) was dissolved in toluene (200 mL). At approximately 15 °C triflic acid (0.50 mL, 98%, 5.6 mmol) was added dropwise within 5 min. Then the reaction mixture was stirred at room temperature for 16 h. By evaporation in vacuo the solution of 4 was reduced to approximately 70 mL. For the synthesis of 5–8, 1,2-dimethoxyethane (40 mL) and LiF (0.25 g, 10 mmol), LiCl (0.40 g), LiBr (1.0 g), or KI (1.7 g) were added at 0 °C. The resulting suspension was stirred at 0 °C for 3 h, and then the solvents were removed in vacuo at 30 °C. Toluene (40 mL) was added, and the salts were removed by filtration and washed with toluene (20 mL). By precipitation from toluene/heptane and drying in vacuo the halotetraphenyltri-*para*-tolylcyclotetrasilanes were obtained as colorless or slightly yellowish powders (90%–95% relative to 2). By NMR spectroscopy only traces of impurities such as the educt or the corresponding difunctional compounds could be observed. The elemental analyses agreed with the calculated compositions. For the synthesis of 9, 7 (3.0 g, 3.9 mmol) was dissolved in 1,2-dimethoxyethane (40 mL) and NaBH_4 (0.2 g, 5.3 mmol) was added at 0 °C. The reaction mixture was stirred at room temperature for 16 h. Then the solvent was removed in vacuo, and toluene was added. The salts were removed by filtration, and drying in vacuo yielded 9 as a colorless powder (2.5 g, 92%). No impurities were observed. For the synthesis of 10, 7 (2.0 g, 2.6 mmol) was dissolved in 1,2-dimethoxyethane (20 mL) and *t*-BuLi (2.6 mmol dissolved in 1.5 mL of pentane) was added at 0 °C. After 2 h of vigorous stirring at 0 °C, the solvents were removed in vacuo and toluene was added. The salts were removed by filtration, and drying in vacuo yielded 10 as a colorless powder (1.8 g, 93%). No impurities were observed. We could not yet crystallize the compounds 4–10; the melting intervals of the amorphously precipitated, powdered substances range around 65–75 °C. The ^{29}Si data are given in Table 1.

Fluoro-1,2,3,4-tetraphenyl-2,3,4-tri-*para*-tolylcyclotetrasilane (5): 713.16 g mol^{-1} . Anal. $\text{C}_{45}\text{H}_{41}\text{FSi}_4$ (found/calcd): C, 75.56/75.79; H, 5.97/5.79. ^{19}F NMR (δ/ppm) –192.05, –192.23, –192.44, –192.51, –192.71, –192.93; $^1J(\text{Si,F}) =$

(17) Marsmann, H. In *NMR Basic Principles and Progress*; Diehl, P., Fluck, E., Kosfeld, R., Eds.; Springer: Berlin, 1981; Vol. 17.

369.7 Hz, $^2J(\text{Si},\text{F}) = 16.6$ Hz. IR (<1000 cm^{-1}) 996 w, 972 m, b, 918 w, 884 m, 797 vs, b, 734 vs, 696 vs, 639 m, 623 s, 615 s, 532 w, 523 w, 491 vs, 465 s, b, 412 w, 388 m, b, 364 m, 329 s, b.

Chloro-1,2,3,4-tetraphenyl-2,3,4-tri-*para*-tolylcyclotetrasilane (6): 729.61 g mol^{-1} . Anal. $\text{C}_{45}\text{H}_{41}\text{ClSi}_4$ (found/calcd): C, 73.93/74.08; H, 5.54/5.66. IR (<1000 cm^{-1}) 996 w, 970 w, b, 965 w, b, 915 vw, 850 sh, 847 w, 798 vs, 777 w, 735 vs, 696 vs, 639 w, 668 vw, 624 s, 615 s, 546 w, 528 w, 493 vs, 465 s, b, 413 w, 387 w, 363 m, 332 sh, 325 s, b, 305 sh, 282 vw, 278 vw.

Bromo-1,2,3,4-tetraphenyl-2,3,4-tri-*para*-tolylcyclotetrasilane (7): 774.06 g mol^{-1} . Anal. $\text{C}_{45}\text{H}_{41}\text{BrSi}_4$ (found/calcd): C, 69.83/69.82; H, 5.24/5.34. IR (<1000 cm^{-1}) 996 m, 971 m, b, 918 w, 891 vw, 849 m, 799 vs, 736 vs, 695 vs, 639 w, 623 w, 616 s, 531 m, 496 vs, 489 w, 467 s, 417 m, 381 m, 362 m, 333 s, 325 sh, 279 vs.

Iodo-1,2,3,4-tetraphenyl-2,3,4-tri-*para*-tolylcyclotetrasilane (8): 821.06 g mol^{-1} . Anal. $\text{C}_{45}\text{H}_{41}\text{ISi}_4$ (found/calcd): C, 65.71/65.83; H, 5.12/5.03. IR (<1000 cm^{-1}) 996 m, 965 m, b, 918 vw, 890 vw, 847 w, 799 vs, 780 sh, 774 vw, 735 vs, 696 vs, 639 vw, 624 s, 615 s, 538 vw, 494 vs, 466 s, 409 m, b, 402 sh, 375 w, 358 w, 328 m, b, 315 sh, 280 vw.

1,2,3,4-Tetraphenyl-1,2,3-tri-*para*-tolylcyclotetrasilane (9): 695.17 g mol^{-1} . Anal. $\text{C}_{45}\text{H}_{42}\text{Si}_4$ (found/calcd): C, 77.63/77.75; H, 5.90/6.09. ^1H NMR (δ/ppm) Si-H, 5.65; aryl-H, 6.75–7.80, 1.92–2.19; $^1J(\text{Si},\text{H}) = 176.7$ Hz. IR (<1000 cm^{-1} , except for $\nu(\text{SiH})$ 2271 s, b, 997 m, 965 w, b, 868 w, 849 m, 798 s, 775 vw, 734 vs, 729 sh, 696 vs, 639 vw, 632 sh, 615 s, 492 vs, b, 477 vw, 468 m, 413 w, 386 w, 357 w.

***tert*-Butyl-1,2,3,4-Tetraphenyl-2,3,4-tri-*para*-tolylcyclotetrasilane (10):** 751.28 g mol^{-1} . Anal. $\text{C}_{48}\text{H}_{50}\text{Si}_4$ (found/calcd): C, 78.16/78.34; H, 6.62/6.71. ^1H NMR (δ/ppm) *t*-Bu-H, 1.18, 1.19, 1.20; aryl-H, 6.70–7.92, 1.90–2.11; ^{13}C NMR (δ/ppm) *t*-Bu-C, 30.7, 24.0, 21.8; aryl-C, 139.6–138.0, 136.4–135.0, 129.7–128.0, 21.6. IR (<1000 cm^{-1}) 997 m, 970 w, b, 917 vw, 868 m, 848 m, b, 798 vs, 735 sh, 728 vs, 695 vs, 667 vw, 639 w, 623 s, 614 s, 515 sh, 491 vs, b, 470 sh, 465 vs, b, 407 m, b, 382 w, 362 m, 340 sh, 333 s, 326 s.

Acknowledgment. The authors thank the Austrian Science Foundation, Vienna, for financial support (Project P 9378-CHE). We also thank Dr. Christa Grogger for performing the electrochemical experiments.

OM950387S

Notes

Mechanism of Photodegradation of Polysilanes: A Relaxed Cross Section of the Conical Intersection Hyperline in 2-Methyltrisilane

Alessandro Venturini,^{*,†} Thom Vreven,[‡] Fernando Bernardi,^{*,‡}
Massimo Olivucci,[‡] and Michael A. Robb[§]

Istituto dei Composti del Carbonio Contenenti Eteroatomi e loro Applicazioni, CNR, via Gobetti 101, 40100 Bologna, Italy, Dipartimento di Chimica "G. Ciamician", Università di Bologna, Via Selmi, 2, 40126 Bologna, Italy, and Department of Chemistry, King's College London, Strand, London WC2 2LS, U.K.

Received February 16, 1995[⊙]

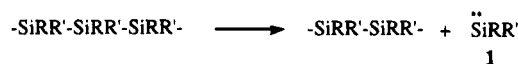
Summary: The potential energy surface of the S_1 state of 2-methyltrisilane has been studied via MC-SCF and multireference MP2 methods. Remarkably, no conventional stationary points appear to exist on this surface. All attempts to minimize the energy with respect to all geometrical coordinates led to a region where the excited and ground states conically intersect and very fast radiationless decay becomes possible. The lowest energy point on the $(n-2)$ -dimensional conical intersection was optimized and lies at a geometry where the system is fragmented. For this reason, a relaxed cross section of the $(n-2)$ -dimensional intersection space was computed between the Franck–Condon region and a point on the conical intersection at a fragmented geometry. The various photodegradation products observed after irradiation of short permethylated silanes can be tentatively rationalized on the basis of the electronic and molecular structures of the points on this relaxed cross section.

Introduction

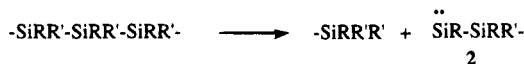
Photodegradation of permethylated polysilanes $-(RR'Si)_n-$ has recently received much attention because of their importance in technology.¹ The observed photodegradation products² are consistent with the production of three different types of intermediates: the silylenes $RR'Si:$ (1) and $-RR'Si-RSi:$ (2) and the Si radical $-RR'Si-RR'Si\cdot$ (3). Remarkably R and R' radical formation has never been detected. Wavelength dependence of photoproduct distribution has also been observed.³ These experimental features have been tentatively explained² via three completely independent mechanisms as shown in Scheme 1.

Scheme 1

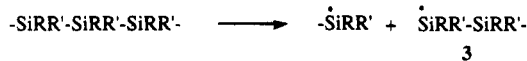
Chain abridgement by 1,1-elimination



Chain cleavage by 1,1-elimination



Homolytic chain scission



Michl and Balaji⁴ have recently reported the result of a MC-SCF+CI study of the three reactions in Scheme 1 using trisilane (Si_3H_8) and methylidisilane ($Si_2H_5CH_3$) as model systems. These computations suggest that formation of the silylenes 1 and 2 occurs via funnels located at avoided crossings between the first excited state and the ground state, and thus the photoproducts are generated via internal conversion at these points. However, the formation of the Si radical 3 was thought to involve intersystem crossing from the singlet S_1 to the triplet T_1 repulsive state followed by separation of a radical pair. In the work of Michl and Balaji,⁴ the excited-state surfaces were documented by scanning the energy surface of the system along distinguished geometrical coordinates. In this paper we have extended the scope of these earlier computations using an optimization method that will locate crossing points (or avoided crossings) in the full space of all the geometric variables. As we shall now discuss, in such a full space, the avoided crossings located by Michl et al.¹ evolve to become real points of crossing on the same $(n-2)$ -dimensional crossing surface.

Results and Discussion

In this paper we use the 2-methyltrisilane ($SiH_3-SiH(CH_3)-SiH_3$) as a model. This molecule provides an

(4) Michl, J.; Balaji, V. *Computational Advances in Organic Chemistry: Molecular Structure and Reactivity*; Ogretir, C., Csizmadia, I. G., Eds.; Kluwer Academic Publishers: Dordrecht, 1991; pp 323–354.

[†] CNR.

[‡] Università di Bologna.

[§] King's College London.

[⊙] Abstract published in *Advance ACS Abstracts*, September 15, 1995.

(1) (a) Miller, R. D.; Michl, J. *Chem. Rev.* **1989**, *89*, 1359. (b) West, R. J. *Organomet. Chem.* **1986**, *300*, 327. (c) Sun, Y.-P.; Hamada, Y.; Huang, L.-M.; Maxka, J. Hsiao, J.-S.; West, R.; Michl, J. *J. Am. Chem. Soc.* **1992**, *114*, 6301. (d) Sun, Y.-P.; Michl, J. *J. Am. Chem. Soc.* **1992**, *114*, 8186.

(2) (a) Trefonas, P., III; West, R.; Miller, R. D. *J. Am. Chem. Soc.* **1985**, *107*, 2737. (b) McKinley, A. J.; Karatsu, T.; Wallraf, G. M.; Miller, R. D.; Sooriyakumaran, R.; Michl, J. *Organometallics* **1988**, *7*, 2567.

(3) See for example: Michl, J.; Downing, J. W.; Karatsu, T.; McKinley, A. J.; Poggi, G.; Wallraf, G. M.; Sooriyakumaran, R.; Miller, R. D. *Pure Appl. Chem.* **1988**, *60*, 959.

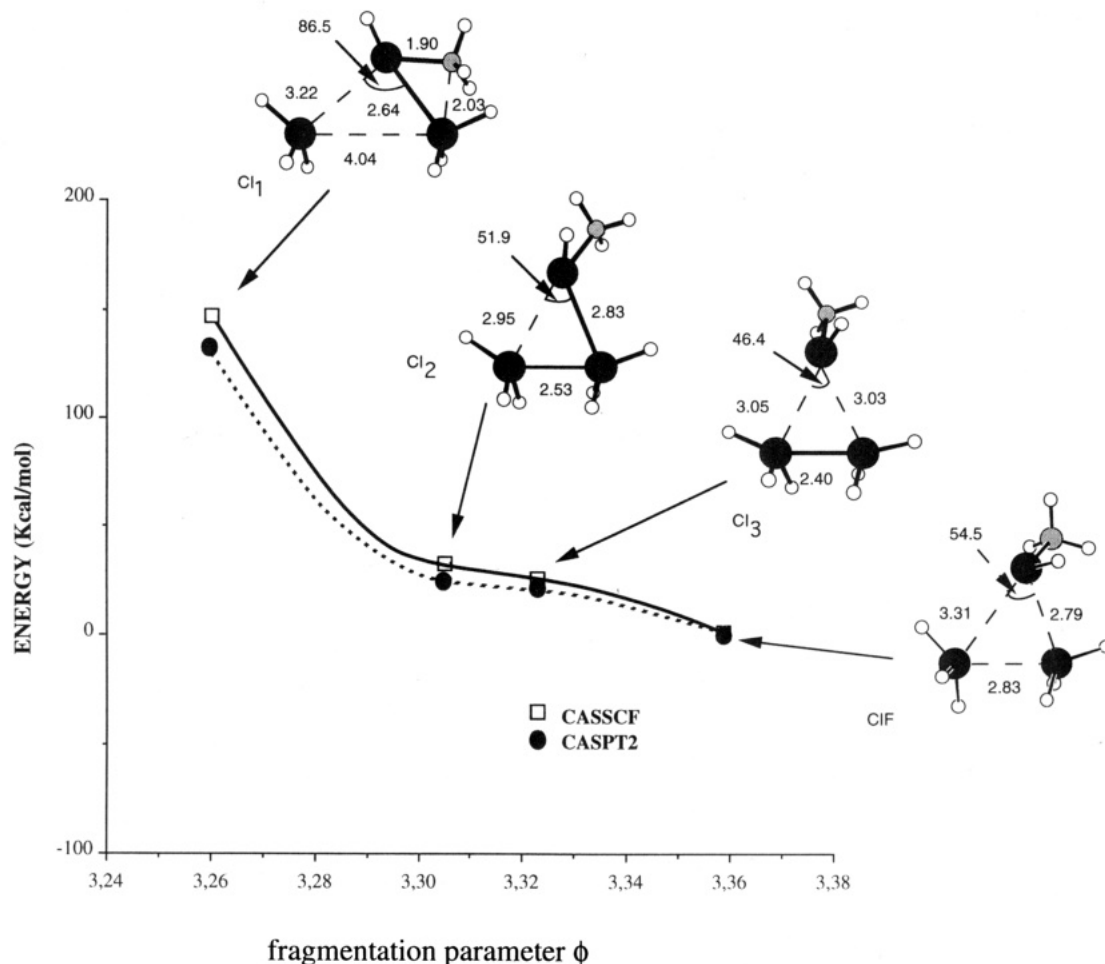


Figure 1. Energy values of the four conical intersections CI₁, CI₂, CI₃, and CIF as a function of the fragmentation parameter ϕ . The energy values are computed at the CAS-SCF/6-31G* optimized structures (full line) and at the CASPT2N/6-31G*/CAS-SCF/6-31G* (dashed line) (the main structural parameters are reported in angstroms and degrees).

improved model system for a methylated silane since the inclusion of a methyl group allows a more realistic investigation of participation of C-sigmatropic shifts in the reaction mechanism. The computations have been carried out using the MC-SCF method (CAS-SCF/6-31G*⁵). The active space used in all computations involves six orbitals and six electrons where the orbitals are the two σ and the two σ^* orbitals describing the silicon framework and the σ and σ^* C-Si orbitals describing the Si-CH₃ bond. The first excited state of the system has been extensively explored via geometry optimization in the full space of its 36 geometrical coordinates. Remarkably, no minima have been located on this surface. All attempts to minimize the energy led to a region where the excited and ground states conically intersect. This intersection region corresponds to a $(n - 2)$ -dimensional hyperline of the coordinate space⁶ spanning infinitely many different configurations of the system where the excited and the ground states

have the same energy. Radiationless decay becomes very fast at these points.⁶ Thus the outcome of silane photodegradation is expected to be related to the molecular structure and energetic accessibility of points on the crossing surface. Conical intersections of this type are similar to those discussed by Yarkony⁷ in the photodissociation of methyl mercaptan.

The system can decay with full efficiency at any point of the $(n - 2)$ -dimensional crossing surface that lies at lower energy than the Franck-Condon energy. We have documented a part of this region by computing a relaxed cross section of this hyperline which starts in the vicinity of the Franck-Condon region and ends at the lowest energy point on the hyperline. (Such computations are performed using a nonstandard method described elsewhere.⁸) All attempts to optimize the lowest energy point on the $n - 2$ hyperline converge only asymptotically at a fully fragmented structure. Thus we have mapped out a segment of the conical intersection line adjacent to the straight line that connects the Franck-Condon structure with a partly fragmented structure that lies on the conical intersection. (Each interpolated structure has then been used as a guess geometry for minimizing the energy difference between the ground and excited states.)

(5) Unless otherwise specified the computations reported in this work have been carried out with the Gaussian 92 series of programmes: Gaussian 92, Revision C.; Frisch, M. J.; Trucks, G. W.; Head-Gordon, M.; Gill, P. M. W.; Wong, M. W.; Foresman, J. B.; Johnson, B. G.; Schlegel, H. B.; Robb, M. A.; Replogle, E. S.; Gomperts, R.; Andres, J. L.; Raghavachari, K.; Binkley, J. S.; Gonzalez, C.; Martin, R. L.; Fox, D. J.; Defrees, D. J.; Baker, J.; Stewart, J. J. P.; Pople, J. A.; Gaussian, Inc.: Pittsburgh, PA, 1992.

(6) (a) Koppel, H.; Domcke, W.; Cederbaum, L. S. *Adv. Chem. Phys.* **1984**, *57*, 59. (b) Whetten, R. L.; Ezra, G. S.; Grant, E. R. *Rev. Phys. Chem.* **1985**, *36*, 277. (c) Manthe, U.; Koppel, H. *J. Chem. Phys.* **1990**, *93*, 1658.

(7) Yarkony, D. R. *J. Chem. Phys.* **1994**, *100*, 3639.

(8) (a) Ragazos, I. N.; Robb, M. A.; Bernardi, F.; Olivucci, M. *Chem. Phys. Lett.* **1992**, *197*, 217. (b) Bearpark, M. J.; Robb, M. A.; Schlegel, H. B. *Chem. Phys. Lett.* **1994**, *223*, 269.

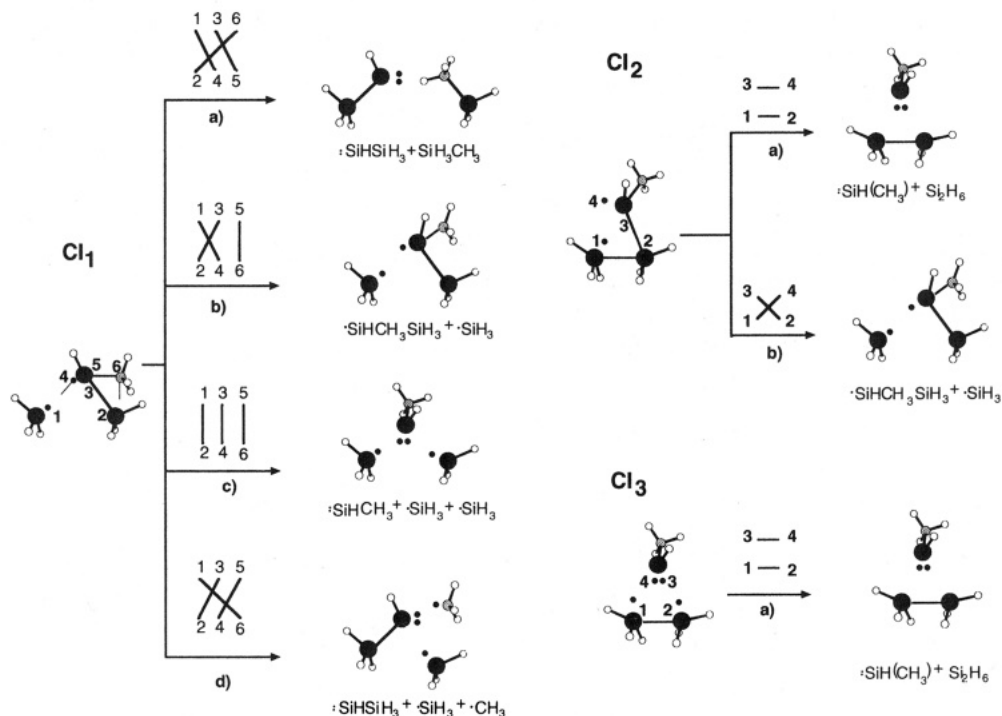


Figure 2. Schematic representation of the possible electron-recoupling processes occurring during the ground-state relaxation from the conical intersections CI_1 , CI_2 , and CI_3 , respectively.

In Figure 1 we show a curve in which the energy is plotted against the fragmentation parameter ϕ^9 of the three intermediate optimized structures (CI_1 , CI_2 , and CI_3) and of the lowest structure (CIF).¹⁰ Each point lies on the $(n - 2)$ -dimensional conical intersection hyperline and thus represents a possible starting point for photodegradation. The structures are all partly fragmented (the normal Si-Si σ -bond length is 2.3 Å, and the Si-C σ -bond length is 1.9 Å) in one or more coordinates. Single-point multireference MP2 computations (CASPT2N¹¹), also shown in Figure 1, indicate that the energy profile and the degeneracy associated with the conical intersection are unaffected by dynamic correlation.

Analysis of the electronic wave function shows that S_0 and S_1 are both covalent states. At each conical intersection point, in the system with six active orbitals, two electrons are fully coupled to a singlet, while the four remaining electrons (in a quasitetraradical) can be coupled in two different ways to yield two singlet states, S_1 and S_0 . The origin of the conical intersection in this

(9) (a) The parameter ϕ (denoted as the fragmentation parameter) is intended to describe the degree of fragmentation of a molecular system with reference to the reactant 2-methyltrisilane. It is taken as the weighted average of the heavy-atom distances and is defined by the following formula:

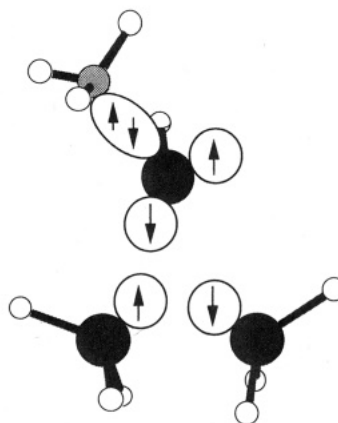
$$\phi = \sum_i f_i g_i / \sum_i f_i$$

where the f_i and g_i denote the interatomic distances at the reactant (reference geometry) and at the various CI, respectively.

(10) At the CAS-SCF/6-31G* level of theory the energies of CIF, CI_3 , CI_2 , and CI_1 are 0.0, 27.8, 33.6 and 162.8 kcal mol⁻¹, respectively (relative to CIF, whose energy is -910.28403 au). At the CASPT2N/6-31G*/CAS-SCF/6-31G* level, the energies of CIF, CI_3 , CI_2 , and CI_1 are 0.0, 24.0, 28.3, and 147.4 kcal mol⁻¹ (relative to CIF, whose energy is -910.67487 au). However, these quantities are expected to be sensitive to both the increase in the computational accuracy and the increase in the chain length of the system.

(11) MOLCAS, Version 3; Andersson, K.; Blomberg, M. R. A.; Fülcher, M. P.; Kellö, V.; Lindh, R.; Malmqvist, P. Å.; Noga, J.; Olsen, J.; Roos, B. O.; Sadlej, A. J.; Siegbahn, P. E. M.; Urban, M.; Widmark, P.-O. University of Lund: Lund, Sweden, 1994.

Scheme 2



context has been discussed elsewhere.¹² An example of this type of electronic structure is shown in Scheme 2 for CI_2 or CI_3 . In this case, in the system with six active orbitals, two electrons are fully coupled in the Si-CH₃ σ -bond, leaving the two possible spin couplings for the remaining four electrons. Thus the driving force which controls the generation of ground-state photoproducts is expected to be provided by recoupling these four electrons in the partly fragmented bonds that occur when the system decays. Thus, as the system begins to relax on the ground-state potential energy surface, the wave function rapidly loses its tetraradical character as the electrons recouple, and the associated bond formation provides the driving force for ground-state relaxation. The different ground-state channels originating from the decay points are located along coordinates which describe the evolution of the molecular structure of the system during electron recoupling.

The different photodegradation modes of polysilanes can thus be correlated with various recoupling schemes

(12) Bernardi, F.; Olivucci, M.; Robb, M. A. *Isr. J. Chem.* **1993**, *33*, 265.

as illustrated in Figure 2. In each case, one pair of electrons are fully coupled and the remaining four electrons can be recoupled. For the case of CI_1 , we are close to the starting geometry (that of the ground-state minimum) and we are in a high-energy region. Route **a** leads to production of silylene **2** via recoupling of electrons 1,4 and 3,5, and with chain cleavage via $\cdot CH_3$ radical 1,2 shift (coupling of electrons 2,6). The route **b** corresponds to the same mechanism but without the $-CH_3$ migration and yields the Si radicals **3** (recoupling of electrons 2,3 and 5,6). Routes **c** and **d** lead to complete fragmentation and suggest the same silylene products **1** and **2** with the formation of $\cdot CH_3$ and $\cdot SiH_3$ radicals. The shorter distance between the SiH_3 centers in CI_3 suggests that silylene **1** is the most probable photoproduct from this decay point. Conversely, the pair of radicals **3** are more easily formed from CI_1 due to the larger Si-Si separation which makes a recoupling of electrons 1,4 (route **b**) less likely. Finally CI_2 results to be an intermediate point in the direction of the recoupling scheme of CI_3 . It suggests two recoupling routes, **a** and **b**, respectively, leading to silylene **1** and Si radicals **3**.

The electronic nature of the conical intersections found in this study is not expected to change much upon proceeding to longer Si chains. In analogy with polyenes,¹³ for long enough chains, critical points can appear in the excited state, and therefore we can expect that there will be barriers that may separate minima from the conical intersection region. We expect also that these barriers are larger for the high-energy region, and therefore the lower energy conical intersections such as CI_2 and CI_3 can become more relevant.

Conclusions

Our results reported above provide an improved mechanistic insight in the singlet photodegradation of polysilanes. The avoided crossings first located by Michl et al.¹ turn out to be points of real crossing (when fully geometry optimization is performed). Thus the reaction mechanism involves fully efficient radiationless decay in the vicinity of the points of the crossing region.

(13) (a) Olivucci, M.; Ragazos, J. N.; Bernardi, F.; Robb, M. A. *J. Am. Chem. Soc.* **1993**, *115*, 3710. (b) Olivucci, M.; Bernardi, F.; Celani, P.; Ragazos, J. N.; Robb, M. A. *J. Am. Chem. Soc.* **1994**, *116*, 1077.

Consequently, the type, quantum yield, and wavelength dependence of the observed photoproducts will depend on the accessibility of these points after reactant photoexcitation. Extensive fragmentation is possible in the proximity of the CI_1 crossing point where the system decays with high energy. If the system evolves to the lowest energy channel, then the silylene **1** is the most probable photoproduct of the reaction. A second factor affecting photoproduct formation must be the geometrical structure of the system at the decay point. This structure affects the initial electron-recoupling process which necessarily occurs soon after the ground-state relaxation begins. While we expect the main features of the crossing surface to be invariant to detailed structure of individual polysilanes, the degree of the accessibility of the various points on it must depend on their relative stability⁴ and on the details of the reactant evolution through different potential energy surfaces after photoexcitation. As previously suggested,⁴ the chain length of the system may affect the accessibility by changing the energy gap between the singlet states involved in the reaction.

The mechanism for photodegradation suggested in the present paper shows that all types of photoproducts can be obtained through the $(n - 2)$ -dimensional conical intersections between the excited S_1 and the ground S_0 states. In particular also the Si radicals **3** can be obtained in this way and not only through an intersystem crossing between the S_1 and the T_1 repulsive states, as suggested in ref 4.

Acknowledgment. This research has been supported in part by the SERC (U.K.) under Grant No. GR/J 25123 and GR/H 58070. All calculations were run on an IBM RISC 6000 at I.Co.C.E.A and at King's College.

Supporting Information Available: Full set of the state-averaged CAS-SCF/6-31G* optimized Cartesian coordinates (\AA) and CAS-SCF/6-31G* and CASPT2N/6-31G**//CAS-SCF/6-31G* absolute energies (au) for the conical intersection structures (CI_1 , CI_2 , CI_3 , and CF) discussed in the paper (3 pages). Ordering information is given on any current masthead page.

OM950129V

A New, Convenient Synthetic Route to Tetramethylethano-Bridged Chromocene Complexes

David Ming Jin Foo and Pamela Shapiro*

Department of Chemistry, University of Idaho, Moscow, Idaho 83844-2343

Received June 26, 1995*

Summary: The reaction of $(\text{CH}_3)_4\text{C}_2[\eta^5\text{-C}_5\text{H}_4]_2\text{Ca}$ with CrCl_2 in the presence of 1 equiv of *tert*-butyl isocyanide affords $(\text{CH}_3)_4\text{C}_2[\eta^5\text{-C}_5\text{H}_4]_2\text{Cr}(\text{C}\equiv\text{NtBu})$, offering a new and convenient synthetic entry into this *ansa*-chromocene system. The isocyanide complex undergoes ligand substitution with CO to form the previously reported $(\text{CH}_3)_4\text{C}_2[\eta^5\text{-C}_5\text{H}_4]_2\text{CrCO}$, which may also be prepared by reacting $(\text{CH}_3)_4\text{C}_2[\eta^5\text{-C}_5\text{H}_4]_2\text{Ca}$ with CrCl_2 in the presence of an atmosphere of carbon monoxide.

Introduction

Since the discovery of ferrocene in the early 1950's, metallocene complexes have played a major role in the development of organotransition-metal chemistry. Bent-sandwich metallocene derivatives of group 3-6 metals have received the greatest amount of attention since a number of fundamentally interesting as well as synthetically useful reactions occur within the "equatorial wedge" of these electronically unsaturated bent-metalocene fragments. Conspicuously absent from this list, however, is the chemistry of bent-sandwich chromocene derivatives. Despite its electronic unsaturation, chromocene prefers a parallel ring geometry akin to that of ferrocene. It is resistant toward the coordination of ligands, such as carbon monoxide,¹ and readily undergoes ring loss upon incorporating additional ligands.² The strategy we have chosen to gain entry into the chemistry of bent-sandwich chromocene complexes is to constrain the geometry about the metal to be bent by linking the rings together with a short, heteroannular bridge. In addition to enforcing a bent geometry in the chromocene complexes, due to a chelation effect, the heteroannular bridge is expected to reduce the tendency of these complexes to undergo ring loss.

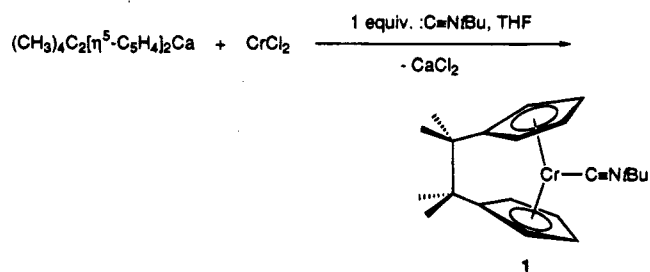
The effectiveness of using a heteroannular bridge to stabilize bent-sandwich chromocene complexes has already been demonstrated in the successful preparation of $(\text{CH}_3)_4\text{C}_2[\eta^5\text{-C}_5\text{H}_4]_2\text{CrCO}$ by Brintzinger and co-workers.³ In contrast to the parent chromocene carbonyl complex, the carbonyl adduct of this *ansa*-chromocene complex is quite stable. In fact, the carbon monoxide remains coordinated even upon one electron oxidation

of the complex.⁴ Encouraged by these results, we wished to explore the synthesis of additional derivatives of the tetramethylethanyl-bridged chromocene fragment. However, we sought a more facile synthetic entry into this system which would afford us with an adequate supply of starting material for pursuing further chemistry.

Results and Discussion

In our hands, the calcium metallocene $(\text{CH}_3)_4\text{C}_2[\eta^5\text{-C}_5\text{H}_4]_2\text{Ca}$ ⁵ recently reported by Edelman and co-workers is a more convenient and reliable reagent for the synthesis of the corresponding *ansa*-chromocene system than the di-Grignard $(\text{CH}_3)_4\text{C}_2[\eta^5\text{-C}_5\text{H}_4]_2\text{Mg}_2\text{Cl}_2\cdot\text{THF}$ ⁶ originally used by Brintzinger and co-workers. We find the calcium reagent to be more convenient since either commercially available CrCl_2 or material prepared by reducing $\text{CrCl}_3(\text{THF})_3$ *in situ* with zinc dust may be used with this reagent for the preparation of compounds **1** and **2**, whereas Brintzinger's method for preparing **2** calls for the use of $\text{CrCl}_2(\text{THF})_2$. We find the calcium metallocene to be more reliable since we are able to prepare it more consistently than the di-Grignard and our yields of compounds **1** and **2** have been consistently 30% and 40%, respectively, using this reagent. Our yields of **2** using the Brintzinger method were never better than 25% and were usually much worse.

Preparation of compound **1** is accomplished by simply combining the calcium metallocene with CrCl_2 in tetrahydrofuran in the presence of an equivalent amount of *tert*-butyl isocyanide (eq 1). Part of the loss in our



product yield may be attributed to the formation of an additional chromium species due to a persistent impurity in our preparations of $(\text{CH}_3)_4\text{C}_2[\eta^5\text{-C}_5\text{H}_4]_2\text{Ca}$. The impurity has been identified by ¹H NMR to be an isopropylcyclopentadienylcalcium species which probably arises from a proton abstraction by the dimethyl-

* Abstract published in *Advance ACS Abstracts*, September 15, 1995.

(1) (a) Wong, K. L. T.; Brintzinger, H. H. *J. Am. Chem. Soc.* **1975**, *97* (18), 5143. (b) Brintzinger, H. H.; Lohr, L. L.; Wong, K. L. T. *J. Am. Chem. Soc.* **1975**, *97*, 5146. (c) Simpson, K. M.; Rettig, M. F.; Wing, R. M. *Organometallics* **1992**, *11*, 4363.

(2) (a) Sneed, R. P. A. *Organochromium Compounds*; Academic Press: New York, 1975; p 171. (b) Davis, R.; Kane-Maguire, L. A. P. In *Comprehensive Organometallic Chemistry*; Wilkinson, G., Stone, F. G. A., Abel, E. W., Eds.; Pergamon: Oxford, U.K., 1982; Vol. 3, Chapter 26.2. (c) Chisholm, M. H.; Gallagher, T. D. *Syn. React. Inorg. Metal-Organ. Chem.* **1977**, *7* (3), 279. (d) Cotton, F. A.; Rice, G. W. *Inorg. Chim. Acta* **1978**, *27*, 75. (e) Kalousová, J.; Votinsky, J.; Klikorka, J.; Nádovnik, M. *J. Organomet. Chem.* **1980**, *184*, 351.

(3) Schwemlein, H.; Zsolnai, L.; Huttner, G.; Brintzinger, H. H. *J. Organomet. Chem.* **1983**, *256*, 285.

(4) van Raaij, E. U.; Monkeberg, S.; Kiesele, H.; Brintzinger, H. H. *J. Organomet. Chem.* **1988**, *356*, 307.

(5) Rieckhoff, M.; Pieper, U.; Stalke, D.; Edelman, F. T. *Angew. Chem., Int. Ed. Engl.* **1993**, *32*, 1079.

(6) Schwemlein, H.; Brintzinger, H. H. *J. Organomet. Chem.* **1983**, *254*, 69.

fulvenyl radical anion intermediate. Despite the use of rigorously dried solvents and dimethylfulvene, we have not been able to reduce this impurity below 25% of the total material as determined from the ^1H NMR integration. Nevertheless, the desired *ansa*-chromocene isonitrile complex may be isolated cleanly from the crude reaction product by fractional crystallization.

The ^1H NMR, ^{13}C NMR, and IR data for the compound are consistent with structure shown in eq 1. Although we have been unable to obtain X-ray-quality crystals of the compound, its molecular weight was determined to be 352 g/mol (theoretical: 347 g/mol) by ebulliometric methods, also confirming this structure. This result also indicates that dissociation of the isocyanide ligand from the metal does not occur to any appreciable extent in solution. The only other examples of stable, bent-sandwich chromocene isocyanide complexes reported to date are of the half-open chromocenes $(\text{C}_5\text{H}_5)(\text{C}_5\text{H}_7)\text{Cr}$ and $(\text{C}_5\text{H}_5)(\text{C}_7\text{H}_{11})\text{Cr}$.⁷

Compound **2** is prepared by reacting $(\text{CH}_3)_4\text{C}_2[\eta^5\text{-C}_5\text{H}_4]_2\text{Ca}$ with CrCl_2 in the presence of an atmosphere of carbon monoxide. Alternatively, this complex can be formed through substitution of the isocyanide ligand by carbon monoxide. An enhancement of the ^{13}C resonance of the carbonyl at δ 183.4 was observed when a benzene- d_6 solution of the *ansa*-chromocene carbonyl compound was placed under an atmosphere of ^{13}CO in a sealed NMR tube, indicating that carbonyl exchange occurs as well in this system.

We suspect that the prearrangement of the ligand in a metallocene geometry about the calcium assists in the transfer of the ligand to a single chromium center as opposed to two chromiums in these syntheses. Polymer formation, presumably due to bridging of the ligand between chromium centers, is encountered when these *ansa*-chromocene syntheses are carried out in the absence of a trapping ligand and appears to be the cause of our low yields of **2** when using the di-Grignard reagent. The higher solubility of the calcium reagent in tetrahydrofuran relative to the di-Grignard probably also contributes to its better performance. Our attempts to prepare the analogous *ansa*-chromocene methyl isocyanide, trimethylphosphine, and trifluorophosphine complexes have been unsuccessful. The stability of the *ansa*-chromocene compound appears to be highly sensitive to the nature of the ligand in the equatorial wedge.

Summary

In summary, we have discovered a more convenient and reliable synthetic entry into tetramethylethanyl-bridged metallocene complexes of Cr(II) involving the use of the corresponding calcium *ansa*-metallocene as a ligand source. Besides carbon monoxide and *tert*-butyl isocyanide, we wish to introduce hydride, alkyl, oxo, imido, and other formally oxidizing ligands into the equatorial wedge of this *ansa*-chromocene system. The fact that chromium has been able to assume +3 and +4 oxidation states when sandwiched between cyclopentadienyl-like carborane rings⁸ suggests the possibility of such higher oxidation state *ansa*-chromocene derivatives. We are interested in these derivatives as

potential catalysts for olefin oxidation and olefin polymerization, among other uses. We also intend to introduce other types of bridges between the cyclopentadienyl rings of the chromocene. For best results, chelated ligand transfer reagents similar to the calcium metallocene will be employed in these synthetic efforts.

Experimental Section

General Considerations. All manipulations were performed using a combination of glovebox, high-vacuum, or Schlenk techniques. All solvents were distilled under nitrogen over sodium benzophenone ketyl (THF) or CaH_2 (petroleum ether, hexane). The solvents were then stored in line-pots from which they were vacuum transferred from sodium benzophenone ketyl or cannulated directly. Benzene- d_6 was dried over activated 4 Å molecular sieves. Argon was purified by passage over oxy tower BASF catalyst (Aldrich) and 4 Å molecular sieves. *tert*-Butyl isocyanide, CaCl_2 , and zinc dust were used as received from Aldrich. $(\text{CH}_3)_4\text{C}_2[\eta^5\text{-C}_5\text{H}_4]_2\text{Ca}$ ⁵ and $\text{CrCl}_3(\text{THF})_3$ ⁹ were prepared as described in the literature.

NMR spectra were recorded on an IBM NR-300 (300.13 MHz ^1H , 74.43 MHz ^{13}C) and an IBM NR-200 (200.13 MHz ^1H , 50.327 MHz ^{13}C). All chemical shifts are reported in ppm and referenced to solvent. IR spectra were obtained on a Perkin-Elmer 1310 spectrophotometer. Elemental analyses were determined by Desert Analytics.

$(\text{CH}_3)_4\text{C}_2[\eta^5\text{-C}_5\text{H}_4]_2\text{Cr}(\text{C}\equiv\text{NtBu})$ (1). Method a. Tetrahydrofuran (70 mL) and *tert*-butyl isocyanide (0.33 mL, 2.9 mmol) were added to a flask containing $(\text{CH}_3)_4\text{C}_2[\eta^5\text{-C}_5\text{H}_4]_2\text{Ca}$ (0.72 g, 2.8 mmol) and CrCl_2 (0.35 g, 2.8 mmol) and cooled at -78°C . The reaction mixture was allowed to warm gradually to room temperature, and the resulting burgundy red solution was stirred for 12 h. The volatiles were removed *in vacuo*, and the residue was taken up in ca. 30 mL of petroleum and filtered to removed the CaCl_2 , which was washed repeatedly with petroleum ether to extract the soluble reaction product. Concentrating and cooling the filtrate at -78°C afforded the desired product as a red-brown solid (yield: 0.31 g, 30%).

Method b. Tetrahydrofuran (75 mL) was added to a flask containing the combined solids of $\text{CrCl}_3(\text{THF})_3$ (0.51 g, 1.4 mmol) and zinc dust (0.10 g, 1.5 mmol) and cooled at -78°C . The reaction mixture was allowed to warm slowly over 4 h to room temperature, producing a light blue slurry. The slurry was cannulated into a second flask cooled at -78°C and containing $(\text{CH}_3)_4\text{C}_2[\eta^5\text{-C}_5\text{H}_4]_2\text{Ca}$ (0.35 g, 1.4 mmol). After *tert*-butyl isocyanide (0.20 mL, 1.8 mmol) was admitted to the flask, the reaction mixture was allowed to warm slowly with constant stirring to room temperature. The reaction was stirred for another 12 h at room temperature. The resulting burgundy red solution was then dried under vacuum. The reaction residue was taken up in ca. 30 mL of petroleum and filtered to removed the CaCl_2 and excess zinc dust, which were washed repeatedly with petroleum ether to extract the soluble reaction product. Concentration of the filtrate and cooling to -78°C afforded 0.12 g of **1** (yield: 25%). ^1H NMR (C_6D_6): δ 4.61, 3.95 (m, 8H, C_5H_4), 1.21 (s, 12H, $\text{C}_2(\text{CH}_3)_4$), 1.01 (s, 9H, $\{\text{CH}_3\}_3\text{-CNC}$). ^{13}C NMR (C_6D_6): δ 206.8 ($\{\text{CH}_3\}_3\text{CNC}$), 79.9, 75.2 (C_5H_4), 31.2 ($\text{C}_2(\text{CH}_3)_4$), 27.4 ($\{\text{CH}_3\}_3\text{CNC}$). IR (KBr plates, Nujol mull, cm^{-1}): 1835 ($\nu(\text{C}\equiv\text{N})$). Anal. Calcd for $\text{C}_{21}\text{H}_{28}\text{-CrN}$: C, 72.59; H, 8.41; N, 4.03. Found: C, 72.61; H, 8.55; N, 3.90.

$(\text{CH}_3)_4\text{C}_2[\eta^5\text{-C}_5\text{H}_4]_2\text{Cr}(\text{C}\equiv\text{NtBu})$ (2). Method a. An atmosphere of carbon monoxide was admitted to a flask containing $(\text{CH}_3)_4\text{C}_2[\eta^5\text{-C}_5\text{H}_4]_2\text{Ca}$ (0.50 g, 2.0 mmol) and CrCl_2 (0.24 g, 2.0 mmol) in 50 mL of tetrahydrofuran cooled at -78°C . The reaction mixture turned from green to red as it was allowed to warm to room temperature over 4 h, and the reaction was stirred at room temperature overnight. The

(7) Freeman, J. W.; Hallinan, N. C.; Arif, A. M.; Gedridge, R. W.; Ernst, R. D.; Basolo, F. *J. Am. Chem. Soc.* **1991**, *113*, 6509.

(8) Oki, A. R.; Zhang, H.; Maguire, J. A.; Hosmane, N. S.; Ro, H.; Hatfield, W. E. *Organometallics* **1991**, *10*, 2996.

volatiles were removed *in vacuo*, and the residue was taken up in *ca.* 20 mL of hexane and filtered to removed the CaCl_2 , which was washed repeatedly with hexane to extract the soluble reaction product. Concentrating and cooling the filtrate at -78°C afforded **2** as a red precipitate (yield: 0.23 g, 40%). The ^1H and ^{13}C NMR data for the compound were consistent with that reported in ref 3.

Method b. A solution of **1** (0.50 g, 1.4 mmol) in petroleum ether (50 mL) was stirred for 12 h under an atmosphere of carbon monoxide. The solution was concentrated to 20 mL and cooled to -78°C to afford $(\text{CH}_3)_4\text{C}_2[\eta^5\text{-C}_5\text{H}_4]_2\text{CrCO}$ as a

red powder (0.18 g, 45%). The identity of the compound was established by comparison of its benzene- d_6 ^1H NMR spectrum with that of compound which was prepared as originally reported in ref 3.

Acknowledgment. Financial support from the University of Idaho and from the donors of the Petroleum Research Fund, administered by the American Chemical Society, is gratefully acknowledged.

OM9504967

Geometry of the SiOCN Linkage. Crystal Structure of $(\text{Me}_3\text{Si})_2(\text{PhMe}_2\text{Si})\text{CSiMe}_2\text{OCN}$

G. Adefikayo Ayoko, Colin Eaborn,* and Peter B. Hitchcock

School of Chemistry and Molecular Sciences, University of Sussex, Brighton BN1 9QJ, U.K.

Received May 25, 1995[®]

Summary: The first accurate determination of the structure of a silicon cyanate has yielded the following parameters for the SiOCN linkage: $d(\text{Si}-\text{O})$, 1.738(3) Å; $d(\text{O}-\text{C})$, 1.250(5) Å; $d(\text{C}-\text{N})$, 1.163(6) Å; $\angle\text{Si}-\text{O}-\text{C}$, 126.7(3)°; $\angle\text{N}-\text{C}-\text{O}$, 176.5(5)°.

Until now no accurate experimental information has been available on the geometry of the SiOCN linkage, though ab initio calculations were recently carried out for H_3SiOCN .¹ The first silicon cyanate, $(\text{Me}_3\text{Si})_3\text{CSiMe}_2\text{OCN}$, was isolated in 1982,² and its chemical properties and those of some related cyanates have been studied,³ but its crystals did not yield significant X-ray diffraction data, probably because the near-spherical shape of the molecule gives rise to plastic crystal behavior. We recently obtained approximate data for the compound $(\text{Me}_3\text{Si})_2(\text{Ph}_2\text{MeSi})\text{CSiMe}_2\text{OCN}$ (as a methylcyclohexane solvate), but serious disorder in the crystal meant that only an approximate estimate ($124 \pm 6^\circ$) could be given for the most interesting parameter, the angle $\text{Si}-\text{O}-\text{C}$.⁴ We have now obtained good-quality data for the title compound, **1**, as described below.

Compound **1** was made by treatment of the corresponding iodide $(\text{Me}_3\text{Si})_2(\text{PhMe}_2\text{Si})\text{CSiMe}_2\text{I}$ with AgOCN in CH_2Cl_2 . A single-crystal X-ray diffraction study at low temperature showed it to have the structure depicted in Figure 1. Atomic coordinates are shown in Table 1 and relevant bond lengths and angles for the SiOCN linkage in Table 2, along with the less accurate data previously obtained for $(\text{Me}_3\text{Si})_2(\text{Ph}_2\text{MeSi})\text{CSiMe}_2\text{OCN}$ (**2**) and those calculated for H_3SiOCN .¹



1



2

It can be seen that the value of the $\text{Si}-\text{O}-\text{C}$ angle, 126.7(3)°, is in reasonable agreement with that calculated for H_3SiOCN .¹ (In contrast, the calculated equilibrium value, 179.88°,¹ for the $\text{Si}-\text{N}-\text{C}$ angle in H_3SiNCO is markedly different from the available experimental values for solid silicon isocyanates, including H_3SiNCO , which all fall within the range 155.5–163°.^{4,5} However, the calculated potential energy curve for the the $\text{Si}-\text{N}-\text{C}$ bond is flat near the minimum and

Table 1. Atomic Coordinates ($\times 10^4$) and Equivalent Isotropic Displacement Parameters ($\text{\AA}^2 \times 10^3$) for **1**

	<i>x</i>	<i>y</i>	<i>z</i>	<i>U</i> (eq)
Si(1)	3438(1)	1076(1)	514(1)	23(1)
Si(2)	3654(1)	62(1)	2122(1)	20(1)
Si(3)	3104(1)	-1099(1)	585(1)	23(1)
Si(4)	6122(1)	-145(1)	902(1)	24(1)
O	4012(3)	2027(2)	1086(2)	30(1)
N	3183(6)	3672(3)	1073(3)	57(1)
C(1)	3580(5)	2879(3)	1058(2)	29(1)
C(2)	1843(4)	617(3)	2372(2)	23(1)
C(3)	1678(5)	1611(3)	2418(3)	32(1)
C(4)	376(6)	2020(4)	2648(3)	39(1)
C(5)	-755(5)	1443(4)	2857(3)	39(1)
C(6)	-618(5)	460(4)	2845(3)	34(1)
C(7)	679(4)	55(3)	2605(2)	27(1)
C(8)	4058(4)	-16(3)	1043(2)	17(1)
C(9)	1465(5)	1239(3)	415(3)	35(1)
C(10)	4255(5)	1343(3)	-434(2)	31(1)
C(11)	3652(5)	-1155(3)	2600(2)	30(1)
C(12)	4988(5)	824(3)	2650(3)	32(1)
C(13)	1193(4)	-1230(3)	921(2)	29(1)
C(14)	2940(5)	-1019(4)	-486(2)	34(1)
C(15)	4041(5)	-2267(3)	801(3)	33(1)
C(16)	6964(5)	-1012(3)	1590(3)	32(1)
C(17)	7099(4)	1029(3)	1003(3)	33(1)
C(18)	6610(5)	-620(3)	-71(3)	33(1)

^a *U*(eq) is defined as one-third of the trace of the orthogonalized U_{ij} tensor.

Table 2. Bond Lengths (Å) and Angles (deg) for the SiOCN Linkage in **1 and **2** and Calculated Values for That in H_3SiOCN**

	1	2	H_3SiOCN ¹
Si-O	1.738(3)	1.756(10)	1.720
O-C	1.250(5)	1.27(2)	1.300
C-N	1.163(6)	1.12(2)	1.185
Si-O-C	126.7(3)	124 ± 6	120.43
O-C-N	176.5(5)	175(1)	178.43

so the results of the calculations cannot be regarded as inconsistent with the experimental observations.) Like the $\text{N}-\text{C}-\text{O}$ linkage in isocyanates,⁴ the $\text{O}-\text{C}-\text{N}$ linkage in **1** is not quite linear.

The $\text{Si}-\text{O}$ bond in **1** (1.738(3) Å) is notably long, the great majority of $\text{Si}-\text{O}$ bonds having lengths of < 1.68 Å,⁶ but it is comparable with those in the *p*-toluenesulfonate $(\text{Me}_3\text{Si})_3\text{CSiPh}(\text{H})(\text{OSO}_2\text{C}_6\text{H}_4\text{Me}-p)$ (1.717(8) Å),⁷ the trifluoroacetate $(\text{Me}_3\text{Si})_3\text{CSi}(\text{OH})_2\text{OCOCF}_3$ (1.716(6) Å),⁸ and particularly the perchlorate $\text{Ph}_3\text{SiOCIO}_3$ (1.744(4) Å).⁹ It is of interest that the leaving-group abilities of OCIO_3 and OCN are exceptionally high and are rather similar to one another in solvolysis of

(6) Lukevics, E.; Pudova, O.; Sturkovich, R. *Molecular Structure of Organosilicon Compounds*; Horwood: Chichester, U.K., 1989; pp 175–220.

(7) Al-Juaid, S. S.; Al-Nasr, A. A. K.; Eaborn, C.; Hitchcock, P. B. *J. Organomet. Chem.* **1993**, *455*, 57.

(8) Al-Juaid, S. S.; Eaborn, C.; Hitchcock, P. B. *J. Organomet. Chem.* **1992**, *423*, 5.

[®] Abstract published in *Advance ACS Abstracts*, August 1, 1995.

(1) Fehér, M.; Pasinszki, T.; Veszprémi, T. *J. Phys. Chem.* **1993**, *97*, 1538.

(2) Eaborn, C.; Lickiss, P. D.; Marquina-Chidsey, G.; Thorli, E. Y. *J. Chem. Soc., Chem. Commun.* **1982**, 1326.

(3) Eaborn, C.; El-Kaddar, Y. Y.; Lickiss, P. D. *Inorg. Chim. Acta* **1992**, *198–200*, 337. El-Kaddar, Y. Y.; Eaborn, C.; Lickiss, P. D.; Reed, D. E. *J. Chem. Soc., Perkin Trans. 2* **1992**, 1753.

(4) Al-Juaid, S. S.; Al-Nasr, A. A. K.; Ayoko, G. A.; Eaborn, C.; Hitchcock, P. B. *J. Organomet. Chem.* **1995**, *488*, 155.

(5) Glidewell, C.; Robiette, A. G.; Sheldrick, G. M. *Chem. Phys. Lett.* **1972**, *16*, 526.

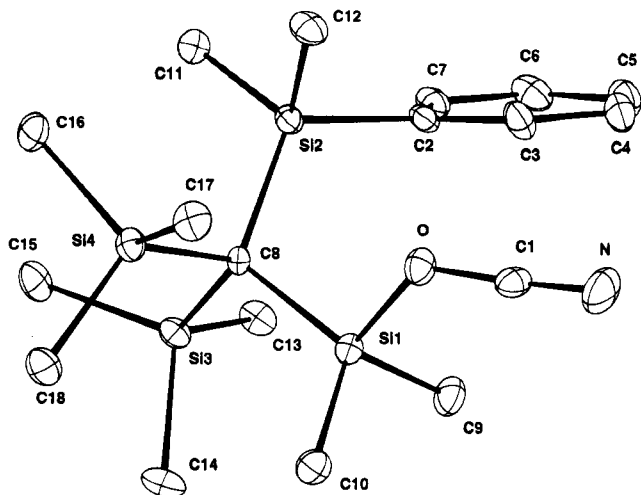


Figure 1. Molecular structure of **1** with atom numbering.

compounds of the type $(\text{Me}_3\text{Si})_3\text{CSiMe}_2\text{X}$,¹⁰ and it is reasonable to associate this with the long and similar lengths of the Si–OCIO₃ and Si–OCN bonds.

It could be argued that the geometry of the SiOCN linkage in **1** may be somewhat affected by the crowding in the molecule, but we note that there is no significant change in the parameters for the SiNCO linkage on going from H₃SiNCO to the highly crowded compound $(\text{PhMe}_2\text{Si})_3\text{CSiMe}_2\text{NCO}$.⁴ In any case it is unlikely that data will become available in the foreseeable future for simple cyanates such as H₃SiOCN, Me₃SiOCN, and Ph₃SiOCN, since even if they could be generated they would probably isomerize rapidly to the isocyanates.

It is noteworthy that the geometry of the OCN group in **1** is fairly similar to that in a representative aryl cyanate, 4-chloro-3,5-dimethylphenyl cyanate, for which the relevant bond lengths and angles are as follows: O–C, 1.27 Å; C–N, 1.14 Å; C–O–C, 118.3°; O–C–N, 173.5°.¹¹

Other features of the structure of **1**, viz. large C(8)–Si(1)–C(9) and C(8)–Si(1)–C(10) angles (mean 117.6°), small O–Si(1)–C(9) and O–Si(1)–C(10) angles (mean 104.4°), and long C(8)–Si(2), C(8)–Si(3), and C(8)–Si(4) bonds (mean 1.928 Å), can be attributed mainly to

steric effects of and within the bulky $(\text{Me}_3\text{Si})_2(\text{PhMe}_2\text{Si})\text{C}$ group.¹²

Experimental Section

A mixture of $(\text{Me}_3\text{Si})_2(\text{PhMe}_2\text{Si})\text{CSiMe}_2\text{I}^{13}$ (0.30 g) and AgOCN (0.15 g) in CH₂Cl₂ (20 mL) was stirred for 2 h at room temperature and then filtered. The solvent was evaporated from the filtrate, and the residue was recrystallized from pentane to give $(\text{Me}_3\text{Si})_2(\text{PhMe}_2\text{Si})\text{CSiMe}_2\text{OCN}$ (0.20 g, 81%). ¹H NMR (CDCl₃): δ 0.30 (s, SiMe₃), 0.43 (s, SiMe₂O), 0.62 (s, SiMe₂Ph) and 5.3–7.8 (m, Ph). MS (EI): *m/z* 393 (7%, M⁺), 378 (25%, M – Me), 73 (100, SiMe₃). Recrystallization from heptane gave crystals suitable for the X-ray diffraction study.

Structure Determination. Crystal data: C₁₈H₃₅NOSi₄, *M_r* = 393.8, orthorhombic, space group *P*2₁2₁2₁ (No. 19), *a* = 9.300(2) Å, *b* = 13.888(5) Å, *c* = 17.411(4) Å, *V* = 2248.8 Å³, *Z* = 4, *D_c* = 1.16 g cm⁻³, *F*(000) = 856, Mo Kα radiation, λ = 0.710 73 Å, μ = 2.7 cm⁻¹. Data were collected on a CAD diffractometer at 173 K from a crystal of size 0.40 × 0.30 × 0.25 mm; 3055 reflections with 2 < θ < 28° were collected, and all were used for the structure analysis. Refinement was by full-matrix least squares based on *F*² with anisotropic temperature factors for non-hydrogen atoms and with hydrogen atoms in the riding mode with *U*_{iso} = 1.2[*U*_{eq}(C)]. Methyl groups were fixed at idealized geometry but with the torsion angle defining the H atom positions refined. The absolute structure was determined by refinement of the Flack parameter.¹⁴ Final *R* indices for 2532 data with *I* > 2σ(*I*) were *R*1 = 0.048, *wR*2 = 0.111 and for all data were *R*1 = 0.065 and *wR*2 = 0.122. The SHELXS-86 program was used for the structure solution, the SHELXL-93 program¹⁵ for the structure refinement, and the CAMERON program¹⁶ for the molecular diagram.

Acknowledgment. We thank the SERC (now EPSRC) for support and the University of Papua New Guinea for granting research leave to G.A.A.

Supporting Information Available: Tables of crystal data and structure refinement details, atomic coordinates, bond lengths and angles, and anisotropic displacement parameters (7 pages). Ordering information is given on any current masthead page.

OM950388K

(12) See, e.g.: Eaborn, C.; Hitchcock, P. B.; Lickiss, P. D. *J. Organomet. Chem.* **1981**, *271*, 13. Eaborn, C.; El-Kheli, M. N. A.; Hitchcock, P. B.; Smith, J. D. *J. Organomet. Chem.* **1984**, *272*, 1. Al-Juaid, S. S.; Dhaher, S. M.; Eaborn, C.; Hitchcock, P. B.; Smith, J. D. *J. Organomet. Chem.* **1985**, *325*, 117.

(13) Eaborn, C.; Jones, K. L.; Lickiss, P. D. *J. Organomet. Chem.* **1994**, *466*, 35.

(14) Flack, H. D. *Acta Crystallogr.* **1983**, *A39*, 876.

(15) Sheldrick, G. M. SHELX-93: Program for Crystal Structure Refinement; University of Göttingen, Göttingen, Germany, 1993.

(16) Pearce, L. J.; Watkins, D. J. CAMERON, An Interactive Graphics Editor; University of Oxford, Oxford, U.K., 1992.

(9) Prakash, G. K. S.; Keyaniyan, S.; Anisfeld, R.; Heiliger, L.; Olah, G. A.; Stevens, R. C.; Choi, H.-K.; Bau, R. *J. Am. Chem. Soc.* **1987**, *109*, 5123.

(10) El-Kaddar, Y. Y.; Eaborn, C.; Lickiss, P. D.; Reed, D. E. *J. Chem. Soc., Perkin Trans. 2* **1992**, 1753.

(11) Kutshabsky, L.; Schrauber, H. *Z. Chem.* **1971**, *11*, 347; *Krist. Tech.* **1973**, *8*, 217.

Reactions of Methoxyallene and of Phenylallene with $\text{RhH}(\text{CO})(\text{PPh}_3)_3$. Insertion of a C=C Bond into an Rh-H Bond, Giving $(\pi\text{-Allyl})\text{rhodium}(\text{I})$ Complexes

Kohtaro Osakada,* Jun-Chul Choi, Take-aki Koizumi, Isao Yamaguchi, and Takakazu Yamamoto*

Research Laboratory of Resources Utilization, Tokyo Institute of Technology, 4259 Nagatsuta, Midori-ku, Yokohama 226, Japan

Received May 15, 1995[®]

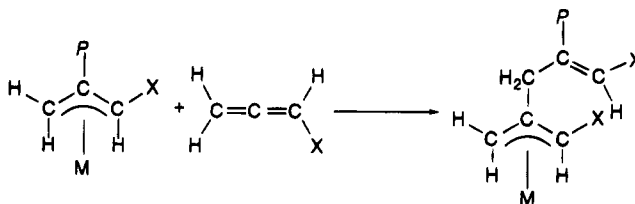
Summary: Methoxyallene and phenylallene react with $\text{RhH}(\text{CO})(\text{PPh}_3)_3$ to give $\text{Rh}(\eta^3\text{-CH}_2\text{CHCHOMe})(\text{CO})(\text{PPh}_3)_2$ (**1**) and $\text{Rh}(\eta^3\text{-CH}_2\text{CHCHPh})(\text{CO})(\text{PPh}_3)_2$ (**2**), respectively. X-ray crystallography shows molecular structures having an allylic ligand with syn OMe and Ph groups. The complexes undergo exchange of two CH_2 allylic hydrogens on the NMR time scale through $\pi\text{-}\sigma\text{-}\pi$ rearrangement of the ligand. NMR studies on reaction mixtures of phenylallene and $\text{RhD}(\text{CO})(\text{PPh}_3)_3$ as well as of **2** and $\text{RhD}(\text{CO})(\text{PPh}_3)_3$ reveal irreversible insertion of a C=C bond of phenylallene into an Rh-H or Rh-D bond to give **2**.

Introduction

Several organotransition-metal complexes catalyze polymerization¹ of allene and substituted allene to give polymers having unique $-\text{C}(\text{=CH}_2)-$ or $-\text{C}(\text{=CHR})-$ structural units in the main chain as well as syntheses of cyclic oligomers of these substrates.² $(\pi\text{-Allyl})\text{nickel}(\text{II})$ and $-\text{palladium}(\text{II})$ complexes are active catalysts for polymerization of monosubstituted allene to give products with high molecular weight or narrow polydispersity.^{1c,d} The reaction is believed to proceed through repeated insertion of a double bond of allene into the bond between the metal center and the π -allylic end of the polymer chain (Scheme 1), because π -allyl complexes initiate the polymerization and also because a $(\pi\text{-allyl})\text{-nickel}$ complex catalyzes the living polymerization of alkoxyallene with almost quantitative catalyst efficiency.^{1d}

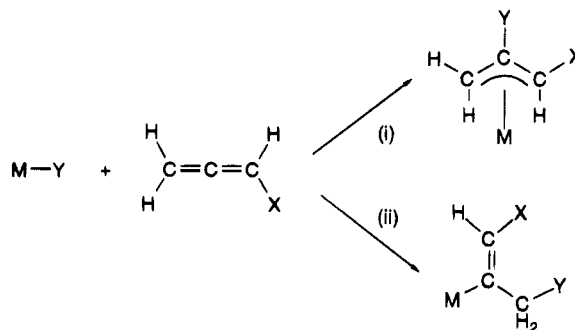
Organorhodium(I) complexes also catalyze polymerization and oligomerization of allene.^{1b,2b,e} Stoichiometric reaction of allene with $\text{RhH}(\text{CO})(\text{PPh}_3)_3$ was briefly reported to give $\text{Rh}(\eta^3\text{-C}_3\text{H}_5)(\text{CO})(\text{PPh}_3)_2$ ³ through insertion of a double bond into the Rh-H bond. Low stability of the $(\pi\text{-allyl})\text{rhodium}$ product prevents a further investigation into the crystal structure of the complex

Scheme 1. Proposed Mechanism for Polymerization of Monosubstituted Allene Catalyzed by $(\pi\text{-Allyl})\text{nickel}(\text{II})$ and $-\text{palladium}(\text{II})$ Complexes^a



^a P = polymer chain.

Scheme 2. Possible Pathways for Insertion of Allene into an M-Y Bond



as well as that on the detailed pathway of the reaction. Studies on the insertion of a double bond of allene into an M-X bond to give a π -allylic complex (path i in Scheme 2),⁴ including the above reaction with $\text{RhH}(\text{CO})(\text{PPh}_3)_3$, seem to leave several mechanistic issues unclarified, such as whether the reaction gives rise to a minor amount of vinylic complexes through insertion in another direction (path ii in Scheme 2) and whether the insertion of a double bond is reversible.

In this paper we report the results of reaction of monosubstituted allenes with $\text{RhH}(\text{CO})(\text{PPh}_3)_3$ to give stable Rh complexes with π -allylic ligands. Full characterizations of the products and deuterium labeling experiments to reveal mechanistic details of the reaction as well as further reaction of the $(\pi\text{-allyl})\text{rhodium}$ complex with phenylallene are also described.

(4) (a) Powell, P. Synthesis of $\eta^3\text{-Allyl}$ Complexes. In *The Chemistry of the Metal-Carbon Bond*; Hartley, F. R., Patai, S., Eds.; Wiley: New York, 1982; pp 355-357. (b) Deeming, J. A.; Johnson, B. F. G.; Lewis, J. J. *J. Chem. Soc. D* **1970**, 598. (c) Chisholm, M. H.; Johns, W. S. *Inorg. Chem.* **1975**, *14*, 1189. (d) Stevens, R. R.; Shier, G. D. *J. Organomet. Chem.* **1970**, *21*, 495. (e) Hughes, R. P.; Powell, J. J. *J. Organomet. Chem.* **1972**, *34*, C51. (f) Hughes, R. P.; Powell, J. J. *J. Organomet. Chem.* **1973**, *60*, 409. (g) May, C. J.; Powell, J. J. *J. Organomet. Chem.* **1980**, *184*, 385.

[®] Abstract published in *Advance ACS Abstracts*, September 1, 1995.

(1) (a) Otsuka, S.; Mori, K.; Iwazumi, F. *J. Am. Chem. Soc.* **1965**, *87*, 3017. (b) Otsuka, S.; Nakamura, A. *J. Polym. Sci., Polym. Lett. Ed.* **1967**, *5*, 973. (c) Ghalamkar-Moazzam, M.; Jacobs, T. L. *J. Polym. Sci., Polym. Chem. Ed.* **1978**, *16*, 615. (d) Tomita, I.; Kondo, Y.; Takagi, K.; Endo, T. *Macromolecules* **1994**, *27*, 4413.

(2) (a) Baker, R. *Chem. Rev.* **1973**, *73*, 487. (b) Otsuka, S.; Nakamura, A.; Minamida, H. *J. Chem. Soc. D* **1969**, 191. (c) Hoover, F. W.; Lindsney, R. V., Jr. *J. Org. Chem.* **1969**, *34*, 3051. (d) Scholten, J. P.; van der Ploeg, H. J. *Tetrahedron Lett.* **1972**, 1685. (e) Otsuka, S.; Nakamura, A.; Yamagata, T.; Tani, K. *J. Am. Chem. Soc.* **1972**, *94*, 1037. (f) Baker, G. K.; Green, M.; Howard, J. A. K.; Spencer, J. L.; Stone, F. G. A. *J. Chem. Soc., Dalton Trans.* **1978**, 1839. (g) Hegedus, L. S.; Kambe, N.; Tamura, R.; Woodgate, P. D. *Organometallics* **1983**, *2*, 1658.

(3) Brown, C. K.; Mowat, W.; Yagupsky, G.; Wilkinson, G. *J. Chem. Soc. A* **1971**, 850.

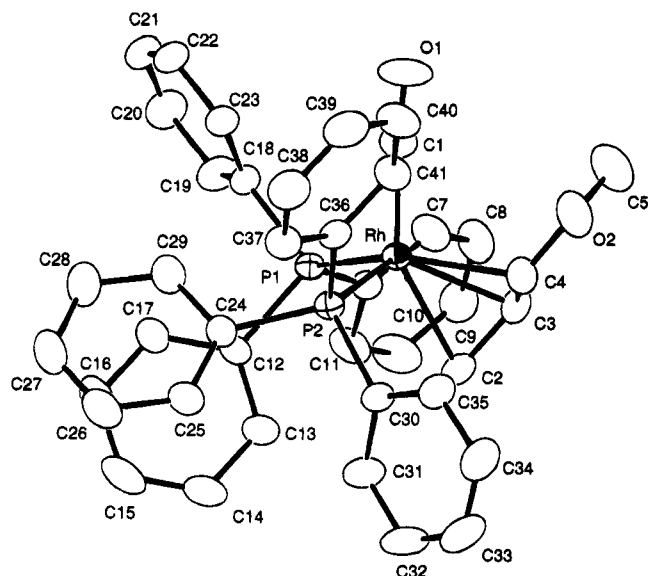
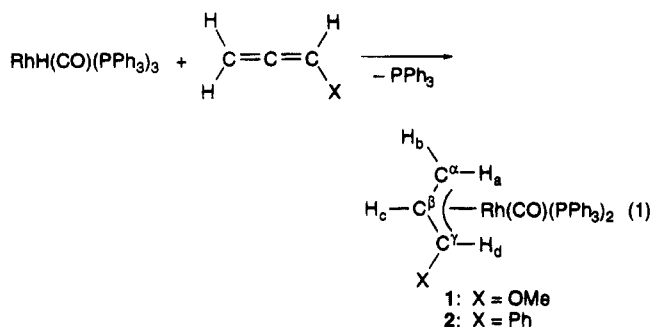


Figure 1. ORTEP drawing of **1** at the 50% ellipsoid level.

Results and Discussion

Reactions of methoxyallene and phenylallene with $\text{RhH}(\text{CO})(\text{PPh}_3)_3$ proceed smoothly to give the corresponding $(\pi\text{-allyl})\text{rhodium(I)}$ complexes $\text{Rh}(\eta^3\text{-CH}_2\text{-CHCHOMe})(\text{CO})(\text{PPh}_3)_2$ (**1**) and $\text{Rh}(\eta^3\text{-CH}_2\text{CHCHPh})(\text{CO})(\text{PPh}_3)_2$ (**2**), respectively.



Reactions of 1.2 equiv of phenylallene to the Rh complex at room temperature and of 3.0 equiv of phenylallene at -30°C result in formation of complex **2** in high yields, while the reaction of 3.0 equiv of phenylallene at room temperature is accompanied by formation of small amounts of uncharacterized Rh complexes and oligomers of the substrates formed probably from further reaction of **2** in the reaction mixture with phenylallene.

Molecular structures of **1** and **2** determined by X-ray crystallography are shown in Figures 1 and 2, respectively. Both complexes have structures quite similar to each other and contain one CO ligand, two PPh_3 ligands, and a π -allylic ligand with the usual Rh-P or Rh-C bond distances. The CO and PPh_3 ligands as well as central carbons of the allylic ligand constitute tetrahedral coordination around the Rh center. The allylic ligands of **1** and **2** have OMe and Ph substituents with syn orientations similar to many monosubstituted allyl complexes of transition metals. Selected bond distances and angles are summarized in Table 1. Two carbon-carbon bonds in the allylic ligand of **1** are similar to each other (1.407(5) Å and 1.393(5) Å), while the C3-C4 bond distance (1.404(5) Å) of **2** is significantly shorter than the C2-C3 bond distance (1.438(5)

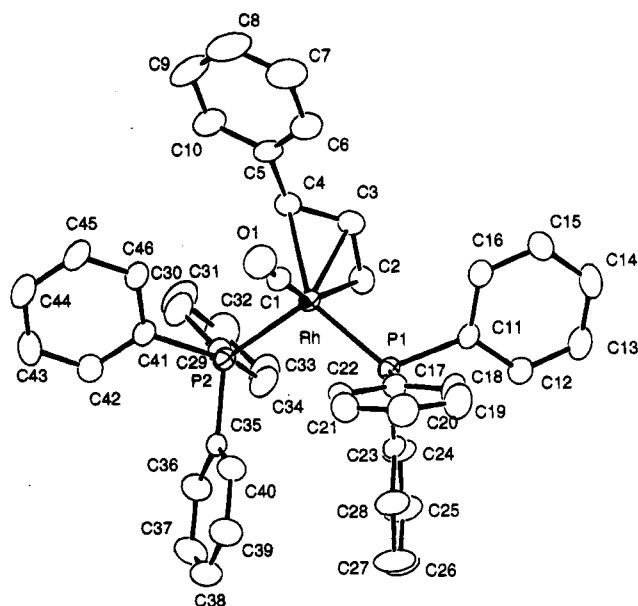


Figure 2. ORTEP drawing of **2** at the 50% ellipsoid level.

Table 1. Selected Bond Distances and Angles of **1** and **2**

	1	2
Distances (Å)		
Rh-P1	2.309(2)	2.306(1)
Rh-P2	2.399(1)	2.401(1)
Rh-C1	1.869(4)	1.876(4)
Rh-C2	2.179(4)	2.181(4)
Rh-C3	2.145(4)	2.132(4)
Rh-C4	2.233(4)	2.258(4)
C2-C3	1.407(5)	1.438(5)
C3-C4	1.393(5)	1.404(5)
C4-O2	1.379(4)	
O2-C5	1.392(5)	
C4-C5		1.484(5)
Angles (deg)		
P1-Rh-P2	109.69(4)	111.17(4)
P1-Rh-C1	97.7(1)	96.8(1)
P1-Rh-C2	90.2(1)	90.7(1)
P1-Rh-C3	111.6(1)	108.8(1)
P1-Rh-C4	148.6(1)	145.1(1)
P2-Rh-C1	106.7(1)	104.5(1)
P2-Rh-C2	99.5(1)	97.4(1)
P2-Rh-C3	117.8(1)	119.3(1)
P2-Rh-C4	93.3(1)	97.8(1)
C1-Rh-C2	148.1(2)	152.4(2)
C1-Rh-C3	111.5(2)	114.0(2)
C1-Rh-C4	95.7(2)	94.4(1)
C2-C3-C4	114.3(4)	116.0(4)
C3-C4-O2(C5)	125.6(4)	122.9(4)

Å). The difference between the Rh-C2 and Rh-C4 bond distances of **2** (0.077 Å) is larger than that of **1** (0.054 Å). The above difference in the structural parameters between **1** and **2** can be attributed to significant π -conjugation of the C3-C4 bond of **2** with a phenyl group on the allyl ligand.

Figure 3 shows the ^1H NMR spectra of **1** at 25°C and at -70°C . The signals due to two CH hydrogens of the allyl ligand, H_d and H_c , appear at 25°C as two multiplets at 4.63 and 4.45 ppm, respectively, while a broad peak due to CH_2 hydrogens is observed at 0.9 ppm. The ^1H NMR spectra as well as the $^{13}\text{C}\{^1\text{H}\}$ NMR spectrum, showing one set of the peaks due to allylic and OMe carbons, indicate the presence of a single isomer in the solution. It can be assigned to the isomer with a syn OMe substituent on the basis of the crystal structure of the complex. The peak at 0.9 ppm is

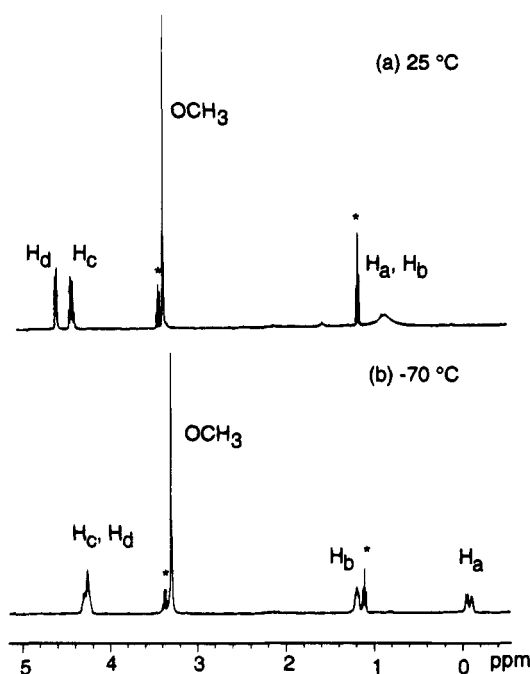


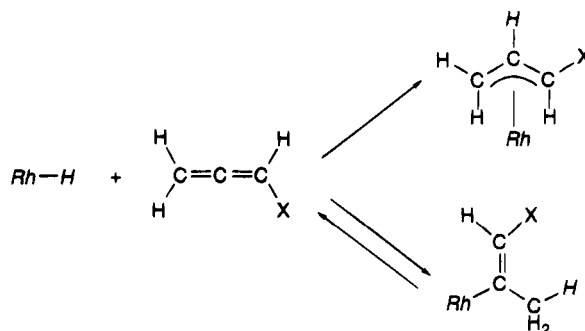
Figure 3. ^1H NMR (CD_2Cl_2 , 400 MHz) of **1** (a) at 25 °C and (b) at -70 °C. Peaks with asterisks are due to Et_2O contained in the sample.

separated into two signals at 1.20 and -0.08 ppm on cooling the solution to -70 °C. The temperature-dependent change of the NMR spectra is attributed to exchange of two CH_2 hydrogens through π - σ - π rearrangement of the allylic ligand on the NMR time scale. Although similar rearrangement through a (σ -1-methoxyallyl)rhodium intermediate would cause isomerization from a syn to an anti structure, the NMR spectra do not show peaks due to an anti isomer, indicating much lower stability of the structure than syn isomer. The ^1H and ^{13}C NMR spectra of **2** show peaks due to allylic hydrogens and carbons at positions similar to those of **1**. A $J(\text{H}_c\text{H}_d)$ value (9 Hz) larger than the $J(\text{H}_b\text{H}_c)$ value (6 Hz) at -70 °C indicates a syn orientation of the phenyl group in the allylic ligand unambiguously.

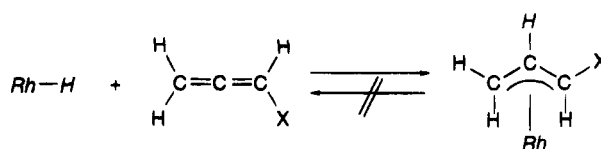
Although the insertion of a double bond of phenylallene and methoxyallene into an $\text{Rh}-\text{H}$ bond gives the π -allylic complex exclusively, the above results are not sufficient to exclude partial formation of a propenylrhodium complex at the initial stage of the reaction followed by its conversion into the final product through β -hydrogen elimination and reinsertion of a double bond into the $\text{Rh}-\text{H}$ bond (Scheme 3).

Previously we have revealed that allylic aryl sulfides react with $\text{RhH}(\text{PPh}_3)_4$ to undergo rapid and reversible insertion and deinsertion of the $\text{C}=\text{C}$ double bond into the $\text{Rh}-\text{H}$ bond.⁵ Facile or reversible β -hydrogen elimination of alkylrhodium complexes is very common also.⁶ In order to examine the reversibility of the insertion of a double bond of allene, deuterium labeling experiments were carried out by using $\text{RhD}(\text{CO})(\text{PPh}_3)_3$. Reactions of methoxyallene and of phenylallene with $\text{RhD}(\text{CO})(\text{PPh}_3)_3$ give $\text{Rh}(\eta^3\text{-CH}_2\text{CDHOME})(\text{CO})(\text{PPh}_3)_2$ (**1-d**) and $\text{Rh}(\eta^3\text{-CH}_2\text{CDCHPh})(\text{CO})(\text{PPh}_3)_2$ (**2-d**), respectively. Deuterium is incorporated exclusively at the

Scheme 3. Possible Scheme for the Reaction of Substituted Allene Involving Reversible Insertion and Deinsertion of a Double Bond



Scheme 4^a



^a $\text{Rh} = \text{Rh}(\text{CO})(\text{PPh}_3)_n$; $\text{X} = \text{OMe}, \text{Ph}$.

central carbon of the π -allyl ligand, as is confirmed by ^1H NMR spectra of the complexes showing no peak due to the central hydrogen as well as by the ^2H NMR spectrum of **2-d** showing a peak at 5.2 ppm at 25 °C. The appearance of the ^1H NMR peaks due to CHOME and CHPh hydrogens as singlets also indicates selective deuteration at the central carbon of the allylic ligand. Reaction of equimolar **2** and $\text{RhD}(\text{CO})(\text{PPh}_3)_3$ for 5 h at room temperature does not cause deuteration of allylic hydrogens of **2** at all, indicating that no liberation of phenylallene from **1** through deinsertion occurs under the conditions. All these results agree with Scheme 4, involving irreversible insertion of a double bond of methoxyallene and phenylallene into the $\text{Rh}-\text{H}$ bond to give (π -allyl)rhodium complexes.

The difference in reactivity toward deinsertion of a $\text{C}=\text{C}$ double bond between alkyl and π -allyl ligands bonded to a Rh center is attributed to high thermodynamic stability of π -allylic coordination preventing elimination of allene from a π -allylic ligand. A Ni complex having both ethyl and η^3 -allyl ligands, $\text{Ni}(\eta^3\text{-C}_3\text{H}_5)\text{Et}(\text{PPh}_3)$, causes β -hydrogen elimination of an ethyl ligand rather than degradation of the allyl ligand to give $\text{Ni}(\eta^3\text{-C}_3\text{H}_5)\text{H}(\text{PPh}_3)$, which undergoes subsequent coupling of hydrido and allyl ligands.⁷

Both $\text{RhH}(\text{CO})(\text{PPh}_3)_3$ and **2** show similar activities as catalysts for the polymerization of phenylallene. Reactions of phenylallene in the presence of 5 mol % of the complexes at 60 °C give a MeOH-insoluble off-white solid. The ^1H NMR spectrum of the product shows somewhat broadened peaks at 6.3 and 2.9 ppm in a ca. 1:2 peak area ratio, indicating the structure $-\text{[CH}_2\text{C}-$

(6) (a) Werner, H.; Fraser, R. *Angew. Chem., Int. Ed. Engl.* **1979**, *18*, 157. (b) Werner, H.; Fraser, R. *J. Organomet. Chem.* **1982**, *232*, 351. (c) Byrne, J. W.; Blaser, H. J.; Osborn, J. A. *J. Am. Chem. Soc.* **1975**, *97*, 3871. (d) Byrne, J. W.; Kress, J. R.; Osborn, J. A.; Picard, L.; Weiss, R. E. *J. Chem. Soc., Chem. Commun.* **1977**, 662. (e) Yamamoto, T.; Miyashita, S.; Naito, Y.; Komiya, S.; Ito, T.; Yamamoto, A. *Organometallics* **1982**, *1*, 808. (f) Brookhart, M.; Lincoln, D. M.; Bennett, M. A.; Pelling, S. *J. Am. Chem. Soc.* **1990**, *112*, 2691. (g) Brookhart, M.; Hauptman, E.; Lincoln, D. M. *J. Am. Chem. Soc.* **1992**, *114*, 10394.

(7) Bönemann, H.; Grard, C.; Kopp, W.; Wilke, G. *Pure Appl. Chem.* **1971**, *23*, 265.

(5) Osakada, K.; Matsumoto, K.; Yamamoto, T.; Yamamoto, A. *Organometallics* **1985**, *4*, 857.

Table 2. Crystal Data and Details of the Structure Refinement

	1	2
formula	C ₄₁ H ₃₇ O ₂ P ₂ Rh	C ₄₆ H ₃₉ OP ₂ Rh
mw	726.60	772.67
cryst size (mm)	0.30 × 0.35 × 0.40	0.35 × 0.40 × 0.40
cryst syst	triclinic	triclinic
space group	P1 (No. 2)	P1 (No. 2)
a (Å)	11.938(7)	12.078(3)
b (Å)	15.725(8)	15.690(4)
c (Å)	10.216(6)	10.958(2)
α (deg)	90.85(5)	99.14(2)
β (deg)	106.47(5)	109.15(2)
γ (deg)	107.16(4)	77.14(2)
V (Å ³)	1746	1904
Z	2	2
T (°C)	23	23
λ (Å)	0.710 69	0.710 69
d _{calcd} (g cm ⁻³)	1.381	1.348
μ (cm ⁻¹)	6.03	5.66
F(000)	748	796
R	0.034	0.035
R _w ^a	0.030	0.028
no. of variables	415	451
no. of unique rflns	6152	6700
no. of obsd rflns	4902	4915
(I > 3σ(I))		

$$^a w = [\sigma(F_o)]^{-2}.$$

(=CHPh)_n-. GPC traces of the polymers show that M_n and M_w are 1.8 and 2.0×10^3 based on a polystyrene standard. Similar results between the reactions using RhH(CO)(PPh₃)₃ and **2** indicate that RhH(CO)(PPh₃)₃-catalyzed polymerization of phenylallene involves initial formation of **2** through insertion of a double bond into the Rh-H bond.

Experimental Section

Materials and Measurement. All the manipulations of the complexes were carried out under nitrogen or argon using standard Schlenk techniques. The solvents were dried by the usual method, distilled, and stored under nitrogen. IR spectra were recorded on a JASCO IR810 spectrophotometer. NMR spectra (¹H and ¹³C) were recorded on JEOL EX-90 and -400 spectrometers. Elemental analyses were carried out on a Yanagimoto Type MT-2 CHN autocorder. Phenylallene, methoxyallene, and RhH(CO)(PPh₃)₃ were prepared according to the literature.^{8,9} RhD(CO)(PPh₃)₃ was prepared by NaBD₄ reduction of RhCl(CO)(PPh₃)₃ in EtOD according to the procedure for preparation of RhH(CO)(PPh₃)₃. ¹H and ²H NMR spectra of the complex in C₆D₆ indicated deuteration higher than 90% and no H-D scrambling between the hydrido ligand and PPh₃ hydrogens in benzene solution.

Reaction of RhH(CO)(PPh₃)₃ with Methoxyallene. To a toluene (8 mL) solution of RhH(CO)(PPh₃)₃ (290 mg, 0.32 mmol) was added methoxyallene (33 mg, 0.48 mmol) at room temperature. After the reaction mixture was stirred for 2 h, the solvent was removed under vacuum. The resulting oily material was washed repeatedly with hexane to give **1** as a yellow solid (160 mg, 69%). Similar reaction of the complex and methoxyallene in a 1:3 molar ratio at -30 °C gave **1** in higher yield (92%). IR (KBr): 1925 cm⁻¹ (ν(CO)). ¹H NMR (400 MHz in CD₂Cl₂ at 25 °C): δ 7.7–7.0 (m, 30H, C₆H₅), 4.63

(dd, 1H, H_d, J(H_dH_c) = 7 Hz, J(H_dRh) = 2 Hz), 4.45 (dddd, 1H, H_e, J(H_eH_d) = J(H_eH_a) = J(H_eH_b) = 7 Hz, J(H_eRh) = 2 Hz), 3.39 (s, 3H, OCH₃), 0.9 (br, 2H, H_a and H_b). ¹H NMR (400 MHz in CD₂Cl₂ at -70 °C): δ 7.7–7.0 (m, 30H, C₆H₅), 4.30 (m, 1H, H_e), 4.26 (br, 1H, H_d), 3.30 (s, 3H, OCH₃), 1.20 (dd, 1H, H_b, J(H_bH_c) = 6 Hz, J(H_bP) = 9 Hz), -0.08 (dd, 1H, H_a, J(H_aH_c) = 8 Hz, J(H_aP) = 23 Hz). ¹³C{¹H} NMR (100 MHz in C₆D₆ at 25 °C): δ 201.9 (CO, J(CRh) = 72 Hz), 111.4 (CHO, J(CH) = 184 Hz), 69.4 (CH, J(CH) = 173 Hz), 58.1 (OCH₃, J(CH) = 143 Hz), 35.2 (CH₂, J(CH) = 153 Hz). The ¹H and ¹³C{¹H} COSY NMR spectra agreed well with the above assignment of the ¹H and ¹³C{¹H} NMR peaks. Anal. Found (calcd) for C₄₁H₃₇O₂P₂Rh: C, 67.6 (67.8); H, 5.3 (5.1).

Reaction of RhH(CO)(PPh₃)₃ with Phenylallene. To a toluene (10 mL) solution of RhH(CO)(PPh₃)₃ (430 mg, 0.47 mmol) was added phenylallene (65 mg, 0.56 mmol) at room temperature. After the reaction mixture was stirred for 2 h, the solvent was removed under vacuum. The resulting oily material was washed repeatedly with hexane to give **2** as a yellow solid (310 mg, 85%). IR (KBr): 1945 cm⁻¹ (ν(CO)). ¹H NMR (90 MHz in C₆D₆ at 25 °C): δ 7.5–6.7 (m, 35H, C₆H₅), 5.15 (dddd, 1H, H_e, J(H_eH_d) = 9 Hz, J(H_eH_a) = J(H_eH_b) = 7 Hz, J(H_eRh) = 2 Hz), 3.70 (d, 1H, H_d, J(H_dH_c) = 9 Hz), 1.6 (br, 2H, H_a and H_b). ¹H NMR (400 MHz in CD₂Cl₂ at -70 °C): δ 7.7–7.0 (m, 35H, C₆H₅), 4.61 (br, H_c), 3.18 (ddd, H_d, J(H_dH_c) = 9 Hz, J(H_dP) = 15 and 7 Hz), 1.53 (dd, H_b, J(H_bH_c) = 6 Hz, J(H_bP) = 10 Hz), 0.54 (dd, H_a, J(H_aH_c) = 8 Hz, J(H_aP) = 21 Hz). ¹³C{¹H} NMR (100 MHz in C₆D₆ at 25 °C): δ 201.0 (CO, J(CRh) = 72 Hz), 83.9 (CHPh), 71.1 (CH), 42.9 (CH₂). Anal. Found (calcd) for C₄₅H₃₉O₂P₂Rh: C, 71.0 (71.5); H, 4.4 (5.1).

X-ray Crystallographic Study. Crystals of **1** and **2** suitable for crystallography were obtained by recrystallization from Et₂O at -20 °C. Crystal data and results of structural refinement were summarized in Table 2. The data were collected on a Rigaku AFC5R diffractometer at ambient temperature (23 °C) using the ω scan mode (2θ ≤ 50°). Correction for Lorentz and polarization effects and an empirical absorption correction (ψ scan) were applied. The structure was solved by a common combination of direct methods (SAPI 91) and subsequent Fourier techniques. The positional and thermal parameters of non-hydrogen atoms were refined anisotropically, while hydrogen atoms were located by assuming the ideal geometry.

Polymerization of Phenylallene. To a toluene (4 mL) solution of RhH(CO)(PPh₃)₃ (46 mg, 0.050 mmol) and PPh₃ (26 mg, 0.10 mmol) was added phenylallene (120 mg, 1.0 mmol) at room temperature. After the reaction mixture was stirred at 60 °C for 19 h, the solvent was reduced to ca. 1 mL under vacuum. The resulting reaction mixture was slowly poured into MeOH (ca. 150 mL) with stirring. The resulting off-white solid was filtered, washed with MeOH repeatedly and dried in vacuo (44 mg, 38%).

Polymerization using **2** as the catalyst gave the polymer product in 47% yield.

Acknowledgment. This work was supported by a Grant-in-Aid for Scientific Research from the Ministry of Education, Science, and Culture of Japan. We are grateful to Dr. Masako Tanaka for the crystallographic study.

Supporting Information Available: Tables giving crystallographic data for complexes **1** and **2** (35 pages). This material is contained in many libraries on microfiche, immediately follows this article in the microfilm version of the journal, and can be ordered from the ACS; see any current masthead page for ordering information.

OM9503510

(8) Hallman, P. S.; Evans, D.; Osborn, J. A.; Wilkinson, G. *J. Chem. Soc., Chem. Commun.* **1967**, 305.

(9) (a) Moreau, J. L.; Gaudemar, M. *J. Organomet. Chem.* **1976**, *108*, 159. (b) Roppe, W. *Justus Liebigs Ann. Chem.* **1955**, *74*, 596. (c) Hoff, S.; Brandsma, L.; Arens, J. K. *Recl. Trav. Chim. Pays-Bas* **1974**, *27*, 295.

Alkyl(hydrido)platinum(IV) Complexes: The Mechanism of Pt-C Bond Protonolysis

Geoffrey S. Hill, Louis M. Rendina, and Richard J. Puddephatt*

Department of Chemistry, The University of Western Ontario,
London, Ontario, Canada N6A 5B7

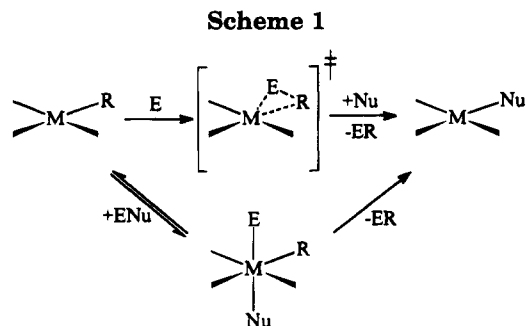
Received May 31, 1995*

Summary: The complexes $[\text{PtMe}_2(\text{N}-\text{N})]$ $\{\text{N}-\text{N} = \textit{t}\text{bu}_2\text{-bpy}$ (4,4'-di-*tert*-butyl-2,2'-bipyridine), *bpy* (2,2'-bipyridine), or *phen* (1,10-phenanthroline) $\}$ react with HX ($\text{X} = \text{Cl, Br, I, O}_2\text{CCF}_3, \text{SO}_3\text{CF}_3$) to yield $[\text{PtXMe}(\text{N}-\text{N})]$ and CH_4 , by an oxidative addition/reductive elimination mechanism. The new alkyl(hydrido)platinum(IV) intermediates $[\text{PtCl}(\text{H})\text{Me}_2(\textit{t}\text{bu}_2\text{bpy})]$ (1), $[\text{PtBr}(\text{H})\text{Me}_2(\textit{t}\text{bu}_2\text{bpy})]$ (2), $[\text{PtH}(\text{I})\text{Me}_2(\textit{t}\text{bu}_2\text{bpy})]$ (3), and $[\text{PtCl}(\text{H})\text{Me}_2(\textit{t}\text{bu}_2\text{bpy})]$ (4), formed by *trans* oxidative addition of HX , have been fully characterized at -78°C by ^1H NMR spectroscopy. Rapid reductive elimination of CH_4 ensues at higher temperatures to yield the corresponding organoplatinum(II) products $[\text{PtXMe}(\text{N}-\text{N})]$. The thermal stability of the platinum(IV) intermediates follows the sequence $\text{X} = \text{Cl} > \text{Br} > \text{I} > \text{O}_2\text{CCF}_3, \text{SO}_3\text{CF}_3$.

Introduction

The cleavage of metal-carbon σ -bonds by electrophiles is of fundamental importance in organometallic chemistry, and the mechanism of this process has been the subject of several thorough investigations.¹ With non-transition metals, the cleavage is believed to occur *via* the $\text{S}_{\text{E}}2$ mechanism which involves direct electrophilic attack at the M-C bond.¹ In alkyltransition metal complexes, the highest occupied molecular orbital (HOMO) may be either the M-C bonding orbital or a nonbonding d-orbital. Attack at the M-C bond gives cleavage by the classical $\text{S}_{\text{E}}2$ mechanism, but the same product can be obtained by attack at the metal center (oxidative addition) followed by reductive elimination of the corresponding alkane (Scheme 1).¹ In the case of protonolysis of alkylplatinum(II) bonds, arguments have been put forward in favor of both mechanisms.¹ For example, in the case of $[\text{PtR}_2(\text{PR}_3)_2]$, studies of selectivity in cleavage of alkyl or aryl groups from platinum(II) support an oxidative addition/reductive elimination mechanism^{1d} whereas kinetic studies indicate an $\text{S}_{\text{E}}2$ mechanism.^{1b} The most definitive evidence for the oxidative addition mechanism would be the detection of the proposed alkyl(hydrido)platinum(IV) intermediate, but this has proved difficult owing to the facile reductive elimination of the alkane.

There are few examples of hydridoplatinum(IV) complexes in the literature,² and the first alkyl(hydrido)-



platinum(IV) complexes $\{[\text{PtX}(\text{H})\text{R}_2(\text{dmphen})], \text{X} = \text{Cl, Br}; \text{R} = \text{Me, 4-MeOC}_6\text{H}_4; \text{dmphen} = 2,9\text{-dimethyl-1,10-phenanthroline}\}$ were reported very recently.^{2a,f} In this paper, we describe the reactions of $[\text{PtMe}_2(\text{N}-\text{N})]$ $\{\text{N}-\text{N} = \textit{t}\text{bu}_2\text{bpy}$ (4,4'-di-*tert*-butyl-2,2'-bipyridine), *bpy* (2,2'-bipyridine), or *phen* (1,10-phenanthroline) $\}$ with HX ($\text{X} = \text{Cl, Br, I, O}_2\text{CCF}_3, \text{SO}_3\text{CF}_3$) to ultimately yield $[\text{PtMeX}(\text{N}-\text{N})]$ and CH_4 . In several cases, the alkyl(hydrido)platinum(IV) intermediate proposed in Scheme 1 was detected and fully characterized by low-temperature ^1H NMR spectroscopy. This work therefore provides further support for the oxidative addition/reductive elimination mechanism for the electrophilic cleavage of metal-carbon σ -bonds.

Experimental Section

All ^1H NMR spectra were recorded at -78°C using a Varian Gemini 300 MHz spectrometer and are referenced to the residual protons of the deuterated solvents. Chemical shifts are reported in ppm relative to TMS.

The complexes $[\text{PtMe}_2(\textit{t}\text{bu}_2\text{bpy})]$ ³ and $[\text{PtMe}_2(\textit{t}\text{bu}_2\text{bpy})]$ ⁴ were prepared by the literature methods. The complexes $[\text{PtClMe}(\textit{t}\text{bu}_2\text{bpy})]$,⁶ $[\text{PtClMe}(\textit{t}\text{bu}_2\text{bpy})]$,⁵ $[\text{PtBrMe}(\textit{t}\text{bu}_2\text{bpy})]$,⁶ and $[\text{PtIme}(\textit{t}\text{bu}_2\text{bpy})]$ ⁶ were characterized by comparing their ^1H NMR spectra to those of authentic samples.

Reaction of $[\text{PtMe}_2(\textit{t}\text{bu}_2\text{bpy})]$ with HCl . To a 5 mm NMR tube charged with a solution of $[\text{PtMe}_2(\textit{t}\text{bu}_2\text{bpy})]$ (0.030g,

(2) For example, see: (a) De Felice, V.; De Renzi, A.; Panunzi, A.; Tesaro, D. *J. Organomet. Chem.* **1995**, *488*, C13. (b) Wehman-Ooyevaar, I. C. M.; Grove, D. M.; de Vaal, P.; Dedieu, A.; van Koten, G. *Inorg. Chem.* **1992**, *31*, 5484. (c) Ebsworth, E. A. V.; Marganian, V. M.; Reed, F. J. S. *J. Chem. Soc., Dalton Trans.* **1978**, 1167. (d) Ebsworth, E. A. V.; Rankin, D. W. H. *J. Chem. Soc., Dalton Trans.* **1973**, 854. (e) Bentham, J. E.; Craddock, S.; Ebsworth, E. A. V. *J. Chem. Soc. A* **1971**, 587. (f) Stahl, S. S.; Labinger, J. A.; Bercaw, J. E. *J. Am. Chem. Soc.*, in press.

(3) Achar, S.; Scott, J. D.; Vittal, J. J.; Puddephatt, R. J. *Organometallics* **1993**, *12*, 4592.

(4) Monaghan, P. K.; Puddephatt, R. J. *Organometallics* **1984**, *3*, 444.

(5) Rendina, L. M.; Vittal, J. J.; Puddephatt, R. J. *Organometallics* **1995**, *14*, 1030.

(6) Note that under rigorously anhydrous conditions oxidative addition of the Si-X bond occurs, but this is much slower. Levy, C. J.; Puddephatt, R. J.; Vittal, J. J. *Organometallics* **1994**, *13*, 1559, and unpublished results.

* Abstract published in *Advance ACS Abstracts*, September 15, 1995.

(1) (a) Alibrandi, G.; Minniti, D.; Romeo, R.; Uguagliati, P.; Calligaro, L.; Belluco, U. *Inorg. Chim. Acta* **1986**, *112*, L15. (b) Alibrandi, G.; Minniti, D.; Romeo, R.; Uguagliati, P.; Calligaro, L.; Belluco, U.; Crociani, B. *Inorg. Chim. Acta* **1985**, *100*, 107. (c) Belluco, U.; Michelin, R. A.; Uguagliati, P.; Crociani, B. *J. Organomet. Chem.* **1983**, *250*, 565. (d) Jawad, J. K.; Puddephatt, R. J.; Stalteri, M. A. *Inorg. Chem.* **1982**, *21*, 332. (e) Uguagliati, P.; Michelin, R. A.; Belluco, U.; Ros, R. *J. Organomet. Chem.* **1979**, *169*, 115. (f) Johnson, M. D. *Acc. Chem. Res.* **1978**, *11*, 57. (g) Romeo, R.; Minniti, D.; Lanza, S.; Uguagliati, P.; Belluco, U. *Inorg. Chem.* **1978**, *17*, 2813. (h) Belluco, U.; Giustiniani, M.; Graziani, M. *J. Am. Chem. Soc.* **1967**, *89*, 6494. (i) Belluco, U.; Croatto, U.; Uguagliati, P.; Peitropolo, R. *Inorg. Chem.* **1967**, *6*, 718. (j) Falk, C. D.; Halpern, J. *J. Am. Chem. Soc.* **1965**, *87*, 3523.

Table 1. Selected ^1H NMR^a Spectroscopic Data for Complexes 1–4

complex	^1H δ			
	N–N aromatic	<i>bu</i>	Pt–Me	Pt–H
1	8.75 [d, 2H, $^3J_{\text{H}^6\text{H}^5} = 5.8$, H ⁶], 8.17 [br s, 2H, H ³], 7.63 [br d, 2H, $^3J_{\text{H}^6\text{H}^5} = 5.8$, H ⁵]	1.37 [s, 18H]	1.23 [s, 6H, $^2J_{\text{PtH}} = 67.0$]	-21.80 [s, 1H, $^1J_{\text{PtH}} = 1589.7$]
2	8.76 [d, 2H, $^3J_{\text{H}^6\text{H}^5} = 5.7$, H ⁶], 8.14 [br s, 2H, H ³], 7.61 [br d, 2H, $^3J_{\text{H}^6\text{H}^5} = 5.7$, H ⁵]	1.35 [s, 18H]	1.34 [s, 6H]	-20.90 [s, 1H, $^1J_{\text{PtH}} = 1630.5$]
3	8.77 [d, 2H, $^3J_{\text{H}^6\text{H}^5} = 5.9$, H ⁶], 8.14 [br s, 2H, H ³], 7.60 [br d, 2H, $^3J_{\text{H}^6\text{H}^5} = 5.9$, H ⁵]	1.39 [s, 18H]	1.41 [s, 6H, $^2J_{\text{PtH}} = 67.5$]	-19.16 [s, 1H, $^1J_{\text{PtH}} = 1655.5$]
4	8.78 [br m, 2H], 8.26 [br m, 2H], 8.10 [br m, 2H], 7.63 [br m, 2H]		1.28 [s, 6H, $^2J_{\text{PtH}} = 68.3$]	-21.65 [s, 1H, $^1J_{\text{PtH}} = ca. 1591$]

^a In CD_2Cl_2 at -78 °C. Quoted multiplicities do not include ^{195}Pt satellite signals. Coupling constants are given in Hz.

0.061 mmol) in CD_2Cl_2 at -78 °C was added Me_3SiCl (7.70 μL , 0.061 mmol). Distilled H_2O (1.1 μL , 0.061 mmol) was added to the cold solution, thus hydrolyzing the Me_3SiCl to afford 1 equiv of HCl. The progress of the reaction was followed by ^1H NMR spectroscopy, and, within 5 min, the presence of $[\text{PtCl}(\text{H})\text{Me}_2(\text{bu}_2\text{bpy})]$ (1) was detected. ^1H NMR of 1 in CD_2Cl_2 : $\delta = 8.75$ [d, 2H, $^3J_{\text{H}^6\text{H}^5} = 5.8$ Hz, H⁶], 8.17 [br s, 2H, H³], 7.63 [br d, 2H, $^3J_{\text{H}^6\text{H}^5} = 5.8$ Hz, H⁵], 1.37 [s, 18H, *bu*], 1.23 [s, 6H, $^2J_{\text{PtH}} = 67.0$ Hz, Pt–Me], -21.80 [s, 1H, $^1J_{\text{PtH}} = 1589.7$ Hz, Pt–H]. Compound 1 was indefinitely stable at -78 °C, but it decomposed rapidly at 0 °C to give CH_4 and $[\text{PtClMe}(\text{bu}_2\text{bpy})]$.⁵

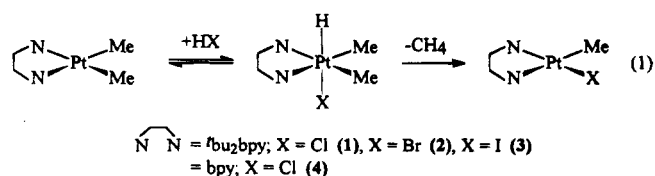
Reaction of $[\text{PtMe}_2(\text{bu}_2\text{bpy})]$ with HBr. In a similar reaction to that described above, $[\text{PtMe}_2(\text{bu}_2\text{bpy})]$, Me_3SiBr , and distilled H_2O were reacted in CD_2Cl_2 at -78 °C to afford $[\text{PtBr}(\text{H})\text{Me}_2(\text{bu}_2\text{bpy})]$ (2) within 5 min. ^1H NMR of 2 in CD_2Cl_2 : $\delta = 8.76$ [d, 2H, $^3J_{\text{H}^6\text{H}^5} = 5.7$ Hz, H⁶], 8.14 [br s, 2H, H³], 7.61 [br d, 2H, $^3J_{\text{H}^6\text{H}^5} = 5.7$ Hz, H⁵], 1.35 [s, 18H, *bu*], 1.34 [s, 6H, ^{195}Pt satellite signals are obscured, Pt–Me], -20.90 [s, 1H, $^1J_{\text{PtH}} = 1630.5$ Hz, Pt–H]. Compound 2 decomposed to the yellow $[\text{PtBrMe}(\text{bu}_2\text{bpy})]$ ⁶ within 10 min at -78 °C.

Reaction of $[\text{PtMe}_2(\text{bu}_2\text{bpy})]$ with HI. In a similar reaction to that described above, $[\text{PtMe}_2(\text{bu}_2\text{bpy})]$, Me_3SiI , and distilled H_2O were reacted in CD_2Cl_2 at -78 °C to afford $[\text{PtI}(\text{H})\text{Me}_2(\text{bu}_2\text{bpy})]$ (3). ^1H NMR of 3 in CD_2Cl_2 : $\delta = 8.77$ [d, 2H, $^3J_{\text{H}^6\text{H}^5} = 5.9$ Hz, H⁶], 8.14 [br s, 2H, H³], 7.60 [br d, 2H, $^3J_{\text{H}^6\text{H}^5} = 5.9$ Hz, H⁵], 1.41 [s, 6H, $^2J_{\text{PtH}} = 67.5$ Hz, Pt–Me], 1.39 [s, 18H, *bu*], -19.16 [s, 1H, $^1J_{\text{PtH}} = 1655.5$ Hz, Pt–H]. Complex 3 decomposed to the yellow $[\text{PtI}(\text{Me})_2(\text{bu}_2\text{bpy})]$ ⁶ within 5 min at -78 °C.

Reaction of $[\text{PtMe}_2(\text{bpy})]$ with HCl. To a 5 mm NMR tube charged with a solution of $[\text{PtMe}_2(\text{bpy})]$ (0.005 g, 0.013 mmol) in CD_2Cl_2 at -78 °C was added Me_3SiCl (1.60 μL , 0.013 mmol). Distilled H_2O (0.2 μL , 0.013 mmol) was added to the cold solution, thus hydrolyzing the Me_3SiCl to afford 1 equiv of HCl. The progress of the reaction was followed by ^1H NMR spectroscopy, and, within 5 min, the presence of $[\text{PtCl}(\text{H})\text{Me}_2(\text{bpy})]$ (4) was clearly detected. ^1H NMR of 4 in CD_2Cl_2 : $\delta = 8.78$ [br m, 2H], 8.26 [br m, 2H], 8.10 [br m, 2H], 7.63 [br m, 2H], 1.28 [s, 6H, $^2J_{\text{PtH}} = 68.3$ Hz, Pt–Me], -21.65 [s, 1H, $^1J_{\text{PtH}} = ca. 1591$ Hz, Pt–H]. Compound 4 was indefinitely stable at -78 °C, but it decomposed by reductive elimination of CH_4 at 0 °C to afford $[\text{PtClMe}(\text{bpy})]$.⁶

Results and Discussion

The reaction of Me_3SiX (X = Cl, Br, I) and H_2O (to generate HX *in situ*) with $[\text{PtMe}_2(\text{N–N})]$ (N–N = *bu*₂bpy, bpy) affords the novel alkyl(hydrido)platinum(IV) complexes 1–4 (eq 1).⁶ Compounds 1–4 are all unstable



at room temperature owing to the easy decomposition by reductive elimination of CH_4 to give the corresponding platinum(II) complex $[\text{PtMeX}(\text{N–N})]$, and so they were characterized by ^1H NMR spectroscopy at -78 °C. The evolution of CH_4 was confirmed by GC–MS.

Selected ^1H NMR spectroscopic data for complexes 1–4 are presented in Table 1. The ^1H NMR spectrum of 1 is presented in Figure 1. The proposed *trans* stereochemistry for the alkyl(hydrido)platinum(IV) complexes 1–4 is strongly supported by ^1H NMR spectroscopic evidence. The spectra of 1–3 show the expected three sets aromatic resonances due to the equivalent nature of the two pyridyl moieties of the *bu*₂bpy ligand. Similarly, the spectrum of 4 displays four sets of aromatic signals. In each of the complexes only one Pt–Me resonance is observed at high field, again only consistent with the *trans* stereochemistry. These Pt–Me resonances possess ^{195}Pt satellite signals with the magnitude of $^2J_{\text{PtH}}$ (67.0–68.3 Hz) indicative of an organoplatinum(IV) center.^{5,9} There is only one *tert*-butyl resonance in each of the ^1H NMR spectra of complexes 1–3, thus further supporting a *trans* arrangement of HX about the platinum. In contrast to our results, the only other examples of six-coordinate alkyl(hydrido)platinum(IV) species in the literature ($[\text{PtX}(\text{H})\text{R}_2(\text{dmphen})]$, X = Cl, Br; R = Me, 4-MeOC₆H₄; dmphen = 2,9-dimethyl-1,10-phenanthroline) possess *cis* stereochemistry of the H and X ligands about the metal center.^{2a} This difference is certainly a consequence of the diimine ligand employed. The bulky methyl groups of dmphen introduce large interligand steric constraints in the platinum–(N–N) plane that are absent when *bu*₂bpy and bpy are employed.¹⁰ We believe that these constraints most likely promote the *cis* geometry observed in complexes of the type $[\text{PtX}(\text{H})\text{R}_2(\text{dmphen})]$, since the hydride occupies a more sterically encumbered site. The ^1H NMR spectra of 1–4 show the expected low-frequency hydride resonances with ^{195}Pt satellite signals. The large $^1J_{\text{PtH}}$ (1589.7–1655.5 Hz) is similar to that reported in the literature for related compounds,^{2a,b} and, as expected, its magni-

(7) Collman, J. P.; Hegedus, L. S.; Norton, J. R.; Finke, R. G. *Principles and Applications of Organotransition Metal Chemistry*; University Science Books: Mill Valley, CA, 1987; p 326.

(8) (a) Borkovskii, N. B.; Kovrilov, A. B.; Lipnitskii, I. V.; Umreiko, D. S. *Koord. Khim.* **1982**, *8*, 523. (b) Mortimer, C. T.; Wilkinson, M. P.; Puddephatt, R. J. *J. Organomet. Chem.* **1979**, *165*, 269.

(9) For example, see: (a) Anderson, C. M.; Crespo, M.; Jennings, M. C.; Lough, A. J.; Ferguson, G.; Puddephatt, R. J. *J. Organometallics* **1991**, *10*, 2672. (b) Monaghan, P. K.; Puddephatt, R. J. *J. Chem. Soc., Dalton Trans.* **1988**, 595. (c) Crespo, M.; Puddephatt, R. J. *J. Organometallics* **1987**, *6*, 2548. (d) Jawad, J.; Puddephatt, R. J. *J. Chem. Soc., Dalton Trans.* **1977**, 1466. (e) Kuyper, J. *Inorg. Chem.* **1977**, *16*, 2171. (f) Jawad, J.; Puddephatt, R. J. *J. Organomet. Chem.* **1976**, *117*, 297.

(10) Albano, V. G.; Natile, G.; Panunzi, A. *Coord. Chem. Rev.* **1994**, *133*, 67.

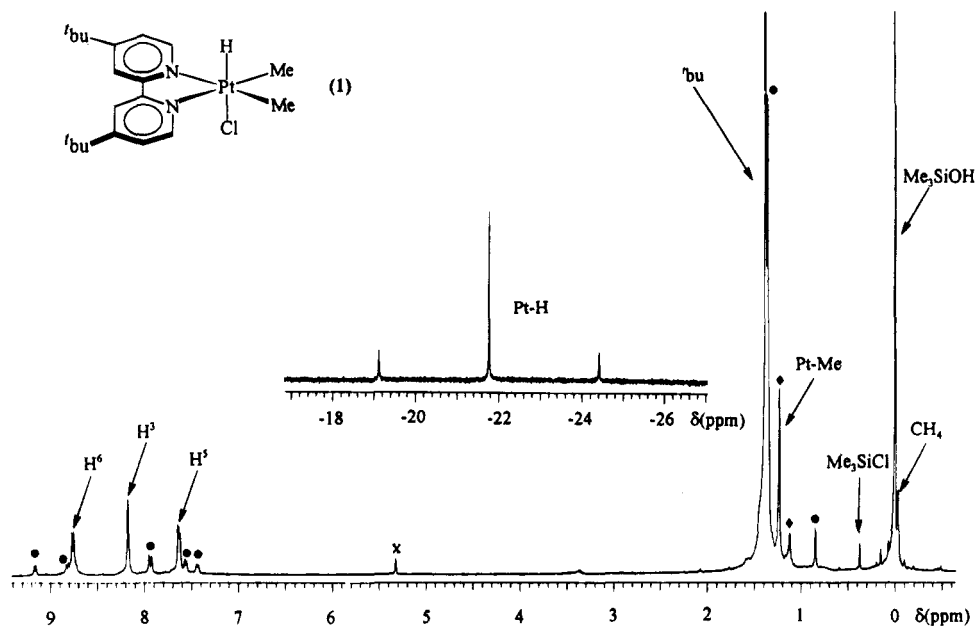


Figure 1. The ^1H NMR spectrum of **1** in CD_2Cl_2 at -78°C . The x and the ● denote the residual protons of the solvent and $[\text{PtClMe}(\text{tert}\text{-bu})_2\text{bpy}]$, respectively.

tude is strongly dependent on the ligand *trans* to the hydride (X). For complexes **1–4**, the magnitude of $^1J_{\text{PtH}}$ follows a similar trend to that reported in the literature and increases as the nature of X is changed from Cl to Br to I.^{2d,11}

Studies with $[\text{PtMe}_2(\text{N–N})]$ (N–N = bpy, X = Br, I; N–N = phen, X = Cl, Br, I) complexes were more difficult or impossible owing to the low solubilities of both the reactants and products at low temperatures. Indeed, the *tert*-butyl groups in *tert*-bu₂bpy greatly assist in the solubility of both the intermediates and the products in CD_2Cl_2 .

The stability of the organoplatinum(IV) species toward reductive elimination appears to be largely a function of the nature of the ligand *trans* to the hydride, i.e., the X group. Qualitatively, the observed rate of reductive elimination for the platinum(IV) species follows the order $1 \approx 4 < 2 < 3$. In addition, attempts to detect the hydridoplatinum(IV) intermediate in reactions of $[\text{PtMe}_2(\text{tert}\text{-bu})_2\text{bpy}]$ with HX (X = O_2CCF_3 , SO_3CF_3), in which cases the anion X[–] is a poor ligand for platinum, have been unsuccessful even in reactions carried out at -90°C . Hence, the first step of the

reductive elimination is most likely to be the dissociation of the Pt–X bond, yielding a five-coordinate intermediate $[\text{PtHMe}_2(\text{N–N})]^+$, which then undergoes reductive elimination;⁷ the rate then follows the order of Pt–X bond strengths, namely $\text{Pt–Cl} > \text{Pt–Br} > \text{Pt–I} > \text{Pt–O}_2\text{CCF}_3$, $\text{Pt–O}_3\text{SCF}_3$.^{6,8}

In conclusion, the reactions of HX with a series of $[\text{PtMe}_2(\text{N–N})]$ compounds to ultimately afford CH_4 and $[\text{PtXMe}(\text{N–N})]$ complexes were studied as a function of X and N–N. In several cases, alkyl(hydrido)platinum(IV) complexes were detected and fully characterized by low-temperature ^1H NMR spectroscopy. These compounds possess exclusively *trans* stereochemistry of the H and X ligands about the metal center. Complexes of this type are proposed intermediates in the mechanism of platinum(II)–carbon σ -bond protonolysis, and their detection provides further insight into this fundamentally important area of organometallic chemistry.

Acknowledgment. We thank the NSERC (Canada) for financial support to R.J.P., for a Canada International Fellowship to L.M.R., and for a Postgraduate Scholarship to G.S.H.

OM950404D

(11) Appleton, T. G.; Clark, H. C.; Manzer, L. E. *Coord. Chem. Rev.* **1973**, *10*, 335.